Knot Floer Homology, Folding Automata, *and the* Connect-Sum of Trefoils

Kevin Yeh

A Dissertation submitted to the Faculty of the

Department of Mathematics

in partial fulfillment of the requirements for the degree of

Doctor of Philosophy

Boston College

Morrissey College of Arts and Sciences

Graduate School

May, 2026

© Copyright 2026 Kevin Yeh

Knot Floer Homology, Folding Automata,
and the Connect-Sum of Trefoils

Kevin Yeh

Advisor: Prof. Dr. John A. Baldwin

We prove that knot Floer homology detects the connect-sum of two right-handed trefoil knots, $T_{2,3}\#T_{2,3}$ (the granny knot). This is the first detection result in knot Floer homology for a composite knot, and the second detection result for a knot of genus greater than one.

The proof proceeds by ruling out, in turn, each of the three Nielsen-Thurston classes that the monodromy of a hypothetical knot K with $\widehat{HFK}(K) \cong \widehat{HFK}(T_{2,3}\#T_{2,3})$ could occupy. The torus knot case is dispatched by a direct Alexander polynomial comparison. The bulk of the work is devoted to the hyperbolic case, which requires the systematic study of pseudo-Anosov maps on the six-marked disk via the theory of train tracks and folding automata.

To facilitate this analysis, we introduce the `autofolder` algorithm, a computational framework that, given a stratum of mapping classes on the n-punctured disk, exhaustively generates the complete directed graph of standard train tracks connected by elementary folding operations. The algorithm answers a call of Los for a generalized, algorithmic method to construct folding automata, and serves as an independent contribution to low-dimensional topology and topological dynamics.

Using the `autofolder` output, together with tight splitting, the Trace Lemma, and the Absorption Obstruction, we enumerate all candidate pseudo-Anosov mapping classes carried by the jointless standard train tracks in the relevant non-orientable strata $(3; 1^6; 3)$ and $(2; 1^6; 3^2)$. We then apply two homological filters — the zero-surgery condition and the Alexander polynomial condition — to eliminate every candidate. This rules out the possibility

that K is hyperbolic.

The remaining satellite case is handled by Schubert's formula and the classification of Thurston reducing systems, which restrict the pattern and companion of K to trefoil knots and the algebraic winding number to one. A short case analysis on the canonical reducing system, together with the fractional Dehn twist coefficient bound of Hedden–Mark and the right-veering criterion of Honda–Kazez–Matić, eliminates every remaining configuration except the connect-sum of two right-handed trefoils, completing the proof.

As a second result, the same toolkit applied to the cable target Alexander polynomial $\Phi_{12}(t) = t^4 - t^2 + 1$ yields a partial detection theorem for the $(2, 1)$-cable of the right-handed trefoil, $C_{2,1}(T_{2,3})$: any knot with the same knot Floer homology is isotopic to $C_{2,1}(T_{2,3})$ unless it is hyperbolic and the disk braid associated to its monodromy belongs to one of an explicitly enumerated finite list of candidate braid families.

List of Symbols

$\mathbb{Z}$	The integers
$\mathbb{F}_2$	The field with two elements; coefficient ring for $\widehat{\mathrm{HFK}}$
$\mathbb{Q}$	The rational numbers
$\mathbb{R}$	The real numbers
$\mathbb{C}$	The complex numbers
$\Sigma_{g,n}$	Orientable surface of genus g with n boundary components
D_n	The n-punctured disk
$\mathrm{Mod}(\Sigma)$	Mapping class group of the surface Σ
$\mathrm{PMod}(\Sigma)$	Pure mapping class group fixing punctures setwise
Tw_γ	Right-handed Dehn twist about the simple closed curve γ
τ	A train track on a surface
β	A branch of a train track

$\mathcal{Q}(\kappa)$	Stratum of quadratic differentials of singularity profile κ
$\mathcal{T}$	The set of standard train tracks in a fixed stratum
f_β	The folding (train-track) map of a pseudo-Anosov β
$f_\beta(e)$	Image of a branch e under the folding map
$\mathrm{Aut}(\tau)$	Folding automaton on standard train tracks
$\mathrm{Rule}(\beta)^\times$	Folding rule applied to β on the disk
$\mathrm{Abso}(a,b)^\times$	Absorption operator on neighboring branches
$K \subset S^3$	A knot
$T_{p,q}$	The (p,q)-torus knot
$T_{2,3}$	The right-handed trefoil knot $T_{2,3}$
$T_{2,3}\#T_{2,3}$	The granny knot, connect-sum of two trefoils
$C_{p,q}(K)$	The (p,q)-cable of K with respect to the Seifert framing
B_n	The braid group on n strands
ρ_n	The reduced Burau representation of B_n
$\Delta_K(t)$	The Alexander polynomial of K
$\Phi_n(t)$	The n-th cyclotomic polynomial

$\Phi_{12}(t)$	$t^4 - t^2 + 1$, governing $C_{2,1}(T_{2,3})$
$\widehat{\mathrm{HF}}(Y)$	Hat Heegaard Floer homology of a 3-manifold Y
$\widehat{\mathrm{HFK}}(K)$	Hat knot Floer homology of a knot K with $\mathbb{F}_2$ coefficients
$\widehat{\mathrm{HFK}}_d(K, s)$	Bigraded summand at Maslov grading d and Alexander grading s
$\tau(K)$	The Ozsváth–Szabó concordance invariant
$\mathrm{Spin}^{\mathrm{c}}(Y)$	The set of $\mathrm{Spin}^{\mathrm{c}}$ structures on Y
$\mathrm{FDTC}(K)$	Fractional Dehn twist coefficient of a fibered knot K
$\operatorname{rank} A$	Rank of an abelian group or $\mathbb{F}_2$-vector space A
g^{-1}	The inverse of g
id	The identity map
$\pitchfork$	Transverse intersection

Contents

List of Symbols **ii**

Acknowledgements **xxiii**

1 Introduction **1**

1.1 Summary of Results . . . 1

1.1.1 From Topology to Dynamics . . . 2

1.1.2 The Dynamical Obstruction . . . 3

1.1.3 Eliminating the Hyperbolic Case . . . 4

1.1.4 Eliminating the Satellite Case . . . 8

1.1.5 A Partial Detection Theorem for the $(2,1)$-Cable . . . 9

1.2 Applications . . . 11

1.2.1 Botany of Genus-Two Fibered Knots . . . 11

1.2.2 The Granny as the Unique Composite Almost L-Space Knot . . . 12

1.2.3 Enumerating Pseudo-Anosovs of Bounded Dilatation . . . 13

1.3 Outline of the Chapters . . . 14

2 Preliminaries **17**

2.1 Notation and Conventions . . . 18

2.2 Fibered Knots and Knot Floer Homology . . . 19

2.3 Pseudo-Anosov Maps . . . 26

2.3.1 Fractional Dehn Twist Coefficient . . . 28

2.4 Fibered Hyperbolic Knots . . . 29

2.5 The Birman-Hilden Correspondence and Monodromy Descent . . . 33

2.5.1 Fixed Point Dynamics of the Capped Monodromy . . . 35

2.5.2 The Induced Map on the Disk . . . 37

2.5.3 The Fixed-Point-Free Lift ϕ_Φ . . . 38

2.5.4 General Framework: Braids and Prongs . . . 39

2.6 Strata . . . 42

2.6.1 Two prongs on z and p . . . 45

2.6.2 Three prongs on z and p . . . 45

2.6.3 Four prongs on z and p 45
2.7 Summary 46

3 Train Tracks **48**
3.1 Train Tracks on a Compact Surface 49
3.1.1 The Underlying Graph 50
3.2 Train Track Maps and Dynamics 51
3.2.1 Carrying and Fibered Neighborhoods 51
3.2.2 Train Paths and Maps 52
3.3 Relationship to Invariant Foliations 57
3.4 Real and Infinitesimal Edges 58
3.5 Standard Train Tracks on the Marked Disk 61
3.6 Jointless Train Tracks 63
3.7 Lifting Train Track Maps 65
3.7.1 Geometric Lifting of Standard Tracks 65
3.7.2 Smoothing Infinitesimal Polygons at Branch Points 68
3.7.3 The Trace Lemma 69

4 The Hyperbolic Case: The Strata $(2;1^4,2^2;\emptyset)$, $(4;1^6;\emptyset)$, and $(2;1^6;4)$ on the Disk **73**
4.1 Introduction 73
4.2 Orientability of Train Tracks 75
4.3 Application to $T_{2,3}\#T_{2,3}$ 80
4.4 Conclusion 81

5 Folding Automata on the Disk **85**
5.1 Folding and The Folding Automaton 86
5.1.1 Elementary Folding 86

5.1.2 The Standardizing Braid . . . 89
5.1.3 The Folding Automaton . . . 90
5.1.4 Proof of Completeness and Termination . . . 95
5.2 Computational Implementation: `autofolder` . . . 98
5.2.1 Combinatorial Structure and Equivalence . . . 98
5.2.2 Data Structures . . . 101
5.2.3 Implementation of Detecting Combinatorial Equivalence . . . 102
5.2.4 Implementation of the Folding Operation . . . 103
5.2.5 Extended Automaton Capabilities . . . 105
5.2.6 The `autofolder` Enumeration Algorithm . . . 105
5.3 Conclusion . . . 107

6 Tight Splitting and Jointless Tracks 108
6.1 Splitting Standard Train Tracks . . . 109
6.1.1 Branches at a switch . . . 110
6.1.2 Tight Splitting and Stability . . . 111
6.1.3 Dynamics and the Transition Matrix . . . 113
6.2 Switch Rigidity and Existence of Splits . . . 116
6.2.1 Ruling out splitting loops . . . 117
6.3 Conclusion . . . 123

7 The Hyperbolic Case: The Strata $(3;1^6;3)$ and $(2;1^6;3^2)$ on the Disk 125
7.1 Introduction . . . 125
7.2 Topological Constraints on Train Track Maps . . . 127
7.2.1 The Trace Lemma . . . 127
7.2.2 The Absorption Obstruction . . . 129
7.2.3 The Case Analysis Procedure . . . 131
7.2.4 Path Notation and The Two Triangles . . . 133

7.3 Homological Filtering of Candidate Braids . . . 155
7.3.1 The Action on Homology . . . 156
7.3.1.1 Explicit Matrix Representation . . . 157
7.3.2 Invariance Properties of the Filters . . . 159
7.3.3 Verification via Zero-Surgery . . . 160
7.3.4 Verification via the Alexander Polynomial . . . 160
7.4 The Stratum $(3; 1^6; 3)$ . . . 162
7.4.1 Reducing Candidate Train Tracks via Splitting . . . 163
7.4.2 Enumeration of Train Track Maps and Braids . . . 164
7.4.3 Proof of the Main Elimination Theorem . . . 165
7.5 The Stratum $(2; 1^6; 3^2)$ . . . 166
7.5.1 Reducing Candidate Train Tracks via Splitting . . . 166
7.5.2 Enumeration of Train Track Maps and Braids . . . 168
7.5.3 Proof of the Main Elimination Theorem . . . 169

8 The Satellite Case 176

8.1 Schubert's Formula on the Alexander polynomial of a Satellite Knot . . . 178
8.2 Thurston Reducing System . . . 182

9 Proof of the Main Theorem 198

9.1 Proof of Theorem 1.1 . . . 199
9.2 Summary . . . 205

10 Detection of the (2,1)-Cable of the Trefoil 207

10.1 Statement of the Result . . . 207
10.2 Initial Reductions and the Trichotomy . . . 210
10.2.1 The torus knot case . . . 210
10.2.2 The satellite knot case . . . 211

10.2.3 The hyperbolic knot case . . . 213
10.3 Homological Filtering for the Cable Target . . . 215
10.4 Discussion of the Residual Hyperbolic Candidates . . . 217
10.5 Implications for Almost L-Space Knots . . . 217

11 Conclusion and Future Directions **218**
11.1 Summary of Results . . . 218
11.2 Direct Consequences . . . 219
11.2.1 Almost L-space rigidity . . . 219
11.2.2 The autofolder as a stand-alone contribution . . . 220
11.3 Future Directions . . . 220
11.3.1 Closing the cable detection gap . . . 220
11.3.2 Detection beyond genus two . . . 222
11.3.3 Khovanov detection of the granny knot . . . 224
11.3.4 Knot Floer homology and Khovanov homology on the Hedden-Watson pretzel family . . . 226
11.3.5 Generalizing the autofolder . . . 227
11.4 Closing Remarks . . . 227

A Splitting Sequences for the Stratum $(2; 1^6; 3^2)$ **230**

B Appendix: Case Analysis Preliminaries **243**
B.1 Primary Obstructions . . . 243
B.1.1 The Trace Lemma . . . 243
B.1.2 The Absorption Obstruction . . . 244
B.2 Trace Constraints for the Central Edge d . . . 245
B.3 Named Configurations and Their Contradictions . . . 245
B.3.1 Situation α . . . 246

B.3.2 Situation β . . . 246
B.3.3 Path Mills . . . 247
B.4 Notation and Common Phrases . . . 248

C Train Track Case Analysis: The Candelabra 250

C.0.1 NHT . . . 254
C.0.1.1 Jehu . . . 257
C.0.1.2 Kexy . . . 260
C.0.2 CMJ . . . 260
C.0.2.1 Mome . . . 261
C.0.2.2 Nesh . . . 264
C.0.3 WST . . . 278
C.0.3.1 Whid . . . 279
C.0.3.2 Dido . . . 282
C.0.4 PPG . . . 283
C.0.4.1 Fash . . . 283
C.0.4.2 Gley . . . 288
C.0.5 WVL . . . 289
C.0.5.1 Birl . . . 289
C.0.5.2 Darg . . . 294
C.0.5.3 Busk . . . 304
C.1 Figures . . . 311

D Appendix: Train Track Case Analysis: Track 0 495

D.1 Case A: Triangles fixed . . . 496
D.1.1 AVX . . . 496
D.1.1.1 Phil . . . 497
D.1.1.2 Test . . . 502

D.1.2 ACK 511
D.1.2.1 Dram 511
D.1.2.2 Lugs 528
D.1.2.3 Haze 529
D.1.3 Quip 530
D.1.4 Zest 531
D.1.4.1 Omen 531
D.1.4.2 Axe 533
D.1.5 Lox 534
D.1.5.1 Lava 535
D.1.5.2 Drop 544
D.1.5.3 Rage 544
D.1.6 Lake 545
D.1.6.1 Join 546
D.2 Case B,C,D: Triangles Swapped 570
D.2.1 ATL 570
D.2.2 LAX 571
D.2.2.1 Jolt 572
D.2.2.2 Mile 573
D.2.3 CDG 597
D.2.4 SYD 599
D.2.4.1 Ride 601
D.2.4.2 Clam 605
D.2.5 DXB 628
D.2.5.1 Zero 630
D.2.5.2 Dome 631
D.2.6 PHX 632

D.2.7 MIA 632
D.2.8 NRT 632
D.2.9 ARN 633
D.2.9.1 Corf 635
D.2.9.2 Woad 636
D.2.10ICN 636
D.2.11SIN 637
D.2.12PRG 637
D.3 Figures 639

E Train Track Case Analysis: Track 1 **945**

E.1 Case A: Triangles fixed 945
E.1.1 VIE 945
E.1.1.1 Iris 947
E.1.1.2 Ruby 960
E.1.2 GRR 960
E.1.2.1 Bree 961
E.1.2.2 Scud 965
E.1.3 IPC 996
E.1.3.1 Etui 997
E.1.3.2 Snee 997
E.1.3.3 Zarf 998
E.1.4 HND 1005
E.1.4.1 Froe 1005
E.1.4.2 Moxa 1005
E.1.4.3 Erne 1006
E.1.5 USH 1006

E.1.5.1 Torc 1006
E.1.5.2 Yegg 1007
E.1.5.3 Kief 1007
E.1.6 LXA 1007
E.1.6.1 Xama 1008
E.1.6.2 Zoea 1011
E.2 Case B,C,D: Triangles Swapped 1012
E.2.1 OMG 1012
E.2.2 SUX 1012
E.2.3 DIE 1012
E.2.4 ULN 1013
E.2.5 NAN 1013
E.2.6 GOH 1014
E.2.7 PPT 1015
E.2.8 BOD 1015
E.2.9 MAA 1016
E.2.10XNB 1016
E.2.10.1Qadi 1017
E.2.10.2Iwis 1022
E.2.11QRO 1023
E.2.11.1Burl 1023
E.2.11.2Kyat 1024
E.2.12WVB 1025
E.2.12.1Nard 1026
E.2.12.2Drek 1026
E.2.13ZFB 1027
E.2.13.1Aery 1028

E.3 Figures 1030

F Train Track Case Analysis: Track 8 **1232**

F.1 Case A: Triangles fixed 1232

F.1.1 YOW 1232

F.1.1.1 Bubo 1234

F.1.1.2 Gurn 1240

F.1.2 BRR 1247

F.1.2.1 Agog 1248

F.1.2.2 Dory 1248

F.1.3 Mien 1250

F.1.4 NUK 1250

F.1.5 GAY 1251

F.1.5.1 Ogee 1251

F.1.5.2 Tret 1256

F.1.6 OGG 1260

F.1.7 SME 1261

F.1.7.1 Barm 1262

F.1.7.2 Nary 1263

F.2 Case B,C,D: Triangles Swapped 1266

F.2.1 FUN 1266

F.2.2 XOY 1268

F.2.3 FAT 1268

F.2.4 KNH 1269

F.2.5 MZG 1269

F.2.6 GUM 1270

F.2.7 WAK 1270

F.2.8 MAU 1271
F.2.9 EEN 1271
F.2.10 MYU 1273
F.2.11 QBC 1273
F.2.12 OWD 1274
F.2.13 BFI 1274
F.2.14 CQD 1274
F.2.15 KYD 1275
F.2.16 FHR 1275
F.2.16.1 Eyas 1276
F.2.16.2 Fard 1276
F.3 Figures 1280

G Train Track Case Analysis: Track 12 **1440**

G.1 Case A: Triangles Fixed 1441
G.1.1 BKG 1441
G.1.2 CNM 1442
G.1.3 LGU 1444
G.1.4 CXH 1444
G.1.5 SXM 1445
G.1.6 GIB 1448
G.1.7 TEX 1449
G.1.8 LYR 1449
G.2 Case B,C,D: Triangles Swapped 1449
G.2.1 TGU 1449
G.2.2 XNA 1450
G.2.3 WYS 1451

G.2.4 HTI 1451
G.2.5 SEZ 1452
G.2.6 PBH 1454
G.2.7 CVF 1454
G.2.8 BRW 1454
G.2.9 TRK 1455
G.3 Figures 1456

H Train Track Case Analysis: Track 13 1503

H.1 Case A: Triangles Fixed 1504
H.1.1 RNT 1505
H.1.1.1 Bort 1507
H.1.1.2 Cess 1508
H.1.2 PWK 1508
H.1.2.1 Dowl 1508
H.1.2.2 Fubs 1509
H.1.3 BAF 1510
H.1.3.1 Grig 1511
H.1.3.2 Harl 1520
H.1.4 SEN 1522
H.1.4.1 Marl 1522
H.1.4.2 Peen 1523
H.1.5 HUN 1526
H.2 Case B,C,D: Triangles Swapped 1526
H.2.1 GUW 1527
H.2.2 CPX 1528
H.2.3 SCC 1528

H.2.4 LKE 1534
H.2.5 YVQ 1538
H.2.6 SOB 1538
H.2.7 BAM 1539
H.2.8 PIZ 1539
H.2.8.1 Nurl 1540
H.2.8.2 Oast 1541
H.2.8.3 Pilf 1541
H.2.8.4 Risp 1543
H.2.9 RUT 1544
H.2.10ART 1545
H.2.11WOT 1545
H.2.12ORE 1546
H.2.13BTV 1548
H.2.14AFN 1549
H.2.15CSS 1549
H.2.16UUU 1549
H.2.17GTK 1552
H.2.18CGI 1552
H.2.19GLD 1553
H.2.20UGN 1553
H.3 Figures 1555

I Train Track Case Analysis: Track 17 1726

I.1 Case A: Triangles Fixed 1726
I.1.1 VSF 1726
I.1.1.1 Bawn 1727

I.1.1.2 Blet 1738
I.1.2 HLE 1739
I.1.2.1 Dree 1739
I.1.2.2 Moke 1739
I.1.3 UAH 1741
I.1.3.1 Oche 1742
I.1.3.2 Roop 1745
I.1.4 GKA 1748
I.1.5 WGA 1748
I.1.6 LUA 1749
I.2 Case B,C,D: Triangles Swapped 1749
I.2.1 GBR 1749
I.2.1.1 Boke 1754
I.2.1.2 Clat 1757
I.2.2 MMU 1758
I.2.3 TKE 1763
I.2.4 RKD 1764
I.3 Figures 1765

J Appendix: Candidate Braids for the Candelabra 1913

J.1 Summary of Candidate Braid Families 1913
J.2 The Auxiliary Braid H 1917
J.3 Candidate 1 1919
J.4 Candidate 1.1 1922
J.5 Candidate Family 1.2 1924
J.6 Candidate 2 1926
J.7 Candidate Family 3 1928

J.8 Candidate Family 4 1930
J.9 Candidate Family 5 1932
J.10 Candidate Family 6 1934
J.11 Candidate Family 7 1936
J.12 Candidate Family 8 1938
J.13 Candidate Family 9 1940
J.14 Candidate Family 10 1942
J.15 Candidate Family 11 1944
J.16 Candidate Family 12 1946
J.17 Candidate 13 1948
J.18 Candidate Family 14 1950
J.19 Candidate Family 15 1952
J.20 Candidate Family 16 1954
J.21 Candidate Family 17 1956

K Appendix: Candidate Braids for Track 0 1958

K.1 Summary of Candidate Braid Families 1958
K.2 Base Braids Λ_6 and J 1961
K.3 Candidate Family 1 (Loblolly) 1962
K.4 Candidate Family 2 (Sloom) 1964
K.5 Candidate Family 3 (Mooncalf) 1967
K.6 Candidate Family 4 (Faffel) 1969
K.7 Candidate Family 5 (Balance) 1971
K.8 Candidate Family 6 (Fiasco) 1974
K.9 Candidate Family 7 (Briefing) 1976
K.10 Candidate Family 8 (Briefing) 1979
K.11 Candidate Family 9 (Quail) 1982

K.12 Candidate Family 10 (Quail) 1984
K.13 Candidate Family 11 (Jubilant) 1986
K.14 Candidate Family 12 (Jubilant) 1988
K.15 Candidate Family 13 (Treasure) 1990

L Appendix: Candidate Braids for Track 1 **1992**

L.1 Summary of Candidate Braid Families 1992
L.2 Base Braids Λ_6 and J 1995
L.3 Candidate Family 1 (Flute) 1996
L.4 Candidate Family 2 (Dolphin) 1998
L.5 Candidate Family 3 (Magpie) 2000
L.6 Candidate Family 4 (Bezoar) 2002
L.7 Candidate Family 5 (Abscond) 2004
L.8 Candidate Family 6 (Abscond) 2006
L.9 Candidate Family 7 (Fervent) 2008
L.10 Candidate Family 8 (Panorama) 2010
L.11 Candidate Family 9 (Pristine) 2012
L.12 Candidate Family 10 (Gingham) 2014
L.13 Candidate Family 11 (Dossier) 2016
L.14 Candidate Family 12 (Querulous) 2018
L.15 Candidate Family 13 (Querulous) 2020
L.16 Candidate Family 14 (Sybaritic) 2022
L.17 Candidate Family 15 (Leverage) 2024
L.18 Candidate Family 16 (Guddle) 2026
L.19 Candidate Family 17 (Popjoy) 2028

M Appendix: Candidate Braids for Track 8 **2030**

M.1 Summary of Candidate Braid Families 2030

M.2 Base Braids Λ_6 and J 2032
M.3 Candidate Family 1 (Anomy) 2033
M.4 Candidate Family 2 (Diatree) 2035
M.5 Candidate Family 3 (Fulmine) 2037
M.6 Candidate Family 4 (Chine) 2039
M.7 Candidate Family 5 (Quaint) 2041
M.8 Candidate Family 6 (Lacuna) 2043
M.9 Candidate Family 7 (Aulic) 2045
M.10 Candidate Family 8 (Oread) 2047
M.11 Candidate Family 9 (FAT) 2049

N Appendix: Candidate Braids for Track 13 **2051**

N.1 Summary of Candidate Braid Families 2051
N.2 Base Braids Λ_6 and L 2052
N.3 Candidate Family 1 (Chirk) 2053
N.4 Candidate Family 2 (Cagmag) 2055
N.5 Candidate Family 3 (Boofus) 2057
N.6 Candidate Family 4 (SCC) 2059

O Appendix: Candidate Braids for Track 17 **2061**

O.1 Summary of Candidate Braid Families 2061
O.2 Base Braids Λ_6 and P 2062
O.3 Candidate Family 1 (Cudden) 2063
O.4 Candidate Family 2 (Flisky) 2065
O.5 Candidate Family 3 (Wanion) 2067
O.6 Candidate Family 4 (Roop) 2069
O.7 Candidate Family 5 (Boke) 2072
O.8 Candidate Family 6 (Boke) 2075

P Verdict Tables for the Granny Detection **2078**

P.1 Stratum $(3;1^6;3)$: The Candelabra 2079

P.2 Stratum $(2;1^6;3^2)$: The Two-Triangle Tracks 2081

P.2.1 Track 0 (13 families) 2081

P.2.2 Track 1 (17 families) 2082

P.2.3 Track 8 (9 families) 2082

P.2.4 Track 13 (4 families) 2083

P.2.5 Track 17 (6 families) 2083

P.3 Summary 2084

Q Residual Hyperbolic Candidates for the Cable Detection **2085**

Q.1 Surviving Families 2085

Q.2 Excluded Families 2087

Q.3 Discussion 2087

Acknowledgements

First and foremost, I would like to thank my advisor, Prof. John A. Baldwin, for supervising me throughout this journey and for his patient guidance through every stage of the work.

To Dr. Braeden Reinoso, for proposing this dissertation project and for laying the groundwork on which my entire dissertation rests. Braeden, I consider you my unofficial co-advisor; your generosity with your time and your ideas has shaped this thesis in ways I cannot easily measure.

To Melody, thank you for your steady support throughout, and to Tor and Gary for being there as well.

To my dearest friends Rafael, Ana, and Nate, for the company and the conversations that kept me going.

To my mother, my sister, and Steve, thank you for your love and for the opportunities that made this possible.

Kevin, May 2026

A
NEW AND COMPLETE DISQUISITION

concerning the

KNOT INVARIANTS OF OZSVÁTH AND SZABÓ,

in which the

SINGULAR ABILITY

of said

HOMOLOGY THEORY

to Detect the

CONNECTED SUM OF TWO TREFOILS

is

RIGOROUSLY DEMONSTRATED;

The Whole being Elucidated by means of

FOLDING AUTOMATA, TRAIN TRACKS,

and

SUNDRY DEMONSTRATIONS

touching upon the

FIBERED NATURE

of the

COMPOSITE KNOT.

CHAPTER ONE

Introduction

The primary objective of this dissertation is to establish that knot Floer homology detects the *granny knot* $T_{2,3}\#T_{2,3}$, the connect-sum of two right-handed trefoil knots. While knot Floer homology is known to detect the unknot [OS04a], the trefoil [Ghi08], and the cinquefoil [Rei23], the detection of $T_{2,3}\#T_{2,3}$ is, to our knowledge, the first detection result for a composite knot.

1.1 Summary of Results

Our main result is the following detection theorem:

Theorem 1.1. Let $K \subset S^3$ be a knot. If there is an isomorphism of bigraded vector spaces

$$\widehat{HFK}(K;\mathbb{F}) \cong \widehat{HFK}(T_{2,3}\#T_{2,3};\mathbb{F})$$

over the field $\mathbb{F} = \mathbb{Z}/2\mathbb{Z}$, then K is isotopic to $T_{2,3}\#T_{2,3}$.

The Alexander polynomial of $T_{2,3}\#T_{2,3}$ is the square of the Alexander polynomial of the trefoil, which, combined with the rank of $\widehat{HFK}$, dictates a highly specific grading distribution.

The complexity of the proof lies in rigorously eliminating all other knots that possess this homological profile.

1.1.1 From Topology to Dynamics

Our strategy to prove Theorem 1.1 exploits the fact that knot Floer homology detects both the genus and fiberedness of a knot [Ni07; Juh08]. The connect-sum $T_{2,3}\#T_{2,3}$ is a fibered knot of genus two, and this information is recorded directly in the top Alexander grading of $\widehat{HFK}(T_{2,3}\#T_{2,3})$. Consequently, any knot K satisfying the hypothesis of Theorem 1.1 must also be a genus-two fibered knot.

This fundamental observation allows us to translate the topological problem of knot classification into a dynamical one involving the mapping class group. A genus-two fibered knot is determined by its monodromy, a surface homeomorphism $h\colon \Sigma_2^1 \to \Sigma_2^1$ of the genus-two fiber, which fixes the boundary. The knot Floer homology of K constrains this monodromy in two powerful ways:

1. **Homological constraint:** The Alexander polynomial of K is determined by the Euler characteristic of $\widehat{HFK}$. Thus any hypothetical knot sharing the same knot Floer homology as that of $T_{2,3}\#T_{2,3}$ must share the same Alexander polynomial:

$$\Delta_K(t) = \Delta_{T_{2,3}\#T_{2,3}}(t) = (t^2 - t + 1)^2.$$

   Thus any monodromy of such a hypothetical knot must induce this Alexander polynomial on homology.

2. **Fixed-point constraint:** The work of Ghiggini [Ghi08], and independently of Ni [Ni07], shows that the number of fixed points of the monodromy of a fibered knot is constrained by the next-to-top Alexander grading of knot Floer homology. This directly requires h to have a specific number of fixed points.

1.1.2 The Dynamical Obstruction

Our case analysis is organized entirely by the *knot* trichotomy of Theorem 2.3: a hypothetical knot K satisfying the hypothesis of Theorem 1.1 is a torus knot, a satellite knot, or a hyperbolic knot, and these three possibilities are mutually exclusive at the level of the knot exterior $E(K)$. We stress at the outset that the case division is by knot type (Theorem 2.3, exclusive), never by the Nielsen-Thurston type of the monodromy; the dynamical classification of the monodromy enters only as a tool within the individual geometric cases, and the proof makes no use of any exclusivity among the periodic, reducible, and pseudo-Anosov surface classes.

(0) Reduction to genus-two fibered knots. Since $\widehat{HFK}$ detects fiberedness (Ni [Ni07]) and the Seifert genus (Ozsváth-Szabó [OS04a]), any such K is a fibered knot of genus two, with Alexander polynomial

$$\Delta_K(t) = \Delta_{T_{2,3}\#T_{2,3}}(t) = (t^2 - t + 1)^2.$$

(1) Torus case. The Alexander polynomials of the torus knots are completely classified, and none equals $(t^2-t+1)^2$; equivalently, no torus knot carries the rank profile of $\widehat{HFK}(T_{2,3}\#T_{2,3})$. This case is eliminated by the Alexander polynomial (equivalently the $\widehat{HFK}$ rank) alone, with no reference whatsoever to the monodromy.

(2) Hyperbolic case. If K is hyperbolic then, K being fibered, Thurston's fibered hyperbolization (Theorem 2.4) forces the monodromy $h \in \mathrm{Mod}(\Sigma_2^1)$ to be pseudo-Anosov. We descend h through the Birman-Hilden correspondence to a six-marked disk braid and, via the train-track and `autofolder` machinery of Chapters 3–7, enumerate every pseudo-Anosov candidate compatible with the homological data; a homological filtering pipeline then eliminates them all. This is the technical heart of the dissertation, developed in the next subsection.

(3) Satellite case. If K is a satellite then $E(K)$ is toroidal. Because K is then not a torus knot, its monodromy is not periodic, and the essential torus is the suspension of an h-invariant essential multicurve; hence the canonical reducing system Γ of h is nonempty (Chapter 8). Schubert's formula [Sch53] forces both the pattern and the companion to be trefoils of winding number one, and the reducing-system analysis (Case A / Case B) narrows the possibilities to the connect-sum of two trefoils. The bigraded structure of $\widehat{HFK}$ finally isolates the granny knot $T_{2,3}\#T_{2,3}$ from the square knot and the mirror granny.

1.1.3 Eliminating the Hyperbolic Case

The hyperbolic case is the technical heart of the dissertation. To analyze it, we descend the genus-two monodromy of K to a braid mapping class on the marked disk via the **Birman-Hilden correspondence**. The key geometric fact is that the hyperelliptic involution ι is central in the mapping class group $\mathrm{Mod}(\Sigma_2^0)$, so every monodromy on the closed genus-two surface commutes with ι and descends through the quotient $\Sigma_2^0 \to \Sigma_2^0/\iota \cong S^2_{0,6}$, branched over six points. Beginning with the pseudo-Anosov representative $\phi_h\colon \Sigma_2^1 \to \Sigma_2^1$ of the monodromy of K (which has exactly one interior fixed point z), we cap off the boundary $\partial\Sigma_2^1$ with a disk to obtain a pseudo-Anosov map $\hat{\phi}_h\colon \Sigma_2^0 \to \Sigma_2^0$ on the closed surface, with two fixed points $\{z, p\}$ swapped by ι. Descending through the involution yields a pseudo-Anosov map $\phi_b\colon S^2_{0,6} \to S^2_{0,6}$ with a single non-marked fixed point r, the common image of z and p. A real blow-up at r then produces a pseudo-Anosov map $\phi_\beta\colon D^2 \to D^2$ on the six-marked disk, whose mapping class $\beta \in \mathrm{Mod}(D_6)$ we refer to as the *disk braid* associated to K. The canonical lift of β to the genus-two surface with two boundary components Σ_2^2 (the double cover of D^2 branched over the six marked points) is fixed-point-free in its interior, by construction. We develop this correspondence in detail in Chapter 2, Section 2.5.

Having reduced the topological classification problem on S^3 to a dynamical question about a pseudo-Anosov 6-braid whose lift is fixed-point-free, we now bring the theory of train tracks

to bear. The Euler-Poincaré formula restricts β to one of finitely many admissible singularity strata, each specified by the prong structure of the invariant foliations of ϕ_β. Within each stratum, β may be analyzed via the dynamics of its action on train tracks; however, the state space of such train tracks is in general too large for feasible analysis. Producing such an enumeration is a long-standing problem in topological dynamics: in his foundational paper on estimating the entropy of braids, Los [Los93] explicitly called for the development of a generalized, algorithmic method to construct exhaustive folding automata for train tracks on punctured disks, noting that ad-hoc constructions were a major bottleneck in dynamical classifications.

In response to this, we introduce the `autofolder` algorithm. This computational tool takes as input a stratum of mapping classes and exhaustively generates the complete directed graph of standard train tracks connected by elementary folding operations.

Theorem 1.2. The `autofolder` algorithm provides a complete, finite classification of all standard train tracks and their valid elementary folds for any specified stratum of pseudo-Anosov braids on the n-punctured disk.

In particular, for each admissible stratum on the 6-marked disk, the `autofolder` outputs a finite list of standard train tracks with the property that every pseudo-Anosov 6-braid in that stratum is carried by one of the tracks on the list. This list serves as the starting point for our subsequent case analysis.

Although the `autofolder` is developed here as the computational backbone for the hyperbolic case of Theorem 1.1, the algorithm operates on arbitrary strata of the marked disk and stands as an independent contribution to the field of low-dimensional topology and topological dynamics. We discuss these broader applications in Section 1.2.3.

With the `autofolder` in hand, we eliminate the hyperbolic case as follows. For each admissible

stratum we generate the complete folding automaton; by the carrying theorem of Ko-Los-Song [SKL02], every pseudo-Anosov 6-braid in that stratum is carried by one of the finitely many standard train tracks appearing as its vertices. Whenever a stratum carries an interior singularity of at least two prongs, the refinement of Farber-Reinoso-Wang [FRW24] applies: every such braid is in fact carried by a *jointless* standard track. Their tight-splitting operation — the inverse of the elementary folds recorded by the automaton — removes the joints from any standard track, so we may discard every track carrying a joint and reduce each such stratum to a short, explicit list of jointless standard tracks.

The obstructions we then impose are conditions not on the braids in the abstract, but on the induced *train-track maps* $f_\beta \colon \tau \to \tau$ that these tracks carry — equivalently, on the edge-image words of f_β and the transition matrix $M(f_\beta)$ they determine. Each translates the requirement that the canonical lift $\phi_\Phi \colon \Sigma_2^2 \to \Sigma_2^2$ be interior fixed-point-free into a combinatorial condition on f_β: the Trace Lemma forces $\operatorname{tr} M(f_\beta) = 0$, which in the jointless setting means that no real edge incident to a marked monogon occurs in its own image; and the Absorption Obstruction, a consequence of the injectivity of the surface homeomorphism inducing f_β, forbids any edge-image from being absorbed into the cone spanned by two adjacent edge-images at a switch. We carry out the resulting enumeration in full: for every jointless track in each such stratum we exhaustively generate the train-track maps f_β consistent with the track's combinatorics and test each one against both obstructions, either eliminating it or recording the parametric braid family to which it belongs. This program yields the following positive classification of the pseudo-Anosov 6-braids whose canonical lift to the genus-two surface with two boundary components Σ_2^2 is interior fixed-point-free:

Theorem 1.3. Let $\beta \in \mathrm{Mod}(D_6)$ be a pseudo-Anosov 6-braid whose canonical lift $\phi_\beta \colon \Sigma_2^2 \to \Sigma_2^2$ is fixed-point-free in its interior. Then the singularity type of β lies in one of the five admissible strata

$$(2; 1^4, 2^2; \emptyset), \quad (4; 1^6; \emptyset), \quad (2; 1^6; 4), \quad (3; 1^6; 3), \quad (2; 1^6; 3^2).$$

In the orientable strata $(2; 1^4, 2^2; \emptyset)$, $(4; 1^6; \emptyset)$, and $(2; 1^6; 4)$, the invariant foliations of ϕ_β on Σ_2^2 are orientable. In the non-orientable strata $(3; 1^6; 3)$ and $(2; 1^6; 3^2)$, β or β^{-1} is conjugate, up to a power of the full twist Δ^2, to a member of one of finitely many explicit braid families. These families are enumerated in Appendices J–O.

The three orientable strata are eliminated at once: an orientable invariant foliation would force the dilatation of ϕ_β to appear as a real root of $\Delta_{T_{2,3}\#T_{2,3}}(t) = (t^2 - t + 1)^2$, a polynomial with no real roots, so no pseudo-Anosov braid can inhabit these strata (Chapter 4). For the two non-orientable strata, the candidate families remain; we evaluate their reduced homological action matrices and apply the homological filter.

Theorem 1.4. None of the fixed-point-free pseudo-Anosov mapping classes generated by the standard train tracks in the admissible strata induce both an Alexander polynomial equal to $\Delta(t) = (t^2 - t + 1)^2$ and a 3-manifold (the underlying space of the associated open book) that is an integer homology sphere.

Corollary 1.5. No hyperbolic knot $K \subset S^3$ satisfies $\widehat{HFK}(K; \mathbb{F}) \cong \widehat{HFK}(T_{2,3}\#T_{2,3}; \mathbb{F})$ as bigraded vector spaces over $\mathbb{F} = \mathbb{Z}/2\mathbb{Z}$.

Combined with the elimination of the periodic case (corresponding to torus knots, cf. the Alexander polynomial check above), Corollary 1.5 together with the Nielsen-Thurston trichotomy forces the monodromy of K to be *reducible*.

1.1.4 Eliminating the Satellite Case

Having ruled out the torus and hyperbolic cases, K must be a satellite knot. Schubert's formula for the Alexander polynomial of a satellite knot constrains the structure of the satellite decomposition:

$$\Delta_K(t) \doteq \Delta_{P(U)}(t) \cdot \Delta_C(t^w),$$

where C is the companion knot, P is the pattern (with winding number w), and $P(U)$ is the pattern realized in the unknot. The constraint $\Delta_K = (t^2 - t + 1)^2$, together with the requirement that both C and $P(U)$ be fibered, forces the pattern $P(U)$ to be a trefoil, the companion C to be a trefoil, and the winding number to be $|w| = 1$.

The geometric content of the satellite structure is then captured by the Thurston reducing system on the genus-two fiber: the canonical reducing curves divide the fiber into pieces with restricted geometric types. Following the framework of Baldwin and Sivek, the outermost piece of this decomposition has one of two topological types, leading to two cases:

- **Case A (pair of pants):** The Baldwin-Sivek classification yields either a composite knot or a (p, q)-cable knot; a cable knot has winding number at least two, contradicting $|w| = 1$, so K is composite. The only composite genus-two fibered knot consistent with $\Delta_K = (t^2 - t + 1)^2$ is a connect-sum of two trefoils.

- **Case B (genus-one piece):** The outer monodromy is either periodic or pseudo-Anosov. The periodic sub-case forces K to be a cable knot whose winding number contradicts $|w| = 1$; the pseudo-Anosov sub-case is eliminated by a fractional-Dehn-twist-coefficient analysis using the Hedden-Mark bound and the Honda-Kazez-Matić right-veering criterion applied to the L-space contact invariant.

The satellite case therefore reduces to a connect-sum of two trefoils:

Corollary 1.6. If $K \subset S^3$ is a non-trivial satellite knot with

$$\widehat{HFK}(K;\mathbb{F}) \cong \widehat{HFK}(T_{2,3}\#T_{2,3};\mathbb{F})$$

as bigraded vector spaces over $\mathbb{F} = \mathbb{Z}/2\mathbb{Z}$, then K is isotopic to a connect-sum of two trefoils.

It remains to resolve the chirality of the two trefoil summands. The candidates are $T_{2,3}\#T_{2,3}$ (the granny knot, homochiral), $T_{2,3}\#\overline{T}_{2,3}$ (the square knot, heterochiral), and $\overline{T}_{2,3}\#\overline{T}_{2,3}$ (the mirror granny). All three share the same Alexander polynomial $(t^2 - t + 1)^2$ and the same total $\widehat{HFK}$ rank, but their bigraded (M, A) supports differ. Mirroring a knot reverses both gradings, $(M, A) \mapsto (-M, -A)$; the square knot is amphichiral and so has a centrally symmetric support, while the granny and the mirror granny have supports that are central reflections of one another. The three supports are therefore distinct, and the bigraded isomorphism in the hypothesis of Theorem 1.1 selects exactly one of them, namely $T_{2,3}\#T_{2,3}$. This completes the proof of Theorem 1.1; we discuss the chirality-resolution aspect further in Section 1.2.

1.1.5 A Partial Detection Theorem for the $(2, 1)$-Cable

Beyond the granny knot, another natural target within the satellite class is the $(2, 1)$-cable of the right-handed trefoil, $C_{2,1}(T_{2,3})$. This is a genus-two fibered satellite knot with Alexander polynomial

$$\Delta_{C_{2,1}(T_{2,3})}(t) \;=\; \Delta_{T_{2,3}}(t^2) \;=\; t^4 - t^2 + 1,$$

which differs from the granny's $(t^2 - t + 1)^2$, so the cable is not a candidate for K in Theorem 1.1. Both $C_{2,1}(T_{2,3})$ and the granny knot are *almost L-space knots* in the sense of Baldwin and Sivek [BS24]: the cable is realized as a $(2, 4g - 3)$-cable of the L-space knot $T_{2,3}$, and Binns [Bin23] showed that all such cables are almost L-space knots. Binns further

showed that $T_{2,3}\#T_{2,3}$ is the unique composite almost L-space knot [Bin23].

It is therefore natural to ask: does $\widehat{HFK}$ itself detect $C_{2,1}(T_{2,3})$? The same machinery developed for the granny detection — the `autofolder` algorithm, tight splitting, the Trace Lemma, the Absorption Obstruction, and homological filtering — can be applied to the cable target Alexander polynomial $t^4 - t^2 + 1$. This analysis dispatches the torus and satellite cases entirely, but the homological filter is less effective at the cable target than at the granny target: a small number of candidate braid families survive both filters at certain non-negative integer parameter values. We thus obtain the following partial result:

Theorem 1.7. Let $K \subset S^3$ be a knot such that

$$\widehat{HFK}(K;\mathbb{F}) \cong \widehat{HFK}(C_{2,1}(T_{2,3});\mathbb{F})$$

as bigraded vector spaces over $\mathbb{F} = \mathbb{Z}/2\mathbb{Z}$. Then either K is isotopic to $C_{2,1}(T_{2,3})$, or K is hyperbolic and the disk braid associated to its monodromy under the Birman-Hilden correspondence (cf. Chapter 2, Section 2.5) belongs to one of an explicitly enumerated finite list of parametric families.

The residual hyperbolic candidates are tabulated in Appendix Q, and avenues for closing the gap are discussed in Section 10.4. As an immediate corollary that is fully proved, we have:

Corollary 1.8. Knot Floer homology detects $C_{2,1}(T_{2,3})$ among non-hyperbolic knots: any non-hyperbolic knot K with $\widehat{HFK}(K) \cong \widehat{HFK}(C_{2,1}(T_{2,3}))$ as bigraded vector spaces is isotopic to $C_{2,1}(T_{2,3})$.

1.2 Applications

In this section, we discuss the topological and geometric implications of our main result, Theorem 1.1, which establishes that knot Floer homology detects the connect-sum of two right-handed trefoil knots, $T_{2,3}\#T_{2,3}$ (the granny knot). We also address the implications of Theorem 1.7, our partial detection result for the satellite knot $C_{2,1}(T_{2,3})$ (the $(2,1)$-cable of the right-handed trefoil).

These results contribute to the classification of genus-two fibered knots and to the rigidity theory of *almost L-space knots* in the sense of Baldwin and Sivek.

1.2.1 Botany of Genus-Two Fibered Knots

Following the framework of Hedden and Watson [HW18], the central organizing questions of knot Floer homology in any given genus split into two complementary problems:

- *Geography:* which bigraded groups arise as $\widehat{HFK}(K)$ for some knot $K \subset S^3$?
- *Botany:* given a bigraded group V that does arise, which knots K satisfy $\widehat{HFK}(K) \cong V$?

Detection results are precisely positive botany results: they assert that a particular bigraded group is realized by a unique knot. The two results in this dissertation, Theorems 1.1 and 1.7, are botany results in genus two, the same setting addressed by Reinoso [Rei23] for the cinquefoil $T_{2,5}$.

Genus-two fibered knots in S^3 fall into three Nielsen-Thurston classes: torus, satellite, and hyperbolic. The torus case is fully resolved by Reinoso's detection of $T_{2,5}$ and its mirror, the only non-trivial genus-two fibered torus knots in S^3. The hyperbolic case remains open — no genus-two hyperbolic fibered knot is currently known to be detected by $\widehat{HFK}$. Theorems

1.1 and 1.7 of this dissertation address the satellite class in two complementary sub-cases: the granny knot (composite) and the cable $C_{2,1}(T_{2,3})$ (prime). Together with Reinoso's torus result, these constitute the first systematic progress on the botany problem for genus-two fibered knots, leaving the hyperbolic class as the principal open frontier.

1.2.2 The Granny as the Unique Composite Almost L-Space Knot

A knot $K \subset S^3$ is termed an *L-space knot* if there exists an integer n with $|n| \geq 2g(K) - 1$ such that $S^3_n(K)$ is an L-space—a rational homology sphere Y with the simplest possible Heegaard Floer homology, satisfying $\dim \widehat{HF}(Y) = |H_1(Y; \mathbb{Z})|$.

Generalizing this notion, Baldwin and Sivek define a knot K to be an *almost L-space knot* if K is not itself an L-space knot and there exists an integer n with $|n| \geq 2g(K) - 1$ such that

$$\dim \widehat{HF}(S^3_n(K)) = |n|+2,$$

i.e., large Dehn surgeries on K yield 3-manifolds with Heegaard Floer homology of next-to-minimal rank [BS24]. Both the granny knot and the cable $C_{2,1}(T_{2,3})$ are almost L-space knots [Bin23], and natural topological constraints — compositeness, primeness within a given satellite pattern, fixed Alexander polynomial — often force a knot in this class to be uniquely determined. Our detection results combine cleanly with such structural constraints.

- **The granny knot.** Binns has shown that $T_{2,3}\#T_{2,3}$ is the unique composite almost L-space knot [Bin23]. Consequently, Theorem 1.1 implies that $\widehat{HFK}$ detects the unique composite almost L-space knot.

- **The cable $C_{2,1}(T_{2,3})$.** Corollary 1.8 provides the first non-trivial detection result by $\widehat{HFK}$ for an almost L-space knot beyond the L-space-knot torus class: any non-hyperbolic knot with $\widehat{HFK}$ matching that of $C_{2,1}(T_{2,3})$ is $C_{2,1}(T_{2,3})$ itself.

Combining Binns' uniqueness theorem with Theorem 1.1, we obtain the following corollary:

Corollary 1.9. Knot Floer homology detects the unique composite almost L-space knot.

1.2.3 Enumerating Pseudo-Anosovs of Bounded Dilatation

Beyond its role in the proof of Theorem 1.1, the `autofolder` algorithm provides a tool for the systematic enumeration of pseudo-Anosov mapping classes by dilatation. By the framework of Ko, Los, and Song [SKL02], every pseudo-Anosov braid in a given stratum is conjugate to one represented by a closed cycle in the folding automaton for that stratum, and the dilatation of the braid is the spectral radius of the product of transition matrices recorded along the cycle. The `autofolder` algorithm explicitly produces this automaton, with the transition matrix attached to every edge, making the dilatation of any cycle directly computable from the automaton data.

A bound on the dilatation translates, via Perron-Frobenius theory, into a bound on the length of cycles that need to be examined. Indeed, the transition matrix associated to a cycle is a product of the elementary folding matrices recorded along its edges, so longer cycles produce matrices with larger entries. Since each elementary folding matrix contributes a fixed amount to the total entry sum, the entry sum $|M|$ of the transition matrix of a cycle grows linearly in the cycle length. The Perron-Frobenius inequality

$$\lambda^n \geq |M| - n + 1,$$

valid for any $n \times n$ Perron-Frobenius matrix with leading eigenvalue $\lambda > 1$ ([HS07, Lemma 3.1]), then converts an upper bound $\lambda \leq \lambda_0$ into an upper bound on $|M|$, and thereby into an upper bound on the cycle length. Consequently, for any fixed stratum $\mathcal{S}$ and any $\lambda_0 > 1$, the enumeration of pseudo-Anosov mapping classes in $\mathcal{S}$ with dilatation at most λ_0 reduces to traversing a finite portion of the `autofolder` automaton. This is the same strategy used

by Ham and Song to determine the minimum dilatation of pseudo-Anosov 5-braids [HS07], carried out by hand for that single stratum; the `autofolder` framework turns this approach into an algorithmic computation applicable to any stratum.

This procedure is particularly well-suited to investigating questions about fixed-point structure and dilatation in specific strata, an area which has seen recent activity from a number of directions [AFT25].

1.3 Outline of the Chapters

This dissertation is structured to systematically eliminate topological candidates for the knot K, moving from algebraic algorithms to geometric dynamics.

In **Chapter 2**, we provide the necessary background on knot Floer homology, the Birman-Hilden correspondence, and the Nielsen-Thurston classification of surface homeomorphisms. We rigorously establish the bounds placed on the geometric monodromy by the knot Floer homology of $T_{2,3}\#T_{2,3}$, and dispatch the torus knot case via an elementary Alexander polynomial check.

In **Chapter 3**, we develop the theory of train tracks on punctured disks and surfaces with boundary, including standard and jointless train tracks, the Birman-Hilden lift, and the Trace Lemma which encodes fixed-point information of the lifted monodromy.

In **Chapter 4**, we introduce the primary technique for ruling out mapping classes based on the orientability of their invariant foliations. We show that for three specific strata, the lifted invariant foliations on Σ_2^2 are orientable, forcing the dilatation of the monodromy to appear as a real root of $\Delta_{T_{2,3}\#T_{2,3}}(t) = (t^2 - t + 1)^2$. Since this polynomial has no real roots greater than 1, these strata are eliminated.

In **Chapter 5**, we detail the theoretical construction of folding automata and our algorithmic

realization. We prove Theorem 1.2 and demonstrate how the `autofolder` algorithm explicitly generates the finite, exhaustive list of standard train tracks in each stratum required for the dynamical classification.

In **Chapter 6**, we introduce the tight-splitting operation, which prunes the `autofolder`'s output to a small set of jointless standard train tracks carrying the same pseudo-Anosov maps. We prove that this reduction terminates (Theorem 6.14) and that, up to conjugation and mirroring, every pseudo-Anosov braid in the non-orientable strata is carried by one of finitely many terminal tracks — the Candelabra in the stratum $(3; 1^6; 3)$, and six tracks in $(2; 1^6; 3^2)$.

In **Chapter 7**, we deploy this machinery to eliminate the remaining non-orientable strata. Using the reduced list of jointless tracks, the Trace Lemma, and the Absorption Obstruction, we enumerate all valid train track maps on the 6-marked disk and apply homological filters to rule out every hyperbolic candidate.

In **Chapter 8**, having eliminated all torus and hyperbolic knot candidates, we analyze the remaining reducible (satellite) case. We utilize Schubert's formula and Thurston reducing systems to definitively prove that K must be the connect-sum of two right-handed trefoil knots.

In **Chapter 9**, we assemble the preceding results into a complete proof of Theorem 1.1, including the chirality discharge that distinguishes the granny knot from the square knot and from the mirror granny knot via the bigraded structure of $\widehat{HFK}$.

In **Chapter 10**, we adapt the framework to the $(2, 1)$-cable of the trefoil. We prove the partial detection theorem for $C_{2,1}(T_{2,3})$ (Theorem 10.2), enumerating the residual list of hyperbolic candidates that survive the homological filters and discussing avenues for closing the resulting gap.

Finally, in **Chapter 11**, we summarize the principal results, discuss broader implications, and identify directions for future research, including the extension of the autofolder framework to higher-genus detection problems and to Khovanov-homology analogues.

CHAPTER TWO

Preliminaries

In this chapter, we establish the foundational topological and geometric machinery required to prove our main detection result, Theorem 1.1.

To achieve this, we must translate a problem in three-dimensional topology into one of surface dynamics. Because the knot $T_{2,3}\#T_{2,3}$ is fibered, any knot sharing its knot Floer homological profile must also be fibered. This shifts the focus of our proof from the geometry of the knot to the mapping class group of its fiber surface. Consequently, our argument relies on weaving together the algebraic constraints of knot Floer homology with the dynamical rigidity of surface homeomorphisms.

We structure this background material as follows. In Section 2.1, we fix the notational conventions used throughout the dissertation. In Section 2.2, we review the basics of fibered knots and knot Floer homology, highlighting the pivotal theorems of Ozsváth–Szabó and Ni which demonstrate that $\widehat{HFK}$ detects the Seifert genus and fiberedness of a knot. We then introduce the Nielsen-Thurston classification of surface mapping classes and its three-dimensional analogue, Thurston's geometric classification of knots.

In Section 2.3, we delve into the geometry of pseudo-Anosov mapping classes, which cor-

respond precisely to hyperbolic knots. We detail their invariant singular foliations and characterize their twisting behavior near the boundary via the fractional Dehn twist coefficient. In Section 2.4, we restrict our focus to hyperbolic fibered knots sharing the knot Floer homological profile of $T_{2,3}\#T_{2,3}$, drawing on recent work of Ghiggini-Spano and Ni in knot Floer homology to bound the fixed points and boundary prongs of their monodromies.

Finally, in Section 2.5, we invoke the Birman-Hilden correspondence. This machinery allows us to project monodromies on the genus-two surface down to the punctured sphere and disk. This descent directly sets the stage for the combinatorial enumeration of pseudo-Anosov strata, which we carry out at the conclusion of the chapter.

2.1 Notation and Conventions

Throughout this dissertation we adopt the following conventions; later chapters refer back to this section.

Surfaces. We denote by Σ_g^b the compact, oriented surface of genus g with $b \geq 0$ boundary components and no marked points. When marked points are present, we write $\Sigma_{g,n}^b$ for the surface of genus g with b boundary components and n marked points in its interior. When $b = 0$, the marked-point notation reduces to $\Sigma_{g,n}$. The n-marked closed disk is denoted D_n, and we identify D_n throughout with the closed unit disk in $\mathbb{C}$ together with n designated marked points. The n-marked sphere is denoted $S_{0,n}^2$, or simply S_n^2 when no confusion arises.

Mapping classes. The mapping class group of a surface Σ is denoted $\mathrm{Mod}(\Sigma)$, and consists of isotopy classes of orientation-preserving homeomorphisms fixing $\partial\Sigma$ pointwise and preserving the set of marked points. The mapping class of a homeomorphism f is denoted $[f]$. We use letters such as h, $\hat{h}$, b, β, Φ for mapping classes, and the corresponding ϕ-decorated symbols (ϕ_h, $\hat{\phi}_h$, ϕ_b, ϕ_β, ϕ_Φ) for chosen geometric (typically pseudo-Anosov) representatives.

The hyperelliptic involution. The hyperelliptic involution of Σ_2^0 is denoted ι throughout this dissertation. We reserve the symbol τ for train tracks (Chapters 5–7); these two notational roles are kept strictly disjoint.

Field of coefficients. Unless explicitly stated otherwise, all knot Floer homology groups in this dissertation are taken with coefficients in the field $\mathbb{F} := \mathbb{Z}/2\mathbb{Z}$. The detection results of Ghiggini [Ghi08], Ni [Ni07], and Juhász [Juh08] were originally established over $\mathbb{Q}$ but extend to $\mathbb{F}$; see the discussion in [BHS25, §2] for the relevant coefficient-ring considerations.

The Birman-Hilden correspondence data. A central object in this dissertation is the ordered tuple

$$(h, \phi_h, \hat{h}, \hat{\phi}_h, b, \phi_b, \beta, \phi_\beta, \Phi, \phi_\Phi),$$

which we shall refer to as the *Birman-Hilden correspondence data* associated to a hyperbolic fibered knot K satisfying $\widehat{HFK}(K) \cong \widehat{HFK}(T_{2,3}\#T_{2,3})$. The construction and properties of this tuple are developed in detail in Section 2.5.

2.2 Fibered Knots and Knot Floer Homology

Let $K \subset S^3$ be a knot and let $N(K)$ denote its open tubular neighborhood. We say that K is **fibered** if the knot exterior $E(K) = S^3 \setminus N(K)$ admits the structure of a fiber bundle over the circle S^1. More precisely, there exists a smooth submersion

$$\pi : E(K) \to S^1$$

such that for every $\theta \in S^1$, the preimage

$$\Sigma_\theta = \pi^{-1}(\theta)$$

is a compact, orientable surface with boundary $\partial\Sigma_\theta = K$. The fiber $\Sigma_\theta \cong \Sigma_g^1$ (where g is the Seifert genus of K) is a minimal genus Seifert surface for K, and the fibration is entirely determined by the monodromy diffeomorphism

$$h : \Sigma_g^1 \to \Sigma_g^1,$$

which is defined up to isotopy fixing the boundary pointwise.

The knot exterior is thus homeomorphic to the mapping torus

$$M_h = (\Sigma_g^1 \times [0,1])/\sim,$$

where $(x,1) \sim (h(x),0)$ for $x \in \Sigma_g^1$ and $(x,s) \sim (x,t)$ for $x \in \partial\Sigma_g^1$ and all $s,t \in [0,1]$.

Knot Floer Homology

Knot Floer homology, introduced by Ozsváth and Szabó [OS04b], and independently by Rasmussen [Ras03], provides a powerful knot invariant for distinguishing topological properties of K, including its genus and fiberedness. There are several flavors of knot Floer homology; however, in this thesis, we shall exclusively utilize the "hat" version with coefficients in the field $\mathbb{F} = \mathbb{Z}/2\mathbb{Z}$, denoted $\widehat{HFK}(K)$. This invariant is a bigraded vector space over $\mathbb{F}$:

$$\widehat{HFK}(K) = \bigoplus_{M,A} \widehat{HFK}_M(K,A), \tag{2.1}$$

where M denotes the **Maslov grading** and A denotes the **Alexander grading**. The Euler characteristic of this homology theory recovers the classical Alexander polynomial $\Delta_K(t)$:

$$\Delta_K(t) = \sum_{M,A} (-1)^M \dim_{\mathbb{F}} (\widehat{HFK}_M(K,A)) t^A. \tag{2.2}$$

A seminal result of Ozsváth and Szabó establishes that knot Floer homology detects the Seifert genus of the knot, denoted $g(K)$. Specifically, the width of the homology in the Alexander grading is completely determined by the genus:

$$g(K) = \max\{A \mid \widehat{HFK}(K, A) \neq 0\}. \tag{2.3}$$

Of central importance to this work is the ability of knot Floer homology to detect fibered knots. While it is well-known that the Alexander polynomial provides a necessary condition for fiberedness—namely, that $\Delta_K(t)$ must be monic—it is not sufficient (for example, any non-trivial untwisted Whitehead double possesses a trivial Alexander polynomial but is never fibered[1]). On the other hand, knot Floer homology provides a necessary and sufficient condition. This detection result was established by Ghiggini [Ghi08] for genus-one knots and by Ni [Ni07] for arbitrary genus.

Theorem 2.1 (Ni [Ni07])**.** A knot $K \subset S^3$ is fibered if and only if

$$\dim_{\mathbb{F}} \widehat{HFK}(K, g(K)) = 1. \tag{2.4}$$

In other words, K is fibered if and only if the knot Floer homology in the top Alexander grading is one-dimensional. Consequently, for a fibered knot, the top-graded component is supported in a single Maslov grading. This theorem reduces the deeply topological question of the existence of a fibration to a computation in knot Floer homology.

The complete bi-graded knot Floer homology of $T_{2,3}\#T_{2,3}$ is shown in Figure 2.1.

[1]The trivial polynomial $\Delta(t) = 1$ *is* monic, so the monic-Alexander test alone fails to detect non-fiberedness; non-fiberedness in this case is detected only by the finer Heegaard Floer criterion below.

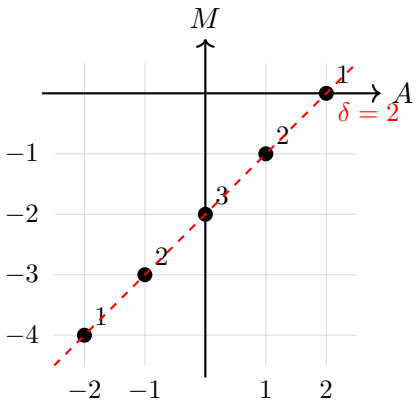


Figure 2.1: The bigraded knot Floer homology $\widehat{HFK}(T_{2,3}\#T_{2,3};\mathbb{F}_2)$. Each dot represents a generator at bigrading (A, M); the integer beside each dot is the rank $\dim_{\mathbb{F}} \widehat{HFK}_M(T_{2,3}\#T_{2,3}, A)$. The top Alexander grading is 2, of rank 1, thus this knot is fibered of genus 2. Also, all generators lie on the diagonal $A - M = 2$, exhibiting the so-called *thinness* of the granny knot.

The Monodromy and the Nielsen-Thurston Classification

As a consequence of Theorem 2.1, if a hypothetical knot K satisfies the hypothesis of Theorem 1.1:

$$\widehat{HFK}(K) \cong \widehat{HFK}(T_{2,3}\#T_{2,3})$$

as bigraded vector spaces, then it is immediate that K is a fibered knot of genus two. The bulk of the work required to prove Theorem 1.1 involves the rigorous study of the monodromy $h\colon \Sigma_2^1 \to \Sigma_2^1$ of such a fibered knot.

A simple closed curve on $\Sigma_{g,n}^b$ is **essential** if it does not bound a disk, a once-punctured disk, or an annulus cobounding a boundary component of $\Sigma_{g,n}^b$. A **multicurve** is a finite collection of disjoint, pairwise non-isotopic, essential simple closed curves.

The Nielsen-Thurston Classification Theorem provides a fundamental structural trichotomy for elements of the mapping class group.

Theorem 2.2 (Nielsen-Thurston Classification [Thu88])**.** Let Σ be a compact, orientable surface with negative Euler characteristic. Every mapping class $[h] \in \mathrm{Mod}(\Sigma)$ is of at least one of the following three types:

- **Periodic:** There exists an integer $m > 0$ such that $[h]^m = [\mathrm{id}]$. Equivalently, by the Nielsen Realization Theorem, $[h]$ contains a representative homeomorphism f such that $f^m = \mathrm{id}$ pointwise.
- **Reducible:** There exists a multicurve $\Gamma = \{\gamma_1, \ldots, \gamma_k\}$ on Σ that is invariant under $[h]$; that is, $h(\Gamma)$ is isotopic to Γ.
- **Pseudo-Anosov:** The mapping class $[h]$ contains a unique geometric representative ϕ_h (up to conjugacy by isometries) that preserves a pair of transverse, measured singular foliations: the stable foliation $(\mathcal{F}_s, \mu_s)$ and the unstable foliation $(\mathcal{F}_u, \mu_u)$. Furthermore, there exists a real number $\lambda > 1$, called the *dilatation*, such that $\phi_h(\mathcal{F}_s, \mu_s) = (\mathcal{F}_s, \lambda^{-1}\mu_s)$ and $\phi_h(\mathcal{F}_u, \mu_u) = (\mathcal{F}_u, \lambda\mu_u)$.

A pseudo-Anosov class is neither periodic nor reducible. The periodic and reducible types, by contrast, are *not* a priori disjoint: a periodic class may fix an essential multicurve and so also qualify as reducible in the sense above. The genuine trichotomy — a partition of $\mathrm{Mod}(\Sigma)$ into three pairwise-disjoint types — is recovered only after refining the reducible class by means of the *canonical reducing system*, which we develop in Chapter 8 (Theorem 8.5): there the reducible type is characterized by a nonempty canonical reducing system and the periodic and pseudo-Anosov types by an empty one. We make no use of disjointness among these surface types in the present chapter.

We will refer to the mapping class $[h]$ as periodic, reducible, or pseudo-Anosov according to the geometric type of its representative. More details on pseudo-Anosov maps will be provided in Section 2.3.

Thurston's Trichotomy for Knots

The *Thurston classification of knots* is the three-dimensional counterpart of the Nielsen-Thurston classification of surface mapping classes: for a fibered knot, the dynamical type of the monodromy on the fiber translates directly into a geometric description of the knot exterior. For a fibered knot $K \subset S^3$ with fiber Σ_g^1 and monodromy h, the knot exterior $E(K)$ is homeomorphic to the mapping torus M_h.

The dynamical properties of the mapping class $[h]$ directly dictate the three-dimensional topology and geometry of M_h. Thurston demonstrated that every knot $K \subset S^3$ falls into exactly one of three categories, which perfectly mirror the two-dimensional classification:

Theorem 2.3 (Thurston's Classification of Knots [Thu82])**.** Every knot $K \subset S^3$ is exactly one of the following three types, according to the geometry of its exterior $E(K)$:

- a **torus knot**, for which $E(K)$ is atoroidal and Seifert fibered;
- a **satellite knot**, for which $E(K)$ is toroidal — it contains an essential (incompressible, non-boundary-parallel) torus;
- a **hyperbolic knot**, for which $E(K)$ is atoroidal and not Seifert fibered, and so admits a complete hyperbolic metric of finite volume.

These three types are mutually exclusive and exhaustive: the trichotomy is a genuine partition of all knots, read directly off the geometric decomposition of the knot exterior, and it requires no analysis of the surface dynamics of any monodromy.

For a fibered knot, the geometry of the mapping torus $M_h = E(K)$ is governed by the Nielsen-Thurston type of the monodromy h, and this is the bridge we use as a tool within each knot-level case. The dictionary is as follows; we caution that the three knot types are exclusive (Theorem 2.3), whereas the surface types on the right are taken in the genuine

sense fixed by the canonical reducing system Γ (Chapter 8), so that "reducible" means $\Gamma \neq \emptyset$:

- **Torus Knots (Periodic):** If $[h]$ is periodic, the mapping torus M_h admits a Seifert fibered structure. In S^3, the only fibered knots with Seifert fibered complements are the torus knots $T_{p,q}$, which can be embedded on the surface of an unknotted torus.

- **Satellite Knots (reducible, $\Gamma \neq \emptyset$):** If h is reducible in the genuine sense — equivalently, its canonical reducing system Γ is nonempty — the invariant multicurve $\Gamma \subset \Sigma_g^1$ sweeps out a finite union of incompressible, non-boundary-parallel tori $\Gamma \times S^1$ in the mapping torus M_h. The existence of such a torus in the knot exterior $E(K)$ is the defining condition for K to be a satellite knot; we provide more details in Chapter 8.

- **Hyperbolic Knots (Pseudo-Anosov):** If $[h]$ is pseudo-Anosov, the invariant measured foliations on Σ_g^1 can be suspended to construct a complete Riemannian metric of constant negative curvature on the interior of M_h. Thus, $S^3 \setminus K$ is a hyperbolic 3-manifold of finite volume.

The proof of Theorem 1.1 is organized by the *knot* trichotomy of Theorem 2.3, which is exclusive at the level of the knot exterior; the dictionary above is invoked only as a tool inside the individual cases, and the argument makes no use of any exclusivity among the periodic, reducible, and pseudo-Anosov surface classes. We assume in turn that K is a torus knot, a hyperbolic knot, or a satellite knot, and eliminate all distinct candidates in each. The torus case is immediate: the Alexander polynomials of torus knots are completely classified, and none coincides with the observed polynomial $\Delta_K(t) = (t^2 - t + 1)^2$. Thus the remaining work rests on eliminating the hyperbolic and satellite cases.

2.3 Pseudo-Anosov Maps

The case where K is assumed to be a hyperbolic knot will be the most technically involved and will constitute the bulk of this thesis. As established by the trichotomy correspondence above:

Theorem 2.4 (Thurston [Thu98])**.** Let K be a fibered knot with monodromy h. The knot complement $S^3 \setminus K$ admits a complete hyperbolic metric of finite volume if and only if $[h]$ is pseudo-Anosov. In other words, K is hyperbolic if and only if h is freely isotopic to a pseudo-Anosov map ϕ_h.

Let $\phi\colon \Sigma_{g,n}^b \to \Sigma_{g,n}^b$ be a pseudo-Anosov homeomorphism permuting the marked points $\mathcal{P}$. The stable and unstable singular foliations $(\mathcal{F}_s, \mu_s)$ and $(\mathcal{F}_u, \mu_u)$ have singularities in the interior of $\Sigma_{g,n}^b$ that are required to be "k-pronged saddles" with $k \geq 3$. Each foliation must have at least one singularity on every boundary component. For marked points, the foliations are permitted to have 1-pronged singularities. Note that the singularities of $\mathcal{F}_s$ and $\mathcal{F}_u$ perfectly coincide and exhibit the identical number of prongs with respect to both foliations.

We illustrate the local models for these allowable singularities in Figure 2.2. As depicted, non-marked interior singularities must exhibit three or more prongs, corresponding to the traditional saddle points of the invariant foliations. In contrast, marked points (or punctures) may host 1-pronged or 2-pronged configurations, as the foliation is permitted to terminate or pass smoothly through these designated points. Similarly, a boundary component can support any integer number of prongs $k \geq 1$, with the invariant leaves terminating at the boundary curve.

Locally, one should view a pseudo-Anosov map ϕ as stretching the surface in the direction of $\mathcal{F}_u$ and shrinking it in the transverse direction described by $\mathcal{F}_s$. Because the invariant foliations are set-wise preserved by ϕ, the map must always permute singular points that

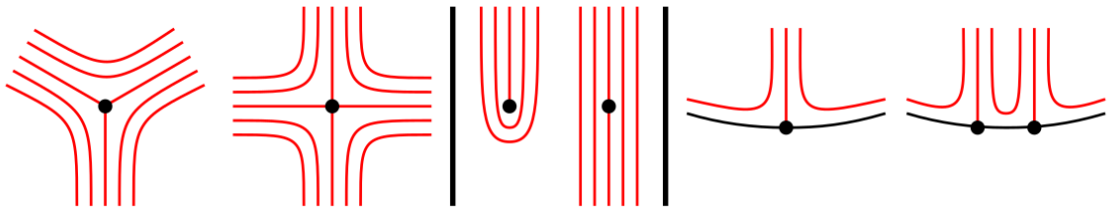


Figure 2.2: The allowable singularities in the invariant foliations of a pseudo-Anosov map. Non-marked interior singularities must have at least 3 prongs. Left: a 3-pronged and a 4-pronged singularity. Center: a 1-pronged and a 2-pronged singularity at a marked point. Right: a 1-pronged and a 2-pronged boundary component. Image courtesy of Braeden Reinoso [Rei24].

possess the same number of prongs.

Singularity Types

Following the convention of Farber, Reinoso, and Wang [FRW24], we utilize the following notation. The *singularity type* of a pseudo-Anosov map ϕ is the tuple recording the number of prongs at each singularity:

$$(b_1, \ldots, b_r;\, m_1, \ldots, m_n;\, k_1, \ldots, k_s)$$

where the ith boundary component of ϕ has b_i prongs; the ith marked point has m_i prongs; and the ith non-marked interior singularity has k_i prongs. We use $\emptyset$ if there are no singularities of a certain type, and exponents to denote multiple singularities possessing the same number of prongs.

For example, the tuple $(2; 1^6; 3^2)$ indicates that the foliations have a 2-pronged singularity at the unique boundary component; six 1-pronged singularities at marked points; and two 3-pronged non-marked interior singularities. If the surface has an empty boundary, we suppress the b_i entries entirely. For instance, the stratum $(1^6; 3^2)$ on the sphere S^2 indicates six 1-pronged singularities at marked points and two 3-pronged interior singularities.

2.3.1 Fractional Dehn Twist Coefficient

The **fractional Dehn twist coefficient**, denoted $c(h)$, is a rational number that quantifies the amount of twisting of the monodromy near the boundary $\partial\Sigma_g^1$.

Definition 2.5. Let $h \in \mathrm{Mod}(\Sigma_g^1)$ be a mapping class with pseudo-Anosov representative ϕ_h. The fractional Dehn twist coefficient $c(h)$ is defined as

$$c(h) = n + \frac{m}{k},$$

where:

- $n \in \mathbb{Z}$ is the number of full Dehn twists h performs near $\partial\Sigma_g^1$ relative to ϕ_h.
- $k \geq 1$ is the number of singular points (prongs) of the invariant foliations on $\partial\Sigma_g^1$.
- The geometric map ϕ_h permutes these k singular points on the boundary by a fractional rotation of m steps in the counter-clockwise direction.

Although Definition 2.5 is phrased in terms of the chosen geometric representative ϕ_h, the resulting rational number $c(h)$ depends only on the mapping class $[h]$. The following theorem of Reinoso, building on the work of Honda-Kazez-Matić [HKM07] and Ito-Kawamuro, records the conjugation invariance of $c(h)$ as well as the linear behavior under composition with a boundary Dehn twist.

Theorem 2.6 ([Rei24, Theorem 2.1.4])**.** Let Σ be a compact surface, possibly with marked points, and let $h \in \mathrm{Mod}(\Sigma)$ be a pseudo-Anosov mapping class. Then:

1. $c(h)$ is preserved under conjugation within $\mathrm{Mod}(\Sigma)$.
2. $c(\mathrm{id}) = 0$ and $c(T_{\partial\Sigma}^n \circ h) = n + c(h)$, where $T_{\partial\Sigma}$ is a positive boundary Dehn twist.

Given a fibered knot K, we define $c(K) \coloneqq c(h)$ where (Σ_g^1, h) is the open book associated to K. The monodromy of a fibered knot is determined up to conjugation in $\mathrm{Mod}(\Sigma_g^1)$ (different choices of fiber surface in the same fibration give monodromies that differ by conjugation), so the conjugation invariance in part (1) of the theorem is exactly what makes $c(K)$ a well-defined knot invariant.

2.4 Fibered Hyperbolic Knots

To prove our main result, we must rule out the existence of a distinct hyperbolic knot K whose knot Floer homology coincides with $T_{2,3}\#T_{2,3}$. Let K be a hyperbolic knot such that

$$\widehat{HFK}(K) \cong \widehat{HFK}(T_{2,3}\#T_{2,3})$$

as bigraded vector spaces. By the discussion in Section 2.2, K is immediately known to be fibered and of genus two. Let

$$h\colon \Sigma_2^1 \to \Sigma_2^1$$

denote the monodromy of K. By Theorem 2.4, $[h]$ is pseudo-Anosov. Let ϕ_h be its geometric representative.

Fixed Points

The work of Ghiggini-Spano, and independently of Ni, establishes that the next-to-top Alexander grading of K severely bounds the number of fixed points of ϕ_h:

Theorem 2.7 ([GS22, Theorem 1.2], [Ni22])**.** Let Y be a closed, oriented 3-manifold, and $K \subset Y$ be a hyperbolic fibered knot with fiber Σ and monodromy h. If

$$\dim_{\mathbb{F}} \widehat{HFK}(Y, K, [\Sigma], g(\Sigma) - 1) = r,$$

then h is freely isotopic to a pseudo-Anosov map ϕ_h with at most $r - 1$ fixed points.

In our case, the next-to-top Alexander grading is of rank two (cf. Figure 2.1):

$$\dim_{\mathbb{F}} \widehat{HFK}(S^3, K, [\Sigma_2^1], 1) = \dim_{\mathbb{F}} \widehat{HFK}(S^3, T_{2,3}\#T_{2,3}, [\Sigma_2^1], 1) = 2.$$

Hence ϕ_h has at most one fixed point. The work of Farber, Reinoso, and Wang [FRW24] eliminates the possibility that there are no fixed points:

Lemma 2.8 (Farber–Reinoso–Wang [FRW24])**.** Let K be a hyperbolic, fibered knot with monodromy h, and suppose $\widehat{HFK}(K) \cong \widehat{HFK}(T_{2,3}\#T_{2,3})$. Then ϕ_h has exactly one fixed point in the interior of Σ_2^1.

Proof. Farber, Reinoso, and Wang [FRW24] showed that the cinquefoil $T(2,5)$ is the only fibered genus-two knot in S^3 whose monodromy is fixed-point-free. The cinquefoil has a completely different knot Floer homology from $T_{2,3}\#T_{2,3}$, as is immediate from the fact that $\Delta_{T(2,5)}(t) = t^4 - t^3 + t^2 - t + 1 \neq (t^2 - t + 1)^2$. Hence K is not the cinquefoil, so ϕ_h is not fixed-point-free; combined with the bound of at most one interior fixed point, ϕ_h has exactly one. □

Capping Off

The work of Baldwin-Hu-Sivek [BHS25] demonstrates that when there is more than one prong on the boundary of Σ_2^1, the geometric map ϕ_h extends naturally to a "capped-off"

pseudo-Anosov map

$$\hat{\phi}_h \colon \Sigma_2^0 \to \Sigma_2^0$$

on the closed genus-two surface Σ_2^0, obtained by capping $\partial\Sigma_2^1$ with a disk. The invariant foliations extend to stable and unstable foliations $\hat{\mathcal{F}}^s$ and $\hat{\mathcal{F}}^u$, where the n-prongs on $\partial\Sigma_2^1$ meet at a newly formed singularity p in the capping disk. The point p is necessarily a fixed point of $\hat{\phi}_h$: since the geometric monodromy ϕ_h fixes $\partial\Sigma_2^1$ pointwise, the capped-off map $\hat{\phi}_h$ fixes the entire capping disk setwise; the boundary prongs of ϕ_h extend as a singular foliation pattern centered at p, and the only point on the capping disk left invariant by the local pseudo-Anosov dynamics around the prongs is the singular point p itself.

We now show that ϕ_h must have more than one prong on the boundary $\partial\Sigma_2^1$, allowing for such a capping off and extension of the foliations. The following argument follows Baldwin-Hu-Sivek closely, but with more details:

Thinness and the τ invariant A knot K is called *(Floer-)thin* if $\widehat{HFK}(K)$ is supported on a single diagonal $\delta := A - M$. The composite knot $T_{2,3}\#T_{2,3}$ is alternating (the trefoil is alternating, and a connect-sum of alternating knots is alternating), and Ozsváth and Szabó showed that every alternating knot is thin [OS03]; more generally, Manolescu and Ozsváth established that the larger class of quasi-alternating knots is thin [**ManolescuOzsvath2008**]. For an alternating knot the homology is concentrated on the diagonal $\delta = -\sigma(K)/2$, where $\sigma(K)$ is the classical knot signature. For the granny, $\sigma(T_{2,3}\#T_{2,3}) = -4$ (additivity under connect-sum, with $\sigma(T_{2,3}) = -2$), so all generators lie on $\delta = 2$ — this is visible in Figure 2.1, where every dot lies on the dashed red line. Since $\widehat{HFK}(K) \cong \widehat{HFK}(T_{2,3}\#T_{2,3})$, K is also thin and supported on $\delta = 2$. For thin knots, the spectral sequence from $\widehat{HFK}$ to $\widehat{HF}(S^3)$ collapses immediately, so the Ozsváth-Szabó concordance invariant $\tau(K)$ is determined entirely by the grading support: it equals the Alexander grading of the unique generator in Maslov grading 0. From Figure 2.1, this generator lies at $(A, M) = (2, 0)$, giving

$\tau(T_{2,3}\#T_{2,3}) = 2$, and hence

$$\tau(K) = g(K) = 2.$$

Strong quasipositivity By the work of Hedden [Hed10], a fibered knot K satisfies $\tau(K) = g(K)$ if and only if K is strongly quasipositive. In terms of contact topology, this implies the open book decomposition of S^3 with binding K supports the standard tight contact structure ξ_{std}.

Right-veering monodromy The monodromy h inherits two pieces of contact-theoretic information from the previous paragraph. First, Honda, Kazez, and Matić [HKM07] proved that the contact structure supported by an open book (Σ_2^1, h) is tight if and only if h is *right-veering*, a positivity condition on the action of h on properly embedded arcs near $\partial\Sigma_2^1$. Combined with their characterization h right-veering $\iff$ $c(h) \geq 0$, this gives $c(h) \geq 0$ for the monodromy of K. Second, Honda-Kazez-Matić show that a right-veering pseudo-Anosov mapping class with $c(h) = 0$ must be reducible. Since K is hyperbolic, h is pseudo-Anosov and irreducible, ruling out $c(h) = 0$. We conclude $c(h) > 0$.

Prongs of the invariant foliation Recall that $c(h) = n + \frac{m}{k}$, where k is the number of prongs on the boundary. A result of Hedden-Mark (Proposition 2.9 below) implies that for fibered hyperbolic knots, $|c(h)| < 1$.

Proposition 2.9 ([HM18, Remark 2.7])**.** If $K \subset S^3$ is a fibered hyperbolic knot with monodromy h, then $|c(h)| < 1$.

Since $0 < c(h) < 1$, the coefficient is strictly non-integer, meaning the singularity at the boundary cannot be 1-pronged. Therefore, the invariant foliation must possess $k \geq 2$ prongs on the boundary.

Remark 2.10. Remark 2.7 of Hedden-Mark states the result of Proposition 2.9 for an

arbitrary fibered knot in an L-space without assuming hyperbolicity. They cite a result of Honda-Kazez-Matić [HKM07] that when $|c(h)|\geq 1$, the L-space admits a taut foliation. However, this cited result strictly requires the assumption of hyperbolicity.

2.5 The Birman-Hilden Correspondence and Monodromy Descent

In this section, we establish the geometric machinery required to relate the monodromy of the knot K to a braid on the sphere, and subsequently to a braid on the disk. This relationship relies on the geometric symmetries of the closed genus-two surface, which, as in the capping-off construction of Section 2.4, should be thought of as arising from capping off the monodromy of the hyperbolic knot K.

Recall that for the closed genus-two surface Σ_2^0, the mapping class group $\mathrm{Mod}(\Sigma_2^0)$ contains a distinguished element $[\iota]$, known as the **hyperelliptic involution**. Algebraically, $[\iota]$ is the unique non-trivial element in the center of $\mathrm{Mod}(\Sigma_2^0)$. Consequently, for any mapping class $[\hat{\phi}_h] \in \mathrm{Mod}(\Sigma_2^0)$, we have the commutation relation:

$$[\hat{\phi}_h][\iota] = [\iota][\hat{\phi}_h]. \tag{2.5}$$

We call a geometric representative $\iota\colon \Sigma_2^0 \to \Sigma_2^0$ a hyperelliptic involution if it belongs to the class $[\iota]$.

The geometric utility of this involution is captured by the Birman-Hilden correspondence. Broadly speaking, this classical correspondence establishes an algebraic relationship between the subgroup of mapping classes that commute with a branched covering involution (the *symmetric* mapping class group) and the mapping class group of the quotient surface marked by the branch data.

For the closed genus-two surface Σ_2^0, the hyperelliptic involution $[\iota]$ generates the center of $\mathrm{Mod}(\Sigma_2^0)$. Because every mapping class commutes with the center, *every* mapping class on Σ_2^0 is symmetric, that is, lies in the symmetric mapping class group $\mathrm{SMod}(\Sigma_2^0)$. The Birman-Hilden theorem asserts an isomorphism between the symmetric mapping class group modulo the involution and the mapping class group of the quotient surface (with the branch points marked); since in our genus-two setting the symmetric subgroup is everything, this specializes to the cleaner statement

$$\mathrm{Mod}(\Sigma_2^0)/\langle[\iota]\rangle \;\cong\; \mathrm{Mod}(S_{0,6}^2),$$

the mapping class group of the sphere with six marked points (the images of the six Weierstrass points of Σ_2^0 under the quotient map).

This algebraic isomorphism has profound geometric implications for surface dynamics. It guarantees that any pseudo-Anosov mapping class on Σ_2^0 can be projected down to a well-defined pseudo-Anosov map on the marked sphere. For our purposes, this descent is made precise by the following lemma of Baldwin, Hu, and Sivek:

Lemma 2.11 ([BHS25, Lemma 3.7])**.** Let $\hat{h} \in \mathrm{Mod}(\Sigma_2^0)$ be a pseudo-Anosov mapping class with geometric representative $\hat{\phi}_h \colon \Sigma_2^0 \to \Sigma_2^0$. Then there exists a branched double covering

$$\pi \colon \Sigma_2^0 \to S^2,$$

branched along six points $q_1, \ldots, q_6 \in S^2$, such that $\hat{\phi}_h$ is a lift of a pseudo-Anosov map

$$\phi_b \colon (S^2, q_1, \ldots, q_6) \to (S^2, q_1, \ldots, q_6),$$

representing a class $b \in \mathrm{Mod}(S_{0,6}^2)$. Furthermore, the invariant foliations of $\hat{\phi}_h$ are lifts of those of ϕ_b.

The construction in the proof of Lemma 2.11 is the following. One starts with any branched double covering $\pi\colon \Sigma_2^0 \to S^2$, whose covering involution is necessarily a hyperelliptic involution of Σ_2^0. Although the given representative $\hat{\phi}_h$ need only commute with ι *up to isotopy*, Baldwin-Hu-Sivek use the fact (originally due to Goldsmith, see also [FM11, Theorem 4.1]) that $\hat{\phi}_h$ is isotopic to a representative that commutes with ι *on the nose*:

$$\hat{\phi}_h \circ \iota = \iota \circ \hat{\phi}_h.$$

After this adjustment, $\hat{\phi}_h$ descends through the quotient map π to a homeomorphism ϕ_b on the marked sphere $S^2_{0,6}$, whose marked points are the six branch points $q_1, \ldots, q_6$. The fixed points of the involution ι are exactly the preimages of these branch points; denoting these preimages by $p_i = \pi^{-1}(q_i)$, we have $\mathrm{Fix}(\iota) = \{p_1, \ldots, p_6\}$. These six points are called the **Weierstrass points** of Σ_2^0.

2.5.1 Fixed Point Dynamics of the Capped Monodromy

Recall that our hypothetical knot K is fibered of genus two. Let $h \in \mathrm{Mod}(\Sigma_2^1)$ denote its monodromy class on the surface with one boundary component, and let $\phi_h\colon \Sigma_2^1 \to \Sigma_2^1$ be its unique pseudo-Anosov geometric representative.

By Lemma 2.8, we know that the original monodromy ϕ_h possesses exactly one fixed point in the interior of the surface, which we shall denote by z.

When extending ϕ_h to the closed surface Σ_2^0 by capping the boundary with a disk, we introduce exactly one new fixed point, p (the center of the capping disk). Thus, the capped-off pseudo-Anosov map $\hat{\phi}_h$ has exactly two fixed points, $\{z, p\}$. The geometric fate of these two points under the branched covering is then dictated by the hyperelliptic involution, as established in the following proposition. This proposition is the principal new geometric input of this dissertation at the level of the Birman-Hilden setup: the parallel result of

Baldwin-Hu-Sivek [BHS25] for L-space knots starts from a monodromy with *zero* interior fixed points, in which case $\hat{\phi}_h$ has only the single capping fixed point and the swap-versus-fix dichotomy below does not arise.

Proposition 2.12 (Capping Off)**.** Let K be a hyperbolic, genus-two knot with monodromy class h and pseudo-Anosov representative ϕ_h. Suppose

$$\widehat{HFK}(K) \cong \widehat{HFK}(T_{2,3}\#T_{2,3}).$$

The capped-off monodromy $\hat{\phi}_h\colon \Sigma_2^0 \to \Sigma_2^0$ is a pseudo-Anosov homeomorphism with exactly two fixed points, and the hyperelliptic involution ι swaps these two fixed points.

Proof. By Lemma 2.8, ϕ_h has exactly one interior fixed point on Σ_2^1, which we denote z. Capping the boundary introduces one further fixed point p at the center of the capping disk, so $\mathrm{Fix}(\hat{\phi}_h) = \{z, p\}$.

Since ι and $\hat{\phi}_h$ commute, ι preserves the fixed point set of $\hat{\phi}_h$. Thus, ι must either fix both z and p pointwise, or swap them.

Suppose, for the sake of contradiction, that $\iota(z) = z$ and $\iota(p) = p$. Then z and p are Weierstrass points and descend to branch points on S^2, say $\pi(z) = q_5$ and $\pi(p) = q_6$.

We now follow the construction of Baldwin-Hu-Sivek [BHS25, Proof of Theorem 3.1], adapted to our setting. Remove the point p from Σ_2^0 and the corresponding branch point q_6 from S^2. The restriction of π gives a branched double cover

$$\pi'\colon \Sigma_2^0 \setminus \{p\} \to S^2 \setminus \{q_6\},$$

still branched along the five remaining points $q_1, \ldots, q_5$. We identify the punctured genus-two surface $\Sigma_2^0 \setminus \{p\}$ with the interior of Σ_2^1 (the genus-two surface with one boundary component),

and the punctured sphere $S^2 \setminus \{q_6\}$ with the interior of D^2. Under these identifications, the restriction of $\hat{\phi}_h$ to $\Sigma_2^0 \setminus \{p\}$ is freely isotopic to the original monodromy h on Σ_2^1, and π' extends to a branched double cover $\bar{\pi}\colon \Sigma_2^1 \to D^2$ along $\{q_1, \ldots, q_5\}$. The descended map $\phi_b|_{S^2 \setminus \{q_6\}}$ extends continuously to a homeomorphism $\phi_\beta\colon D^2 \to D^2$ fixing ∂D^2 pointwise (the boundary arising from the puncture), representing a 5-braid mapping class

$$\beta \in \mathrm{Mod}(D_5), \qquad \beta\colon (D^2, q_1, \ldots, q_5) \to (D^2, q_1, \ldots, q_5).$$

Let $\sigma_\beta \in S_5$ denote the permutation of the indices $\{1, \ldots, 5\}$ induced by ϕ_β on the marked points. Under our assumption, $z \in \Sigma_2^0$ descends to the branch point $q_5 \in S^2$, and z is fixed by $\hat{\phi}_h$, so q_5 is fixed by ϕ_β. Hence σ_β fixes the index 5. Consequently, the fifth strand of the braid forms a distinct link component L_1 of the closure $\hat{\beta}$, while the remaining strands form at least one other component. Thus, the closure $B = \hat{\beta}$ is a link with $\mu(B) \geq 2$ components.

The braid β specifies an open book decomposition of S^3 whose branch set is B. The covering map $\bar{\pi}$ extends to a branched double covering between the manifolds $M_h \to M_\beta$. Since K is a knot in S^3, we have $M_h \cong \Sigma(S^3, B) \cong S^3$. However, $b_1(\Sigma(S^3, B)) \geq \mu(B) - 1 > 1$, which implies M_h cannot be S^3, a contradiction.

Therefore, the involution ι cannot fix z and p. It must swap them: $\iota(z) = p$ and $\iota(p) = z$. $\square$

2.5.2 The Induced Map on the Disk

As a consequence of Proposition 2.12, z and p descend to a single point $r \in S^2$ that is *not* a branch point. Since z and p are fixed by $\hat{\phi}_h$, r is a fixed point of the spherical pseudo-Anosov map ϕ_b.

We perform a **real blow-up** at r: we replace r by its unit tangent circle, identifying $S^2 \setminus \{r\}$ with $\mathrm{int}(D^2)$ and adjoining ∂D^2 as a new boundary circle. The six branch points become

marked points in $\mathrm{int}(D^2)$, and ϕ_b extends to a pseudo-Anosov homeomorphism $\phi_\beta\colon D^2 \to D^2$ fixing ∂D^2 setwise, whose mapping class we denote $\beta \in \mathrm{Mod}(D_6)$. The blow-up produces a genuine self-map of D^2 precisely because $\phi_b(r) = r$: at a non-fixed point it would instead carry the blow-up at r to the blow-up at $\phi_b(r)$, a different surface. (Puncturing at r would serve the same purpose; we use the blow-up so as to land in the compact marked disk, the natural setting for the braid and train-track machinery of Chapter 3.)

Remark 2.13. The mapping class $\beta \in \mathrm{Mod}(D_6)$ is well-defined only up to powers of the full twist Δ_6^2. Fixing r, the representative ϕ_b determines a class in the pointed mapping class group $\mathrm{Mod}(S^2_{0,6}, r)$, and β is a preimage under the surjection $\mathrm{Mod}(D_6) \twoheadrightarrow \mathrm{Mod}(S^2_{0,6}, r)$ that collapses ∂D^2 to r. The kernel of this surjection is generated by the boundary-parallel Dehn twist Δ_6^2, central in $\mathrm{Mod}(D_6)$, giving the short exact sequence

$$1 \to \mathbb{Z}\langle\Delta_6^2\rangle \to \mathrm{Mod}(D_6) \to \mathrm{Mod}(S^2_{0,6}, r) \to 1,$$

so any two choices of β differ by a power of Δ_6^2. This ambiguity is harmless: the train-track enumeration of Chapter 3 operates on the quotient $\mathrm{Mod}(D_6)/\langle\Delta_6^2\rangle$, as a consequence of Corollary 3.9.

2.5.3 The Fixed-Point-Free Lift ϕ_Φ

We now lift the disk homeomorphism ϕ_β back to the genus-two surface, with two boundary components. Let Σ_2^2 denote the compact surface obtained from Σ_2^0 by performing a real blow-up at the two points z and p. Topologically, Σ_2^2 is a genus-two surface with two boundary components, which we denote ∂_z and ∂_p respectively (the unit tangent circles at z and p).

The branched covering $\pi\colon \Sigma_2^0 \to S^2$ restricts to a map $\Sigma_2^0 \setminus \{z, p\} \to S^2 \setminus \{r\}$, and after identifying the punctured surfaces with the interiors of Σ_2^2 and D^2, this extends continuously to a branched double covering

$$\tilde{\pi}\colon \Sigma_2^2 \to D^2,$$

branched along the six marked points $q_1, \ldots, q_6$ in $\mathrm{int}(D^2)$, with $\tilde{\pi}(\partial_z) = \tilde{\pi}(\partial_p) = \partial D^2$. The disk map ϕ_β then admits a lift under $\tilde{\pi}$ to a homeomorphism

$$\phi_\Phi \colon \Sigma_2^2 \to \Sigma_2^2.$$

The two lifts of ϕ_β under $\tilde{\pi}$ differ by the covering involution ι, which swaps ∂_z and ∂_p; we take ϕ_Φ to be the lift that preserves each boundary component. It is pseudo-Anosov, since being pseudo-Anosov is detected by the invariant foliations, and these lift through the branched cover. Under the identification of $\mathrm{int}(\Sigma_2^2)$ with $\Sigma_2^0 \setminus \{z, p\}$, this is precisely the lift agreeing with $\hat{\phi}_h$ (the other lift swaps z and p). Since $\mathrm{Fix}(\hat{\phi}_h) = \{z, p\}$ are exactly the blown-up points, $\hat{\phi}_h$ has no fixed points on $\Sigma_2^0 \setminus \{z, p\}$, and hence ϕ_Φ is fixed-point-free in the interior of Σ_2^2.

2.5.4 General Framework: Braids and Prongs

The constructions above yield what we shall term the *Birman-Hilden correspondence data*, an ordered tuple completely capturing the algebraic and geometric descent of the monodromy:

$$(h, \phi_h, \hat{h}, \hat{\phi}_h, b, \phi_b, \beta, \phi_\beta, \Phi, \phi_\Phi)$$

1. $h \in \mathrm{Mod}(\Sigma_2^1)$ is the original monodromy class of the hyperbolic knot K.

2. $\phi_h \colon \Sigma_2^1 \to \Sigma_2^1$ is the unique pseudo-Anosov representative of h. It has exactly one interior fixed point, z.

3. $\hat{h} \in \mathrm{Mod}(\Sigma_2^0)$ is the capped-off mapping class on the closed surface.

4. $\hat{\phi}_h \colon \Sigma_2^0 \to \Sigma_2^0$ is the pseudo-Anosov representative of $\hat{h}$. It possesses exactly two fixed points: the inherited point z, and the new capping center p.

5. $b \in \mathrm{Mod}(S_{0,6}^2)$ is the spherical mapping class obtained by descending $\hat{h}$ via the hyperel-

liptic involution.

6. $\phi_b \colon S^2 \to S^2$ is the pseudo-Anosov representative of b. It permutes the six branch points and has exactly one non-marked fixed point r, which is the geometric descent of z and p.

7. $\beta \in \mathrm{Mod}(D_6)$ is the 6-braid mapping class on the disk, obtained by performing a real blow-up of S^2 at the fixed point r.

8. $\phi_\beta \colon D^2 \to D^2$ is the pseudo-Anosov representative of β, fixing the boundary ∂D^2 set-wise and permuting the six marked points.

9. $\Phi \in \mathrm{Mod}(\Sigma_2^2)$ is the mapping class obtained by lifting β back to the genus-two surface with two boundary components (the real blow-up of z and p).

10. $\phi_\Phi \colon \Sigma_2^2 \to \Sigma_2^2$ is the pseudo-Anosov representative of Φ. It is strictly fixed-point-free in its interior.

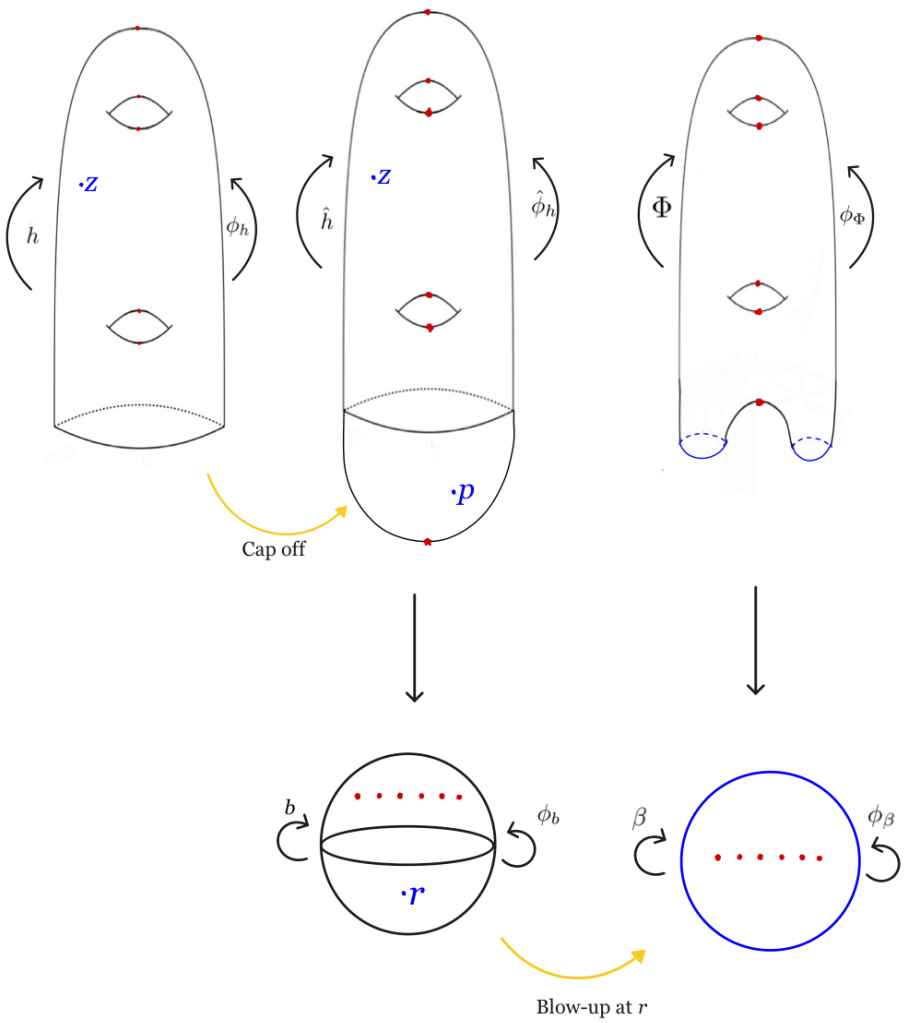


Figure 2.3: The Birman-Hilden Correspondence data. Top left: original knot monodromy h and its geometric representative ϕ_h, with one interior fixed point z. Top middle: Capped-off monodromy $\hat{h}$ and its geometric representative $\hat{\phi}_h$, with one additional fixed point p. Bottom Middle: Descent of capped-off monodromy b and its geometric representative ϕ_b, with a single fixed point r that is the descent of z and p. Bottom right: Blow-up at r to obtain a disk braid β and its geometric representative ϕ_β, no interior fixed points. Top right: lifting β to obtain Φ and its geometric representative ϕ_Φ, no interior fixed points. Capping off one of the boundaries of the top right recovers the original monodromy.

When h is pseudo-Anosov, its invariant foliations descend to the disk D^2. To understand the

geometric relationship between the singularities of ϕ_β and ϕ_h, we must examine the local behavior of the branched covering map π. As detailed by Reinoso [Rei24, Section 2.2], away from the branch locus, π is a local diffeomorphism; pulling back a singular foliation through a local diffeomorphism preserves the number of prongs but duplicates the singularity in the cover. Conversely, at the branch points, the covering map behaves locally like the complex map $w = z^2$. Pulling back a measured foliation through this purely quadratic map doubles the cone angle, effectively doubling the number of prongs.

Consequently, the geometric singularities relate via the following rigid dictionary:

- A k-pronged singularity of ϕ_β at a marked point (the branch locus) lifts to a single $2k$-pronged singularity of $\hat{\phi}_h$ because the covering map branches over these points, doubling the cone angle.
- A k-pronged singularity of ϕ_β on the boundary ∂D^2 (the blown-up unbranched point r) lifts to two distinct k-pronged boundaries ∂_z and ∂_p on Σ_2^2, which correspond to k-pronged singularities at z and p on Σ_2^0.
- A k-pronged singularity of ϕ_β in the interior of the disk (away from branch points) lifts to two distinct k-pronged singularities of $\hat{\phi}_h$, which are necessarily permuted by the hyperelliptic involution ι.

2.6 Strata

With this geometric dictionary established, we are now equipped to classify all possible Birman-Hilden correspondence data where h is the monodromy of a hyperbolic knot K satisfying $\widehat{HFK}(K) \cong \widehat{HFK}(T_{2,3}\#T_{2,3})$. We first enumerate all possible singularity structures (strata) that $\hat{\phi}_h$ can exhibit on Σ_2^0.

Proposition 2.14 (Euler-Poincaré Formula, [FM11, Proposition 11.4])**.** Let Σ be a surface with a singular foliation. Let P_s denote the number of prongs at a singular point s. Then

$$2\chi(\Sigma) = \sum_s (2 - P_s)$$

where the sum is over all singular points.

Applying this to the capped-off pseudo-Anosov $\hat{\phi}_h \colon \Sigma_2^0 \to \Sigma_2^0$, we obtain

$$-4 = \sum_s (2 - P_s). \tag{2.6}$$

The possible sets of prongs ($P_s > 2$) that satisfy this sum are:

- {3, 3, 3, 3}
- {3, 3, 4}
- {4, 4}
- {5, 3}
- {6}

We can immediately eliminate the $\{5, 3\}$ case. Since ι swaps z and p (Proposition 2.12) and is a homeomorphism, the local foliation pictures at z and p are identical; in particular, z and p must have the *same* prong count. The configuration $\{5, 3\}$ assigns distinct prong counts to its two interior singularities, so they cannot both be in $\{z, p\}$. But $\hat{\phi}_h$ permutes singularities of equal prong count, and each of the two singularities in $\{5, 3\}$ is the unique one of its prong count, so $\hat{\phi}_h$ must fix both. This would give at least three interior fixed points of $\hat{\phi}_h$ (the 5-pronged singularity, the 3-pronged singularity, and one of z, p), contradicting

$\text{Fix}(\hat{\phi}_h) = \{z, p\}$.

We can also eliminate $\{3, 3, 4\}$ and $\{6\}$ by the same mechanism. In $\{3, 3, 4\}$: because z and p have equal prong count, they can together account for the two 3-pronged singularities, but then the 4-pronged singularity remains alone with no partner of equal prong count. As $\hat{\phi}_h$ must permute equal-prong singularities, the unique 4-pronged singularity must be *fixed* by $\hat{\phi}_h$, contributing a third fixed point in the interior. Alternatively, if z and p are not the two 3-pronged singularities, then they would need to be the lone 4-pronged singularity together — but there is only one of those, so this case is impossible. Either way, $\{3, 3, 4\}$ forces a third interior fixed point, contradicting $\text{Fix}(\hat{\phi}_h) = \{z, p\}$.

The case $\{6\}$ is similar: the single 6-pronged singularity is unique in its prong count, so $\hat{\phi}_h$ must fix it. It cannot be either z or p, since z and p are required to share a prong count and there is only one 6-pronged singularity available. So the 6-pronged singularity would be a third interior fixed point, again a contradiction.

Thus, the only valid sets of singularities are $\{3, 3, 3, 3\}$ and $\{4, 4\}$. Bearing in mind that p and z must have the exact same number of prongs (which could also be 2, meaning they are smooth points), the possible configurations are summarized in Table 2.1.

Prongs on p	Prongs on z	Prongs on other Singularities
2	2	{4,4} or {3,3,3,3}
3	3	{3,3}
4	4	$\emptyset$

Table 2.1: Possible singularity configurations satisfying the Euler-Poincaré formula.

We analyze each case to determine the precise strata on Σ_2^0, S^2, and D^2.

2.6.1 Two prongs on z and p

If z and p are 2-pronged (smooth) points, then by Table 2.1 the remaining singularities form either $\{4,4\}$ or $\{3,3,3,3\}$; we determine the resulting strata according to whether these singularities lie at the Weierstrass (marked) points or at unmarked points.

For the stratum $(4,4;\emptyset)$, two marked points are 4-pronged singularities. ι fixes them, and $\hat{\phi}_h$ swaps them. This descends to $(2^2,1^4;2)$ on S^2, which corresponds to $(2;1^4,2^2;\emptyset)$ on D^2.

For $(\emptyset;4,4)$, two unmarked points are 4-pronged. ι swaps them, and $\hat{\phi}_h$ swaps them. This descends to $(1^6;4)$ on S^2, corresponding to $(2;1^6;4)$ on D^2.

For the $\{3,3,3,3\}$ case, marked points cannot be odd-pronged, leaving only $(\emptyset;3,3,3,3)$. The four 3-pronged unmarked points are permuted without fixed points. This descends to $(1^6;3^2)$ on S^2, corresponding to $(2;1^6;3^2)$ on D^2.

Stratum on Σ_2^0	Stratum on S^2	Stratum on D^2
$(4,4;\emptyset)$	$(2^2,1^4;2)$	$(2;1^4,2^2;\emptyset)$
$(\emptyset;4,4)$	$(1^6;4)$	$(2;1^6;4)$
$(\emptyset;3,3,3,3)$	$(1^6;3^2)$	$(2;1^6;3^2)$

Table 2.2: The strata with two prongs on z and p.

2.6.2 Three prongs on z and p

Here, z and p are 3-pronged, leaving two additional unmarked 3-pronged singularities. This is stratum $(\emptyset;3,3,3,3)$, where z and p are among the set. ι and $\hat{\phi}_h$ both swap the extra two singularities. This descends to $(1^6;3,3)$ on S^2, corresponding to $(3;1^6;3)$ on D^2.

2.6.3 Four prongs on z and p

If z and p are 4-pronged, there are no additional singularities. This is stratum $(\emptyset;4,4)$. It descends to $(1^6;4)$ on S^2, corresponding to $(4;1^6;\emptyset)$ on D^2.

Stratum on Σ_2^0	Stratum on S^2	Stratum on D^2
$(\emptyset; 3, 3, 3, 3)$	$(1^6; 3, 3)$	$(3; 1^6; 3)$

Table 2.3: The strata with three prongs on z and p.

Stratum on Σ_2^0	Stratum on S^2	Stratum on D^2
$(\emptyset; 4, 4)$	$(1^6; 4)$	$(4; 1^6; \emptyset)$

Table 2.4: The strata with four prongs on z and p.

2.7 Summary

We close this chapter by recording the framework that the rest of the dissertation will inhabit.

Starting from a knot $K \subset S^3$ with $\widehat{HFK}(K) \cong \widehat{HFK}(T_{2,3}\#T_{2,3})$, the genus and fiberedness detection results of Ozsváth-Szabó and Ni place K in the class of genus-two fibered knots. Thurston's classification of knots (Theorem 2.3) then partitions the remaining possibilities into torus, satellite, and hyperbolic, exclusively at the level of the knot exterior. The torus case is eliminated at once by the Alexander polynomial; the satellite case is treated separately in Chapter 8; the bulk of this dissertation is devoted to ruling out a distinct hyperbolic representative.

In the hyperbolic case, the monodromy class $h \in \mathrm{Mod}(\Sigma_2^1)$ has a unique pseudo-Anosov representative ϕ_h. The thinness and signature input force $\tau(K) = g(K) = 2$, which by Hedden's theorem characterizes K as strongly quasipositive, hence the associated open book supports the tight contact structure; Honda-Kazez-Matić then yields $0 < c(h) < 1$, and the fractional Dehn twist coefficient analysis shows the boundary singularity of ϕ_h has at least two prongs. The Ghiggini-Spano fixed-point bound combined with the Farber-Reinoso-Wang classification of zero-fixed-point monodromies then forces ϕ_h to have exactly one interior fixed point z.

Capping the boundary disk introduces a second fixed point p, so the closed-surface map $\hat{\phi}_h \colon \Sigma_2^0 \to \Sigma_2^0$ has $\mathrm{Fix}(\hat{\phi}_h) = \{z, p\}$. The centrality of the hyperelliptic involution ι in $\mathrm{Mod}(\Sigma_2^0)$ forces ι to commute with $\hat{\phi}_h$, and Proposition 2.12 shows that ι *swaps* z and p. From here, the Birman-Hilden machinery produces the correspondence data

$$(h, \phi_h, \hat{h}, \hat{\phi}_h, b, \phi_b, \beta, \phi_\beta, \Phi, \phi_\Phi),$$

in which the hyperbolic problem is repackaged as a question about a six-marked disk braid $\beta \in \mathrm{Mod}(D_6)$ and its fixed-point-free lift ϕ_Φ to Σ_2^2.

Finally, the Euler-Poincaré formula together with the constraint that z and p have identical prong counts cuts down the possible singularity types of $\hat{\phi}_h$ to five strata on Σ_2^0, and these descend to five strata on the disk D_6. The remainder of the dissertation is structured around these five strata: in Chapters 3–7 we develop the train-track machinery and the autofolder algorithm that allows us to enumerate the candidate pseudo-Anosov braids in each stratum, and in Chapter 9 we eliminate every candidate by a homological filtering pipeline. The satellite case, deferred from this chapter, is handled separately in Chapter 8, and the cable variant of the main theorem is treated in Chapter 10.

CHAPTER THREE

Train Tracks

In this chapter, we introduce the theory of train tracks, which together with the folding automata of Chapter 5 serve as the primary combinatorial engines for resolving the hyperbolic case of our main result. The ultimate goal of developing this machinery is to rigorously classify the pseudo-Anosov maps that can inhabit the singularity strata identified in Chapter 2. By translating the continuous topological dynamics of a surface homeomorphism into a discrete train track map, we can algorithmically constrain its behavior. Specifically, in Chapter 5 we will construct and utilize train track automata—directed graphs where paths correspond to sequences of valid folding operations—to systematically output the complete, finite list of standard train tracks that must be considered within each stratum.

Historically, the theory of train tracks was originally introduced by Thurston [Thu88] to study the dynamics of surface homeomorphisms and the classification of mapping classes. This geometric framework was later formalized combinatorially by Penner and Harer [PH92], providing a rigorous calculus for studying laminations on surfaces. Specifically, they formalized the notion of *carrying*, by which they proved that measured laminations can be identified with non-negative weight systems on a train track.

The problem of effectively constructing a train track representative for a given pseudo-Anosov

map was subsequently solved by Bestvina and Handel [BH95]. They introduced an algorithm that computes the invariant train track by iteratively folding a graph carried by the surface, a method that serves as the basis for the computational techniques used in this work.

We follow the conventions established by Reinoso [Rei24], who derived them from the work of Song, Ko, and Los [SKL02] and Ham and Song [HS07].

3.1 Train Tracks on a Compact Surface

Let S be a compact surface, possibly with non-empty boundary, and containing a set Q of n marked points. We first provide the general topological definition of a train track on S.

Definition 3.1 (Train Track)**.** A *train track* on S is a smooth, branched 1-submanifold $\tau \subset S$ satisfying the following conditions:

1. τ is contained in the interior $S \setminus \partial S$.
2. The branch points of τ, referred to as *switches*, have valence at least 3.
3. **Tangency:** At every switch v, the tangent vectors of the incident branches are collinear. Consequently, there is a well-defined tangent line $T_v\tau$ in the tangent space T_vS.
4. **Cusps:** If two branches incident to a switch v share the same ray of the tangent line (i.e., their tangent vectors point in the same direction), we say they form a *cusp*.
5. **Complementary Regions:** Every component of the complement $S \setminus \tau$ is either an unmarked polygon with $k \geq 3$ sides or a marked polygon (containing exactly one marked point) with $k \geq 1$ sides (where "sides" are branches of τ and "vertices" are switches).

We consider two train tracks τ_1 and τ_2 to be **equivalent** if they are smoothly isotopic relative to the marked points Q. Formally, there exists a smooth family of embeddings $h_t : \tau \to S$ for $t \in [0, 1]$ such that $h_0(\tau) = \tau_1$, $h_1(\tau) = \tau_2$, and for all t, $h_t(\tau)$ is a valid train track disjoint from Q. From this point on, unless otherwise stated, we speak of train tracks on a surface up to equivalency.

3.1.1 The Underlying Graph

It will be necessary to separately consider certain combinatorial data of a train track from its smooth embedding.

Definition 3.2 (Underlying Graph)**.** The *underlying graph* of a train track τ, denoted G_τ, is the 1-dimensional CW-complex obtained by forgetting the C^1 tangency structure at the switches.

- The vertex set $V(G_\tau)$ consists of the switches of τ.
- The edge set $E(G_\tau)$ consists of the branches of τ.

Two train tracks τ_1 and τ_2 have isomorphic underlying graphs if there is a graph isomorphism $\varphi : G_{\tau_1} \to G_{\tau_2}$.

Remark 3.3. An isomorphism of underlying graphs does not imply the train tracks are equivalent, as the graph G_τ itself does not encode the embedding information into the surface S. In the terminology of [SKL02], the graph G_τ corresponds to the *skeleton*, while the train track τ constitutes a specific *marking* (embedding) of that skeleton which encodes the cusp data.

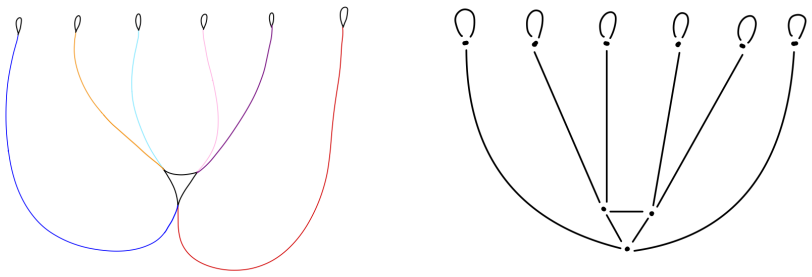


Figure 3.1: A train track and its underlying graph.

3.2 Train Track Maps and Dynamics

Having established the geometric structure of train tracks, we now define the notion of carrying and the dynamics of maps on the track. We follow the definitions provided in Reinoso [Rei24, Section 2.2].

3.2.1 Carrying and Fibered Neighborhoods

To relate train tracks to surface homeomorphisms formally, we use the notion of a fibered neighborhood.

Definition 3.4 (Fibered Neighborhood)**.** A *fibered neighborhood* $F(\tau) \subset S$ is a tubular neighborhood of the train track τ equipped with a singular foliation by vertical fibers. The leaves of this foliation are transverse to the branches of τ and are singular only at the switches (corresponding to the corners of the polygonal complementary regions).

Now we are ready to define what it means for a train track to "carry" a surface homeomorphism.

Definition 3.5 (Carrying)**.** A homeomorphism $\phi_h : S \to S$ is said to be *carried* by τ if $\phi_h(\tau)$ can be isotoped into the interior of $F(\tau)$ such that the image is everywhere transverse to the vertical fibers.

We say that a mapping class $h \in \mathrm{Mod}(S)$ is carried by τ if its geometric representative ϕ_h is carried by τ.

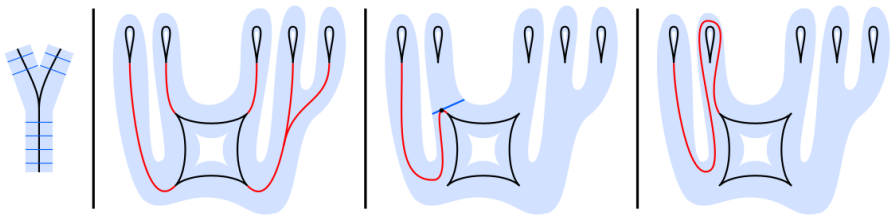


Figure 3.2: An example fibered neighborhood, and transversality of a train track map. Left: A switch of a train track τ (black) inside its fibered neighborhood $F(\tau)$ (blue), with the vertical fibers (blue, transverse to the branches) singular at the switch. Center, Right: The image of a train path (red) on a train track, drawn first transverse to the vertical fibers and then collapsed back onto τ. The middle panel shows the carrying condition: $\phi_h(\tau) \subset F(\tau)$ is transverse to the vertical fibers; the rightmost panel shows the resulting train track map $f_h : \tau \to \tau$ obtained by projecting along fibers. Image courtesy of Braeden Reinoso [Rei24].

3.2.2 Train Paths and Maps

When ϕ_h is carried by τ, we can project the image $\phi_h(\tau)$ along the fibers of $F(\tau)$ back onto τ. This projection induces a combinatorial map on the track itself. To make this more precise, we make use of the following definitions:

Definition 3.6 (Train Path)**.** A *train path* on τ is a smooth immersion $\gamma : [0, 1] \to \tau$ mapping endpoints to switches. Crucially, γ must respect the tangent structure: it may pass through a switch smoothly, but it may not turn back at a cusp (i.e., it cannot backtrack against the flow).

Definition 3.7 (Train Track Map)**.** A *train track map* is a continuous surjection $f : \tau \to \tau$ such that:

1. f maps switches to switches.

2. For any train path γ, the composition $f \circ \gamma$ is a valid train path.

This definition ensures that the map f does not "fold" the track back onto itself arbitrarily; it preserves the smooth directionality of the branches. The geometric content of the carrying definition — the transverse fiber structure of $F(\tau)$ and the requirement that $\phi_h(\tau)$ lie transverse to the vertical fibers — is illustrated in Figure 3.2.

When ϕ_h is carried by a train track τ, there is naturally an induced train track map $f_h\colon \tau \to \tau$, determined by the image $\phi_h(\tau)$ under ϕ_h. For an edge e of τ, we define $f_h(e)$ to be the train path that the image $\phi_h(e) \subset F(\tau)$ collapses onto under the natural deformation retraction $F(\tau) \to \tau$.

Figure 3.3 shows an example of an illustration of a train track map. On the left is a train track τ, where we have named six of the edges: b, o, s, i, p, r and given them (arbitrary) orientations, all oriented toward the monogons. The image of each of these colored edges is the following:

$$f_\beta(b) = s$$

$$f_\beta(o) = i$$

$$f_\beta(s) = ppr$$

$$f_\beta(i) = bbo$$

$$f_\beta(p) = b$$

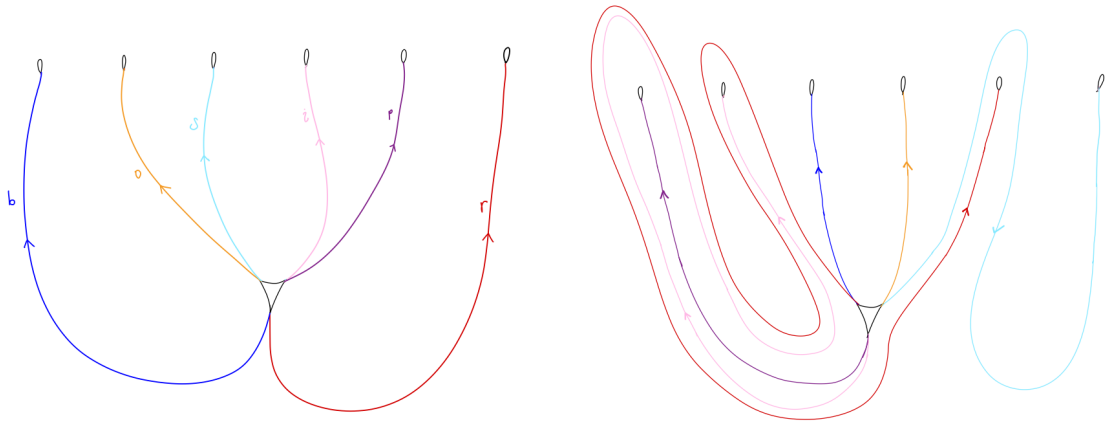


Figure 3.3: Left: A train track τ. Right: A train track map $f\colon \tau \to \tau$.

$$f_\beta(r) = bboosp$$

The image of the black edges making up the polygons can be inferred from the image of the above edges.

An important result of Bestvina-Handel is the fact that a geometric representative ϕ_h of a mapping class $h \in \mathrm{Mod}(S)$ is completely determined by its induced train track map on a train track that carries ϕ_h:

Theorem 3.8 ([BH95], [Rei24, Theorem 2.2.1])**.** Let $h, g \in \mathrm{Mod}(S)$ be two mapping classes with geometric representatives ϕ_h, ϕ_g, respectively. Suppose that h and g are carried by the same train track τ, and induce maps $f_h, f_g\colon \tau \to \tau$. If $f_h = f_g$, then h and g are freely isotopic and $\phi_h = \phi_g$.

Applying Theorem 3.8 to the specific case of maps on the n-marked disk, we have the

following corollary:

Corollary 3.9 ([Rei24, Corollary 2.2.2])**.** Let $\alpha, \beta \in \mathrm{Mod}(D_n)$ be two n-braids which are carried by the same track τ and induce the same train track map $f_\alpha = f_\beta : \tau \to \tau$. Then, we have

$$\phi_\alpha = \phi_\beta,$$

and

$$\alpha = \Delta^{2k}\beta$$

for some $k \in \mathbb{Z}$, where $\Delta^2 = (\sigma_1 \dots \sigma_{n-1})^n$ is a full twist about ∂D_n.

Corollary 3.9 resolves the full-twist ambiguity in the Birman-Hilden disk braid noted in Remark 2.13. The disk braid $\beta \in \mathrm{Mod}(D_6)$ associated to a hyperbolic fibered knot K via the Birman-Hilden correspondence is well-defined only up to powers of Δ_6^2. By the corollary, two braids carried by the same train track and inducing the same train-track map differ exactly by a power of Δ_6^2. The train-track framework therefore captures each disk braid at precisely the resolution at which it is canonically defined: a coset of $\langle \Delta_6^2 \rangle$ in $\mathrm{Mod}(D_6)$, represented by a unique train-track map. All downstream obstructions in this dissertation — the orientability obstruction of Chapter 4, the homological filter of Chapter 7, and the trace and absorption obstructions of Chapter 7 — depend on the disk braid only through its train-track signature, and therefore factor through the quotient $\mathrm{Mod}(D_6)/\langle \Delta_6^2 \rangle$ automatically.

We formalize the relationship between a mapping class and its combinatorial representation through the concept of *geometric data*. For a mapping class $h \in \mathrm{Mod}(S)$, the geometric data is defined as the tuple

$$(h, \phi_h, \tau, f_h),$$

comprising the mapping class h, its geometric representative ϕ_h, a train track τ that carries h, and the induced train track map $f_h : \tau \to \tau$.

While a single mapping class may be carried by a variety of distinct train tracks, the induced map f_h is uniquely determined by the choice of τ. It is important to distinguish this structure from general train tracks; an arbitrary train track does not necessarily carry a mapping class, nor does every train track map on a track correspond to a surface homeomorphism. However, when this data exists—particularly in the pseudo-Anosov case—the train track τ effectively encodes the geometry of the mapping class, as the following proposition shows:

Proposition 3.10 ([BH95])**.** Let h be a pseudo-Anosov mapping class carried by τ. If N is a connected interior (resp. peripheral) component of $S \setminus \tau$, then τ has p cusps along ∂N if and only if ϕ_h has a p-pronged singularity in the interior of N (resp. a p-pronged boundary in N).

For an illustration of Proposition 3.10, consider once again the train track τ shown on the left of Figure 3.3. This is the *candelabra* track on D_6: six 1-cusped monogons each enclosing a marked point, plus one 3-cusped interior infinitesimal triangle. If this track carries a pseudo-Anosov braid (which it does — the map shown on the right of Figure 3.3 is precisely such a train-track map), then by the proposition the singularity type is forced. The six marked monogons each contribute one 1-pronged singularity at a marked point. The interior triangle contributes one 3-pronged interior singularity. The remaining peripheral region adjacent to ∂D^2 must absorb the remaining prong structure; the Euler-Poincaré count for the disk shows that it has exactly three cusps, contributing a 3-pronged boundary singularity. Thus the candelabra carries pseudo-Anosov braids in precisely the stratum $(3; 1^6; 3)$, one of the five admissible disk strata enumerated in Chapter 2.

Remark 3.11 (Terminology in the literature)**.** We note that in the broader literature on surface dynamics (e.g., Penner-Harer [PH92], Bestvina-Handel [BH95]), a train track τ satisfying the condition that $f_h(\tau)$ is carried by τ in an efficient manner (specifically, with a non-negative transition matrix) is typically referred to as an *invariant train track*.

In this work, we follow the conventions of Reinoso [Rei24], where this invariance property is intrinsic to the definition of *geometric data* for a pseudo-Anosov mapping class. Consequently, we will generally avoid the term "invariant train track" and instead refer to the tuple (h, ϕ_h, τ, f_h) as the geometric data associated with the map.

3.3 Relationship to Invariant Foliations

The utility of train tracks in studying pseudo-Anosov homeomorphisms arises from their relationship with the invariant measured foliations. Recall from the definition of a pseudo-Anosov map $\phi\colon \Sigma \to \Sigma$, that it preserves a pair of transverse measured singular foliations: the unstable foliation $\mathcal{F}^u$ (which is expanded by a factor $\lambda > 1$) and the stable foliation $\mathcal{F}^s$ (which is contracted by $1/\lambda$).

Following Thurston [Thu88] and the formalization by Penner and Harer [PH92], a train track τ carrying a pseudo-Anosov ϕ can be understood as a C^1 *smoothing* of the singular foliation $\mathcal{F}^u$. This creates a correspondence between the invariant foliations of a pseudo-Anosov ϕ_h and a train track that carries it. This is made explicit in the construction of Bestvina and Handel [BH95] (also see Reinoso [Rei24]), and is rigorous in the following sense:

The algorithm developed by Bestvina and Handel provides a systematic method for constructing a train track τ that carries a pseudo-Anosov homeomorphism ϕ_h. Central to this construction is the concept of an *efficient fibered surface* $F \subset S$, which acts as a deformation retract of the surface S. The surface F admits a decomposition into rectangular *strips* and disk-like *junctions*, where the strips connect the junctions and are foliated by arcs parallel to the junction boundaries.

To pass from this fibered surface to the train track τ, one performs a controlled collapse of the decomposition. While the strips collapse to form the *real edges* of the track, the junctions are not merely collapsed to vertices; rather, they are refined into a complex of *infinitesimal*

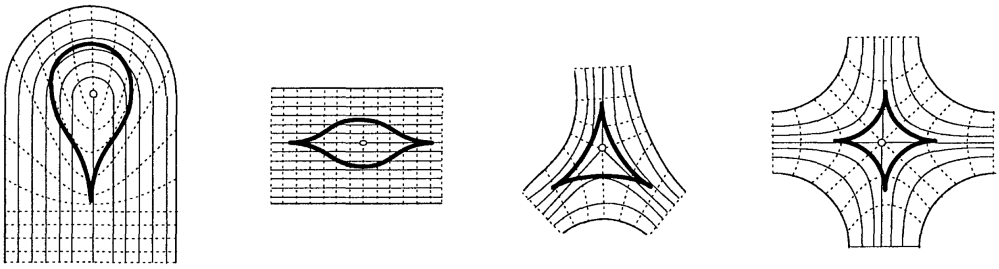


Figure 3.4: Local models of k-pronged singularities ($k = 1, 2, 3, 4$). The solid lines, tangent to the boundaries of the central complementary regions, represent the leaves of the unstable foliation $\mathcal{F}^u$. The transverse dotted lines represent the leaves of the stable foliation $\mathcal{F}^s$.

edges determined by the local dynamics of ϕ_h. This structure ensures that the induced train track map $f_h : \tau \to \tau$ restricts to an automorphism on the subgraph of infinitesimal edges. Consequently, the topological characteristics of the complementary regions within the junctions—referred to as *infinitesimal polygons*—are preserved. Specifically, f_h maps any infinitesimal polygon to an image with an identical number of cusps.

On the other hand, given a train track τ that carries ϕ_h, one can recover the invariant foliations (up to isotopy), so that τ lies tangent to $\mathcal{F}^u$ and transverse to $\mathcal{F}^s$. By Proposition 3.10, each connected interior/peripheral region is a k-sided polygon, with a k-pronged singularity within. In this way, there exists an embedding of the unstable foliation $\mathcal{F}^u$ into the fibered neighborhood $N(\tau)$. Under this embedding, every regular leaf of $\mathcal{F}^u$ is everywhere transverse to the vertical fibers of $N(\tau)$. Consequently, the branches of τ are isotopic to the leaves of $\mathcal{F}^u$ away from the singularities. See Figure 3.4.

3.4 Real and Infinitesimal Edges

Since the details of the Bestvina-Handel construction are not of central importance to our work, it suffices for us to take the following equivalent notion of *infinitesimal edges* and *real edges*. For us, it is merely a matter of combinatorial convenience in distinguishing those

edges of a train track that enclose an interior singularity to form polygons, from those edges which connect these polygons.

- **Infinitesimal Edges ($E_{\mathbf{inf}}$):** Edges that lie on the boundary of the connected regions of $S \setminus \tau$ containing the marked points and interior non-marked singularities. In the context of the invariant foliation, these correspond to the separatrices near these singularities and carry zero transverse measure. We refer to the polygons they make up as *marked infinitesimal polygons* or *unmarked infinitesimal polygons*, depending on whether they enclose a marked point or a non-marked interior singularity.

- **Real Edges ($E_{\mathbf{real}}$):** All edges of τ not in E_{inf}. These edges connect the infinitesimal regions and carry the dynamics of the map.[1]

These two edge types are illustrated by the candelabra track of Figure 3.3 (left). The six colored edges $\{b, o, s, i, p, r\}$ are the real edges; the unlabeled black edges are the infinitesimal edges. There are seven infinitesimal polygons: six marked monogons (each enclosing one marked point) and one unmarked triangle in the interior (enclosing a 3-pronged interior singularity).

Remark 3.12 (Marked points versus punctures)**.** We pause to fix terminology. Following Farb and Margalit [FM11, Chapter 1], a *puncture* is a point removed from a compact surface; the resulting surface is non-compact, with an end at the missing point. A *marked point* is a distinguished interior point of a compact surface that is preserved (as a point) by all homeomorphisms and isotopies under consideration. The two carry the same topological information for purposes of mapping class groups, and the literature is generally cavalier about the distinction. In this dissertation we work with the *closed disk* $D_n = D^2$ together with n marked points, since the train-track framework requires the compact disk with its true boundary ∂D^2. Hence we use *marked point* throughout and reserve *puncture* for cases

[1] Ham and Song [HS07] refer to these as "expanding edges," a term highlighting their role in the Markov partition. We retain Reinoso's terminology for consistency.

where we genuinely need to refer to a removed point (as in the discussion of puncturing versus real blow-up in Chapter 2, Section 2.5).

The Transition Matrix

With the distinction between real and infinitesimal edges in place, we can encode the combinatorial dynamics of a train-track map in a single matrix. The idea is that a train-track map $f_h : \tau \to \tau$ sends each edge to a train path traversing a sequence of edges, and we record how many times each edge is traversed. Because the infinitesimal edges carry zero transverse measure — they contribute nothing to the lengths used by the pseudo-Anosov to compute its dilatation — we ignore them and track only the real edges. This gives a square matrix indexed by the real edges, whose (i, j) entry counts the number of times $f_h(e_j)$ traverses the real edge e_i. The matrix encodes all the dynamical content of the map at the level of real edges: its spectral radius is the dilatation of ϕ_h, and its trace bounds the fixed-point count via the Perron-Frobenius theorem stated below. For full details, see Bestvina-Handel [BH95].

Definition 3.13 (Transition Matrix)**.** Let $E_{\text{real}}(\tau) = \{e_1, \ldots, e_m\}$ be the set of *real edges* of a train track τ. The *transition matrix* $M(f_h)$ is the $m \times m$ non-negative integer matrix where the entry M_{ij} records the number of times the image $f_h(e_j)$ traverses the edge e_i in either direction.

Example 3.14 (Transition matrix of the candelabra)**.** Returning to Figure 3.3, with the labeling $E_{\text{real}}(\tau) = \{b, o, s, i, p, r\}$ in this order, the train-track map is recorded by

$$f(b) = s, \quad f(o) = i, \quad f(s) = ppr, \quad f(i) = bbo, \quad f(p) = b, \quad f(r) = bboosp.$$

The transition matrix $M(f)$ in this basis is

$$M(f) = \begin{pmatrix} 0 & 0 & 0 & 2 & 1 & 2 \\ 0 & 0 & 0 & 1 & 0 & 2 \\ 1 & 0 & 0 & 0 & 0 & 1 \\ 0 & 1 & 0 & 0 & 0 & 0 \\ 0 & 0 & 2 & 0 & 0 & 1 \\ 0 & 0 & 1 & 0 & 0 & 0 \end{pmatrix},$$

where the row indexed by an edge e_i records, across the columns, how many times each $f(e_j)$ passes over e_i. Note that $\mathrm{tr}(M(f)) = 0$ — no real edge appears in its own image. By the Trace Lemma (Section 3.7), this is consistent with the lifted surface map being fixed-point-free, a necessary condition for this train-track map to arise from the lift of a hyperbolic genus-two fibered knot satisfying our hypotheses.

Theorem 3.15 (Perron-Frobenius [BH95; Rei24])**.** Let h be a pseudo-Anosov mapping class carried by τ, with geometric representative ϕ_h, inducing the train track map $f_h : \tau \to \tau$. Then the transition matrix $M(f_h)$ is a Perron-Frobenius matrix. The spectral radius of $M(f_h)$ is exactly the dilatation $\lambda(\phi_h)$ of the pseudo-Anosov map. In this case, the dilatation $\lambda(\phi_h)$ is the largest eigenvalue of $M(f_h)$, and the number of fixed points of ϕ_h is bounded in terms of the trace of $M(f_h)$:

$$\mathrm{tr}(M(f_h)) \leq |\mathrm{Fix}(\phi_h)|.$$

3.5 Standard Train Tracks on the Marked Disk

We now restrict our attention to the unit disk D_n with n marked points $Q = \{q_1, \ldots, q_n\}$. We utilize the subclass of *standard train tracks* defined by Ko-Los-Song [SKL02], Farber-Reinoso-Wang [FRW24], and Reinoso [Rei24]. A result of Ko-Los-Song ensures that every

pseudo-Anosov map on D_n is carried by such a track.

Definition 3.16 (Standard Train Track)**.** A train track $\tau \subset D_n$ is *standard* if:

1. **Infinitesimal Polygons:** Every component of $D_n \setminus \tau$ disjoint from ∂D_n is an *infinitesimal polygon*. Its boundary consists entirely of infinitesimal edges.

2. **Switches:** The set of switches coincides with the vertices of these infinitesimal polygons.

3. **Tangency Structure:**

   - Two adjacent infinitesimal edges at a switch share a common tangent (forming a smooth boundary for the polygon).

   - Two adjacent real edges at a switch share a common tangent.

   - A real edge and an infinitesimal edge at a switch are never tangent; they meet at a cusp.

4. **Vertical Marking:** For each marked point q_i, there is exactly one infinitesimal edge of τ passing vertically above q_i. No other edge intersects the vertical ray extending upwards from q_i.

Condition 4 is essential for identifying the mapping class group of the marked disk with the braid group B_n. It ensures the track is "pinned" in a canonical way relative to the standard braid generator positions.

The candelabra track of Figure 3.3 (left) is an example of a standard train track on D_6. Every interior complementary region (the six monogons and the central triangle) is infinitesimal — bounded entirely by infinitesimal edges; every switch sits on one of these polygons; the tangency structure is exactly the cusp/smooth pattern required by condition 3; and each

marked point sits below exactly one infinitesimal edge of its enclosing monogon, satisfying the vertical-marking condition.

Proposition 3.17 ([SKL02])**.** Every pseudo-Anosov map on a marked disk is carried by a standard train track.

3.6 Jointless Train Tracks

While Proposition 3.17 ensures that every pseudo-Anosov map on the disk is carried by a standard train track, this carrying track is not strictly unique. To obtain a canonical representative—and specifically one that facilitates the algorithmic detection of fixed points—we can restrict our attention to a well-behaved subclass of standard tracks by eliminating localized regions of combinatorial complexity known as *joints*.

Definition 3.18 (Joint)**.** Let τ be a standard train track. A *joint* is a switch v located on an infinitesimal monogon (a region surrounding a single marked point) such that v is incident to at least two real edges.

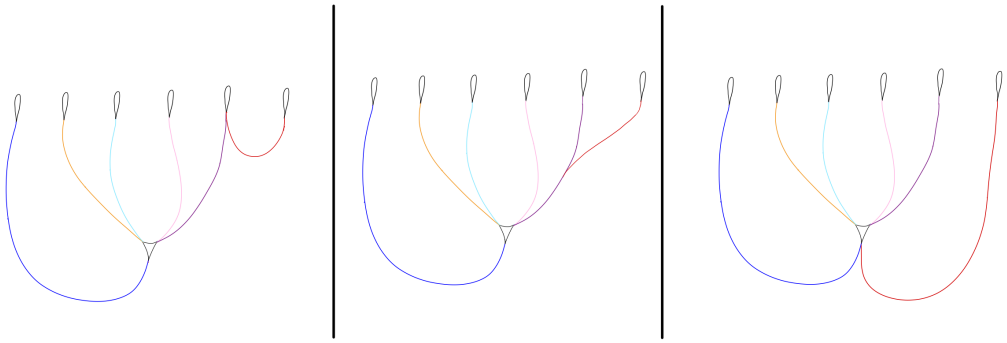


Figure 3.5: Some train tracks in the stratum $(3; 1^6; 3)$ on D_6. **Left:** a standard track with a joint — the red edge forms a real arc between two adjacent marked monogons, and the switch from the second monogon from the right is incident to two real edges (the purple and red edges entering the same monogon). **Center:** a non-standard track (with no joints) — the red edge meets the rest of the track away from a switch on an infinitesimal polygon, violating the tangency and switch-location conditions for a standard track. **Right:** a standard, jointless track, the *candelabra* of Figure 3.3, in which every marked monogon has exactly one real edge incident to its single switch.

Figure 3.5 illustrates the joint condition and contrasts it with two other types of track in the same stratum. The left panel is a standard track with a joint at the marked monogon on the right; the center panel is jointless but fails the standard-track conditions; the right panel is the candelabra of Figure 3.3, which is both standard and jointless, and serves as the running example throughout the dissertation.

Reinoso [Rei24] showed that for a broad class of pseudo-Anosov maps, these joints can be systematically eliminated through a graph-refinement operation known as *tight splitting*.

The formal mechanics of tight splitting will be rigorously defined and utilized in Chapter 6 to systematically reduce the list of train tracks to consider. For the purposes of our foundational setup, it suffices to rely on the following guarantee by Reinoso, which assures us that tight splitting will always successfully yield a jointless representative for the maps we care about:

Theorem 3.19 ([Rei24, Theorem C])**.** Let ϕ_β be a pseudo-Anosov representative of a braid β on the marked disk. Assume that the invariant foliations of ϕ_β have at least one k-pronged singularity away from the boundary with $k \geq 2$. Then, ϕ_β is carried by a standard train track τ with no joints.

Corollary 3.20 ([Rei24, Corollary 6.2.9])**.** Let ϕ_β be a pseudo-Anosov homeomorphism on the n-marked disk D_n. Suppose that the invariant foliations of ϕ_β have at least one k-pronged singularity in the interior of D_n (away from the boundary) with $k \geq 2$. Then ϕ_β is carried by a standard train track τ that has no joints.

Because the monodromy of our hypothetical genus-two knot necessarily involves 3-pronged or 4-pronged interior singularities (as classified in Table 2.1), we safely satisfy the hypothesis of Corollary 3.20. Consequently, we may strictly restrict our attention to jointless standard train tracks moving forward. In such tracks, every marked point is enclosed by a monogon incident to exactly one real edge, or is part of a larger polygon (cf. Figure 3.5, right).

3.7 Lifting Train Track Maps

To bridge the gap between the combinatorial dynamics of braids on the disk and the topology of genus-two knots in 3-manifolds, we consider the Birman-Hilden correspondence as described in Section 2.5 (with the surface conventions of Section 2.1). Under this correspondence, train tracks, as well as their associated maps on the disk, can be lifted back to the genus-two surface.

3.7.1 Geometric Lifting of Standard Tracks

To analyze the fixed-point properties of the surface map $\phi_\Phi \colon \Sigma_2^2 \to \Sigma_2^2$, we lift standard train tracks from the disk to the surface Σ_2^2 via the branched double covering map π. Let $\tau \subset D^2$ be a standard train track carrying the pseudo-Anosov braid β. Since τ is embedded in D^2,

its full preimage $\tilde{\tau} = \pi^{-1}(\tau)$ yields a graph embedded in Σ_2^2 which is inherently invariant under the hyperelliptic involution ι.

The geometric construction of the lifted track $\tilde{\tau}$ is strictly dictated by the local behavior of the covering map, which we illustrate in Figure 3.6. There are two regimes to consider: away from the branch points, π is a local diffeomorphism, and components lift in duplicate; at the branch points (the marked points $q_1, \ldots, q_6$ where the involution ι has fixed-point preimages), π behaves locally like $w = z^2$, which doubles the cone angle. The components of τ lift as follows:

1. **Real Edges:** Each real edge of τ avoids the branch points and therefore lifts to two distinct real edges in $\tilde{\tau}$, which are interchanged by ι.

2. **Interior Singularities (away from branch points):** An infinitesimal polygon with k sides in the interior of D^2 that does *not* enclose a marked point (i.e., it surrounds a non-marked interior pseudo-Anosov singularity, away from the branch locus of π) lies in the unbranched region of the cover. It therefore lifts to a pair of disjoint k-sided polygons in $\tilde{\tau}$, swapped by ι.

3. **Boundary Behavior:** The boundary of the disk ∂D^2 lifts to the two boundary components of Σ_2^2, denoted ∂_z and ∂_p, which are swapped by ι. An infinitesimal k-gon adjacent to ∂D^2 lifts to a $2k$-gon bounding ∂_z and a $2k$-gon bounding ∂_p, reflecting the local doubling of the cone angle.

The remaining case — infinitesimal polygons enclosing the *marked* points (the branch locus of π) — requires a separate analysis, since here the cover is branched. We treat this in the next subsection.

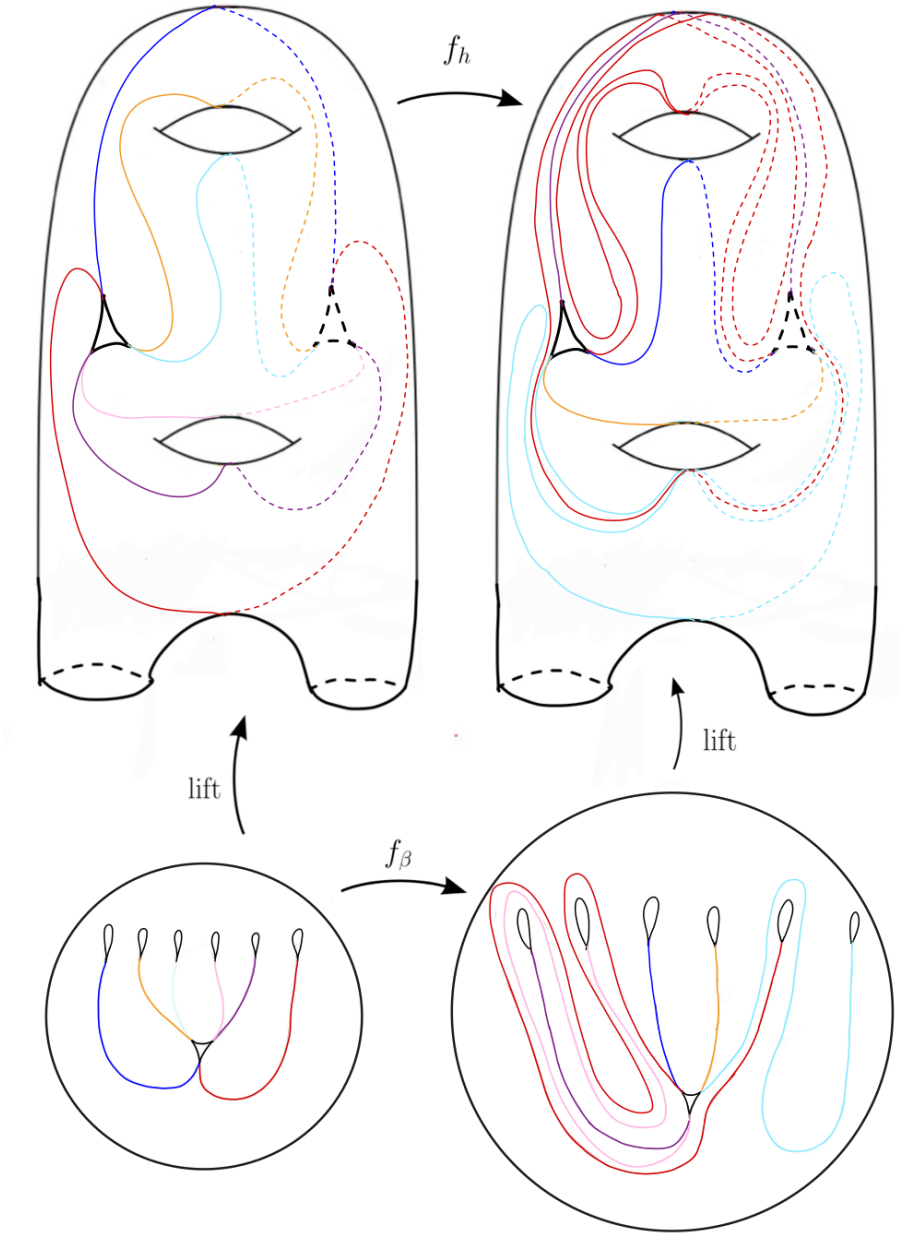


Figure 3.6: Lifting a train track and train track map from D_6 to Σ_2^2. Dashed edges indicate the back side of the surface.

3.7.2 Smoothing Infinitesimal Polygons at Branch Points

A necessary local modification to the lifted train track occurs at the branch points themselves. In a standard track on the disk, a marked point q_i may be surrounded by an infinitesimal k-gon (where $k \geq 1$), which represents a k-pronged singularity in the invariant foliation. Because the branched covering map π behaves locally like the complex map $w = z^2$ at the branch points, the strict topological preimage of this k-gon is an infinitesimal $2k$-gon enclosing the lifted Weierstrass point in Σ_2^2.

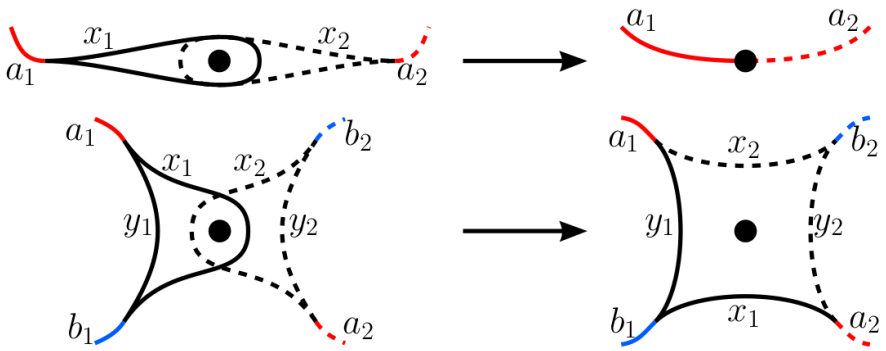


Figure 3.7: The local smoothing operation at branch points. Top: An infinitesimal monogon ($k = 1$) lifts to a bigon, which is smoothed into a regular real edge. Bottom: An infinitesimal bigon ($k = 2$) at a branch point lifts to a 4-gon with pinched internal cusps, which is smoothed into a proper 4-sided polygonal complementary region. Image courtesy of Braeden Reinoso [Rei24].

While this $2k$-gon correctly captures the doubled cone angle of the lifted foliation, the raw geometric lift retains "pinched" internal cusps where the lifted infinitesimal edges meet. To ensure the lifted track efficiently carries the pseudo-Anosov map ϕ_Φ and correctly acts as a C^1 smoothing of the unstable foliation, we must apply a local *smoothing* operation to these regions. This operation flattens the inward-pointing cusps, merging the infinitesimal edges into a continuous boundary. We illustrate the two distinct geometric outcomes of this operation in Figure 3.7:

1. **The $k = 1$ Case (Top):** If the original marked point was enclosed by a monogon, it

lifts to a 2-cusped bigon. In the theory of measured foliations, a 2-pronged singularity is geometrically degenerate; it corresponds merely to a regular, smooth point. Smoothing flattens the two cusps, merging the incident real edges into a single continuous line and entirely deleting the switches associated with the branch point.

2. **The $k \geq 2$ Case (Bottom):** If the original marked point was enclosed by a higher-order polygon (e.g., a bigon lifting to a 4-gon, as shown), the $2k$-pronged singularity is retained. The smoothing operation flattens the internal cusps, "opening up" the center to form a standard smooth polygonal complementary region with $2k$ sides, accurately bounding the $2k$-pronged saddle.

3.7.3 The Trace Lemma

Suppose the braid β is carried by τ via the train track map $f_\beta : \tau \to \tau$. While the lifted track $\tilde{\tau}$ is uniquely determined by the geometry described above, the map f_β does not lift uniquely as a train-track map on $\tilde{\tau}$. There are exactly two train-track maps

$$\tilde{f}, \tilde{g} \colon \tilde{\tau} \to \tilde{\tau}$$

satisfying the covering relation $\pi \circ \tilde{f} = \pi \circ \tilde{g} = f_\beta \circ \pi$. These two lifts are related by the covering involution: $\tilde{g} = \iota \circ \tilde{f}$.

To carry out the trace-lemma analysis, we must single out one of these two lifts as the geometrically meaningful one — the one whose dynamics actually correspond to the surface monodromy ϕ_Φ. Following Reinoso [Rei24, Section 2.3.2], the construction is as follows. The edges of $\tilde{\tau}$ come in pairs $\{e_1, e_2\}$ with $\iota(e_1) = e_2$, the two lifts of a single real edge e of τ. A standard track on D_n has a unique infinitesimal edge above each marked point inside the enclosing monogon; we call these the *side-swapping edges*, because a train path that crosses one switches between the two "sides" of $\tilde{\tau}$ (i.e., between e_1-type and e_2-type edges).

Given $f_\beta(e) = e(1)\cdots e(n)$, the lift $\tilde{f}_h$ is the unique lift for which, on each e_i, the image $\tilde{f}_h(e_i) = e(1)_{i_1}\cdots e(n)_{i_n}$ is the lift of $f_\beta(e)$ that starts on the same side of $\tilde{\tau}$ as the surface monodromy $\phi_\Phi(e_i)$ does. We refer to this as the **canonical lift** of f_β.

Remark 3.21 (Equivalent characterization via ∂_p)**.** The canonical lift admits a useful equivalent description in our setting. The two boundary components ∂_z, ∂_p of Σ_2^2 are swapped by ι (Proposition 2.12), so the two lifts $\tilde{f}_h, \iota\circ\tilde{f}_h$ differ on the boundary: one preserves the pair $\{\partial_z, \partial_p\}$ component by component, while the other swaps them. The geometric monodromy ϕ_h of the knot fixes its boundary $\partial\Sigma_2^1$ pointwise; identifying ∂_p with this boundary, the canonical lift is the one that preserves ∂_p as a set. This boundary-preserving formulation agrees with Reinoso's same-side formulation after tracing side-information through the smoothing operation. We use the boundary-preserving formulation in the rest of the dissertation.

A key utility of the canonical lift is the ability to relate the fixed points of the surface homeomorphism ϕ_Φ to the combinatorial properties of the disk map f_β. In particular, the presence of fixed points for ϕ_Φ can often be detected strictly by the trace of the transition matrix of the disk map. We encapsulate this relationship in the following lemma, due to Reinoso, which is essential for our detection arguments.

Lemma 3.22 (The Trace Lemma, [Rei24, Lemma 2.3.2])**.** Let $\beta \in \mathrm{Mod}(D_n)$ be a pseudo-Anosov braid carried by a standard train track τ, with induced train-track map $f_\beta : \tau \to \tau$ and canonical lift $\tilde{f}_h$. If the pseudo-Anosov representative ϕ_Φ is fixed-point free in the interior of Σ_2^2, then for any real edge e of τ, between any two occurrences of e in $f_\beta(e)$ the image path $f_\beta(e)$ contains an even number of side-swapping edges. In particular, $\mathrm{tr}(M(f_\beta)) = 0$.

For the train tracks used in this dissertation, the marked points are always enclosed by jointless monogons (Corollary 3.20), and in this case the trace lemma admits a much cleaner form.

Corollary 3.23 (Trace Lemma for jointless monogons, [Rei24, Corollary 2.3.3])**.** Retain the same notation and assumptions as Lemma 3.22. If e is a real edge of τ incident to a jointless monogon at a marked point, then e does not appear in $f_\beta(e)$.

Proof sketch of Lemma 3.22. The fixed points of ϕ_Φ are contained in the preimage of the fixed points of ϕ_β. For an efficient train-track map, fixed points of the map on the graph correspond to fixed points of the homeomorphism.

Suppose $\mathrm{tr}(M(f_\beta)) > 0$. Then f_β has a fixed point on the interior of some real edge $e \in \tau$. This edge lifts to a pair of edges e_1, e_2 in $\tilde{\tau}$ which are swapped by ι. A fixed point $x \in e$ lifts to a pair $\{y, \iota(y)\}$ in $\tilde{\tau}$, and the canonical lift $\tilde{f}_h$ must map this fiber to itself.

The two lifts $\tilde{f}_h$ and $\iota \circ \tilde{f}_h$ act differently on this fiber: one fixes each point individually, while the other swaps them. By the canonical-lift condition (equivalently, by the same-side characterization or the ∂_p-preservation), the canonical lift fixes each point of the fiber individually. Consequently, both y and $\iota(y)$ are fixed points of $\tilde{f}_h$, and they correspond to fixed points of the geometric representative ϕ_Φ in the interior of Σ_2^2.

Thus, if the trace is non-zero, ϕ_Φ retains an interior fixed point, contradicting the FPF hypothesis. The vanishing of the trace — equivalently, the no-self-appearance condition for real edges — is therefore necessary for ϕ_Φ to be FPF. The full "even number of side-swapping edges between adjacent occurrences" refinement is Reinoso's strengthening of this no-self-appearance condition, which we will use in the case analysis of Chapter 7. □

We will use the Trace Lemma to rule out pseudo-Anosov candidates for the monodromy of our knot. Because Heegaard Floer homology constraints imply that our hypothetical knot must have exactly one fixed point corresponding to the original un-capped surface (which we factored out into the boundary of Σ_2^2), we can immediately eliminate any braid β for which

$M(f_\beta)$ has non-zero trace.

CHAPTER FOUR

The Hyperbolic Case: The Strata $(2; 1^4, 2^2; \emptyset)$, $(4; 1^6; \emptyset)$, and $(2; 1^6; 4)$ on the Disk

4.1 Introduction

In this chapter, we analyze the specific strata of pseudo-Anosov homeomorphisms on the 6-marked disk defined by the singularity data $(2; 1^4, 2^2; \emptyset)$, $(4; 1^6; \emptyset)$, and $(2; 1^6; 4)$. We aim to rigorously eliminate these cases by proving the following result:

Theorem 4.1. Let $K \subset S^3$ be a hyperbolic knot satisfying $\widehat{HFK}(K) \cong \widehat{HFK}(T_{2,3}\#T_{2,3})$, and let

$$(h, \phi_h, \hat{h}, \hat{\phi}_h, b, \phi_b, \beta, \phi_\beta, \Phi, \phi_\Phi)$$

be the associated Birman-Hilden correspondence data induced by the monodromy of K. Furthermore, let

$$(\beta, \phi_\beta, \tau, f_\beta)$$

be the geometric data associated with the disk braid, where τ is a standard train track. Then the pseudo-Anosov representative $\phi_\beta \colon D^2 \to D^2$ (and consequently the invariant train track τ) cannot belong to the strata $(2; 1^4, 2^2; \emptyset)$, $(4; 1^6; \emptyset)$, or $(2; 1^6; 4)$.

To achieve this, our primary objective is to establish that the invariant foliations associated with the lifted pseudo-Anosov map on the genus-two surface with two boundary components Σ_2^2 in these strata are orientable. This will immediately imply that the original monodromy of K also possesses orientable invariant foliations.

Establishing orientability allows us to invoke the homological arguments utilized by Baldwin, Hu, and Sivek [BHS25] for their detection result on the cinquefoil. Specifically, once orientability is shown, we apply a theorem of Thurston [Thu88], as reformulated by Baldwin-Hu-Sivek, to identify the dilatation λ of the pseudo-Anosov map with the spectral radius of its action on the first homology of the branched cover. This action is completely determined by the Alexander polynomial of the knot K. We will demonstrate that for $T_{2,3}\#T_{2,3}$, the Alexander polynomial possesses no real roots $\lambda > 1$. This leads to a strict algebraic contradiction, thereby proving that the knot cannot support a pseudo-Anosov monodromy associated with these specific strata.

4.2 Orientability of Train Tracks

We begin by examining the combinatorial structure of the train tracks carrying the pseudo-Anosov maps in the specified strata. Let $\phi_\beta : D^2 \to D^2$ be a pseudo-Anosov homeomorphism of the 6-marked disk, and let τ be a train track carrying ϕ_β. Note that by Theorem 3.19, we may assume τ is a jointless standard train track.

Let $\tilde{\tau}$ denote the lift of τ to the double branched cover Σ_2^2. As described in Section 3.7, $\tilde{\tau}$ carries the lifted mapping class Φ with pseudo-Anosov representative ϕ_Φ. The lifted train track $\tilde{\tau}$ can be viewed geometrically as two copies of the planar train track τ, connected via the lifts of the marked points.

In the planar track τ, the marked points reside in the interior of infinitesimal polygons. Upon lifting to the double cover, these marked points lift to the Weierstrass points of the hyperelliptic surface. Each of these Weierstrass points is enclosed by infinitesimal polygons obtained by the smoothing procedure described in Section 3.7. In the specific strata under consideration, the marked points on the disk are enclosed by either monogons (1-pronged) or bigons (2-pronged).

Because the covering map acts locally as $w = z^2$, these infinitesimal polygons at the branch locus lift to regions with exactly double the number of sides. The bigons lift to 4-gons. The monogons lift to bigons, which are subsequently smoothed into regular points on the track (eliminating the cusps entirely). Similarly, on the boundary of the lift, the peripheral regions—which are 2-gons and 4-gons on the disk—lift to 4-gons and 8-gons, respectively. Finally, for the stratum $(2; 1^6; 4)$, the un-marked 4-pronged singularity (4-gon) lies in the unbranched interior of the disk; thus, it lifts cleanly to two distinct 4-gons on Σ_2^2 which are swapped by the hyperelliptic involution.

An equivalent description of the correspondence between τ and $\tilde{\tau}$ is as follows. Consider the

disk D^2 embedded in $\mathbb{C}$, with the marked points positioned on the real line. By assumption, τ is standard, hence only a single side-swapping edge passes vertically above each marked point. We may isotope τ so that every edge except for the side-swapping edges lies in the upper half-plane; hence the intersection of the underlying graph of τ with the lower half-plane is a union of disjoint arcs. We can then construct $\tilde{\tau}$ by taking the mirror image of this upper-half-plane graph across the real line and applying the required smoothing procedure at the marked points. This symmetric union is exactly the underlying graph of $\tilde{\tau}$. See Figure 4.1 (top and middle panels) for an illustration of this construction on a track in the stratum $(2; 1^4, 2^2; \emptyset)$ — the same underlying track whose lift was depicted (in a different schematic) in Figure 3.6, here redrawn in the reflection-and-smoothing presentation.

Lemma 4.2. In the strata $(2; 1^4, 2^2; \emptyset)$, $(4; 1^6; \emptyset)$, and $(2; 1^6; 4)$ on D^2, every complementary region of the lifted invariant train track $\tilde{\tau}$ on Σ_2^2 is an even-sided polygon.

Proof. By Proposition 3.10, the complementary regions of τ on the disk correspond to the singularities of the foliation.

- In the stratum $(2; 1^4, 2^2; \emptyset)$, the complementary regions are 1-gons, 2-gons, and a peripheral 2-gon.
- In $(4; 1^6; \emptyset)$, they are 1-gons and a peripheral 4-gon.
- In $(2; 1^6; 4)$, they are 1-gons, an interior 4-gon, and a peripheral 2-gon.

Since the double branched covering doubles the cone angle at the branch points and the boundary, the 1-gons smooth into 0-gons (regular lines), while the peripheral 2-gons and 4-gons lift strictly to 4-gons and 8-gons on Σ_2^2. The interior 4-gon in the unbranched region simply lifts to two distinct 4-gons. Therefore, all surviving complementary regions in $\tilde{\tau}$ have an even number of sides. □

We now establish a procedure to specify an orientation for the invariant foliations on Σ_2^2 by orienting the train track itself.

Definition 4.3 (Consistent Orientation)**.** Let τ be a train track. We call an orientation of the edges of τ (real and infinitesimal alike) **consistent** if for every switch v of τ:

- Any two edges forming a cusp at v are both oriented into, or both oriented out of, v.
- If two incident edges form a valid smooth train path through v, they must be oriented so that the train path flows continuously (one entering v, one leaving v).

It is immediately clear from this definition that any train track possessing odd-sided polygons (such as monogons or triangles) cannot be consistently oriented. Every polygon has cusps as its corners. Choosing an orientation for an edge incident to a polygon forces orientations on all adjacent edges along the boundary of that region. Since the orientation must flow either strictly into or strictly out of a cusp, it forces an alternating sequence of orientations at each subsequent cusp along the polygon. A cusp whose edges point inward must be adjacent to a cusp whose edges point outward. Consequently, a polygon with an odd number of corners yields an alternating parity contradiction and cannot admit a consistent orientation.

Conversely, this alternating property ensures that a train track whose complementary regions are strictly even-sided can always be consistently oriented. The argument is direct propagation: fix an arbitrary edge e_0 of $\tilde{\tau}$ and an arbitrary orientation on it. Then propagate orientations to all neighboring edges using the two rules of Definition 4.3—across a cusp, the two edges point the same direction; across a smooth switch, they point opposite directions. Because every complementary region has an even number of cusps, traversing the boundary of any region returns the orientation to itself without contradiction. Since $\tilde{\tau}$ is connected and embedded in the orientable surface Σ_2^2, this local propagation rule extends uniquely to a

global consistent orientation on the entire track. An example of this construction is shown in the bottom panel of Figure 4.1, with the consistent orientation indicated by red arrows on every edge of $\tilde{\tau}$.

Proposition 4.4. The invariant foliations of a pseudo-Anosov map ϕ_β belonging to the strata $(2; 1^4, 2^2; \emptyset)$, $(4; 1^6; \emptyset)$, and $(2; 1^6; 4)$ are orientable upon lifting to Σ_2^2.

Proof. Orientability of the foliation on Σ_2^2 corresponds directly to the existence of a consistent orientation of the edges of the lifted train track $\tilde{\tau}$. By Lemma 4.2, every complementary region in $\tilde{\tau}$ is an even-sided polygon, so by the direct propagation argument above, $\tilde{\tau}$ admits a globally consistent orientation. It remains to verify that this consistent orientation on the track edges extends to an orientation of the foliation $\mathcal{F}^u$ across the polygonal complementary regions.

Considering $\tilde{\tau}$ as embedded in Σ_2^2, the interior of every $2k$-sided infinitesimal polygon is foliated by the unstable foliation $\mathcal{F}^u$ as described in Section 3.3. Specifically, the well-defined tangent line at each cusp is parallel to a leaf extending to the interior singularity, forming the $2k$ prongs at the singularity. These separatrices can be oriented in direct accordance with the consistent orientation of the bounding track edges. This partitions the region into $2k$ sectors, each foliated by leaves parallel to the corresponding side. We orient these subregions smoothly in accordance with the consistent orientation of the polygon. This procedure extends the orientation across every interior region of each infinitesimal polygon without contradiction. See Figure 4.2.

It remains to show that the peripheral regions can be oriented in a compatible way. This is an identical procedure, except that the edges forming the periphery consist of both real edges and portions of the boundary components ∂_z, ∂_p. There are $2r$ cusps forming the corners of the peripheral region. The tangent line at each cusp is parallel to a leaf extending to

the boundary components, forming the r prongs at each of the two boundary components. These leaves can be oriented in accordance with the locally consistent orientation of the cusps. Because $\tilde{\tau}$ is globally consistently oriented, these paths connect without orientation clashes. We orient the foliations on the surrounding disk by extending the orientation of these paths smoothly towards the boundary. Thus, $\mathcal{F}^u$ is globally orientable. □

Corollary 4.5. Let K be a hyperbolic knot such that $\widehat{HFK}(K) \cong \widehat{HFK}(T_{2,3}\#T_{2,3})$, and suppose

$$(h, \phi_h, \hat{h}, \hat{\phi}_h, b, \phi_b, \beta, \phi_\beta, \Phi, \phi_\Phi)$$

is the corresponding Birman-Hilden correspondence data. If the disk map $\phi_\beta \colon D^2 \to D^2$ belongs to the strata $(2; 1^4, 2^2; \emptyset)$, $(4; 1^6; \emptyset)$, or $(2; 1^6; 4)$, then the invariant foliations of the original monodromy ϕ_h are orientable.

Proof. By Proposition 4.4, the invariant foliations of the fixed-point-free lift ϕ_Φ on Σ_2^2 are orientable; that is, the unstable foliation $\widetilde{\mathcal{F}}^u$ admits a global transverse orientation on Σ_2^2.

To recover the invariant foliations of the original knot monodromy ϕ_h on Σ_2^1, we cap off the boundary component ∂_z of Σ_2^2, collapsing it to the interior point z of Σ_2^1 (cf. Figure 2.3, where capping off one of the boundaries of the top-right surface recovers the original monodromy of the top-left). This recovers $\hat{\phi}_h$ on $\Sigma_2^0 \setminus \{p\}$, and restricting to Σ_2^1 by deleting a small disk around p produces the original monodromy $\phi_h \colon \Sigma_2^1 \to \Sigma_2^1$. Throughout this operation, the transverse orientation of $\widetilde{\mathcal{F}}^u$ in a neighborhood of ∂_z descends without sign flips or leaf crossings to a transverse orientation of $\hat{\mathcal{F}}^u$ in a punctured neighborhood of z, which in turn restricts to a transverse orientation of $\mathcal{F}^u$ on Σ_2^1. Thus the invariant foliation of ϕ_h on Σ_2^1 is orientable. □

Having established that the pseudo-Anosov representative ϕ_h in these strata must have

orientable invariant foliations, we can now strictly relate its dilatation to the homological invariants of the knot. We employ the argument formalized by Baldwin, Hu, and Sivek [BHS25], in which the dilatation $\lambda(\phi_h)$ manifests as an eigenvalue of the action of the map on the first homology.

Theorem 4.6 (Thurston [Thu88]; see also [LT11, Theorem 2.2])**.** If a pseudo-Anosov homeomorphism ϕ on a surface Σ preserves an orientable foliation, then its dilatation $\lambda > 1$ is a root of the characteristic polynomial of the induced map on homology:

$$\det(\lambda I - \phi_*) = 0, \tag{4.1}$$

where $\phi_* : H_1(\Sigma; \mathbb{R}) \to H_1(\Sigma; \mathbb{R})$. In particular, λ is a real eigenvalue of ϕ_*.

In the context of the monodromy of a knot, the map $\phi = \phi_h$ is the geometric representative of h, the monodromy of the fibration associated with the knot K. Consequently, the characteristic polynomial of the homological action ϕ_* is identified exactly with the Alexander polynomial of the knot.

Corollary 4.7. For a fibered knot K, if the monodromy ϕ_h lies in a stratum with orientable invariant foliations, then the dilatation $\lambda(\phi_h) > 1$ must be a real root of the Alexander polynomial $\Delta_K(t)$.

4.3 Application to $T_{2,3}\#T_{2,3}$

We now apply this algebraic restriction to our specific case: the candidate knot $K = T_{2,3}\#T_{2,3}$. The Alexander polynomial for the right-handed trefoil $T_{2,3}$ is given by $\Delta_{T_{2,3}}(t) = t^2 - t + 1$, and the Alexander polynomial of the connect-sum is the product of the individual polynomials:

$$\Delta_K(t) = \Delta_{T_{2,3}}(t) \cdot \Delta_{T_{2,3}}(t) = (t^2 - t + 1)^2. \tag{4.2}$$

The discriminant of the quadratic factor $t^2 - t + 1$ is $\Delta = (-1)^2 - 4(1)(1) = -3 < 0$. Hence the roots of $t^2 - t + 1$ are the primitive sixth roots of unity,

$$t = \frac{1 \pm i\sqrt{3}}{2} = e^{\pm i\pi/3},$$

which are strictly complex. Consequently, $\Delta_K(t) = (t^2 - t + 1)^2$ has no real roots.

4.4 Conclusion

We now assemble the preceding results to formally prove our main theorem.

Proof of Theorem 4.1. Assume, for the sake of contradiction, that the knot K admits a monodromy ϕ_h corresponding to a disk map ϕ_β belonging to the strata $(2; 1^4, 2^2; \emptyset)$, $(4; 1^6; \emptyset)$, or $(2; 1^6; 4)$. By Proposition 4.4, the invariant foliations of the lifted map ϕ_Φ on Σ_2^2 are orientable. By Corollary 4.5, the invariant foliations of the original knot monodromy ϕ_h on Σ_2^1 are likewise orientable.

Therefore, by Corollary 4.7, the dilatation $\lambda(\phi_h) > 1$ must be a real root of the Alexander polynomial $\Delta_K(t) = (t^2 - t + 1)^2$. However, as established in the preceding section, $\Delta_K(t)$ has strictly complex roots and no real roots, contradicting the requirement that λ be a real root exceeding 1.

Thus, no pseudo-Anosov representative for the knot K exists within these orientable strata. □

This elimination constitutes a critical step in the classification of the fiber surface monodromy, demonstrating that knot Floer homology severely restricts the topological dynamics of K. By eliminating these three strata using only the orientability obstruction, we reduce our remaining task to the analysis of the non-orientable strata $(3; 1^6; 3)$ and $(2; 1^6; 3^2)$, which

we treat in Chapter 7 via the more delicate Trace Lemma and Absorption Obstruction machinery.

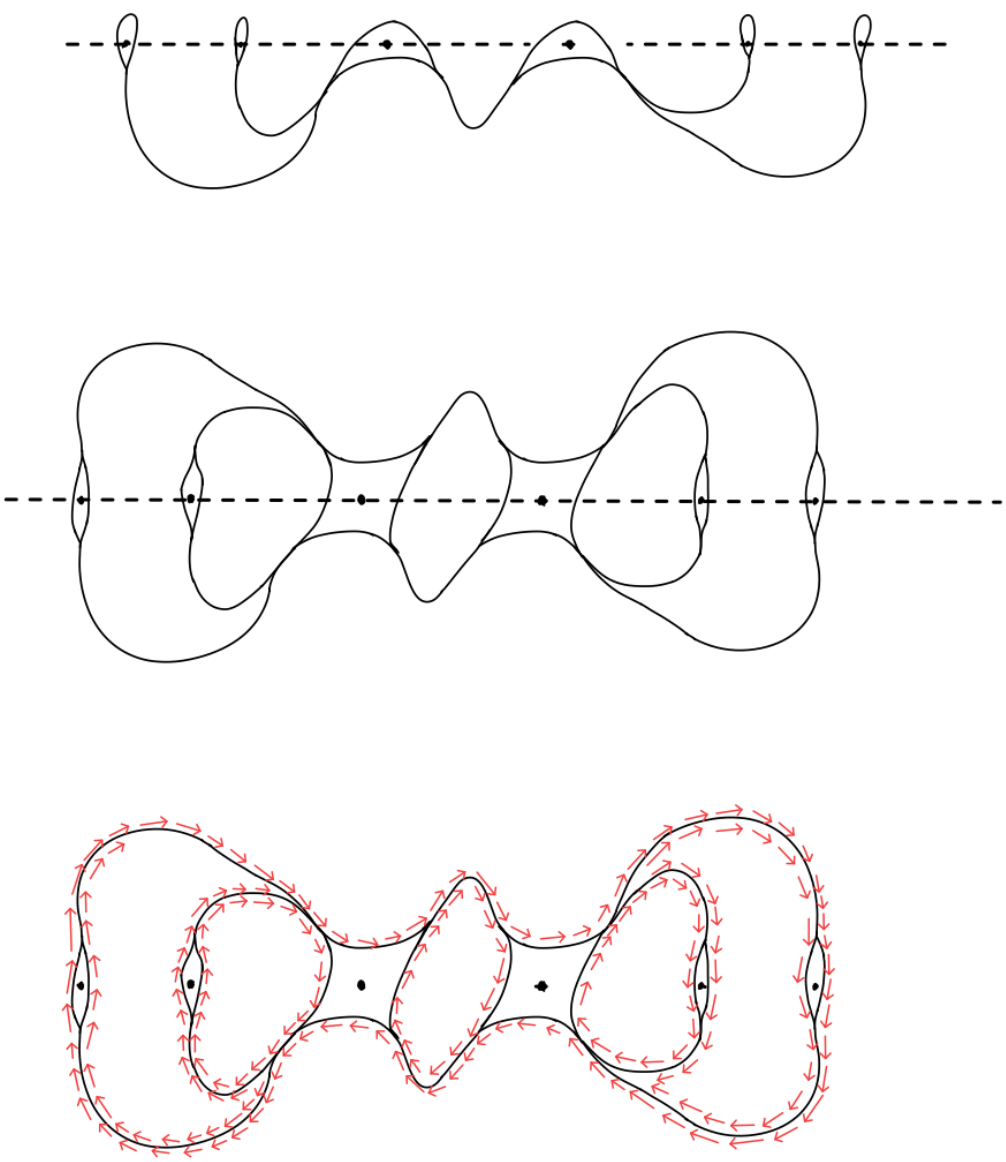


Figure 4.1: Top: A train track τ in the stratum $(2; 1^4, 2^2; \emptyset)$, drawn with its marked points on the real line (dashed). Middle: Reflecting τ across the real line and resolving the polygons via the smoothing procedure of Section 3.7 produces the lifted track $\tilde{\tau}$ on Σ_2^2. (This is the same lifted track depicted, in a different schematic, in Figure 3.6.) Bottom: A consistent orientation on $\tilde{\tau}$ (red arrows on every edge), possible because every complementary region is even-sided.

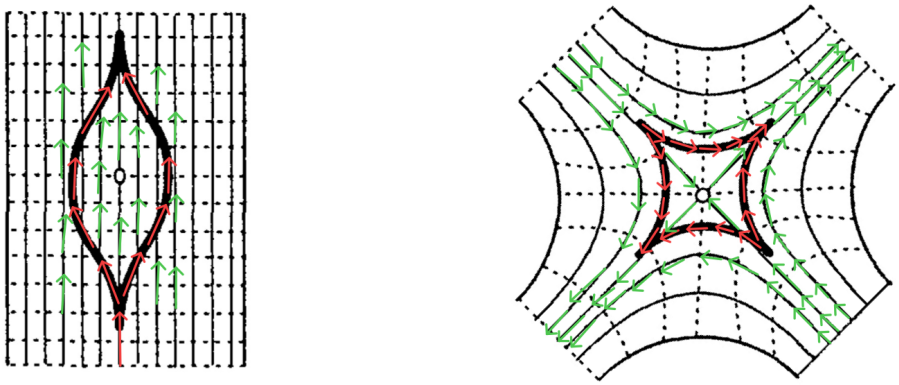


Figure 4.2: Near a singularity, a consistent orientation of the surrounding train track (red arrows) induces a globally consistent orientation on the leaves of the unstable foliation (green arrows).

CHAPTER FIVE

Folding Automata on the Disk

In Chapter 4, we successfully eliminated the pseudo-Anosov strata $(2; 1^4, 2^2; \emptyset)$, $(4; 1^6; \emptyset)$, and $(2; 1^6; 4)$ by exploiting the global orientability of their lifted invariant foliations. The remaining possible strata for the disk monodromy—specifically those containing odd-pronged internal singularities, namely $(2; 1^6; 3^2)$ and $(3; 1^6; 3)$—do not admit orientable foliations. To eliminate these final candidates, we cannot rely on the Alexander polynomial. Instead, in Chapter 7 we will directly construct the valid train track maps within these strata and manually apply the Trace Lemma established in Chapter 3.

This topological case analysis requires a finite, exhaustive list of candidate standard train tracks to serve as the starting point. While the existence of an invariant train track is guaranteed by the Bestvina-Handel algorithm [BH95], we require a systematic enumeration of all possible tracks within our specific strata.

To achieve this, we utilize the concept of the *folding automaton*, introduced by Ko, Los, and Song [SKL02]. A folding automaton is a directed graph where vertices represent isomorphism classes of train tracks and edges represent folding operations. For the purposes of this thesis, we utilize the automaton strictly as an **enumeration engine**. By generating the complete automaton for a given stratum, the set of vertices provides the exact, finite catalog

of standard train tracks required for our subsequent analysis.

In this chapter, we describe the theory of folding automata on the n-punctured disk D_n. We then present our computational implementation of the "genauto" algorithm proposed by Ham and Song [HS07], which we have developed in the software package `autofolder` to systematically output the candidate tracks for our remaining strata.

5.1 Folding and The Folding Automaton

Ko, Los, and Song [SKL02] defined the folding automaton $\mathcal{A}_n$ for the braid group B_n. This structure encodes all possible standard train tracks (of a fixed complexity) and the transitions between them. First, we must define the procedure of *folding* a train track.

5.1.1 Elementary Folding

To rigorously define the folding operation, we adopt the terminology of Reinoso [Rei24], who adapts the notion of elementary folding from Ham and Song [HS07].

Definition 5.1 (Markov Map)**.** Let τ and τ' be standardly embedded train tracks on D_n. A **Markov map** is a graph map $p : \tau \to \tau'$ that maps vertices to vertices and is locally injective away from the preimages of vertices.

Definition 5.2 (Elementary Folding Map)**.** An **elementary folding map** is a smooth Markov map $p : \tau \to \tau'$ satisfying the following conditions:

1. **Edge Lengths:** There exists exactly one real edge $\alpha \in E(\tau)$ such that its image $p(\alpha)$ has word length 2 in the edge basis of τ'. For all other edges $e \in E(\tau) \setminus \{\alpha\}$, the image $p(e)$ has word length 1.

2. **Cusp Condition:** The distinguished edge α must belong to a cusp of τ. Specifically, if α and β form a cusp at a switch v, then $p(\alpha)$ is of the form $p(\beta) \cdot \delta$ (or $\delta \cdot p(\beta)$), effectively "zipping" α along β.

In this context, *smoothness* implies that p preserves the tangent structure at the switches, mapping cusps to cusps or smoothing them into arcs, strictly preserving the train track embedding.

The transition matrix M_p of an elementary folding map (with respect to the basis of real edges, in the convention of Section 3.2) has a simple structure. All real edges except α map to a single real edge under p, contributing a single 1 to their column. The distinguished edge α maps to a real-edge word of length two, namely $p(\alpha) = p(\beta) \cdot a$ (where a is the real edge joined to $p(\beta)$ by an intermediate infinitesimal edge), contributing a 1 in the row of $p(\beta)$ and a 1 in the row of a. We may therefore write

$$M_p = P + E,$$

where P is a permutation matrix (the column of α assigns it to the destination real edge a, and all other columns implement the bijection p acts on the remaining real edges) and E is an elementary matrix — zero except for a single 1 in position $(p(\beta), \alpha)$ — recording the extra traversal of $p(\beta)$ in the image of α.

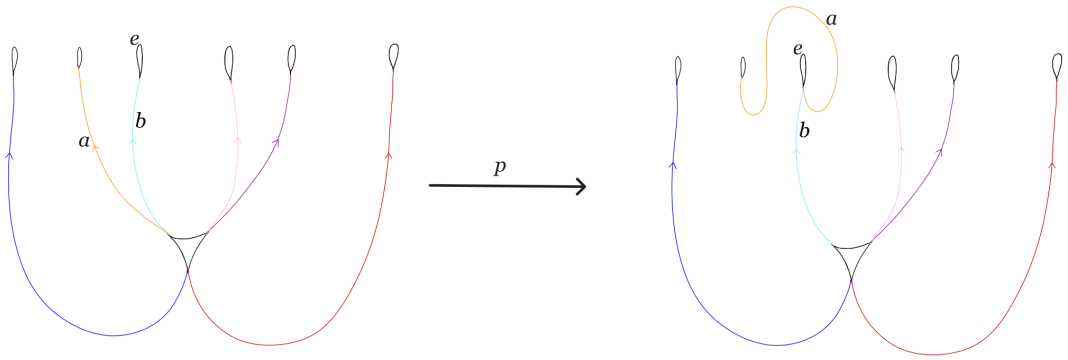


Figure 5.1: An example of an elementary folding map. The map p is the identity except at the edge a, which is mapped as a directed path to $b \cdot e \cdot a$.

Geometric Description. Visually, the folding operation takes place at a **cusp**—a switch v where two *real* edges, say a and b, meet tangentially. In the local cyclic ordering at v, these real edges are separated by an infinitesimal edge e, which represents the boundary of a punctured region.

To fold a onto b, we slide the vertex v along the edge b. This action identifies a with a segment of b ("zipping" them together) and simultaneously drags the endpoint of the edge a along the fold path. The fold terminates when v reaches the vertex at the other end of e. At this point, the modified a connects to the infinitesimal edge located at that destination vertex, completing the topological transition. For an example, see Figure 5.1, which shows an elementary folding of a onto b at the cusp formed between the two edges.

Remark 5.3 (Why Real Edges?)**.** It is important to note that a valid cusp must involve two *real* edges (or at least one real edge, depending on the specific standard definitions used). A cusp formed purely by two infinitesimal edges is forbidden in a standard train track. Dynamically, such a fold would be trivial (mapping zero measure to zero measure). Topologically, two infinitesimal edges meeting at a cusp would imply a singularity on the

boundary of a puncture that is not connected to the interior foliation; such a configuration is unstable and can be removed by isotopy.

5.1.2 The Standardizing Braid

While an elementary folding map $p : \tau \to \tau'$ preserves the foliation data, the resulting graph τ' often fails to satisfy the vertical marking condition of a standard train track. For example, the folding operation in Figure 5.1 produces a non-standard train track. Recall from Definition 3.16, the vertical marking condition requires that for each marked point, there is exactly one infinitesimal edge of τ passing vertically above it. In practice, this infinitesimal edge belongs to the infinitesimal polygon surrounding the marked point.

After an elementary fold starting from a standard train track τ, the folded track τ' often violates the vertical marking condition; however, Ko-Los-Song [SKL02] show that τ' is at most *almost standard*. That is, τ' has at most one offending infinitesimal edge. In other words, there is at most one marked point having two infinitesimal edges lying above it. We can perform a homeomorphism of the disk to transform the embedding of the folded train track so that it becomes standard. This choice of homeomorphism fixes the boundary pointwise, is orientation-preserving, and respects the marked points (permutes them), and thus can be thought of as a braid. We call such a braid a *standardizing braid*. This standardizing braid is non-unique for a given almost standard train track. However, it can be taken to be of a certain form[1]:

[1]Recall that braid words are read from left to right.

Lemma 5.4 ([SKL02, Lemma 1])**.** Let τ' be an almost standard train track on D_n. Then there exists an n-braid $\beta \in B_n$ of the form

$$\beta = \delta_{[l,m]}^{\pm 1},$$

where

$$\delta_{[l,m]} = \sigma_{m-1}\sigma_{m-2}\cdots\sigma_l,$$

is the n-braid written in standard Artin generators, so that $\beta(\tau')$ is a standard train track on D_n.

Figure 5.2 shows an example of a standardizing operation following an elementary fold.

5.1.3 The Folding Automaton

A pseudo-Anosov braid β induces a train track map $f_\beta : \tau \to \tau$ on a standard train track τ. By the work of Bestvina-Handel and others, f_β admits a decomposition into a sequence of elementary folding maps followed by a train track isomorphism:

$$f_\beta \simeq \psi \circ p_k \circ \ldots \circ p_1, \tag{5.1}$$

where each $p_i : \tau_{i-1} \to \tau_i$ is an elementary folding map and $\psi : \tau_k \to \tau_0$ is an isomorphism, that is, a train track map induced by an orientation-preserving pointed homeomorphism of the disk.

It is further shown that the folding decomposition of Equation (5.1) can be rewritten so that it implies that the braid β decomposes as the composition of standardizing braids associated to the elementary folding operations p_i, along with a braid inducing the isomorphism ψ:

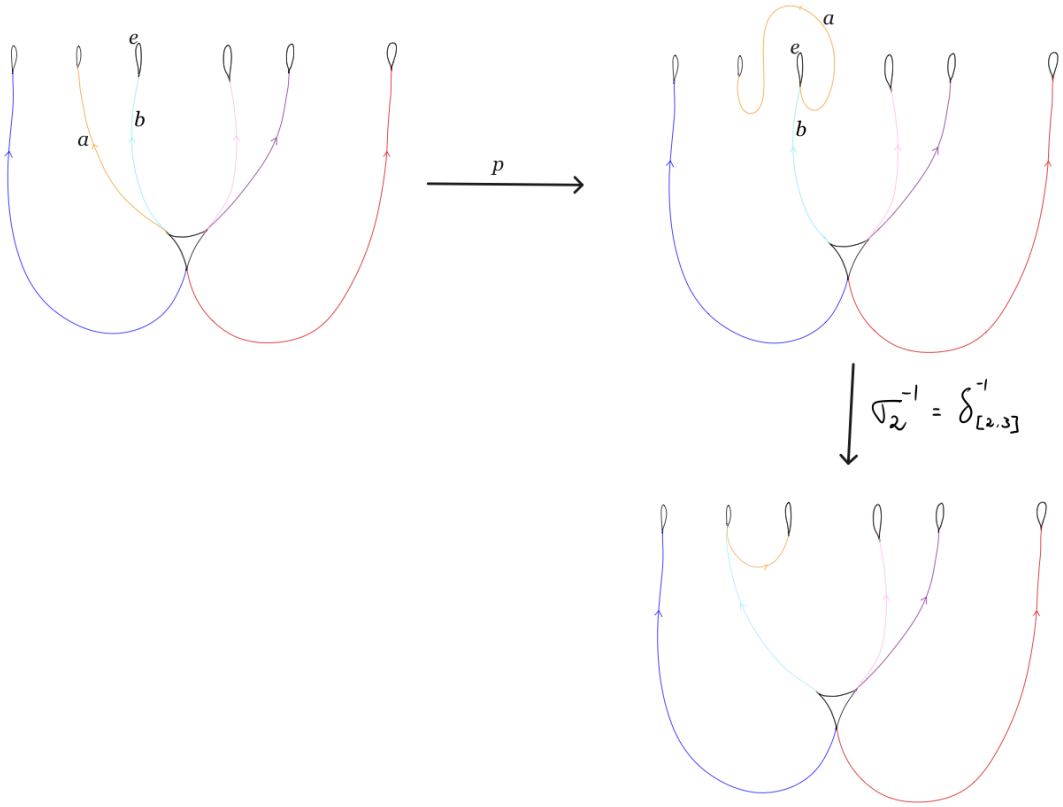


Figure 5.2: The braid $\delta_{[2,3]}^{-1} = \sigma_2^{-1}$ standardizes the folded train track.

$$\beta = \Delta_n^{2m} \Psi \circ \beta_{p_k} \circ \ldots \circ \beta_{p_1}. \tag{5.2}$$

Here Ψ is a braid inducing the train track isomorphism $\psi \colon \tau_k \to \tau_0$; the term Δ_n^{2m} accounts for an ambiguity arising from the Dehn twists along the outer boundary. This motivates the following definition:

Definition 5.5. Let τ and τ' be train tracks on D_n (not necessarily standard). We say τ and τ' are *isomorphic* if there exists a braid inducing a train track isomorphism between the two train tracks.

Geometrically, this definition is equivalent to saying that τ and τ' are ambient isotopic relative to the boundary, via an isotopy that is permitted to permute the marked points.

We are now ready to give the formal definition of the folding automaton:

Definition 5.6 (Folding Automaton)**.** The folding automaton $\mathcal{A}$ is a directed graph defined as follows:

- **Vertices:** The set of vertices $V(\mathcal{A})$ consists of isomorphism classes of standard train tracks on D_n. In other words, each vertex represents an orbit of standard tracks under the action of the braid group B_n.
- **Edges:** A directed edge exists from a class $[\tau_1]$ to $[\tau_2]$ if there exists a standard train track $\tau \in [\tau_1]$ and a valid cusp c such that folding τ at c and standardizing yields a track $\tau' \in [\tau_2]$.
- **Labels:** The directed edge is labeled by the standardizing braid $\beta_{std} \in B_n$ required to return the folded track to standard form.

Stratum Specificity It is important to emphasize that in our context, an automaton is constructed for a **single, fixed stratum** of the space of measured foliations $\mathcal{PMF}(D_n)$. The stratum is determined by the number and type of singularities of the foliations carried by the tracks. This restriction to a single stratum is a natural consequence of the folding operation itself. Geometrically, the complementary regions of a standard train track correspond precisely to the singularities of the measured foliations it carries; the cusps along the boundary of each complementary region count the prongs of the corresponding singularity (Proposition 3.10). An elementary folding map modifies the embedding of τ only locally near the folded edge α, replacing α with a path that forms a bigon with the original edge inside its enclosing complementary region. This local modification fixes the boundary of every complementary region setwise and preserves the cusp count along each boundary. Therefore folding leaves the

singularity stratum invariant: if a track τ decomposes the disk into a specific configuration of k-gons, every track reachable from τ via folding decomposes the disk into exactly the same set of k-gons.

Corollary 5.7. Let $(\beta, \phi_\beta, \tau, f_\beta)$ be geometric data of a pseudo-Anosov n-braid. Then τ appears as a vertex in the folding automaton associated to the particular stratum ϕ_β belongs to.

Corollary 5.8. Let β be a pseudo-Anosov n-braid. Up to conjugacy, a decomposition of β in the form of Equation (5.2) appears as a cycle in the folding automaton.

Proof. By Proposition 3.17, β is carried by a standard train track τ, and the isomorphism class of τ must exist as a vertex in the folding automaton. □

Figure 5.3 shows an example of a folding automaton of the 4-marked disk, on the stratum $(1; 1^4; 1)$. The solid lines represent folding operations, where "ROL fold" means **Right-Over-Left fold**. This indicates that the edge on the right-hand side of the cusp (facing toward the mouth of the cusp) is folded over the edge on the left-hand side. Since there is a single cusp in this example, this is sufficient to specify the particular folding operation. The analogous **Left-Over-Right Fold** is represented by "LOR fold".

The dotted lines are standardizing operations and thus represent isomorphisms. Consequently, this specific automaton is a directed graph with three vertices and six directed edges.

In general, the folding automaton of a particular stratum can become extremely complicated as soon as the disk under consideration has 5 or 6 marked points, making it impracticable to reproduce graphically.

Ham and Song [HS07] proposed an algorithm for generating the folding automaton, which they termed `genauto`. The theoretical version of this algorithm, as described in the appendix

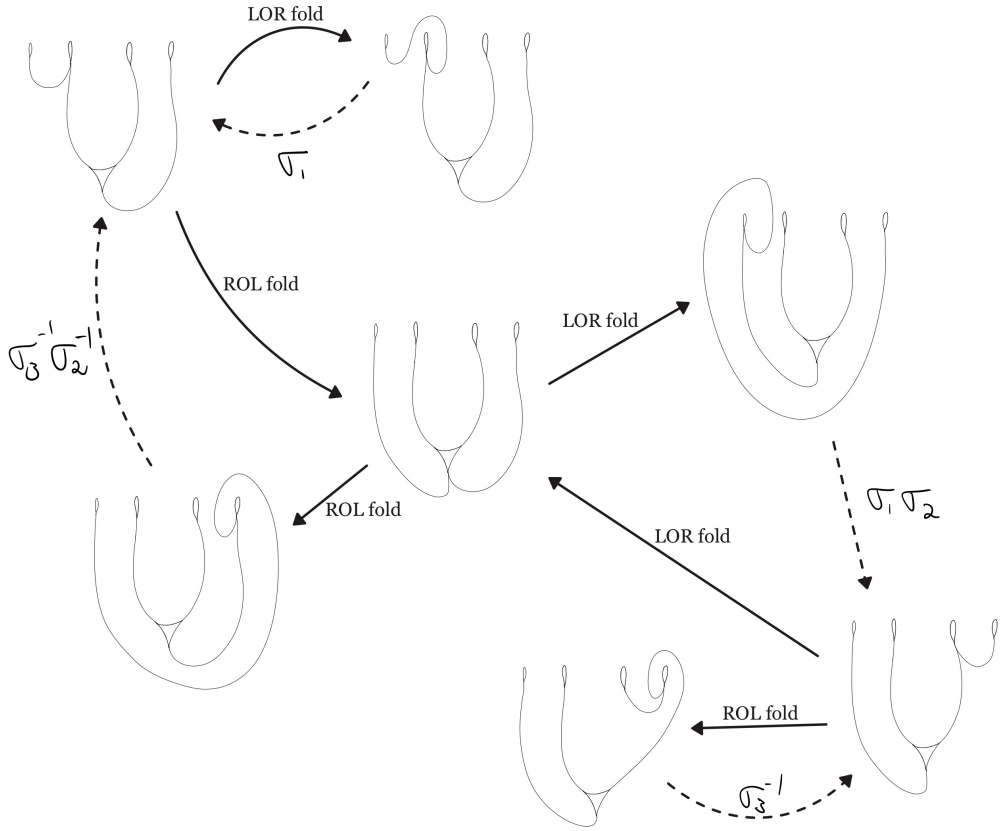


Figure 5.3: The folding automaton of the stratum $(1; 1^4; 1)$ on the 4-marked disk.

of their work, is presented below. It requires a "seed" standard train track belonging to the stratum of interest. That is, suppose we would like to generate the folding automaton of the stratum

$$(b_1, \ldots, b_r; m_1, \ldots, m_n; k_1, \ldots, k_s),$$

then we must choose a seed standard train track τ whose peripheral region $D_n \setminus \tau$ is an r-gon; whose ith marked point is enclosed by an m_i-gon; and whose ith non-marked polygon is k_i-sided. The algorithm will then proceed to identify all of the cusps available to perform folding operations. Each time it performs a folding operation and obtains a new train track, it checks against the list of current train tracks (which initializes to a set only containing τ).

If it finds it in the list, a directed edge is created pointing to it, and the edge is decorated by a standardizing braid. If it does not find it in the list, the new train track is added to the list, with a directed edge pointing to it, again decorated with a standardizing braid. The algorithm exhausts every possible folding operation on every train track in the list.

Algorithm 1 genauto (Theoretical [HS07])

Let S be a set of standard train tracks, initialized with a seed track: $S \leftarrow \{\tau_{seed}\}$.
Let N be the set of new tracks found in the current iteration.
repeat
    $N \leftarrow \emptyset$
    for every track $\tau \in S$ **do**
        for every valid cusp c in τ **do**
            $\tau' \leftarrow \text{Fold}(\tau, c)$
            $\tau_{std} \leftarrow \text{Standardize}(\tau')$
            if τ_{std} is not isomorphic to any track in S **then**
                $N \leftarrow N \cup \{\tau_{std}\}$
            end if
        end for
    end for
    $S \leftarrow S \cup N$
until $N = \emptyset$
return The graph with vertices S and edges determined by the folds.

5.1.4 Proof of Completeness and Termination

In the Introduction, we stated Theorem 1.2, asserting that the algorithmic realization of the folding automaton provides a complete and finite classification of all standard train tracks for a given stratum. The proof has two parts: *exhaustiveness* (the algorithm visits

every isomorphism class of standard tracks in the stratum) and *finiteness* (the algorithm terminates). Exhaustiveness rests on a connectivity theorem of Penner and Harer; finiteness rests on a counting bound for standard tracks on the punctured disk.

Theorem 5.9 (Completeness of the `genauto` algorithm)**.** Let $\mathcal{S}$ be a connected stratum of the space of measured foliations on D_n. Given a seed standard train track $\tau_{seed} \in \mathcal{S}$, the `genauto` algorithm terminates and returns the complete, finite list of isomorphism classes of standard train tracks in $\mathcal{S}$.

Proof. Exhaustiveness. The exhaustiveness argument relies on a connectivity result of Penner and Harer phrased in terms of *splitting*, the topological inverse of folding. We will define splitting more carefully and use it heavily in Chapter 7; for the present proof, it suffices to know that a split is a local move on a train track that reverses an elementary fold — if a track τ folds to τ', then τ' splits to τ. A split is permitted at a switch where the local geometry admits an inverse-fold configuration; not every switch can be split, but every fold can be undone by a split.

With this, we may state the relevant Penner-Harer connectivity result [PH92]: the space of measured laminations $\mathcal{ML}_0(D_n)$ admits a cellular decomposition whose cells correspond to standard train tracks, and any two equivalent positively measured standard tracks (τ_1, μ_1) and (τ_2, μ_2) admit a common refinement (τ, μ), in the sense that each (τ_i, μ_i) splits (and isotopes) to (τ, μ) [PH92, Theorem 2.3.1]. Consequently, any two standard tracks in the same stratum are related by a finite sequence of splits and inverse splits (i.e., folds) modulo isotopy.

To translate this geometric statement into the combinatorial language of folding automata:

- **Splitting is inverse folding:** As stated above, splitting and folding are mutually inverse local moves. A splitting move corresponds to traversing a directed edge of the

automaton backwards.

- **Connectivity of the automaton:** Since any two tracks in the stratum are related by a sequence of splits and folds, the folding automaton is connected as an *undirected* graph.

The `genauto` algorithm performs a breadth-first search on the directed automaton starting from τ_{seed}. Because the underlying undirected graph is connected, every vertex is reachable from τ_{seed} by some directed path: any sequence of splits and folds connecting τ_{seed} to a target τ' may be rewritten as a sequence of folds (possibly through intermediate vertices not on the shortest path). Hence the BFS exhausts every isomorphism class of standard tracks in the stratum.

Finiteness. A standard train track on the n-marked disk is a finite graph G whose switches have valence at least 3 (Definition 3.1), and whose vertex and edge counts are bounded by the stratum's singularity data via the Euler-Poincaré formula. The number of switches and real edges admits a uniform bound depending only on n and the singularity profile (specifically, the sum of cusp counts $\sum b_i + \sum m_j + \sum k_l$, which determines the total switch valence and hence both the switch and edge counts up to the polygon structure). The cyclic ordering at each switch admits only finitely many configurations, and only finitely many labelings of edges as real or infinitesimal are compatible with a given polygon structure. Therefore the set of isomorphism classes of standard tracks in a fixed stratum is finite.

The algorithm checks each newly generated track against the registry of previously discovered isomorphism classes (Algorithm 2). If a fold yields an isomorphism class already in the registry, it is not enqueued for further exploration. Since the state space is finite, the BFS frontier must eventually empty, and the algorithm terminates.

Combining the two parts, the algorithm produces a finite, exhaustive enumeration of the

standard tracks in the stratum. □

5.2 Computational Implementation: `autofolder`

The relevance of folding automata to our work on the detection of the connect-sum of trefoils lies in our analysis of the non-orientable strata $(3; 1^6; 3)$ and $(2; 1^6; 3^2)$ on D_6. Specifically, having an implementation of the `genauto` algorithm will allow us to generate all possible isomorphism classes of standard train tracks $[\tau]$ that may fit into geometric data $(\beta, \phi_\beta, \tau, f_\beta)$ belonging to those strata.

To that end, we implemented a robust version of the `genauto` algorithm in Python. Our software, `autofolder`, constructs the folding automaton for specified strata on the punctured disk. The implementation handles the complexities of graph isomorphism and explicit folding mechanics.

5.2.1 Combinatorial Structure and Equivalence

When the algorithm generates a new track (Algorithm 2, Line 9), it must determine if this track corresponds to a state already existing in the automaton. To perform this check algorithmically, we rely on the discrete data of the graph structure.

Definition 5.10 (Combinatorial Structure)**.** The *combinatorial structure* of a train track τ is the tuple $\mathcal{C}(\tau) = (G, \mathcal{O}, \ell)$, where:

- $G = (V, E)$ is the underlying graph.
- $\mathcal{O} = \{\sigma_v : v \in V\}$ is the set of cyclic permutations recording the counter-clockwise ordering of edges at each switch.
- $\ell : E \to \{\text{real, infinitesimal}\}$ is the labeling function distinguishing edge types.

Definition 5.11 (Combinatorial Equivalence)**.** Let τ and τ' be two train tracks with combinatorial structures $\mathcal{C}(\tau) = (G, \mathcal{O}, \ell)$ and $\mathcal{C}(\tau') = (G', \mathcal{O}', \ell')$.

We say that τ and τ' are **combinatorially equivalent** if there exists a graph isomorphism $\phi : G \to G'$ satisfying:

1. **Structure Preserving:** The isomorphism ϕ respects the cyclic ordering of edges at every vertex. That is, for every vertex $v \in V(G)$, the cyclic permutation at the image vertex $\phi(v)$ is the conjugation of the permutation at v by ϕ:

$$\sigma'_{\phi(v)} = \phi \circ \sigma_v \circ \phi^{-1}$$

2. **Label Preserving:** The isomorphism ϕ respects the edge labelings:

$$\ell'(\phi(e)) = \ell(e) \quad \text{for all } e \in E(G).$$

In this case, we write $\mathcal{C}(\tau) \cong \mathcal{C}(\tau')$ and say that the train tracks define the same combinatorial state.

We now prove that checking combinatorial equivalence is sufficient to establish train track isomorphism, thereby providing a rigorous method for state detection in the `genauto` algorithm.

Proposition 5.12. Let τ_1 and τ_2 be standard train tracks on D_n. Then τ_1 and τ_2 are isomorphic (i.e., differ by a braid) if and only if they are combinatorially equivalent.

Proof. ($\Rightarrow$) Suppose τ_1 and τ_2 are isomorphic. By definition, there exists an orientation-preserving diffeomorphism $h : D_n \to D_n$ (representing a braid β) such that $h(\tau_1)$ is isotopic

to τ_2. Since h is a diffeomorphism, it induces a graph isomorphism $\phi = h|_{\tau_1} \colon \tau_1 \to \tau_2$. Because h is orientation-preserving, it strictly respects the cyclic ordering of edges at every vertex. Furthermore, as an isomorphism of train tracks, h maps real edges to real edges and infinitesimal edges to infinitesimal edges. Thus, ϕ is a combinatorial equivalence and $\mathcal{C}(\tau_1) \cong \mathcal{C}(\tau_2)$.

($\Leftarrow$) Suppose $\phi : \mathcal{C}(\tau_1) \to \mathcal{C}(\tau_2)$ is a combinatorial equivalence. We construct the required braid β in three steps.

Step 1: Constructing a homeomorphism between fibered neighborhoods. The tuple $(G, \mathcal{O})$ defines a unique ribbon graph structure. Following Penner and Harer [PH92, Section 1.1], this combinatorial data uniquely determines an oriented surface with boundary $N(\tau_i)$ obtained by thickening the ribbon graph; in our setting, $N(\tau_i)$ is the fibered neighborhood of τ_i. Since ϕ preserves the cyclic ordering $\mathcal{O}$, it induces an orientation-preserving homeomorphism $h' : N(\tau_1) \to N(\tau_2)$ that carries τ_1 onto τ_2 and respects the vertical-fiber structure.

Step 2: Extending across the complementary regions. The complement $D_n \setminus N(\tau_i)$ is a disjoint union of polygons: marked infinitesimal polygons (containing one marked point each), unmarked infinitesimal polygons (containing one non-marked singularity each), and a single peripheral region (adjacent to ∂D_n). The combinatorial equivalence ϕ induces a bijection between these polygons preserving cusp counts and edge labels, so it sends each polygon of τ_1 to a polygon of τ_2 of the same combinatorial type. We extend h' across each polygon by the Alexander trick (any orientation-preserving homeomorphism of the boundary of a disk extends to a homeomorphism of the disk; the extension is unique up to isotopy rel boundary).

Marked polygons. For a marked k-gon enclosing the marked point $q_i \in \tau_1$, the boundary map specified by h' extends to a homeomorphism sending q_i to the corresponding marked point $q_{\phi(i)} \in \tau_2$ (since the vertical infinitesimal edge above each marked point is preserved by ϕ,

the marked point is determined by the polygon structure).

Peripheral region. For the peripheral region P (adjacent to ∂D_n), the boundary ∂P consists of ∂D_n together with a portion of τ_i. We choose the Alexander-trick extension on P to be the identity on ∂D_n. This is permissible because $\partial D_n \subset \partial P$ is one of the boundary components of P, and the Alexander extension is free to be the identity on any single boundary component.

The composite map $h : D_n \to D_n$ is an orientation-preserving homeomorphism, satisfying $h(\tau_1) = \tau_2$ as embedded subsets of D_n, fixing ∂D_n pointwise, and permuting the marked points.

Step 3: Defining the braid. Since h is an orientation-preserving homeomorphism of D_n fixing ∂D_n pointwise and permuting the marked points, it represents an element $\beta = [h] \in \mathrm{Mod}(D_n) \cong B_n$. The action of β on isotopy classes of embedded subsets of D_n sends $[\tau_1]$ to $[h(\tau_1)] = [\tau_2]$. That is, $\beta(\tau_1)$ is isotopic to τ_2 as embedded train tracks, so τ_1 and τ_2 are isomorphic in the sense of the chapter. □

5.2.2 Data Structures

To implement the `genauto` algorithm, we must encode the combinatorial structure of the tracks and the auxiliary data required for the folding operations.

The core data structure in our software is the `StandardTrainTrack` class, which inherits from a base `TrainTrack` class. This class encodes the train track τ combinatorially as a decorated graph structure $\mathcal{C}(\tau) = (G, \mathcal{O}, \ell)$ along with embedding data:

- **Graph Representation (`graph`):** The underlying graph G is stored using the SageMath `Graph` class, which provides optimized methods for standard graph invariants.
- **Cyclic Ordering (`vert_orders`):** A dictionary representing $\mathcal{O}$, mapping each vertex

v to the counter-clockwise list of its incident edges. This encodes the ribbon graph structure required to define the surface.

- **Singularity Data (`infpoly`):** The labeling function ℓ is encoded via the `infpoly` dictionary, which lists the sequences of vertices bounding each infinitesimal polygon (puncture). Edges connecting consecutive vertices in these lists are identified as *infinitesimal*, while all other edges are *real*.

- **Cusp Information (`cusps`):** A list of `cusp` objects, enabling the `fold` method to iterate efficiently over valid folding sites.

5.2.3 Implementation of Detecting Combinatorial Equivalence

A significant challenge in generating the automaton is detecting when two distinct `StandardTrainTrack` objects represent the same vertex in the automaton. Recall that vertices correspond to tracks equivalent up to the action of the braid group. In our implementation, this check is performed by the method `is_isomorphic_to`:

- **Graph Isomorphism Check:** The function first verifies if the underlying graphs are isomorphic using computationally cheap invariants (vertex and edge counts) and the SageMath `is_isomorphic` method.

- **Permutation Search (The Braid Action):** If the underlying graphs match, the algorithm must verify if the cyclic orderings and singularity data can be aligned. Crucially, to account for the action of the braid group (which acts by permuting the marked points), the algorithm iterates through all valid permutations of the singularity types. It returns `True` if there exists a permutation σ of the polygons such that relabeling the graph according to σ yields a match in both the adjacency structure and the cyclic ordering $\mathcal{O}$.

5.2.4 Implementation of the Folding Operation

The engine of the automaton generation is the `fold` method. It transforms the combinatorial structure of a track τ into a new track τ' according to the topological definition of an elementary fold. It takes as input a specific cusp object c and a direction $d \in \{0, 1\}$ (representing Right-over-Left or Left-over-Right).

The procedure executes the following algorithmic steps, modifying the track data in place:

1. **Cusp and Edge Identification:** The algorithm first retrieves the local geometry of the cusp c. Let v_{cusp} be the cusp vertex, and let e_L, e_R be the incident left and right real edges connecting v_{cusp} to vertices v_L and v_R, respectively. Based on the folding direction d, we identify an *intermediate vertex* v_{int} and the specific *infinitesimal edge* e_{inf} that the fold will traverse. Before proceeding, the method validates that e_{inf} is indeed an infinitesimal edge. If e_{inf} is a real edge, the fold is illegal, and the operation returns failure.

2. **Graph Surgery (Topological Transition):** The folding operation is realized combinatorially by "zipping" one branch of the cusp along the infinitesimal edge. Let v_{far} be the vertex at the other end of e_{inf}. The algorithm updates the graph G by essentially moving the endpoint of the folded edge from v_{int} to v_{far}. This rewiring corresponds to the topological quotient map where the infinitesimal interval e_{inf} is collapsed into the train track.

3. **Updating Cyclic Orderings:** The algorithm modifies the ribbon structure $\mathcal{O}$ to reflect the new embedding. The new edge must be inserted into the cyclic order $\mathcal{O}_{v_{far}}$ immediately adjacent to e_{inf}, preserving the planar embedding. At the folded vertex, the old edge is removed from the ordering, and the new edge is inserted in its place.

4. **Cusp Evolution:** Finally, the algorithm updates the list of cusps for the new track.

The folding operation destroys the original cusp c and creates a new cusp at v_{far}.

The method returns a mutated `StandardTrainTrack` object representing the folded track.

See Figure 5.4 for an example.

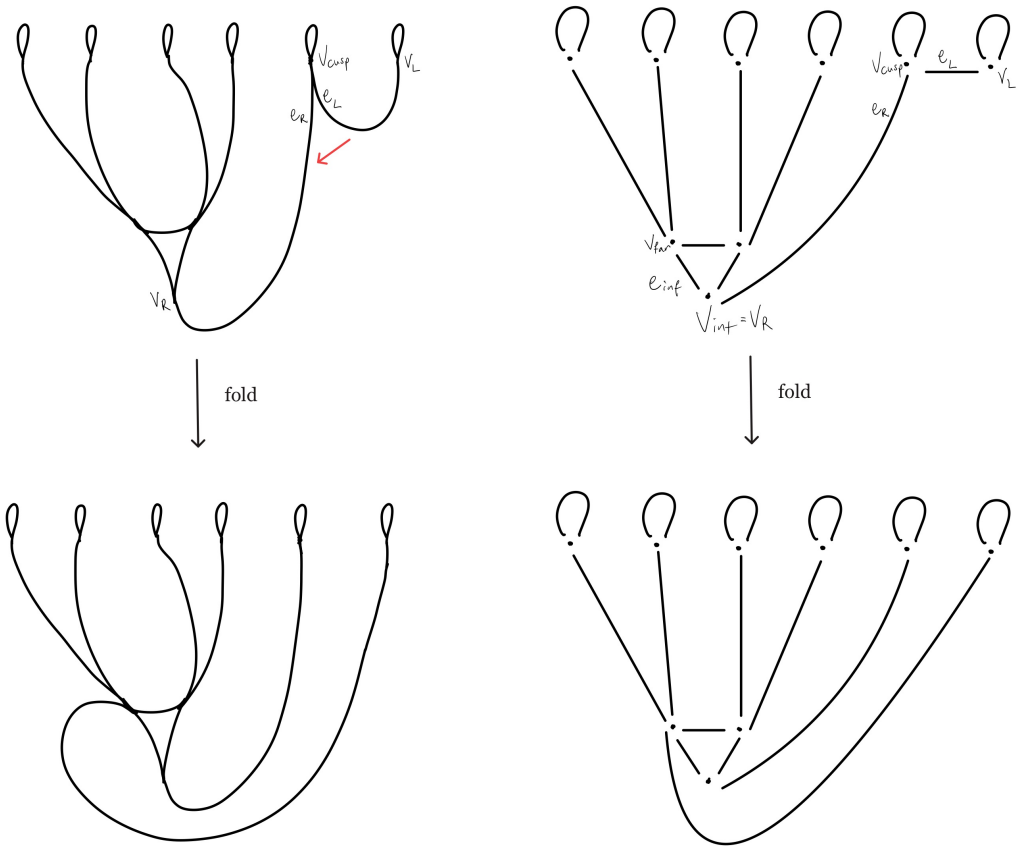


Figure 5.4: Left: A left-to-right folding at the cusp located at v_{cusp}. Right: The equivalent operation performed by the algorithm on a `StandardTrainTrack` object. The algorithm deletes e_L, then attaches a new edge between v_L and v_{far} at the appropriate position in the cyclic ordering. The graph information, cyclic ordering, and cusp information are updated for the newly created `StandardTrainTrack` object.

5.2.5 Extended Automaton Capabilities

A complete theoretical folding automaton encodes not only the set of standard train tracks (the vertices), but also the exact standardizing braids and transition matrices associated with the folding maps between them (the directed edges).

Our software package, `autofolder`, is fully equipped to compute this edge data. It features a robust standardization module that analyzes the global connectivity of a folded strand (identifying how it "swings" and "winds" around puncture clusters) to automatically derive the specific Artin braid generators required to return the track to standard form. Furthermore, it strictly tracks the permutation of real edges to compute the exact linear transition matrices induced on the space of transverse measures.

However, because the primary objective of this thesis is to classify pseudo-Anosov maps via manual topological case analysis and the Trace Lemma, we strictly require only the exhaustive list of candidate standard train tracks generated by the automaton. The complex cycle structure, explicit braid words, and transition matrices of the automaton's edges are not necessary for our obstruction. Consequently, we omit the dense algorithmic details of the standardization and matrix computations here, and focus our algorithm specifically on the Breadth-First Search mechanism used to exhaustively discover the state space (the vertices).

5.2.6 The `autofolder` Enumeration Algorithm

We now present the streamlined pseudo-code for our implementation, focused specifically on state enumeration. By leveraging the combinatorial equivalence checks detailed in Section 5.2.1, the algorithm efficiently generates the finite catalog of train tracks for any given stratum.

Algorithm 2 autofolder: Train Track Enumeration

Require: An initial "seed" standard train track τ_{seed} belonging to stratum $\mathcal{S}$.

Ensure: The exhaustive list L of all isomorphism classes of standard train tracks in $\mathcal{S}$.

$L \leftarrow$ **List**$(\{\tau_{seed}\})$ ▷ Ordered list of discovered isomorphism classes
$Q \leftarrow$ **Queue**$(\{\tau_{seed}\})$ ▷ Queue for BFS exploration
while Q is not empty **do**
    $\tau_{curr} \leftarrow$ DEQUEUE(Q)
    $\mathcal{K} \leftarrow \tau_{curr}$.`cusps`
    for each cusp $c \in \mathcal{K}$ **do**
        for each direction $d \in \{\text{Right-over-Left}, \text{Left-over-Right}\}$ **do**
            ▷ 1. Perform the combinatorial fold
            $\tau_{folded} \leftarrow$ FOLD(τ_{curr}, c, d)
            if τ_{folded} is Invalid **then continue**
            end if
            ▷ 2. Linear Search for Isomorphism
            $is_new_state \leftarrow$ **True**
            for $\tau_{ex} \in L$ **do**
                if ISISOMORPHIC$(\tau_{folded}, \tau_{ex})$ **then**
                    $is_new_state \leftarrow$ **False**
                    break
                end if
            end for
            ▷ 3. Record new tracks
            if is_new_state **then**
                ENQUEUE(Q, τ_{folded})
                APPEND(L, τ_{folded})
            end if
        end for
    end for
end while
return L

5.3 Conclusion

In this chapter, we formalized the theory of folding automata and provided a complete algorithmic realization of the enumeration framework originally theorized by Ko, Los, and Song [SKL02]. As noted by Los [Los08], a systematic study of all pseudo-Anosov homeomorphisms within a given stratum requires the rigorous development of its specific train-track automata theory. Furthermore, Los anticipated that because such automata are practically immense, an explicit algorithmic description is strictly necessary to make the state space tractable.

For the remaining non-orientable strata on the disk—specifically $(2; 1^6; 3^2)$ and $(3; 1^6; 3)$—our `autofolder` implementation fulfills this exact requirement. It provides a sufficient list of standard train tracks within each stratum, from which we can systematically hunt for valid train track maps.

However, executing this algorithmic enumeration reveals an immediate practical challenge: just as Los predicted, the raw topological output of the automaton is massive. The unrestricted state space contains a vast number of standard tracks, many of which possess localized, topologically redundant complexities known as *joints*. Attempting to manually construct maps and apply the Trace Lemma across this entire, unpruned space would remain analytically intractable.

To bridge the gap between algorithmic enumeration and manual topological analysis, we apply, in Chapter 7, the geometric operation of *tight splitting*. By applying tight splitting to our enumerated tracks, we resolve these localized complexities and strictly reduce the automaton's massive output to a minimal, canonical set of jointless standard train tracks. It is upon this highly refined, manageable set of candidate tracks that our final Trace Lemma arguments are executed.

CHAPTER SIX

Tight Splitting and Jointless Tracks

For the purpose of classifying all pseudo-Anosov braids on D_6 in the strata $(3; 1^6; 3)$ and $(2; 1^6; 3^2)$ which lift to fixed-point-free pseudo-Anosov maps, we utilize the `autofolder` program to output all standard train track isomorphism classes for these strata. For each of these isomorphism classes, the program provides one standard train track representative; thus, for each of the two strata, we obtain a finite list of standard train tracks (encoded as `StandardTrainTrack` objects). By Proposition 3.17, every pseudo-Anosov 6-braid β in each stratum is carried by one of these standard train tracks.

We can further reduce the number of standard train tracks to consider by invoking Reinoso's Theorem C [Rei24], which builds on the broader framework of Farber, Reinoso, and Wang [FRW24]: in any stratum possessing an interior singularity with at least two prongs—in particular both strata above—every pseudo-Anosov map is conjugate to one carried by a *jointless* train track. A *joint* is a loop switch (a switch at a marked monogon) incident to at least two real edges. The mechanism behind this reduction is an operation called *tight splitting* on standard train tracks. As mentioned previously, there is a more general operation of splitting, due to Penner and Harer [PH92], which can be viewed as the geometric inverse of folding; tight splitting is the specific instance that inverts the elementary folding defined

in Chapter 5.

Crucially, a tight splitting preserves the carried dynamics: the resulting train track carries the same pseudo-Anosov ϕ_β up to conjugation by a braid, even though the induced train-track map is a new map on a new track. Iterating this, Reinoso shows that all joints of a standard train track τ carrying ϕ_β can be removed by a finite sequence of tight splittings at loop switches, producing a jointless train track τ' that still carries ϕ_β up to conjugation.

We utilize this strategy to reduce the number of standard train tracks to consider from the `autofolder` output. We demonstrate that for the majority of standard train tracks in the list, a finite sequence of tight splittings leads to a select subset of tracks. Consequently, up to conjugation, any pseudo-Anosov braid is carried by this smaller set of train tracks. Furthermore, for the purpose of identifying the knot monodromy h associated with the braid via the Birman-Hilden correspondence, we may consider braids up to mirroring. This allows for a further reduction by identifying pairs of standard jointless train tracks that are mirror images of one another and selecting a single representative from each pair.

Notation reminder. Throughout this chapter we fix a pseudo-Anosov braid $\beta \in \mathrm{Mod}(D_n)$ with geometric data $(\beta, \phi_\beta, \tau, f_\beta)$, in the sense of Chapter 3: β is the braid (mapping class), $\phi_\beta \colon D_n \to D_n$ is its pseudo-Anosov representative, τ is a standard train track carrying ϕ_β, and $f_\beta \colon \tau \to \tau$ is the induced train-track map. This is the data on which all of the splitting operations below act. The associated lift (Φ, ϕ_Φ) to Σ_2^2 via the Birman-Hilden correspondence (Chapter 2) is what ultimately matters for the knot-detection argument, but the train-track operations themselves take place entirely on the disk level.

6.1 Splitting Standard Train Tracks

The goal of tight splitting is to reverse the elementary folding process (Definition 5.2) in a manner that preserves the property of carrying a specific pseudo-Anosov map. To achieve

this, we first rigorously define the local coordinates and orientation at a switch.

6.1.1 Branches at a switch

To formalize the splitting operation, we require precise notation for the local geometry of the train track $\tau \subset D_n$ near a switch.

Definition 6.1 (Incoming Real Edges)**.** Let v be a switch of τ. We adopt the convention that real edges incident to v are oriented **towards** v. We denote the set of incoming real edges at v by $R(v)$. Since τ is standardly embedded in the oriented disk D_n, the set $R(v)$ admits a natural linear ordering induced by the counter-clockwise orientation of the tangent space at v. This linear ordering is a subset of the ordering described in the definition of the combinatorial structure $\mathcal{C}(\tau) = (G, \mathcal{O}, \ell)$ of τ, where $\mathcal{O}$ records the cyclic ordering at each switch (both infinitesimal and real).

Definition 6.2 (Left and Right Edges)**.** Let v be a switch with $R(v) \neq \emptyset$.

1. We define $l(v) \in R(v)$ to be the minimal element of $R(v)$ with respect to the local ordering. We refer to $l(v)$ as the **leftmost incoming edge** at v.

2. We define $r(v) \in R(v)$ to be the maximal element of $R(v)$. We refer to $r(v)$ as the **rightmost incoming edge** at v.

Definition 6.3 (Source Switches and Composite Notation)**.** For the distinguished edges $l(v)$ and $r(v)$, we denote their source vertices as follows:

- Let v_l denote the source vertex of $l(v)$ (i.e., $l(v)$ is directed from v_l to v).

- Let v_r denote the source vertex of $r(v)$ (i.e., $r(v)$ is directed from v_r to v).

Consequently, the notation $r(v_l)$ refers to the rightmost incoming edge at the switch v_l, and $l(v_r)$ refers to the leftmost incoming edge at the switch v_r.

6.1.2 Tight Splitting and Stability

With these local coordinates established, we define the tight splitting operation.

Definition 6.4 (Tight Splitting)**.** Let $\tau \hookrightarrow D_n$ be a standardly embedded train track, let v be a switch of τ, and fix a train track map $f\colon \tau \to \tau$. We say that v **splits tightly to the left** (or ***l*-splits**) if for every real edge $x \subseteq \tau$, the following conditions hold regarding the image path $f(x)$:

1. Whenever the edge $l(v)$ appears in the train path $f(x)$, it is immediately followed by the edge $r(v_l)$ (traversed against its orientation).

2. Whenever the edge $l(v)$ appears in the train path $f(x)$, it is immediately preceded by the edge $r(v_l)$ (traversed along its orientation).

Similarly, we say that v **splits tightly to the right** (or ***r*-splits**) if the analogous conditions hold with the roles of "left" and "right" reversed (i.e., replacing $l(v)$ with $r(v)$ and $r(v_l)$ with $l(v_r)$).

If a switch v splits tightly, we construct a new train track τ_v^l (in the case of an l-split) which maps to τ via an elementary folding map. We use the notation τ_v^t to refer generically to the result of either an l-split or an r-split.

Construction of the Split Track τ_v^l. Suppose v l-splits. We define τ_v^l to be the standardly embedded train track obtained from τ by deleting the edge $l(v)$ and replacing it with a new real edge α satisfying the following conditions:

1. As a directed edge, the source and target of α are given by $\alpha(0) = l(v)(0)$ and $\alpha(1) = r(v_l)(1)$.

2. The edge α forms a bigon (a two-cusped disk) with the train path $l(v) \cdot \overline{r(v_l)}$, and

there is an isotopy relative to the punctures of D_n such that α lies transverse to the measured foliation.

The construction of τ_v^r (when v r-splits) is symmetric.

This construction is the precise geometric inverse of the elementary folding operation described in Chapter 5. Specifically, the transformation $\tau \to \tau_v^l$ corresponds to the inverse of the elementary folding map

$$p\colon \tau_v^l \to \tau,$$

where the folding operation maps the edge α onto $l(v)$ and $r(v_l)$ (effectively folding the "new" branch back into the "old" branch).

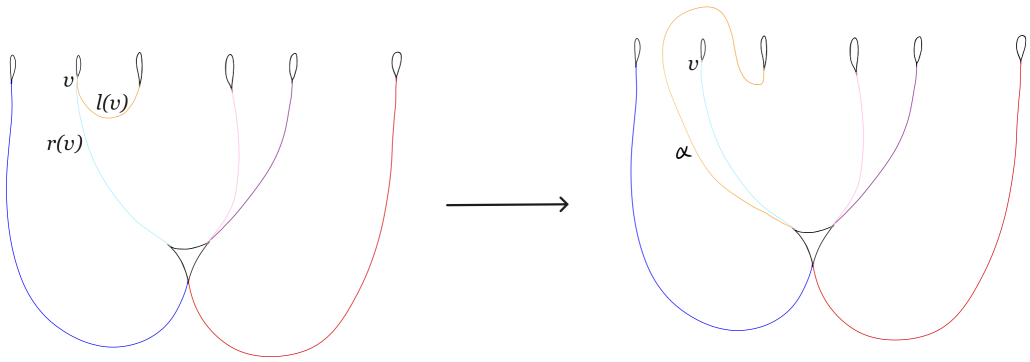


Figure 6.1: An l-split at the vertex v. Notice this is the exact inverse of the folding operation p of Figure 5.1.

Remark 6.5. While the geometric construction of the split track τ_v^t can be performed at any switch v with sufficient valence, the definition of a *tight* splitting requires the existence of a compatible train track map $f\colon \tau \to \tau$ that respects the local folding structure.

6.1.3 Dynamics and the Transition Matrix

The primary utility of tight splitting is encapsulated in the following results, which ensure that the dynamic properties of the map (such as the dilatation) are preserved.

Proposition 6.6 ([Rei24, Proposition 6.1.7])**.** Retain the notation $(\beta, \phi_\beta, \tau, f_\beta)$ from above, with τ a standard train track carrying the pseudo-Anosov ϕ_β. Suppose τ splits tightly to the left at a switch v to produce the train track τ_v^l. Then, up to conjugacy by a braid, ϕ_β is carried by τ_v^l. We denote the associated train track map on τ_v^l by

$$f_{\beta,v}^l \colon \tau_v^l \to \tau_v^l.$$

An analogous result holds if τ splits tightly to the right.

In the language of folding automata, a tight splitting implies that traversing a cycle representing a pseudo-Anosov map corresponds to a reverse traversal of elementary foldings. The transition matrices of the split and original tracks are related by conjugation via the folding matrix.

Proposition 6.7 ([Rei24, Proposition 6.1.8])**.** Retain the notation of Proposition 6.6. Suppose that τ l-splits at v, and let M and M_v be the transition matrices of $f_\beta\colon \tau \to \tau$ and $f^l_{\beta,v}\colon \tau^l_v \to \tau^l_v$ respectively. Then

$$M_v = P^{-1}MP,$$

where P is the transition matrix of the elementary folding map

$$p\colon \tau^l_v \to \tau$$

associated with the inverse of the tight splitting. Concretely, if $l(v)$ is the jth real edge of τ and $r(v_l)$ is the ith real edge, then

$$P = I_n + D_{i,j},$$

where $D_{i,j}$ is the elementary matrix with a 1 in entry (i, j) and zeros elsewhere.

The tight splitting condition imposes a strict inequality on the invariant measure (the weights) of the branches involved.

Proposition 6.8 ([Rei24, Corollary 6.1.9])**.** Retain the notation $(\beta, \phi_\beta, \tau, f_\beta)$ for a pseudo-Anosov braid carried by a standardly embedded train track. Let M be the transition matrix for $f_\beta\colon \tau \to \tau$, and let λ be the dilatation of f_β. Fix a positive right λ-eigenvector μ of M representing the transverse measure. If v l-splits, then $\mu_v = P^{-1}\mu$ is a positive right λ-eigenvector of M_v. Consequently, the weights satisfy the inequality:

$$\mu(l(v)) < \mu(r(v_l)).$$

Similarly, if v r-splits, then $\mu(r(v)) < \mu(l(v_r))$.

The utility of Proposition 6.8 becomes apparent when analyzing a tight splitting at a switch where the resulting track is isomorphic to the original. This situation arises, in particular, at loop switches (switches at a marked monogon), but it also occurs at switches incident to higher-order infinitesimal polygons in the splitting diagrams of Section 6.2.

Corollary 6.9. Suppose a switch v of a standard train track τ carrying a pseudo-Anosov ϕ_β l-splits, such that the resulting train track τ_v^l is isomorphic to τ. Let $\varphi\colon \tau_v^l \to \tau$ be the isomorphism (given by a braid). Then the weight of the branch corresponding to $r(v_l)$ strictly decreases. That is, if μ is the invariant measure on τ and μ_v is the measure on τ_v^l, then:

$$\mu_v(r(v_l)_{new}) < \mu(r(v_l)_{old}).$$

The analogous statement holds for r-splits, with $r(v_l)$ replaced by $l(v_r)$.

Proof. Let $p\colon \tau_v^l \to \tau$ be the elementary folding map associated with the tight splitting. This map identifies the new edge α with $l(v)$ and the new branch $r(v_l)_{new}$ with $r(v_l)_{old}$. The relationship between the transverse measures is given by the pullback of p, which satisfies the additivity equation:

$$\mu(r(v_l)_{old}) = \mu_v(r(v_l)_{new}) + \mu_v(\alpha).$$

By Proposition 6.8, the eigenvector μ_v is well-defined and positive. Furthermore, the proposition establishes that for the splitting to be valid (tight), the weights must satisfy the strict inequality $\mu(l(v)) < \mu(r(v_l)_{old})$.

Since the splitting operation assigns the weight of the removed edge $l(v)$ to the new edge α (i.e., $\mu_v(\alpha) = \mu(l(v))$), and since μ is a positive eigenvector for a pseudo-Anosov map, we have $\mu_v(\alpha) > 0$.

Substituting this back into the additivity equation yields:

$$\mu_v(r(v_l)_{new}) = \mu(r(v_l)_{old}) - \mu(l(v)).$$

Because $\mu(l(v))$ is strictly positive, it follows immediately that:

$$\mu_v(r(v_l)_{new}) < \mu(r(v_l)_{old}).$$

Thus, under the isomorphism φ which maps the edge $r(v_l)_{new}$ back to $r(v_l)_{old}$, the weight associated with this edge orbit strictly decreases. □

Remark 6.10. Corollary 6.9 should not be read as a termination statement. A tight splitting that returns to an isomorphic track strictly decreases a weight, but a strictly decreasing sequence of positive weights may converge to a positive limit or to 0 without any term vanishing; positivity of the transverse measure is therefore not violated. Indeed, the canonical (renormalization) splitting sequence of a pseudo-Anosov is genuinely infinite and eventually periodic, returning to an isomorphic track infinitely often while scaling the transverse measure by λ^{-1} at each period. Such periodic recurrence is not an obstruction to be excluded but the defining feature of a pseudo-Anosov: a closed loop in the folding automaton, read as a braid, *is* a pseudo-Anosov mapping class, with dilatation equal to the spectral radius of the product of transition matrices around the loop [Los08]. Consequently, finiteness of our reduction cannot be obtained from weight monotonicity alone; it is established loop-by-loop in Section 6.2, using a bounded-below integer for loops that retain a joint (Reinoso's Theorem C) and the Nielsen–Thurston type of the loop braid for loops that return to a jointless track.

6.2 Switch Rigidity and Existence of Splits

The following proposition of Reinoso [Rei24, Corollary 6.2.9], building on the broader work of Farber-Reinoso-Wang [FRW24], is instrumental in their proof that every train track map

is carried by a jointless train track, essentially showing that any joint at a loop switch can be split.

Proposition 6.11 (Existence of Splittable Switches, [Rei24, Corollary 6.2.9])**.** Let n_k denote the maximal real valence of a switch at an infinitesimal k-gon of τ, where $k \geq 1$. If $n_k > 1$, then there exists a switch of valence n_k at such a k-gon which l-splits or r-splits. In particular, if the train track has any switch with valence greater than 1, there exists at least one switch that l-splits or r-splits.

For our purposes, the result provides a sufficient condition to guarantee a switch can be split. This provides the inductive step for our reduction procedure: at every k-gon, a unique switch of maximal valence can always be split.

It is worth emphasising at the outset that Proposition 6.11 does *not* cause our reduction to run forever, even though it guarantees a splittable switch at every track with a switch of valence greater than 1. The point is that "a splittable switch always exists" and "the reduction terminates" are not in tension: one never runs out of splittable switches, but one does run out of *joints*. Reinoso's reduction halts precisely when every loop switch has valence one (the jointless condition), at which stage non-loop switches of higher valence typically remain and are still splittable. Pushing the reduction past the jointless stage—as we do at the infinitesimal triangles below—re-enters the regime in which splitting may continue indefinitely along a loop. We control this regime in the next subsection.

6.2.1 Ruling out splitting loops

A **splitting diagram** is a finite directed graph whose nodes are isomorphism classes of standard train tracks and whose edges are tight l- and r-splits, emanating from a fixed starting track. (The finiteness of the node set is Theorem 1.2: there are only finitely many isomorphism classes of standard tracks in a fixed stratum.) A **splitting loop** is a directed

cycle $\mathcal{C}$ in this graph, i.e. a sequence of tight splits returning to a track isomorphic to its starting track. Each edge of $\mathcal{C}$ carries a *standardizing braid* identifying the split track with its standard representative; the ordered product of these braids around $\mathcal{C}$ is the **loop braid** $\gamma_{\mathcal{C}}$, well defined up to conjugacy and multiplication by a full twist Δ^2.

Suppose a pseudo-Anosov ϕ_β carried by a track on $\mathcal{C}$ has a tight-splitting sequence that is eventually periodic with periodic part the cycle $\mathcal{C}$; we say ϕ_β **traverses $\mathcal{C}$ infinitely often**. By the closed-path correspondence for folding automata [Los08], the periodic part realizes ϕ_β, up to conjugacy and up to passing to a power, as the loop mapping class $\gamma_{\mathcal{C}}$; in particular the dilatation of ϕ_β is a positive power of $\lambda(\gamma_{\mathcal{C}})$ (or vice versa), and ϕ_β has the same Nielsen–Thurston type as $\gamma_{\mathcal{C}}$. The two lemmas below rule out infinite traversals in the two ways a loop can arise, according to whether the loop returns to a jointless track.

Lemma 6.12 (Loops with a non-pseudo-Anosov loop braid)**.** Let $\mathcal{C}$ be a splitting loop whose loop braid $\gamma_{\mathcal{C}}$ is not pseudo-Anosov—for instance, periodic or reducible—and suppose this remains the case after multiplication by any full twist. Then no pseudo-Anosov train-track map can traverse $\mathcal{C}$ infinitely often.

Proof. Suppose, for contradiction, that a pseudo-Anosov ϕ_β traverses $\mathcal{C}$ infinitely often. By the closed-path correspondence, ϕ_β is conjugate to a power $\gamma_{\mathcal{C}}^m$ with $m \geq 1$ (after absorbing the finite pre-periodic part of the splitting sequence into a conjugating braid). Nielsen–Thurston type is invariant under conjugacy and under passage to nonzero powers, and a nonzero power of a non-pseudo-Anosov mapping class is again non-pseudo-Anosov; equivalently, $\lambda(\phi_\beta) = \lambda(\gamma_{\mathcal{C}})^m = 1^m = 1$. This contradicts $\lambda(\phi_\beta) > 1$. Since the loop braid is only defined up to a full twist and the hypothesis is stable under that ambiguity, the conclusion is independent of the representative chosen. □

Lemma 6.13 (Jointed loops, via Reinoso's Theorem C)**.** Let $\mathcal{C}$ be a splitting loop all of whose tracks carry a joint. Then no pseudo-Anosov train-track map can traverse $\mathcal{C}$ infinitely often.

Proof. Every track on $\mathcal{C}$ has joint number $J = \sum_v (|R(v)|-1) \geq 1$, where v ranges over the loop switches. An infinite traversal of $\mathcal{C}$ would produce an infinite tight-splitting sequence, all of whose tracks carry the fixed pseudo-Anosov ϕ_β and hence share its dilatation λ. By the argument in Reinoso's proof of Theorem C [Rei24, §6.3], only finitely many transition matrices can occur in such a sequence (each is an integer Perron–Frobenius matrix of size n with spectral radius λ, and there are finitely many such by his counting lemma), so some transition matrix recurs. Simplicity of λ then pins the transverse measure up to scale across the recurrence, and the strict per-split weight reduction of Corollary 6.9 forces a stem incident to a marked monogon to be split over, which strictly decreases the nonnegative integer J. As J cannot decrease indefinitely, the sequence must leave $\mathcal{C}$ after finitely many splits, contradicting infinite traversal. □

The contrast between the two lemmas is exactly the point of Remark 6.10. A loop that retains a joint carries a bounded-below *integer* ($J \geq 1$), which Reinoso's mechanism drives down. A loop that returns to a jointless track carries no such integer—J merely oscillates between 0 and a positive value—so termination there cannot come from a monovariant at all; it comes from the Nielsen–Thurston type of the loop braid.

Splitting Diagram

We now illustrate how Proposition 6.11 (existence of a splittable switch) together with Lemmas 6.12 and 6.13 (no infinite traversal of a splitting loop) combine in practice to constrain which train tracks must carry a given pseudo-Anosov map. The following diagram traces all possible tight splittings emanating from a particular standard jointless train track

labeled (1.) in the stratum $(3; 1^6; 3)$. The upshot is that any train track map carried by (1.) must, after a finite sequence of tight splittings, be carried by one of two specific terminal tracks — labeled (12.) and (0.) in the diagram.

Figure 6.2 shows a sequence of splittings starting from the standard jointless train track labeled (1.). We implicitly assume that there is a train track map carried by this train track (1.). Consider the triangle, i.e., the 3-gon, on the left of this train track. The maximal real valence of a switch at this infinitesimal 3-gon is 2. Specifically, the switch v is the unique switch of maximal real valence.

By Proposition 6.11, v must either l-split or r-split. If it l-splits, we traverse to the left-hand side of the diagram to a standard train track with a joint labeled v again. Invoking Proposition 6.11 once more, this train track either l-splits or r-splits. For the r-split case, we arrive at a train track labeled (12.). For the l-split case, we arrive at a train track at the bottom left of the diagram, which is isomorphic to the original train track (1.).

Going back to the initial splitting of (1.), the r-split scenario yields a train track which l-splits to itself, and r-splits to the train track (0.).

At each bifurcation, Proposition 6.11 guarantees that at least one of an l-split or an r-split occurs, but not necessarily both. The diagram contains exactly two splitting loops, which we rule out in turn.

The left loop. Starting from (1.), the composite l-split followed by l-split returns to a track isomorphic to the *jointless* track (1.). The first l-split already lands in standard embedded position—the resulting (jointed) track *is* the standard representative of its isomorphism class—so no standardizing braid is required, and the loop braid is carried entirely by the second split, namely $\sigma_2^{-1}\sigma_1^{-1}$. (Whether a split requires a standardizing braid depends only on whether the constructed track is already standard, not on whether it carries a joint.)

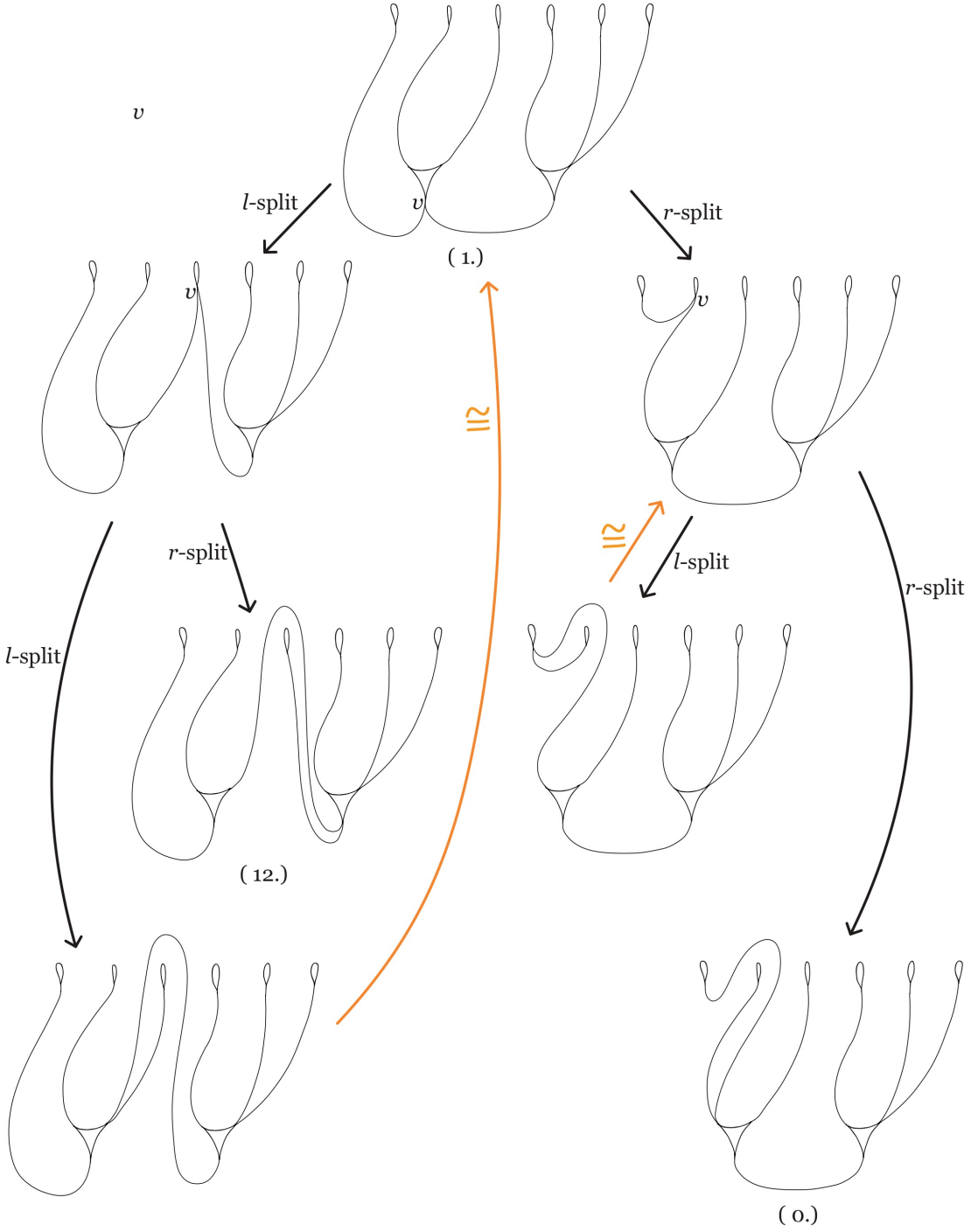


Figure 6.2: This splitting diagram shows that any train track map carried by train track (1.) must also be carried by train track (12.) or (0.), up to the action of a braid.

Hence, up to conjugacy and full twists, the loop braid is

$$\gamma_{\mathcal{C}_{\text{left}}} = \sigma_2^{-1}\sigma_1^{-1} = \delta^{-1},$$

the inverse of the canonical periodic generator $\delta = \sigma_1\sigma_2$ of the three-strand sub-braid group. Since $\delta^3 = \Delta^2$ on the relevant sub-disk, every full-twist representative $\sigma_2^{-1}\sigma_1^{-1}\Delta^{2k} = \delta^{3k-1}$ is again a power of δ, hence periodic. Because the loop returns to a jointless track, Lemma 6.13 does not apply; instead, Lemma 6.12 forbids any pseudo-Anosov from traversing this loop infinitely often. The tight-splitting sequence must therefore r-split out of the loop, arriving at the terminal track (12.).

The right loop. The r-split of (1.) produces a track carrying a joint, on which an l-split returns to an isomorphic *jointed* track (standardizing braid σ_1^{-1}). Since every track on this loop carries a joint, Lemma 6.13 forbids an infinite traversal: a pseudo-Anosov whose splitting sequence remained on the loop would carry the joint forever, contradicting the strict decrease of the bounded-below integer J guaranteed by Reinoso's Theorem C. The sequence must therefore r-split out of the loop, arriving at the terminal track (0.).

In either branch, the tight-splitting sequence of any pseudo-Anosov carried by (1.) terminates at (12.) or (0.) after finitely many splits. Therefore, given any train track map f carried by train track (1.), f is also carried by train track (12.) or (0.), up to an action by a braid.

We record the general conclusion as the main result of the chapter.

Theorem 6.14 (Termination of tight splitting)**.** Let τ be a standard jointless train track in the stratum $(3; 1^6; 3)$ or $(2; 1^6; 3^2)$, and let ϕ_β be a pseudo-Anosov map carried by τ. Then, after finitely many tight splittings, ϕ_β is carried by one of the finitely many terminal tracks of the splitting diagram of τ; in particular, no tight-splitting sequence traverses a splitting loop indefinitely.

Proof. Each splitting diagram is a finite directed graph, so the only obstruction to termination is a splitting loop. Every loop is of one of two types. A loop that retains a joint cannot be traversed indefinitely by Lemma 6.13: Reinoso's Theorem C forces the bounded-below joint number to strictly decrease along it. A loop that returns to a jointless track carries the periodic loop braid $\sigma_2^{-1}\sigma_1^{-1} = \delta^{-1}$ and is ruled out by Lemma 6.12, since a pseudo-Anosov cannot be conjugate to a periodic braid. As no other loop type occurs, the splitting sequence exits every loop after finitely many steps and terminates at a terminal track. □

We call a diagram such as Figure 6.2 a **splitting diagram**. In our analysis of the non-orientable strata $(3; 1^6; 3)$ and $(2; 1^6; 3^2)$, we aim to classify all train track maps in these strata lifting to fixed-point-free pseudo-Anosov maps. As will be shown, we make use of these splitting diagrams to drastically reduce the number of candidate train tracks to consider in our final topological analysis. The remaining splitting diagrams for the stratum $(2; 1^6; 3^2)$ are collected in Appendix A. Their loops fall into the same two types analysed above, and in fact both types are dispatched uniformly. Every loop that returns to a jointless track has standardizing data composing to the single loop braid $\sigma_2^{-1}\sigma_1^{-1} = \delta^{-1}$ (up to conjugacy and full twists), which is periodic; Lemma 6.12 therefore rules out all such loops at once. Every loop that retains a joint is ruled out by Lemma 6.13 via Reinoso's Theorem C. No other loop type occurs, so in every diagram the tight-splitting sequence of a pseudo-Anosov terminates at the indicated terminal tracks.

6.3 Conclusion

In this chapter, we addressed the proliferation of redundant states inherent in the unrestricted folding automaton. Because the `autofolder` algorithm exhaustively executes every valid elementary fold at every available cusp, it generates a state space that contains many valid but topologically redundant standard train tracks — specifically those burdened by joints. By deploying the tight splitting operation, we established a rigorous reduction procedure

to mathematically prune this state space for our non-orientable strata. The first stage of this reduction, the elimination of joints at loop switches (i.e., switches incident to a marked monogon), was established by Reinoso in his thesis [Rei24]; we then go further, applying tight splittings at non-loop switches (e.g., the switches of maximal real valence on infinitesimal triangles) to prune the resulting list of jointless tracks even more.

This second stage re-enters the regime in which splitting may continue indefinitely, so its finiteness does not follow from a single monovariant. Instead, each splitting diagram is a finite directed graph whose only obstruction to termination is a splitting loop, and we showed that every such loop is ruled out: loops retaining a joint are eliminated by Reinoso's Theorem C via the bounded-below joint number (Lemma 6.13), and loops returning to a jointless track—all of which, in our strata, carry the single periodic loop braid $\sigma_2^{-1}\sigma_1^{-1} = \delta^{-1}$—are eliminated by the periodicity (more generally, the non-pseudo-Anosov type) of that loop braid (Lemma 6.12). Consequently every pseudo-Anosov carried by a starting track is carried, after finitely many tight splits, by one of the finitely many terminal tracks of its splitting diagram.

In Chapter 7, we will execute this procedure, utilizing the splitting diagrams introduced above to systematically collapse the raw output of our `autofolder` algorithm. Through this reduction, we will demonstrate that any pseudo-Anosov mapping class belonging to the strata $(3; 1^6; 3)$ or $(2; 1^6; 3^2)$ on D_6 must, up to braid conjugation and mirroring, be carried by a small, manageable number of jointless standard train tracks. Once this finite collection is established, we will explicitly enumerate, by hand, all possible train track maps carried by each such track, and apply the Trace Lemma (Lemma 3.22) and its jointless-monogon corollary (Corollary 3.23) directly to each candidate train-track map to rule out the existence of a fixed-point-free lift, thereby completing the proof of our main detection theorem.

CHAPTER SEVEN

The Hyperbolic Case: The Strata $(3; 1^6; 3)$ and $(2; 1^6; 3^2)$ on the Disk

7.1 Introduction

In this chapter, we detail the classification of pseudo-Anosov 6-braids belonging to the strata $(3; 1^6; 3)$ and $(2; 1^6; 3^2)$ whose canonical lifts to the surface Σ_2^2 are fixed-point-free. These strata cannot be eliminated using the orientable foliations technique developed in Chapter 4 because their invariant train tracks contain odd-sided unmarked polygons (specifically 3-gons). Consequently, their invariant foliations are non-orientable, meaning we cannot apply the Alexander polynomial obstruction directly to the geometric data. Instead, we must explicitly enumerate and analyze the specific train track maps carried by the allowable standard train tracks in these strata.

Our analysis proceeds in several steps. First, the finite list of candidate standard train tracks is generated by the `autofolder` algorithm, and among these we retain the ones which are jointless. By utilizing the tight splitting sequences established in Chapter 6, we further reduce the number of tracks that need to be considered. We further reduce the number by identifying train tracks that are vertical mirror images of each other; since the mirror of

a braid inducing a map on one track induces a symmetric map on the other, it suffices to analyze a single representative from each mirror pair.

For the stratum $(3; 1^6; 3)$, this reduction process isolates a single standard jointless train track, which we refer to as *The Candelabra* (see Figure 7.19). For the stratum $(2; 1^6; 3^2)$, the tight splitting sequences reduce the candidate list to exactly six tracks. Therefore, up to conjugation, mirroring, and the addition of full twists, every fixed-point-free pseudo-Anosov 6-braid in these two strata must be carried by one of these specific train tracks.

We then exhaustively analyze all possible train track maps that can be carried by each of these refined tracks. The analysis proceeds edge by edge, enumerating the admissible image paths $f_\beta(e)$ subject to two combinatorial obstructions: the Trace Lemma (which forbids self-occurrence at jointless monogon edges and imposes parity constraints at the central edge d of two-triangle tracks) and the Absorption Obstruction (which forbids image paths from entering geometrically inaccessible regions near vertices). When neither obstruction can be satisfied, the configuration falls into one of three named patterns—Situation α, Situation β, or a path mill—each of which produces a contradiction; we collect these in Appendix B. This procedure successfully prunes the infinite space of maps down to a finite list of eligible train track map *families* for each track. For each surviving family, we produce explicit braid words β that induce those maps.

Finally, to verify if such a braid β can properly fit into the Birman-Hilden correspondence data

$$(h, \phi_h, \hat{h}, \hat{\phi}_h, b, \phi_b, \beta, \phi_\beta, \Phi, \phi_\Phi)$$

induced by the monodromy h of a hyperbolic fibered knot K satisfying $\widehat{HFK}(K) \cong \widehat{HFK}(T_{2,3}\#T_{2,3})$, we apply two homological filters. We compute the action of the open book decomposition induced by β on the first homology to ensure it bounds the correct ambient manifold, and we extract its Alexander polynomial. We demonstrate that none of

the candidate braid families generated by the train track analysis satisfy these necessary homological conditions, allowing us to definitively rule out both strata.

7.2 Topological Constraints on Train Track Maps

Fixing a stratum of pseudo-Anosov maps on the 6-marked disk (either $(3; 1^6; 3)$ or $(2; 1^6; 3^2)$), the `autofolder` algorithm produces a finite list of standard train tracks. Among these, we restrict our attention solely to the jointless standard train tracks, as any pseudo-Anosov map in this stratum is guaranteed to be carried by one such track (Corollary 3.20).

Let τ be one such jointless standard train track. We aim to enumerate all possible train track maps f_β carried by τ, subject to the strict topological condition that any 6-braid β inducing f_β must lift to a fixed-point-free pseudo-Anosov map on the genus-two surface Σ_2^2. This topological condition places severe combinatorial constraints on the underlying train track map on the disk.

7.2.1 The Trace Lemma

The relationship between the transition matrix of a train track map on the disk and the fixed-point theory of its lift is encapsulated by the Trace Lemma, which was established as Lemma 3.22 in Chapter 3 (with its jointless-monogon refinement, Corollary 3.23). For the convenience of the reader and to fix the notation used throughout this chapter, we restate both results below in the form most useful for our case analysis. The lemma and corollary stated here are precisely Lemma 3.22 and Corollary 3.23 of Chapter 3, respectively, applied to the standard tracks on the disk that arise in our setting.

Recall that a standard train track on the marked disk possesses a unique edge belonging to the infinitesimal polygon incident to each marked point. We refer to these as **side-swapping edges** (as introduced in Section 3.7 of Chapter 3). The geometric significance of such an

edge is that because the double cover is branched exactly over the marked points, whenever a train path on the disk traverses a side-swapping edge, its canonical lift to the surface strictly transitions to the "other sheet" of the cover.

Lemma 7.1 (The Trace Lemma, Lemma 3.22 of Chapter 3)**.** Let $(\beta, \phi_\beta, \tau, f_\beta)$ be the geometric data of a pseudo-Anosov braid with Birman-Hilden lift $(h, \phi_h, \tilde{\tau}, \tilde{f}_h)$ on the surface Σ_2^2. Suppose that τ is a standard train track and that the canonical lift ϕ_h has no interior fixed points on Σ_2^2. Then, for any real edge e of τ, any sub-word of the image path $f_\beta(e)$ bounded by two occurrences of e must contain an **even** number of side-swapping edges.

Proof. If the canonical lift ϕ_h has no interior fixed points, the transition matrix $M(\tilde{f}_h)$ must be traceless by Lemma 3.22 of Chapter 3. Consequently, for any real edge e_i in the lifted track $\tilde{\tau}$, the edge e_i cannot appear in its own image $\tilde{f}_h(e_i)$.

Consider the image path $f_\beta(e)$ on the disk. Every traversal of a side-swapping edge causes the image $\tilde{f}_h(e_i)$ of either lift of e to cross to the opposite sheet of the branched cover. If e appeared in $f_\beta(e)$ separated by an odd number of side-swapping edges, then the lifted image $\tilde{f}_h(e_1)$ would necessarily map back onto e_1 (and similarly for e_2). This would force a non-zero diagonal entry of $M(\tilde{f}_h)$, contradicting the tracelessness established above. □

In our context, the standard train tracks generated for these strata feature jointless monogons at the marked points. This specific local geometry allows for a highly restrictive corollary, which is Corollary 3.23 of Chapter 3 restated in our notation.

Corollary 7.2 (Trace Lemma for Jointless Monogons, Corollary 3.23 of Chapter 3)**.** Retain the notation and assumptions of Lemma 7.1. If e is a real edge of τ which is directly incident to a jointless monogon at a marked point, then e cannot appear anywhere in its own image path $f_\beta(e)$.

Proof. Suppose, for the sake of contradiction, that e appears in $f_\beta(e)$. Because e is incident to a jointless monogon (which has only one real edge attached to it), any path entering the monogon via e must immediately exit via e, effectively "turning around". This forces two adjacent, consecutive appearances of e in the word $f_\beta(e)$. Since there are zero side-swapping edges between these two occurrences, it violates the parity condition of Lemma 7.1.

Alternatively, if the path $f_\beta(e)$ terminates entirely upon reaching e, it implies that the vertex corresponding to the monogon is mapped to itself. This local invariance generates an interior fixed point at the singularity in the lifted surface, which again contradicts the assumption that ϕ_h is fixed-point-free. Thus, e cannot appear in $f_\beta(e)$. □

In the stratum $(3; 1^6; 3)$, all of the real edges of the train tracks under consideration are incident to a jointless monogon, thus Corollary 7.2 applies. In the stratum $(2; 1^6; 3^2)$, all but a single real edge d connecting the two unmarked triangles are incident to a jointless monogon. Thus Corollary 7.2 applies to all real edges except d. Consequently, in our enumeration of possible train track maps, the image path of real edges except d cannot contain itself.

7.2.2 The Absorption Obstruction

While the Trace Lemma places strict algebraic restrictions on the transition words, we must also ensure the geometric validity of the map f_β. Because f_β is induced by a genuine, injective surface homeomorphism ϕ_β, it must preserve the injectivity of train paths. This requirement imposes local geometric rigidity near the vertices of τ, formalized through the concept of *absorption*.

Definition 7.3. Let a and b be two real edges of τ adjacent at an initial vertex v. The initial segments of the mapped edges $\phi_\beta(a)$ and $\phi_\beta(b)$ determine a convex cone extending from $\phi_\beta(v)$, denoted $X_v(a, b)$, lying transverse to the invariant foliations of the surface.

Lemma 7.4 (The Absorption Obstruction, [Rei24, Lemma 4.2.5])**.** For any real edge c of τ, the image path $\phi_\beta(c)$ cannot intersect the interior of the convex cone $X_v(a, b)$.

Proof. By the injectivity of the diffeomorphism ϕ_β, the path $\phi_\beta(c)$ cannot cross the boundary of the cone, which is formed strictly by the paths $\phi_\beta(a)$ and $\phi_\beta(b)$. Suppose, for the sake of contradiction, that $\phi_\beta(c)$ enters the interior of $X_v(a, b)$.

Since $\phi_\beta(c)$ cannot cross the boundary to exit, it must either terminate strictly inside the cone, or exit by backtracking through the vertex $\phi_\beta(v)$. Backtracking is impossible for a valid train track map. Furthermore, in a standard train track, the endpoints of real edges lie at switches on the boundaries of infinitesimal polygons (the polygons enclosing marked points or unmarked singularities), and these polygons are permuted by ϕ_β. Hence the only way for $\phi_\beta(c)$ to terminate is at one of these polygons. The local structure at $\phi_\beta(v)$ prescribes a strict cyclic ordering of the incident edges. If c is distinct from a and b, its image cannot essentially land "between" $\phi_\beta(a)$ and $\phi_\beta(b)$ without violating the preservation of this cyclic order or destroying the planar embedding of the graph. Thus, $\phi_\beta(c)$ cannot enter the cone $X_v(a, b)$. The forbidden configuration is illustrated in Figure 7.1. □

When the theoretical transition word $f_\beta(c)$ implies that the path $\phi_\beta(c)$ enters $X_v(a, b)$, we say that $f_\beta(c)$ is **absorbed** between $f_\beta(a)$ and $f_\beta(b)$ (illustrated in Figure 7.1). We denote such a disallowed scenario in our hypothetical image paths with an $\times$ superscript:

$$f_\beta(c) = \ldots \mathrm{Abso}(f_\beta(a), f_\beta(b))^{\times} \ldots$$

The existence of such an absorption immediately invalidates the transition word. By systematically applying the Absorption Obstruction alongside the algebraic parity constraints of the Trace Lemma, we can definitively prune the space of possible transition matrices.

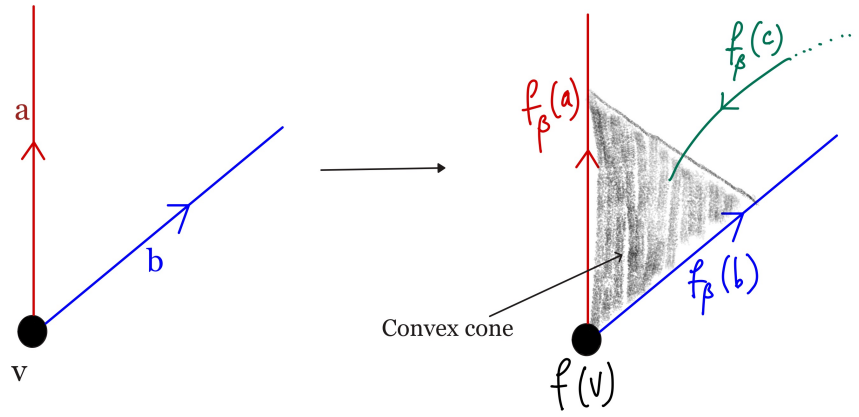


Figure 7.1: An invalid geometric configuration where $\phi_\beta(c)$ is absorbed between $\phi_\beta(a)$ and $\phi_\beta(b)$, violating injectivity.

7.2.3 The Case Analysis Procedure

Given a jointless standard train track τ, we enumerate the families of train track maps f_β carried by τ via the following procedure. Steps 1–6 below constitute the content of the per-track case analyses in Appendices C, D, E, F, G, H, and I; Step 7 is the content of the corresponding braid-extraction appendices.

1. **Initial labeling.** Label and orient the real edges of τ toward their adjacent monogons. For two-triangle tracks, identify the central edge d connecting the two infinitesimal triangles and its symmetric companion $\bar{d}$.

2. **Triangle permutation case split.** For two-triangle tracks, branch the analysis into Cases A, B, C, D according to how f_β permutes the two infinitesimal triangles, as described in Section 7.2.4.

3. **Initial-letter enumeration.** For each real edge e of τ, enumerate the possible first letters of $f_\beta(e)$, subject to Corollary 7.2 (the letter e does not appear in $f_\beta(e)$) and, in Case A, the parity constraint of Assumption A applied to $f_\beta(d)$ and $f_\beta(\bar{d})$.

4. **Forced continuations.** For each partial image path, determine the next admissible letters by checking the Trace Lemma (for paths at the central edge d, the parity of the number of letters between consecutive d-crossings) and the Absorption Obstruction (at each vertex traversed, the image path must not enter a cone formed by adjacent edge images, as in Lemma 7.4).

5. **Termination or contradiction.** Continue Step 4 until either (i) the path terminates with a $\circ$-decoration at a marked point, yielding a candidate, or (ii) the path is forced into Situation α, Situation β, a path mill, or a direct tracing or absorption violation, eliminating the case. See Appendix B for the precise definitions of Situations α, β, and path mills, together with worked examples of each contradiction pattern.

6. **Parameterization.** Group surviving paths into families parameterized by the number of internal twists k between adjacent edges, accommodating the fact that an edge image may twist between two adjacent edges an arbitrary number of times before terminating.

7. **Braid extraction.** For each surviving family, reverse-engineer a braid word β inducing the family by isotoping the image train track back to τ. This is illustrated explicitly for the candelabra example below and for the Jehu family in Appendix J.

We now demonstrate this procedure with two worked examples: first on the candelabra (one infinitesimal triangle, no central edge d), then on Track 0 (two infinitesimal triangles, with the central edge analysis in full).

7.2.4 Path Notation and The Two Triangles

In both strata under consideration, the six marked points are each enclosed by jointless monogons — single-cusped infinitesimal polygons each adjoining only one real edge. The other endpoint of each such real edge lies at a switch on the boundary of an infinitesimal triangle (the central singularity in the candelabra, or one of the two triangles in the two-triangle tracks). The central edge d (and its symmetric companion $\bar{d}$) in the two-triangle tracks connect the two triangles to each other rather than to a monogon, so they form the unique exception. We adopt the convention that every real edge incident to a jointless monogon is *oriented toward its monogon*; the central edges $d, \bar{d}$ are oriented arbitrarily but consistently throughout.

This orientation convention is what makes the turning notation below sensible: when the image $f_\beta(e)$ runs over a real edge other than d or $\bar{d}$, that traversal must end at the corresponding jointless monogon, after which the next leg of the image path must either round the monogon clockwise, round it counter-clockwise, or terminate at the marked point inside. We encode these three options by decorations on the letter.

Following the conventions established by Reinoso [Rei24], we describe the image of a real edge under the train track map f_β as a sequence of real edges decorated with turn information. Let τ be a standard train track. The image path $f_\beta(e)$ is represented as a word in the real edges $\{x_1, \ldots, x_k\}$ of τ.

Each letter is equipped with a decoration from $\{+, -, \circ\}$ indicating the behavior of the path at the vertex reached after traversing that edge:

- x^+ indicates the path traverses edge x and turns in the **positive** direction (typically left relative to the orientation) at the vertex to enter the next edge.
- x^- indicates the path traverses edge x and turns in the **clockwise** direction to enter

the next edge.

- x° indicates the path traverses edge x and **terminates** at the marked point inside the associated polygon. This decoration appears only on the final edge of the path.

As noted previously, the invariant train tracks carrying our candidate pseudo-Anosov braids fall into two distinct geometric categories based on their central singularities. The single track in stratum $(3; 1^6; 3)$ (*The Candelabra*) possesses only one infinitesimal triangle, while the five candidate tracks in $(2; 1^6; 3^2)$ feature a central edge d connecting exactly **two** infinitesimal triangles. The constraints arising on the image $f_\beta(d)$ in the two-triangle setting depend on how f_β permutes the two triangles — a case split that we defer until Example 2 below, where the two-triangle geometry is in front of us.

Example 1: The Candelabra

We illustrate the procedure on the candelabra (Figure 7.19), the unique jointless standard train track in the stratum $(3; 1^6; 3)$ (as will be established in Section 7.4). The candelabra has six real edges b, o, s, i, p, r, each incident to a jointless monogon, and a single central infinitesimal triangle. Because there is no central edge d, Step 2 of the procedure (the triangle permutation case split) does not arise here.

Step 1 (Initial labeling). We label and orient the six real edges toward their respective monogons, as shown in Figure 7.19.

Step 3 (Initial letters). By Corollary 7.2, the letter e cannot appear in $f_\beta(e)$ for any of the six edges. This already constrains the first letter of each image path: for instance, $f_\beta(b)$ cannot begin with b, so it must begin with one of o, s, i, p, r (with an appropriate decoration). Combined with the local cyclic order at each vertex, this immediately implies that the triangle must be rotated by f_β; otherwise at least one of $f_\beta(b)$ or $f_\beta(r)$ would immediately trace. Thus the complete case analysis must consider separately the case in

which $f_\beta(r)$ and $f_\beta(b)$ begin with the pair $\{o^*, s^*\}$ in some order, and the case in which they begin with $\{i^*, p^*\}$ in some order. For the purpose of this example, we treat the former case. In this situation, $f_\beta(o)$ and $f_\beta(s)$ begin with the pair $\{i^*, p^*\}$ in some order, while $f_\beta(i)$ and $f_\beta(p)$ begin with the pair $\{b^*, r^*\}$ in some order. The complete case analysis enumerates all such possibilities; here we restrict to the following subcase:

$$f_\beta(p) = b^\circ, \qquad f_\beta(i) = r^\circ,$$

$$f_\beta(r) = o^* \ldots, \qquad f_\beta(b) = o^* \ldots,$$

$$f_\beta(o) = p^* \ldots, \qquad f_\beta(s) = p^* \ldots.$$

This initial state is shown in Figure 7.2.

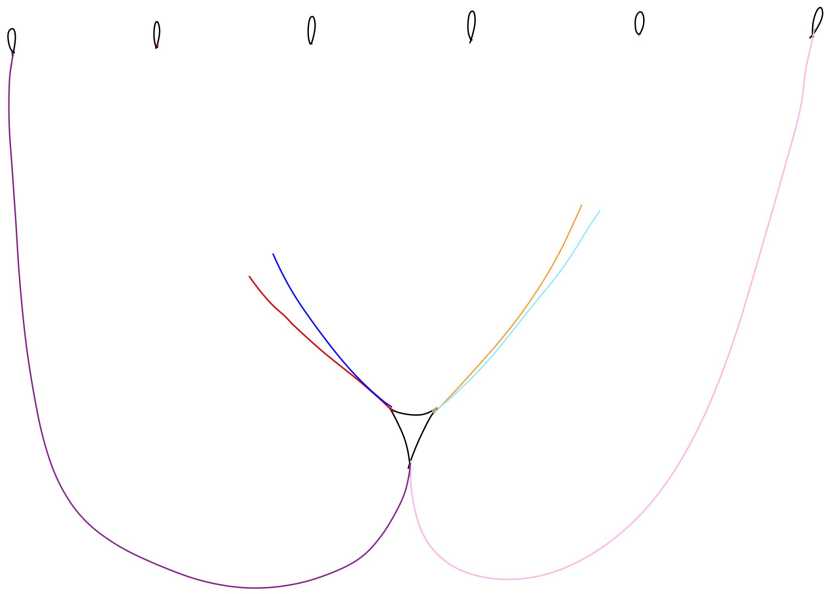


Figure 7.2: Initial subcase under consideration: $f_\beta(p) = b^\circ$, $f_\beta(i) = r^\circ$, with $f_\beta(r)$ and $f_\beta(b)$ both beginning at o, and $f_\beta(o)$ and $f_\beta(s)$ both beginning at p.

Step 4 (Forced continuations and absorption). Within this subcase, the case analysis further branches on the decoration of each first letter. Let us first consider $f_\beta(r)$. If it were to begin with o° (meaning it terminates immediately) or o^+ (a counterclockwise turn), then because $f_\beta(b)$ lies to the right of $f_\beta(r)$, $f_\beta(b)$ would in both cases be forced to begin with o^+, and would then immediately trace:

$$f_\beta(b) = o^+ b^\times,$$

as shown in Figures 7.3 and 7.4.

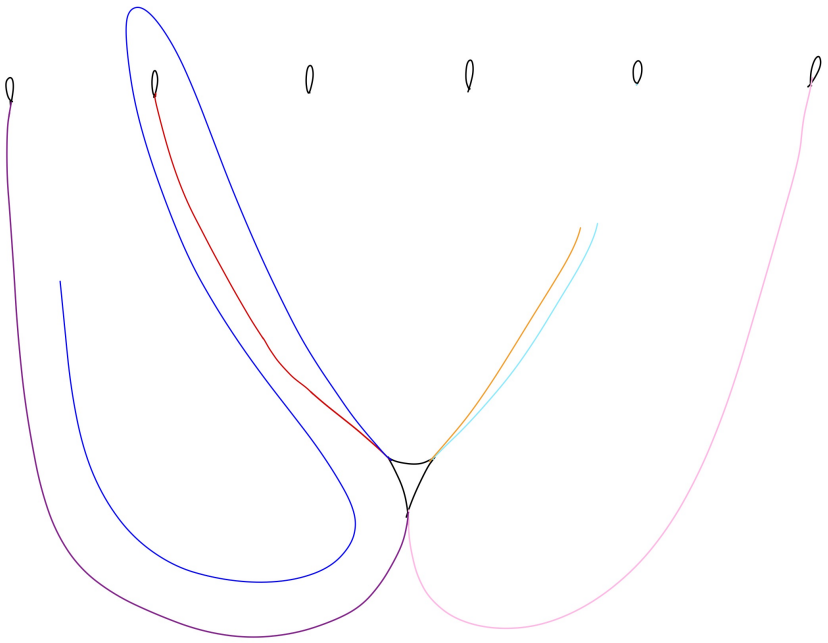


Figure 7.3: Failure of the $f_\beta(r) = o^\circ$ branch: $f_\beta(b)$ is forced to begin with o^+ and traces immediately at $b^\times$.

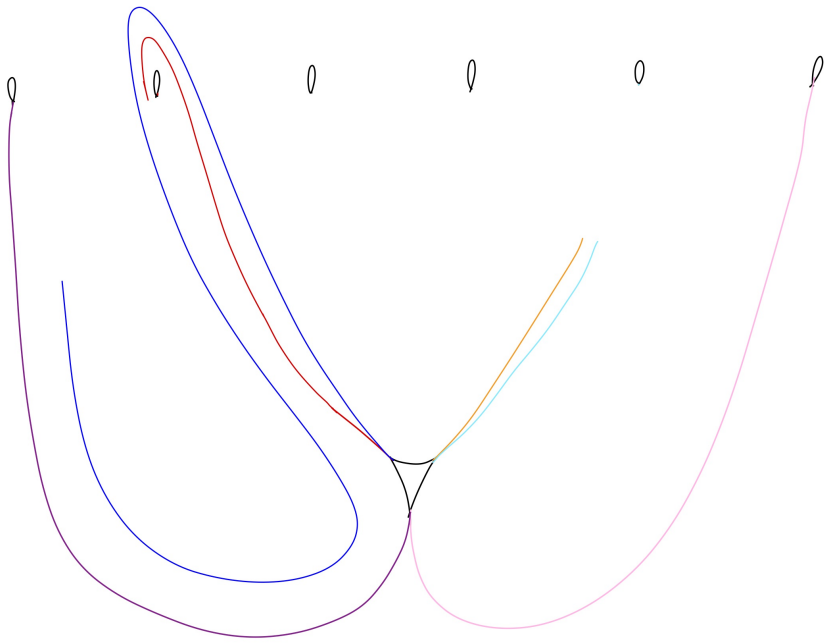


Figure 7.4: Failure of the $f_\beta(r) = o^+$ branch: $f_\beta(b)$ is again forced into $o^+b^\times$, tracing immediately.

The only remaining possibility is for $f_\beta(r)$ to begin with o^-, entering to the right of $f_\beta(b)$ after the clockwise turn:

$$f_\beta(r) = o^- \ldots,$$

as shown in Figure 7.5. The next letter can then be either i^* or p^*.

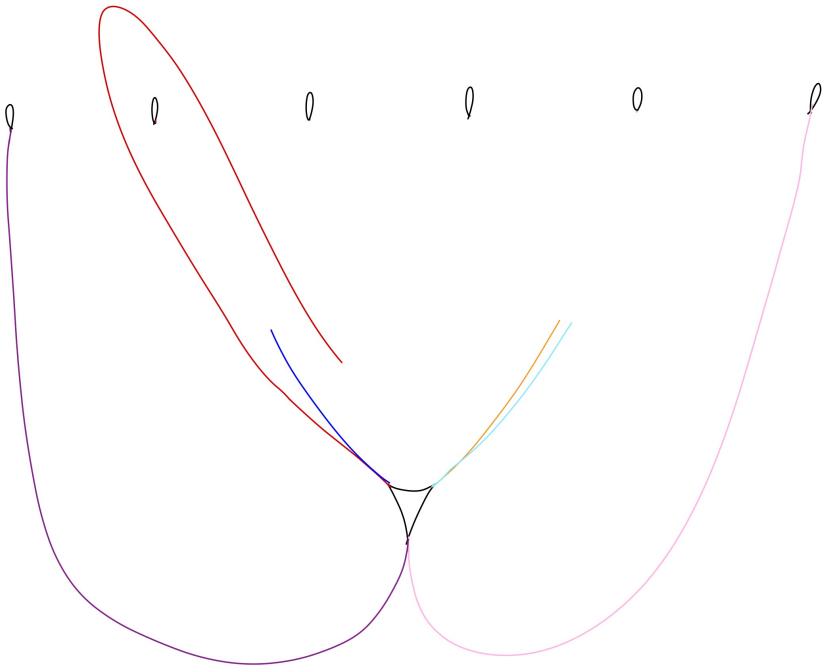


Figure 7.5: The only admissible decoration: $f_\beta(r) = o^- \ldots$, with $f_\beta(r)$ entering to the right of $f_\beta(b)$ after the clockwise turn.

Let us now turn to $f_\beta(s)$. If it were to begin with p° or p^-, then because $f_\beta(o)$ lies to the left of $f_\beta(s)$, $f_\beta(o)$ would be forced to begin with p^- and would be absorbed:

$$f_\beta(o) = p^- r^- \operatorname{Abso}(f_\beta(p), f_\beta(i))^\times,$$

as shown in Figure 7.6.



Figure 7.6: Failure of the $f_\beta(s) = p^\circ$ and $f_\beta(s) = p^-$ branches: $f_\beta(o)$ is forced to begin with p^- and is absorbed between $f_\beta(p)$ and $f_\beta(i)$.

We must therefore have instead $f_\beta(s) = p^+ \ldots$, and the next letter can be either o^* or s^*. To avoid tracing, it must be the former:

$$f_\beta(s) = p^+ o^* \ldots .$$

This is Figure 7.7. Note that $f_\beta(s)$ must go to the left of $f_\beta(r)$; otherwise $f_\beta(s)$ would continue traversing the outer perimeter and be absorbed between $f_\beta(p)$ and $f_\beta(i)$.

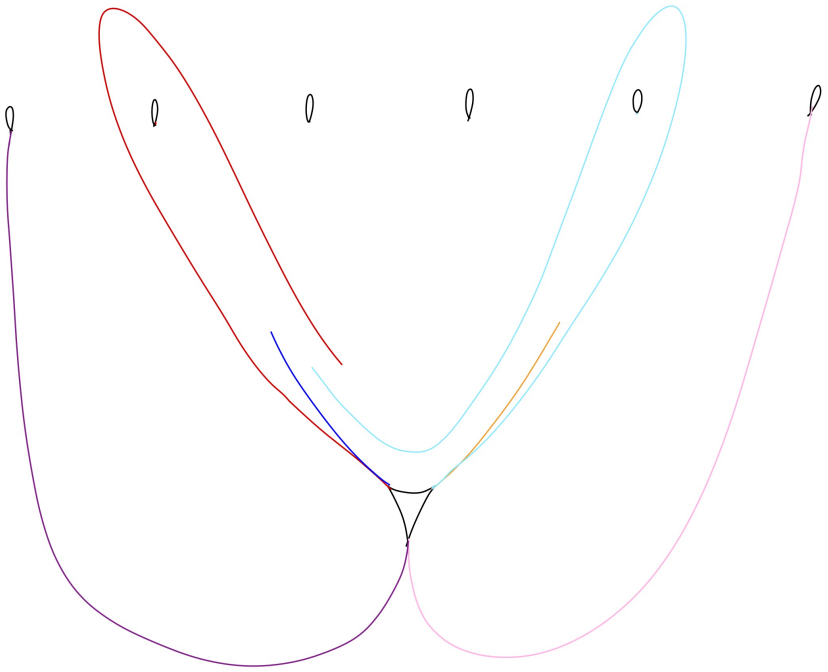


Figure 7.7: Forced continuation: $f_\beta(s) = p^+ o^* \ldots$, with $f_\beta(s)$ passing to the left of $f_\beta(r)$ to avoid the outer-perimeter absorption.

We can now return to $f_\beta(r)$. In this situation, if $f_\beta(r)$ continued with p^*, then it would traverse above $f_\beta(s)$ and wrap around to be absorbed:

$$f_\beta(r) = o^- p^- r^- \operatorname{Abso}(f_\beta(p), f_\beta(i))^\times,$$

as shown in Figure 7.8.

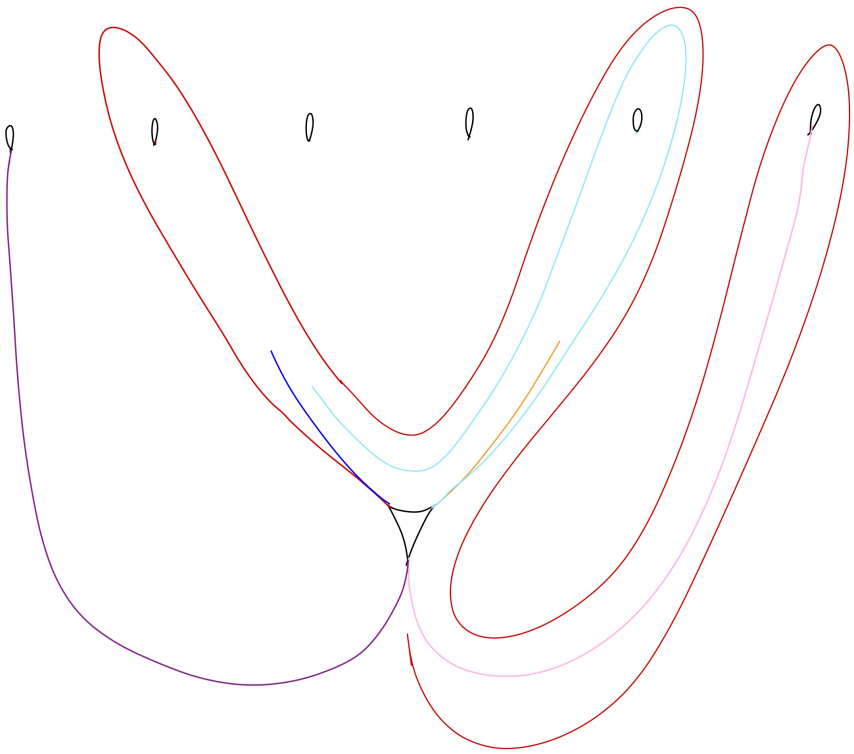


Figure 7.8: Failure of the $f_\beta(r) = o^- p^* \ldots$ branch: $f_\beta(r)$ traverses above $f_\beta(s)$, wraps around r^-, and is absorbed between $f_\beta(p)$ and $f_\beta(i)$.

We must therefore have

$$f_\beta(r) = o^- i^* \ldots,$$

as shown in Figure 7.9.

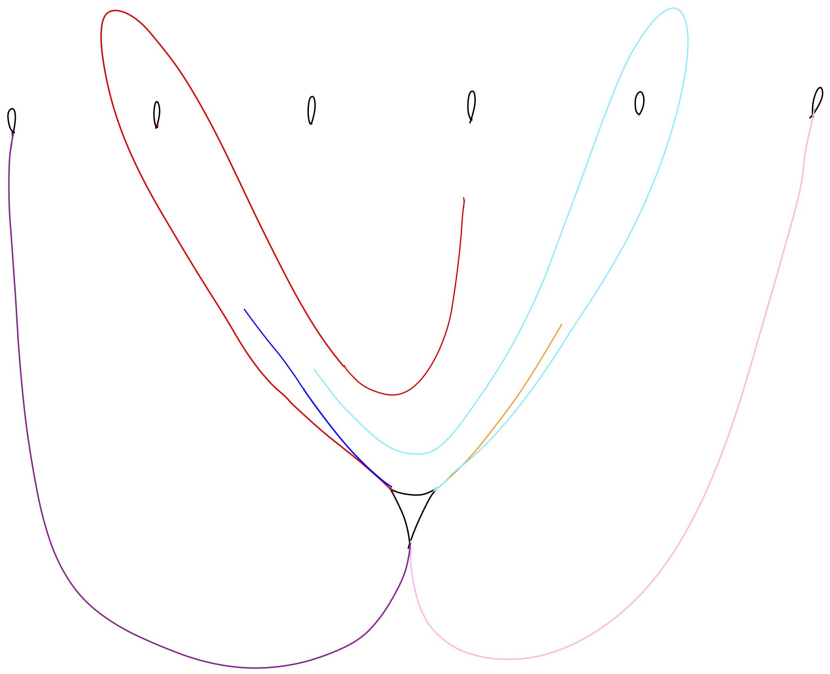


Figure 7.9: Forced continuation: $f_\beta(r) = o^- i^* \ldots$, the only remaining admissible route.

Now consider $f_\beta(b)$. Beginning with o^+ is ruled out by immediate absorption. On the other hand, if $f_\beta(b)$ began with o°, the incoming $f_\beta(s)$ would then traverse o^+ and be absorbed. We must therefore have

$$f_\beta(b) = o^- i^* \ldots,$$

as shown in Figure 7.10.

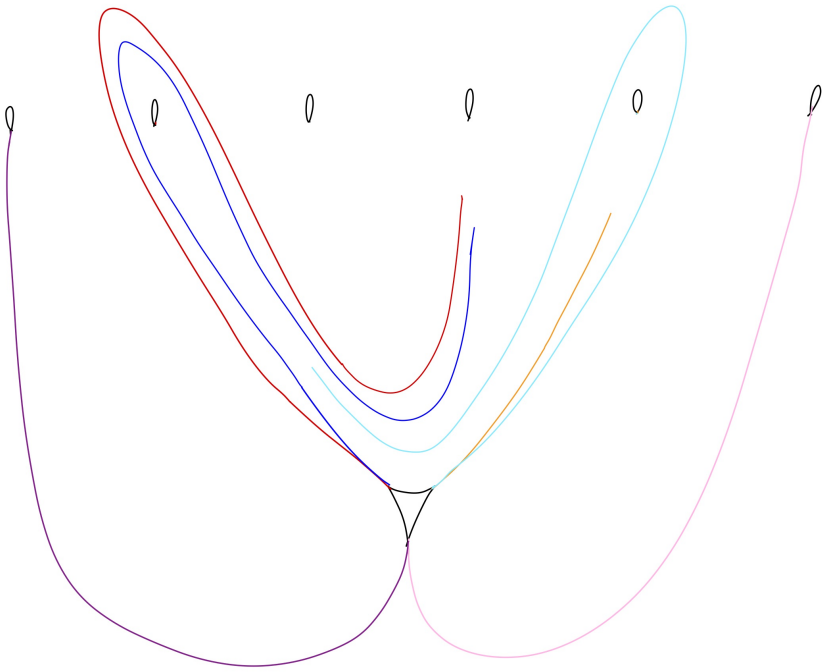


Figure 7.10: Forced continuation: $f_\beta(b) = o^- i^* \ldots$, after ruling out $f_\beta(b) = o^+ \ldots$ (immediate absorption) and $f_\beta(b) = o^\circ$ (which would absorb the incoming $f_\beta(s)$).

Consider next the sub-branch in which $f_\beta(s)$ terminates at o°:

$$f_\beta(s) = p^+ o^\circ.$$

(The complete case analysis verifies that if $f_\beta(s)$ did not terminate here, the resulting configuration would eventually produce a contradiction, but the argument requires extensive further branching that we omit.) The situation is shown in Figure 7.11.

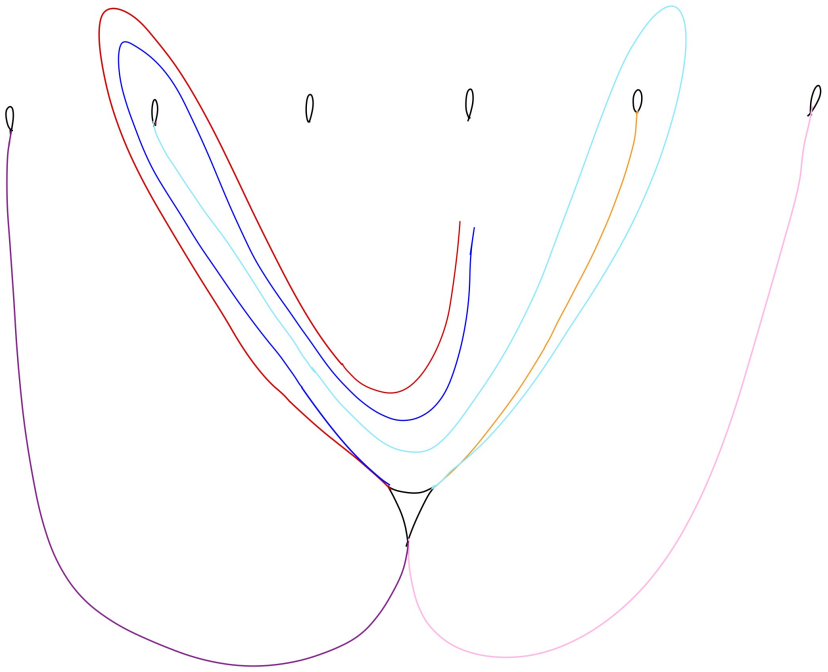


Figure 7.11: The subcase $f_\beta(s) = p^+o^\circ$ (terminating at o), together with the forced $f_\beta(o) = p^\circ$ in this configuration.

In this situation, $f_\beta(o)$ must terminate immediately: if it did not, the next letter could only be o^*, which would trace. Thus

$$f_\beta(o) = p^\circ.$$

It remains to determine the continuations of $f_\beta(b)$ and $f_\beta(r)$. Here $f_\beta(b)$ cannot continue with i° or i^-: either choice would force $f_\beta(r)$ to continue with i^-, which would then be absorbed:

$$f_\beta(r) = o^-i^-o^+p^- \operatorname{Abso}(f_\beta(o), f_\beta(s))^\times,$$

as shown in Figure 7.12.

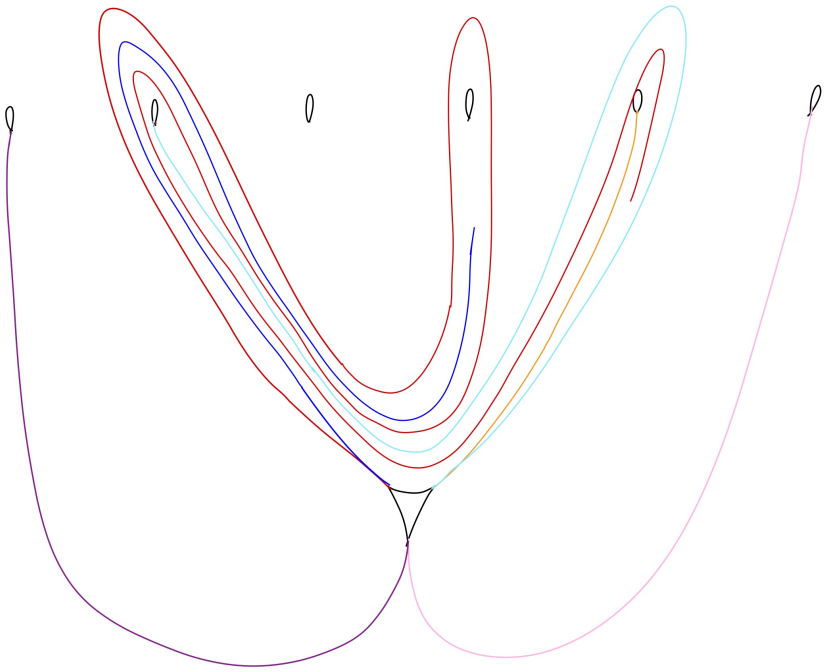


Figure 7.12: Failure of the $f_\beta(b) = o^- i^\circ$ and $f_\beta(b) = o^- i^-$ branches: $f_\beta(r)$ is forced into $o^- i^- o^+ p^-$ and absorbed between $f_\beta(o)$ and $f_\beta(s)$.

We must therefore have

$$f_\beta(b) = o^- i^+ s^* \ldots,$$

as shown in Figure 7.13.

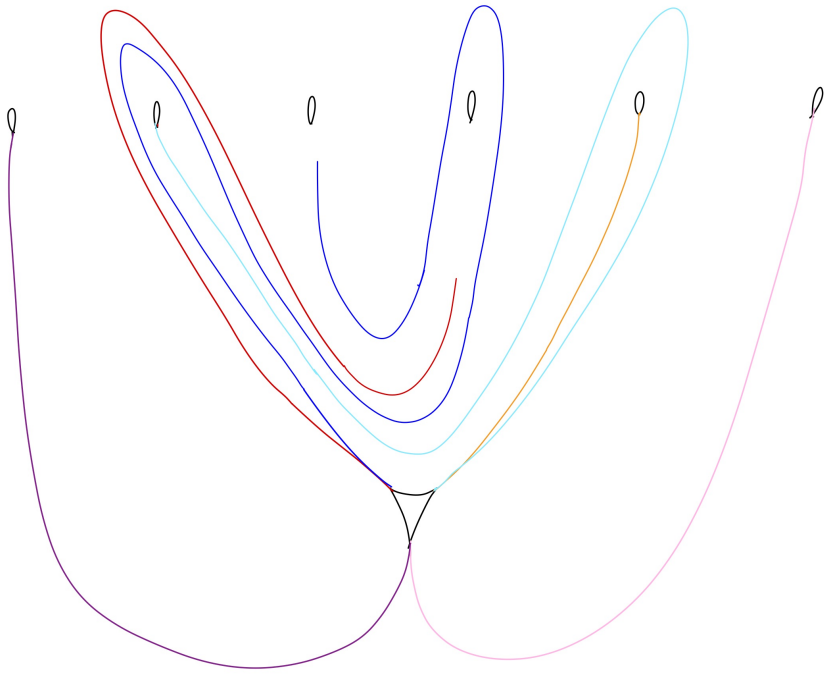


Figure 7.13: Forced continuation: $f_\beta(b) = o^- i^+ s^* \ldots$, the only remaining admissible route.

At this point, $f_\beta(b)$ and $f_\beta(r)$ may both terminate, or they may twist between s^* and i^* some number of times before terminating. Figures 7.14 and 7.15 show two examples of such twisting. Neither $f_\beta(b)$ nor $f_\beta(r)$ can escape this region between s and i without eventually being absorbed or tracing; both must terminate at one of the two letters after finitely many twists.

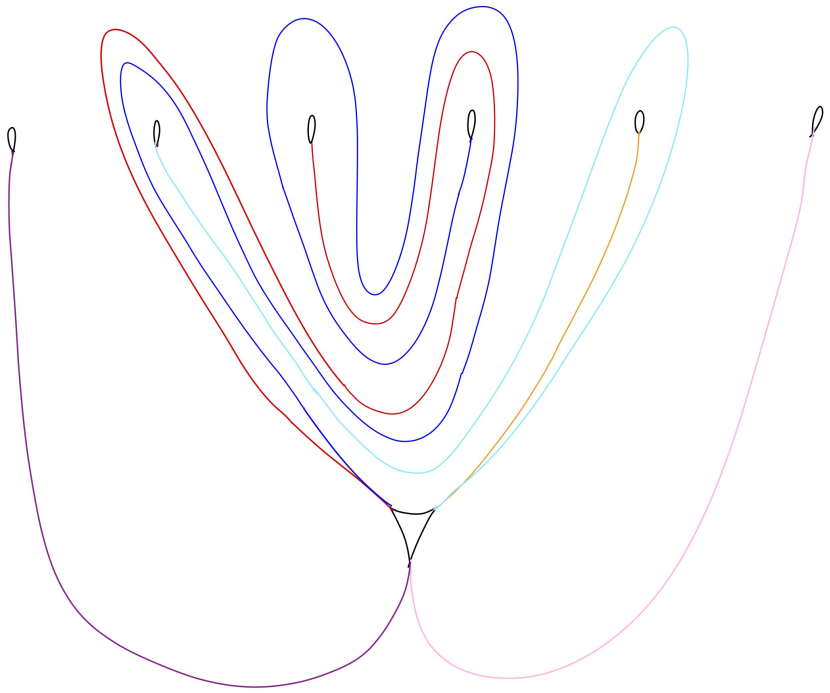


Figure 7.14: The surviving family with one twist ($k = 1$) of $f_\beta(b)$ and $f_\beta(r)$ between s and i before termination.

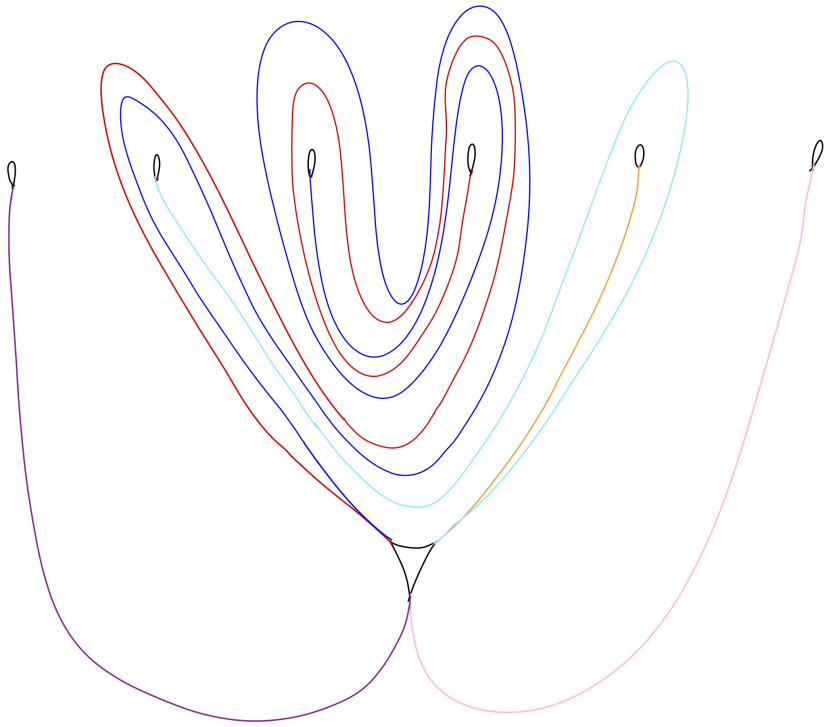


Figure 7.15: The surviving family with two twists ($k = 2$). The general case admits an arbitrary $k \geq 0$ number of twists, with one of $f_\beta(b), f_\beta(r)$ ending at s° and the other at i°.

Step 5–6 (Image paths and parameterization). In conclusion, the resulting image paths are:

$$f_\beta(p) = b^\circ,$$

$$f_\beta(o) = p^\circ,$$

$$f_\beta(i) = r^\circ,$$

$$f_\beta(s) = p^+ o^\circ,$$

together with the twisting pair $f_\beta(r)$ and $f_\beta(b)$, which twist between s and i an arbitrary $k \geq 0$ number of times, with one terminating at s and the other at i. Precisely, we have either

$$f_\beta(r) = o^- (i^+ s^+)^k i^\circ \quad \text{and} \quad f_\beta(b) = o^- i^+ (s^+ i^+)^k s^\circ,$$

or

$$f_\beta(r) = o^- i^+ (s^+ i^+)^k s^\circ \quad \text{and} \quad f_\beta(b) = o^- (i^+ s^+)^k i^\circ.$$

This family appears as Candidate Family 2 of the Candelabra train track in our full case analysis (Appendix C).

Step 7 (Braid extraction). For each $k \geq 0$, this family is induced by a 6-braid of the form

$$\beta = \Delta^{2i} (\sigma_3^k \cdot G_1 \cdot G_2)^{-1},$$

where $i \in \mathbb{Z}$ is an arbitrary number of full twists (see Corollary 3.9) and the two intermediate braid factors are

$$\begin{aligned} G_1 &= \sigma_2^{-1} \sigma_3^{-1} \sigma_4, \\ G_2 &= \sigma_3^{-1} \sigma_4^{-1} \sigma_2^{-1} \sigma_3^{-1} \sigma_1^{-1} \sigma_2^{-1} \sigma_3^{-1} \sigma_4^{-1} \sigma_3 \sigma_4^{-1} \sigma_5^{-1} \sigma_4^{-1} \sigma_3^{-1} \sigma_4 \sigma_5 \sigma_2^{-1} \sigma_1^{-1} \sigma_1^{-1} \sigma_2^{-1} \sigma_1^{-1} \sigma_1^{-1} \\ &\quad \cdot \sigma_5 \sigma_4 \sigma_3 \sigma_2 \sigma_1 \sigma_2 \sigma_3 \sigma_4 \sigma_5 \sigma_5 \sigma_4 \sigma_3 \sigma_2 \sigma_3 \sigma_4 \sigma_5 \sigma_5 \sigma_4 \sigma_3 \sigma_4 \sigma_5 \sigma_5 \sigma_4 \sigma_5 \sigma_5. \end{aligned}$$

The derivation matches the stages described visually in Figure J.8 of Appendix J: the factor σ_3^k unwinds the k twists between $f_\beta(r)$ and $f_\beta(b)$; the factor $G_1 = \sigma_2^{-1}\sigma_3^{-1}\sigma_4$ then transforms the unwound image to a standardized intermediate configuration; finally, G_2 transforms this intermediate back to the candelabra, as illustrated step by step in Figure J.2. The inverse of the product gives the candidate braid. We remind the reader that throughout this thesis, braid words are read from left to right.

By Corollary 3.9, every 6-braid that induces this same family of train track maps differs from β by a number of full twists. Up to conjugation, these braids represent candidates β which can fit into the Birman-Hilden correspondence data.

Example 2: A Two-Triangle Track

We now illustrate the procedure on a two-triangle track to demonstrate the additional features of Step 2 (the Cases A, B, C, D split) and Assumption A. We work on Track 0 (Figure 7.21), one of the six irreducible jointless tracks in the stratum $(2; 1^6; 3^2)$. Track 0 has five real edges b, i, o, p, r each incident to a jointless monogon, plus the central edge d (and its symmetric companion $\bar{d}$) connecting the two infinitesimal triangles.

The triangle permutation case split. For two-triangle tracks, the constraints on the image $f_\beta(d)$ are governed entirely by how f_β permutes the two infinitesimal triangles downstairs, and how the canonical lift $\tilde{f}_h$ permutes their preimages upstairs. Because the surface Σ_2^2 is a double cover branched over the marked points (not over the triangles), each triangle has two preimage triangles in the cover, labeled $\{p_1, p_2\}$ (preimages of the first triangle) and $\{p_3, p_4\}$ (preimages of the second). We can partition the admissible behavior of f_β into four exhaustive cases based on the resulting triangle permutation:

- **Case A (Triangles Fixed):** The infinitesimal triangles are fixed by f_β downstairs. Under the lift, this occurs iff the lifts of each triangle are swapped (sent to the opposite side of $\tilde{\tau}$) by $\tilde{f}_h$.

  Trace Constraint (Assumption A): For $\tilde{f}_h$ to prevent the lifted edge $\tilde{d}$ from mapping over itself on the same sheet, every occurrence of d or $\bar{d}$ in $f_\beta(d)$ must occur after an **even** number of preceding letters.

- **Case B (Triangles Swapped — Both Same Side):** The triangles are swapped downstairs, and both of their lifts are sent to the same side of $\tilde{\tau}$.

Trace Constraint: Because the boundary points of d are exchanged, the path must switch its sheet parity to avoid an interior fixed point on $\tilde{d}$. Thus, at least one of $f_\beta(d)$ or $f_\beta(\bar{d})$ must pass over d or $\bar{d}$ after an **odd** number of letters.

- **Cases C & D (Triangles Swapped — Mixed Sides):** The triangles are swapped downstairs; one lift is sent to the same side, and the other to the opposite side. Subject to the exact same **odd** parity constraint as Case B.

For the purpose of this example, we focus on *Case A* (triangles fixed). The analysis for Cases B, C, D proceeds analogously with odd parity replacing even at d-crossings.

Step 1 (Initial labeling). The real edges b, i, o, p, r are oriented toward their monogons; d runs between the two triangles, with $\bar{d}$ its symmetric companion.

Step 2 (Triangle permutation). We work in Case A: f_β fixes the two infinitesimal triangles.

Step 3 (Initial letters under Assumption A). *Assumption A* is the parity constraint above: every occurrence of d or $\bar{d}$ in $f_\beta(d)$ must be preceded by an even number of letters (and likewise for $f_\beta(\bar{d})$). The Trace Lemma applied to b, i, o, p, r (each jointless-monogon-incident) forbids any of these edges from appearing in its own image path. For the central edge d, Assumption A requires that the first occurrence of d in $f_\beta(d)$ be preceded by an even number of letters. Consider, for instance, an attempted start

$$f_\beta(d) = r^+ d \dots$$

This places the first crossing of d after a single letter (r^+), violating Assumption A. The same applies to any attempt to put d in the second position of $f_\beta(d)$. The first d-crossing

must therefore occur in an even position, so the start of $f_\beta(d)$ has the form

$$f_\beta(d) = x^{\pm}\, y^{\pm}\, d \dots$$

or with more preceding letters (still in even count). The same parity constraint applies to $f_\beta(\bar{d})$.

Step 4 (Forced continuations). Suppose we are exploring a branch in which

$$f_\beta(d) = b^- p^- d \dots, \qquad f_\beta(\bar{d}) = i^+ s^+ \bar{d} \dots$$

(Each begins with two letters preceding the central edge crossing, in agreement with Assumption A.) After the d-crossing in $f_\beta(d)$, the next letter is constrained by both the Trace Lemma and the Absorption Obstruction. The Trace Lemma requires that the next occurrence of d in $f_\beta(d)$ be again preceded by an even number of letters since the previous d; equivalently, d cannot reappear after a single letter. So a continuation of the form

$$f_\beta(d) = b^- p^- d \cdot z^{\pm}\, d \dots$$

is forbidden, where $z^{\pm}$ is any single letter.

Independently, the Absorption Obstruction may forbid certain geometric routings of the continuation. Suppose the next letter is being chosen at a vertex where $f_\beta(i)$ and $f_\beta(o)$ have already established initial segments forming the cone $X_v(f_\beta(i), f_\beta(o))$. Then Lemma 7.4 forbids $f_\beta(d)$ from continuing into the interior of this cone:

$$f_\beta(d) = b^- p^- d\ \mathrm{Abso}(f_\beta(i), f_\beta(o))^{\times} \dots$$

is invalid, and we record this with the absorption symbol $\times$.

Step 5 (Termination, contradictions, or survival). Continuing the case analysis at each branching point eventually either:

1. produces a complete candidate image word terminating with a $\circ$-decoration, or

2. forces the dotted lines $f_\beta(d)$ and $f_\beta(\bar{d})$ to fail to join in the interior of the configuration. In the latter case, the dotted lines must continue around the outer perimeter of the train track, each successive d-crossing necessarily at an even position—but they continue indefinitely, never terminating. This is *Situation* α, and it produces a non-termination contradiction (Appendix B).

A third possibility is that the dotted lines do join in the interior but are forced into a region of the configuration from which they cannot escape without an odd-parity return to d. This is *Situation* β, also called the bagged serpent.

Step 6 (Parameterization) and Step 7 (Braid extraction). The surviving image paths organize into families parameterized by twist counts $k, m, j, \ldots$ between adjacent edges, exactly as in the candelabra example. For Track 0, the full case analysis (Appendix D) produces 13 such families, of which the family labeled *Jubilant* provides one of the two F1-passing candidates in the homological filtering of Section 7.3. Each surviving family is then turned into an explicit candidate braid word by the same reverse-isotopy procedure used in Example 1.

We do not attempt to walk through Track 0's complete case analysis here; the per-track appendix (Appendix D) is approximately 100 pages of step-by-step forced-letter reasoning across all four cases. The miniature derivation above shows the typical local move—enumerate next letters at each vertex, eliminate by the Trace Lemma or Absorption Obstruction, classify any failures as Situation α, β, or path mill, and continue. For a worked instance of the resulting Jubilant family with concrete parameter values, see Figure D.264 of Appendix D.

7.3 Homological Filtering of Candidate Braids

Once the topological constraints from Section 7.2 isolate a finite list of candidate braid families $\beta \in B_6$ on the disk D_6 for a given stratum, we must determine which, if any, of these candidates can possibly correspond to the monodromy of a hyperbolic fibered knot K satisfying $\widehat{HFK}(K) \cong \widehat{HFK}(T_{2,3}\#T_{2,3})$. To do this, we apply two filters, both of which are homological in nature. These tests utilize the Birman-Hilden correspondence to relate the action of the lifted braid to the topological invariants of the resulting knot complement.

Notation reminder. As established in Chapter 2, the Birman-Hilden correspondence relates the geometric data of the knot K on its genus-2 fiber to a 6-braid on the marked disk:

$$(h, \phi_h, \hat{h}, \hat{\phi}_h, b, \phi_b, \beta, \phi_\beta, \Phi, \phi_\Phi).$$

Here $\beta \in \mathrm{Mod}(D_6)$ is the disk braid mapping class, ϕ_β is its pseudo-Anosov representative carried by some standard train track τ via geometric data $(\beta, \phi_\beta, \tau, f_\beta)$, and $\Phi \in \mathrm{Mod}(\Sigma_2^2)$ is the lift to the genus-two surface with two boundary components via the Birman-Hilden correspondence, with pseudo-Anosov representative ϕ_Φ. The candidate braid families produced by the case analysis of Section 7.2 give us specific words representing the disk-level mapping class β; what we filter is the homological action of the lifted Φ on $H_1(\Sigma_2^2)$, ultimately reduced to the action on the closed genus-2 surface $H_1(\Sigma_2)$.

Recall that our topological analysis determines the candidate braid only up to specific equivalences:

1. **Conjugacy:** The combinatorial train track data identifies the conjugacy class of the braid, not a unique word.

2. **Full Twists:** The mapping class is determined up to composition with powers of the

full twist Δ^2 (the generator of the center of B_6, corresponding to a Dehn twist along the boundary of the disk).

3. **Chirality (Mirroring):** The analysis deliberately does not distinguish between β and its mirror image β^{-1}.

Under the Birman-Hilden correspondence, these braids lift to a diffeomorphism Φ on the double branched cover Σ_2^2. We will explicitly derive the action of this lift on the homology of the surface and compute the characteristic polynomial of the induced map. Crucially, this filtering process is well-defined on the equivalence classes described above. As we will formally establish, the characteristic polynomial is invariant under matrix conjugation, the full twist lifts to the identity map on the relevant homology group, and the symplectic nature of the action ensures that mirroring leaves the polynomial unchanged. Consequently, it suffices to test a single representative braid word for each candidate family.

7.3.1 The Action on Homology

A candidate braid β lifts to a diffeomorphism Φ on the double cover of the disk branched over the six marked points. This cover is a genus-2 surface with two boundary components, denoted Σ_2^2. The map $\Phi\colon \Sigma_2^2 \to \Sigma_2^2$ induces a linear action on the first homology:

$$\Phi_*\colon H_1(\Sigma_2^2;\mathbb{Z}) \to H_1(\Sigma_2^2;\mathbb{Z}).$$

The first homology group $H_1(\Sigma_2^2;\mathbb{Z})$ has rank 5 and splits as $V \oplus \partial V$, where $V \cong \mathbb{Z}^4$ is the symplectic subspace generated by the handles of the surface, and ∂V is the subspace generated by the boundary cycles ∂_1, ∂_2 (modulo the relation $\partial_1 + \partial_2 = 0$).

To compute the homological action, we translate the braid generators on the disk into matrices. Each standard braid generator σ_i on D_6 swaps two adjacent marked points via a

half-twist. In the double branched cover, the preimage of the arc connecting these points is a simple closed curve γ_i. The lift of the half-twist is a full Dehn twist T_{γ_i} along this curve. Because the standard braid generators are supported entirely in the interior of the disk, their lifts are supported in the interior of Σ_2^2, meaning they fix the boundary components pointwise.

Since the action acts as the identity on ∂V, the matrix representation of Φ_* with respect to a basis adapted to the decomposition $V \oplus \mathbb{Z}\langle\partial_1\rangle$ takes the block upper-triangular form:

$$\Phi_* = \begin{pmatrix} A_{\text{red}} & * \\ 0 & 1 \end{pmatrix}.$$

We define the *reduced action* A_{red} as the map induced on the quotient space:

$$H_1(\Sigma_2^2)/\langle\partial_1, \partial_2\rangle \cong H_1(\Sigma_2; \mathbb{Z}).$$

Geometrically, this corresponds to "capping off" both boundary components with disks to obtain the closed genus-2 surface Σ_2, and computing the action on the homology of this closed manifold.

7.3.1.1 Explicit Matrix Representation

We identify the reduced homology $H_1(\Sigma_2; \mathbb{Z})$ with the standard lattice $\mathbb{Z}^4$ by fixing a symplectic basis $\mathcal{B} = \{e_1, e_2, e_3, e_4\}$. Geometrically, this basis corresponds to the standard system of curves on the genus-2 surface, where e_1, e_3 represent the meridians (a-cycles) and e_2, e_4 represent the dual longitudes (b-cycles) of the two handles. These elements satisfy the standard algebraic intersection relations:

$$\langle e_1, e_2\rangle = \langle e_3, e_4\rangle = 1, \quad \text{and} \quad \langle e_i, e_j\rangle = 0 \text{ otherwise.}$$

The action of a Dehn twist T_{γ_i} on a homology class x is given by the Picard-Lefschetz formula:

$$T_{\gamma_i}(x) = x + \langle x, [\gamma_i] \rangle [\gamma_i]. \tag{7.1}$$

By applying this formula to each basis vector e_j, we derive the explicit symplectic matrices $M_i \in \mathrm{Sp}(4, \mathbb{Z})$ representing the action of the lifted generators σ_i on the closed surface Σ_2:

$$M_1 = \begin{pmatrix} 1 & -1 & 0 & 0 \\ 0 & 1 & 0 & 0 \\ 0 & 0 & 1 & 0 \\ 0 & 0 & 0 & 1 \end{pmatrix}, \qquad M_2 = \begin{pmatrix} 1 & 0 & 0 & 0 \\ 1 & 1 & -1 & 0 \\ 0 & 0 & 1 & 0 \\ 0 & 0 & 0 & 1 \end{pmatrix}, \tag{7.2}$$

$$M_3 = \begin{pmatrix} 1 & 0 & 0 & 0 \\ 0 & 1 & 0 & 0 \\ 0 & 1 & 1 & -1 \\ 0 & 0 & 0 & 1 \end{pmatrix}, \qquad M_4 = \begin{pmatrix} 1 & 0 & 0 & 0 \\ 0 & 1 & 0 & 0 \\ 0 & 0 & 1 & 0 \\ 0 & 0 & 1 & 1 \end{pmatrix}, \tag{7.3}$$

$$M_5 = \begin{pmatrix} 1 & 0 & 0 & -1 \\ 0 & 1 & 0 & 0 \\ 0 & 0 & 1 & -1 \\ 0 & 0 & 0 & 1 \end{pmatrix}. \tag{7.4}$$

For any representative braid word $\beta = \sigma_{i_1}^{k_1} \dots \sigma_{i_m}^{k_m}$, the action on the reduced homology is given exactly by the matrix product:

$$A_{\mathrm{red}} = \prod_{j=1}^{m} M_{i_j}^{k_j}. \tag{7.5}$$

7.3.2 Invariance Properties of the Filters

Both filters defined below — the zero-surgery condition $|\det(I - A_{\text{red}})| = 1$ and the Alexander polynomial condition $\det(tI - A_{\text{red}}) = (t^2 - t + 1)^2$ — are well-defined on the equivalence classes (conjugacy, full twists, mirroring) of our candidate braids. We record the invariance properties here, before stating either filter, since both rely on them.

- **Conjugacy:** Both $\det(I - A_{\text{red}})$ and the characteristic polynomial $\det(tI - A_{\text{red}})$ are similarity invariants: $\det\big(I - PAP^{-1}\big) = \det(I - A)$ and similarly for $\det(tI - A)$. Conjugate braids yield identical values for both filters.

- **Full Twists:** The central element Δ^2 corresponds to a Dehn twist along the boundary of D_6. Upon lifting and capping to Σ_2, this becomes a Dehn twist along a trivial curve (bounding a disk), which is isotopic to the identity. Algebraically, the half-twist Δ lifts to the hyperelliptic involution ι, which acts as $-I$ on $H_1(\Sigma_2; \mathbb{Z})$. Consequently, the full twist Δ^2 acts as $(-I)^2 = I$. Thus, A_{red} itself is invariant under the addition of full twists, and hence both filters are.

- **Mirroring:** Mirroring β (replacing each σ_i with σ_i^{-1}) replaces A_{red} with A_{red}^{-1}. For the Alexander polynomial: since A_{red} is a symplectic matrix, its characteristic polynomial is reciprocal, $P(t) = t^4 P(t^{-1})$, so the characteristic polynomials of A_{red} and A_{red}^{-1} agree. For the zero-surgery condition: $\det\big(I - A^{-1}\big) = \det\big(A^{-1}\big)\det(A - I) = (\det A^{-1}) \cdot (-1)^4 \det(I - A) = \det A^{-1} \cdot \det(I - A) = \det(I - A)$ (since $\det A = 1$ for $A \in \mathrm{Sp}(4, \mathbb{Z})$). Both filters are thus insensitive to chirality.

Consequently, for each candidate braid family, it suffices to test a single representative braid word against both filters.

7.3.3 Verification via Zero-Surgery

The first filter verifies that the candidate braid produces a knot embedded in the correct ambient manifold, specifically the 3-sphere S^3.

Let Y be the 3-manifold associated with the open book decomposition defined by the page Σ_2^2 and the lifted monodromy Φ. The binding of this open book is a two-component link $L = L_1 \cup L_2$, corresponding to the two boundary components of the surface. We identify one component, say L_1, as the candidate for the knot K.

Topologically, capping off the boundary component corresponding to L_2 is equivalent to performing zero-surgery on L_2. This operation yields a new manifold Y' containing the single knot L_1. For L_1 to be a valid candidate for the knot $K \subset S^3$, the ambient manifold Y' must be an integer homology sphere (such that $H_1(Y'; \mathbb{Z}) = 0$).

Using the exact sequence for the mapping torus, the order of the first homology is determined by the determinant of $(I - h_*)$, where h_* is the monodromy acting on the fiber. In our reduced basis, this condition dictates that for Y' to be a homology sphere, we require:

$$|\det(I - A_{\text{red}})| = 1. \tag{7.6}$$

If this determinant evaluates to anything other than ± 1, the resulting manifold Y' possesses non-trivial torsion (e.g., it may be a Lens space), which implies the knot L_1 cannot reside in S^3. Any candidate braid family failing this condition is immediately eliminated.

7.3.4 Verification via the Alexander Polynomial

The second, finer filter compares the induced characteristic polynomial of the surviving candidates to that of the target knot. The Alexander polynomial $\Delta_K(t)$ is the characteristic polynomial of the monodromy acting on the symplectic homology of the fiber. For $K =$

$T_{2,3}\#T_{2,3}$, this is exactly:

$$\Delta_K(t) = (t^2 - t + 1)^2.$$

A technical subtlety arises because the candidate braids are defined on the disk (lifting to the surface with boundary Σ_2^2), while the standard Alexander polynomial is an invariant of the closed fiber. We rely on the following lemma to justify comparing the polynomial computed from our reduced matrices M_i directly to $\Delta_K(t)$.

Lemma 7.5. Let $f\colon \Sigma_g^n \to \Sigma_g^n$ be a homeomorphism that preserves the boundary components pointwise. Let A be the matrix of f_* on $H_1(\Sigma_g^n;\mathbb{Z})$ and A_{red} be the matrix of the induced map on the capped closed surface Σ_g. Then:

$$\det(tI - A) = (t-1)^n \det(tI - A_{\text{red}}).$$

Proof. We decompose the first homology group $H_1(\Sigma_g^n;\mathbb{Z})$ as $V \oplus \partial V$, where $V \cong H_1(\Sigma_g;\mathbb{Z}) \cong \mathbb{Z}^{2g}$ is the symplectic subspace generated by the handles, and $\partial V \cong \mathbb{Z}^n$ is the subspace generated by the boundary cycles. Since f fixes the boundary components pointwise, the induced map f_* acts as the identity on ∂V. Furthermore, since f preserves the boundary, it maps the subspace V into $V \oplus \partial V$. With respect to a basis reflecting this decomposition, the matrix A representing f_* takes the block upper-triangular form:

$$A = \begin{pmatrix} A_{\text{red}} & * \\ 0 & I_n \end{pmatrix},$$

where A_{red} is the matrix of the map induced on the quotient $H_1(\Sigma_g^n)/\partial V \cong H_1(\Sigma_g)$, and I_n is the $n \times n$ identity matrix. Because the characteristic polynomial of a block triangular matrix is the product of the characteristic polynomials of its diagonal blocks, we obtain:

$$\det(tI - A) = \det(tI - A_{\text{red}}) \cdot \det(tI - I_n) = \det(tI - A_{\text{red}}) \cdot (t-1)^n.$$

□

Remark 7.6. Geometrically, capping a boundary is equivalent to trivializing the homology cycle corresponding to that boundary loop. Before capping, these trivial actions manifest as factors of $(t-1)$ in the characteristic polynomial because the boundary components are strictly fixed by the monodromy.

Since we have explicitly computed A_{red} using the matrices M_i (which correspond to the action on the closed surface), we have effectively removed the boundary artifacts described in Lemma 7.5. Therefore, the characteristic polynomial must match the standard Alexander polynomial $\Delta_K(t)$ exactly, without any additional factors of $(t-1)$. We verify if:

$$\det(tI - A_{\text{red}}) = (t^2 - t + 1)^2. \tag{7.7}$$

Any candidate braid failing this exact equality is eliminated, concluding our obstruction.

7.4 The Stratum $(3; 1^6; 3)$

We now apply our geometric and algebraic machinery to the first of the two non-orientable strata. Our ultimate goal for this section is to rigorously establish the following elimination theorem:

Theorem 7.7. Let $K \subset S^3$ be a hyperbolic knot satisfying $\widehat{HFK}(K) \cong \widehat{HFK}(T_{2,3}\#T_{2,3})$, and let

$$(h, \phi_h, \hat{h}, \hat{\phi}_h, b, \phi_b, \beta, \phi_\beta, \Phi, \phi_\Phi)$$

be the associated Birman-Hilden correspondence data induced by the monodromy of K. Then the pseudo-Anosov 6-braid β on the disk cannot belong to the stratum $(3; 1^6; 3)$.

To prove this theorem, we must traverse the full obstruction pipeline: generating the state

space, pruning it via tight splitting, enumerating the valid mapping classes, and applying homological filters.

7.4.1 Reducing Candidate Train Tracks via Splitting

We begin by demonstrating that any pseudo-Anosov map in this stratum must be carried by a single specific train track.

Lemma 7.8. Let β be a pseudo-Anosov 6-braid in the stratum $(3; 1^6; 3)$ that lifts to a fixed-point-free mapping class on Σ_2^2. If β is carried by a standard train track τ, then up to conjugation and mirroring, τ is the Candelabra train track (Figure 7.19).

Proof. Running the `autofolder` algorithm on the stratum $(3; 1^6; 3)$ yields an exhaustive train track automaton configured as a directed graph with 138 vertices and 706 directed edges. Among these 138 standard train tracks, there are exactly 4 which are jointless. These are shown in Figure 7.16. By Corollary 3.20, up to conjugation, we only need to consider these four tracks.

We construct splitting diagrams for these candidate tracks. Figure 7.17 shows that Train Track 3 eventually splits to Train Track 1 or 2. Figure 7.18 shows that Train Track 1 eventually splits to the Candelabra (Track 0), or Train Track 2.

Observe that Train Tracks 1 and 2 are vertical mirrors of each other. By mirroring the entire splitting sequence of Figure 7.18, we obtain a valid splitting sequence for Train Track 2, which necessarily shows that Train Track 2 eventually splits to the Candelabra or back to Train Track 1. By the termination of tight splitting (Theorem 6.14), this cyclic pattern cannot repeat indefinitely. Therefore, both Train Track 1 and Train Track 2 must eventually split to the Candelabra.

In conclusion, any pseudo-Anosov map carried by Tracks 1, 2, or 3 is ultimately carried by

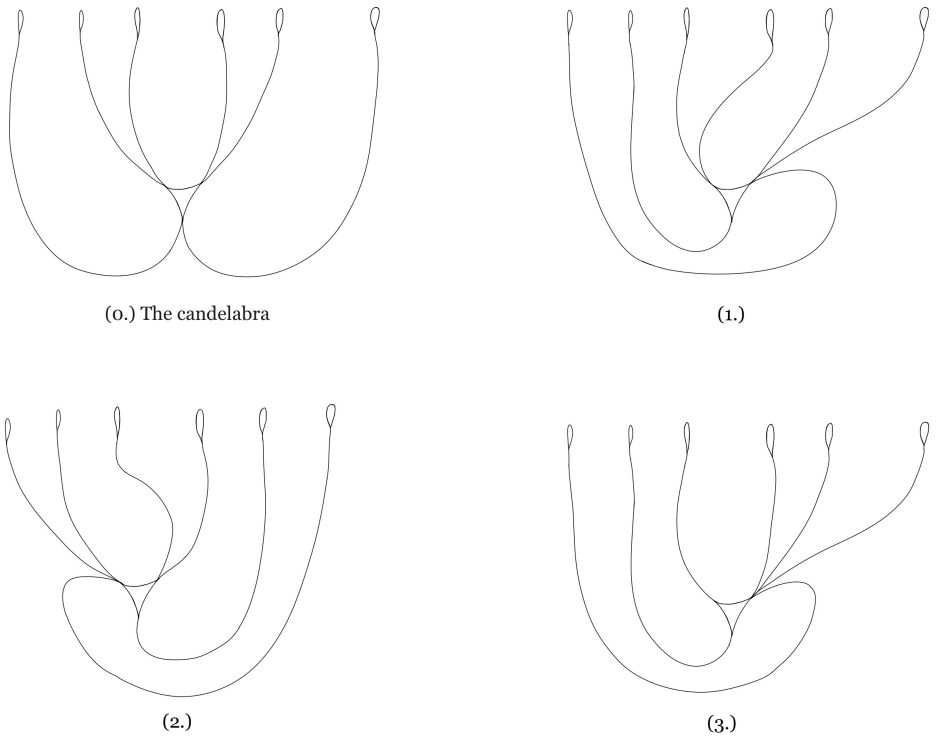


Figure 7.16: The four jointless standard train tracks in the stratum $(3; 1^6; 3)$. Track 0 is the Candelabra.

the Candelabra. Thus, we may assume τ is strictly the Candelabra train track. □

7.4.2 Enumeration of Train Track Maps and Braids

Having reduced our geometric search space to the Candelabra, we execute the case analysis procedure of Section 7.2.3. With no central edge d in this stratum, Cases B, C, D and Assumption A do not arise; the dominant obstruction is Corollary 7.2 (the no-self-occurrence rule for jointless-monogon edges), with the Absorption Obstruction handling most remaining geometric routing decisions. The complete derivation of the surviving maps, together with the rotational symmetry argument that relates the two initial rotational states of the central

triangle, is presented in Appendix C. The corresponding braid words are listed in Appendix J, yielding the following proposition:

Proposition 7.9. Let $\Phi\colon \Sigma_2^2 \to \Sigma_2^2$ be a pseudo-Anosov mapping class corresponding to the stratum $(3; 1^6; 3)$ on the disk. If the pseudo-Anosov representative ϕ_Φ has no interior fixed points, then Φ is conjugate to the lift of one of the 38 braid families explicitly enumerated in Appendix J.

7.4.3 Proof of the Main Elimination Theorem

We are now equipped to definitively prove Theorem 7.7.

Proof of Theorem 7.7. Suppose, for the sake of contradiction, that the geometric braid representative β associated with the knot K belongs to the stratum $(3; 1^6; 3)$. Since the knot complement is hyperbolic, β lifts to a pseudo-Anosov map on Σ_2^2 that must be fixed-point-free in its interior.

By Lemma 7.8, up to conjugation and mirroring, β must be carried by the Candelabra train track. By Proposition 7.9, the topological restriction that its lift is fixed-point-free further forces β to belong to one of the 38 specific braid families enumerated in Appendix J.

To determine if any of these 38 braid families can correspond to the monodromy of K, we apply the homological filters detailed in Section 7.3. For each of the 38 families, we computationally extract the reduced homological action matrix A_{red}. We test each matrix against the zero-surgery condition (requiring $|\det(I - A_{\text{red}})| = 1$ to ensure the ambient manifold is S^3) and the Alexander polynomial condition (requiring $\det(tI - A_{\text{red}}) = (t^2 - t + 1)^2$).

Our computational verification demonstrates that **none** of the 38 families simultaneously satisfy both homological requirements. Since the finite, exhaustive list of topological candidates has been entirely eliminated by algebraic obstruction, no such braid β can exist. This

concludes the proof. □

7.5 The Stratum $(2; 1^6; 3^2)$

We now turn our attention to the second non-orientable stratum. As in the previous section, our objective is to rigorously eliminate all pseudo-Anosov mapping classes within this stratum as candidates for our specific Birman-Hilden correspondence.

We aim to establish the following elimination theorem:

Theorem 7.10. Let $K \subset S^3$ be a hyperbolic knot satisfying $\widehat{HFK}(K) \cong \widehat{HFK}(T_{2,3}\#T_{2,3})$, and let

$$(h, \phi_h, \hat{h}, \hat{\phi}_h, b, \phi_b, \beta, \phi_\beta, \Phi, \phi_\Phi)$$

be the associated Birman-Hilden correspondence data induced by the monodromy of K. Then the pseudo-Anosov 6-braid β on the disk cannot belong to the stratum $(2; 1^6; 3^2)$.

7.5.1 Reducing Candidate Train Tracks via Splitting

Because the geometric complexity of this stratum involves two interior 3-pronged singularities, the initial state space generated by the folding automaton is significantly larger than that of the Candelabra. We rely heavily on tight splitting and symmetries to reduce this to a computable set.

Lemma 7.11. Let β be a pseudo-Anosov 6-braid in the stratum $(2; 1^6; 3^2)$ that lifts to a fixed-point-free mapping class on Σ_2^2. If β is carried by a standard train track τ, then up to conjugation and mirroring, τ is one of exactly six specific standard train tracks (Tracks 0, 1, 8, 12, 13, and 17).

Proof. Running the `autofolder` algorithm on the stratum $(2; 1^6; 3^2)$ outputs a folding

automaton structured as a directed graph with 110 vertices and 412 directed edges. This corresponds to 110 standard train track isomorphism classes. By Corollary 3.20, we may strictly restrict our analysis to the jointless train tracks within this automaton. There are exactly 20 such jointless tracks, depicted in Figure 7.20.

To simplify the analysis, we identify pairs of train tracks that are vertical mirror images of one another. Any pseudo-Anosov braid carried by a given track can simply be mirrored to be carried by its partner. Among the 20 jointless tracks, we identify the following mirror pairs:

- (1) and (4)
- (2) and (3)
- (5) and (6)
- (7) and (11)
- (8) and (10)
- (12) and (14)
- (15) and (16)
- (17) and (18)

By selecting one representative from each pair, we reduce the space to 12 base tracks: (0), (1), (2), (5), (7), (8), (9), (12), (13), (15), (17), and (19).

Finally, we deploy the tight splitting operation. Because each train track possesses two infinitesimal triangles (3-gons), an initial tight splitting can occur at either of the two corresponding loop switches. We compute the exhaustive splitting sequences for these 12 base tracks, the complete diagrams for which are provided in Appendix A.

As demonstrated in the appendix, the splitting sequences for tracks (19), (17), (15), (13), (12), (9), (8), (7), (5), (2), and (1) recursively terminate by splitting into one of the following six base tracks: (0), (1), (8), (12), (13), and (17). Therefore, up to conjugation and mirroring, any pseudo-Anosov map in this stratum must be carried by one of these final six tracks, shown in Figure 7.21. □

7.5.2 Enumeration of Train Track Maps and Braids

With the geometric state space reduced to six invariant tracks, we execute the case analysis procedure of Section 7.2.3 on each. The parity constraints on $f_\beta(d)$ and $f_\beta(\bar{d})$ (the Trace Lemma applied to the central edge in its four-case form) become the decisive obstruction in this stratum: Situation α produces the bulk of non-termination eliminations (the dotted lines circle the outer perimeter without joining), and Situation β produces the bulk of direct-violation eliminations (the dotted lines are trapped in a pocket forcing an odd-parity return). Path mills arise as a secondary non-termination obstruction for the non-dotted edges.

For Track 12, this analysis yields no surviving train track maps: every candidate transition word is excluded either by a tracing violation of Corollary 7.2 or by absorption between adjacent edge images. The full case analysis for Track 12 is included in Appendix G for completeness. Consequently, no fixed-point-free pseudo-Anosov braid in the stratum $(2; 1^6; 3^2)$ is carried by Track 12, and the analysis below treats only the remaining five tracks where surviving candidates exist.

This combinatorial exhaustion yields a finite set of surviving train track map families on the five remaining tracks. The step-by-step derivation and the explicit extraction of their corresponding braid words are detailed in Appendices K, L, M, N, and O. This analysis establishes the following proposition:

Proposition 7.12. Let $\Phi: \Sigma_2^2 \to \Sigma_2^2$ be a pseudo-Anosov mapping class corresponding to the stratum $(2; 1^6; 3^2)$ on the disk. If the pseudo-Anosov representative ϕ_Φ has no interior fixed points, then Φ is conjugate to the lift of one of the finite braid families enumerated for Tracks 0, 1, 8, 13, and 17 (Appendices K, L, M, N, O).

7.5.3 Proof of the Main Elimination Theorem

With our topological candidates isolated, we arrive at the final algebraic obstruction.

Proof of Theorem 7.10. Suppose, for the sake of contradiction, that the geometric braid representative β associated with the knot K belongs to the stratum $(2; 1^6; 3^2)$. Because the target knot complement is hyperbolic, β lifts to a pseudo-Anosov map on Σ_2^2 that is fixed-point-free in its interior.

By Lemma 7.11, β must be carried by one of the six irreducible train tracks. By Proposition 7.12, the Trace Lemma forces β to belong to one of the specific braid families enumerated in the corresponding track appendices.

We route these surviving candidates through the homological filters detailed in Section 7.3. For each candidate family, we compute the reduced homological action matrix A_{red}. We test these matrices against the zero-surgery requirement ($|\det(I - A_{\text{red}})| = 1$) and the Alexander polynomial requirement ($\det(tI - A_{\text{red}}) = (t^2 - t + 1)^2$).

Computation demonstrates that none of the candidate families from these appendices simultaneously satisfy both necessary conditions. Because the finite set of topological candidates has been entirely eliminated, no such braid β can correspond to the monodromy of K. This completes the proof. □

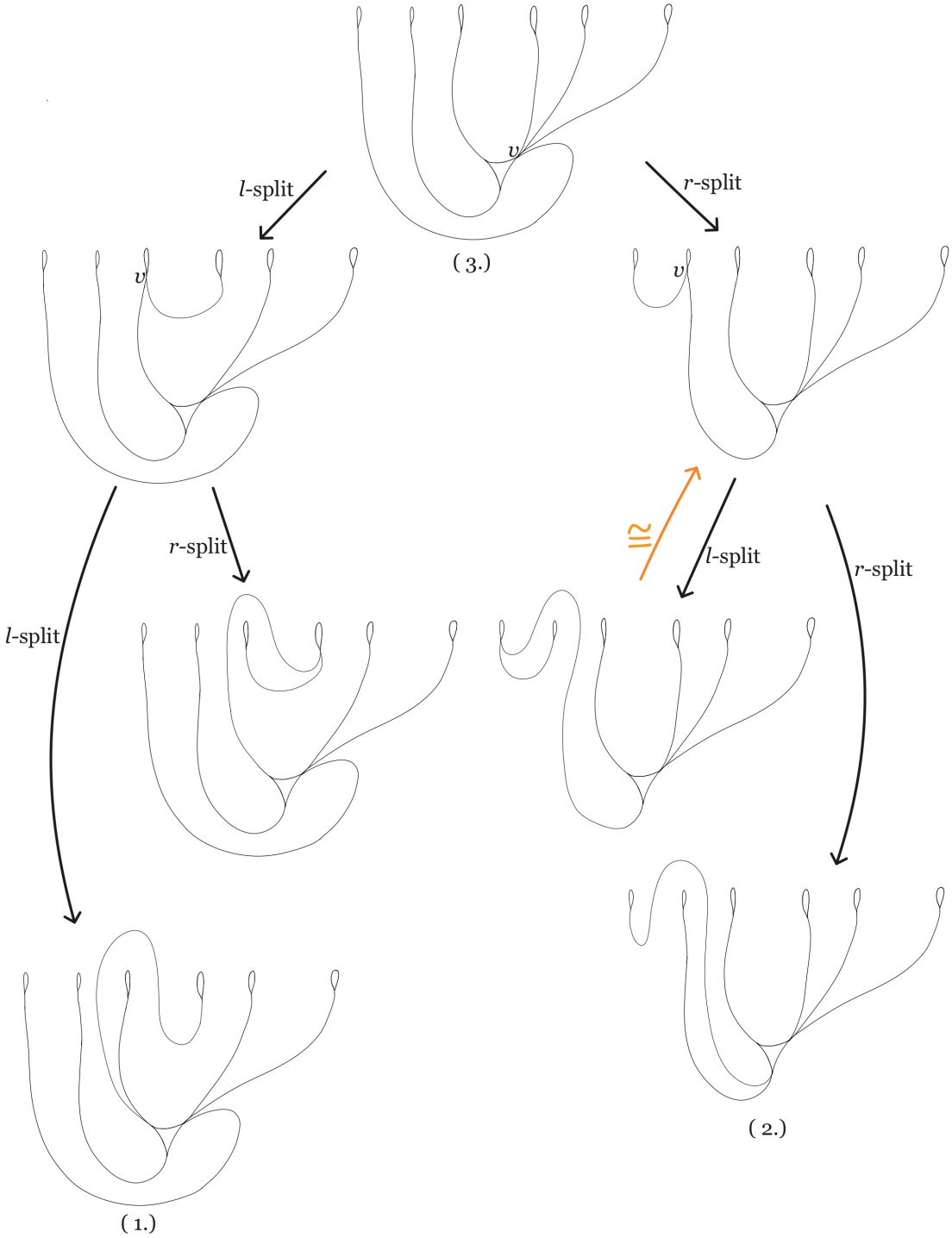


Figure 7.17: Train Track 3 eventually splits to Train Track 1 or the Candelabra.

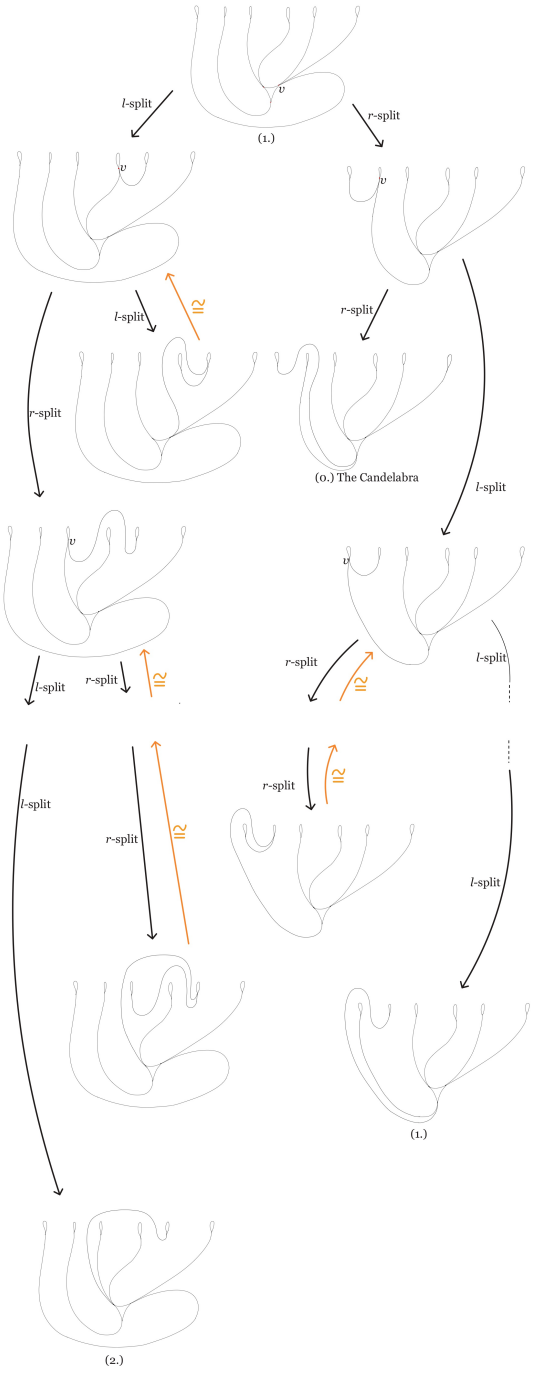


Figure 7.18: Train Track 1 eventually splits to Train Track 2 or the Candelabra. Mirroring this figure demonstrates that Train Track 2 eventually splits to Train Track 1 or the Candelabra.

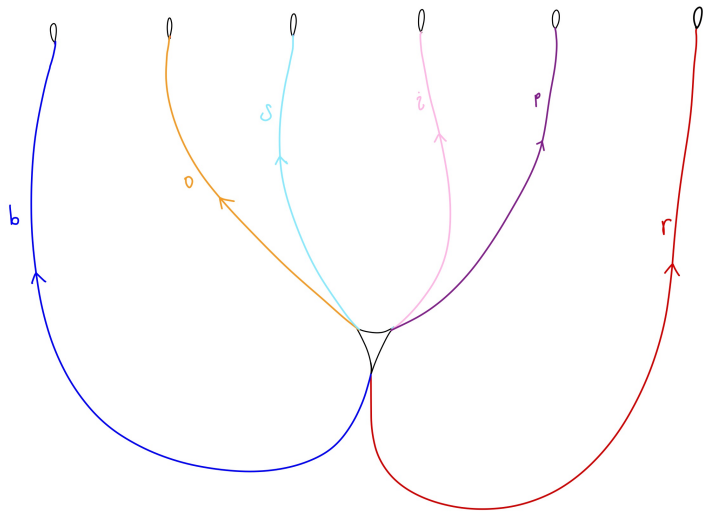


Figure 7.19: The Candelabra train track.

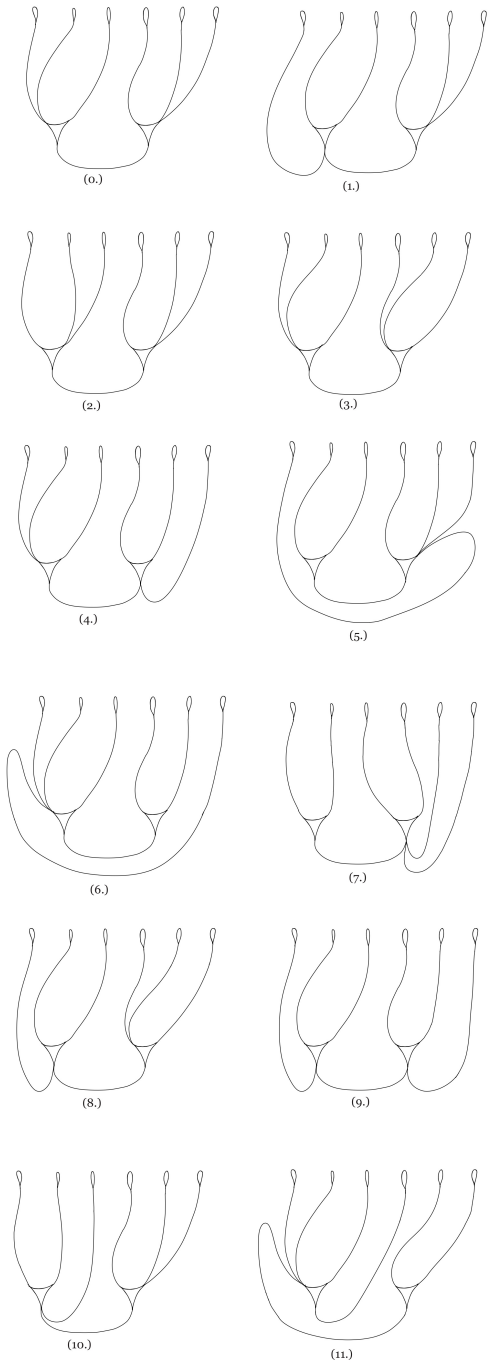


Figure 7.20: The 20 standard jointless train tracks in the stratum $(2; 1^6; 3^2)$.

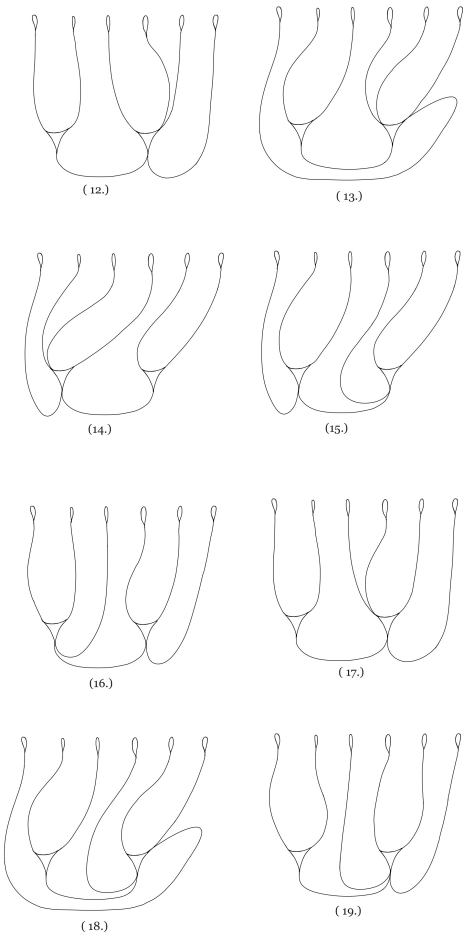


Figure 7.20: The 20 standard jointless train tracks in the stratum $(2; 1^6; 3^2)$ (continued).

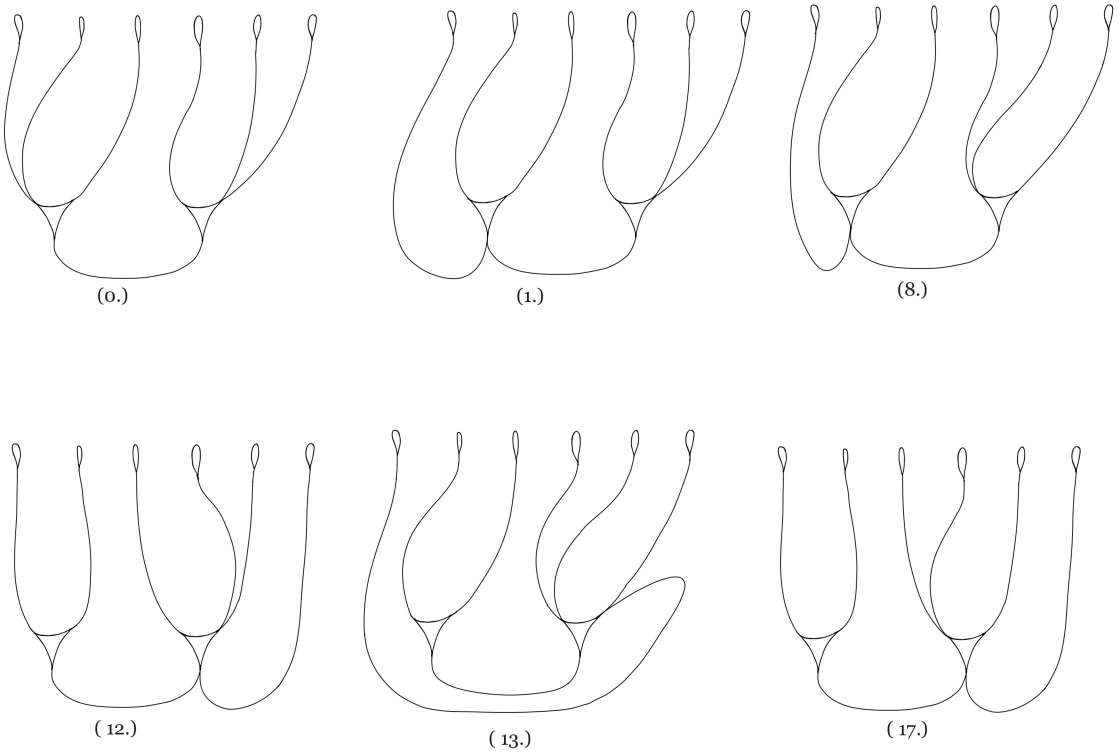


Figure 7.21: The six irreducible standard train tracks for the stratum $(2; 1^6; 3^2)$. Up to equivalence, all valid maps must be carried by one of these tracks.

CHAPTER EIGHT

The Satellite Case

In this chapter, we establish the following result:

Theorem 8.1. Suppose K is a satellite knot satisfying the assumptions of Theorem 1.1, that is, there is an isomorphism of bigraded vector spaces

$$\widehat{HFK}(K;\mathbb{F}) \cong \widehat{HFK}(T(2,3)\#T(2,3);\mathbb{F}).$$

Then K is isotopic to $T(2,3)\#T(2,3)$.

The argument proceeds in several stages. We first apply Schubert's formula to constrain the Alexander polynomials of the pattern and companion of K, forcing both to be trefoils and the algebraic winding number to be one (Lemma 8.4). We then invoke the Thurston reducing system framework to classify the canonical reducing curves of the monodromy h, isolating two non-trivial possibilities (Case A: Σ_0 is a pair of pants; Case B: Σ_0 is genus one with one reducing curve, in Lemma 8.7). For each of these cases, we systematically eliminate sub-cases using a combination of Baldwin-Sivek's classification of periodic outer maps, the fractional Dehn twist coefficient bound of Hedden-Mark, and the Honda-Kazez-Matić right-veering criterion, leaving only the connect-sum of two right-handed trefoils. Finally, we briefly address

the degenerate $(2,1)$-cable configuration via a direct Alexander polynomial calculation.

We begin by reviewing the definition of a satellite knot.

Let

$$P \subset S^1 \times D^2$$

be a knot in S^3 lying non-trivially inside an unknotted solid torus, by which we mean that P is not allowed to be inside a 3-ball in the solid torus, and P is not allowed to be isotopic to the core curve of the solid torus. This knot P is called the **pattern** of the satellite knot. Fix an embedding

$$f\colon S^1 \times D^2 \to S^3.$$

The satellite knot K is defined to be the knot $f(P)$. The core curve of the solid torus $S^1 \times D^2$ is sent to a knot C, which is called the **companion** of the satellite knot. We will sometimes denote the satellite knot K as $P(C)$.

The **winding number** of the satellite knot $P(C)$ is the winding number of the pattern inside the solid torus:

Definition 8.2. Let $K = P(C)$ be a satellite knot, where

$$P \subset V = S^1 \times D^2,$$

an unknotted solid torus. The **(algebraic) winding number** w of K is the algebraic intersection number of P with a meridional disk of V. The **wrapping number** (or **geometric winding number**) m of K is the minimum number of geometric intersection points between P with a meridional disk of V, where the minimum is taken over all ambient isotopies of P within V. It is clear that

$$m \geq |w|.$$

We would like to sometimes consider the pattern P as a knot in S^3, by which we mean the image of P under the natural embedding of $S^1 \times D^2$ into S^3. We will denote this knot as $P(U)$. The notation is indicative of the fact that this knot is equivalent to a satellite knot construction with pattern P, and f is the embedding that sends the core curve to the unknot.

8.1 Schubert's Formula on the Alexander polynomial of a Satellite Knot

A well-known formula originally due to Schubert[Sch53] relates the Alexander polynomials of K and that of $P(U)$ and C:

Theorem 8.3 (Schubert, 1953 [Sch53])**.** Let K be a satellite knot with companion knot C and pattern knot P, and let w denote the winding number, and m the wrapping number of K. Then the following relations hold:

1. The Alexander polynomials satisfy

$$\Delta_K(t) \doteq \Delta_P(t) \cdot \Delta_C(t^w) \tag{8.1}$$

   where $\doteq$ denotes equality up to multiplication by a unit $\pm t^k$ in the ring of Laurent polynomials $\mathbb{Z}[t, t^{-1}]$.

2. The Seifert genus g satisfies the inequalities

$$g(K) \geq g(P(U)) + m \cdot g(C) \geq g(P(U)) + |w| \cdot g(C).$$

For the situation where we assume that K is a knot such that

$$\widehat{HFK}(K) \cong \widehat{HFK}(T(2,3)\#T(2,3)),$$

the left-hand side of (8.1), namely $\Delta_K(t)$, is the Alexander polynomial of the connected sum of trefoils. This allows us to constrain what could be the Alexander polynomials of pattern and companion, and further argue that the winding number must be one:

Lemma 8.4. Let $K = P(C)$ be a satellite knot satisfying the assumptions of Theorem 1.1. Then the pattern $P(U)$ and C are both trefoils, and K has winding number 1.

Proof. By assumption K has the following symmetrized Alexander polynomial:

$$\Delta_K(t) = t^2 - 2t + 3 - 2t^{-1} + t^{-2}.$$

Since K is fibered, the algebraic winding number is non-zero, so we may assume $|w| \geq 1$. (Indeed, if $w = 0$, then Schubert's formula gives $\Delta_K(t) \doteq \Delta_{P(U)}(t) \cdot \Delta_C(1) \doteq \pm\Delta_{P(U)}(t)$, so Δ_K degenerates to depend only on the pattern. By Hirasawa, Murasugi, and Silver [HMS08, Theorem 1], a satellite knot with winding number zero and non-trivial companion is not fibered, contradicting our hypothesis.) Furthermore, both the companion C and the pattern in the unknot $P(U)$ must also be fibered [BZ03, Corollary 4.15, Proposition 5.5]. The Alexander polynomials of these knots are related by the formula from Theorem 8.3:

$$\Delta_K(t) = \Delta_{P(U)}(t) \cdot \Delta_C(t^w).$$

Because C is a fibered knot, the maximum degree of its symmetrized Alexander polynomial strictly equals its Seifert genus $g(C)$. Consequently, $\Delta_C(t^w)$ is a nontrivial polynomial with maximum degree $|w| \cdot g(C) \geq 1$.

Now $\Delta_K(t)$ can only be factored either trivially, i.e., $\Delta_{P(U)}(t) = 1$; or it must split symmetrically, i.e., $\Delta_{P(U)}(t) = \Delta_C(t^w) = t - 1 + t^{-1}$.

Suppose it is the former case. Since $P(U)$ is fibered, $\Delta_{P(U)}(t) = 1$ occurs only when $P(U)$ is the unknot. On the other hand, we now have

$$\Delta_K(t) = \Delta_C(t^w).$$

Since $\Delta_K(t)$ has degree 2, $\Delta_C(t^w)$ must also have degree 2, meaning $|w| \cdot g(C) = 2$. This leaves two possibilities: $|w| = 1$ (and $g(C) = 2$) or $|w| = 2$ (and $g(C) = 1$).

If $|w| = 2$, then $\Delta_C(t)$ has degree 1, meaning $\Delta_C(t) = at + b + at^{-1}$. Substituting t^2 yields $\Delta_C(t^2) = at^2 + b + at^{-2}$, which has zero coefficients for the $t^{\pm 1}$ terms. This contradicts our explicit formula for $\Delta_K(t)$, which contains $-2t$ and $-2t^{-1}$. This strictly forces $|w| = 1$.

Since the winding number is one and $P(U)$ is the unknot, a result of Hirasawa, Murasugi,

and Silver [HMS08, Corollary 1] states that $K = P(C)$ can only be fibered if P is isotopic to the core $S^1 \times \{0\} \subset S^1 \times D^2$. But this implies K is isotopic to C, contradicting the assumption that K is a non-trivial satellite knot.

Thus, it must be that $\Delta_K(t)$ splits symmetrically, i.e.,

$$\Delta_{P(U)}(t) = \Delta_C(t^w) = t - 1 + t^{-1}.$$

Since $\Delta_C(t^w)$ has degree one, we have

$$1 = |w| \cdot g(C) \geq 1,$$

which implies $|w| = 1$ and $g(C) = 1$.

Applying the genus inequality from Theorem 8.3:

$$g(K) \geq |w| \cdot g(C) + g(P(U))$$

to the case at hand, we have

$$2 \geq 1 \cdot 1 + g(P(U)).$$

Thus $P(U)$ must either be genus zero or genus one. If it were genus zero, it would be the unknot, which has a trivial Alexander polynomial, contradicting $\Delta_{P(U)}(t) = t - 1 + t^{-1}$. Hence $P(U)$ must be a genus-one knot. By Hirasawa-Murasugi-Silver [HMS08], both C and $P(U)$ are fibered. The only fibered genus-one knots are the figure-eight knot and the trefoils. Since the figure-eight knot has $\Delta(t) = t - 3 + t^{-1}$, the Alexander polynomial restricts $P(U)$ to being one of the trefoils. Similarly, since $\Delta_C(t) = t - 1 + t^{-1}$ and C is a genus-one fibered knot, the companion C is also one of the trefoils. □

8.2 Thurston Reducing System

The previously mentioned Thurston's classification of surface homeomorphisms (Theorem 2.2) has in fact a more refined statement in terms of "reducing systems". Wherein the surface can be divided into pieces by a finite set of curves, and the map restricted to each piece can be classified. More precisely:

Theorem 8.5 (Thurston [Thu88])**.** Let $h\colon \Sigma \to \Sigma$ be a homeomorphism of a compact oriented surface with possibly empty boundary. The map h is isotopic rel boundary to a map $\phi_h\colon \Sigma \to \Sigma$ such that

1. there exists a possibly empty reducing system $\Gamma \subset \Sigma$ consisting of a finite disjoint union of simple closed curves which is fixed setwise by ϕ_h;

2. if S is a component of $\Sigma \setminus \Gamma$ and n is the smallest positive integer such that $\phi_h^n(S) = S$, then $\phi_h^n|_S$ is freely isotopic to a periodic or pseudo-Anosov map. When $n = 1$, we refer to this map and S as a periodic or pseudo-Anosov component of h or $\Sigma \setminus \Gamma$, accordingly.

As explained in Thurston's work, we may, and will assume that Γ is minimal with respect to inclusion, in which case it is unique up to isotopy [BLM83, Theorem C] and is called the **canonical reducing system** for h. We refer to the pair (ϕ_h, Γ) as the **Nielsen-Thurston form of** h.

Remark 8.6 (The global Nielsen-Thurston type is read off Γ)**.** The canonical reducing system Γ records the *global* Nielsen-Thurston type of h: it is empty precisely when h is periodic or pseudo-Anosov, and nonempty precisely when h is reducible in the genuine (infinite-order) sense. Thus, for the monodromy of a fibered knot,

$$h \text{ is reducible} \iff \Gamma \neq \emptyset,$$

and this is the only sense of "reducible" used in the proof; in particular we never invoke disjointness among the periodic, reducible, and pseudo-Anosov classes of the surface classification (Theorem 2.2).

It is worth recording how the granny knot itself sits inside this framework, since at first sight it appears to straddle the periodic and reducible types. Its monodromy is reducible with two *periodic* pieces — the order-six monodromies of the two trefoil summands, carried by the once-punctured tori that Γ cuts off — and yet the *global* class $[h]$ is non-periodic. This is forced geometrically: were $[h]$ periodic, the mapping torus $M_h = E(T_{2,3}\#T_{2,3})$ would be Seifert fibered and hence atoroidal, contradicting the essential swallow-follow torus that exhibits the granny as a satellite. Consequently $[h]$ has infinite order, $\Gamma \neq \emptyset$, and the granny lands in the satellite case purely at the level of the knot exterior — consistent with its periodic pieces and requiring no appeal to surface-level exclusivity.

Let us now consider the case where

$$h\colon \Sigma_2^1 \to \Sigma_2^1$$

is the monodromy of a genus-two fibered satellite knot K, and suppose (ϕ_h, Γ) is its Nielsen-Thurston form.

Following Baldwin-Sivek[BS25], let Σ_0 be the component of $\Sigma_2^1 \setminus \Gamma$ containing $\partial\Sigma_2^1$. We call Σ_0 the **outermost component** of $\Sigma \setminus \Gamma$. Note that ϕ_h fixes Σ_0 set-wise, and its restriction to Σ_0 is freely isotopic to a map

$$\phi_0\colon \Sigma_0 \to \Sigma_0$$

which is either periodic or pseudo-Anosov.

Lemma 8.7. Suppose

$$h\colon \Sigma_2^1 \to \Sigma_2^1$$

is the monodromy of a genus-two fibered knot K, and (ϕ_h, Γ) the Nielsen-Thurston form of h. Then up to homeomorphism of the surface and isotopy of Γ, the only possibilities of Γ are

1. $\Gamma = \emptyset$;
2. Case A: $\Gamma = \gamma_1 \cup \gamma_2$. The outer surface Σ_0 is a pair of pants with boundary components K, γ_1, and γ_2; or
3. Case B: $\Gamma = \gamma$, a single curve. The outer surface Σ_0 is genus one with boundary components K and γ.

Case A and Case B are shown in Figure 8.1.

Proof. By a result of Baldwin and Sivek [BS26], for a fibered knot in an L-space, every curve in the canonical reducing system Γ is separating. Furthermore, by definition, Γ is a minimal collection of disjoint, essential, and non-boundary-parallel simple closed curves.

The surface Σ_2^1 has genus $g = 2$ and one boundary component $\partial\Sigma = K$. We analyze the possible components of $\Sigma_2^1 \setminus \Gamma$ based on the number of curves in Γ.

Suppose $\Gamma \neq \emptyset$, and let $\gamma \in \Gamma$. Because γ is separating, cutting Σ_2^1 along γ yields two disconnected subsurfaces, S_1 and S_2. Since the original surface has exactly one boundary component K, exactly one of these subsurfaces must contain K. Let S_1 be the subsurface containing K, meaning $\partial S_1 = K \cup \gamma$. The other subsurface, S_2, has exactly one boundary component, $\partial S_2 = \gamma$.

The sum of the genera of the subsurfaces must equal the genus of the original surface, so

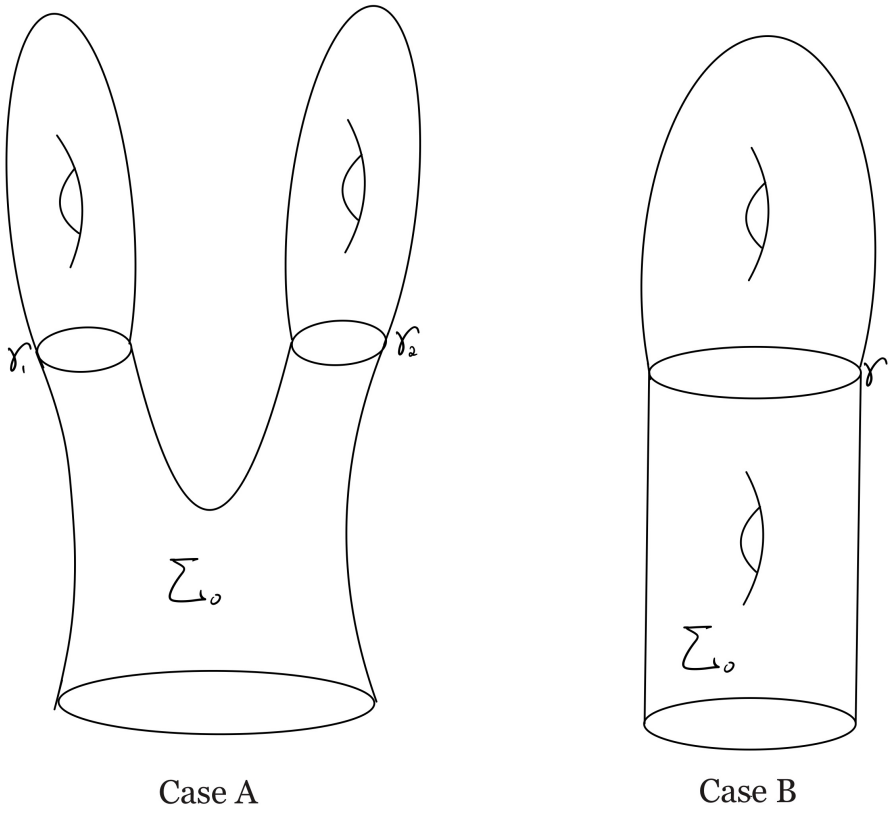


Figure 8.1: The two non-trivial cases of Γ.

$g(S_1) + g(S_2) = g(\Sigma_2^1) = 2$. We can rigorously determine the genera of these pieces:

- Since γ is an essential curve, it cannot bound a disk. Therefore, the one-boundary surface S_2 cannot be a disk, which strictly forces $g(S_2) \geq 1$.

- Since γ is not boundary-parallel to K, the two-boundary surface S_1 cannot be an annulus. Therefore, $g(S_1) \neq 0$, which strictly forces $g(S_1) \geq 1$.

The only integer solution to $g(S_1) + g(S_2) = 2$ given these constraints is $g(S_1) = 1$ and $g(S_2) = 1$. Consequently, any single separating curve $\gamma \in \Gamma$ must decompose Σ_2^1 into $S_1 \cong \Sigma_1^2$ (a genus-one surface with two boundaries) and $S_2 \cong \Sigma_1^1$ (a once-punctured torus).

We now classify Γ by its size:

Case 1: $|\Gamma| = 1$**.** If $\Gamma = \{\gamma\}$, the outermost component Σ_0 is precisely the subsurface containing K. As shown above, $\Sigma_0 = S_1 \cong \Sigma_1^2$. Thus, the outer surface is genus one with boundary components K and γ. This corresponds exactly to **Case B**.

Case 2: $|\Gamma| = 2$**.** Suppose $\Gamma = \{\gamma_1, \gamma_2\}$. The curves are disjoint, so γ_2 must lie entirely within S_1 or S_2 (defined by cutting along γ_1). It is a standard topological fact that a once-punctured torus (Σ_1^1) contains no essential, non-boundary-parallel separating curves; any separating curve on Σ_1^1 must bound a disk or be parallel to the boundary puncture. Therefore, S_2 cannot contain γ_2.

Thus, γ_2 must lie inside S_1. Since $\gamma_2 \in \Gamma$, it is also a separating curve for the global surface Σ_2^1, meaning it must cut off another once-punctured torus (Σ_1^1) from S_1. By cutting the genus-one surface S_1 along γ_2, we subtract a genus-one piece, leaving a remainder of genus zero. This remaining outermost component Σ_0 now contains three boundaries: the knot K, the cut γ_1, and the cut γ_2. A genus-zero surface with three boundaries is a pair of pants (Σ_0^3). This corresponds exactly to **Case A**.

Case 3: $|\Gamma| \geq 3$**.** If there were a third curve γ_3, it would have to reside within one of the components of $\Sigma_2^1 \setminus \{\gamma_1, \gamma_2\}$. Those components are two once-punctured tori and one pair of pants. None of these subsurfaces can contain an essential, non-boundary-parallel simple closed curve. Thus, Γ can contain at most two curves.

Therefore, up to homeomorphism, the only possibilities for Γ are the empty set, Case A, or Case B. □

The following Proposition of Baldwin-Sivek gives a classification result of K when the outer map is periodic.

Proposition 8.8 ([BS25] Proposition 2.3)**.** If ϕ_0 is periodic, then either

- $\Gamma = \emptyset$ and K is a (p, q)-torus knot, or
- $\Gamma \neq \emptyset$ and either
  - K is a composite knot and Σ_0 is a planar surface, or
  - K is a (p, q)-cable knot of some other knot in S^3 and Σ_0 has genus $g(T_{p,q})$

In each case above, $q \geq 2$ and $\gcd(p, q) = 1$.

We isolate one further fact, relating the genus of the outermost piece to the genus of the pattern in the unknot. It underlies both the granny analysis below and the cable detection of Chapter 10, and it is the hinge that determines which reducing-system configuration a given satellite occupies.

Lemma 8.9. Let $K = P(C)$ be a fibered satellite knot with companion solid torus V and satellite torus $T = \partial V$, and suppose the pattern-in-the-unknot $P(U)$ is fibered. Let Σ be the fiber of K, isotoped so as to meet T in the minimal number of curves, which is then the wrapping number m of K, and let $\Sigma_0 = \Sigma \cap V$ be the outermost piece, with boundary $\partial\Sigma_0 = K \cup (\Sigma \cap T)$. Then capping off the m curves of $\Sigma \cap T$ with disks in the standardly embedded solid torus yields the fiber of $P(U)$, and this operation preserves genus, so

$$g(\Sigma_0) = g(P(U)).$$

Proof. Embed V standardly in S^3, so that its core is unknotted. This is precisely the change of ambient space that carries the satellite $K = P(C)$ to the pattern-in-the-unknot $P(U)$, and it leaves the piece $\Sigma_0 \subset V$ unchanged. Under the standard embedding the curves $\Sigma \cap T$ bound meridional disks of the complementary solid torus; attaching these m disks to Σ_0

produces a surface $\widehat{\Sigma}_0$ whose only boundary component is K. Since K and $P(U)$ are fibered and the global monodromy preserves T, the surface $\widehat{\Sigma}_0$ is the fiber of $P(U)$.

Capping a surface with m disks raises the Euler characteristic by m while removing m boundary components. Writing $\chi = 2 - 2g - b$ for a surface of genus g with b boundary components, and noting that Σ_0 has $b = m + 1$ boundary components while $\widehat{\Sigma}_0$ has one,

$$1 - 2g(\widehat{\Sigma}_0) = \chi(\widehat{\Sigma}_0) = \chi(\Sigma_0) + m = (1 - 2g(\Sigma_0) - m) + m = 1 - 2g(\Sigma_0),$$

so $g(\widehat{\Sigma}_0) = g(\Sigma_0)$. Hence $g(\Sigma_0) = g(\widehat{\Sigma}_0) = g(P(U))$. □

We shall need one more proposition before we are ready to prove the main result of this chapter.

Proposition 8.10. Let $K = P(C)$ be a fibered satellite knot with Seifert genus $g(K) = 2$ and algebraic winding number $w = 1$, where the companion C and the pattern knot in the unknot $P(U)$ are both trefoils. Let $h\colon \Sigma \to \Sigma$ be the monodromy of K. Suppose the Nielsen-Thurston form of h is Case B as in Lemma 8.7. The outer map

$$\phi_0\colon \Sigma_0 \to \Sigma_0$$

can be capped off at the boundary component γ with a disk. The resulting map on the surface $\widehat{\Sigma}_0 \cong \Sigma_1^1$:

$$\widehat{\phi}_0\colon \widehat{\Sigma}_0 \to \widehat{\Sigma}_0$$

is precisely the monodromy of the trefoil $P(U)$.

Proof. Let V be the solid torus containing the pattern P, and let $T = \partial V$ be its boundary. In the satellite construction, V is embedded in S^3 such that its core is the companion knot

C. The boundary T forms an essential JSJ torus in the knot exterior.

Let m be the wrapping number of K. By Schubert's geometric genus inequality (Theorem 8.3), the genera must satisfy

$$g(K) \geq g(P(U)) + m \cdot g(C).$$

Substituting our known values yields $2 \geq 1 + m \cdot 1$, which simplifies to $m \leq 1$. However, by definition, the geometric wrapping number must be at least the absolute value of the algebraic winding number, so $m \geq |w| = 1$. These two inequalities strictly force the geometric wrapping number to be $m = 1$. Consequently, the fiber surface Σ can be isotoped to intersect the JSJ torus T in exactly one simple closed curve, which is our Thurston reducing curve γ.

This curve γ splits Σ into two compact subsurfaces. By our convention, the "outer" surface $\Sigma_0 = \Sigma \cap V$ resides entirely inside the solid torus. Its boundary consists of exactly two components: $\partial\Sigma_0 = K \cup \gamma$.

We construct a new surface by capping off strictly the boundary component γ. Abstractly, we attach a 2-disk D^2 to γ, forming the surface

$$\widehat{\Sigma}_0 = \Sigma_0 \cup_\gamma D^2.$$

The only remaining boundary of this new surface is the knot K.

Capping off γ in this abstract way corresponds, geometrically, to changing the ambient 3-manifold. The curve γ is a longitude of V — it lies on $T = \partial V$ and runs once longitudinally around the solid torus. Inside V, the curve γ does not bound a disk (it is essential in $\pi_1 V$), so the capping disk cannot live inside the original S^3. Instead, the capping operation corresponds to *unknotting* the companion: we replace the knotted complement $S^3 \setminus \mathring{V}$ with a standardly embedded solid torus, which has a meridional disk whose boundary is precisely

the relevant longitude. Equivalently, this is the change of ambient space that takes the satellite knot $K = P(C)$ to the pattern-in-the-unknot $P(U)$.

Under this change of ambient space, the embedding of V becomes standard, and the satellite knot $K = P(C)$ is transformed into the pattern knot in the unknot, $P(U)$. Therefore, the capped-off surface $\widehat{\Sigma}_0$ is a Seifert surface for $P(U)$. By Lemma 8.9, $g(\Sigma_0) = g(P(U)) = 1$, so $\widehat{\Sigma}_0$ is exactly the minimal-genus fiber of the trefoil $P(U)$.

The global monodromy h preserves the JSJ torus T and thus restricts to an automorphism

$$\phi_0 \colon \Sigma_0 \to \Sigma_0$$

that fixes both boundary components K and γ pointwise.

When we cap off γ with the disk D^2, the homeomorphism ϕ_0 extends naturally to the disk by the identity, yielding a well-defined homeomorphism $\widehat{\phi}_0 \colon \widehat{\Sigma}_0 \to \widehat{\Sigma}_0$ that fixes the boundary K.

Because capping off γ unties the companion and transforms the ambient fibration into the standard fibration of the unknotted solid torus, this extended map $\widehat{\phi}_0$ is precisely the geometric monodromy of the resulting knot. Since $P(U)$ is a trefoil, $\widehat{\phi}_0$ is the geometric monodromy of the trefoil. □

We are now ready to prove the main result of this chapter, Theorem 8.1.

Proof of Theorem 8.1. By Theorem 2.1, K is fibered; and by Equation 2.3, of genus two. Let

$$h \colon \Sigma_2^1 \to \Sigma_2^1$$

be the monodromy of K. Let (ϕ_h, Γ) be the Nielsen-Thurston form of the monodromy.

If $\Gamma = \emptyset$, then $\Sigma_0 = \Sigma_2^1$, and

$$\phi_0 \colon \Sigma_0 \to \Sigma_0.$$

is periodic. Otherwise, K would be a hyperbolic knot, and not a satellite knot by Theorem 2.3. Hence Proposition 8.8 applies, in particular K is a (p, q)-torus knot. However, the knot Floer homology of torus knots is well-known, and none coincides with that of $T(2,3)\#T(2,3)$. Specifically, all torus knots are L-space knots (or mirrors of L-space knots). A defining property of L-space knots is that the rank of their knot Floer homology in any fixed Alexander grading a is at most 1. Thus, if $K = T_{p,q}$, then

$$\widehat{HFK}(T(2,3)\#T(2,3)) \cong \widehat{HFK}(K) \cong \widehat{HFK}(T(p,q)),$$

and we must have

$$\operatorname{rank} \widehat{HFK}(K, a) \leq 1$$

for all $a \in \mathbb{Z}$. But this is a contradiction, as it is known that the rank of the second-to-top Alexander grading of $\widehat{HFK}(T(2,3)\#T(2,3))$ is 2.

Hence $\Gamma \neq \emptyset$, and this can be either Case A or Case B, by Lemma 8.7.

Suppose the fiber Σ_2^1 and its reducing system is of Case A. Then Σ_0 is homeomorphic to a pair of pants, which is known to not support pseudo-Anosov homeomorphisms (see, e.g., Farb-Margalit[FM12]). This follows from the observation that every essential simple closed curve on the pair of pants is boundary-parallel; thus, every homeomorphism preserves a multicurve (the boundary itself) and is therefore reducible. Hence in this case $\phi_0 \colon \Sigma_0 \to \Sigma_0$ must be periodic, thus Proposition 8.8 applies, specifically the case for when $\Gamma \neq \emptyset$.

Consider first the cable knot sub-case, i.e., that K is a (p, q)-cable knot. A cable knot has winding number at least 2: its pattern is a non-trivial torus knot on ∂V, whose longitudinal wrapping is the parameter $q \geq 2$ of Proposition 8.8. This contradicts Lemma 8.4, which

forces the winding number of K to be 1. Hence the cable sub-case cannot occur. (We note for contrast that this is precisely the configuration occupied by the $(2,1)$-cable $C_{2,1}(T_{2,3})$ of Chapter 10, whose winding number is 2; it is excluded here only because the granny target forces winding number 1.)

Thus it must be the sub-case that K is a composite knot. In other words, K is a genus-two satellite knot that is a connect-sum of two genus-one knots. The only genus-one knots are the trefoils and the figure-eight knot. The Alexander polynomial of the connect-sum of one of the trefoils (either the left- or right-handed) and the figure-eight knot is the product of their respective Alexander polynomials:

$$\begin{aligned}\Delta_{3_1\#4_1}(t) &= \Delta_{\bar{3}_1\#4_1}(t)\\ &= \Delta_{3_1}(t)\cdot\Delta_{4_1}(t)\\ &= (t-1+t^{-1})\cdot(-t+3-t^{-1})\\ &= -t^2+4t-5+4t^{-1}-t^{-2}.\end{aligned}$$

Which differs from that of $T(2,3)\#T(2,3)$, hence that of K. Therefore, K must be the connect-sum of trefoils, and it must be in fact the connect-sum of the right-handed trefoils since the $\widehat{HFK}$ of the square knot $\overline{T(2,3)}\#T(2,3)$ and of $\overline{T(2,3)}\#\overline{T(2,3)}$ both differ from

$$\widehat{HFK}(T(2,3)\#T(2,3)) \cong \widehat{HFK}(K)$$

as bigraded vector spaces.

Now suppose that the fiber Σ_2^1 and its reducing system is of Case B. There are two possibilities: either the outermost map ϕ_0 is periodic, or it is pseudo-Anosov.

Suppose ϕ_0 is periodic. Then since $\Gamma \neq \emptyset$ and Σ_0 is not planar, Proposition 8.8 implies

that K is a (p,q)-cable knot of a knot in S^3 and Σ_0 has genus $g(T_{p,q})$, where $q \geq 2$ and $\gcd(p,q) = 1$. Since Σ_0 of Case B has genus one, we have

$$g(\Sigma_0) = g(T_{p,q}) = 1.$$

The only genus one torus knots are the trefoils, hence K is a cable knot with trefoil pattern, where the trefoils are embedded in the solid torus as torus knots (as required by the definition of a cable knot). However, this is a contradiction, as the presentation of the trefoils as torus knots yields winding number 2 if presented as $T(2,3)$ on the solid torus, and winding number 3 if presented as $T(3,2)$ on the solid torus. This contradicts Lemma 8.4 which states that the winding number of K must be 1.

So suppose ϕ_0 is pseudo-Anosov. Then Proposition 8.8 does not apply. However, from Lemma 8.4, it is still known that $K = P(C)$ satisfies $P(U)$ and C are trefoils, and the winding number w is 1.

Let us consider the capped-off map

$$\widehat{\phi}_0 \colon \widehat{\Sigma}_0 \to \widehat{\Sigma}_0$$

of ϕ_0. That is, capping off Σ_0 along $\Gamma = \gamma$ with a disk and extending ϕ_0 to the identity along the capping disk to obtain $\widehat{\phi}_0$. This map is in fact the monodromy of the trefoil $P(U)$ by Proposition 8.10, which is known to be not pseudo-Anosov (since the trefoils are not hyperbolic). Consequently, the number of prongs on Σ_0 located at Γ must be 1. Otherwise, the capped off map would still be pseudo-Anosov. We claim that on the other boundary component, which we denote by $\partial\Sigma$, there is also only one prong. Indeed, the map ϕ_0 commutes with the hyperelliptic involution ι. By construction, ι exchanges the two boundary components of Σ_0. Since ι is a diffeomorphism preserving the invariant foliation, it must map the singularity at Γ to the singularity at $\partial\Sigma$. Consequently, the number of prongs at

both boundaries must be identical.

This implies that the fractional Dehn twist coefficient $c(K)$ is at least one and an integer:

$$|c(K)|\geq 1, \quad |c(K)|\in \mathbb{Z}.$$

On the other hand, since K is a fibered knot in S^3 and S^3 is an L-space, the theorem of Hedden and Mark[HM18] bounds the fractional Dehn twist coefficient by

$$|c(K)|\leq 1.$$

Therefore, the only possibility is

$$|c(K)|= 1.$$

We show that this is not possible. Suppose by way of contradiction that

$$c(K) = 1.$$

Let $-Y$ denote the manifold defined by the open book decomposition (Σ_2^1, ϕ_h), which must be S^3, with reverse orientation:

$$-Y = -Y_{(\Sigma_2^1,\phi_h)} \cong S^3.$$

Let $-Y_1(K)$ denote the result of performing 1-surgery along the binding K on $-Y$, and let $-Y_0(K)$ denote the result of performing 0-surgery. The 1-surgery is equivalent to the open book decomposition obtained by composing ϕ_h with a right-handed Dehn twist along the boundary:

$$-Y_1(K) \cong -Y_{(\Sigma_2^1,\phi_h\circ T_\partial)}.$$

Let ξ_1 denote the contact structure on $-Y_1(K)$ supported by this open book.

The triple $(-Y_1(K), -Y, -Y_0(K))$ fits into a surgery exact triangle of Ozváth-Szabó, with twisted coefficients on the 0-surgery term (cf. Hedden-Mark[HM18], Section 5):

$$\ldots \longrightarrow HF^+(-Y_1(K);\mathbb{F}) \xrightarrow{H} HF^+(-Y;\mathbb{F}) \xrightarrow{G} HF^+(-Y_0(K);\mathbb{F}[C_1]) \xrightarrow{F} HF^+(-Y_1(K);\mathbb{F}) \longrightarrow \ldots$$

All maps in this triangle are $\mathbb{F}[U]$-equivariant, where U is the formal variable of degree -2 in the $\mathbb{F}[U]$-module structure on HF^+.

We focus on the canonical spin^c structure $\mathfrak{s}_{1-g}$ on $-Y_0(K)$, namely the one cobordant through the surgery cobordism to $\mathfrak{s}_{\xi_1}$ and satisfying $\langle c_1(\mathfrak{s}_{1-g}), [\widehat{S}]\rangle = 2-2g$ on the capped-off fiber. By Lemma 2.1 of Hedden-Mark[HM18], the corresponding summand satisfies

$$HF^+(-Y_0(K), \mathfrak{s}_{1-g}; \mathbb{F}[C_1]) \cong \mathbb{F}[C_1] \cong \mathbb{F},$$

on which U acts as zero.

Let G_{1-g} and F_{1-g} denote the components of G and F corresponding to this summand:

$$HF^+(-Y;\mathbb{F}) \xrightarrow{G_{1-g}} \mathbb{F} \xrightarrow{F_{1-g}} HF^+(-Y_1(K), \mathfrak{s}_{\xi_1}; \mathbb{F}).$$

Claim: The map G_{1-g} is zero.

Proof of claim. Since $-Y \cong S^3$ is an L-space (indeed, the simplest one),

$$HF^+(-Y;\mathbb{F}) \cong \mathcal{T}^+ := \mathbb{F}[U, U^{-1}]/U \cdot \mathbb{F}[U],$$

the tower module. On $\mathcal{T}^+$, the action of U is *surjective*: for every $U^{-k} \in \mathcal{T}^+$ with $k \geq 0$, we have $U \cdot U^{-(k+1)} = U^{-k}$. Therefore, every element $x \in HF^+(-Y)$ may be written as $x = U \cdot y$ for some $y \in HF^+(-Y)$. By $\mathbb{F}[U]$-equivariance of G_{1-g} and the fact that U acts

as zero on the target $\mathbb{F}$,

$$G_{1-g}(x) = G_{1-g}(U \cdot y) = U \cdot G_{1-g}(y) = 0.$$

Hence $G_{1-g} \equiv 0$, as claimed. □

By exactness of the surgery triangle restricted to the $\mathfrak{s}_{1-g}$ summand,

$$\ker(F_{1-g}) = \mathrm{im}(G_{1-g}) = 0,$$

so F_{1-g} is injective. Since its source $\mathbb{F}$ is non-zero, F_{1-g} is non-trivial.

By Proposition 2.4 of Hedden-Mark[HM18], non-triviality of F on the $\mathfrak{s}_{1-g}$ summand implies that the contact invariant

$$c(\xi_1) \in HF^+(-Y_1(K); \mathbb{F})$$

is non-zero. By Theorem 1.4 of Ozváth-Szabó[OS04c], this implies that ξ_1 is *tight*.

On the other hand, by assumption $c(\phi_h) = 1$, so composition with a right-handed boundary Dehn twist gives

$$c(\phi_h \circ T_\partial) = 0.$$

Since $\phi_h \circ T_\partial$ is pseudo-Anosov and has vanishing fractional Dehn twist coefficient on its (single) boundary component, Proposition 3.1 of Honda-Kazez-Matić[HKM07] implies that $\phi_h \circ T_\partial$ is *not* right-veering. By Theorem 1.1 of the same paper, the contact structure ξ_1 supported by $(\Sigma_2^1, \phi_h \circ T_\partial)$ is therefore *overtwisted*, contradicting the tightness established above.

For the case of

$$c(K) = -1,$$

the same argument works with Y in place of $-Y$, and a left-handed Dehn twist in place of the right-handed Dehn twist. $\square$

Remark 8.11. The satellite analysis above eliminates every candidate for K, and we have not had occasion to consider the $(2,1)$-cable of the right-handed trefoil, $C_{2,1}(T_{2,3})$, as a candidate: Lemma 8.4 already excludes it on two counts (its winding number is 2, not 1, and its pattern $P(U) = T_{2,1}$ is the unknot rather than a trefoil). Nevertheless, $C_{2,1}(T_{2,3})$ is itself a fibered satellite knot of genus two, and one may ask whether its knot Floer homology is detected by $\widehat{HFK}$ in the same spirit as our main theorem. We establish a corresponding detection result for $C_{2,1}(T_{2,3})$—namely, that any knot $K' \subset S^3$ with $\widehat{HFK}(K';\mathbb{F}) \cong \widehat{HFK}(C_{2,1}(T_{2,3});\mathbb{F})$ and satisfying additional hyperbolic-monodromy hypotheses must in fact be $C_{2,1}(T_{2,3})$—in Chapter 10.

CHAPTER NINE

Proof of the Main Theorem

Having developed in the preceding chapters all of the topological, dynamical, and homological machinery required to constrain the monodromy of a hypothetical knot sharing the knot Floer homology of $T_{2,3}\#T_{2,3}$, we now assemble these results into a proof of the primary result of this dissertation, Theorem 1.1.

The argument proceeds along Thurston's classification of knots (Theorem 2.3): the knot K is a torus knot, a hyperbolic knot, or a satellite knot, and these three possibilities are mutually exclusive at the level of the knot exterior $E(K)$. The case division is by knot type throughout; the Nielsen-Thurston type of the monodromy is used only as a tool inside the hyperbolic and satellite cases, and at no point do we appeal to exclusivity among the periodic, reducible, and pseudo-Anosov surface classes. We eliminate the torus and hyperbolic cases entirely and use the satellite analysis of Chapter 8 to identify the remaining case with the connect-sum of two trefoils, with the residual chirality question resolved inline by inspection of the Maslov-grading support of $\widehat{HFK}$.

9.1 Proof of Theorem 1.1

Proof of Theorem 1.1. Let $K \subset S^3$ be a knot such that

$$\widehat{HFK}(K;\mathbb{F}) \cong \widehat{HFK}(T_{2,3}\#T_{2,3};\mathbb{F})$$

as bigraded vector spaces over $\mathbb{F} = \mathbb{Z}/2\mathbb{Z}$. We must show that K is isotopic to $T_{2,3}\#T_{2,3}$.

Initial Reductions. The Euler characteristic of $\widehat{HFK}$ recovers the Alexander polynomial:

$$\Delta_K(t) = \sum_{M,A} (-1)^M \dim_{\mathbb{F}} \widehat{HFK}_M(K,A) \cdot t^A = (t^2 - t + 1)^2.$$

By Theorem 2.1 and the genus-detection result of Ozsváth–Szabó (Equation (2.3)), the rank profile of $\widehat{HFK}(K)$ in its top Alexander grading forces K to be a fibered knot of genus exactly $g = 2$. Let

$$h\colon \Sigma_2^1 \to \Sigma_2^1$$

denote its monodromy, defined up to isotopy fixing $\partial\Sigma_2^1$ pointwise.

By Thurston's classification of knots (Theorem 2.3), K is exactly one of three types: a torus knot, a hyperbolic knot, or a satellite knot. This exclusive partition is read off the geometry of the exterior $E(K)$ — atoroidal Seifert-fibered, atoroidal non-Seifert-fibered, or toroidal — and is the sole source of exclusivity in what follows. Within each case we will, where convenient, invoke the Nielsen-Thurston type of h as a tool, via the correspondence between the geometry of the mapping torus $M_h = E(K)$ and the dynamics of h; but we never use the surface classification (Theorem 2.2) to *partition* the cases, and in particular we never assume the periodic, reducible, and pseudo-Anosov types to be mutually exclusive. We treat each knot type in turn.

Case 1: K is a torus knot. Suppose K is a torus knot, $K = T_{p,q}$ for some coprime integers p, q with $|p|, |q| \geq 2$. Every torus knot in S^3 is an L-space knot (or the mirror of one), and a defining property of L-space knots is that their knot Floer homology has rank at most 1 in every Alexander grading:

$$\dim_{\mathbb{F}} \widehat{HFK}(T_{p,q}, a) \leq 1 \quad \text{for all } a \in \mathbb{Z}.$$

However, an explicit calculation of $\widehat{HFK}(T_{2,3}\#T_{2,3})$ shows that the next-to-top Alexander grading has rank exactly 2:

$$\dim_{\mathbb{F}} \widehat{HFK}(T_{2,3}\#T_{2,3}, 1) = 2.$$

Since the bigraded isomorphism $\widehat{HFK}(K) \cong \widehat{HFK}(T_{2,3}\#T_{2,3})$ would force $\dim_{\mathbb{F}} \widehat{HFK}(K, 1) = 2$, K cannot be a torus knot.

Case 2: K is a hyperbolic knot. Suppose K is hyperbolic, so that $S^3 \setminus K$ admits a complete hyperbolic metric of finite volume. Since K is fibered, Thurston's fibered hyperbolization (Theorem 2.4) then forces the monodromy h to be pseudo-Anosov; let ϕ_h denote its unique pseudo-Anosov representative.

By Lemma 2.8, ϕ_h has exactly one fixed point in the interior of Σ_2^1. By the capping-off construction (Proposition 2.12) and the Birman-Hilden correspondence (Section 2.5), this monodromy descends to a 6-braid mapping class $\beta \in \mathrm{Mod}(D_6)$ on the marked disk, whose canonical lift to the genus-two surface with two boundary components Σ_2^2 is fixed-point-free in its interior. Concretely, the data of K thus assembles into the Birman-Hilden correspondence tuple

$$(h, \phi_h, \hat{h}, \hat{\phi}_h, b, \phi_b, \beta, \phi_\beta, \Phi, \phi_\Phi).$$

The Euler-Poincaré analysis carried out in Section 2.6 of the Preliminaries restricts the

singularity stratum of ϕ_β on the disk to one of five possibilities:

$$(2; 1^4, 2^2; \emptyset), \quad (4; 1^6; \emptyset), \quad (2; 1^6; 4), \quad (3; 1^6; 3), \quad (2; 1^6; 3^2).$$

We have eliminated all five strata across Chapters 4 and 7:

- By Theorem 4.1, the orientable strata $(2; 1^4, 2^2; \emptyset)$, $(4; 1^6; \emptyset)$, and $(2; 1^6; 4)$ are eliminated by an Alexander polynomial obstruction: any such stratum forces the lifted invariant foliations on Σ_2^2 to be orientable, but $\Delta_K(t) = (t^2-t+1)^2$ has no real roots, contradicting Thurston's identification of the dilatation with a real eigenvalue of the homological action.

- By Theorem 7.7, the non-orientable stratum $(3; 1^6; 3)$ is eliminated: the `autofolder` algorithm together with tight splitting reduces the candidate train tracks to the Candelabra, and exhaustive enumeration via the Trace Lemma and the Absorption Obstruction produces 38 candidate braid families. Homological filtering—requiring both $|\det(I - A_{\text{red}})| = 1$ (so that the underlying 3-manifold of the open book is an integer homology sphere) and $\det(tI - A_{\text{red}}) = (t^2 - t + 1)^2$ (matching Δ_K)—eliminates all 38 (Appendix P).

- By Theorem 7.10, the non-orientable stratum $(2; 1^6; 3^2)$ is eliminated by the parallel analysis: tight splitting reduces the 20 candidate jointless tracks to six (one of which, Track 12, admits no surviving train track maps), exhaustive enumeration on the remaining five tracks produces 49 candidate braid families in total (13 for Track 0, 17 for Track 1, 9 for Track 8, 4 for Track 13, and 6 for Track 17), and the same homological filters eliminate them all (Appendix P).

These results combine to establish the obstruction theorem promised in the introduction:

Theorem 9.1 (1.4, restated)**.** None of the fixed-point-free pseudo-Anosov mapping classes generated by the standard train tracks in the admissible strata $(2; 1^4, 2^2; \emptyset)$, $(4; 1^6; \emptyset)$, $(2; 1^6; 4)$, $(3; 1^6; 3)$, and $(2; 1^6; 3^2)$ on the 6-marked disk induce both an Alexander polynomial equal to $\Delta(t) = (t^2 - t + 1)^2$ and a 3-manifold (the underlying space of the associated open book) that is an integer homology sphere.

Proof. The orientable strata are dispatched by Theorem 4.1. The non-orientable strata $(3; 1^6; 3)$ and $(2; 1^6; 3^2)$ are dispatched by Theorems 7.7 and 7.10, respectively. By the Euler-Poincaré classification of Section 2.6, these are exhaustive. □

Consequently, no pseudo-Anosov mapping class ϕ_β on D_6 with the required fixed-point structure can correspond to the monodromy of K. This contradicts the assumption that h is pseudo-Anosov, so K is not hyperbolic.

Case 3: K is a satellite knot. Having eliminated the torus and hyperbolic cases, Thurston's classification of knots (Theorem 2.3), exclusive at the level of the knot exterior, leaves only the possibility that K is a satellite knot. We stress that this conclusion uses the knot trichotomy directly, not any exclusivity among the surface Nielsen-Thurston types; we do *not* argue that h is reducible by eliminating the periodic and pseudo-Anosov classes.

Being a satellite, K is not a torus knot (Theorem 2.3), so its monodromy h is not periodic and the mapping torus $M_h = E(K)$ is not Seifert fibered. The essential torus furnished by the satellite structure is therefore isotopic to a vertical torus — the suspension of an h-invariant essential multicurve — so the canonical reducing system Γ of h is nonempty (the fibered correspondence: for aperiodic h, an essential torus in M_h is equivalent to a nonempty canonical reducing system; see Theorem 8.5 and Remark 8.6). With $\Gamma \neq \emptyset$ in hand, Theorem 8.1, established in Chapter 8, shows that the only satellite configuration consistent with

$\Delta_K(t) = (t^2 - t + 1)^2$ and the genus-two fiberedness constraint is the connect-sum of two trefoils.

Remark 9.2. A parallel detection question for the $(2, 1)$-cable $C_{2,1}(T_{2,3})$ — which is itself a fibered genus-two satellite knot — is taken up separately in Chapter 10, where we establish a partial detection theorem for that knot. Note that the $(2, 1)$-cable is not a candidate for K in the present proof, because Lemma 8.4 excludes it (its winding number is 2, not 1, and its pattern $P(U) = T_{2,1}$ is the unknot rather than a trefoil).

The remaining configuration is the connect-sum of two trefoils. The detailed argument of Chapter 8 proceeds as follows. Schubert's formula (Theorem 8.3) and the explicit factorization of $\Delta_K(t) = (t^2 - t + 1)^2 = t^2 - 2t + 3 - 2t^{-1} + t^{-2}$ force the algebraic winding number to equal 1 and identify both the pattern $P(U)$ and the companion C as trefoils (Lemma 8.4). The classification of canonical reducing systems (Lemma 8.7) presents two non-trivial geometric configurations: Case A (the outer surface Σ_0 is a pair of pants) and Case B (the outer surface is genus one). The pair-of-pants case admits no pseudo-Anosov outer map, forcing the outer map to be periodic; combined with Baldwin-Sivek's Proposition 8.8 and the genus-two constraint, this yields the connect-sum of two genus-one knots, of which only the trefoil-trefoil connect sum (up to chirality of the two factors) has the correct Alexander polynomial. The genus-one case is eliminated by a fractional Dehn twist coefficient analysis: the Hedden-Mark bound $|c(K)| \leq 1$ forces $|c(K)| = 1$, but the contact-invariant argument via Honda-Kazez-Matić rules out integer twist coefficients.

Therefore, K is isotopic to a connect-sum of two trefoils, taken with some choice of chirality. The three candidates are $T_{2,3}\#T_{2,3}$ (the granny knot, homochiral), $T_{2,3}\#\overline{T}_{2,3}$ (the square knot, heterochiral), and $\overline{T}_{2,3}\#\overline{T}_{2,3}$ (the mirror granny), shown in Figure 9.1.

All three share the Alexander polynomial $(t^2 - t + 1)^2$ and the total $\widehat{HFK}$-rank of 9, so the unbigraded $\widehat{HFK}$ does not distinguish them. However, the Künneth formula combined

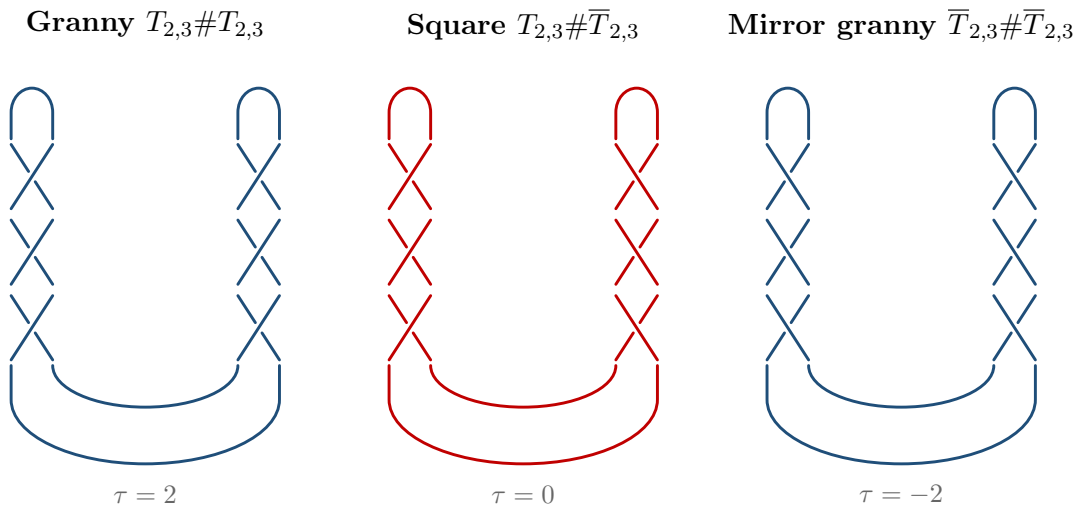


Figure 9.1: The three candidate connect-sums of trefoils consistent with $\Delta_K(t) = (t^2 - t + 1)^2$: the granny knot $T_{2,3}\#T_{2,3}$ (left), the square knot $T_{2,3}\#\overline{T}_{2,3}$ (centre), and the mirror granny $\overline{T}_{2,3}\#\overline{T}_{2,3}$ (right). The three knots have identical total $\widehat{HFK}$ rank but distinct Maslov-grading supports in the top Alexander grading; the values of the Ozsváth-Szabó tau invariant are $\tau = 2, 0, -2$ respectively. The bigraded hypothesis of Theorem 1.1 selects the granny.

with the mirror duality $\widehat{HFK}_M(\overline{K}, A) \cong \widehat{HFK}_{-M}(K, -A)$ [OS04b] shows that the top Alexander grading $A = 2$ is supported in Maslov grading 0 for $T_{2,3}\#T_{2,3}$, in Maslov grading 2 for $T_{2,3}\#\overline{T}_{2,3}$, and in Maslov grading 4 for $\overline{T}_{2,3}\#\overline{T}_{2,3}$; equivalently, the Ozsváth-Szabó concordance invariant τ takes the values 2, 0, and -2 respectively. Since the bigraded isomorphism $\widehat{HFK}(K) \cong \widehat{HFK}(T_{2,3}\#T_{2,3})$ matches Maslov gradings, only the homochiral case is compatible with the hypothesis. Therefore

$$K \cong T_{2,3}\#T_{2,3}.$$

This concludes the proof. □

9.2 Summary

We have established the full strength of Theorem 1.1: any knot $K \subset S^3$ whose knot Floer homology agrees with that of the granny knot $T_{2,3}\#T_{2,3}$ as a bigraded vector space over $\mathbb{F} = \mathbb{Z}/2\mathbb{Z}$ is isotopic to $T_{2,3}\#T_{2,3}$ itself. The proof rests on the following structural pillars:

1. The genus-and-fiberedness detection results of Ozsváth-Szabó, Ni, and Juhász, which transfer the question from three-dimensional topology to surface dynamics.

2. The Birman-Hilden correspondence, which descends the genus-two monodromy to a 6-braid on the disk.

3. The autofolder algorithm and tight splitting (Chapters 5, 7), which generate and prune the finite list of candidate train tracks for each non-orientable stratum.

4. The Trace Lemma and Absorption Obstruction (Chapters 3, 7), which encode fixed-point and injectivity constraints on the train track maps.

5. The orientability obstruction of Chapter 4, which dispatches the orientable strata via the absence of real Alexander roots.

6. The homological filtering pipeline (Section 7.3), which eliminates the candidate braid families via $|\det(I - A_{\mathrm{red}})| = 1$ and $\det(tI - A_{\mathrm{red}}) = (t^2 - t + 1)^2$, with the verdicts catalogued in Appendix P.

7. The satellite analysis of Chapter 8, which combines Schubert's formula, the Baldwin-Sivek classification of canonical reducing systems, and the Hedden-Mark / Honda-Kazez-Matić contact-invariant arguments to identify the connect-sum of two trefoils as the unique surviving satellite candidate.

A parallel partial detection theorem for the $(2,1)$-cable of the trefoil, $C_{2,1}(T_{2,3})$, is established

in Chapter 10, where the same machinery—autofolder, Trace Lemma, Absorption Obstruction, and homological filtering—is deployed against the cable target Alexander polynomial $t^4 - t^2 + 1$.

CHAPTER TEN

Detection of the (2,1)-Cable of the Trefoil

In this chapter, we apply the machinery developed in Chapters 3–8 to the detection problem for $C_{2,1}(T_{2,3})$, the $(2,1)$-cable of the right-handed trefoil. Our principal result is a partial detection theorem: we show that any knot $K \subset S^3$ with $\widehat{HFK}(K) \cong \widehat{HFK}(C_{2,1}(T_{2,3}))$ is either isotopic to $C_{2,1}(T_{2,3})$ or, if hyperbolic, must arise from one of an explicitly enumerated finite list of candidate braid families that survive both the homology-sphere filter and the Alexander polynomial filter.

10.1 Statement of the Result

Let $C = C_{2,1}(T_{2,3})$ denote the $(2,1)$-cable of the right-handed trefoil knot $T_{2,3}$. This is a genus-two fibered satellite knot in S^3 with Alexander polynomial

$$\Delta_C(t) = t^2 - 1 + t^{-2},$$

which after clearing denominators becomes the cyclotomic polynomial

$$t^2 \cdot \Delta_C(t) = t^4 - t^2 + 1 = \Phi_{12}(t).$$

The complete bigraded knot Floer homology of $C_{2,1}(T_{2,3})$ over $\mathbb{F} = \mathbb{Z}/2\mathbb{Z}$, computed using the SnapPy implementation of Szábó's algorithm [**szabo2017knotfloercalculator**], is shown in Figure 10.1. The total rank is 7, with two Alexander gradings ($A = \pm 1$) carrying rank 2 and the remaining three ($A = 0, \pm 2$) carrying rank 1.

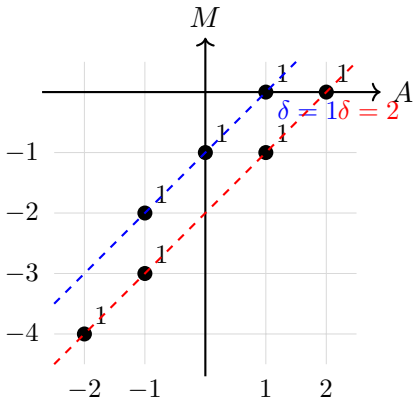


Figure 10.1: The bigraded knot Floer homology $\widehat{HFK}(C_{2,1}(T_{2,3}); \mathbb{F}_2)$. Each dot represents a generator at bigrading (A, M); the integer beside each dot is the rank $\dim_{\mathbb{F}} \widehat{HFK}_M(C_{2,1}(T_{2,3}), A)$. The top Alexander grading is 2, of rank 1, so this knot is fibered of genus 2. Two generators sit at bigrading $(0, -1)$ and $(1, 0)$ on the diagonal $\delta = A - M = 1$; the remaining five lie on the diagonal $\delta = 2$, so the knot fails to be thin. In particular, the next-to-top Alexander grading $A = 1$ has rank 2, exceeding the L-space bound, so $C_{2,1}(T_{2,3})$ is not an L-space knot. The Ozsváth-Szabó concordance invariant is $\tau(C_{2,1}(T_{2,3})) = 2$, the Alexander grading of the unique generator in Maslov grading 0 along the $\delta = 2$ diagonal.

The knot C is an almost L-space knot in the sense of Baldwin and Sivek [BS24].

Remark 10.1 (Derivation of $\tau(C_{2,1}(T_{2,3})) = 2$)**.** The value $\tau(C_{2,1}(T_{2,3})) = 2$ asserted above can be read directly from the bigraded rank table of Figure 10.1, but it also admits a structural derivation independent of the explicit computation. Hom's cabling formula for the τ-invariant [Hom14] gives

$$\tau(K_{p,q}) \;=\; p \cdot \tau(K) \;+\; \frac{(p-1)(q-1)}{2}$$

whenever the companion K satisfies $\varepsilon(K) = 1$, where ε denotes Hom's epsilon invariant. The

right-handed trefoil $T_{2,3}$ is an L-space knot, and every L-space knot satisfies $\varepsilon = 1$; combined with $\tau(T_{2,3}) = 1$, the formula gives

$$\tau(C_{2,1}(T_{2,3})) \;=\; 2 \cdot \tau(T_{2,3}) \;+\; \frac{(2-1)(1-1)}{2} \;=\; 2 \cdot 1 \;+\; 0 \;=\; 2.$$

In particular, $\tau(C_{2,1}(T_{2,3})) = g(C_{2,1}(T_{2,3})) = 2$, so by Hedden's characterization of strong quasipositivity for fibered knots [Hed10], the cable $C_{2,1}(T_{2,3})$ is strongly quasipositive. This identity $\tau = g$ is used in Section 10.2.3 to invoke the right-veering monodromy property in the hyperbolic case.

Theorem 10.2 (Partial cable detection)**.** Let $K \subset S^3$ be a knot such that

$$\widehat{HFK}(K;\mathbb{F}) \cong \widehat{HFK}(C_{2,1}(T_{2,3});\mathbb{F})$$

as bigraded vector spaces over $\mathbb{F} = \mathbb{Z}/2\mathbb{Z}$. Then one of the following holds:

1. $K \cong C_{2,1}(T_{2,3})$, or
2. K is hyperbolic, and the disk braid $\beta \in \mathrm{Mod}(D_6)$ associated to the monodromy of K via the Birman-Hilden correspondence — obtained by capping off the pseudo-Anosov monodromy on Σ_2^1 to Σ_2^0, descending to the marked sphere $S^2_{0,6}$, and blowing up the canonical fixed point — belongs to one of the finitely many parametric families enumerated in Appendix Q.

The residual hyperbolic candidates of case (2) constitute the obstruction to a complete detection theorem. We discuss this gap and possible avenues for closing it in Section 10.4.

Remark 10.3. Theorem 10.2 should be contrasted with the complete detection result for $T_{2,3}\#T_{2,3}$ established in Theorem 1.1. The granny knot analysis succeeds because every candidate braid family with $|\det(I - A_{\mathrm{red}})| = 1$ either has the wrong characteristic

polynomial outright or admits no non-negative integer parameter values yielding the granny target $(t^2 - t + 1)^2$. The cable target $\Phi_{12}(t) = t^4 - t^2 + 1$ is comparatively well-aligned with several of the parametric polynomials produced by the candidate braids on the disk, leaving a small but non-trivial residue of unresolved cases.

10.2 Initial Reductions and the Trichotomy

Let K satisfy the hypotheses of Theorem 10.2. The Euler characteristic computation gives $\Delta_K(t) = t^2 - 1 + t^{-2}$, so K has genus exactly 2. By the fiberedness criterion of Ni [Ni07], K is fibered. Let

$$h\colon \Sigma^1_2 \to \Sigma^1_2$$

denote its monodromy.

By Thurston's classification of knots, K falls into one of three geometric categories. We treat each in turn.

10.2.1 The torus knot case

If h is periodic, then K is a torus knot $T_{p,q}$. Every torus knot is an L-space knot (or the mirror of one), and L-space knots satisfy

$$\dim_{\mathbb{F}} \widehat{HFK}(K, a) \leq 1 \quad \text{for all } a \in \mathbb{Z}.$$

However, the rank table of Figure 10.1 shows that

$$\dim_{\mathbb{F}} \widehat{HFK}(C, 1) = 2,$$

and the hypothetical isomorphism $\widehat{HFK}(K) \cong \widehat{HFK}(C)$ would force $\dim_{\mathbb{F}} \widehat{HFK}(K, 1) = 2$ as well. Hence K is not a torus knot.

10.2.2 The satellite knot case

Suppose h is reducible, so that K is a satellite knot. We invoke the classification framework established in Chapter 8: by Schubert's formula and the Hirasawa-Murasugi-Silver criterion [HMS08], any genus-two fibered satellite knot has one of two structures, classified by the type of the canonical reducing system.

Lemma 10.4. If K is a fibered genus-two satellite knot with Alexander polynomial $\Delta_K(t) = t^2 - 1 + t^{-2}$, then $K \cong C_{2,1}(T_{2,3})$.

Proof. We adapt the satellite analysis of Chapter 8; as the genus computation below shows, the reducing-system dichotomy resolves differently for the cable target than for the granny target. Schubert's formula gives

$$\Delta_K(t) = \Delta_{P(U)}(t) \cdot \Delta_C(t^w),$$

where P is the pattern (with winding number w), C is the companion, $P(U)$ is the satellite of the unknot by the same pattern. Both C and $P(U)$ are fibered [BZ03, Corollary 4.15, Proposition 5.5].

Since K is fibered, the algebraic winding number is non-zero, so $|w| \geq 1$. Furthermore, because C is a fibered knot, the maximum degree of its symmetrized Alexander polynomial strictly equals its Seifert genus $g(C)$. Consequently, $\Delta_C(t^w)$ is a nontrivial symmetric Laurent polynomial of maximum degree $|w| \cdot g(C) \geq 1$.

Now $\Delta_K(t) = t^2 - 1 + t^{-2}$ has maximum degree 2 as a symmetric Laurent polynomial. The factorization above forces $|w| \cdot g(C) + \deg \Delta_{P(U)} = 2$, where deg denotes the maximum degree of the symmetrized polynomial. Since both factors have non-negative degree, we obtain three cases.

Case $|w|= 2$, $g(C) = 1$, $\Delta_{P(U)} = 1$. Then $\Delta_C(t^2) = t^2 - 1 + t^{-2}$ forces $\Delta_C(t) = t - 1 + t^{-1}$, the Alexander polynomial of the trefoil; as C is a genus-one fibered knot, $C \cong T_{2,3}$. Since $\Delta_{P(U)} = 1$ and $P(U)$ is fibered, $P(U)$ is the unknot, so $g(P(U)) = 0$.

We determine the reducing-system configuration. Schubert's geometric genus inequality (Theorem 8.3) gives $2 = g(K) \geq g(P(U)) + m \cdot g(C) = m$, while $m \geq |w|= 2$ always; hence the wrapping number is $m = |w|= 2$. Moreover, by Lemma 8.9 the outermost piece satisfies $g(\Sigma_0) = g(P(U)) = 0$. A planar outermost surface occurs only in Case A of Lemma 8.7, where Σ_0 is a pair of pants; equivalently, the fiber meets the satellite torus in $m = 2$ curves. (Case B is impossible here, as it requires $g(\Sigma_0) = 1$.)

A pair of pants admits no pseudo-Anosov homeomorphism, so the outer map ϕ_0 is periodic, and Baldwin–Sivek's classification (Proposition 8.8) applies: K is a torus knot, a composite knot (with Σ_0 planar), or a (p, q)-cable knot. The torus case is excluded in Section 10.2.1. A composite knot of genus two is a connect-sum of two genus-one fibered knots, each a trefoil or figure-eight; the three possible products of their Alexander polynomials have $t^{\pm 1}$-coefficients -2, 4, and -6, none equal to the vanishing $t^{\pm 1}$-coefficient of $\Delta_K(t) = t^2 - 1 + t^{-2}$, so the composite case is excluded. Hence K is a cable knot, and the pattern P is a torus-knot pattern $T_{a,b}$ with $P(U) = T_{a,b}$ and winding number a. From $|w|= 2$ we obtain $a = 2$, and from $P(U) = T_{2,b}$ being the unknot we obtain $|b|= 1$. Therefore P is the $(2, 1)$-cable pattern, the companion is $C \cong T_{2,3}$, and $K \cong C_{2,1}(T_{2,3})$ up to chirality.

The identification $|b|= 1$ also follows independently of the unknottedness of $P(U)$: for $|b|\geq 3$, the torus knot $T_{2,b}$ is an L-space knot, and cabling preserves the L-space property over the L-space companion $T_{2,3}$ [Hed09], which would force K to be an L-space knot, contradicting the rank-2 Alexander grading of Figure 10.1.

Case $|w|= 1$, $g(C) = 2$, $\Delta_{P(U)} = 1$. Then $\Delta_C(t) = t^2 - 1 + t^{-2}$ and $P(U)$ is the unknot (the only fibered knot with trivial Alexander polynomial). By Hirasawa-Murasugi-Silver [HMS08],

a fibered satellite $K = P(C)$ with winding number 1 and P isotopic to the core (which is forced when $P(U)$ is the unknot and $|w|= 1$) satisfies $K \cong C$; that is, the satellite operation is trivial. This contradicts our assumption that K is a non-trivial satellite.

Case $|w|= 1$, $g(C) = 1$, $\deg \Delta_{P(U)} = 1$. Then $\Delta_C(t)$ has degree 1 and $\Delta_{P(U)}(t)$ has degree 1, with their product equal to $t^2 - 1 + t^{-2}$. Symmetric Laurent polynomials of degree 1 have the form $at + b + at^{-1}$, so their product has constant coefficient sum $2a_1a_2 + b_1b_2$. The polynomial $t^2 - 1 + t^{-2}$ has zero $t^{\pm 1}$ coefficients, forcing $a_1b_2 + a_2b_1 = 0$. Combined with the coefficient of t^2 being $a_1a_2 = 1$, we obtain $a_1 = a_2 = \pm 1$ and $b_1 = -b_2$. Then the constant term is $2 - b_1^2 = -1$, so $b_1^2 = 3$, which has no integer solution. Hence this case is excluded.

This concludes the proof: the only allowable satellite structure is Case 1, giving $K \cong C_{2,1}(T_{2,3})$. □

10.2.3 The hyperbolic knot case

Suppose h is pseudo-Anosov, so that K is hyperbolic. The rank table of Figure 10.1 shows $\dim_{\mathbb{F}} \widehat{HFK}(K, 1) = \dim_{\mathbb{F}} \widehat{HFK}(C, 1) = 2$, so by the theorem of Ni-Ghiggini-Spano (Theorem 2.1), the pseudo-Anosov representative ϕ_h has at most 1 interior fixed point on Σ_2^1. The Farber-Reinoso-Wang classification [FRW24] then rules out the case of zero interior fixed points: the cinquefoil $T_{2,5}$ is the only fibered genus-two knot in S^3 whose monodromy is fixed-point-free, and its Alexander polynomial $t^2 - t + 1 - t^{-1} + t^{-2}$ differs from $\Delta_C(t) = t^2 - 1 + t^{-2}$, so $K \neq T_{2,5}$. Hence ϕ_h is not fixed-point-free and has exactly one interior fixed point.

Before invoking the capping-off construction, we verify that its hypotheses are met for K, even though K is not thin. The cable $C = C_{2,1}(T_{2,3})$ has $\tau(C) = 2 = g(C)$ (see Figure 10.1); since τ and g are read off from the bigraded $\widehat{HFK}$ structure, the isomorphism $\widehat{HFK}(K) \cong \widehat{HFK}(C)$ forces $\tau(K) = 2 = g(K)$ as well. By Hedden [Hed10], a fibered knot

$K \subset S^3$ satisfying $\tau(K) = g(K)$ is strongly quasipositive, and its open book decomposition supports the standard tight contact structure ξ_{std} on S^3. By Honda-Kazez-Matić [HKM07], the monodromy of an open book supporting a tight contact structure is right-veering. Hence ϕ_h is right-veering and the fractional Dehn twist coefficient satisfies $c(\phi_h) \geq 0$; since ϕ_h is pseudo-Anosov (in particular, irreducible), Honda-Kazez-Matić further yield $c(\phi_h) > 0$. This is the hypothesis on the monodromy required by the capping-off construction, and so the construction applies to K in the same form as it does in the granny case — the absence of thinness (in the sense of $\widehat{HFK}$ supported on a single diagonal) plays no role in the capping-off argument.

By the capping-off construction (Proposition 2.12) and the Birman-Hilden correspondence (Section 2.5), this monodromy descends to a 6-braid mapping class $\beta \in \text{Mod}(D_6)$ on the marked disk, whose canonical lift to the genus-two surface with two boundary components Σ_2^2 is fixed-point-free in its interior. The Euler-Poincaré stratum analysis from Chapter 2 then restricts β to one of the five admissible strata

$$(2; 1^4, 2^2; \emptyset), \quad (4; 1^6; \emptyset), \quad (2; 1^6; 4), \quad (3; 1^6; 3), \quad (2; 1^6; 3^2).$$

The orientability obstruction of Chapter 4 eliminates the three orientable strata for any target Alexander polynomial without real roots. The roots of the symmetrized cable polynomial $t^4 - t^2 + 1 = \Phi_{12}(t)$ are the primitive twelfth roots of unity $\zeta_{12}^{\pm 1}, \zeta_{12}^{\pm 5}$, none of which are real. Hence the orientable strata are excluded for the cable target as they were for the granny target.

The non-orientable strata $(3; 1^6; 3)$ and $(2; 1^6; 3^2)$ require the non-trivial train-track analysis of Chapter 7. The same `autofolder` enumeration, tight-splitting reduction, Trace Lemma, and Absorption Obstruction all apply unchanged in the cable setting, since these geometric and combinatorial constraints depend only on the assumption that the canonical lift is

fixed-point-free, which we have established above.

Therefore the same finite list of 87 candidate braid families (across the Candelabra and the five surviving two-triangle tracks) constitutes the residual list of topological candidates for the cable monodromy.

10.3 Homological Filtering for the Cable Target

We now apply the homological filters of Section 7.3, retargeted to the cable's Alexander polynomial.

Lemma 10.5. The reduced homological action A_{red} associated with the cable monodromy of K satisfies

$$\det(tI - A_{\text{red}}) = t^4 - t^2 + 1 = \Phi_{12}(t).$$

Proof. Lemma 7.5 relates $\det(tI - A)$ on the bordered surface Σ_2^2 to the closed-surface action via $\det(tI - A) = (t-1)^2 \det(tI - A_{\text{red}})$. Since the standard Alexander polynomial of the closed monodromy on Σ_2 equals the (cleared-denominator) Alexander polynomial $t^2\Delta_C(t) = t^4 - t^2 + 1$ of K, the result follows. □

The zero-surgery Filter 1, requiring $|\det(I - A_{\text{red}})| = 1$, is unchanged. The Alexander polynomial Filter 2 now requires

$$\det(tI - A_{\text{red}}) = t^4 - t^2 + 1.$$

Proposition 10.6. Let β be a candidate 6-braid from one of the 87 families enumerated in Propositions 7.9 and 7.12. Let $A_{\text{red}}(\beta)$ denote its reduced homological action. Then β satisfies both

$$|\det(I - A_{\text{red}}(\beta))| = 1 \quad \text{and} \quad \det(tI - A_{\text{red}}(\beta)) = t^4 - t^2 + 1$$

at non-negative integer values of the family's parameters $k, m, j \geq 0$ if and only if β belongs to one of the following families and parameter values:

Track	Family	Surviving non-negative parameter values
Candelabra	16 Kieve	$(j,k,m) = (0,3,4),\ (0,7,0),\ (1,2,0)$
Track 0	7 Briefing	infinite family of (j,k,m) pairs
Track 0	8 Briefing	$(k,m) = (1,2),\ (2,1)$
Track 0	10 Quail	infinite family of (j,k,m) pairs
Track 0	13 Treasure	$(k,m) = (2,1)$
Track 8	9 FAT	$k = 2$

All other 81 candidate families are excluded by either Filter 1 or Filter 2 at every non-negative integer parameter value.

Proof. The reduced action $A_{\text{red}}(\beta)$ is computed via the same matrices $M_1, \ldots, M_5$ defined in Section 7.3, applied to the candidate braid words of Appendices J–O. We then evaluate the determinant $|\det(I - A_{\text{red}})|$ and the characteristic polynomial $\det(tI - A_{\text{red}})$ as functions of the family's parameters and check whether non-negative integer values exist for which both filters return their target values.

The complete computation, performed via the implementation of the homological filter described in Section 7.3, reproduces the determinant and polynomial expressions tabulated for the granny case (since these depend only on β and not on the chosen target polynomial). Cross-checking the polynomial against the cable target $t^4 - t^2 + 1$ then identifies the residual

list above; the verdict for each individual family is recorded in Appendix Q. □

10.4 Discussion of the Residual Hyperbolic Candidates

The six families isolated in Proposition 10.6 represent the gap between Theorem 10.2 and a complete detection result. Closing this gap requires invoking obstructions beyond the simple polynomial equality at the level of the reduced homological action. Several concrete approaches to eliminating the residual list are discussed in the Conclusion (Section 11.3, "Closing the cable detection gap"), where they are framed alongside related future-work directions. A complete cable detection theorem along these lines is the subject of ongoing work and is not included in this dissertation.

10.5 Implications for Almost L-Space Knots

While Theorem 10.2 is partial, it does suffice to establish the following corollary, which contributes to the rigidity theory of almost L-space knots.

Corollary 10.7. Knot Floer homology detects $C_{2,1}(T_{2,3})$ among non-hyperbolic knots. More precisely, any non-hyperbolic knot $K \subset S^3$ with $\widehat{HFK}(K) \cong \widehat{HFK}(C_{2,1}(T_{2,3}))$ as bigraded vector spaces is isotopic to $C_{2,1}(T_{2,3})$.

Proof. By Theorem 10.2, alternative (2) is excluded under the hypothesis that K is non-hyperbolic, leaving alternative (1). □

In the language of Baldwin-Sivek, Corollary 10.7 says that $C_{2,1}(T_{2,3})$ is rigidly identified by its $\widehat{HFK}$ within the class of torus and satellite genus-two fibered knots, complementing Theorem 1.1's identification of $T_{2,3}\#T_{2,3}$ within the same class.

CHAPTER ELEVEN

Conclusion and Future Directions

We have established that knot Floer homology detects the granny knot $T_{2,3}\#T_{2,3}$ as a bigraded vector space over $\mathbb{F} = \mathbb{Z}/2\mathbb{Z}$, providing the first detection result for a composite knot. Along the way, we developed the `autofolder` algorithm — a complete, algorithmic realization of the folding-automaton framework theorized by Ko, Los, and Song — and a partial detection result for the $(2, 1)$-cable of the trefoil. In this concluding chapter, we summarize the principal results, discuss their broader implications, and identify directions for future research.

11.1 Summary of Results

The principal results of this dissertation are the following.

Theorem 11.1 (Theorem 1.1)**.** Let $K \subset S^3$ be a knot. If $\widehat{HFK}(K;\mathbb{F}) \cong \widehat{HFK}(T_{2,3}\#T_{2,3};\mathbb{F})$ as bigraded vector spaces, then K is isotopic to $T_{2,3}\#T_{2,3}$.

Theorem 11.2 (Theorem 1.2)**.** The `autofolder` algorithm provides a complete, finite classification of all standard train tracks and their valid elementary folds for any specified stratum of pseudo-Anosov braids on the n-punctured disk.

Theorem 11.3 (Theorem 10.2)**.** Let $K \subset S^3$ be a knot with $\widehat{HFK}(K) \cong \widehat{HFK}(C_{2,1}(T_{2,3}))$ as bigraded vector spaces. Then either $K \cong C_{2,1}(T_{2,3})$, or K is hyperbolic and the disk braid $\beta \in \mathrm{Mod}(D_6)$ associated to the monodromy of K via the Birman-Hilden correspondence (capping off to Σ_2^0, descent to $S^2_{0,6}$, blowup at the canonical fixed point) belongs to one of finitely many parametric families enumerated in Appendix Q. In particular, $\widehat{HFK}$ detects $C_{2,1}(T_{2,3})$ among non-hyperbolic knots.

The proof strategy throughout combines three threads. First, the genus and fiberedness detection results of Ozsváth-Szabó, Ni, and Juhász translate the topological classification problem into a problem about surface monodromies. Second, the Birman-Hilden correspondence descends the genus-two monodromy to a 6-braid on the disk, where train track methods become applicable. Third, the explicit machinery developed in this dissertation — the `autofolder`, tight splitting, the Trace Lemma, the Absorption Obstruction, and the homological filtering pipeline — exhaustively eliminates candidate mapping classes within each topological stratum.

11.2 Direct Consequences

11.2.1 Almost L-space rigidity

The granny knot is the unique composite almost L-space knot, by a theorem of Binns [Bin23]. Combined with our Theorem 1.1, this establishes:

Corollary 11.4. Knot Floer homology detects the unique composite almost L-space knot.

For the cable, our partial result already establishes detection within the non-hyperbolic class:

Corollary 11.5. Among non-hyperbolic knots in S^3, the cable $C_{2,1}(T_{2,3})$ is uniquely identified by its bigraded knot Floer homology.

These results contribute to the program of using $\widehat{HFK}$ as a detector of certain distinguished knot classes, complementing Reinoso's classification of genus-two L-space knots [Rei23], from which $\widehat{HFK}$-detection of $T(2,5)$ follows, and Baldwin-Hu-Sivek's Khovanov-homology detection of $T(2,5)$ [BHS25].

11.2.2 The autofolder as a stand-alone contribution

The `autofolder` algorithm, while developed here in service of Theorem 1.1, is independently useful. Los [Los93] explicitly called for an algorithmic realization of the folding-automaton machinery to make the state space of pseudo-Anosov mapping classes tractable; the `autofolder` provides this. Beyond the specific strata analyzed in Chapters 4 and 7, the algorithm operates on arbitrary strata of the marked disk and outputs the complete folding automaton.

We anticipate that the algorithm will be a useful tool for future detection problems on genus-two and higher fibered knots, for the explicit construction of pseudo-Anosov braids of small dilatation, and for the experimental investigation of singularity strata that have not yet been analyzed by hand.

11.3 Future Directions

11.3.1 Closing the cable detection gap

The most immediate open problem left by this dissertation is closing the gap in Theorem 10.2: eliminating the residual finite list of candidate braid families that pass both the homology-sphere filter and the Alexander polynomial filter at non-negative integer parameter values. The six families isolated in Proposition 10.6 represent precisely this gap. Closing it

requires obstructions beyond polynomial equality at the level of the reduced homological action. We outline two complementary avenues.

(A) Pseudo-Anosov degeneration at boundary parameter values. The candidate train track maps in the residual families are parametrized by integer twists. At certain parameter values — particularly $k = 0$ or $m = 0$ — the corresponding braid may degenerate into a non-pseudo-Anosov mapping class (periodic or reducible), in which case the topological enumeration assumption is violated. A direct check of the dilatation (Perron-Frobenius eigenvalue of the train track transition matrix) at each surviving parameter value would either confirm the braid is pseudo-Anosov or exclude that parameter from consideration. This is a strictly local refinement to the existing case analysis and would yield a smaller residual list.

(B) Direct knot reconstruction and $\widehat{HFK}$ comparison. A more ambitious avenue is to bypass the homological filter entirely and directly compute the knot corresponding to each surviving braid family, then compute its knot Floer homology and compare against the cable target. The pipeline is:

1. For each candidate braid word β and parameter assignment, close up the braid lift on Σ_2^2 to obtain a fibered three-manifold, and identify the knot component K_β that plays the role of the candidate for our knot K;

2. Use SnapPy [**SnapPy**] (which handles braid closures, computes hyperbolic structures, and identifies knots from their hyperbolic invariants) to recognize K_β as a specific knot in S^3;

3. Compute $\widehat{HFK}(K_\beta)$ directly — either from known catalogues if K_β is identified as a tabulated knot, or via dedicated knot Floer software for novel knots — and compare against the target $\widehat{HFK}(C_{2,1}(T_{2,3}))$, including the full bigraded structure rather than

just the Alexander polynomial.

This is in principle a complete obstruction: if K_β is not isotopic to $C_{2,1}(T_{2,3})$, the comparison will detect it. The practical challenge is the computational handling of step (1) — mapping from a train-track-map braid word on the disk through the Birman-Hilden lift to a concrete knot in S^3 that SnapPy can ingest — which requires either careful manual reconstruction or further automation built on top of the `autofolder` infrastructure. The bigraded comparison in step (3) captures Maslov-grading information beyond the Alexander polynomial and would, in principle, resolve any residual ambiguity that the polynomial filter misses.

Either avenue, if it successfully eliminates all residual candidates, would close the gap and yield a complete cable detection theorem.

11.3.2 Detection beyond genus two

The strategy of this dissertation — Birman-Hilden descent to a braid on the disk, and exhaustive train-track elimination of candidate mapping classes — extends to higher-genus fibered knots only under an important structural constraint.

In genus two, the hyperelliptic involution ι is central in the mapping class group $\mathrm{Mod}(\Sigma_2)$, so *every* monodromy of a genus-two fibered knot automatically commutes with ι and therefore descends to a $(2g+2) = 6$-braid on the disk via the Birman-Hilden correspondence. For genus $g \geq 3$, the picture changes: the hyperelliptic mapping class group

$$\mathcal{H}_g \;=\; C_{\mathrm{Mod}(\Sigma_g)}(\iota)$$

is a *proper* subgroup of $\mathrm{Mod}(\Sigma_g)$, and Birman-Hilden descent applies only to monodromies in $\mathcal{H}_g$ — the so-called **hyperelliptic** (or **symmetric**) monodromies. Consequently, the framework developed here generalizes naturally to fibered knots of genus $g \geq 3$ *whose monodromy is hyperelliptic*, but not directly to general genus-g fibered knots.

Even within the hyperelliptic class, the principal computational obstruction in genus three is the rapid growth in complexity of the train-track state space: the Euler-Poincaré stratum analysis admits substantially more strata, and the `autofolder`'s output graphs grow correspondingly.

A symmetric detection schema. These considerations suggest the following template for detection results beyond genus two, in which a symmetry hypothesis on the monodromy of the unknown knot replaces the symmetry that is automatic in genus two.

Conjecture 11.6 (Symmetric detection schema)**.** Let $K_0 \subset S^3$ be a fibered knot of genus g whose monodromy is hyperelliptic, and let $K \subset S^3$ be a fibered knot whose monodromy is likewise hyperelliptic — for instance, a 2-bridge knot. If

$$\widehat{HFK}(K) \;\cong\; \widehat{HFK}(K_0)$$

as bigraded vector spaces, then $K \cong K_0$.

Two of the three hypotheses placed on K are in fact intrinsic to $\widehat{HFK}$ and need not be assumed separately: that K is fibered and that it has genus g both follow from the isomorphism, by the genus and fiberedness detection of Ozsváth–Szabó and Ni [Ni07]. The single genuinely additional hypothesis is that the monodromy of K be hyperelliptic. This is exactly the condition that licenses the Birman–Hilden descent of the monodromy to a braid on the $(2g+2)$-marked disk, after which the train-track elimination of Chapters 3 and 7 and the homological filtering of Section 7.3 apply, in principle, without modification. In genus two the hypothesis is vacuous — the hyperelliptic involution is central in $\mathrm{Mod}(\Sigma_2)$ — and Conjecture 11.6 specializes to the unconditional detection results of this dissertation. Removing the hyperelliptic hypothesis, so as to detect K_0 among *all* genus-g fibered knots, is the deeper problem: it would require controlling non-symmetric monodromies, to which the disk-braid machinery does not directly apply.

The torus knot $T_{2,7}$ as a first target. The natural first test of this schema beyond genus two is the genus-three torus knot $T_{2,7}$, a 2-bridge knot whose Alexander polynomial is the cyclotomic polynomial

$$\Delta_{T_{2,7}}(t) \;=\; \Phi_{14}(t) \;=\; t^6 - t^5 + t^4 - t^3 + t^2 - t + 1.$$

A knot K with $\widehat{HFK}(K) \cong \widehat{HFK}(T_{2,7})$ is, by genus and fiberedness detection, a genus-three fibered knot; the periodic case of the Nielsen–Thurston trichotomy returns $T_{2,7}$ through the Alexander polynomial, and the reducible case is controlled by Schubert's satellite formula, as in Chapter 8. The hyperbolic case is where the genus-three program would be carried out, and here one expects a genuine simplification relative to the granny: the next-to-top fixed-point bound of Ghiggini–Spano and Ni [GS22; Ni22] — the same bound that constrained the granny monodromy — forces a hyperbolic representative sharing the knot Floer homology of $T_{2,7}$ to be *fixed-point-free*, since the next-to-top knot Floer group of $T_{2,7}$ has rank one. Unlike the granny case — where the monodromy carries a single interior fixed point that must first be located and capped off — there is then no fixed point to remove, and under the hyperelliptic hypothesis the analysis could be carried out directly on the eight-marked disk D_8: paralleling Reinoso's treatment of the cinquefoil [Rei23], the `autofolder` would enumerate the candidate pseudo-Anosov train-track maps on the relevant strata of D_8. Confirming that none of these survives the homological filters would establish a conditional detection of $T_{2,7}$ and the first instance of Conjecture 11.6 beyond genus two.

11.3.3 Khovanov detection of the granny knot

The detection of the granny knot by knot Floer homology raises the natural question of whether Khovanov homology detects $T_{2,3}\#T_{2,3}$ as well. Khovanov homology is currently known to detect the unknot, the two trefoils, the figure-eight, the cinquefoils $T(\pm 2, 5)$, 5_2, and the Whitehead doubles $\mathrm{Wh}^{\pm}(T_{2,3}, 2)$, but is not known to detect any composite knot. A

Khovanov-side analog of Theorem 1.1 would be the first such detection result.

We outline the natural strategy here, adapted from the Khovanov detection of the figure-eight knot by Baldwin, Dowlin, Levine, Lidman, and Sazdanovic [Bal+21]. The granny knot has the following relevant invariants:

- $\dim_{\mathbb{Q}} \widetilde{Kh}(T_{2,3}\#T_{2,3}) = 9$, since reduced Khovanov homology is multiplicative under connect sum and $\dim_{\mathbb{Q}} \widetilde{Kh}(T_{2,3}) = 3$;
- $T_{2,3}\#T_{2,3}$ is thin (a connect sum of thin knots is thin);
- $T_{2,3}\#T_{2,3}$ is strongly quasipositive, and $\tau(T_{2,3}\#T_{2,3}) = g(T_{2,3}\#T_{2,3}) = 2$.

Let $K \subset S^3$ be a knot whose reduced Khovanov homology over $\mathbb{Q}$ is isomorphic to $\widetilde{Kh}(T_{2,3}\#T_{2,3};\mathbb{Q})$ as a bigraded vector space. The proposed argument proceeds in three steps:

1. *Khovanov thinness.* The bigraded isomorphism implies K is thin (Khovanov-thinness is a property of the bigraded structure).
2. *Spectral sequence collapse.* Dowlin's spectral sequence [Dow24] from reduced Khovanov homology to $\widehat{HFK}$ degenerates at the E_2-page for thin knots, yielding

$$\widehat{HFK}(K;\mathbb{Q}) \cong \widehat{HFK}(T_{2,3}\#T_{2,3};\mathbb{Q})$$

   as bigraded vector spaces.
3. *$\widehat{HFK}$-detection.* Theorem 1.1 (extended from $\mathbb{F}_2$ to $\mathbb{Q}$ coefficients) concludes $K \cong T_{2,3}\#T_{2,3}$.

The principal subtlety in this strategy is the extension of Theorem 1.1 from $\mathbb{F}_2$ to $\mathbb{Q}$ coefficients, which requires verifying that the fixed-point obstructions used in the proof remain valid in

characteristic zero. We do not pursue this in the present work.

A natural further question is whether the strategy above could be adapted to detect the *square knot* $T_{2,3}\#\overline{T}_{2,3}$, which is the most prominent composite knot with the same Alexander polynomial as the granny. Here Step 3 fails: $\tau(T_{2,3}\#\overline{T}_{2,3}) = 0 \neq g(T_{2,3}\#\overline{T}_{2,3}) = 2$, so the square knot is not strongly quasipositive, and the strong-quasipositive simplifications used in the granny case fail. The square knot in fact lies in an infinite $\widehat{HFK}$-equivalence class (Subsection 11.3.4 below), placing it genuinely beyond the reach of $\widehat{HFK}$-driven detection. Khovanov detection of the square knot would therefore require a different mechanism, and would yield the first Khovanov detection result for a composite knot.

11.3.4 Knot Floer homology and Khovanov homology on the Hedden-Watson pretzel family

The square knot $T_{2,3}\#\overline{T}_{2,3}$ is the central member of the infinite Hedden-Watson pretzel family $\{P(3,-3,2n)\}_{n\in\mathbb{Z}}$ shown in Figure 11.1. All members of this family share the same knot Floer homology and the same instanton knot Floer homology [HW18; Wan22], with $P(3,-3,0)$ being the square knot. In the geography/botany framework of §1.2, this family is a negative botany result for genus two: the bigraded $\widehat{HFK}$ profile of the square knot is realized by infinitely many distinct knots, and consequently no positive botany result — no detection theorem — can ever be obtained for the square knot via $\widehat{HFK}$ alone. The natural follow-up question is whether the family itself is detectable as a collection.

This picture raises two complementary conjectures about how $\widehat{HFK}$ and Khovanov homology interact with the family:

> **Conjecture (Coarse HFK detection of the family).** *If* $\widehat{HFK}(K) \cong \widehat{HFK}(P(3,-3,2n))$ *for some (equivalently, every)* n*, then* $K = P(3,-3,2m)$ *for some* $m \in \mathbb{Z}$*.*
>
> **Conjecture (Khovanov refinement).** *The members of the family* $\{P(3,-3,2n)\}_{n\in\mathbb{Z}}$

have pairwise non-isomorphic Khovanov homology.

If both conjectures hold, $\widehat{HFK}$ and Khovanov homology together detect each $P(3,-3,2n)$ as a knot: $\widehat{HFK}$ identifies membership in the family, and Khovanov refines that identification to a specific member. This would be a clean complementarity between the two invariants on a family where $\widehat{HFK}$ alone cannot suffice, being constant on the family. Both conjectures are structural questions about the interaction of $\widehat{HFK}$ and Khovanov homology, naturally raised by the existence of the Hedden-Watson pretzel family but not directly addressed by the techniques of this dissertation.

11.3.5 Generalizing the autofolder

The `autofolder` as currently implemented enumerates standard train tracks on the marked disk. Two natural extensions are:

- **Closed surfaces of higher genus.** Train track theory on closed surfaces (rather than on the disk) is well-developed, but the algorithmic enumeration is more delicate. An autofolder operating directly on Σ_g would give a valuable contribution.

- **Activating the edge data.** The current `autofolder` outputs the vertex set of the folding automaton; the edge set, encoding standardizing braids and transition matrices, is computed by the package but not utilized in our obstruction. The dilatation-enumeration applications of this edge data are discussed in the introduction (Section 1.2.3); other potential uses include the study of finer dynamical invariants of pseudo-Anosov mapping classes within each stratum.

11.4 Closing Remarks

The detection of the granny knot by knot Floer homology demonstrates that the bigraded structure of $\widehat{HFK}$ is sufficiently rich to identify a knot uniquely even in the presence

of essential tori in its complement, where geometric obstructions of the hyperbolic kind are unavailable. The combination of monodromy descent via Birman-Hilden, train-track classification via the `autofolder`, and homological filtering via the characteristic polynomial of the lifted action provides a template for future detection results in low-dimensional topology.

We hope that the methods developed in this dissertation — particularly the algorithmic infrastructure for navigating the geometry of mapping class groups — will serve as a springboard for further work on the rigidity of knot invariants and the classification of pseudo-Anosov mapping classes.

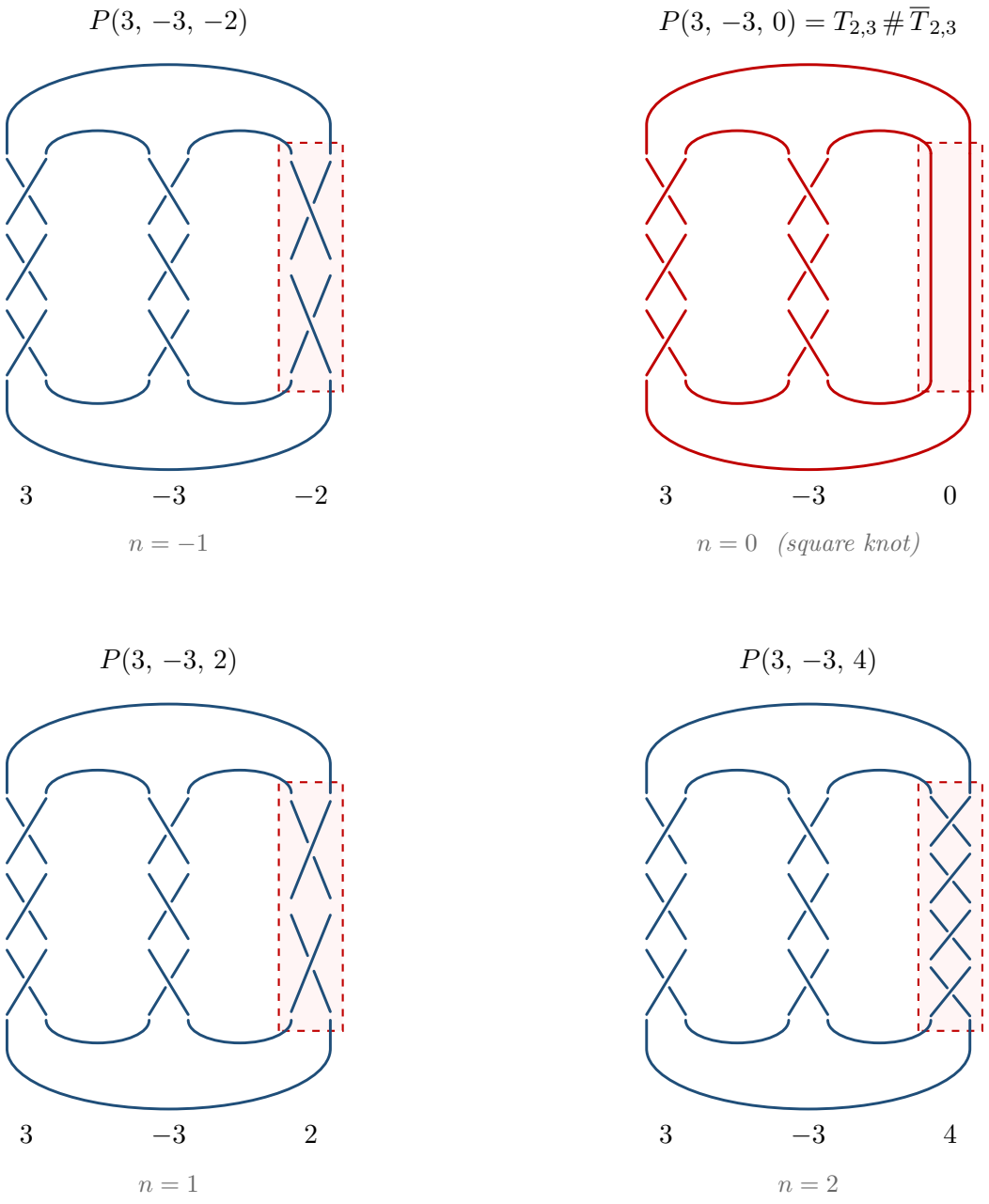


Figure 11.1: The Hedden-Watson pretzel family $P(3,-3,2n)$, due to an unpublished observation of Rasmussen and formalized in [HW18]. All four members shown above have isomorphic knot Floer homology. The member $P(3,-3,0)$ (top right) is the square knot $T_{2,3}\,\#\,\overline{T}_{2,3}$; twisting the third tangle (highlighted) by n full twists yields the further members $P(3,-3,2n)$, each carrying the same $\widehat{HFK}$. This infinite family is the canonical obstruction to $\widehat{HFK}$ detection of the square knot. The analogous construction with two right-handed trefoils, $P(3,3,2n)$, fails to produce a $\widehat{HFK}$-equivalent family for the granny knot: the four-ball genus bound $|\tau(K)|\leq g_4(K)$ gives $g_4(T_{2,3}\#T_{2,3}) \geq 2$, so the granny is not slice and hence not a band sum of two unknots.

APPENDIX ONE

Splitting Sequences for the Stratum $(2; 1^6; 3^2)$

This appendix collects the exhaustive tight-splitting diagrams for the base train tracks of the stratum $(2; 1^6; 3^2)$ that arise in the proof of Lemma 7.11 of Chapter 7 (Figures A.1–A.11). Together with the mirror-pair identification carried out there, these diagrams establish the second stage of the reduction of the geometric state space, from the jointless `autofolder` output for this stratum to the six surviving standard train tracks $(0), (1), (8), (12), (13), (17)$ recorded in Figure 7.21.

What the diagrams show. Each figure depicts a single train track τ (numbered by its label in the `autofolder` output for the stratum) together with the tree of tight splittings emanating from τ. The root of each tree is τ itself; the leaves are the tracks reached after a finite sequence of tight splittings. By Proposition 6.6, a tight splitting preserves the carrying property: any pseudo-Anosov map carried by τ is carried, up to conjugation by a braid, by each track in the splitting tree; by Proposition 6.7 the associated dynamics (transition matrix, and hence dilatation) are preserved as well. Consequently, classifying the pseudo-Anosov maps carried by τ reduces to classifying those carried by the leaves of its tree.

How to read the diagrams. Each diagram is a splitting diagram in the sense of Section 6.2: a finite directed graph of tight l- and r-splits rooted at τ. A diagram may contain splitting loops, but by the analysis of that section every such loop is excluded. A loop returning to a jointless track carries the periodic loop braid $\delta^{-1} = \sigma_2^{-1}\sigma_1^{-1}$ (up to conjugacy and full twists) and is ruled out by Lemma 6.12; a loop retaining a joint is ruled out by Reinoso's Theorem C (Lemma 6.13). The leaves recorded in each caption are therefore the tracks reached upon exiting every loop. Each such leaf is either one of the six surviving tracks $(0), (1), (8), (12), (13), (17)$, the root of another diagram in this appendix, or the vertical mirror image of such a track. Tracing the diagrams transitively and identifying mirror pairs (as in the proof of Lemma 7.11), every base track of the stratum reduces to one of the six surviving tracks.

Consequences for the enumeration. Combined with the mirror-pair identification of Lemma 7.11, the splitting diagrams collected here establish that, up to conjugation and mirroring, every pseudo-Anosov mapping class in the stratum $(2; 1^6; 3^2)$ is carried by one of the six surviving tracks of Figure 7.21. This is the geometric reduction underlying Proposition 7.12 and the enumeration of candidate braid families that follows.

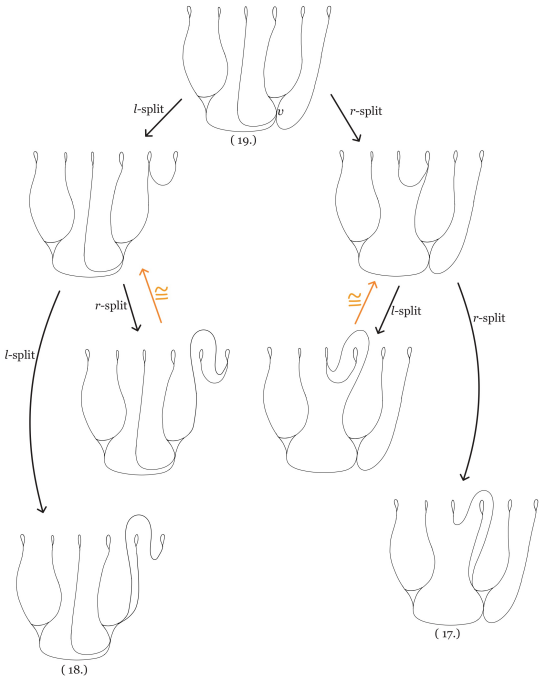


Figure A.1: Tight-splitting diagram of train track (19.). After excluding the splitting loops (Lemmas 6.12 and 6.13), the diagram terminates at the tracks (18.) and (17.).

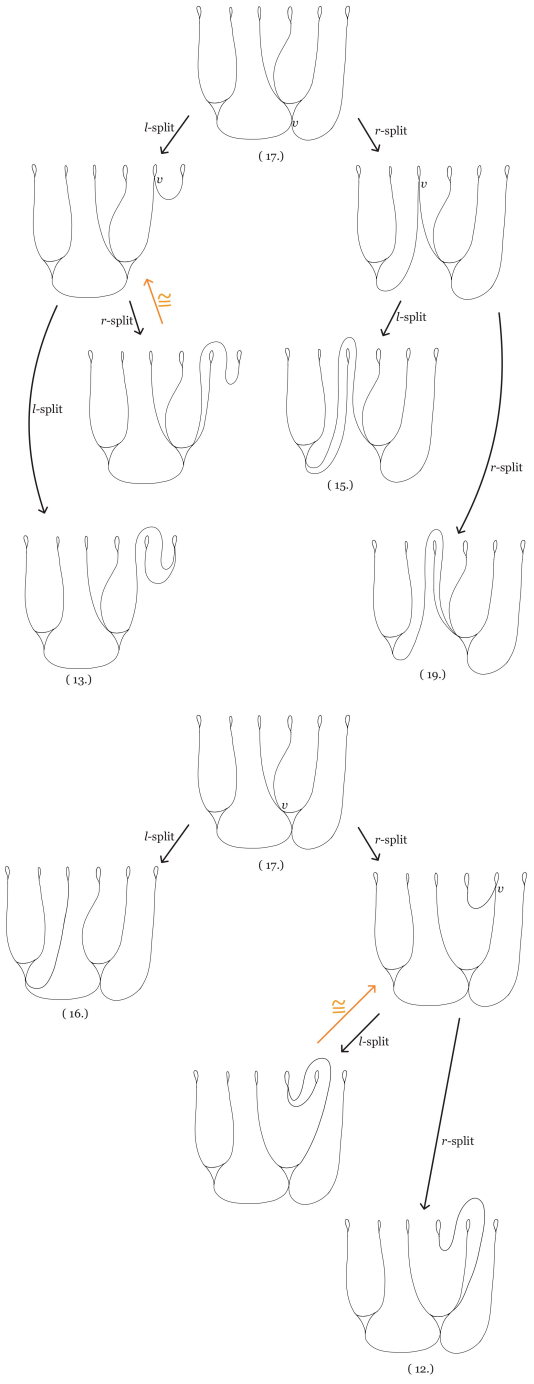


Figure A.2: Tight-splitting diagram of train track (17.). After excluding the splitting loops (Lemmas 6.12 and 6.13), the diagram terminates at the tracks (19.), (13.), (16.), and (12.).

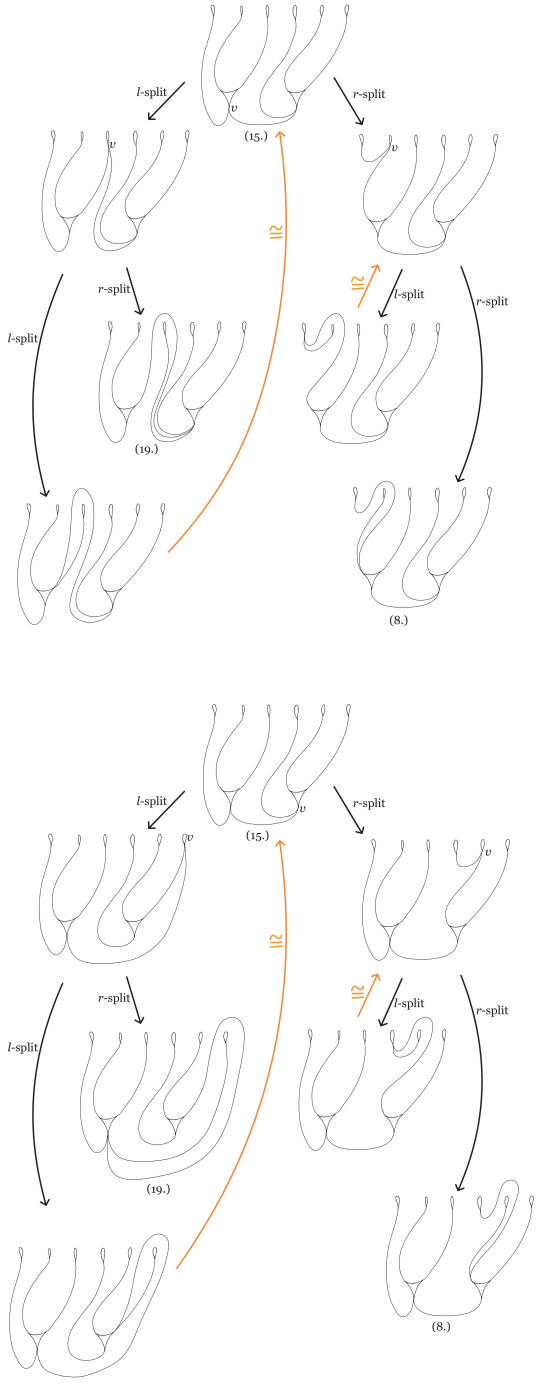


Figure A.3: Tight-splitting diagram of train track (15.). After excluding the splitting loops (Lemmas 6.12 and 6.13), the diagram terminates at the tracks (19.) and (8.).

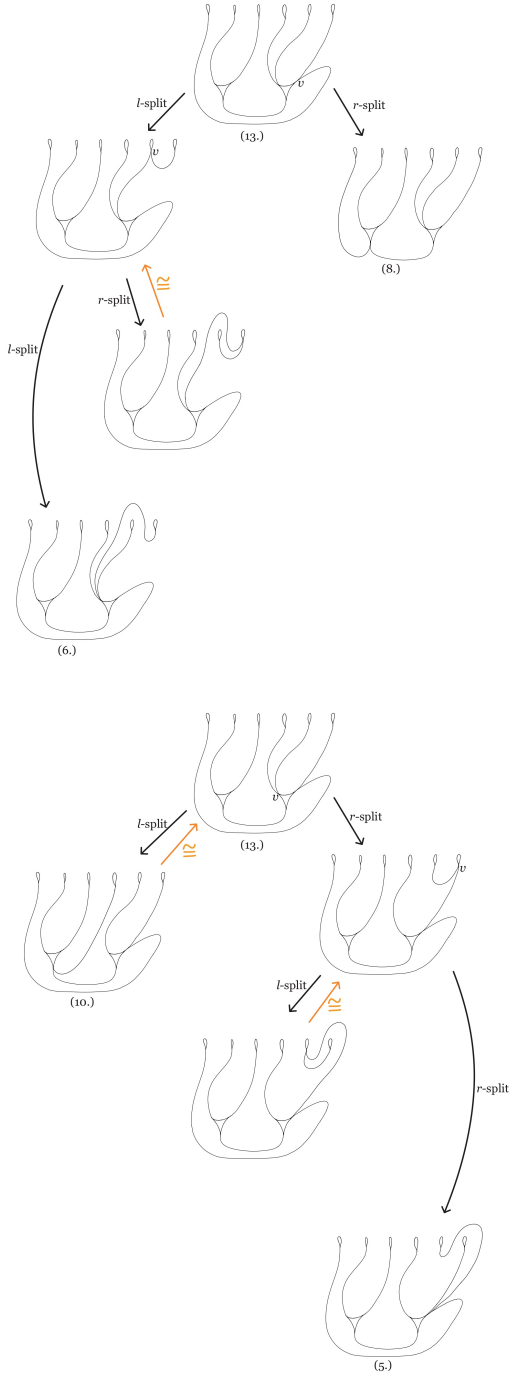


Figure A.4: Tight-splitting diagram of train track (13.). After excluding the splitting loops (Lemmas 6.12 and 6.13), the diagram terminates at the tracks (8.), (6.), (10.), and (5.).

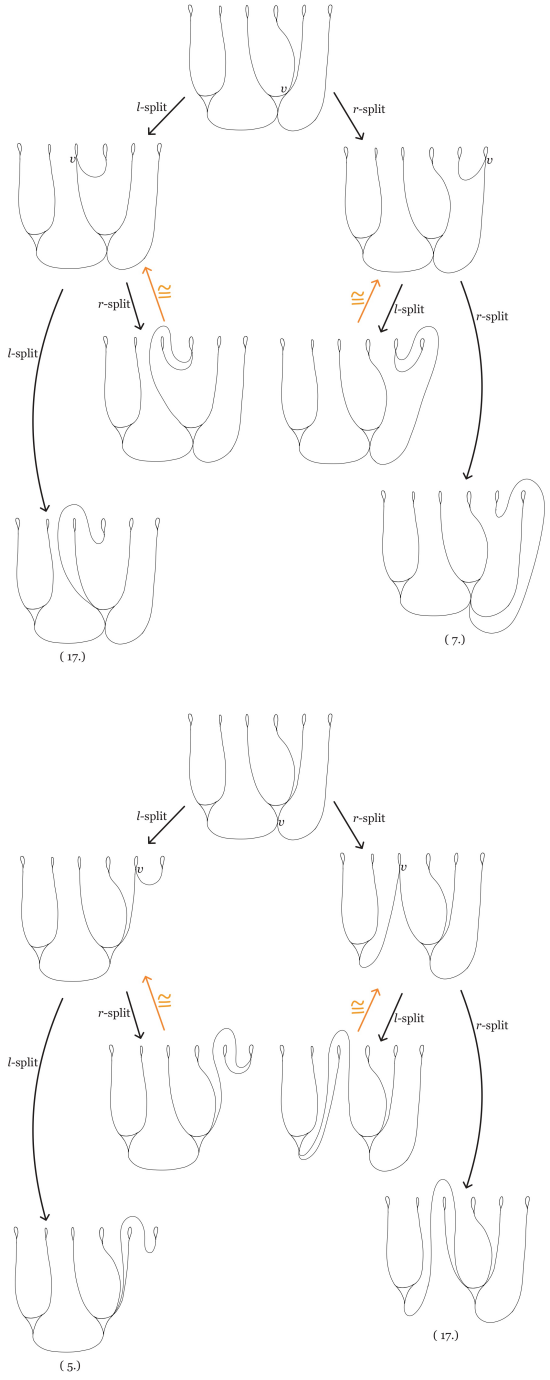


Figure A.5: Tight-splitting diagram of train track (12.). After excluding the splitting loops (Lemmas 6.12 and 6.13), the diagram terminates at the tracks (17.), (7.), and (5.).

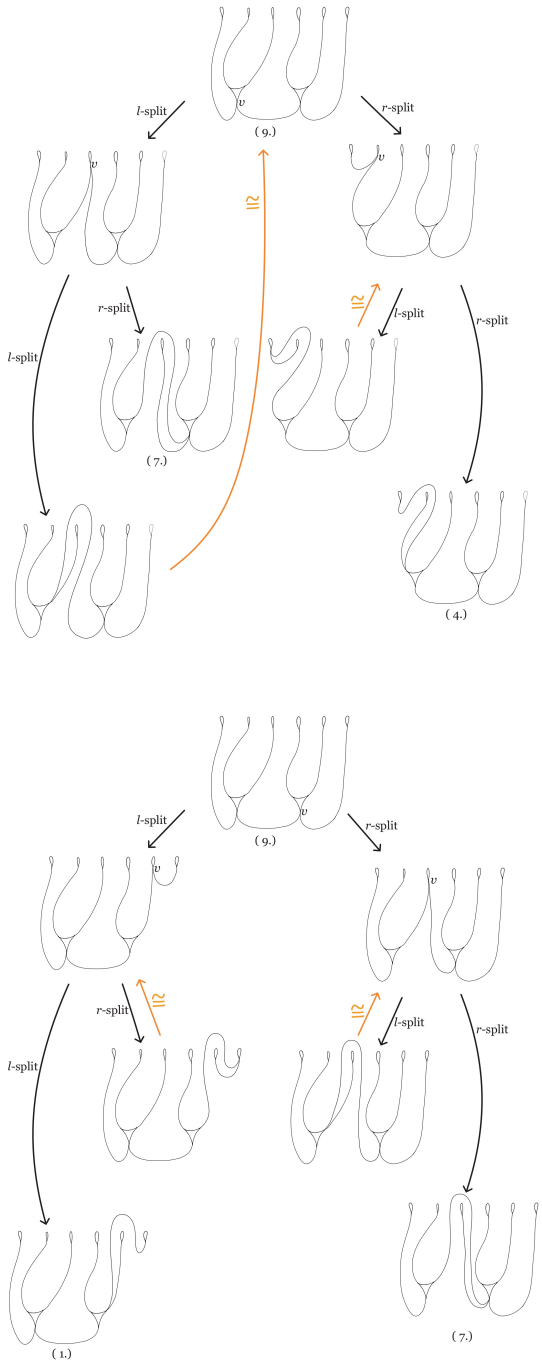


Figure A.6: Tight-splitting diagram of train track (9.). After excluding the splitting loops (Lemmas 6.12 and 6.13), the diagram terminates at the tracks (7.), (4.), and (1.).

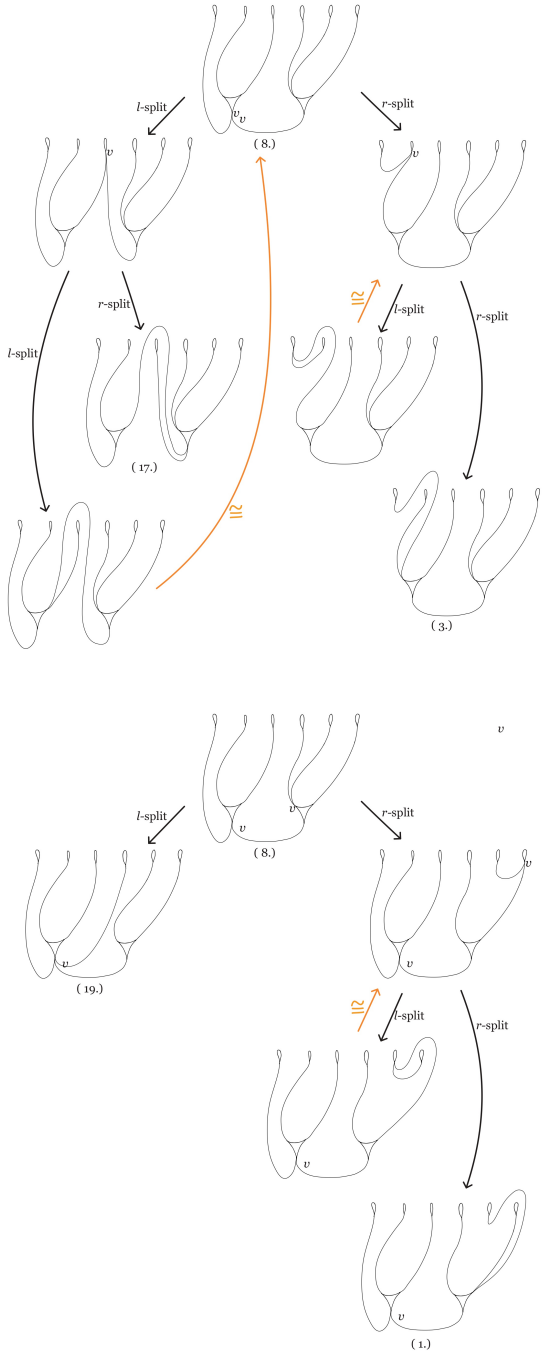


Figure A.7: Tight-splitting diagram of train track (8.). After excluding the splitting loops (Lemmas 6.12 and 6.13), the diagram terminates at the tracks (17.), (3.), (19.), and (1.).

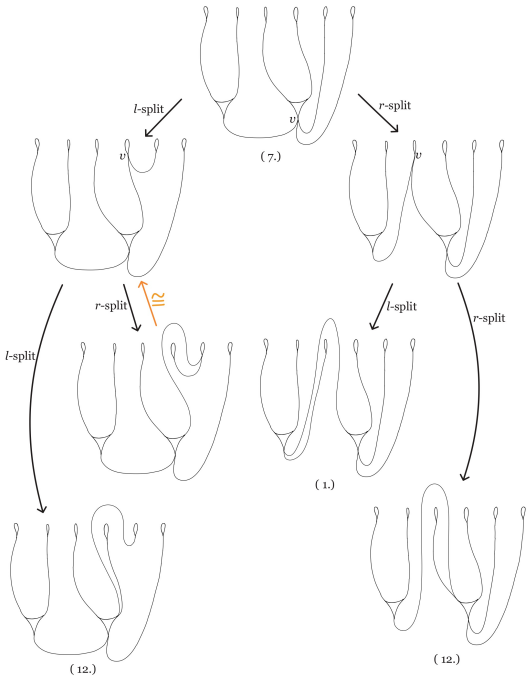


Figure A.8: Tight-splitting diagram of train track (7.). After excluding the splitting loops (Lemmas 6.12 and 6.13), the diagram terminates at the tracks (12.) and (1.).

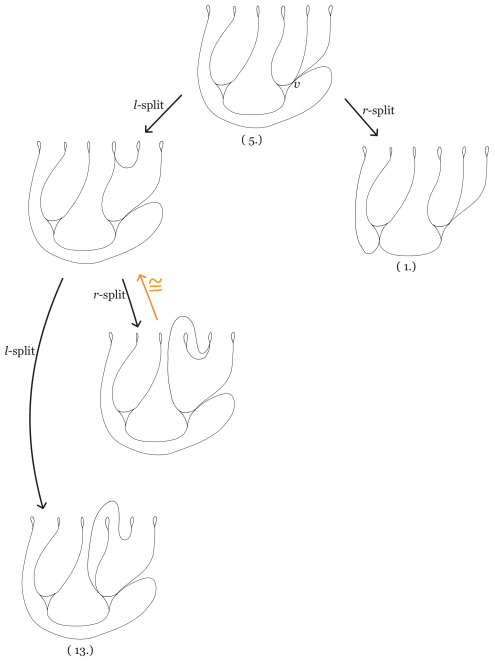


Figure A.9: Tight-splitting diagram of train track (5.). After excluding the splitting loops (Lemmas 6.12 and 6.13), the diagram terminates at the tracks (13.) and (1.).

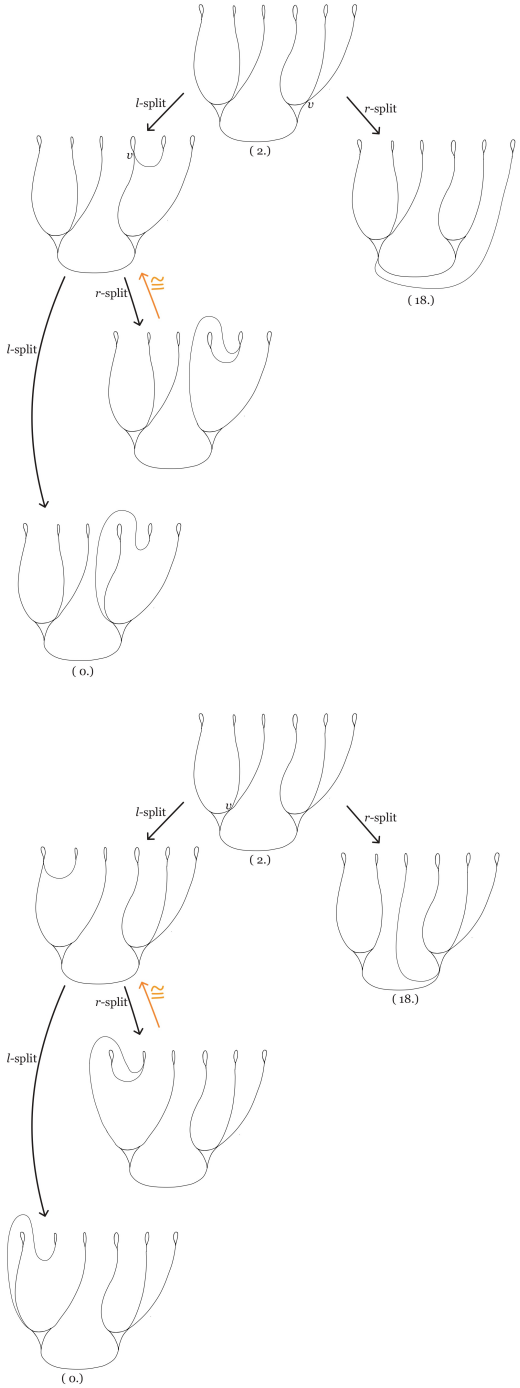


Figure A.10: Tight-splitting diagram of train track (2.). After excluding the splitting loops (Lemmas 6.12 and 6.13), the diagram terminates at the tracks (18.) and (0.).

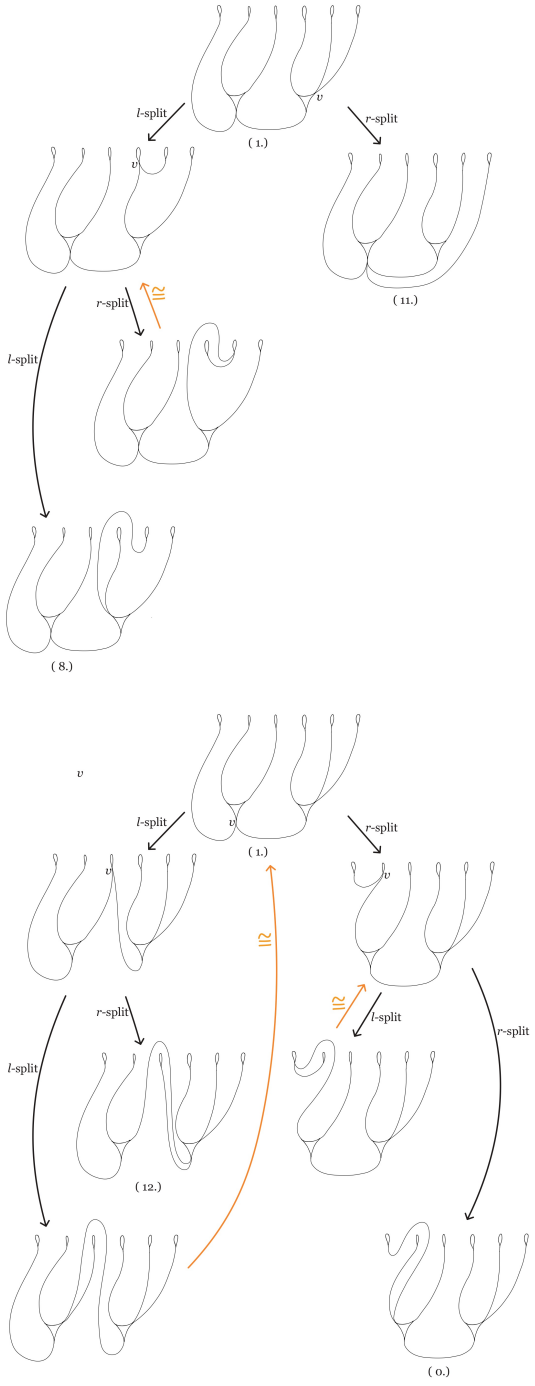


Figure A.11: Tight-splitting diagram of train track (1.). After excluding the splitting loops (Lemmas 6.12 and 6.13), the diagram terminates at the tracks (11.), (8.), (12.), and (0.).

APPENDIX TWO

Appendix: Case Analysis Preliminaries

The case analyses presented in Appendices C, D, E, F, G, H, and I all turn on a small number of recurring obstructions and named configurations established in Chapter 7. This appendix collects these into a single reference and explains the language and patterns of argument that appear repeatedly across the per-track case analyses.

B.1 Primary Obstructions

B.1.1 The Trace Lemma

The fundamental algebraic constraint on the image words $f_\beta(e)$ is the Trace Lemma, established as Lemma 7.1 and its strong consequence Corollary 7.2, which we restate here for reference.

Lemma B.1 (Trace Lemma, restated from Lemma 7.1)**.** Suppose the canonical lift ϕ_h has no interior fixed points on Σ_2^2. Then, for any real edge e of the standard train track τ, any sub-word of the image path $f_\beta(e)$ bounded by two occurrences of e must contain an even number of side-swapping edges.

Corollary B.2 (Trace Lemma for Jointless Monogons, restated from Corollary 7.2)**.** If e is a real edge of τ which is directly incident to a jointless monogon, then e cannot appear anywhere in its own image path $f_\beta(e)$.

In the Candelabra (stratum $(3; 1^6; 3)$), every real edge b, o, s, i, p, r is incident to a jointless monogon, so Corollary B.2 applies to all six real edges. In the two-triangle strata (stratum $(2; 1^6; 3^2)$, Tracks 0, 1, 8, 12, 13, 17), Corollary B.2 applies to all five monogon-incident edges b, i, o, p, r, but it does *not* apply to the central edge d (and its symmetric companion $\bar{d}$), which is incident to two infinitesimal triangles rather than a monogon. For d and $\bar{d}$, only the more general Lemma B.1 applies, in the form of the parity constraints recalled below.

We refer to a violation of Corollary B.2 as **tracing**: an image path $f_\beta(e)$ traces if it contains the letter e. The phrase "$f_\beta(e)$ will trace immediately" indicates that the next forced letter in the image word would produce a self-occurrence of e.

B.1.2 The Absorption Obstruction

The Trace Lemma supplies the algebraic restriction; the geometric restriction is the Absorption Obstruction (Lemma 7.4). Recall: at any vertex v where two real edges a and b are adjacent, the initial segments of $\phi_\beta(a)$ and $\phi_\beta(b)$ bound a convex cone $X_v(a, b)$ in the disk; for any real edge c, the image path $\phi_\beta(c)$ cannot enter the interior of this cone.

When the case analysis arrives at a hypothetical image word for $f_\beta(c)$ whose induced path enters $X_v(a, b)$, we say $f_\beta(c)$ is **absorbed** between $f_\beta(a)$ and $f_\beta(b)$, and we record this in image words with the notation

$$f_\beta(c) = \ldots \mathrm{Abso}(f_\beta(a), f_\beta(b))^\times \ldots$$

following the convention introduced in Section 7.2.2. Such an absorption immediately

invalidates the candidate word.

B.2 Trace Constraints for the Central Edge d

For Tracks 0, 1, 8, 12, 13, and 17, the analysis subdivides into Cases A, B, C, and D based on how f_β permutes the two infinitesimal triangles (see the discussion of Cases A, B, C, D in Section "Path Notation and the Two Triangles of Chapter efchap:stratatraintrackanalysis). The Trace Lemma yields the following parity constraints, which we use throughout the per-track case analyses.

- **Case A (Triangles Fixed).** Every occurrence of d in $f_\beta(d)$, and every occurrence of $\bar{d}$ in $f_\beta(\bar{d})$, must follow an *even* number of preceding letters. In particular, the *first* occurrence of d in $f_\beta(d)$ is preceded by an even number of letters.

- **Cases B, C, D (Triangles Swapped).** At least one of $f_\beta(d)$ or $f_\beta(\bar{d})$ must pass over d or $\bar{d}$ after an *odd* number of letters.

In what follows, we refer to the parity constraint in Case A as **Assumption A**.

Assumption B.3 (Assumption A)**.** In Case A, the first occurrence of d in $f_\beta(d)$ is preceded by an even number of letters, and likewise for the first occurrence of $\bar{d}$ in $f_\beta(\bar{d})$.

B.3 Named Configurations and Their Contradictions

The per-track case analyses repeatedly arrive at one of three named configurations, each of which produces a contradiction with the obstructions above. We distinguish two flavors of contradiction:

- **Non-termination contradictions.** The image word would need to continue indefinitely to satisfy all rules. Since each $f_\beta(e)$ is a finite word, this is impossible.

- **Direct violation contradictions.** The image word cannot continue at all without immediately violating the Trace Lemma or being absorbed.

B.3.1 Situation α

Definition B.4 (Situation α)**.** A pair of image paths $f_\beta(d)$ and $f_\beta(\bar{d})$ are in *Situation* α if they fail to join in the interior of the configuration and are instead forced to traverse the outer perimeter of the train track indefinitely, with each successive crossing of d in either word at the parity required by the Trace Lemma (Case A) or its odd-parity analog (Cases B, C, D).

The contradiction produced by Situation α is of the *non-termination* type: each individual perimeter crossing is consistent with the Trace Lemma, but the resulting image word $f_\beta(d)$ has no finite length, contradicting the requirement that $f_\beta(d)$ be a finite word in the letters of the train track.

A clean instance of Situation α appears in subsection Yaffle of Appendix D, depicted in Figure D.29: the dotted lines have no interior route by which to join, and so continue clockwise around the outer perimeter of the train track without termination.

B.3.2 Situation β

Definition B.5 (Situation β)**.** A dotted line $f_\beta(d)$ (or $f_\beta(\bar{d})$) is in *Situation* β if, after a crossing of d (or $\bar{d}$), it is trapped inside a region of the configuration enclosed by another edge-path—typically $f_\beta(b)$, $f_\beta(i)$, $f_\beta(o)$, $f_\beta(p)$, or $f_\beta(r)$—such that every escape route from this region forces the next return to d (or $\bar{d}$) after an odd number of letters.

The contradiction produced by Situation β is of the *direct violation* type: every geometrically available continuation produces an odd-parity return to d, violating Lemma B.1 for the central edge.

The colloquial name for Situation β that appears in some passages of the case analyses is the "bagged serpent," reflecting the geometric picture of a dotted line coiled inside an enclosing pocket without a parity-respecting exit. A clean instance of Situation β appears in subsection Fangle of Appendix D, depicted in Figure D.12: the dotted lines cannot traverse above $f_\beta(p)$ without subsequently violating the Trace Lemma on their return to d.

B.3.3 Path Mills

Definition B.6 (Path Mill)**.** A *k-way path mill* is a configuration in which k image paths $f_\beta(e_1), \ldots, f_\beta(e_k)$, with the e_i among $\{b, i, o, p, r, s\}$, become stuck in a rotational pattern between two fixed vertices of the train track. At each step, $k-1$ of the $f_\beta(e_i)$ are positioned at one vertex while the remaining one is at the other; the edge image that just arrived is then forced by Corollary B.2 and the Absorption Obstruction (Lemma 7.4) to traverse to the opposite vertex, joining the others there, after which the pattern repeats. The cycle never terminates.

The contradiction produced by a path mill is of the *non-termination* type: the image words of the involved edges would need to continue indefinitely, which is impossible.

At each step in the cycle, an edge image that fails to continue along the prescribed route is forced either to trace (violating Corollary B.2) or to be absorbed by one of the other edges (violating Lemma 7.4), both of which are forbidden. Hence the cycle has no escape.

The cleanest illustration is the three-way path mill between vertices b and o appearing in subsection SYD of Appendix D, depicted in Figures D.215–D.219. We reproduce the key passage here:

> The edges $f_\beta(s)$, $f_\beta(i)$, and $f_\beta(r)$ are in a three-way counterclockwise path mill between b and o. At each step there is always a pair from the three positioned at b or o, while the third edge is at the other. Looking at the pair at each step, the edge on the right is always forced to continue counterclockwise and to traverse to the left of the edge on the left—otherwise the left edge would be forced either

to trace, or to be absorbed in some way. Thus the right edge traverses to the other vertex (b or o) to join the third edge, forming the new pair, and the pattern repeats indefinitely.

Four-way path mills arise occasionally; see for example subsection LKE of Appendix H (Figure H.114) and subsection MMU of Appendix I (Figure I.130). The forcing mechanism generalizes from the three-way case in the obvious manner.

B.4 Notation and Common Phrases

We collect here the meanings of recurring shorthand used throughout the per-track case analyses.

Dotted lines. Refers to the two image paths $f_\beta(d)$ and $f_\beta(\bar{d})$, which together depict the image of the central edge between the two infinitesimal triangles in Tracks 0, 1, 8, 12, 13, 17. These are drawn as dashed or dotted curves in the figures of the per-track appendices, to distinguish them from the five monogon-incident edges.

Joining in the middle. Two image paths $f_\beta(d)$ and $f_\beta(\bar{d})$ are said to *join in the middle* if they meet at a common interior point of the train track configuration. Joining in the middle is the desired outcome at each branching choice in the case analysis: the alternative—failing to join—is what produces Situation α or Situation β.

Tracing. An image path $f_\beta(e)$ *traces* (or *traces itself*) when its image word contains the letter e. By Corollary B.2, this is a contradiction whenever e is incident to a jointless monogon. The phrase "$f_\beta(e)$ will trace immediately" indicates that the next forced letter in the candidate word would produce a self-occurrence of e.

Absorbed. An image path $f_\beta(c)$ is *absorbed* between $f_\beta(a)$ and $f_\beta(b)$ when it is forced to enter the convex cone $X_v(a, b)$ near a vertex v, in violation of Lemma 7.4. Absorption is

distinct from tracing but is similarly fatal to the case at hand. In displayed image words, absorption is recorded with the notation $\mathrm{Abso}(f_\beta(a), f_\beta(b))^\times$.

Initial twists. An image path $f_\beta(d)$ has *initial twists* if it begins with one or more letters before the first crossing of d. By Assumption B.3, in Case A the number of initial twists must be even.

Exit routes 1, 2, 3. The figures in the case analyses label the possible local continuations of an image path at a branching point with small numbers (e.g. "goes into 1, 2, or 3"). These numbers correspond to the local choice of direction at the vertex shown in the figure; the case analysis then enumerates which of these routes survives the constraints imposed by the Trace Lemma, the Absorption Obstruction, and the trace constraints of Section B.2.

Outer perimeter. The boundary loop of the train track polygon, traversed in either the clockwise or counterclockwise direction. An image path circling the outer perimeter without termination is the geometric signature of Situation α.

APPENDIX THREE

Train Track Case Analysis: The Candelabra

This is the Candelabra:

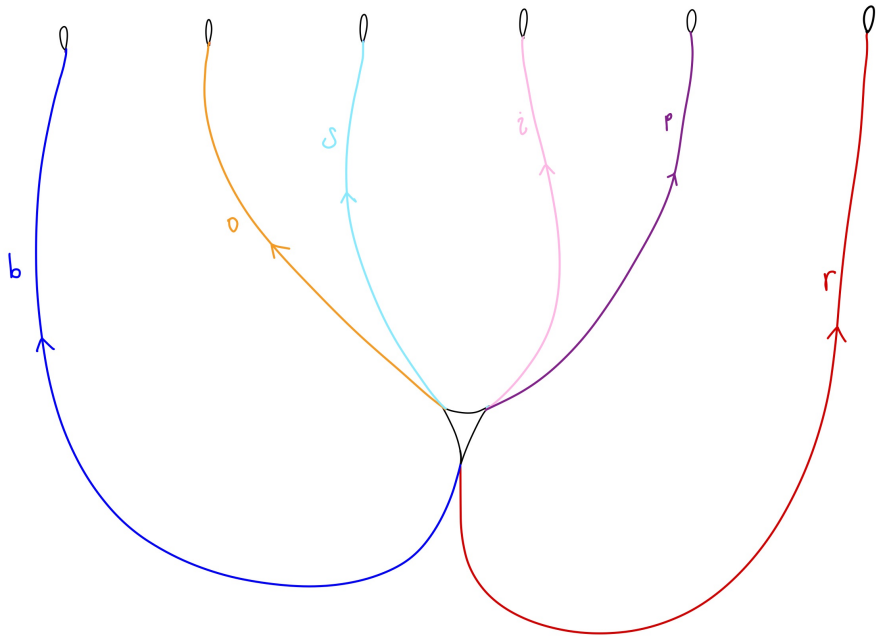


Figure C.1: The Candelabra train track.

First notice that the triangle must be rotated by f_β, otherwise the image of all of the real edges will trace. There are two possible rotations of the triangle, one is the result of a single clockwise rotation, and the other is the result of two clockwise rotations.

First we assume that the triangle is rotated once clockwise. Thus, $f_\beta(i)$ begins with r^*, but could only be r° or r^+, and $f_\beta(p)$ begins with b^*. On the other hand, $f_\beta(r)$ and $f_\beta(b)$ begin with o^* or s^*, while $f_\beta(o)$ and $f_\beta(s)$ begin with i or p. As shown in Figure C.2.

Figure C.3 shows the starting position of the situation where the triangle is rotated twice clockwise. In this situation, $f_\beta(o)$ begins with r^*, but could only be r° or r^+, and $f_\beta(s)$

begins with b^*. On the other hand, $f_\beta(i)$ and $f_\beta(p)$ begin with o^* or s^*, while $f_\beta(r)$ and $f_\beta(b)$ begin with i or p.

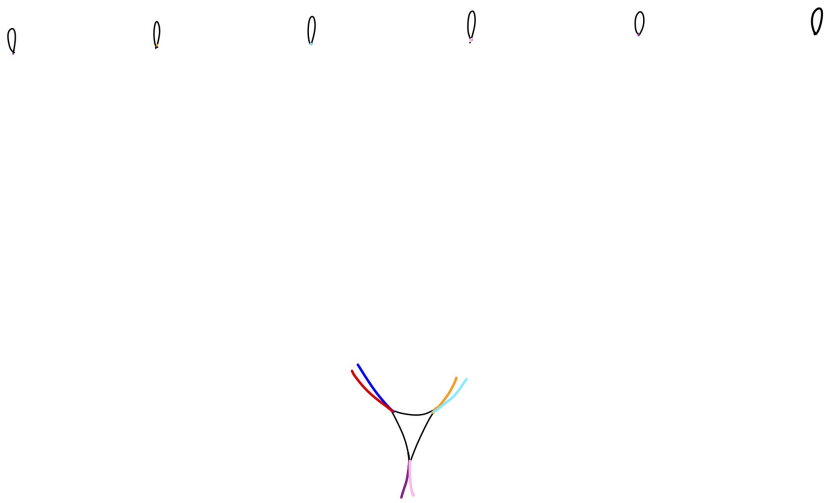


Figure C.2: Starting position when the triangle is rotated one "click" clockwise.

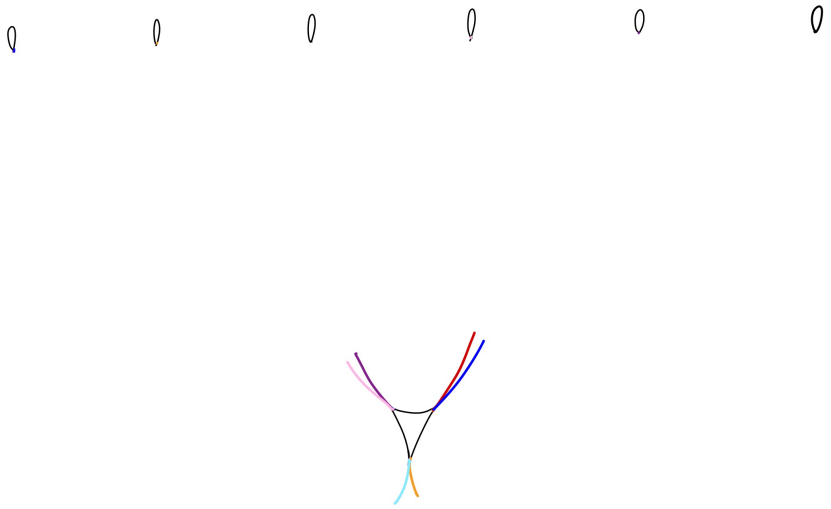


Figure C.3: Starting position when the triangle is rotated two "clicks" clockwise.

We carry out the full case analysis only under the assumption that the triangle is rotated one click clockwise. The two-click case is recovered from the one-click case by precomposition with a single braid G, as the following argument shows.

Remark C.1 (Rotational symmetry of the two initial cases)**.** The two starting configurations depicted in Figures C.2 and C.3 correspond to the two possible non-trivial rotational states of the central triangle under f_β ("one click clockwise" versus "two clicks clockwise"). The candelabra is rotationally symmetric with respect to the cyclic permutation of its six real edges

$$b \to o, \quad o \to i, \quad i \to r, \quad r \to s, \quad s \to p, \quad p \to b,$$

and this permutation interchanges the two initial configurations: applying it to the one-click starting configuration yields exactly the two-click starting configuration. Crucially, this permutation of the edges is itself realized by a specific braid G in B_6, namely the braid extracted from Train Track Candidate 1 (the "NHT" family; see Section J.3).

Consequently, the entire case analysis is symmetric between the two initial configurations. If the one-click case analysis yields candidate families $1, 2, \ldots, n$ with braid representatives $\beta_1, \beta_2, \ldots, \beta_n$, then the two-click case analysis mechanically yields a parallel set of candidate families $1', 2', \ldots, n'$ with braid representatives $\beta_1 \cdot G, \beta_2 \cdot G, \ldots, \beta_n \cdot G$. (Equivalently: applying the edge permutation above to a one-click candidate map produces a two-click candidate map whose representing braid differs by composition with G.) The primed candidate braids are recorded alongside the unprimed in Appendix J, and the homological filter is applied to both in Appendix P.

It therefore suffices to present the case analysis under the one-click assumption. We proceed with this assumption for the remainder of this appendix.

C.0.1 NHT

Suppose

$$f_\beta(i) = r^\circ$$

and

$$f_\beta(p) = b^\circ$$

Suppose further that

$$f_\beta(r) = o^\circ$$

and

$$f_\beta(s) = i^\circ$$

This is Figure C.4.

This then forces $f_\beta(b)$ to begin with either s° or s^-, so suppose it were the former. Then

$$f_\beta(o) = i^\circ$$

is forced.

This is Figure C.5. This is Candidate 1.

So suppose now

$$f_\beta(b) = s^- ...$$

This is Figure C.6.

Here $f_\beta(b)$ must continue with i^-, to give us

$$f_\beta(b) = s^- i^- s^* ...$$

But now $f_\beta(o)$ will be absorbed:

$$f_\beta(o) = i^+ s^+ \,\mathrm{Abso}(f_\beta(r), f_\beta(b))^\times$$

shown in Figure C.7.

So now suppose

$$f_\beta(s) = p^+ ...$$

The next letter must be o^* or it will trace, but now both $f_\beta(b)$ and $f_\beta(s)$ will be absorbed, shown in Figure C.8.

So now assume

$$f_\beta(r) = o^- ...$$

This is Figure C.9.

Here $f_\beta(r)$ can continue with i or p.

C.0.1.1 Jehu

Suppose

$$f_\beta(r) = o^- i^* ...$$

This is Figure C.10.

Here the next letter can be i° or i^+. Suppose it were the former.

Here both $f_\beta(o)$ and $f_\beta(s)$ cannot both begin with i^+, or one of them will immediately trace. So suppose

$$f_\beta(o) = i^+ ...$$

while

$$f_\beta(s) = p^* ...$$

This is Figure C.11.

Here $f_\beta(s)$ must immediately end otherwise it will be absorbed. Similarly, $f_\beta(o)$ must immediately end, or it will be absorbed:

$$f_\beta(o) = i^+ s^- i^- \, \mathrm{Abso}(f_\beta(o), f_\beta(s))^\times$$

or trace:

$$f_\beta(o) = i^+ s^+ i^- o^\times$$

So we must have

$$f_\beta(o) = i^+ s^\circ$$

Finally, $f_\beta(b)$ is then forced to also end, or it either traces:

$$f_\beta(b) = o^- i^+ o^+ b^\times$$

or is absorbed

$$f_\beta(b) = o^- i^+ s^- i^- \operatorname{Abso}(f_\beta(o), f_\beta(s))^\times$$

Thus we have the train track Candidate 1.1, shown in Figure C.12.

Going back to considering the starting letter of $f_\beta(o)$ and $f_\beta(s)$, now suppose both begin with p^*. Then in fact $f_\beta(s)$ must begin with p^+ and to the left of $f_\beta(o)$. Otherwise, $f_\beta(o)$ would be forced to begin with p^- and be absorbed:

$$f_\beta(o) = p^- r^- \operatorname{Abso}(f_\beta(p), f_\beta(i))^\times$$

Thus we have the situation depicted in Figure C.13.

Here $f_\beta(b)$ is forced to begin with o^- and to the right of the incoming $f_\beta(s)$:

$$f_\beta(b) = o^- i^+ s^* ...$$

as shown in Figure C.13.

Here $f_\beta(s)$ must end. Otherwise it either traces:

$$f_\beta(s) = p^+ o^- i^+ s^\times$$

or, if it continued with o^+ then be absorbed between itself and $f_\beta(o)$. Thus we have

$$f_\beta(s) = p^+ o^\circ$$

This then forces $f_\beta(b)$ to end, or be absorbed between $f_\beta(o)$ and $f_\beta(s)$.

This is Figure C.15, which is a valid train track map candidate; however, it will be subsumed in Candidate Family 2, to come shortly.

Now we go back to the situation depicted in Figure C.10, and suppose the next letter for $f_\beta(r)$ is $i^+/$ Suppose further that $f_\beta(s)$ begins with p^* while $f_\beta(o)$ begins with i^*. Then $f_\beta(s)$ must immediately end or be absorbed.

This is Figure C.16.

Here $f_\beta(o)$ must continue with s^+ and to the left of $f_\beta(r)$, or $f_\beta(r)$ will be absorbed between $f_\beta(o)$ and $f_\beta(s)$. This gives Figure C.17. Here $f_\beta(o)$ twist between i and s and must end there as if it were to escape it either escapes to the outer perimeter and eventually is absorbed, or it escapes to o and trace. Suppose here $f_\beta(o)$ twist for k times. Then $f_\beta(r)$ and $f_\beta(b)$ twist among themselves between the two remaining edge paths m times. This gives Candidate Family 1.2.

Now suppose instead both $f_\beta(s)$ and $f_\beta(o)$ begin with p^*. Then we have Figure C.18. Here $f_\beta(b)$ is forced to begin with o^- and to the right of the incoming $f_\beta(s)$. So we have Figure C.19. Here $f_\beta(o)$ immediately ends or it immediately trace; while $f_\beta(s)$ also ends or it either traces:

$$f_\beta(s) = p^+ o^- i^+ s^\times$$

or be absorbed between itself and $f_\beta(o)$.

This is Figure C.20.

Here $f_\beta(b)$ then continue with s^+ and to the left of $f_\beta(r)$. Otherwise, $f_\beta(r)$ would be absorbed between $f_\beta(o)$ and $f_\beta(s)$. Then $f_\beta(b)$ and $f_\beta(r)$ twist k times between i and s, and eventually end there, giving Candidate Family 2, shown in Figure C.21.

C.0.1.2 Kexy

Back to the end of NHT C.0.1. Suppose

$$f_\beta(r) = o^- p^* ...$$

Then we have Figure C.22.

Here $f_\beta(r)$ must continue with r^- and to the right of both $f_\beta(o)$ and $f_\beta(s)$. Otherwise, at least one of $f_\beta(o)$ or $f_\beta(s)$ will trace. But now it traces immediately:

$$f_\beta(r) = o^- i^- r^\times$$

This finishes the situation under NHT C.0.1.

C.0.2 CMJ

Suppose

$$f_\beta(i) = r^+ ...$$

and

$$f_\beta(p) = b^\circ$$

This is Figure C.23.

Here $f_\beta(i)$ can continue with p° or p^+.

C.0.2.1 Mome

Suppose

$$f_\beta(i) = r^+p^\circ$$

This is the situation depicted in Figure C.24.

Here $f_\beta(r)$ must begin with s or o. We claim that the former cannot occur. Indeed, if $f_\beta(r) = s^*....$ then $f_\beta(b)$ also starts with s. But then $f_\beta(r)$ must in fact start with s^- and to the right of $f_\beta(b)$ otherwise $f_\beta(b)$ will trace, but then we have Figure C.25. Here if $f_\beta(r)$ continued with i° or i^+ then $f_\beta(o)$ and $f_\beta(s)$ will be absorbed between $f_\beta(p)$ and $f_\beta(i)$; but then if $f_\beta(r)$ continued with i^- then it immediately traces.

Thus we must have

$$f_\beta(r) = o^\circ$$

or

$$f_\beta(r) = o^-...$$

C.0.2.1.1 Kedge

Suppose

$$f_\beta(r) = o^\circ$$

Then we must have

$$f_\beta(b) = s^*...$$

This is Figure C.26.

Here $f_\beta(b)$ either ends at s° or continues with s^-.

C.0.2.1.1.1 Dindle

Suppose

$$f_\beta(b) = s^\circ$$

This is Figure C.27.

Here $f_\beta(s)$ can either end at i° or continue with i^-. Suppose

$$f_\beta(s) = i^\circ$$

Then we have Figure C.28, which is forced. This is a candidate train track map that will be subsumed in Candidate Family 3, to follow.

Suppose instead

$$f_\beta(s) = i^- ...$$

Then we have Figure C.29. Here $f_\beta(o)$ and $f_\beta(s)$ twist clockwise between r and i, and end there. This gives Candidate Family 3.

C.0.2.1.1.2 Jirble

Back to the end of Kedge C.0.2.1.1. Suppose

$$f_\beta(b) = i^- ...$$

Then we have Figure C.30.

Here both $f_\beta(o)$ and $f_\beta(b)$ must continue with i^- and to the right of $f_\beta(s)$. Otherwise, $f_\beta(s)$

will be forced to begin with i^+ and immediately trace.

Thus we have

$$f_\beta(o) = i^- ...$$

and

$$f_\beta(b) = s^- i^- ...$$

This is Figure C.31.

Here $f_\beta(b)$ must continue with r^-, otherwise $f_\beta(o)$ will be forced to continue with r^+ and to the left of $f_\beta(b)$. In which case it will be absorbed:

$$f_\beta(o) = i^- \hat{r}^+ p^- r^- \, \mathrm{Abso}(f_\beta(p), f_\beta(i))^\times$$

or

$$f_\beta(o) = i^- \hat{r}^+ i^+ s^+ \, \mathrm{Abso}(f_\beta(r), f_\beta(b))^\times$$

Thus we must have

$$f_\beta(b) = s^- i^- \hat{r}^- i^* ...$$

which forces

$$f_\beta(s) = i^- r^* ...$$

This is Figure C.32.

Now notice that $f_\beta(b)$, $f_\beta(o)$, and $f_\beta(s)$ are stuck in a three-way clockwise path mill between i and r.

This is a contradiction.

C.0.2.1.2 Mulse

Back to the end of Mome C.0.2.1. Suppose

$$f_\beta(r) = o^- ...$$

This is Figure C.33.

Here if $f_\beta(r)$ were to end with i° or continue with i^+, then $f_\beta(o)$ and $f_\beta(s)$ would both begin with i^+, but then either

$$f_\beta(s) = i^+ s^\times$$

or

$$f_\beta(o) = i^+ o^\times$$

would occur. Thus we must have $f_\beta(r)$ continue with i^- and to the right of $f_\beta(o)$ and $f_\beta(s)$. But then it traces:

$$f_\beta(r) = o^- i^- r^\times$$

This is a contradiction.

C.0.2.2 Nesh

Back to the end of CMJ C.0.2. Suppose

$$f_\beta(i) = r^+ p^+ ...$$

This is Figure C.34.

Here $f_\beta(i)$ can continue with r^*, s^*, or o^*.

C.0.2.2.1 Nudzh

Suppose $f_\beta(i)$ continued with r^*. This forces

$$f_\beta(i) = i^*...$$

and

$$f_\beta(o) = i^*...$$

where for $f_\beta(o)$ the first letter could either be i° or i^- (it cannot be i^+ as either itself would trace or $f_\beta(s)$ would).

Suppose

$$f_\beta(o) = i^\circ$$

This forces Figure C.35.

Here $f_\beta(r)$ and $f_\beta(b)$ must begin with o^- and to the right of $f_\beta(s)$. Otherwise, $f_\beta(s)$ would be absorbed:

$$f_\beta(s) = i^+\hat{o}^+b^+ \operatorname{Abso}(f_\beta(p), f_\beta(i))^\times$$

But now $f_\beta(r)$ will trace:

$$f_\beta(r) = o^-i^-r^\times$$

Back to the situation depicted in Figure C.35. Suppose

$$f_\beta(o) = i^-...$$

This is Figure C.36.

Here we claim that $f_\beta(r)$ must begin and end at o°. Indeed, if it began with o^+ then it will be absorbed:

$$f_\beta(r) = o^+ b^+ \,\mathrm{Abso}(f_\beta(p), f_\beta(i))^\times$$

If it began with o^- it would trace:

$$f_\beta(r) = o^- i^- r^\times$$

If it began with s^*, then $f_\beta(b)$ would also begin with s^*. But then $f_\beta(b)$ must begin with s^+ and to the left of $f_\beta(r)$ otherwise $f_\beta(r)$ would again trace. But then we have

$$f_\beta(b) = s^+ b^\times$$

Therefore, we must have

$$f_\beta(r) = o^\circ$$

which forces $f_\beta(b) = s^\circ$ or $f_\beta(b) = s^-$...

This is Figure C.37.

Here $f_\beta(b)$ can either begin and end at s°, or begin with s^-.

C.0.2.2.1.1 Keffel

Suppose

$$f_\beta(b) = s^\circ$$

This is Figure C.38.

Here $f_\beta(s)$ can begin and end at i°, or begin with i^-. In the former case, $f_\beta(i)$ and $f_\beta(o)$

then twist between r and p, giving Candidate Family 4. This is Figure C.39.

Suppose it were the latter case:

$$f_\beta(s) = i^- ...$$

Then we have Figure C.40.

Here $f_\beta(i)$ twist between r and p and end there as it cannot escape or it will trace. Then $f_\beta(s)$ and $f_\beta(o)$ twist clockwise between i and r/p (depending on which is left), and end there as well. This gives Candidate Family 5. An example is shown in Figure C.41.

C.0.2.2.1.2 Mizzle

Back to the end of NudzhC.0.2.2.1. Suppose

$$f_\beta(b) = s^- ...$$

and it continues:

$$f_\beta(b) = s^- i^- r^* ...$$

This is Figure C.42.

Here $f_\beta(s)$ can either begin and end at i°, or begin with $i^-...$

Suppose it were the former. Then we have Figure C.43. Here both $f_\beta(b)$ and $f_\beta(o)$ must continue with r^+ and to the left of $f_\beta(i)$, otherwise $f_\beta(i)$ will immediately trace. This gives Figure C.44. Here $f_\beta(b)$, $f_\beta(o)$, and $f_\beta(i)$ are in a three-way counterclockwise path mill between p and r. This is a contradiction.

Suppose it were the latter case:

$$f_\beta(s) = i^- ...$$

This forces the situation depicted in Figure C.45.

Here $f_\beta(b)$, $f_\beta(o)$, and $f_\beta(s)$ all have to continue with r^+ and to the left of $f_\beta(i)$, otherwise $f_\beta(i)$ will be forced to continue with r^- and immediately trace,

This is Figure C.46.

Here $f_\beta(i)$ must eventually end at r or p, possible after twisting between the two. But then $f_\beta(b)$, $f_\beta(o)$, and $f_\beta(s)$ will be stuck in a three-way clockwise path mill between which ever is left (r or p), and i.

This is a contradiction.

C.0.2.2.2 Snirt

Back to the end of Nesh C.0.2.2. Suppose $f_\beta(i)$ continues with o^*:

$$f_\beta(i) = r^+ p^+ \hat{o}^* ...$$

This is Figure C.47.

Here $f_\beta(i)$ can either continue with o° or o^+.

C.0.2.2.2.1 Tittup

Suppose $f_\beta(i)$ continued with o°:

$$f_\beta(i) = r^+ p^+ \hat{o}^\circ$$

This is Figure C.48.

Here if $f_\beta(s)$ were to begin with i^+, then we have

$$f_\beta(s) = i^+ o^- i^* ...$$

Here the third letter cannot be p as in that case it would be absorbed:

$$f_\beta(s) = i^+ o^- \hat{p}^- r^- \,\mathrm{Abso}(f_\beta(p), f_\beta(i))^\times$$

Thus we have Figure C.49.

Here $f_\beta(s)$ must continue with i^+ and to the left of both $f_\beta(r)$ and $f_\beta(b)$. Otherwise, $f_\beta(r)$ would be forced to continue with i^-, in which case it would trace:

$$f_\beta(r) = o^- \hat{i}^- o^+ p^- r^\times$$

Thus we must have

$$f_\beta(s) = i^+ o^- \hat{i}^+ ...$$

but now it either traces:

$$f_\beta(s) = i^+ o^- \hat{i}^+ s^\times$$

or is absorbed:

$$f_\beta(s) = i^+ o^- \hat{i}^+ o^+ b^+ \,\mathrm{Abso}(f_\beta(p), f_\beta(i))^\times$$

Therefore, in the situation depicted in Figure C.48, $f_\beta(o)$ must begin with p^- and to the right of $f_\beta(s)$:

$$f_\beta(o) = p^- r^* ...$$

This gives Figure C.50.

Here $f_\beta(o)$ can either end at r° or continue with r^-.

C.0.2.2.2.1.1 Epigone

Suppose $f_\beta(o)$ ends at r°:

$$f_\beta(o) = p^- r^\circ$$

This forces

$$f_\beta(s) = p^\circ$$

as otherwise $f_\beta(s)$ wither traces:

$$f_\beta(s) = p^- r^+ p^+ o^- i^+ s^\times$$

or it is absorbed:

$$f_\beta(s) = p^- r^+ p^+ o^- p^- r^- \text{ Abso}(f_\beta(p), f_\beta(i))^\times$$

Thus we must have Figure C.51.

Here $f_\beta(b)$ and $f_\beta(r)$ twist between s and i k times and end there, giving us Candidate Family 6.

C.0.2.2.2.1.2 Farrago

Back to the end of Tittup C.0.2.2.2.1. Suppose $f_\beta(o)$ were to continue with r^-:

$$f_\beta(o) = p^- r^- p^* ...$$

which forces:

$$f_\beta(s) = p^- r^* ...$$

This is Figure C.52.

Here $f_\beta(o)$ and $f_\beta(s)$ must end at r or p after possibly twisting among themselves m times. The two cannot escape p and r as either they would trace or be absorbed. On the other hand $f_\beta(b)$ and $f_\beta(r)$ also twist k times between s and i and end there. This gives us Candidate Family 7.

C.0.2.2.2.2 Ullage

Back to the end of Snirt. Suppose $f_\beta(i)$ continued with o^+:

$$f_\beta(i) = r^+p^+\hat{o}^+p^*...$$

This is Figure C.53.

Here $f_\beta(i)$ must continue with p^- and to the right of $f_\beta(o)$ and $f_\beta(s)$. Otherwise, $f_\beta(o)$ will be forced to begin with p^+, after which it will immediately trace.

Thus we must have

$$f_\beta(i) = r^+p^+o^+\hat{p}^-r^*...$$

This is Figure C.54.

Here $f_\beta(s)$ can either begin and end at i°, or begin with i^-, or i^+.

Suppose

$$f_\beta(s) = p^\circ$$

Then this forces

$$f_\beta(o) = p^-r^*...$$

This is the situation depicted in Figure C.55.

Here if $f_\beta(i)$ were to continue with r° or r^+, then $f_\beta(o)$ is forced to continue with r^+, but then it will trace:

$$f_\beta(o) = p^- \hat{r}^+ p^+ o^\times$$

Thus $f_\beta(i)$ must continue with r^- and to the right of $f_\beta(o)$. But then it will be absorbed:

$$f_\beta(i) = ...r^- p^+ \,\mathrm{Abso}(f_\beta(o), f_\beta(s))^\times$$

This is a contradiction.

So suppose instead

$$f_\beta(s) = p^+ ...$$

then it continues:

$$f_\beta(s) = p^+ o^- i^* ...$$

This is Figure C.56.

Here if $f_\beta(b)$ were to continue with i° or i^+ then $f_\beta(s)$ must continue with i^+, in which case it either immediately traces or is absorbed between $f_\beta(p)$ and $f_\beta(i)$. Hence, $f_\beta(b)$ and $f_\beta(r)$ must both continue with i^- and to the right of $f_\beta(s)$. But now r will trace:

$$f_\beta(r) = o^- \hat{i}^- o^+ p^- r^\times$$

This is a contradiction.

Thus it must be the case that

$$f_\beta(s) = p^- r^* ...$$

which forces

$$f_\beta(o) = p^- r^* ...$$

This is Figure C.57.

Here $f_\beta(i)$ must continue with r^- and to the right of $f_\beta(o)$ and $f_\beta(s)$. Otherwise, $f_\beta(o)$ will be forced to continue with r^+, in which case it will trace:

$$f_\beta(o) = p^- \hat{r}^+ p^+ o^\times$$

This gives Figure C.58.

Here $f_\beta(i)$, $f_\beta(o)$, and $f_\beta(s)$ are in a three-way clockwise path mill between p and r.

This is a contradiction.

C.0.2.2.3 Quire

Back to the end of Nesh C.0.2.2. Suppose $f_\beta(i)$ continued with s^*:

$$f_\beta(i) = r^+ p^+ s^* ...$$

This is Figure C.59.

Here $f_\beta(r)$ can begin with s^*, or o^*.

C.0.2.2.3.1 Yepsen

Suppose

$$f_\beta(r) = s^*...$$

Then in fact must be s^- and to the right of $f_\beta(b)$, otherwise $f_\beta(b)$ would be absorbed. After s^-, the next letter must be i. Indeed, otherwise it either traces:

$$f_\beta(r) = s^- p^- r^\times$$

or it would force $f_\beta(i)$ to be absorbed:

$$f_\beta(i) = r^+ p^+ o^+ b^+ \operatorname{Abso}(f_\beta(p), f_\beta(i))^\times$$

This gives Figure C.60.

This then forces

$$f_\beta(b) = s^- i^*...$$

This is Figure C.61.

Here $f_\beta(i)$ can either continue with s°, or s^+. Whereas s^- is not possible as that would mean it either immediately traces, or eventually absorbed:

$$f_\beta(i) = ...s^- p^- r^- \operatorname{Abso}(f_\beta(p), f_\beta(i))^\times$$

C.0.2.2.3.2 Gubbins

Suppose $f_\beta(i)$ ends at s°:

$$f_\beta(i) = r^+ p^+ s^\circ$$

This forces Figure C.62.

Here $f_\beta(b)$ cannot continue with i° or i^-, otherwise $f_\beta(r)$ will be forced to continue with i^-. In which case $f_\beta(r)$ will trace:

$$f_\beta(r) = s^- \hat{i}^- s^+ p^- r^\times$$

Thus we must have

$$f_\beta(b) = s^- \hat{i}^+ ...$$

but then it will trace:

$$f_\beta(b) = s^- \hat{i}^+ s^+ b^\times$$

shown in Figure C.63.

This is a contradiction.

C.0.2.2.3.3 Ignavia

Back to the end of YepsenC.0.2.2.3.1. Suppose $f_\beta(i)$ continues with s^+:

$$f_\beta(i) = r^+ p^+ \hat{s}^+ p^* ...$$

This is Figure C.64.

Here again $f_\beta(r)$ is forced to continue with i^- otherwise $f_\beta(b)$ will be absorbed.

This gives Figure C.65.

Here $f_\beta(r)$ must continue with p^- and to the right of $f_\beta(s)$. Otherwise, $f_\beta(s)$ will be forced to continue with p^+ and immediately trace. But then $f_\beta(r)$ traces:

$$f_\beta(r) = s^- i^- s^+ \hat{p}^- r^\times$$

This is a contradiction.

C.0.2.2.3.4 Zoilus

Back to the end of Quire C.0.2.2.3. Suppose

$$f_\beta(r) = o^* ...$$

This is Figure C.66.

Here $f_\beta(i)$ can continue with s° or s^+.

C.0.2.2.3.4.1 Jumbuck

Suppose $f_\beta(i)$ continued with s°:

$$f_\beta(i) = r^+ p^+ s^\circ$$

This is Figure C.67.

Here if $f_\beta(s)$ were to begin with p^+, then we would have Figure C.68. But here $f_\beta(r)$ must begin with o^- and to the right of $f_\beta(o)$ to prevent $f_\beta(o)$ from being absorbed. But then $f_\beta(r)$ will trace:

$$f_\beta(r) = o^- p^- r^\times$$

Hence, $f_\beta(s)$ must begin with p° or p^-, which means $f_\beta(o)$ must begin with p^-. This forces

$$f_\beta(r) = o^\circ$$

as otherwise $f_\beta(r)$ will trace. This in turn forces

$$f_\beta(b) = s^- i^* ....$$

This is Figure C.69.

Here $f_\beta(b)$ can either end at i° or continue with i^-.

Suppose it ended at i°:

$$f_\beta(b) = s^- i^\circ$$

Then we have the situation depicted in Figure C.70, where $f_\beta(s)$ and $f_\beta(o)$ twist k times between p and r and end there, giving Candidate Family 8.

Now suppose instead

$$f_\beta(b) = s^- i^- ...$$

then it continues:

$$f_\beta(b) = s^- i^- s^+ p^- r^* ...$$

This is Figure C.71.

Here $f_\beta(s)$, $f_\beta(b)$, and $f_\beta(o)$ are stuck in a three-way clockwise path mill between p and r.

This is a contradiction.

C.0.2.2.3.4.2 Nithing

Back to the end of Zoilus C.0.2.2.3.4. Suppose $f_\beta(i)$ were to continue with s^+. Then it continues:

$$f_\beta(i) = r^+ p^+ \hat{s}^+ p^- r^* ...$$

This is Figure C.72.

Here as before we must have $f_\beta(o)$ begin with p^-. Otherwise, $f_\beta(s)$ will begin with p^+, in which case it will then force $f_\beta(r)$ to begin with o^- and then trace.

Thus we have the situation depicted in Figure C.73.

Here $f_\beta(s)$ must end at either p or r, possibly after twisting m times between the two. It can never escape or it will trace. Once it ends, $f_\beta(i)$ must then end at either s or p/r, possibly after twisting k times. Once this is decided, $f_\beta(b)$ and $f_\beta(o)$ must immediately end without more twisting, as otherwise one of them will eventually escape to the outer perimeter and therefore be absorbed. An example of such a situation is shown in Figure C.74, where one can see $f_\beta(b)$ will eventually escape to the outer perimeter.

This gives Candidate Family 9.

This finishes the analysis under the assumptions of CMJ C.0.2.

C.0.3 WST

Suppose

$$f_\beta(i) = r^\circ$$

and

$$f_\beta(p) = b^- ...$$

This is Figure C.75.

here $f_\beta(p)$ can continue with o^* or s^*.

C.0.3.1 Whid

Suppose $f_\beta(p)$ continued with o^*. Then it is either o° or o^-.

C.0.3.1.1 Tilly

Suppose

$$f_\beta(p) = b^- o^\circ$$

This forces

$$f_\beta(b) = s^* ...$$

and

$$f_\beta(r) = s^- ...$$

This is Figure C.76.

Here the next letter for $f_\beta(r)$ is either i^* or p^*.

Suppose it were the former:

$$f_\beta(r) = s^- i^\cdot ..$$

Then both $f_\beta(s)$ and $f_\beta(o)$ must begin at p^*. Indeed, otherwise, $f_\beta(s)$ would be forced to begin with p^+, which it would trace; or $f_\beta(r)$ would continue with p^-, in which case it would trace.

This is Figure C.77.

Then $f_\beta(s)$ must in fact begin with p^+, otherwise $f_\beta(o)$ would be absorbed. But then $f_\beta(s)$ immediately traces.

So suppose instead $f_\beta(r)$ continued with p^*. This is Figure C.78.

Here if $f_\beta(r)$ were to continue with p° or p^+, then $f_\beta(s)$ will begin with p^+, in which case it will immediately trace. But this means $f_\beta(r)$ must continue with p^-, in which case it immediately traces.

This is a contradiction.

C.0.3.1.2 Whelm

Back to the end of Whid C.0.3.1. Suppose

$$f_\beta(p) = b^- o^- ...$$

This is Figure C.79.

Here $f_\beta(o)$ can either begin with i^* or p^*.

C.0.3.1.2.1 Bodger

Suppose

$$f_\beta(o) = i^* ...$$

This forces the situation depicted in Figure C.80.

Here $f_\beta(o)$ must end at s or i, possibly after some twisting between the two. Then $f_\beta(b)$ will end at o or s/i possibly after twisting. But now at least one of $f_\beta(p)$ or $f_\beta(r)$ will be forced to escape to the outer perimeter, thereby eventually absorbed. An example is shown in Figure C.81. Here $f_\beta(r)$ must continue with s^+, or $|fbp$ will be absorbed between $f_\beta(r)$

and $f_\beta(b)$. But now $f_\beta(r)$ will escape to the outer perimeter:

$$f_\beta(r) = o^- i^+ \hat{s}^+ i^- o^+ ...$$

or

$$f_\beta(r) = o^- i^+ \hat{s}^+ i^- s^- ...$$

C.0.3.1.2.2 Callid

Back to the end of Whelm C.0.3.1.2. Suppose

$$f_\beta(o) = p^* ...$$

Then it must in fact be

$$f_\beta(o) = p^\circ$$

Otherwise it would immediately trace or be absorbed.

Then this forces

$$f_\beta(s) = p^+ o^* ...$$

which forces

$$f_\beta(b) = o^- ...$$

This is Figure C.82.

Here if $f_\beta(s)$ were to end at o°, then $f_\beta(p)$, $f_\beta(r)$, and $f_\beta(b)$ will be stuck in a three-way counterclockwise path mill between i and s.

So suppose $f_\beta(s)$ here continued with o^-...

This is Figure C.83.

Here $f_\beta(p)$, $f_\beta(r)$, and $f_\beta(b)$ must contiue with i^- and to the right of $f_\beta(s)$. Otherwise, $f_\beta(s)$ will trace.

This is Figure C.84.

Here $f_\beta(s)$ must eventually end at i or o after possibly twisting between the two. But then $f_\beta(p)$, $f_\beta(b)$, and $f_\beta(r)$ will be stuck in a three-way path mill.

This is a contradiction.

C.0.3.2 Dido

Back to the end of WST C.0.3. Suppose $f_\beta(p)$ were to continue with s^*.

This is Figure C.85.

Here $f_\beta(r)$ and $f_\beta(p)$ must continue with s^- and to the right of $f_\beta(b)$. Otherwise, $f_\beta(b)$ will trace. Here $f_\beta(r)$ can either continue with p^* or i^*. If it were the former, then we have Figure C.86. Here if $f_\beta(r)$ were to continue with p° or p^+ then $f_\beta(s)$ will immediately trace; but then if $f_\beta(r)$ continued with p^- it will immediately trace. Thus $f_\beta(r)$ must continue with i^*. This is Figure C.87.

Here both $f_\beta(o)$ and $f_\beta(s)$ must begin with p^*, otherwise either $f_\beta(p)$ will be absorbed:

$$f_\beta(p) = b^- s^- \hat{i}^- r^- \,\mathrm{Abso}(f_\beta(p), f_\beta(i))^\times$$

or $f_\beta(s)$ will trace:

$$f_\beta(s) = i^+ s^\times$$

But now if $f_\beta(s)$ began with p° or p^-, then $f_\beta(o)$ will begin with p^- and be absrobed:

$$f_\beta(o) = p^\circ r^- \operatorname{Abso}(f_\beta(p), f_\beta(i))^\times$$

But then this means $f_\beta(s)$ begins with p^+, which mean it will immediately trace:

$$f_\beta(s) = p^+ s^\times$$

This is a contradiction.

This completes the analysis of the scanario under the assumptions of WST C.0.3.

C.0.4 PPG

Suppose

$$f_\beta(i) = r^+ ...$$

and

$$f_\beta(p) = b^- ...$$

This is Figure C.88.

Here $f_\beta(p)$ can continue with o^* or s^*.

C.0.4.1 Fash

Suppose $f_\beta(p)$ continued with o^*. It can either be o° or o^-.

On the other hand, $f_\beta(i)$ can either continue with p° or p^+.

Suppose

$$f_\beta(p) = b^- o^\circ$$

and

$$f_\beta(i) = r^+ p^\circ$$

This is Figure C.89.

Here $f_\beta(o)$ must begin with i^- and to the right of $f_\beta(s)$. Otherwise, $f_\beta(s)$ will be forced to begin with i^+ in which case it immediately traces.

Now we have Figure C.90.

Now if $f_\beta(r)$ began with s° or s^+, $f_\beta(b)$ will begin with s^+ and immediately trace. But then if $f_\beta(r)$ began with s^-, then it also traces;

$$f_\beta(r) = s^- i^- r^\times$$

So suppose instead

$$f_\beta(p) = b^- o^- ...$$

and

$$f_\beta(i) = r^+ p^\circ$$

This is Figure C.91.

Here if $f_\beta(p)$ were to continue with i^*, then we will have the situation depicted in Figure C.92.

Here $f_\beta(s)$ must begin with i° or i^-, or it will immediately trace. But this will force $f_\beta(r)$

to continue with i^- and immediately trace.

So suppose instead $f_\beta(p)$ were to continue with b^*. This gives Figure C.93.

Here again $f_\beta(s)$ must begin with i° or i^-, but again $f_\beta(r)$ will trace.

So suppose instead

$$f_\beta(p) = b^- o^- ...$$

and

$$f_\beta(i) = r^+ p^+ ...$$

This is Figure C.94.

Here $f_\beta(i)$ can continue with o^* or s^*.

C.0.4.1.1 Xeric

Suppose $f_\beta(i)$ continued with o^*:

$$f_\beta(i) = r^+ p^+ o^* ...$$

This forces the situation depicted in Figure C.95.

Here $f_\beta(r)$ can continue into 1. or 2.

Suppose it continued into 1. Then we have Figure C.96.

Here if $f_\beta(r)$ were to continue with p° or p^+, then $f_\beta(o)$ will be forced to begin with p^+ and it will immediately trace. So then $f_\beta(r)$ must continue with p^- but then it immediately traces. Thus $f_\beta(r)$ cannot go into 1.

Suppose it continued into 2. Then it forces

$$f_\beta(b) = o^- ...$$

This is the situation depicted in Figure C.97.

Here $f_\beta(i)$ can either continue with o° or o^+.

C.0.4.1.1.1 Fizgig

Suppose $f_\beta(i)$ were to continue with o°:

$$f_\beta(i) = r^+ p^+ o^\circ$$

This gives Figure C.98.

Here $f_\beta(o)$ can either continue with r° or r^-.

C.0.4.1.1.1.1 Quiddit

Suppose $f_\beta(o)$ continue with r°:

$$f_\beta(o) = p^- r^\circ$$

This forces

$$f_\beta(s) = p^\circ$$

This is Figure C.99.

But here $f_\beta(b)$ must eventually end at s or i after possibly twisting between the two. But then at least one of $f_\beta(p)$ and $f_\beta(r)$ will then escape to the outer perimeter and thus eventually

absorbed.

This is a contradiction.

C.0.4.1.1.1.2 Rudesby

Back to the end of C.0.4.1.1.1. Suppose $f_\beta(o)$ continued with r^-.

This is Figure C.100.

Here $f_\beta(s)$ and $f_\beta(o)$ twist between p and r and eventually end there, since if either were to escape they would trace. Then as before, $f_\beta(b)$ must eventually end at s or i after possibly twisting between the two. But then at least one of $f_\beta(p)$ and $f_\beta(r)$ will then escape to the outer perimeter and thus eventually absorbed.

This is a contradiction.

C.0.4.1.1.2 Bawbee

Back to the end of Xeric C.0.4.1.1. Suppose $f_\beta(i)$ continued with o^+.

This forces Figure C.101.

Here $f_\beta(o)$, $f_\beta(i)$, and $f_\beta(i)$ are stuck in a three-way clockwise path mill between p and r.

This is a contradiction.

C.0.4.1.2 Bavin

Back to the end of Fash C.0.4.1. Suppose $f_\beta(i)$ continued with s^*. Then we must have

$$f_\beta(p) = b^- o^\circ$$

otherwise if the second letter of $f_\beta(p)$ were o^- then it would immediately trace.

This is Figure C.102.

Then in order for $f_\beta(b)$ to not trace, we must have the situation depicted in Figure C.103, then continue with Figure C.104. Here $f_\beta(i)$, $f_\beta(r)$, and $f_\beta(b)$ are stuck in a three-way clockwise path mill between s and i.

This is a contradiction.

C.0.4.2 Gley

Back to the end of PPG C.0.4. Suppose $f_\beta(p)$ continued with s^*. It cannot be s° as that would force $f_\beta(b)$ to begin with s^+ and immediately trace. So we must have

$$f_\beta(p) = b^- s^- i^* ...$$

This is Figure C.105.

Here in order to prevent $f_\beta(b)$ from tracing, $f_\beta(r)$ must begin with s^- to give us Figure C.106.

Here $f_\beta(r)$ can either continue with p^* or i^*. Suppose it were the former.

This is Figure C.107.

But here if $f_\beta(r)$ continued with p° or p^+ then $f_\beta(s)$ will immediately trace; whereas if $f_\beta(r)$ were to continue with p^- then it immediately traces. This is a contradiction.

So suppose $f_\beta(r)$ continued with i^*. This is Figure C.108. Here $f_\beta(s)$ can either begin with i^* or p^*. Suppose it were the former. Then this is Figure C.109.

Here if $f_\beta(r)$ were to continue with i° or i^+, then $f_\beta(s)$ will immediately trace; whereas if $f_\beta(r)$ were to continue with i^- then it also immediately traces. This is a contradiction.

Thus suppose $f_\beta(s)$ began with p^*. Then $f_\beta(o)$ can begin with either i^* or p^*. Suppose it were the former. This is Figure C.110.

Here if $f_\beta(p)$ continued into 1. or 2. then either $f_\beta(r)$ or $f_\beta(o)$ will be absorbed between $f_\beta(p)$ and $f_\beta(i)$. If $f_\beta(p)$ continued into 3 then it immediately is absorbed.

Thus it must be the case that $f_\beta(o)$ begins with p. This is Figure C.111.

Here $f_\beta(b)$, $f_\beta(p)$, and $f_\beta(r)$ are stuck in a three-way clockwise path mill between s and i.

This is a contradiction.

This concludes the case analysis for the assumptions under PPG C.0.4.

C.0.5 WVL

Suppose

$$f_\beta(p) = b^*...$$

and

$$f_\beta(i) = b^*...$$

This is Figure C.112.

Here $f_\beta(i)$ can end at b° immediately, or continue with b^-. Whereas b^+ is impossible a that would force $f_\beta(p)$ to continue with b^+ as well, and at least one of these will then immediately trace.

C.0.5.1 Birl

Suppose

$$f_\beta(i) = b^\circ$$

Then we have the situation depicted in Figure C.113.

Here $f_\beta(b)$ can either begin with o^* or s^*. Suppose it were the former. Then $f_\beta(r)$ must begin with o^- so as to not cause $f_\beta(b)$ to trace:

$$f_\beta(r) = o^- i^* ...$$

Here it must continue with i^-. Otherwise, either $f_\beta(o)$ or $f_\beta(s)$ will immediately trace.

This is Figure C.114.

Here we see that if $f_\beta(r)$ continued with r then it trace, but if it continued with b^- then it will circle back to the same position, so it cannot indefinitely continue with b^-. This is a contradiction.

Thus it must be the case that

$$f_\beta(b) = s^* ...$$

This forces $f_\beta(o)$ to begin with i^-. Otherwise, $f_\beta(s)$ will immediately trace.

This is Figure C.115.

Here $f_\beta(s)$ must begin with i^-, which means $f_\beta(o)$ must continue with r^* or at least one of $f_\beta(s)$ or $f_\beta(o)$ will trace.

This is Figure C.116.

Here $f_\beta(r)$ can begin with o^* or s^-.

C.0.5.1.1 Eisel

Suppose

$$f_\beta(r) = o^* ...$$

Now $f_\beta(s)$ can either continue with b^* or o^*. Suppose it were the former. Then we have Figure C.117.

Here $f_\beta(r)$ must begin with o^+ and to the left of $f_\beta(s)$ or else $f_\beta(s)$ is immediately absorbed. But then $f_\beta(r)$ itself will be absorbed:

$$f_\beta(r) = o^+ b^+ i^+ \,\mathrm{Abso}(f_\beta(o), f_\beta(s))^\times$$

This is a contradiction. Thus $f_\beta(s)$ must continue with r^*.

This is Figure C.118.

Here $f_\beta(o)$ can continue with r° or r^+, in which case $f_\beta(s)$ continues with r^+; or $f_\beta(o)$ can continue with r^-.

C.0.5.1.1.1 Chouse

Suppose $f_\beta(o)$ continued with r° or r^+, thus $f_\beta(s)$ continues with r^+.

Then $f_\beta(s)$ continues with $p^*...$ in order to not trace.

This is Figure C.119.

Here $f_\beta(b)$ can begin with s^- or s°. If it were the former, then we have

$$f_\beta(b) = s^- i^- r^* ...$$

which forces $f_\beta(o)$ to continue with r^+:

$$f_\beta(o) = i^- \hat{r}^+ p^* ...$$

and thus

$$f_\beta(s) = i^- r^+ \hat{p}^+ ...$$

This is Figure C.120.

Here $f_\beta(b)$, $f_\beta(s)$, and $f_\beta(o)$ are stuck in a three-way counterclockwise path mill between p and r. This is a contradiction.

Thus we must have

$$f_\beta(b) = s^\circ$$

This gives us Figure C.121. Here $f_\beta(s)$ and $f_\beta(o)$ twist k times between p and r k times to give us Candidate Family 10.

C.0.5.1.1.2 Fardel

Back to the end of Eisel C.0.5.1.1. Suppose $f_\beta(o)$ continued with r^-.

This is Figure C.122.

Here $f_\beta(p)$ must continue with i^-. Otherwise, $f_\beta(o)$ will be forced to continue with i^+, in which case it will be absorbed between $f_\beta(i)$ and $f_\beta(p)$. Thus we have

$$f_\beta(p) = b^+ \hat{i}^- r^* ...$$

This is Figure C.123.

Here $f_\beta(b)$ can either begin with s^-, or begin and end with s°. Suppose it were the former case. Then it continues:

$$f_\beta(b) = s^- i^- r^- i^* ...$$

This is Figure C.124.

Here $f_\beta(s)$ must continue with r^- and to the right of $f_\beta(p)$. Otherwise $f_\beta(p)$ will be forced to continue with r^+ and then be absorbed between $f_\beta(o)$ and $f_\beta(s)$.

This leads to the situation depicted in Figure C.125. Here $f_\beta(p)$ must twist between r and i and eventually end at either one; or it could end at s after escaping. However, regardless which scenario, the remaining three strands, $f_\beta(b)$, $f_\beta(o)$ and $f_\beta(s)$ will be stuck in a three-way path mill. This is a contradiction.

Thus we must have

$$f_\beta(b) = s^\circ$$

This is Figure C.126.

Here $f_\beta(p)$ must continue with i^- in order to prevent $f_\beta(o)$ from being absorbed.

This is Figure C.127.

Here $f_\beta(p)$ twist m times between $f_\beta(i)$ and $f_\beta(r)$ before ending at one of these as it cannot escape. Then the remaining $f_\beta(o)$ and $f_\beta(s)$ twist between p and i or r k times and end there.

This gives Candidate Family 11.

C.0.5.1.2 Glaur

Back to the end of Birl C.0.5.1. Suppose

$$f_\beta(r) = s^-...$$

But here $f_\beta(r)$ immediately traces.

This is a contradiction.

C.0.5.2 Darg

Back to the end of WVL C.0.5. Suppose $f_\beta(i)$ began with b^-.

This is Figure C.128.

Here $f_\beta(p)$ can end immediately at b°, or continue with b^-.

C.0.5.2.1 Halse

Suppose

$$f_\beta(p) = b^\circ$$

This is Figure C.129.

Here $f_\beta(i)$ can continue with o^* or s^*.

C.0.5.2.1.1 Kittle

Suppose $f_\beta(i)$ were to continue with o^*. This is Figure C.130.

Here it can be o°, o^-, or o^+.

####### C.0.5.2.1.1.1 Tantivy

Suppose $f_\beta(i)$ continued with o°:

$$f_\beta(i) = b^- o^\circ$$

This is Figure C.131.

Here $f_\beta(s)$ can either begin with i^* or p^*.

Suppose $f_\beta(s)$ began with i^*. Then $f_\beta(o)$ also begins with i^*, and in fact

$$f_\beta(o) = i^- r^* ...$$

This is Figure C.132.

Now consider $f_\beta(r)$. If it were to begin with s^*, then it must be s^- or $f_\beta(b)$ will trace. But then the next letter will need to be s^- and to the right of $f_\beta(s)$. Otherwise, $f_\beta(s)$ will immediately trace. But then $f_\beta(r)$ will trace:

$$f_\beta(r) = s^- i^- r^\times$$

Thus we must have

$$f_\beta(r) = o^+ b^+ i^* ...$$

which forces

$$f_\beta(s) = i^- r^* ...$$

This is Figure C.133.

Here we claim that $f_\beta(r)$ must end here at i°. Otherwise it will either trace:

$$f_\beta(r) = o^+ b^+ \hat{i}^- r^\times$$

or will be absorbed:

$$f_\beta(r) = o^+ b^+ \hat{i}^+ b^- o^+ b^+ \,\mathrm{Abso}(f_\beta(p), f_\beta(i))^\times$$

Thus we must have

$$f_\beta(r) = o^+ b^+ \hat{i}^\circ$$

This is Figure C.134.

Here $f_\beta(b)$ can either end immediately at s° or begin with s^-.

Suppose it were the latter, then we have

$$f_\beta(b) = s^- i^- r^* ...$$

This is Figure C.135.

Here $f_\beta(o)$ and $f_\beta(s)$ continue with r^+ and to the left of $f_\beta(b)$, otherwise $f_\beta(b)$ will eventually trace.

This is Figure C.136.

But here $f_\beta(o)$, $f_\beta(s)$, and $f_\beta(b)$ are stuck in a three-way couterclockwise path mill between p and r.

Thus it must be the former case, that

$$f_\beta(b) = s^\circ$$

This is Figure C.137.

Here $f_\beta(s)$ and $f_\beta(o)$ twist between p and r k times and eventually end there. This gives us Candidate Family 12.

Now back to the situation depicted in Figure C.131. Suppose instead $f_\beta(s)$ began with p^*.

Then $f_\beta(o)$ can either begin with i^* or also begin with p^*. Suppose it were the former case:

$$f_\beta(o) = i^*...$$

Then we have Figure C.138.

Here we claim that $f_\beta(r)$ cannot begin with s. Indeed, if it did then it would have to be s^-, in which case the next letter must be i^*. If it were i° or i^+, then $f_\beta(o)$ will trace; if it were i^- then $f_\beta(r)$ itself is immediately absorbed. Thus we must have

$$f_\beta(r) = o^+b^+p^*...$$

which forces

$$f_\beta(s) = p^-r^*...$$

This is Figure C.139.

Here $f_\beta(r)$ must end. Otherwise, it either trace:

$$f_\beta(r) = ...p^-r^\times$$

or is absorbed:

$$f_\beta(r) = ...p^+b^-o^-b^+ \,\mathrm{Abso}(f_\beta(p), f_\beta(i))^\times$$

On the other hand, $f_\beta(b)$ and $f_\beta(o)$ both must also end, as there is no possible way for them to twist without at least one of them being immediately absorbed. Then $f_\beta(s)$ must also end.

This gives Figure C.140, which is Candidate 13.

Now suppose it were the case that $f_\beta(o)$ began with p^*. This is Figure C.141.

Here we claim that $f_\beta(r)$ cannot begin with o^+. Indeed, if it did, then it must be

$$f_\beta(r) = o^+ b^+ p^* ...$$

which forces

$$f_\beta(s) = p^- r^* ...$$

This is Figure C.142. But here $f_\beta(r)$ must end, otherwise it would either immediately trace if continuing with p^-, or eventually absorbed if continuing with p^+. But then $f_\beta(s)$ must continue with r^+ and to the left of $f_\beta(o)$. Otherwise $f_\beta(o)$ will be absorbed. Now $f_\beta(s)$ will trace:

$$f_\beta(s) = p^- \hat{r}^+ p^+ s^\times$$

Thus we must have

$$f_\beta(r) = s^- ...$$

and the next letter must be i^*.

This is Figure C.143.

Here suppose further that $f_\beta(o)$ continued with r^+:

$$f_\beta(o) = p^- \hat{r}^+ p^+ s^* ...$$

which forces

$$f_\beta(b) = s^- ...$$

if the next letter were r^-, then we have Figure C.144, where $f_\beta(s)$ must begin with p^-:

$$f_\beta(s) = p^- r^+ p^+ s^\times$$

So this cannot occur. Suppose instead the next letter for $f_\beta(b)$ were i^*. Then we have Figure C.145, where $f_\beta(o)$, $f_\beta(r)$, and $f_\beta(b)$ are stuck in a three-way clockwise path mill between s and i.

Back to the situation depicted in Figure C.143. Suppose $f_\beta(o)$ were to end there:

$$f_\beta(o) = p^- r^\circ$$

This forces $f_\beta(s)$ to end immediately otherwise it will eventually trace. This gives Figure C.146. Here $f_\beta(b)$ and $f_\beta(r)$ twist between s and i k times and eventually end there, giving a candidate that will be subsumed in Candidate Family 15 to follow.

Back to the situation depicted in Figure C.143. Suppose $f_\beta(o)$ continued with r^-:

$$f_\beta(o) = p^- r^- p^* ...$$

This forces

$$f_\beta(s) = p^- r^* ...$$

This is Figure C.147.

Here $f_\beta(o)$ and $f_\beta(s)$ twist k times between p and r times and end there; while $f_\beta(r)$ twist m times between s and i k times and end there. This gives Candidate Family 14.

C.0.5.2.1.1.2 Wherret

Back to the end of Kittle C.0.5.2.1.1. Suppose $f_\beta(i)$ were to continue with o^-. Then $f_\beta(o)$ and $f_\beta(s)$ must begin with p^*, and $f_\beta(r)$ must begin with

$$f_\beta(r) = o^- p^* ...$$

This is Figure C.148.

Here $f_\beta(r)$ and $f_\beta(i)$ must continue with p^- and to the right of $f_\beta(o)$ and $f_\beta(s)$. Otherwise, $f_\beta(s)$ would begin with p^+ in which case it would immediately trace. Thus we have

$$f_\beta(r) = s^- \hat{p}^- b^- o^- i^* ...$$

and

$$f_\beta(i) = b^- o^- \hat{p}^- r^* ...$$

This is Figure C.149.

Here $f_\beta(s)$ must begin with p^+, otherwise $f_\beta(o)$ would trace. Thus we have

$$f_\beta(s) = p^+ o^* ...$$

which forces

$$f_\beta(b) = o^- p^- b^\times$$

This is a contradiction.

C.0.5.2.1.1.3 Xiphias

Back to the end of Kittle C.0.5.2.1.1. Suppose $f_\beta(i)$ were to continue with o^+.

This is Figure C.150.

Here $f_\beta(r)$ can begin with o^+ or s^*.

Suppose it were the former:

$$f_\beta(r) = o^+ b^+ p^* ...$$

Here $f_\beta(s)$ can either begin with i^+ or p^*. Suppose it were the former, then it forces $f_\beta(b)$ to begin with o^+, and then immediately trace. As shown in Figure C.151. Thus $f_\beta(s)$ must begin with p^*. Now $f_\beta(o)$ can begin with i^* or p^*. Suppose it were the former. Then it must in fact be

$$f_\beta(o) = i^\circ$$

Otherwise it would cause $f_\beta(b)$ to be absorbed. This is Figure C.152.

Here $f_\beta(s)$ continues to give us Figure C.153.

Here $f_\beta(r)$ cannot continue with p°. This would imply that $f_\beta(i)$ continus with $p^- o^* ...$, and then forcing $f_\beta(s)$ to continue with $o^- ...$, as shown in Figure C.154. Here $f_\beta(s)$ will eventually be absorbed in between $f_\beta(p)$ and $f_\beta(i)$. On the other hand, it is clear that $f_\beta(r)$ cannot continue with p^- as that would mean it either immediately trace, or escape to the outer perimeter and absorbed between itself and $f_\beta(b)$. So it must continue with p^+, as shown in Figure C.155.

Here we claim that $f_\beta(s)$ must end at o°. Indeed, suppose it did not; then it continues with o^-, to give us the situation depicted in Figure C.156. But now $f_\beta(r)$, $f_\beta(s)$, and $f_\beta(i)$ are

stuck in a three-way counterclockwise path mill between o and p. Thus we must have

$$f_\beta(s) = p^- o^\circ$$

to give us Figure C.157.

Here $f_\beta(r)$ and $f_\beta(i)$ can twist between p and o (traversing counterclockwise) k times and must end at either of those locations. This gives us Candidate Family 15.

Suppose now that $f_\beta(o)$ began with p^*.

This is Figure C.158.

Here $f_\beta(o)$ must continue with p^- and to the right of $f_\beta(r)$. Otherwise, $f_\beta(s)$ will be forced to begin with i^+ and immediately trace. This then also forces $f_\beta(s)$ to begin with p^-. Otherwise, $f_\beta(i)$ and $f_\beta(r)$ will be absorbed between $f_\beta(o)$ and $f_\beta(s)$.

This is Figure C.159.

Here $f_\beta(o)$ must continue with r^- and to the right of $f_\beta(s)$. Otherwise, $f_\beta(s)$ will be forced to continue with r^+ and trace:

$$f_\beta(s) = p^- \hat{r}^+ p^+ s^\times$$

Thus we have Figure C.160.

Here if $f_\beta(r)$ continued with p° or p^+ then $f_\beta(o)$ will trace:

$$f_\beta(o) = ...p^+ b^- o^\times$$

But if $f_\beta(r)$ continued with p^- it immediately traces.

This is a contradiction.

Back to the situation depicted in Figure C.150. Suppose $f_\beta(r)$ began with s^*.

This is Figure C.161.

Here $f_\beta(o)$ can begin with i or p. Suppose it were the former, then it must be s^- otherwise $f_\beta(s)$ will immediately trace. But now $f_\beta(o)$ traces:

$$f_\beta(o) = i^- b^- o^\times$$

Thus we must have

$$f_\beta(o) = p^- r^* ...$$

This gives Figure C.162.

But here $f_\beta(i)$, $f_\beta(o)$, and $f_\beta(s)$ are stuck in a three-way clockwise path mill between p and r. This is a contradiction.

C.0.5.2.1.2 Nidder

Back to the end of Halse C.0.5.2.1. Suppose $f_\beta(i)$ continued with s^*:

$$f_\beta(i) = b^- s^* ...$$

This is Figure C.163.

Here $f_\beta(r)$ and $f_\beta(i)$ must continue with s^- and to the right of $f_\beta(b)$. Otherwise, $f_\beta(b)$ would begin with s^+ and immediately trace.

This is Figure C.164.

Here $f_\beta(o)$ and $f_\beta(r)$ must continue with p^- and to the right of $f_\beta(s)$. Otherwise, $f_\beta(s)$

would begin with p^+ and then immediately trace.

This gives us Figure C.165.

Here notice that $f_\beta(r)$ circles the outer perimeter clockwise some number of times, and eventually it must go up to i^*, as the only other choice is r, but then it would trace.

Figure C.166 shows an example. While $f_\beta(r)$ circles, $f_\beta(i)$ will follow. Once $f_\beta(r)$ goes up to i^*, then $f_\beta(i)$ must then go to r, otherwise it would follow r to i^* and trace.

Now $f_\beta(o)$ cannot also go up to i^*, since in that case, either $f_\beta(r)$ continued with i° or i^+, forcing $f_\beta(o)$ to continue with i^+, then it will be eventually absorbed; but then if $f_\beta(r)$ went i^-, then $f_\beta(r)$ will eventually be absorbed as well. This can be seen in Figure C.166.

Thus we must be in the situation depicted in Figure C.167. But here if $f_\beta(o)$ continued with r° or r^+, forcing $f_\beta(i)$ to continue with r^+, then $f_\beta(i)$ will be absorbed:

$$f_\beta(i) = ...r^+p^+s^+b^+p^+s^+b^+p^+s^+ \operatorname{Abso}(f_\beta(r), f_\beta(b))^\times$$

On the other hand, if $f_\beta(o)$ continued with o^-, then it would also be absorbed:

$$f_\beta(o) = ...r^-p^+s^+b^+p^+s^+b^+ \operatorname{Abso}(f_\beta(p), f_\beta(i))^\times$$

This is a contradiction.

C.0.5.3 Busk

Back to the end of WVL C.0.5. Suppose $f_\beta(i)$ and $f_\beta(p)$ both began with b^-

$$f_\beta(i) = b^-...$$

and

$$f_\beta(p) = b^- ...$$

This is Figure C.168.

Suppose $f_\beta(i)$ continued with $s*$. Then $f_\beta(i)$ will trace, as depicted in Figure C.169.

So $f_\beta(i)$ must continue with o^*. On the other hand $f_\beta(p)$ can continue with o^* as well or continue with s^* in stead. Suppose it were the former.

This is Figure C.170.

Here $f_\beta(b)$ can begin with o^* or s^*. Suppose it were the former case. But now $f_\beta(i)$ traces, as shown in Figure C.171.

So $f_\beta(b)$ must begin with s^*, and $f_\beta(r)$ can also begin with s^* or begin with o^*.

C.0.5.3.1 Kieve

Suppose $f_\beta(r)$ began with s^*. Then it must be s^-, otherwise $f_\beta(b)$ would trace. The second letter can be p^* or i^*. Suppose it were the former. Then this forces

$$f_\beta(s) = p^* ...$$

and

$$f_\beta(o) = p^- r^* ...$$

This is Figure C.172.

But now $f_\beta(r)$ trace.

So it must be

$$f_\beta(r) = s^- i^* ...$$

Now $f_\beta(s)$ can begin with i^* or p^*. Suppose it were the former. Then this forces

$$f_\beta(o) = i^- ...$$

and the next letter cannot be r or it would force $f_\beta(r)$ to trace. Thus we must have the situation depicted in Figure C.173.

But now $f_\beta(o)$ will trace:

$$f_\beta(o) = s^- b^- o^\times$$

Thus $f_\beta(s)$ must begin with p^*. Then $f_\beta(o)$ can either begin with i^+, or also begin with p^*. Suppose it were the former. Then it must do so to the left of the incoming $f_\beta(r)$, otherwise $f_\beta(r)$ would be immediately absorbed. This forces the situation depicted in Figure C.174. Here $f_\beta(o)$, $f_\beta(i)$, and $f_\beta(p)$ are stuck in a three-way path mill between b and o. This is a contradiction.

Thus we must have

$$f_\beta(o) = p^- r^* ...$$

This gives Figure C.175.

Here three are three twisting pairs: $f_\beta(i)$ and $f_\beta(p)$ twist k times between b and o; $f_\beta(b)$ and $f_\beta(r)$ twist m times between s and i; and $f_\beta(s)$ and $f_\beta(o)$ twist j times between p and r. Each of the image paths of these pairs cannot escape and enter into another pair, as that would immediately create a three-way path mill. This gives us Candidate Family 16.

C.0.5.3.2 Oorie

Back to the end of Busk C.0.5.3. Suppose and $f_\beta(r)$ began with o^*. Then it must be

$$f_\beta(r) = b^+...$$

otherwise $f_\beta(i)$ and $f_\beta(p)$ will immediately trace. This is Figure C.176.

The next letter cannot be i, as this would force the situation depicted in Figure C.177, where $f_\beta(o)$ must begin with i° or i^+ or it will eventually trace; but then this forces $f_\beta(s)$ to begin with i^+ and immediately trace.

Thus we must have

$$f_\beta(r) = o^+b^+p^*...$$

Now again $f_\beta(s)$ cannot begin with i^* for the reason as before, thus it must begin with p^*, and continue:

$$f_\beta(s) = p^-r^*...$$

Now $f_\beta(o)$ can begin with i^* or p^* as well. Suppose it were the former.

This is Figure C.178.

Then it must be the case that

$$f_\beta(b) = s^\circ$$

and

$$f_\beta(o) = i^\circ$$

Indeed, otherwise, one of $f_\beta(b)$ and $f_\beta(o)$ would force the other to be immediately absorbed.

This is Figure C.179.

Now we claim that $f_\beta(s)$ must end here at r°. Suppose that were not the case, then it must continue with r^-, then it continues:

$$f_\beta(s) = ...r^- i^+ b^- o^* ...$$

This is Figure C.180.

Here $f_\beta(p)$ will twist between o and b and eventually end there, as escaping would force it to trace. But once it ends, the remaining $f_\beta(s)$, $f_\beta(i)$, and $f_\beta(r)$ will be stuck in a three-way path mill.

For example, Figure C.181 shows a scenario where it is clear that they are stuck in a counterclockwise path mill. The other situations will be the same except with more twisting of $f_\beta(p)$ before it ends.

Thus we must have

$$f_\beta(s) = p^- r^\circ$$

This is Figure C.182.

Here again $f_\beta(p)$ twist between b and o some number of times, say k times. Then $f_\beta(i)$ and $f_\beta(r)$ twist m times between p and o or b, k times and end there.

This is Candidate Family 17.

Figure C.183 shows an example.

Now suppose $f_\beta(o)$ began with p^*. Then it must be p^- as to not make $f_\beta(s)$ trace.

This forces the situation depicted in Figure C.184.

Here $f_\beta(r)$ must continue with p° or p^+, or it will immediately trace. But then this forces $f_\beta(o)$ to continue with p^+, and it will trace:

$$f_\beta(o) = p^- r^- \hat{p}^+ b^- o^\times$$

This is a contradiction.

C.0.5.3.3 Quank

Back to the middle part of Busk C.0.5.3. Suppose

$$f_\beta(i) = b^- o^* ...$$

and

$$f_\beta(p) = b^- s^* ...$$

This is Figure C.185.

Here $f_\beta(s)$ can begin with i^* or p^*. Suppose it were the former. Then this forces

$$f_\beta(o) = i^- r^* ...$$

which then forces

$$f_\beta(p) = b^- s^- i^- r^* ...$$

This is Figure C.186.

But now $f_\beta(r)$ will trace.

Thus we must have

$$f_\beta(s) = p^* ...$$

and $f_\beta(o)$ can either begin with i^* or p^*. Suppose it were the former. Then it continues and is absorbed:

$$f_\beta(o) = i^+ s^+ b^+ \operatorname{Abso}(f_\beta(p), f_\beta(i))^\times$$

Thus we must have

$$f_\beta(o) = p^- r^* ...$$

This is Figure C.187.

Here $f_\beta(r)$ must continue with $i^*...$, but then this forces $f_\beta(p)$ to continue with i^- and to the right of the incoming $f_\beta(i)$. But now $f_\beta(b)$, $f_\beta(r)$, and $f_\beta(p)$ are stuck in a three-way clockwise path mill between s and i, shown in Figure C.187.

This finishes the case analysis for the Candelabra.

C.1 Figures

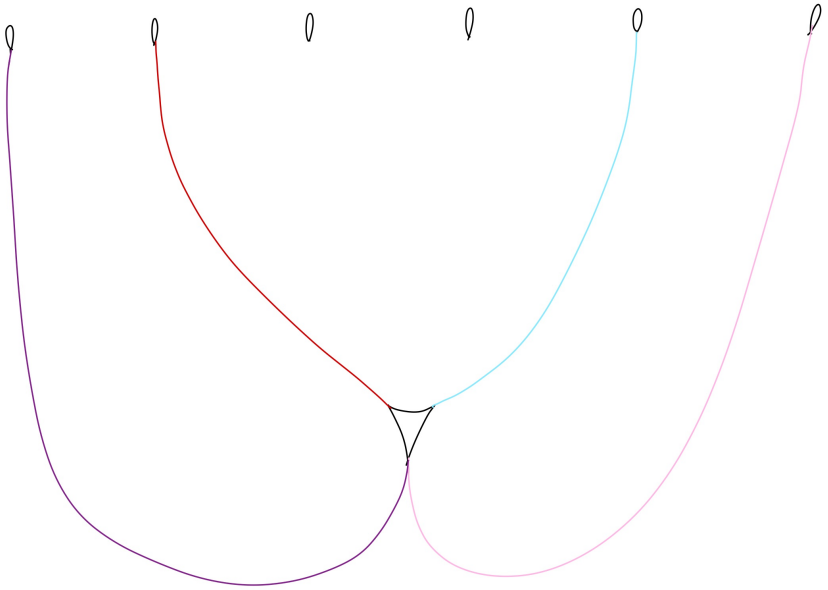


Figure C.4: NHT1

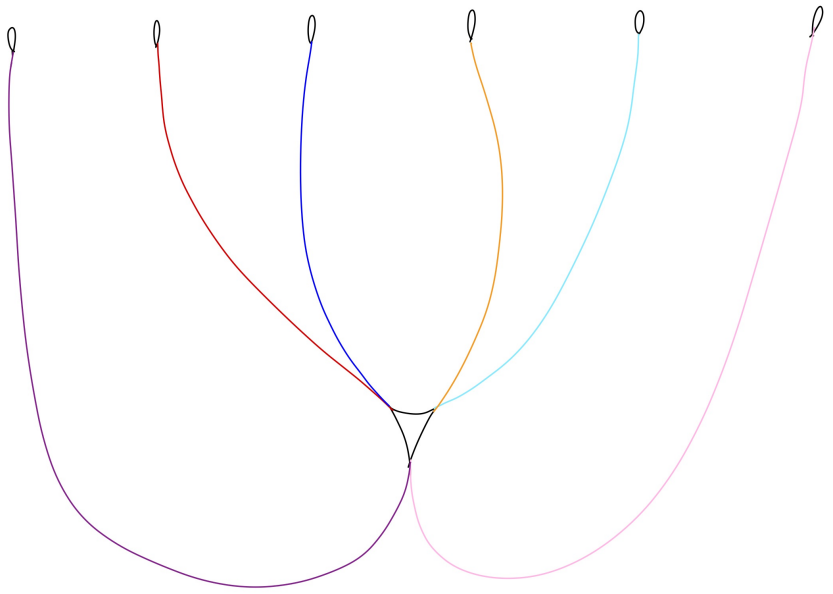


Figure C.5: NHT2

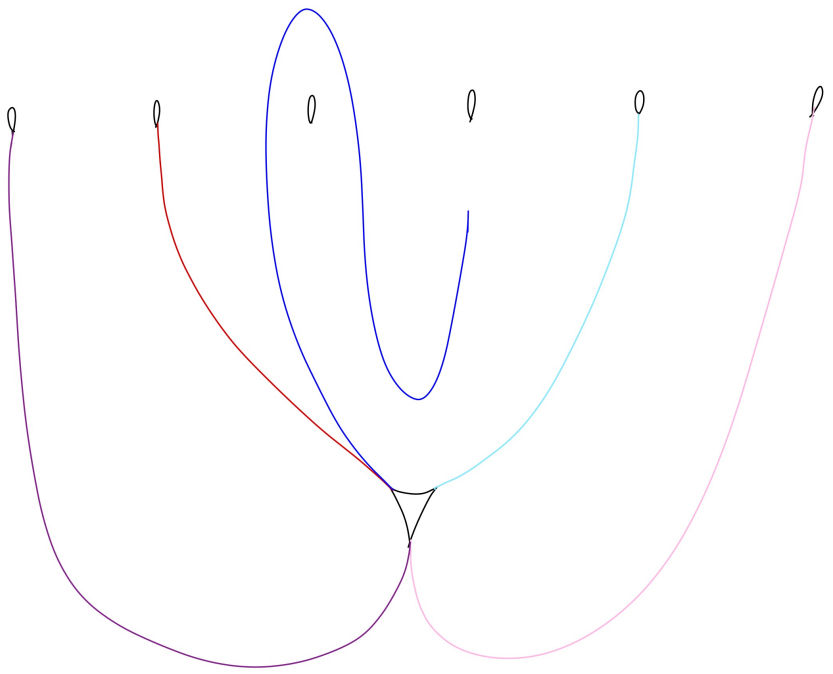


Figure C.6: NHT3

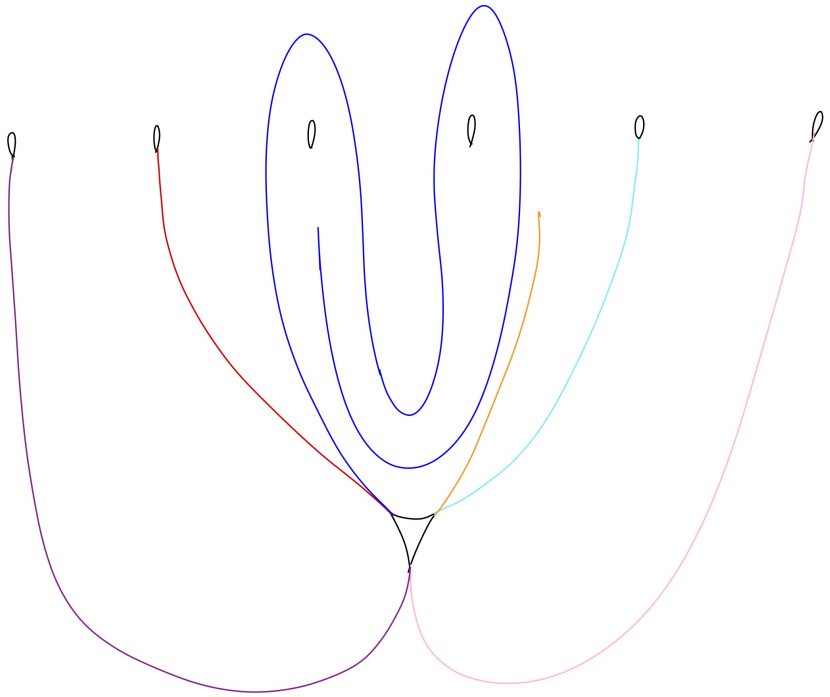


Figure C.7: NHT4

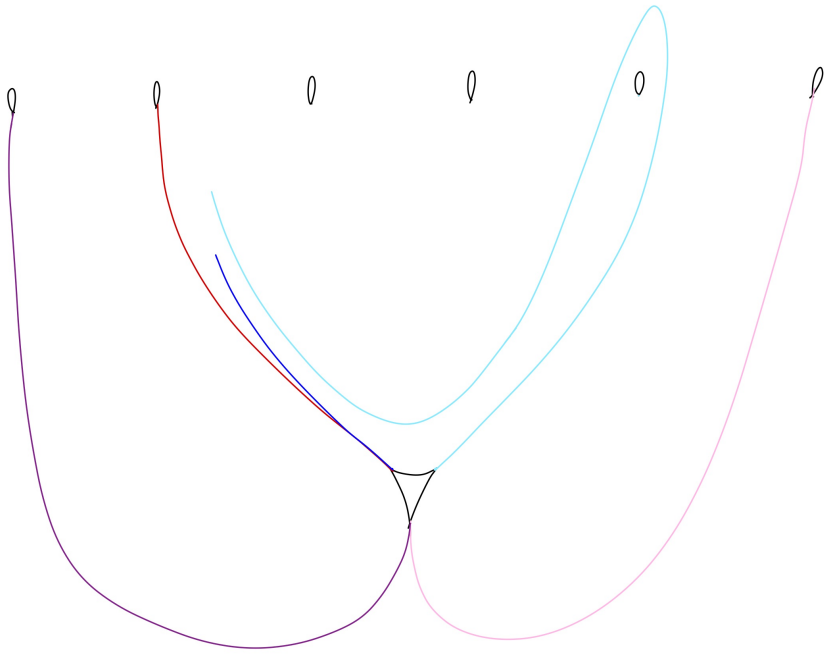


Figure C.8: NHT5

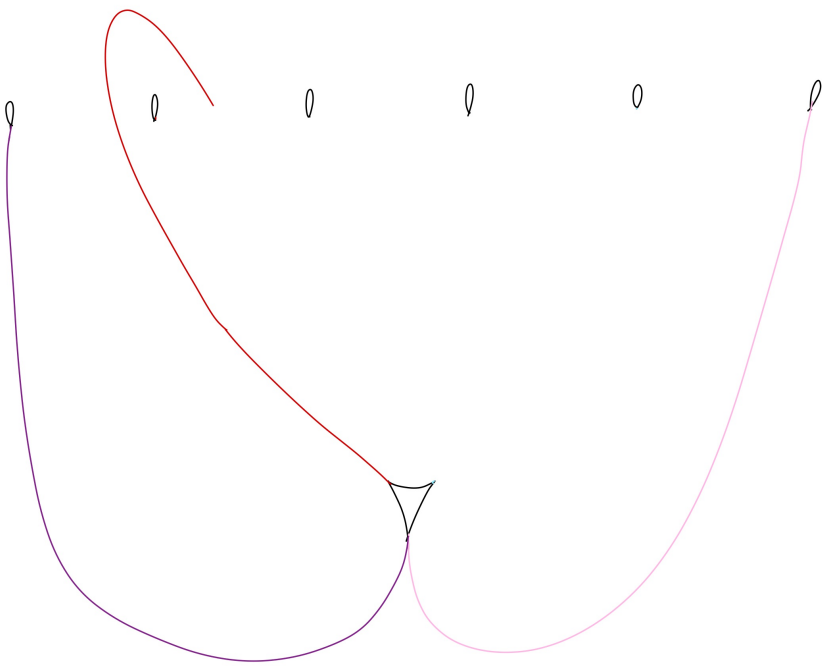


Figure C.9: NHT6

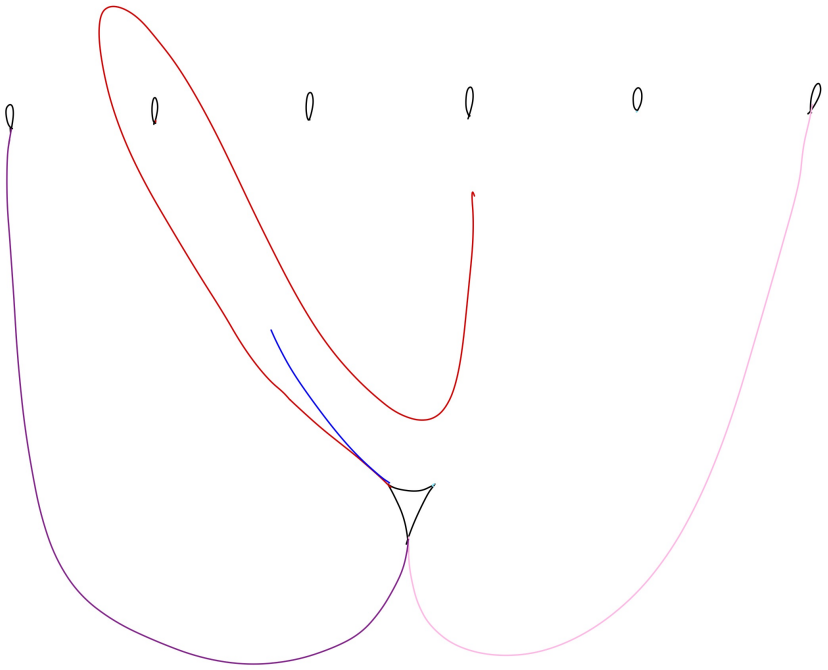


Figure C.10: Jehu1

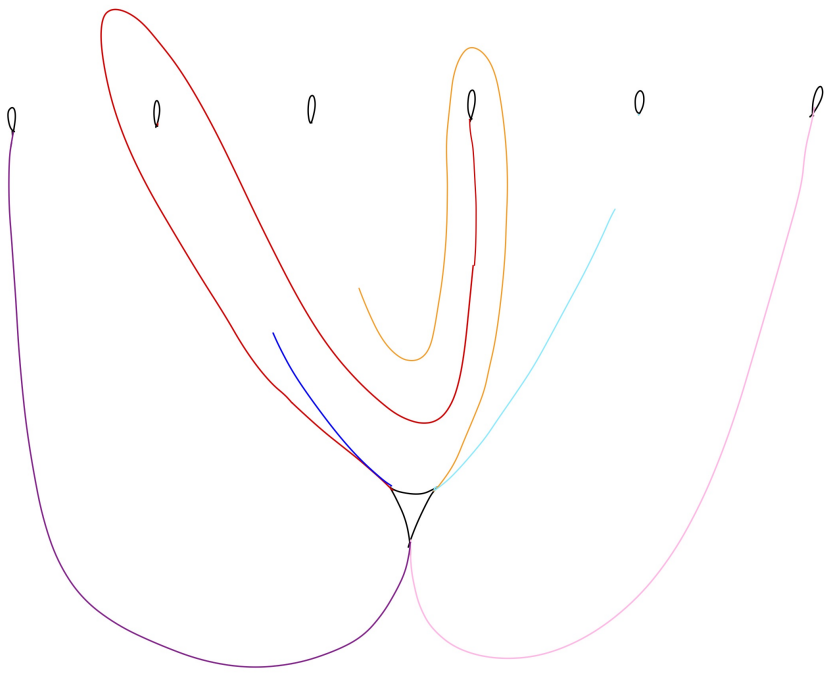


Figure C.11: Jehu2

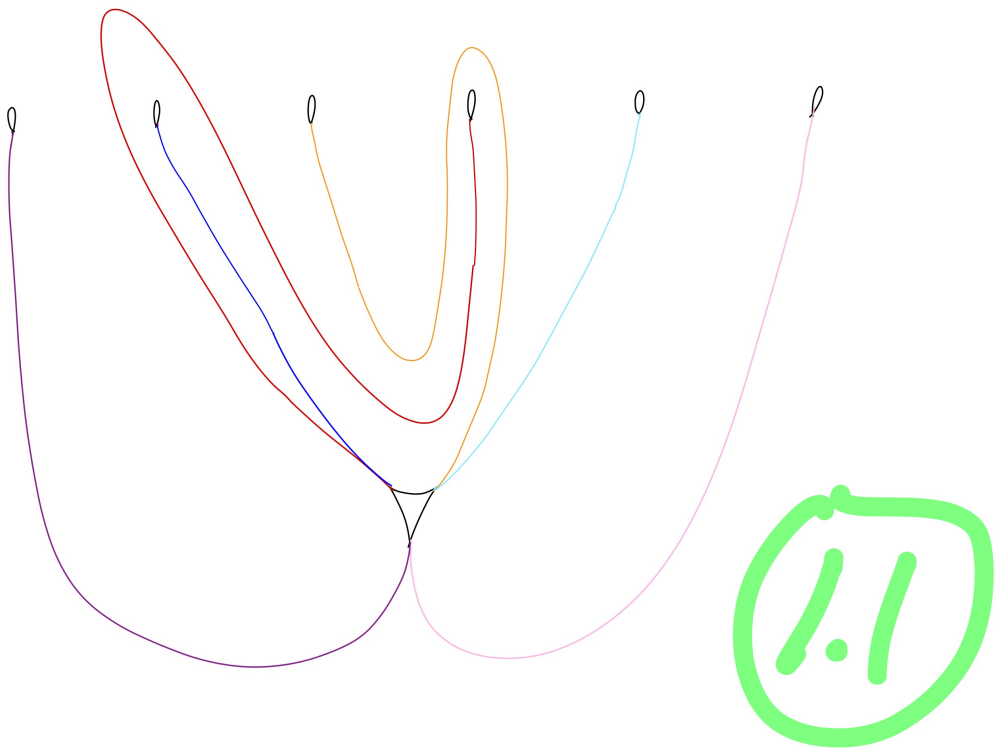


Figure C.12: Jehu3

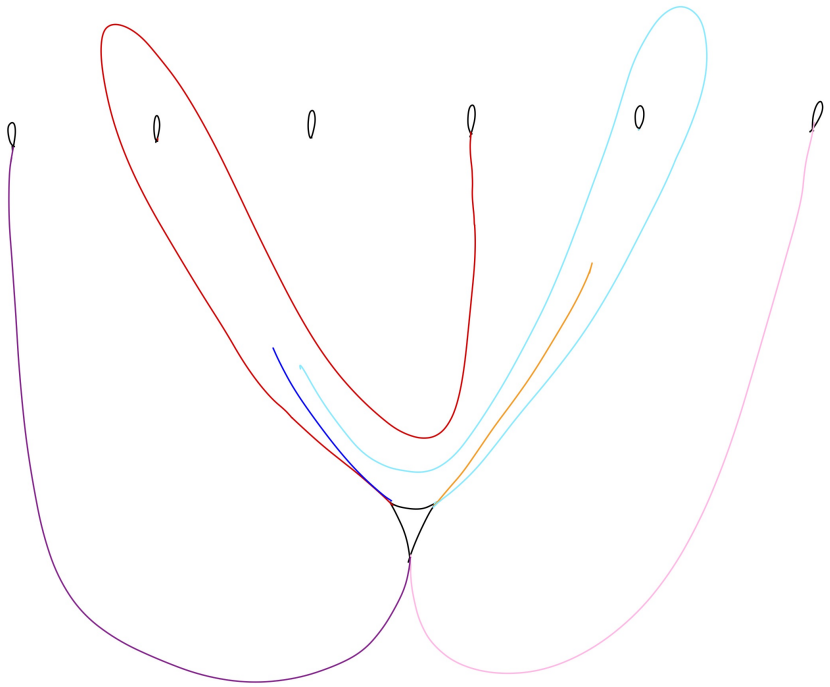


Figure C.13: Jehu4

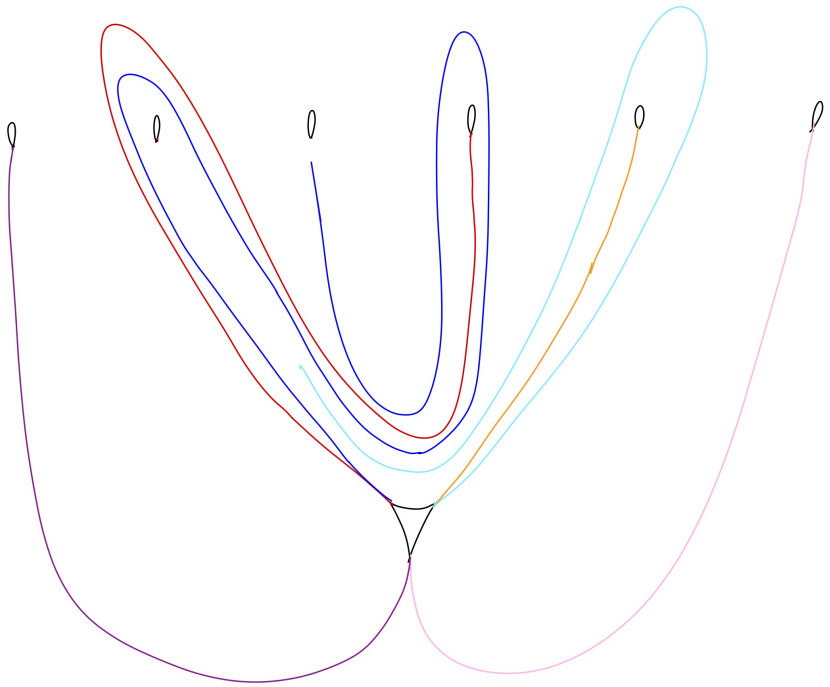


Figure C.14: Jehu5

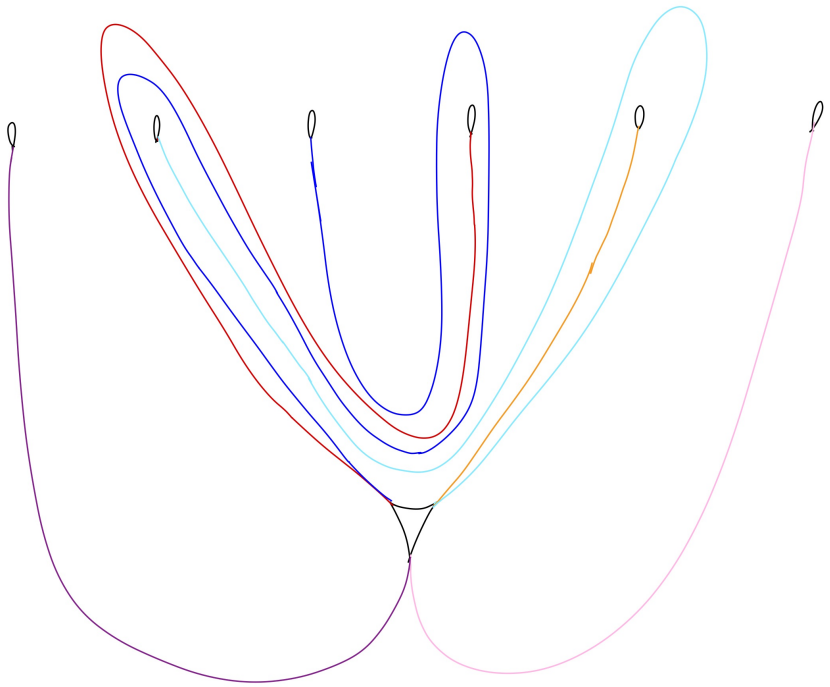


Figure C.15: Jehu6

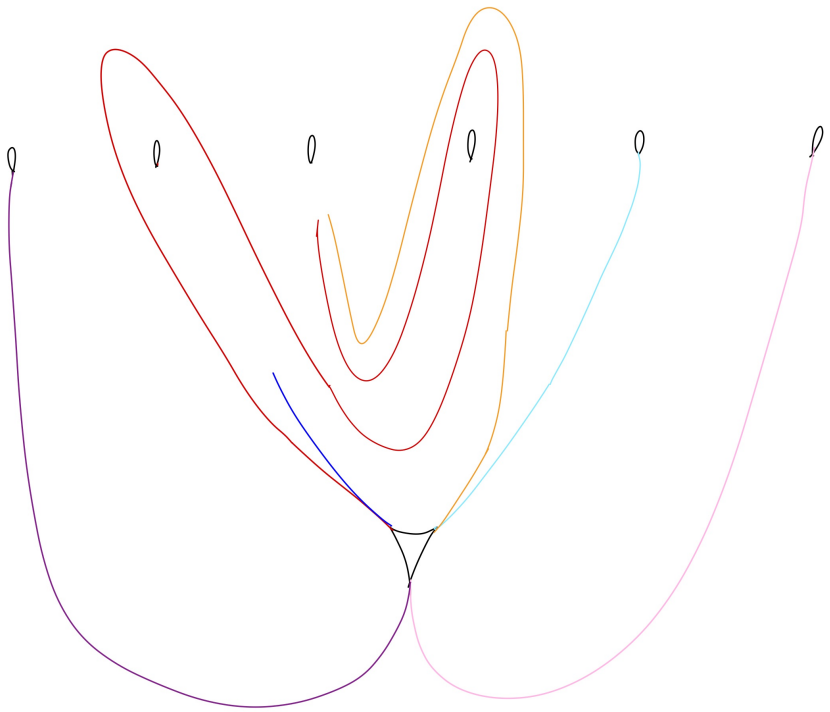


Figure C.16: Jehu7

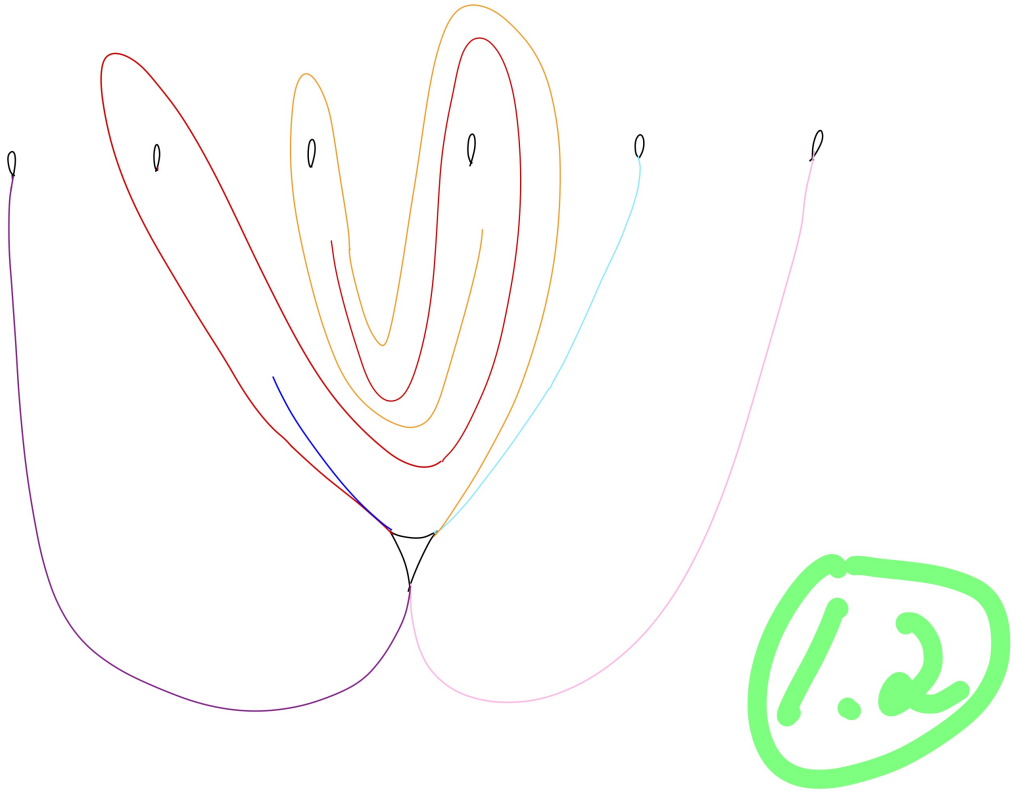


Figure C.17: Jehu8

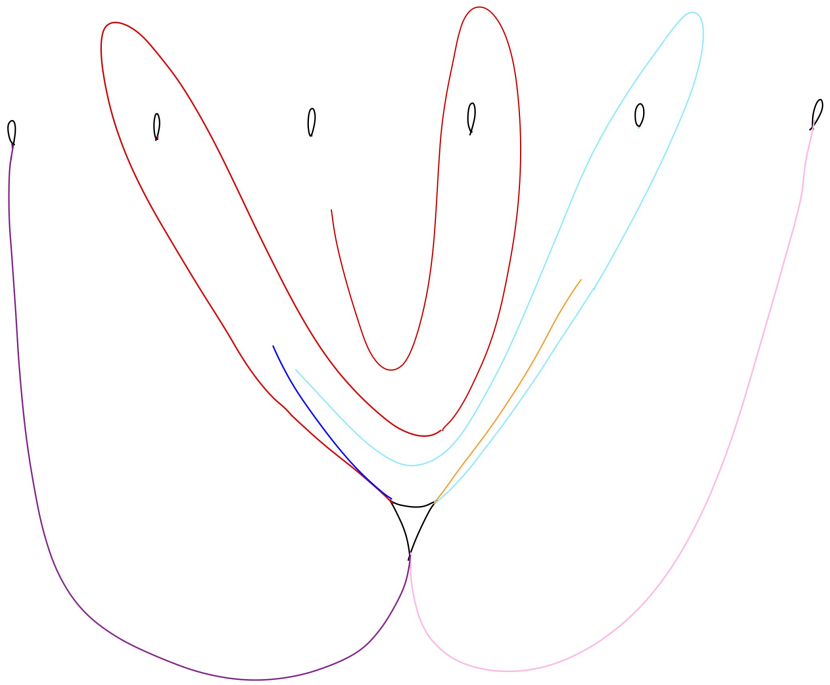


Figure C.18: Jehu9

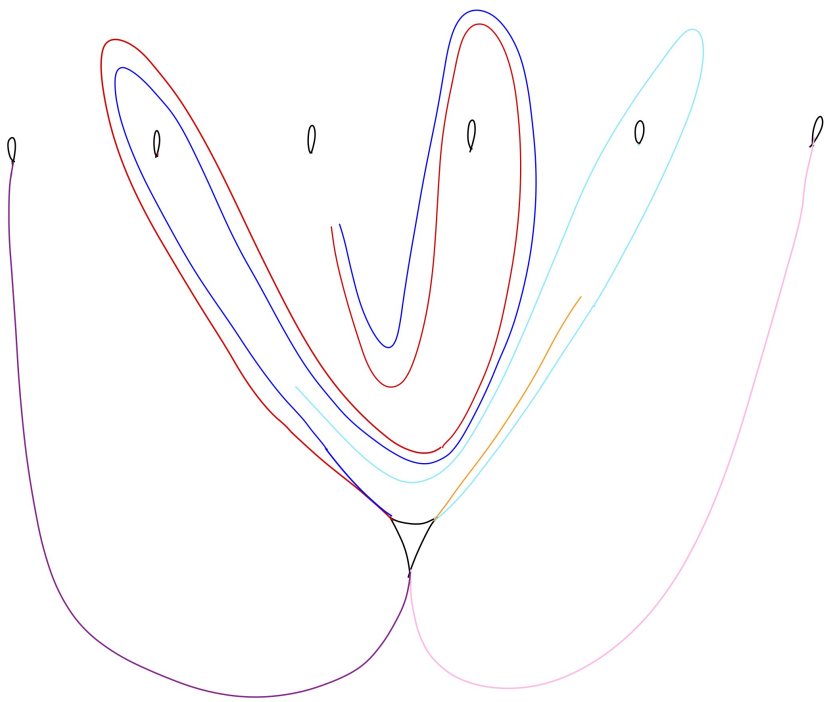


Figure C.19: Jehu10

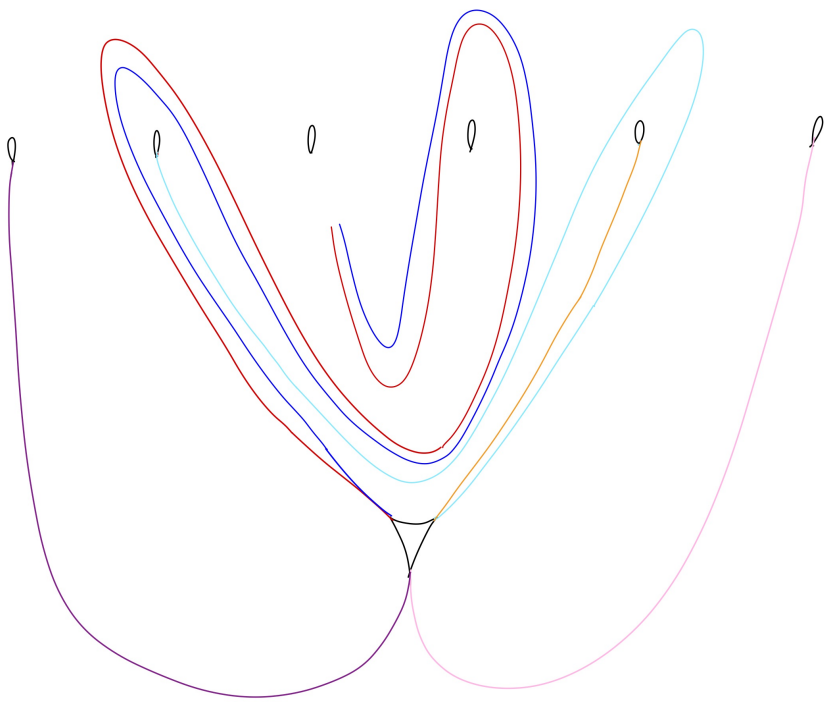


Figure C.20: Jehu11

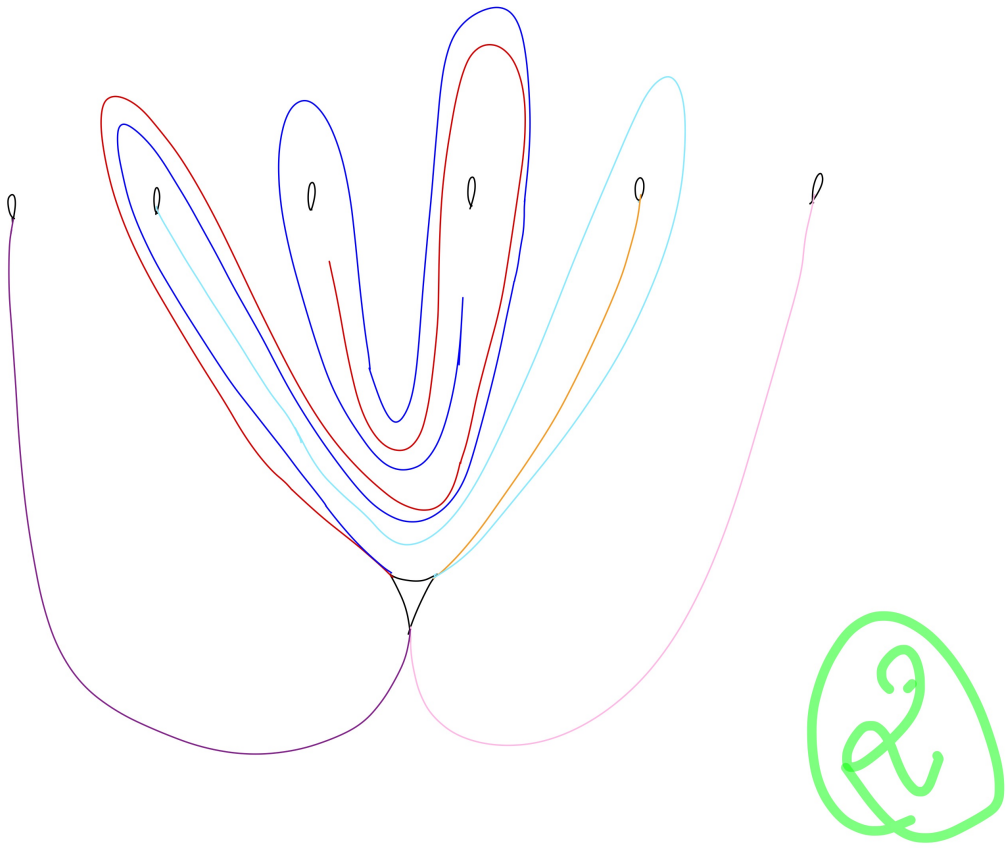


Figure C.21: Jehu12

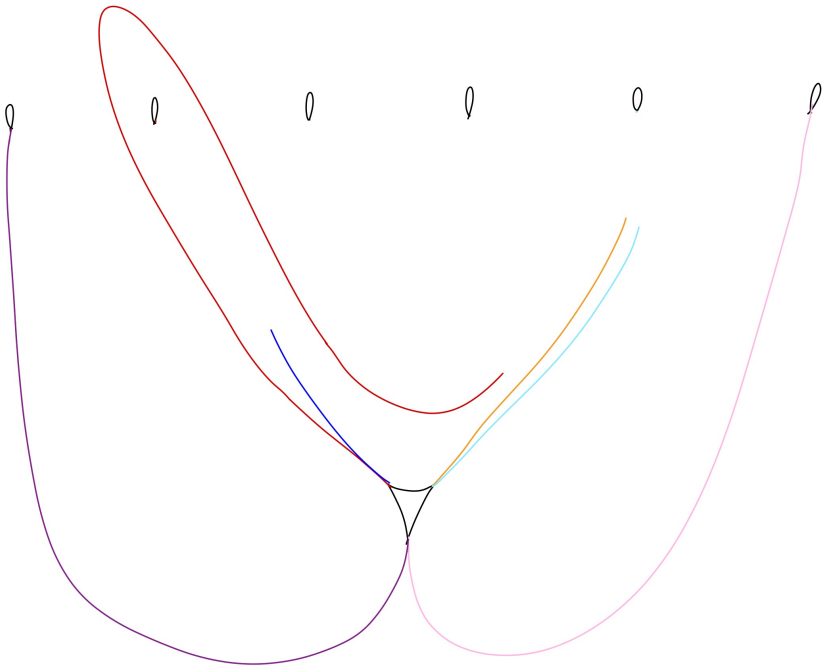


Figure C.22: Kexy1

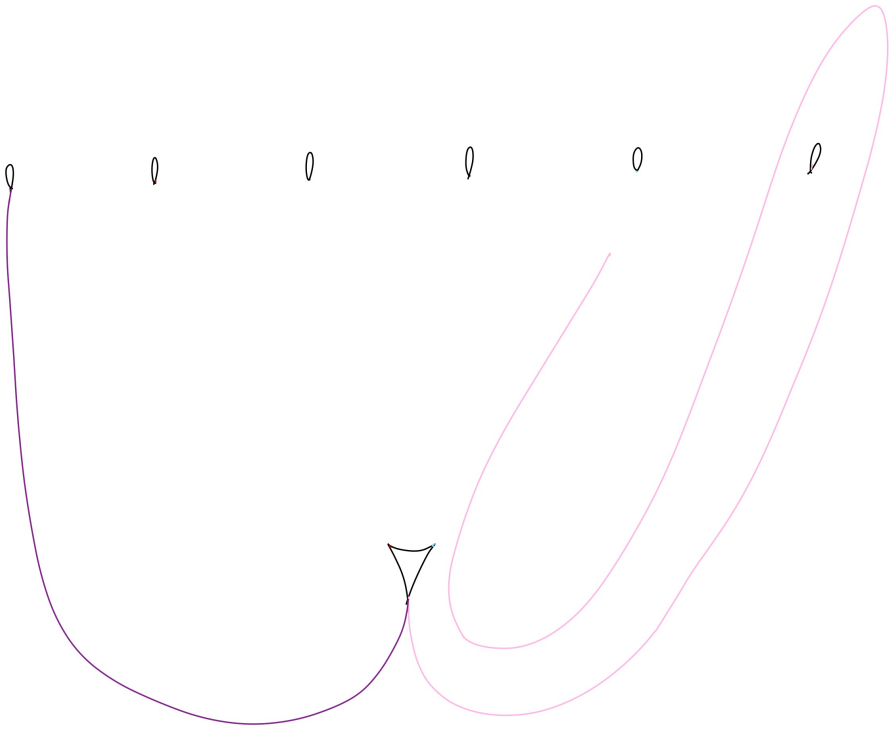


Figure C.23: CMJ1

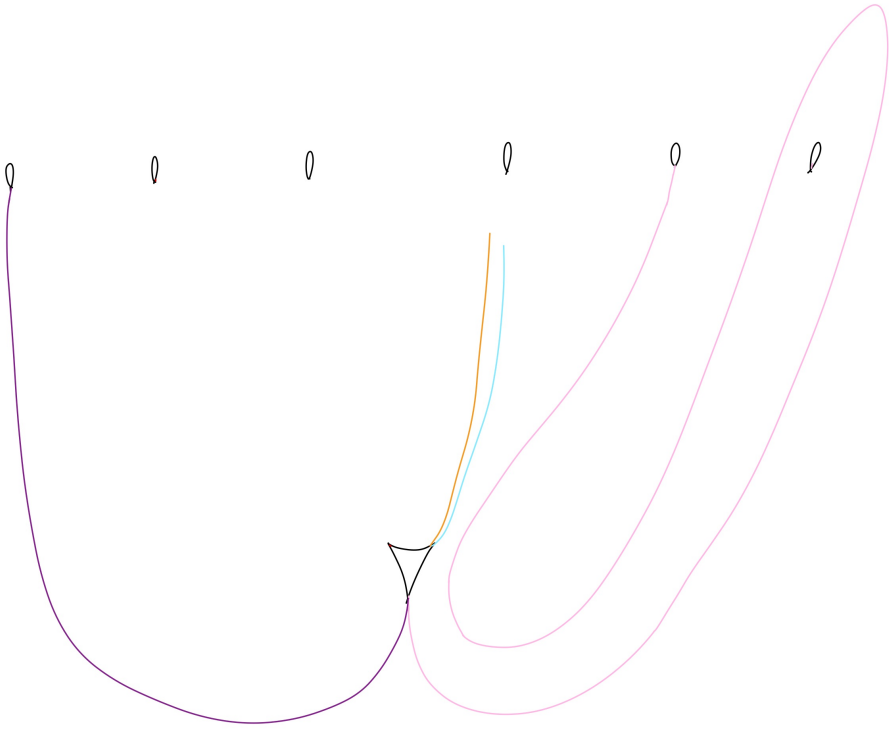


Figure C.24: Mome1

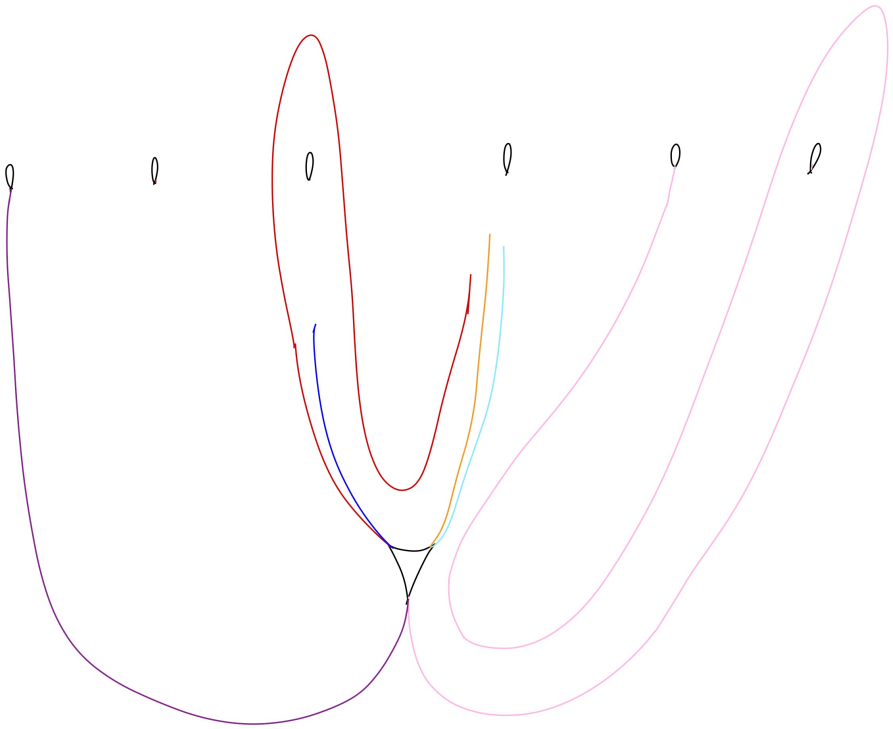


Figure C.25: Mome2

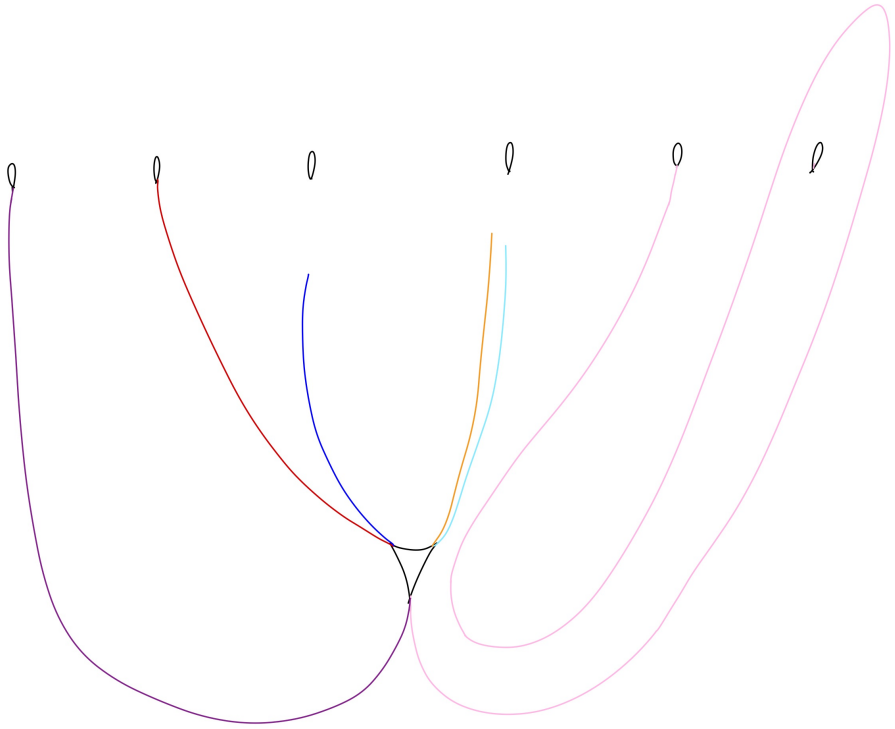


Figure C.26: Kedge1

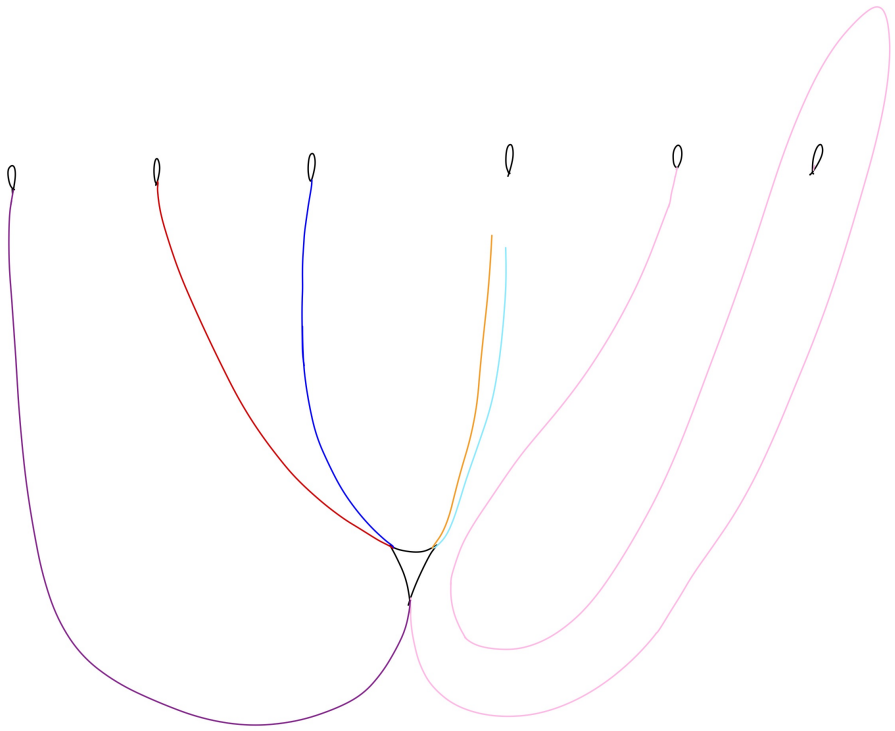


Figure C.27: Dindle1

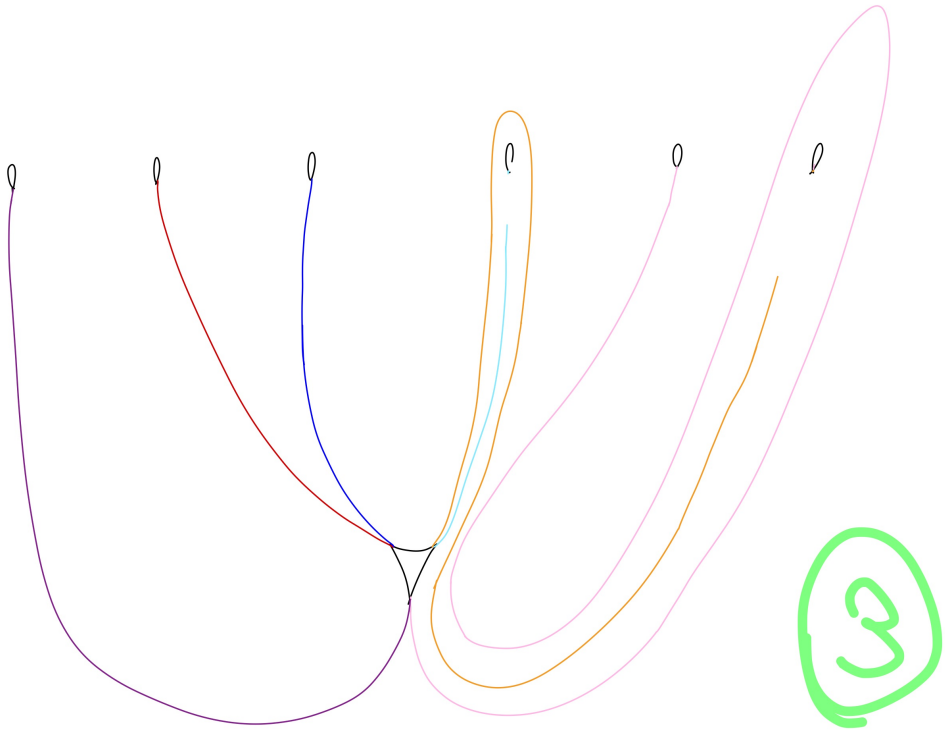


Figure C.28: Dindle2

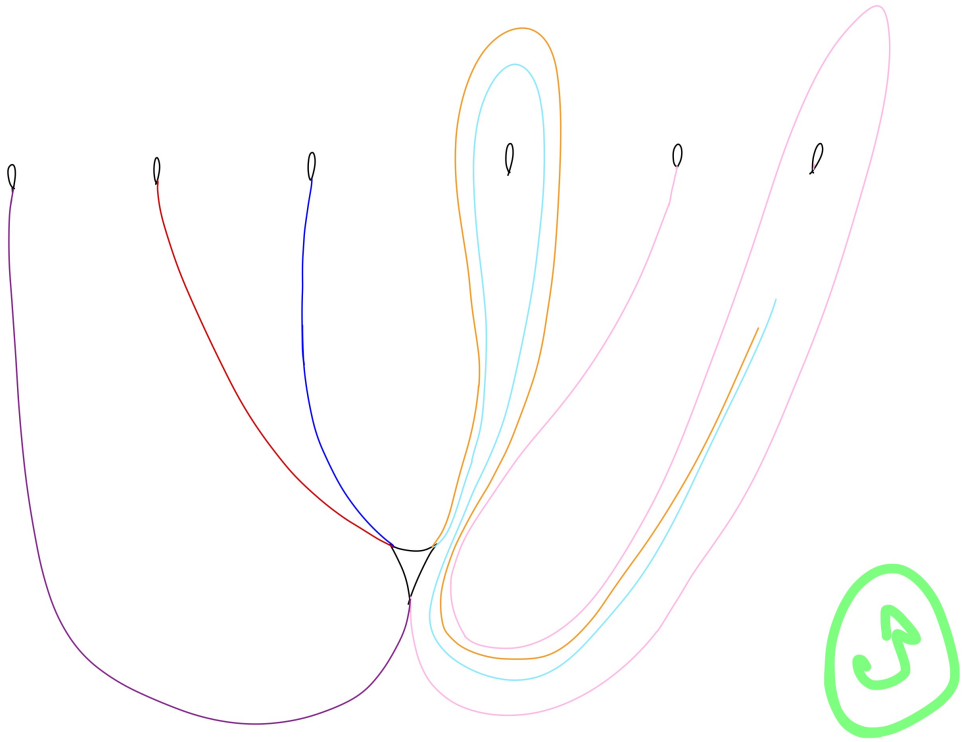


Figure C.29: Dindle3

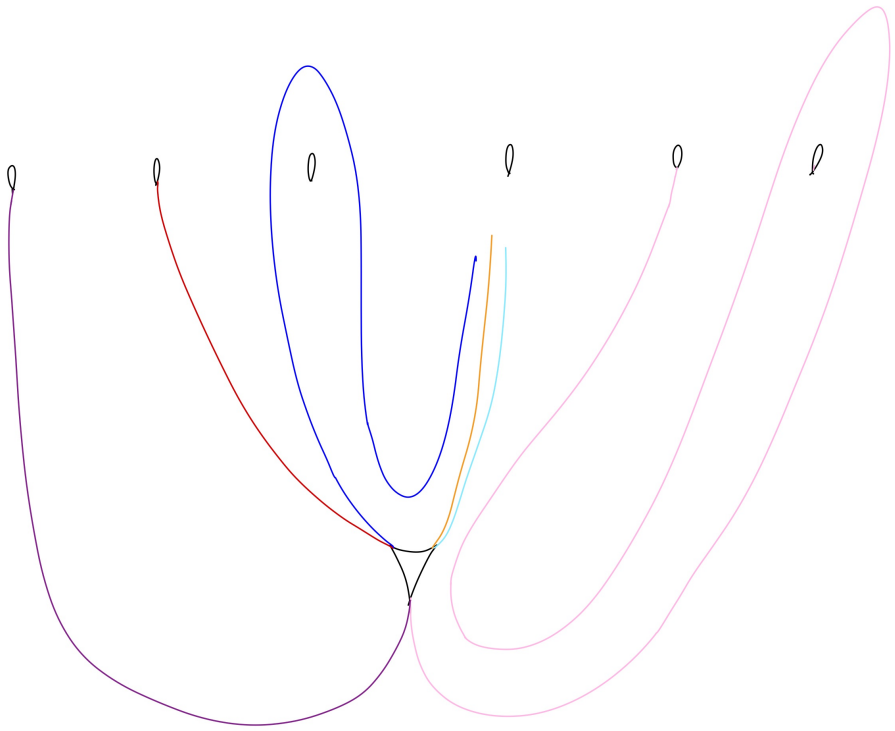


Figure C.30: Jirble1

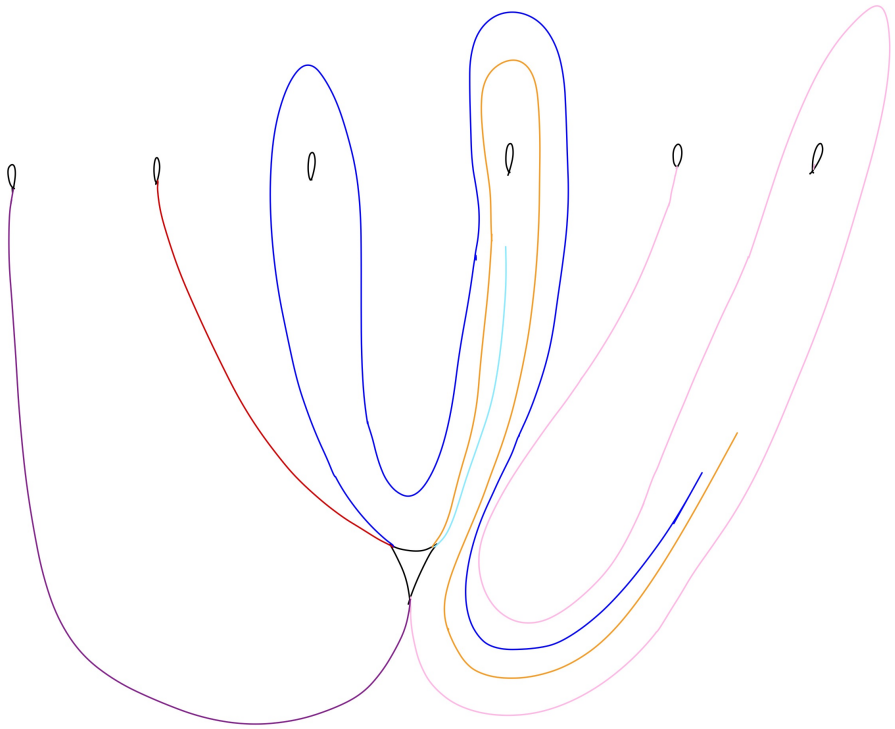


Figure C.31: Jirble2

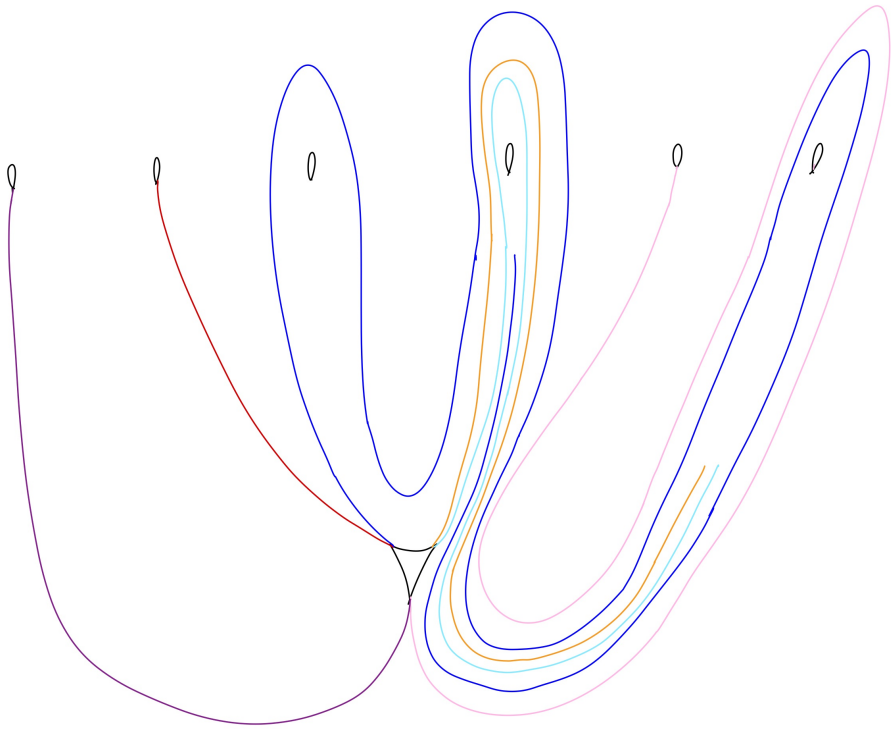


Figure C.32: Jirble3

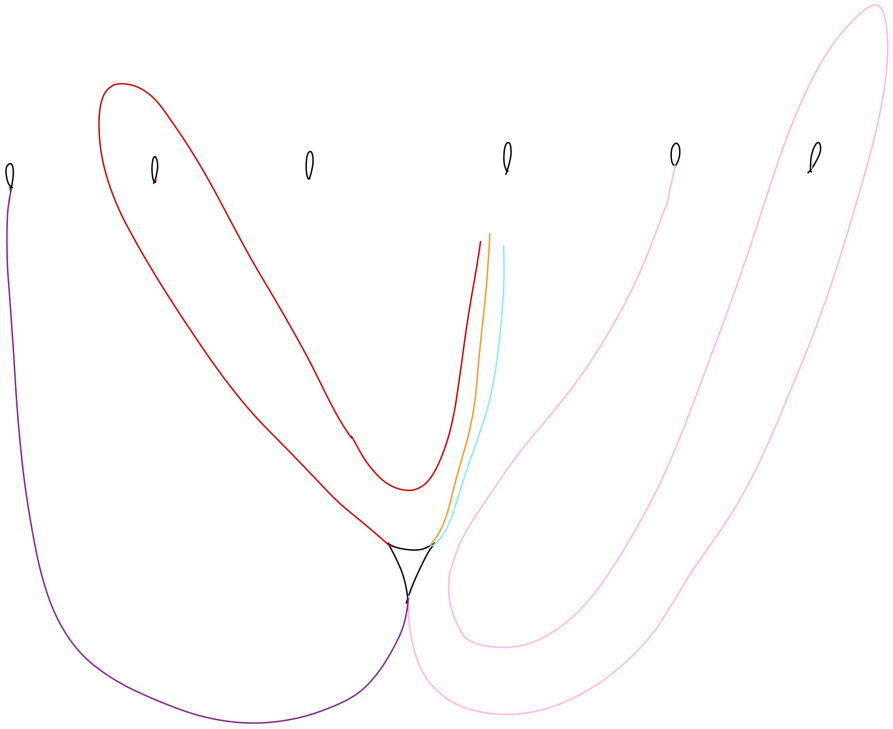


Figure C.33: Mulse1

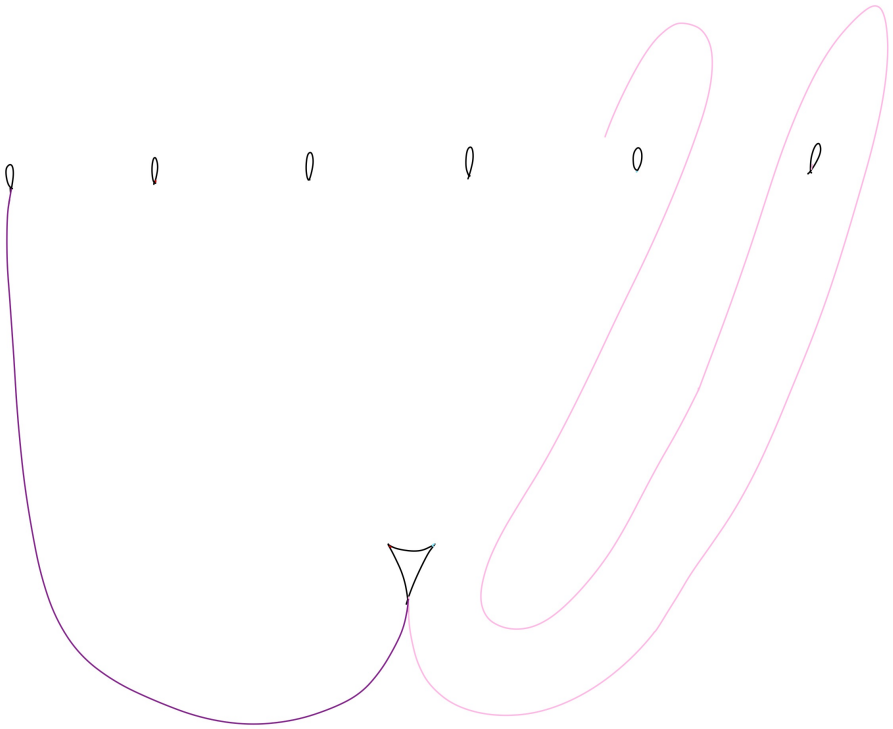


Figure C.34: Nesh1

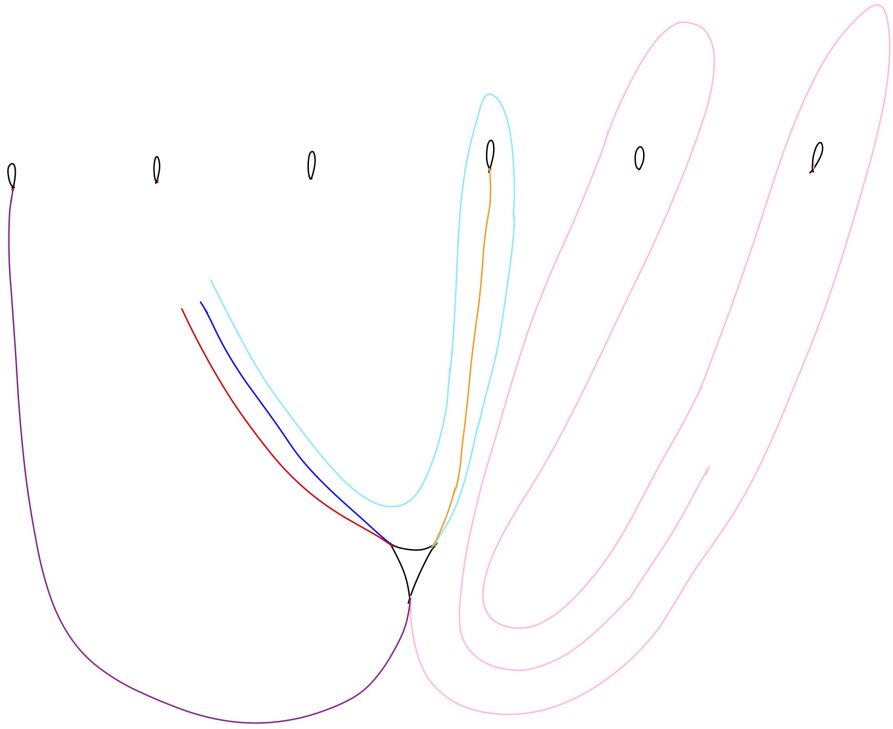


Figure C.35: Nudzh2

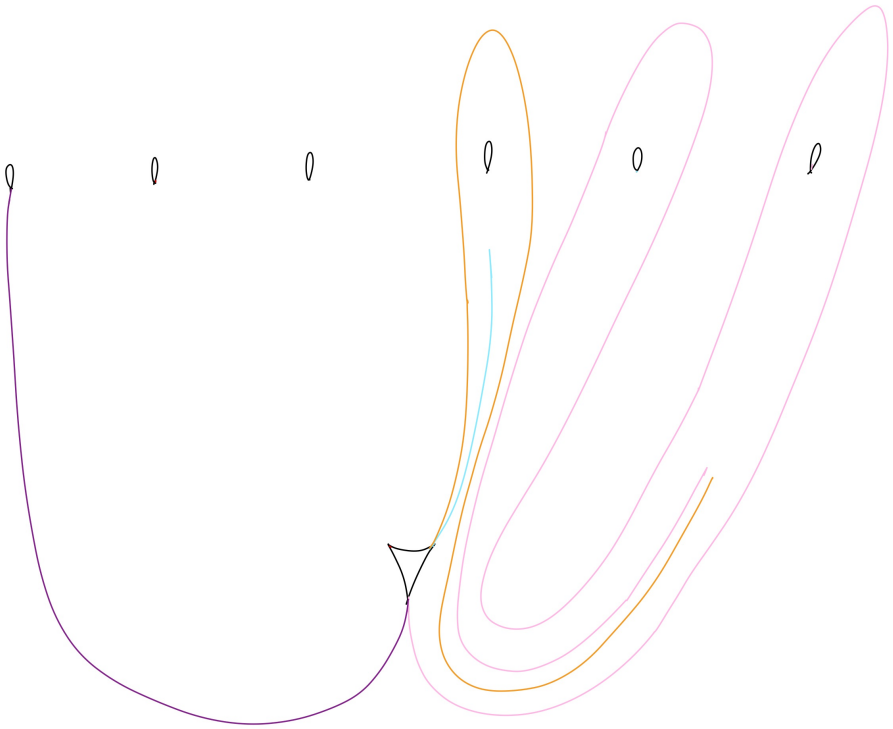


Figure C.36: Nudzh3

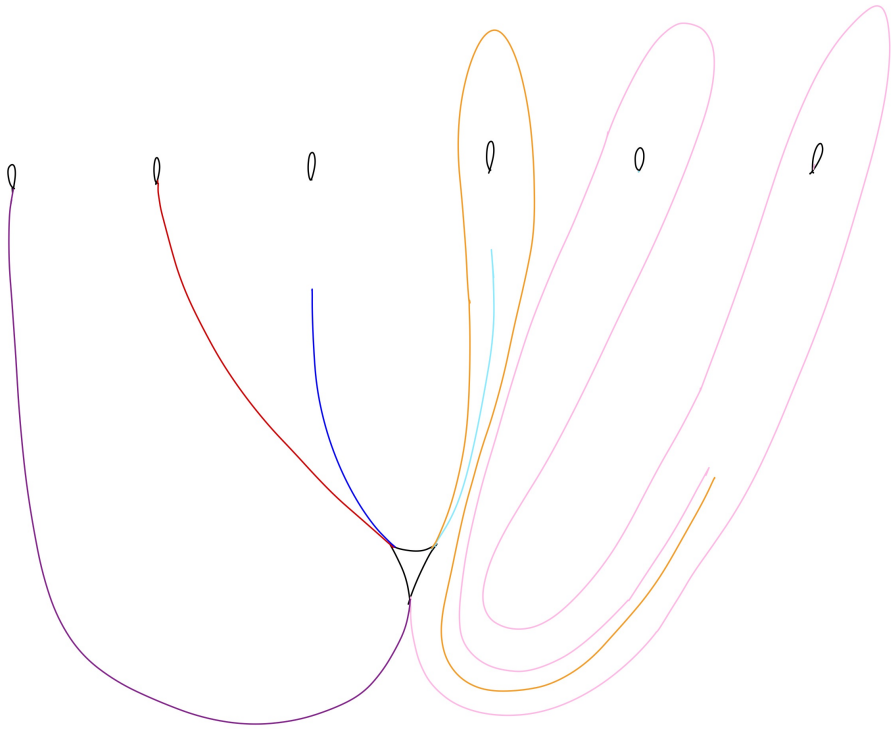


Figure C.37: Nudzh4

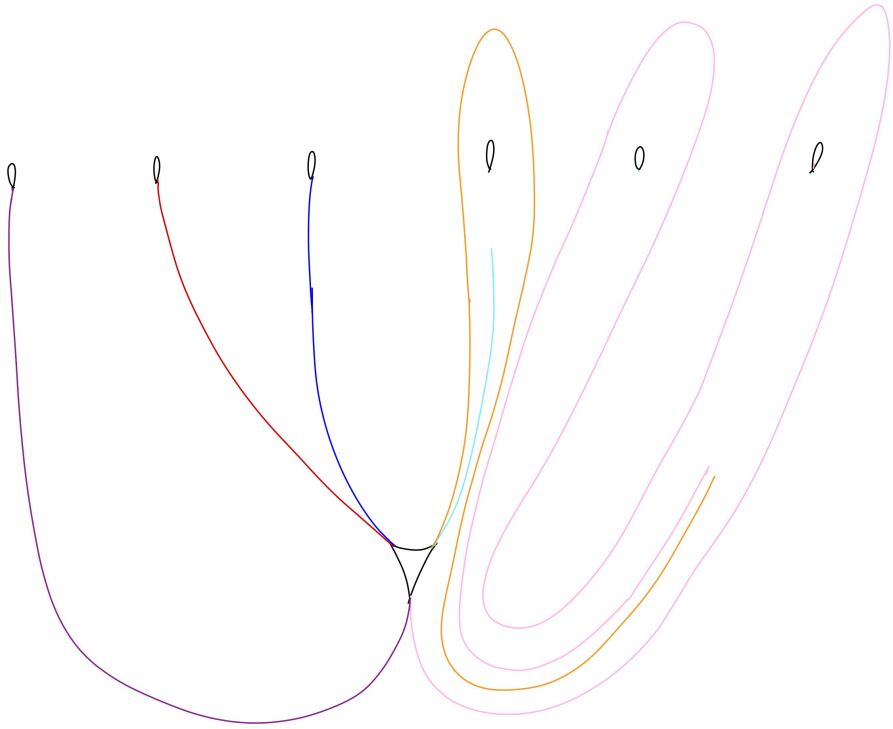


Figure C.38: Keffel1

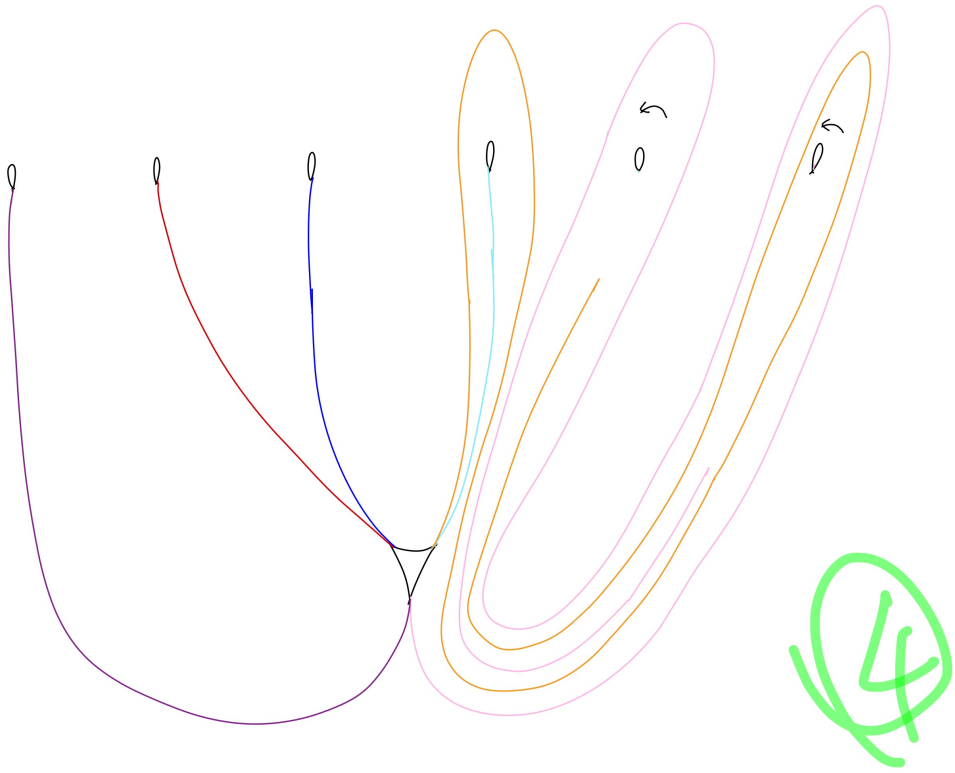


Figure C.39: Keffel2

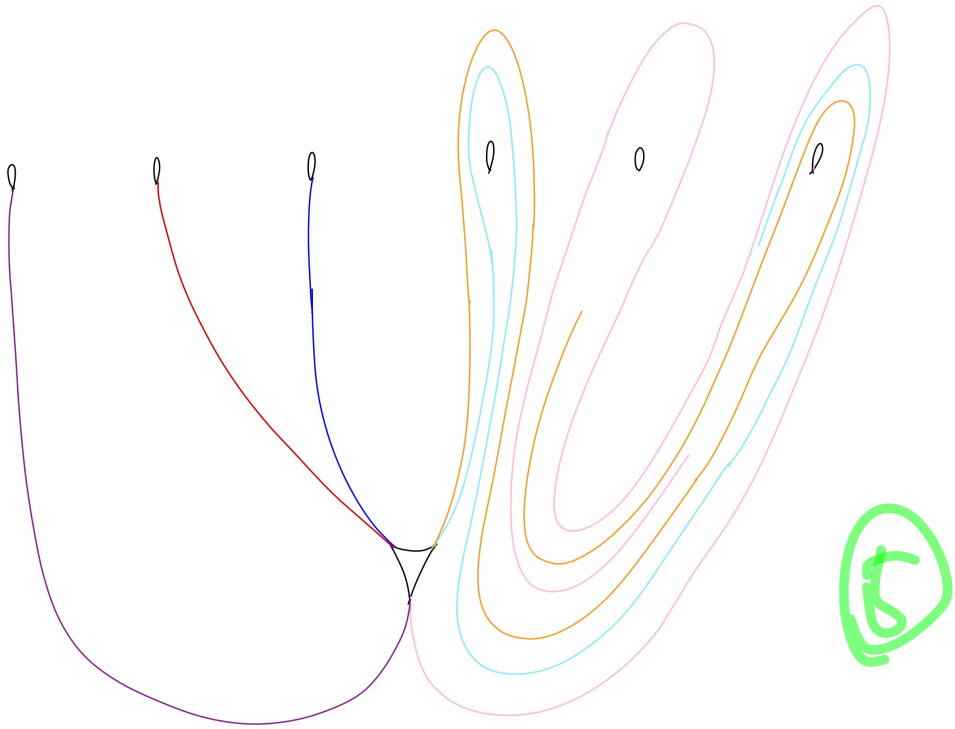


Figure C.40: Keffel3

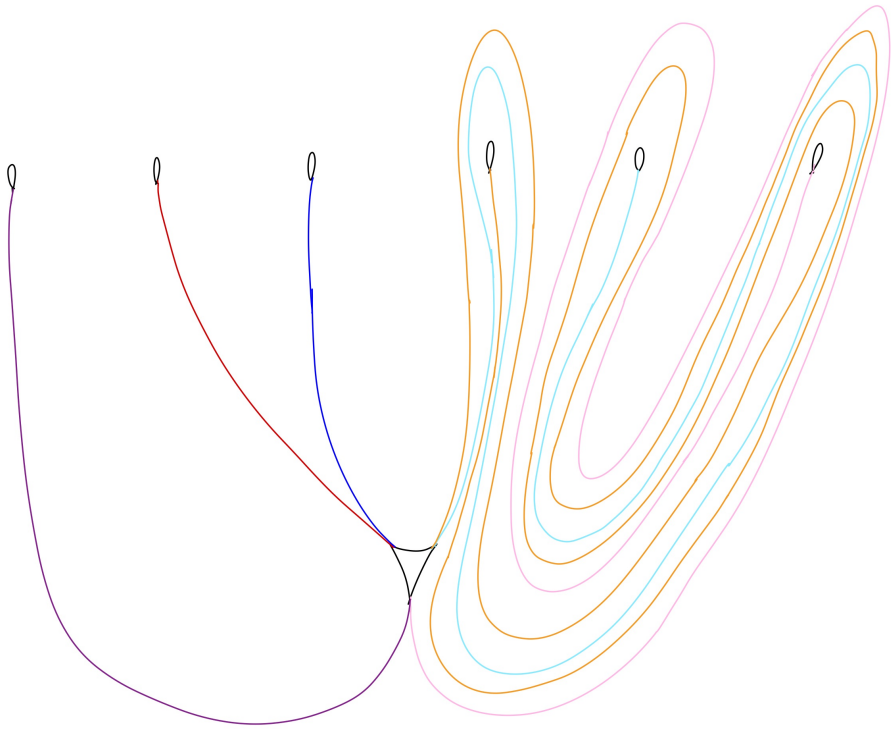


Figure C.41: Keffel4

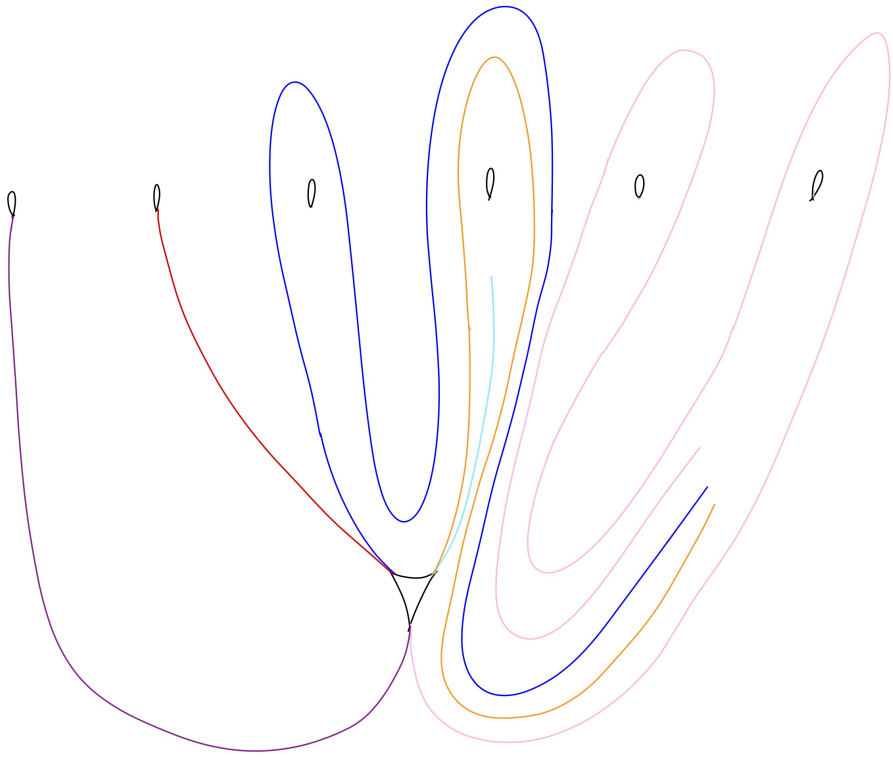


Figure C.42: Mizzle1

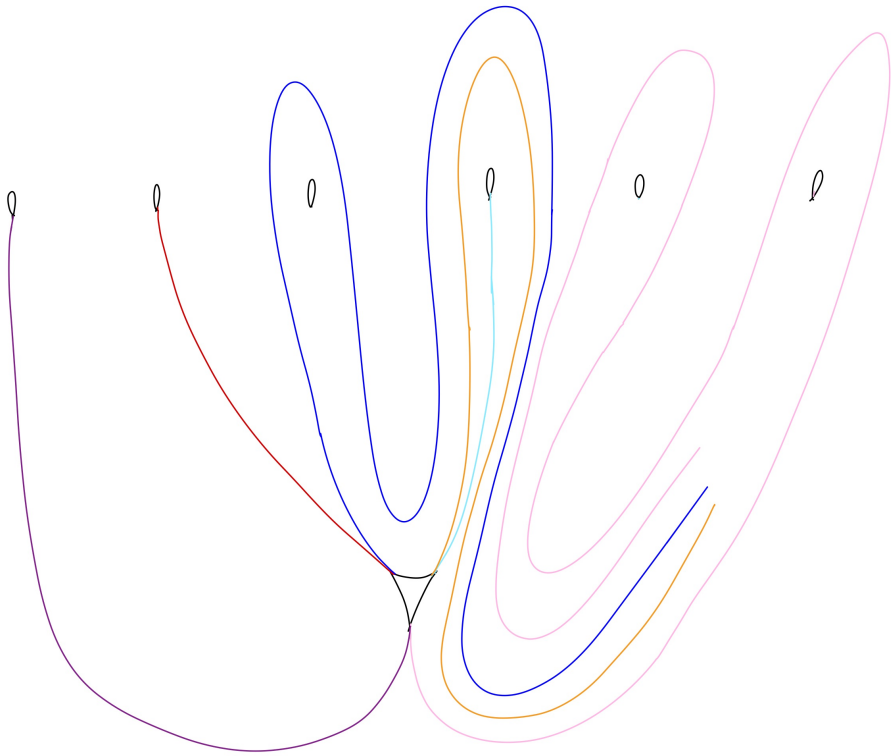


Figure C.43: Mizzle2

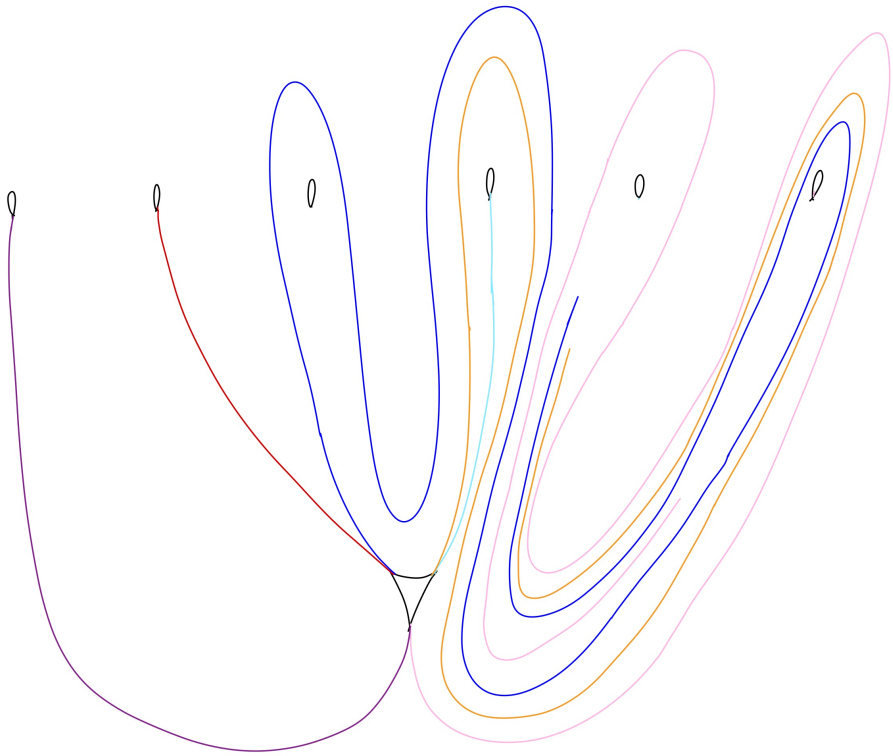


Figure C.44: Mizzle3

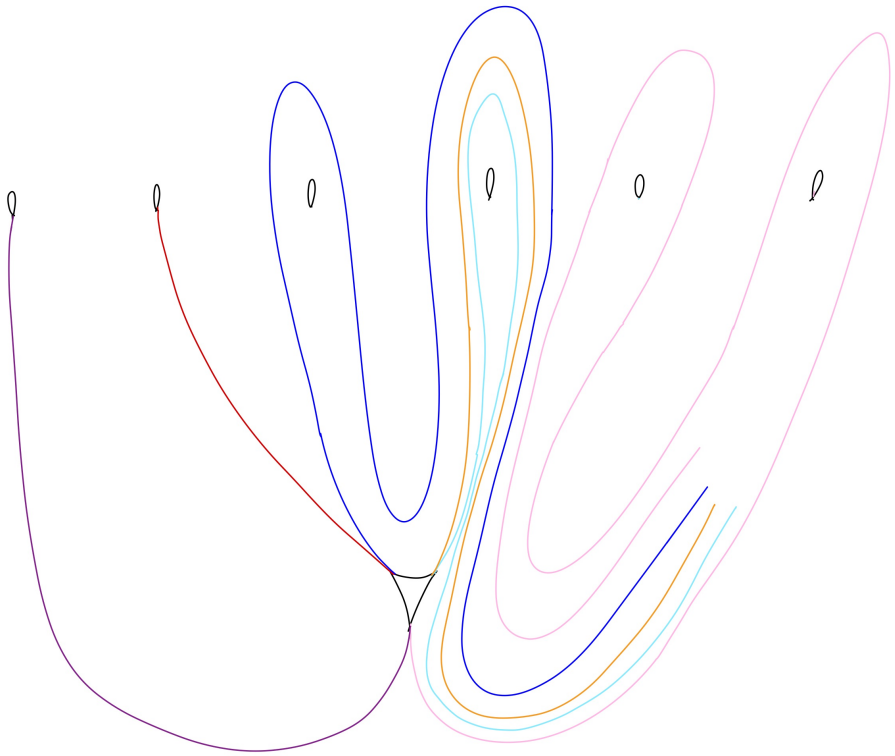


Figure C.45: Mizzle4

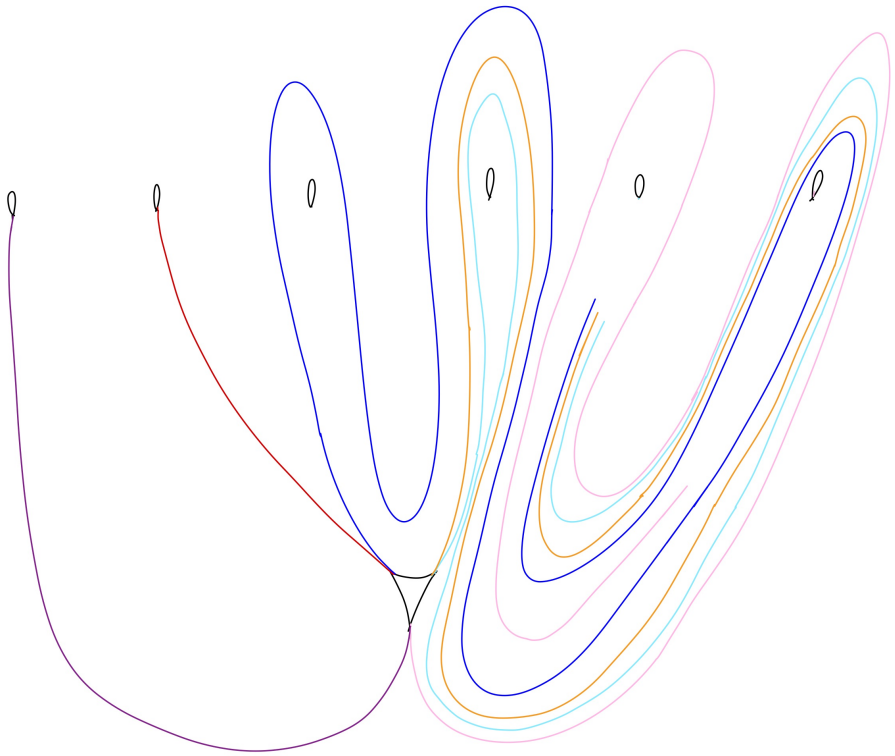


Figure C.46: Mizzle5

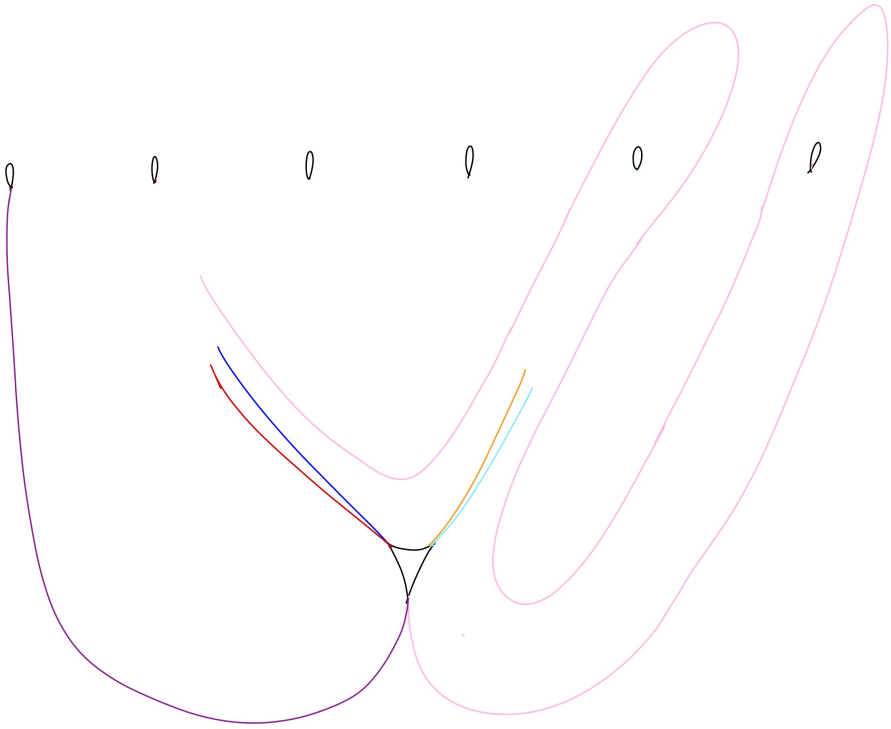


Figure C.47: Snirt1

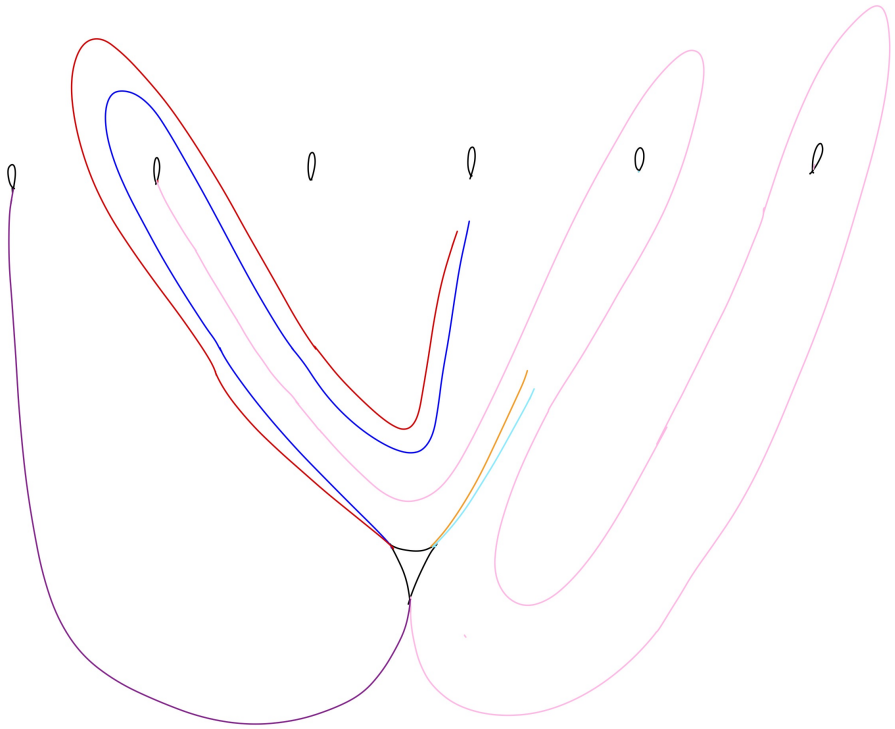


Figure C.48: Tittup1

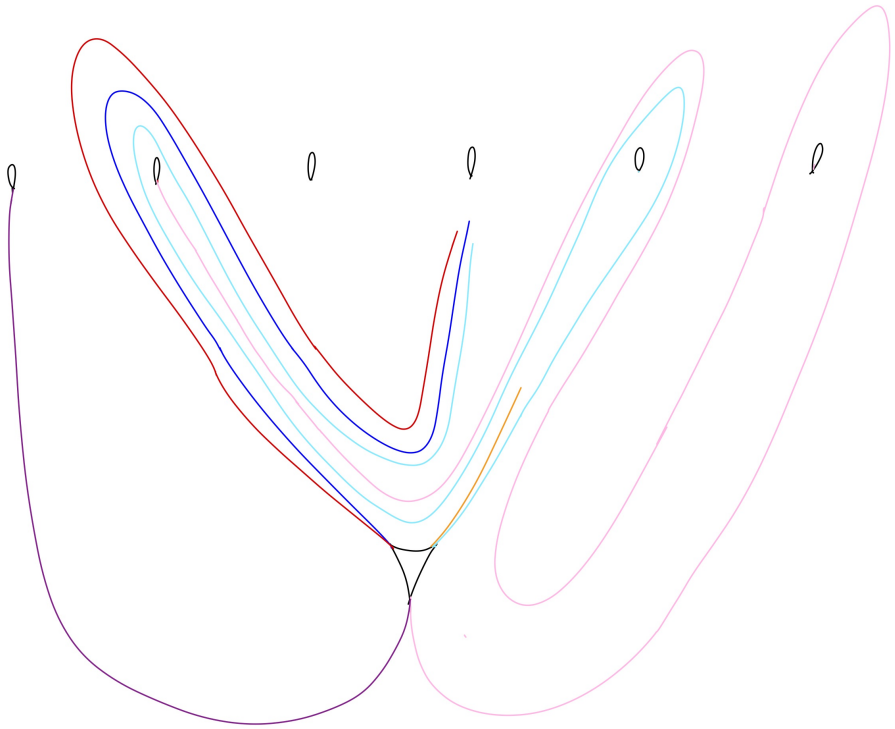


Figure C.49: Tittup2

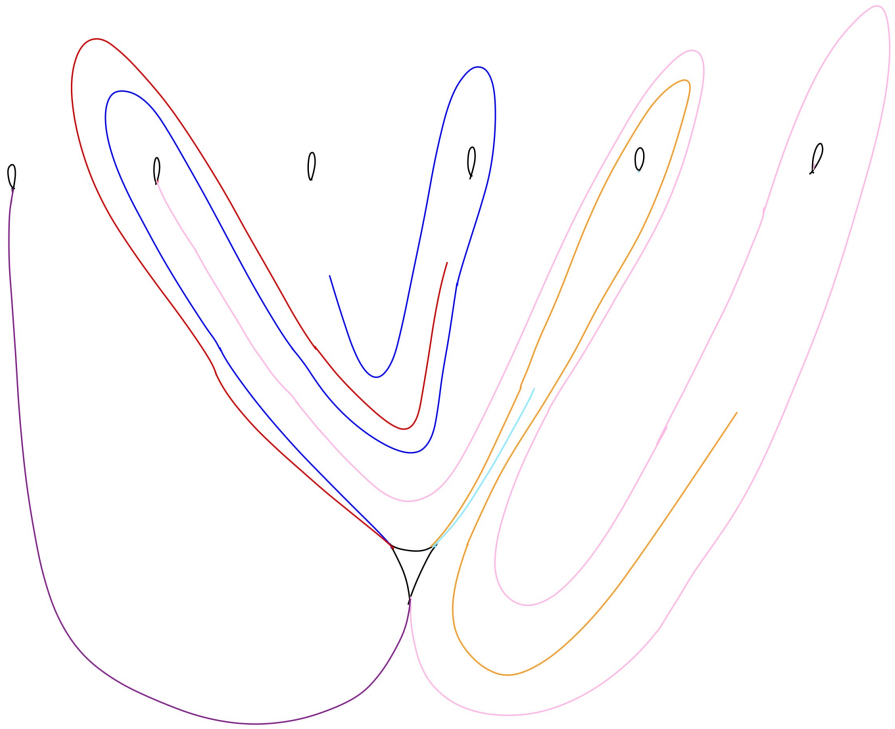


Figure C.50: Tittup3

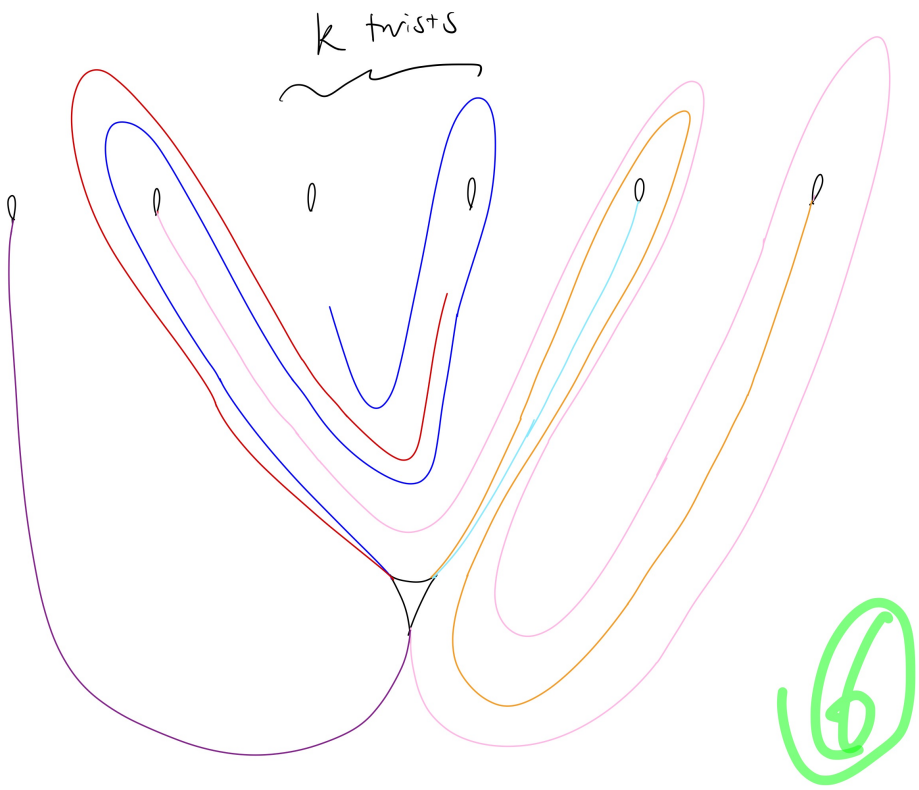


Figure C.51: Epigone1



Figure C.52: Farrago1

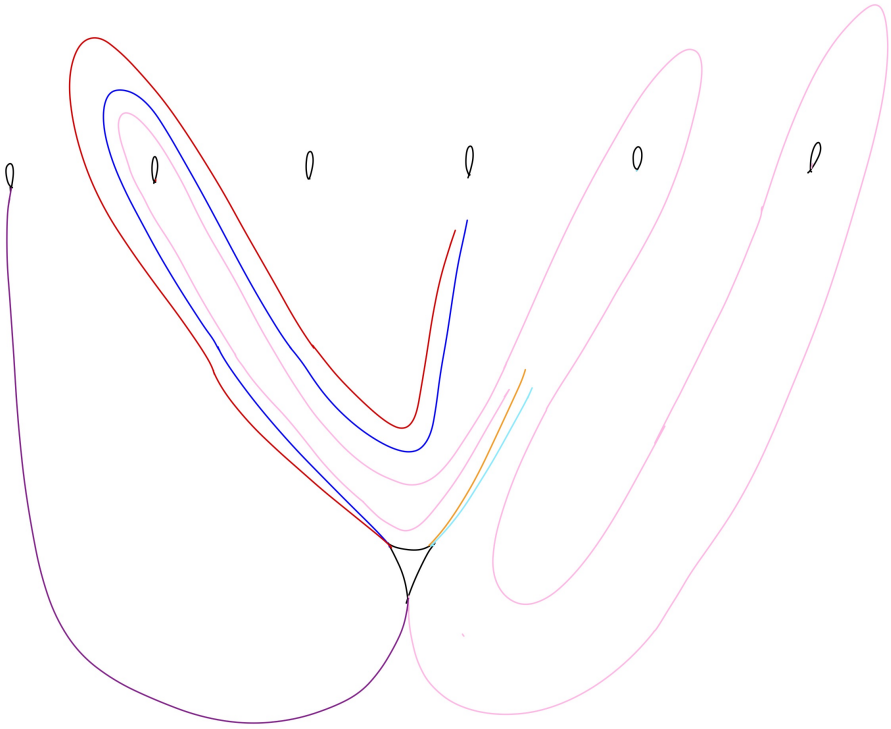


Figure C.53: Ullage1

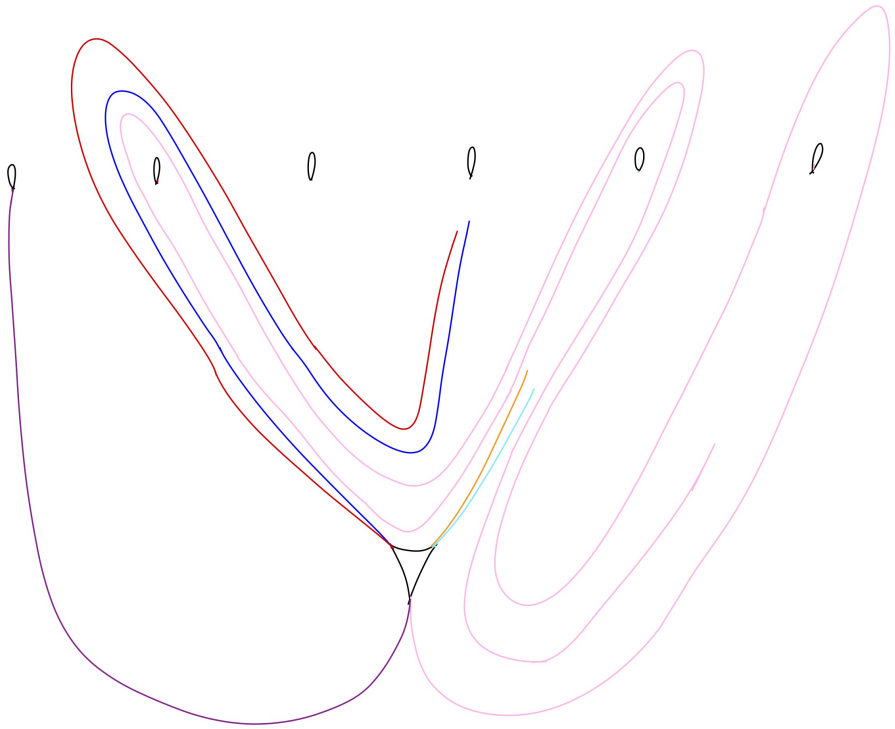


Figure C.54: Ullage2

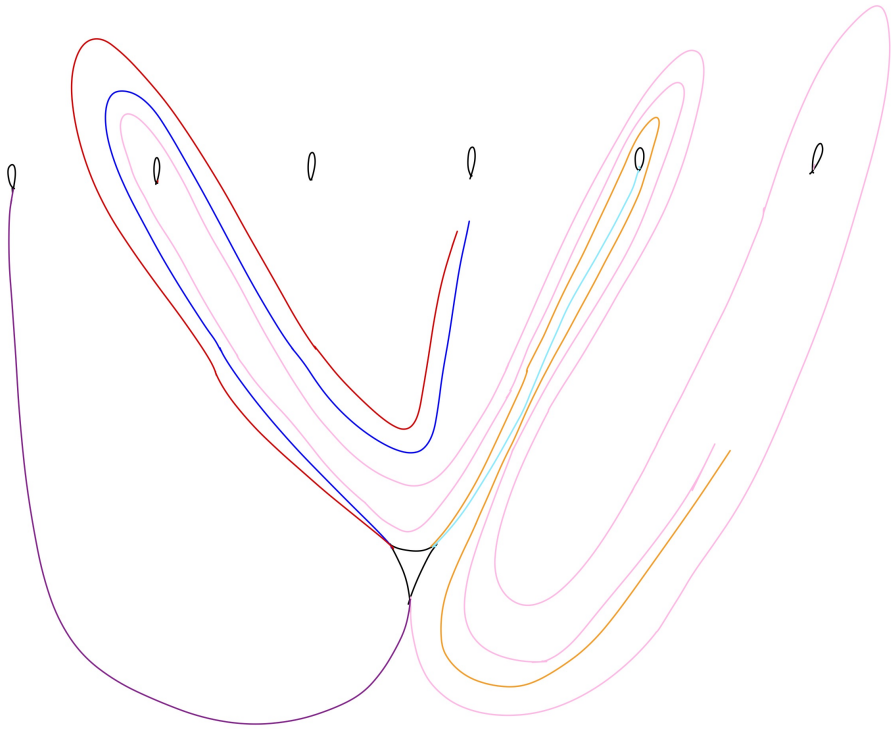


Figure C.55: Ullage3

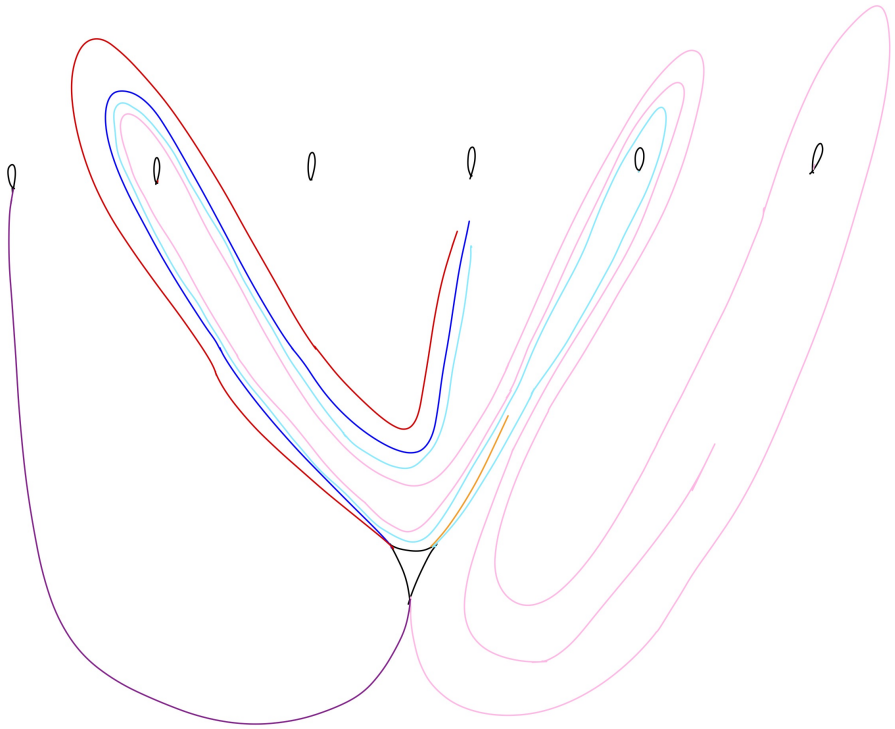


Figure C.56: Ullage4

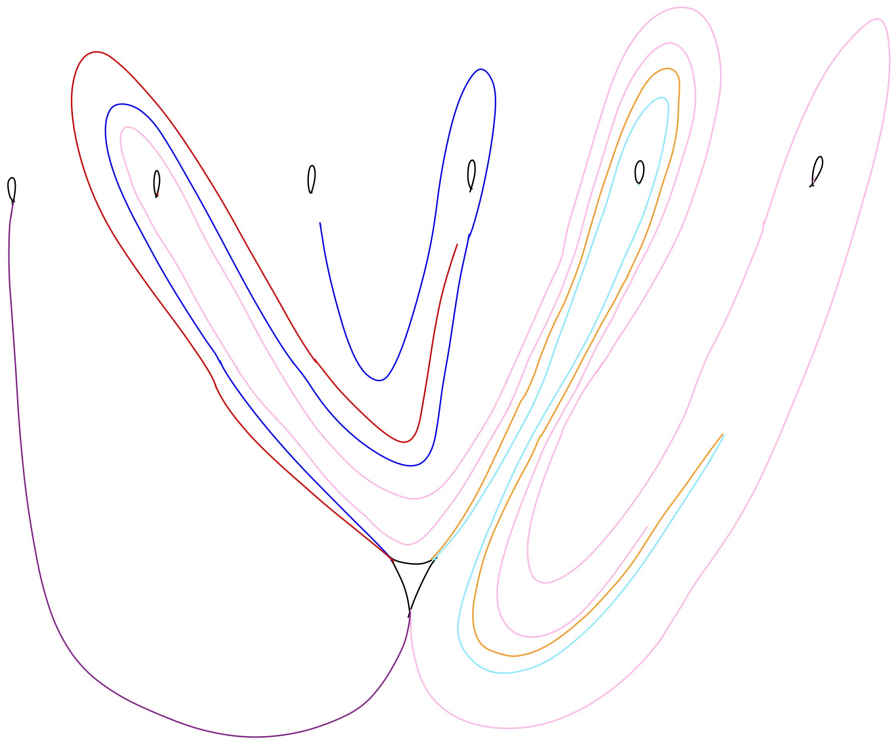


Figure C.57: Ullage5

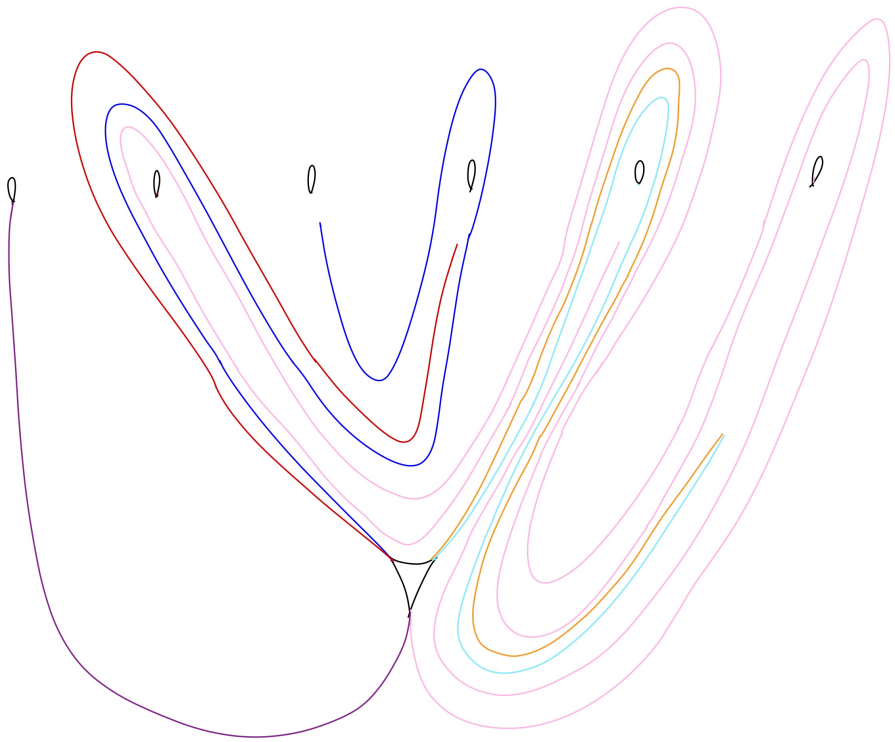


Figure C.58: Ullage6

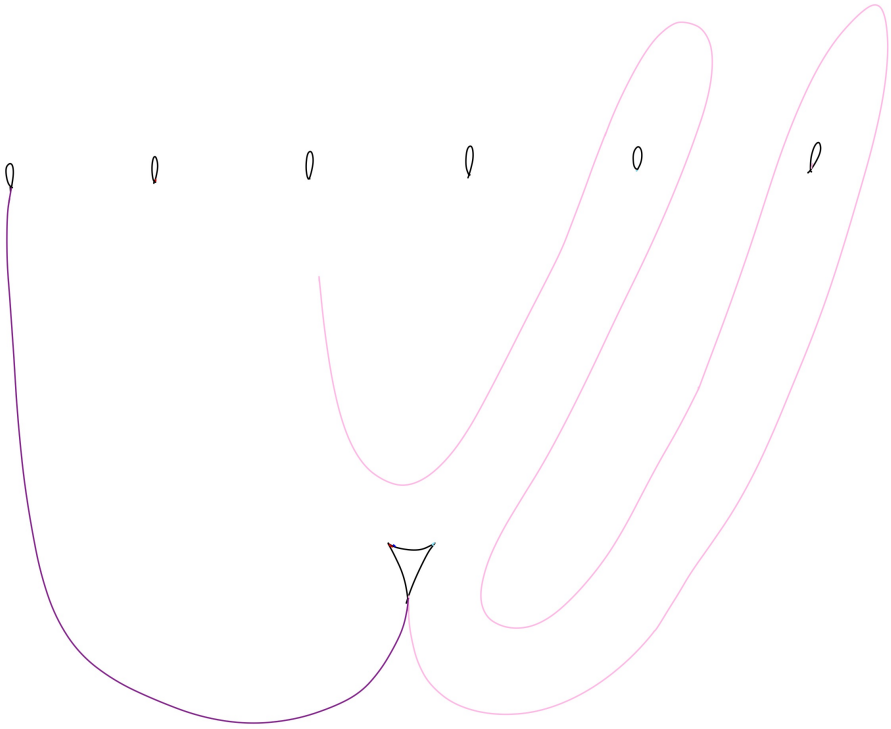


Figure C.59: Quire1

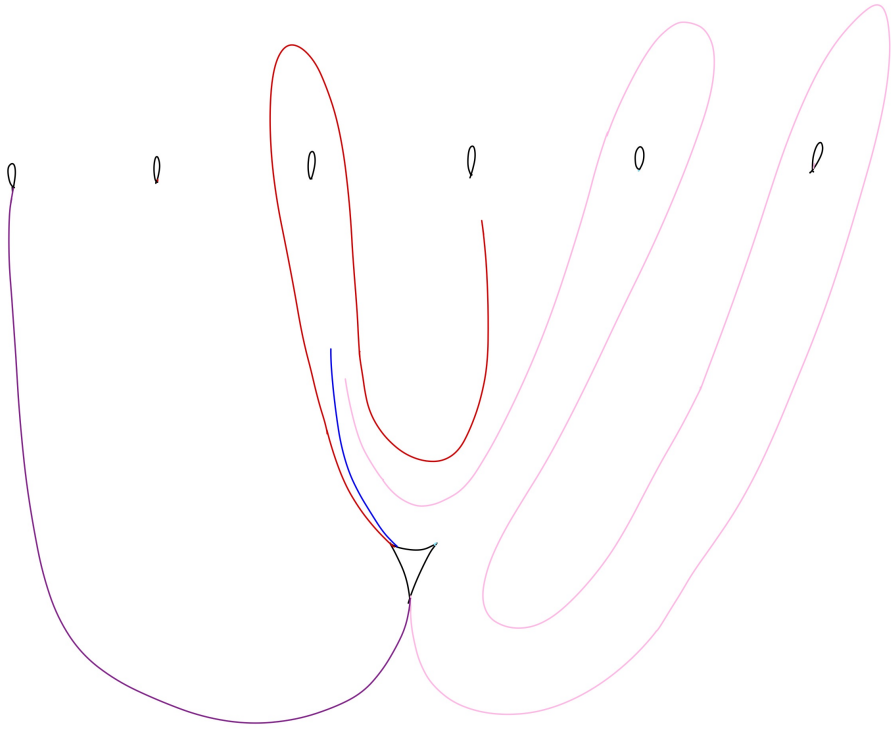


Figure C.60: Yepsen1

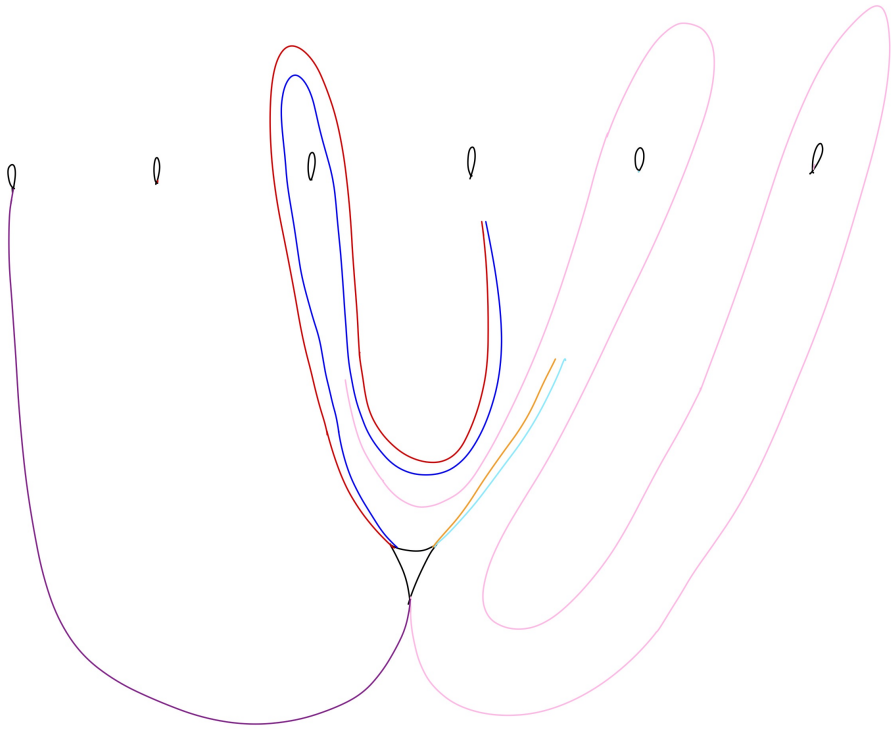


Figure C.61: Yepsen2

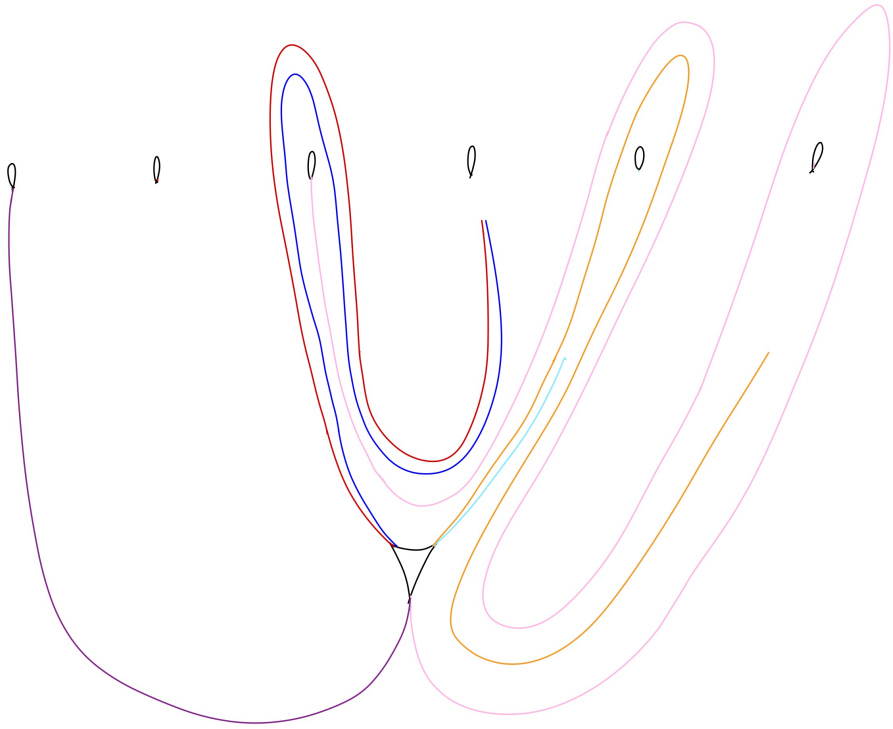


Figure C.62: Gubbins1

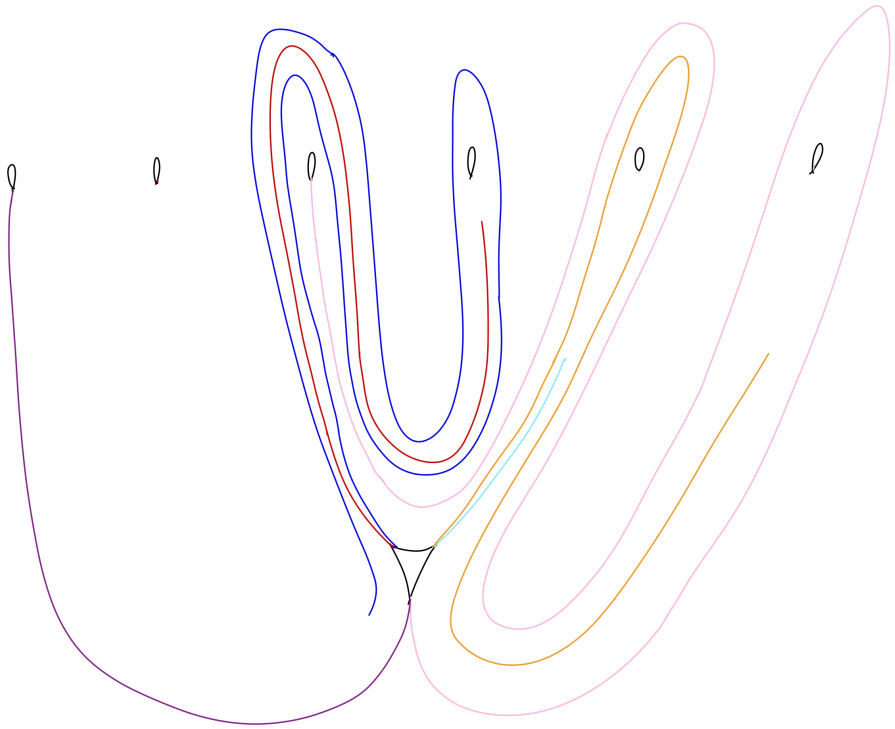


Figure C.63: Gubbins2

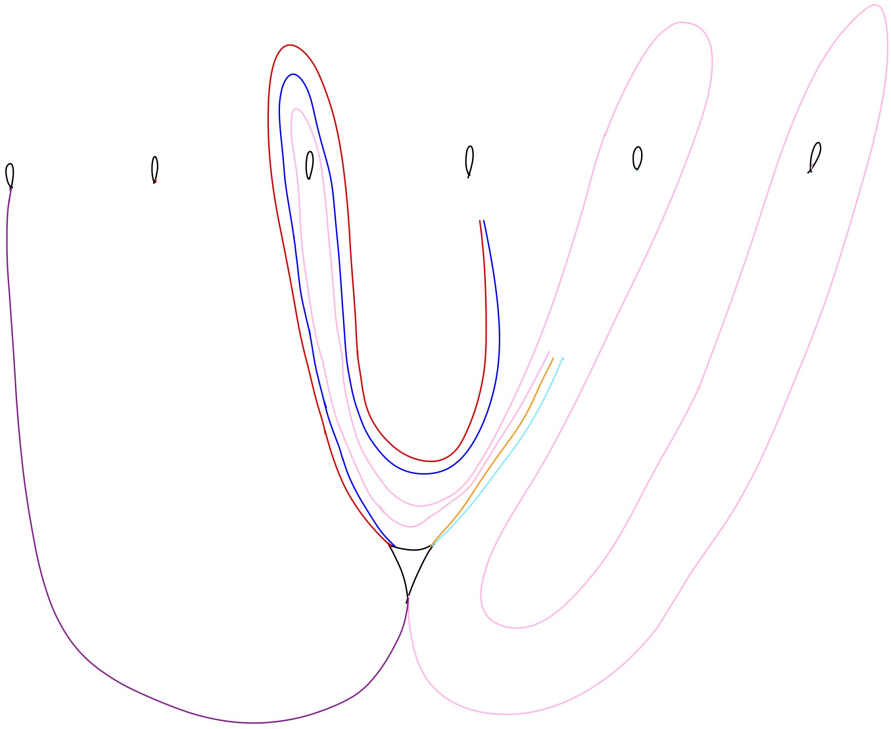


Figure C.64: Ignavia1

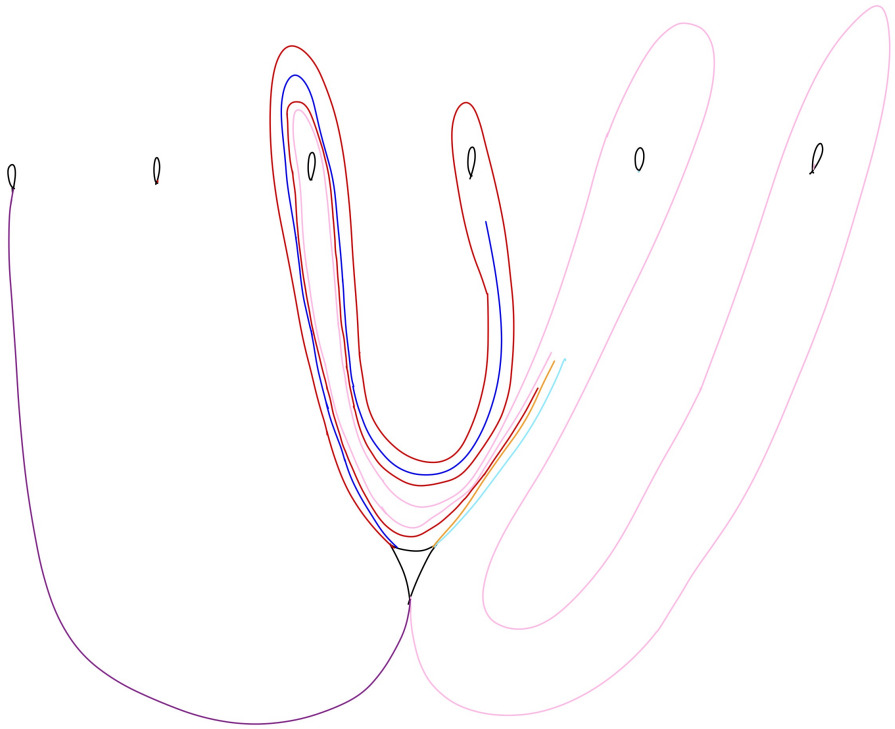


Figure C.65: Ignavia2

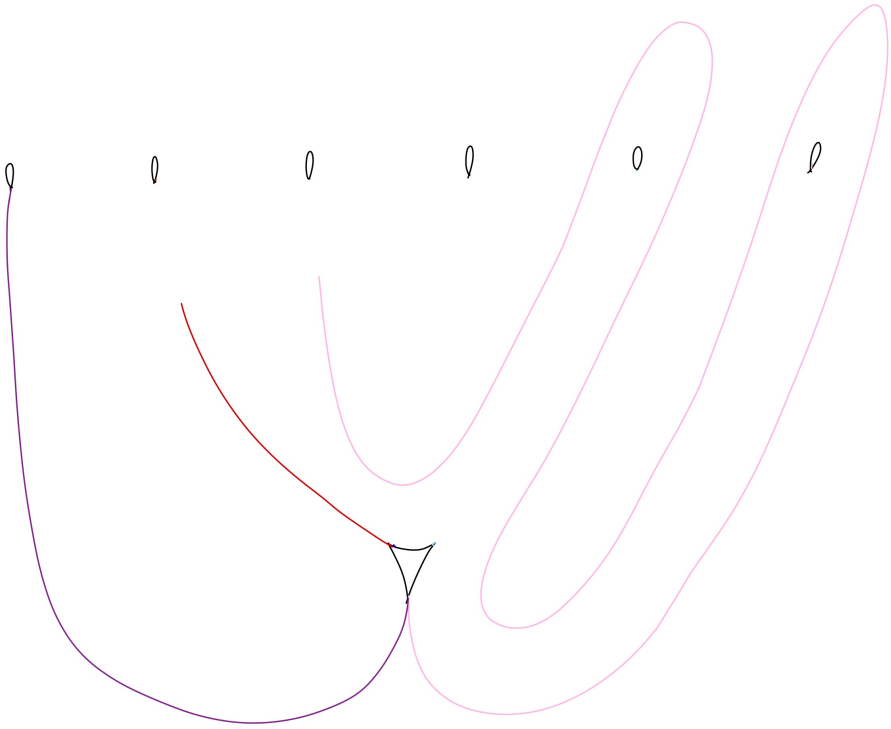


Figure C.66: Zoilus1

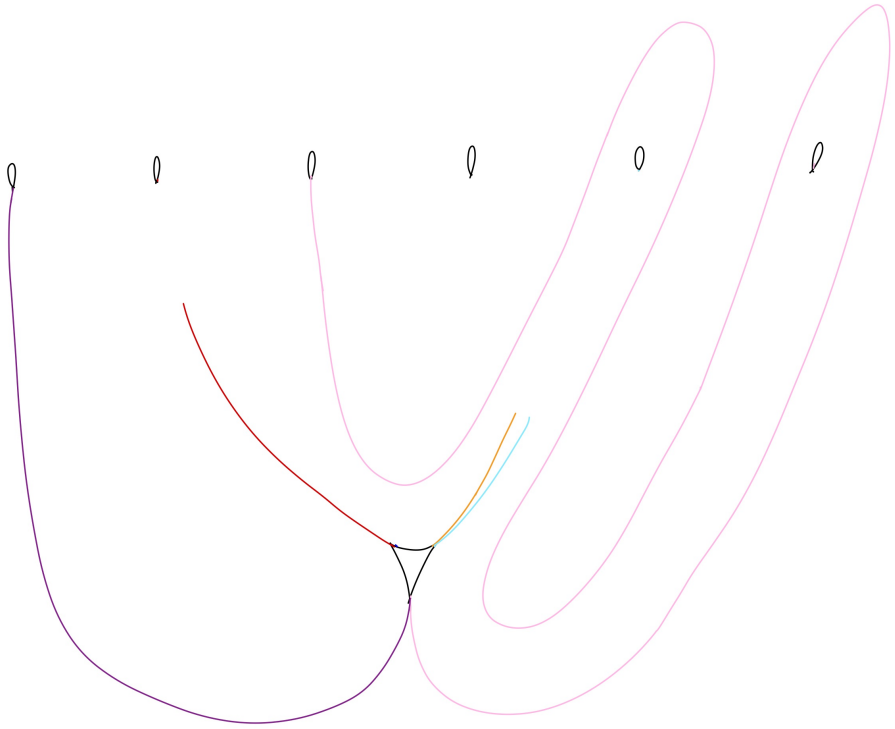


Figure C.67: Jumbuck1

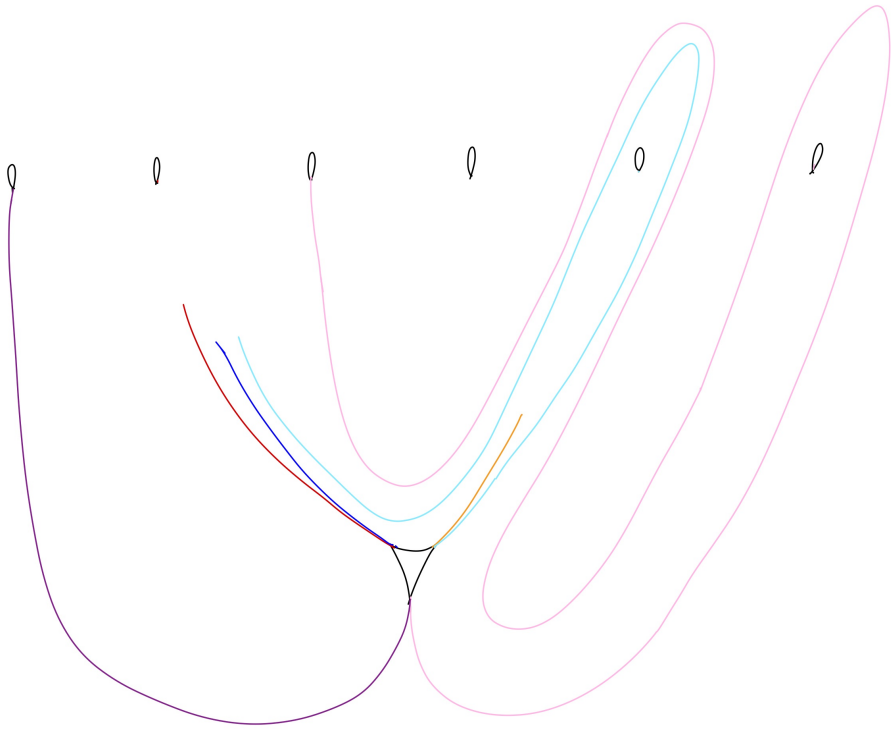


Figure C.68: Jumbuck2

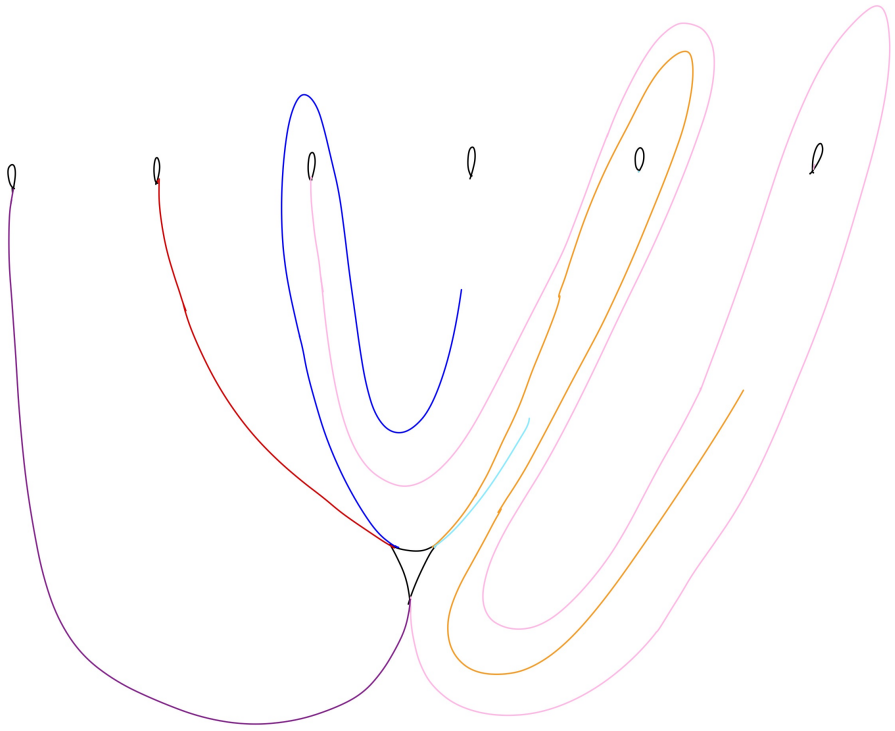


Figure C.69: Jumbuck3

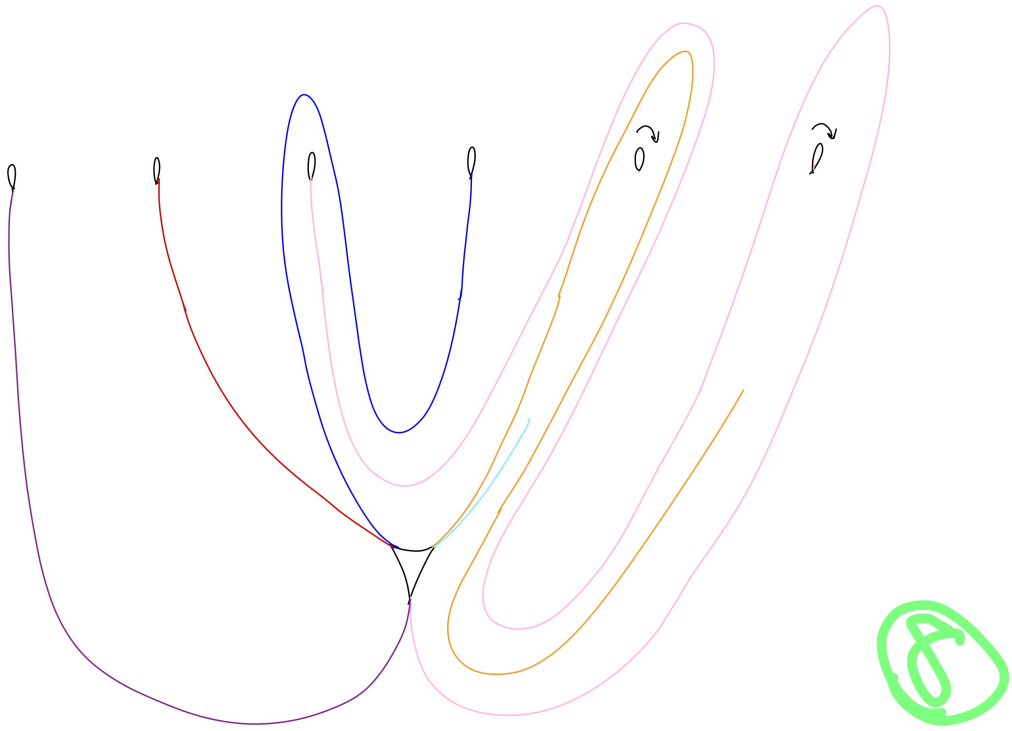


Figure C.70: Jumbuck4

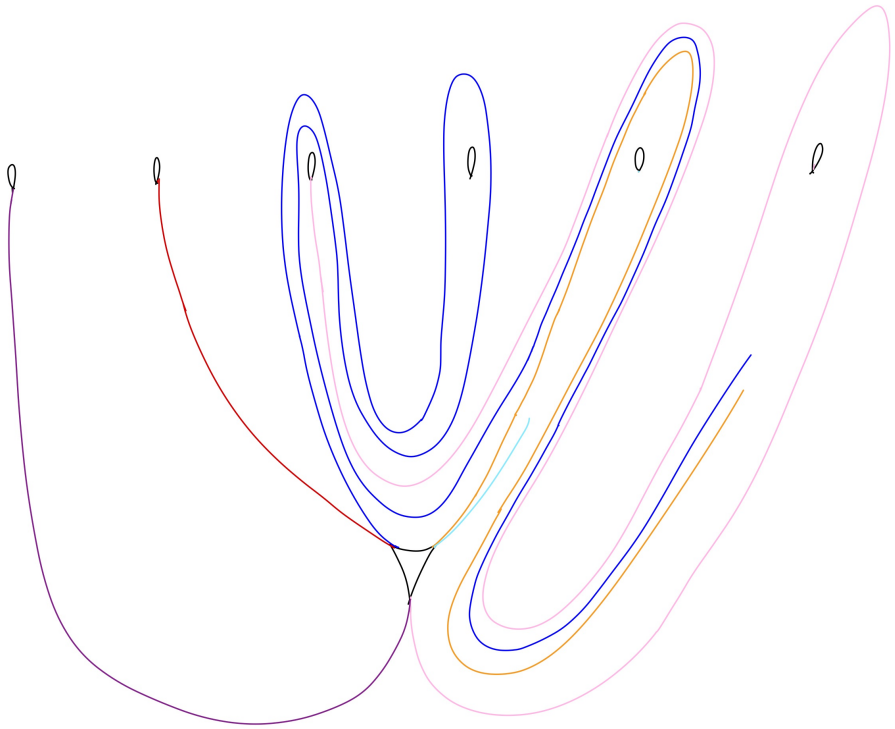


Figure C.71: Jumbuck5

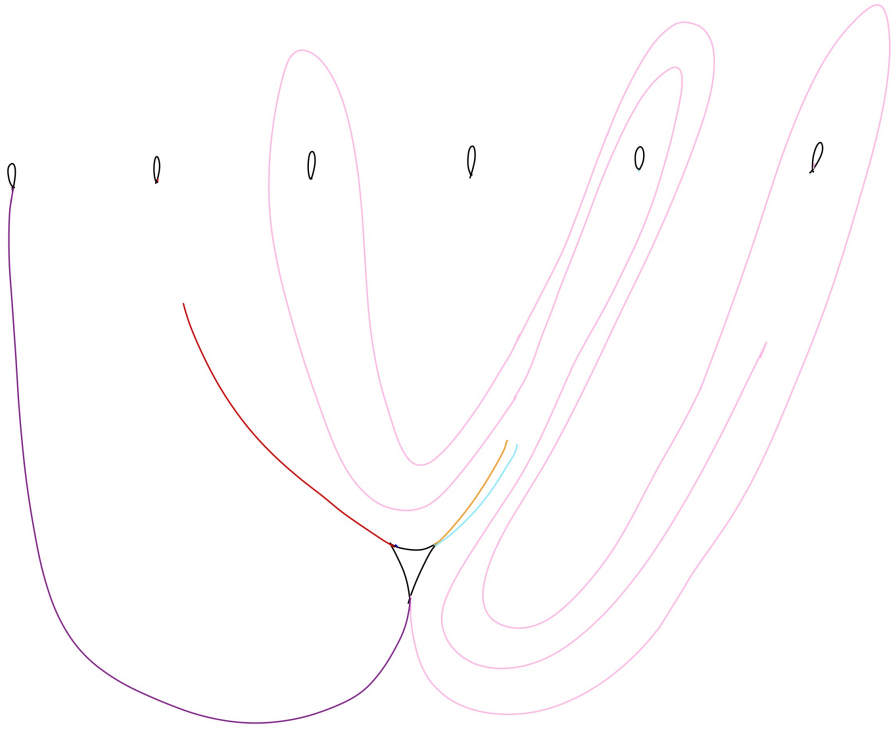


Figure C.72: Nithing1

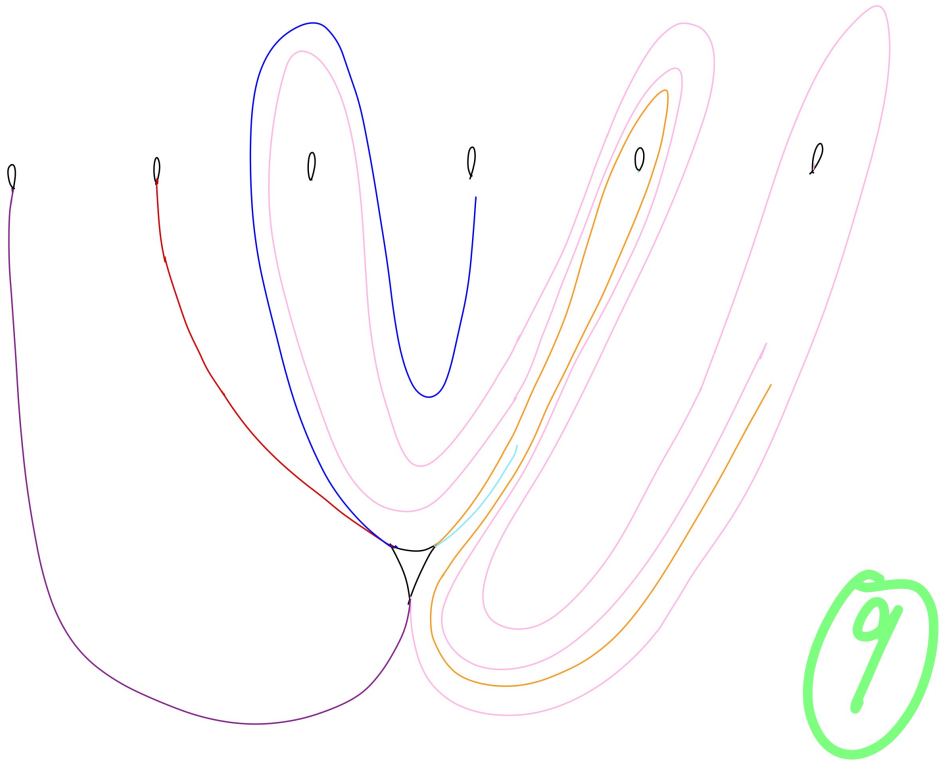


Figure C.73: Nithing2

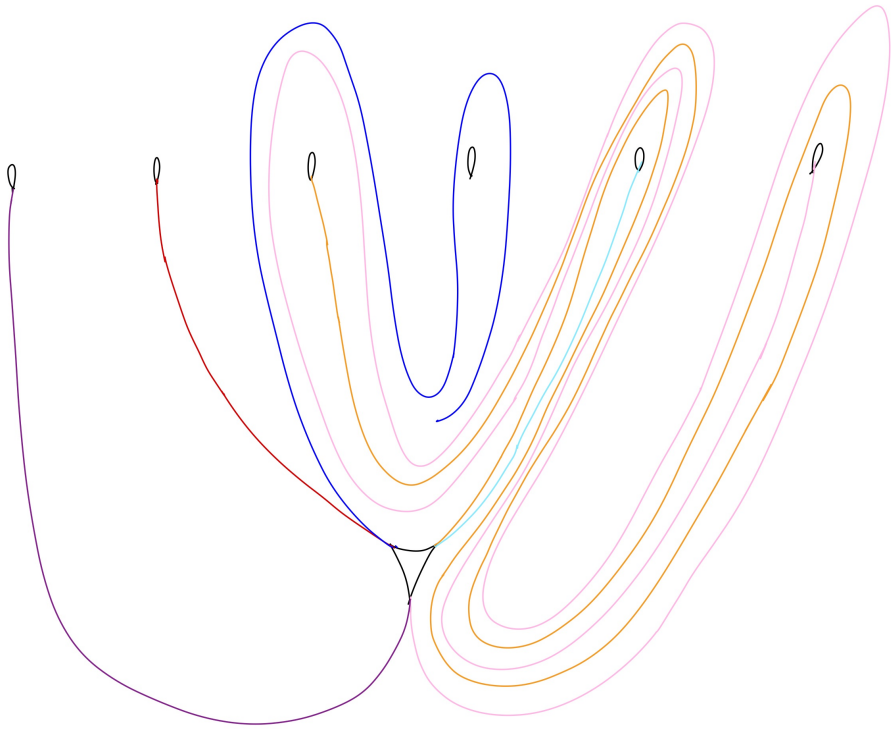


Figure C.74: Nithing3

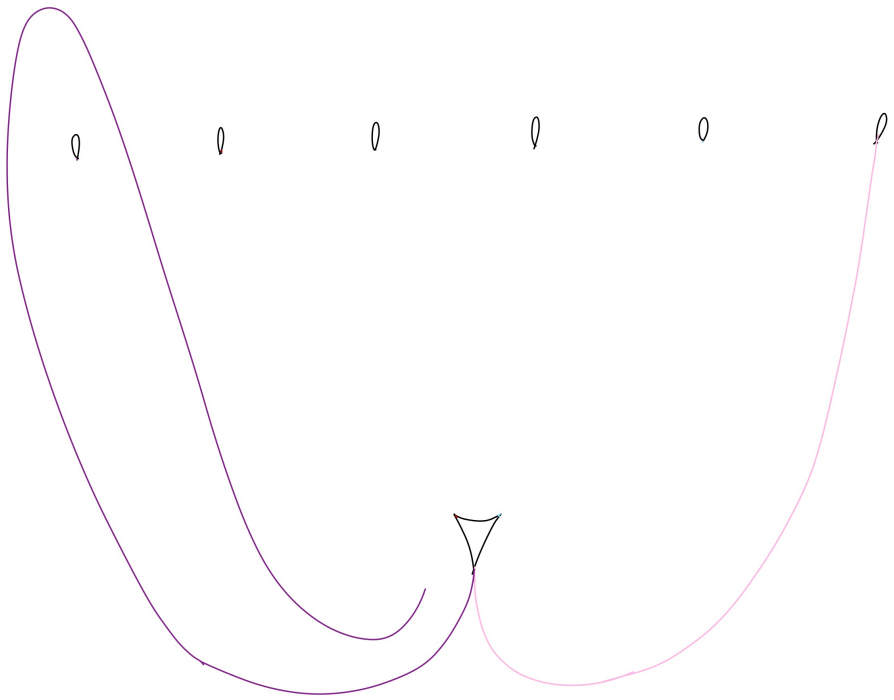


Figure C.75: WST1

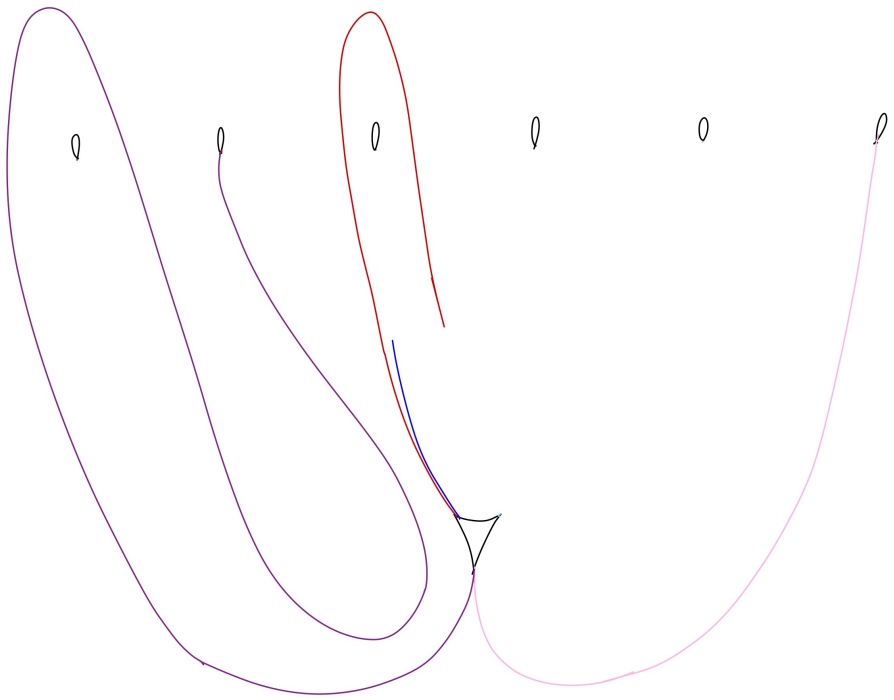


Figure C.76: Tilly1

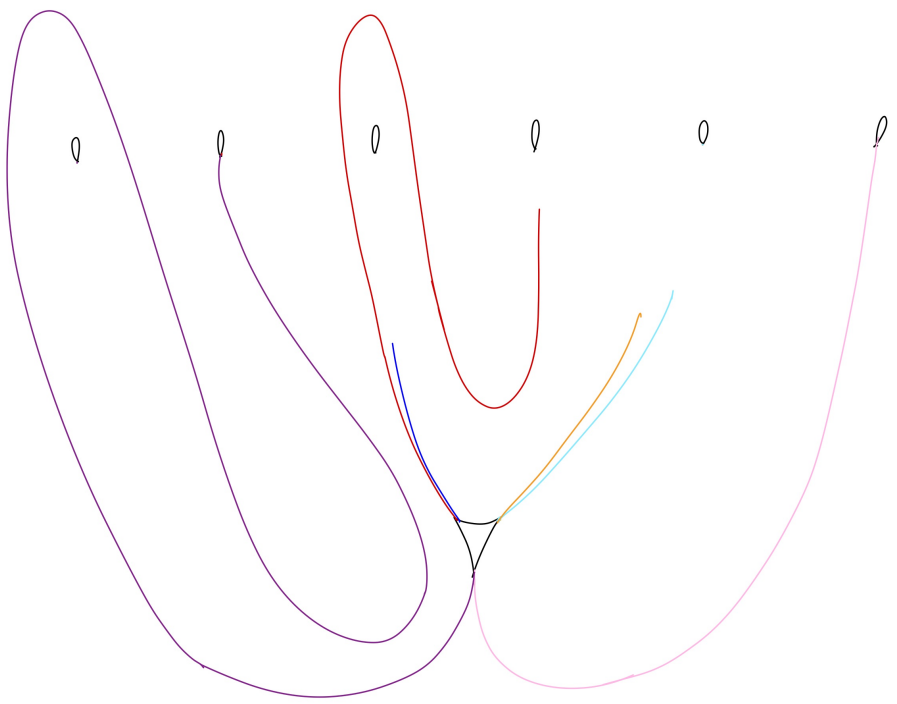


Figure C.77: Tilly2

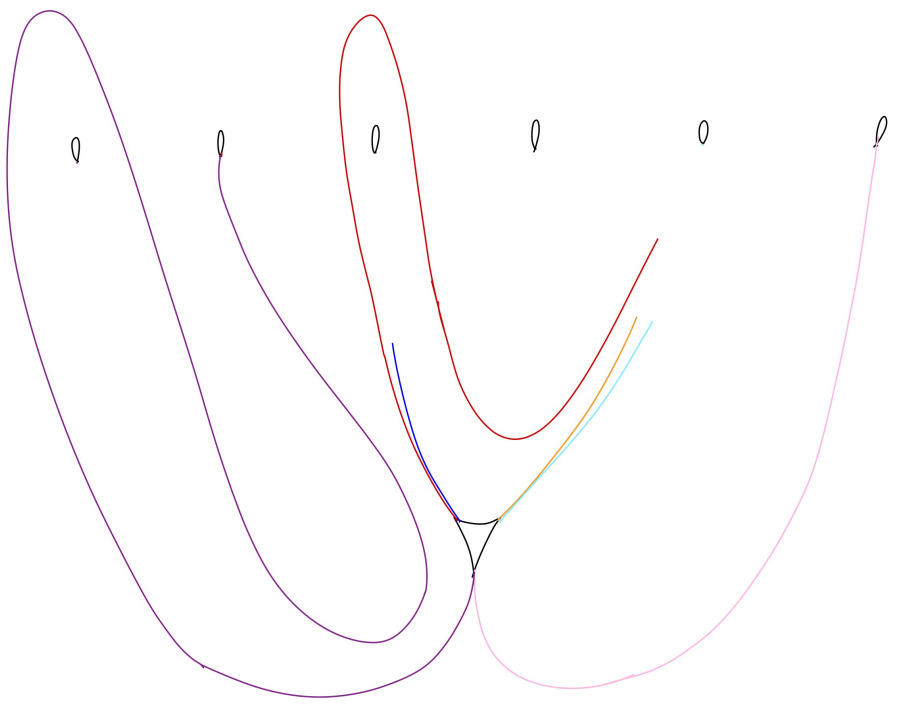


Figure C.78: Tilly3

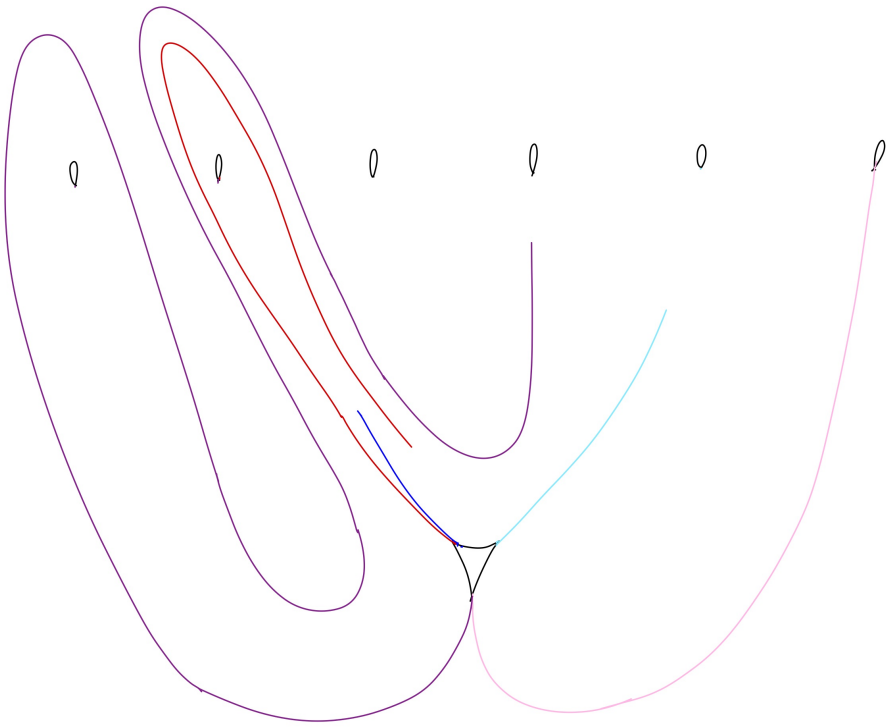


Figure C.79: Whelm1

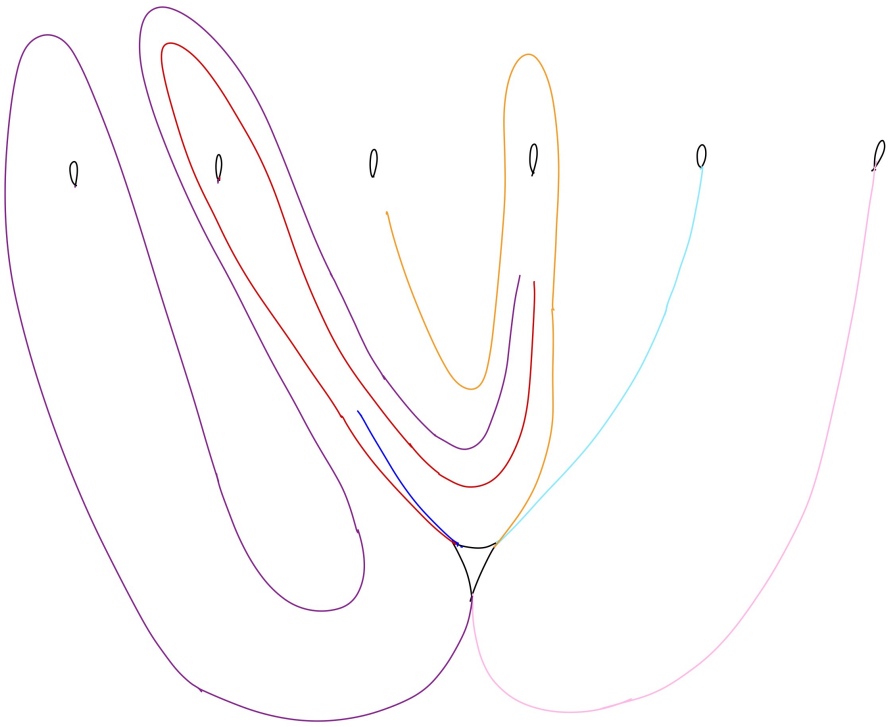


Figure C.80: Bodger1

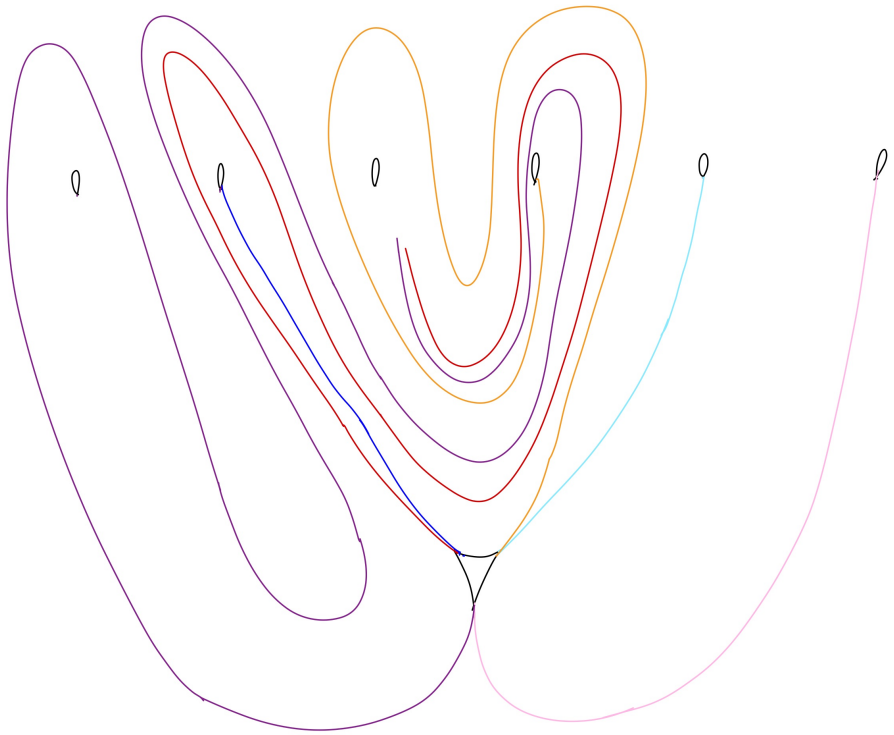


Figure C.81: Bodger2

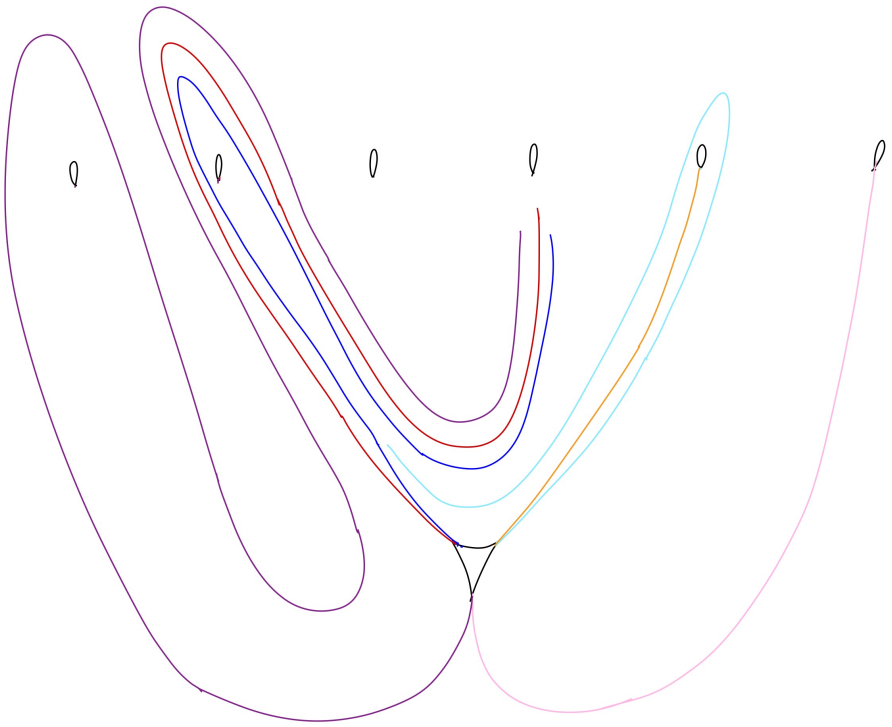


Figure C.82: Callid2

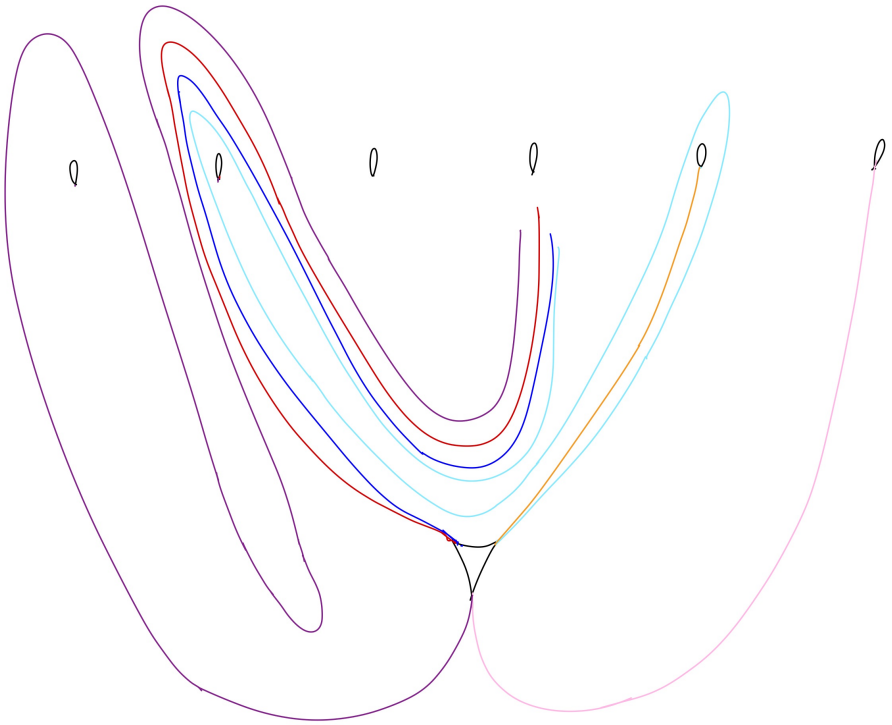


Figure C.83: Callid3

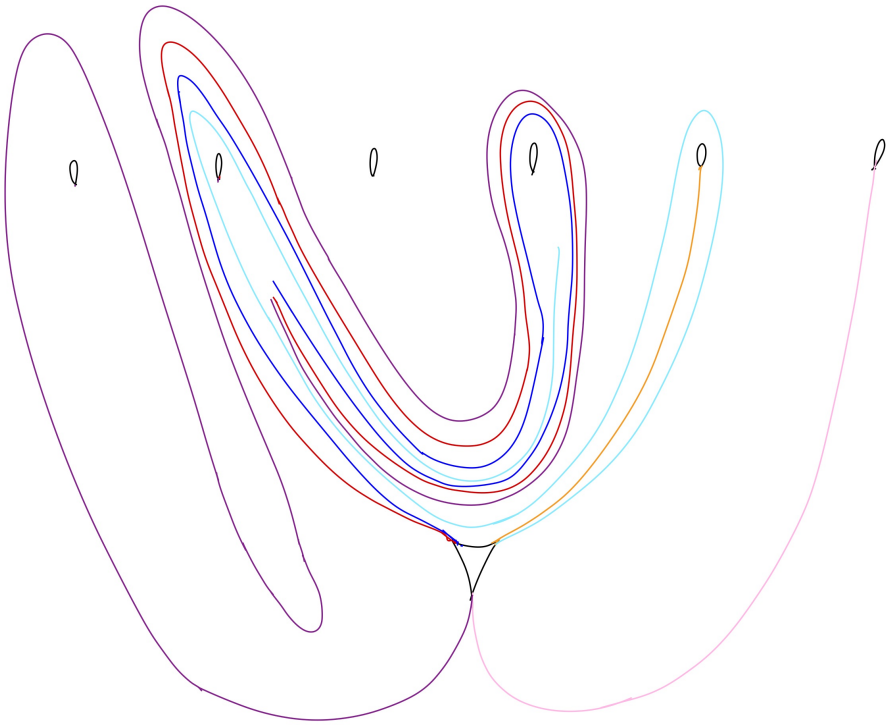


Figure C.84: Callid4

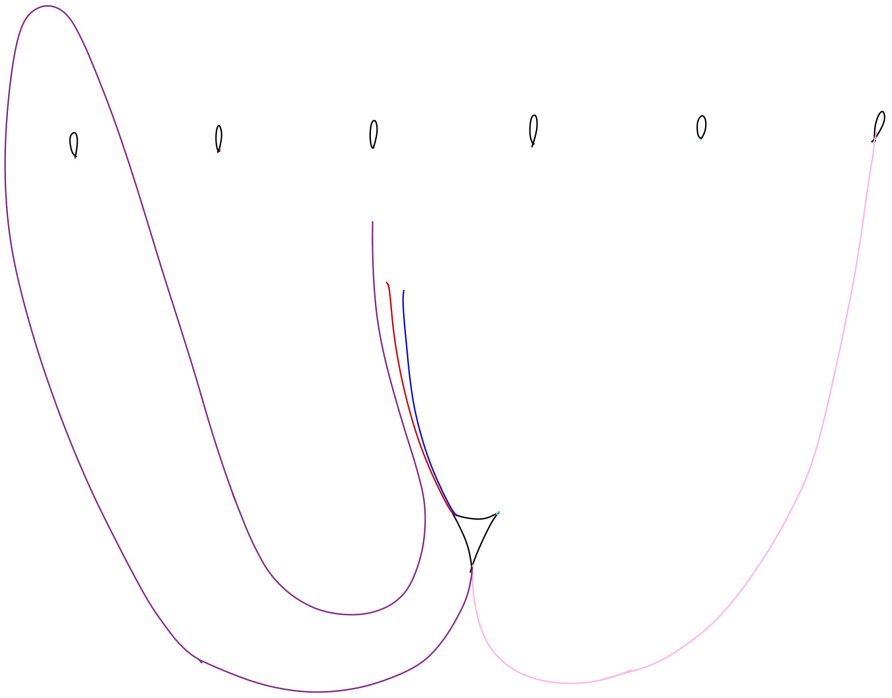


Figure C.85: Dido1

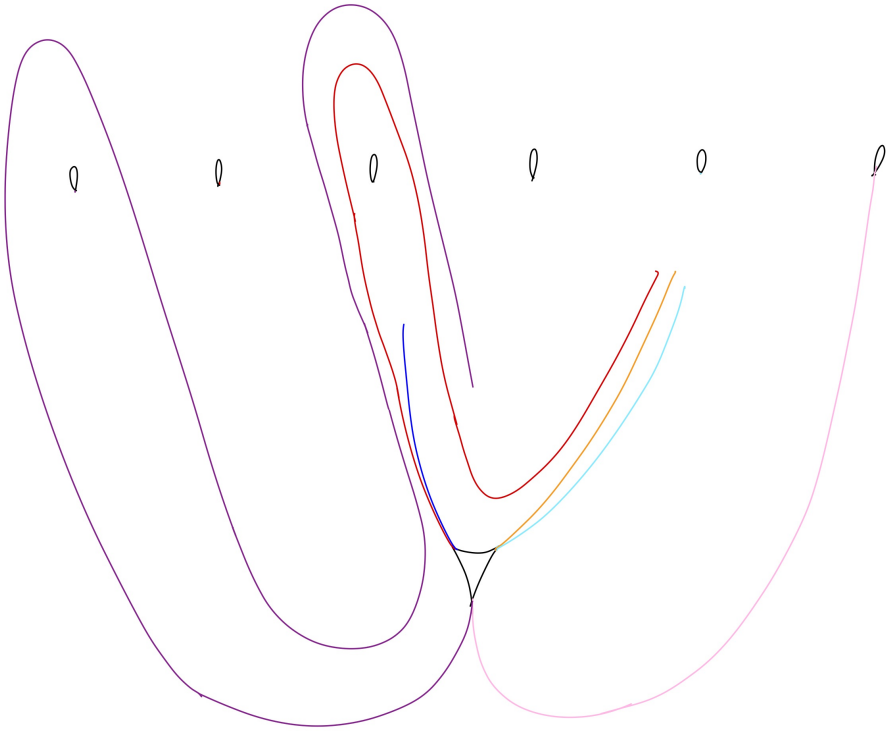


Figure C.86: Dido2

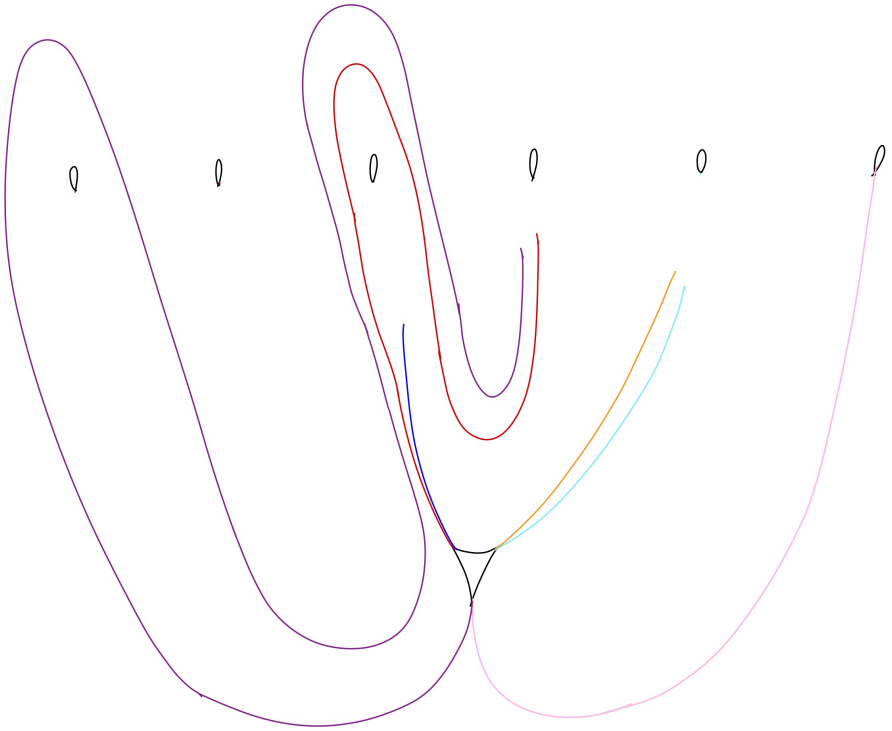


Figure C.87: Dido3

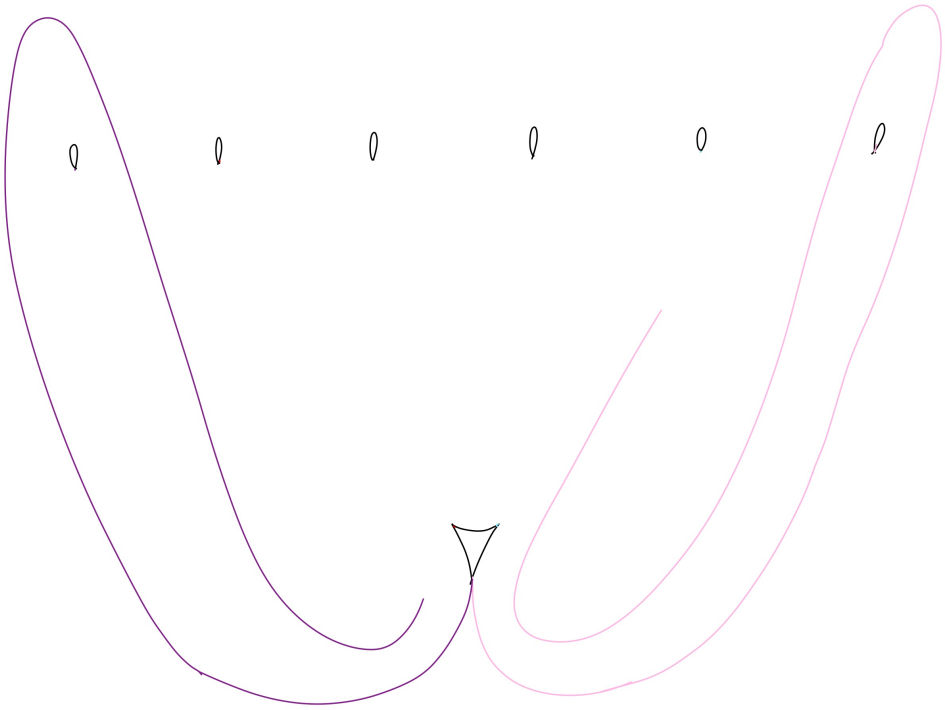


Figure C.88: PPG1

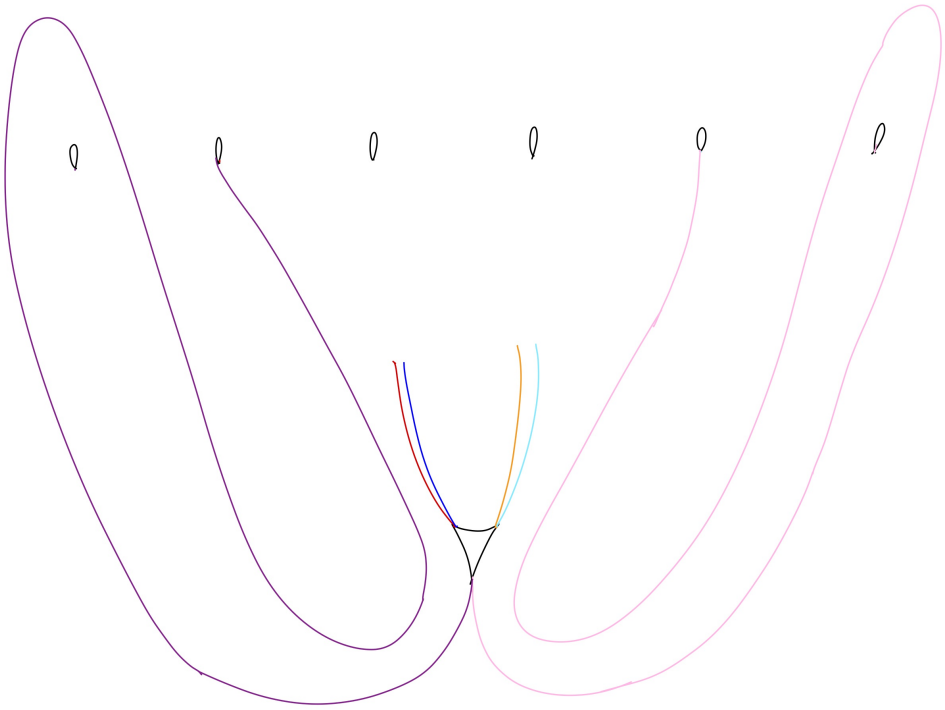


Figure C.89: Fash1

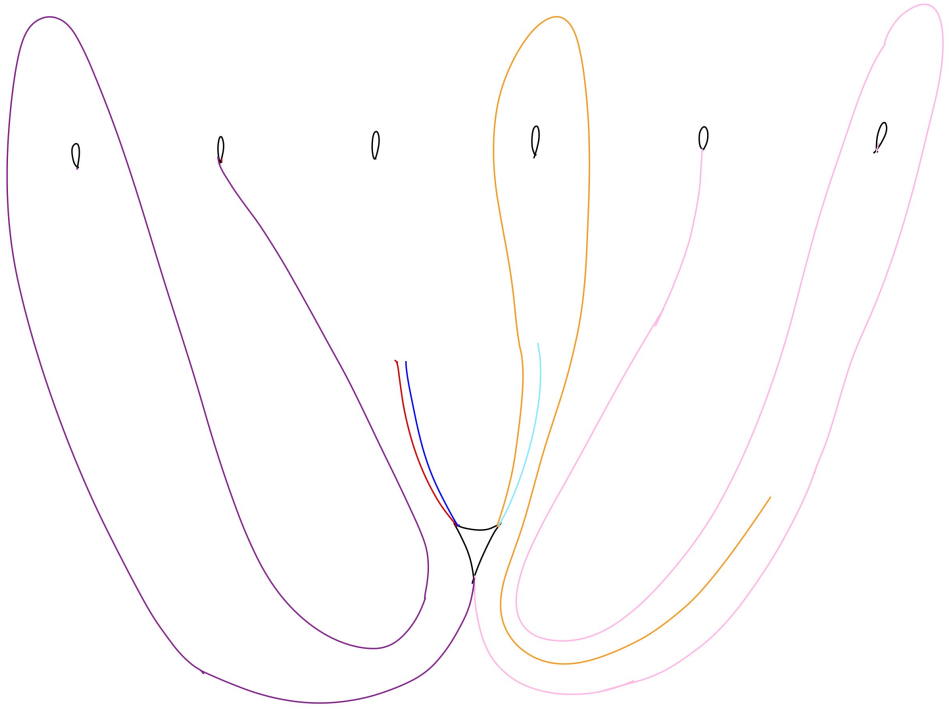


Figure C.90: Fash2

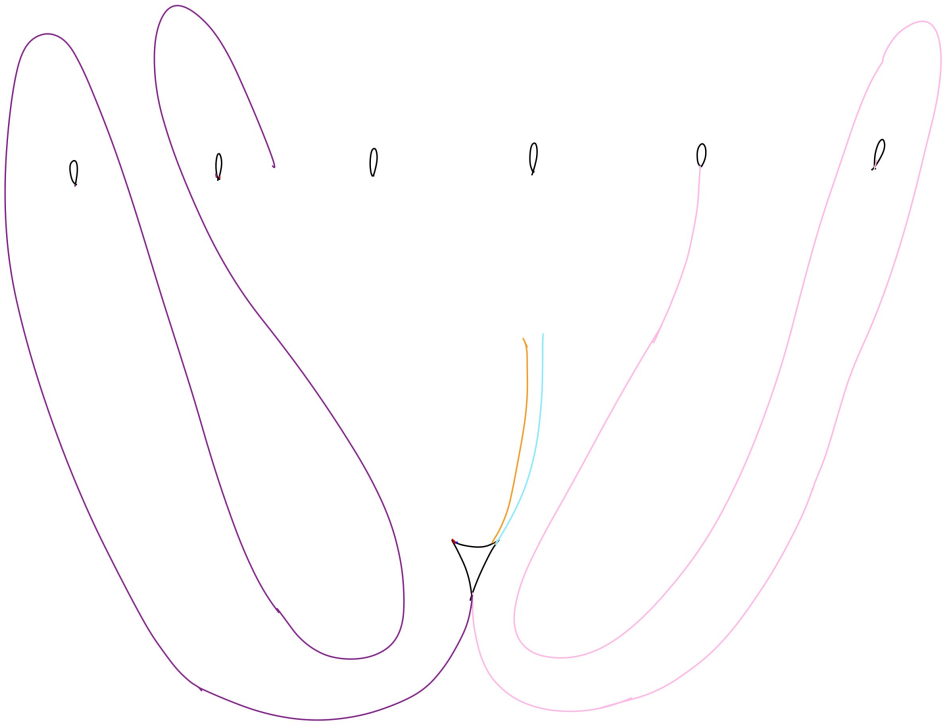


Figure C.91: Fash3

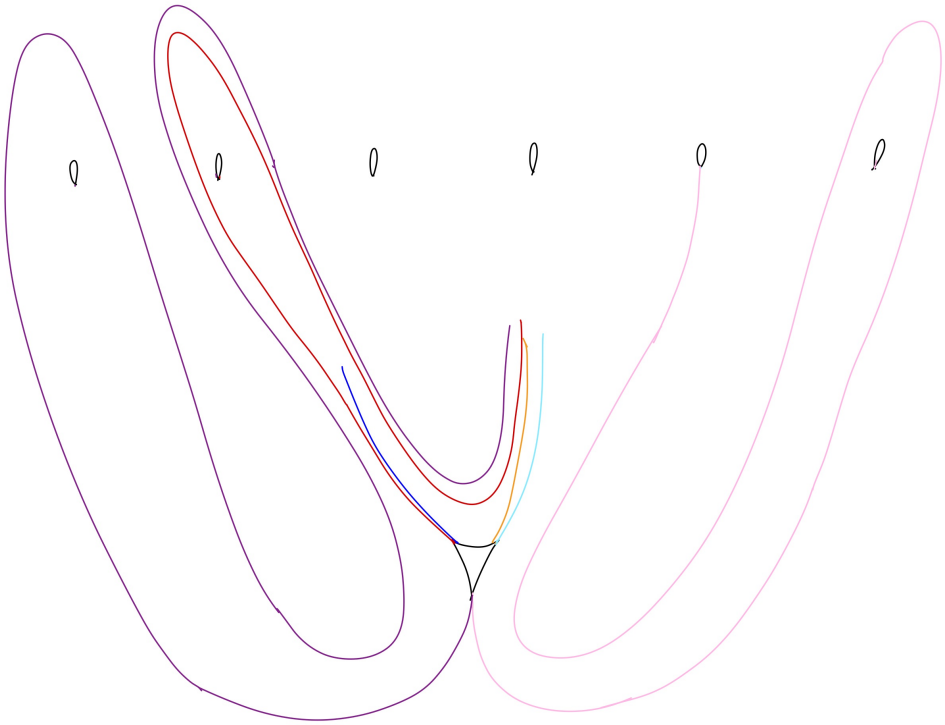


Figure C.92: Fash4

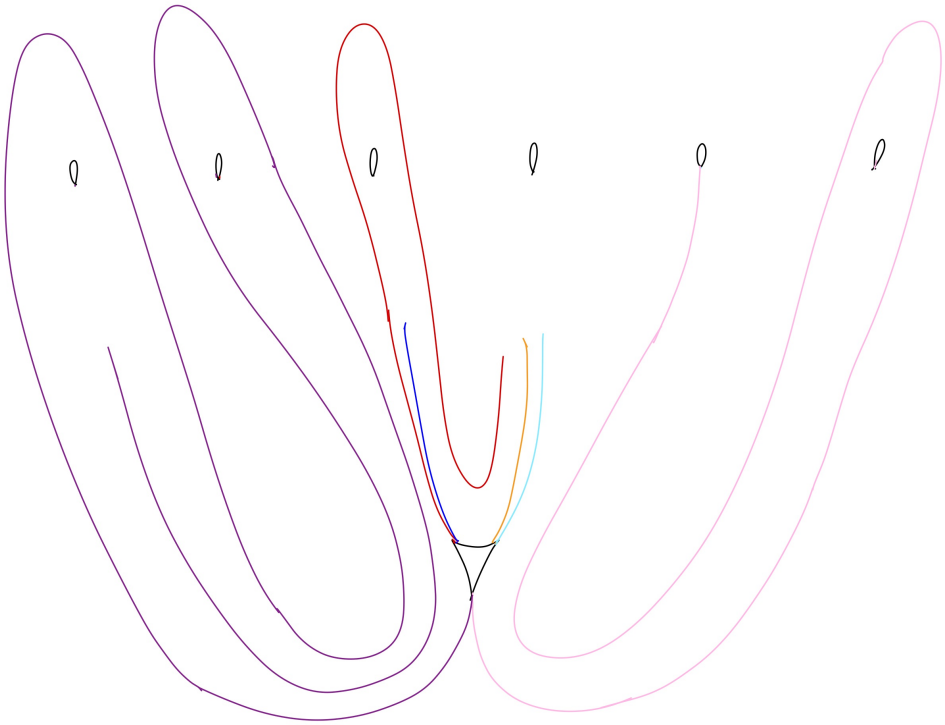


Figure C.93: Fash5

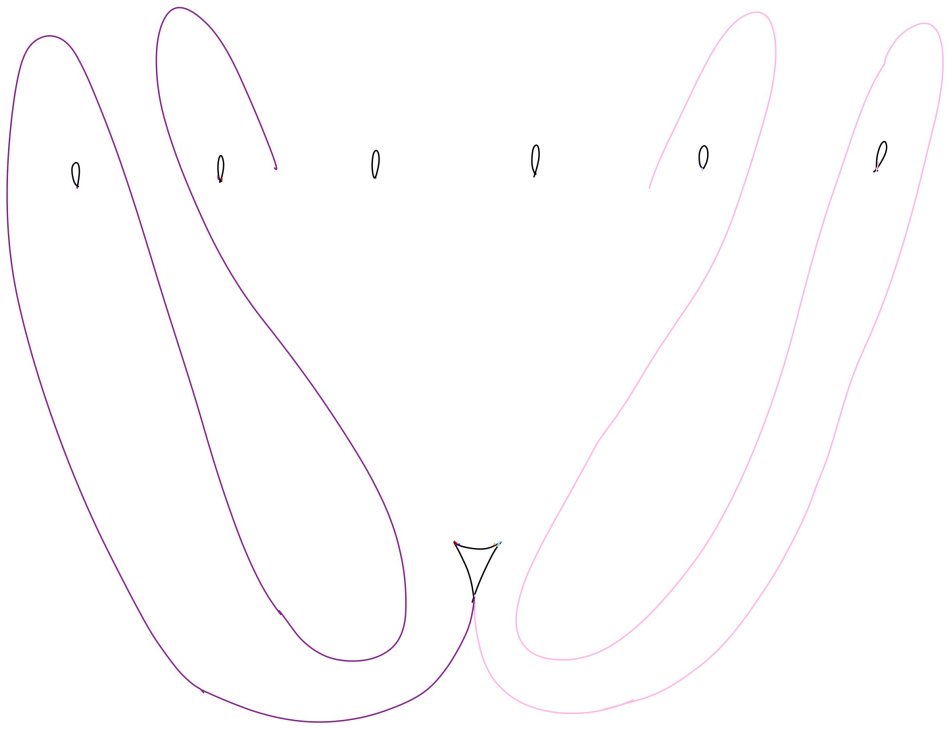


Figure C.94: Fash6

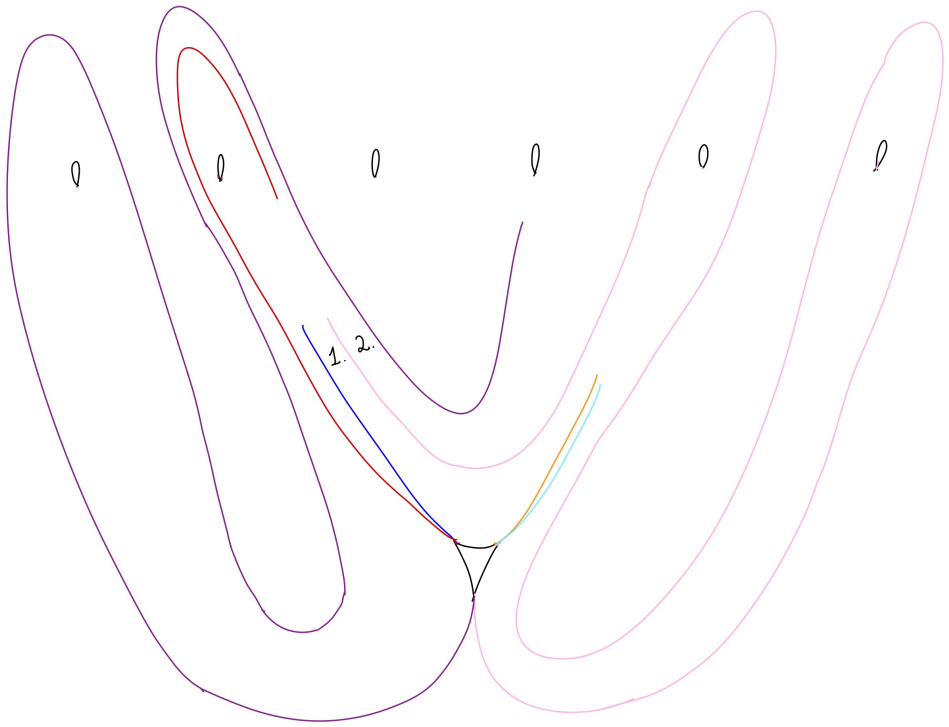


Figure C.95: Xeric1

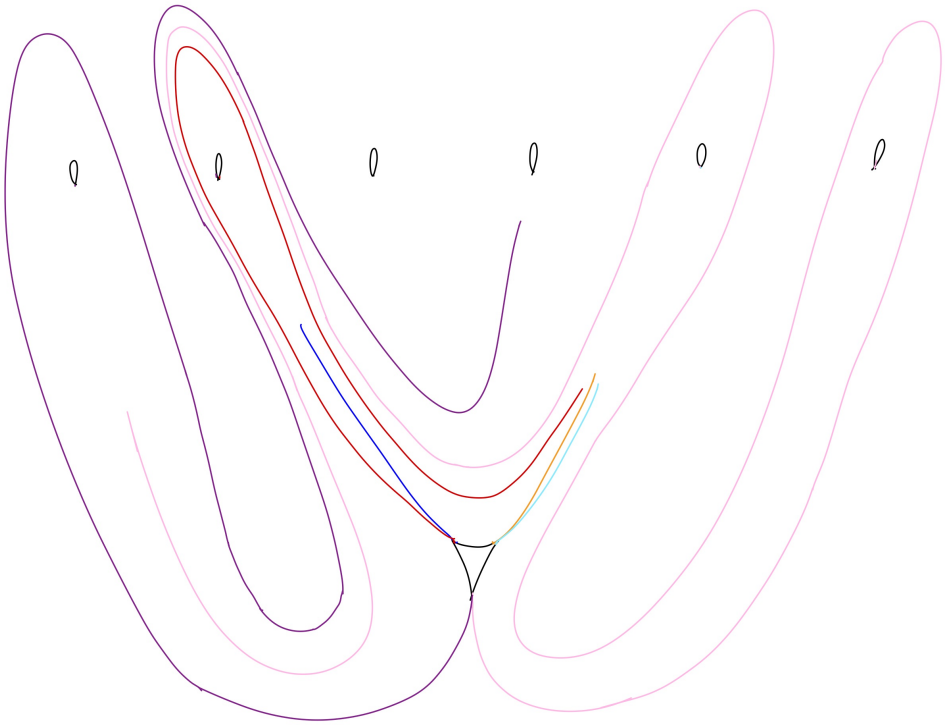


Figure C.96: Xeric2

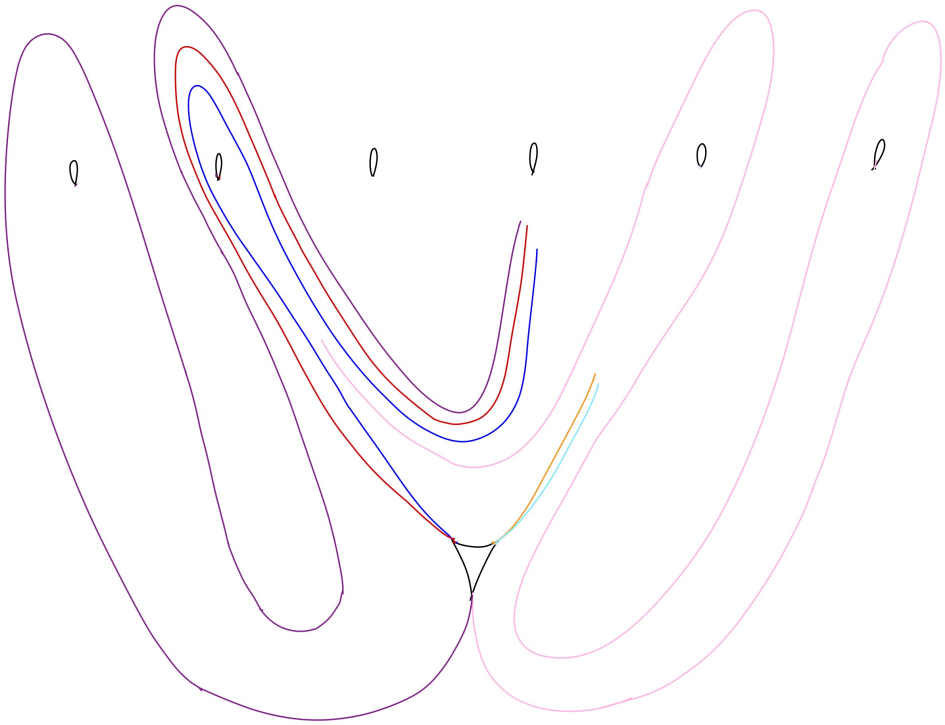


Figure C.97: Xeric3

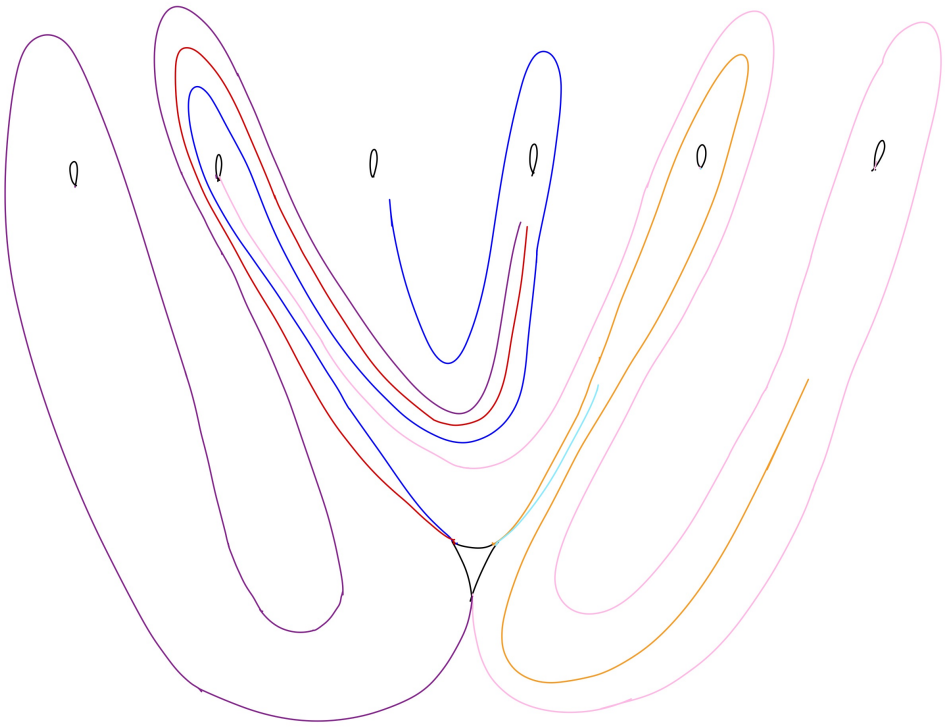


Figure C.98: Fizgig1

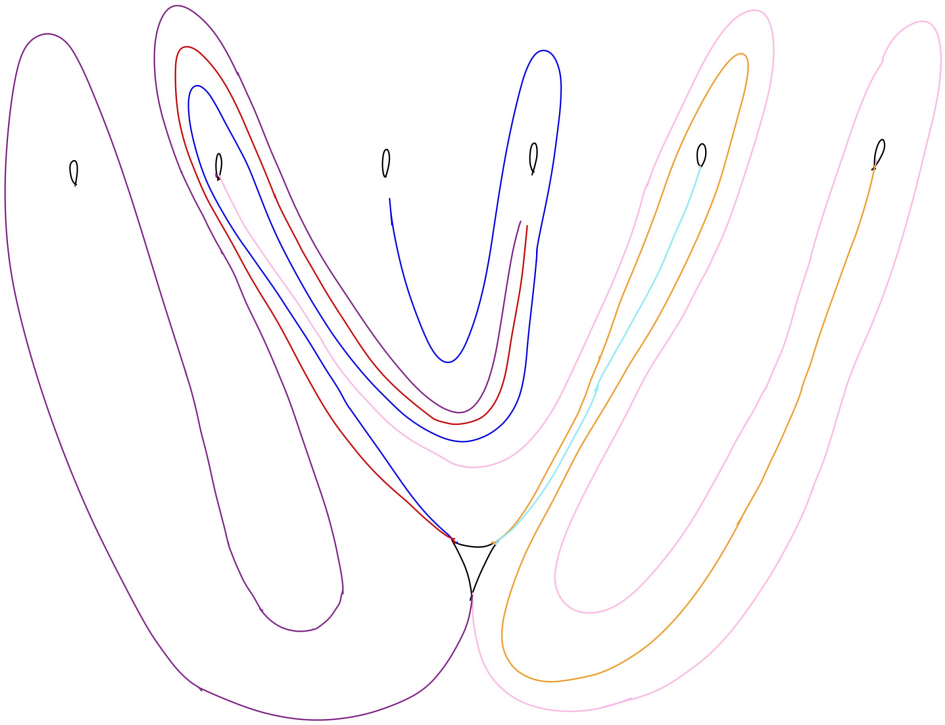


Figure C.99: Quiddit1

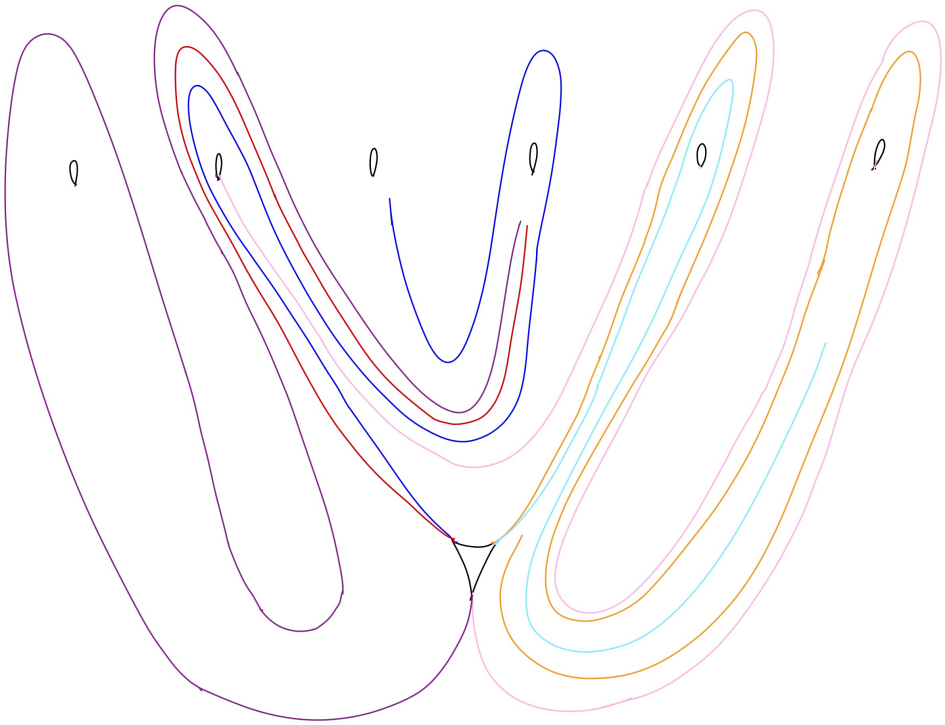


Figure C.100: Rudesby1

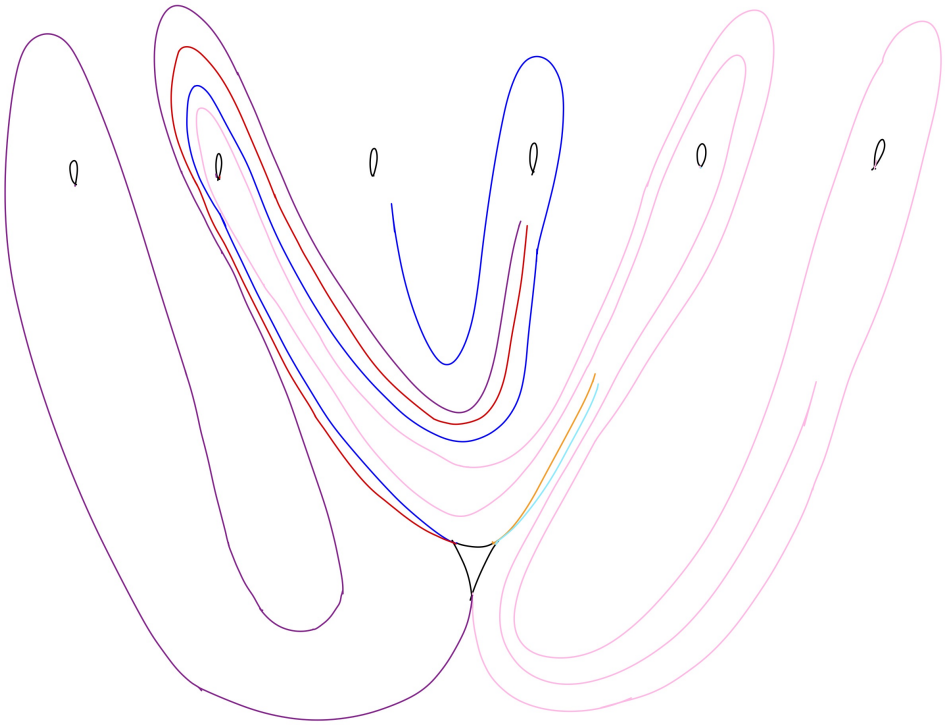


Figure C.101: Bawbee2

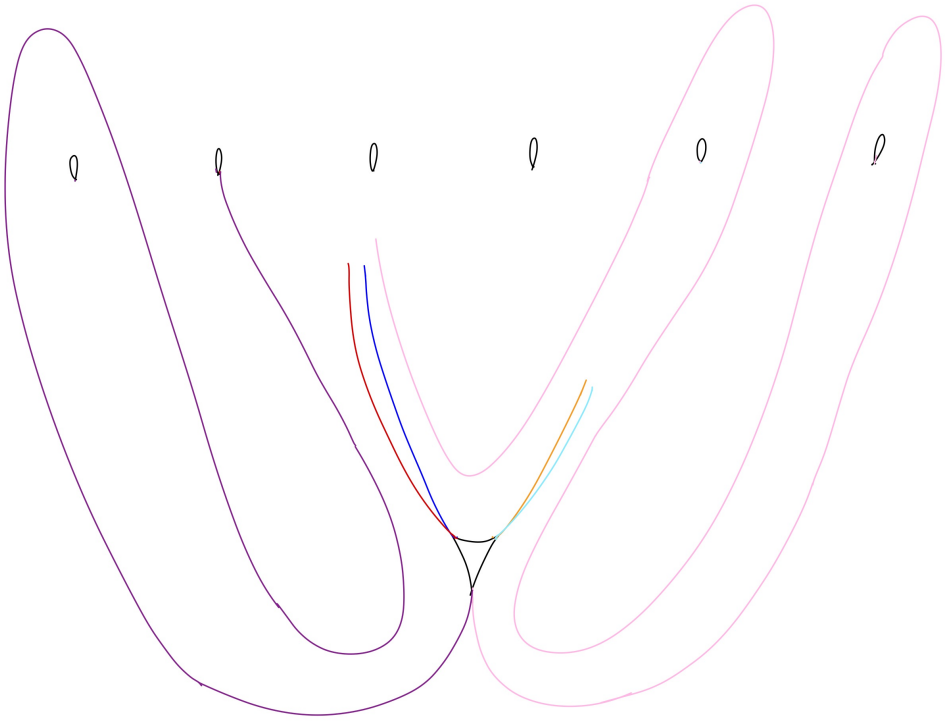


Figure C.102: Bavin1

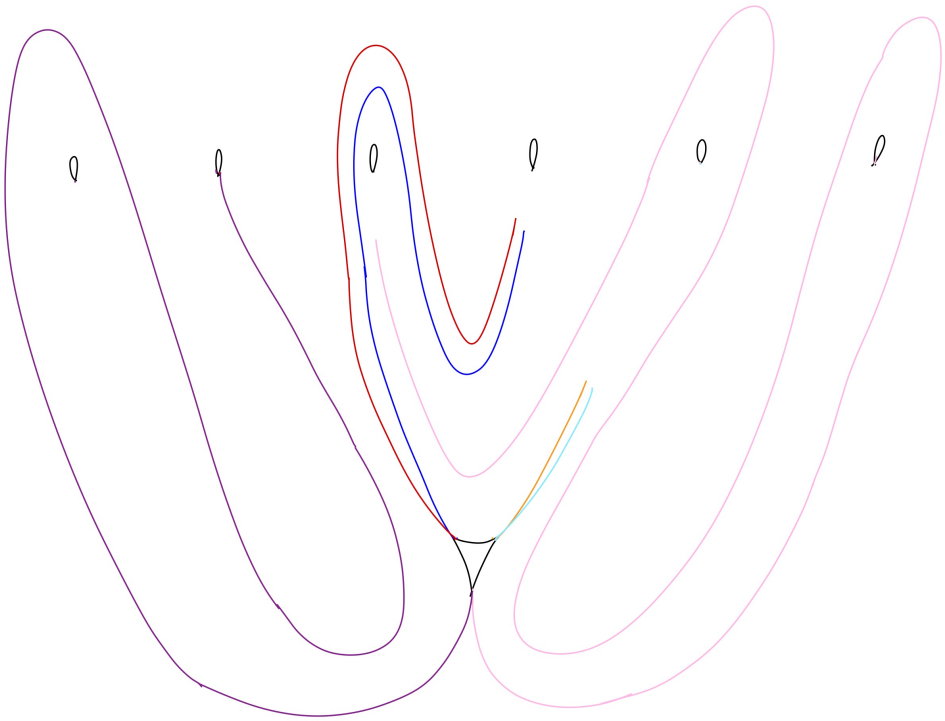


Figure C.103: Bavin2

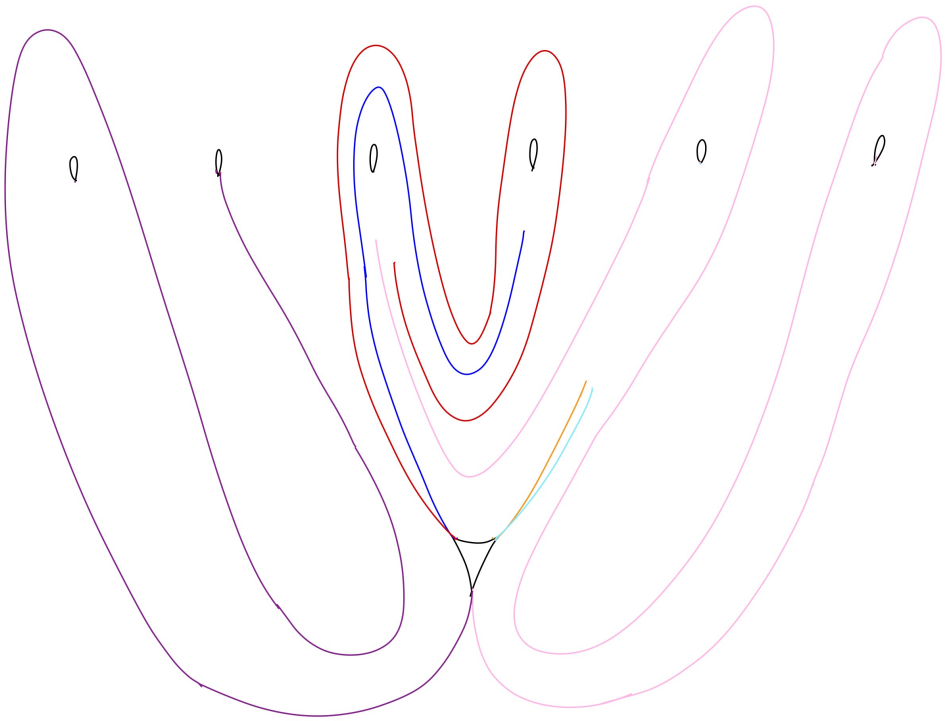


Figure C.104: Bavin3

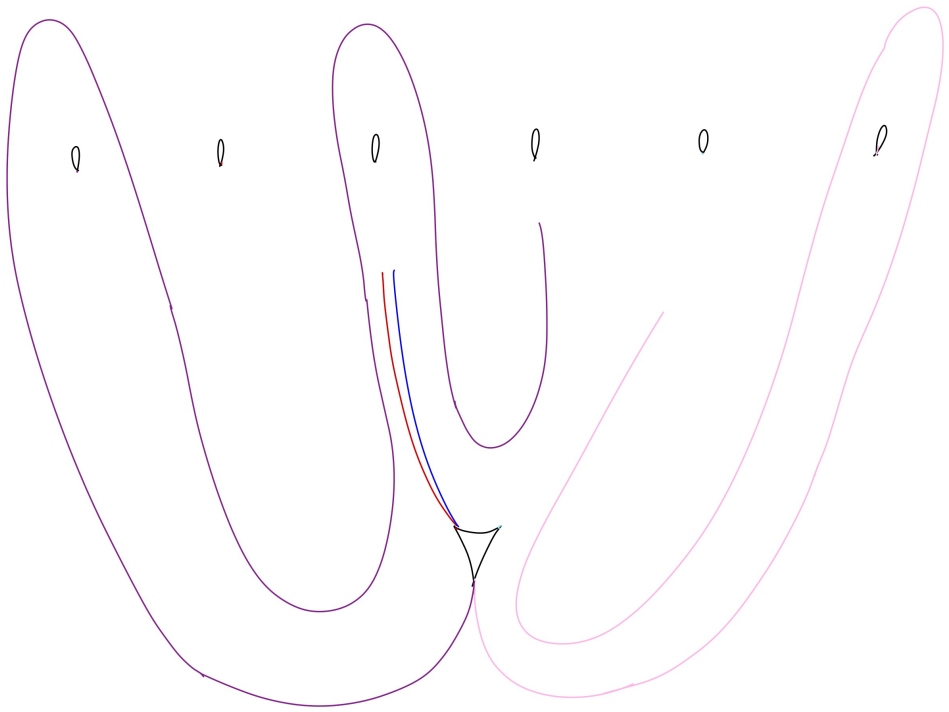


Figure C.105: Gley1

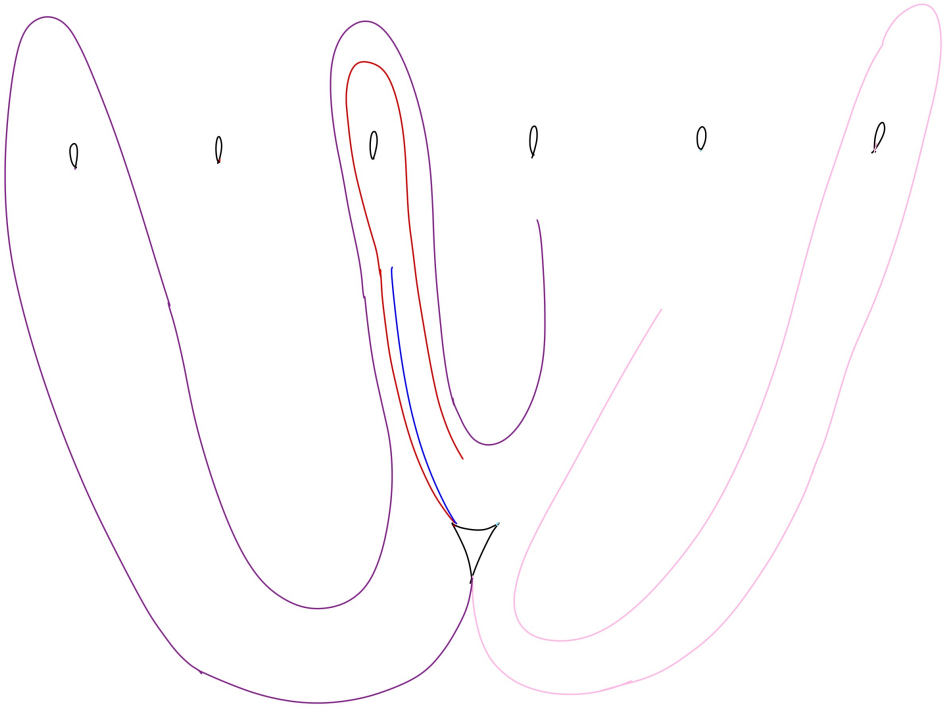


Figure C.106: Gley2

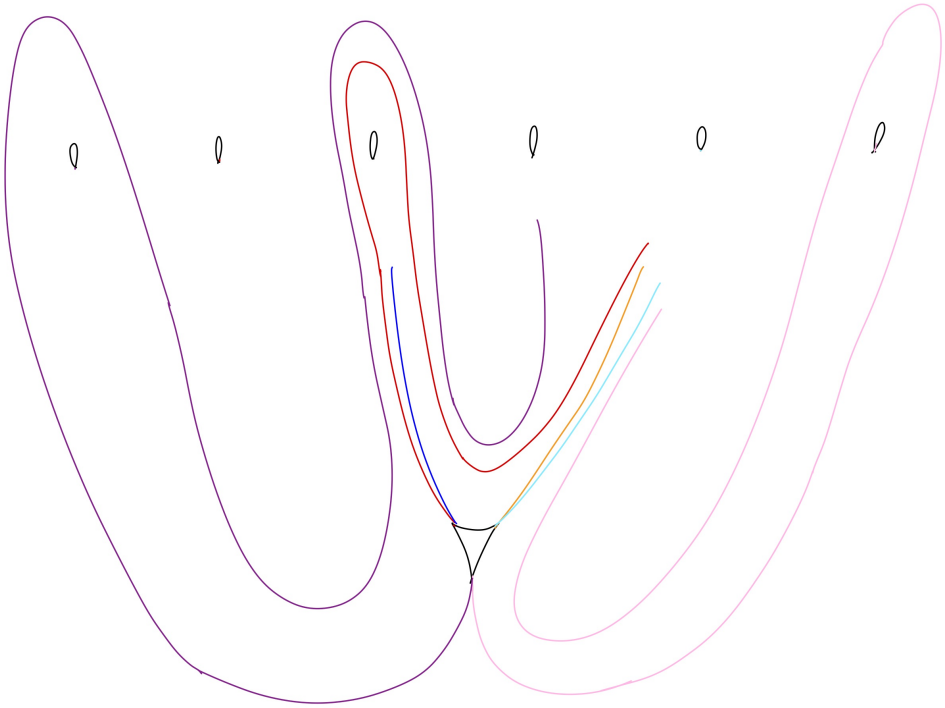


Figure C.107: Gley3

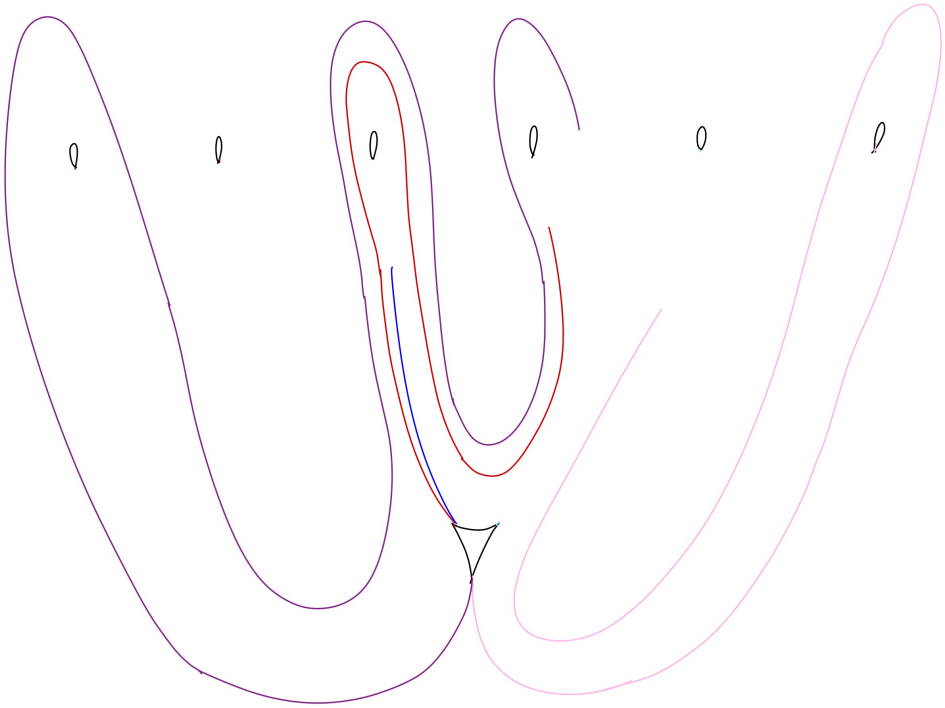


Figure C.108: Gley4

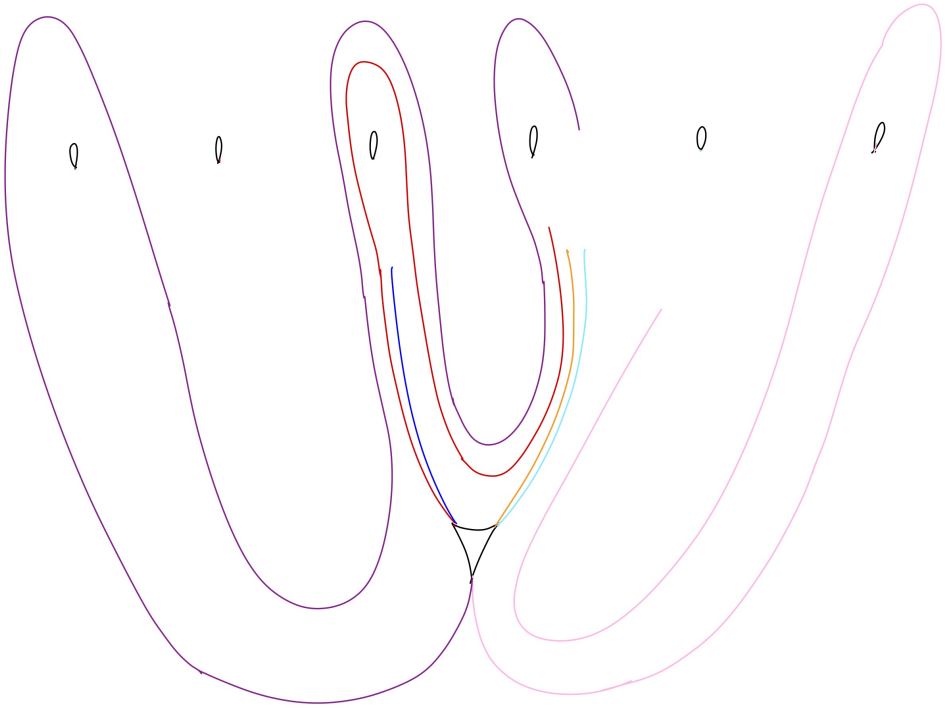


Figure C.109: Gley5

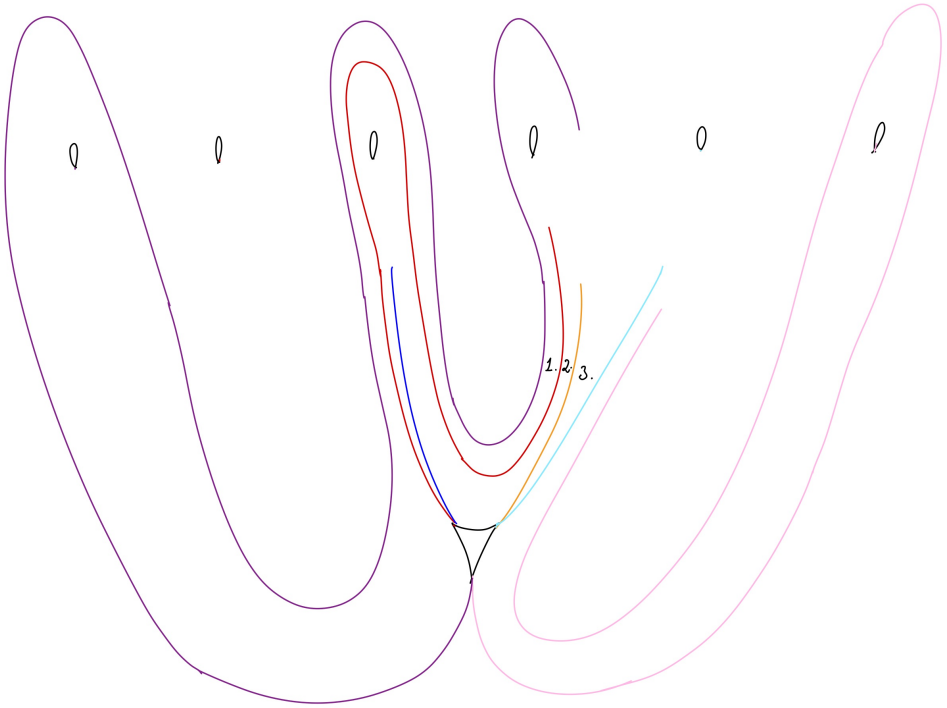


Figure C.110: Gley6

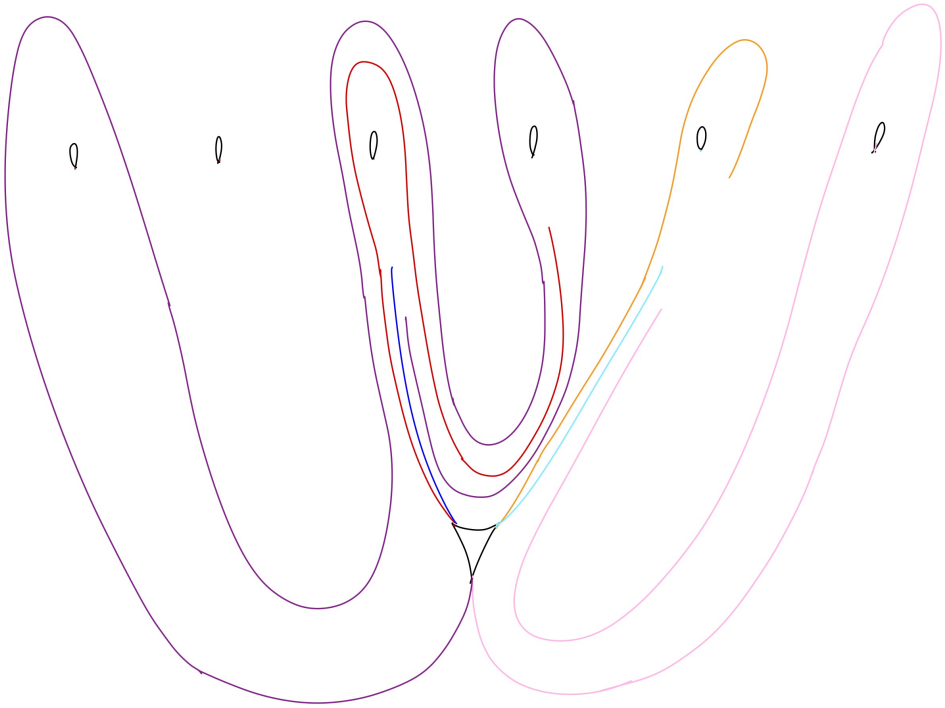


Figure C.111: Gley7

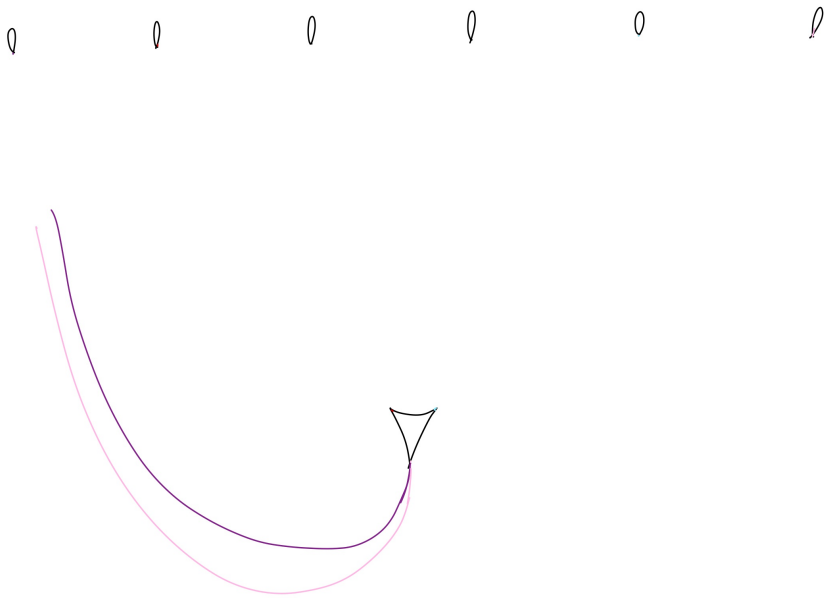


Figure C.112: WVL1

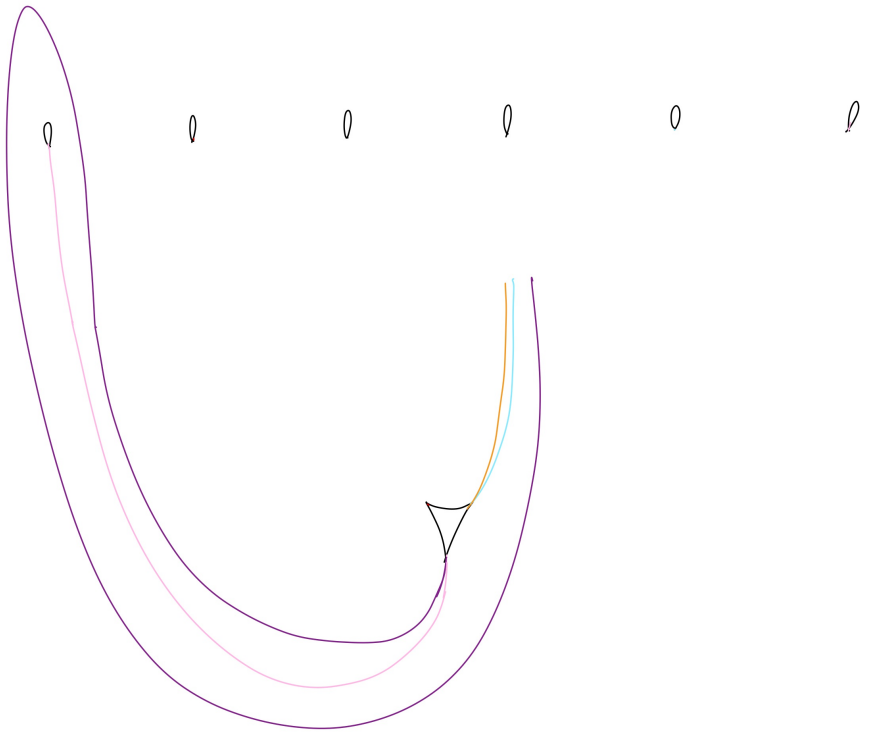


Figure C.113: Birl1

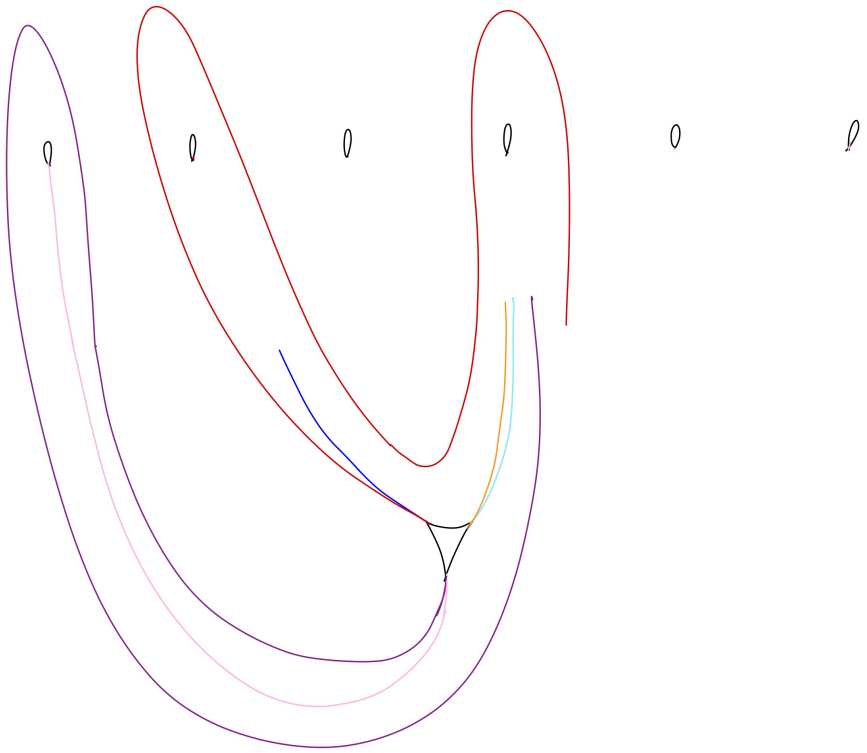


Figure C.114: Birl2

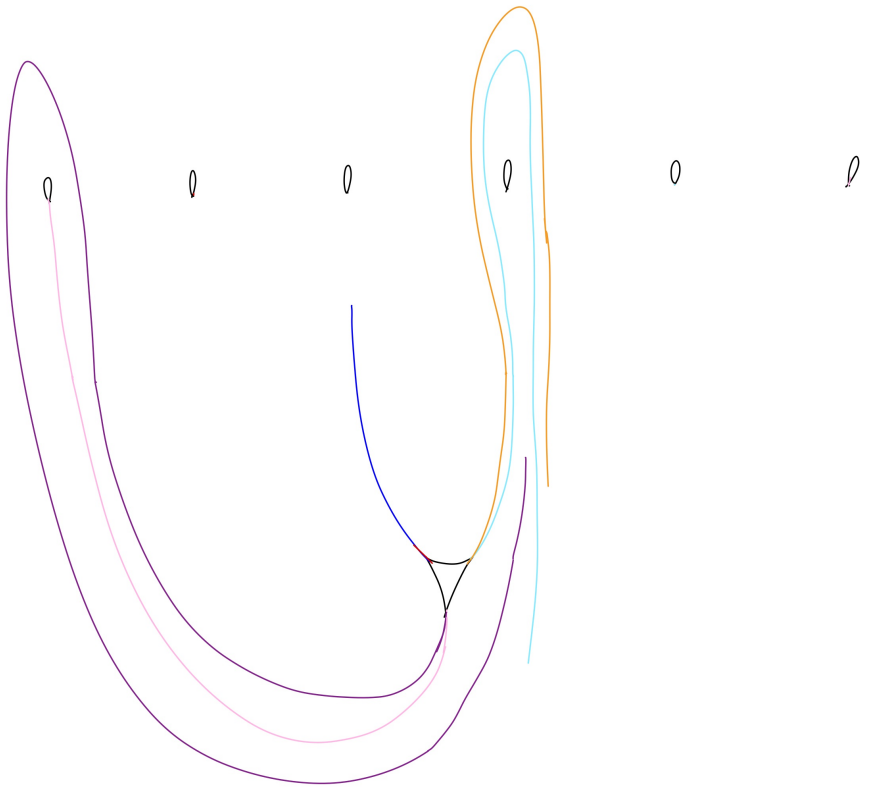


Figure C.115: Birl3

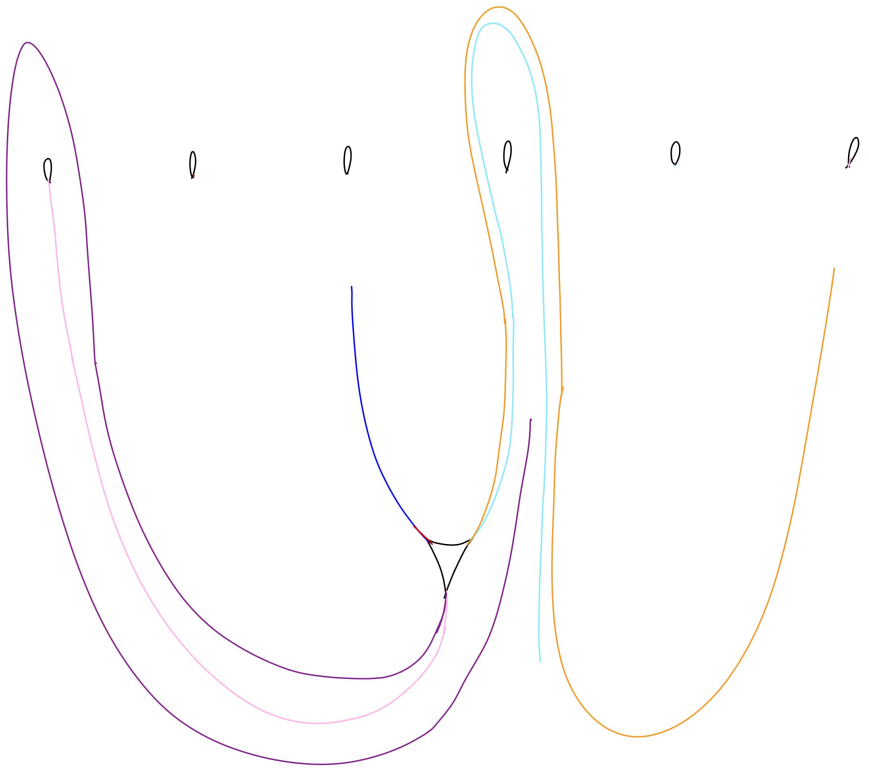


Figure C.116: Birl4

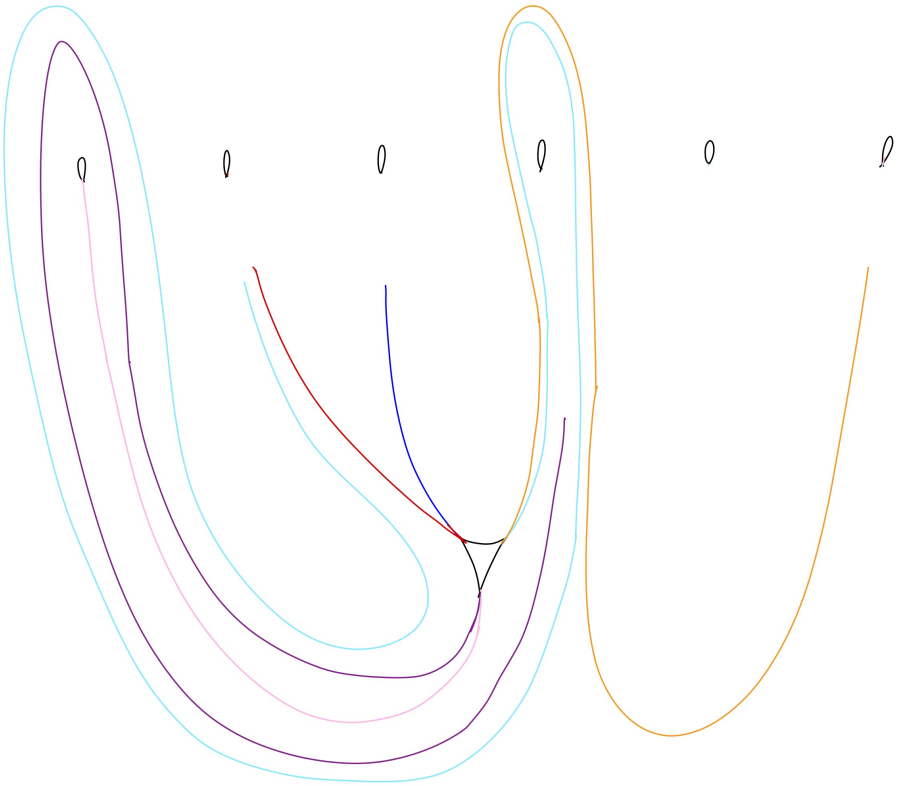


Figure C.117: Eisel1

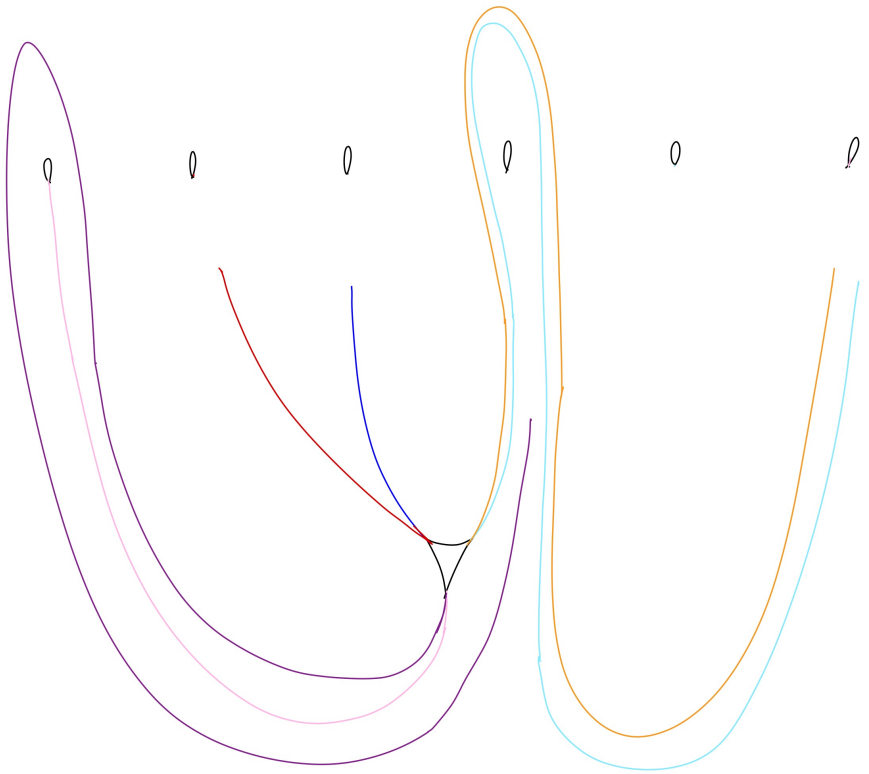


Figure C.118: Eisel2

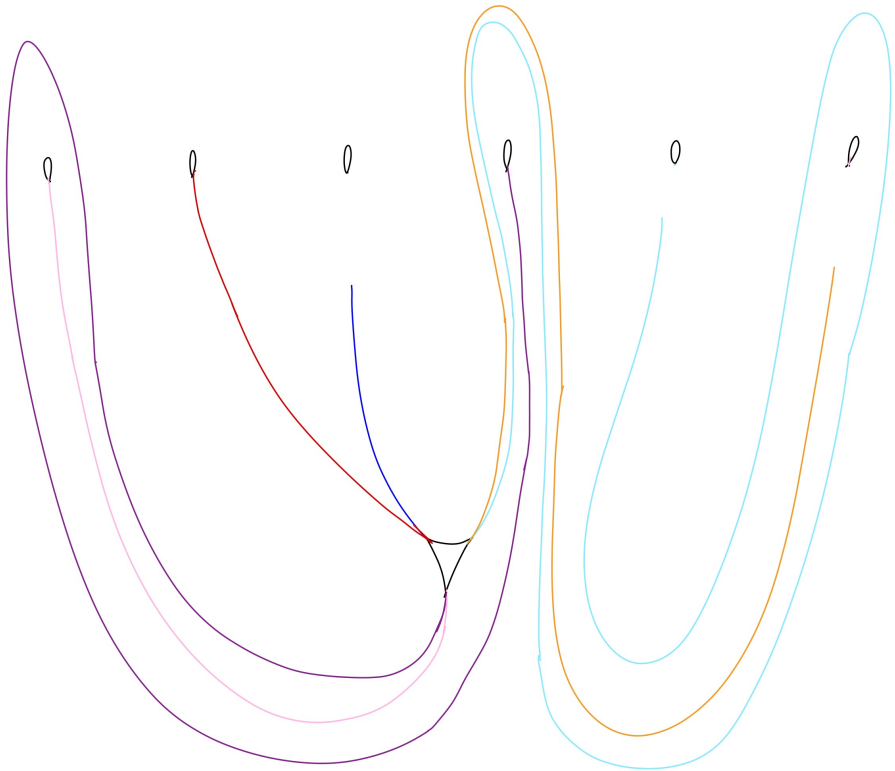


Figure C.119: Chouse1

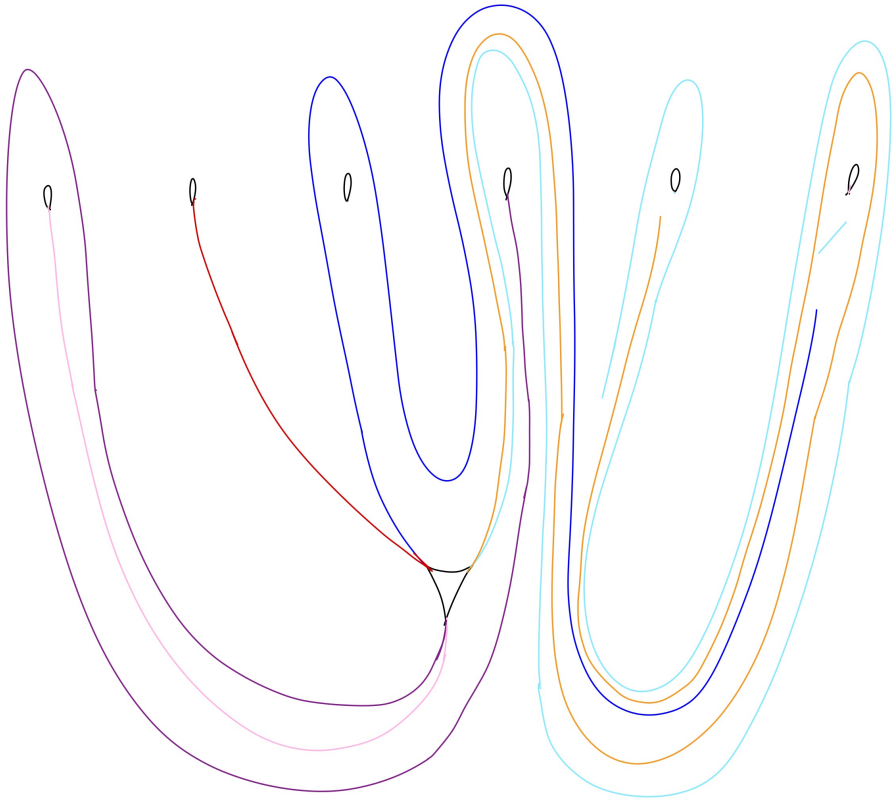


Figure C.120: Chouse2

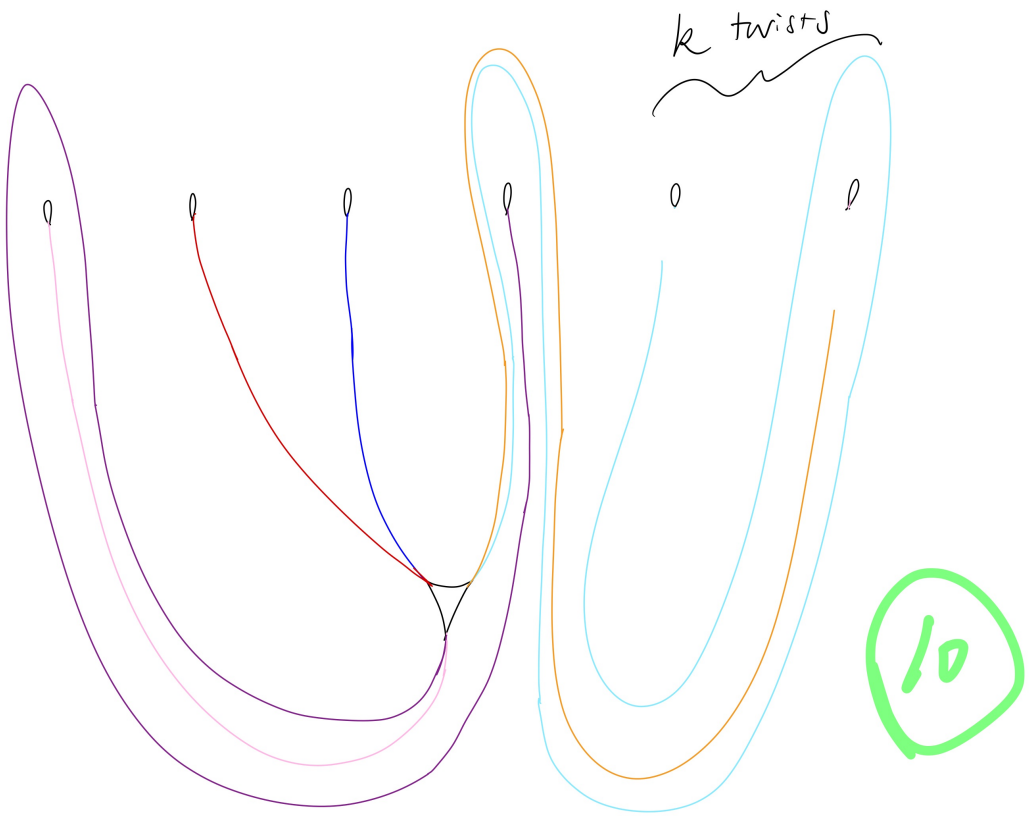


Figure C.121: Chouse3

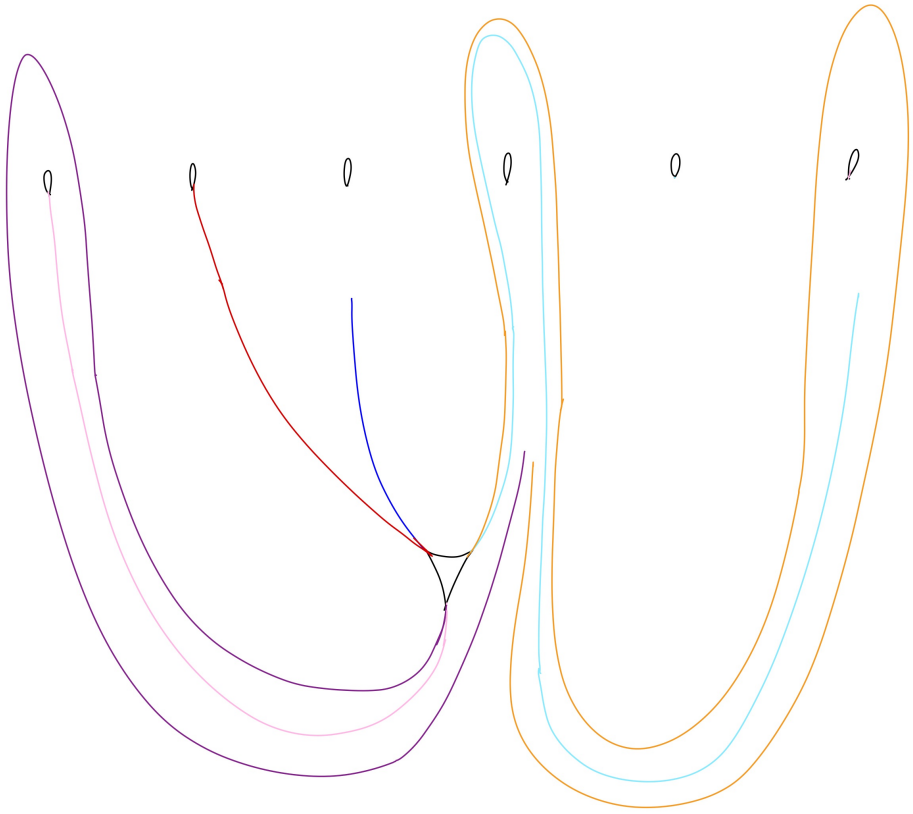


Figure C.122: Fardel1

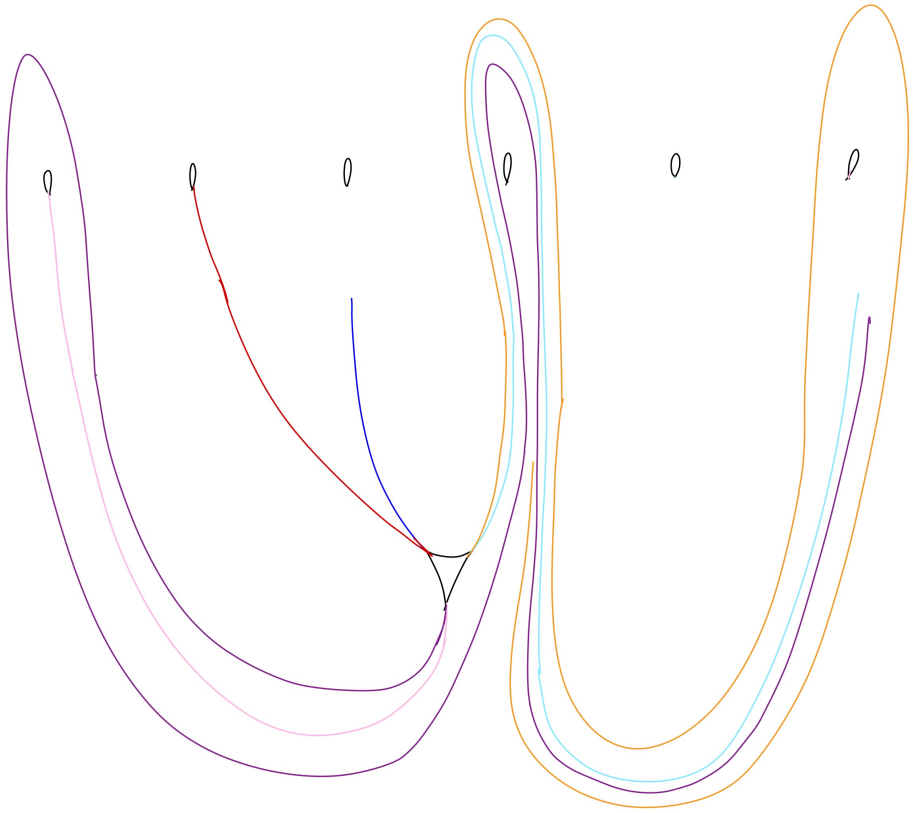


Figure C.123: Fardel2

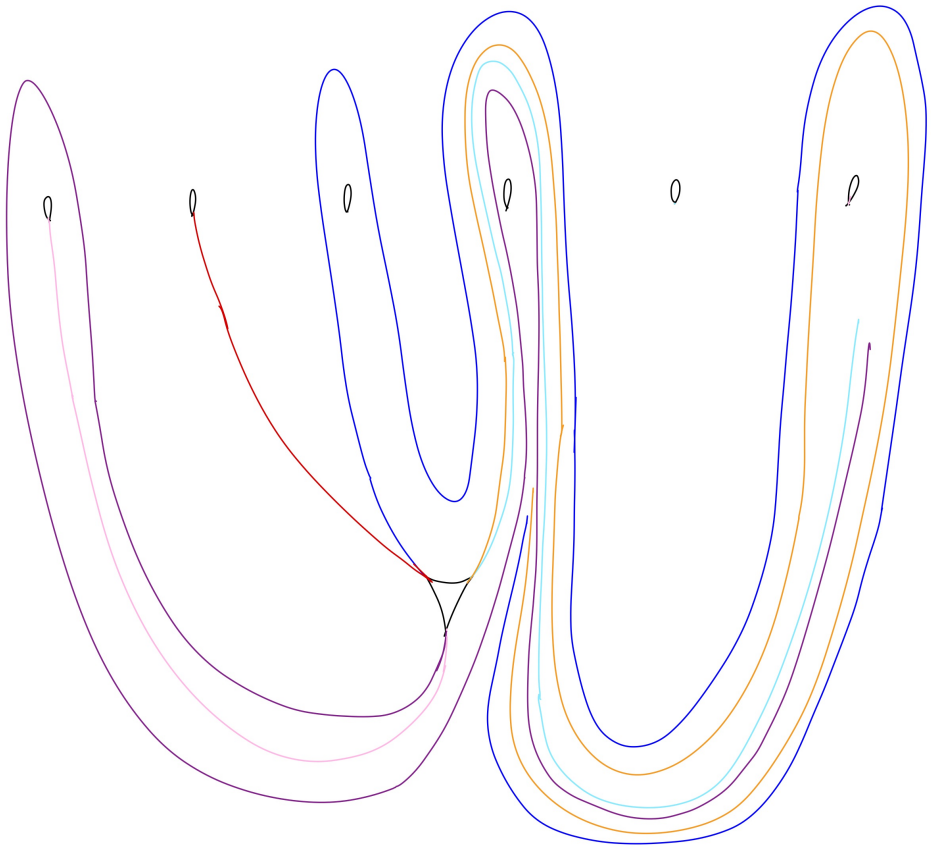


Figure C.124: Fardel3

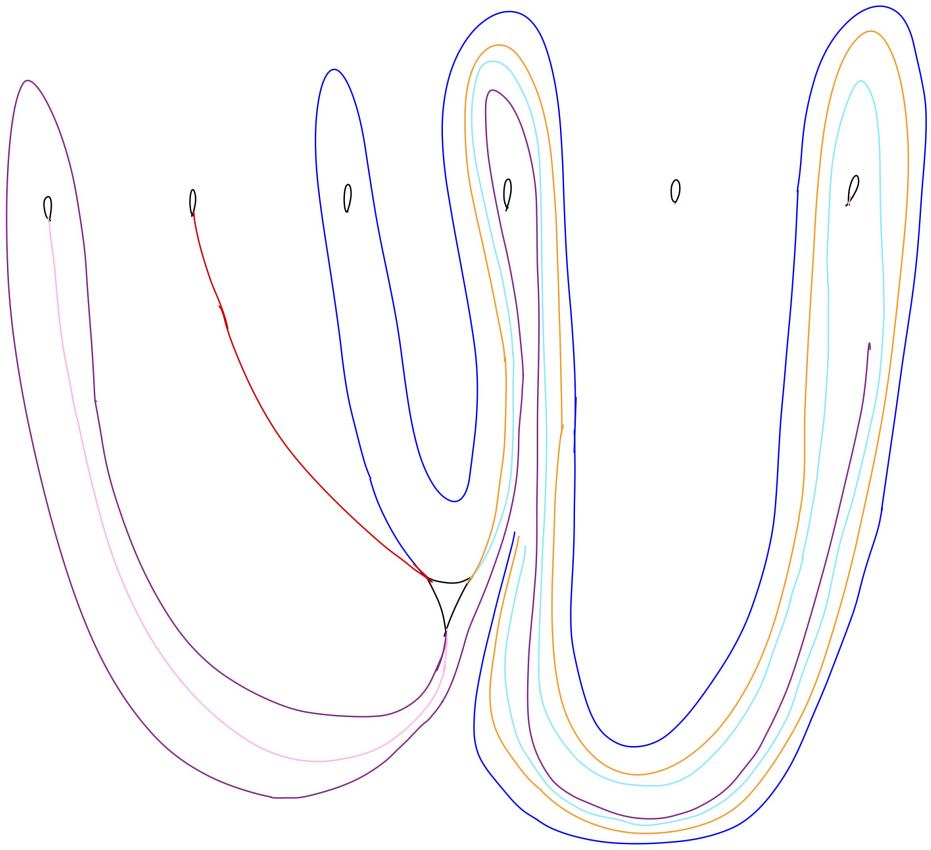


Figure C.125: Fardel4

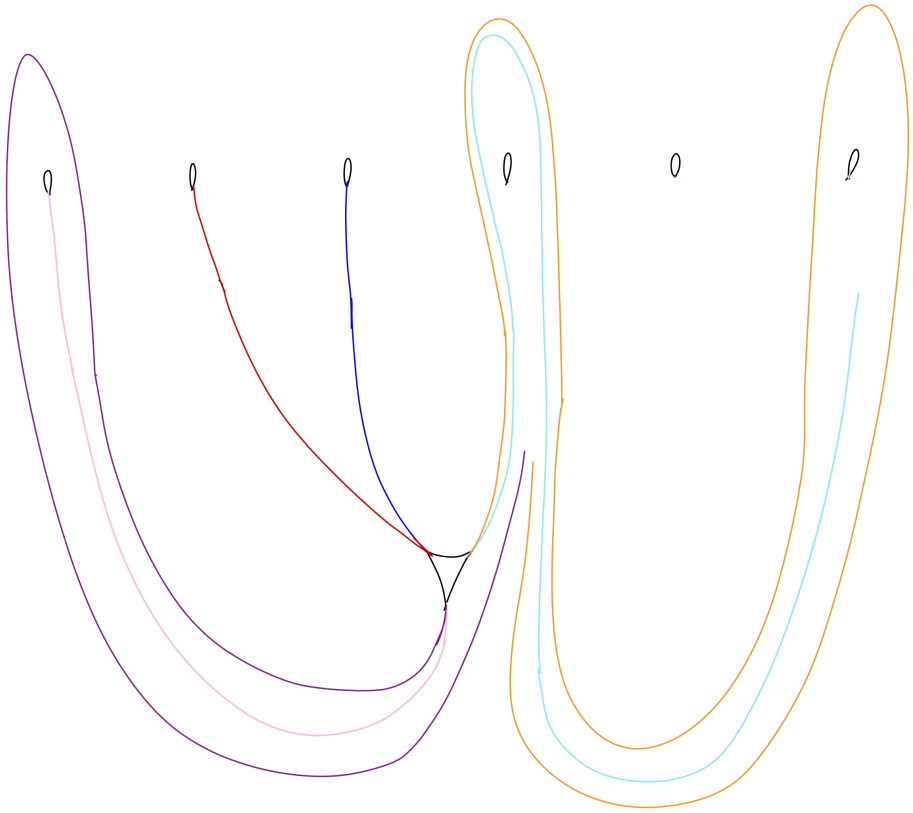


Figure C.126: Fardel5

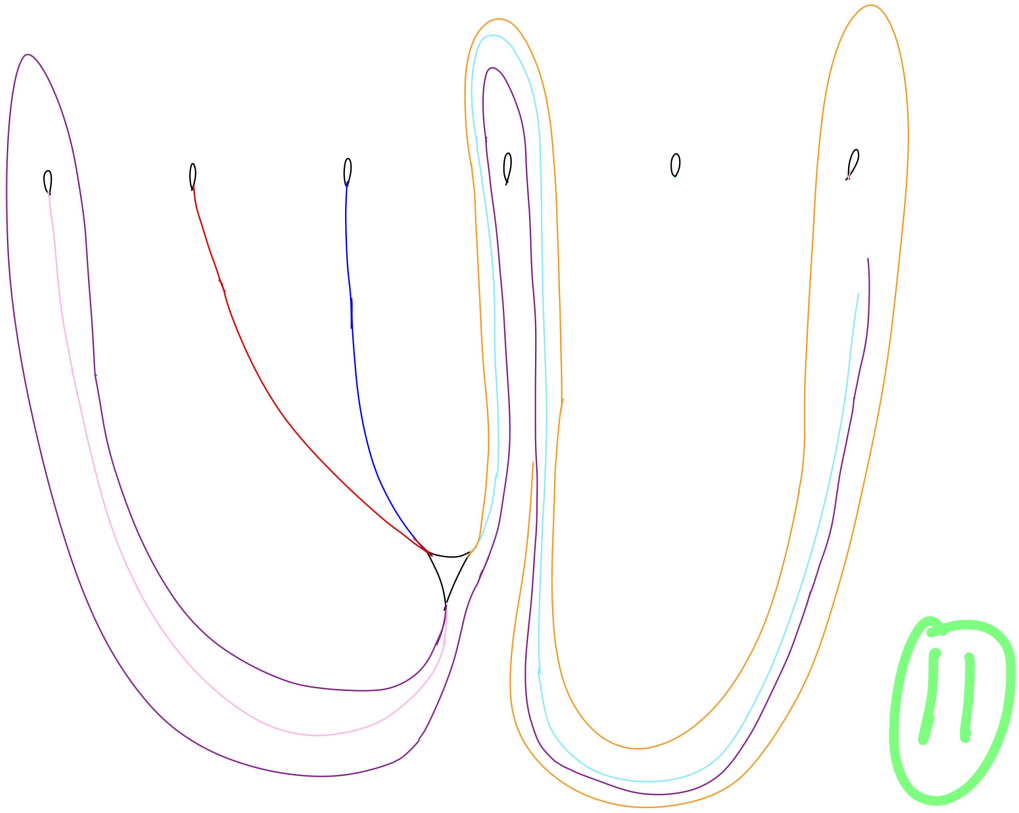


Figure C.127: Fardel6

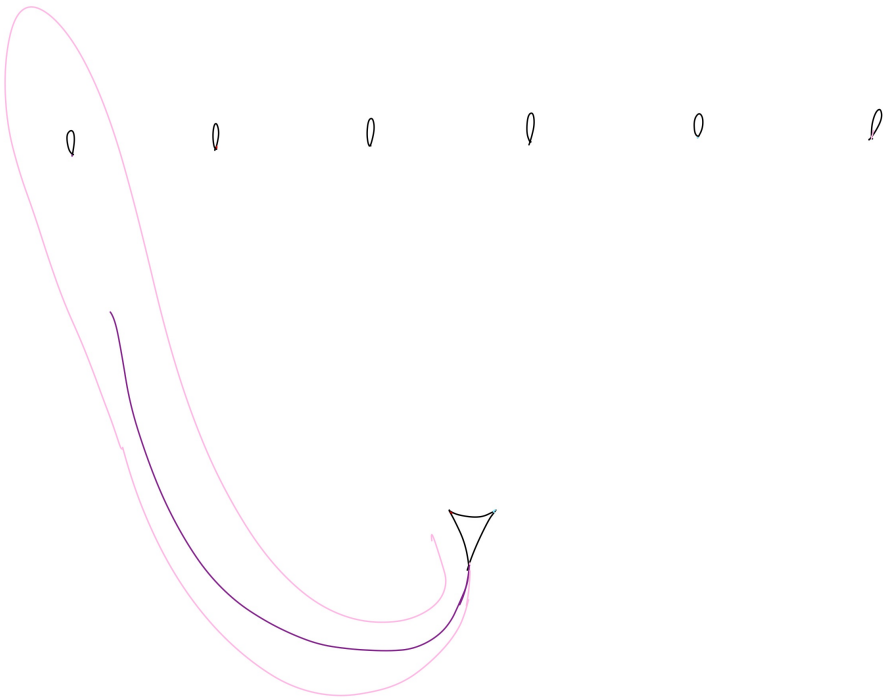


Figure C.128: Darg1

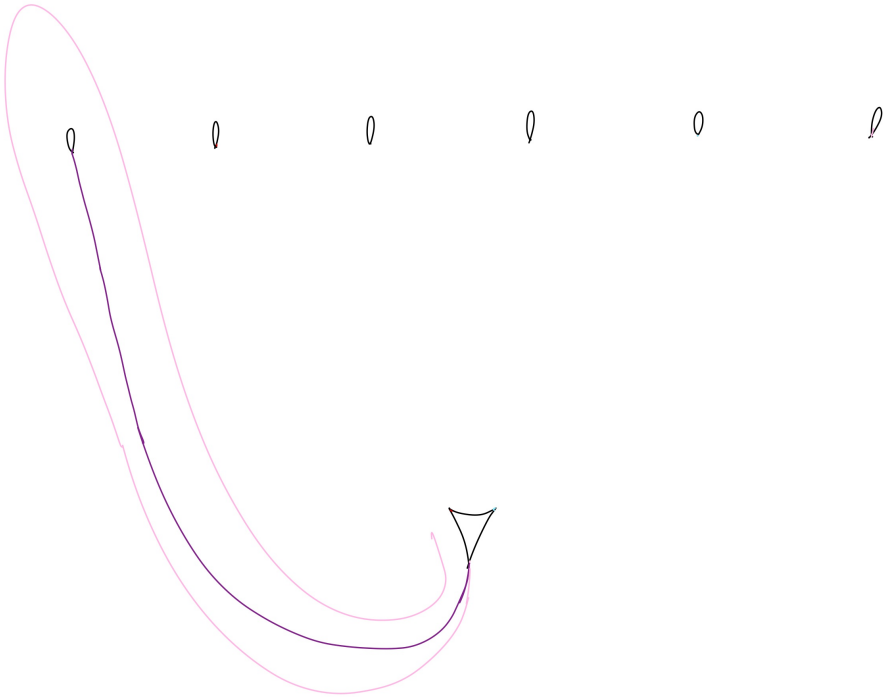


Figure C.129: Halse1

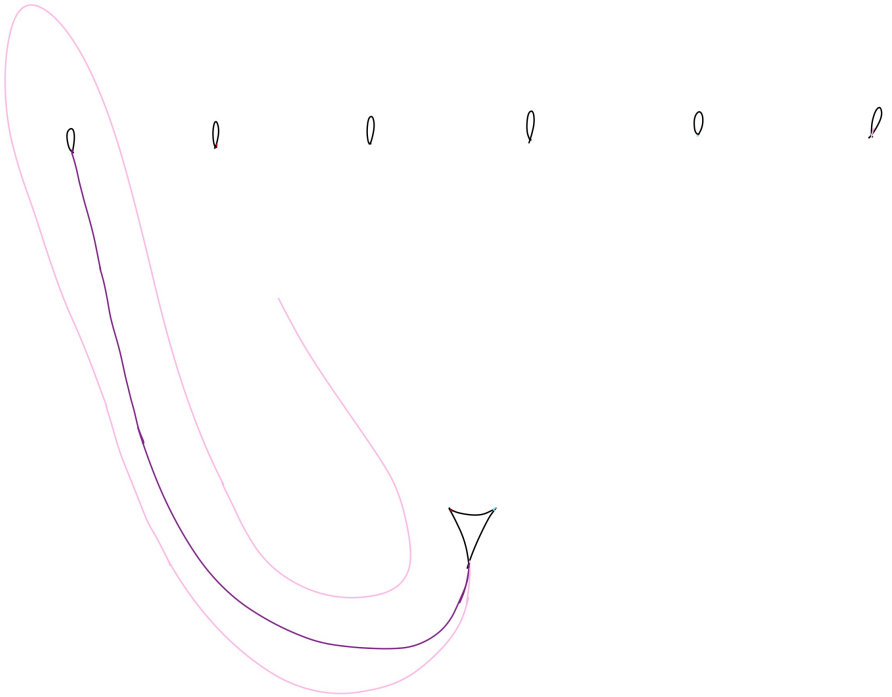


Figure C.130: Kittle1

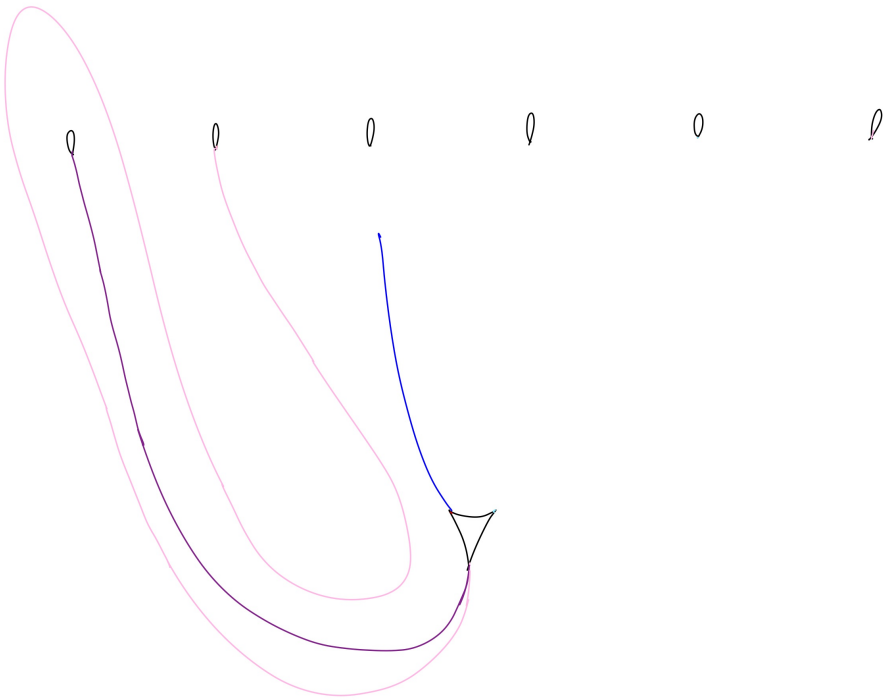


Figure C.131: Tantivy1

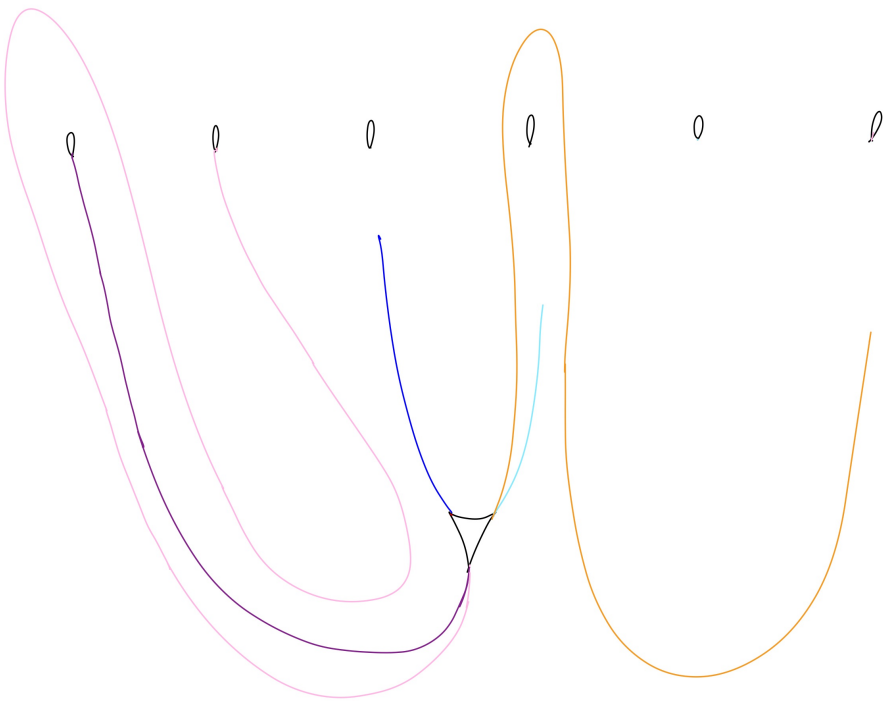


Figure C.132: Tantivy2

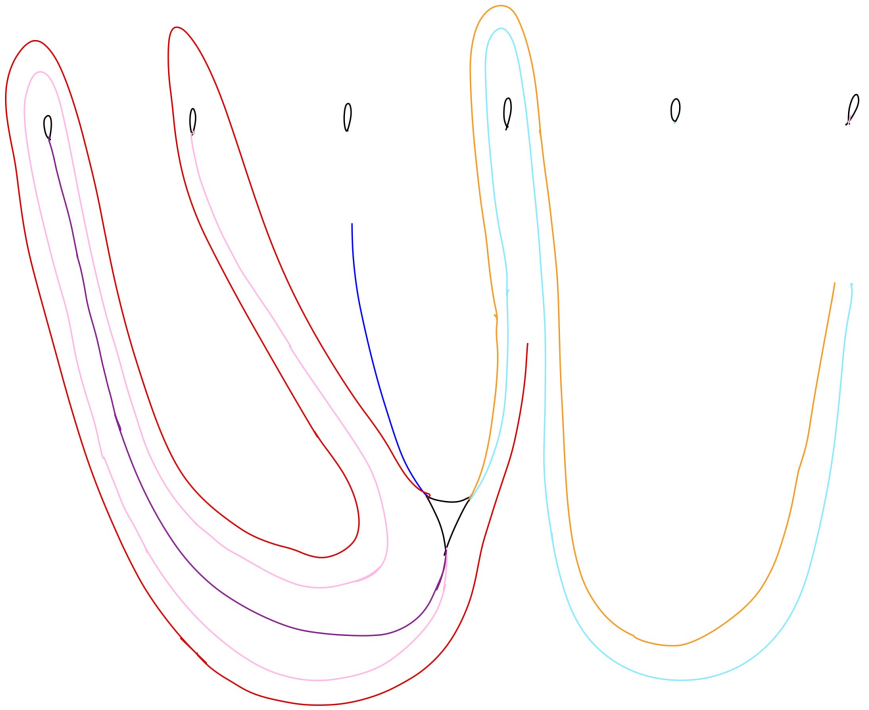


Figure C.133: Tantivy3

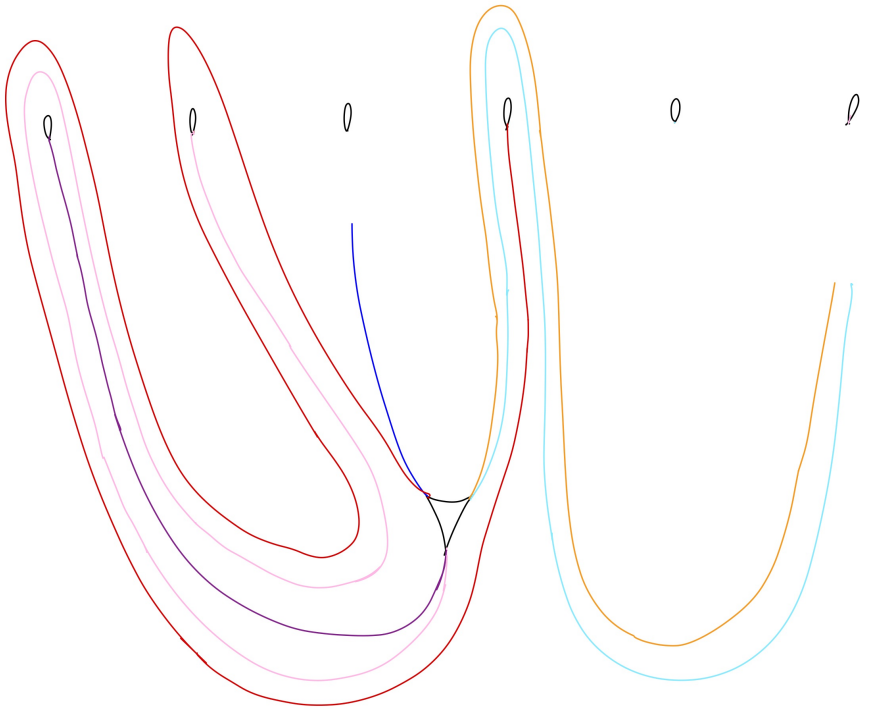


Figure C.134: Tantivy4

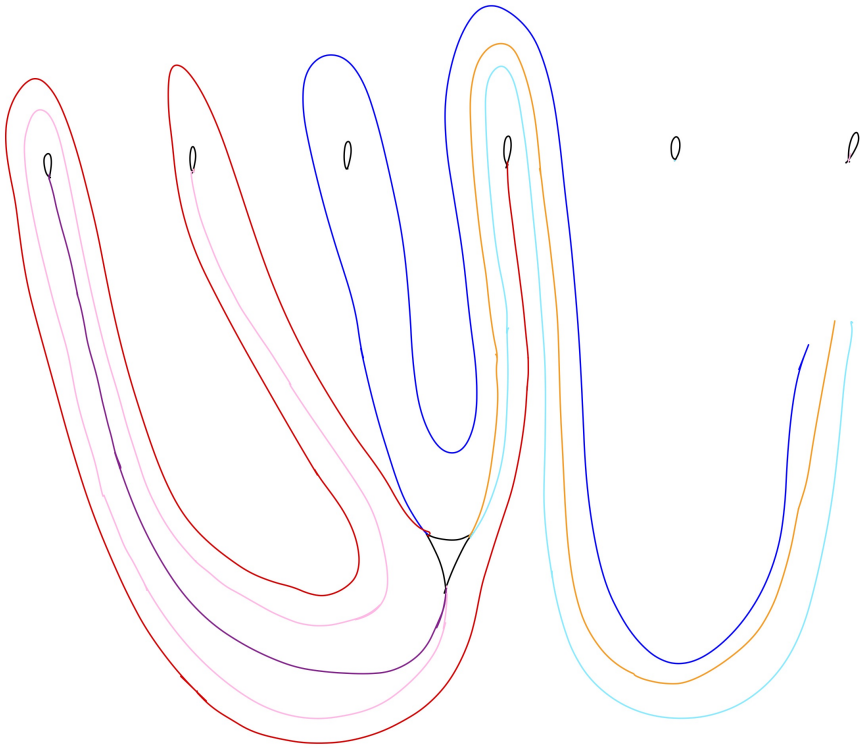


Figure C.135: Tantivy5

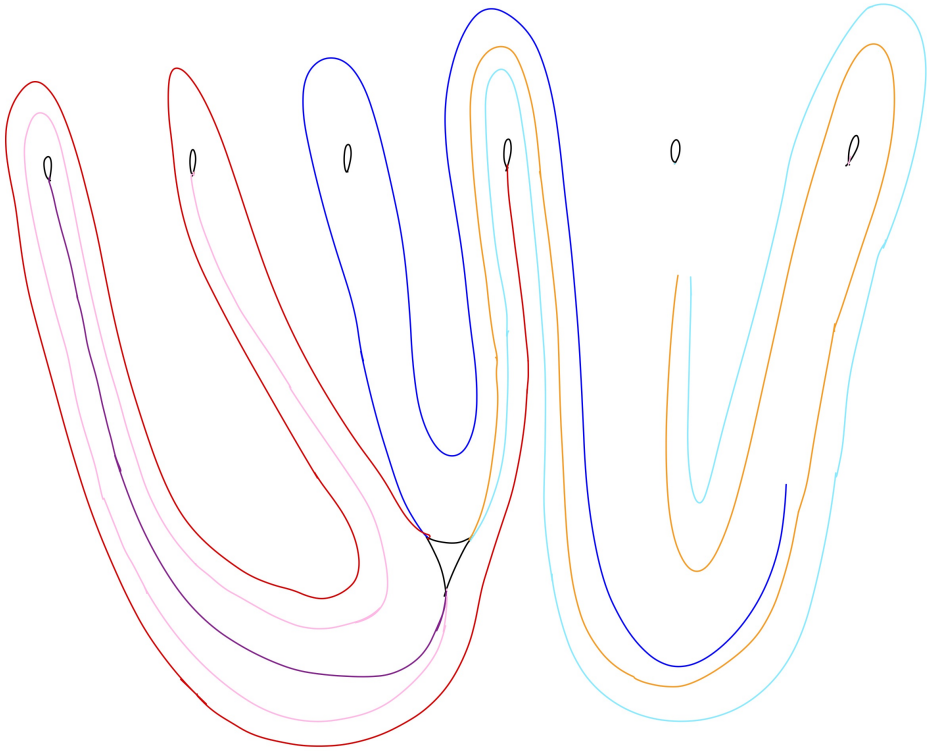


Figure C.136: Tantivy6

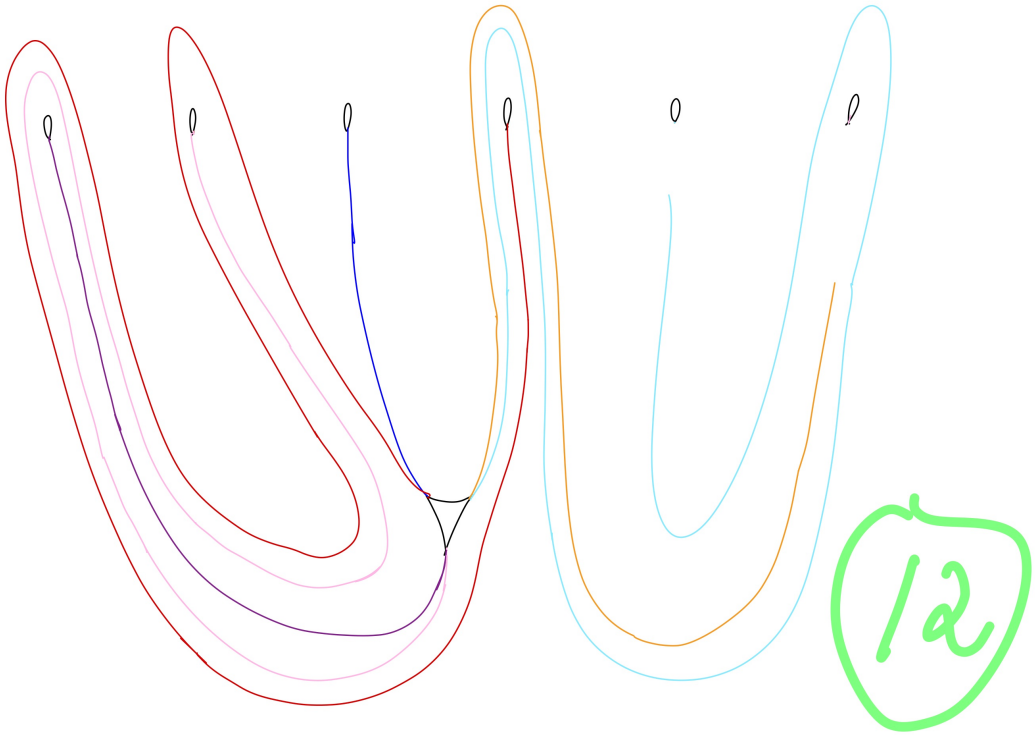


Figure C.137: Tantivy7

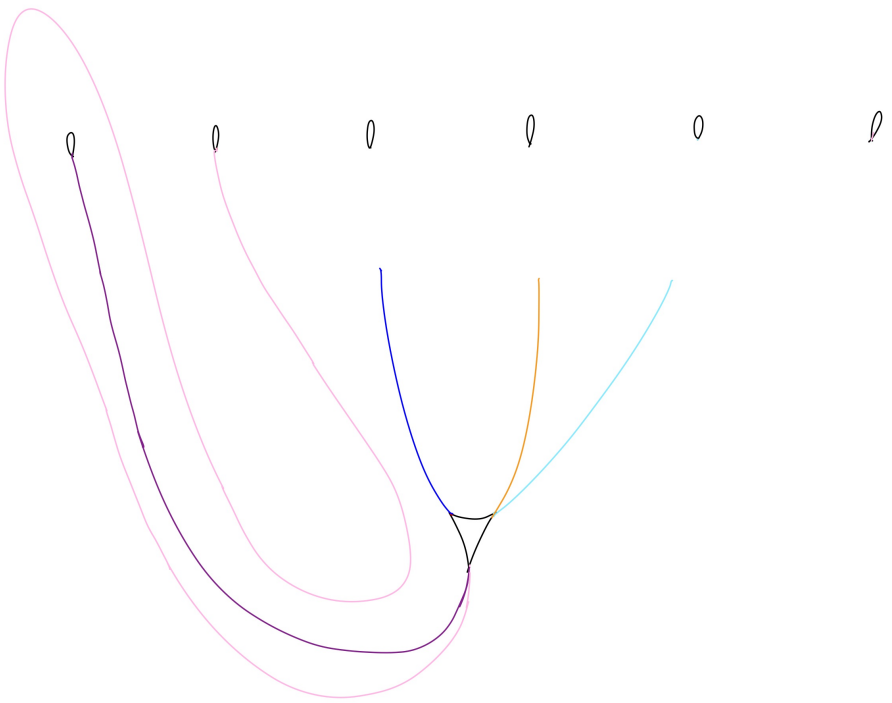


Figure C.138: Tantivy8

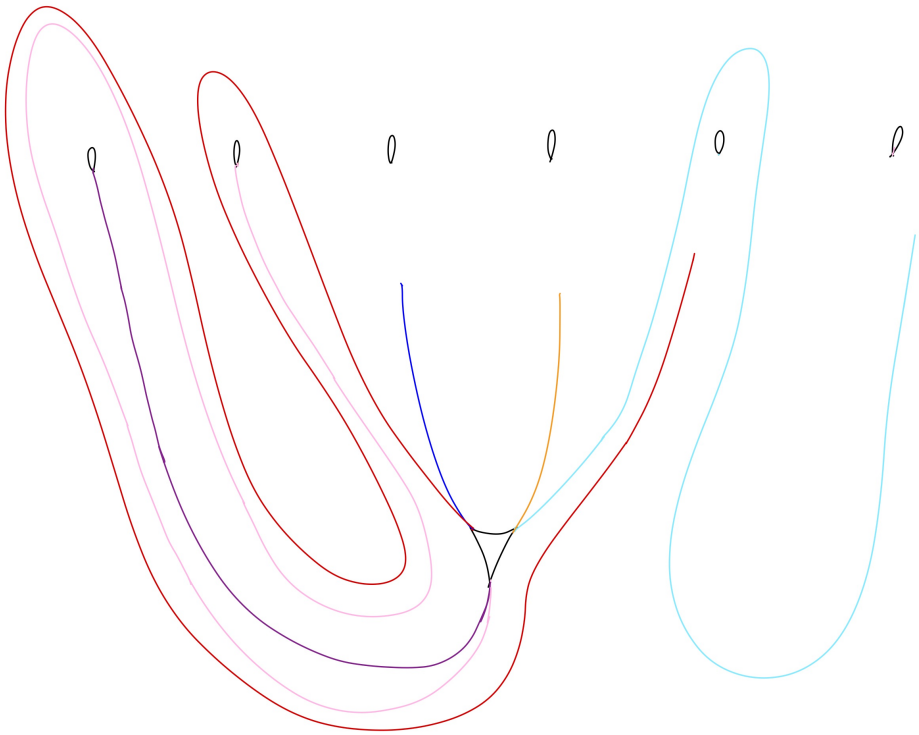


Figure C.139: Tantivy9

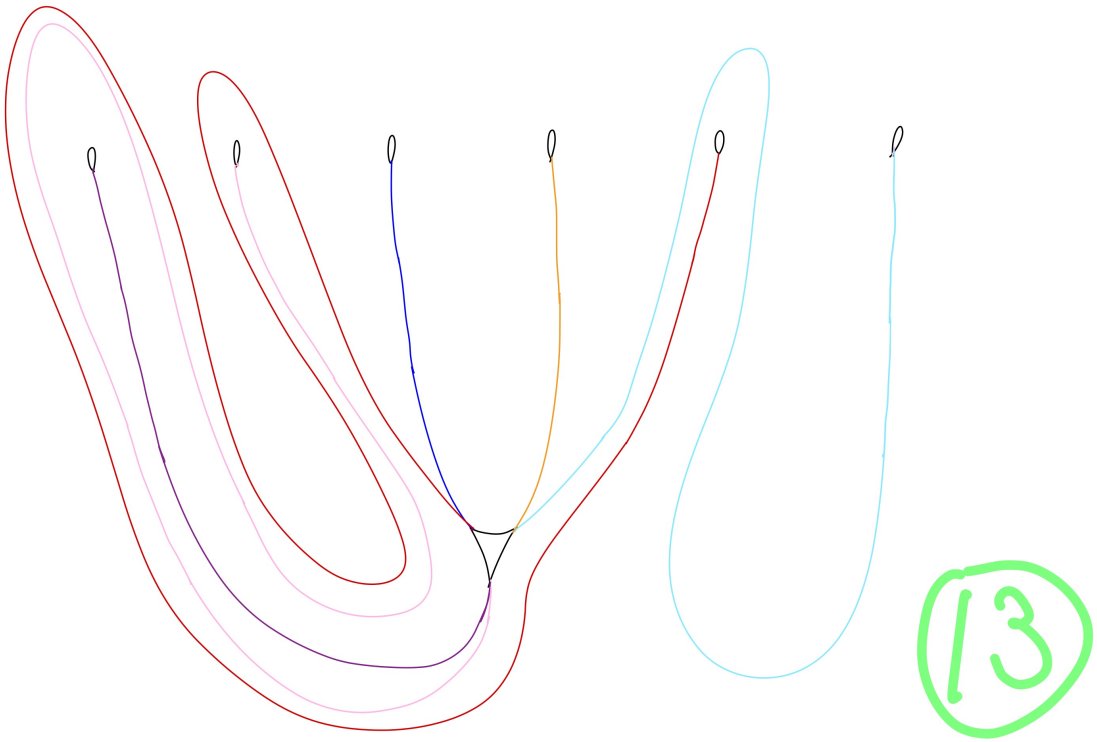


Figure C.140: Tantivy10

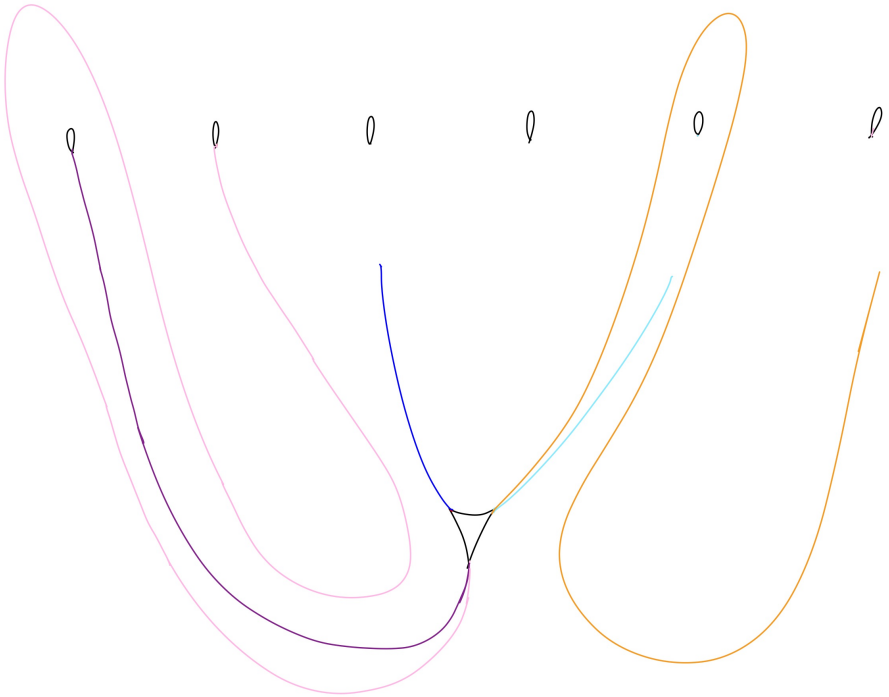


Figure C.141: Tantivy11

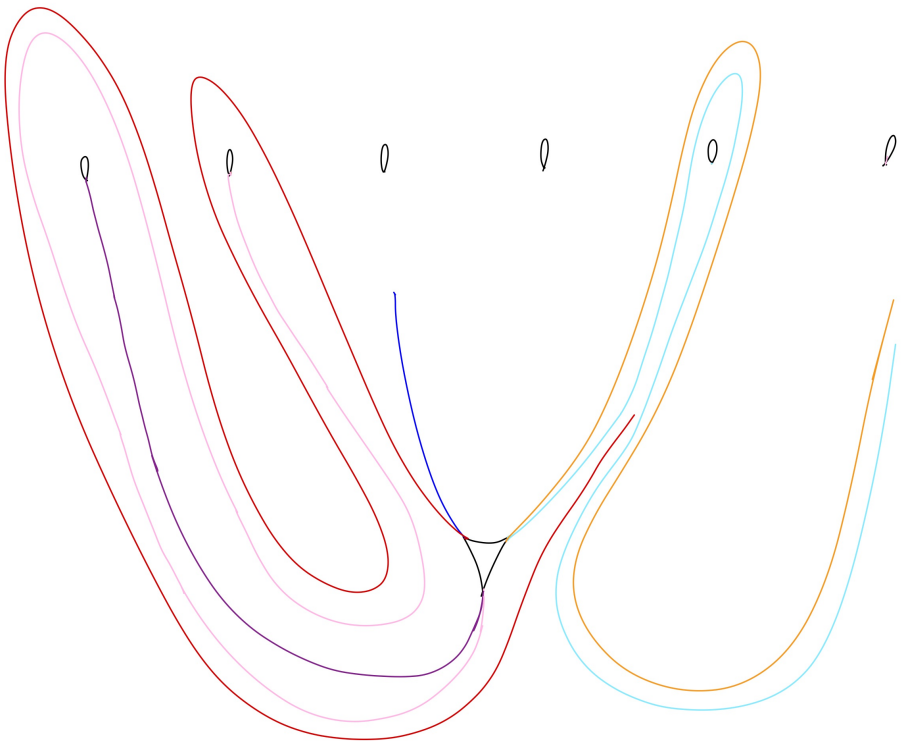


Figure C.142: Tantivy12

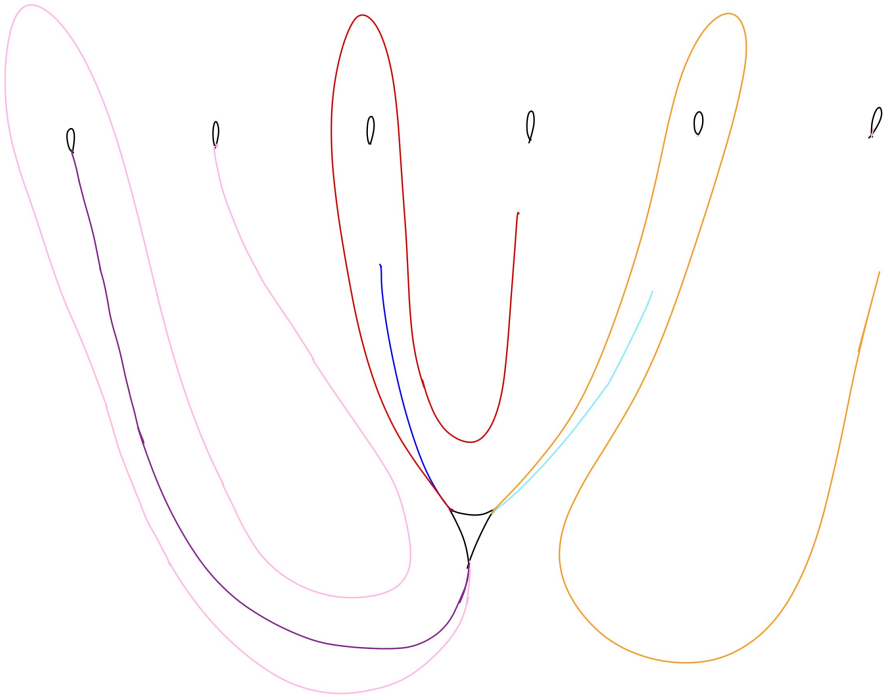


Figure C.143: Tantivy13

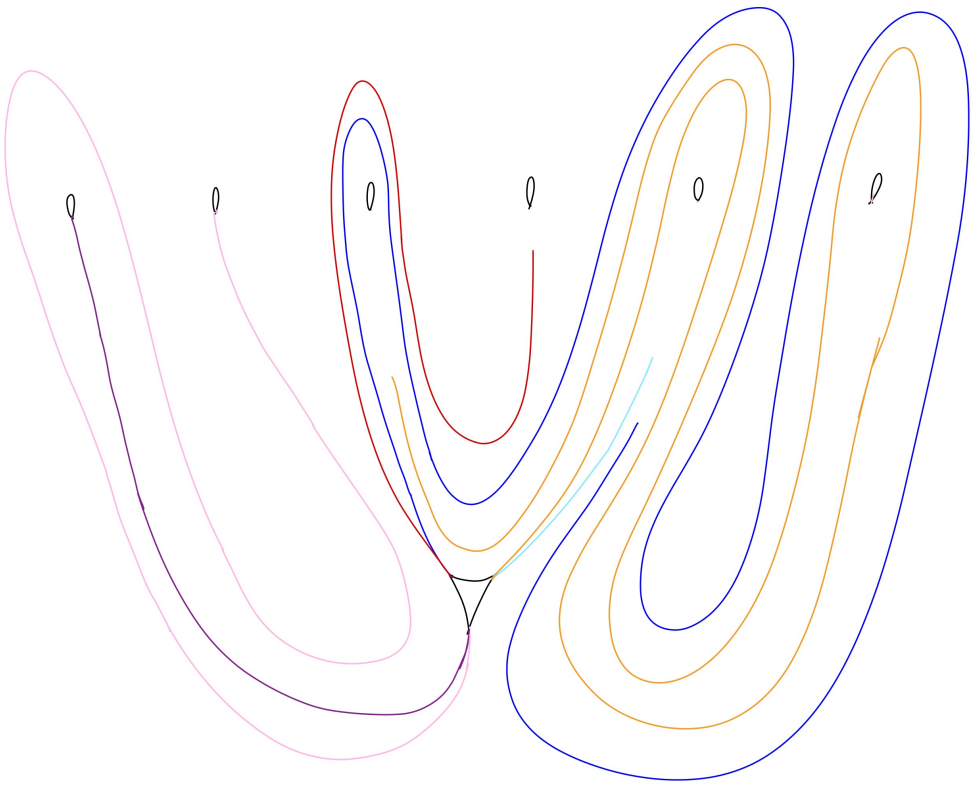


Figure C.144: Tantivy14

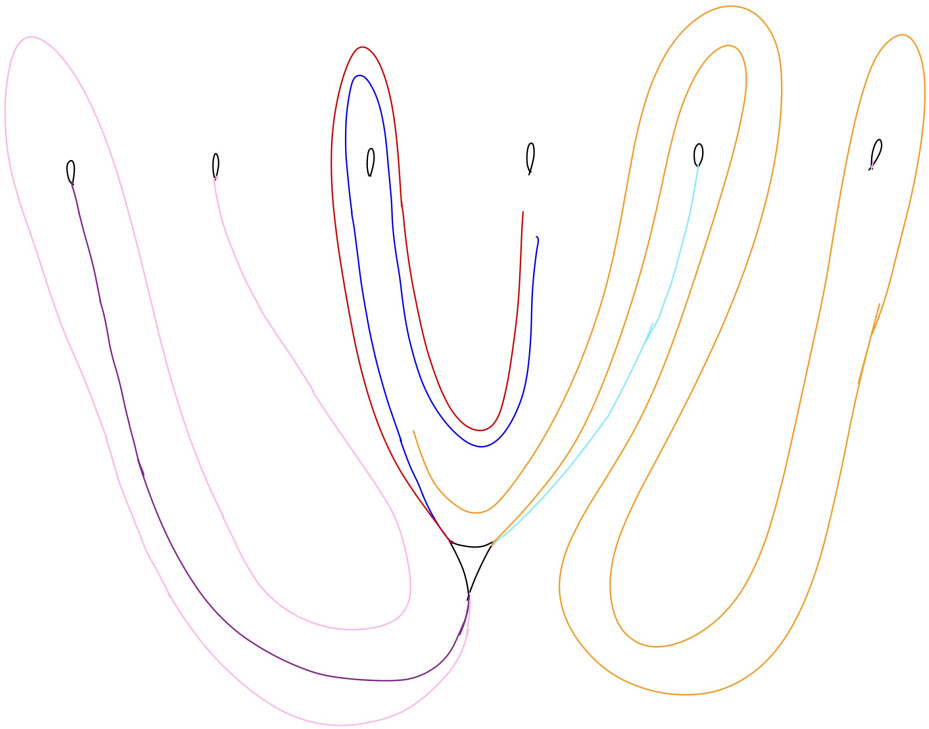


Figure C.145: Tantivy15

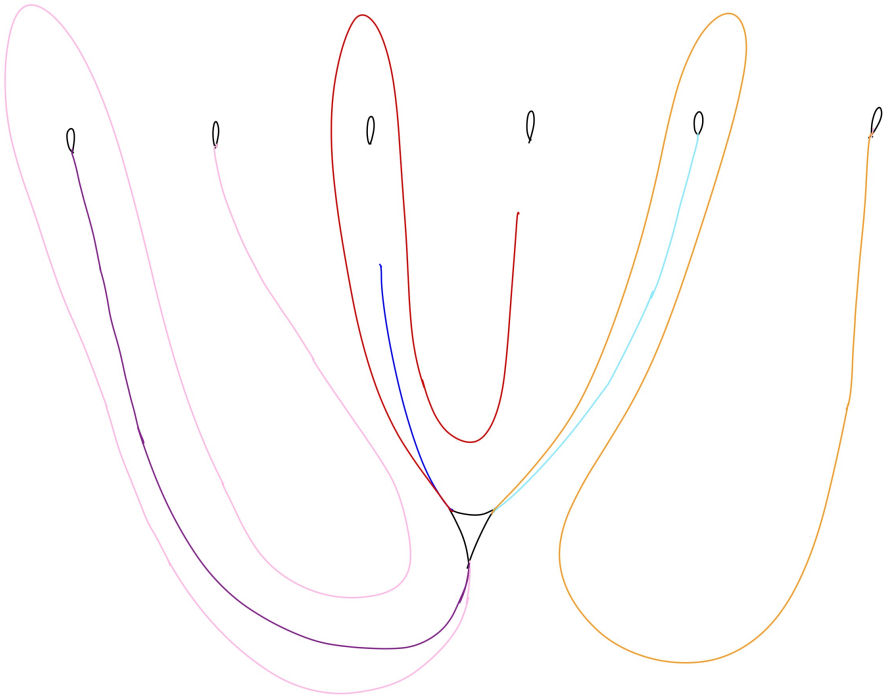


Figure C.146: Tantivy16

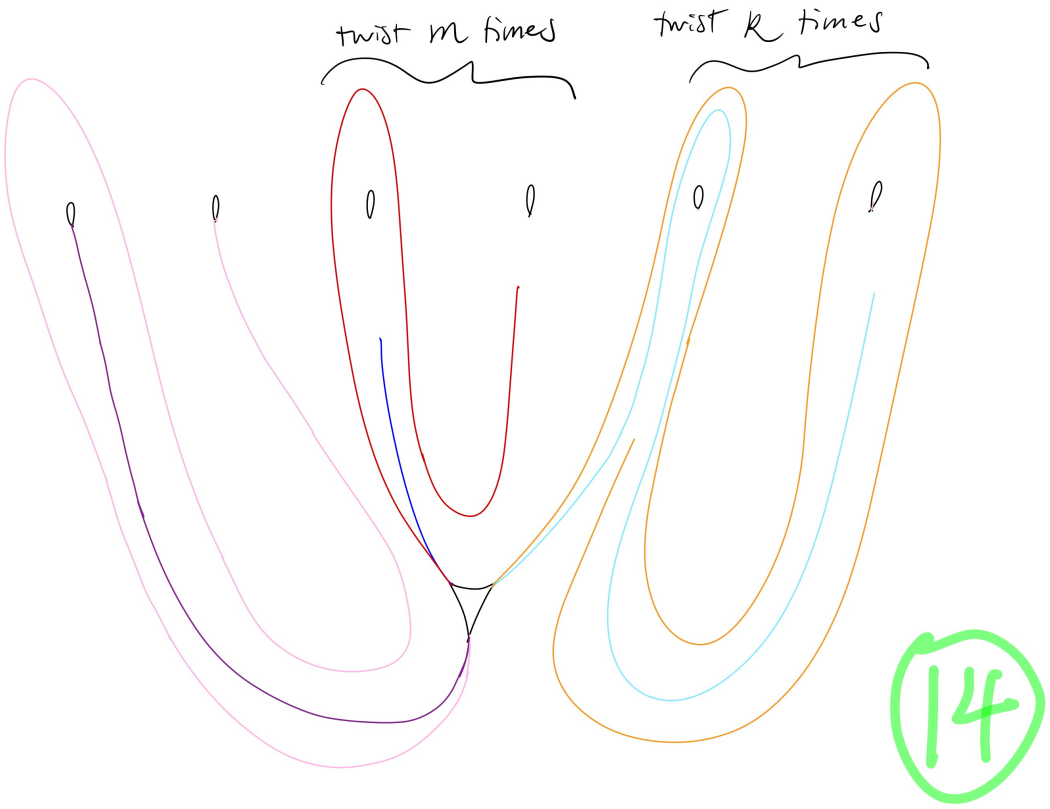


Figure C.147: Tantivy17

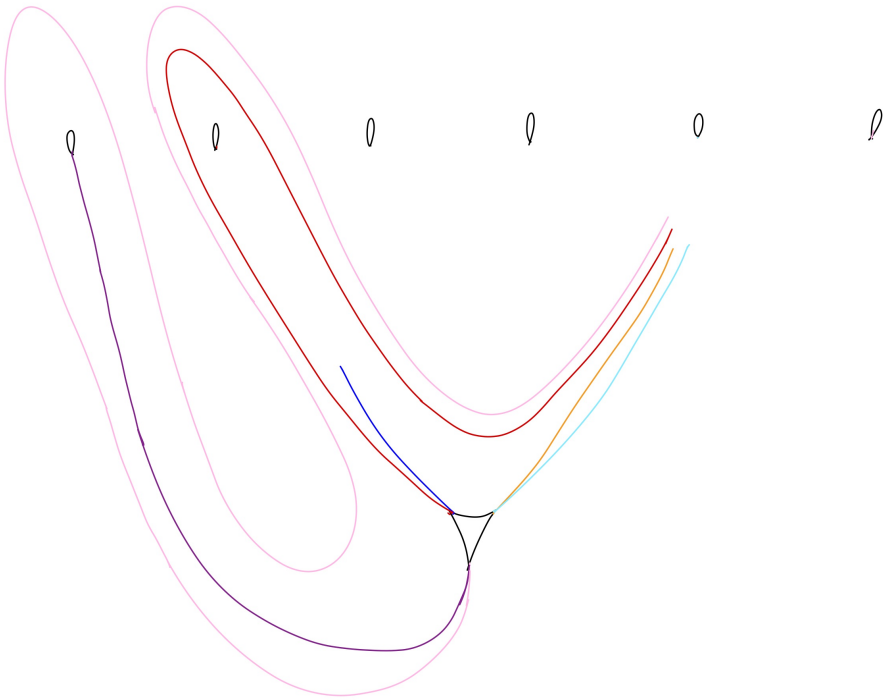


Figure C.148: Wherret1

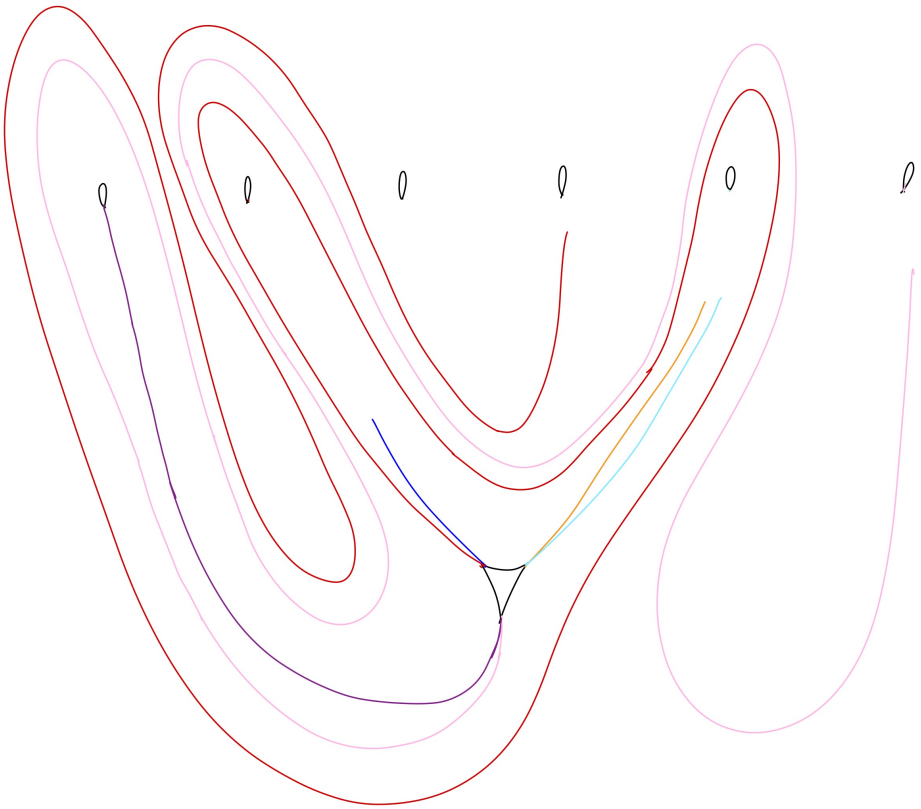


Figure C.149: Wherret2

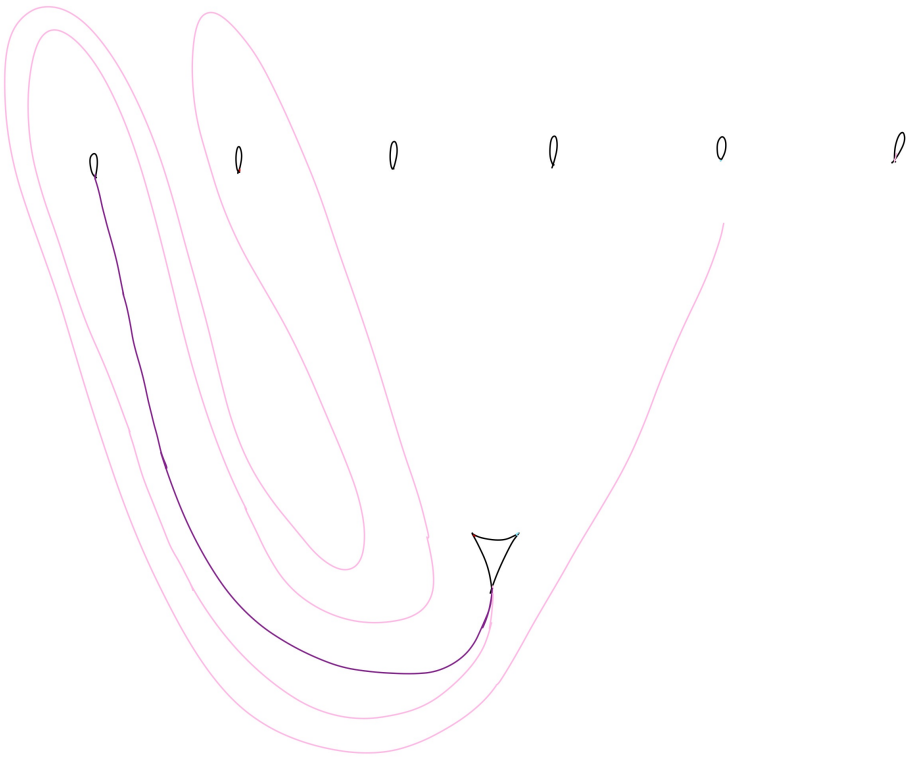


Figure C.150: Xiphias1

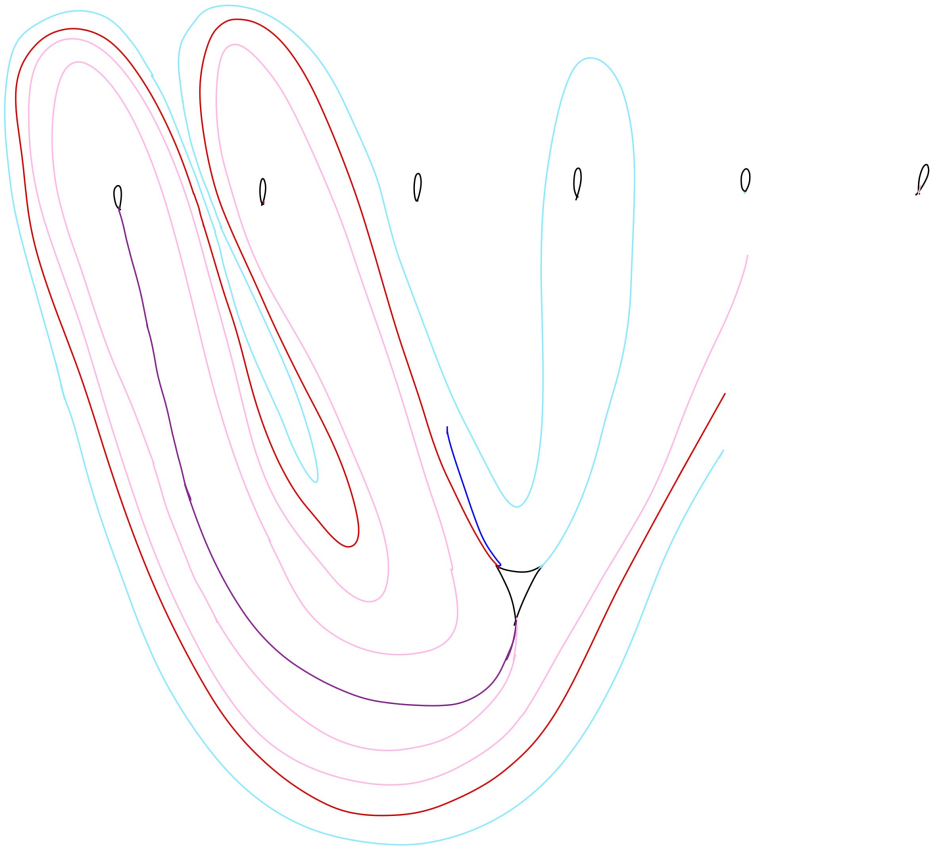


Figure C.151: Xiphias2

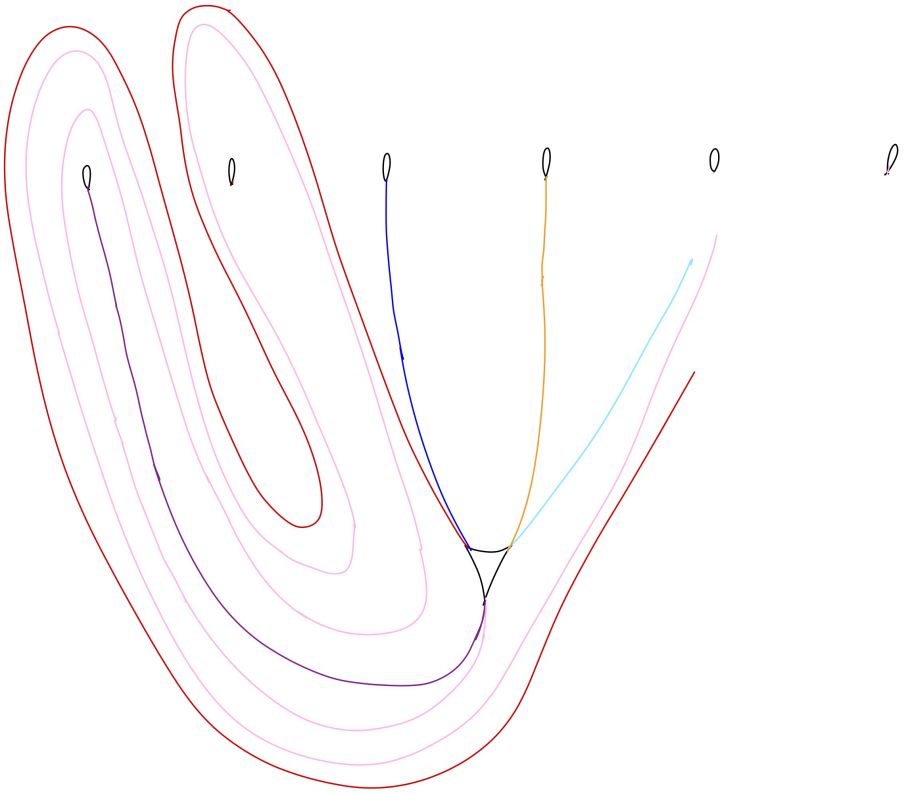


Figure C.152: Xiphias3

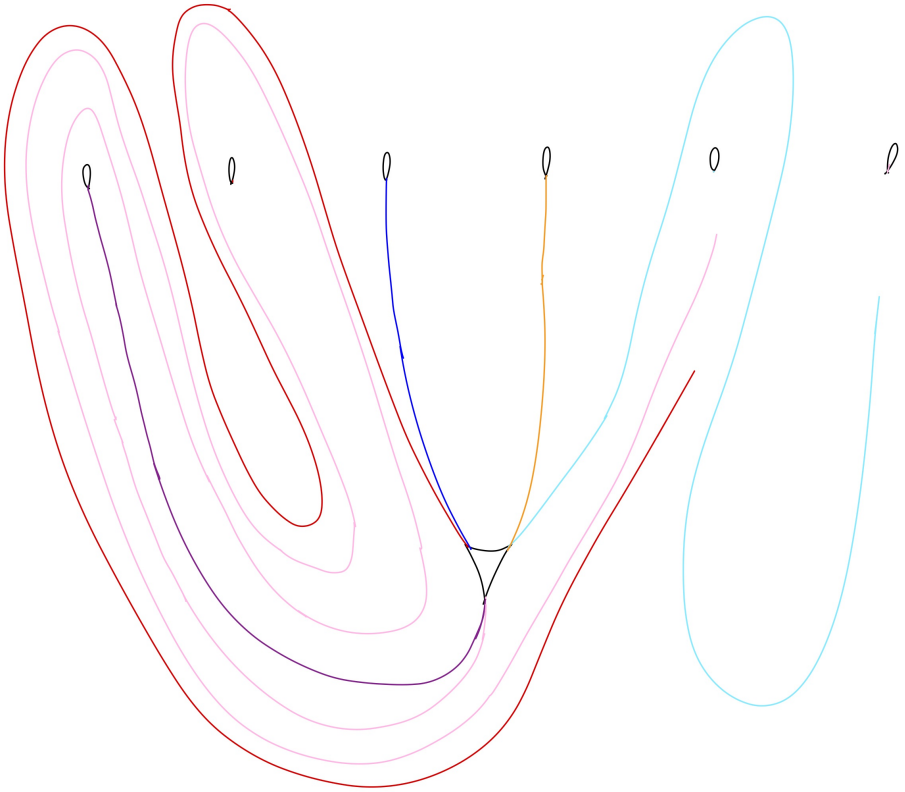


Figure C.153: Xiphias4

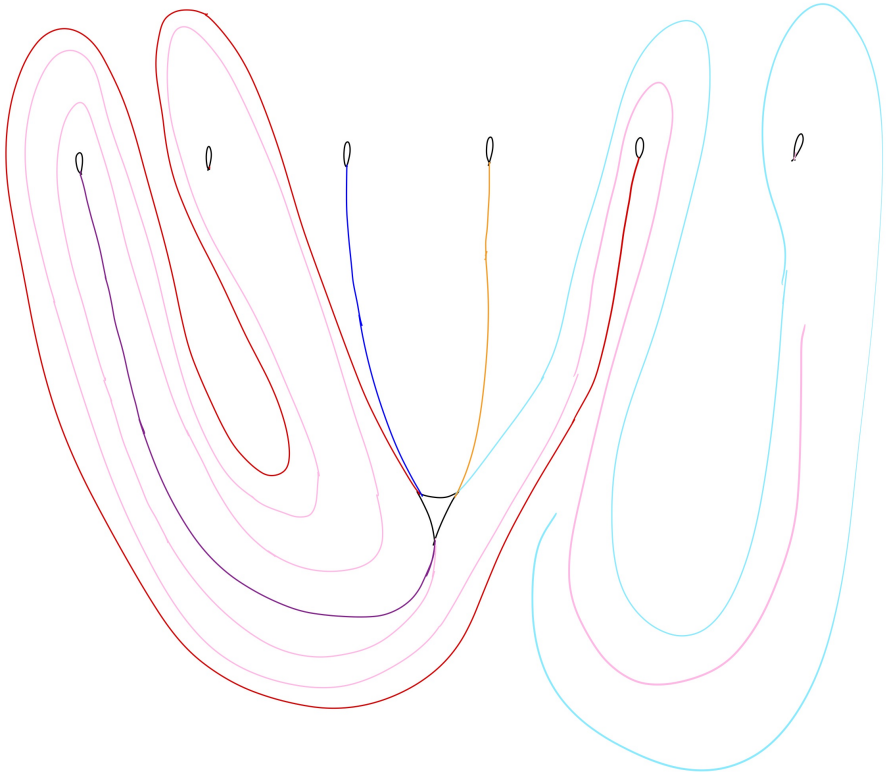


Figure C.154: Xiphias5

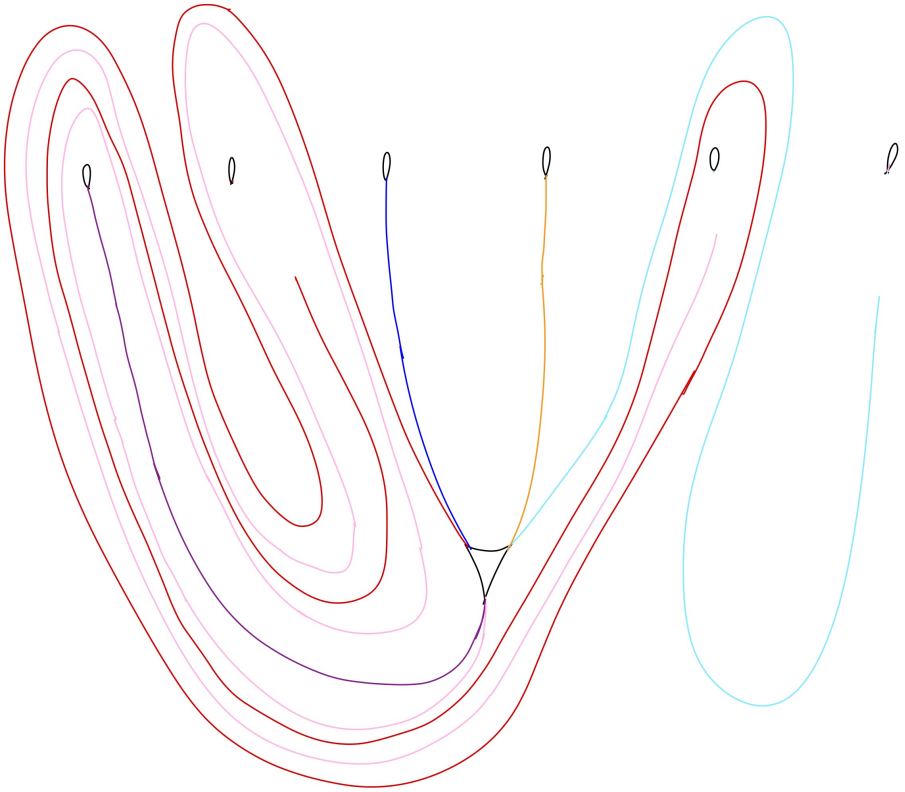


Figure C.155: Xiphias6

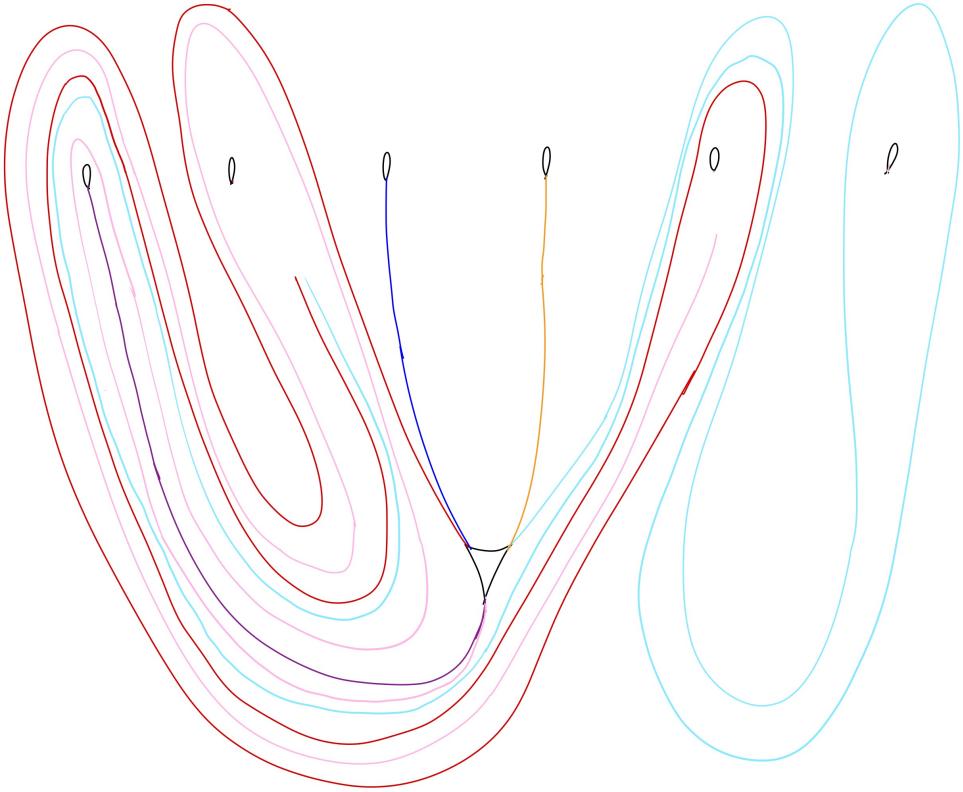


Figure C.156: Xiphias7

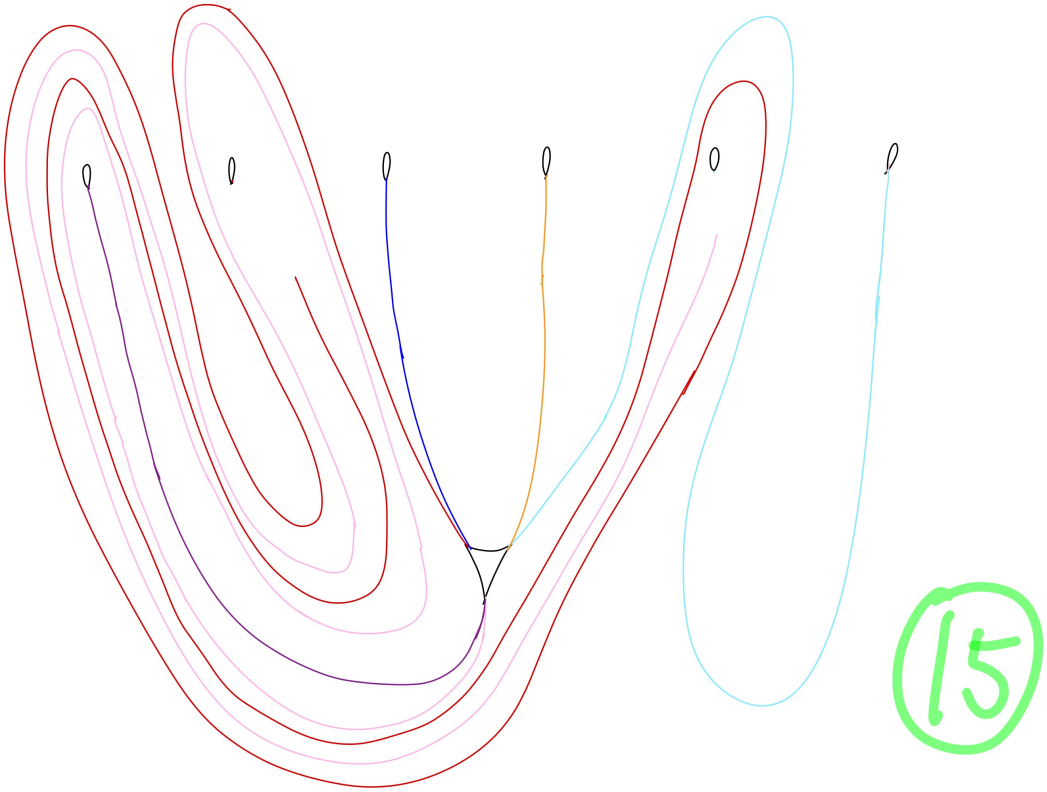


Figure C.157: Xiphias8

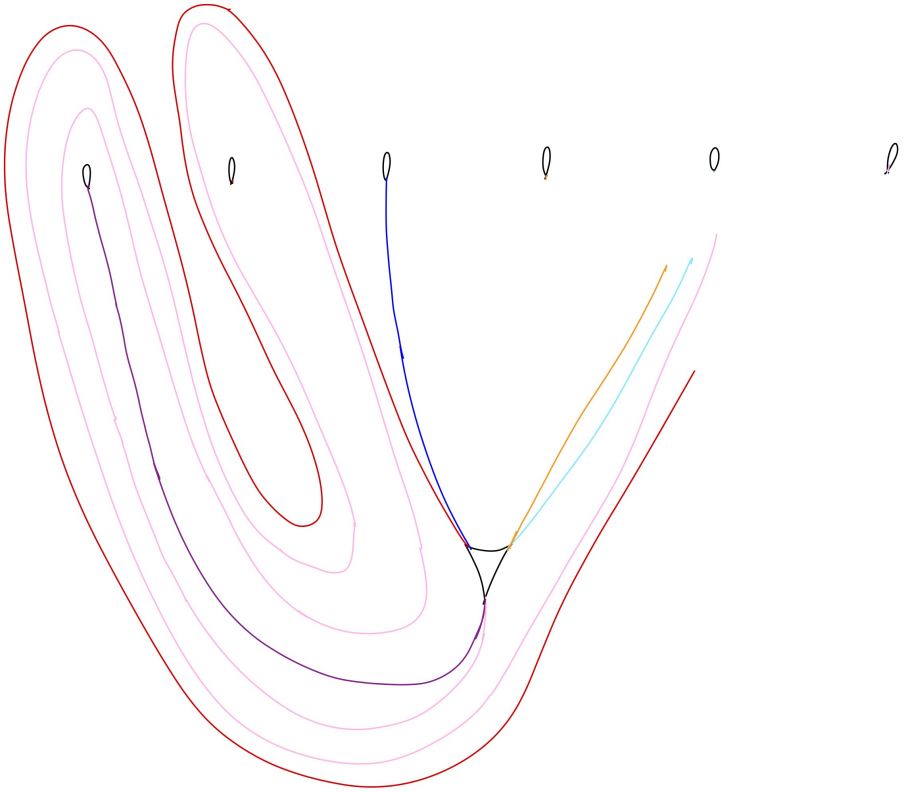


Figure C.158: Xiphias9

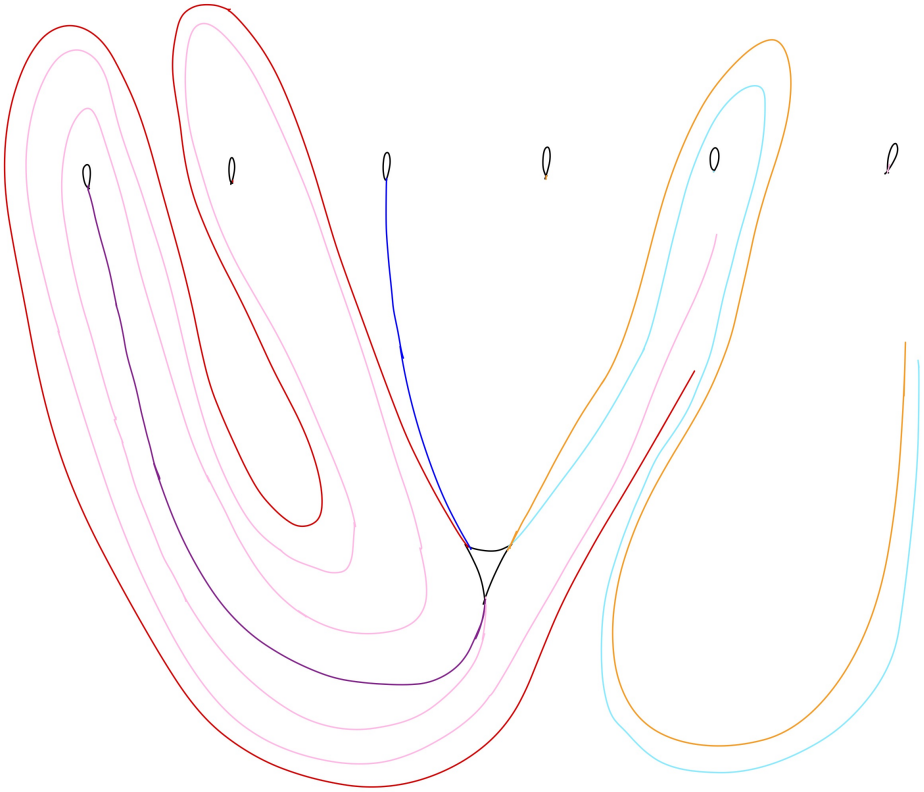


Figure C.159: Xiphias10

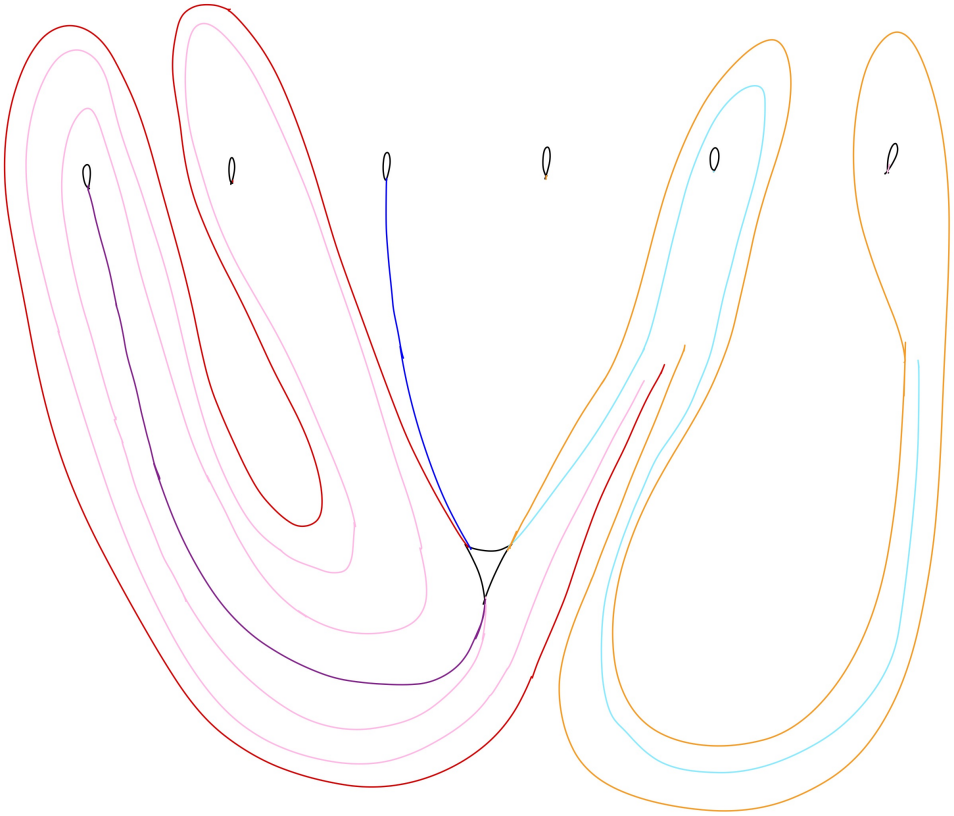


Figure C.160: Xiphias11

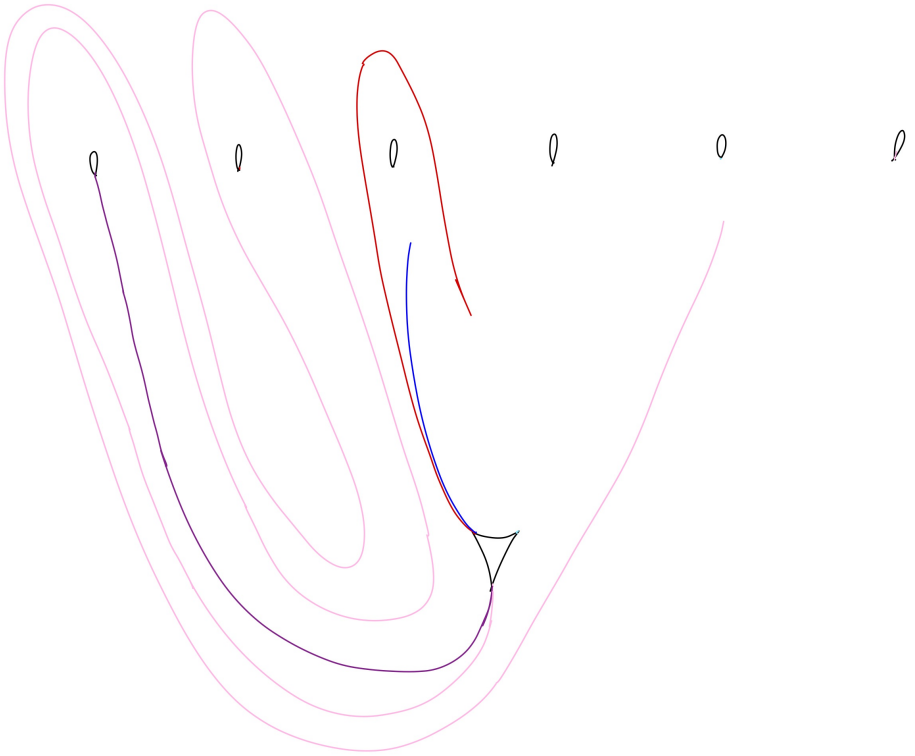


Figure C.161: Xiphias12

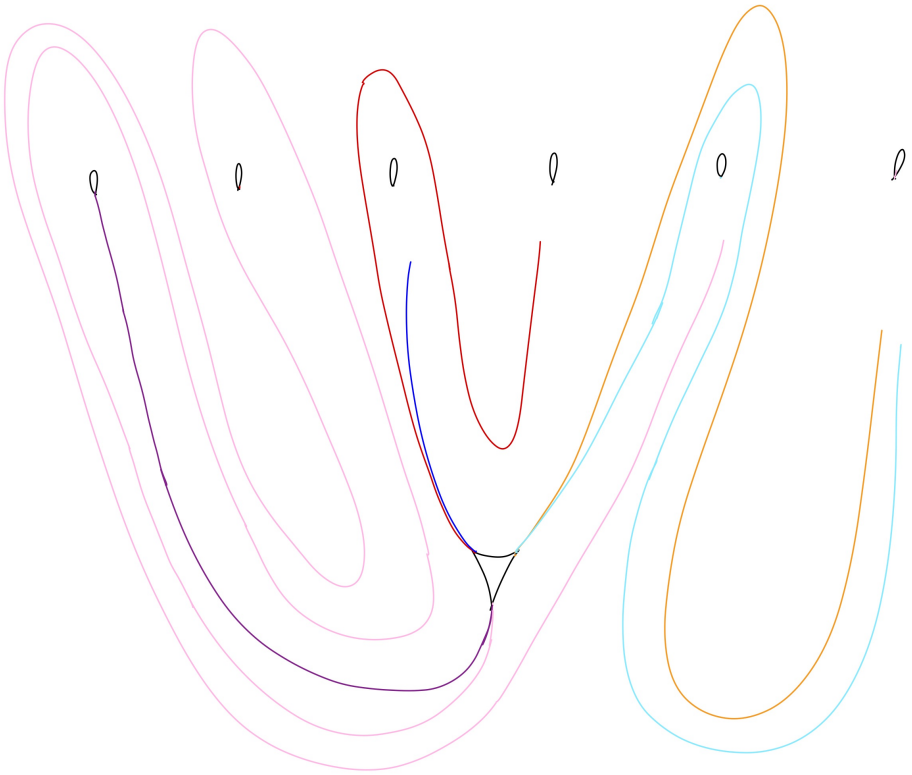


Figure C.162: Xiphias13

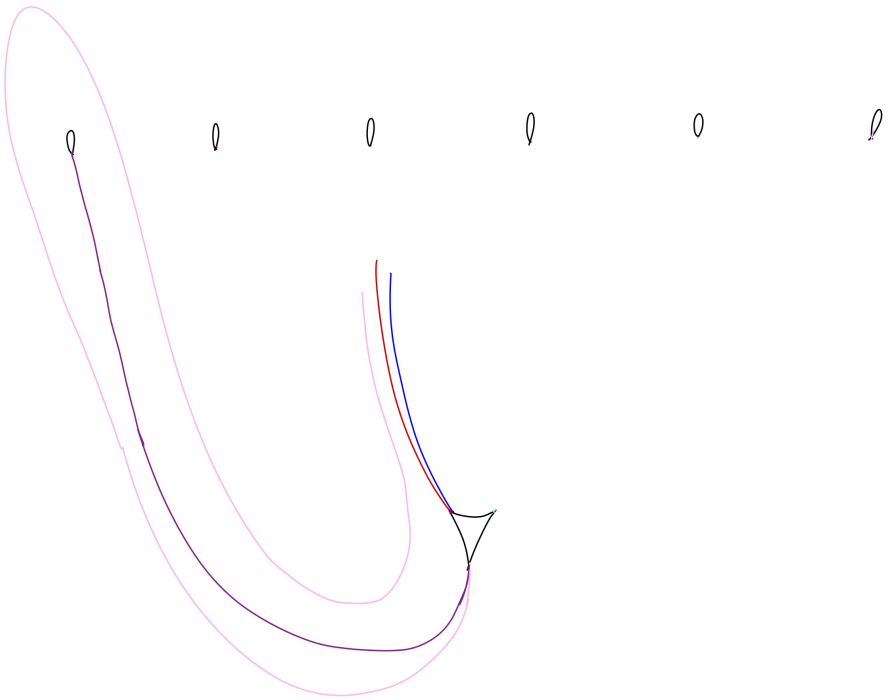


Figure C.163: Nidder1

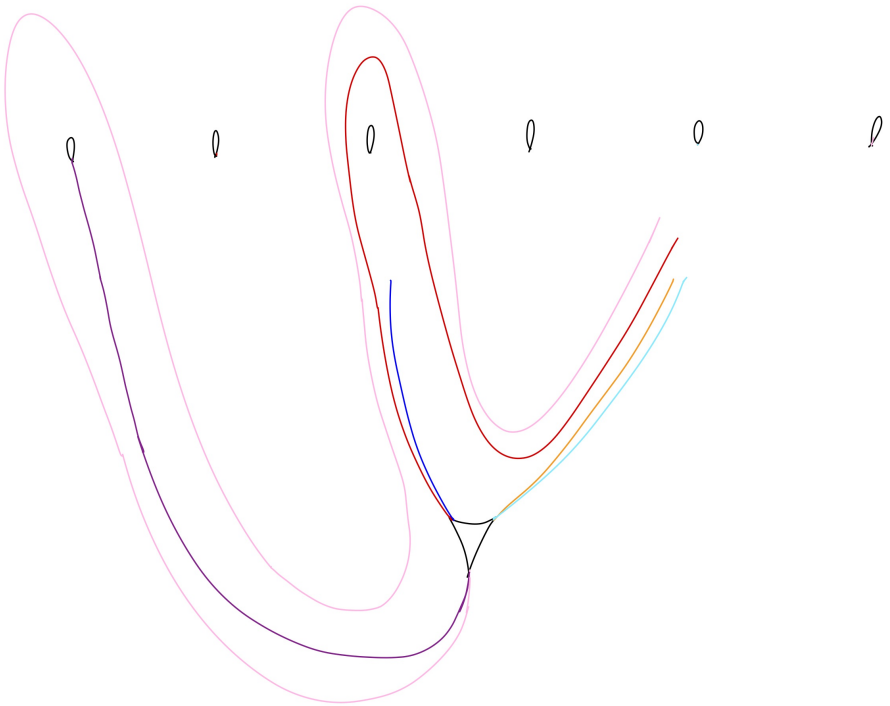


Figure C.164: Nidder2

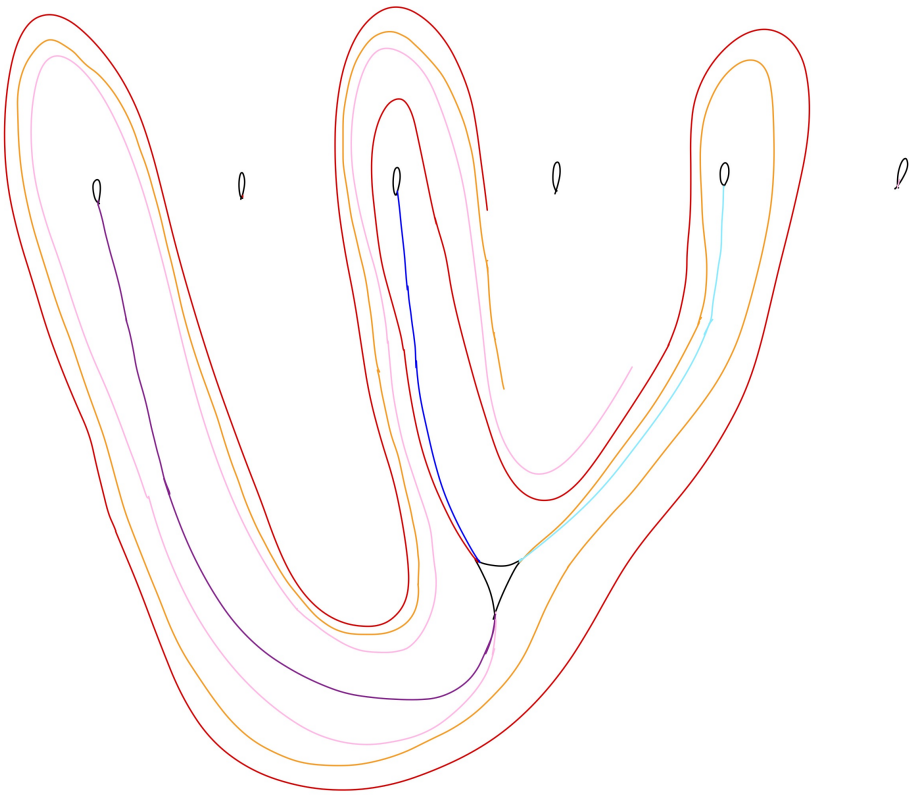


Figure C.165: Nidder3

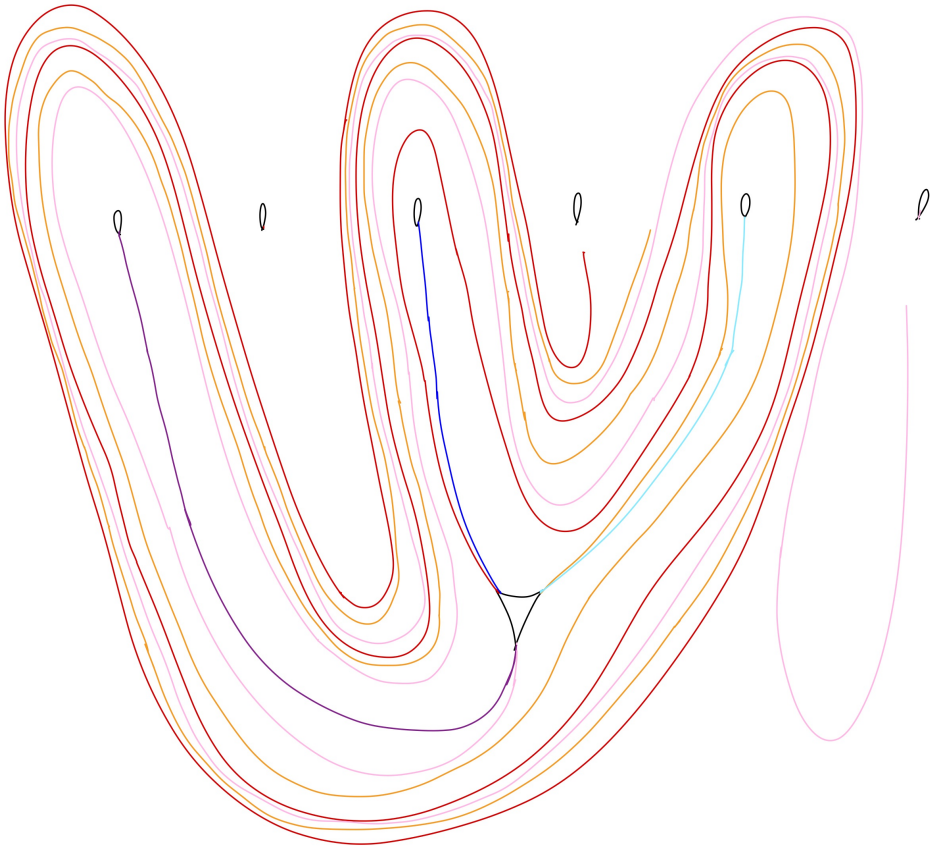


Figure C.166: Nidder4

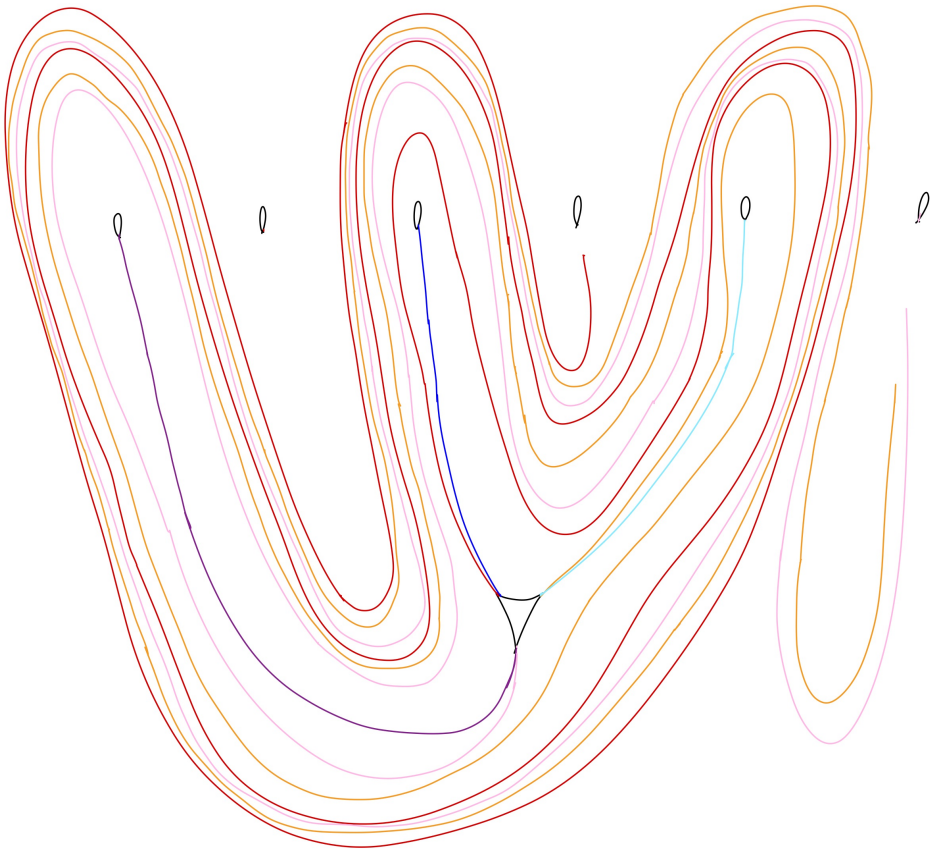


Figure C.167: Nidder5

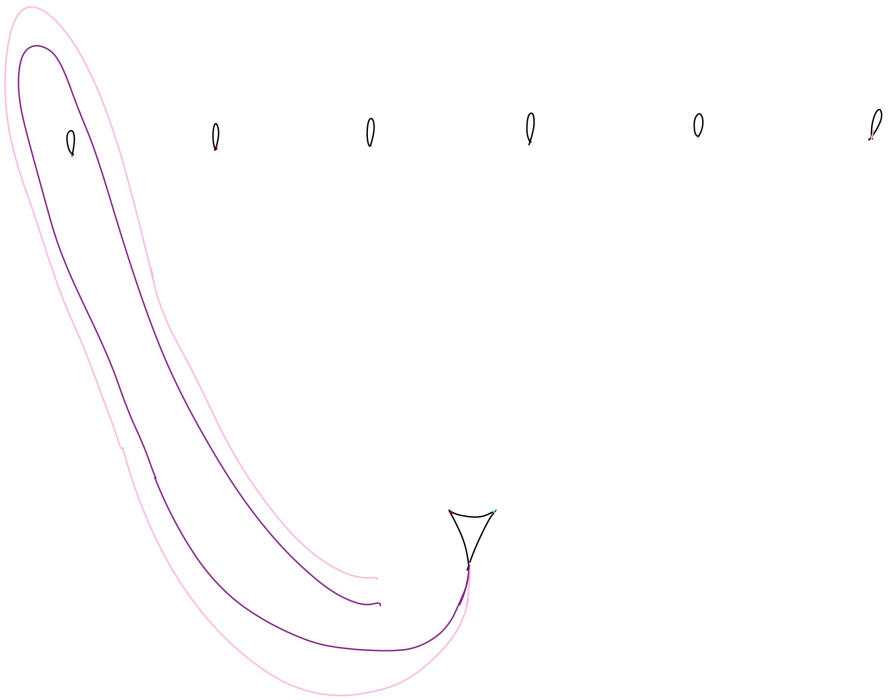


Figure C.168: Busk1

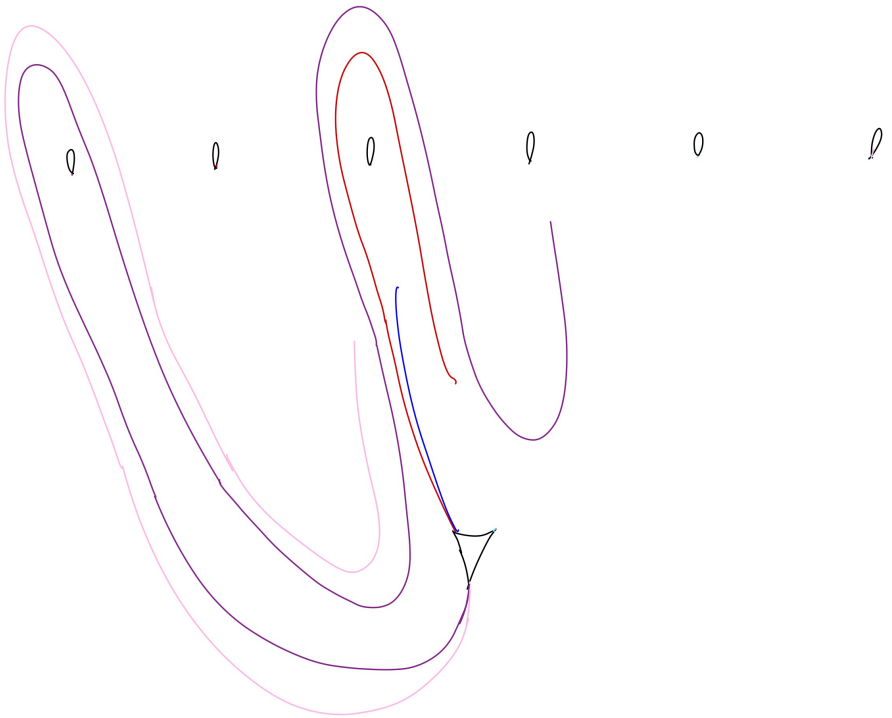


Figure C.169: Busk2

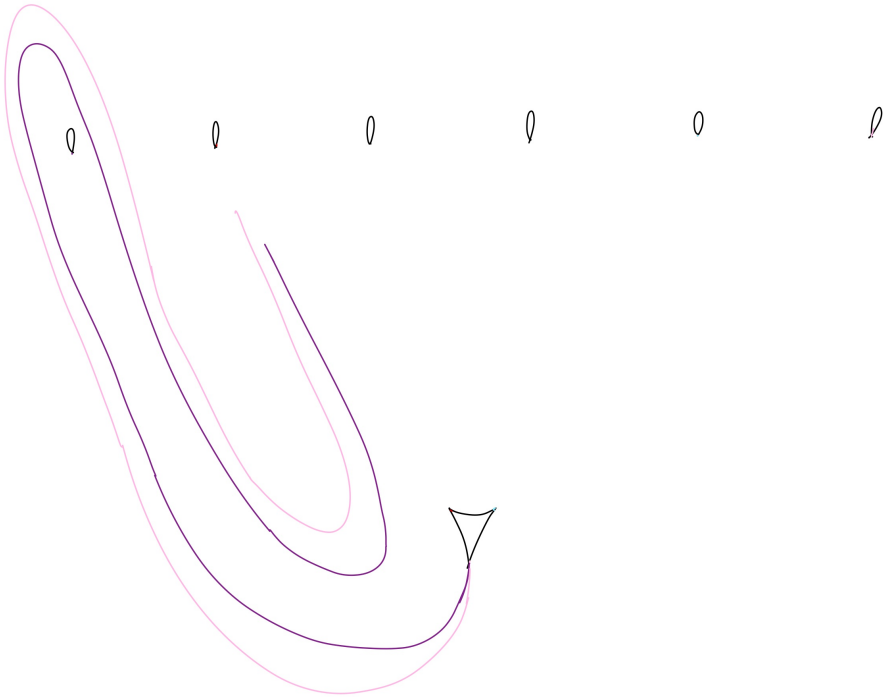


Figure C.170: Busk3

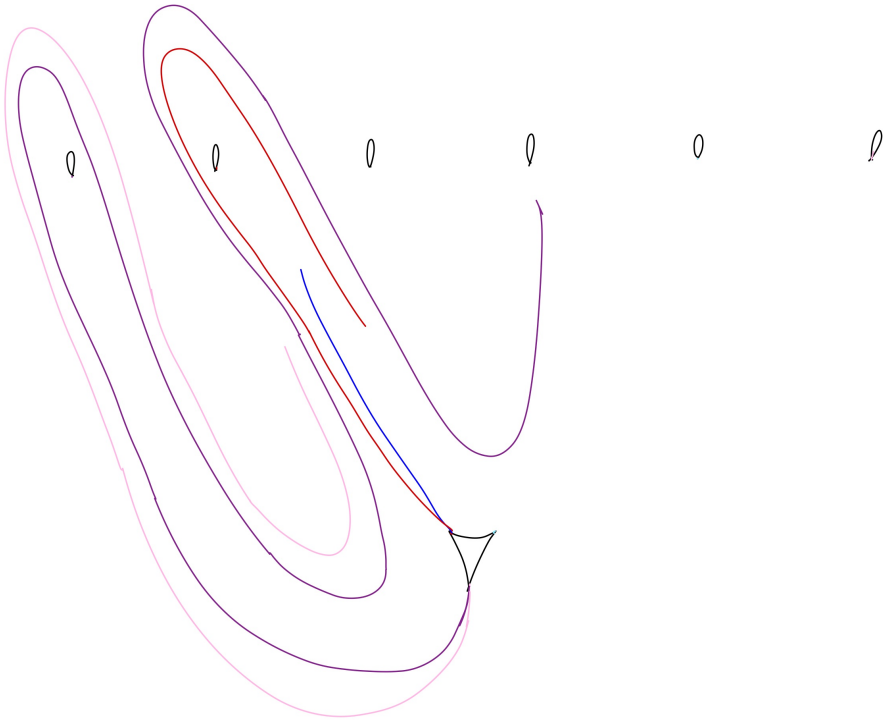


Figure C.171: Busk4

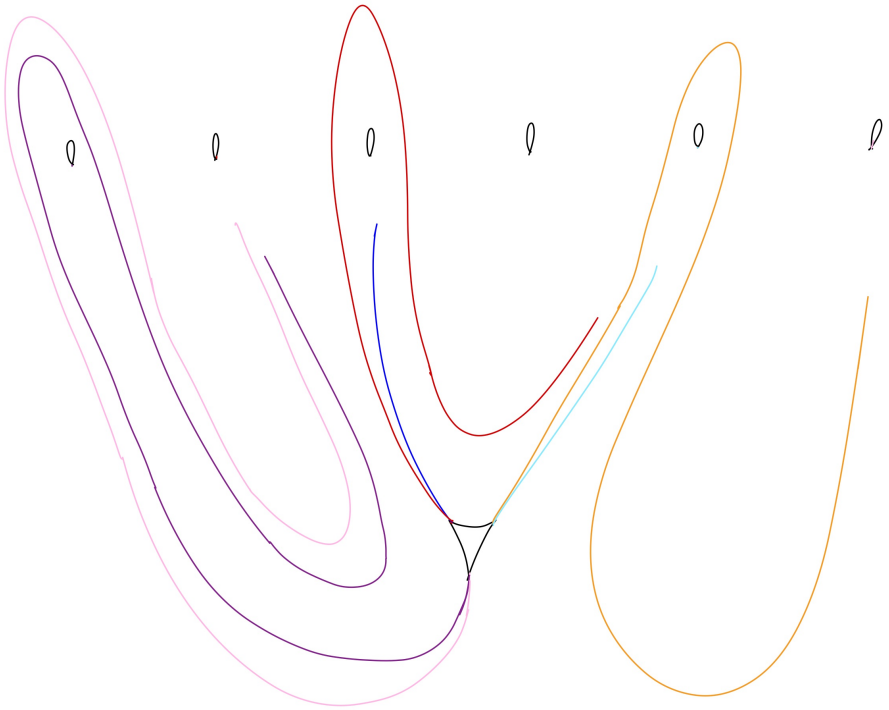


Figure C.172: Kieve1

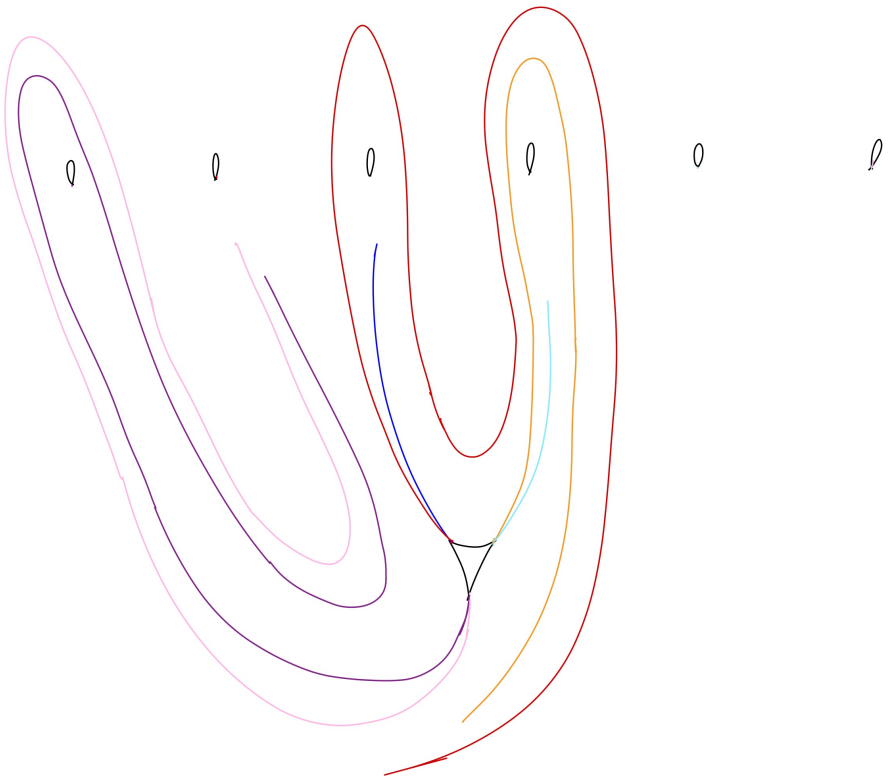


Figure C.173: Kieve2

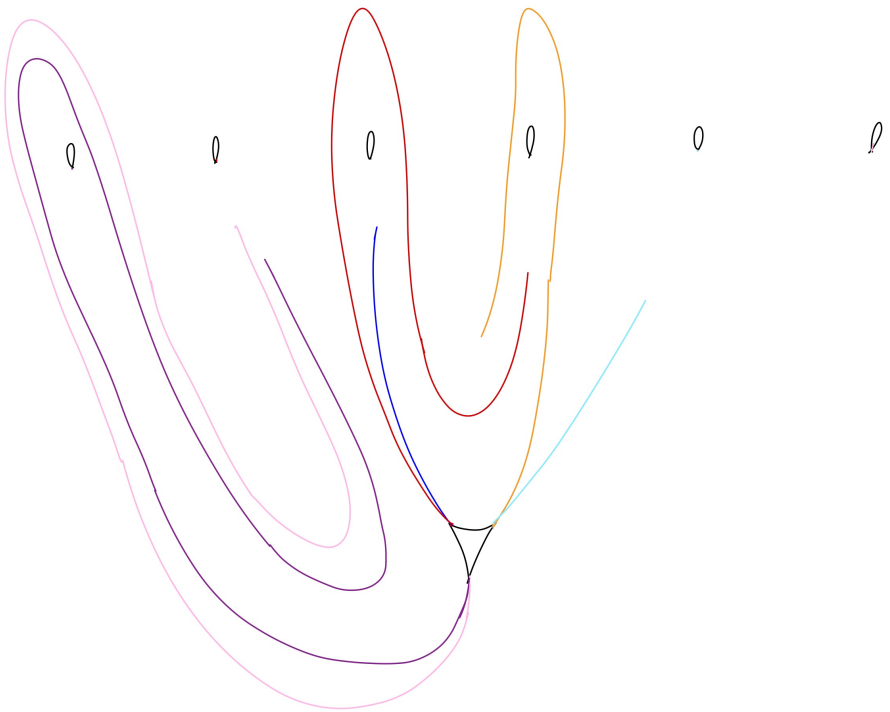


Figure C.174: Kieve3

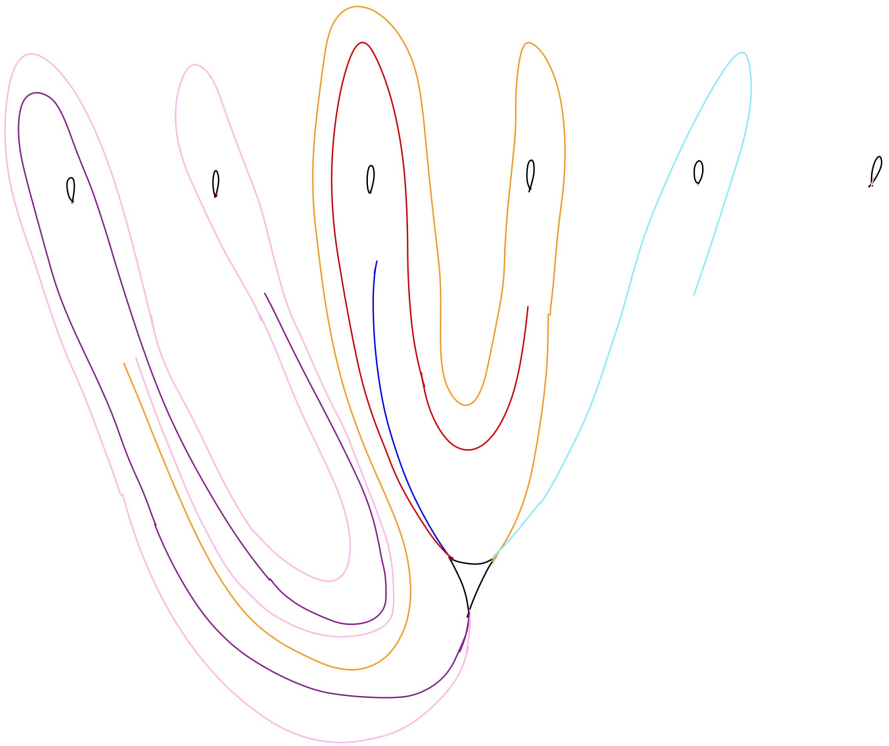


Figure C.175: Kieve4

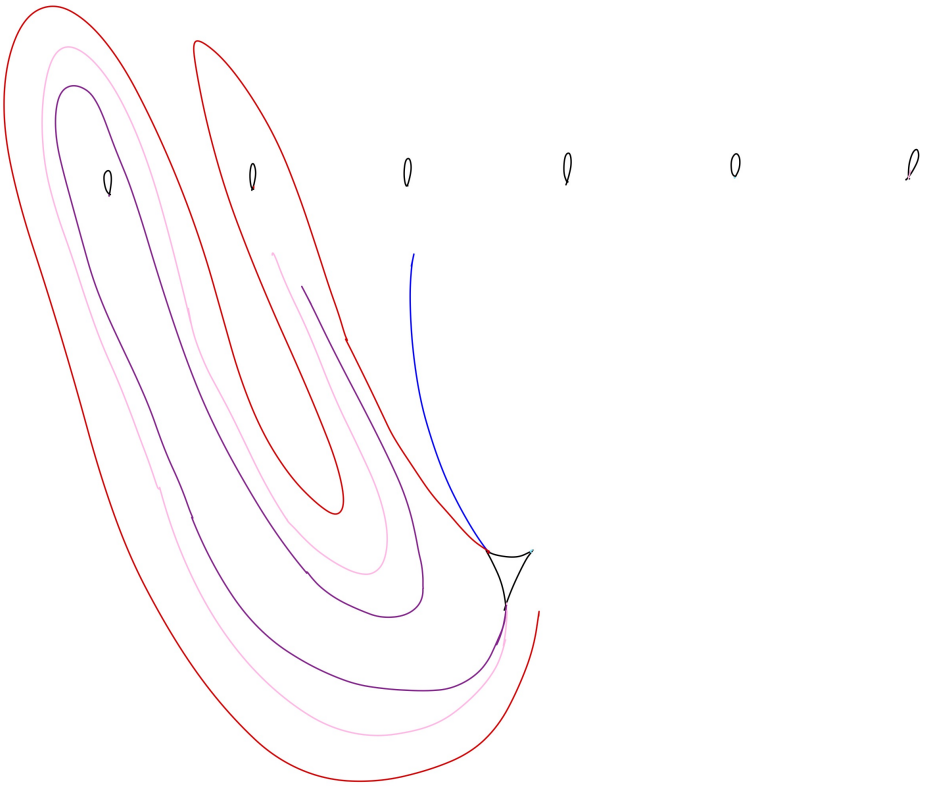


Figure C.176: Oorie1

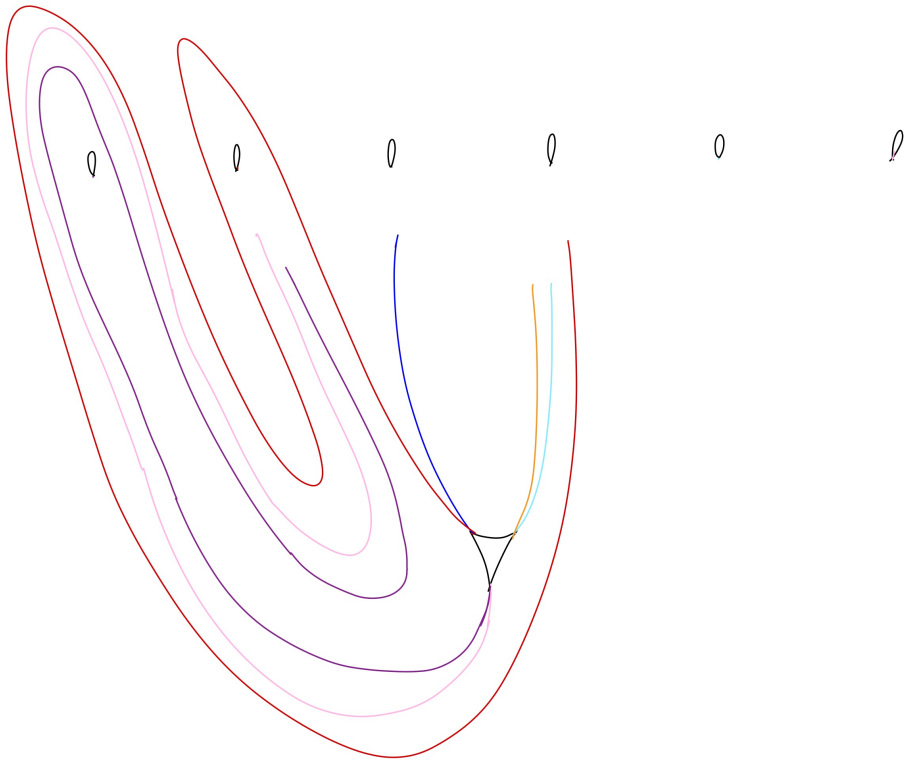


Figure C.177: Oorie2

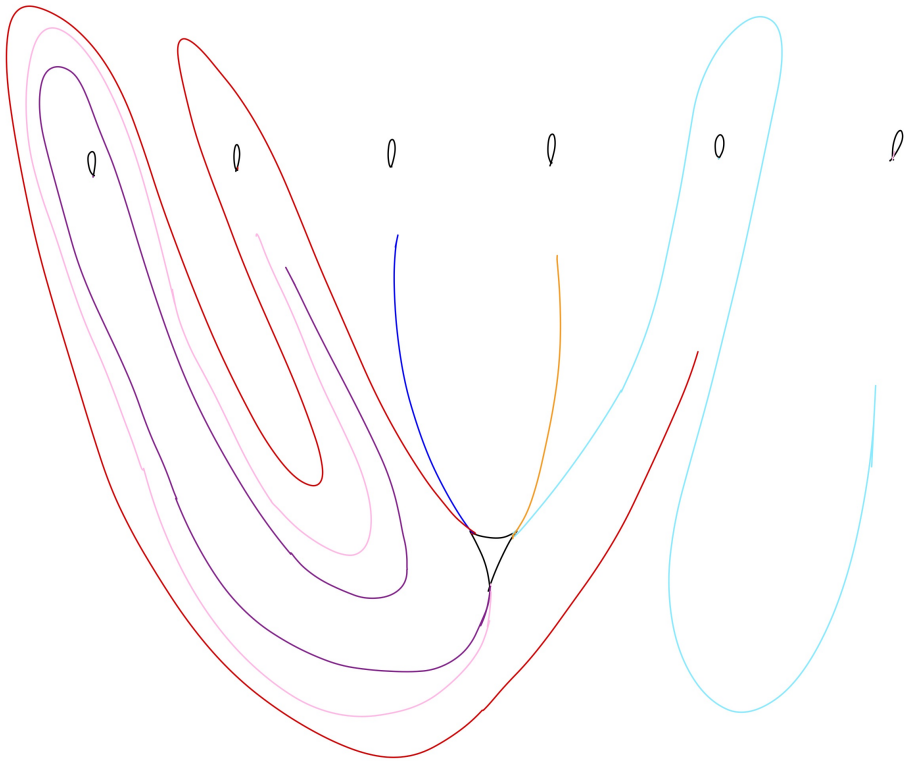


Figure C.178: Oorie3

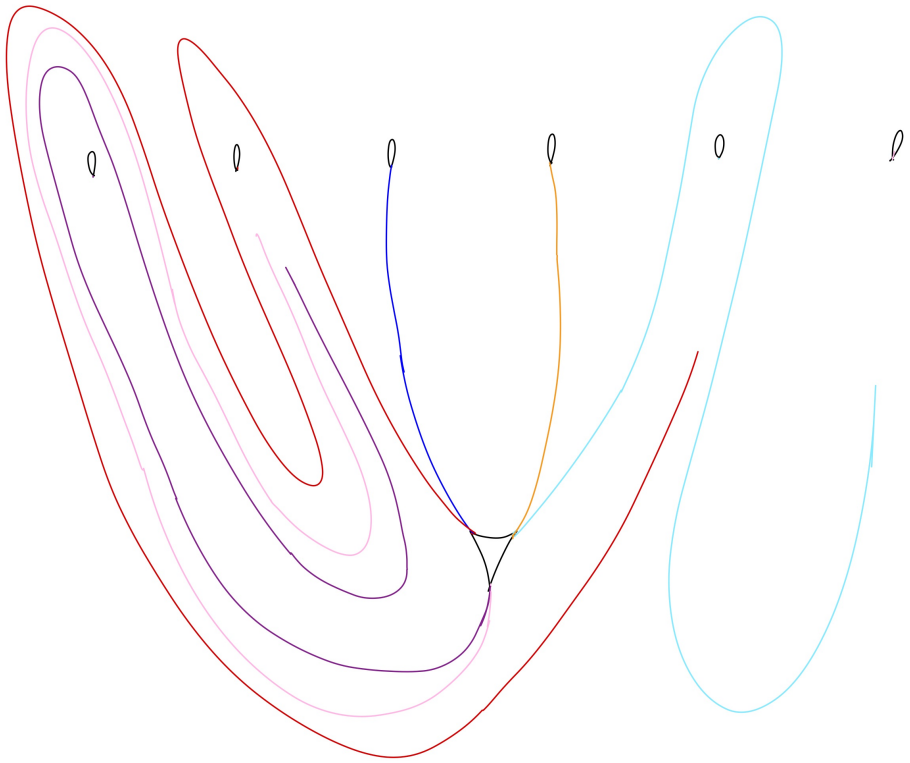


Figure C.179: Oorie4

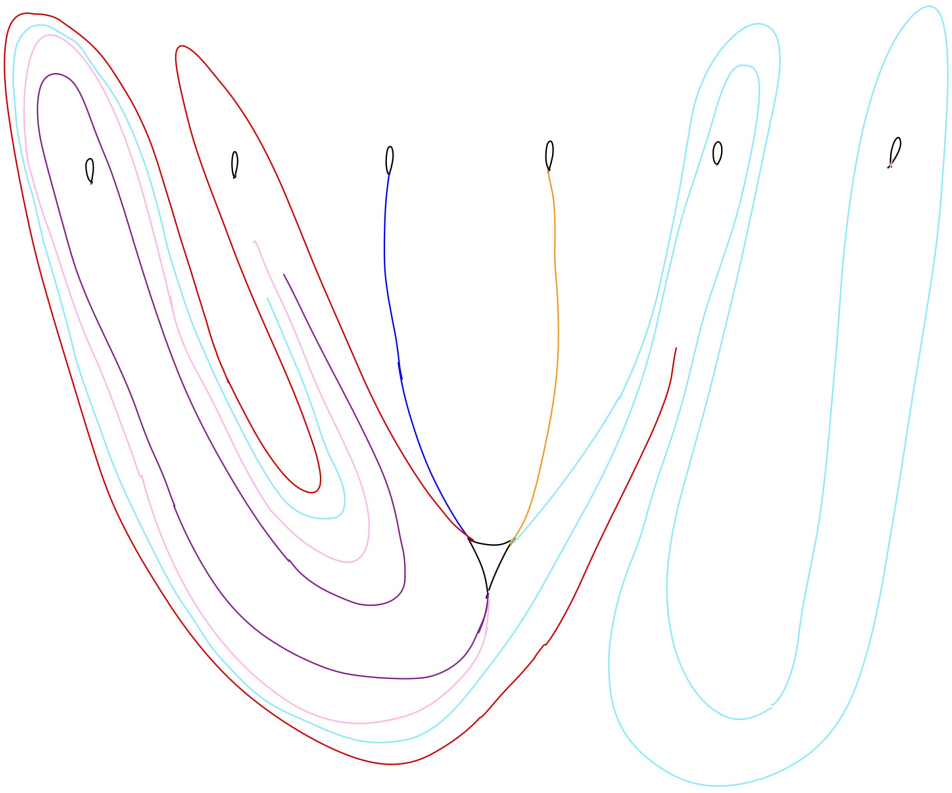


Figure C.180: Oorie5

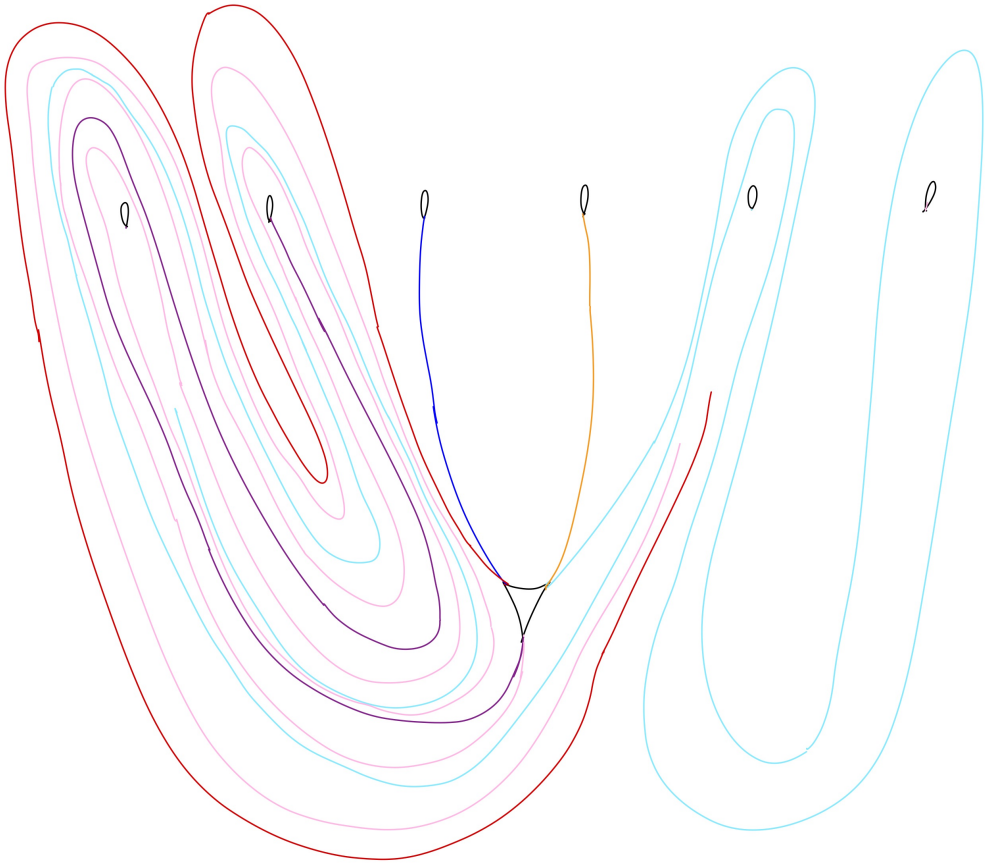


Figure C.181: Oorie6

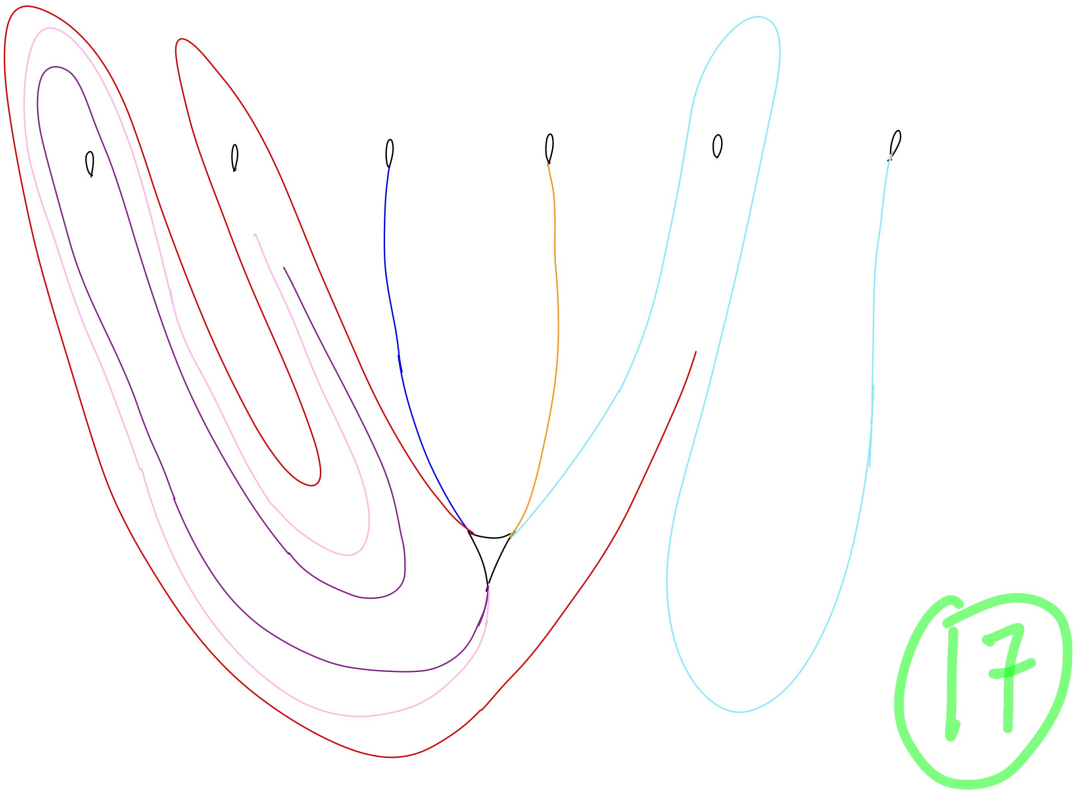


Figure C.182: Oorie7

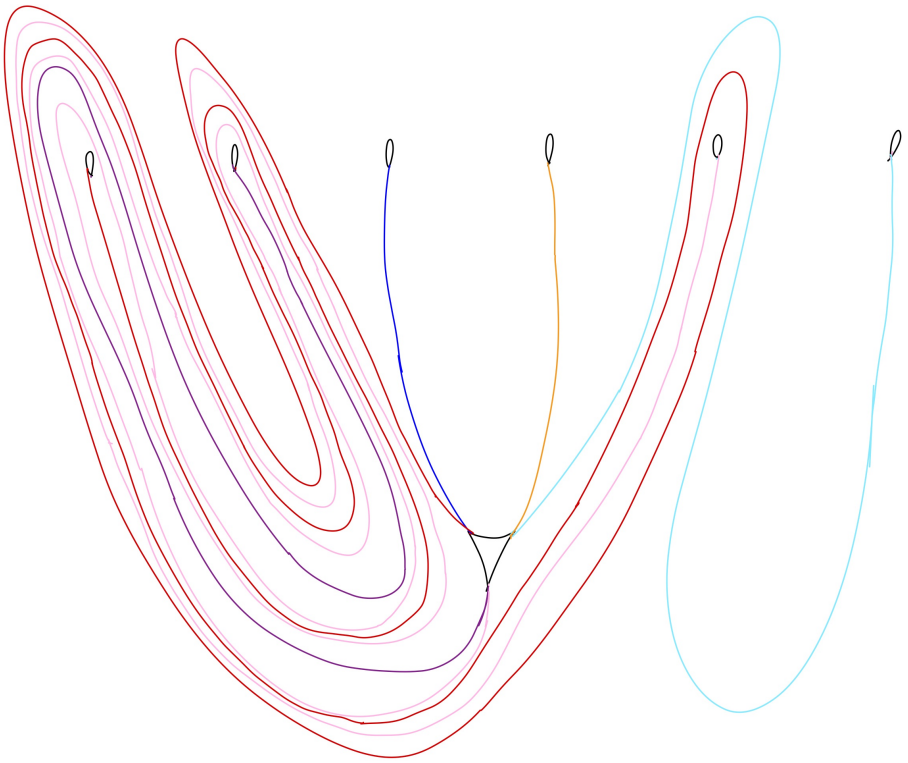


Figure C.183: Oorie8

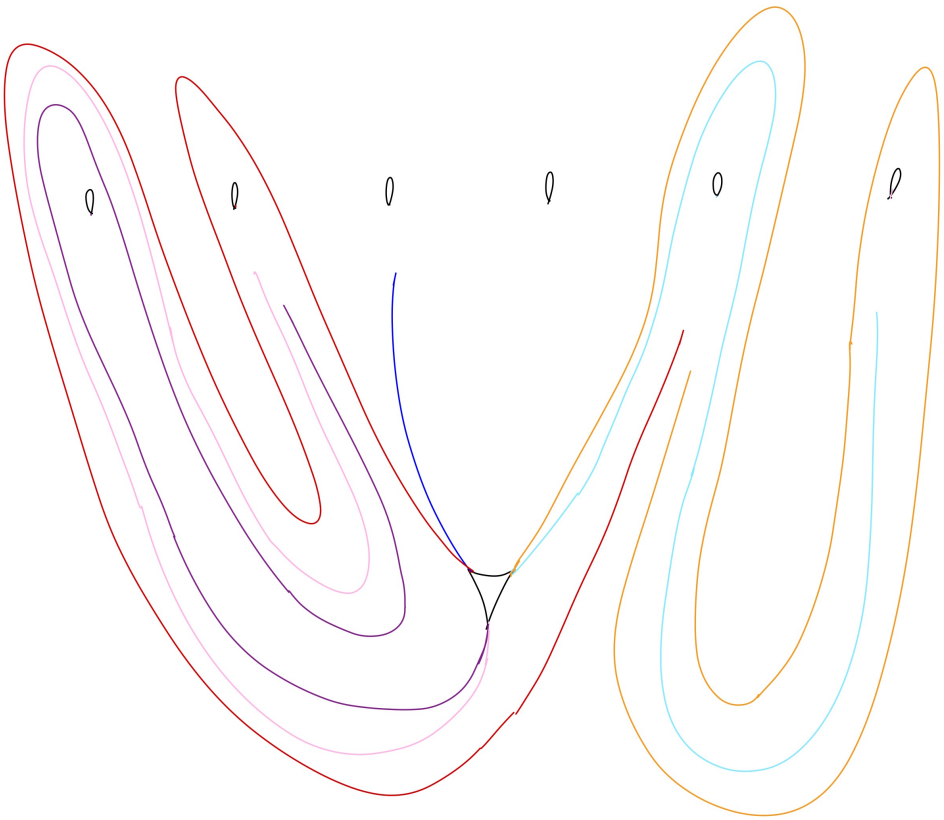


Figure C.184: Oorie9

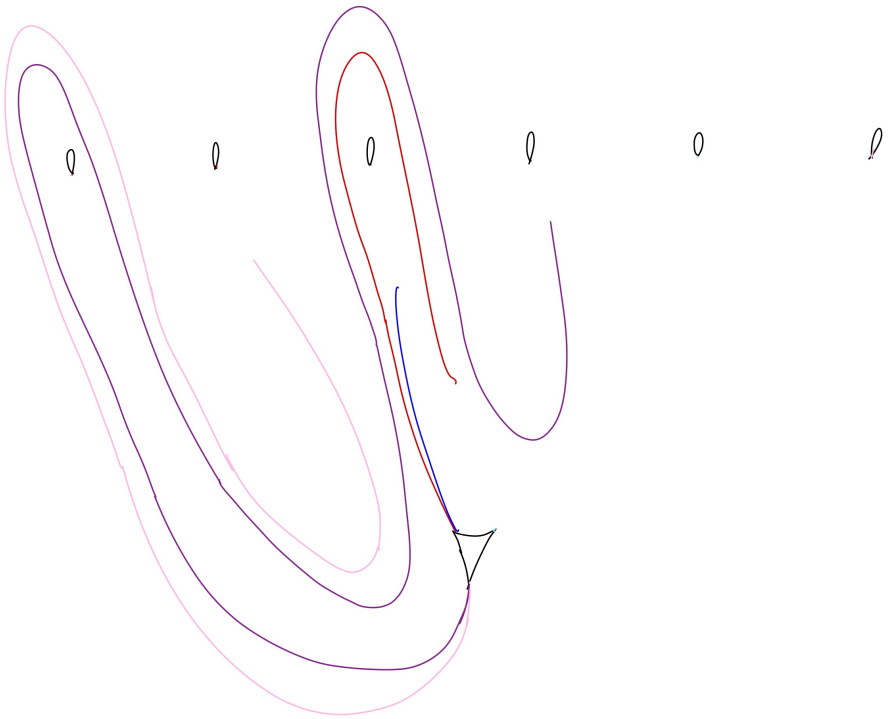


Figure C.185: Quank1

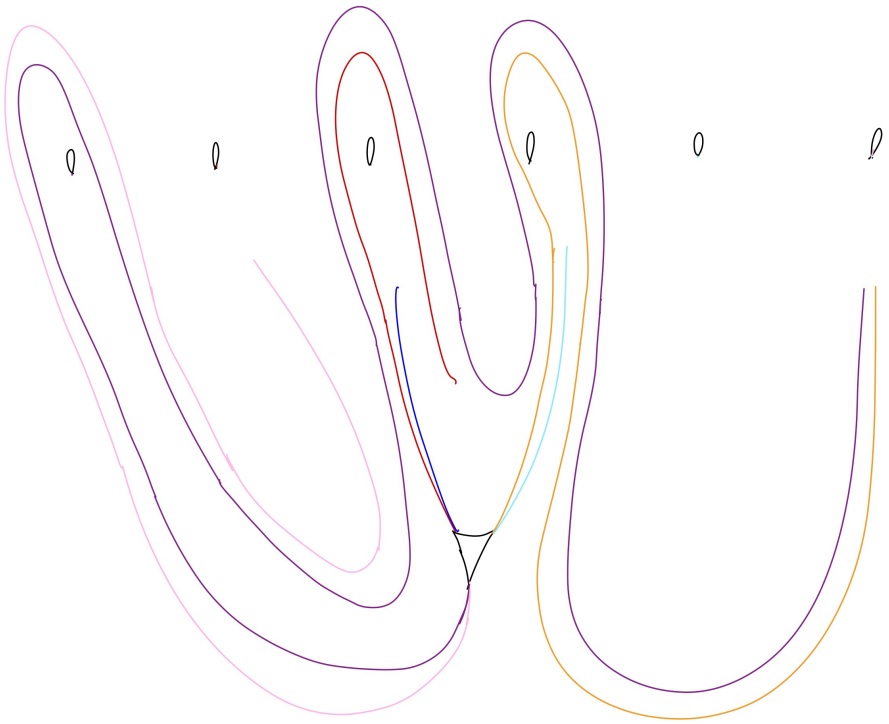


Figure C.186: Quank2

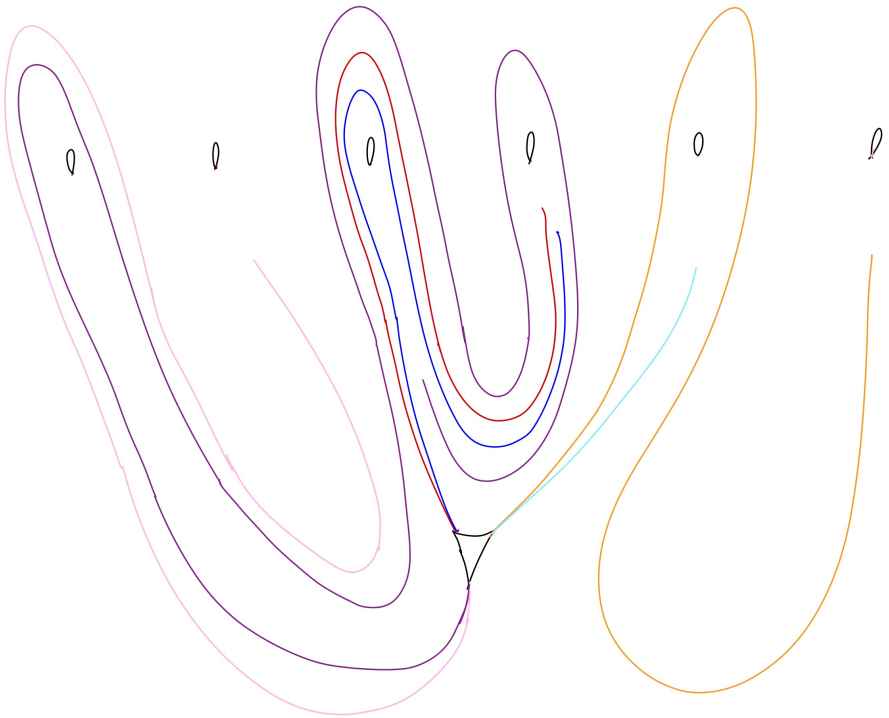


Figure C.187: Quank5

APPENDIX FOUR

Train Track Case Analysis: Track 0

Here is Track 0:

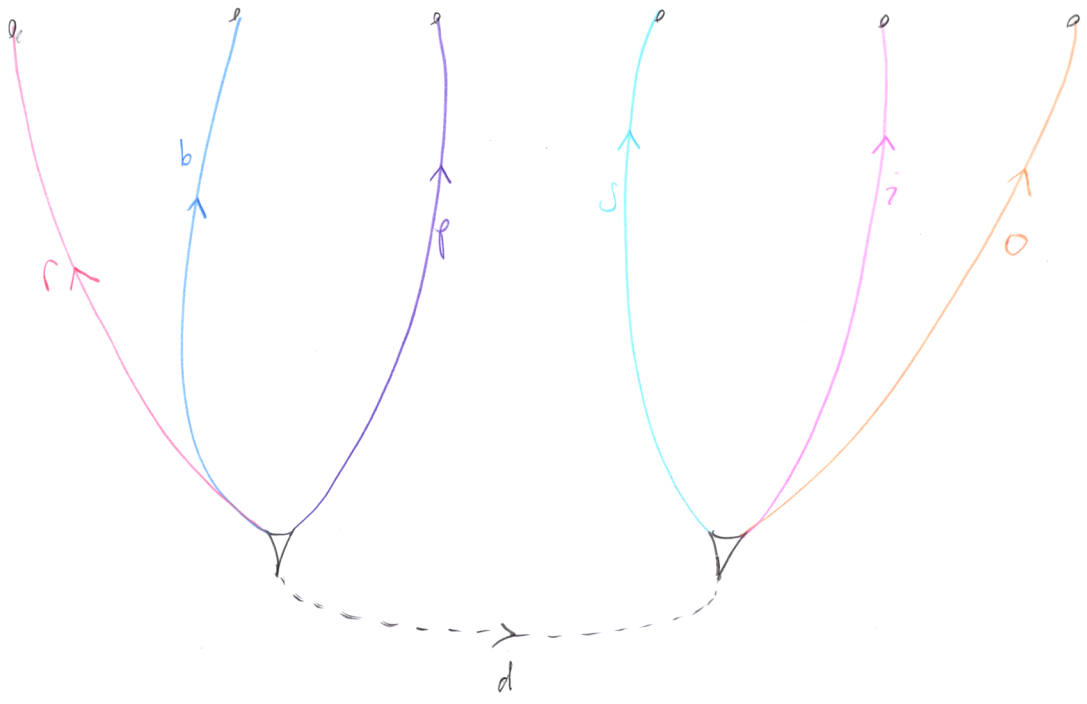


Figure D.1: Track 0

D.1 Case A: Triangles fixed

Triangles are fixed, and $f_\beta(d)$ and $f_\beta(\overline{d})$ both pass over d after an even number of letters, we will call this *Assumption A*. We know f_β does not start at d, and $f_\beta(\overline{d})$ does not start at $\overline{d}$, otherwise p and s would pass over themselves.

Thus $f_\beta(d)$ must start at r, b, or p; and $f_\beta(\overline{d})$ must start at s, i, or o.

Furthermore, notice that Track 0 is isomorphic to its own mirror, so there is the following symmetry: a train track map, carried by a braid β yields from among the case analysis under the assumption that $f_\beta(d)$ begins with r and $f_\beta(\bar{d})$ begins with i if and only if one carried by $\bar{\beta}$ yields from among the case analysis under the assumption that $f_\beta(d)$ begins with b and $f_\beta(\bar{d})$ begins with o.

Indeed, it is clear that β also carries a train track map on the mirror of Track 0,

D.1.1 AVX

Suppose $f_\beta(d)$ starts at r and $f_\beta(\bar{d})$ starts at s.

This is Figure D.2.

Here notice that $f_\beta(d)$ must eventually traverse $p^- d...$ in order to meet Assumption A, and in fact it must do so without any prior initial twists with b. Otherwise it would bring $f_\beta(b)$ along and cause it to trace. So we must have

$$f_\beta(d) = r^- p^- d...$$

as depicted in Figure D.3.

Notice also that $f_\beta(\bar{d})$ must begin with s^- to meet Assumption A.

Here $f_\beta(r)$ can begin with p^- or p°

D.1.1.1 Phil

Suppose $f_\beta(r)$ begins with p^-. Then we have Figure D.4.

Here $f_\beta(\bar{d})$ can continue with i^- or o^-.

D.1.1.1.1 Linen

Suppose $f_\beta(\bar{d})$ continues with i^-. Then we must have

$$f_\beta(\bar{d}) = s^- o^- \bar{d}...$$

This is Figure D.5.

Here the dotted lines can either join, or $f_\beta(d)$ must continue into 1., 2., or 3. labeled in the diagram. Note here that $f_\beta(d)$ cannot continue between $f_\beta(o)$ and $f_\beta(i)$ (the orange and pink edges) since it will be absorbed.

D.1.1.1.1.1 Bibble

Suppose dotted lines join. Then $f_\beta(r)$ is forced to continue with $di^*...$, and it cannot go to o^* after crossing d, as that would force wither itself to trace if it goes o^-, or forcing $f_\beta(p)$ to trace. Then $f_\beta(r)$ continues with $s^+\bar{d}p^+b^*$. So we have

$$f_\beta(r) = p^- di^+ s^+ \bar{d} p^+ b^*...$$

This forces $f_\beta(p)$ to end at o°:

$$f_\beta(p) = do^\circ$$

or else it will trace.

On the other hand, $f_\beta(i)$ has to be

$$f_\beta(i) = \overline{d}p^+...$$

and continue with r^* or b^*.

This is Figure D.6.

D.1.1.1.1.1.1 Bawcock

Suppose $f_\beta(i)$ continue with r^*. Then the following is forced:

Figure D.7.

Here $f_\beta(i)$ is forced to go

$$f_\beta(i) = \overline{d}p^+r^+do^+\overline{d}...$$

Thus $f_\beta(b)$ cannot simply be $f_\beta(p^\circ)$ because then $f_\beta(i)$ will be absorbed; nor can it start with $f_\beta(b) = p^+$ because then itself will be absorbed. Hence we have $f_\beta(b) = p^-...$ and continues with $f_\beta(b) = p^-d....$ At this point it can continue with either o^- or i^+ but the former will trace, so it continues with o^-:

$$f_\beta(b) = p^-do^-\overline{d}r^-p^-...$$

but now it is absorbed.

and $f_\beta(b)$ is absorbed. This is a contradiction.

D.1.1.1.1.1.2 Chaffer

Back to the end of Bibble D.1.1.1.1.1. Suppose $f_\beta(i)$ continues with b^*.

This is Figure D.8.

In this case it has to be in fact b°, otherwise it will trace. So we have

$$f_\beta(i) = \bar{d}p^+b^\circ.$$

This forces the situation depicted in Figure D.9.

Now consider $f_\beta(s)$, which starts with i^*. It cannot start with i^+, or it will immediately trace. We claim that it can also not start with i^-. Suppose it did. Then the following is forced:

$$f_\beta(s) = i^-\bar{d}p^+r^+do^+p^*...$$

At this point $f_\beta(b)$ is forced to begin with p^-, or $f_\beta(s)$ will be absorbed. So we have

$$f_\beta(b) = p^-di^*$$

And now $f_\beta(o)$, which we know at this point is

$$f_\beta(o) = \overline{d}p^+b^+p^+di^*$$

must continue with i^-, otherwise $f_\beta(b)$ will trace. Thus we have

$$f_\beta(o) = \overline{d}p^+b^+p^+di^-...$$

but now $f_\beta(o)$ will trace as the following is forced:

$$f_\beta(o) = \overline{d}p^+b^+p^+di^-\bar{d}p^+r^+do^*$$

This is a contradiction. Thus $f_\beta(s)$ must start (and end) with i°:

$$f_\beta(s) = i^\circ.$$

This is Figure D.10.

Here $f_\beta(o)$ must continue with s^- and to the right of $f_\beta(r)$. Otherwise, $f_\beta(r)$ would continue with s^+ and to the left of $f_\beta(o)$, in which case, it would be absorbed:

$$f_\beta(r) = ...s^+i^-\bar{d}p^+b^-p^-d\,\mathrm{Abso}(f_\beta(o), f_\beta(i))^\times$$

So we must have

$$f_\beta(o) = ...s^-i^-\bar{d}p^+b^-p^-ds^-i^-\bar{d}p^*...$$

as shown in Figure D.11.

Here the incoming $f_\beta(o)$ forces $f_\beta(b)$ to begin with p^- and to the right of $f_\beta(o)$. But now it will trace:

$$f_\beta(b) = p^-di^+s^+\bar{d}p^+b^\times$$

This is a contradiction.

D.1.1.1.1.2 Fangle

Back to the end of Linen D.1.1.1.1 . Suppose dotted lines do not join, and suppose $f_\beta(d)$ goes into 1.

This is Figure D.12.

Here neither of the dotted lines can traverse above $f_\beta(p)$, or they would enter into Situation

β. So they circle the perimeter, and will be in Situation α.

This is a contradiction.

D.1.1.1.1.3 Hallan

Back to the end of Linen D.1.1.1.1. Suppose dotted lines do not join, and suppose $f_\beta(d)$ goes into 2. But in this case, $f_\beta(d)$ is immediately in Situation β.

This is a contradiction.

D.1.1.1.1.4 Jargle

Back to the end of Linen D.1.1.1.1. Suppose dotted lines do not join, and suppose $f_\beta(d)$ goes into 3.

Then the situation is shown in Figure D.13.

Where $f_\beta(d)$ must continue with p^+ after crossing d and not o to not violate the Trace Lemma.

Here $f_\beta(d)$ continues with $\bar{d}p^+$, and the next letter cannot be b^* or it would violate the Trace Lemma. So the next letter must be r^+, and then:

$$f_\beta(\bar{d}) = s^- i^- \bar{d} p^+ \hat{r}^+ d o^+ ...$$

where it just violated the Trace Lemma.

This is a contradiction.

D.1.1.1.2 Kench

Back to D.1.1.1 Phil. Suppose $f_\beta(\bar{d})$ continues with o^-.

This is Figure D.14.

Here if $f_\beta(\bar{d})$ went above $f_\beta(p)$ in the middle, then $f_\beta(p)$ will trace:

$$f_\beta(p) = do^+s^+\bar{d}p^\times$$

So $f_\beta(\bar{d})$ msut go below $f_\beta(p)$ to give the situation in Figure D.15.

Here both dotted lines cannot go below $f_\beta(o)$ and $f_\beta(i)$ or they would enter Situation β. So they go above, and will be in Situation α.

This is a contradiction.

D.1.1.2 Test

Back to the end of AVX D.1.1. Suppose

$$f_\beta(r) = p^\circ$$

This is Figure D.16.

Similar to the previous situations, here $f_\beta(\bar{d})$ can continue with i^- or o^-.

D.1.1.2.1 Pugil

Suppose $f_\beta(\bar{d})$ continues with i^-.

This is Figure D.17.

Here the dotted lines can join in the middle or $f_\beta(d)$ goes into 1. or 2. Note that it is impossible for it to go in between $f_\beta(i)$ and $f_\beta(\bar{d})$ as that would cause it to enter Situation β.

D.1.1.2.1.1 Limmer

Suppose the dotted lines join in the middle.

This is Figure D.18.

Consider $f_\beta(p)$. After $f_\beta(p) = d...$, we must have

$$f_\beta(p) = do^*$$

as $f_\beta(p) = di$ will cause it to trace. In fact, it must be

$$f_\beta(p) = do^\circ$$

since both do^- and do^+ will cause $f_\beta(p)$ to trace.

Now consider $f_\beta(o)$. We must have

$$f_\beta(o)\bar{d}p^+b^*...$$

Here it cannot go $f_\beta(o)\bar{d}pr^*...$ as it will then trace.

Now consider $f_\beta(i)$. We have either

$$f_\beta(i) = \bar{d}p^+r^*...$$

or

$$f_\beta(i) = \bar{d}p^+b^*...$$

D.1.1.2.1.1.1 Costard

Suppose

$$f_\beta(i) = \bar{d}p^+r^*...$$

Then $f_\beta(i)$ continues:

$$f_\beta(i) = \bar{d}p^+r^+do^+\bar{d}p^+r^*$$

This is Figure D.19.

Consider $f_\beta(b)$. We have

$$f_\beta(b) = p^+r^*...$$

and here if $f_\beta(b) = p^+r^\circ$ or $f_\beta(b) = p^+r^+$ will cause $f_\beta(i)$ to be absorbed between $f_\beta(r)$ and $f_\beta(b)$. Hence we must have $f_\beta(b) = p^+r^-...$, and continue with

$$f_\beta(b) = p^+r^-p^-do^-\bar{d}p^-...$$

but now $f_\beta(b)$ is absorbed between $f_\beta(o)$ and $f_\beta(i)$.

This is a contradiction

D.1.1.2.1.1.2 Daddock

Back to the end of Limmer D.1.1.2.1.1 Suppose

$$f_\beta(i) = \bar{d}p^+b^*...$$

Then in fact $f_\beta(i)$ must end there:

$$f_\beta(i) = \bar{d}p^+b^\circ.$$

This is because both $f_\beta(i) = \bar{d}p^+b^+$ and $f_\beta(i) = \bar{d}p^+b^-$ will cause it to trace, or absorbed:

$$f_\beta(i) = \bar{d}p^+b^+p^-di^\times$$

$$f_\beta(i) = \bar{d}p^+b^-p^-ds^-i^\times$$

or

$$f_\beta(i) = \bar{d}p^+b^-p^-\times$$

So we have the situation depicted in Figure D.20.

Consider $f_\beta(o)$. We have

$$f_\beta(o) = \bar{d}p^+b^+p^-di^*...$$

Consider $f_\beta(s)$. We cannot have $f_\beta(s) = i^+...$ because it will immediately trace. Thus we must have either

$$f_\beta(s) = i^-$$

or

$$f_\beta(s) = i^\circ$$

D.1.1.2.1.1.2.1 Cordwain

Suppose

$$f_\beta(s) = i^- ...$$

Then right after i^-, $f_\beta(s)$ must go to the right of $f_\beta(o)$ or else it will eventually be absorbed between $f_\beta(o)$ and $f_\beta(i)$. Continuing, we have

$$f_\beta(s) = i^- \bar{d}p^+ ...$$

Here it cannot go up b: $f_\beta(s) = i^- \bar{d}p^+ b^- ...$, as this would make it eventually trace:

$$f_\beta(s) = i^- \bar{d}p^+ b^- p^- ds^\times$$

Thus we must have

$$f_\beta(s) = i^- \bar{d}p^+ r^+ do^+ \bar{d}p^+ r^* ...$$

This is Figure D.21.

Now consider $f_\beta(b)$. We have

$$f_\beta(b) = p^+ r^*$$

and here if we have $f_\beta(b) = p^+ r^\circ$ or $f_\beta(b) = p^+ r^+$, then $f_\beta(s)$ will be forced to continue with $f_\beta(s) = i^- \bar{d}p^+ r^+ do^+ \bar{d}p^+ r^+ ...$, which would immediately lead to $f_\beta(s)$ being absorbed between $f_\beta(r)$ and $f_\beta(b)$. Thus we must have $f_\beta(b) = p^+ r^- ...$, and continue to the right side of $f_\beta(s)$ as it comes down.

Now the following is forced, and it is eventually absorbed:

$$f_\beta(b) = p^+ r^- p^- do^- \bar{d}r^- p^- di^*$$

This is Figure D.22.

Consider $f_\beta(o)$. Here $f_\beta(o)$ cannot continue with i° or i^+ as this will force $f_\beta(b)$ to continue with i^+ as well, and it will be absorbed:

$$f_\beta(b) = p^+ r^- p^- do^- \bar{d} r^- p^- di^+ \bar{d} p^+ b^- p^- d \,\mathrm{Abso}(f_\beta(o), f_\beta(i))^\times$$

Similarly, $f_\beta(o)$ cannot continue with i^+ or it will also be absorbed between itself and $f_\beta(i)$:

$$f_\beta(o) = \bar{d} p^+ b^+ p^- di^+ \bar{d} p^+ b^- p^- d \,\mathrm{Abso}(f_\beta(o), f_\beta(i))^\times$$

This is a contradiction.

D.1.1.2.1.1.2.2 Loblolly

Back to end of Daddock D.1.1.2.1.1.2. Suppose

$$f_\beta(s) = i^\circ$$

Then $f_\beta(o)$ continues with i^+:

$$f_\beta(o) = \bar{d} p^+ b^+ p^- di^+ s^*$$

The situation now is shown in Figure D.23.

Here $f_\beta(o)$ cannot continue with s^+ or it will be absorbed:

$$f_\beta(o) = \bar{d} p^+ b^+ p^- di^+ s^+ i^- \bar{d} p^+ b^- p^- d \,\mathrm{Abso}(f_\beta(o), f_\beta(i))^\times$$

Also, $f_\beta(b)$ cannot continue with r^+ or it will be absorbed:

$$f_\beta(b) = p^+ r^+ p^- \,\mathrm{Abso}(f_\beta(o), f_\beta(b))^\times$$

Thus we must have

$$f_\beta(o) = \bar{d}p^+ b^+ p^- d i^+ s^{\circ}_{-} ...$$

and

$$f_\beta(b) = p^+ r^{\circ}_{-} ...$$

However, suppose $f_\beta(o)$ goes s^-, then we have

$$f_\beta(o) = f_\beta(o) = \bar{d}p^+ b^+ p^- d i^+ s^- i^- \bar{d}p^+ b^- p^+ d s^- i^- \bar{d}p^+ r^* ...$$

and now this forces $f_\beta(b)$ to go r^-, as ending with r° here will force $f_\beta(o)$ to be absorbed. But now we have

$$f_\beta(b) = p^+ r^- p^+ d i^+ s^+ i^- \bar{d}p^+ b^- p^- d \,\mathrm{Abso}(f_\beta(o), f_\beta(i))^\times$$

Thus $f_\beta(o)$ cannot go s^-, and so we must have

$$f_\beta(o) = f_\beta(o) = \bar{d}p^+ b^+ p^- d i^+ s^\circ$$

This is Figure D.24.

But now this also forces $f_\beta(b)$ to end with r°; as going r^- now will be absorbed:

$$f_\beta(b) = po^+ r^- p^- d i^+ s^+ i^- \bar{d}p^+ b^- p^- d \,\mathrm{Abso}(f_\beta(o), f_\beta(i))^\times$$

The conclusion is that we must have

$$f_\beta(o) = f_\beta(o) = \bar{d}p^+b^+p^-di^+s^\circ$$

and

$$f_\beta(b) = p^+r^\circ$$

This gives Candidate 1. Shown in Figure D.25.

D.1.1.2.1.2 Smouch

Back to the end of Pugil D.1.1.2.1. Suppose $f_\beta(s)$ goes into 1.

This is Figure D.26.

Here both $f_\beta(d)$ and $f_\beta(\bar{d})$ in the middle cannot go above $f_\beta(p)$ or it would enter Situation β. So they both continue with r^- and will be in Situation α.

This is a contradiction.

D.1.1.2.1.3 Thwite

Back to the end of Pugil D.1.1.2.1. Suppose $f_\beta(s)$ goes into 2, after which it must go up i and not o, or it will have to cross $\bar{d}$ again immediately, which is not allowed. Then we have

$$f_\beta(d) = r^-p^-di^+s^+\bar{d}p^+...$$

and

$$f_\beta(\bar{d}) = s^-i^-\bar{d}p^+...$$

as shown in Figure D.27.

At this point neither of these can go up b, as that will force them to violate the Trace Lemma. Hence both have to continue clockwise, with $...r^+do....$

But then they will cross d and then traverse $o^+\bar{d}$, thereby violating the Trace Lemma.

This is a contradiction.

D.1.1.2.2 Quarl

Back to end of Test D.1.1.2. Suppose $f_\beta(\bar{d})$ continue with o^-, so we have the situation shown in Figure D.28.

Here the dotted lines can join, or $f_\beta(d)$ goes into 1 or 2. Again it cannot go in between $f_\beta(i)$ and $f_\beta(\bar{d})$ or it would be in Situation β.

D.1.1.2.2.1 Wamble

Suppose the dotted lines join, or $f_\beta(d)$ goes into 2. In both cases we have

$$f_\beta(p) = do^+s^+\bar{d}p^\times$$

This is a contradiction.

D.1.1.2.2.2 Yaffle

Back to end of Quarl (D.1.1.2.2). Suppose $f_\beta(d)$ goes into 1. In this case $f_\beta(\bar{d})$ has to go under $f_\beta(p)$ otherwise it would enter Situation β.

Now $f_\beta(d)$ continues:

$$f_\beta(d) = r^-p^-ds^-o^-\bar{d}...$$

Giving us Figure D.29.

But now the dotted lines have no means of joining, and they continue clockwise in the outer perimeter indefinitely, they are in Situation α.

This is a contradiction.

D.1.2 ACK

Back to the end of Case A (D.1). Suppose $f_\beta(d)$ begins with r, and $f_\beta(\bar{d})$ begins with i. We remind the reader that Assumption A must still be held, that is, both $f_\beta(d)$ and $f_\beta(\bar{d})$ must go over an even number of letters before crossing.

The situation is shown in Figure D.30.

Notice that both $f_\beta(d)$ and $f_\beta(\bar{d})$ traverse only twice before crossing, since any additional twists would cause tracing.

Here the dotted lines can join, or $f_\beta(d)$ can go into 1 or 2.

D.1.2.1 Dram

Suppose the dotted lines join.

This is Figure D.31.

Here $f_\beta(s)$ cannot go below $f_\beta(p)$, or it would trace:

$$f_\beta(s) = \bar{d}r^- p^- d s^\times$$

So we have

$$f_\beta(s) = \bar{d}p^*$$

Separately, consider $f_\beta(p)$. It starts with d, and cannot continue with i, or it will trace:

$$f_\beta(p) = di^+s^+\bar{d}p^\times$$

Thus we must have

$$f_\beta(p) = do^*$$

Here, if it is o^+, then $f_\beta(p)$ traces:

$$f_\beta(p) = do^+\bar{d}p^\times$$

Similarly, if it is o^-, $f_\beta(p)$ also traces:

$$f_\beta(p) = do^-\bar{d}r^-p^\times$$

Therefore we must have

$$f_\beta(p) = do^\circ$$

This is Figure D.32.

Consider $f_\beta(r)$ and $f_\beta(b)$. They both start with p:

$$f_\beta(r) = p^*...$$

$$f_\beta(b) = p^*...$$

Consider $f_\beta(o)$. We have

$$f_\beta(o) = s^+\bar{d}p^*$$

and here is we have p° or p^{-}, $f_{\beta}(s)$ will be forced to go p^{-}, and it will trace:

$$f_{\beta}(s) = \bar{d}p^{-}ds^{\times}$$

Thus we must have

$$f_{\beta}(o) = s^{+}\bar{d}p^{+}...$$

and $f_{\beta}(o)$ then goes into 1 or 2.

D.1.2.1.1 Sloom

Suppose $f_{\beta}(o)$ continues into 1. Then it continues with the following:

$$f_{\beta}(o) = s^{+}\bar{d}p^{+}di^{+}s^{+}\bar{d}p^{+}...$$

Here the next letter cannot be r, or we will trace:

$$f_{\beta}(o) = s^{+}\bar{d}p^{+}di^{+}s^{+}\bar{d}p^{+}r^{+}do^{\times}$$

Thus we must have

$$f_{\beta}(o) = s^{+}\bar{d}p^{+}di^{+}s^{+}\bar{d}p^{+}b^{*}...$$

Now consider $f_{\beta}(r)$ and $f_{\beta}(b)$. They both start out similarly:

$$f_{\beta}(r) = p^{-}ds^{-}i^{*}...$$

$$f_{\beta}(b) = p^{-}ds^{-}i^{*}...$$

This is Figure D.33.

Consider $f_\beta(s)$. It must end at p°. Indeed, if after $\bar{d}$ it goes p^- it will trace almost immediately:

$$f_\beta(s) = \bar{d}p^- ds^\times$$

Similarly, if it goes p^+:

$$f_\beta(s) = \bar{d}p^+ di^+ s^\times$$

Hence we have

$$f_\beta(s) = \bar{d}p^\circ$$

This is Figure D.34.

Consider $f_\beta(i)$. It must end immediately at s°. Indeed, $f_\beta(i) = s^-...$ will immediately cause it to be absorbed between itself and $f_\beta(o)$; if it starts with s^+, then

$$f_\beta(i) = s^+ \bar{d}p^+ di\times$$

Therefore we must have

$$f_\beta(i) = s^\circ$$

The situation now is depicted in Figure D.35.

Here $f_\beta(b)$ can either end with i° or continue with i^+. It cannot continue with i^- as that would cause it to escape to the outer perimeter and eventually trace, due to the position of $f_\beta(o)$.

Suppose it ended at i°. Then $f_\beta(r)$ continues:

$$f_\beta(r) = ...i^- s^+ \bar{d}p^+ di^+ s^+ \bar{d}p^+ b^*...$$

as shown in Figure D.36.

Here if $f_\beta(o)$ continue with b° or b^+, forcing $f_\beta(r)$ to continue with b^+, then $f_\beta(r)$ would eventually be absorbed:

$$f_\beta(r) = ...b^+p^-ds^-i^-\bar{d}p^-ds^- \text{ Abso}(f_\beta(i), f_\beta(o))^\times$$

So $f_\beta(o)$ must continue with b^- and to the right of $f_\beta(r)$. But now it will be absorbed:

$$f_\beta(o) = ...b^-p^-ds^-i^-\bar{d}p^-ds^-i^+s^+\bar{d}p^+ \text{ Abso}(f_\beta(r), f_\beta(b))^\times$$

So in fact $f_\beta(b)$ cannot end at i°. So suppose it continued with i^+. Then we have

$$f_\beta(b) = p^-ds^-\hat{i}^+s^+\bar{d}p^+r^*...$$

as shown in Figure D.37.

Here $f_\beta(r)$ must end immediately, as continuing otherwise would cause it to follow $f_\beta(b)$ and trace eventually.

This in turn forces $f_\beta(b)$ to end as well. As otherwise it would either be absorbed between $f_\beta(b)$ and $f_\beta(r)$, or escape to the outer perimeter.

Lastly, these two ending this forces $f_\beta(o)$ to end as well. Otherwise, it would traverse back and eventually be absorbed.

This gives us Candidate 2.

D.1.2.1.2 Thrum

Back to end of Dram (D.1.2.1). Suppose $f_\beta(o)$ goes into 2. Then

$$f_\beta(o) = s^+ \bar{d} p^+ r^* ...$$

This is Figure D.38.

Here

$$f_\beta(i) = s^+$$

or

$$f_\beta(i) = s^\circ$$

D.1.2.1.2.1 Dwammy

Suppose $f_\beta(i) = s^+ ....$

Then

$$f_\beta(i) = s^+ \bar{d} p^+ ...$$

Here if it were p° or p^- then $f_\beta(s)$ will trace. Continuing:

$$f_\beta(i) = s^+ \bar{d} p^+ r^* ...$$

This is Figure D.39.

Now consider $f_\beta(o)$. At this moment we have

$$f_\beta(o) = s^+ \bar{d} p^+ r^* ...$$

Here if it were r° or r^-, $f_\beta(i)$ will be forced to go r^- and eventually trace:

$$f_\beta(i) = s^+\bar{d}p^+r^-p^-ds^-i^\times$$

Hence we must have

$$f_\beta(o) = s^+\bar{d}p^+r^+...$$

and continuing:

$$f_\beta(o) = s^+\bar{d}p^+r^+p*...$$

This is Figure D.40.

Here if it were p° or p^+, then $f_\beta(r)$ will be forced to start with p^+, which would force it to immediately trace. Thus we must have

$$f_\beta(o) = s^+\bar{d}p^+r^+p^-...$$

This situation is depicted in Figure D.41, and here $f_\beta(o)$ can go into 1 or 2 (it cannot go into the left of $f_\beta(r)$ as that would again force $f_\beta(r)$ to immediately trace).

D.1.2.1.2.1.1 Macarize

Suppose $f_\beta(o)$ goes into 1. Then it continues:

$$f_\beta(o) = s^+\bar{d}p^+r^+p^-di^+s^+\bar{d}p^+b^*...$$

Here at the end it has to go to b and not r^+ or it will trace.

This is Figure D.42.

Now consider $f_\beta(s)$. We have

$$f_\beta(s) = \bar{d}p^+r^*...$$

Consider $f_\beta(i)$. Recall we have

$$f_\beta(i) = s^+ \bar{d} p^+ r^* ...$$

Here if it were r° or r^-, then $f_\beta(s)$ will be forced to go r^- and will trace:

$$f_\beta(s) = \bar{d} p^+ r^- p^- d s^\times$$

So it must be r^+. But now $f_\beta(i)$ traces:

$$f_\beta(i) = s^+ \bar{d} p^+ r^+ p^- d i^\times$$

This is a contradiction.

D.1.2.1.2.1.2 Mooncalf

Back to end of Dwammy (D.1.2.1.2.1). Suppose $f_\beta(o)$ goes into 2. Then it continues:

$$f_\beta(o) = s^+ \bar{d} p^+ r^+ p^- d s^* ...$$

The situation is depicted in Figure D.43.

Now consider $f_\beta(r)$. It cannot start with p^+ or it will immediately trace. If it starts with p°, then $f_\beta(s)$ will be forced to continue with p^+ as well and eventually trace:

$$f_\beta(s) = \bar{d} p^+ r^- p^- d s^\times$$

Thus, $f_\beta(r)$ starts with p^-:

$$f_\beta(r) = p^- d s^* ...$$

and note that it has to go to the right of $f_\beta(s)$ to not cause $f_\beta(s)$ to trace again.

This is Figure D.44.

Now consider $f_\beta(b)$. It cannot start with p^+, as the position of $f_\beta(r)$ (which is starting with p^-) prevents it from doing do without one of them getting absorbed immediately. It cannot start with p° either, as that would force $f_\beta(s)$ to be absorbed immediately between $f_\beta(r)$ and $f_\beta(b)$. Thus $f_\beta(b)$ also must start with p^- as well, and also to the right of $f_\beta(s)$ to not cause it to be absorbed:

$$f_\beta(b) = p^- ds^* ...$$

This is Figure D.45.

Now consider $f_\beta(s)$. It must now end at p°. Indeed, if it continues with either $p^+ d$ or $p^- d$ now it will immediately trace. Therefore we have

$$f_\beta(s) = \bar{d} p^\circ$$

This is Figure D.46.

Now consider $f_\beta(o) = s^+ \bar{d} p^+ r^+ p^- ds^* ....$ If it were s° or s^+, then $f_\beta(r)$ will trace:

$$f_\beta(r) = p^- ds^+ \bar{d} p^+ r \times$$

Thus it must be s^- here. Then it continues:

$$fbo = s^+ \bar{d} p^+ r^+ p^- ds^- \bar{d} p^+ di^+ s^+ \bar{d} p^+ ...$$

and here the next letter must be $b*$, and not r^+ since that will force it to go under $f_\beta(p)$

and as a result go up to o with $f_\beta(p)$ and tracing. Thus we have

$$f_\beta(o) = s^+ \bar{d}p^+ r^+ p^- ds^- \bar{d}p^+ di^+ s^+ \bar{d}p^+ b^* ...$$

This is Figure D.47.

Now consider $f_\beta(i)$. We have

$$f_\beta(i) = s^+ \bar{d}p^+ r^* ...$$

Now if it were r^- here, then it will be absorbed:

$$bi = s^+ \bar{d}p^+ r^- p^- ds^- \, \text{Abso}(f_\beta(i), f_\beta(o))^\times$$

and if it were r^+, it traces:

$$f_\beta(i) = s^+ \bar{d}p^+ r^+ p^- ds^- \bar{d}p^+ di^\times$$

Therefore $f_\beta(i)$ ends at r°:

$$f_\beta(i) = s^+ \bar{d}p^+ r^\circ$$

This is Figure D.48.

The situation now is depicted in Mind.

Now let us consider $f_\beta(r)$ and $f_\beta(b)$ again. We claim that $f_\beta(r)$ must end here at s°. Suppose the contrary, then it cannot continue with s^+, as that would cause it to trace:

$$f_\beta(r) = p^- ds^+ \bar{d}p^+ r^\times$$

so in this case it has to continue with s^-. Suppose that were the case, then it has to go to

the right of $f_\beta(b)$ as it comes down from r^- otherwise it enters in between itself and $f_\beta(b)$ and thus will be absorbed eventually. Continuing, we have

$$f_\beta(r) = p^- ds^- \bar{d}p^+ d...$$

and here the next letter must be i^+ and not o^- otherwise $f_\beta(r)$ will trace. Continuing:

$$f_\beta(r) = p^- ds^- \bar{d}p^+ di^+ s^+ \bar{d}p^+ b^*...$$

Now consider $f_\beta(b) = p^- ds^*....$ If here it were s^+ then it will be absorbed between itself and $f_\beta(r)$. If it were s^- then it will follow $f_\beta(r)$ and continue with

$$f_\beta(b) = p^- ds^- \bar{d}p^+ d...$$

but here the next letter must be o^- or it will continue to follow $f_\beta(r)$ and eventually trace. But now we have

$$f_\beta(b) = p^- ds^- \bar{d}p^+ do^- \bar{d}r^- p^- ds^- o^- \bar{d}p^- ds^+ \bar{d}p^+ r^- p^- ds^- \,\mathrm{Abso}(f_\beta(i), f_\beta(o))^\times$$

Therefore, we must have $f_\beta(r)$ ending at s°:

$$f_\beta(r) = p^- ds^\circ$$

This is Figure D.49.

Then this forces $f_\beta(b)$ to continue:

$$f_\beta(b) = f_\beta(b) = p^- ds^+ \bar{d}p^+ r^- p^- ds^- o^*...$$

Now at this point, we claim that $f_\beta(b)$ has to end here at o°. Suppose not, and suppose it were o^+ instead. Then we have

$$f_\beta(b) = f_\beta(b) = p^- ds^+ \bar{d}p^+ r^- p^- ds^- o^+ s^+ \bar{d}p^+ r^+ p^- ds^- \bar{d}p^+ \operatorname{Abso}(f_\beta(r), f_\beta(b))^\times$$

and similarly if it were o^-:

$$f_\beta(b) = p^- ds^+ \bar{d}p^+ r^- p^- ds^- o^- s^+ \bar{d}p^+ r^+ p^- ds^- \bar{d}p^+ d...$$

and here it cannot continue with i^+ or it will follow $f_\beta(o)$ and trace. So instead it must continue with o^-, but then it will be absorbed:

$$\begin{aligned} f_\beta(b) =& p^- ds^+ \bar{d}p^+ r^- p^- ds^- o^- s^+ \bar{d}p^+ r^+ p^- ds^- \bar{d}p^+ d \\ & o^- \bar{d}r^- p^- ds^- o^- \bar{d}p^- ds^+ \bar{d}p^+ r^- p^- ds^- \operatorname{Abso}(f_\beta(i), f_\beta(o))^\times \end{aligned}$$

Therefore, $f_\beta(b)$ has to end at i°:

$$f_\beta(b) = f_\beta(b) = p^- ds^+ \bar{d}p^+ r^- p^- ds^- o^\circ$$

This is Figure D.50.

Finally, let us consider $f_\beta(o)$. Recall we have

$$f_\beta(o) = s^+ \bar{d}p^+ r^+ p^- ds^- \bar{d}p^+ di^+ s^+ \bar{d}p^+ b^* ...$$

Now we claim that $f_\beta(o)$ has to end here at b°. Indeed, if in the contrary it were b^+ here,

then it will be absorbed:

$$f_\beta(o) = ...b^+p^-ds^-i^-\bar{d}p^-ds^+\bar{d}p^+r^-p^-ds^- \text{Abso}(f_\beta(i), f_\beta(o))^\times$$

On the other hand, if it were b^- instead, it will eventually follow $f_\beta(b)$ and thus trace:

$$f_\beta(o) = ...b^-p^-ds^-i^-\bar{d}p^-ds^+\bar{d}p^+r^-p^-ds^-o^\times$$

In conclusion, we have Candidate 3 shown in Figure D.51.

D.1.2.1.2.2 Faffel

Back to the end of Thrum (D.1.2.1.2). Suppose $f_\beta(i) = s^\circ$. This is depicted in Figure D.52.

Consider $f_\beta(o)$. We have

$$f_\beta(o) = s^+\bar{d}p^-r^*...$$

and now this forces $f_\beta(s)$ to also continue with p^-. Indeed, if it continues with p° or p^+ instead, then both $f_\beta(b)$ and $f_\beta(b)$ will be absorbed between $f_\beta(i)$ and $f_\beta(o)$. So we have

$$f_\beta(s) = \bar{d}p^+r^*...$$

Now the situation is depicted in Figure D.53.

Now consider $f_\beta(o)$ again. Here it cannot continue with r° or r^-, as both will force $f_\beta(s)$ to continue with r^-, but that will force it to trace:

$$f_\beta(s) = f_\beta(s) = \bar{d}p^+r^-p^-ds^\times$$

Thus, we must have

$$f_\beta(o) = s^+ \bar{d}p^+ \hat{r}^+ p^- di^+ s^+ \bar{d}p^+ b^* ...$$

and here it must go up b^* and not r^+, or it will trace: $...r^+ do^\times$.

This is depicted in Figure D.54.

Now consider $f_\beta(s)$. We claim that it has to end here at r°. Suppose by the contrary, that it continues with r^-. Then we have

$$f_\beta(s) = \bar{d}p^+ r^- p^- ds^\times$$

Similarly, if it continues with r^+, then we have

$$f_\beta(s) = \bar{d}p^+ r^+ p^- ds^\times$$

So we must have

$$f_\beta(s) = \bar{d}p^+ r\circ$$

This is depicted in Figure D.55.

Now consider $f_\beta(o)$ again. If here it continues with b^+, then it will be absorbed:

$$f_\beta(o) = s^+ \bar{d}p^- r^+ p^- di^+ s^+ \bar{d}p^+ b^+ p^- ds^- i^- \bar{d}p^+ r^- p^- ds^- \,\mathrm{Abso}(f_\beta(i), f_\beta(o))^\times$$

On the other hand, if it continues with b^-, then we have

$$f_\beta(o) = ...\hat{b}^- p^- ds^- i^- \bar{d}p^* ...$$

This is depicted in Figure D.56.

Now it cannot continue with p° or p^-, as that would force both $f_\beta(b)$ and $f_\beta(r)$ to continue with p^-, and both will then continue "inside" $f_\beta(o)$, and eventually $f_\beta(b)$ will trace. On the other hand, if $f_\beta(o)$ were to continue with p^+ here, then it has to go to the left of $f_\beta(b)$ to not be absorbed, so then we have

$$f_\beta(o) = s^+\bar{d}p^-r^+p^-di^+s^+\bar{d}p^+b^-p^-ds^-i^-\bar{d}\hat{p}^+r^-p^-ds^-i^*...$$

This is depicted in Figure D.57.

Now consider $f_\beta(b)$. If it starts with p° or p^-, then $f_\beta(r)$ will start with p^- (and to the right of $f_\beta(b)$ to not be absorbed immediately):

$$f_\beta(r) = p^-d...$$

Now the next letter can be o^- or i^+, but the former will make it trace:

$$f_\beta(r) = p^-do^-\bar{d}r^\times$$

so the next letter must be i^+; but now it traces as well:

$$f_\beta(r) = p^-di^+s^+\bar{d}p^+b^+p^-ds^-i^-\bar{d}p^+r^\times$$

Therefore, in the situation depicted in Figure D.57, $f_\beta(b)$ has to start with p^+, and this forces $f_\beta(r)$ to end at p immediately in order to not trace or be absorbed:

$$f_\beta(r) = p^\circ$$

and $f_\beta(b)$ continues:

$$f_\beta(b) = p^+ r^- p^- ds^- i^* ...$$

Now the situation is depicted in Figure D.58.

Now if $f_\beta(b)$ continues with i° or i^+, then $f_\beta(o)$ continues with i^+, and it will be absorbed:

$$f_\beta(o) = ...\hat{i}^+ s^+ \bar{d} p^+ r^+ p^- \text{ Abso}(f_\beta(r), f_\beta(b))^\times$$

So in this situation depicted in Figure D.58, $f_\beta(b)$ must continue with i^-, and to the right of $f_\beta(o)$, otherwise $f_\beta(o)$ will still be absorbed. But now $f_\beta(b)$ traces:

$$f_\beta(b) = p^+ r^- p^- ds^- \hat{i}^- s^+ \bar{d} p^+ r^+ p^- di^+ s^+ \bar{d} p^+ b^\times$$

Therefore, we can conclude that in the situation depicted in Figure D.55, $f_\beta(o)$ must end there at b°.

Now the situation depicted in Figure D.59 is forced.

Consider $f_\beta(r)$. It cannot start with p^+ or it will immediately trace. So suppose it starts with p^-, and to the right of $f_\beta(b)$ to not be absorbed. Then we have

$$f_\beta(r) = p^- d...$$

Here the next letter can be either o^- or i^+. The former will make $f_\beta(r)$ trace:

$$f_\beta(r) = p^- do^- \bar{d} r^\times$$

so it must be the latter; but that also forces $f_\beta(r)$ to trace:

$$f_\beta(r) = p^- di^+ s^+ \bar{d}p^+ b^+ p^- ds^- i^- \bar{d}p^+ r\times$$

Therefore, we must have, in the situation depicted in Figure D.59, $f_\beta(r)$ starts and ends at p°:

$$f_\beta(r) = p^\circ$$

Now this forces $f_\beta(b)$ to start with p^+ and continue:

$$f_\beta(b) = p^+ r^- p^- ds^- i^* ...$$

This is depicted in Figure D.60.

Now we claim that in fact $f_\beta(b)$ must end here at i°. Suppose the contrary, and suppose $f_\beta(b)$ continues with i^+. Then we have

$$f_\beta(b) = p^+ r^- p^- ds^- \hat{i}^+ s^+ \bar{d}p^+ r^+ p^- \text{ Abso}(f_\beta(b), f_\beta(r))^\times$$

So suppose instead it continues with i^-. Then we have

$$f_\beta(b) = p^+ r^- p^- ds^- \hat{i}^- s^+ \bar{d}p^+ r^+ p^- d...$$

and here the next letter can be either i^+ or o^+, but the former will force it to trace:

$$f_\beta(b) = p^+ r^- p^- ds^- \hat{i}^- s^+ \bar{d}p^+ r^+ p^- di^+ s^+ \bar{d}p^+ b^\times$$

so it must be the latter; but then it will be absorbed:

$$f_\beta(b) = ...\hat{i}^- s^+ \bar{d} p^+ r^+ p^- d o^- \bar{d} r^- p^- d s^- i^- \bar{d} p^+ r^- p^- d s^- \operatorname{Abso}(f_\beta(i), f_\beta(o))^\times$$

In conclusion, in the situation depicted in Figure D.60, $f_\beta(b)$ must end there at i°:

$$f_\beta(b) = p^+ r^- p^- d s^- i^\circ$$

This gives us our Candidate train track map 4. Depicted in Figure D.61.

D.1.2.2 Lugs

Back to end of ACK (D.1.2). Suppose $f_\beta(d)$ go into 1.

The situation is depicted in Figure D.62.

Here $f_\beta(d)$ cannot go above $f_\beta(p)$ or it would enter into Situation β. So it must go below $f_\beta(p)$. On the other hand, $f_\beta(s)$ cannot go below $f_\beta(p)$ or it would trace:

$$f_\beta(s) = \bar{d} r^- p^- d s^\times$$

Then

$$f_\beta(p) = d s^- i^- \bar{d} r^- p^\times$$

This is depicted in Figure D.63.

This is a contradiction.

D.1.2.3 Haze

Back to end of ACK (D.1.2). Suppose $f_\beta(d)$ goes into 2.

The situation is depicted in Figure D.64.

Consider $f_\beta(p) = do^*$.... If here it were o^-, then it traces:

$$f_\beta(p) = do^-\bar{d}r^-p^\times$$

Similarly, if it were o^+, it also traces:

$$f_\beta(p) = do^+\bar{d}p^\times$$

Thus it must be o°:

$$f_\beta(p) = do^\circ$$

Now we are at Figure D.65.

Consider either of the two dotted lines. They both have to continue with p^+, and then either b^* or r^+. If it were the former, then it will go over an odd number of letters before crossing d again. This is because there are only two possibilities:

$$...\bar{d}p^+b^+p^-d...$$

or

$$...\bar{d}p^+b^-p^-d...$$

On the other hand, if it instead continues with r^+, then we have

$$...r^+do^+\bar{d}...$$

and again here it goes over a single letter o^+ before crossing $\bar{d}$ again.

This is a contradiction.

D.1.3 Quip

Back to the end of Case A D.1. Consider the case of $f_\beta(d)$ starts at r, and $f_\beta(\bar{d})$ starts at o. This is Figure D.66. Again $f_\beta(d)$ has to start with

$$f_\beta(d) = r^-p^-d...$$

to not violate Assumption A. Similarly, $f_\beta(\bar{d})$ must start with

$$f_\beta(\bar{d}) = o^+s^-\bar{d}...$$

The situation is depicted in Figure D.66.

Here if $f_\beta(p)$ were to go above $f_\beta(s)$ as it traverses toward the right, $f_\beta(s)$ will trace:

$$f_\beta(s) = \bar{d}r^-p^-s^\times$$

On the other hand, if $f_\beta(p)$ were to go below $f_\beta(s)$, then $f_\beta(p)$ will trace:

$$f_\beta(p) = do^+s^+\bar{d}p^\times$$

This is a contradiction.

D.1.4 Zest

Back to the end of Case A D.1. Consider the case of $f_\beta(d)$ starts at b, and $f_\beta(\bar{d})$ starts at s. Here $f_\beta(d)$ has to start with

$$f_\beta(d) = b^- p^- d...$$

to not violate Assumption A, since if it were to start with b^+, then the next letter will have to be d.

Consider $f_\beta(r) = p^*....$ If it starts with either p° or p^+, then $f_\beta(b)$ will be forced to start with p^+, and so $f_\beta(b)$ will immediately trace. Thus, we must have

$$f_\beta(r) = p^- d...$$

We are now in Figure D.67.

Consider $f_\beta(\bar{d})$. It must start with s^-, in order to not immediately violate Assumption A. There are two choices after the initial letter:

$$f_\beta(\bar{d}) = s^- i^- ...$$

or

$$f_\beta(\bar{d}) = s^- o^- ...$$

Here, both i and o can only be clockwise because otherwise the third and fourth letters will be forced to be $s^+\bar{d}$, which contradicts the Trace Lemma.

D.1.4.1 Omen

Suppose $f_\beta(\bar{d}) = s^- i^- ....$

This is Figure D.68.

Here $f_\beta(d)$ can go into 1, 2, or 3, or it can join with $f_\beta(\bar{d})$.

If it were to go into 1, then we have Figure D.69. But now neither of the dotted lines can ever go up to p, or else we will be in Situation β. This means both of them will continue with $r^\pm$, or b^0 and continue circling clockwise. The former will violate Assumption A, as right after $r^\pm$ has to be d. On the other hand, the latter results in Situation α. Thus $f_\beta(d)$ cannot go into 1.

If it were to go into 2, then we are immediately in Situation β.

Suppose it were to go into 3. Then then next letter cannot be $o^\pm$, since the letter after that would have to be $\bar{d}$, which would violate Assumption A. So then it continues with i^+:

$$f_\beta(d) = b^- p^- d i^+ s^+ \bar{d} p^+ b^+ d i^+ ...$$

again here at the end it has to be i^+ and not $o^\pm$ for the same reason.

This is Figure D.70.

But now, if we consider $f_\beta(i)$, it now has to follow $f_\beta(d)$, and we have

$$f_\beta(i) = \bar{d} p^+ b^+ d i^\times$$

This is shown in Figure D.71.

This is a contradiction.

Therefore, going back to Figure D.68, we must have the dotted lines join in the middle. This is Figure D.72.

Now consider $f_\beta(i) = \bar{d}$. It continues:

$$f_\beta(i) = \bar{d}p^+b^+do^*...$$

here the last letter has to be o^*, as the only other possibility is i^+, which will trace.

Now consider $f_\beta(o) = \bar{d}$.... The location of $f_\beta(i)$ now will force it to trace:

$$f_\beta(o) = \bar{d}p^+b^+do^\times$$

This is Figure D.73.

This is a contradiction.

D.1.4.2 Axe

Back to the end of Zest (D.1.4). Suppose

$$f_\beta(\bar{d}) = s^-o^-...$$

This is Figure D.74.

Here if $f_\beta(d)$ were to go below $f_\beta(o)$, then $f_\beta(o)$ will trace:

$$f_\beta(o) = \bar{d}p^+b^+do^\times$$

Thus $f_\beta(o)$ can only go above $f_\beta(o)$ here. Then it continues:

$$f_\beta(d) = b^-p^-d\hat{s}^-...$$

and here the next letter can either be $i^{\pm}$ or o^{-}. This is Figure D.75.

However, $i^{\pm}$ will cause $f_\beta(d)$ to violate Assumption A:

$$f_\beta(d) = b^- p^- d s^- \hat{i}^+ s^+ \bar{d} ...$$

or

$$f_\beta(d) = b^- p^- d s^- \hat{i}^- s^+ \bar{d} ...$$

Thus $f_\beta(d)$ continues with o^-:

$$f_\beta(d) = b^- p^- d s^- \hat{o}^- \bar{d} ...$$

This is Figure D.76.

But now we are in Situation α. Indeed, the next letter for $f_\beta(d)$ and $f_\beta(\bar{d})$ can either be $r\pm$ or b^-. But the former necessitates d to immediately follow. Thus it has to be b^-. But then both $f_\beta(d)$ continues in the outer perimeter, coming back to $\bar{d}$, repeating indefinitely.

This is a contradiction

D.1.5 Lox

Back to the end of Case A D.1. Consider the case of $f_\beta(d)$ starting at b, and $f_\beta(\bar{d})$ starting at i. Then again $f_\beta(d)$ has to start with

$$f_\beta(d) = b^- p^- d ...$$

to not violate Assumption A; and similarly, $f_\beta(\bar{d})$ has to start with

$$f_\beta(\bar{d}) = i^+ s^+ \bar{d} ...$$

Consider $f_\beta(r)$. It has to start with p^-, otherwise $f_\beta(b)$ will be forced to start with p^+ which will make it immediately trace.

The situation is depicted in Figure D.77.

Here $f_\beta(d)$ cannot go in between $f_\beta(\bar{d})$ and $f_\beta(s)$, as that would become Situation β. Hence, $f_\beta(\bar{d})$ can an join with $f_\beta(\bar{d})$, or go into 1, or 2.

D.1.5.1 Lava

Suppose the dotted lines join. This is depicted in Figure D.78.

Here $f_\beta(p)$ can go above, or go below $f_\beta(s)$.

D.1.5.1.1 Query

Suppose $f_\beta(p)$ goes above $f_\beta(s)$. Then it continues:

$$f_\beta(p) = d s^* ...$$

Now consider $f_\beta(o) = s^*...$. It has to start with $s^+...$, otherwise $f_\beta(i)$ will be forced to start with s^-, but then it will immediately trace.

Now consider $f_\beta(s) = \bar{d}...$. The next letter can be b^- or r^*. The former will make it trace:

$$f_\beta(s) = \bar{d} b^- p^- s^\times$$

Thus it must be the latter:

$$f_\beta(s) = \bar{d}r^*...$$

We are now in Figure D.79.

Here $f_\beta(o) = s^-...$ can go into 1,2, or 3. Note that it cannot go into the right of $f_\beta(i)$ as it would then be absorbed between $f_\beta(i)$ and $f_\beta(o)$.

D.1.5.1.1.0.1 Depth

Suppose $f_\beta(o) = s^-...$ goes into 1. Then it continues:

$$f_\beta(o) = s^-\bar{d}p^+r^*...$$

Consider $f_\beta(i) = s^*....$ If it were to start with s°, then both $f_\beta(r)$ and $f_\beta(p)$ will be absorbed between $f_\beta(i)$ and $f_\beta(o)$. If it were to start with s^- then itself will be absorbed as well. Thus it has to start with s^+.

This is Figure D.80.

Now $f_\beta(i)$ has to go to the left of $f_\beta(r)$ and $f_\beta(p)$, otherwise again they will be absorbed. So $f_\beta(i)$ continues:

$$f_\beta(i) = s^+\bar{d}p^+r^*...$$

This is Figure D.81.

Now consider $f_\beta(r)$. If it were to continue here with s° or s^+, then $f_\beta(p)$ will be forced to continue with s^+, but then it will trace:

$$f_\beta(p) = d\hat{s}^+\bar{d}p^\times$$

Thus $f_\beta(r)$ has to continue with s^- here, and go to the right of $f_\beta(p)$:

$$f_\beta(r) = p^- d\hat{s^-}\bar{d}...$$

and here the next letter has to be b^-, and not r^*, to prevent trace; however, it will still eventually trace:

$$f_\beta(r) = p^- d\hat{s^-}\bar{d}\hat{b}^- p^- ds^- i^- \bar{d} r^\times$$

This is depicted in Figure D.82.

This is a contradiction

D.1.5.1.1.0.2 Kiosk

Back to the end of Query D.1.5.1.1. $f_\beta(o) = s^-...$ goes into 2. Then it continues:

$$f_\beta(o) = s^+ \bar{d} p^*...$$

This is Figure D.83.

Now consider $f_\beta(b) = p^-$. It has to start with p^- and to the right of $f_\beta(o)$; otherwise $f_\beta(o)$, or itself, will be absorbed in between $f_\beta(r)$ and $f_\beta(b)$. It continues:

$$f_\beta(b) = p^- ds^- i^*...$$

This is Figure D.84.

Here $f_\beta(r) = p^- ds^- i^*...$ has to continue with i^- and to the right of $f_\beta(b)$. Indeed, if instead it continued with i° or i^+, then $f_\beta(b)$ will be forced to continue with i^+, but then it will

trace:

$$f_\beta(b) = p^- ds^- i^+ s^+ \bar{d}p^+ b^\times$$

Now $f_\beta(r)$ continues after i^-:

$$f_\beta(r) = p^- ds^- \hat{i}^- s^+ \bar{d}p^* ...$$

Now consider $f_\beta(i) = s^* ....$ It must start with s^+ and to the left of $f_\beta(p)$, or else itself or $f_\beta(p)$ will be absorbed between $f_\beta(i)$ and $f_\beta(o)$. So we have

$$f_\beta(i) = s^+ \bar{d}p^* ...$$

We are now in the situation depicted in Figure D.85.

Now consider $f_\beta(o)$ again. Here if it continues with p° or p^-, then $f_\beta(i)$ will be forced to continue with p^-, but then it will trace (regardless if it goes to the left or right of $f_\beta(r)$):

$$f_\beta(i) = s^+ \bar{d}\hat{p}^- ds^- i^\times$$

Thus, $f_\beta(o)$ must continue with p^+, and to the left of $f_\beta(i)$:

$$f_\beta(o) = s^+ \bar{d}\hat{p}^+ ds^* ...$$

This is Figure D.86.

Here $f_\beta(o)$ cannot continue with s° or s^+, as that would force $f_\beta(p)$ to continue with s^+,

but then it will trace:

$$f_\beta(p) = ds^+ \bar{d}p^\times$$

Thus here $f_\beta(o)$ must continue with s^- and to the right of $f_\beta(p)$:

$$f_\beta(o) = s^+ \bar{d}\hat{p}^+ d\hat{s}^- \bar{d}...$$

This is Figure D.87.

Now here $f_\beta(o)$ can continue with r^* or b^-.

D.1.5.1.1.0.2.1 Abacus

Suppose $f_\beta(o)$ continues with r^*. Then it cannot be r° or r^-, a that would force $f_\beta(s)$ to continue with r^-, and it will trace:

$$f_\beta(s) = \bar{d}r^- ds^t imes$$

Thus we have

$$f_\beta(o) = s^+ \bar{d}\hat{p}^+ d\hat{s}^- \bar{d}\hat{r}^+ di^+ s^+ \bar{d}p^+ b^+ ...$$

This is Figure D.88.

Now consider $f_\beta(s) = \bar{d}r^*$.... Here it must end at r°. Indeed, if it were to continue with r^+, then it will trace:

$$f_\beta(s) = \bar{d}\hat{r}^+ di^+ s^\times$$

Similarly, if it were to continue with r^-, it also traces:

$$f_\beta(s) = \bar{d}\hat{r}^- ds^\times$$

Hence we must have

$$f_\beta(s) = \bar{d}r^\circ$$

This is Figure D.89.

Now consider

$$f_\beta(r) = p^- ds^- \hat{i}^- s^+ \bar{d}p^* ...$$

It now continues:

$$f_\beta(r) = p^- ds^- \hat{i}^- s^+ \bar{d}\hat{p}^+ ds^* ...$$

This is Abscus3.

Now if $f_\beta(r)$ were to end here at s°, or continue with s^+, then $f_\beta(p)$ will be forced to continue with p^+, and it will then trace:

$$f_\beta(p) = ds^+ \bar{d}p^\times$$

Thus, here $f_\beta(r)$ must continue with s^-:

$$f_\beta(r) = p^- ds^- \hat{i}^- s^+ \bar{d}\hat{p}^+ ds^- ...$$

This is Figure D.91.

Here $f_\beta(r)$ can continue into 1,2, or 3.

If it were to continue into 1, then $f_\beta(p)$ will again trace.

If it were to continue into 2, then we have

$$f_\beta(r) = p^- ds^- \hat{i}^- s^+ \bar{d}\hat{p}^+ ds^- \bar{d}...$$

and the next letter has to be b^-, or it will trace immediately; but now it traces anyway:

$$f_\beta(r) = p^- ds^- \hat{i}^- s^+ \bar{d}\hat{p}^+ ds^- \bar{d}b^- p^- ds^- i^- \bar{d}r^\times$$

If it were to continue into 3, then it traces almost immediately:

$$f_\beta(r) = p^- ds^- \hat{i}^- s^+ \bar{d}\hat{p}^+ ds^- \bar{d}r^\times$$

This is a contradiction.

D.1.5.1.1.0.2.2 Banana

Back to the end of Kiosk D.1.5.1.1.0.2. Suppose $f_\beta(o)$n continues with b^-. Then it continues:

$$f_\beta(o) = s^+ \bar{d}\hat{p}^+ d\hat{s}^- \bar{d}b^- p^- ds^- i^- \bar{d}r^*...$$

This is Figure D.92.

Now consider $f_\beta(p) = ds^*$. Here it has to end at s°. Indeed, if it were to instead continue with s^+, then it traces:

$$f_\beta(p) = d\hat{s}^+ p^\times$$

Similarly, if it were to continue with s^-, it also traces:

$$f_\beta(p) = d\hat{s}^- \bar{d}b^- p^\times$$

This is Figure D.93.

Now consider

$$f_\beta(r) = p^- ds^- i^+ s^+ \bar{d}p^* ...$$

It continues, and will eventually trace:

$$f_\beta(r) = p^- ds^- i^+ s^+ \bar{d}\hat{p}^+ ds^- \bar{d}b^- p^- ds^- i^- \bar{d}r^\times$$

This is show in Figure D.94.

This is a contradiction.

D.1.5.1.1.1 Cloud

Back to the end of Query D.1.5.1.1. Suppose $f_\beta(o) = s^-$ goes into 3.

This is Figure D.95.

Consider $f_\beta(r) = p^- ds^* ....$ It continues:

$$f_\beta(r) = p^- d\hat{s}^- i^* ...$$

Consider $f_\beta(p) = ds^* ....$ It continues:

$$f_\beta(p) = d\hat{s}^- i^* ...$$

This is Figure D.96.

Now consider $f_\beta(r)$ again. Here it cannot continue with i° or i^+, as that would force $f_\beta(p)$ to continue with i^+, in which case it would trace:

$$f_\beta(p) = ds^-\hat{i}^+s^+\bar{d}p^\times$$

Hence $f_\beta(r)$ must continue with i^-, and to the right of $f_\beta(p)$:

$$f_\beta(r) = p^-ds^-\hat{i}^-s^+\bar{d}...$$

and here the next letter has to be b^- to not trace; but then it will still eventually trace:

$$f_\beta(r) = p^-ds^-i^-s^+\bar{d}\hat{b}^-p^-ds^-i^-\bar{d}r^\times$$

This is Figure D.97.

This is a contradiction.

D.1.5.1.2 Bold

Back to the end of Lava D.1.5.1. Suppose $f_\beta(p)$ goes below $f_\beta(s)$. Here notice that the (partial) train track map as depicted in Figure D.78 is symmetrical. Thus in all the previous arguments for the non-existence of a suitable train track map, for the case of $f_\beta(p)$ continuing above $f_\beta(s)$, we can make the appropriate substitutions to adapt them into arguments for the non-existence of a suitable train track map, for the case of $f_\beta(p)$ continuing below $f_\beta(s)$.

More specifically, we can interchange every instance of $f_\beta(r)$ with $f_\beta(o)$, $f_\beta(b)$ with $f_\beta(p)$, and $f_\beta(p)$ with $f_\beta(s)$, $f_\beta(d)$ with $f_\beta(\bar{d})$; and replace every instance of $+$ with $-$. In this way, the previous argument will give an argument for the desired result.

D.1.5.2 Drop

Back to the end of Lox D.1.5. Suppose $f_\beta(d)$ goes into 1. Then $f_\beta(d)$ continues:

$$f_\beta(d) = b^- p^- d\hat{s}^- i^- \bar{d}...$$

This is Figure D.98.

Now the next letter for $f_\beta(d)$ cannot be r^*, as the letter after that would have to be d, so the Trace Lemma would be violated. Thus the next letter is either b^- or p^*. If it were b^- then it continues:

$$f_\beta(d) = b^- p^- d\hat{s}^- i^- \bar{d}\hat{b}^- p^- d s^- i^- \bar{d}...$$

and now again it can go to r^* or b^-, it cannot be the former for the same reason as before, and the latter will just repeat the process again.

If it were p^*, then we are in Situation β.

This is a contradiction.

D.1.5.3 Rage

Back to the end of Lox D.1.5. Suppose $f_\beta(\bar{d})$ goes into 2.

Here we have

$$f_\beta(d) = b^- p^- d...$$

and the next letter can be i^+ or o^*, but if it were the latter then the letter after that would have to be $\bar{d}$ which would violate the Trace Lemma. Thus the next letter has to be i^+:

$$f_\beta(d) = b^- p^- d i^+...$$

This is Figure D.99.

Now consider $f_\beta(s) = \bar{d}$.... It continues:

$$f_\beta(s) = \bar{d}p^+b^+d...$$

and the next letter is either i^+ or o^*. If it were i^+ then it will trace

$$f_\beta(s) = \bar{d}p^+b^+di^+s^\times$$

Thus the next letter has to be o^*:

$$f_\beta(s) = \bar{d}p^+b^+do^*$$

Now consider $f_\beta(o) = s^+$.... It continues, and because of the position of $f_\beta(s)$ now it will trace:

$$f_\beta(o) = s^+\bar{d}p^+b^+do^\times$$

This is shown in Figure D.100.

This is a contradiction.

D.1.6 Lake

back to the end of Case A D.1. Consider the case of $f_\beta(d)$ starting at p and $f_\beta(\bar{d})$ starting at s.

The situation is depicted in Figure D.101.

Here $f_\beta(d)$ has to start with p^+ in order to not immediately go over d after p, which would

violate Assumption A. So we have

$$f_\beta(d) = p^+...$$

Now consider $f_\beta(\bar{d}) = s^*....$ Similar to $f_\beta(d)$ (but just mirrored), we must have

$$f_\beta(\bar{d}) = s^-...$$

in order to not immediately violate Assumption A.

Continuing, the next letter for $f_\beta(d) = p^+...$ can either be b^* or r^*:

$$f_\beta(d) = p^+b^*...$$

or

$$f_\beta(d) = p^+r^*...$$

D.1.6.1 Join

Suppose

$$f_\beta(d) = p^+b^*...$$

Here we claim that the second letter has to be b^+. Indeed, if it were b^-, then the Trace Lemma will be violated again, as we would have $f_\beta(d) = p^+b^-d....$ Thus we must have

$$f_\beta(d) = p^+b^+...$$

The next letter can either be d, or p^*. However, if it were to continue with p^*, then we are

in Situation β. Thus the next letter has to be d. So we have

$$f_\beta(d) = p^+b^+d...$$

Now this forces

$$f_\beta(p) = b^*...$$

This is depicted in Figure D.102.

Now consider $f_\beta(\bar{d}) = s^-....$ The next letter can be i^* or o^*:

$$f_\beta(\bar{d}) = s^-i^*...$$

or

$$f_\beta(\bar{d}) = s^-o^*...$$

D.1.6.1.1 Jolly

Suppose

$$f_\beta(\bar{d}) = s^-i^*...$$

Then in fact it has to be i^-, as if it were i^+ the Trace Lemma will be violated:

$$f_\beta(\bar{d}) = s^-i^+s^+\bar{d}...$$

Thus,

$$f_\beta(\bar{d}) = s^-i^-...$$

And now the next letter can be $\bar{d}$ or s^*. This is the same situation as that of $f_\beta(d)$ earlier,

but simply mirrored. So similarly, if the next letter were s^* then we would be in Situation β. Hence the next letter must be $\bar{d}$:

$$f_\beta(\bar{d}) = s^- i^- \bar{d}...$$

This forces

$$f_\beta(s) = i^*...$$

This is Figure D.103.

Here the dotted lines can join in the middle. Alternatively, $f_\beta(d)$ (on the left) can go above $f_\beta(o)$ and $f_\beta(i)$; it cannot go between $f_\beta(i)$ and $f_\beta(\bar{d})$ as that would put it in Situation β.

Finally, $f_\beta(d)$ could also go under $f_\beta(\bar{d})$. In this case $f_\beta(\bar{d})$ has to go above $f_\beta(r)$ and $f_\beta(b)$, and not below them as that would again lead to Situation β.

Suppose $f_\beta(d)$ goes above $f_\beta(o)$ and $f_\beta(i)$. Then it continues:

$$f_\beta(d) = p^+ b^+ d s^- i^- \bar{d}...$$

Now consider $f_\beta(r) = d....$ It continues:

$$f_\beta(r) = d s^- i^- \bar{d}...$$

and the next letter has to be b^+ to not trace:

$$f_\beta(r) = d s^- i^- \bar{d} \hat{r}^+ ...$$

Now consider $f_\beta(b)$. It will follow $f_\beta(r)$ and eventually trace:

$$f_\beta(b) = ds^- i^- \bar{d} b^\times$$

This is shown in Figure D.104.

So now suppose $f_\beta(d)$ goes under $f_\beta(\bar{d})$, and os $f_\beta(\bar{d})$ has to go above $f_\beta(r)$ and $f_\beta(b)$. Then this is the same situation but mirrored. We have

$$f_\beta(\bar{d}) = s^- i^- \bar{d} p^+ b^+ d...$$

Now consider $f_\beta(o) = \bar{d}...$. It continues:

$$f_\beta(o) = \bar{d} p^+ b^+ d i^*...$$

where it has to go up i^* to not trace. Now consider $f_\beta(i) = \bar{d}...$, which will follow $f_\beta(o)$ and trace:

$$f_\beta(i) = \bar{d} p^+ b^+ d i^\times$$

This is shown in Figure D.105.

Therefore, in the situation depicted in Figure D.103, the dotted lines must join.

This is Figure D.106.

But now the $f_\beta(r)$ and $f_\beta(b)$ pair on the left has to either go above or below the $f_\beta(o)$ and $f_\beta(i)$ pair on the right. If the left pair goes above the right pair, then this again leads to $f_\beta(b)$ tracing, identical to the situation before. This is depicted in Figure D.107.

Similarly, if the left pair goes below the right pair, we will again have $f_\beta(i)$ tracing, as before.

This is depicted in Figure D.108.

This is a contradiction.

D.1.6.1.2 Eager

Back to the end of Join D.1.6.1. Suppose

$$f_\beta(\bar{d}) = s^- o^* ...$$

This forces

$$f_\beta(s) = o^* ...$$

This is Figure D.109.

Now here the dotted lines are forced to join. The argument for this is identical to that in D.1.6.1.1.

This is Figure D.110.

Now here if the pair on the right, $f_\beta(o)$ and $f_\beta(i)$ were to go above the pair on the left, $f_\beta(r)$ and $f_\beta(b)$, then $f_\beta(o)$ will trace:

$$f_\beta(o) = \bar{d} p^+ b^+ d o^\times$$

Thus the pair on the right has to go below the pair on the left.

Now $f_\beta(b)$ and $f_\beta(r)$ will continue:

$$f_\beta(b) = d s^- ...$$

and

$$f_\beta(r) = ds^- ...$$

This is Figure D.111.

Now here the next letter for $f_\beta(b)$ can be o^-, or i^*.

Suppose the next letter were o^-. Then we have

$$f_\beta(b) = ds^- \hat{o}^- \bar{d} r^* ...$$

and thus $f_\beta(r)$ will have to go up i^* to not trace:

$$f_\beta(r) = ds^- i^* ...$$

This is shown in Figure D.112.

Here, we claim that in fact $f_\beta(b)$ has to end. Indeed, if it were to continue with r^-, it will trace:

$$f_\beta(b) = ds^- \hat{o}^- \bar{d} r^- do^+ s^+ \bar{d} b^\times$$

and if it were to continue with r^+ it will be absorbed:

$$f_\beta(b) = ds^- \hat{o}^- \bar{d} r^+ do^+ s^+ \bar{d}\, \mathrm{Abso}(f_\beta(r), f_\beta(b))^\times$$

Consider $f_\beta(i)$. Here if it were to continue with b° or b^+ then $f_\beta(o)$ will be forced to continue with b^+ and thus it will trace:

$$f_\beta(o) = \bar{d} b^+ do^\times$$

Thus we have

$$f_\beta(i) = \bar{d}b^- ...$$

This is Figure D.113.

Now here $f_\beta(i)$ can continue into either 1, 2, or 3, The case of 1 will still make $f_\beta(o)$ trace as above. The case of 2 will make it be absorbed:

$$f_\beta(i) = \bar{d}b^- ds^- p^- \bar{d} ...$$

and here the next letter has to be r^+ otherwise it will eventually trace. So it continues:

$$f_\beta(i) = \bar{d}b^- ds^- p^- \bar{d}\hat{r}^+ do^+ s^+ \bar{d}\,\mathrm{Abso}(f_\beta(r), f_\beta(b))^\times$$

This is Figure D.114.

Thus we consider if $f_\beta(i)$ goes into 3.

Consider $f_\beta(o)$. It it were to continue here with b° or b^+ then that would force $f_\beta(p)$ to continue with b^+, but then it will immediately be absorbed:

$$f_\beta(p) = p^+ d\,\mathrm{Abso}(f_\beta(o), f_\beta(i))^\times$$

Thus we must have $f_\beta(o)$ continuing with b^- and to the right of $f_\beta(p)$.

This is Figure D.115.

Now consider $f_\beta(i)$ again. Here if it were to continue with p° or p^+ then $f_\beta(o)$ will be forced

to continue with p^+ here, and that would cause it to trace:

$$f_\beta(o) = \bar{d}b^- p^+ b^+ do^\times$$

Thus here $f_\beta(i)$ has to continue with p^-, and to the right of $f_\beta(o)$:

$$f_\beta(i) = \bar{d}b^- p^- b^* ...$$

This is Figure D.116.

Now here consider $f_\beta(p)$. If $f_\beta(p)$ continues with b° or b^+, then $f_\beta(i)$ is forced to continue with b^+ here and it will be absorbed eventually:

$$f_\beta(i) = \bar{d}b^- p^- b^+ ds^- o^- \bar{d}r^+ do^+ s^+ d\,\mathrm{Abso}(f_\beta(r), f_\beta(b))^\times$$

Thus here $f_\beta(p)$ has to continue with b^- and to the right of $f_\beta(i)$. But now $f_\beta(p)$ immediately traces.

This is Figure D.117.

Thus gonig back to the situation depicted in Figure D.111, we must have $f_\beta(b)$ continue with i^*, and not o^-, and $f_\beta(r)$ will follow:

$$f_\beta(b) = ds^- i^* ...$$

and

$$f_\beta(r) = ds^- i^* ...$$

This is Figure D.118.

Now here if $f_\beta(r)$ were to continue with i° or i^+ then $f_\beta(b)$ will be forced to continue with i^+ here, and it will trace:

$$f_\beta(b) = ds^- i^+ \bar{d}p^+ b^\times$$

Thus here $f_\beta(r)$ continues with i^- and to the right of $f_\beta(b)$. It continues:

$$f_\beta(r) = ds^- \hat{i}^- s^+ \bar{d}b^* ...$$

Consider $f_\beta(b)$ again. Notice here that it has to end at i°. Indeed if it were to continue with i^+, it will be absorbed:

$$f_\beta(b) = ds^- \hat{i}^+ s^+ \,\mathrm{Abso}(f_\beta(r), f_\beta(b))^\times$$

And if it were to continue with i^- will trace:

$$f_\beta(b) = ds^- \hat{i}^- s^+ \bar{d}b^\times$$

Thus we must have

$$f_\beta(b) = ds^- \hat{i}^\circ$$

This is Figure D.119.

Now her consider $f_\beta(i)$. If it were to continue with b° or b^+, then $f_\beta(o)$ will be forced to continue with b^+, and that will cause it to trace:

$$f_\beta(o) = \bar{d}b^+ do^\times$$

Thus we have

$$f_\beta(i) = \bar{d}b^- ...$$

This is Figure D.120.

Here $f_\beta(i)$ can go into 1, 2, 3, or 4. It cannot be 1 as that would cause it to be immediately absorbed between $f_\beta(o)$ and $f_\beta(i)$. So it goes into 2, 3, or 4.

D.1.6.1.2.1 Global

Suppose $f_\beta(i)$ goes into 2.

Then it continues:

$$f_\beta(i) = \bar{d}b^- ds^- ...$$

This is Figure D.121.

Now the next letter cannot be i^+ to not trace, and so the only choice is o^-. Then it continues:

$$f_\beta(i) = \bar{d}b^- ds^- \hat{o}^- \bar{d} ...$$

Now the next letter can be b^- or r^*. If it were the former it will trace:

$$f_\beta(i) = \bar{d}b^- ds^- o^- \bar{d}\hat{b}^- p^- ds^- i^\times$$

Thus the next letter has to be r^*:

$$f_\beta(i) = \bar{d}b^- ds^- o^- \bar{d}\hat{r}^* ...$$

Now consider $f_\beta(o) = \bar{d}b^* ....$ Here if it were to continue with b^+ it will immediately be

absorbed between $f_\beta(o)$ and itself. If it were to continue with b^-, then it will trace, due to the position of $f_\beta(i)$:

$$f_\beta(o) = \bar{d}b^- ds^- o^\times$$

Thus $f_\beta(o)$ must end here:

$$f_\beta(o) = \bar{d}b^\circ$$

Now consider $f_\beta(r) = ds^- i^- s^+ \bar{d}$.... It continues:

$$f_\beta(r) = ds^- i^- s^+ \bar{d}\hat{b}^+ do^* ...$$

Similarly, consider $f_\beta(p) = b^*$.... It continues:

$$f_\beta(p) = b^+ do^* ...$$

We are now in Figure D.122.

Now consider $f_\beta(s) = o^*$.... Here the first letter can be o°, or it can be o^-. Whereas o^+ would cause it to immediately trace. So we have

$$f_\beta(s) = o^\circ$$

or

$$f_\beta(s) = o^-$$

D.1.6.1.2.1.1 Balance

Suppose $f_\beta(s) = o^\circ$.

This is Figure D.123.

Then $f_\beta(r)$ and $f_\beta(p)$ continue with o^+:

$$f_\beta(r) = ds^- i^- s^+ \bar{d} b^+ d\hat{o}^+ s^* ...$$

and

$$f_\beta(p) = b^+ d\hat{o}^+ s^* ...$$

This is Figure D.124.

Here we claim that $f_\beta(p)$ has to end. Suppose the contrary that $f_\beta(p)$ continues with s^-, then it traces:

$$f_\beta(p) = b^+ d\hat{o}^+ s^- o^- \bar{d} b^- p^\times$$

Suppose it continues with s^+, then it has to go to the left of $f_\beta(r)$, otherwise it'll eventually be absorbed between $f_\beta(r)$ and $f_\beta(b)$, so we have:

$$f_\beta(p) = b^+ d\hat{o}^+ s^+ o^- \bar{d} b^- ds^- ...$$

and here the next letter has to be o^- and not i^+ otherwise it'll eventually trace. So we have

$$f_\beta(p) = b^+ do^+ s^+ o^- \bar{d} b^- ds^- \hat{o}^- \bar{d} r^* ...$$

This is Figure D.125.

Now consider $f_\beta(r)$. It must end here at s°. Indeed, if it were to continue with s^-, then it will be absorbed:

$$f_\beta(r) = ds^- i^- s^+ \bar{d} b^+ do^+ \hat{s}^- o^- \bar{d} b^- ds^- i^+ s^+ \bar{d}\, \mathrm{Abso}(f_\beta(r), f_\beta(b))^\times$$

If it were to continue with i^+, then it will trace due to the position of $f_\beta(p)$:

$$f_\beta(r) = ds^- i^- s^+ \bar{d}b^+ do^+ \hat{s}^+ o^- b^- ds^- o^- \bar{d}r^\times$$

Thus we must have

$$f_\beta(r) = ds^- i^- s^+ \bar{d}b^+ do^+ \hat{s}^\circ$$

This is Figure D.126.

Now consider $f_\beta(p)$ again. We claim that it has to end here at r°. Suppose instead it continues with r^- and to the right of $f_\beta(i)$. Then it will be absorbed:

$$f_\beta(p) = b^+ do^+ s^+ o^- \bar{d}b^- ds^- \hat{o}^- \bar{d}\hat{r}^- do^+ s^+ \bar{d}b^+ d\,\mathrm{Abso}(f_\beta(o), f_\beta(i))^\times$$

If instead it continues with r^- and goes to the left of $f_\beta(i)$, then it will trace:

$$f_\beta(p) = b^+ do^+ s^+ o^- \bar{d}b^- ds^- \hat{o}^- \bar{d}\hat{r}^- do^+ s^+ \bar{d}b^+ do^+ s^- o^- \bar{d}b^- p^\times$$

If instead it continues with r^+, then it will be absorbed:

$$f_\beta(p) = b^+ do^+ s^+ o^- \bar{d}b^- ds^- \hat{o}^- \bar{d}\hat{r}^+ do^+ s^+ \bar{d}b^+ do^+ s^- o^- \bar{d}b^- ds^- i^+ s^+ \bar{d}\,\mathrm{Abso}(f_\beta(r), f_\beta(b))^\times$$

Thus $f_\beta(p)$ must end here. So we have

$$f_\beta(p) = b^+ do^+ s^+ o^- \bar{d}b^- ds^- \hat{o}^- \bar{d}\hat{r}^\circ$$

This is Figure D.127.

Now consider $f_\beta(i)$. It continues with r^+, but now it will trace:

$$f_\beta(i) = \bar{d}b^- ds^- o^- \bar{d}\hat{r}^+ do^+ s^+ \bar{d}b^+ do^+ s^- o^- \bar{d}b^- ds^- i^\times$$

This is Figure D.128.

Therefore going back to the situation depicted in Figure D.124, $f_\beta(p)$ has to end there at s°.

This is Figure D.129.

Now $f_\beta(r)$ continues with s^-:

$$f_\beta(r) = ds^- i^- s^+ \bar{d}b^+ d\hat{o}^+ s^- o^- \bar{d}b^- p^* ...$$

This is Figure D.130.

Consider $f_\beta(r)$ again.

Now here if $f_\beta(r)$ were to continue with p^-, then it gets absorbed:

$$f_\beta(r) = ds^- i^- s^+ \bar{d}b^+ d\hat{o}^+ s^- o^- \bar{d}b^- \hat{p}^- b^+ do^+ s^+ o^- \bar{d}b^- ds^- i^+ s^+ \bar{d}\,\mathrm{Abso}(f_\beta(r), f_\beta(b))^\times$$

On the other hand if $f_\beta(r)$ were to continue with p^+, then it will also be absorbed:

$$f_\beta(r) = ds^- i^- s^+ \bar{d}b^+ d\hat{o}^+ s^- o^- \bar{d}b^- \hat{p}^+ b^+ do^+ s^+ o^- \bar{d}b^- ds^- ...$$

here the next letter cannot be o^- or it will trace due to the position of $f_\beta(i)$. Thus the next

letter can only be i^+:

$$f_\beta(r) = ds^- i^- s^+ \bar{d}b^+ d\hat{o}^+ s^- o^- \bar{d}b^- \hat{p}^+ b^+ do^+ s^+ o^- \bar{d}b^- ds^- \hat{i}^+ s^+ \bar{d}p^+ b^+ do^+ s^+ \bar{d}b^+ d\,\mathrm{Abso}(f_\beta(o), f_\beta(i))^\times$$

Thus $f_\beta(r)$ must end at p° in the situation depicted in Figure D.130.

This gives us Figure D.131.

Finally, we consider $f_\beta(i)$ now.

We claim that it has to end here at r° as well. Indeed, if it were to continue with r^+, it will be absorbed:

$$f_\beta(i) = \bar{d}b^- ds^- o^- \bar{d}\hat{r}^+ do^+ s^+ \bar{d}b6 + do^+ s^- o^- \bar{d}b^- p^- b^+ do^+ s^+ o^- \bar{d}b^- ds^- i^+ s^+ \bar{d}\,\mathrm{Abso}(f_\beta(r), f_\beta(b))^\times$$

While if it were to continue with r^-, it will also be absorbed:

$$f_\beta(i) = \bar{d}b^- ds^- o^- \bar{d}\hat{r}^- do^+ s^+ \bar{d}b^+ d\,\mathrm{Abso}(f_\beta(o), f_\beta(i))^\times$$

Thus we must have

$$f_\beta(i) = \bar{d}b^- ds^- o^- \bar{d}\hat{r}^\circ$$

This gives Candidate 5. Depicted in Figure D.132.

D.1.6.1.2.1.2 Machine

Back to the end of Global D.1.6.1.2.1. Suppose

$$f_\beta(s) = o^- ...$$

This is Figure D.133.

Here $f_\beta(s)$ can continue into 1, 2, or 3. However, both 1 and 2 will lead to it tracing:

$$f_\beta(s) = o^- \bar{d} b^- ds^\times$$

Thus it has to continue into 3:

$$f_\beta(s) = o^- \bar{d} b^- p^* ...$$

This is Figure D.134.

Consider $f_\beta(i)$. We claim that $f_\beta(i)$ has to end here at r°. Indeed, suppose instead it continues with r^-, then it will be absorbed:

$$f_\beta(i) = \bar{d} b^- ds^- o^- \bar{d} \hat{r}^- do^+ s^+ \bar{d} b^+ d \,\mathrm{Abso}(f_\beta(o), f_\beta(i))^\times$$

So suppose instead it continues with r^+:

$$f_\beta(i) = \bar{d} b^- ds^- o^- \bar{d} \hat{r}^+ do^+ s^+ \bar{d} b^+ do^* ...$$

This is Figure D.135.

Now here if $f_\beta(i)$ were to continue with o° or o^+, then $f_\beta(r)$ will be forced to continue with o^+, and this will cause it to trace:

$$f_\beta(r) = ds^- i^- s^+ \bar{d} b^+ d\hat{o}^+ \bar{d} b^- ds^- o^- \bar{d} r^\times$$

Thus here $f_\beta(i)$ has to continue with o^-:

$$f_\beta(i) = \bar{d}b^- ds^- o^- \bar{d}\hat{r}^+ do^+ s^+ \bar{d}b^+ do^- ...$$

This is Figure D.136.

Here $f_\beta(i)$ can continue into 1, 2, or 3. However, 1 would lead to the same situation as before where $f_\beta(r)$ traces. If it goes into 2, then it will trace:

$$f_\beta(i) = \bar{d}b^- ds^- o^- \bar{d}\hat{r}^+ do^+ s^+ \bar{d}b^+ do^- \bar{d}b^- ds^- i^\times$$

Thus it can only go into 3, and continues:

$$f_\beta(i) = \bar{d}b^- ds^- o^- \bar{d}\hat{r}^+ do^+ s^+ \bar{d}b^+ do^- \bar{d}b^- p^* ...$$

This is Figure D.137.

Now consider $f_\beta(r)$. If it continues with o° or o^+, then $f_\beta(p)$ will be forced to continue with o^+, in which case it will be absorbed:

$$f_\beta(p) = b^+ d\hat{o}^+ \bar{d}b^- ds^- ...$$

and here the next letter has to be o^- otherwise it will trace; so it continues:

$$f_\beta(p) = b^+ do^+ \bar{d}b^- ds^- \hat{o}^- \bar{d}r^- do^+ s^+ \bar{d}b^+ d\,\mathrm{Abso}(f_\beta(o), f_\beta(i))^\times$$

Thus $f_\beta(r)$ can only continue with o^-, and to the right of $f_\beta(p)$:

$$f_\beta(r) = ds^- i^- s^+ \bar{d}b^+ d\hat{o}^- \bar{d}b^- p^* ...$$

This is Figure D.138.

Consider $f_\beta(p)$. Here it has to end at i°. Indeed, if it were to continue with i^+, then it will be absorbed:

$$f_\beta(p) = b^+ d\hat{i}^+ \bar{d}b^- ds^- i^+ s^+ \bar{d}\,\mathrm{Abso}(f_\beta(r), f_\beta(b))^\times$$

If it were to continue with i^-, then it will trace:

$$f_\beta(p) = b^+ d\hat{i}^- \bar{d}b^- p^\times$$

Thus we must have

$$f_\beta(p) = b^+ d\hat{i}^\circ$$

This is Figure D.139.

Now consider $f_\beta(s)$. If it were to continue with p^+, it will trace:

$$f_\beta(s) = o^- \bar{d}b^- p^+ b^+ do^+ s^\times$$

If it were to continue with p^-, it can then continue into 1, 2, or 3.

Suppose it continues into 2. Then it traces:

$$f_\beta(s) = i^- \bar{d}b^- \hat{p}^- b^+ do^+ \bar{d}b^- ds^\times$$

Suppose it continues into 3. Then it also traces:

$$f_\beta(s) = i^- \bar{d}b^- \hat{p}^- b6 + do^+ \bar{d}b^- ds^\times$$

Therefore at this point the remaining possibility for $f_\beta(s)$ is to continue with p^- into 1, or end with p°. Both of these possibilities will force $f_\beta(i)$ and $f_\beta(r)$ to continue with p^+.

This is shown in Figure D.140, where we have drawn both possibilities for $f_\beta(s)$.

Now $f_\beta(i)$ and $f_\beta(r)$ continue:

$$f_\beta(i) = \bar{d}b^- ds^- o^- \bar{d}\hat{r}^+ do^+ s^+ \bar{d}b^+ do^- \bar{d}b^- \hat{p}^+ b^+ do^+ s^* ...$$

and

$$f_\beta(r) = ds^- i^- s^+ \bar{d}b^+ do^- \bar{d}b^- \hat{p}^+ b^+ do^+ s^* ...$$

This is Figure D.141.

Now here if $f_\beta(i)$ continues with s° or s^+, then $f_\beta(r)$ will be forced to continue with s^+. But then it will trace, due to the position of $f_\beta(i)$:

$$f_\beta(r) = ds^- i^- s^+ \bar{d}b^+ do^- \bar{d}b^- p^+ b^+ do^+ \hat{s}^+ o^- \bar{d}p^- b^+ do^+ \bar{d}b^- ds^- o^- \bar{d}r^\times$$

Hence $f_\beta(i)$ has to continue with s^- and to the right of $f_\beta(r)$. However, now it will be absorbed:

$$f_\beta(r) = ds^- i^- s^+ \bar{d}b^+ do^- \bar{d}b^- p^+ b^+ do^+ \hat{s}^- o^- \bar{d}p^- b^+ do^+ \bar{d}b^- ds^- i^+ s^+ \,\mathrm{Abso}(f_\beta(r), f_\beta(b))^\times$$

This is a contradiction.

D.1.6.1.2.2 Iguana

Back to the end of Eager D.1.6.1.2. Suppose $f_\beta(i)$ goes into 3. Then it will be absorbed:

$$f_\beta(i) = \bar{d}b^- ds^- i^+ s^+ \bar{d}\,\mathrm{Abso}(f_\beta(r), f_\beta(b))^\times$$

This is Figure D.142.

This is a contradiction.

D.1.6.1.2.3 Fiasco

Back to the end of Eager D.1.6.1.2. Suppose $f_\beta(i)$ goes into 4.

This is Figure D.143.

Here consider $f_\beta(o)$. If it were to continue with b° or b^+, then both $f_\beta(r)$ and $f_\beta(p)$ will be forced to continue with b^+ and they will then immediately be absorbed between $f_\beta(o)$ and $f_\beta(i)$.

Thus we have

$$f_\beta(o) = \bar{d}b^- p^* ...$$

and to the right of $f_\beta(p)$.

This is Figure D.144.

Here if $f_\beta(i)$ were to continue with p° or p^+, then $f_\beta(o)$ will be forced to continue with p^+, and it will trace:

$$f_\beta(o) = \bar{d}b^- p^+ b^+ do^\times$$

Thus $f_\beta(i)$ has to continue with p^- and to the right of $f_\beta(o)$:

$$f_\beta(o) = \bar{d}b^-p^-b^*...$$

and here it has to continue with b^+ and to the left of $f_\beta(p)$ or else $f_\beta(p)$ will immediately trace. So we have

$$f_\beta(o) = \bar{d}b^-p^-b^+...$$

This is Figure D.145.

Here $f_\beta(i)$ can continue into 1 or 2. But if it continues into 2 then it will trace:

$$f_\beta(o) = \bar{d}b^-p^-b^+ds^-i^\times$$

Hence it has to go into 1:

$$f_\beta(o) = \bar{d}b^-p^-b^+ds^-o^-\bar{d}...$$

and here the next letter has to be r^* and not b^-, or it will trace. So we have

$$f_\beta(o) = \bar{d}b^-p^-b^+ds^-o^-\bar{d}r^*...$$

This is Figure D.146.

Now consider $f_\beta(o) = \bar{d}b^-p^*....$ It has to end here at p°. Indeed, if it continues with p^+, it will trace:

$$f_\beta(o) = \bar{d}b^-p^+b^+do^\times$$

Similarly, if it continues with p^-, it will also trace:

$$f_\beta(o) = \bar{d}b^- p^- b^+ ds^- o^\times$$

Thus we have

$$f_\beta(o) = \bar{d}b^- p^\circ$$

This is Figure D.147.

Now consider $f_\beta(s) = o^*$.... We claim that it has to end here immediately at o°. Indeed, if it starts with o^+ then it will immediately trace. On the other hand, if it starts with o^-, then we have

$$f_\beta(s) = o^- \bar{d}b^- p^- b^+ ...$$

This is Figure D.148.

Now it can continue into 1 or 2. But both will cause it to trace:

$$f_\beta(s) = o^- \bar{d}b^- p^- b^+ ds^\times$$

Thus we must have

$$f_\beta(s) = o^\circ$$

This is Figure D.149.

Now consider $f_\beta(i)$. We claim that it has to end here at r°. Suppose it did not. Then if it

were to continue with r^-, then it will be absorbed:

$$f_\beta(i) = \bar{d}b^- p^- b^+ ds^- o^- \bar{d}\hat{r}^- do^+ s^+ \bar{d}b^- p^+ b^+ d\,\mathrm{Abso}(f_\beta(o), f_\beta(i))^\times$$

If it were to instead continue with r^+, then we have

$$f_\beta(i) = \bar{d}b^- p^- b^+ ds^- o^- \bar{d}\hat{r}^+ do^+ s^+ \bar{d}b^* ...$$

This is Figure D.150.

But now if $f_\beta(i)$ were to continue with b° or b^+, then $f_\beta(r)$ will be forced to continue with b^+, and it will trace:

$$f_\beta(r) = ds^- i^- s^+ \bar{d}b^+ ds^- o^- r^\times$$

Thus $f_\beta(i)$ can only continue with b^-, and then continue into 1, or 2 as depicted in Figure D.150.

If it goes into 1, then it will be absorbed eventually:

$$f_\beta(i) = \bar{d}b^- p^- b^+ ds^- o^- \bar{d}r^+ do^+ s^+ \bar{d}\hat{b}^- ds^- ...$$

and here the next letter has to be o^- or it will trace:

$$f_\beta(i) = \bar{d}b^- p^- b^+ ds^- o^- \bar{d}r^+ do^+ s^+ \bar{d}b^- ds^- \hat{o}^- \bar{d}r^- do^+ s^+ \bar{d}b^- p^+ b^+ d\,\mathrm{Abso}(f_\beta(o), f_\beta(i))^\times$$

If instead it continues into 2, then it will also be absorbed:

$$f_\beta(i) = \bar{d}b^- p^- b^+ ds^- o^- \bar{d}r^+ do^+ s^+ \bar{d}\hat{b}^- ds^- i^+ s^+ \bar{d}\,\mathrm{Abso}(f_\beta(r), f_\beta(b))^\times$$

Therefore, we have established that in the situation depicted in Figure D.149, $f_\beta(i)$ has to end at r°:

$$f_\beta(i) = \bar{d}b^- p^- b^+ ds^- o^- \bar{d}r^\circ$$

This is Figure D.151.

Now consider $f_\beta(p)$. We claim it has to start and here at b°. It cannot start with b^- or it will trace immediately. If it were to start with b^+, then it has to continue into 1, or 2. Suppose it goes into 1, then it will be absorbed:

$$f_\beta(p) = b^+ ds^- o^- \bar{d}r^- do^+ s^+ \bar{d}b^- p^+ b^+ d\,\mathrm{Abso}(f_\beta(o), f_\beta(i))^\times$$

If it were to go into 2, then it also gets absorbed:

$$f_\beta(p) = b^+ ds^- i^+ s^+ \bar{d}\,\mathrm{Abso}(f_\beta(r), f_\beta(b))^\times$$

Hence $f_\beta(p)$ has to start and end at b°:

$$f_\beta(p) = b^\circ$$

This forced $f_\beta(r)$ to continue with b^-:

$$f_\beta(r) = ds^- i^- s^+ \bar{d}b^- p^+ b^+ do^+ s^* ...$$

This is Figure D.152.

Here we claim that $f_\beta(r)$ has to end at s°. Indeed, suppose instead it continued with s^+.

Then it will be absorbed:

$$f_\beta(r) = f_\beta(r) = ds^- i^- s^+ \bar{d} b^- p^+ b^+ do^+ \hat{s}^+ o^- \bar{d} b^- p^- b^+ ds^- i^+ s^+ \bar{d} p^+ b^+ do^+ s^+ \bar{d} b^- p^+ b^+ d \,\mathrm{Abso}(f_\beta(o), f_\beta(i))^\times$$

Suppose instead it continued with s^-. Then it will again be absorbed:

$$f_\beta(r) = f_\beta(r) = ds^- i^- s^+ \bar{d} b^- p^+ b^+ do^+ \hat{s}^- o^- \bar{d} b^- p^- b^+ ds^- i^+ s^+ \bar{d} \,\mathrm{Abso}(f_\beta(r), f_\beta(b))^\times$$

Thus $f_\beta(r)$ must end at s°:

$$f_\beta(r) = f_\beta(r) = ds^- i^- s^+ \bar{d} b^- p^+ b^+ do^+ \hat{s}^\circ$$

This establishes the train track map Candidate 6 depicted in Figure D.143.

D.2 Case B,C,D: Triangles Swapped

At least one of $f_\beta(d)$ or $f_\beta(\bar{d})$ passes over d or $\bar{d}$ after an odd number of letters.

We assume $f_\beta(\bar{d})$ passes over d after an odd number of letters. My symmetry, this turns out to be the only one to check.

We know that $f_\beta(\bar{d})$ must start at r, b, p, or d. On the other hand, $f_\beta(\bar{d})$ cannot start at d by the assumption; hence it must start at b, r, or p.

D.2.1 ATL

Suppose $f_\beta(\bar{d})$ starts at p, and $f_\beta(d)$ starts at s.

Recall that $f_\beta(\bar{d})$ needs to pass over an odd number of letters and then cross d, so it must

do so in the following way:

$$f_\beta(p) = p^- d...$$

or

$$f_\beta(p) = p^+ ... p^- d...$$

We will refer to the former as $f_\beta(p)$ "having no initial twists", and the latter as $f_\beta(p)$ "having initial twists" (we will use this terminology from now on for similar situations to come).

This is to say, the preceding letter before crossing d must be p^-. It is not possible for this preceding letter to be r^*, as it is impossible to do so with an odd number of letters before crossing.

We also have $f_\beta(s)$ starting with d, and $f_\beta(p)$ starting with $\bar{d}$; and here $f_\beta(p)$ has to go under $f_\beta(s)$ or it will immediately trace.

The situation is depicted in Figure D.153.

Now we see that $f_\beta(s)$ will immediately trace:

$$f_\beta(s) = ds^\times$$

This is a contradiction.

D.2.2 LAX

Back to the end of Case B,C,D D.2. Suppose $f_\beta(\bar{d})$ starts at p and $f_\beta(d)$ starts at i.

Now again the starting behavior of $f_\beta(\bar{d})$ is the same.

We have Figure D.154.

Consider $f_\beta(d) = i^*....$ It needs to cross $\bar{d}$ at some point, to join with $f_\beta(\bar{d})$, and it can do this in two ways: the letter immediately preceding $\bar{d}$ can be either i or s.

D.2.2.1 Jolt

Suppose the former case, $f_\beta(d)$ goes over i then cross $\bar{d}$, and it may or may not have initial twists:

$$f_\beta(d) = i^*...i^-\bar{d}...$$

or

$$f_\beta(d) = i^-\bar{d}...$$

This is Figure D.155.

Now the pair $f_\beta(b)$ and $f_\beta(r)$ on the right-hand side has to go below $f_\beta(\bar{d})$ on the left-hand side. Otherwise, either $f_\beta(b)$ or $f_\beta(r)$ will trace after they go over p^+.

This immediately implies that the starting sequence for $f_\beta(\bar{d})$ has to be

$$f_\beta(\bar{d}) = p^-ds^*...$$

That is, $f_\beta(\bar{d})$ cannot start with p^+ and have initial twists before crossing d. Moreover, it has to continue with s^-, as either s° or s^+ will force $f_\beta(p)$ to start with s^+, and thus trace:

$$f_\beta(p) = s^+\bar{d}p^\times$$

Thus we must have

$$f_\beta(\bar{d}) = p^-ds^-...$$

Now consider $f_\beta(s)$. It has to go above $f_\beta(d)$ on the right, otherwise $f_\beta(d)$ will enter into

Situation β. This immediately means $f_\beta(s)$ has to continue with i^* after crossing d:

$$f_\beta(s) = di^*...$$

and hence, $f_\beta(d)$ cannot have initial twists, as that would force $f_\beta(s)$ to trace as any initial twists must bring $f_\beta(s)$ along, and any such twists must go over s.

We are now in Figure D.156.

Now $f_\beta(d)$ continues with i^-:

$$f_\beta(\bar{d}) = p^- ds^- \hat{i}^- \bar{d}$$

This is Figure D.157.

Now we are in Situation α, in a clockwise manner.

This is a contradiction.

D.2.2.2 Mile

Back to the end of LAX D.2.2. Suppose $f_\beta(d)$ goes over s and then cross $\bar{d}$.

Then the only way this could occur is

$$f_\beta(d) = i^+ s^+ \bar{d}...$$

That is, $f_\beta(d)$ cannot have any initial twists, as any such twists will lead to it going over i^- before crossing $\bar{d}$.

This is Figure D.158.

Consider $f_\beta(s)$. It must go below the pair $f_\beta(b)$ and $f_\beta(r)$, otherwise it will immediately trace. Thus we have

$$f_\beta(s) = do^*...$$

The pair $f_\beta(b)$ and $f_\beta(r)$ on the right must go below $f_\beta(\bar{d})$ on the left, otherwise at least one of them will trace, irregardless of whether $f_\beta(\bar{d})$ has any initial twists or not.

This is Figure D.159.

Now consider $f_\beta(\bar{d})$. Since the pair $f_\beta(b)$ and $f_\beta(r)$ must go up p, $f_\beta(\bar{d})$ is now forced to not have any initial twists, as any such twist will bring the pair along, and will have to go over one of r or b, thus tracing.

Now consider $f_\beta(d)$ and $f_\beta(\bar{d})$ in the middle. If they do not join in the middle, then one of them will be in Situation β: If $f_\beta(\bar{d})$ goes above $f_\beta(d)$ then $f_\beta(d)$ will be in Situation β, and vice versa.

We are in Figure D.160.

Here $f_\beta(o)$ can start with r or b:

$$f_\beta(o) = r^*...$$

or

$$f_\beta(o) = b^*...$$

D.2.2.2.1 Night

Suppose

$$f_\beta(o) = r^*...$$

Then $f_\beta(i)$ also starts with r^*. Furthermore, if $f_\beta(i)$ were to start with r° or r^+, then $f_\beta(o)$

will start with r^+, and it will trace:

$$f_\beta(o) = r^+ do^\times$$

Thus we must have

$$f_\beta(i) = r^- ...$$

But now it will trace:

$$f_\beta(i) = r^- p^= ds^- i^\times$$

This is Figure D.161.

This is a contradiction.

D.2.2.2.2 Shade

Back to the end of Mile D.2.2.2. Suppose

$$f_\beta(o) = b^* ...$$

Then $f_\beta(i)$ can start with r or b:

$$f_\beta(i) = r^* ...$$

or

$$f_\beta(i) = b^* ...$$

D.2.2.2.2.1 Adieu

This is Figure D.162.

Here $f_\beta(i)$ can start with r^+ or r° (r^- is not possible as it will be immediately absorbed.).

D.2.2.2.2.1.1 Sizzle

Suppose $f_\beta(i)$ starts with r^+. Then it continues:

$$f_\beta(i) = r^+ do^* ...$$

This is Figure D.163.

Now here it must continue with o^+ and to the left of $f_\beta(s)$. Indeed, if instead it were to continue with o° or o^-, then $f_\beta(s)$ will be forced to continue with o^- and to the right of $f_\beta(i)$, which would force it to be absorbed:

$$f_\beta(s) = d\hat{o}^- \bar{d}r^- \text{ Abso}(f_\beta(i), f_\beta(p))^\times$$

Thus we have

$$f_\beta(i) = r^+ d\hat{o}^+ \bar{d}p^* ...$$

This is Figure D.164.

Here $f_\beta(p)$ can continue with p°, or p^+, or p^-.

Suppose it continues with p°. Then $f_\beta(b)$ and $f_\beta(r)$ continue with p^+:

$$f_\beta(b) = \bar{d}\hat{p}^+ do^* ...$$

$$f_\beta(r) = \bar{d}p^+ do^* ...$$

This is Figure D.165.

Now here $f_\beta(s)$ has to continue with o^+ and to the left of $f_\beta(r)$, otherwise $f_\beta(r)$ will be

forced to continue with o^- and to the right of $f_\beta(s)$, and will trace:

$$f_\beta(r) = \bar{d}p^+ do^- \bar{d}r^\times$$

But now $f_\beta(s)$ will be absorbed:

$$f_\beta(s) = d\hat{o}^+ \bar{d}p^- d...$$

here the next letter has to be o^- or it will trace. So we have

$$f_\beta(s) = do^+ \bar{d}p^- d\hat{o}^- \bar{d}r^- \text{ Abso}(f_\beta(i), f_\beta(o))^\times$$

This is Figure D.166.

Now back to the situation in Figure D.164, suppose $f_\beta(p)$ continues with p^+. Then $f_\beta(r)$ and $f_\beta(b)$ follow with p^+ as well. So we have:

$$f_\beta(i) = r^+ do^+ \bar{d}\hat{p}^+ do^* ...$$

$$f_\beta(r) = \bar{d}b^+ do^* ...$$

$$f_\beta(b) = \bar{d}b^+ do^* ...$$

This is Figure D.167.

Here $f_\beta(s)$ must continue with o^+ otherwise $f_\beta(r)$ will be forced to continue with o^- and to the right of $f_\beta(s)$ and will trace. Furthermore, $f_\beta(s)$ has to do so while doing to the left of $f_\beta(r)$ (so $f_\beta(r)$ does not still trace), and to the left of $f_\beta(i)$ (if it went in between $f_\beta(r)$ and

$f_\beta(i)$ then it will be absorbed). So we have

$$f_\beta(s) = d\hat{o}^+ \bar{d}p^* ...$$

This is Figure D.168.

Now for the same reason, $f_\beta(b)$ must continue with o^+ and to the left of $f_\beta(i)$:

$$f_\beta(b) = \bar{d}b^+ dhato^+ \bar{d}p^* ...$$

This is Figure D.169.

Now $f_\beta(r)$ must also do the same, continue with o^+ and to the left of $f_\beta(i)$, otherwise $f_\beta(i)$ will be forced to continue with o^- and be absorbed:

$$f_\beta(i) = r^+ do^+ \bar{d}p^+ d\hat{o}^- \bar{d}p^- d\,\mathrm{Abso}(f_\beta(b), f_\beta(r))^\times$$

So we must have

$$f_\beta(r) = \bar{d}p^+ do^+ \bar{d}p^* ...$$

This is Figure D.170.

Here $f_\beta(s)$ must continue with p^+ and to the left of $f_\beta(r)$, otherwise $f_\beta(r)$ will be forced to continue with p^- and to the right of $f_\beta(s)$, which will make $f_\beta(r)$ trace:

$$f_\beta(r) = \bar{d}p^+ do^+ \bar{d}\hat{p}^- do^- \bar{d}r^\times$$

Thus we must have

$$f_\beta(s) = do^+ \bar{d}p^+ do^* ...$$

This is Figure D.171.

At this point, observe that we are repeating the pattern. That is, we are back in the situation depicted in Figure D.164, but just with more twists.

In other words, here if $f_\beta(i)$ were to continue with p° then it will be a repeat of a previous case for Figure D.164, but with more twists. If it continues with p^+ again then it repeats this process again but with more twists. It may however, continue here with p^-.

Therefore, it suffices now to eliminate the case of $f_\beta(i)$ continuing with p^- in the situation depicted in Figure D.164.

So consider the situation depicted in Figure D.164 once more, and let us consider the case when $f_\beta(i)$ continues with p^-.

This is Figure D.172. Here it can go into 1, 2, or 3. If it goes into 1, then both $f_\beta(r)$ and $f_\beta(b)$ will continue with p^+ to the right of $f_\beta(i)$, which will make $f_\beta(b)$ trace:

$$f_\beta(b) = \bar{d}p^+ d...$$

here the next letter cannot be o^- or it will be absorbed. So we have

$$f_\beta(b) = \bar{d}p^+ d\hat{i}^+ s^+ \bar{d}p^+ b^\times$$

If instead $f_\beta(i)$ goes into 2, then it is immediately absorbed.

So it can only go into 3:

$$f_\beta(i) = r^+ do^+ \bar{d}p^- ds^* ...$$

This is Figure D.173.

Here, $f_\beta(i)$ must continue with s^- and to the right of $f_\beta(p)$, otherwise $f_\beta(p)$ will be forced to continue with s^+, and it will trace:

$$f_\beta(p) = s^+ \bar{d}p^\times$$

but now $f_\beta(i)$ will trace:

$$f_\beta(i) = r^+ do^+ \bar{d}p^- d\hat{s}^- i^\times$$

This is a contradiction. This eliminates the possibility of $f_\beta(i)$ continuing with p^- in the situation depicted in Figure D.164, and thereby eliminating the possibility of p^+ as well.

D.2.2.2.2.1.2 Fleshy

Back to the end of Adieu D.2.2.2.2.1 . Suppose $f_\beta(i)$ starts with r°:

$$f_\beta(i) = r^\circ$$

This is Figure D.174.

Here $f_\beta(o)$ can start with b^- or b°.

D.2.2.2.2.1.2.1 Keyboard

Suppose

$$f_\beta(o) = b^- ...$$

Then it continues:

$$f_\beta(o) = b^- p^- d s^- i^- \bar{d} p^* ...$$

This is Figure D.175.

Here $f_\beta(o)$ can continue with p^+, or p°, or p^-.

Suppose $f_\beta(o)$ continues with p^+. Then it continues:

$$f_\beta(o) = b^- p^- d s^- i^- \bar{d} p^+ d ...$$

Here the next letter cannot be i^+, or it will be absorbed:

$$f_\beta(o) = b^- p^- d s^- i^- \bar{d} p^+ d i^+ s^+ \bar{d} p 6 + \text{Abso}(f_\beta(r), f_\beta(b))^\times$$

But the only other choice for the next letter is o^*, which will trace.

Thus $f_\beta(o)$ cannot continue with p^+.

So suppose instead $f_\beta(o)$ continues with p°:

$$f_\beta(o) = b^- p^- d s^- i^- \bar{d} p^\circ$$

Then $f_\beta(s)$ must end at o°. Indeed, if instead it continues with o^-, then it will be absorbed:

$$f_\beta(s) = d o^- \bar{d} r^- \text{Abso}(f_\beta(r), f_\beta(o))^\times$$

If instead it continues with o^+, it will either trace:

$$f_\beta(s) = d\hat{o}^+ \bar{d}p^- ds^\times$$

or

$$f_\beta(s) = d\hat{o}^+ \bar{d}p^- di^+ s^\times$$

or it will be absorbed:

$$f_\beta(s) = d\hat{o}^+ \bar{d}p^- \text{Abso}(f_\beta(b), f_\beta(r))^\times$$

depending on which gap it continues into after p^-.

Thus $f_\beta(o)$ cannot continue with p°.

So suppose $f_\beta(o)$ continues with p^-. This is Figure D.176. Here it can continue into 1, 2, or 3.

Suppose it continues into 1. Then it continues:

$$f_\beta(o) = b^- p^- ds^- i^- \bar{d}\hat{p}^- di^+ s^+ \bar{d}p^+ b^* ...$$

Now consider $f_\beta(s)$. It must end at o°. If instead it were to continue with o^-, it will be absorbed between $f_\beta(i)$ and $f_\beta(o)$. If instead it were to continue with o^+, then it will either trace or be absorbed between $f_\beta(b)$ and $f_\beta(r)$.

This is Figure D.177.

Now $f_\beta(b)$ will trace:

$$f_\beta(b) = \bar{d}\hat{p}^+ d...$$

here the next letter cannot be o^- or it will be absorbed. So we must have:

$$f_\beta(b) = \bar{d}\hat{p}^+ d\hat{i}^+ s^+ \bar{d}p^+ b^\times$$

Thus $f_\beta(o)$ cannot continue into 1. Suppose it continues into 2, then it will be immediately absorbed.

So suppose it continues into 3. It continues:

$$f_\beta(o) = b^- p^- ds^- i^- \bar{d}\hat{p}^- d...$$

and here the next letter must be s^- otherwise $f_\beta(p)$ will be forced to continue with s^+ and will trace. So we have:

$$f_\beta(o) = b^- p^- ds^- i^- \bar{d}p^- d\hat{s}^- i^*...$$

Consider $f_\beta(s)$. It must end at o°. Indeed if it were to continue with o^- it will be absorbed as before; and if it were to continue with o^+, due to the position of $f_\beta(o)$ now, it will trace:

$$f_\beta(s) = do^+ \bar{d}p^- ds^\times$$

Thus we must have

$$f_\beta(s) = do^\circ$$

This is Figure D.178.

Now consider $f_\beta(r)$. If it were to continue with p° or p^+, then $f_\beta(b)$ will be forced to continue with p^+ and to the left of $f_\beta(r)$. But then it will trace:

$$f_\beta(b) = \bar{d}p^+ di^+ s^+ \bar{d}p^+ b^\times$$

Thus here $f_\beta(r)$ must continue with p^- and to the right of $f_\beta(b)$:

$$f_\beta(r) = \bar{d}p^- ds^* ...$$

and here it must continue with s^- and to the right of $f_\beta(p)$ otherwise $f_\beta(p)$ will trace:

$$f_\beta(r) = \bar{d}p^- d\hat{s}^- i^* ...$$

This is Figure D.179.

Now consider $f_\beta(o)$. If it were to continue with i° or i^+, then $f_\beta(r)$ will be forced to continue with i^+, and it will either be absorbed:

$$f_\beta(r) = \bar{d}p^- ds^- \hat{i}^+ s^+ \bar{d}p^+ di^+ s^+ \bar{d}p^+ b^+ \,\mathrm{Abso}(f_\beta(r), f_\beta(b))^\times$$

or trace:

$$f_\beta(r) = \bar{d}p^- ds^- \hat{i}^+ s^+ \bar{d}p^+ do^- \bar{d}r^\times$$

Therefore, we must have

$$f_\beta(o) = b^- p^- ds^- i^- \bar{d}p^- ds^- i^- s^* ...$$

This is Figure D.180.

Here $f_\beta(p)$ can start with s° or s^-. Suppose it starts with p°. Then $f_\beta(o)$ continues:

$$f_\beta(o) = b^- p^- ds^- i^- \bar{d}p^- ds^- i^- \hat{s}^+ \bar{d}p^* ...$$

This is Figure D.181.

Here $f_\beta(b)$ must continue with p^- and to the right of $f_\beta(o)$. Otherwise, $f_\beta(o)$ will be forced to continue with p^+ and to the left of $f_\beta(b)$, and $f_\beta(o)$ will be immediately absorbed.

So we have

$$f_\beta(b) = \bar{d}p^- ds^- i^* ...$$

This is Figure D.182.

Here $f_\beta(r)$ must continue with i^- and to the right of $f_\beta(b)$. Otherwise, $f_\beta(b)$ will be forced to continue with i^+ and to the left of $f_\beta(r)$. In which case it will trace:

$$f_\beta(b) = \bar{d}p^- ds^- \hat{i}^+ s^+ \bar{d}p^+ d...$$

here the next letter cannot be o^- or it will be absorbed. So instead we have

$$f_\beta(b) = \bar{d}p^- ds^- i^+ s^+ \bar{d}p^+ d\hat{i}^+ s^+ \bar{d}p^+ b^\times$$

Therefore $f_\beta(r)$ must continue with i^-:

$$f_\beta(r) = \bar{d}p^- ds^- i^- s^+ \bar{d}p^* ...$$

This is Figure D.183.

Here $f_\beta(o)$ must continue with p^- and to the right of $f_\beta(r)$. Otherwise, $f_\beta(r)$ will be forced to continue with p^+ and to the left of $f_\beta(o)$, in which case it will either be absorbed:

$$f_\beta(r) = \bar{d}p^- ds^- i^- s^+ \bar{d}p^+ ds^- i^+ s^+ \bar{d}p^+ di^+ s^+ \bar{d}p^+ b^+ \,\mathrm{Abso}(f_\beta(b), f_\beta(p))^\times$$

or trace:

$$f_\beta(r) = \bar{d}p^- ds^- i^- s^+ \bar{d}p^+ ds^- i^+ s^+ \bar{d}p^+ do^- \bar{d}r^\times$$

Therefore, $f_\beta(o)$ must continue with p^- and to the right of $f_\beta(r)$:

$$f_\beta(o) = b^- p^- ds^- i^- \bar{d}p^- ds^- i^- s^+ \bar{d}\hat{p}^- ds^- i^* ...$$

This is Figure D.184.

Here $f_\beta(b)$ must continue with i^- and to the right of $f_\beta(o)$. Otherwise, $f_\beta(o)$ will be forced to continue with i^+ and to the left of $f_\beta(b)$. But then $f_\beta(o)$ will be absorbed:

$$f_\beta(o) = b^- p^- ds^- i^- \bar{d}p^- ds^- i^- s^+ \bar{d}p^- ds^- i^+ s6 + \bar{d}p^+ d\,\mathrm{Abso}(f_\beta(b), f_\beta(r))^\times$$

Therefore $f_\beta(b)$ must continue with i^- and to the right of $f_\beta(o)$:

$$f_\beta(b) = \bar{d}p^- ds^- i^- s^+ \bar{d}p^* ...$$

This is Figure D.185.

Here $f_\beta(r)$ must continue with p^- and to the right of $f_\beta(b)$. Otherwise, $f_\beta(b)$ will be forced to continue with p^+ and to the left of $f_\beta(r)$. But then it will trace:

$$f_\beta(b) = \bar{d}p^- ds^- i^- s^+ \bar{d}p^+ ds^- i^+ s^+ \bar{d}p^+ di^+ s^+ \bar{d}p^+ b^\times$$

Therefore $f_\beta(r)$ must continue with p^- and to the right of $f_\beta(b)$:

$$f_\beta(r) = \bar{d}p^- ds^- i^- s^+ \bar{d}p^- ds^- i^* ...$$

This is Figure D.186.

Here $f_\beta(o)$ must continue with i^- and to the right of $f_\beta(r)$. Otherwise, $f_\beta(r)$ will be forced to continue with i^+ and to the left of $f_\beta(o)$. But now $f_\beta(r)$ will be absorbed:

$$f_\beta(r) = \bar{d}p^- ds^- i^- s^+ \bar{d}p^- ds^- \hat{i}^+ s^+ \bar{d}p^+ ds^- i^+ s^+ \bar{d}p^+ di^+ s^+ \bar{d}p^+ b^+ \operatorname{Abso}(f_\beta(i), f_\beta(b))^\times$$

or trace:

$$f_\beta(r) = \bar{d}p^- ds^- i^- s^+ \bar{d}p^- ds^- \hat{i}^+ s^+ \bar{d}p^+ ds^- i^+ s^+ \bar{d}p^+ do^- \bar{d}r^\times$$

This is Figure D.187.

Now notice we have returned to the same situation as depicted in Figure D.181, but simply with more twists. Notice we have $f_\beta(b)$ to the left of $f_\beta(o)$ on p^*, and $f_\beta(r)$ on i^*, exactly as they were in Figure D.181. In particular, we can repeat all of the steps from that point on wards, except with additional twists added in for each mapping that appears in the argument. This process will then repeat indefinitely, and so none of the remaining edges have anywhere to end.

This is a contradiction.

So back to the situation depicted in Figure D.180. Suppose $f_\beta(p)$ starts with s^-. Then we have

$$f_\beta(p) = s^- i^* ...$$

This is Figure D.188.

Now here $f_\beta(r)$ must continue with i^- and to the right of $f_\beta(p)$. Otherwise, $f_\beta(p)$ will be

forced to continue with i^+, and it will immediately trace after crossing $\bar{d}$. Thus we have

$$f_\beta(p) = s^- \hat{i}^- s^* ...$$

This is Figure D.189.

Now $f_\beta(o)$ must continue with s^- and to the right of $f_\beta(r)$. Otherwise $f_\beta(r)$ will be forced to continue with s^+ and it will eventually be absorbed:

$$f_\beta(r) = \bar{d}p^- ds^- i^- \hat{s}^+ \bar{d}p^+ di^+ s^+ \bar{d}p^+ b^+ \,\mathrm{Abso}(f_\beta(r), f_\beta(b))^\times$$

or trace:

$$\bar{d}p^- ds^- i^- \hat{s}^+ \bar{d}p^+ do^- \bar{d}r^\times$$

Thus we must have

$$f_\beta(o) = b^- p^- ds^- i^- \bar{d}p^- ds^- i^- s^- i^* ...$$

This is Figure D.190.

Here $f_\beta(b)$ can end at p° or continue with p^-; whereas p^+ will cause it to immediately be absorbed. Suppose it continues with p°:

$$f_\beta(b) = \bar{d}b^\circ$$

This is Figure D.191.

Here $f_\beta(p)$ must continue with i^- and to the right of $f_\beta(o)$. Otherwise, $f_\beta(o)$ will be forced

to continue with i^+ and to the left of $f_\beta(p)$, and it will eventually be absorbed:

$$f_\beta(o) = b^- p^- ds^- i^- \bar{d}p^- ds^- i^- s^- i^+ s^+ \bar{d}p^+ d \,\mathrm{Abso}(f_\beta(b), f_\beta(r))^\times$$

Thus we must have

$$f_\beta(p) = s^- i^- s^* ...$$

This is Figure D.192.

Here $f_\beta(r)$ must continue with s^- and to the right of $f_\beta(p)$. Otherwise, $f_\beta(p)$ will be forced to continue with s^+ and to the left of $f_\beta(r)$, and it will trace:

$$f_\beta(p) = s^- i^- \hat{s}^+ i^+ s^+ \bar{d}p^\times$$

Thus we must have

$$f_\beta(r) = \bar{d}p^- ds^- i^- \hat{s}^- i^* ...$$

This is Figure D.193.

Here $f_\beta(o)$ must continue with i^- and to the right of $f_\beta(r)$. Otherwise, $f_\beta(r)$ will be forced to continue with i^+ and to the left of $f_\beta(o)$, and it will either be absorbed:

$$f_\beta(r) = \bar{d}p^- ds^- i^- s^- \hat{i}^+ s^+ i^+ s^+ \bar{d}p^+ di^+ s^+ \bar{d}p^+ b^+ \,\mathrm{Abso}(f_\beta(r), f_\beta(b))^\times$$

or trace:

$$f_\beta(r) = \bar{d}p^- ds^- i^- s^- \hat{i}^+ s^+ i^+ s^+ \bar{d}p^+ do^- \bar{d}r^\times$$

Thus we must have

$$f_\beta(o) = b^- p^- d s^- i^- \bar{d} p^- d s^- i^- s^- \hat{i}^- s^* ...$$

This is Figure D.194.

Here $f_\beta(p)$ must continue with s^- and to the right of $f_\beta(o)$. Otherwise, $f_\beta(o)$ will be forced to continue with s^+ and to the left of $f_\beta(p)$, in which case it will be absorbed:

$$f_\beta(o) = b^- p^- d s^- i^- \bar{d} p^- d s^- i^- s^- i^- s^+ i^+ s^+ \bar{d} p^+ d \, \mathrm{Abso}(f_\beta(b), f_\beta(r))^\times$$

Thus we must have

$$f_\beta(p) = s^- i^- \hat{s}^- i^* ...$$

This is Figure D.195.

Now notice we are now repeating the situation depicted in Figure D.189, except with more twists, and $f_\beta(b)$ having already ended at p°. This means that the pattern repeats indefinitely, creating more twists, but never ends.

This is a contradiction.

Thus going back to the situation depicted in Figure D.190, let us suppose $f_\beta(b)$ does not end at p° but instead continues with p^-. Then it continues:

$$f_\beta(b) = \bar{d} p^- d s^- i^* ...$$

This is Figure D.196.

Here $f_\beta(b)$ must continue with i^-. Otherwise, $f_\beta(p)$ will be forced to continue with i^+, in

which case it will immediately trace after crossing $\bar{d}$. Thus we have

$$f_\beta(b) = \bar{d}p^- ds^- \hat{i}^- ...$$

This is Figure D.197.

Now $f_\beta(b)$ must continue into the space labeled 3. Indeed, if instead it were to continue into 1, then $f_\beta(p)$ still traces; and if it were to continue into 2, then itself will trace:

$$f_\beta(b) = \bar{d}p^- ds^- \hat{i}^- s^+ i^+ s^+ \bar{d}p^+ di^+ s^+ \bar{d}p^+ b^\times$$

So it must go into 3. Thus we have

$$f_\beta(b) = \bar{d}p^- ds^- i^- s^* ...$$

This is Figure D.198.

Now consider $f_\beta(p)$. It must end either at i° or s°, possibly with some number of twists between the two before ending. This is the only possibility it can continue, as any deviation from such twisting would necessitate it to leave this region of the train track, and the only way to do so is to trace p after $\bar{d}$. Suppose $f_\beta(p)$ were to end at i°. We will consider the specific case of when it immediately ends here as depicted in Figure D.198. The cases for when it may have some twisting with s before ending at i° is similar but simply with more redundant twisting in our argument.

So we suppose

$$f_\beta(p) = s^- i^\circ$$

Then $f_\beta(o)$ will be forced to continue with i^+:

$$f_\beta(o) = b^- p^- ds^- i^- \bar{d}p^- ds^- i^- s^- i^+ s^+ \bar{d}p^* ...$$

This is Figure D.199.

Now $f_\beta(r)$ must continue with s^- and to the right of $f_\beta(b)$. Otherwise, $f_\beta(b)$ will be forced to continue with s^+ and to the left of $f_\beta(r)$, in which case it will trace:

$$f_\beta(b) = \bar{d}p^- ds^- i^- \hat{s}^+ i^+ s^+ \bar{d}p^+ di^+ s^+ \bar{d}p^+ b^\times$$

Thus we must have

$$f_\beta(r) = \bar{d}p^- ds^- i^- \hat{s}^- i^+ s^+ \bar{d}p^* ...$$

This is Figure D.200.

Now here $f_\beta(o)$ must continue with p^- and to the right of $f_\beta(r)$. Otherise, $f_\beta(r)$ will be forced to continuew with p^+ and to the left of $f_\beta(o)$, in which case it will be absorbed:

$$f_\beta(r) = \bar{d}p^- ds^- i^- s^- i^+ s^+ \bar{d}p^+ ds^- i^- s^+ i^+ s^+ \bar{d}p^+ di^+ s^+ \bar{d}p^+ b^+ \,\mathrm{Abso}(f_\beta(r), f_\beta(b))^\times$$

or trace:

$$f_\beta(r) = \bar{d}p^- ds^- i^- s^- i^+ s^+ \bar{d}p^+ ds^- i^- s^+ i^+ s^+ \bar{d}p^+ do^= \bar{d}r^\times$$

Thus we must have

$$f_\beta(o) = b^- p^- ds^- i^- \bar{d}p^- ds^- i^- s^- i^+ s^+ \bar{d}\hat{p}^- ds^- i^- s^* ...$$

This is Figure D.201.

Now here $f_\beta(b)$ must continue with s^- and to the right of $f_\beta(o)$. Otherwise, $f_\beta(o)$ will be forced to continue with s^+ and to the left of $f_\beta(b)$, but then it will be absorbed:

$$f_\beta(o) = b^- p^- d s^- i^- \bar{d} p^- d s^- i^- s^- i^+ s^+ \bar{d} p^- d s^- i^- s^+ i^+ s^+ \bar{d} p^+ d \,\mathrm{Abso}(f_\beta(b), f_\beta(r))^\times$$

Thus we must have

$$f_\beta(b) = \bar{d} p^- d s^- i^- s^- i^+ s^+ d p^* ...$$

This is Figure D.202.

If we continue this process, at every step there will be a pair among $f_\beta(r)$, $f_\beta(b)$, and $f_\beta(o)$ situated at p^* or at s^*. The one not among the pair will be situated also at p^* if the pair is at s^* and vice versa. Observing the pair, whichever is on the left must continue counterclockwise and to the right of the one of the right. The argument will always be the following: Suppose the edge of hte left were to not behave like such, then the edge on the right will be forced to continue with counterclockwise and to the left of the left edge. If this edge on the right is $f_\beta(r)$, then it will inevitably "escape" the twisting through $\bar{d}$and be absorbed via traversing the outer perimeter counterclockwise, or trace if it traverses clockwise. If this edge on the right is $f_\beta(b)$, then it will eventually be absorbed between $f_\beta(b)$ and $f_\beta(r)$. If this edge on the right is $f_\beta(o)$, then it will also eventually be absorbed between $f_\beta(b)$ and $f_\beta(r)$.

Therefore this process can never terminate.

This is a contradiction.

Now we go back to the situation depicted in Figure D.198. Let us consider the case when $f_\beta(p)$ ends at s°. We will consider the case when it ends immediately after continuing with

i^-, with the understanding that it could possibly have more twisting.

This situation is shown in Figure D.205.

Now $f_\beta(r)$ and $f_\beta(b)$ will continue with s^- to give us

$$f_\beta(r) = \bar{d}p^- ds^- i^- s^- i^* ...$$

and

$$f_\beta(b) = \bar{d}p^- ds^- i^- s^- i^* ...$$

This is Figure D.206.

Here $f_\beta(o)$ must continue with i^- and to the right of both $f_\beta(r)$ and $f_\beta(b)$. Otherwise, $f_\beta(b)$ will be forced to continue with i^+ and to the left of $f_\beta(o)$, in which case it will eventually trace.

Thus we have

$$f_\beta(o) = f_\beta(o) = b^- p^- ds^- i^- \bar{d}p^- ds^- i^- s^- i^- s^+ \bar{d}p^* ...$$

This is Figure D.207.

Now we are in a similar situation as before, where we have three edges $f_\beta(o)$, $f_\beta(r)$, and $f_\beta(b)$ twisting between p and i. More precisely, at each step a pair among the three will be situated at either p or i, while the lone edge is situated at the other. In each of these steps, the one of the left will need to continue clockwise and to the right of the edge next to it otherwise that edge will eventually trace or be absorbed.

This process never ends.

This is a contradiction.

D.2.2.2.2.1.3 Briefing

Suppose

$$f_\beta(o) = b^\circ$$

This is Figure D.208.

Here $f_\beta(s)$ can continue with o^+ or o° (o^- will cause it to be absorbed between $f_\beta(i)$ and $f_\beta(o)$).

Suppose $f_\beta(s)$ continues with o^+:

$$f_\beta(s) = do^+...$$

Then it continues:

$$f_\beta(s) = do^-\bar{d}p^*...$$

This forces both $f_\beta(b)$ and $f_\beta(r)$ to continue with p^+ and to the left of $f_\beta(s)$. Otherwise, $f_\beta(s)$ will be forced to continue with p^- and to the right of $f_\beta(b)$, which would cause $f_\beta(s)$ to immediately trace. Thus we have

$$f_\beta(r) = \bar{d}p^+do^*..$$

and

$$f_\beta(b) = \bar{d}p^+do^*..$$

This is Figure D.209.

Consider $f_\beta(s)$. It must end at either p° or o°, possibly after some twisting between the two in the form of repeated iterations of p^+o^+ until it ends at one of p° or o°. It cannot possibly

end at s for obvious reasons, and if it were to end at i it will need to pass through s first. Furthermore, if it ever "escapes" the twisting between p and o, if will either be absorbed in some way, either between $f_\beta(b)$ and $f_\beta(r)$, or if it escaped to the outer perimeter, between $f_\beta(i)$ and $f_\beta(o)$, or it traces itself. Let us say $f_\beta(s)$ twist k times.

On the other hand, $f_\beta(p)$ must end at either s or i, also possibly with a number of twists between the two before ending. Let us say $f_\beta(p)$ twist m times.

Once the path of these two edges, $f_\beta(s)$ and $f_\beta(p)$ have been settled, the remaining two: $f_\beta(r)$ and $f_\beta(b)$ will end at the remaining two positions, also possibly with j number of twisting before ending.

This is Candidate Family 7. Shown in Figure D.209.

Now let us go back to the situation depicted in Figure D.208, and suppose $f_\beta(s)$ continues with o°.

Now $f_\beta(r)$ must continue with p^- and to the right of $f_\beta(b)$. Otherwise, $f_\beta(b)$ will be forced to continue with p^+ and to the left of $f_\beta(r)$, which means it will escape to the outer perimeter and will either trace or be absorbed between $f_\beta(i)$ and $f_\beta(o)$.

Thus we have

$$f_\beta(r) = \bar{d}p^- ds^- i^* ...$$

Here note that it must continue with s^- after d, otherwise $f_\beta(p)$ will be forced to start with s^+ and it will trace.

This is Figure D.210.

Here $f_\beta(p)$ must end at either s or i, possibly with k number of twisting between the two before ending. It can never escape this unless it crosses $\bar{d}$, but then it will trace immediately

after. Once the path for $f_\beta(p)$ has been determined, the remaining two edges $f_\beta(r)$ and $f_\beta(b)$ will need to end at the remaining two positions, possibly with m number of twists between the two.

This is Candidate Family 8.

D.2.2.2.2.2 Vision

Back to the end of Shade D.2.2.2.2. Suppose

$$f_\beta(i) = b^*...$$

But now $f_\beta(o)$ will be forced to start with b^+ and to the left of $f_\beta(i)$. Otherwise, $f_\beta(i)$ will be forced to start with b^- and to the right of $f_\beta(o)$, in which case it will trace:

$$f_\beta(i) = \hat{b}^- p^- d s^- i^\times$$

So we must have $f_\beta(o) = b^+....$ But now it will trace:

$$f_\beta(o) = b^+ d o^\times$$

This is a contradiction.

D.2.3 CDG

Back to the end of Case B,C,D D.2. Suppose $f_\beta(\bar{d})$ starts at p, and $f_\beta(d)$ starts at o.

This is Figure D.211.

Consider $f_\beta(s)$. It must go under $f_\beta(b)$ and $f_\beta(r)$. Otherwise it will immediately trace after

crossing d. Thus we have

$$f_\beta(s) = do^*...$$

At the same time we have

$$f_\beta(b) = \bar{d}p^*...$$

and

$$f_\beta(r) = \bar{d}p^*...$$

This is Figure D.212.

Now consider $f_\beta(d)$. If it were to start with o^+, then $f_\beta(s)$ will be forced to continue with o^+ with it, but then it will immediately trace. Thus $f_\beta(d)$ has to start with o^- and to the right of $f_\beta(s)$:

$$f_\beta(d) = o^-\bar{d}...$$

This is Figure D.213.

Now consider $f_\beta(\bar{d})$. If it were to have any initial twists with r or b after starting with p^+, then it could force $f_\beta(r)$ and $f_\beta(b)$ to follow such twists, and at least one of them will trace. Therefore $f_\beta(\bar{d})$ cannot have initial twists, and must start with p^-:

$$f_\beta(\bar{d}) = p^-d...$$

Here the next letter must be s^- and to the right of $f_\beta(p)$. Otherwise $f_\beta(p)$ will be forced to continue with s^+ and will trace immediately after crossing $\bar{d}$. Thus we have

$$f_\beta(\bar{d}) = p^-ds^-...$$

Now the next letter can be i^* or o^-. If it were the former, then after some twisting, it must still eventually at some point continue with o^- to not violate the Trace Lemma. So we have

$$f_\beta(\bar{d}) = p^- d s^- ... o^- \bar{d} ...$$

This is Figure D.214.

But now we are in Situation α.

This is a contradiction.

D.2.4 SYD

Back to the end of Case B,C,D D.2. Suppose $f_\beta(\bar{d})$ starts at p, and $f_\beta(d)$ starts at d.

This is shown in Figure D.215.

Here if the dotted lines do not join, then $f_\beta(d)$ cannot go below $f_\beta(\bar{d})$. Indeed, if $f_\beta(d)$ were to go below $f_\beta(\bar{d})$ and enter in between $f_\beta(\bar{d})$ and $f_\beta(s)$, then it will be in Situation β; if it went under $f_\beta(s)$, then $f_\beta(s)$ will immediately trace.

So suppose the dotted lines do not join, then $f_\beta(d)$ goes above $f_\beta(\bar{d})$. Then it continues:

$$f_\beta(d) = \bar{d} p^+ r^+ d ...$$

Here, after p^+ it has to continue with r^+ and not b^*; otherwise it will not be able to go over an even number of letters before crossing again.

This is Figure D.216.

Now consider $f_\beta(\bar{d})$. If it were to have any initial twists, then it must be with r (due to the position of $f_\beta(d)$). But then the pair $f_\beta(i)$ and $f_\beta(o)$ will follow the twist, above it, and

then cross d together. However, this will force at least one of $f_\beta(i)$ and $f_\beta(o)$ to trace after crossing because they cross d and exit to the right of the triangle, and thus the following letter after d must be one of i or o; but because $f_\beta(i)$ is above $f_\beta(o)$ one of them will trace.

This is depicted in Figure D.217.

Thus $f_\beta(\bar{d})$ cannot have initial twists. This is Figure D.218.

Now notice that $f_\beta(s)$ is in between $f_\beta(d)$ and $f_\beta(\bar{d})$, both of which are heading to the right-hand side of the train track. Consider $f_\beta(\bar{d})$ (the dotted line above $f_\beta(s)$). If it were to continue with o, it cannot be o^- as that would mean going over a single letter between crossing d. Thus it would have to be o^+, but then the next letter cannot be $\bar{d}$ for the same reason, so the next letter has to be s^*. But this will force $f_\beta(s)$ to trace because $f_\beta(s)$ is being forced to follow $f_\beta(\bar{d})$. Therefore, $f_\beta(\bar{d})$ in this situation cannot continue with o^*. So it can only continue with i^+. Continuing, the next letter has to be s^* (in fact it has to be s^+ but this turns out to be irrelevant):

$$f_\beta(\bar{d}) = p^- d i^+ s^* ...$$

This means $f_\beta(s)$ cannot follow $f_\beta(\bar{d})$ to continue with i^+ or it will trace. Thus $f_\beta(s)$ must continue with o^*. But now $f_\beta(d)$, which is below $f_\beta(s)$ is forced to follow $f_\beta(s)$ towards o^*. Notice now the next letter for $f_\beta(d)$ must be $\bar{d}$ again; it is impossible for the next letter to be i^* due to the position of $f_\beta(\bar{d})$.

This is depicted in Figure D.219.

Therefore, the dotted lines, in the situation depicted in Figure D.215 must join. In this

situation, $f_\beta(s)$ can continue with i^* or o^* after crossing:

$$f_\beta(s) = di^*...$$

or

$$f_\beta(s) = do^*...$$

D.2.4.1 Ride

Suppose

$$f_\beta(s) = di^*...$$

Then $f_\beta(p)$ must start with i^- and to the right of $f_\beta(s)$. Otherwise, $f_\beta(s)$ will have to continue with i^- and to the left of $f_\beta(p)$ and thus immediately trace.

Thus we have

$$f_\beta(p) = i^-\bar{d}...$$

This is Figure D.220.

Now consider $f_\beta(o)$. It can start with r^* or b^*:

$$f_\beta(o) = r^*...$$

or

$$f_\beta(o) = b^*...$$

D.2.4.1.1 Spend

Suppose

$$f_\beta(o) = r^*...$$

This is Figure D.221.

Now consider $f_\beta(p)$:

$$f_\beta(p) = i^- \bar{d} r^* ...$$

Here it must continue with r^-. Indeed, if it were to continue with r° or r^+, then the pair $f_\beta(i)$ and $f_\beta(o)$ will be forced to continue with r^+ and to the left of $f_\beta(p)$. But then at least one of them will trace immediately after they cross d.

Thus we must have

$$f_\beta(p) = i^- \bar{d} r^- ...$$

Moreover, it has to go to the right of the pair $f_\beta(i)$ and $f_\beta(o)$. Otherwise the pair will still trace, as before; or $f_\beta(p)$ itself will be absorbed between the pair. But now $f_\beta(p)$ will trace:

$$f_\beta(p) = i^- \bar{d} r^- p^\times$$

This is Figure D.222.

D.2.4.1.2 Acrid

Back to the end of Ride D.2.4.1. Suppose

$$f_\beta(o) = b^* ...$$

This is Figure D.223.

Here $f_\beta(i)$ can start with r^* or b^*:

$$f_\beta(i) = r^* ...$$

or

$$f_\beta(i) = b^*...$$

D.2.4.1.2.1 Jasper

Suppose

$$f_\beta(i) = r^*...$$

Then $f_\beta(p)$ continues with r^* as well:

$$f_\beta(p) = i^- \bar{d} p^*...$$

This is Figure D.224.

Now $f_\beta(i)$ must in fact start with r^-, and to the left of $f_\beta(p)$. Indeed, if it were to start with r^+ it will be absorbed between itself and $f_\beta(o)$; if it were to start with r° then $f_\beta(p)$ will be forced to continue with p^- and be absorbed as well. Thus we have

$$f_\beta(i) = \hat{r}^- d o^*...$$

Now consider $f_\beta(r)$. It must start with s^- and to the right of $f_\beta(b)$. Otherwise, $f_\beta(b)$ will be forced to start with s^+ and to the left of $f_\beta(r)$, and it will trace:

$$f_\beta(b) = s^+ \bar{d} p^+ b^\times$$

But now $f_\beta(r)$ traces:

$$f_\beta(r) = s^- i^- \bar{d} r^\times$$

This is Figure D.225.

This is a contradiction.

D.2.4.1.2.2 Fledge

Back to the end of Acrid D.2.4.1.2. Suppose

$$f_\beta(i) = b^*...$$

This is Figure D.226.

Consider $f_\beta(r)$. It must start with s^- and to the right of $f_\beta(b)$. Otherwise, $f_\beta(b)$ will be forced to start with s^+ and to the left of $f_\beta(r)$, and it will trace:

$$f_\beta(b) = s^+\bar{d}p^+b^\times$$

Thus we have

$$f_\beta(r) = s^-i^-\bar{d}b^*...$$

This forces $f_\beta(p)$ to continue with b^* as well:

$$f_\beta(p) = i^-\bar{d}\hat{b}^*...$$

This is Figure D.227.

Now consider $f_\beta(i)$. It must start with b^+ and to the left of both $f_\beta(r)$ and $f_\beta(r)$. Otherwise, $f_\beta(p)$ will be forced to continue with b^- and immediately trace; and it has to be to the left of $f_\beta(r)$ otherwise it will trace. This forces $f_\beta(o)$ to follow it, and then both cross d to the

right-hand side:

$$f_\beta(i) = b^+ d...$$

and

$$f_\beta(o) = b^+ d...$$

This is Figure D.228.

But now at least one of $f_\beta(i)$ or $f_\beta(o)$ will trace because $f_\beta(i)$ is to the left of $f_\beta(o)$ and i is to the left of o as well.

This is a contradiction.

D.2.4.2 Clam

Back to the end of SYD D.2.4. Suppoe

$$f_\beta(s) = do^*...$$

This is Figure D.229.

Here $f_\beta(o)$ can start with r^* or b^*:

$$f_\beta(o) = r^*...$$

or

$$f_\beta(o) = b^*...$$

D.2.4.2.1 Quail

Suppose

$$f_\beta(o) = r^*...$$

Then $f_\beta(i)$ must start with r^- and to the right of $f_\beta(o)$. Otherwise, $f_\beta(o)$ will be forced to start with r^+ and to the left of $f_\beta(i)$, which will cause it to trace rigth after crossing d.

Thus

$$f_\beta(i) = r^- ...$$

This is Figure D.230.

Here Consider $f_\beta(\bar{d})$. It can either have initial twists or not. Suppose it had no initial twists. Then $f_\beta(i)$ continues with p^-:

$$f_\beta(i) = r^- \hat{p}^- d s^- o^* ...$$

This forces

$$f_\beta(p) = o^* ...$$

This is Figure D.231.

But now $f_\beta(p)$ must continue with o^- and to the right of $f_\beta(s)$. Otherwise, $f_\beta(s)$ will be forced to continue with o^+, which will force it to immediately trace. But now $f_\beta(p)$ will trace:

$$f_\beta(p) = o^- \bar{d} r^- p^\times$$

Thus $f_\beta(\bar{d})$ must have initial twists, and it must be with b, due to the position of $f_\beta(i)$.

In this case we also have that $f_\beta(r)$ must start with s^- and to the right of $f_\beta(b)$. Otherwise, $f_\beta(b)$ will be forced to start with s^- and to the left of $f_\beta(r)$, which will cause it to trace because now $f_\beta(\bar{d})$ has iniital twists with b.

This is Figure D.232.

Consider $f_\beta(p)$. If it were to begin with o^*, then it cannot be o^- as that would lead to it tracing immediately after crossing $\bar{d}$. But then $f_\beta(s)$ must continue with o^+, which would lead it to trace as well.

Thus $f_\beta(p)$ must start with i^* :

$$f_\beta(p) = i^*...$$

This then forces $f_\beta(r)$ to continue with i^*, and in particular i^- and to the right of $f_\beta(p)$ to not cause $f_\beta(p)$ to trace:

$$f_\beta(r) = s^-\hat{i}^-...$$

This is Figure D.233. It then continues:

$$f_\beta(r) = s^-\hat{i}^-\bar{d}p^+b^*...$$

This is Figure D.234.

Now consider $f_\beta(b)$. We claim it must start (and end) with s°. Indeed, if it did not do so, then it must start with s^-. Then it continues

$$f_\beta(b) = s^-i^*...$$

and here it must continue with i^- and to the right of $f_\beta(p)$, otherwise $f_\beta(p)$ will trace. So we have

$$f_\beta(b) = s^-\hat{i}^-\bar{d}p^+b^\times$$

Thus we must have

$$f_\beta(b) = s^\circ$$

On the other hand, $f_\beta(p)$ must also start (and end) at i°. If it did not, then it must start with i^-, as starting with i^+ will cause it to be absorbed between $f_\beta(r)$ and $f_\beta(b)$. So:

$$f_\beta(p) = i^- \bar{d} p^\times$$

Thus we must have

$$f_\beta(p) = i^\circ$$

This is Figure D.235.

Now for the remainder of this section, we will assume that the initial twist of $f_\beta(\bar{d})$ is the simplest it could be, that is, one twist with b:

$$f_\beta(\bar{d}) = p^+ b^- p^- d$$

This is shown in Figure D.236.

We assume this with the understanding that, if we are able to find any train track candidates, any braid that carries it can be modified by adding powers of $\sigma 2^{-1}$ to account for the same train track map but with more initial twists.

Let us now consider $f_\beta(o)$. Suppose it starts (and ends) at r°.

This is Qauil8.

Now consider $f_\beta(i)$. It can continue with p^+, or p°; whereas p^- will cause it to be absorbed between $f_\beta(i)$ and $f_\beta(o)$. Suppose it continues with p^+. Then it continues:

$$f_\beta(i) = r^- \hat{p}^+ r^+ d o^* ...$$

This is Figure D.238.

Here $f_\beta(i)$ must continue with o^+ and to the left of $f_\beta(s)$. Otherwise, $f_\beta(s)$ will be forced to continue with o^- and to the right of $f_\beta(i)$, in which case it will be eventually absorbed between $f_\beta(i)$ and $f_\beta(o)$.

So we must have:

$$f_\beta(i) = r^- p^+ r^+ do^+ \bar{d} p^+ b^* ...$$

This is Figure D.239.

Here $f_\beta(r)$ must continue with b^+ and to the left of $f_\beta(i)$. Otherwise, $f_\beta(i)$ will be forced to continue with b^- and to the right of $f_\beta(r)$, in which case it will eventually be absorbed between $f_\beta(r)$ and $f_\beta(b)$:

$$f_\beta(i) = r^- p^+ r^+ do^+ \bar{d} p^+ \hat{b}^- p^- di^+ s^+ \,\mathrm{Abso}(f_\beta(r), f_\beta(b))^\times$$

Thus we must have

$$f_\beta(r) = s^- i^- \bar{d} p^+ b^+ p^- do^* ...$$

This is Figure D.240.

Now $f_\beta(s)$ must continue with o^+ and to the right of $f_\beta(r)$. Otherwise, $f_\beta(r)$ will be forced to continue with o^- and to the right of $f_\beta(s)$, in which case it will trace after crossing $\bar{d}$.

Thus we must have

$$f_\beta(s) = do^+ \bar{d} p^+ b^* ...$$

This is Figure D.241.

Notice here $f_\beta(s)$, $f_\beta(i)$, and $f_\beta(r)$ are in a three-way counterclockwise path mill between b and o. Indeed, this process continues and never ends. More specifically, notice that we have three edges $f_\beta(s)$, $f_\beta(i)$, and $f_\beta(r)$, and at each step there is always a pair from the three positioned at b or o, while the third edge at the other (b or o). Looking at the pair at each step, the edge of the right will always need to continue counterclockwise and to the left of the edge on the right. Otherwise, the left edge will be forced to either trace, or be absorbed in some way. Thus the edge on the right traverses to the other edge (b or o) to join the third edge, forming the new pair, and the pattern repeats.

This is a contradiction.

Therefore, in the situation depicted in Figure D.237, $f_\beta(i)$ must end at p°.

This is Figure D.242.

This forms our train track map Candidate Family 9, where $f_\beta(r)$ and $f_\beta(s)$ as depicted in Figure D.242 can twist between b and o k times but eventually they have to end there.

Figure D.243 depicts this family with no such twists.

Figure D.244 depicts this family with one such twist. Notice that as soon as one of $f_\beta(r)$ or $f_\beta(s)$ ends, the other is forced to end as well, so they have to twist the same number of times.

This finishes the situation where $f_\beta(o) = r^\circ$. So going back to the situation depicted in Figure D.236, suppose $f_\beta(o)$ does not end at r, then it has to start with r^-:

$$f_\beta(o) = r^- p^* ...$$

This is Figure D.245.

Now if $f_\beta(o)$ were to continue with p^+ and to the left of $f_\beta(i)$, thereby “escape" to the outer

perimeter, then it must continue with:

$$f_\beta(o) = r^- p^+ b^- p^- d s^- i^- \bar{d} p^+ b^* ...$$

This is Figure D.246.

Here $f_\beta(r)$ must continue with b^+ and to the right of $f_\beta(o)$. Otherwise, $f_\beta(o)$ will be forced to continue with b^- and to the right of $f_\beta(r)$, in which case it will eventually be absorbed between $f_\beta(r)$ and $f_\beta(b)$.

Thus we have

$$f_\beta(r) = s^- i^- \bar{d} p^+ b^+ p^- d o^* ...$$

This is Figure D.247.

Here $f_\beta(o)$, $f_\beta(r)$, and $f_\beta(s)$ are stuck in a three-way counterclockwise path mill between o and b. Indeed, we have another unending repeated pattern involving the path of $f_\beta(r)$, $f_\beta(s)$, and $f_\beta(b)$; at the edges o and b. As before, at each step, a pair will be situated at one of these edge, while the third one at the other. At each step, the edge-path on the right, among the pair, must continue counterclockwise, and to the left of the one on the left. Otherwise, the left edge-path will either be absorbed or trace. The right edge-path continues after going counterclockwise and join the third edge-path at the other edge. The cycle then continues.

This is a contradiction. Thus in the situation depicted in Figure D.245, $f_\beta(o)$ cannot continue with p^+ and thereby escape to the outer perimeter. This means that $f_\beta(o)$ can only end at p or r, possibly with twists between the two. Moreover, we claim that $f_\beta(i)$ is also forced to twist among p or r and also end there (end at whichever one $f_\beta(o)$ does not end at). Indeed if $f_\beta(i)$ were to ever escape (possibly after some twisting), then we have the situation depicted in Figure D.248 (depicted with a couple twists before escaping).

Here $f_\beta(r)$, $f_\beta(s)$, and $f_\beta(i)$ are stuck in a three-way counterclockwise path mill between o and b. Indeed, we have the edge-paths $f_\beta(s)$, $f_\beta(i)$, and $f_\beta(r)$. Similar to the previous one, the right edge-path of the pair must continue counterclockwise, and to the left of the left edge-path, and join the third edge-path to form a new pair. This continues ad infinitum. This is a contradiction, thus $f_\beta(i)$ cannot escape.

Therefore, we have arrived at our next family of candidate train track maps, Candidate Family 10, as depicted in Figure D.249. Here $f_\beta(o)$ and $f_\beta(i)$ twist m times between r and p and end there, with twisting direction indicated by the arrows; and $f_\beta(r)$ and $f_\beta(s)$ twist k times between b and o, and end there, with twisting direction indicated by the arrows.

Notice that Candidate Family 9 is contained in this family, so it suffices to consider this family, although for organizational purposes we keep both. Also recall that any braid that carries a train track map from this family must be modified to include the possibility of $f_\beta(\bar{d})$ having more initial twists. This amounts to pre-concatenating σ_2^{-1} j times to any braid β that carries a train track map from this family.

D.2.4.2.2 Imbue

Back to the end of Clam D.2.4.2. Suppose

$$f_\beta(o) = b^*...$$

This is Figure D.250.

Here $f_\beta(\bar{d})$ can have initial twists with b or have no initial twists. Suppose it did have initial twists with b. Then $f_\beta(o)$ is forced to continue:

$$f_\beta(o) = b^- p^- ds^*...$$

This is Figure D.251.

Here $f_\beta(o)$ has to continue with s^- and to the right of $f_\beta(b)$. Otherwise, $f_\beta(b)$ will be forced to start with s^+, and it will trace:

$$f_\beta(b) = s^+ \bar{d} p^+ b^\times$$

Thus we have

$$f_\beta(o) = b^- p^- d s^- i^* ...$$

Here again, $f_\beta(o)$ must continue with i^- and to the right of $f_\beta(p)$. Otherwise $f_\beta(p)$ will be forced to continue with i^+ and it will trace after crossing $\bar{d}$.

Thus we have

$$f_\beta(o) = b^- p^- d s^- \hat{i}^- \bar{d} p^+ b^* ...$$

This is Figure D.252.

Now consider $f_\beta(r)$. It has to start with s^- and to the right of $f_\beta(b)$. Otherwise, $f_\beta(b)$ will be forced to start with s^+, and it will trace, as before. And again for the same reason as that for $f_\beta(o)$, $f_\beta(r)$ must continue with i^- and to the right of $f_\beta(p)$. So we have

$$f_\beta(r) = s^- i^- \bar{d} p^+ b^* ...$$

Now consider $f_\beta(b)$. If it did not end immediately at s°, then it has to begin with $f_\beta(b) = s^- i^* ....$ But then it has to continue with i^-, otherwise $f_\beta(p)$ will be forced to begin with i^+

and it will be absorbed. So now we have

$$f_\beta(b) = s^- p^- \bar{d} p^+ b^\times$$

Thus we must have

$$f_\beta(b) = s^\circ$$

Now consider $f_\beta(p)$. If it did not end immediately at i°, then we either have

$$f_\beta(p) = i^+ s^+ \operatorname{Abso}(f_\beta(r), f_\beta(b))^\times$$

or

$$f_\beta(p) = i^- \bar{d} p^\times$$

Thus we must have

$$f_\beta(p) = i^\circ$$

This is Figure D.253.

For simplicity, we will assume in the following arguments and diagrams that the initial twists of $f_\beta(\bar{d})$ is minimal, i.e. one twist with b, as depicted in Figure D.254. The arguments will still work for any number of initial twists, except one has to add in more twists for any edge-path that traverses this region.

So consider the situation depicted in Figure D.254. Consider $f_\beta(r)$. It has to continue with b^+ and to the left of $f_\beta(o)$. Otherwise, $f_\beta(o)$ will be forced to continue with b^- and to the

right of $f_\beta(r)$, in which case it will be absorbed:

$$f_\beta(o) = b^- p^- d s^- i^- \bar{d} p^+ \hat{b}^- p^- d i^+ s^+ \,\mathrm{Abso}(f_\beta(r), f_\beta(b))^\times$$

Thus we must have

$$f_\beta(r) = s^- i^- \bar{d} p^+ \hat{b}^+ p^- d o^* ...$$

Note that here the letter after crossing d must be o, otherwise $f_\beta(r)$ will escape to the outer perimeter traversing counterclockwise which will lead to it being absorbed between $f_\beta(i)$ and $f_\beta(o)$.

This is Figure D.255.

Here $f_\beta(s)$ has to continue with o^+ and to the left of $f_\beta(r)$. Otherwise, $f_\beta(r)$ will be forced to continue with o^- and to the right of $f_\beta(s)$, in which case it will trace:

$$f_\beta(r) = s^- i^- \bar{d} p^+ b^+ p^- d \hat{o} o^- \bar{d} r^\times$$

Thus we must have

$$f_\beta(s) = d o^+ \bar{d} p^+ b^* ...$$

This is Figure D.256.

Here $f_\beta(o)$ must continue with b^+ and to the left of $f_\beta(s)$. Otherwise, $f_\beta(s)$ will be forced to continue with b^- and to the right of $f_\beta(o)$, in which case it will be absorbed:

$$f_\beta(s) = d o^+ \bar{d} p^+ b^- p^- d i^+ s^+ \,\mathrm{Abso}(f_\beta(r), f_\beta(b))^\times$$

Thus $f_\beta(o)$ must continue with b^+, but now it will trace:

$$f_\beta(o) = b^- p^- d s^- i^- \bar{d} p^+ b^+ p^- d o^\times$$

This is Figure D.257.

Therefore we can conclude that $f_\beta(\bar{d})$ cannot have any initial twists. Thus we must have the sitaution depicted in Figure D.258.

Here $f_\beta(i)$ can either start with b^* or r^*.

Suppose $f_\beta(i)$ starts with b^*. Then it must in fact be b^- and to the right of $f_\beta(o)$. Otherwise $f_\beta(o)$ will be forced to start with b^+ and to the left of $f_\beta(i)$, in which case it will trace immediately after crossing d. So $f_\beta(i)$ must start with b^-, and continue:

$$f_\beta(i) = b^- p^- d s^* ...$$

Now here it must continue with s^-. Otherwise, $f_\beta(b)$ will be forced to start with s^+ and to the left of $f_\beta(i)$, in which case it will trace:

$$f_\beta(b) = s^+ \bar{d} p 6 + b^\times$$

Thus $f_\beta(i)$ must continue with s^-. But then it will now trace:

$$f_\beta(i) = b^- p^- d \hat{s}^- i^\times$$

Thus we must have

$$f_\beta(i) = r^* ...$$

Here it can be

$$f_\beta(i) = r^\circ$$

or

$$f_\beta(i) = r^+...$$

D.2.4.2.2.1 Zither

Suppose

$$f_\beta(i) = r^\circ$$

This is Figure D.259.

Now consider $f_\beta(r)$. It has to begin with s^- and to the right of $f_\beta(b)$. Otherwise, $f_\beta(b)$ will be forced to begin with s^+ and to the left of $f_\beta(r)$, in which case it will trace:

$$f_\beta(b) = s^+ \bar{d} p^+ b^\times$$

Thus we have

$$f_\beta(r) = s^- i^*...$$

Here $f_\beta(r)$ has to continue with i^- and to the right of $f_\beta(p)$. Otherwise, $f_\beta(p)$ will be forced to begin with i^+ and to the left of $f_\beta(r)$, in which case it will trace:

$$f_\beta(p) = i^+ s^+ \bar{d} p^\times$$

Thus we have

$$f_\beta(r) = s^- \hat{i}^- \bar{d} p^*...$$

This is Figure D.260.

Consider $f_\beta(o)$. It can begin with b°, or b^-.

D.2.4.2.2.1.1 Abandon

Suppose

$$f_\beta(o) = b^\circ$$

This is Figure D.261.

Consider $f_\beta(s)$. It can continue with o°, or o^+ (here o^- is not possible as that would cause it to be absorbed between $f_\beta(i)$ and $f_\beta(o)$).

D.2.4.2.2.1.1.1 Jubilant

Suppose $f_\beta(s)$ continues with o°:

$$f_\beta(s) = do^\circ$$

This is depicted in Figure D.262.

Consider $f_\beta(p)$. It can begin and end at i°, or it can continue with i^+. Here i^- is not possible, as it would trace right after crossing $\bar{d}$:

$$f_\beta(p) = i^- \bar{d} p^\times$$

Suppose

$$f_\beta(p) = i^\circ$$

This is Figure D.263.

Here we have Candidate Family given by Figure D.263, where $f_\beta(r)$ and $f_\beta(b)$ end at p or i, after possibly k twists between the two. In Figure D.264, we have drawn the train track map from this family with one twist, in which case $f_\beta(b)$ ends at p, and $f_\beta(r)$ ends at s.

This is Candidate Family 11.

Now suppose in the situation depicted in Figure D.262, that $f_\beta(p)$ continues with i^+:

$$f_\beta(p) = i^+ s^* ...$$

Now $f_\beta(b)$ must begin with s^- and to the right of $f_\beta(p)$. Otherwise, $f_\beta(p)$ will immediately be absorbed between $f_\beta(r)$ and $f_\beta(b)$. So we have

$$f_\beta(b) = s^- i^- \bar{d} p^* ...$$

This is Figure D.265.

Here $f_\beta(r)$ must continue with p^- and to the right of $f_\beta(b)$. Otherwise, $f_\beta(b)$ will be forced to continue with p^+ and to the left of $f_\beta(r)$, in which case it will escape to the outer perimeter, and will be absorbed:

$$f_\beta(b) = s^- i^- \bar{d} \hat{p}^+ d o^- \bar{d} r^- \, \mathrm{Abso}(f_\beta(i), f_\beta(o))^\times$$

or trace:

$$f_\beta(b) = s^- i^- \bar{d} \hat{p}^+ d i^+ s^+ \bar{d} p^+ b^\times$$

Thus we must have

$$f_\beta(r) = s^- i^- \bar{d} \hat{p}^- d i^+ s^* ...$$

This is Figure D.266.

Here $f_\beta(p)$ must end at either s or i, after possibly twisting between the two. It must end here because if it ever "escapes" this region, it must do so by crossing $\bar{d}$, which would cause it to immediately trace after crossing. So after possibly k number of twisting, $f_\beta(p)$ ends at either s or i; and $f_\beta(r)$ will be forced to twist with it some number of times. The remaining two edge-paths, $f_\beta(r)$ and $f_\beta(b)$ will end at either p, or at the other remaining edge available. The two can possibly also twist m times among the two possibilities before ending. This is train track Candidate Family 12.

In Figure D.267, we have depicted an example of a train track map from this family. In his example, $f_\beta(p)$ twists once, ending at i. On the other hand, $f_\beta(b)$ and $f_\beta(r)$ twist also once, so $f_\beta(b)$ does not end at p, but traverses to s and end there; this forces $f_\beta(r)$ to continue with s^- and traverse to p to end there.

D.2.4.2.2.1.1.2 Emergency

Back to the end of Abandon D.2.4.2.2.1.1. Suppose $f_\beta(s)$ continues with o^+ (in the situation depicted in Figure D.261):

$$f_\beta(s) = d\hat{o}^+\bar{d}p^*...$$

This is Figure D.268.

Here $f_\beta(s)$ can continue with p^-, p°, or p^+.

D.2.4.2.2.1.1.2.1 Landscape

Suppose $f_\beta(s)$ continues with p^-:

$$f_\beta(s) = do^+\bar{d}p^-...$$

Then it has to go to the right of $f_\beta(r)$. Otherwise $f_\beta(s)$ will escape to the outer perimeter and either trace:

$$f_\beta(s) = do^+ \bar{d}\hat{p}^- di^+ s^\times$$

or be absorbed:

$$f_\beta(s) = do^+ \bar{d}\hat{p}^- do^- \bar{d}r^- \text{Abso}(f_\beta(i), f_\beta(o))^\times$$

Thus we must have

$$f_\beta(s) = do^+ \bar{d}\hat{p}^- di^* ...$$

This is Figure D.269.

Now $f_\beta(s)$ has to continue with i^+ and to the left of $f_\beta(p)$. Otherwise $f_\beta(p)$ will be forced to begin with i^- and to the right of $f_\beta(s)$, in which case it will trace after crossing $\bar{d}$. But now $f_\beta(s)$ will trace:

$$f_\beta(s) = do^+ \bar{d}p^- di^+ s^\times$$

This is a contradiction.

D.2.4.2.2.1.1.2.2 Treasure

Back to the end of Emergency D.2.4.2.2.1.1.2 . Suppose $f_\beta(s)$ continues with p°:

$$f_\beta(s) = do^+ \bar{d}p^\circ$$

Then $f_\beta(r)$ is forced to continue with p^+:

$$f_\beta(r) = s^- i^- \bar{d}p^+ do^* ...$$

This is Figure D.270.

Here $f_\beta(p)$ needs to end at either i or s, after possibly twisting k times between the two. Indeed, if it ever escapes this region it would have to do so by crossing $\bar{d}$, in which case it will immediately trace after crossing.

Once $f_\beta(p)$ ends, at either i or s, we will have two remaining edge-paths: $f_\beta(b)$ and $f_\beta(r)$, and two edges remaining that they can end at: $f_\beta(o)$ and i or s, whichever is the one that $f_\beta(p)$ did not end at. Here $f_\beta(b)$ and $f_\beta(r)$ can possibly twist m times between the two edges before ending.

This gives us Candidate family 13.

In Figure D.271, we have depicted a train track map from this family, where $f_\beta(p)$ twists once to end at s, and $f_\beta(b)$ and $f_\beta(r)$ twist once as well.

D.2.4.2.2.1.1.2.3 Education

Back to the end of Emergency D.2.4.2.2.1.1.2. Suppose $f_\beta(s)$ continues with p^+:

$$f_\beta(s) = do^+\bar{d}\hat{p}^+do^*...$$

and $f_\beta(r)$ follows:

$$f_\beta(s) = s^-i^-\bar{d}\hat{p}^+do^*...$$

This is Figure D.272.

Here, as before, $f_\beta(p)$ must end at either i or s, after possibly twisting between the two. On the other hand, $f_\beta(s)$ must end at either o or p, after possibly twisting between the two. Note that it is impossible for $f_\beta(s)$ to end at i without tracing, as that would force $f_\beta(p)$ to exit the region, i.e. cross $f_\beta(\bar{d})$ and thus trace.

Once the paths of $f_\beta(p)$ and $f_\beta(s)$ have been established, $f_\beta(r)$ and $f_\beta(b)$ end at the remaining two available edges, possibly twisting between the two.

In Figure D.273 we have depicted an example train track map from this family..

This is 12 (combined with 11)

D.2.4.2.2.1.2 Hapless

Back to the end of Zither D.2.4.2.2.1. Suppose

$$f_\beta(o) = b^- ...$$

Then it continues:

$$f_\beta(o) = b^- p^- d s^- i^- \bar{d} p^* ...$$

This is Figure D.274.

Here $f_\beta(s)$ can continue with o^+ or o°, as o^- will cause it to be absorbed between $f_\beta(i)$ and $f_\beta(o)$.

Suppose it were to continue with o^+, then

$$f_\beta(s) = d\hat{o}^+ \bar{d} p^* ...$$

This is Figure D.275.

Here it has to continue with p^- and to the right of $f_\beta(o)$. Otherwise $f_\beta(o)$ will be forced to continue with p^+ and to the left of $f_\beta(s)$ and trace immediately after crossing d. Furthermore,

$f_\beta(s)$ as to go to the right of $f_\beta(r)$ as well. Otherwise, $f_\beta(s)$ itself will trace:

$$f_\beta(s) = do^+ \bar{d}\hat{p}^- di^+ s^\times$$

Thus it has to continue with p^- and to the right of both $f_\beta(o)$ and $f_\beta(r)$:

$$f_\beta(s) = do^+ \bar{d}\hat{p}^- di^* ...$$

This is Figure D.276.

Here $f_\beta(p)$ must start with i^- and to the right of $f_\beta(s)$. Otherwise, $f_\beta(s)$ will be forced to continue with i^+ and to the left of $f_\beta(i)$, in which case it will immediately trace. But now $f_\beta(p)$ will trace:

$$f_\beta(p) = i^- \bar{d}p^\times$$

Therefore, in the situation depicted in Figure D.274, we must have

$$f_\beta(s) = do^\circ$$

This is Figure D.277.

Now consider $f_\beta(o)$. It must continue with p^- and to the right of $f_\beta(r)$. Otherwise, $f_\beta(r)$ will be forced to continue with p^+ and to the left of $f_\beta(o)$, in which case it will escape to the outer perimeter and either trace, or be absorbed between $f_\beta(i)$ and $f_\beta(o)$. Thus we have

$$f_\beta(o) = b^- p^- ds^- i^- \bar{d}\hat{p}^- di^* ...$$

This is Figure D.278.

Here $f_\beta(o)$ must continue with i^+ and to the left of $f_\beta(p)$. Otherwise, $f_\beta(p)$ will be forced to start with i^- and to the right of $f_\beta(o)$, in which case it will trace immediately after crossing $\bar{d}$. So we have

$$f_\beta(o) = b^- p^- d s^- i^- \bar{d} p^- d i^+ s^* ...$$

Now $f_\beta(b)$ is forced to start with s^- and to the right of $f_\beta(o)$. Otherwise, $f_\beta(o)$ will be immediately absorbed between $f_\beta(r)$ and $f_\beta(b)$. Thus we must have

$$f_\beta(b) = s^- i^- \bar{d} p^* ...$$

This is Figure D.279.

Here $f_\beta(p)$ must end at i or s after possibly some number of twisting between the two. For the following argument, we assume that $f_\beta(p) = i^\circ$, with the understanding that the argument can be easily modified if there were more twists. Specifically, any image path will follow the twists in this region, and if $f_\beta(p)$ in fact ended at s, then in our argument i is replaced by s.

This is Figure D.280.

Here $f_\beta(r)$ must continue with p^- and to the right of $f_\beta(b)$. Otherwise, $f_\beta(b)$ will be forced to continue with p^+ and to the left of $f_\beta(b)$, in which case it will trace:

$$f_\beta(b) = s^- i^- \bar{d} \hat{p}^+ d i^+ s^+ \bar{d} p^+ b^\times$$

Thus we must have

$$f_\beta(r) = s^- i^- \bar{d} \hat{p}^- d i^+ s^* ...$$

This is Figure D.281.

Here $f_\beta(o)$ must continue with s^- and to the right of $f_\beta(r)$. Otherwise, $f_\beta(r)$ will be forced to continue with s^+ and to the left of $f_\beta(o)$, in which case it will escape to the outer perimeter and thus either trace or be absorbed between $f_\beta(i)$ and $f_\beta(o)$.

This pattern continues and never ends. More specifically, we have three edge-paths situated on two edges: p and s, where a pair among the three at one and the other edge-path at the other edge. The left edge-path among the pair will always continue with clockwise traversal and to the right of the edge-path on the right. Otherwise, the edge-path on the right will be forced to continue with counterclockwise traversal and to the left of the edge-path on the left, in which case this right edge-path will inevitably escape to the outer perimeter and trace or be absorbed. Thus the left-edge path will now join the other lone edge-path at the other edge after traversing clockwise. The cycle then repeats.

This is a contradiction.

D.2.4.2.2.2 Unwary

Back to the end of Imbue D.2.4.2.2. Suppose

$$f_\beta(i) = r^+...$$

Then it continues:

$$f_\beta(i) = r^+do^*...$$

This is Figure D.282.

Here it has to continue with o^+ and to the left of $f_\beta(s)$. Otherwise, $f_\beta(s)$ will be forced to

continue with o^- and to the right of $f_\beta(i)$, and be absorbed:

$$f_\beta(s) = d\hat{o}^- \bar{d}r^- \text{Abso}(f_\beta(i), f_\beta(o))^\times$$

Thus we must have

$$f_\beta(i) = r^+ d\hat{o} + \bar{d}p^* ...$$

This is Figure D.283.

Here $f_\beta(r)$ must continue with p^+ and to the left of $f_\beta(i)$. Otherwise, $f_\beta(i)$ will be forced to continue with p^- and to the right of $f_\beta(r)$, in which case it will trace:

$$f_\beta(i) = f_\beta(i) = r^+ do^+ \hat{p}^- di^\times$$

Thus we must have

$$f_\beta(r) = s^- i^- \bar{d}\hat{p}^+ do^* ...$$

This is Figure D.284.

Here $f_\beta(s)$ must continue with o^+ and to the left of $f_\beta(r)$. Otherwise, $f_\beta(r)$ will be forced to continue with o^- and to the right of $f_\beta(s)$, in which case it will immediately trace after crossing $\bar{d}$.

Thus we must have

$$f_\beta(s) = d\hat{o}^+ \bar{d}p^* ...$$

This is Figure D.285.

Here $f_\beta(i)$ must continue with p^+ and to the left of $f_\beta(s)$. Otherwise, $f_\beta(s)$ will be forced to

continue with p^- and to the right of $f_\beta(i)$, in which case it will escape to the outer perimeter, and either trace, or be absorbed between $f_\beta(i)$ and $f_\beta(o)$.

Thus we must have

$$f_\beta(i) = r^+ do^+ \bar{d}\hat{p}^+ do^* ...$$

This is Figure D.286.

Here $f_\beta(r)$ must continue with o^+ and to the left of $f_\beta(i)$. Otherwise, $f_\beta(i)$ will be forced to continue with o^- and to the right of $f_\beta(r)$, in which case it will trace:

$$f_\beta(i) = r^+ do^+ \bar{d}p^+ do^- \bar{d}p^- di^\times$$

Thus we must have

$$f_\beta(r) = s^- i^- \bar{d}p^+ do^+ \bar{d}o^* ...$$

This pattern continues. We are in a counterclockwise path mill, with edge paths $f_\beta(s)$, $f_\beta(r)$, and $f_\beta(i)$; situated at p and o. If the counterclockwise traversal is not respected, $f_\beta(r)$ and $f_\beta(i)$ could trace, and $f_\beta(s)$ could escape to the outer perimeter.

This is a contradiction.

D.2.5 DXB

Back to the end of Case B,C,D D.2. Suppose $f_\beta(\bar{d})$ starts at b, and $f_\beta(d)$ starts at s.

Here $f_\beta(\bar{d})$ can possibly have initial twists with p, but it must eventually traverse $...b^+d...$ (after an odd number of letters).

This is depicted in Figure D.287.

Here the pair $f_\beta(i)$ and $f_\beta(o)$ must go above $f_\beta(p)$. Otherwise at least one of $f_\beta(i)$ or $f_\beta(o)$ will trace. Thus we have

$$f_\beta(i) = ds^*...$$

and

$$f_\beta(o) = ds^*...$$

Now $f_\beta(p)$ can either go above or below $f_\beta(\bar{d})$. Suppose it went below. Then after crossing it must go to r^*, and not b^-, as the latter would cause it to trace immediately, regardless if $f_\beta(\bar{d})$ has any initial twists.

This is Figure D.288.

Now consider $f_\beta(d)$. It must start with s^+ and to the left of $f_\beta(i)$, otherwise the pair $f_\beta(i)$ and $f_\beta(o)$ will be forced to continue with s^- and to the right of $f_\beta(d)$, and then at least one of the two will trace immediately. Thus we have

$$f_\beta(s) = s^+...$$

This is Figure D.289.

But now notice $f_\beta(\bar{d})$ must continue with s^+ or s^-, both of which will cause it to violate the Trace Lemma, as the next letter will have to be $\bar{d}$ in both situations.

This is a contradiction. Thus $f_\beta(p)$ must go above $f_\beta(\bar{d})$:

$$f_\beta(p) = \bar{d}b^*...$$

This is Figure D.290.

Now this forces $f_\beta(\bar{d})$ to not have any initial twists, as any such twist will bring $f_\beta(p)$ with it to p, tracing it.

This is Figure D.291.

Now $f_\beta(\bar{d})$ can continue with i^* or o^*.

D.2.5.1 Zero

Suppose $f_\beta(\bar{d})$ continues with i^*. Then it in fact has to continue with i^+ in order to not violate the Trace Lemma:

$$f_\beta(\bar{d}) = b^+ d\hat{i}^+ s^+ ...$$

and here it has to go to the left of $f_\beta(i)$ and $f_\beta(o)$, otherwise $f_\beta(i)$ will trace. It continues:

$$f_\beta(\bar{d}) = b^+ d i^+ \hat{s}^+ \bar{d} p^+ ...$$

and here it has to go to the left of $f_\beta(s)$ or $f_\beta(s)$ will trace after crossing d. It continues:

$$f_\beta(\bar{d}) = b^+ d i^+ \hat{s}^+ \bar{d} p^+ b^+ \bar{d} ...$$

This is Figure D.292. Here we are in a situation where $f_\beta(\bar{d})$ continues to circle the outer perimeter counterclockwise and never ends. It cannot go up to o^*, as that would mean violating the Trace Lemma.

This is a contradiction.

D.2.5.2 Dome

Back to the end of DXB. Suppose $f_\beta(\bar{d})$ continues with o^*. Then in fact it has to be o^+ and then s^*, otherwise it will violate the Trace Lemma:

$$f_\beta(\bar{d}) = b^+ d\hat{o}^+ s^* ...$$

This forces both $f_\beta(b)$ and $f_\beta(r)$ to begin with o^*.

This is Figure D.293.

Now $f_\beta(\bar{d})$ must continue with s^+, and to the left of $f_\beta(i)$ and $f_\beta(o)$. Otherwise, both $f_\beta(i)$ and $f_\beta(o)$ will be forced to continue with s^- and to the right of $f_\beta(\bar{d})$, in which case at least one of them will immediately trace. So we must have

$$f_\beta(\bar{d}) = b^+ do^+ \hat{s}^+ \bar{d} p^* ..$$

This is Figure D.294.

Here $f_\beta(\bar{d})$ must continue with p^+ and to the left of $f_\beta(s)$. Otherwise, $f_\beta(s)$ will be forced to start with p^- and to the right of $f_\beta(\bar{d})$, and it will immediately trace after crossing d. Thus we must have

$$f_\beta(\bar{d}) = b^+ do^+ s^+ \bar{d} \hat{p}^+ b^+ d...$$

This is Figure D.295.

Here we see that $f_\beta(\bar{d})$ will continue to traverse the outer perimeter counterclockwise, and never ends.

This is a contradiction.

D.2.6 PHX

Back to the end of Case B,C,D D.2. Suppose $f_\beta(\bar{d})$ starts at b, and $f_\beta(d)$ starts at i.

This is Figure D.296.

Here the pair $f_\beta(b)$ and $f_\beta(r)$ cannot go below the pair $f_\beta(i)$ and $f_\beta(o)$. This is because if that were the case, either $f_\beta(r)$ or $f_\beta(r)$ will immediately trace; if the pair $f_\beta(r)$ and $f_\beta(b)$ went above $f_\beta(\bar{d})$ then $f_\beta(b)$ will trace, while if the pair went below $f_\beta(\bar{d})$ then $f_\beta(r)$ will trace. Therefore, the pair $f_\beta(b)$ and $f_\beta(r)$ must go above the pair $f_\beta(i)$ and $f_\beta(o)$. But now either $f_\beta(i)$ or $f_\beta(o)$ will trace immediatley after crossing d.

This is a contradiction.

D.2.7 MIA

Back to the end of Case B,C,D D.2. Suppose $f_\beta(\bar{d})$ starts at b, and $f_\beta(d)$ starts at o.

This is Figure D.297.

Here the situation is esesentially identical to that of PHX D.2.6. In fact we can repeat the same argument to conclude that no such train track map exist; the difference in the starting position of $f_\beta(d)$ is of no consequence.

D.2.8 NRT

Back to the end of Case B,C,D D.2. Suppose $f_\beta(\bar{d})$ starts at b, and $f_\beta(d)$ starts at d.

This is Figure D.298.

Here $f_\beta(i)$ and $f_\beta(o)$ have to go above $f_\beta(d)$. Otherwise, at leat one of them will immediately trace after crossing d. OS we have

$$f_\beta(i) = ds^*...$$

and

$$f_\beta(o) = ds^*...$$

This is Figure D.299.

Here $f_\beta(r)$ and $f_\beta(b)$ have to start with s^+ and to the left of both $f_\beta(i)$ and $f_\beta(o)$. Otherwise, both $f_\beta(i)$ and $f_\beta(o)$ will be forced to continue with s^- and to the right of $f_\beta(b)$, in which case at least one of $f_\beta(i)$ or $f_\beta(o)$ will trace. Thus we have

$$f_\beta(r) = s^+\bar{d}p^*...$$

and

$$f_\beta(b) = s^+\bar{d}p^*...$$

This is Figure D.300.

Here $f_\beta(b)$ must continue with p^+ and to the left of $f_\beta(s)$. Otherwise, $f_\beta(s)$ will be forced to begin with p^- and to the right of $f_\beta(b)$, and will trace:

$$f_\beta(s) = p^- ds^\times$$

But now $f_\beta(b)$ will trace:

$$f_\beta(b) = s^+\bar{d}\hat{p}^+b^\times$$

This is a contradiction.

D.2.9 ARN

Back to the end of Case B,C,D D.2. Suppose $f_\beta(\bar{d})$ starts at r, and $f_\beta(d)$ starts at s.

This is Figure D.301.

Similar to the previous cases, in order for $f_\beta(\bar{d})$ to run over an odd number of letters before crossing d, it must do so by traversing b^+ right before crossing, possibly after some number of twisting with p and/or b.

Consider $f_\beta(p)$. It must go below the pair $f_\beta(i)$ and $f_\beta(o)$ in order to not immediately trace. On the other hand, it has to also go above $f_\beta(\bar{d})$, otherwise it will trace, regardless if $f_\beta(\bar{d})$ has any initial twists:

$$f_\beta(p) = \bar{d}r^- p^\times$$

Thus we must have

$$f_\beta(p) = \bar{d}r^* ...$$

and

$$f_\beta(i) = ds^* ...$$

and

$$f_\beta(o) = ds^* ...$$

Now notice that due to the position of $f_\beta(p)$, $f_\beta(\bar{d})$ cannot have any initial twists, as any such twists will have to start with r^-, and then twisting with p. This would cause $f_\beta(p)$ to trace since it will have to follow $f_\beta(\bar{d})$.

This is Figure D.302.

Now here $f_\beta(\bar{d})$ can either continue with i^*:

$$f_\beta(\bar{d}) = r^+ di^* ...$$

or continue with o^*:

$$f_\beta(\bar{d}) = r^+ do^* ...$$

D.2.9.1 Corf

Suppose $f_\beta(\bar{d})$ continues with i^*:

$$f_\beta(\bar{d}) = r^+ di^* ...$$

Then it must in fact be i^+ and to the left of $f_\beta(r)$ and $f_\beta(b)$ to not violate the Trace Lemma. It also must It then continues:

$$f_\beta(\bar{d}) = r^+ di^+ s^* ...$$

This is Figure D.303.

Here $f_\beta(\bar{d})$ must continue with s^+ and to the left of $f_\beta(i)$. Otherwise, $f_\beta(i)$ will be forced to continue with s^- and to the right of $f_\beta(\bar{d})$, and will immediately trace.

Thus we must have:

$$f_\beta(\bar{d}) r^+ di^+ \hat{s}^+ \bar{d} p^* ...$$

This is Figure D.304.

Here $f_\beta(\bar{d})$ must continue with p^+ and to the left of $f_\beta(s)$. Otherwise, $f_\beta(s)$ will be forced to begin with p^- and to the right of $f_\beta(\bar{d})$, in which case it will immediately trace right after crossing d.

Thus we must have

$$f_\beta(\bar{d}) = r^+ di^+ s^+ \bar{d} \hat{p}^+ ...$$

This is Figure D.305.

Here in order to not violate the Trace Lemma, $f_\beta(\bar{d})$ must eventually traverse r^+ and cross d, possibly after some twisting between b and p. But now $f_\beta(\bar{d})$ will continue to traverse the outer perimeter counterclockwise, and will never be able to join with $f_\beta(d)$.

This is a contradiction.

D.2.9.2 Woad

Back to the end of ARN D.2.9. Suppose $f_\beta(\bar{d})$ continues with o^*:

$$f_\beta(\bar{d}) = r^+ do^* ...$$

Then in fact it must continue with $o^+ s^* ...$ to not violate the Trace Lemma.

This is Figure D.306.

This situation is very similar to that depicted in Figure D.303; and indeed here we can repeat the arguments of D.2.9.1, starting with the situation depicted in Figure D.303, to eventually conclude that $f_\beta(\bar{d})$ must continue traversing indefinitely the outer perimeter countercloclwise.

This is a contradiction.

D.2.10 ICN

Back to the end of Case B,C,D D.2. Suppose $f_\beta(\bar{d})$ starts at r, and $f_\beta(d)$ starts at i.

This is ICM1.

Here the pair $f_\beta(i)$ and $f_\beta(o)$ must go abnove the pair $f_\beta(r)$ and $f_\beta(b)$. Otherwise, at least

one of $f_\beta(i)$ or $f_\beta(o)$ will immediately trace after crossing d. So we must have

$$f_\beta(i) = ds^*...$$

and

$$f_\beta(o) = ds^*...$$

This is ICM2.

Here the pair $f_\beta(i)$ and $f_\beta(o)$ must continue with s^- and to the right of $f_\beta(p)$. Otherwise, $f_\beta(p)$ will be forced to continue with s^+ and to the left of s, in which case it will immediately trace after crossing $\bar{d}$. But now $f_\beta(i)$ traces.

This is a contradiction.

D.2.11 SIN

Back to the end of Case B,C,D D.2. Suppose $f_\beta(\bar{d})$ starts at r, and $f_\beta(d)$ starts at o.

This is Figure D.307.

Repeat the argument of ICN D.2.10, except for the last sentence, wherein we have $f_\beta(o)$ traces instead.

This is a contradiction.

D.2.12 PRG

Back to the end of Case B,C,D D.2. Suppose $f_\beta(\bar{d})$ starts at r, and $f_\beta(d)$ starts at d.

This is PRA1.

Suppose here that the dotted lines do not join, and $f_\beta(\bar{d})$ on the left goes below $f_\beta(d)$ on

the right. Then $f_\beta(d)$ cannot go below $f_\beta(i)$ and $f_\beta(o)$, as that would cause it to violate the Trace Lemma immediately. Thus it must go above $f_\beta(i)$ and $f_\beta(o)$. But now $f_\beta(i)$ or $f_\beta(o)$ will immediately trace after crossing d. This is a contradiction.

So suppose instead either $f_\beta(\bar{d})$ on the left goes above $f_\beta(d)$ on the right, or the dotted lines join. Then this forces

$$f_\beta(i) = ds^*...$$

and

$$f_\beta(o) = ds^*...$$

This is PRA1.

Here $f_\beta(r)$ and $f_\beta(b)$ must begin with s^+ and to the left of $f_\beta(i)$ and $f_\beta(o)$. Otherwise, $f_\beta(i)$ and $f_\beta(o)$ will be forced to continue with s^- and to the right of $f_\beta(r)$ and $f_\beta(b)$. in which case at least one of $f_\beta(i)$ or $f_\beta(o)$ will immediately trace. Thus we must have

$$f_\beta(r) = s^+\bar{d}p^*...$$

and

$$f_\beta(b) = s^+\bar{d}p^*...$$

This is PRA3.

Here $f_\beta(r)$ and $f_\beta(b)$ must continue with p^+ and to the left of $f_\beta(s)$. Otherwise, $f_\beta(s)$ will be forced to begin with p^- and to the right of $f_\beta(r)$ and $f_\beta(b)$, in which case it will immediately trace right after crossing d. But now at least one of $f_\beta(r)$ or $f_\beta(b)$ will trace.

This is a contradiction.

D.3 Figures

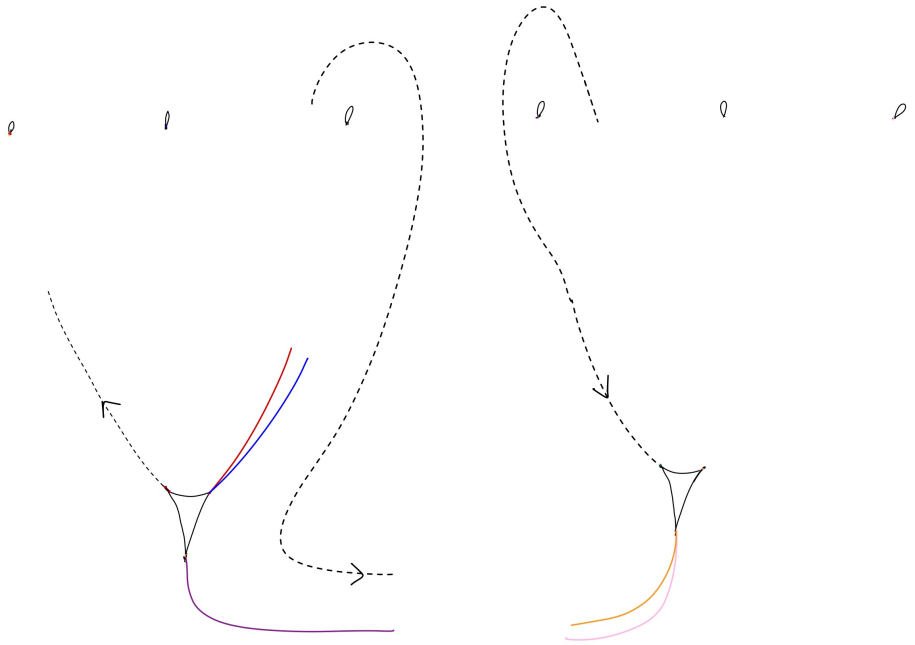


Figure D.2: AVX1

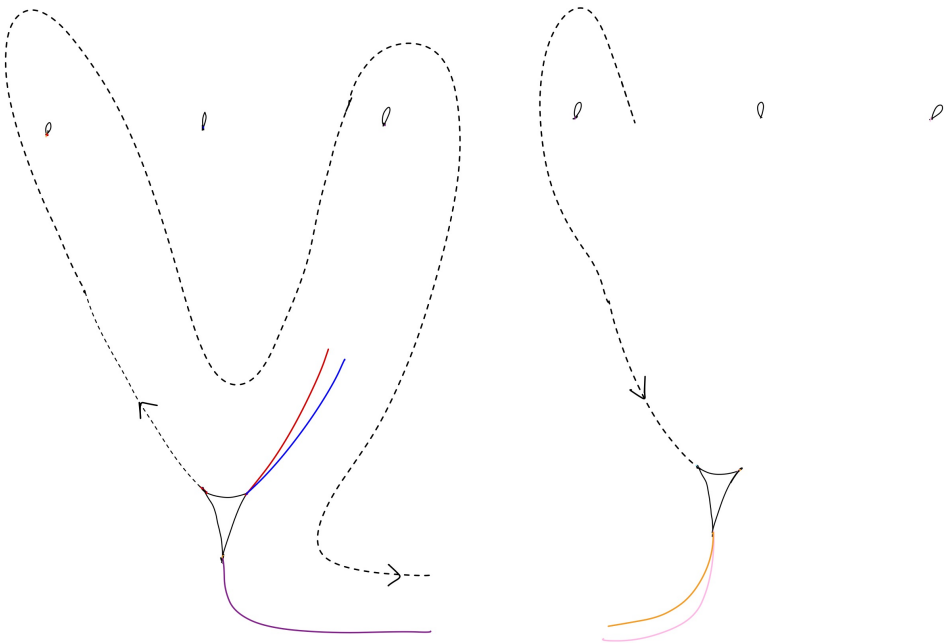


Figure D.3: AVX2

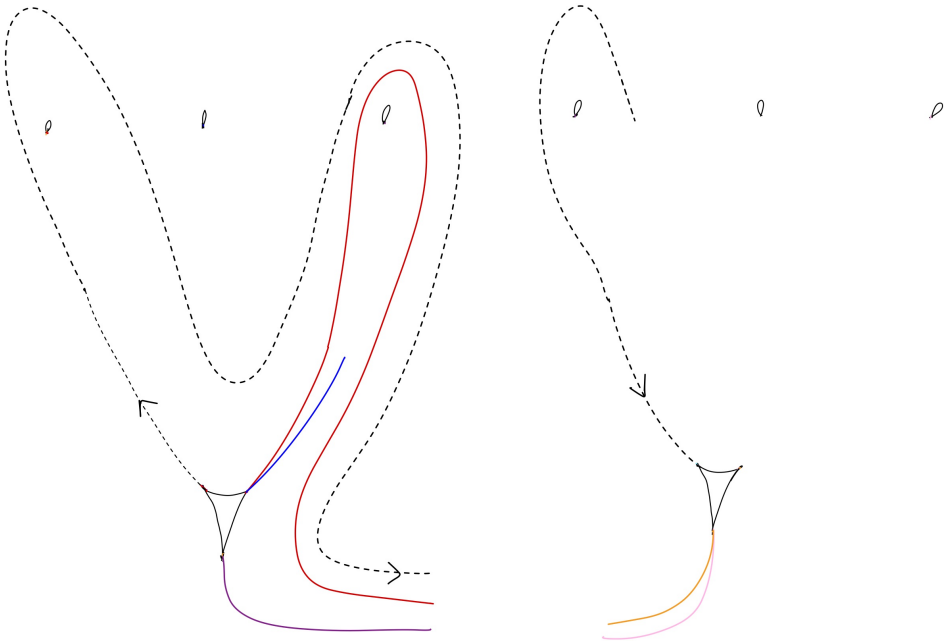


Figure D.4: Phil1

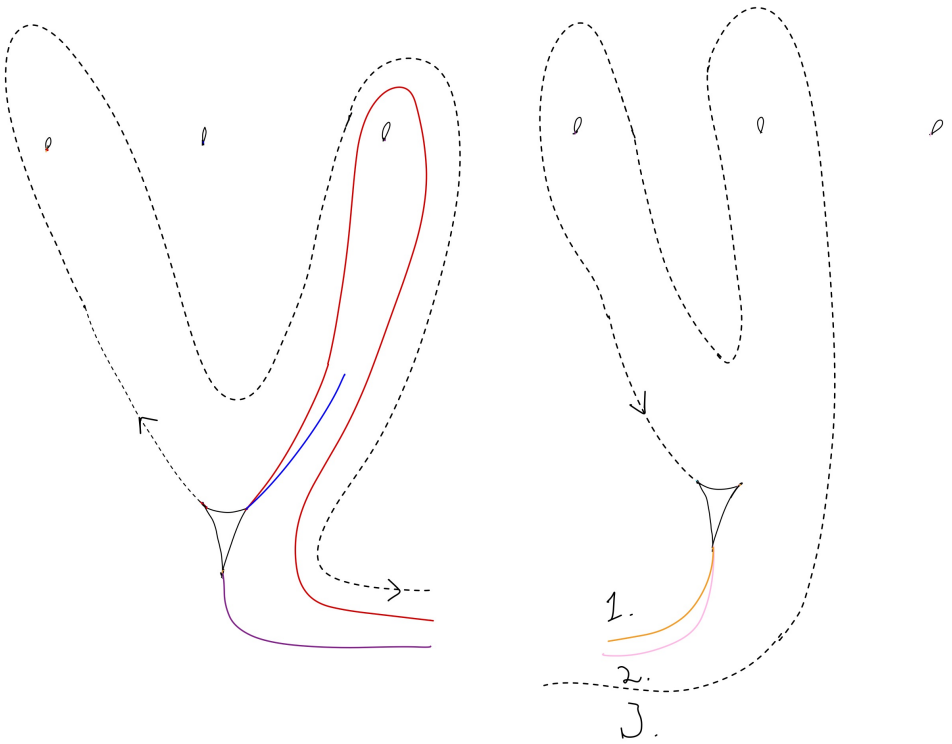


Figure D.5: Linen1

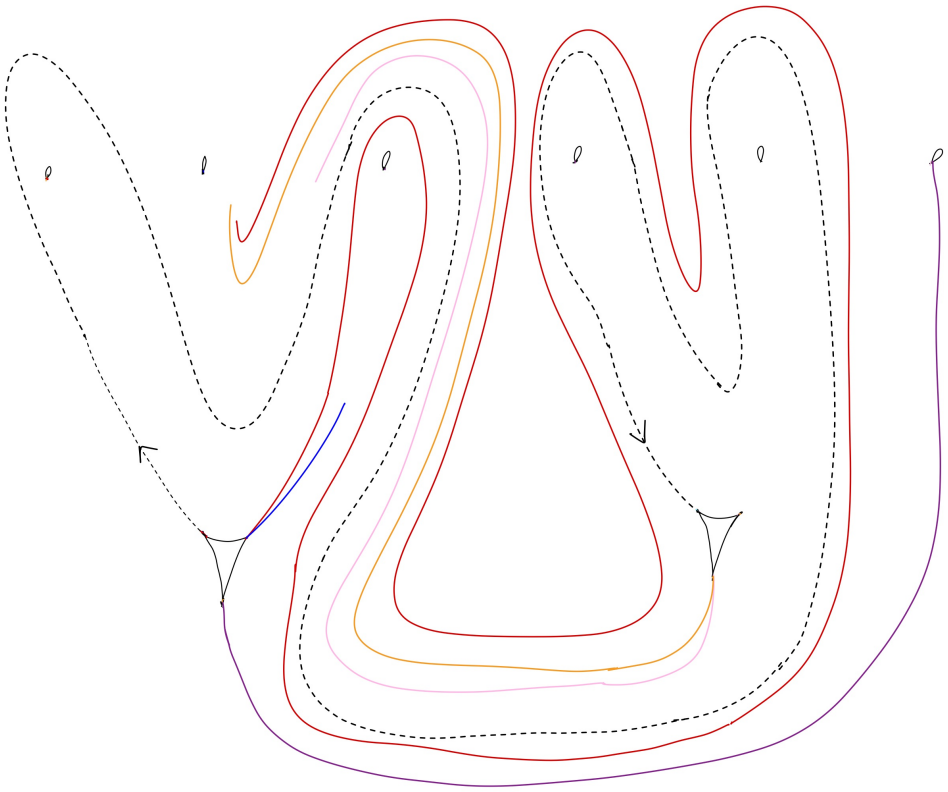


Figure D.6: Bibble1

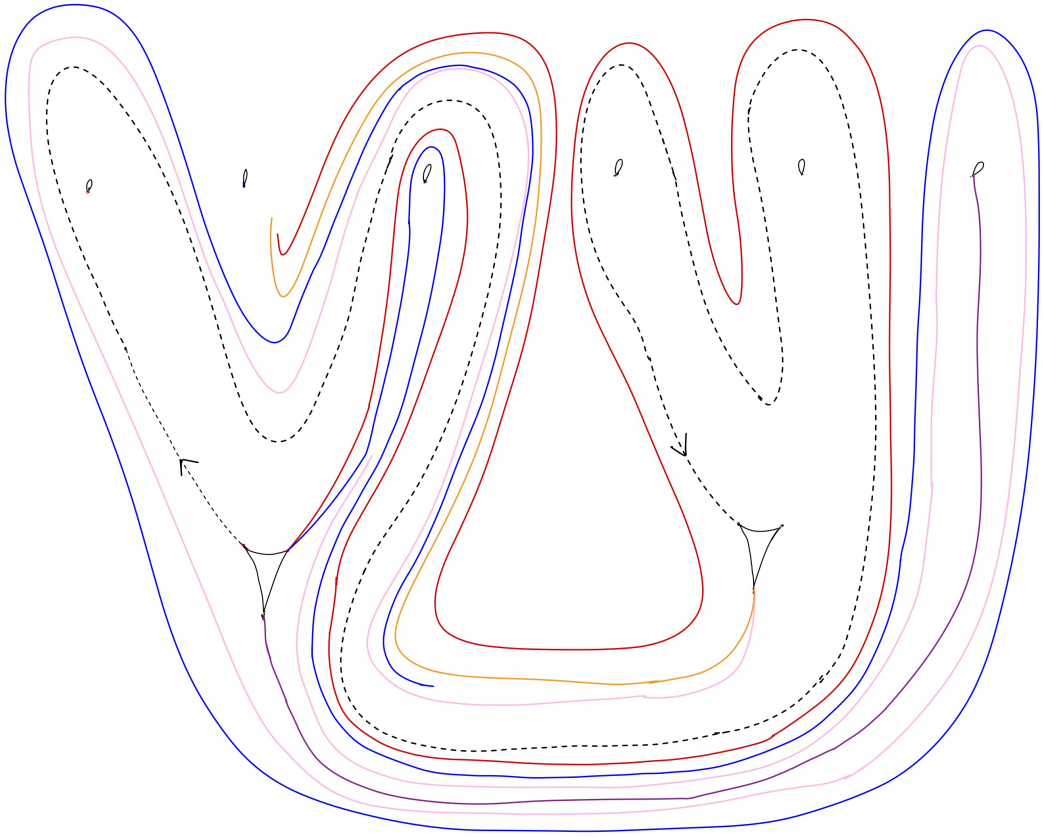


Figure D.7: Bawcock1

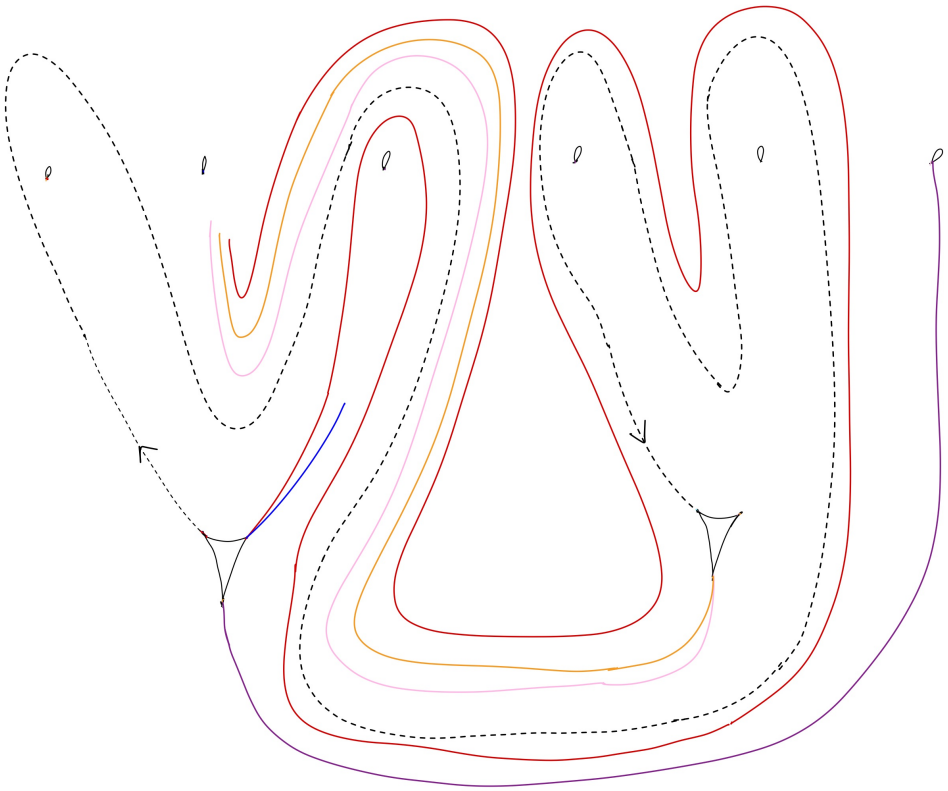


Figure D.8: Chaffer1

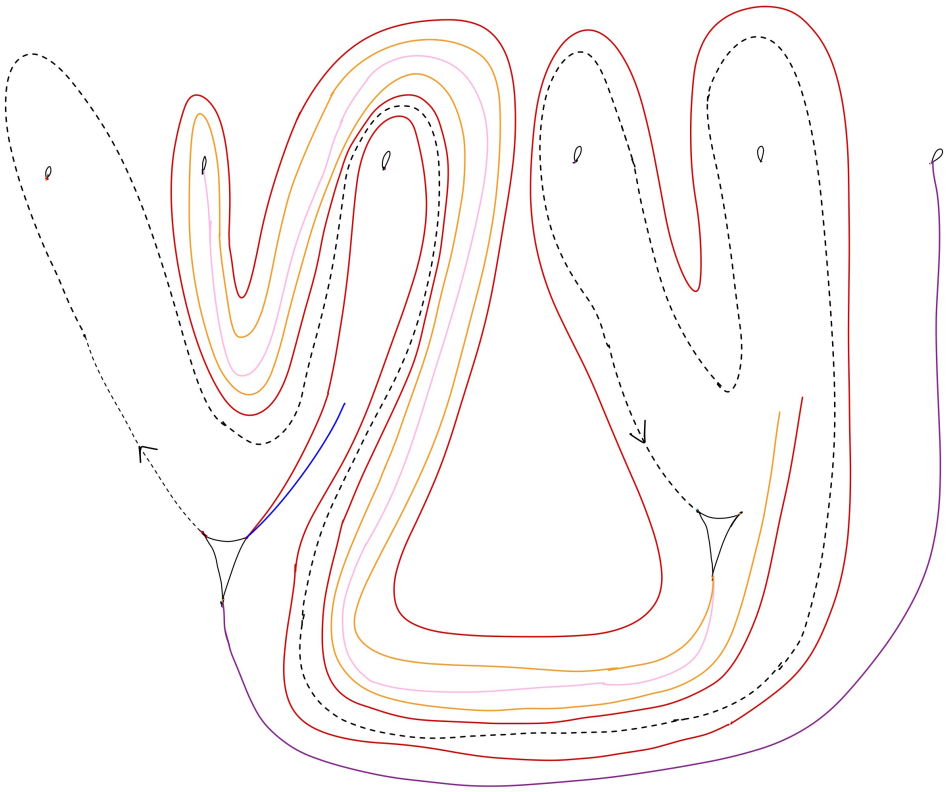


Figure D.9: Chaffer2

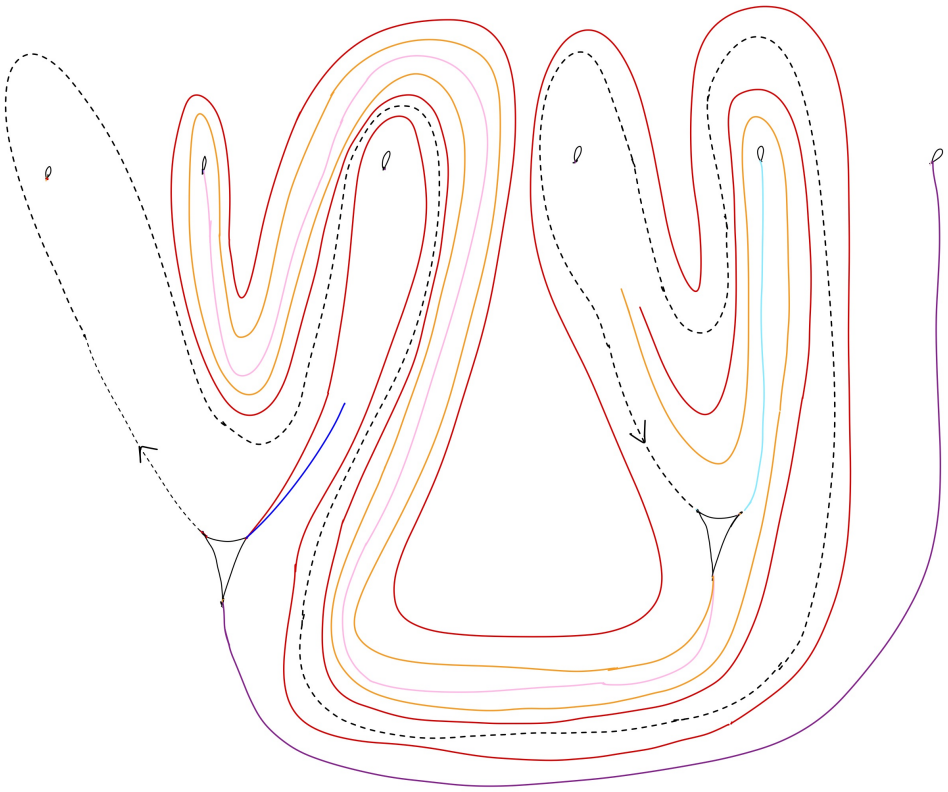


Figure D.10: Chaffer3

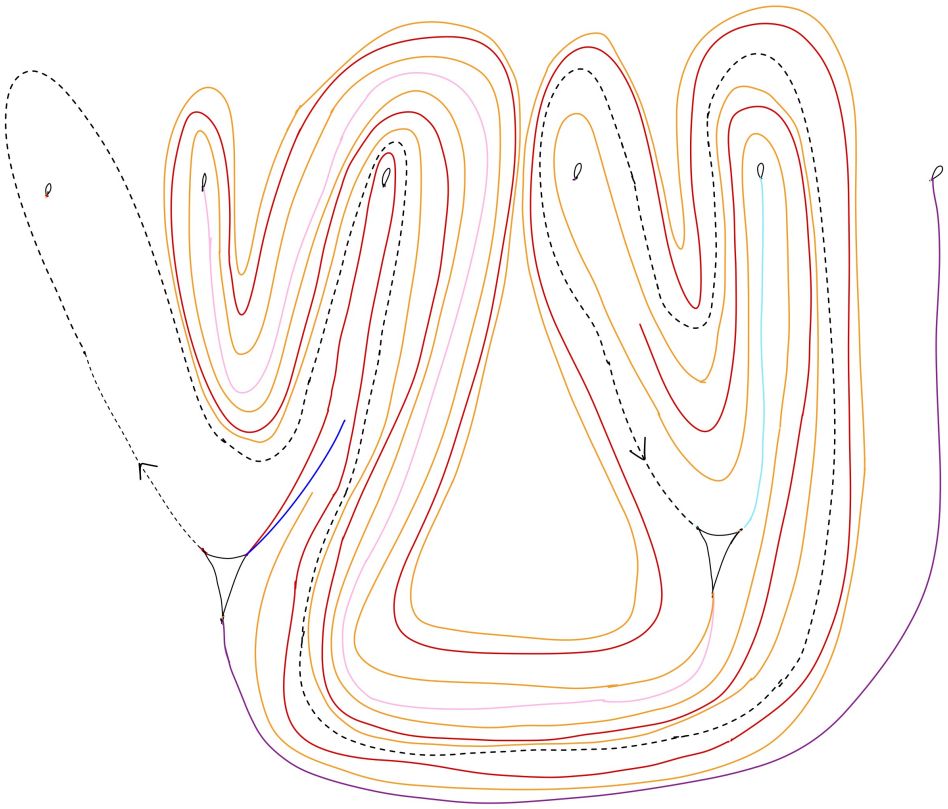


Figure D.11: Chaffer4

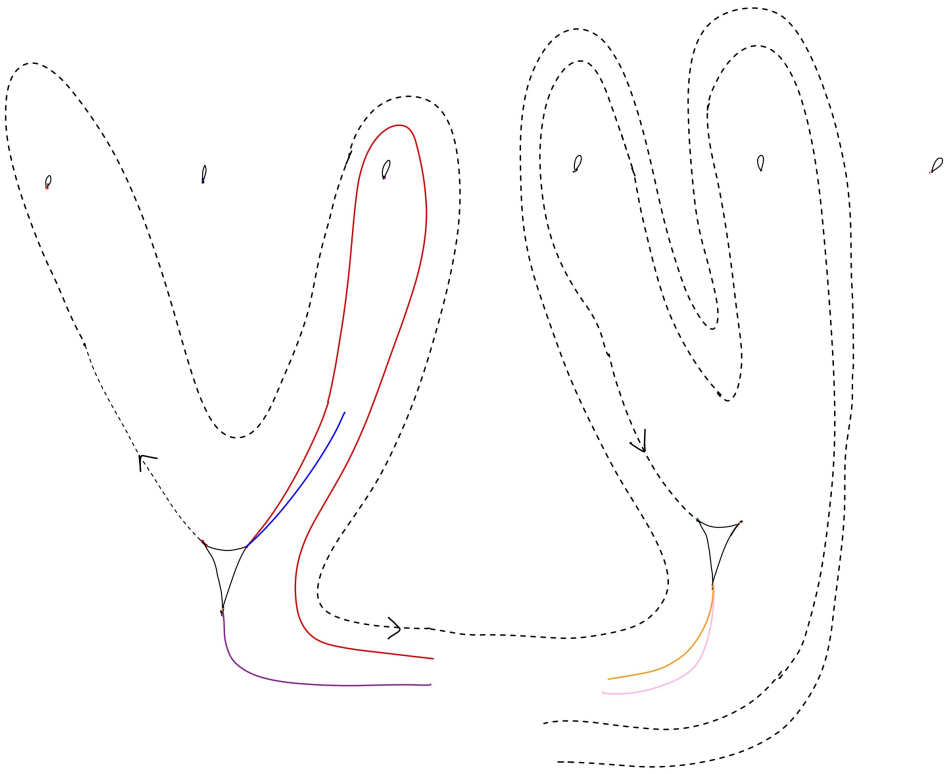


Figure D.12: Fangle1

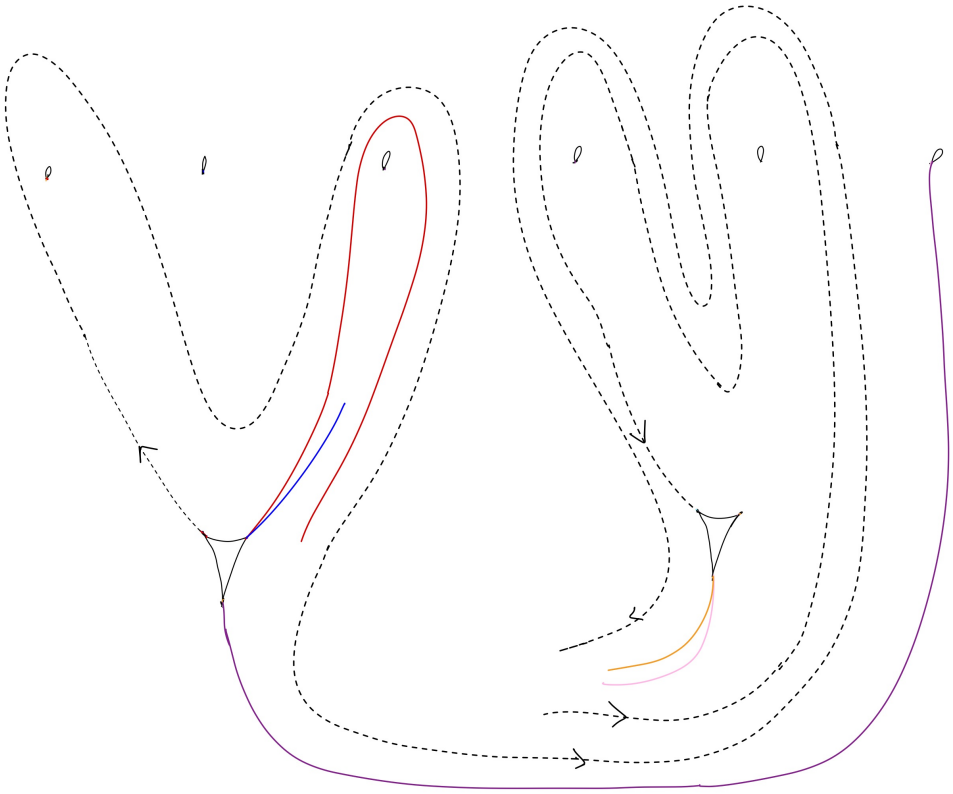


Figure D.13: Jargle1

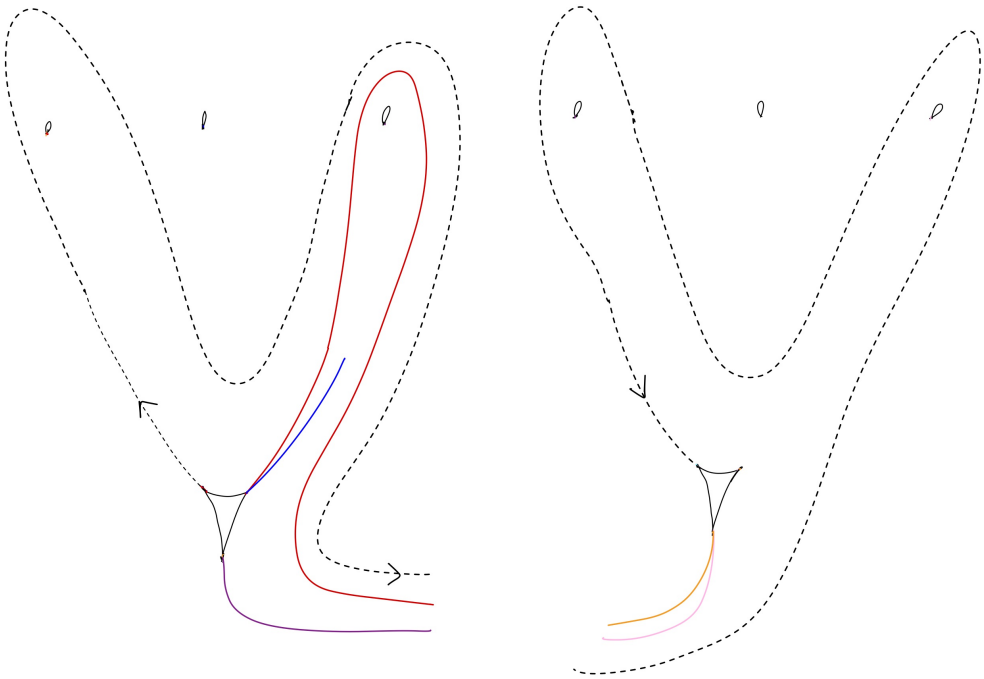


Figure D.14: Kench1

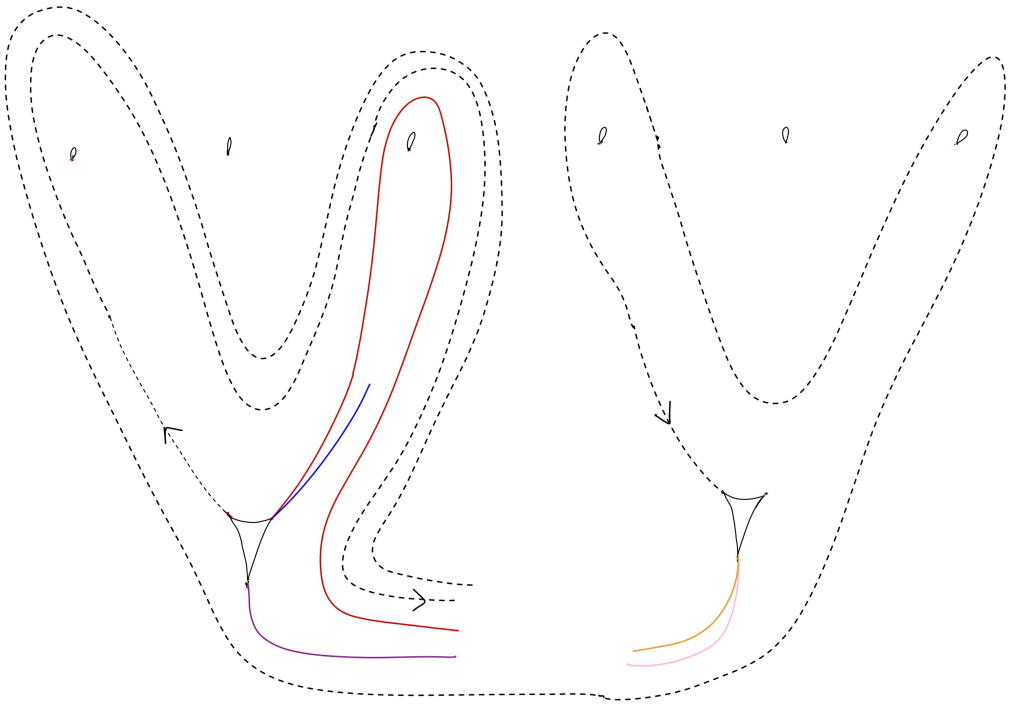


Figure D.15: Kench2

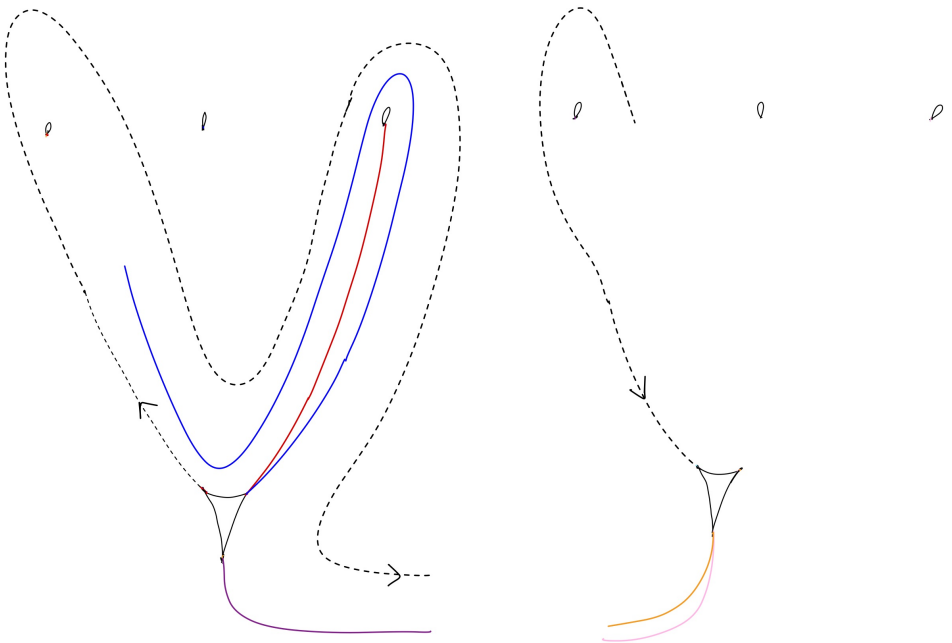


Figure D.16: Test1

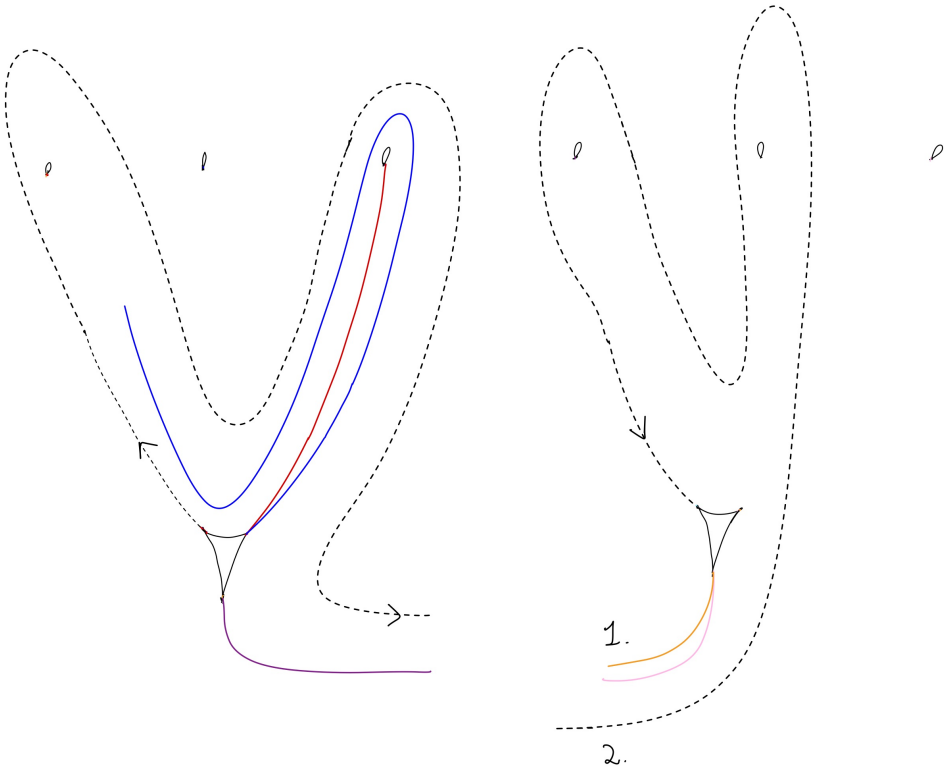


Figure D.17: Pugil1

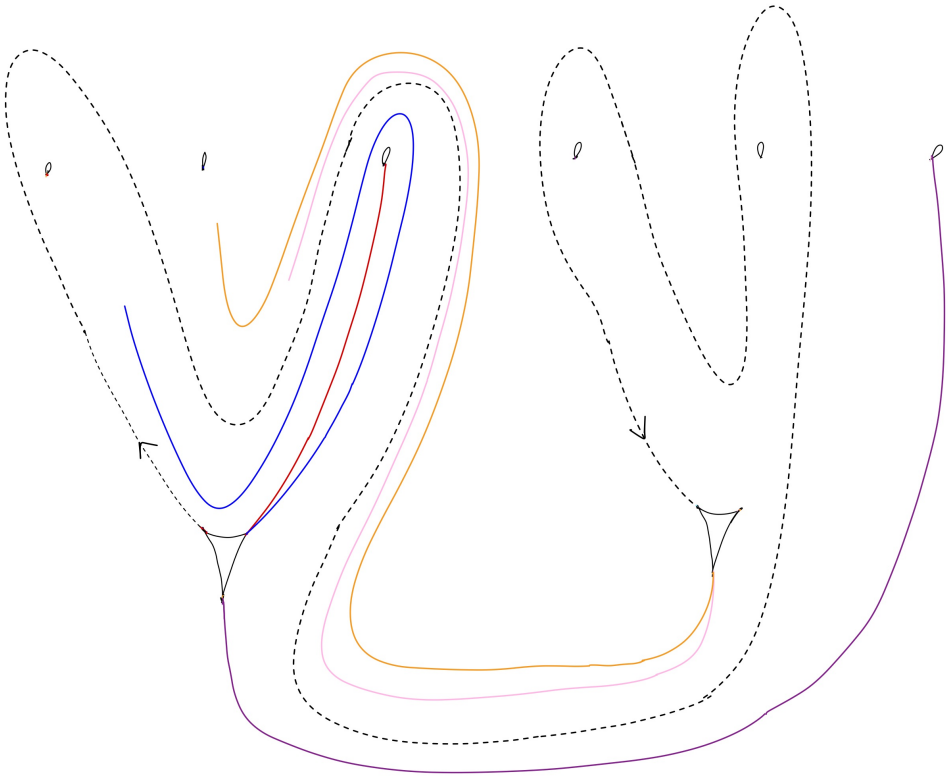


Figure D.18: Limmer1

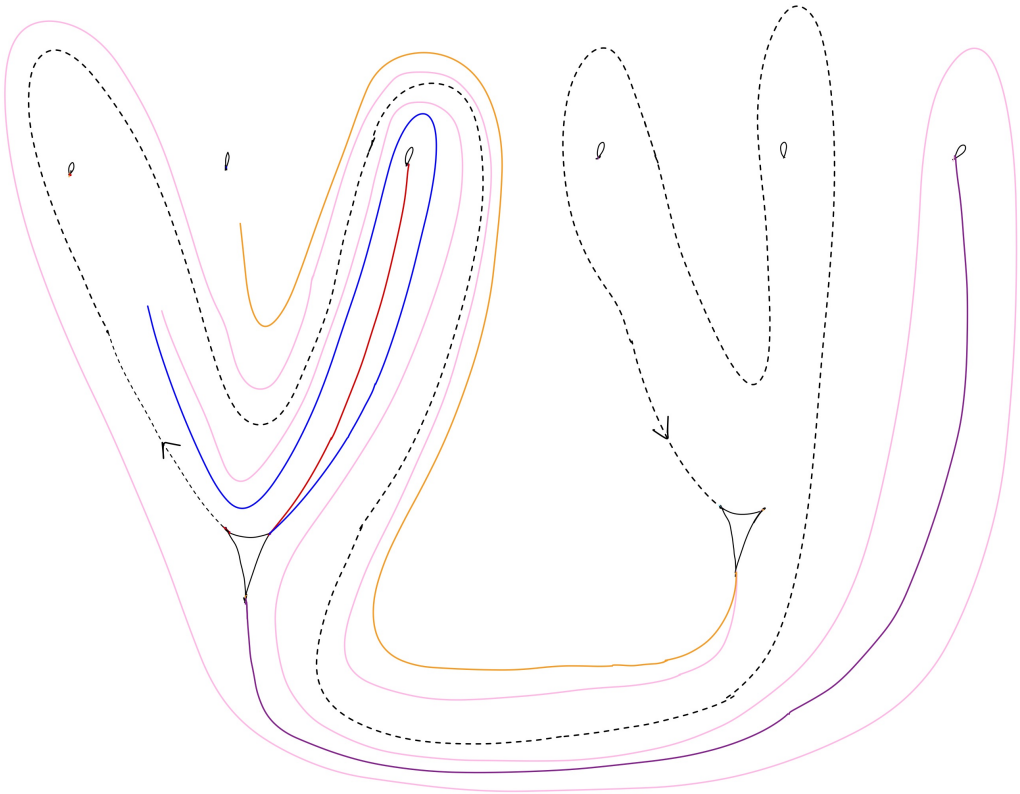


Figure D.19: Costard1

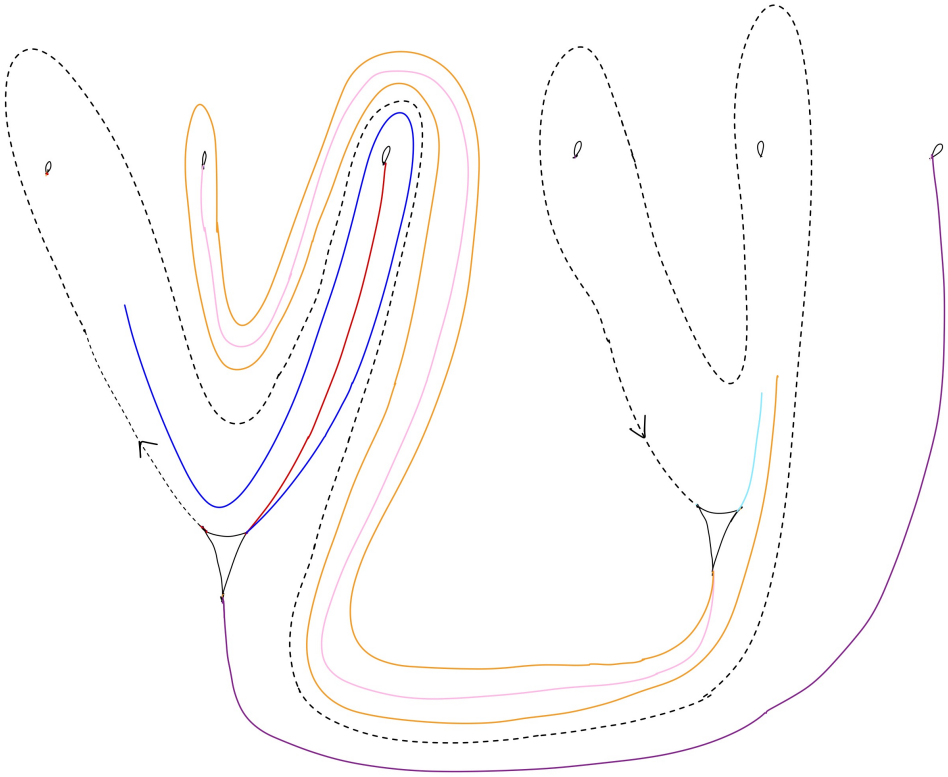


Figure D.20: Daddock1

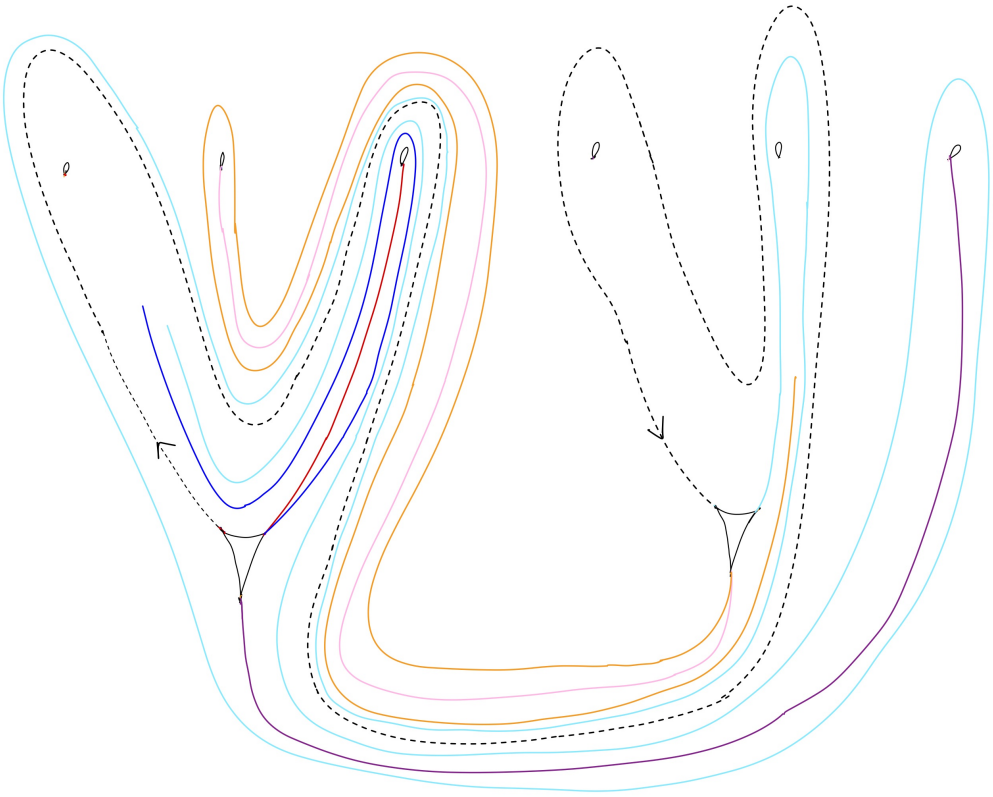


Figure D.21: Cordwain1

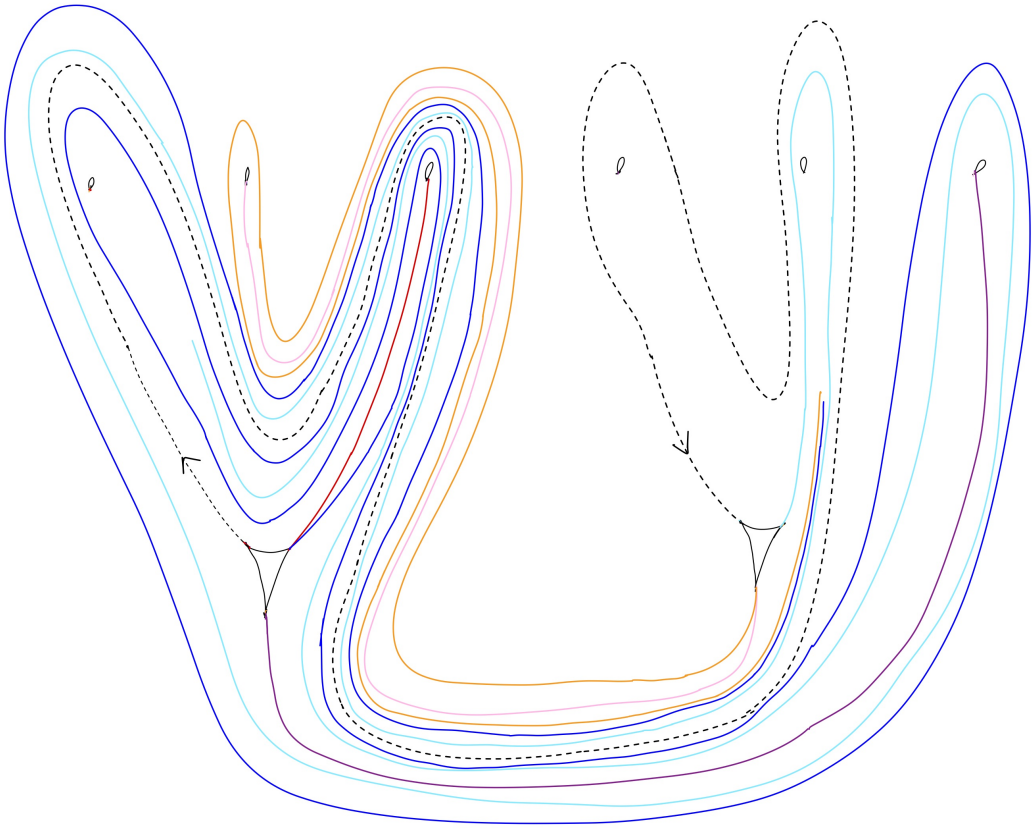


Figure D.22: Cordwain2

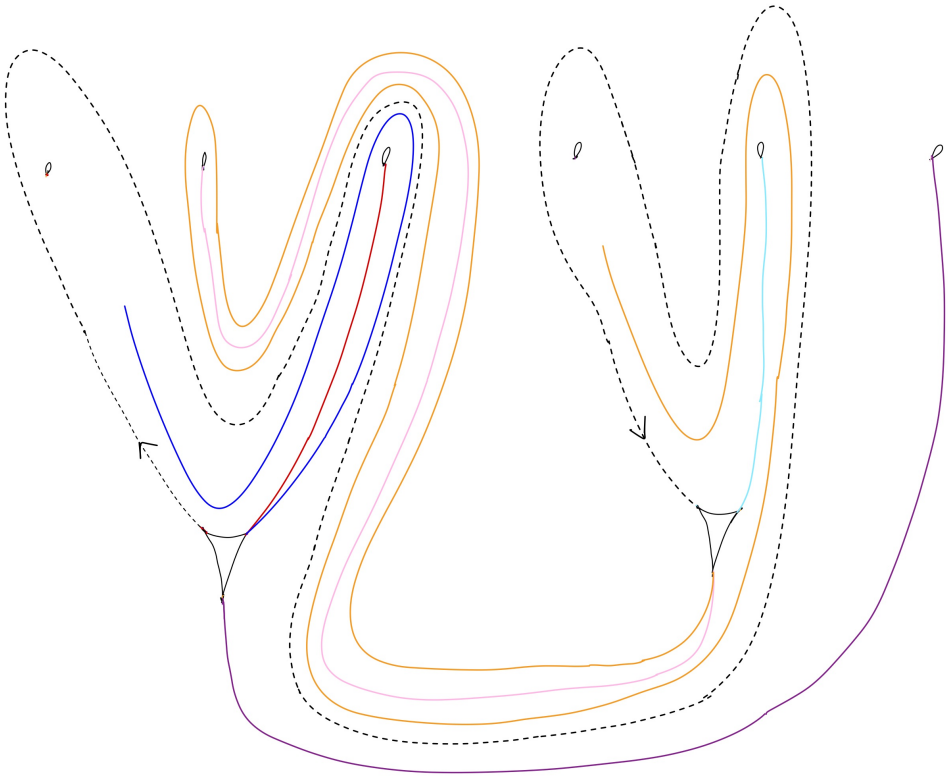


Figure D.23: Loblolly1

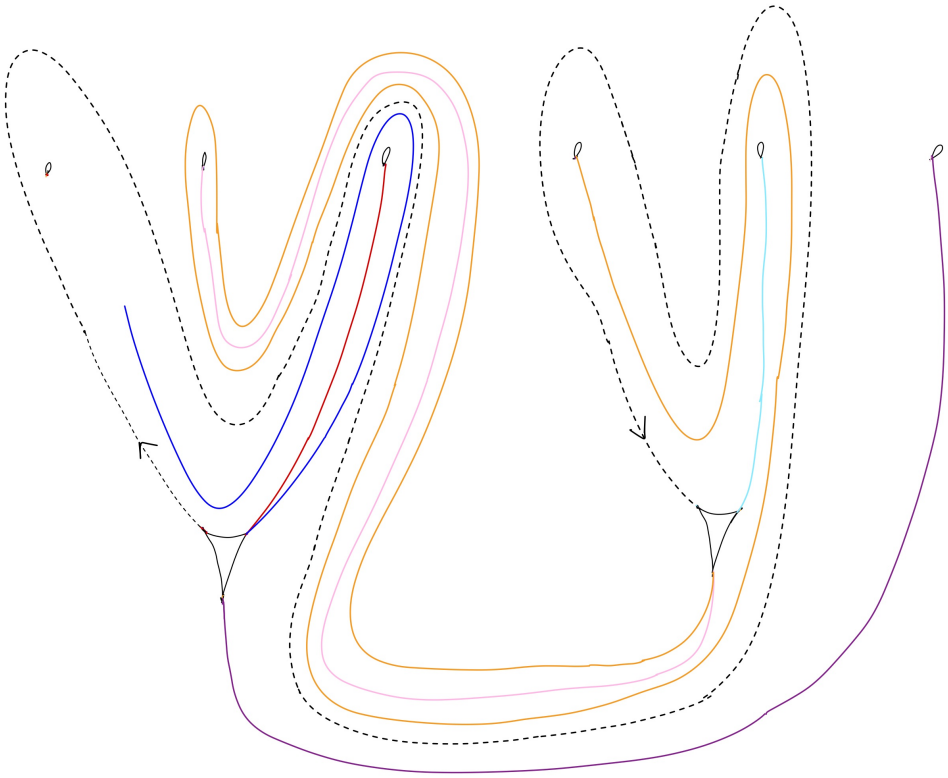


Figure D.24: Loblolly2

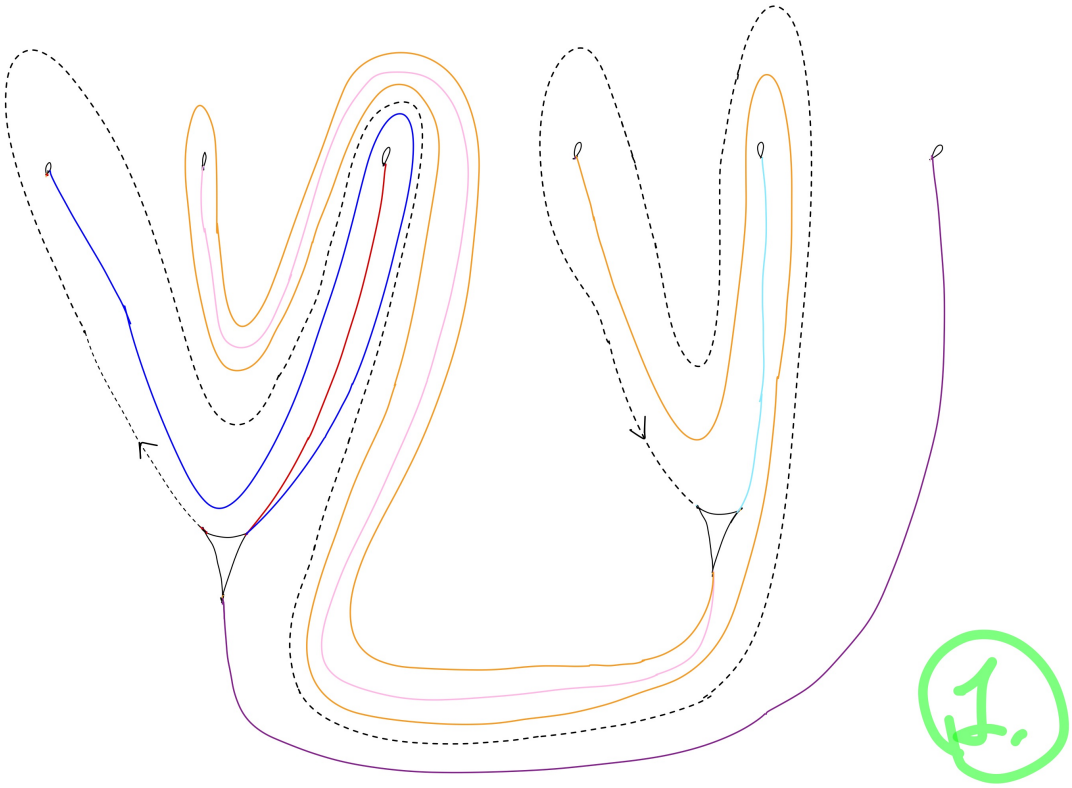


Figure D.25: Loblolly3

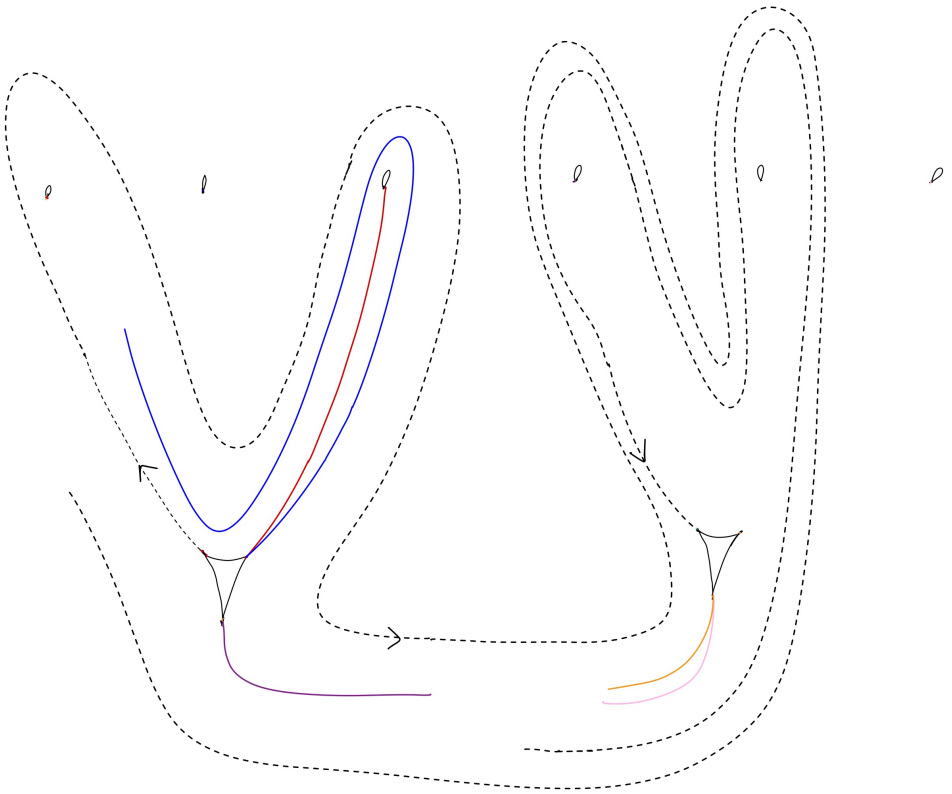


Figure D.26: Smouch1

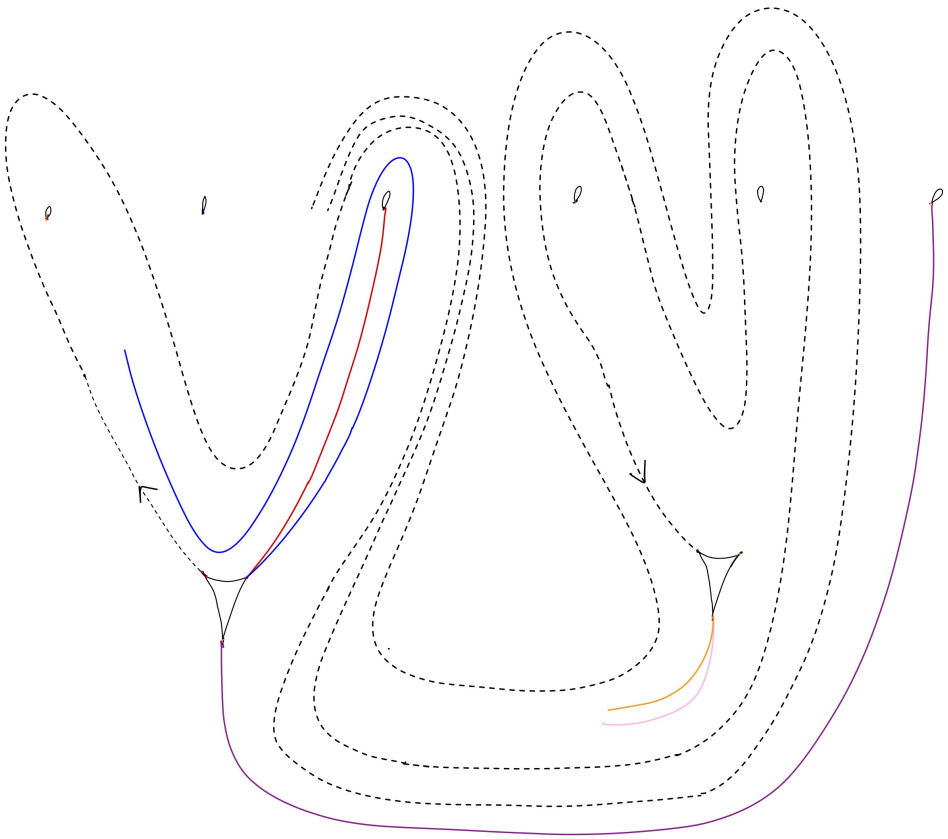


Figure D.27: Thwite1

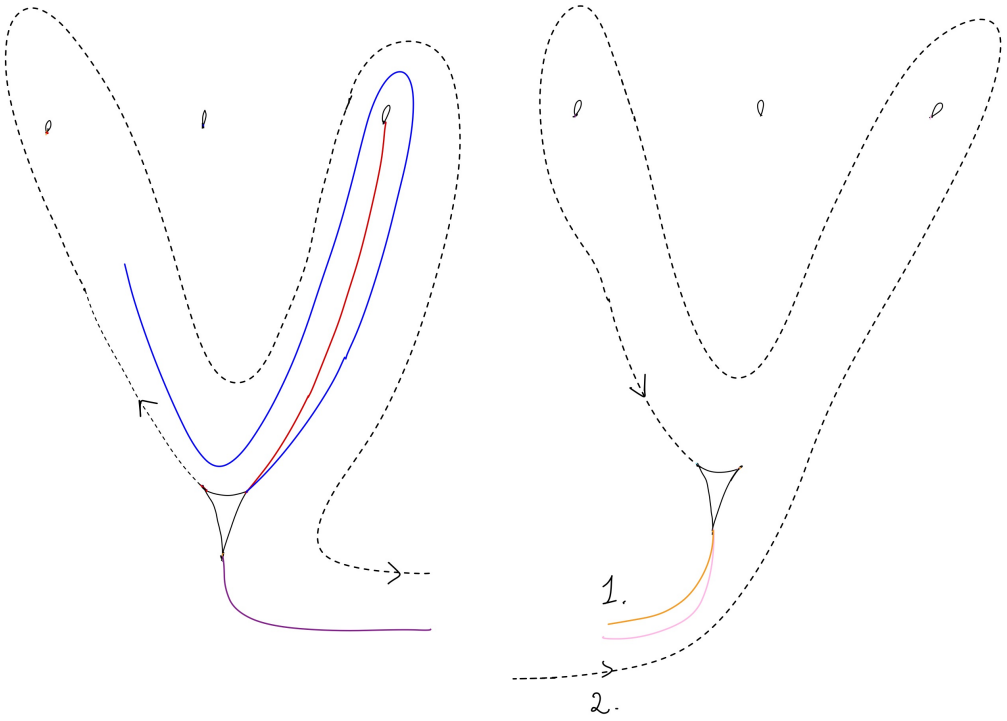


Figure D.28: Quarl1

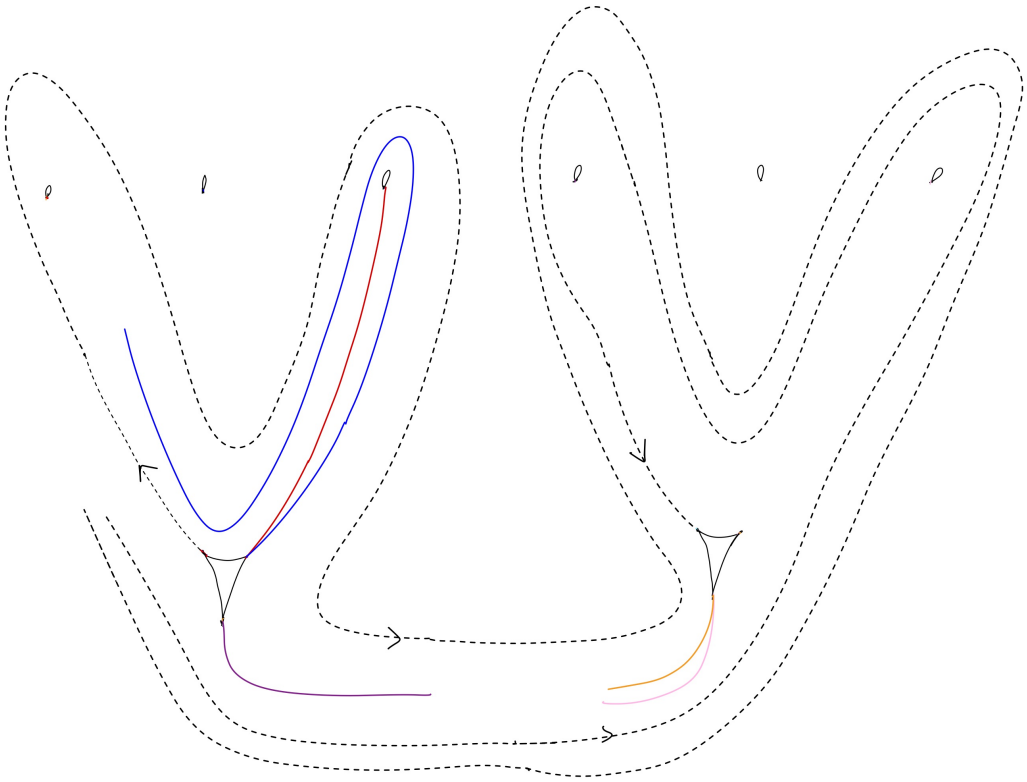


Figure D.29: Yaffle1

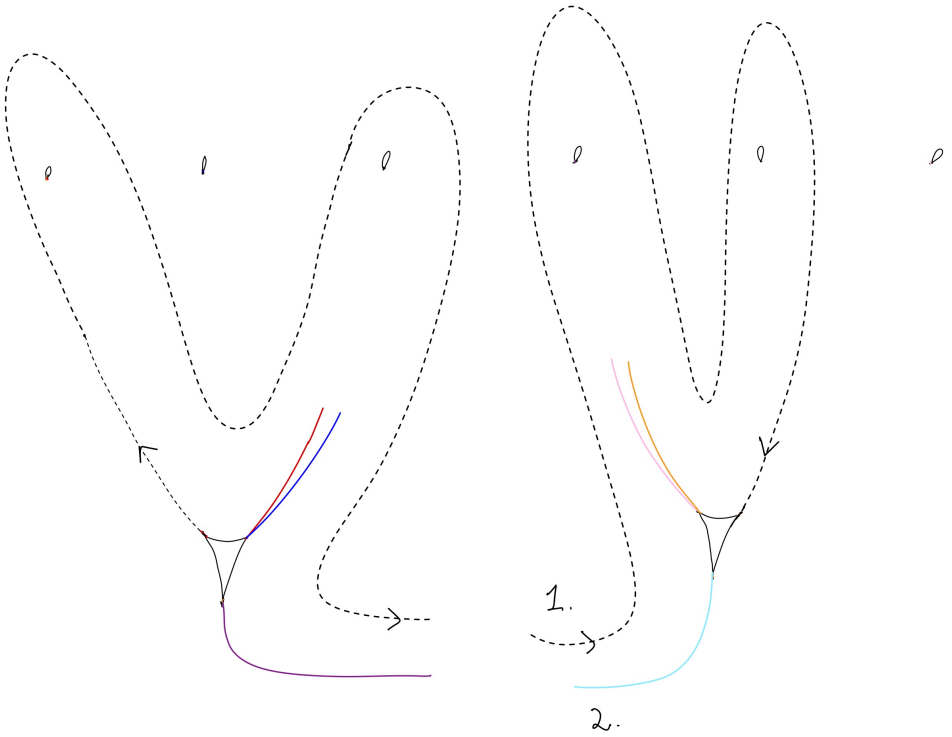


Figure D.30: ACK1

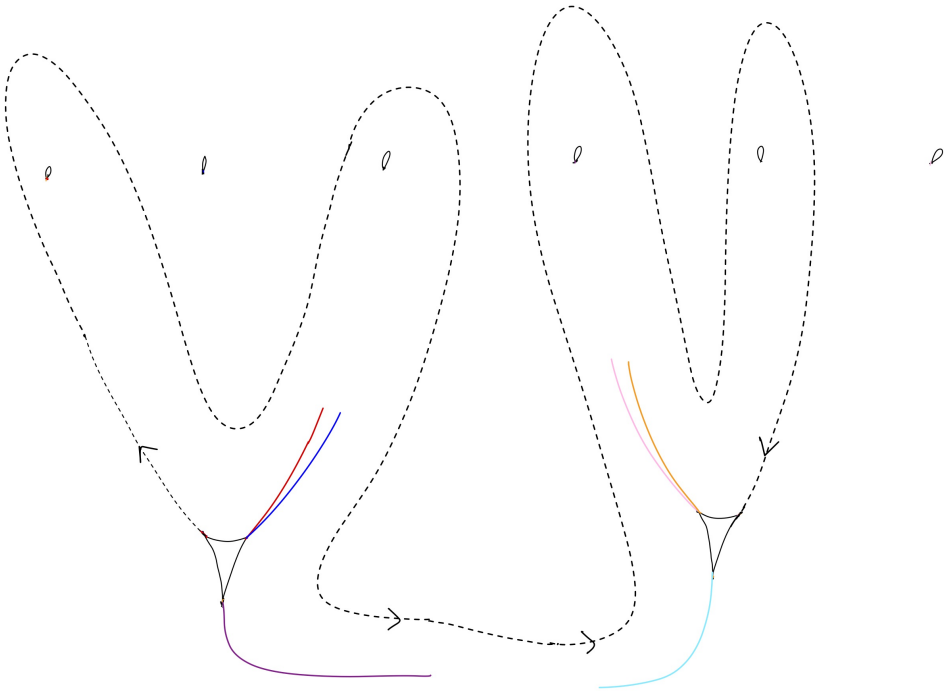


Figure D.31: Dram1

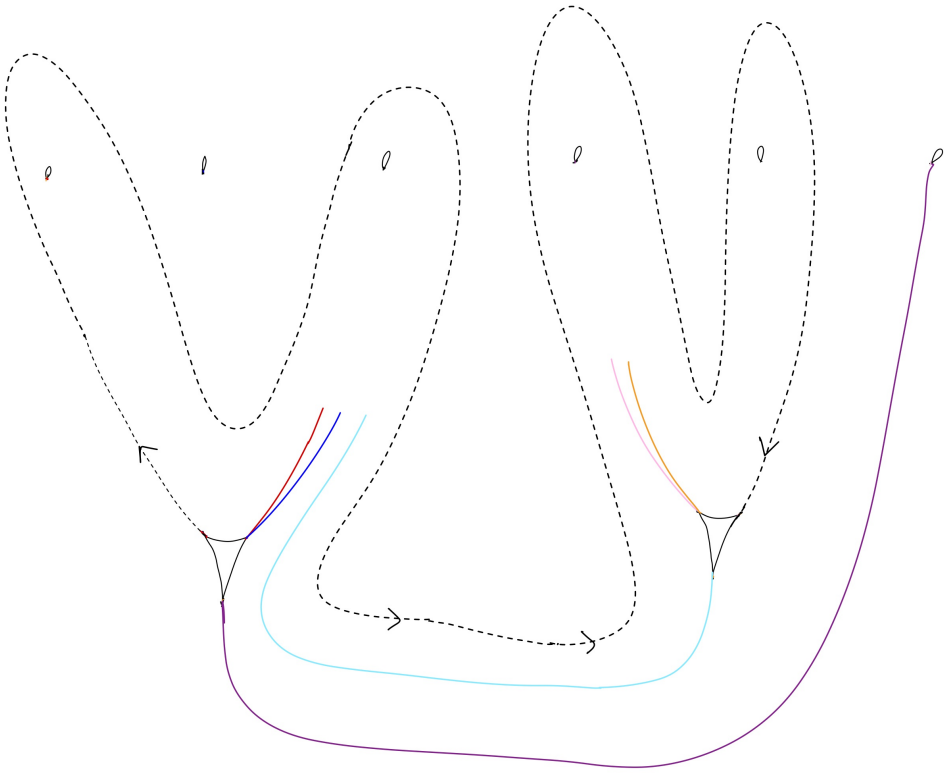


Figure D.32: Dram2

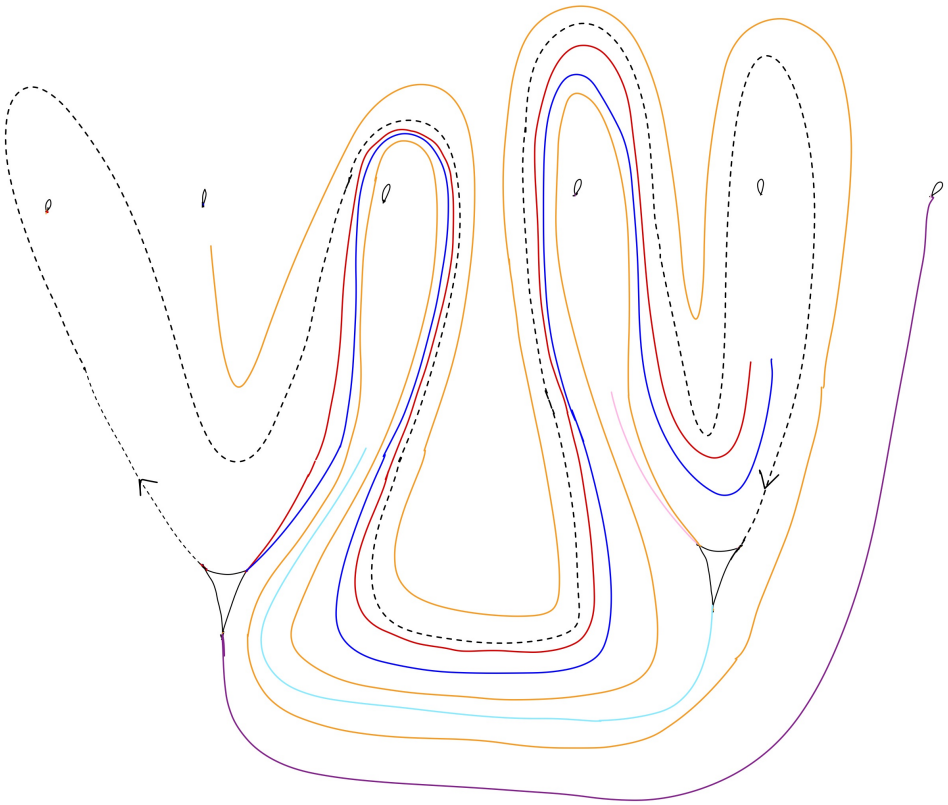


Figure D.33: Sloom1

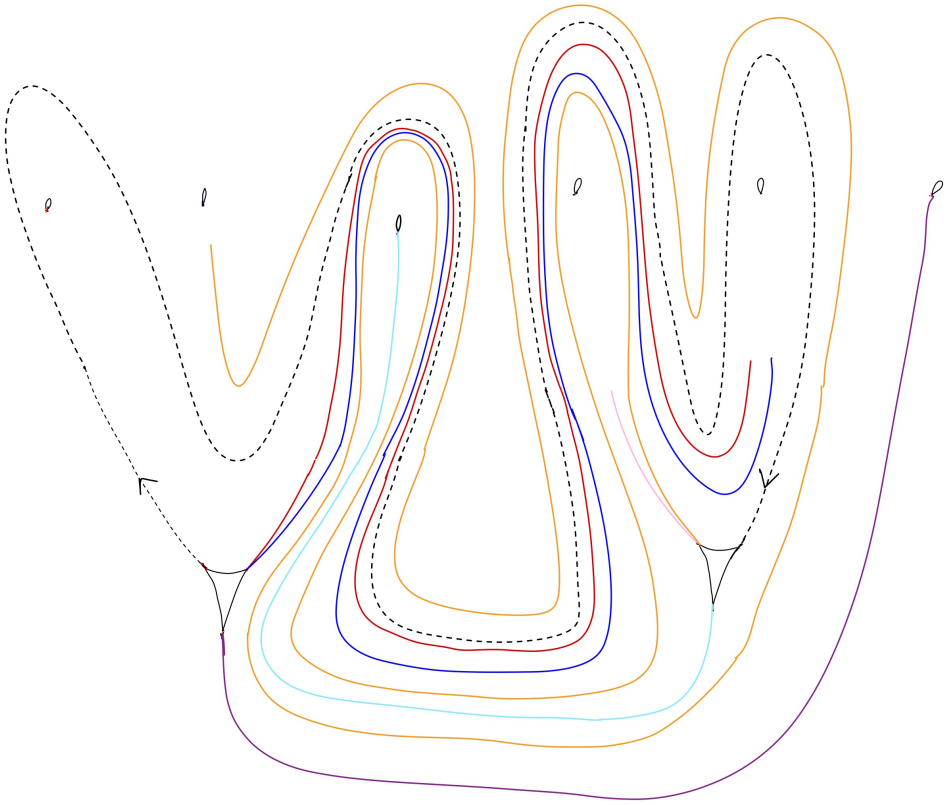


Figure D.34: Sloom2

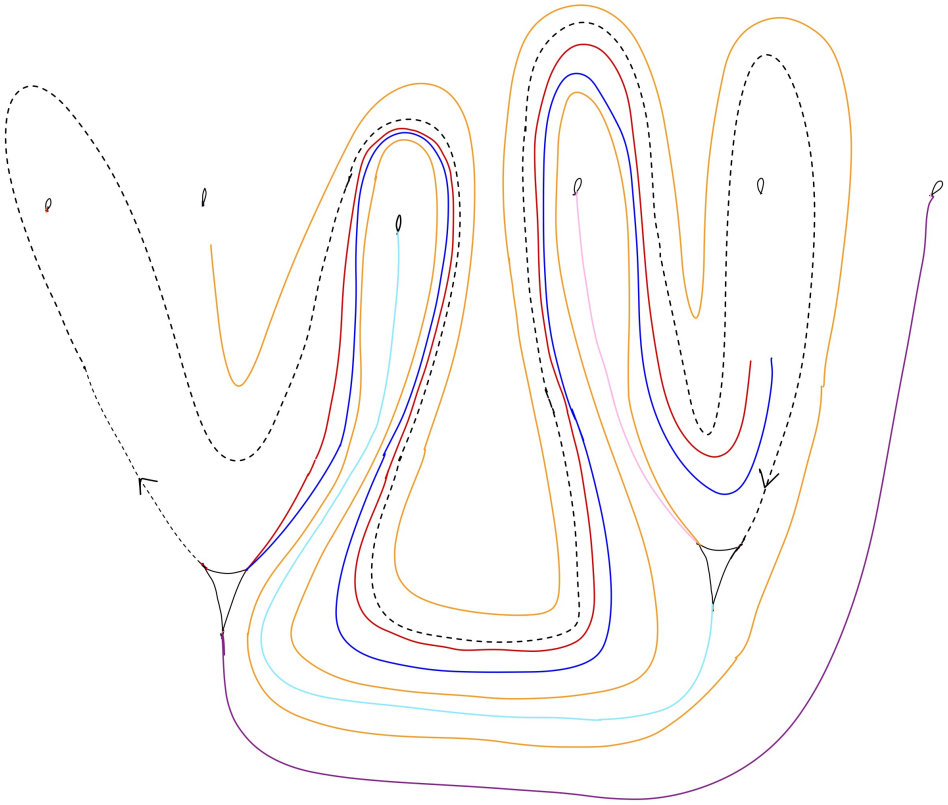


Figure D.35: Sloom3

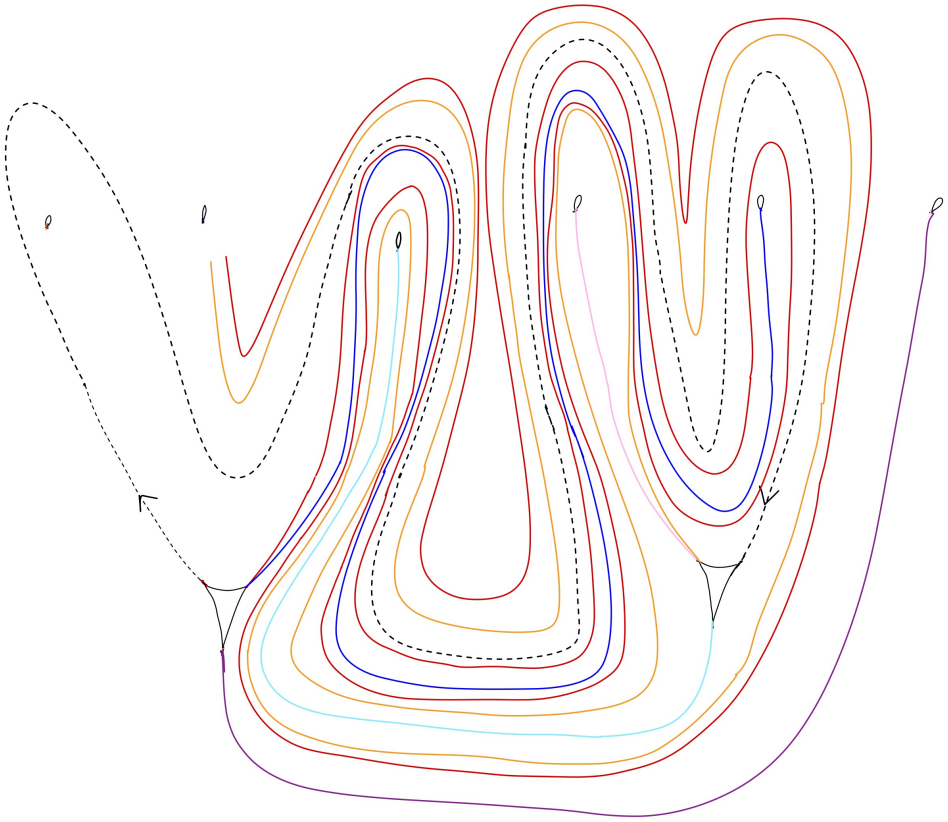


Figure D.36: Sloom4

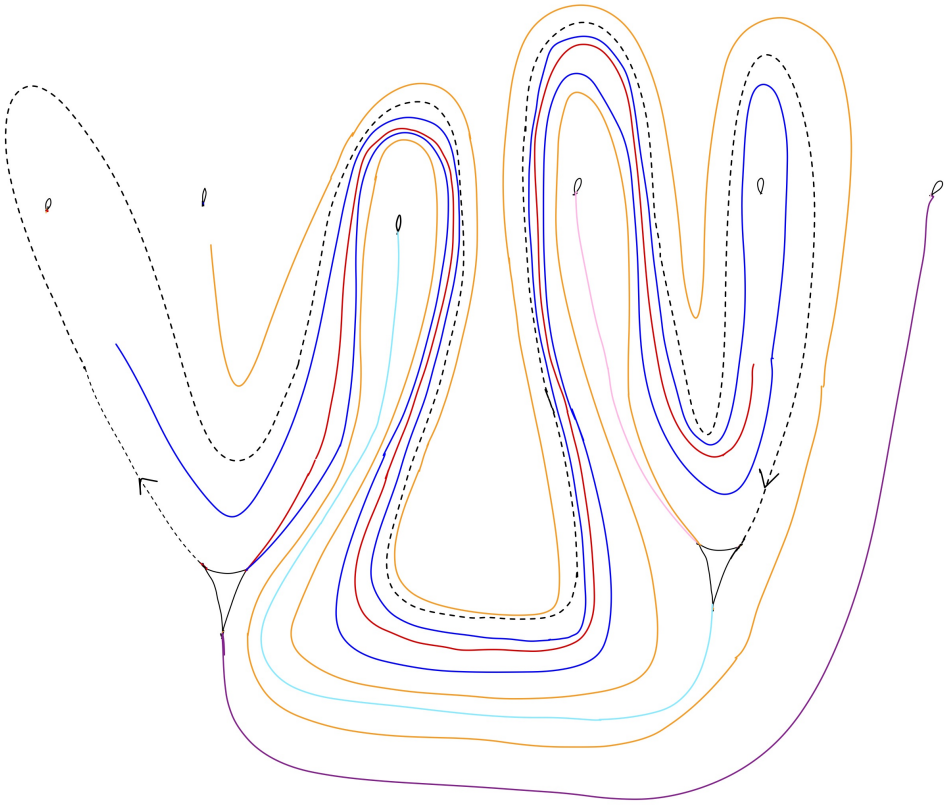


Figure D.37: Sloom5

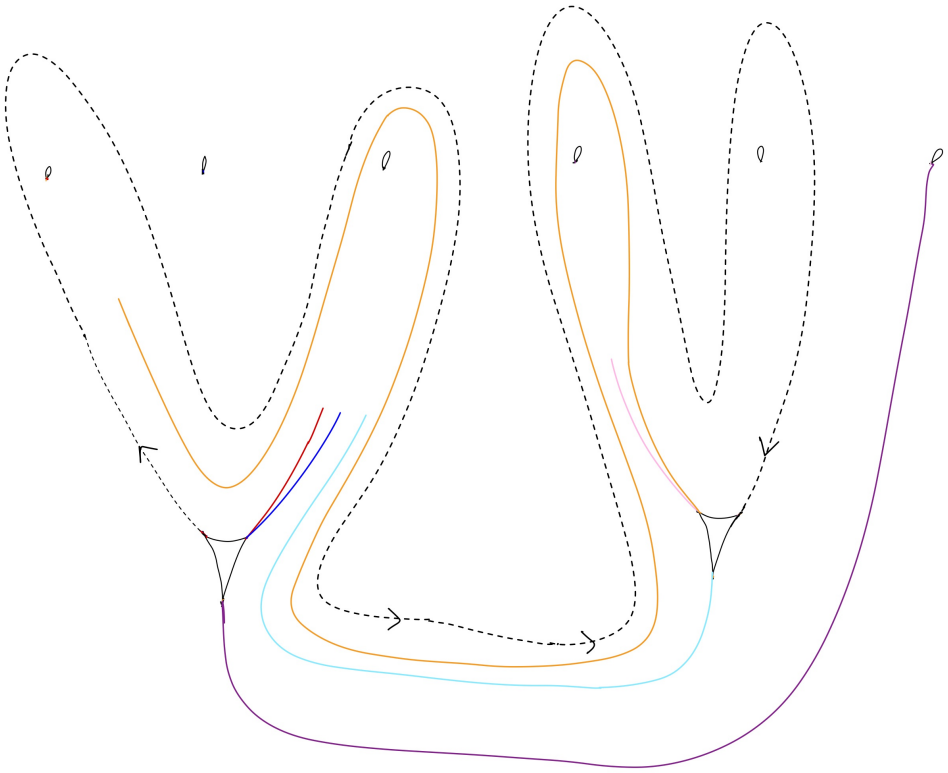


Figure D.38: Thrum1

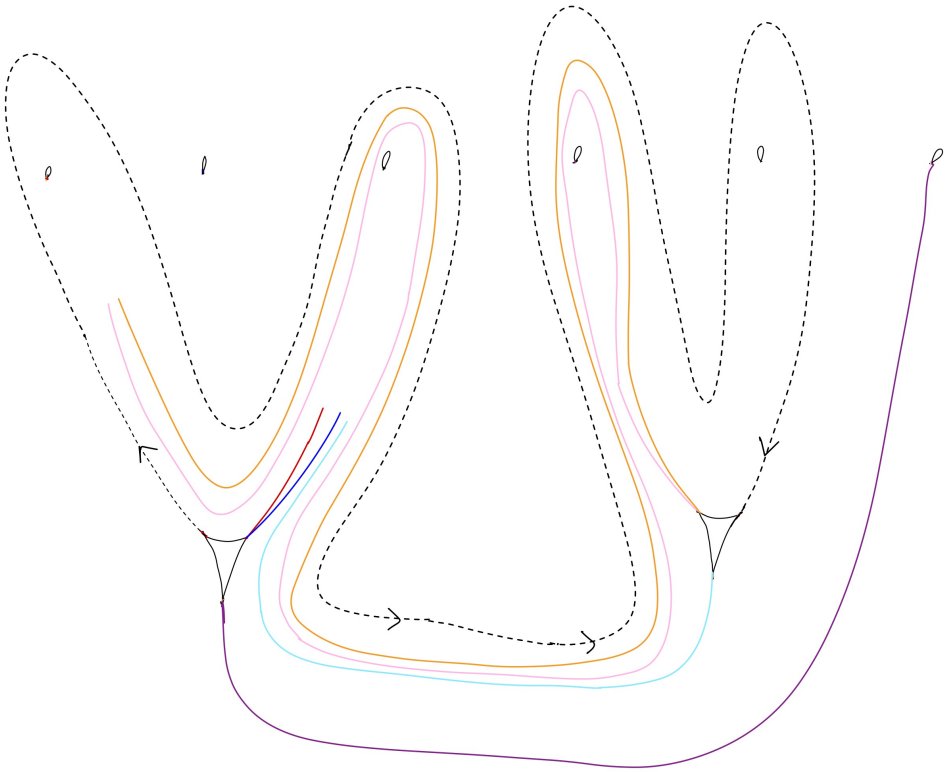


Figure D.39: Dwammy1

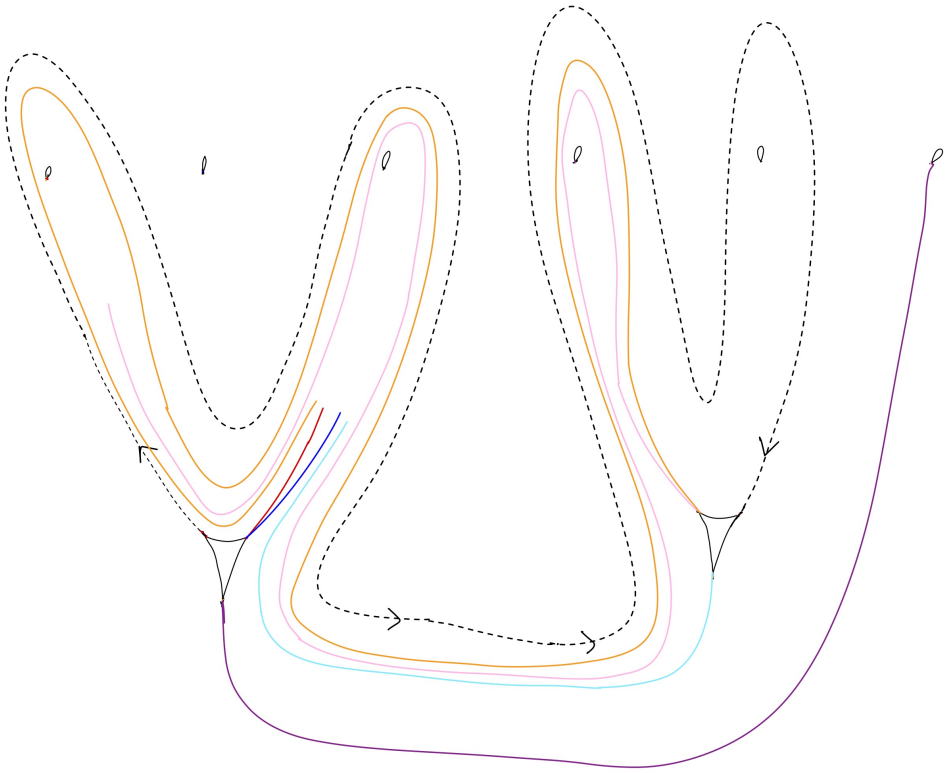


Figure D.40: Dwammy2

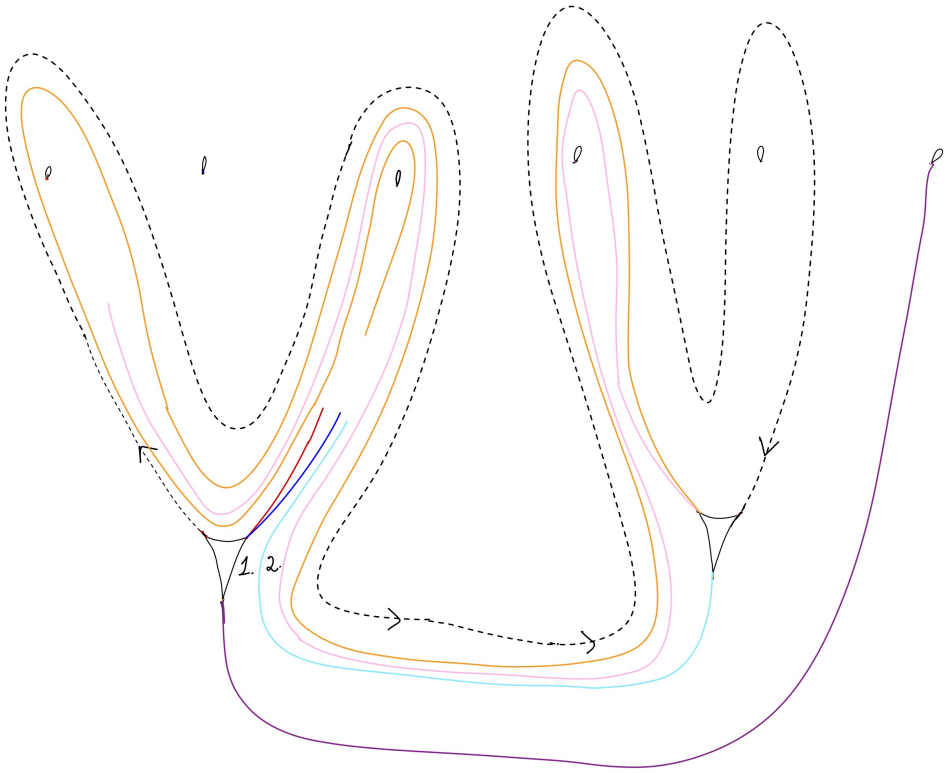


Figure D.41: Dwammy3

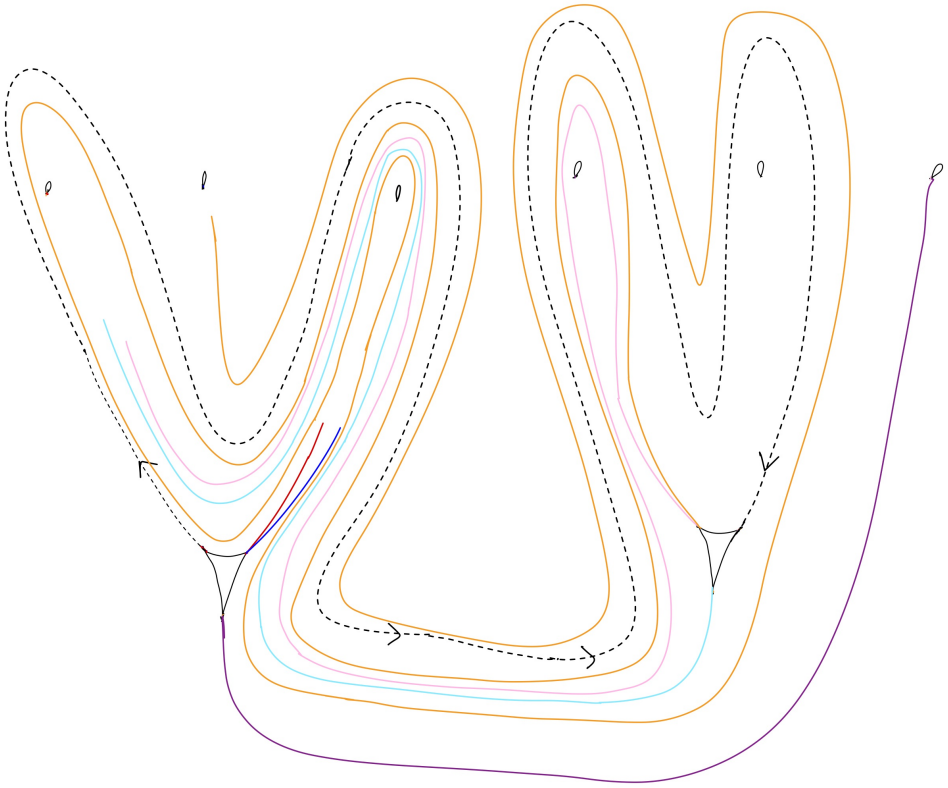


Figure D.42: Macarize1

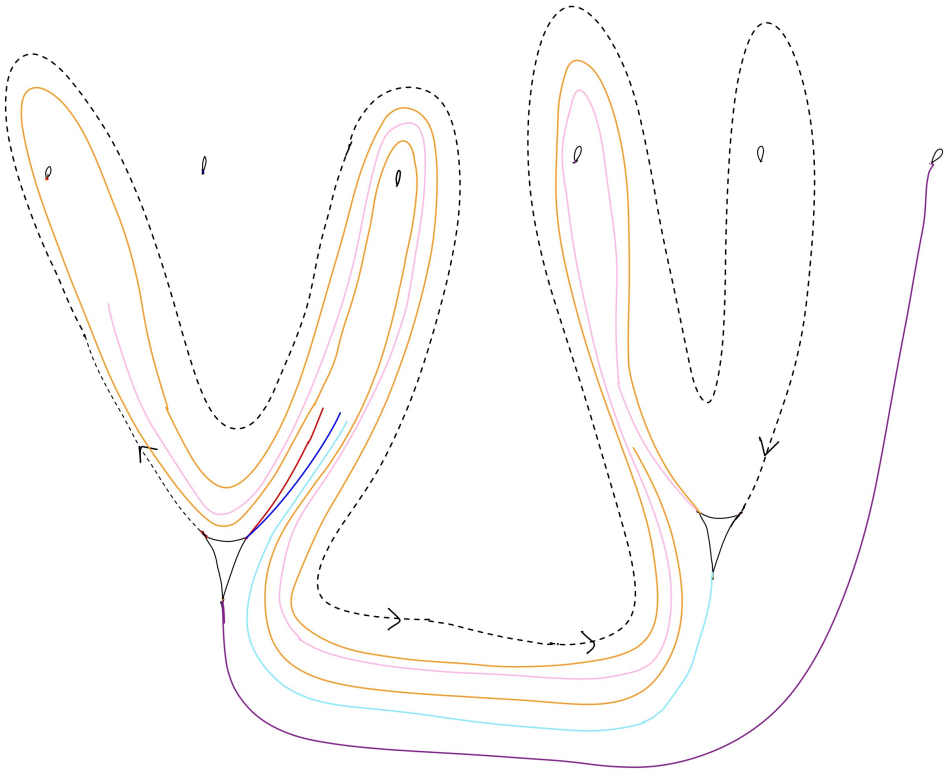


Figure D.43: Mooncalf1

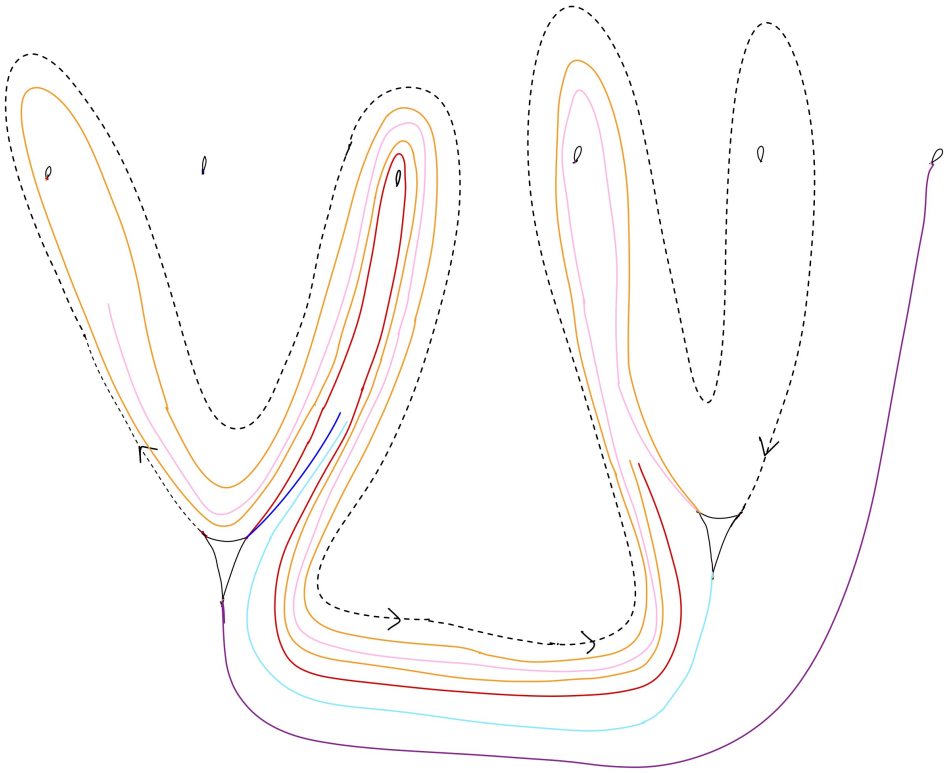


Figure D.44: Mooncalf2

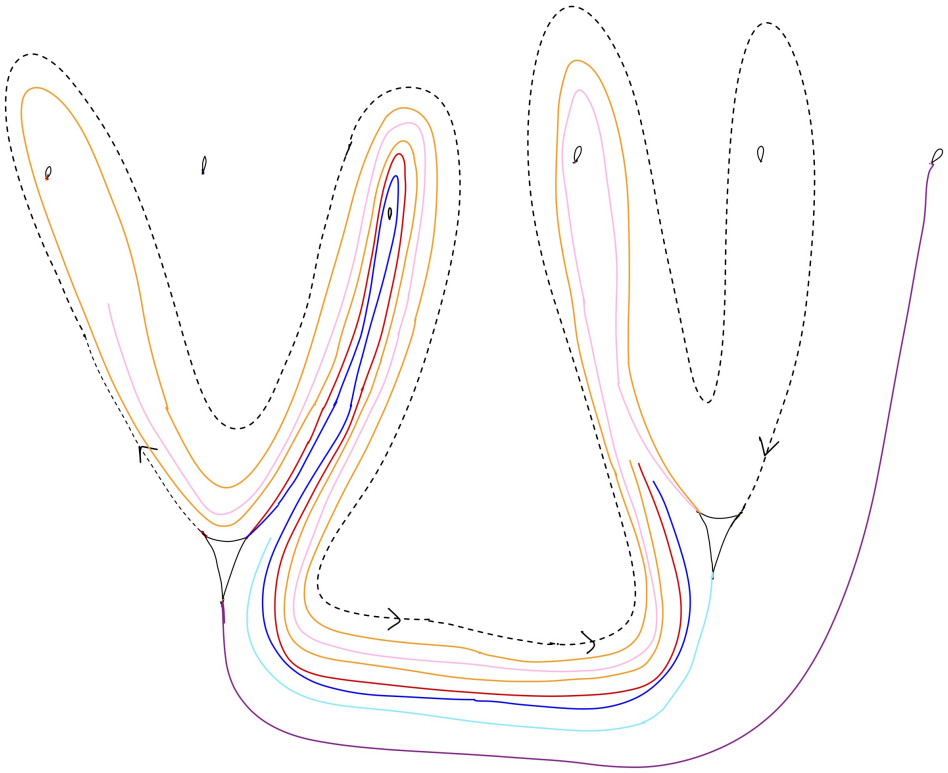


Figure D.45: Mooncalf3

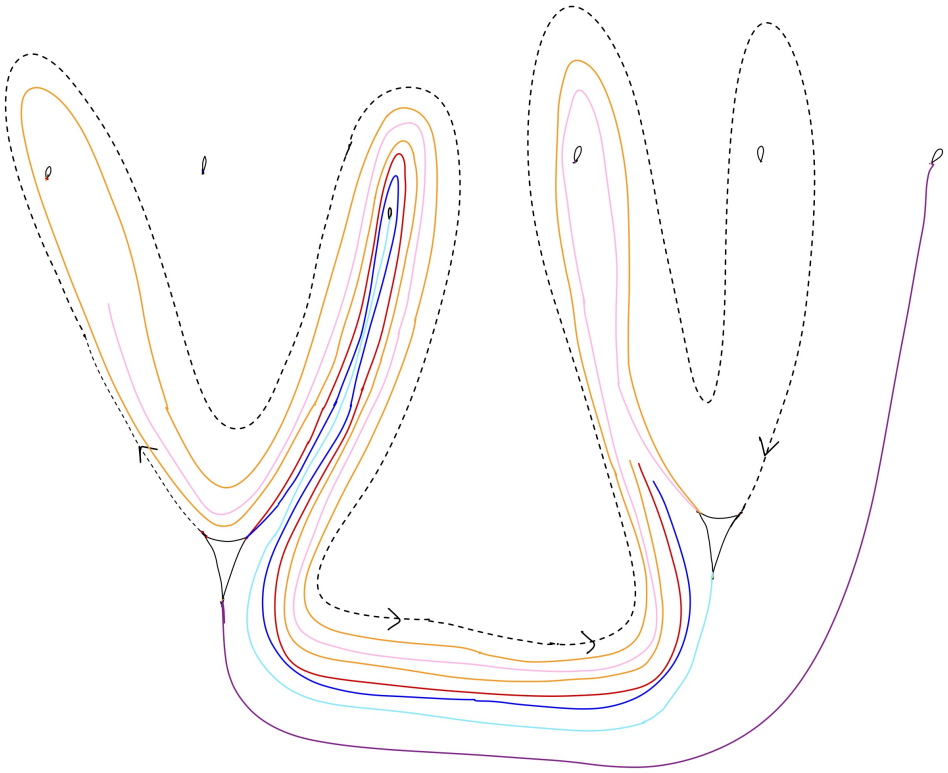


Figure D.46: Mooncalf4

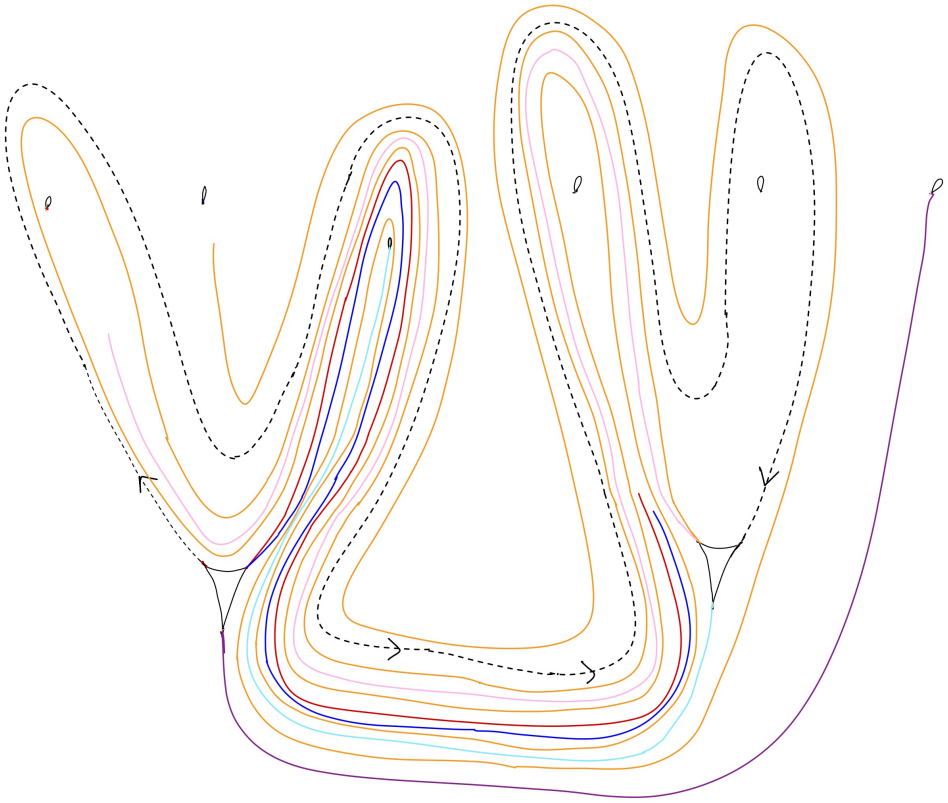


Figure D.47: Mooncalf5

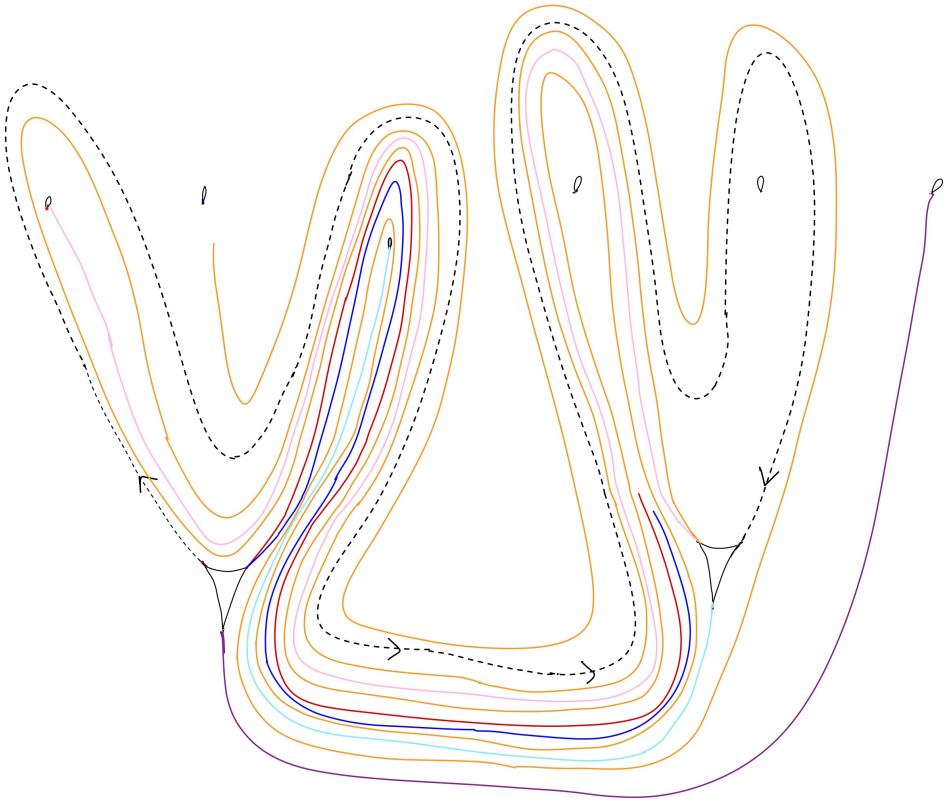


Figure D.48: Mooncalf6

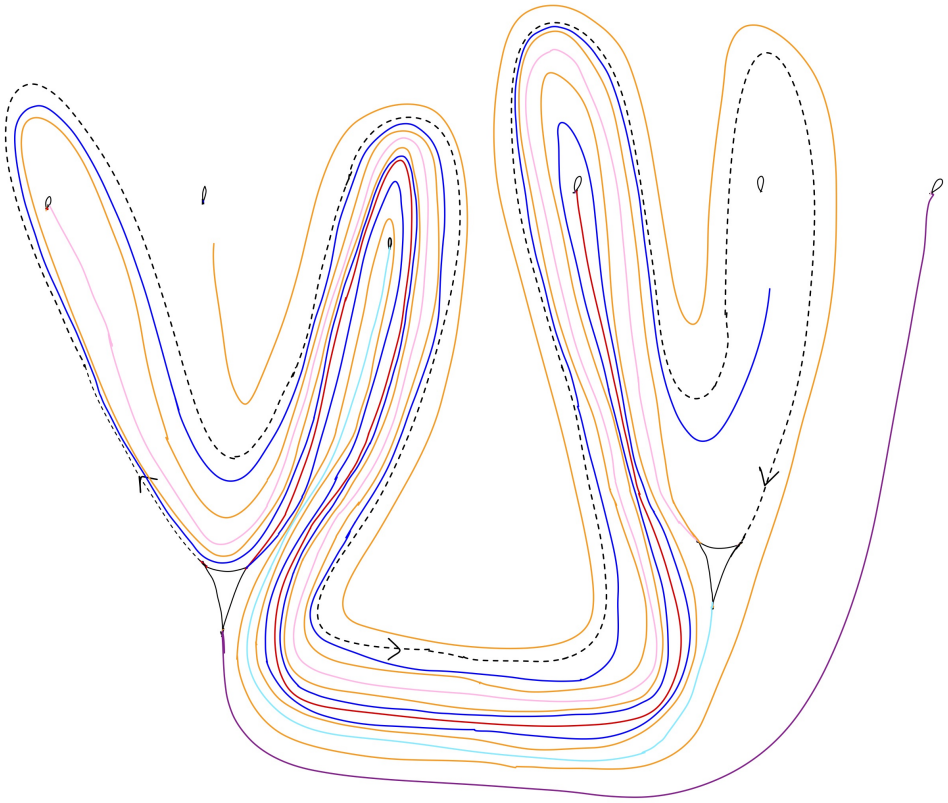


Figure D.49: Mooncalf7

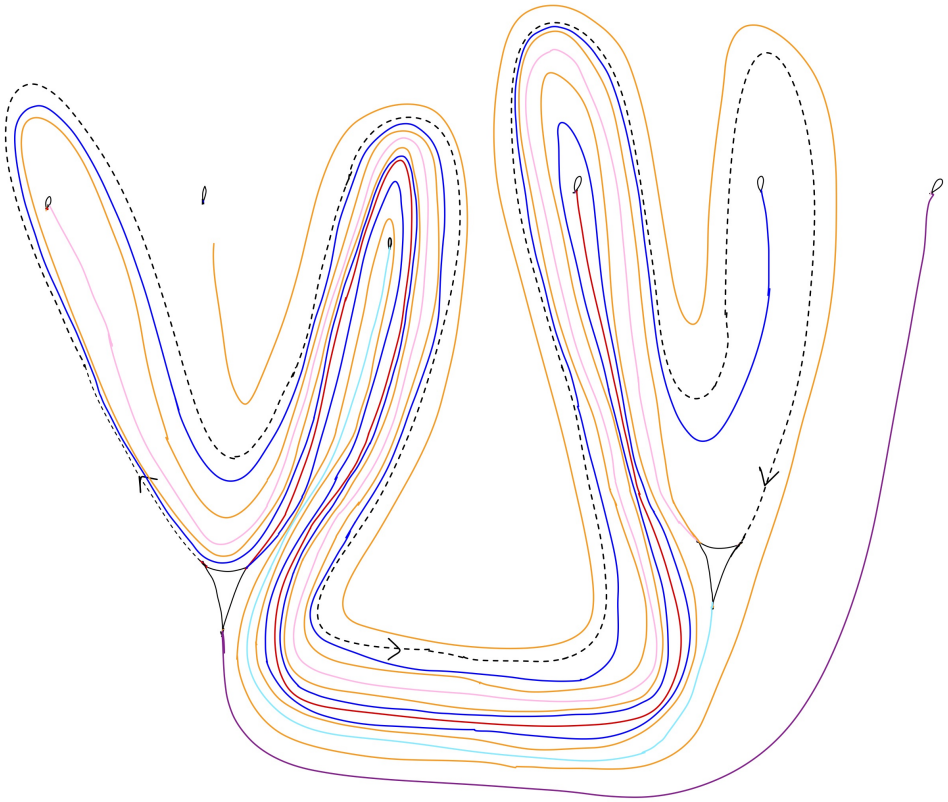


Figure D.50: Mooncalf8

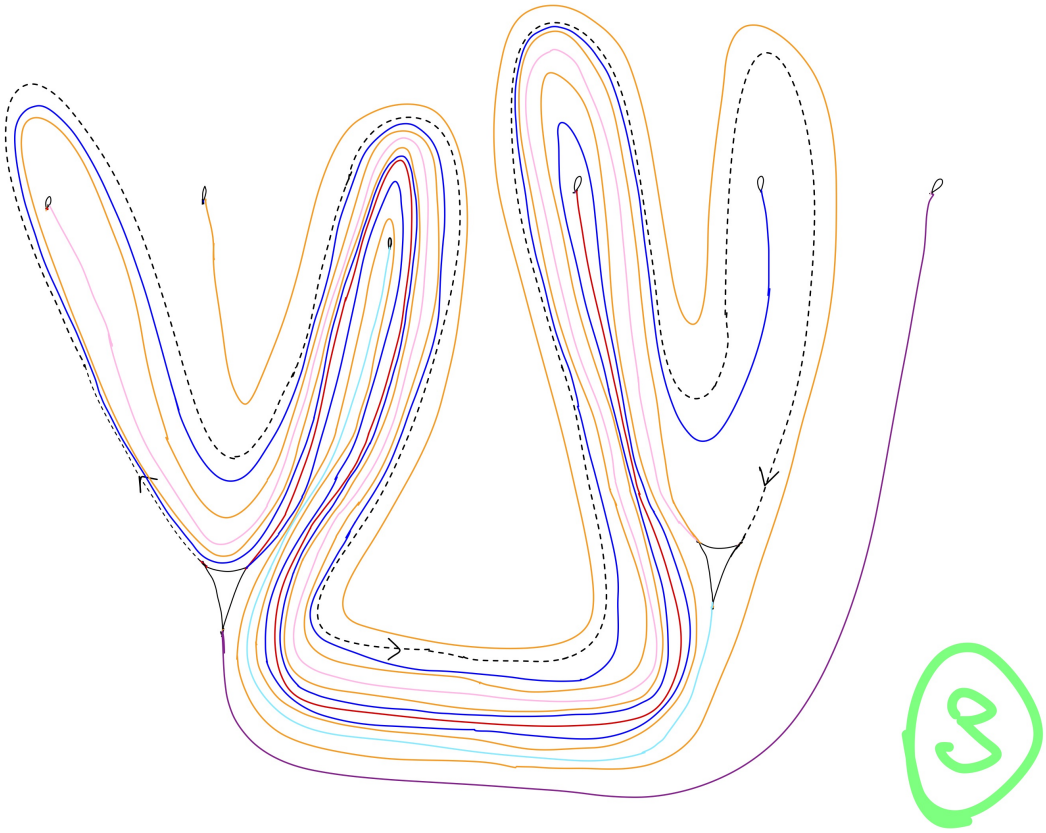


Figure D.51: Mooncalf9

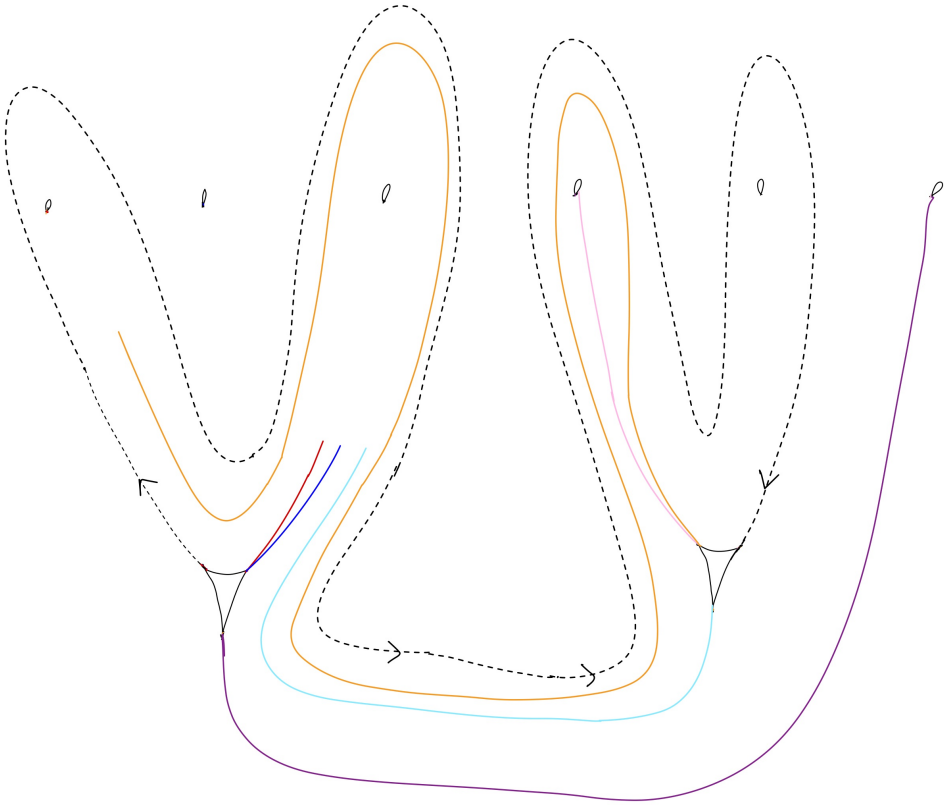


Figure D.52: Faffel1

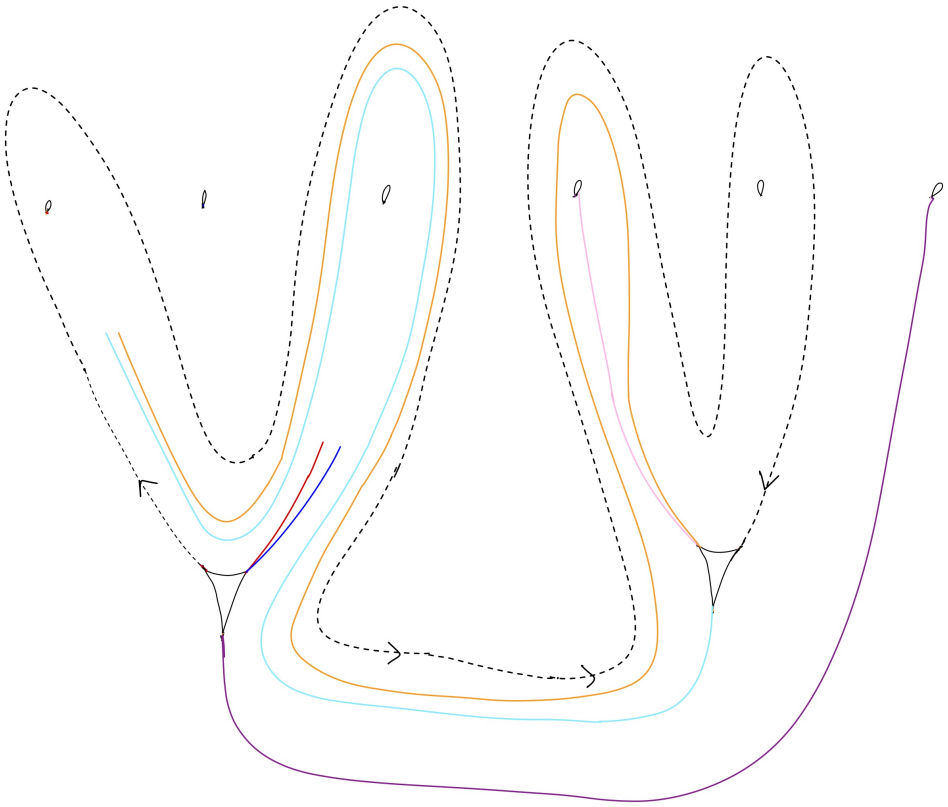


Figure D.53: Faffel2

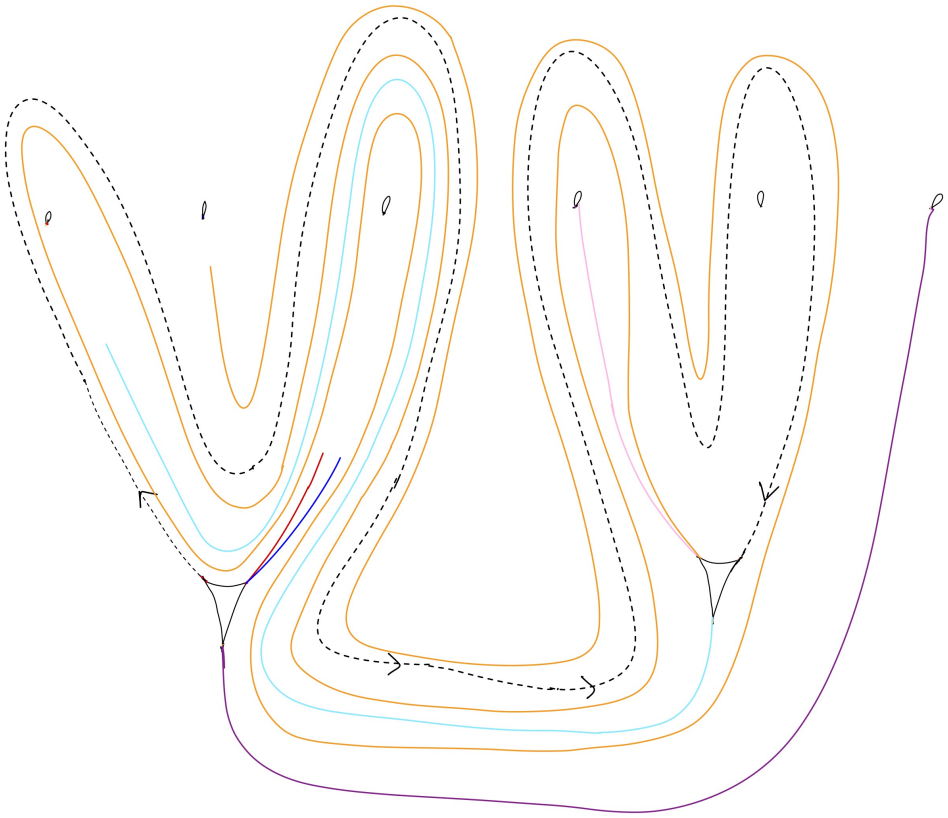


Figure D.54: Faffel3

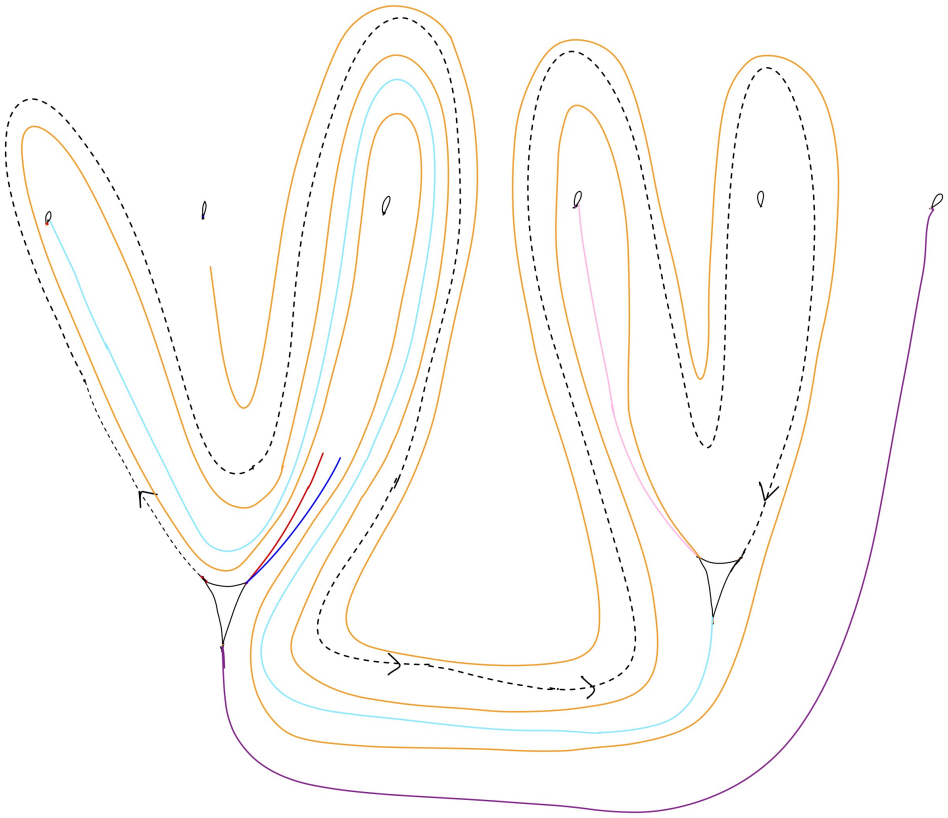


Figure D.55: Faffel4

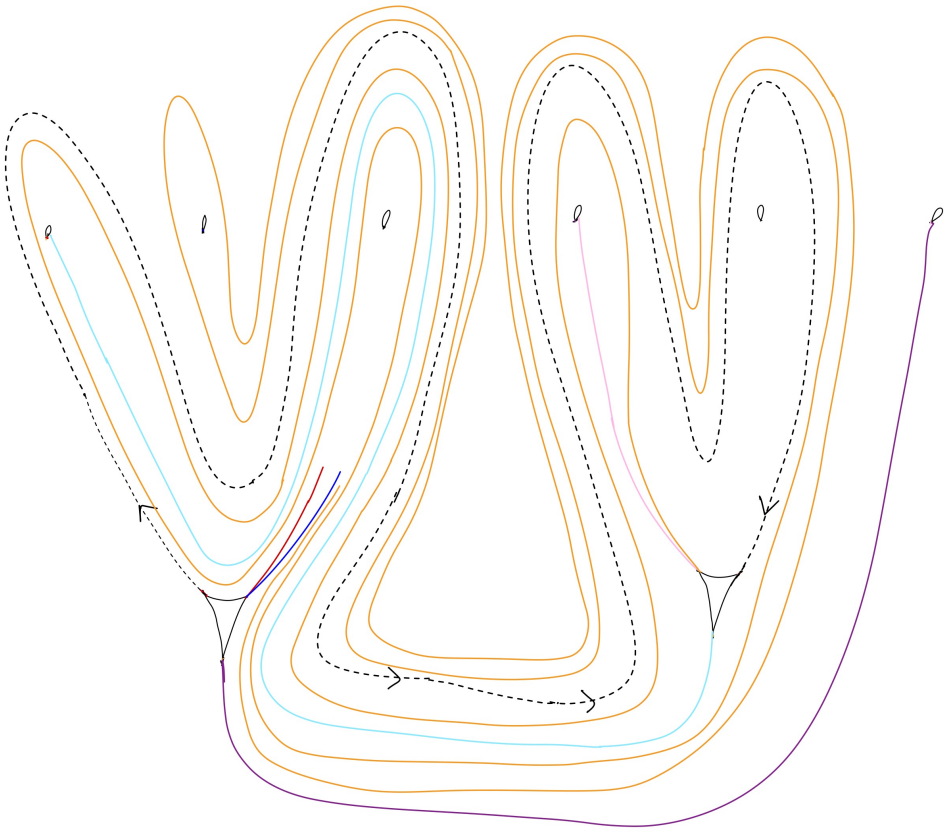


Figure D.56: Faffel5

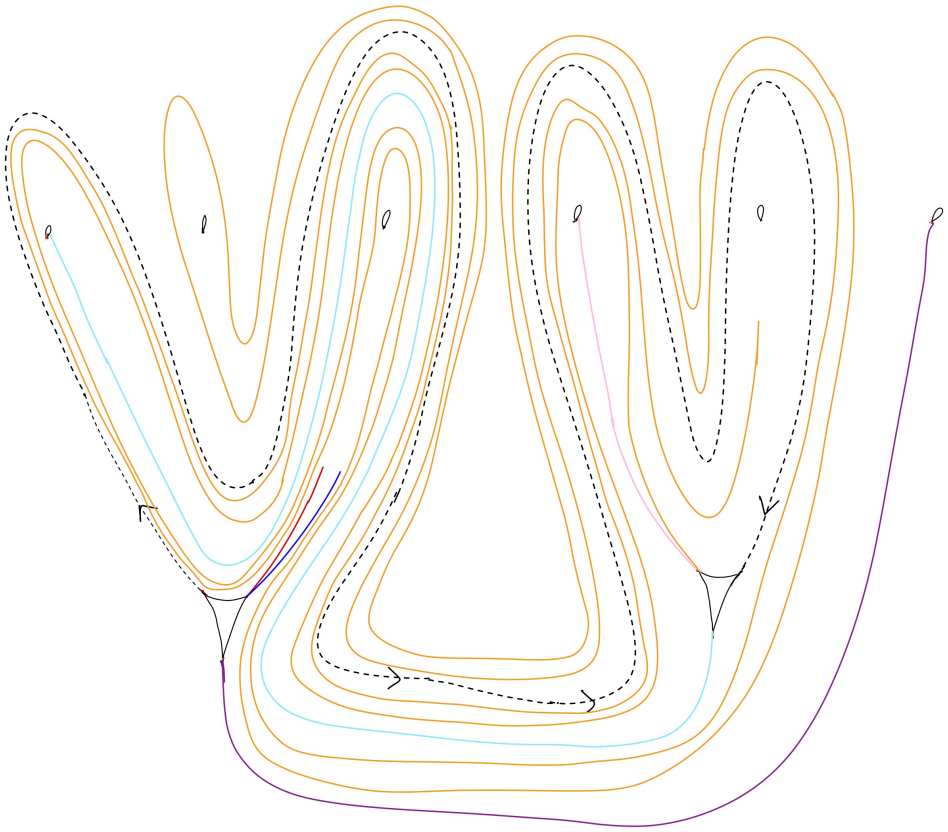


Figure D.57: Faffel6

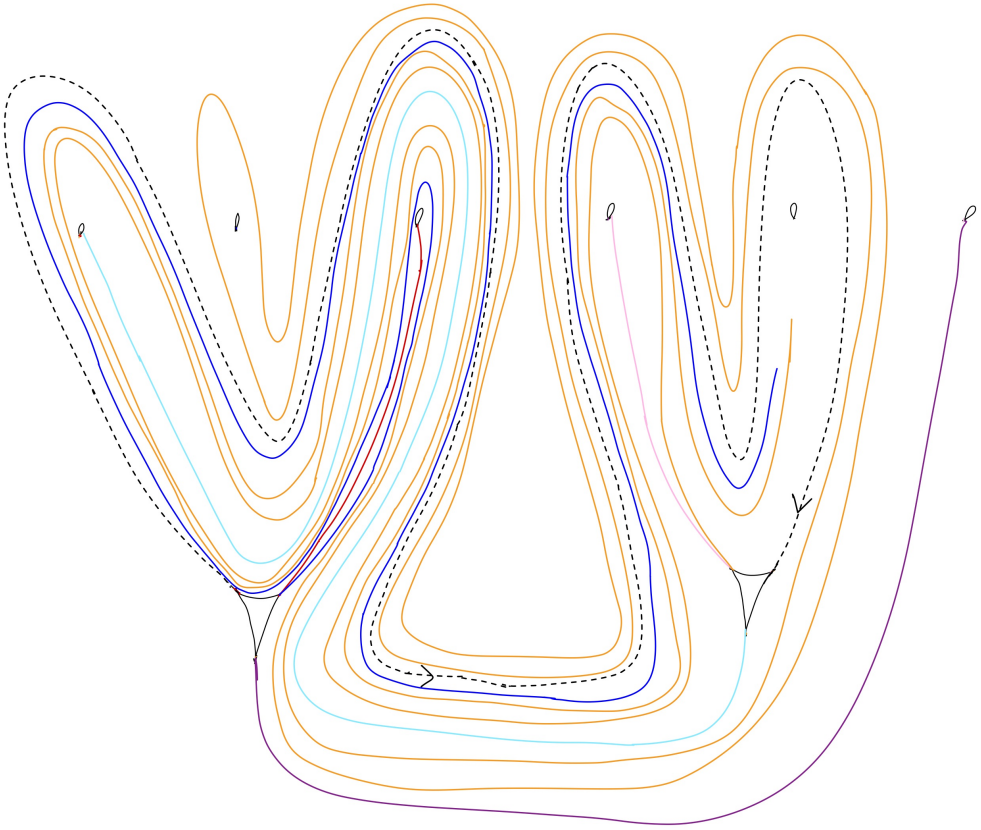


Figure D.58: Faffel7

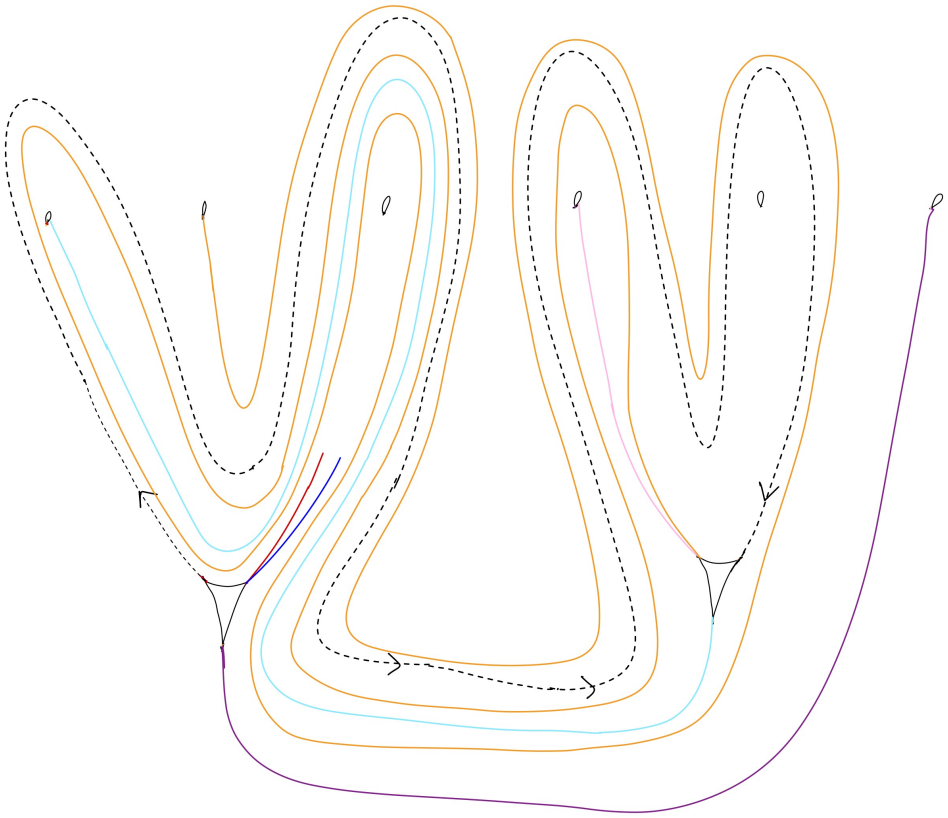


Figure D.59: Faffel8

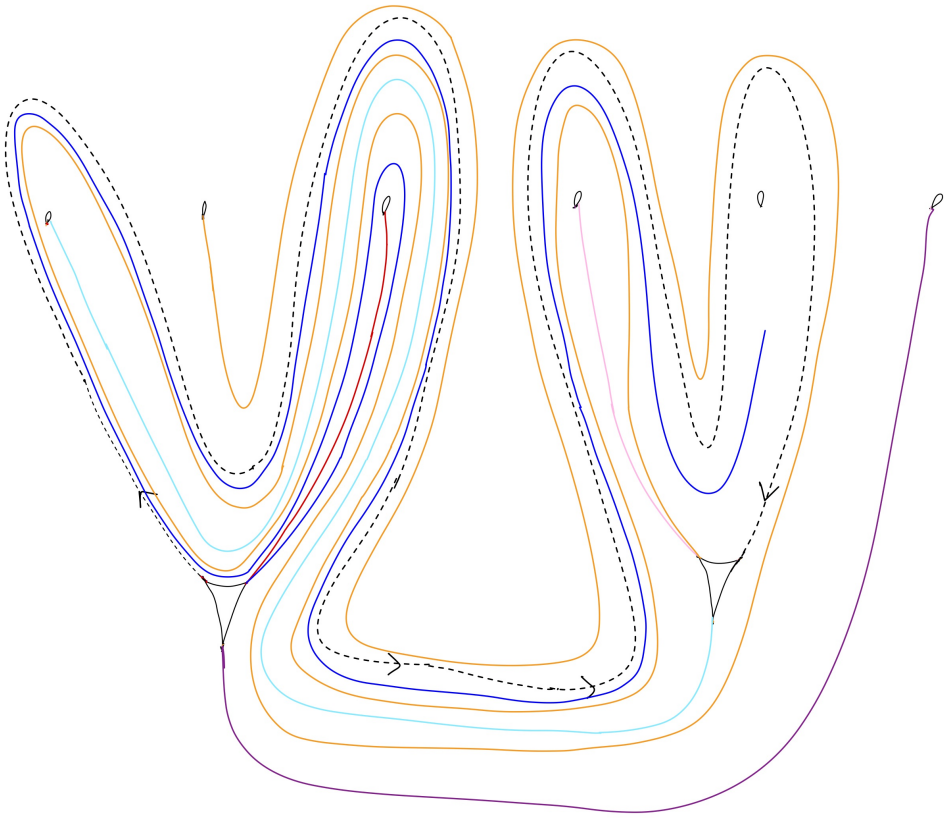


Figure D.60: Faffel9

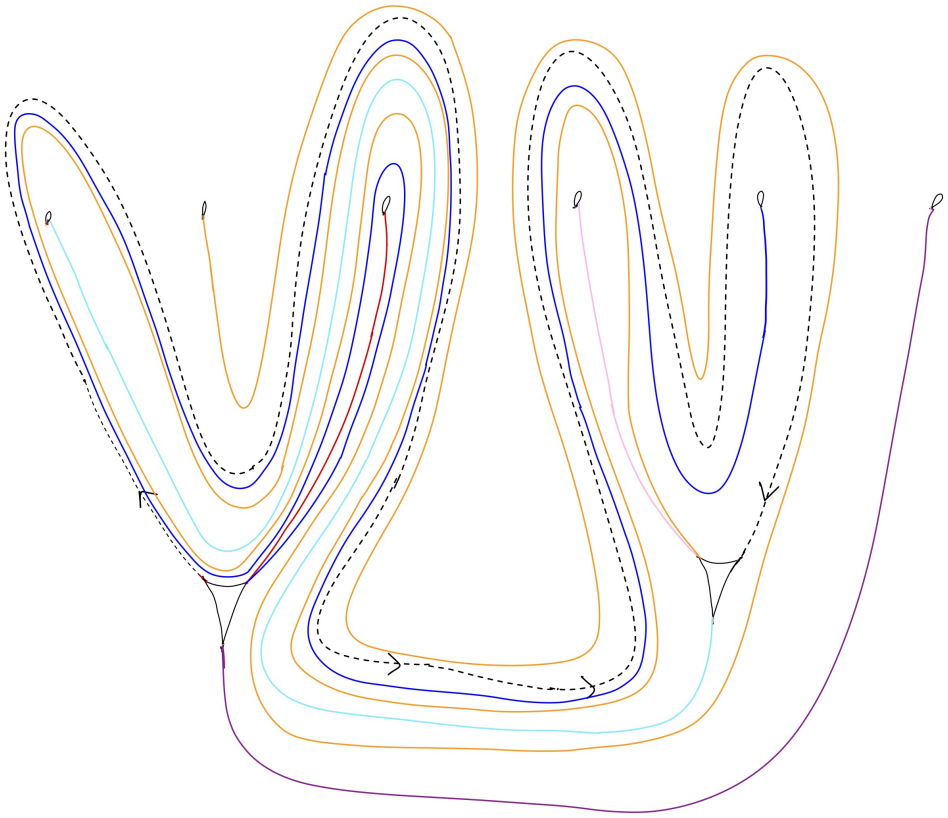


Figure D.61: Faffel10

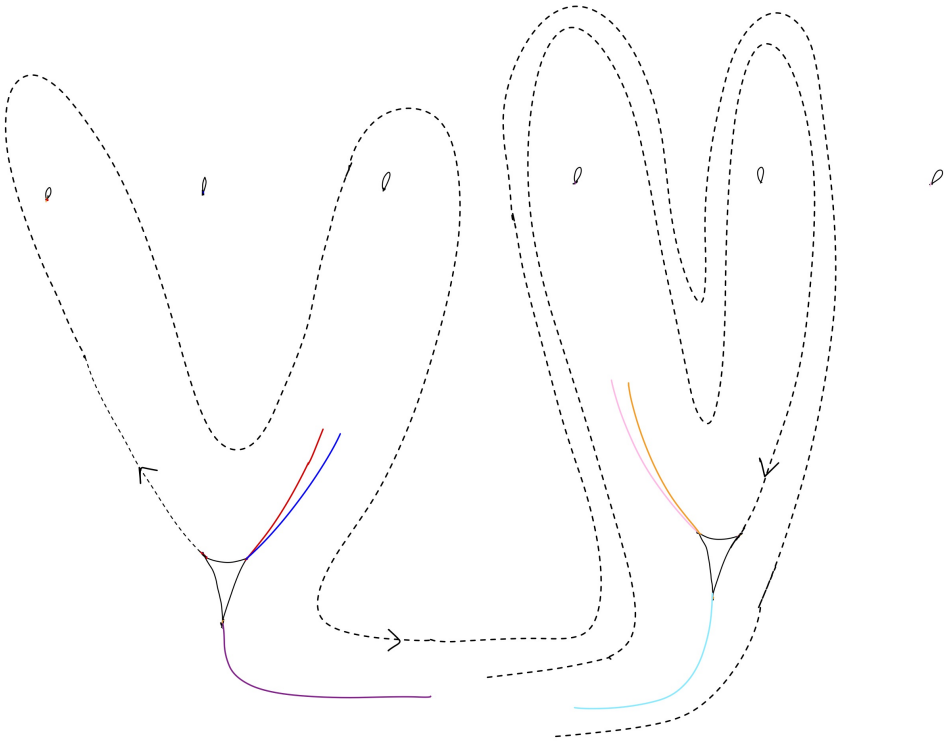


Figure D.62: Lugs1

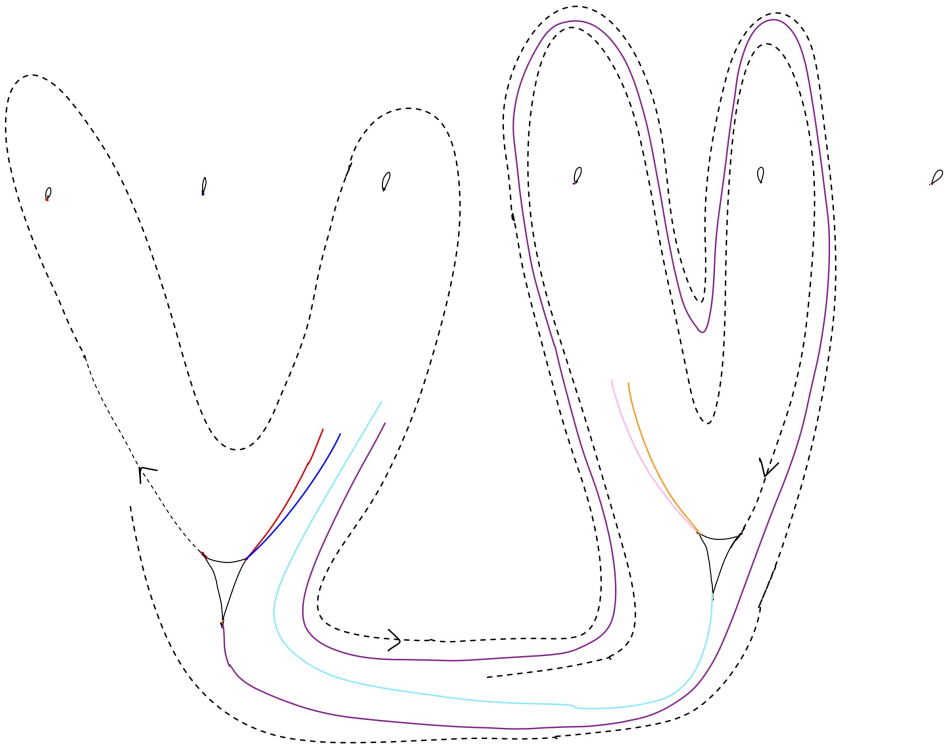


Figure D.63: Lugs2

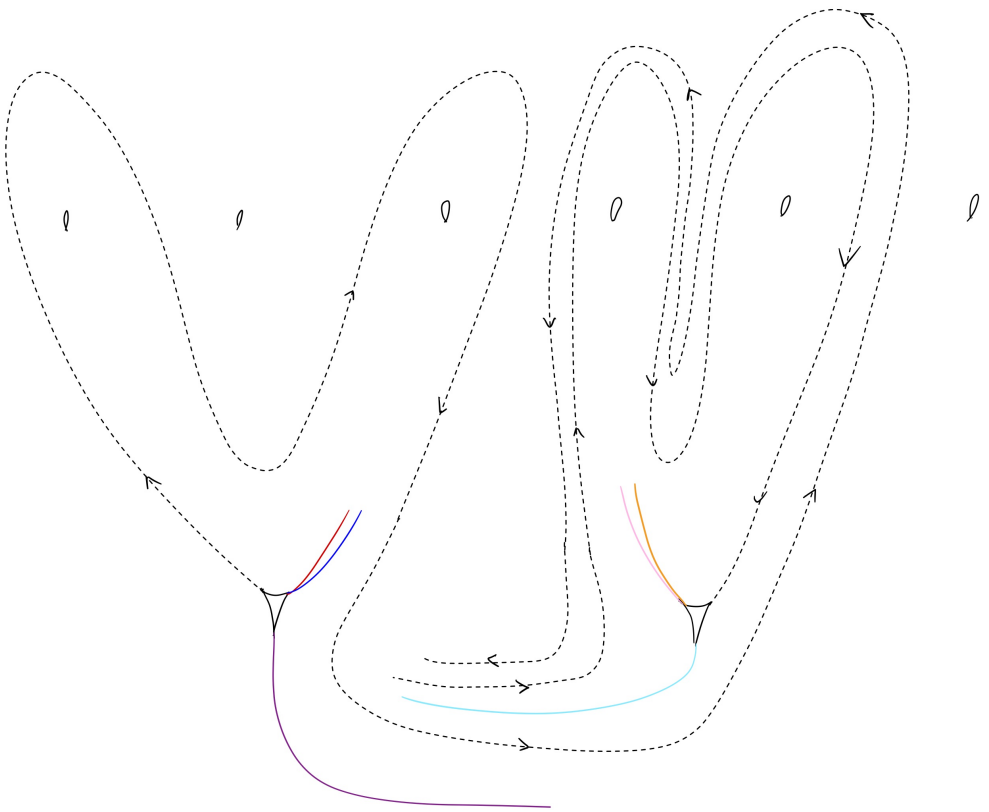


Figure D.64: Haze1

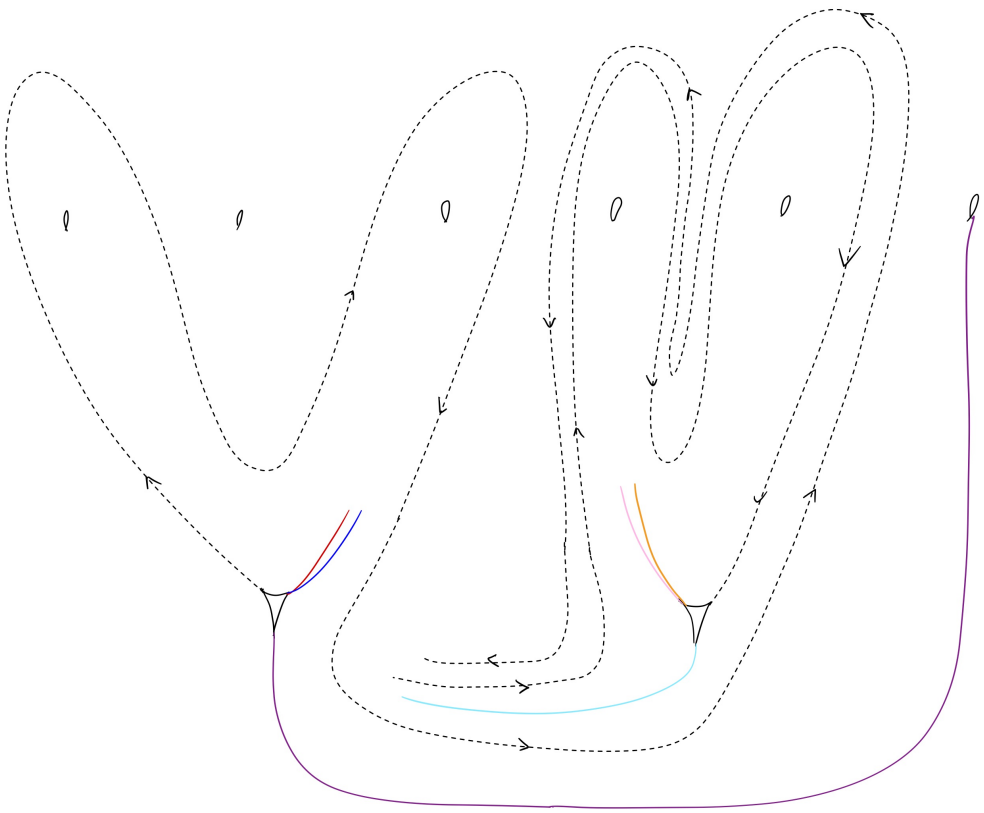


Figure D.65: Haze2

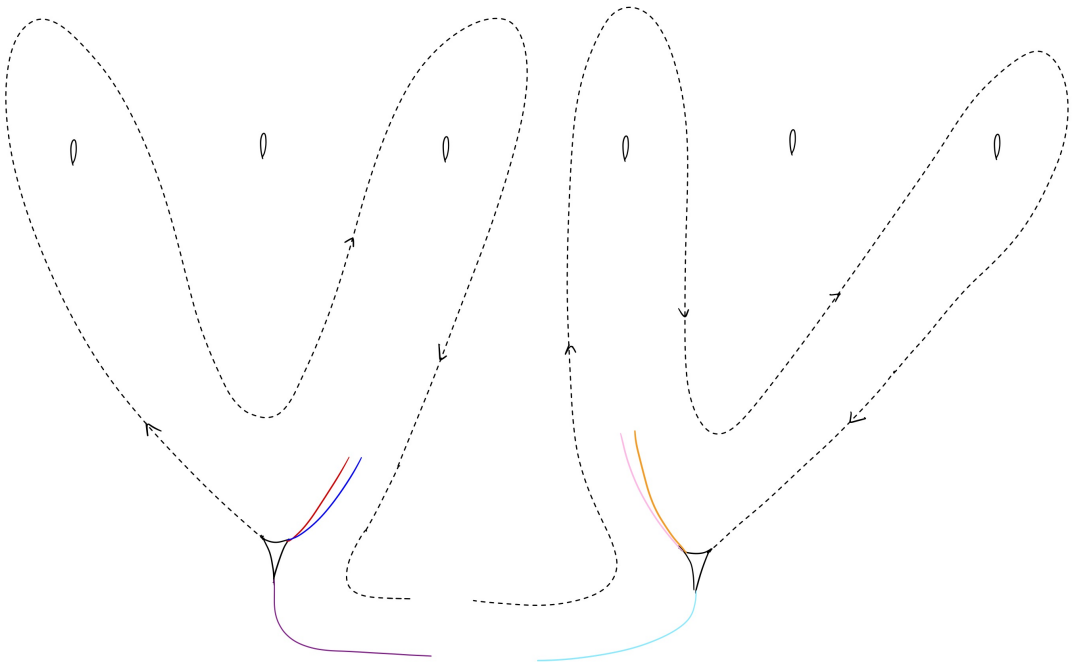


Figure D.66: Quip1

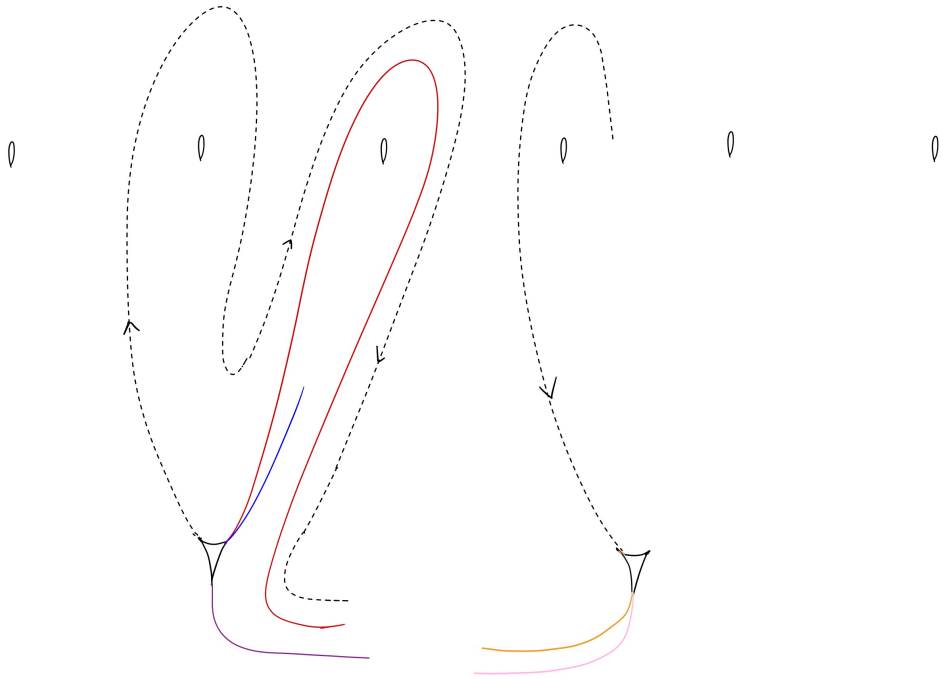


Figure D.67: Zest1

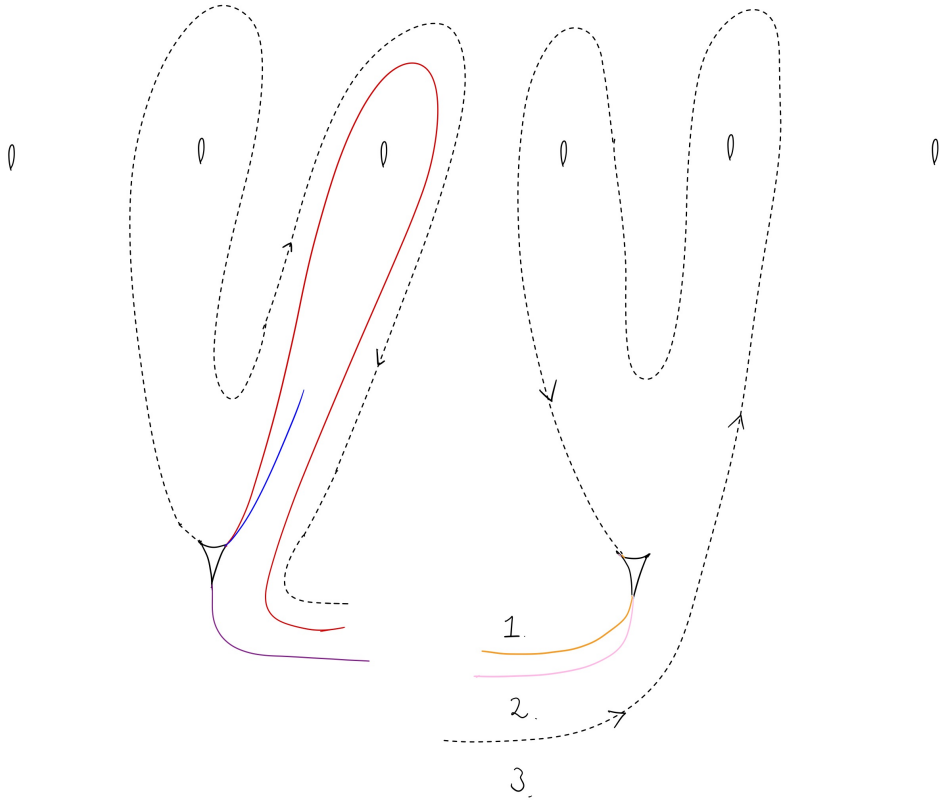


Figure D.68: Omen1

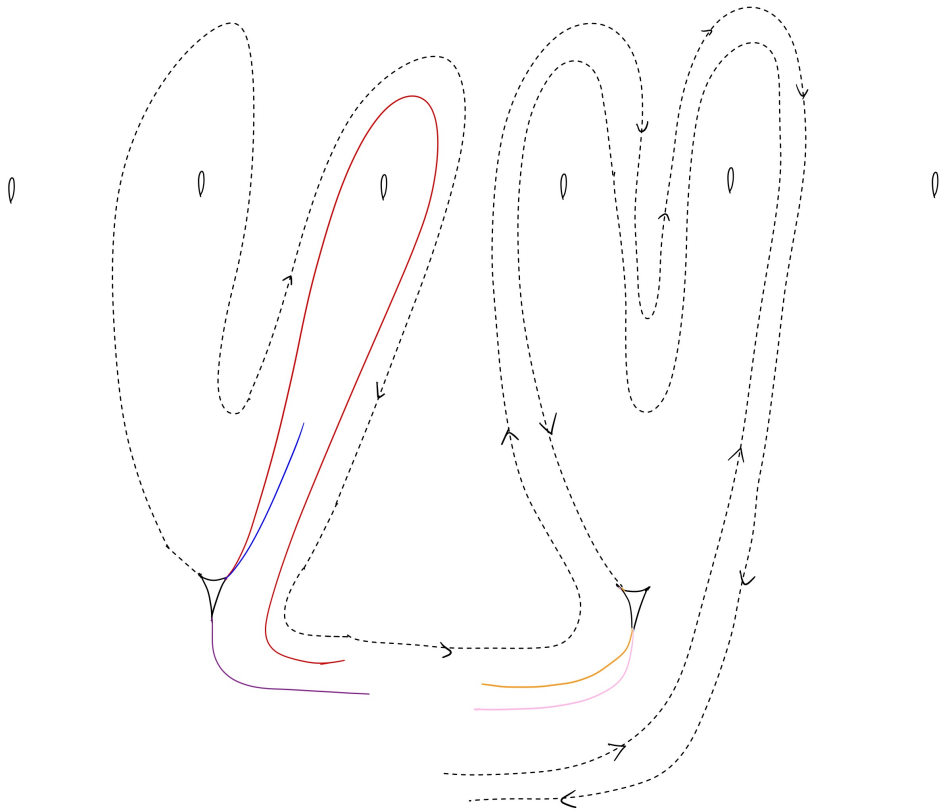


Figure D.69: Omen2

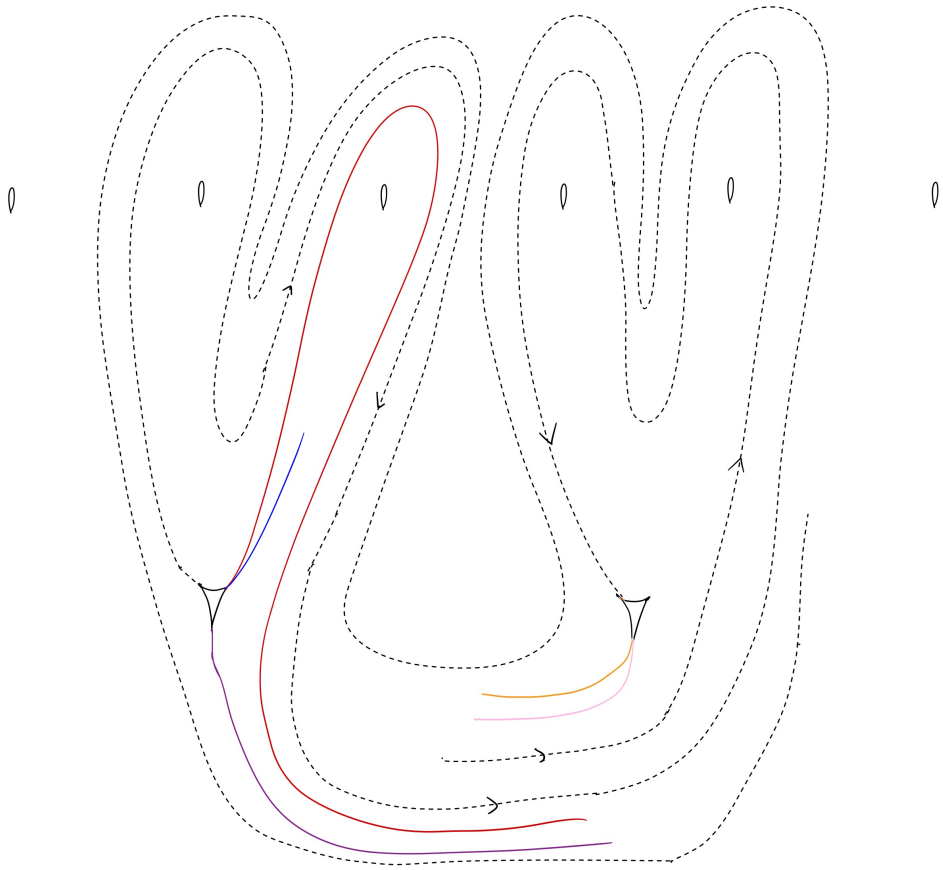


Figure D.70: Omen3

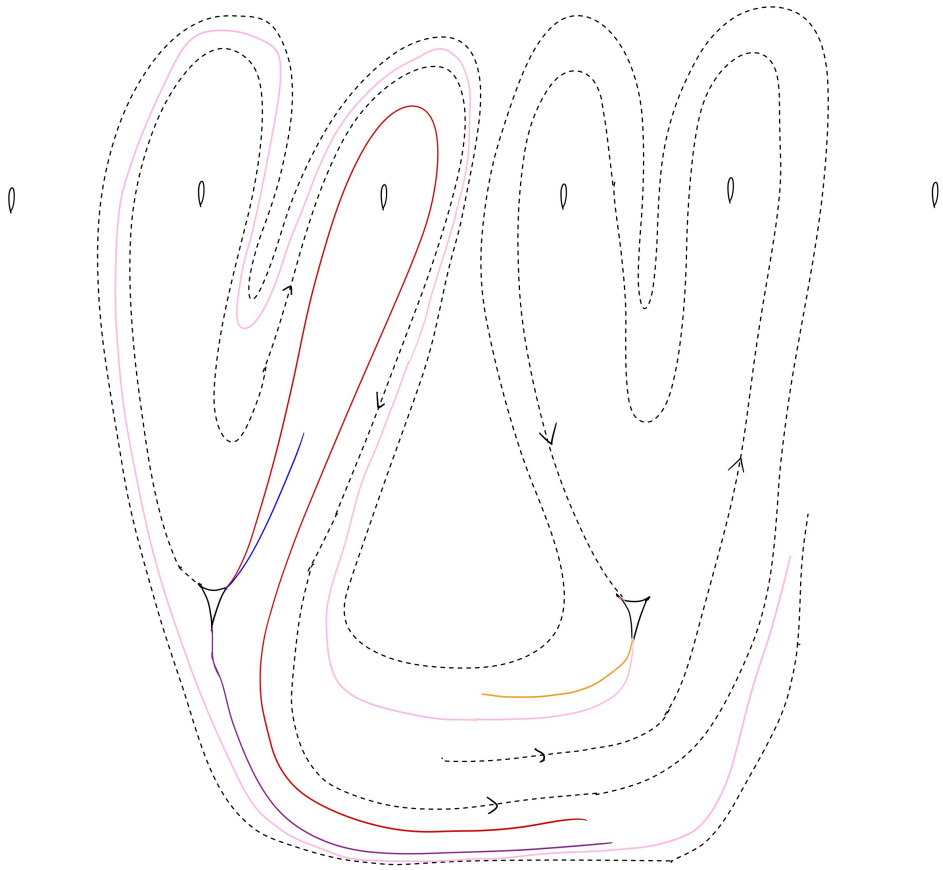


Figure D.71: Omen4

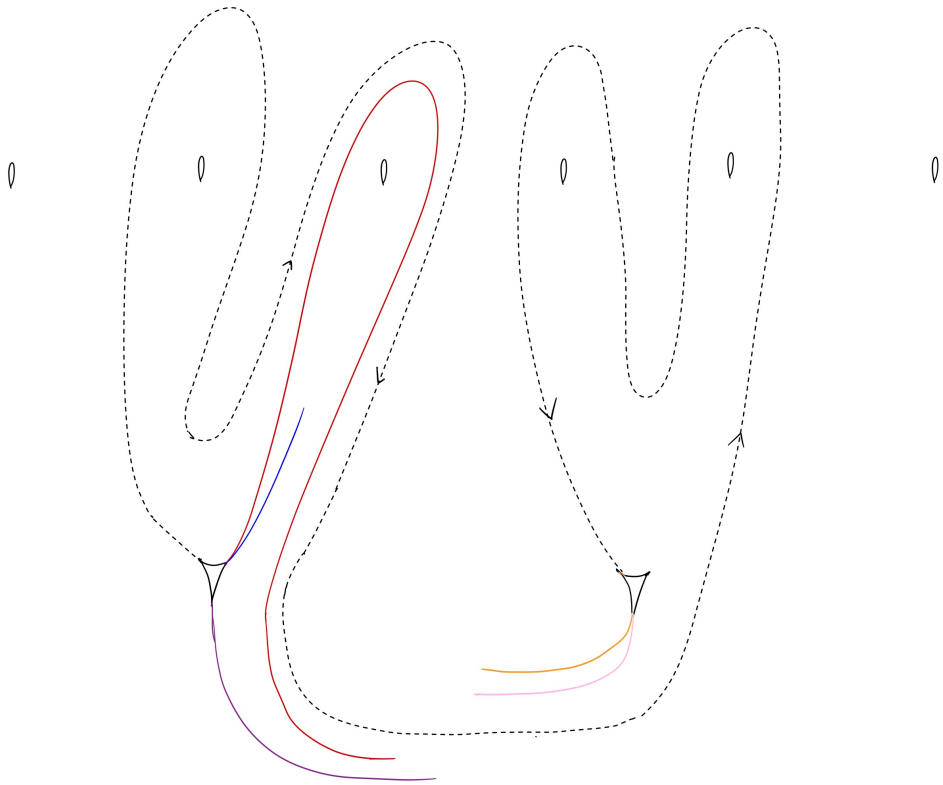


Figure D.72: Omen5

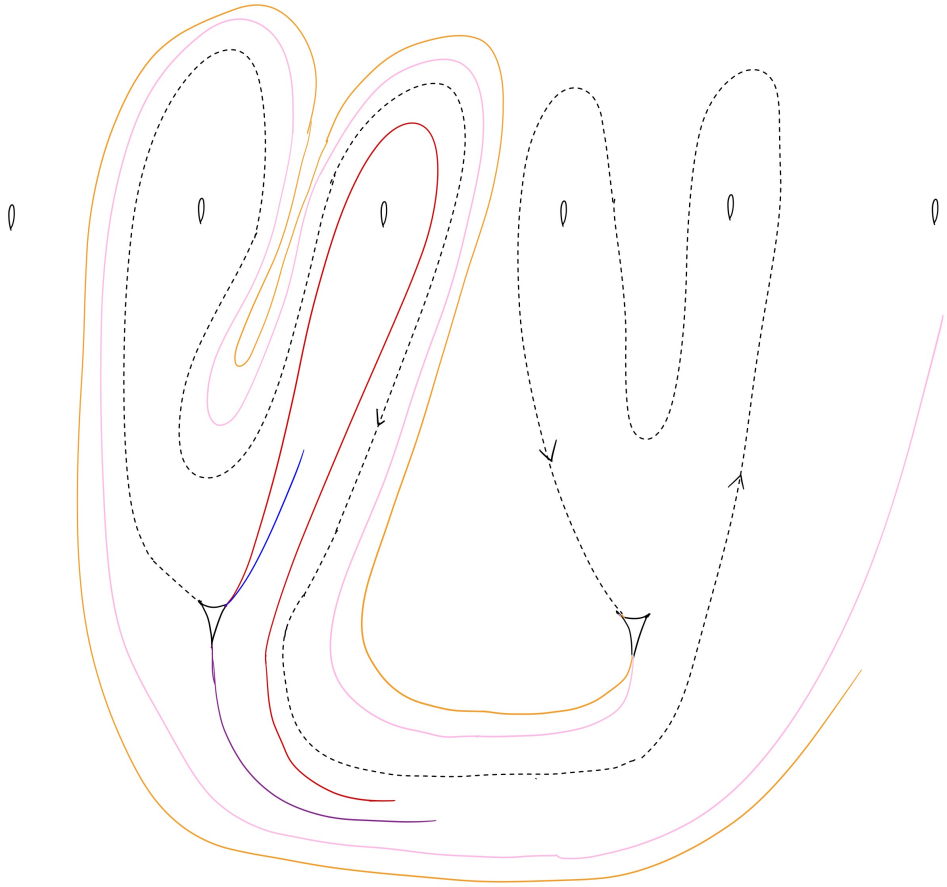


Figure D.73: Omen6

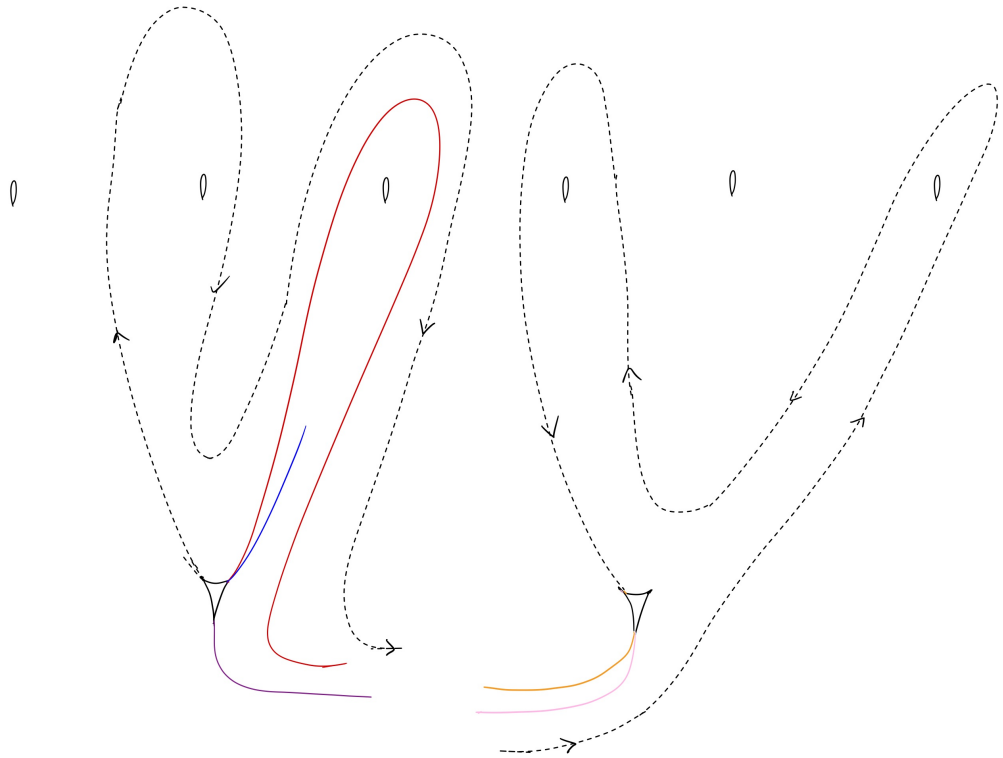


Figure D.74: Axe1

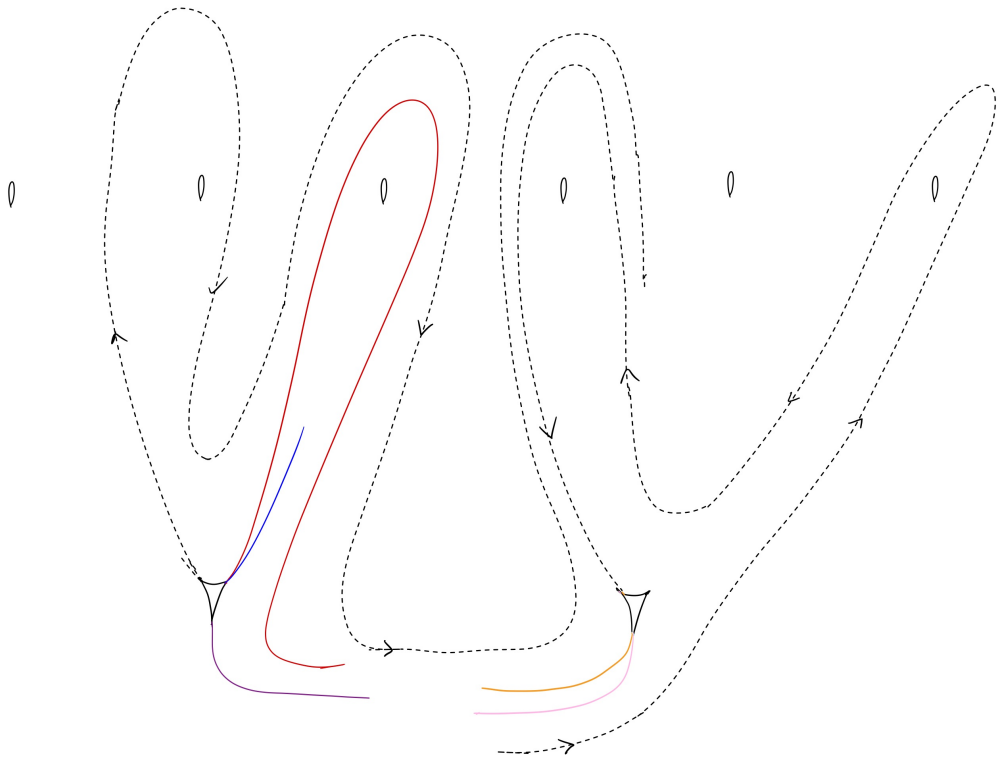


Figure D.75: Axe2

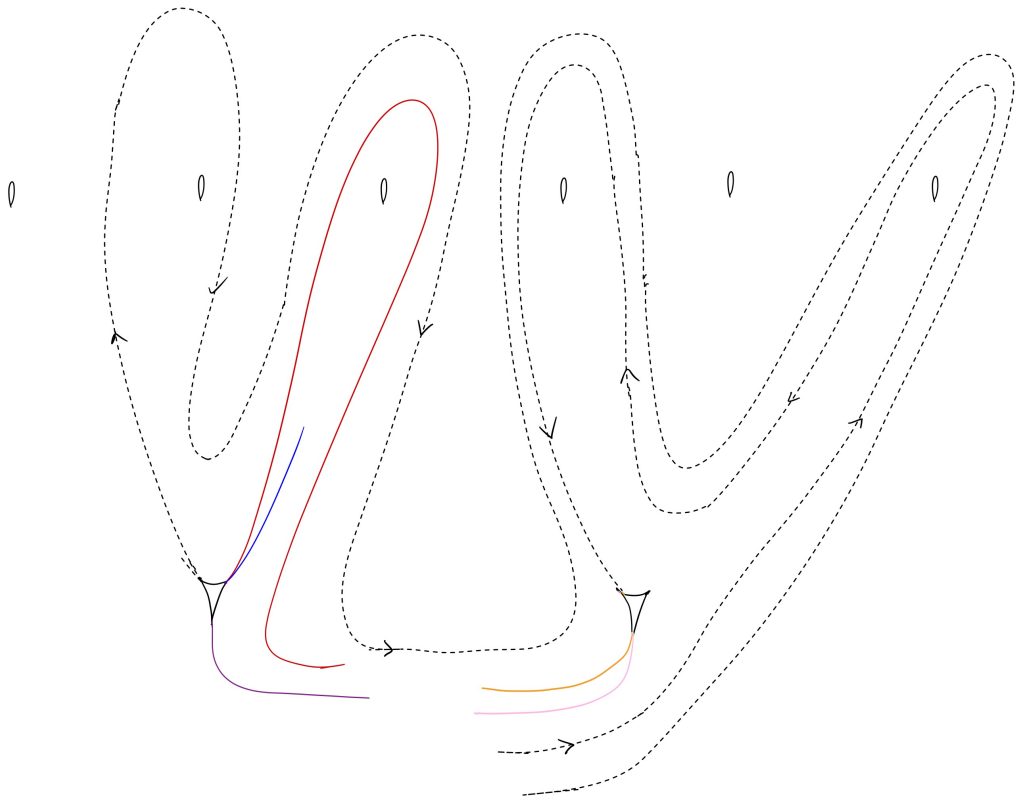


Figure D.76: Axe3

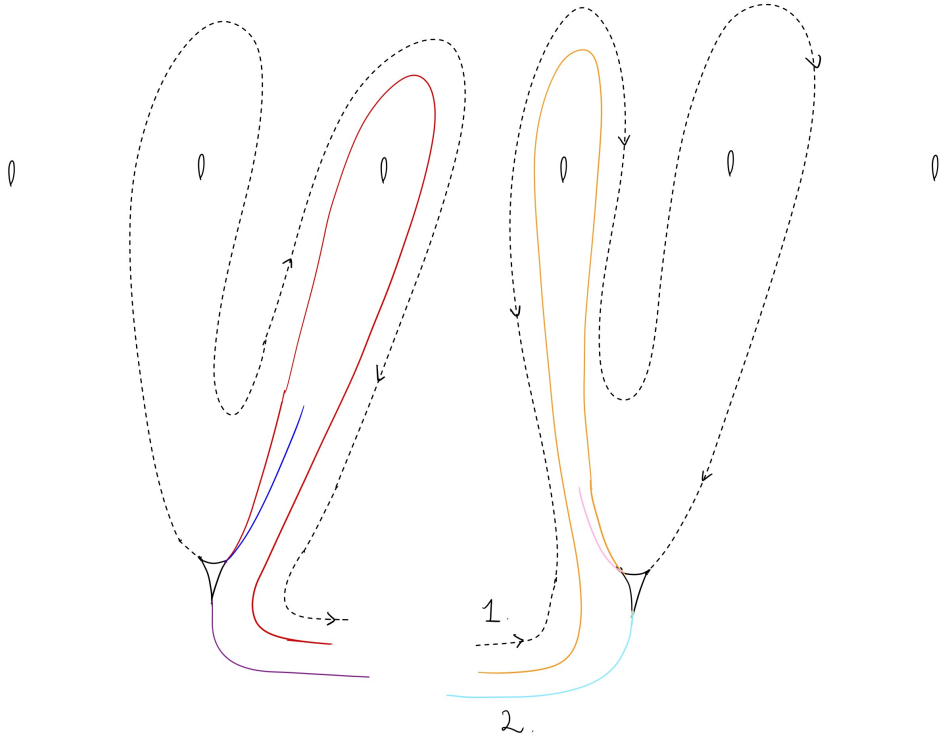


Figure D.77: Lox1

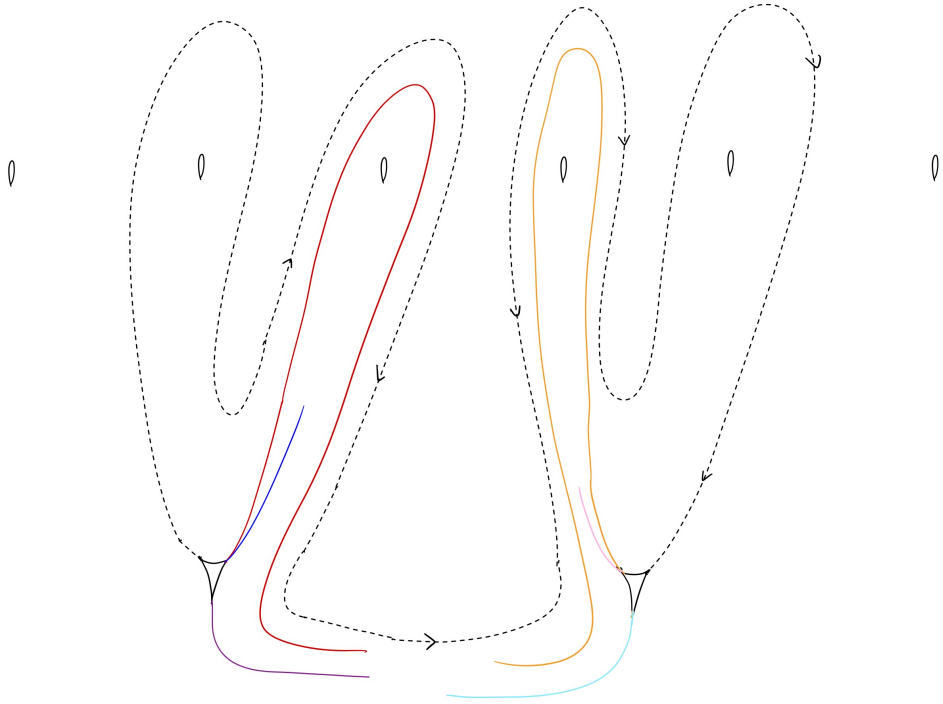


Figure D.78: Lava1

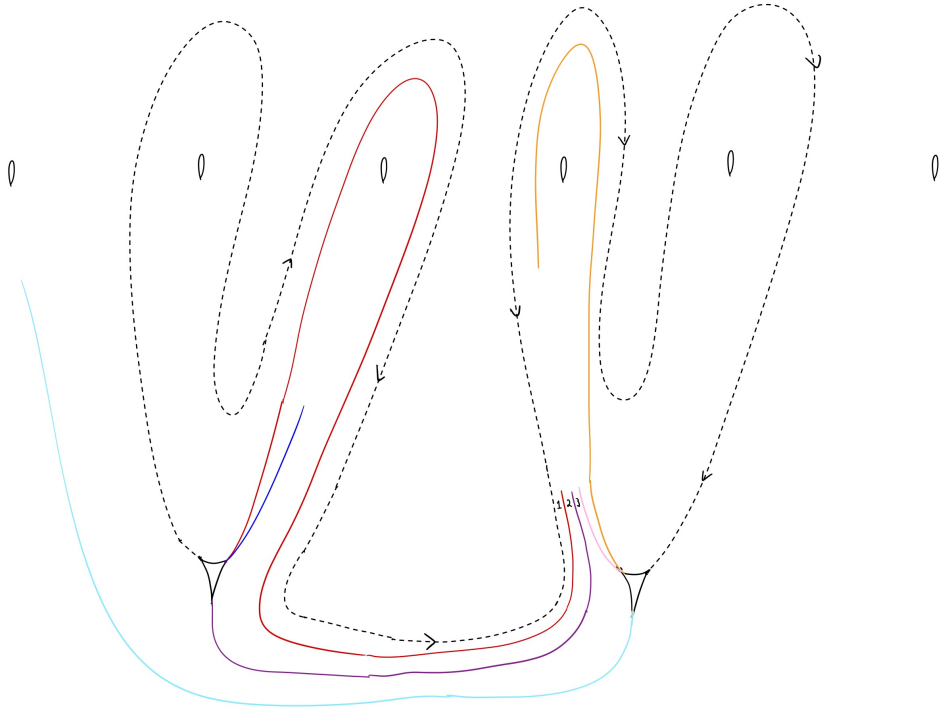


Figure D.79: Query1

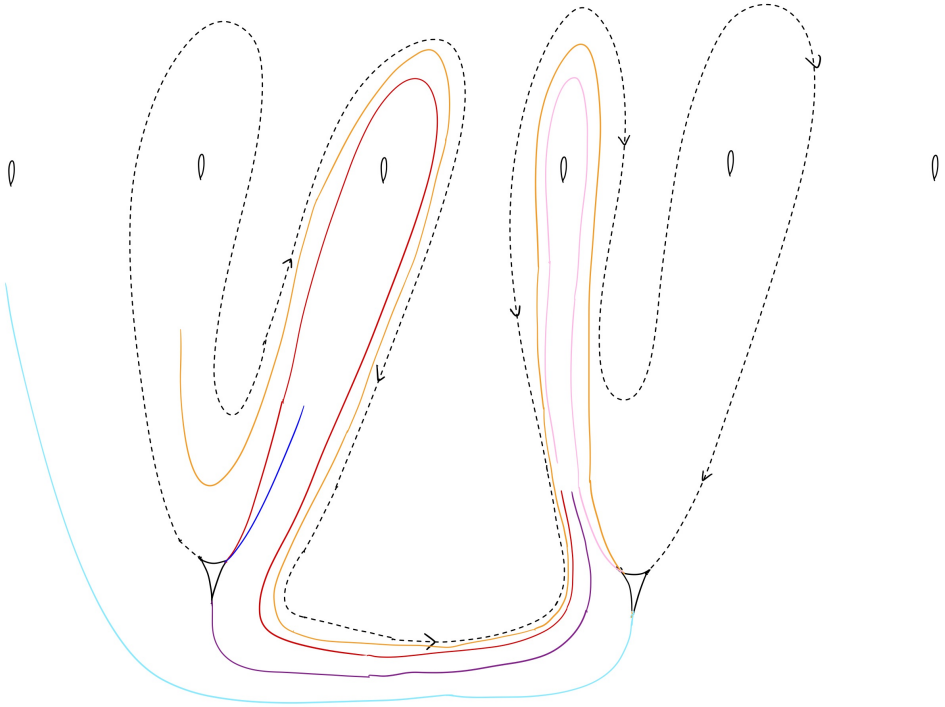


Figure D.80: Depth1

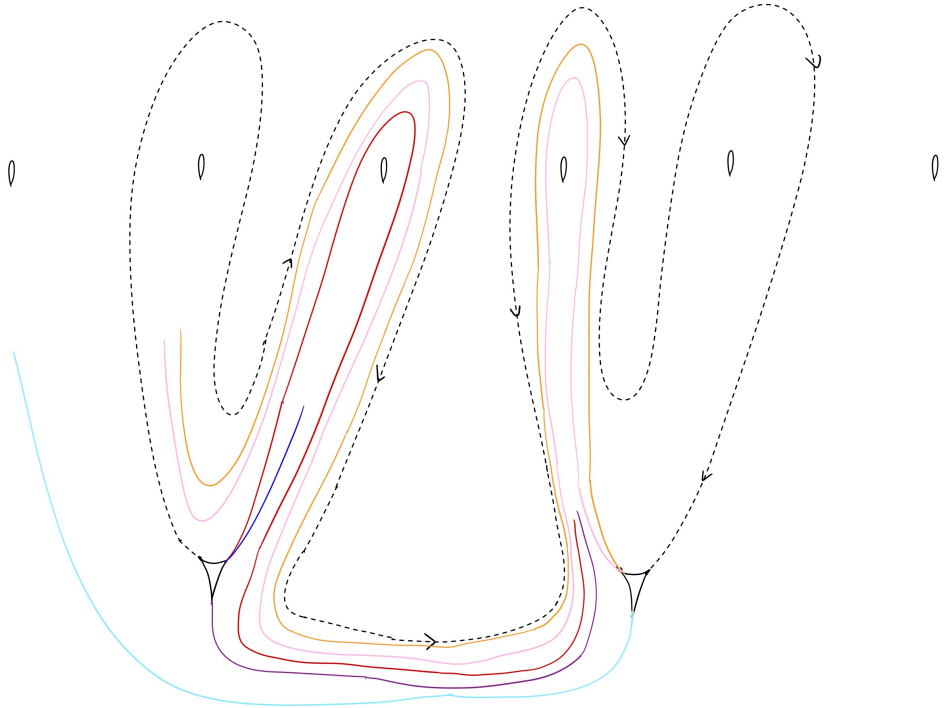


Figure D.81: Depth2

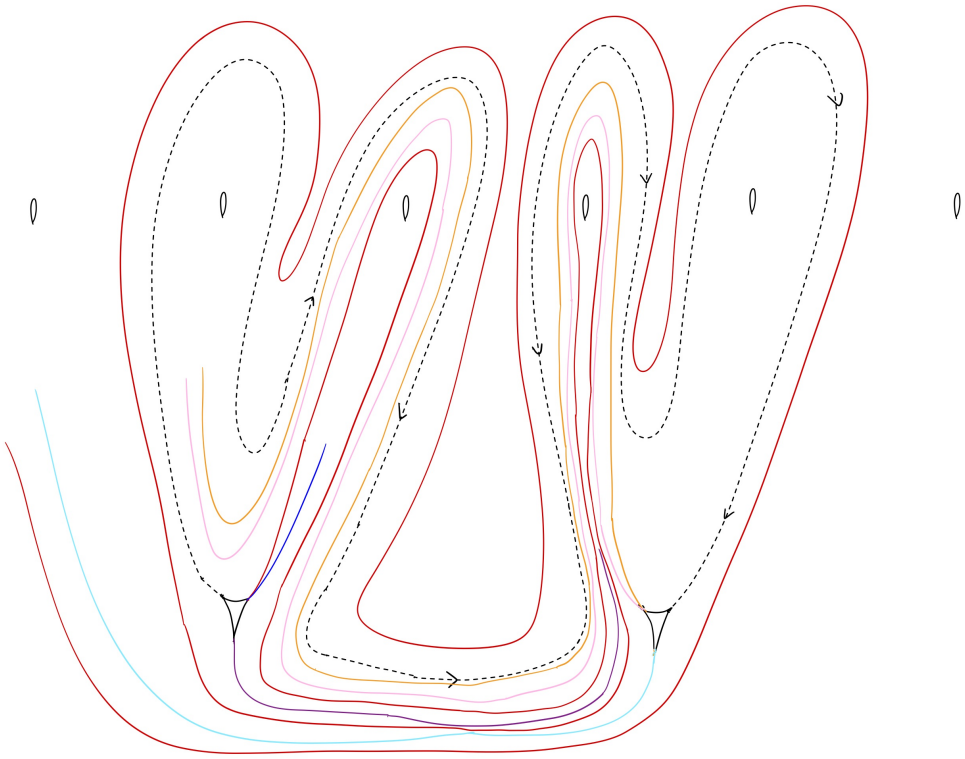


Figure D.82: Depth3

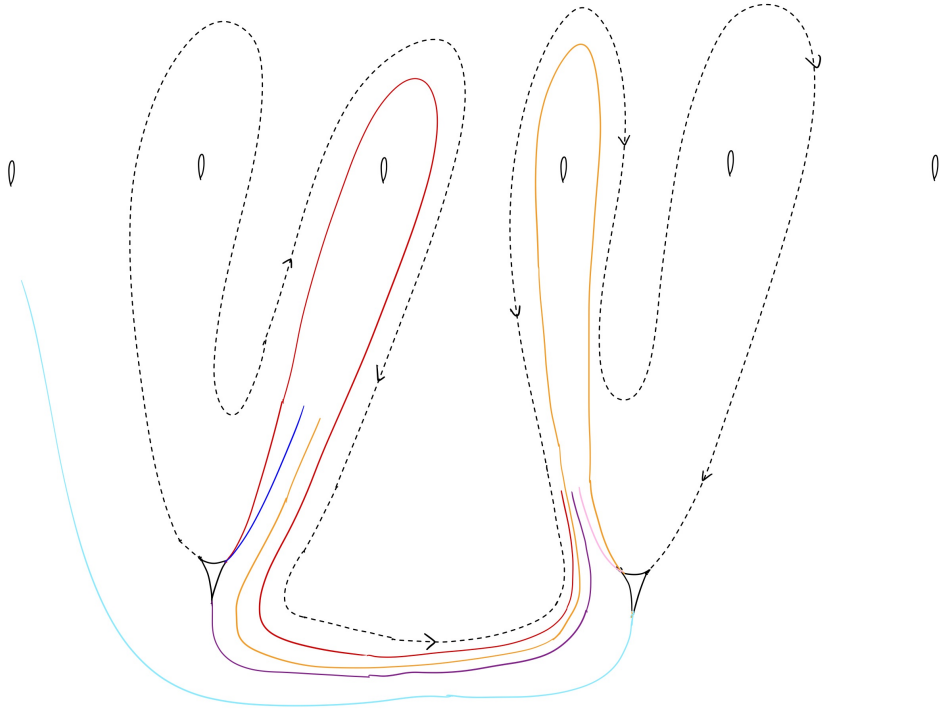


Figure D.83: Kiosk1

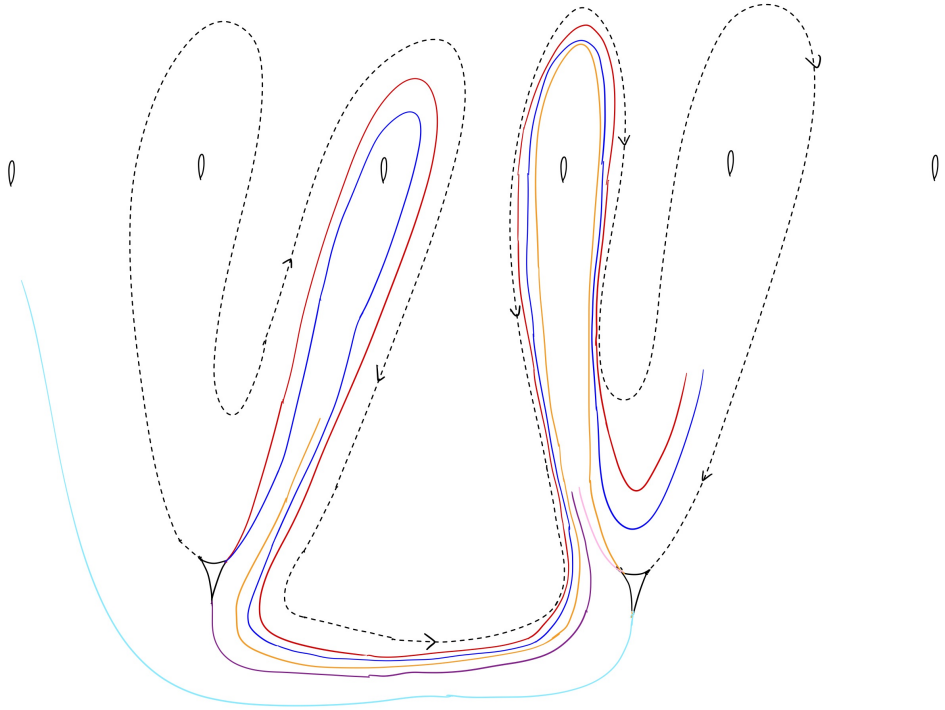


Figure D.84: Kiosk2

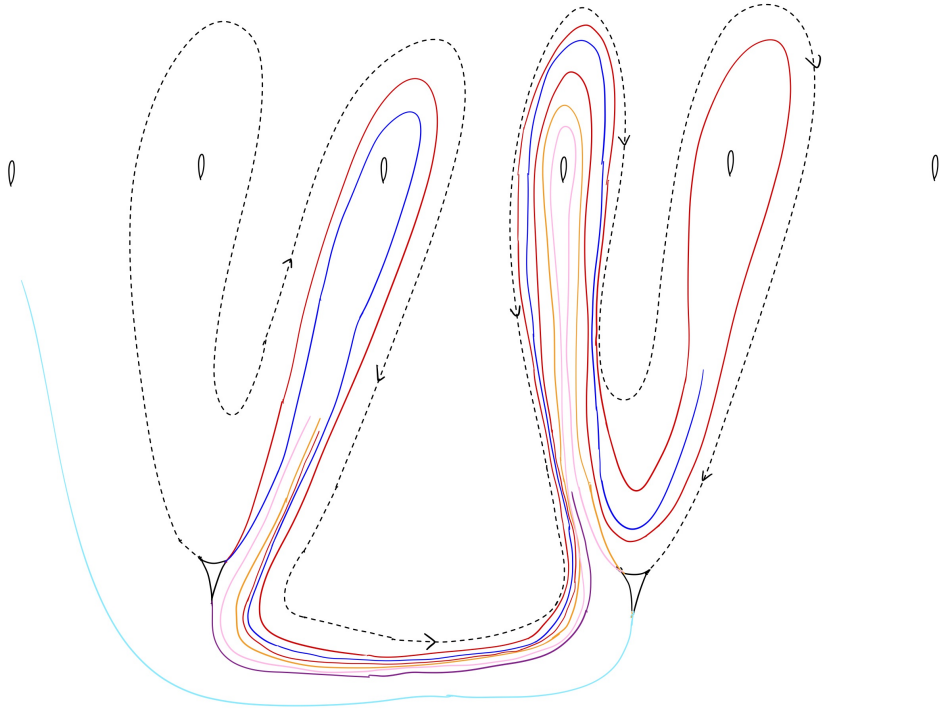


Figure D.85: Kiosk3

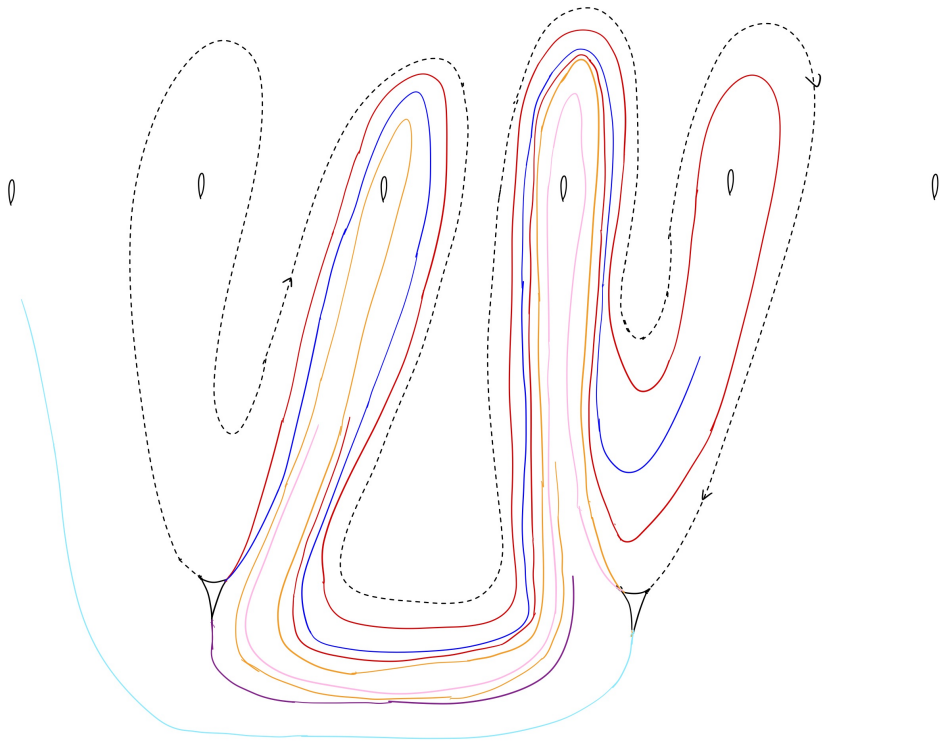


Figure D.86: Kiosk4

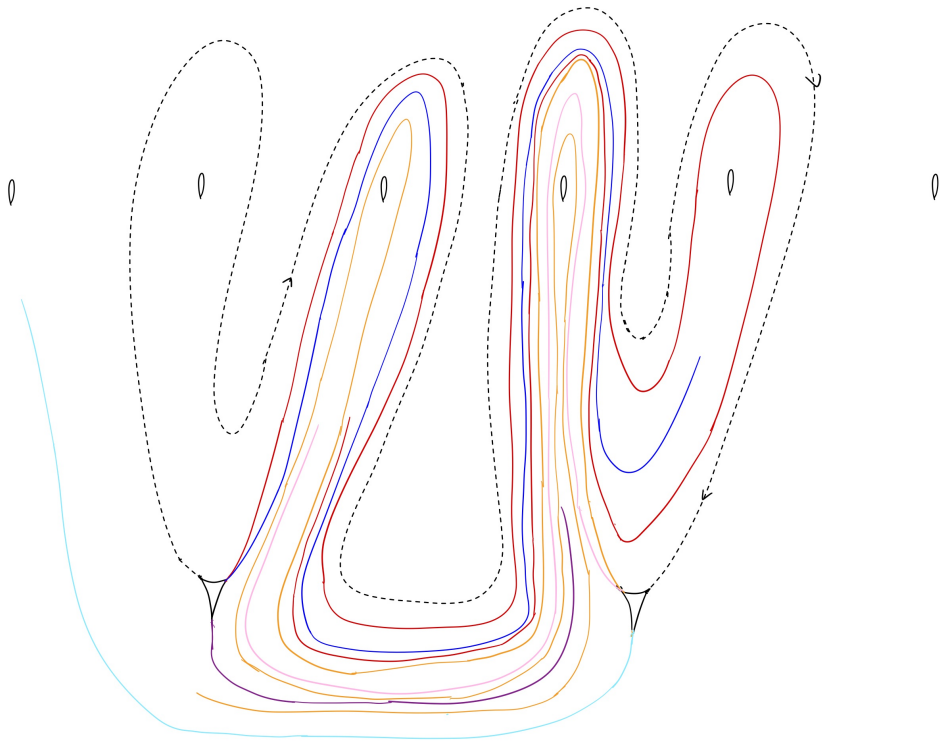


Figure D.87: Kiosk5

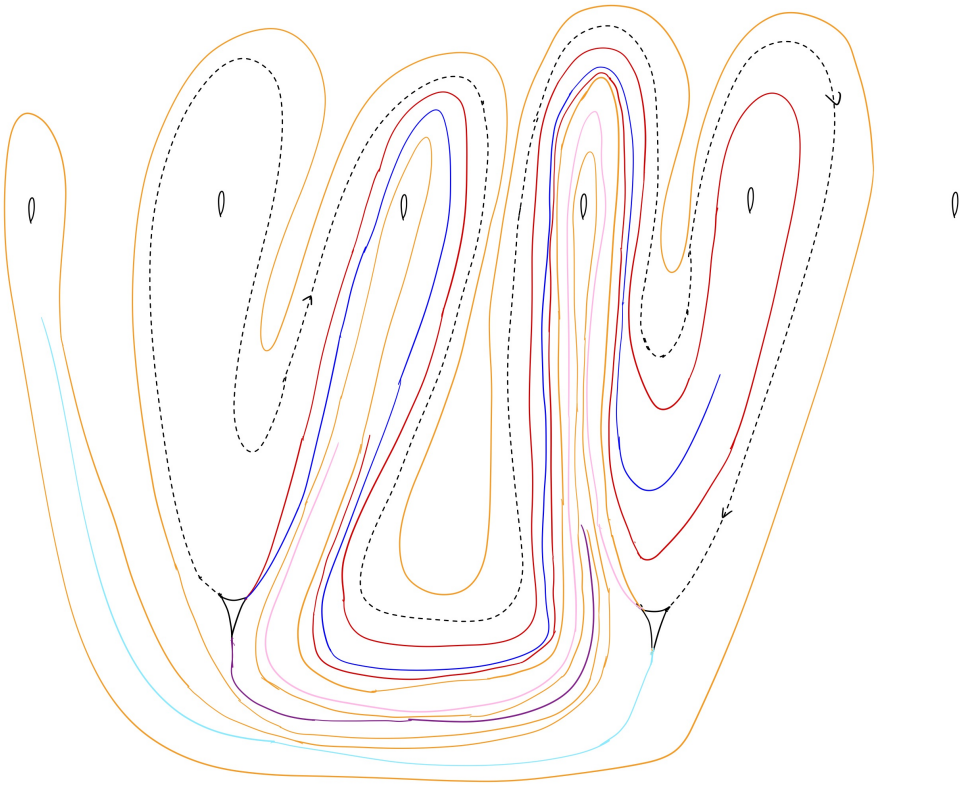


Figure D.88: Abacus1

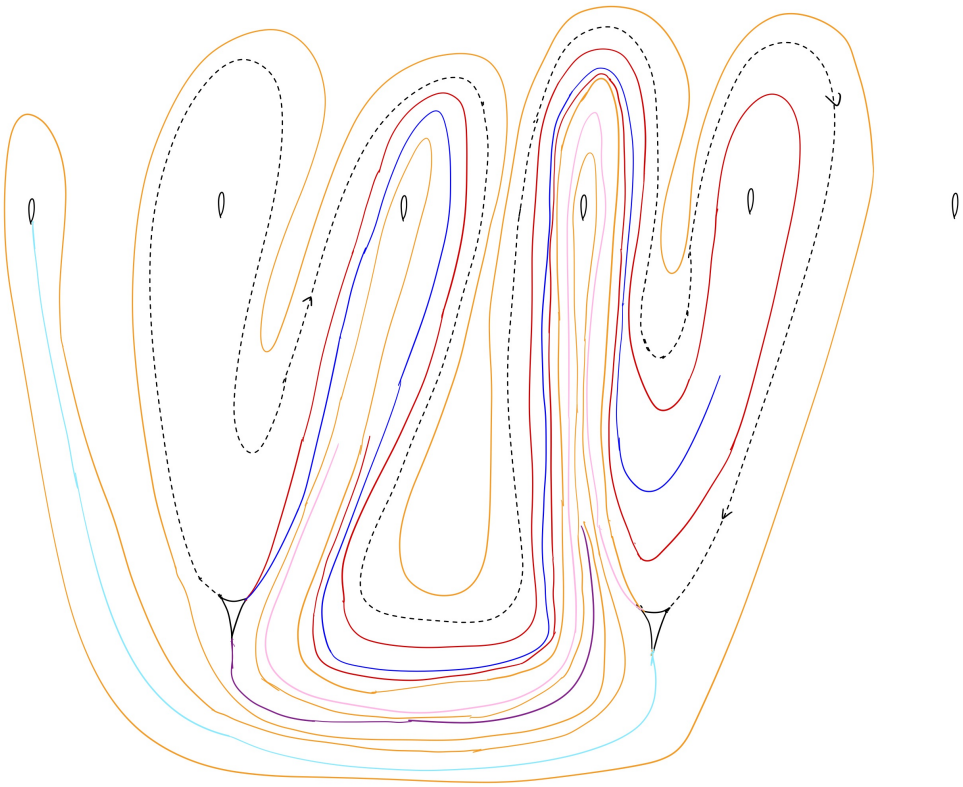


Figure D.89: Abacus2

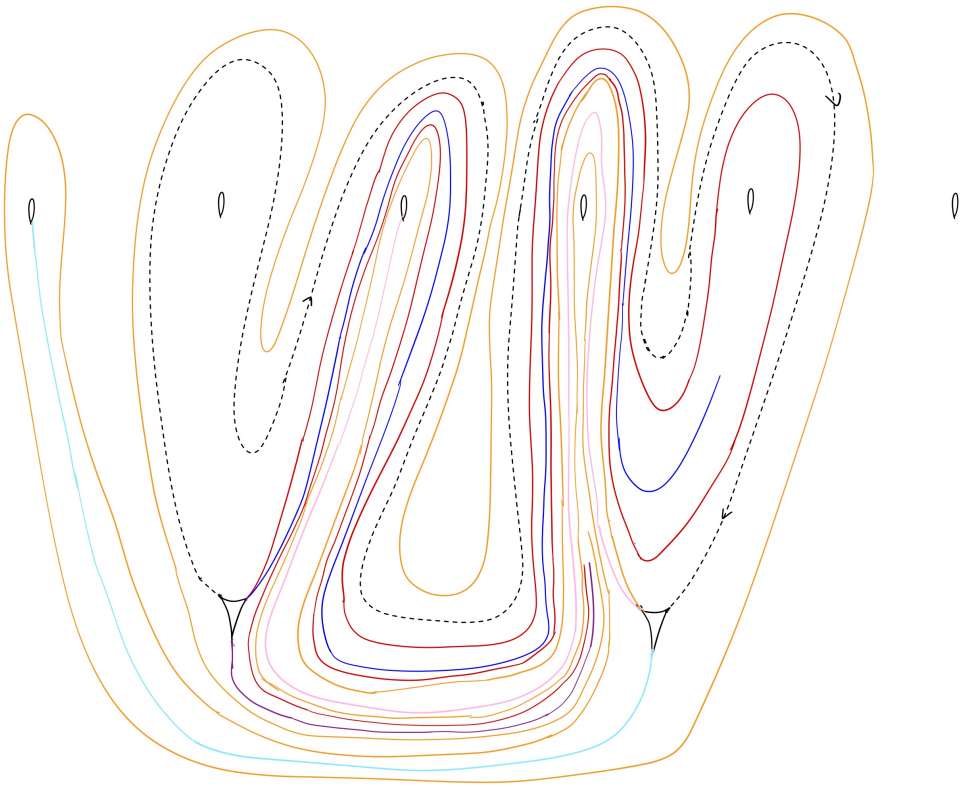


Figure D.90: Abacus3

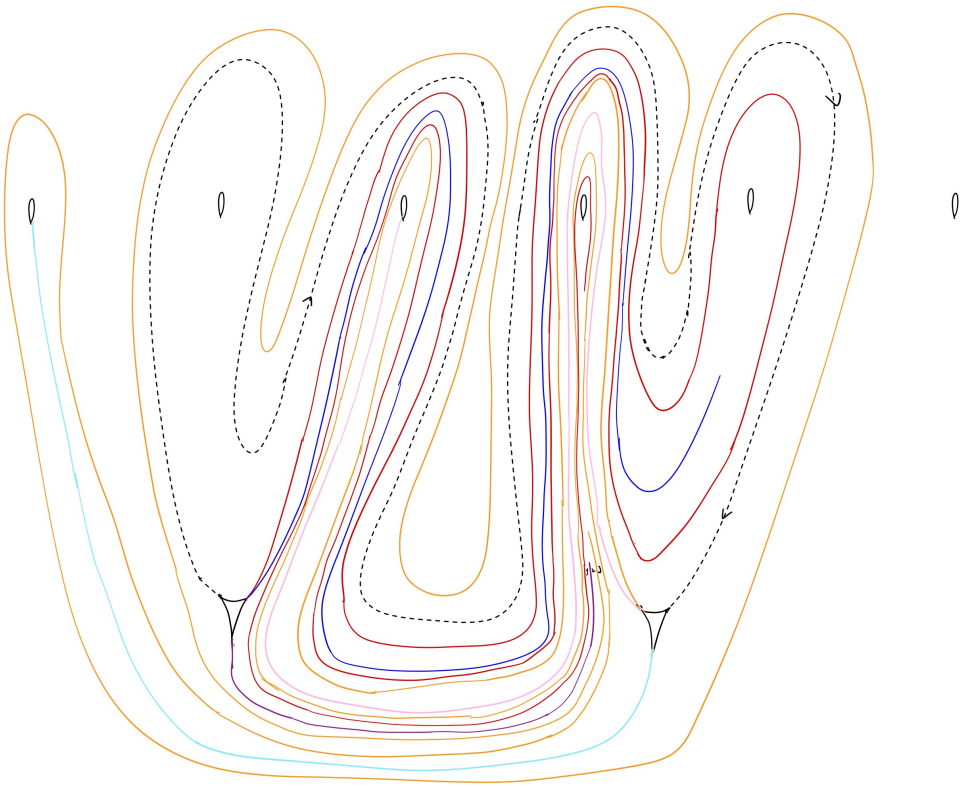


Figure D.91: Abacus4

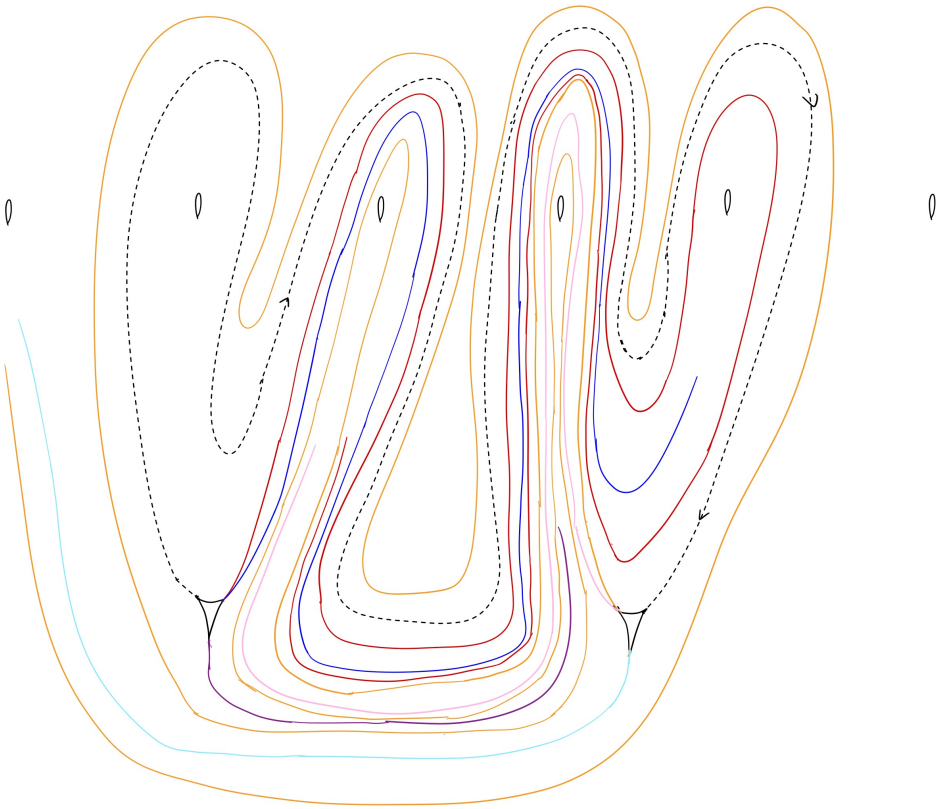


Figure D.92: Banana1

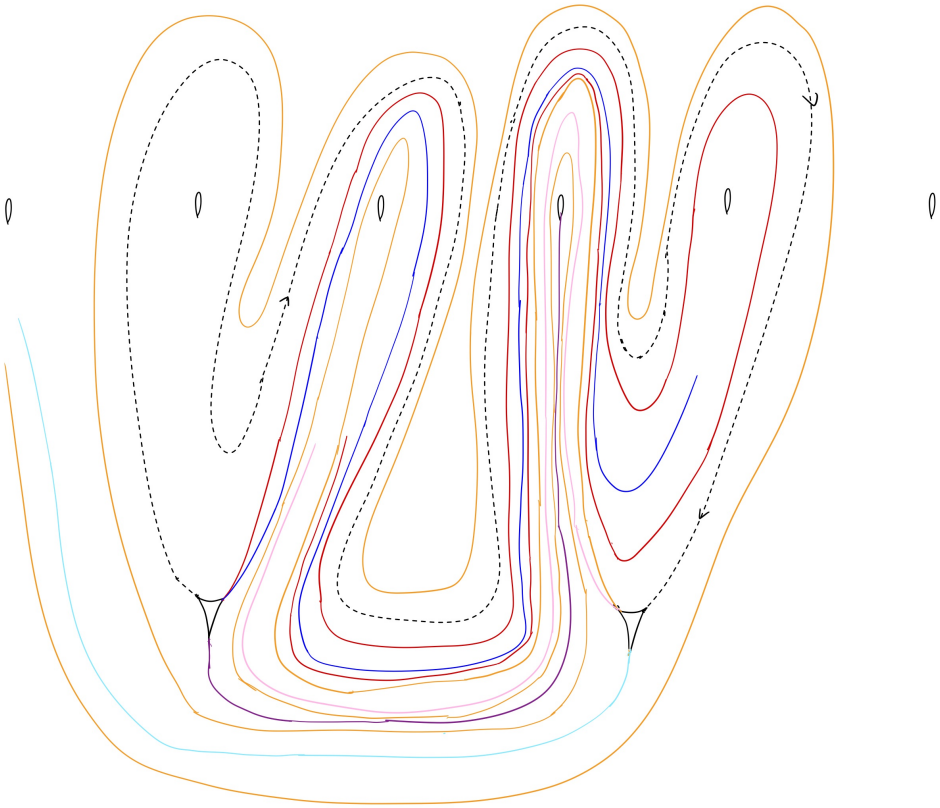


Figure D.93: Banana2

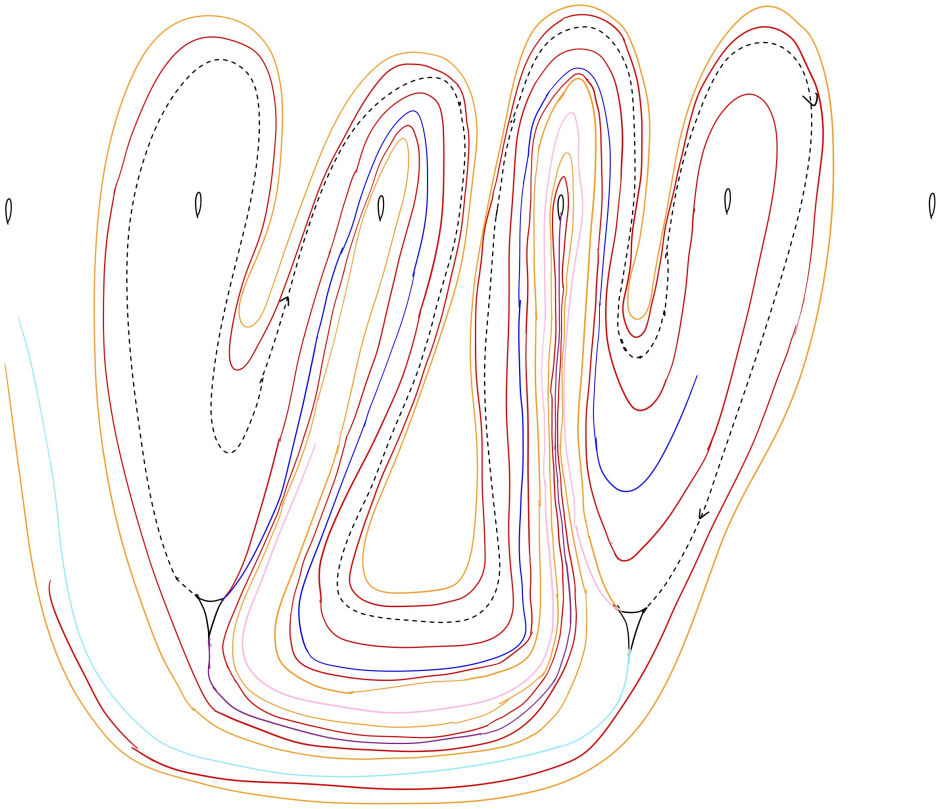


Figure D.94: Banana3

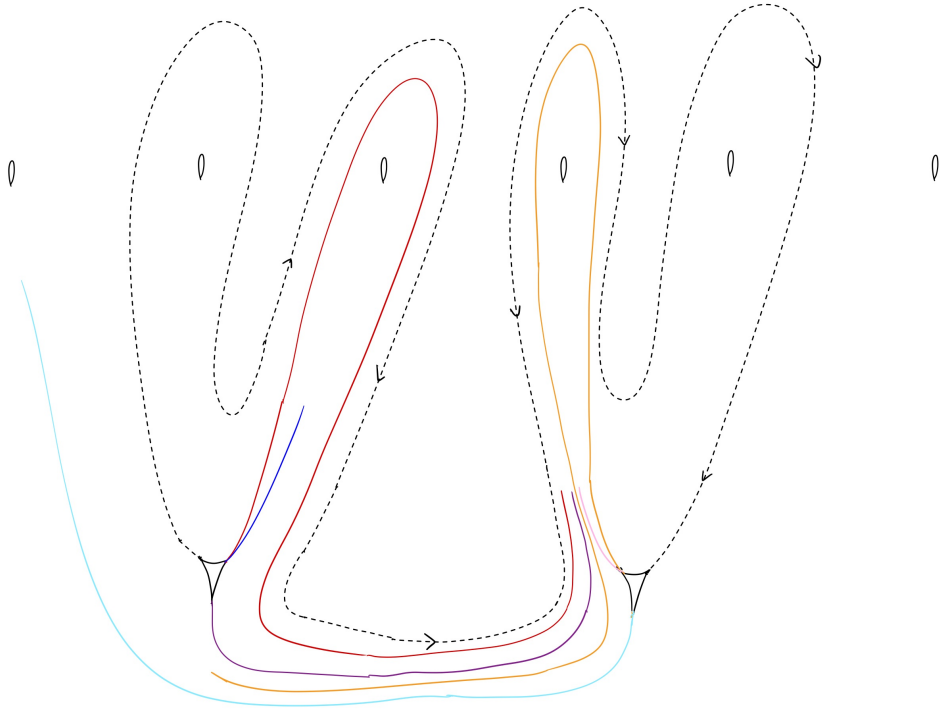


Figure D.95: Cloud1

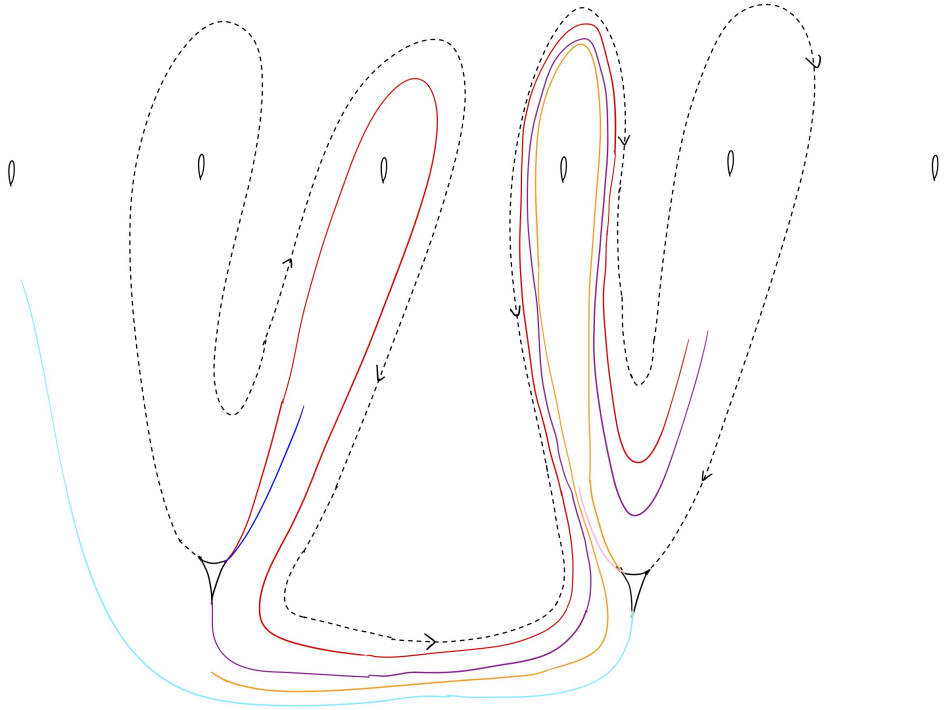


Figure D.96: Cloud2

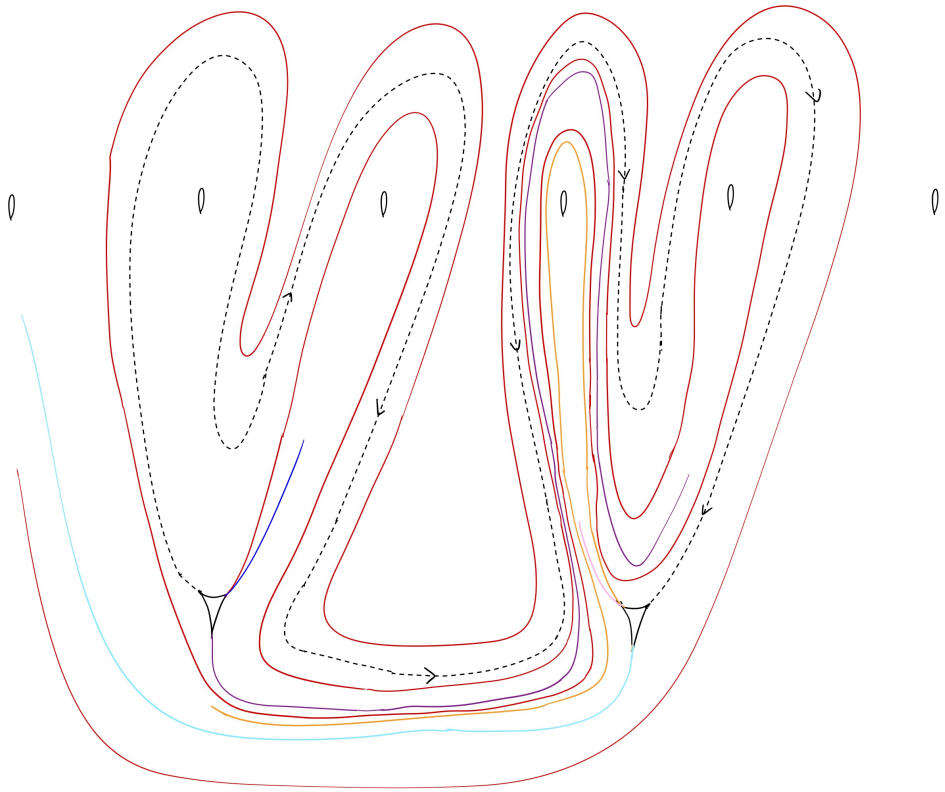


Figure D.97: Cloud3

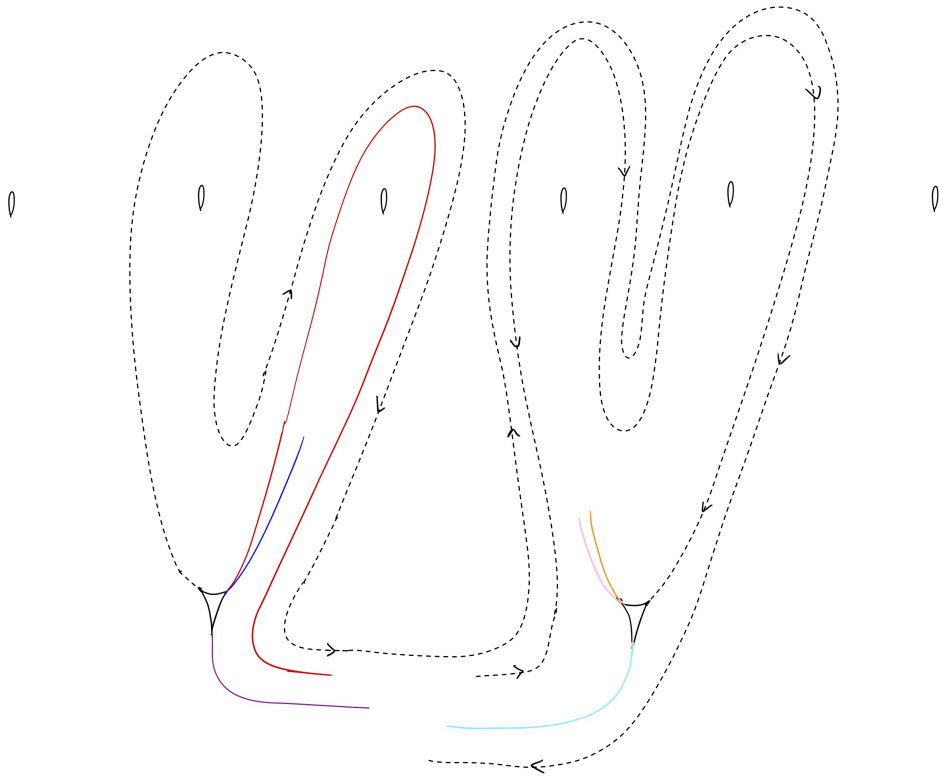


Figure D.98: Drop1

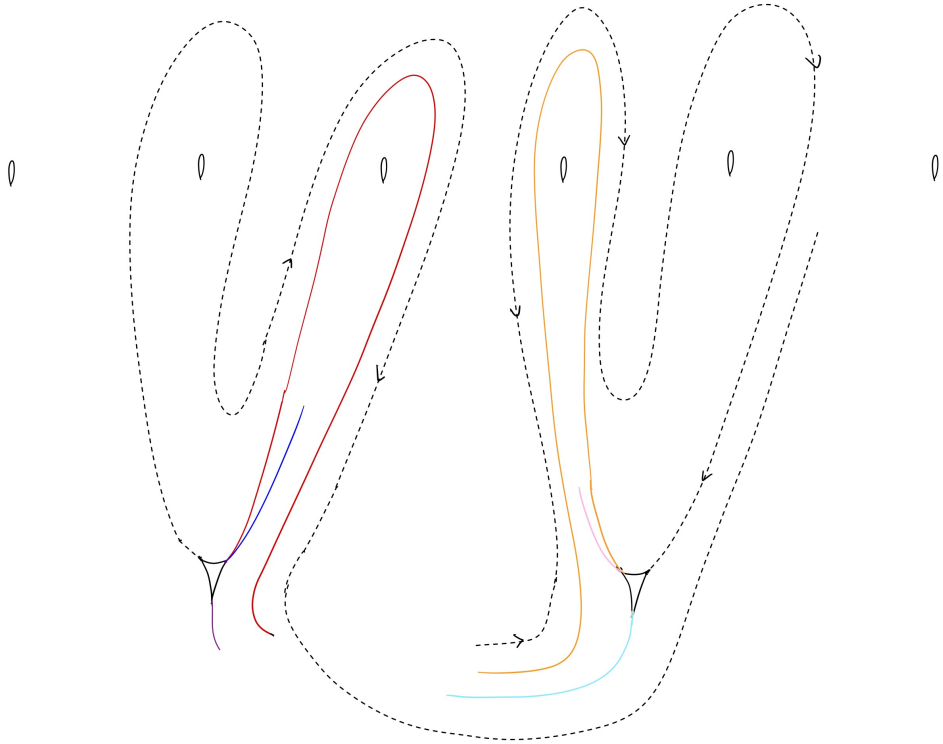


Figure D.99: Rage1

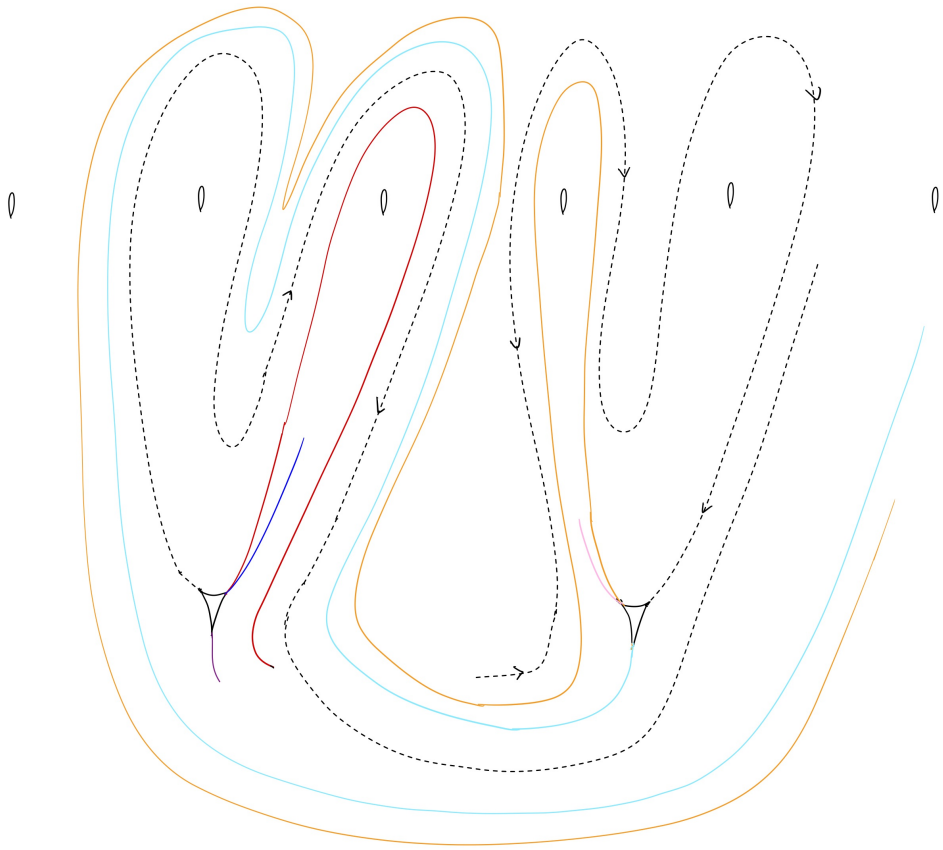


Figure D.100: Rage2

Figure D.101: Lake1

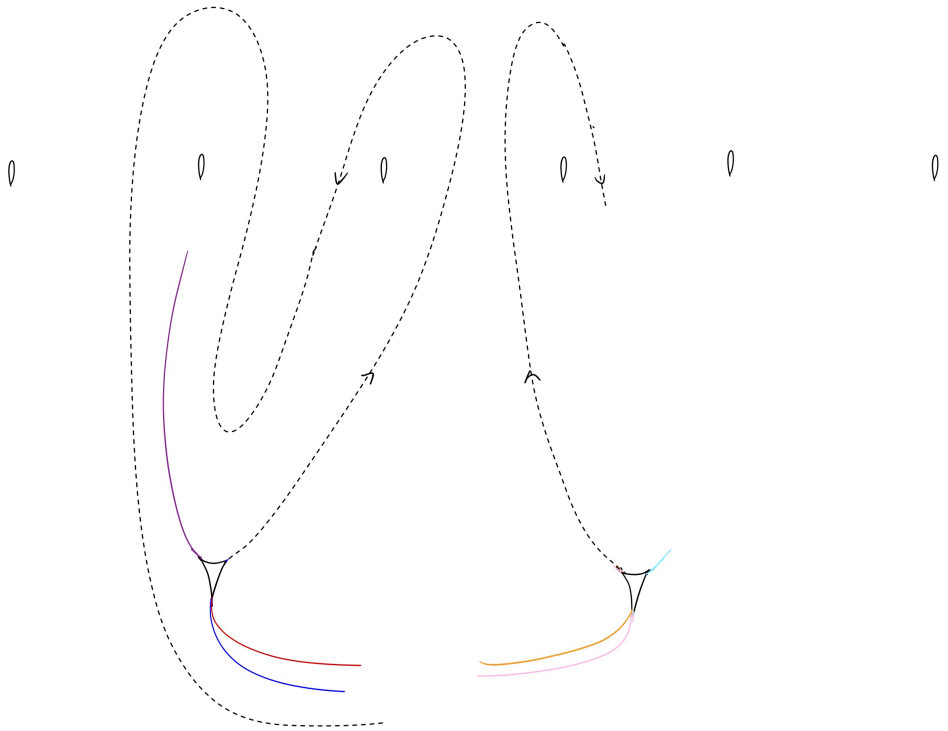


Figure D.102: Join1

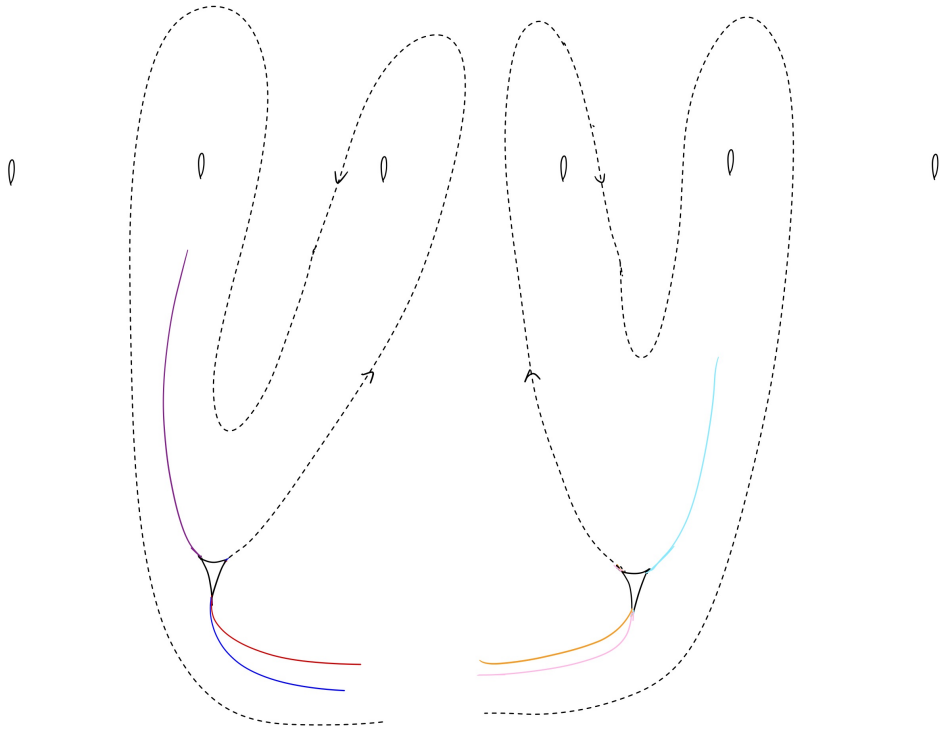


Figure D.103: Jolly1

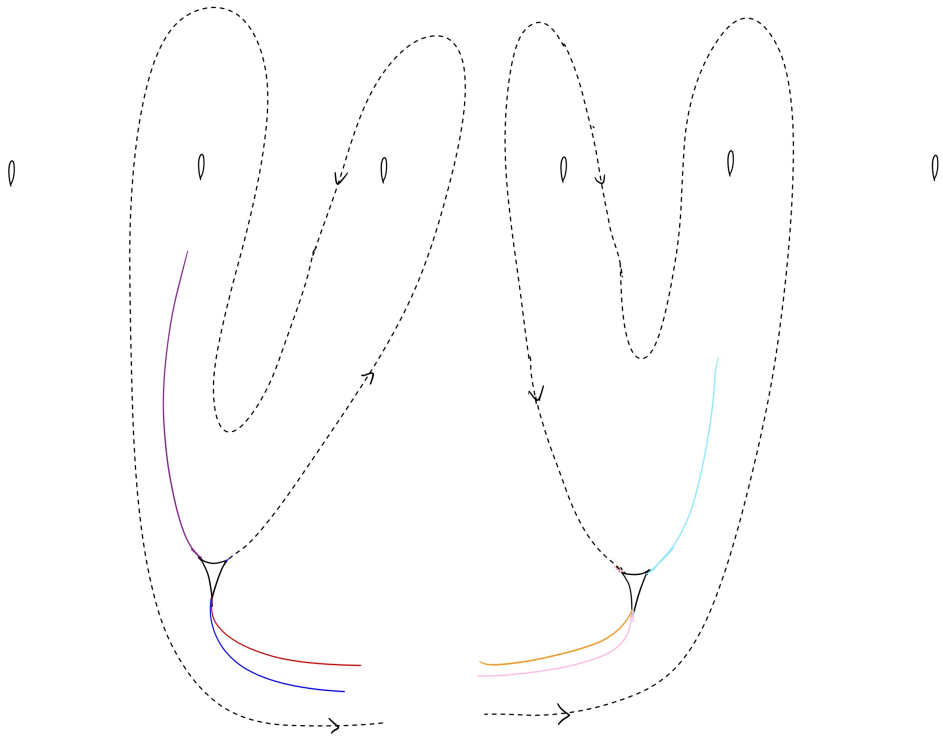


Figure D.104: Jolly2

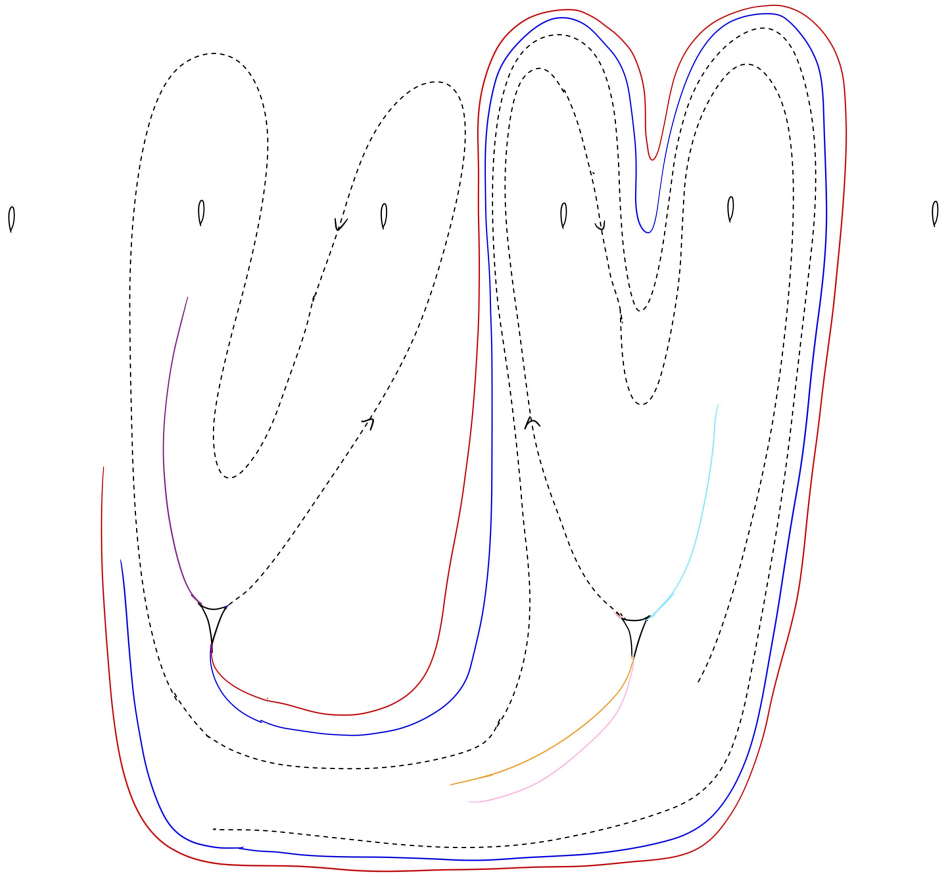


Figure D.105: Jolly3

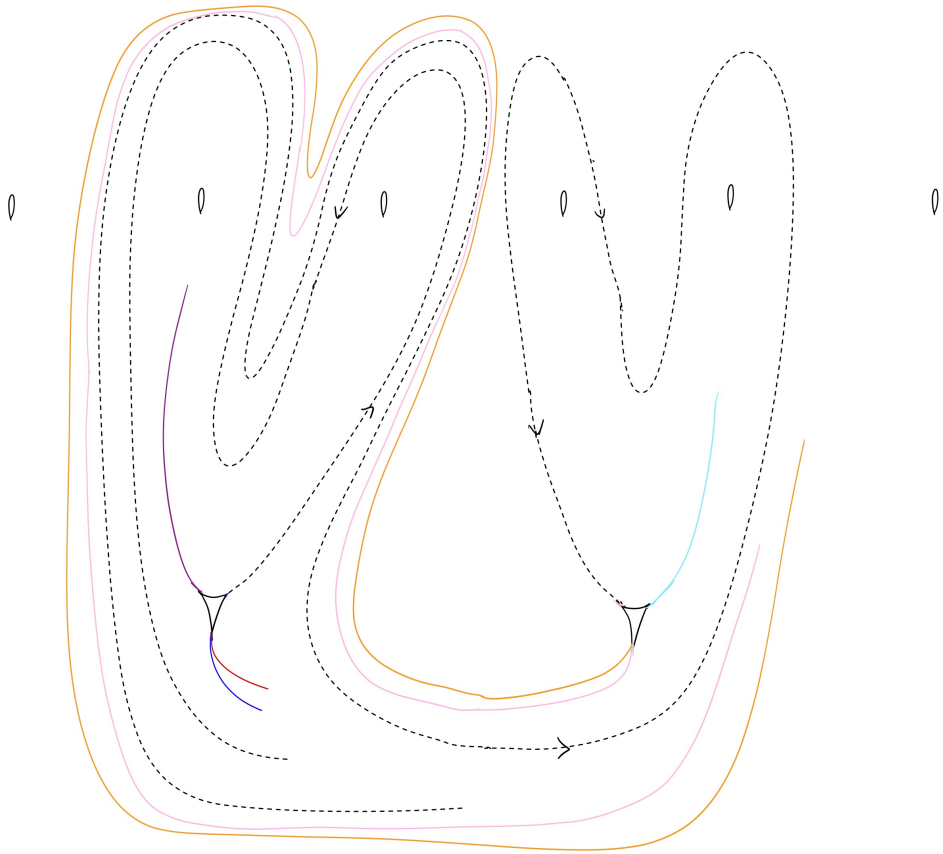


Figure D.106: Jolly4

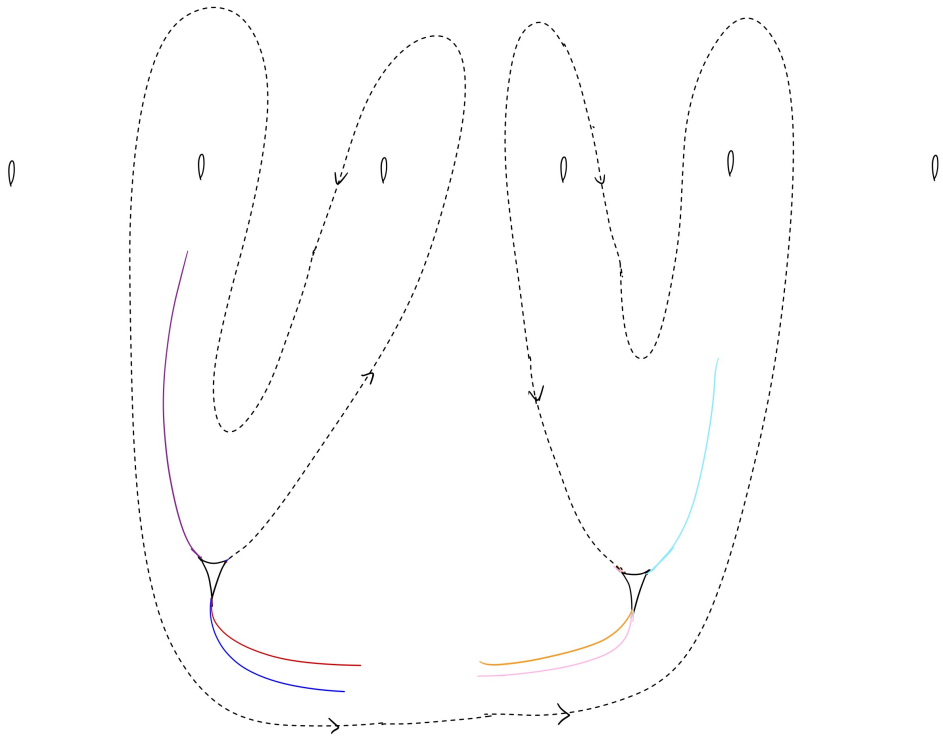


Figure D.107: Jolly5

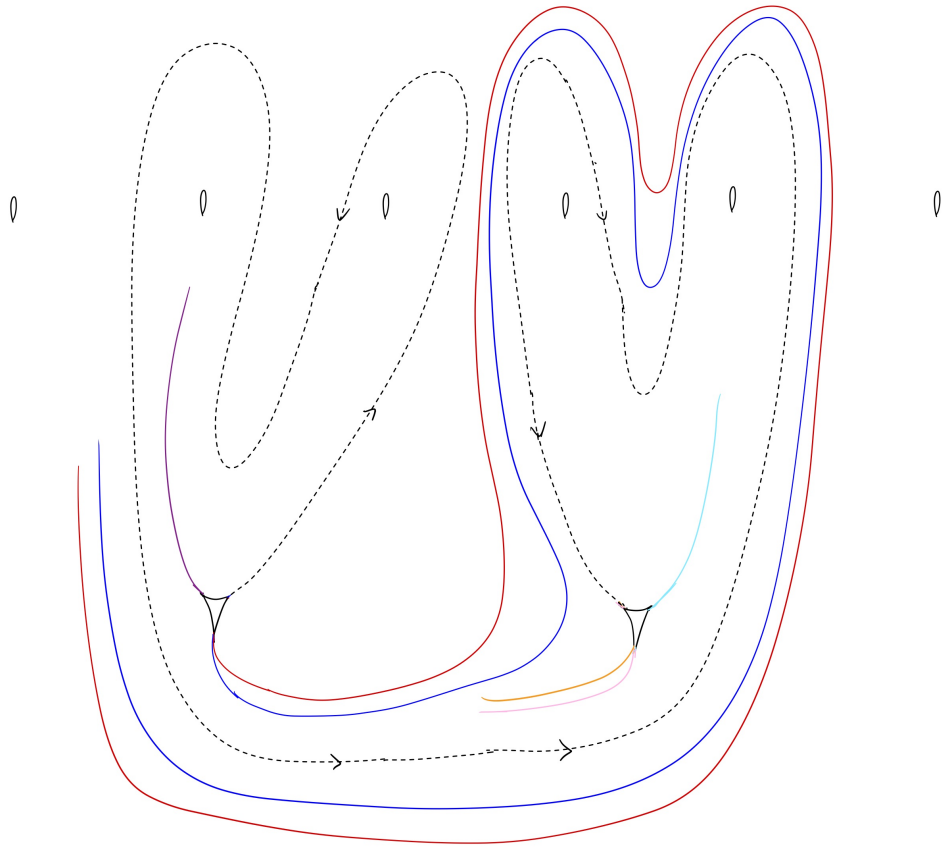


Figure D.108: Jolly6

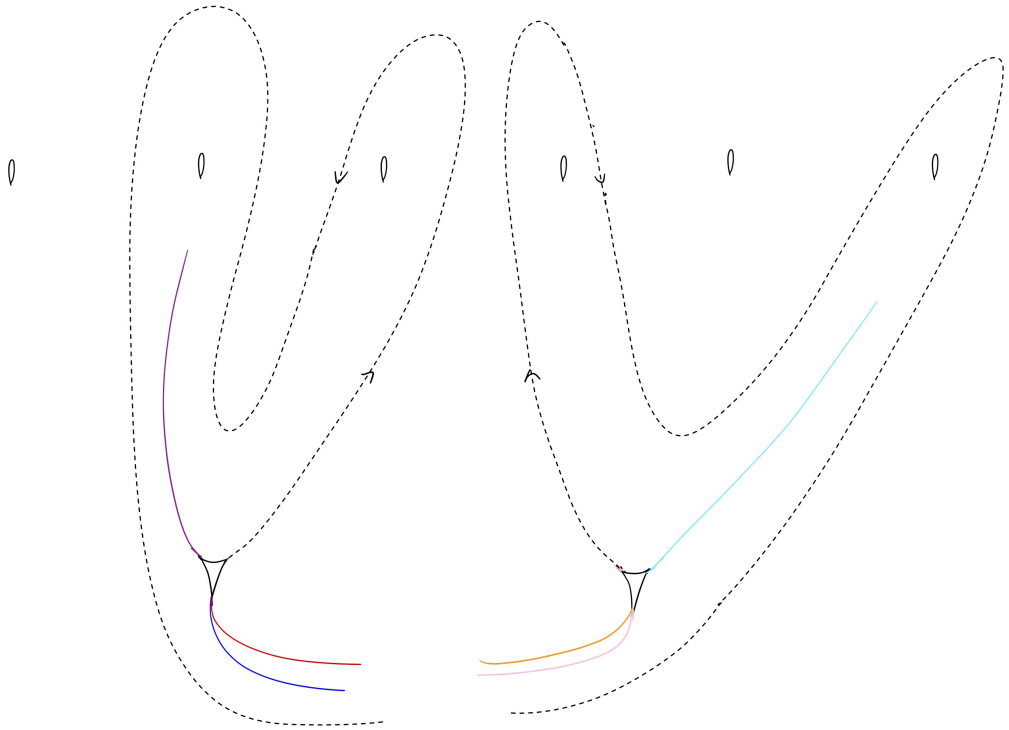


Figure D.109: Eager1

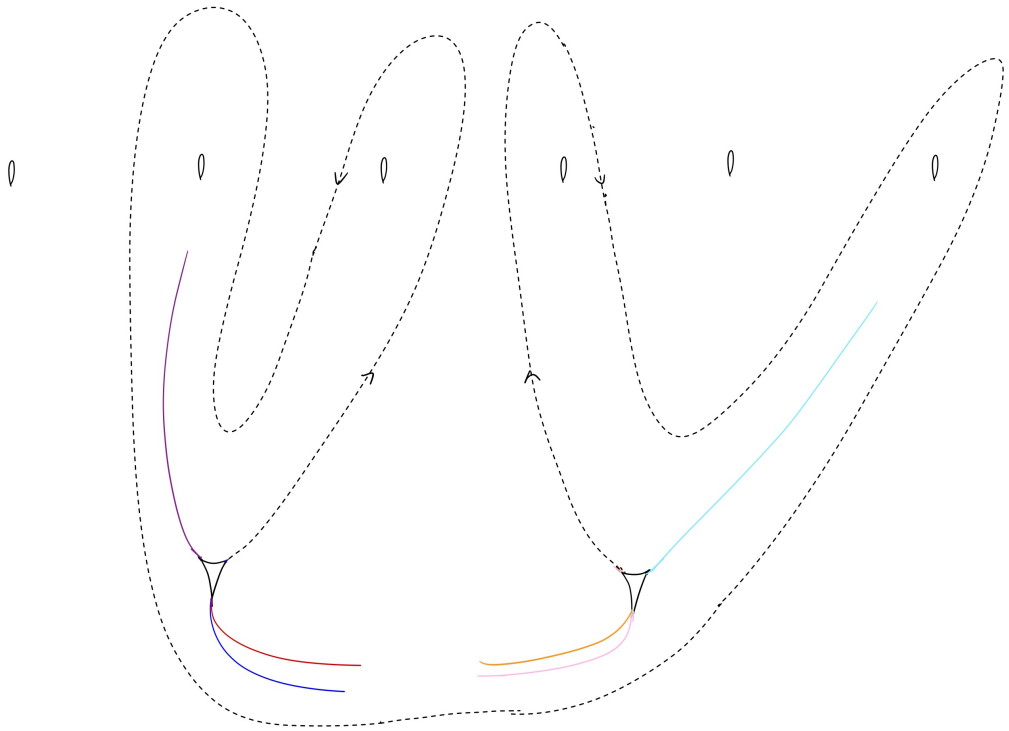


Figure D.110: Eager2

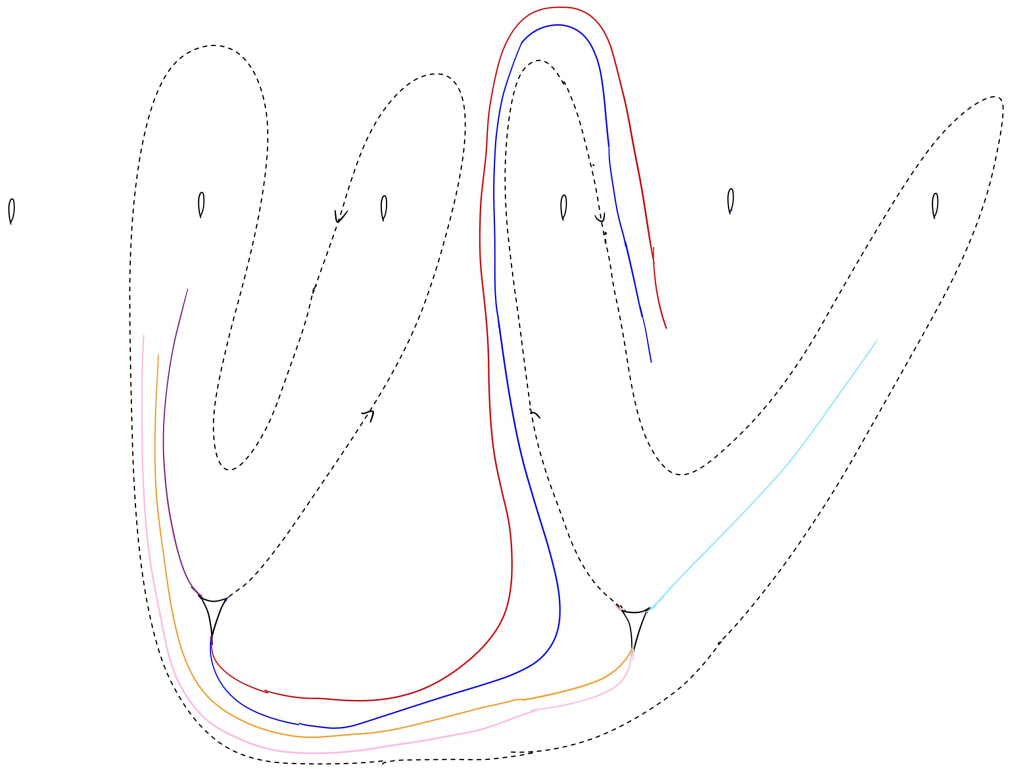


Figure D.111: Eager3

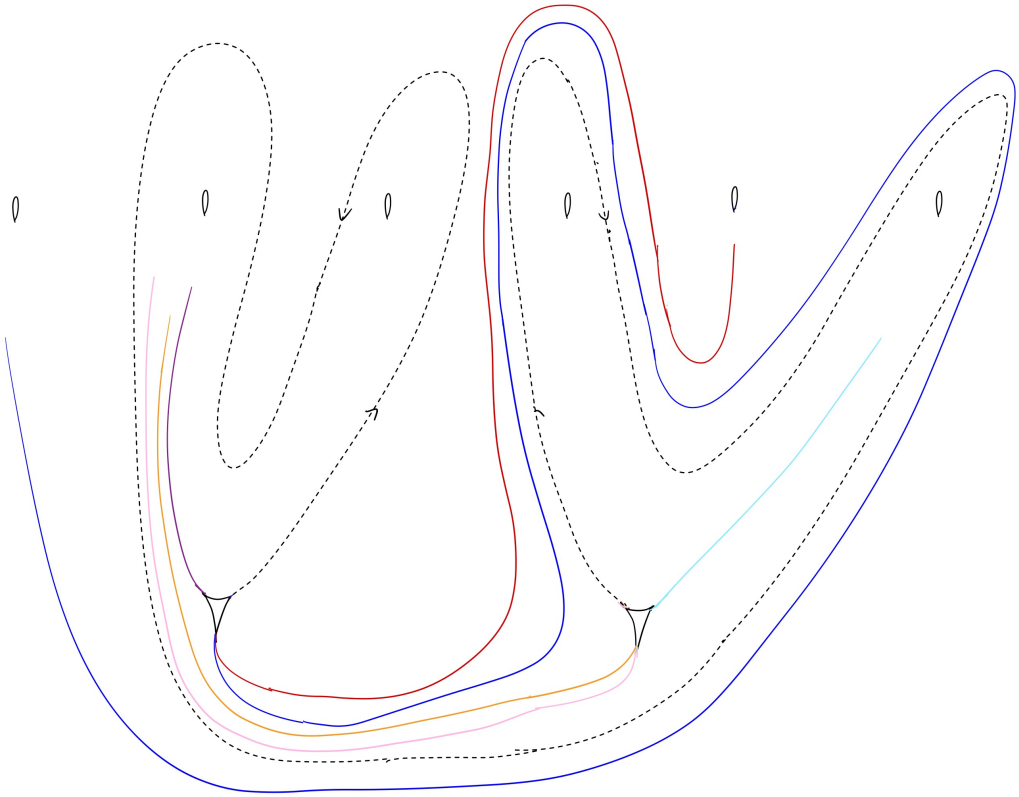


Figure D.112: Eager4

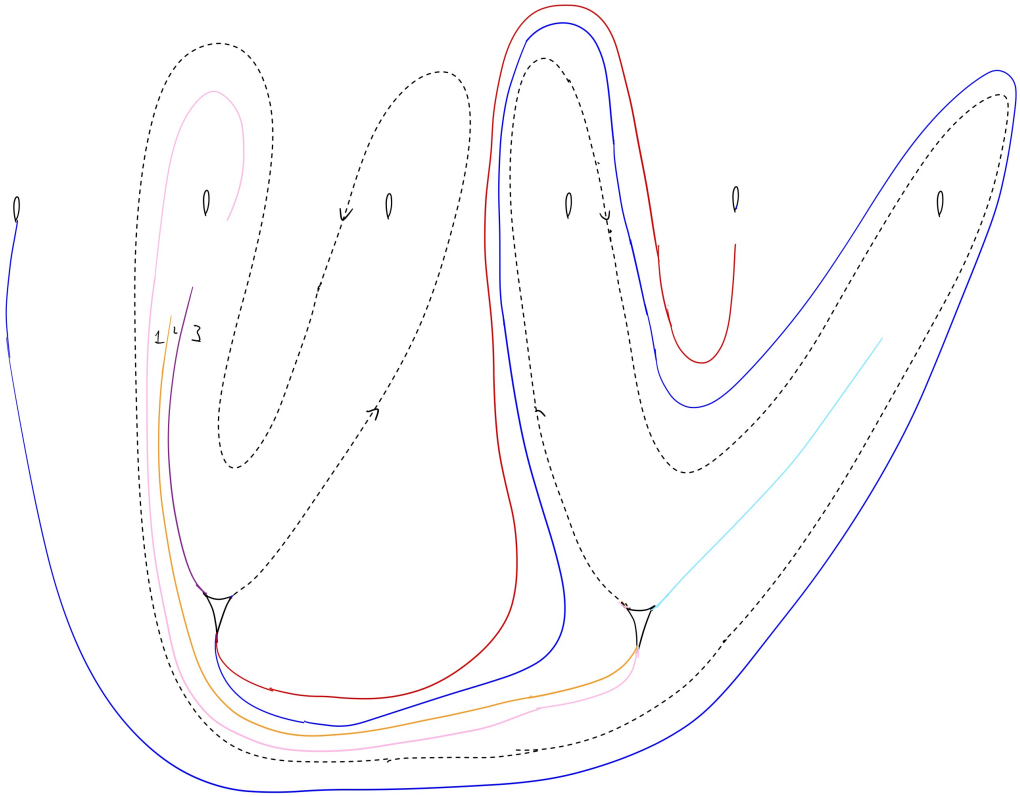


Figure D.113: Eager5

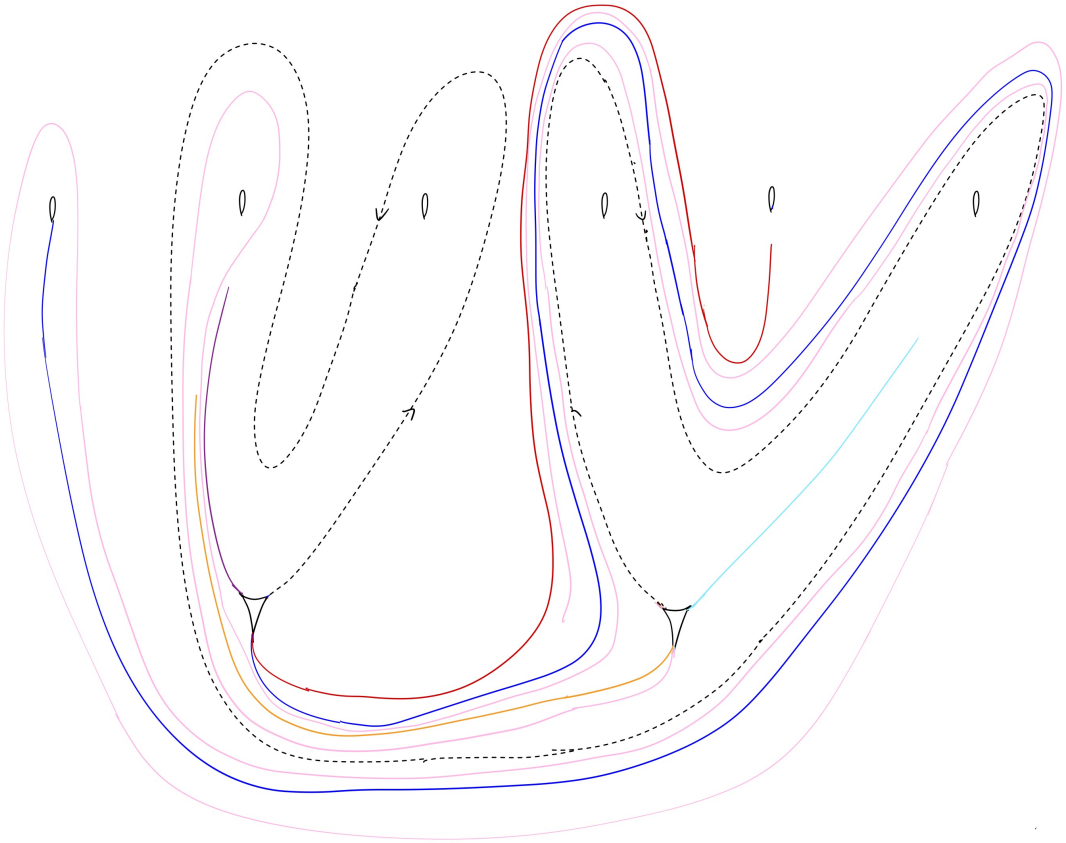


Figure D.114: Eager6

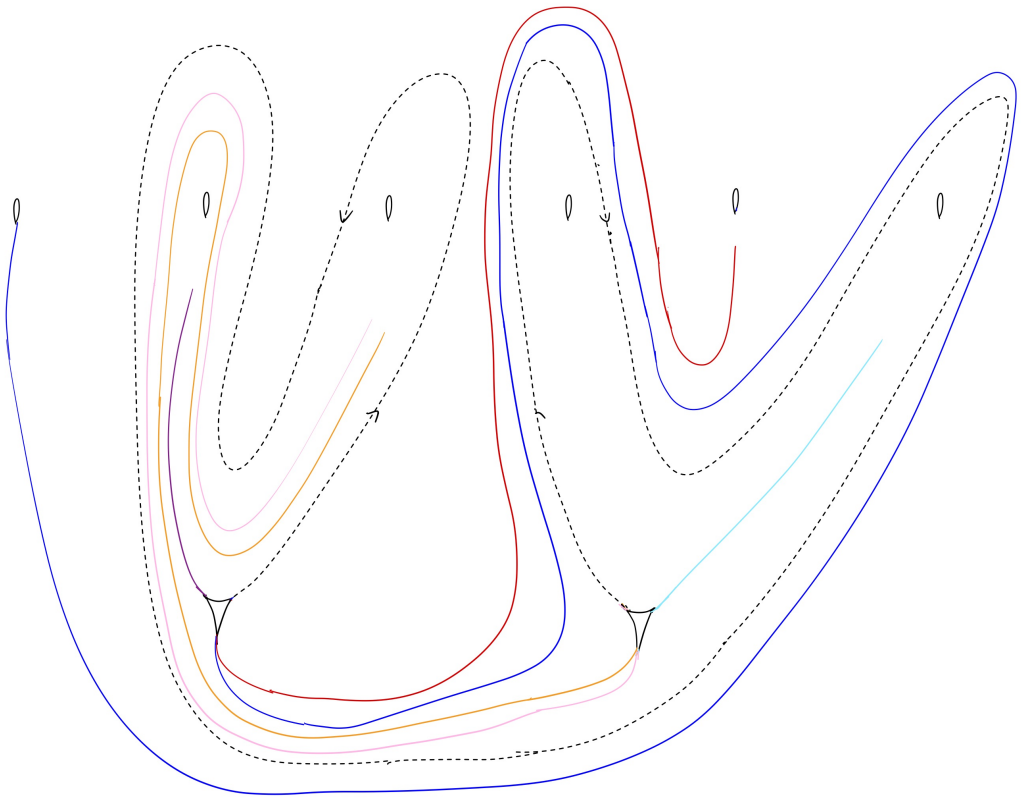


Figure D.115: Eager7

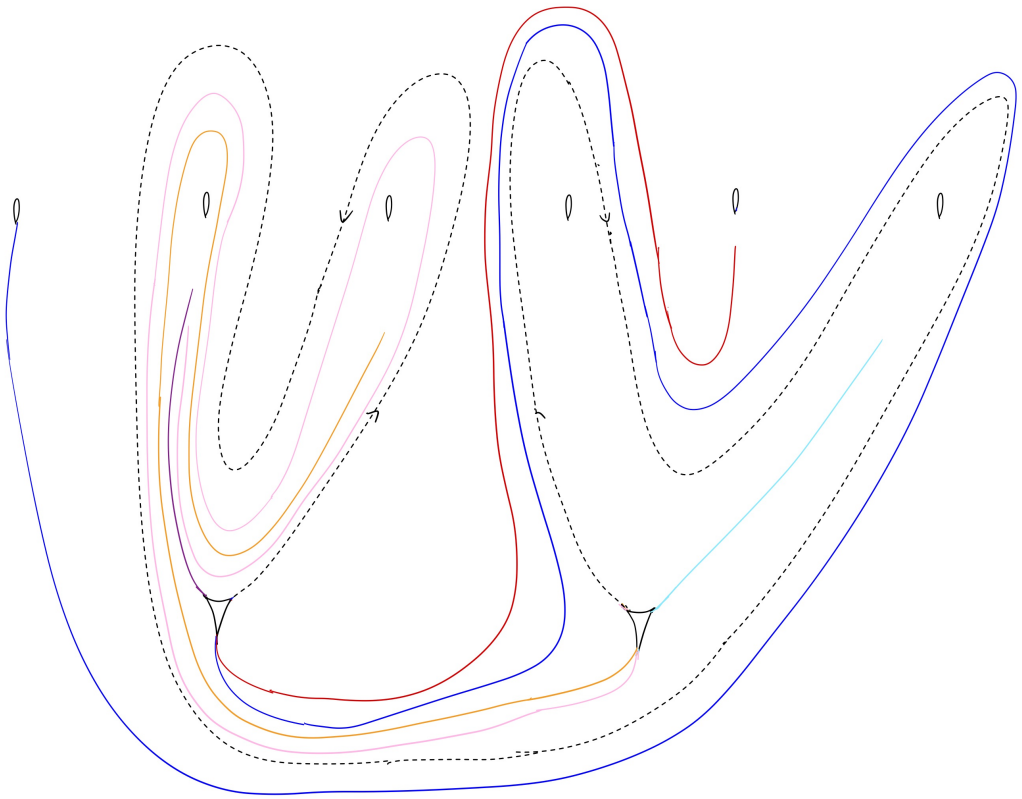


Figure D.116: Eager8

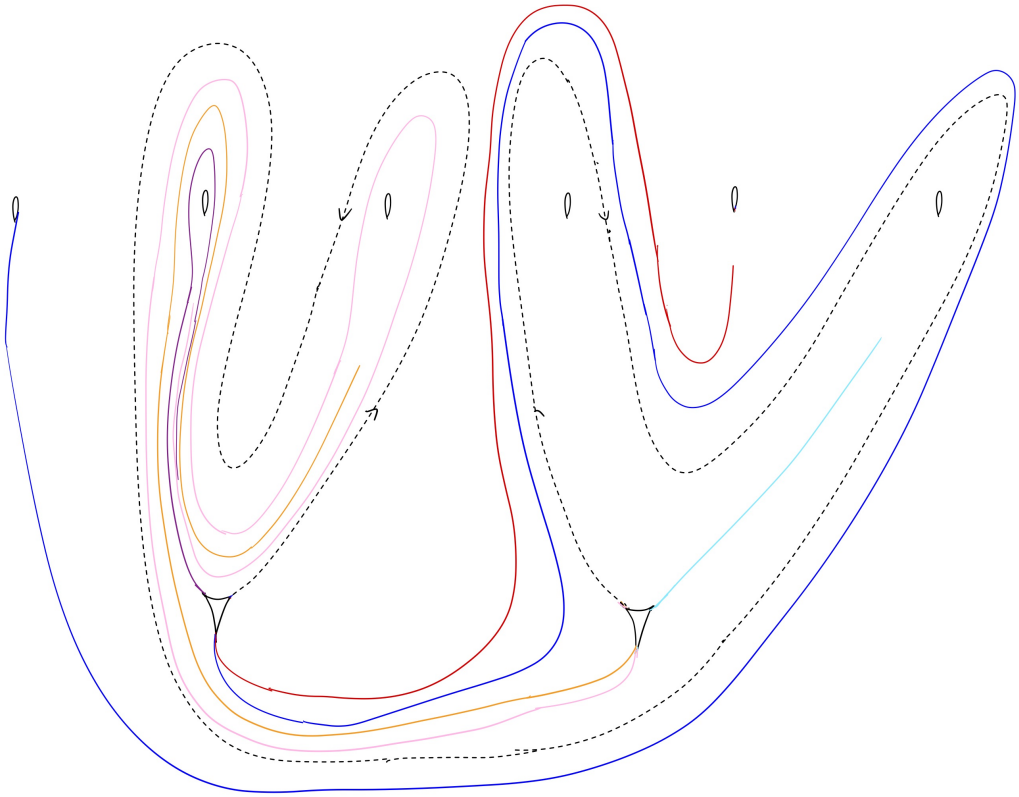


Figure D.117: Eager9

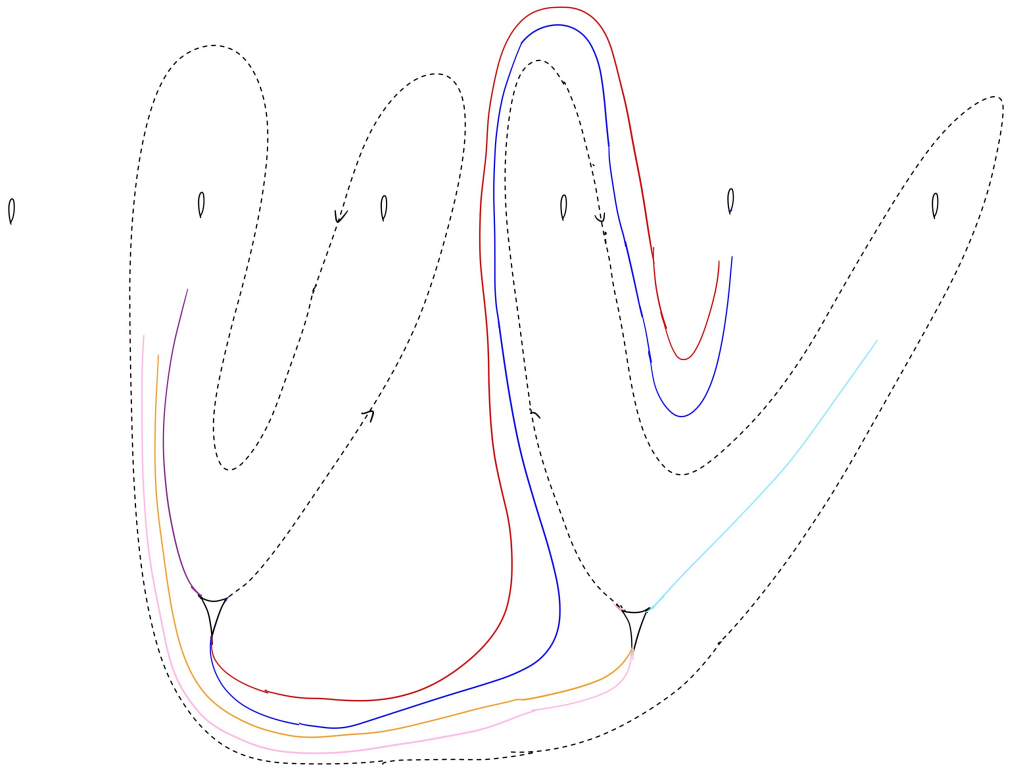


Figure D.118: Eager10

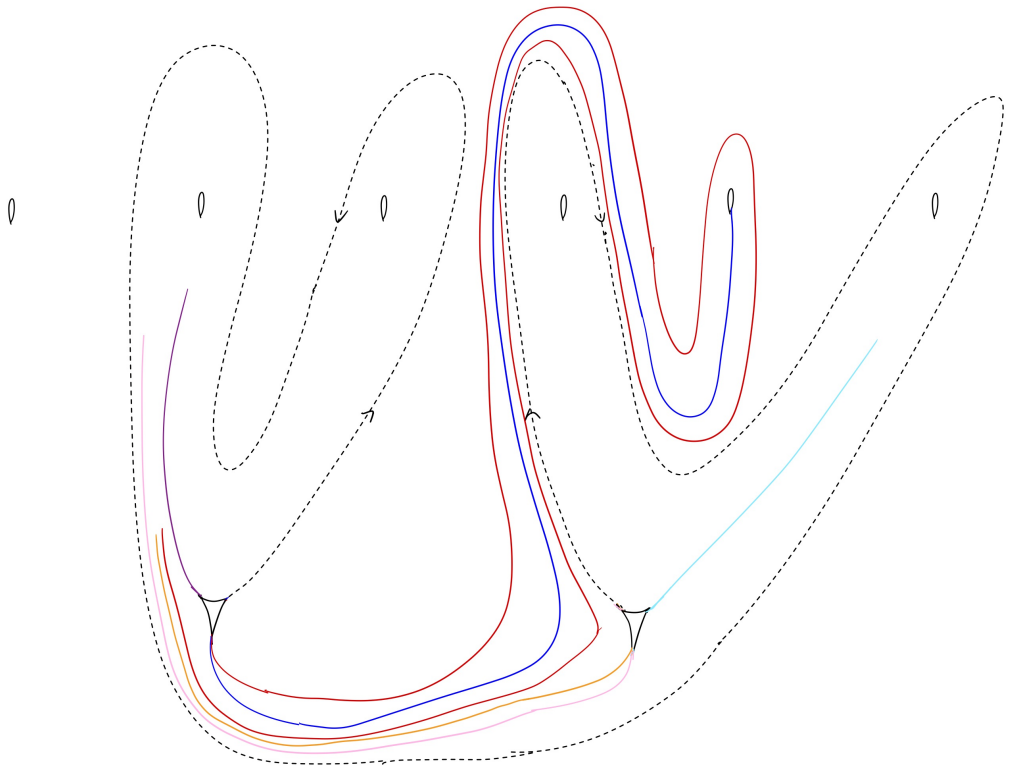


Figure D.119: Eager11

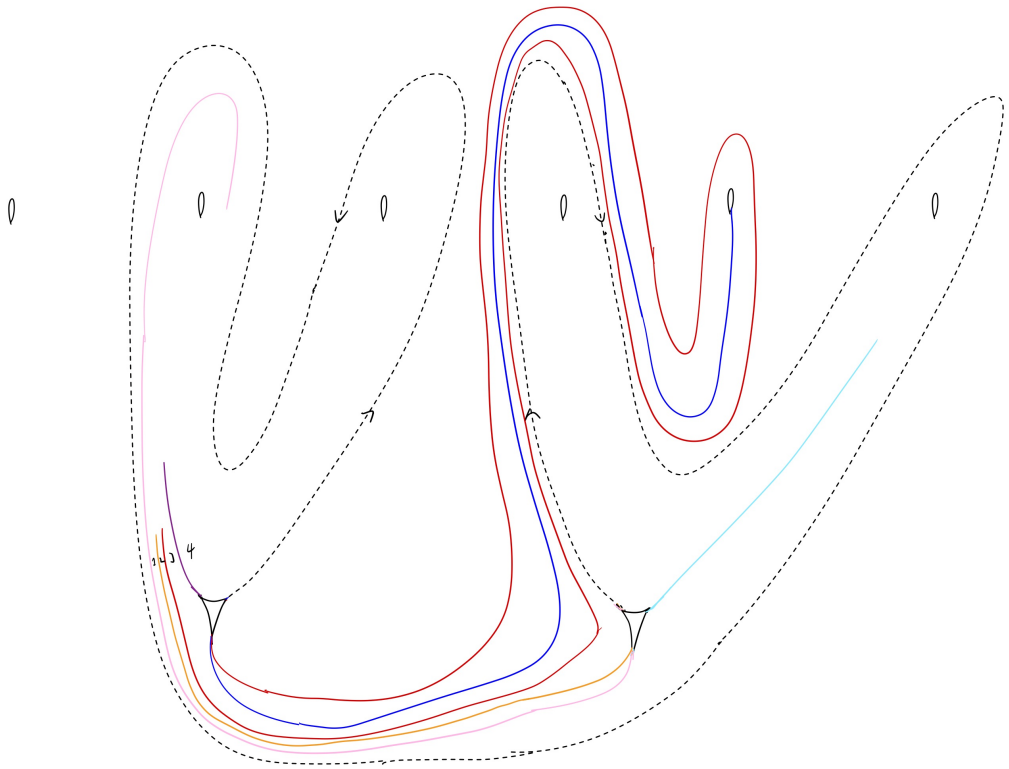


Figure D.120: Eager12

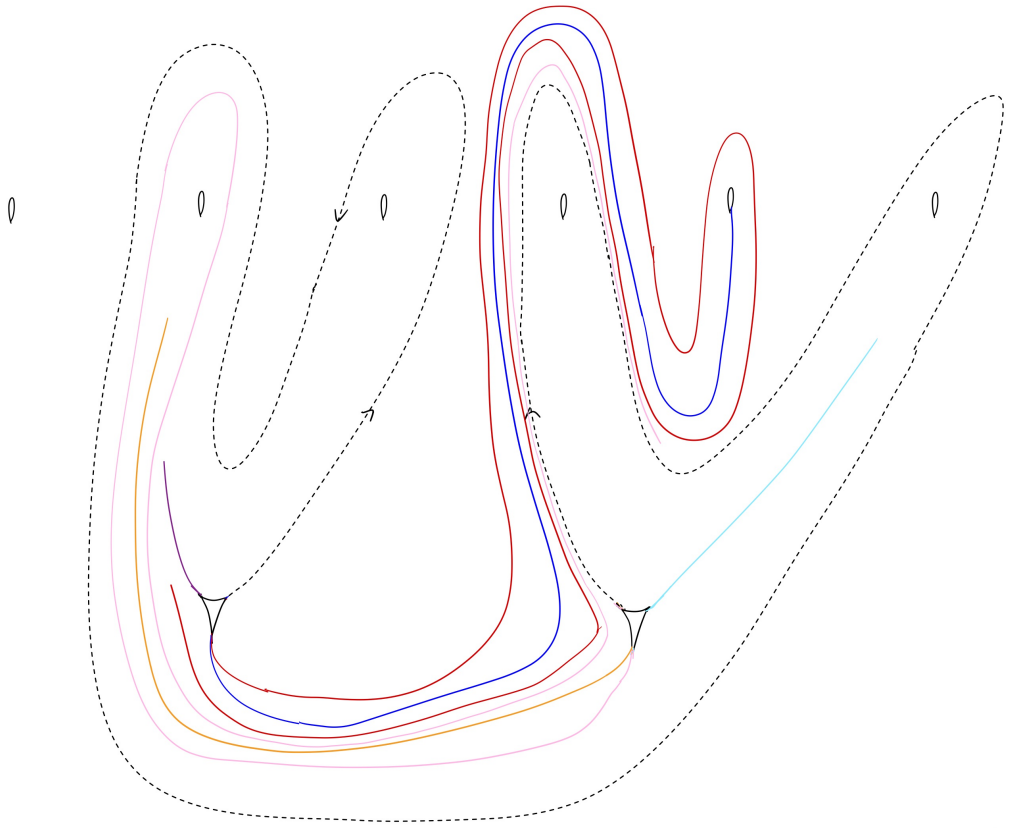


Figure D.121: Global1

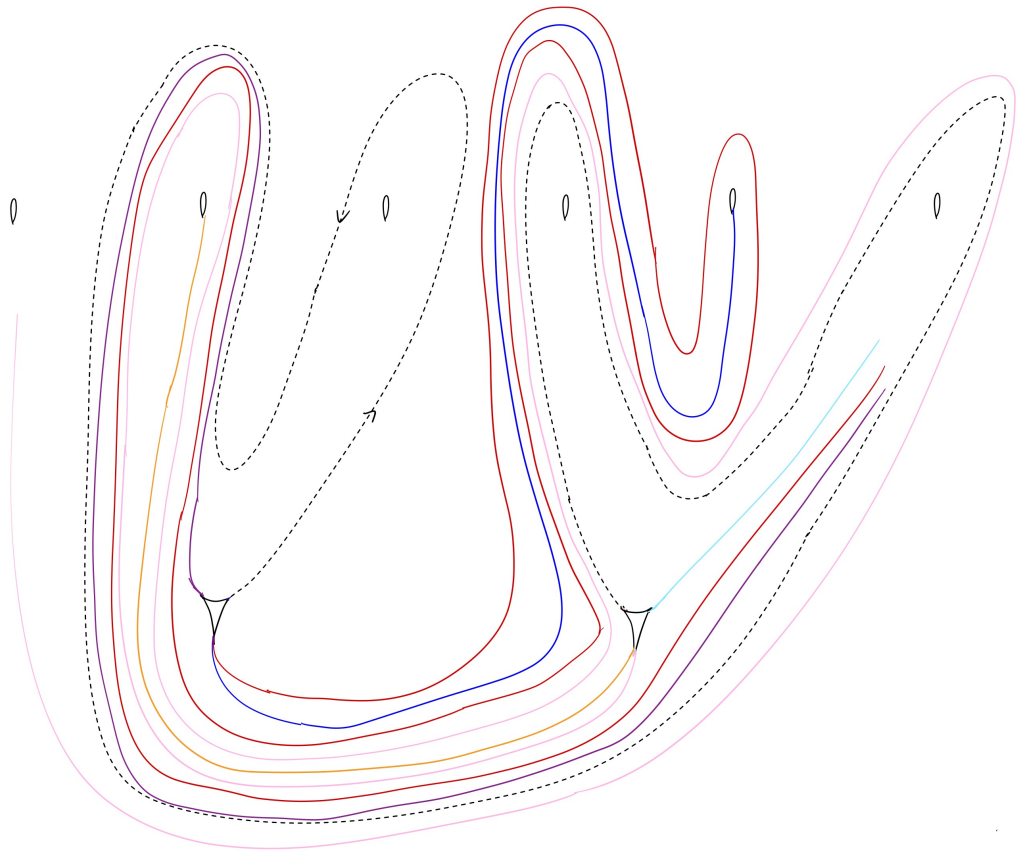


Figure D.122: Global2

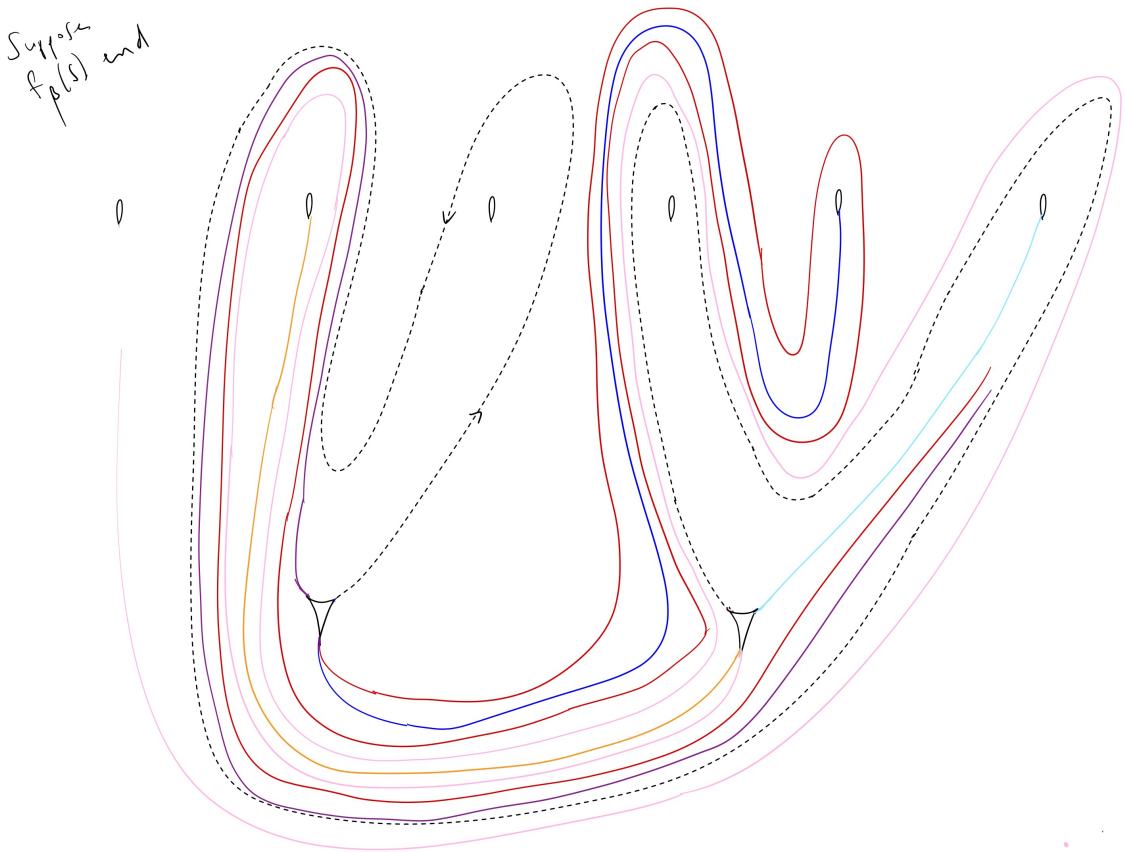


Figure D.123: Balance1

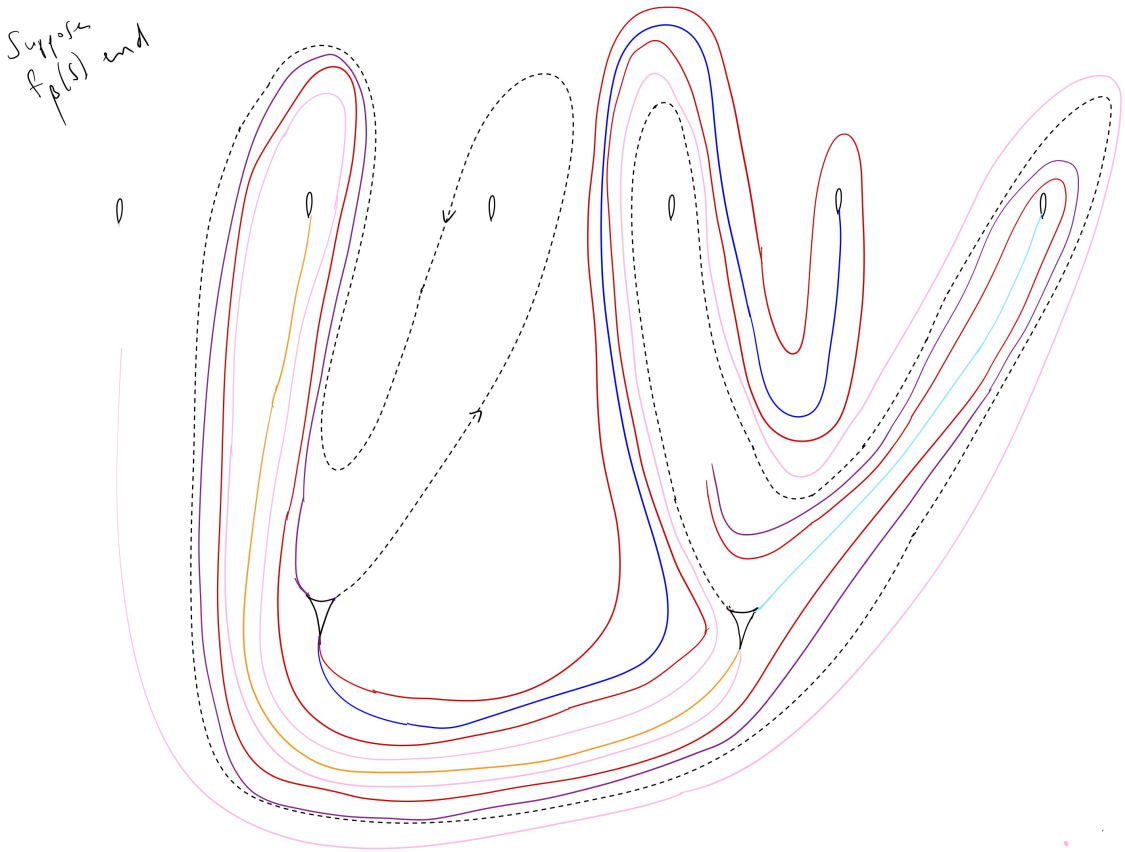


Figure D.124: Balance2

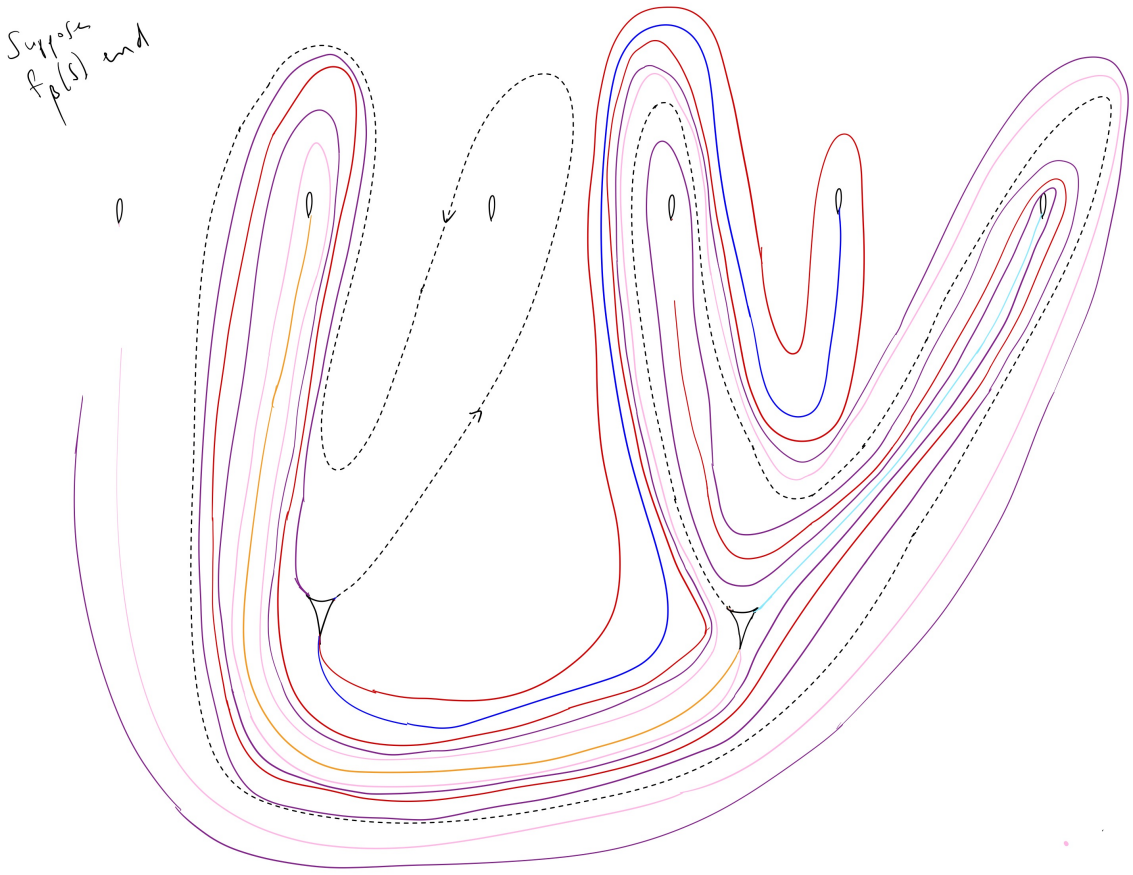


Figure D.125: Balance3

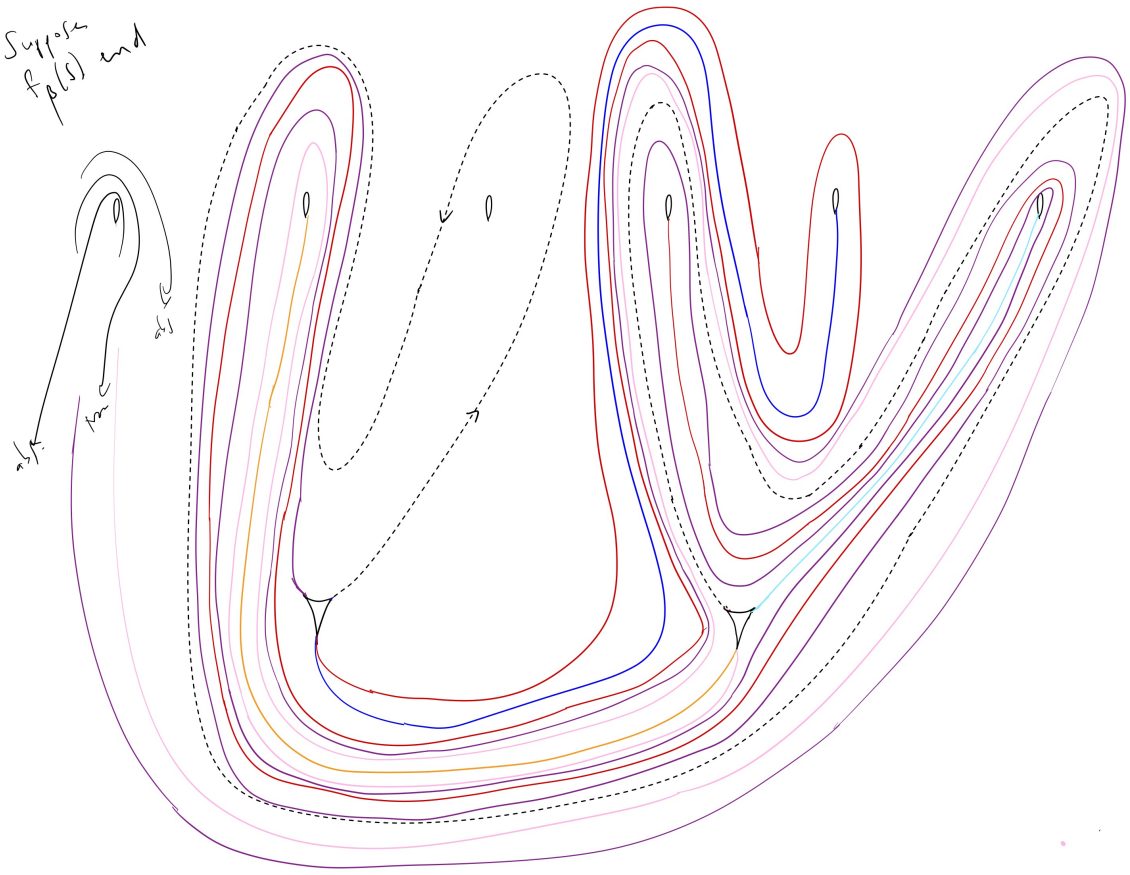


Figure D.126: Balance4

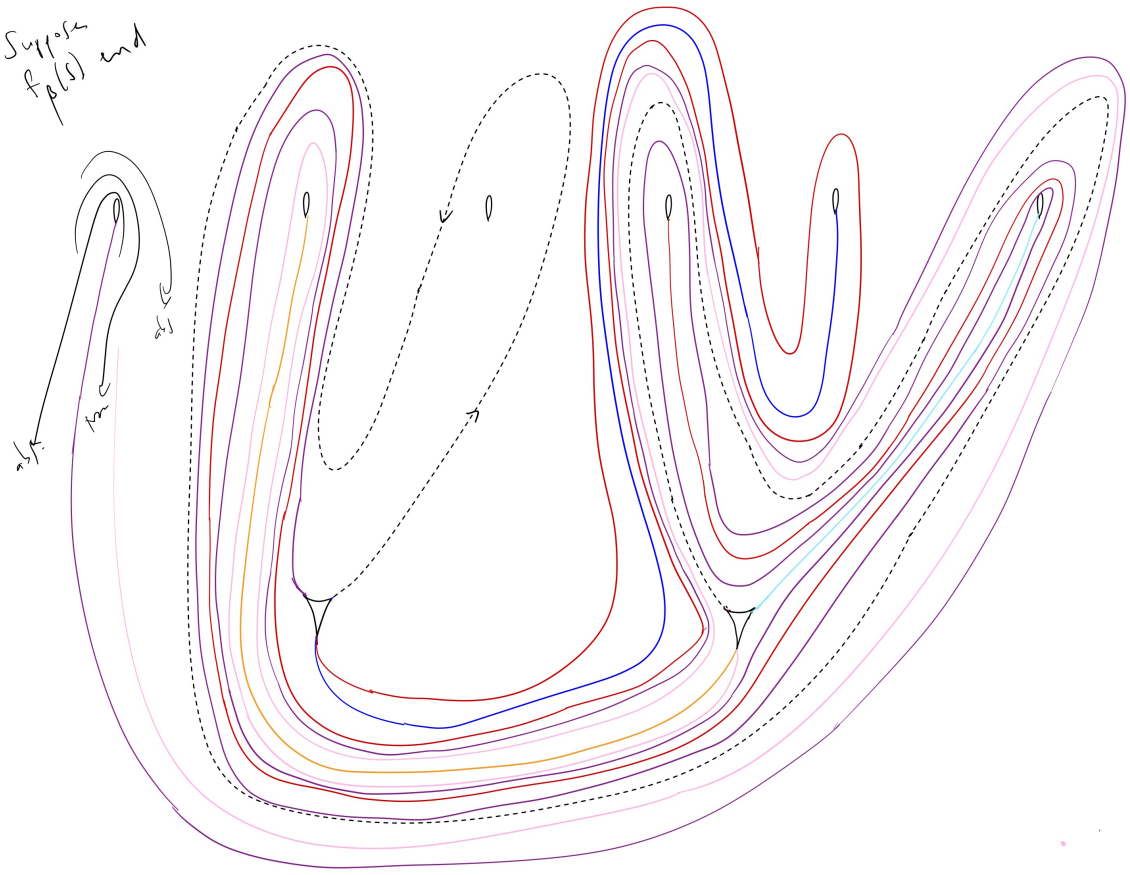


Figure D.127: Balance5

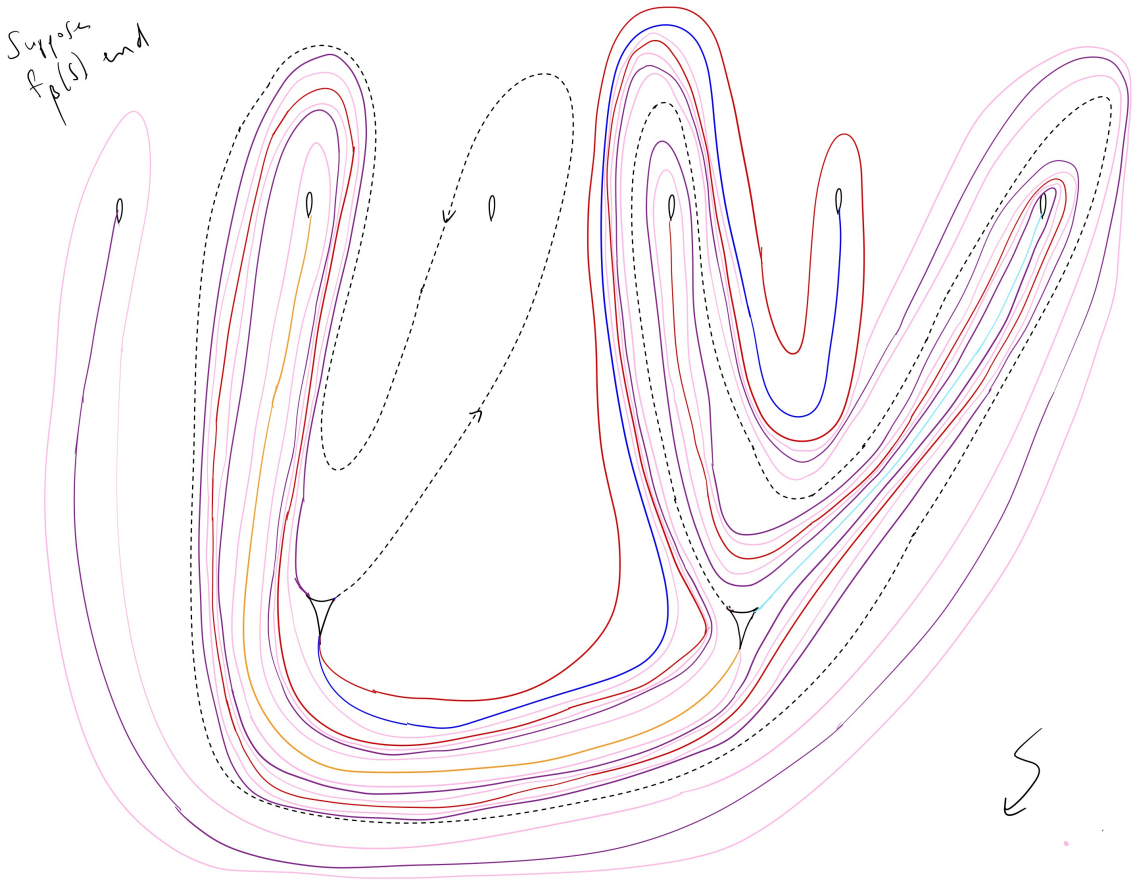


Figure D.128: Balance6

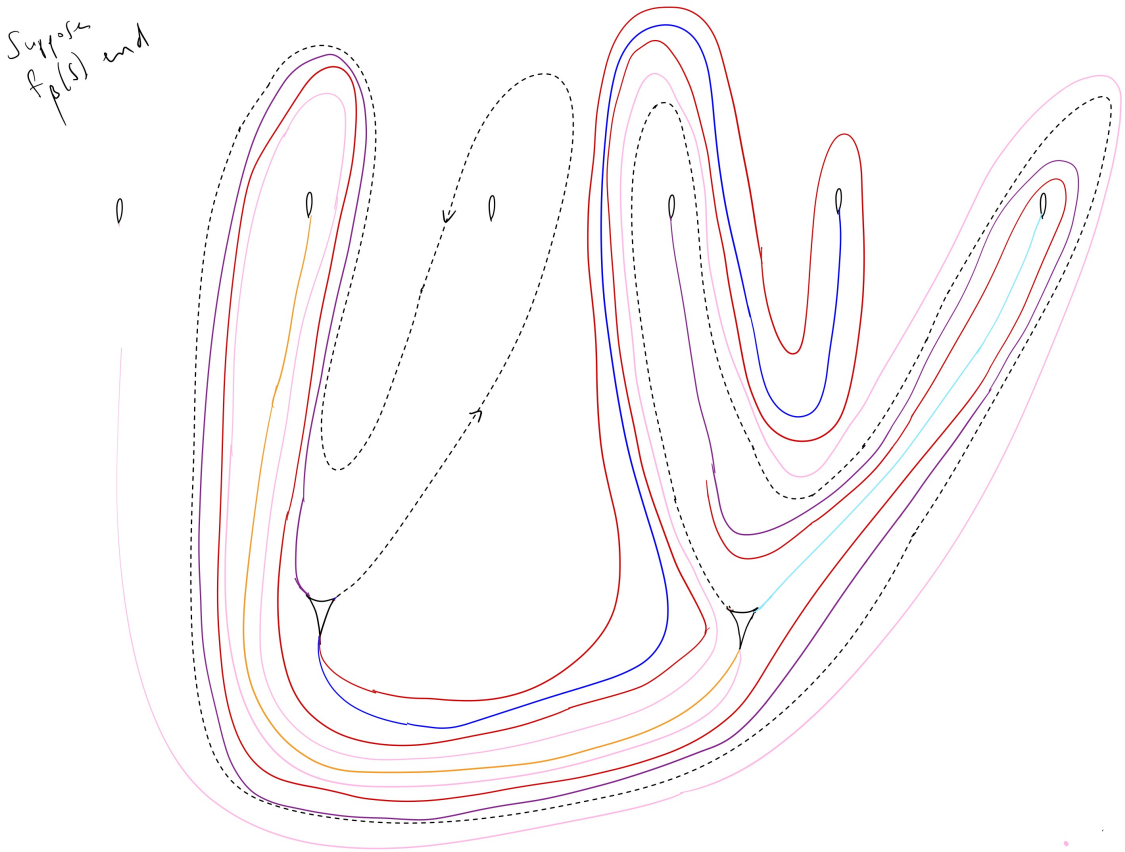


Figure D.129: Balance7

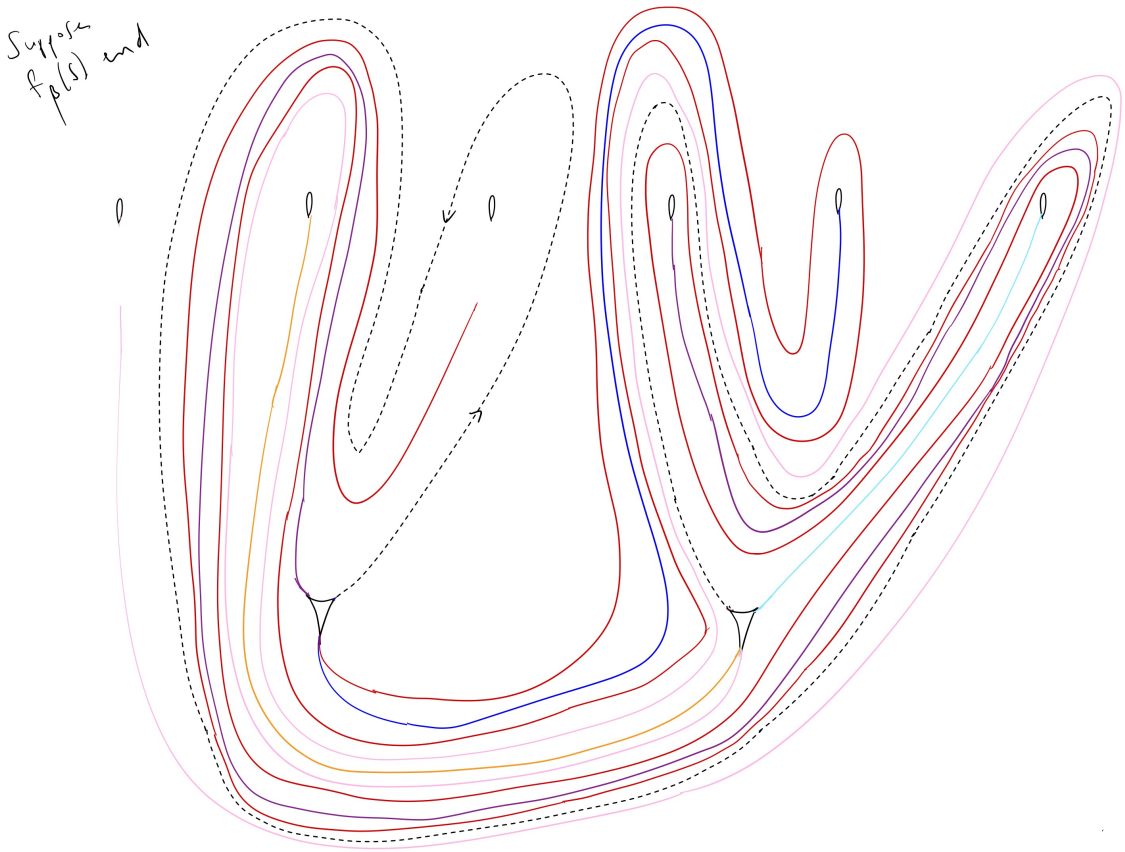


Figure D.130: Balance8

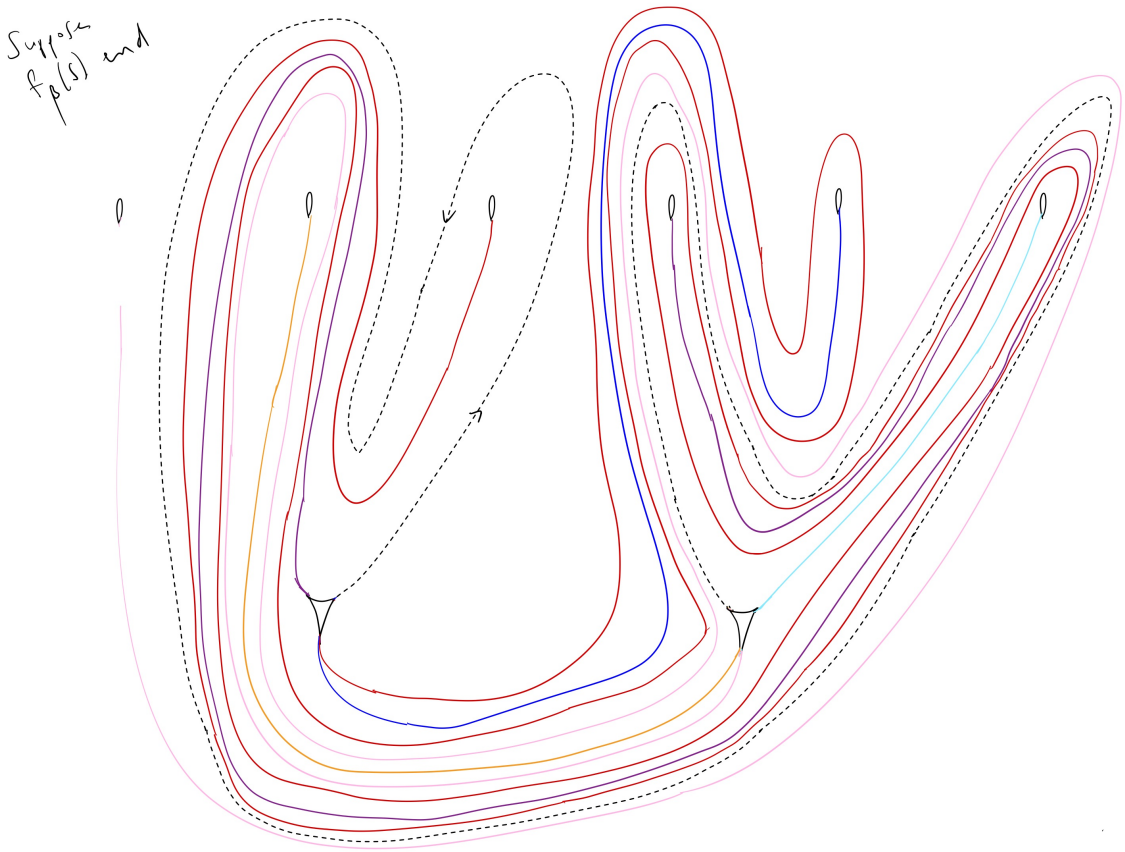


Figure D.131: Balance9

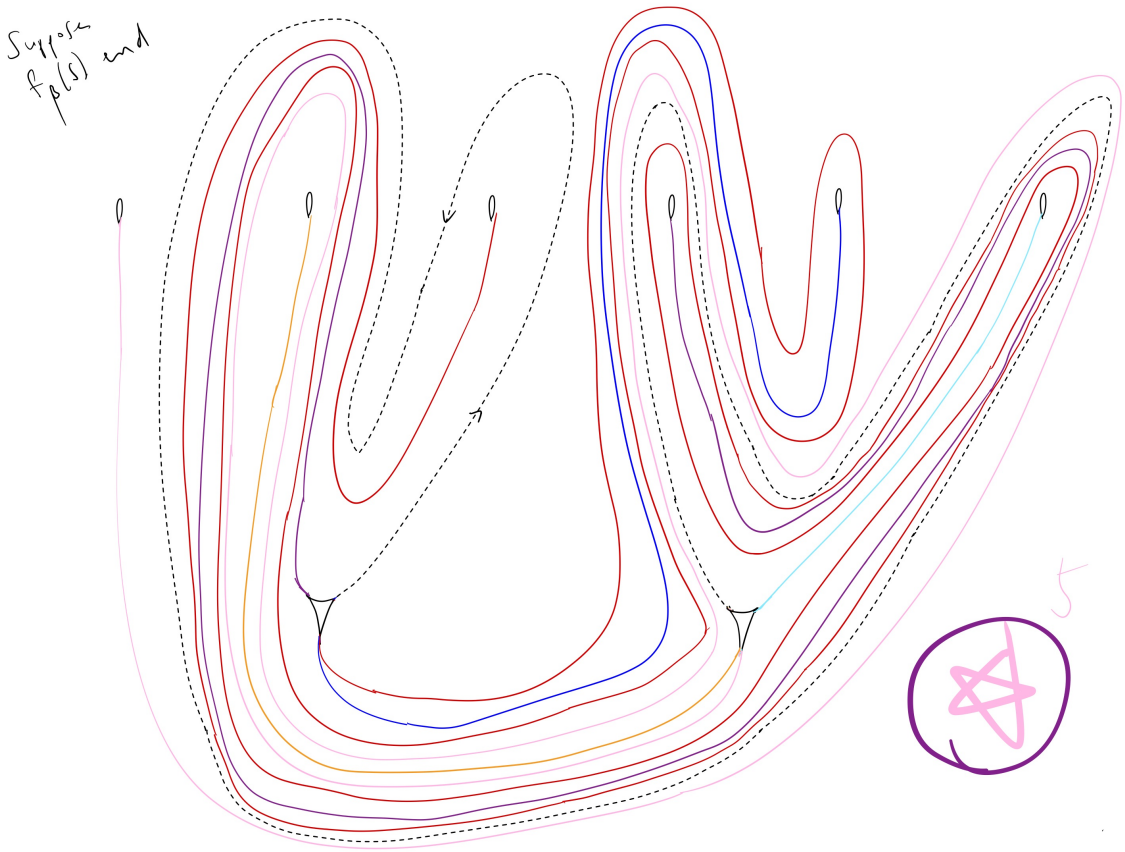


Figure D.132: Balance10

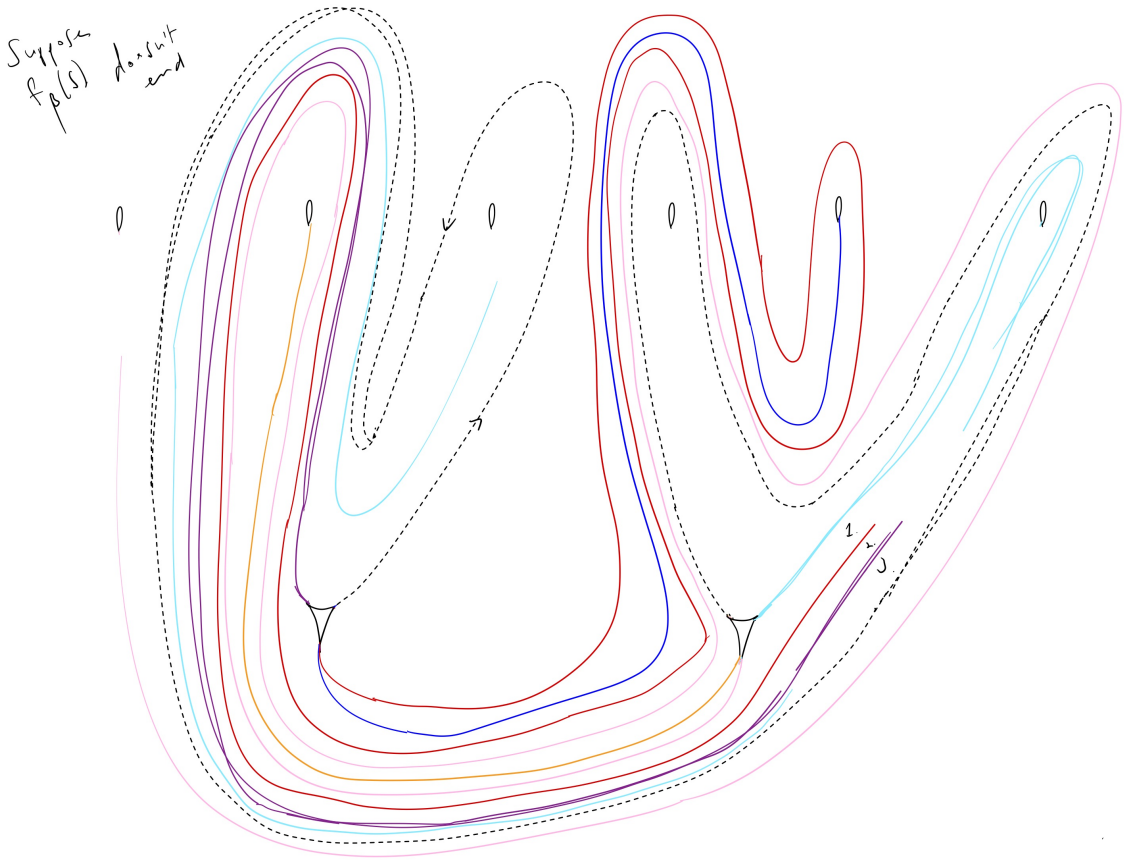


Figure D.133: Machine1

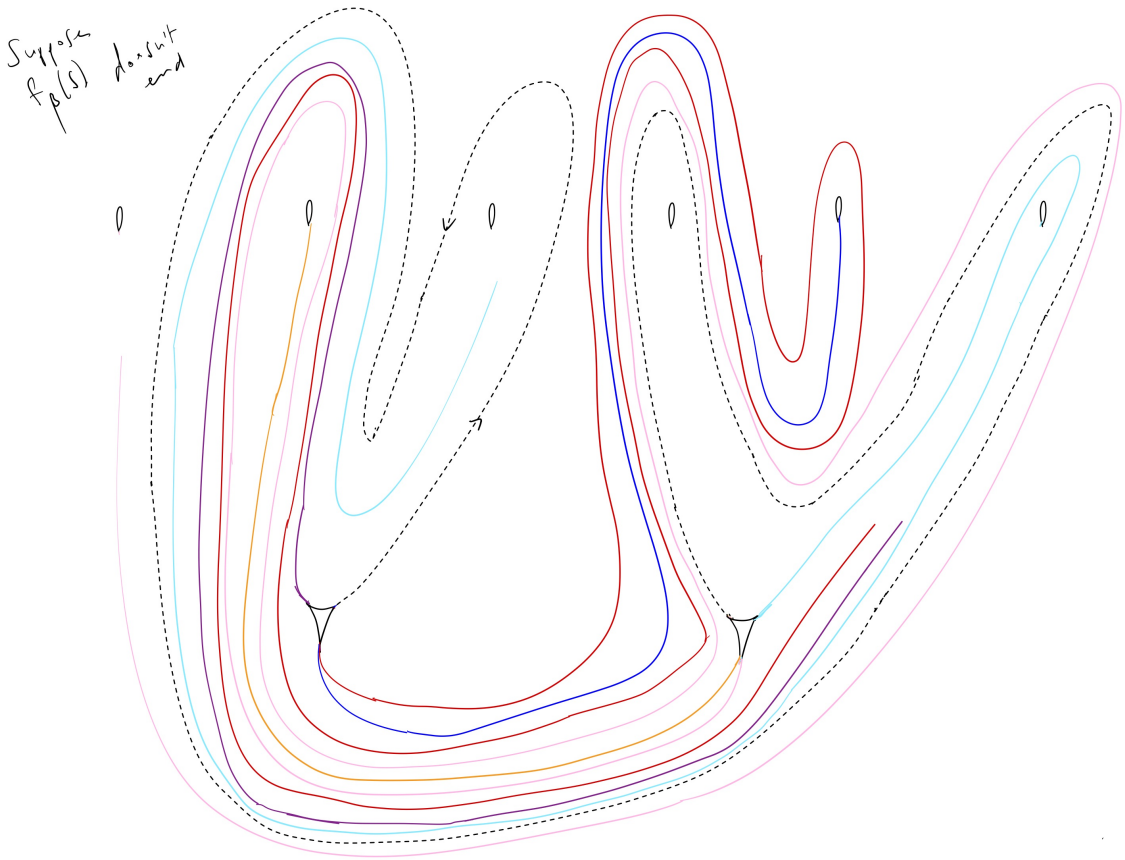


Figure D.134: Machine2

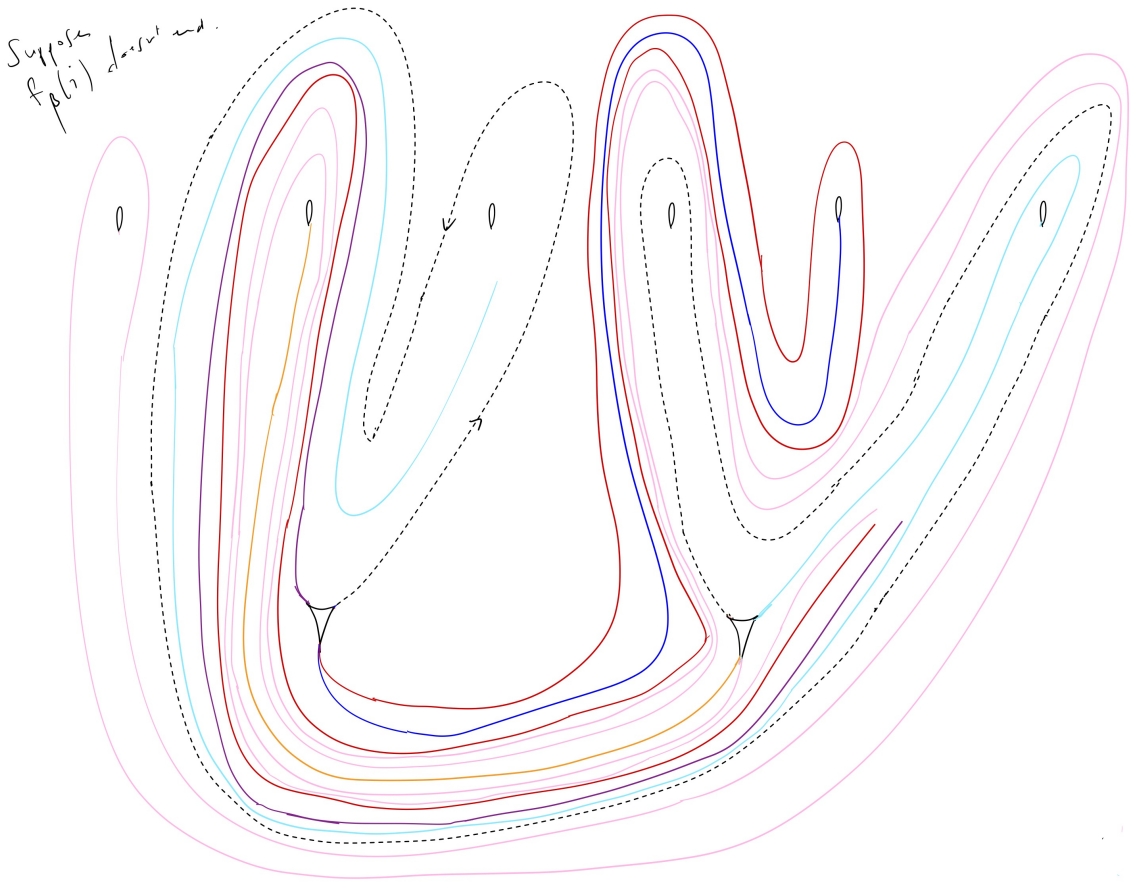


Figure D.135: Machine3

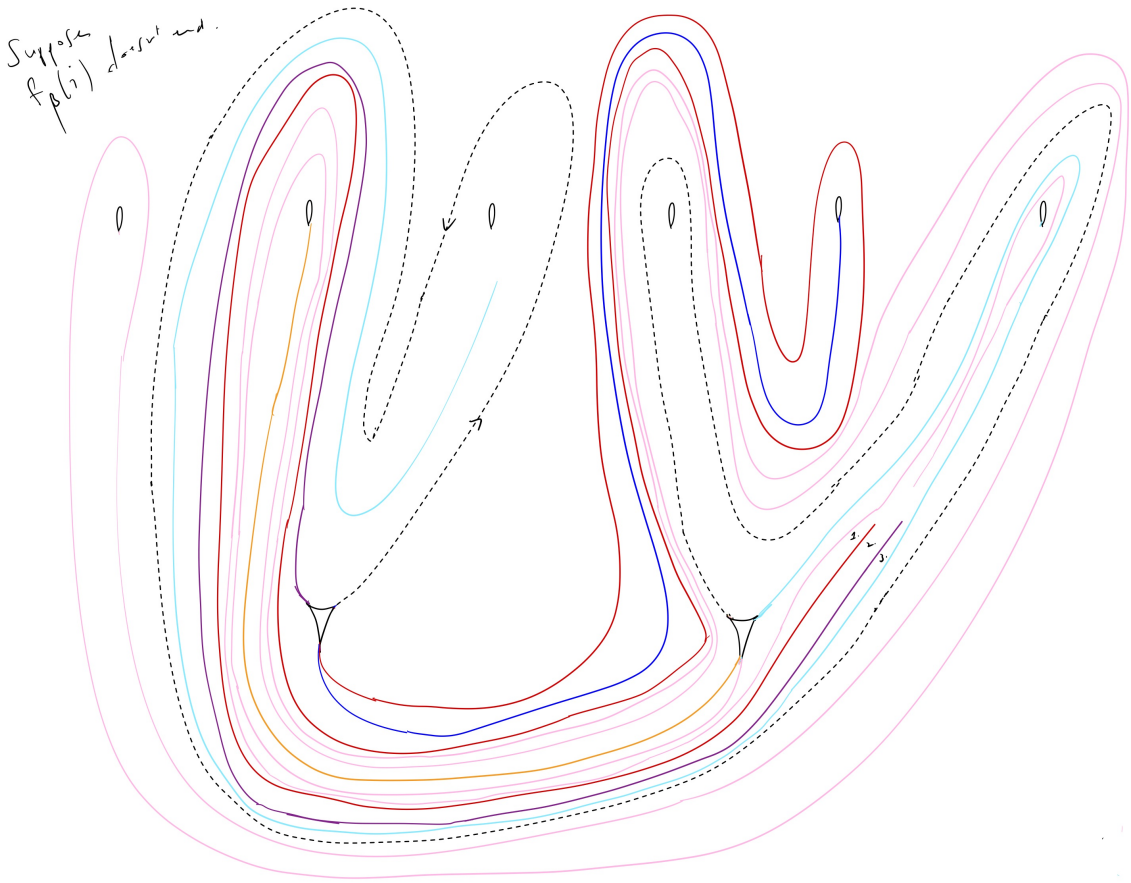


Figure D.136: Machine4

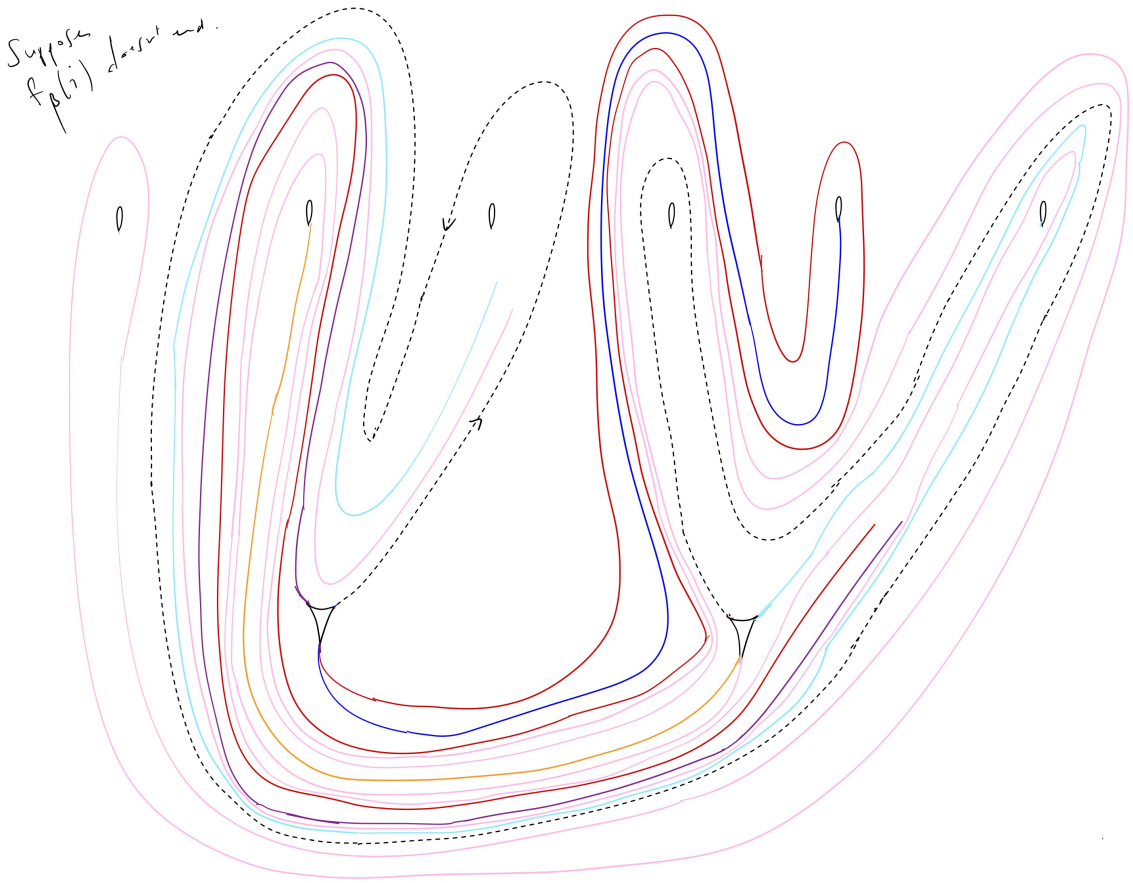


Figure D.137: Machine5

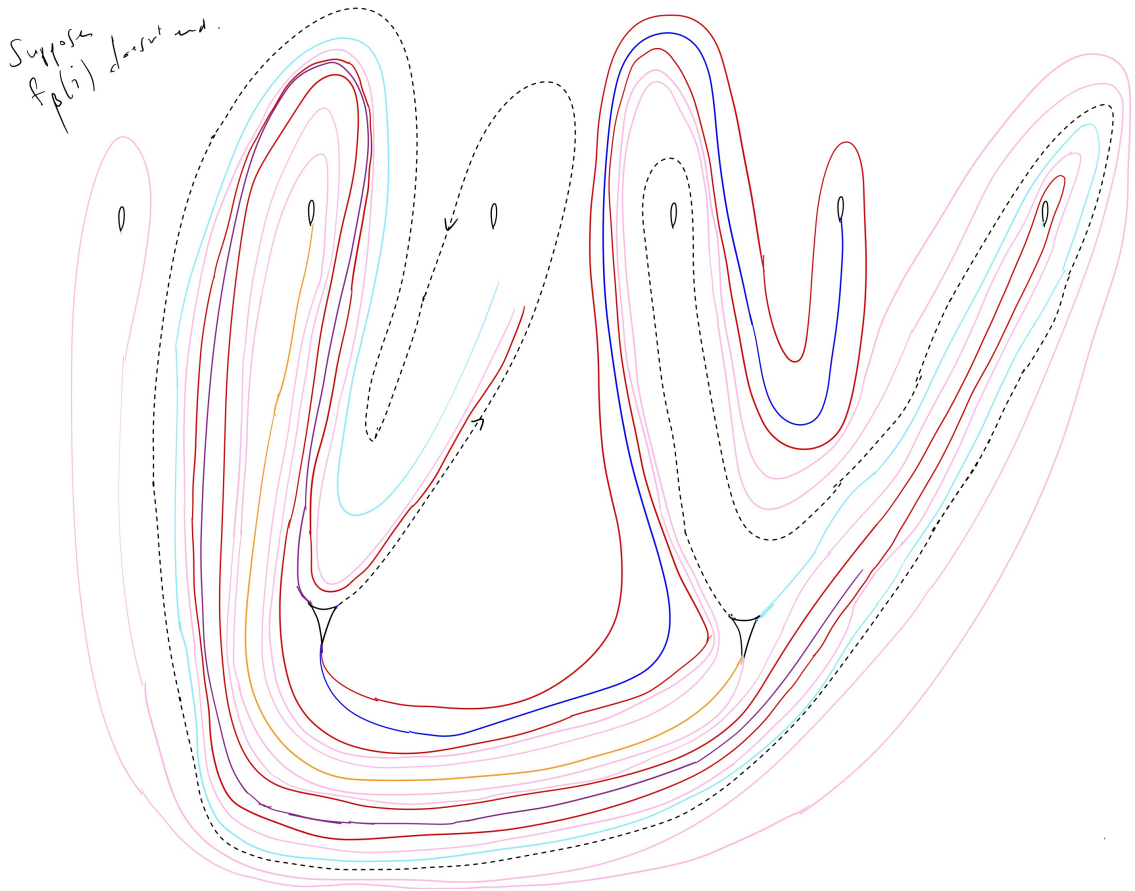


Figure D.138: Machine6

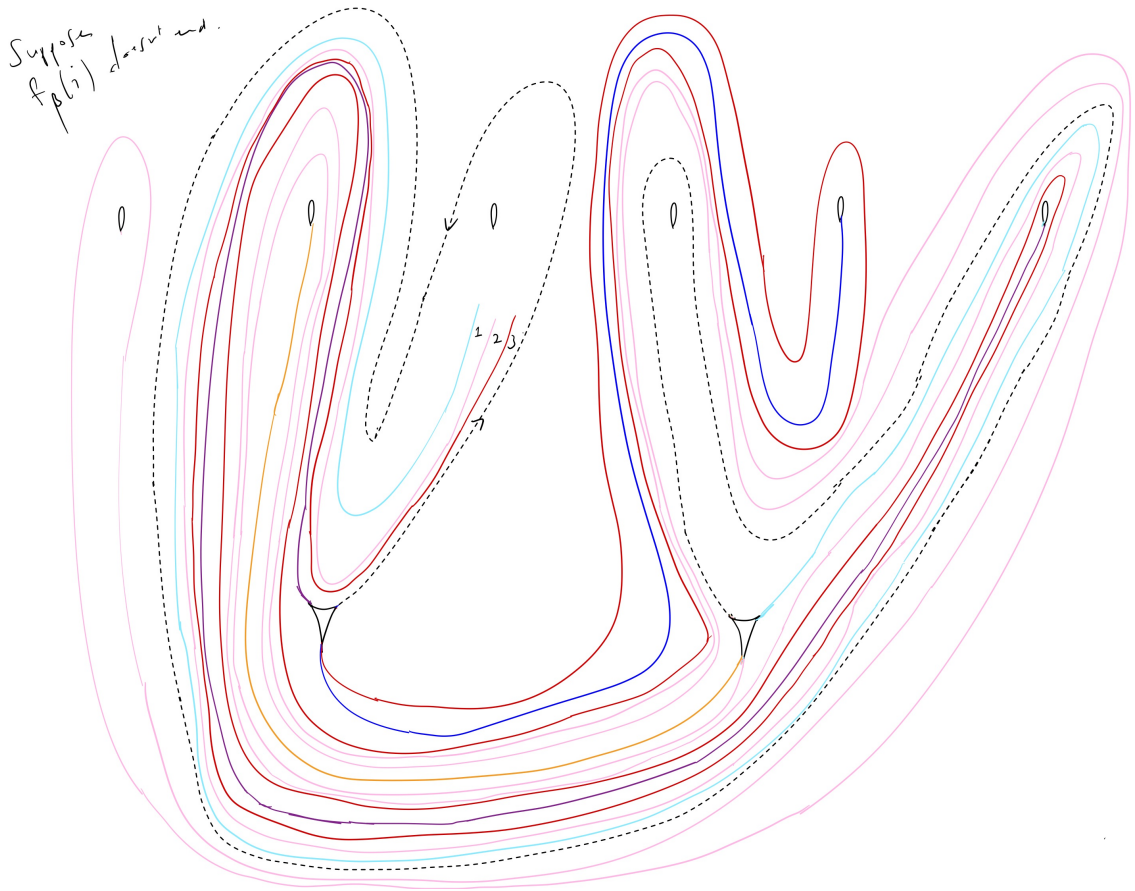


Figure D.139: Machine7

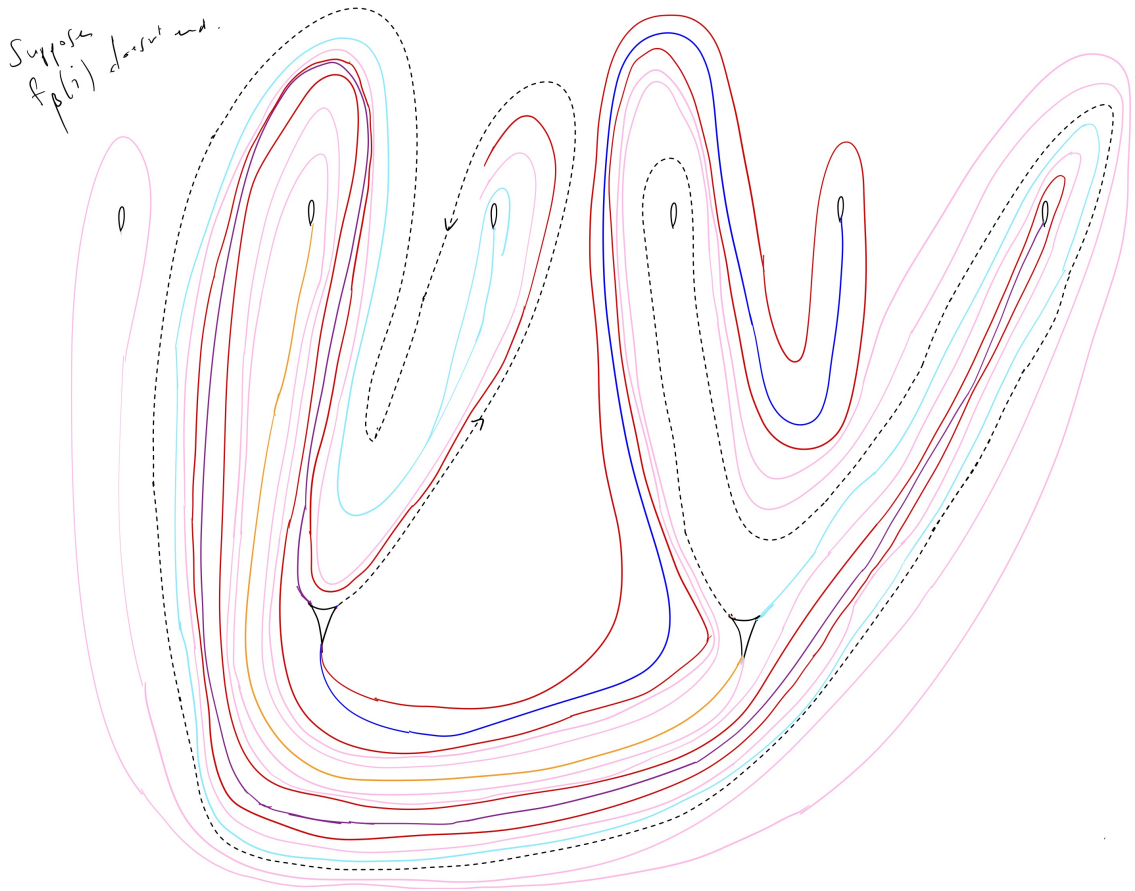


Figure D.140: Machine8

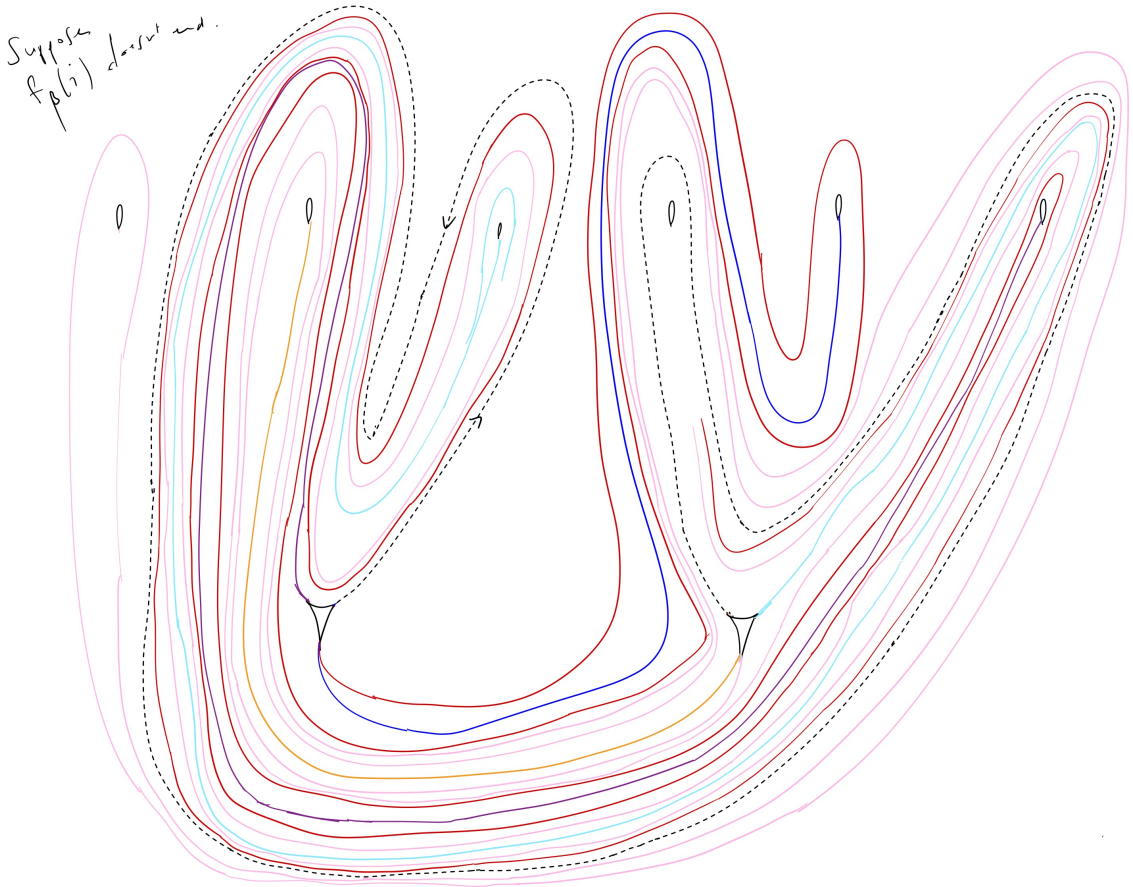


Figure D.141: Machine9

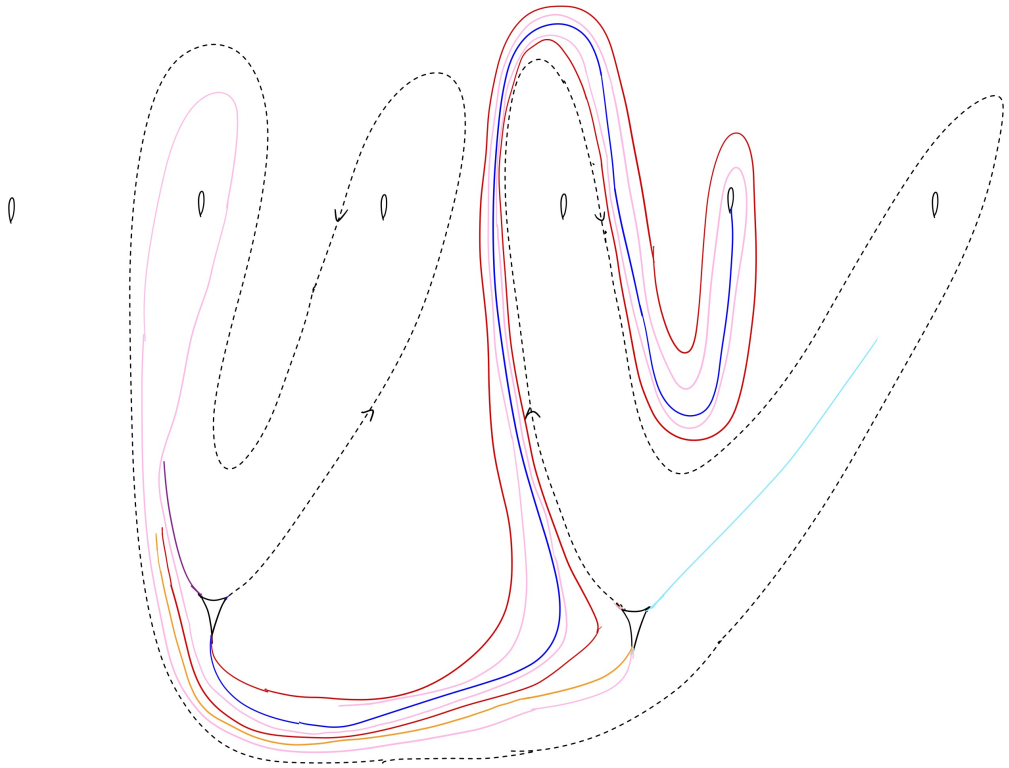


Figure D.142: Iguana1

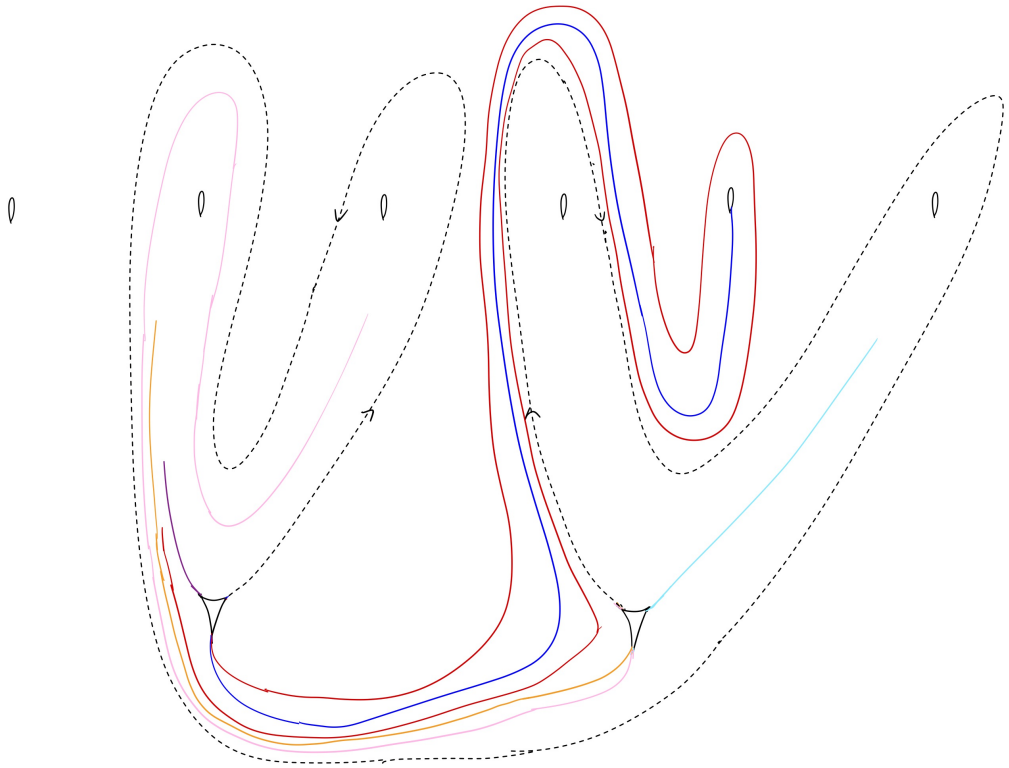


Figure D.143: Fiasco1

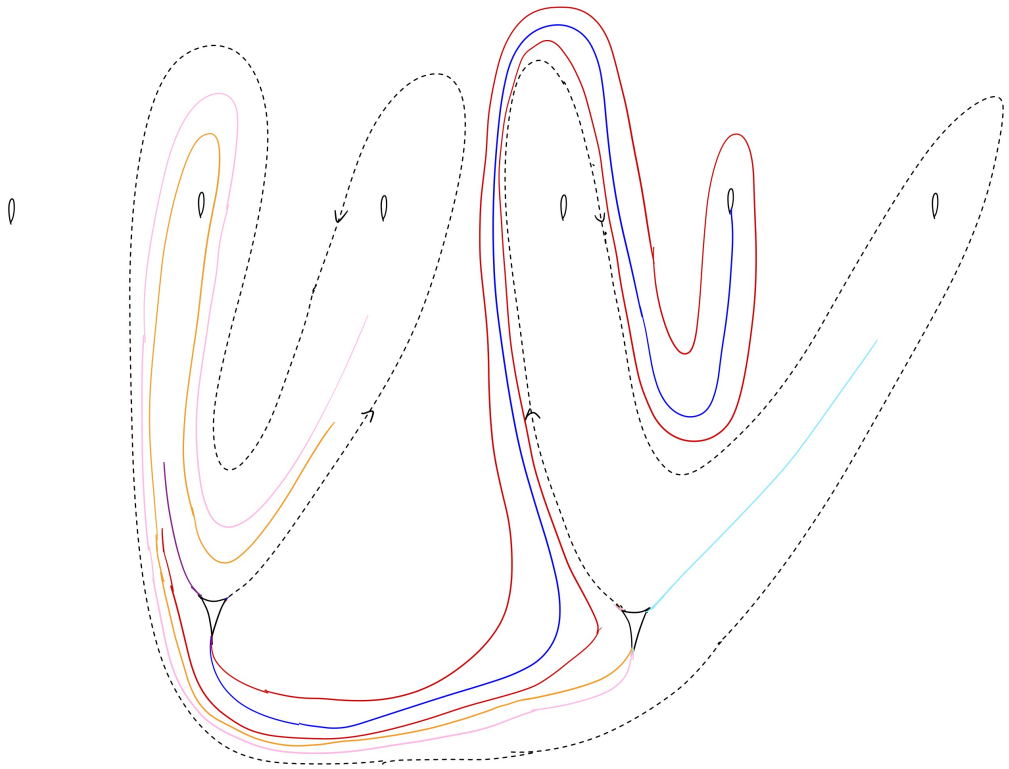


Figure D.144: Fiasco2

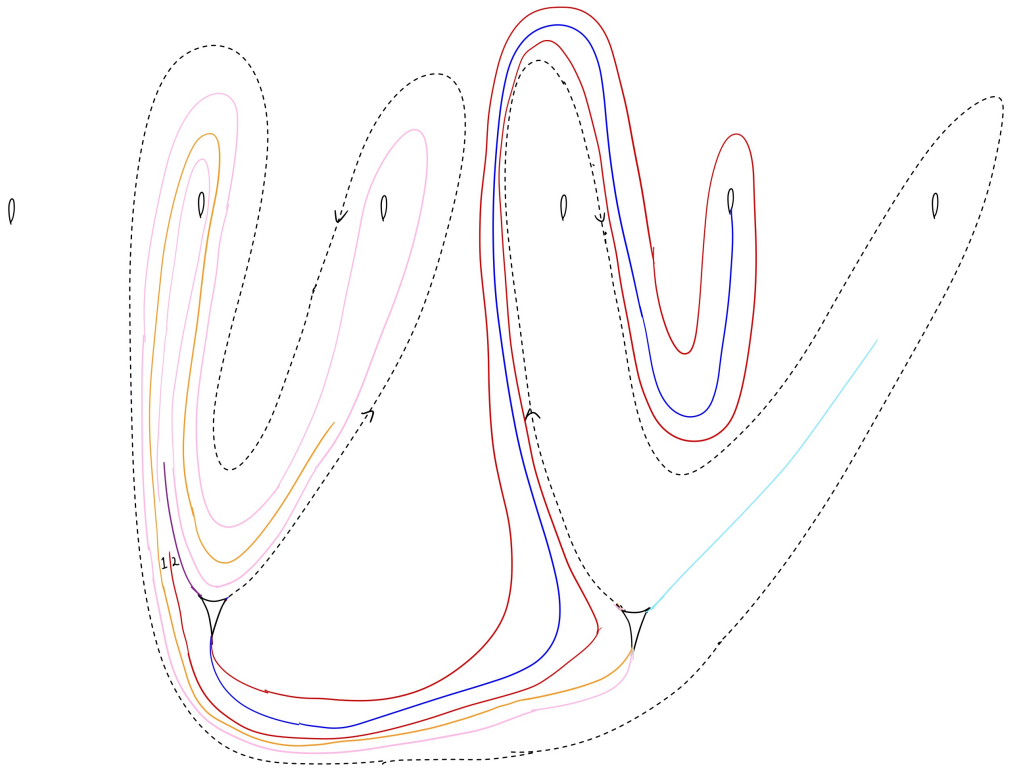


Figure D.145: Fiasco3

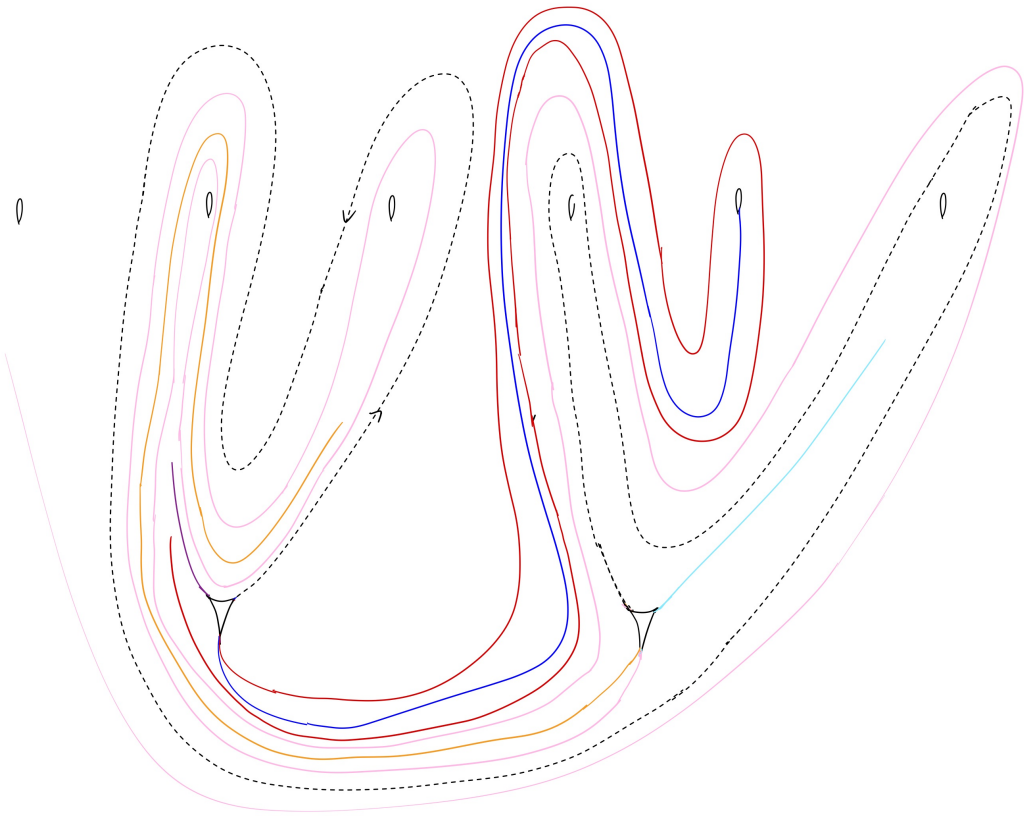


Figure D.146: Fiasco4

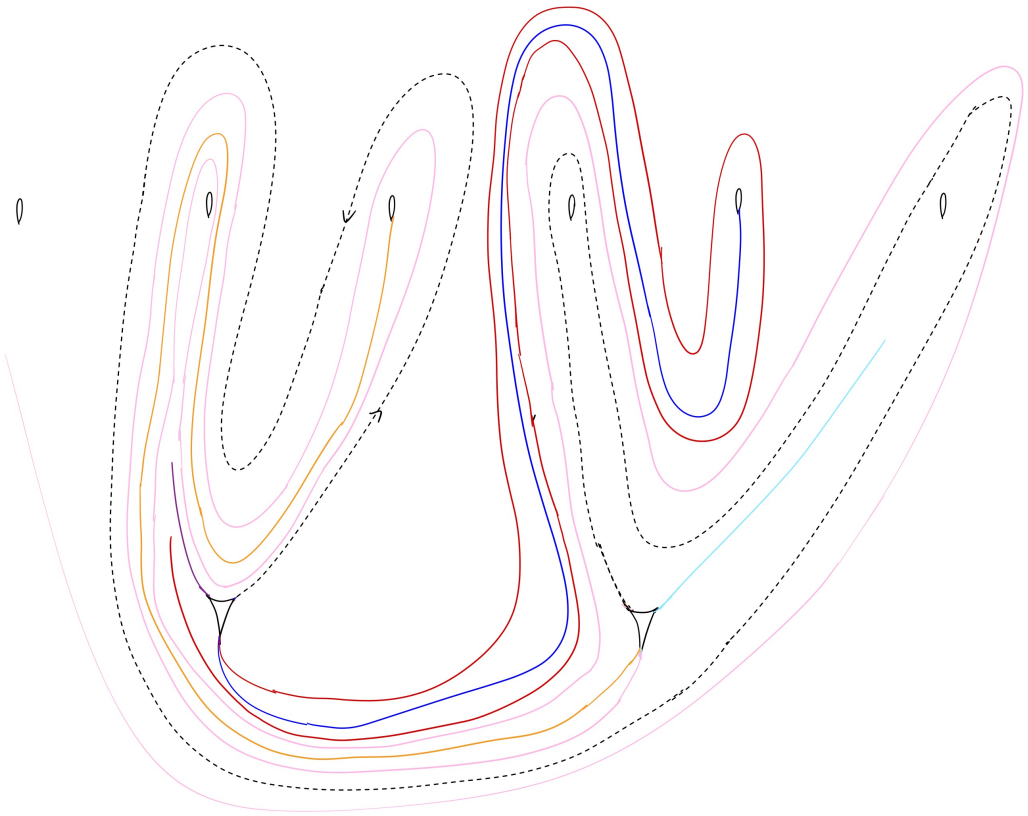


Figure D.147: Fiasco5

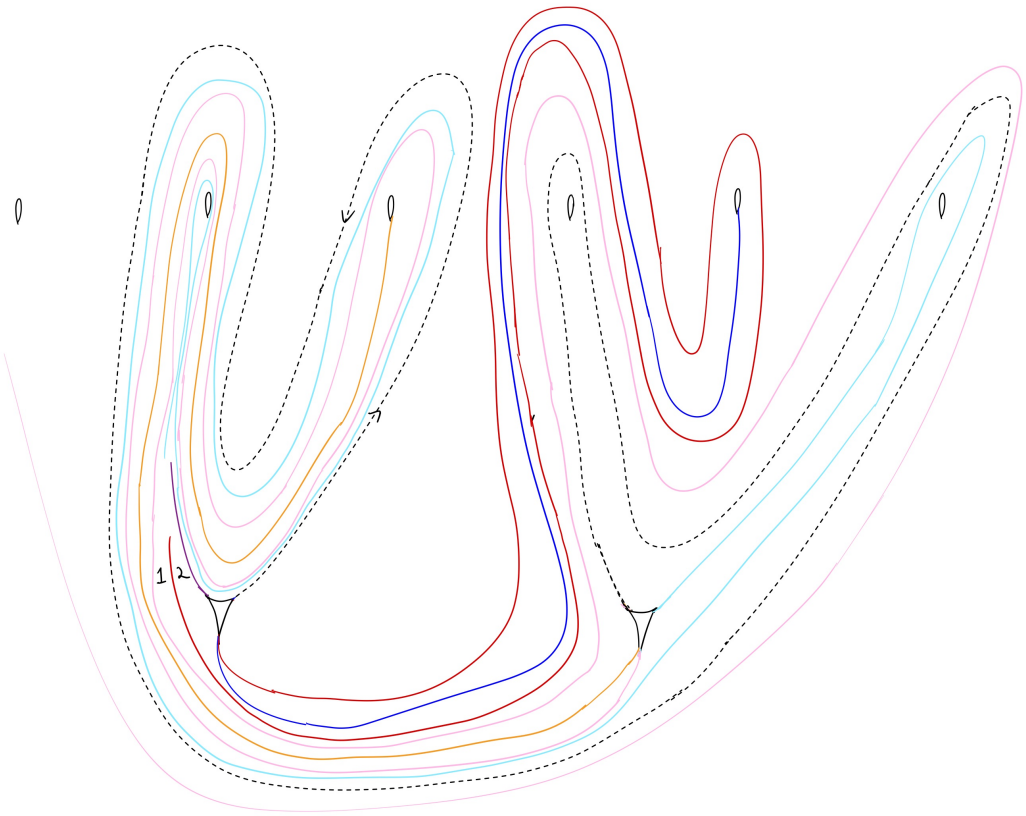


Figure D.148: Fiasco6

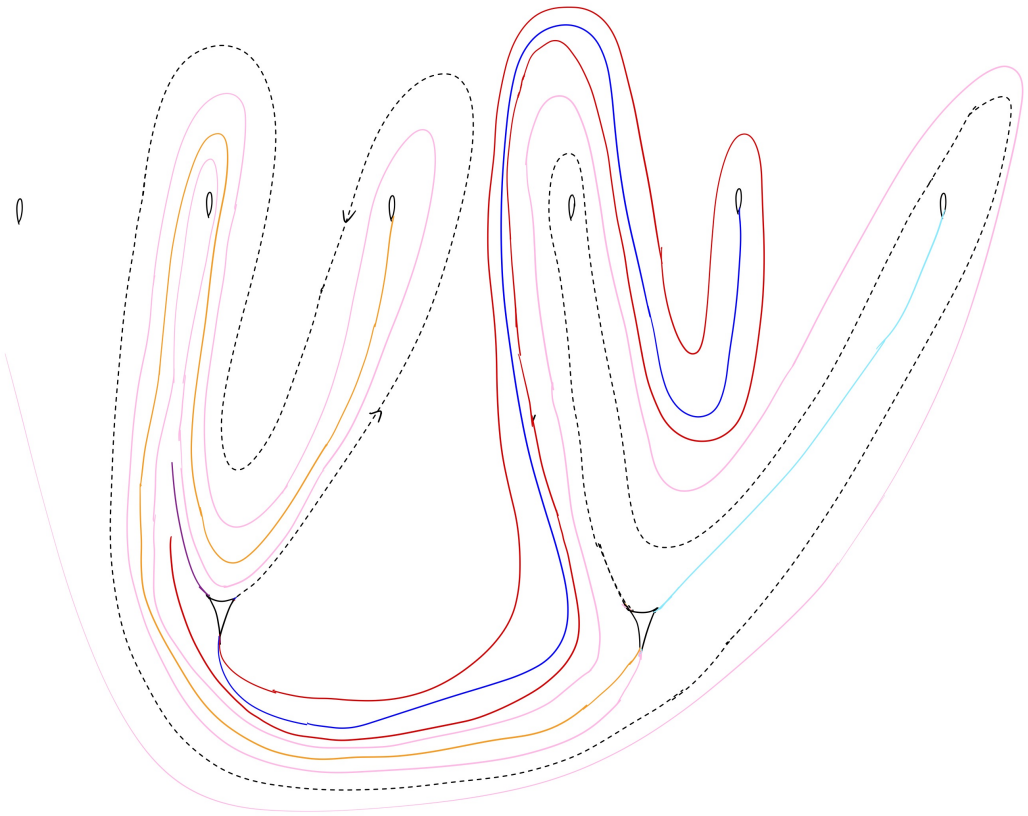


Figure D.149: Fiasco7

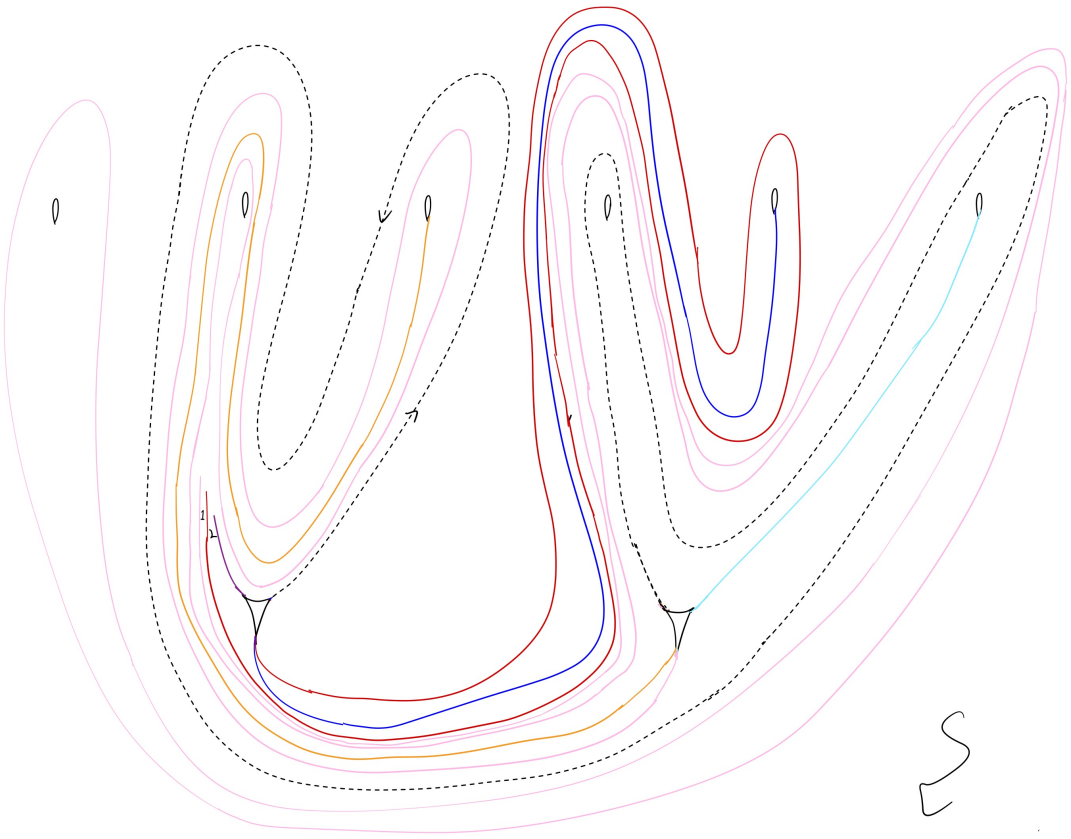


Figure D.150: Fiasco8

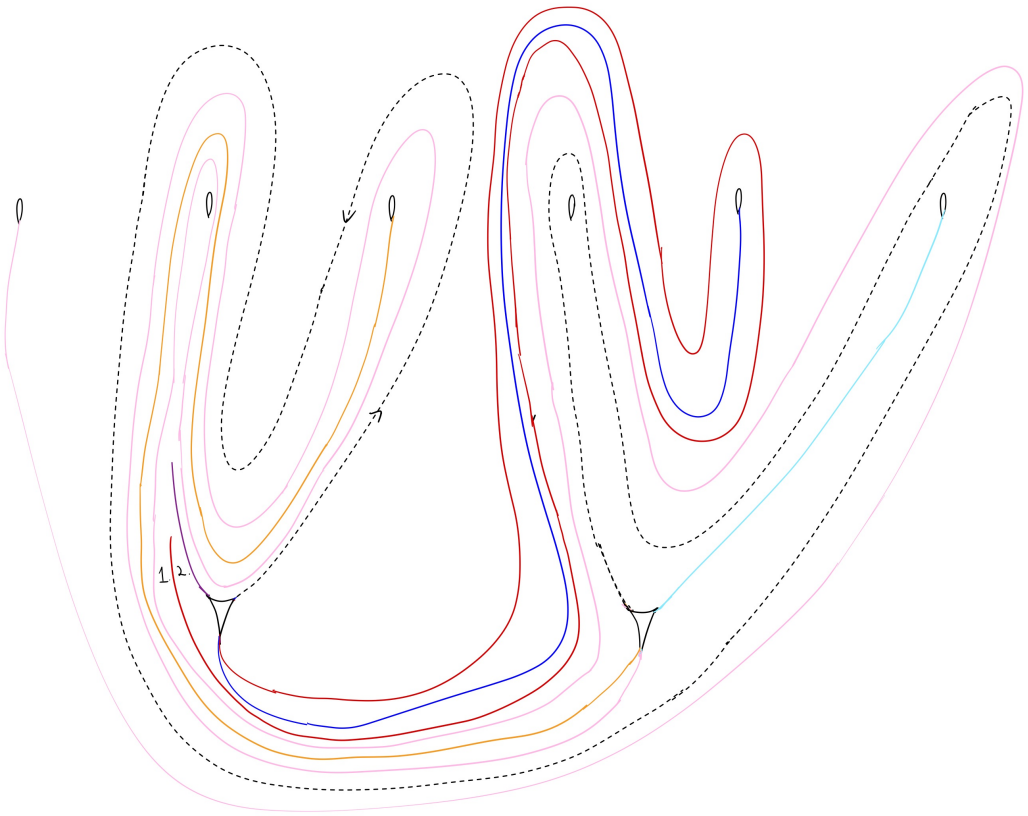


Figure D.151: Fiasco9

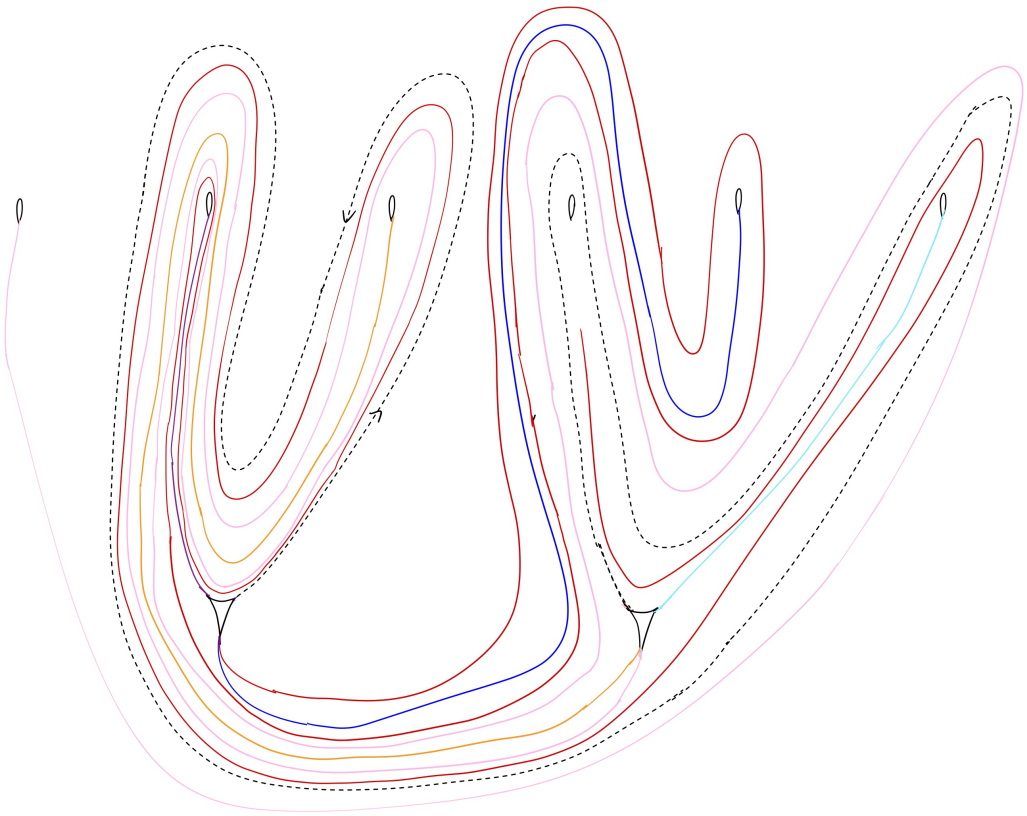


Figure D.152: Fiasco10

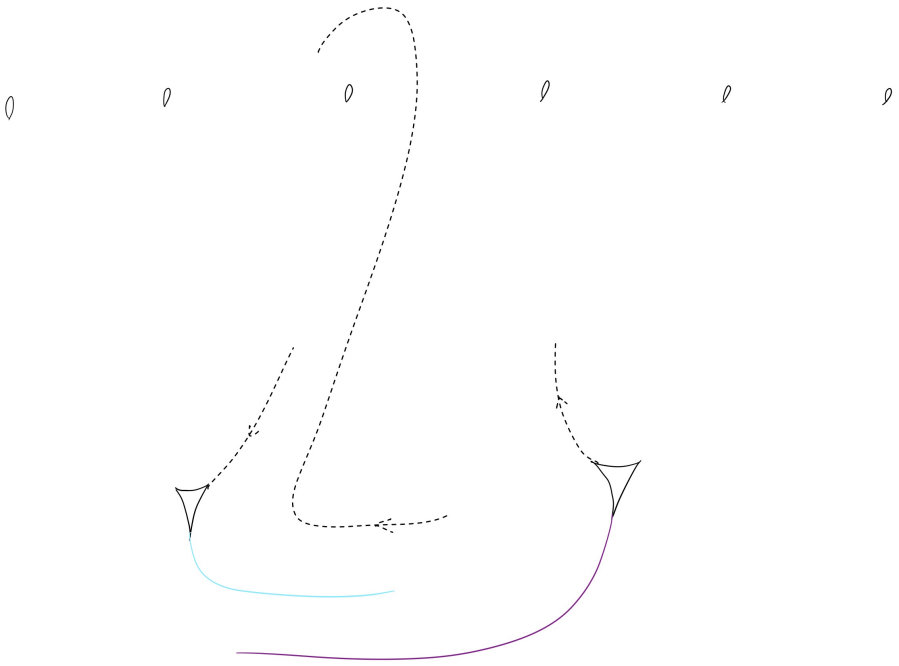


Figure D.153: ATL1

Figure D.154: LAX1

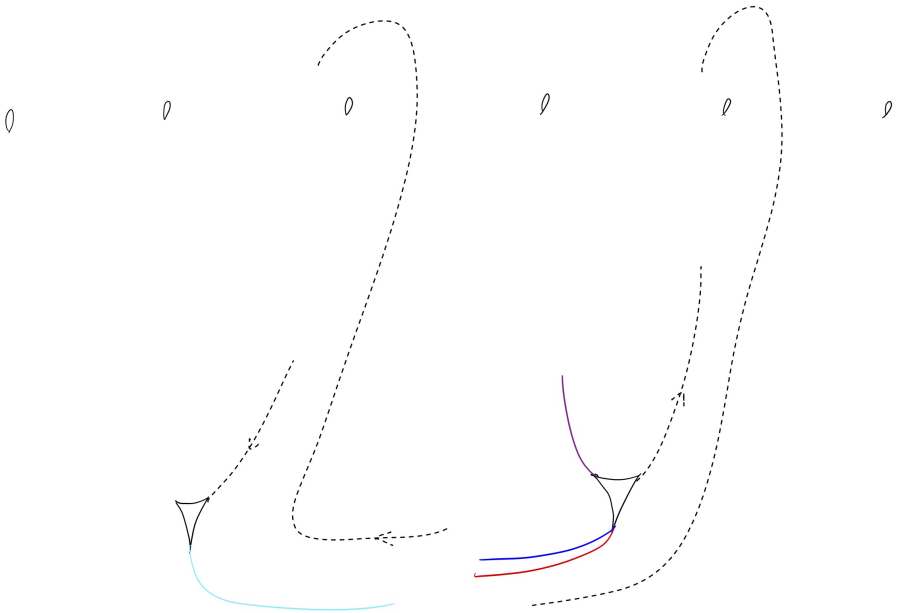


Figure D.155: Jolt1

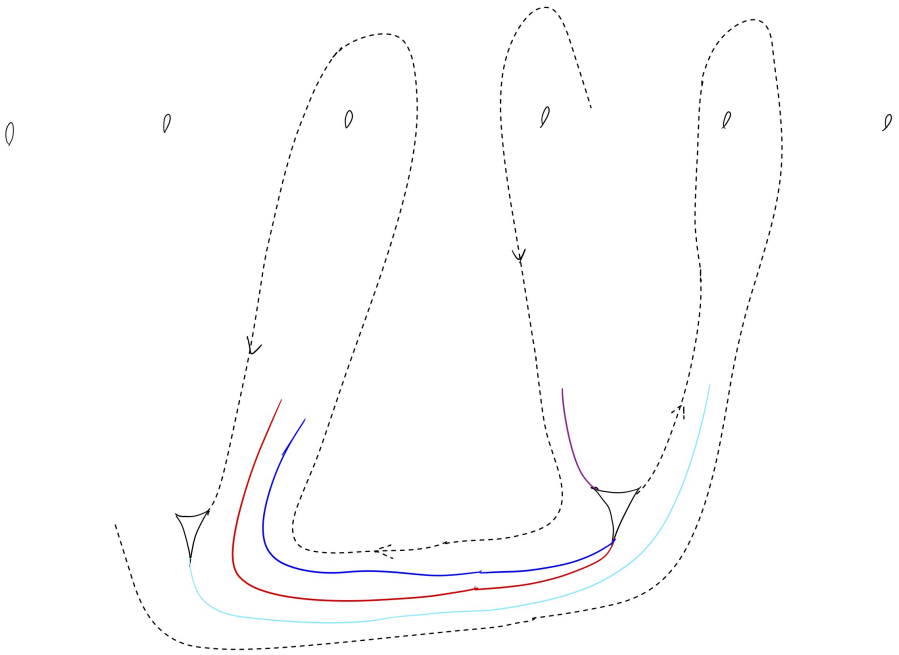


Figure D.156: Jolt2

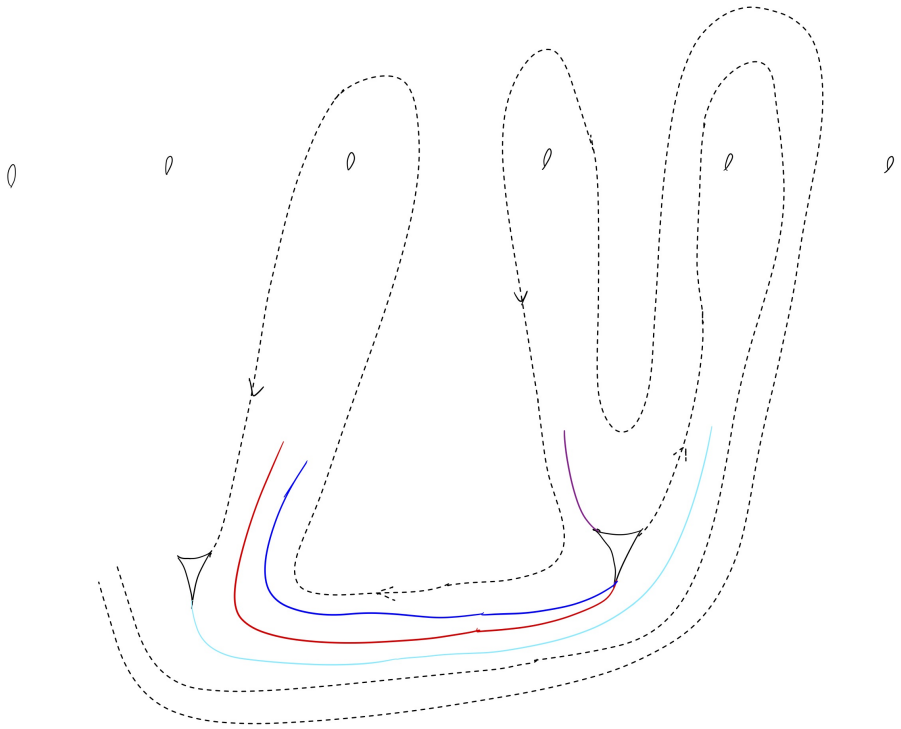


Figure D.157: Jolt3

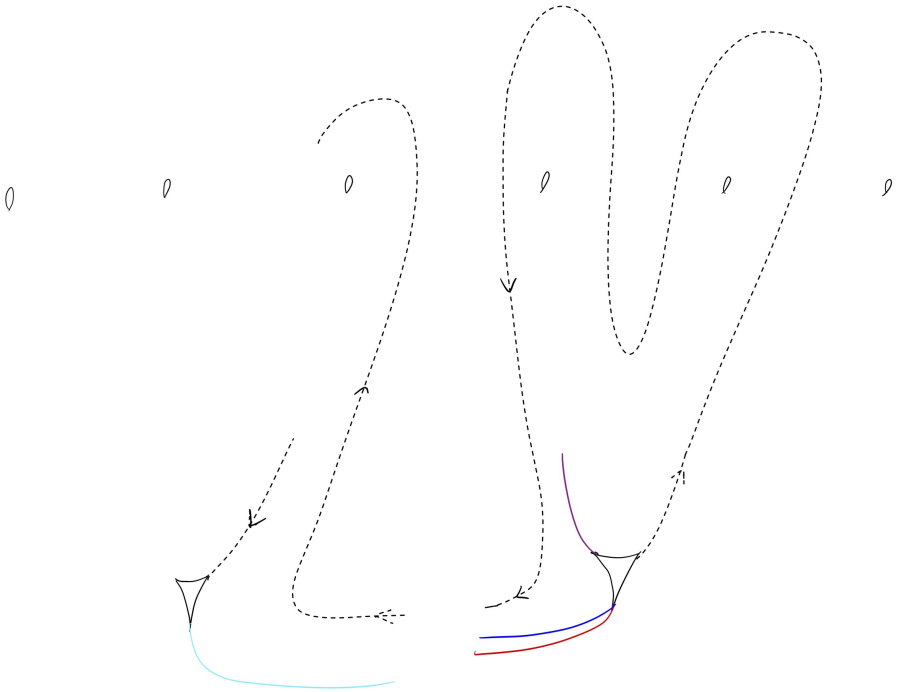


Figure D.158: Mile1

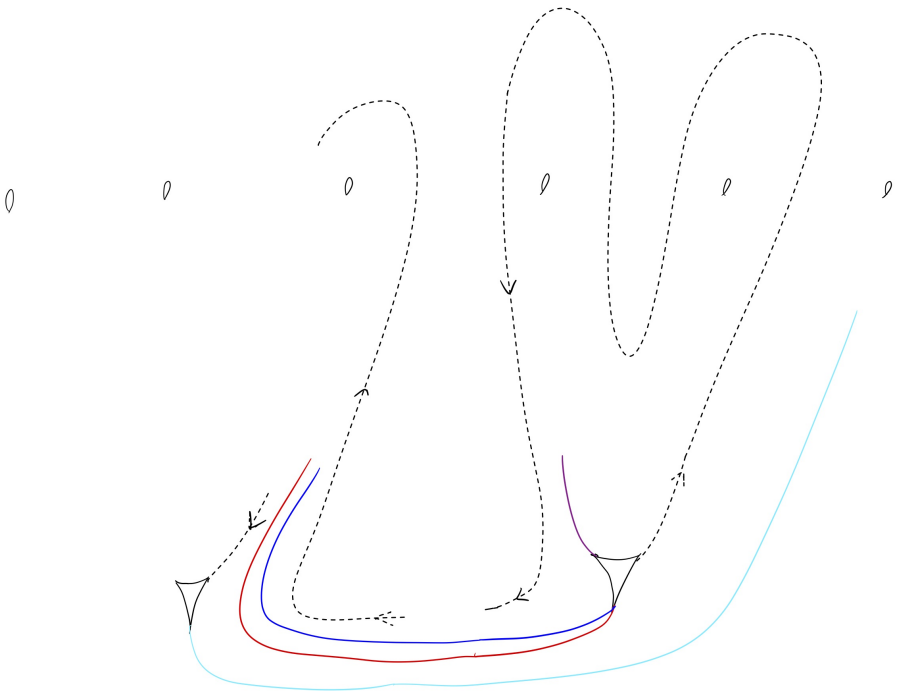


Figure D.159: Mile2

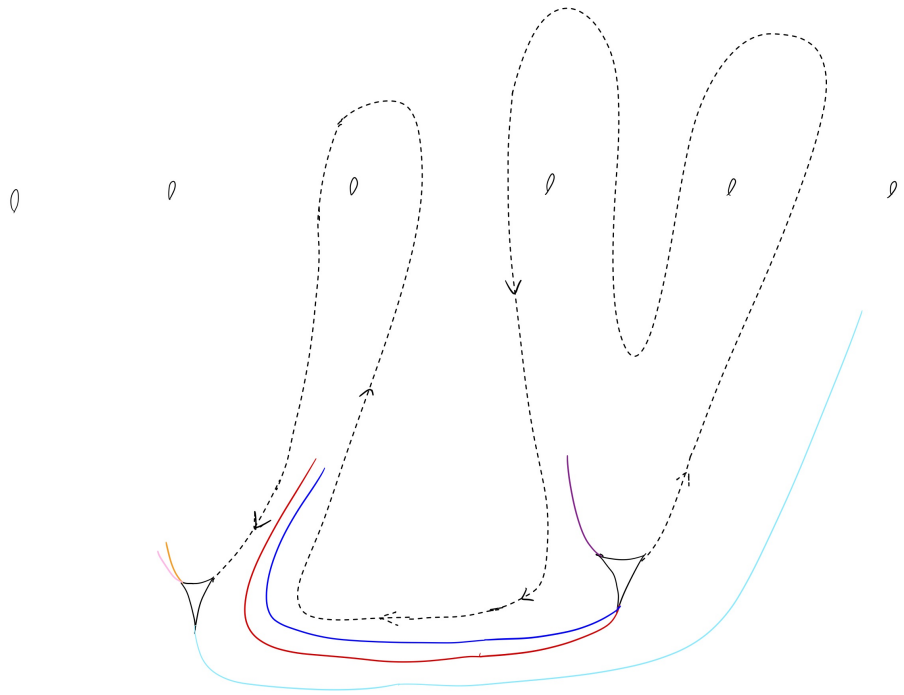


Figure D.160: Mile3

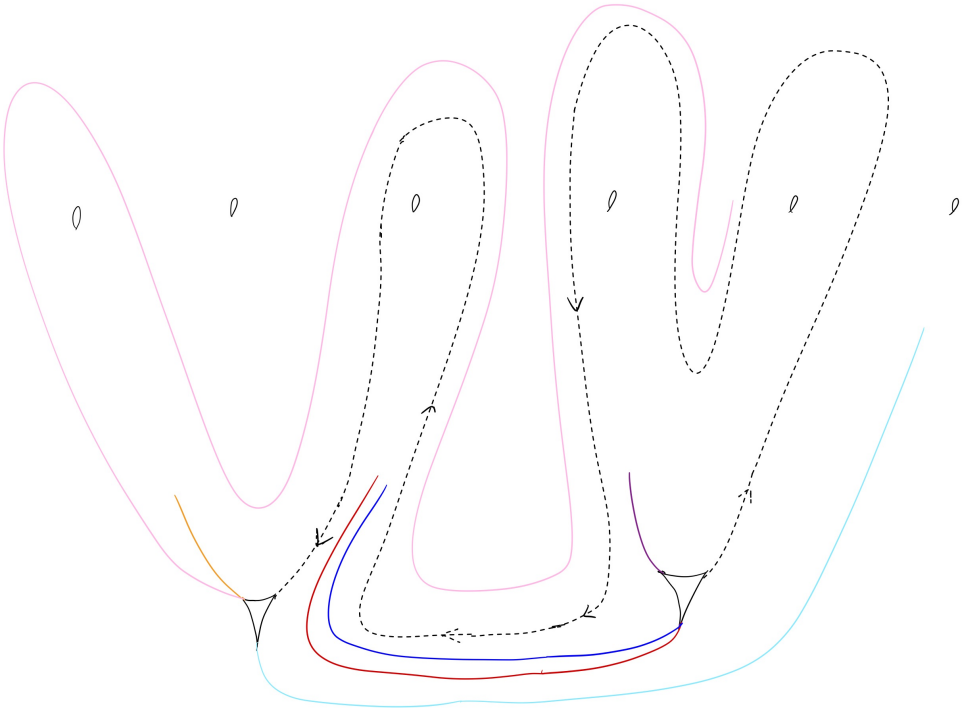


Figure D.161: Night1

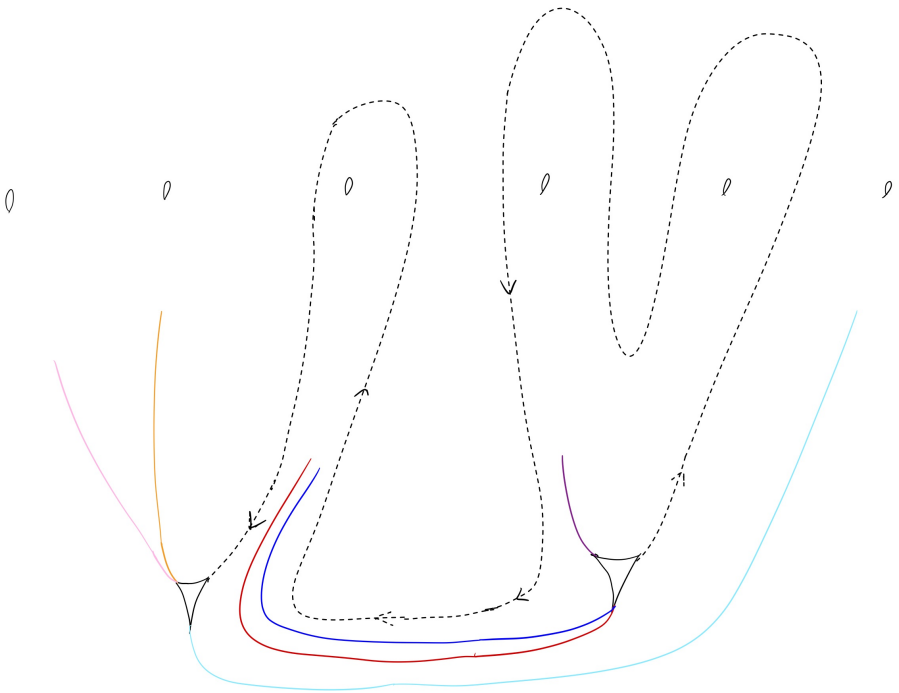


Figure D.162: Adieu1

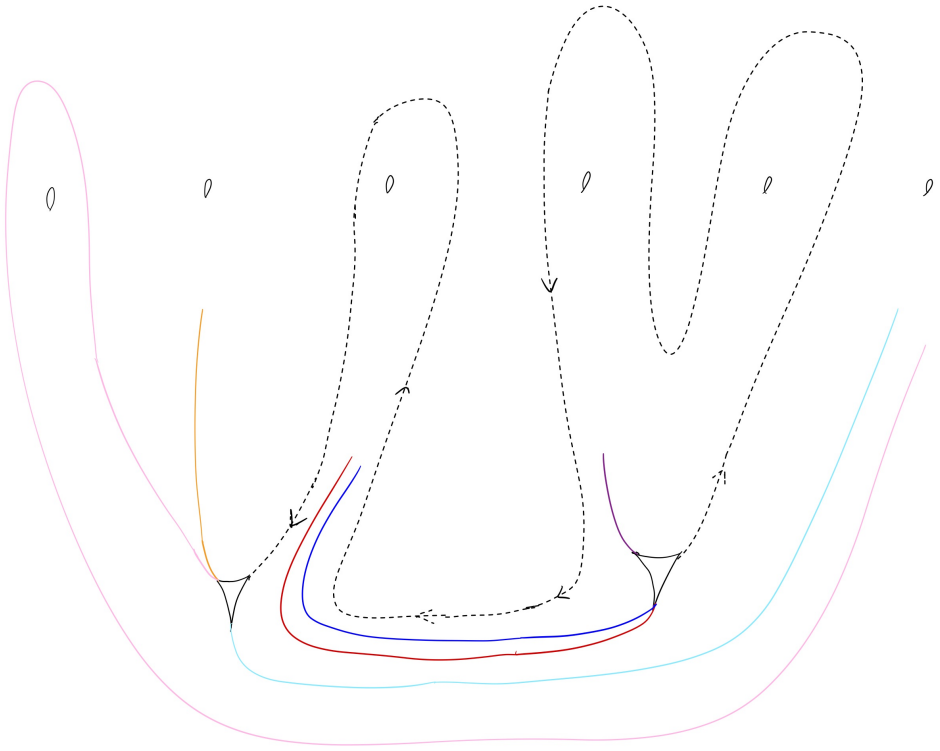


Figure D.163: Sizzle1

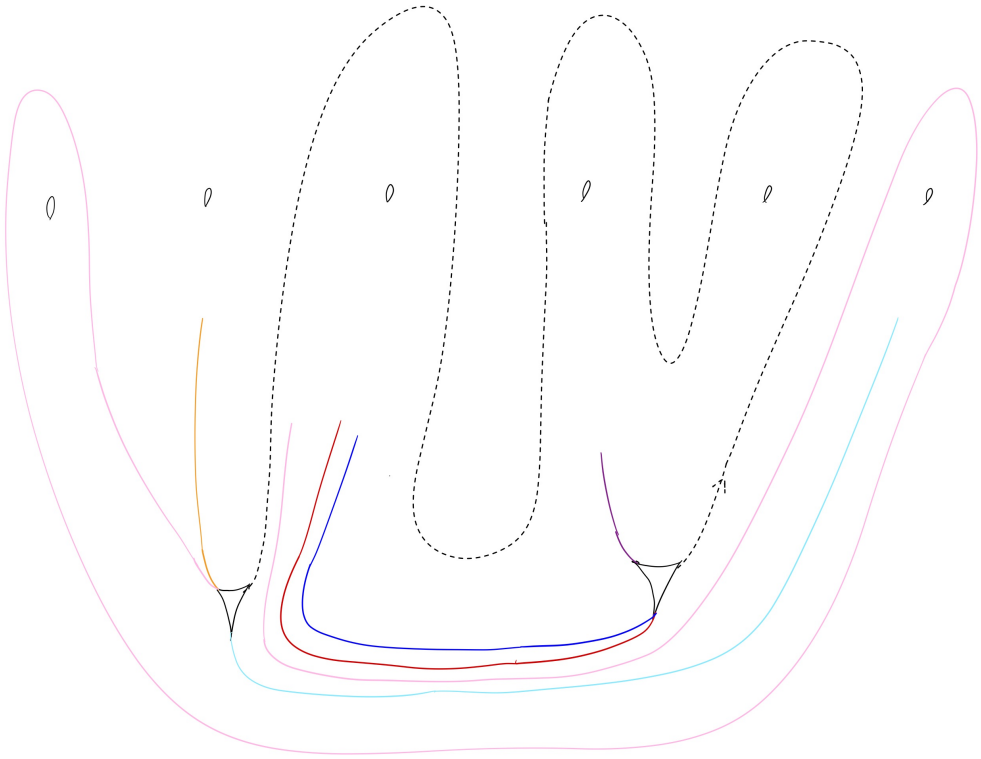


Figure D.164: Sizzle2

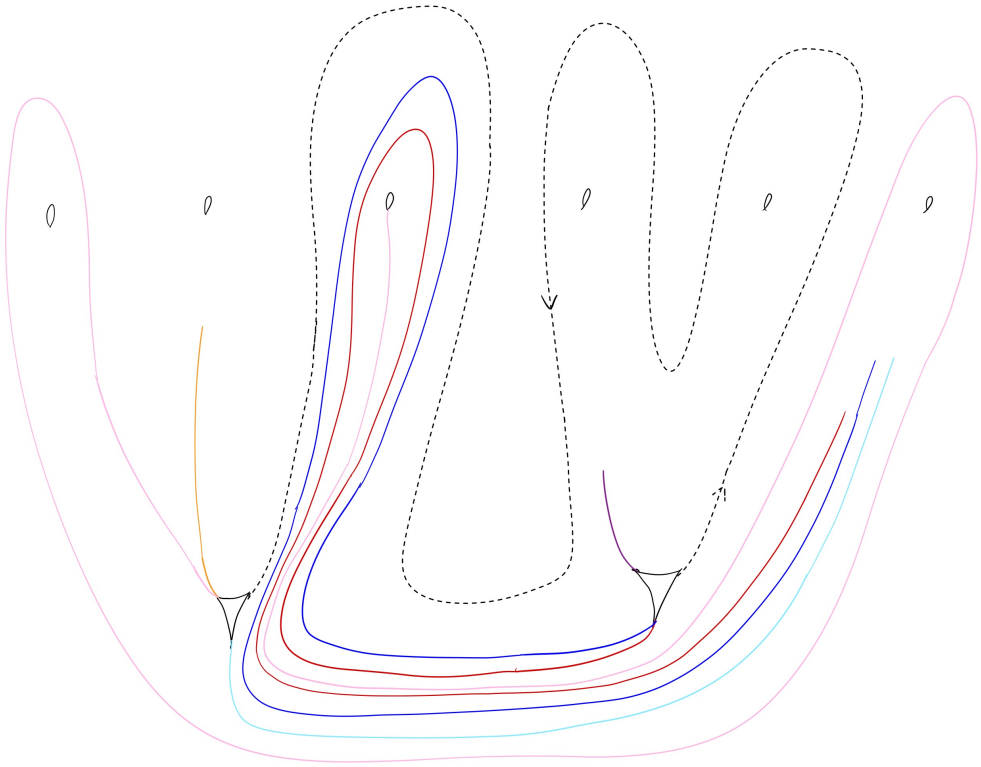


Figure D.165: Sizzle3

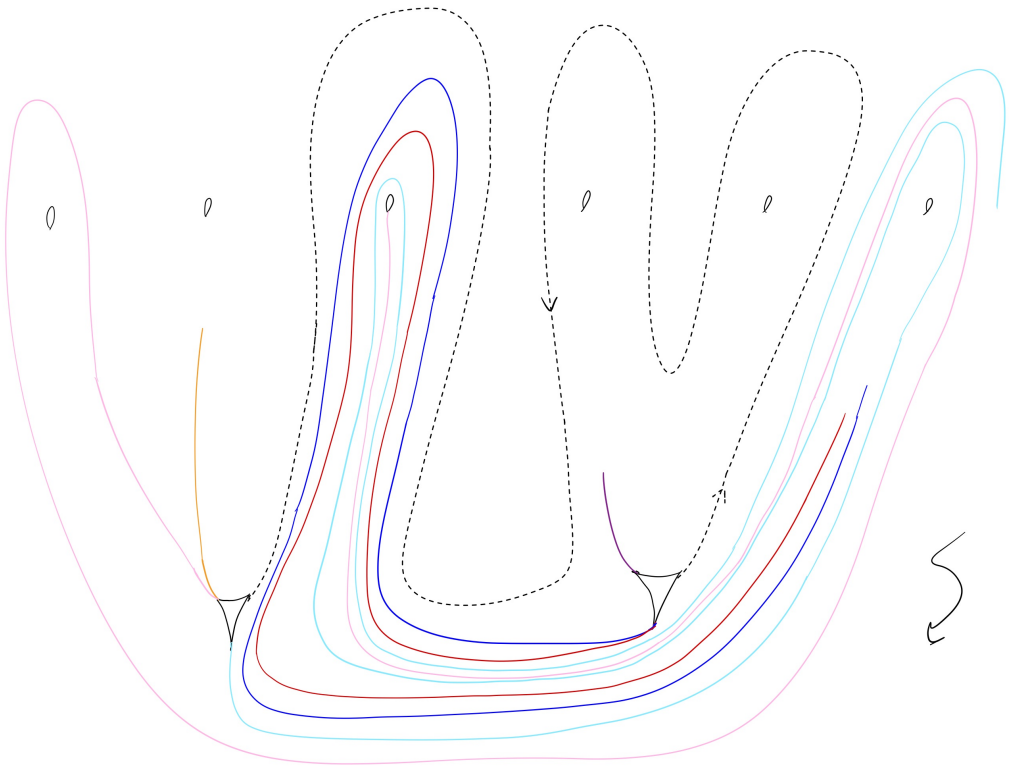


Figure D.166: Sizzle4

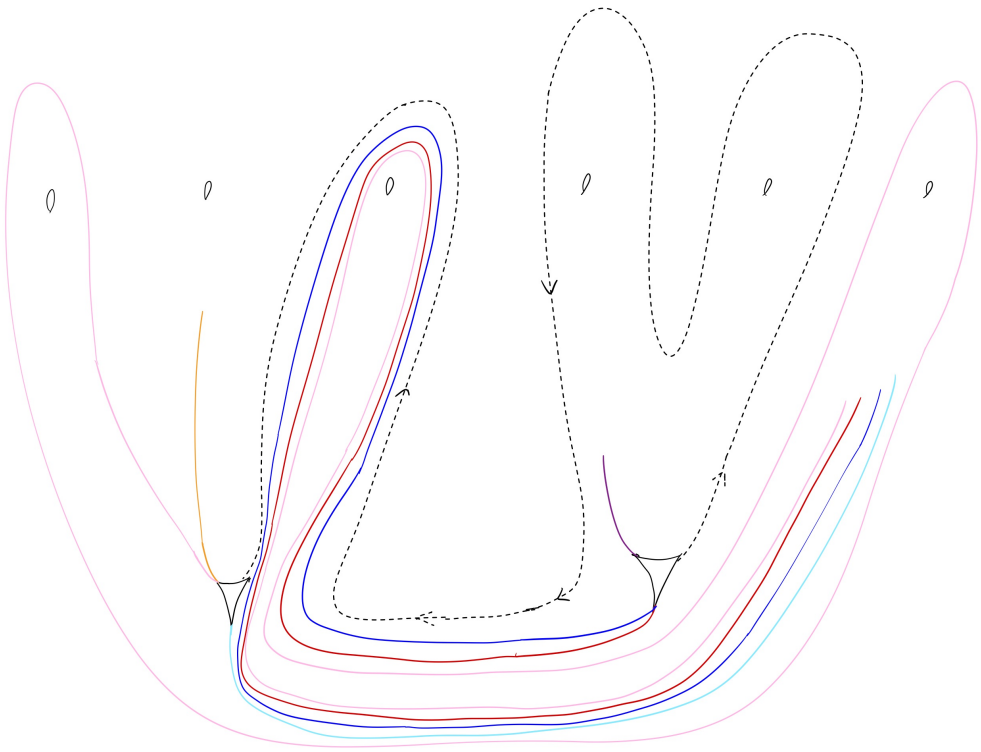


Figure D.167: Sizzle5

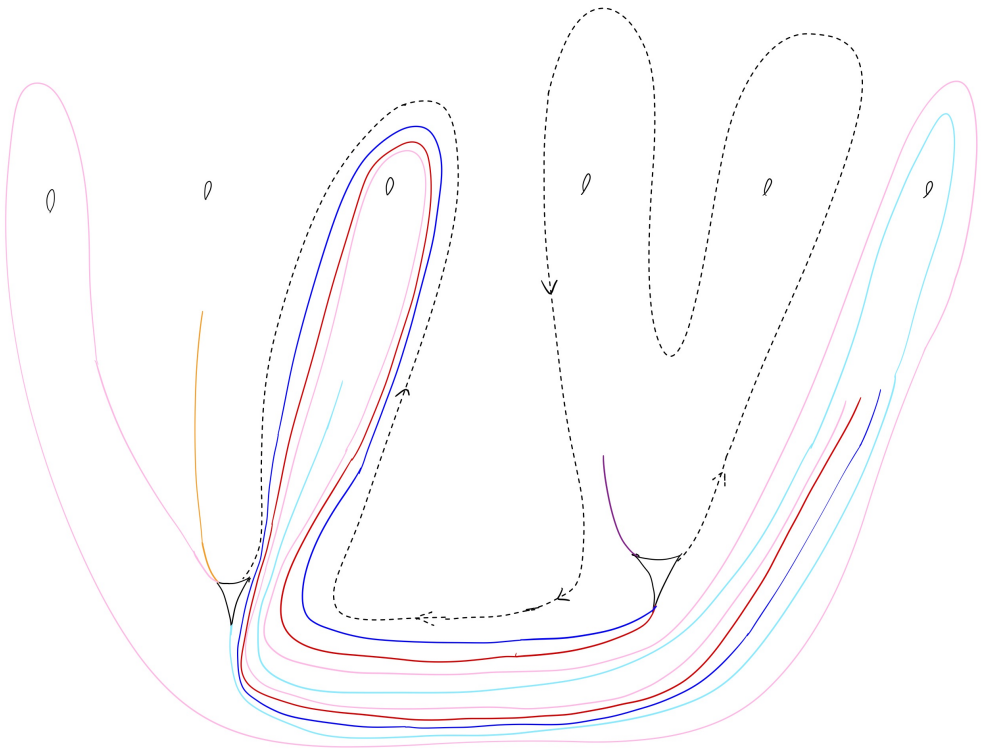


Figure D.168: Sizzle6

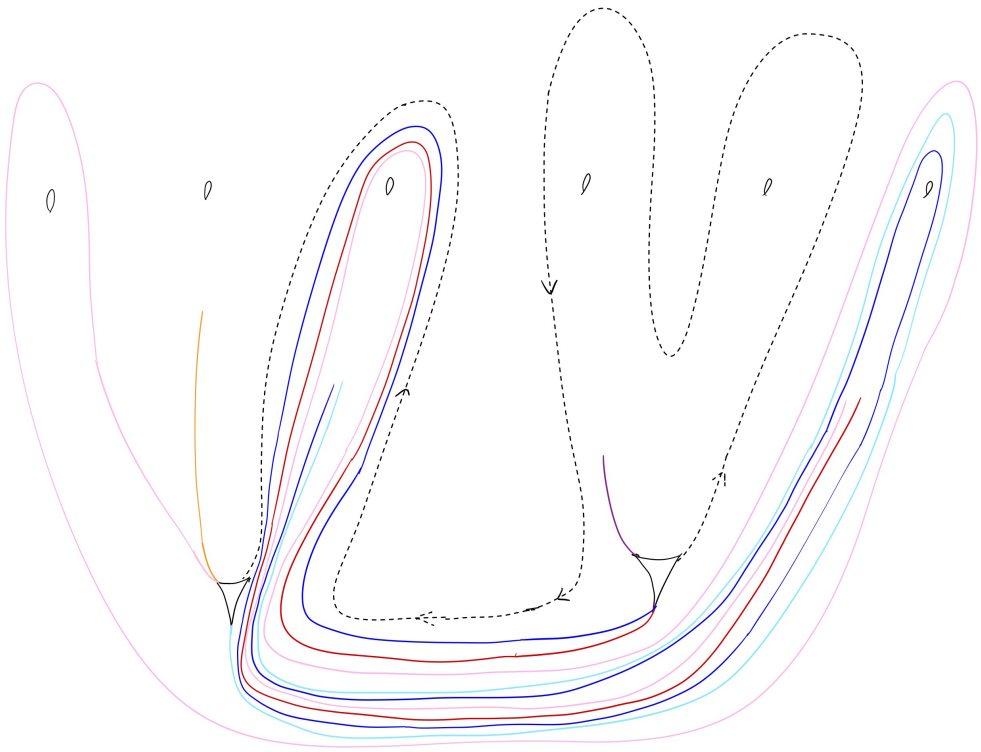


Figure D.169: Sizzle7

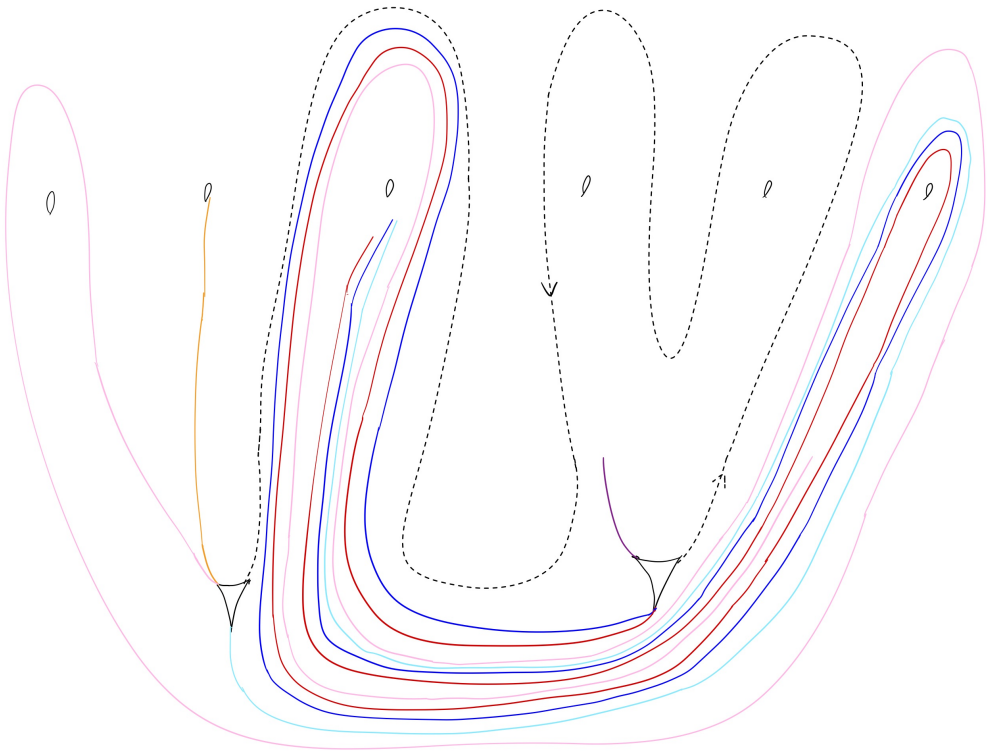


Figure D.170: Sizzle8

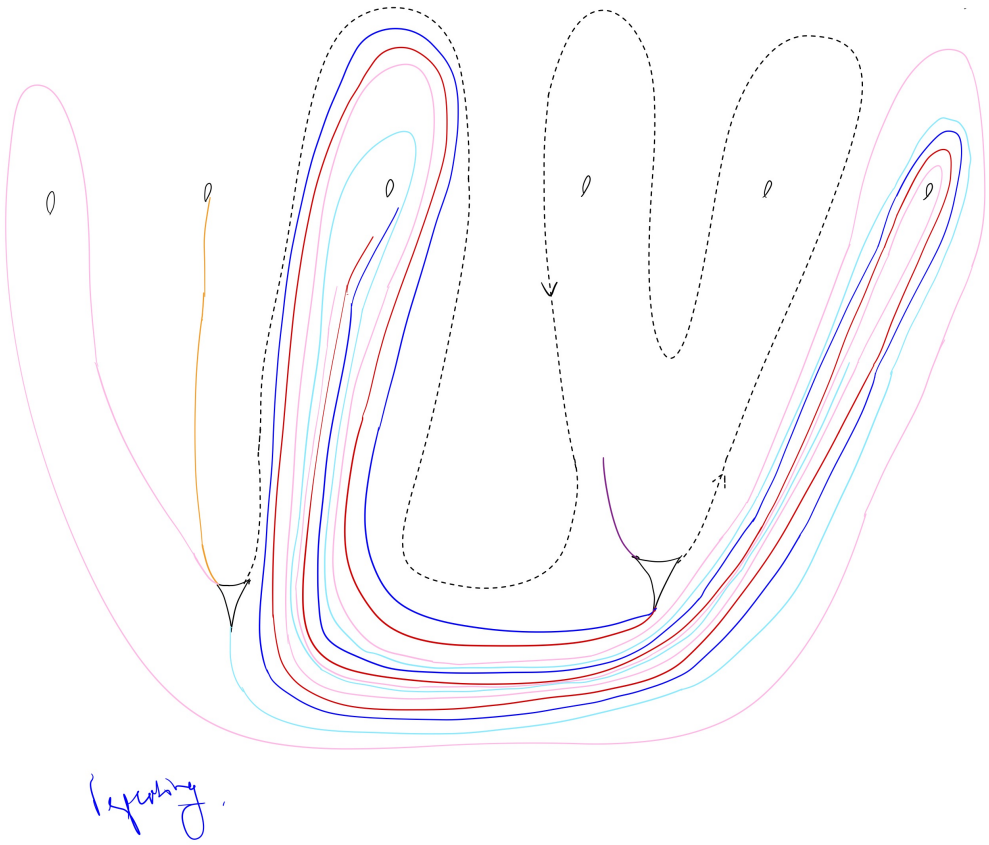


Figure D.171: Sizzle9

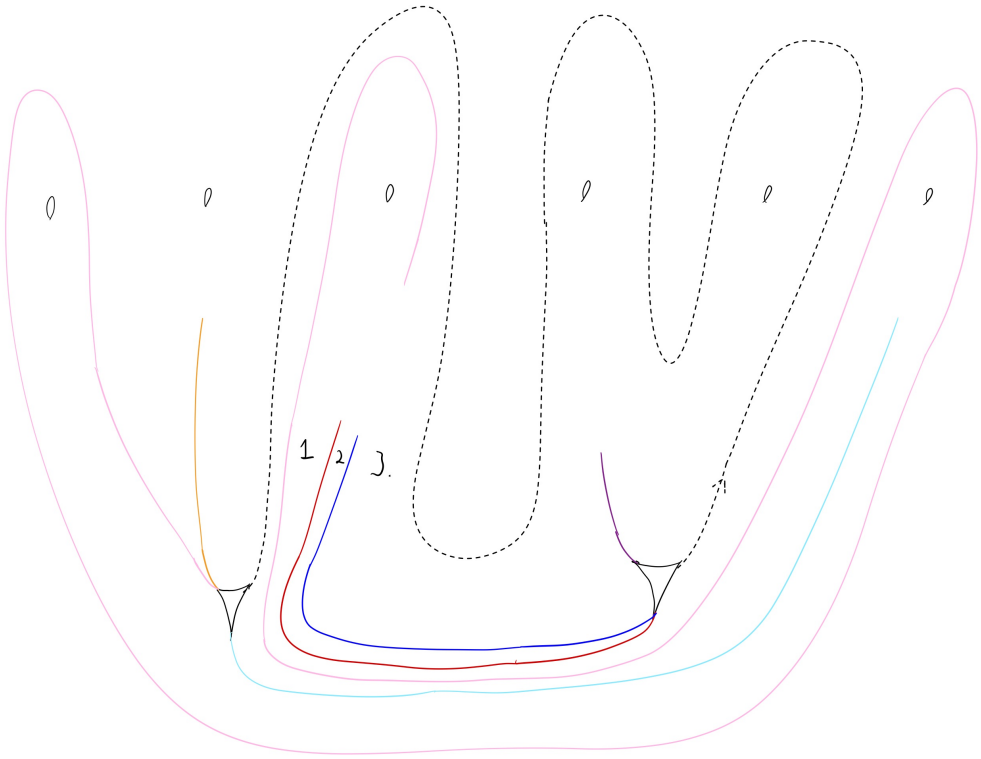


Figure D.172: Sizzle10

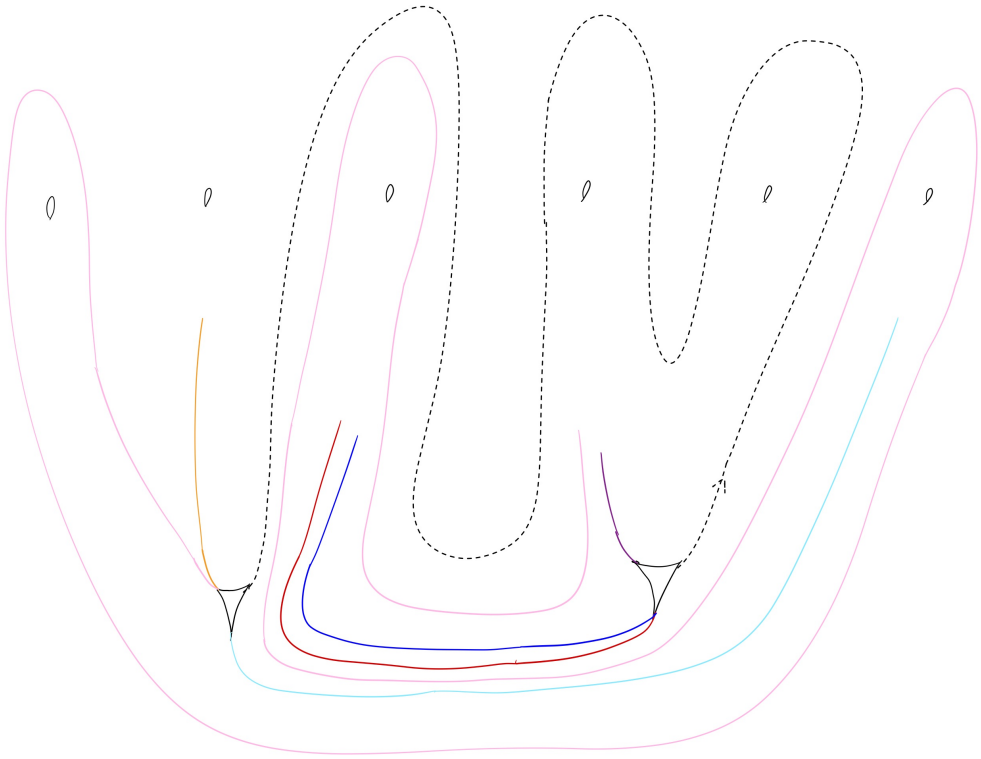


Figure D.173: Sizzle11

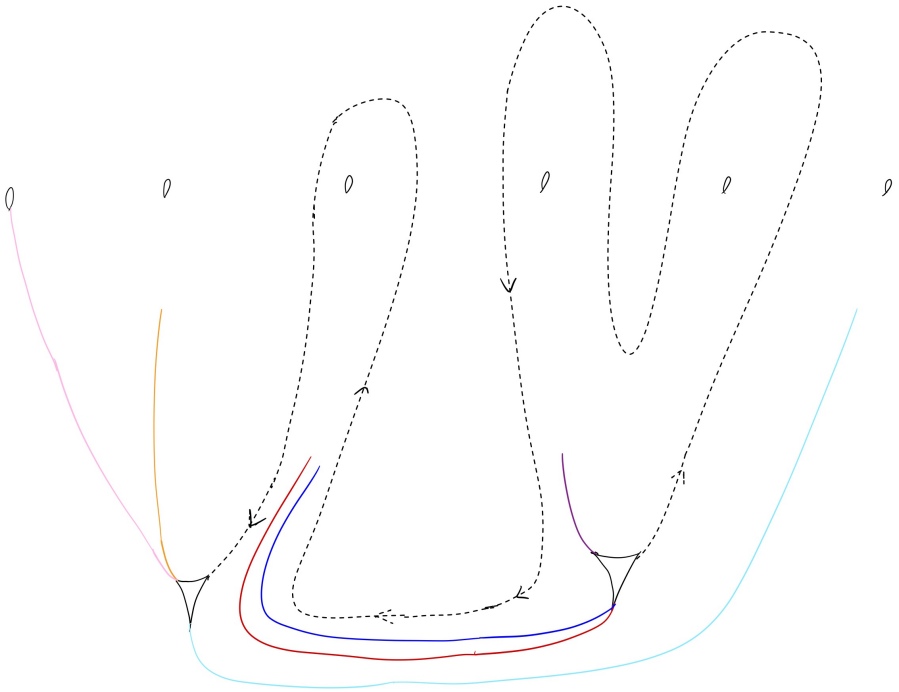


Figure D.174: Fleshy1

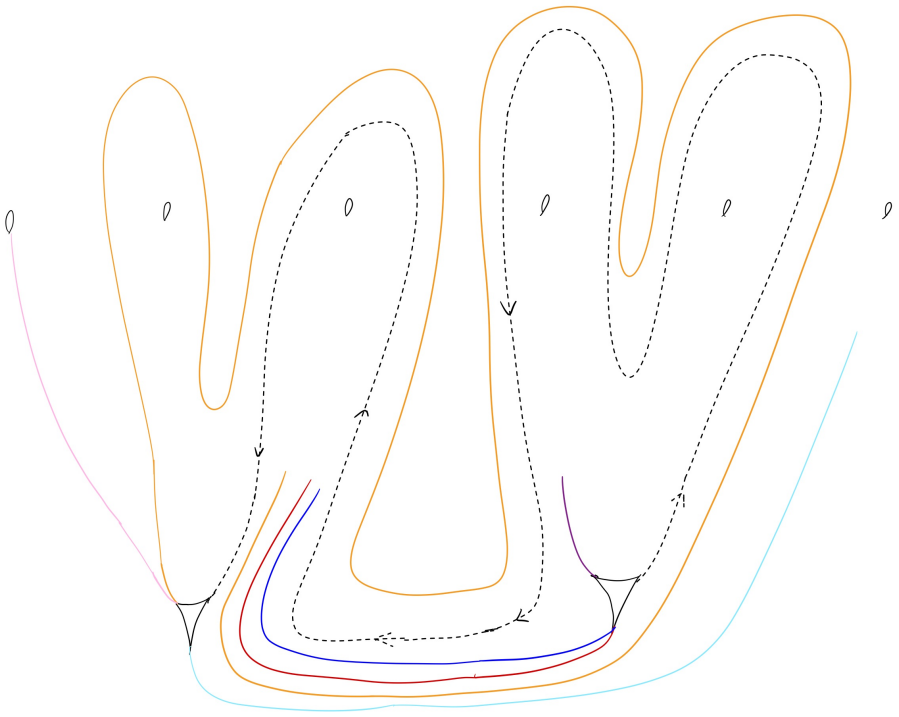


Figure D.175: Keyboard1

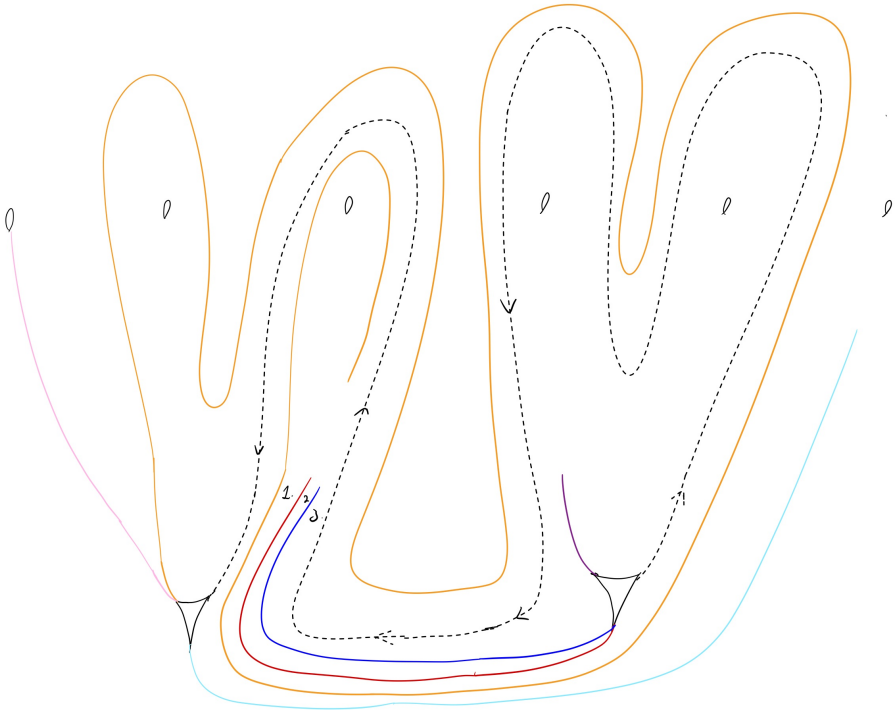


Figure D.176: Keyboard2

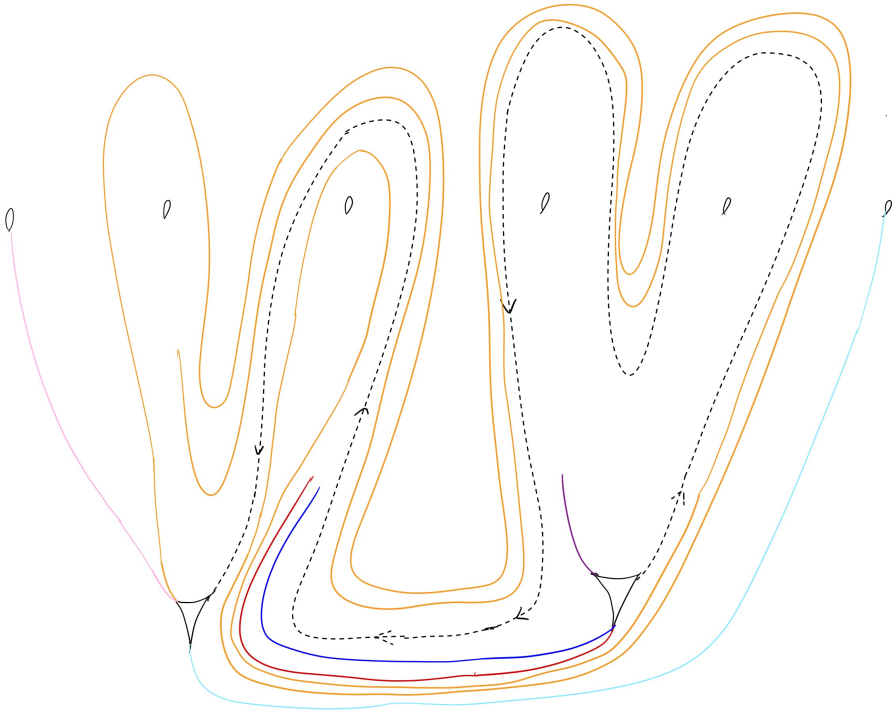


Figure D.177: Keyboard3

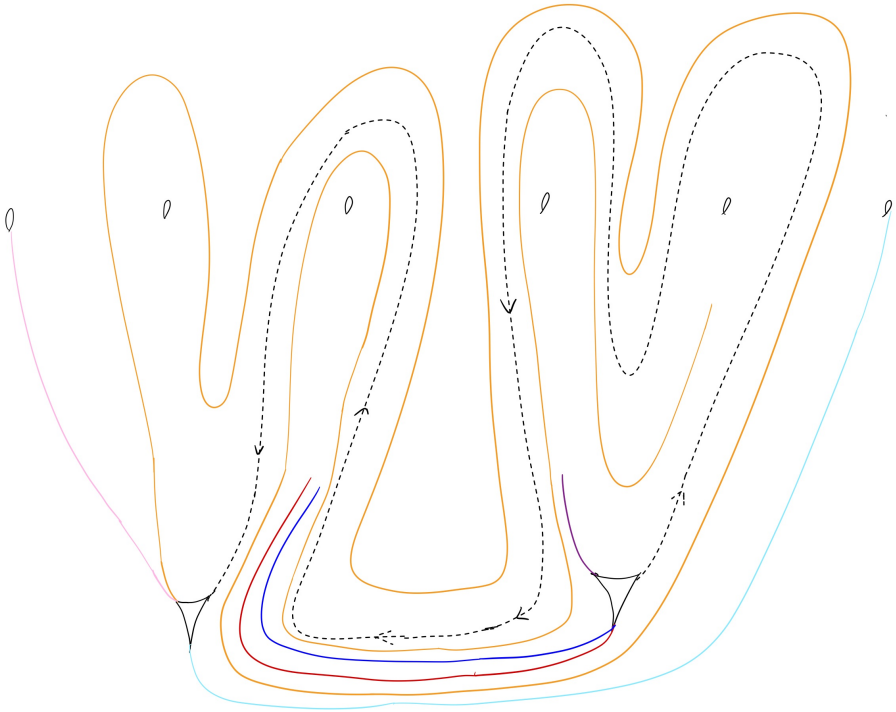


Figure D.178: Keyboard4

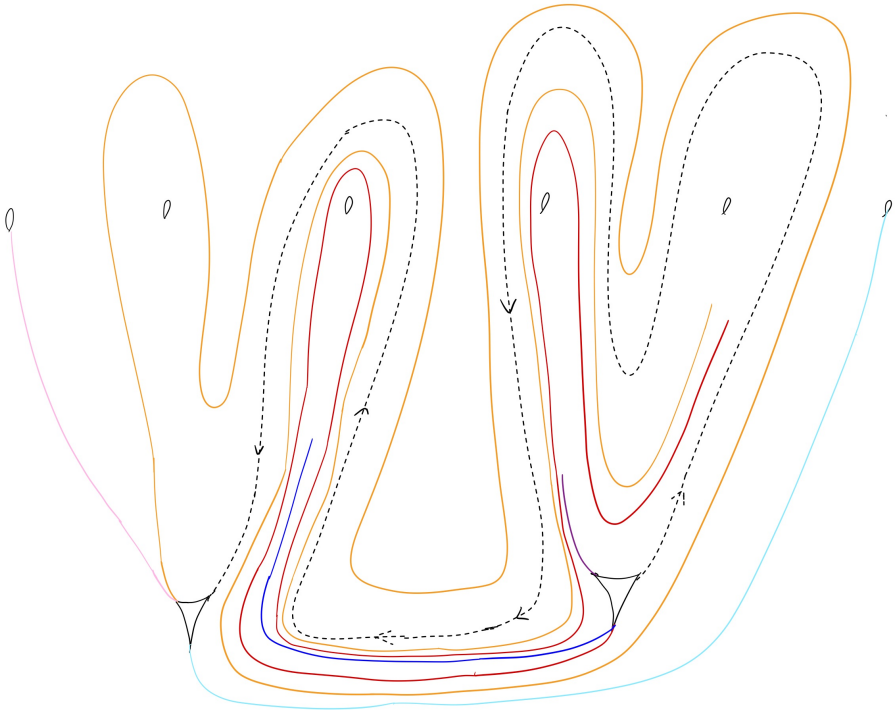


Figure D.179: Keyboard5

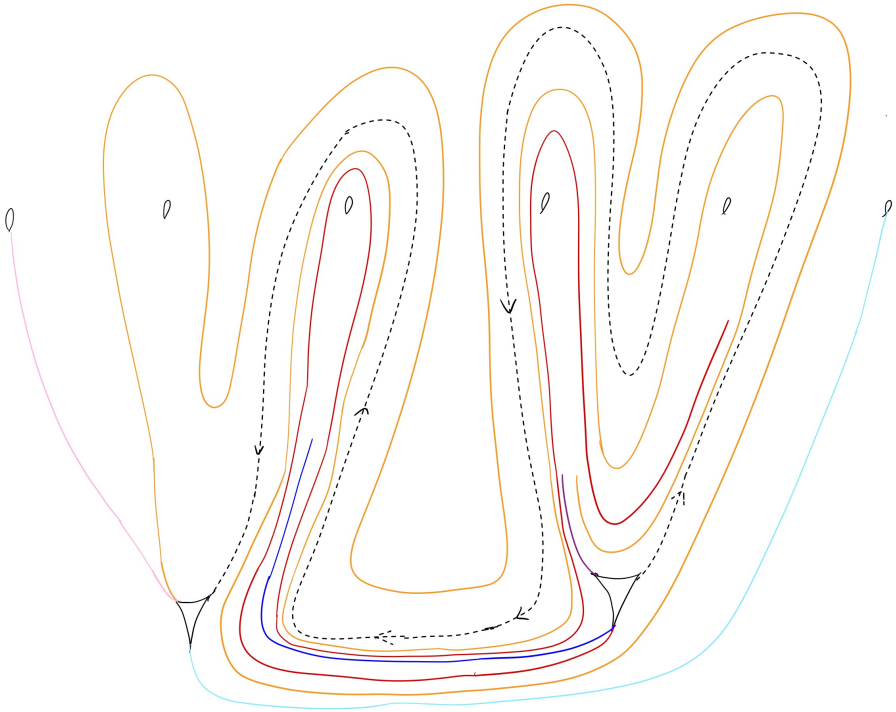


Figure D.180: Keyboard6

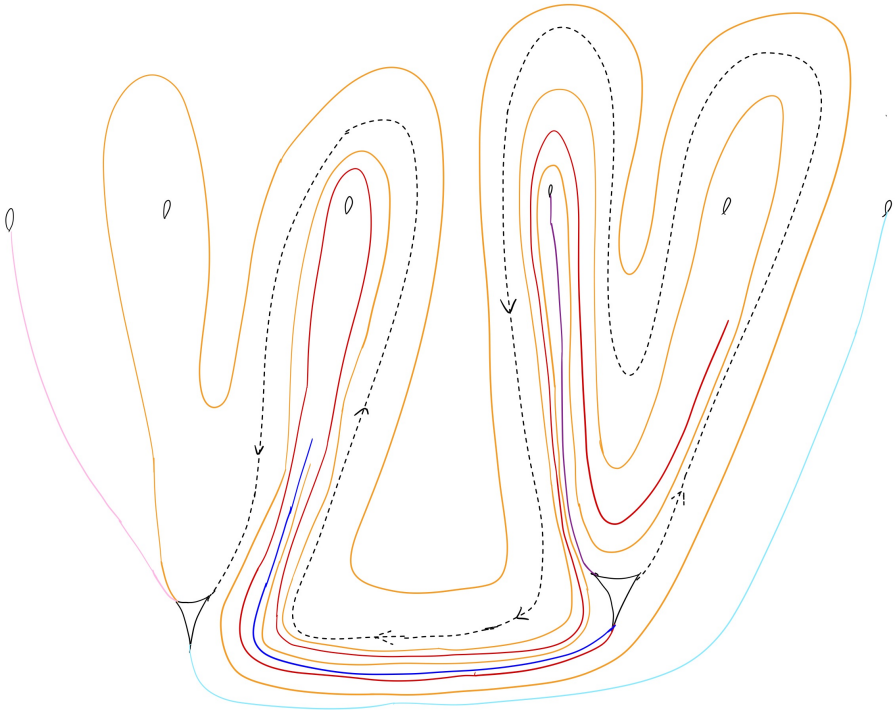


Figure D.181: Keyboard7

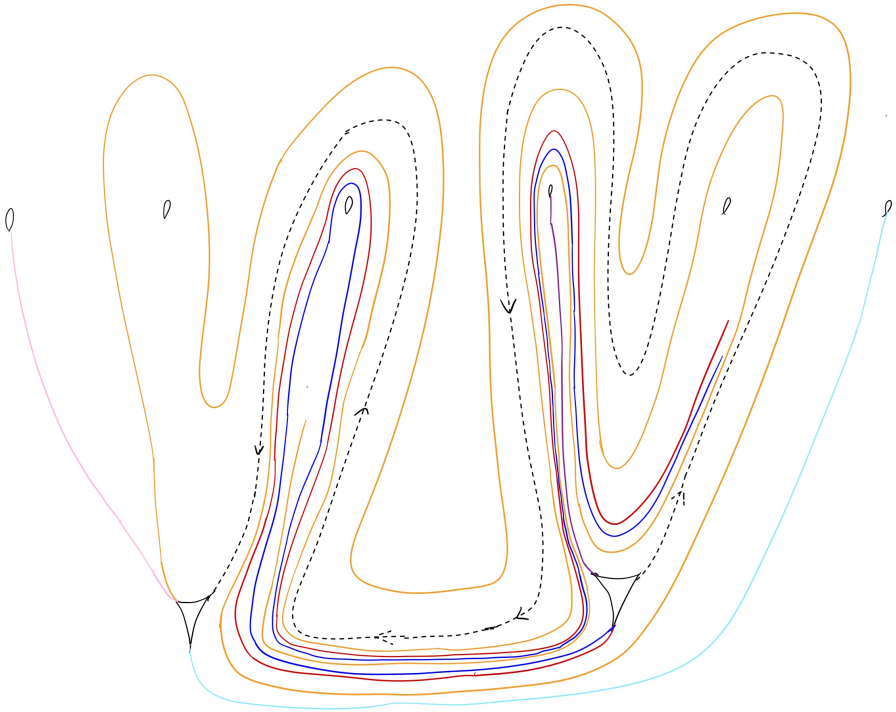


Figure D.182: Keyboard8

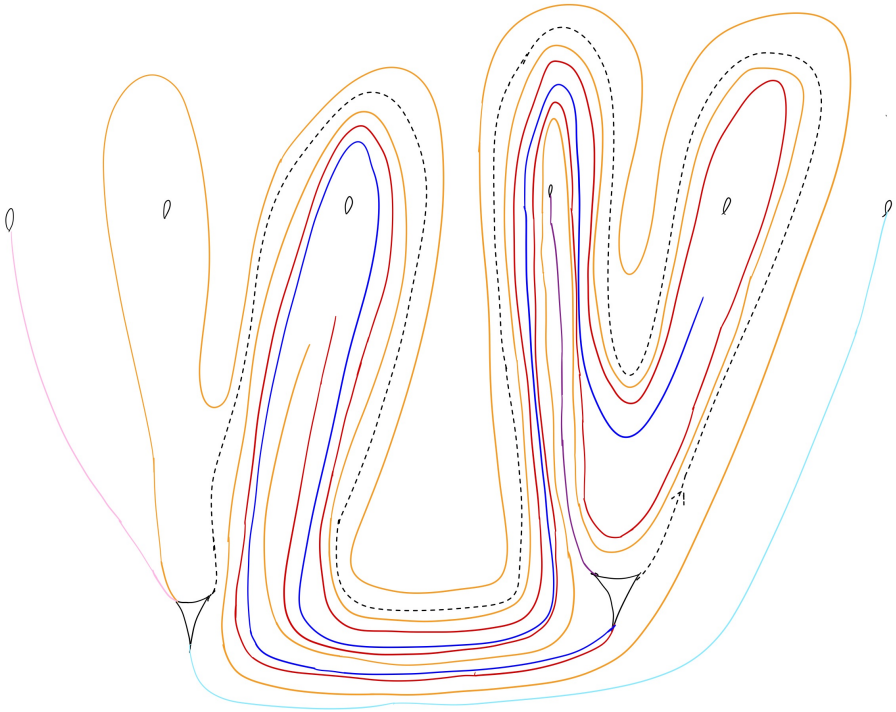


Figure D.183: Keyboard9

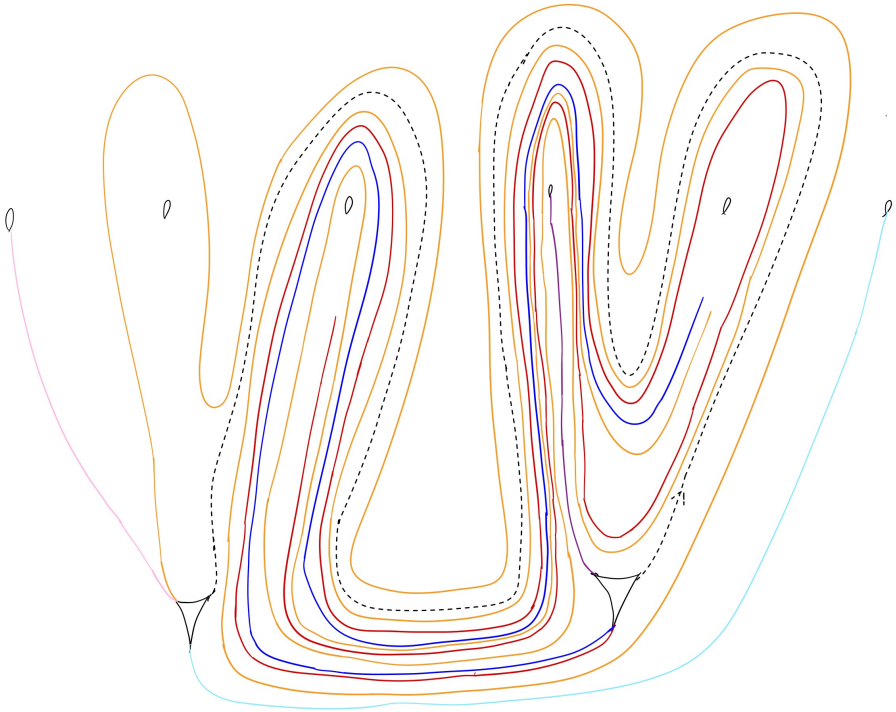


Figure D.184: Keyboard10

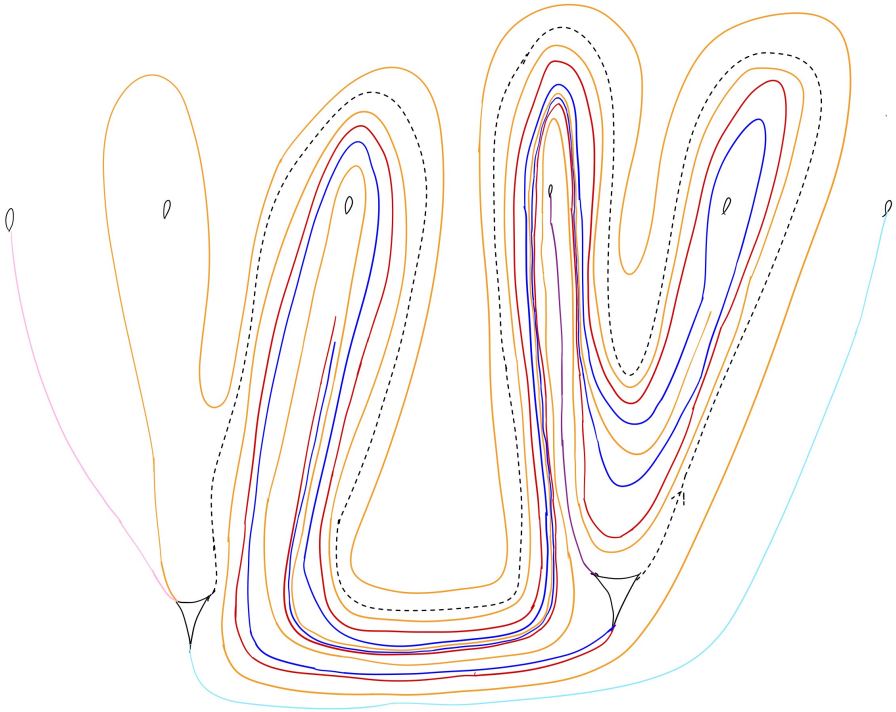


Figure D.185: Keyboard11

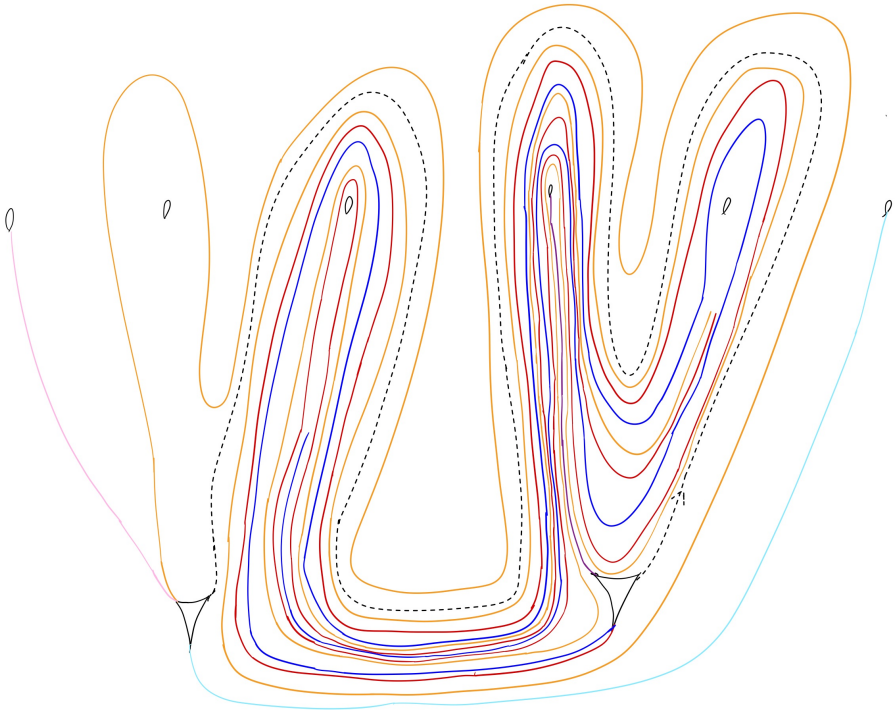


Figure D.186: Keyboard12

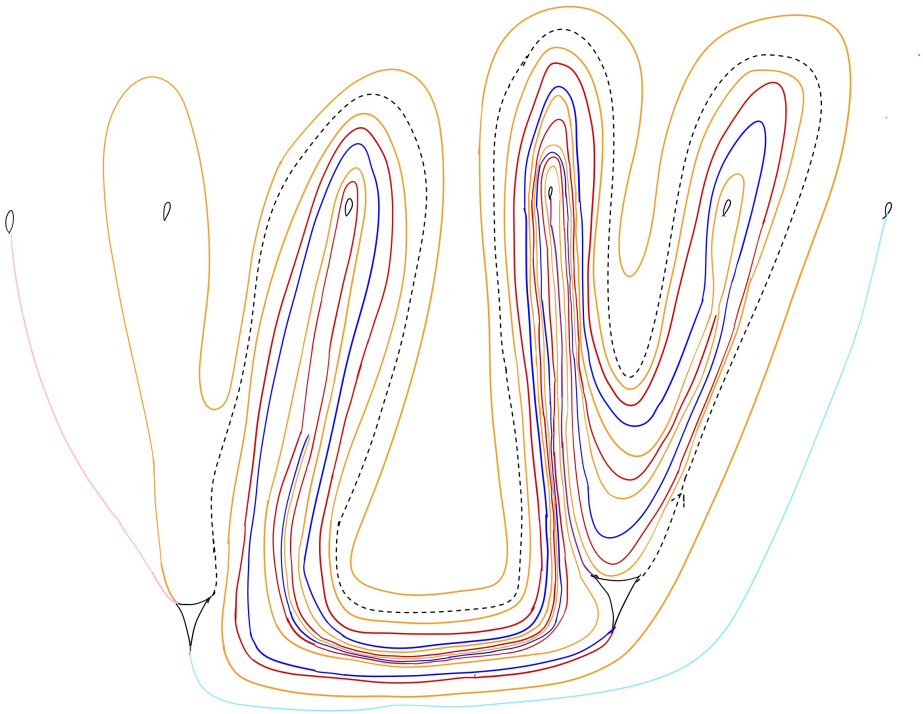


Figure D.187: Keyboard13

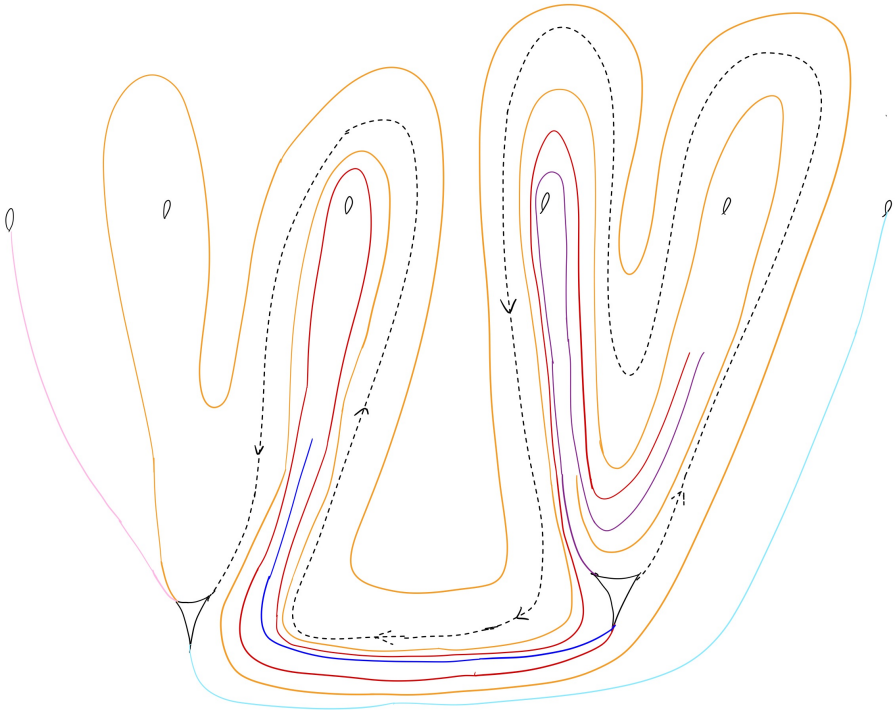


Figure D.188: Keyboard14

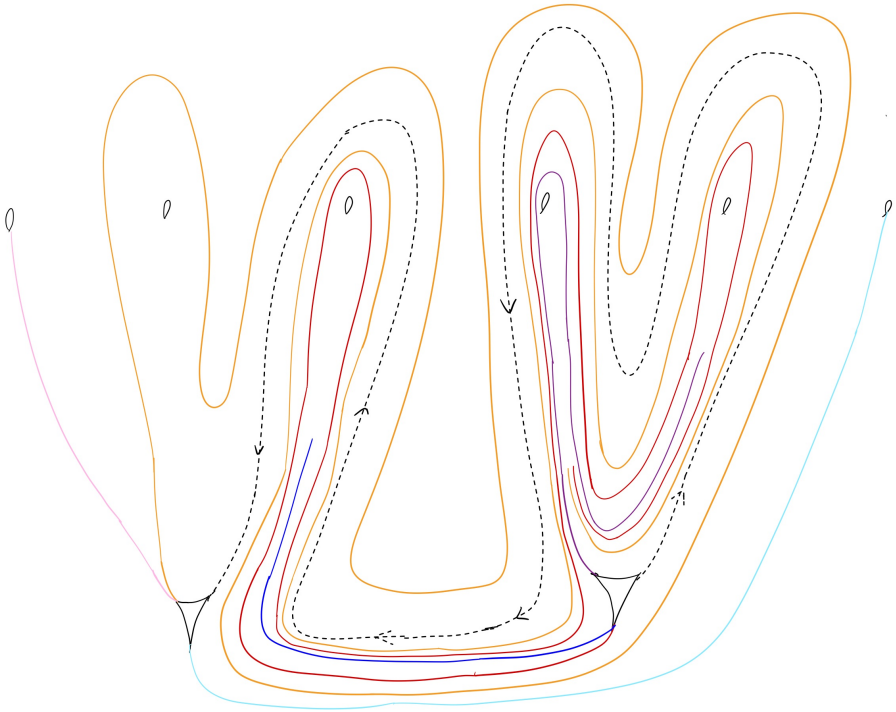


Figure D.189: Keyboard15

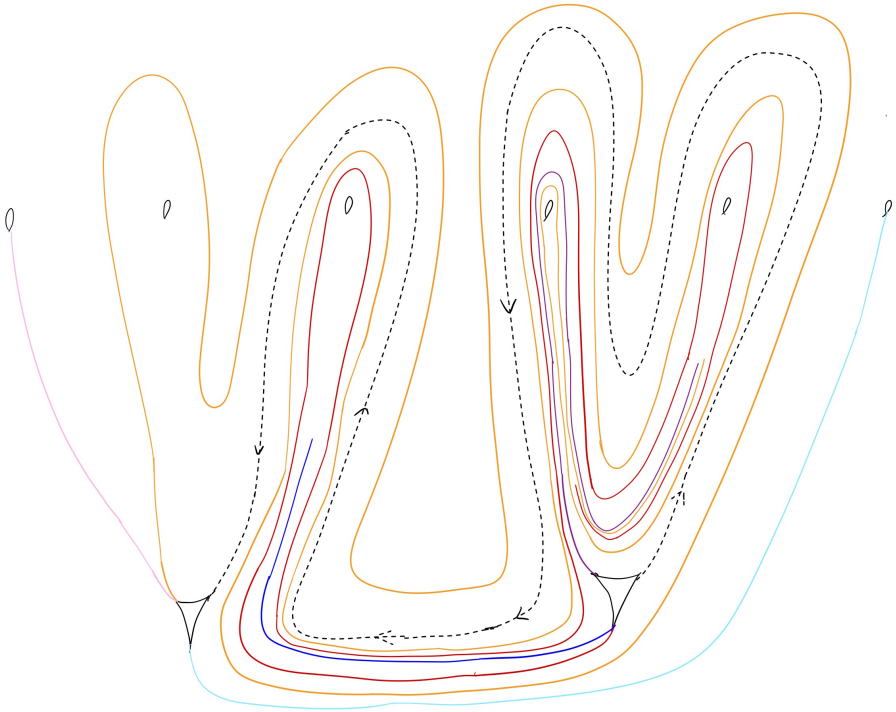


Figure D.190: Keyboard16

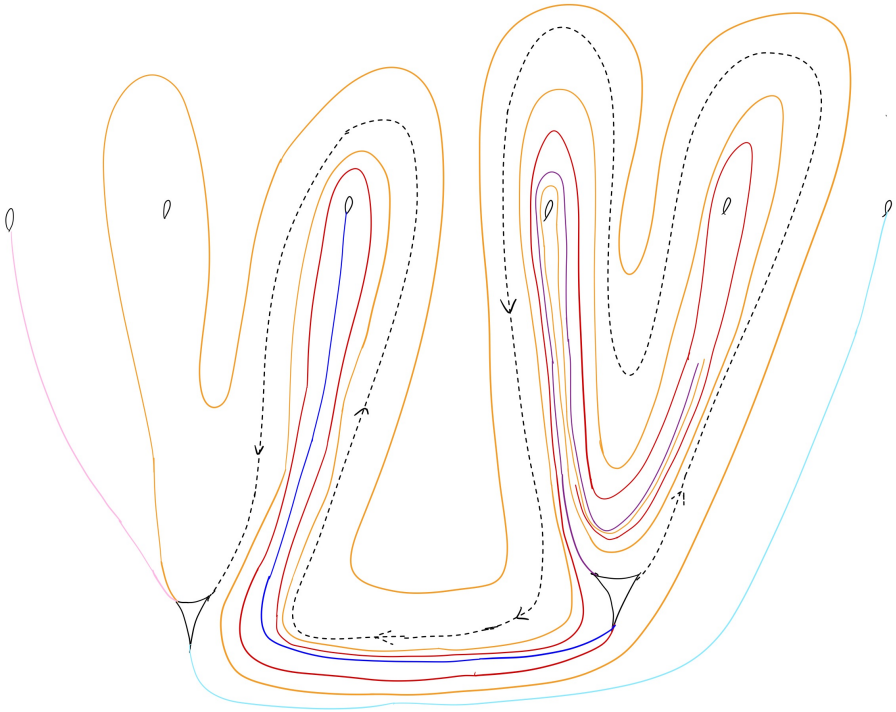


Figure D.191: Keyboard17

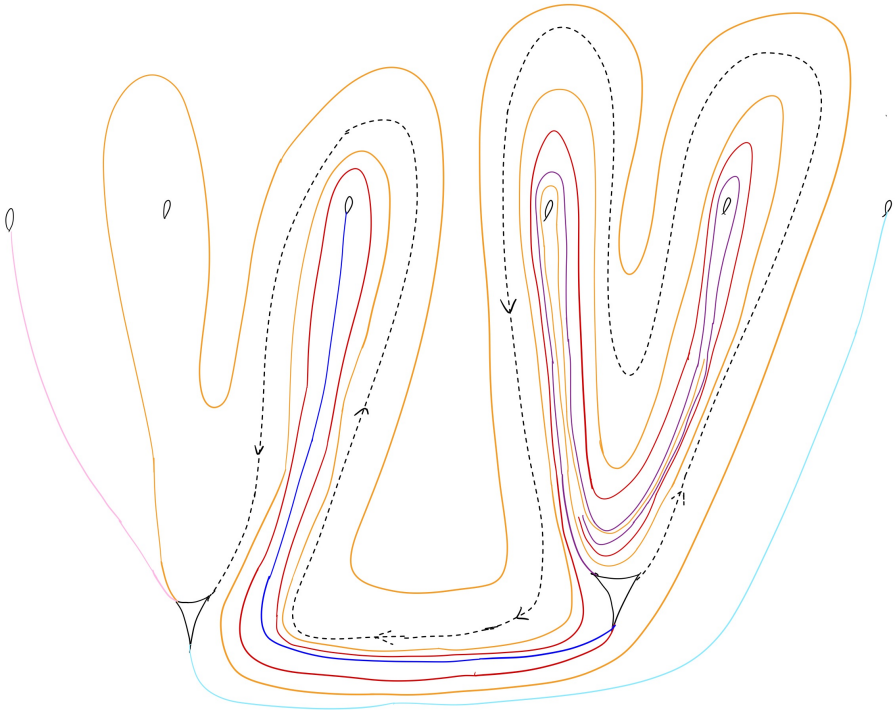


Figure D.192: Keyboard18

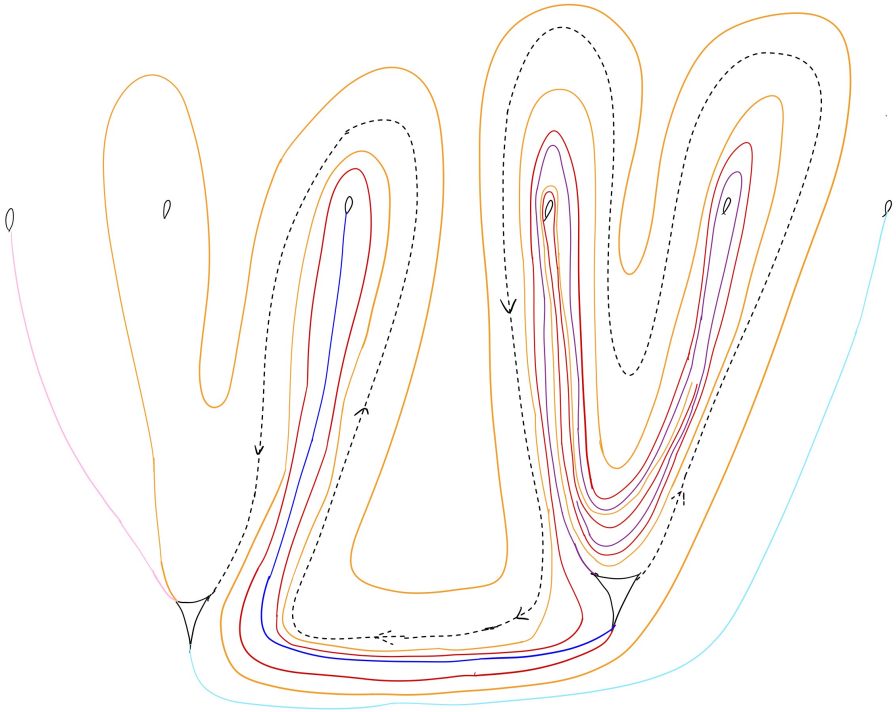


Figure D.193: Keyboard19

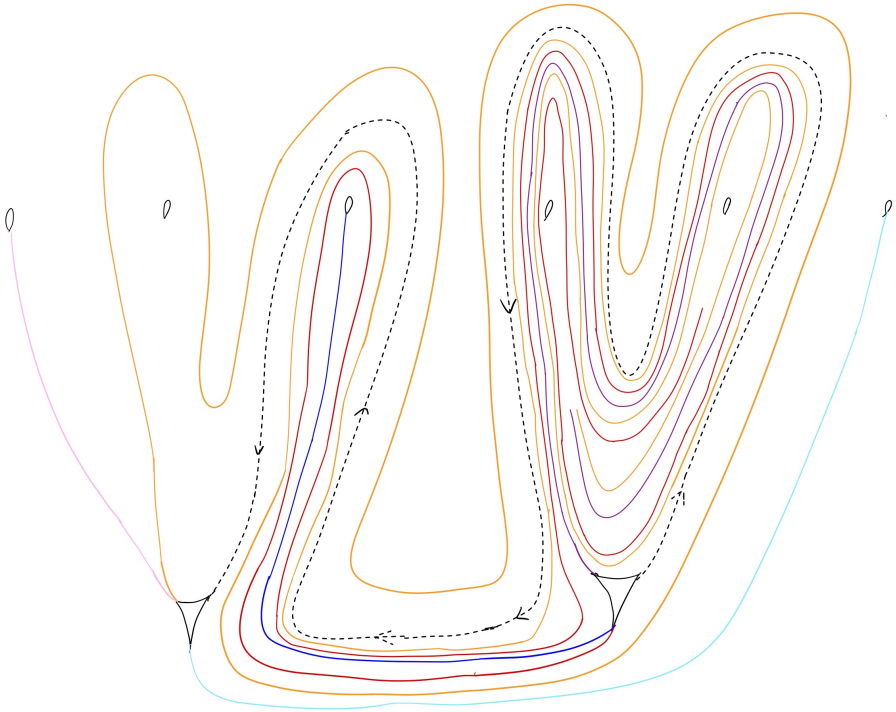


Figure D.194: Keyboard20

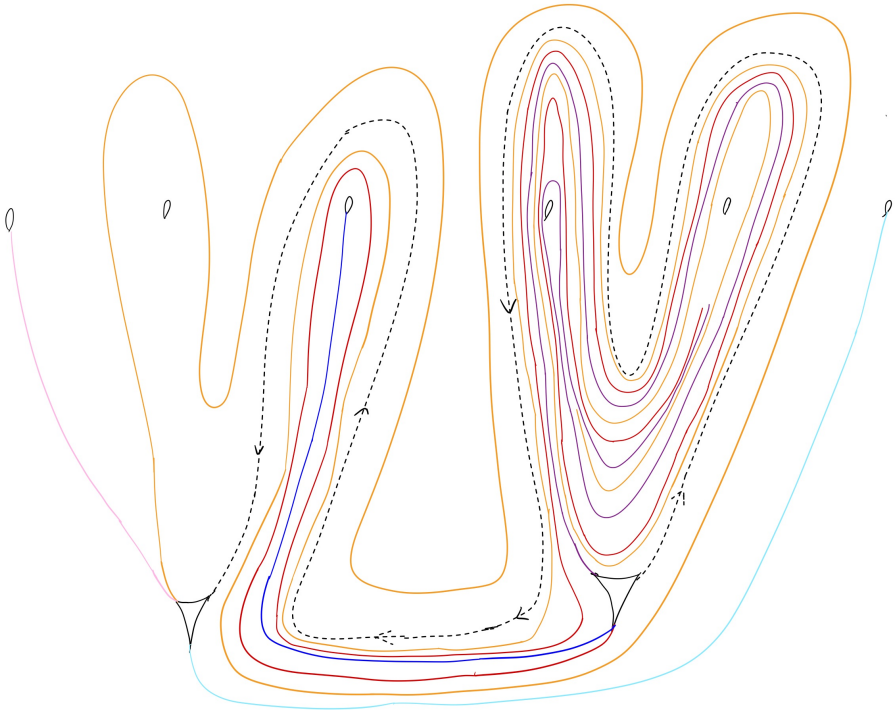


Figure D.195: Keyboard21

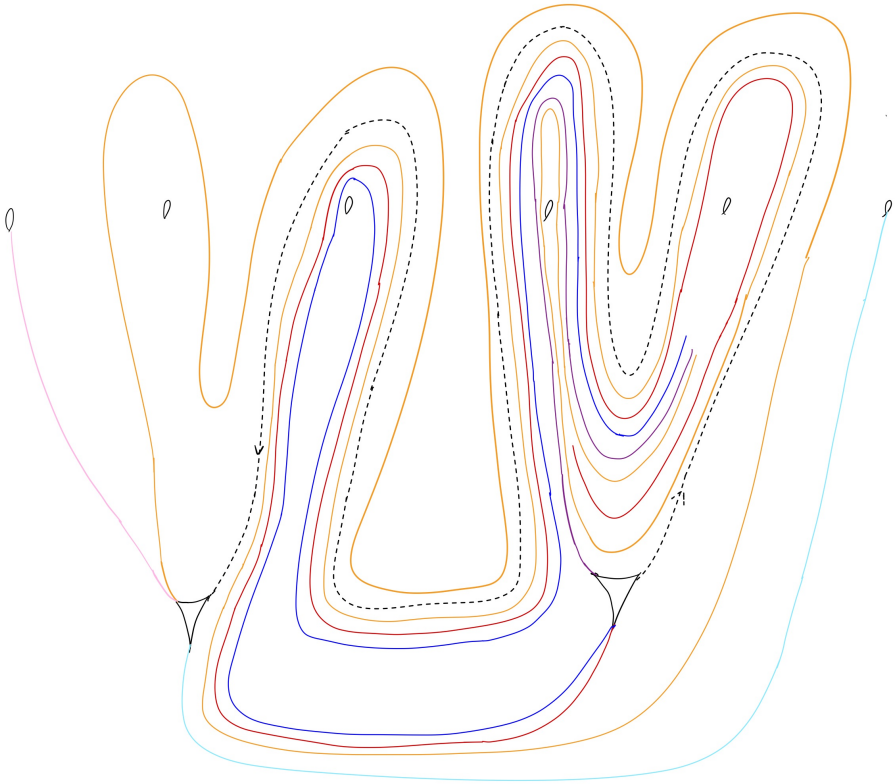


Figure D.196: Keyboard22

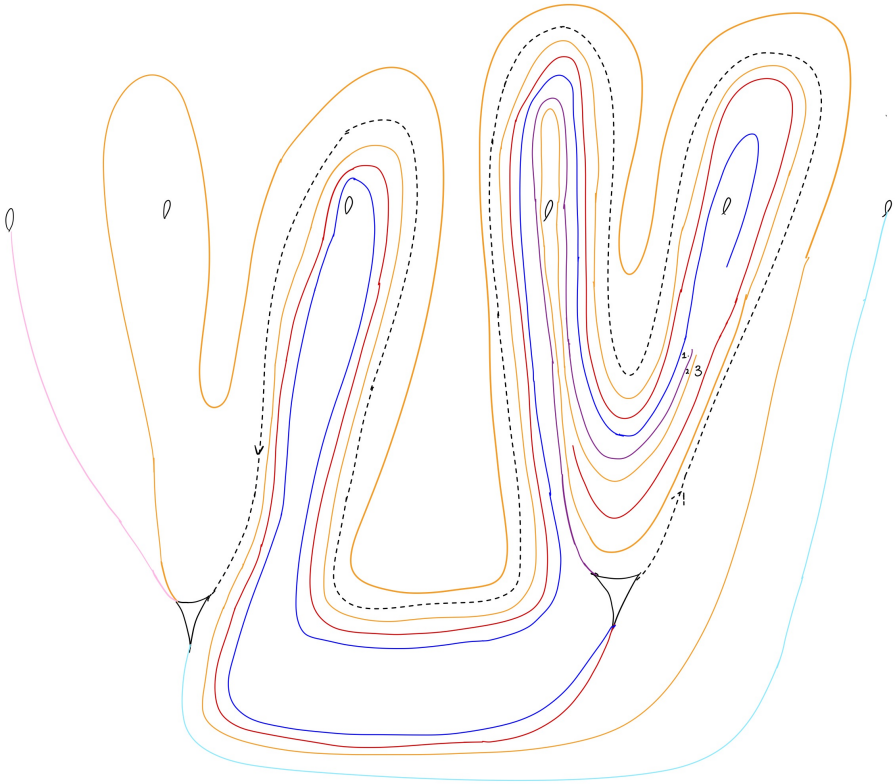


Figure D.197: Keyboard23

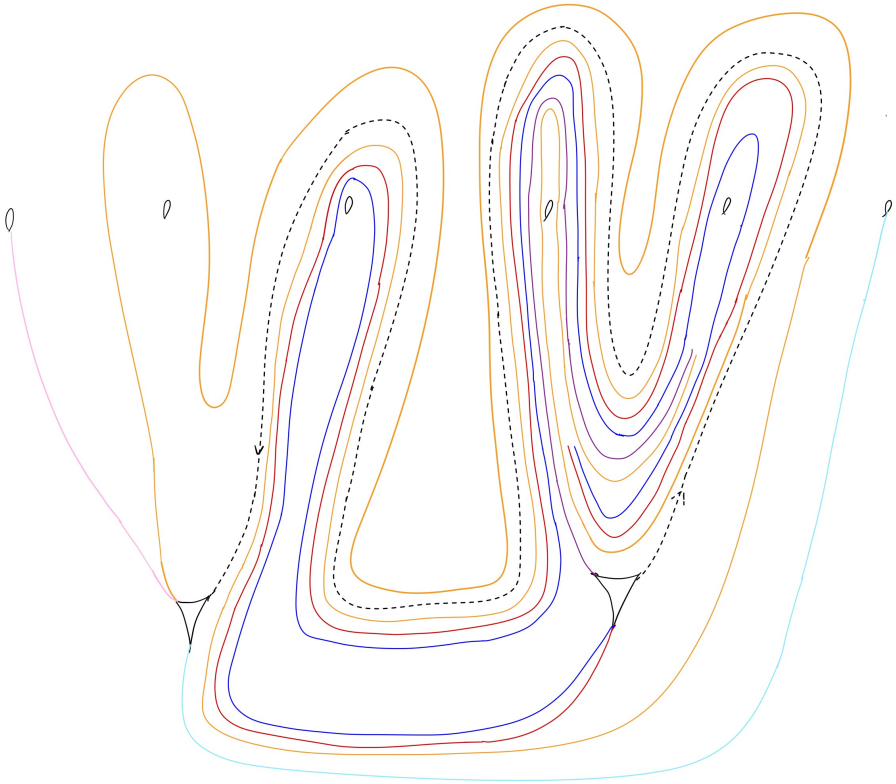


Figure D.198: Keyboard24

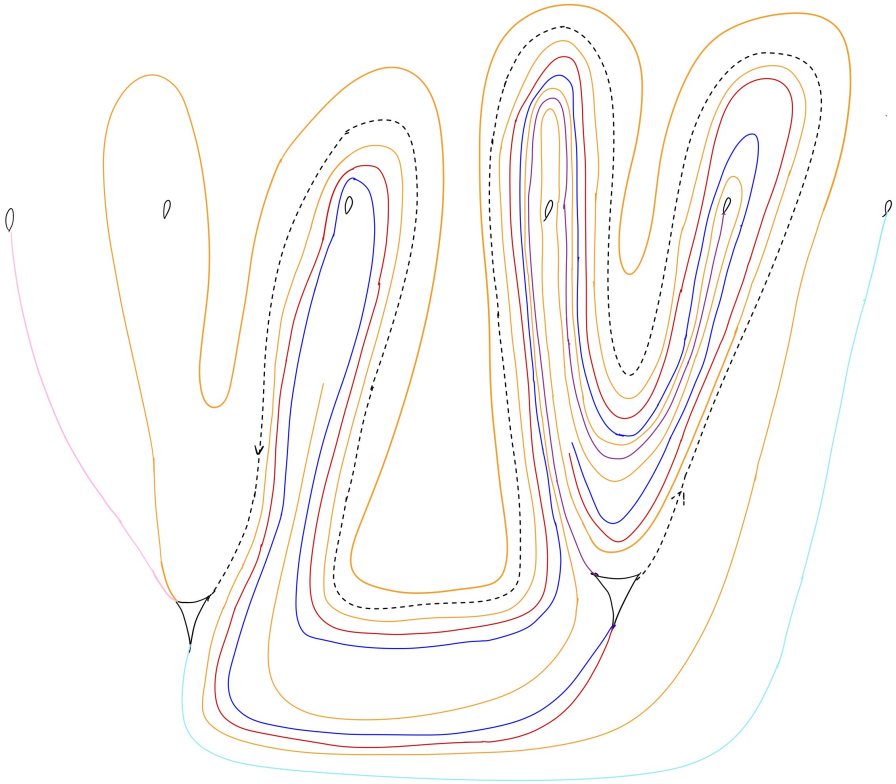


Figure D.199: Keyboard25

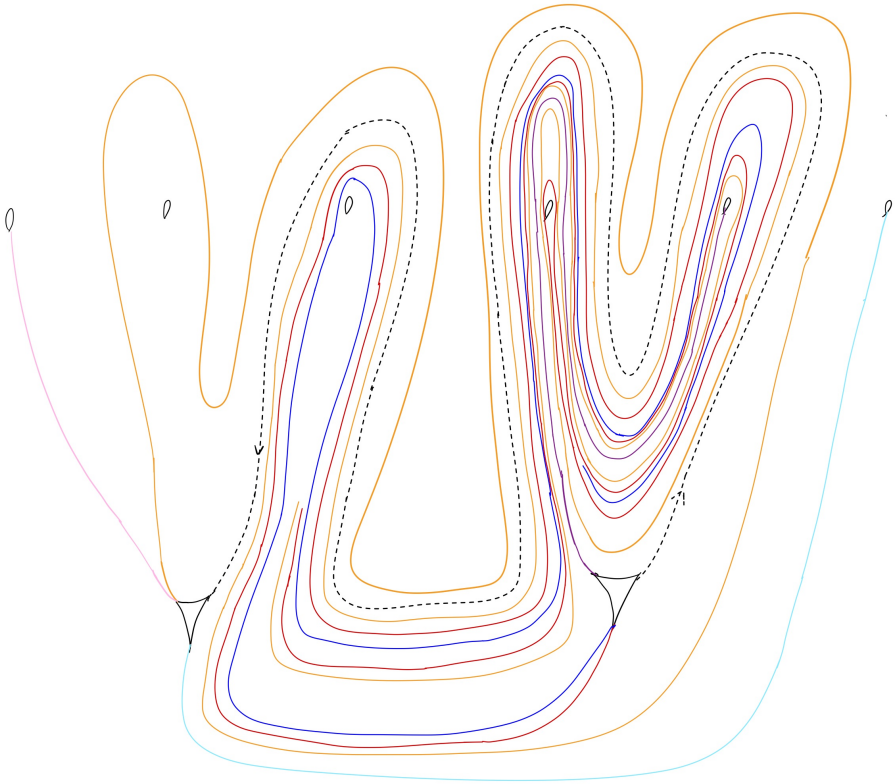


Figure D.200: Keyboard26

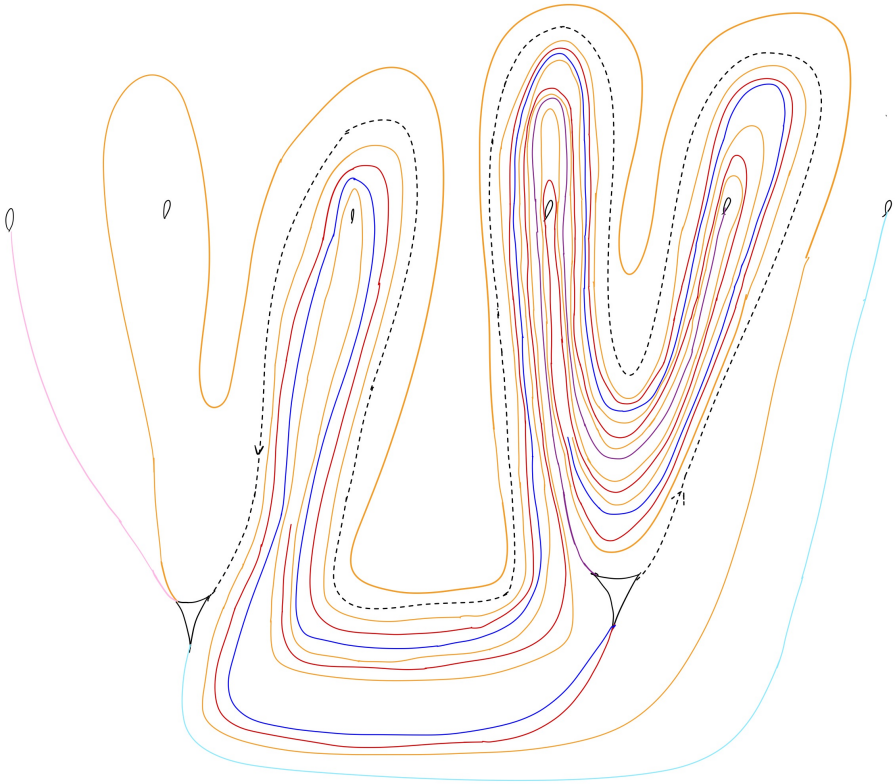


Figure D.201: Keyboard27

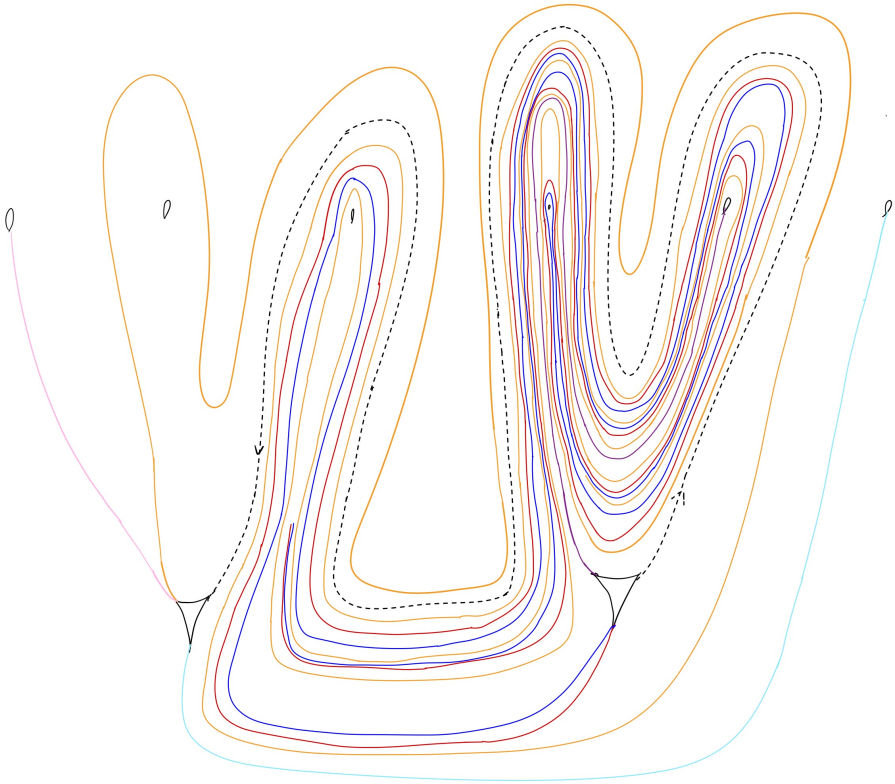


Figure D.202: Keyboard28

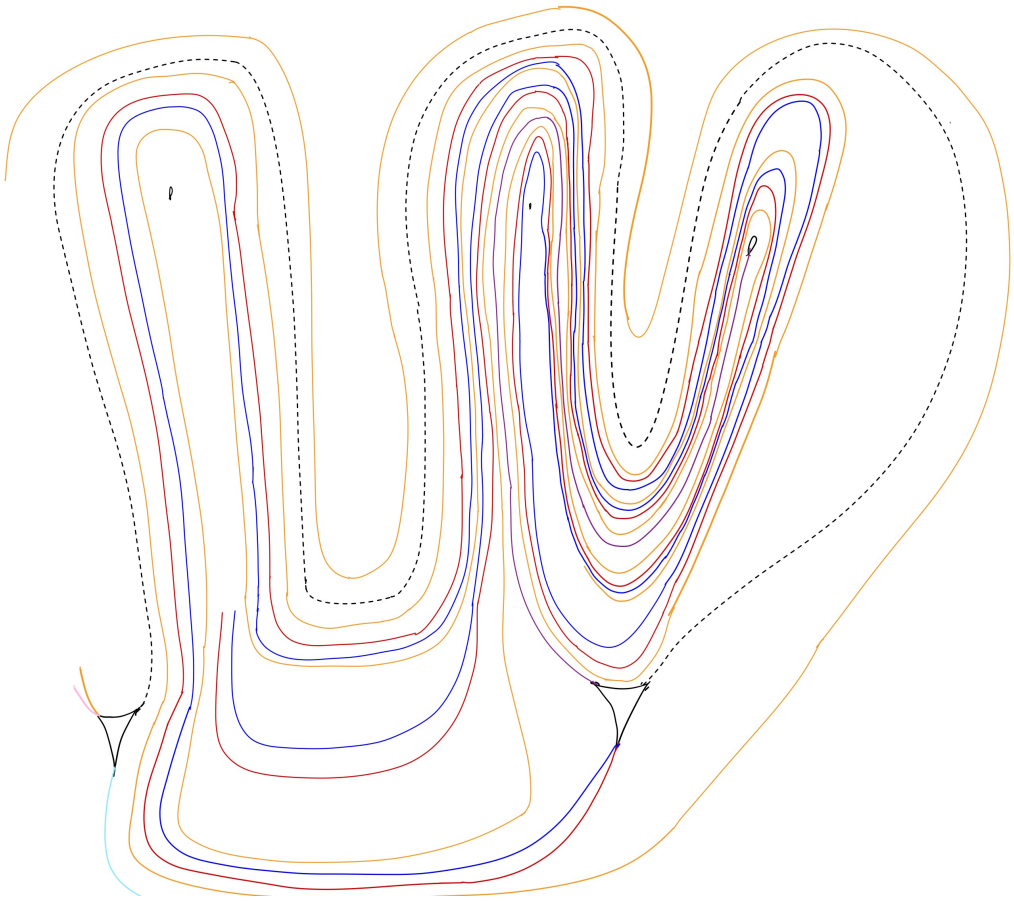


Figure D.203: Keyboard29

Figure D.204: Keyboard30

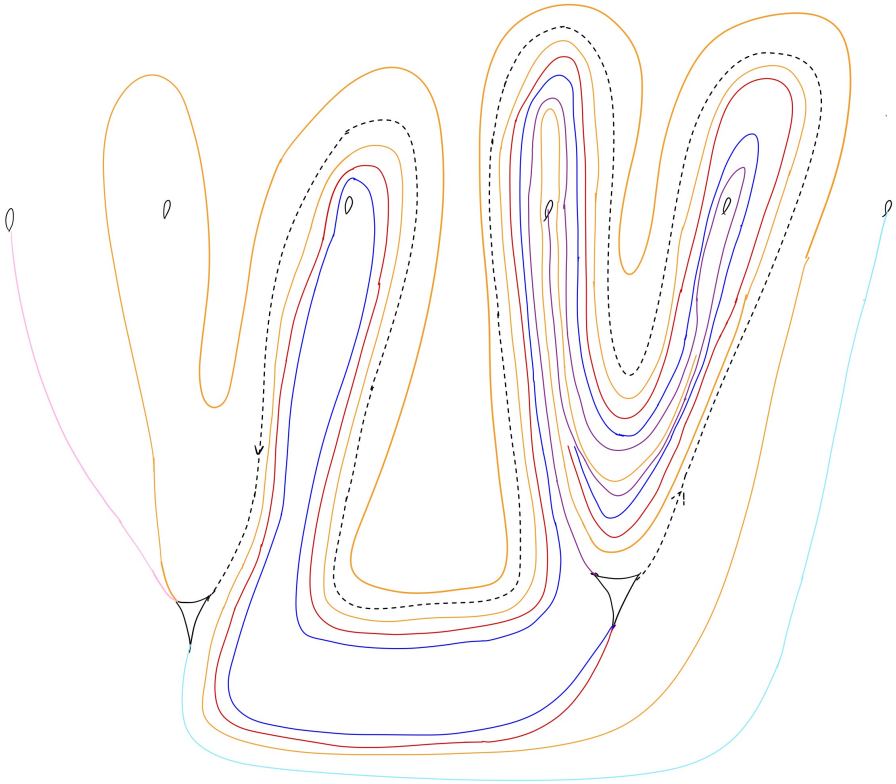


Figure D.205: Keyboard31

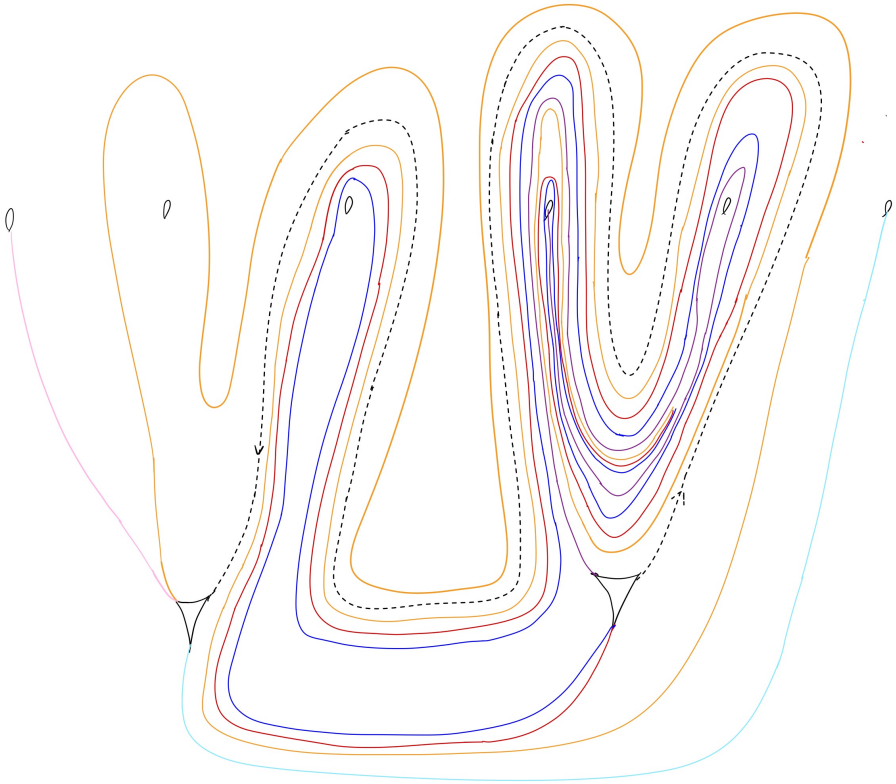


Figure D.206: Keyboard32

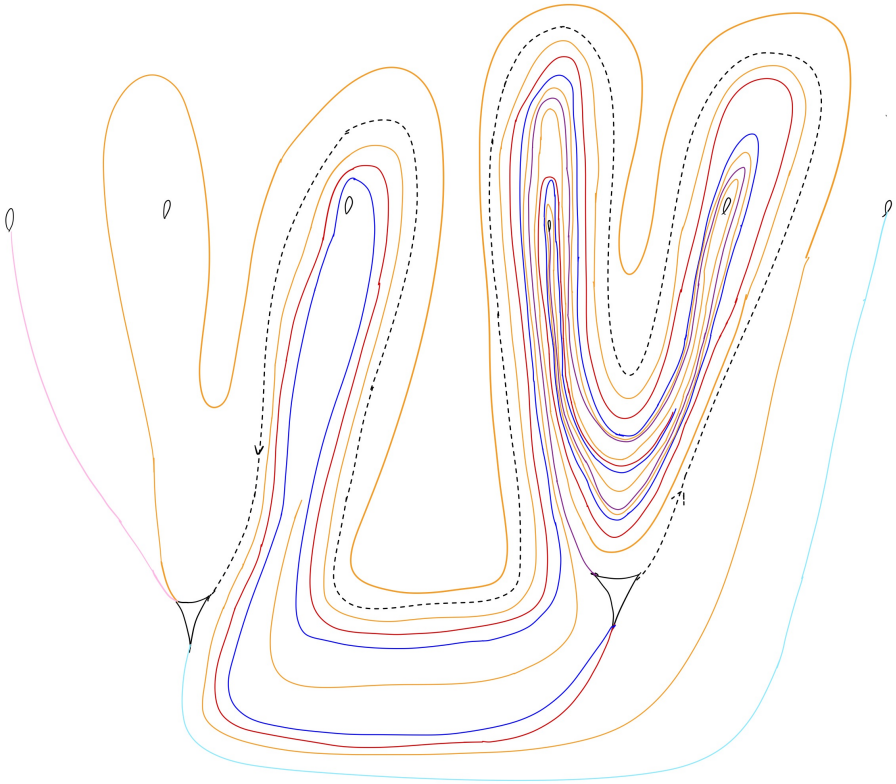


Figure D.207: Keyboard33

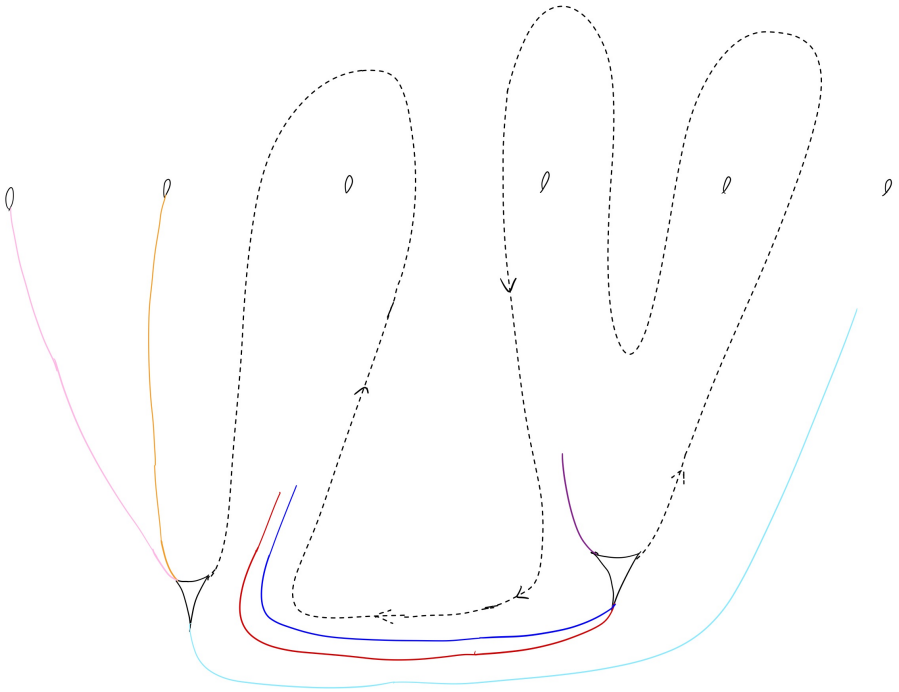


Figure D.208: Briefing1

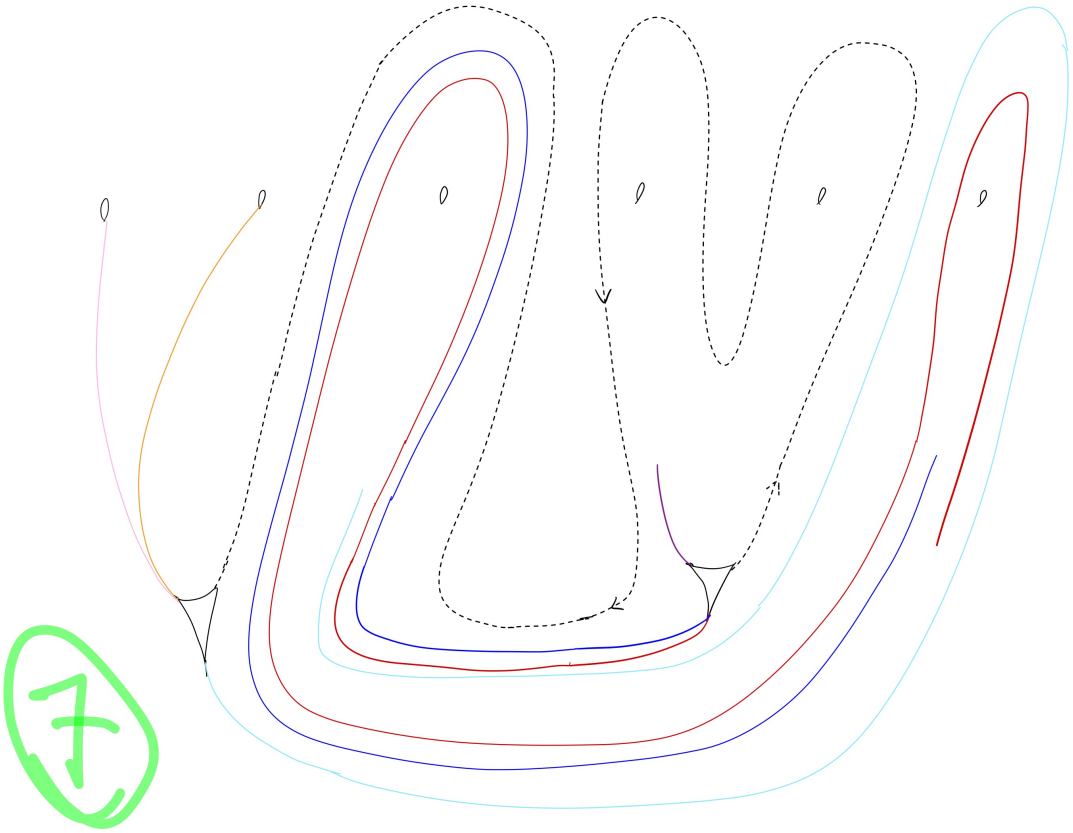


Figure D.209: Briefing2

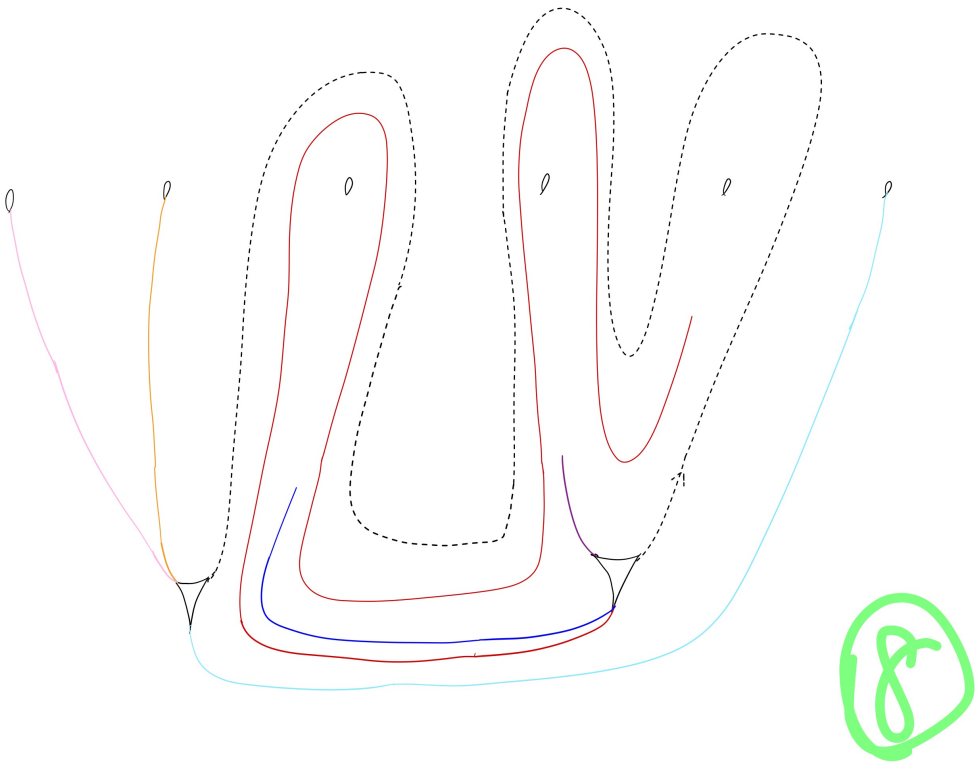


Figure D.210: Briefing3

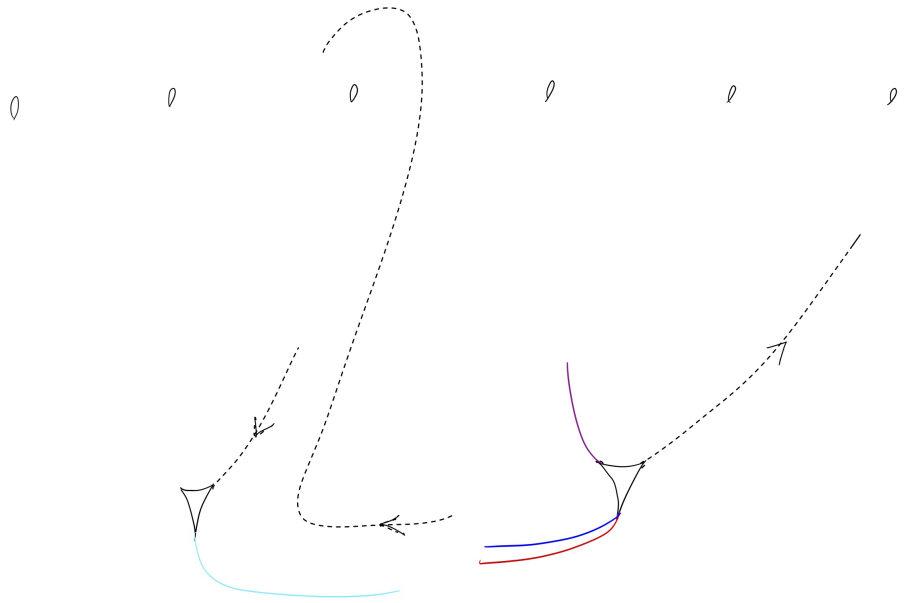


Figure D.211: CDG1

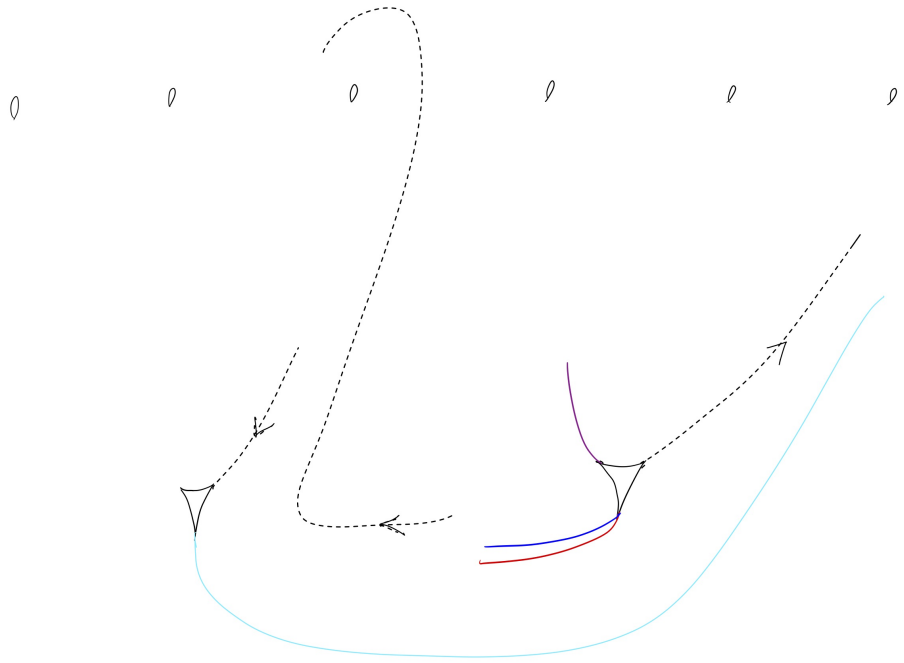


Figure D.212: CDG2

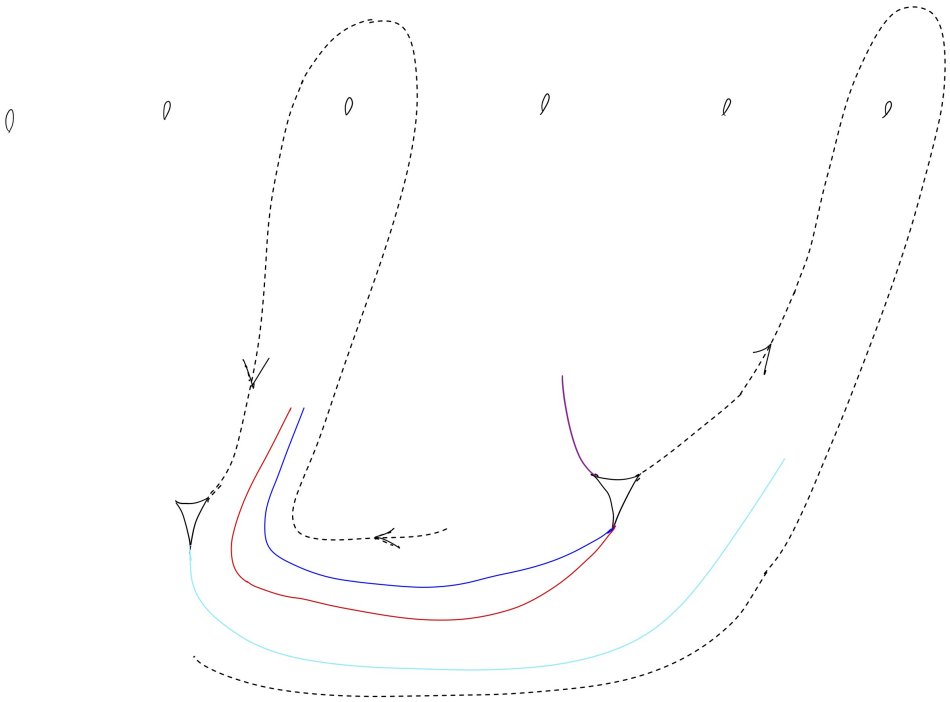


Figure D.213: CDG3

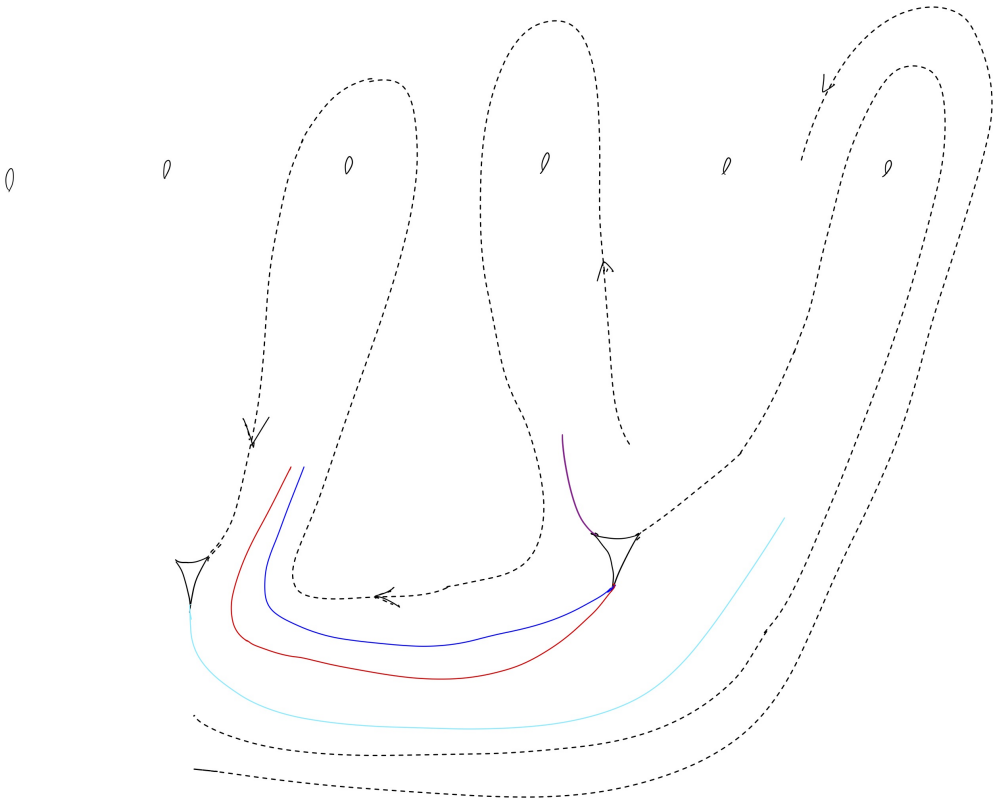


Figure D.214: CDG4

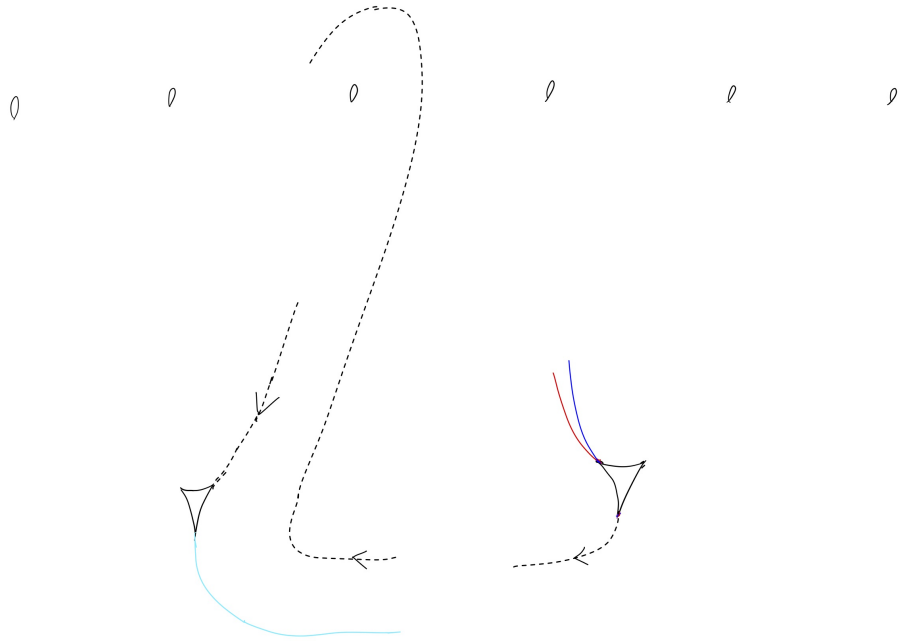


Figure D.215: SYD1

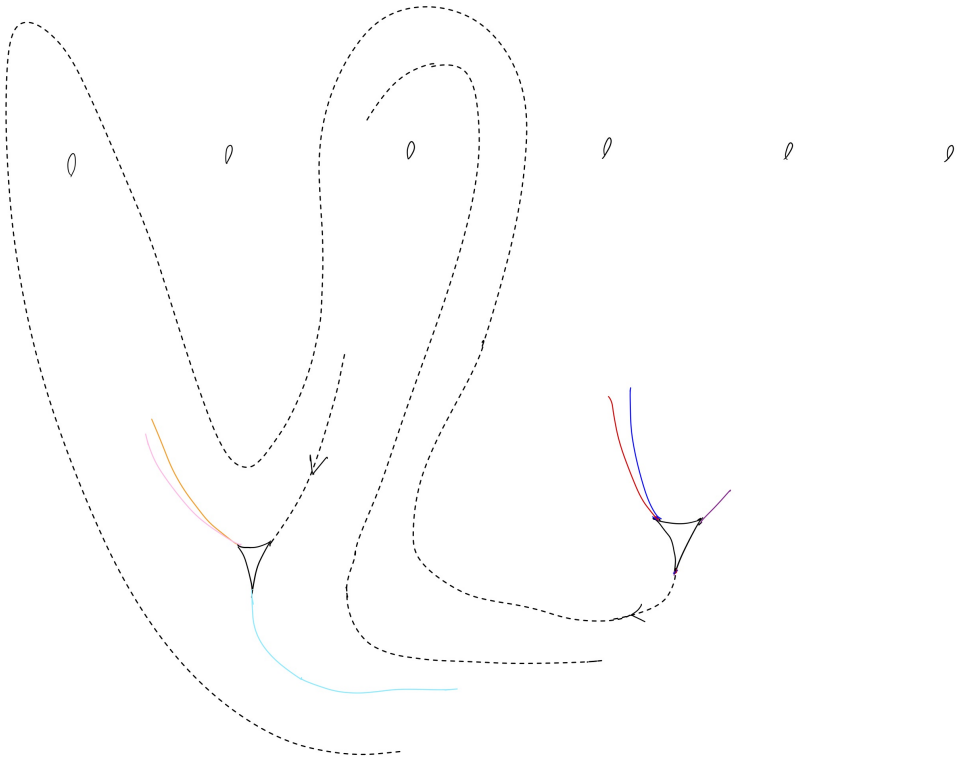


Figure D.216: SYD2

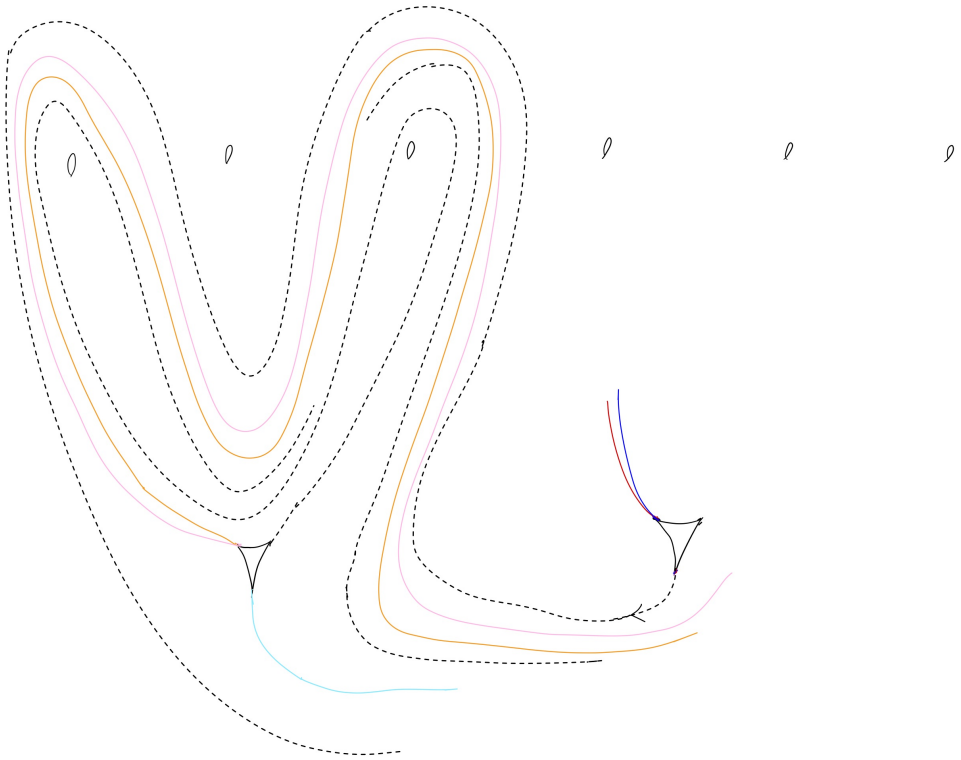


Figure D.217: SYD3

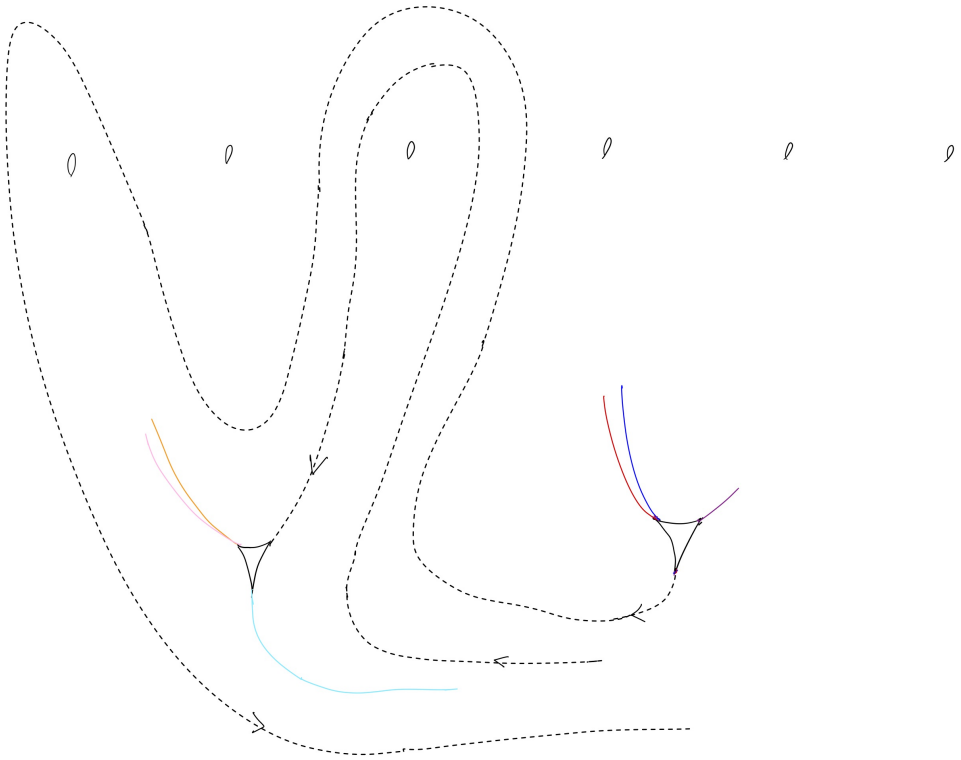


Figure D.218: SYD4

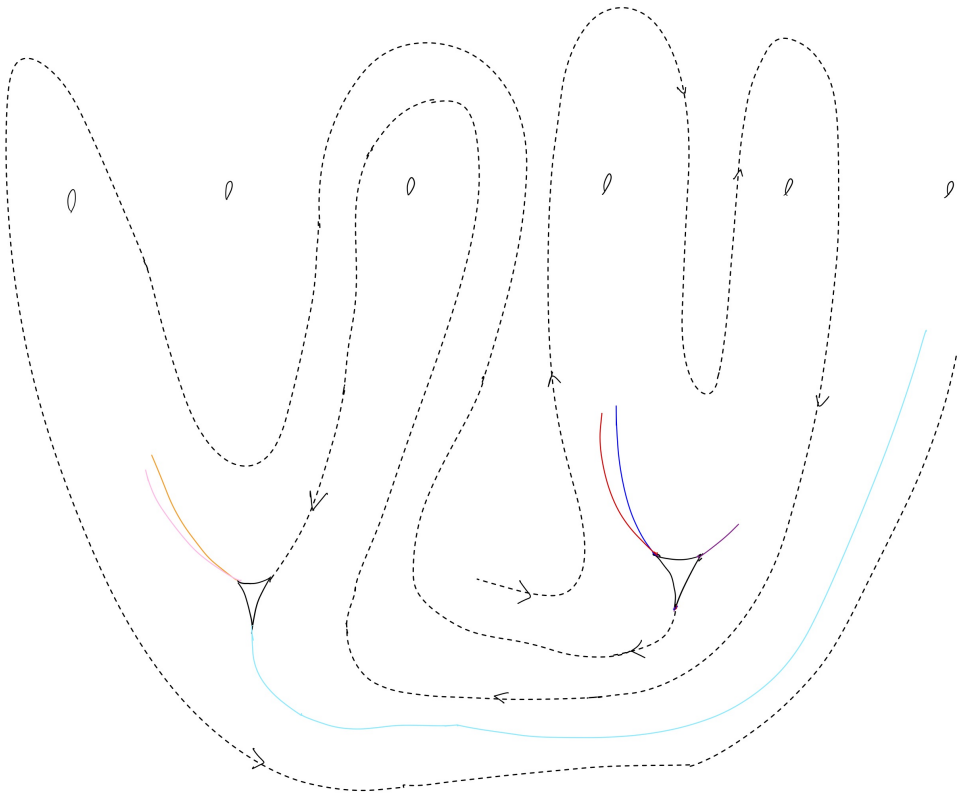


Figure D.219: SYD5

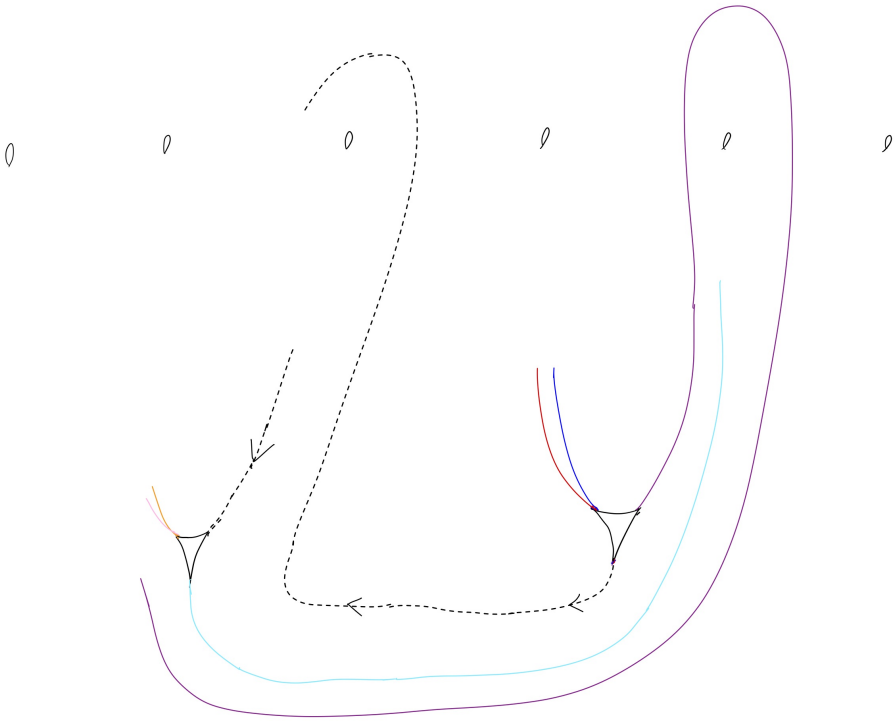


Figure D.220: Ride1

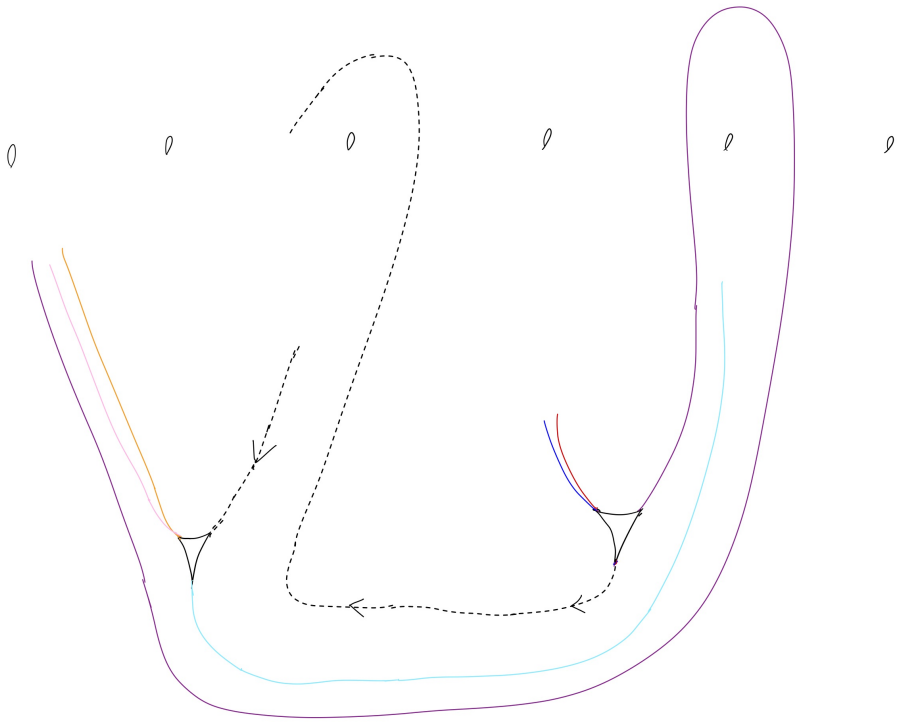


Figure D.221: Spend1

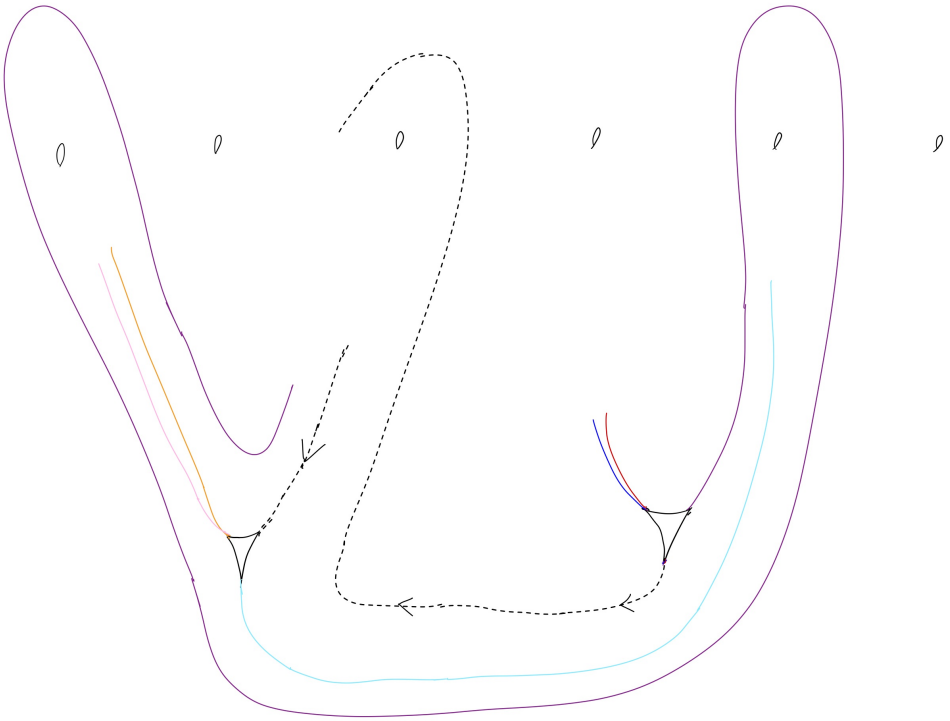


Figure D.222: Spend2

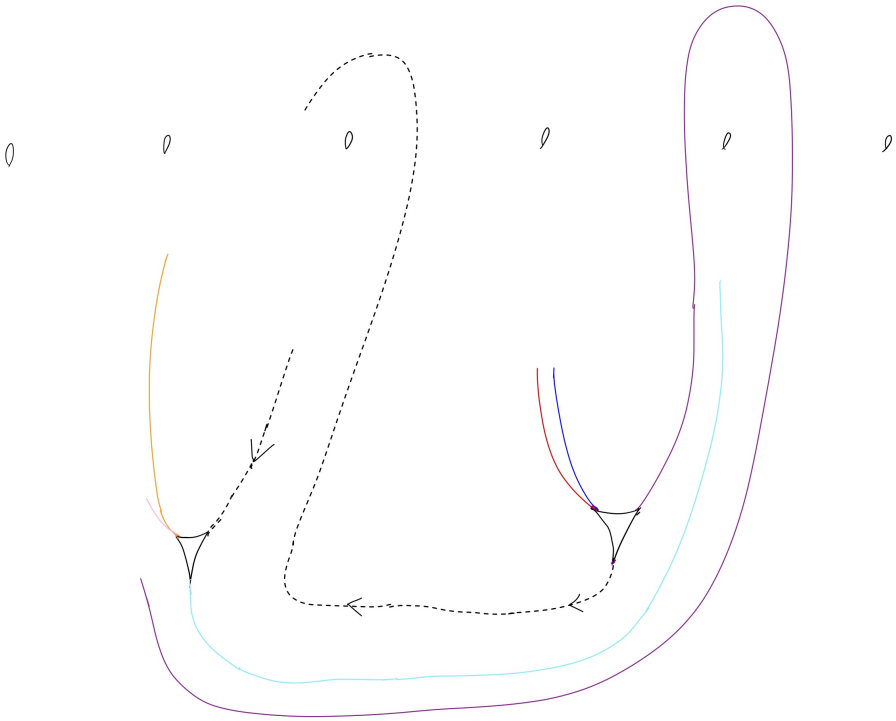


Figure D.223: Acrid1

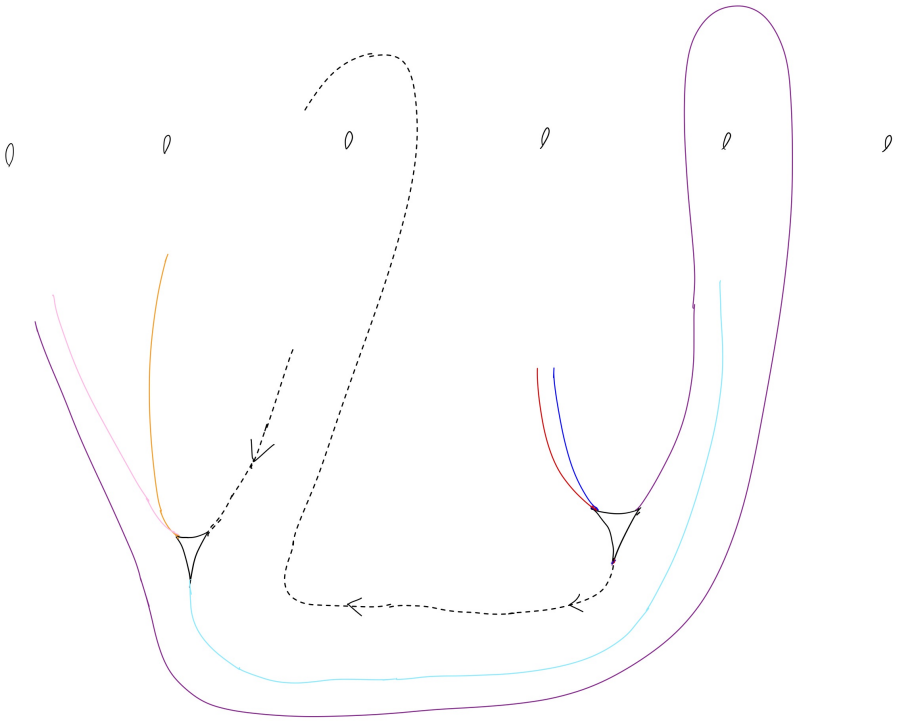


Figure D.224: Jasper1

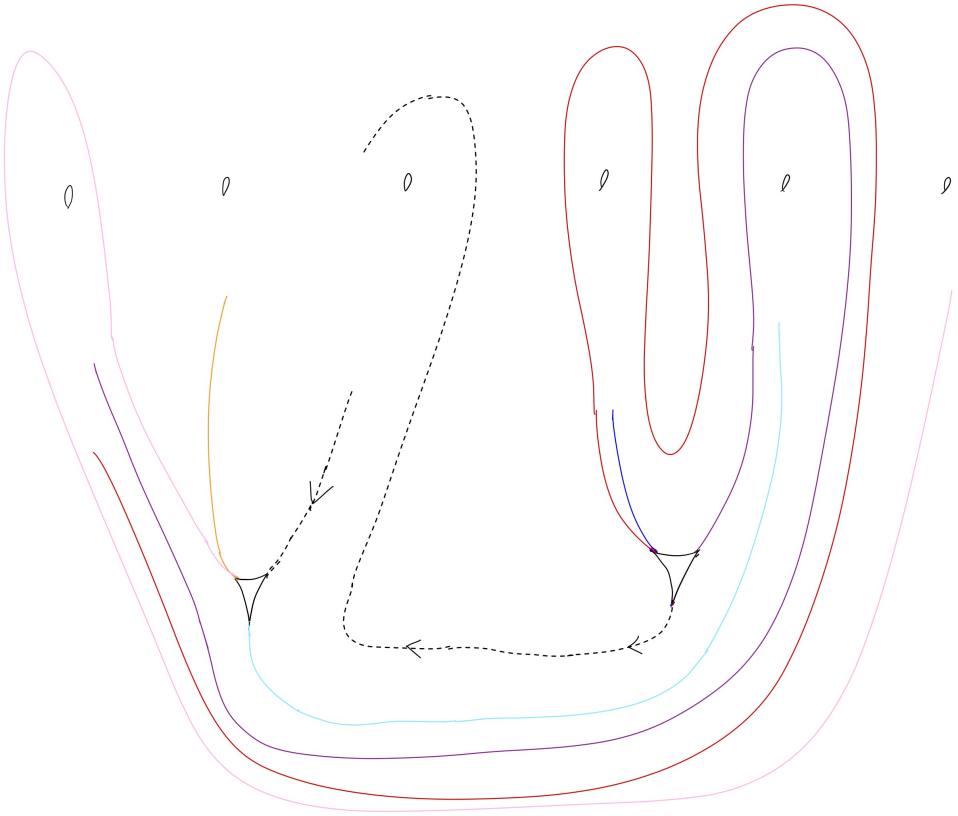


Figure D.225: Jasper2

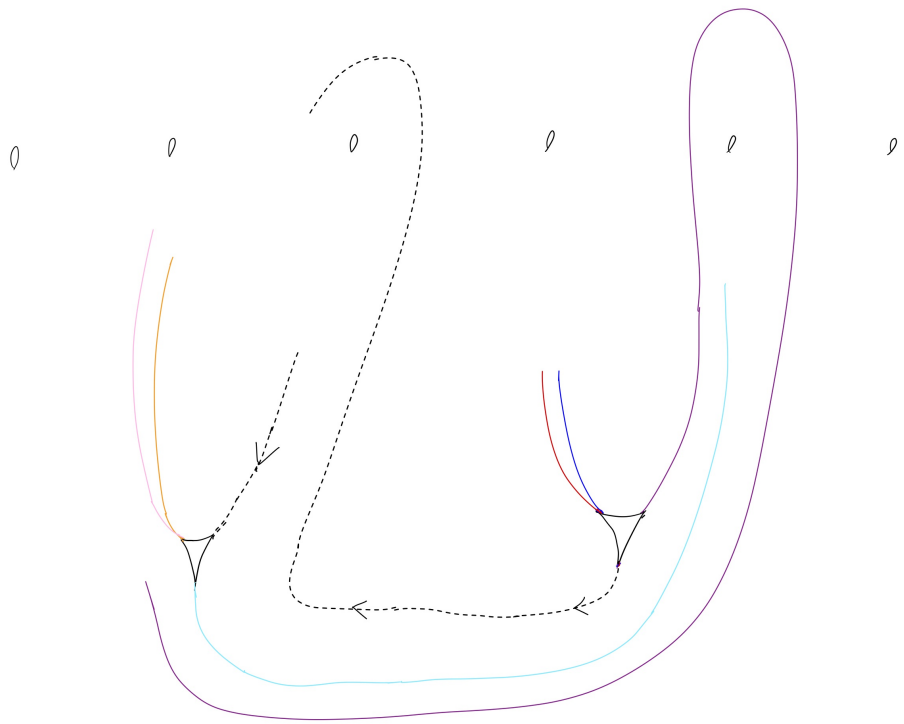


Figure D.226: Fledge1

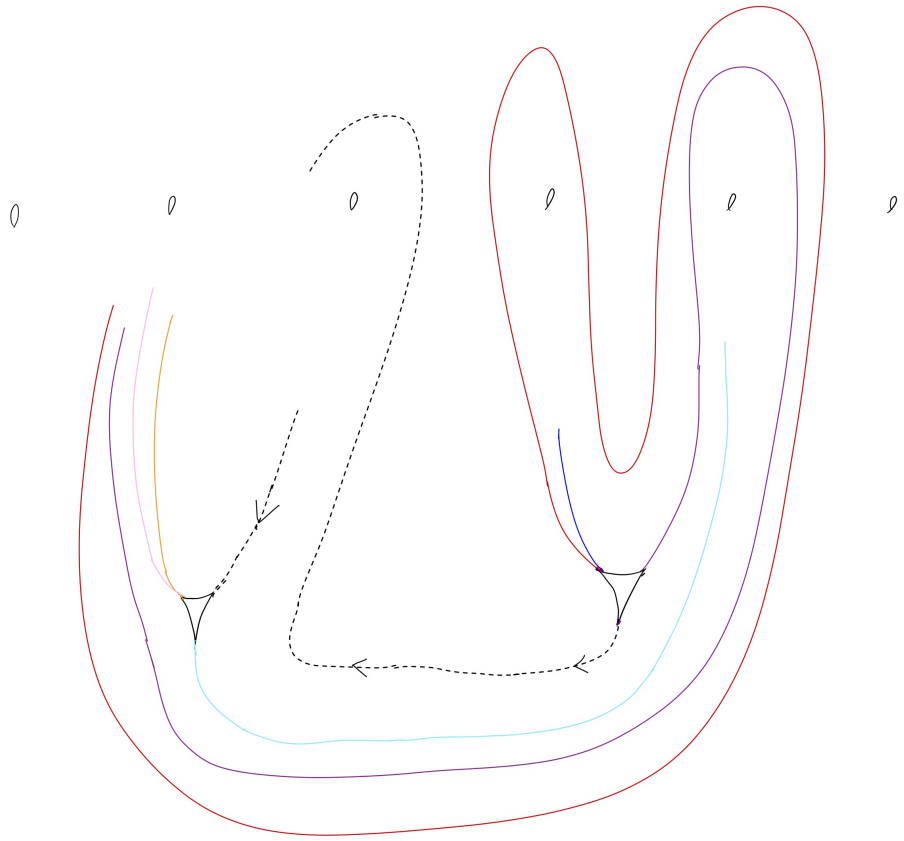


Figure D.227: Fledge2

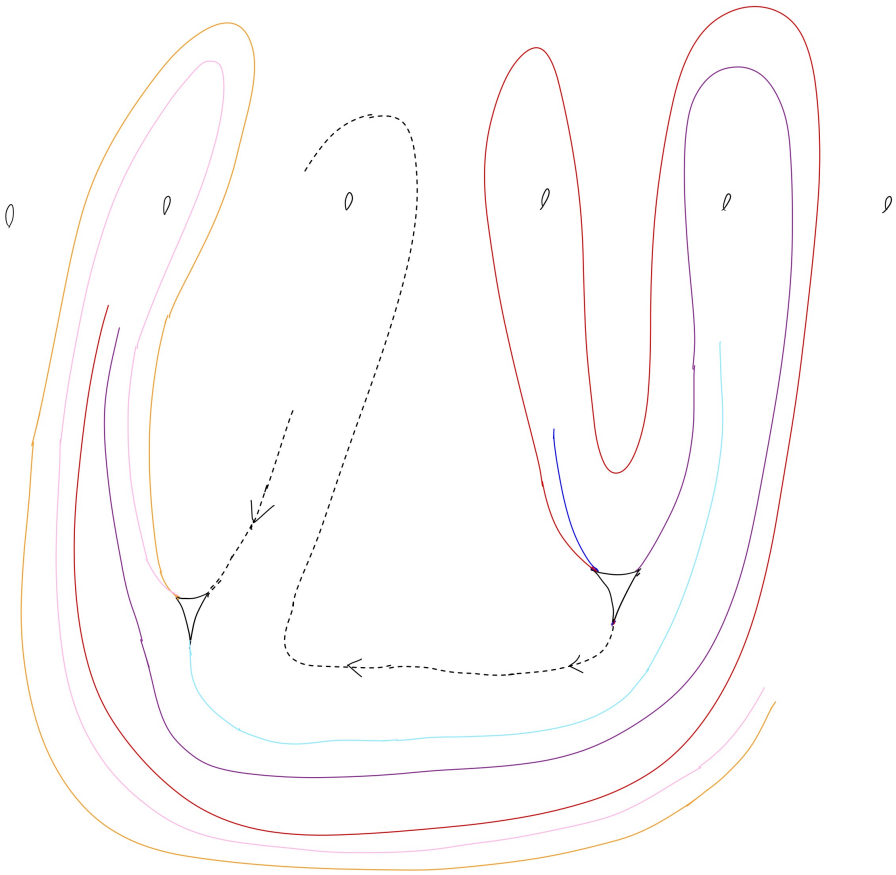


Figure D.228: Fledge3

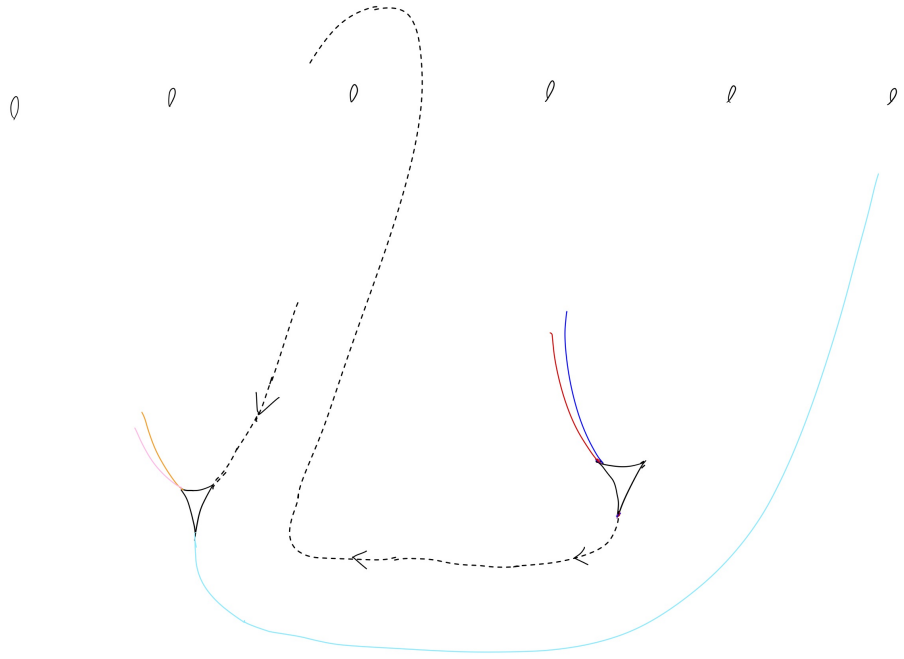


Figure D.229: Clam1

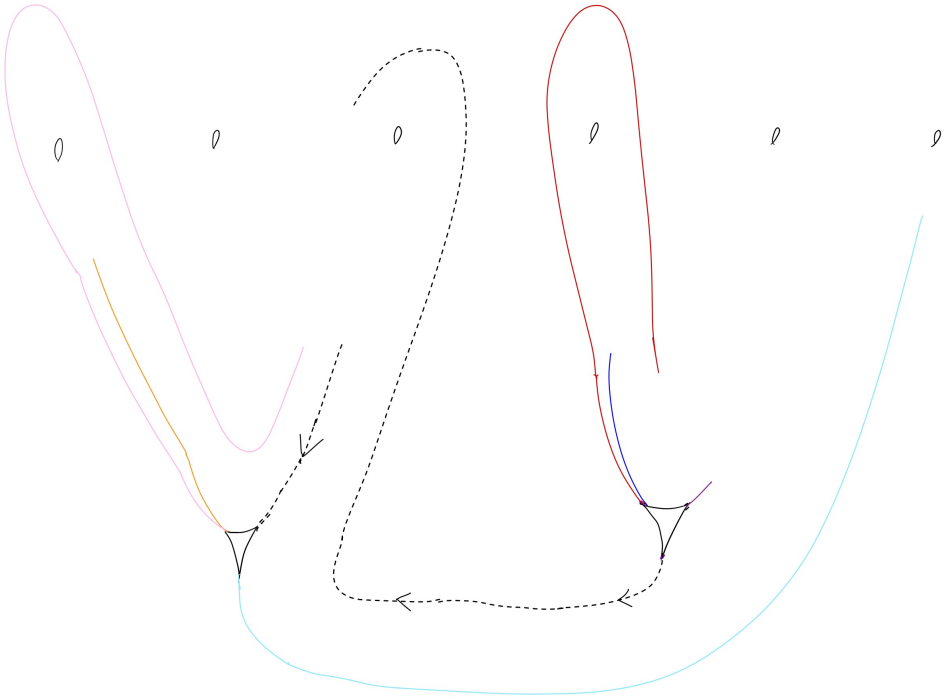


Figure D.230: Quail1

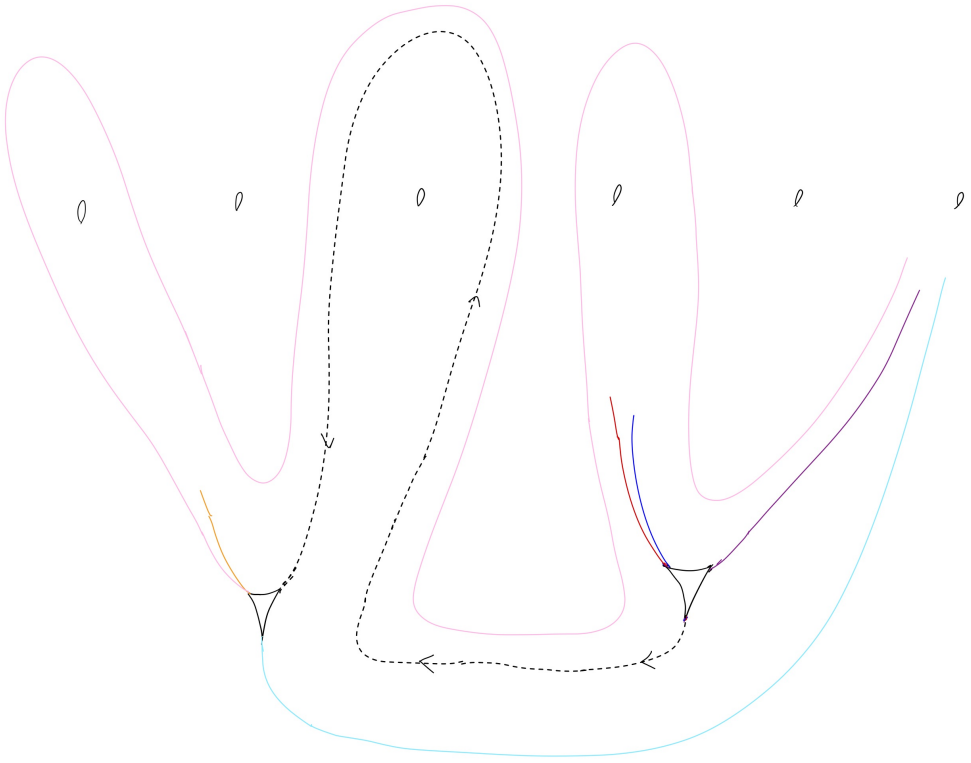


Figure D.231: Quail2

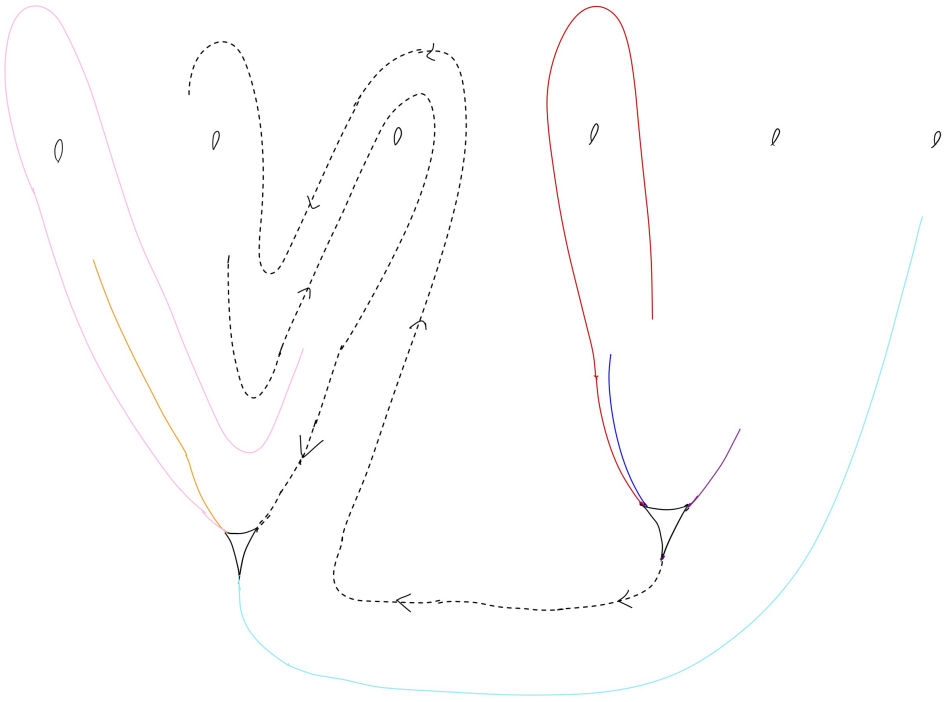


Figure D.232: Quail3

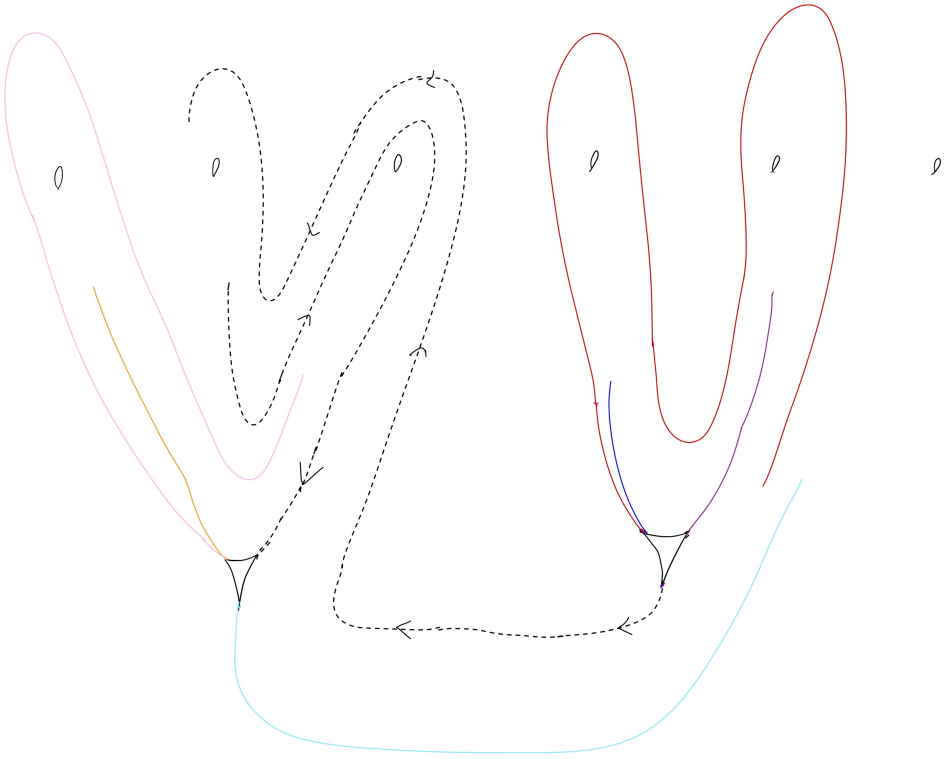


Figure D.233: Quail4

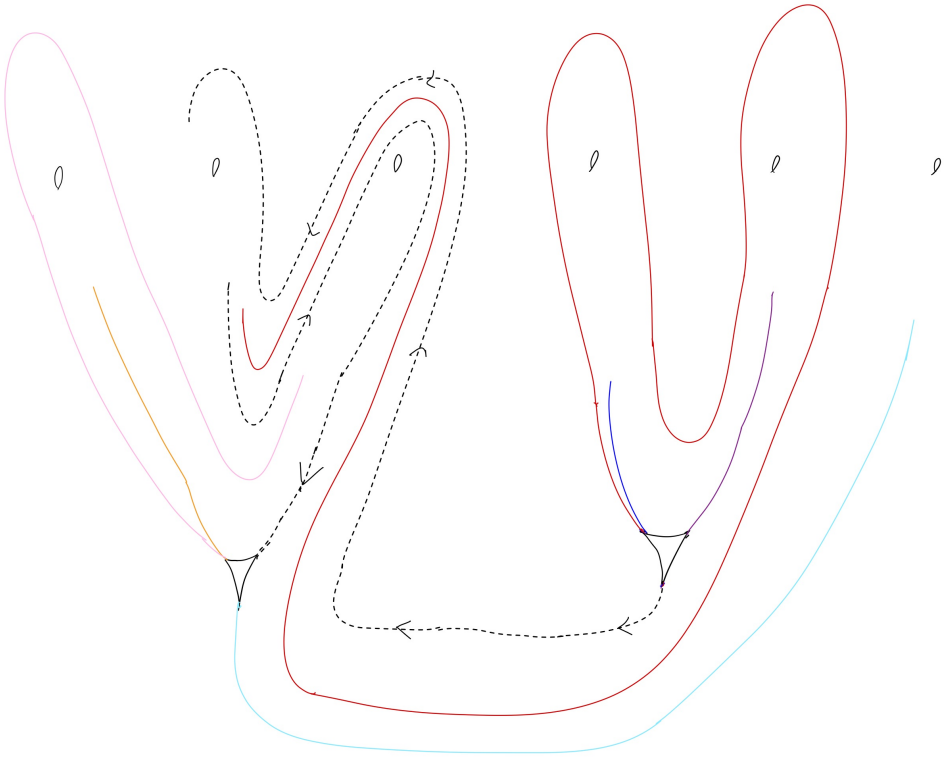


Figure D.234: Quail5

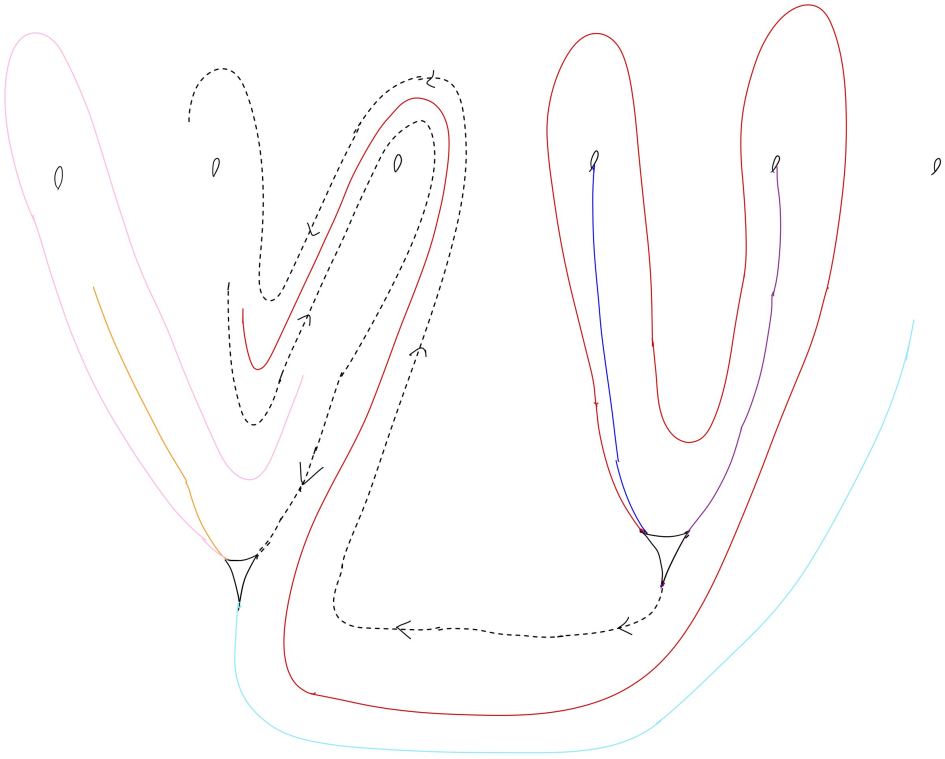


Figure D.235: Quail6

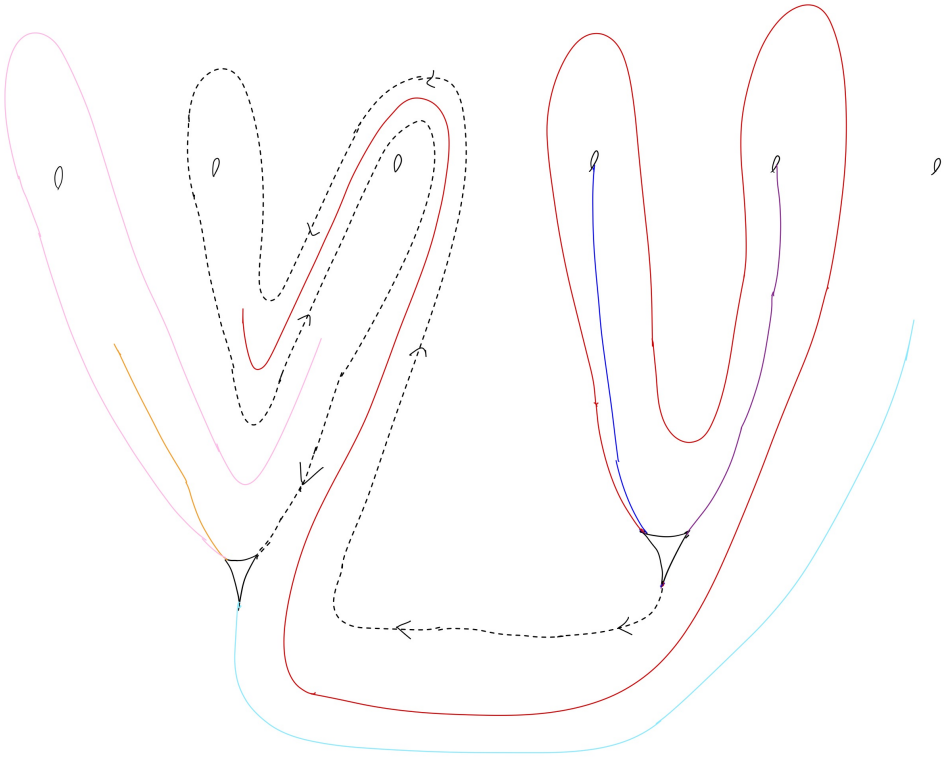


Figure D.236: Quail7

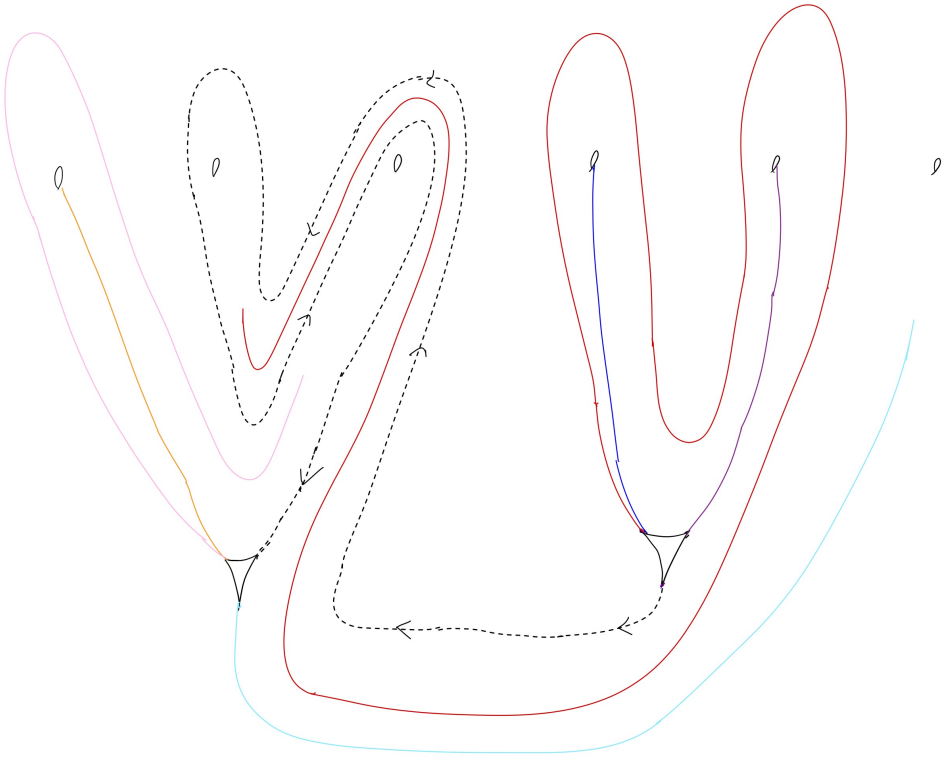


Figure D.237: Quail8

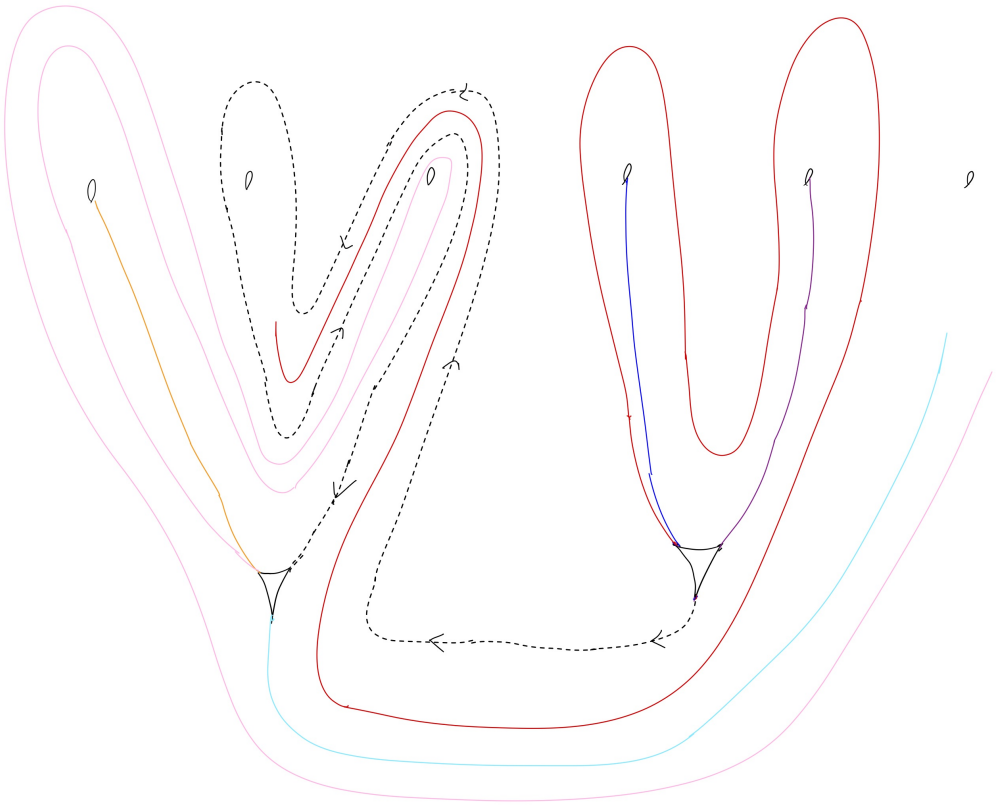


Figure D.238: Quail9

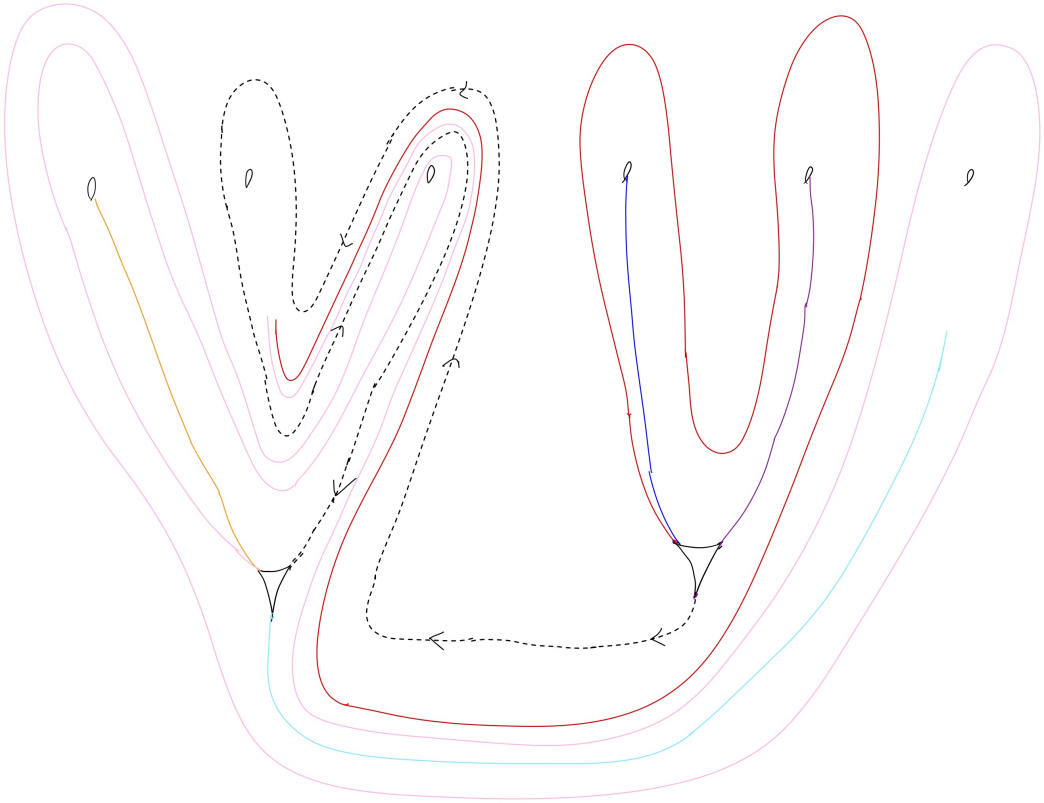


Figure D.239: Quail10

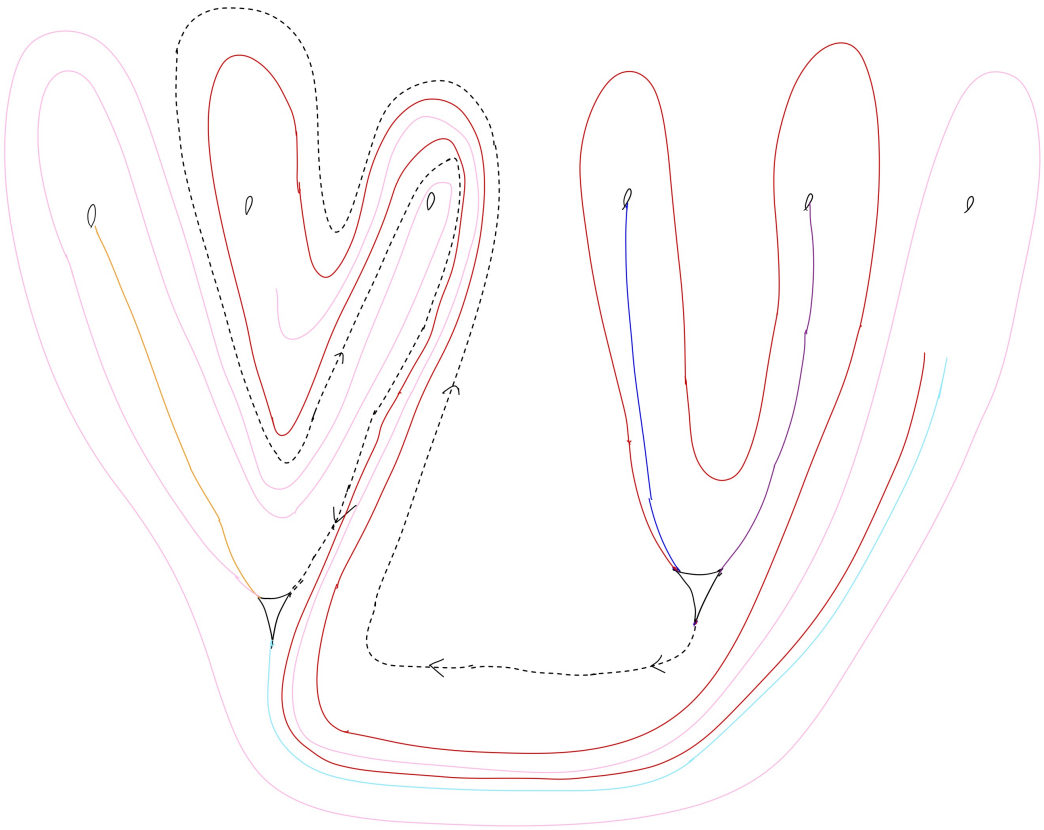


Figure D.240: Quail11

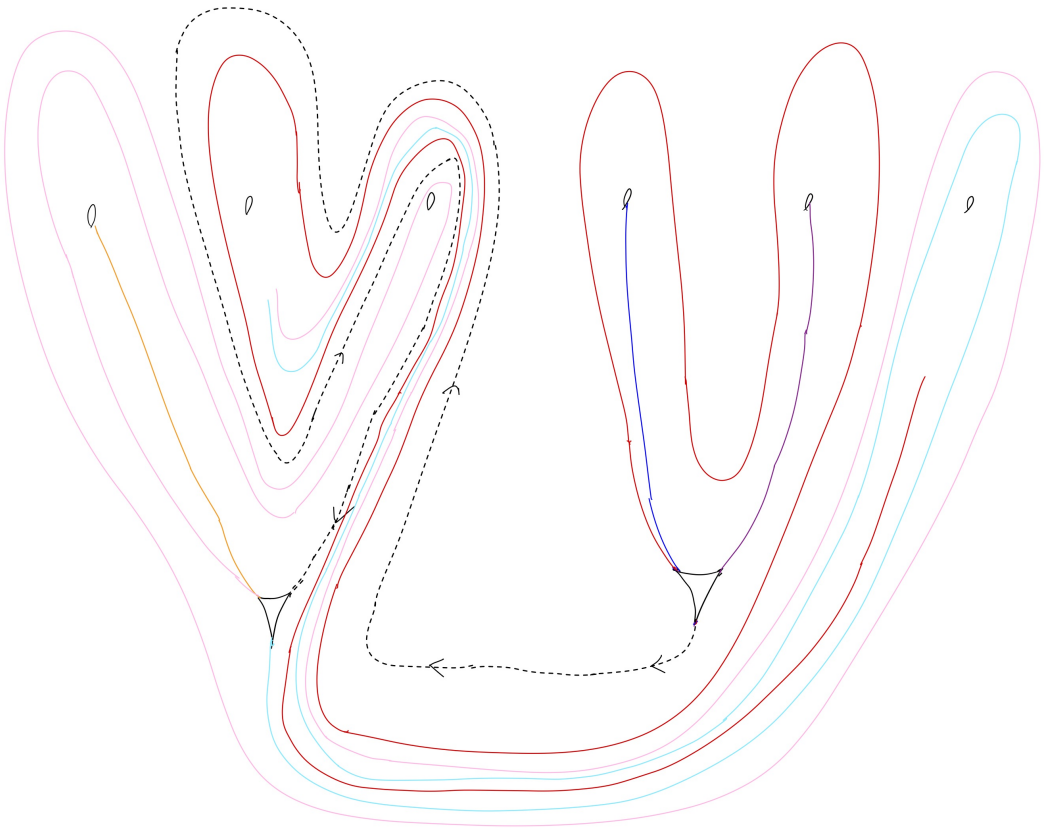


Figure D.241: Quail12

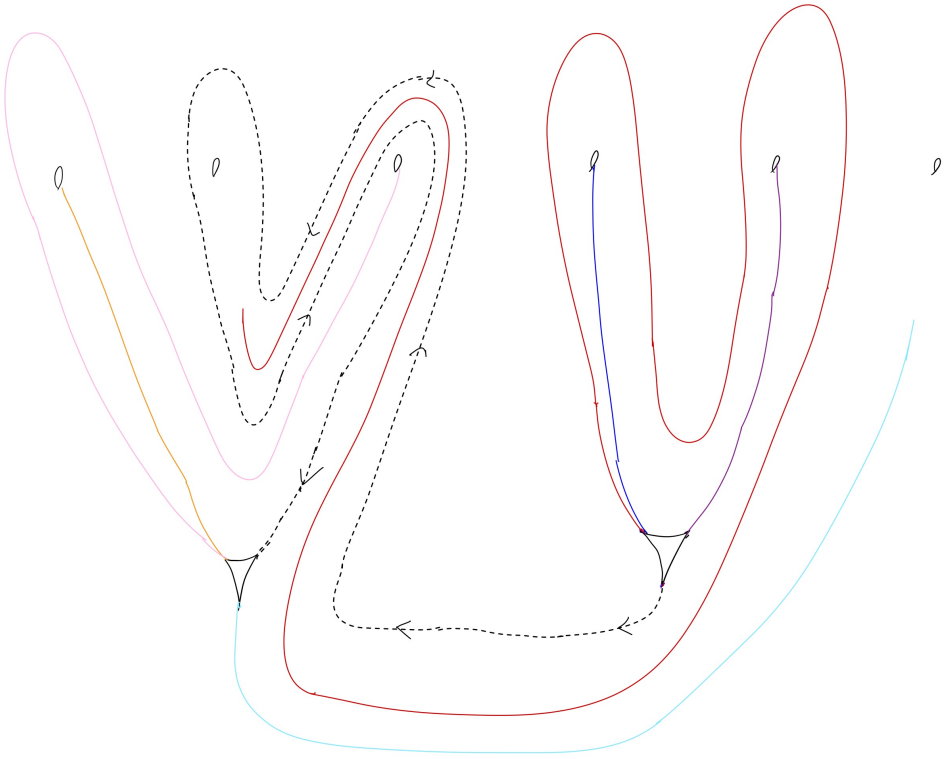


Figure D.242: Quail13

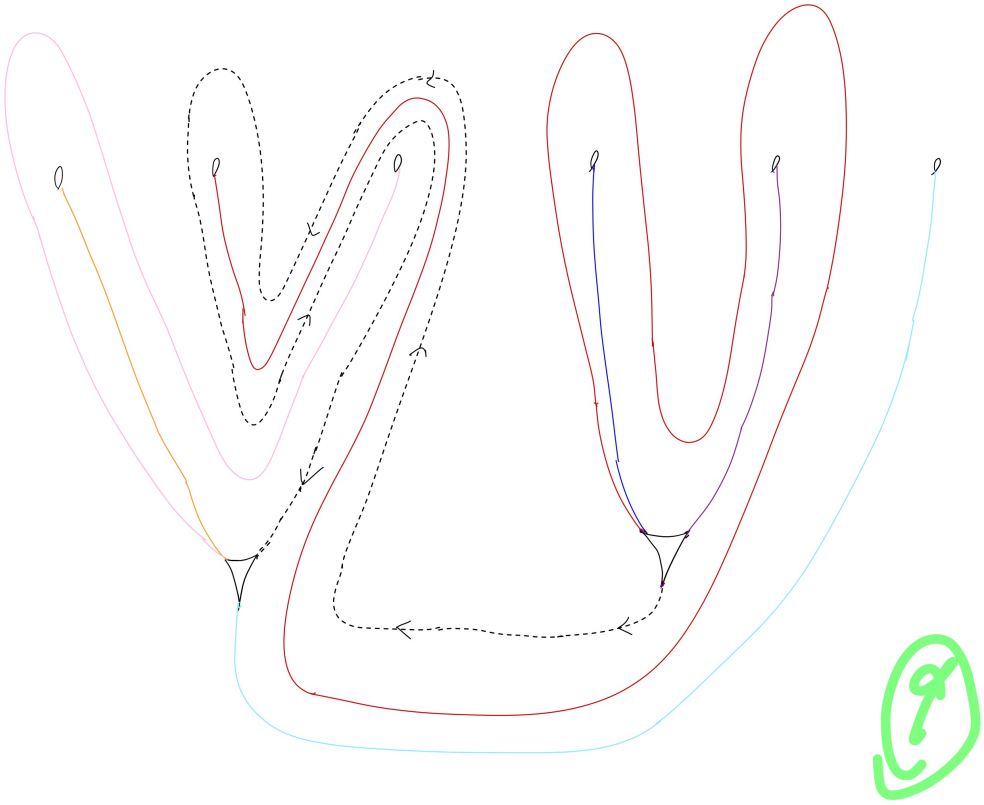


Figure D.243: Quail14

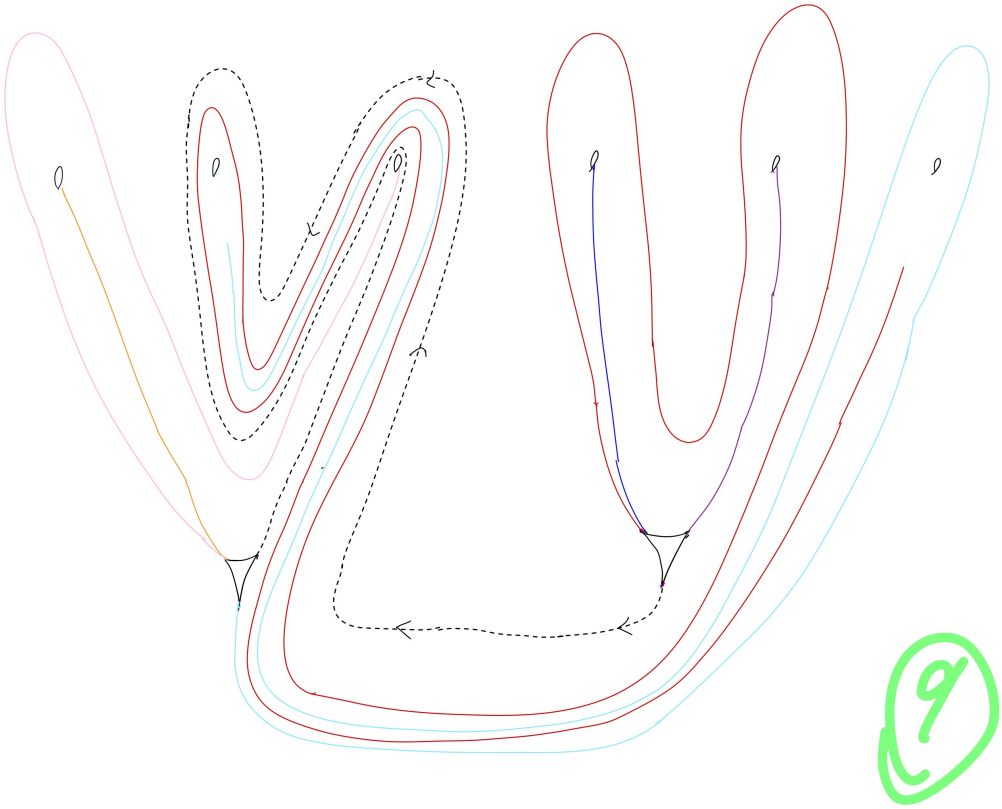


Figure D.244: Quail15

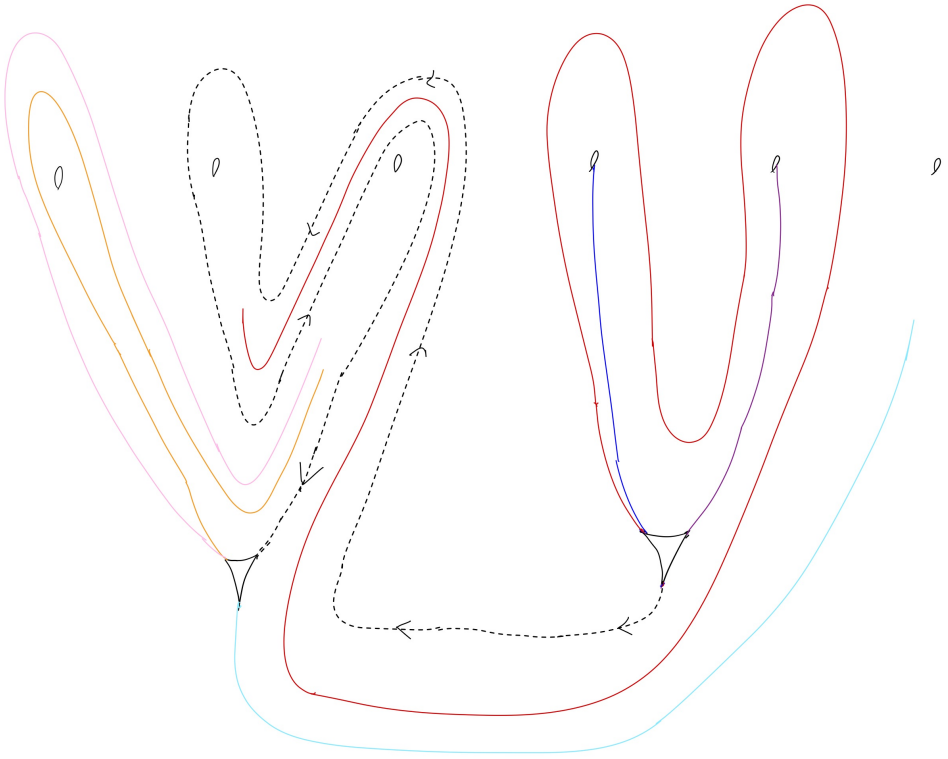


Figure D.245: Quail16

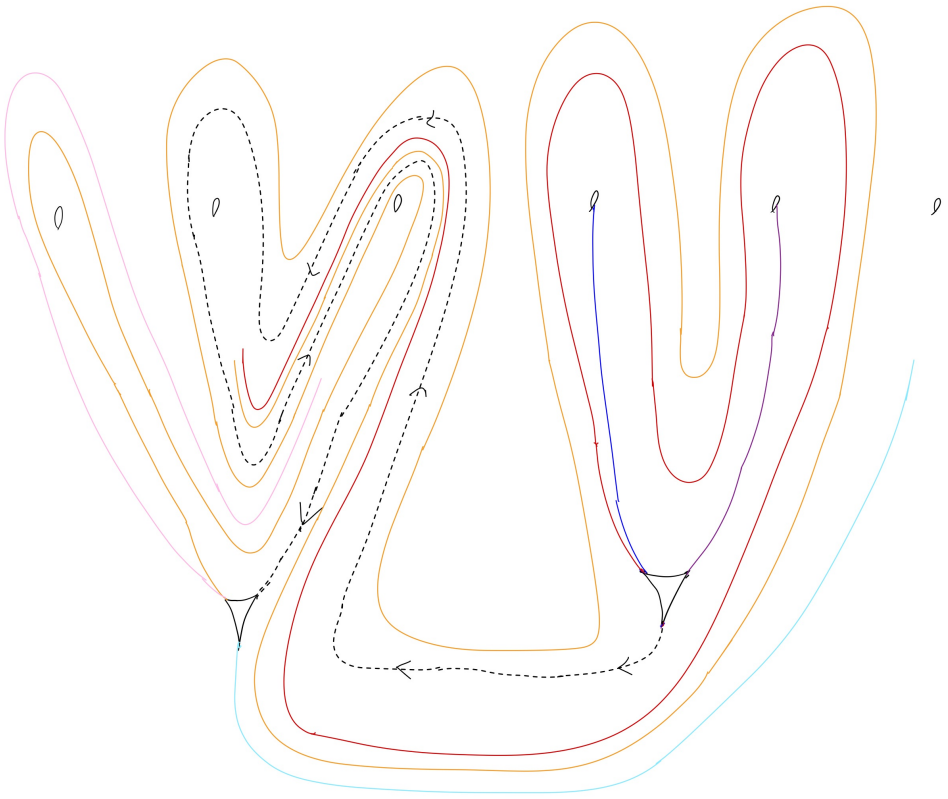


Figure D.246: Quail17

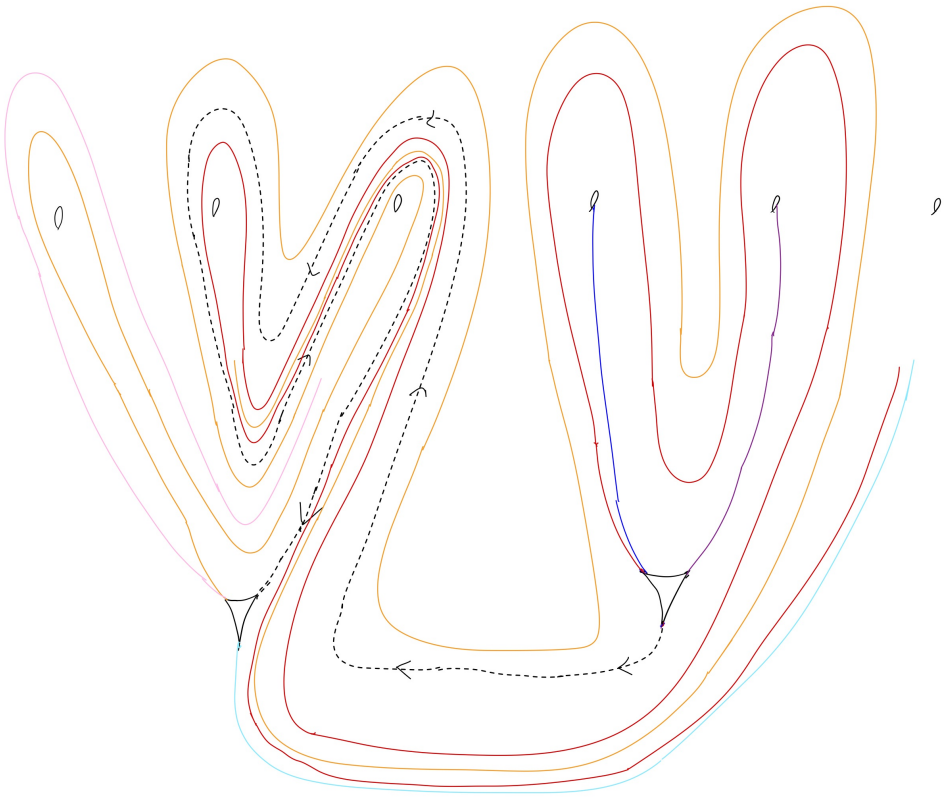


Figure D.247: Quail18

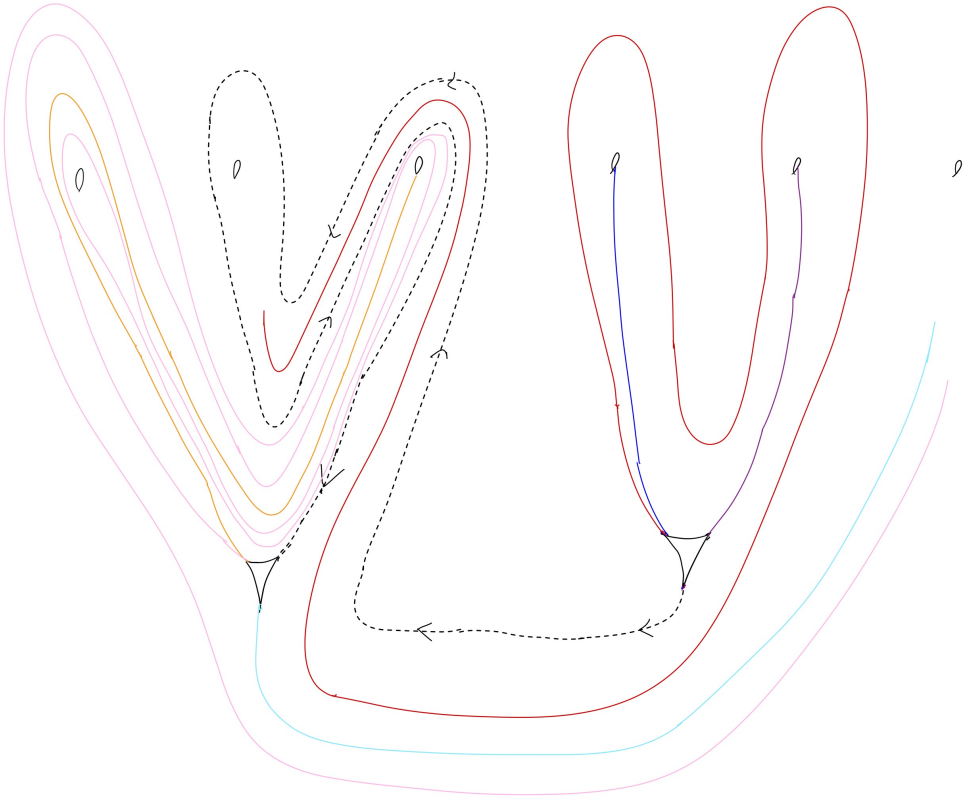


Figure D.248: Quail19

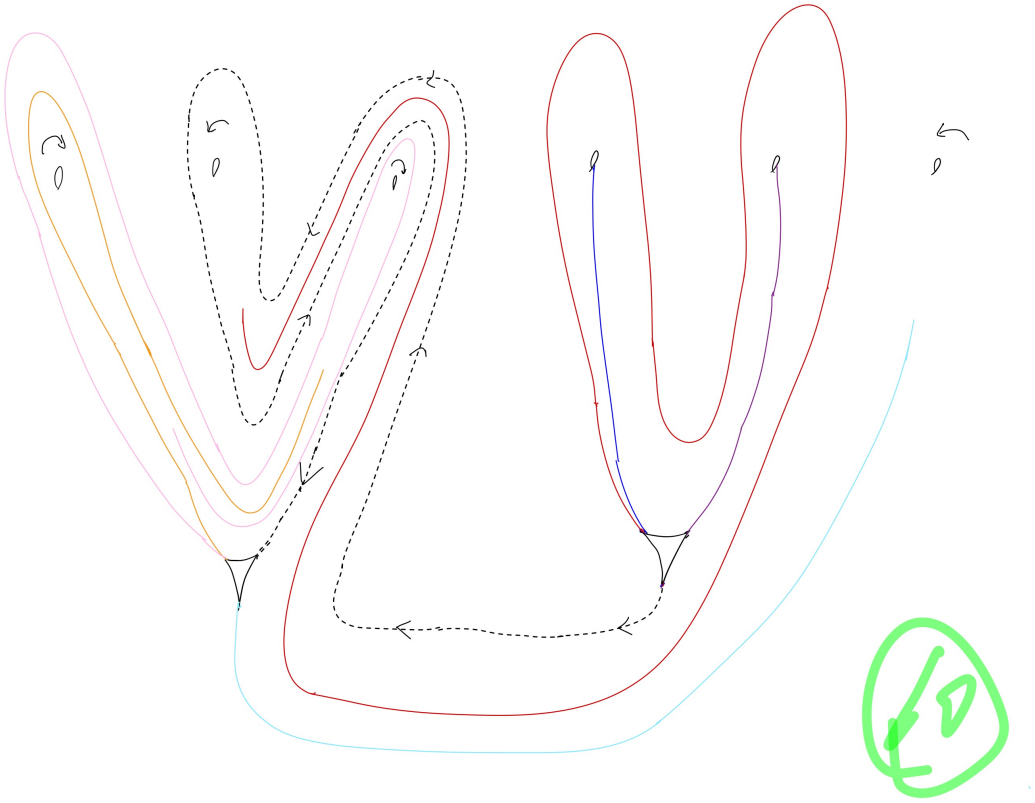


Figure D.249: Quail20

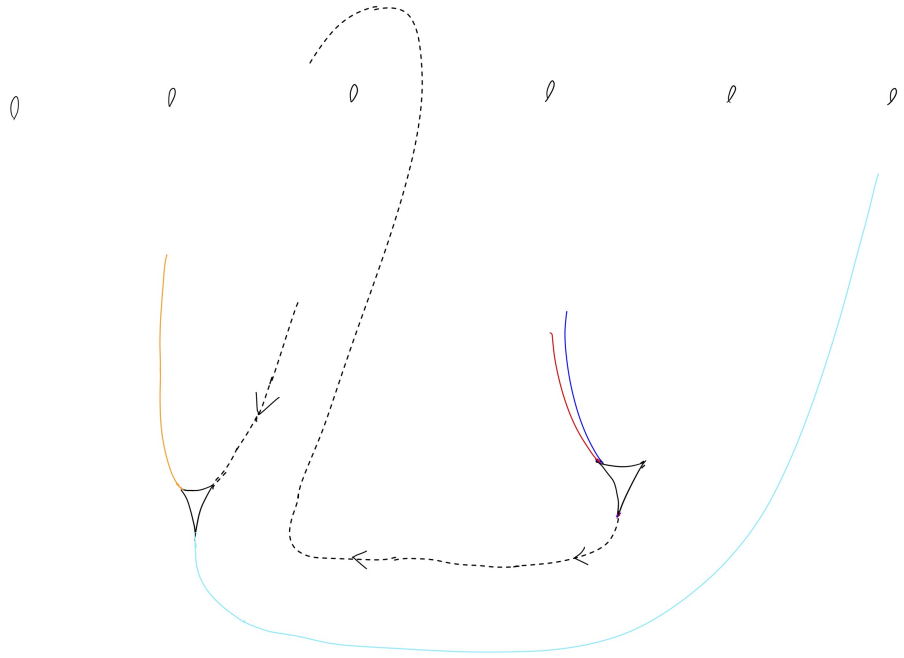


Figure D.250: Imbue1

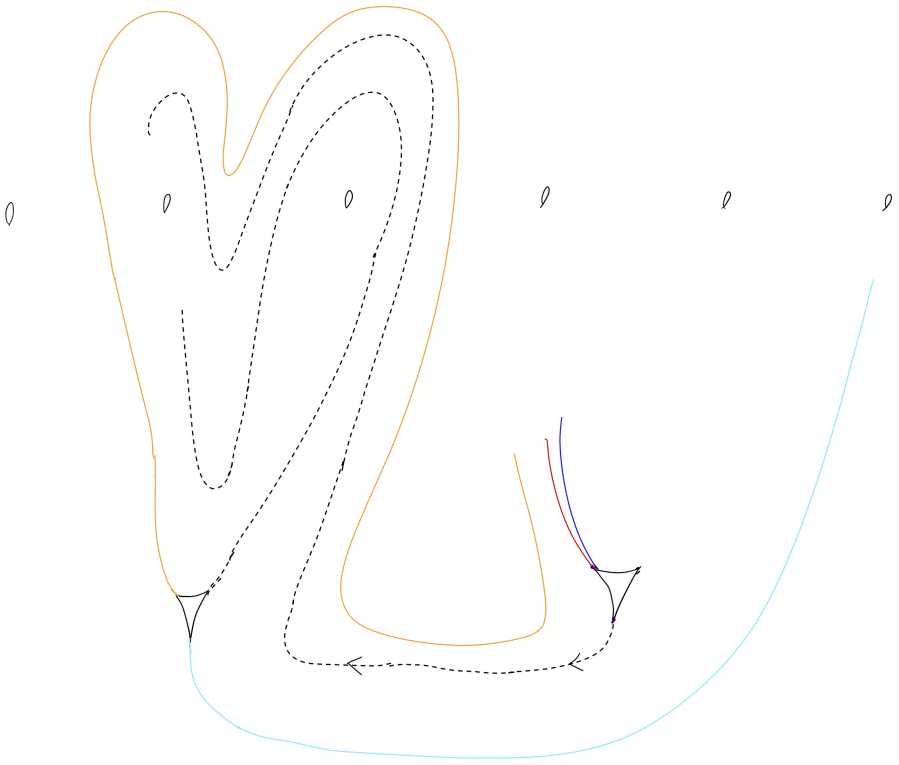


Figure D.251: Imbue2

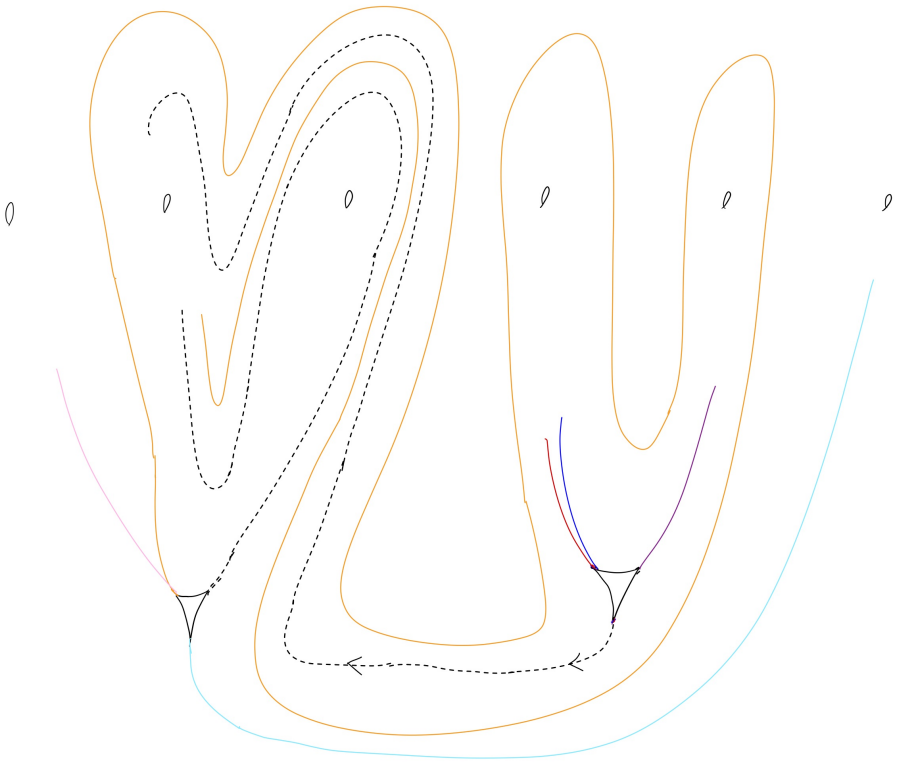


Figure D.252: Imbue3

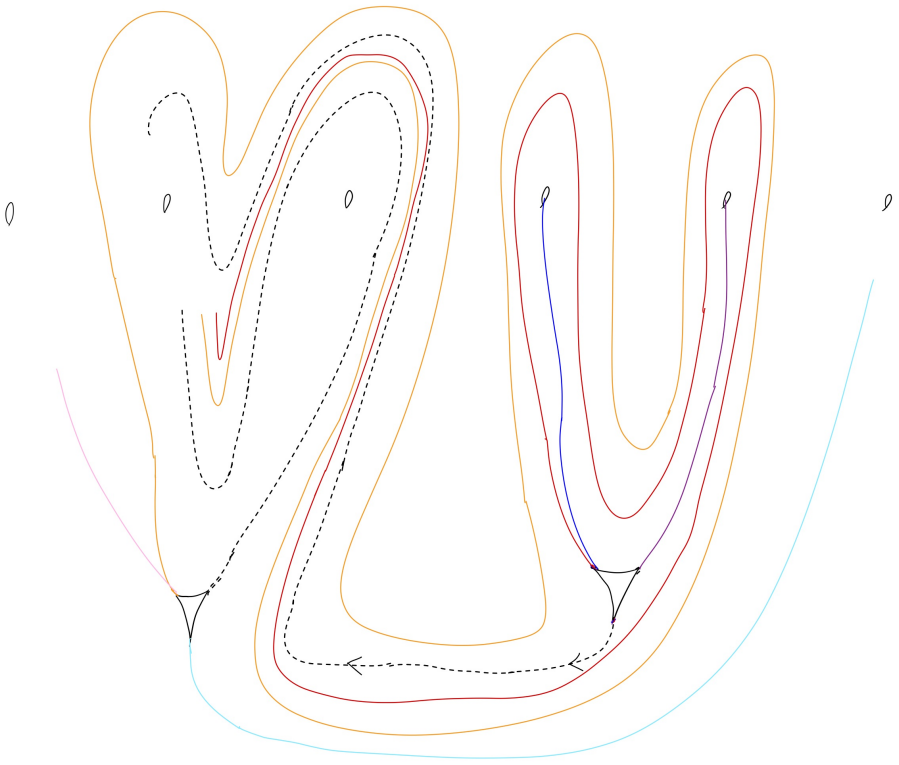


Figure D.253: Imbue4

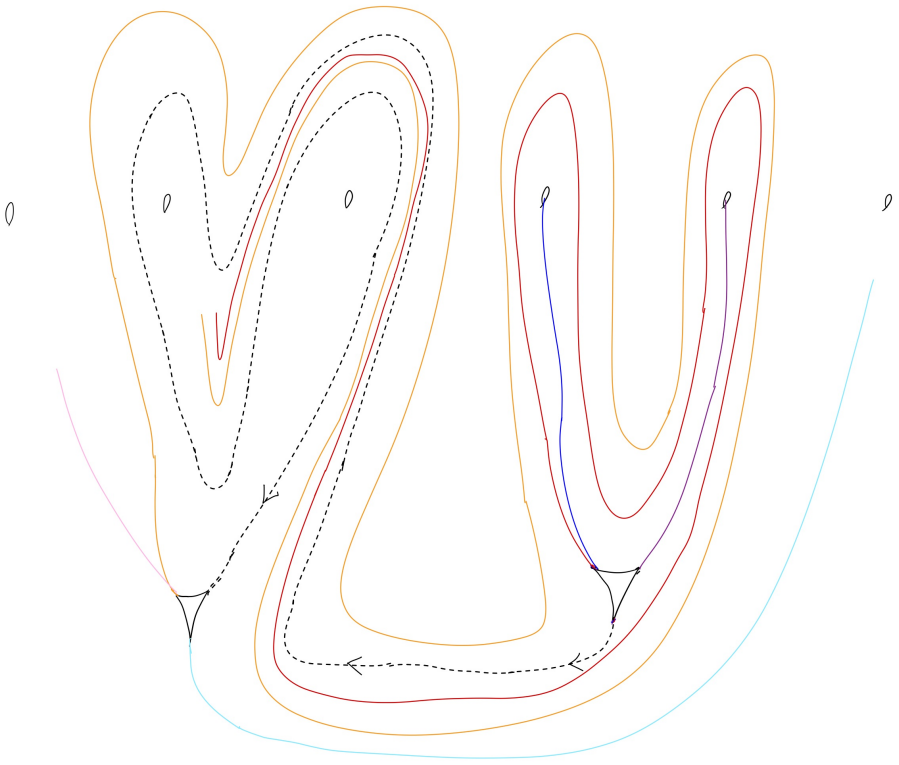


Figure D.254: Imbue5

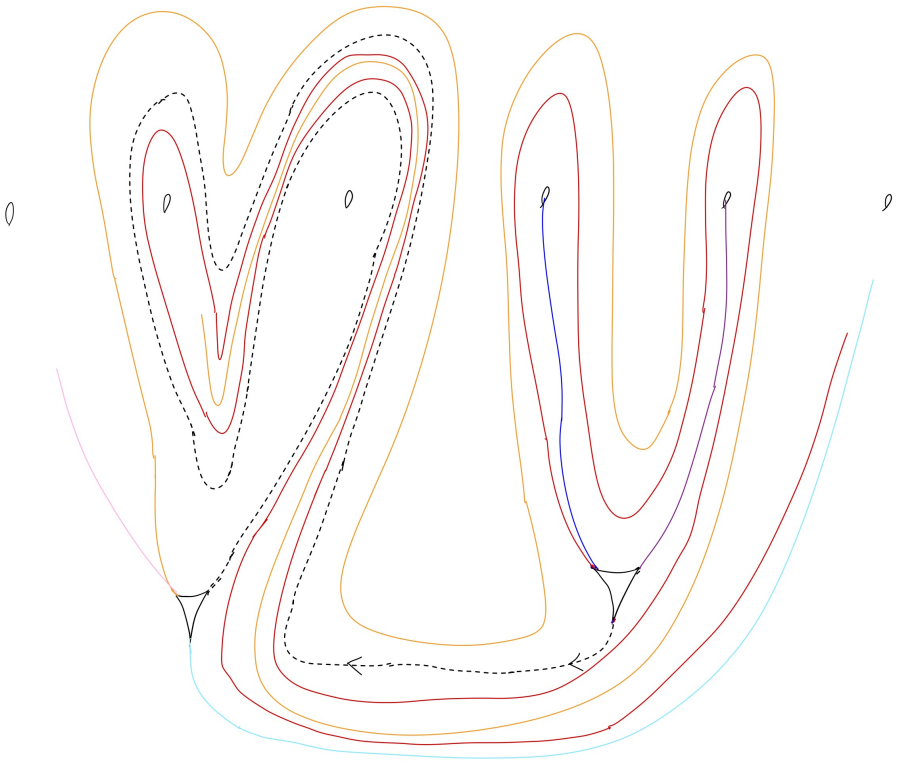


Figure D.255: Imbue6

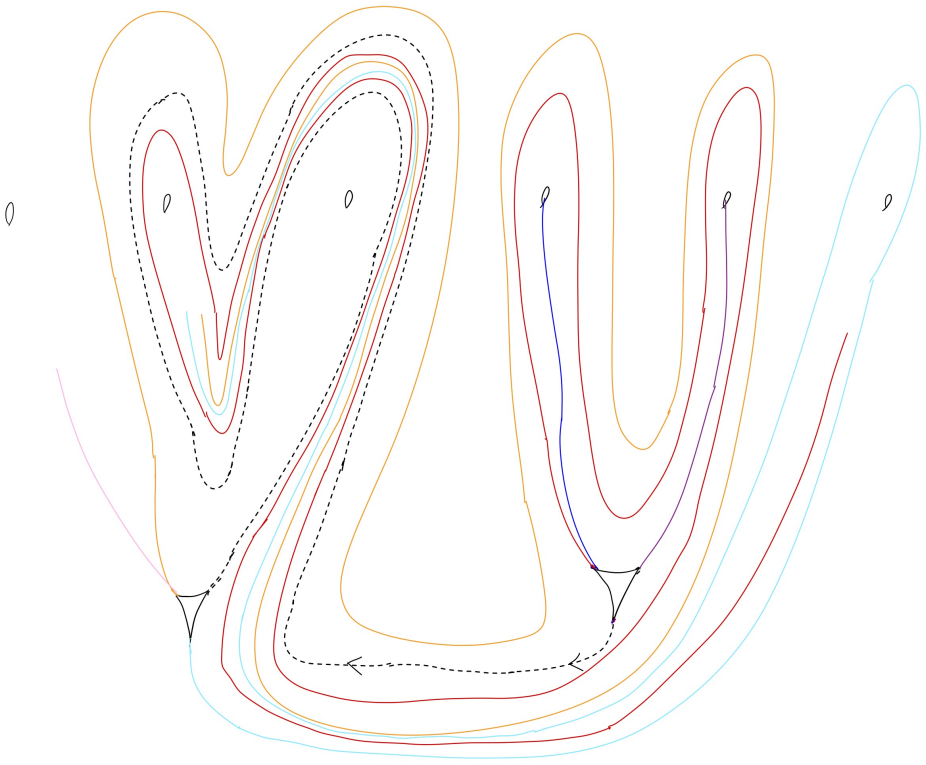


Figure D.256: Imbue7

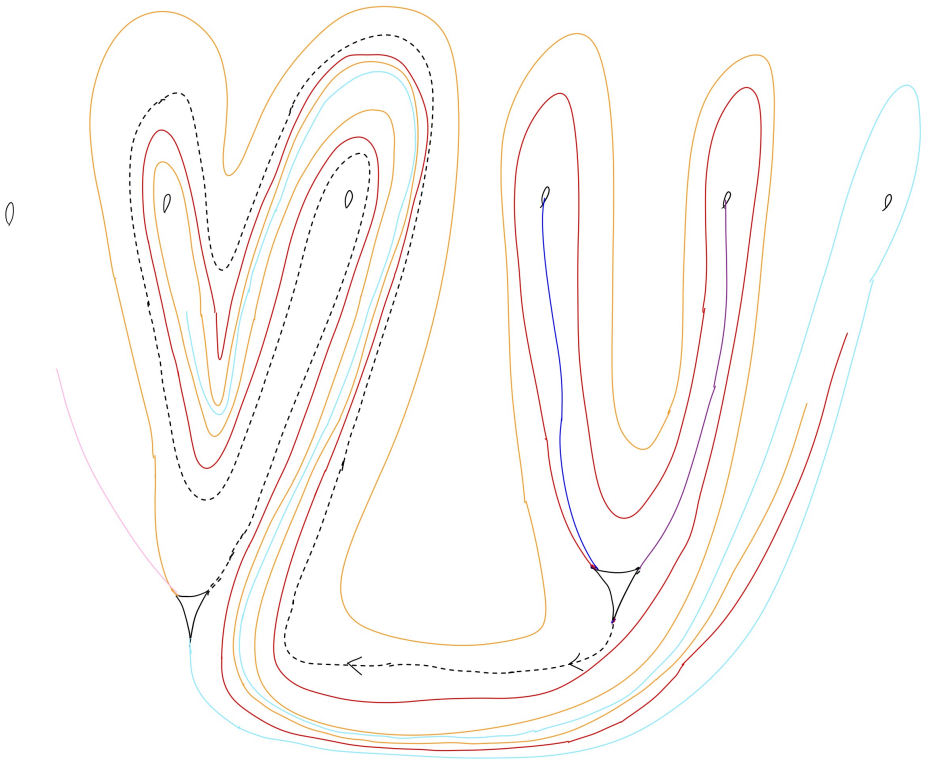


Figure D.257: Imbue8

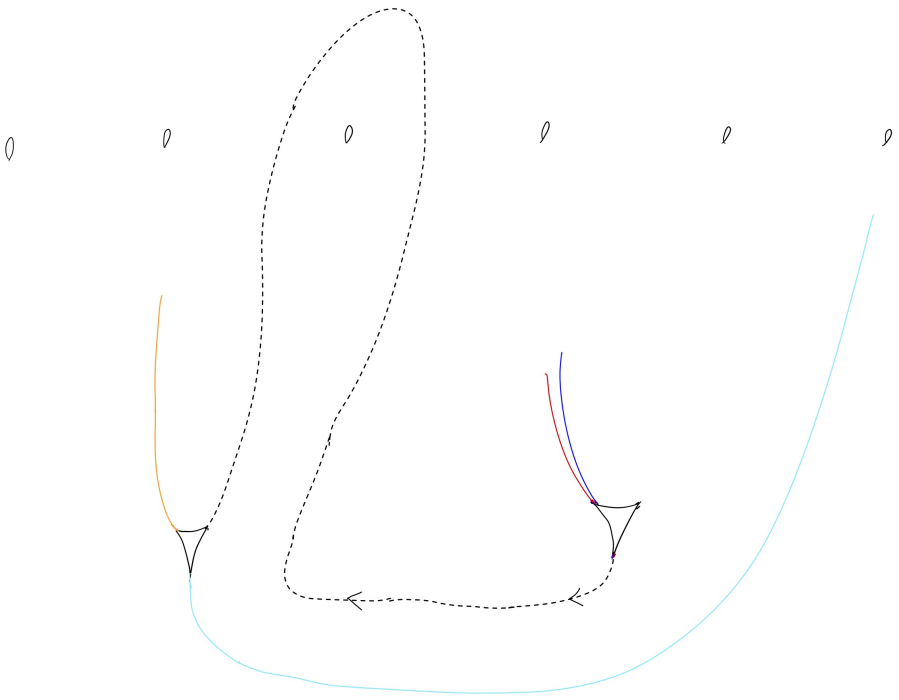


Figure D.258: Imbue9

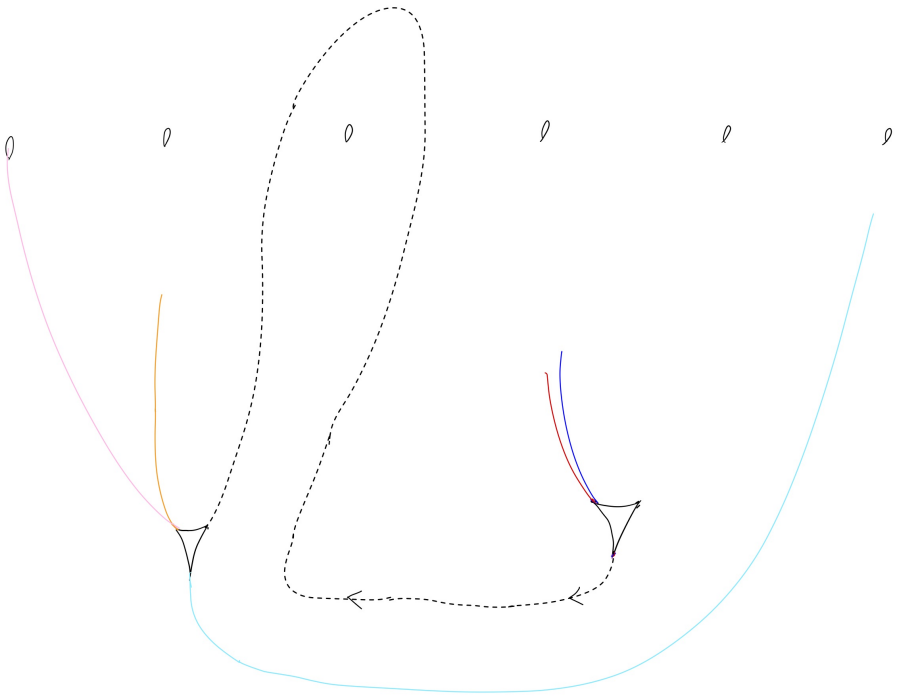


Figure D.259: Zither1

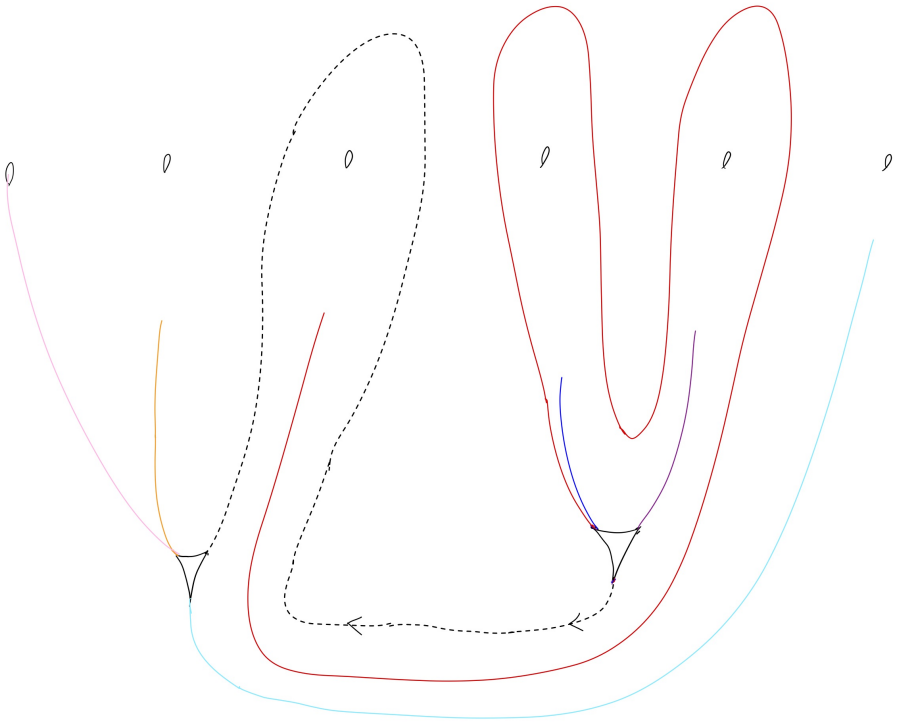


Figure D.260: Zither2

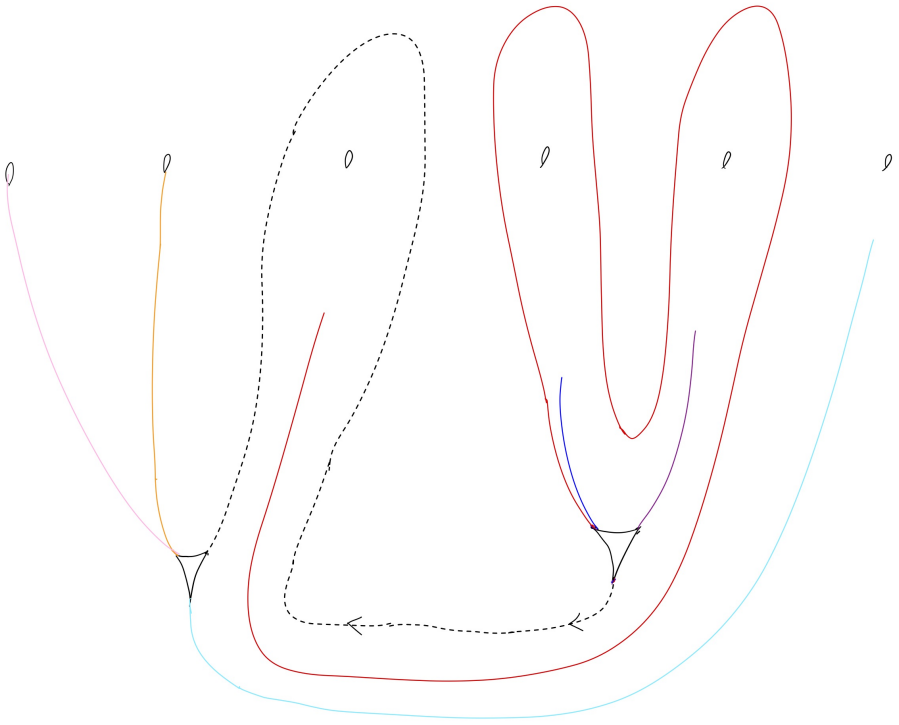


Figure D.261: Abandon1

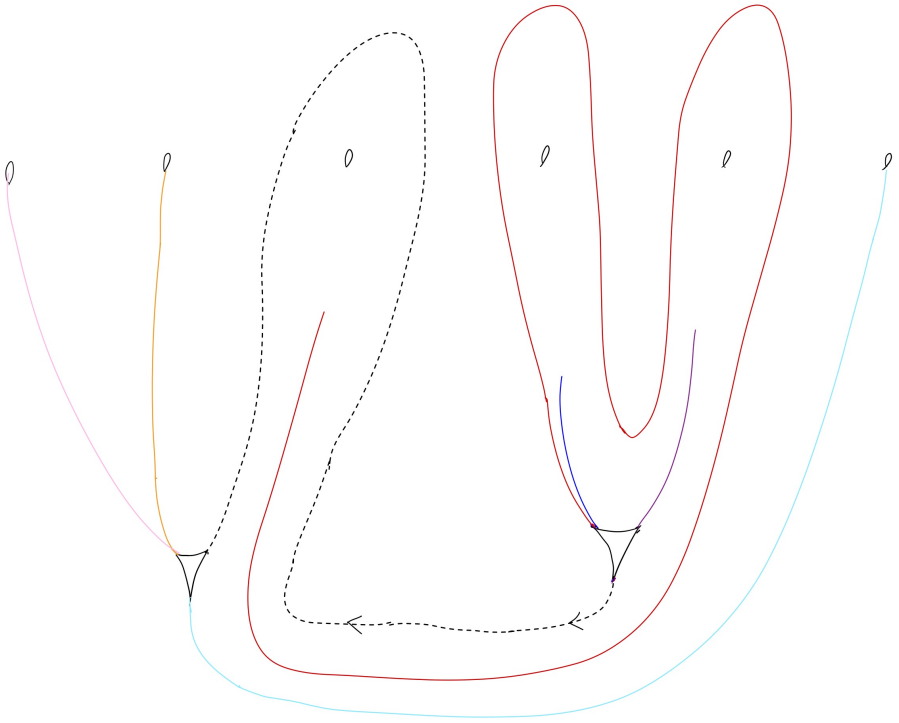


Figure D.262: Jubilant1

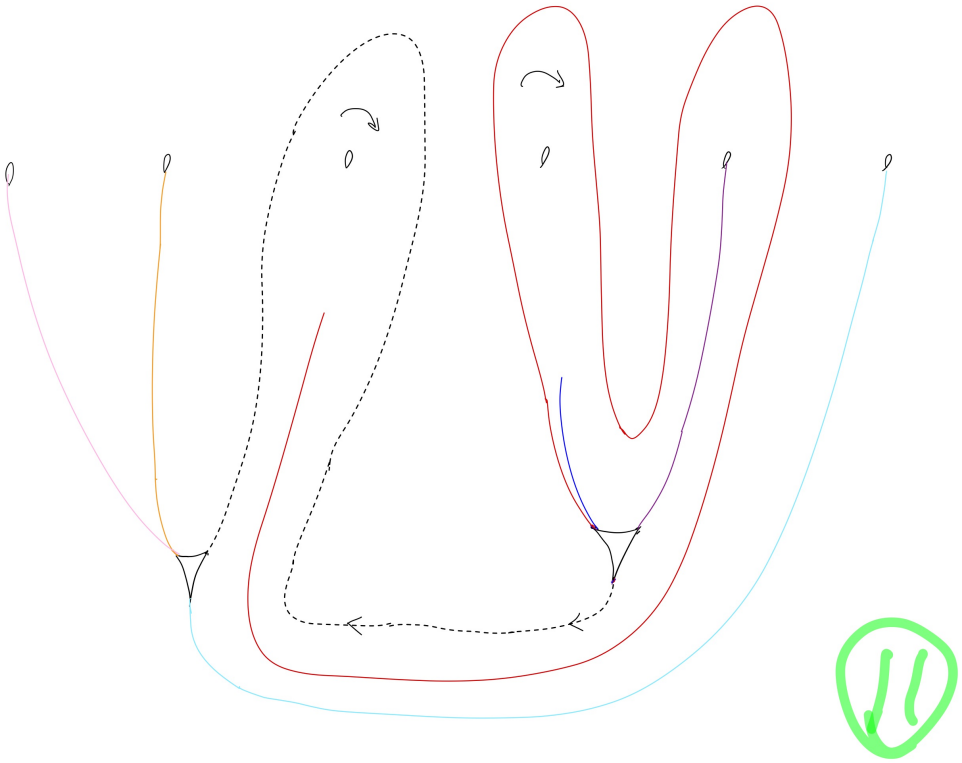


Figure D.263: Jubilant2

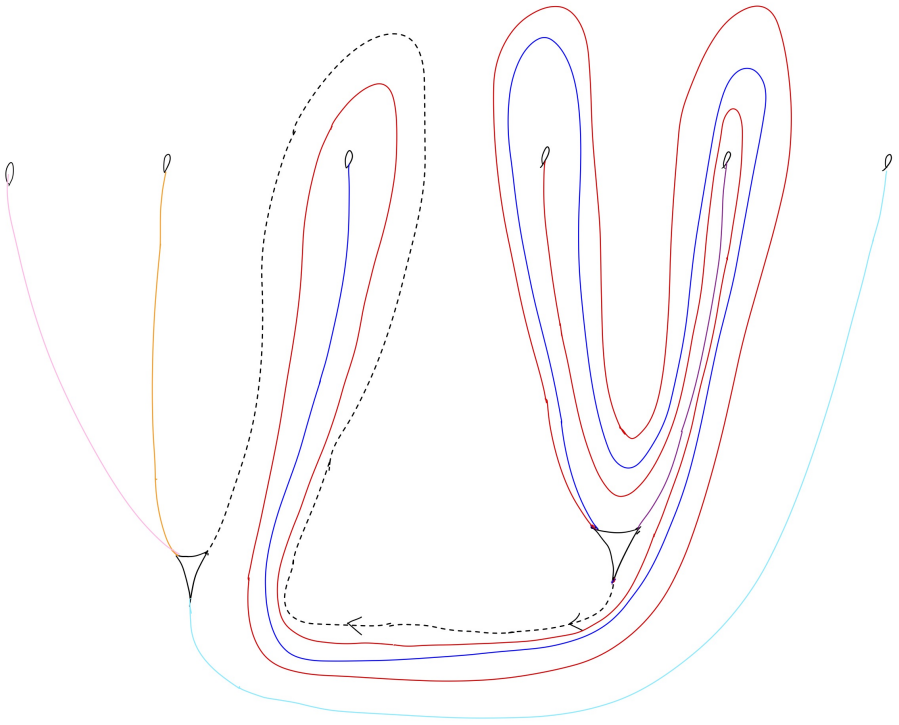


Figure D.264: Jubilant3

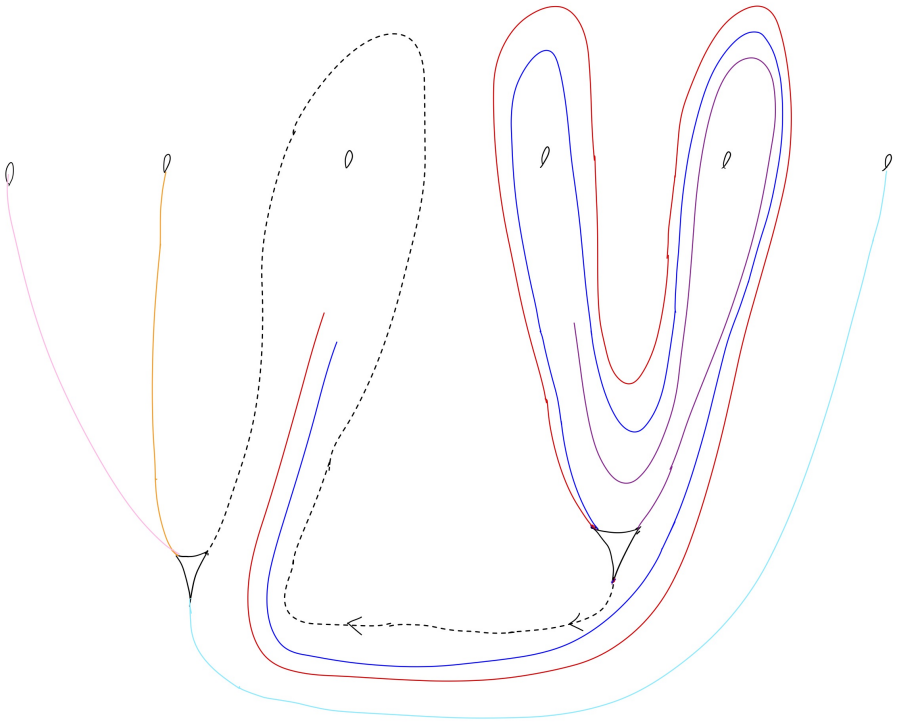


Figure D.265: Jubilant4

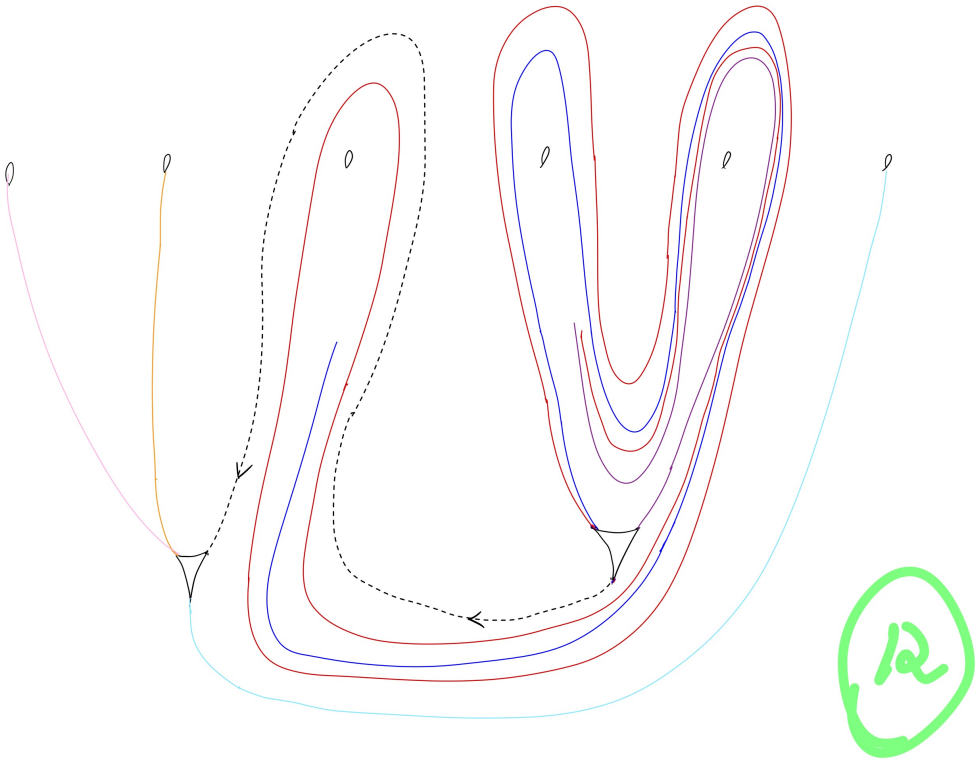


Figure D.266: Jubilant5

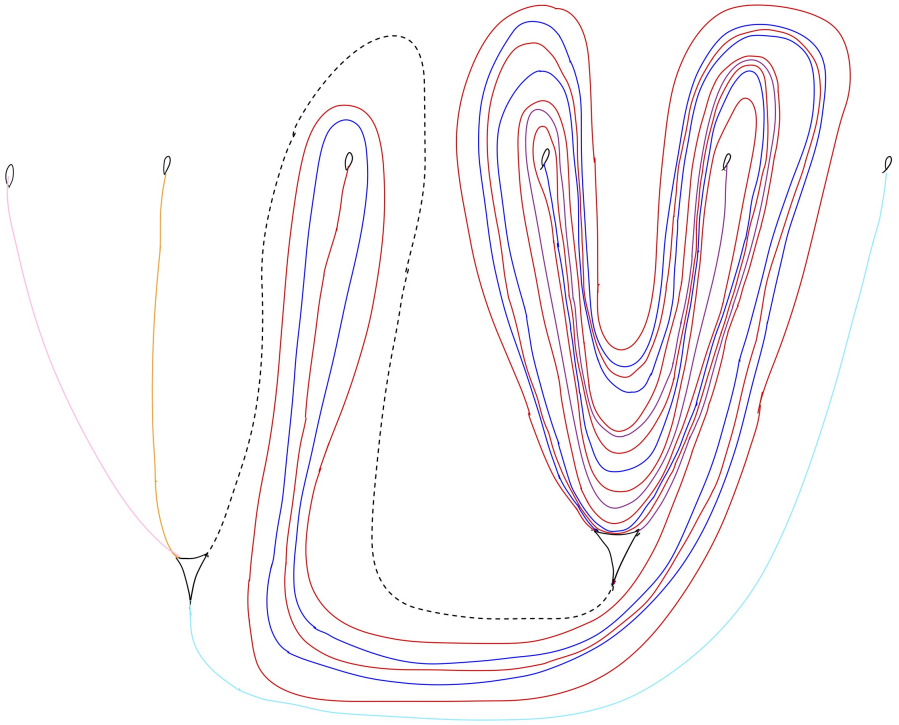


Figure D.267: Jubilant6

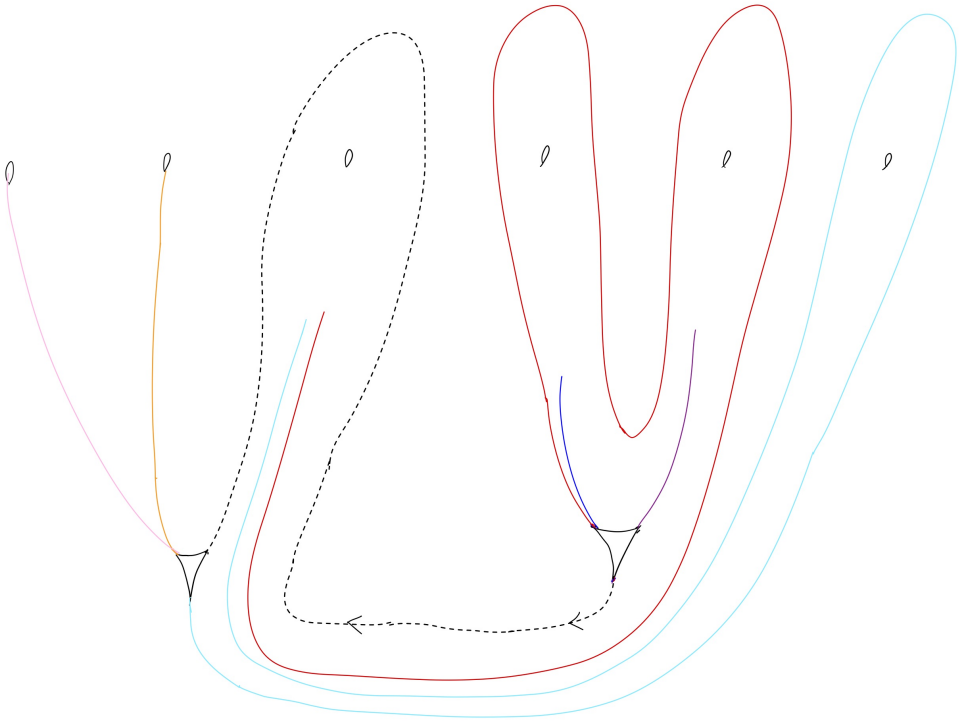


Figure D.268: Emergency1

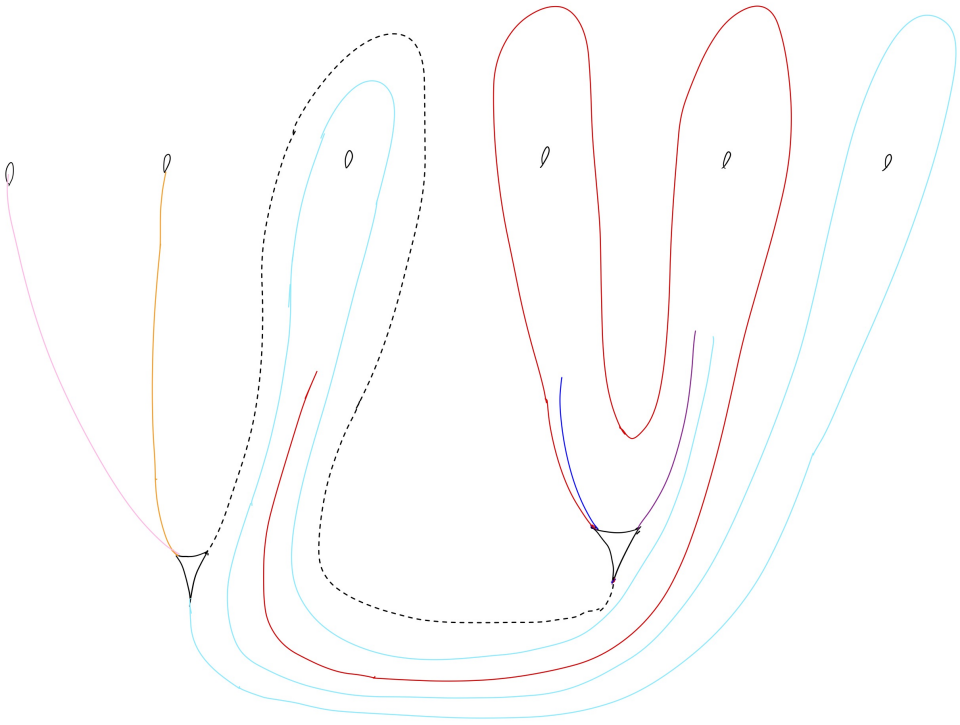


Figure D.269: Landscape1

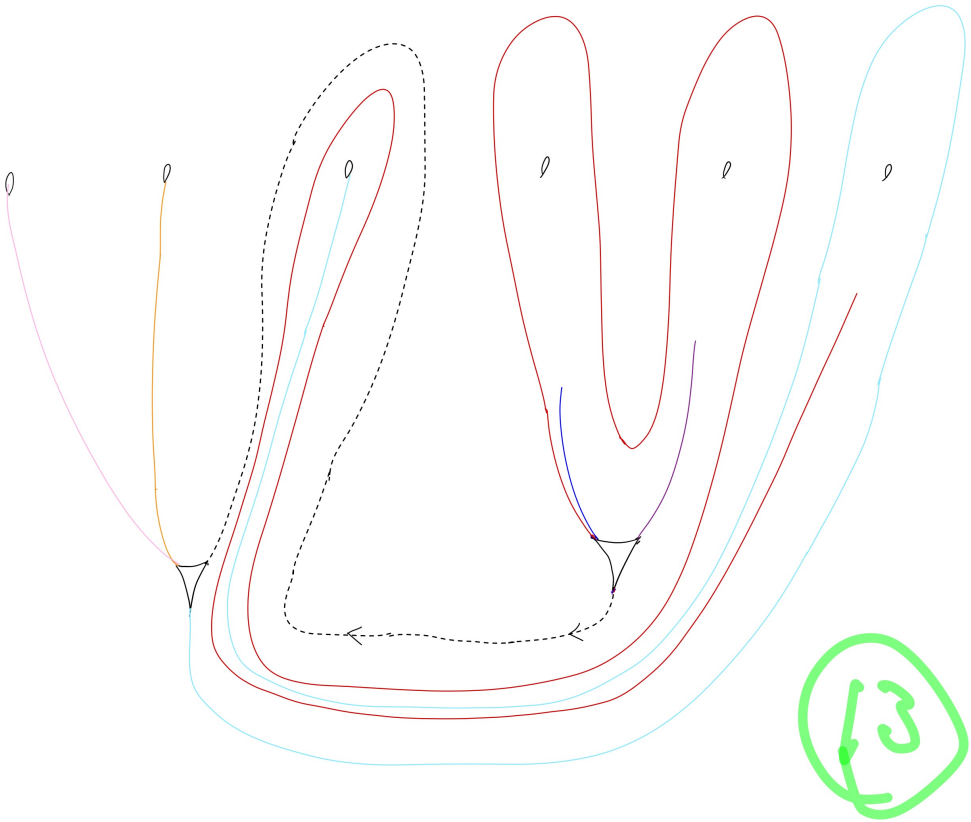


Figure D.270: Treasure1

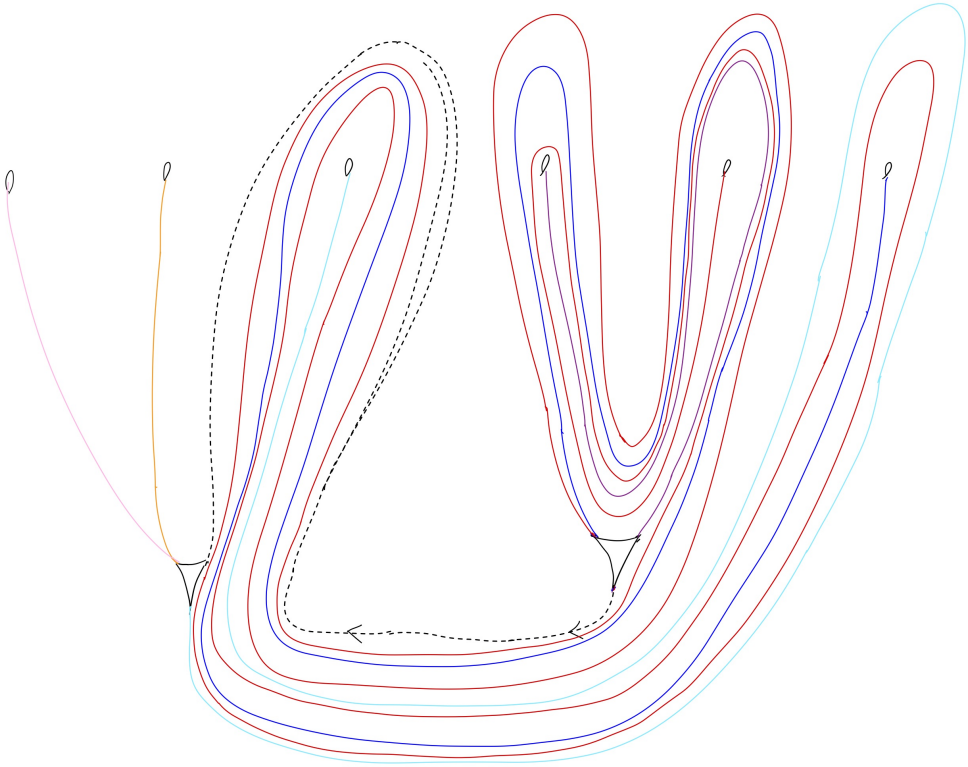


Figure D.271: Treasure2

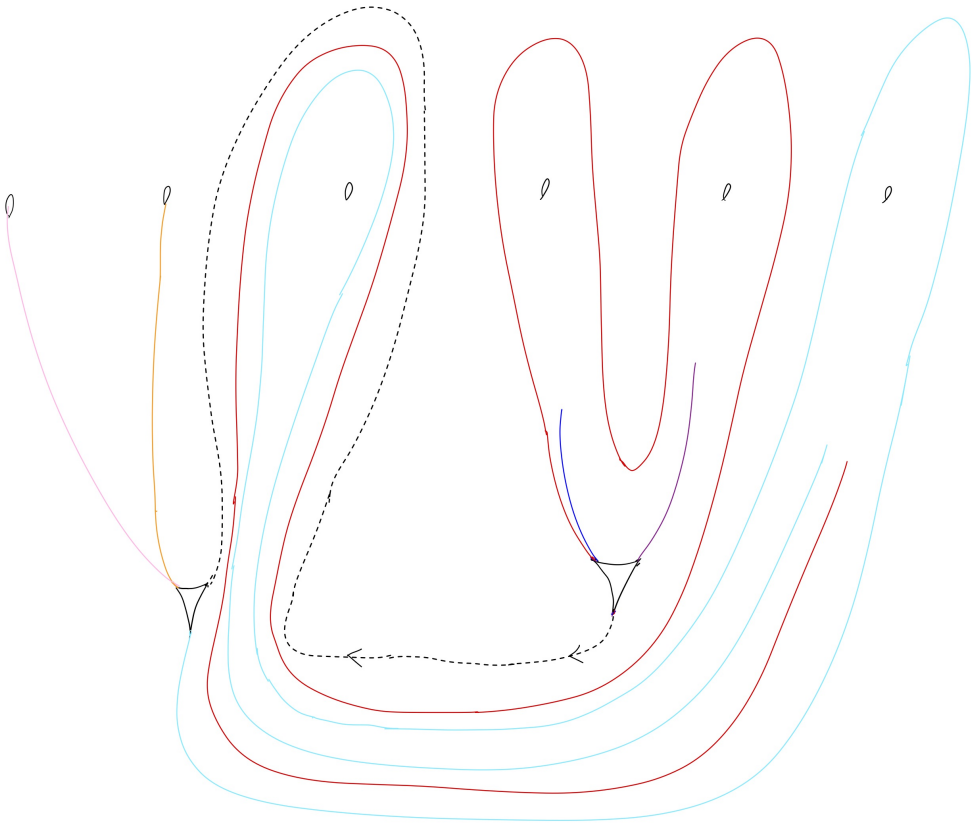


Figure D.272: Education1

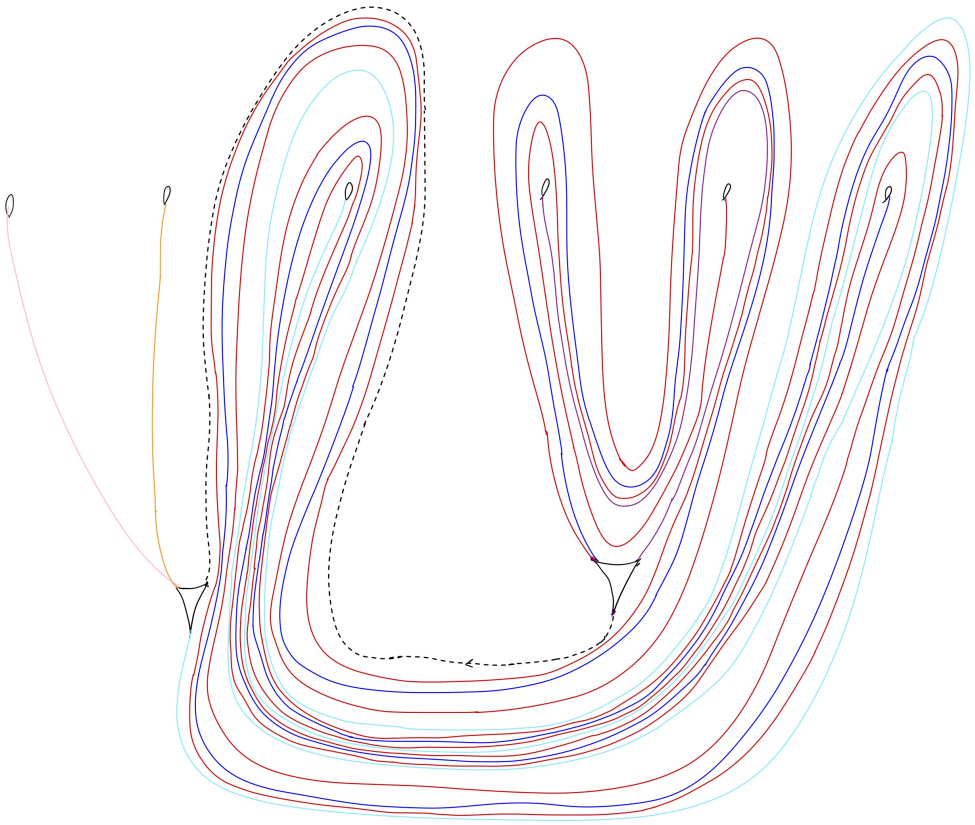


Figure D.273: Education2

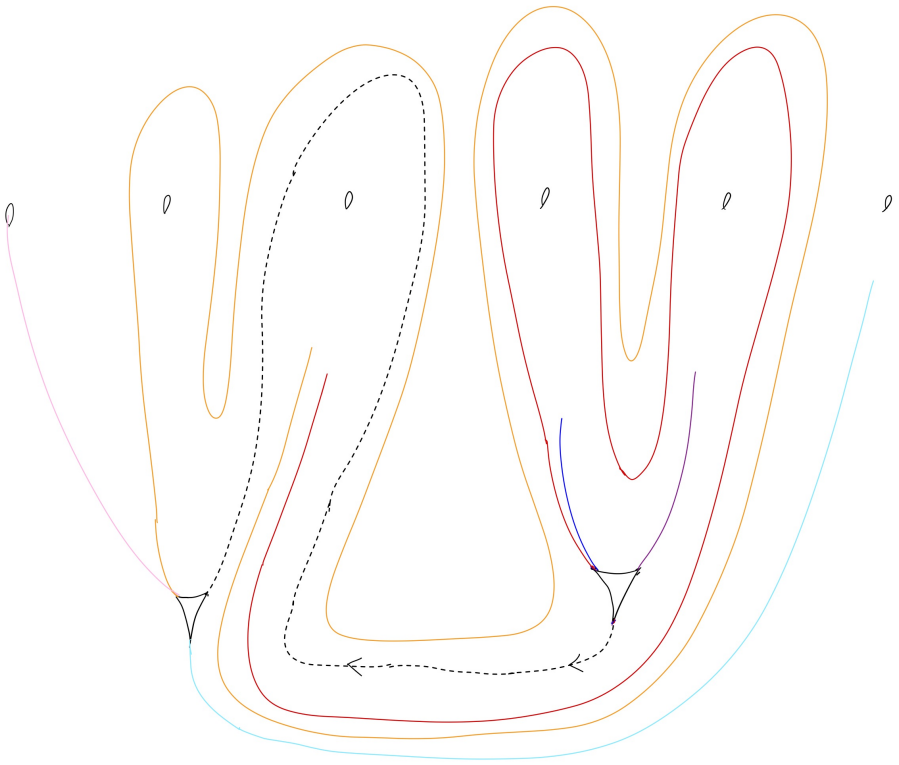


Figure D.274: Hapless1

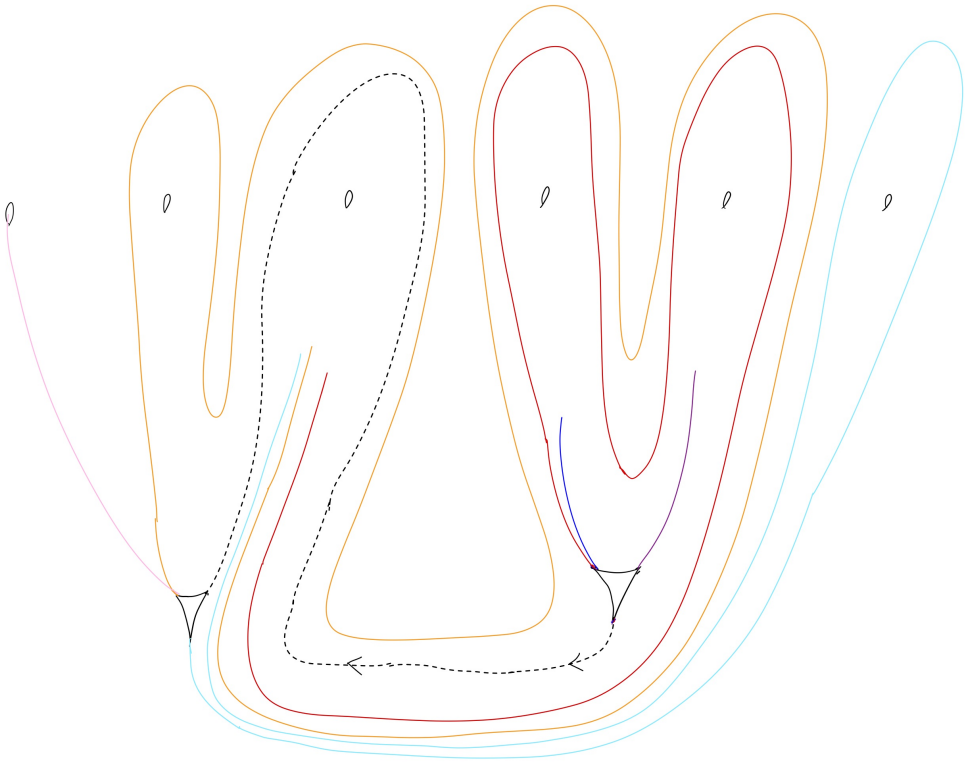


Figure D.275: Hapless2

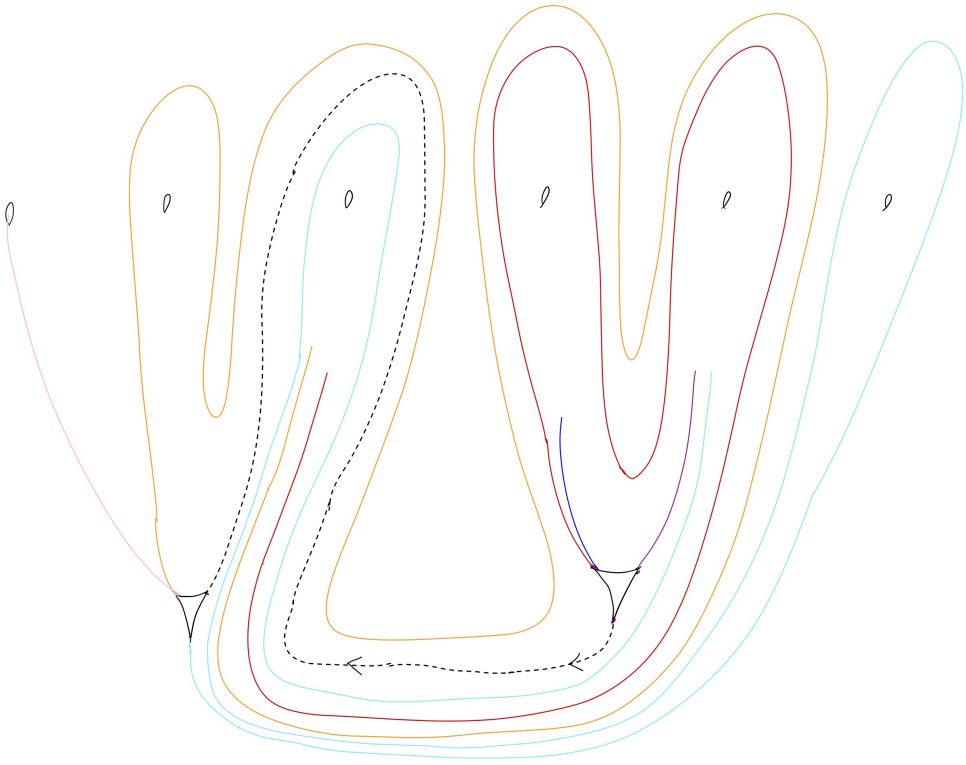


Figure D.276: Hapless3

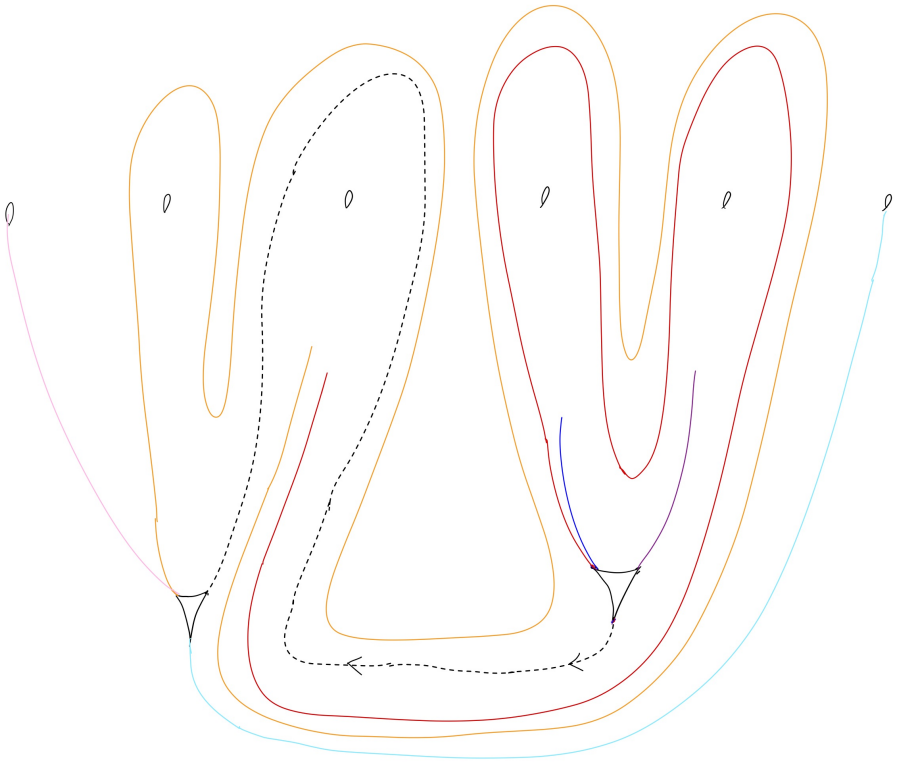


Figure D.277: Hapless4

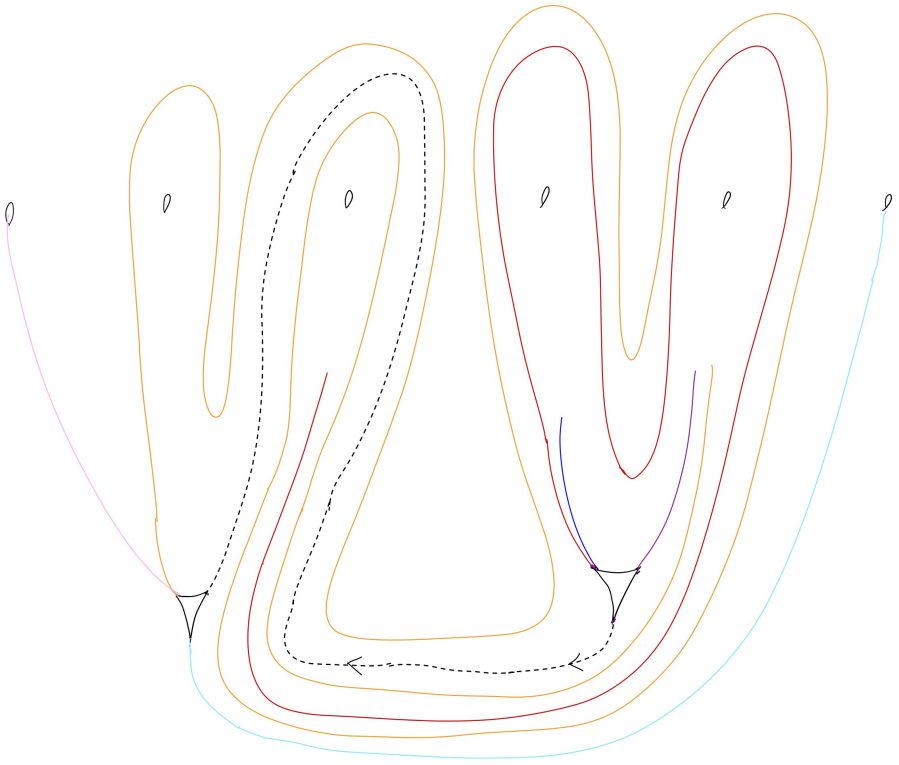


Figure D.278: Hapless5

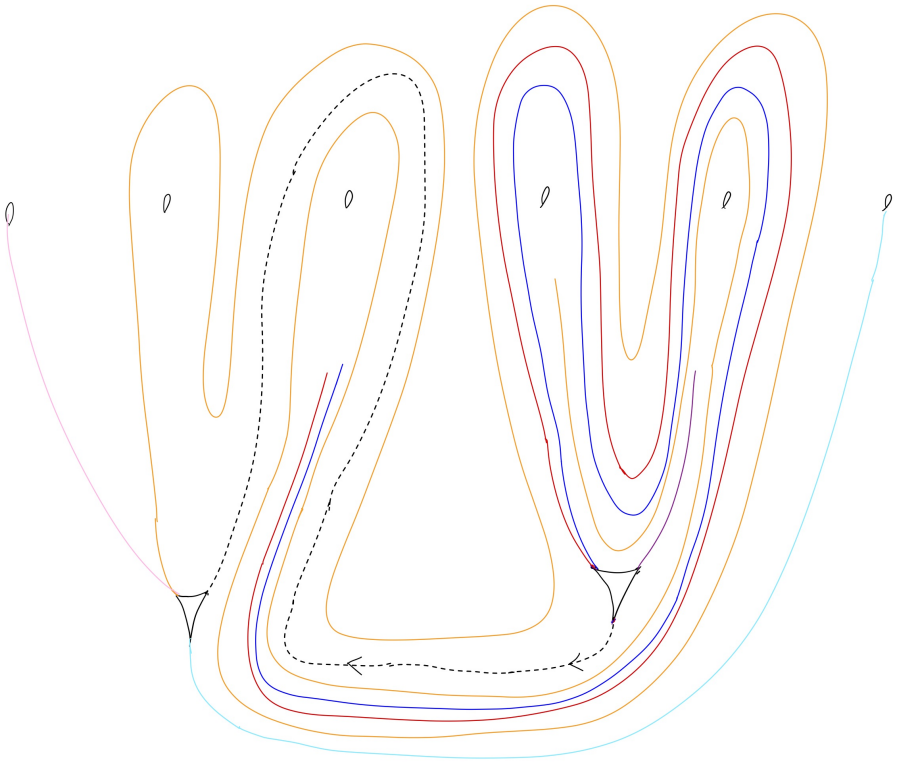


Figure D.279: Hapless6

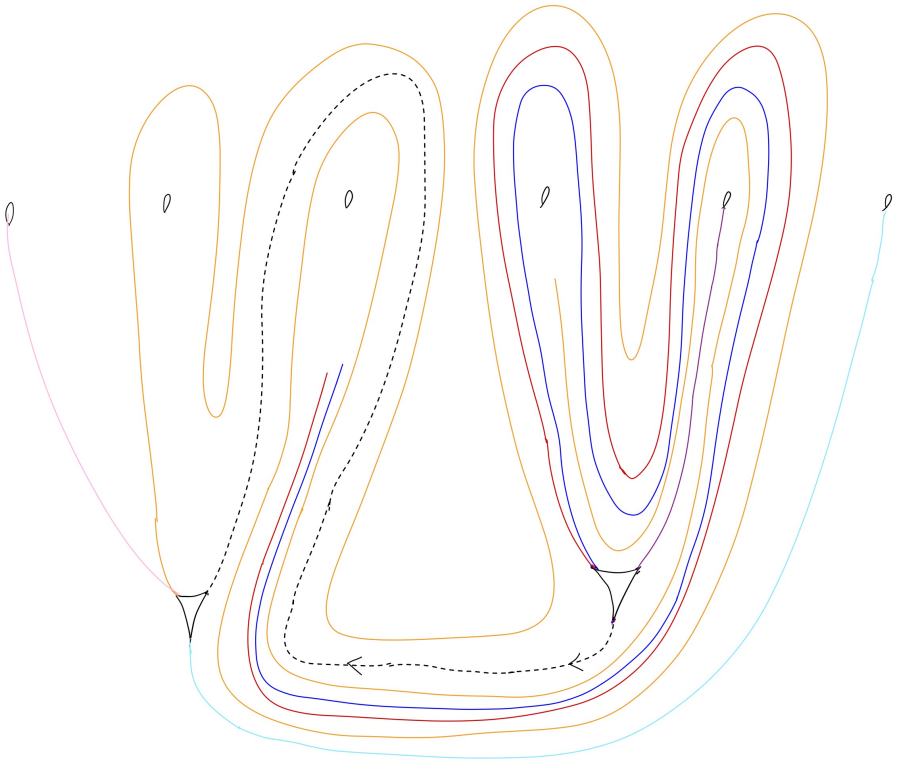


Figure D.280: Hapless7

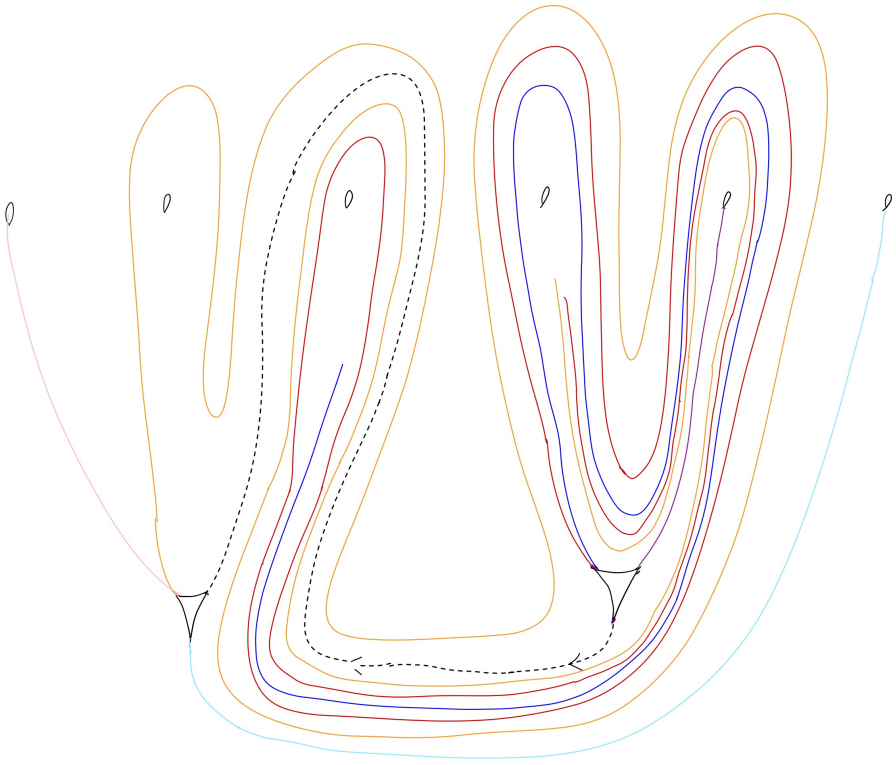


Figure D.281: Hapless8

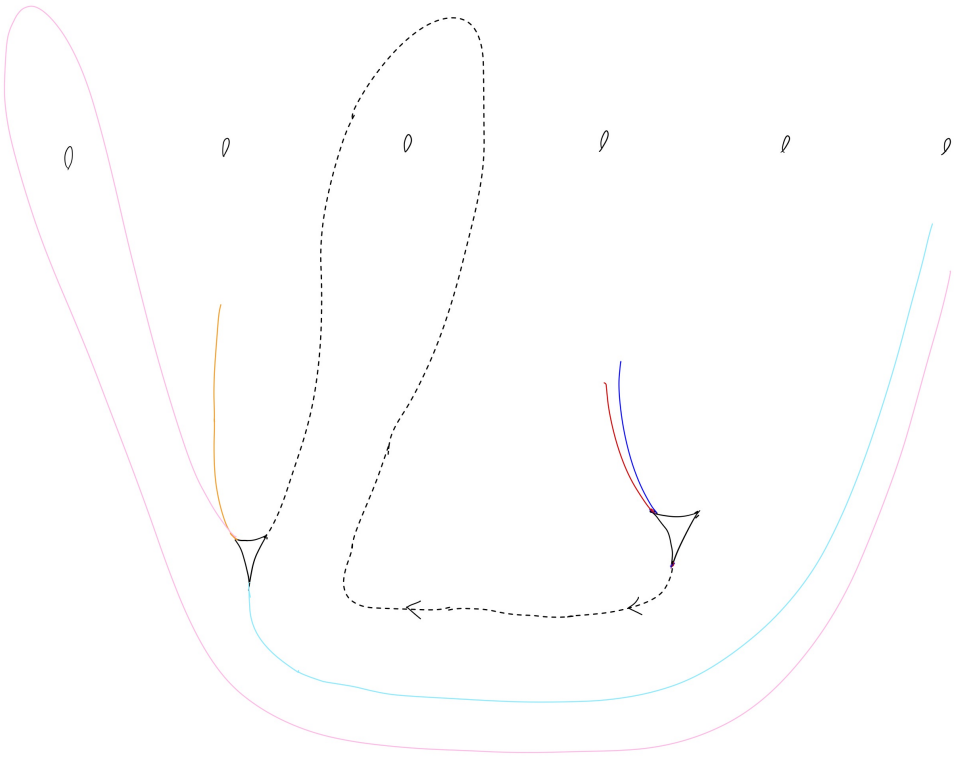


Figure D.282: Unwary1

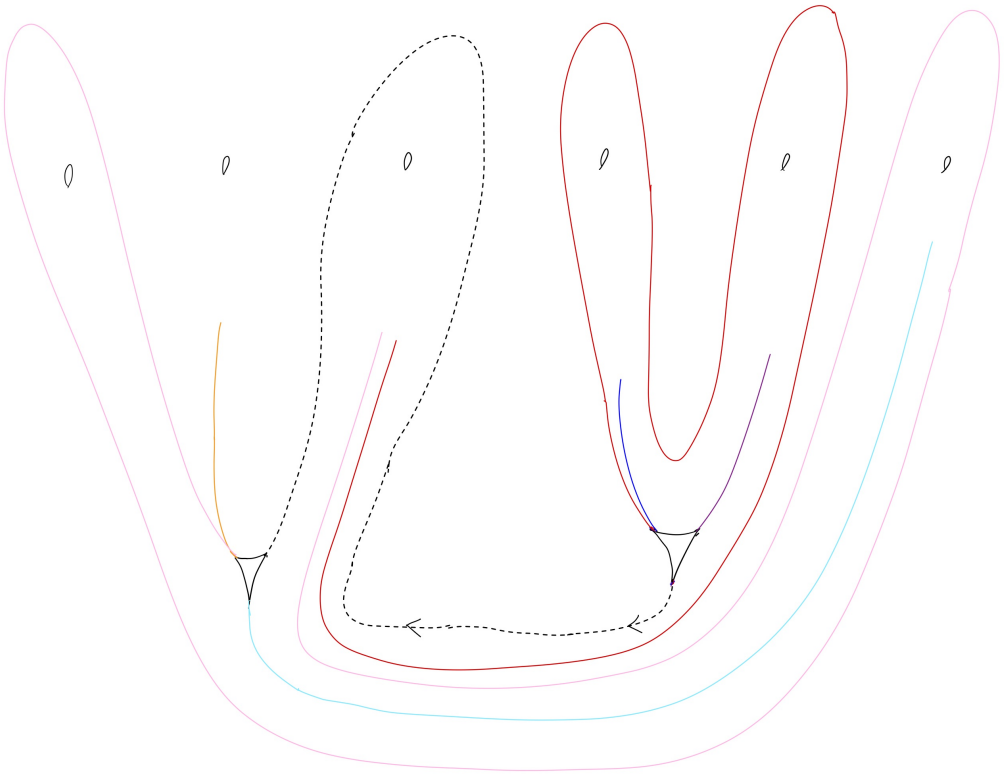


Figure D.283: Unwary2

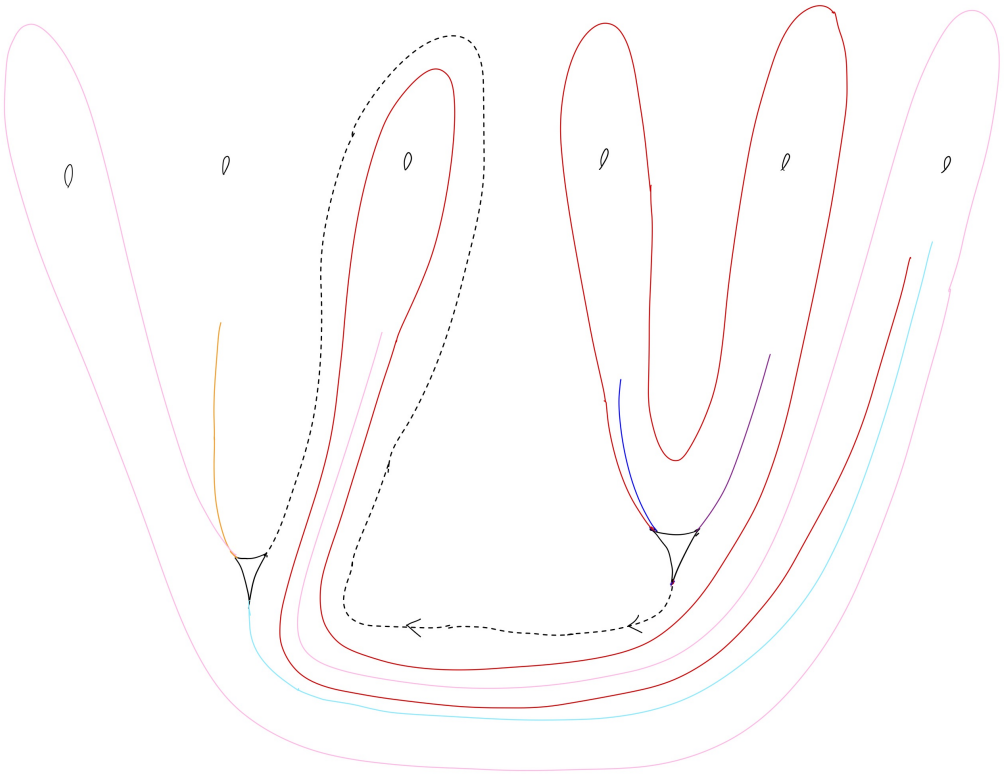


Figure D.284: Unwary3

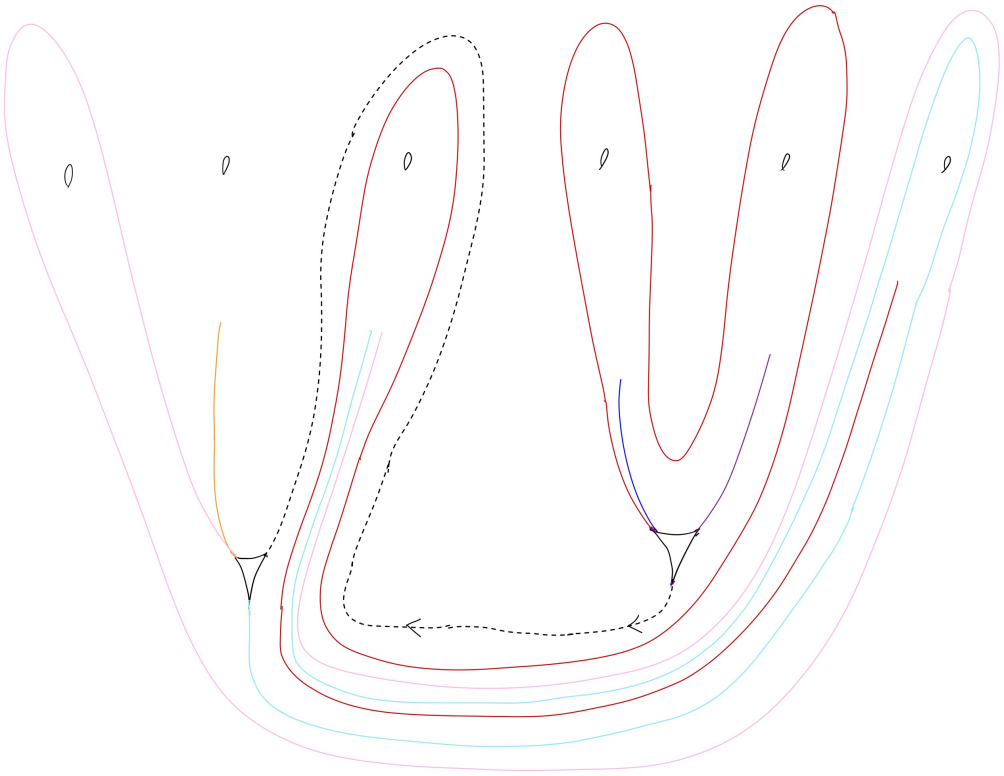


Figure D.285: Unwary4

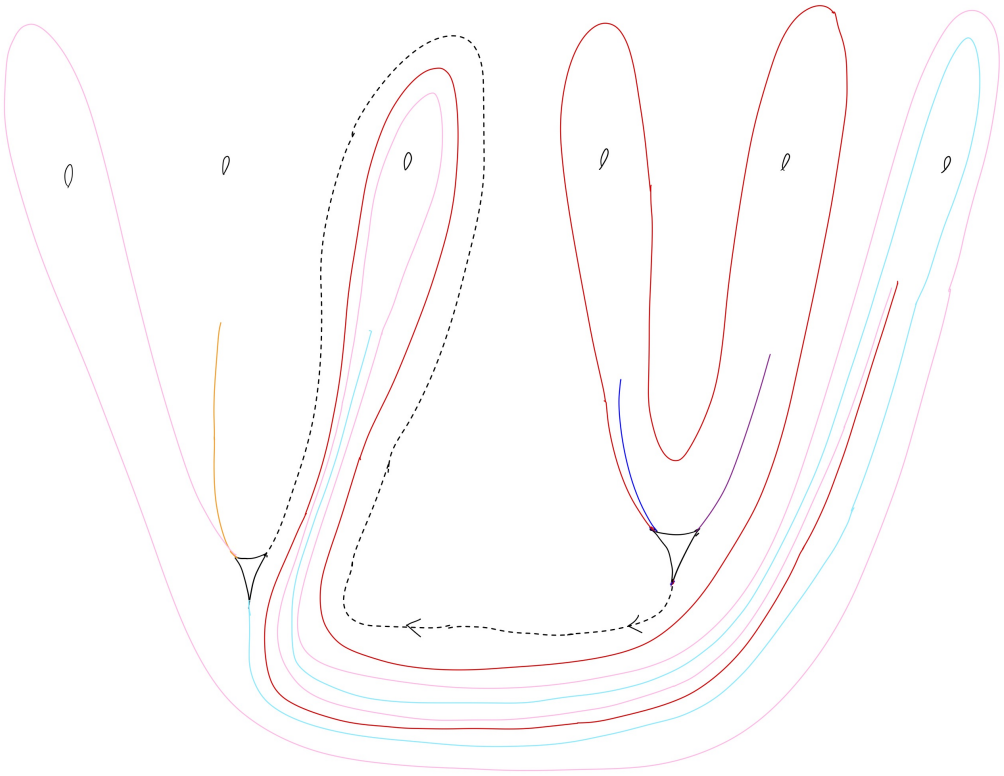


Figure D.286: Unwary5

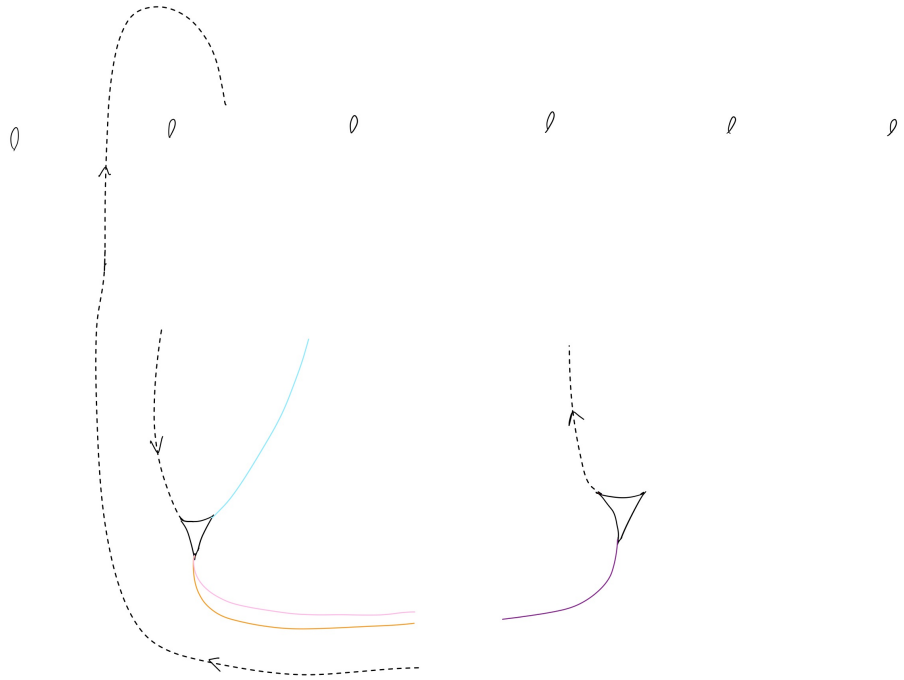


Figure D.287: DXB1

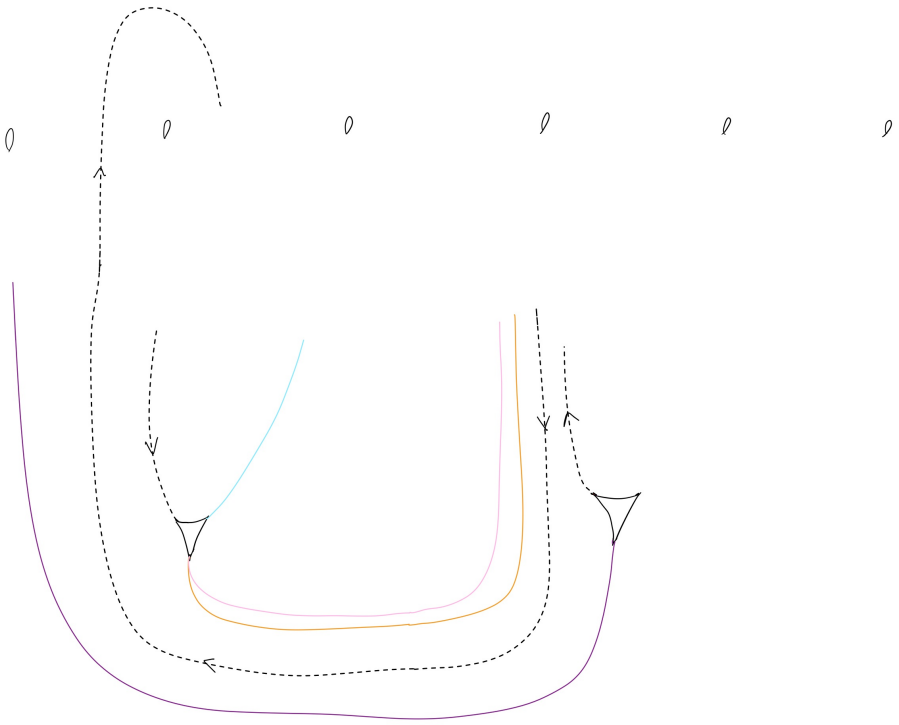


Figure D.288: DXB2

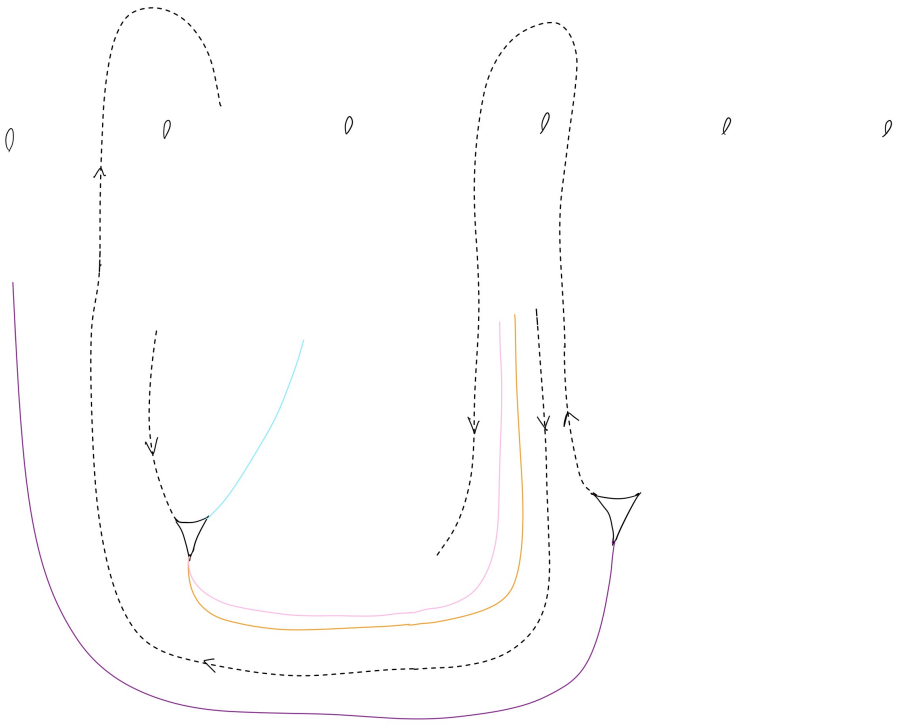


Figure D.289: DXB3

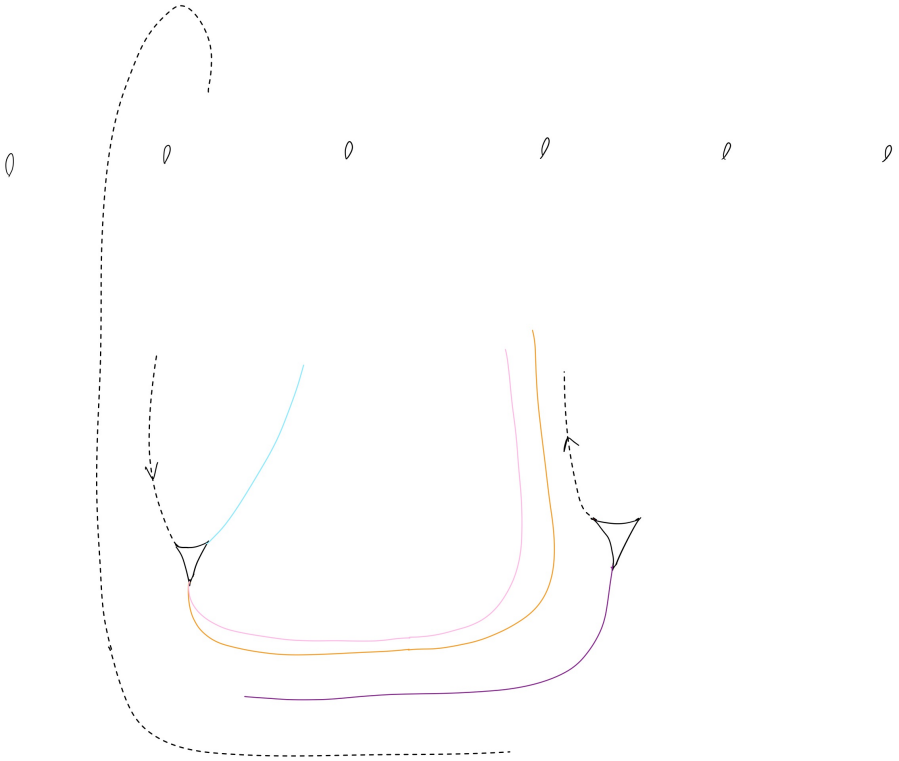


Figure D.290: DXB4

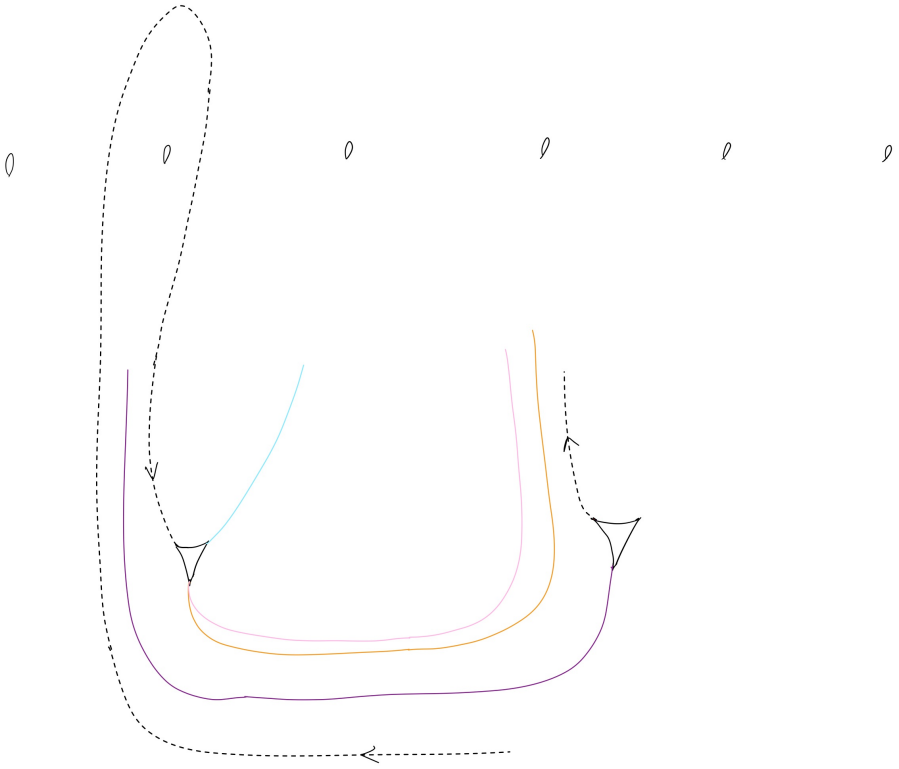


Figure D.291: DXB5

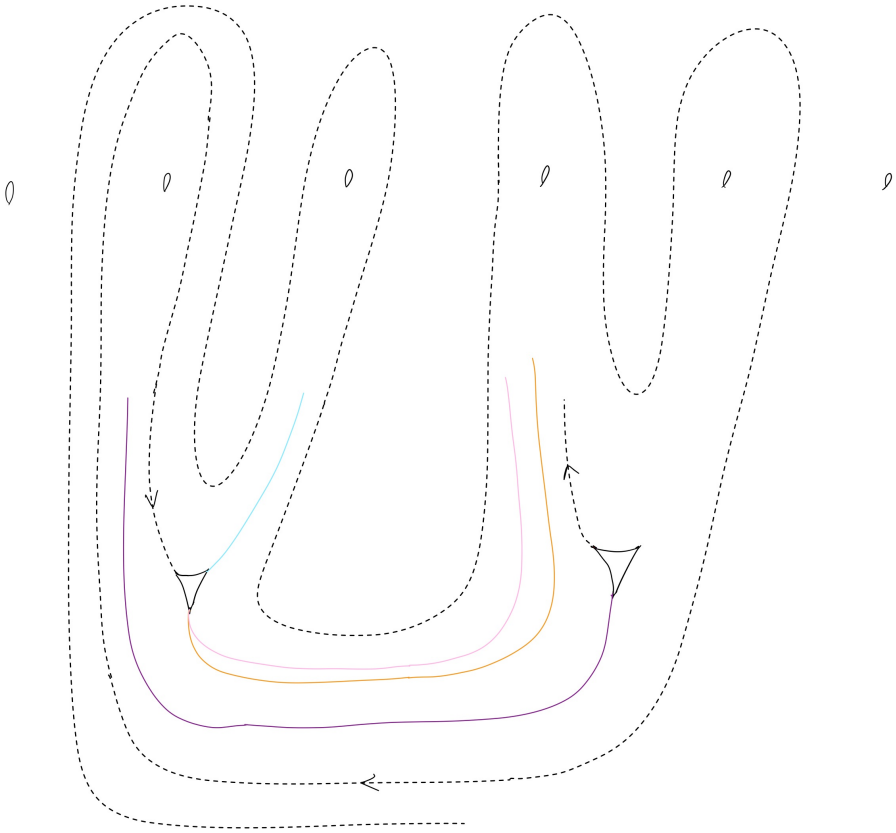


Figure D.292: Zero1

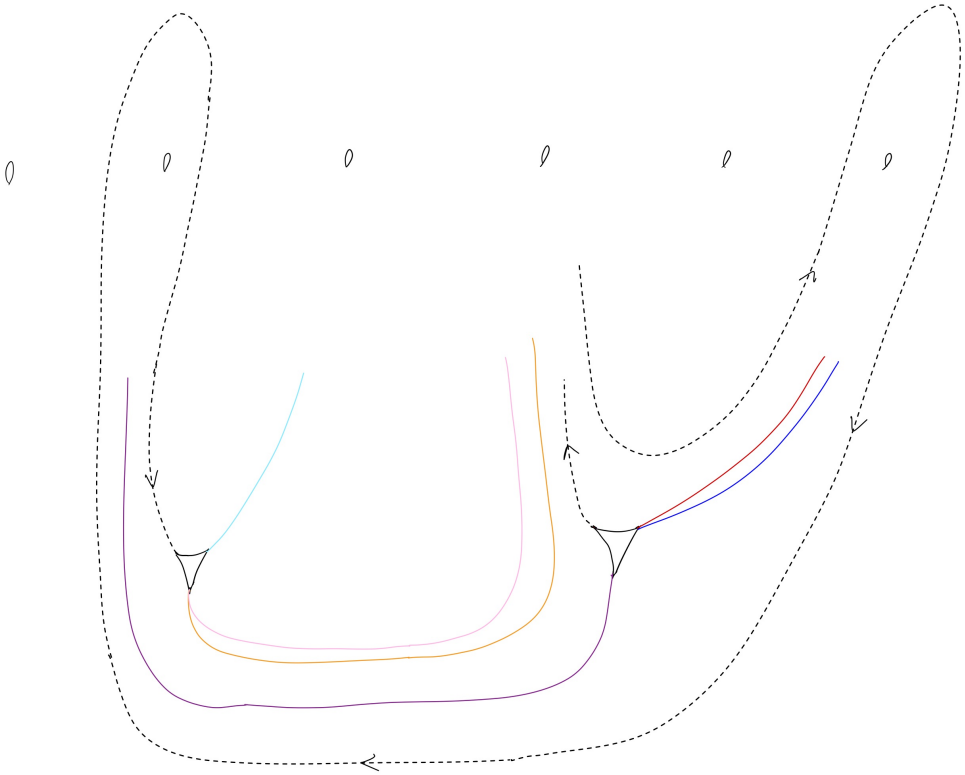


Figure D.293: Dome1

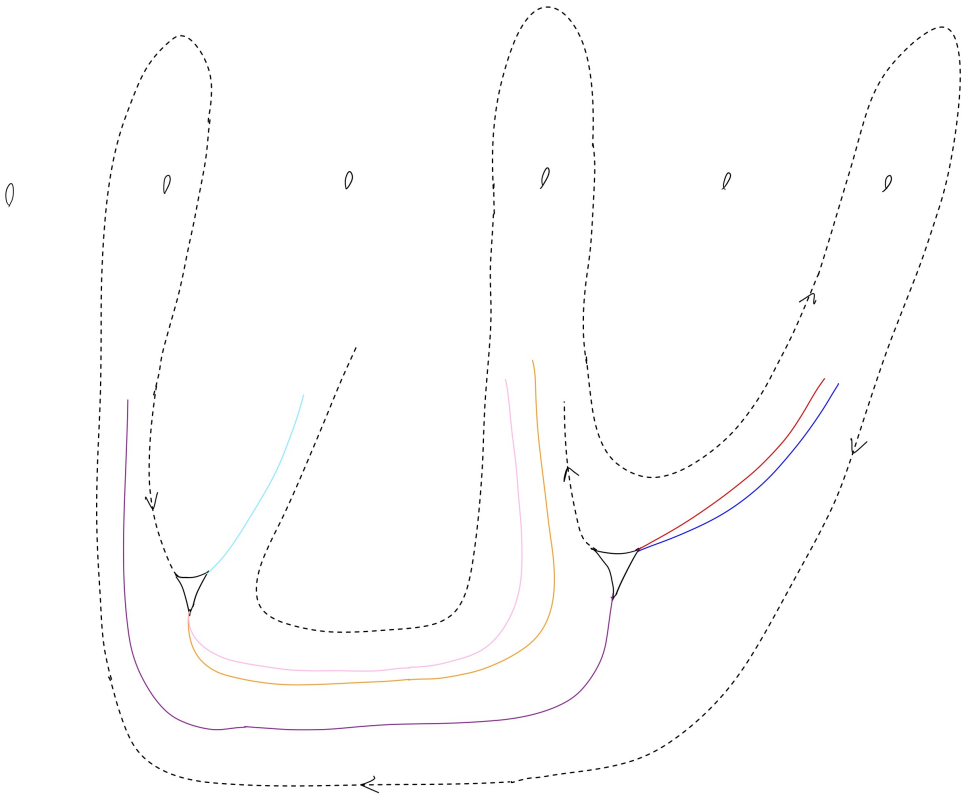


Figure D.294: Dome2

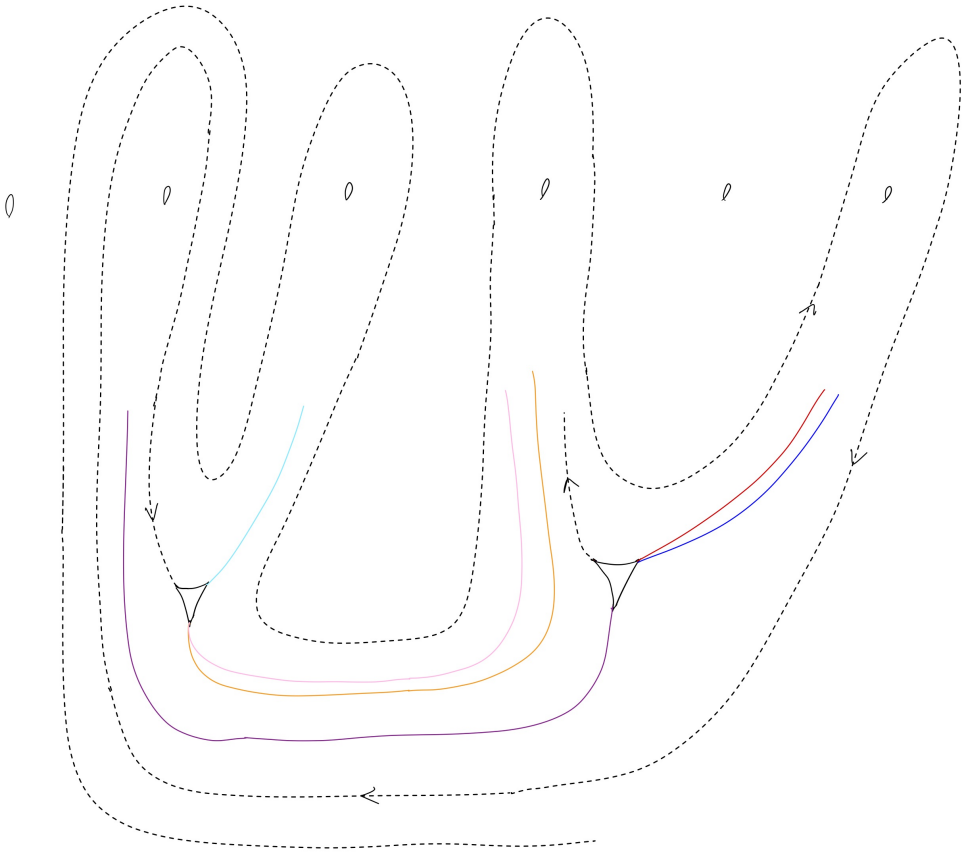


Figure D.295: Dome3

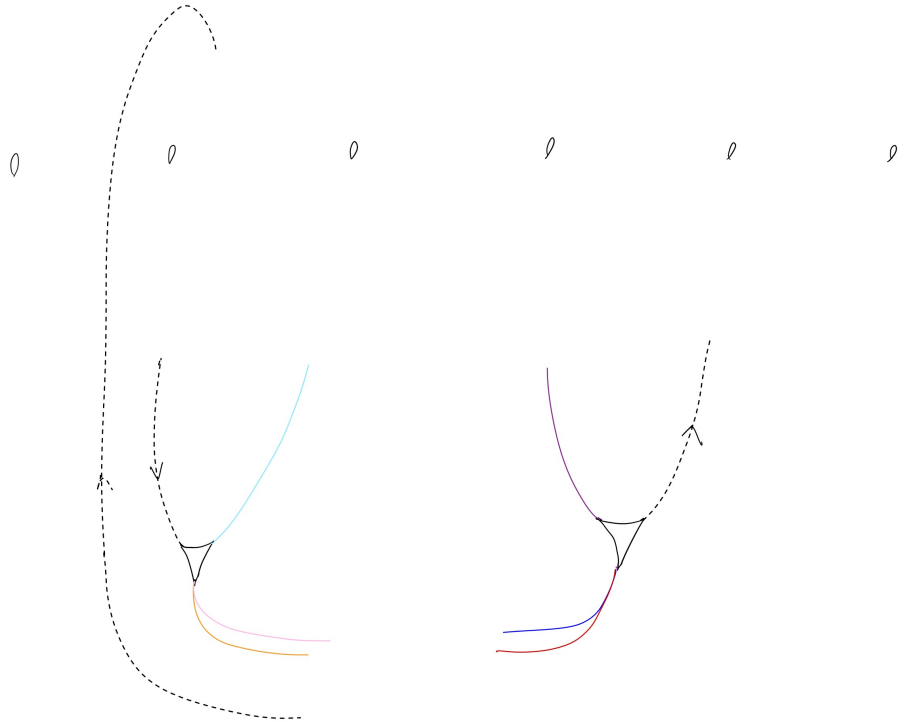


Figure D.296: PHX1

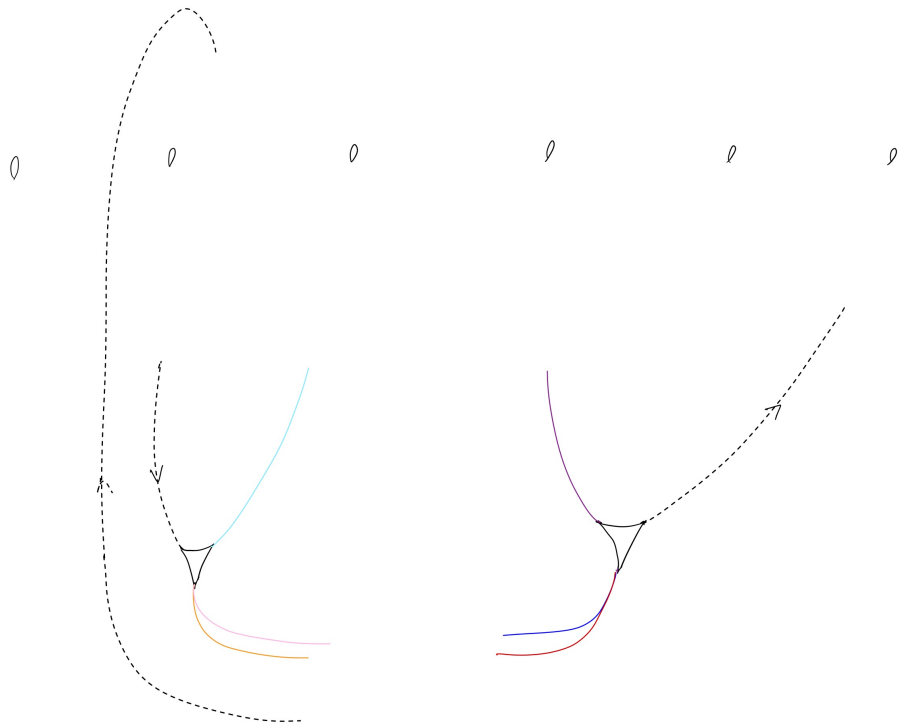


Figure D.297: MIA1

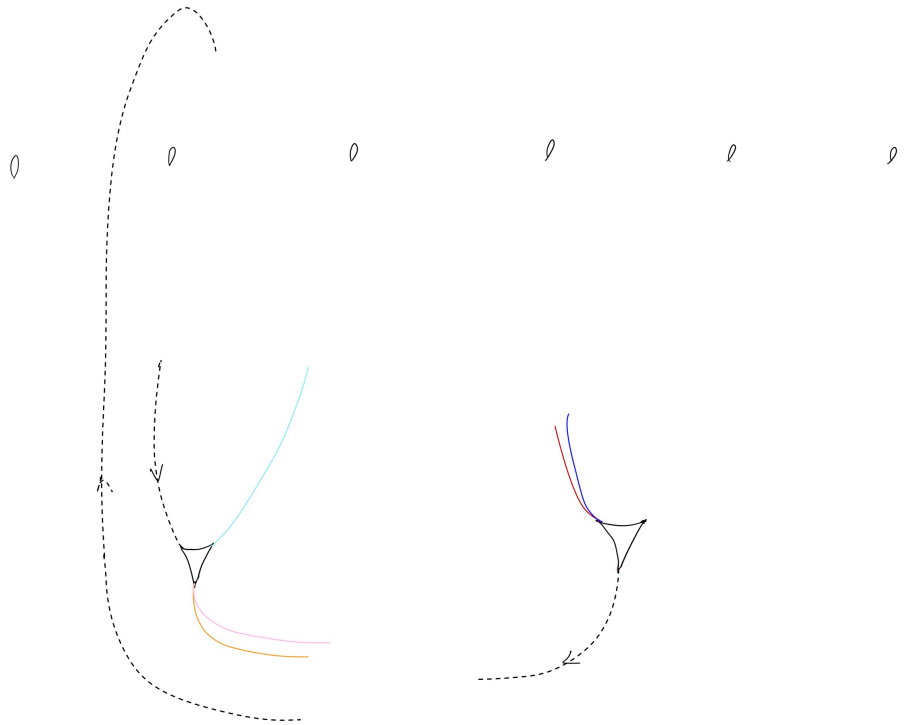


Figure D.298: NRT1

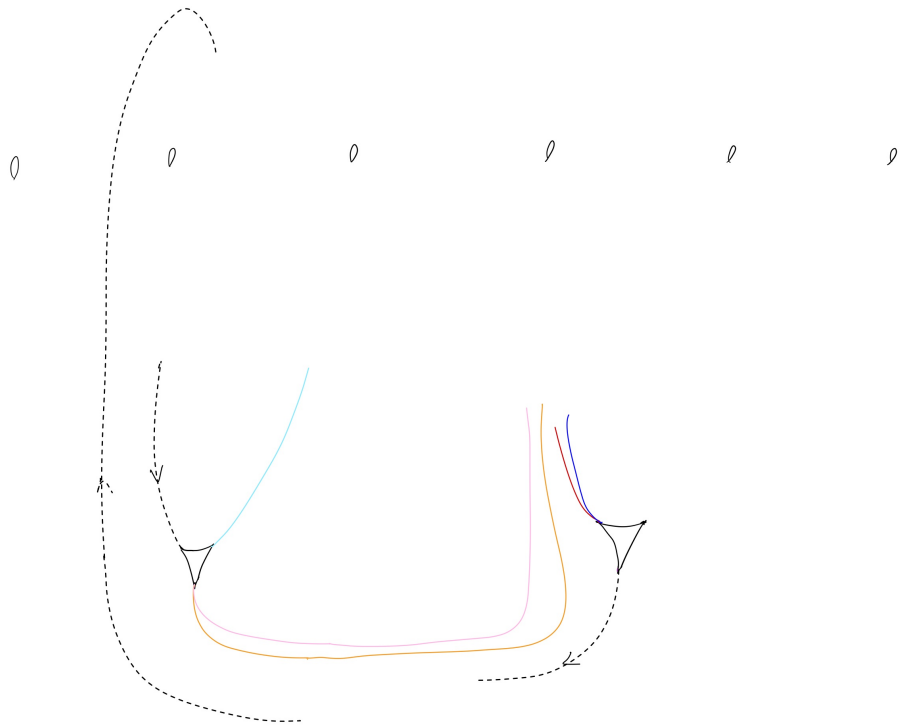


Figure D.299: NRT2

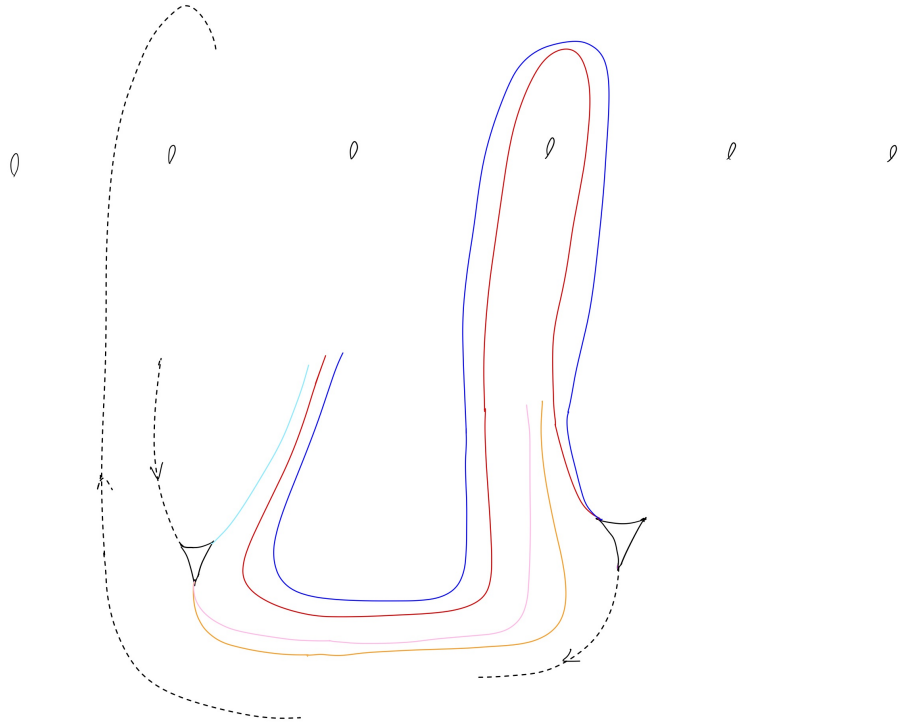


Figure D.300: NRT3

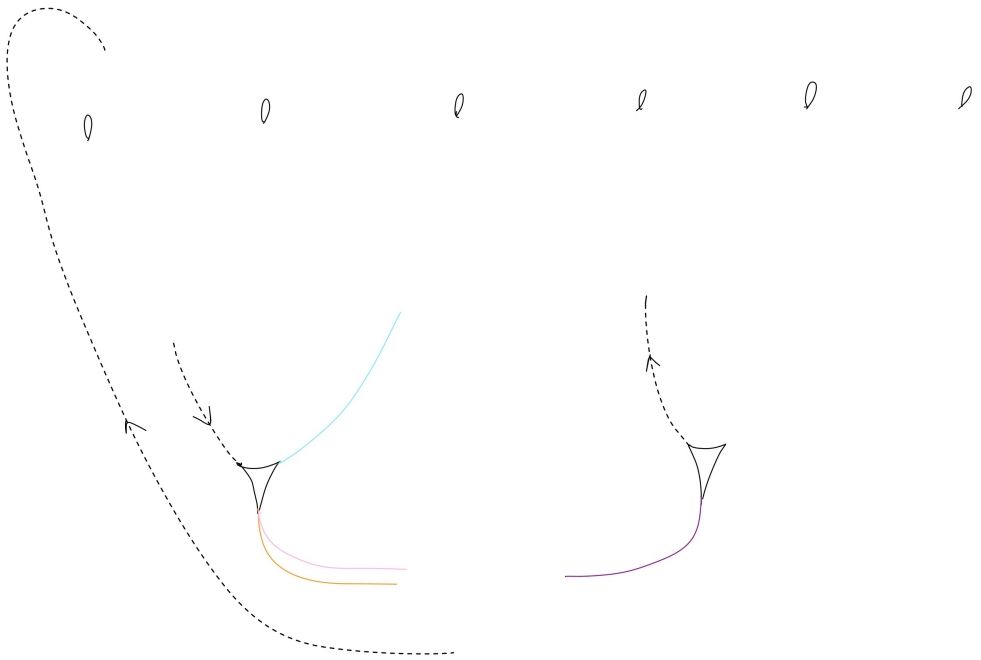


Figure D.301: ARN1

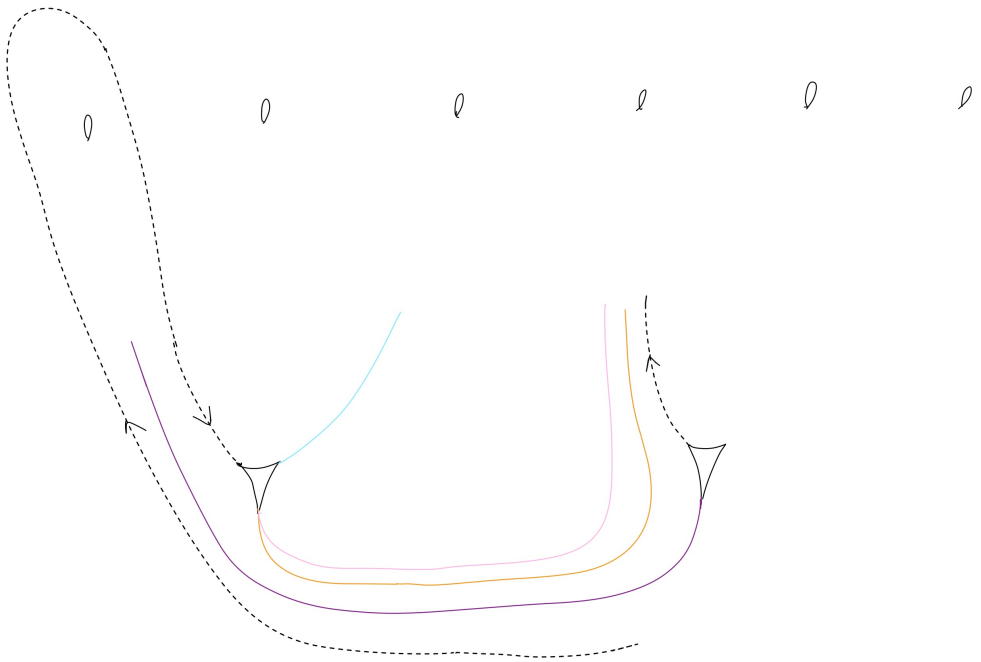


Figure D.302: ARN2

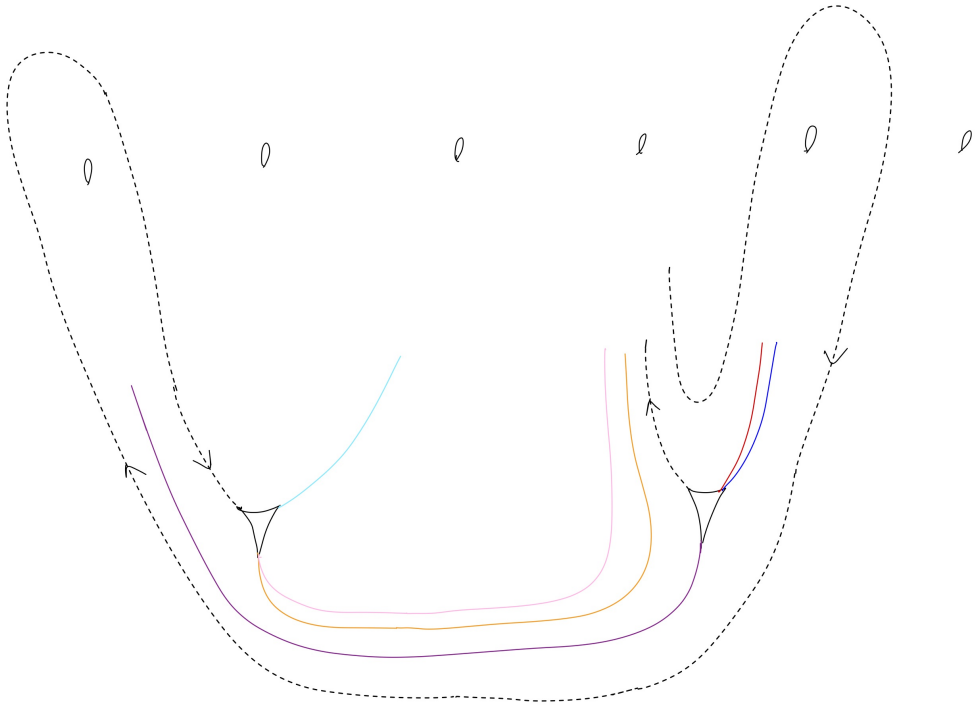


Figure D.303: Corf1

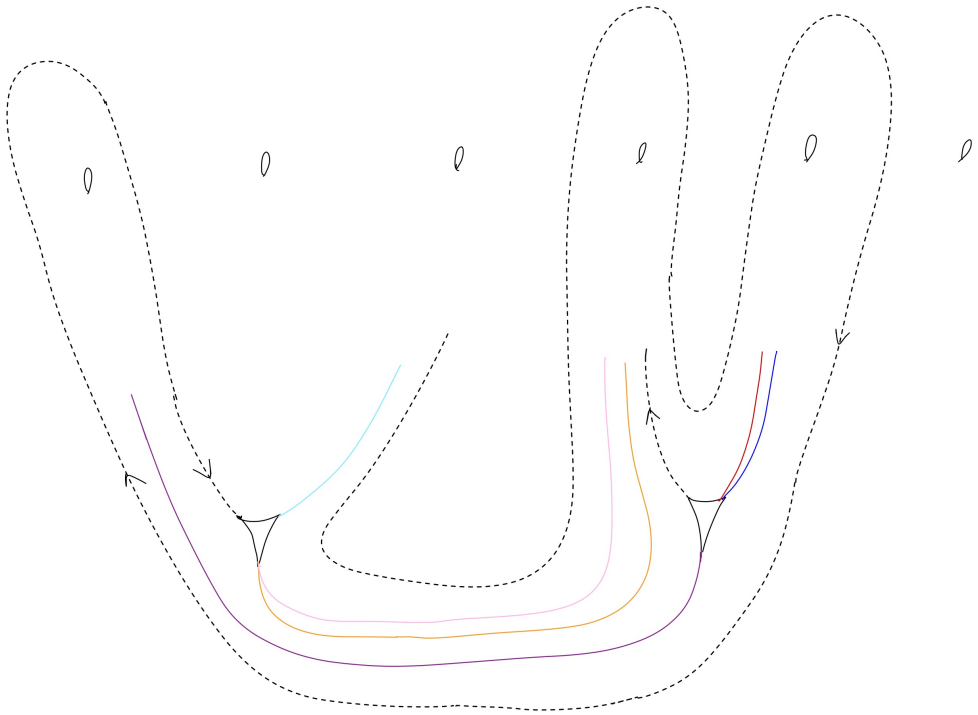


Figure D.304: Corf2

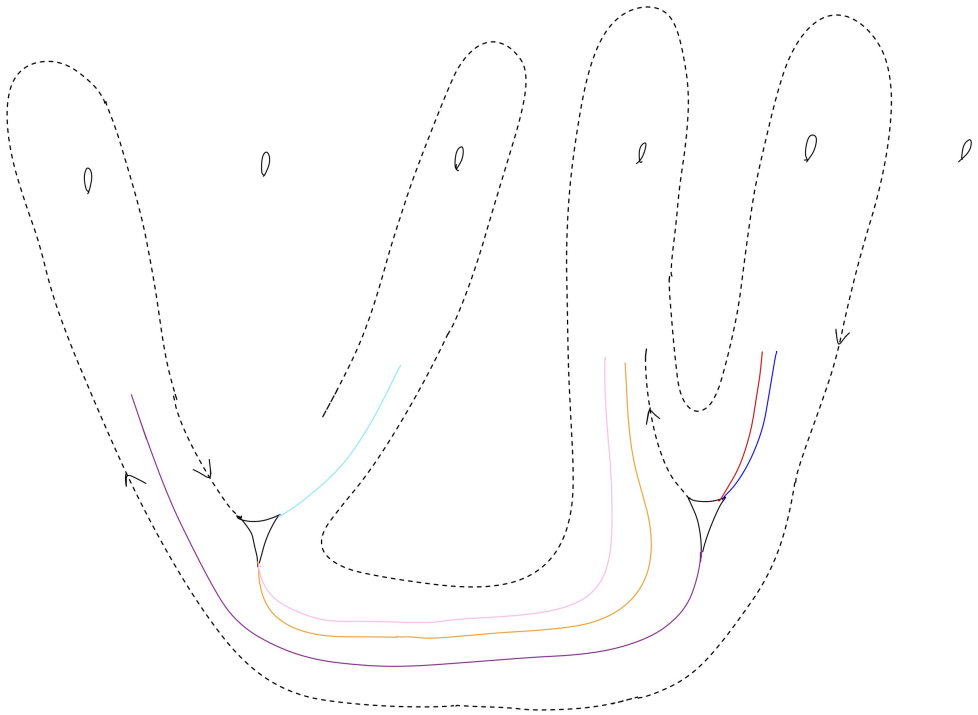


Figure D.305: Corf3

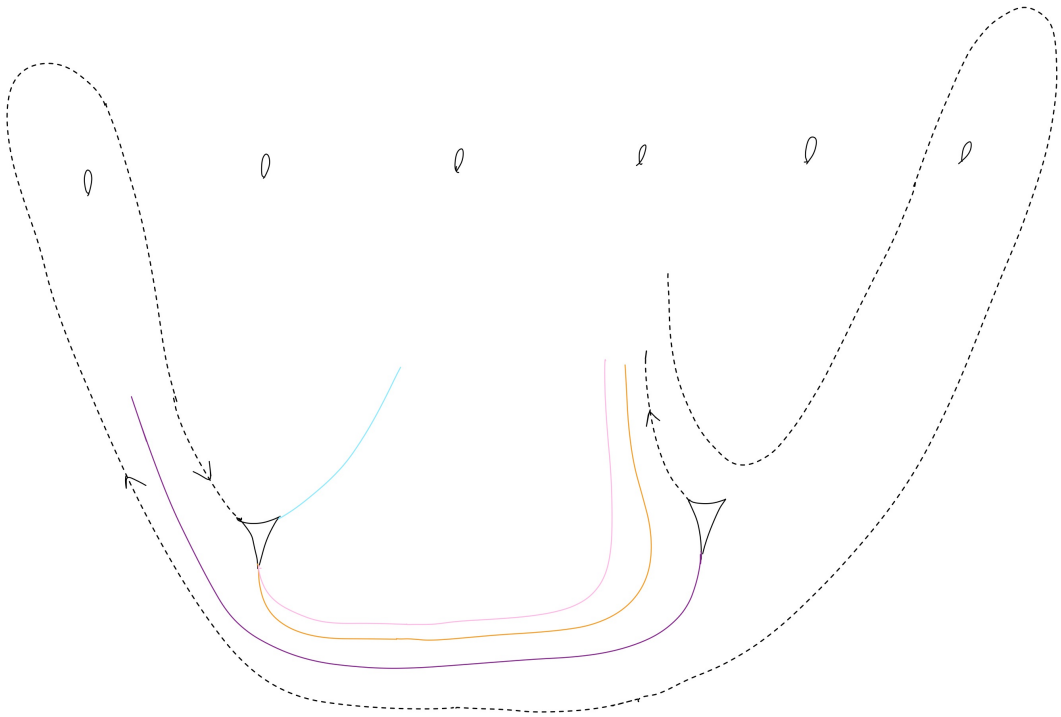


Figure D.306: Woad1

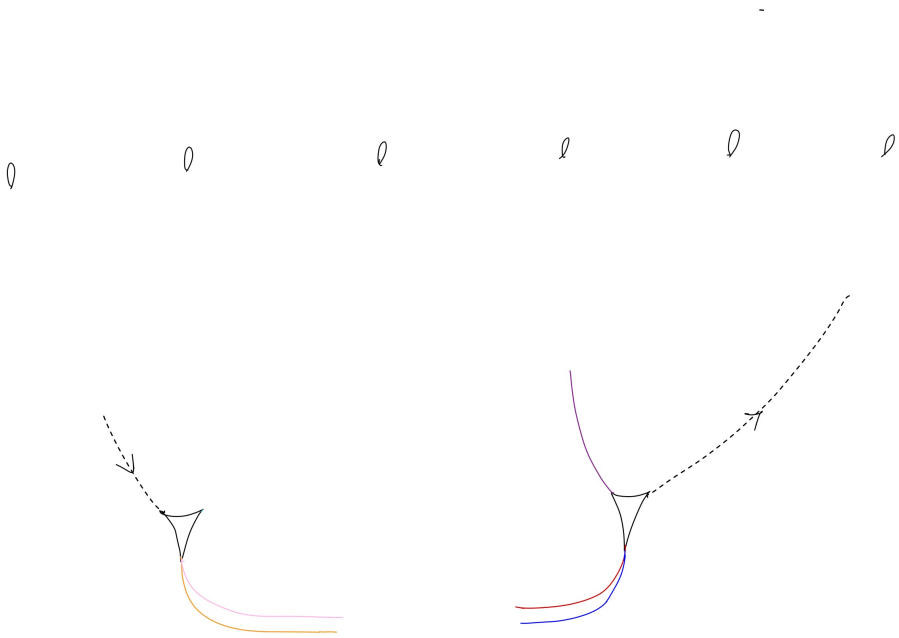


Figure D.307: SIN1

APPENDIX FIVE

Train Track Case Analysis: Track 1

E.1 Case A: Triangles fixed

Let us assume the triangles are fixed by f_β, hence $f_\beta(d)$ and $f_\beta(\bar{d})$ both pass over d or $\bar{d}$ after an even number of letters. We will call this *Assumption A*. We know $f_\beta(d)$ does not start at d or o, as both instances would cause $f_\beta(b)$ and $f_\beta(r)$ to trace. We also know $f_\beta(\bar{d})$ does not start at $\bar{d}$, as that would cause $f_\beta(p)$ and at least one of $f_\beta(s)$ and $f_\beta(i)$ to trace. Therefore, $f_\beta(d)$ must start at b, or r; and $f_\beta(\bar{d})$ must start at i, s, or p.

E.1.1 VIE

Suppose $f_\beta(d)$ starts at b, and $f_\beta(\bar{d})$ starts at i. Then $f_\beta(d)$ must start with b^-, as starting with b^+ would force the next letter to be d, thereby violating Assumption A. In addition, Assumption A necessitates that $f_\beta(d)$ eventually crossing d right after r^-, possibly after some twisting between b, o, and r. This is because it is impossible to cross over d right after b after an even number of letters, assuming that $f_\beta(d)$ starts at b.

This is Figure E.1.

But here notice that if there were in fact initial twists by $f_\beta(\bar{d})$, it must be of the form

$f_\beta(d) = b^- r^+ b^* ...$, which would mean that it takes $f_\beta(b)$ with it and therefore cause it to trace. Thus $f_\beta(d)$ cannot have initial twists.

Consider $f_\beta(\bar{d})$. It must start with i^+ to not violate Assumption A. The next letter must then be p^*. So we have

$$f_\beta(\bar{d}) = i^+ p^* ...$$

It must also cross $\bar{d}$ right after p^+ to not violate Assumption A as well. Similar to the situation for $f_\beta(d)$ above, suppose that $f_\beta(\bar{d})$ were to have initial twists before $...p^+\bar{d}...$, in this case they would be twists between p, s, or i. Then it must be of the form $f_\beta(\bar{d}) = i^+ p^- ...$, and the next letter is s^* or i^*. However, this forces $f_\beta(s)$ and $f_\beta(i)$ to start with p^- and then to s^* or i^* together, thereby tracing. This is a contradiction. Thus $f_\beta(\bar{d})$ cannot have initial twists.

This is Figure E.2.

Consider $f_\beta(r)$. It can start with d or o. If it were to start with d, then it can either do so while going above $f_\beta(p)$ or below $f_\beta(p)$. If it went above $f_\beta(p)$, then $f_\beta(p)$ will trace:

$$f_\beta(p) = \bar{d} b^- r^- d p^\times$$

If instead $f_\beta(r)$ were to go below $f_\beta(p)$, then itself would trace:

$$f_\beta(r) = d i^+ p^+ \bar{d} r^\times$$

Therefore, $f_\beta(r)$ cannot start with d, so it must start with o. In fact, it must start and end there immediately:

$$f_\beta(r) = o^\circ$$

Indeed, if it did not and started with o^+ instead, then it will trace:

$$f_\beta(r) = o^+ r^\times$$

Similarly if it started with o^-:

$$f_\beta(r) = o^- b^- r^\times$$

This is Figure E.3.

Here if the dotted lines can join, or if they do not, $f_\beta(d)$ on the left can go either below or above $f_\beta(\bar{d})$ on the right.

E.1.1.1 Iris

Suppose the dotted lines join in the middle.

This is Figure E.4.

Consider $f_\beta(b)$. We can either have

$$f_\beta(b) = r^\circ$$

or

$$f_\beta(b) = r^- ...$$

E.1.1.1.1 Flute

Suppose

$$f_\beta(b) = r^\circ$$

This forces $f_\beta(p)$ to continue with $r+$:

$$f_\beta(p) = \bar{d}\hat{r}^+ b^* ...$$

This forces $f_\beta(o)$ to start with b^- and to the right of $f_\beta(p)$. Otherwise, $f_\beta(p)$ will be forced to continue with b^+, and be absorbed between $f_\beta(d)$ and $f_\beta(o)$. Thus we must have

$$f_\beta(o) = b^- r^- dp^* ...$$

This is Figure E.5.

Here $f_\beta(o)$ must continue with p^- and to the right of $f_\beta(s)$ and $f_\beta(i)$. Otherwise, $f_\beta(s)$ and $f_\beta(i)$ will be forced to start with p^+ and to the left of $f_\beta(o)$, in which case they will be absorbed between $f_\beta(d)$ and $f_\beta(o)$:

$$f_\beta(s) = f_\beta(i) = p^+ \bar{d} r^+ b^+ \,\mathrm{Abso}(f_\beta(d), o)^\times$$

Thus we must have:

$$f_\beta(o) = b^- r^- d\hat{p}^- i^* ...$$

This is Figure E.6.

Here $f_\beta(i)$ can start and end at p°, or it can start with p^+. It cannot start with p^- as that would cause it to trace immediately.

Suppose

$$f_\beta(i) = p^\circ$$

Then this forces

$$f_\beta(s) = p^- i^* ...$$

This is Figure E.7.

Consider $f_\beta(o)$. If it continued with i° or i^+, then $f_\beta(s)$ is forced to continue with i^+ and to the left of $f_\beta(o)$. But then $f_\beta(s)$ will be absorbed:

$$f_\beta(s) = p^- \hat{i}^+ p^+ \bar{d} r^+ b^+ \operatorname{Abso}(f_\beta(d), f_\beta(o))^\times$$

On the other hand, if $f_\beta(o)$ were to continue with i^-, then if it did so to the left of $f_\beta(s)$ then $f_\beta(s)$ will still be absorbed in the same manner; but if $f_\beta(o)$ went to the right of $f_\beta(s)$, it will be absorbed itself:

$$f_\beta(o) = b^- r^- d p^- \hat{i}^- p^+ \operatorname{Abso}(f_\beta(s), f_\beta(i))^\times$$

This is a contradiction. Thus in the situation depicted in Figure E.6, $f_\beta(i)$ cannot start and end at p°. So suppose instead it starts with p^+. Then we have

$$f_\beta(i) = p^+ \bar{d} r^+ b^* ...$$

This is Figure E.8.

Here $f_\beta(i)$ must continue with b^+ and to the right of $f_\beta(p)$. Otherwise, $f_\beta(p)$ will be forced to continue with b^- and to the right of $f_\beta(i)$, in which case it will trace:

$$f_\beta(p) = \bar{d} r^+ \hat{b}^- r^- d p^\times$$

Thus we must have:

$$f_\beta(i) = p^+ \bar{d} r^+ \hat{b}^+ r^- ...$$

This is Figure E.9.

Here $f_\beta(i)$ can continue with d or o^-. If it were to continue with d, it will trace:

$$f_\beta(i) = p^+ \bar{d} r^+ b^+ r^- \hat{d} i^\times$$

Thus it must continue with o^-:

$$f_\beta(i) = p^+ \bar{d} r^+ b^+ r^- \hat{o}^- b^- r^- d p^- s^* ...$$

This is Figure E.10.

Here consider $f_\beta(p)$. It must end here at b°. Indeed, if it were to continue with b^+, it will trace:

$$f_\beta(p) = \bar{d} r^+ \hat{b}^+ r^- d i^+ p^\times$$

or

$$f_\beta(p) = \bar{d} r^+ \hat{b}^+ r^- b^- b^- r^- d p^\times$$

On the other hand, if it were to continue with b^-, it also traces:

$$f_\beta(p) = \bar{d} r^+ \hat{b}^- r^- d p^\times$$

Thus we must have

$$f_\beta(p) = \bar{d} r^+ \hat{b}^\circ$$

Consider $f_\beta(o)$. It must end here at i°. Indeed, if instead it were to continue with i^+, then:

$$f_\beta(o) = b^- r^- dp^- \hat{i}^+ p^+ \bar{d}r^+ b^+ \,\mathrm{Abso}(f_\beta(d), f_\beta(o))^\times$$

While if instead it were to continue with i^-, we have:

$$f_\beta(o) = b^- r^- dp^- \hat{i}^- p^+ \bar{d}r^+ b^+ r^- o^\times$$

Thus we must have

$$f_\beta(o) = b^- r^- dp^- \hat{i}^\circ$$

This is Figure E.11.

Here let us consider $f_\beta(s)$. It must start and end at p°. Indeed, if it were to start with p^+, then it continues, either

$$f_\beta(s) = \hat{p}^+ \bar{d}r^+ b^+ r^- di^+ p^+ \bar{d}r^+ b^+ o^+ r^+ b^- r^- dp^- i^+ p^+ \bar{d}r^+ b^+ \,\mathrm{Abso}(f_\beta(d), f_\beta(o))^\times$$

or

$$f_\beta(s) = \hat{p}^+ \bar{d}r^+ b^+ r^- o^- b^- r^- dp^- s^\times$$

Hence we must have

$$f_\beta(s) = p^\circ$$

This is Figure E.12.

Here we claim that $f_\beta(i)$ must end at s°. Indeed, suppose it were to continue with s^+, then

$$f_\beta(i) = p^+ \bar{d}r^+ b^+ r^- o^- b^- r^- dp^- \hat{s}^+ p^+ \bar{d}r^+ b^+ o^+ r^+ b^- r^- dp^- \operatorname{Abso}(f_\beta(s), f_\beta(i))^\times$$

While if it were to continue with s^-, we have

$$f_\beta(i) = p^+ \bar{d}r^+ b^+ r^- o^- b^- r^- dp^- \hat{s}^- p^+ \bar{d}r^+ b^+ o^+ r^+ b^- r^- dp^- i^\times$$

Thus we must have

$$f_\beta(i) = p^+ \bar{d}r^+ b^+ r^- o^- b^- r^- dp^- \hat{s}^\circ$$

This is Figure E.13, and this is our Candidate 1.

E.1.1.1.2 Plump

Back to the end of Iris E.1.1.1, suppose

$$f_\beta(b) = r^- ...$$

Then it must do so while going to the right of $f_\beta(p)$, otherwise it will trace:

$$f_\beta(b) = r^- di^+ p^+ \bar{d}r^+ b^\times$$

Thus we have

$$f_\beta(b) = r^- dp^* ...$$

Consider $f_\beta(p)$. It must end here at r°. Indeed, if it were to continue with r^+, then we have

$$f_\beta(p) = \bar{d}r^+ di^+ p^\times$$

or

$$f_\beta(p) = \bar{d}r^+ o^- b^+ r^- dp^\times$$

While if it were to continue with r^-, we have

$$f_\beta(p) = \bar{d}r^- dp^\times$$

Thus we must have

$$f_\beta(p) = \bar{d}r^\circ$$

This is Figure E.14.

Here $f_\beta(b)$ must either end at p°, or continue with p^- and into 1., or 2. Note that p^+ is not possible as it would eventually trace.

E.1.1.1.2.1 Muscle

Suppose $f_\beta(b)$ ends at p°, so we have

$$f_\beta(b) = r^- d\hat{p}^\circ$$

Then $f_\beta(s)$ and $f_\beta(i)$ will start with p^+. So we have

$$f_\beta(s) = p^+ \bar{d}r^+ b^* ...$$

and

$$f_\beta(i) = p^+ \bar{d}r^+ b^* ...$$

This is Figure E.15.

Here $f_\beta(o)$ is forced to start with b^- and to the right of $f_\beta(s)$ and $f_\beta(i)$. Otherwise $f_\beta(s)$ and $f_\beta(i)$ will be immediately absorbed between $f_\beta(d)$ and $f_\beta(o)$.

This is Figure E.16.

Here $f_\beta(i)$ can continue with b° or b^+. Note that b^- is not possible as that would cause it to trace:

$$f_\beta(i) = p^+ \bar{d}r^+ \hat{b}^- r^- dp^- i^\times$$

So suppose it continues with b°:

$$f_\beta(i) = p^+ \bar{d}r^+ \hat{b}^\circ$$

Then $f_\beta(s)$ continues with b^-:

$$f_\beta(s) = p^+ \bar{d}r^+ \hat{b}^- r^- dp^- i^* ...$$

This is Muslce3.

Here $f_\beta(o)$ must continue with i^- and to the right of $f_\beta(s)$. Otherwise, $f_\beta(s)$ will be forced to continue with i^+ and to the left of $f_\beta(o)$, in which case it will be absorbed:

$$f_\beta(s) = p^+ \bar{d}r^+ b^- r^- dp^- \hat{i}^+ p^+ \bar{d}r^+ b^+ \,\mathrm{Abso}(f_\beta(d), f_\beta(o))^\times$$

Thus $f_\beta(o)$ must continue with i^-. But now it will be absorbed:

$$f_\beta(o) = b^- r^- dp^- \hat{i}^- p^+ \bar{d}r^+ b^+ r^- dp^- \text{ Abso}(f_\beta(s), f_\beta(i))^\times$$

This is depicted in Figure E.18.

This is a contradiction. Thus in the situation depicted in Figure E.16, $f_\beta(i)$ cannot end at b°. So $f_\beta(i)$ must continue with b^+ there.

This is Figure E.19.

Here $f_\beta(i)$ can go into 1, or 2.

E.1.1.1.2.1.1 Dolphin

Suppose it goes into 1. Then it continues:

$$f_\beta(i) = p^+ \bar{d}r^+ \hat{b}^+ r^- dp^- \bar{d}r^+ ...$$

This is Figure E.20.

Here it cannot continue with d, or it will trace:

$$f_\beta(i) = p^+ \bar{d}r^+ b^+ r^- dp^- \bar{d}r^+ \hat{d}i^\times$$

Thus it must continue with o^-:

$$f_\beta(i) = p^+ \bar{d}r^+ b^+ r^- dp^- \bar{d}r^+ \hat{o}^- b^- r^- dp^- s^* ...$$

This is Figure E.21.

Here $f_\beta(o)$ must end here at i°. Indeed, if it were to continue with i^+, then we will have:

$$f_\beta(o) = b^- r^- dp^- \hat{i}^+ p^+ \bar{d}r^+ b^+ \operatorname{Abso}(f_\beta(d), f_\beta(o))^\times$$

While if it were to continue with i^-, we will have:

$$f_\beta(o) = b^- r^- dp^- \hat{i}^- p^+ \bar{d}r^+ b^+ r^- dp^- \bar{d}r^+ o^\times$$

Thus we must have $f_\beta(o)$ ending at i°.

This is Figure E.22.

Similarly, $f_\beta(s)$ must end here at b°. Indeed, if it were to continue with b^+, then we will have:

$$f_\beta(s) = p^+ \bar{d}r^+ \hat{b}^+ r^- dp^- \bar{d}r^+ ...$$

and here the next letter cannot be o^- or it will escape to the outer perimeter, and due to the position of $f_\beta(i)$, it will trace. Thus here the next letter must be d:

$$f_\beta(s) = p^+ \bar{d}r^+ b^+ r^- dp^- \bar{d}r^+ \hat{d}t^+ p^+ \bar{d}r^+ b^+ o^+ r^- dp^+ \bar{d}r^+ b^- r^- dp^- i^+ p^+ \bar{d}r^+ b^+ \operatorname{Abso}(f_\beta(d), f_\beta(o))^\times$$

While if $f_\beta(s)$ were to continue with b^-, we will have:

$$f_\beta(s) = p^+ \bar{d}r^+ \hat{b}^- r^- dp^- \operatorname{Abso}(f_\beta(s), f_\beta(i))^\times$$

Thus we must have $f_\beta(s)$ ending at b°.

This is Figure E.23.

Here $f_\beta(i)$ is forced to end at s°. Indeed, if instead it were to continue with s^+, then we will have:

$$f_\beta(i) = p^+\bar{d}r^+b^+r^-dp^-\bar{d}r^+o^-b^-r^-dp^-\hat{s}^+p^+\bar{d}r^+b^+o^+r^-dp^+\bar{d}r^+b^-r^-dp^- \operatorname{Abso}(f_\beta(s), f_\beta(i))^\times$$

]While if it were to continue with s^-, then we will have:

$$f_\beta(i) = p^+\bar{d}r^+b^+r^-dp^-\bar{d}r^+o^-b^-r^-dp^-\hat{s}^-p^+\bar{d}r^+b^+o^+r^-dp^+\bar{d}r^+b^-r^-dp^-i^+p^+\bar{d}r^+b^+ \operatorname{Abso}(f_\beta(d), f_\beta(o))^\times$$

Thus we must have

$$f_\beta(i) = p^+\bar{d}r^+b^+r^-dp^-\bar{d}r^+o^-b^-r^-dp^-\hat{s}^\circ$$

This is Candidate Train Track map 2, depicted in Figure E.24.

E.1.1.1.2.1.2 Cottage

Back to the end of Muscle E.1.1.1.2.1. Suppose $f_\beta(i)$ goes into 2. Then it will trace:

$$f_\beta(i) = p^+\bar{d}r^+\hat{b}^+r^-dp^- \operatorname{Abso}(f_\beta(s), f_\beta(i))^\times$$

This is depicted in Figure E.25.

This is a contradiction.

E.1.1.1.2.2 Magpie

Back to the end of Plump E.1.1.1.2. Suppose $f_\beta(b)$ continues with p^-.

This is Figure E.26.

Here it can continue into 1, or 2. Suppose it continues into 1, then it will trace:

$$f_\beta(b) = r^- d\hat{p}^- \bar{d}r^+ ...$$

Here the next letter cannot be o^-, since the letter following that would be b. Thus here the next letter must be d:

$$f_\beta(b) = r^- dp^- \bar{d}r^+ \hat{d}i^+ p^+ \bar{d}r^+ b^\times$$

This is Figure E.27.

So it must continue into 2. This is Figure E.28.

Here $f_\beta(b)$ must end at i or p, possibly after some number of twisting between the two. It can never escape this region since any such behavior would cause it to trace, even if it escaped to the outer perimeter. For the following argument that leads to the Candidate Train Track family 2a, we will assume $f_\beta(b)$ ends at i, with the understanding that the general family can have more twists, and and other edge path that goes through this region will have the appropriate amount of twisted added.

This is Figure E.29.

Here suppose $f_\beta(s)$ were to begin with p^- and to the right of $f_\beta(i)$. Then it continues:

$$f_\beta(s) = p^- i^+ p^+ \bar{d}r^+ b^* ...$$

This forces $f_\beta(o)$ to begin with b^- and to the right of $f_\beta(s)$:

$$f_\beta(o) = b^- r^- dp^- i^- p^* ...$$

This is Figure E.30.

This forces $f_\beta(i)$ to begin with p^- and to the right of $f_\beta(o)$, which will cause it to immediately trace. This is a contradiction. Thus in the situation depicted in Figure E.29, $f_\beta(s)$ cannot begin with p^- and to the right of $f_\beta(i)$. This means that $f_\beta(i)$ must begin with p^+ and to the left of $f_\beta(s)$. It then continues:

$$f_\beta(i) = p^+ \bar{d}r^+ o^- b^- r^- dp^- s^* ...$$

This is Figure E.31.

Here $f_\beta(o)$ os forced to begin and end with b°. Otherwise, it will trace:

$$f_\beta(o) = b^- r^- dp^- i^- p^+ \bar{d}r^+ o^\times$$

So we must have

$$f_\beta(o) = b^\circ$$

Then this also forces $f_\beta(s)$ to begin and end with p°. Indeed, if it did not, then it will be absorbed:

$$f_\beta(s) = p^+ \bar{d}r^+ di^+ p^+ \bar{d}r^+ b^+ \operatorname{Abso}(f_\beta(d), f_\beta(o))^\times$$

Finally, $f_\beta(i)$ is forced to end at s°. Indeed, if it were to continue with s^+, then we will have:

$$f_\beta(i) = p^+ \bar{d}r^+ o^- b^- r^- dp^- \hat{s}^+ p^+ \bar{d}r^+ b^+ o^+ r^- dp^- \operatorname{Abso}(f_\beta(s), f_\beta(i))^\times$$

While if it were to continue with s^-, we will have

$$f_\beta(i) = p^+\bar{d}r^+o^-b^-r^-dp^-\hat{s}^-p^+\bar{d}r^+b^+o^+r^-dp^-i^+p^+\bar{d}r^+b^+\,\mathrm{Abso}(f_\beta(d), f_\beta(o))^\times$$

Thus we must have

$$f_\beta(i) = p^+\bar{d}r^+o^-b^-r^-dp^-\hat{s}^\circ$$

This gives us the Train Track Map Candidate depicted in Figure E.32, which is part of the Train Track Map Candidates 3, with no twists from $f_\beta(b)$. In general, this Candidate Family includes k twists from $f_\beta(b)$. In Figure E.33, we have illustrated a train track map from this candidate with one twist from $f_\beta(b)$.

E.1.1.2 Ruby

Back to the end of VIE E.1.1. Suppose dotted lines do not join, so $f_\beta(d)$ on the left can go either below or above $f_\beta(\bar{d})$ on the right. If $f_\beta(d)$ went above $f_\beta(d)$, then $f_\beta(d)$ will enter Situation β. Thus this cannot happen. Therefore $f_\beta(d)$ must go below $f_\beta(\bar{d})$. Furthermore, it must go below $f_\beta(p)$ as well, or else it will enter Situation β. It then continues:

$$f_\beta(d) = b^-r^-\hat{d}i^+p^+\bar{d}r^+b^+o^+r^*...$$

This is Figure E.35.

Now it enters Situation β. This is a contradiction.

E.1.2 GRR

Back to the end of Case A E.1, triangles fixed. Suppose $f_\beta(d)$ starts at b, and $f_\beta(\bar{d})$ starts at s. Using the same argument used in VIE E.1.1, we can conclude that neither $f_\beta(d)$, nor

$f_\beta(\bar{d})$ can have initial twists.

This is Figure E.36.

Here $f_\beta(r)$ can start with d or start with o^*.

E.1.2.1 Bree

Suppose $f_\beta(r)$ starts with d. This is shown in Figure E.37.

Here $f_\beta(r)$ must go below $f_\beta(p)$. Otherwise, $f_\beta(p)$ will trace:

$$f_\beta(p) = \bar{d}b^- r^- dp^\times$$

Continuing, $f_\beta(r)$ must go to i^* after crossing, as the other option, s^+, would cause it to trace:

$$f_\beta(r) = d\hat{s}^+ p^+ \bar{d}r^\times$$

So we must have

$$f_\beta(r) = di^*...$$

Here it must in fact end at i°, as both i^+ and i^- would cause it to trace:

$$f_\beta(r) = d\hat{i}^+ \bar{d}r^\times$$

$$f_\beta(r) = d\hat{i}^- \bar{d}b^- r^\times$$

Thus we must have

$$f_\beta(r) = di^\circ$$

This is Figure E.38.

Here consider $f_\beta(i)$. It must begin with p^+ and to the left of $f_\beta(s)$. Otherwise, $f_\beta(s)$ will be forced to begin with p^- and to the right of $f_\beta(i)$, in which case it will immediately trace.

This is Figure E.39.

Here $f_\beta(i)$ must go below $f_\beta(d)$ since if it were to go above, then it will trace:

$$f_\beta(i) = p^+ \hat{\bar{d}} r^+ b^+ di^\times$$

So now we have the situation depicted in Figure E.40.

Now here $f_\beta(i)$ must continue with r^+ and to the left of $f_\beta(p)$. Otherwise $f_\beta(p)$ will be forced to continue with r^-, in which case it will immediately trace after crossing d.

This is Figure E.41.

Here $f_\beta(i)$ can go into 1, or 2. But if it were to go into 2, it will eventually trace:

$$f_\beta(i) = p^+ \bar{d} \hat{r}^+ di^\times$$

or

$$f_\beta(i) = p^+ \bar{d} \hat{r}^+ ds^+ p^+ \bar{d} r^+ b^+ di^\times$$

So it must go into 1. So we have

$$f_\beta(i) = p^+ \bar{d} \hat{r}^+ b^* ...$$

This forces $f_\beta(o)$ to begin with b^-, and continue:

$$f_\beta(o) = b^- r^- d p^- s^* ...$$

This is Figure E.42.

Note that here $f_\beta(o)$ cannot go above $f_\beta(\bar{d})$ as it crosses d, as that would immediately put $f_\beta(\bar{d})$ in Situation β.

Now consider $f_\beta(p)$. It can either end here at r°, or continue with r^+. while r^- would cause it to immediately trace after crossing d. So suppose it ends here at r°:

$$f_\beta(p) = \bar{d} r^\circ$$

Then $f_\beta(b)$ will begin with r^-:

$$f_\beta(b) = r^- d p^* ...$$

This then forces $f_\beta(s)$ to begin with p^+ and to the left of $f_\beta(b)$:

$$f_\beta(s) = p^+ \bar{d} r^+ o^* ...$$

This is Figure E.43.

Here notice that the dotted lines have to join. Otherwise, either going below or above the other would place at least one of $f_\beta(d)$ or $f_\beta(\bar{d})$ in Situation β.

But now we have a counterclockwise path mill, with edge paths $f_\beta(s)$, $f_\beta(i)$, and $f_\beta(b)$; situated at edges b and p.

Spo going back to the situation depicted in Figure E.42, suppose $f_\beta(p)$ does not end there and continues with r^+. Then we have

$$f_\beta(p) = \bar{d}r^+b^*...$$

This is Figure E.44.

Here $f_\beta(i)$ must continue with b^+ and to the left of $f_\beta(p)$. Otherwise, $f_\beta(p)$ will be forced to continue with b^- and to the right of $f_\beta(i)$, in which case it will trace:

$$f_\beta(p) = \bar{d}r^+\hat{b}^-r^-dp^\times$$

So we must have

$$f_\beta(i) = p^+\bar{d}r^+b^+r^*...$$

This is Figure E.45. Here $f_\beta(i)$ must continue with r^- and to the right of $f_\beta(b)$. Otherwise, $f_\beta(b)$ will be forced to begin with r^+, and it will immediately trace. But now $f_\beta(i)$ will eventually trace:

$$f_\beta(i) = p^+\bar{d}r^+b^+\hat{r}^-di^\times$$

or

$$f_\beta(i) = p^+\bar{d}r^+b^+\hat{r}^-ds^+p^+\bar{d}r^+b^+di^\times$$

This is a contradiction.

E.1.2.2 Scud

Back to the end of GRR E.1.2. Suppose $f_\beta(r)$ starts with o^*. Then in fact it must also end there or it will trace:

$$f_\beta(r) = o^+ r^\times$$

$$f_\beta(r) = o^- b^- r^\times$$

Thus we must have

$$f_\beta(r) = o^\circ$$

This is Figure E.46.

Here the dotted lines can either join, or if not, the only possibility would be if $f_\beta(d)$ went below $f_\beta(p)$. If instead $f_\beta(d)$ went above $f_\beta(p)$ but below $f_\beta(\bar{d})$, then it will be in Situation β; if it went above $f_\beta(\bar{d})$, then $f_\beta(\bar{d})$ will be in Situation β.

So suppose the dotted lines join. Consider $f_\beta(i)$. It must begin with p^+, and to the left of $f_\beta(s)$. Otherwise, $f_\beta(s)$ will be forced to begin with p^- and to the right of $f_\beta(i)$, in which case it will immediately trace. So we must have

$$f_\beta(i) = p^+ \bar{d} r^* ...$$

This is Figure E.47.

Here $f_\beta(i)$ must continue with r^+ and into 1, or 2. If it did not, $f_\beta(p)$ will be forced to continue with r^- and to the right of $f_\beta(i)$, in which case it will trace immediately after crossing d.

E.1.2.2.1 Swale

Suppose $f_\beta(i)$ goes into 1. Then $f_\beta(b)$ is forced to begin with r^-, and it continues:

$$f_\beta(b) = r^- dp^- s^* ...$$

This is Figure E.48.

Here $f_\beta(b)$ can continue with s^- or s°. It cannot continue with s^+ as that would cause it to trace:

$$f_\beta(b) = r^- dp^- \hat{s}^+ p^+ \bar{d} r^+ b^\times$$

E.1.2.2.1.1 Bezoar

Suppose $f_\beta(b)$ continues with s^-. Then it continues:

$$f_\beta(b) = r^- dp^- \hat{s}^- p^+ \bar{d} r^+ ...$$

This is Figure E.49.

Here $f_\beta(b)$ cannot continue with o^-, or it will trace immediately. Thus it must continue with d. The next letter after d must be i^*, and not s^+, as that would make it traverse counterclockwise at the outer perimeter, thereby tracing. Thus we have:

$$f_\beta(b) = r^- dp^- s^- p^+ \bar{d} r^+ \hat{d} i^* ...$$

This is Figure E.50.

Here $f_\beta(i)$ is forced to continue with d, and continues:

$$f_\beta(i) = p^+ \bar{d} r^+ \hat{d} s^+ p^+ \bar{d} r^+ b^+ o^+ r^- dp^- s^* ...$$

Consider $f_\beta(p)$. It must end here at r°. Indeed, if not then it will trace:

$$f_\beta(p) = \bar{d} \hat{r}^+ ds^+ p^\times$$

or

$$f_\beta(p) = \bar{d} \hat{r}^- dp^\times$$

So we must have

$$f_\beta(p) = \bar{d} r^\circ$$

This is Figure E.51.

Consider $f_\beta(s)$. It must end her eat p°. Indeed, if not, then it must begin with p^+, in which case it will trace:

$$f_\beta(s) = p^+ \bar{d} r^+ ds^\times$$

So we must have

$$f_\beta(s) = p^\circ$$

This is Figure E.52.

Consider $f_\beta(i)$. It cannot continue with s^+, as that would cause it to be absorbed:

$$f_\beta(i) = p^+ \bar{d} r^+ ds^+ p^+ \bar{d} r^+ b^+ o^+ r^- dp^- \hat{s}^+ p^+ \bar{d} r^+ o^- b^- r^- dp^- s^- \bar{d} r^- dp^- \text{ Abso}(f_\beta(s), f_\beta(i))^\times$$

So it must either continue with s^- or s°. Suppose it continues with s^-, then it continues

$$f_\beta(i) = p^+\bar{d}r^+ds^+p^+\bar{d}r^+b^+o^+r^-dp^-\hat{s}^-p^+\bar{d}r^+b^*...$$

This forces $f_\beta(o)$ to begin with b^- and to the right of the incoming $f_\beta(i)$. But now it will trace:

$$f_\beta(p) = b^-r^-dp^-s^-p^+\bar{d}r^+ds^+p^+\bar{d}r^+b^+o^\times$$

Thus $f_\beta(i)$ must end at s°:

$$f_\beta(i) = p^+\bar{d}r^+ds^+p^+\bar{d}r^+b^+o^+r^-dp^-\hat{s}^\circ$$

This is Figure E.53.

Here consider $f_\beta(b)$. If it did not end here at i°, it will trace:

$$f_\beta(b) = r^-dp^-s^-p^+\bar{d}r^+d\hat{i}^+\bar{d}r^-dp^-s^+p^+\bar{d}r^+b^\times$$

or

$$f_\beta(b) = r^-dp^-s^-p^+\bar{d}r^+d\hat{i}^-\bar{d}r^-dp^-s^+p^+\bar{d}r^+o^-b^\times$$

Thus we must have

$$f_\beta(b) = r^-dp^-s^-p^+\bar{d}r^+d\hat{i}^\circ$$

Now consider $f_\beta(o)$. If it were to not begin and end immediately at b°, it will trace:

$$f_\beta(o) = b^-r^-dp^-s^-p^+\bar{d}r^+ds^+p^+\bar{d}r^+b^+o^\times$$

or

$$f_\beta(o) = b^- r^- dp^- s^- p^+ \bar{d}r^+ di^- \bar{d}r^- dp^- s^+ p^+ \bar{d}r^+ o^\times$$

So we must have

$$f_\beta(o) = b^\circ$$

This establishes candidate train track map 4. Shown in Figure E.54.

E.1.2.2.1.2 Efface

Back to the end of Swale E.1.2.2.1, suppose $f_\beta(b)$ continues with s°:

$$f_\beta(b) = r^- dp^- \hat{s}^\circ$$

This is Figure E.55.

Here $f_\beta(i)$ can continue with o^- or d.

E.1.2.2.1.2.1 Abscond

Suppose $f_\beta(i)$ continues with o^-. Then it continues:

$$f_\beta(i) = p^+ \bar{d}r^+ \hat{o}^- b^- r^- dp^- s^- \bar{d}r^* ...$$

Then this forces $f_\beta(o)$ to begin and end immediately at b°. If it did not, then it will trace:

$$f_\beta(o) = b^- r^- dp^- s^- p^+ \bar{d}r^+ o^\times$$

This is Figure E.56.

Here $f_\beta(s)$ can either begin (and end with) p°, or p^+. Suppose it were the former:

$$f_\beta(s) = p^\circ$$

Then $f_\beta(p)$ must continue with r^+ and to the left of $f_\beta(i)$, otherwise $f_\beta(i)$ will be forced to continue with r^- and to the right of $f_\beta(p)$ in which case it will be absorbed between $f_\beta(s)$ and $f_\beta(i)$. So we must have

$$f_\beta(p) = \bar{d}r^+ di^* ...$$

This is Figure E.57.

Now $f_\beta(i)$ must end at r°. Indeed, if it were to continue with r^+, we would have:

$$f_\beta(i) = p^+ \bar{d}r^+ o^- b^- r^- dp^- s^- \bar{d}\hat{r}^+ ds^+ p^+ \bar{d}r^+ b^+ o^+ r^- dp^- \,\mathrm{Abso}(f_\beta(s), f_\beta(i))^\times$$

On the other hand, if it were to continue with r^-, then we would have:

$$f_\beta(i) = p^+ \bar{d}r^+ o^- b^- r^- dp^- s^- \bar{d}\hat{r}^- ds^+ p^+ \bar{d}r^+ b^+ o^+ r^- dp^- s^+ p^+ \bar{d}r^+ b^+ \,\mathrm{Abso}(f_\beta(d), f_\beta(o))^\times$$

So we must have

$$f_\beta(i) = p^+ \bar{d}r^+ o^- b^- r^- dp^- s^- \bar{d}\hat{r}^\circ$$

This then forces $f_\beta(p)$ to also end at $f_\beta(i)$, or else it will trace:

$$f_\beta(p) = \bar{d}r^+ \hat{di}^+ \bar{d}r^- ds^+ p^\times$$

or

$$f_\beta(p) = \bar{d}r^+ d\hat{i}^- \bar{d}r^- dp^\times$$

So we must have

$$f_\beta(p) = \bar{d}r^+ d\hat{i}^\circ$$

This establishes a Train Track Map Candidate, depicted in Figure E.58. We will call this Candidate 5.

Going back to the situation depicted in Figure E.56, suppose $f_\beta(s)$ were to begin instead with p^+.

Here $f_\beta(p)$ either ends at r°, or continue with $r^+ di^*$.... It must end at either i or r at some point, possibly after twisting k times between the two. Here, as soon as $f_\beta(p)$ ends, $f_\beta(i)$ must also end, as otherwise it would escape to the outer perimeter and trace. Thus $f_\beta(s)$ must also end.

This is Candidate Family 6. Figure E.61 shows $f_\beta(p)$ ending immediately at r.

E.1.2.2.1.2.2 Fervent

Back to the end of Efface E.1.2.2.1.2, suppose $f_\beta(i)$ continues with d. Then it continues:

$$f_\beta(i) = p^+ \bar{d}r^+ \hat{d}s^+ p^+ \bar{d}r^+ b^+ o^+ r^- dp^- s^- p^+ \bar{d}r^+ b^* ...$$

This is Figure E.62.

This forces $f_\beta(o)$ to begin with b^-:

$$f_\beta(o) = b^- r^- dp^- s^- p^+ \bar{d}r^+ di^* ...$$

Now consider $f_\beta(s)$. It must begin and end at p°. Indeed, if it were to begin instead with p^+, then:

$$f_\beta(s) = p^+ \bar{d}r^+ ds^\times$$

Thus we must have

$$f_\beta(s) = p^\circ$$

This is Figure E.63.

Here consider $f_\beta(i)$. We claim that it must end here at b°. Indeed, otherwise we would have

$$\begin{aligned} f_\beta(i) =& p^+ \bar{d}r^+ \hat{d}s^+ p^+ \bar{d}r^+ b^+ o^+ r^- dp^- s^- p^+ \bar{d}r^+ \hat{b}^+ \\ & r^- dp^- s^- p^+ \bar{d}r^+ o^- b^- r^- dp^- s^- \bar{d}r^- dp^- \operatorname{Abso}(f_\beta(s), f_\beta(i))^\times \end{aligned}$$

$$\begin{aligned} f_\beta(i) =& p^+ \bar{d}r^+ \hat{d}s^+ p^+ \bar{d}r^+ b^+ o^+ r^- dp^- s^- p^+ \bar{d}r^+ \hat{b}^- r^- dp^- s^- p^+ \\ & \bar{d}r^+ o^- b^- r^- dp^- s^- \bar{d}r^- dp^- s^+ p^+ \bar{d}r^+ b^+ \operatorname{Abso}(f_\beta(d), f_\beta(o))^\times \end{aligned}$$

or

Thus we must have

$$f_\beta(i) = p^+ \bar{d}r^+ \hat{d}s^+ p^+ \bar{d}r^+ b^+ o^+ r^- dp^- s^- p^+ \bar{d}r^+ \hat{b}^\circ$$

This then forces $f_\beta(o)$ to also end at i°. Indeed, if it continued with i^- it would trace:

$$f_\beta(o) = b^- r^- dp^- s^- p^+ \bar{d}r^+ d\hat{i}^- \bar{d}r^- dp^- s^+ p^+ \bar{d}r^+ b^+ r^- dp^- s^- p^+ \bar{d}r^+ o^\times$$

While if it were to continue with i^+, it would be absorbed:

$$f_\beta(o) = b^- r^- dp^- s^- p^+ \bar{d}r^+ d\hat{i}^+ \bar{d}r^- dp^- s^+ p^+ \bar{d}r^+ b^+ \operatorname{Abso}(f_\beta(d), f_\beta(o))^\times$$

This gives us Candidate 7, depicted in Figure E.64.

E.1.2.2.2 Ombre

Back to the end of Scud E.1.2.2. Suppose $f_\beta(i)$ goes into 2.

This then forces $f_\beta(o)$ to begin with b^-:

$$f_\beta(o) = b^- r^- dp^- s^* ...$$

This is Figure E.65.

Here $f_\beta(b)$ can begin with r° or r^-.

E.1.2.2.2.1 Satire

Suppose $f_\beta(b)$ begins with r°. This then forces $f_\beta(p)$ to continue with r^+:

$$f_\beta(p) = \bar{d}r^+ b^* ...$$

This is Figure E.66.

Here $f_\beta(i)$ must continue with b^+ and to the left of $f_\beta(p)$. Otherwise, $f_\beta(p)$ will be forced to continue with b^- and to the right of $f_\beta(i)$, in which case it will trace after crossing d.

So we must have

$$f_\beta(i) = p^+ \bar{d}r^+ \hat{b}^+ r^- ...$$

This is Figure E.67.

Here $f_\beta(i)$ can continue with o^- or d.

E.1.2.2.2.1.1 Abdomen

Suppose $f_\beta(i)$ continues with o^-. Then it continues:

$$f_\beta(i) = p^+ \bar{d}r^+ b^+ r^- \hat{o}^- b^- r^- dp^- s^- \bar{d}r^+ b^* ...$$

Here consider $f_\beta(o)$. We claim it must end here at s°. Indeed, if instead it were to continue with s^+, it would be absorbed:

$$f_\beta(o) = b^- r^- dp^- \hat{s}^+ p^+ \bar{d}r^+ b^+ \operatorname{Abso}(f_\beta(d), f_\beta(o))^\times$$

While if instead it were to continue with s^-, it would trace:

$$f_\beta(o) = b^- r^- dp^- \hat{s}^- p^+ \bar{d}r^+ b^+ r^- o^\times$$

Thus we must have

$$f_\beta(o) = b^- r^- dp^- \hat{s}^\circ$$

This is Figure E.68.

Now consider $f_\beta(p)$. It can continue with b° or b^+.

E.1.2.2.2.1.1.1 Panorama

Suppose $f_{\beta}(p)$ continues with b°. Then $f_{\beta}(i)$ continues with b^{-}:

$$f_{\beta}(i) = p^{+}\bar{d}r^{+}b^{+}r^{-}o^{-}b^{-}r^{-}dp^{-}s^{-}\bar{d}r^{+}\hat{b}^{-}r^{-}dp^{*}...$$

This is Figure E.69.

Here $f_{\beta}(s)$ is forced to begin with p^{+} and to the left of the incoming $f_{\beta}(i)$:

$$f_{\beta}(s) = p^{+}\bar{d}r^{+}b^{+}r^{-}di^{*}...$$

This is Figure E.70.

Here we claim that $f_{\beta}(i)$ must end at p°. Indeed, if instead it were to continue with p^{+}, then we have:

$$\begin{aligned} f_{\beta}(i) =& p^{+}\bar{d}r^{+}b^{+}r^{-}o^{-}b^{-}r^{-}dp^{-}s^{-}\bar{d}r^{+}b^{-}r^{-}d\hat{p}^{+}\bar{d}r^{+}b^{+}r^{-}ds^{+}p^{+} \\ & \bar{d}r^{+}b^{+}o^{+}r^{+}b^{-}r^{-}dp^{+}\,\mathrm{Abso}(f_{\beta}(s), f_{\beta}(i))^{\times} \end{aligned}$$

On the other hand, if it were to continue with p^{-}, then we have

$$\begin{aligned} f_{\beta}(i) =& p^{+}\bar{d}r^{+}b^{+}r^{-}o^{-}b^{-}r^{-}dp^{-}s^{-}\bar{d}r^{+}b^{-}r^{-}d\hat{p}^{-}\bar{d}r^{+}b^{+}r^{-}ds^{+}p^{+} \\ & \bar{d}r^{+}b^{+}o^{+}r^{+}b^{-}r^{-}dp^{-}s^{+}p^{+}\bar{d}r^{+}b^{+}\,\mathrm{Abso}(f_{\beta}(d), f_{\beta}(o))^{\times} \end{aligned}$$

Thus we must have

$$f_\beta(i) = p^+ \bar{d}r^+ b^+ r^- o^- b^- r^- dp^- s^- \bar{d}r^+ b^- r^- d\hat{p}^\circ$$

This then forces $f_\beta(s)$ to also end at i°, as one can check if it did not it would either trace:

$$f_\beta(s) = p^+ \bar{d}r^+ b^+ r^- d\hat{i}^+ \bar{d}r^+ b^- r^- dp^- \bar{d}r^+ b^+ r^- ds^\times$$

or be absorbed:

$$f_\beta(s) = p^+ \bar{d}r^+ b^+ r^- d\hat{i}^- \bar{d}r^+ b^- r^- dp^- \text{ Abso}(f_\beta(s), f_\beta(i))^\times$$

Thus we must have

$$f_\beta(s) = p^+ \bar{d}r^+ b^+ r^- d\hat{i}^\circ$$

This gives us Candidate 8, shown in Figure E.71.

E.1.2.2.2.1.1.2 Pristine

Back to the end of Abdomen E.1.2.2.2.1.1. Suppose $f_\beta(p)$ continues with b^+. Then it must do so by going to the left of $f_\beta(i)$. Otherwise, it would trace. So we must have

$$f_\beta(p) = \bar{d}r^+ \hat{b}^+ r^- di^* ...$$

This is Figure E.72.

Here we claim that $f_\beta(i)$ must end at b°. Indeed, if instead it were to continue with b^-, then

$$\begin{aligned} f_\beta(i) =& p^+\bar{d}r^+b^+r^-o^-b^-r^-dp^-s^-\bar{d}r^+\hat{b}^-r^-ds^+p^+\bar{d}r^+b^+o^+r^+b^- \\ & r^-dp^-s^+p^+\bar{d}r^+b^+ \operatorname{Abso}(f_\beta(d), f_\beta(o))^\times \end{aligned}$$

On the other hand, if it were to continue with b^+, then we would have:

$$f_\beta(i) = p^+\bar{d}r^+b^+r^-o^-b^-r^-dp^-s^-\bar{d}r^+\hat{b}^+r^-ds^+p^+\bar{d}r^+b^+o^+r^+b^-r^-dp^*...$$

and this forces $f_\beta(s)$ to begin with p^+ and to the left of the incoming $f_\beta(i)$:

$$f_\beta(s) = p^+\bar{d}r^+b^+r^-o^-b^-r^-dp^-s^\times$$

Thus we must have

$$f_\beta(i) = p^+\bar{d}r^+b^+r^-o^-b^-r^-dp^-s^-\bar{d}r^+\hat{b}^\circ$$

This is Figure E.73.

Here consider $f_\beta(p)$. We claim it must end here at i°. Indeed, if instead it were to continue with i^+, then we would have:

$$f_\beta(p) = \bar{d}r^+b^+r^-d\hat{i}^+\bar{d}r^+b^-r^-ds^+p^\times$$

If instead it were to continue with i^-, then we would have:

$$f_\beta(p) = \bar{d}r^+b^+r^-d\hat{i}^-\bar{d}r^+b^-r^-dp^\times$$

Thus we must have

$$f_\beta(p) = \bar{d}r^+b^+r^-d\hat{i}^\circ$$

Now consider $f_\beta(s)$. It must begin/end at p°. Indeed if it did not, then it must begin with p^+:

$$f_\beta(s) = p^+\bar{d}r^+b^+r^-di^+\bar{d}r^+b^-r^-ds^\times$$

Thus we must have

$$f_\beta(s) = p^\circ$$

This gives us Candidate Family 9.

E.1.2.2.2.1.2 Gingham

Back to the end of Satire E.1.2.2.2.1. Suppose $f_\beta(i)$ continues with d. Then it continues:

$$f_\beta(i) = p^+\bar{d}r^+b^+r^-\hat{d}s^+p^+\bar{d}r^+b^+o^+r^+b^-r^-dp^-s^*...$$

This is Figure E.74.

Here $f_\beta(o)$ must continue with s^- and to the right of the incoming $f_\beta(i)$. Indeed, otherwise $f_\beta(i)$ will be forced to continue with s^+ and to the left of $f_\beta(o)$, in which case it will be absorbed:

$$f_\beta(i) = p^+\bar{d}r^+b^+r^-ds^+p^+\bar{d}r^+b^+o^+r^+b^-r^-dp^-\hat{s}^+p^+\bar{d}r^+b^+\,\mathrm{Abso}(f_\beta(d), f_\beta(o))^\times$$

Thus we must have

$$f_\beta(o) = b^-r^-dp^-\hat{s}^-p^+\bar{d}r^+b^+r^-di^*...$$

This is Figure E.75.

Here $f_\beta(p)$ has to end here at b°, as both continuing with b^+ or b^- causes it to trace.

Here $f_\beta(s)$ has to also end at p°. Indeed, if it did not, then it has to begin with p^+, in which case it will trace:

$$f_\beta(s) = p^+ \bar{d}r^+ b^+ r^- ds^\times$$

Thus we must have

$$f_\beta(s) = p^\circ$$

This is Figure E.76.

Here $f_\beta(i)$ must end at s°. Indeed, if it did not, then we would have

$$f_\beta(i) = p^+ \bar{d}r^+ b^+ r^- ds^+ p^+ \bar{d}r^+ b^+ o^+ r^+ b^- r^- dp^- \hat{s}^+ p^+ \bar{d}r^+ b^+ r^- o^- b^- r^- dp^- s^- \bar{d}r^+ b^- r^- dp^- \operatorname{Abso}(f_\beta(s), f_\beta(i))^\times$$

or

$$f_\beta(i) = p^+ \bar{d}r^+ b^+ r^- ds^+ p^+ \bar{d}r^+ b^+ o^+ r^+ b^- r^- dp^- \hat{s}^- p^+ \bar{d}r^+ b^+ r^- di^\times$$

Thus we must have

$$f_\beta(i) = p^+ \bar{d}r^+ b^+ r^- ds^+ p^+ \bar{d}r^+ b^+ o^+ r^+ b^- r^- dp^- \hat{s}^\circ$$

This is Figure E.77.

Here $f_\beta(o)$ must end at i°. Indeed, if it did not, then we would have

$$f_\beta(o) = b^- r^- dp^- s^- p^+ \bar{d}r^+ b^+ r^- d\hat{i}^+ \bar{d}r^+ b^- r^- dp^- s^+ p^+ \bar{d}r^+ b^+ r^- o^\times$$

or

$$f_\beta(o) = b^- r^- dp^- s^- p^+ \bar{d}r^+ b^+ r^- d\hat{i}^- \bar{d}r^+ b^- r^- dp^- s^+ p^+ \bar{d}r^+ b^+ r^- o^\times$$

Thus we must have

$$f_\beta(o) = b^- r^- dp^- s^- p^+ \bar{d}r^+ b^+ r^- d\hat{i}^\circ$$

This is Figure E.78. This is Candidate 10.

E.1.2.2.2.2 Kismet

Back to the end of Ombre E.1.2.2.2. Suppose $f_\beta(b)$ begins with r^-.

This is Figure E.79.

Here $f_\beta(b)$ can go into 1 or 2.

E.1.2.2.2.2.1 Dossier

Suppose $f_\beta(b)$ goes into 1. Then it must continue with d and not o^-, or else it would trace:

$$f_\beta(b) = r^- di^*, , ,$$

Now $f_\beta(p)$ is forced to continue with r^+ so we have

$$f_\beta(p) = \bar{d}r^+ b^* ...$$

This is Figure E.80.

Here $f_\beta(i)$ must continue with b^+ and to the left of $f_\beta(p)$, otherwise $f_\beta(p)$ will be forced to

continue with b^- and to the right of $f_\beta(i)$, in which case it will trace:

$$f_\beta(p) = \bar{d}r^+b^-r^-dp^\times$$

Thus we must have

$$f_\beta(i) = p^+\bar{d}r^+b^+r^-ds^+p^+\bar{d}r^+b^+o^+r^*...$$

This is Figure E.81.

Here $f_\beta(p)$ must end at b°. Indeed, otherwise we would have either

$$f_\beta(p) = \bar{d}r^+\hat{b}^+r^-ds^+p\times$$

or

$$f_\beta(p) = \bar{d}r^+\hat{b}^-r^-dp^\times$$

Thus we must have

$$f_\beta(p) = \bar{d}r^+\hat{b}^\circ$$

This forces $f_\beta(s)$ to begin and end at p°. Indeed, otherwise, we would have

$$f_\beta(s) = p^+\bar{d}r^+b^+r^-ds^\times$$

Thus we must have

$$f_\beta(s) = p^\circ$$

Now consider $f_\beta(i)$. If it did not end here at r°, and suppose it continued with r^+, we would

have

$$f_\beta(i) = p^+\bar{d}r^+b^+r^-ds^+p^+\bar{d}r^+b^+o^+\hat{r}^+o^-b^-r^-dp^-s^-\bar{d}r^+b^-r^-dp^- \text{ Abso}(f_\beta(s), f_\beta(i))^\times$$

If instead it were to continue with r^-, then we would have:

$$f_\beta(i) = p^+\bar{d}r^+b^+r^-ds^+p^+\bar{d}r^+b^+o^+\hat{r}^-o^-b^-r^-dp^-s^-\bar{d}r^+b^-r^-dr^+b^-r^-dp^-s^*...$$

This is Figure E.82.

Now here $f_\beta(i)$ cannot continue with s^+, or it will eventually be absorbed between $f_\beta(d)$ and $f_\beta(o)$. This means it must either end there at s° or s^-, in either case this forces $f_\beta(o)$ to continue with s^-, but this will lead to it tracing:

$$f_\beta(o) = b^-r^-dp^-s^-p^+\bar{d}r^+b^+r^-o^\times$$

Thus, we must have

$$f_\beta(i) = p^+\bar{d}r^+b^+r^-ds^+p^+\bar{d}r^+b^+o^+\hat{r}^\circ$$

after all.

This is Figure E.83.

Now here $f_\beta(b)$ must end at i° or it will trace:

$$f_\beta(b) = r^-\bar{\hat{d}}i^+\bar{d}r^+b^\times$$

or

$$f_\beta(b) = r^-\bar{\hat{d}}i^-\bar{d}r^+b^-b^\times$$

Thus we must have

$$f_\beta(b) = r^- \bar{di}^\circ$$

And finally, this also forces $f_\beta(o)$ to end at s°, otherwise we would have:

$$f_\beta(o) = b^- r^- dp^- \hat{s}^+ p^+ \bar{d}r^+ b^+ \text{Abso}(f_\beta(d), f_\beta(o))^\times$$

or

$$f_\beta(o) = b^- r^- dp^- \hat{s}^- p^+ \bar{d}r^+ b^+ r^- di^- r^+ o^\times$$

Thus we must have

$$f_\beta(o) = b^- r^- dp^- \hat{s}^\circ$$

This is Candidate 11, shown in Dossier 5.

E.1.2.2.2.2.2 Perplex

Back to the end of Kismet E.1.2.2.2.2. Suppose $f_\beta(b)$ goes into 2. Then it continues:

$$f_\beta(b) = r^- dp^* ...$$

This is Perlpex1.

This forces $f_\beta(s)$ to begin with p^+ and to the left of the incoming $f_\beta(b)$, otherwise $f_\beta(b)$ will be absorbed. Thus we have

$$f_\beta(s) = p^+ \bar{d}r^+ b^* ...$$

This is Figure E.85.

Here $f_\beta(i)$ must continue with b^+ and to the left of the incoming $f_\beta(s)$, otherwise $f_\beta(s)$ will

be forced to continue with b^- and to the right of $f_\beta(i)$, in which case it will trace:

$$f_\beta(s) = p^+ \bar{d}r^+ \hat{b}^- r^- dp^- s^\times$$

Thus we must have

$$f_\beta(i) = p^+ \bar{d}r^+ \hat{b}^+ r^- dp^* ...$$

This is Figure E.86.

Here $f_\beta(i)$ must continue with p^- and to the right of $f_\beta(b)$, otherwise, $f_\beta(b)$ will be forced to continue with p^+ and to the left of the incoming $f_\beta(i)$, in which case it will trace:

$$f_\beta(b) = r^- d\hat{p}^+ \bar{d}r^+ b^\times$$

Thus we must have

$$f_\beta(i) = p^+ \bar{d}r^+ b^+ r^- d\hat{p}^- \bar{d}r^* ...$$

This is Figure E.87.

Here $f_\beta(p)$ can either end at p°, or continue with r^+. It is not possible for it to continue with r^-, as then it would trace immediately after crossing d.

E.1.2.2.2.2.2.1 Zugzwang

Suppose $f_\beta(p)$ end here at p°. This forces $f_\beta(i)$ to continue with r^+:

$$f_\beta(i) = p^+ \bar{d}r^+ b^+ r^- dp^- \bar{d}\hat{r}^+ ...$$

Here $f_\beta(o)$ can either end at s° or continue with s^-. It cannot continue with s^+ as that

would cause it to be absobed between $f_\beta(d)$ and $f_\beta(o)$.

E.1.2.2.2.2.2.1.1 Querulous

Suppose $f_\beta(o)$ ends at s°. This is Querelous1.

Here $f_\beta(s)$ can either continue with b^+, or end at b°. Continuing with b^- is not possible as then it would be absorbed:

$$f_\beta(s) = p^+ \bar{d}r^+ \hat{b}^- r^- dp^- \text{ Abso}(f_\beta(s), f_\beta(i))^\times$$

So suppose it continues with b^+:

$$f_\beta(s) = p^+ \bar{d}r^+ \hat{b}^+ r^- dp^- \bar{d}r^+ ...$$

This is Figure E.89.

Consider $f_\beta(b)$. It must end here at p°. Indeed, if it were to continue with p^+, it would trace:

$$f_\beta(b) = r^- d\hat{p}^+ \bar{d}r^+ b^\times$$

Whereas if it were to continue with p^-, we would have

$$f_\beta(b) = r^- d\hat{p}^- \bar{d}r^+ di^* ...$$

and here this forces $f_\beta(i)$ and $f_\beta(s)$ to both continue with d, and in order for $f_\beta(i)$ to not trace, they both then continue with s, but that forces s to trace.

Thus we must have

$$f_\beta(b) = r^- d\hat{p}^\circ$$

This is Figure E.90.

Now consider $f_\beta(i)$. If it continued with d, then it will force s to trace, as before. So it must continue with o^-, and $f_\beta(s)$ must continue with $di...$, to not trace. So we must have

$$f_\beta(s) = p^+\bar{d}r^+b^+r^-dp^-\bar{d}r^+di^*...$$

and

$$f_\beta(i) = p^+\bar{d}r^+b^+r^-dp^-\bar{d}r^+\hat{o}^-b^-r^-dp^-s^-\bar{d}r^-dp^+\bar{d}r^+b^*...$$

This is Figure E.91.

Here $f_\beta(i)$ must end at b°. Indeed, if not then we either have

$$f_\beta(i) = ...\hat{b}^-r^-dp\bar{d}r^+ds^+p^+\bar{d}r^+b^+\,\mathrm{Abso}(f_\beta(d), f_\beta(o))^\times$$

or

$$f_\beta(i) = ...\hat{b}^+r^-dp^-\bar{d}r^+ds^+p^+\bar{d}r^+b^+o^+r^-dp^+\bar{d}r^+b^-r^-r^+dp^-\,\mathrm{Abso}(f_\beta(s), f_\beta(i))^\times$$

Thus we must have

$$f_\beta(i) = p^+\bar{d}r^+b^+r^-dp^-\bar{d}r^+\hat{o}^-b^-r^-dp^-s^-\bar{d}r^-dp^+\bar{d}r^+\hat{b}^\circ$$

This forces $f_\beta(s)$ to end at i°, Indeed, other we would have either

$$f_\beta(s) = p^+\bar{d}r^+b^+r^-dp^-\bar{d}r^+d\hat{i}^-\bar{d}r^-dp^+\bar{d}r^+b^-r^-dp^-\,\mathrm{Abso}(f_\beta(s), f_\beta(i))^\times$$

or

$$f_\beta(s) = p^+\bar{d}r^+b^+r^-dp^-\bar{d}r^+d\hat{i}^+\bar{d}r^-dp^+\bar{d}r^+b^-r^-dp^-\bar{d}r^+ds^\times$$

Thus we must have

$$f_\beta(s) = p^+\bar{d}r^+b^+r^-dp^-\bar{d}r^+d\hat{i}^\circ$$

This gives us Candidate 12, shown in Figure E.92.

Back to the situation depicted in Figure E.88. Suppose $f_\beta(s)$ ends at b°.

This is Figure E.93.

Then $f_\beta(i)$ cannot continue with o^-, or it will be absorbed:

$$f_\beta(i) = ...\hat{o}^-b^-b^-r^-dp^-s^-\bar{d}r^-dp^+\bar{d}r^+b^-r^-dp^-\,\text{Abso}(f_\beta(s), f_\beta(i))^\times$$

Thus $f_\beta(i)$ must continue with d:

$$f_\beta(i) = ...\hat{d}s^+p^+\bar{d}r^+b^+o^+r^-dp^*...$$

This is Figure E.94.

Consider $f_\beta(b)$ here. We claim it must continue with p^-. Indeed, if it conitnued with p^+ then it will trace:

$$f_\beta(b) = r^-d\hat{p}^+\bar{d}r^+b^\times$$

On the other hand, suppose it ended at p°:

$$f_\beta(b) = r^-d\hat{p}^\circ$$

Then this forces $f_\beta(i)$ to continue with p^+:

$$f_\beta(i) = ...\hat{p}^+\bar{d}r^+b^-r^-dp^-s^+p^+\bar{d}r^+b^+ \operatorname{Abso}(f_\beta(d), f_\beta(o))^\times$$

This is a contradiction. Thus $f_\beta(b)$ must continue with p^-, and to the right of $f_\beta(i)$:

$$f_\beta(b) = r^-d\hat{p}^-\bar{d}r^+di^*...$$

This is Figure E.95.

Now consider $f_\beta(i)$. We claim it must end here at p°. Indeed, if not we would either have

$$f_\beta(i) = ...\hat{p}^-\bar{d}r^+o^-b^-r^-dp^-s^-\bar{d}r^-dp^+\bar{d}r^+b^-r^-dp^-s^+p^+\bar{d}r^+b^+ \operatorname{Abso}(f_\beta(d), f_\beta(o))^\times$$

or

$$f_\beta(i) = ...\hat{p}^+\bar{d}r^+o^-b^-r^-dp^-s^-\bar{d}r^+ds^+p^+\bar{d}b^-r^-dp^- \operatorname{Abso}(f_\beta(s), f_\beta(i))^\times$$

Thus we must have

$$f_\beta(i) = ...\hat{p}^\circ$$

Next, consider $f_\beta(b)$. Here $f_\beta(b)$ must end at i°. Indeed, if it were to continue with either i^+ or i^-, it would trace:

$$f_\beta(b) = ...\hat{i}^+\bar{d}r^-dp^+\bar{d}r^+b^\times$$

$$f_\beta(b) = ...\hat{i}^-\bar{d}r^-dp^+r^+o^-b^\times$$

Thus we must have

$$f_\beta(b) = ...\hat{i}^\circ$$

This gives Candidate 13, shown in Figure E.96.

E.1.2.2.2.2.2.1.2 Sybaritic

Back to the end of Zugzwang E.1.2.2.2.2.2.1. Suppose $f_\beta(o)$ continues with s^-. Then it continues:

$$f_\beta(o) = ...\hat{s}^- p^+ \bar{d}r^+ b^+ r^- dp^* ...$$

This is Figure E.97.

Here $f_\beta(o)$ must continue with p^- and to the right of the incoming $f_\beta(b)$. Indeed, otherwise $f_\beta(b)$ will be forced to continue with p^+ and to the left of the incoming $f_\beta(o)$, in which case $f_\beta(b)$ will trace:

$$f_\beta(b) = r^- d\hat{p}^+ \bar{d}r^+ b^\times$$

Thus we must have

$$f_\beta(o) = ...\hat{p}^- \bar{d}r^+ di^* ...$$

This forces $f_\beta(i)$ to continue with d:

$$f_\beta(i) = ...\hat{d}s^+ p^+ \bar{d}r^+ b^+ o^+ r^- dp^* ...$$

This is Figure E.98.

Consider $f_\beta(s)$. It must end here at b°. Indeed, otherwise we would have either

$$f_\beta(s) = p^+ \bar{d}r^+ \hat{b}^+ r^- dp^- \bar{d}r^+ ds^\times$$

or

$$f_\beta(s) = p^+ \bar{d} r^+ \hat{b}^- r^- dp^- \text{ Abso}(f_\beta(s), f_\beta(i))^\times$$

Thus we must have

$$f_\beta(s) = p^+ \bar{d} r^+ \hat{b}^\circ$$

This is Figure E.99.

Here $f_\beta(b)$ can either end at p° or continue with p^-. Suppose it ends here at p°.

Then $f_\beta(i)$ is forced to continue with p^+:

$$f_\beta(i) = ...\hat{p}^+ \bar{d} r^+ b^- r^- dp^- s^* ...$$

This is Figure E.100.

Here $f_\beta(i)$ is forced to end at s°. Indeed, otherwise we either have

$$\begin{aligned} f_\beta(i) =& ...\hat{s}^+ p^+ \bar{d} r^+ b^+ r^- dp^- \bar{d} r^+ o^- b^- r^- dp^- s^- \bar{d} r^- dp^+ \bar{d} \\ & r^+ b^- r^- dp^- \text{ Abso}(f_\beta(s), f_\beta(i))^\times \end{aligned}$$

or

$$\begin{aligned} f_\beta(i) =& ...\hat{s}^- p^+ \bar{d} r^+ b^+ r^- dp^- \bar{d} r^+ o^- b^- r^- dp^- s^- \bar{d} r^- dp^+ \bar{d} r^+ \\ & b^- r^- dp^- s^+ p^+ \bar{d} r^+ b^+ \text{ Abso}(f_\beta(d), f_\beta(o))^\times \end{aligned}$$

Thus we must have

$$f_\beta(o) = ...\hat{s}^\circ$$

This then forces $f_\beta(o)$ to end at i°. Indeed, otherwise we either have

$$f_\beta(o) = ...\hat{i}^+ \bar{d}r^- dp^+ \bar{d}r^+ b^- r^- dp^- s^+ p^+ \bar{d}r^+ b^+ \,\mathrm{Abso}(f_\beta(d), f_\beta(o))^\times$$

or

$$f_\beta(o) = ...\hat{i}^- \bar{d}r^- dp^+ \bar{d}r^+ b^- r^- dp^- s^+ p^+ \bar{d}r^+ b^+ r^- dp^- \bar{d}r^+ o^\times$$

Thus we must have

$$f_\beta(o) = ...\hat{i}^\circ$$

This is Figure E.101.

This is Candidate 14.

Back to the situation depicted in Figure E.99. Suppose $f_\beta(b)$ continues with p^-. Then it must do so to the right of $f_\beta(i)$, otherwise it will trace:

$$f_\beta(b) = ...\hat{p}^- \bar{d}r^+ o^- b^\times$$

Thus it continues to the right of $f_\beta(i)$:

$$f_\beta(b) = ...\hat{p}^- \bar{d}r^+ di^*...$$

This is Figure E.102.

Consider $f_\beta(i)$. If it were to continue with p^+ here, then it will be absorbed:

$$f_\beta(i) = ...\hat{p}^+ \bar{d}r^+ b^- b^- r^- dp^- s^- \bar{d}r^- dp^+ \bar{d}r^+ b^- r^- dp^- \,\mathrm{Abso}(f_\beta(s), f_\beta(i))^\times$$

While if it were to continue with p^-, then it will again be absorbed:

$$f_\beta(i) = ...\hat{p}^- \bar{d}r^+ o^- b^- r^- dp^- s^- r^- dp^+ \bar{d}r^+ b^- r^- dp^- s^+ p^+$$
$$\bar{d}r^+ b^+ \text{Abso}(f_\beta(d), f_\beta(o))^\times$$

Thus we must have

$$f_\beta(i) = ...\hat{p}^\circ$$

This is Figure E.103.

Consider $f_\beta(o)$. It must continue with i^- and to the right of $f_\beta(b)$. Otherwise, $f_\beta(b)$ will be forced to continue with i^+ and to the left of $f_\beta(o)$, in which case it will trace:

$$f_\beta(b) = ...\hat{i}^+ \bar{d}r^- dp^+ \bar{d}r^+ b^\times$$

Thus $f_\beta(o)$ must continue with i^- and to the right of $f_\beta(b)$, but then it will trace:

$$f_\beta(o) = ...i^- \bar{d}r^- dp^+ \bar{d}r^+ o^\times$$

This is a contradiction.

E.1.2.2.2.2.2.2 Leverage

Back to the end of Perplex E.1.2.2.2.2.2. Suppose $f_\beta(p)$ continues with r^+. Then it continues with d, and not o^-, or it will trace. Thus we must have

$$f_\beta(p) = \bar{d}\hat{r}^+ di^* ...$$

This is Figure E.104.

This forces $f_\beta(i)$ to continue with r^+:

$$f_\beta(i) = ...\hat{r}^+ o^- b^- r^- dp^- s^- \bar{d}r^* ...$$

This is Figure E.105.

Consider $f_\beta(p)$. It can either continue with i^+, or i°; while i^- will cause it to trace:

$$f_\beta(p) = \bar{d}r^+ d\hat{i}^- \bar{d}r^- dp^\times$$

So suppose it continues with i^+. Then we have

$$f_\beta(p) = \bar{d}r^+ d\hat{i}^+ \bar{d}r^* ...$$

Here it must continue with r^- and to the right of $f_\beta(i)$, otherwise $f_\beta(i)$ will be forced to continue with r^+ and to the left of the incoming $f_\beta(p)$, in which case $f_\beta(i)$ will immediately trace after crossing d. Thus we must have

$$f_\beta(p) = \bar{d}r^+ di^+ \bar{d}\hat{r}^- dp^\times$$

Thus it must be the case that $f_\beta(p)$ ends at i°:

$$f_\beta(p) = \bar{d}r^+ d\hat{i}^\circ$$

This is Figure E.106.

Here consider $f_\beta(b)$. It must end here at p°. Indeed, otherwise it will trace:

$$f_\beta(b) = r^- d\hat{p}^+ \bar{d}r^+ b^\times$$

or

$$f_\beta(b) = r^- d\hat{p}^- \bar{d}r^+ o^- b^\times$$

Thus we must have

$$f_\beta(b) = r^- d\hat{p}^\circ$$

This is Figure E.107.

Here consider $f_\beta(o)$. It must end here at s°. Indeed, otherwise we would either have

$$f_\beta(o) = ...\hat{s}^+ p^+ \bar{d}r^+ b^+ \operatorname{Abso}(f_\beta(d), f_\beta(o))^\times$$

or

$$f_\beta(o) = ...\hat{s}^- p^+ \bar{d}r^+ b^+ r^- dp^- \bar{d}r^+ o^\times$$

Thus we must have

$$f_\beta(o) = b^- r^- dp^- \hat{s}^\circ$$

This is Figure E.108.

Here consider $f_\beta(i)$. It can only continue with r^+ or r°, otherwise it will trace immediately after crossing d. So suppose it continues with r^+. Then we have

$$f_\beta(i) = ...r^+ ds^+ p^+ \bar{d}r^+ b^+ o^+ r^- dp^+ \bar{d}r^+ b^*...$$

This is Figure E.109.

Here $f_\beta(i)$ must continue with b^- and to the right of $f_\beta(s)$. Otherwise, $f_\beta(s)$ will be forced to continue with b^+ and to the left of $f_\beta(i)$, which would force it to eventually trace:

$$f_\beta(s) = ...b^+r^-dp^-\bar{d}r^+o^-r^-r^-dp^-s^\times$$

But then we must have

$$f_\beta(i) = ...b^-r^-dp^-\,\mathrm{Abso}(f_\beta(s), f_\beta(i))^\times$$

Hence in the situated depicted in Figure E.108, $f_\beta(i)$ must end at b°.

Here $f_\beta(s)$ is forced to end at b°. Indeed, otherwise it will be absorbed:

$$f_\beta(s) = ...b^-r^-d\,\mathrm{Abso}(f_\beta(s), f_\beta(i))^\times$$

or trace:

$$f_\beta(s) = ...b^+r^-dp^-\bar{d}r^+o^-r^-r^-dp^-s^\times$$

$$f_\beta(s) = ...b^+r^-dp^-\bar{d}r^+di^+\bar{d}r^-ds^\times$$

This gives Candidate Train Track Map 15, shown in Figure E.110.

E.1.2.2.3 Jumar

Back to the situation depicted in Figure E.46, and suppose the dotted lines do not join. Then $f_\beta(d)$ on the left hand side must go under $f_\beta(p)$ on the right hand side. Then we have

$$f_\beta(p) = \bar{d}r^+b^+o^+r^*...$$

This is Jamar2.

We also must have

$$f_\beta(d) = b^- r^- d s^+ p^+ \bar{d} r^+ b^+ o^+ r^* ...$$

and

$$f_\beta(\bar{d}) = s^+ p^+ \bar{d} r^+ b^+ o^+ r^* ...$$

This is Jamar3.

Here both $f_\beta(d)$ and $f_\beta(\bar{d})$ must continue with r^-. Otherwise, continuing with r^+ will force either of them to violate the Trace Lemma. But then they either circle the perimeter counterclockwise and back at r^* again, and repeat, or they both go up to i^*. But in that case, they both violate Rule F! since after i they must cross $\bar{d}$. This is a contradiction.

E.1.3 IPC

Back to the end of Case A E.1, triangles fixed. Suppose $f_\beta(d)$ starts at b, and $f_\beta(\bar{d})$ starts at p.

If $f_\beta(d)$ were to have any initial twists, and it does so starting with b^+, then $f_\beta(o)$ will immediately trace. If the initial twists starts wit b^-, then it must be

$$f_\beta(d) = b^- r^+ b^+ o^- b^- r^- ...$$

But in this case, $f_\beta(b)$ is forced to follow $f_\beta(d)$, which will force it to trace. Thus $f_\beta(d)$ cannot have any initial twists. Thus we must have

$$f_\beta(d) = b^- r^- d ...$$

This is Figure E.111.

Here $f_\beta(\bar{d})$ can begin with no initial twists, which has two possibilities:

$$f_\beta(\bar{d}) = p^- s^- ...$$

or

$$f_\beta(\bar{d}) = p^- i^- ...$$

It can also begin with initial twists, in which case it must be

$$f_\beta(\bar{d}) = p^- s^- (p^- s^+)^n p^+ i^- \bar{d} ...$$

f On the other hand, $f_\beta(\bar{d})$ in the middle can go under $f_\beta(r)$, above $f_\beta(d)$, or join with $f_\beta(d)$. It cannot go in between $f_\beta(d)$ and $f_\beta(r)$ or it will violate the Trace Lemma.

E.1.3.1 Etui

Suppose $f_\beta(\bar{d})$ goes under $f_\beta(r)$.

This is Figure E.112. Here regardless of whether $f_\beta(\bar{d})$ has any initial twists, the pair $f_\beta(d)$ and $f_\beta(\bar{d})$ on the left must go above the pair $f_\beta(i)$ and $f_\beta(s)$. Indeed, otherwise both $f_\beta(d)$ and $f_\beta(\bar{d})$ will violate the Trace Lemma. But now we are in Situation α. This is a contradiction.

E.1.3.2 Snee

Back to the end of IPC. Suppose $f_\beta(\bar{d})$ on the right goes above $f_\beta(d)$. Then we have

$$f_\beta(\bar{d}) = ... \bar{d} r^+ b^+ d ...$$

and

$$f_\beta(s) = \bar{d}r^+b^+d...$$

and

$$f_\beta(i) = \bar{d}r^+b^+d...$$

This is Figure E.113.

Here at least one of $f_\beta(s)$ and $f_\beta(i)$ will trace immediately after crossing d, regardless of whether $f_\beta(\bar{d})$ has any initial twists or not. This is a contradiction.

E.1.3.3 Zarf

Back to the end of IPC E.1.3. Suppose the dotted lines join in the middle. Then we have

$$f_\beta(s) = \bar{d}r^+b^+...$$

$$f_\beta(i) = \bar{d}r^+b^+o^*...$$

and

$$f_\beta(r) = di^*...$$

Here $f_\beta(r)$ must go up i and not s since in that case, regardless whether $f_\beta(\bar{d})$ has any initial twists, $f_\beta(r)$ will be forced to continue with

$$...s^+p6 + \bar{d}r^\times$$

Hence it must go up to i^*....

This is Figure E.114.

Here we claim that $f_\beta(\bar{d})$ cannot have any initial twists. Indeed, if it did, then $f_\beta(s)$ cannot cross d to the right hand side, otherwise it will trace due to the twisting. So $f_\beta(s)$ must continue with o^*.... But now $f_\beta(i)$ cannot end at o° or continue with o^- because that would then force $f_\beta(s)$ to continue with o^-, and it will trace:

$$f_\beta(i) = \bar{d}r^+b^+\hat{o}^-b^-r^-dp^-s^\times$$

Hence $f_\beta(i)$ must continue with o^+, but then it will either be absorbed:

$$f_\beta(i) = \bar{d}r^+b^+\hat{o}^+b^-r^-d\,\mathrm{Abso}(f_\beta(i), f_\beta(s))^\times$$

or trace:

$$f_\beta(i) = \bar{d}r^+b^+\hat{o}^+b^-r^-di^\times$$

This shows that $f_\beta(\bar{d})$ cannot have any initial twists. In which case we must have

$$f_\beta(\bar{d}) = p^-s^-\bar{d}r - b^-$$

and not

$$f_\beta(\bar{d}) = p^-i^-...$$

because in this case $f_\beta(d)$ will be forced to go up i and violate the Trace Lemma.

This means we are in the situation depicted in Figure E.115.

Here $f_\beta(r)$ must end at i° or it will trace:

$$f_\beta(r) = di^+\bar{d}r^\times$$

or

$$f_\beta(r) = di^- \bar{d}b^- r^\times$$

Thus we must have

$$f_\beta(r) = di^\circ$$

Now $f_\beta(s)$ can either continue with d or o^*.

E.1.3.3.1 Xebec

Suppose $f_\beta(s)$ continues with d. Then we have

$$f_\beta(s) = \bar{d}r^+ b^+ \hat{d}i^+ \bar{d}r^* ...$$

This is Figure E.116.

Here $f_\beta(s)$ must continue with r^+ and to the left of $f_\beta(b)$. Otherwise, $f_\beta(b)$ must begin with r^- and to the right of $f_\beta(s)$, in which case it will trace:

$$f_\beta(b) = r^- di^- \bar{d}b^\times$$

or

$$f_\beta(b) = r^- ds^+ p^+ \bar{d}r^+ b^\times$$

Thus we must have

$$f_\beta(s) = ...r^+ b^* ...$$

which immediately forces $f_\beta(o)$ to begin with b^- and to the right of the incoming $f_\beta(s)$. But

now it either is absorbed or traces:

$$f_\beta(p) = b^- r^- d i^- \bar{d} b^- r^- d \,\mathrm{Abso}(f_\beta(i), f_\beta(s))^\times$$

or

$$f_\beta(o) = b^- r^- d s^+ p^+ \bar{d} r^+ b^+ o^\times$$

This is a contradiction.

E.1.3.3.2 Vuggy

Back to the end of Zarf E.1.3.3. We must have $f_\beta(s)$ continues with o^*....

This is Figure E.117.

In fact, it must end here at o°. Indeed, otherwise it traces:

$$f_\beta(s) = \bar{d} r^+ b^+ \hat{o}^+ b^- r^- d s^\times$$

or

$$f_\beta(s) = \bar{d} r^+ b^+ \hat{o}^- b^- r^- d p^- s^\times$$

Or it is absorbed:

$$f_\beta(s) = \bar{d} r^+ b^+ \hat{o}^+ b^- r^- d \,\mathrm{Abso}(f_\beta(i), f_\beta(s))^\times$$

Thus we must have

$$f_\beta(s) = \bar{d} r^+ b^+ \hat{o}^\circ$$

Which forces:

$$f_\beta(i) = \bar{d} r^+ b^+ \hat{o}^+ b^- r^- d s^* ...$$

This is Figure E.118.

Here $f_\beta(b)$ must end immediately at r°. Indeed, otherwise it traces:

$$f_\beta(b) = r^- di^- b^\times$$

or

$$f_\beta(b) = r^- ds^+ p^+ \bar{d}r^+ b^\times$$

Thus we must have

$$f_\beta(b) = r^\circ$$

Here $f_\beta(o)$ can either end with b° or begin with b^-.

E.1.3.3.2.1 Guddle

Suppose

$$f_\beta(o) = b^\circ$$

Consider $f_\beta(i)$. It must continue with s^+ and to the left of $f_\beta(p)$. Otherwise, $f_\beta(p)$ will be forced to continue with s^- and to the right of $f_\beta(i)$, in which case it will either trace:

$$f_\beta(p) = s^- \bar{d}r^+ b^+ o^- b^- r^- dp^\times$$

or be absorbed:

$$f_\beta(p) = s^- \bar{d}r^+ b^+ di^+ r^+ b^+ \,\mathrm{Abso}(f_\beta(d), f_\beta(o))^\times$$

Thus we must have

$$f_\beta(i) = ...s^+...$$

and here $f_\beta(p)$ must end at s°. Otherwise it will be absorbed:

$$f_\beta(p) = s^- \bar{d} r^+ b^+ o^- r^- r^- d \, \mathrm{Abso}(f_\beta(i), f_\beta(s))^\times$$

Thus we must have

$$f_\beta(p) = s^\circ$$

This is Figure E.119.

Here $f_\beta(i)$ must end at p°. Otherwise, it will be absorbed:

$$f_\beta(i) = ...p^- s^- \bar{d} r^+ b^+ d i^+ \bar{d} r^+ b^+ \, \mathrm{Abso}(f_\beta(d), f_\beta(o))^\times$$

or

$$f_\beta(i) = ...p^+ s^- \bar{d} r^+ b^+ o^+ b^- r^- d \, \mathrm{Abso}(f_\beta(i), f_\beta(s))^\times$$

This gives us Candidate Train Track map 16, shown in Figure E.120.

E.1.3.3.2.2 Fipple

Back to the end of Vuggy E.1.3.3.2. Suppose $f_\beta(i)$ begins with b^-. Thus we have

$$f_\beta(o) = b^- r^- d i^- \bar{d} b^- r^- d s^* ...$$

This is Figure E.121.

Here $f_\beta(p)$ can either end at s°, or begin with s^- and into 1., 2., or 3.

E.1.3.3.2.2.1 Macumba

Suppose $f_\beta(p)$ ends at s°. Then we have the situation depicted in Figure E.122.

Here $f_\beta(i)$ must continue with p^- and to the right of $f_\beta(o)$. Otherwise, $f_\beta(o)$ will be forced to continue with p^+ and to the left of $f_\beta(i)$, in which case it will trace:

$$f_\beta(o) = ...p^+s^-\bar{d}r^+b^+o^\times$$

Thus $f_\beta(i)$ must continue with p^- and to the right of $f_\beta(o)$. But then it will eventually trace:

$$f_\beta(i) = ...p^-s^-\bar{d}r^+b^+di^\times$$

E.1.3.3.2.2.2 Fopdoodle

Back to the end of Fipple E.1.3.3.2.2. Suppose $f_\beta(p)$ beings with s^-, and suppose it enters into 1. Then it reduces to the same argument concerning $f_\beta(i)$ and $f_\beta(o)$ in Macumba E.1.3.3.2.2.1, which leads to a contradiction. So suppose it goes into 2. Then it will be absorbed:

$$f_\beta(p) = s^-\bar{d}r^+b^+di^+\bar{d}r^+b^+ \operatorname{Abso}(f_\beta(d), f_\beta(o))^\times$$

So suppose it goes into 3, then we have

$$f_\beta(p) = s^-\bar{d}r^+b^+di^+\bar{d}r^+b^*...$$

This is Figure E.123.

Here $f_\beta(i)$ must continue with s^- and to the right of $f_\beta(o)$. Otherwise, $f_\beta(o)$ will be forced to continue with s^+ and the left of $f_\beta(i)$, in which case it will trace:

$$f_\beta(o) = ...s^+\bar{d}r^+b^+o^times$$

But then we have

$$f_\beta(i) = ...d^- \bar{d} r^+ b^+ d i^\times$$

E.1.4 HND

Back to the end of Case A E.1, triangles fixed. Suppose $f_\beta(d)$ starts at r, and $f_\beta(\bar{d})$ starts at i.

The situation is depicted in Figure E.124.

Here $f_\beta(\bar{d})$ cannot go in between $f_\beta(d)$ and $f_\beta(b)$ or it will violate the Trace Lemma; nor can it go in between $f_\beta(d)$ and $f_\beta(o)$ or it will be absorbed between $f_\beta(d)$ and $f_\beta(o)$. So it must go into 1., 2., or join with $f_\beta(d)$ in the middle.

E.1.4.1 Froe

Suppose $f_\beta(\bar{d})$ goes into 1. Then we haave

$$f_\beta(\bar{d}) = i^+ p^+ \bar{d} r^+ b^+ d...$$

This is Figure E.125.

Here the pair $f_\beta(d)$ and $f_\beta(\bar{d})$, and $f_\beta(o)$ in between them on the left hand side are in Situation α. This is a contradiction.

E.1.4.2 Moxa

Back to the end of E.1.4. Suppose $f_\beta(\bar{d})$ goes into 2. Then we have

$$f_\beta(\bar{d}) = i^+ p^+ \bar{d} b^- r^- d...$$

This is Figure E.126.

Here $f_\beta(p)$ will trace:

$$f_\beta(p) = \bar{d}b^- r^- dp^\times$$

E.1.4.3 Erne

Back to the end of E.1.4. Suppose the dotted lines join in the middle.

This is Figure E.127.

But now $f_\beta(p)$ must continue nuder $f_\beta(o)$ or be absorbed between $f_\beta(d)$ and $f_\beta(o)$; but then it traces:

$$f_\beta(p) = \bar{d}b^- r^- dp^\times$$

E.1.5 USH

Back to the end of Case A E.1, triangles fixed. Suppose $f_\beta(d)$ starts at r, and $f_\beta(\bar{d})$ starts at s.

The situation is depicted in Figure E.128.

Here $f_\beta(\bar{d})$ cannot go into 2., or it will be in Situation β. It cannot go into 3., or it will be absorbed between $f_\beta(d)$ and $f_\beta(o)$. So $f_\beta(\bar{d})$ can only go into 1., 4., or join with $f_\beta(d)$ in the middle.

E.1.5.1 Torc

Suppose $f_\beta(\bar{d})$ goes into 1.

This is Figure E.129.

Here the pair $f_\beta(d)$ and $f_\beta(\bar{d})$, together with $f_\beta(o)$ in between them, are in Situation α.

E.1.5.2 Yegg

Back to the end of USH E.1.5. Suppose $f_\beta(\bar{d})$ goes into 4. But now $f_\beta(p)$ traces, as depicted in Vegg1.

E.1.5.3 Kief

Back to the end of USH E.1.5. Suppose $f_\beta(\bar{d})$ and $f_\beta(d)$ join in the middle. But now $f_\beta(b)$ will trace:

$$f_\beta(b) = dp^- s^- \bar{d} b^\times$$

as shown in Figure E.130.

E.1.6 LXA

Back to the end of Case A E.1, triangles fixed. Suppose $f_\beta(d)$ starts at r, and $f_\beta(\bar{d})$ starts at p.

This is Figure E.131.

Here $f_\beta(\bar{d})$ will cross $\bar{d}$ right after it comes down via s^-, or i^-, possibly with initial twists.

Suppose it comes down on s^- before crossing. Then it cannot have any initial twisting. This is shown in Figure E.132.

Here if $f_\beta(b)$ were to go above the pair $f_\beta(i)$ and $f_\beta(s)$ on the right, then it will trace:

$$f_\beta(b) = dp^- s^- \bar{d} b^\times$$

While if instead the pair $f_\beta(i)$ and $f_\beta(s)$ were to go above $f_\beta(b)$ on the left, then after they cross again:

$$f_\beta(i) = \bar{d} r^+ b^+ d ...$$

and

$$f_\beta(s) = \bar{d}r^+b^+d...$$

at least one of them will trace. This is a contradiction.

Thus, $f_\beta(\bar{d})$ must go down via i before crossing. Then $f_\beta(\bar{d})$ can either have no initial twists or have initial twists.

E.1.6.1 Xama

Suppose $f_\beta(\bar{d})$ has no initial twists. The situation is depicted in Figure E.133.

Here $f_\beta(\bar{d})$ can go into 1, 2., or join with $f_\beta(d)$. It cannot go in between $f_\beta(b)$ and $f_\beta(d)$ as that would be Situation β; and it cannot go in between $f_\beta(d)$ and $f_\beta(o)$ or it will be absorbed between the two.

Suppose it goes into 1. This is Figure E.134. Here $f_\beta(d)$ and $f_\beta(\bar{d})$, together with $f_\beta(o)$ in between them, are in Situation α.

So suppose $f_\beta(\bar{d})$ goes into 2. This is Figure E.134. Here $f_\beta(\bar{d})$ has to go above the pair $f_\beta(i)$ and $f_\beta(s)$, or it will go into Situation β. Similarly, $f_\beta(d)$ has to go above the pair, and therefore $f_\beta(b)$ as well.

This is Figure E.135.

Here the pair $f_\beta(d)$ and $f_\beta(\bar{d})$, together with $f_\beta(b)$ in between them, are in Situation α. This is a contradiction.

So suppose in the situation depicted in Figure E.133, the dotted lines joint in the middle.

This is Figure E.136.

Here $f_\beta(b)$ can only go into 1., or 2. If it were to go in between $f_\beta(o)$ and $f_\beta(i)$ then it will

eventually trace after crossing $\bar{d}$.

If it goes into 2., then $f_\beta(i)$, $f_\beta(s)$, and $f_\beta(o)$ go above $f_\beta(b)$. Then we have

$$f_\beta(i) = \bar{d}r^+b^+o^*...$$

Here it cannot go $f_\beta(i) = f_\beta r^+b^+d...$ a the next letter would trace. But now $f_\beta(o)$ traces;

$$f_\beta(o) = r^+b^+di^+p^+\bar{d}r^+b^+o^\times$$

THis is Figure E.137.

Thus going back to the situation depicted in Figure E.136, $f_\beta(b)$ must go into 1. Then we must have

$$f_\beta(b) = dp^-s^\circ$$

It must end here at s° since either s^+ and s^- would lead it to eventually trace.

This is Figure E.138.

Here $f_\beta(r)$ can either end at b°, or begin with b^+.

E.1.6.1.1 Zaxes

Suppose $f_\beta(r)$ ends at b°:

$$f_\beta(r) = b^\circ$$

Then we have

$$f_\beta(i) = \bar{d}b^-r^*...$$

and

$$f_\beta(s) = \bar{d}b^- r^* ...$$

Now $f_\beta(i)$ must continue with r^+ and to the left of $f_\beta(s)$. otherwise $f_\beta(s)$ will be forced to continue with r^- and to the right of $f_\beta(i)$, which would force it to trace:

$$f_\beta(s) = \bar{d}b^- \hat{r}^- b^+ dp^- i^- \bar{d}b^- r^- dp^- s^\times$$

But now we have

$$f_\beta(i) = \bar{d}b^- \hat{r}^+ di^\times$$

This is Figure E.139.

E.1.6.1.2 Qophs

Back to the end of Xama E.1.6.1. Suppose

$$f_\beta(r) = b^+ di^* ...$$

This is Figure E.140.

Here $f_\beta(s)$ must continue with b^- and to the right of $f_\beta(i)$ and $f_\beta(o)$. Otherwise, $f_\beta(i)$ will be forced to continue iwth b^+ and trace immediately after scrossing d. It must go to the right of $f_\beta(o)$ as well since if it were t ogo in between $f_\beta(i)$ and $f_\beta(o)$ (i.e. to the left of $f_\beta(o)$), then it will be absorbed:

$$f_\beta(s) = \bar{d}b^- dp^- i^- \bar{d}b^- r^- \,\mathrm{Abso}(f_\beta(d), f_\beta(o))^\times$$

But no it is still forced to trace:

$$f_\beta(s) = \bar{d}b^- dp^- i^- \bar{d}b^- r^- dp^- s^\times$$

E.1.6.2 Zoea

Back to the end of LXAE.1.6. Suppose $f_\beta(\bar{d})$ has initial twisting, and comes down on i right before crossing $\bar{d}$.

This is Figure E.141, where we've depicted one twisting between s and p before going to i^- and crossing $\bar{d}$.

Here $f_\beta(s)$ must continue with b^- and to the right of $f_\beta(r)$. Otherwise $f_\beta(i)$ will be forced to continue with b^+ and to the left of $f_\beta(s)$, in which case it will immediately trace after crossing d. Further, $f_\beta(s)$ must go to the right of $f_\beta(r)$ or it will trace:

$$f_\beta(s) = \bar{d}b^- dp^- s^\times$$

Thus we must continue with the situation depicted in Figure E.142.

Here $f_\beta(s)$ must continue with r^- and to the right of $f_\beta(i)$. Otherwise, $f_\beta(i)$ will be forced to continue with r^+ and immediately trace right after crossing d.

Thus we have the situation depicted in Figure E.143. Here again $f_\beta(s)$ is forced to continue with b^+ and to the left of $f_\beta(r)$. Otherwise, $f_\beta(r)$ will immediately trace.

But now $f_\beta(s)$ will trace:

$$f_\beta(s) = ...b^+ dp^- s^\times$$

This is a contradiction.

E.2 Case B,C,D: Triangles Swapped

Now we assume the triangles are swapped by f_β. Hence at least one of $f_\beta(d)$ or $f_\beta(\bar{d})$ passes over d or $\bar{d}$ after an odd number of letters.

We first assume $f_\beta(\bar{d})$ passes over d after an odd number of letters.

E.2.1 OMG

Assuming $f_\beta(\bar{d})$ passes over d after an odd number of letters, and let us assume $f_\beta(\bar{d})$ starts at o, and $f_\beta(d)$ starts at p.

But in this situation $f_\beta(r)$ traces, as shown in Figure E.144.

E.2.2 SUX

Assuming $f_\beta(\bar{d})$ passes over d after an odd number of letters, and let us assume $f_\beta(\bar{d})$ starts at o, and $f_\beta(d)$ starts at s.

This is Figure E.145.

Here both $f_\beta(s)$ and $f_\beta(i)$ must continue with r^- and to the right of $f_\beta(b)$. Otherwise, $f_\beta(b)$ will trace.

This is Figure E.146.

Here again both $f_\beta(s)$ and $f_\beta(i)$ must continue with p^- and to the right of $f_\beta(r)$. Otherwise $f_\beta(r)$ will trace immediately after crossing $\bar{d}$. But now $f_\beta(s)$ traces.

E.2.3 DIE

Assuming $f_\beta(\bar{d})$ passes over d after an odd number of letters, and let us assume $f_\beta(\bar{d})$ starts at o, and $f_\beta(d)$ starts at i.

The same argument in SUX E.2.2 shows this cannot happen. Except at the very last step, $f_\beta(i)$ traces in stead of $f_\beta(s)$.

E.2.4 ULN

Assuming $f_\beta(\bar{d})$ passes over d after an odd number of letters, and let us assume $f_\beta(\bar{d})$ starts at o, and $f_\beta(d)$ starts at $\bar{d}$.

This is Figure E.147.

Here $f_\beta(d)$ must continue with r^+ and to the left of $f_\beta(s)$ and $f_\beta(i)$. Otherwise, both $f_\beta(i)$ and $f_\beta(b)$ cross d, and then continue with p^- (or $f_\beta(b)$ will trace after crossing $\bar{d}$). But then at least one of $f_\beta(s)$ or $f_\beta(i)$ will trace. So we must have

$$f_\beta(s) = \bar{d}r^+b^+o^*...$$

This is Figure E.148.

Now consider $f_\beta(o)$. It must continue with r^+ and to the left of $f_\beta(s)$ and $f_\beta(i)$. Otherwise the two will be abssorbed between $f_\beta(i)$ and $f_\beta(o)$. Now we have the situation depicted in Figure E.149.

Here $f_\beta(o)$ must continue with b^+ and to the left of $f_\beta(p)$. Otherwise $f_\beta(p)$ also woud be absorbed. But now $f_\beta(o)$ traces.

This is a contradiction.

E.2.5 NAN

Assuming $f_\beta(\bar{d})$ passes over d after an odd number of letters, and let us assume $f_\beta(\bar{d})$ starts at b, and $f_\beta(d)$ starts at p.

Consider $f_\beta(r) = \bar{d}$.... The next letter must be b or else it will trace:

$$f_\beta(r) = \bar{d}b^*...$$

This forces both $f_\beta(i)$ and $f_\beta(s)$ to begin with d:

$$f_\beta(s) = dp^*...$$

$$f_\beta(i) = dp^*...$$

This is Figure E.150.

Here $f_\beta(d)$ must begin with p^+ otherwise either $f_\beta(s)$ or $f_\beta(i)$ will trace. This gives Figure E.151.

Both $f_\beta(d)$ and $f_\beta(o)$ must continue with r^+ otherwise $f_\beta(p)$ will trace immediately after crossing d. This gives Figure E.152.

Here $f_\beta(o)$ must continue with b^+ and to the left of $f_\beta(r)$. Otherwise, $f_\beta(r)$ will trace. This gives Figure E.153.

Here $f_\beta(d)$ and $f_\beta(\bar{d})$ cannot join or $f_\beta(r)$ will trace. Thus they both must continue with b^+ and to the left of $f_\beta(r)$. But now $f_\beta(d)$ and $f_\beta(\bar{d})$ are in Situation α.

This is a contradiction.

E.2.6 GOH

Assuming $f_\beta(\bar{d})$ passes over d after an odd number of letters, and let us assume $f_\beta(\bar{d})$ starts at b, and $f_\beta(d)$ starts at s.

his is Figure E.154.

Here $f_\beta(b)$ must go above $f_\beta(s)$ and $f_\beta(i)$. Otherwise it will tace immediately after crossing $\bar{d}$. but now either $f_\beta(s)$ or $f_\beta(i)$ will trace immediately after crossing d.

This is a contradiction.

E.2.7 PPT

Assuming $f_\beta(\bar{d})$ passes over d after an odd number of letters, and let us assume $f_\beta(\bar{d})$ starts at b, and $f_\beta(d)$ starts at i.

The same argument as that of GOH E.2.6 gives a contradiction.

E.2.8 BOD

Assuming $f_\beta(\bar{d})$ passes over d after an odd number of letters, and let us assume $f_\beta(\bar{d})$ starts at b, and $f_\beta(d)$ starts at $\bar{d}$.

This is Figure E.155.

Here $f_\beta(s)$ and $f_\beta(i)$ must go above $f_\beta(o)$. Otherwise, either $f_\beta(s)$ or $f_\beta(i)$ will trace immediately after crossing d.

This is Figure E.156.

Here $f_\beta(b)$ must being with p^+ and to the left of $f_\beta(s)$ and $f_\beta(i)$. Otherwise, again either of those would trace. Then after crossing $f_\beta(\bar{d})$, $f_\beta(b)$ must continue with r^+ and to the left of $f_\beta(p)$ otherwise $f_\beta(p)$ will trace right after crossing d. But now $f_\beta(b)$ traces;

$$f_\beta(b) = p^+ \bar{d} r^+ b^\times$$

E.2.9 MAA

Assuming $f_\beta(\bar{d})$ passes over d after an odd number of letters, and let us assume $f_\beta(\bar{d})$ starts at r, and $f_\beta(d)$ starts at p.

This is Figure E.157.

Here $f_\beta(r)$ must go below $f_\beta(p)$ otherwise $f_\beta(r)$ will trace immediately after crossing $\bar{d}$. But now $f_\beta(p)$ will trace immediately right after crossing d.

This is a contradiction.

E.2.10 XNB

Assuming $f_\beta(\bar{d})$ passes over d after an odd number of letters, and let us assume $f_\beta(\bar{d})$ starts at r, and $f_\beta(d)$ starts at s.

This is Figure E.158.

Here $f_\beta(\bar{d})$ must come down on r before crossing d, and it cannot have any initial twists otherwise $f_\beta(d)$ will be forced to cross d with it, and thereby trace. So we must have

$$f_\beta(\bar{d}) = r^- d ...$$

Here it must go above $f_\beta(b)$. Otherwise $f_\beta(b)$ will trace. On the other hand $f_\beta(b)$ must go above $f_\beta(p)$ otherwise $f_\beta(p)$ will trace.

This is Figure E.159.

Here $f_\beta(i)$ must begin with b^+ and to the left of $f_\beta(s)$. Otherwise $f_\beta(s)$ is forced to begin with b^-, and thereby trace:

$$f_\beta(s) = b^- r^- d p^- s^\times$$

In fact $f_\beta(i)$ must then continue with o^* otherwise it would force $f_\beta(p)$ to cross with it and then go up s, which would force $f_\beta(p)$ to trace.

This is Figure E.160.

Here $f_\beta(\bar{d})$ either join with $f_\beta(d)$, or $f_\beta(\bar{d})$ must continue with s^- and to the right of $f_\beta(p)$.

E.2.10.1 Qadi

Suppose the dotted lines join.

This is Figure E.161.

Here $f_\beta(p)$ can continue with d or o^*. Suppose it were to continue with d. Then

$$f_\beta(p) = do^*...$$

This forces $f_\beta(o)$ to begin with i^- and to the right of $f_\beta(p)$. So we have

$$f_\beta(o) = i^-\bar{d}b^*...$$

This is Figure E.162.

This forces $sf_\beta(s)$ to go b^+ and to the left of the incoming $f_\beta(p)$:

$$f_\beta(s) = b^+o^*...$$

Which thereby forces $f_\beta(i)$ to continue with o^+ and to the left of $f_\beta(s)$. Otherwise $f_\beta(s)$ would trace:

$$f_\beta(s) = b^+o^-b^-r^-dp^-s^\times$$

Thus we must have

$$f_\beta(i) = b^+\hat{o}^+b^*...$$

This is Figure E.163.

Here $f_\beta(i)$ must continue with b^- and to the right of $f_\beta(o)$. Otherwise, $f_\beta(o)$ would immediately trace. But now $f_\beta(i)$ will trace:

$$f_\beta(i) = b^+o^+\hat{b}^-di^\times$$

Back to the situation depicted in Figure E.161. SUppose $f_\beta(p)$ continues with o^*.

This is Figure E.164.

Here $f_\beta(o)$ can continue with i^- or i°.

E.2.10.1.1 Agora

Suppose $f_\beta(o)$ continues with i^-. So we have

$$f_\beta(o) = o^-\bar{d}r^*...$$

This is Figure E.165.

Here $f_\beta(i)$ must continue with r^- and to the right of the incoming $f_\beta(o)$. Otherwise $f_\beta(o)$ would be forced to continue with r^+ and to the left of $f_\beta(i)$, and would immediately trace.

So we have

$$f_\beta(i) = ...r^-dp^*...$$

and it must continue with p^- and to the right of $f_\beta(r)$. Otherwise, $f_\beta(r)$ would trace

immediately after crossing $\bar{d}$.

This is Figure E.166.

Here $f_\beta(o)$ is forced to continue with r^- and to the right of $f_\beta(b)$. Otherwise $f_\beta(b)$ is forced to continue with r^+ and either gets absorbed:

$$f_\beta(b) = \bar{d}\hat{r}^+ di^+ \,\mathrm{Abso}(f_\beta(d), f_\beta(o))^\times$$

or trace:

$$f_\beta(b) = \bar{d}\hat{r}^+ o^- b^\times$$

Thus we must have

$$f_\beta(o) = ...r^- dp^- s^*...$$

This is Figure E.167.

Here $f_\beta(i)$ must continue with s^- and to the right of $f_\beta(o)$.

This is Figure E.168.

Here both $f_\beta(p)$ and $f_\beta(s)$ must end immediately or they would both eventually trace. So we have

$$f_\beta(p) = o^\circ$$

and

$$f_\beta(s) = b^\circ$$

This is Figure E.169.

Here $f_\beta(r)$ and either continue with p° or p^-.

E.2.10.1.1.1 Byssus

Suppose

$$f_\beta(r) = p^\circ$$

This is Figure E.170.

This forces $f_\beta(i)$ to continue

$$f_\beta(i) = ...p^+\bar{d}r^*...$$

But now $f_\beta(i)$, $f_\beta(b)$, and $f_\beta(o)$ are in a clockwise path mill. this is a contradiction.

E.2.10.1.1.2 Zareba

Back to the end of Agora E.2.10.1.1. Suppose $f_\beta(r)$ continue with p^-.

This is Figure E.171.

Here $f_\beta(r)$, $f_\beta(o)$, and $f_\beta(i)$ are in a clockwise path mill between s and p.

This is a contradiction.

E.2.10.1.2 Bokeh

Back to the end of Qadi E.2.10.1. Suppose

$$f_\beta(o) = i^\circ$$

This is Figure E.172.

Here $f_\beta(s)$ can begin with b° or b^+.

E.2.10.1.2.1 Popjoy

Suppose

$$f_\beta(s) = b^\circ$$

This is Figure E.173.

Here $f_\beta(p)$ can either begin with o° or o^+. Suppose

$$f_\beta(p) = o^\circ$$

Then $f_\beta(i)$ is forced to continue with r^- and to the right of $f_\beta(b)$. Otherwise $f_\beta(b)$ would be forced to be absorbed between $f_\beta(s)$ and $f_\beta(i)$. After crossing d, it must go p^- and to the right of $f_\beta(r)$, or $f_\beta(r)$ will trace. So we have

$$f_\beta(i) = r^+ o^+ \hat{r}^- p^- s^* ...$$

This is Figure E.174.

Here $f_\beta(r)$ must end at p or s after possibly twisting k times between the two. Then $f_\beta(i)$ and $f_\beta(b)$ twist m times between s and r, and end there.

This is Candidate Train Track Map Family 17.

E.2.10.1.2.2 Archon

Back to the end of Bokeh E.2.10.1.2. suppose

$$f_\beta(s) = b^+ o^* ...$$

This is Arhcon1.

Here $f_\beta(s)$ is forced to continue with o^+ and to the left of $f_\beta(p)$. Otherwise $f_\beta(p)$ will be absorbed.

This is Figure E.176.

Here $f_\beta(b)$ is forced to continue with r^+ and to the left of $f_\beta(s)$. Otherwise, $f_\beta(s)$ is forced to continue with r^- and after crossing d, p^- and to the right of $f_\beta(r)$ (otherwise $f_\beta(r)$ will trace), but then $f_\beta(s)$ itself traces.

This is Figure E.177.

Here $f_\beta(i)$, $f_\beta(b)$, $f_\beta(p)$, and $f_\beta(s)$ are in a four-strand counterclockwise path mill between o and r.

This is a contradiction.

E.2.10.2 Iwis

Back to the end of XNB E.2.10. Suppose $f_\beta(\bar{d})$ does not join with $f_\beta(d)$ in the situation depicted in Figure E.160, but instead continue with s^- and to the right of $f_\beta(p)$. Then it continues as shown in Figure E.178.

here $f_\beta(s)$ must begin with b^+ and to the left of the incoming $f_\beta(\bar{d})$.

This is Figure E.179.

Here $f_\beta(i)$ must continue with o^+ and to the left of $f_\beta(\bar{d})$. Otherwise, $f_\beta(s)$ will be forced to continue with o^- and eventually trace.

This is Figure E.180.

Here $f_\beta(\bar{d})$, $f_\beta(s)$, and $f_\beta(i)$ are in a counter clockwise path mill between o and b.

This is a contradiction.

E.2.11 QRO

Assuming $f_\beta(\bar{d})$ passes over d after an odd number of letters, and let us assume $f_\beta(\bar{d})$ starts at r, and $f_\beta(d)$ starts at i.

This is Figure E.181.

Here $f_\beta(d)$ can either begin with p^+ or p^-.

E.2.11.1 Burl

Suppose

$$f_\beta(d) = p^+...$$

Here $f_\beta(p)$ must begin with o^*. Otherwise, it would trace:

$$f_\beta(p) = di^+p^\times$$

Thus we must have

$$f_\beta(p) = o^*...$$

Now consider $f_\beta(i)$. It must continue with o^+ and to the left of the incoming $f_\beta(p)$. Otherwise, $f_\beta(p)$ will be forced to continue with o^- and to the right of $f_\beta(i)$, in which case it will trace immediately after crossing d. So we have

$$f_\beta(i) = ...o^+r^*...$$

Here $f_\beta(i)$ must continue with r^- and to the right of $f_\beta(b)$. If not, then $f_\beta(b)$ will be forced to continue with r^+, which would put $f_\beta(b)$, $f_\beta(p)$, $f_\beta(i)$ in a conuter clockwise path mill between o and r, as depicted in Figure E.182.

Thus we must have the situation depicted in Figure E.183.

Here we claim that $f_\beta(i)$ must continue with p^- and then s^*, as depicted in Figure E.184. Indeed, if it continues instead with p° or p^+, then $f_\beta(r)$ is forced to begin with p^+ and to the left of $f_\beta(i)$, in which case it will trace immediately after crossing $\bar{d}$.

Thus we are in the situation depicted in Figure E.183. But now $f_\beta(\bar{d})$ must continue with s^- and to the right of $f_\beta(i)$, and not s^+; otherwise, it would violate the Trace Lemma. But then we have the situation depicted in Figure E.185.

Here $f_\beta(r)$ must begin with p^- and continue in between $f_\beta(i)$ and $f_\beta(\bar{d})$, as depicted in Figure E.186.

Here $f_\beta(i)$ must continue with s^- and to the right of $f_\beta(r)$. Otherwise, $f_\beta(r)$ will be forcde to continue with s^+ and to the left of $f_\beta(i)$, in which case it will trace after crossing $\bar{d}$.

This is Figure E.187.

Now $f_\beta(r)$, $f_\beta(i)$, and the triplet $f_\beta(d)/f_\beta(o)/f_\beta(\bar{d})$ are in a clockwise path mill between p and s.

This is a contradiction.

E.2.11.2 Kyat

Back to the end of QRO E.2.11. Suppose

$$f_\beta(d) = p^- ...$$

This is Figure E.188.

Here $f_\beta(d)$ must continue with b^+. Otherwise, if it went to r^*, or b^-, it would violate the Trace Lemma. Thus we must have

$$f_\beta(d) = i^- \bar{d} \hat{b}^+ o^* ...$$

This forces

$$f_\beta(s) = b^+ o^* ...$$

and

$$f_\beta(p) = d i^* ...$$

This is Figure E.189.

Here $f_\beta(o)$ is forced to begin with i^- and to the right of $f_\beta(p)$. But now it will trace:

$$f_\beta(o) = i^- \bar{d} b^+ o^\times$$

As depicted in Figure E.190.

This is a contradiction.

E.2.12 WVB

Assuming $f_\beta(\bar{d})$ passes over d after an odd number of letters, and let us assume $f_\beta(\bar{d})$ starts at r, and $f_\beta(d)$ starts at $\bar{d}$.

This is Figure E.191.

Here $f_\beta(\bar{d})$ can have no initial twists, or have initial twists with b.

E.2.12.1 Nard

Suppose $f_\beta(\bar{d})$ has no initial twists. Then we have

$$f_\beta(\bar{d}) = r^- d...$$

This is Figure E.192.

Here $f_\beta(d)$ on the right hand side can either go above $f_\beta(d)$ on the left hand side, or go below, or the two can join in the middle.

Suppose $f_\beta(d)$ goes above $f_\beta(\bar{d})$. Then this forces the situation depicted in Figure E.193.

Here $f_\beta(d)$ must continue with b^+ and to the left of $f_\beta(s)$ and $f_\beta(i)$. Otherwise b^- would cause $f_\beta(d)$ to violate the Trace Lemma. Then $f_\beta(d)$ must then cross d, again to not violate the Trace Lemma. At the same time $f_\beta(o)$ follows $f_\beta(\bar{d})$ to not trace.

This is Figure E.194.

Here the pair $f_\beta(d)$ and $f_\beta(\bar{d})$ sandwich $f_\beta(p)$ in between them. Now the pair cannot continue with s^+ or i^+, as that would either bring p to trace, or violate the Trace Lemma. However, neither can the pair continue with s^- or i^- as those choices immediately violate the Trace Lemma.

This is a contradiction.

E.2.12.2 Drek

back to the end of WVB E.2.12. Suppose $f_\beta(\bar{d})$ has initial twists.

This is Figure E.195

Then the initial twists cannot include o, such as depicted in Figure E.196. Here either $f_\beta(o)$ will be forced to trace, or $f_\beta(p)$ will be forced to trace.

Thus the initial twists can only occur between r and b, such as the one depicted in Figure E.197, which depicts one twist.

Here the pair $f_\beta(s)$ and $f_\beta(i)$ either continue below the pair $f_\beta(o)$ and $f_\beta(d)$, in which case at least one of $f_\beta(s)$ or $f_\beta(i)$ will immediately trace; or the pair $f_\beta(s)$ and $f_\beta(i)$ go above the pair $f_\beta(o)$ and $f_\beta(d)$, in which case they must continue with p^- and to the right of $f_\beta(b)$, otherwise $f_\beta(b)$ will trace. But now $f_\beta(i)$ or $f_\beta(s)$ will trace. This is depicted in Figure E.198.

This is a contradiction.

E.2.13 ZFB

Now we assume $f_\beta(\bar{d})$ passes over d after an even number of letters, in which case $f_\beta(d)$ must cross $\bar{d}$ after an odd number of letters.

In order to go over an even number of letters before crossing, the only possible places to start for $f_\beta(\bar{d})$ is o or b.

Let us assume $f_\beta(\bar{d})$ starts at o. Then the only possibility for $f_\beta(\bar{d})$ to go over an even number of letters is

$$f_\beta(\bar{d}) = o^+(r^+b^-)^k r^- d...$$

where k is some number of twisting, Figure Figure E.199 shows $k = 1$.

Indeed, if $f_\beta(\bar{d})$ were to begin with o^- instead, then the following is forced:

$$f_\beta(\bar{d}) = o^- b^- r^- ...$$

as shown in Figure E.200.

But it cannot cross d here, so it must continue with b^*... But now it is in Situation β (the bagged serpent)

Regardless of the number of twisting, neither b nor r can start at $\bar{d}$, or they will trace after crossing. Hence $f_\beta(d)$ can only start at $\bar{d}$.

This is Figure E.201.

Here the dotted lines can either join or $f_\beta(d)$ on the right must go above $f_\beta(\bar{d})$ on the left.

E.2.13.1 Aery

Suppose the dotted lines join.

This is Figure E.202.

Here if $f_\beta(\bar{d})$ had no twists, i.e.

$$f_\beta(\bar{d}) = o^+ r^- d^\circ$$

then this forces

$$f_\beta(o) = \bar{d} r^+ b^* ...$$

which forces both $f_\beta(s)$ and $f_\beta(i)$ both to begin with b^- and to the right of the incoming $f_\beta(o)$, otherwise $f_\beta(o)$ will trace.

Then we have

$$f_\beta(i) = b^- r^- d p^- ...$$

and

$$f_\beta(s) = b^- r^- d p^- ...$$

Here both must go with p^- and to the right of $f_\beta(b)$ or $f_\beta(b)$ will trace immediately after crossing $f_\beta(\bar{d})$. But now at least one of $f_\beta(i)$ or $f_\beta(s)$ must trace.

Hence $f_\beta(\bar{d})$ must have twisting. However, the situation is the same, as $f_\beta(s)$ and $f_\beta(i)$ are still forced to begin with

$$f_\beta(i) = b^- r^- dp^- ...$$

and

$$f_\beta(s) = b^- r^- dp^- ...$$

This is a contradiction.

E.3 Figures

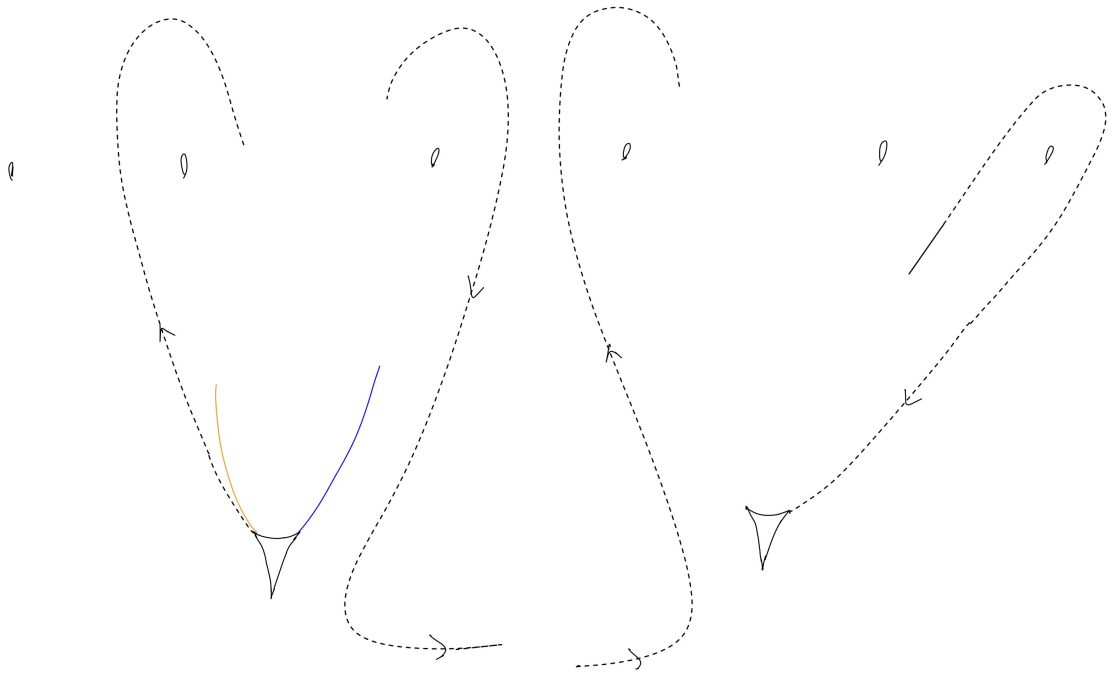


Figure E.1: VIE1

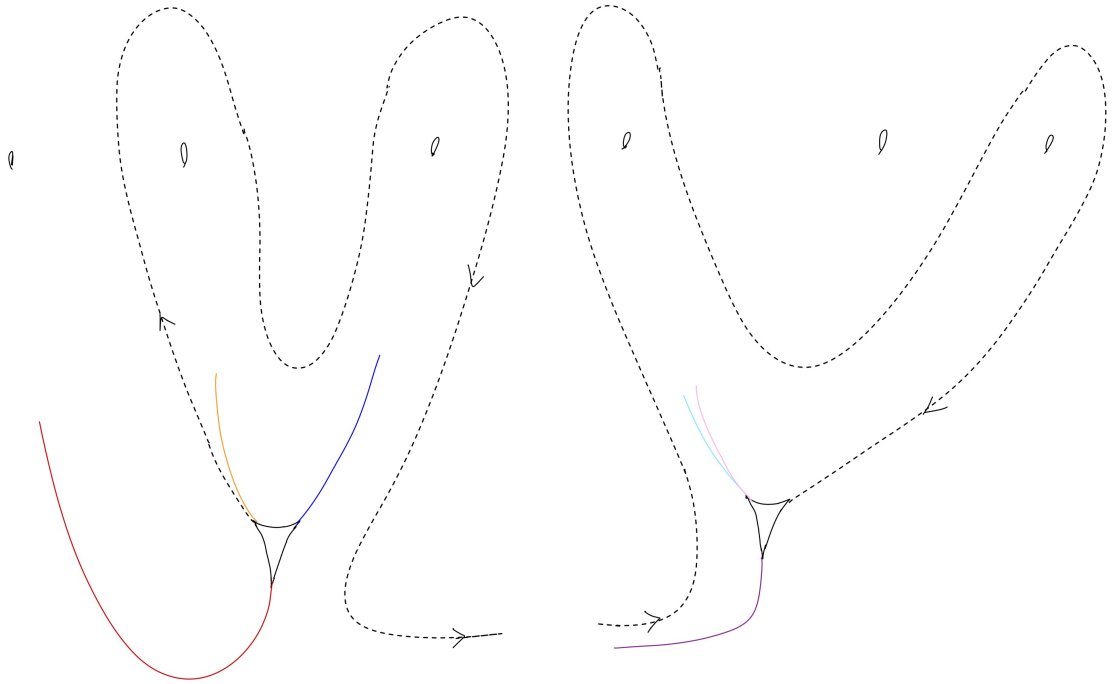


Figure E.2: VIE2

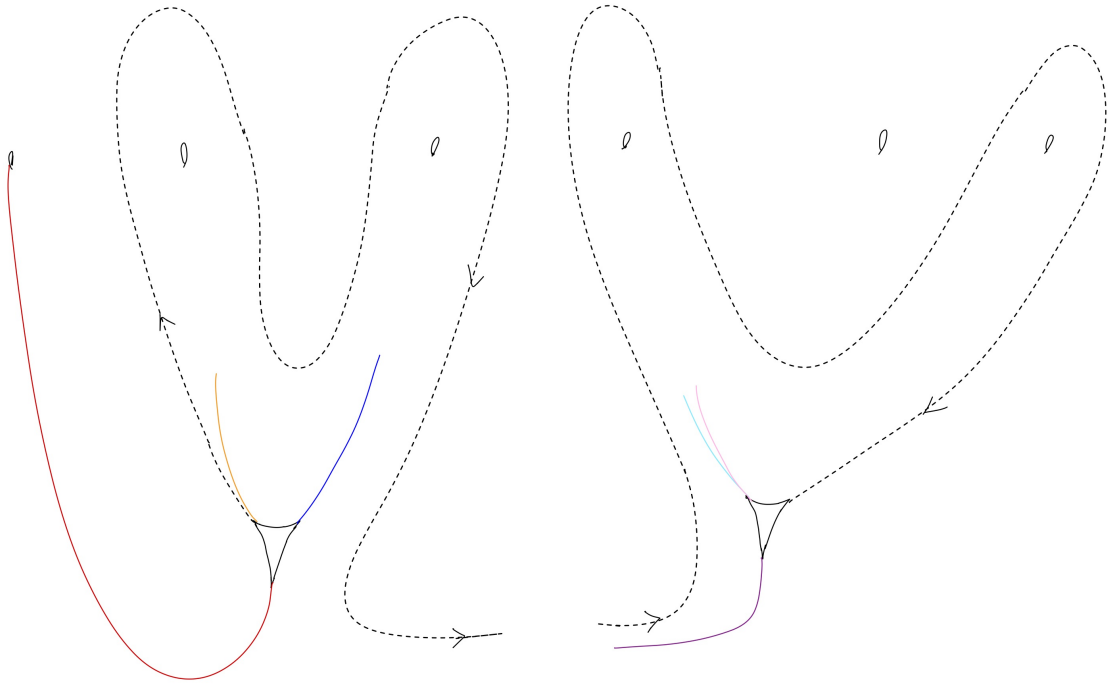


Figure E.3: VIE3

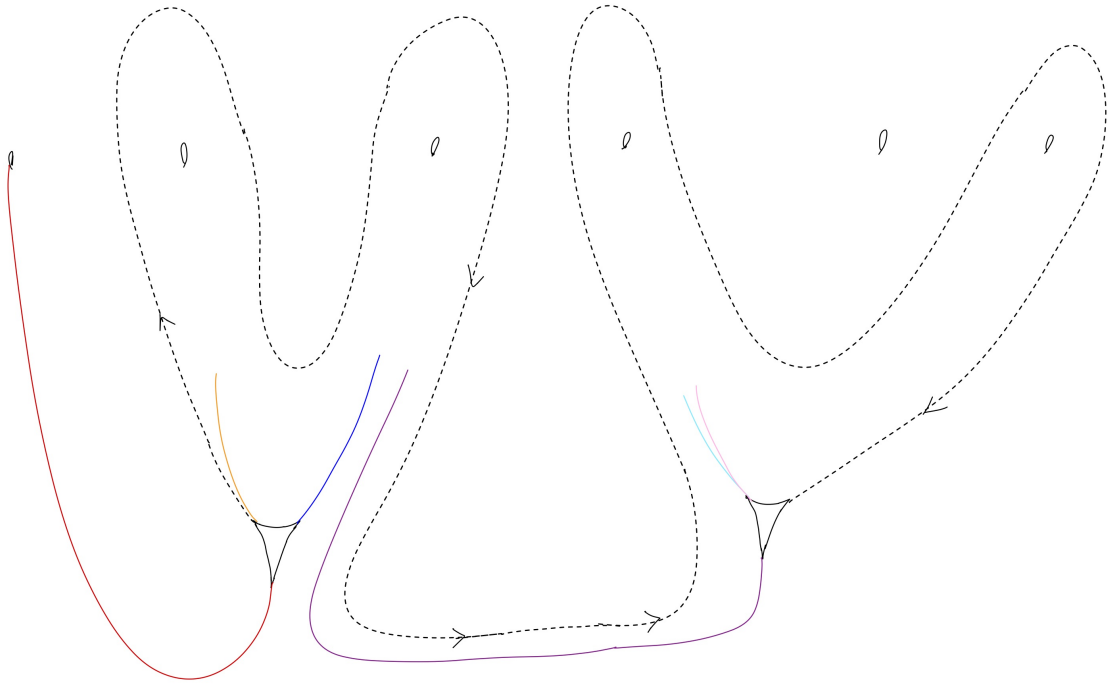


Figure E.4: Iris1

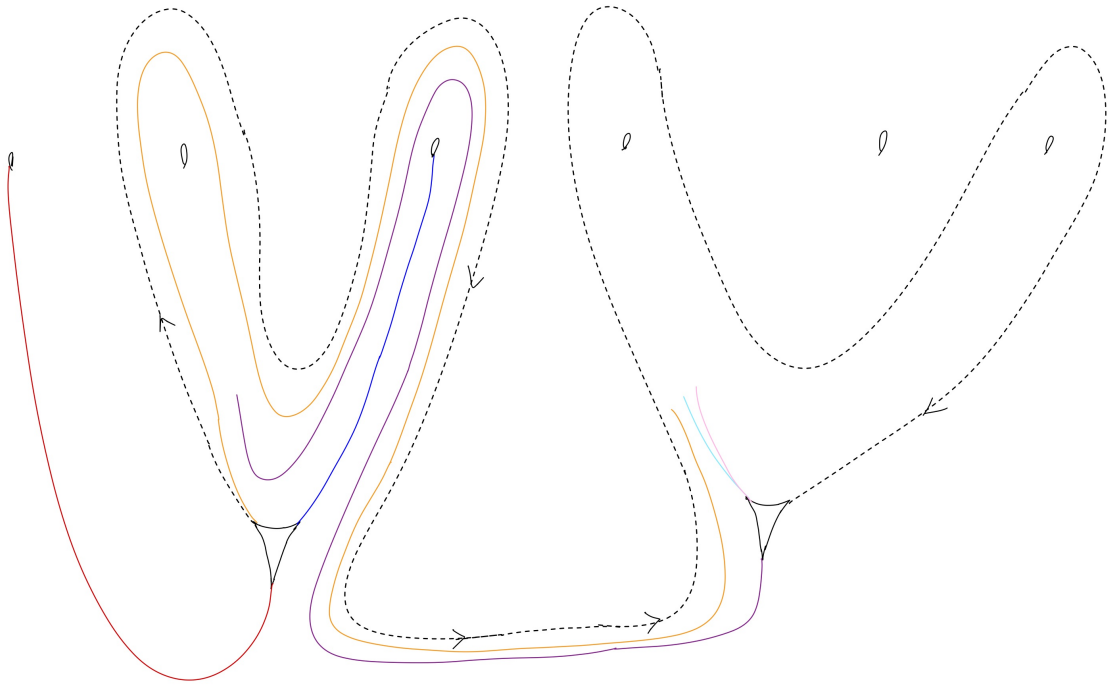


Figure E.5: Flute1

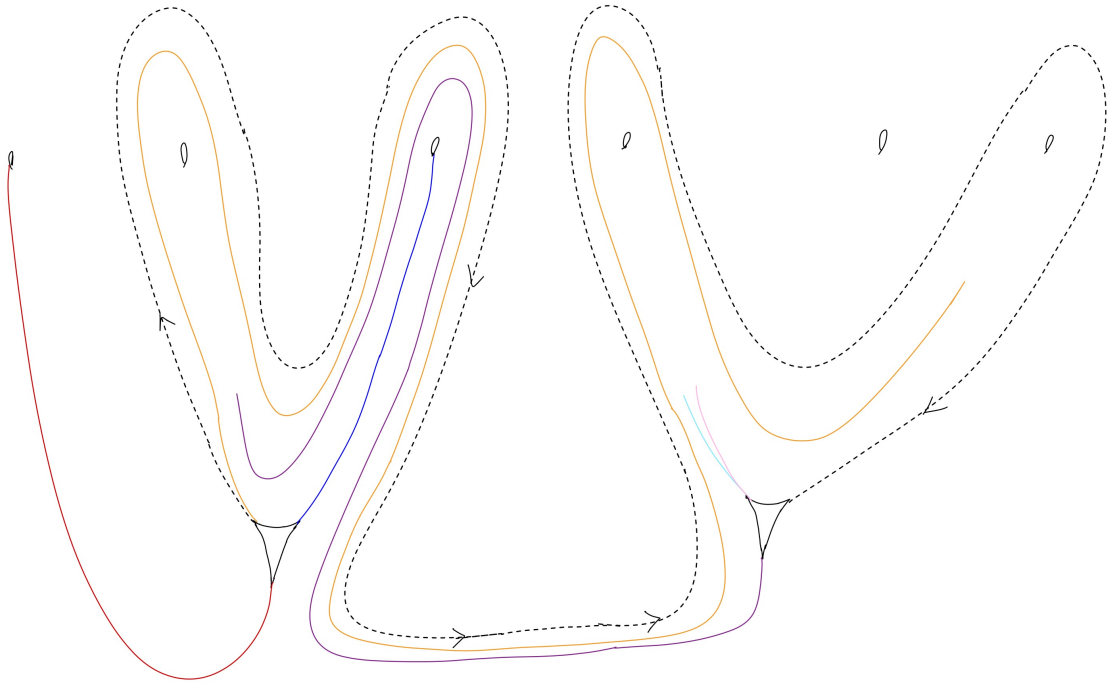


Figure E.6: Flute2

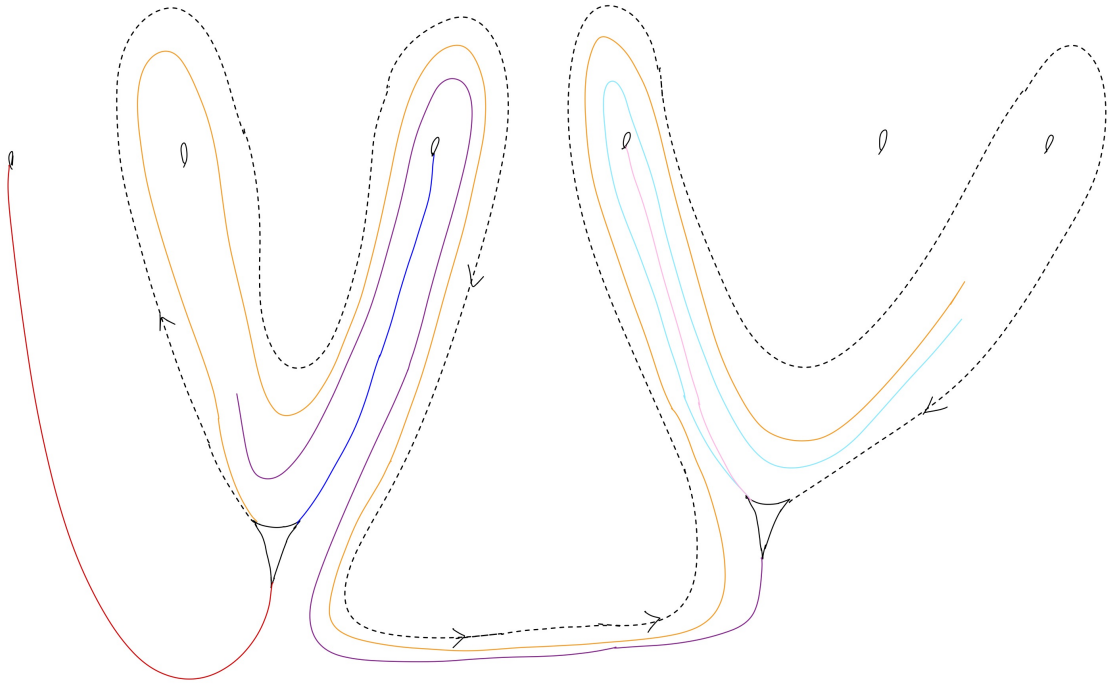


Figure E.7: Flute3

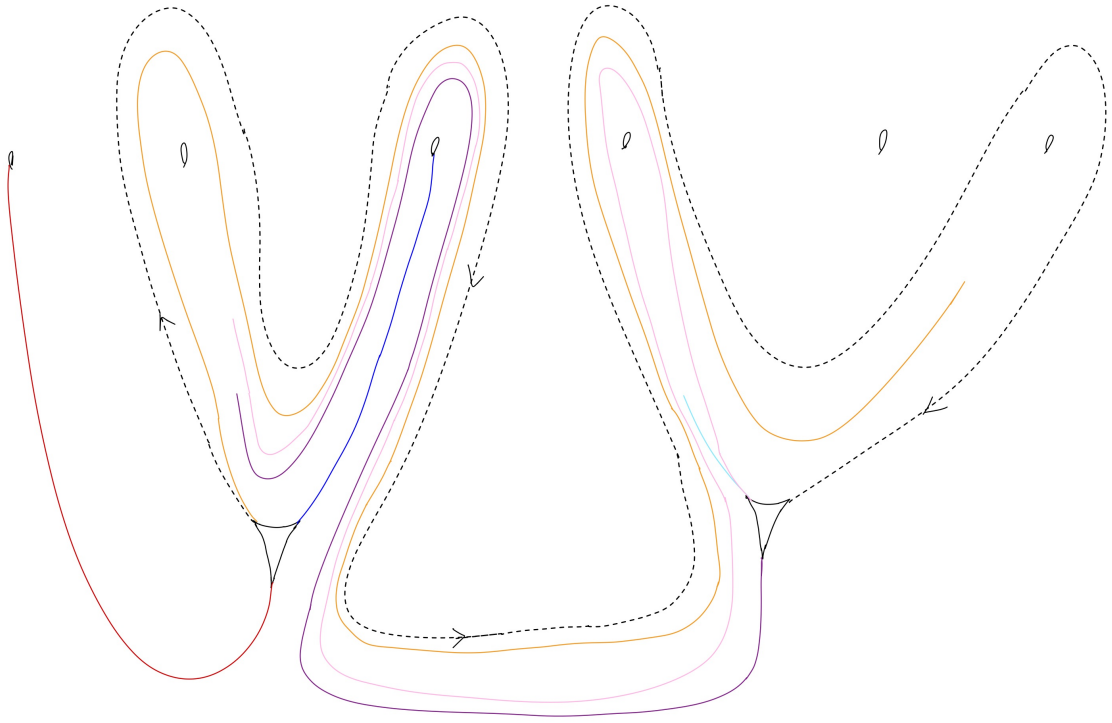


Figure E.8: Flute4

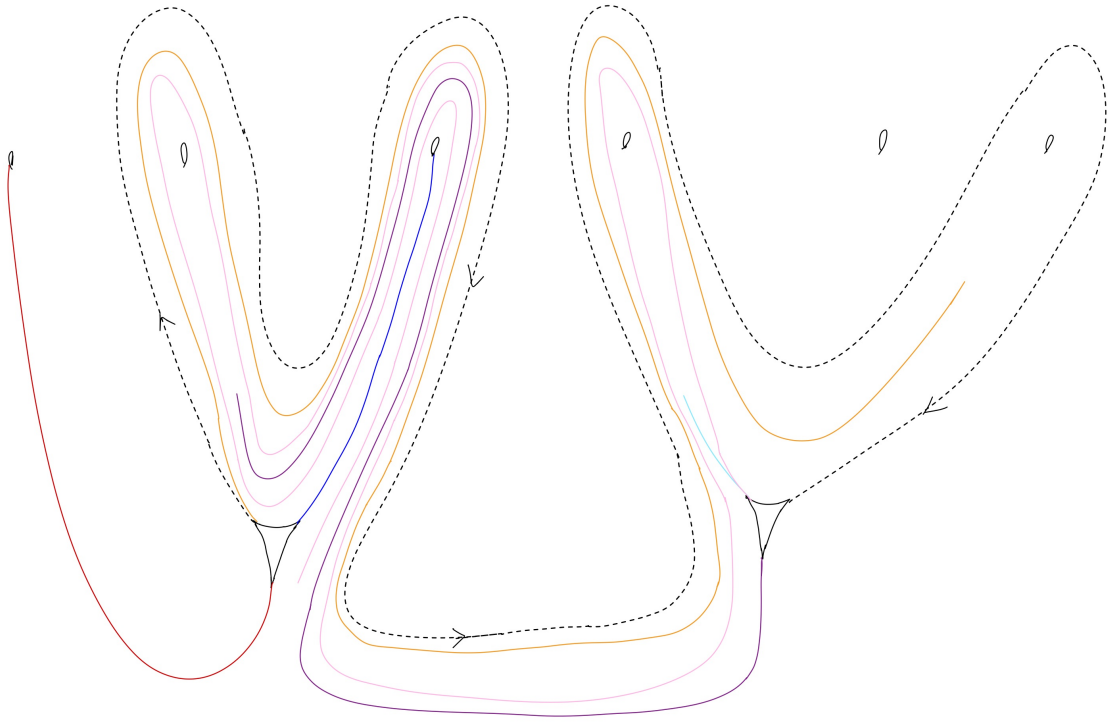


Figure E.9: Flute5

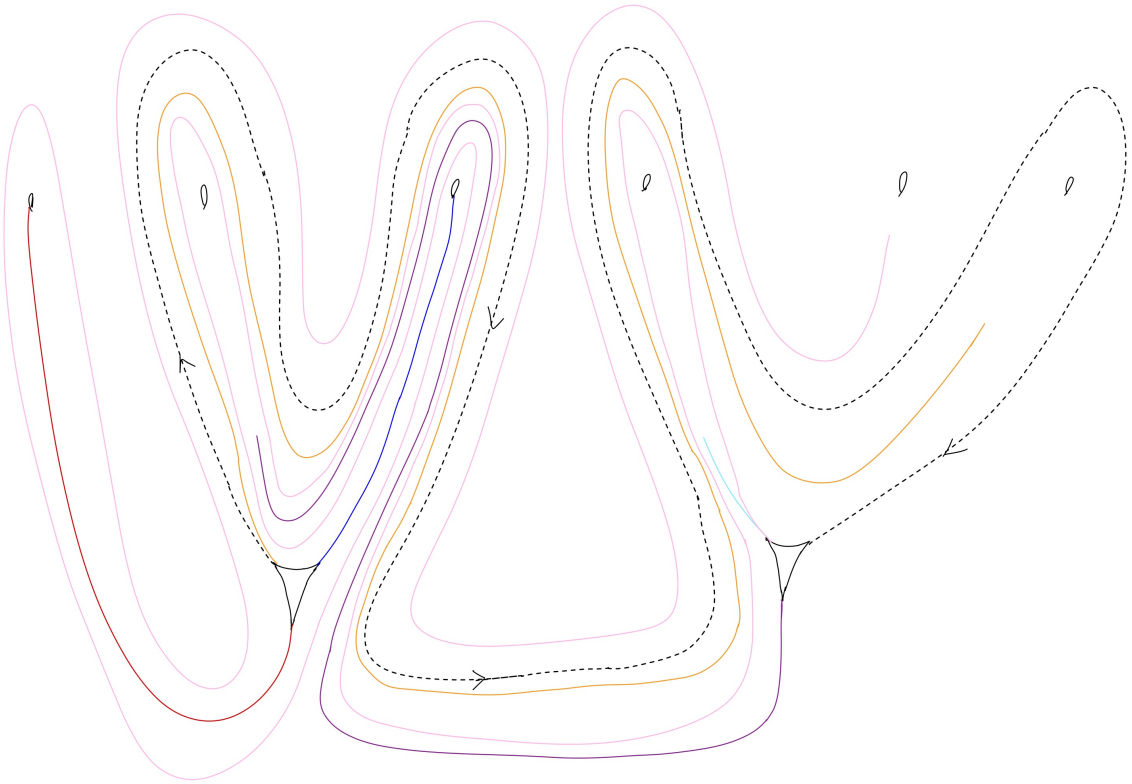


Figure E.10: Flute6

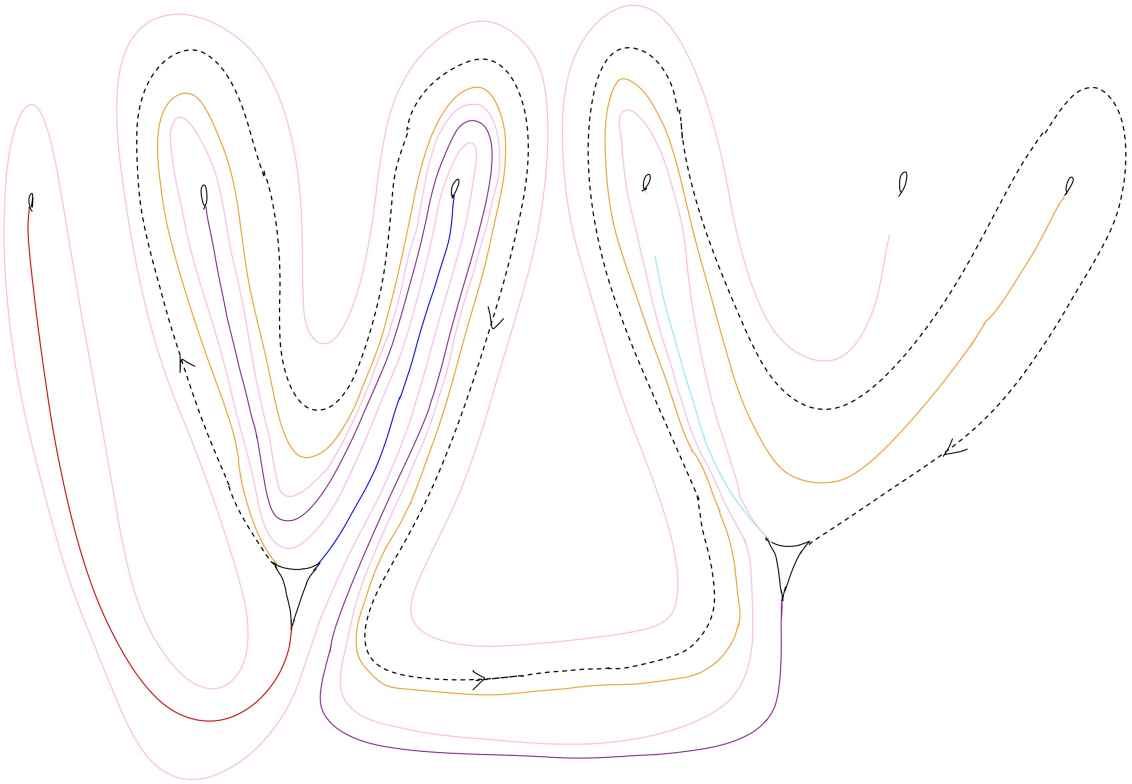


Figure E.11: Flute7

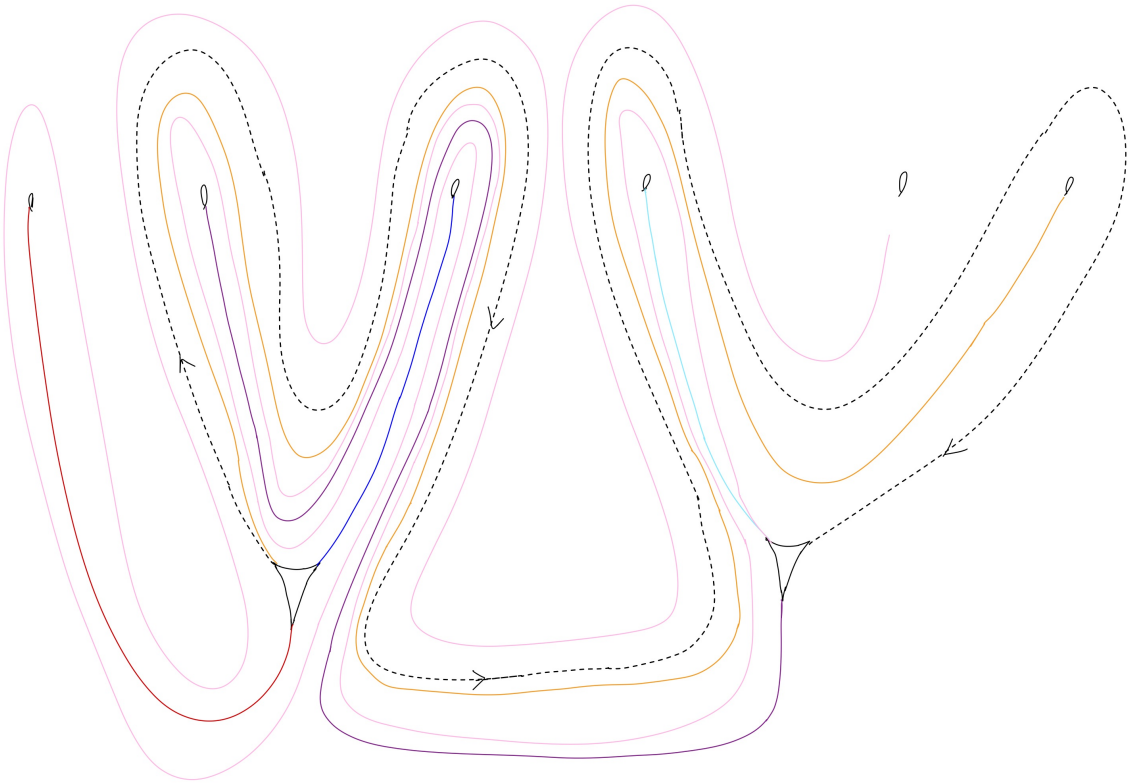


Figure E.12: Flute8

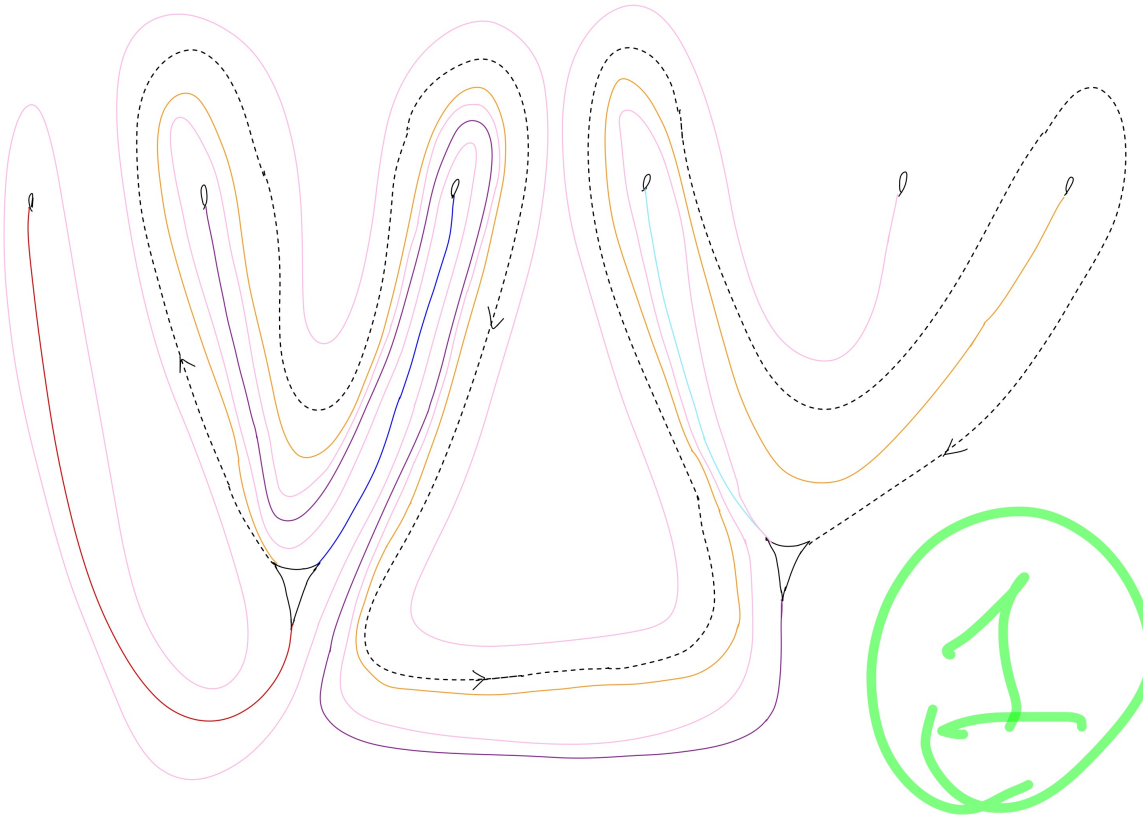


Figure E.13: Flute9

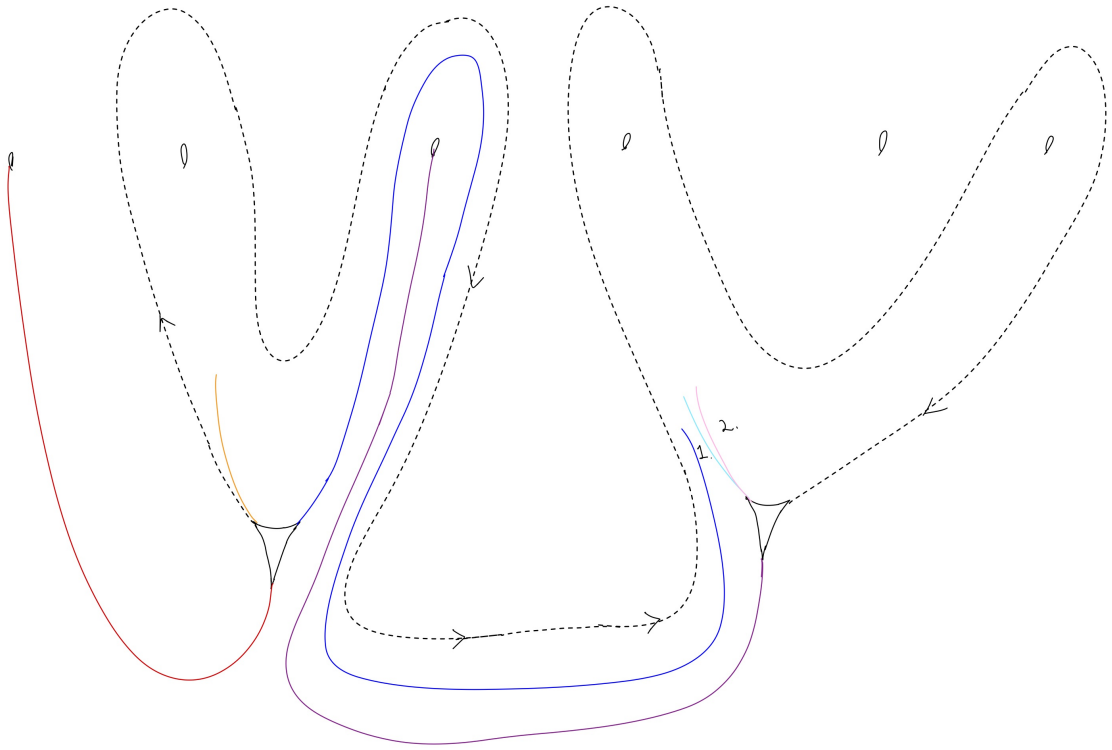


Figure E.14: Plump1

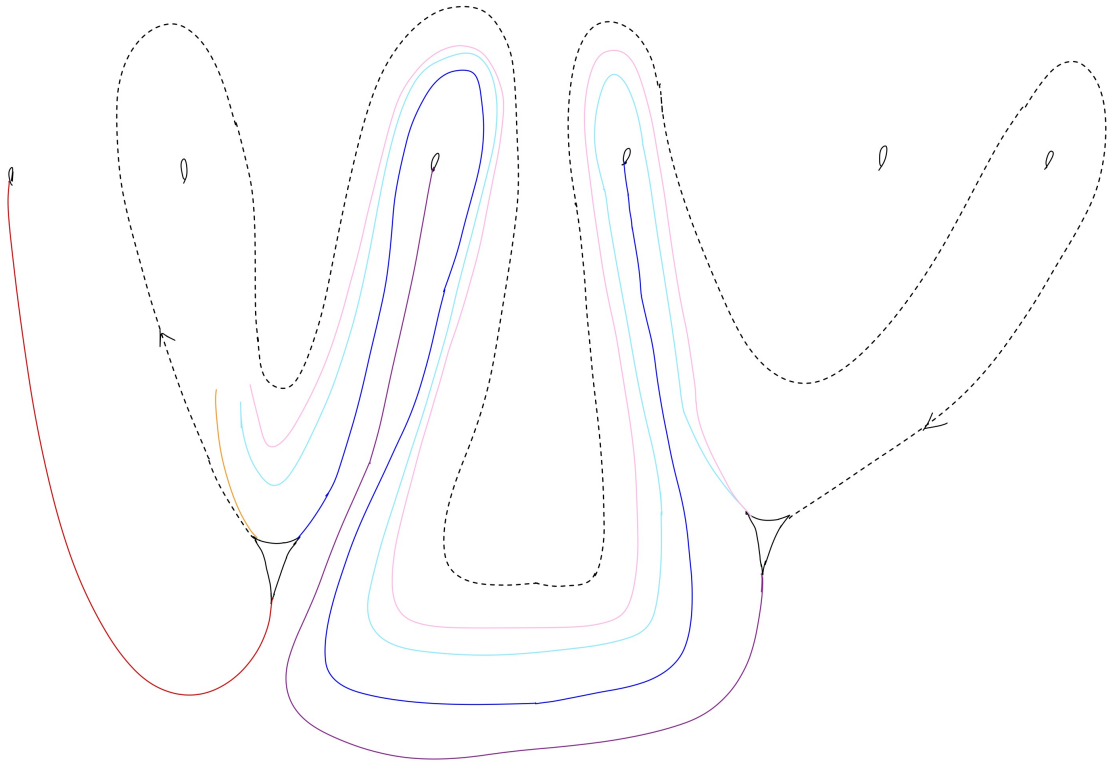


Figure E.15: Muscle1

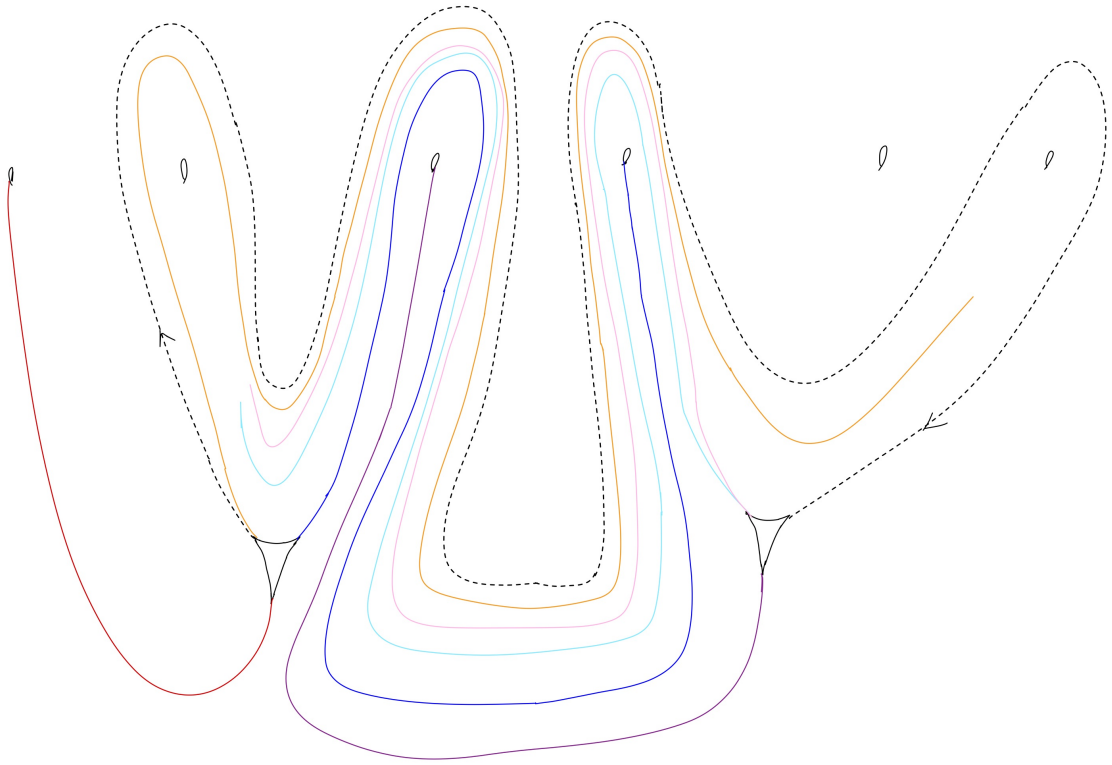


Figure E.16: Muscle2

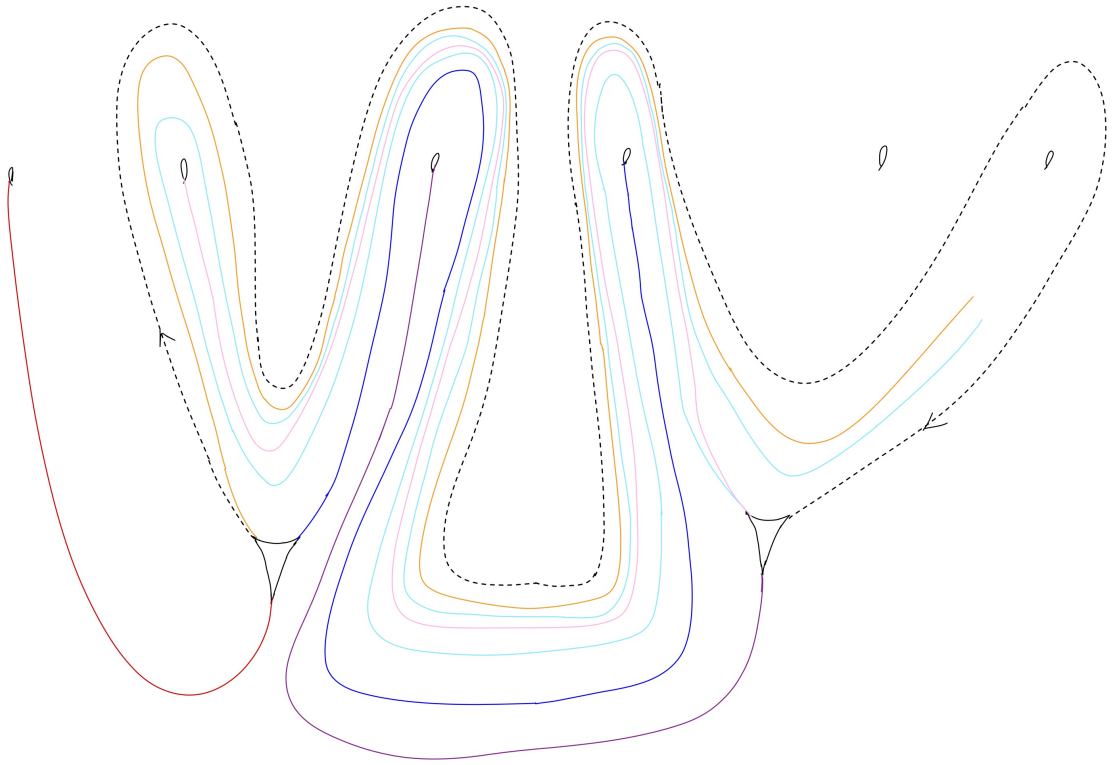


Figure E.17: Muscle3

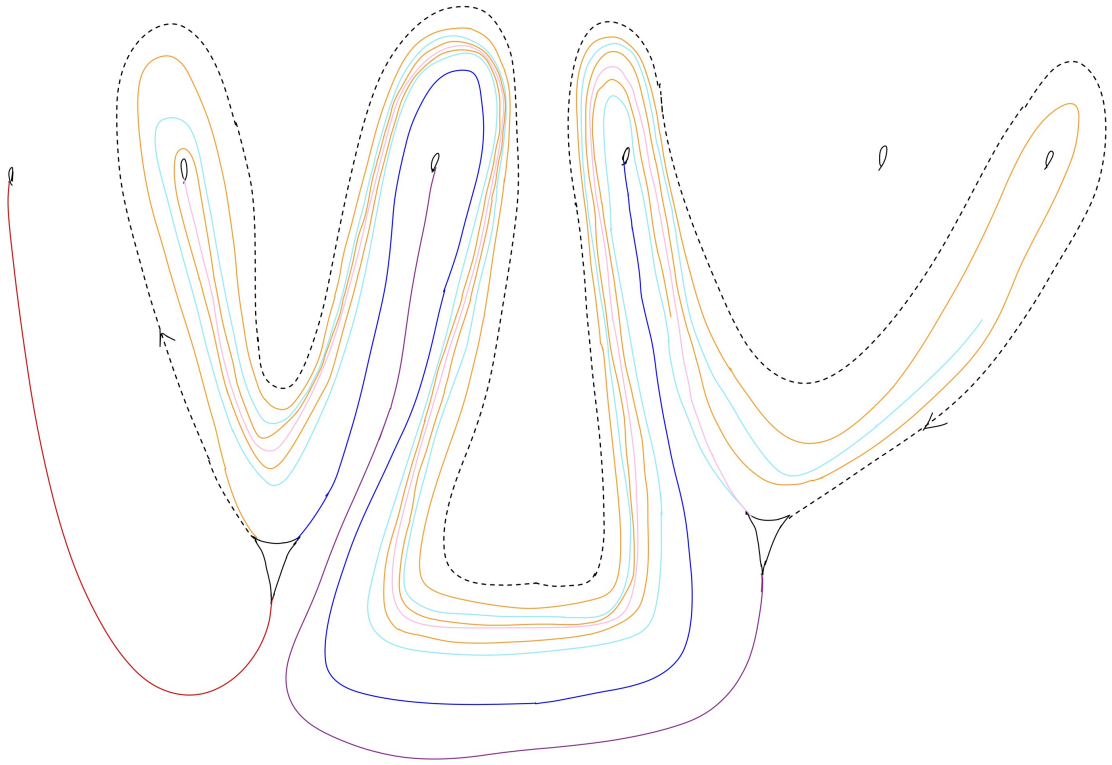


Figure E.18: Muscle4

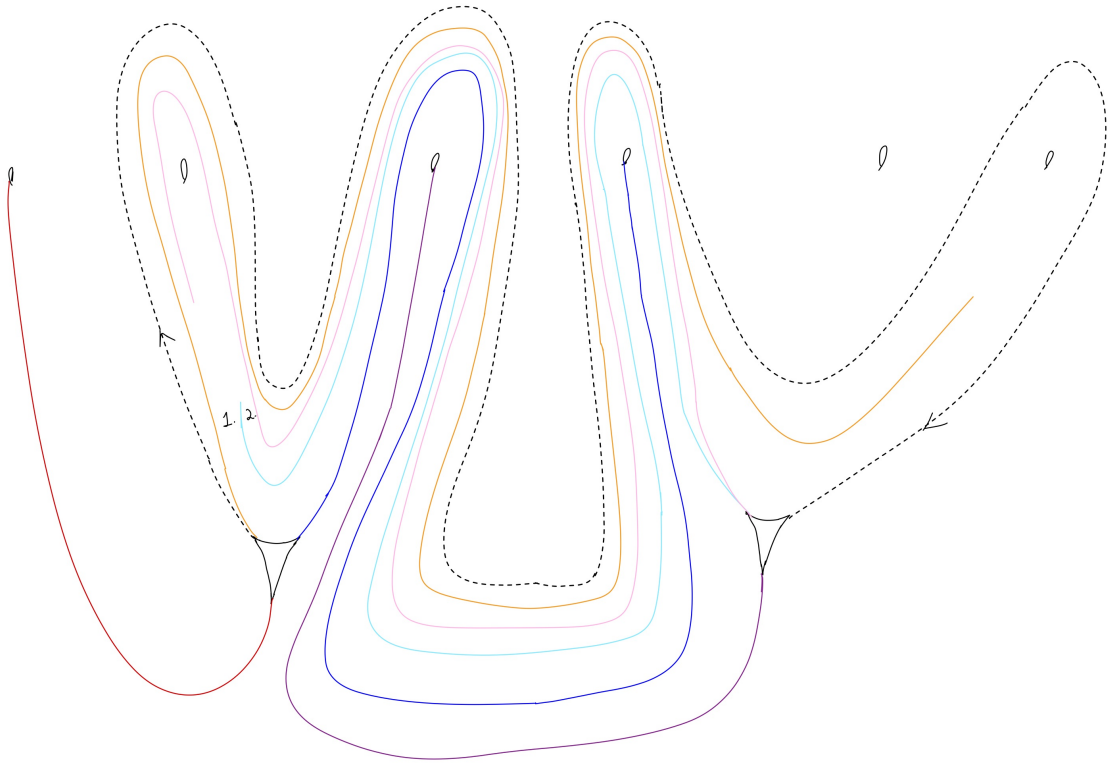


Figure E.19: Muscle5

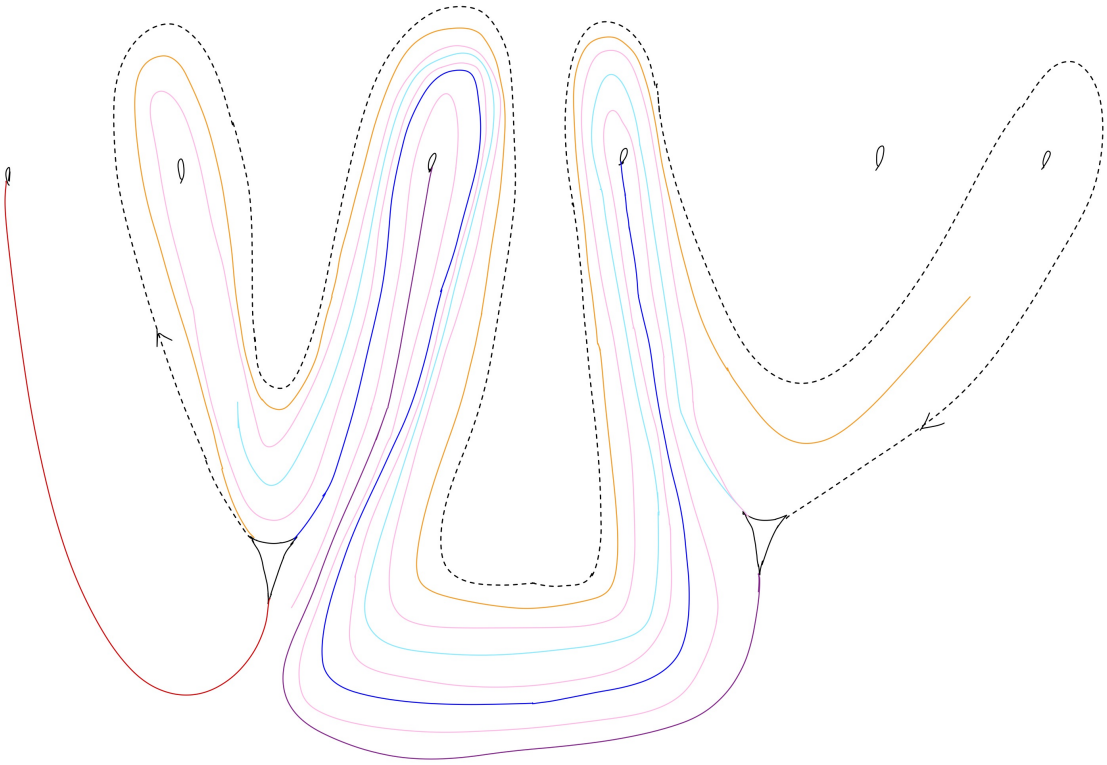


Figure E.20: Dolphin1

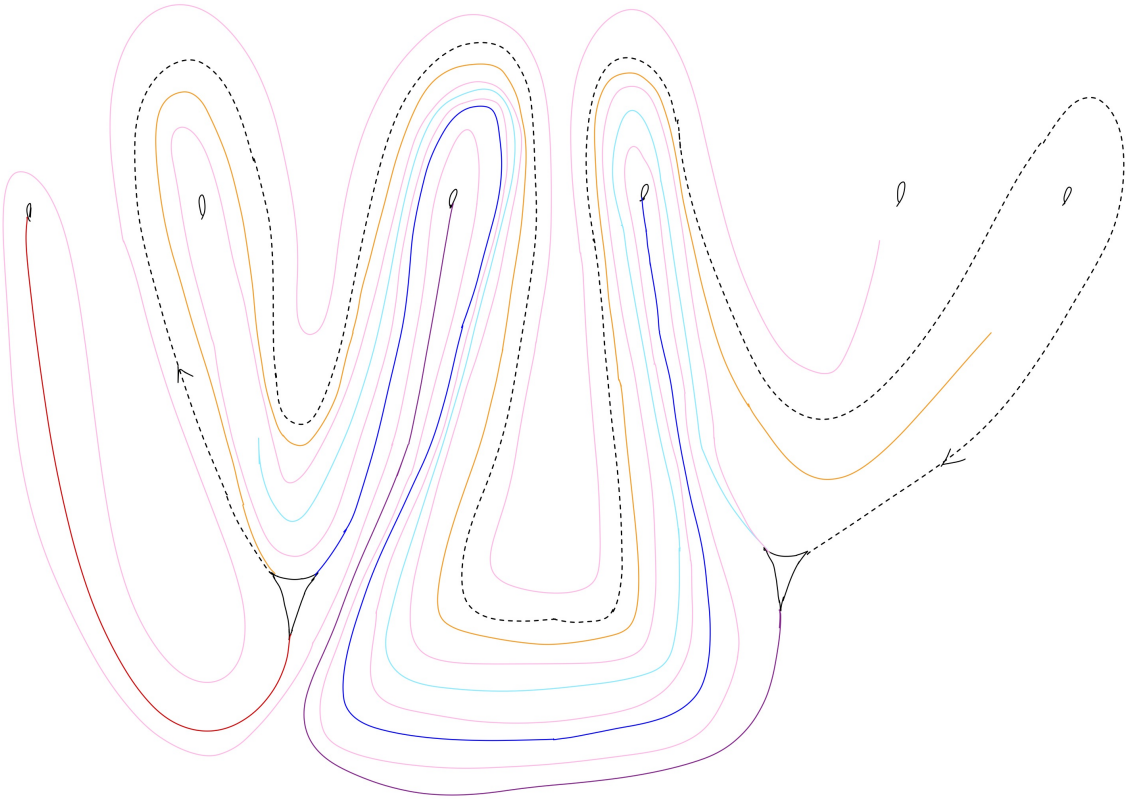


Figure E.21: Dolphin2

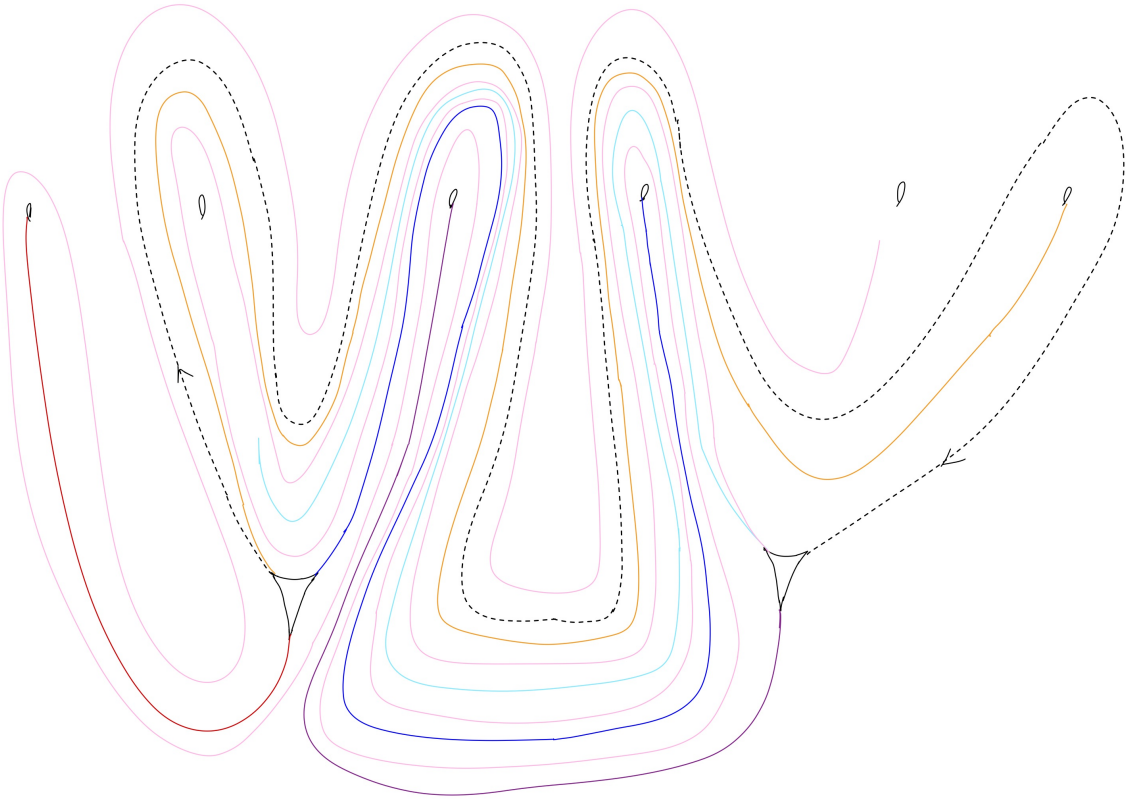


Figure E.22: Dolphin3

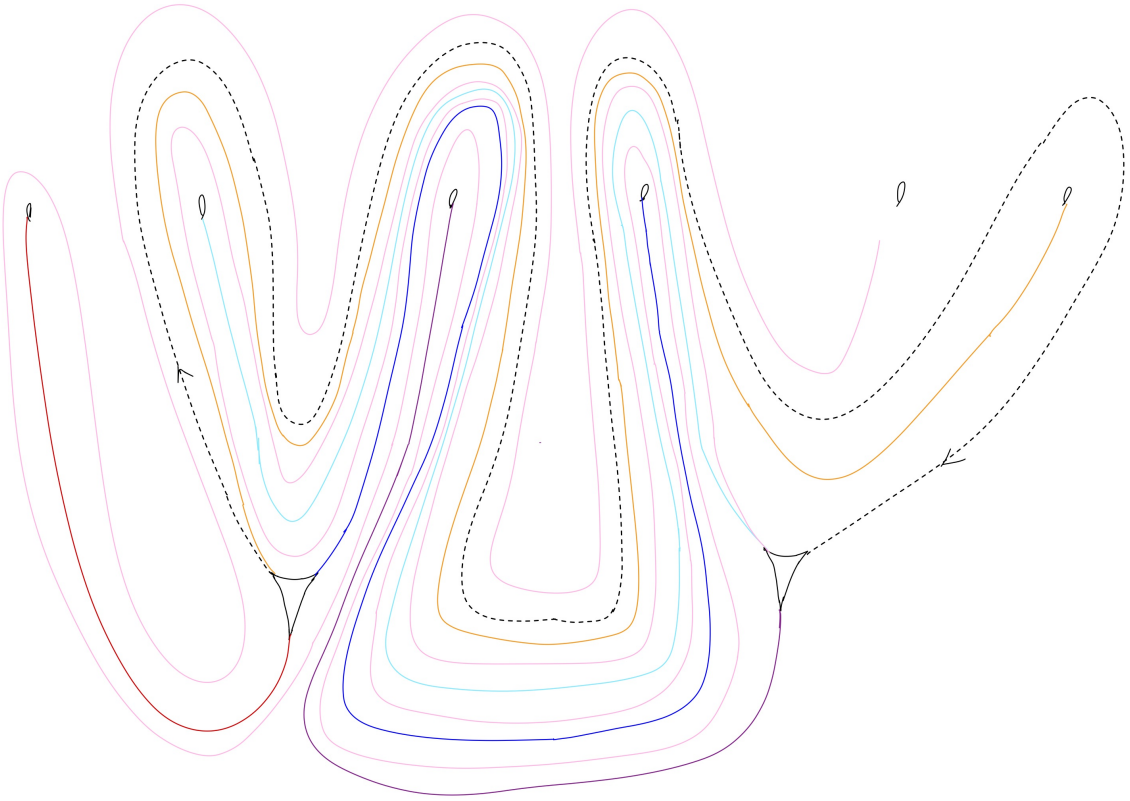


Figure E.23: Dolphin4

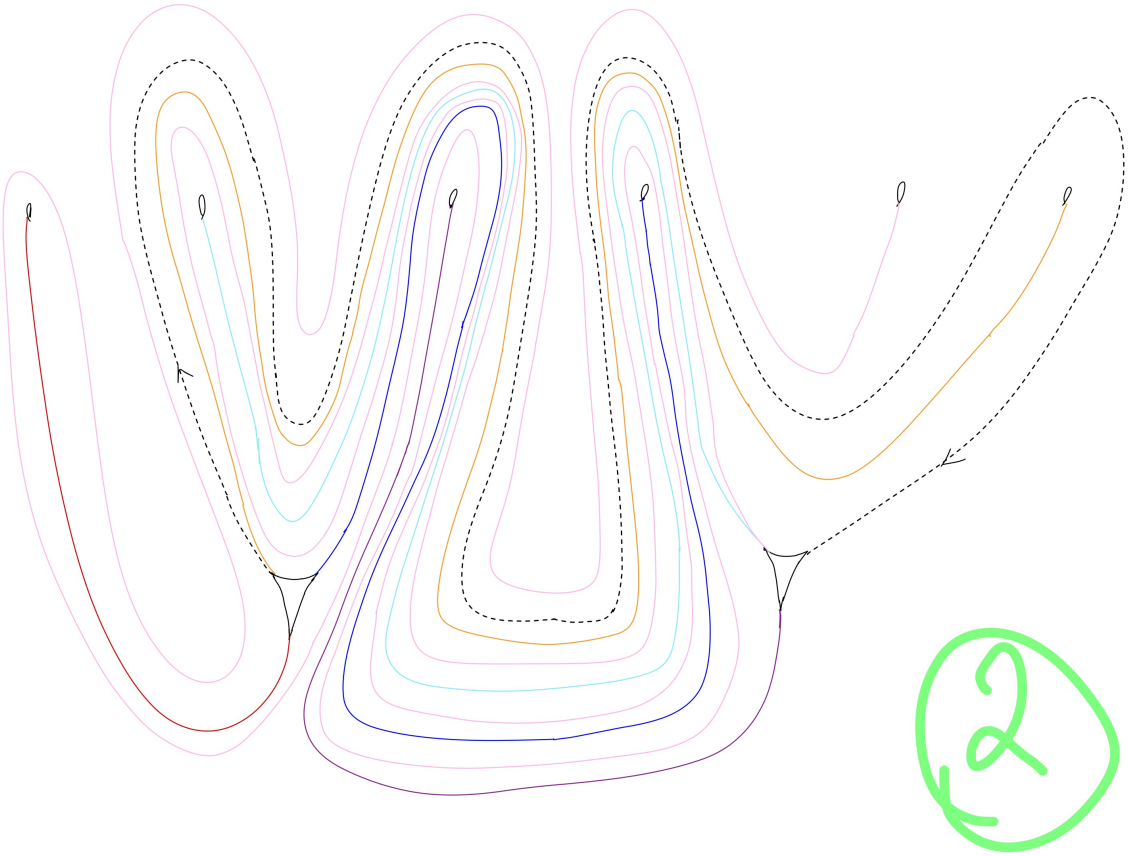


Figure E.24: Dolphin5

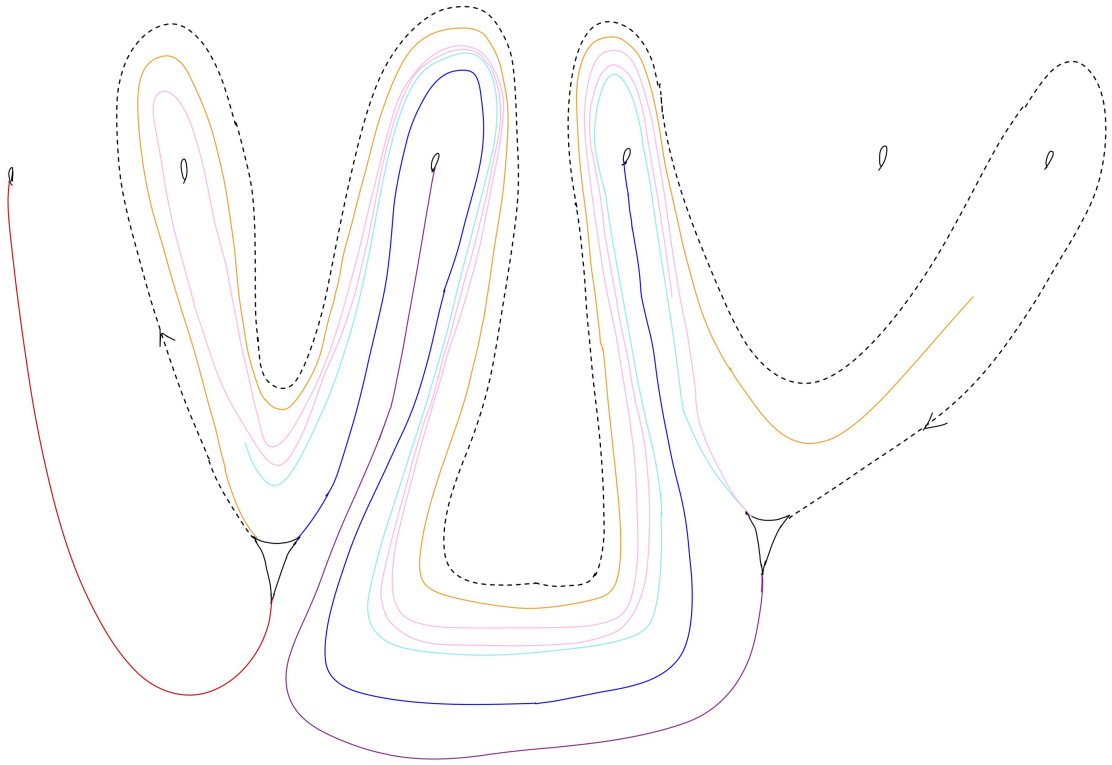


Figure E.25: Cottage1

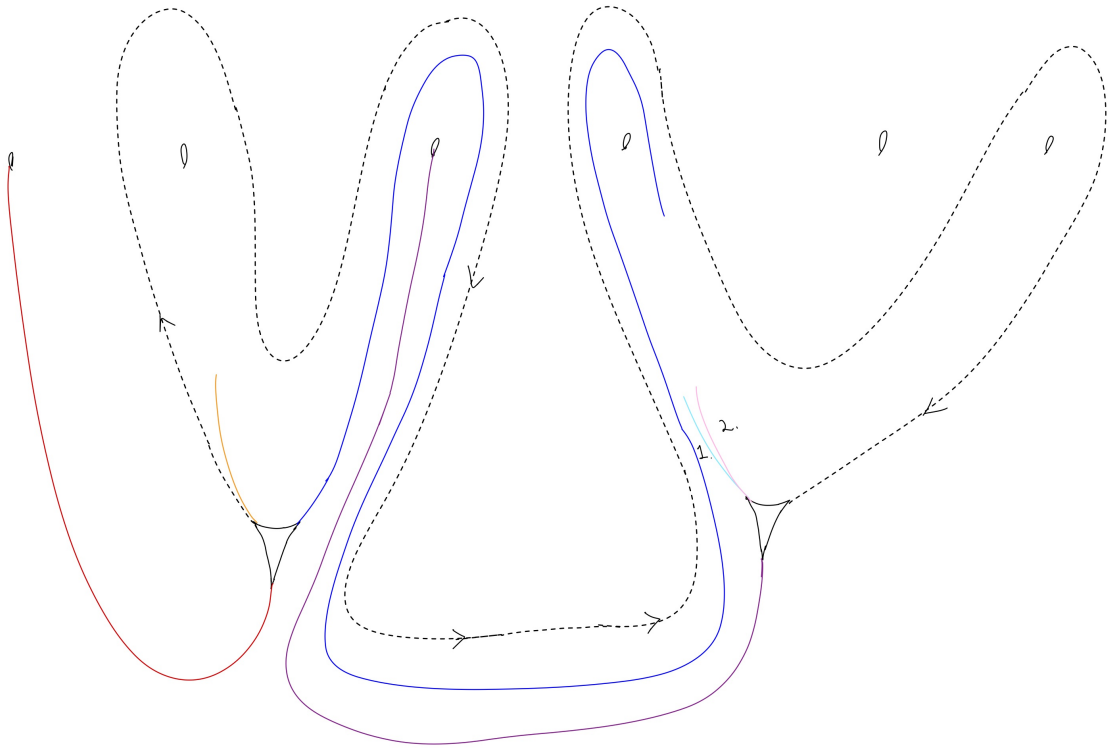


Figure E.26: Magpie1

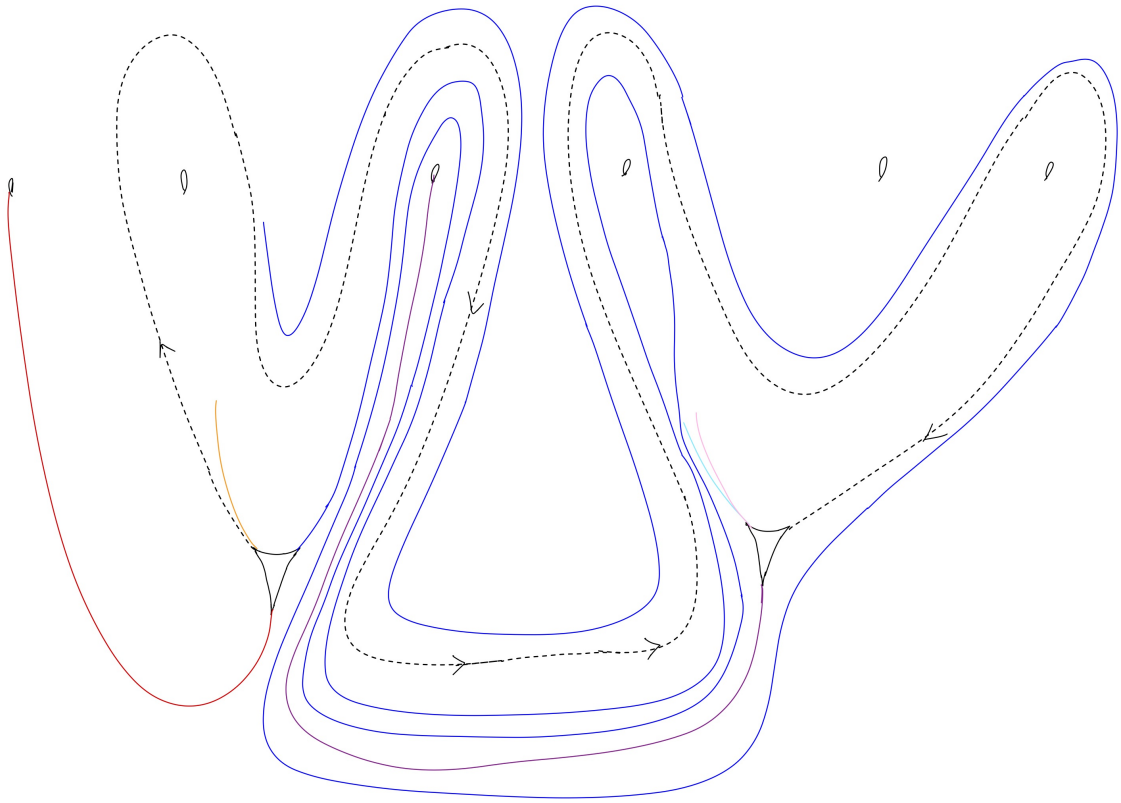


Figure E.27: Magpie2

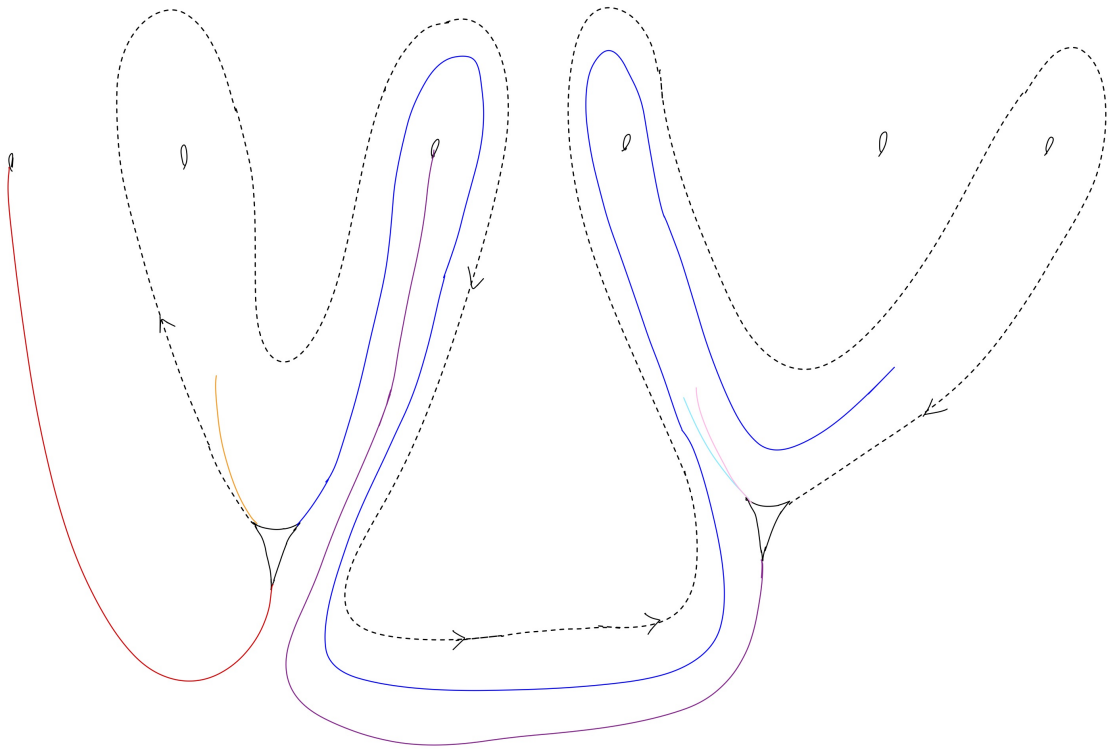


Figure E.28: Magpie3

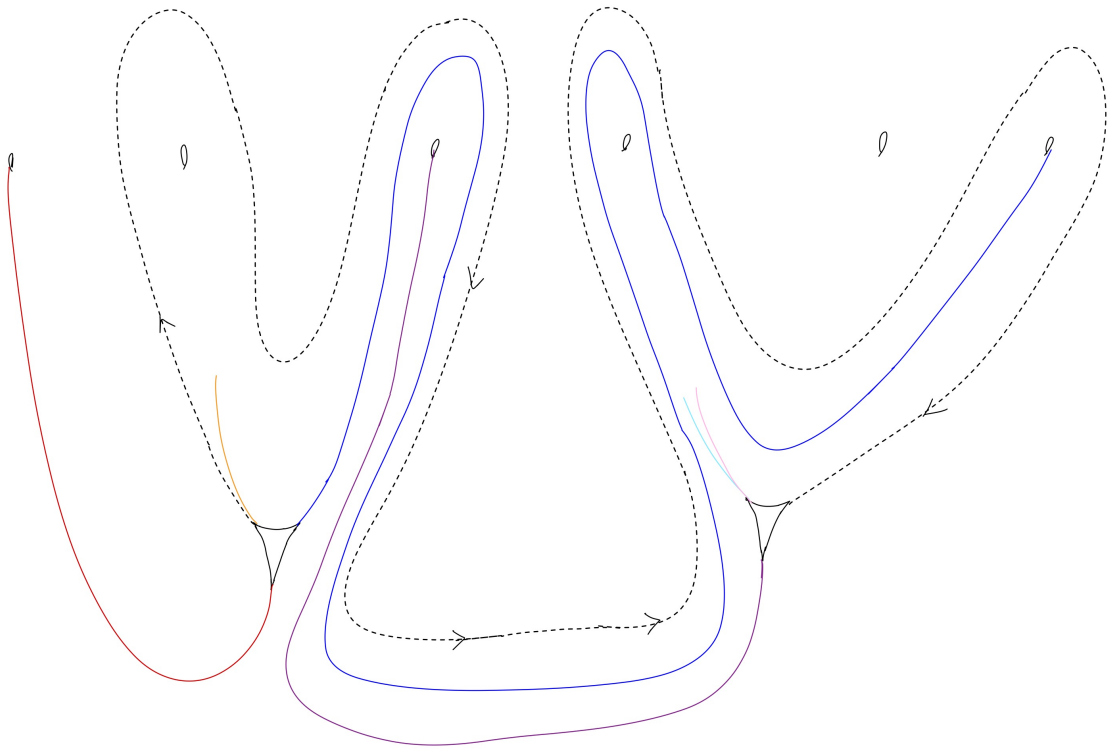


Figure E.29: Magpie4

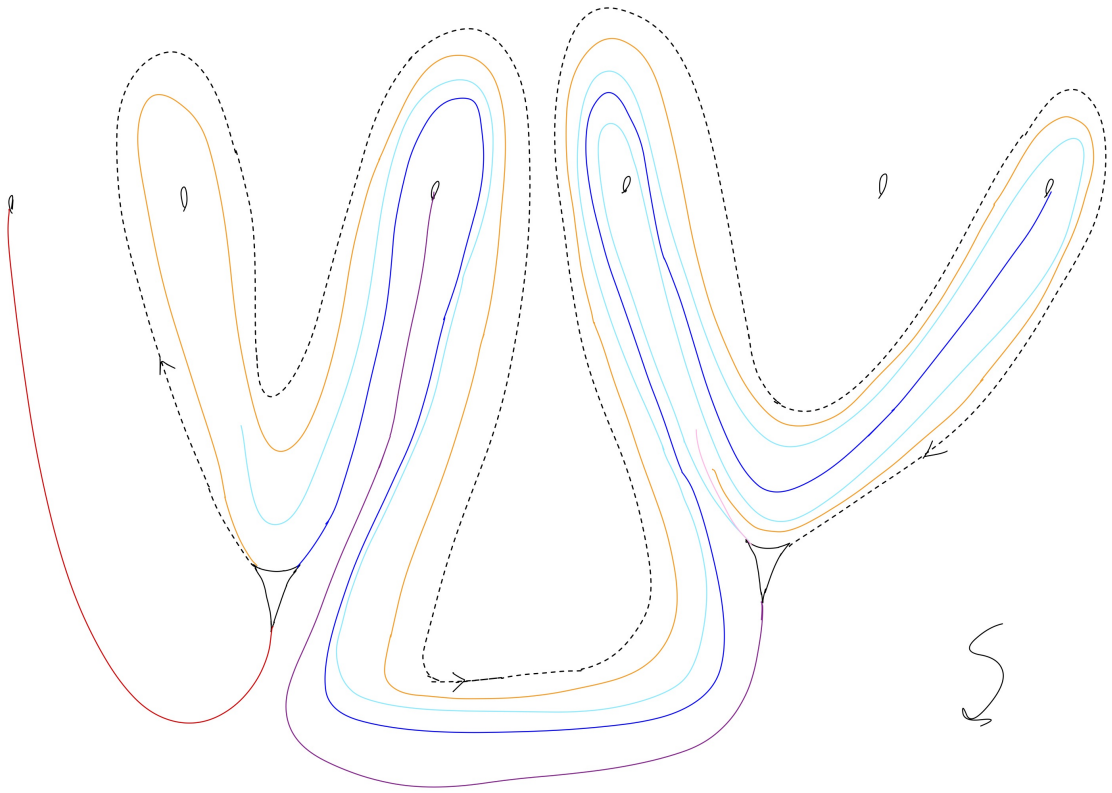


Figure E.30: Magpie5

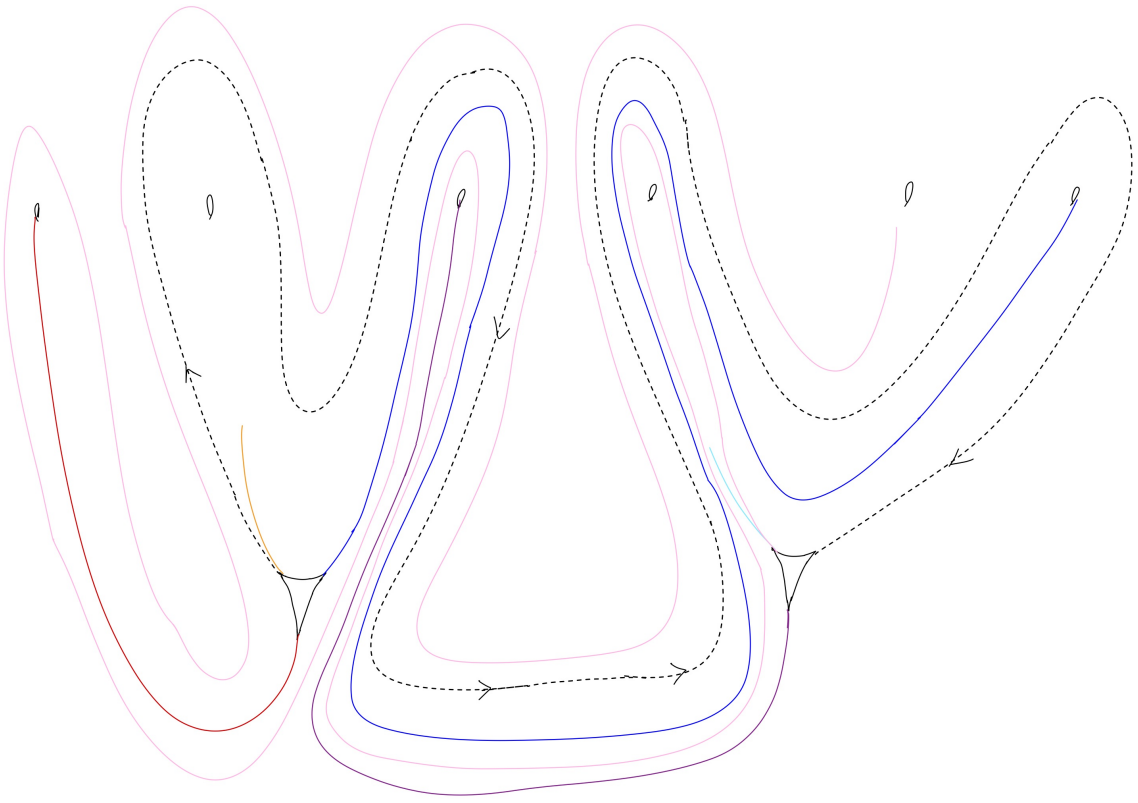


Figure E.31: Magpie6

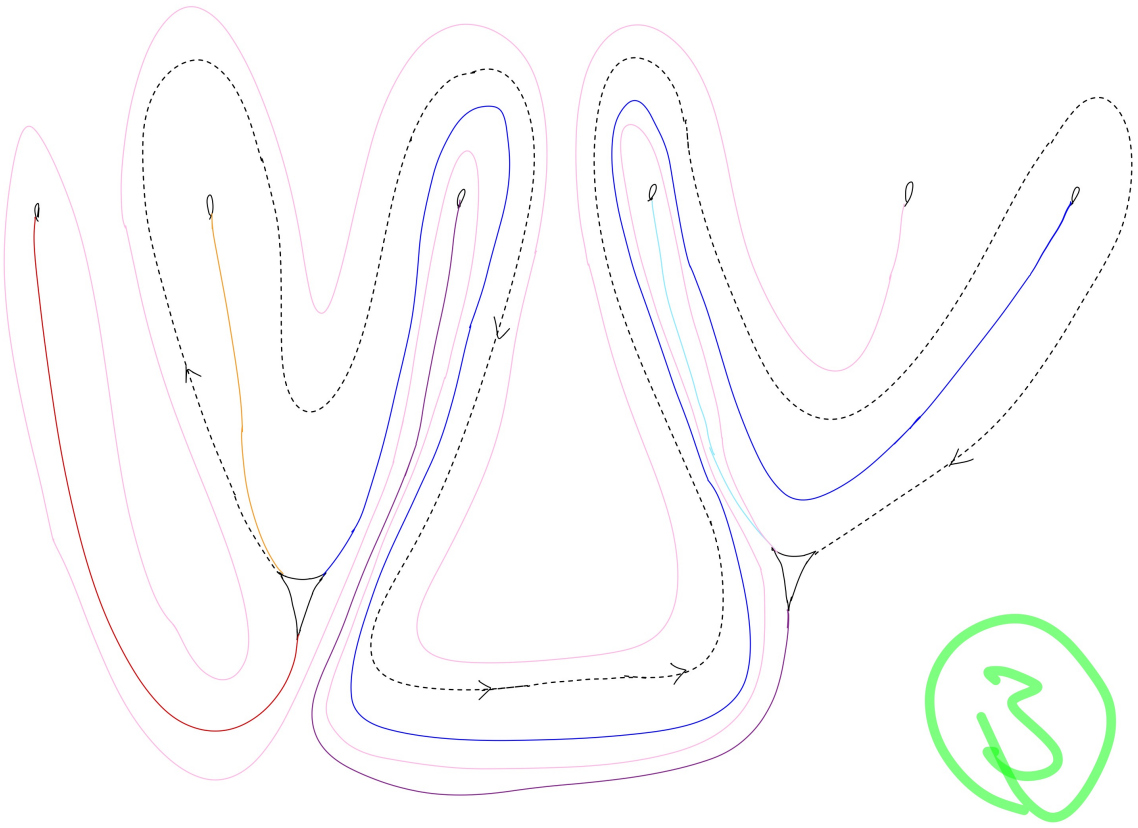


Figure E.32: Magpie7

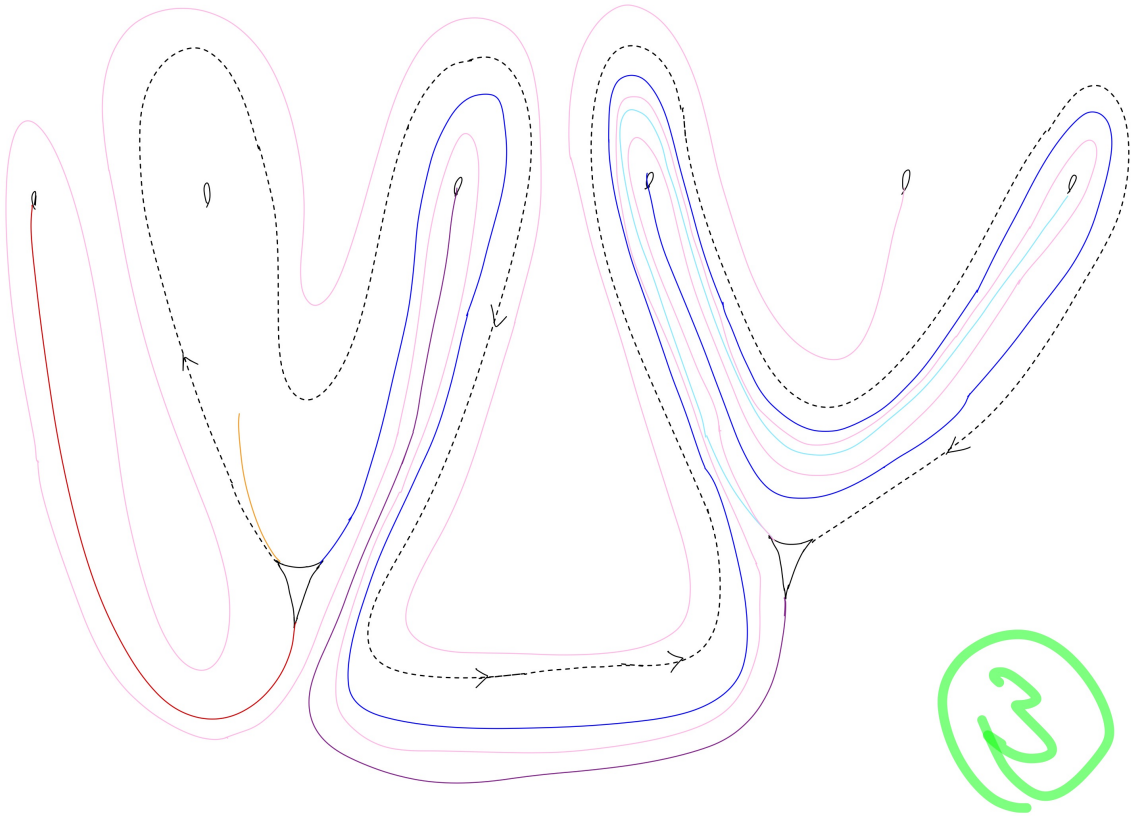


Figure E.33: Magpie8



Figure E.34: Ruby1

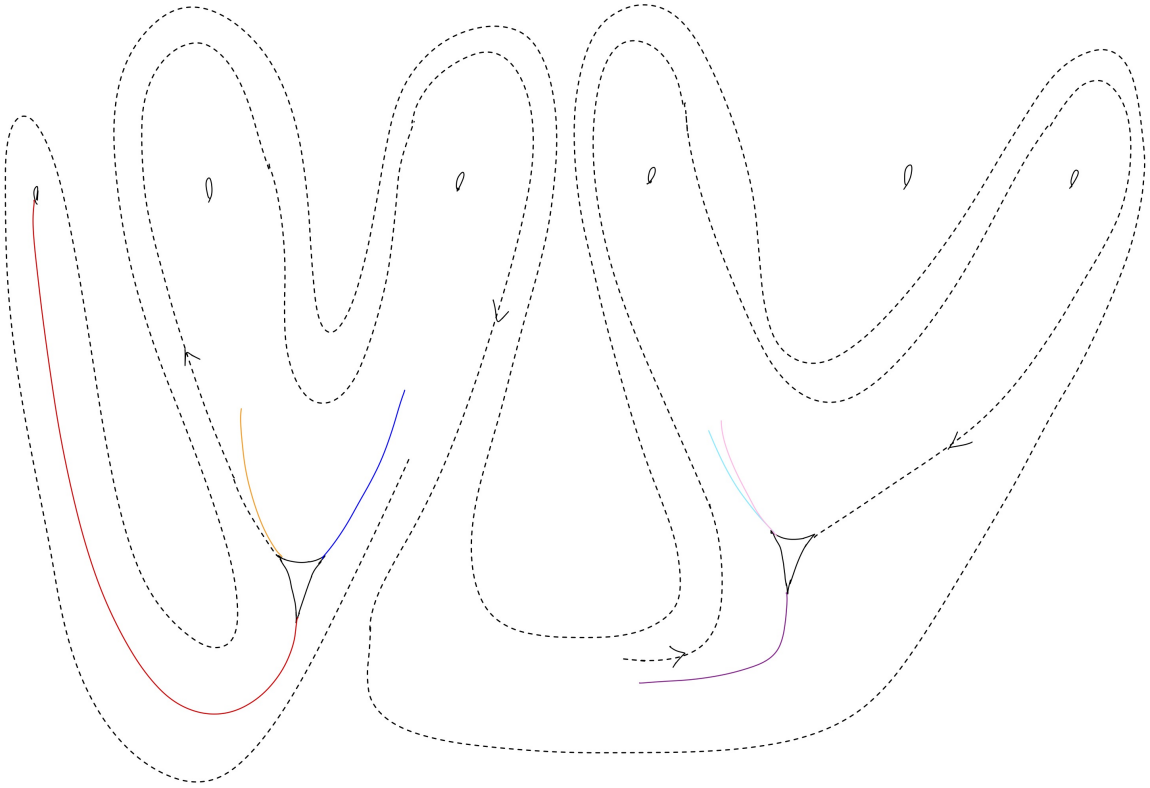


Figure E.35: Ruby2

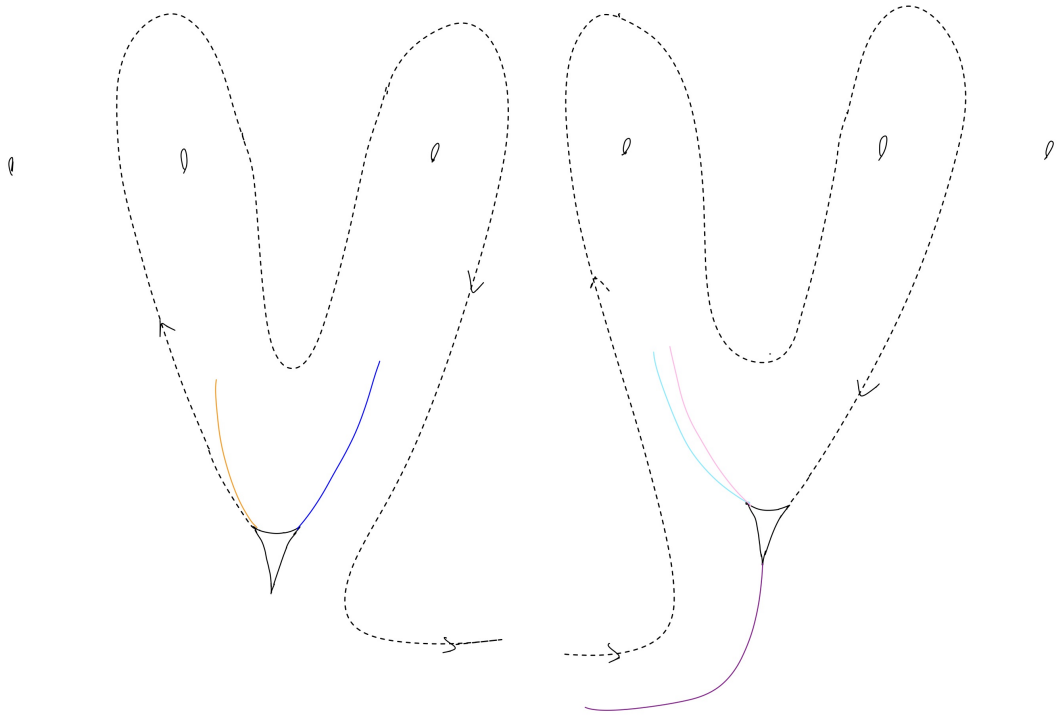


Figure E.36: GRR1

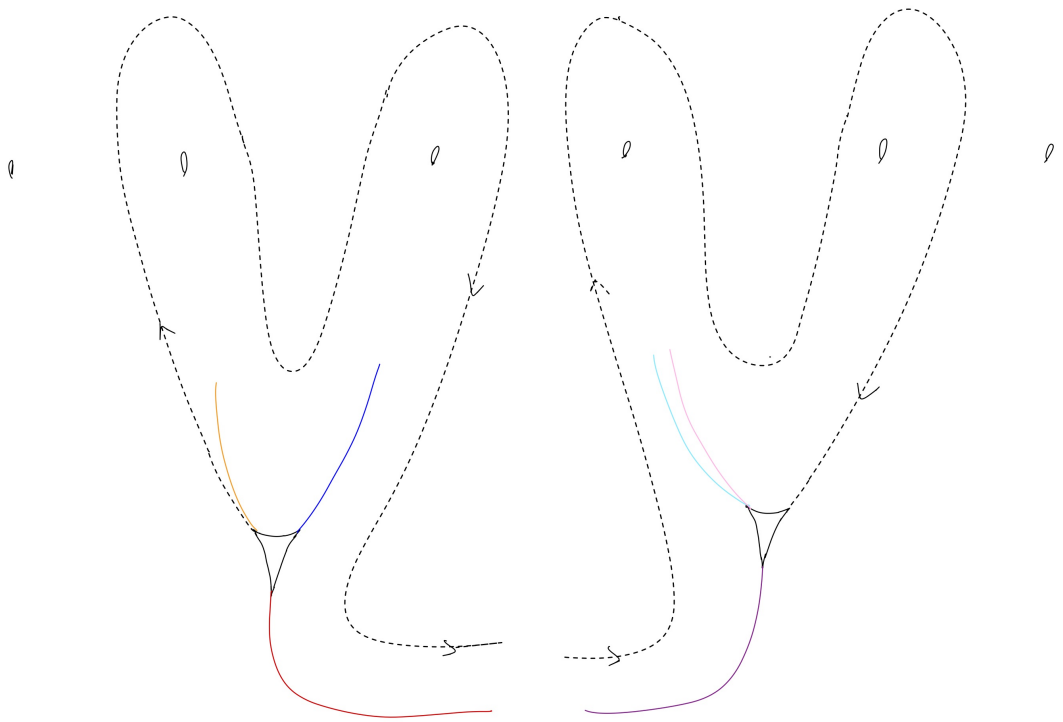


Figure E.37: Bree1

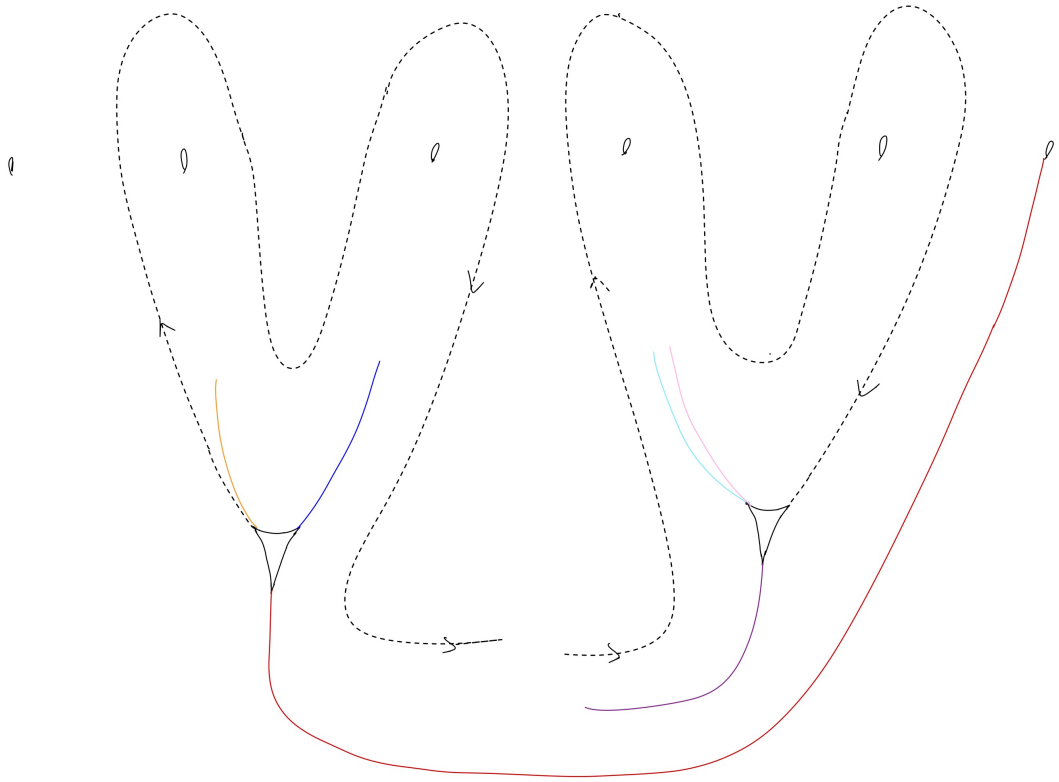


Figure E.38: Bree2

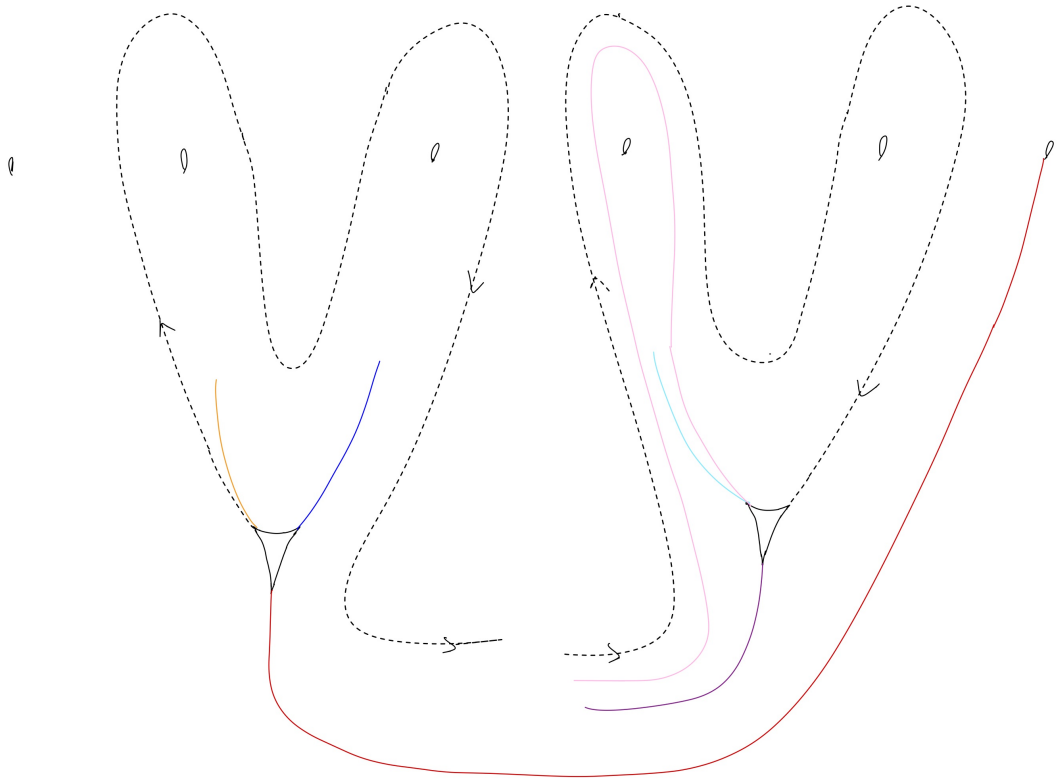


Figure E.39: Bree3

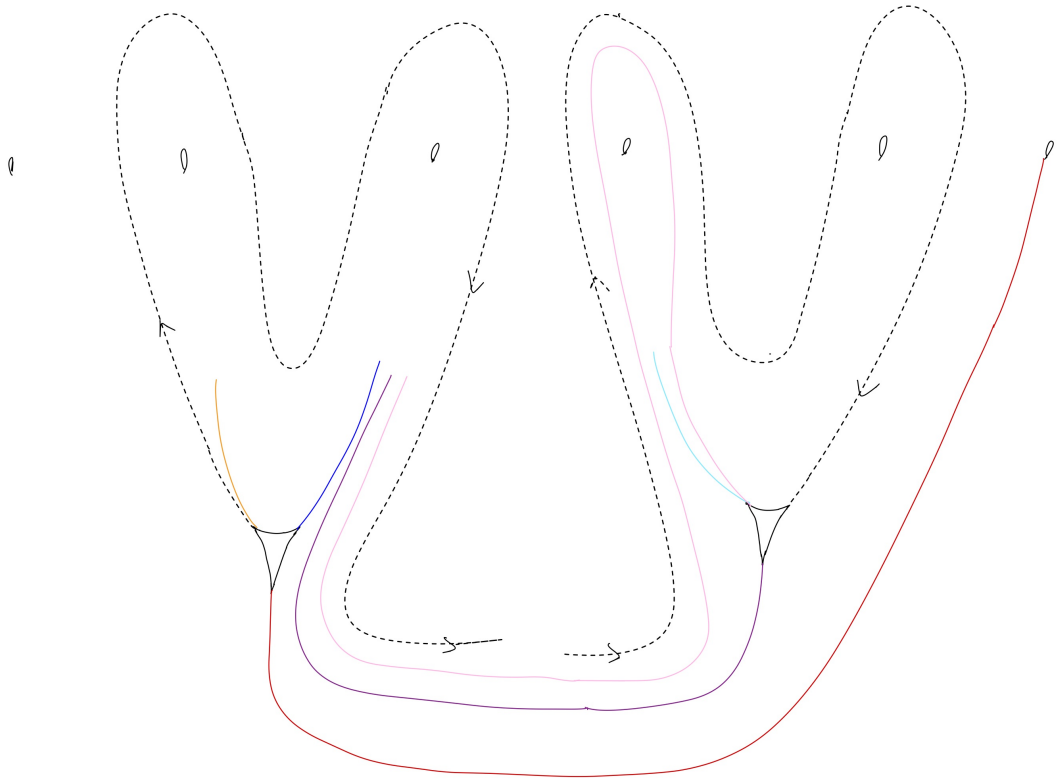


Figure E.40: Bree4

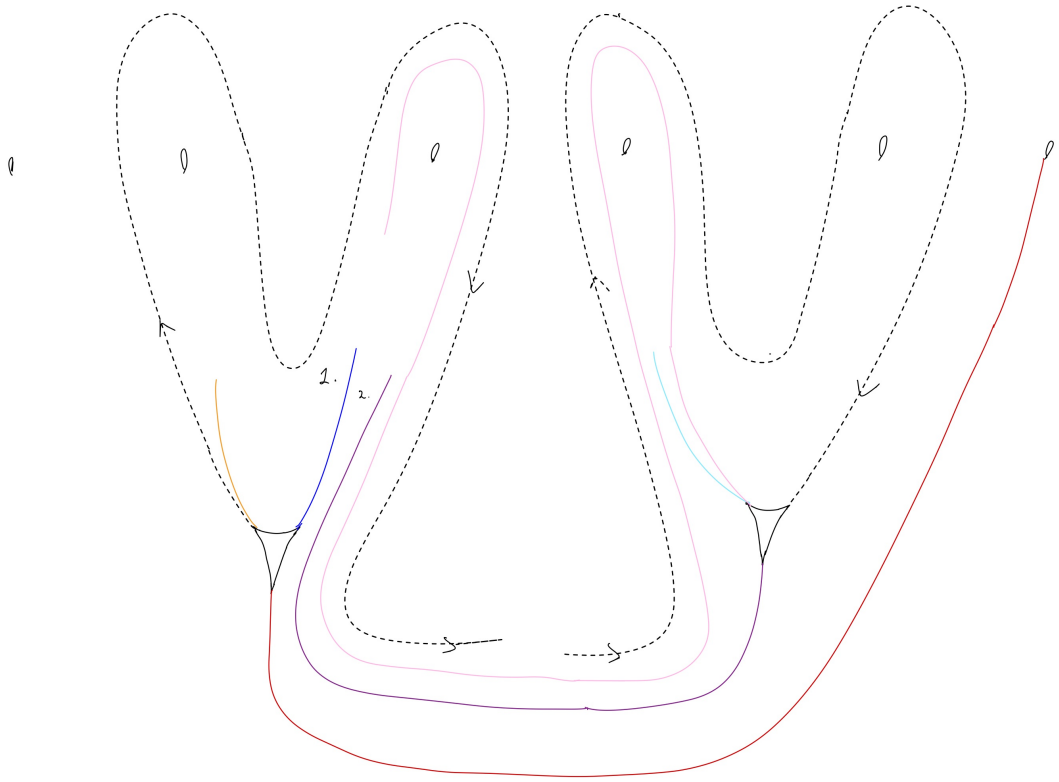


Figure E.41: Bree5

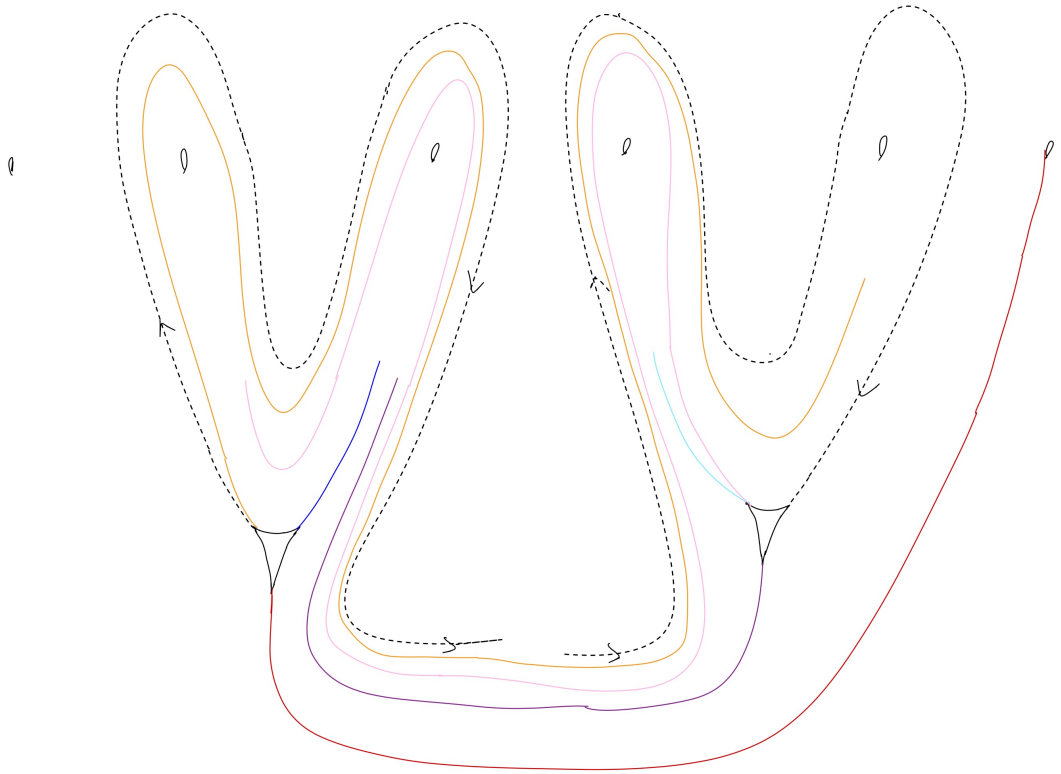


Figure E.42: Bree6

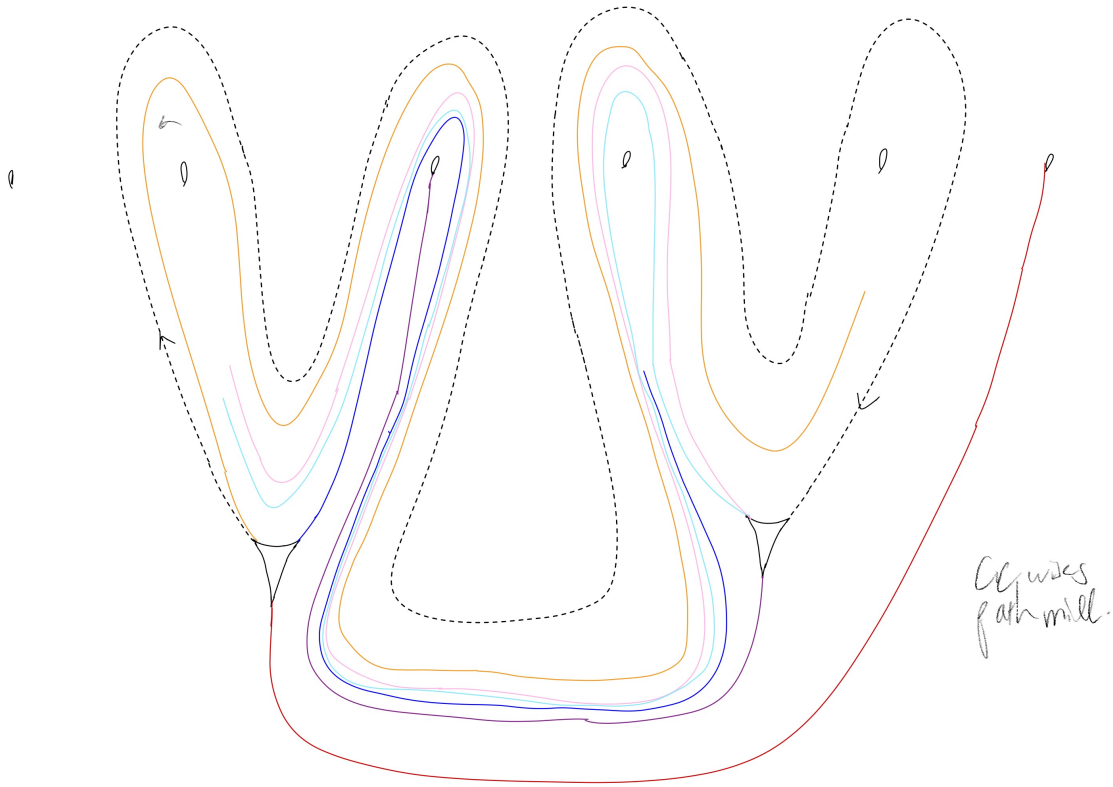


Figure E.43: Bree7

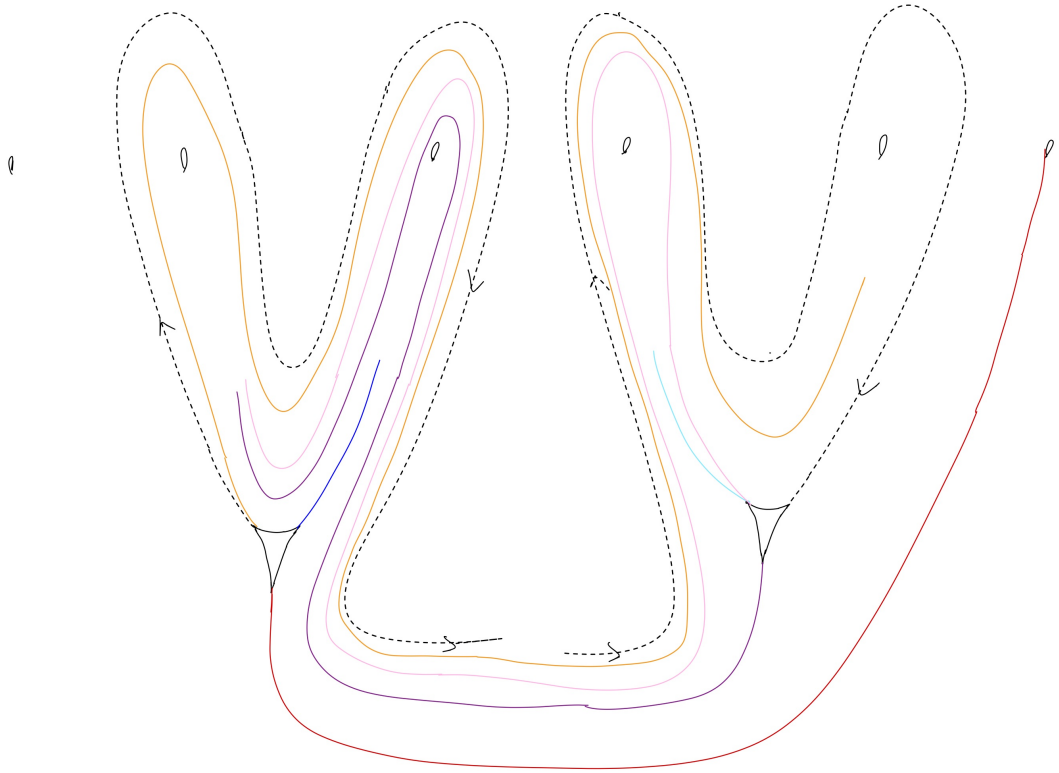


Figure E.44: Bree8

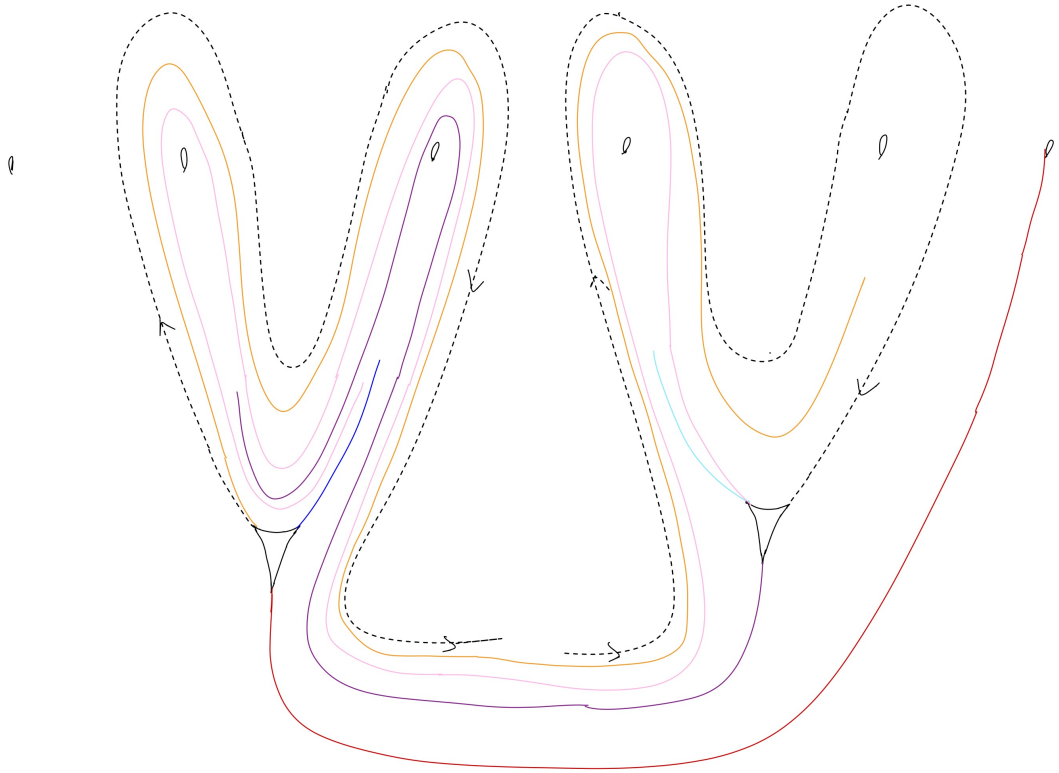


Figure E.45: Bree9

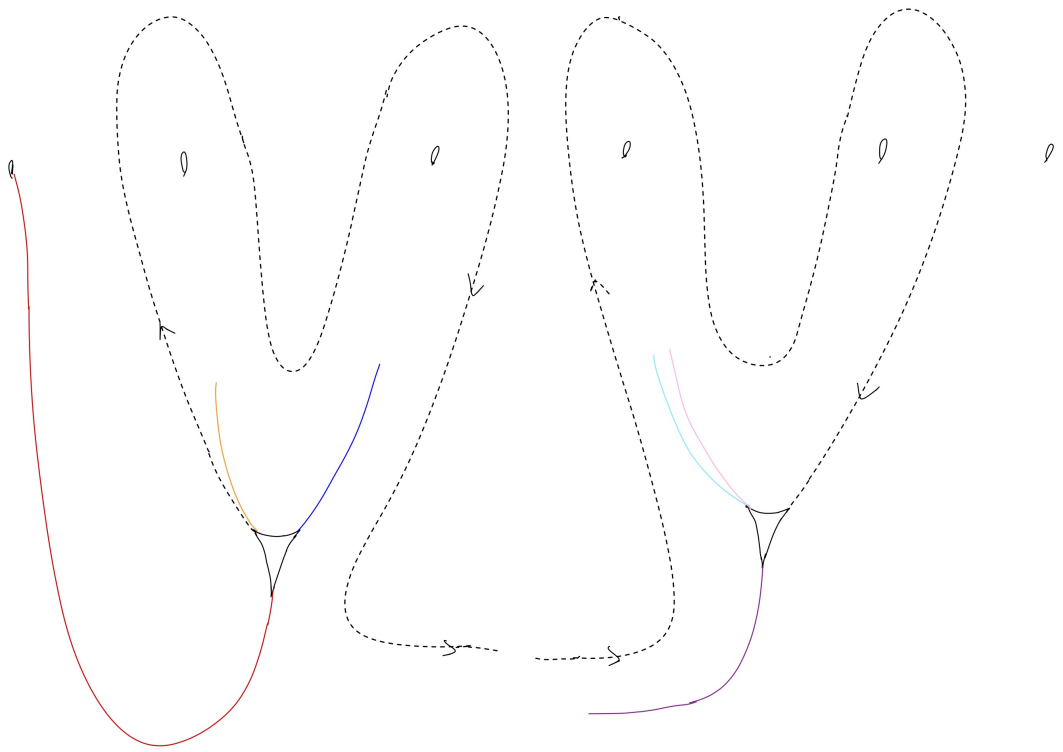


Figure E.46: Scud1

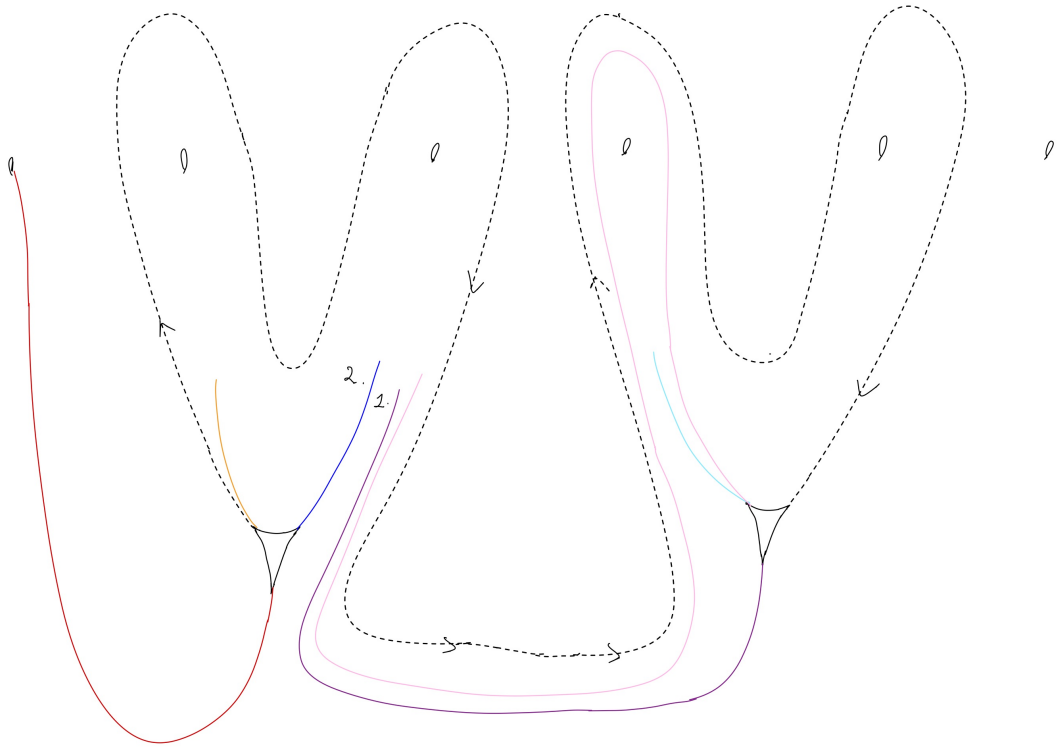


Figure E.47: Scud2

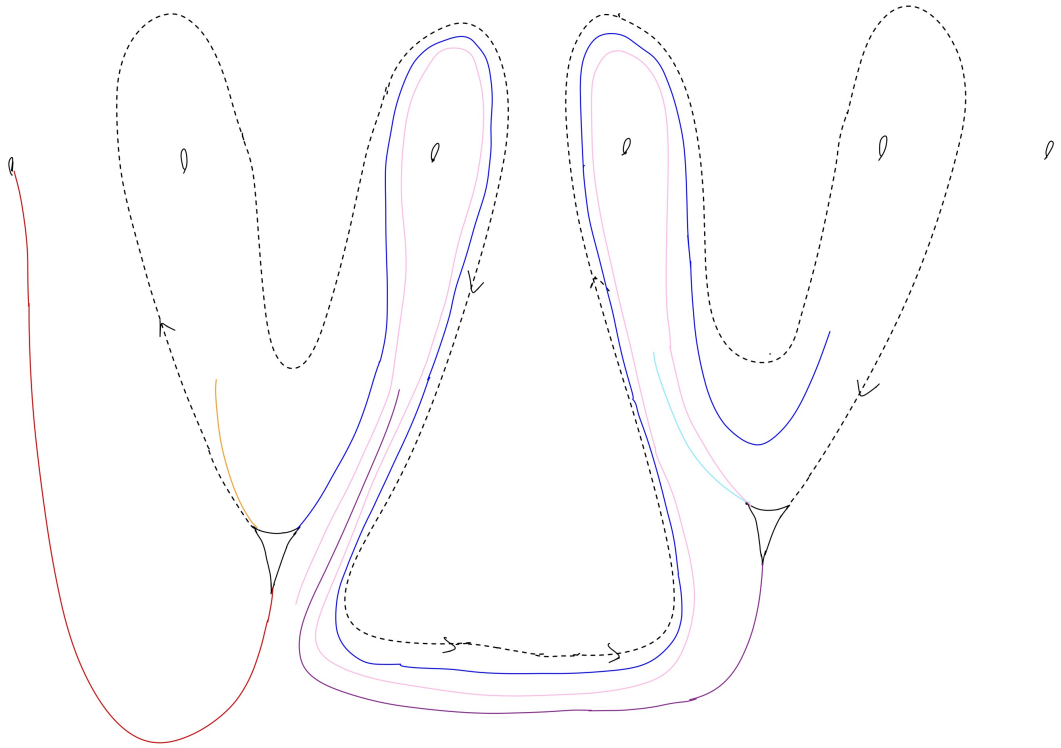


Figure E.48: Swale1

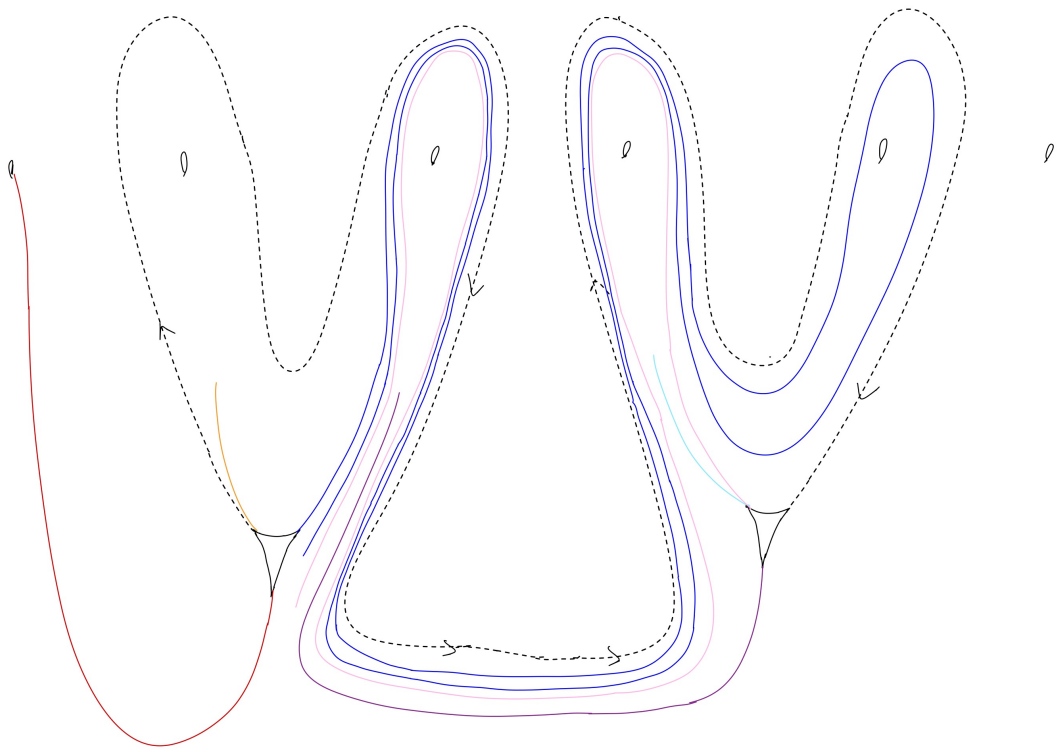


Figure E.49: Bezoar1

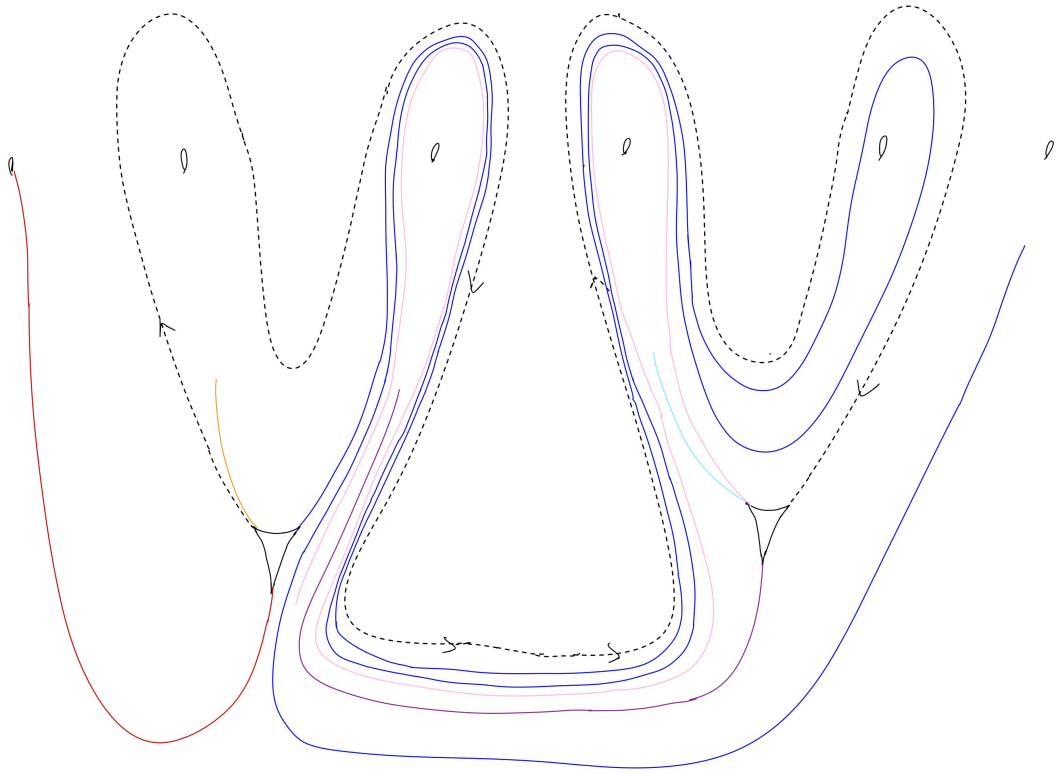


Figure E.50: Bezoar2

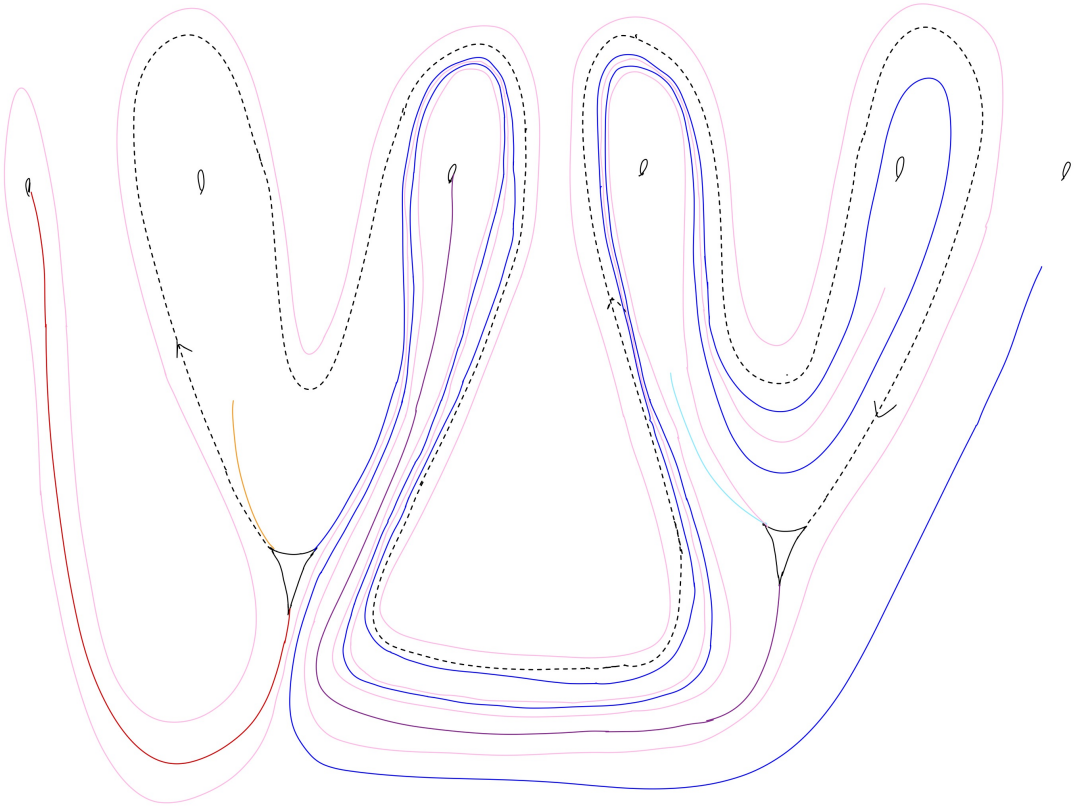


Figure E.51: Bezoar3

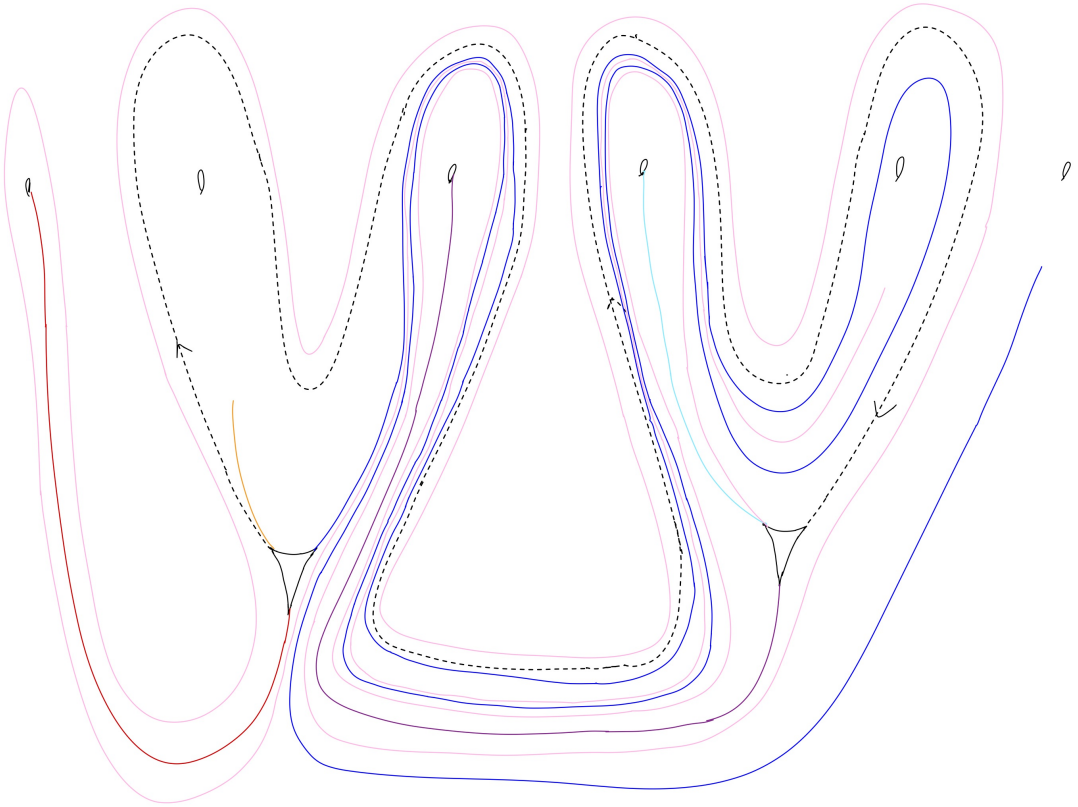


Figure E.52: Bezoar4

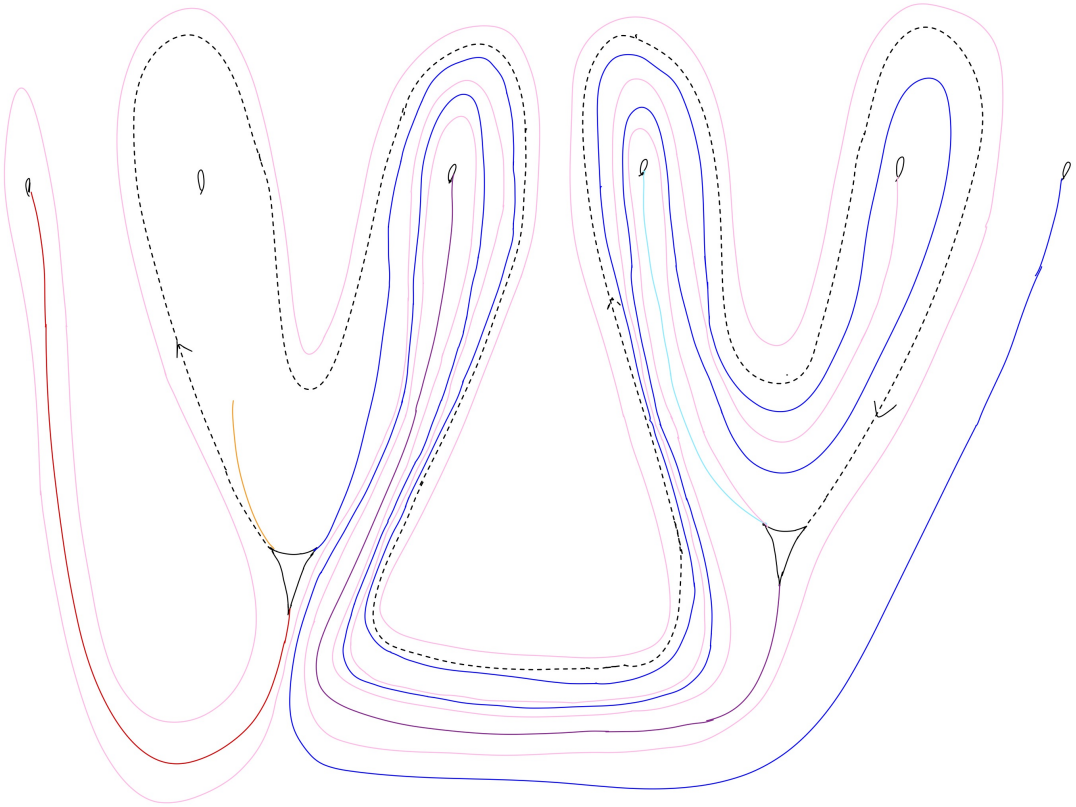


Figure E.53: Bezoar5

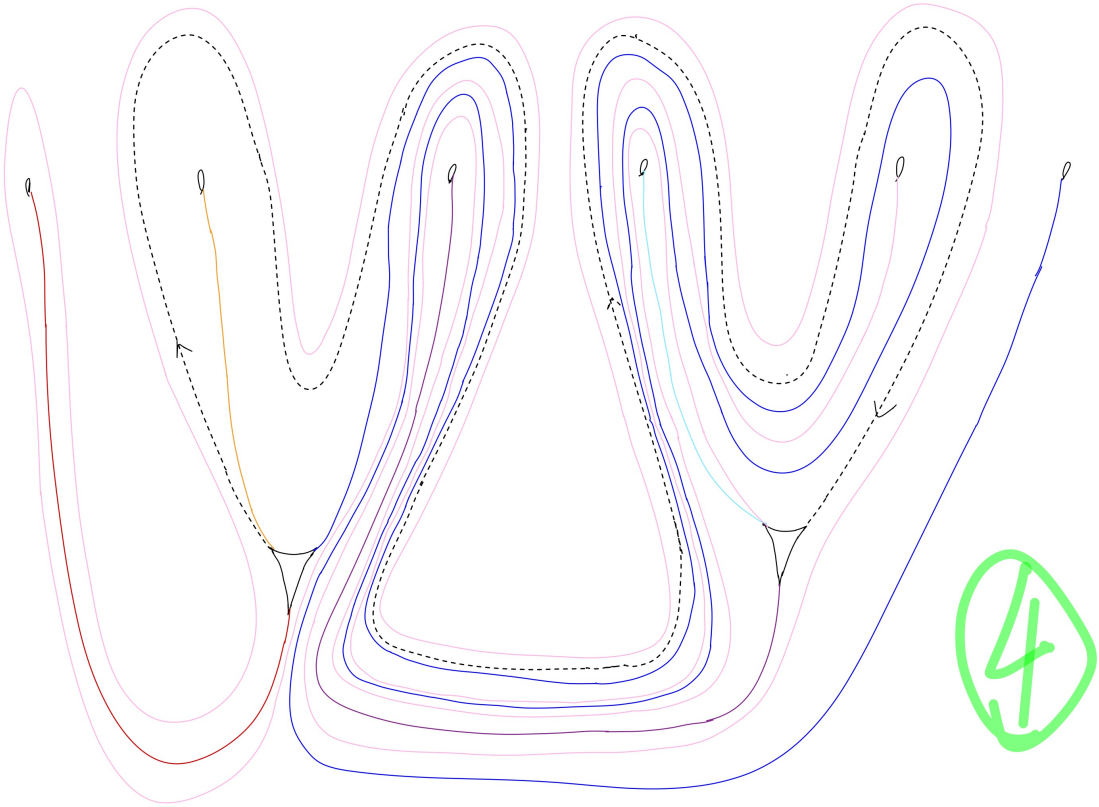


Figure E.54: Bezoar6

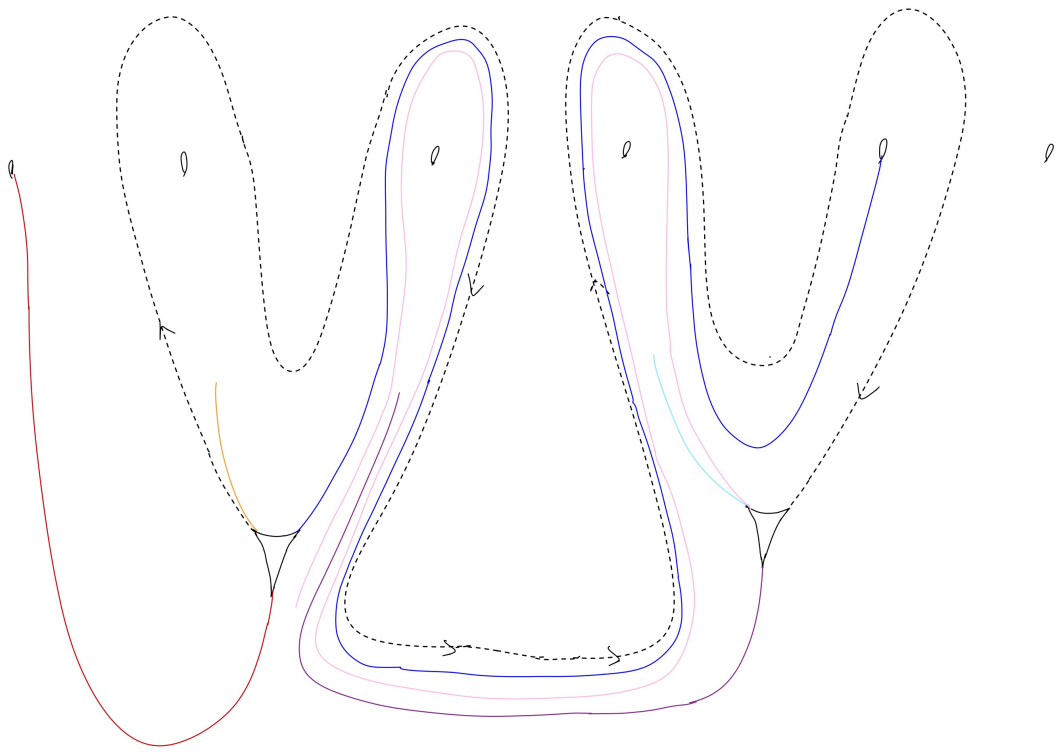


Figure E.55: Efface1

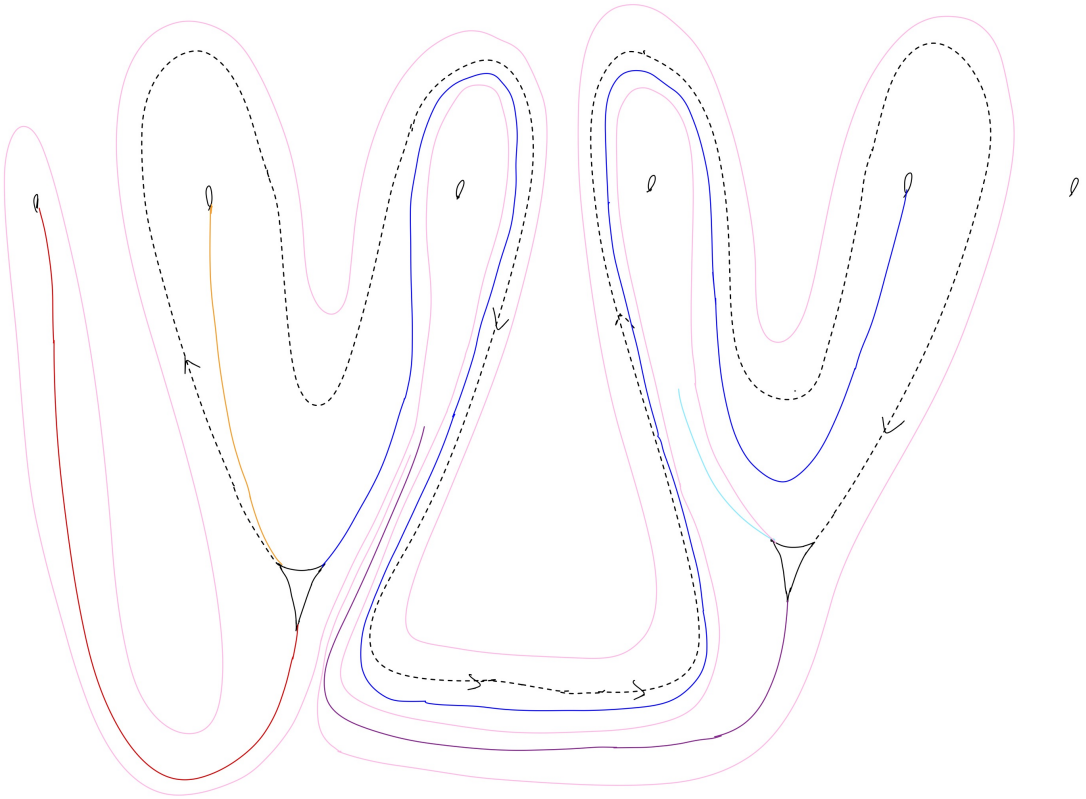


Figure E.56: Abscond1

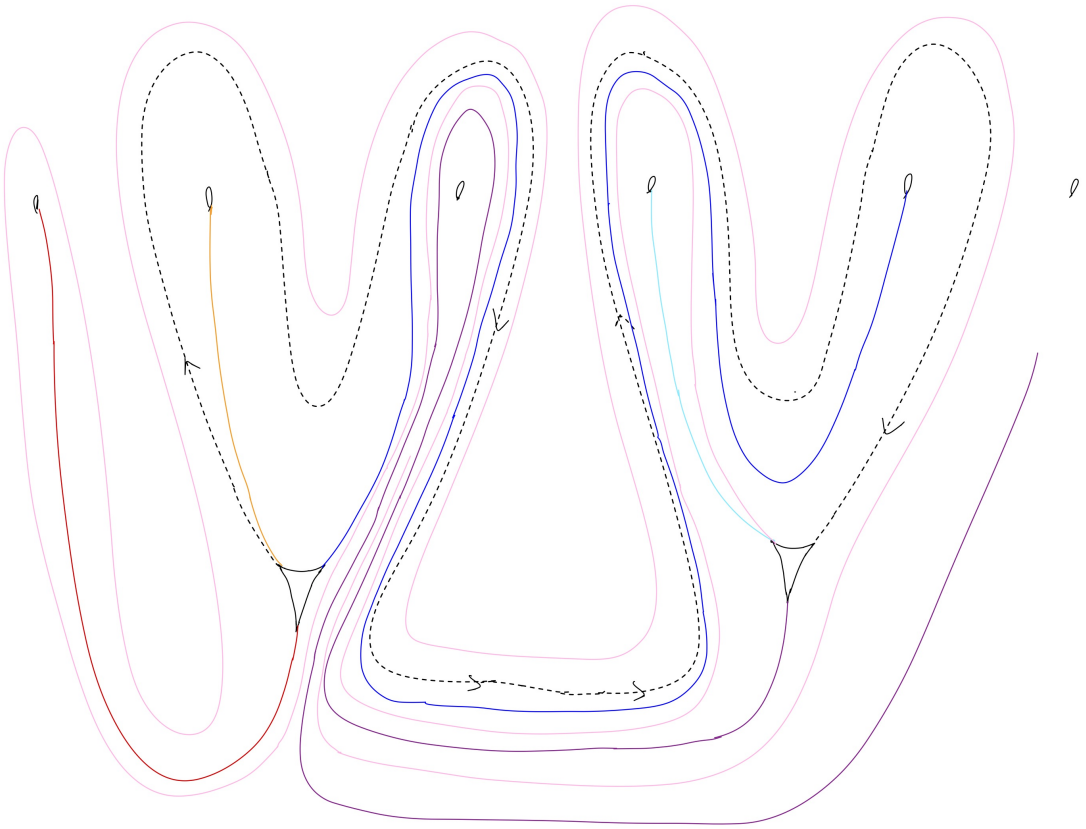


Figure E.57: Abscond2

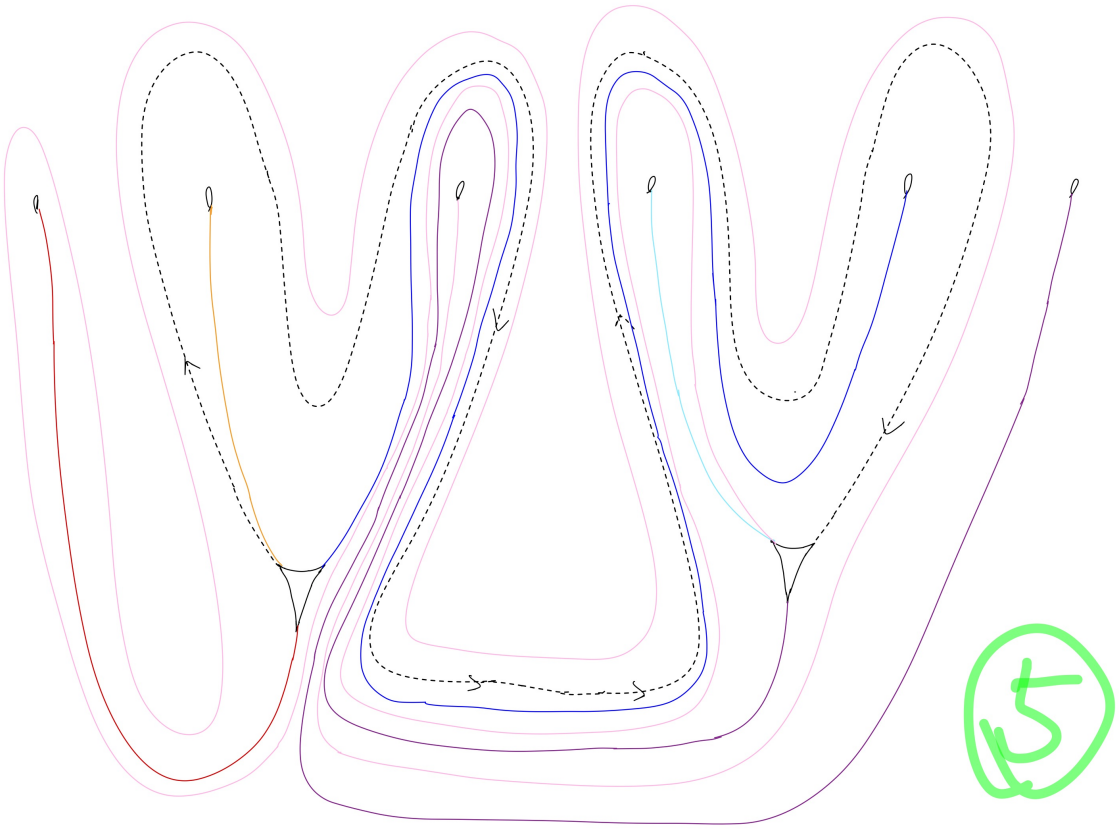


Figure E.58: Abscond3

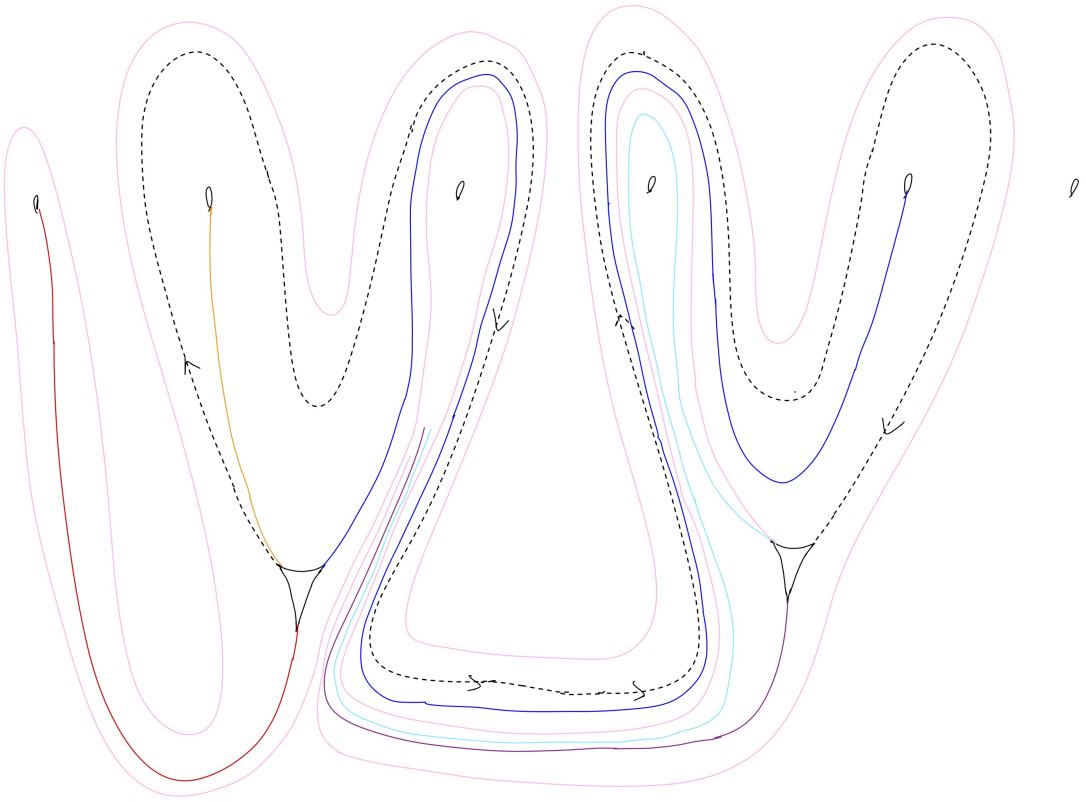


Figure E.59: Abscond4

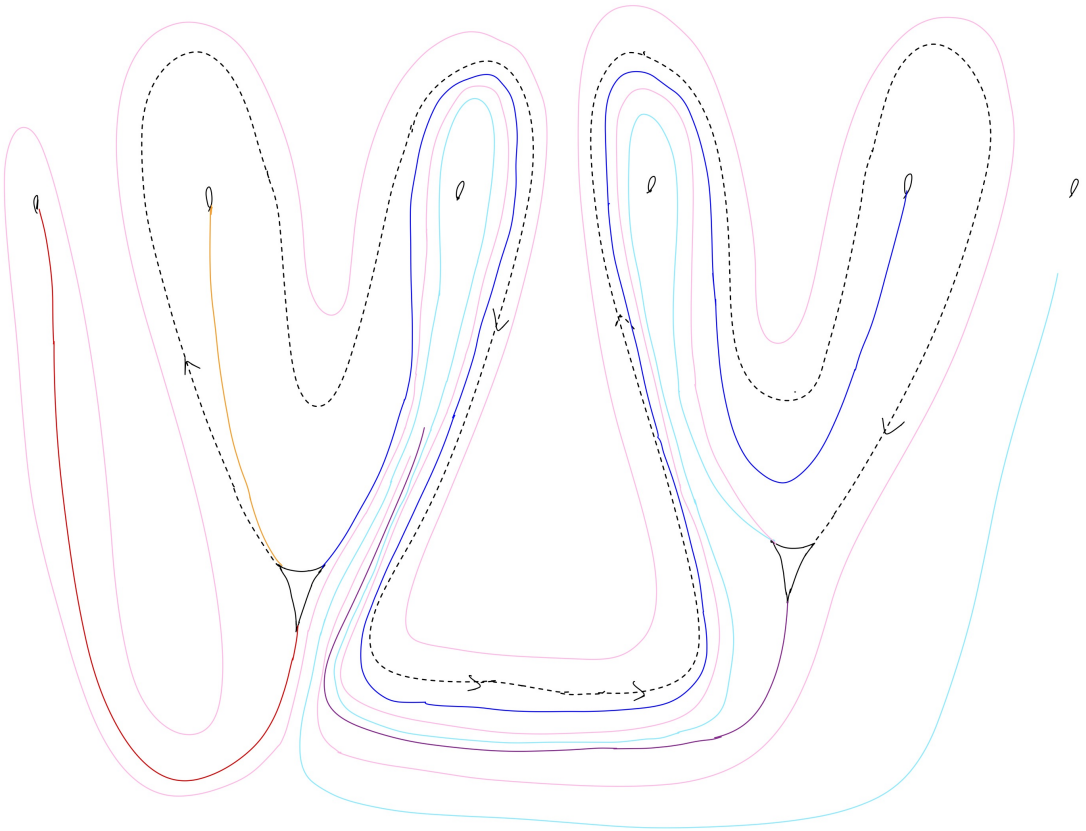


Figure E.60: Abscond5

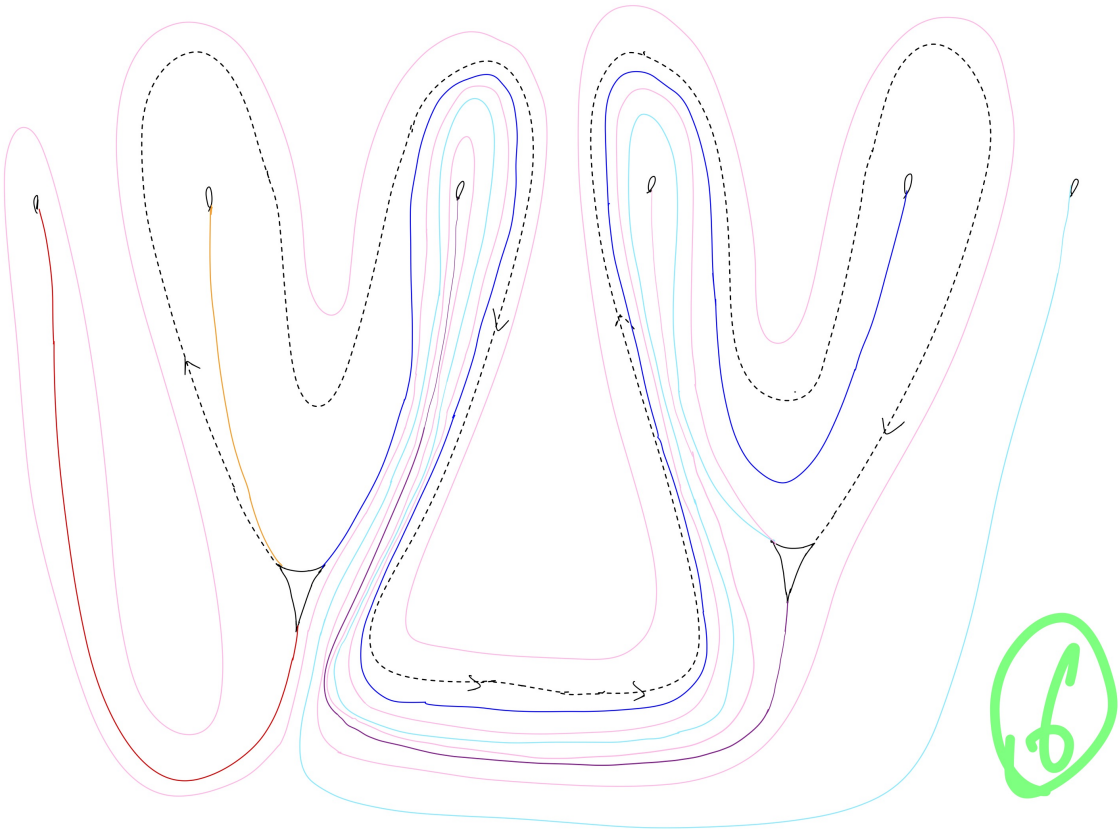


Figure E.61: Abscond6

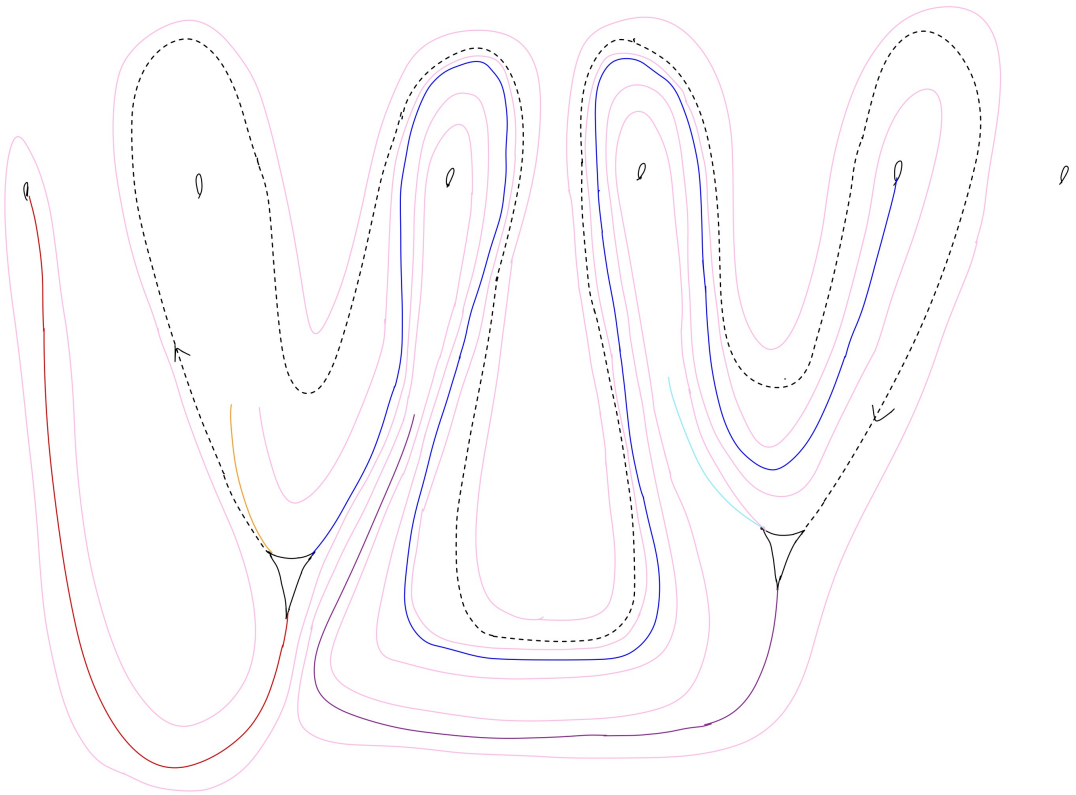


Figure E.62: Fervent1

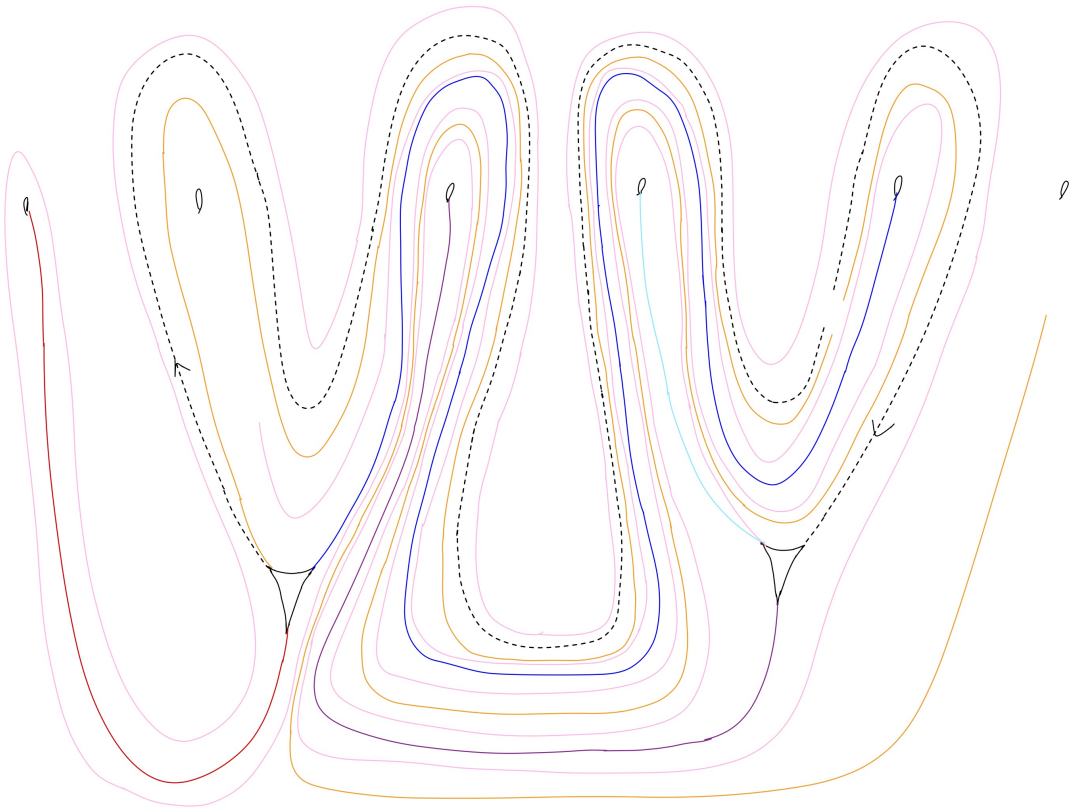


Figure E.63: Fervent2

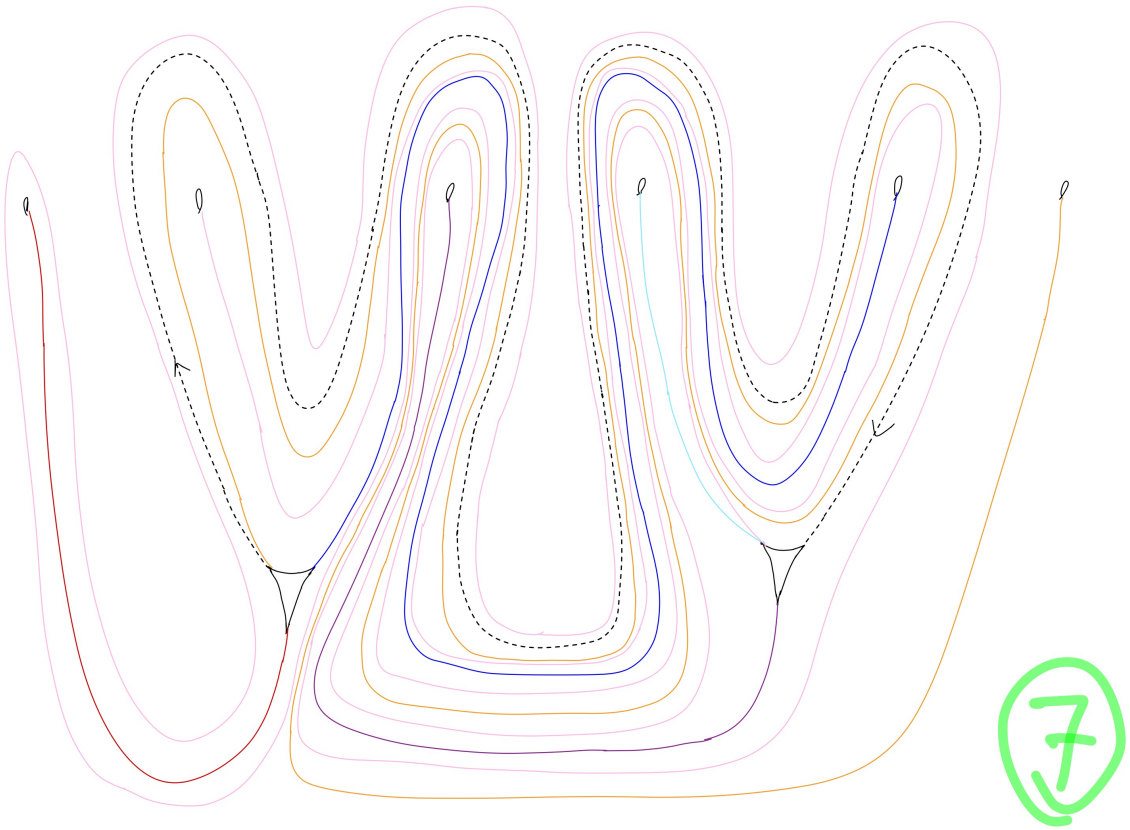


Figure E.64: Fervent3

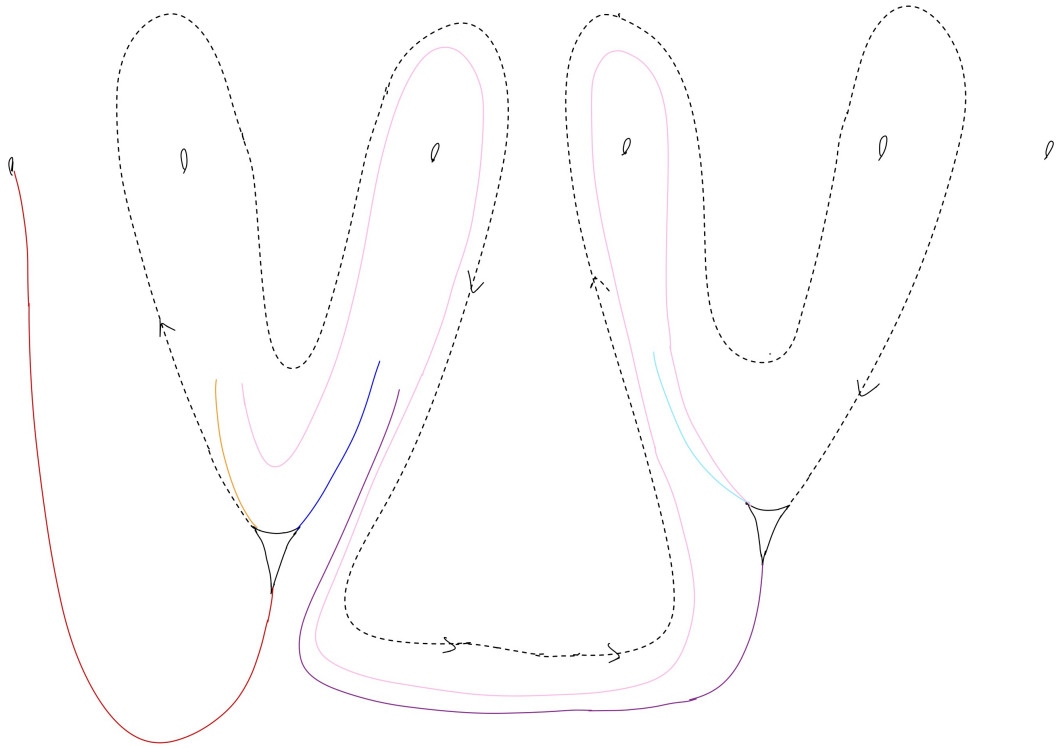


Figure E.65: Ombre1

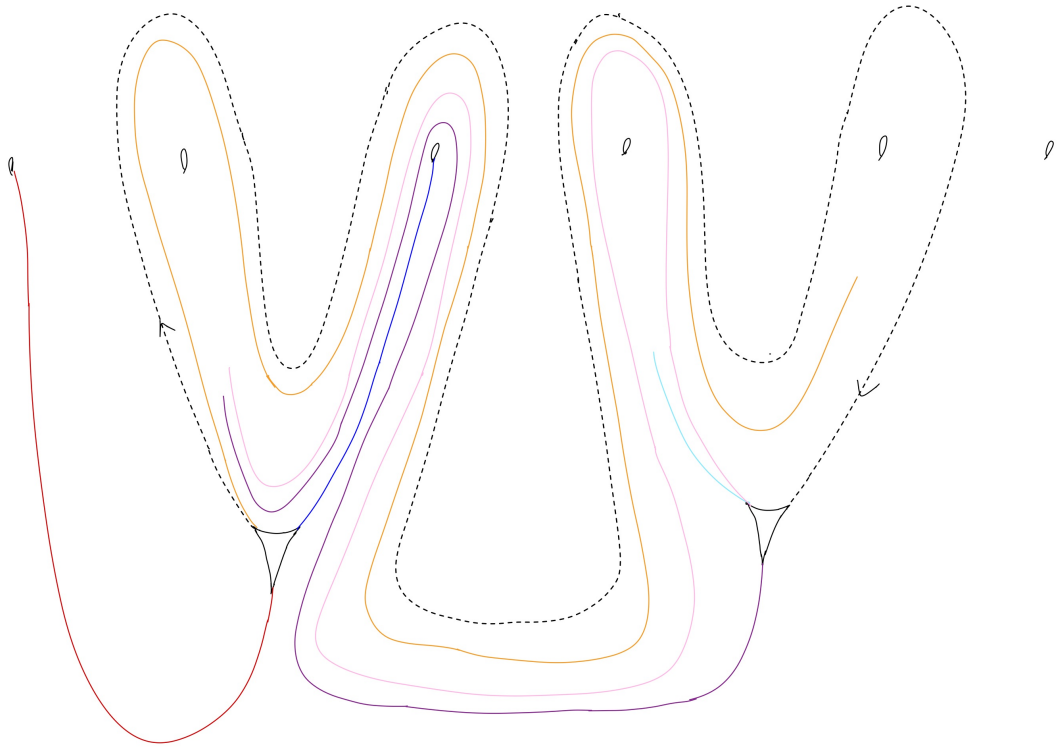


Figure E.66: Satire1

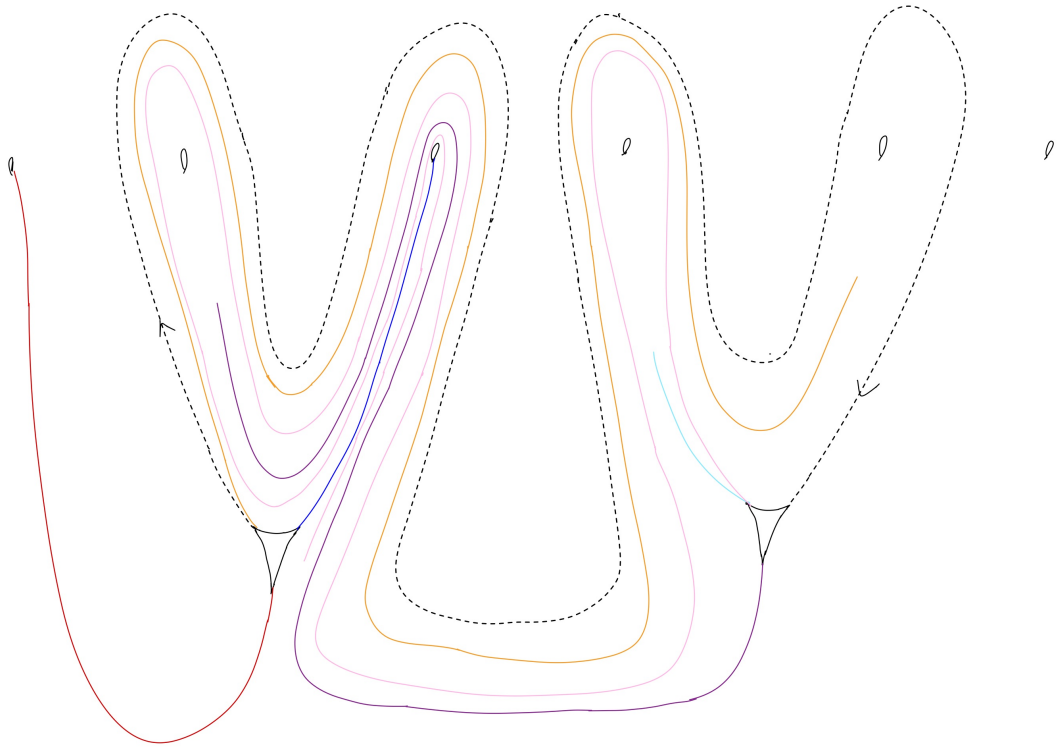


Figure E.67: Satire2

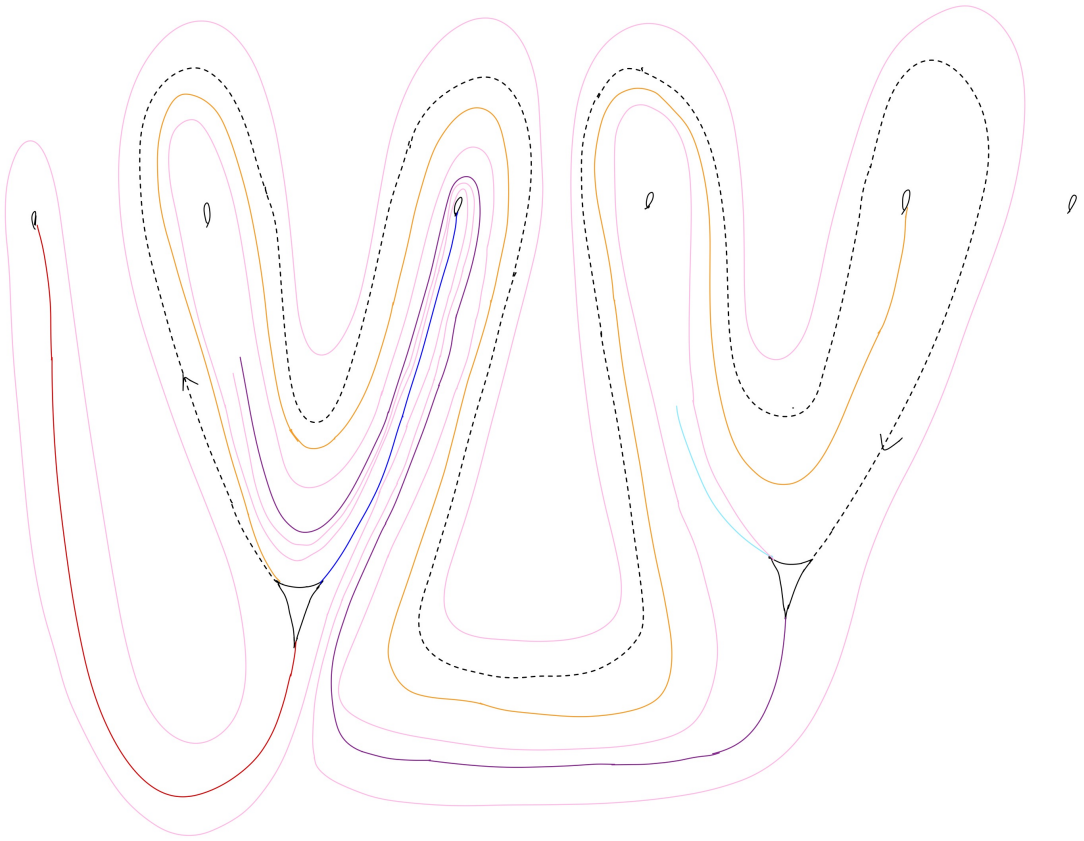


Figure E.68: Abdomen1

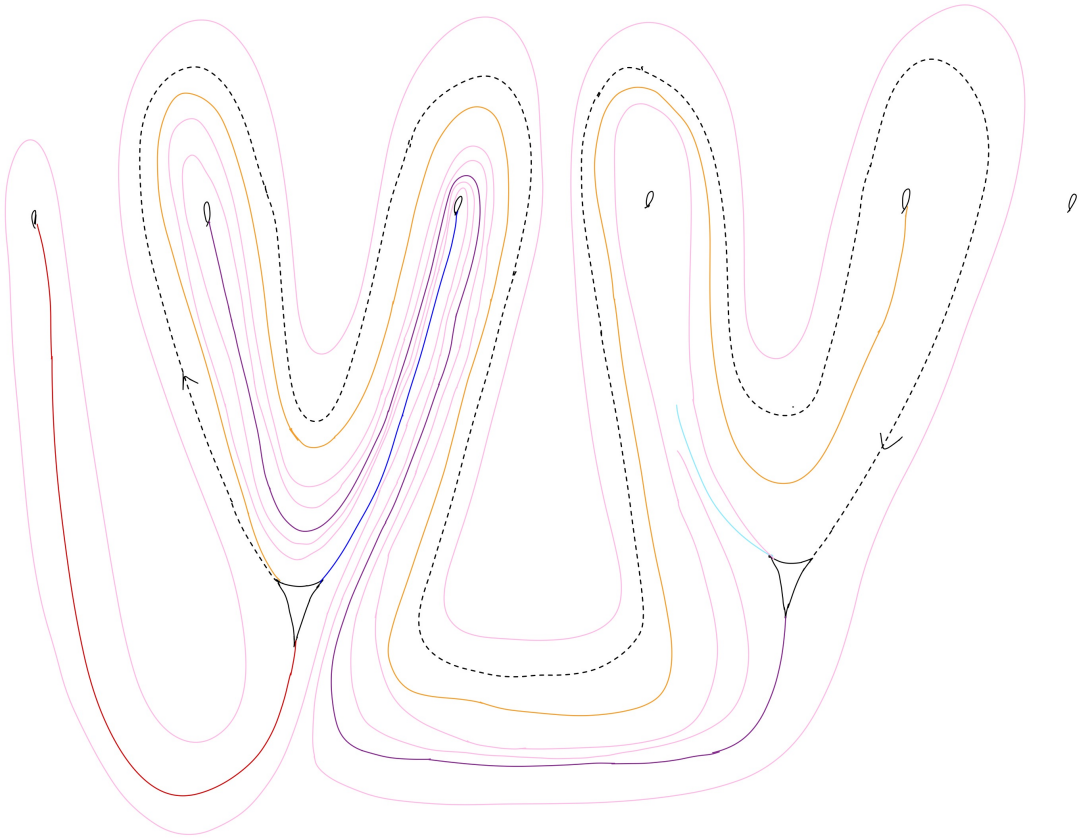


Figure E.69: Panorama1

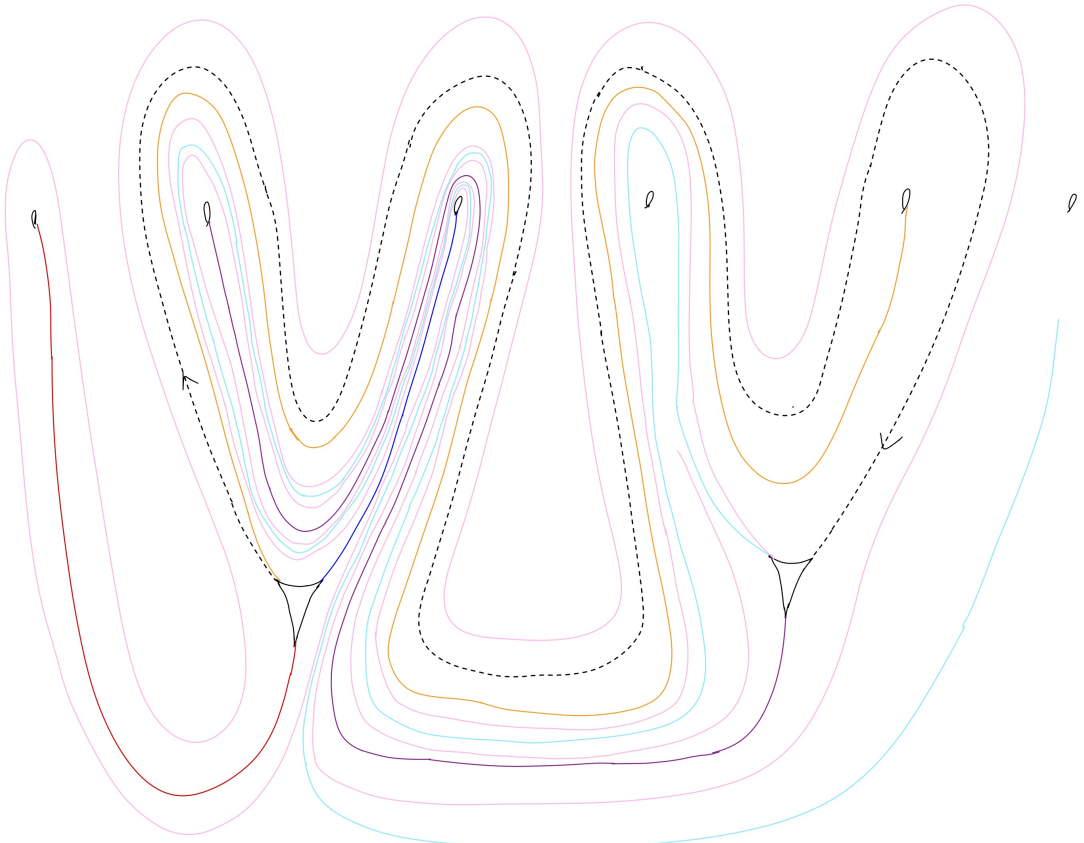


Figure E.70: Panorama2

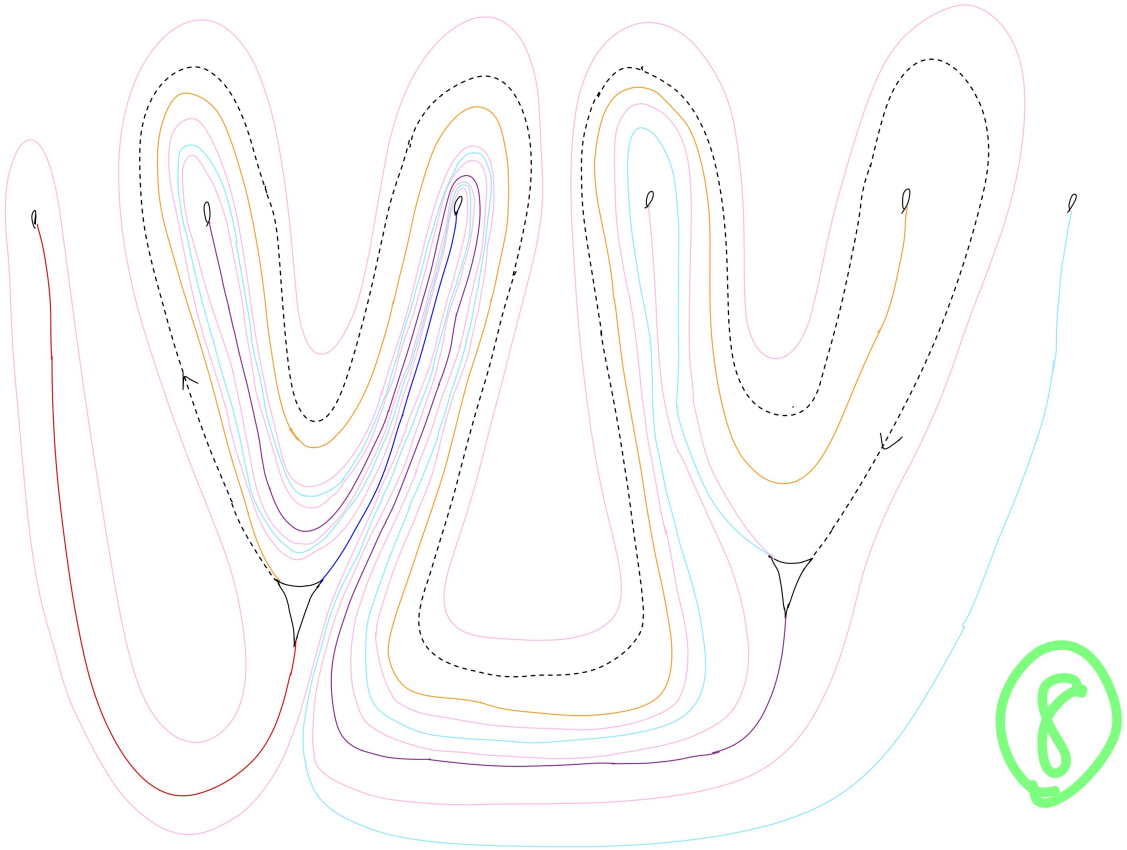


Figure E.71: Panorama3

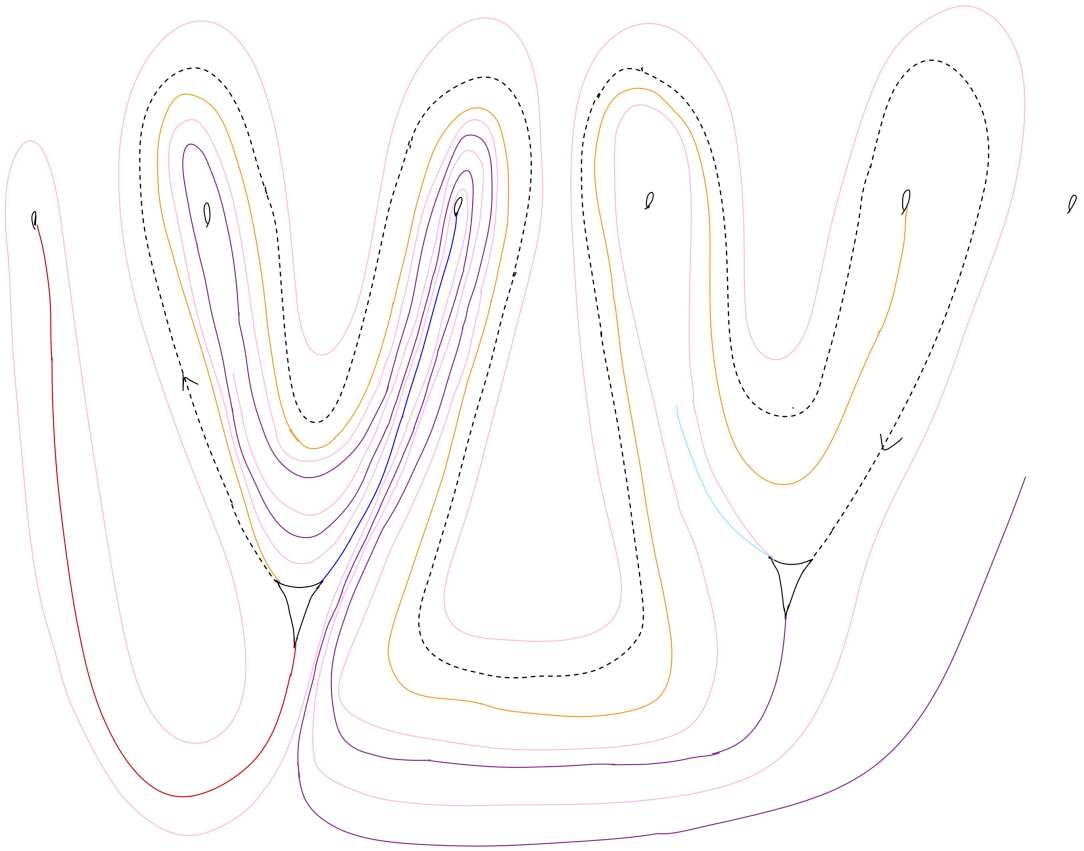


Figure E.72: Pristine1

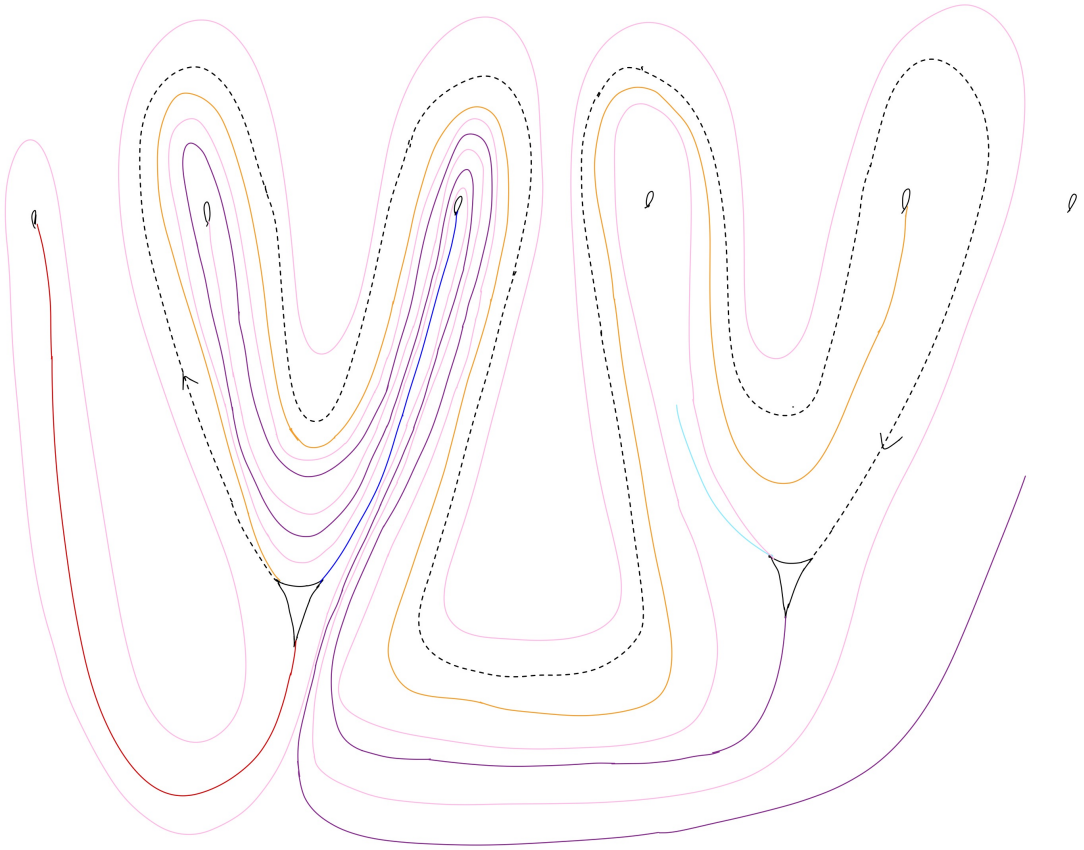


Figure E.73: Pristine2

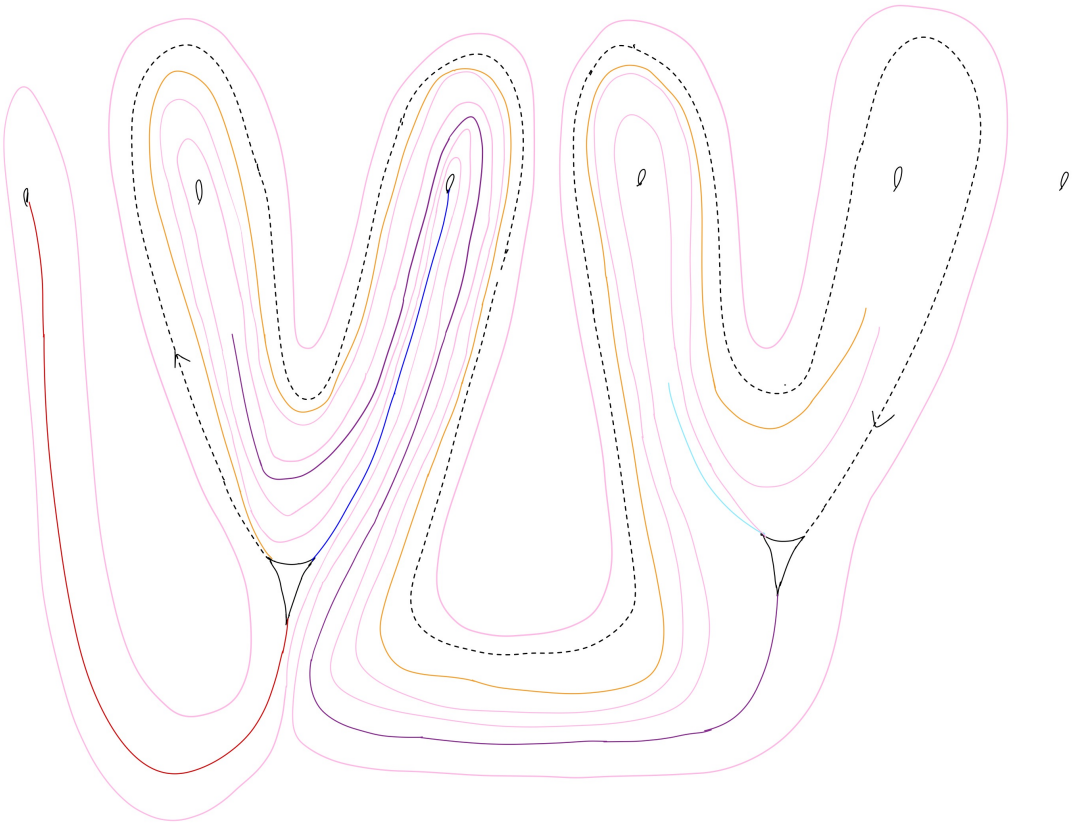


Figure E.74: Gingham1

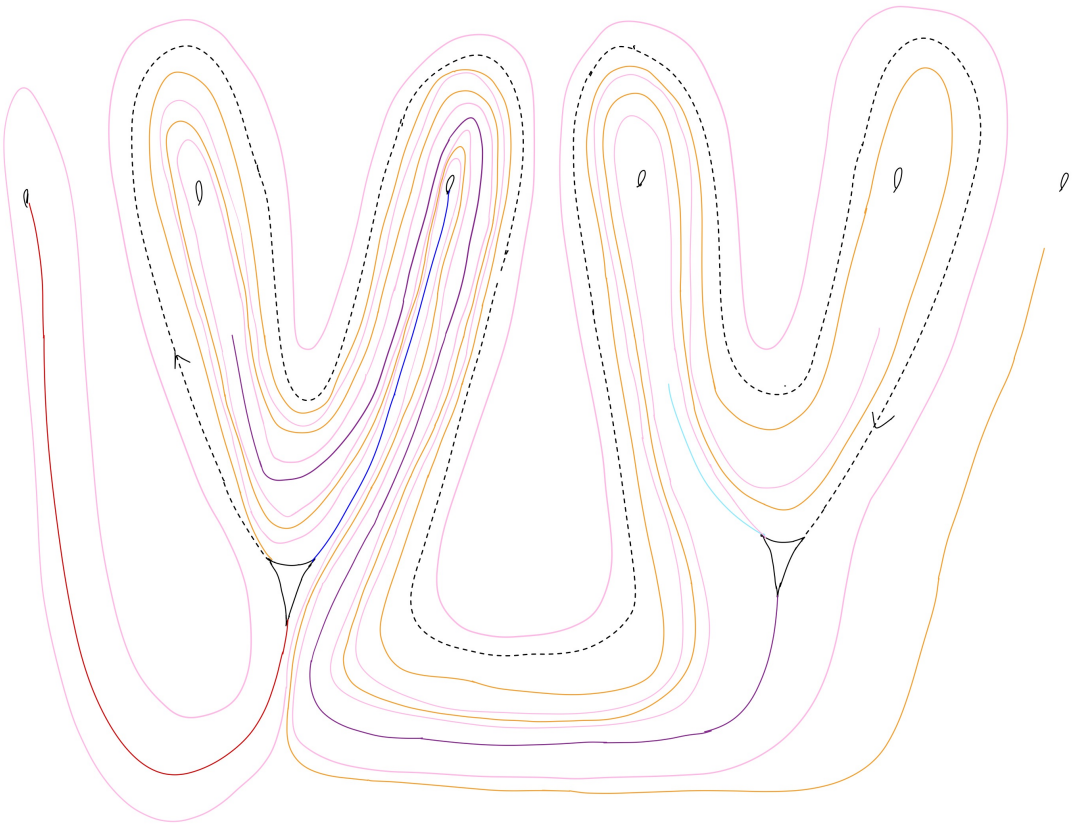


Figure E.75: Gingham2

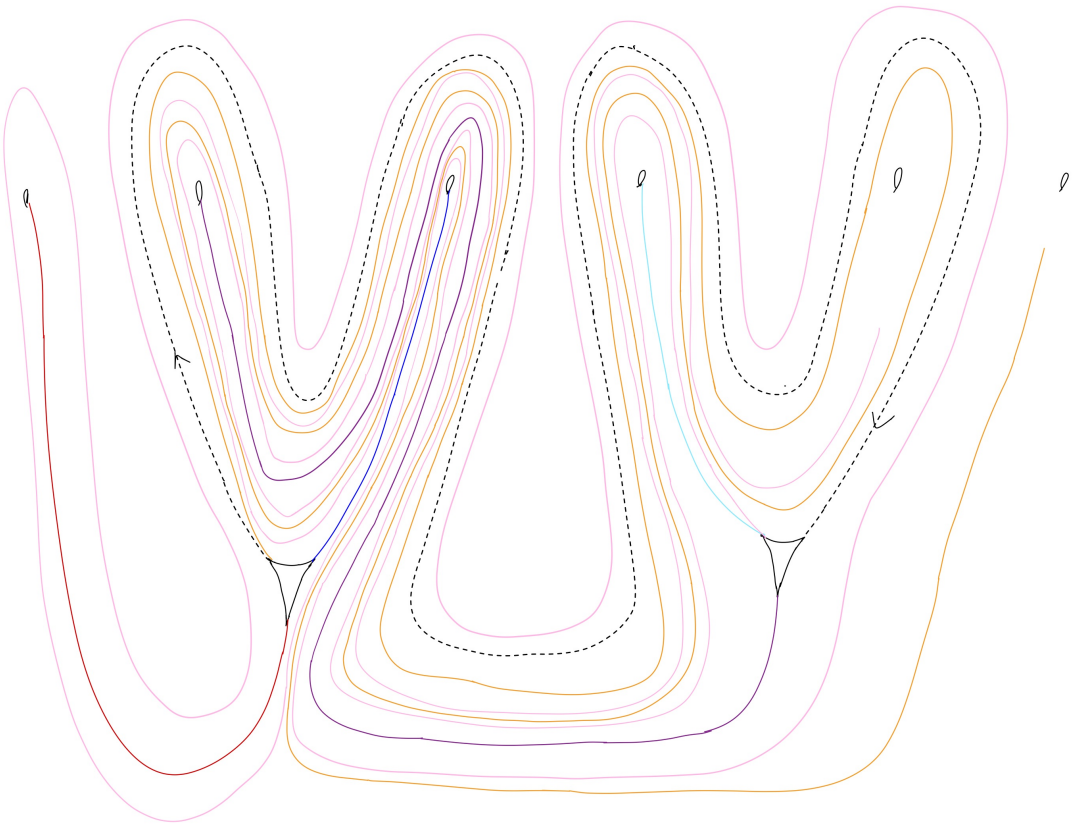


Figure E.76: Gingham3

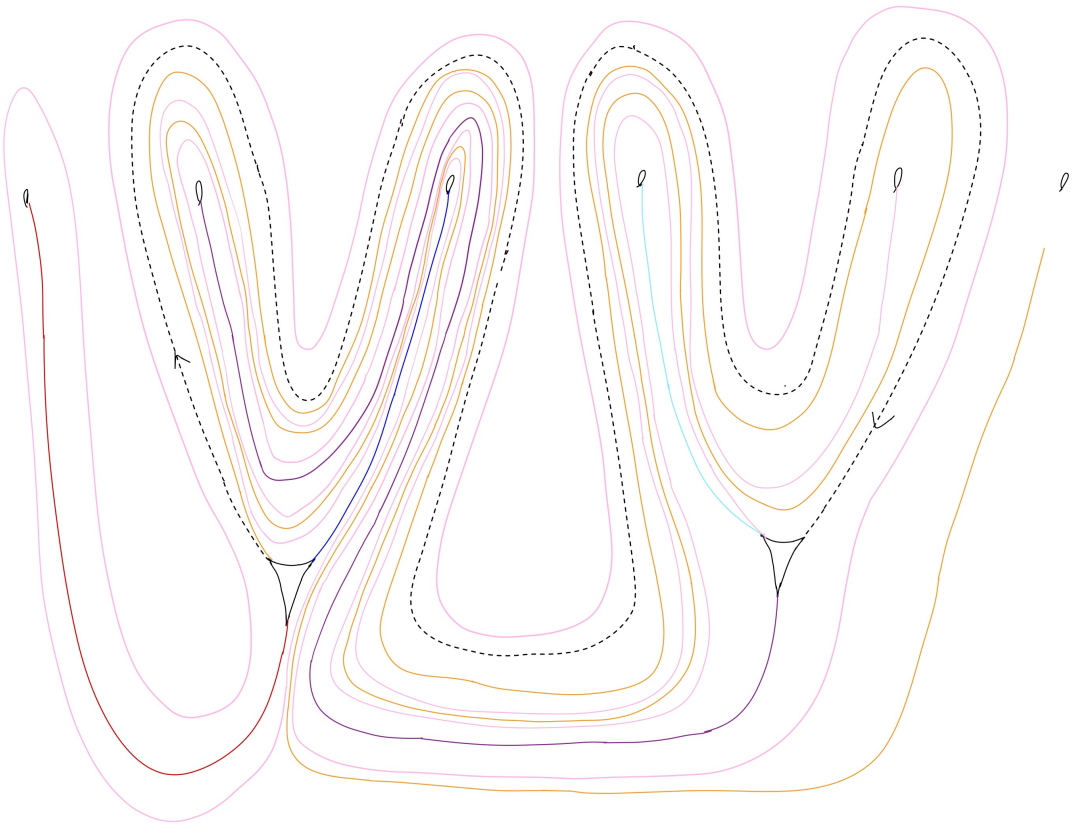


Figure E.77: Gingham4

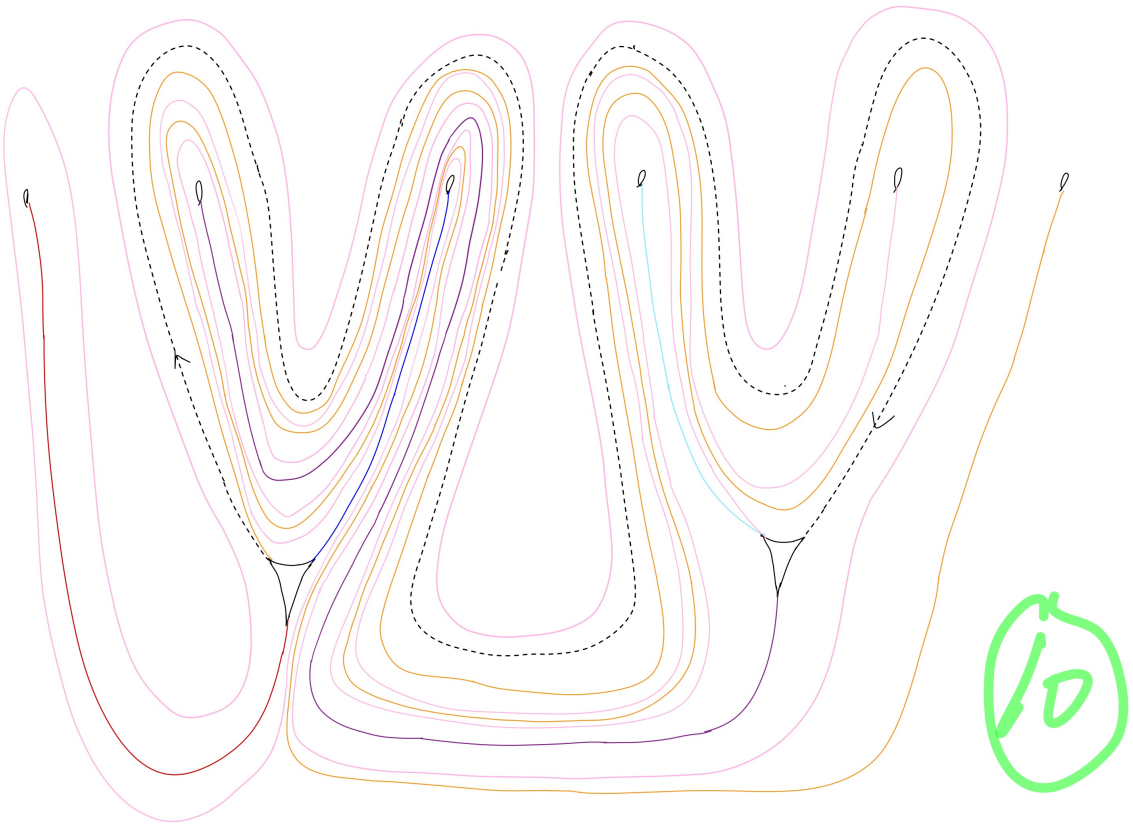


Figure E.78: Gingham5

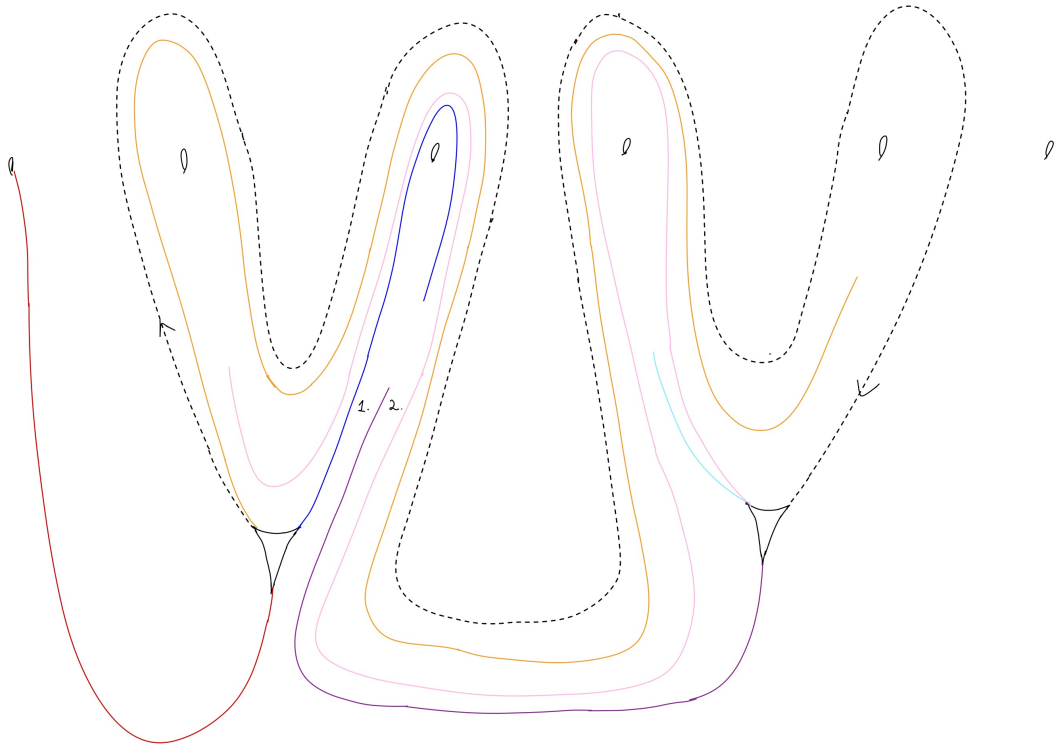


Figure E.79: Kismet1

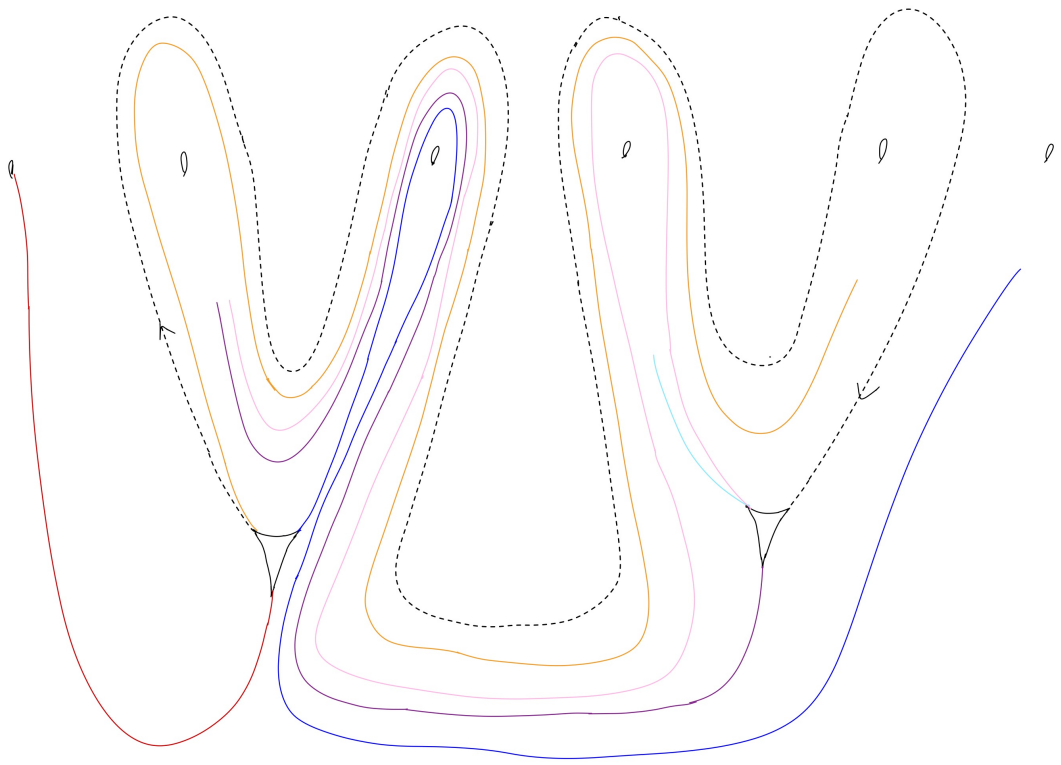


Figure E.80: Dossier1

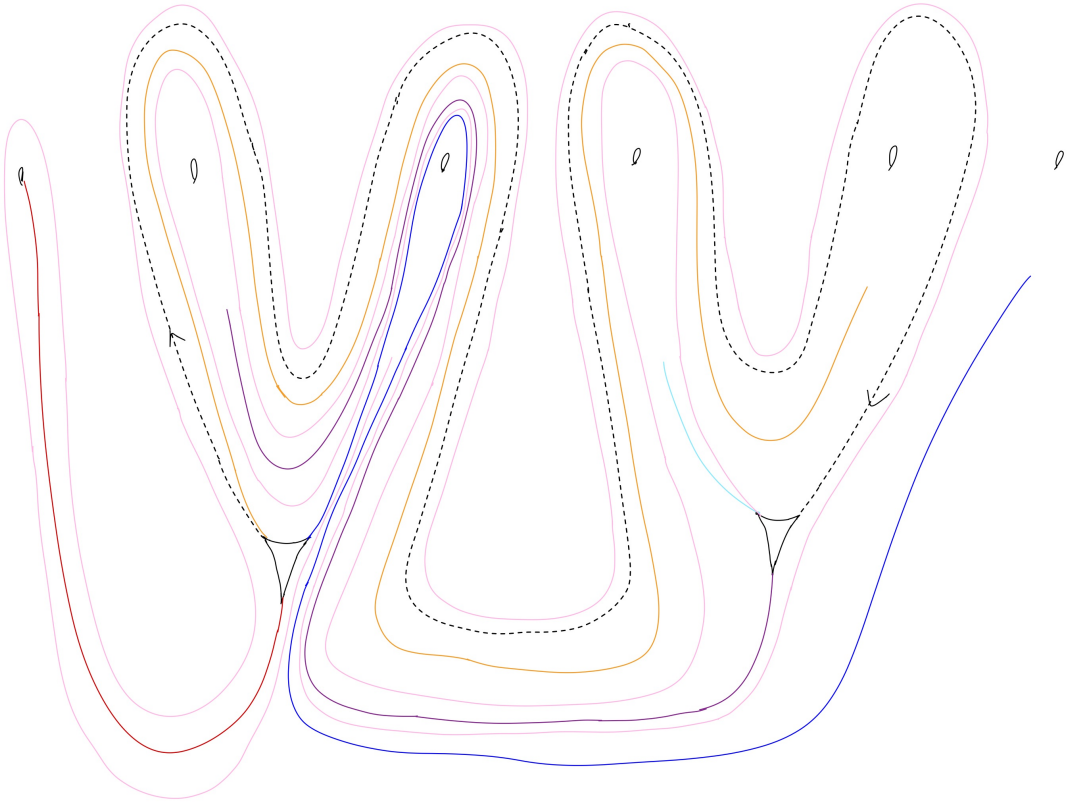


Figure E.81: Dossier2

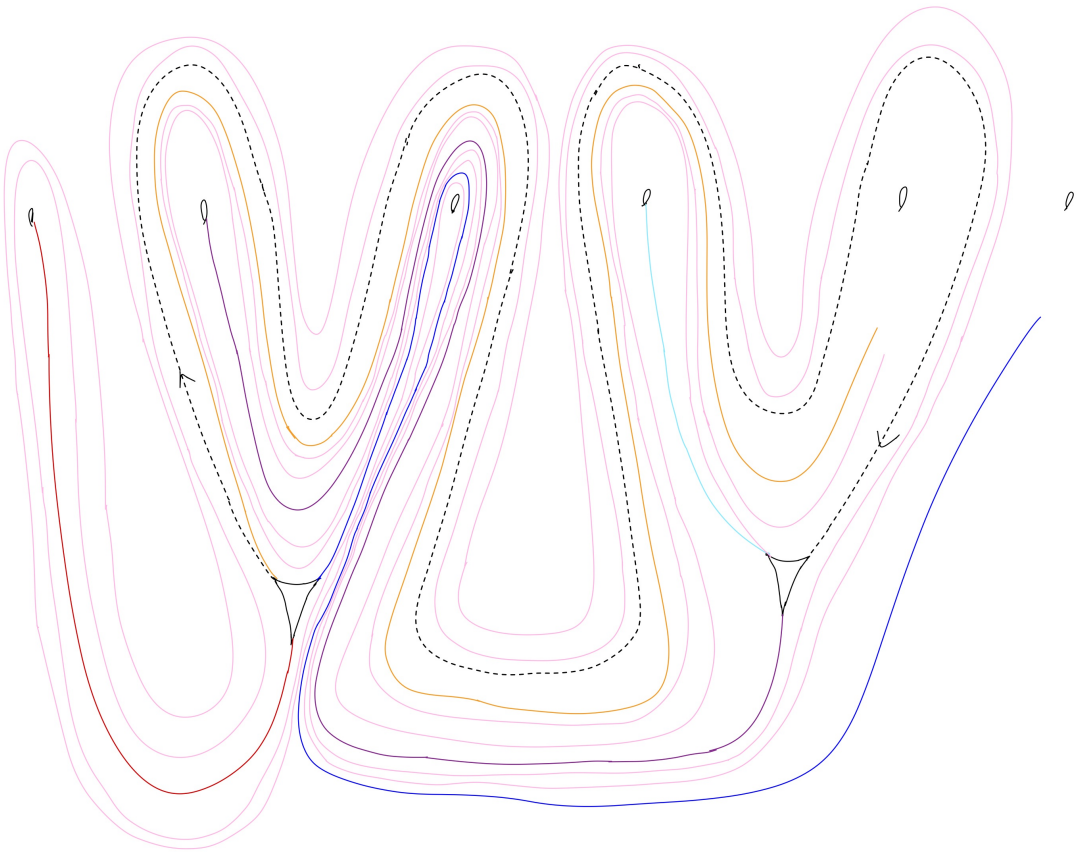


Figure E.82: Dossier3

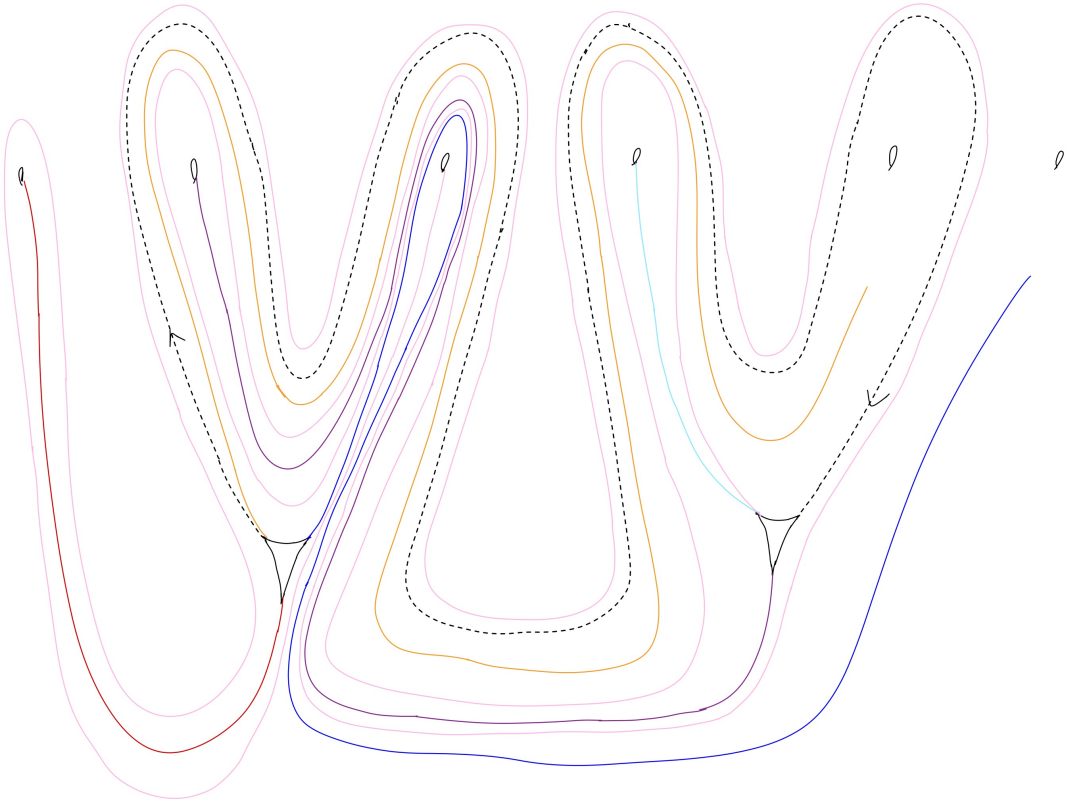


Figure E.83: Dossier4

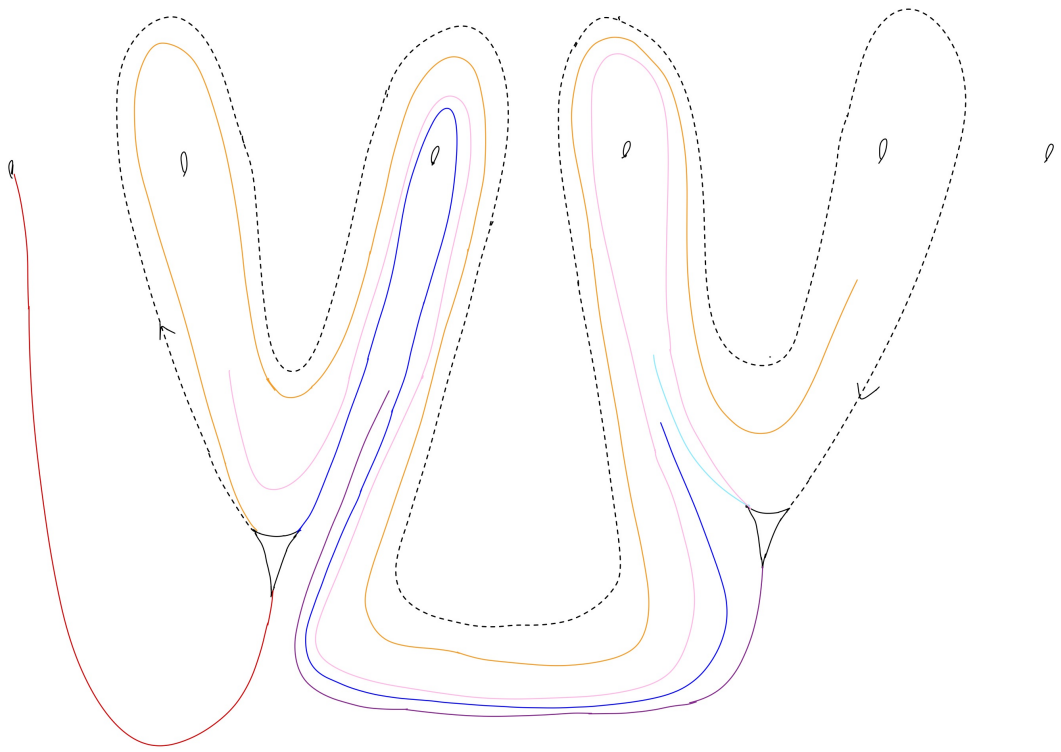


Figure E.84: Perplex1

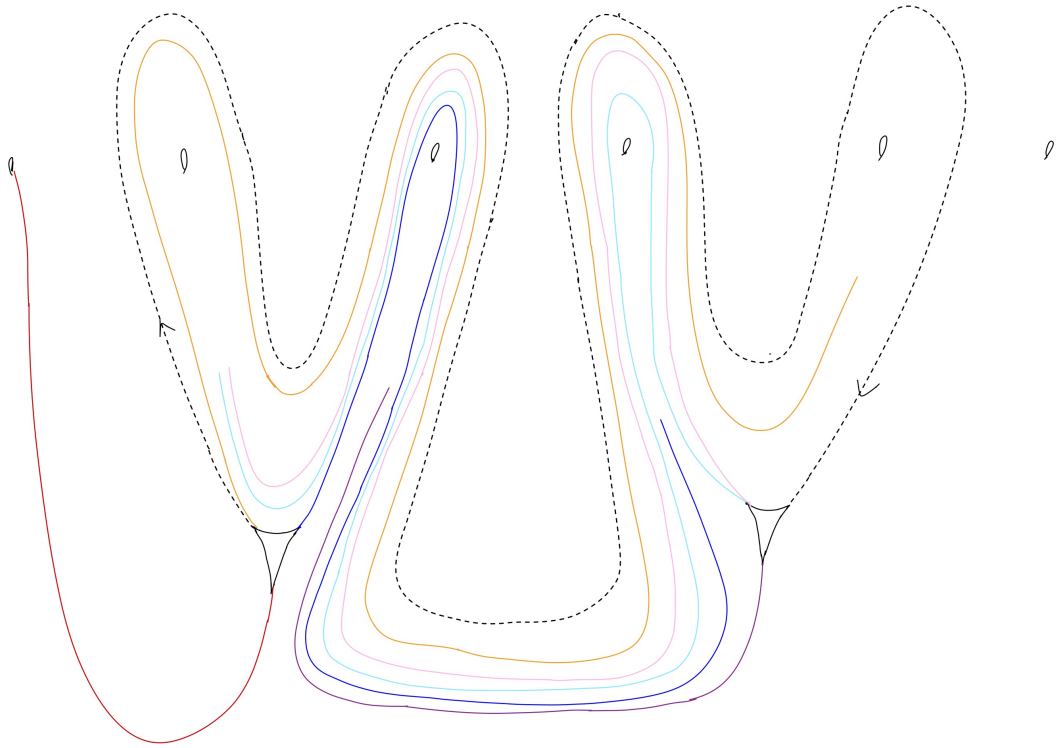


Figure E.85: Perplex2

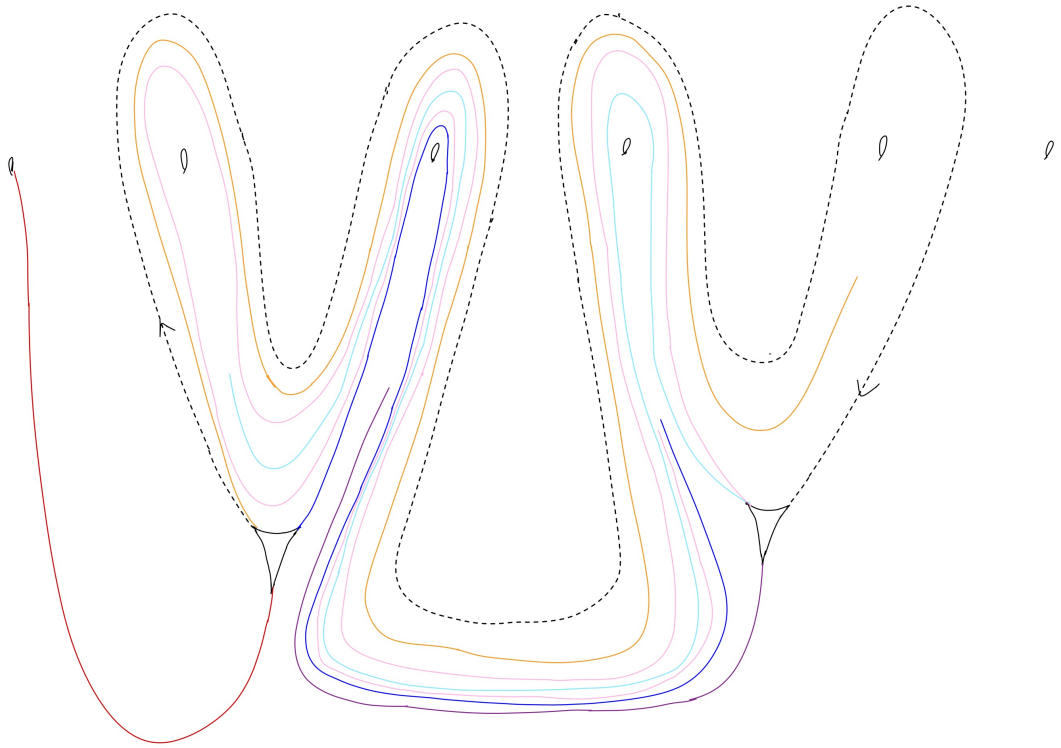


Figure E.86: Perplex3

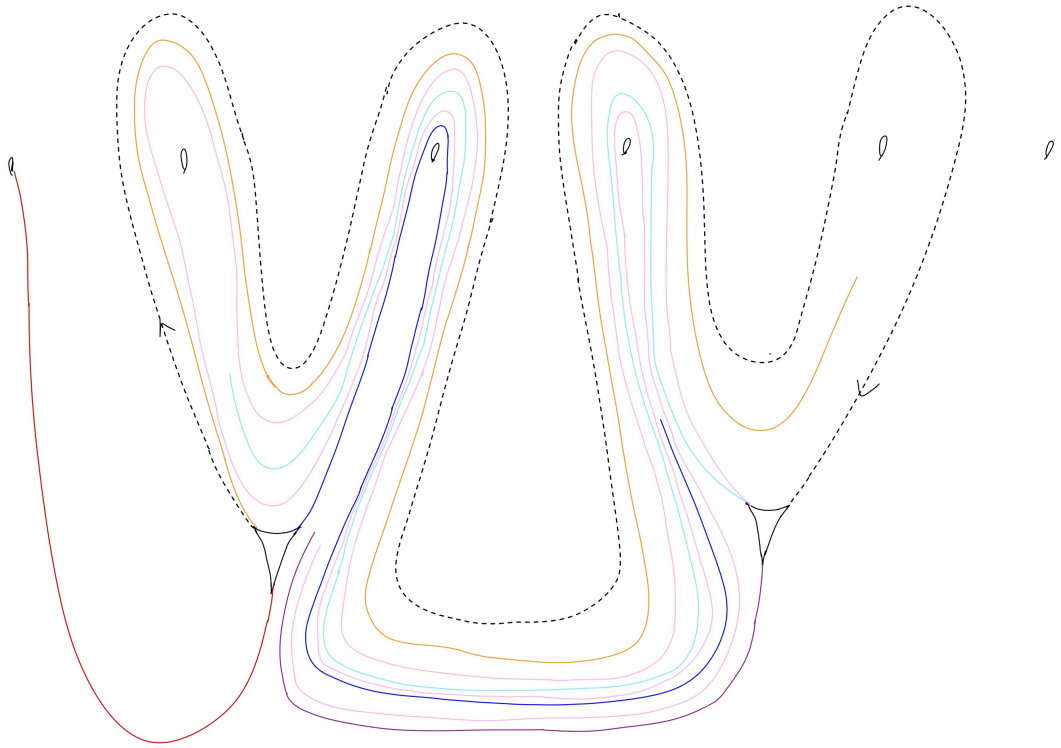


Figure E.87: Perplex4

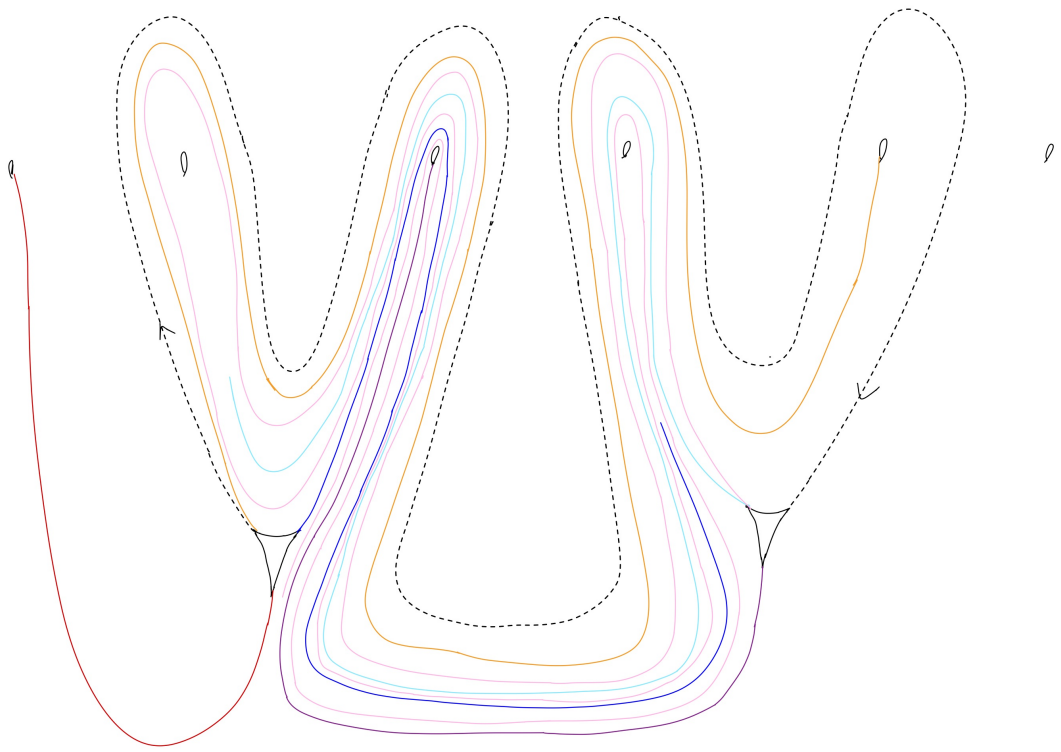


Figure E.88: Querulous1

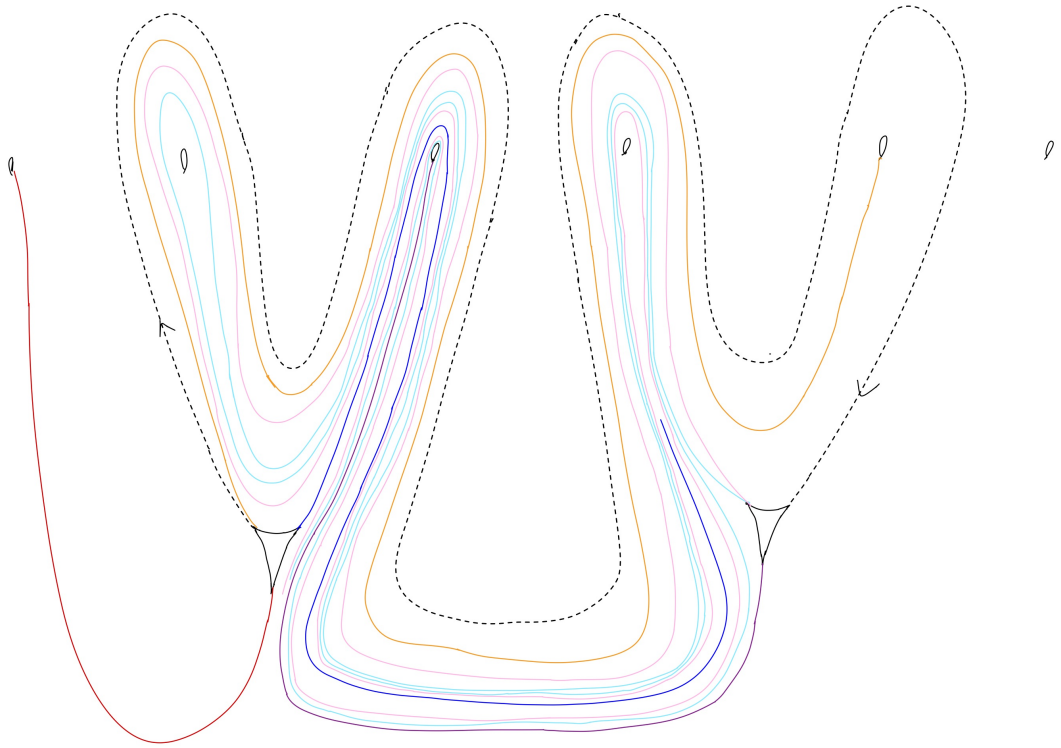


Figure E.89: Querulous2

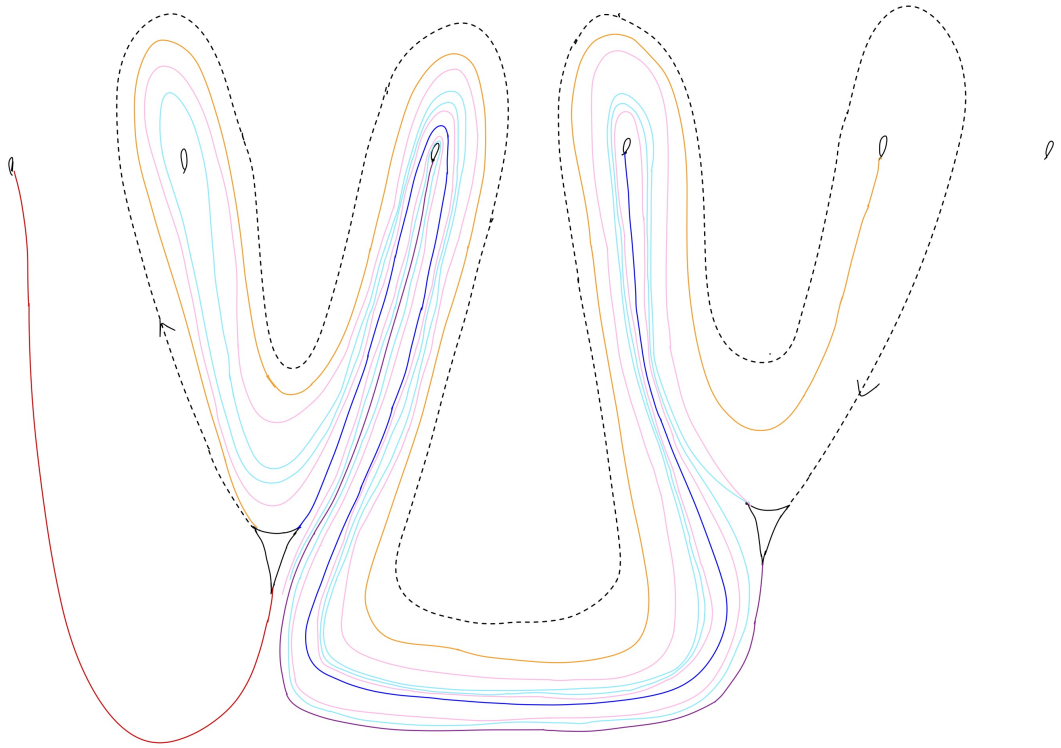


Figure E.90: Querulous3

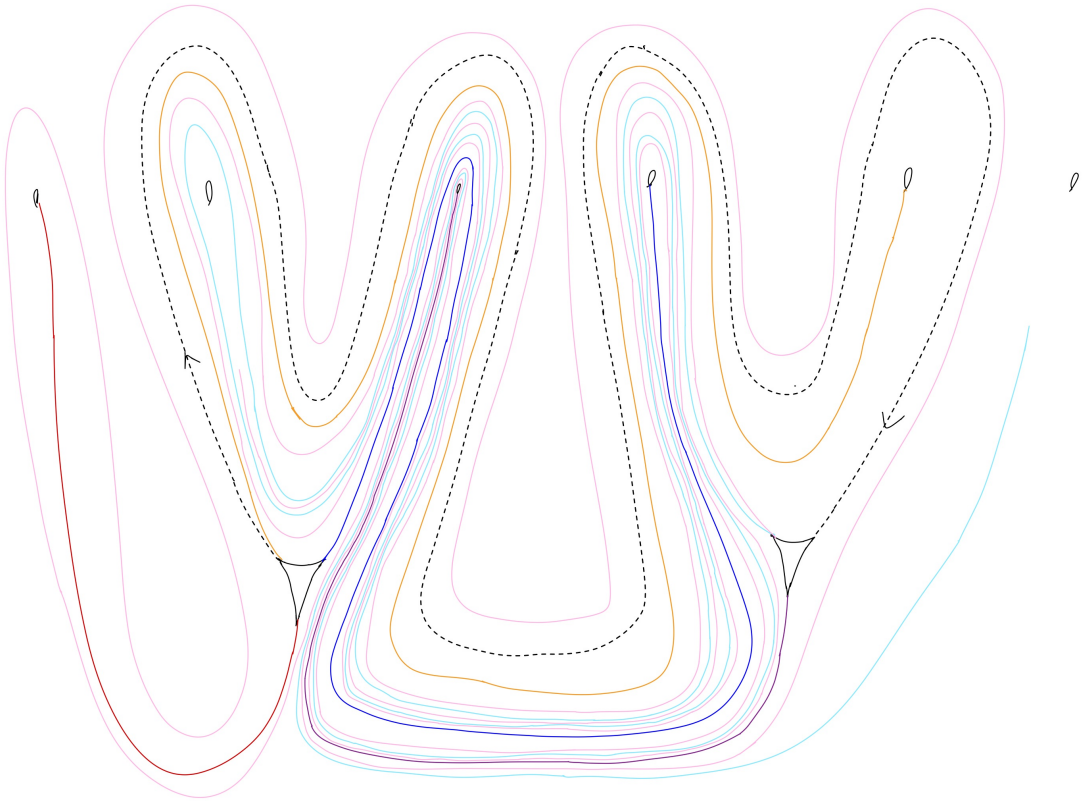


Figure E.91: Querulous4

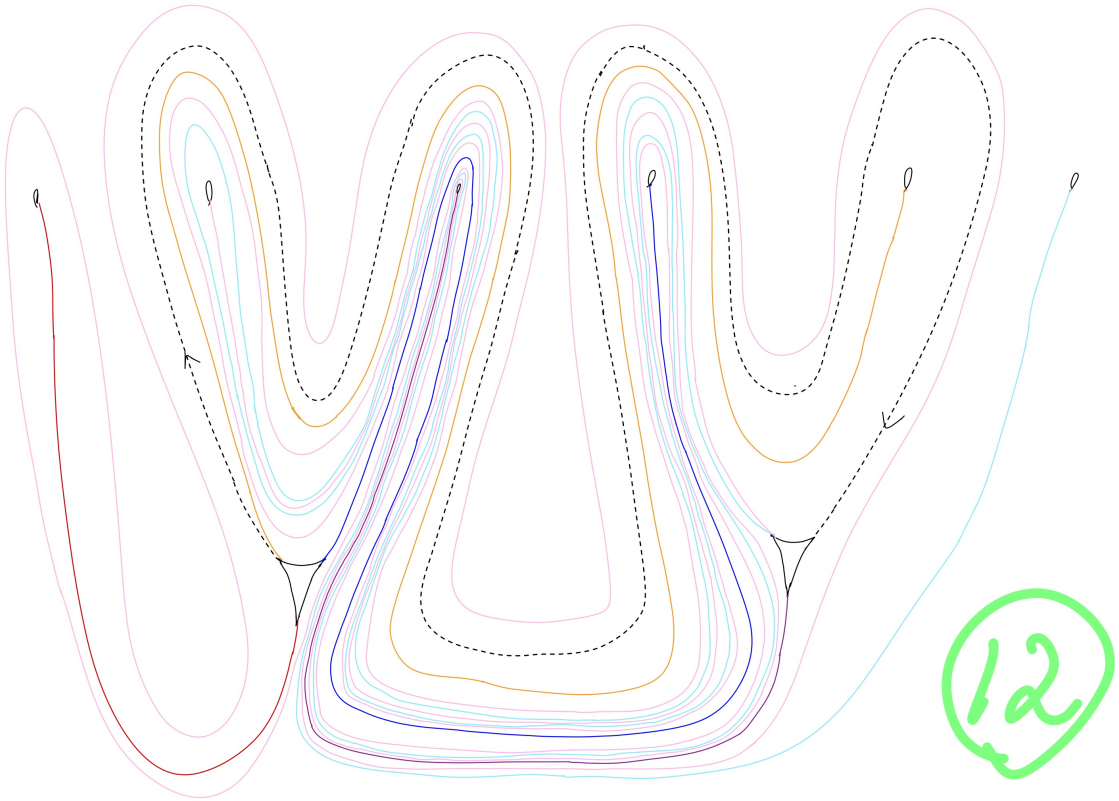


Figure E.92: Querulous5

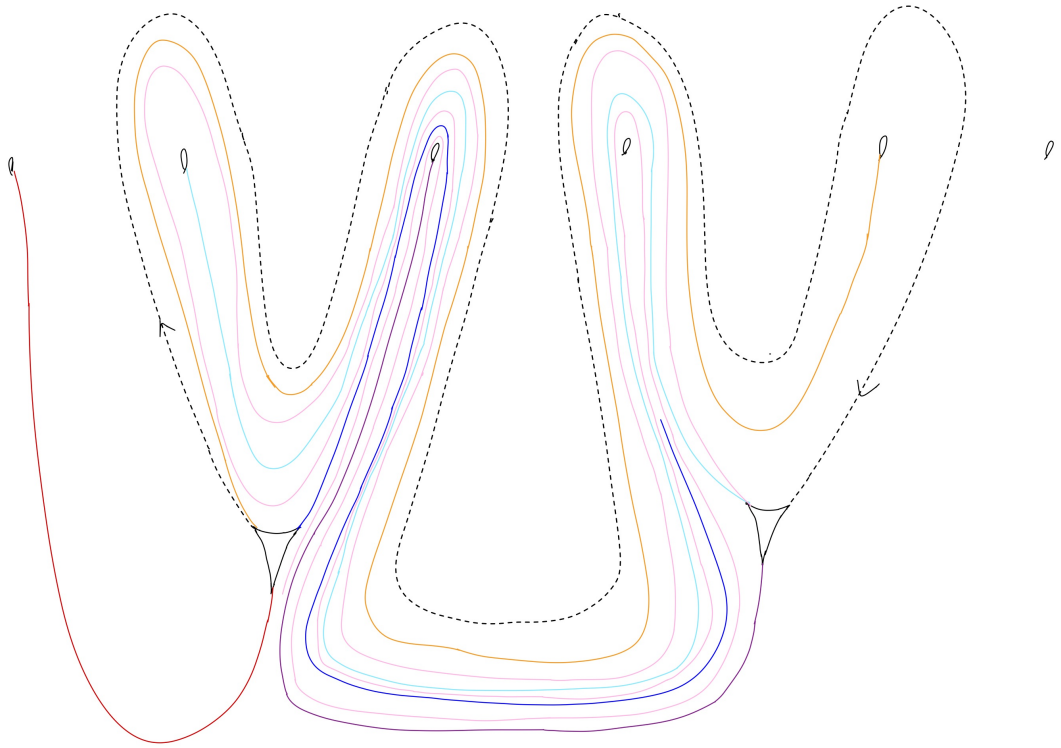


Figure E.93: Querulous6

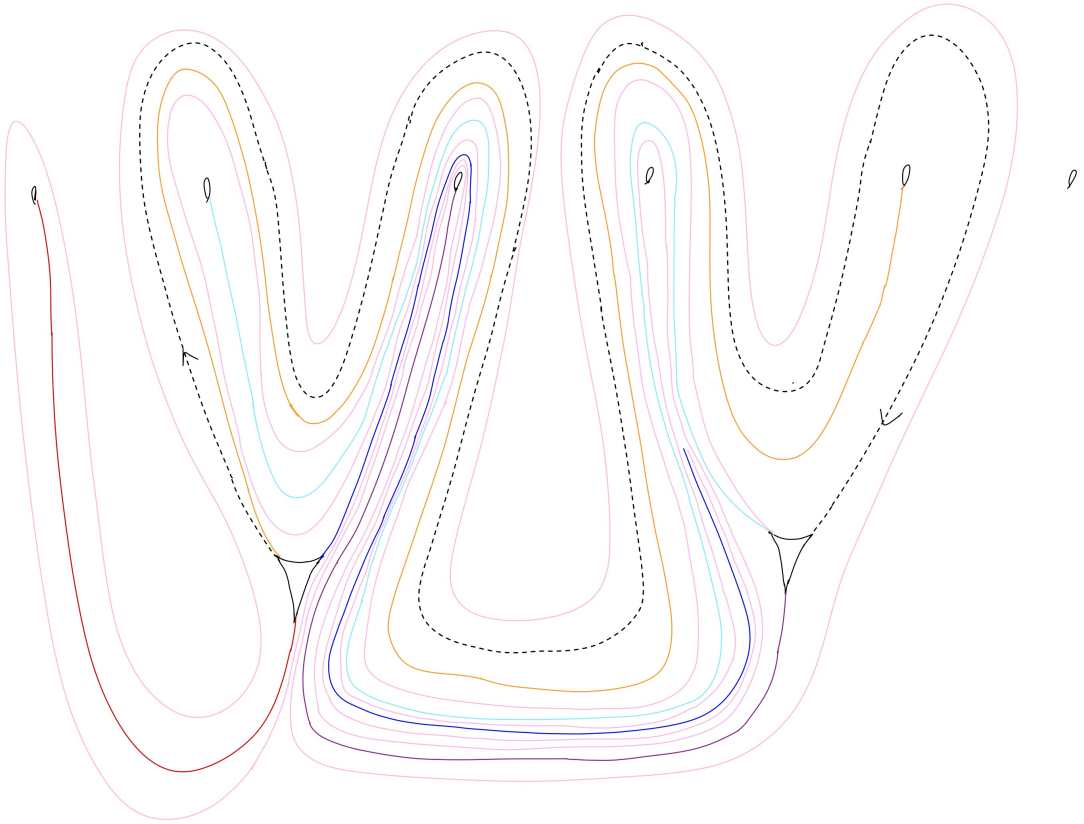


Figure E.94: Querulous7

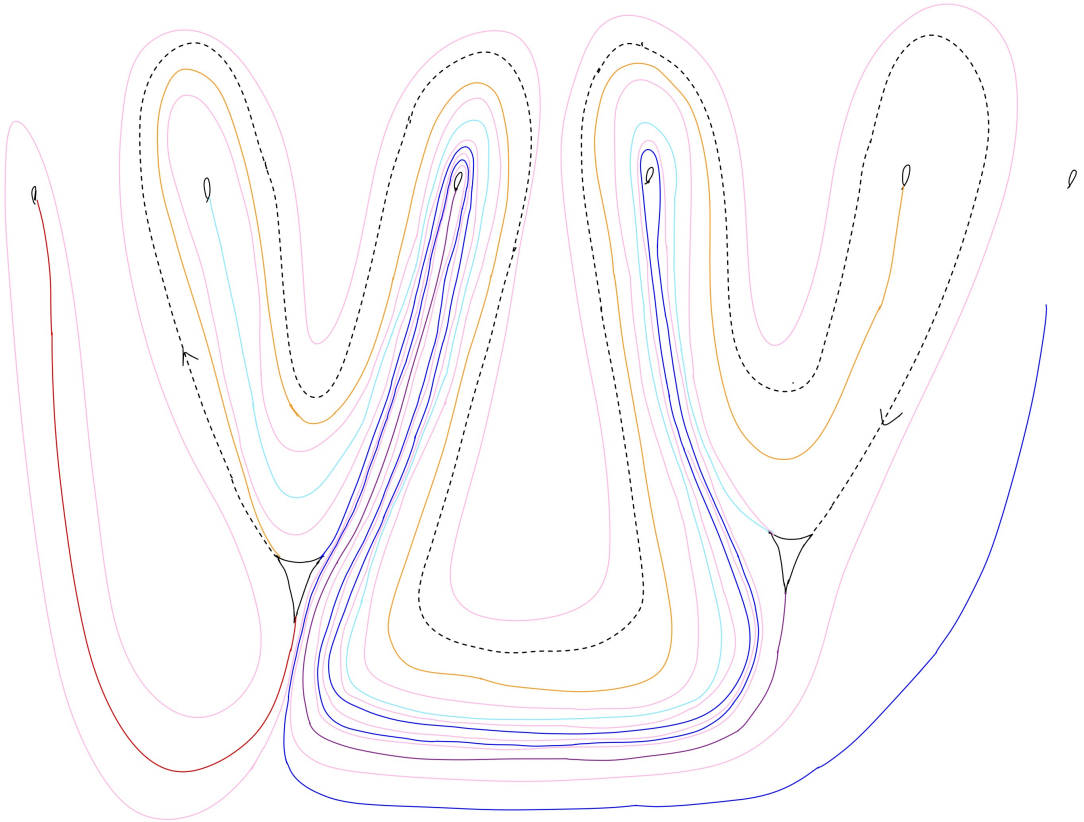


Figure E.95: Querulous8

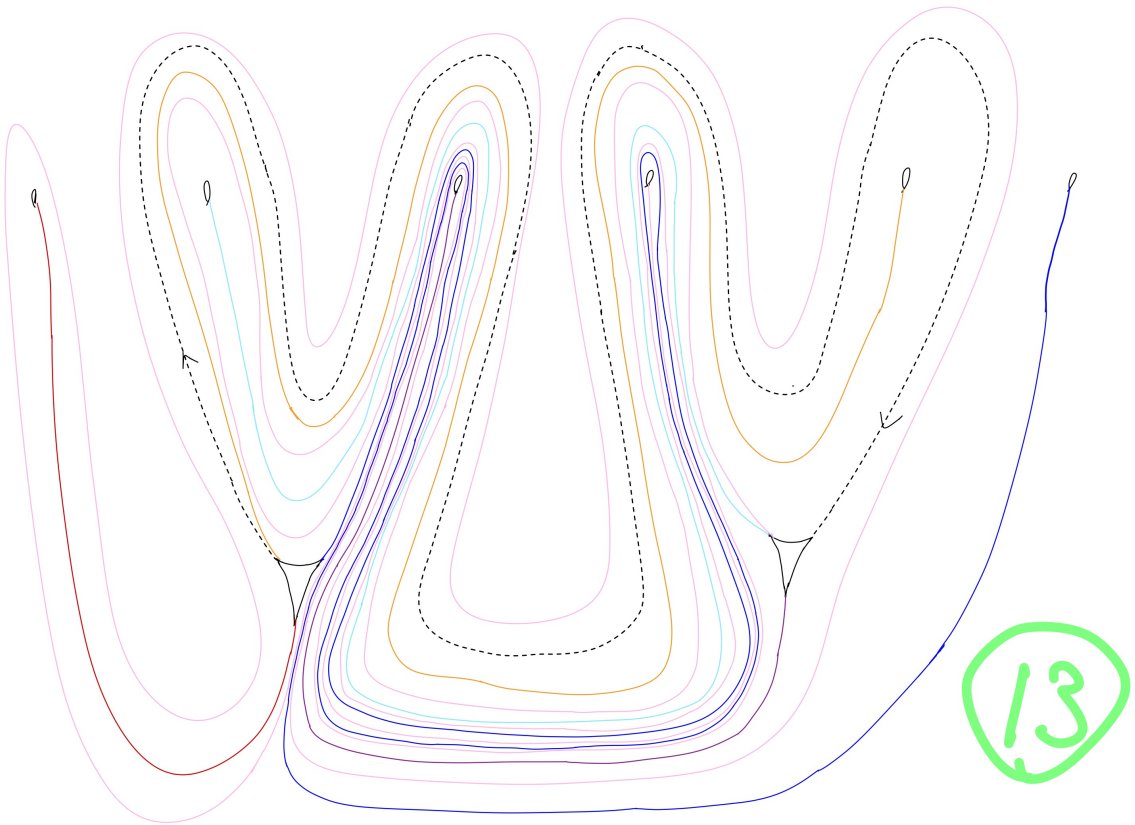


Figure E.96: Querulous9

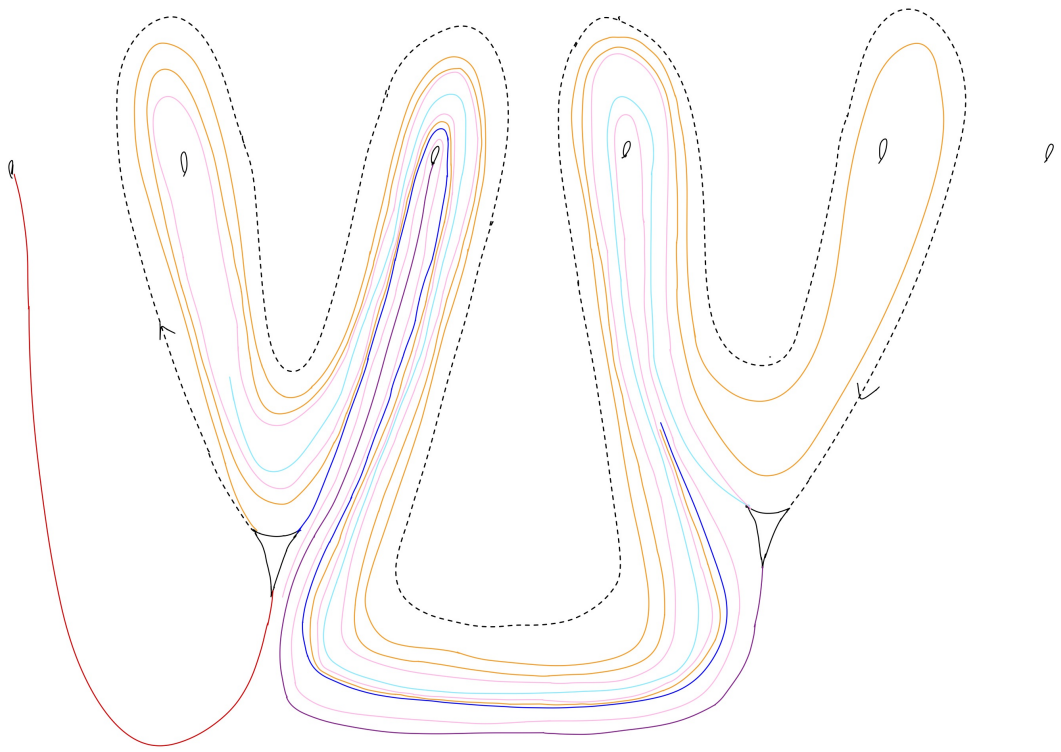


Figure E.97: Sybaritic1

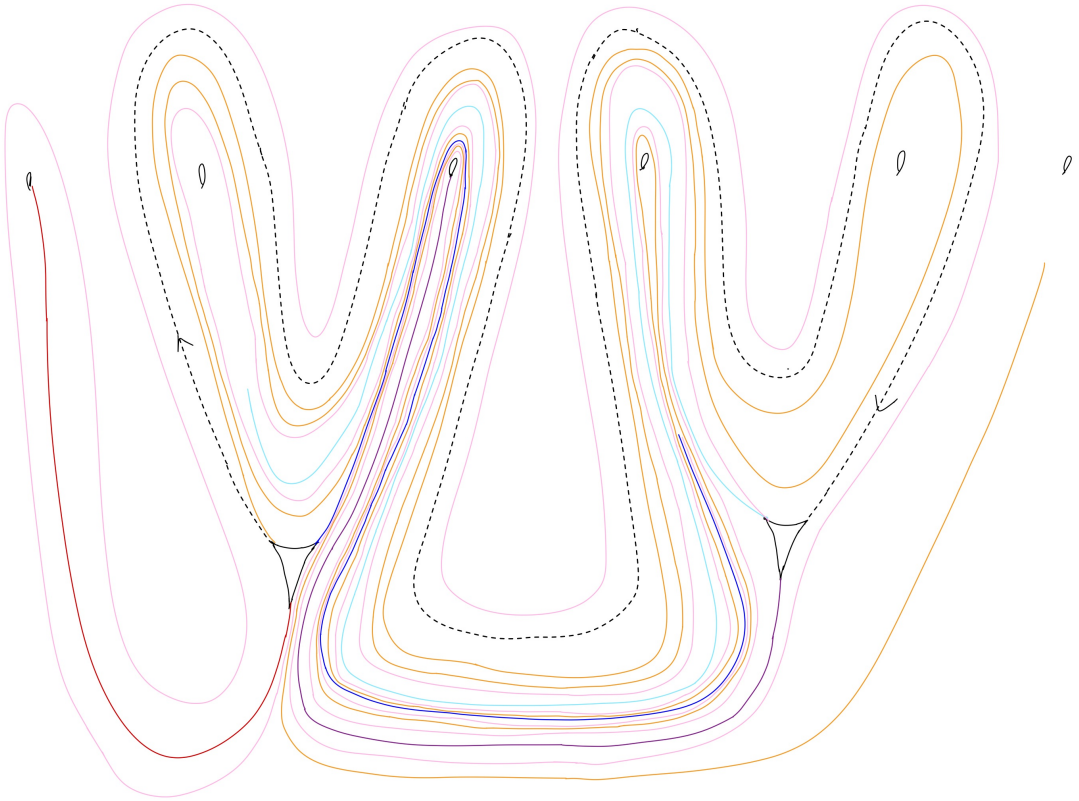


Figure E.98: Sybaritic2

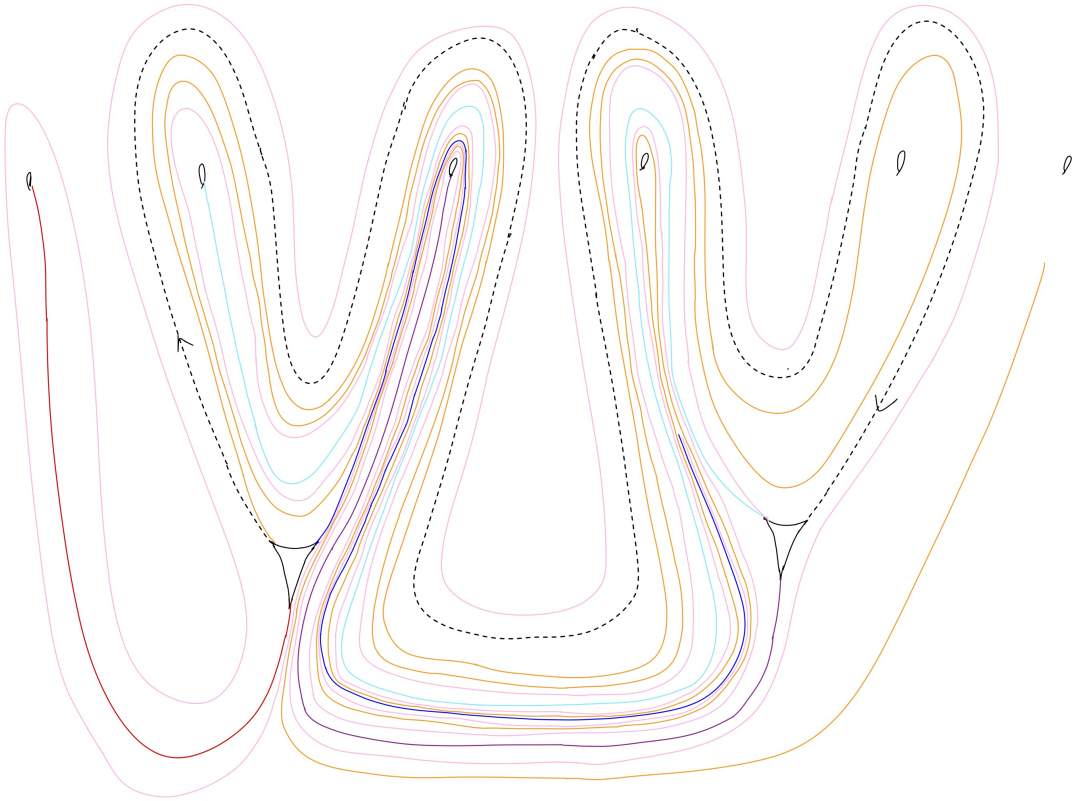


Figure E.99: Sybaritic3

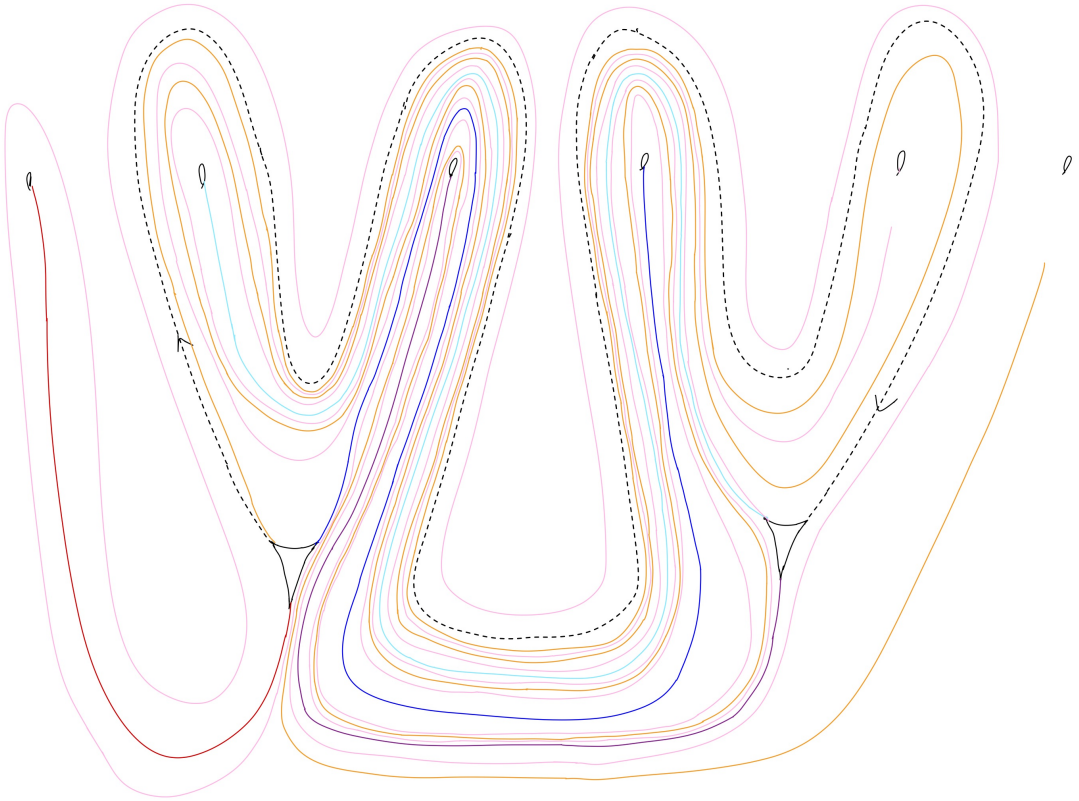


Figure E.100: Sybaritic4

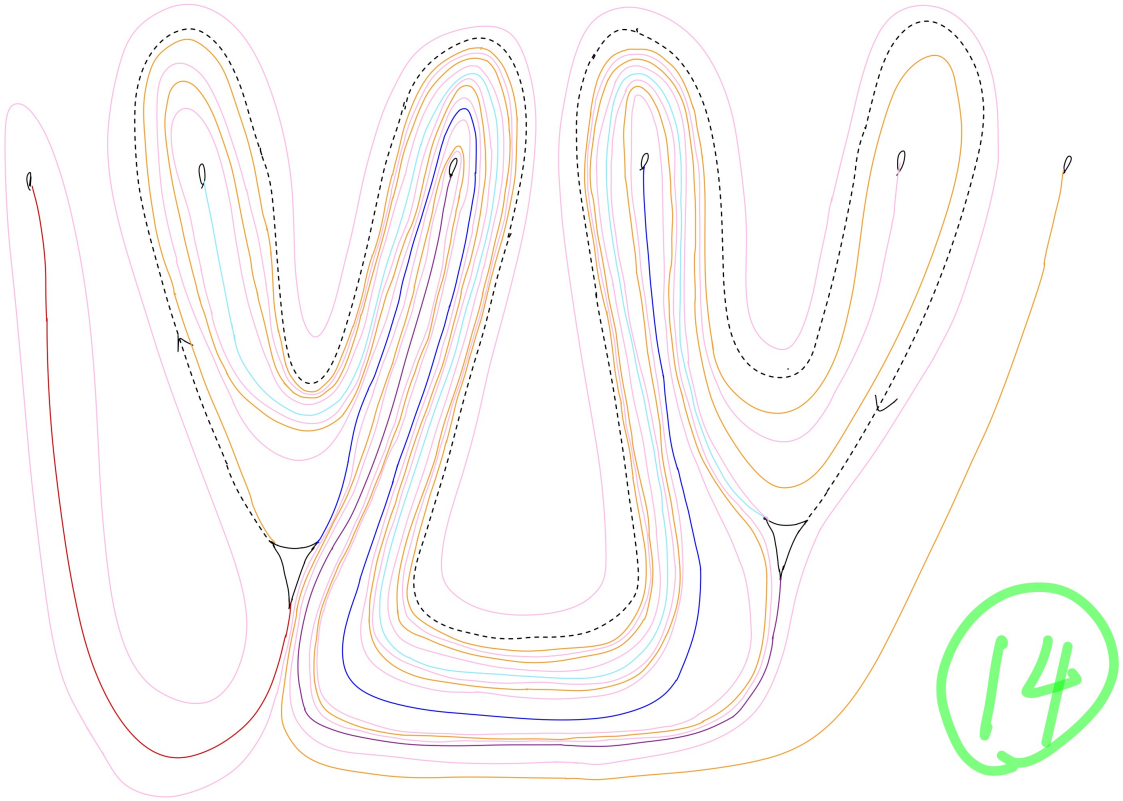


Figure E.101: Sybaritic5

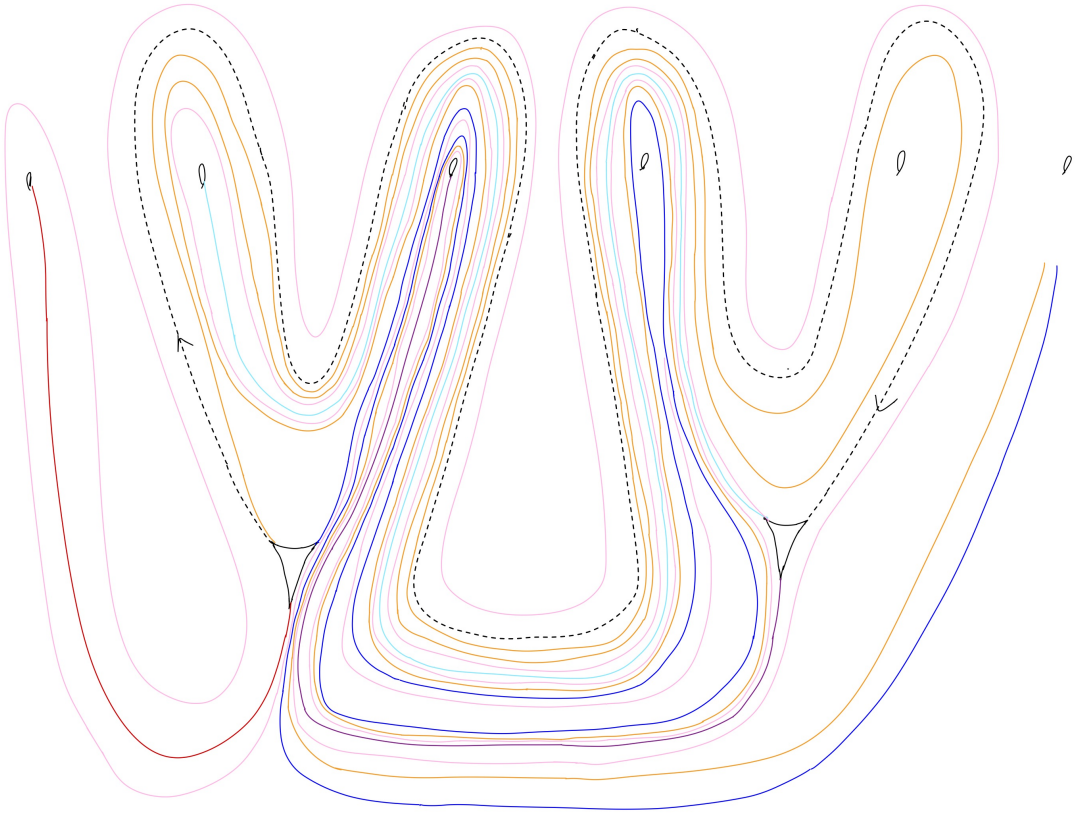


Figure E.102: Sybaritic6

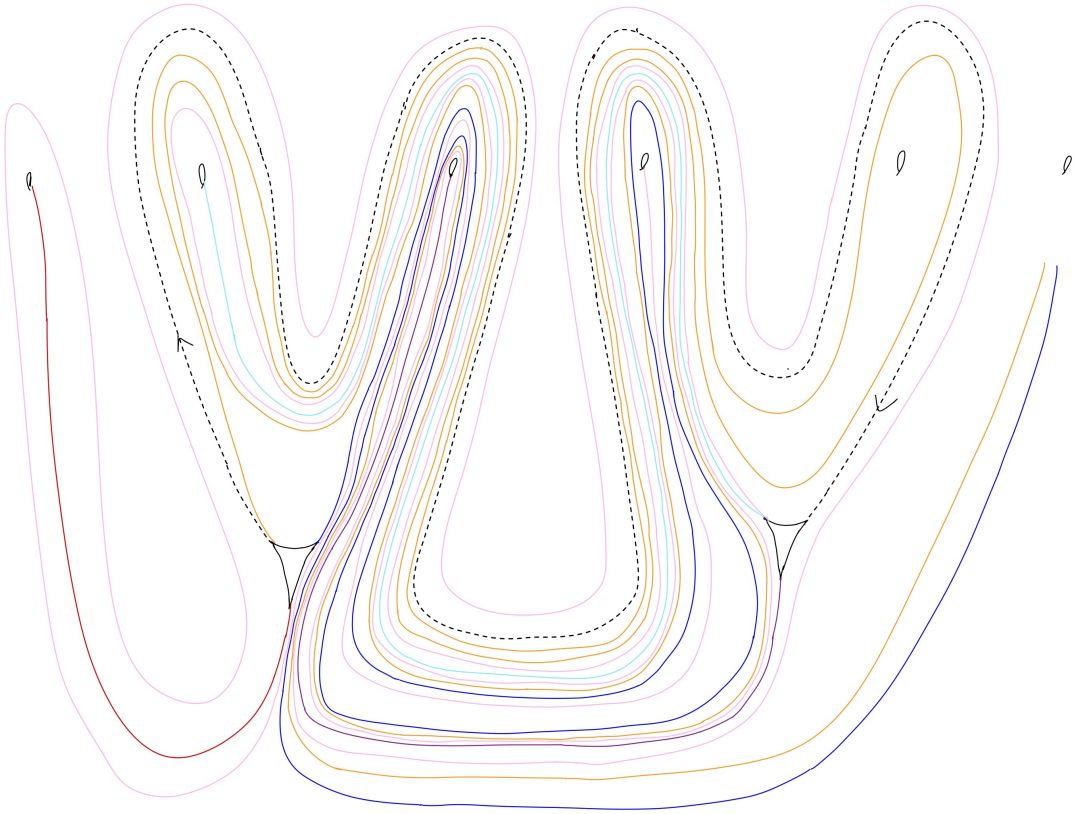


Figure E.103: Sybaritic7

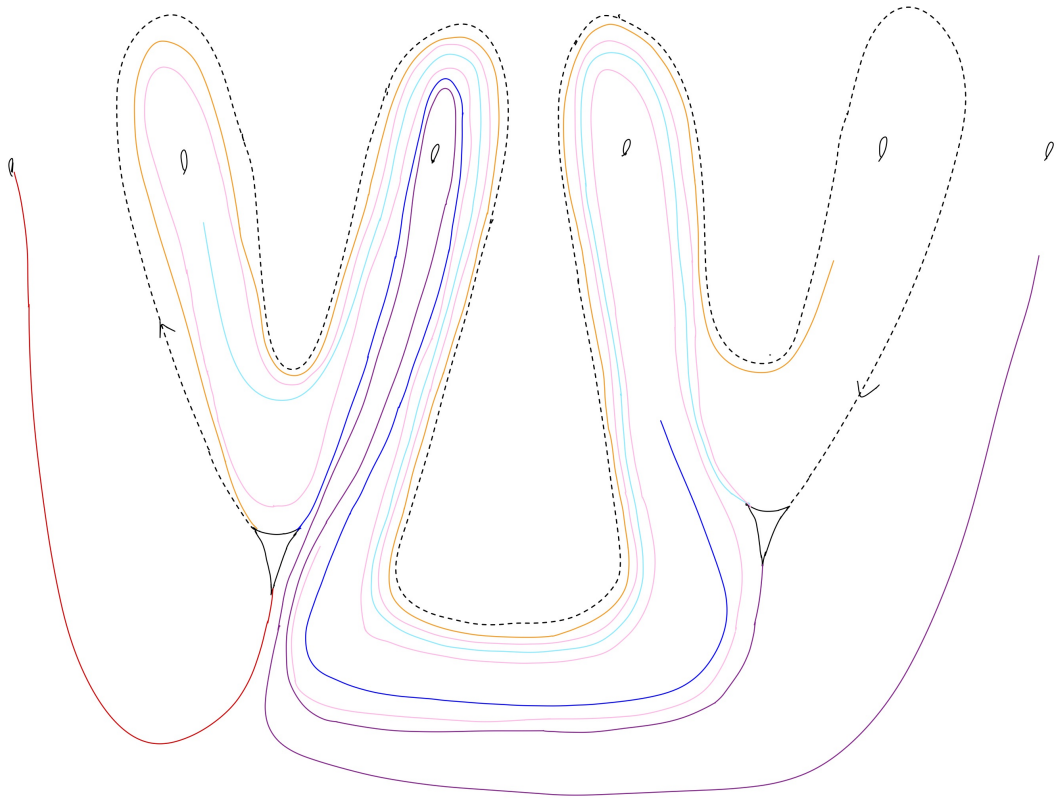


Figure E.104: Leverage1

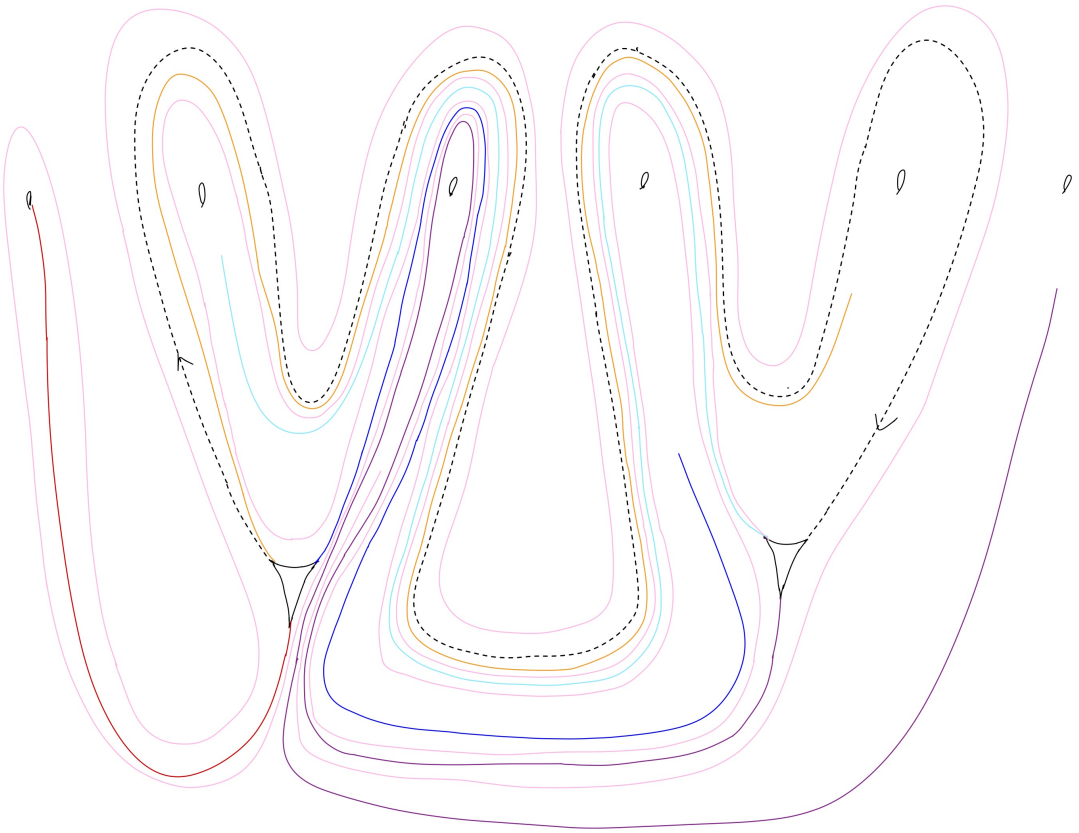


Figure E.105: Leverage2

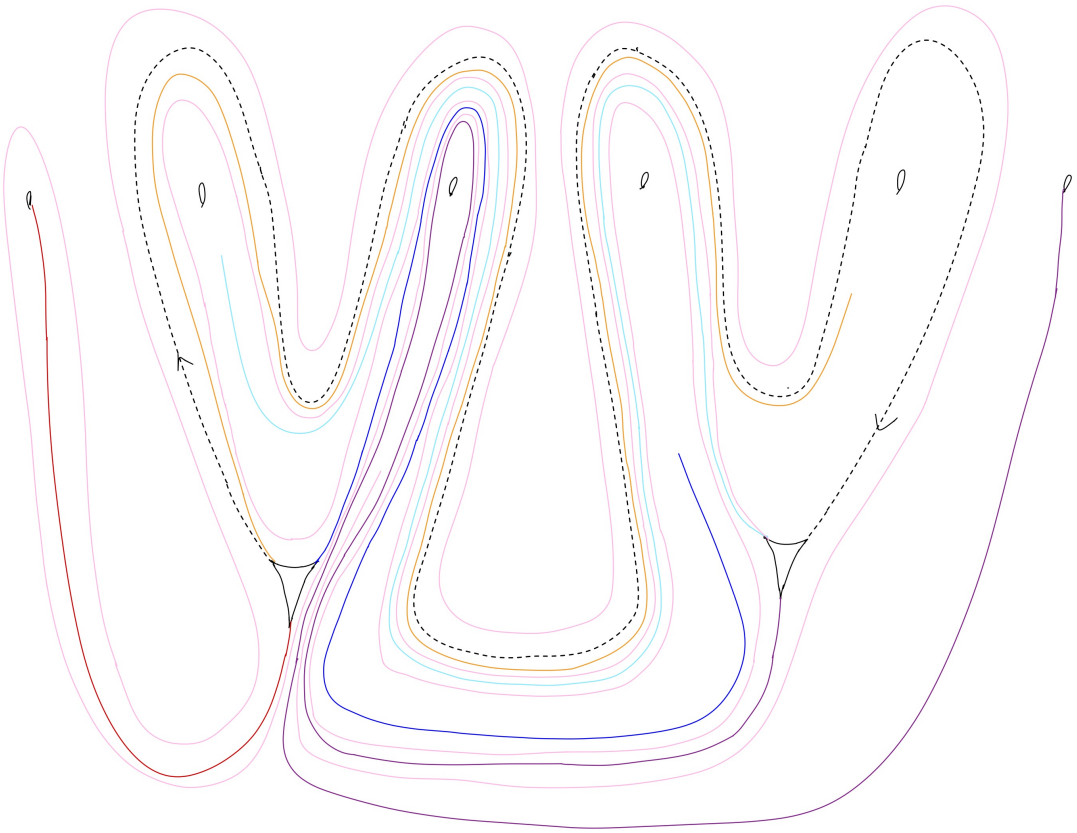


Figure E.106: Leverage3

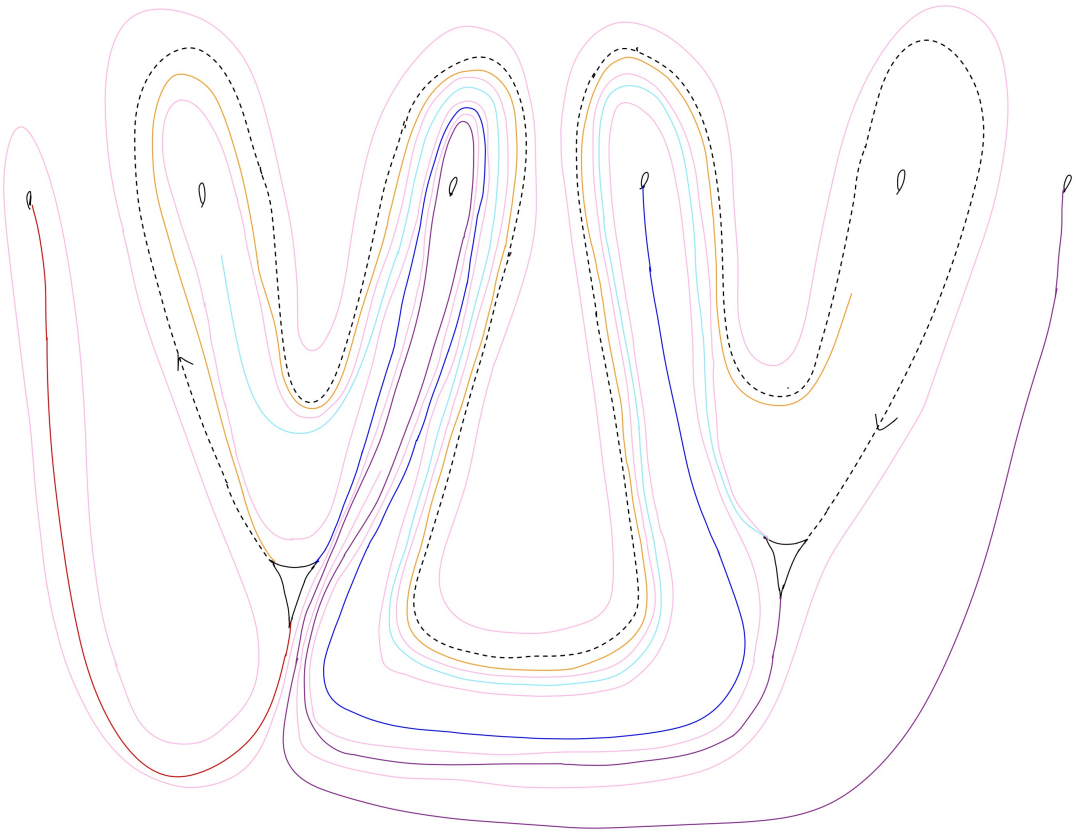


Figure E.107: Leverage4

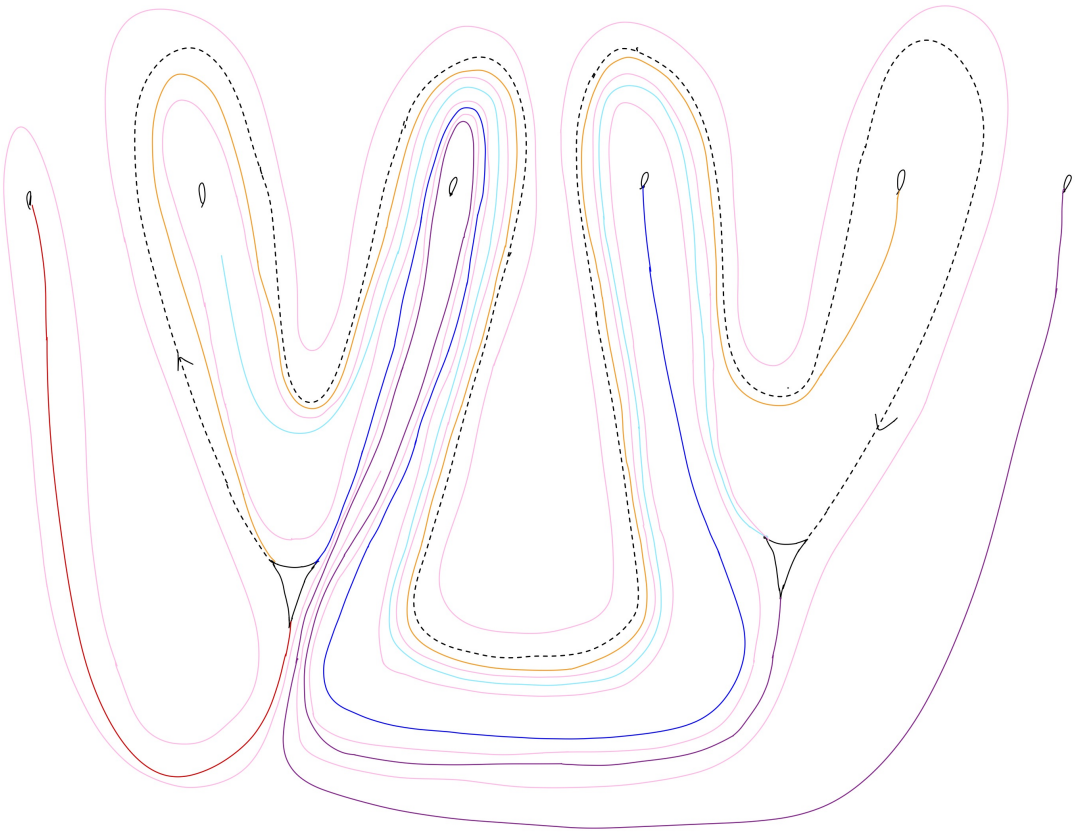


Figure E.108: Leverage5

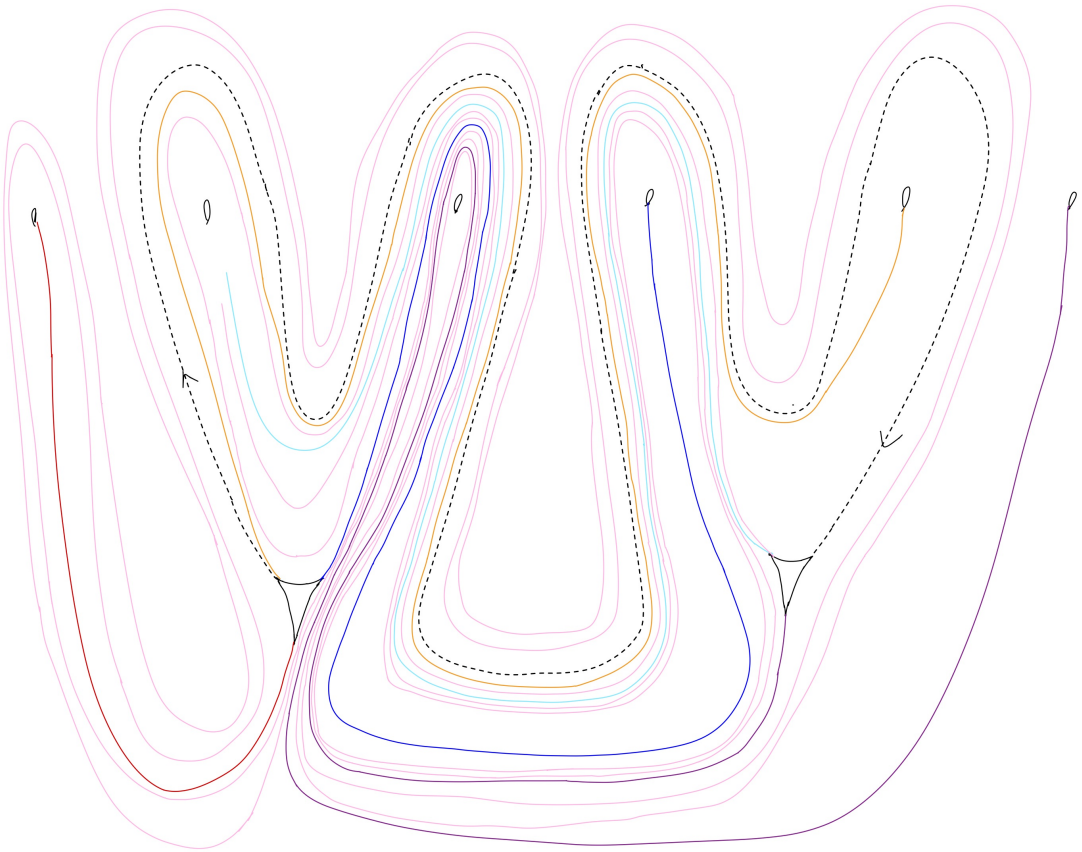


Figure E.109: Leverage6

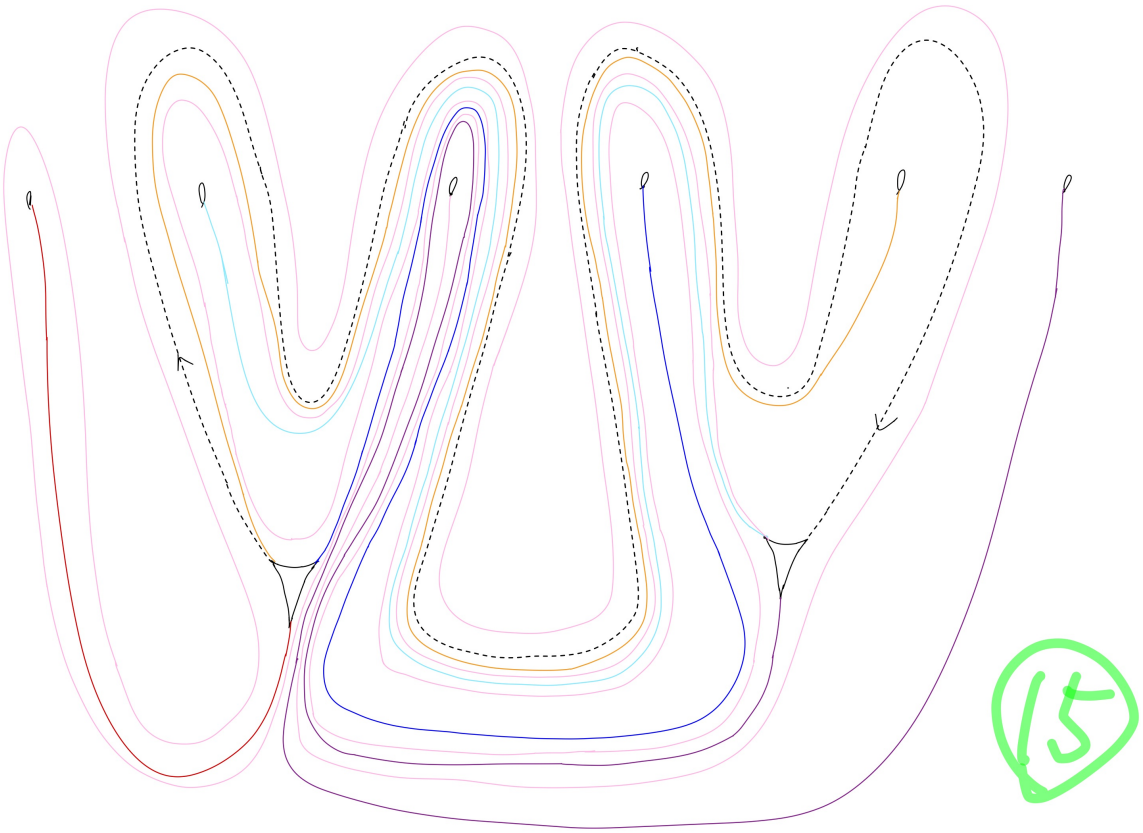


Figure E.110: Leverage7

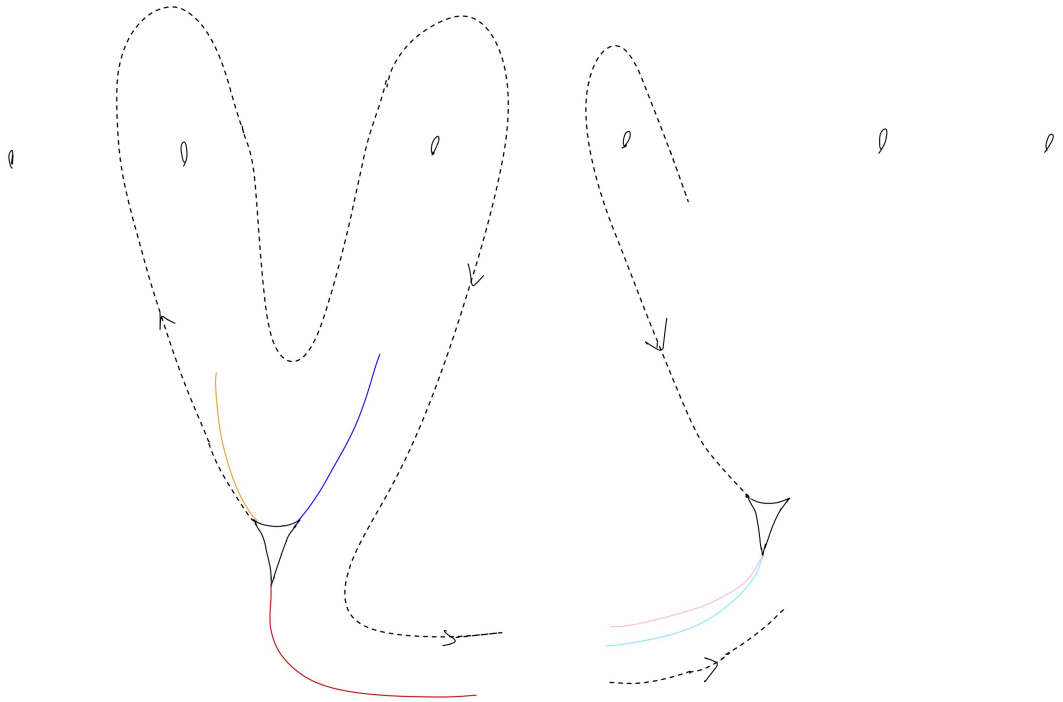


Figure E.111: IPC1

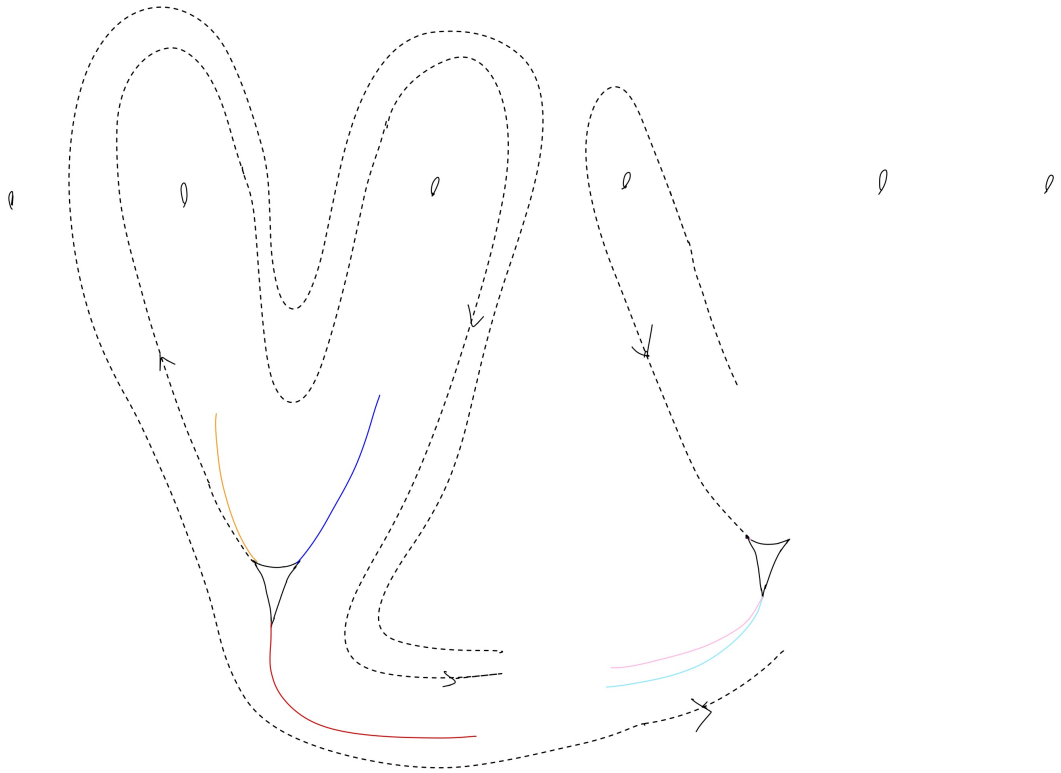


Figure E.112: Etui1

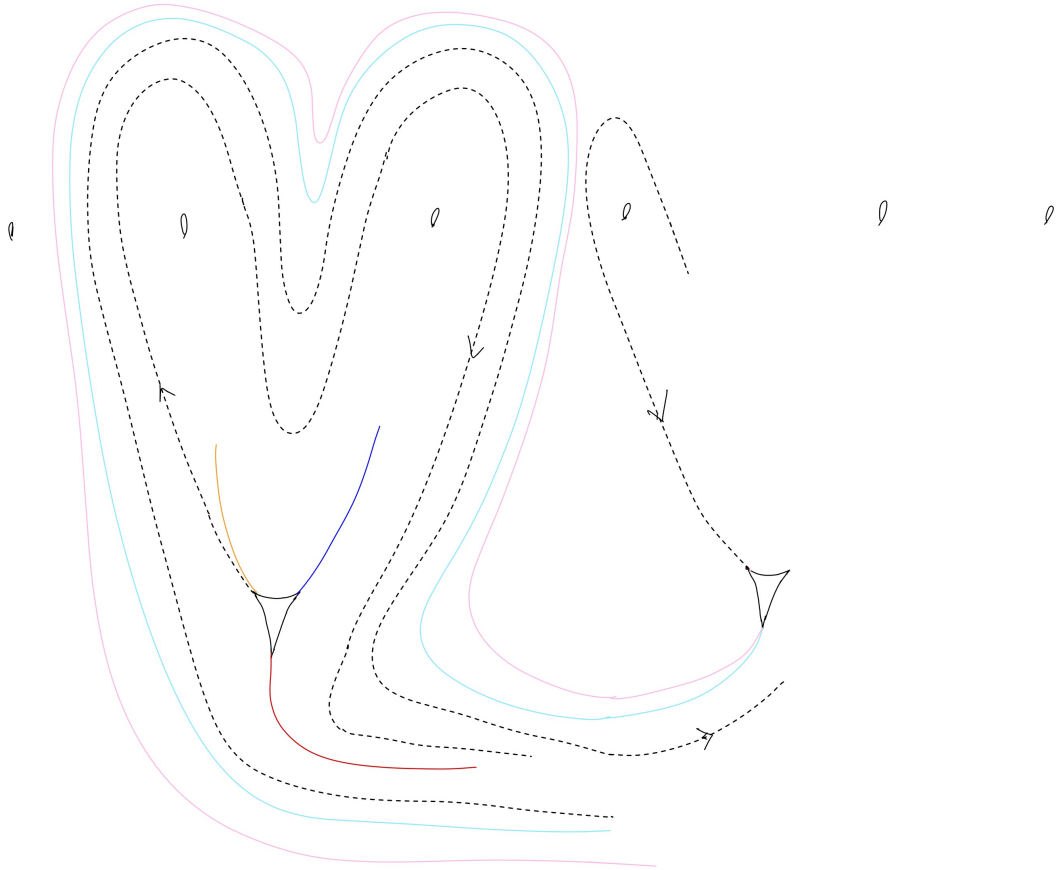


Figure E.113: Snee1

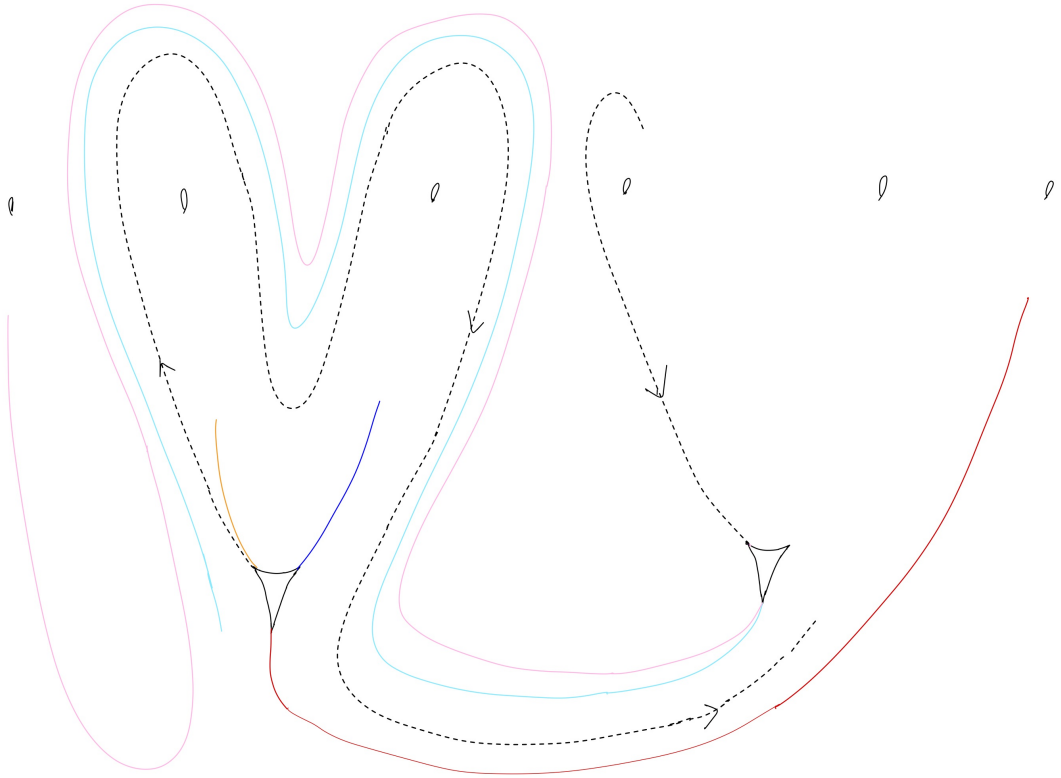


Figure E.114: Zarf1

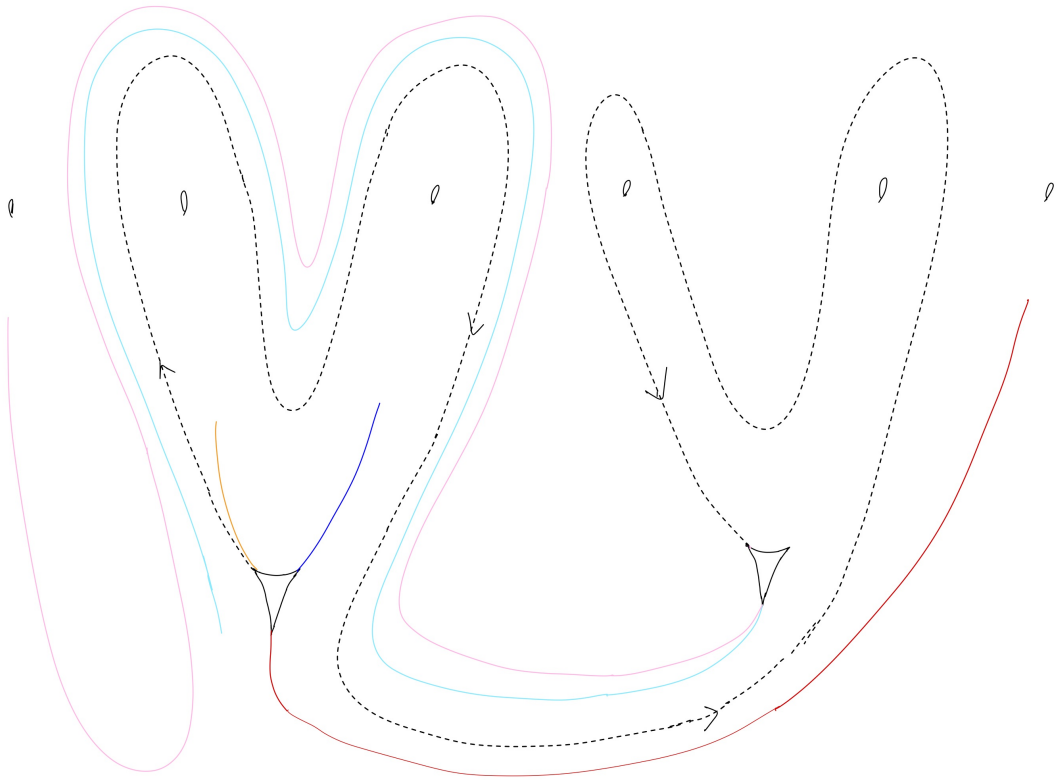


Figure E.115: Zarf2

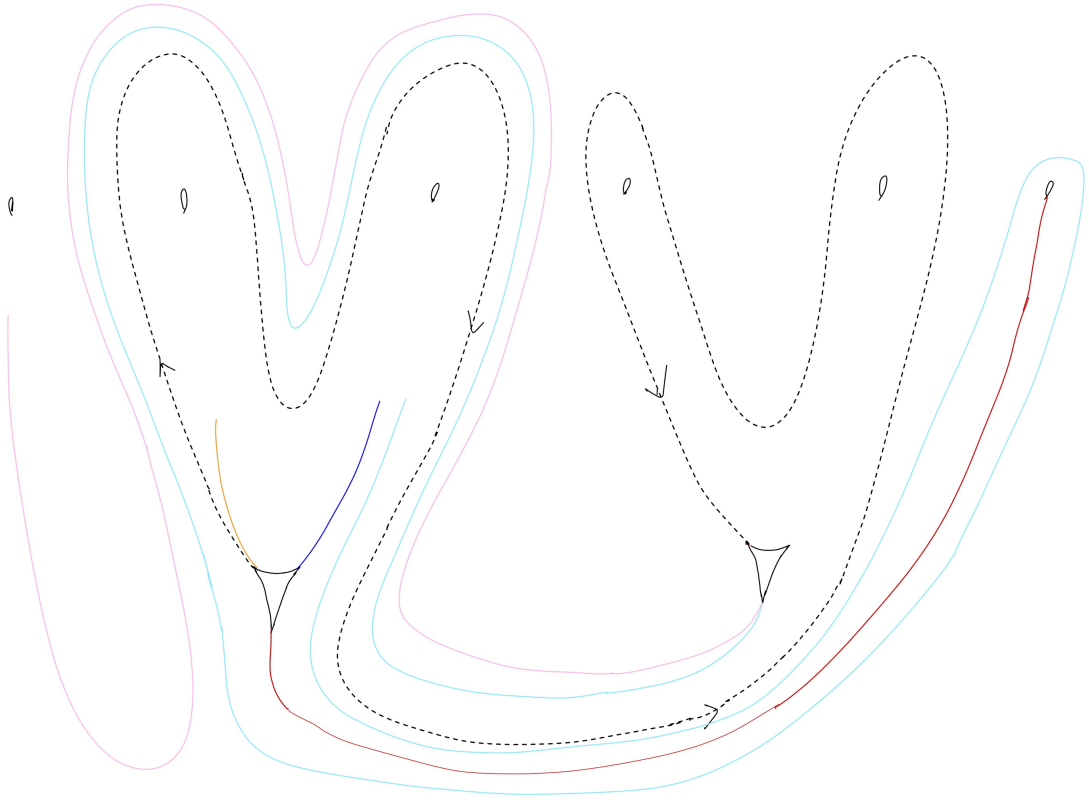


Figure E.116: Xebec1

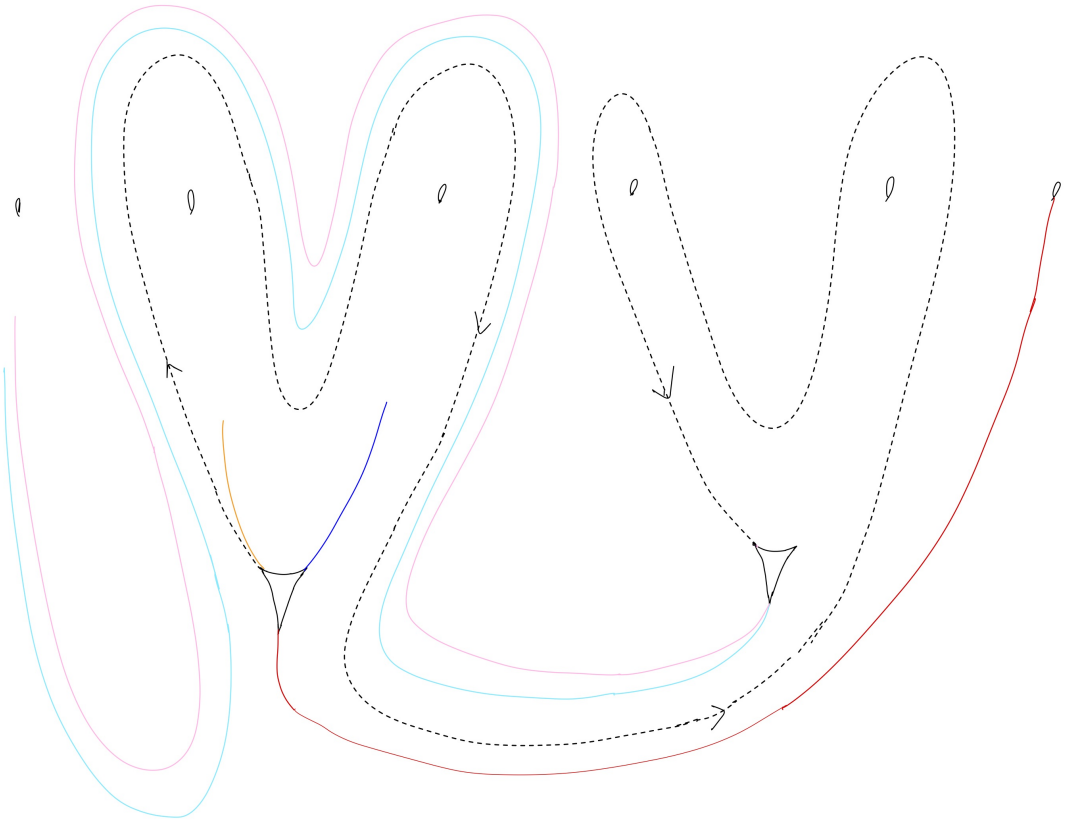


Figure E.117: Vuggy1

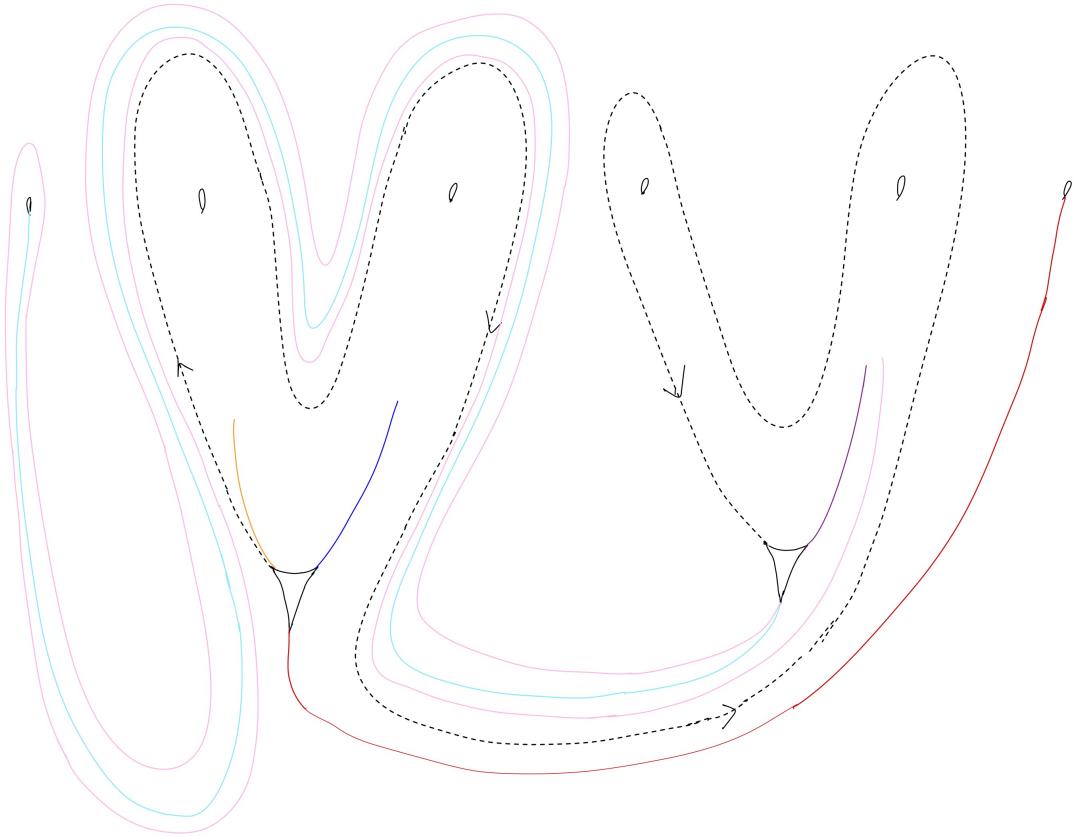


Figure E.118: Vuggy2

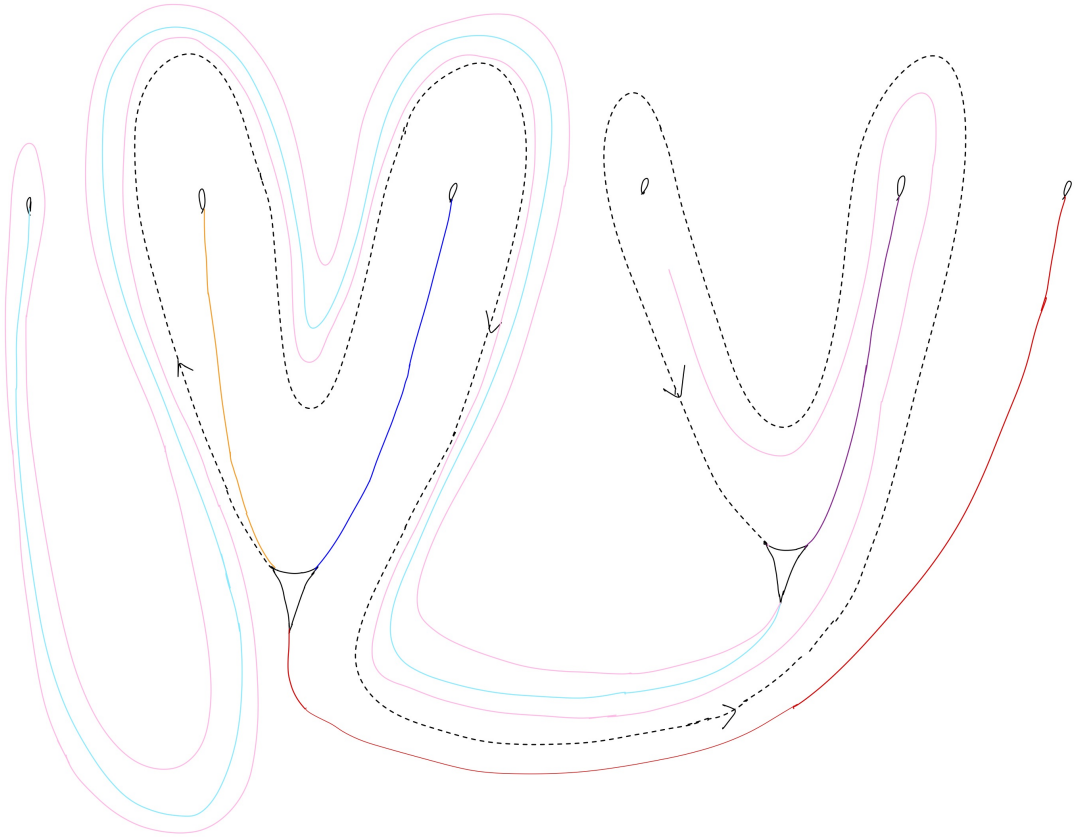


Figure E.119: Guddle1

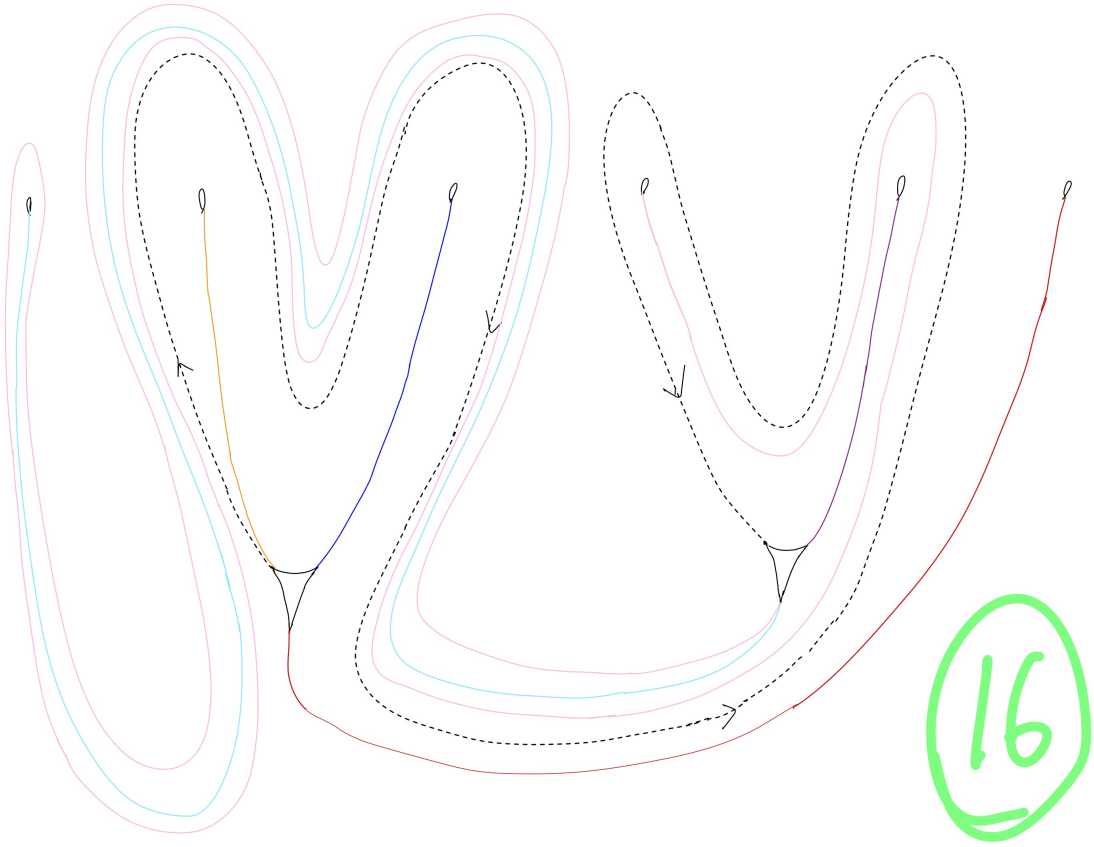


Figure E.120: Guddle2

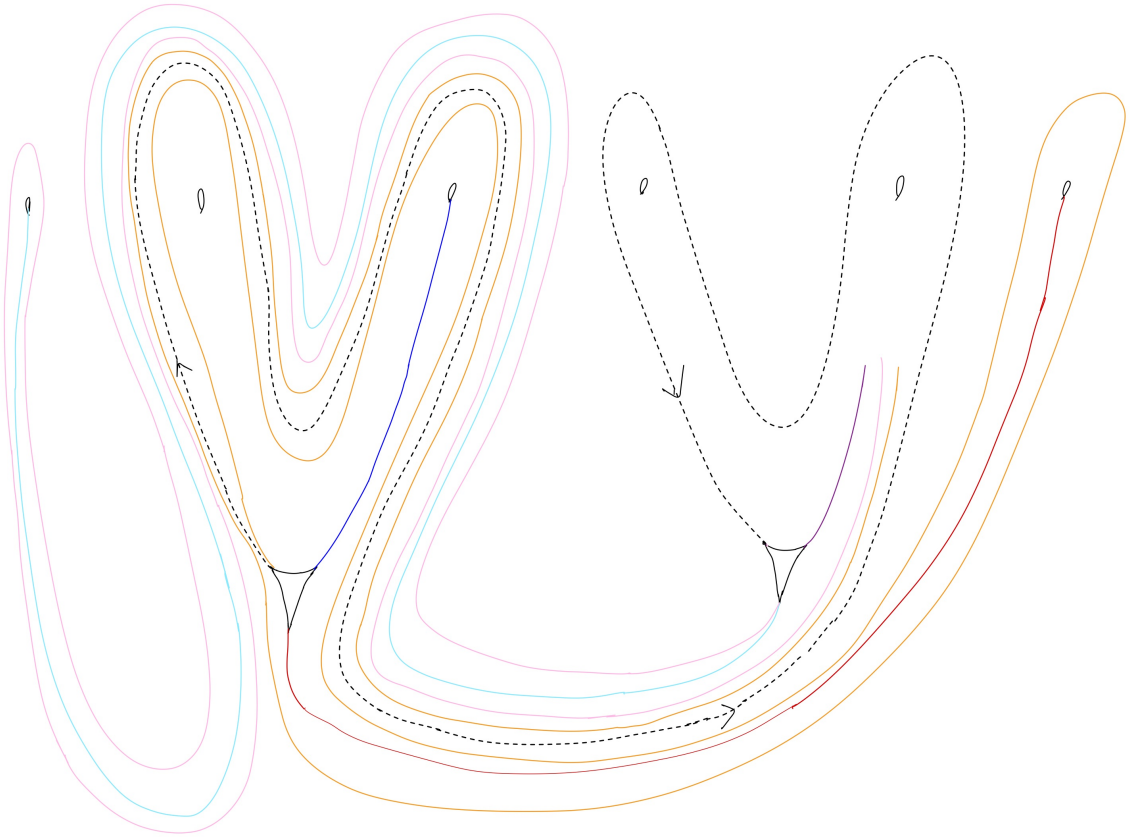


Figure E.121: Fipple1

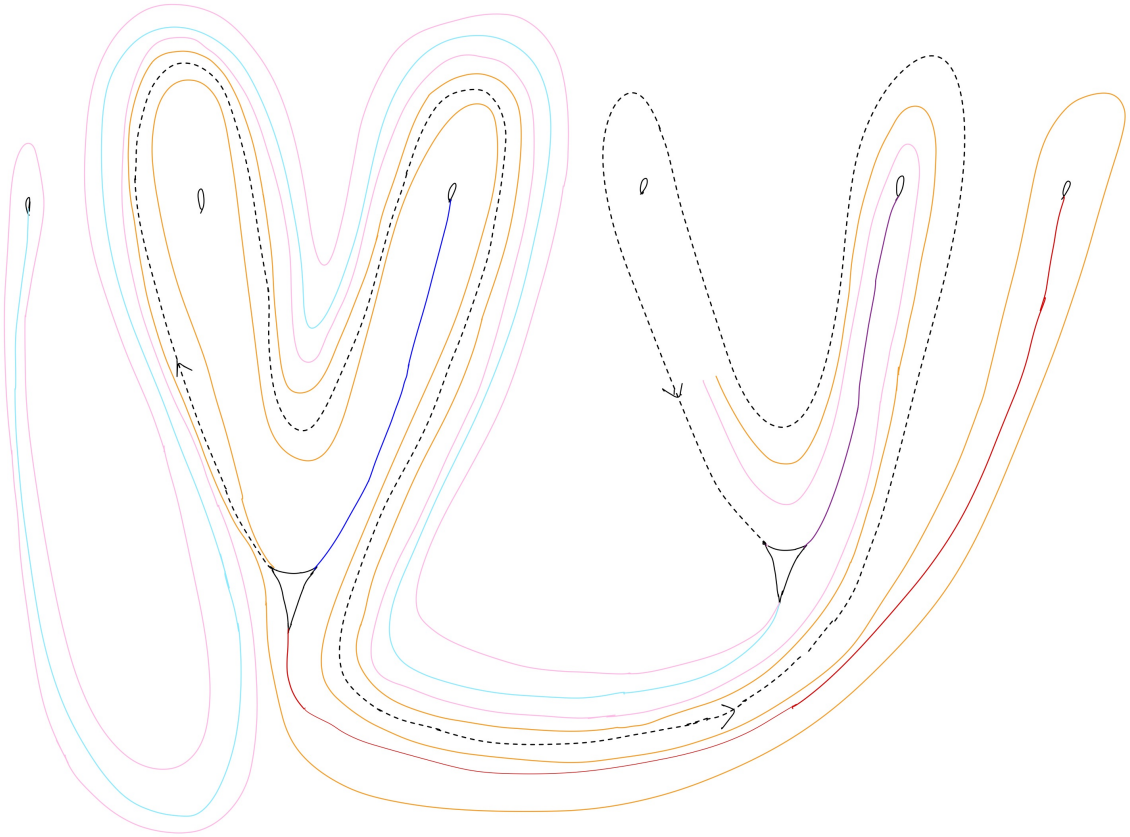


Figure E.122: Macumba1

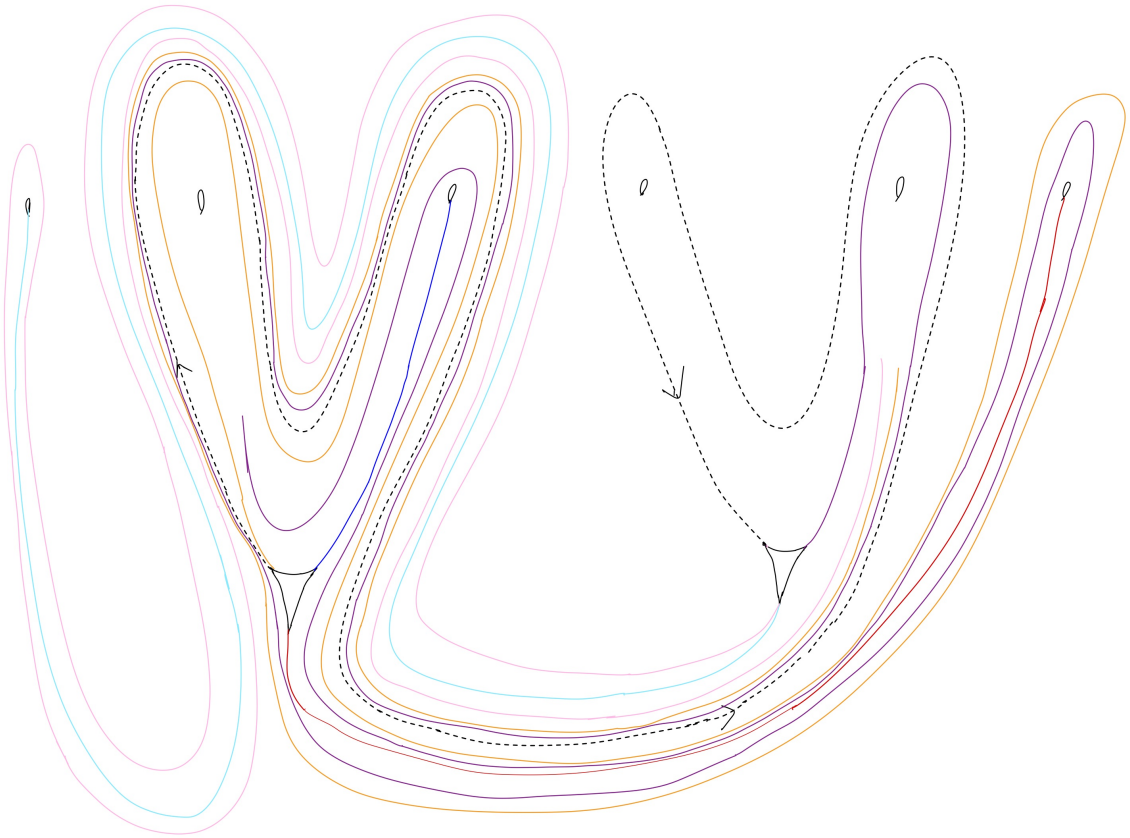


Figure E.123: Fopdoodle1

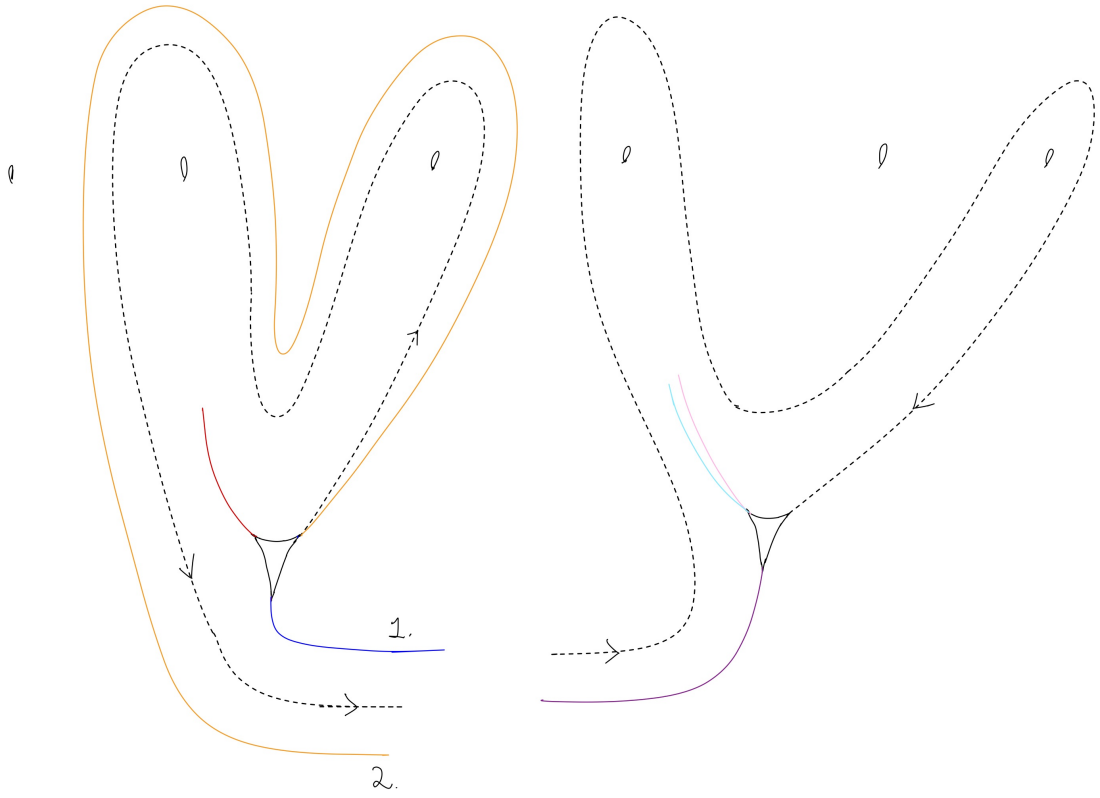


Figure E.124: HND1

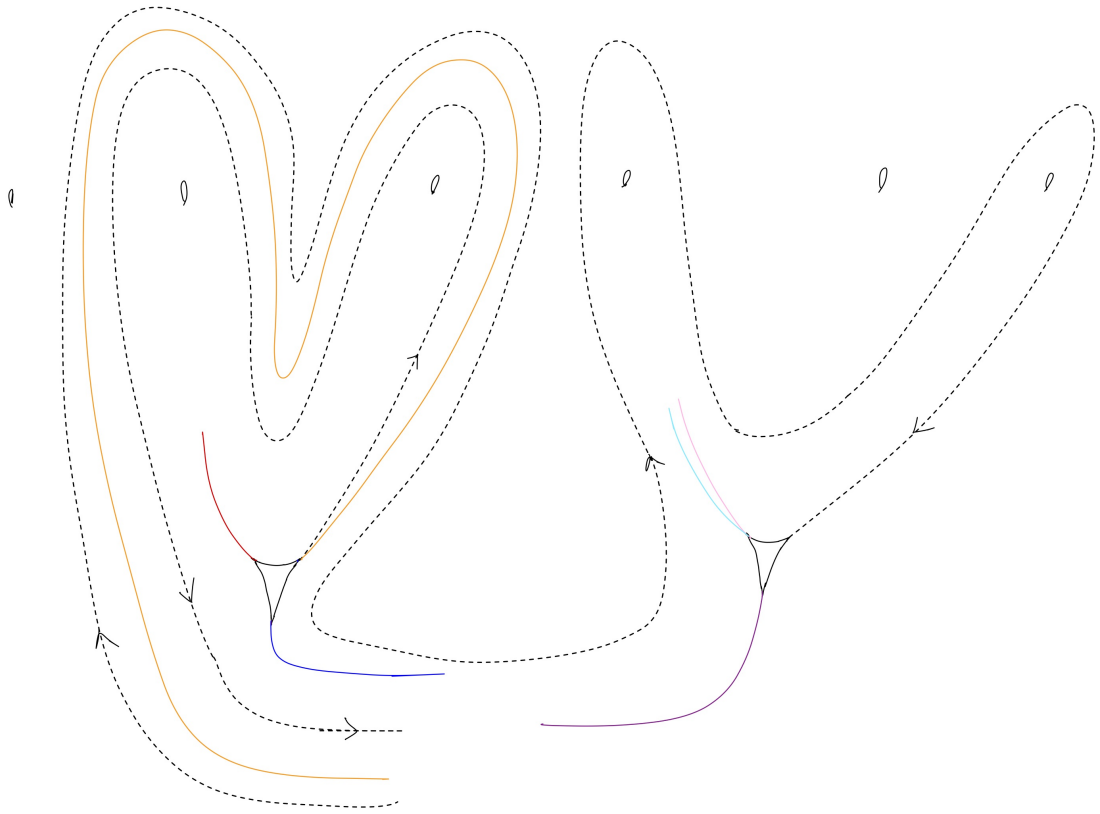


Figure E.125: Froe1

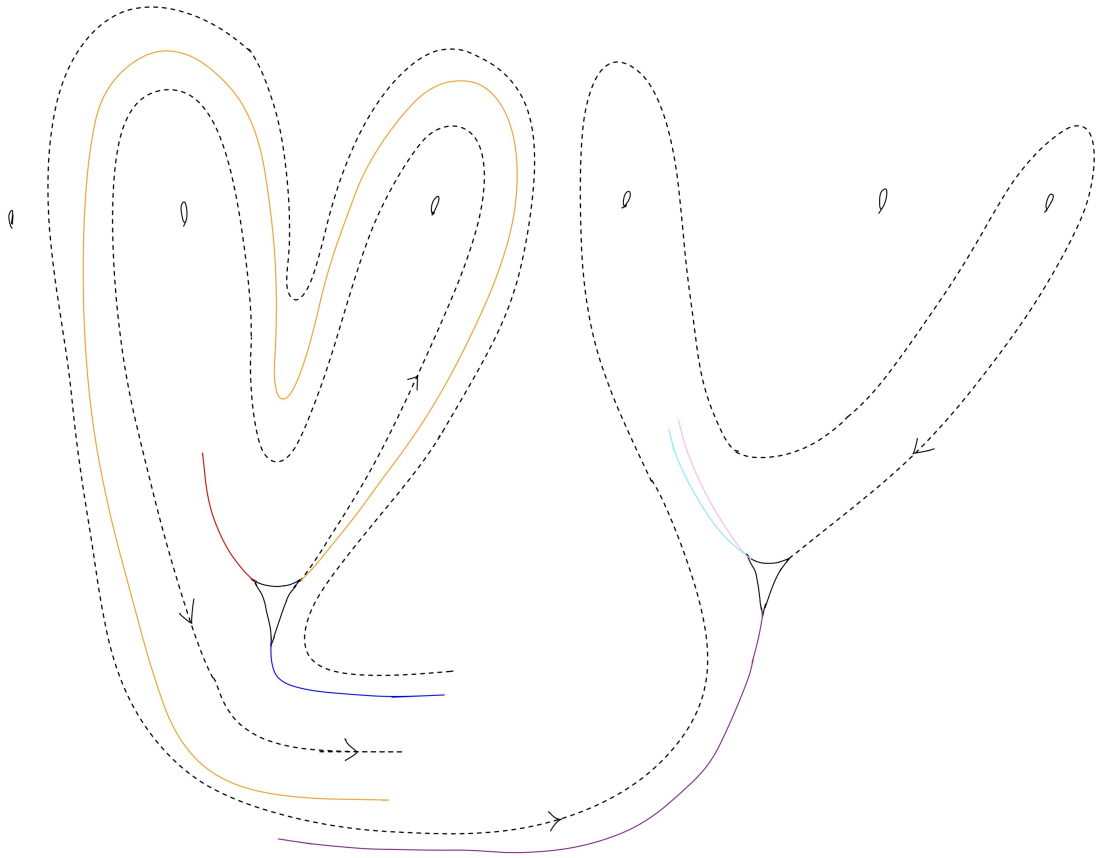


Figure E.126: Moxa1

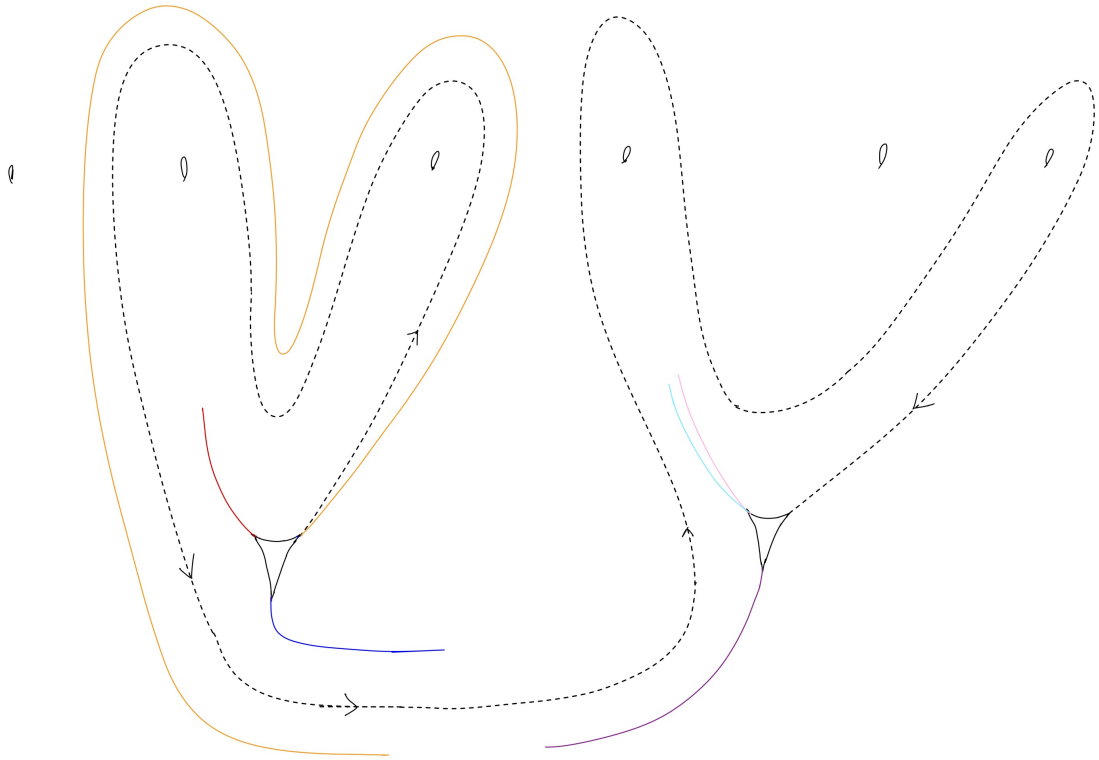


Figure E.127: Erne1

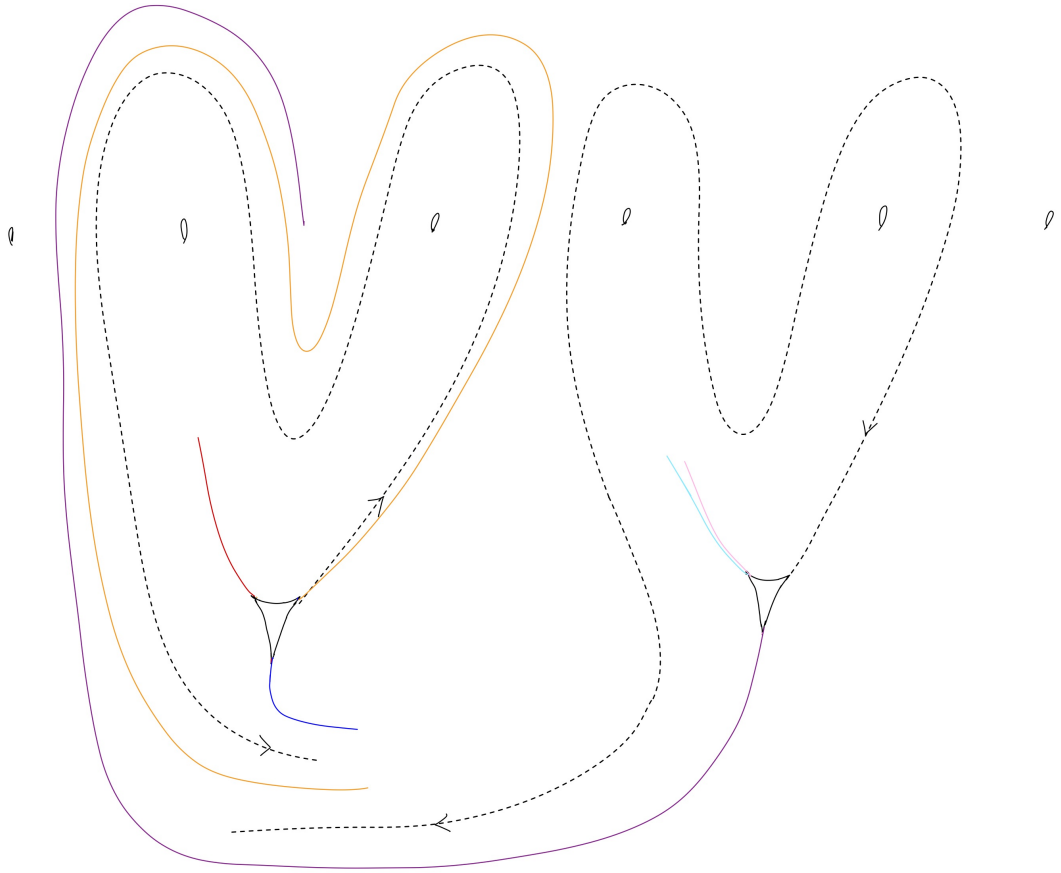


Figure E.128: USH1

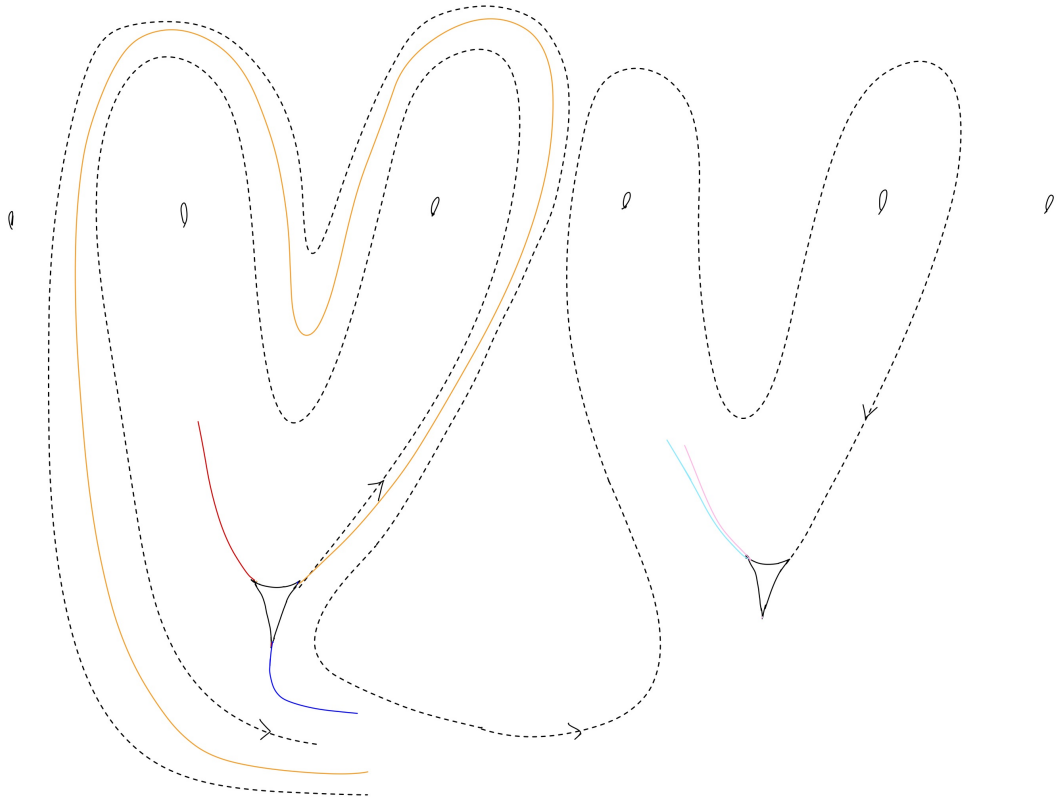


Figure E.129: Torc1

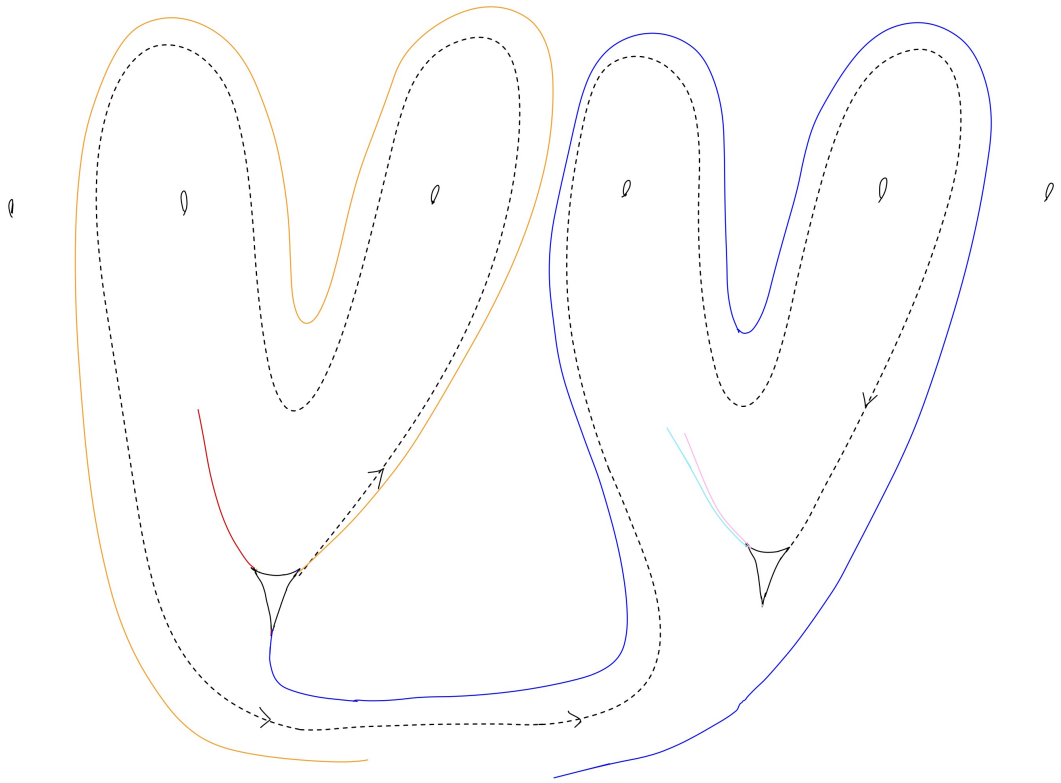


Figure E.130: Kief1

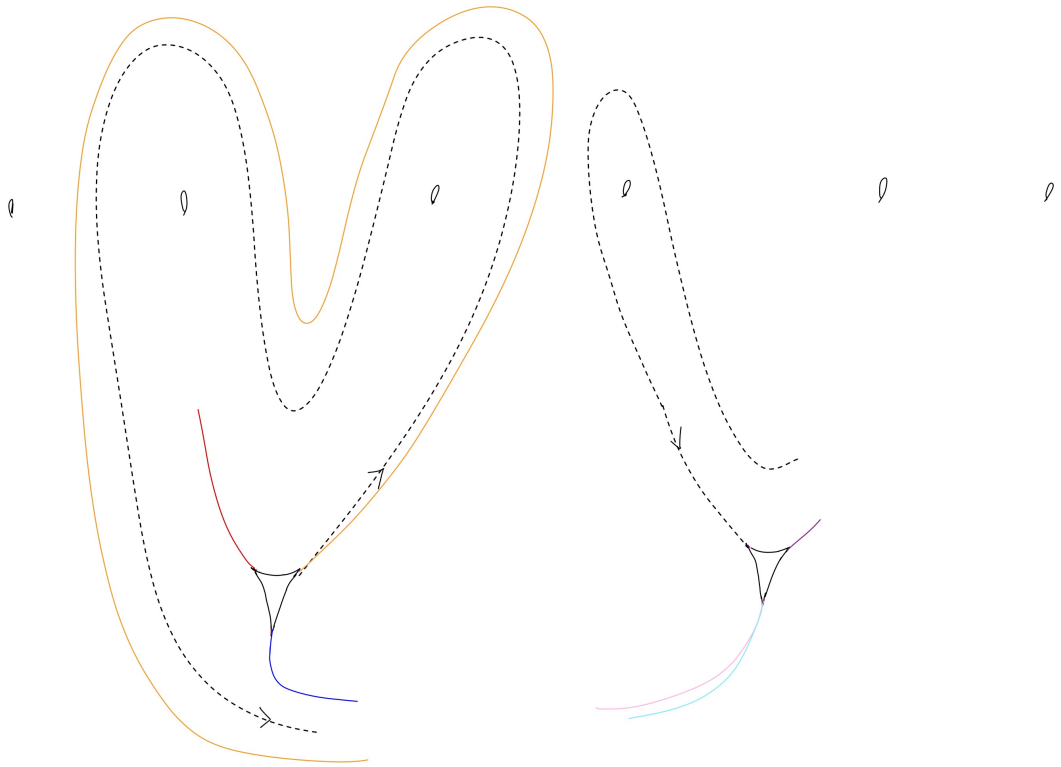


Figure E.131: LXA1

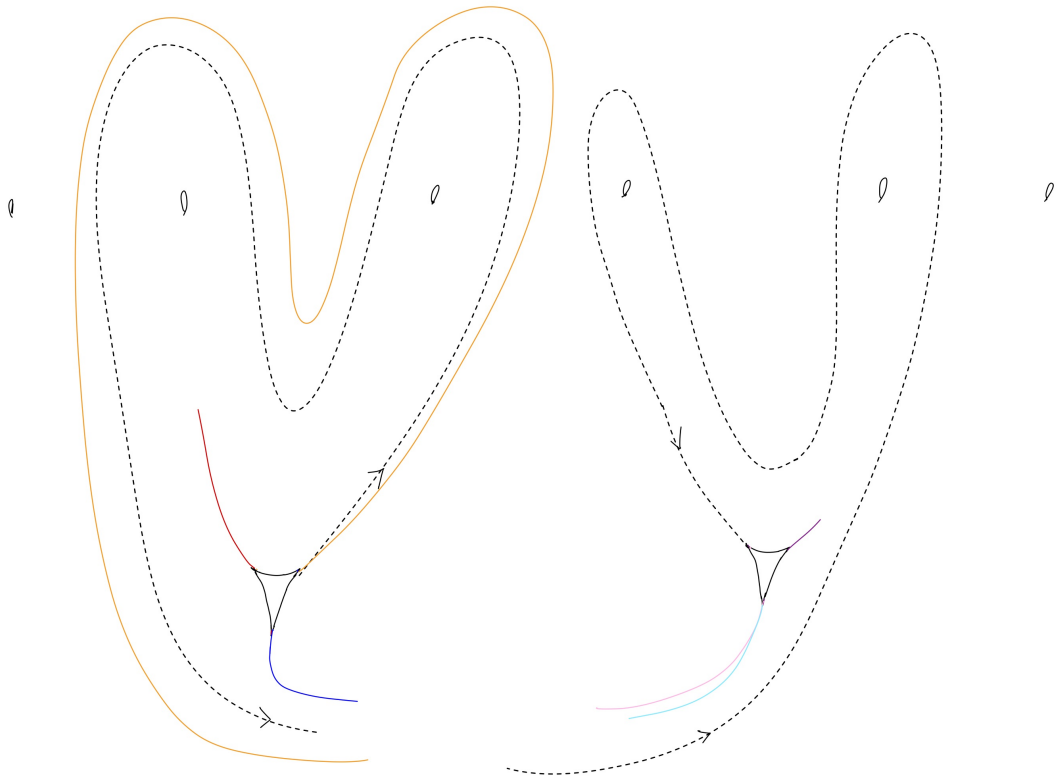


Figure E.132: LXA2

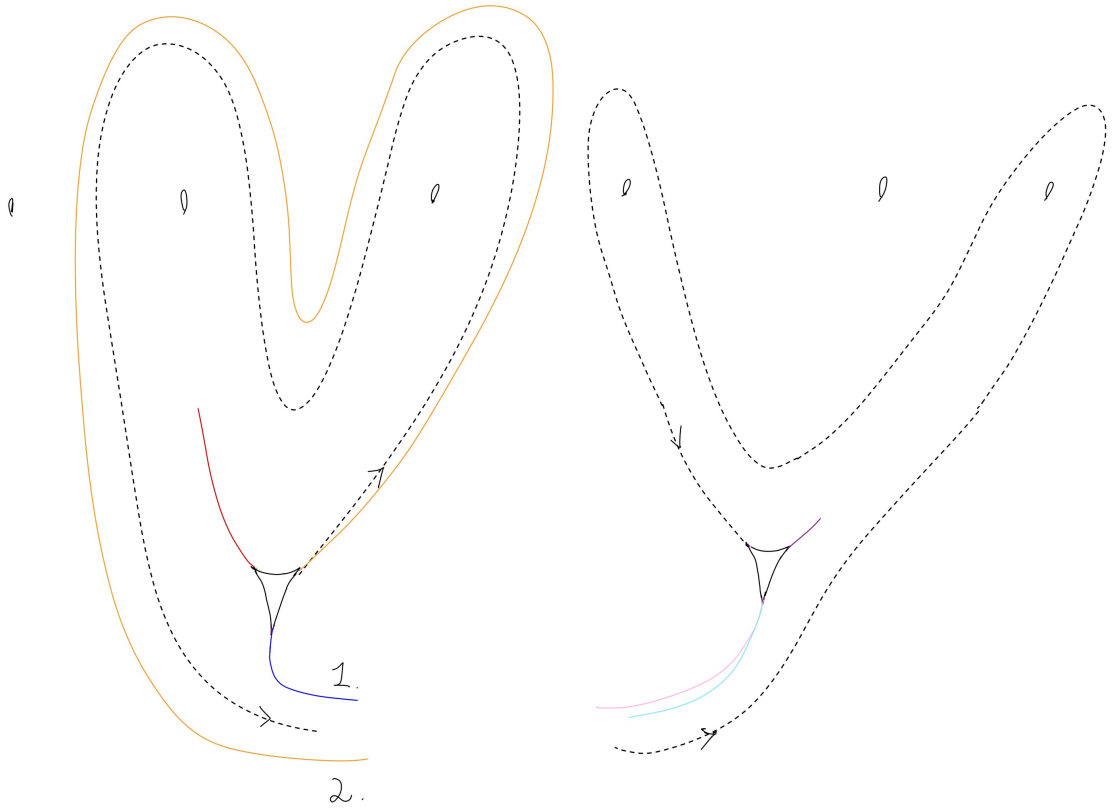


Figure E.133: Xama1

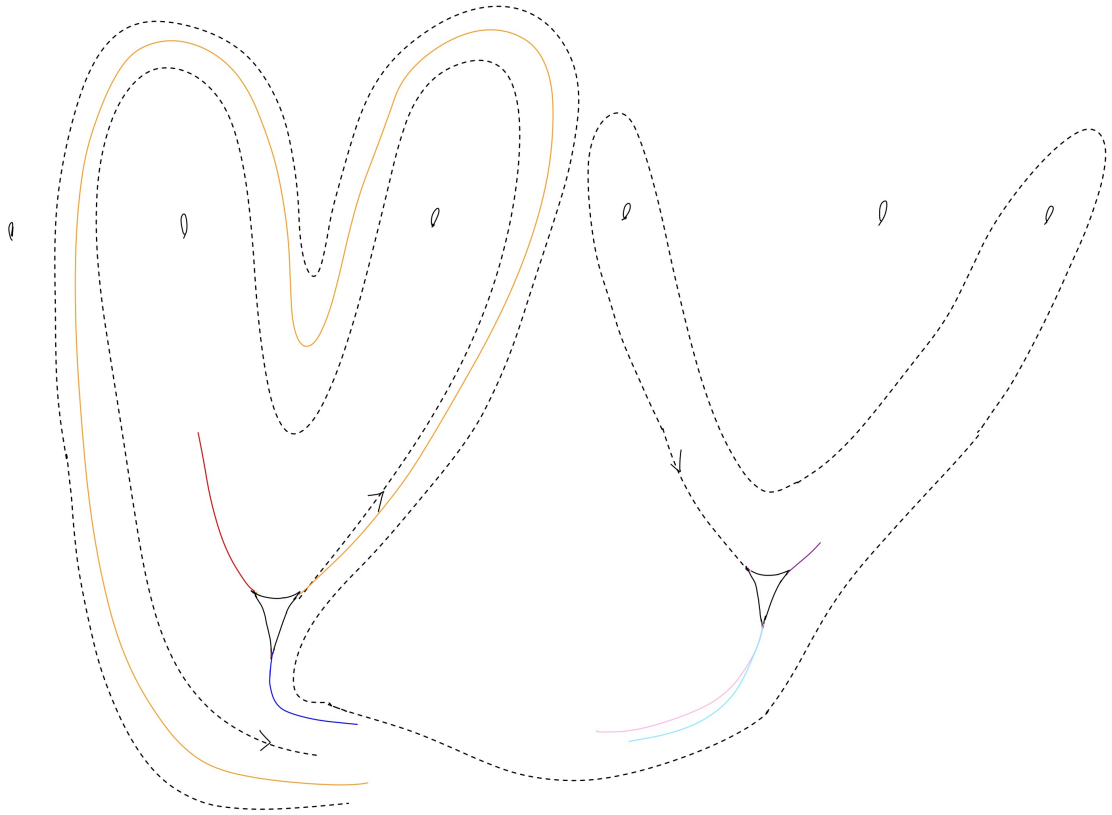


Figure E.134: Xama2

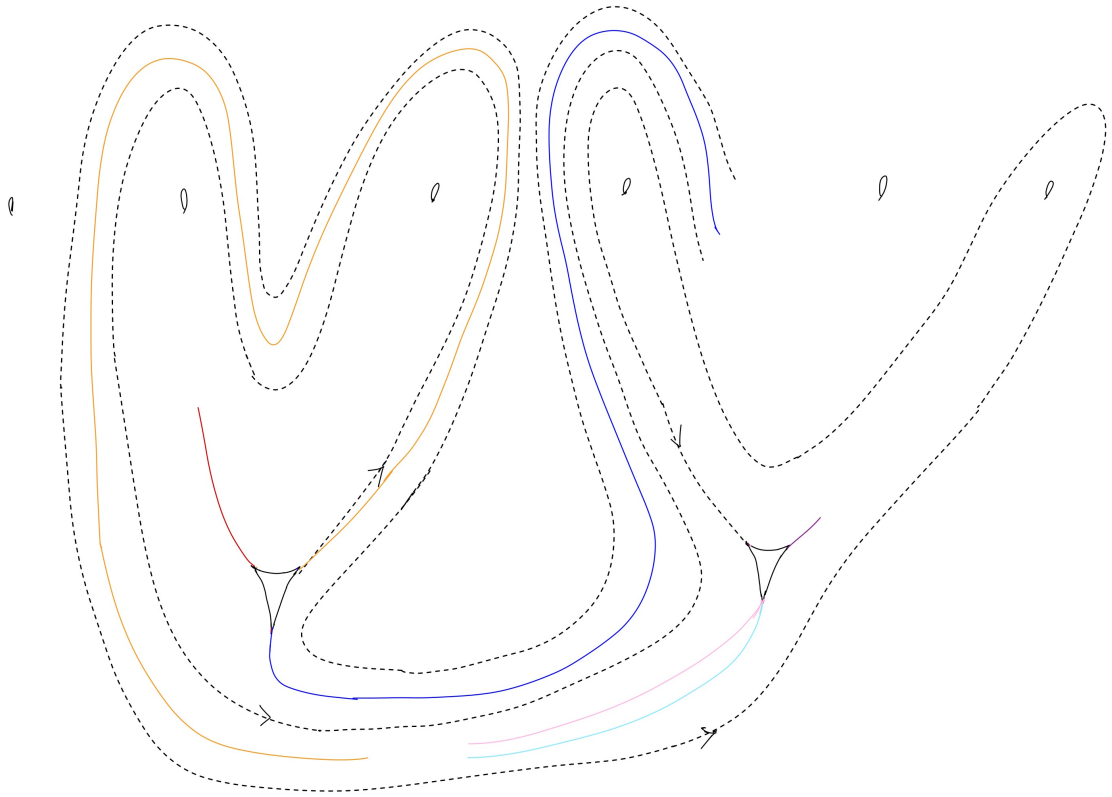


Figure E.135: Xama3

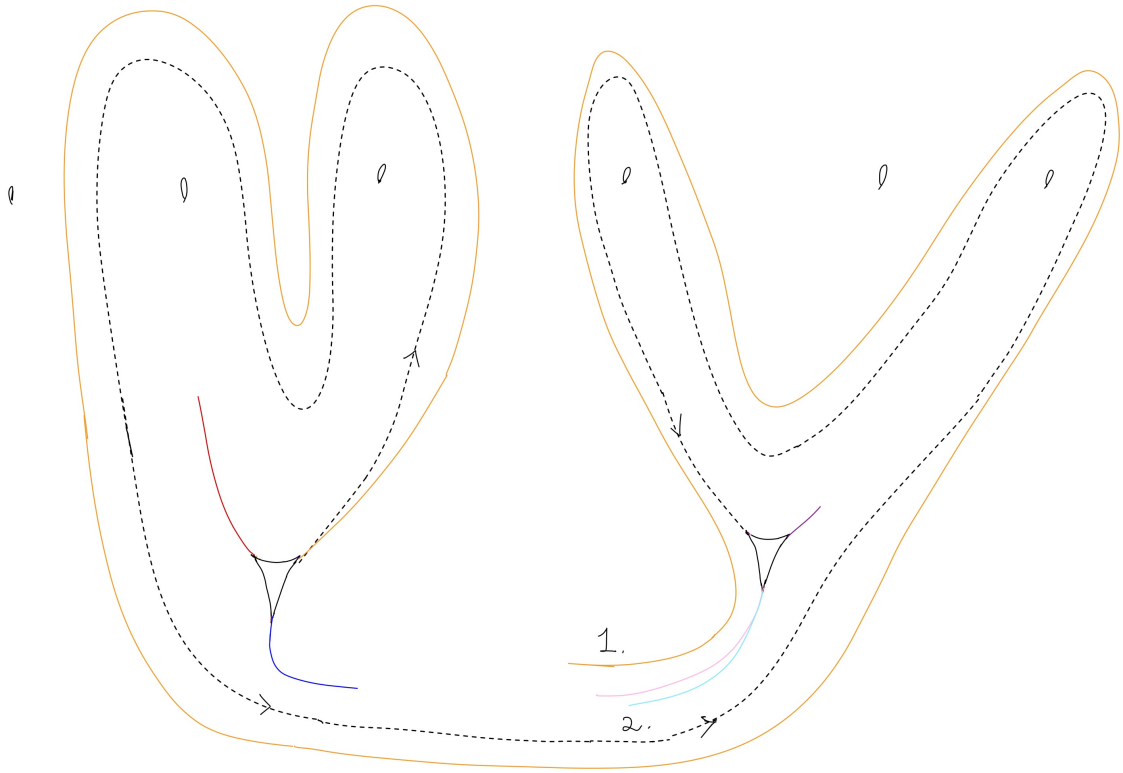


Figure E.136: Xama4

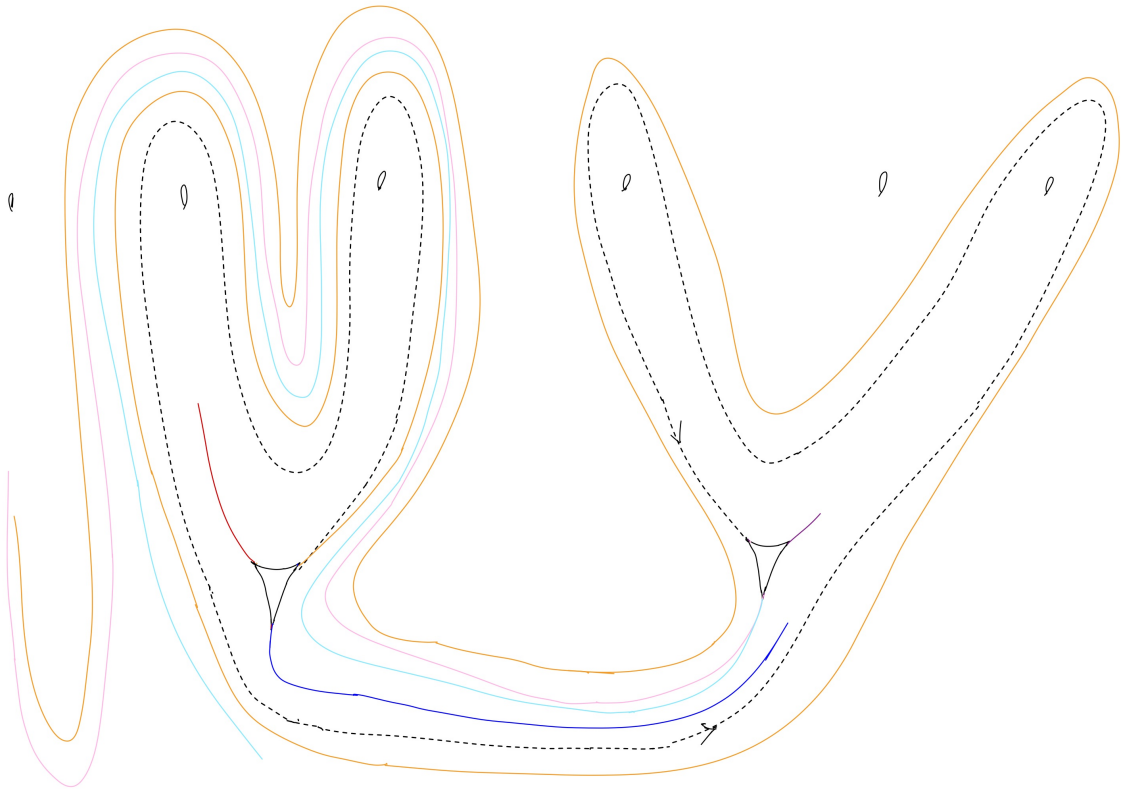


Figure E.137: Xama5

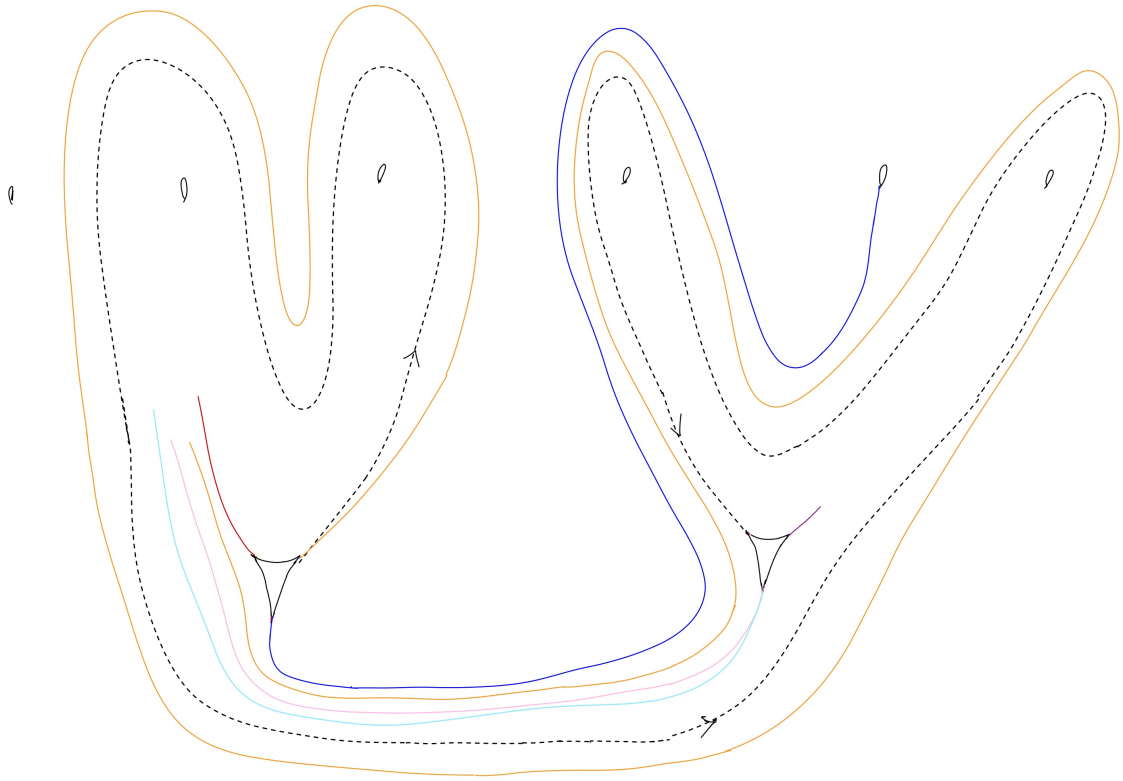


Figure E.138: Xama6

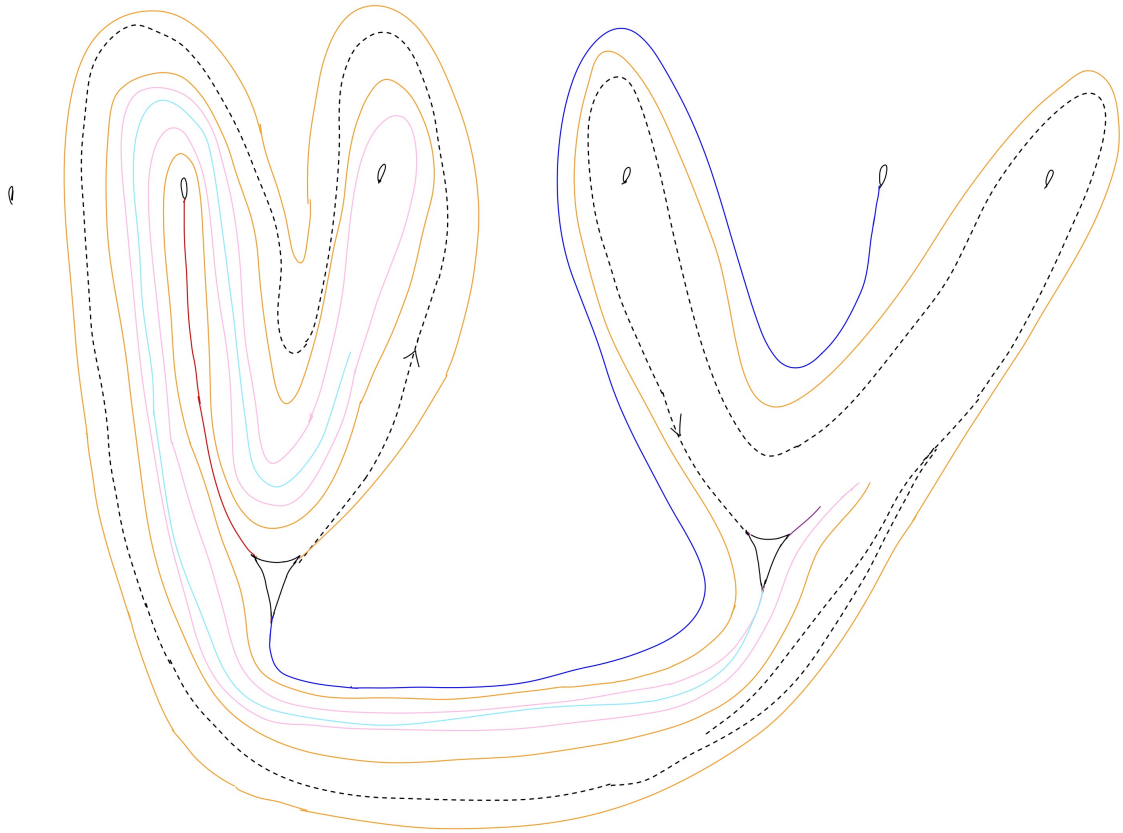


Figure E.139: Zaxes1

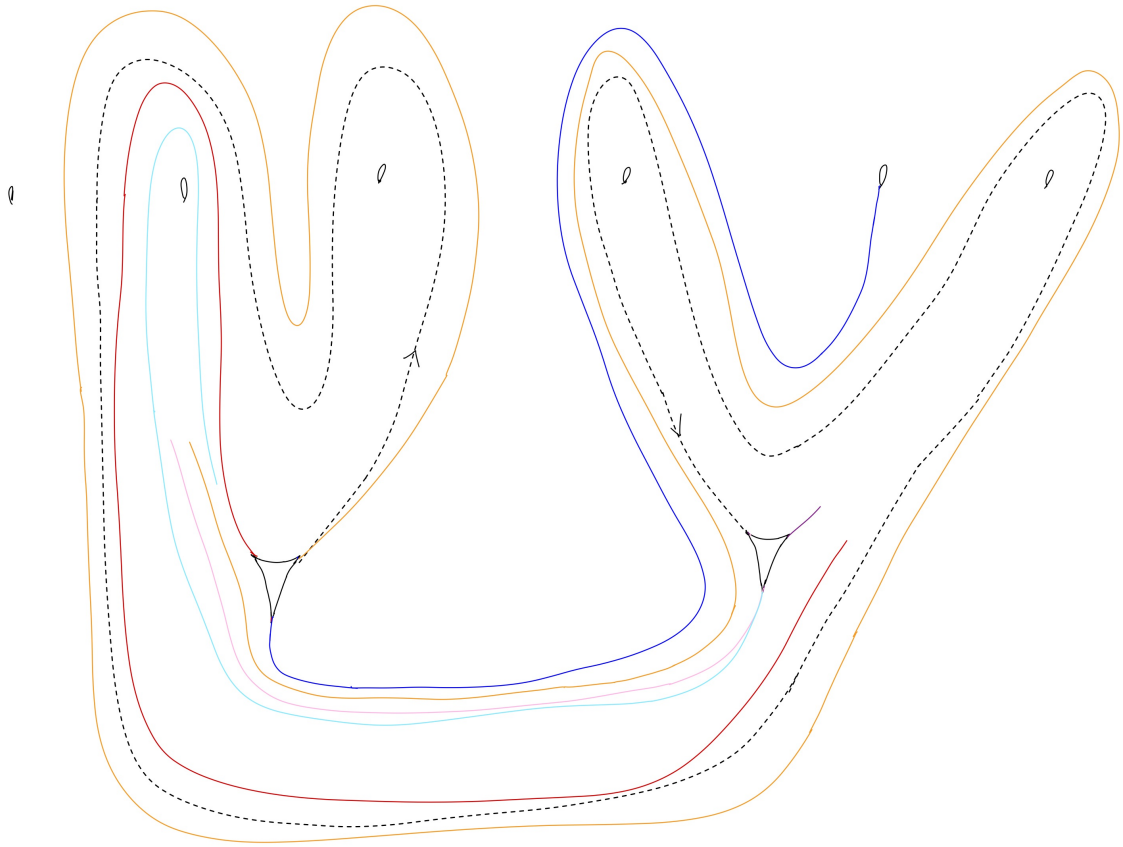


Figure E.140: Qophs1

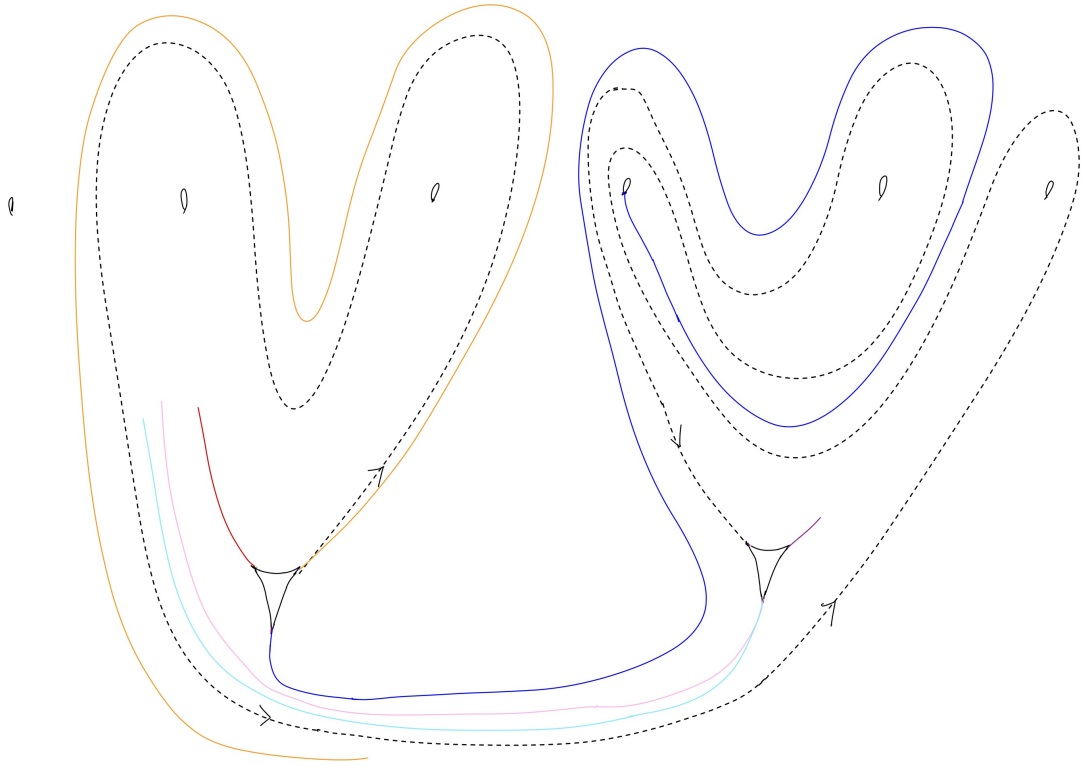


Figure E.141: Zoea1

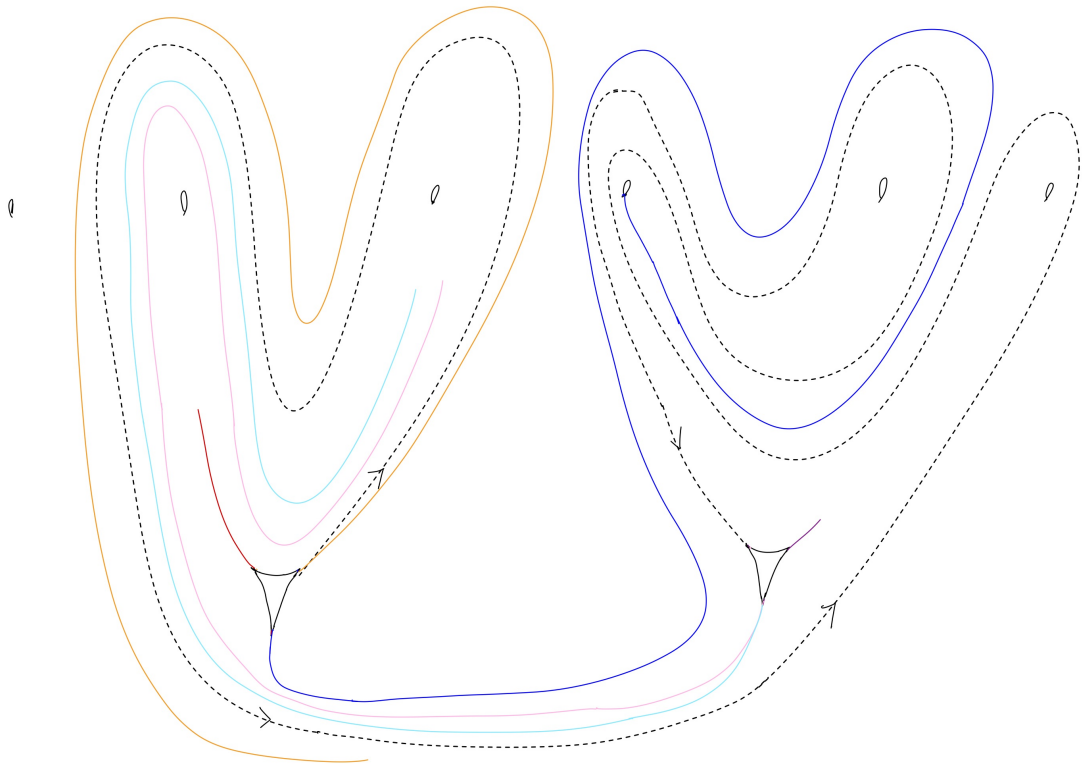


Figure E.142: Zoea2

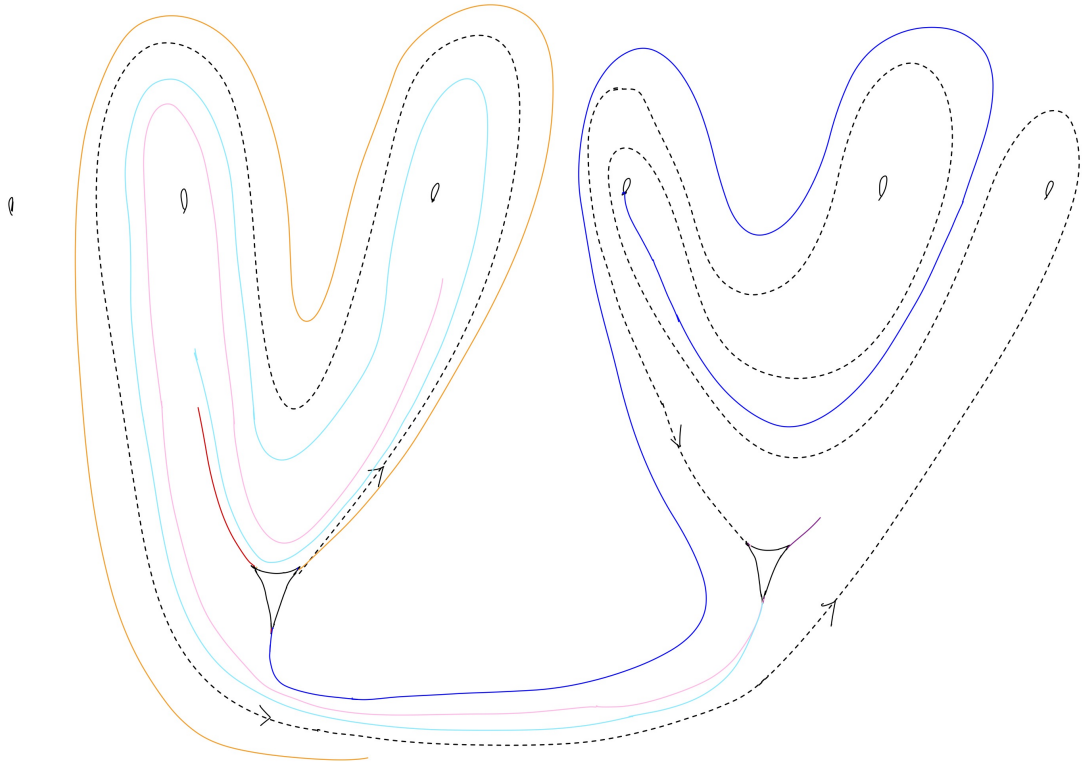


Figure E.143: Zoea3

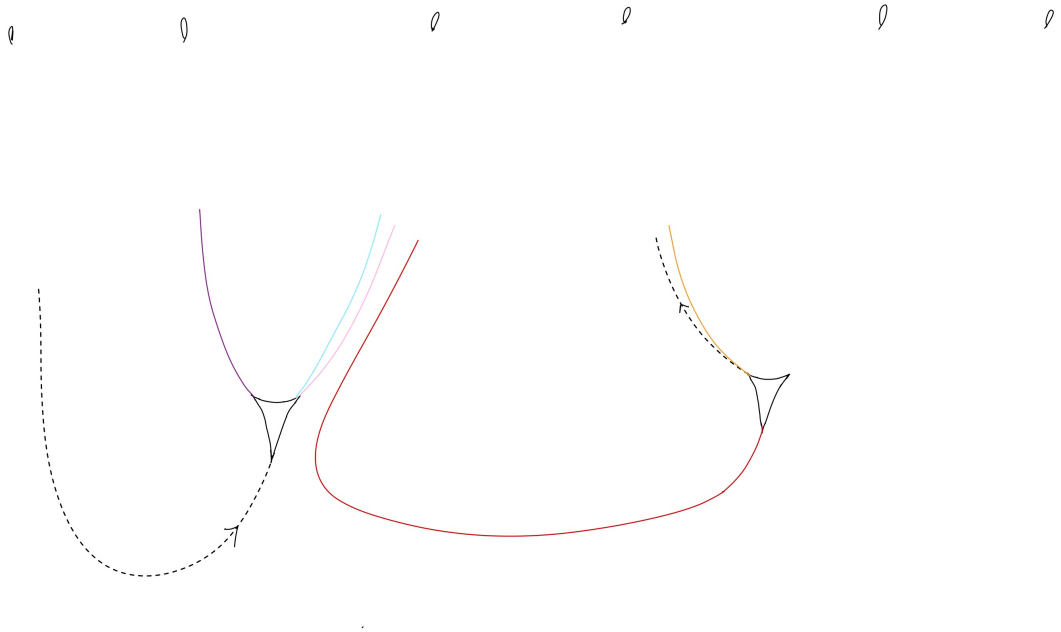


Figure E.144: OMG1

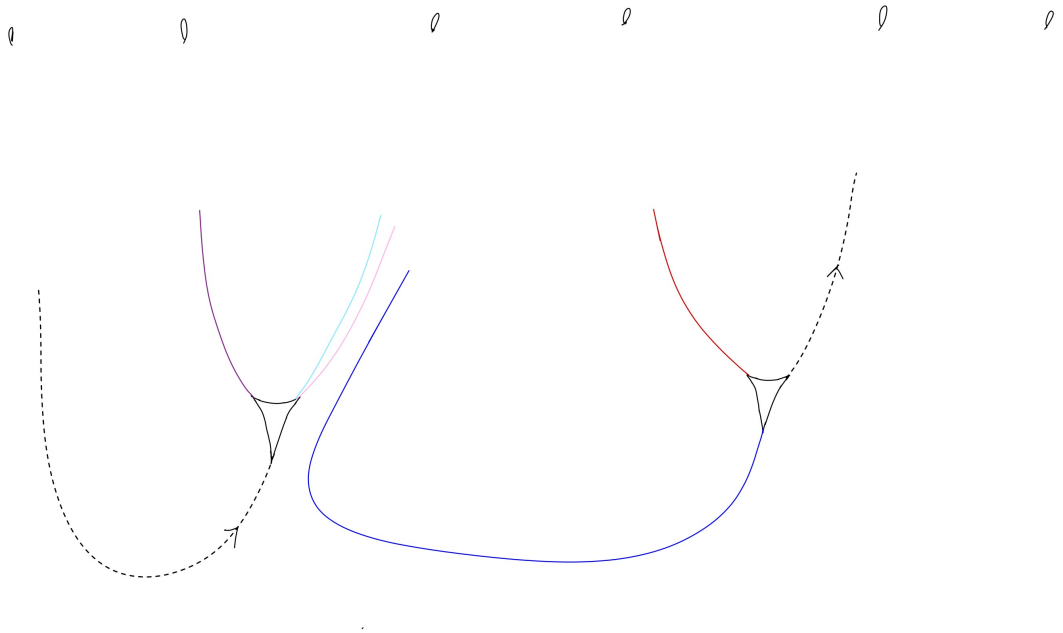


Figure E.145: SUX1

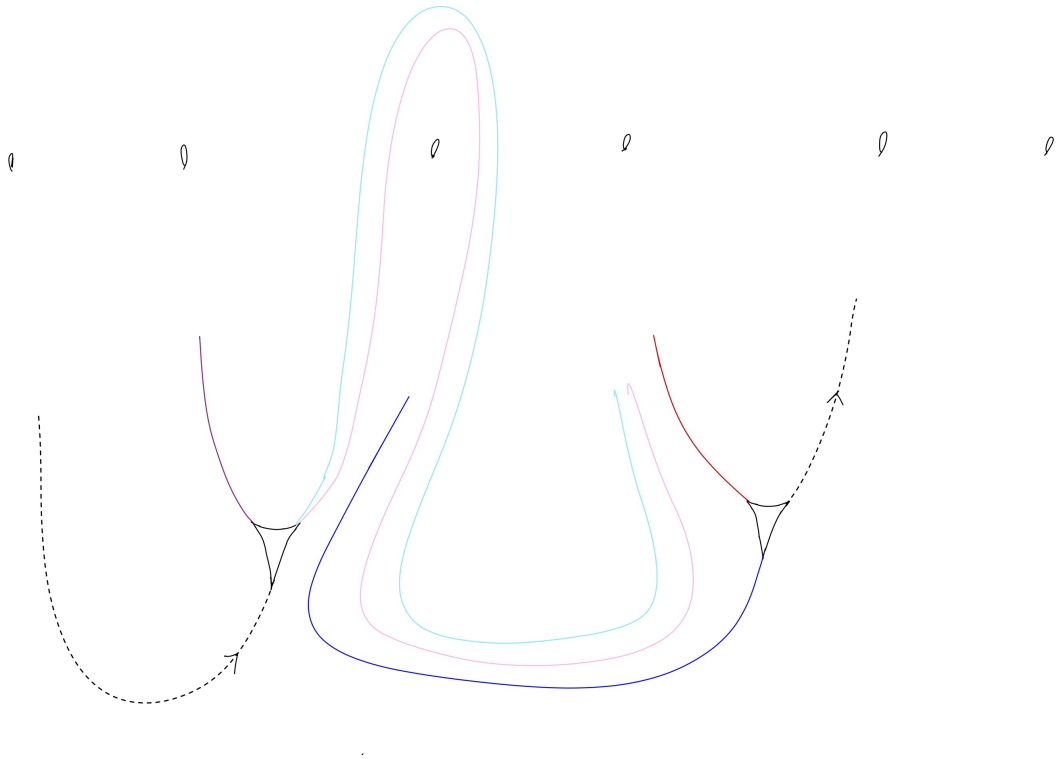


Figure E.146: SUX2

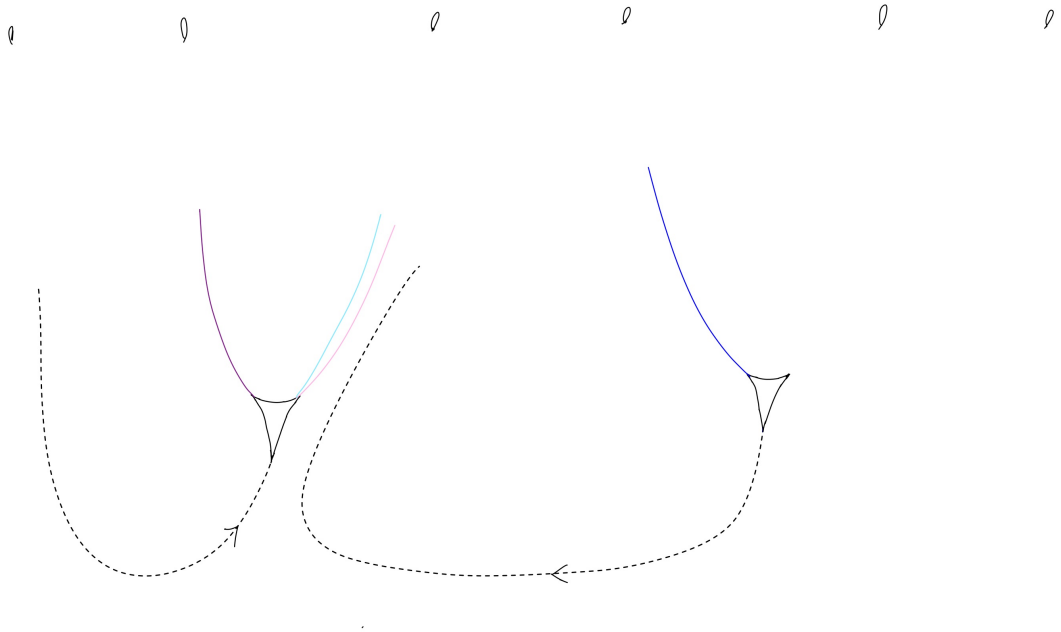


Figure E.147: ULN1

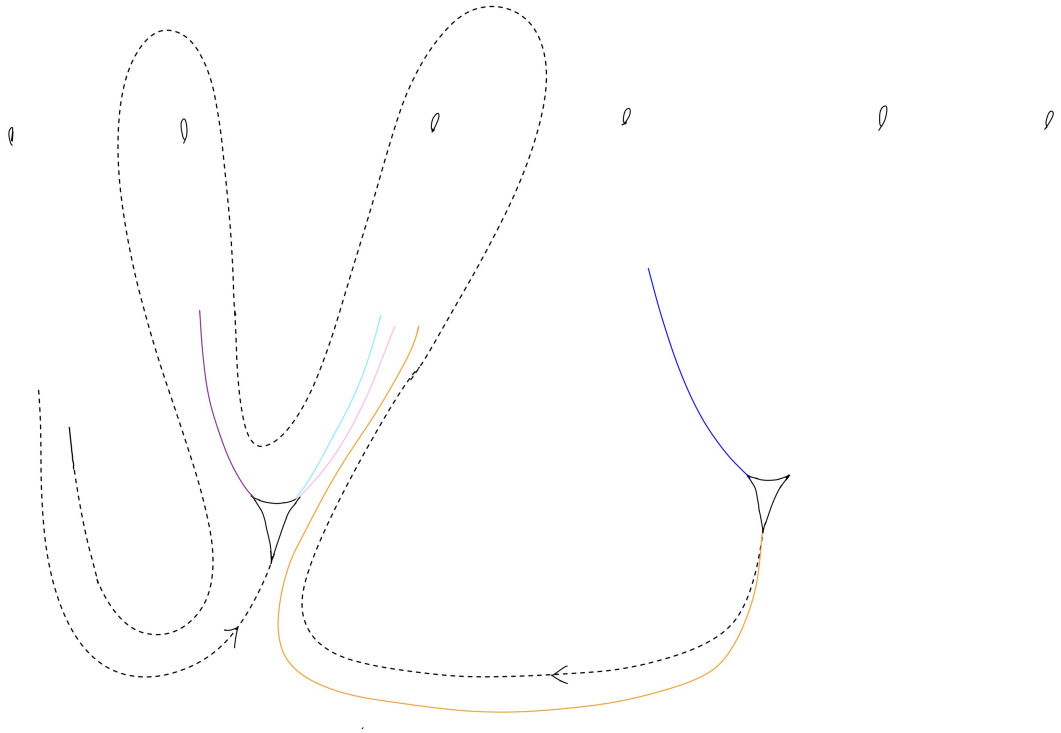


Figure E.148: ULN2

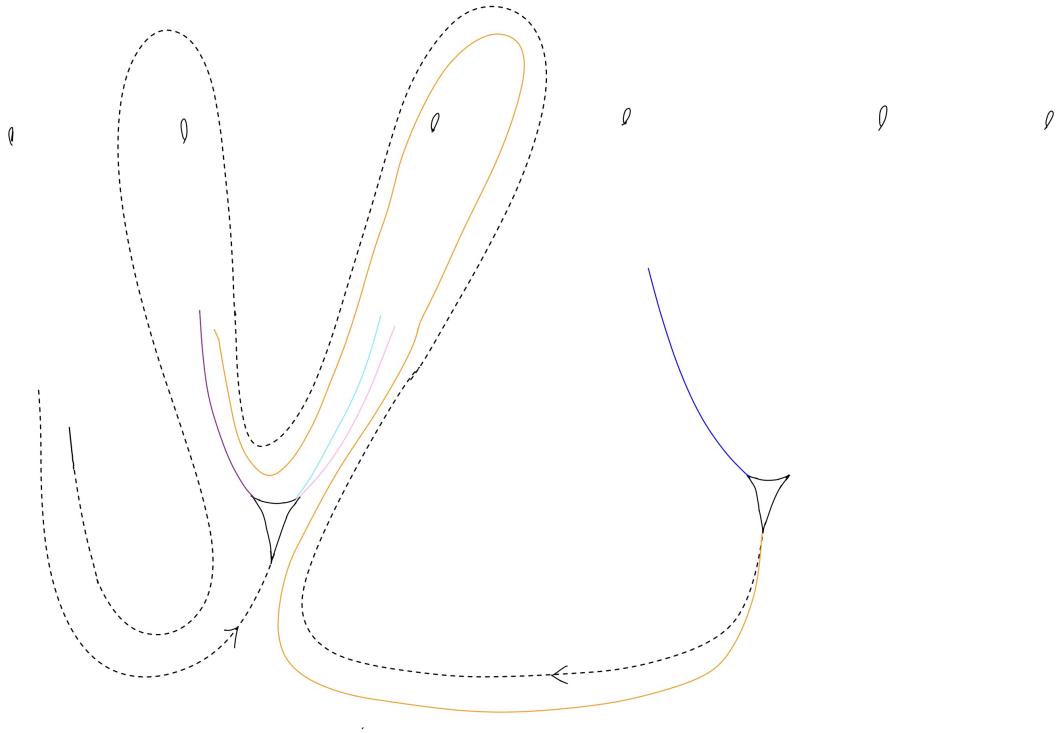


Figure E.149: ULN3

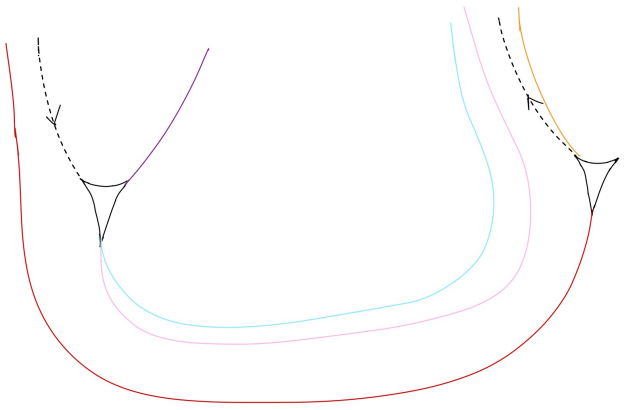


Figure E.150: NAN1

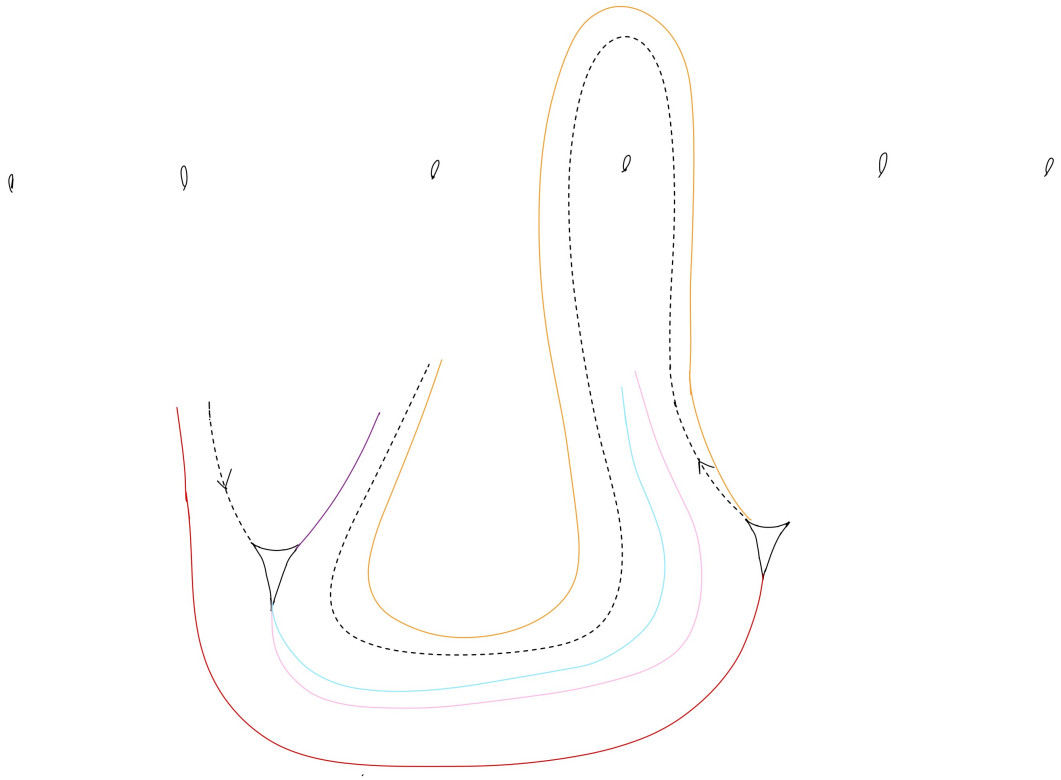


Figure E.151: NAN2

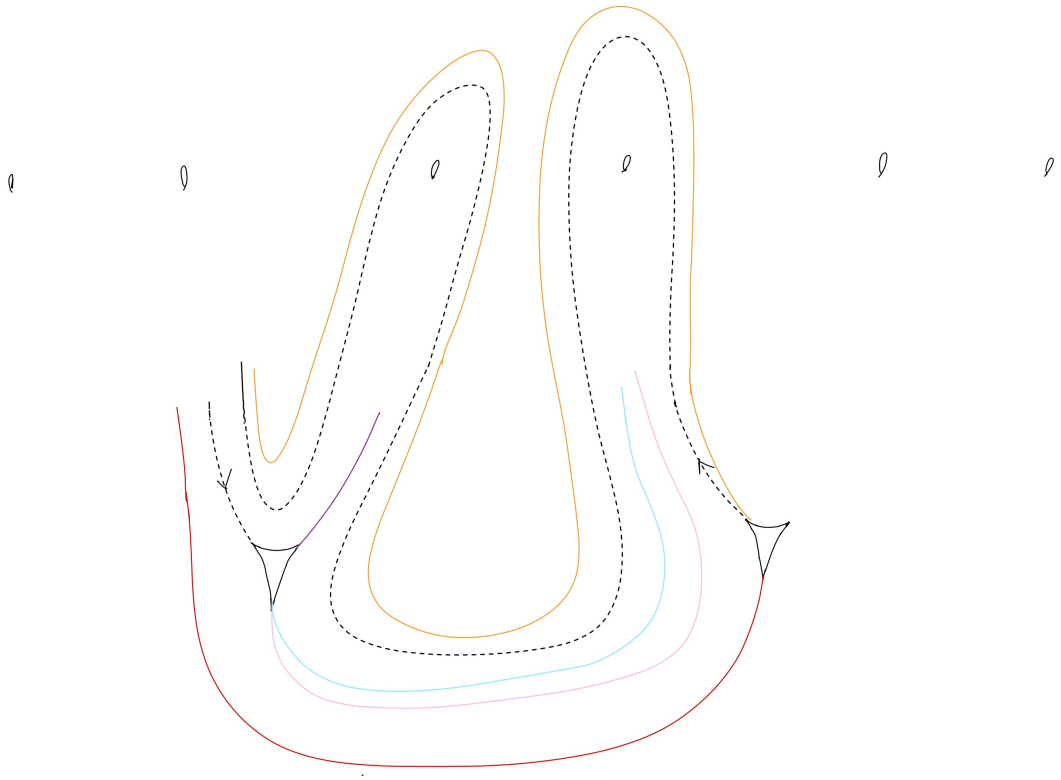


Figure E.152: NAN3

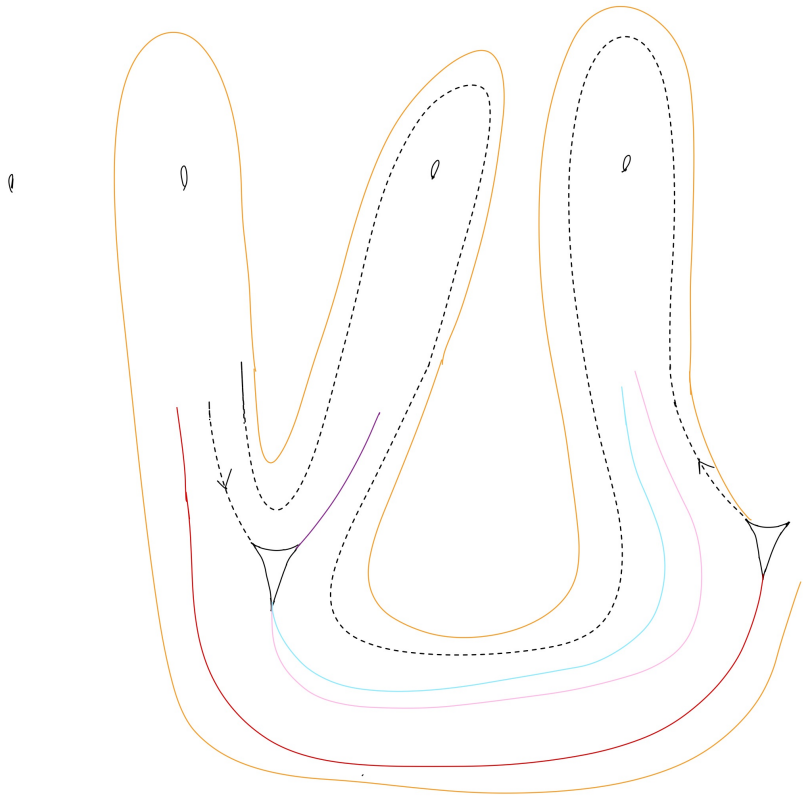


Figure E.153: NAN4

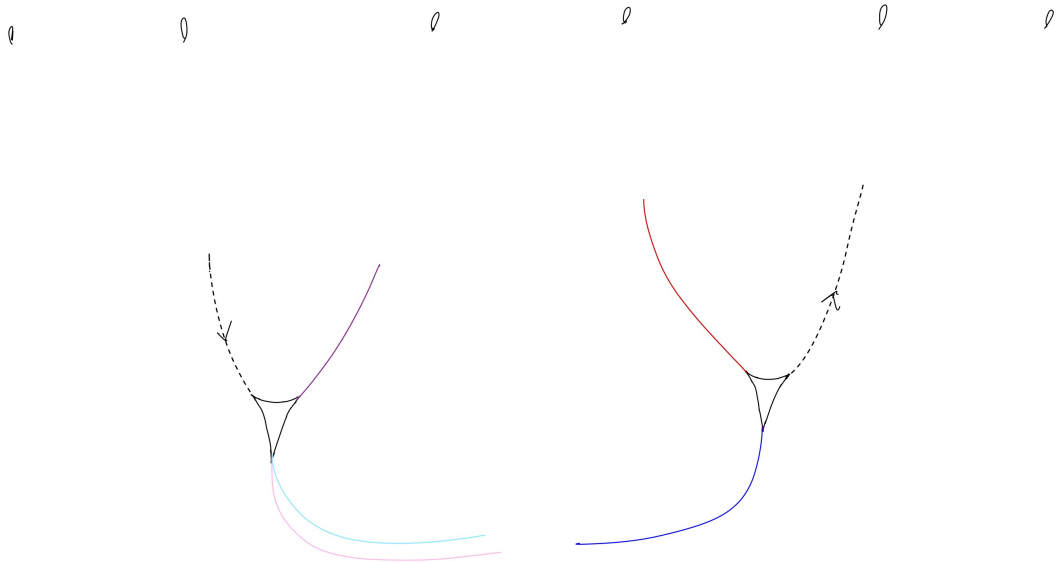


Figure E.154: GOH1

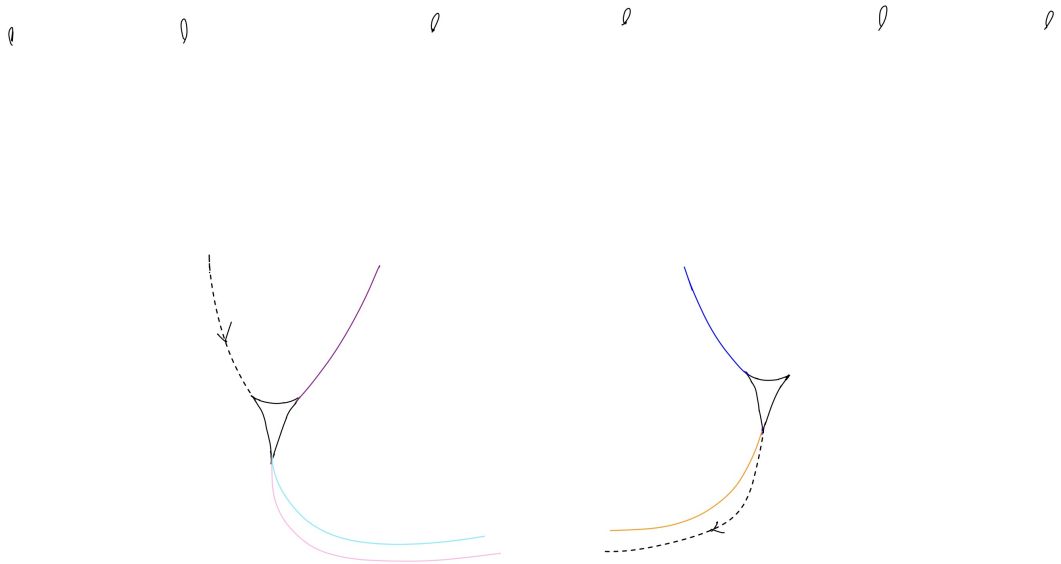


Figure E.155: BOD1

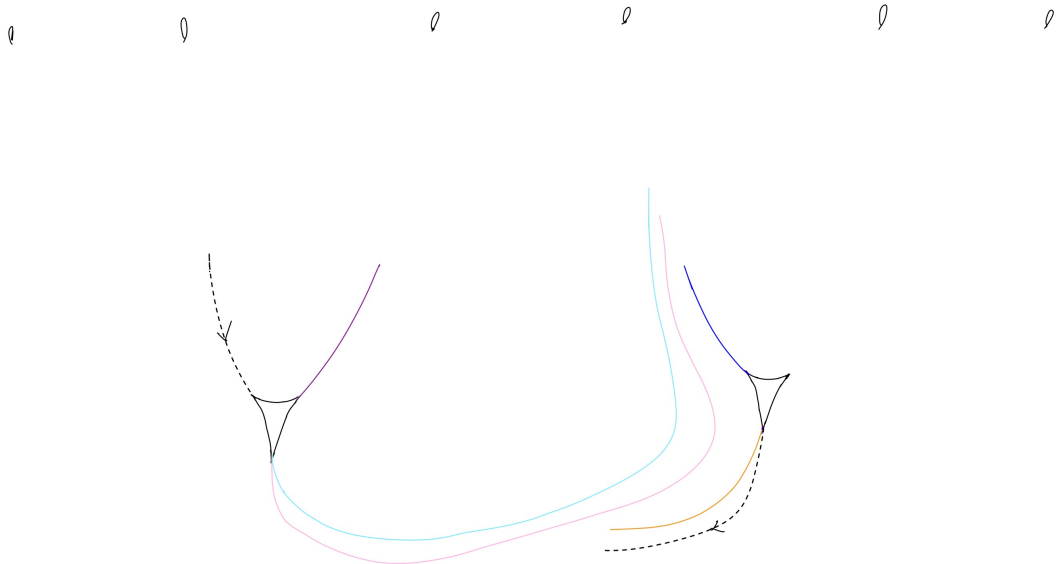


Figure E.156: BOD2

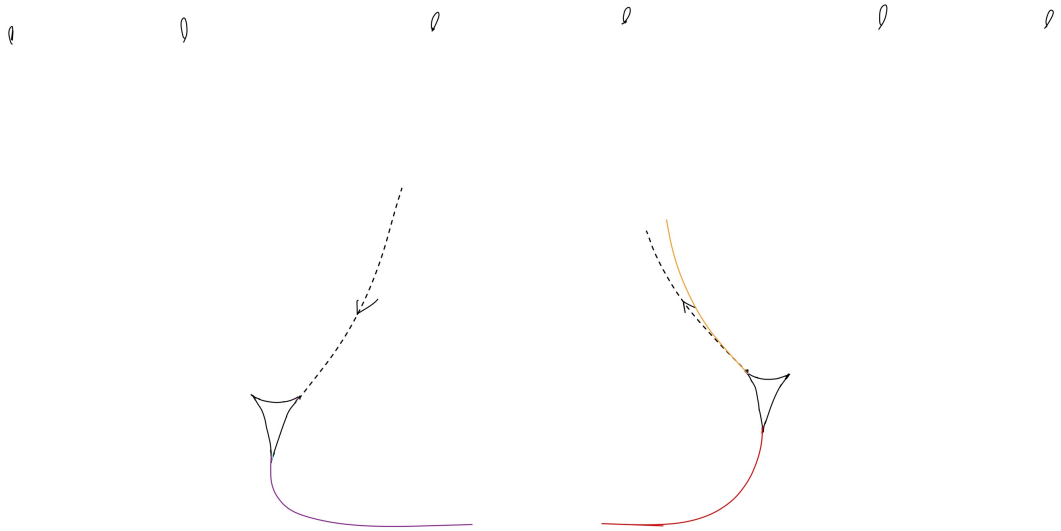


Figure E.157: MAA1

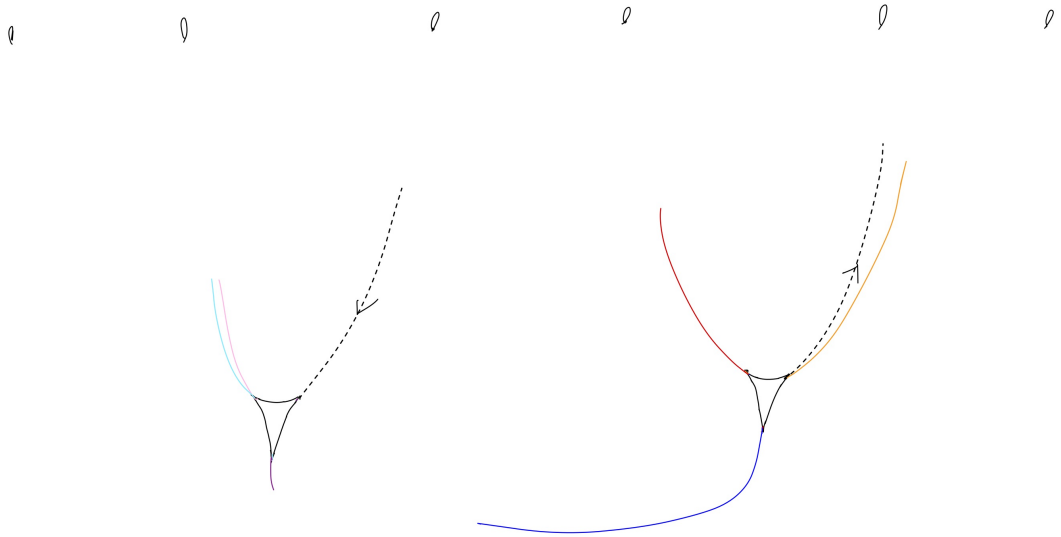


Figure E.158: XNB1

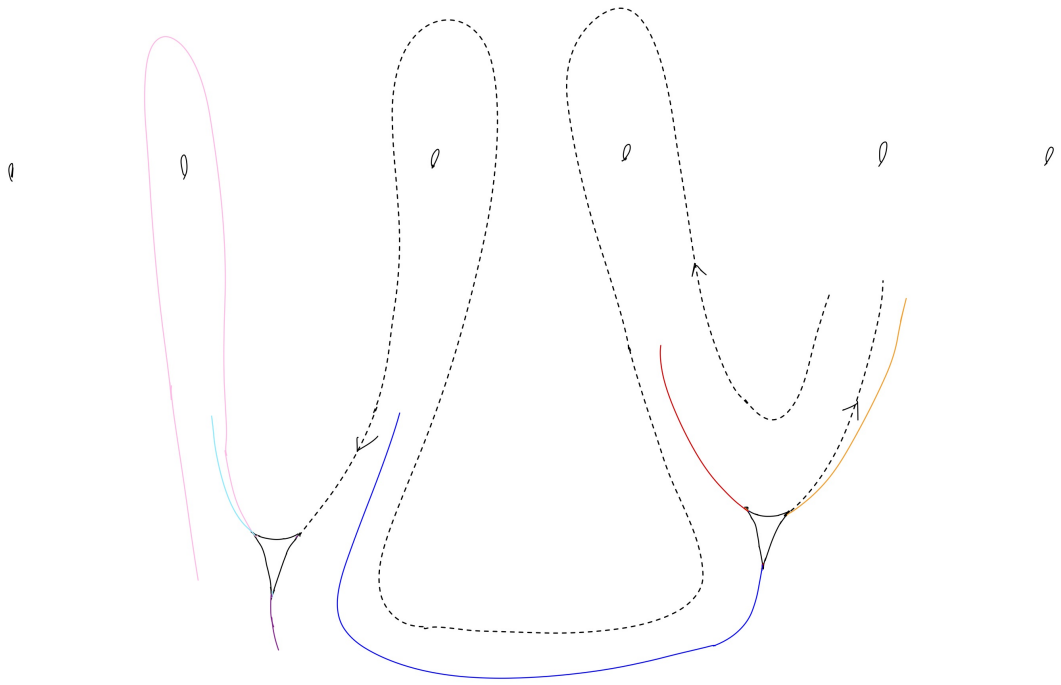


Figure E.159: XNB2

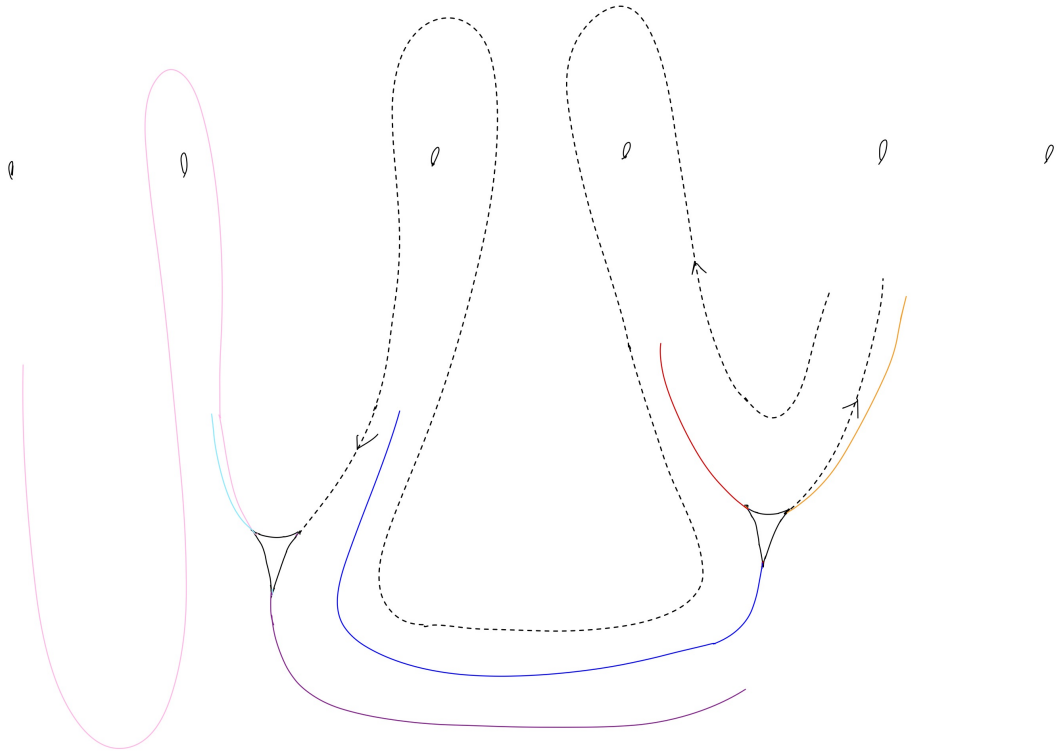


Figure E.160: XNB3

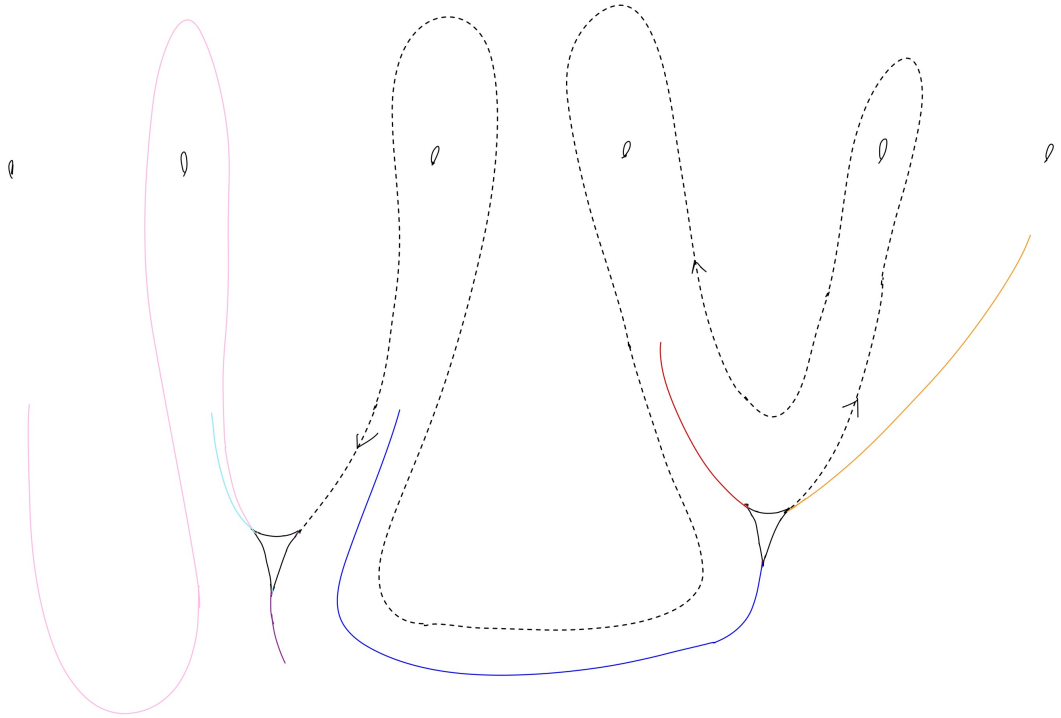


Figure E.161: Qadi1

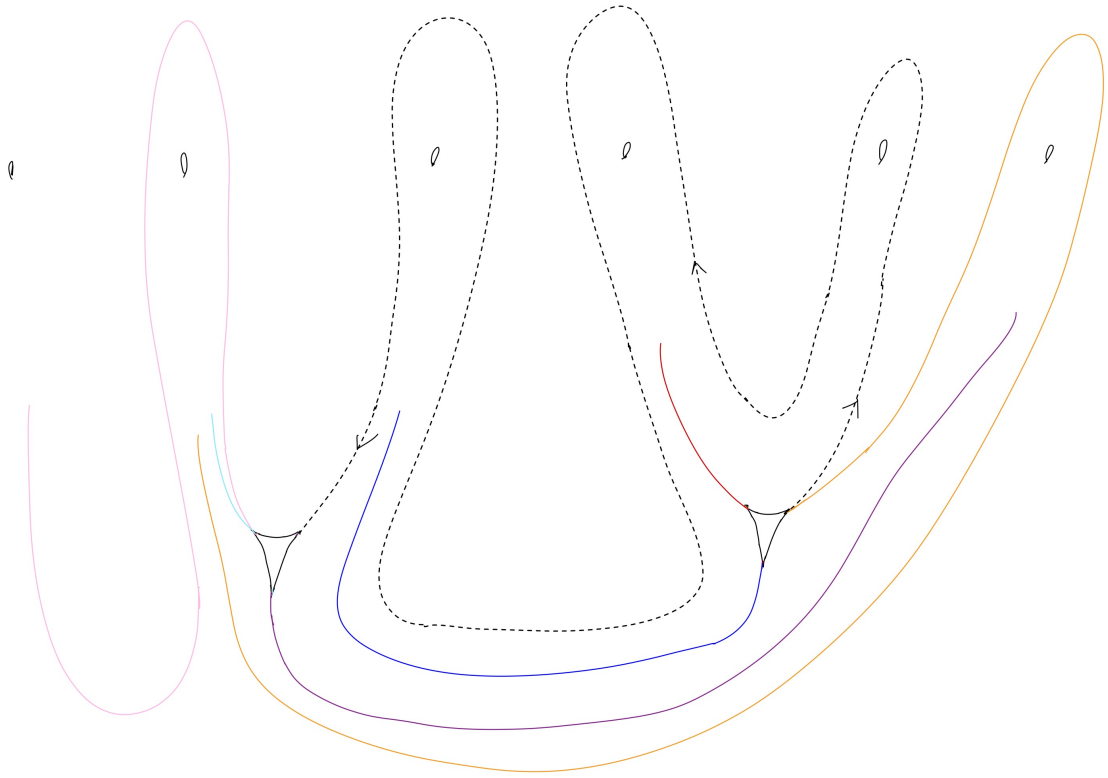


Figure E.162: Qadi2

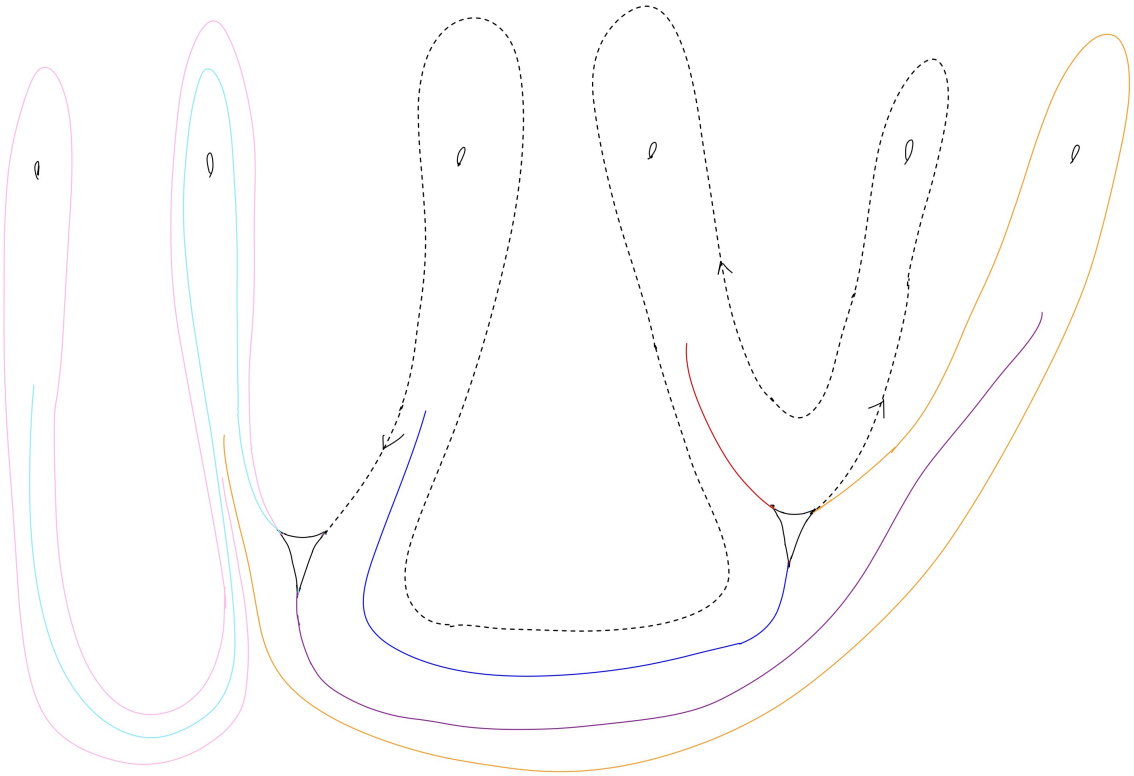


Figure E.163: Qadi3

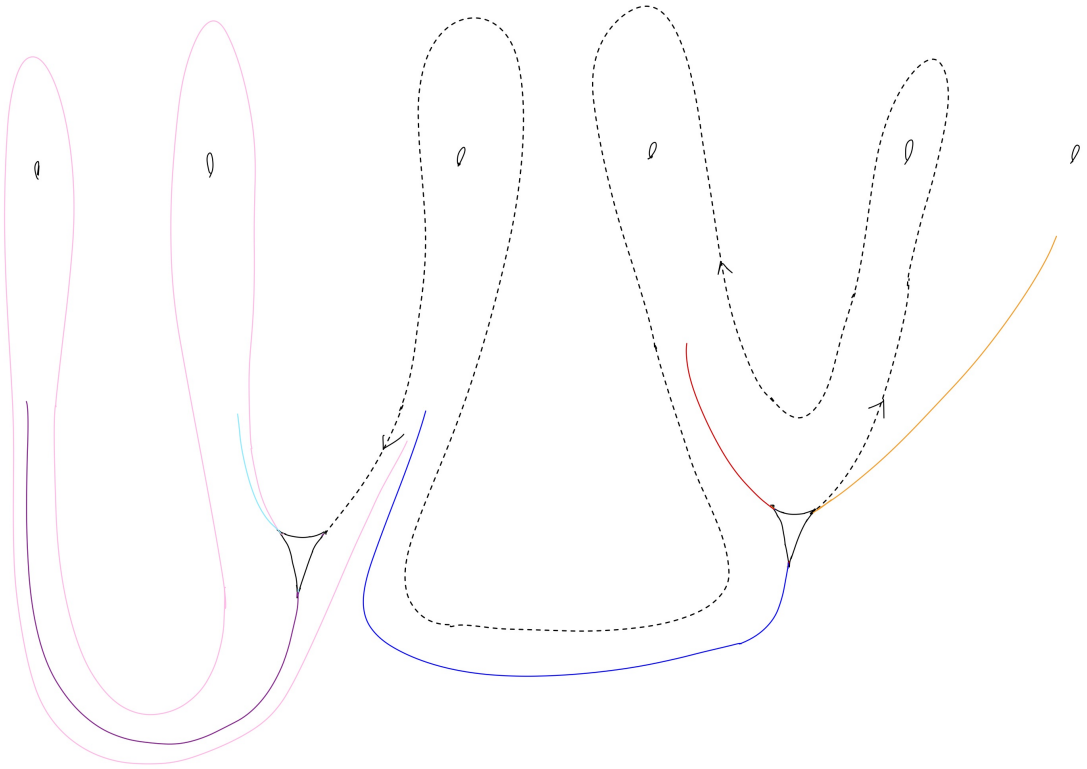


Figure E.164: Qadi4

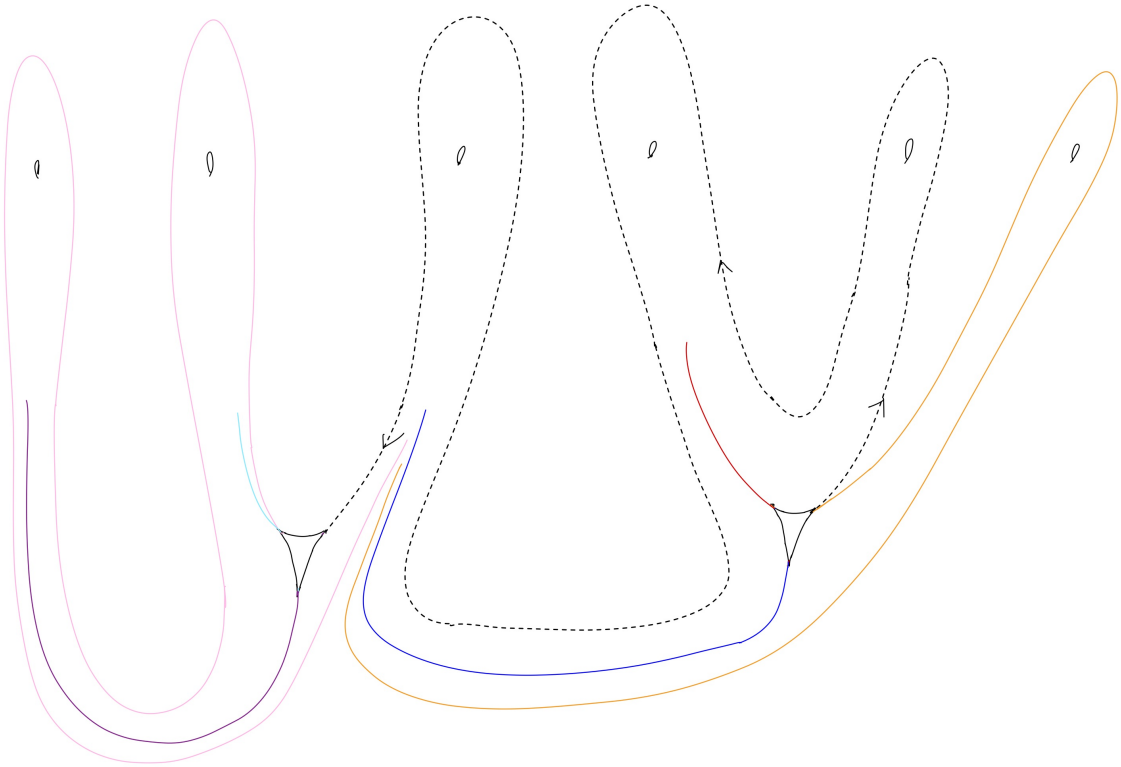


Figure E.165: Agora1

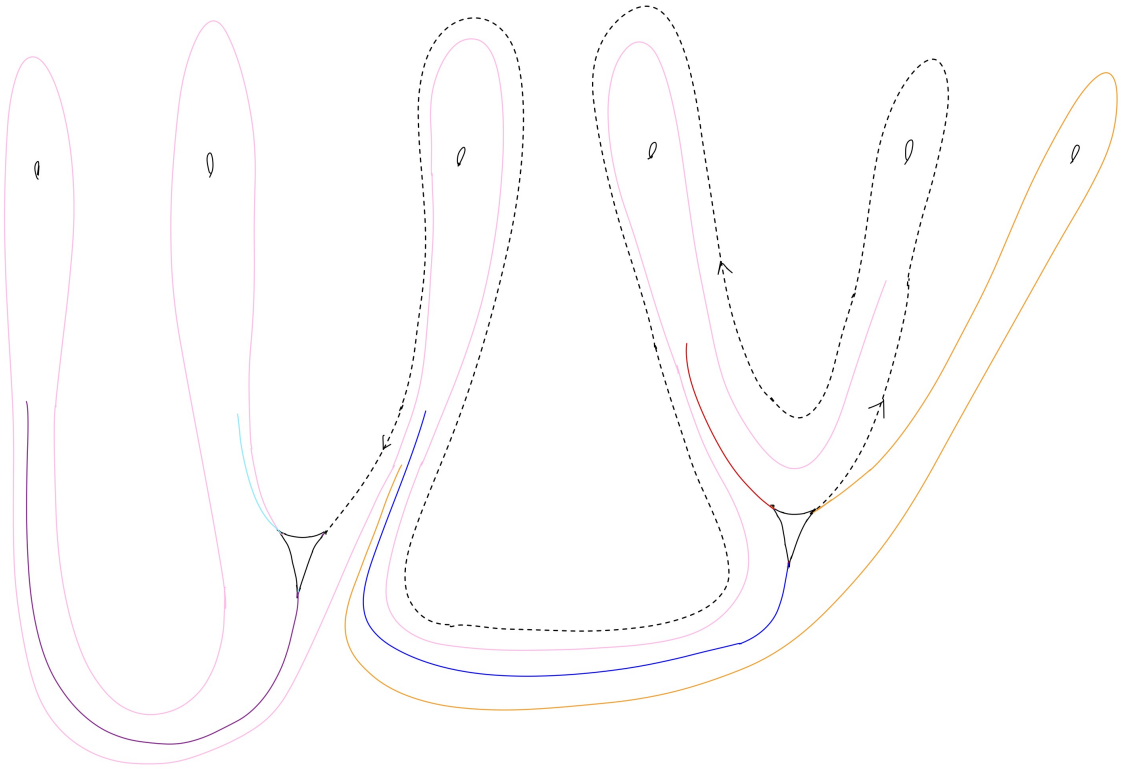


Figure E.166: Agora2

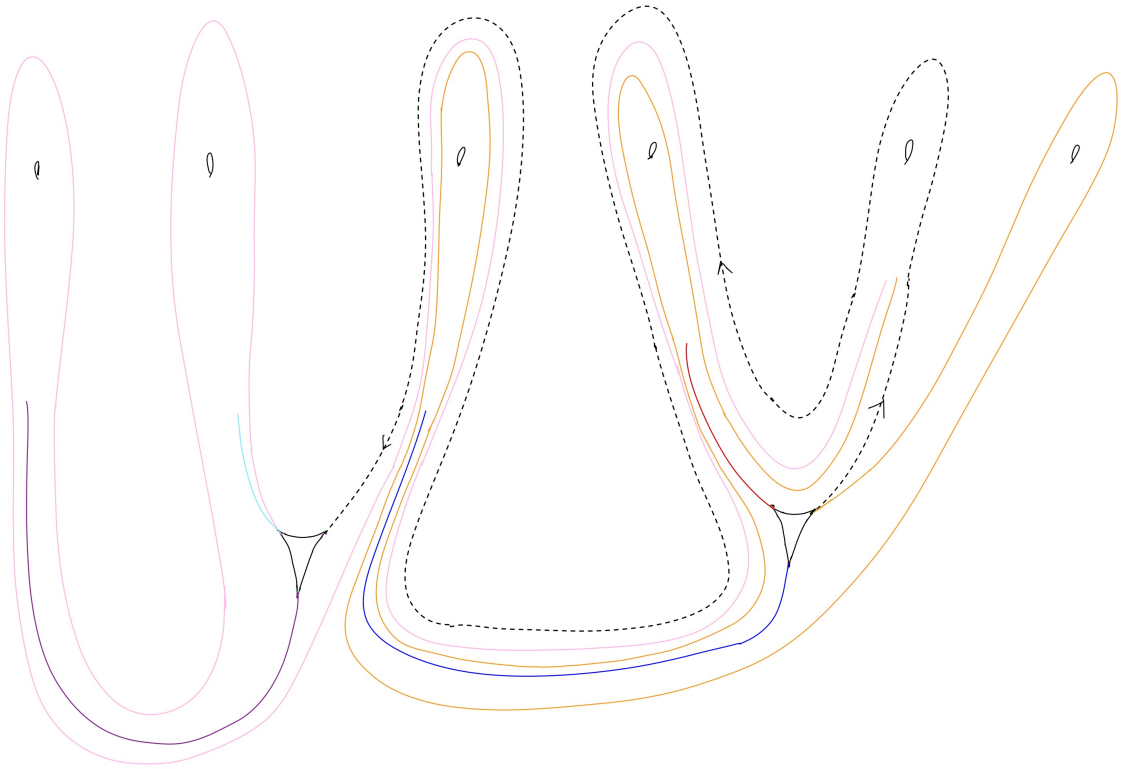


Figure E.167: Agora3

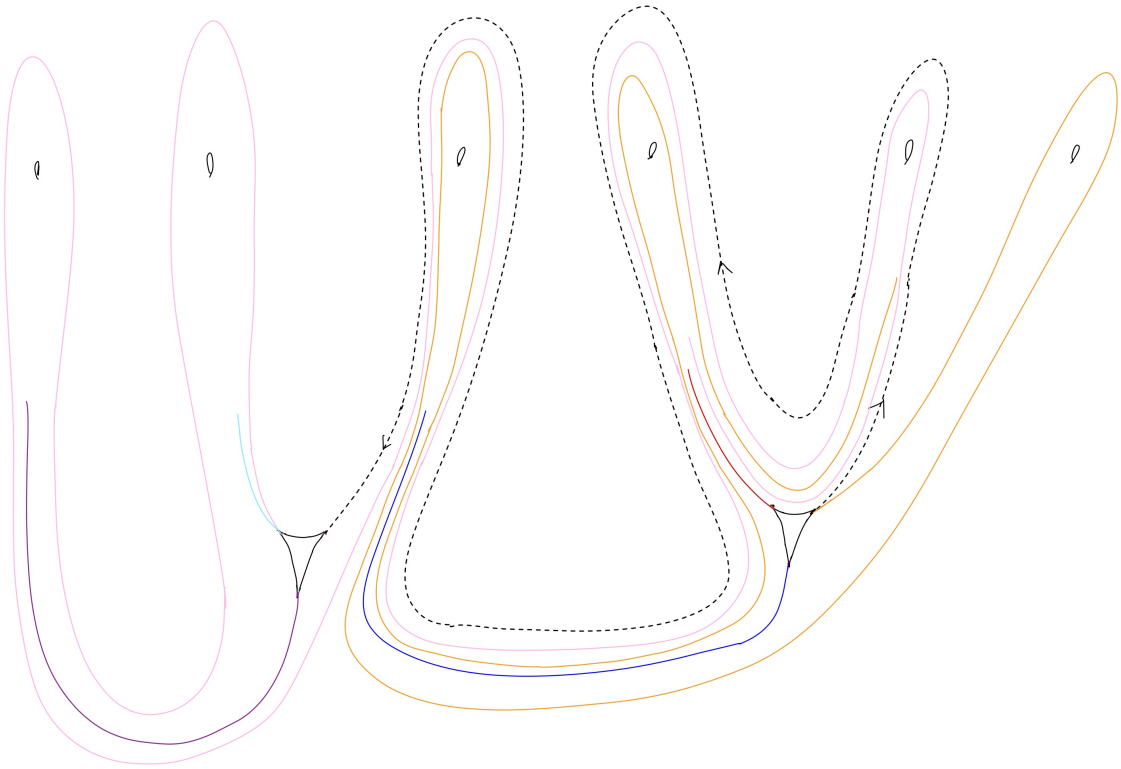


Figure E.168: Agora4

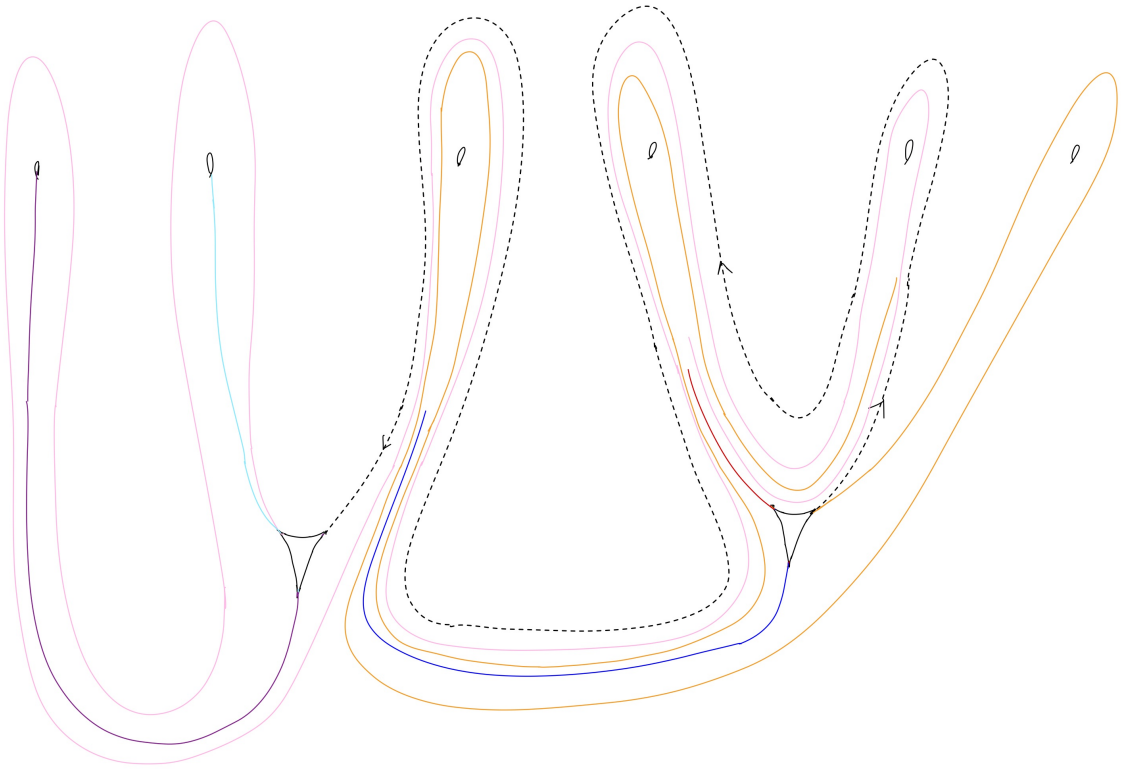


Figure E.169: Agora5

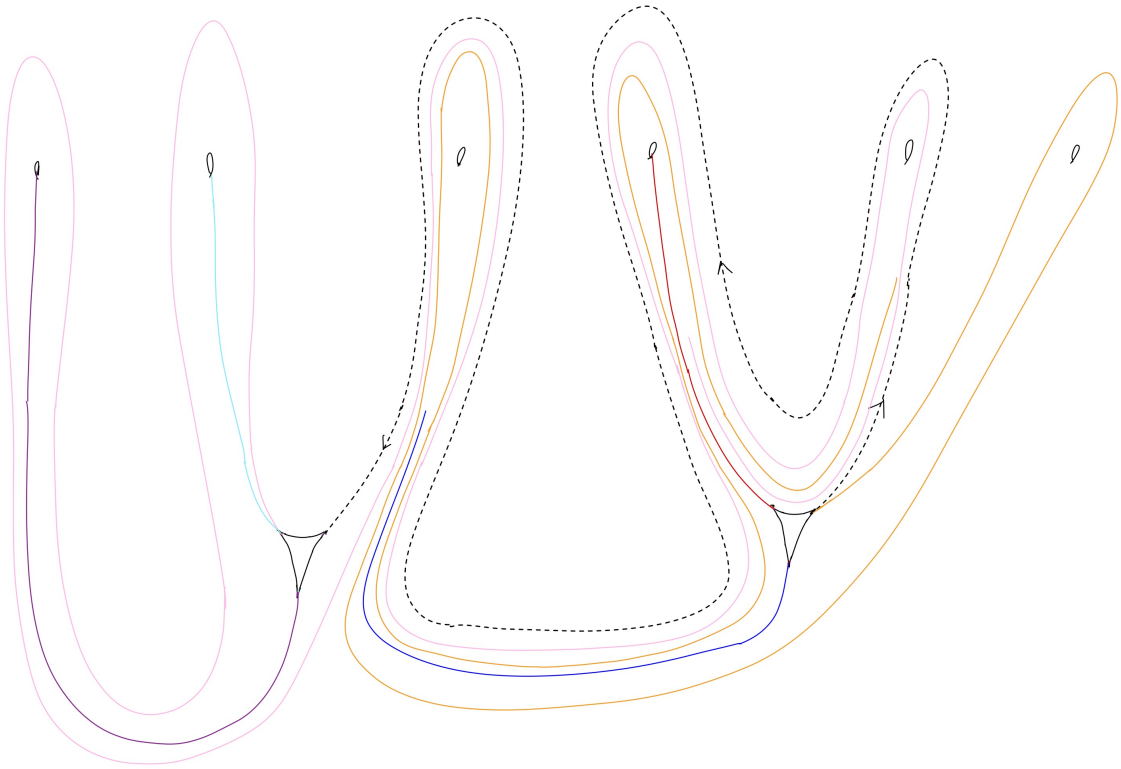


Figure E.170: Byssus1

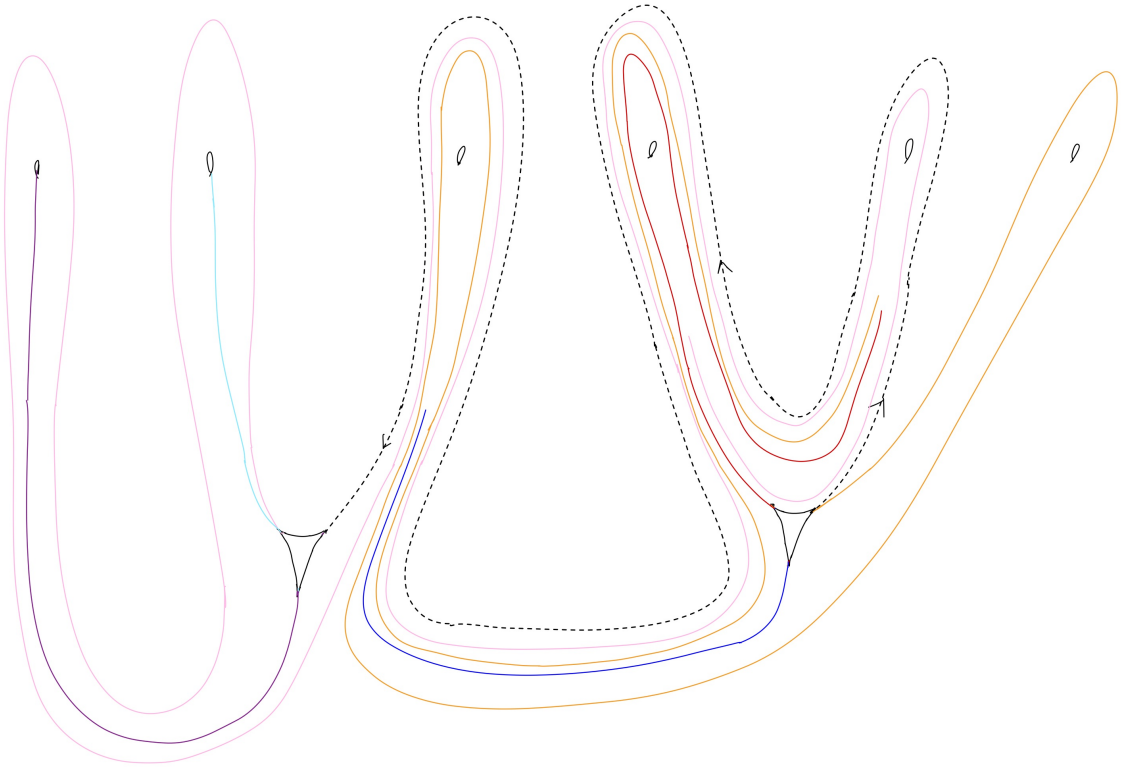


Figure E.171: Zareba1

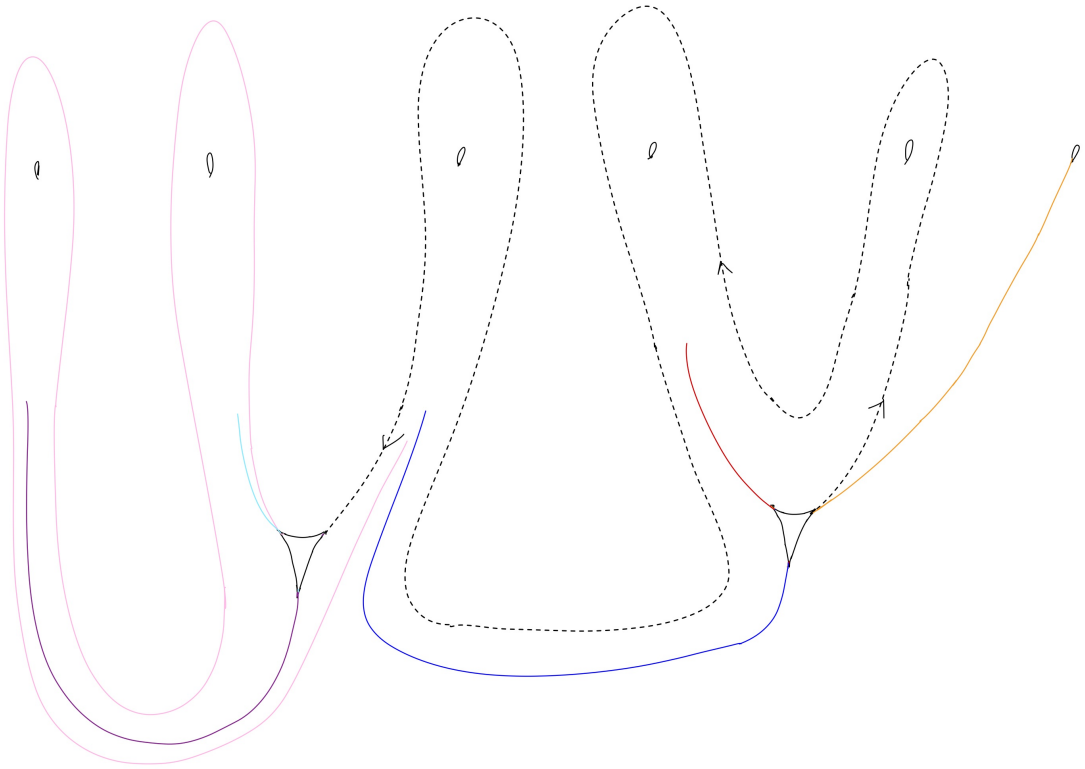


Figure E.172: Bokeh1

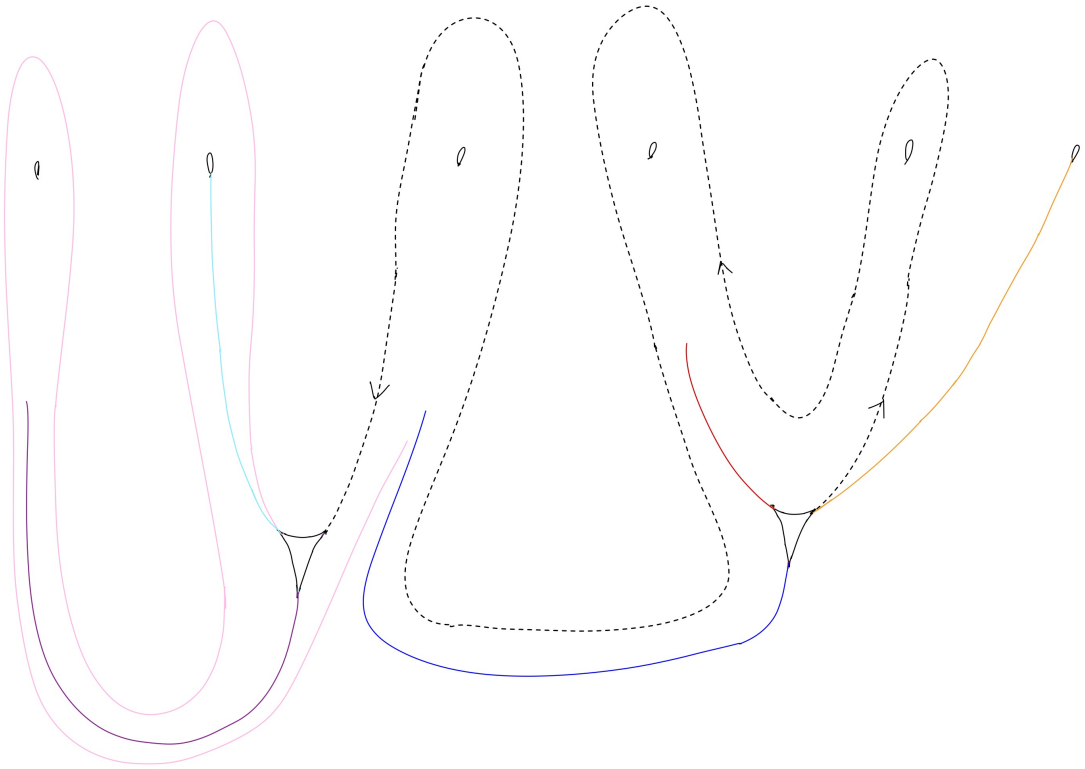


Figure E.173: Popjoy1

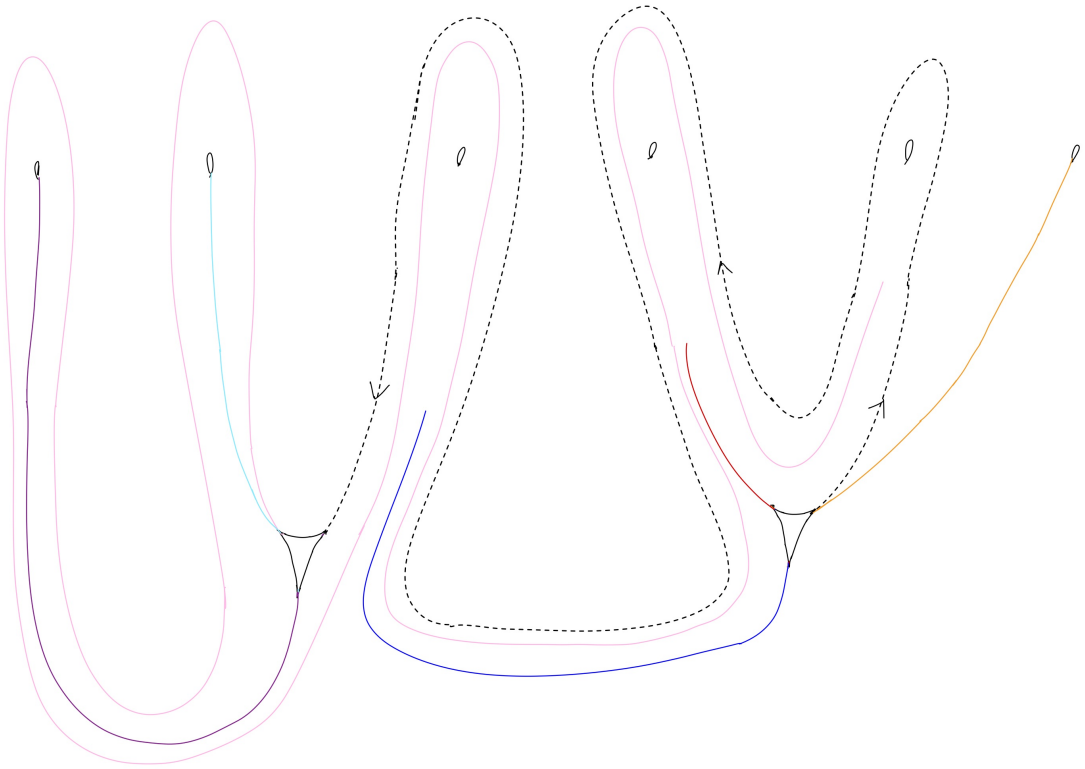


Figure E.174: Popjoy2

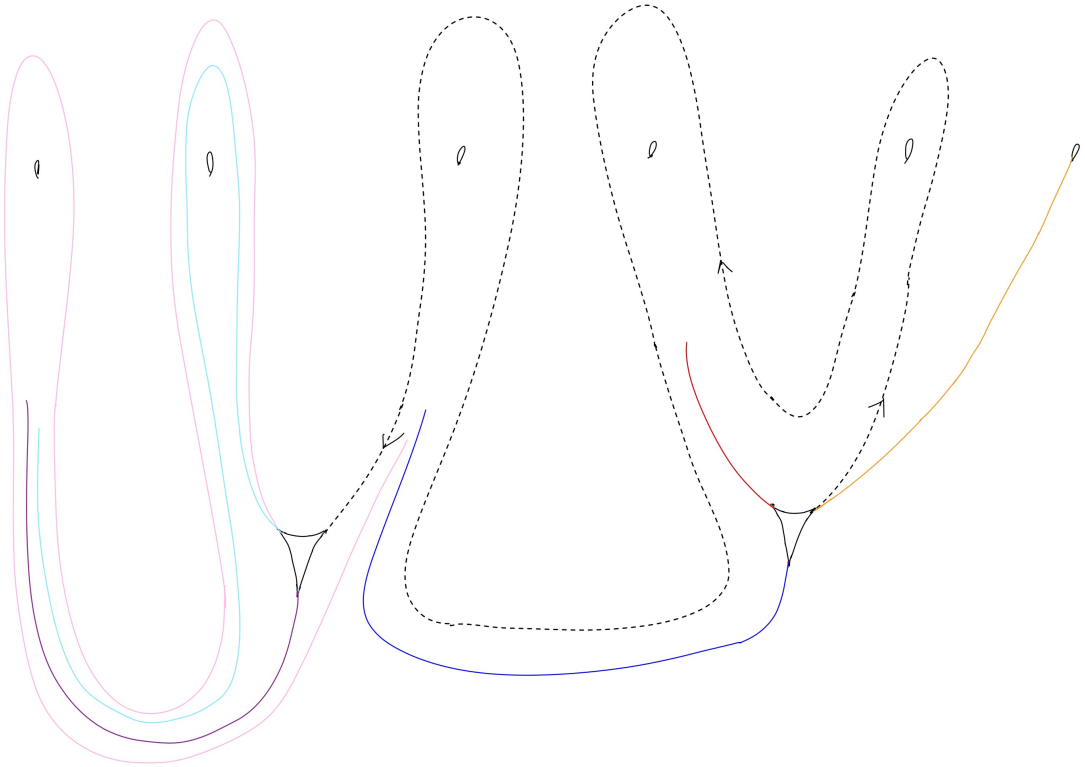


Figure E.175: Archon1

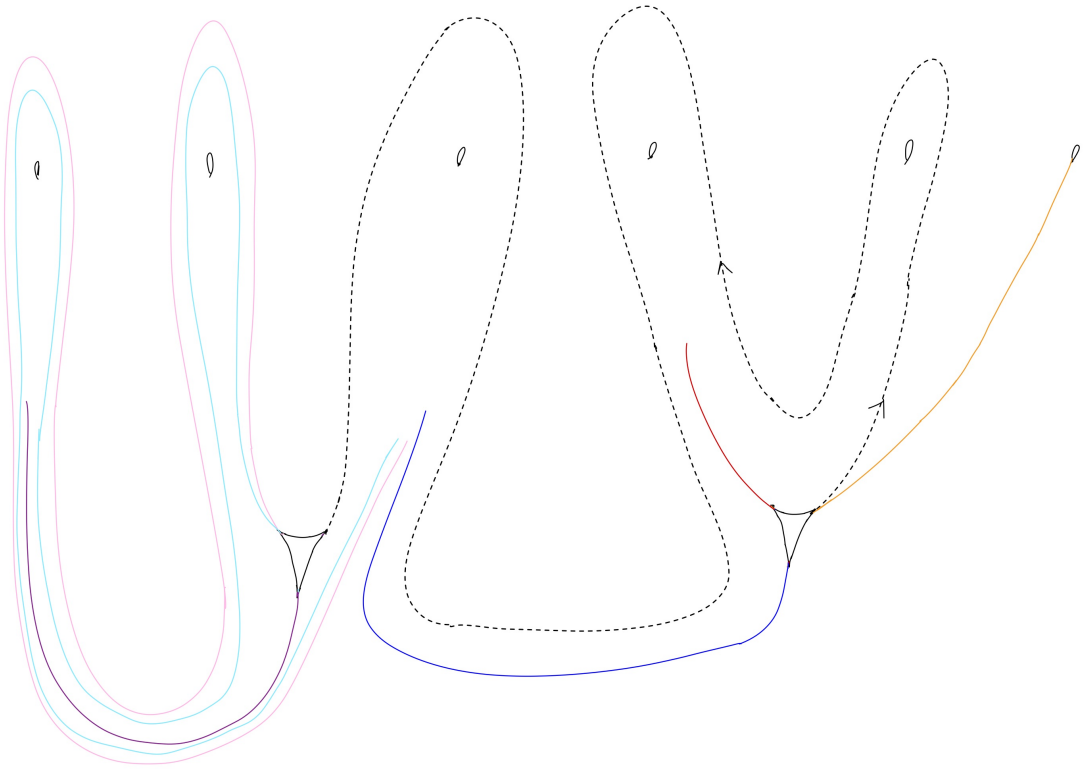


Figure E.176: Archon2

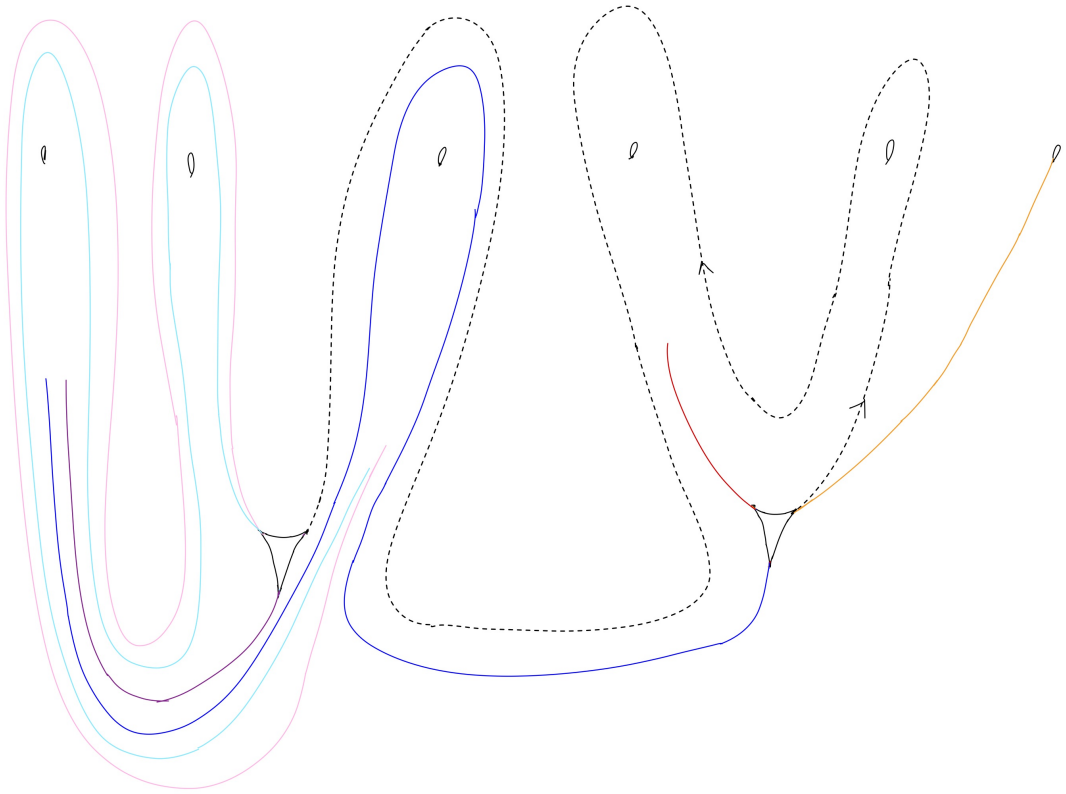


Figure E.177: Archon3

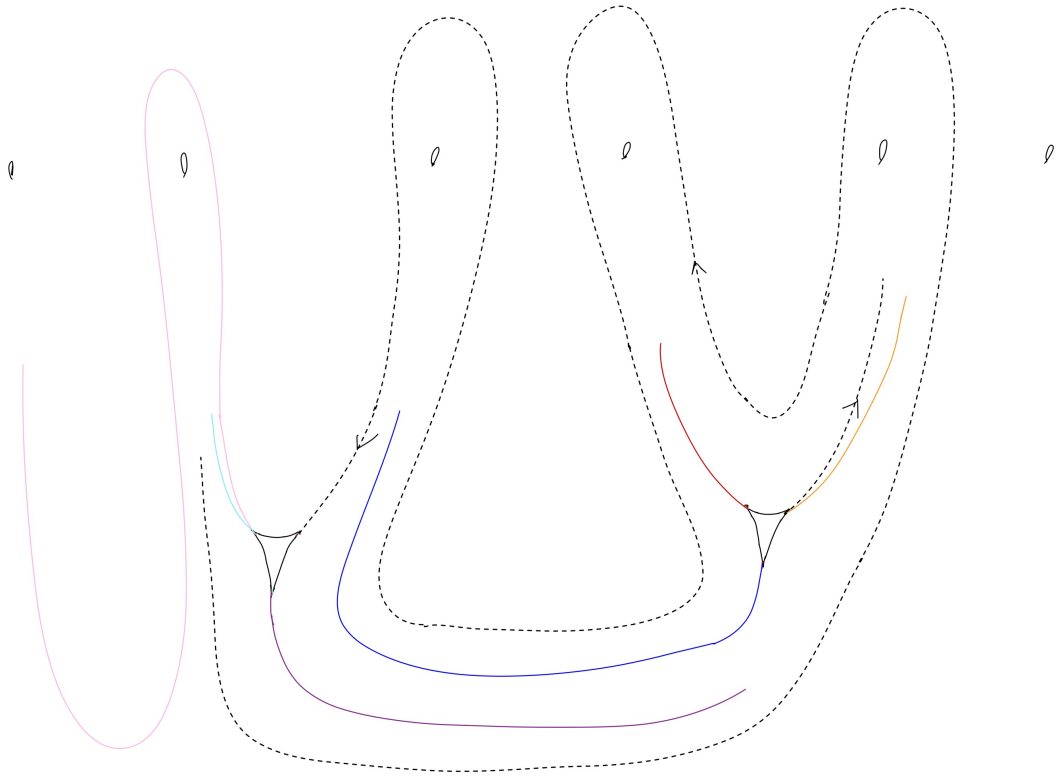


Figure E.178: Iwis1

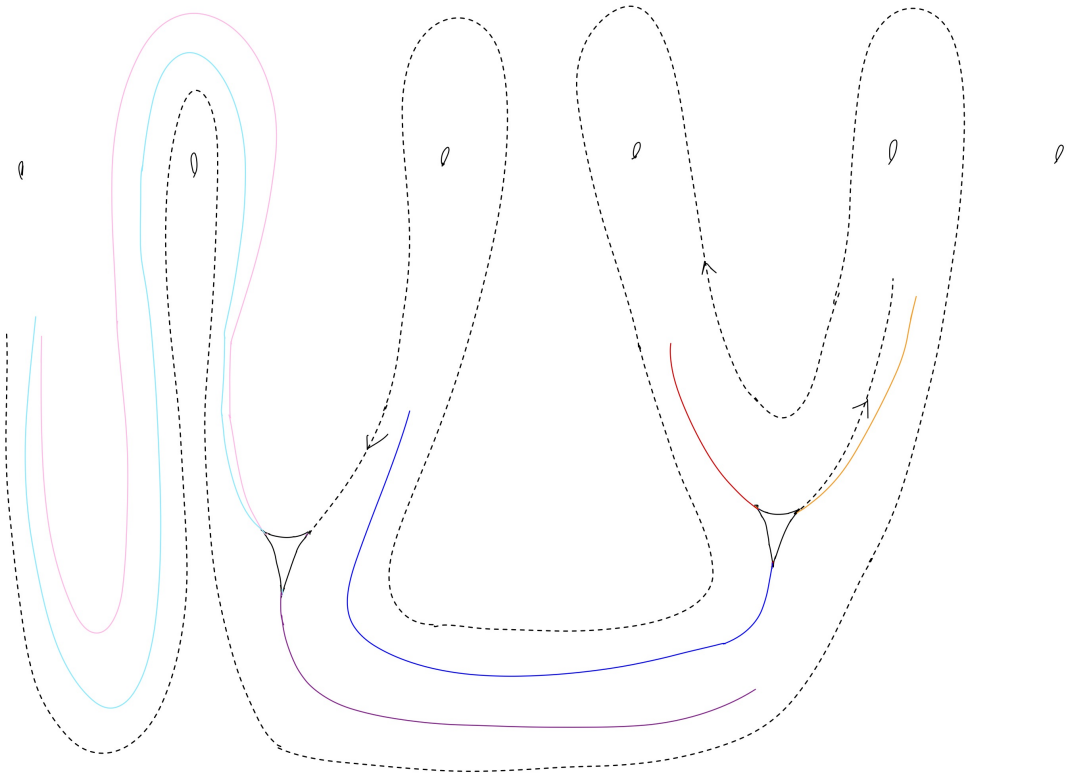


Figure E.179: Iwis2

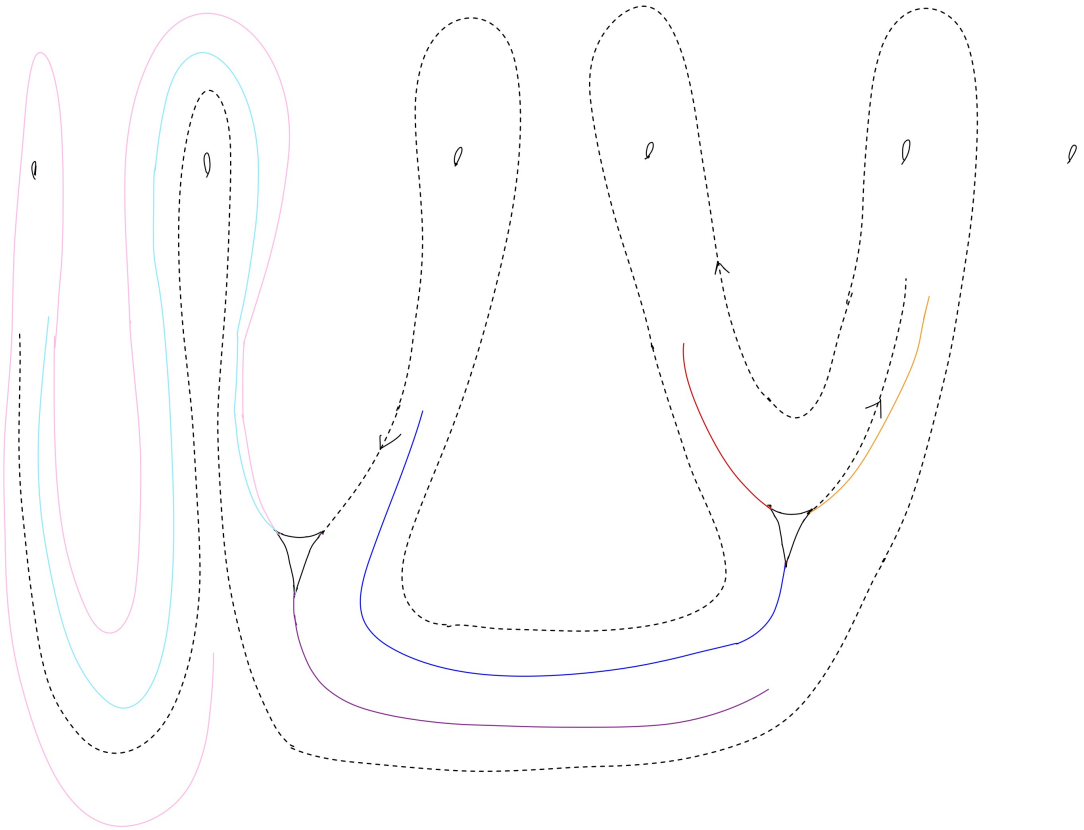


Figure E.180: Iwis3

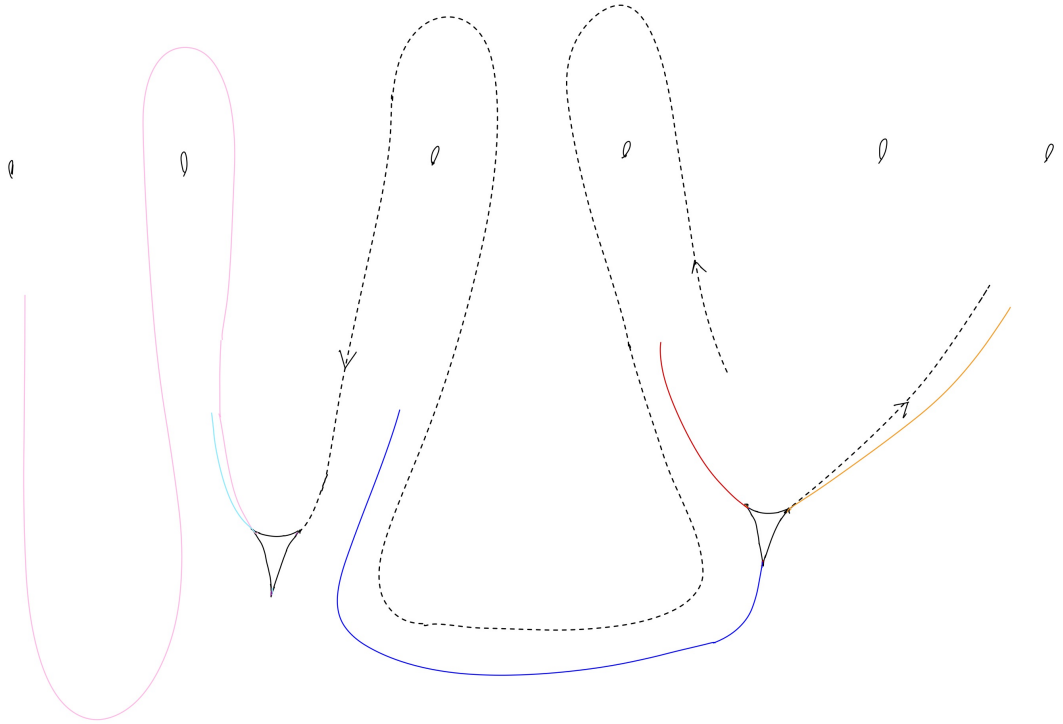


Figure E.181: QRO1

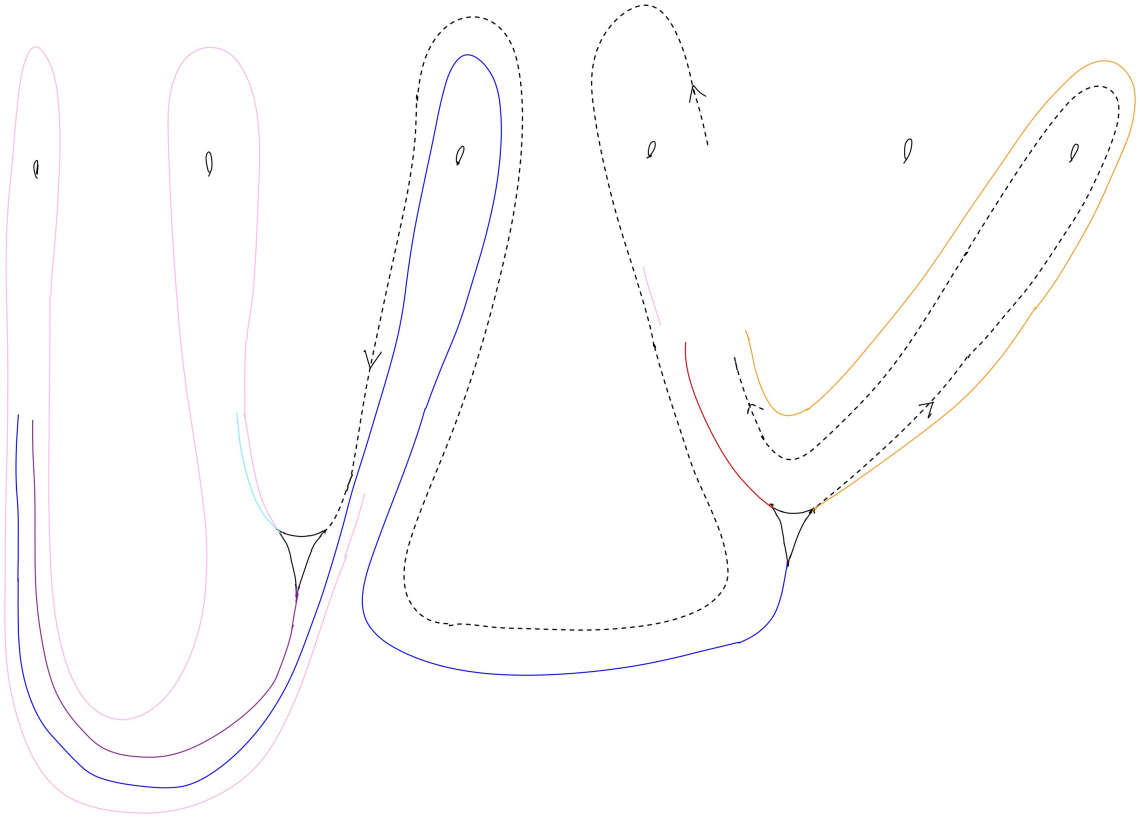


Figure E.182: Burl1

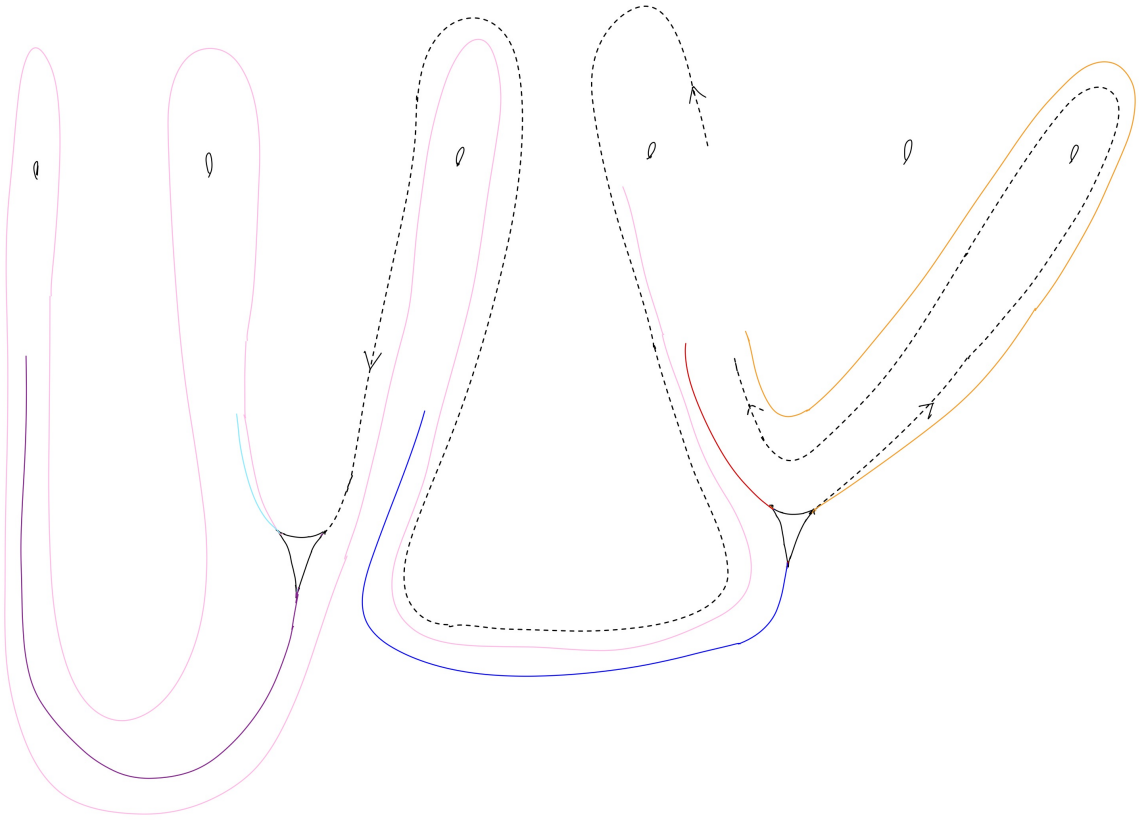


Figure E.183: Burl2

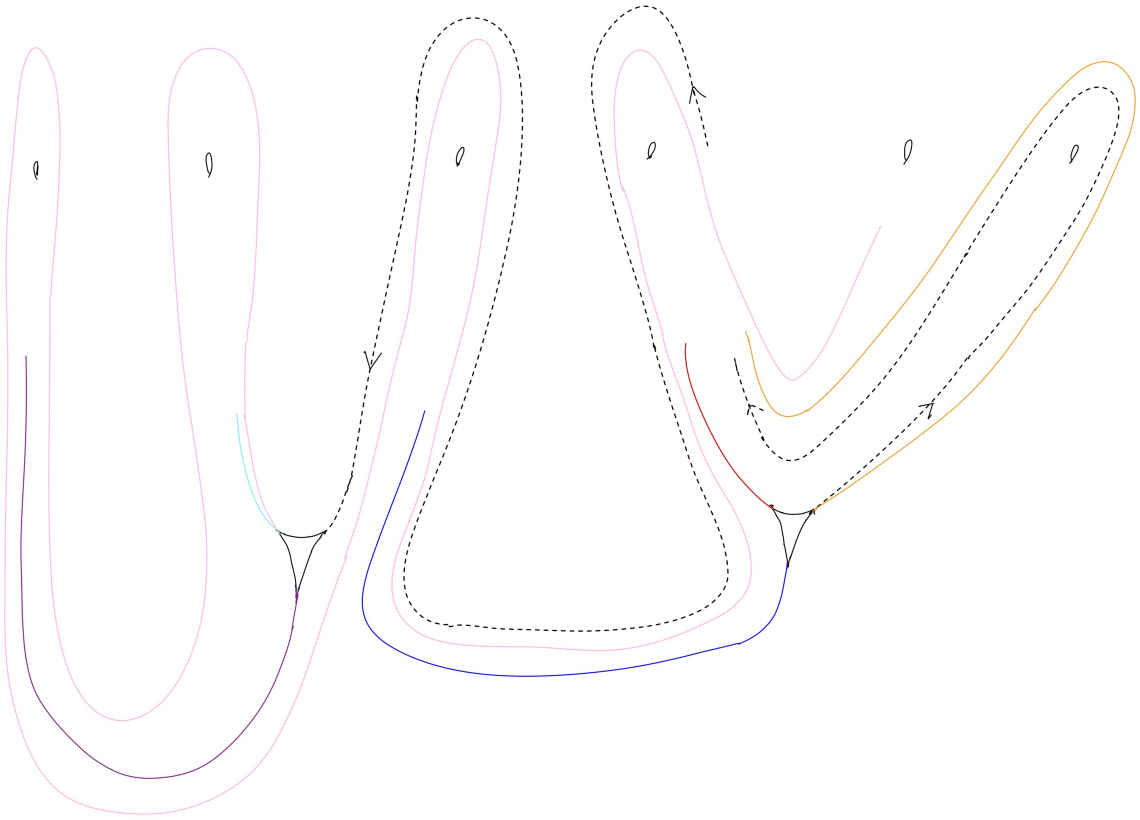


Figure E.184: Burl3

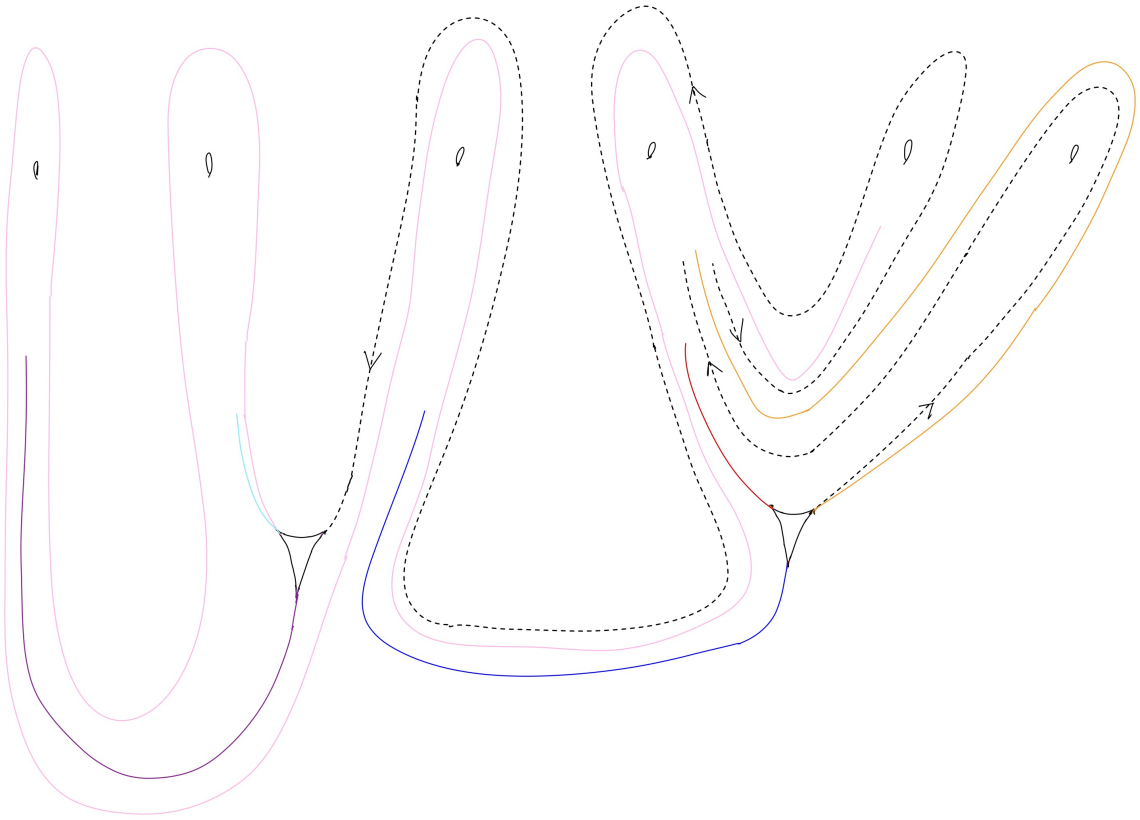


Figure E.185: Burl4

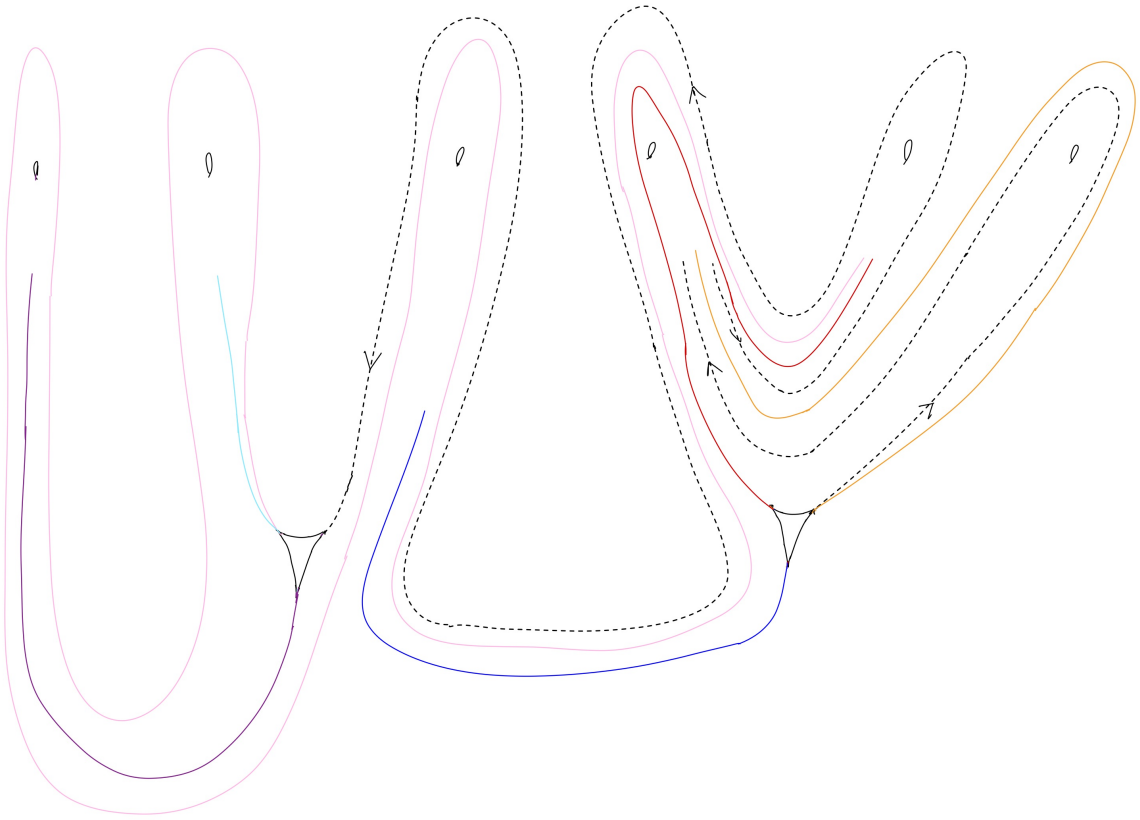


Figure E.186: Burl5

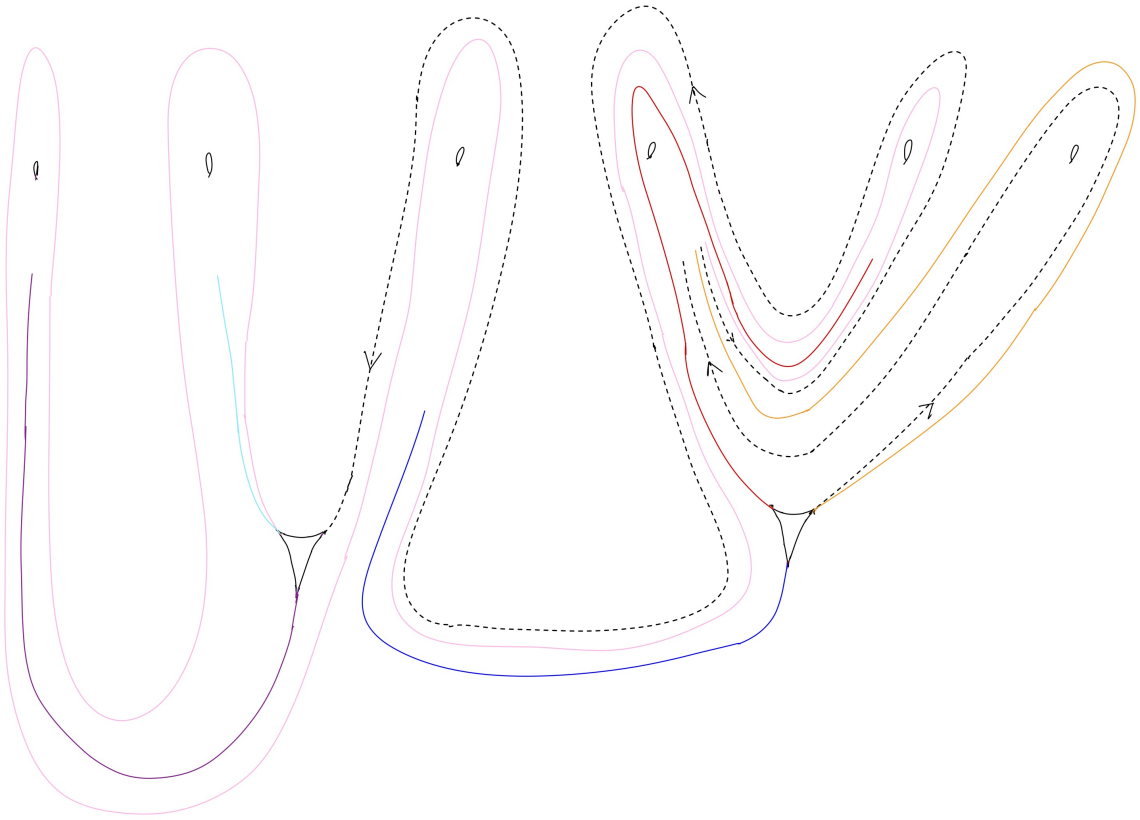


Figure E.187: Burl6

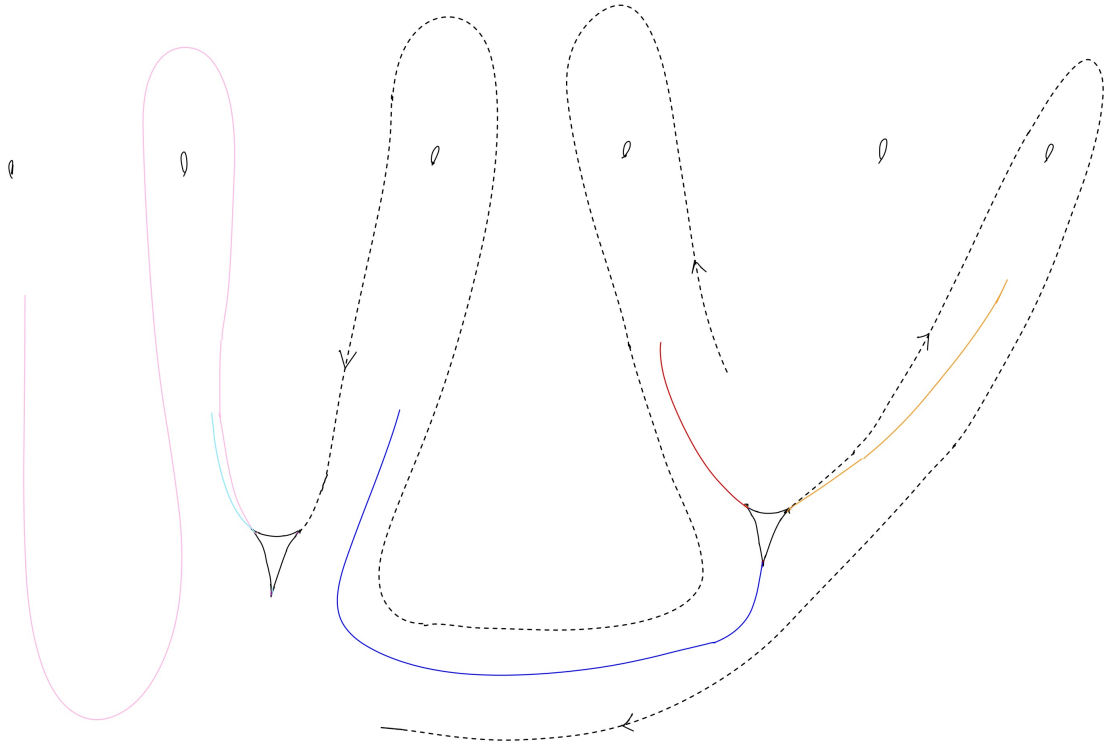


Figure E.188: Kyat1

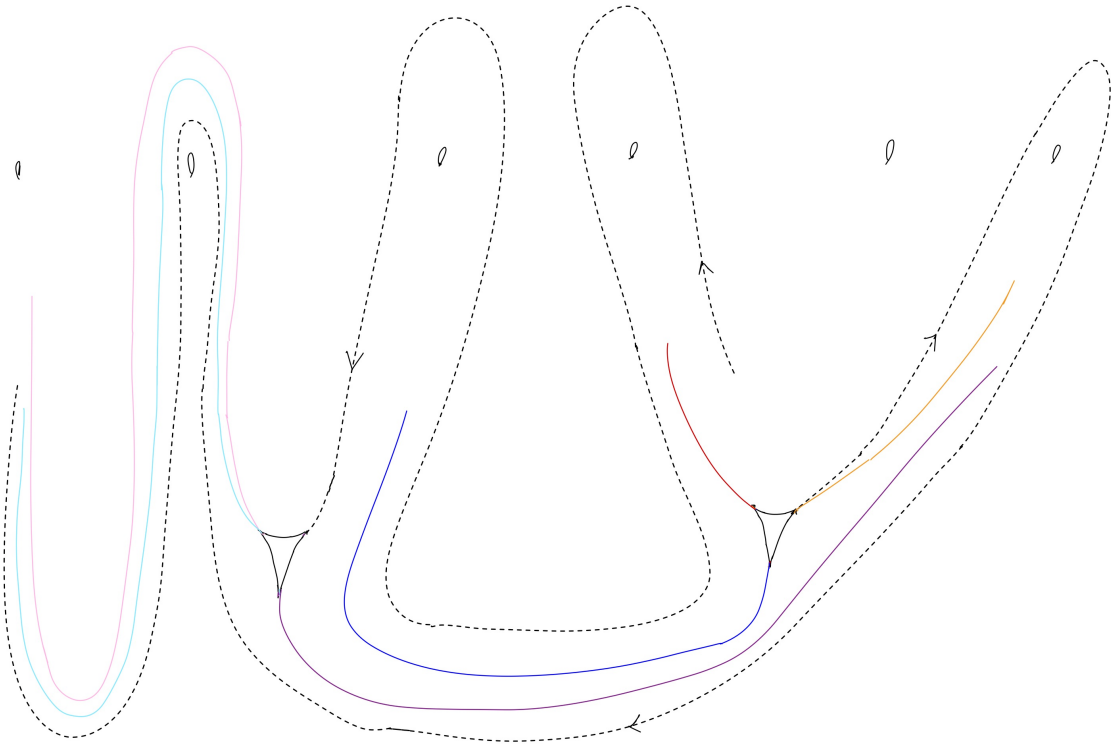


Figure E.189: Kyat2

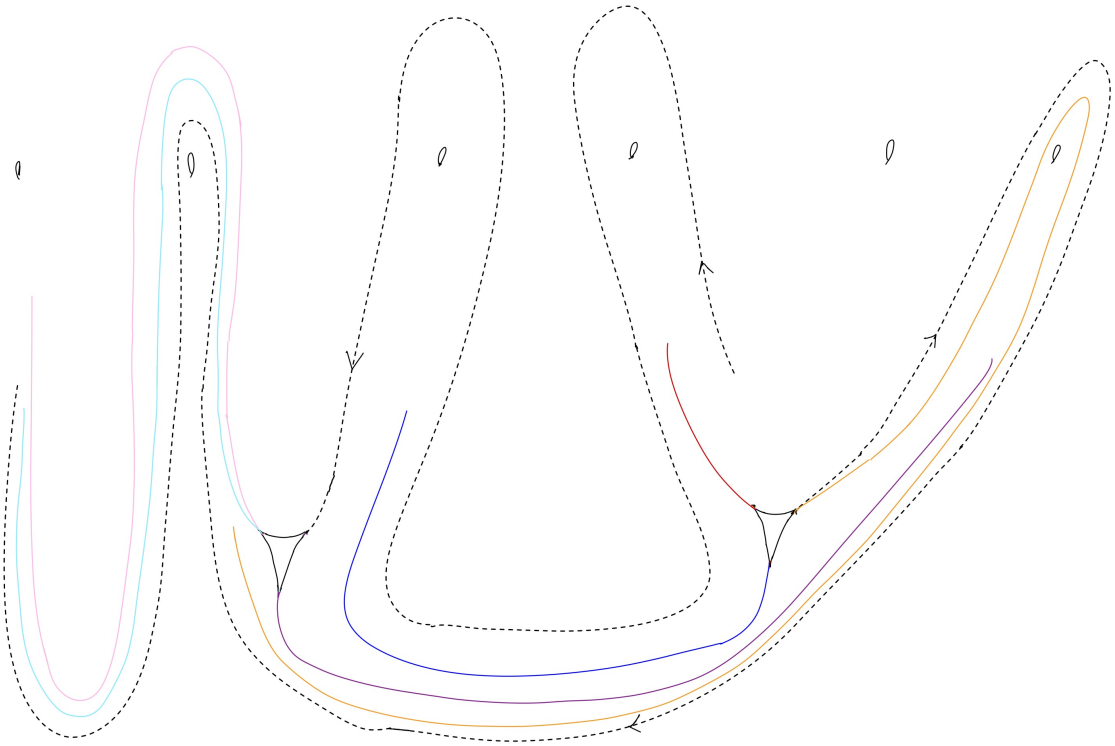


Figure E.190: Kyat3

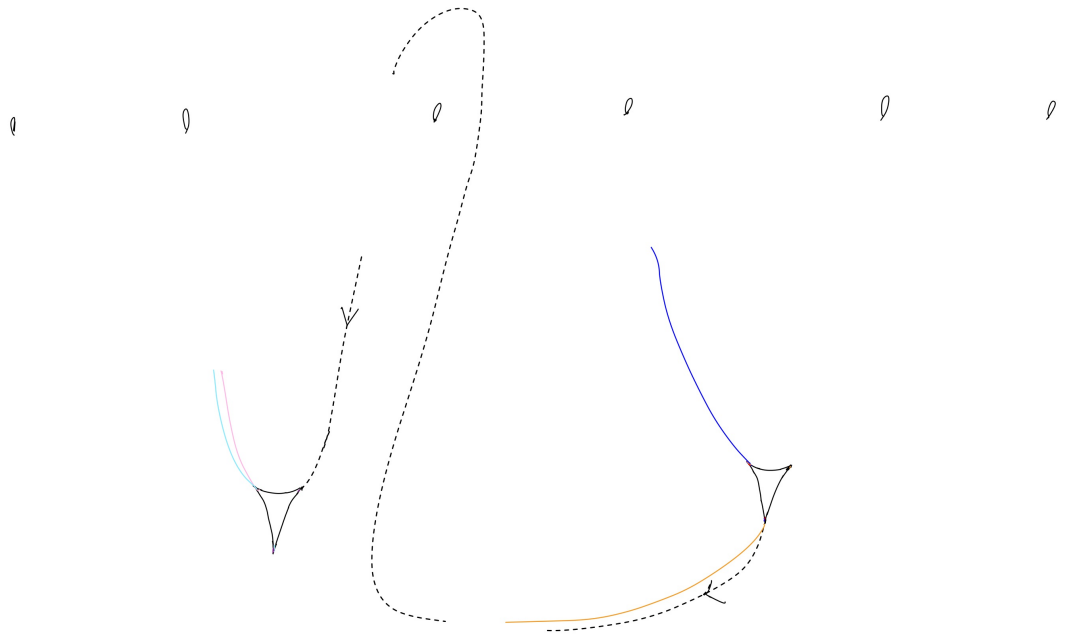


Figure E.191: WVB1

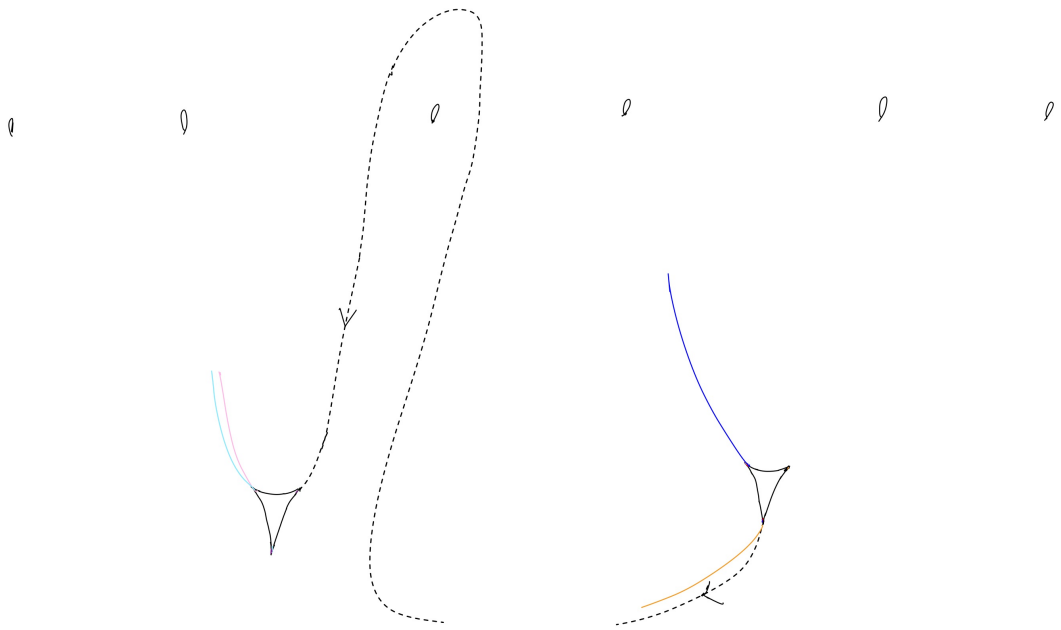


Figure E.192: Nard1

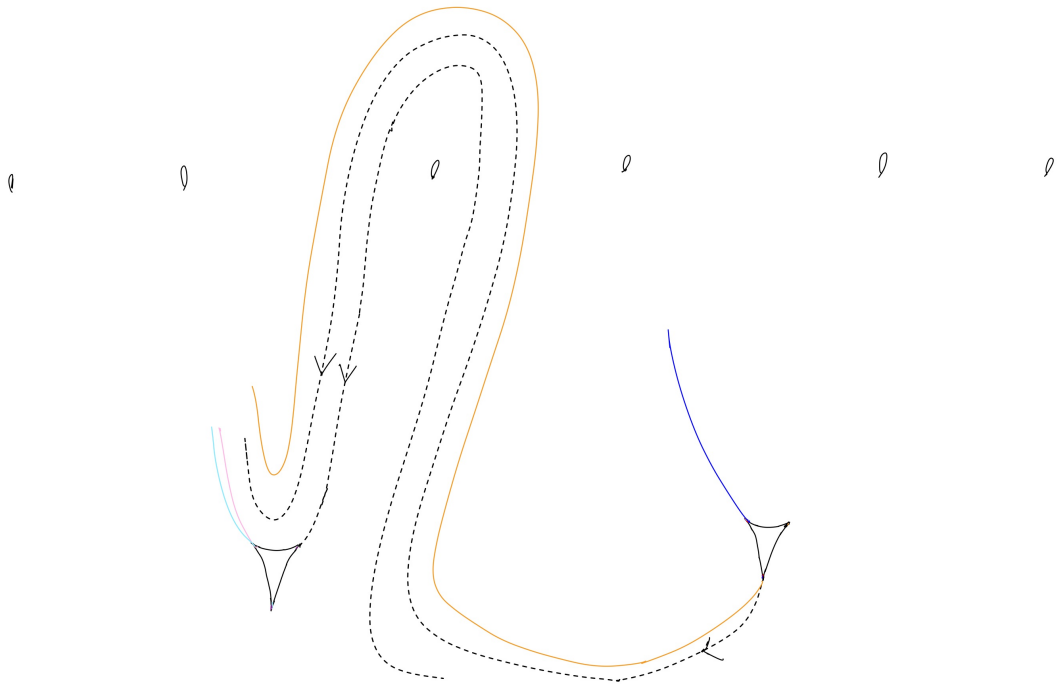


Figure E.193: Nard2

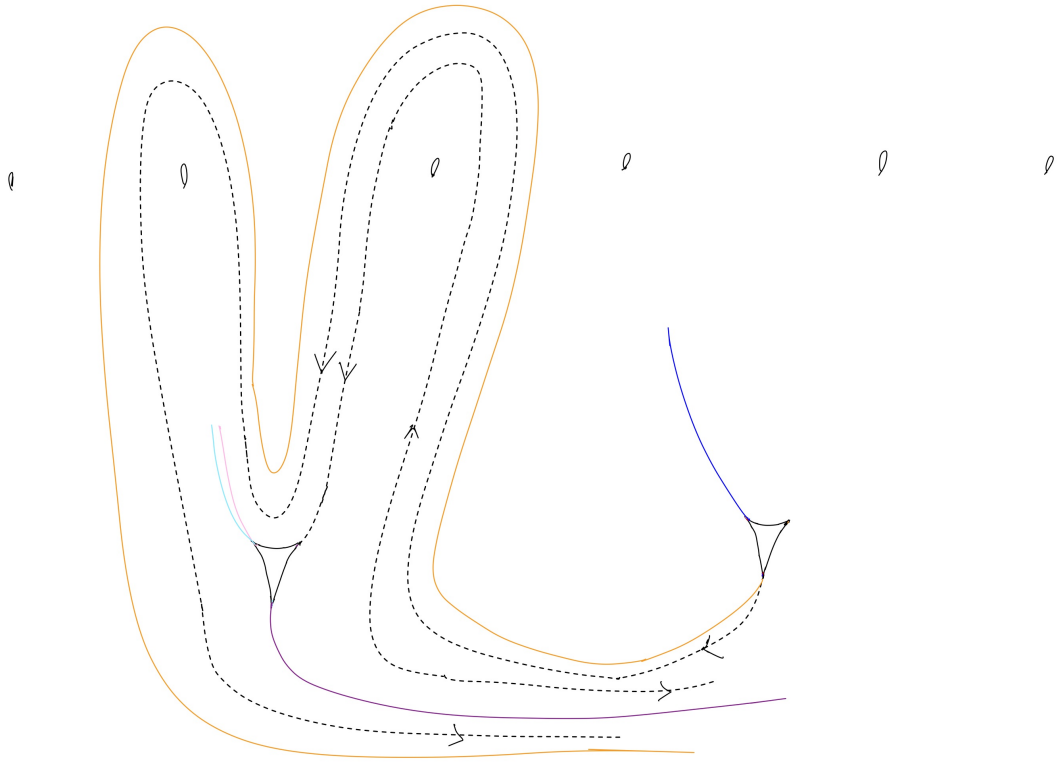


Figure E.194: Nard3

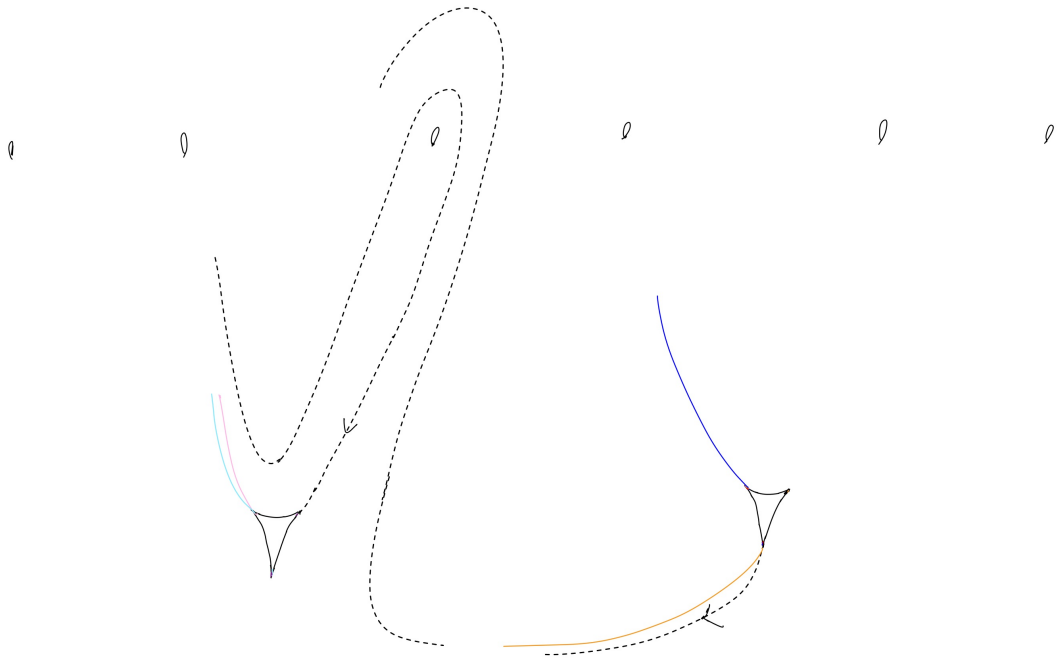


Figure E.195: Drek1

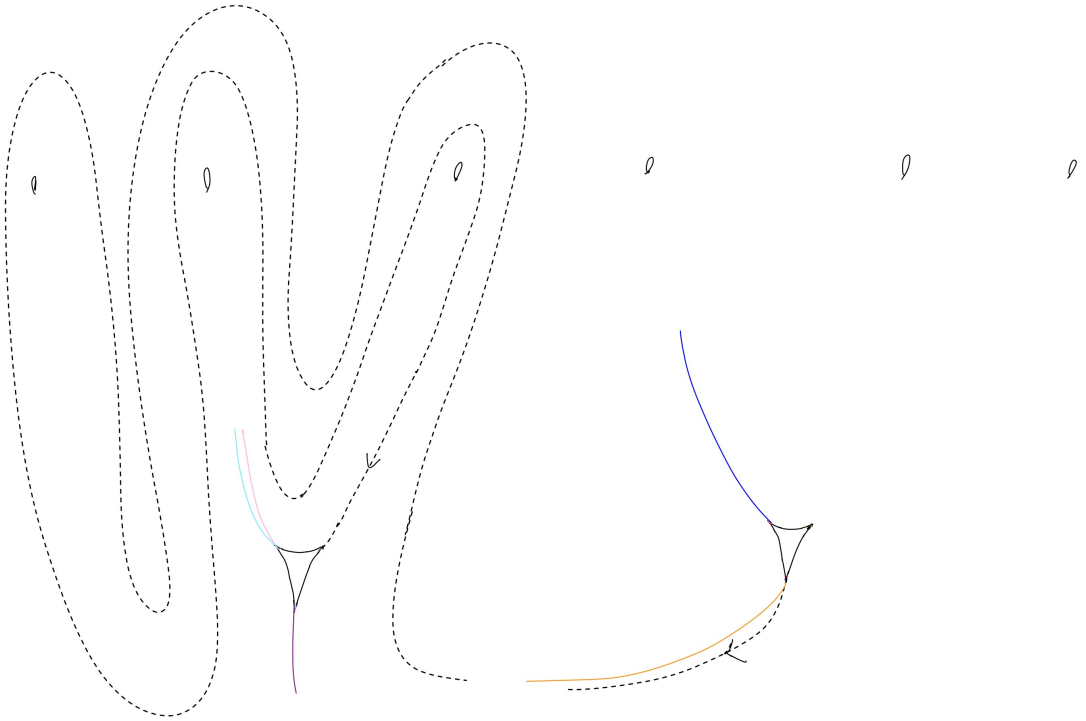


Figure E.196: Drek2

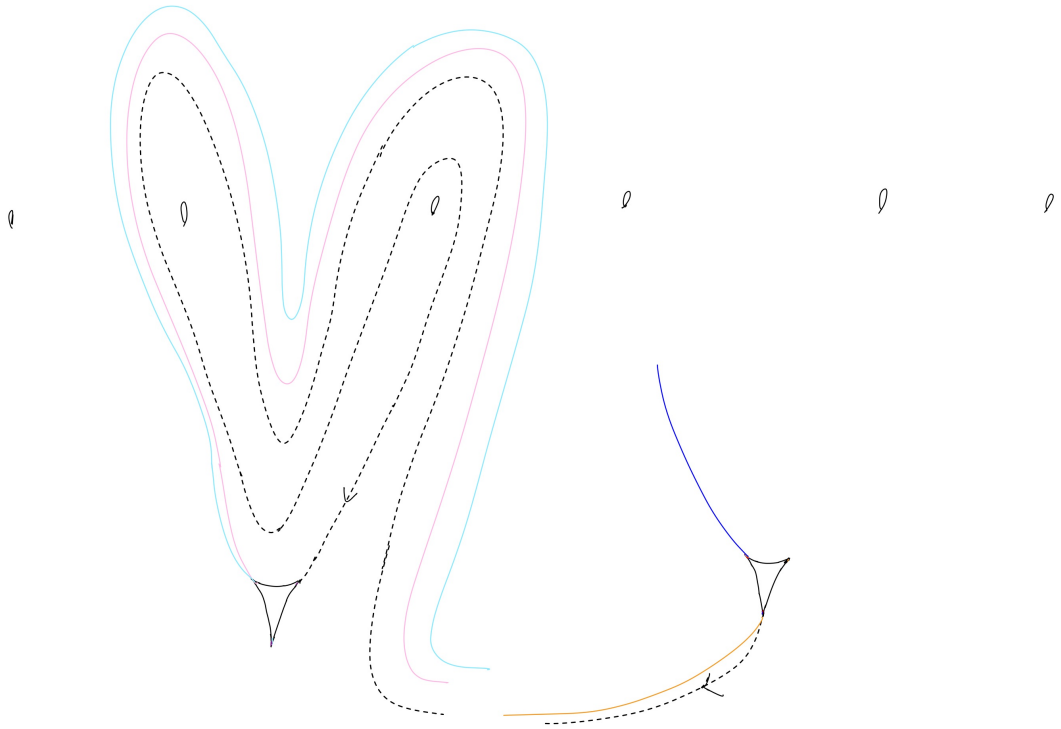


Figure E.197: Drek3

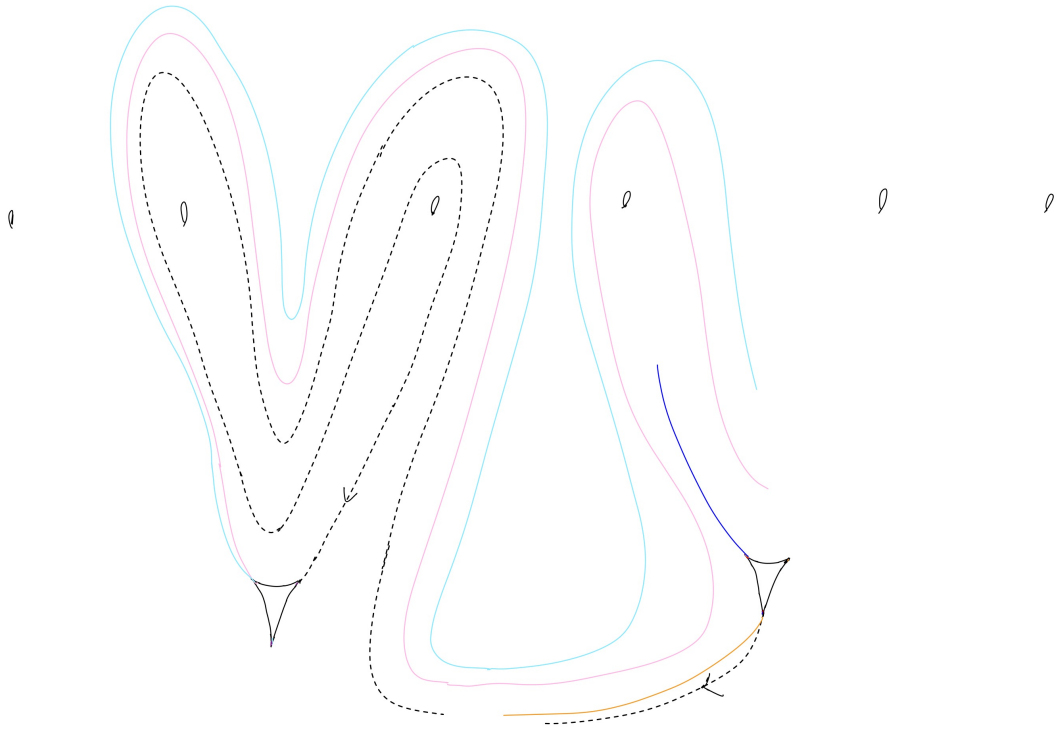


Figure E.198: Drek4

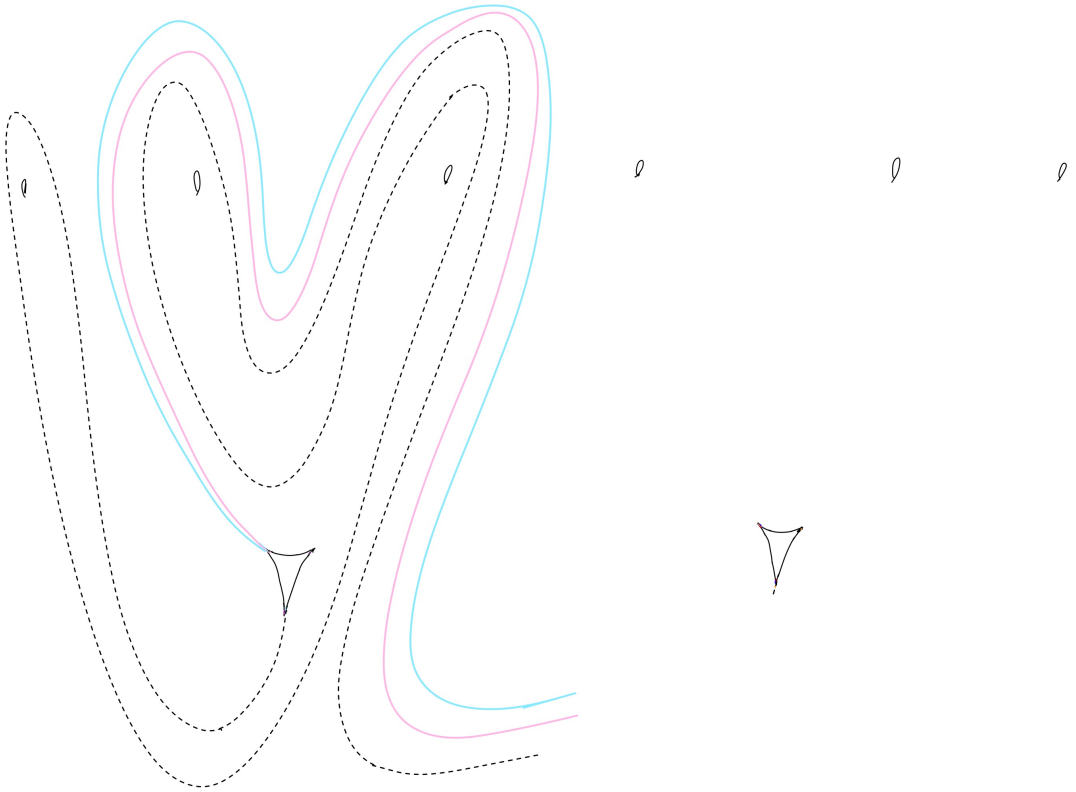


Figure E.199: ZFB1

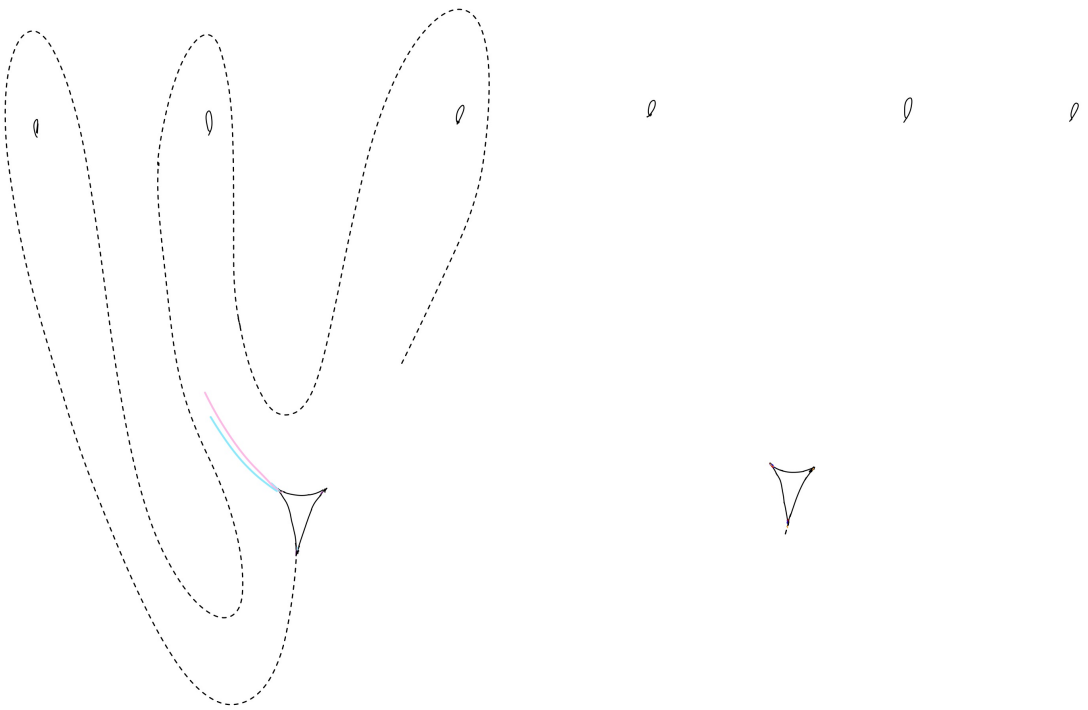


Figure E.200: ZFB2

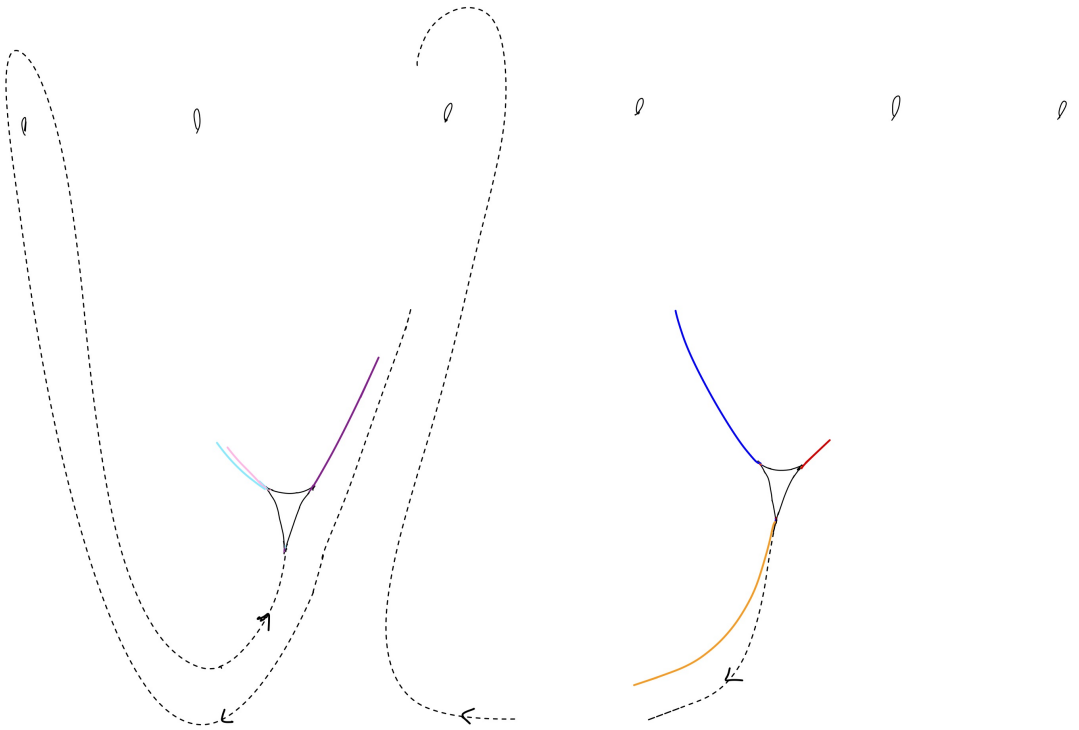


Figure E.201: ZFB3

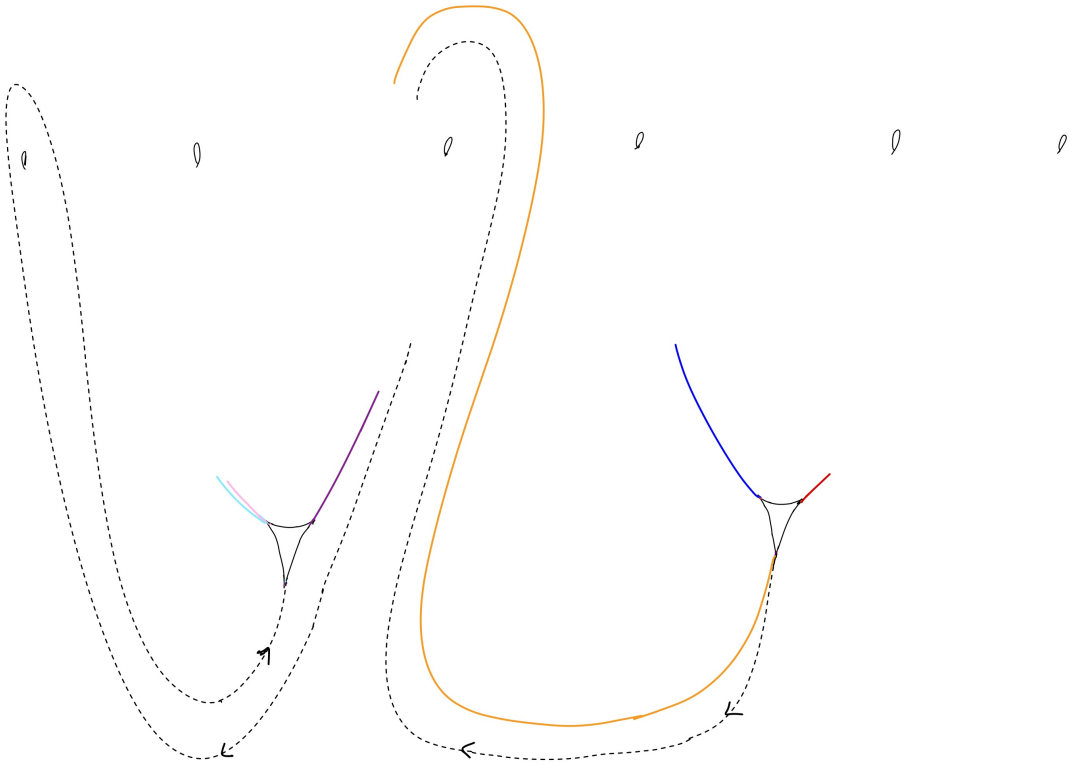


Figure E.202: Aery1

APPENDIX SIX

Train Track Case Analysis: Track 8

F.1 Case A: Triangles fixed

Let us assume the triangles are fixed by f_β, hence $f_\beta(d)$ and $f_\beta(\bar{d})$ both pass over d or $\bar{d}$ after an even number of letters. We will call this *Assumption A*.

F.1.1 YOW

Suppose $f_\beta(d)$ starts at r, and $f_\beta(\bar{d})$ starts at p. In this case, in order to not violate Assumption A, both $f_\beta(d)$ and $f_\beta(\bar{d})$ must not have any initial twists, and thus

$$f_\beta(d) = r^+ b^+ d...$$

and

$$f_\beta(\bar{d}) = p^- i^- \bar{d}...$$

This is Figure F.1.

Here the dotted lines must join. Indeed, if $f_\beta(\bar{d})$ on the right were to go below $f_\beta(d)$ on the

left, then it must be the case that $f_\beta(i)$ also must go below $f_\beta(d)$, otherwise we will be in Situation β. However, in this case $f_\beta(i)$ will necessarily trace:

$$f_\beta(i) = \bar{d}b^- r^- dp^- i^\times$$

On the other hand, if $f_\beta(\bar{d})$ on the right were to go above $f_\beta(d)$ on the left, then similarly $f_\beta(b)$ must also go below $f_\beta(\bar{d})$. Then in order for $f_\beta(b)$ to not trace, we must have

$$f_\beta(b) = di^+ s^* ...$$

which forces:

$$f_\beta(d) = r^+ b^+ di^+ s^* ...$$

But now $f_\beta(d)$ will violate the Trace Lemma (odd cross)

Hence the dotted lines must join.

This is Figure F.2.

here $f_\beta(b)$ must go below $f_\beta(i)$. Otherwise, $f_\beta(b)$ will eventually trace:

$$f_\beta(b) = dp^- i^- \bar{d}b^\times$$

Thus we have the situation depicted in Figure F.3.

Now $f_\beta(o)$ is forced to the following:

$$f_\beta(o) = r^+ b^+ di^+ s^* ...$$

This is Figure F.3.

Here $f_\beta(o)$ can continue with s^- or s°. It cannot continue with s^+, as that would force it be absorbed:

$$f_\beta(o) = r^+ b^+ di^+ \hat{s}^+ i^- \bar{d}b^- r^- \text{ Abso}(f_\beta(d), f_\beta(o))^\times$$

F.1.1.1 Bubo

Suppose $f_\beta(o)$ continues with s^-. thus we have

$$f_\beta(o) = r^+ b^+ di^+ \hat{s}^- i^- \bar{d}b^- r^- di^* ...$$

This is Figure F.4.

Here $f_\beta(p)$ cannot start with i^+, as it would immediately trace. Thus $f_\beta(p)$ either starts with i° or i^-.

F.1.1.1.1 Gnash

Suppose

$$f_\beta(p) = i^\circ$$

Then we have Figure F.5.

Here $f_\beta(b)$ must end at p°. Otherwise, it would trace:

$$f_\beta(b) = di^+ \hat{p}^+ i^- \bar{d}b^\times$$

or

$$f_\beta(b) = di^+ \hat{p}^+ i^- \bar{d}r^+ b^\times$$

or

$$f_\beta(b) = di^+\hat{p}^-i^-\bar{d}b^\times$$

Thus we must have

$$f_\beta(b) = di^+\hat{p}^\circ$$

This forces

$$f_\beta(o) = ...p^-i^-\bar{d}b^*...$$

This is Figure F.6.

Here $f_\beta(r)$ must end at b°. Otherwise, it would trace:

$$f_\beta(r) = b^-r^\times$$

or

$$f_\beta(r) = b^+di^+p^+i^-\bar{d}r^\times$$

Thus we must have

$$f_\beta(r) = b^\circ$$

This forces $f_\beta(o)$ to continue as shown in Figure F.7.

Now consider $f_\beta(s)$, we must have

$$f_\beta(s) = i^+p^-i^-\bar{d}b^-r^*...$$

This is Figure F.8.

Here $f_\beta(s)$ must continue with r^- and to the right of $f_\beta(o)$. Otherwise, $f_\beta(o)$ will be forced to continue with r^+ and to the left of $f_\beta(s)$, in which case it would eventually be absorbed:

$$f_\beta(o) = ...r^+b^+di^+p^+i^-\bar{d}r^+b^+di^+s^+i^-\bar{d}b^-r^- \text{ Abso}(f_\beta(d), f_\beta(o))^\times$$

Thus we must have

$$f_\beta(s) = i^+p^-i^-\bar{d}b^-r^-...$$

but now it will trace, as shown in Figure F.9.

This is a contradiction.

F.1.1.1.2 Inert

Back to the end of Bubo F.1.1.1. Suppose

$$f_\beta(p) = i^-...$$

Consider $f_\beta(i)$. It must end here at o°, otherwise it would trace:

$$f_\beta(i) = \bar{d}r^+b^+\hat{o}^+b^-r^-di^\times$$

or

$$f_\beta(i) = \bar{d}r^+b^+\hat{o}^-b^-r^-dp^-i^\times$$

Thus we must have

$$f_\beta(i) = \bar{d}r^+b^+\hat{o}^\circ$$

This is Figure F.10.

Here $f_\beta(p)$ cannot continue into the path marked with $\times$, as that would lead to it tracing:

$$f_\beta(p) = i^- \bar{d} r^+ b^+ o^- b^- r^- dp^\times$$

or

$$f_\beta(p) = i^- \bar{d} r^+ b^+ di^+ s^+ i^- \bar{d} b^- r^- \text{Abso}(f_\beta(d), f_\beta(o))^\times$$

Hence, in the situation depicted in Intert1, $f_\beta(p)$ must go into 1 or 2.

F.1.1.1.2.1 Callow

Suppose $f_\beta(p)$ goes into 1.

This is Figure F.11.

But now notice that $f_\beta(s)$ must continue with i^- and to the right of the incoming $f_\beta(o)$ to prevent $f_\beta(o)$ from being absorbed. But now $f_\beta(s)$ will trace:

$$f_\beta(s) = i^- \bar{d} r^+ b^+ di^+ s^\times$$

This is a contradiction.

F.1.1.1.2.2 Ennui

Back to the end of Inert F.1.1.1.2. Suppose $f_\beta(p)$ goes into 2.

This is Figure F.12.

Here consider $f_\beta(s)$. It must begin with i^- and to the right of $f_\beta(b)$, otherwise both $f_\beta(b)$ and $f_\beta(o)$ will be absorbed between $f_\beta(p)$ and $f_\beta(s)$.

Thus we must have Figure F.13.

Here $f_\beta(b)$ is forced to end at i°, as either i^+ or i^- would cause it to trace immediately after crossing $\bar{d}$. Thus we have

$$f_\beta(b) = di^\circ$$

This is Figure F.14.

Consider $f_\beta(p)$. It cannot continue with b^+, then it would trace immediately after crossing d. So it must either end at b° or continue with b^-.

F.1.1.1.2.2.1 Brumous

Suppose it ends at b°, so we have

$$f_\beta(p) = i^-\bar{d}b^\circ$$

This is Figure F.15.

This forces $f_\beta(s)$, $f_\beta(o)$, and $f_\beta(r)$ to continue with b^+.

This is Figure F.16.

Here $f_\beta(r)$ must end at p°. Indeed, if it continued with i^- then it would trace:

$$f_\beta(r) = b^+di^+\hat{p}^-i^-\bar{d}b^-r^\times$$

While if it continued with p^+ it either gets absorbed, if it goes to the left of $f_\beta(s)$:

$$f_\beta(r) = b^+di^+\hat{p}^+i^-\bar{d}b^-di^+\,\mathrm{Abso}(f_\beta(p), f_\beta(i))^\times$$

or trace:

$$f_\beta(r) = b^+di^+\hat{p}^+i^-\bar{d}b^-di^+\bar{d}r^\times$$

Thus we must have

$$f_\beta(r) = b^+ di^+ \hat{p}^\circ$$

This gives us Figure F.17.

Here $f_\beta(s)$ cannot continue with r° or r^+, since in that case $f_\beta(o)$ will be forced to continue with r^+. But then it will be absorbed:

$$f_\beta(o) = ...r^+ b^+ di^+ p^+ i^- \bar{d} b^- di^+ \text{ Abso}(f_\beta(p), f_\beta(s))^\times$$

Hence $f_\beta(s)$ must continue with r^- and to the right of $f_\beta(o)$. But now it will trace:

$$f_\beta(s) = ...r^- b^+ di^+ p^+ i^- \bar{d} b^- di^+ \bar{d} r^+ b^+ di^+ s^\times$$

This is a contradiction.

F.1.1.1.2.2.2 Coterie

Back to the end of Ennui F.1.1.1.2.2. Suppose

$$f_\beta(p) = i^- \bar{d} \hat{b}^- ...$$

Here $f_\beta(p)$ must continue with b^- and to the right of $f_\beta(r)$, which forces $f_\beta(r)$ to end at b°:

$$f_\beta(r) = b^\circ$$

which in tuen forces $f_\beta(p)$ to end as well:

$$f_\beta(p) = i^- \bar{d} b^- \hat{r}^\circ$$

This is Figure F.18.

Now $f_\beta(s)$ and $f_\beta(o)$ continue to give Figure F.19.

Here $f_\beta(o)$ cannot continue with p° or p^-, as that would force $f_\beta(s)$ to continue with p^- and to the right of $f_\beta(o)$, in which case it will trace:

$$f_\beta(s) = ...p^- i^- \bar{d} b^- r^- b^+ d i^+ \bar{d} r^+ b^+ d i^+ s^\times$$

Hence $f_\beta(o)$ must continue with p^+ and to the left of $f_\beta(s)$, but then it will be absorbed:

$$f_\beta(s) = ...p^+ i^- \bar{d} b^- r^- b^+ d i^+ \operatorname{Abso}(f_\beta(p), f_\beta(s))^\times$$

This is a contradiction.

F.1.1.2 Gurn

Back to the end of YOW F.1.1. Suppose $f_\beta(o)$ ends at s°:

$$f_\beta(o) = r^+ b^+ d i^+ s^\circ$$

This is Figure F.20.

Here $f_\beta(p)$ can begin and end at i°, or it can continue with i^-.

F.1.1.2.1 Anomy

Suppose

$$f_\beta(p) = i^\circ$$

This is Figure F.21.

Here $f_\beta(b)$ must end at p°, or it will trace:

$$f_\beta(b) = si^+\hat{p}^+i^-\bar{d}r^+b^\times$$

or

$$f_\beta(b) = si^+\hat{p}^-i^-\bar{d}b^\times$$

Thus we must have

$$f_\beta(b) = si^+\hat{p}^\circ$$

This is Figure F.22.

Here $f_\beta(r)$ must begin and end at b°:

$$f_\beta(r) = b^\circ$$

Indeed, if it were to begin with b^- it would immediately trace; if it were to begin with b^+ it would either be absorbed, if it goes to the left of $f_\beta(s)$:

$$f_\beta(r) = b^+di^+p^+i^- \operatorname{Abso}(f_\beta(p), f_\beta(s))^\times$$

or trace, if it goes to the right of $f_\beta(s)$:

$$f_\beta(r) = b^+di^+p^+i^-\bar{d}r^\times$$

This gives us Figure F.23.

Consider $f_\beta(i)$. It must end here at o°. Indeed, otherwise it would trace:

$$f_\beta(i) = \bar{d}r^+b^+\hat{o}^-b^-r^-dp^-i^\times$$

or

$$f_\beta(i) = \bar{d}r^+b^+\hat{o}^+b^-r^-di^\times$$

Thus we must have

$$f_\beta(i) = \bar{d}r^+b^+\hat{o}^\circ$$

Now consider $f_\beta(s)$. It must end here at r°. Indeed, otherwise it would be absorbed:

$$f_\beta(s) = ...r^+b^+di^+p^+i^- \text{ Abso}(f_\beta(p), f_\beta(s))^\times$$

or

$$f_\beta(s) = ...r^-b^+di^+p^+i^-\bar{d}r^+b^+o^-b^-r^-dp^-i^-\bar{d}b^-r^- \text{ Abso}(f_\beta(d), f_\beta(o))^\times$$

This gives us Candidate 1, shown in Figure F.24.

F.1.1.2.2 Bruit

Back to the end of Gurn F.1.1.2. Suppose $f_\beta(p)$ continues with i^-. Again $f_\beta(i)$ must end here at o° or it will trace.

This is Figure F.25.

Here $f_\beta(p)$ must go to the right of $f_\beta(b)$. Indeed, if it were to go into the left of $f_\beta(b)$, it would either trace:

$$f_\beta(p) = i^-\bar{d}r^+b^+o^-b^-r^-dp^\times$$

or be absorbed:

$$f_\beta(p) = i^- \bar{d} r^+ b^+ d i^+ s^+ i^- \bar{d} b^- r^- \operatorname{Abso}(f_\beta(d), f_\beta(o))^\times$$

Thus we must have the situation depicted in Figure F.26.

Here $f_\beta(b)$ must end at i°. Otherwise, it would trace:

$$f_\beta(b) = i^+ \bar{d} r^+ b^\times$$

or

$$f_\beta(b) = i^- \bar{d} b^\times$$

Thus we must have

$$f_\beta(b) = i^\circ$$

Here $f_\beta(r)$ can begin and end with b°, or begin with b^+.

F.1.1.2.2.1 Diatree

Suppose

$$f_\beta(r) = b^\circ$$

This is Figure F.27.

Here $f_\beta(p)$ must end at r°. Indeed, otherwise it would either trace:

$$f_\beta(p) i^- \bar{d} b^- \hat{r}^+ b^+ d i^+ p^\times$$

or absorbed:

$$f_\beta(p)i^-\bar{d}b^-\hat{r}^-b^+di^+\bar{d}r^+b^+di^+s^+i^-\bar{d}b^-r^-\,\mathrm{Abso}(f_\beta(d),f_\beta(i))^\times$$

or

$$f_\beta(p)i^-\bar{d}b^-\hat{r}^-b^+di^+\,\mathrm{Abso}(f_\beta(p),f_\beta(s))^\times$$

Thus we must have

$$f_\beta(p)i^-\bar{d}b^-\hat{r}^\circ$$

This is Figure F.28.

Here $f_\beta(s)$ must end at p°. Indeed, if it were to continue with p^+, it will be absorbed:

$$f_\beta(s)=...p^+i^-dbarb^-r^-b^+di^+\,\mathrm{Abso}(f_\beta(p),f_\beta(s))^\times$$

While if it were t continue with p^-, it is either traces:

$$f_\beta(s)=...p^-i^-\bar{d}b^-r^-b^+di^+\bar{d}r^+b^+di^+s^\times$$

or is absorbed:

$$f_\beta(s)=...p^-i^-r^-b^+r^-di^+\bar{d}r^+b^+o^-b^-r^-dp^-i^-\bar{d}b^-r^-\,\mathrm{Abso}(f_\beta(s),f_\beta(o))^\times$$

Thus we must have Figure F.29, which is Candidate 2.

F.1.1.2.2.2 Fulmine

Back to the end of Bruit F.1.1.2.2. Suppose $f_\beta(r)$ begins with b^+. Then it must do so to the left of $f_\beta(p)$. Otherwise, it is either absorbed:

$$f_\beta(r) = b^+ di^+ \operatorname{Abso}(f_\beta(p), f_\beta(s))^\times$$

or trace:

$$f_\beta(r) = di^+ \bar{d}r^\times$$

Thus we must have the situation depicted in Figure F.30.

Here $f_\beta(p)$ must end at b°. Indeed, if it continued with b^+, then it would trace:

$$f_\beta(p) = i^- \bar{\hat{d}} b^+ di^+ p^\times$$

While if it continued with b^-, it either is absorbed, if to the left of $f_\beta(s)$:

$$f_\beta(p) = i^- \bar{\hat{d}} b^- di^+ \operatorname{Abso}(f_\beta(p), f_\beta(s))^\times$$

or if to the right of $f_\beta(s)$, either it traces:

$$f_\beta(p) = i^- \bar{\hat{d}} b^- di^+ \bar{d}r^+ b^+ o^- b^- r^- dp^\times$$

or absorbed:

$$f_\beta(p) = i^- \bar{\hat{d}} b^- di^+ \bar{d}r^+ b^+ di^+ s^+ i^- \bar{d} b^- r^- \operatorname{Abso}(f_\beta(d), f_\beta(o))^\times$$

Thus we must have

$$f_\beta(p) = i^- \bar{d}\hat{b}^\circ$$

This gives Figure F.31.

Here $f_\beta(r)$ must end at p°. Indeed, if it were to continue with p^-, it would trace:

$$f_\beta(r) = b^+ di^+ \hat{p}^- i^- \bar{d} b^- r^\times$$

While if it were to continue with p^+, if to the left of $f_\beta(s)$, it would be absorbed:

$$f_\beta(r) = b^+ di^+ \hat{p}^+ i^- \bar{d} b^- di^+ \,\mathrm{Abso}(f_\beta(p), f_\beta(s))^\times$$

and if to the right of $f_\beta(s)$, it would trace:

$$f_\beta(r) = b^+ di^+ \hat{p}^+ i^- \bar{d} b^- di^+ \bar{d} r^\times$$

Thus we must have

$$f_\beta(r) = b^+ di^+ \hat{p}^\circ$$

This is Figure F.32.

Here $f_\beta(s)$ must end at r°. Indeed, if it were to continue with r^+, it would be absorbed:

$$f_\beta(s) = ...r^+ b^+ di^+ p^+ i^- \bar{d} b 6 - di^+ \,\mathrm{Abso}(f_\beta(p), f_\beta(s))^\times$$

While if it were to continue with r^-, it would either trace:

$$f_\beta(s) = ...r^- b^+ di^+ p^+ i^- \bar{d} b^- di^+ \bar{d} r^+ b^+ di^+ s^\times$$

or be absorbed:

$$f_\beta(s) = ...r^- b^+ d i^+ p^+ i^- \bar{d} b^- d i^+ \bar{d} r^+ b^+ o^- b^- r^- d p^- i^- \bar{d} b^- r^- \text{ Abso}(f_\beta(d), f_\beta(o))^\times$$

Thus we have Candidate 3, shown in Figure F.33.

F.1.2 BRR

Back to the end of Case A: Triangles fixed F.1. Suppose $f_\beta(d)$ starts at r, $f_\beta(\bar{d})$ starts at s. We remind the reader we are still holding Assumption A.

This is Figure F.34.

Here the same reasoning as that of YOW F.1.1 necessitates that the dotted lines must join. Here $f_\beta(b)$ can either go above $f_\beta(i)$, or belwo $f_\beta(i)$.

Suppose it went above $f_\beta(i)$. Then we must have

$$f_\beta(b) = dp^\circ$$

Otherwise, it would trace if it continued with either p^-, p^+, or s^-.

This is Figure F.35.

Here $f_\beta(p)$ must begin with i^- and to the right of $f_\beta(s)$, otherwise $f_\beta(s)$ would be forced to begin with i^+ and thus immediately trace.

This is Figure F.36.

Here $f_\beta(r)$ can either begin and end at b°, or begin with b^+.

F.1.2.1 Agog

Suppose

$$f_\beta(r) = b^\circ$$

This is Figure F.37.

Here $f_\beta(p)$ cannot continue with r° or r^+, otherwise $f_\beta(i)$ will be forced to continue with r^+ and to the left of $f_\beta(p)$, which would force it to trace:

$$f_\beta(i) = \bar{d}b^-\hat{r}^+b^+di^\times$$

Thus we must have

$$f_\beta(p) = i^-\bar{d}b^-\hat{r}^-...$$

It cannot continue into the right of $f_\beta(o)$, or it will trace after crossing; neither can it go in between $f_\beta(i)$ and $f_\beta(o)$ for the same reason. But then it can only go into the left of $f_\beta(i)$, but then $f_\beta(i)$ would still trace.

This is a contradiction.

F.1.2.2 Dory

Back to the end of BRR F.1.2. Suppose $f_\beta(r)$ continues with r^+.

This is Figure F.38.

Here $f_\beta(r)$ can go into 1,2,3, or 4.

If it were to go into 4 then we are in the same situation as Agog F.1.2.1, which leads to a contradiction. If it were to go into 3 then it would immediately trace after crossing d, as is

the case if it were to go into 1. So suppose it goes into 2.

This is Figure F.39.

Here $f_\beta(s)$ is forced to begin with i^- and to the right of the incoming $f_\beta(r)$.

Then the situation depicted in Figure F.40 is forced.

Here $f_\beta(p)$ is forced to continue with r^- and to the right of $f_\beta(s)$, otherwise $f_\beta(s)$ will be forced to continue with r^+ and to the left of $f_\beta(p)$, in which case it would be absorbed:

$$f_\beta(s) = ...r^+b^+di^+ \,\mathrm{Abso}(f_\beta(p), f_\beta(s))^\times$$

Thus we have Figure F.41.

Here $f_\beta(p)$ must continue with i^+ and to the left of $f_\beta(r)$. Otherwise, $f_\beta(r)$ would be forced to continue with i^- and to the right of $f_\beta(p)$, in which case it would trace:

$$f_\beta(r) = b^+di^- \,\hat{}\, \hat{b}^-\not{m}^\times$$

Thus we have Figure F.42.

Here $f_\beta(o)$ must continue with b^+ and to the left of $f_\beta(p)$. Otherwise, $f_\beta(p)$ would be forced to continue with b^- and to the right of $f_\beta(o)$, in which case it would trace immediately after crossing.

Thus we have Figure F.43.

Now $f_\beta(p)$ must continue with b^- and to the right of $f_\beta(i)$. Otherwise, $f_\beta(i)$ would be forced to continue with b^+ and to the left of $f_\beta(p)$, in which case it would trace immediately after crossing. But now if $f_\beta(p)$ continued with b^-, it would also trace immediately after crossing.

This is a contradiction.

F.1.3 Mien

Back to the situation depicted in Figure F.34. We now assume $f_\beta(b)$ goes below $f_\beta(i)$.

But now $f_\beta(o)$ will trace, as shown in Figure F.44.

F.1.4 NUK

Back to the end of Case A: Triangles fixed F.1. Suppose $f_\beta(d)$ starts at r, $f_\beta(\bar{d})$ starts at i.

The situation is depicted in Figure F.45.

Here $f_\beta(o)$ must go below $f_\beta(p)$. Otherwise, we would have

$$f_\beta(s) = \bar{d}b^- r^- d...$$

and

$$f_\beta(p) = \bar{d}b^- r^- d...$$

in which case at least one of these will trace.

This is Figure F.46.

Here $f_\beta(\bar{d})$ must come down on p before crossing $\bar{d}$ in order to adhere to Assumption A (possibly after some number of twisting with s).

After crossing, it must go above $f_\beta(b)$ otherwise it would be in Situation β (the bagged serpent). But now it is in Situation β

This is a contradiction.

F.1.5 GAY

Back to the end of Case A: Triangles fixed F.1. Suppose $f_\beta(d)$ starts at b, $f_\beta(\bar{d})$ starts at p.

Here $f_\beta(r)$ can either begin with o^* or d.

F.1.5.1 Ogee

Suppose

$$f_\beta(r) = o^*...$$

This is Figure F.47.

Here $f_\beta(d)$ must begin with b^- otherwise $f_\beta(o)$ would trace.

This is Figure F.48.

Here $f_\beta(r)$ must end at o° to trace. Here we claim that the dotted lines must join. Indeed, if instead $f_\beta(d)$ continues with r^+ towards the left of $f_\beta(\bar{d})$, then we have the situation shown in Figure F.49. But now the dotted lines are in Situation α.

On the other hand, in the situation depicted in Figure F.48, if $f_\beta(d)$ continues with r^+ towards the right of $f_\beta(\bar{d})$, then we have Figure F.50. Here the dotted lines cannot join or the Trace Lemma will be violated. Also, $f_\beta(d)$ must contiue with r^- and to the right of $f_\beta(b)$ or $f_\beta(b)$ will trace.

So now we have Figure F.51.

But now $f_\beta(d)$ is in Situation β

Thus in the situation depiated in Figure F.48, the dotted lines must join (and $f_\beta(r)$ must end).

This is Figure F.52.

Here $f_\beta(o)$ can either begin and end at b°, or begin with b^-.

F.1.5.1.1 Chine

Suppose

$$f_\beta(o) = b^\circ$$

This forces

$$f_\beta(b) = r^- di^+ s^* ...$$

and $f_\beta(i)$ must end at r°.

This is Figure F.53.

Here $f_\beta(b)$ must end at s°. Otherwise it would trace:

$$f_\beta(b) = r^- di^+ \hat{s}^+ i^- \bar{d} r^+ b^\times$$

and

$$f_\beta(b) = r^- di^+ \hat{s}^- i^- \bar{d} r^+ o^- b^\times$$

Thus we must have

$$f_\beta(b) = r^- di^+ \hat{s}^\circ$$

This is Figure F.54.

Here $f_\beta(p)$ cannot begin with i^-, as it would either trace:

$$f_\beta(p) = i^- \bar{d} r^+ b^+ o^+ r^- o^- b^- r^- d^\times$$

or be absorbed:

$$f_\beta(p) = i^- \bar{d} r^+ b^+ o^+ r^- d i^+ s^+ i^- \bar{d} r^+ b^+ \operatorname{Abso}(f_\beta(d), f_\beta(o))^\times$$

On the other hand, it cannot begin with i^+ as it would immediately trace. Thus we must have

$$f_\beta(p) = i^\circ$$

This then forces

$$f_\beta(s) = i^+ p^\circ$$

This gives Candidate 4. Shown in Figure F.55.

F.1.5.1.2 Droit

Back to the end of Ogee F.1.5.1. Suppose

$$f_\beta(o) = b^- ...$$

This forces

$$f_\beta(o) = b^- r^- d i^+ s^* ...$$

This is Figure F.56.

Here $f_\beta(b)$ can either begin and end at r° or begin with r^-.

F.1.5.1.2.0.1 Quaint

Suppose

$$f_\beta(b) = r^\circ$$

This is Figure F.57.

Here $f_\beta(i)$ is forced to end at b°, otherwise it would trace:

$$f_\beta(i) = ...b^+r^-o^-b^-r^-di^\times$$

or

$$f_\beta(i) = ...b^-r^-di^\times$$

or

$$f_\beta(i) = ...b^-o^-b^-r^-dp^-i^\times$$

Thus we must have Figure F.58.

Now $f_\beta(o)$ is forced to end here at s°. Otherwise it would either be absorbed:

$$f_\beta(o) = ...s^+i^-\bar{d}r^+b^+ \text{Abso}(f_\beta(d), f_\beta(o))^\times$$

or trace:

$$f_\beta(o) = ...s^-i^-\bar{d}r^+b^+r^-o^\times$$

Thus we must have

$$f_\beta(o) = b^-r^-di^+s^\circ$$

This is Figure F.59.

Now if $f_\beta(p)$ were to begin with i^-, then it would either trace:

$$f_\beta(p) = i^=\bar{d}r^+b^+o^+r^+b^-r^-o^-b^-r^-dp^times$$

or be absorbed:

$$f_\beta(p) = i^{=}\bar{d}r^{+}b^{+}o^{+}r^{+}b^{-}r^{-}di^{+}s^{+}i^{-}\bar{d}r^{+}b^{+}\,\mathrm{Abso}(f_\beta(d), f_\beta(o))^{\times}$$

On the other hand starting with i^+ would immediately trace. Thus we must have

$$f_\beta(p) = i^{\circ}$$

This then forces $f_\beta(s)$ to begin with i^+ and to end there.

This is Figure F.60, which is Candidate5.

F.1.5.1.2.1 Abscis

Back to the end of Droit F.1.5.1.2. Suppose

$$f_\beta(b) = r^{-}...$$

Then we have Figure F.61. here $f_\beta(i)$ is forced to end.

But now $f_\beta(o)$ cannot continue with s° or s^+, otherwise $f_\beta(b)$ will be forced to continue with s^+ and to the left of $f_\beta(o)$ which would lead it to trace:

$$f_\beta(b) = ...s^{+}i^{-}\bar{d}r^{+}b^{\times}$$

But then if $f_\beta(o)$ were to continue with s^- and to the right of $f_\beta(b)$, then it would trace:

$$f_\beta(o) = ...s^{-}i^{-}\bar{d}r^{+}o^{\times}$$

This is a contradiction.

F.1.5.2 Tret

Back to the end of GAY F.1.5. Suppose $f_\beta(r)$ begins with d.

This is Figure F.62.

Here $f_\beta(d)$ must come down at r right before crossing, and with no initial twisting otherwise o will trace.

This is Figure F.63.

Here $f_\beta(r)$ cannot go above $f_\beta(i)$, otherwise it would trace:

$$f_\beta(r) = dp^- i^- \bar{d} b^- r^\times$$

If $f_\beta(r)$ were to go in between $f_\beta(i)$ and $f_\beta(\bar{d})$, then the dotted lines are in Situation β shown in Figure F.64.

So suppose $f_\beta(r)$ goes below $f_\beta(\bar{d})$. Then we must have

$$f_\beta(r) = di^+ s^* ...$$

This is Figure F.65.

In fact it must be

$$f_\beta(r) = di^+ s^\circ$$

as otherwise it would trace:

$$f_\beta(r) = di^+ \hat{s}^+ i^- \bar{d} r^\times$$

or

$$f_\beta(r) = di^+\hat{s}^-i^-\bar{d}b^-r^\times$$

This is Figure F.66.

Here the dotted lines can either join, or $f_\beta(d)$ goes below $f_\beta(\bar{d})$.

F.1.5.2.1 Fosse

Suppose the dotted lines join. Then this forces

$$f_\beta(i) = \bar{d}r^+b^+o^\circ$$

This is Figure F.67.

Here $f_\beta(b)$ must end at r°. Otherwise it would trace:

$$f_\beta(b) = r^+b^\times$$

or

$$f_\beta(b) = r^-di^+p^+\bar{d}r^+b^\times$$

or

$$f_\beta(b) = r^-di^+s^-i^-\bar{d}b^\times$$

Thus we must have

$$f_\beta(b) = r^\circ$$

This is Figure F.68.

Here $f_\beta(o)$ either begins and ends at b° or begins with b^-.

F.1.5.2.1.1 Lacuna

Suppose

$$f_\beta(o) = b^\circ$$

Then $f_\beta(p)$ must begin and end with i°. Otherwise it either traces:

$$f_\beta(p) = i^+ p^\times$$

or is absorbed:

$$f_\beta(p) = i^- \bar{d} r^+ b^+ d i^+ s^+ i^- \bar{d} r^+ b^+ \operatorname{Abso}(f_\beta(d), f_\beta(o))^\times$$

or

$$f_\beta(p) = i^- \bar{d} r^+ b^+ o^- b^- r^- d p^- i^- \bar{d} r^+ b^+ \operatorname{Abso}(f_\beta(d), f_\beta(o))^\times$$

Thus we must have

$$f_\beta(p) = i^\circ$$

This immediately forces

$$f_\beta(s) = i^+ p^c i r c$$

This is Candidate 6, shown in Figure F.69.

F.1.5.2.1.2 Exedra

Back to the end of Fosse F.1.5.2.1. Suppose

$$f_\beta(o) = b^- ...$$

Then the following is forced, shown in Figure F.70.

Here $f_\beta(o)$ must continue with i^+ and to the left of $f_\beta(p)$. Otherwise, $f_\beta(s)$ will be forced to continue with i^- and to the right of $f_\beta(o)$, which would then force it to trace:

$$f_\beta(s) = ...i^-\bar{d}r^+b^+di^+s^\times$$

Then $f_\beta(p)$ is forced to begin and end with i°. Otherwise, it must begin with i^-, then it is either absorbed:

$$f_\beta(p) = i^-\bar{d}r^+b^+di^+s^+i^-\bar{d}r^+b^+\,\mathrm{Abso}(f_\beta(d), f_\beta(o))^\times$$

or trace;

$$f_\beta(p) = i^-\bar{d}r^+b^+b^-b^-r^-dp^\times$$

Thus we must have

$$f_\beta(p) = i^\circ$$

This is Figure F.71.

Now $f_\beta(o)$ cannot continue with p° or p^-, as that would force $f_\beta(s)$ to continue with p^- and to the right of $f_\beta(o)$, in which case it will be trace:

$$f_\beta(s) = i^+\hat{p}^-i^-\bar{d}r^+b^+di^+s^\times$$

So $f_\beta(o)$ must continue with p^+ and to the left of $f_\beta(s)$, but then it will be absorbed:

$$f_\beta(o) = ...p^+i^-\,\mathrm{Abso}(f_\beta(p), f_\beta(o))^\times$$

This is a contradiction.

F.1.5.2.2 Lemur

Back to the end of F.1.5.2. Suppose $f_\beta(d)$ goes below $f_\beta(\bar{d})$.

This forces the situation depicted in Figure F.72. But now the dotted lines are in Situation α.

F.1.6 OGG

Back to the end of Case A: Triangles fixed F.1. Suppose $f_\beta(d)$ starts at b, $f_\beta(\bar{d})$ starts at s.

Here again $f_\beta(r)$ can either begin with o^* or d.

However, the arguments in Ogee F.1.5.1 and its subsections can be repeated to show that $f_\beta(r)$ cannot begin with o^*.

So suppose $f_\beta(r)$ begins with d.

This is Figure F.73.

Here $f_\beta(p)$ must begin with i^- and to the right of the incoming $f_\beta(s)$. Otherwise, $f_\beta(s)$ will be forced to begin with i^+ and to the left of $f_\beta(p)$, in which case it will immediately trace. Thus we must have

$$f_\beta(p) = i^- \bar{d} ...$$

This is Figure F.74.

Here $f_\beta(r)$ cannot go below $f_\beta(\bar{d})$, or it will trace:

$$f_\beta(r) = d i^+ s^+ \bar{d} r^\times$$

Thus we must have the situation depicted in Figure F.75.

But now the dotted lines cannot go below $f_\beta(i)$ or they will be in Situation β (bagged). On the other hand, going above $f_\beta(i)$ puts them in Situation α.

This is a contradiction.

F.1.7 SME

Back to the end of Case A: Triangles fixed F.1. Suppose $f_\beta(d)$ starts at b, $f_\beta(\bar{d})$ starts at i.

This is Figure F.76.

Here $f_\beta(r)$ cannot go above $f_\beta(s)$, as at least one of $f_\beta(s)$ or $f_\beta(p)$ will trace after crossing $f_\beta(d)$ again. Here $f_\beta(r)$ can continue with p^* or s^*.

Suppose it continued with p^*. This is Figure F.78. Now it must in fact end there. Otherwise, it would trace:

$$f_\beta(r) = di^+\hat{p}^+\bar{d}r^\times$$

or

$$f_\beta(r) = di^+\hat{p}^+i^-\bar{d}r^\times$$

or

$$f_\beta(r) = di^+\hat{p}^-i^-\bar{d}b^-r^\times$$

Thus we must have

$$f_\beta(r) = di^+\hat{p}^\circ$$

This is Figure F.79. But now notice $f_\beta(\bar{d})$ will violate Assumption A.

This is contradiction. Thus $f_\beta(r)$ must continue with s^*.

This is Figure F.80.

Here $f_\beta(\bar{d})$ can either continue with s^* or p^*.

F.1.7.1 Barm

Suppose it continued with s^*. Then we have the situation depicted in Figure F.81.

Here $f_\beta(\bar{d})$ must continue with s^+ , and eventually come down on p before crossing $\bar{d}$, possibly after some twisting.

This is Figure F.82.

In Figure F.83 , the situation is shown with no twisting.

Here the dotted lines can either join, or $f_\beta(\bar{d})$ must go below $f_\beta(d)$.

Suppose the dotted lines join. This is shown in Figure F.84. Here $f_\beta(s)$ cannot continue with r° or r^-, otherwise $f_\beta(p)$ would be forced to continue with r^- and to the right of $f_\beta(s)$, in which case it traces immediately after crossing d. Thus $f_\beta(s)$ must continue with r^+ and to the left of $f_\beta(b)$ (it cannot go in between $f_\beta(b)$ and $f_\beta(p)$ or it will itself trace eventually after crossing d). But now $f_\beta(o)$ is forced to begin with b^- and to the right of the incoming $f_\beta(s)$.

This is Figure F.85.

But now $f_\beta(i)$ is forced to begin with p^+ and to the left of the incoming $f_\beta(o)$, and now it will be absorbed:

$$f_\beta(i) = p^+ \bar{d} r^+ b^+ \,\mathrm{Abso}(f_\beta(d), f_\beta(o))^\times$$

This is a contradiction. Thus the dotted lines cannot join so $f_\beta(\bar{d})$ must go above $f_\beta(d)$.

This is Figure F.86.

But now again $f_\beta(i)$ is forced to begin with p^+ and to the left of the incoming $f_\beta(\bar{d})$, and it will be absorbed.

This is a contradiction.

F.1.7.2 Nary

Back to the end of SME F.1.7. Suppose $f_\beta(\bar{d})$ continue with p^*.

This is Figure F.87.

Here $f_\beta(\bar{d})$ must continue with $\bar{d}$ and not to the right of $f_\beta(i)$ or it will be in Situation β. Thus we must have the situation depicted in Figure F.88.

Here the dotted lines must join. Indeed, if $f_\beta(d)$ were to go above $f_\beta(\bar{d})$ then $f_\beta(\bar{d})$ will be in Situation β. If instead $f_\beta(d)$ were to go under $f_\beta(\bar{d})$ and above $f_\beta(s)$, then $f_\beta(d)$ will be in Situation β. If $f_\beta(d)$ were to go under $f_\beta(\bar{d})$ and also under $f_\beta(p)$, then we have the situation depicted in Figure F.89.

But here the dotted lines will necessarily violate the Trace Lemma.

Thus the dotted lines must join. This is Figure F.90.

Here $f_\beta(s)$ cannot continue with r° or r^-, otherwise $f_\beta(p)$ would be forced to continue with r^- and to the right of $f_\beta(s)$, in which case it traces immediately after crossing d. Thus $f_\beta(s)$ must continue with r^+.

This is Figure F.91.

Here $f_\beta(s)$ can either go into 1. or 2.

Suppose $f_\beta(s)$ were to go into 1. Then we have the situation depicted in Figure F.92.

Here $f_\beta(p)$ must end at r°. Otherwise, it is either absorbed:

$$f_\beta(p) = \bar{d}\hat{r}^+ d\,\mathrm{Abso}(f_\beta(s), f_\beta(p))^\times$$

or trace:

$$f_\beta(p) = \bar{d}\hat{r}^+ p^\times$$

This is Figure F.93.

Here $f_\beta(o)$ can either begin and end with b°, or begin with b^-.

F.1.7.2.1 Aulic

Suppose

$$f_\beta(o) = b^\circ$$

Then we have Figure F.94.

Here $f_\beta(s)$ can either end at o° or continue with o^-.

If it ends here at o°, then what is left is $f_\beta(i)$ and $f_\beta(b)$ twist k times between s and i and end there, giving us Candidate Family 7. Shown in Figure F.95.

Suppose instead $f_\beta(s)$ continues with o^-. Then we have the situation depicted in Figure F.96 and Figure F.97.

Here if $f_\beta(b)$ were to continue with i° or i^+, then $f_\beta(s)$ continues with i^+ and to the left of $f_\beta(b)$. But then it will be absorbed:

$$f_\beta(s) = ...i6 + p^+\bar{d}r^+ b^+\,\mathrm{Abso}(f_\beta(d), f_\beta(o))^\times$$

On the other hand, if $f_\beta(b)$ were to continue with i^- and to the right of $f_\beta(s)$, then it will trace:

$$f_\beta(b) = ...i^- p^+ \bar{d}r^+ di^+ p^+ \bar{d}r^+ b^\times$$

This is a contradiction.

F.1.7.2.2 Oread

Back to the end of Nary F.1.7.2. Suppose

$$f_\beta(o) = b^- ...$$

This is Figure F.98.

Here $f_\beta(o)$ must continue with p^- and to the right of $f_\beta(i)$. Otherwise, $f_\beta(b)$ will trace.

This is Figure F.99.

Here $f_\beta(i)$ can either begin and end here at p°, or begin with p^+. Suppose

$$f_\beta(i) = p^\circ$$

This is Figure F.100.

Here $f_\beta(o)$ must continue with i^- and to the right of $f_\beta(b)$. Otherwise $f_\beta(b)$ must continue with i^+, and it will trace.

But now either $f_\beta(o)$ traces:

$$f_\beta(o) = ...i^- p^+ \bar{d}r^+ di^+ p^+ \bar{d}r^+ b^+ o^\times$$

or it is absorbed:

$$f_\beta(o) = ...i^- p^+ \bar{d} r^+ d i^+ s^- i^- \bar{d} b^- r^- d p^- i^- \bar{d} r^- d \,\mathrm{Abso}(f_\beta(s), f_\beta(p))^\times$$

Thus we must have

$$f_\beta(i) = p^+ ...$$

This is Figure F.101.

This eventually forces the situation depicted in Figure F.102, and then Figure F.103 which is Candidate 8.

F.2 Case B,C,D: Triangles Swapped

Now we assume the triangles are swapped.

We first assume that $f_\beta(d)$ passes $\bar{d}$ after an odd number of letters.

F.2.1 FUN

Supposing $f_\beta(d)$ passes $\bar{d}$ after an odd number of letters. Suppose $f_\beta(d)$ starts at p, and suppose $f_\beta(\bar{d})$ starts at d. Then after possibly twisting with i, $f_\beta(d)$ must come down on p^+ immediately before crossing.

This is Figure F.104.

Here $f_\beta(p)$ and $f_\beta(s)$ must begin with b^+ and to the left of $f_\beta(r)$. Otherwise, $f_\beta(r)$ will be forced to continue with b^- and immediately trace.

This is Figure F.105.

Now we claim that in fact $f_\beta(d)$ cannot have initial twists. Indeed, if it did then $f_\beta(b)$ would be forced to do the following:

$$f_\beta(b) = i^+ ... p^+ \bar{d} r^* ...$$

and here it must continue with r° or r^- to not immediately trace. But then this forces

$$f_\beta(i) = r^- d p^- i^\times$$

Thus there cannot be initial twists.

This is Figure F.106.

Consider the dotted lines $f_\beta(d)$ and $f_\beta(\bar{d})$. Here they can either join, or $f_\beta(d)$ must go below $f_\beta(\bar{d})$ in order to not put $f_\beta(\bar{d})$ in Situation β. If it were the latter case, then we would have the situation depicted in Figure F.107.

But now, the dotted lines are in Situation α. Thus the dotted lines must join. This is Figure F.108.

Here $f_\beta(o)$ must continue with r^+ and to the left of $f_\beta(i)$, or $f_\beta(i)$ will be forced to begin with r^- and to the right of $f_\beta(o)$, in which case it will trace:

$$f_\beta(i) = r^- d p^- i^\times$$

Thus the situation depicted in Figure F.109 is forced.

Now $f_\beta(b)$ must begin with i^- and to the right of both $f_\beta(p)$ and $f_\beta(s)$. Otherwise $f_\beta(p)$ and $f_\beta(s)$ will be forced to continue with i^+ and thus at least one of them will then immediately trace. But now $f_\beta(b)$ will trace:

$$f_\beta(b) = i^- \bar{d} b^\times$$

This is a contradiction.

F.2.2 XOY

Supposing $f_\beta(d)$ passes $\bar{d}$ after an odd number of letters. Suppose $f_\beta(d)$ starts at p, and suppose $f_\beta(\bar{d})$ starts at o.

This case is impossible as $f_\beta(r)$ would immediately trace:

$$f_\beta(r) = \bar{d}r^\times$$

F.2.3 FAT

Supposing $f_\beta(d)$ passes $\bar{d}$ after an odd number of letters. Suppose $f_\beta(d)$ starts at p, and suppose $f_\beta(\bar{d})$ starts at b.

This is Fat1.

Here $f_\beta(d)$ must begin with b^+ or $f_\beta(r)$ will trace. Similarly $f_\beta(\bar{d})$ must continue with r^+ or $f_\beta(p)$ will trace.

Thus we have Figure F.111.

Here $f_\beta(s)$ must begin with r^+ and to the left of $f_\beta(p)$ or $f_\beta(p)$ will trace.

This gives Figure F.112.

Then the situation in Figure F.113 is forced. Here because $f_\beta(p)$ cannot escape the left hand side, it twists between r and o k times and end there. Then $f_\beta(s)$ is forced to end at whichever r or o is left. Then $f_\beta(i)$ is forced to end at p°.

This is Candidate Family 9.

F.2.4 KNH

Supposing $f_\beta(d)$ passes $\bar{d}$ after an odd number of letters. Suppose $f_\beta(d)$ starts at p, and suppose $f_\beta(\bar{d})$ starts at r.

Then we must have the situation in Figure F.114, where $f_\beta(p)$ must go below $f_\beta(r)$ to not trace. But now $f_\beta(r)$ must trace.

This is a contradiction.

F.2.5 MZG

Supposing $f_\beta(d)$ passes $\bar{d}$ after an odd number of letters. Suppose $f_\beta(d)$ starts at s, and suppose $f_\beta(\bar{d})$ starts at d.

This is Figure F.115.

Here $f_\beta(p)$ and $f_\beta(s)$ must begin with b^+ and to the left of $f_\beta(r)$ or $f_\beta(r)$ will trace.

Then we have Figure F.116.

Here $f_\beta(p)$ can continue with d or o^*.

Suppose $f_\beta(p)$ were to continue with o^*. Then this is Figure F.117. Here the dotted lines must join. Indeed, if not the only possibility is $f_\beta(d)$ goes below $f_\beta(\bar{d})$, otherwise $f_\beta(\bar{d})$ will be in Situation β. But then we would have

$$f_\beta(d) = ...db^+o^-b^-r^-d...$$

which would then put the dotted lines in Situation α

So we must have the situation depicted in Figure F.117.

Here let us assume that $f_\beta(d)$ has no initial twists. Then we have the situation depicted in Figure F.118.

Here $f_\beta(p)$ must continue with o^+ and to the left of $f_\beta(r)$, otherwise $f_\beta(r)$ will be absorbed between $f_\beta(p)$ and $f_\beta(s)$. This gives us Figure F.119.

Here we claim that $f_\beta(p)$ cannot continue with b^-. Indeed, if it did then we would be in the situation depicted in Figure F.120. But here $f_\beta(p)$, $f_\beta(i)$, and $f_\beta(o)$ are stuck in a counterclockwise path mill.

Thus in the situation depicted in Figure F.119, we must have $f_\beta(p)$ continue with b° or b^+, thus $f_\beta(s)$ must continue with b^+. But now $f_\beta(r)$, $f_\beta(p)$, and $f_\beta(s)$ are stuck in a counterclockwise path mill.

Thus we must assume that $f_\beta(d)$ has initial twists. This forces $f_\beta(b)$ to cross d after twisting. But this then forces the situation depicted in Figure F.121.

Here notice $f_\beta(d)$ is in Situation β.

This is a contradiction.

F.2.6 GUM

Supposing $f_\beta(d)$ passes $\bar{d}$ after an odd number of letters. Suppose $f_\beta(d)$ starts at s, and suppose $f_\beta(\bar{d})$ starts at o.

This case cannot occur as $f_\beta(r)$ will immediately trace after crossing.

F.2.7 WAK

Supposing $f_\beta(d)$ passes $\bar{d}$ after an odd number of letters. Suppose $f_\beta(d)$ starts at s, and suppose $f_\beta(\bar{d})$ starts at b.

This is Figure F.122.

Here $f_\beta(\bar{d})$ must begin with b^+ otherwise $f_\beta(r)$ will trace. Also here $f_\beta(i)$ can either go above $f_\beta(d)$ or below $f_\beta(d)$.

Suppose it were to go above. Then Figure F.123 is forced. But now $f_\beta(d)$ must have initial twists, otherwise $f_\beta(o)$ will eventually trace. This gives Figure F.124. But now $f_\beta(b)$ will eventually trace after crossing:

$$f_\beta(b) = i^+ ... p^+ \bar{d} b^\times$$

Thus $f_\beta(i)$ must go below $f_\beta(d)$. This gives Figure F.125. Here if the dotted lines continue with d, then they would be in Situation β, so they must continue with o^*. But now notice by the same reasoning as before $f_\beta(d)$ must have initial twists otherwise $f_\beta(o)$ will trace after crossing. But then again $f_\beta(o)$ will eventually trace, again by the same reasoning as before.

This is a contradiction.

F.2.8 MAU

Supposing $f_\beta(d)$ passes $\bar{d}$ after an odd number of letters. Suppose $f_\beta(d)$ starts at s, and suppose $f_\beta(\bar{d})$ starts at r.

This is Figure F.126.

But here at least one of $f_\beta(p)$ and $f_\beta(s)$ will immediately trace after crossing.

This is a contradiction.

F.2.9 EEN

Supposing $f_\beta(d)$ passes $\bar{d}$ after an odd number of letters. Suppose $f_\beta(d)$ starts at i, and suppose $f_\beta(\bar{d})$ starts at d. This is Figure F.127, where $f_\beta(d)$ can possible have initial twists.

Here $f_\beta(i)$ must begin with r^- and to the right of $f_\beta(b)$, or $f_\beta(b)$ will trace. This gives Figure F.128.

Here $f_\beta(i)$ must continue with p or s. Suppose $f_\beta(i)$ contiues with p. This is Figure F.129.

Now if $f_\beta(d)$ were to have initial twists, then $f_\beta(r)$ will be forced to follow the path as shown in Figure F.130. This then forces $f_\beta(p)$ to begin with

$$f_\beta(p) = b^+ o^* ...$$

as shown.

But now $f_\beta(p)$, $f_\beta(s)$, and $f_\beta(r)$ are in a three-way path mill.

So $f_\beta(d)$ cannot have initial twists. This is Figure F.131. Here $f_\beta(o)$ can either end at i°, or begin with i^-. Suppose it were to begin with i^-. This is Figure F.132. Then it continues with

$$f_\beta(o) = i^- \bar{d} r^- d ...$$

and here if the next letter were p, then $f_\beta(o)$, $f_\beta(i)$, and $f_\beta(b)$ will be in a three-way clockwise path mill. Thus the next letter must be s^-. So we have

$$f_\beta(o) = i^- \bar{d} r^- d \hat{s}^- i^- \bar{d} ...$$

This forces

$$f_\beta(p) = b^+ o^* ...$$

This is Figure F.133. Now here $f_\beta(p)$, $f_\beta(s)$, and $f_\beta(o)$ are stuck in a three-way couterclockwise path mill.

This is a contradiction.

Thus going back to the situation depicted in Figure F.128, $f_\beta(i)$ must continue with s^*. This is Figure F.134.

But now $f_\beta(i)$ must continue with p^- and to the right of $f_\beta(r)$, or $f_\beta(r)$ will trace immediately after crossing $\bar{d}$. But now $f_\beta(i)$ traces. This is a contradiction.

This concludes the situation where $f_\beta(d)$ passes an odd number of letters before crossing. Now we assume $f_\beta(d)$, Now, suppose instead that $f_\beta(d)$ passes over $\bar{d}$ after an even number of letters. From previous arguments, we can then conclude that $f_\beta(\bar{d})$ passes over $\bar{d}$ after an odd number of letters. Then the only possibility for $f_\beta(\bar{d})$ is to start at b, r, or o. While for $f_\beta(d)$ the only possibility is to start at p, s, or i.

F.2.10 MYU

Supposing both $f_\beta(d)$ passes f_β after an even number of letters. Suppose $f_\beta(d)$ starts at p, and suppose $f_\beta(\bar{d})$ starts at b.

This is Figure F.135. Here $f_\beta(r)$ must go below $f_\beta(i)$ or it will immediately trace. But now $f_\beta(i)$ will trace. As shown in Figure F.136.

This is a contradiction.

F.2.11 QBC

Supposing both $f_\beta(d)$ passes f_β after an even number of letters. Suppose $f_\beta(d)$ starts at p, and suppose $f_\beta(\bar{d})$ starts at o. This is Figure F.137. But now $f_\beta(r)$ will immediately trace after crossing.

This is a contradiction.

F.2.12 OWD

Supposing both $f_\beta(d)$ passes f_β after an even number of letters. Suppose $f_\beta(d)$ starts at p, and suppose $f_\beta(\bar{d})$ starts at r.

Here again $f_\beta(r)$ must continue with b after crossing. But this forces $f_\beta(p)$ to trace, as shown in Figure F.138.

This is a contradiction.

F.2.13 BFI

Supposing both $f_\beta(d)$ passes f_β after an even number of letters. Suppose $f_\beta(d)$ starts at p, and suppose $f_\beta(\bar{d})$ starts at r.

This is a contadiction.

Now suppose $f_\beta(d)$ begins at s. The arguments of MYU F.2.10, QBC F.2.11, OWD F.2.12, and BFI F.2.13 can all be repeated to rule this scenario out.

F.2.14 CQD

Supposing both $f_\beta(d)$ passes f_β after an even number of letters. Suppose $f_\beta(d)$ starts at i, and suppose $f_\beta(\bar{d})$ starts at o.

Then this is Figure F.139.

Here $f_\beta(i)$ is forced to begin with r^- and to the right of $f_\beta(b)$, or $f_\beta(b)$ will trace. This is Figure F.140. Now notice that the next letter of $f_\beta(d)$ must either be s or p, but in the latter case $f_\beta(i)$ will trace. So we must have

$$f_\beta(d) = i^+ s^- \bar{d} ...$$

and

$$f_\beta(i) = r^- dp^* ...$$

But now $f_\beta(d)$ continues with

$$f_\beta(d) = i^+ s^- \bar{d} r^+ o \cdot ..$$

This forces $f_\beta(o)$ to trace. As shown in Figure F.141.

This is a contradiction.

F.2.15 KYD

Supposing both $f_\beta(d)$ passes f_β after an even number of letters. Suppose $f_\beta(d)$ starts at i, and suppose $f_\beta(\bar{d})$ starts at b.

This is Figure F.142.

Here $f_\beta(p)$ and $f_\beta(s)$ must begin with r^- and to the right of $f_\beta(b)$. Otherwise $f_\beta(b)$ will immediately trace. But then notice at least one of $f_\beta(p)$ or $f_\beta(s)$ will immediately trace after crossing d.

This is a contradiction.

F.2.16 FHR

Supposing both $f_\beta(d)$ passes f_β after an even number of letters. Suppose $f_\beta(d)$ starts at i, and suppose $f_\beta(\bar{d})$ starts at r.

This is Figure F.143.

Here we either have

$$f_\beta(d) = i^+ s^+ ...$$

or

$$f_\beta(d) = i^+ p^+ ...$$

F.2.16.1 Eyas

Suppose

$$f_\beta(d) = i^+ s^+ ...$$

Then the situation in Figure F.144 is forced. The dotted lines are forced to connect since otherwise either $f_\beta(\bar{d})$ enters Situation β, or the dotted lines enter Situation α.

Here if $f_\beta(p)$ continued with o^+ and to the left of $f_\beta(s)$, then $f_\beta(p)$, $f_\beta(b)$, and $f_\beta(s)$ will be in a three-way couterclockwise path mill as shown in Figure F.145.

So we must have $f_\beta(s)$ continue with o^-, and $f_\beta(p)$ ending at o°.

This is Figure F.146.

Here we claim that $f_\beta(i)$ cannot continue with p^+ and to the left of $f_\beta(s)$. Indeed, if so then we would have the situation depicted in Figure F.147. But here $f_\beta(i)$ must continue with s^- or $f_\beta(r)$ will trace, but then $f_\beta(i)$ immediately traces as well.

This gives Figure F.148. But here notice that $f_\beta(o)$, $f_\beta(o)$, and $f_\beta(i)$ are in a three-way clockwise path mill.

This is a contradiction,

F.2.16.2 Fard

Back to the end of FHR F.2.16. Suppose

$$f_\beta(d) = i^+ p^+ ...$$

This is Figure F.149.

Here the dotted lines must connect. Otherwise, if $f_\beta(\bar{d})$ went under $f_\beta(d)$, then $f_\beta(\bar{d})$ will be in Situation β. On the other hand, if $f_\beta(d)$ went below $f_\beta(\bar{d})$, then we would have Figure F.150, in which case the dotted lines are in Situation α.

Thus we must have Figure F.151.

Here $f_\beta(p)$ can either begin with d, or begin with o. Suppose

$$f_\beta(p) = d...$$

Then $f_\beta(s)$ must begin with o. This is Figure F.152.

Here $f_\beta(o)$ cannot go up to s because then if $f_\beta(p)$ continued with s° or s^-, $f_\beta(o)$ will be forced to continue with s^-, but then it will be absorbed between $f_\beta(s)$ and $f_\beta(p)$. On the other hand, if $f_\beta(p)$ continued with s^+, then it will be absorbed between $f_\beta(d)$ and $f_\beta(o)$.

Thus we must have the situation depicted in Figure F.153. But now $f_\beta(i)$ must begin with b^- and to the right of $f_\beta(o)$, otherwise $f_\beta(o)$ will immediately trace. But now $f_\beta(i)$ will trace:

$$f_\beta(i) = b^- r^- d p^- i^\times$$

This is a contradiction.

So suppose

$$f_\beta(p) = o^*...$$

This gives the situation depicted in Figure F.154.

Here $f_\beta(i)$ can either begin and end with b°, or begin with b^+.

F.2.16.2.1 Dwaal

Suppose

$$f_\beta(i) = b^\circ$$

This gives Figure F.155.

Here $f_\beta(s)$ must continue with r^- and to the right of $f_\beta(b)$. Otherwise, $f_\beta(b)$, $f_\beta(s)$, and $f_\beta(p)$ will be in a three-way counterclockwise path mill.

Thus we have Figure F.156.

Here $f_\beta(r)$ and $f_\beta(o)$ twist among themselves between p and i and end there, since $f_\beta(r)$ can never escape or it will trace. This then forces $f_\beta(o)$ to end here at s°, and $f_\beta(b)$ to end here at r°.

This gives Cnadidate Family 10.

F.2.16.2.2 Fremd

Back to the end of Fard F.2.16.2. Suppose

$$f_\beta(i) = b^+...$$

This is Figure F.157.

Here $f_\beta(i)$ must continue with o^+ and to the left of $f_\beta(p)$ and $f_\beta(s)$, otherwise $f_\beta(p)$ will trace after crossing d. This is Figure F.158.

Here $f_\beta(b)$ must continue with r^+ and to the left of $f_\beta(i)$, otherwise $f_\beta(i)$ will continue

with d and then p. Then it must continue with p^-, or $f_\beta(r)$ will trace, but then $f_\beta(i)$ itself traces. So we have the situation depicted in Figure F.159. Here $f_\beta(p)$ and $f_\beta(s)$ must continue with o^+ and to the left of $f_\beta(b)$, otherwise $f_\beta(b)$ will immediately trace. So we have Figure F.160. This continues and we see that $f_\beta(p)$, $f_\beta(s)$, $f_\beta(b)$, and $f_\beta(i)$ are in a four-way counterclockwise path mill.

This is a contradiction.

F.3 Figures

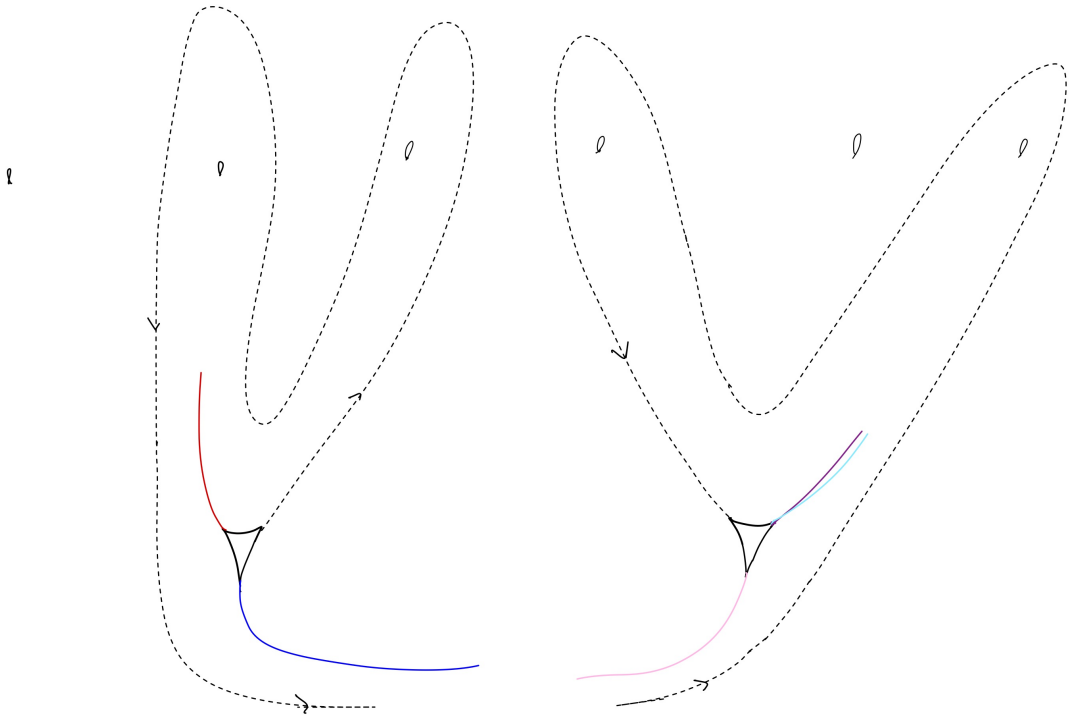


Figure F.1: YOW1

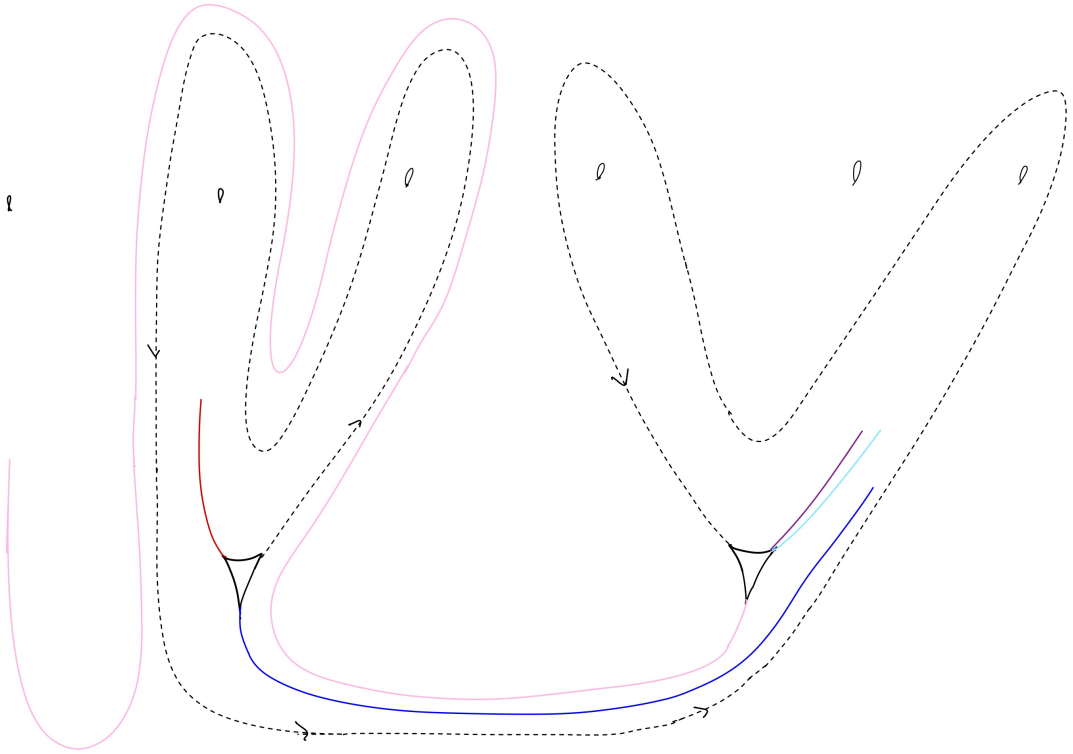


Figure F.2: YOW2

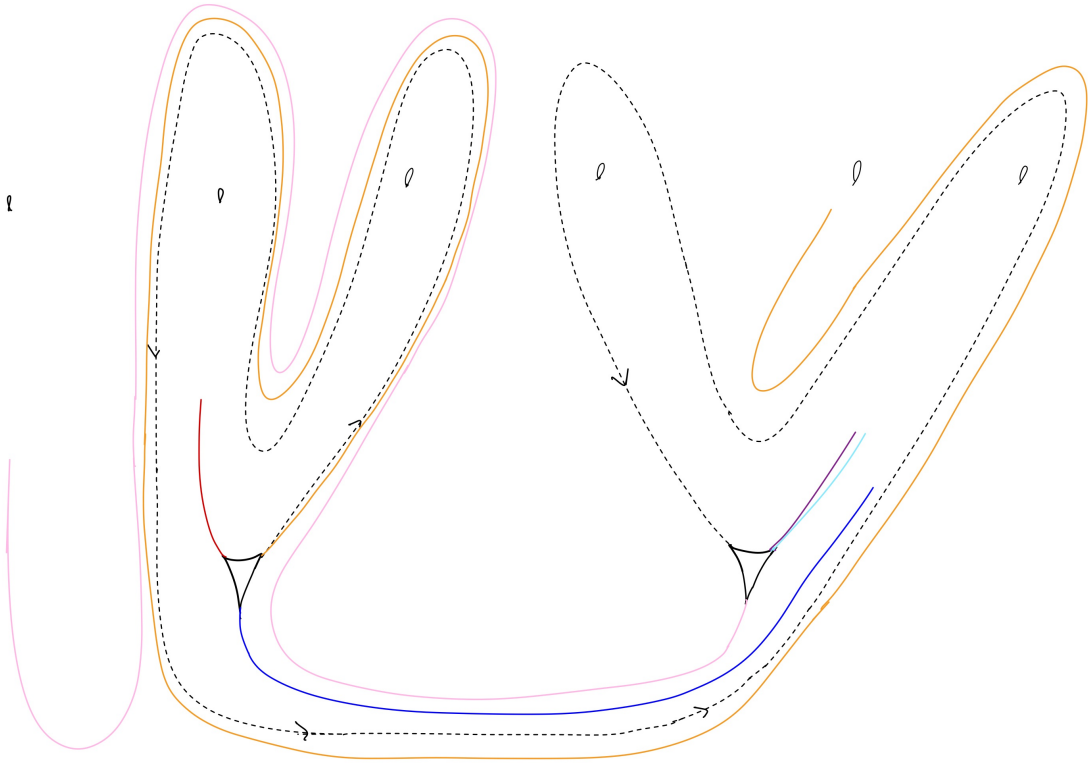


Figure F.3: YOW3

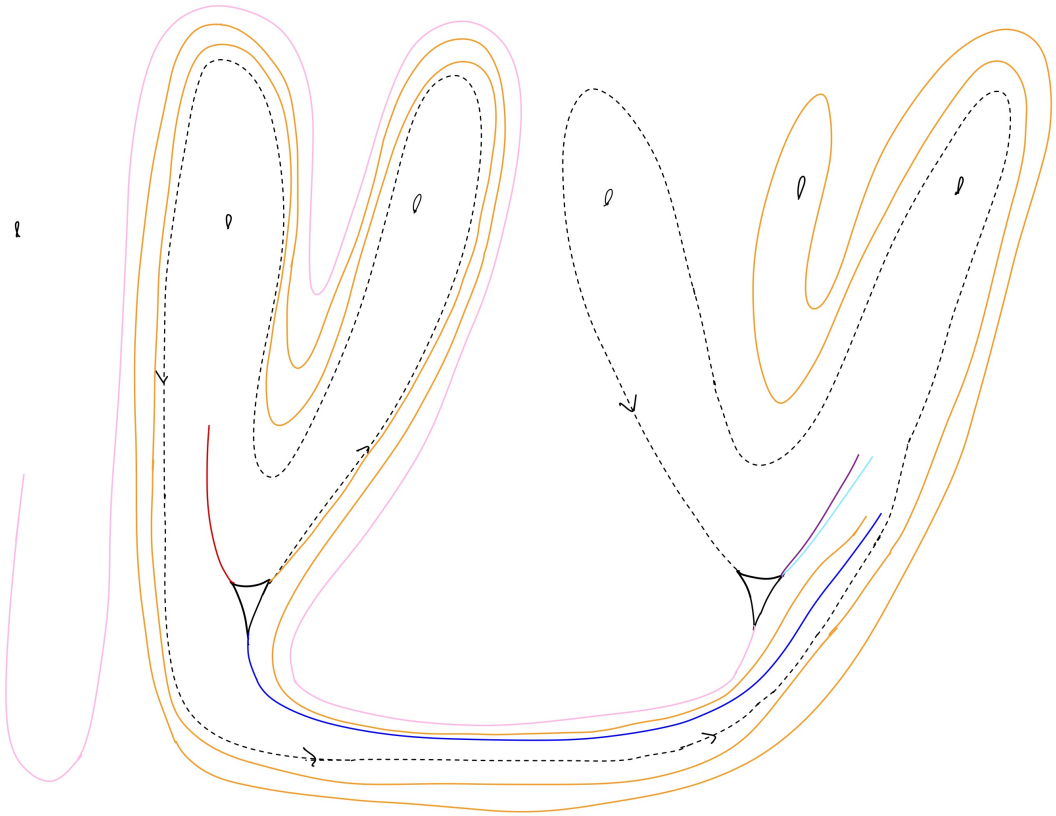


Figure F.4: Bubo1

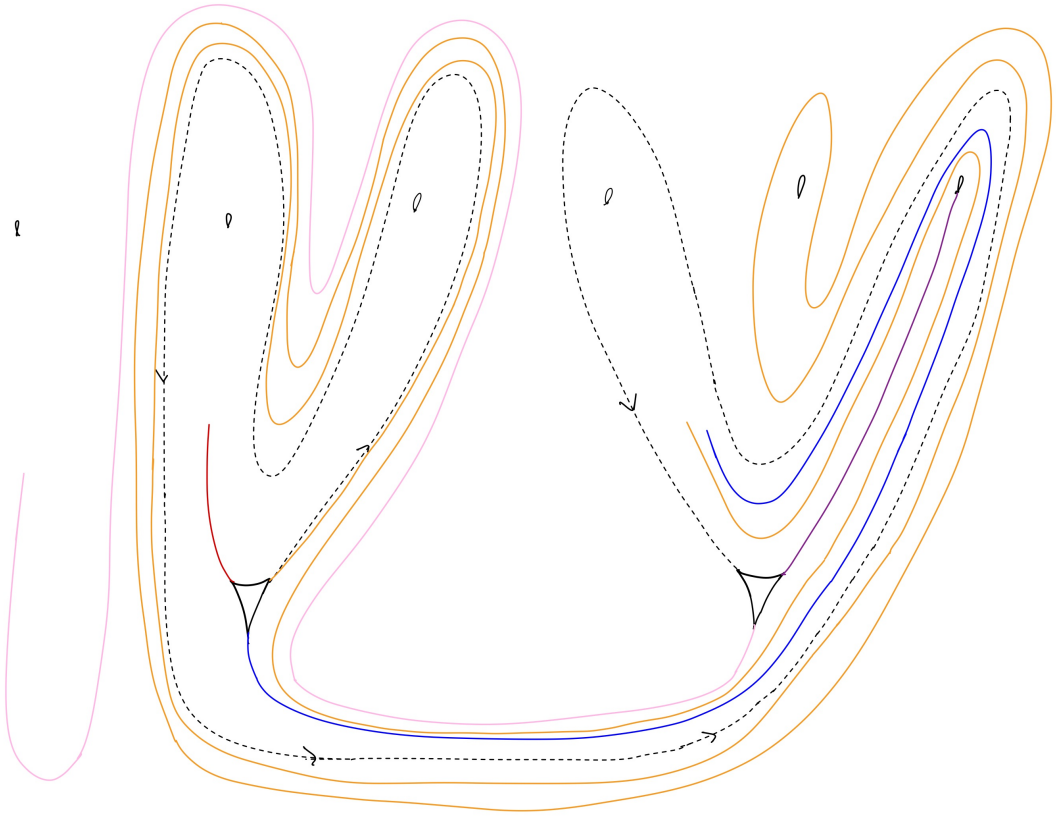


Figure F.5: Gnash1

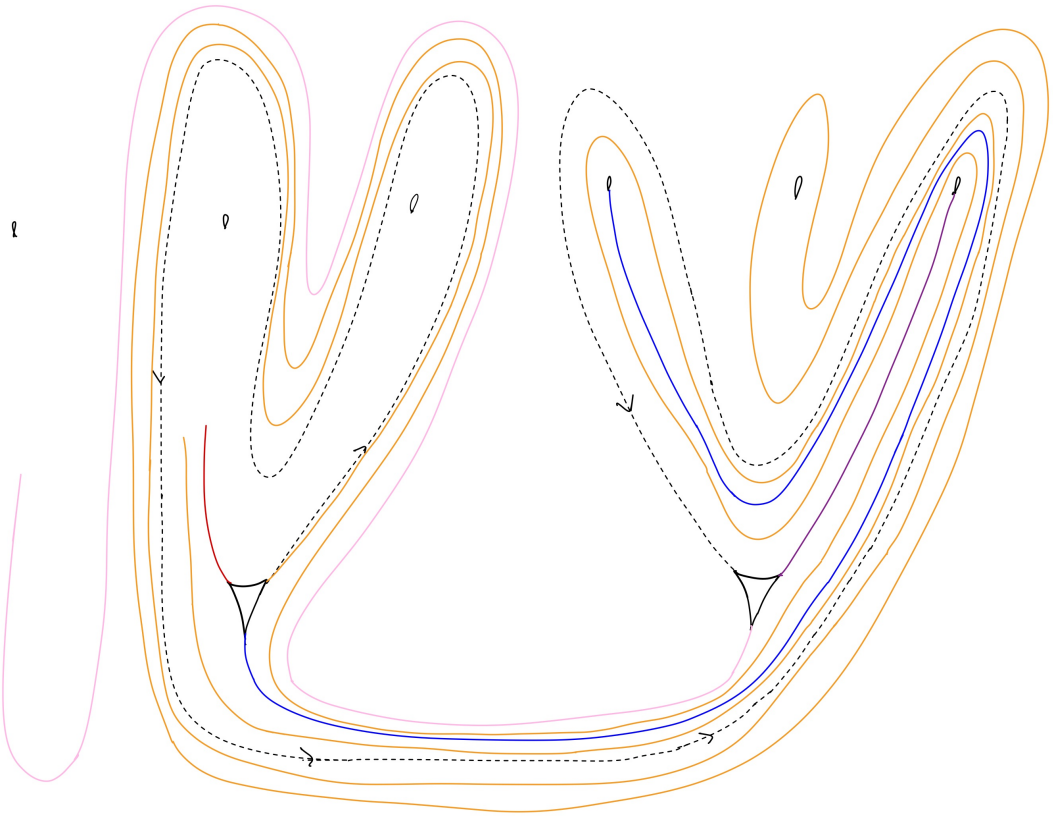


Figure F.6: Gnash2

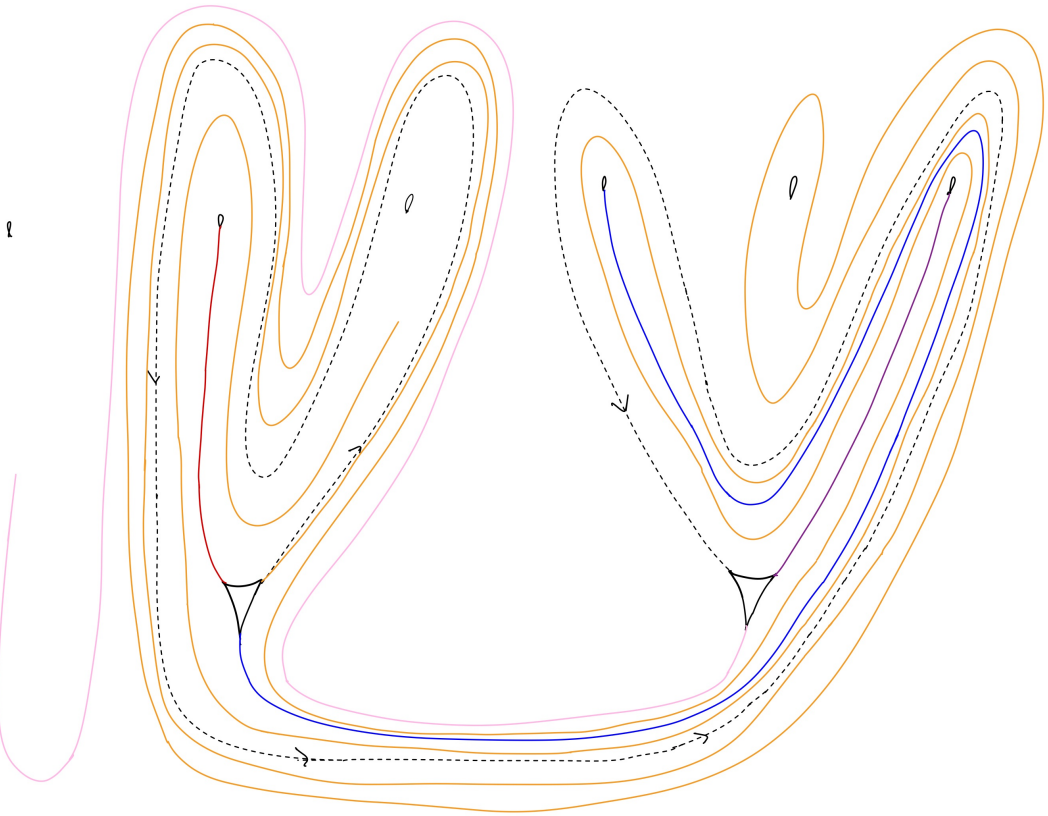


Figure F.7: Gnash3

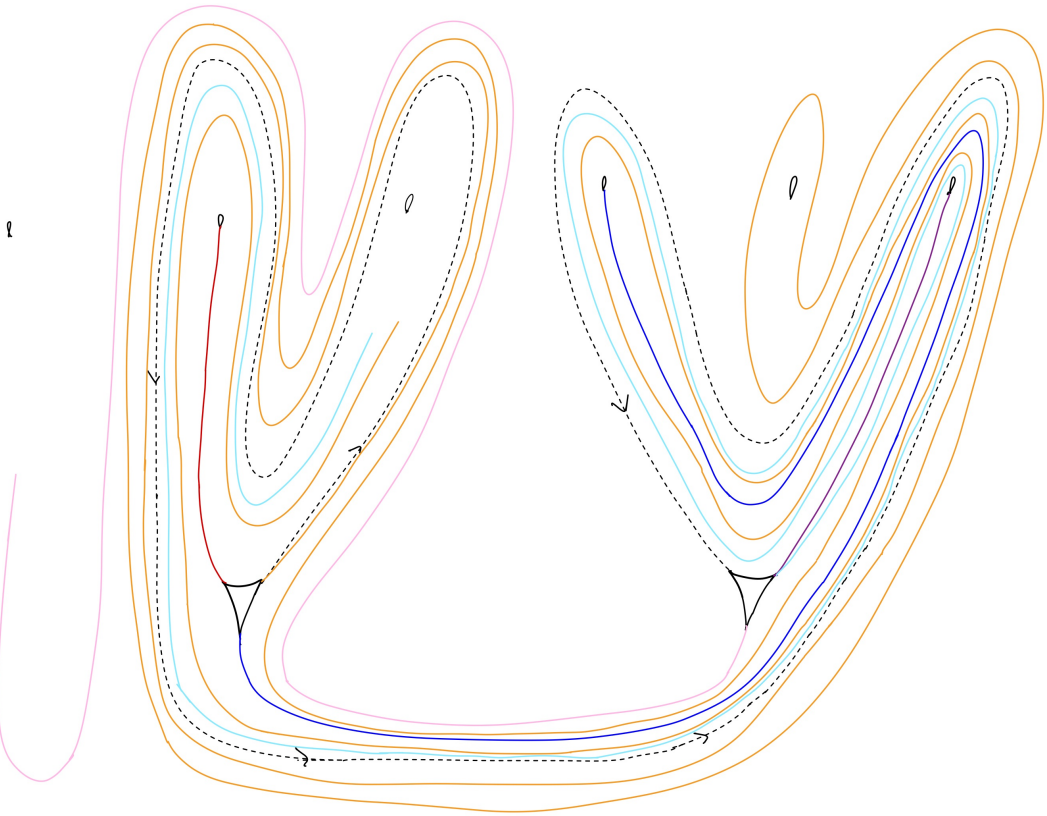


Figure F.8: Gnash4

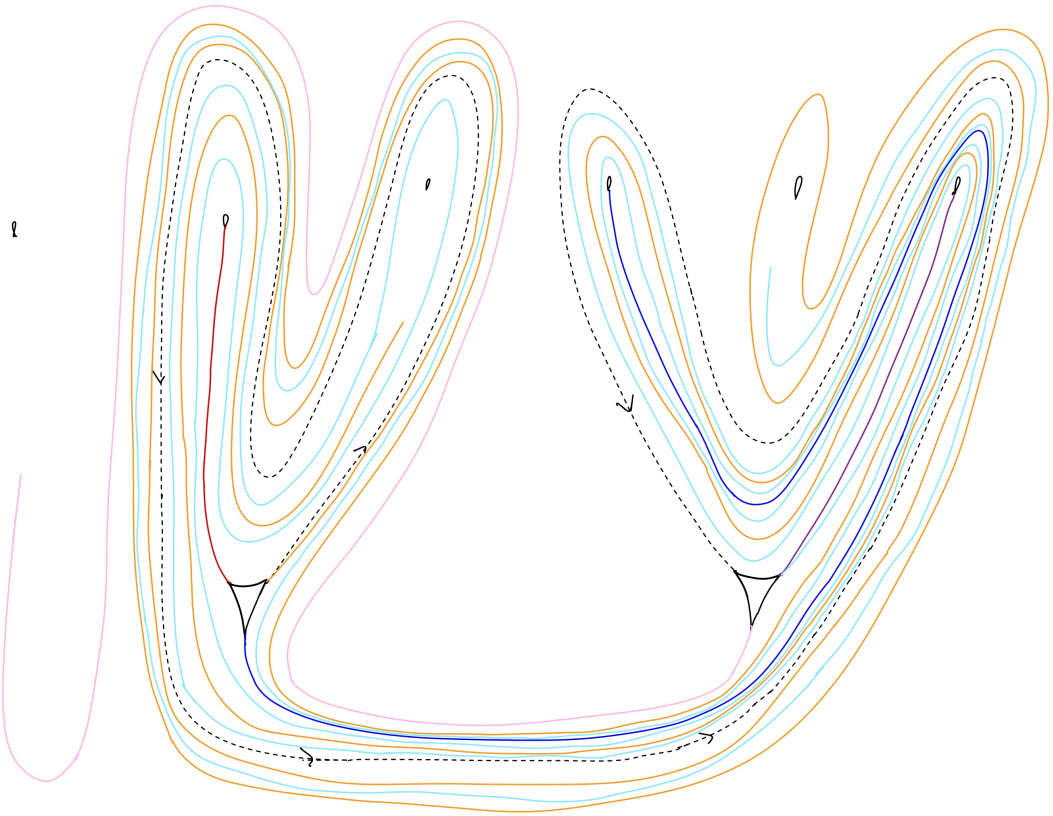


Figure F.9: Gnash5

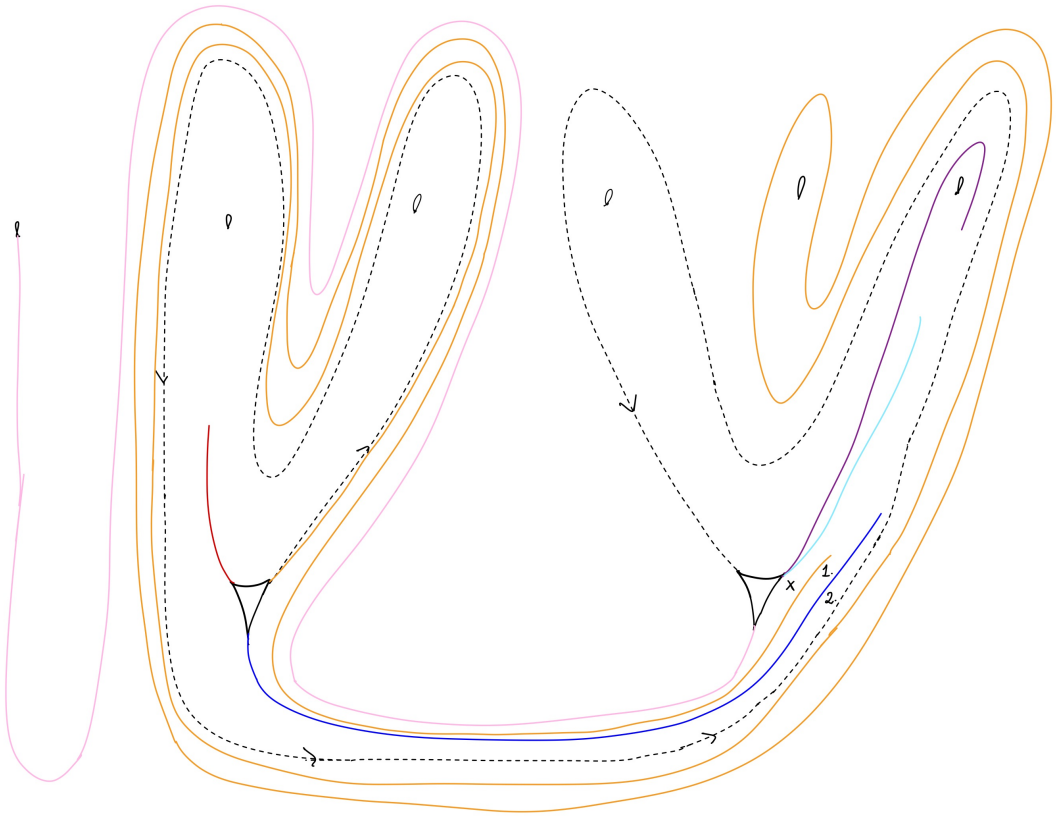


Figure F.10: Inert1

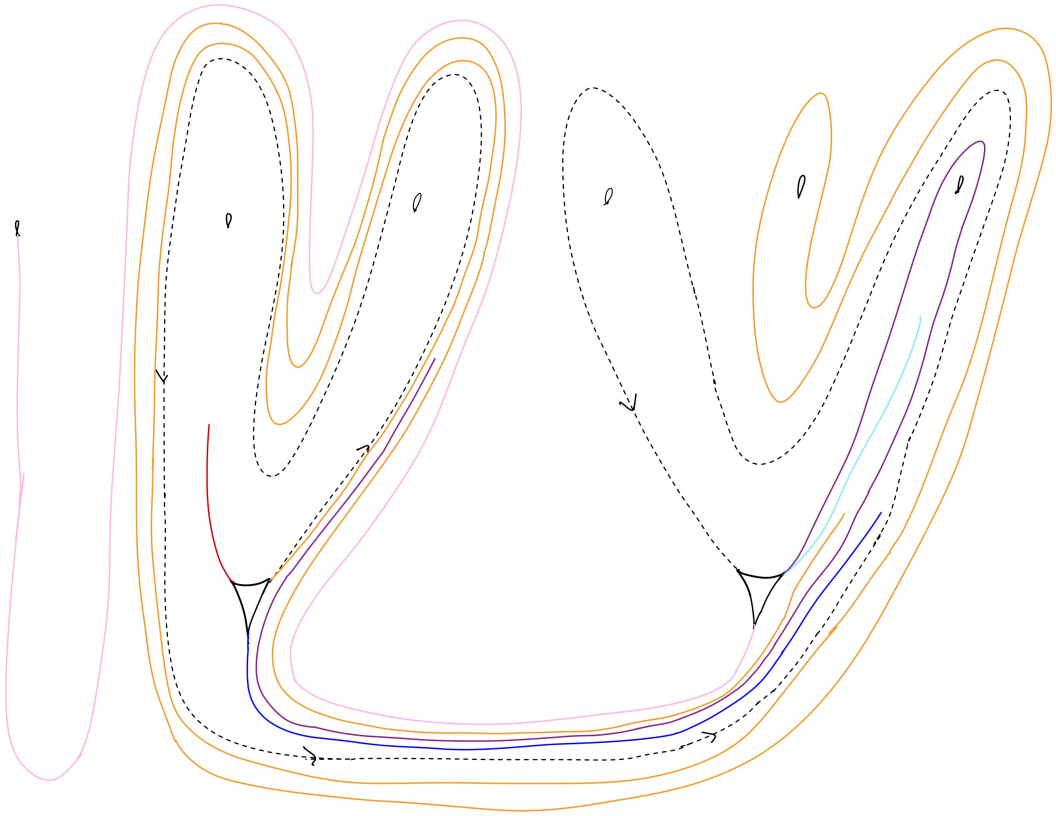


Figure F.11: Callow1

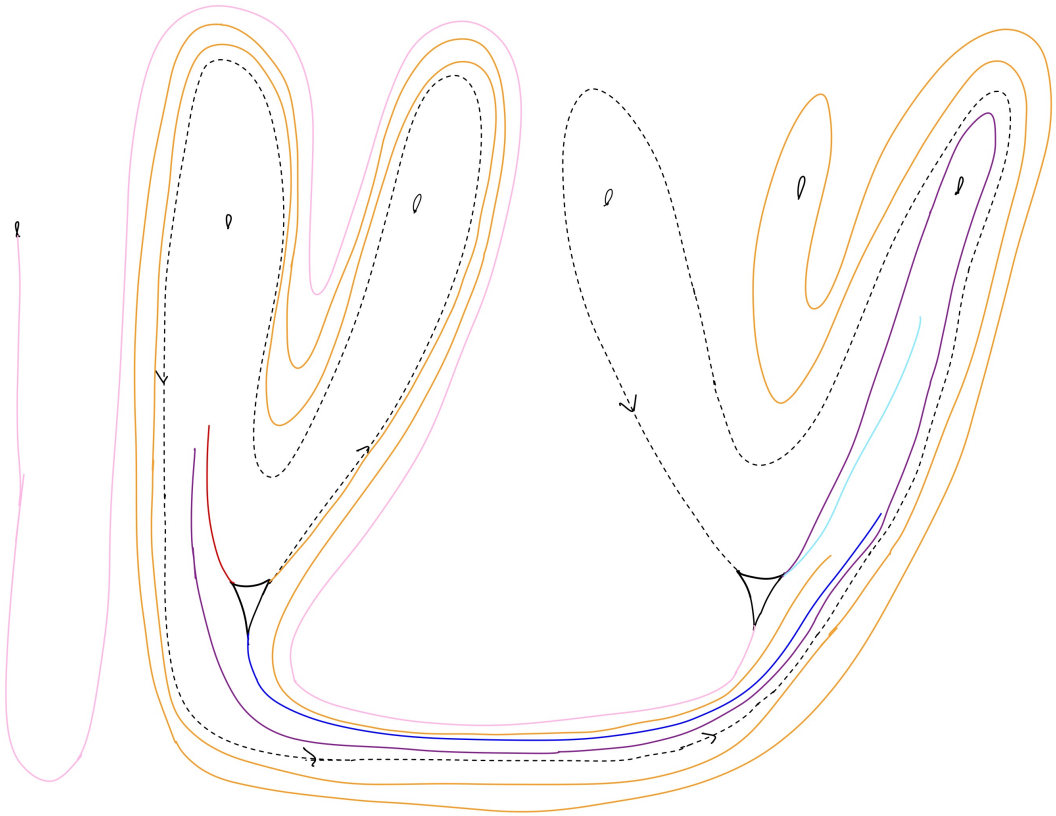


Figure F.12: Ennui1

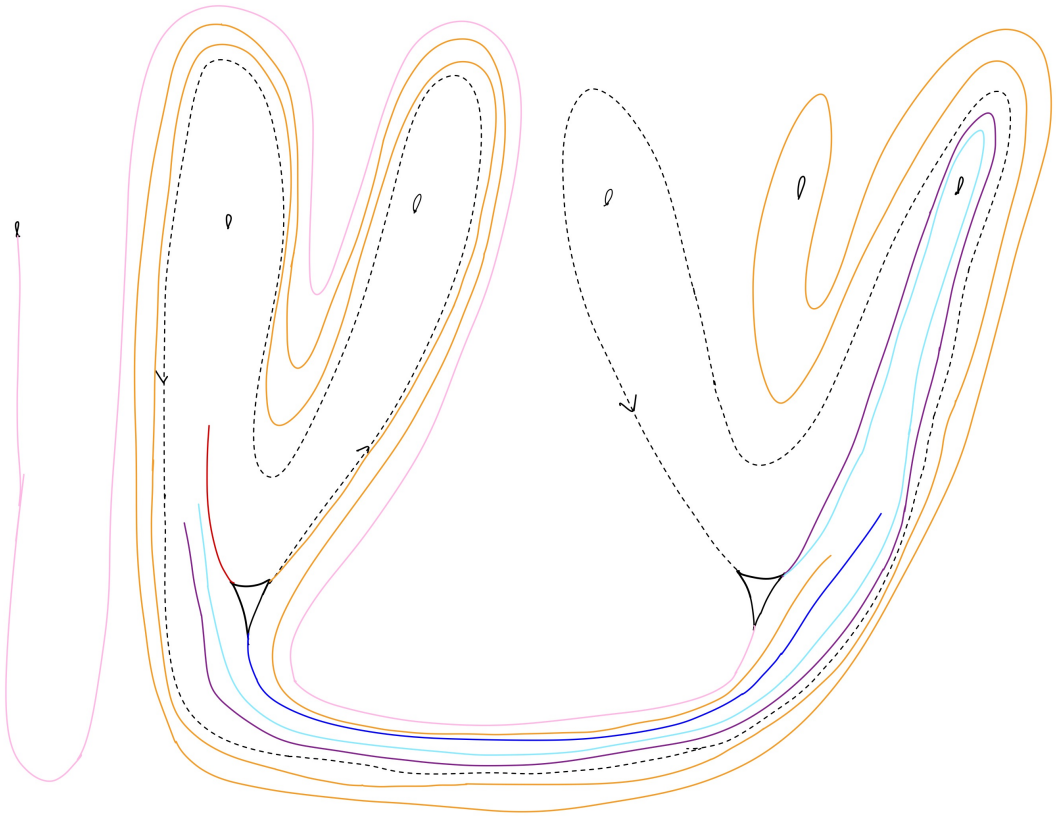


Figure F.13: Ennui2

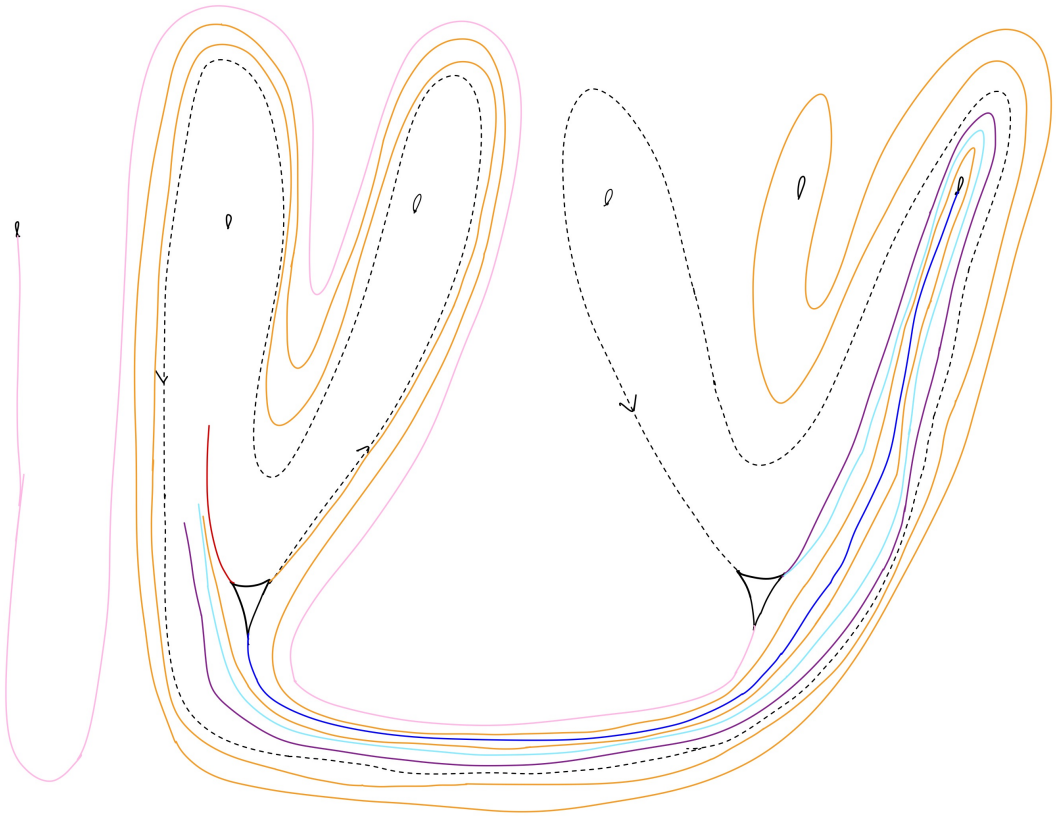


Figure F.14: Ennui3

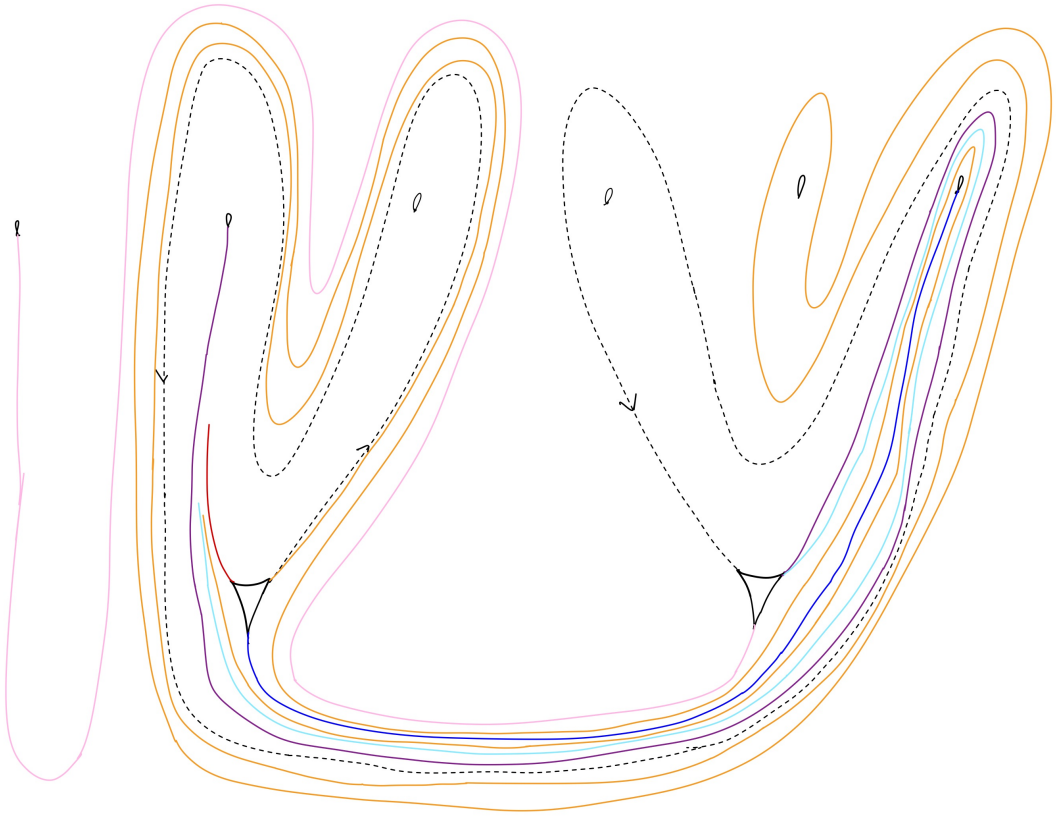


Figure F.15: Brumous1

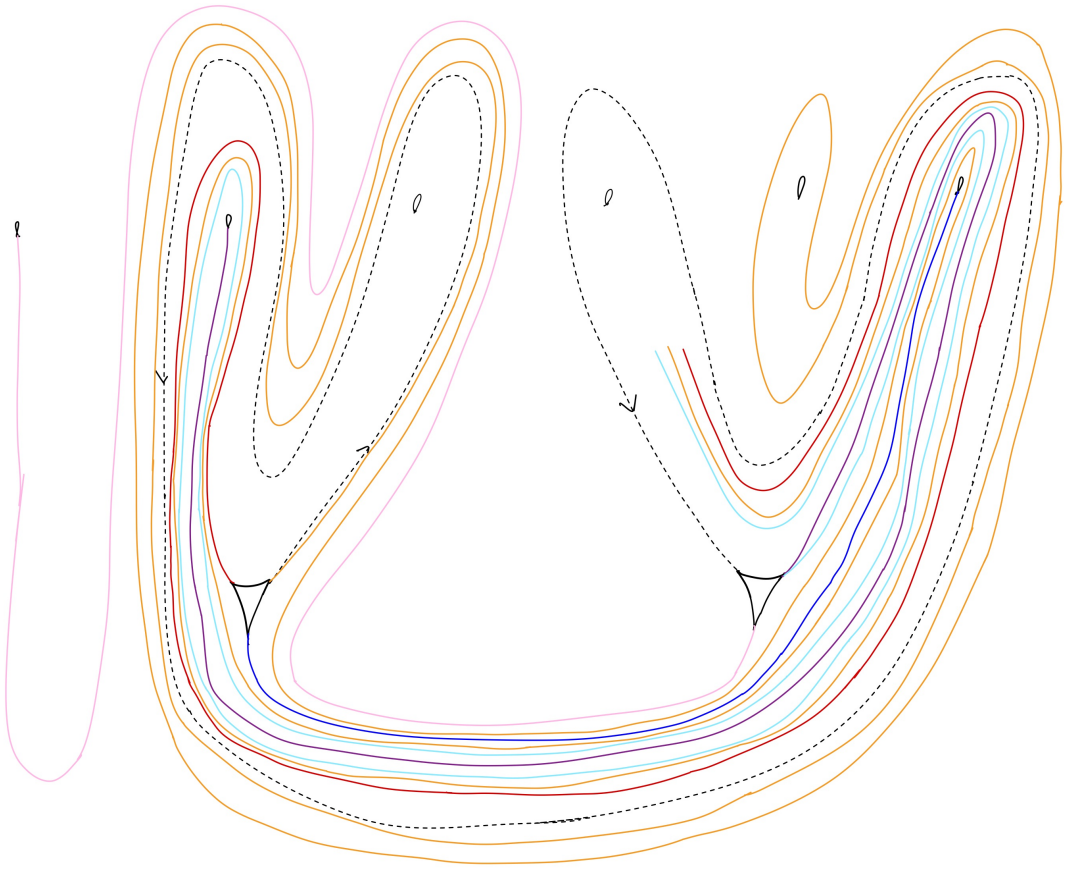


Figure F.16: Brumous2

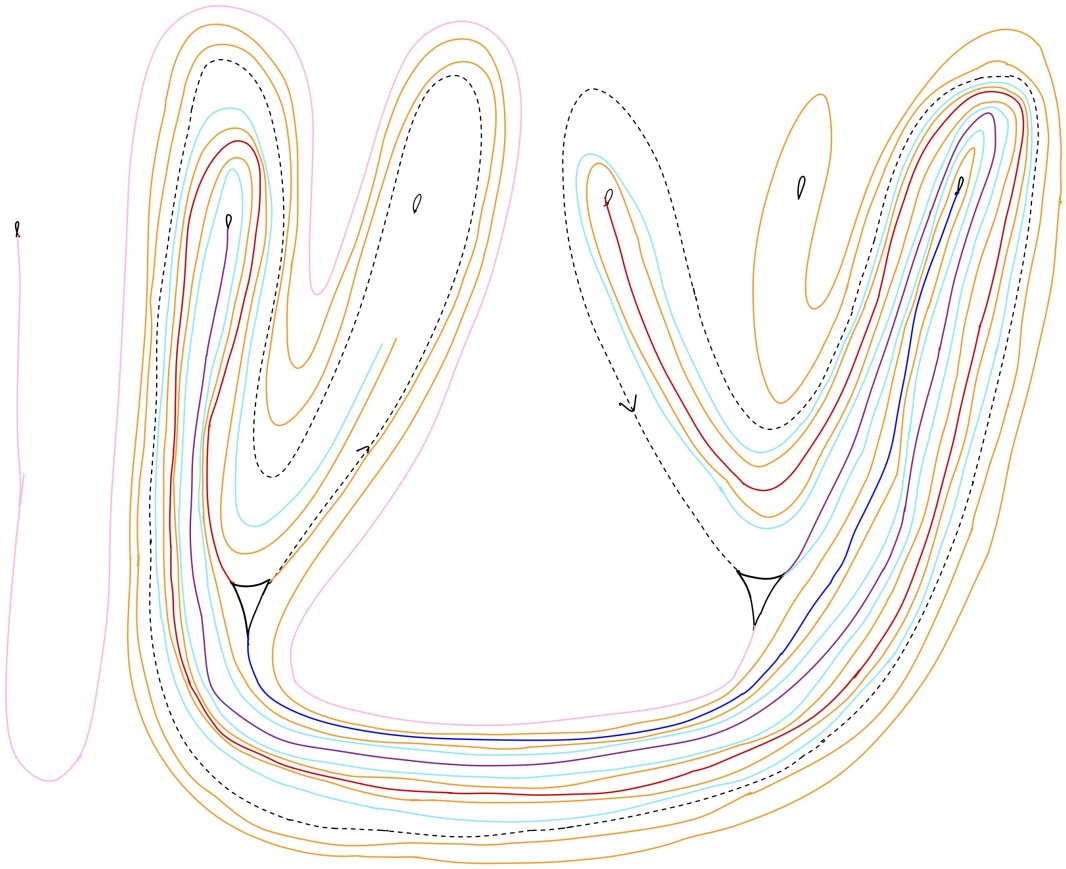


Figure F.17: Brumous3

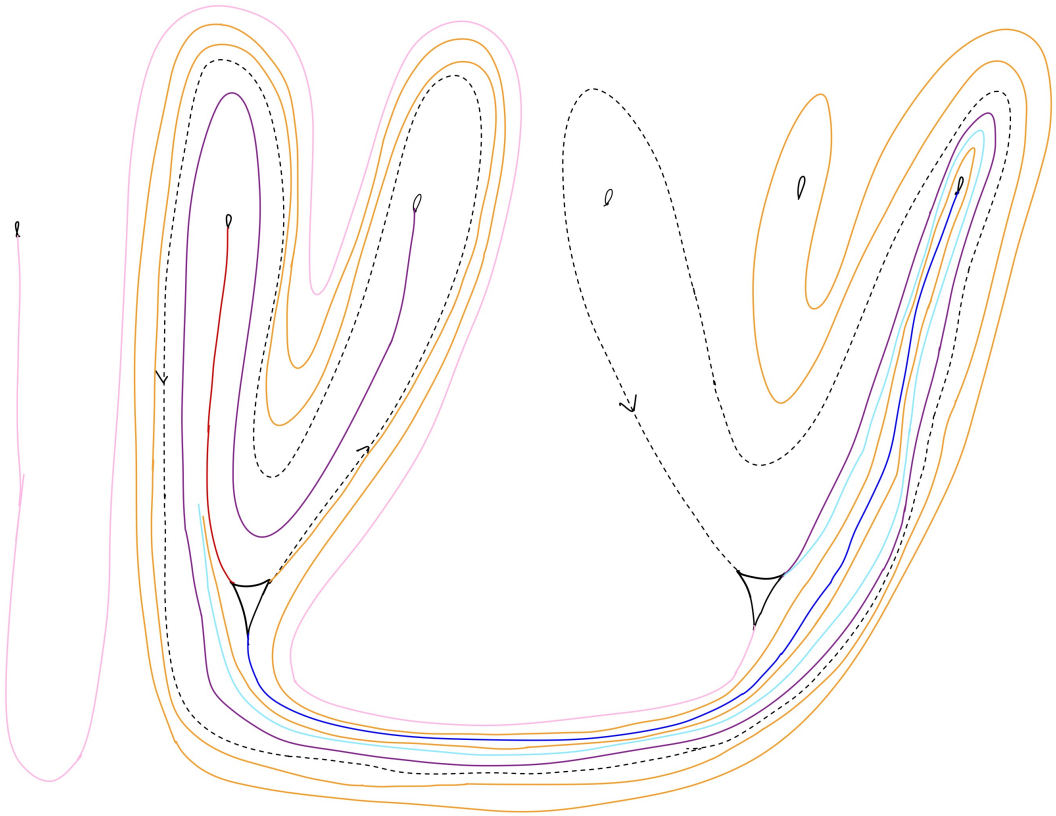


Figure F.18: Coterie1

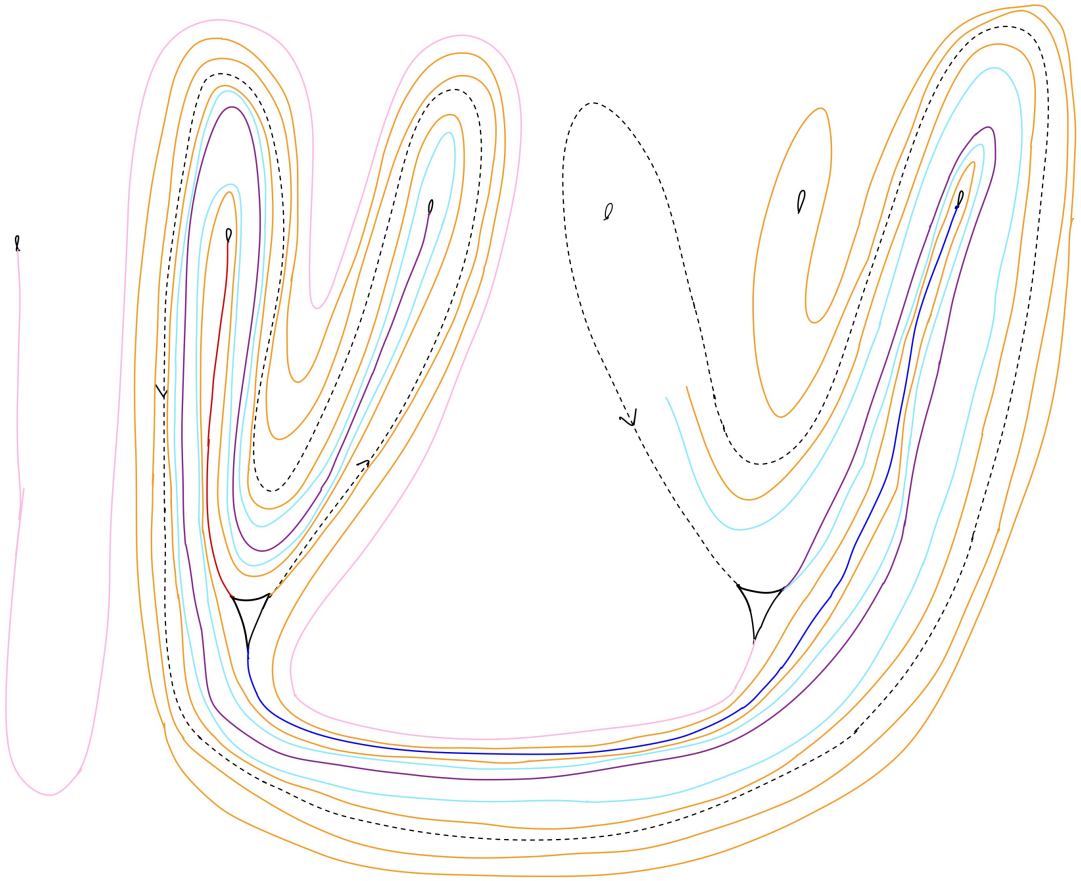


Figure F.19: Coterie2

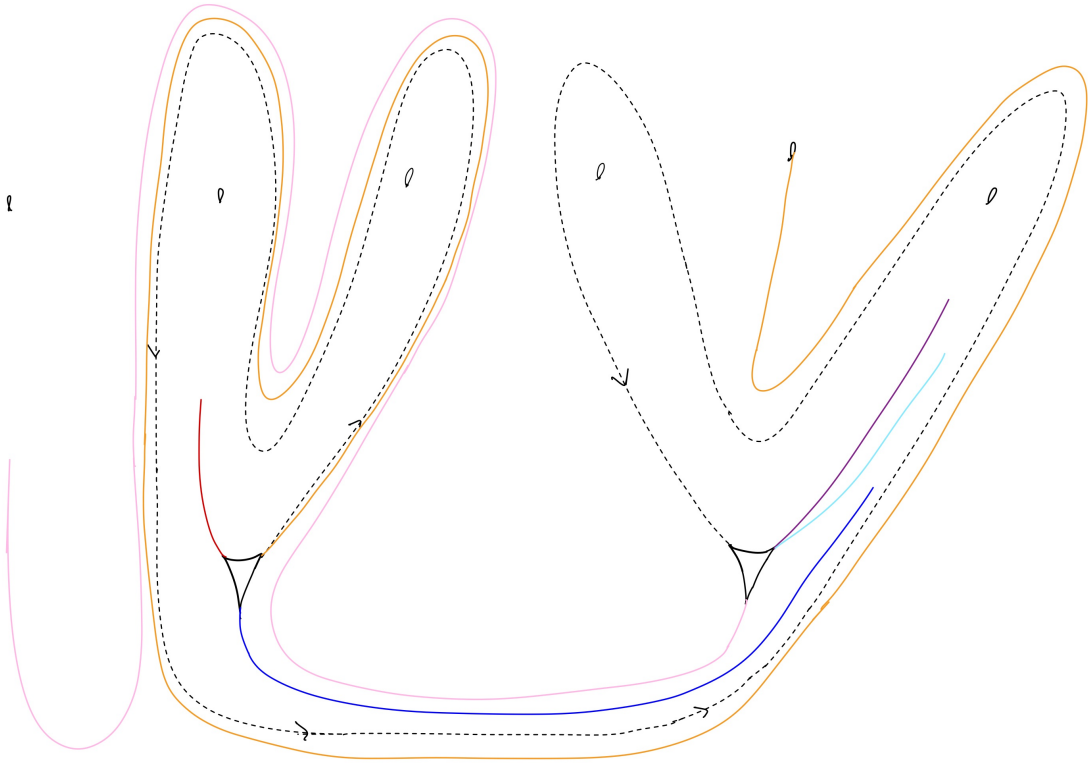


Figure F.20: Gurn1

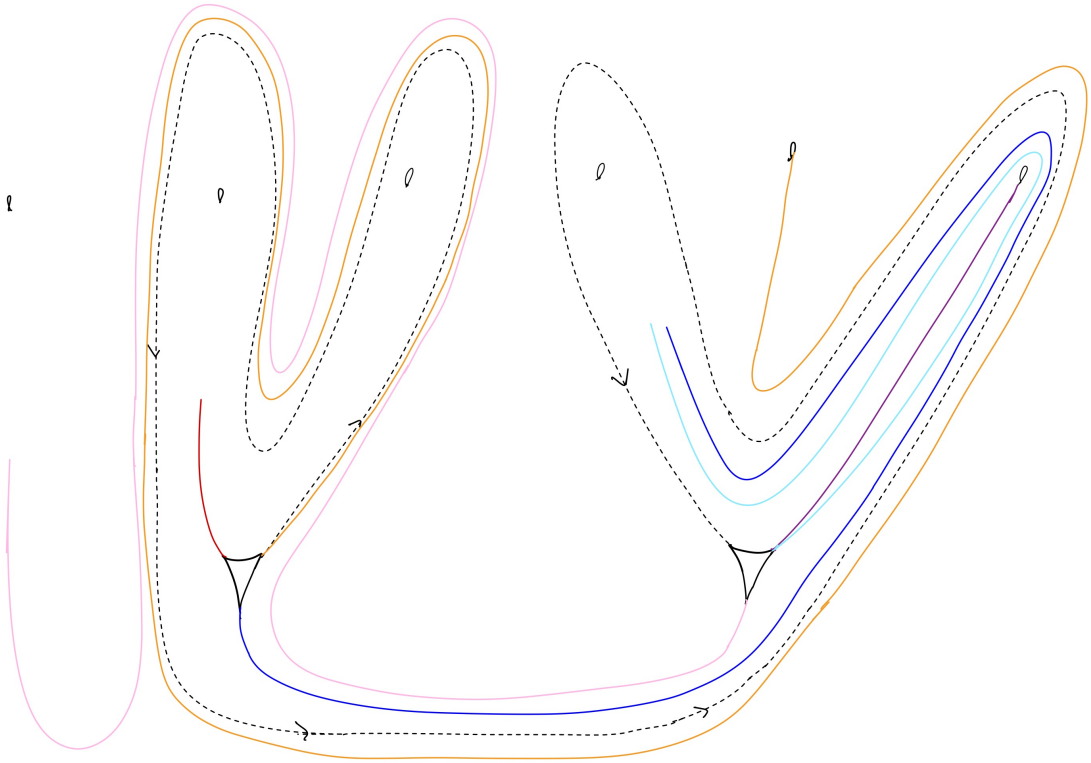


Figure F.21: Anomy1

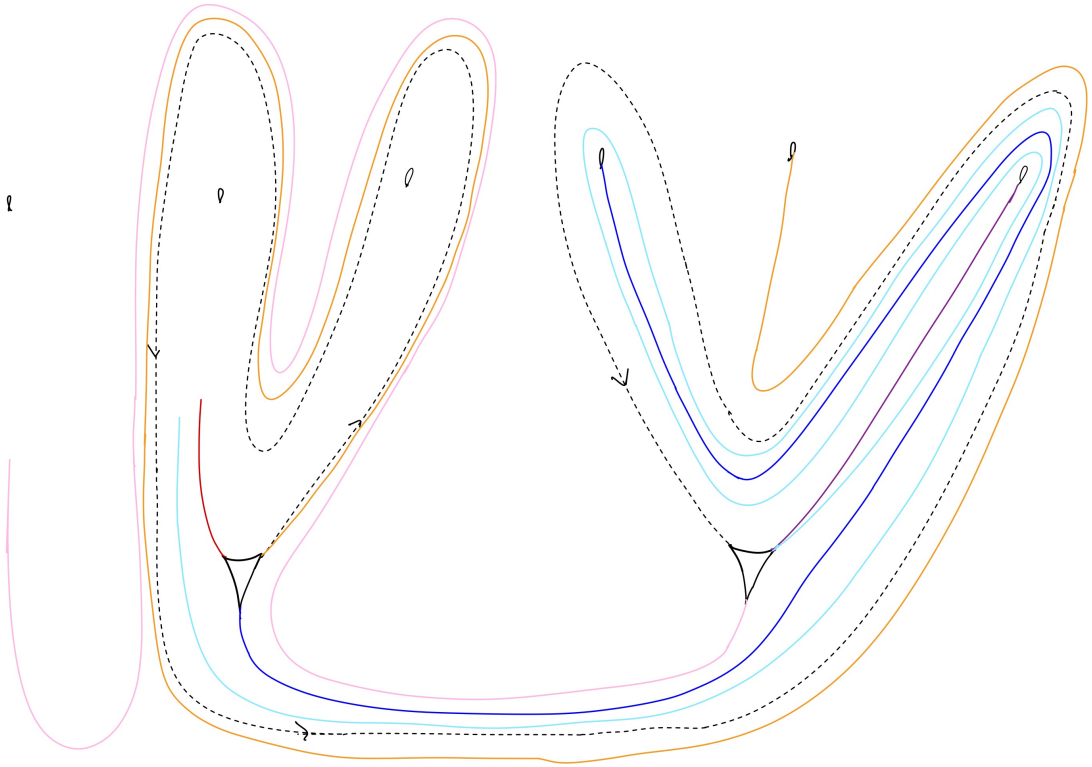


Figure F.22: Anomy2

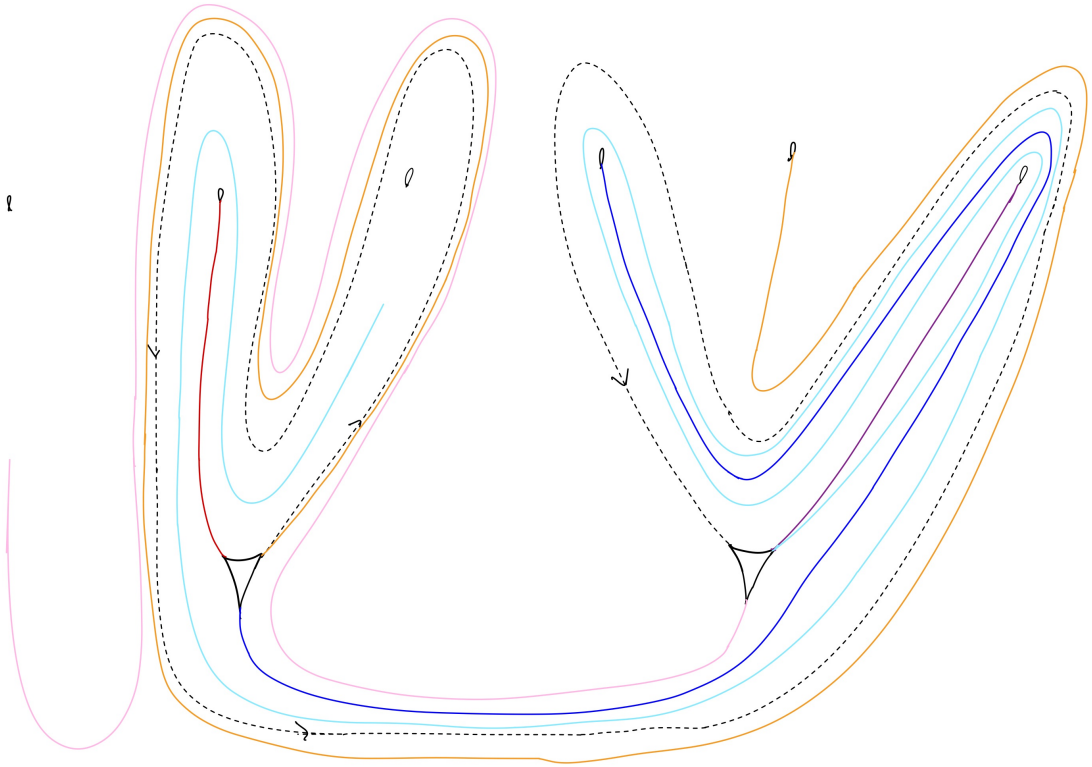


Figure F.23: Anomy3

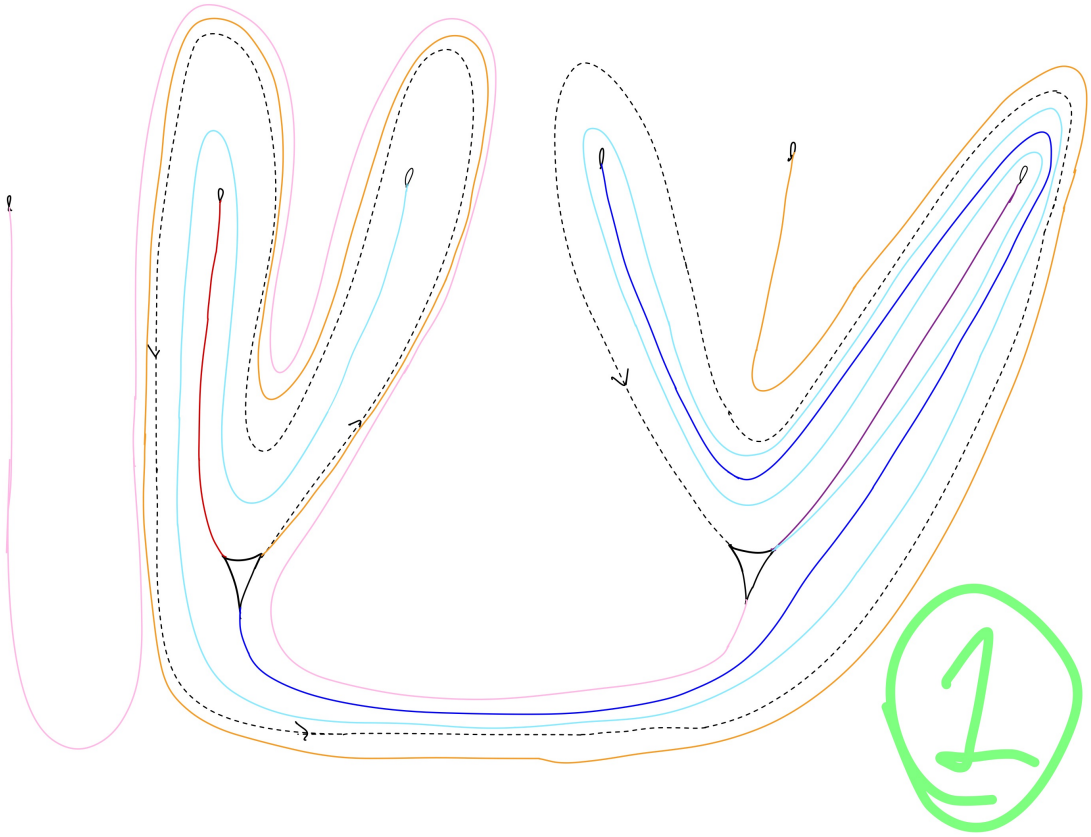


Figure F.24: Anomy4

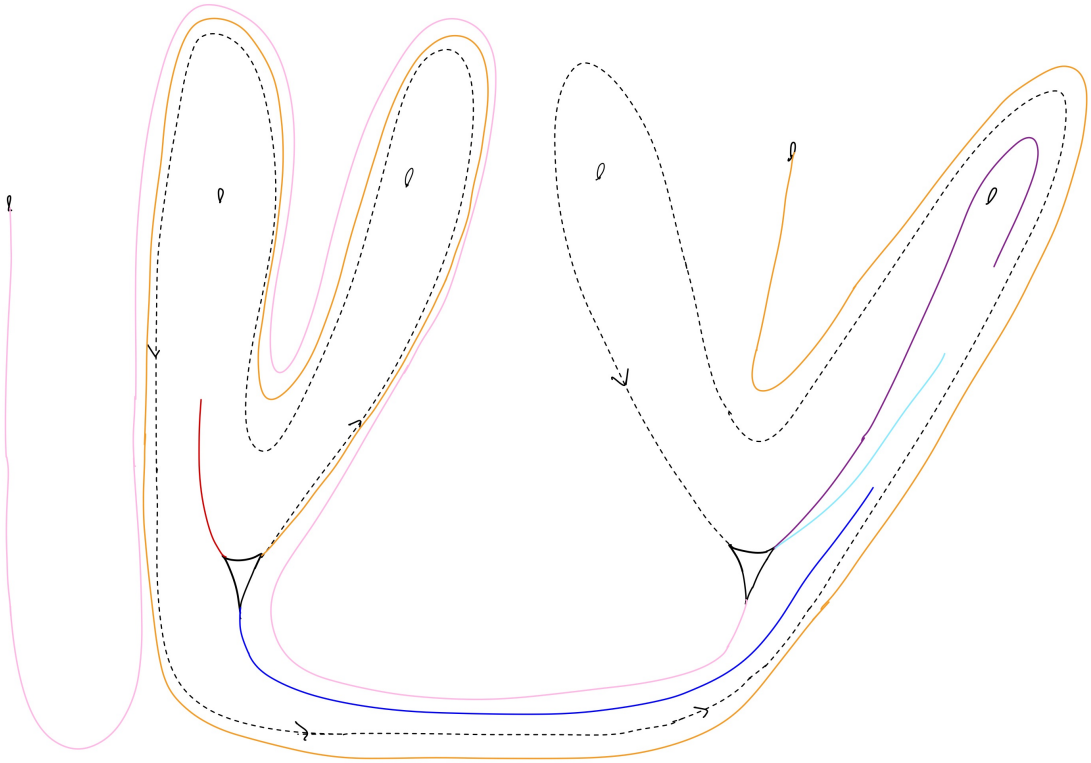


Figure F.25: Bruit1

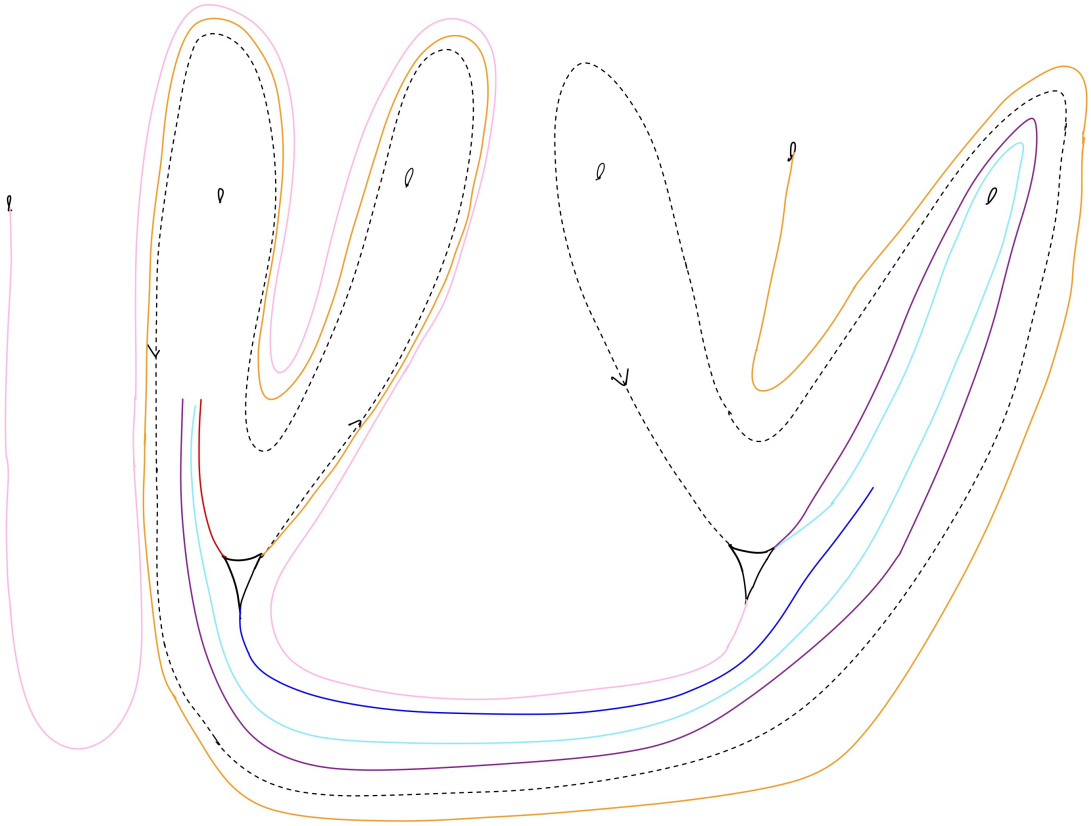


Figure F.26: Bruit2

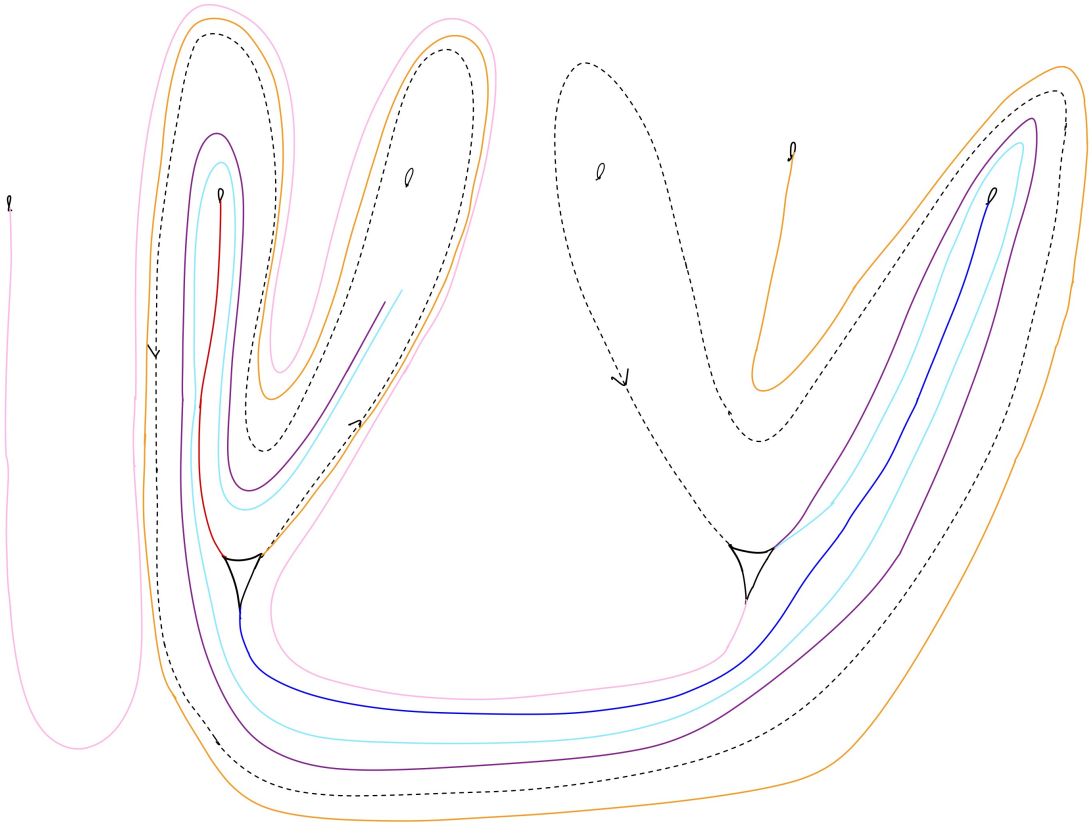


Figure F.27: Diatree1

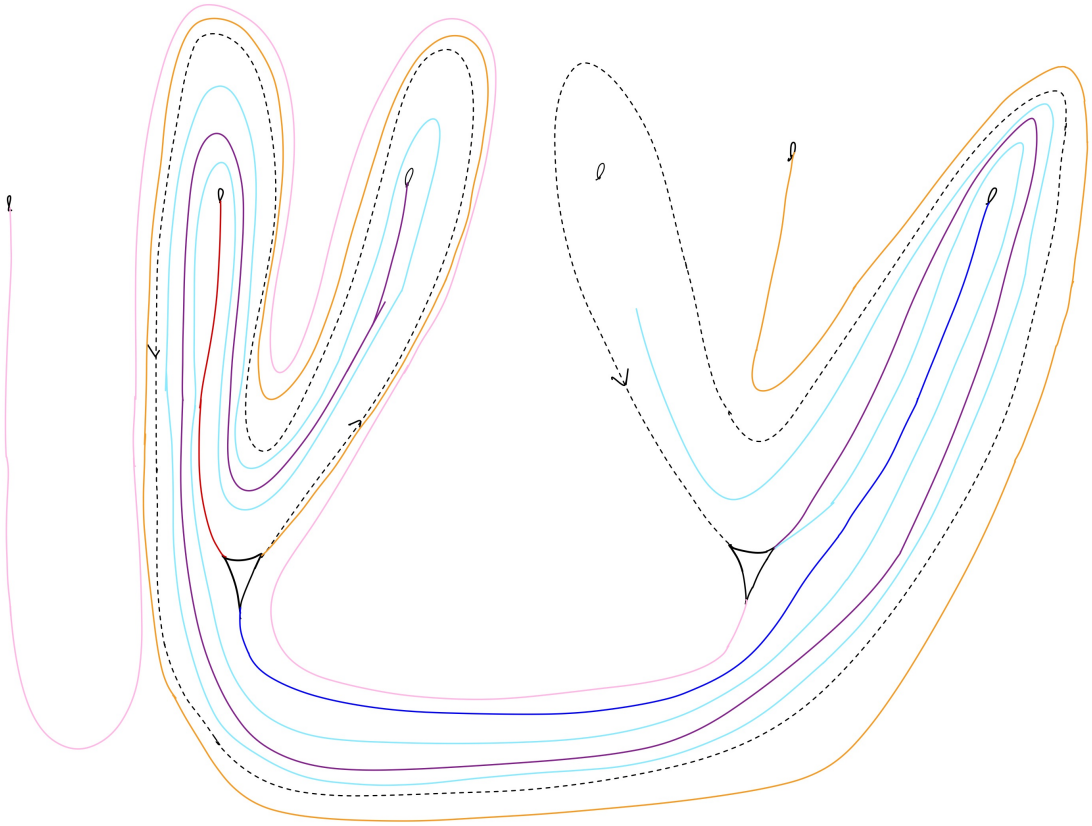


Figure F.28: Diatree2

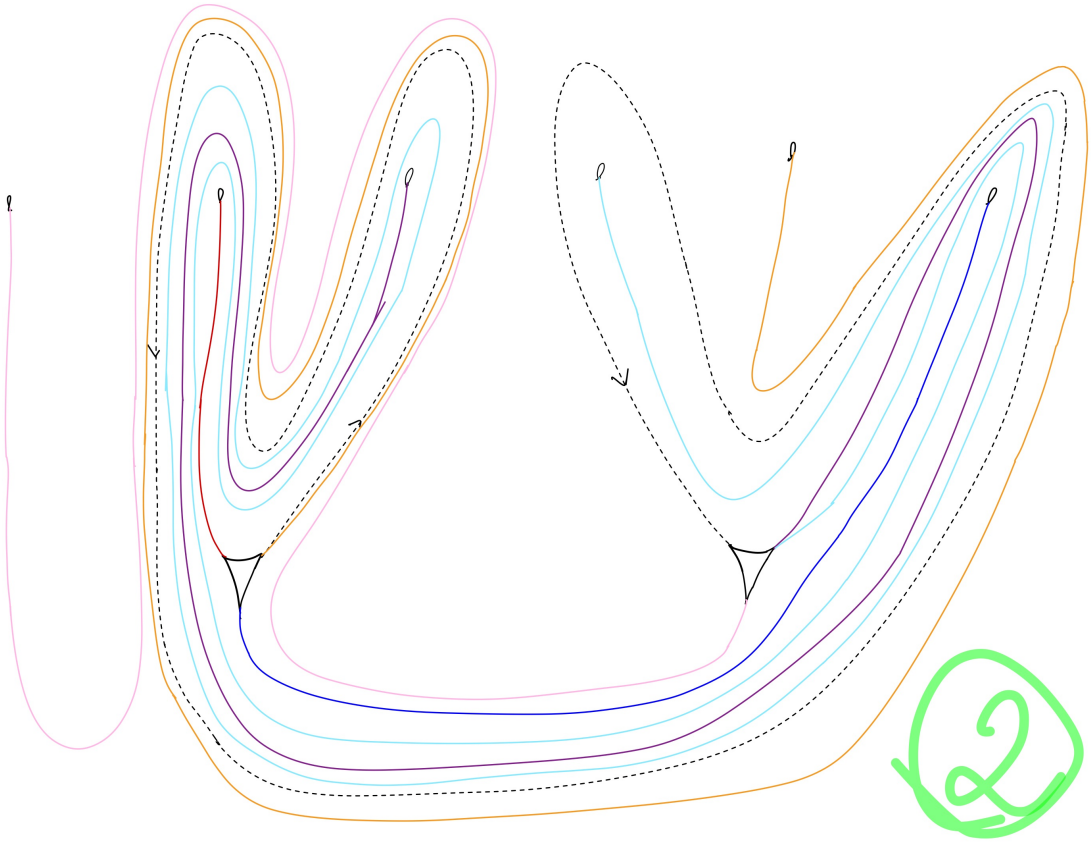


Figure F.29: Diatree3

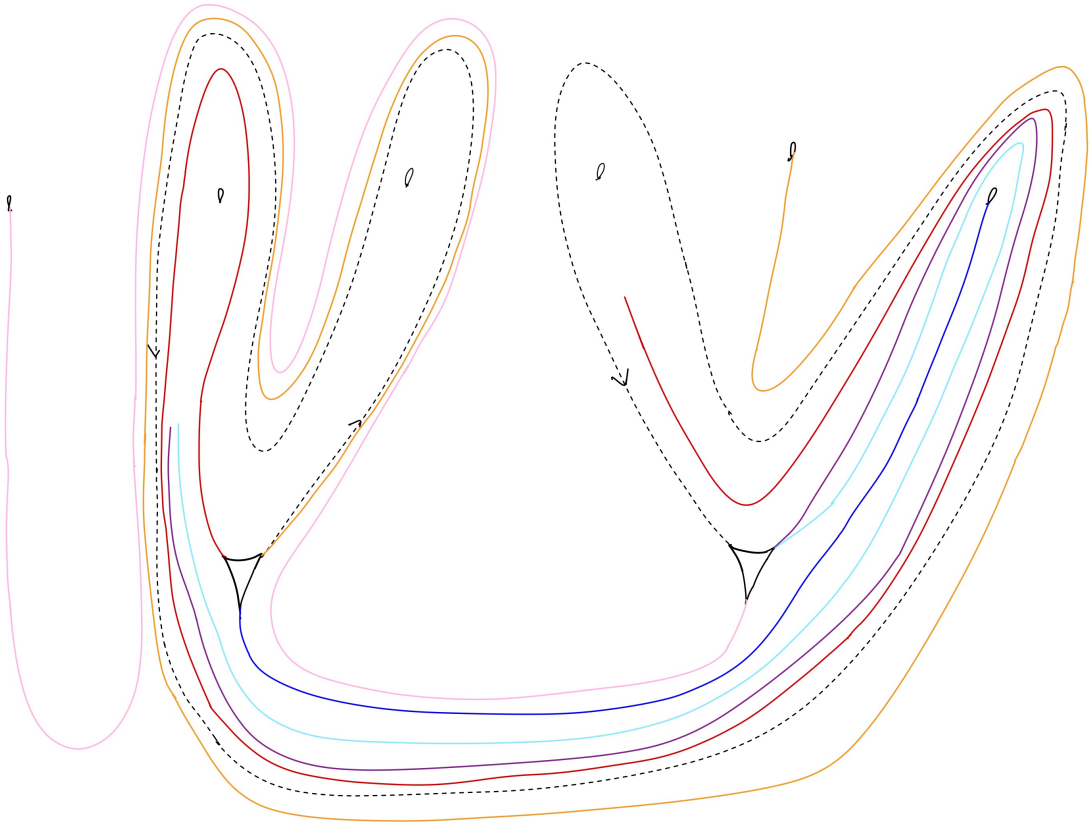


Figure F.30: Fulmine1

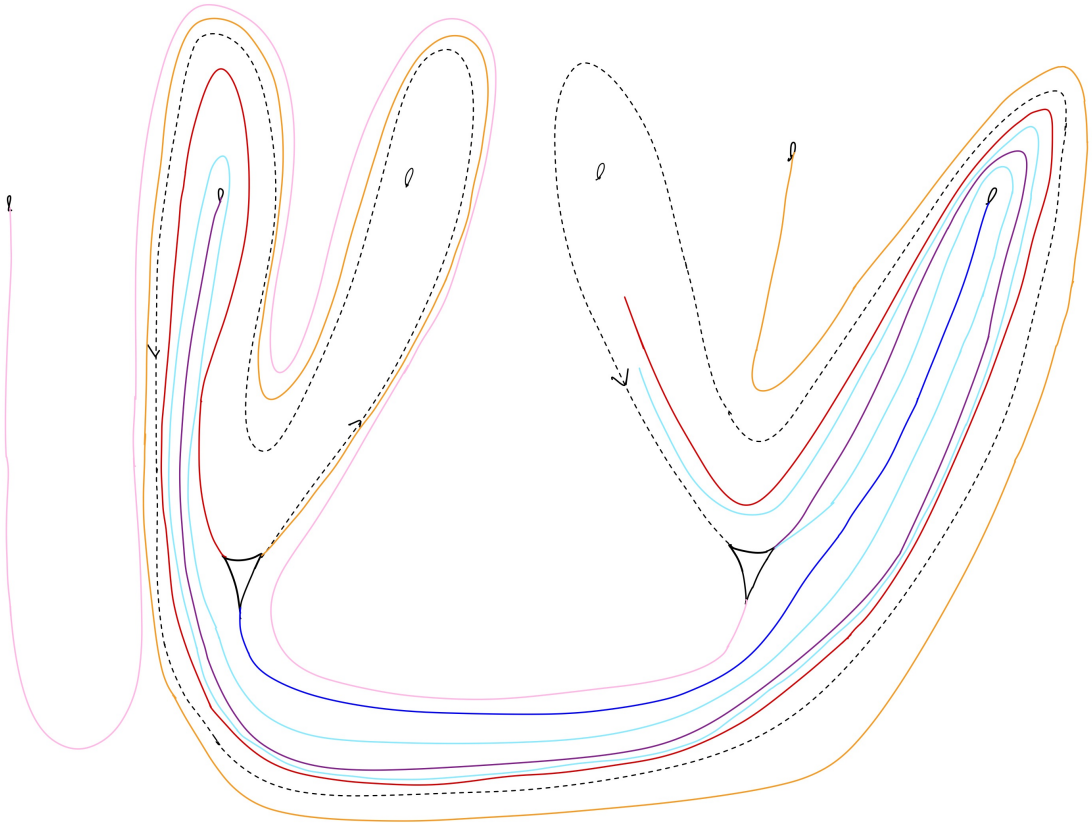


Figure F.31: Fulmine2

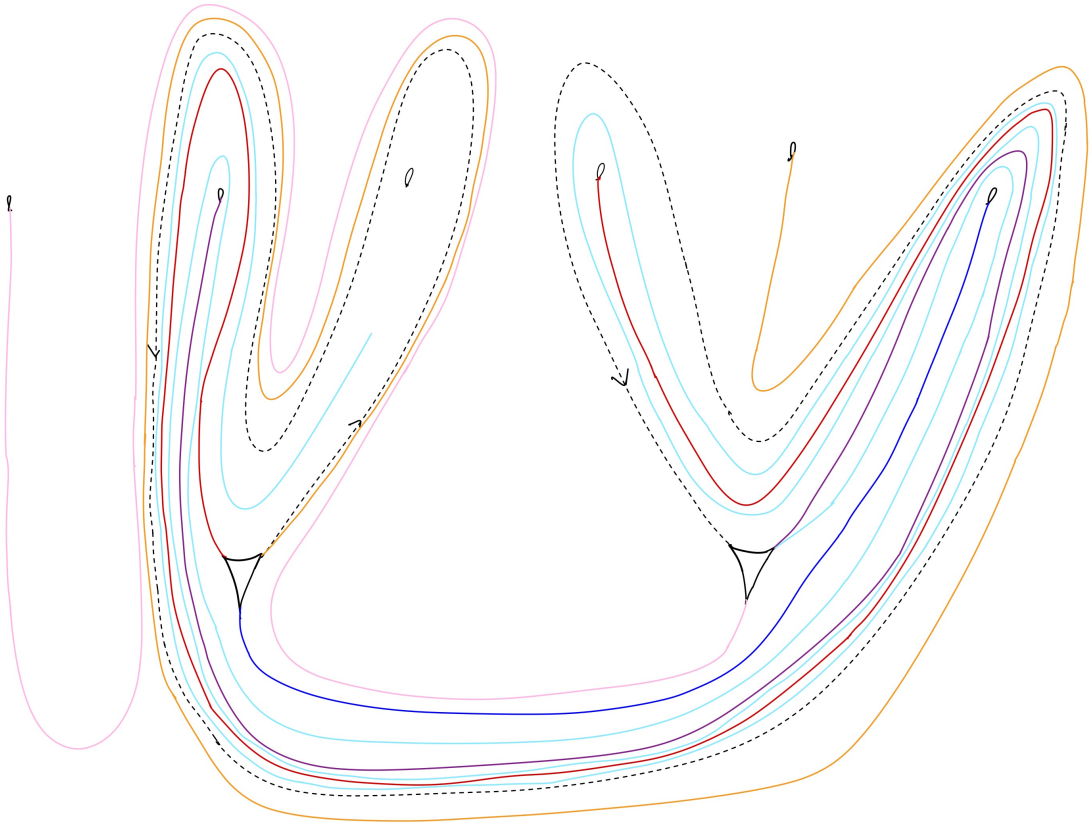


Figure F.32: Fulmine3

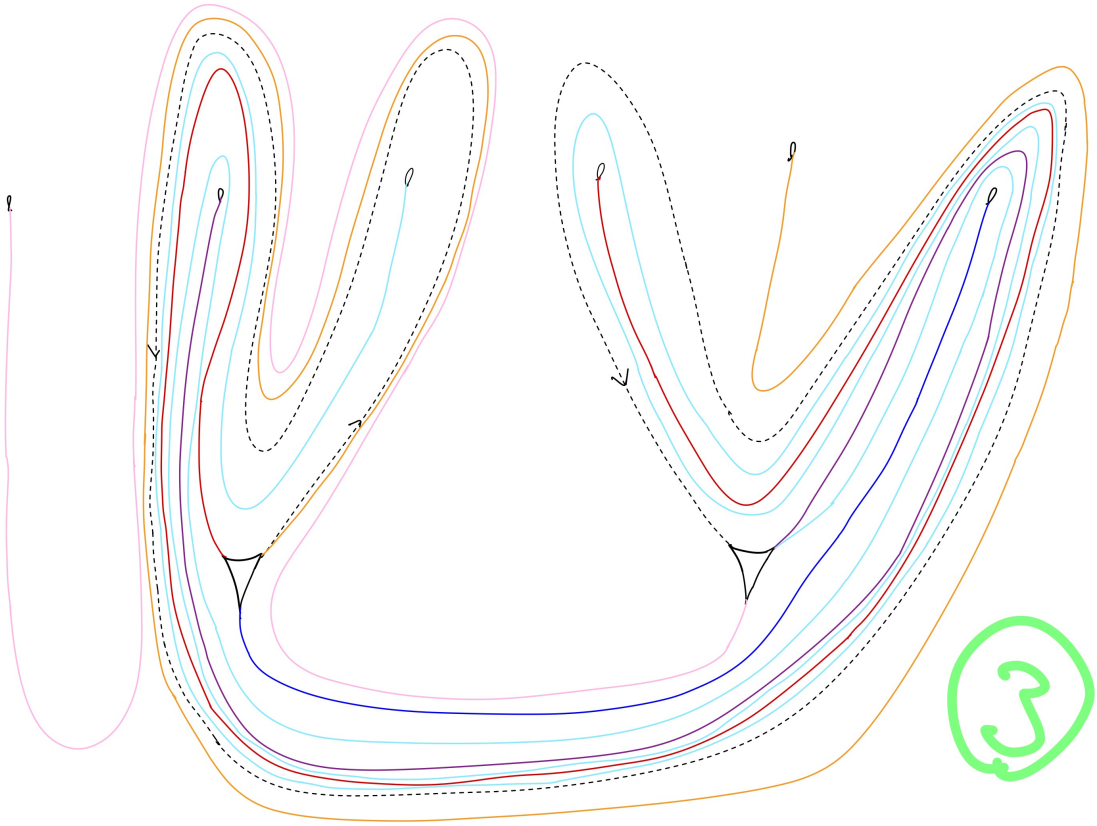


Figure F.33: Fulmine4

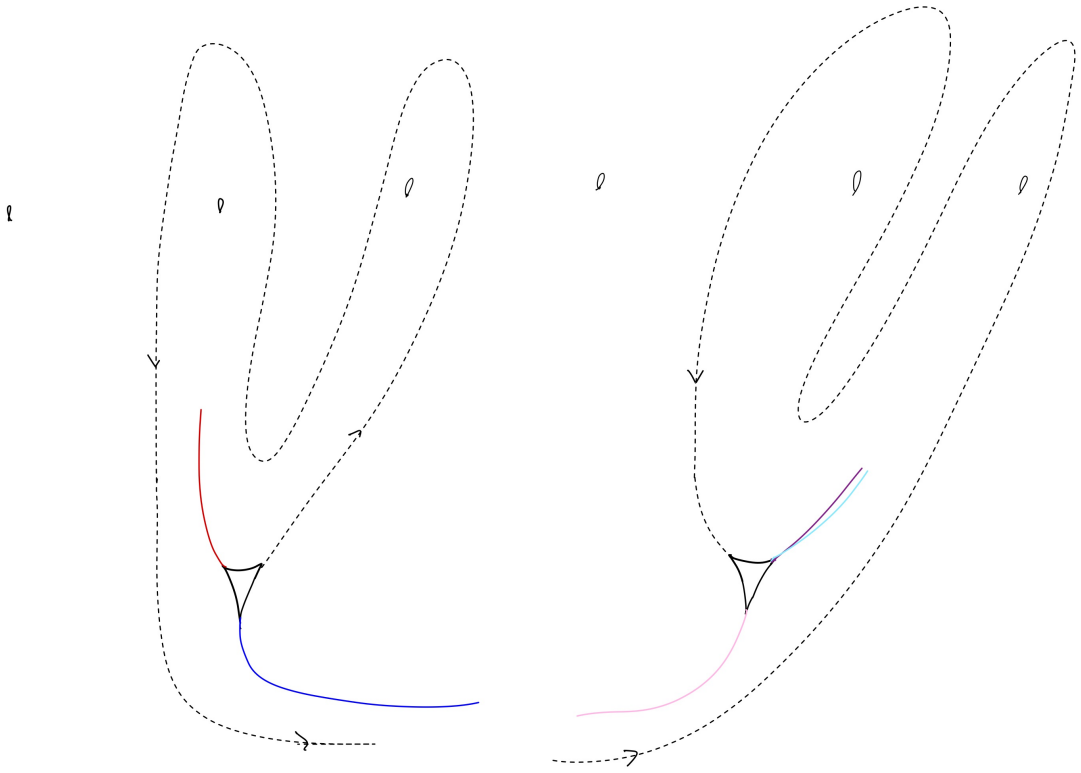


Figure F.34: BRR1

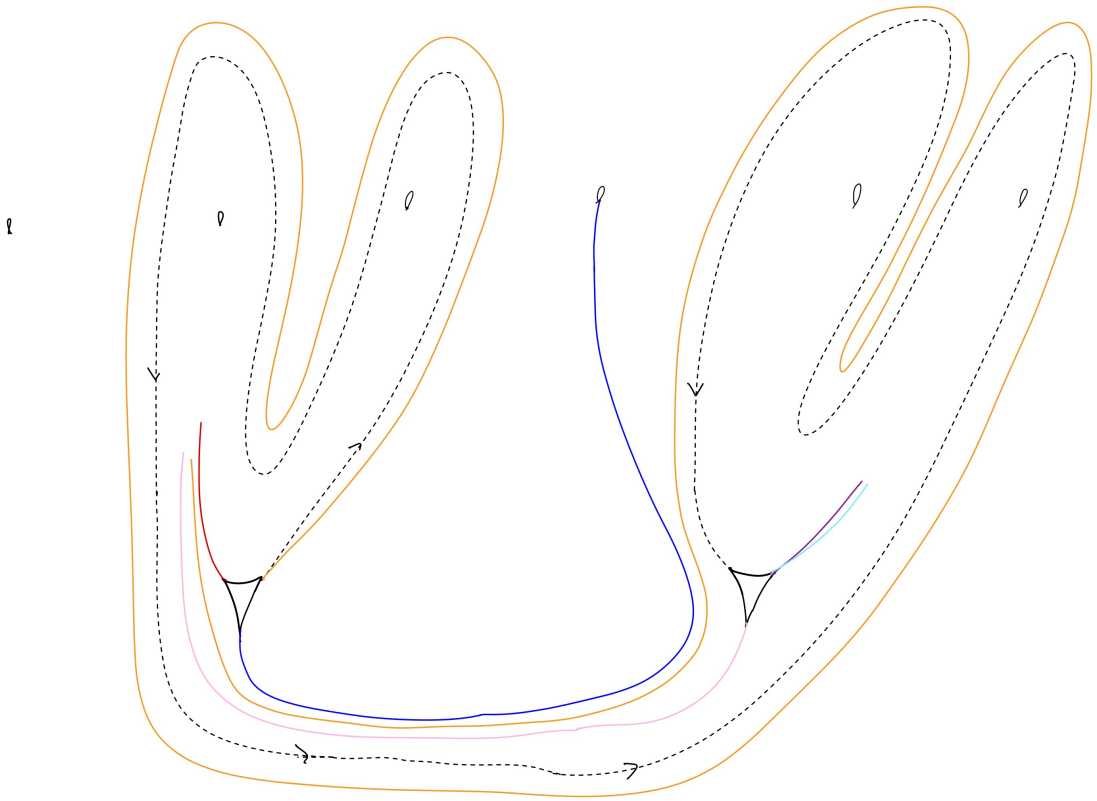


Figure F.35: BRR2

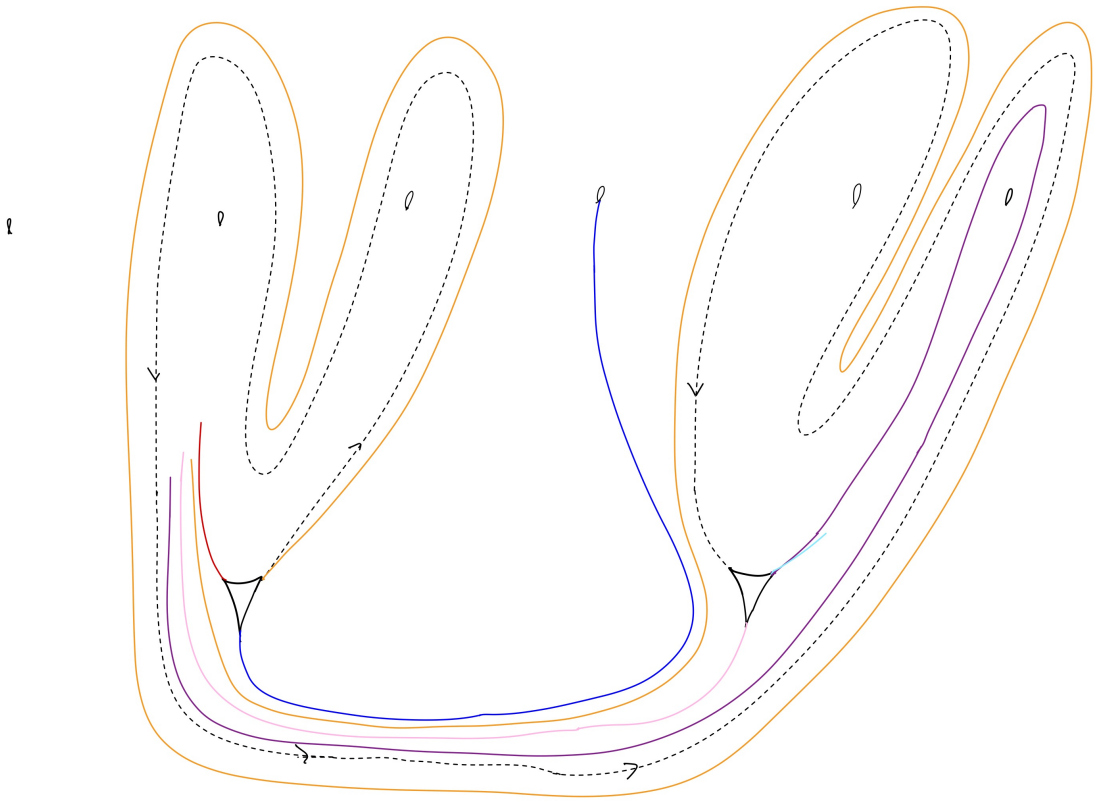


Figure F.36: BRR3

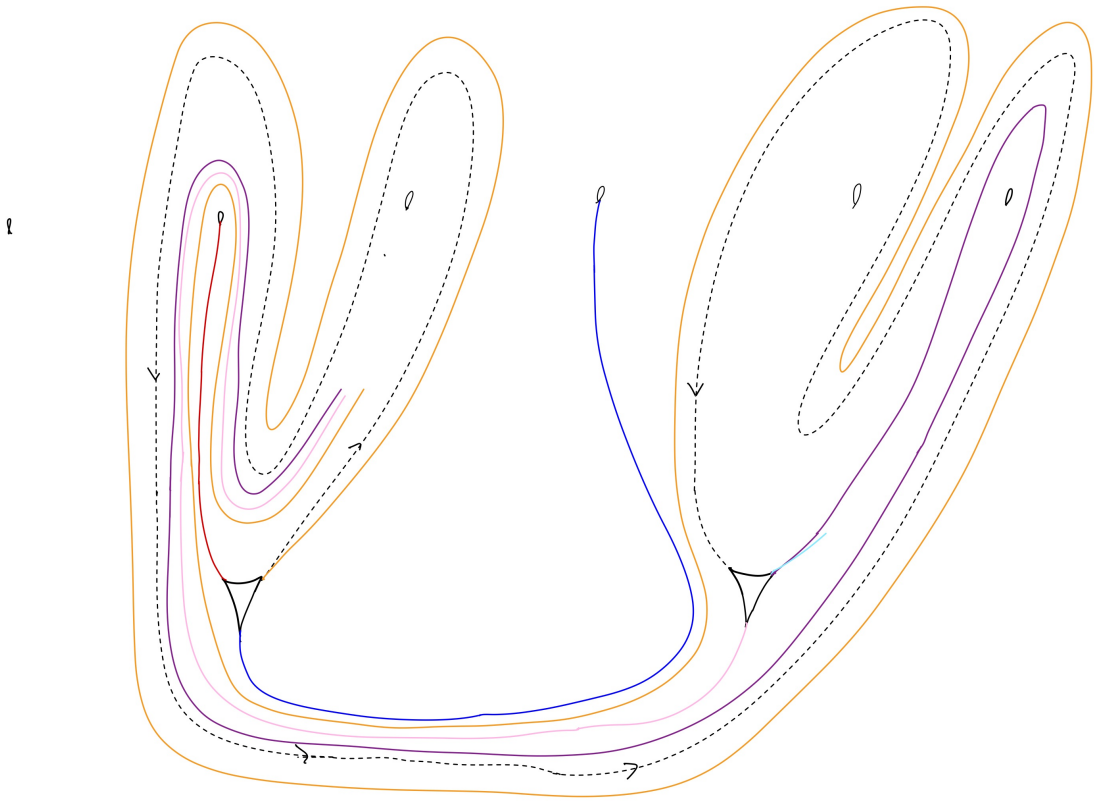


Figure F.37: Agog1

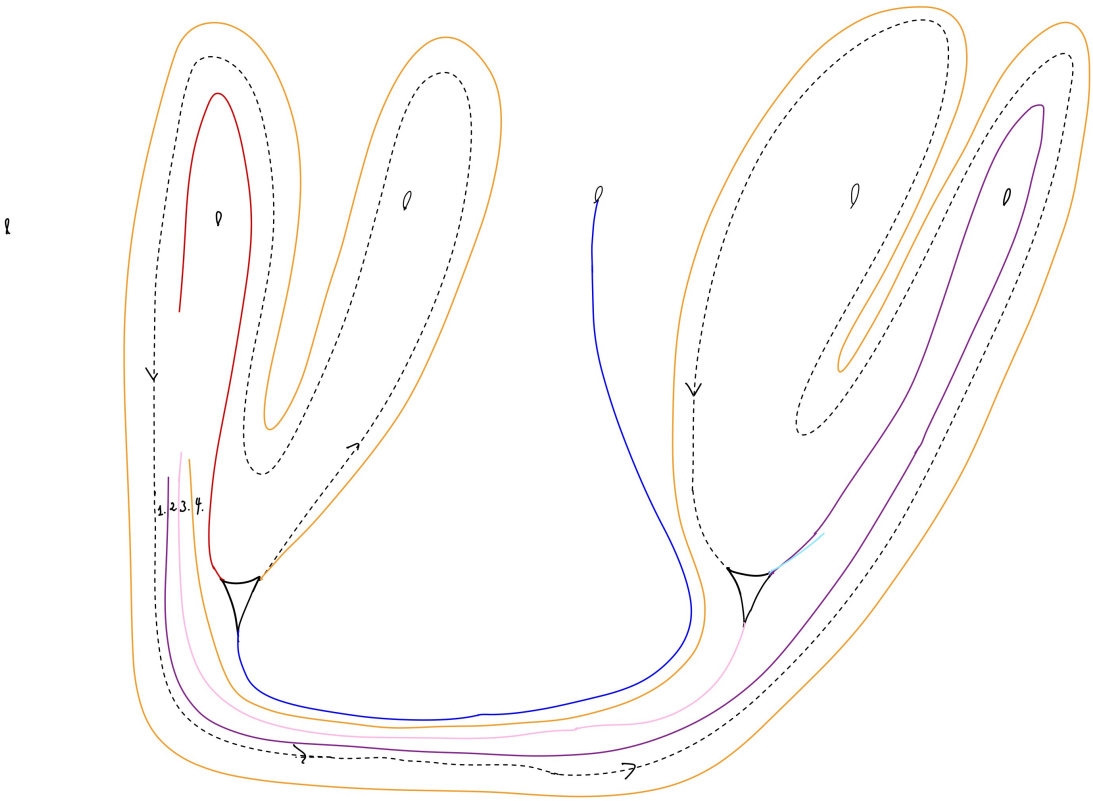


Figure F.38: Dory1

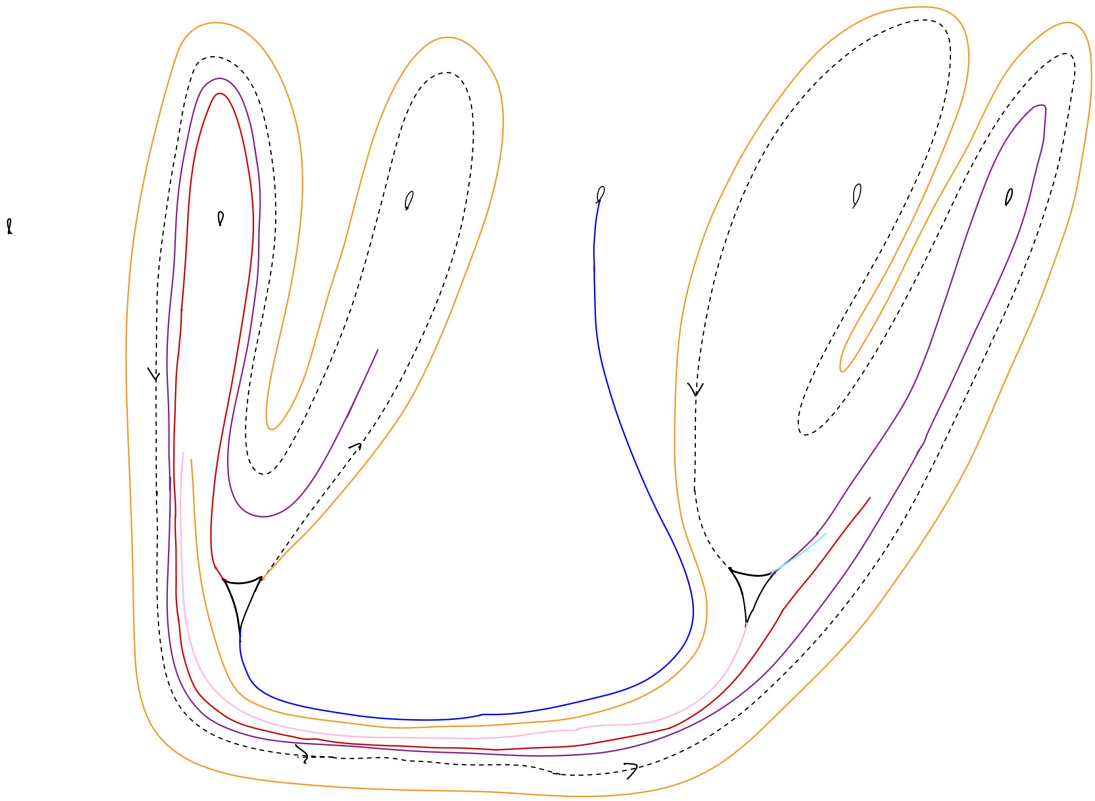


Figure F.39: Dory2

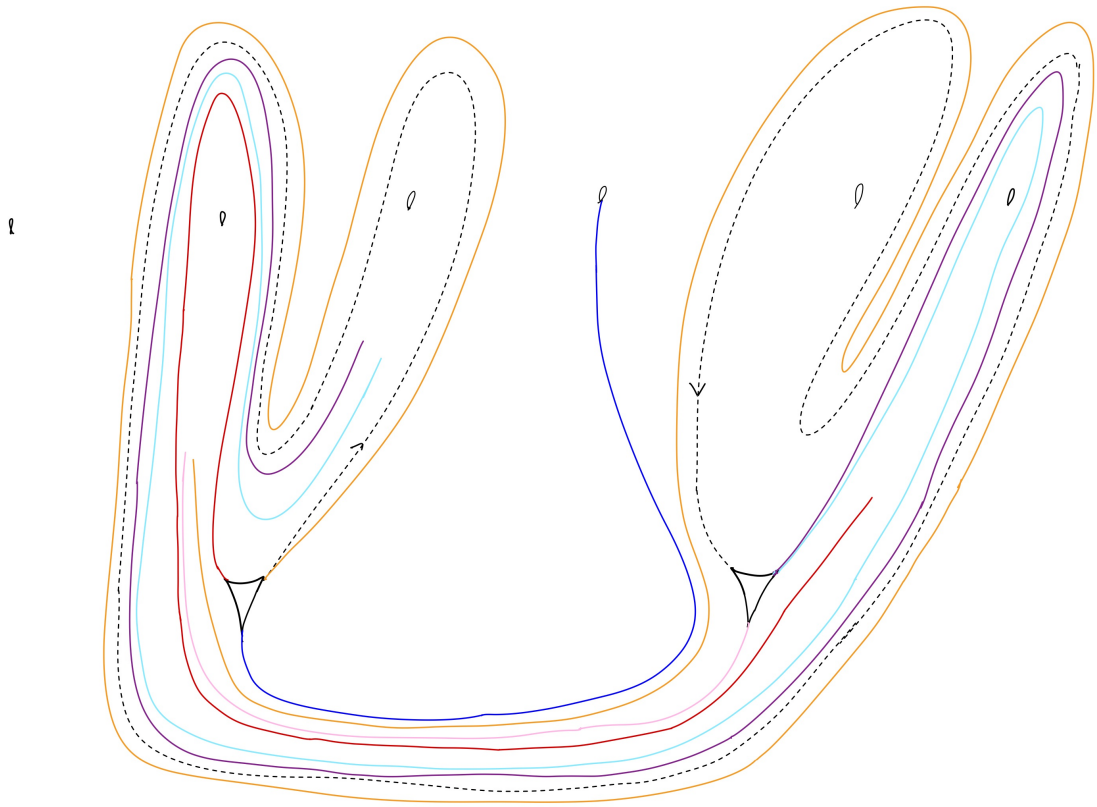


Figure F.40: Dory3

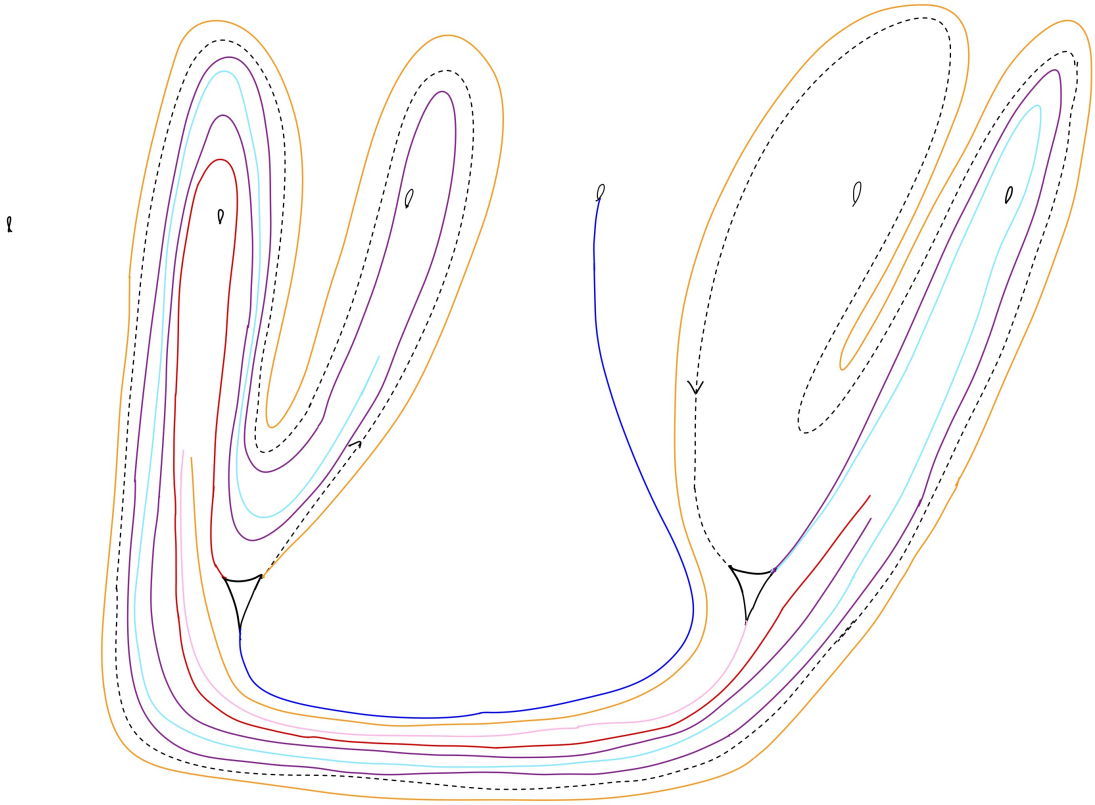


Figure F.41: Dory4

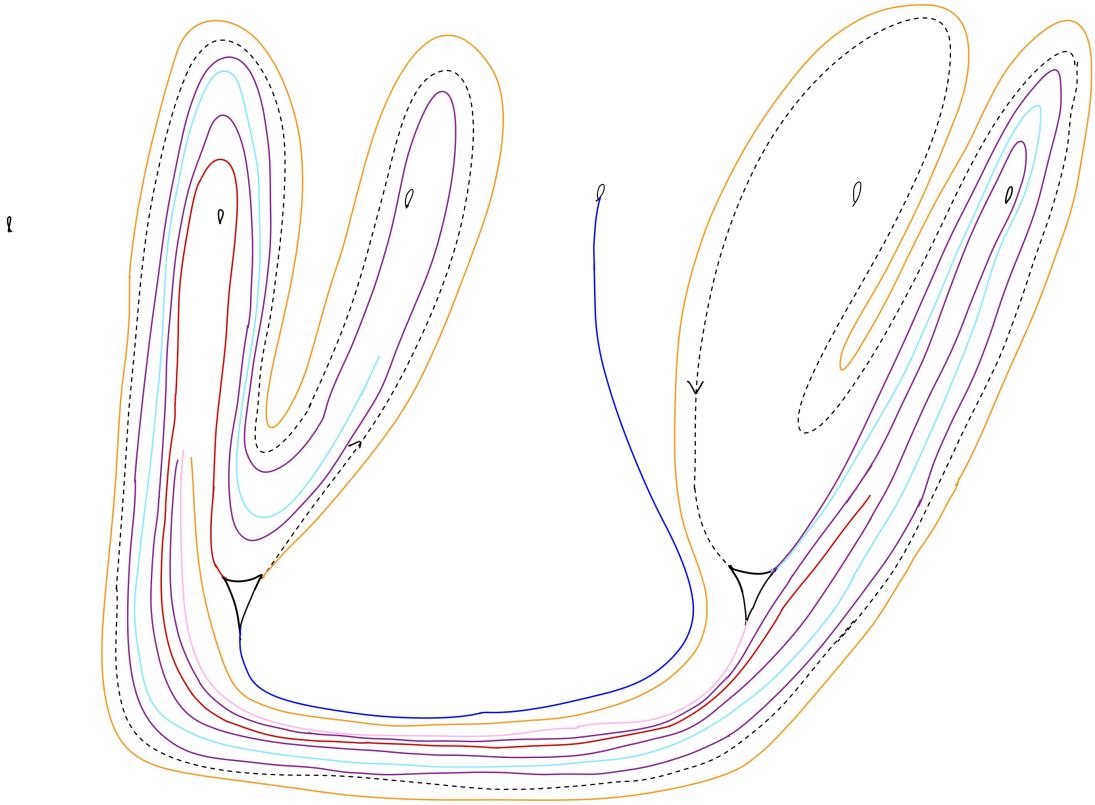


Figure F.42: Dory5

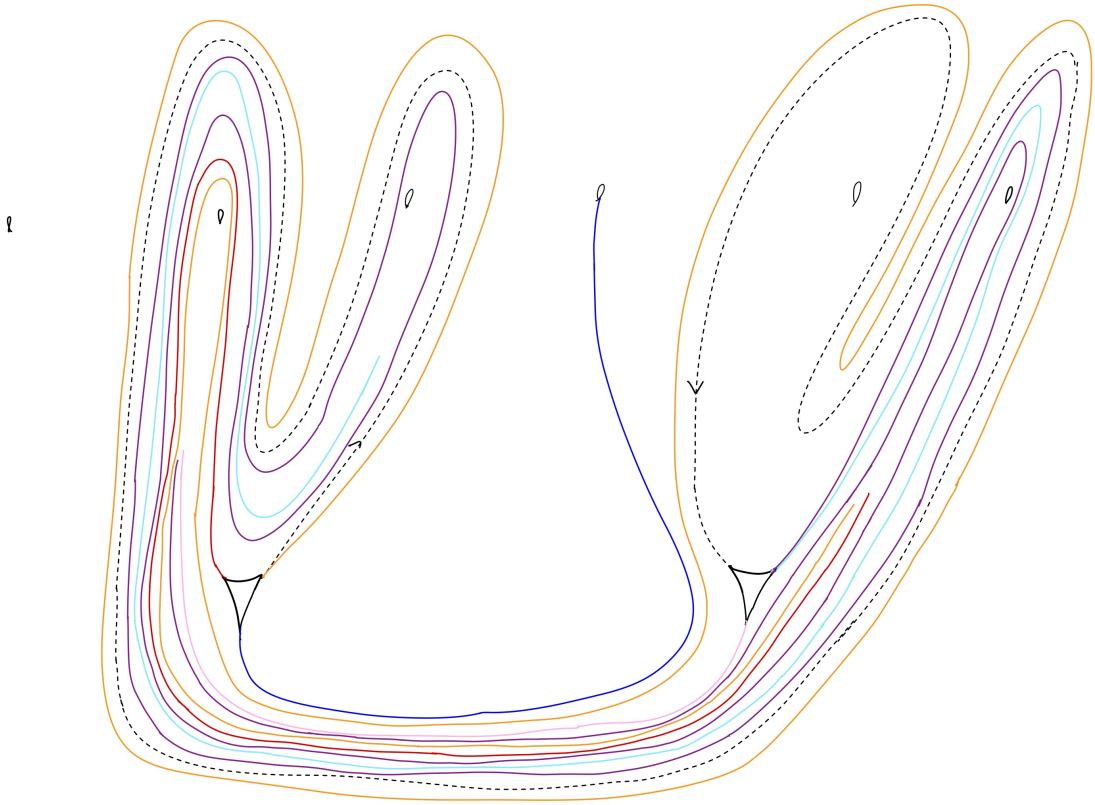


Figure F.43: Dory6

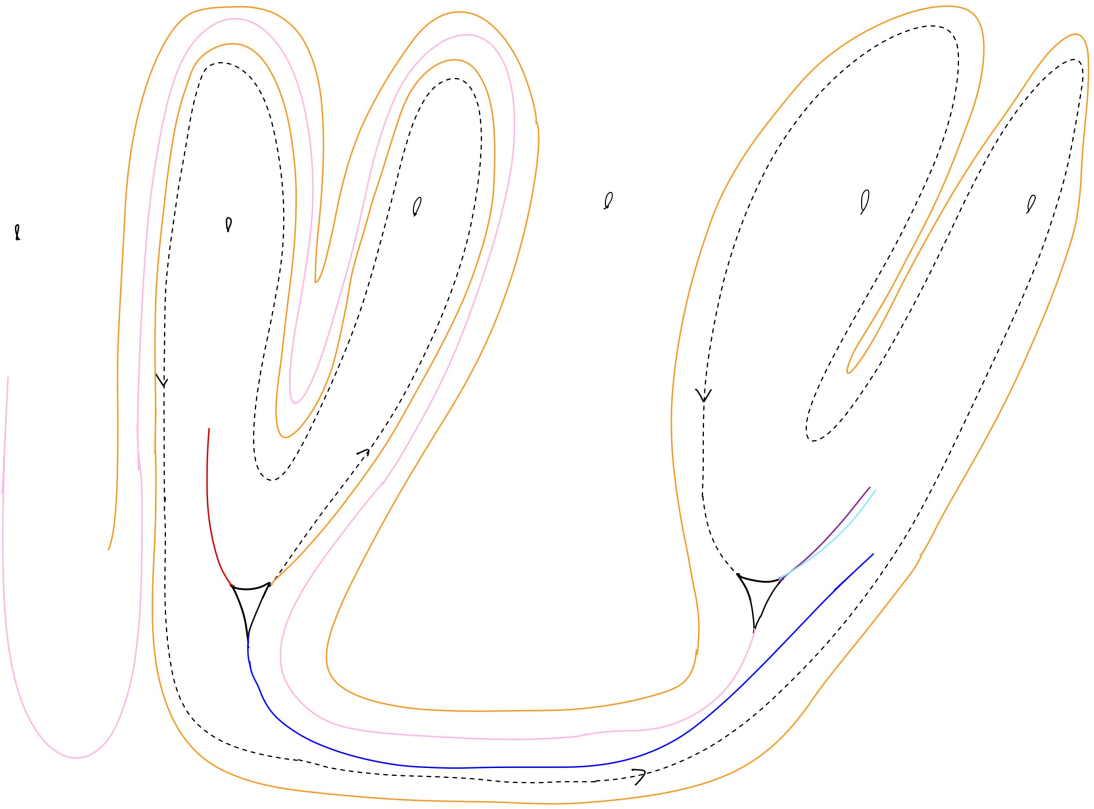


Figure F.44: Mien1

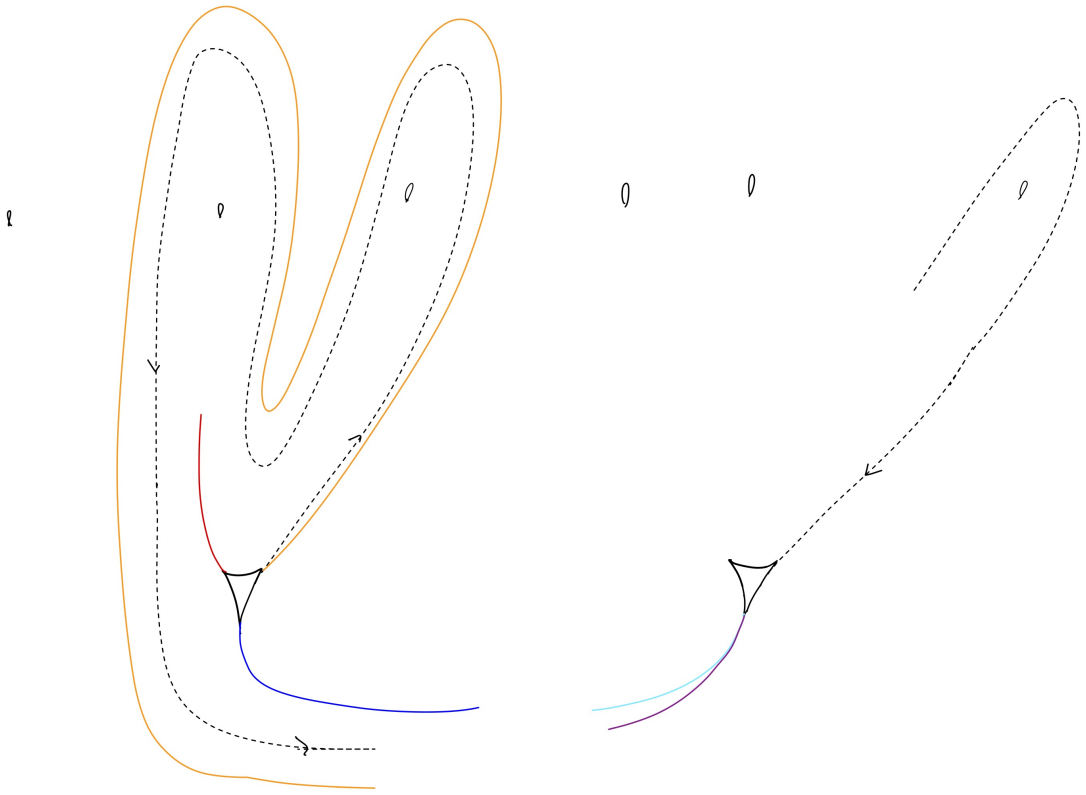


Figure F.45: NUK1

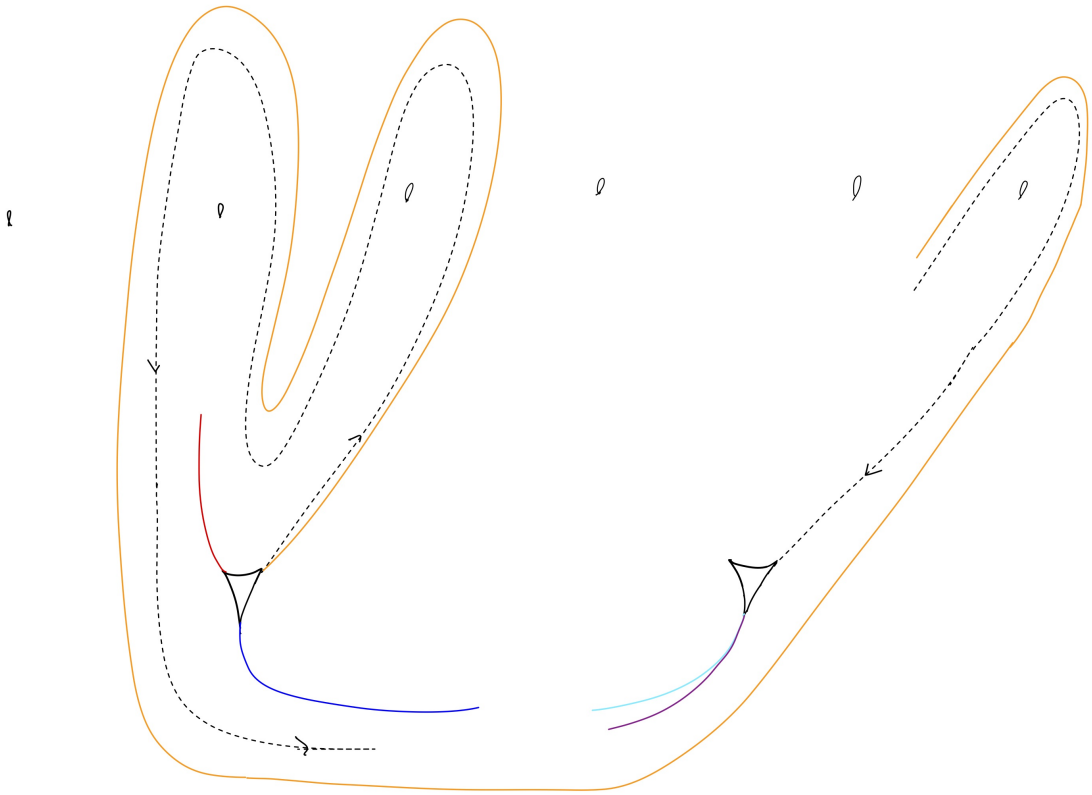


Figure F.46: NUK2

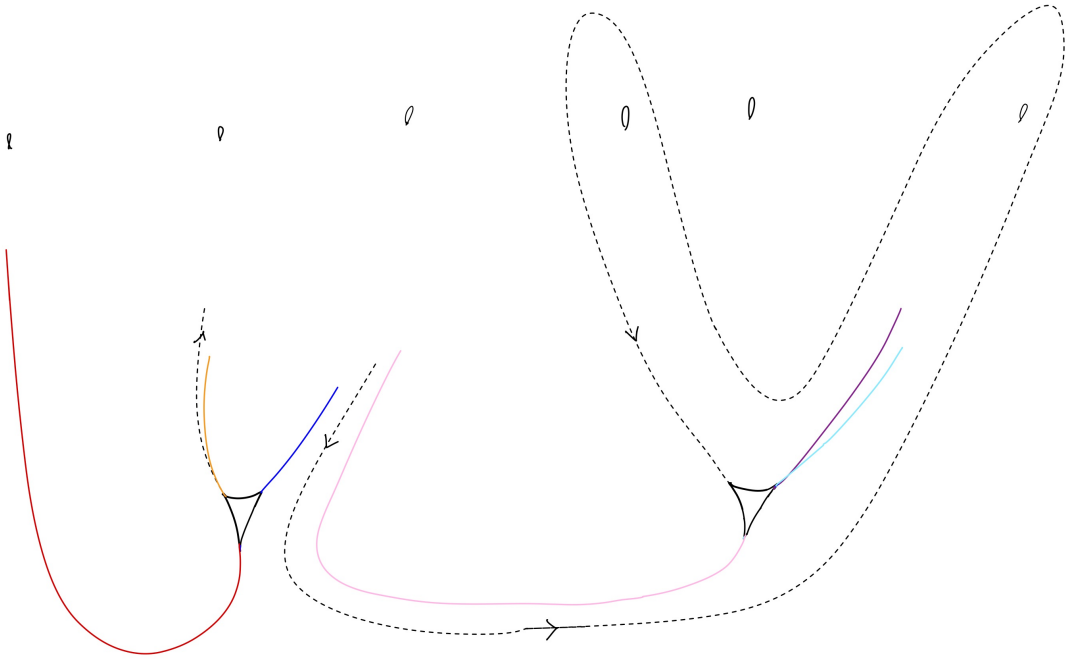


Figure F.47: Ogee1

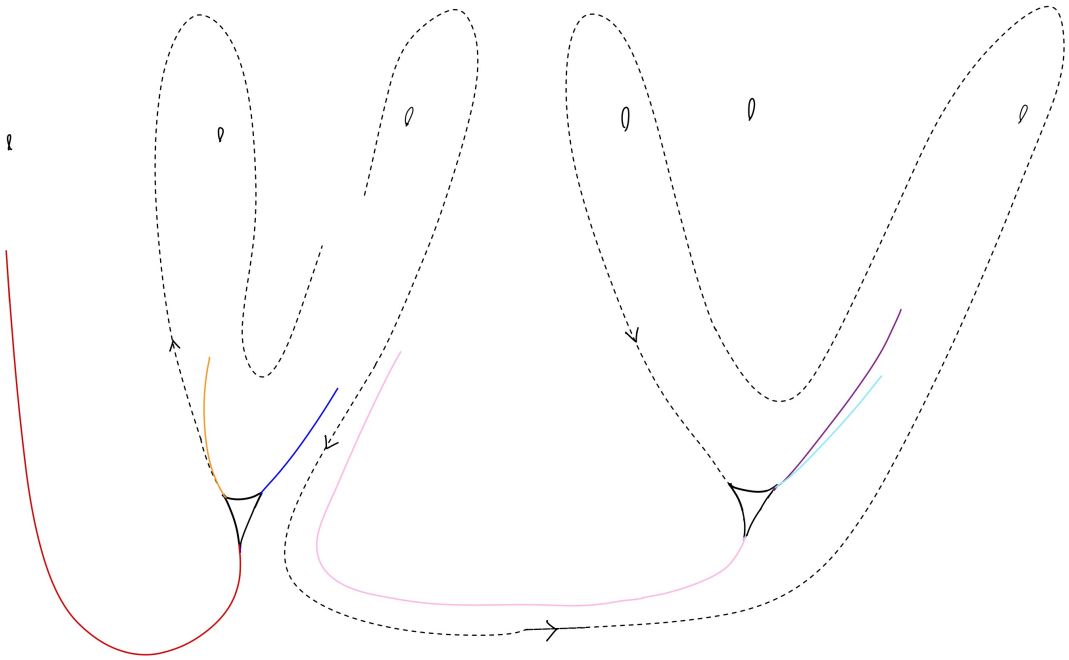


Figure F.48: Ogee2

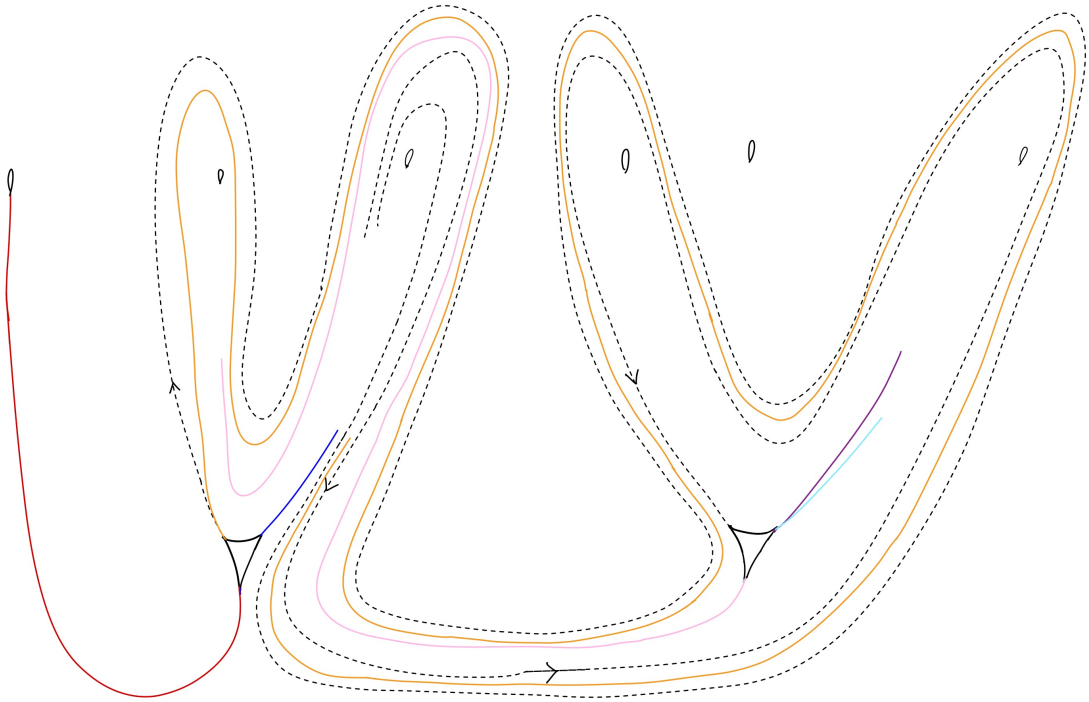


Figure F.49: Ogee3

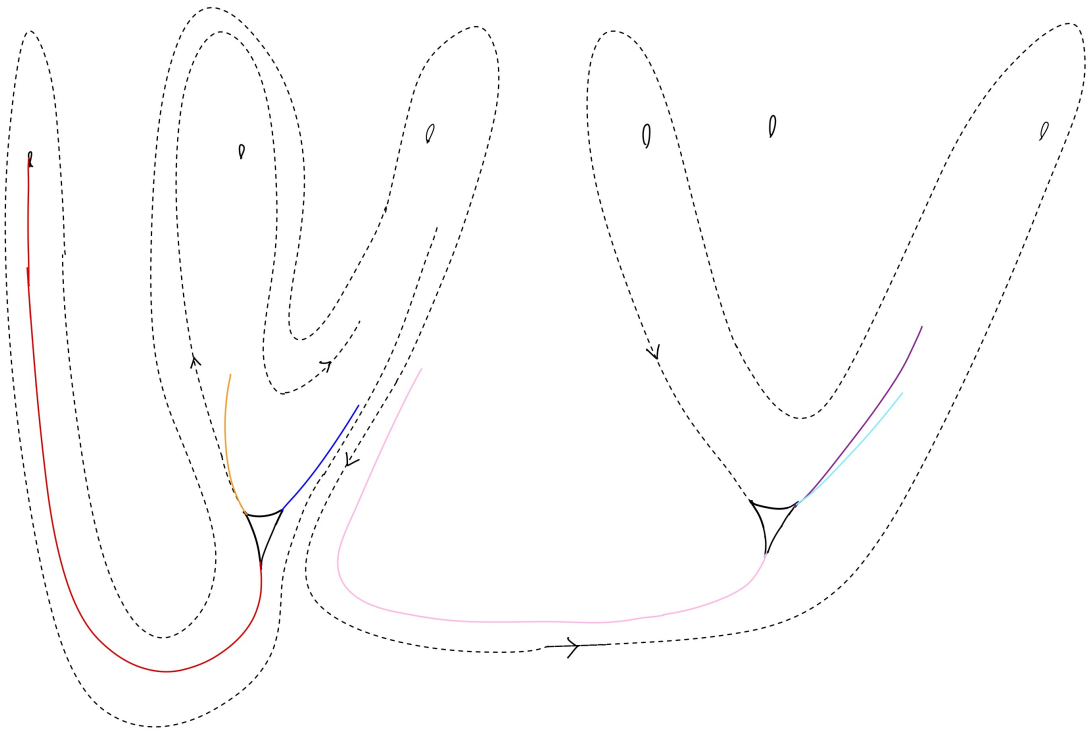


Figure F.50: Ogee4

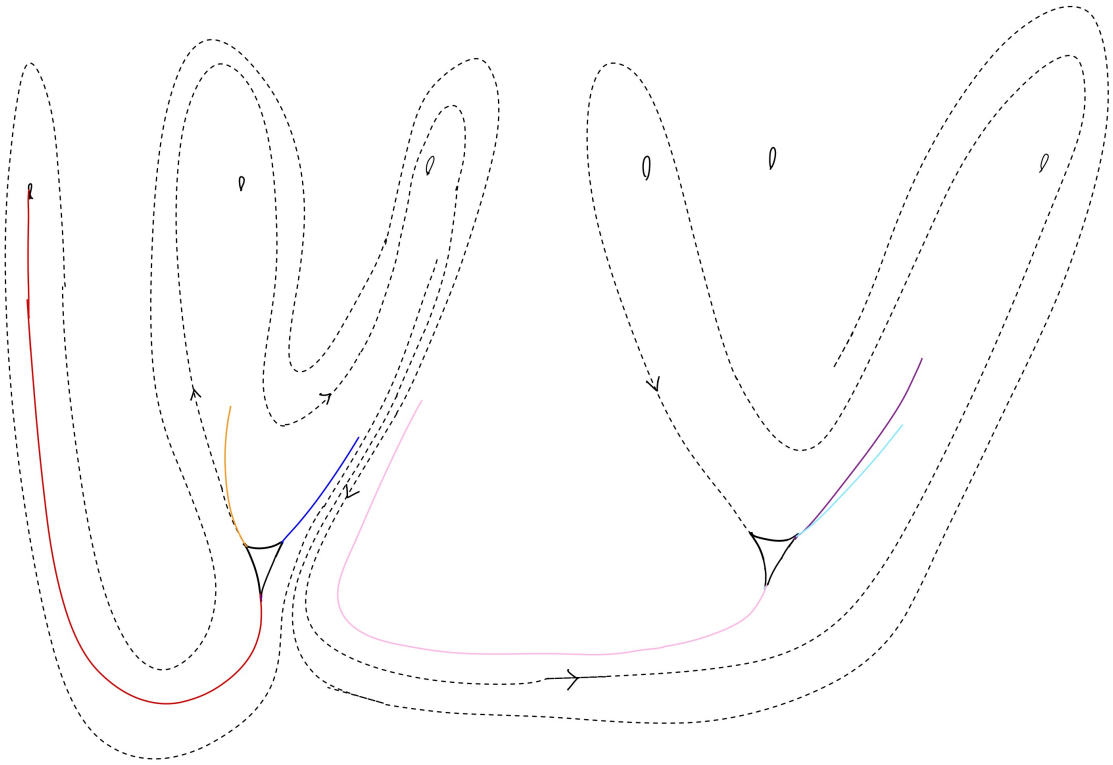


Figure F.51: Ogee5

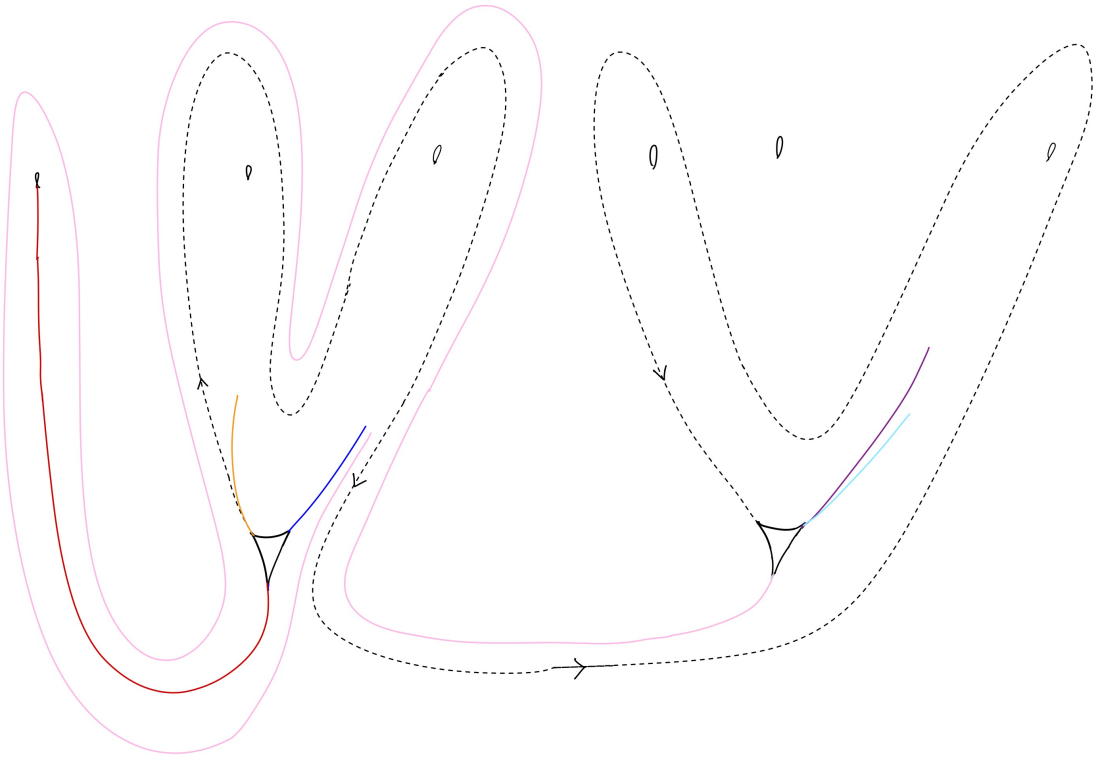


Figure F.52: Ogee6

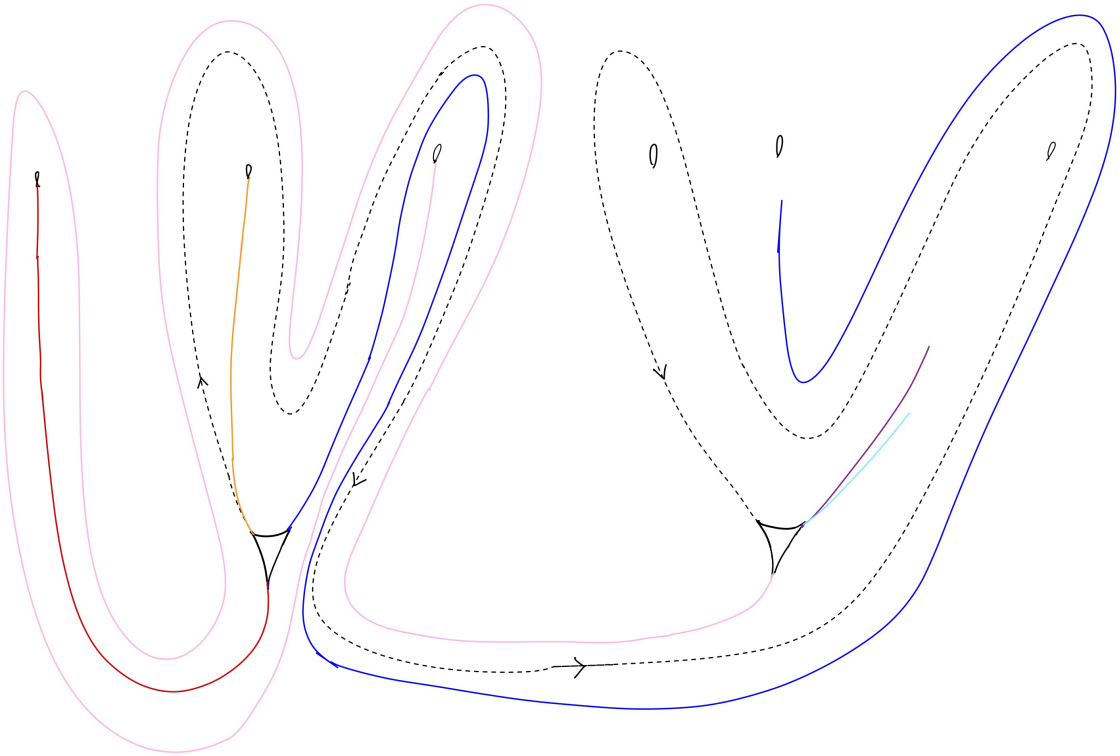


Figure F.53: Chine1

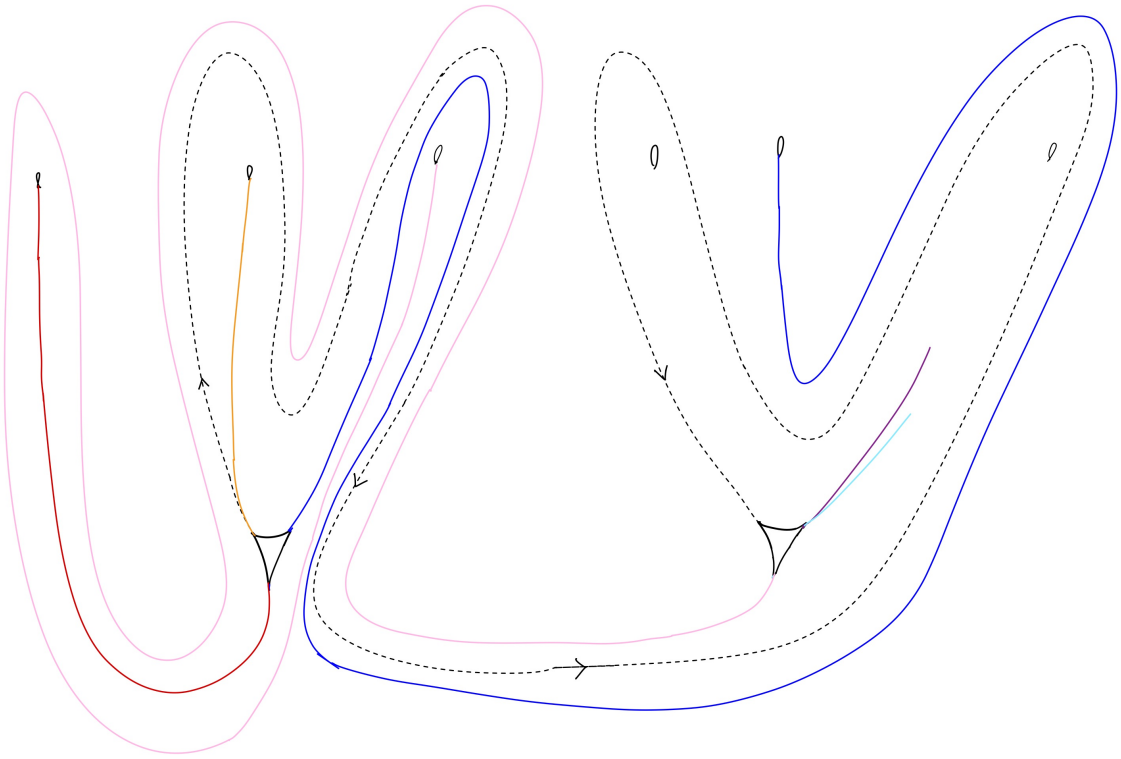


Figure F.54: Chine2

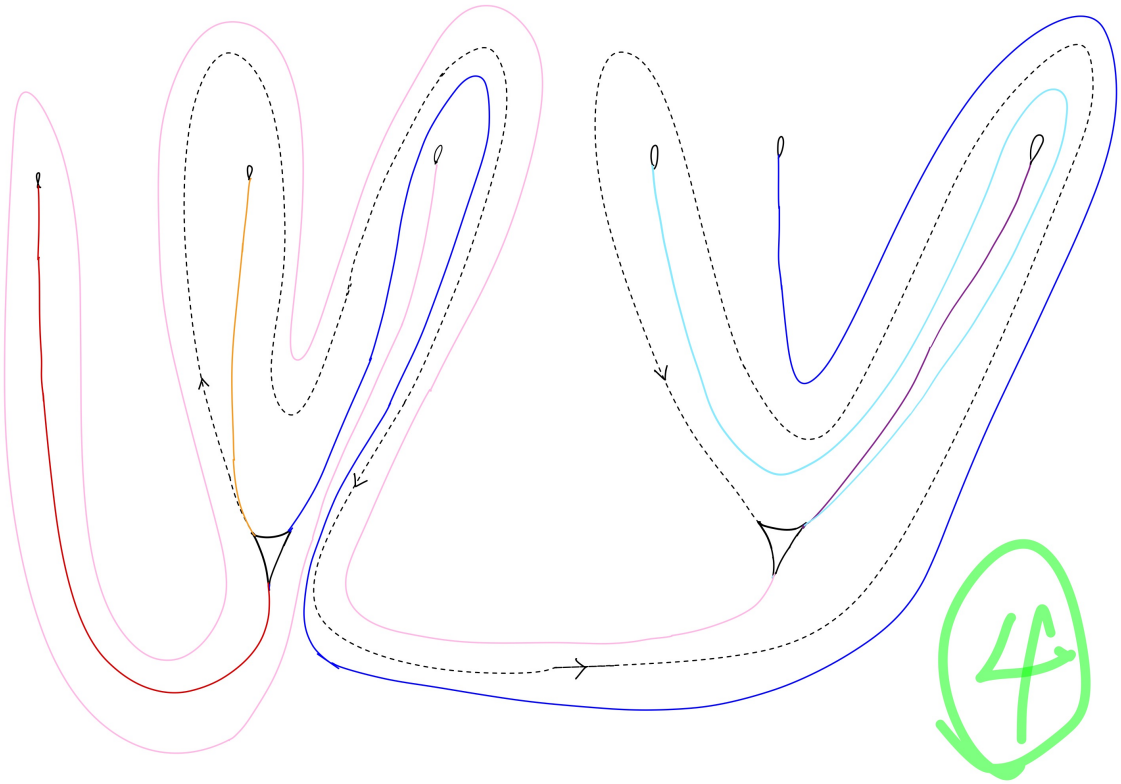


Figure F.55: Chine3

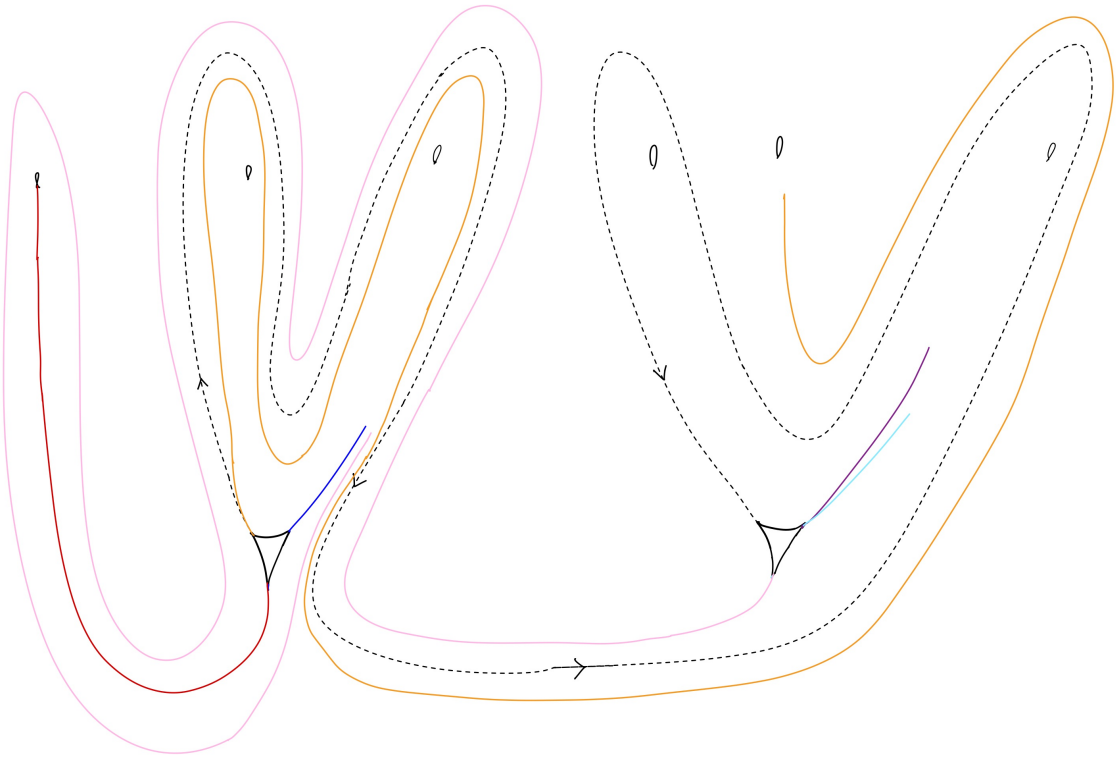


Figure F.56: Droit1

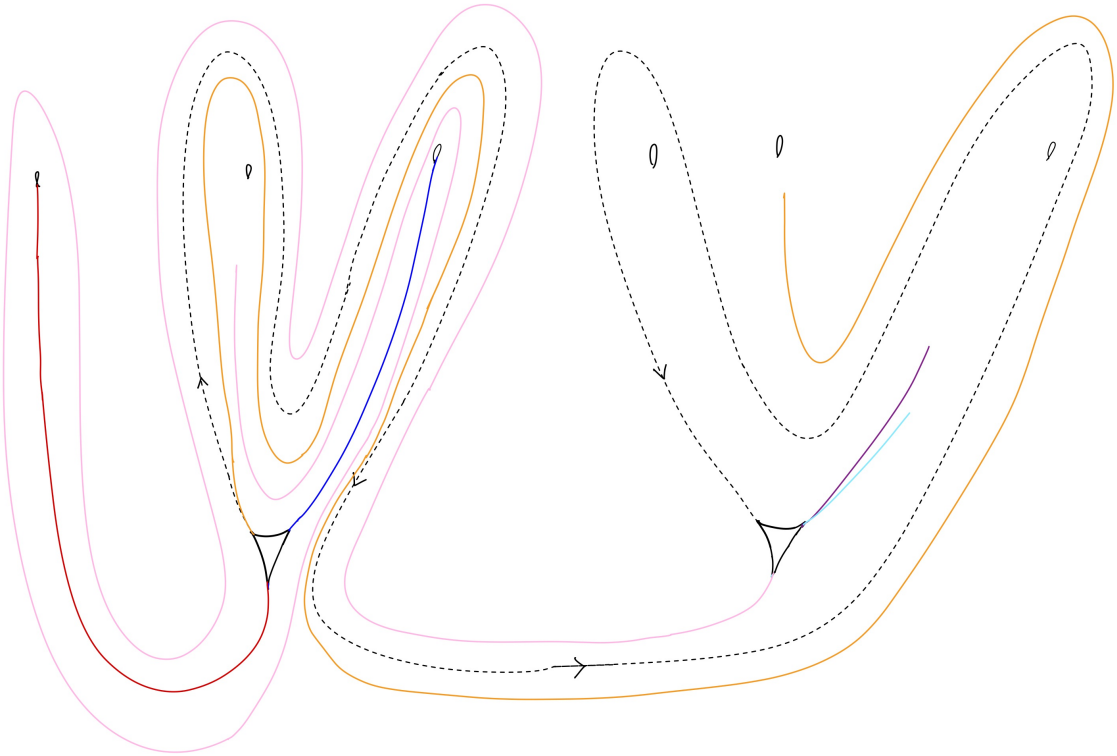


Figure F.57: Quaint1

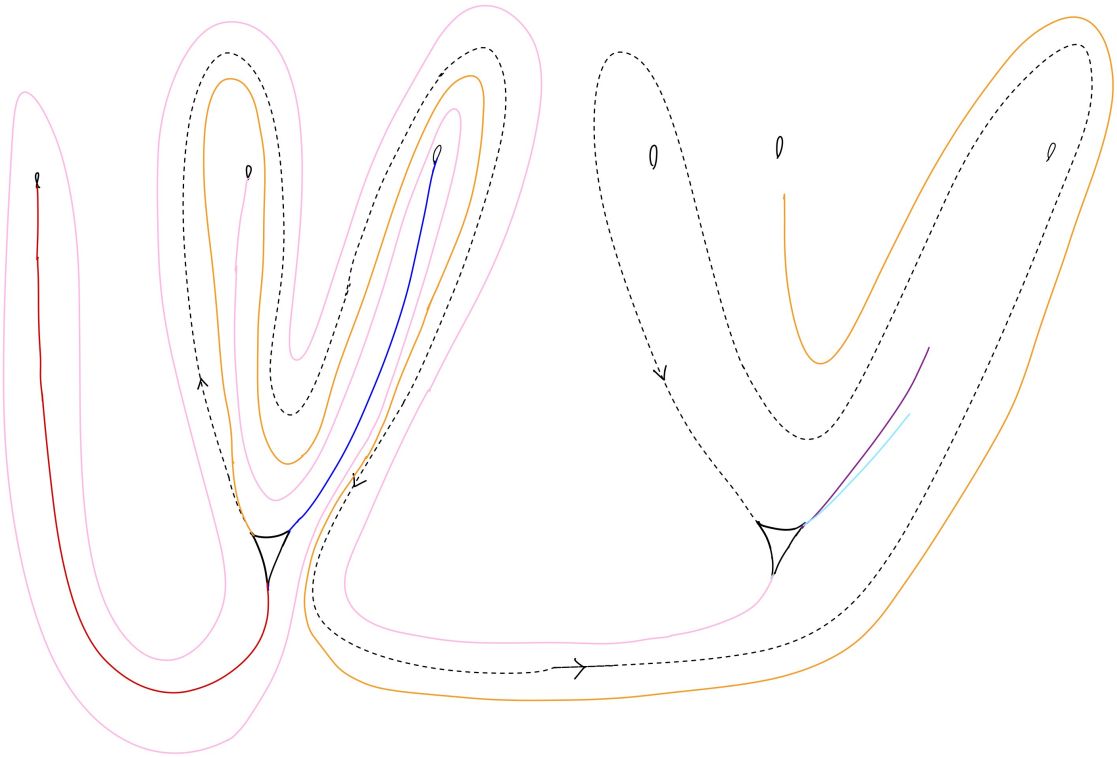


Figure F.58: Quaint2

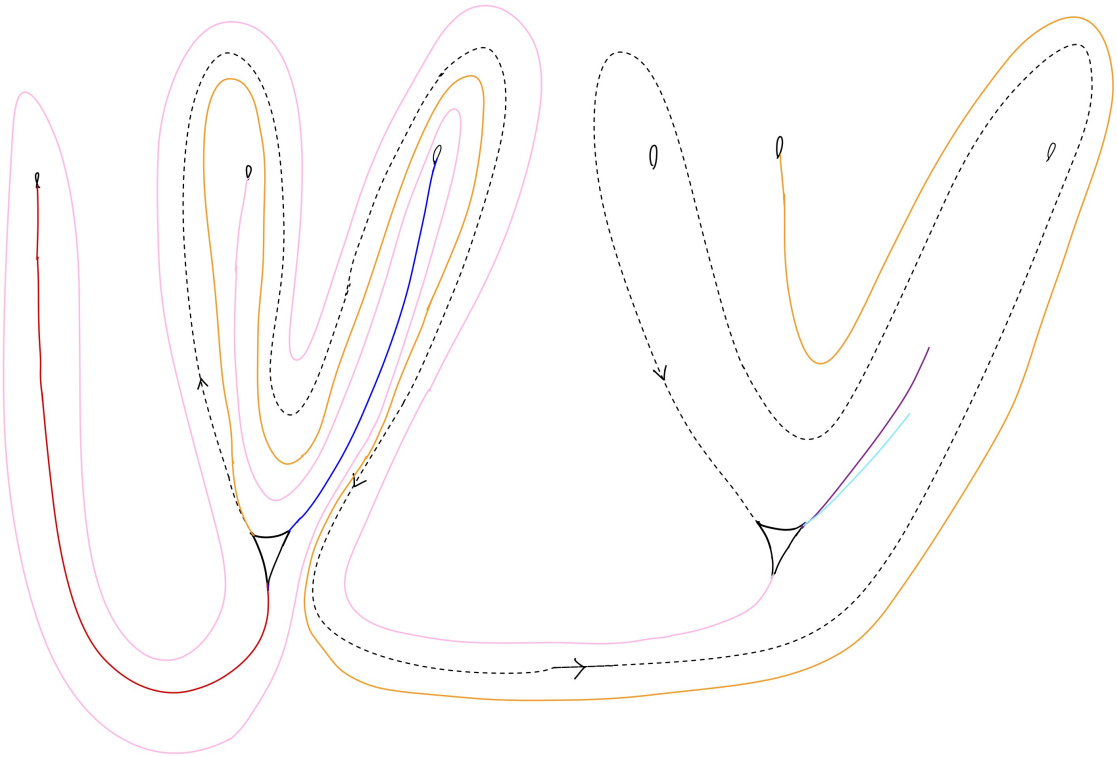


Figure F.59: Quaint3

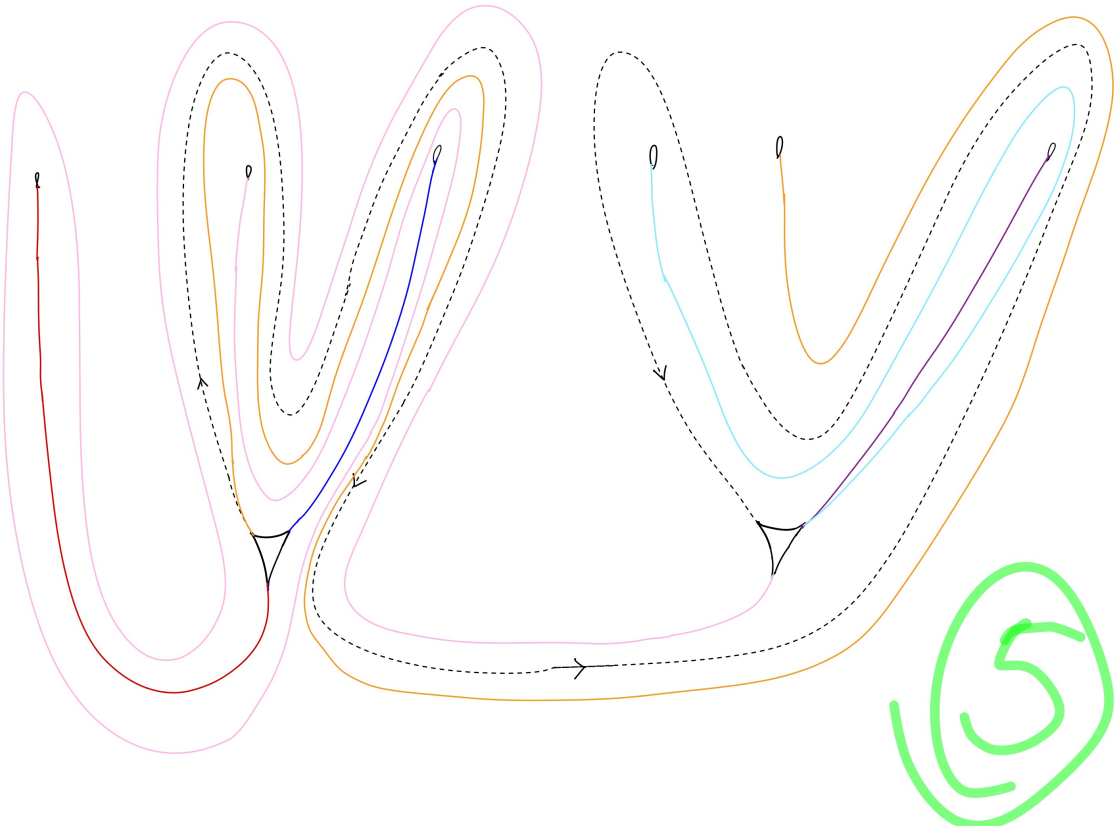


Figure F.60: Quaint4

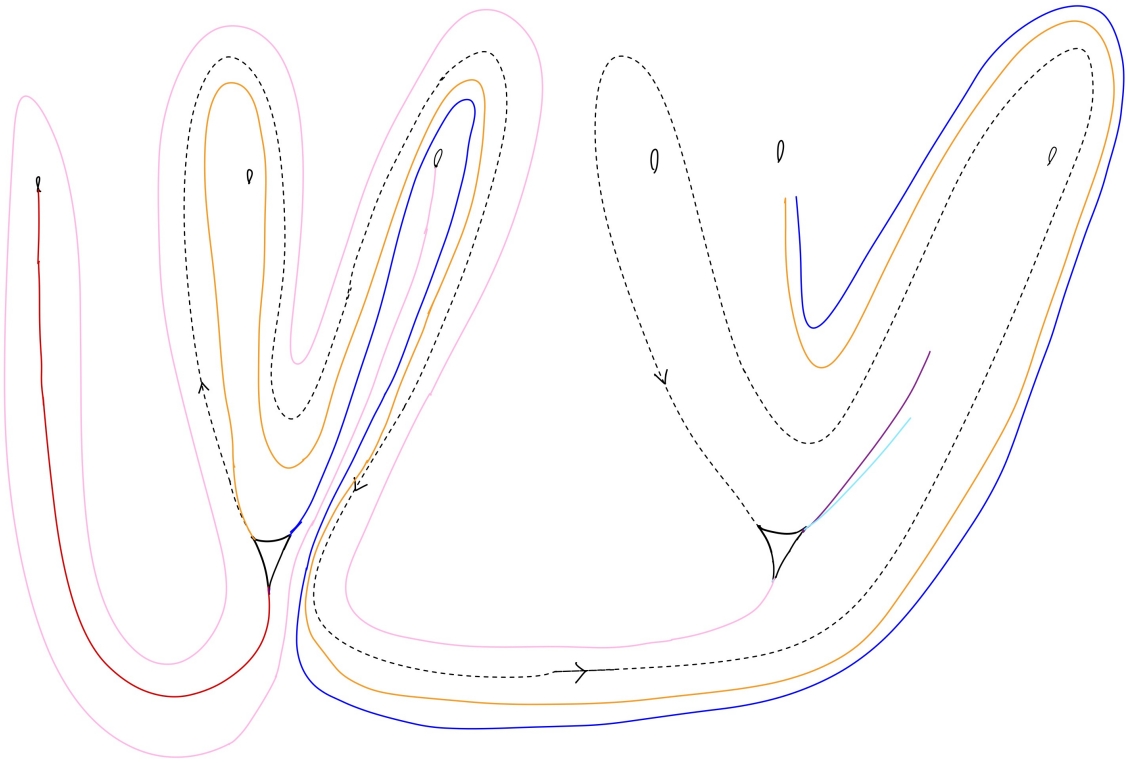


Figure F.61: Abscis1

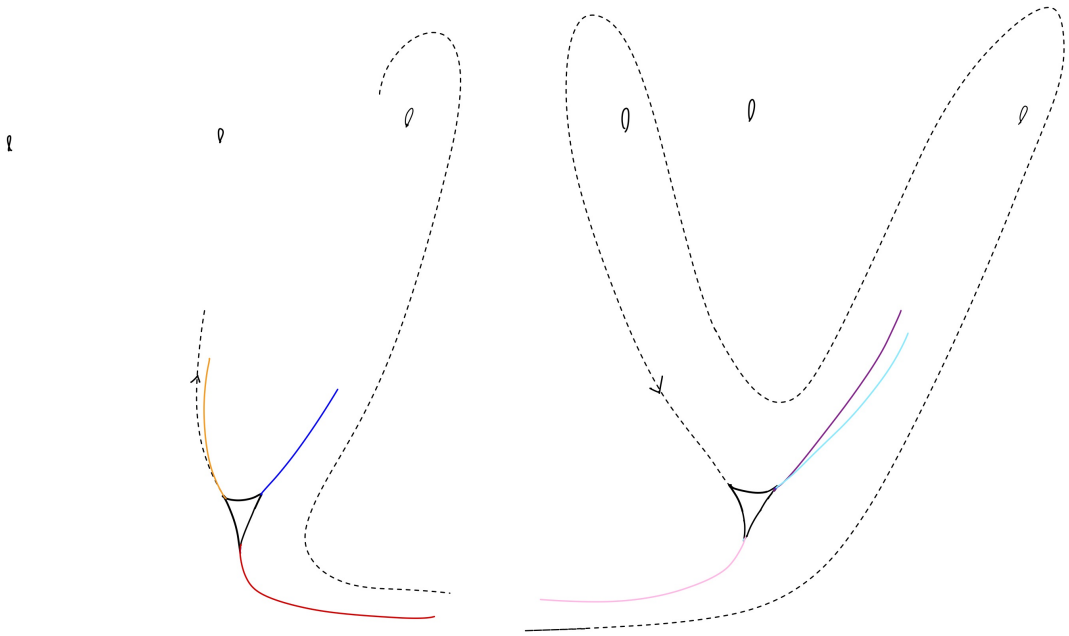


Figure F.62: Tret1

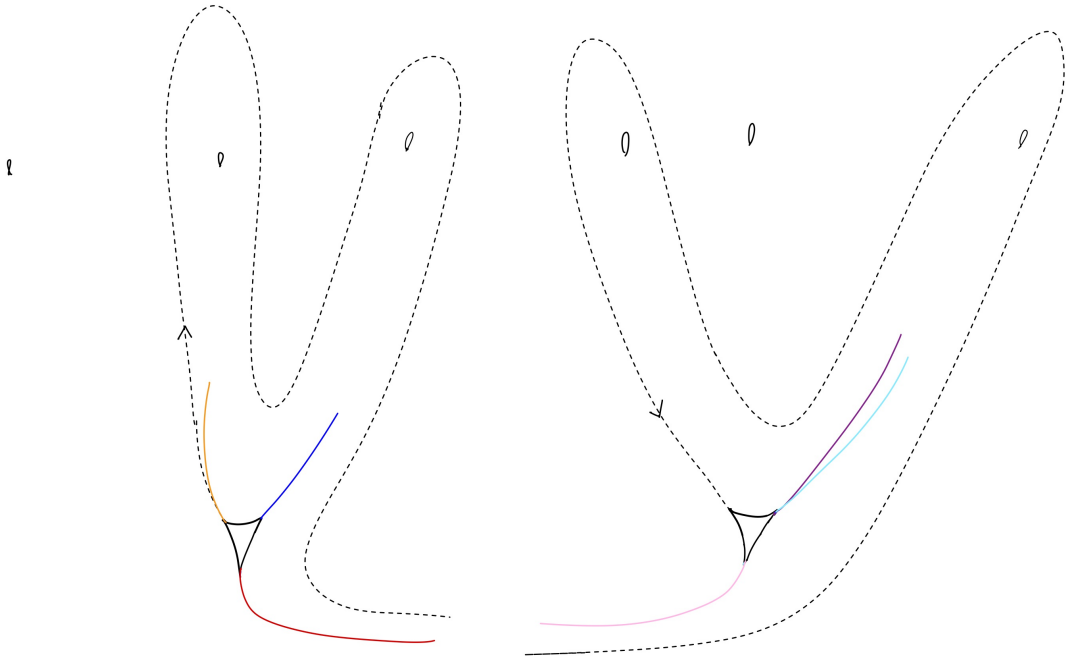


Figure F.63: Tret2

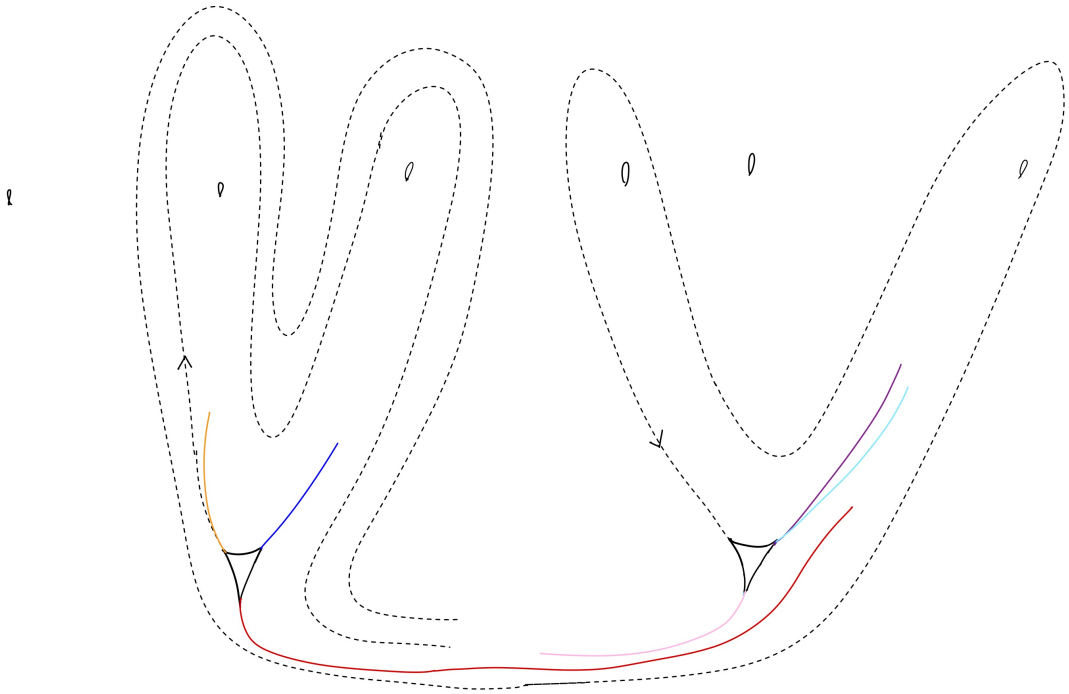


Figure F.64: Tret3

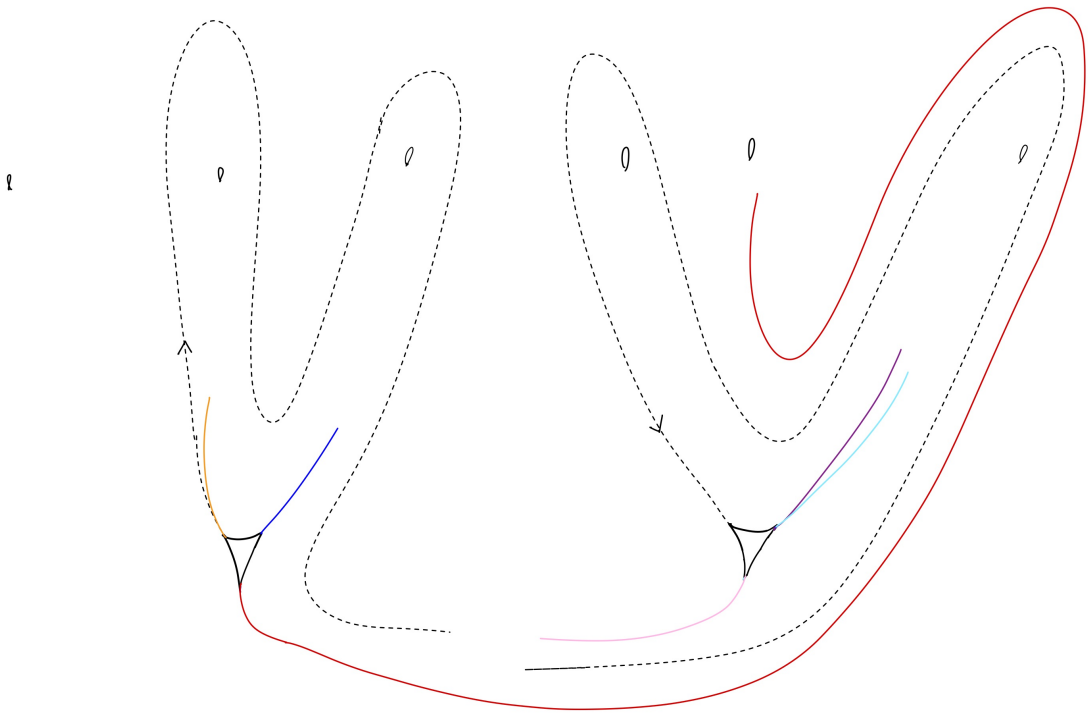


Figure F.65: Tret4

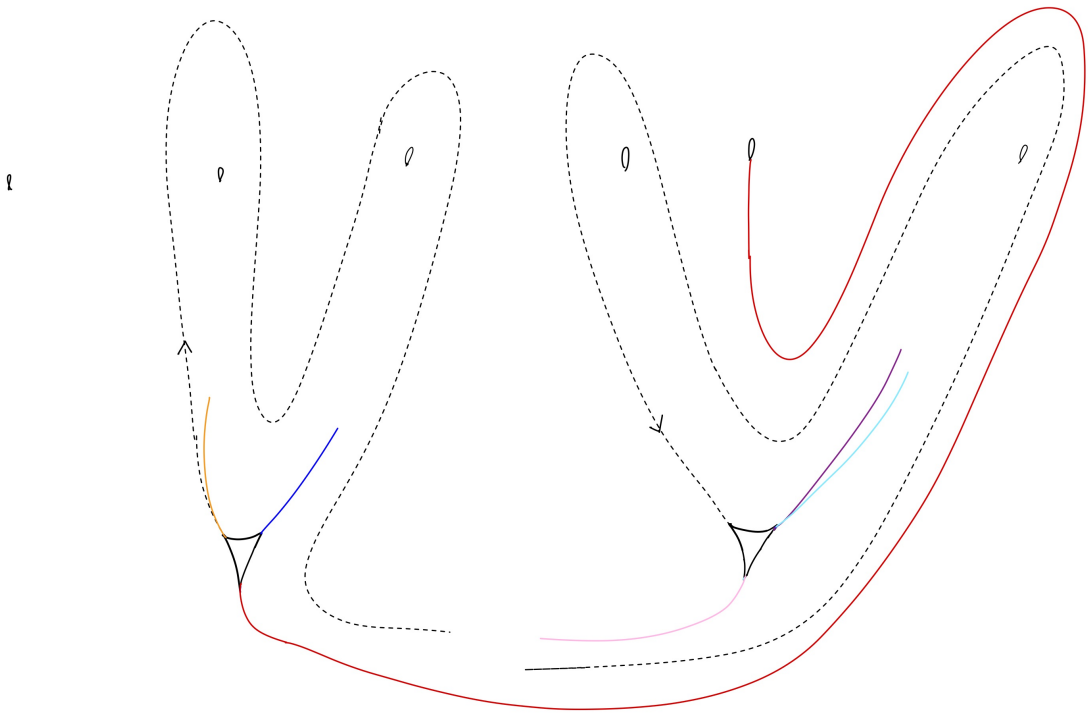


Figure F.66: Tret5

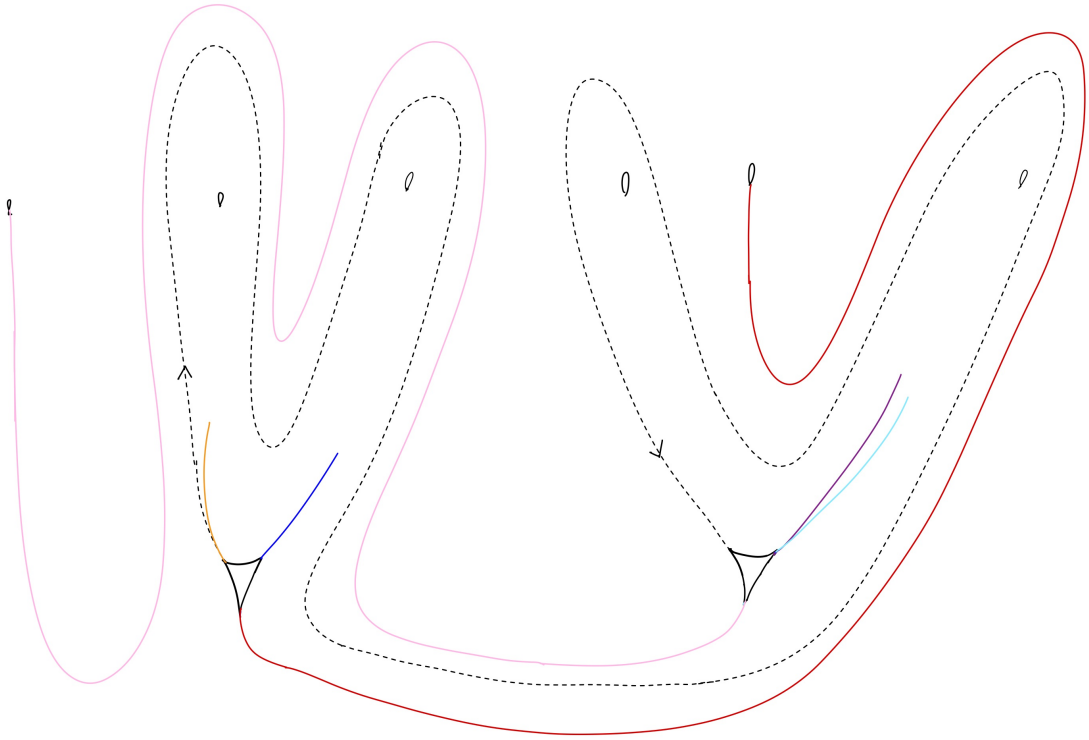


Figure F.67: Fosse1

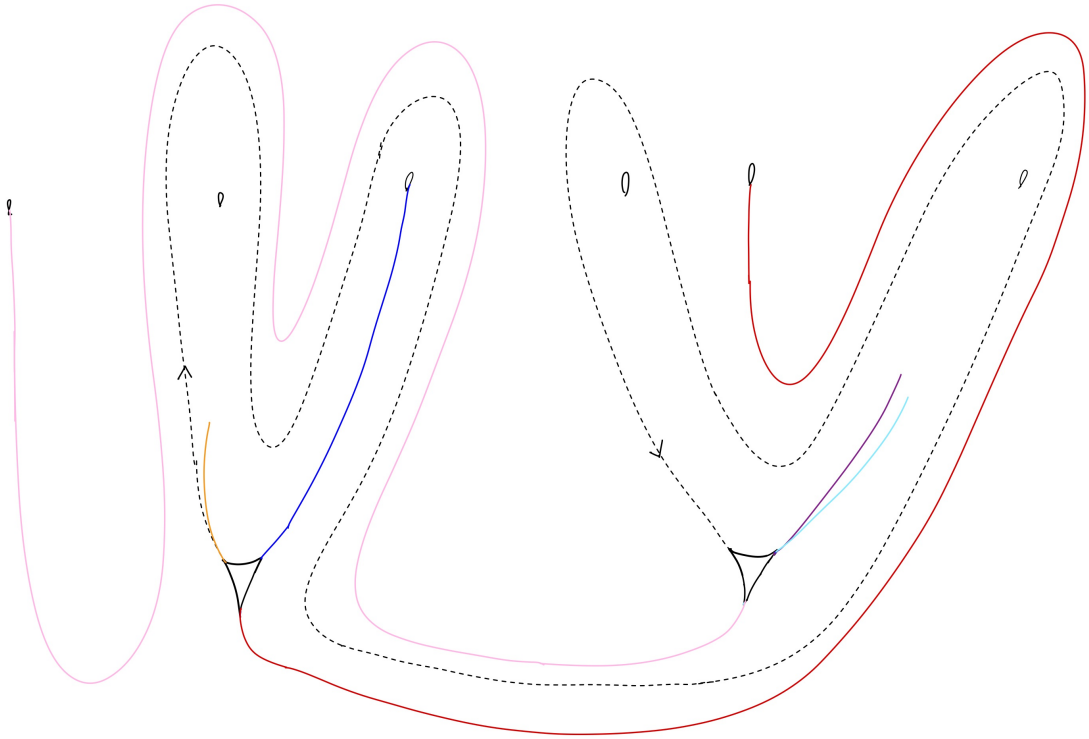


Figure F.68: Fosse2

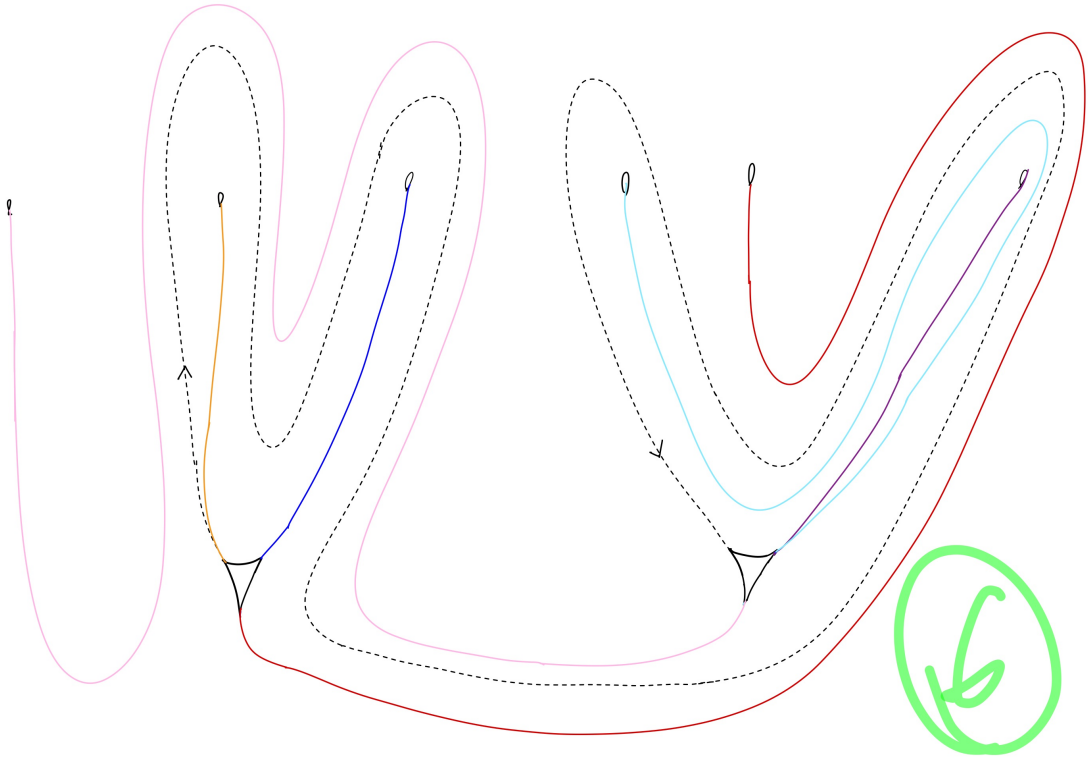


Figure F.69: Lacuna1

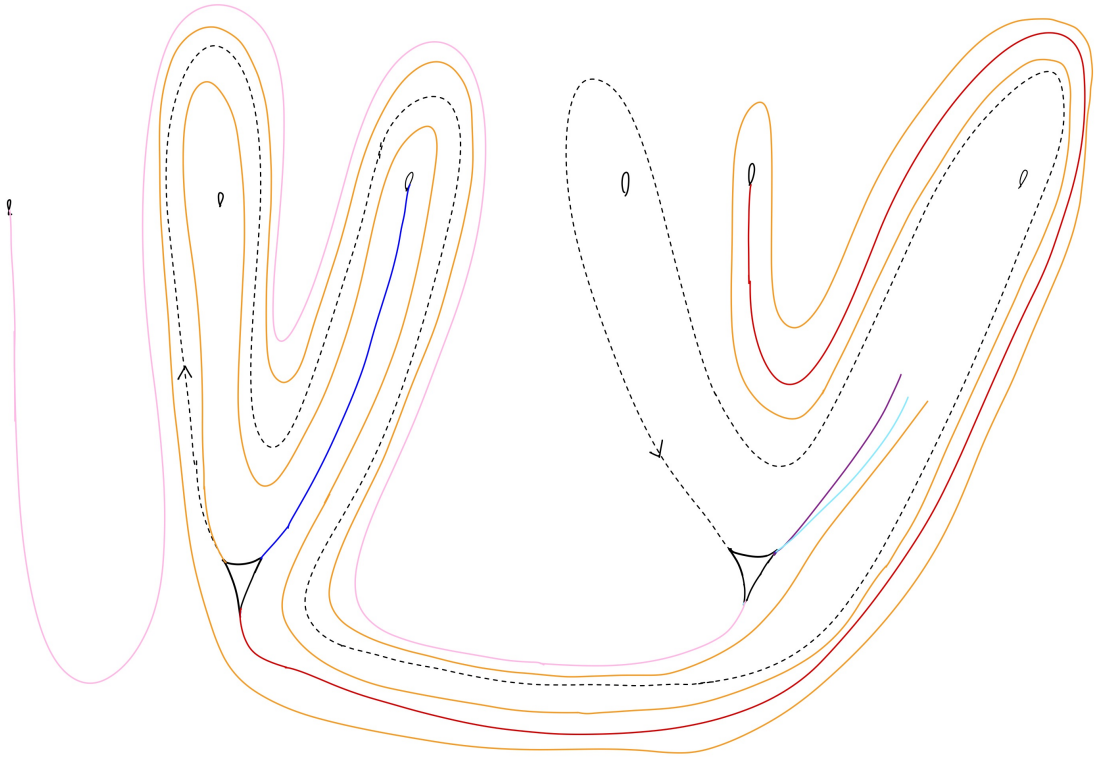


Figure F.70: Exedra1

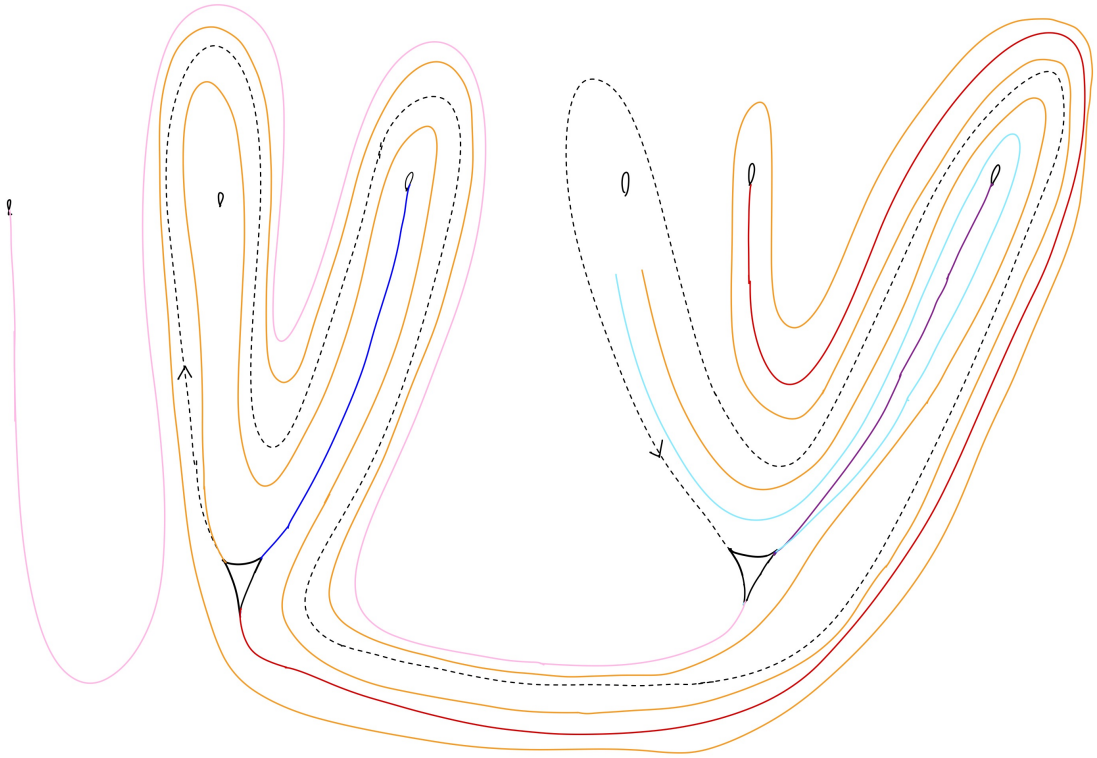


Figure F.71: Exedra2

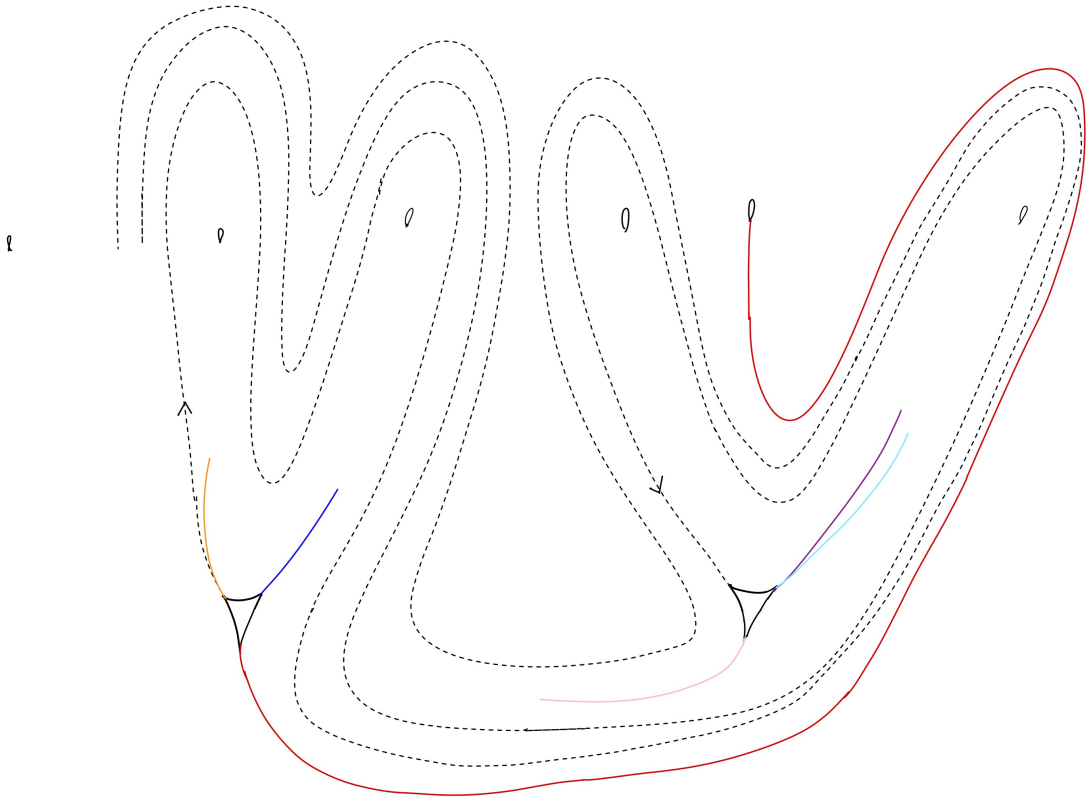


Figure F.72: Lemur1

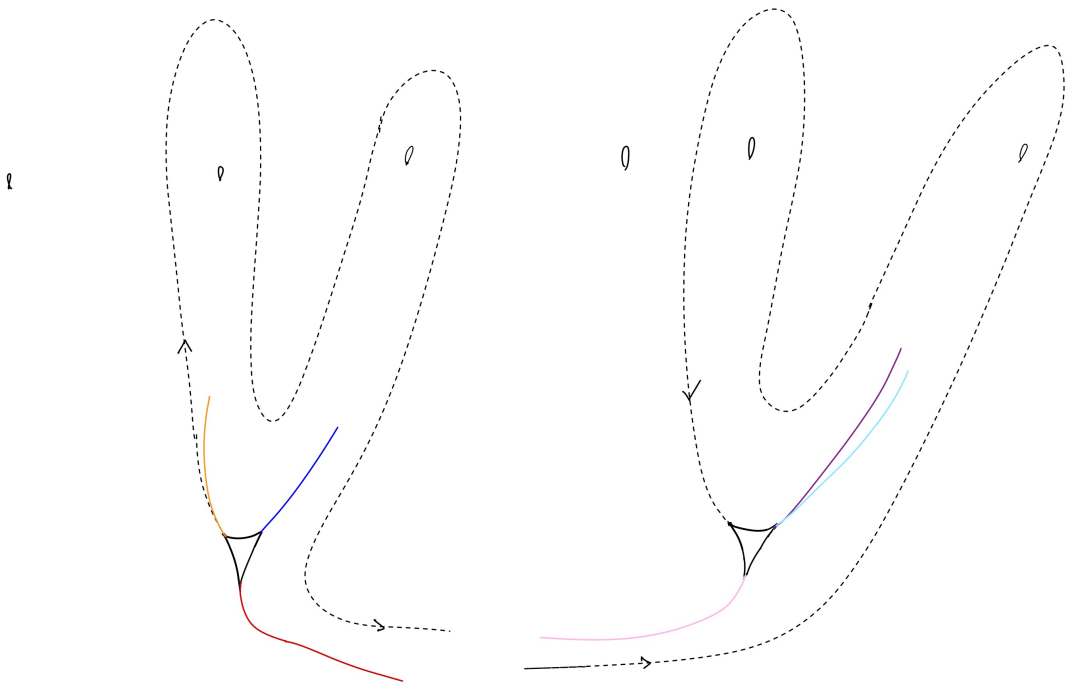


Figure F.73: OGG1

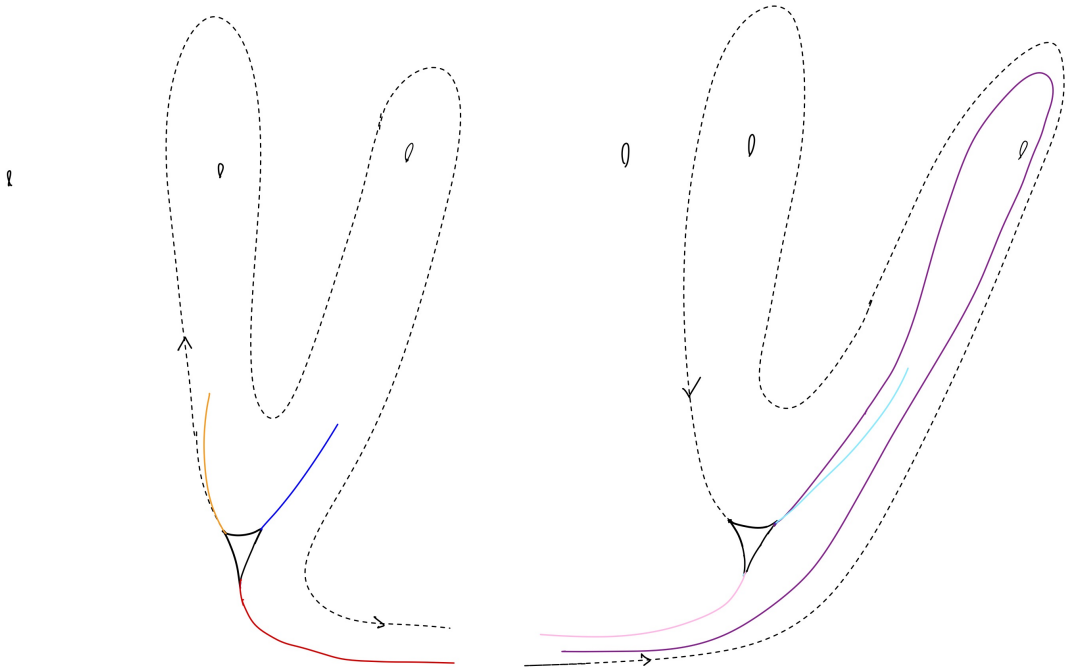


Figure F.74: OGG2

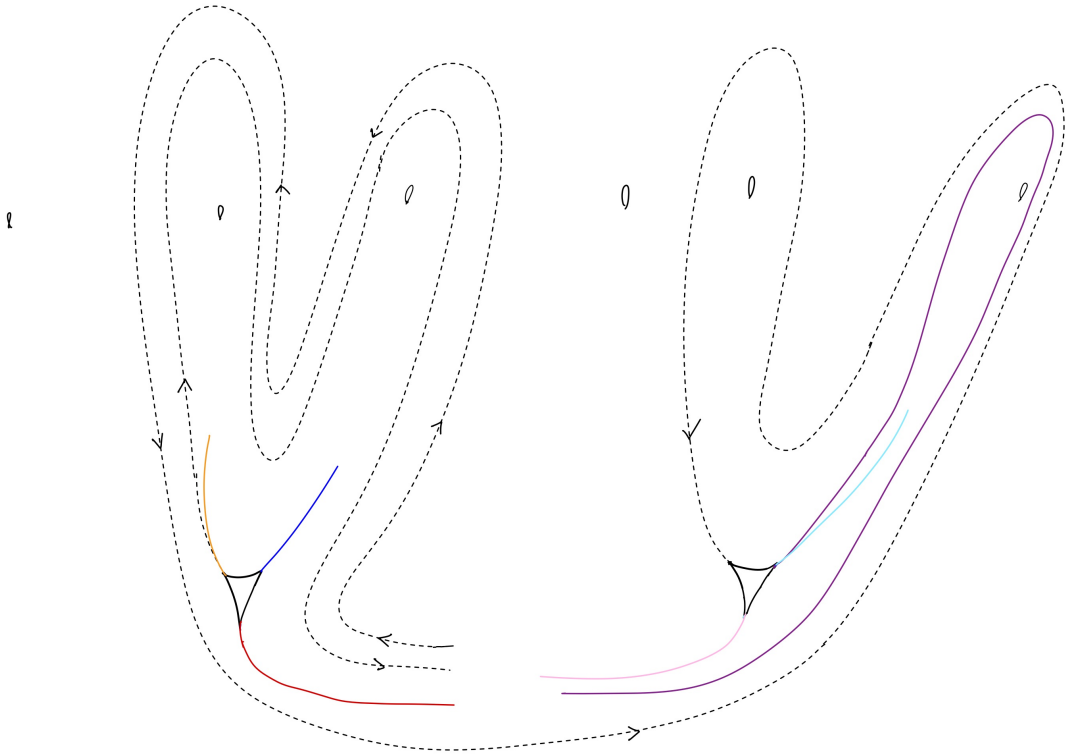


Figure F.75: OGG3

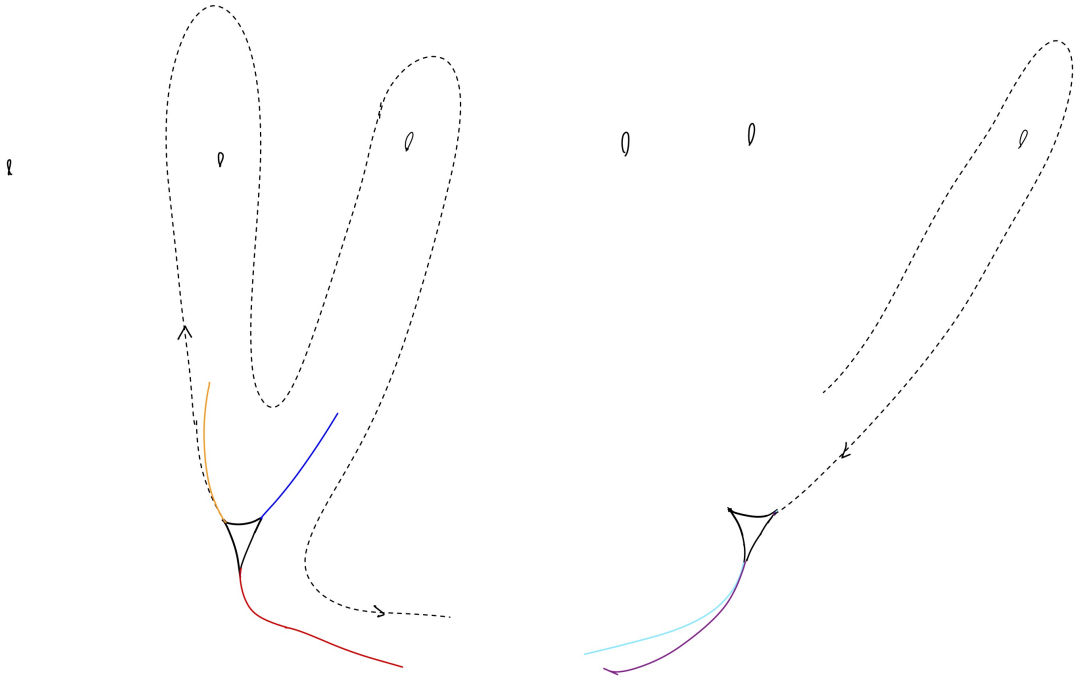


Figure F.76: SME1

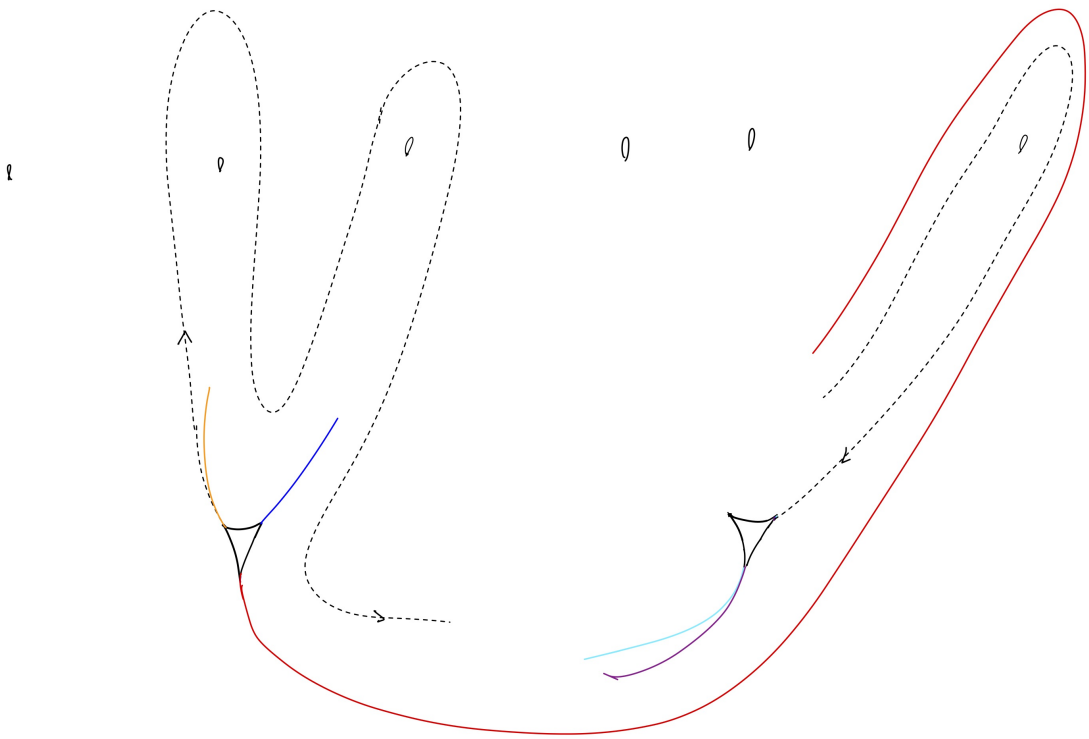


Figure F.77: SME2

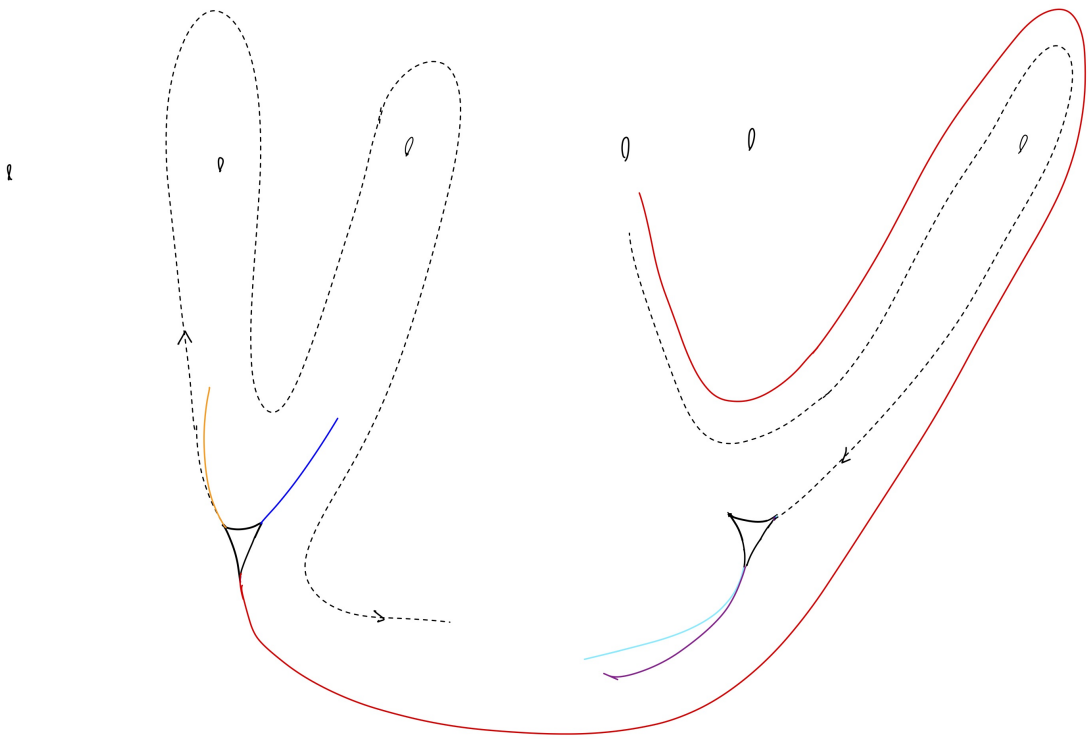


Figure F.78: SME3

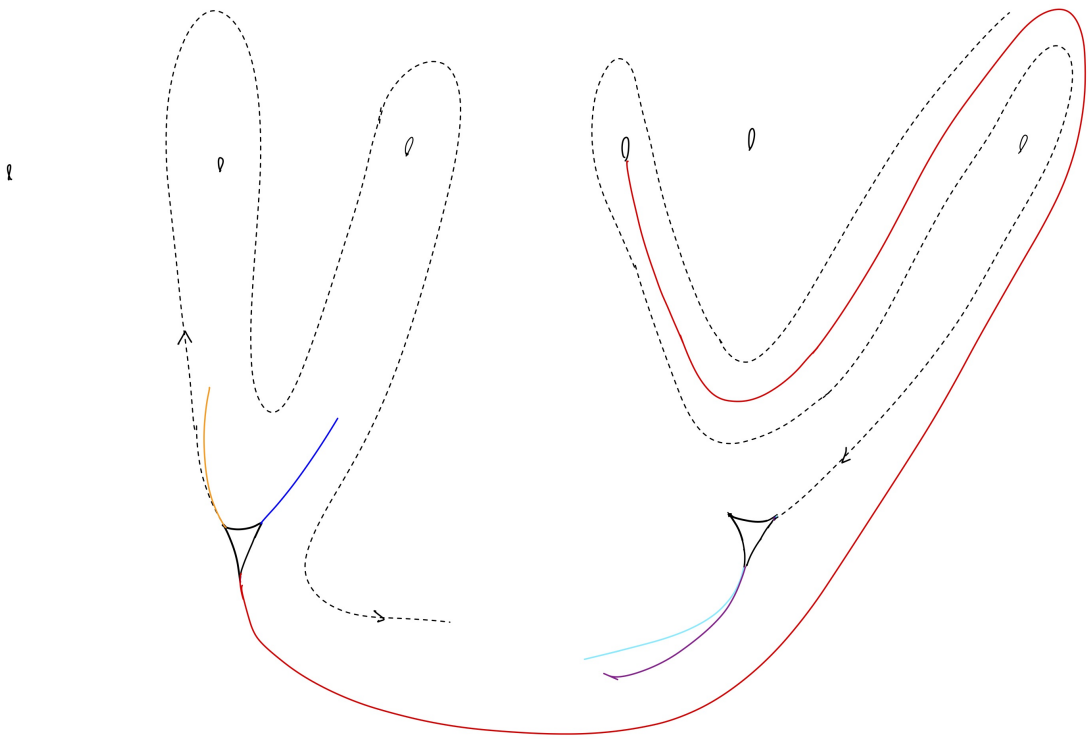


Figure F.79: SME4

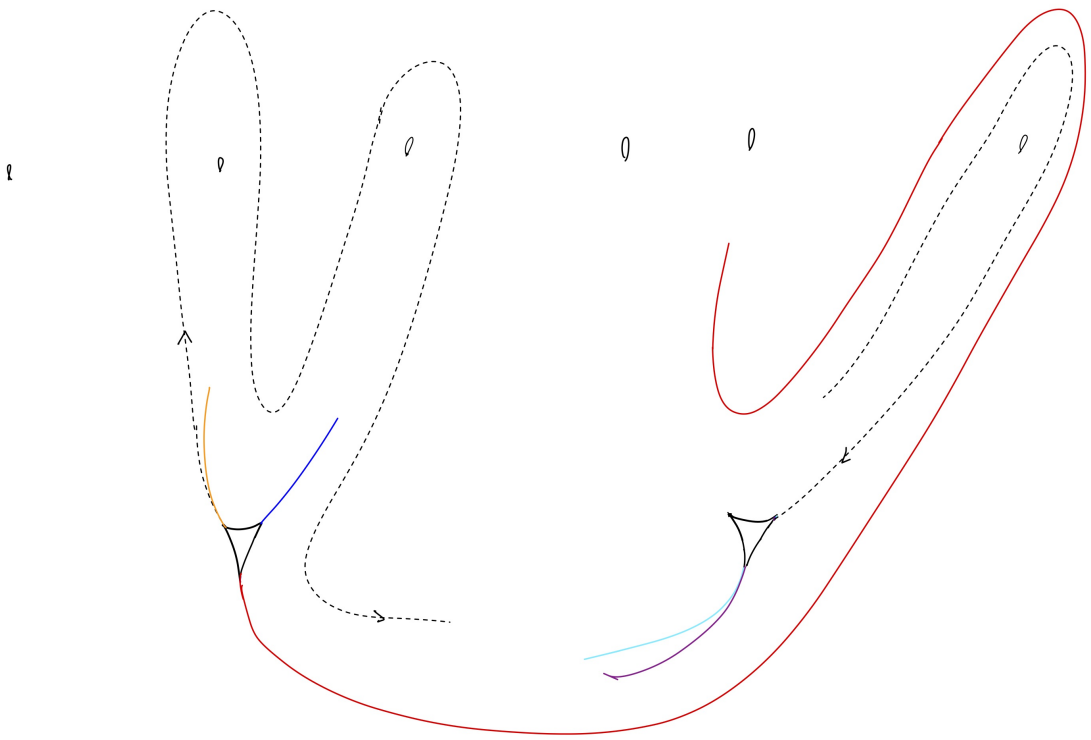


Figure F.80: SME5

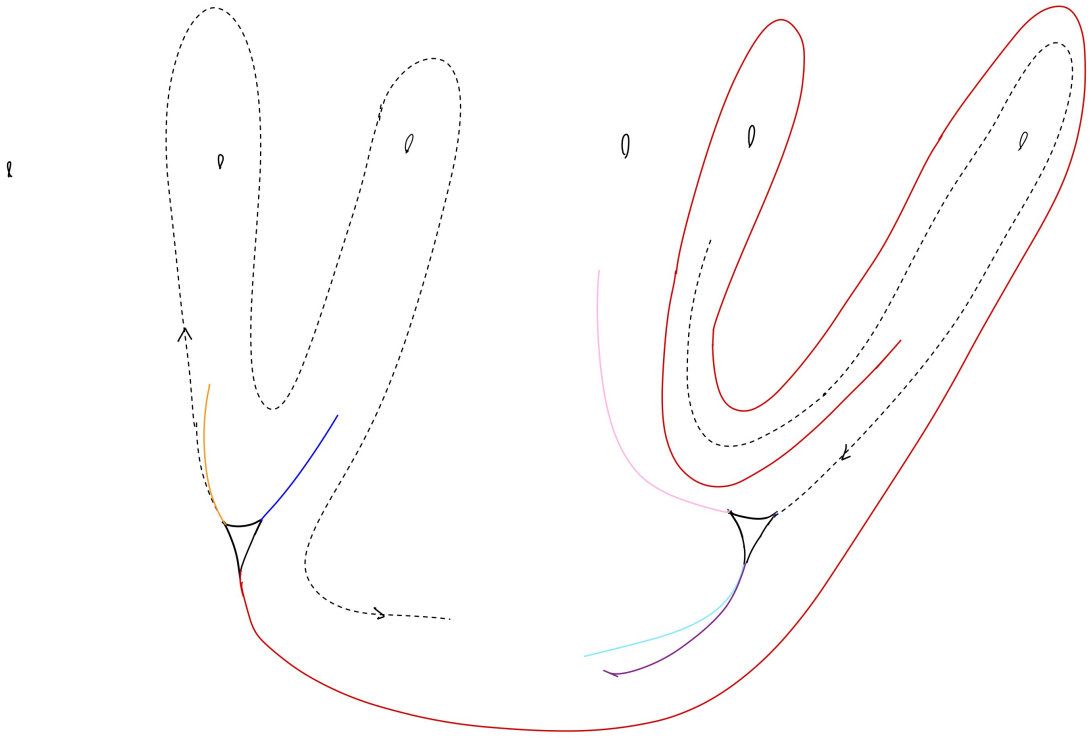


Figure F.81: Barm1

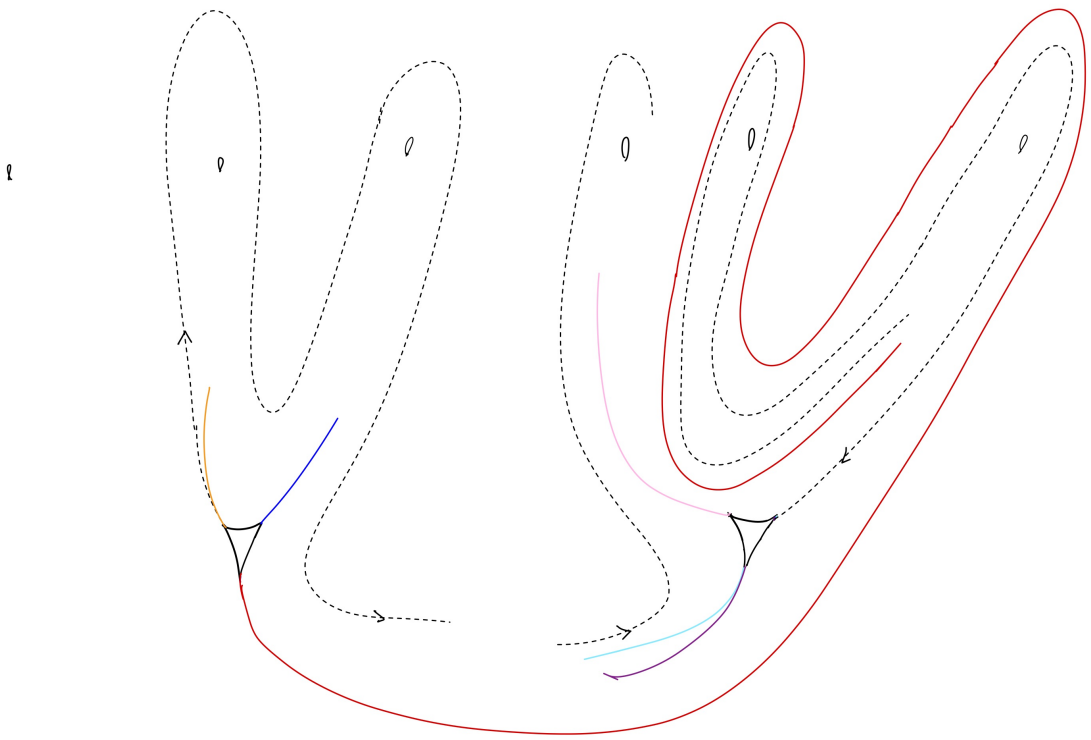


Figure F.82: Barm2

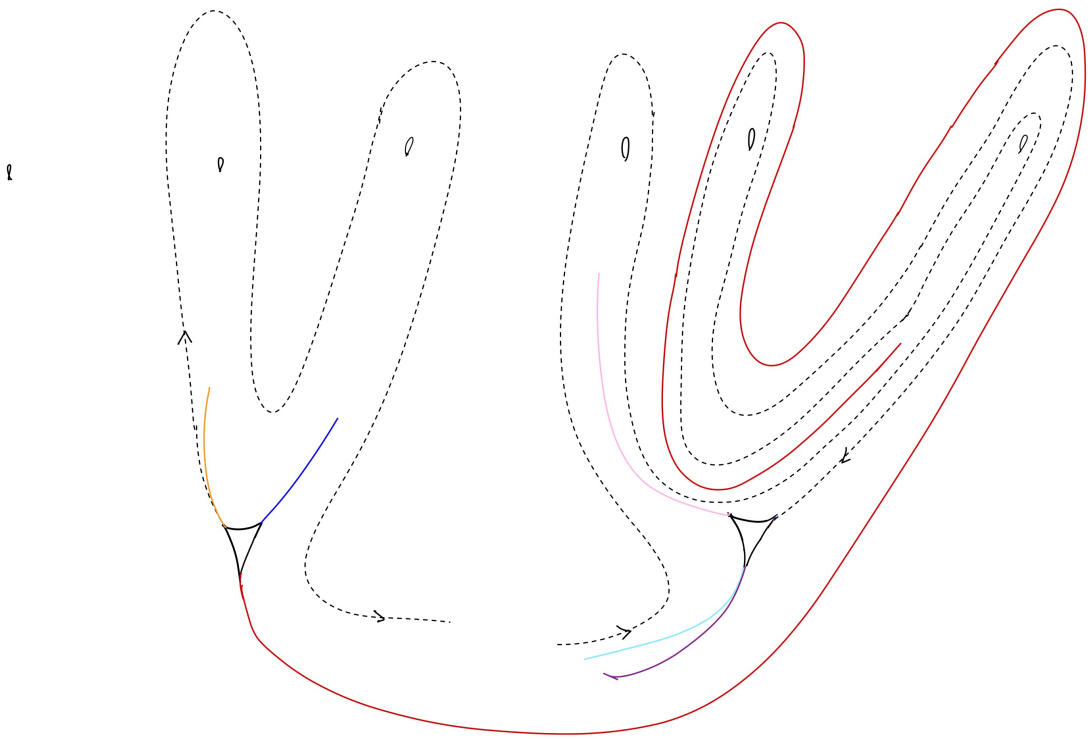


Figure F.83: Barm3

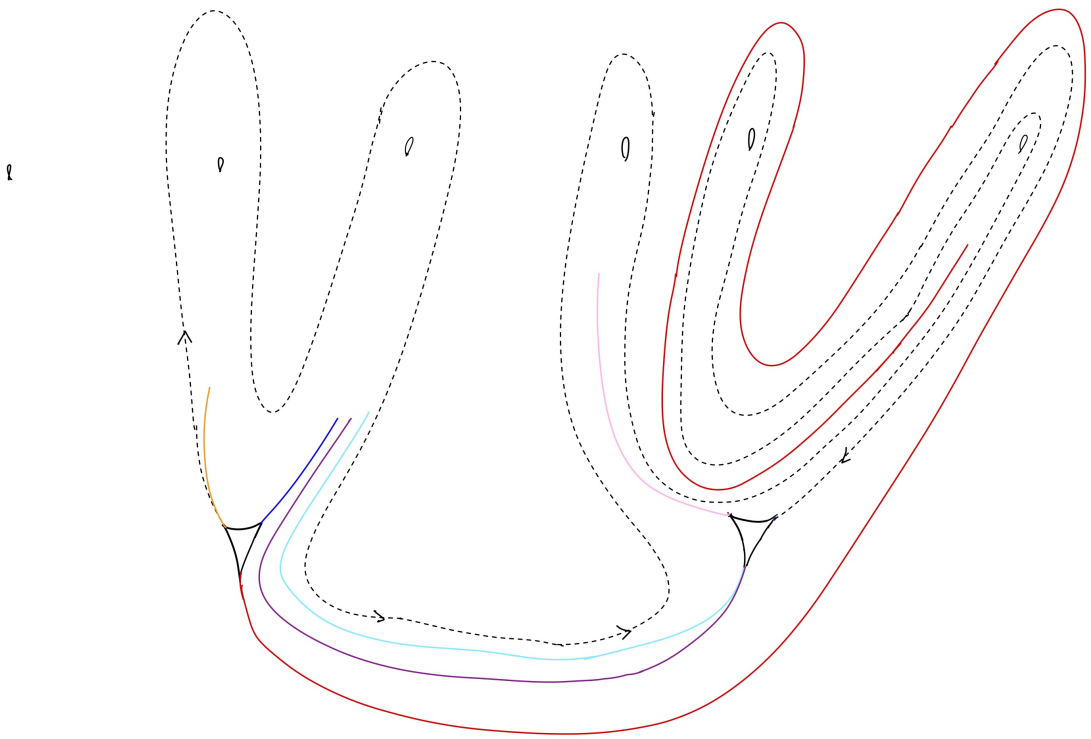


Figure F.84: Barm4

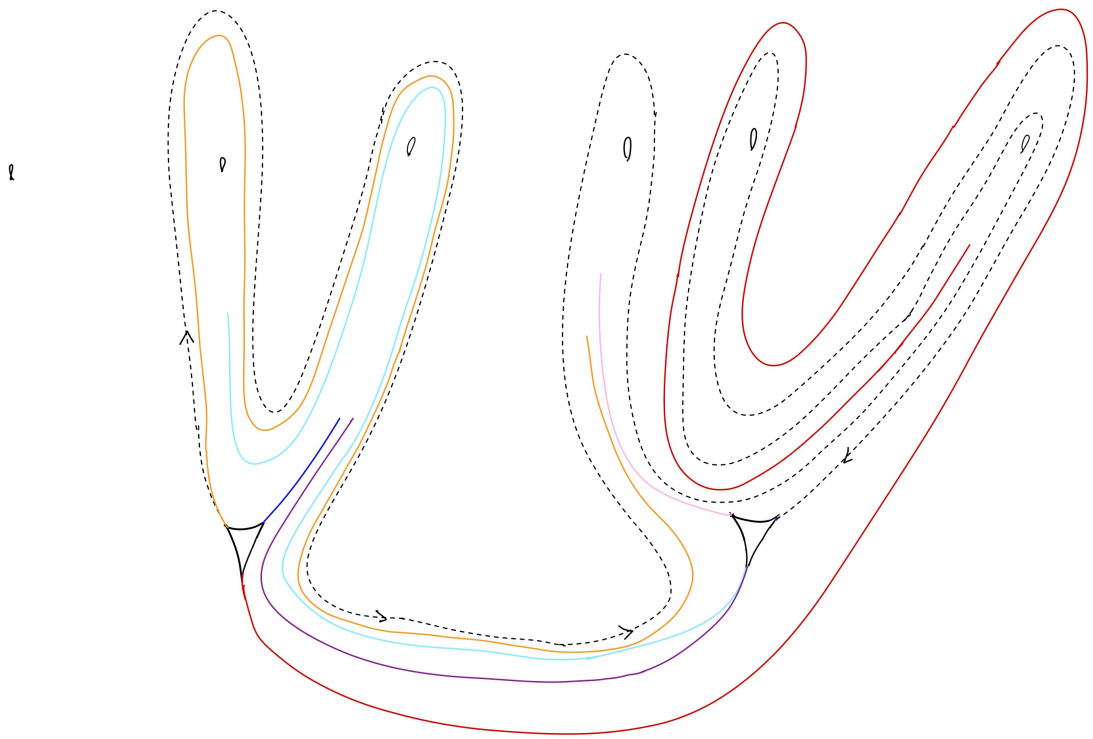


Figure F.85: Barm5

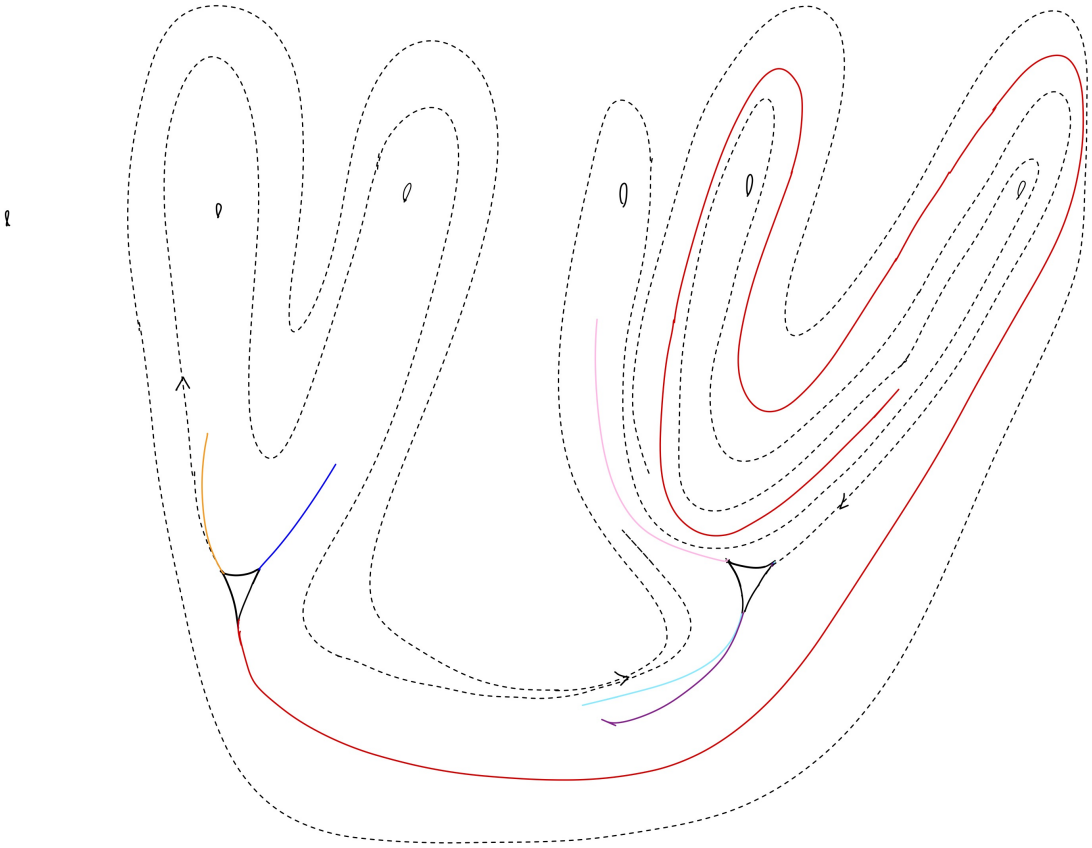


Figure F.86: Barm6

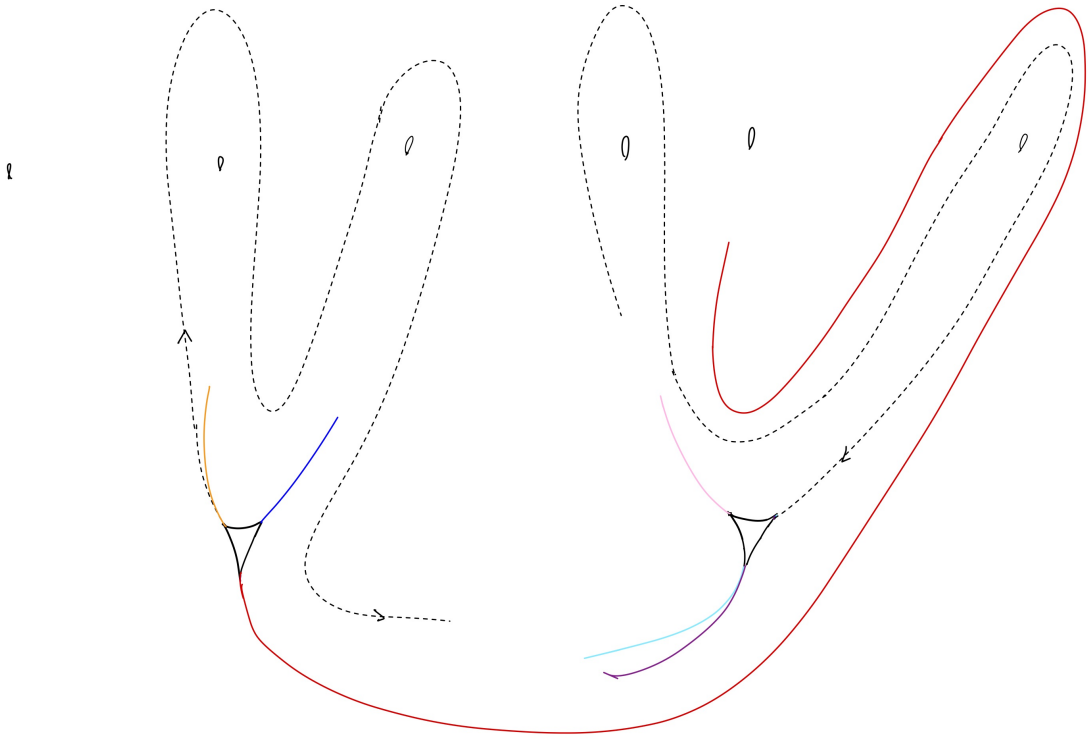


Figure F.87: Nary1

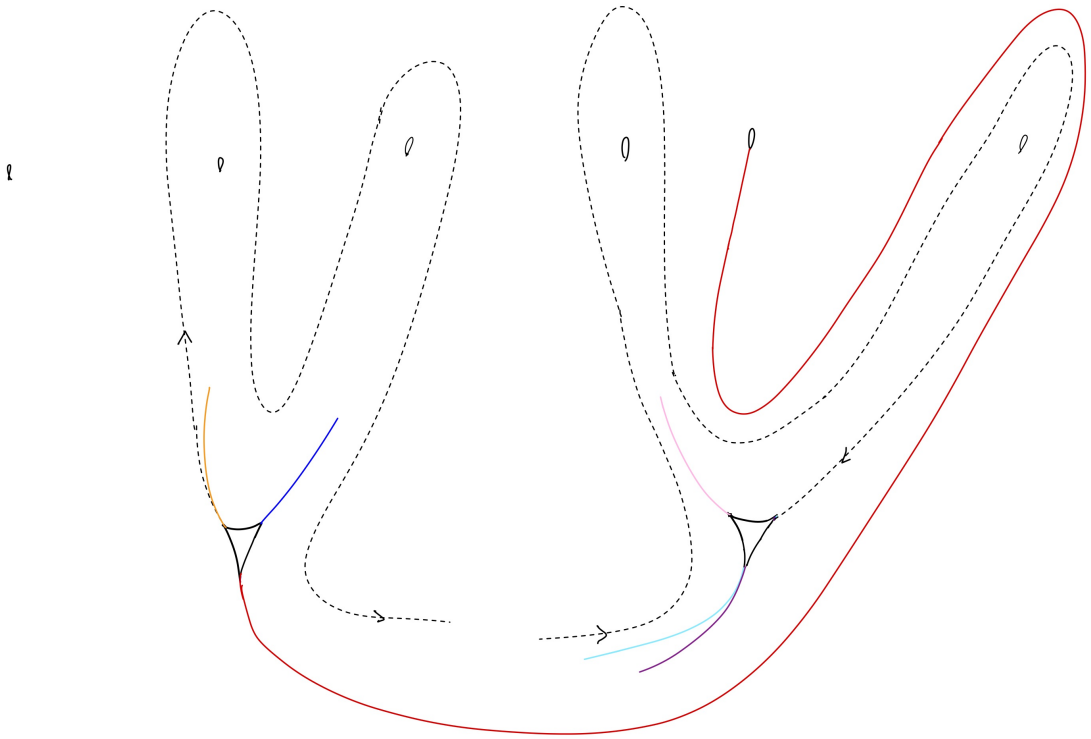


Figure F.88: Nary2

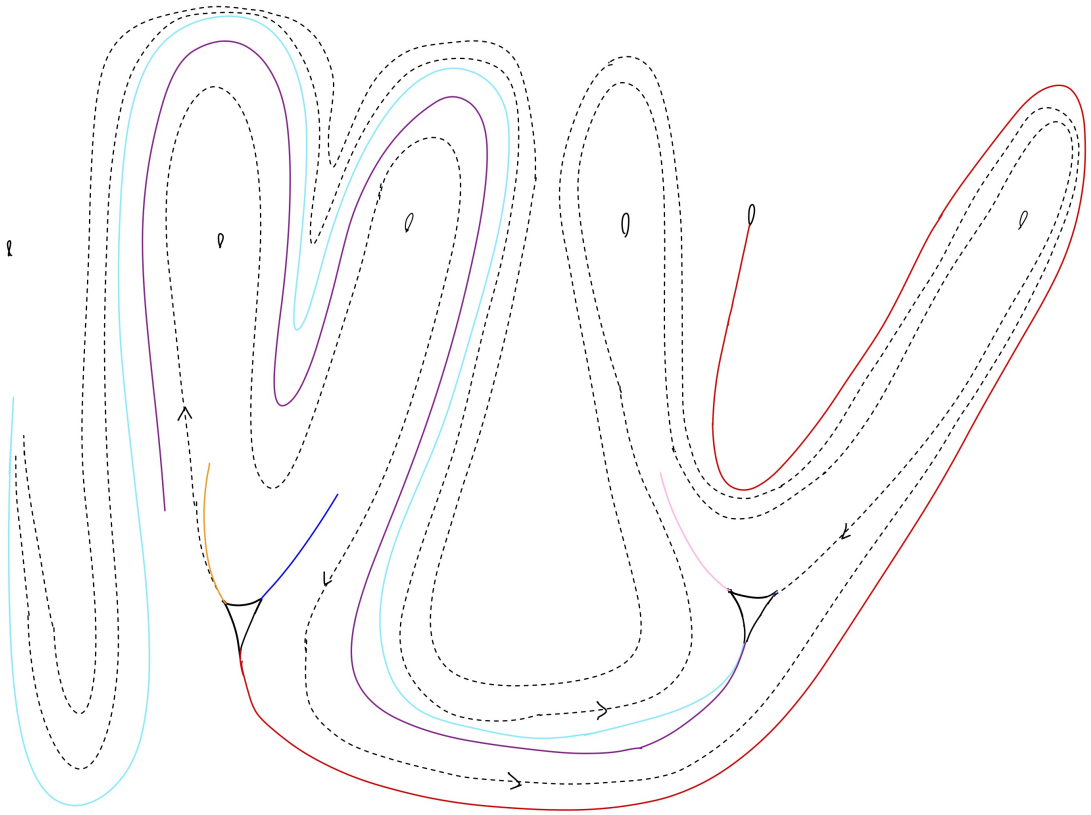


Figure F.89: Nary3

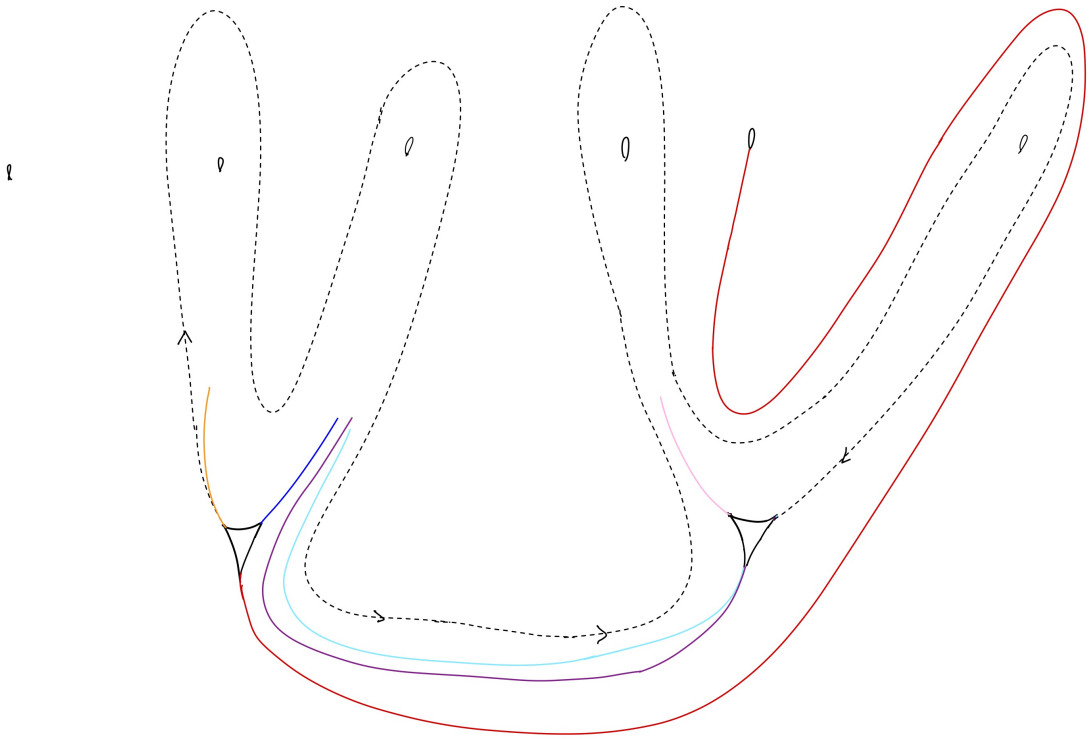


Figure F.90: Nary4

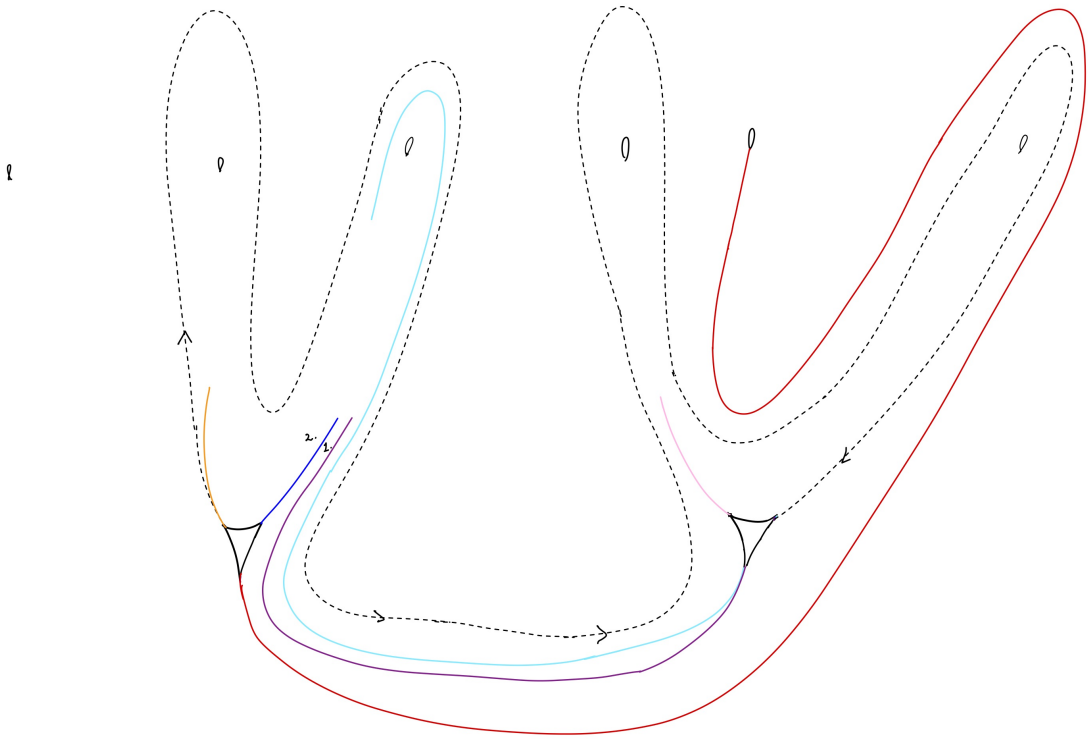


Figure F.91: Nary5

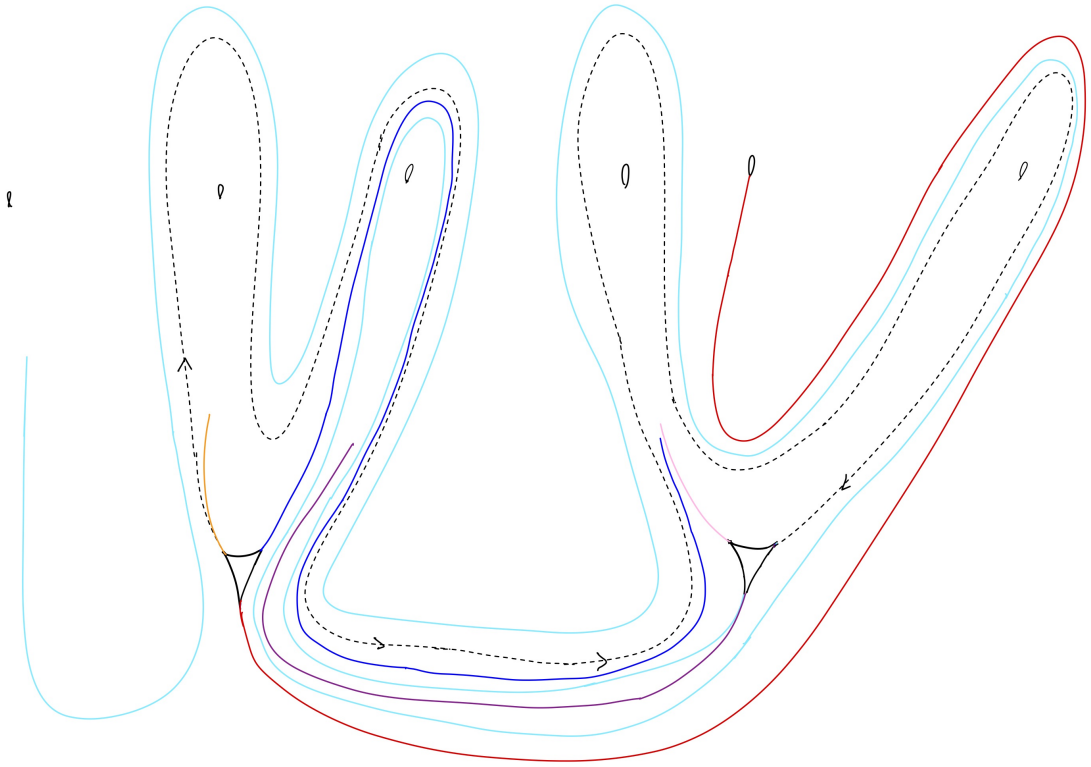


Figure F.92: Nary6

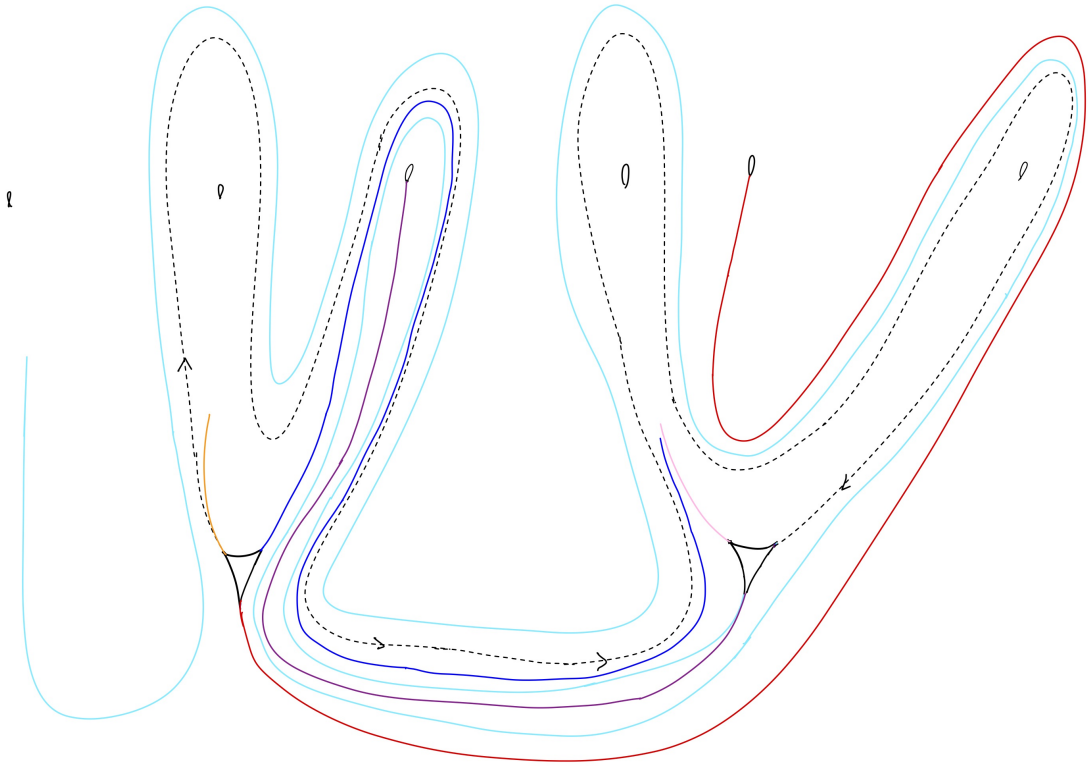


Figure F.93: Nary7

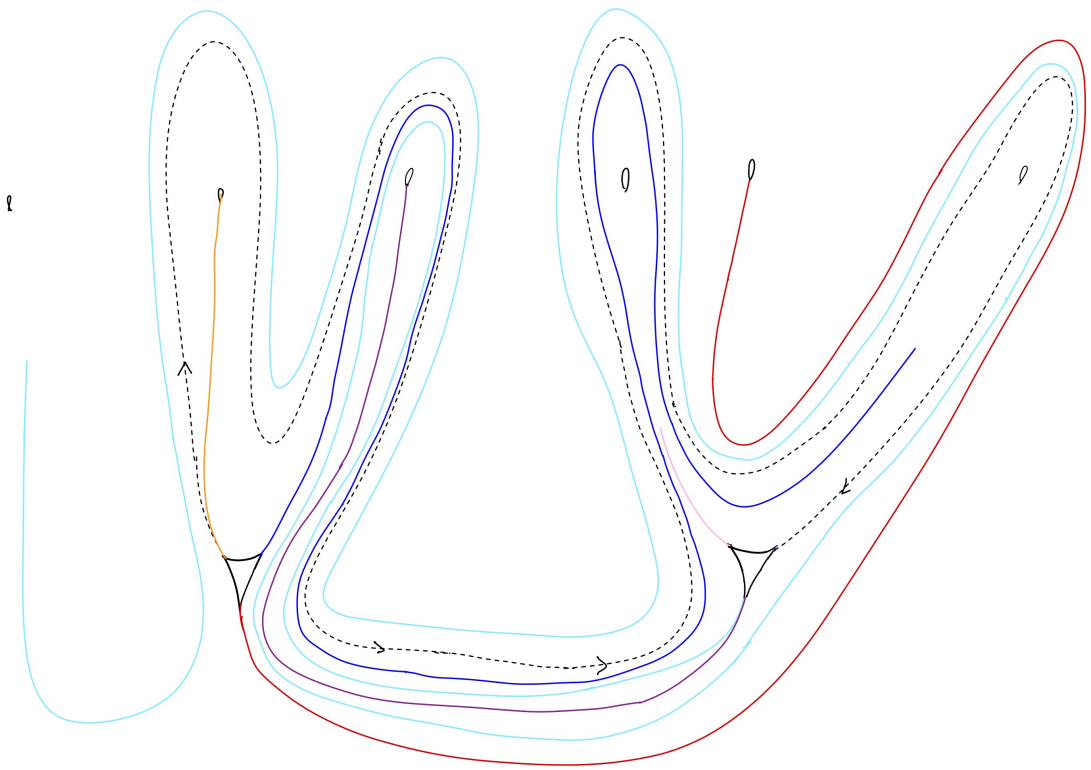


Figure F.94: Aulic1

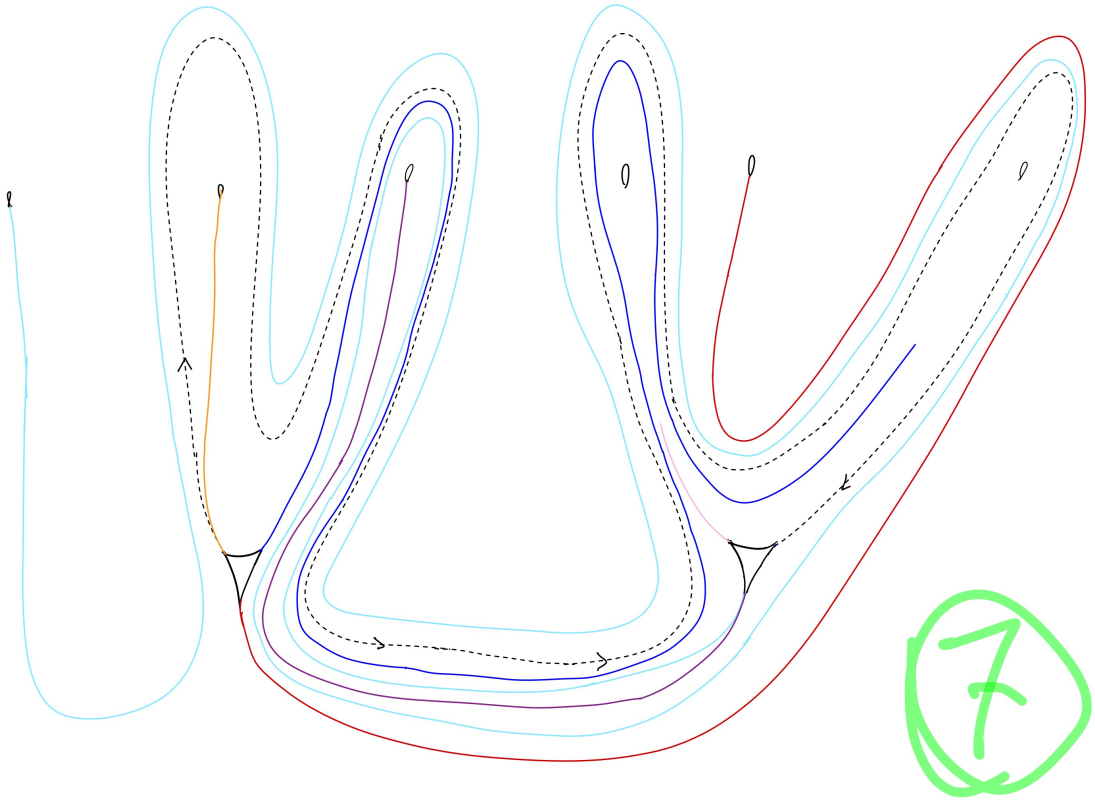


Figure F.95: Aulic2

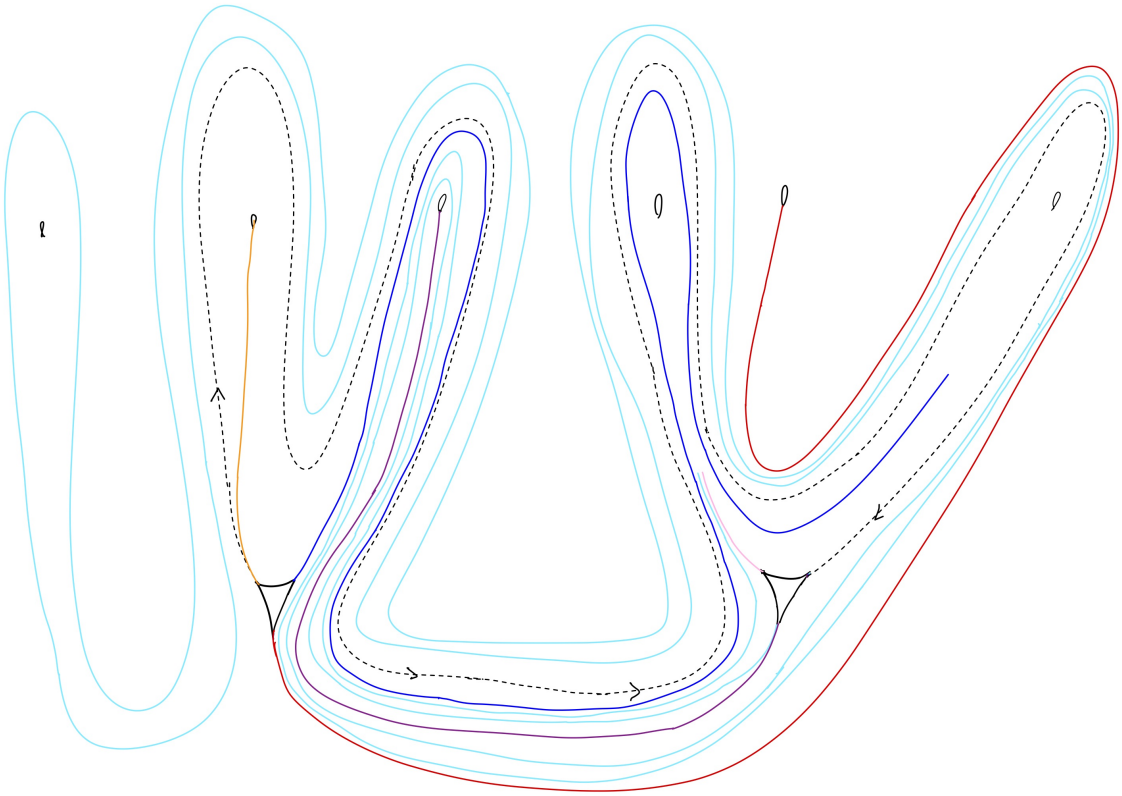


Figure F.96: Aulic3

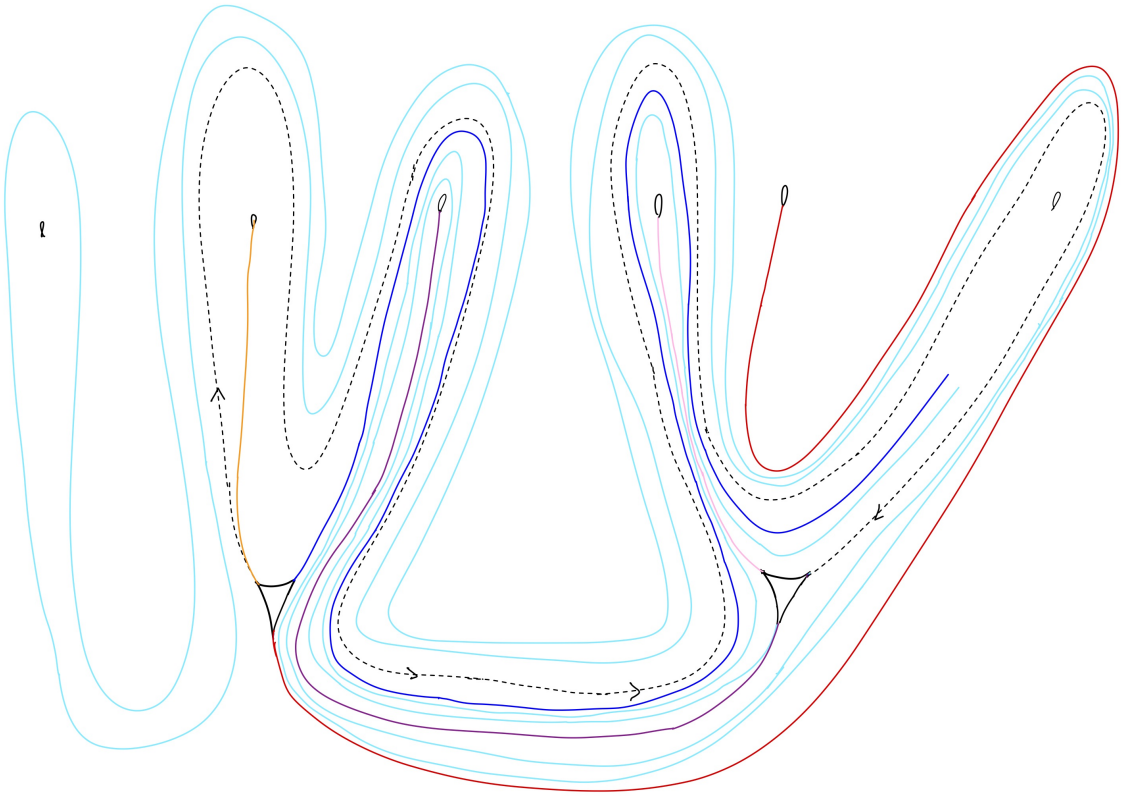


Figure F.97: Aulic4

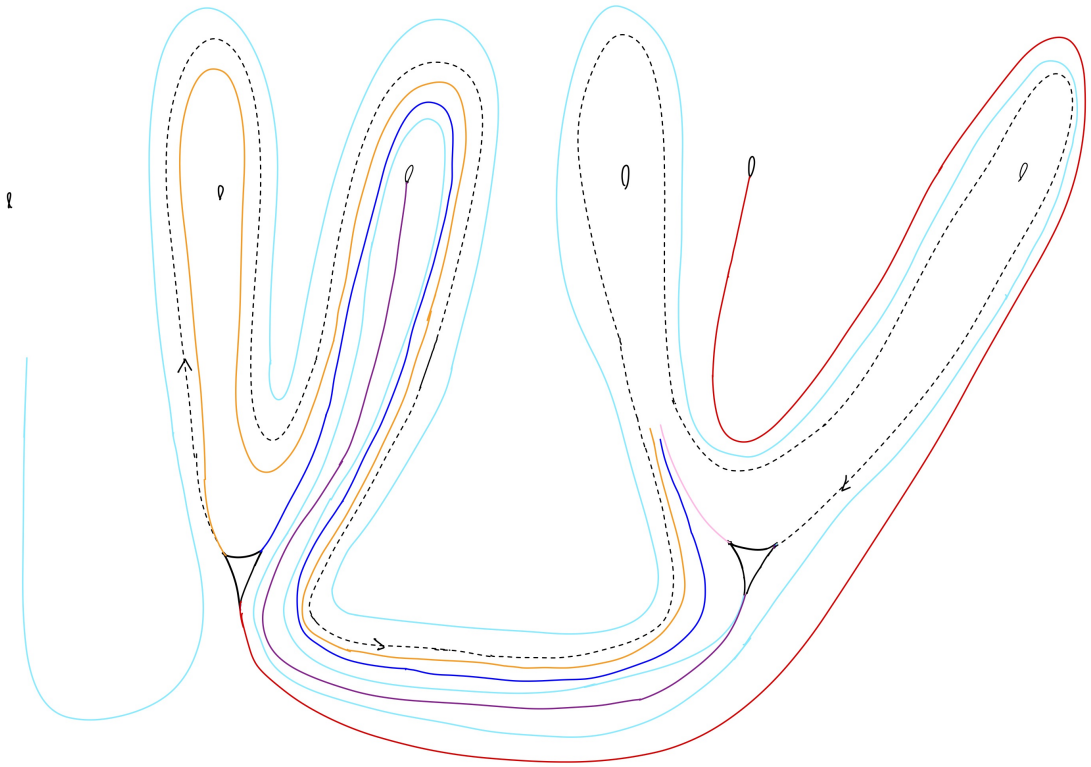


Figure F.98: Oread1

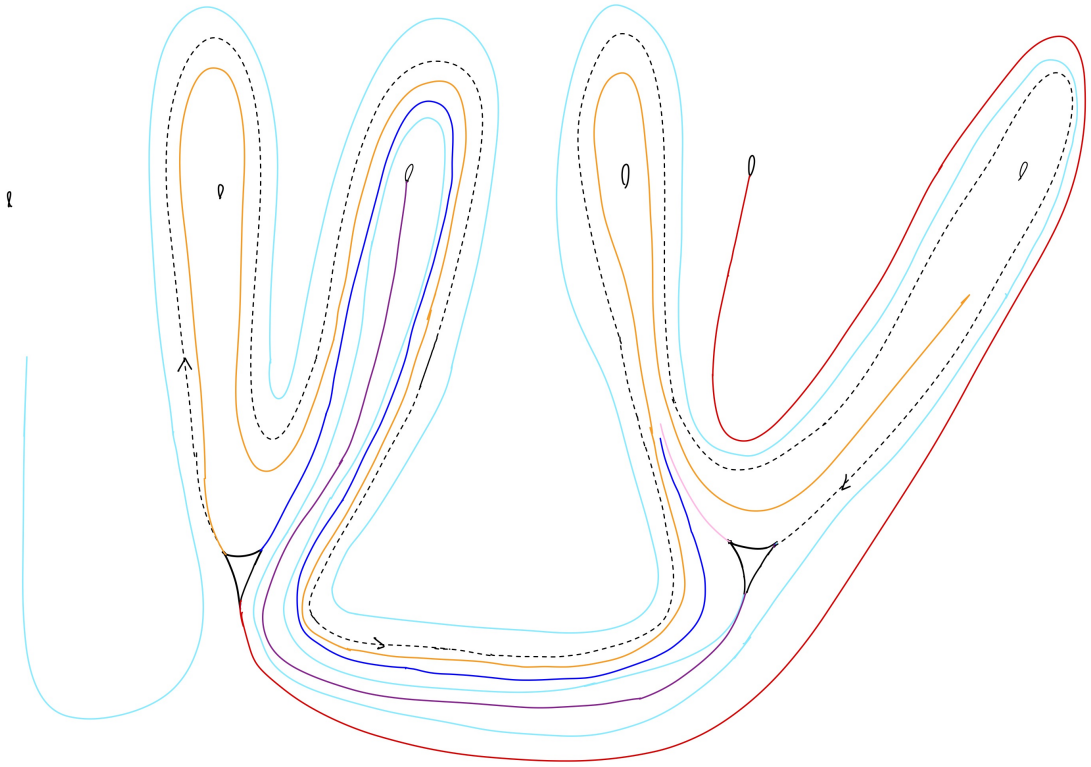


Figure F.99: Oread2

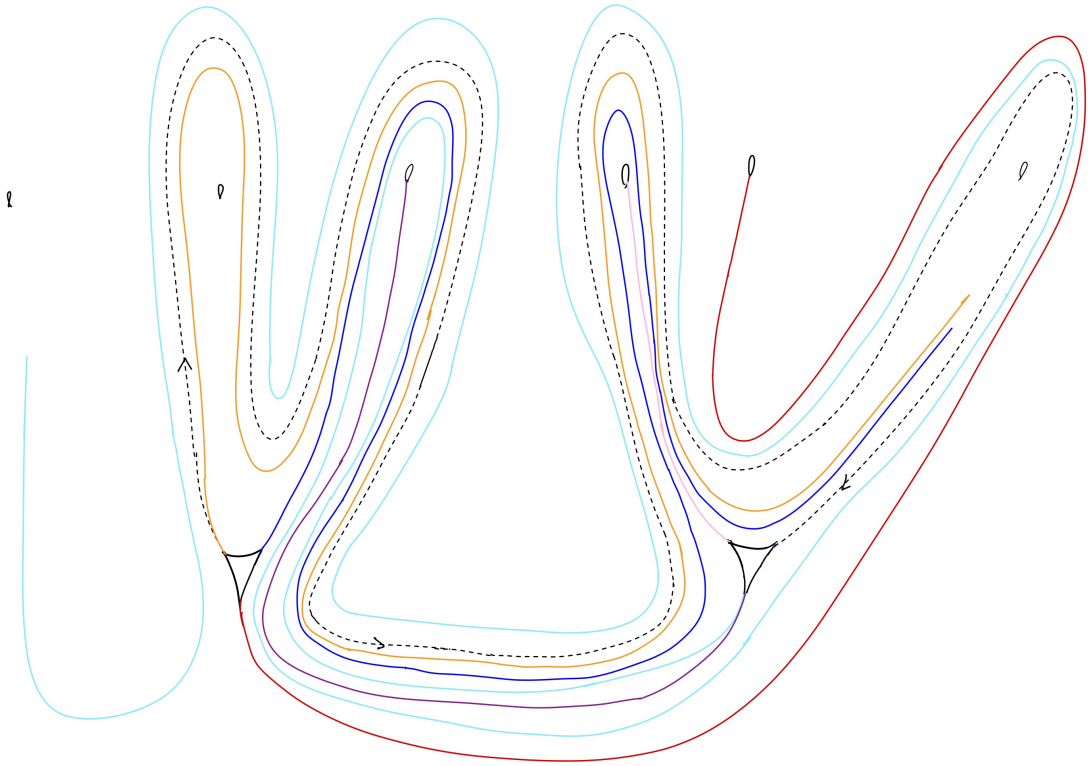


Figure F.100: Oread3

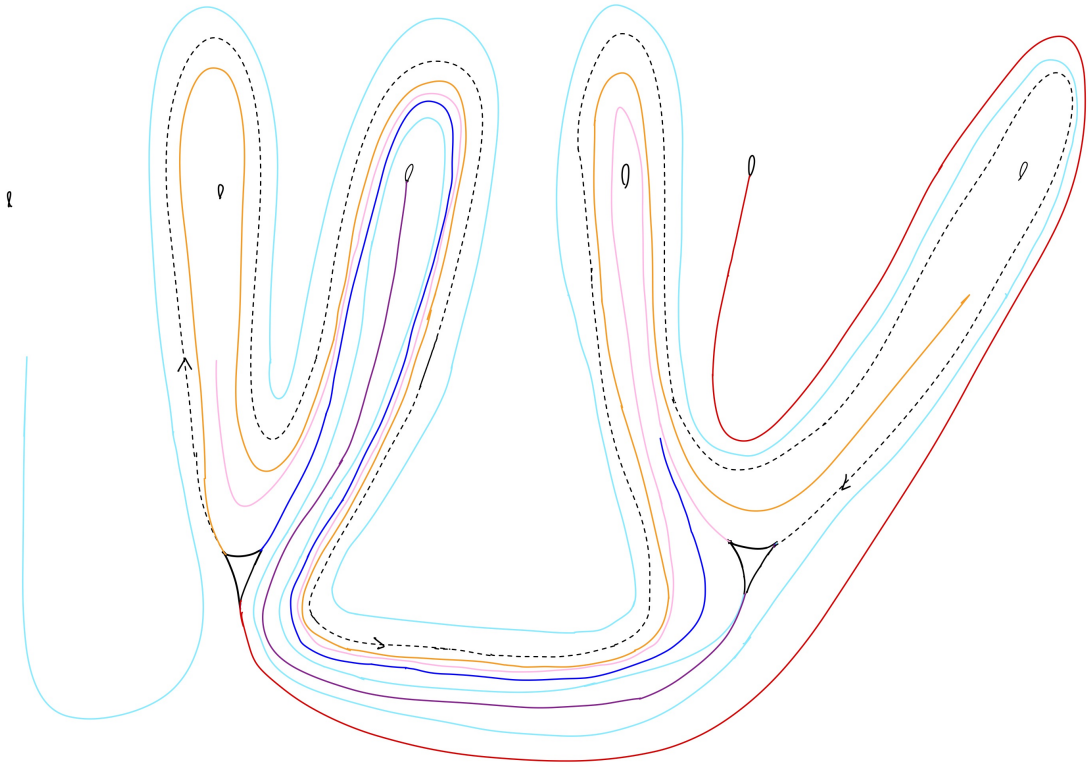


Figure F.101: Oread4

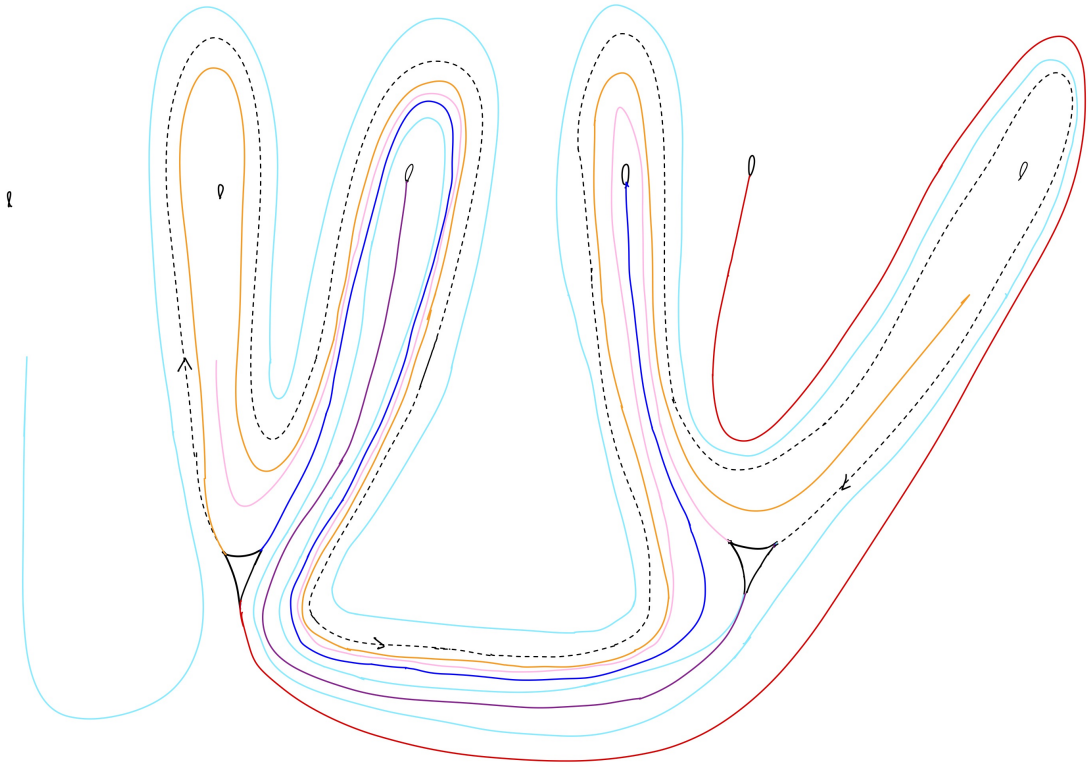


Figure F.102: Oread5

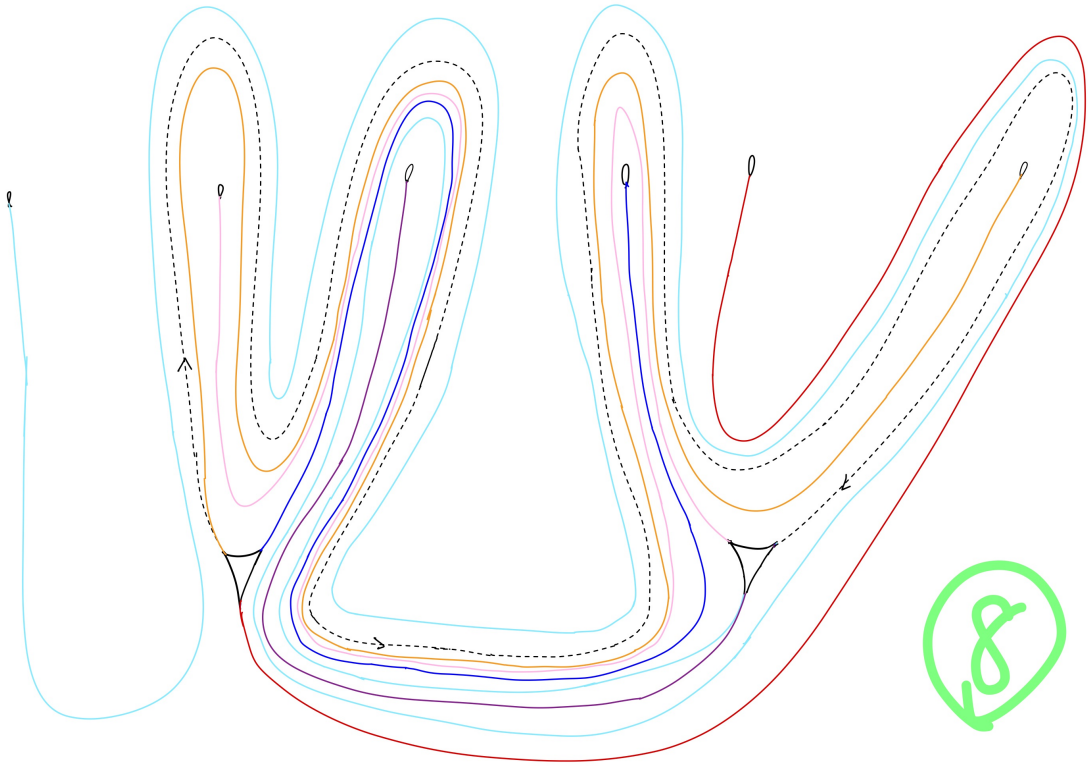


Figure F.103: Oread6

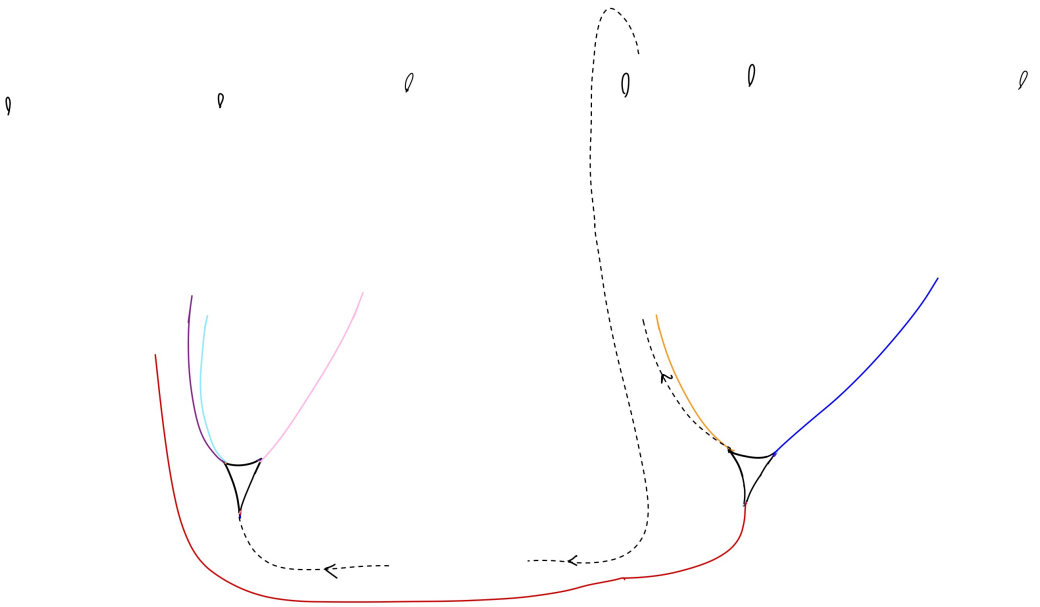


Figure F.104: FUN1

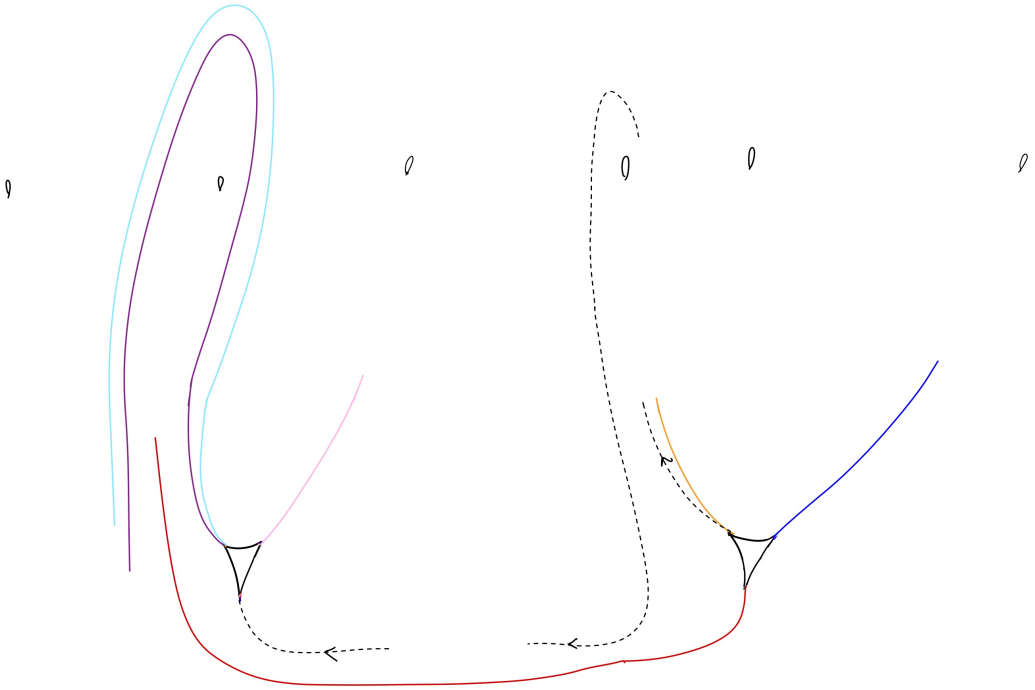


Figure F.105: FUN2

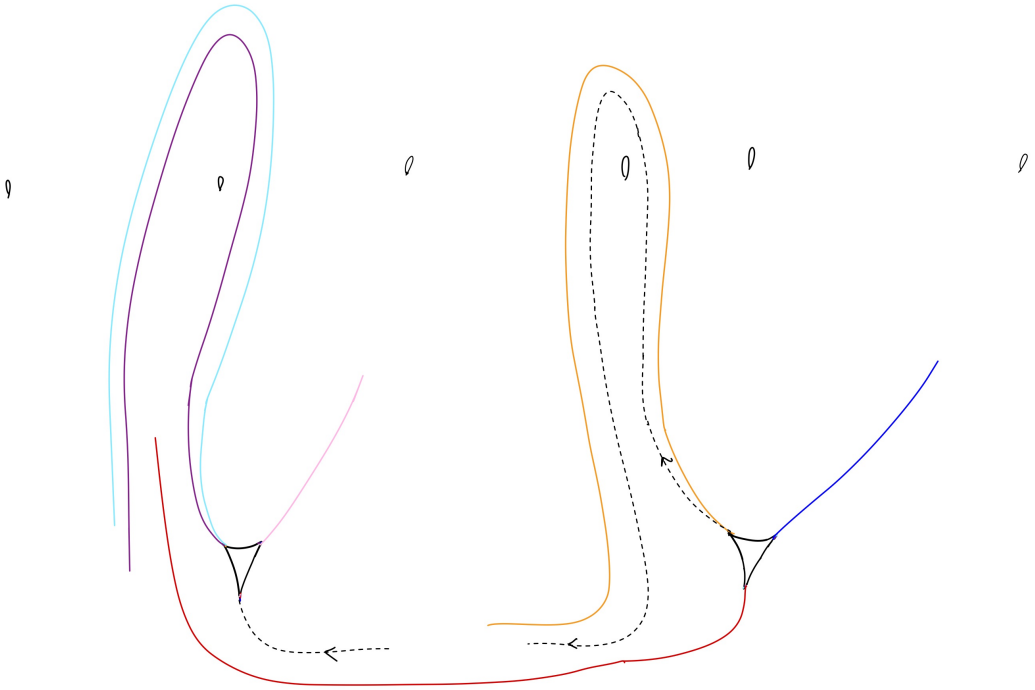


Figure F.106: FUN3

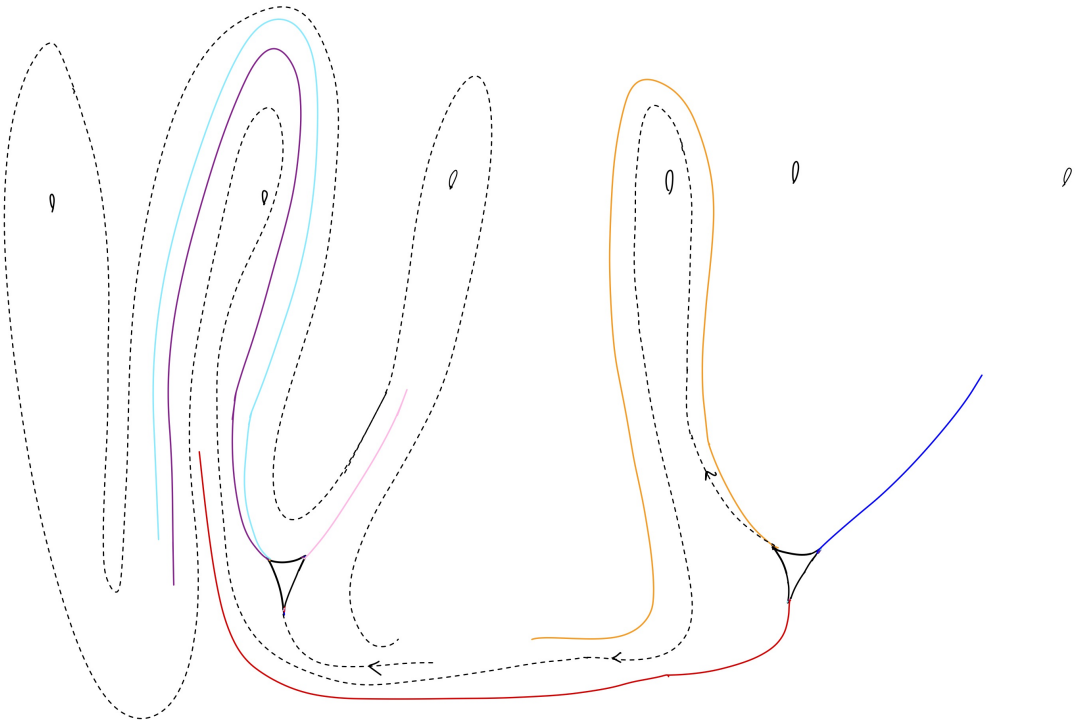


Figure F.107: FUN4

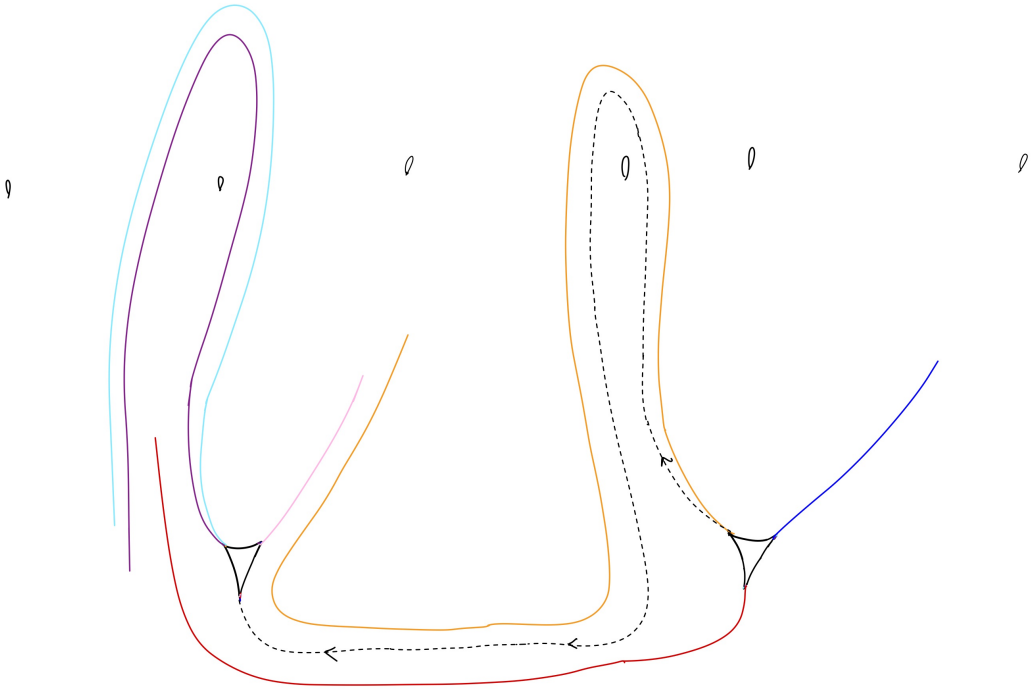


Figure F.108: FUN5

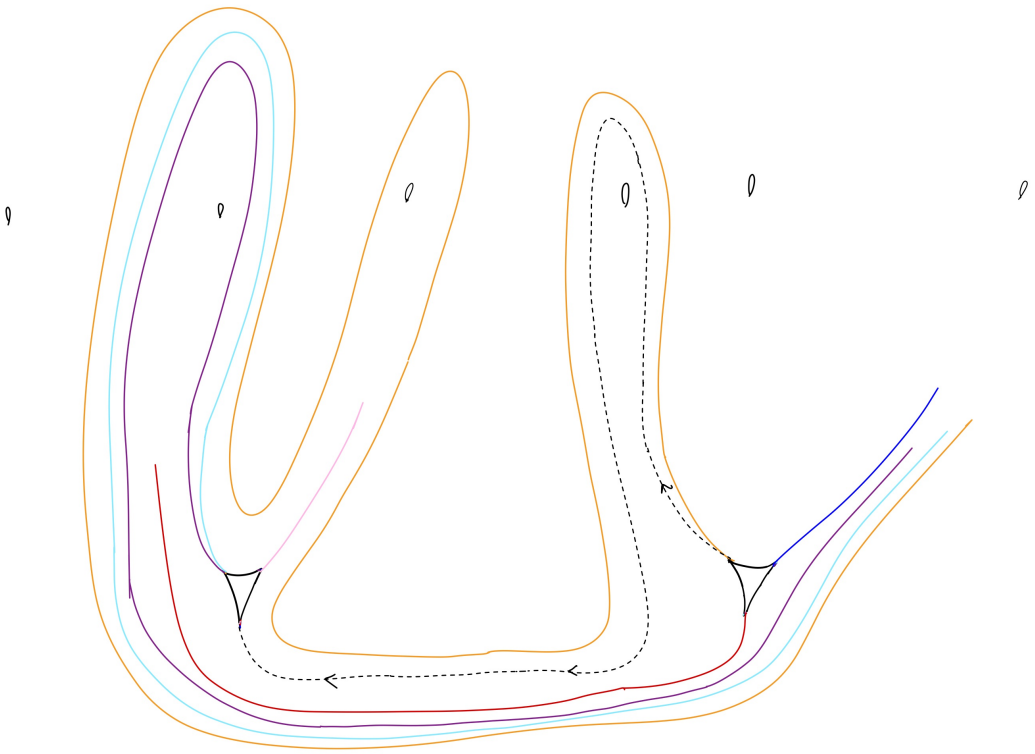


Figure F.109: FUN6

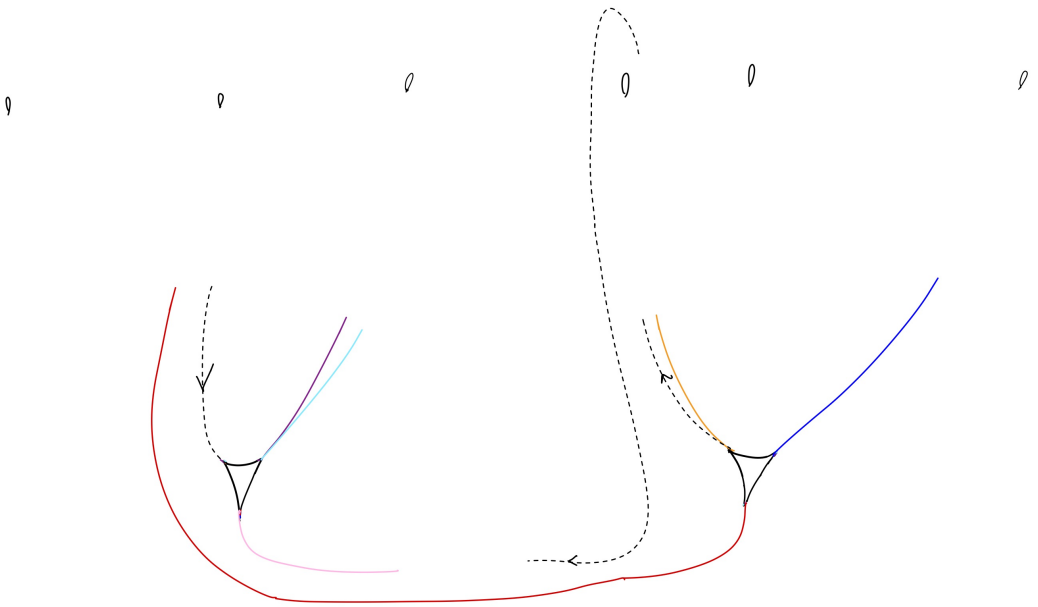


Figure F.110: FAT1

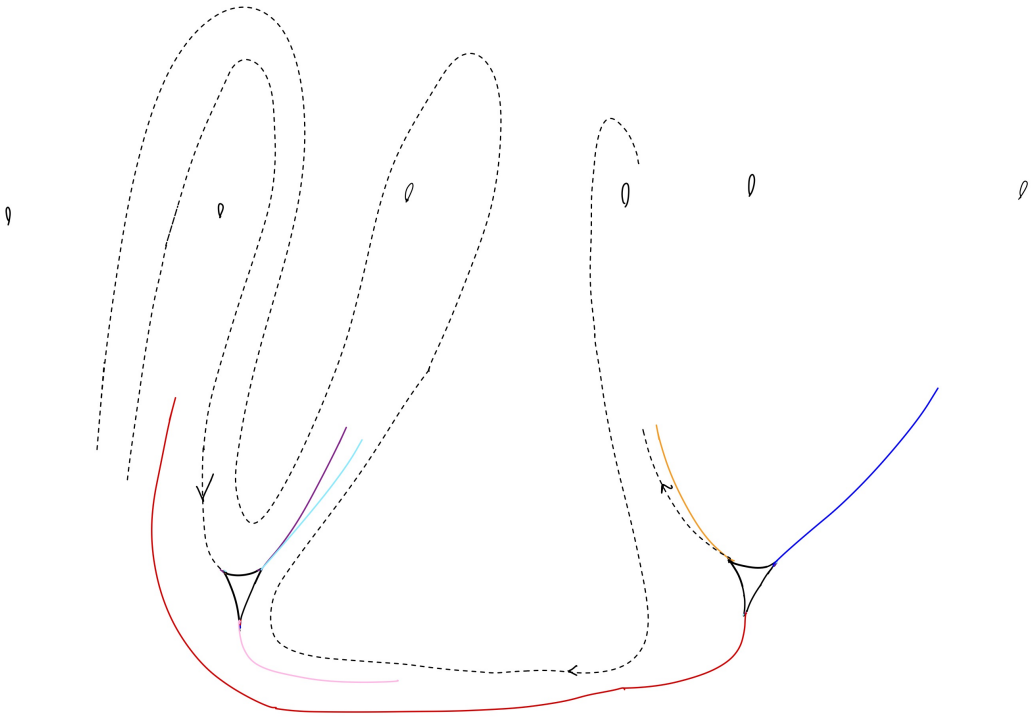


Figure F.111: FAT2

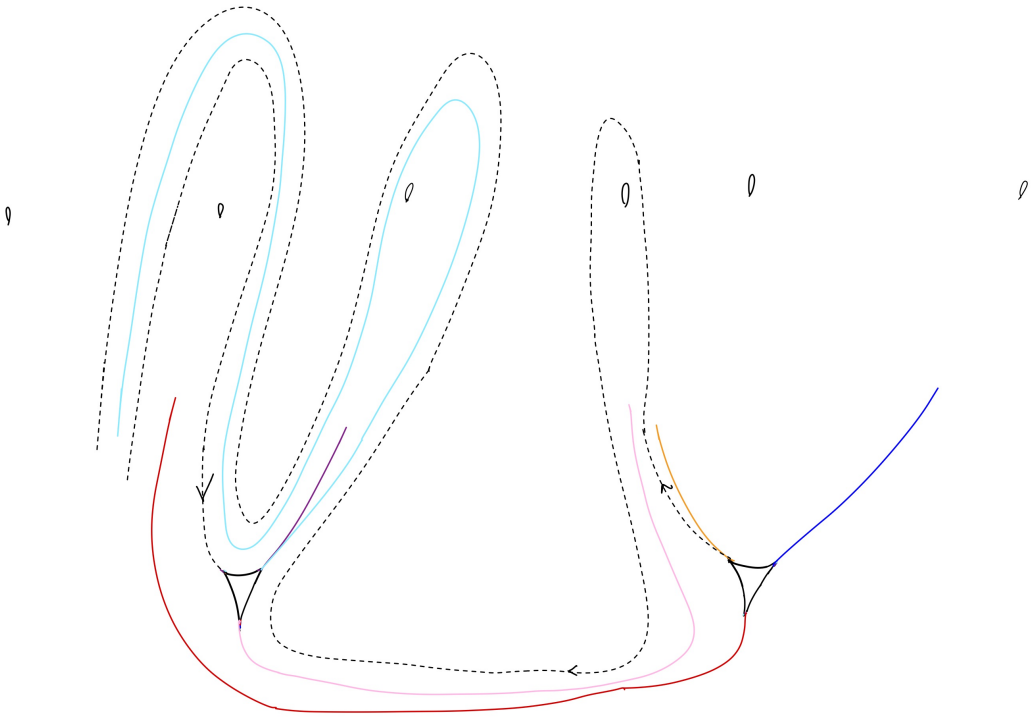


Figure F.112: FAT3

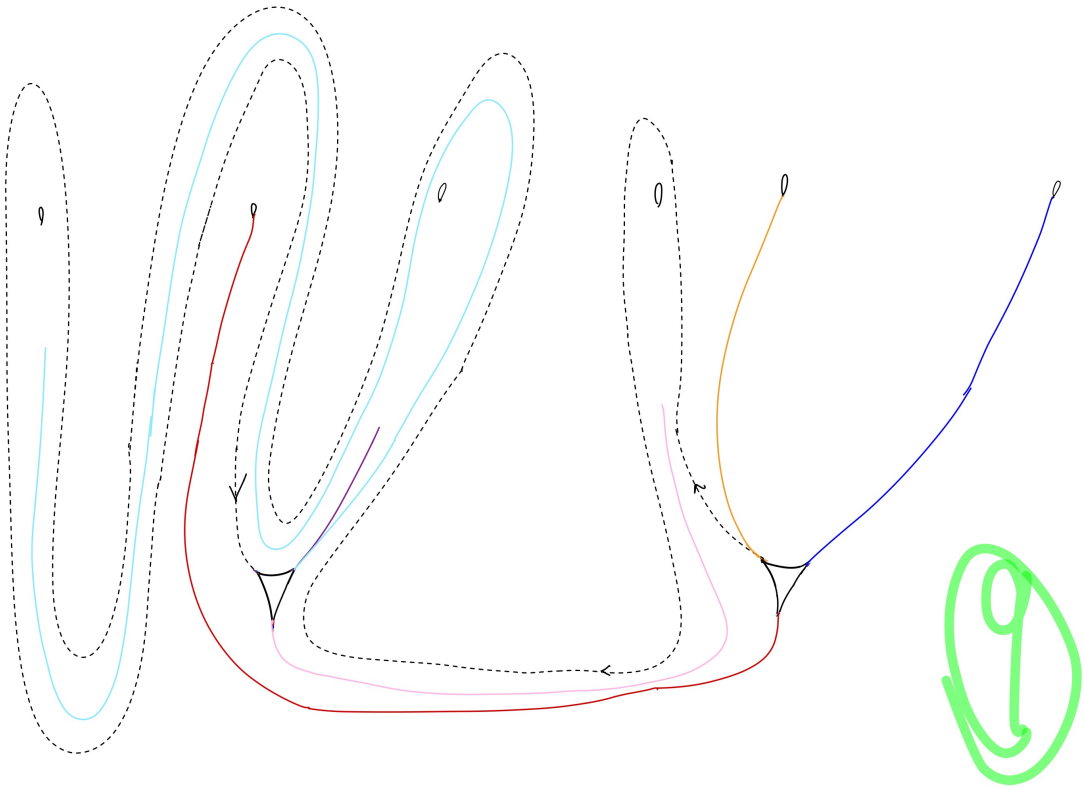


Figure F.113: FAT4

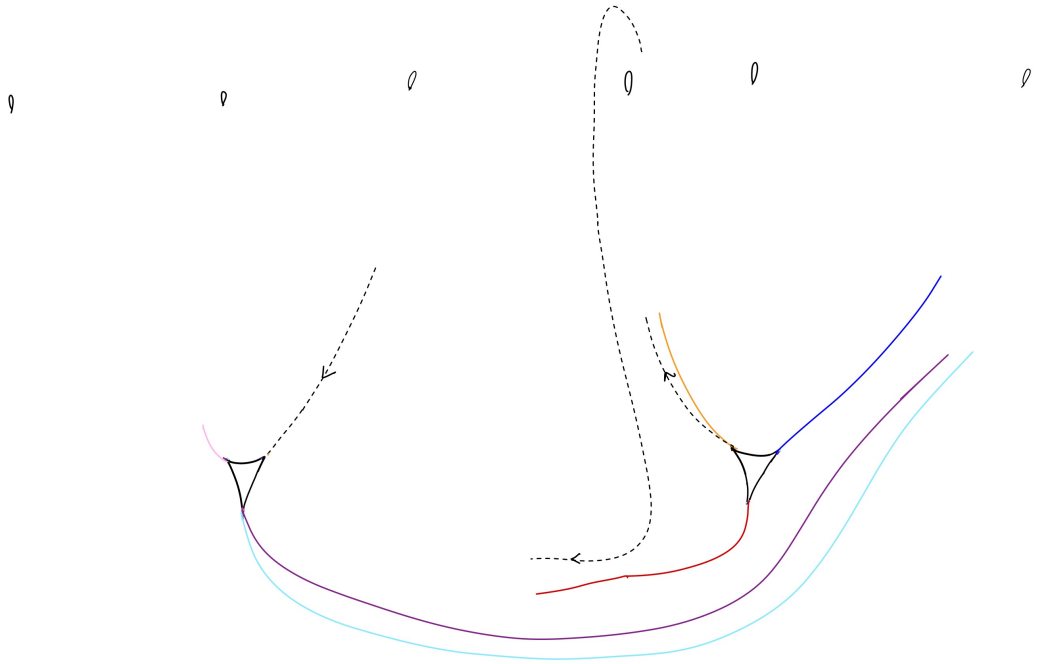


Figure F.114: KNH1

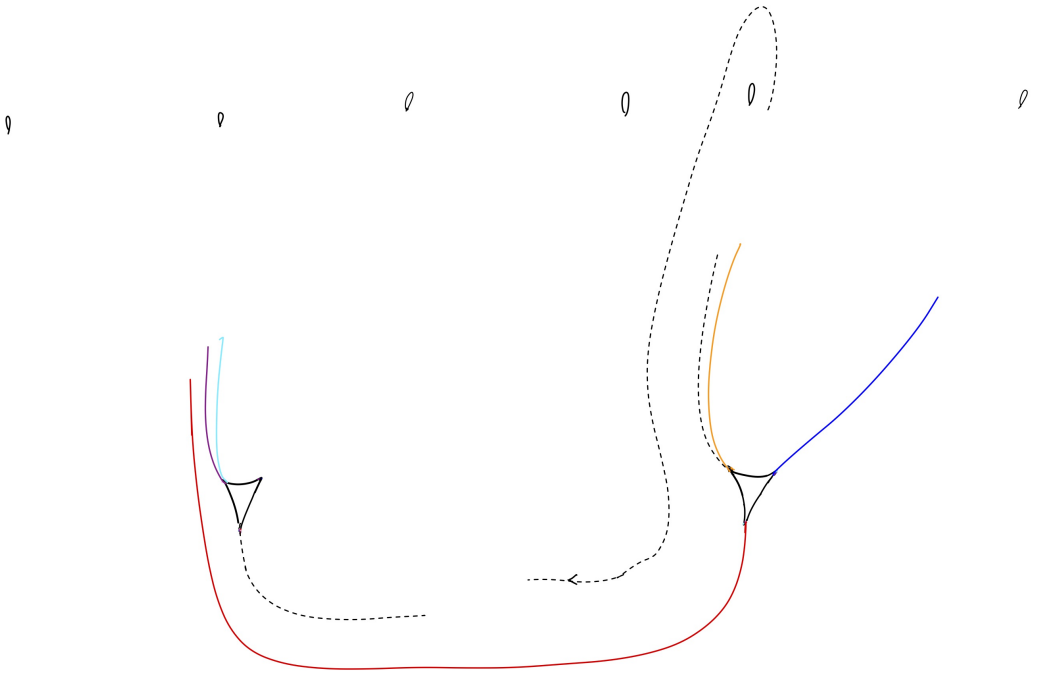


Figure F.115: MZG1

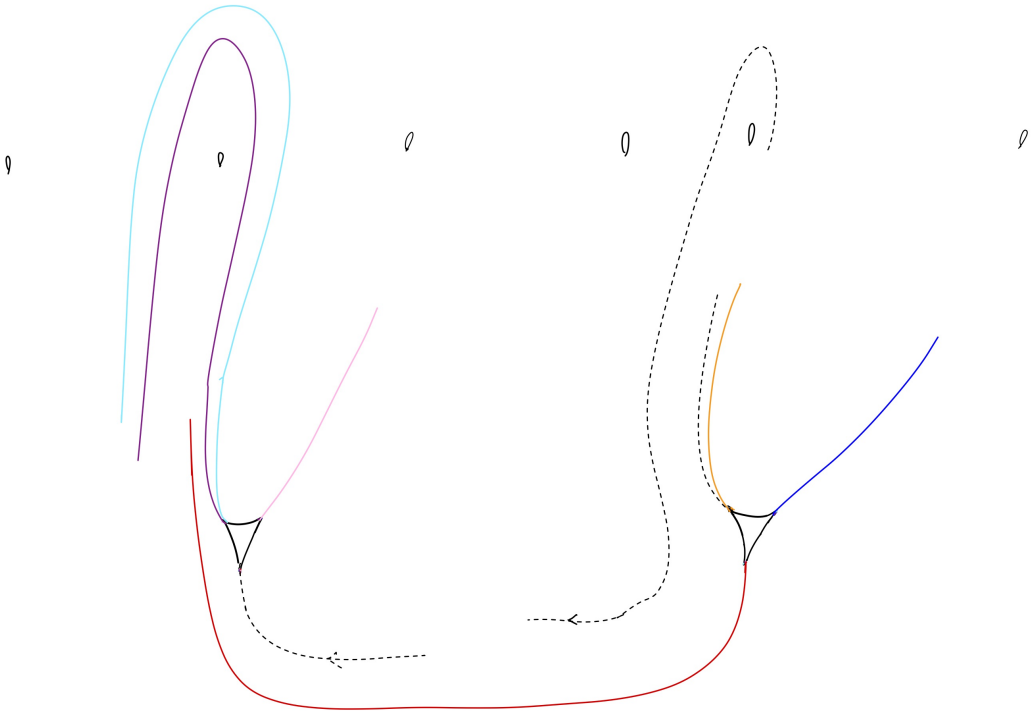


Figure F.116: MZG2

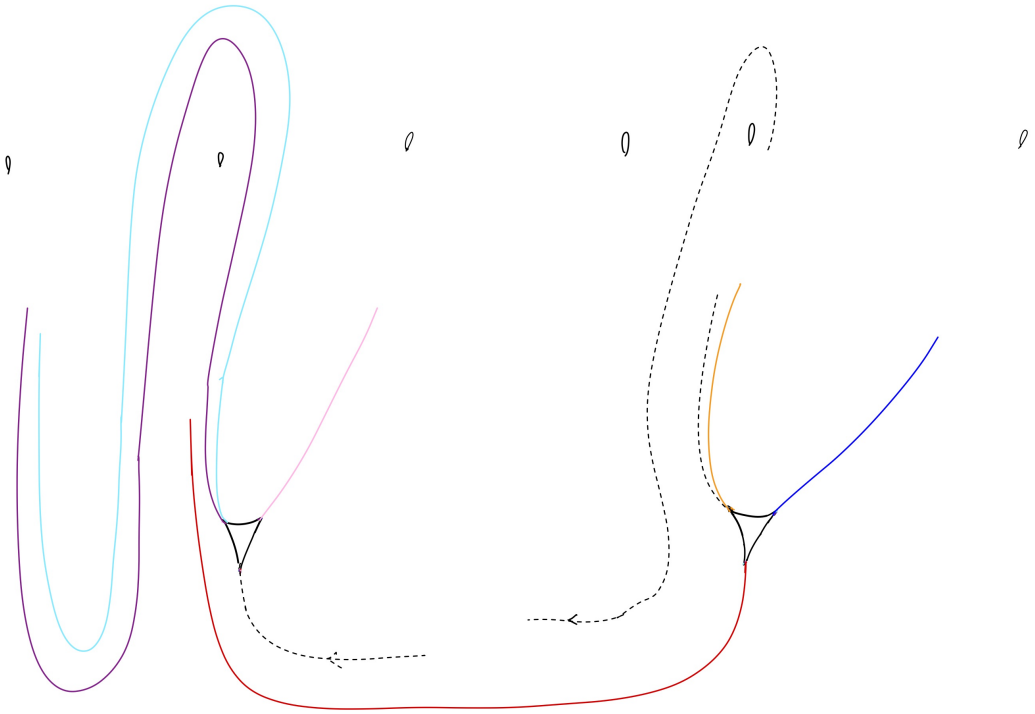


Figure F.117: MZG3

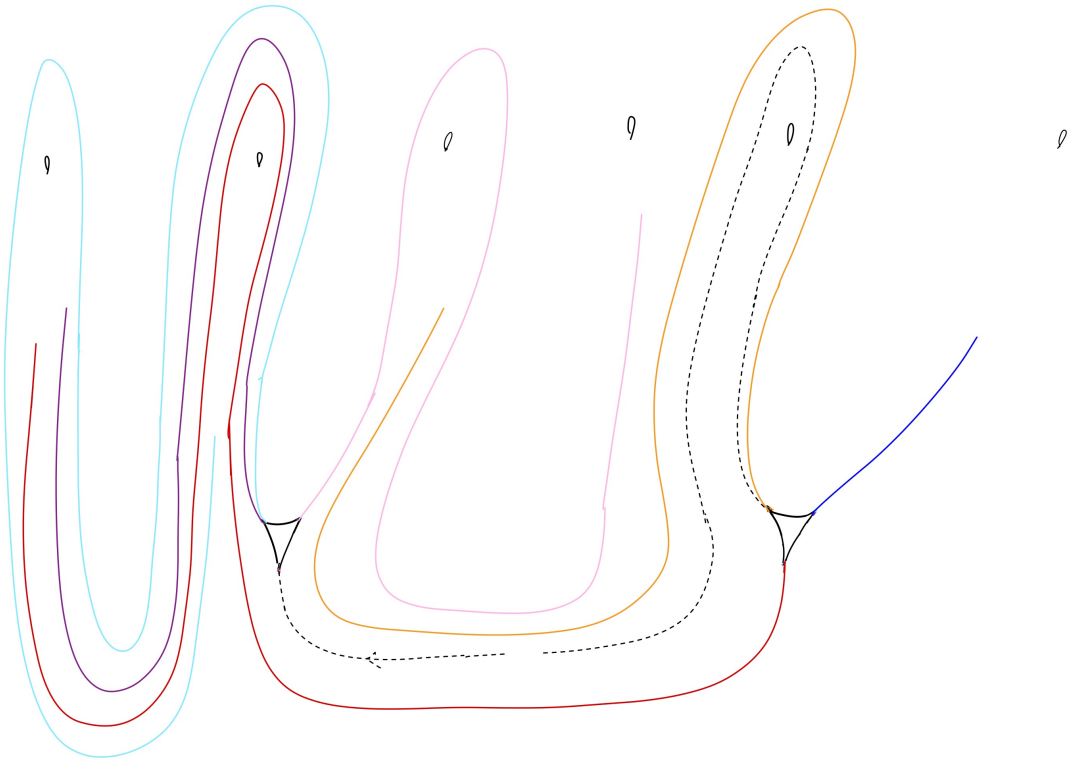


Figure F.118: MZG4

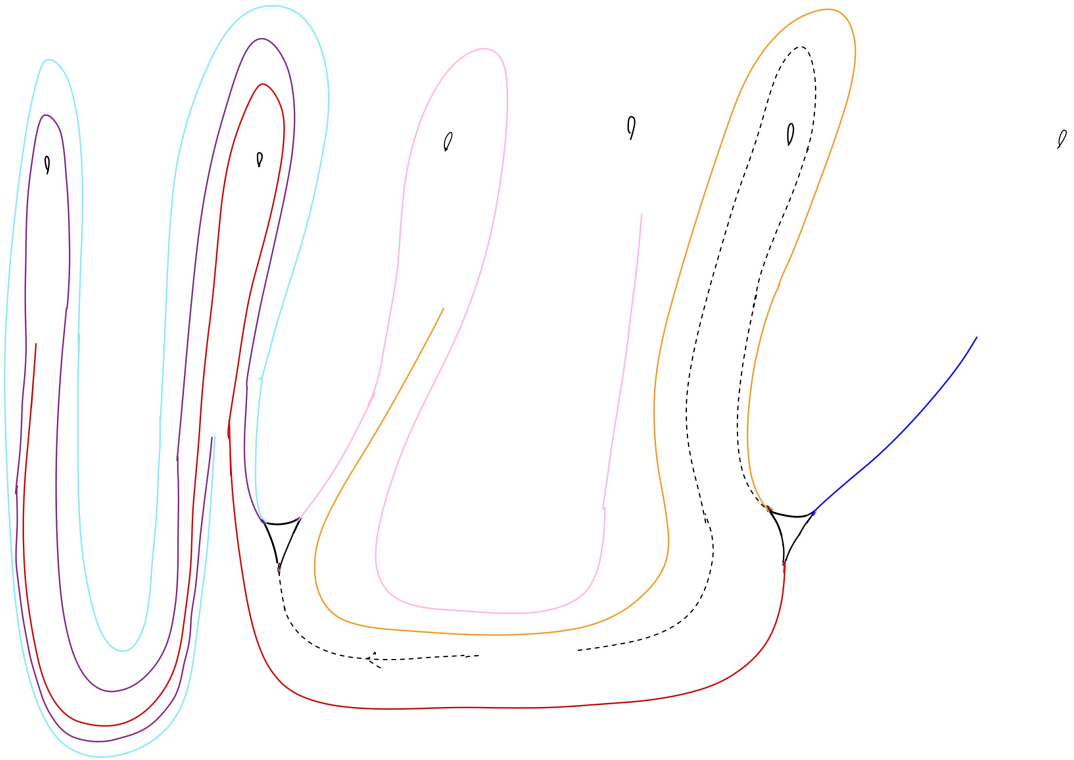


Figure F.119: MZG5

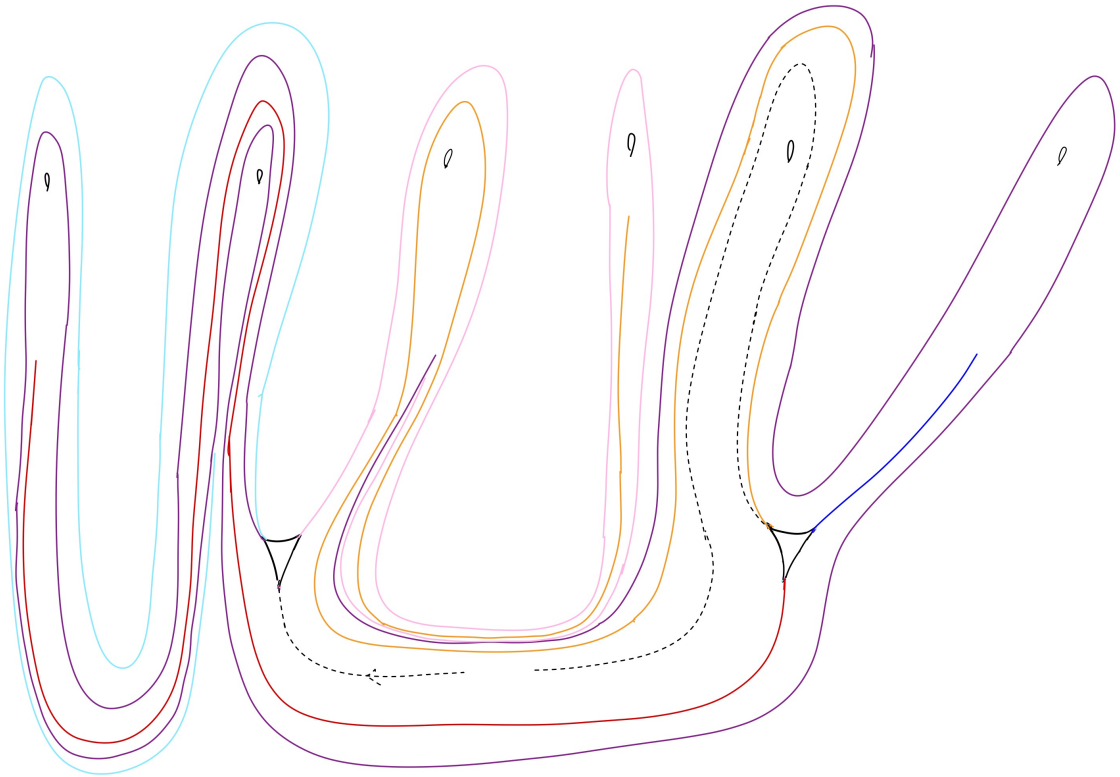


Figure F.120: MZG6

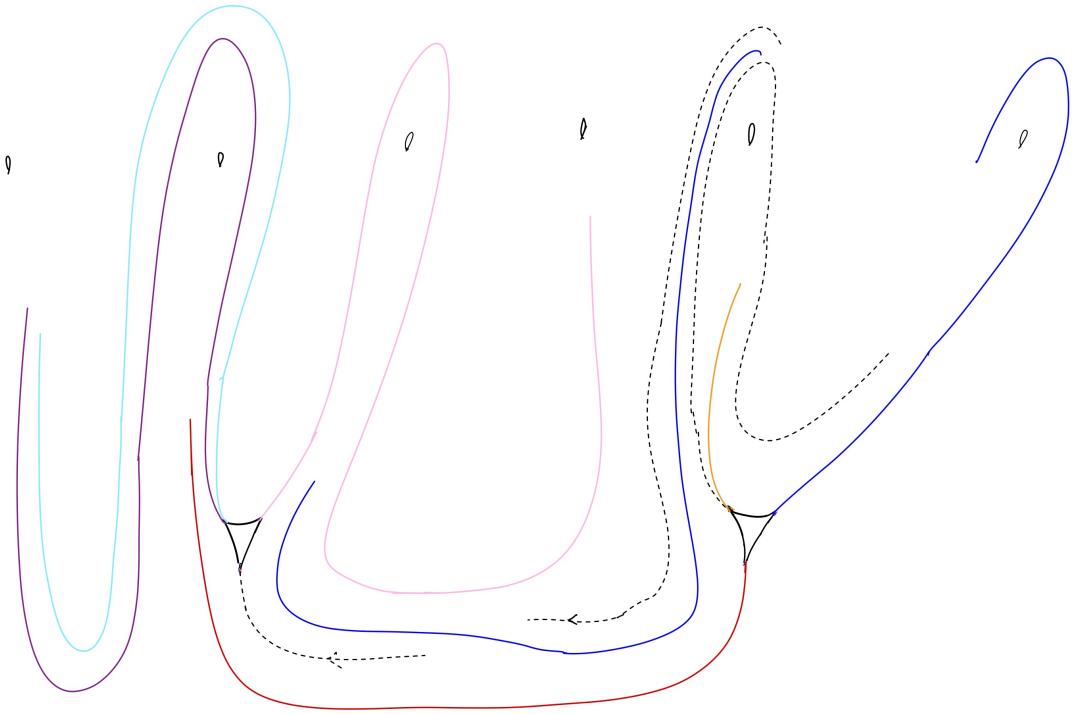


Figure F.121: MZG7

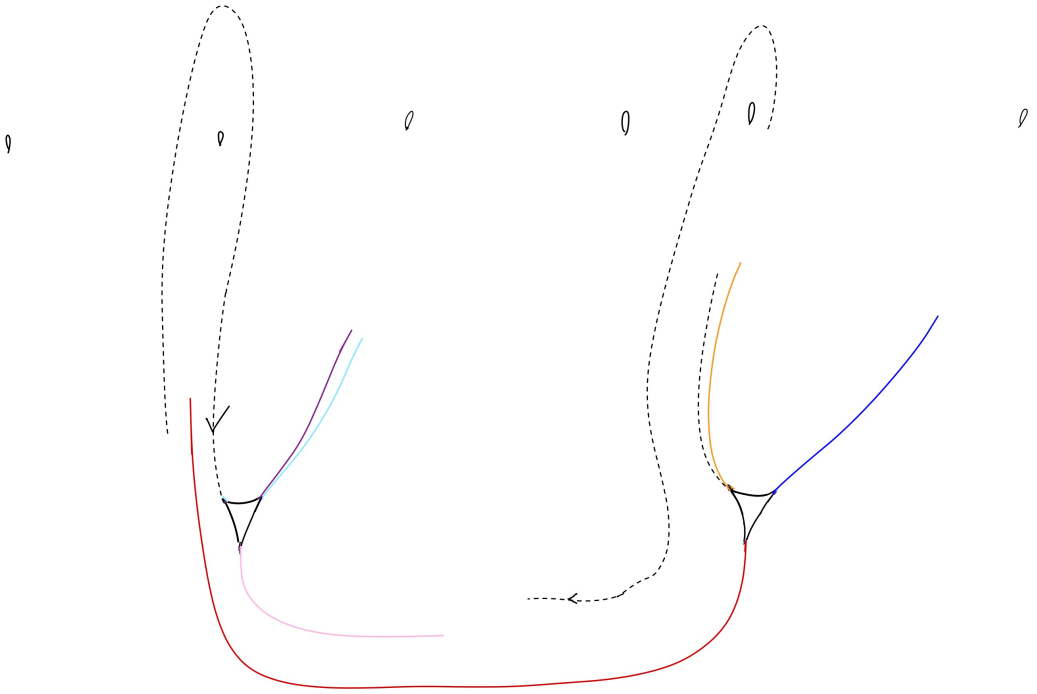


Figure F.122: WAK1

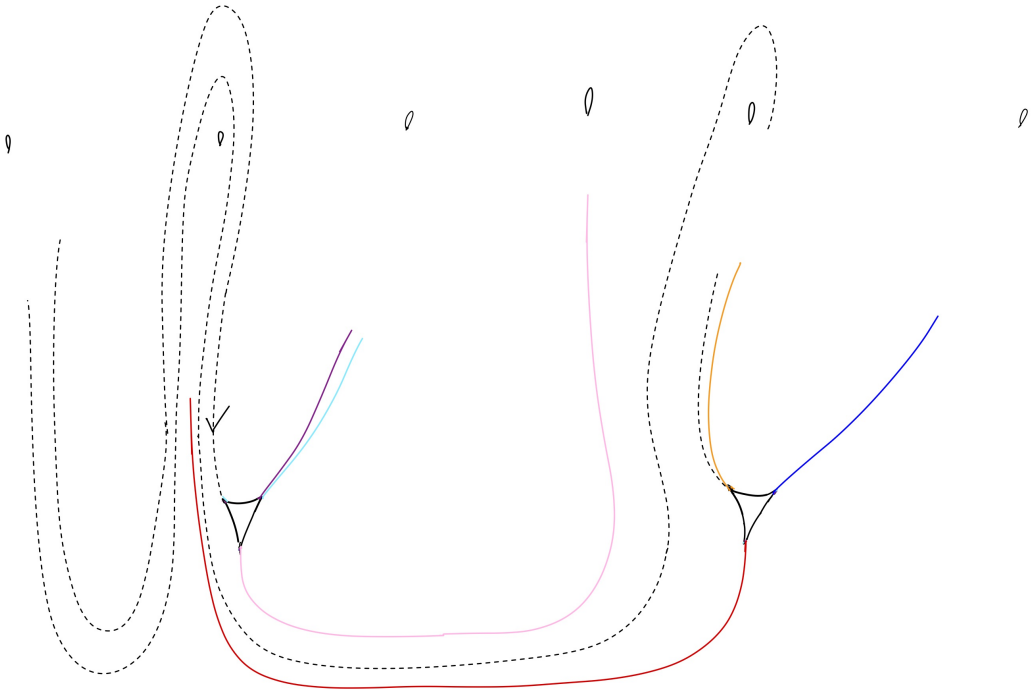


Figure F.123: WAK2

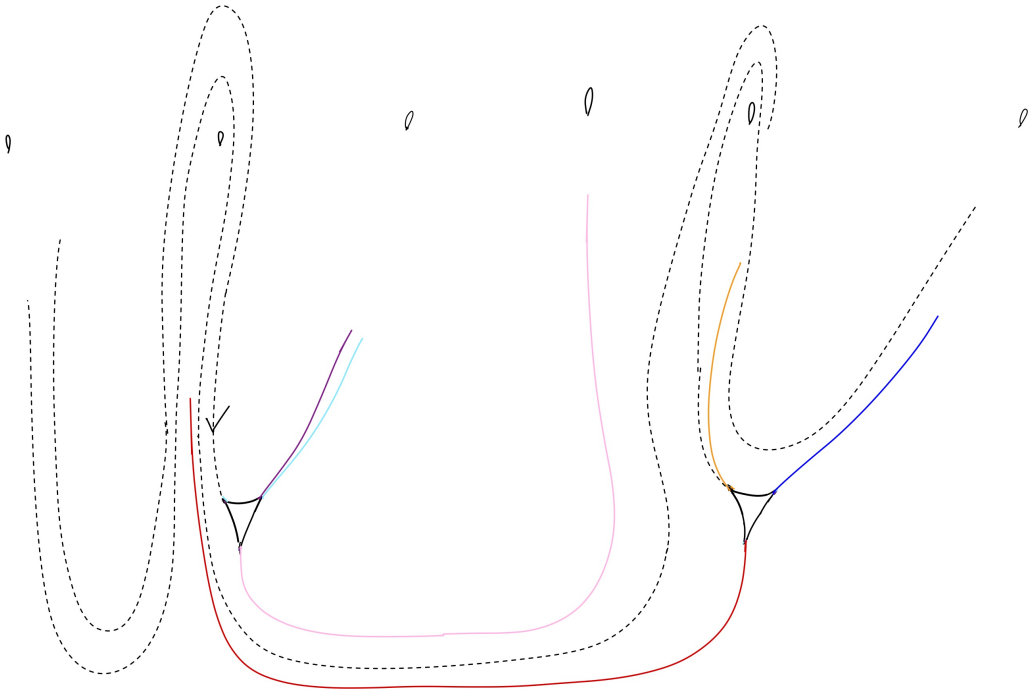


Figure F.124: WAK3

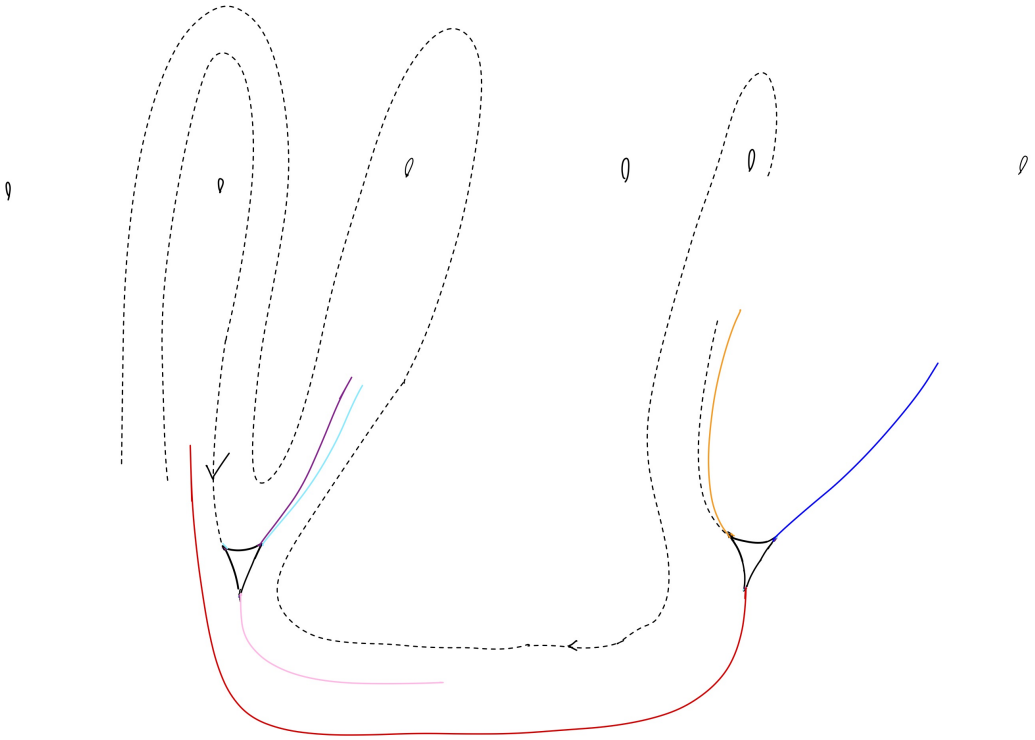


Figure F.125: WAK4

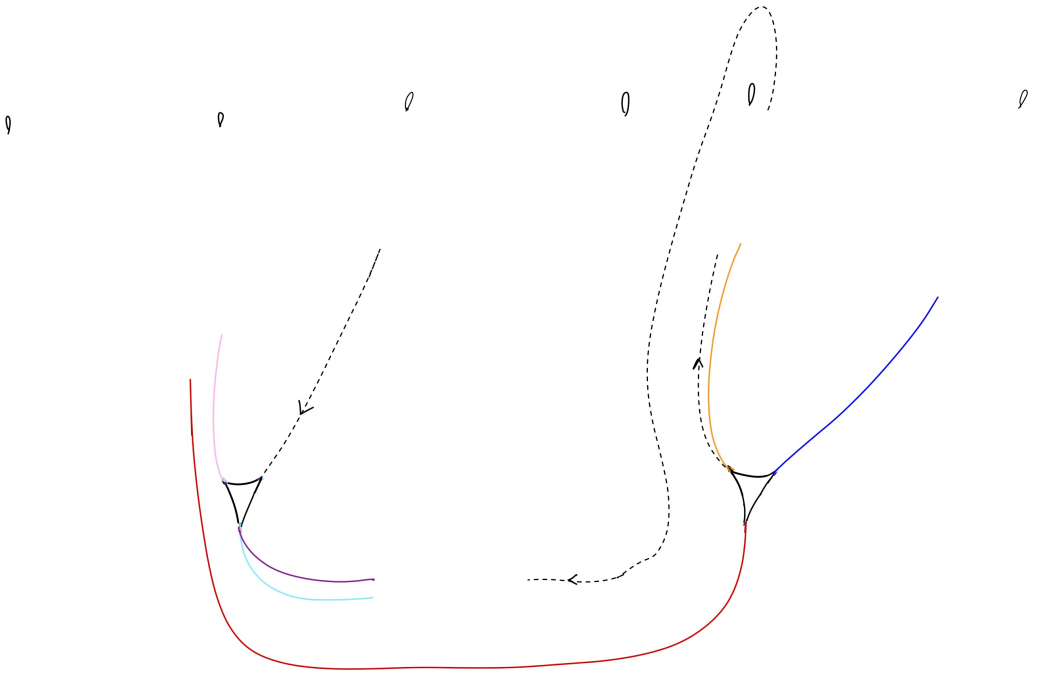


Figure F.126: MAU1

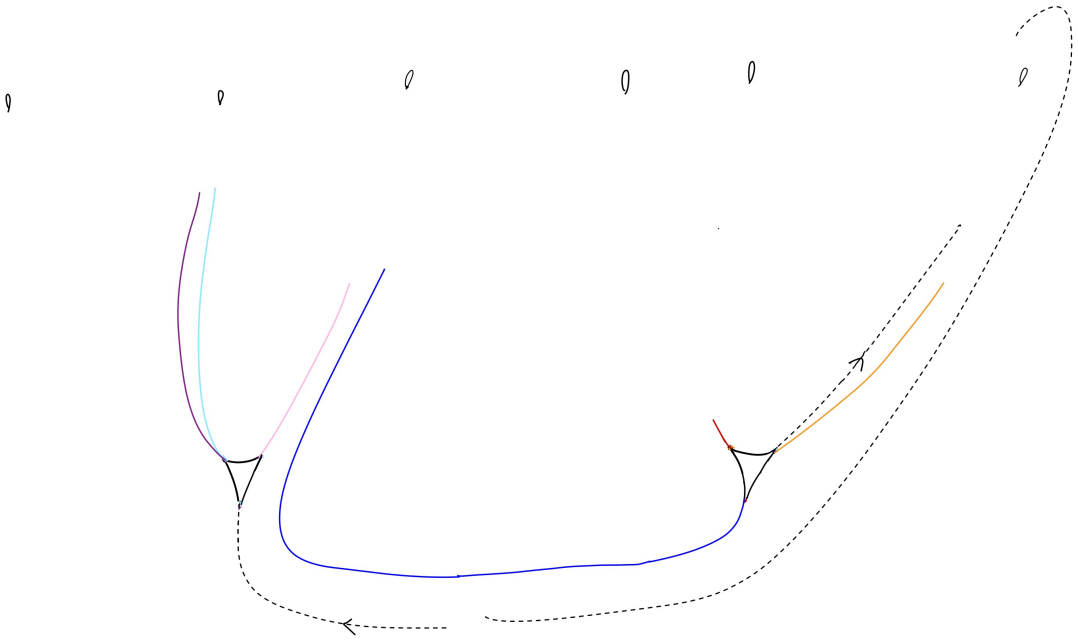


Figure F.127: EEN1

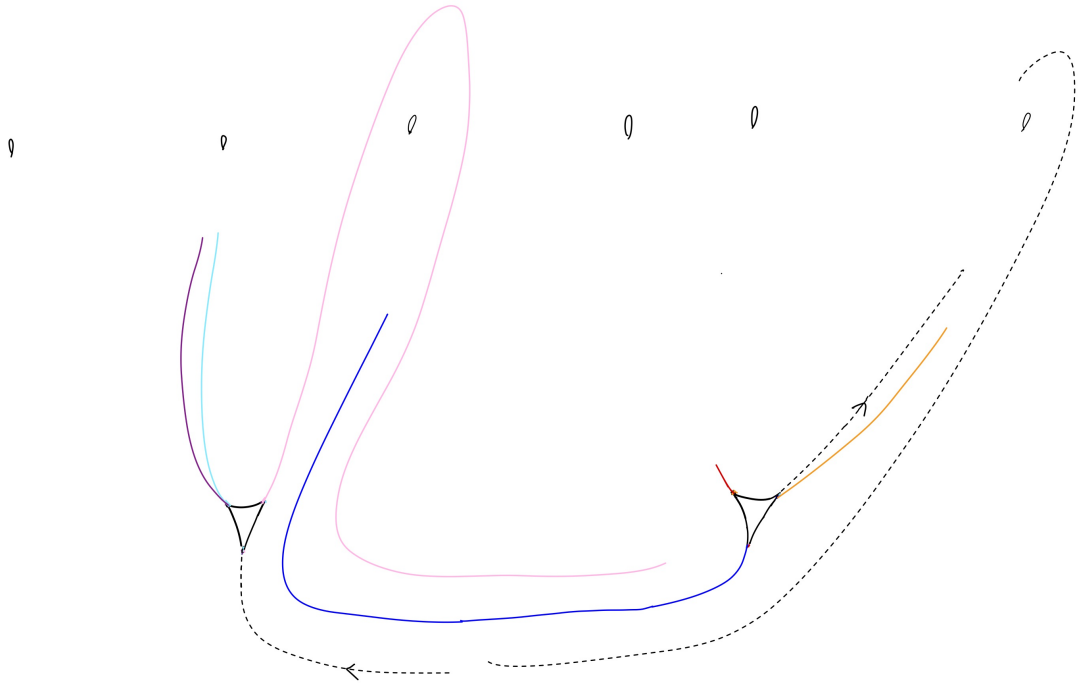


Figure F.128: EEN2

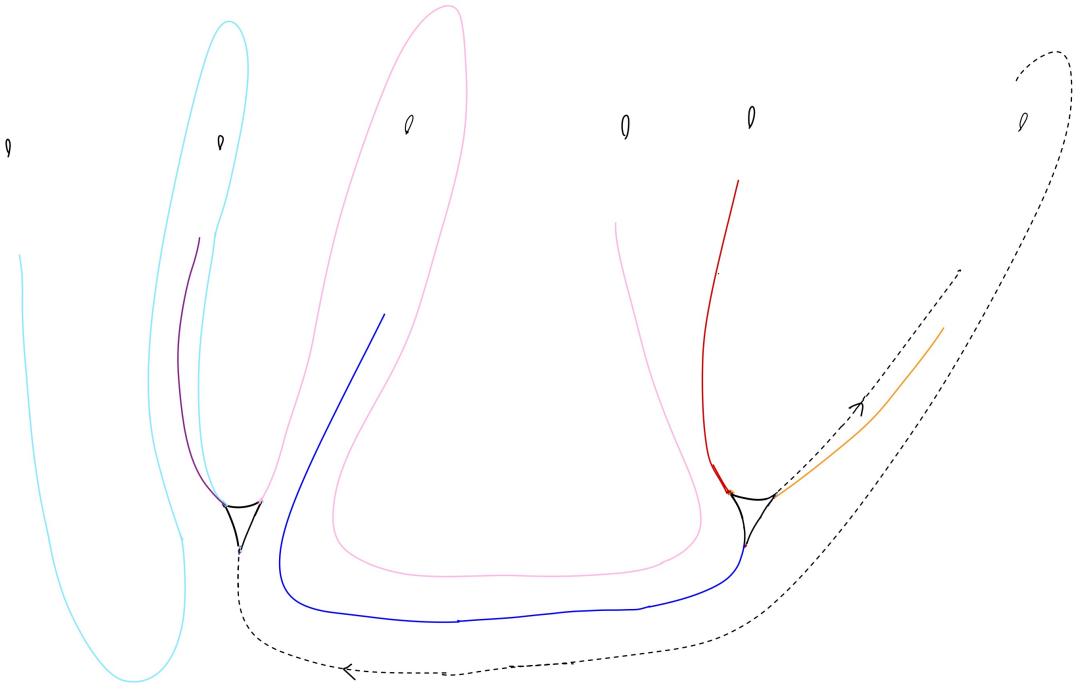


Figure F.129: EEN3

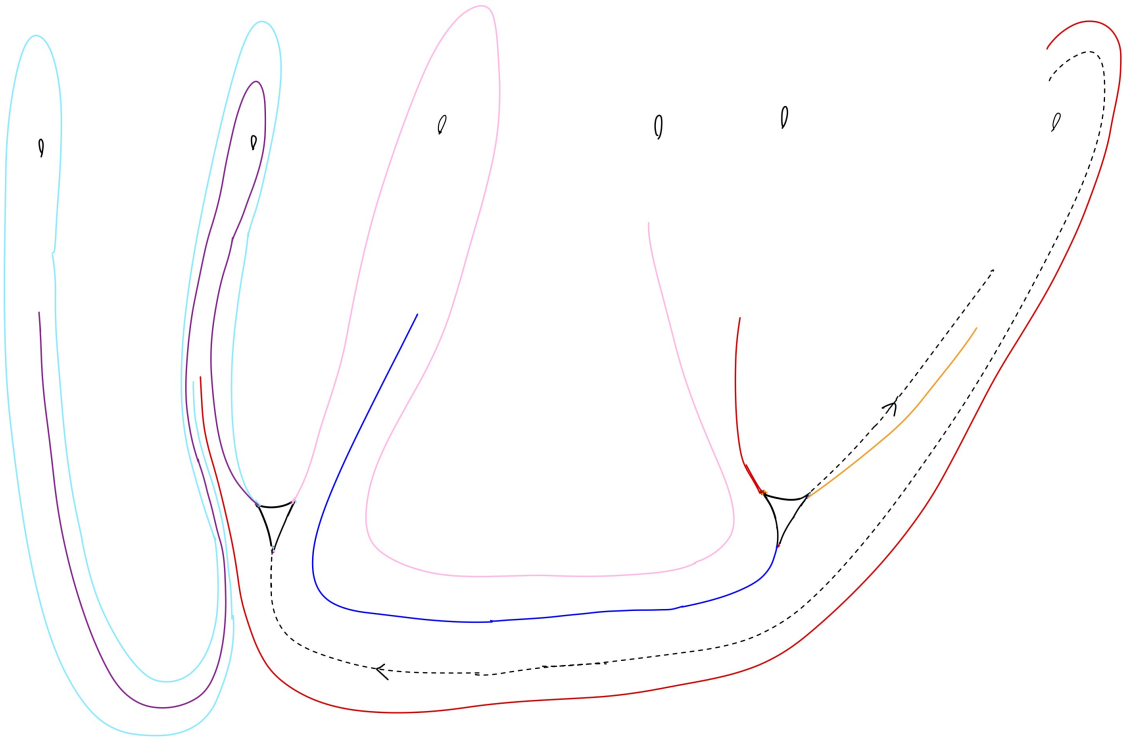


Figure F.130: EEN4

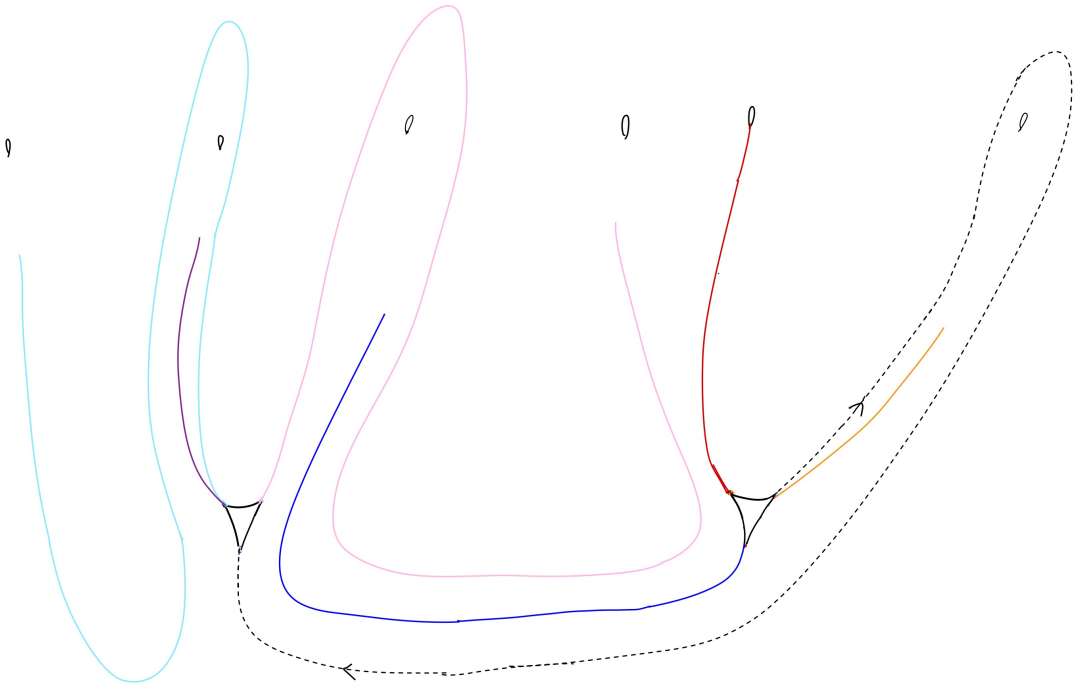


Figure F.131: EEN5

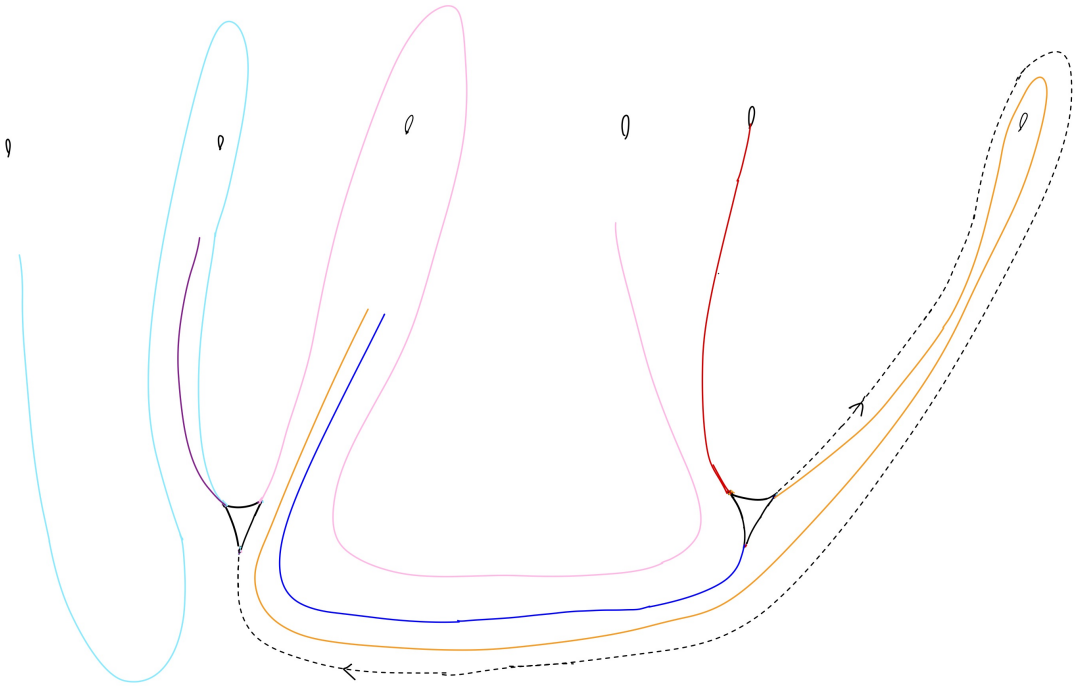


Figure F.132: EEN6

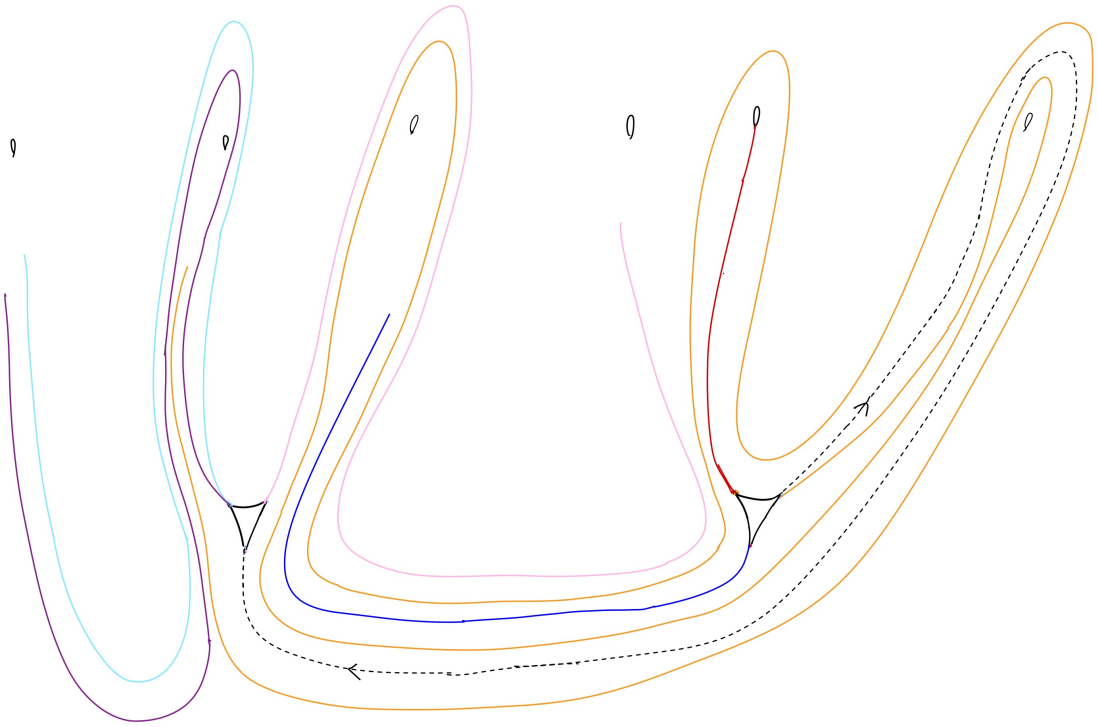


Figure F.133: EEN7

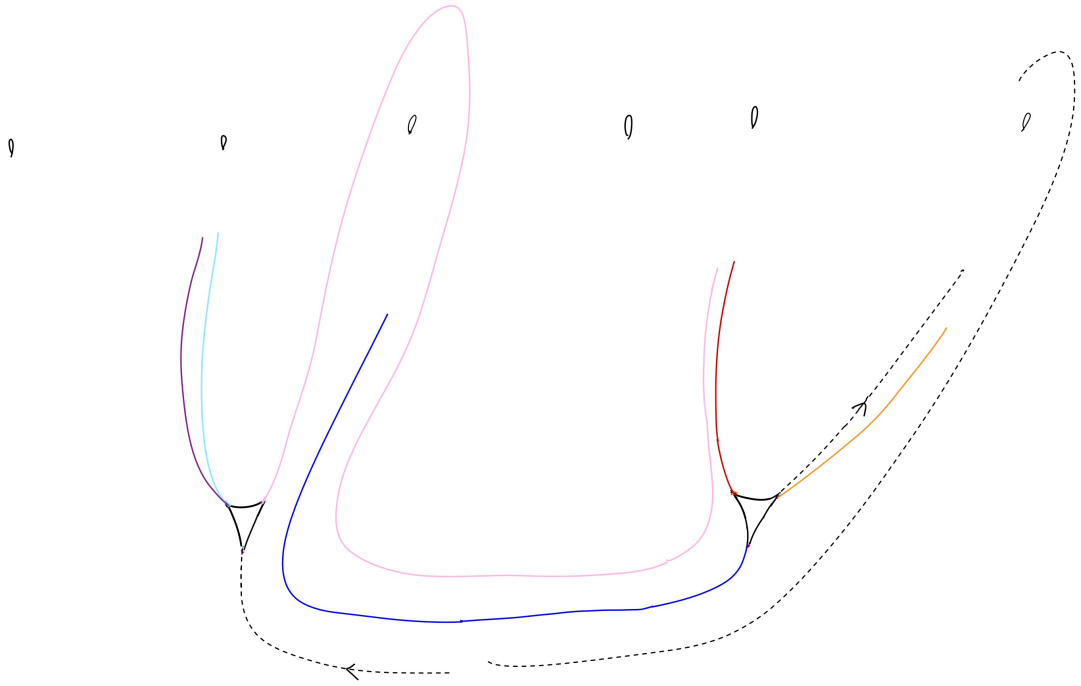


Figure F.134: EEN8

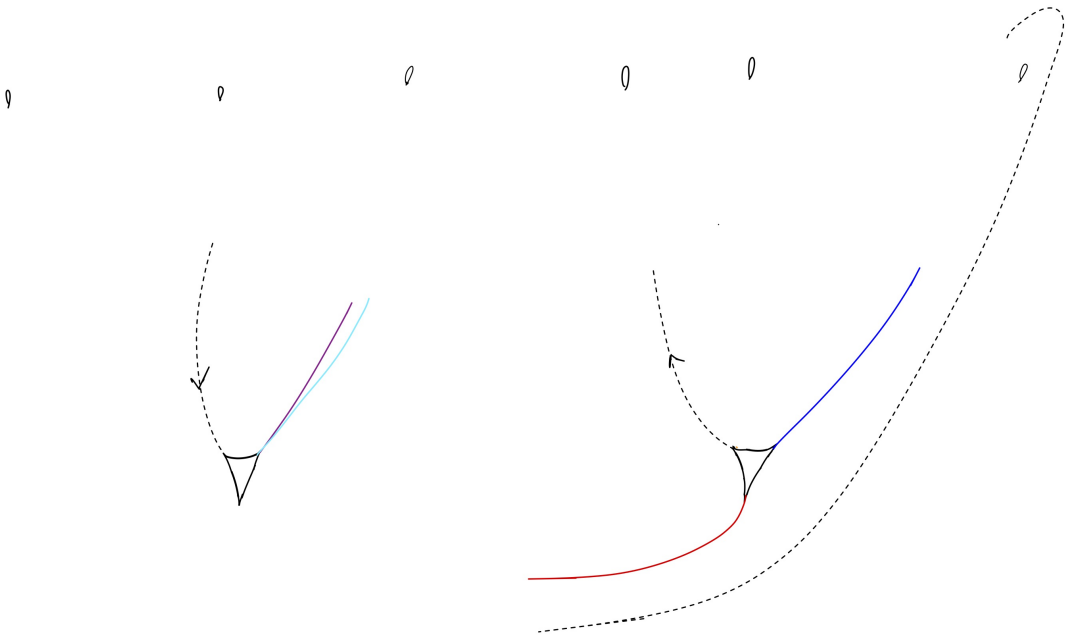


Figure F.135: MYU1

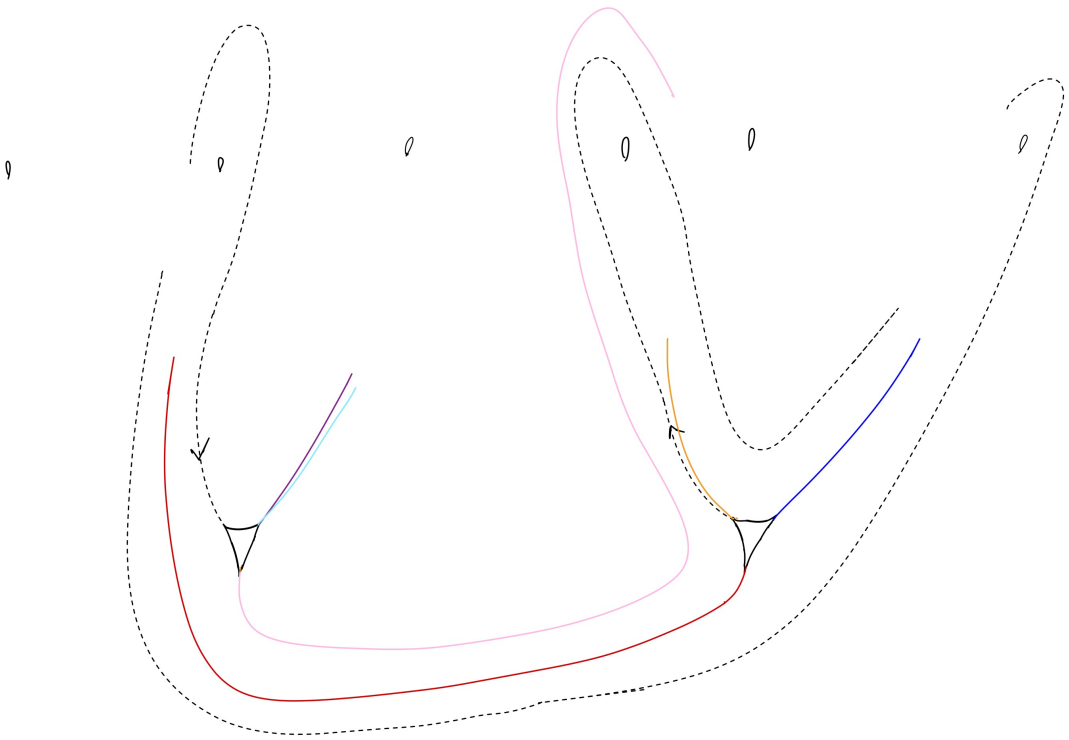


Figure F.136: MYU2

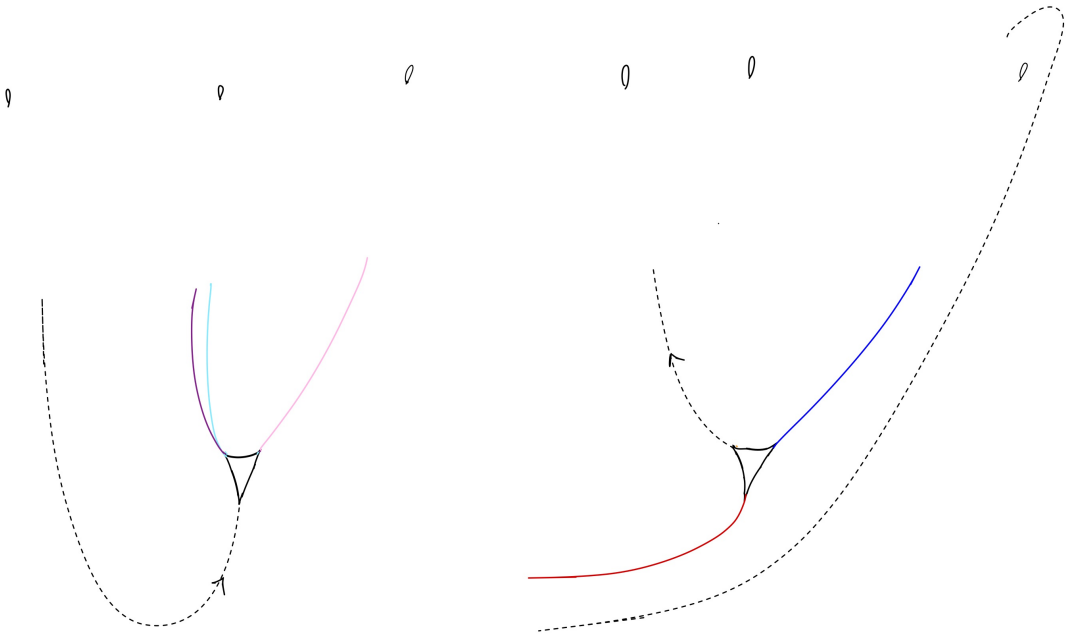


Figure F.137: QBC1

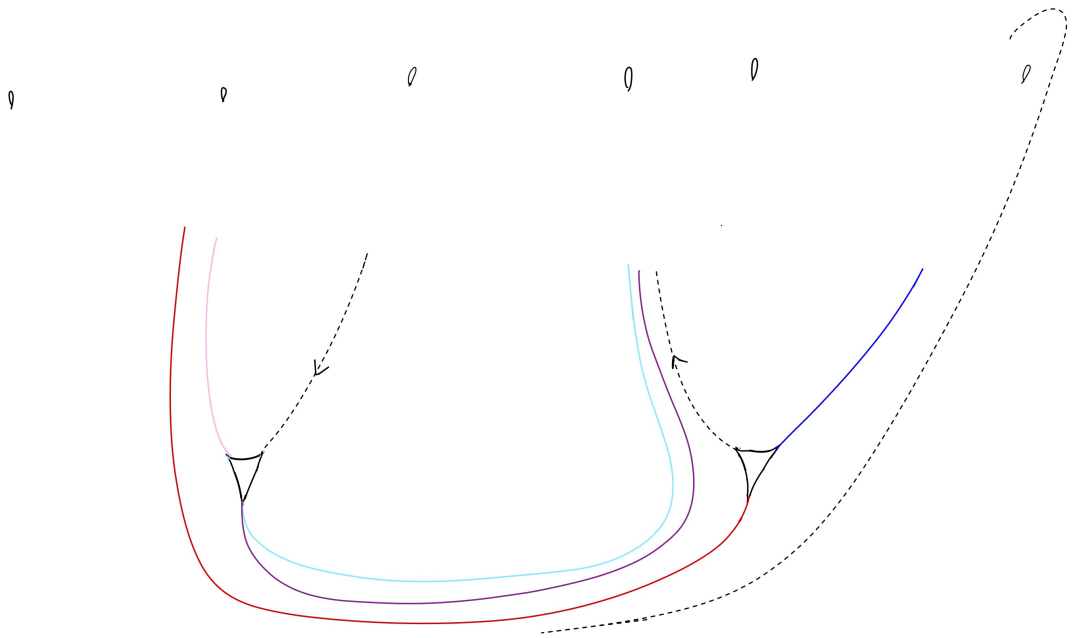


Figure F.138: OWD1

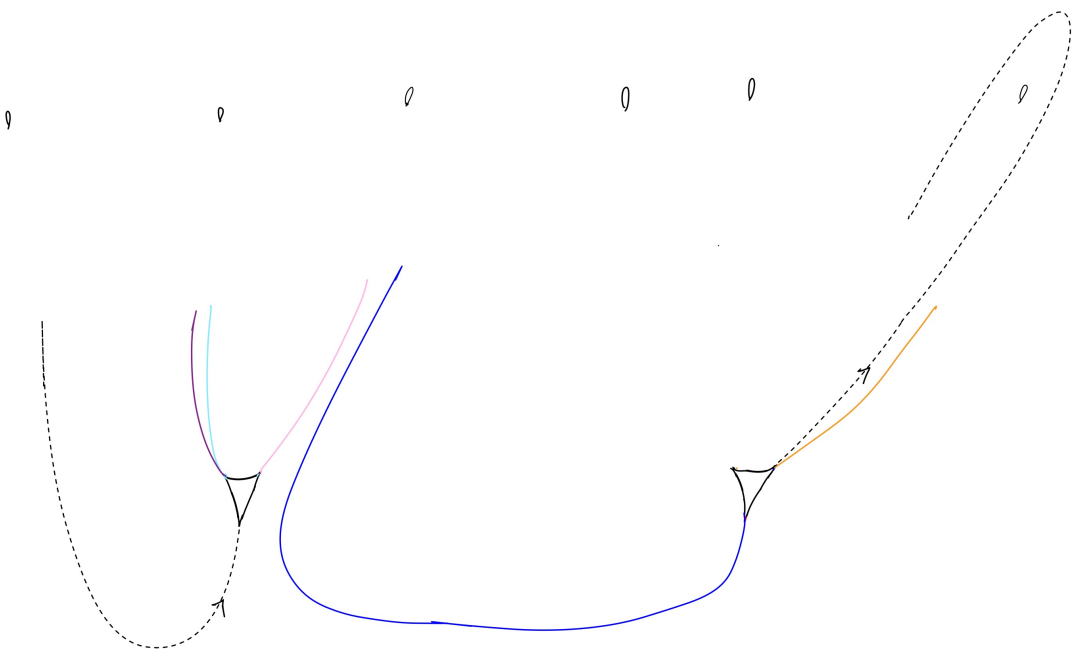


Figure F.139: CQD1

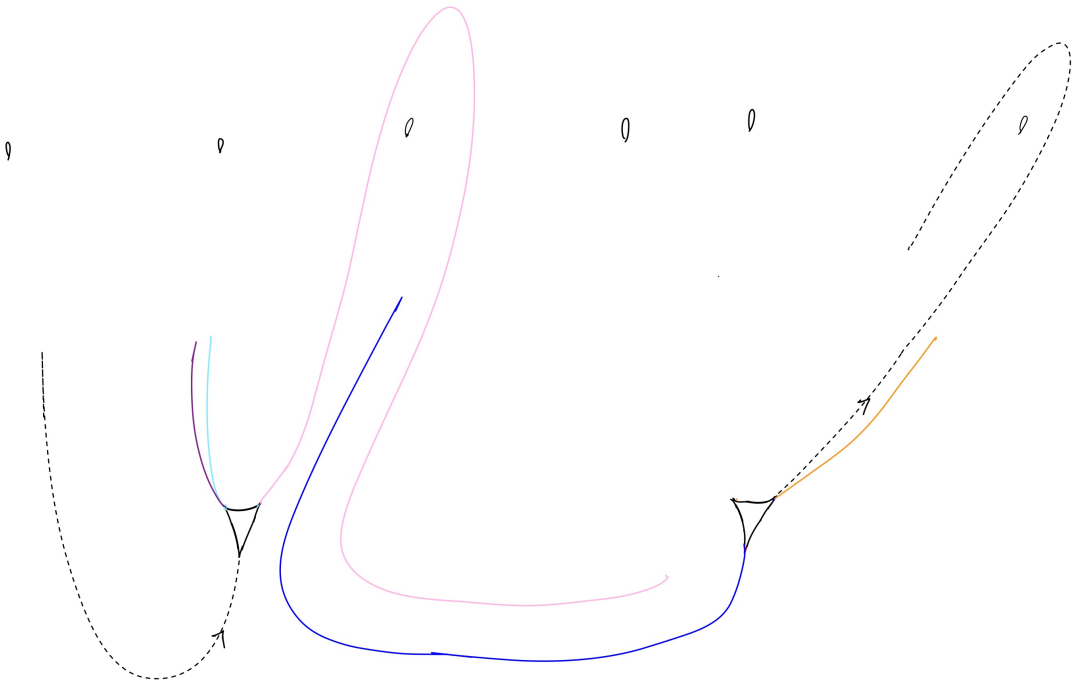


Figure F.140: CQD2

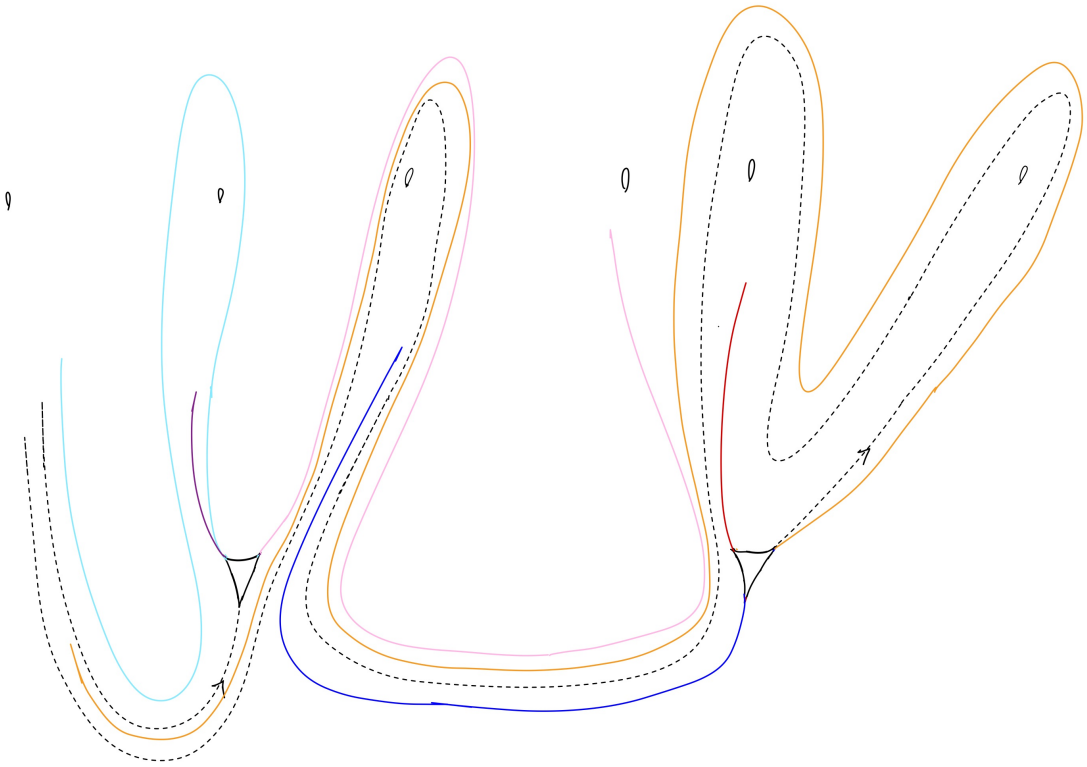


Figure F.141: CQD3

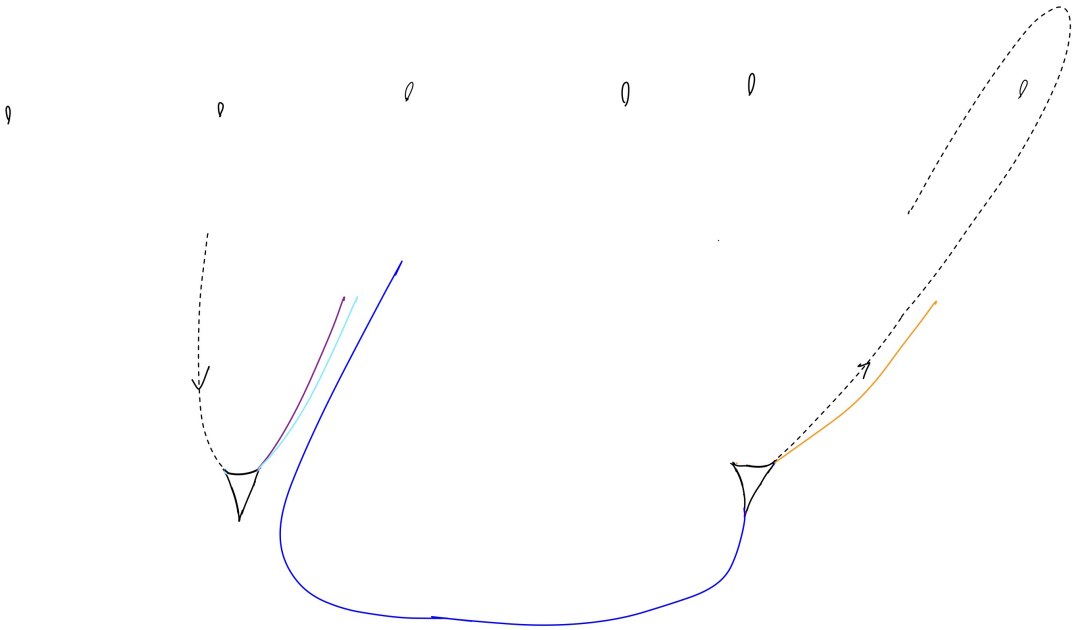


Figure F.142: KYD1

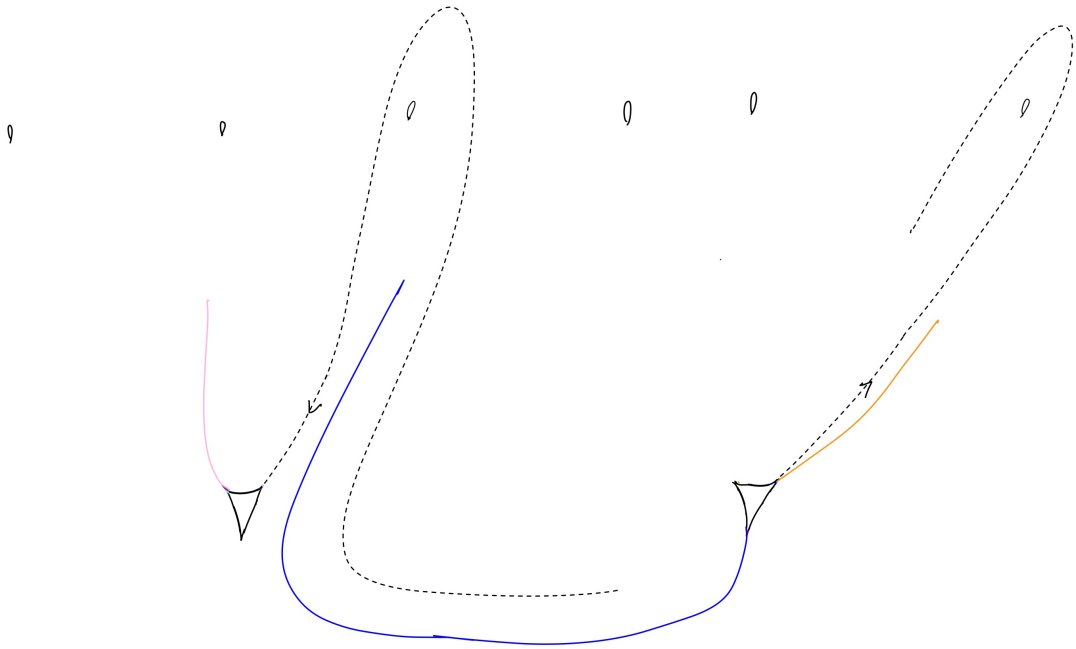


Figure F.143: FHR1

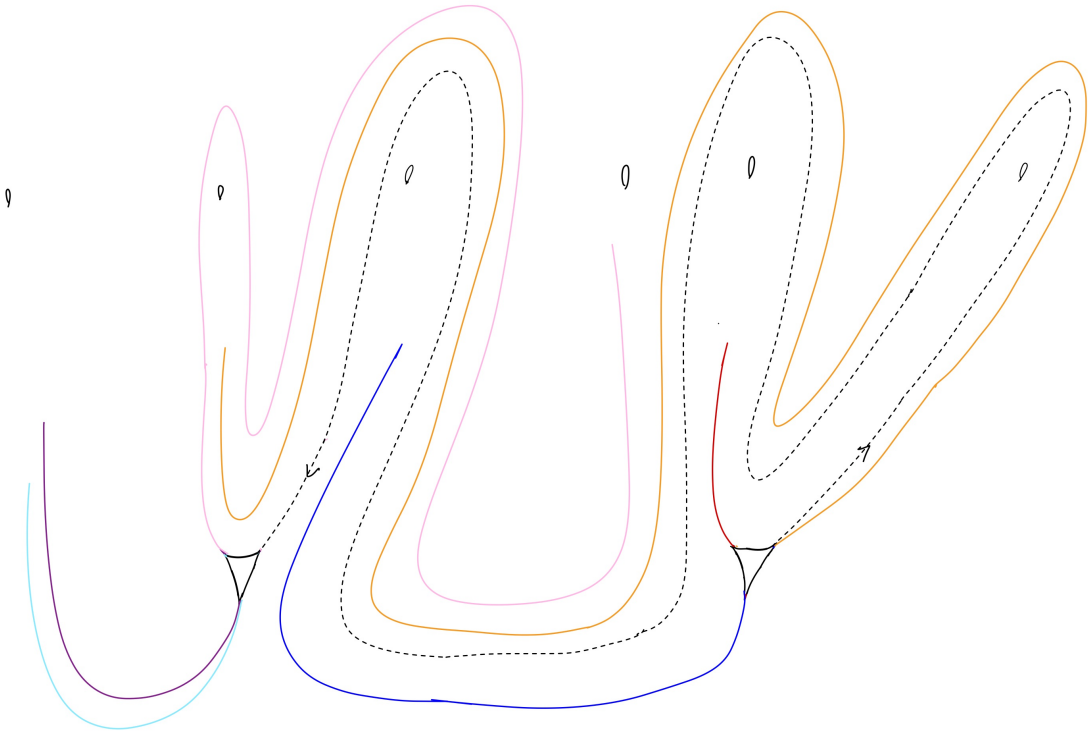


Figure F.144: Eyas1

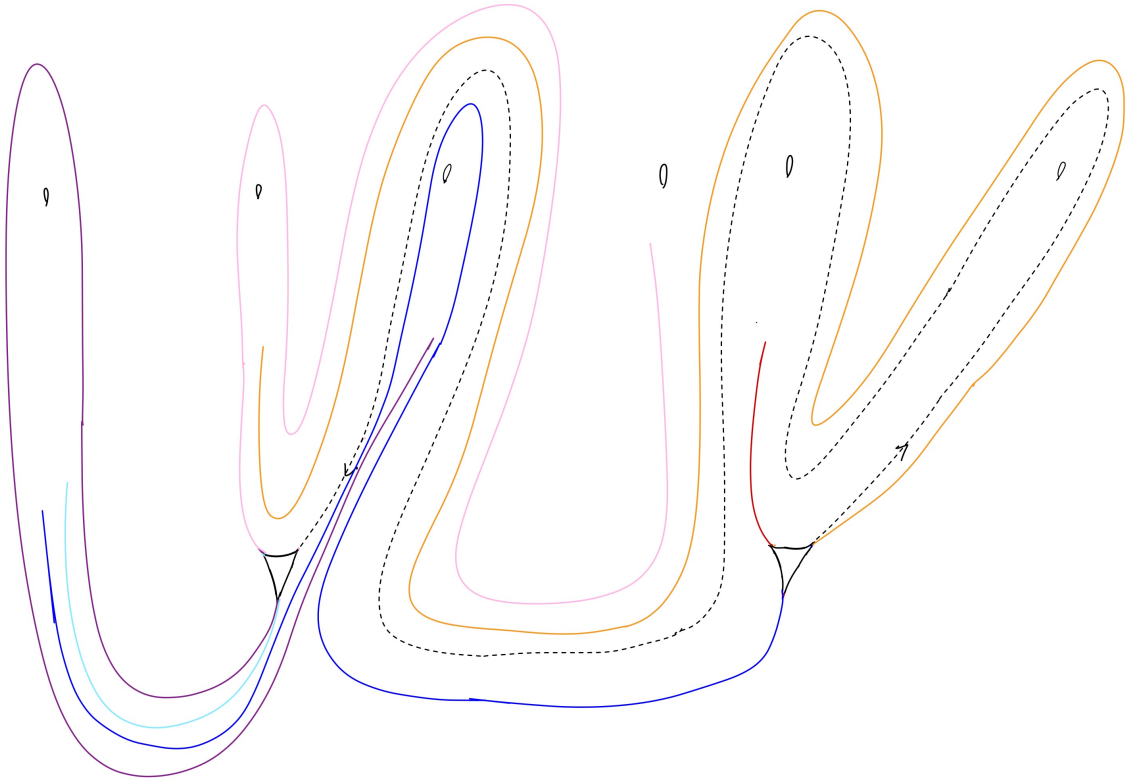


Figure F.145: Eyas2

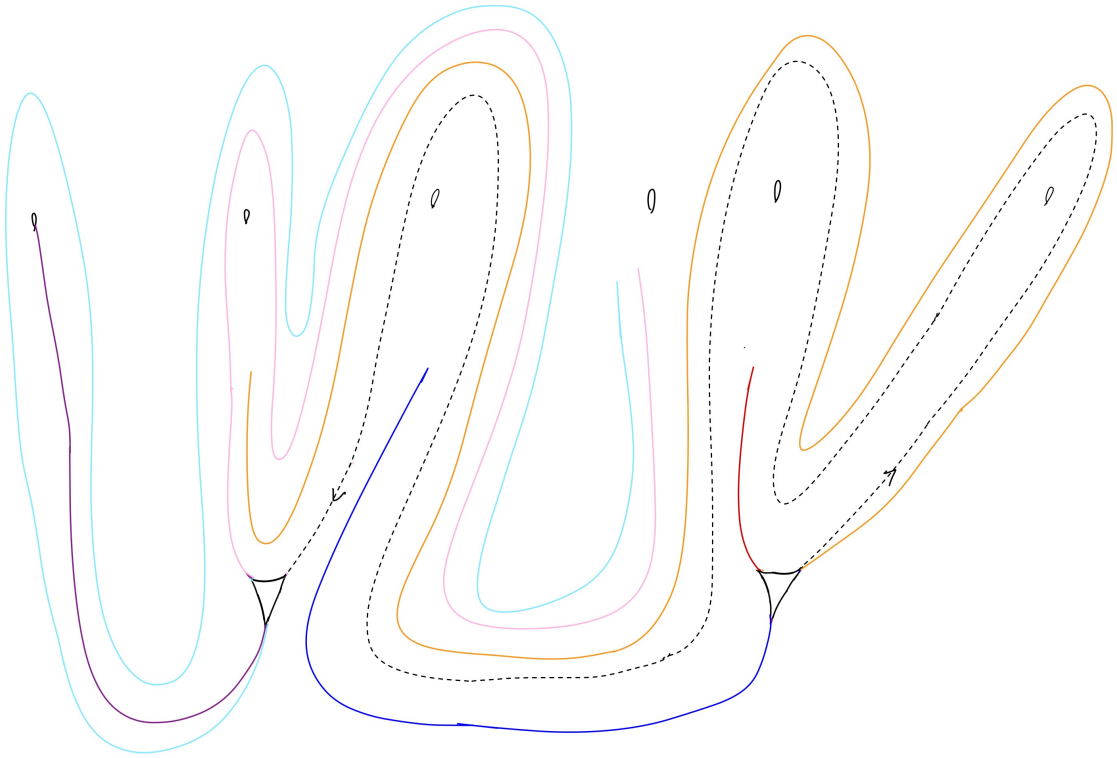


Figure F.146: Eyas3

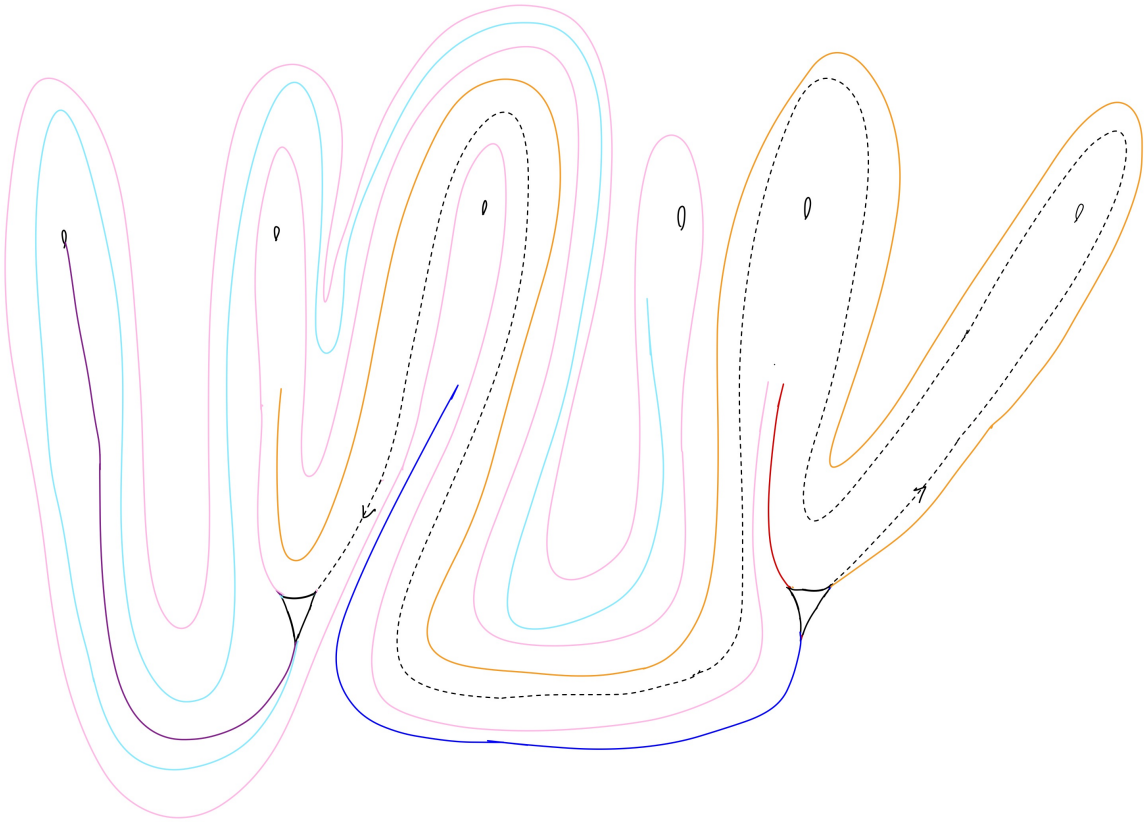


Figure F.147: Eyas4

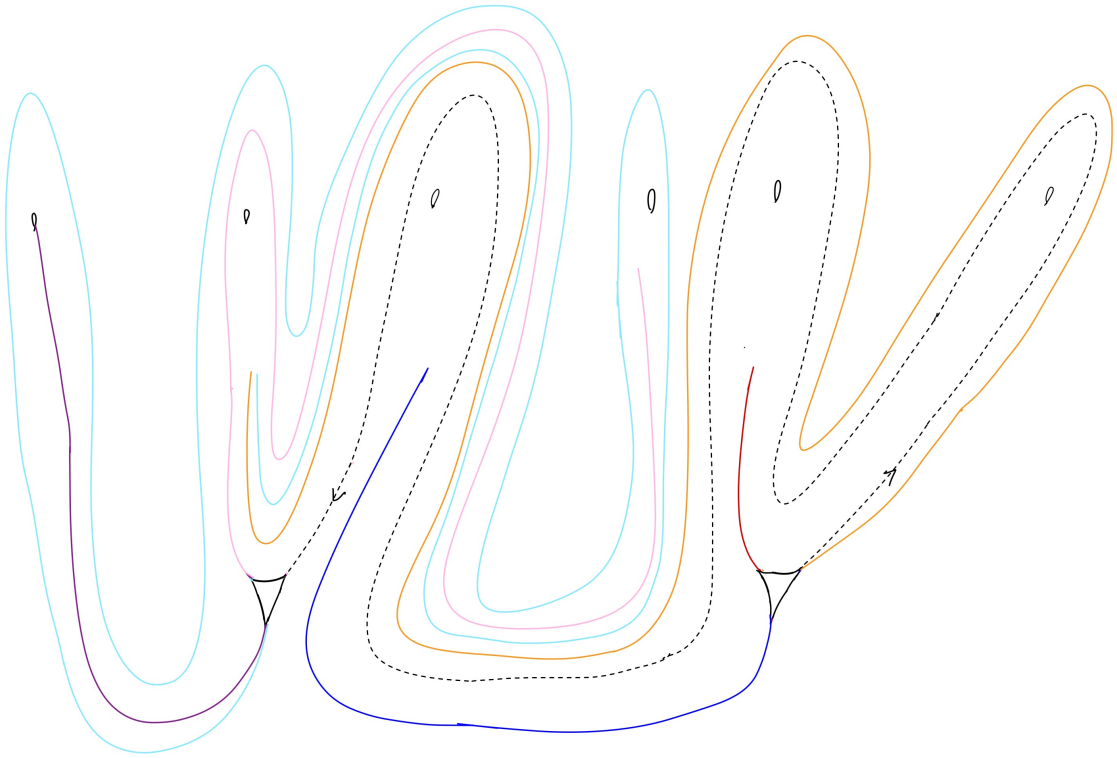


Figure F.148: Eyas5

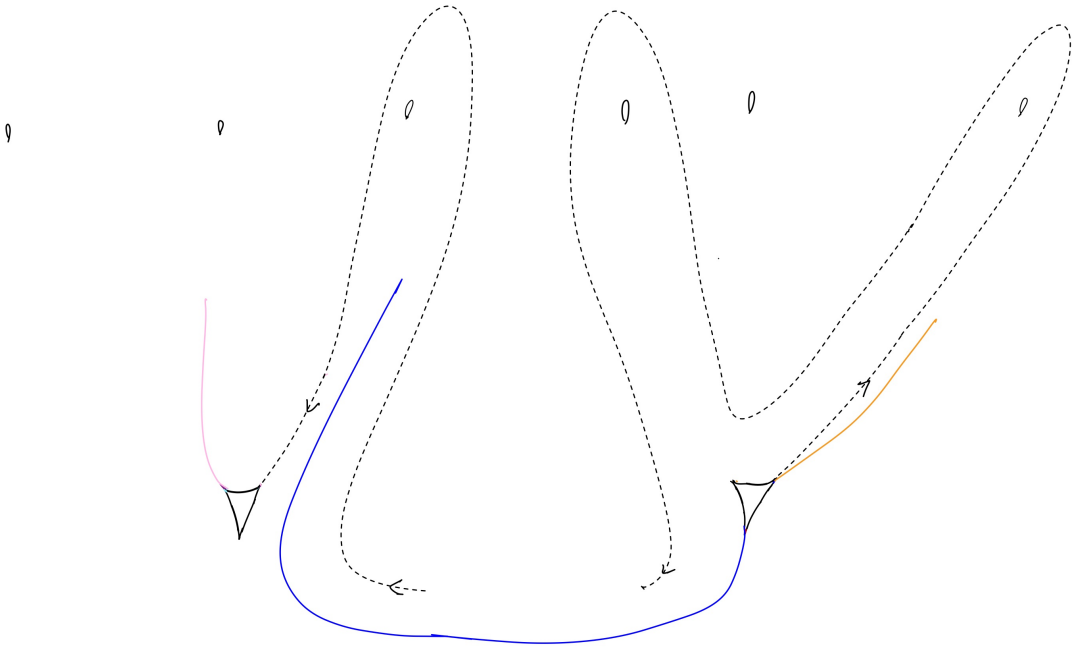


Figure F.149: Fard1

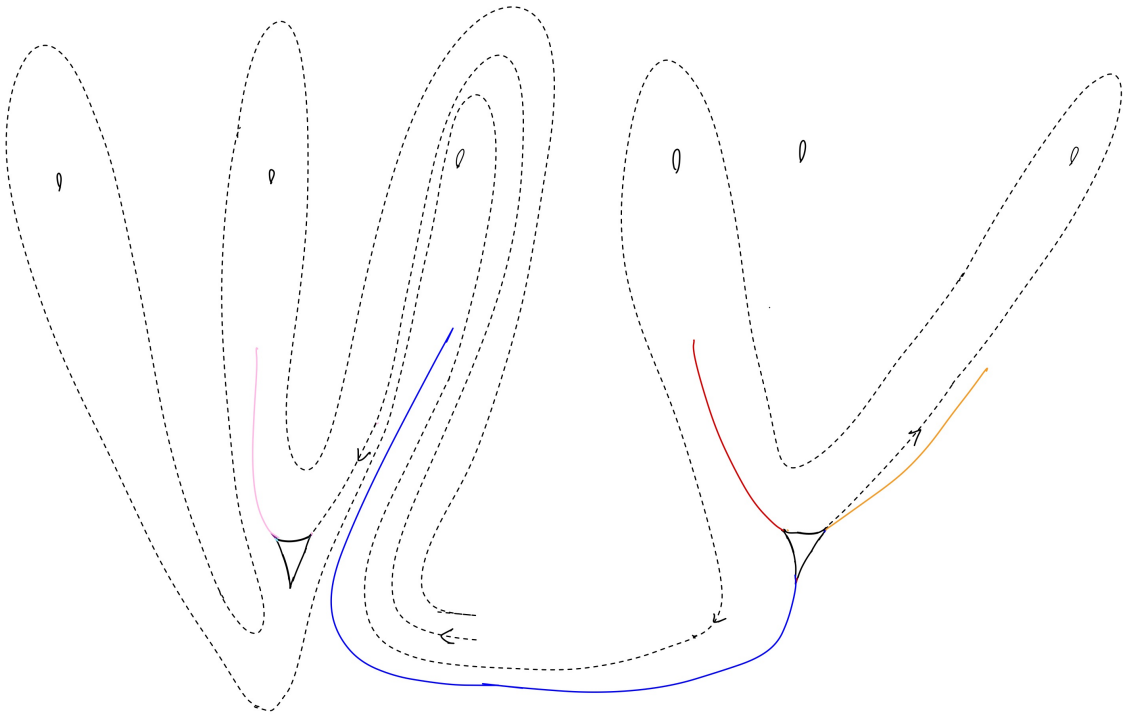


Figure F.150: Fard2

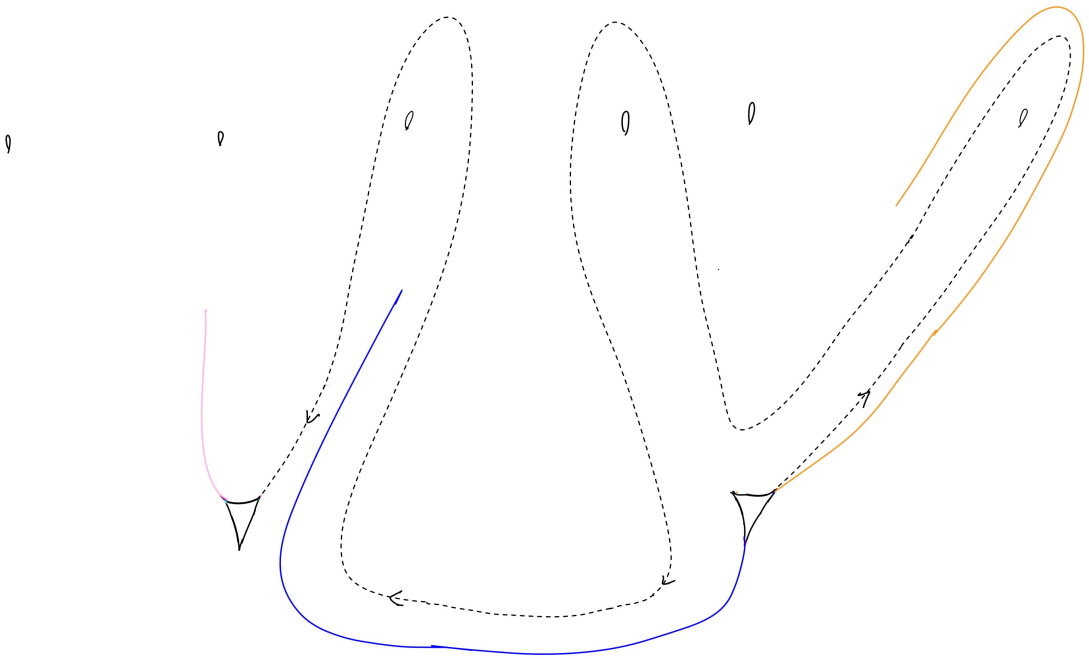


Figure F.151: Fard3

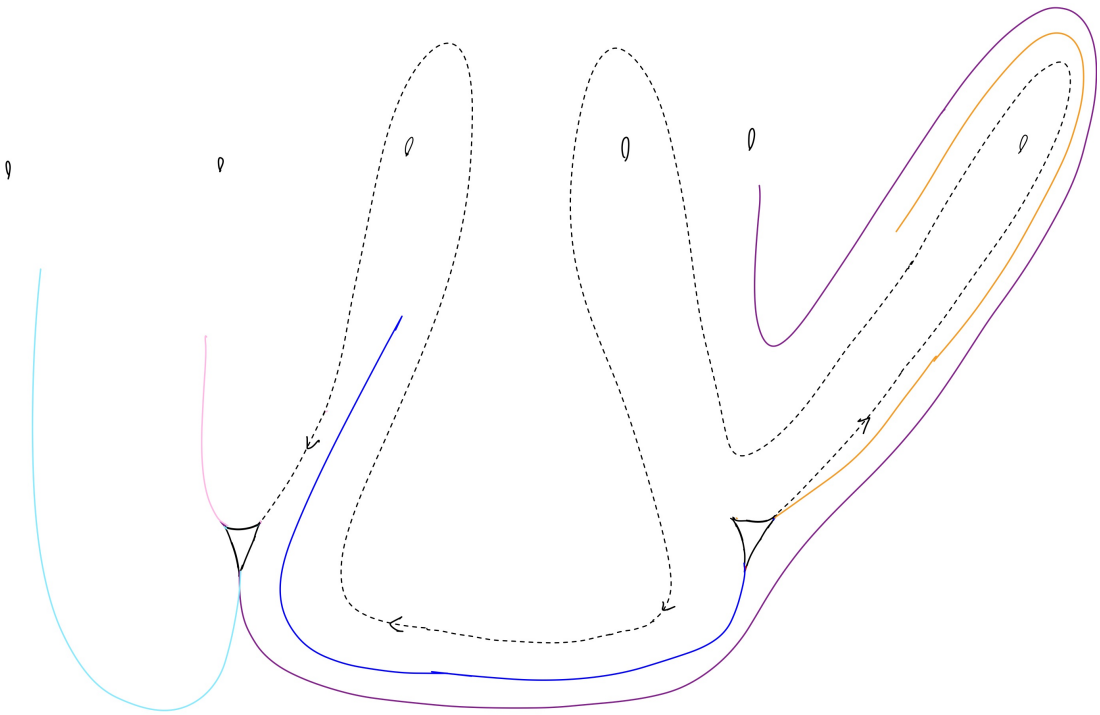


Figure F.152: Fard4

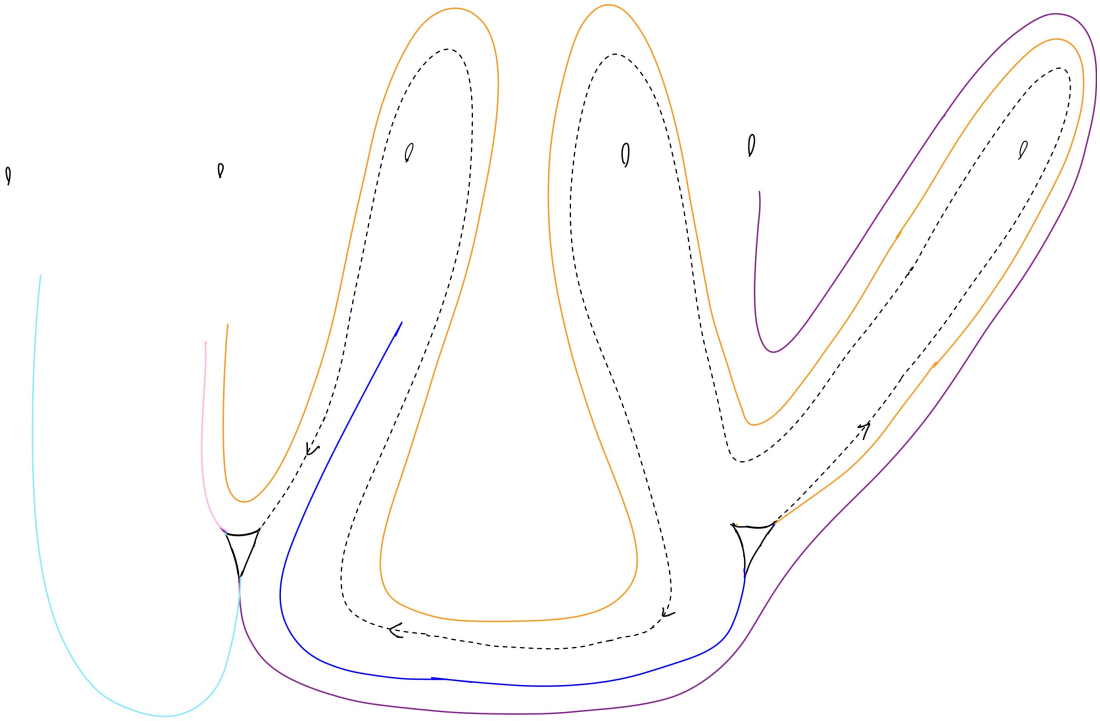


Figure F.153: Fard5

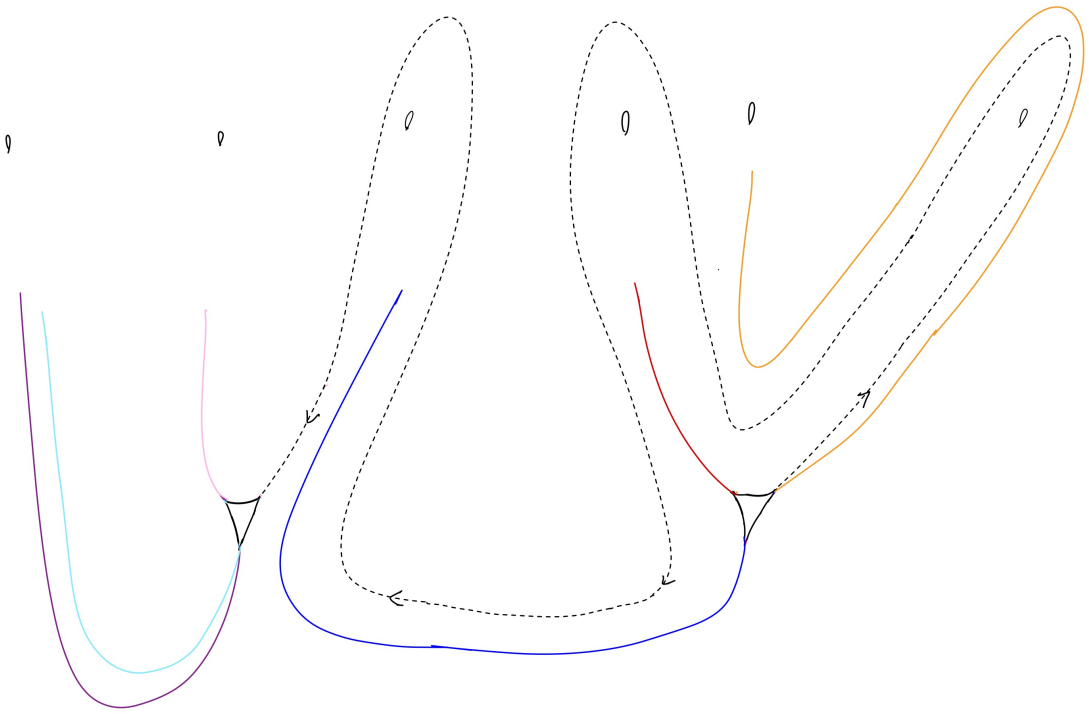


Figure F.154: Fard6

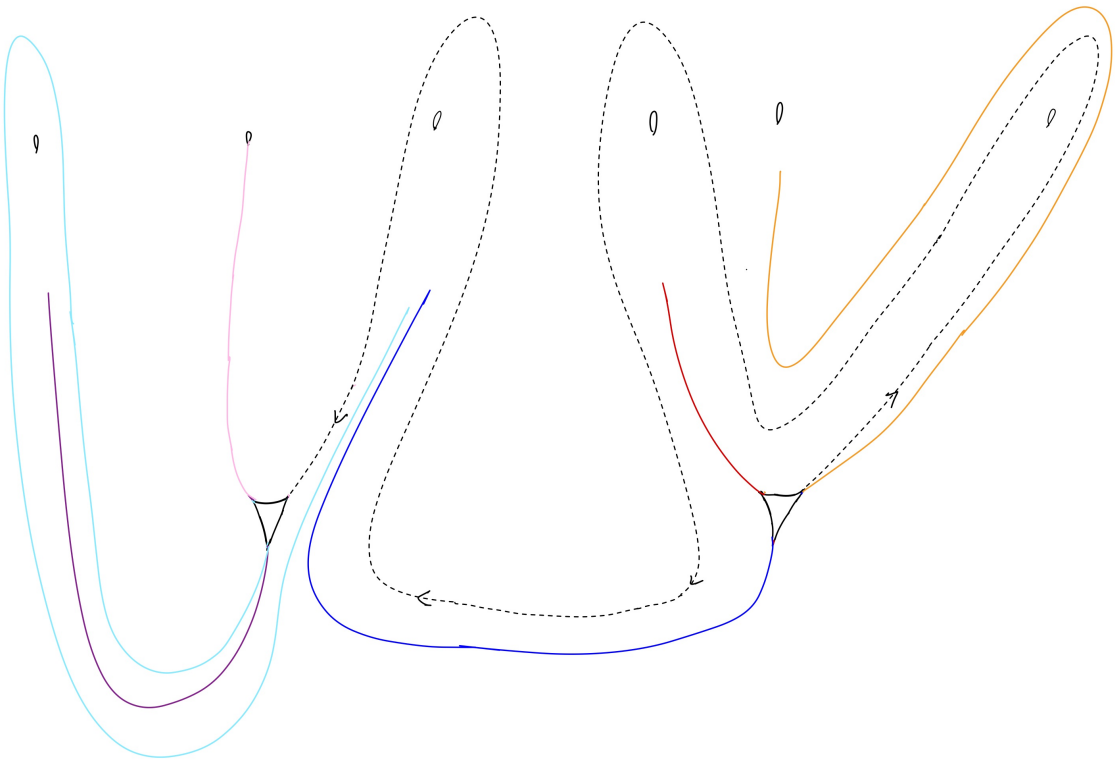


Figure F.155: Dwaal1

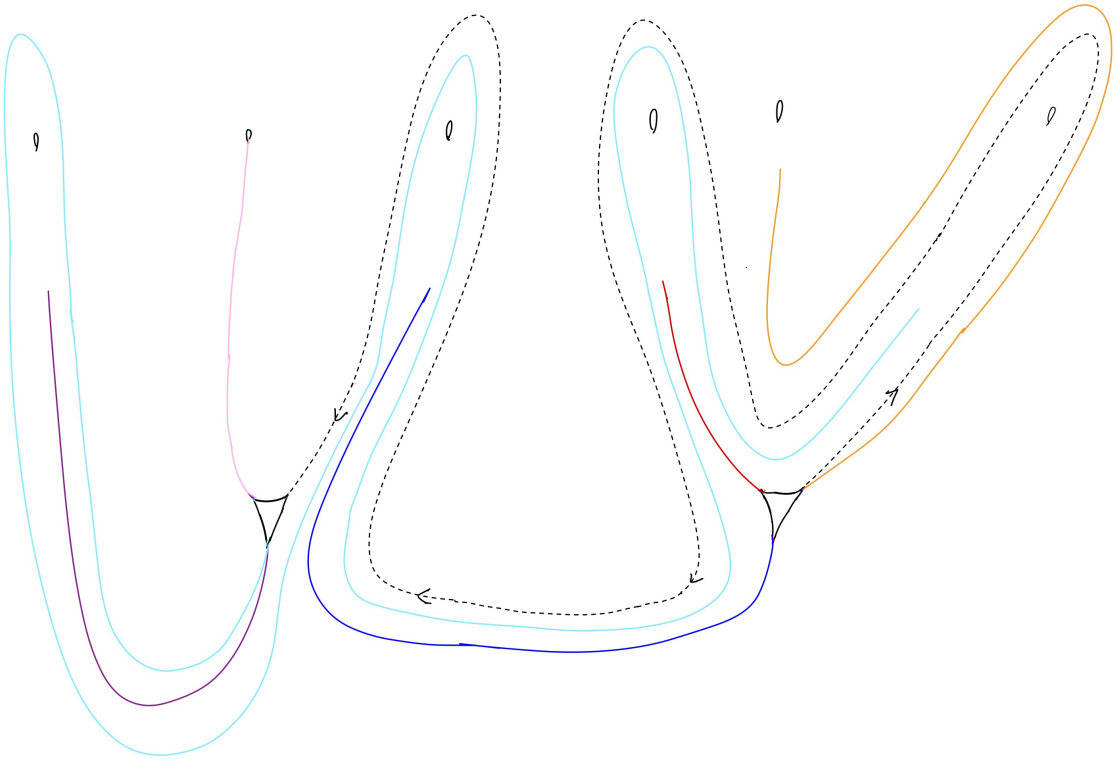


Figure F.156: Dwaal2

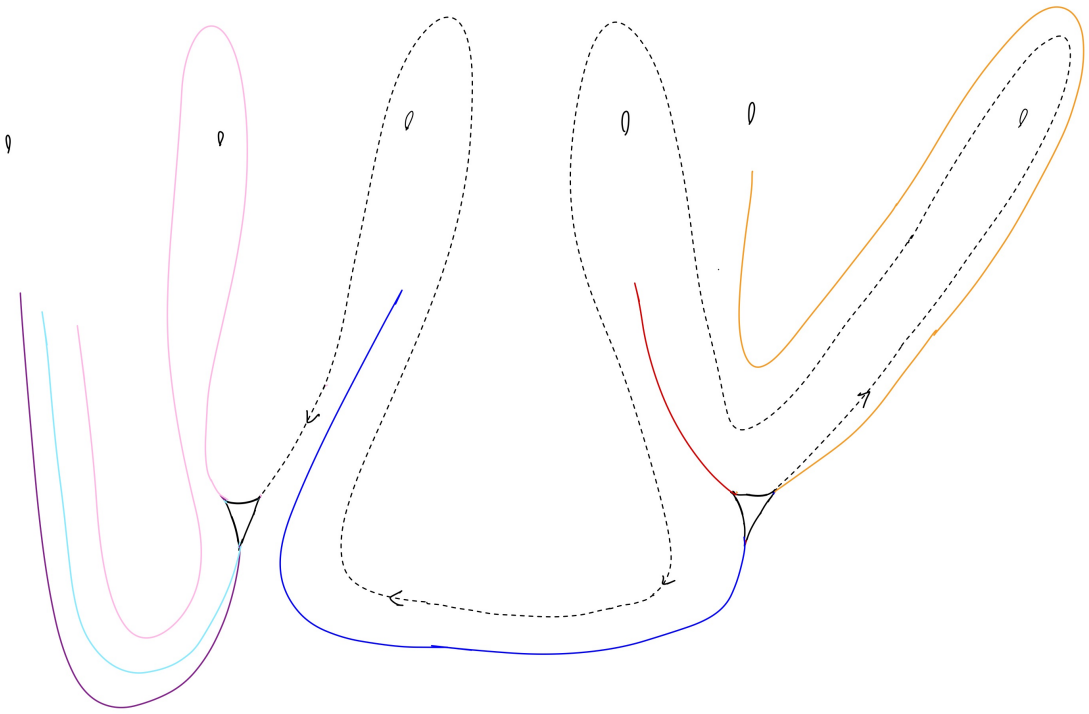


Figure F.157: Fremd1

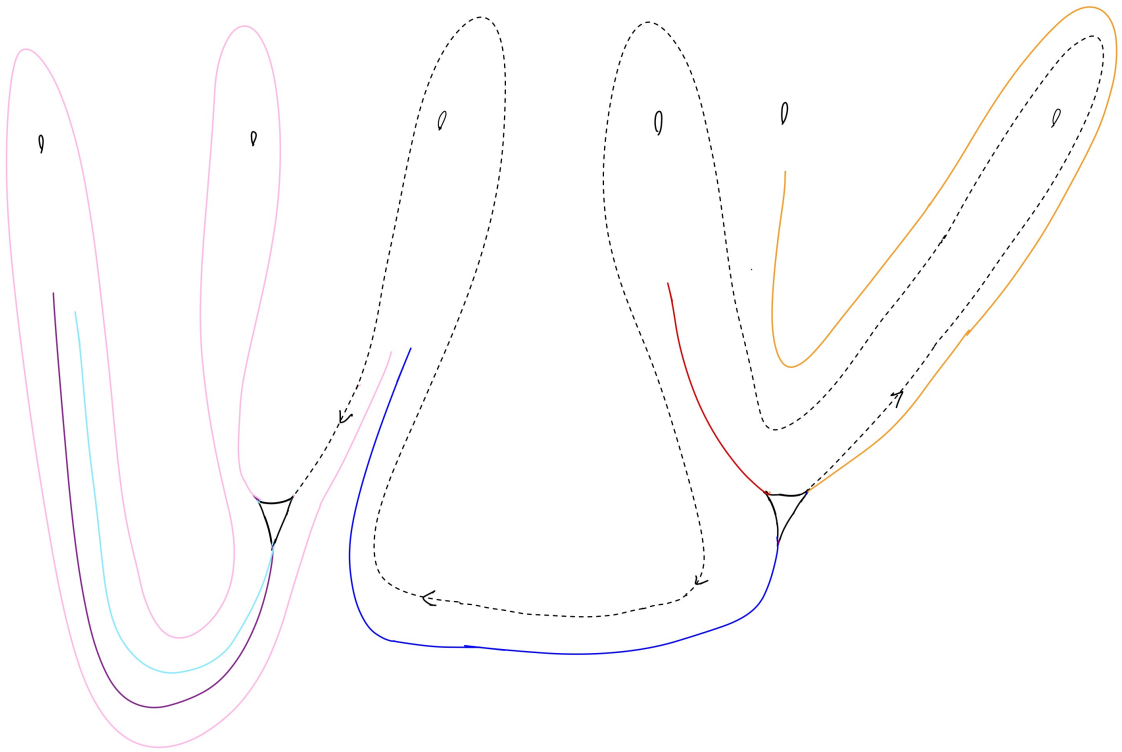


Figure F.158: Fremd2

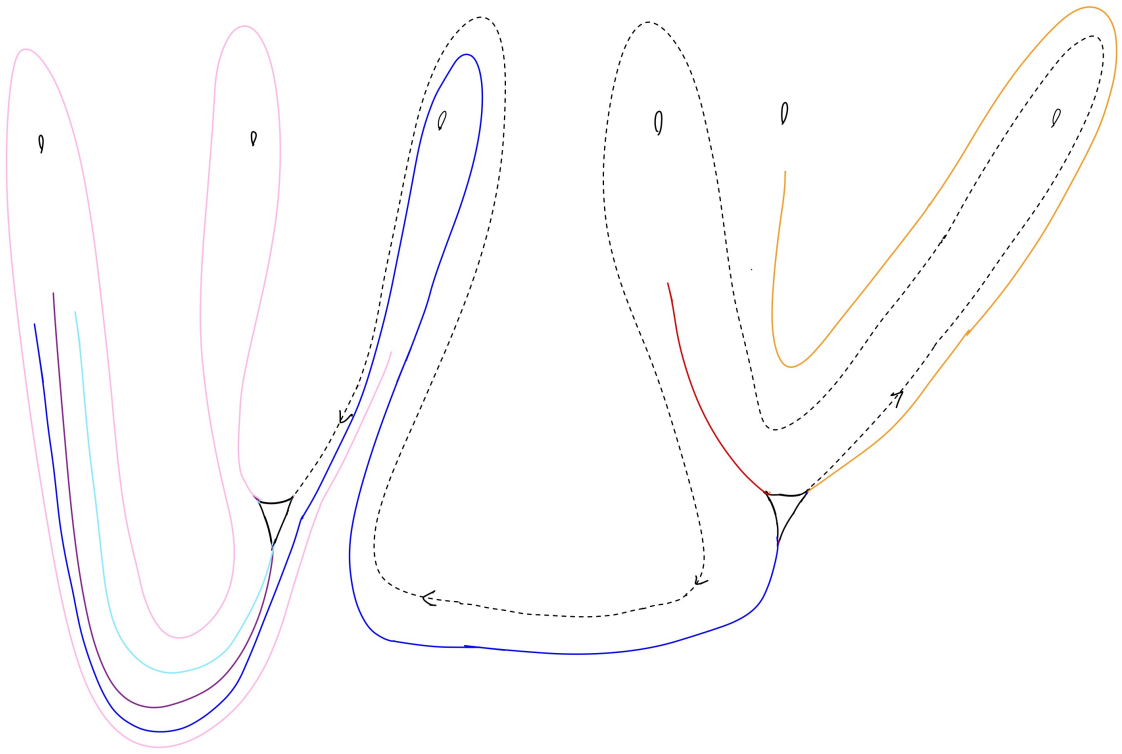


Figure F.159: Fremd3

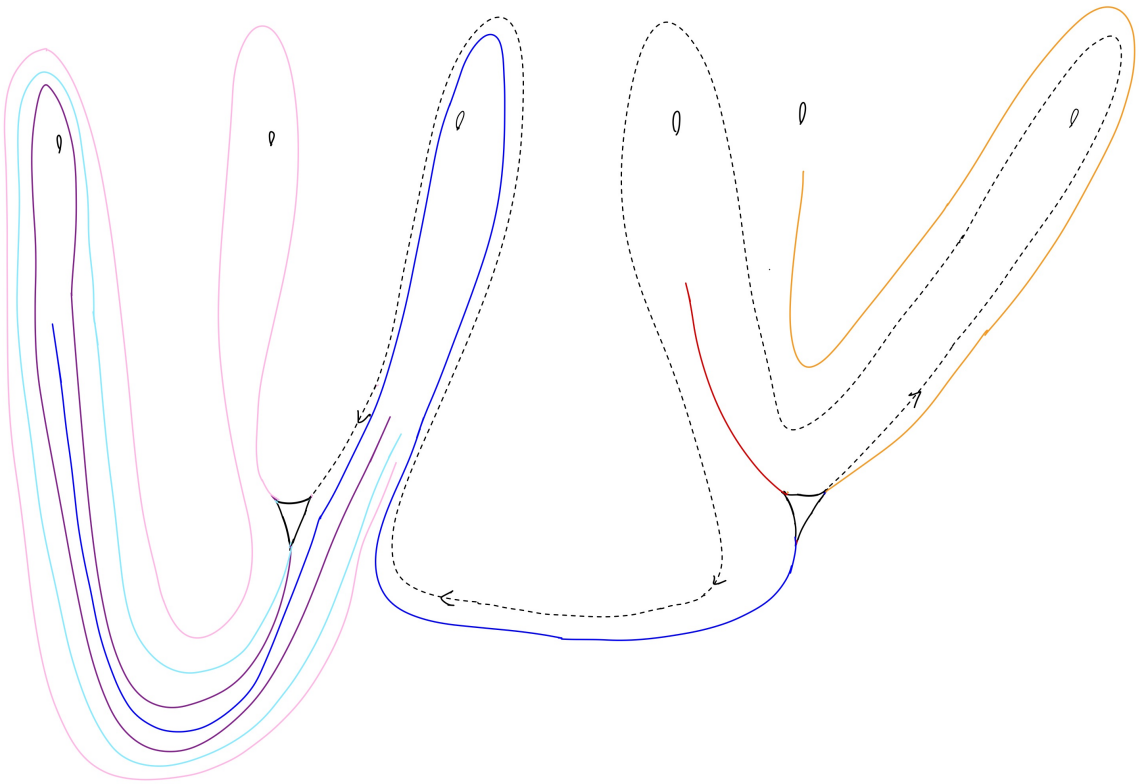


Figure F.160: Fremd4

APPENDIX SEVEN

Train Track Case Analysis: Track 12

This is Track 12:

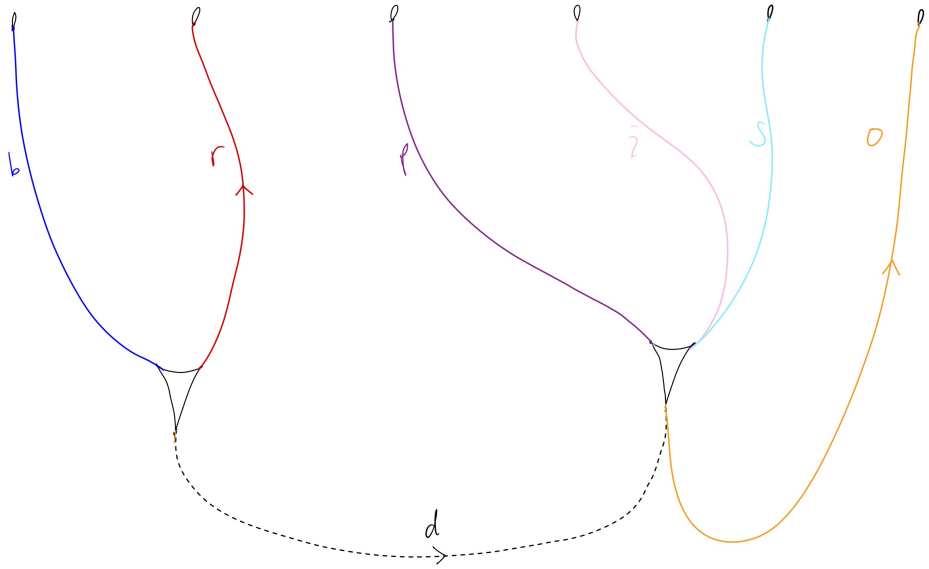


Figure G.1: Track 12

G.1 Case A: Triangles Fixed

Let us assume the triangles are fixed. Hence, both $f_\beta(d)$ and $f_\beta(\bar{d})$ both pass over $d/\bar{d}$ after an even number of letters. We shall call this *Assumption A*. Then $f_\beta(d)$ can begin with b or r, while $f_\beta(\bar{d})$ can begin with s, i, p, or o.

G.1.1 BKG

Suppose $f_\beta(d)$ began with b, and $f_\beta(\bar{d})$ began with s.

This is Figure G.2.

Here in order to meet Assumption A, $f_\beta(\bar{d})$ must eventually traverse p^+ before crossing $\bar{d}$. Before that it would possibly have twisting with o or i.

Here we claim that the dotted lines must join in the middle. Indeed, if they did not, then in order to not put either $f_\beta(d)$ or $f_\beta(\bar{d})$ in Situation β, this can only occur with $f_\beta(\bar{d})$ going below $f_\beta(r)$, or $f_\beta(p)$ going above $f_\beta(d)$. In the former case, this causes $f_\beta(p)$ to trace, as shown in Figure G.3. In the latter case, the dotted lines will be in Situation α, as shown in Figure G.4.

Thus the dotted lines must join, so we have Figure G.5.

Now let us assume that there were no initial twists by $f_\beta(\bar{d})$. Then $f_\beta(r)$ will trace, as shown in Figure G.6.

So let us assume instead that $f_\beta(\bar{d})$ has initial twists with o.

But this means $f_\beta(o)$ will trace, as shown in Figure G.7.

This is a contradiction.

G.1.2 CNM

Suppose $f_\beta(d)$ began with b, and $f_\beta(\bar{d})$ began with i.

The same argument used in BKG G.1.1 to show that the dotted lines in the middle must join applies here.

This is Figure G.8.

Here if $f_\beta(\bar{d})$ were to begin with i^+ then it must continue with p^+ otherwise $f_\beta(i)$ would immediately trace. Moreover, $f_\beta(\bar{d})$ must join with $f_\beta(d)$ here or $f_\beta(d)$ would be in Situation β. So in this scenario we have Figure G.9.

Here $f_\beta(s)$ must begin with p^+ otherwise $f_\beta(i)$ will immediately trace. So it continues:

$$f_\beta(s) = p^+ \bar{d} r^+ ...$$

where it must be r^+ otherwise it would cause $f_\beta(p)$ to trace after crossing.

Here $f_\beta(s)$ cannot go into 2, otherwise it will escape to the outer perimeter and eventually trace due to the position of $f_\beta(r)$. So it goes into 1, which is Figure G.10.

Here $f_\beta(b)$ can either begin with r° or r^-. Suppose it were the former. Then we have $f_\beta(p)$ and $f_\beta(s)$ both continuing with r^+, and $f_\beta(s)$ must then continue with b^-. Otherwise, $f_\beta(p)$ would continue with b^+ and then trace:

$$f_\beta(p) = ...b^+ r^- dp^\times$$

So we have

$$f_\beta(s) = ...b^- r^- d...$$

This is Figure G.11. But here $f_\beta(s)$ escapes to the outer perimeter again and will eventually trace.

So suppose instead that $f_\beta(b)$ began with r^-, as in Figure G.12.

Here it can go into 1 or 2. Suppose it went into 1. Then

$$f_\beta(b) = r^- d s^- o^* ...$$

where it must traverse s^- as to not cause $f_\beta(r)$ to traverse s^+ and thereby trace.

This is Figure G.13.

Here again we must have

$$f_\beta(s) = ...b^- r^- d...$$

and $f_\beta(s)$ will escape to the outer perimeter and trace, as shown in Figure G.14.

So suppose $f_\beta(b)$ went into 2. Then we have the situation depicted in Figure G.15. Here $f_\beta(i)$, $f_\beta(s)$, and $f_\beta(b)$ are stuck in a three-way counterclockwise path mill between $f_\beta(b)$, and $f_\beta(p)$. This is a contradiction.

So going back to the situation depicted in Figure G.8, suppose $f_\beta(\bar{d})$ began with i^-, then

$$f_\beta(\bar{d}) = i^- o^* ...$$

as it cannot cross or it would violate Assumption A. But now $f_\beta(o)$ will follow it and trace.

This is a contradiction.

G.1.3 LGU

Suppose $f_\beta(d)$ began with b, and $f_\beta(\bar{d})$ began with p. Then $f_\beta(\bar{d})$ must begin with p^-, as shown in Figure G.16; and then it must traverse either $i^-\bar{d}$, or $s^-\bar{d}$. In either case, this would cause the dotted lines to be in Situation α, as shown in Figure G.17, and Figure G.18.

This is a contradiction.

G.1.4 CXH

Suppose $f_\beta(d)$ began with b, and $f_\beta(\bar{d})$ began with o. But this forces $f_\beta(o)$ to also begin with o which is impossible.

This concludes the case when we assume $f_\beta(d)$ begins with b. Now we assume $f_\beta(d)$ begins with r, and $f_\beta(\bar{d})$ can begin with p, i, s, or o, as before. Again Assumption A must be

upheld.

G.1.5 SXM

Suppose $f_\beta(d)$ began with r, and $f_\beta(\bar{d})$ began with p. Then we have the situation depicted in Figure G.19.

Here there are four possibilities for $f_\beta(\bar{d})$ to traverse before crossing without violating Assumption A. We have

$$f_\beta(\bar{d}) = p^- i^- \bar{d} ...$$

$$f_\beta(\bar{d}) = p^- s^- \bar{d} ...$$

$$f_\beta(\bar{d}) = p^- s^- o^- (s^- o^+)^k s^+ ...$$

$$f_\beta(\bar{d}) = p^- i^- o^- (i^- o^+)^k i^+ ...$$

where $k = 0, 1, 2, ...$ is a number of possible twisting.

Let us first assume the first case. Notice that in the middle, $f_\beta(b)$ must go above the pair $f_\beta(i)$, and $f_\beta(s)$. Otherwise, the pair would traverse $\bar{d} r^+ b^+ d$, and then either $f_\beta(s)$ or $f_\beta(i)$ would trace. So we have

$$f_\beta(b) = d p^- i^- o^* ...$$

as shown in Figure G.20.

Here if $f_\beta(o)$ were to go above $f_\beta(d)$, then it would force $f_\beta(\bar{d})$ into Situation β, But if it went below $f_\beta(d)$, then it would eventually trace.

So let us assume the second case, that

$$f_\beta(\bar{d}) = p^- s^- \bar{d} ...$$

This is Figure G.21, where again $f_\beta(b)$ must go above $f_\beta(\bar{d})$ for the same reason as before, and the dotted lines must join in the middle otherwise one of them will immediately enter Situation β.

Here $f_\beta(o)$ must continue with i^+ and to the left of $f_\beta(b)$ otherwise $f_\beta(b)$ would trace after crossing $\bar{d}$. But now $f_\beta(o)$ will be absorbed:

$$f_\beta(o) = p^- s^- \bar{d} b^- r^- d p^- \hat{i}^+ p^+ \bar{d} r^+ b^+ d s^+ p^+ \,\mathrm{Abso}(f_\beta(o), f_\beta(\bar{d}))^\times$$

So suppose we have the third case:

$$f_\beta(\bar{d}) = p^- s^- o^- (s^- o^+)^k s^+ ...$$

(in the following analysis for simplicity we draw these cases with $k = 1$. For more twisting the arguments will remain the same with possibly more redundant twisting inserted into each image path)

This forces

$$f_\beta(p) = s^- o^* ...$$

Again the dotted lines must join and $f_\beta(b)$ traverses

$$f_\beta(b) = d p^- i^* ..$$

and also

$$f_\beta(o) = p^- i^* ...$$

And again $f_\beta(o)$ must continue with i^+:

$$f_\beta(o) = p^- i^+ p^+ \bar{d} r^+ b^+ d s^* ...$$

This is Figure G.23.

Here $f_\beta(b)$ must end to give

$$f_\beta(b) = d p^- i^\circ$$

as either continuing with i^+ or i^- would cause it to immediately trace after crossing $\bar{d}$.

This is Figure G.24.

Here consider $f_\beta(r)$. It can either begin with b° or b^+. Suppose it were the former. This is Figure G.25.

Here if $f_\beta(i)$ continued with r° or r^+, forcing $f_\beta(s)$ to continue with r^+, then $f_\beta(s)$ would trace immediately after crossing d. On the other hand, if $f_\beta(i)$ continued with r^-, then it would trace:

$$f_\beta(i) = ... r^- b^+ d p^- i^\times$$

This is a contradiction.

So suppose $f_\beta(r)$ began with b^+. Then it must do so going to the left of $f_\beta(i)$, as otherwise it would either be absorbed, or $f_\beta(i)$ and $f_\beta(s)$ would again be put in the same situation as before. So we have

$$f_\beta(r) = b^+ d s^- o^* ...$$

This is Figure G.26.

Here if $f_\beta(i)$ continued with b° or b^+, forcing $f_\beta(s)$ to continue with b^+, then $f_\beta(s)$ is immediately absorbed. But if $f_\beta(i)$ continued with b^- then it will trace:

$$f_\beta(i) = \bar{d}\hat{b}^- dp^- i^+ p^+ \bar{d}r^+ b^+ ds^\times$$

This is a contradiction.

So now suppose it were the fourth case:

$$f_\beta(\bar{d}) = p^- i^- o^- (i^- o^+)^k i^+ ...$$

But now $f_\beta(o)$ will trace as shown in Figure G.27.

G.1.6 GIB

Suppose $f_\beta(d)$ began with r, and $f_\beta(\bar{d})$ began with i. Then we have the situation depicted in Figure G.28.

Here, as show, in order to meet Assumption A, $f_\beta(\bar{d})$ must eventually traverse p^+ right before crossing, possibly first with some twisting.

Here if the dotted lines do not join, then in order to not put either $f_\beta(d)$ or $f_\beta(\bar{d})$ in Situation β, the only way this could be done is if $f_\beta(p)$ went above $f_\beta(d)$; or $f_\beta(\bar{d})$ went below $f_\beta(d)$.

In the former case, this causes $f_\beta(p)$ to trace, as shown in Figure G.29. In the latter case, the dotted lines will enter Situation α, as shown in Figure G.30.

So the dotted lines must join. But in this case $f_\beta(p)$ still trace, as shown in Figure G.31.

This is a contradiction.

G.1.7 TEX

Suppose $f_\beta(d)$ began with r, and $f_\beta(\bar{d})$ began with s. Then we have the situation depicted in Figure G.28. As in the situation in GIB G.1.6, $f_\beta(\bar{d})$ must eventually traverse p^+ right before crossing.

Here we can repeat the entire argument in GIB G.1.6 to reach a contradiction.

G.1.8 LYR

Suppose $f_\beta(d)$ began with r, and $f_\beta(\bar{d})$ began with o. But this is impossible as this forces $f_\beta(o)$ to also begin with o.

This concludes the case analysis for Case A: Triangles Fixed.

G.2 Case B,C,D: Triangles Swapped

Now suppose the triangles are swapped. Then at least one of $f_\beta(d)$ and $f_\beta(\bar{d})$ must go over an odd number of letters before crossing. We first assume this to be the case for $f_\beta(\bar{d})$, that is, $f_\beta(\bar{d})$ crosses an odd number of letters before crossing d.

Then $f_\beta(\bar{d})$ can begin with r, b; and $f_\beta(d)$ can begin with p, i, i, s or $\bar{d}$.

G.2.1 TGU

Suppose $f_\beta(\bar{d})$ began with r, and $f_\beta(\bar{d})$ began with p. We remind the reader that we are assuming $f_\beta(\bar{d})$ must go over an odd number of letters before crossing. This assumption necessitates that eventually $f_\beta(\bar{d})$ must traverse o^- right before crossing d.

This is Figure G.32.

Here if $f_\beta(r)$ went above $f_\beta(p)$ then $f_\beta(r)$ will immediately trace; if instead $f_\beta(r)$ went below

$f_\beta(p)$ then $f_\beta(p)$ will immediately trace.

This is a contradiction.

G.2.2 XNA

Suppose $f_\beta(\bar{d})$ began with r, and $f_\beta(\bar{d})$ began with i. We remind the reader that we are assuming $f_\beta(\bar{d})$ must go over an odd number of letters before crossing. This assumption necessitates that eventually $f_\beta(\bar{d})$ must traverse o^- right before crossing d.

This is Figure G.33.

Here $f_\beta(b)$ must go above $f_\beta(p)$ to not immediately trace; and in between $f_\beta(p)$ and $f_\beta(\bar{d})$ in order to not trace as well. This forces $f_\beta(\bar{d})$ to not have any initial twists or $f_\beta(b)$ would be brought along and trace.

This is Figure G.34.

Here $f_\beta(\bar{d})$ must continue with p^- after crossing to not violate the Trace Lemma.

Here if $f_\beta(s)$ began with b° or b^-, forcing $f_\beta(i)$ to begin with b^- then $f_\beta(i)$ will trace:

$$f_\beta(i) = b^- r^- d p^- i^\times$$

So $f_\beta(s)$ must begin with b^+:

$$f_\beta(s) = b^+ d i^* ...$$

forcing

$$f_\beta(p) = d i^* ...$$

This is Figure G.35.

Here $f_\beta(d)$ must begin with i^- otherwise $f_\beta(p)$ would trace. Then if $f_\beta(d)$ immediately crosses, it would traverse

$$f_\beta(d) = i^- \bar{d} b^- r^- d p^- ...$$

and then the dotted lines will be in Situation α. So we must have

$$f_\beta(d) = i^- o^* ...$$

instead.

But now as Figure G.36 shows, $f_\beta(o)$ will trace.

This is a contradiction.

G.2.3 WYS

Suppose $f_\beta(\bar{d})$ began with r, and $f_\beta(\bar{d})$ began with s. We remind the reader that we are assuming $f_\beta(\bar{d})$ must go over an odd number of letters before crossing.

This is Figure G.37.

The same arguments used in XNA G.2.2 lead to the conclusion that $f_\beta(s)$ must begin with b^+, but in this instance this means it will immediately trace after crossing, as shown in Figure G.38.

This is a contradiction.

G.2.4 HTI

Suppose $f_\beta(\bar{d})$ began with r, and $f_\beta(\bar{d})$ began with o. We remind the reader that we are assuming $f_\beta(\bar{d})$ must go over an odd number of letters before crossing. This assumption

necessitates that eventually $f_\beta(\bar{d})$ must traverse o^- right before crossing d.

In this case, $f_\beta(p)$ is forced to immediately trace after crossing, as shown in Figure G.39.

This is a contradiction.

G.2.5 SEZ

Suppose $f_\beta(\bar{d})$ began with r, and $f_\beta(\bar{d})$ began with $\bar{d}$. We remind the reader that we are assuming $f_\beta(\bar{d})$ must go over an odd number of letters before crossing. This assumption necessitates that eventually $f_\beta(\bar{d})$ must traverse o^- right before crossing d.

Here $f_\beta(p)$ must go under $f_\beta(d)$ or it would immediately trace.

We have Figure G.40.

Here $f_\beta(p)$ can continue with i or o. Suppose it were the former. Then this forces

$$f_\beta(r) = i^- o^* ...$$

to prvent $f_\beta(p)$ from tracing. Also, we must have

$$f_\beta(i) = b^- r^- d ...$$

to prevent $f_\beta(s)$ from tracing after crossing d.

We have the situation depicted in Figure G.41.

The position of $f_\beta(i)$ here forces $f_\beta(\bar{d})$ to not have any initial twists, so we have

$$f_\beta(\bar{d}) = r^- d ...$$

and

$$f_\beta(o) = r^- d...$$

and here $f_\beta(o)$ must go above $f_\beta(d)$, otherwise if $f_\beta(d)$ went in between $f_\beta(o)$ and $f_\beta(i)$ then it would be in Situation β; while if it went above $f_\beta(i)$, it would cause $f_\beta(i)$ to trace. So now

$$f_\beta(o) = r^- dp^*...$$

and here it must continue with p^- or else $f_\beta(b)$ would trace.

But now we have the situation depicted in Figure G.42, where it is clear that $f_\beta(o)$ will trace.

So suppose instead $f_\beta(p)$ continued with s:

$$f_\beta(p) = ds^*...$$

and if $f_\beta(r)$ also began with s here we would have Figure G.43. Here the same argument as before shows the dotted liens must join. Here $f_\beta(i)$ and $f_\beta(o)$ must continue with p^- otherwise $f_\beta(b)$ would trace after crossing; but then one of $f_\beta(o)$ or $f_\beta(i)$ will trace.

If $f_\beta(r)$ instead began with i, then this is the situation depicted in Figure G.44. Here again $f_\beta(i)$ and $f_\beta(o)$ must continue with p^- otherwise $f_\beta(b)$ would trace after crossing; but then one of $f_\beta(o)$ or $f_\beta(i)$ will trace.

This is contradiction.

This concludes the situation where we assume $f_\beta(\bar{d})$ goes over an odd number of letter before crossing. Now we assume $f_\beta(\bar{d})$ goes over an even number of letters before crossing, which means $f_\beta(d)$ must go over an odd number of letters before crossing.

Hence, $f_\beta(\bar{d})$ can begin with b or r, whicle $f_\beta(d)$ can begin with p, i, s, o.

G.2.6 PBH

Back to the end of Case B,C,D G.2. Suppose $f_\beta(\bar{d})$ began with b, and $f_\beta(\bar{d})$ began with p. We assume $f_\beta(d)$ must go over an even number of letters before crossing, which necessitates that $f_\beta(\bar{d})$ must go over an odd number of letters before crossing.

Here we must have

$$f_\beta(\bar{d}) = b^- r^- d...$$

and thus

$$f_\beta(o) = b^- r^- d...$$

as shown in Figure G.45.

Here no matter where $f_\beta(r)$ continues it will trace.

This is a contradiction.

G.2.7 CVF

Back to the end of Case B,C,D G.2. Suppose $f_\beta(\bar{d})$ began with b, and $f_\beta(\bar{d})$ began with i. We assume $f_\beta(d)$ must go over an even number of letters before crossing, which necessitates that $f_\beta(\bar{d})$ must go over an odd number of letters before crossing.

Here the only way $f_\beta(b)$ can not trace is to go in between $f_\beta(\bar{d})$ and $f_\beta(i)$. But then $f_\beta(i)$ and $f_\beta(s)$ cross, and one of them will immediately trace on the other side.

This is a contradiction.

G.2.8 BRW

Back to the end of Case B,C,D G.2. Suppose $f_\beta(\bar{d})$ began with b, and $f_\beta(\bar{d})$ began with s. We assume $f_\beta(d)$ must go over an even number of letters before crossing, which necessitates

that $f_\beta(\bar{d})$ must go over an odd number of letters before crossing.

The same argument of CVF G.2.7 applies to give a contradiction.

G.2.9 TRK

Back to the end of Case B,C,D G.2. Suppose $f_\beta(\bar{d})$ began with b, and $f_\beta(\bar{d})$ began with o. We assume $f_\beta(d)$ must go over an even number of letters before crossing, which necessitates that $f_\beta(\bar{d})$ must go over an odd number of letters before crossing.

This is Figure G.46.

Then Figure G.47 is immediate.

Here if $f_\beta(b)$ were to begin with p° or p^-, then $f_\beta(i)$ and $f_\beta(s)$ will follow with p^-, but then one of them will immediately trace.

On the other hand, if $f_\beta(b)$ were to begin with p^+, then in order to not trace, it can only do so by going in between $f_\beta(\bar{d})$ and $f_\beta(i)$, as shown in Figure G.48.

Now if it continues with r° or r^-, forcing $f_\beta(p)$ to begin with r^-, then $f_\beta(p)$ will immediately trace after crossing. But then this means $f_\beta(b)$ has to continue with r^+, immediately tracing.

This is a contradiction.

This concludes the cases analysis for Track 12.

G.3 Figures

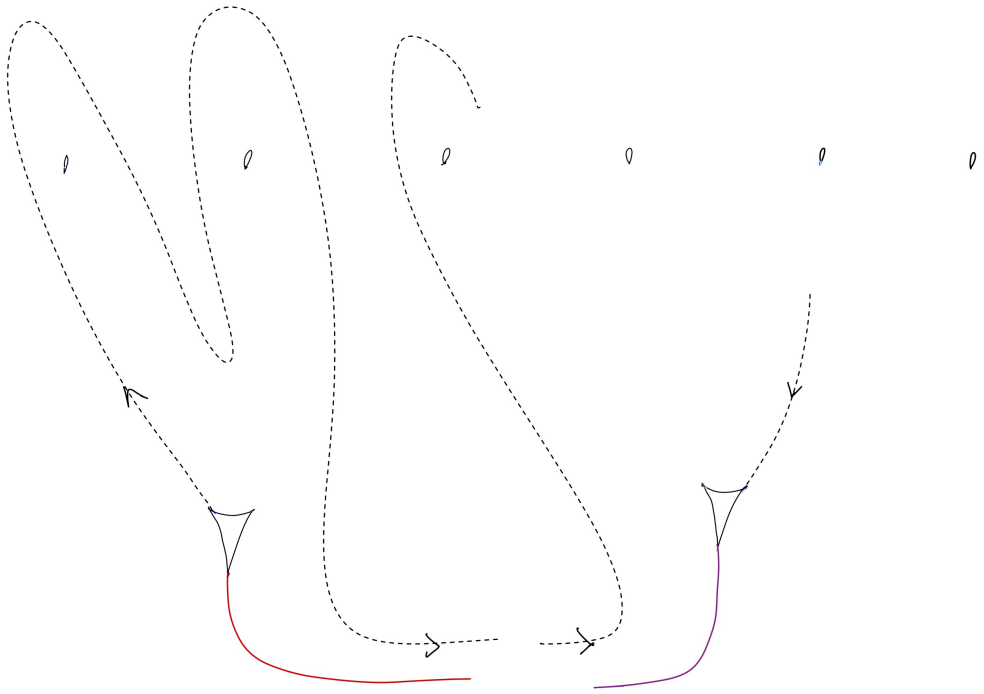


Figure G.2: BKG1

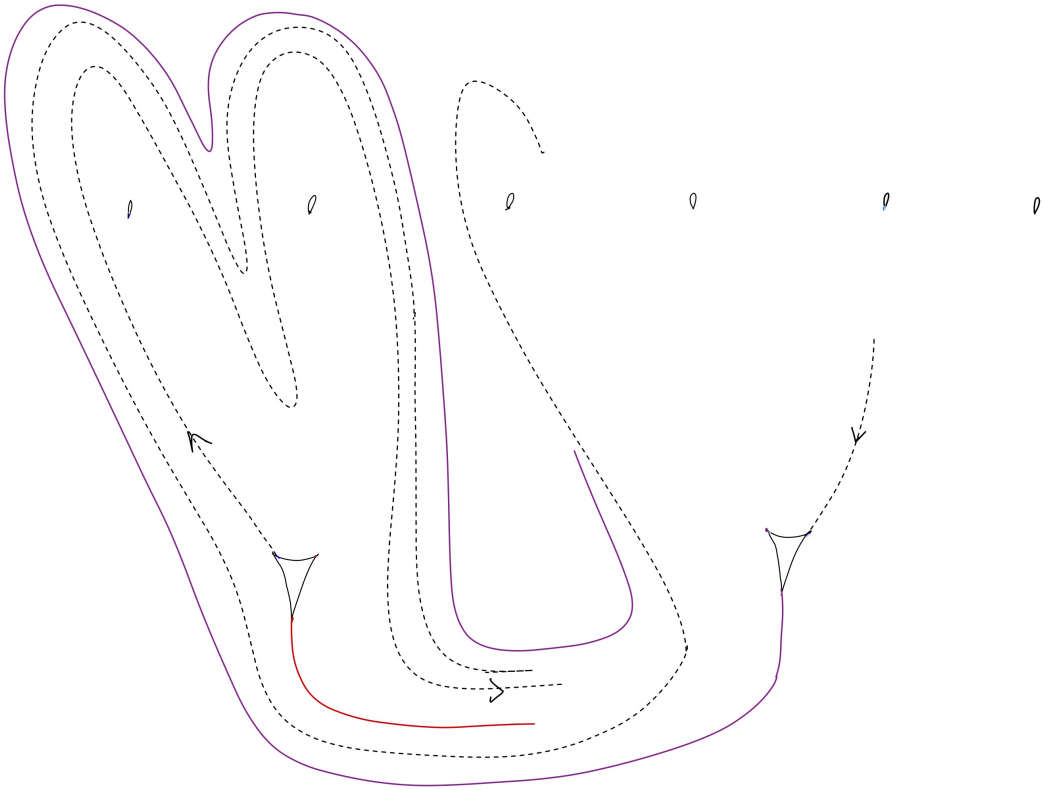


Figure G.3: BKG2

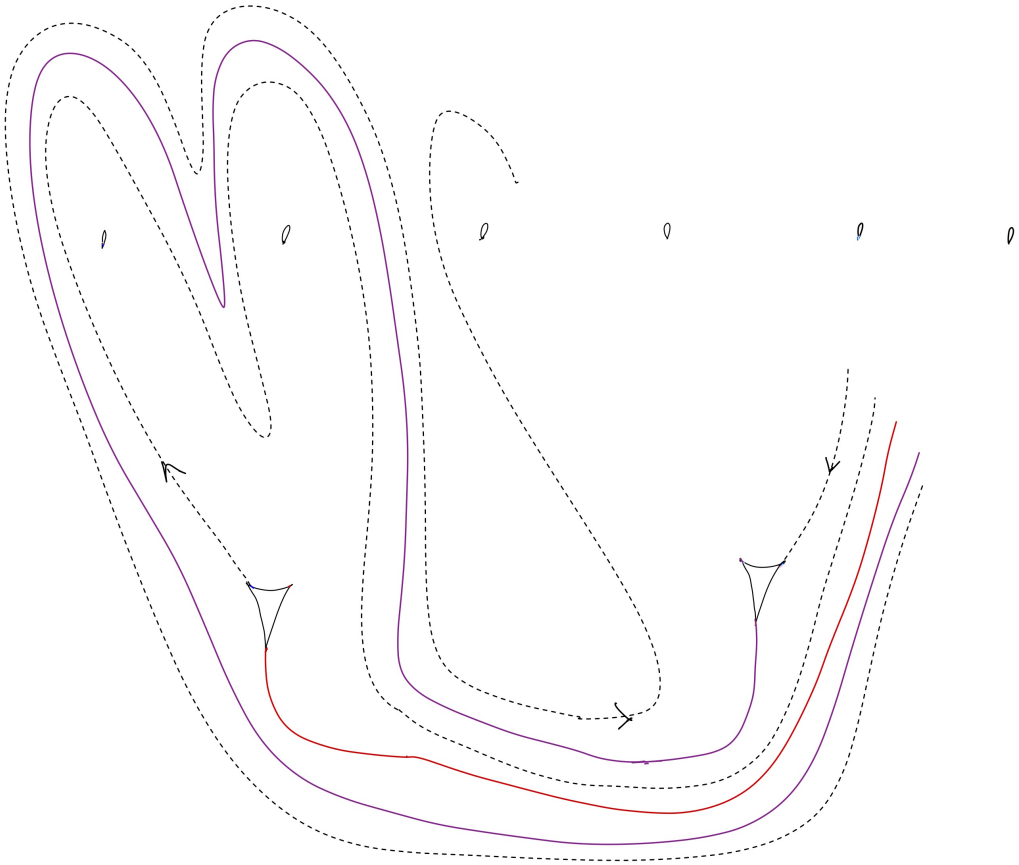


Figure G.4: BKG3

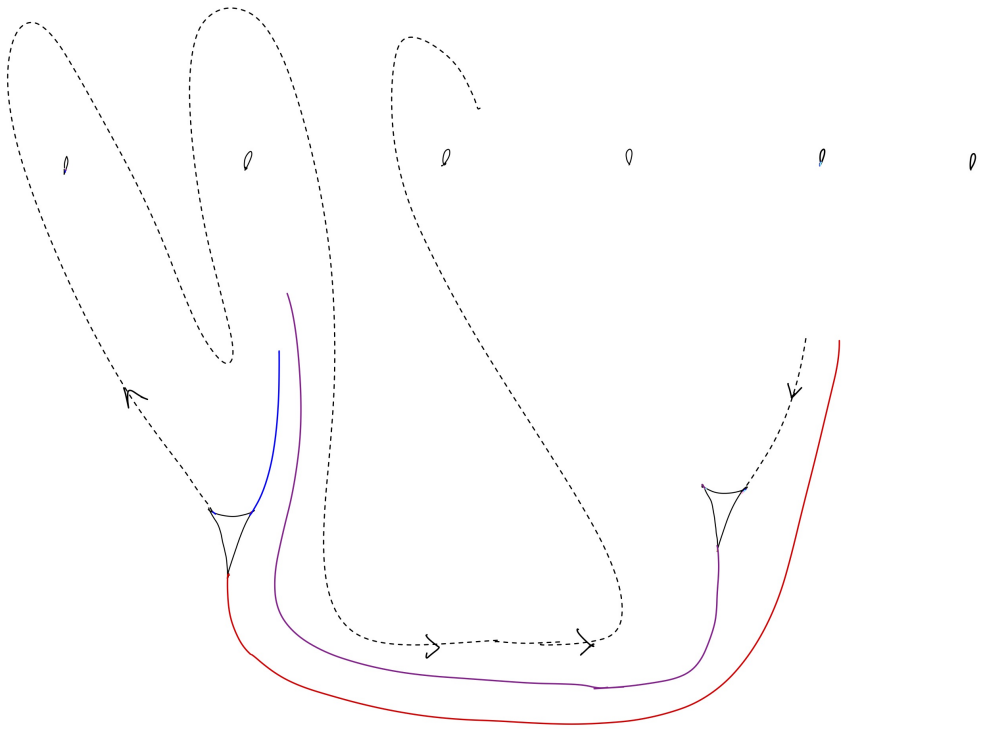


Figure G.5: BKG4

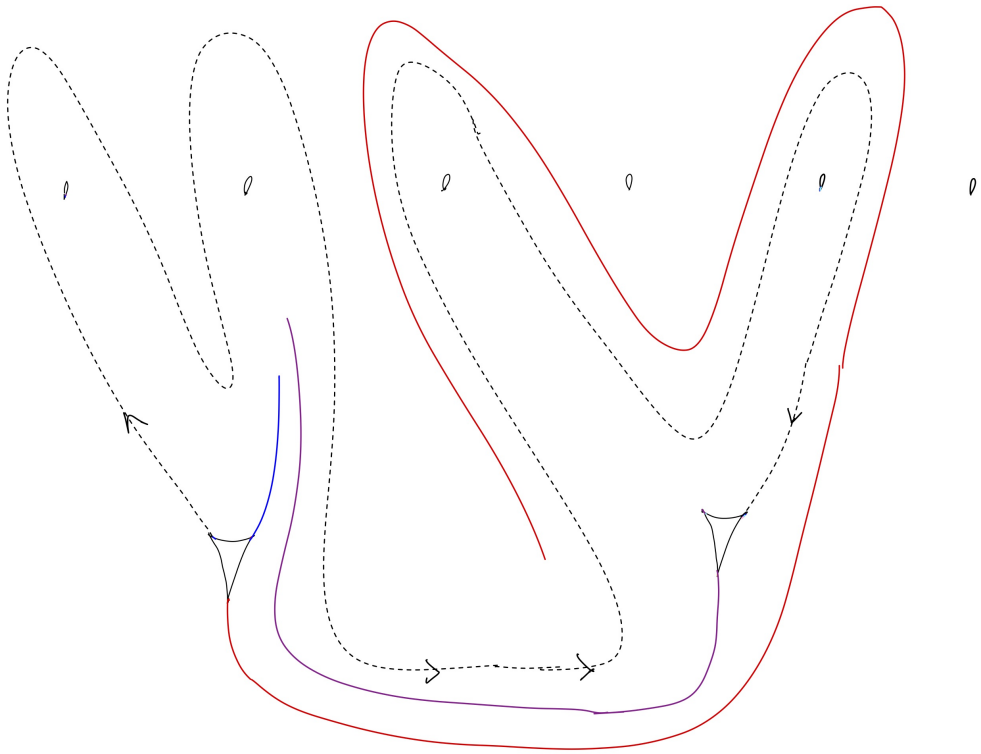


Figure G.6: BKG5

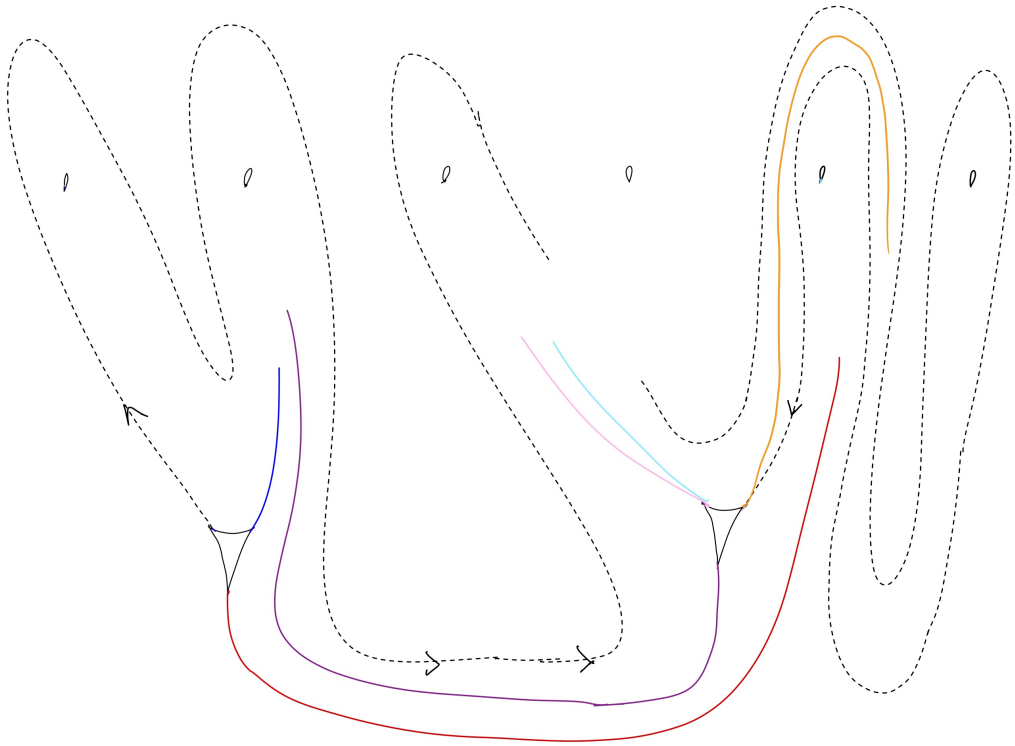


Figure G.7: BKG6

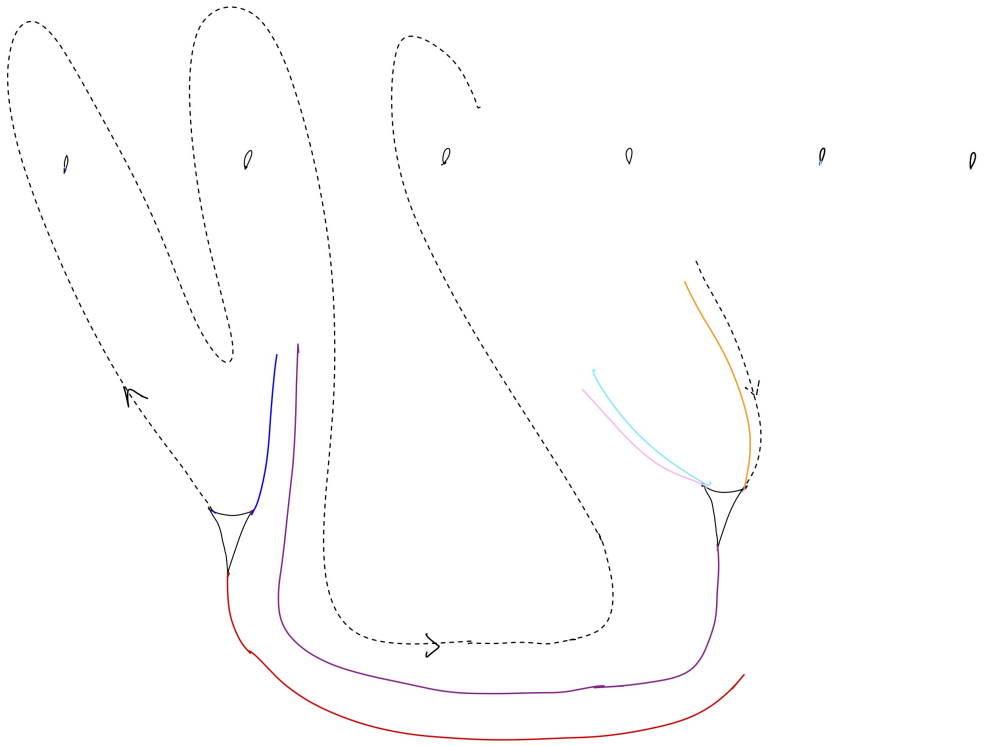


Figure G.8: CNM1

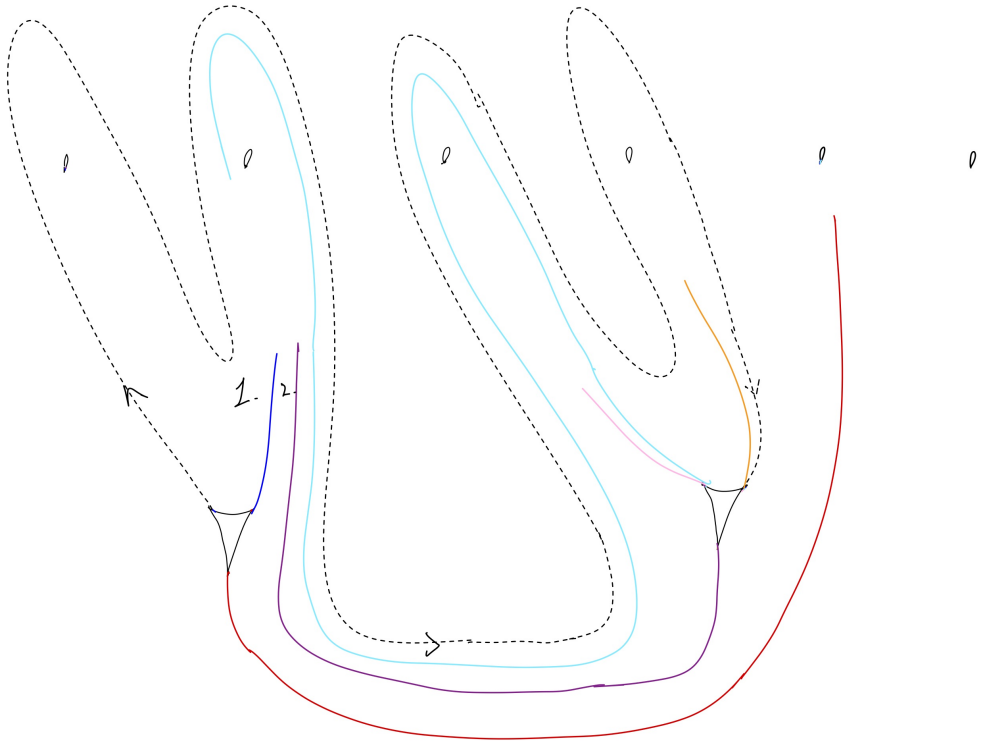


Figure G.9: CNM2

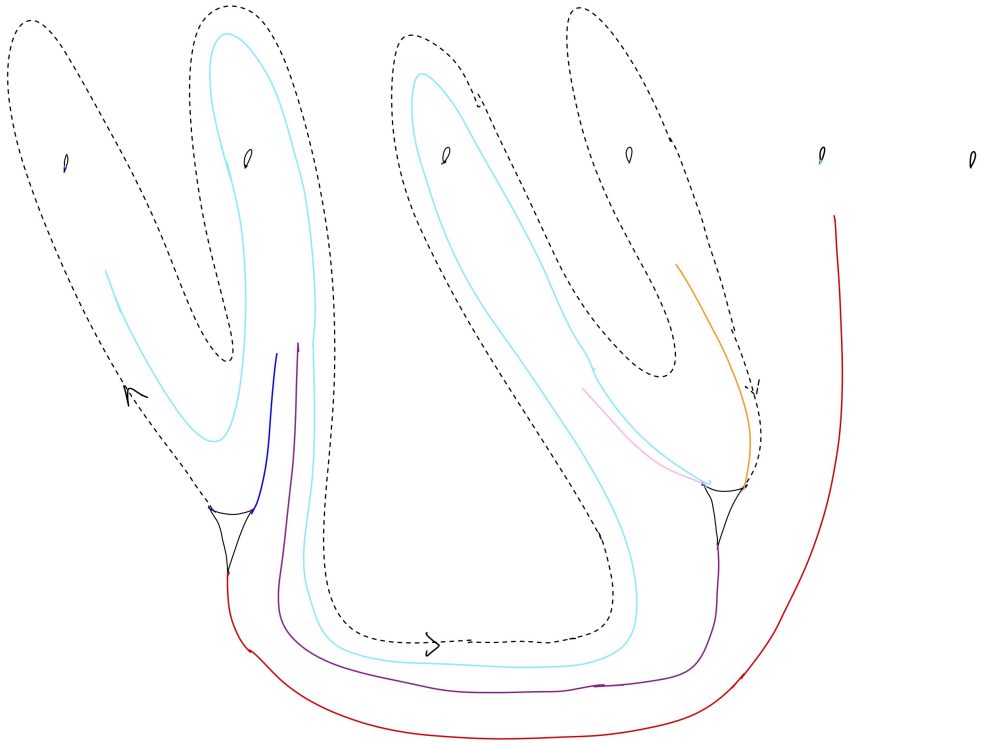


Figure G.10: CNM3

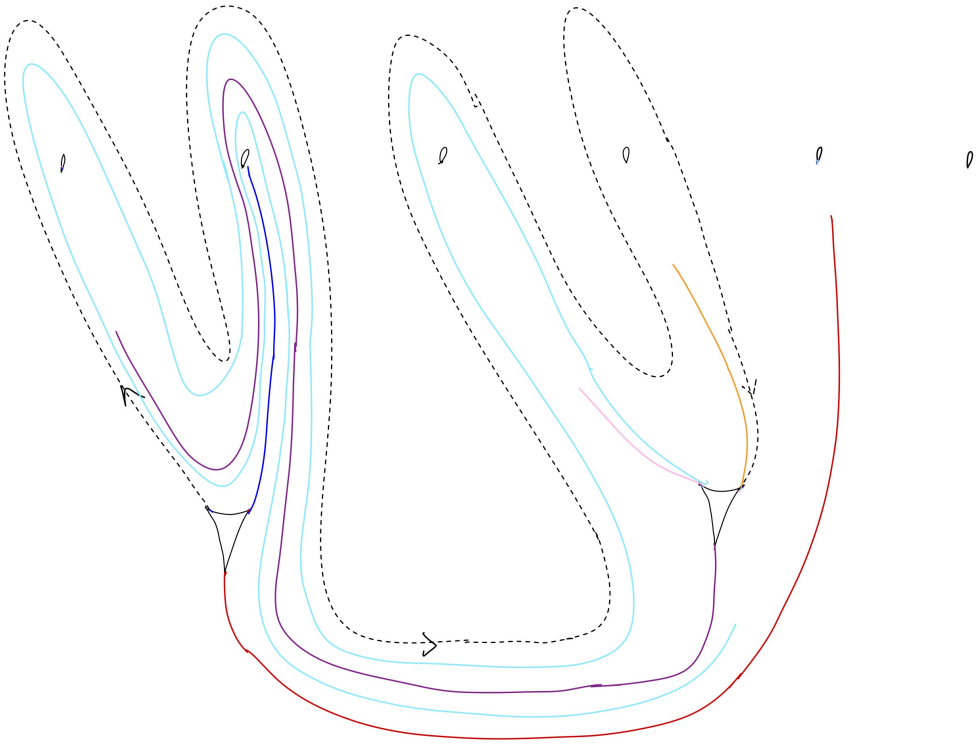


Figure G.11: CNM4

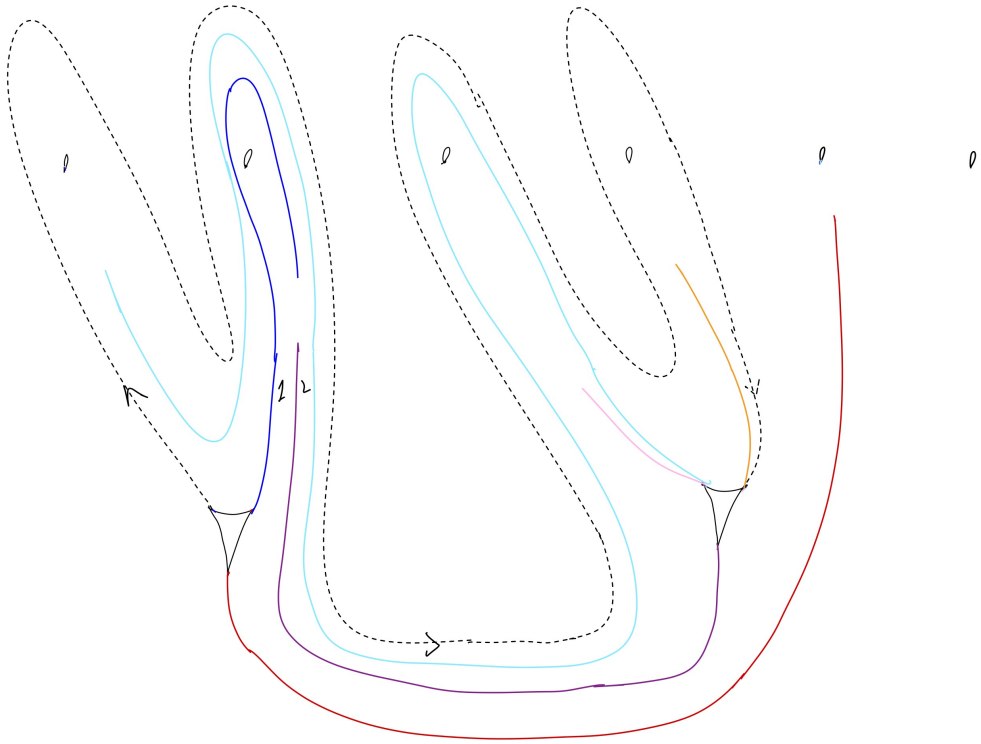


Figure G.12: CNM5

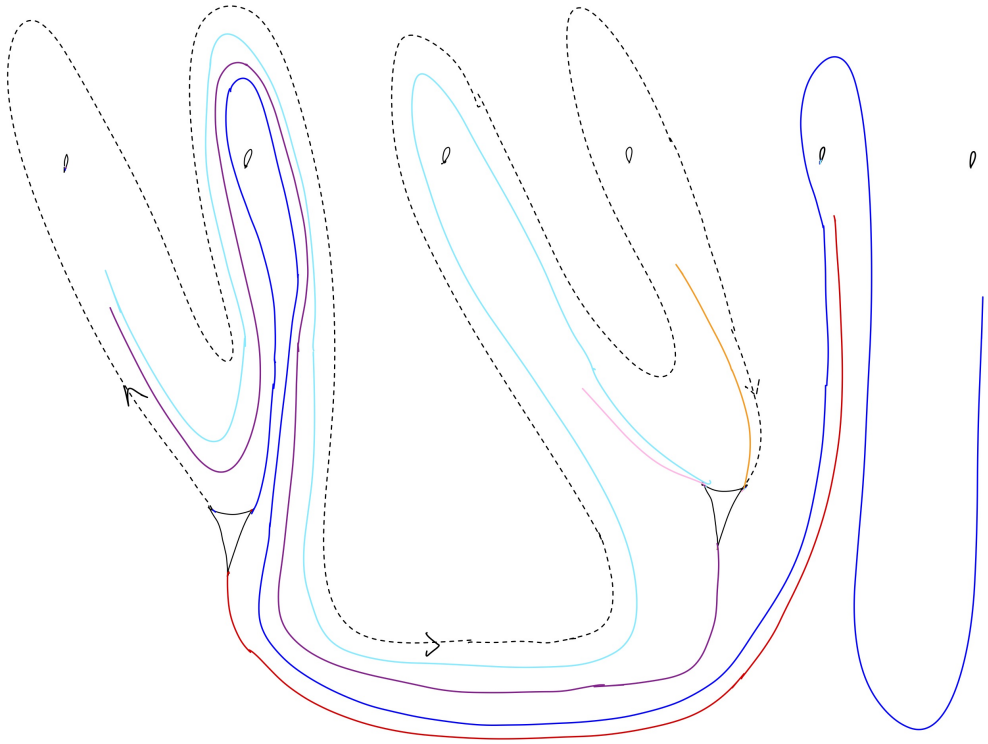


Figure G.13: CNM6

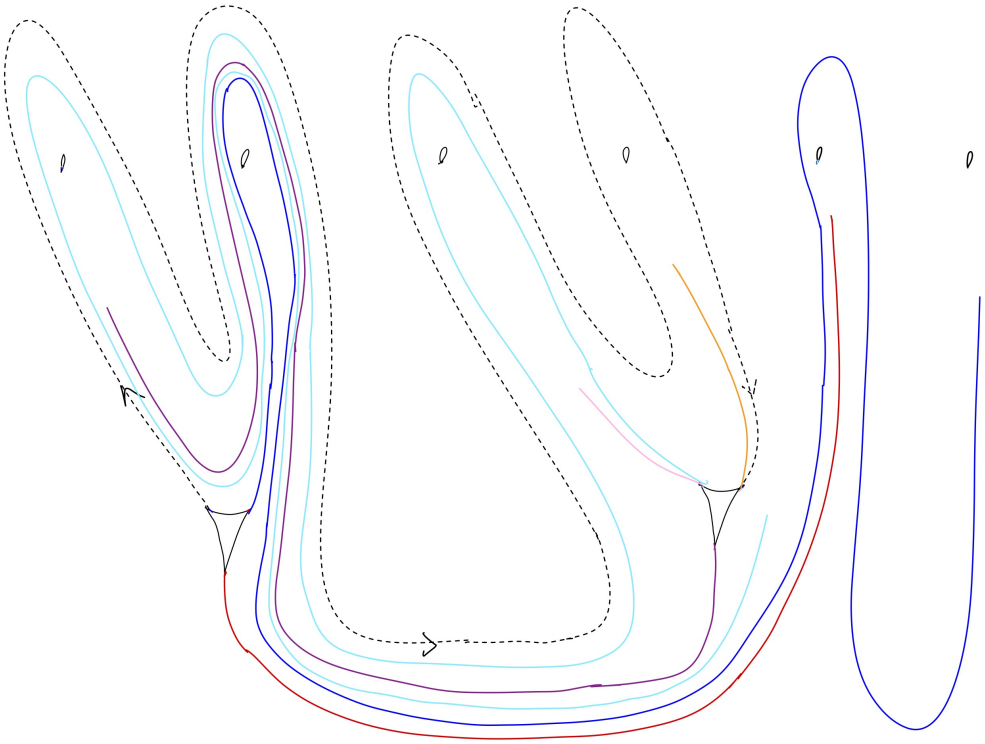


Figure G.14: CNM7

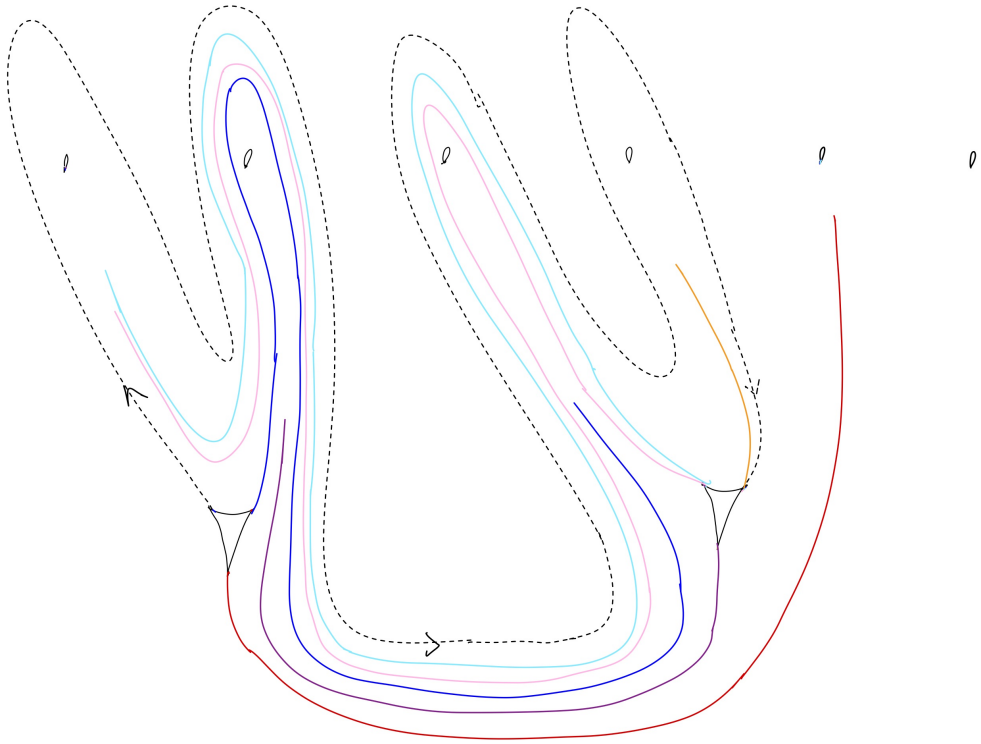


Figure G.15: CNM8



Figure G.16: LGU1

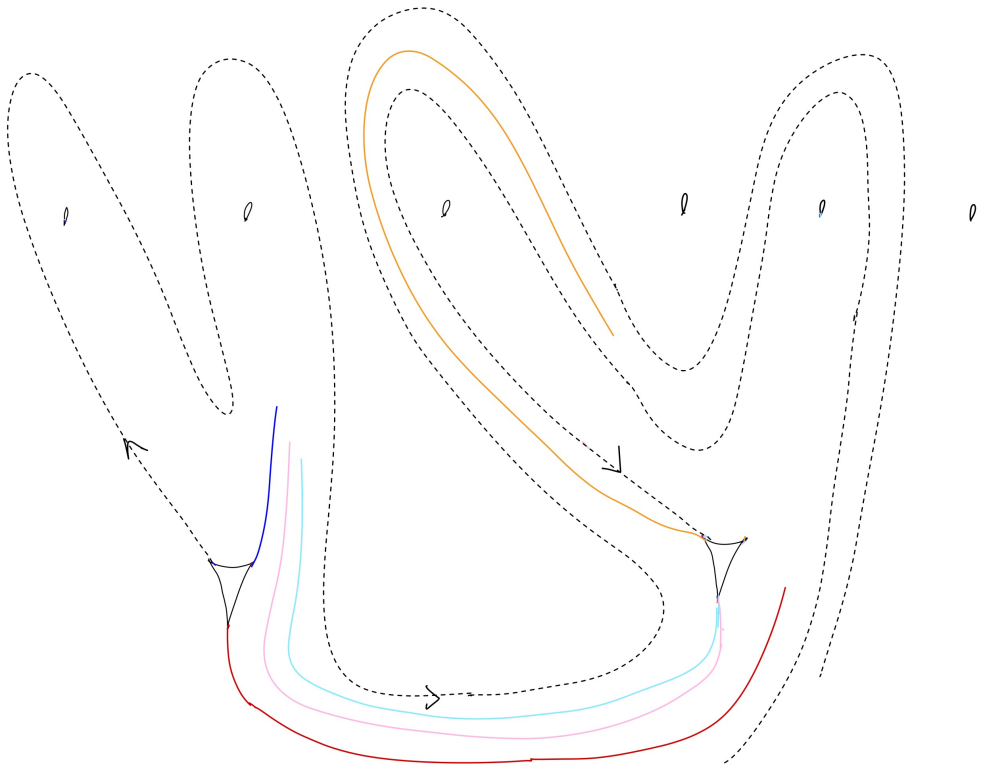


Figure G.17: LGU2

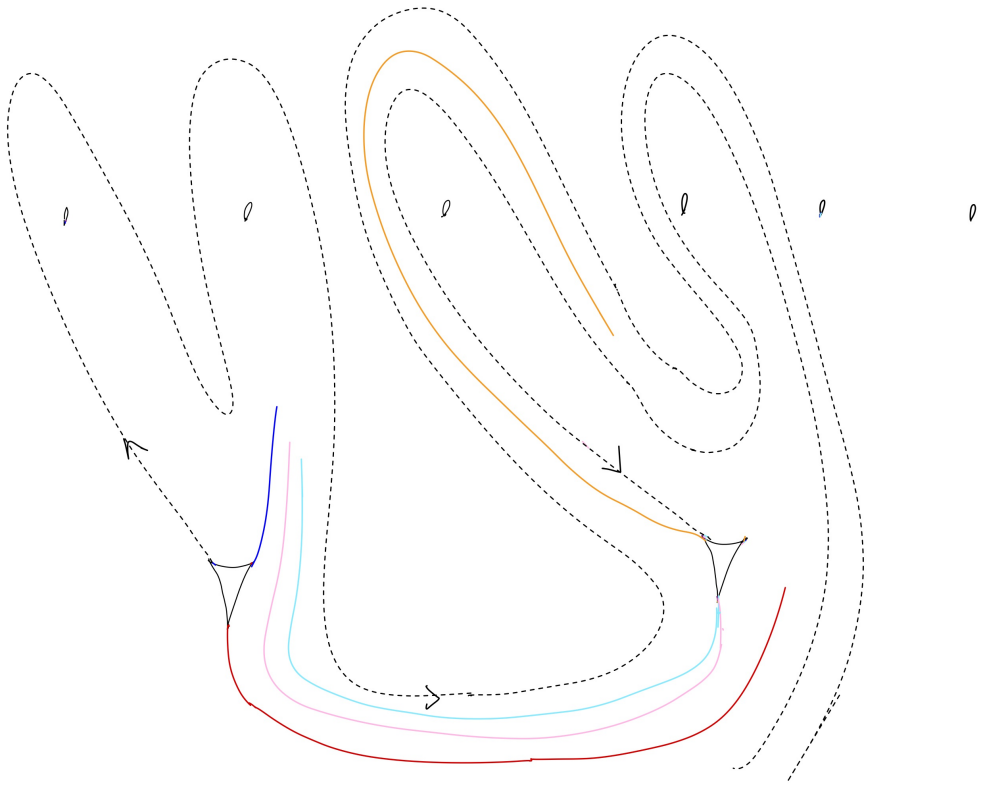


Figure G.18: LGU3

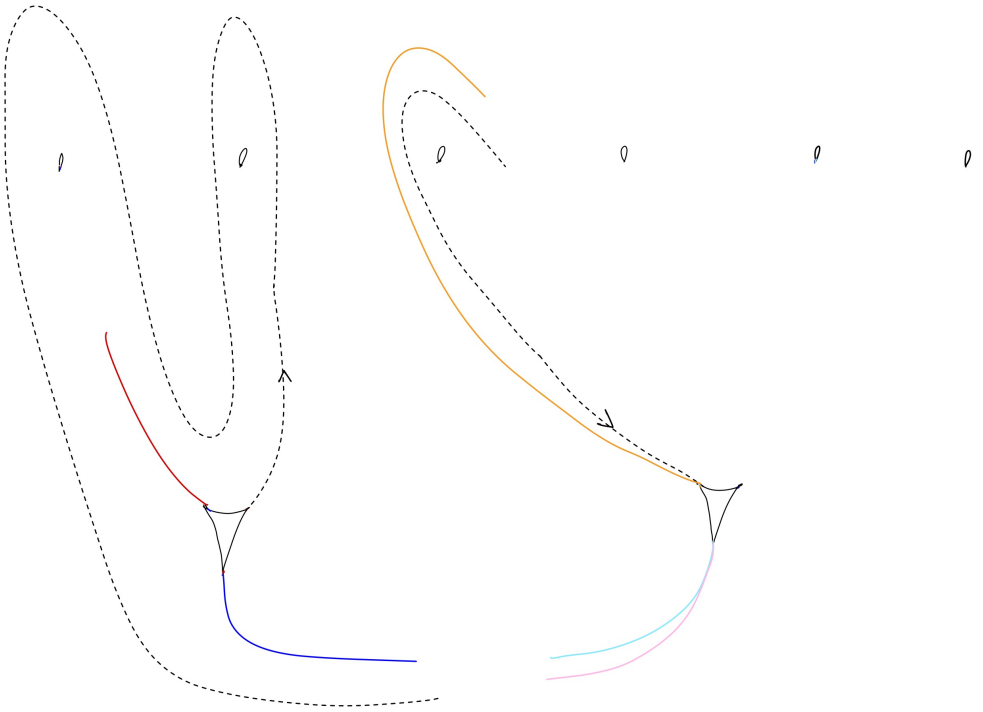


Figure G.19: SXM1

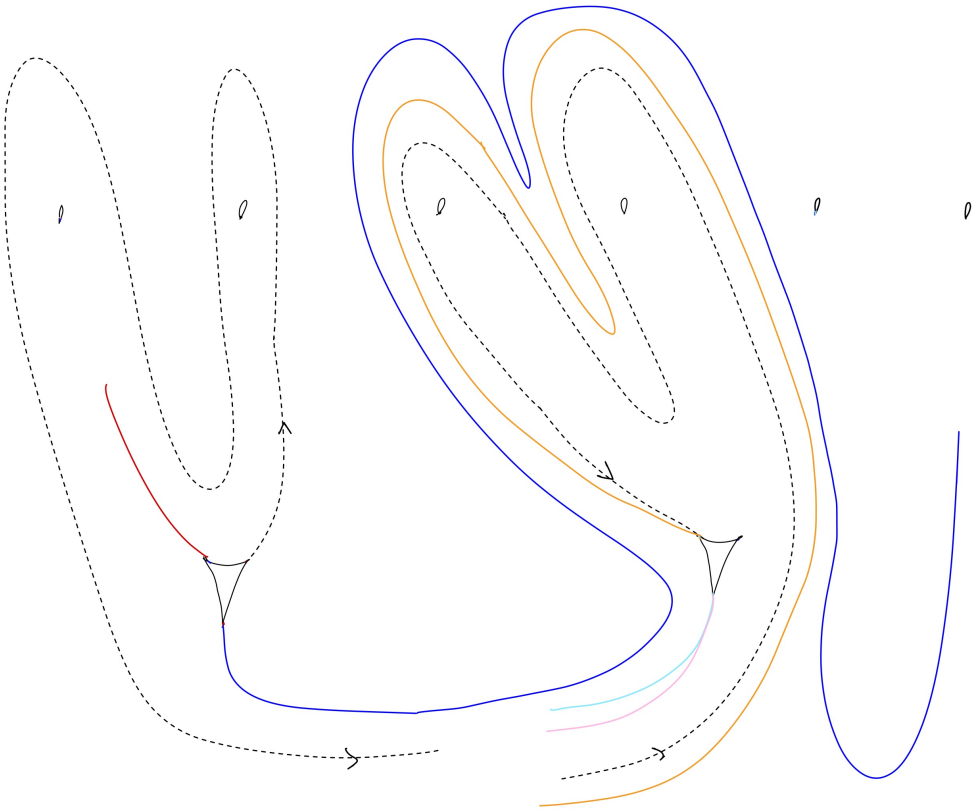


Figure G.20: SXM2

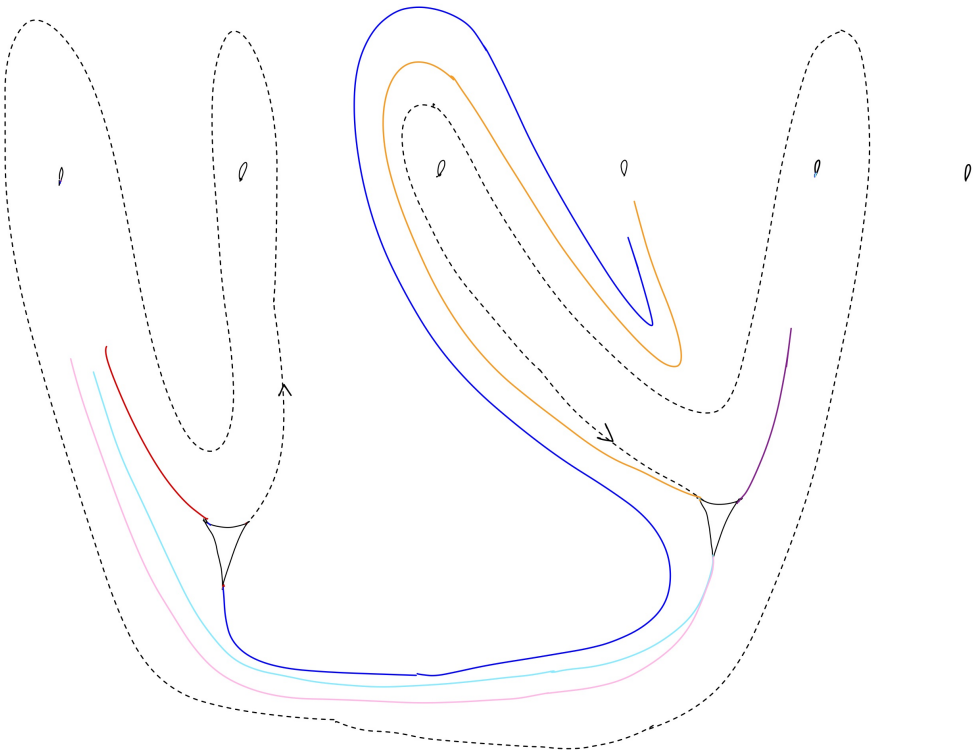


Figure G.21: SXM3

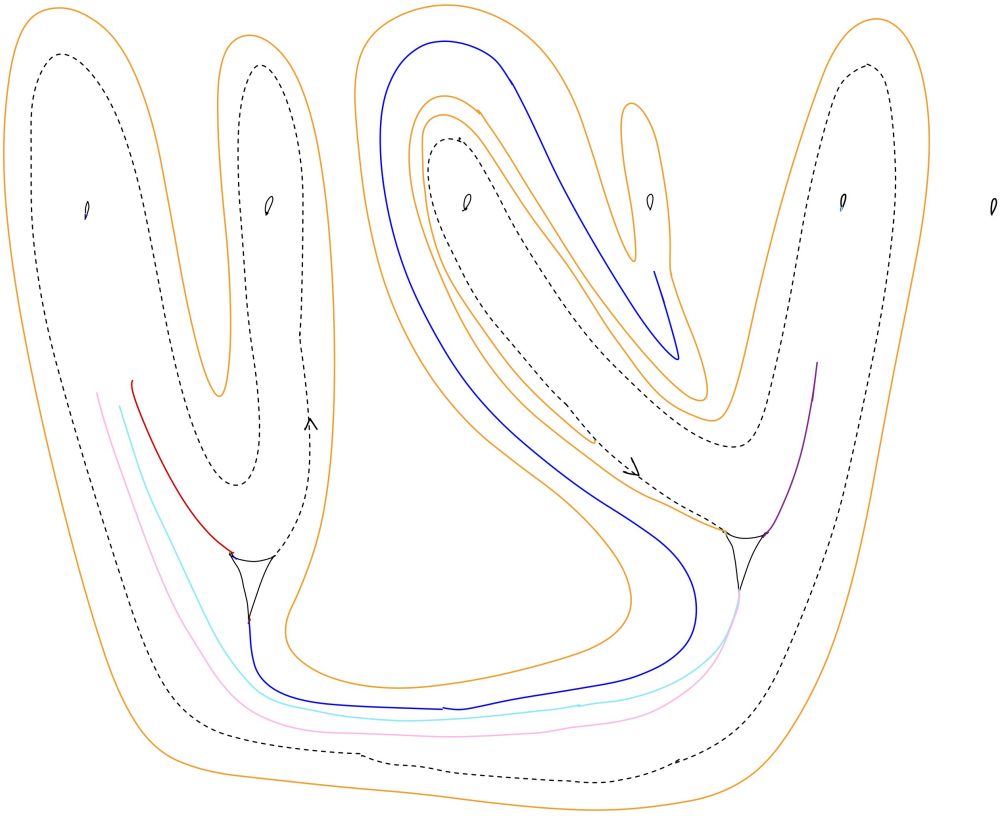


Figure G.22: SXM4

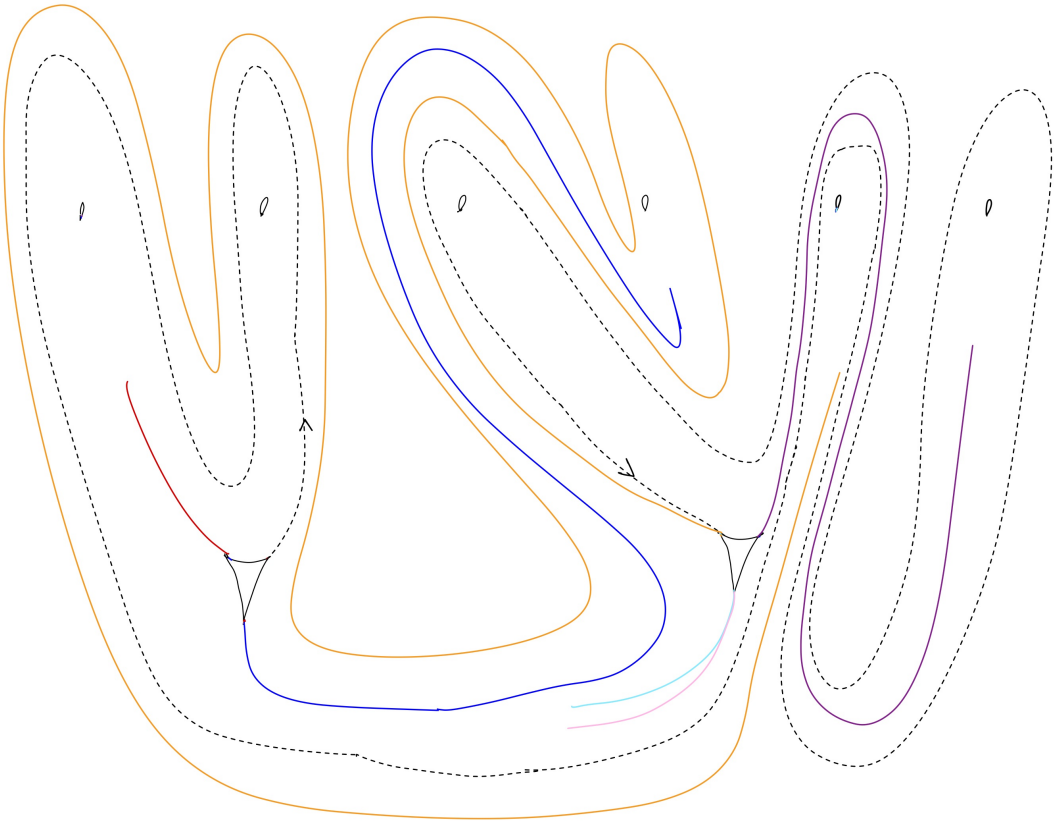


Figure G.23: SXM5

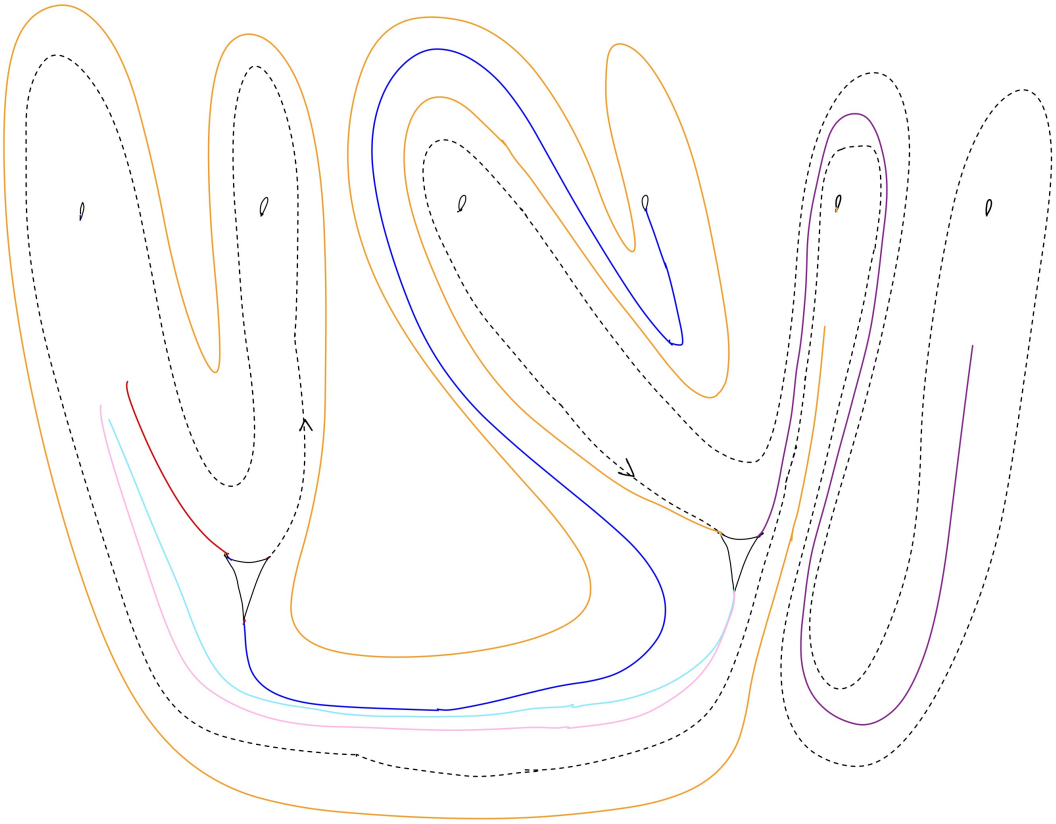


Figure G.24: SXM6

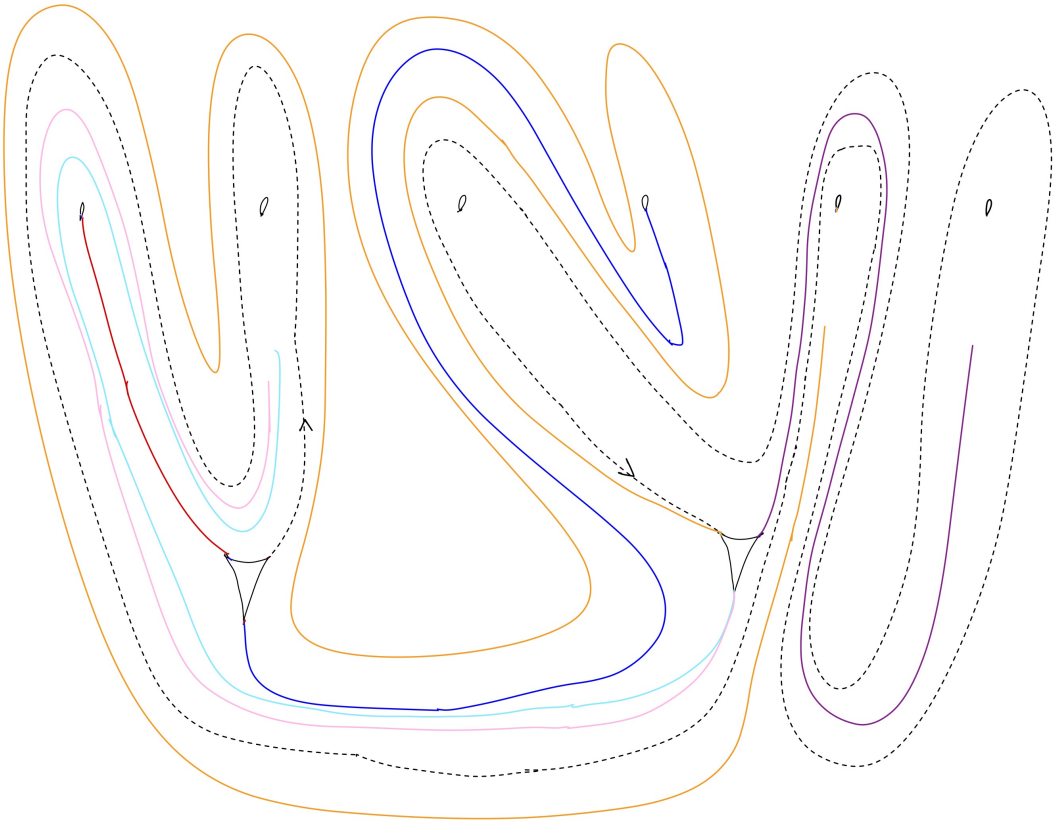


Figure G.25: SXM7

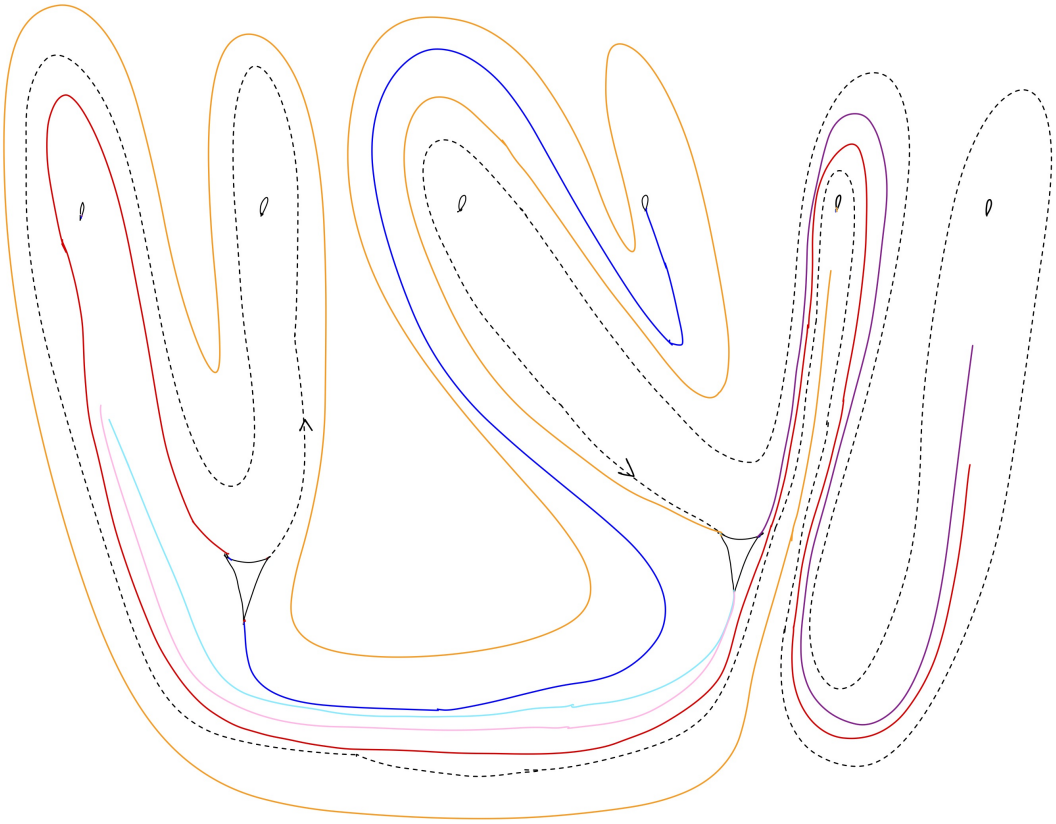


Figure G.26: SXM8

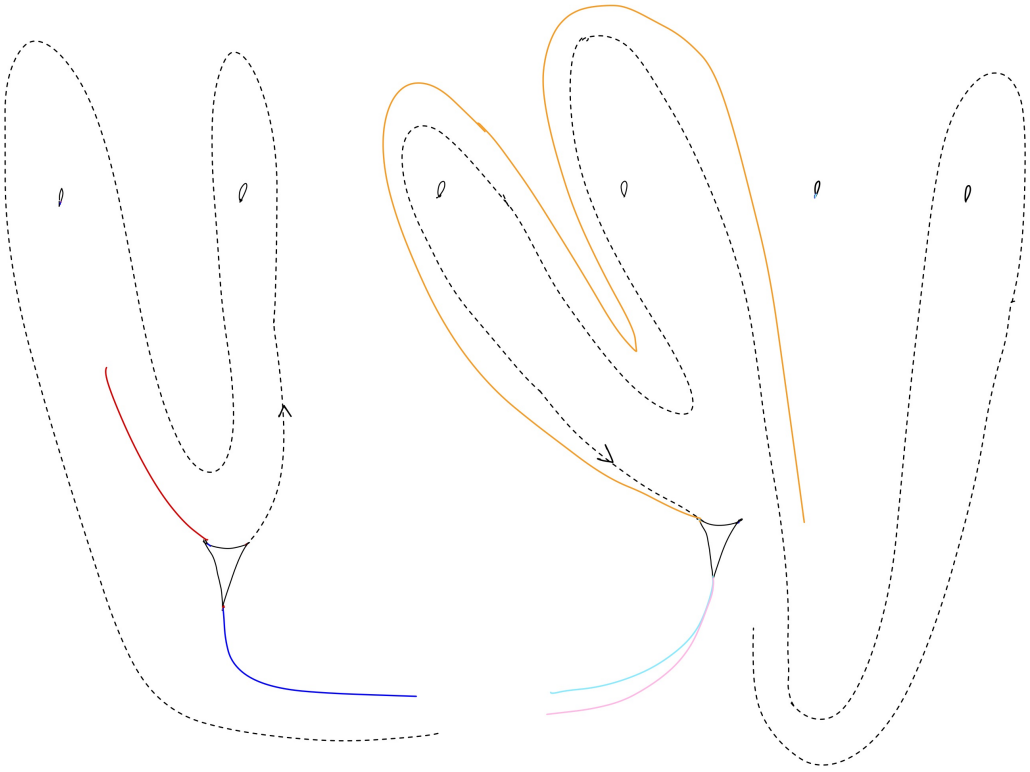


Figure G.27: SXM9



Figure G.28: GIB1

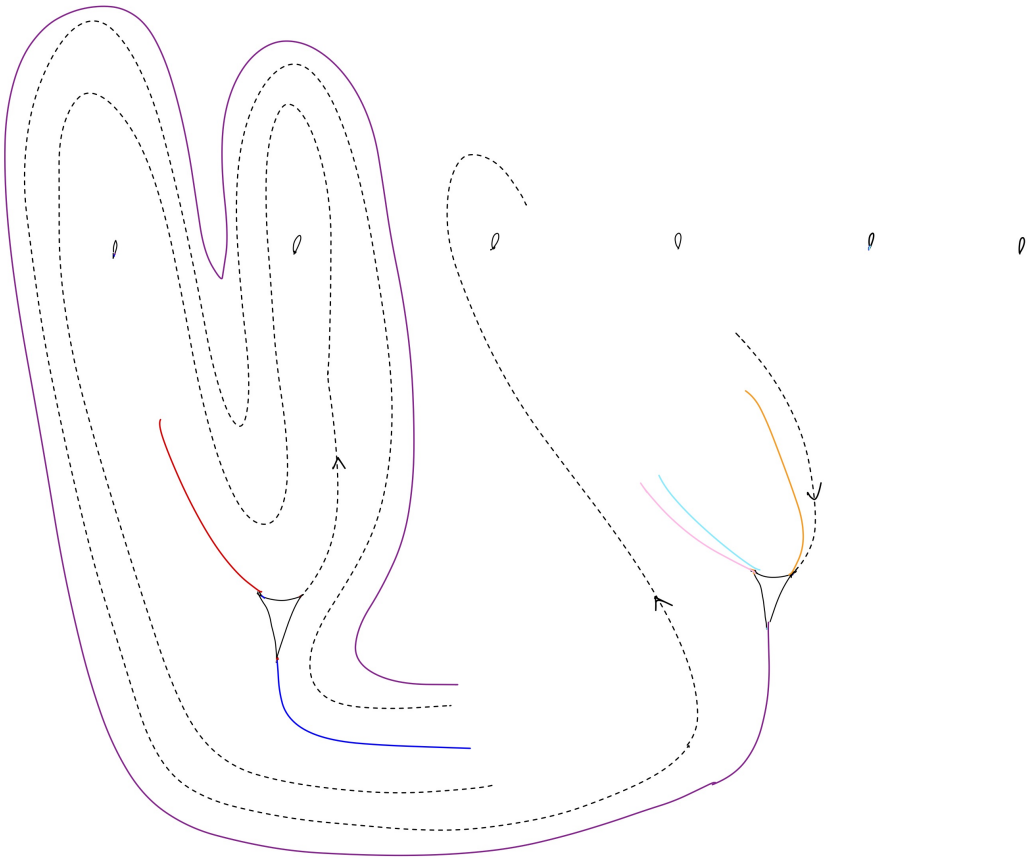


Figure G.29: GIB2

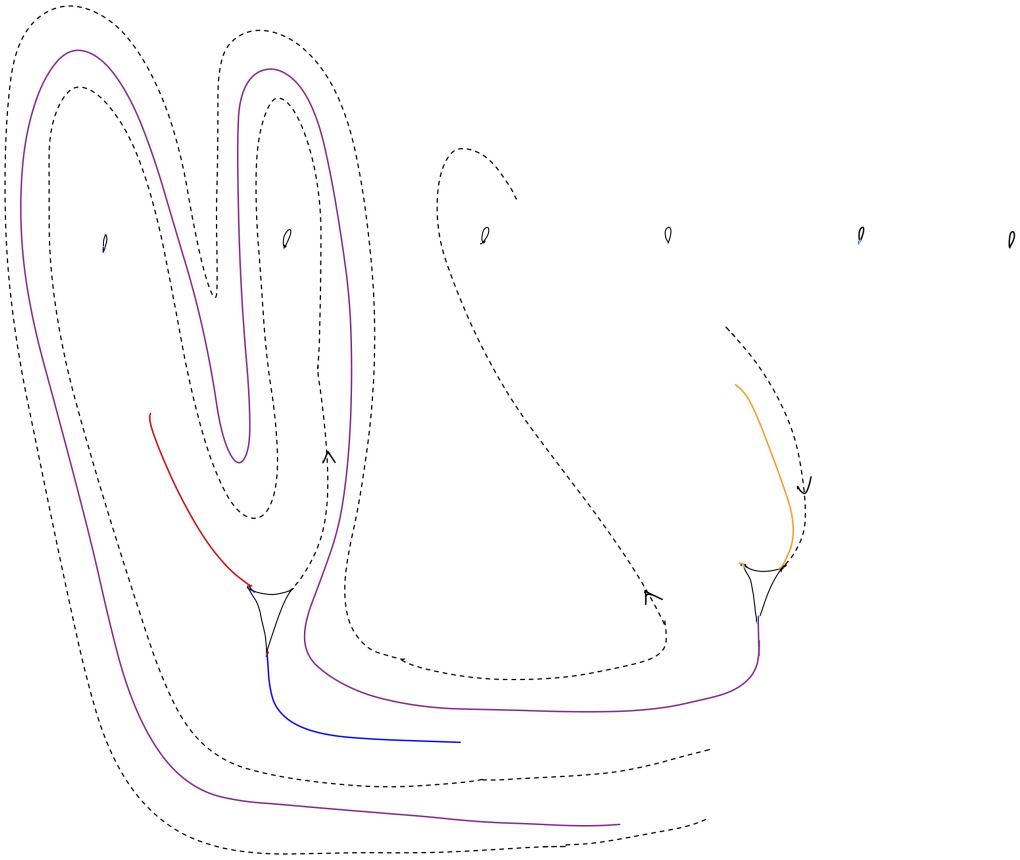


Figure G.30: GIB3



Figure G.31: GIB4

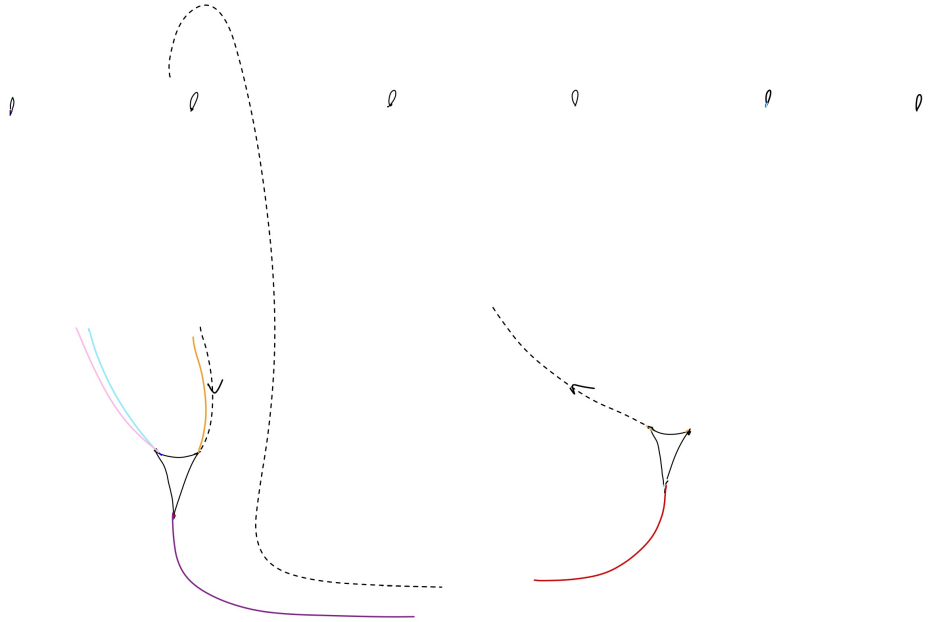


Figure G.32: TGU1

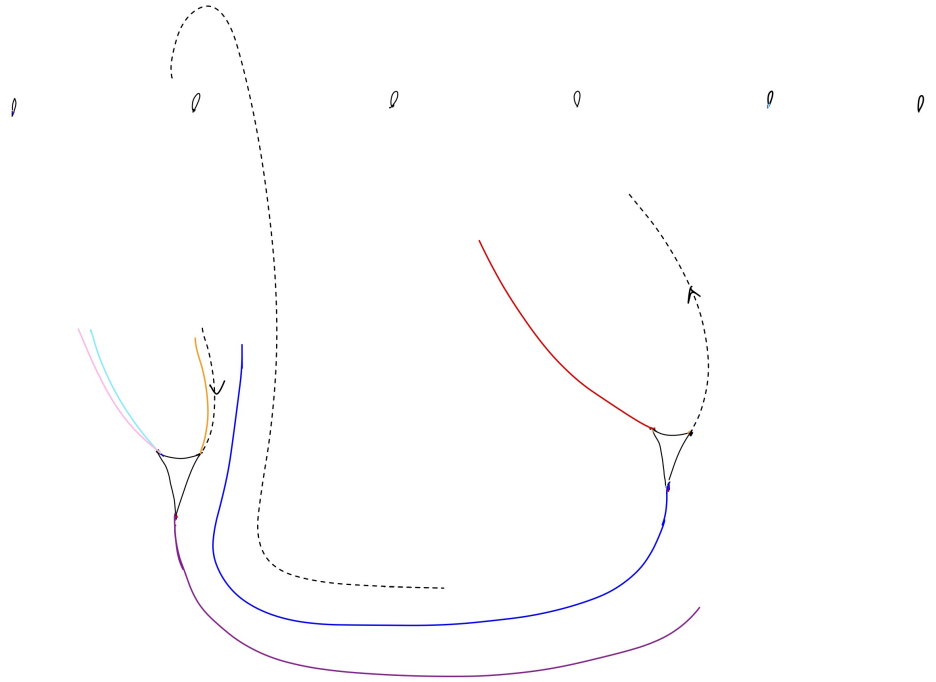


Figure G.33: XNA1

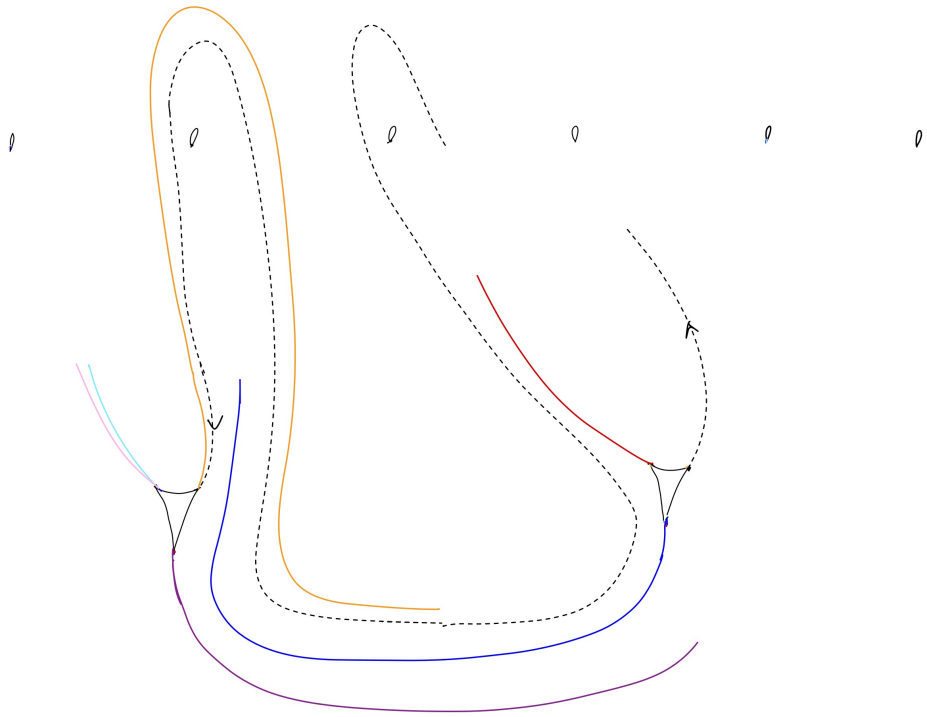


Figure G.34: XNA2

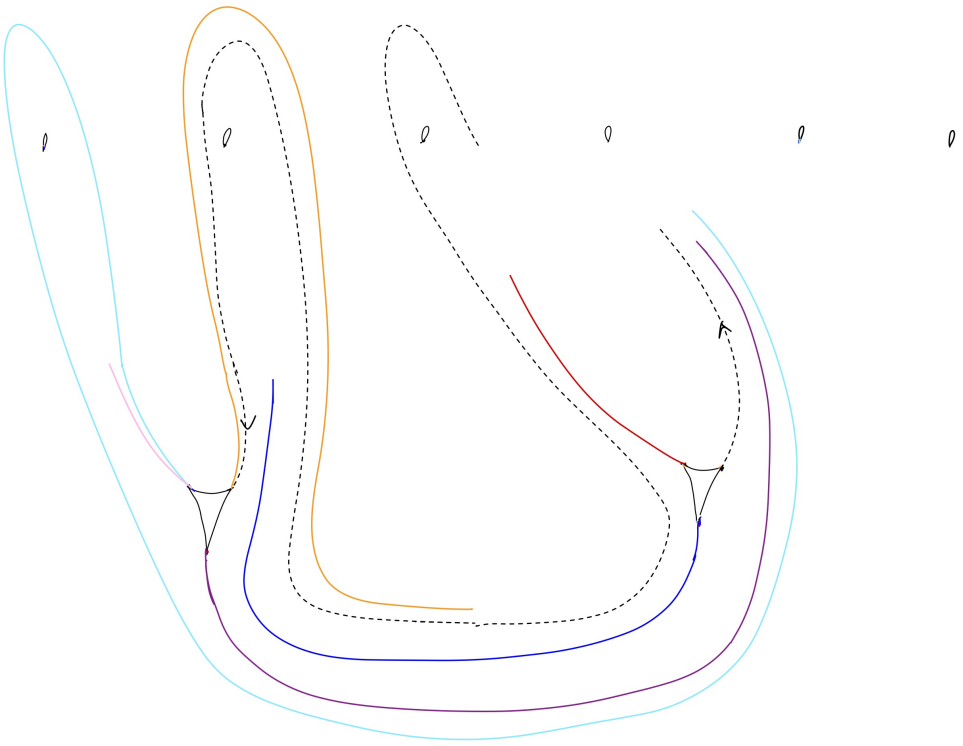


Figure G.35: XNA3

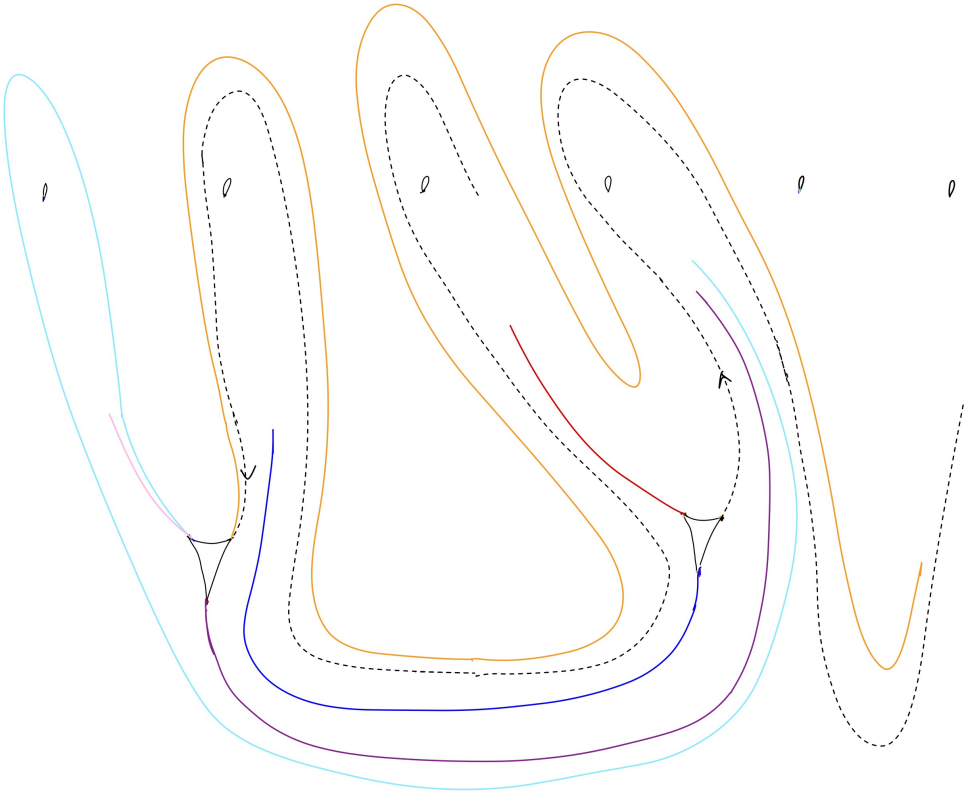


Figure G.36: XNA4

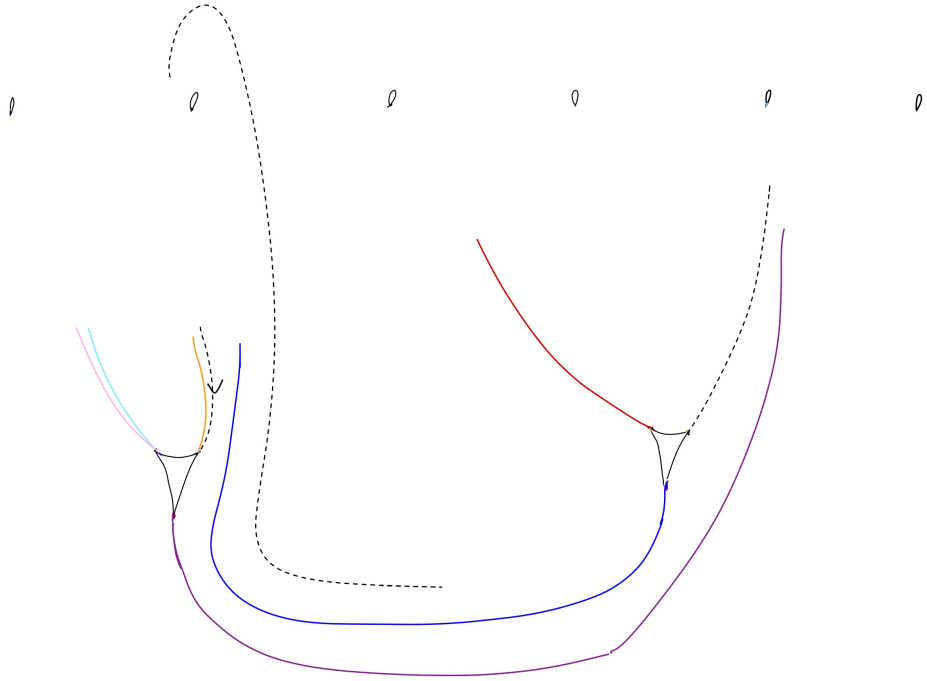


Figure G.37: WYS1

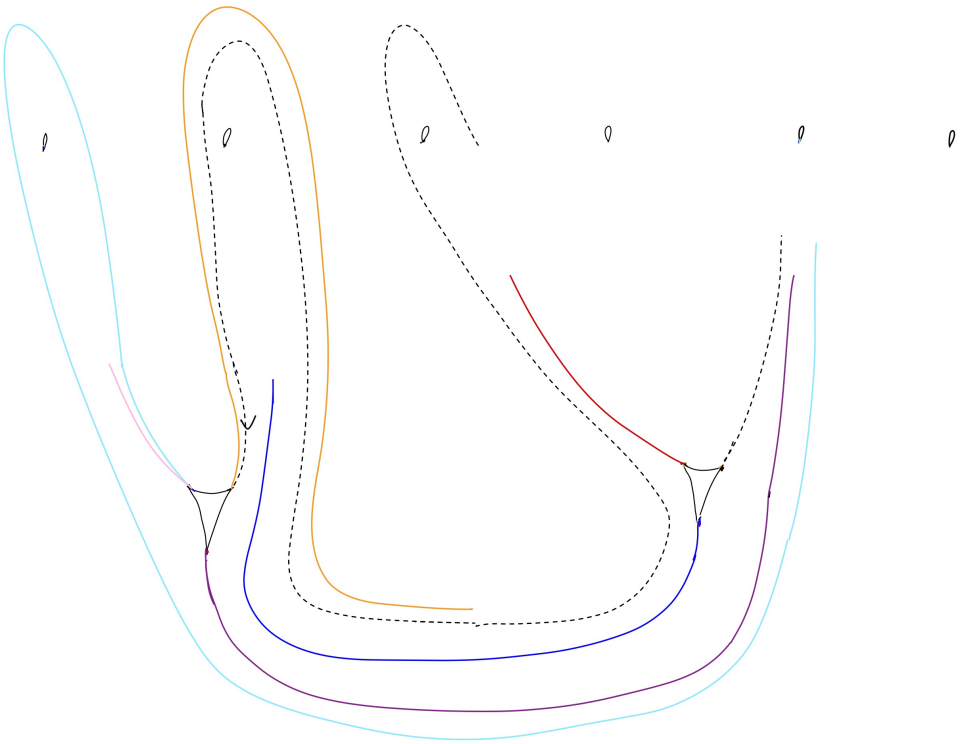


Figure G.38: WYS2

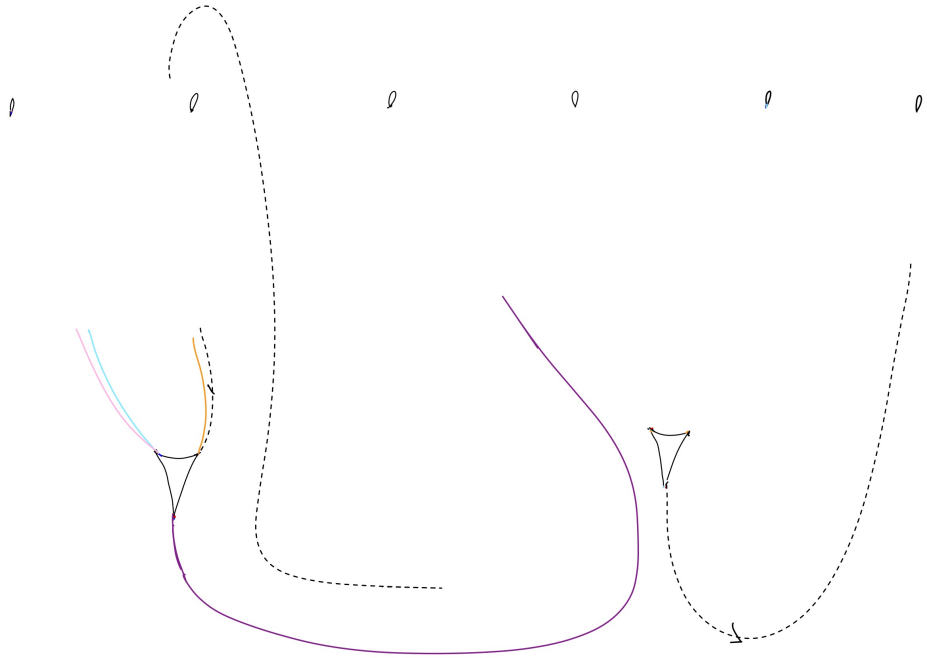


Figure G.39: HTI1

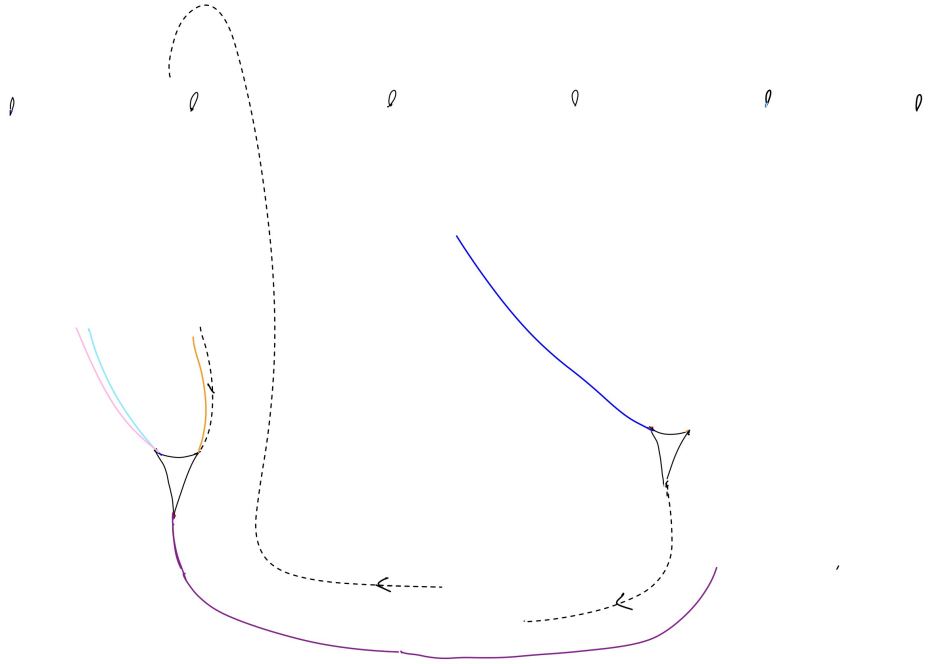


Figure G.40: SEZ1

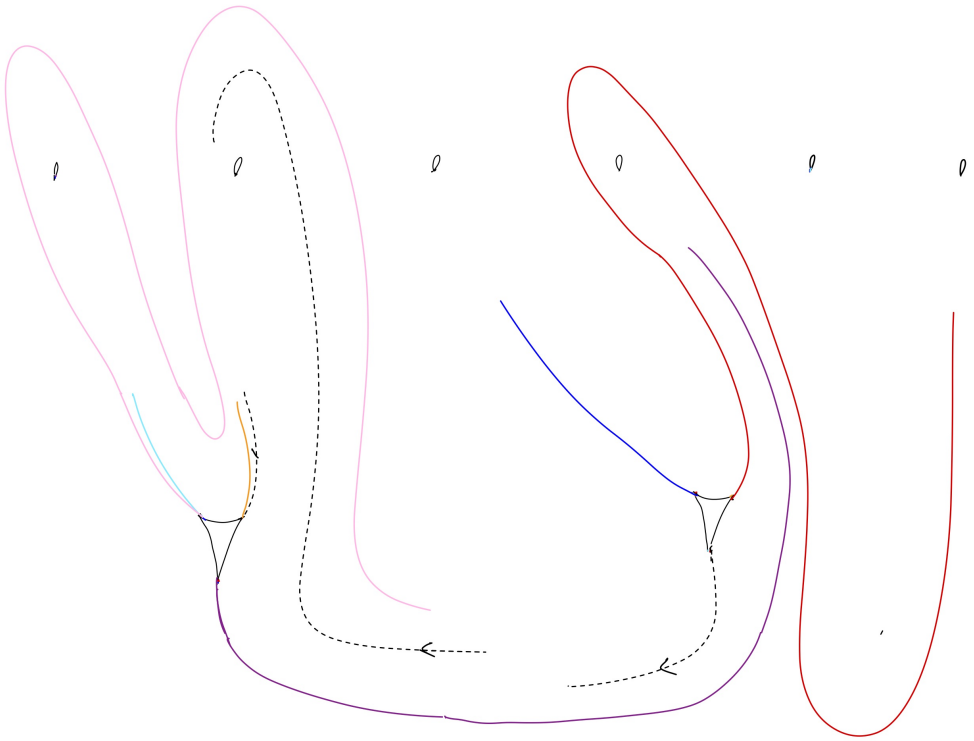


Figure G.41: SEZ2

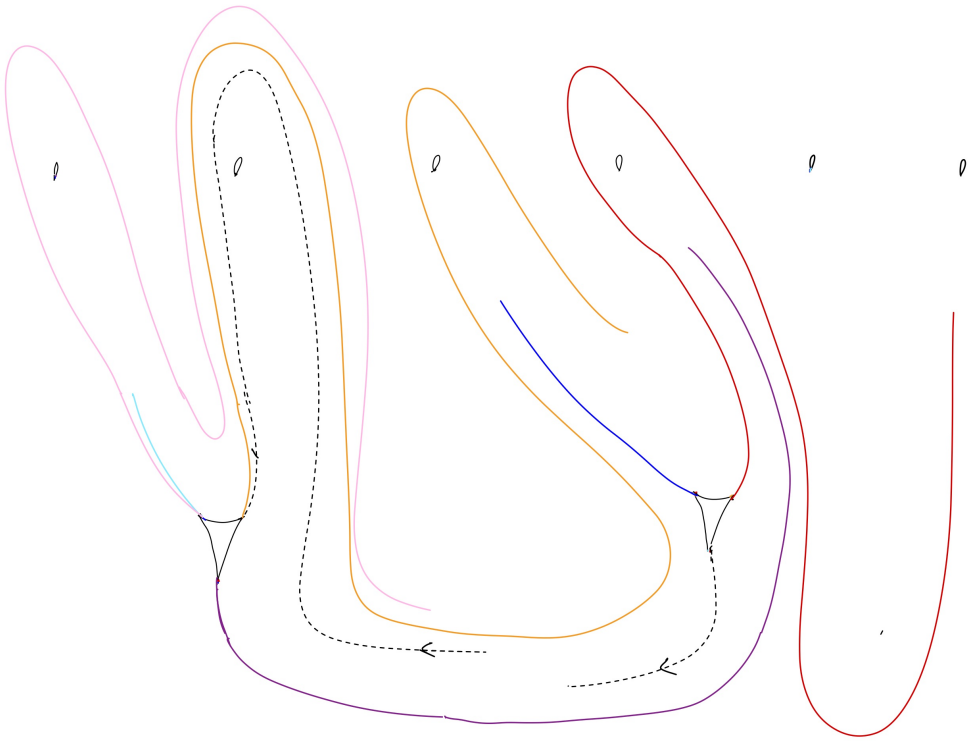


Figure G.42: SEZ3

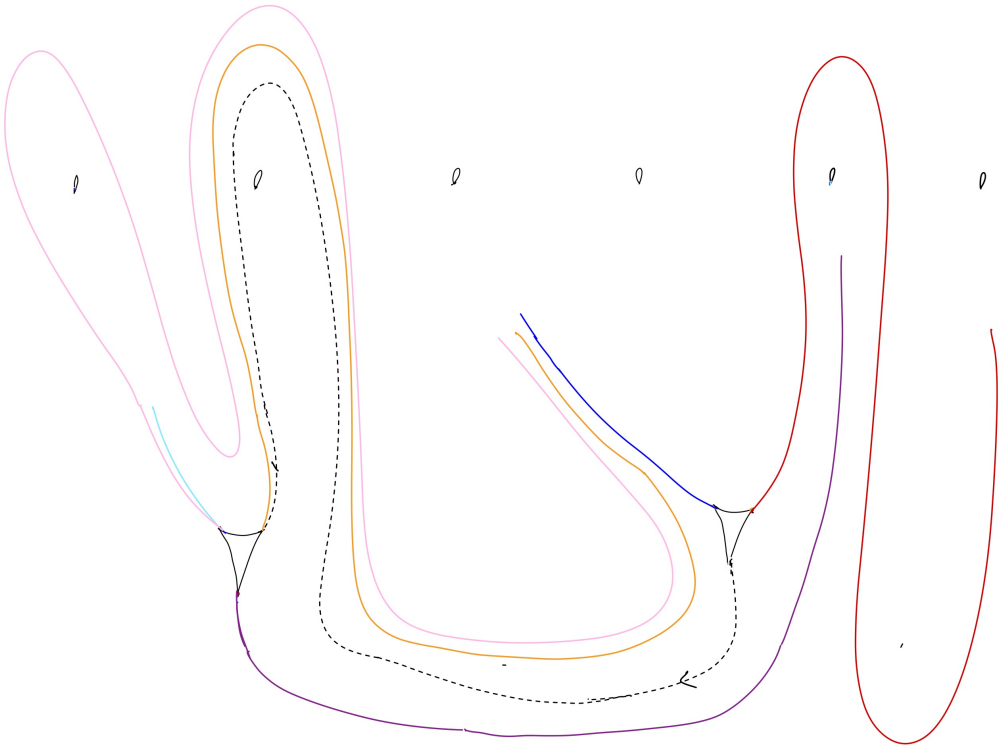


Figure G.43: SEZ4



Figure G.44: SEZ5

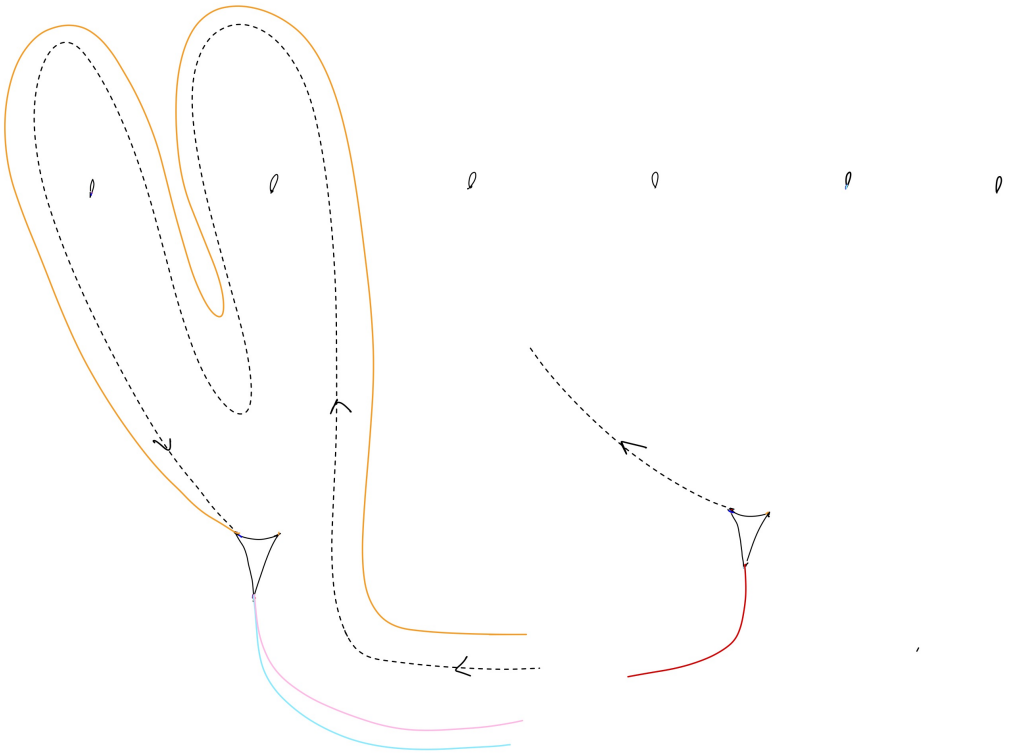


Figure G.45: PBH1

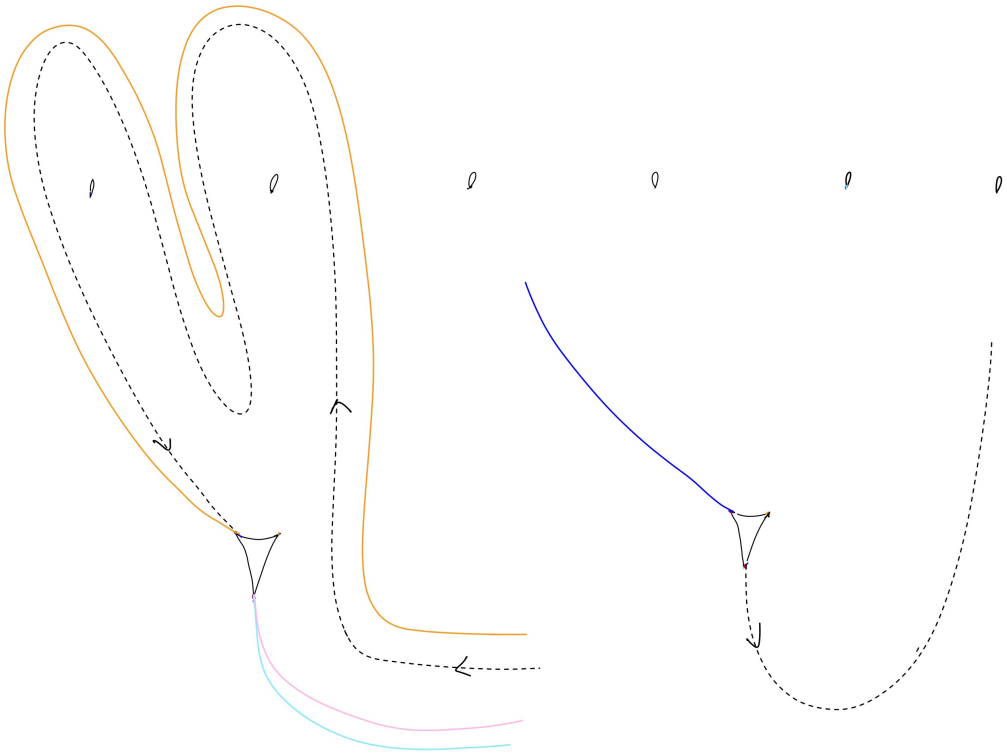


Figure G.46: TRK1

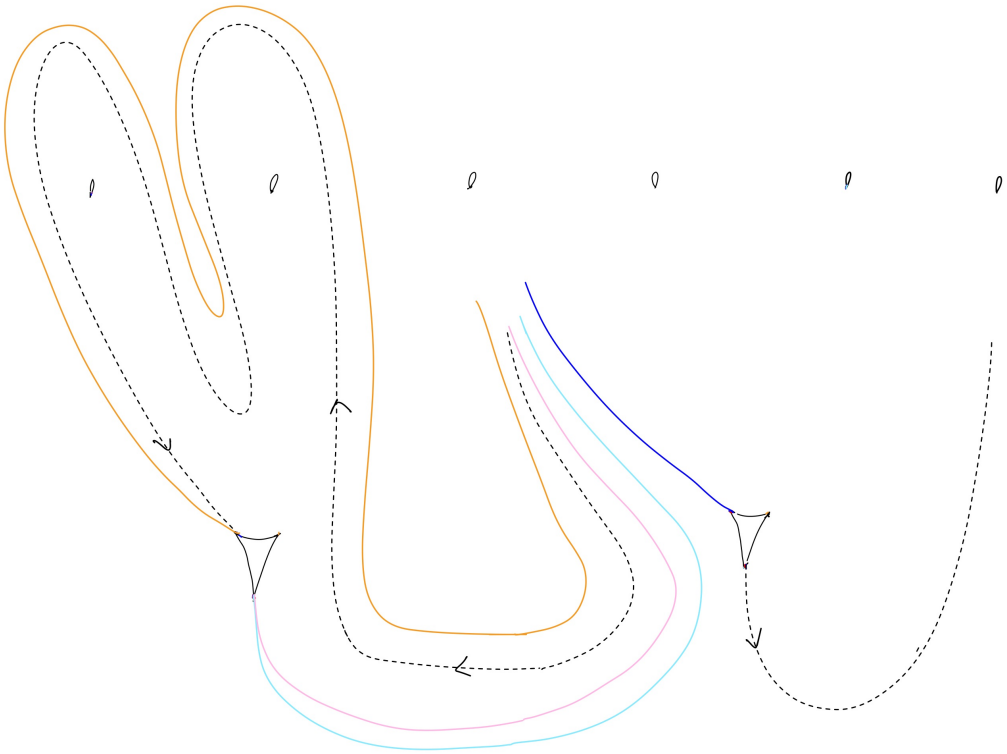


Figure G.47: TRK2

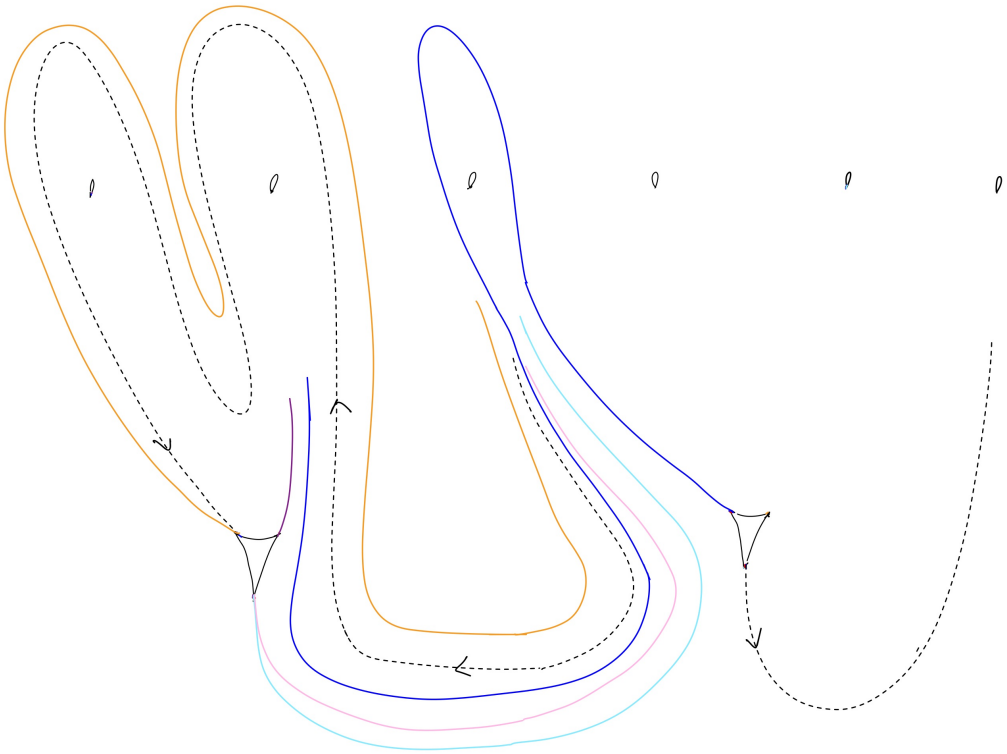


Figure G.48: TRK3

APPENDIX EIGHT

Train Track Case Analysis: Track 13

This is Track 13:

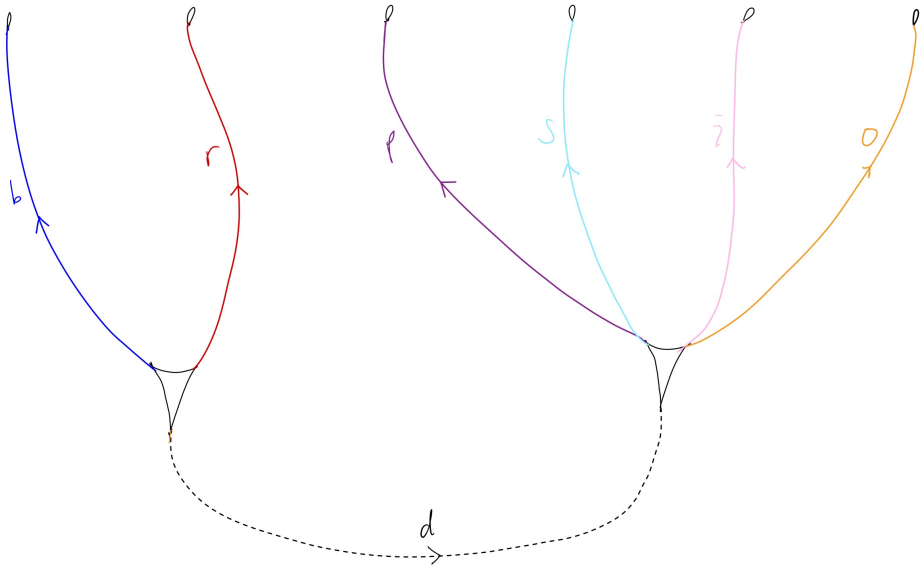


Figure H.1: Track 13

H.1 Case A: Triangles Fixed

Let us assume the triangles are fixed. Hence, both $f_\beta(d)$ and $f_\beta(\bar{d})$ both pass over $d/\bar{d}$ after an even number of letters. We shall call this *Assumption A*. Then $f_\beta(\bar{d})$ can begin with o, i, s, or p; and $f_\beta(d)$ can begin with r or b.

H.1.1 RNT

Suppose that $f_\beta(\bar{d})$ began with o^*. Then it must be o^+:

$$f_\beta(o) = o^+...$$

Then $f_\beta(d)$ can begin with r^+ or b^-.

Suppose also that $f_\beta(d)$ began with r^*. Then it must be r^+, and then b^+:

$$f_\beta(d) = r^+b^+d...$$

This is Figure H.2.

Here the next letter is either p^* or s^*, and there might then be twists with i before going p^+/s^+ right before crossing $\bar{d}$. Suppose it were the former case. Then in fact there cannot be such initial twists as this would force $f_\beta(i)$ to trace.

Thus we must have the situation depicted in Figure H.3.

Here the dotted lines cannot join. Otherwise, $f_\beta(p)$ will trace:

$$f_\beta(p) = \bar{d}b^-r^-dp^\times$$

This is also true in general if $f_\beta(p)$ were to go below $f_\beta(d)$.

On the other hand, if $f_\beta(p)$ were to go above $f_\beta(b)$, then either $f_\beta(p)$ or $f_\beta(s)$ will trace, as shown in Figure H.4.

Thus, the only possibility is for $f_\beta(p)$ and $f_\beta(s)$ to go in between $f_\beta(b)$ and $f_\beta(d)$.

This is Figure H.5.

Here $f_\beta(\bar{d})$ cannot go in between $f_\beta(b)$ and $f_\beta(s)$ or it will be in Situation β. Thus it must be above to give Figure H.6. But now the dotted lines are in Situation α.

This is a contradiction.

Going back to the situation depicted in Figure H.2. Suppose $f_\beta(\bar{d})$ goes down at s before crossing $\bar{d}$. Then again in factr it cannot have any twists with i or $f_\beta(i)$ will trace.

This gives us Figure H.7.

Here the situation is similar to the previous scenario. If $f_\beta(p)$ were to go below $f_\beta(d)$ then $f_\beta(s)$ will trace, as shown in Figure H.8. If $f_\beta(p)$ were to go above $f_\beta(b)$ then again $f_\beta(s)$ traces, as shown in Figure H.9. Thus we must have the situation depicted in Figure H.10, where the dotted lines again are in Situation α.

This is a contradiction.

Back to the beginning of RNT H.1.1. Suppose $f_\beta(d)$ were to begin with b^-:

$$f_\beta(d) = b^- r^- d...$$

This is Figure H.11.

By the same reasoning as before, $f_\beta(\bar{d})$ can either traverse:

$$f_\beta(\bar{d}) = o^+ p^+ \bar{d}...$$

or

$$f_\beta(\bar{d}) = o^+ s^+ \bar{d}...$$

H.1.1.1 Bort

Suppose it were the former case:

$$f_\beta(\bar{d}) = o^+ p^+ \bar{d} ...$$

This is Figure H.12.

Here, by the same reasoning as before, $f_\beta(p)$ and $f_\beta(s)$ can only go in between $f_\beta(d)$ and $f_\beta(r)$, giving us Figure H.13.

Consider $f_\beta(\bar{d})$. If it went below $f_\beta(d)$, then it would be in Situation β. If it went above $f_\beta(d)$, then it would violate the Trace Lemma after crossing d to the right-hand side due to the position of $f_\beta(r)$. Thus the dotted lines must join. On the other hand, $f_\beta(s)$ must continue with r^+ and to the left of $f_\beta(b)$ or else $f_\beta(b)$ will trace immediately after crossing d; and $f_\beta(p)$ must continue with r^+ and to the left of $f_\beta(b)$ as well, or else $f_\beta(b)$ will be absorbed between $f_\beta(s)$ and $f_\beta(p)$.

Thus we have Figure H.14.

Here $f_\beta(s)$ must continue with b^+ and to the left of $f_\beta(b)$. Otherwise, $f_\beta(p)$ would be forced to continue with b^- and to the right of $f_\beta(s)$, and then trace

$$f_\beta(p) = r^+ \hat{b}^- r^- d p^\times$$

Thus we have

$$f_\beta(s) = \bar{d} r^+ \hat{b}^+ r^* ...$$

which forces $f_\beta(b)$ to trace:

$$f_\beta(b) = r^+ b^\times$$

This is a contradiction.

H.1.1.2 Cess

Back to the end of RNT H.1.1. Suppose

$$f_\beta(\bar{d}) = o^+ s^+ \bar{d} ...$$

This is Figure H.15.

Again for the same reasoning as before, $f_\beta(s)$ and $f_\beta(p)$ must go in between $f_\beta(d)$ and $f_\beta(r)$. But now $f_\beta(r)$ will trace:

$$f_\beta(r) = \bar{d} o^+ s^+ \bar{d} r^\times$$

as shown in Figure H.16.

H.1.2 PWK

Back to the end of Case A H.1. Suppose $f_\beta(\bar{d})$ began with i, in which case it must be i^+ as to not violate Assumption A; and suppose $f_\beta(d)$ began with r.

Thus we have the situation depicted in Figure H.17.

Here $f_\beta(\bar{d})$ can either continue with $p^+ \bar{d}$ or $s^+ \bar{d}$.

H.1.2.1 Dowl

Suppose

$$f_\beta(\bar{d}) = i^+ p^+ \bar{d} ...$$

This is Figure H.18.

Here $f_\beta(b)$ cannot go above $f_\beta(\bar{d})$ as it would trace:

$$f_\beta(b) = \bar{d}p^- i^- \bar{d}b^\times$$

So either $f_\beta(b)$ goes in between $f_\beta(\bar{d})$ and $f_\beta(s)$, or it goes below $f_\beta(p)$. If it were the latter, then $f_\beta(d)$ continues:

$$f_\beta(d) = r^+ b^+ di^+ ...$$

here the next letter cannot be s^*, as then it would violate the Trace Lemma. So we have

$$f_\beta(d) = r^+ b^+ di^+ p^+ \bar{d} ...$$

This is Figure H.19.

Here the dotted lines are in Situation α.

So suppose it were the former case, that $f_\beta(b)$ went below $f_\beta(p)$. But then again we have

$$f_\beta(d) = r^+ b^+ di^+ p^+ \bar{d} ...$$

and now this forces $f_\beta(b)$ to trace, as shown in Figure H.20.

This is a contradiction.

H.1.2.2 Fubs

Back to the end of PWK H.1.2. Suppose $f_\beta(\bar{d})$ continued with $s^+\bar{d}$:

$$f_\beta(\bar{d}) = i^+ s^+ \bar{d} ...$$

This is Figure H.21.

Here if $f_\beta(d)$ went below $f_\beta(p)$, then it would cause the dotted lines to be in Situation α, as shown in Figure H.22.

If instead the dotted lines join here, then the following is forced for $f_\beta(b)$:

$$f_\beta(b) = dp^*...$$

as the alternative would cause it to trace:

$$f_\beta(b) = ds^- i^- \bar{d} b^\times$$

But now $f_\beta(p)$ will trace:

$$f_\beta(p) = \bar{d} b^- r^- p^\times$$

as shown in Figure H.22.

This is the same for the case where $f_\beta(d)$ went above $f_\beta(\bar{d})$, as shown in Figure H.23.

This is a contradiction.

H.1.3 BAF

Back to the end of Case A H.1. Suppose $f_\beta(\bar{d})$ began with i, in which case it must be i^+ as to not violate Assumption A; and suppose $f_\beta(d)$ began with b^-.

Thus we have the situation depicted in Figure H.24.

Here again $f_\beta(\bar{d})$ can contiue with

$$f_\beta(\bar{d}) = i^+ p^+ \bar{d}...$$

or

$$f_\beta(\bar{d}) = i^+ s^+ \bar{d} ...$$

H.1.3.1 Grig

Suppose

$$f_\beta(\bar{d}) = i^+ p^+ \bar{d} ...$$

This is Figure H.25.

Here $f_\beta(s)$ and $f_\beta(p)$ cannot go under $f_\beta(r)$. Otherwise, $f_\beta(p)$ will trace:

$$f_\beta(p) \bar{d} b^- r^- d p^\times$$

On the hand, if $f_\beta(p)$ and $f_\beta(s)$ went above $f_\beta(d)$, then we have

$$f_\beta(d) = b^- r^- d i^+ p^+ ...$$

and now the dotted lines are in Situation α, as shown in Figure H.26.

Thus $f_\beta(s)$ and $f_\beta(p)$ must go in between $f_\beta(s)$ and $f_\beta(p)$:

$$f_\beta(p) = \bar{d} r^* ...$$

and

$$f_\beta(s) \bar{d} r^* ...$$

This is Figure H.27.

Here $f_\beta(r)$ must end at o°. Otherwise it would trace:

$$f_\beta(r) = d\hat{o}^+ \bar{d} r^\times$$

or

$$f_\beta(r) = do^- \bar{d} b^- r^\times$$

Here the dotted lines must join. Otherwise, if $f_\beta(d)$ went below $f_\beta(\bar{d})$ then $f_\beta(d)$ immediately enters Situation β. If $f_\beta(d)$ went above $f_\beta(\bar{d})$, then $f_\beta(\bar{d})$ immediately enters Situation β.

This gives us the situation depicted in Figure H.28.

Here $f_\beta(b)$ can begin and end with r°, or begin and continue with b^-.

H.1.3.1.1 Chirk

Suppose

$$f_\beta(b) = r^\circ$$

Then we have Figure H.29.

Here $f_\beta(s)$ and $f_\beta(o)$ must continue with b^+ and to the left of $f_\beta(p)$. Otherwise, $f_\beta(p)$ would be forced to continue with b^-, as it either traces:

$$f_\beta(p) = \bar{d} r^+ \hat{b}^- dp^\times$$

or is absorbed:

$$f_\beta(p) = \bar{d} r^+ \hat{b}^- d \,\mathrm{Abso}(f_\beta(s), f_\beta(p))^\times$$

Then $f_\beta(o)$ continues:

$$f_\beta(o) = p^+ \bar{d} r^+ \hat{b}^+ r^- di^+ s^* ...$$

and $f_\beta(s)$ continues:

$$f_\beta(s) = p^+ \bar{d}r^+ \hat{b}^+ r^- di^+ p^+ \bar{d}r^+ b^+ do^+ \bar{d}r^+ b^- r^- dp^- i^* ...$$

This is Figure H.30.

Here $f_\beta(i)$ must begin and end at p°. Otherwise, it would trace:

$$f_\beta(i) = p^+ \bar{d}r^+ b^+ r^- di^\times$$

Now consider $f_\beta(p)$. It must end at b°. Otherwise, it would be absorbed:

$$f_\beta(p) = ...b^- r^- dp^- \,\mathrm{Abso}(f_\beta(i), f_\beta(o))^\times$$

or trace:

$$f_\beta(p) = ...b^+ r^- di^+ p^\times$$

Now consider $f_\beta(o)$ and $f_\beta(s)$. They both must end. Indeed, otherwise $f_\beta(s)$ will trace:

$$f_\beta(s) = ...i^- r^+ \bar{d}r^+ b^+ r^- di^+ s^\times$$

or be absorbed:

$$f_\beta(s) = ...i^- r^+ \bar{d}r^+ b^+ r^- do^- \bar{d}r^- dp^- i^- \bar{d}r^+ b^- r^- dp^- \,\mathrm{Abso}(f_\beta(i), f_\beta(o))^\times$$

or

$$f_\beta(s) = ...i^+ p^+ \bar{d}r^+ b^+ r^- do^- \bar{d}b^- r^- dp^- i^- \bar{d}r^+ b^- r^- d\,\mathrm{Abso}(f_\beta(s), f_\beta(p))^\times$$

As soon as $f_\beta(s)$ ends, if $f_\beta(o)$ did not also end, it would be absorbed:

$$f_\beta(o) = ...s^+i^-\bar{d}r^+b^-r^-dp^- \operatorname{Abso}(f_\beta(i), f_\beta(o))^\times$$

or trace:

$$f_\beta(o) = ...s^-\bar{d}r^+b^-r^-dp^-i^+p^+\bar{d}r^+b^+r^-do^\times$$

Thus we have Figure H.31, which is Candidate 1.

H.1.3.1.2 Dwalm

Back to the end of Grig H.1.3.1. Suppose Suppose

$$f_\beta(b) = r^-d...$$

This is Figure H.32.

Here $f_\beta(b)$ can go into 1, 2, or 3.

H.1.3.1.2.1 Bocage

Suppose $f_\beta(b)$ went into 1. Then it continues:

$$f_\beta(b) = r^-di^+s^*...$$

This is Figure H.33.

Here $f_\beta(s)$ and $f_\beta(o)$ both must continue with $b^=$ and to the left of $f_\beta(p)$. Otherwise, $f_\beta(p)$ would be forced to continue with b^- and be absorbed:

$$f_\beta(p) = \bar{d}r^+\hat{b}^-d \operatorname{Abso}(f_\beta(s), f_\beta(p))^\times$$

or trace:

$$f_\beta(p) = \bar{d}r^+\hat{b} - dp^\times$$

Then $f_\beta(o)$ continues:

$$f_\beta(o) = p^+\bar{d}r^+\hat{b}^+r^-di^+s^*...$$

and $f_\beta(s)$ continues:

$$f_\beta(s) = \bar{d}r^+\hat{b}^+r^-di^+p^+\bar{d}r^+b^+do^+\bar{d}r^*...$$

This is Figure H.34. Here it is clear that $f_\beta(p)$ and $f_\beta(i)$ must end immediately, otherwise they would trace.

Consider $f_\beta(s)$. If it continued with r^+, it would be absorbed:

$$f_\beta(s) = ...r^+do^-\bar{d}b^-r^-dp^-i^-\bar{d}r^+b^-r^-d\,\mathrm{Abso}(f_\beta(s), f_\beta(p))^\times$$

While it it continued with r^- it would trace:

$$f_\beta(s) = ...r^-di^+s^\times$$

Thus it must end here.

This is Figure H.35.

Here if $f_\beta(o)$ continued with s° or s^+, forcing $f_\beta(b)$ to continue with s^+, then $f_\beta(b)$ would trace:

$$f_\beta(b) = ...s^+i^-\bar{d}r^+b^\times$$

This means $f_\beta(o)$ must continue with s^- and to the right of $f_\beta(b)$. But then it would also

trace:

$$f_\beta(o) = ...s^- \bar{d} r^+ do^\times$$

This is a contradiction.

H.1.3.1.2.2 Cagmag

Back to the end of H.1.3.1.2. Suppose $f_\beta(b)$ went into 2:

$$f_\beta(b) = r^- dp^* ...$$

Then this immediately forces:

$$f_\beta(p) = p^+ \bar{d} r^+ b^* ...$$

This is Figure H.36.

Here $f_\beta(o)$ must continue with b^+ and to the left of $f_\beta(i)$. Otherwise, $f_\beta(i)$ would continue with b^- and trace:

$$f_\beta(i) = ...b^- r^- dp^- i^\times$$

Thus we have

$$f_\beta(o) = p^+ dr^+ b^+ r^- dp^* ...$$

This is Figure H.37.

Here $f_\beta(s)$ cannot continue with r° or r^-, as that would force $f_\beta(p)$ to continue with r^- and then immediately trace after crossing d. So suppose $f_\beta(s)$ continued with r^+ and to the left of $f_\beta(p)$. Then it continues:

$$f_\beta(s) = \bar{d} r^+ d...$$

This is Figure H.38.

Here $f_\beta(s)$ can either continue with o^- or i^+. Suppose it were the former:

$$f_\beta(s) = ...o^- \bar{d}b^- r^- dp^- i^- \bar{d}r^* ...$$

This is Figure H.39.

Here $f_\beta(o)$ cannot continue with p° or p^+ as that would force $f_\beta(b)$ to continue with p^+, and thus trace:

$$f_\beta(b) = r^- d\hat{p}^+ \bar{d}r^+ b^* ...$$

However, if $f_\beta(o)$ continued with p^- and to the right of $f_\beta(b)$, then it also traces:

$$f_\beta(o) = ...p^- \bar{d}r^+ do^\times$$

So suoopose it were the latter case, that $f_\beta(s)$ continued with i^+:

$$f_\beta(s) = ...i^+ p^+ \bar{d}r^+ b^+ do^+ \bar{d}r^* ...$$

Here $f_\beta(p)$ it is clear must end at r° or it will trace. So this forces the next lette for $f_\beta(s)$ to be r^-:

$$f_\beta(s) = ...i^+ p^+ \bar{d}r^+ b^+ do^+ \bar{d}\hat{r}^- dp^* ...$$

This is the situation depicted in Figure H.40. Here $f_\beta(o)$ must continue with p^-. Otherwise, it would force $f_\beta(b)$ to continue with p^+ and immediately trace after crossing $\bar{d}$. Now if $f_\beta(o)$

went in between $f_\beta(b)$ and $f_\beta(s)$ then it would trace:

$$f_\beta(o) = ...p^- \bar{d}r^+ do^\times$$

So it must go in between $f_\beta(s)$ and $f_\beta(i)$.

This is Figure H.41.

Here $f_\beta(i)$ must end. Indeed, otherwise it trace:

$$f_\beta(i) = ...b^+ r^- dp^- \bar{d}r^+ di^\times$$

or

$$f_\beta(i) = ...b^+ r^- dp^- \bar{d}r^+ do^- \bar{d}b^- r^- dp^- i^\times$$

or it it absorbed:

$$f_\beta(i) = ...b^- r^- dp^- \,\mathrm{Abso}(f_\beta(i), f_\beta(s))^\times$$

Thus we have Figure H.42.

Here we claim that $f_\beta(b)$ must end at p°. Indeed, otherwise we either have

$$f_\beta(b) = r^- d\hat{p}^+ \bar{d}r^+ b^\times$$

or it continues with p^+, which is the sitation depicted in Figure H.43. But here $f_\beta(o)$, $f_\beta(b)$, and $f_\beta(s)$ are stuck in a three-way clockwise path mill between s and p. This is a contradiction.

Thus we must have

$$f_\beta(b) = r^- dp^\circ$$

This is Figure H.44.

Here we claim that both $f_\beta(s)$ and $f_\beta(o)$ must end here. Indeed, consider $f_\beta(s)$. If it did not end here, then

$$f_\beta(s) = ...i^+p^+\bar{d}r^+b^+r^-dp^-\bar{d}r^+do^-\bar{d}b^-r^-dp^-i^-\bar{d}r^-d\,\mathrm{Abso}(f_\beta(s), f_\beta(p))^\times$$

or

$$f_\beta(s) = ...i^-p^+\bar{d}r^+b^+r^-dp^+\bar{d}r^+b^-r^-dp^-\,\mathrm{Abso}(f_\beta(i), f_\beta(o))^\times$$

Thus $f_\beta(s)$ must end at i°. This then also force $f_\beta(o)$ to end at s°, otherwise it would eventually trace.

This is Figure H.45, which is Candidate 2.

H.1.3.1.2.3 Boofus

Back to the end of H.1.3.1.2. Suppose $f_\beta(b)$ went into 3:

$$f_\beta(b) = r^-dp^*...$$

This is Figure H.46.

Here $f_\beta(o)$ must continue with r^+ and to the left of $f_\beta(p)$. Otherwise, $f_\beta(p)$ would immediately trace after crossing d. The same is true for $f_\beta(s)$. The two continue to give the situation depicted in Figure H.47.

Here we claim that $f_\beta(p)$ must end at r°. Indeed, otherwise it would trace:

$$f_\beta(p) = \bar{d}\hat{r}^+dp^\times$$

or absorbed:

$$f_\beta(p) = \bar{d}\hat{r}^- d\,\mathrm{Abso}(f_\beta(s), f_\beta(p))^\times$$

Thus

$$f_\beta(p) = \bar{d}r^\circ$$

now consider $f_\beta(i)$. It must end immediately atp°. Otherwise, it would trace:

$$f_\beta(i) = p^+\bar{d}r^+di^\times$$

This is Figure H.48.

Here $f_\beta(s)$ must continue with i^+ and to the left of $f_\beta(b)$. Otherwise, $f_\beta(b)$ would continue with i^- and to the right of $f_\beta(s)$. In which case, we could have the situation depicted in Figure H.49.

Here $f_\beta(s)$ must end or it will eventually trace. Whereas if $f_\beta(o)$ continued with s° or s^+, then $f_\beta(b)$ would eventually be absorbed between $f_\beta(i)$ and $f_\beta(o)$; but if $f_\beta(o)$ continued with s^-, then it would eventually trace.

Thus we must have the situation depicted in Figure H.50, where $f_\beta(s)$ continued with i^+ and $f_\beta(b)$ must end or it will eventually trace. Here $f_\beta(o)$ must end as well or it will eventually trace; and the same is true for $f_\beta(s)$. This gives Candidate 3, shown in Figure H.51.

H.1.3.2 Harl

Back to the end of BAF H.1.3. Suppose

$$f_\beta(\bar{d}) = i^+s^+\bar{d}...$$

This is Figure H.52.

For the same reasoning as that in Grig H.1.3.1, $f_\beta(s)$ and $f_\beta(p)$ cannot go under $f_\beta(r)$.

On the other hand, if $f_\beta(p)$ and $f_\beta(s)$ went above $f_\beta(d)$, then we would similarly have the situation depicted in Figure H.53, where the dotted lines are in Situation α.

So the only possibility is for $f_\beta(s)$ and $f_\beta(p)$ to go in between $f_\beta(d)$ and $f_\beta(r)$.

This gives Figure H.54.

If if the dotted lines do not join, then at least one of the two ($f_\beta(d)$ or $f_\beta(\bar{d})$ will immediately be in Situation β). Thus the dotted lines must join.

Now $f_\beta(o)$ continues:

$$f_\beta(o) = s^+\bar{d}r^+b^+...$$

This is Figure H.55.

Here if $f_\beta(b)$ were to end at r°, then $f_\beta(o)$ is either absorbed:

$$f_\beta(o) = s^+\bar{d}r^+b^+\hat{r}^-d\,\mathrm{Abso}(f_\beta(s), f_\beta(p))^\times$$

or traces:

$$f_\beta(o) = s^+\bar{d}r^+b^+\hat{r}^-do^\times$$

or

$$f_\beta(o) = s^+\bar{d}r^+b^+\hat{r}^-di^+s^+\bar{d}r^+b^+do^\times$$

Thus we must have

$$f_\beta(b) = r^-d...$$

and in between itself and $f_\beta(p)$, otherwise it would be immediately absorbed between $f_\beta(p)$ and $f_\beta(s)$, as shown in Figure H.56. Here notice that regardless of whether the next letter is o^- or i^+, it would eventually trace. This is a contradiction.

H.1.4 SEN

Back to the end of Case A H.1. Suppose $f_\beta(\bar{d})$ began with s, in which case it must be s^- as to not violate Assumption A; and suppose $f_\beta(d)$ began with r^+.

Thus we have the situation depicted in Figure H.57.

Here we claim the dotted lines must join. Indeed, otherwise, either $f_\beta(d)$ or $f_\beta(\bar{d})$ immediately enter Situation β, or the dotted lines enter Situation α.

Now consider $f_\beta(p)$. It must begin with i^- so as to not cause $f_\beta(s)$ to immediately trace. Then it continues:

$$f_\beta(p) = i^-\bar{d}b^*...$$

where it must do so going below $f_\beta(b)$ in the middle, otherwise this forces $f_\beta(o)$ and $f_\beta(i)$ to continue with $...r^+b^+d...$ and thereby causing at least one of them to trace. For the same reason, $f_\beta(b)$ must go above $f_\beta(o)$ and $f_\beta(i)$. This gives us the situation depicted in Figure H.58.

Here $f_\beta(i)$ can continue with b° or b^-.

H.1.4.1 Marl

Suppose it were the former case:

$$f_\beta(i) = \bar{d}\hat{b}^\circ$$

This is Figure H.59.

Here $f_\beta(p)$ cannot continue in between $f_\beta(i)$ and $f_\beta(o)$, or it would be absorbed:

$$f_\beta(p) = i^- \bar{\hat{d}} \bar{b} d \, \mathrm{Abso}(f_\beta(o), f_\beta(i))^\times$$

So suppose it went in between $f_\beta(r)$ and $f_\beta(o)$. Then it continues:

$$f_\beta(p) = i^- \bar{\hat{d}} \bar{b} d s^- i^- \bar{d} b^- r^- p^\times$$

as shown in Figure H.60.

So suppose it went in between $f_\beta(d)$ and $f_\beta(r)$. Then $f_\beta(r)$ and $f_\beta(o)$ continue with $...di^*...$, forcing

$$f_\beta(s) = i^- \bar{d} b^- r^* ...$$

as shown in Figure H.61.

Here $f_\beta(p)$ must continue with r^+ and to the left of $f_\beta(s)$. Otherwise, $f_\beta(s)$ would trace after crossing d. This gives Figure H.62.

Here if $f_\beta(r)$ continued with i° or i^+ then $f_\beta(p)$ would either be absorbed between $f_\beta(o)$ and $f_\beta(i)$, or it would escape to the outer perimeter and eventually trace. But if $f_\beta(r)$ continued instead with r^-, it would trace itself:

$$f_\beta(r) = ...i^- \bar{d} b^- r^\times$$

This is a contradiction.

H.1.4.2 Peen

Back to the end of SEN H.1.4. Suppose $f_\beta(i)$ continued with b^-.

This is Figure H.63.

Here $f_\beta(i)$ can either go into 1 or 2. Note that it cannot go in between $f_\beta(i)$ and $f_\beta(o)$ or it would be immediately absorbed. Note also that $f_\beta(p)$ can only continue with r^* otherwise it would escapte to the outer perimeter and eventually trace.

H.1.4.2.1 Howff

Suppose $f_\beta(i)$ went into 1. Then it continues:

$$f_\beta(i) = \bar{d}b^- dp^* ...$$

and $f_\beta(r)$ continues:

$$f_\beta(r) = b^+ di^* ...$$

which forces

$$f_\beta(s) = i^- \bar{d}b^- r^* ...$$

and

$$f_\beta(p) = i^- \bar{d}b^- r^* ...$$

This is Figure H.64.

Here $f_\beta(i)$ must continue with p^+ and to the left of $f_\beta(b)$. Otherwise, $f_\beta(b)$ would immediately trace after crossing $\bar{d}$. This is Figure H.65.

Here both $f_\beta(b)$ and $f_\beta(r)$ must end. Otherwise, both would eventually trace.

This is Figure H.66.

Now if $f_\beta(p)$ continued with r° or r^+, then $f_\beta(s)$ would continue with r^+ and trace:

$$f_\beta(s) = ...r^+b^+di^+s^\times$$

But then if $f_\beta(p)$ continued with r^-, it would trace:

$$f_\beta(p) = ...r^-b^+di^+\bar{d}b^-dp^\times$$

This is a contradiction.

H.1.4.2.2 Jasey

Back to the end of Peen H.1.4.2. Suppose $f_\beta(i)$ went into 2.

This gives Figure H.67.

Here $f_\beta(r)$ can either end immediately at b°, or continue with b^+.

H.1.4.2.2.1 Gimmer

Suppose

$$f_\beta(r) = b^\circ$$

This gives Figure H.68.

Here $f_\beta(i)$ can either end at r° or continue with r^-. Suppose it were the former. Then $f_\beta(p)$ will continue with r^- and in between $f_\beta(o)$ and $f_\beta(d)$ (going in tween $f_\beta(i)$ and $f_\beta(o)$ would cause it to be absorbed). Then it continues and traces:

$$f_\beta(p) = ...r^-b^+ds^-i^-\bar{d}b^-r^-dp^\times$$

as shown in Figure H.69.

So suppose it were the latter, that $f_\beta(i)$ continued with r^-, as shown in Figure H.70. But here the behavior of $f_\beta(p)$ is identical to the former case. This is a contradiction.

H.1.4.2.2.2 Hantle

Back to the end of Jasey H.1.4.2.2. Suppose $f_\beta(r)$ continued with b^+.

This is shown in Figure H.71.

Here notice that $f_\beta(r)$ will escape to the outer perimeter and eventually trace.

This is a contradiction.

H.1.5 HUN

Back to the end of Case A H.1. Suppose $f_\beta(\bar{d})$ began with s, in which case it must be s^- as to not violate Assumption A; and suppose $f_\beta(d)$ began with b^-.

Thus we have the situation depicted in Figure H.72.

Here if the dotted lines were to join, then $f_\beta(i)$ or $f_\beta(o)$ will eventually trace. For the same reason, the only alternative is for $f_\beta(d)$ to go above $f_\beta(o)$ and $f_\beta(i)$. But now we will have Situation α, as depicted in Figure H.73.

This is a contradiction.

H.2 Case B,C,D: Triangles Swapped

Now suppose the triangles are swapped. Then at least one of $f_\beta(d)$ and $f_\beta(\bar{d})$ must go over an odd number of letters before crossing. We first assume this to be the case for $f_\beta(d)$, that is, $f_\beta(d)$ crosses an odd number of letters before crossing $\bar{d}$.

Then $f_\beta(d)$ can begin with o, i, s, or p; and $f_\beta(\bar{d})$ can begin with r, b, or d.

H.2.1 GUW

Suppose $f_\beta(d)$ began with o, and $f_\beta(\bar{d})$ began with r. We remind the reader that we are assuming $f_\beta(d)$ must go over an odd number of letters before crossing. This assumption necessitates that eventually $f_\beta(d)$ must traverse o^- right before crossing $\bar{d}$.

Now $f_\beta(b)$ must begin with

$$f_\beta(b) = \bar{d}r^*...$$

which forces

$$f_\beta(p) = do^*...$$

and

$$f_\beta(s) = do^*...$$

This is Figure H.74.

Here notice that $f_\beta(d)$ cannot have any initial twists before traversing $o^-\bar{d}...$, as that would cause either $f_\beta(p)$ or $f_\beta(s)$ to trace.

Thus we must have Figure H.75.

Here both dotted lines must continue with r^- otherwise $f_\beta(b)$ would immediately trace. But now the dotted lines are in Situation α, as shown in Figure H.76.

This is a contradiction.

H.2.2 CPX

Back to the end of Case B,C,D H.2. Suppose $f_\beta(d)$ began with o, and $f_\beta(\bar{d})$ began with r. We remind the reader that we are assuming $f_\beta(d)$ must go over an odd number of letters before crossing. This assumption necessitates that eventually $f_\beta(d)$ must traverse o^- right before crossing $\bar{d}$.

Again we must have

$$f_\beta(b) = \bar{d}r^*...$$

which forces $f_\beta(o)$ to trace:

$$f_\beta(o) = do^\times$$

as shown in Figure H.77.

H.2.3 SCC

Back to the end of Case B,C,D H.2. Suppose $f_\beta(d)$ began with o, and $f_\beta(\bar{d})$ began with d. We remind the reader that we are assuming $f_\beta(d)$ must go over an odd number of letters before crossing. This assumption necessitates that eventually $f_\beta(d)$ must traverse o^- right before crossing $\bar{d}$.

We have the situation depicted in Figure H.78.

Now $f_\beta(o)$ and $f_\beta(s)$ must continue with r^- and to the right of $f_\beta(b)$. Otherwise $f_\beta(b)$ would immediately trace.

Here the dotted lines must join. Otherwise, either $f_\beta(d)$ went below $f_\beta(\bar{d})$, which would put $f_\beta(\bar{d})$ in Situation β; or $f_\beta(d)$ went above $f_\beta(\bar{d})$, which would put $f_\beta(d)$ in Situation β. Thus they must join.

This is Figure H.79.

Here $f_\beta(r)$ can begin with p°, s°, p^-, or s^-.

Suppose $f_\beta(r)$ began with p°. Then $f_\beta(s)$ would trace, as shown in Figure H.80.

Suppose $f_\beta(r)$ began with s°. This is Figure H.81.

Here $f_\beta(b)$ must continue with r^- or $f_\beta(s)$ would trace immediately after crossing d.

This is Figure H.82.

Here $f_\beta(i)$ can either end at p° or continue with p^+ or p^-.

Suppose it ended here with p°:

$$f_\beta(i) = r^- dp^\circ$$

Then this is Figure H.83. Here $f_\beta(o)$ must continue with i^- and to the right of $f_\beta(b)$. Otherwise, $f_\beta(b)$ would be absrobed:

$$f_\beta(b) = ...i^+ s^+ \bar{d} r^+ \,\text{Abso}(f_\beta(i), f_\beta(o))^\times$$

This gives us Figure H.84.

Here if $f_\beta(s)$ were to continue with r° or r^+, then $f_\beta(o)$ would continue with r^+ and then trace:

$$f_\beta(o) = ...r^+ ds^- o^\times$$

But if $f_\beta(s)$ continued with r^- and to the right of $f_\beta(o)$, then it would also trace:

$$f_\beta(s) = ...r^- ds^\times$$

This is a contradiction.

So suppose in the situation depicted in Figure H.84, $f_\beta(i)$ continued with p^+. Then it continues:

$$f_\beta(i) = ...p^+\bar{d}r^+b^+do^+s^+\bar{d}...$$

This is Figure H.85. Here if $f_\beta(i)$ went above $f_\beta(o)$ then $f_\beta(o)$ would trace. The same is true if $f_\beta(i)$ went be tween $f_\beta(o)$ and $f_\beta(b)$. Thus $f_\beta(i)$ can only go below $f_\beta(b)$. This gives Figure H.86.

Here $f_\beta(o)$ must continue with i^- and to the right of $f_\beta(b)$. Otherwise, $f_\beta(b)$ would be absorbed:

$$f_\beta(b) = ...i^+s^+\bar{d}r^+ \,\mathrm{Abso}(f_\beta(i), f_\beta(o))^\times$$

Thus $f_\beta(o)$ continues:

$$f_\beta(o) = ...i^-d^+\bar{d}r^*...$$

as shown in Figure H.87.

Here $f_\beta(o)$ cannot continue with r^+, or it will trace after crossing d. Thus $f_\beta(s)$ and $f_\beta(i)$ need to continue with r^- and to the right of $f_\beta(o)$. But then $f_\beta(s)$ traces:

$$f_\beta(s) = ...r^-ds^\times$$

So suppose in the situation depicted in Figure H.84, $f_\beta(i)$ continued with p^-, as in Figure H.88. Again here it must go below $f_\beta(o)$ to not be absorbed eventually between itself and $f_\beta(o)$

Then it continues:

$$f_\beta(i) = ...p^- \bar{d} r^+ do^* ...$$

This is Figure H.89.

Here notice that $f_\beta(s)$ must end immediately at r°. Otherwise, it would immediately trace after crossing d. Now we claim that all of $f_\beta(b)$, $f_\beta(i)$, $f_\beta(o)$, and $f_\beta(p)$ must end immediately.

Suppose by contradiction that $f_\beta(b)$ did not end. Then suppose it continued with i^-, then it will trace:

$$f_\beta(b) = ...i^- p^+ \bar{d} r^+ ds^- o^- \bar{d} b^\times$$

as shown in Figure H.90.

So suppose it continued with i^+, then it continues:

$$f_\beta(b) = ...i^+ s^+ \bar{d} r^+ do^* ...$$

This is Figure H.91.

Here if $f_\beta(b)$ continued with o° or o^+, then $f_\beta(i)$ continues with o^+ and to the left of $f_\beta(b)$. But then it will trace:

$$f_\beta(i) = ...o^+ \bar{d} r^- ds^- i^\times$$

But then if $f_\beta(b)$ continued with o^- and to the right of $f_\beta(o)$, then it continues to give the situation depicted in Figure H.92.

Here if $f_\beta(b)$ continued with p^+ then it will immediately be absorbed right after crossing $\bar{d}$. But then this means $f_\beta(o)$ must continue with p^- and to the right of $f_\beta(b)$, in which case it

would trace:

$$f_\beta(o) = p^- \bar{d} r^+ d o^\times$$

This establishes that $f_\beta(b)$ must end at i°. This is Figure H.93.

Here let us suppose by contradiction that $f_\beta(i)$ did not end. Then suppose it continued with o^+:

$$f_\beta(i) = ...o^+ \bar{d} r^- dp^+ \bar{d} r^+ b^+ do^+ s^+ \bar{d} r^+ ds^- o^- \bar{d} b^* ...$$

This is Figure H.94.

But here $f_\beta(p)$ is forced to begin with b^+, and trace:

$$f_\beta(p) = b^+ do^+ s^+ \bar{d} r^- ds^- o^- \bar{d} b^- r^- dp^\times$$

This is a contradiction. So suppose instead $f_\beta(i)$ continued with o^-:

$$f_\beta(i) = ...o^- \bar{d} r^- dp^* ...$$

This is Figure H.95.

Here if $f_\beta(o)$ continued with p° or p^+, then fbi would continue with p^+ and to the left of $f_\beta(o)$, but then it would immediately be absorbed after crossing $f_\beta(\bar{d})$. But hen if $f_\beta(o)$ continued with p^- and to the right of $f_\beta(i)$, then it would trace immediately after crossing d.

This establishes that $f_\beta(i)$ must end at o°.

This is Figure H.96.

Now suppose by contradiction that $f_\beta(o)$ did not end. Then it could only continue with p^-:

$$f_\beta(o) = ...p^- \bar{d}r^+ do^+ \bar{d}r^- ds^- i^- s^+ \bar{d}r^+ ds^- o^- \bar{d}b^*...$$

This is Figure H.97.

Here this forces $f_\beta(p)$ to begin with b^+, and thereby eventually trace, similar to a previous situation.

This establishes that $f_\beta(o)$ must end at p°.

This is Figure H.98.

Here if by contradiction fbp did not end at b°, then

$$f_\beta(p) = b^+ do^+ s^+ \bar{d}r^- ds^- i^- s^+ \bar{d}r^+ do^- \bar{d}r^- dp^\times$$

Thus we must have

$$f_\beta(p) = b^\circ$$

This establishes Candidate 4, shown in Figure H.99.

Now back to the Situation depicted in Figure H.79. Suppose $f_\beta(r)$ began with p^-:

$$f_\beta(r) = p^-...$$

But this forces $f_\beta(i)$ to trace, as shown in Figure H.100.

So suppose $f_\beta(r)$ began with s^-:

$$f_\beta(r) = s^-...$$

Then $f_\beta(d)$ cannot have any initial twists. On the other hand, $f_\beta(i)$ must continue with p^*...:

$$f_\beta(i) = r^- dp^* ...$$

Here $f_\beta(s)$ cannot continue with b^+ or it would trace after crossing:

$$f_\beta(s) = b^+ do^+ s^\times$$

This means that $f_\beta(p)$ must begin with b^- and to the right of $f_\beta(s)$, but then it will trace:

$$\bar{d}_\beta(p) = b^- r^- dp^\times$$

This is shown in Figure H.101.

H.2.4 LKE

Back to the end of Case B,C,D H.2. Suppose $f_\beta(d)$ began with i, and $f_\beta(\bar{d})$ began with r. We remind the reader that we are assuming $f_\beta(d)$ must go over an odd number of letters before crossing. This assumption necessitates that eventually $f_\beta(d)$ must traverse i^- right before crossing $\bar{d}$.

We have the situation depicted in Figure H.102.

Here the dotted lines must join. Otherwise, either $f_\beta(d)$ or $f_\beta(\bar{d})$ would immediately enter Situation β.

This is Figure H.103.

Here $f_\beta(r)$ cannot begin with p° or p^-, as in that case $f_\beta(o)$ or $f_\beta(s)$ would immediately trace after crossing and after p^-. On the other hand, $f_\beta(r)$ also cannot begin with p^+ or s^+

as then it would immediately trace after crossing $\bar{d}$.

So it can only begin with s° or s^{-}.

Suppose it were the former. Then this forces $f_{\beta}(d)$ to not have any initial twists. Also, $f_{\beta}(i)$ must continue with p^{*}, otherwise it would trace. This then forces $f_{\beta}(s)$ to traverse:

$$f_{\beta}(s) = b^{+}do^{*}...$$

otherwise $f_{\beta}(p)$ would begin with b^{-}, and immediately trace after crossing.

This is Figure H.104.

Here $f_{\beta}(o)$ can either continue with p^{*}, or with s^{-}. Suppose it were the former. Then it cannot continue with p^{+}, or it would trace:

$$f_{\beta}(o) = ...p^{+}\bar{d}r^{+}b^{+}do^{\times}$$

This means $f_{\beta}(i)$ must continue with p^{-} and to the right of $f_{\beta}(o)$, and continue:

$$f_{\beta}(i) = r^{-}p^{-}\bar{d}r^{*}...$$

This is Figure H.105.

Here $f_{\beta}(b)$, $f_{\beta}(o)$, and $f_{\beta}(i)$ are stuck in a three-way clockwise path mill between r and p.

So suppose $f_{\beta}(o)$ continued with s^{-}. Then it continues:

$$f_{\beta}(o) = r^{-}d\hat{s}^{-}i^{-}\bar{d}b^{*}...$$

forcing

$$f_\beta(p) = b^+ d...$$

This is Figure H.106.

Here if the next letter for $f_\beta(p)$ were o^*, then $f_\beta(s)$ must continue with o^+. Otherwise, $f_\beta(p)$ would continue with o^- and eventually trace. So we have

$$f_\beta(s) = b^+ d\hat{o}^+ \bar{d}b^*...$$

This is Figure H.107. Here $f_\beta(s)$, $f_\beta(o)$, and $f_\beta(p)$ are stuck in a three-way counterclockwise path mill between b and o.

So suppose the next letter for $f_\beta(p)$ were i, then it would be absorbed:

$$f_\beta(p) = b^+ d\hat{i}^+ s^+ \bar{d}r^+ \,\mathrm{Abso}(f_\beta(i), f_\beta(o))^\times$$

as shown in Figure H.108.

Going back to the situation depicted in Figure H.103. Suppose $f_\beta(r)$ began with s^-.

This is Figure H.109.

Here $f_\beta(d)$ may have initial twists with s before traversing $i^-\bar{d}$. On the other hand, $f_\beta(r)$ must necessarily continue:

$$f_\beta(r) = s^- i^- \bar{d}b^*...$$

and this is irregardless whether $f_\beta(d)$ has any initial twists.

Also, $f_\beta(s)$ must begin with b^+ and to the left of $f_\beta(p)$, otherwise $f_\beta(p)$ would trace

immediately after crossing d. So we have

$$f_\beta(s) = b^+ do^* ...$$

Now consider $f_\beta(p)$, the incoming $f_\beta(r)$ forces:

$$f_\beta(p) = b^+ d ...$$

We now have Figure H.110.

Here $f_\beta(p)$ can either continue with o^*, or i^+. Suppose it were the former. Then it forces $f_\beta(s)$ to continue with o^+ and to the left of $f_\beta(p)$. Otherwise, $f_\beta(p)$ would eventually trace. This gives us Figure H.111.

Here $f_\beta(s)$, $f_\beta(r)$, and $f_\beta(p)$ are stuck in a three-way counterclockwise path mill between b and o.

So suppose instead $f_\beta(p)$ continued with i^+:

$$f_\beta(p) = b^+ d\hat{i}^+ s^+ dr^* ...$$

This is Figure H.112.

Here suppose $f_\beta(p)$ continued with r° or r^-, forcing $f_\beta(b)$ to continue with r^-. This gives Figure H.115.

Here boyth $f_\beta(i)$ and $f_\beta(o)$ must continue with p^- and to the right of $f_\beta(b)$. Otherwise, $f_\beta(b)$ would continue with p^+ and then trace. This gives Figure H.114. Here $f_\beta(p)$, $f_\beta(i)$, $f_\beta(o)$, and $f_\beta(b)$ are stuck in a four-way clockwise path mill between r and p. This is a

contradiction.

So suppose instead that $f_\beta(p)$ continued with r^+ and to the left of $f_\beta(b)$.

This is Figure H.115.

Here $f_\beta(o)$ cannot continue with p^*, as that would then force either $f_\beta(o)$ or $f_\beta(i)$ to eventually trace, whichever possible continuation $f_\beta(i)$ and $f_\beta(o)$ were to take. So $f_\beta(o)$ must continue with s^-, but then it will trace, as shown in Figure H.116.

This is a contradiction.

H.2.5 YVQ

Back to the end of Case B,C,D H.2. Suppose $f_\beta(d)$ began with i, and $f_\beta(\bar{d})$ began with b. We remind the reader that we are assuming $f_\beta(d)$ must go over an odd number of letters before crossing. This assumption necessitates that eventually $f_\beta(d)$ must traverse i^- right before crossing $\bar{d}$.

We have the situation depicted in Figure H.117.

But now at either $f_\beta(o)$ or $f_\beta(i)$ will immediately trace after crossing d

This is a contradiction.

H.2.6 SOB

Back to the end of Case B,C,D H.2. Suppose $f_\beta(d)$ began with i, and $f_\beta(\bar{d})$ began with r. We remind the reader that we are assuming $f_\beta(d)$ must go over an odd number of letters before crossing. This assumption necessitates that eventually $f_\beta(d)$ must traverse i^- right before crossing $\bar{d}$.

We have the situation depicted in Figure H.118.

Here $f_\beta(d)$ must go below $f_\beta(s)$ and $f_\beta(p)$, or it will be in Situation β. So we have Figure H.119.

This then indicates that $f_\beta(d)$ cannot have initial twists, as that would cause either $f_\beta(p)$ or $f_\beta(s)$ to trace. So we have Figure H.120.

Here the dotted lines are in Situation α.

This is a contradiction.

H.2.7 BAM

Back to the end of Case B,C,D H.2. Suppose $f_\beta(d)$ began with s, and $f_\beta(\bar{d})$ began with r. We remind the reader that we are assuming $f_\beta(d)$ must go over an odd number of letters before crossing. This assumption necessitates that eventually $f_\beta(d)$ must traverse s^+ right before crossing $\bar{d}$.

Then we must have

$$f_\beta(r) = \bar{d}b^*...$$

We have the situation depicted in Figure H.121. Here it is clear that $f_\beta(p)$ will trace.

This is a contradiction.

H.2.8 PIZ

Back to the end of Case B,C,D H.2. Suppose $f_\beta(d)$ began with s, and $f_\beta(\bar{d})$ began with d. We remind the reader that we are assuming $f_\beta(d)$ must go over an odd number of letters before crossing. This assumption necessitates that eventually $f_\beta(d)$ must traverse s^+ right before crossing $\bar{d}$.

We have the situation depicted in Figure H.122.

Here the dotted lines must join. Otherwise, either $f_\beta(d)$ or $f_\beta(\bar{d})$ would immediately be in Situation β.

This gives Figure H.123.

Here $f_\beta(p)$ can continue with o°, o^-, o^+, or i^+. Whereas i° and i^- would cause $f_\beta(b)$ to begin with i^- and then trace immediately after crossing $\bar{d}$.

H.2.8.1 Nurl

Suppose $f_\beta(p)$ continued with o°:

$$f_\beta(p) = b^+ d o^\circ$$

Then $f_\beta(s)$ is forced to continue with o^+:

$$f_\beta(s) = b^+ d \hat{o}^+ b^* ...$$

This gives Figure H.124.

Here if $f_\beta(r)$ continued with b° or b^- then $f_\beta(s)$ will trace immediately after crossing d. But then if $f_\beta(r)$ continued with b^+ and to the left of $f_\beta(s)$, then it would be absorbed:

$$f_\beta(r) = \bar{d}\hat{\bar{b}}^+ d o^- \bar{d} b^- \operatorname{Abso}(f_\beta(p), f_\beta(s))^\times$$

This is a contradiction.

H.2.8.2 Oast

Back to the end of PIZ H.2.8. Suppose $f_\beta(p)$ continued with o^-:

$$f_\beta(p) = b^+ d o^- ...$$

Then it continues:

$$f_\beta(p) = b^+ d o^- \bar{d} \bar{b}^- ...$$

This is Figure H.125.

Here $f_\beta(p)$ and $f_\beta(i)$ must continue with r^- and to the right of $f_\beta(o)$. Otherwise, $f_\beta(o)$ would begin with r^+ and immediately trace after crossing d.

Then $f_\beta(p)$ continues with s^- after crossing, forcing $f_\beta(i)$ to do the same. But now $f_\beta(i)$ must trace, irregardless of whether $f_\beta(d)$ has any initial twists, as shown in Figure H.126.

This is a contradiction.

H.2.8.3 Pilf

Back to the end of PIZ H.2.8. Suppose $f_\beta(p)$ continued with o^+:

$$f_\beta(p) = b^+ d o^+ ...$$

This is Figure H.127.

Here $f_\beta(p)$ must continue with $\bar{d}$ and not s^*, otherwise $f_\beta(s)$ would trace. Thus we have Figure H.128.

Here similarly $f_\beta(s)$ must continue with $\bar{d}$ to give Figure H.129.

Here $f_\beta(r)$ must continue with b^+ and to the left of $f_\beta(p)$ and $f_\beta(s)$. Otherwise, $f_\beta(s)$ would trace immediately after crossing.

This is Figure H.130.

Here we claim that $f_\beta(p)$, $f_\beta(s)$, and $f_\beta(r)$ are stuck in a three-way counterclockwise path mill between b and o. Indeed, suppose instead that here $f_\beta(p)$ continued with b^- and threby escape to the outer perimeter. Then we note that $f_\beta(b)$ must begin with i^+ or i°, and so $f_\beta(p)$ continues:

$$f_\beta(p)b^- do^+ s^+ \bar{d} r^* ...$$

to give us Figure H.131. This is regardless whether $f_\beta(d)$ has any initial twists or not. Now here if $|fbo$ were to continue with p^*, then $f_\beta(i)$ will be forced to continue with p^- and to the right of the incoming $f_\beta(o)$, otherwise $|fbo$ will eventually trace. This is Figure H.132.

But here it is clear that $f_\beta(p)$, $f_\beta(i)$, and $f_\beta(o)$ are stuck in a clockwise three-way path mill between r and p.

So instead suppose $|fbo$ continued with $s^- =:$

$$f_\beta(o) = ...s^- i^- \bar{d} b^* ...$$

This is shown in Figure H.133.

Here it is clear that $f_\beta(s)$, $f_\beta(o)$,and $f_\beta(r)$ are stuck in a three-way counterclockwise path mill between b and o. Hence, it must not be possible for $f_\beta(p)$ to escape to the outer perimeter.

Hence the situation depicted in Figure H.130 is indeed a path mill, as it is clear that $f_\beta(s)$ could not escape to the outer perimeter or it will trace, and similarly for r; and we just

showed this as well for p.

This is a contradiction.

H.2.8.4 Risp

Back to the end of PIZ H.2.8. Suppose $f_\beta(p)$ continued with i^+:

$$f_\beta(p) = b^+ d^+ ...$$

This is Figure H.134.

Here $f_\beta(i)$ must continue with

$$f_\beta(i) = r^- dp^* ...$$

and the incoming $f_\beta(p)$ forces

$$f_\beta(o) = r^- d ...$$

as shown in Figure H.135.

Here $f_\beta(o)$ can continue with p^* or s^-. Suppose it were the former. Then this forces $f_\beta(i)$ to continue with p^- and to the right of the incoming $f_\beta(o)$. Otherwise $f_\beta(o)$ would be forced to continue with p^+ and eventually trace.

This is Figure H.136.

Here $f_\beta(p)$, $f_\beta(i)$, and $f_\beta(o)$ are struck in a three-way clockwise path mill between r and p.

So suppose instead $f_\beta(o)$ continued with s^-. But now it will be absorbed:

$$f_\beta(o) = r^- d\hat{s}^- i^- \bar{d}b^- \, \text{Abso}(f_\beta(p), f_\beta(s))^\times$$

as shown in Figure H.137.

This is a contradiction.

H.2.9 RUT

Back to the end of Case B,C,D H.2. Suppose $f_\beta(d)$ began with s, and $f_\beta(\bar{d})$ began with b. We remind the reader that we are assuming $f_\beta(d)$ must go over an odd number of letters before crossing. This assumption necessitates that eventually $f_\beta(d)$ must traverse s^+ right before crossing $\bar{d}$.

We have the situation depicted in Figure H.138.

Here $f_\beta(\bar{d})$ must begin with b^+ and to the left of $f_\beta(r)$. Otherwise $f_\beta(r)$ would immediately trace.

This is Figure H.139.

Here $f_\beta(d)$ must go above $f_\beta(o)$ and $f_\beta(i)$ or it will be in Situation β.

This is Figure H.140.

Here $f_\beta(d)$ must continue with r^+ and to the left of $f_\beta(p)$ and $f_\beta(s)$. Otherwise, $f_\beta(p)$ or $f_\beta(s)$ will trace immediately after crossing d.

This gives us Figure H.141.

Here we see that the dotted lines are in Situation α.

This is a contradiction.

H.2.10 ART

Back to the end of Case B,C,D H.2. Suppose $f_\beta(d)$ began with p, and $f_\beta(\bar{d})$ began with r. We remind the reader that we are assuming $f_\beta(d)$ must go over an odd number of letters before crossing. This assumption necessitates that eventually $f_\beta(d)$ must traverse p^+ right before crossing $\bar{d}$.

We have the situation depicted in Figure H.142.

Here $f_\beta(p)$ will trace immediately after crossing d.

This is a contradiction.

H.2.11 WOT

Back to the end of Case B,C,D H.2. Suppose $f_\beta(d)$ began with p, and $f_\beta(\bar{d})$ began with b. We remind the reader that we are assuming $f_\beta(d)$ must go over an odd number of letters before crossing. This assumption necessitates that eventually $f_\beta(d)$ must traverse p^+ right before crossing $\bar{d}$.

We have the situation depicted in Figure H.143.

Here $f_\beta(s)$ must begin with r^+ otherwise $f_\beta(p)$ would trace immediately after crossing d. Then $f_\beta(s)$ must continue with b^+ otherwise $f_\beta(r)$ would immediately trace. So we have

$$f_\beta(s) = r^+ b^+ d...$$

This is Figure H.144.

Here $f_\beta(d)$ must go above $f_\beta(o)$ and $f_\beta(i)$. Otherwise, it would immediately be in Situation

β. It then continues:L

$$f_\beta(\bar{d}) = ...\bar{d}r^+b^+d...$$

This is Figure H.145.

Now consider $f_\beta(\bar{d})$. It must begin with b^+ and to the left of $f_\beta(r)$. Otherwise, $f_\beta(r)$ would immediately trace. So we have

$$f_\beta(\bar{d}) = b^+d...$$

This is Figure H.146.

Here the dotted lines are in Situation α.

This is a contradiction.

H.2.12 ORE

Back to the end of Case B,C,D H.2. Suppose $f_\beta(d)$ began with p, and $f_\beta(\bar{d})$ began with d. We remind the reader that we are assuming $f_\beta(d)$ must go over an odd number of letters before crossing. This assumption necessitates that eventually $f_\beta(d)$ must traverse p^+ right before crossing $\bar{d}$.

We have the situation depicted in Figure H.147.

Here both $f_\beta(p)$ and $f_\beta(s)$ must begin with b^+ and to the left of the incoming $f_\beta(r)$. Otherwise, $f_\beta(r)$ would immediately trace.

This is Figure H.148.

Here the dotted lines must join. Otherwise, either $f_\beta(d)$ or $f_\beta(\bar{d})$ will immediately enter into Situation β.

So we have Figure H.149.

Here $f_\beta(p)$ can continue with o^* or i^*. Suppose it were the former case. Then $f_\beta(s)$ also continues with o^*. This means that $f_\beta(i)$ must begin with r^- and to the right of $f_\beta(o)$. Otherwise $f_\beta(o)$ would trace:

$$f_\beta(o) = r^+ b^+ d o^\times$$

So we must have

$$f_\beta(i) = r^- d p^- o^* ...$$

as shown in Figure H.150.

Here $f_\beta(b)$ is forced to begin with o^*, as shown in Figure H.151.

Now if $f_\beta(b)$ continued with o° or o^+ then $f_\beta(p)$ or $f_\beta(s)$ would continue with o^+ and one of them will immediately trace. But if $f_\beta(b)$ instead continued with o^- it would immediately trace after crossing $\bar{d}$.

So suppose instead $f_\beta(p)$ continued with i^*, then it must in fact be i^+, otherwise $f_\beta(b)$ would begin with i^- and then trace immediately after crossing $\bar{d}$. Then it must continue with s^* to not trace:

$$f_\beta(p) = b^+ d i^+ s^* ...$$

This forces $f_\beta(s)$ to continue with o^* to not trace:

$$f_\beta(s) = b^+ d o^* ...$$

Now consider $f_\beta(i)$. If it began with r° or r^+ then it would force $f_\beta(o)$ to begin with r^+ and

then eventually trace due to the position of $f_\beta(s)$:

$$f_\beta(o) = r^+ b^+ d o^\times$$

Thus we must have

$$f_\beta(i) = r^- ...$$

but then it will trace:

$$f_\beta(i) = r^- d p^- i^\times$$

This is a contradiction.

This completes the case analysis for when we assume $f_\beta(d)$ must go over an odd number of letters before crossing.

We now assume triangle are swapped, and that $f_\beta(d)$ must go over an even number of letters before crossing, which necessitates that $f_\beta(\bar{d})$ must go over an odd number of letters before crossing.

The possible places to start for $f_\beta(d)$ are p, s, i, and o; while $f_\beta(\bar{d})$ can only start at b or r.

H.2.13 BTV

Back to the end of Case B,C,D H.2. Suppose $f_\beta(d)$ began with p, and $f_\beta(\bar{d})$ began with r. We assume $f_\beta(d)$ must go over an even number of letters before crossing, which necessitates that $f_\beta(\bar{d})$ must go over an odd number of letters before crossing.

We have the situation depicted in Figure H.152.

Here due to the assumption that $f_\beta(d)$ go over an even number of letters before crossing, it

must begin with p^-. But now it is clear that $f_\beta(p)$ will trace.

This is a contradiction.

H.2.14 AFN

Back to the end of Case B,C,D H.2. Suppose $f_\beta(d)$ began with p, and $f_\beta(\bar{d})$ began with b. We assume $f_\beta(d)$ must go over an even number of letters before crossing, which necessitates that $f_\beta(\bar{d})$ must go over an odd number of letters before crossing.

We have the situation depicted in Figure H.153.

Here due to the assumption that $f_\beta(d)$ go over an even number of letters before crossing, it must begin with p^-. But now it is clear that either $f_\beta(o)$ or $f_\beta(i)$ will trace.

This is a contradiction.

H.2.15 CSS

Back to the end of Case B,C,D H.2. Suppose $f_\beta(d)$ began with s, and $f_\beta(\bar{d})$ began with r. We assume $f_\beta(d)$ must go over an even number of letters before crossing, which necessitates that $f_\beta(\bar{d})$ must go over an odd number of letters before crossing.

We have the situation depicted in Figure H.154.

Here it is clear that wither $f_\beta(p)$ or $f_\beta(s)$ will immediately trace after crossing d.

This is a contradiction.

H.2.16 UUU

Back to the end of Case B,C,D H.2. Suppose $f_\beta(d)$ began with s, and $f_\beta(\bar{d})$ began with b. We assume $f_\beta(d)$ must go over an even number of letters before crossing, which necessitates

that $f_\beta(\bar{d})$ must go over an odd number of letters before crossing.

This is Figure H.155.

Here $f_\beta(s)$ must begin with r^+ and to the left of $f_\beta(p)$. Otherwise, $f_\beta(p)$ would force $f_\beta(o)$ and $f_\beta(i)$ to cross and then continue with s^-, and one of them will trace, as shown in Figure H.156.

Also, $f_\beta(\bar{d})$ must begin with b^+ and to the left of $f_\beta(r)$ or $f_\beta(r)$ will immediately trace. This gives us Figure H.157.

Here $f_\beta(\bar{d})$ can continue with o^* or i^*. Suppose it were the former, then it must continue with $o^+s^*...$, as to not violate the Trace Lemma. But then $f_\beta(s)$ will trace, as shown in Figure H.158.

So suppose instead $f_\beta(\bar{d})$ continued with i^+. This is Figure H.159.

Here if the dotted lines do not join, then it must do so with $f_\beta(\bar{d})$ to the right of $f_\beta(d)$, as to not put $f_\beta(\bar{d})$ in Situation β, as in Figure H.160. But now we see $f_\beta(\bar{d})$ still enters Situation β on the left hand side.

So the dotted lines must join, as shown in Figure H.161.

Now $f_\beta(o)$ can either continue with p^*, or s^-. Suppose it were the former,then $f_\beta(i)$ is forced to continue with p^- otherwise $f_\beta(o)$ would trace after crossing d. This gives Figure H.162. Here $f_\beta(r)$, $f_\beta(i)$, and $f_\beta(o)$ are stuck in a three-way clockwise path mill between b and p.

So suppose $f_\beta(o)$ continued with s^-. Then it continues:

$$f_\beta(o) = ds^-i^-\bar{d}b^-r^*...$$

forcing

$$f_\beta(p) = r^+ b^+ d...$$

as shown in Figure H.163.

Here $f_\beta(p)$ can continue with o or i^+. Suppose it were the former. Then this forces $f_\beta(s)$ to continue with o^+ and to the left of the incoming $f_\beta(p)$. Otherwise, $f_\beta(p)$ would continue with o^- and then trace:

$$f_\beta(p) = ...o^- \bar{d} b^- r^- dp^\times$$

So we have

$$f_\beta(s) = o^+ \bar{d} b^- r^* ...$$

This is Figure H.164.

Here if $f_\beta(s)$ were to continue with r° or r^+, then $f_\beta(o)$ would continue with r^+ and to the left of $f_\beta(s)$. In which case, it would trace:

$$f_\beta(o) = ...r^+ b^+ do^\times$$

However, if instead $f_\beta(s)$ continued with r^- and to the right of $f_\beta(o)$, then it would trace:

$$f_\beta(s) = r^- b^+ d i^+ s^\times$$

So suppose $f_\beta(p)$ continued with i^+:

$$f_\beta(p) = r^+ b^+ d\hat{i}^+ s^+ \,\mathrm{Abso}(f_\beta(i), f_\beta(o))^\times$$

as shown in Figure H.165.

This is a contradiction.

H.2.17 GTK

Back to the end of Case B,C,D H.2. Suppose $f_\beta(d)$ began with i, and $f_\beta(\bar{d})$ began with b. We assume $f_\beta(d)$ must go over an even number of letters before crossing, which necessitates that $f_\beta(\bar{d})$ must go over an odd number of letters before crossing.

This is Figure H.166..

But here $f_\beta(b)$ must continue with r° or r^- otherwise it would immediately trace. However, this means

$$f_\beta(p) = r^- d...$$

and

$$f_\beta(s) = r^- d...$$

and one of these will immediately trace.

This is a contradiction.

H.2.18 CGI

Back to the end of Case B,C,D H.2. Suppose $f_\beta(d)$ began with i, and $f_\beta(\bar{d})$ began with r. We assume $f_\beta(d)$ must go over an even number of letters before crossing, which necessitates that $f_\beta(\bar{d})$ must go over an odd number of letters before crossing.

This is Figure H.167.

Here $f_\beta(\bar{d})$ must begin with r^- and to the right of $f_\beta(b)$, otherwise $f_\beta(b)$ would immediately trace. This gives us Figure H.168.

Here $f_\beta(d)$ can continue with either $s^+\bar{d}...$, or $p^+\bar{d}...$ One can check that there are no other

possibilities without violating the assumption that it must go over an even number of letters before crossing.

But in both cases, this forces

$$f_\beta(o) = b^+ do^\times$$

as if it were to begin with b° or b^- then $f_\beta(i)$ would begin with b^- and then eventually trace.

This is shown in Figure H.169, and Figure H.170.

H.2.19 GLD

Back to the end of Case B,C,D H.2. Suppose $f_\beta(d)$ began with o, and $f_\beta(\bar{d})$ began with b. We assume $f_\beta(d)$ must go over an even number of letters before crossing, which necessitates that $f_\beta(\bar{d})$ must go over an odd number of letters before crossing.

This is Figure H.171.

But here it is immediately clear that $f_\beta(o)$ will trace.

H.2.20 UGN

Back to the end of Case B,C,D H.2. Suppose $f_\beta(d)$ began with o, and $f_\beta(\bar{d})$ began with r. We assume $f_\beta(d)$ must go over an even number of letters before crossing, which necessitates that $f_\beta(\bar{d})$ must go over an odd number of letters before crossing.

This is Figure H.172.

Here we must have

$$f_\beta(p) = do^+ ...$$

and

$$f_{\beta}(s) = do^{+}...$$

But now one of them will immediately trace.

This concludes the case analyses for Track 13.

H.3 Figures

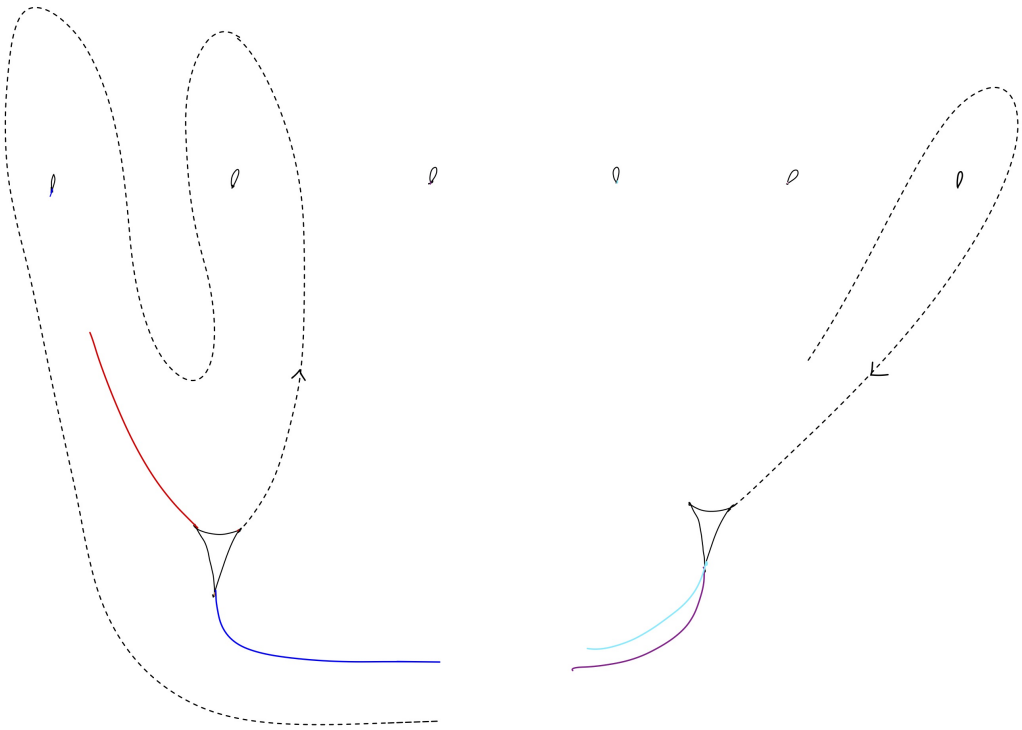


Figure H.2: RNT1

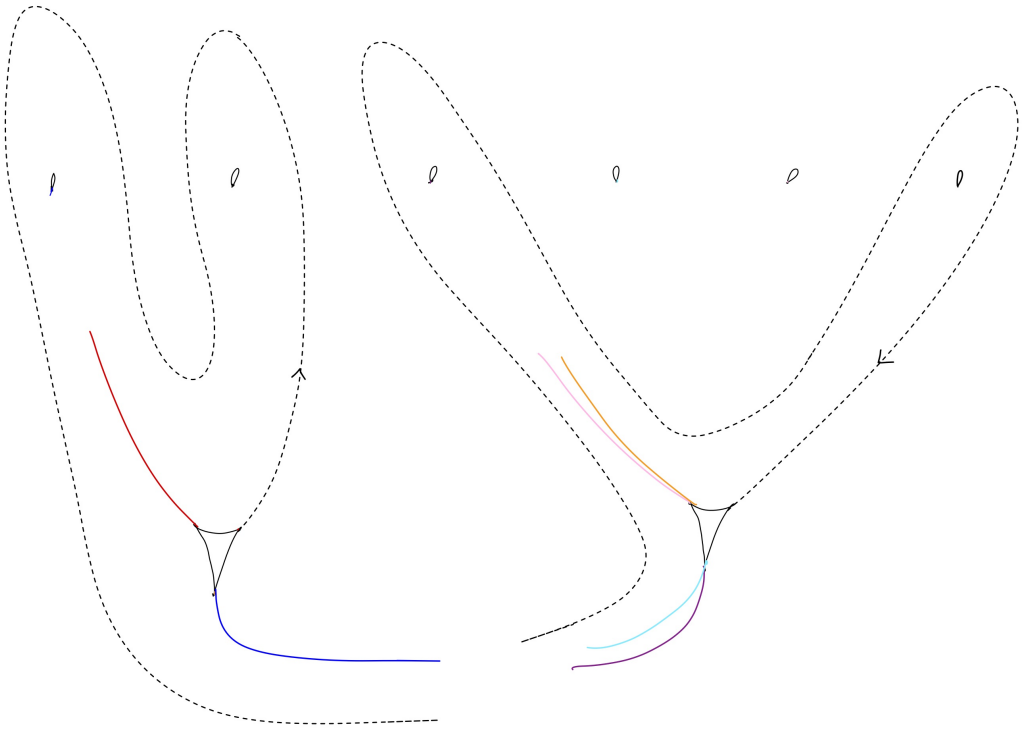


Figure H.3: RNT2

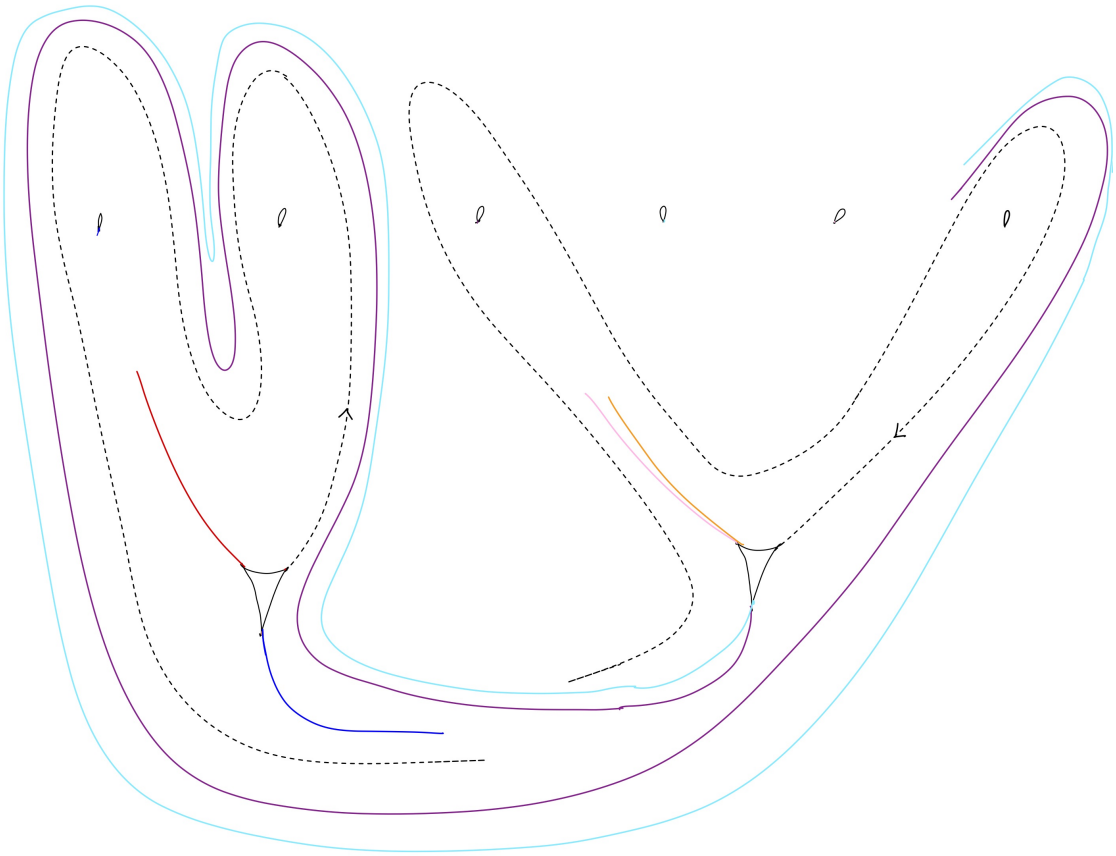


Figure H.4: RNT3

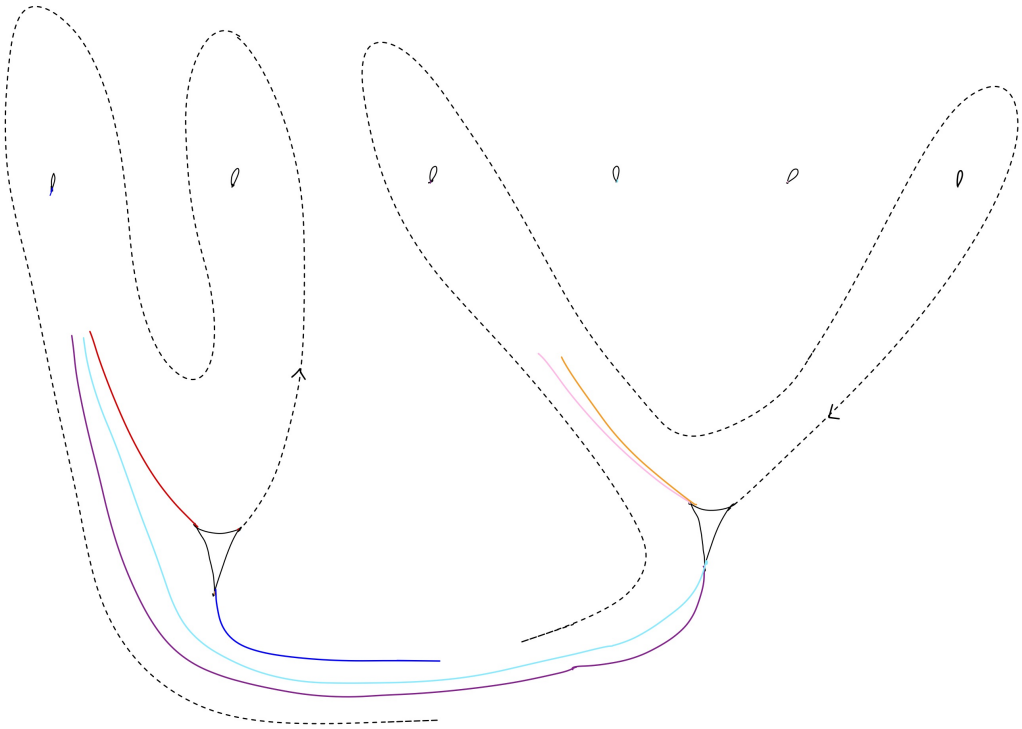


Figure H.5: RNT4

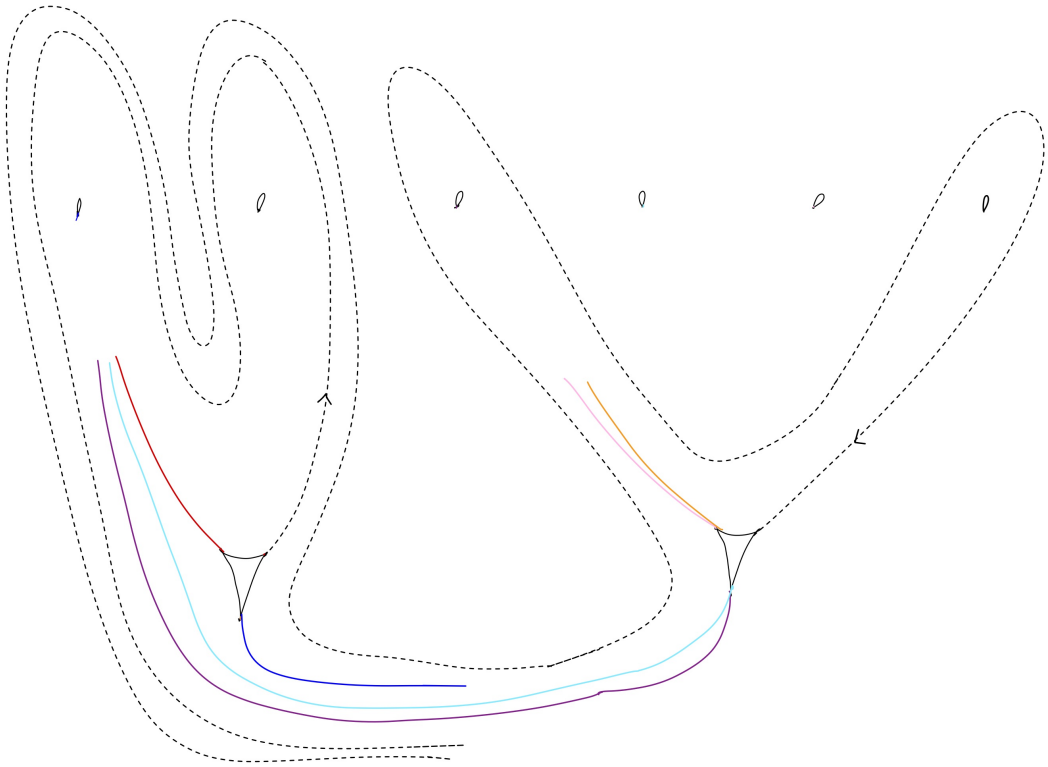


Figure H.6: RNT5

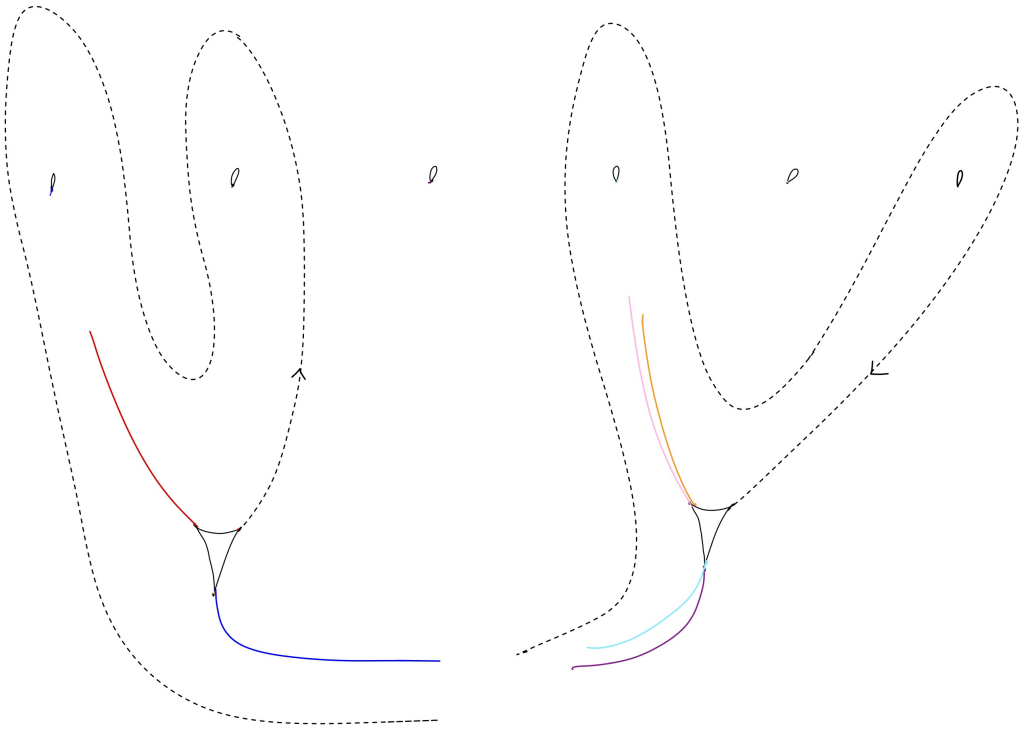


Figure H.7: RNT6

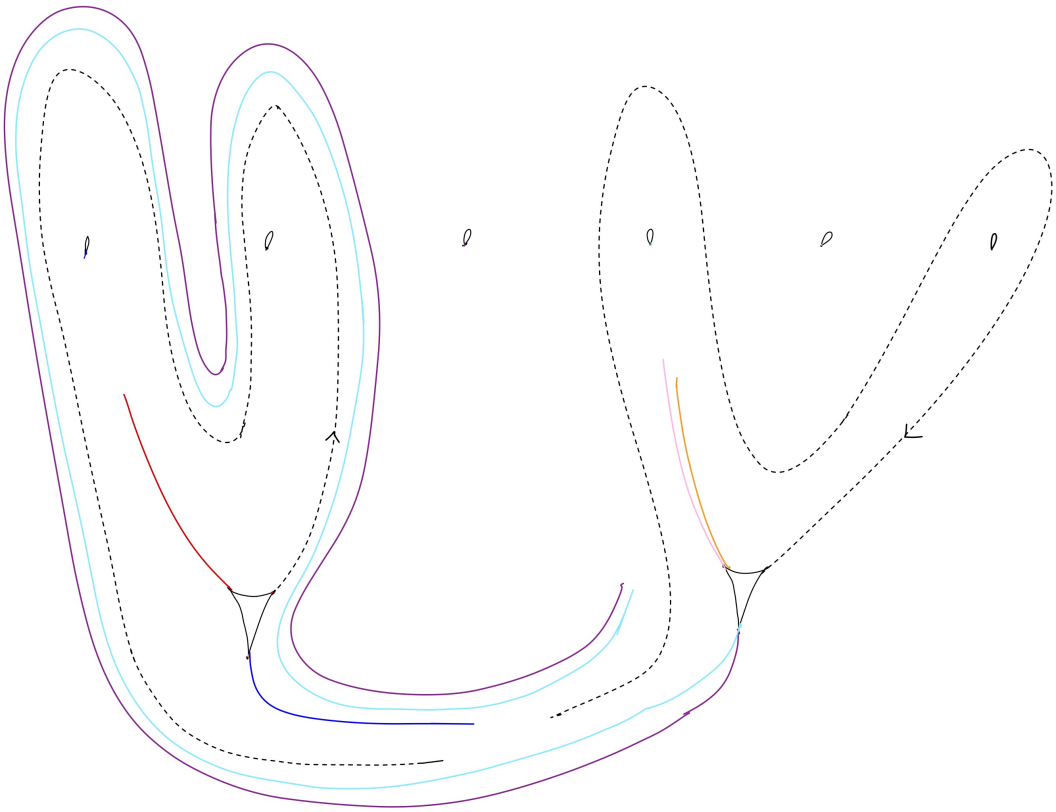


Figure H.8: RNT7

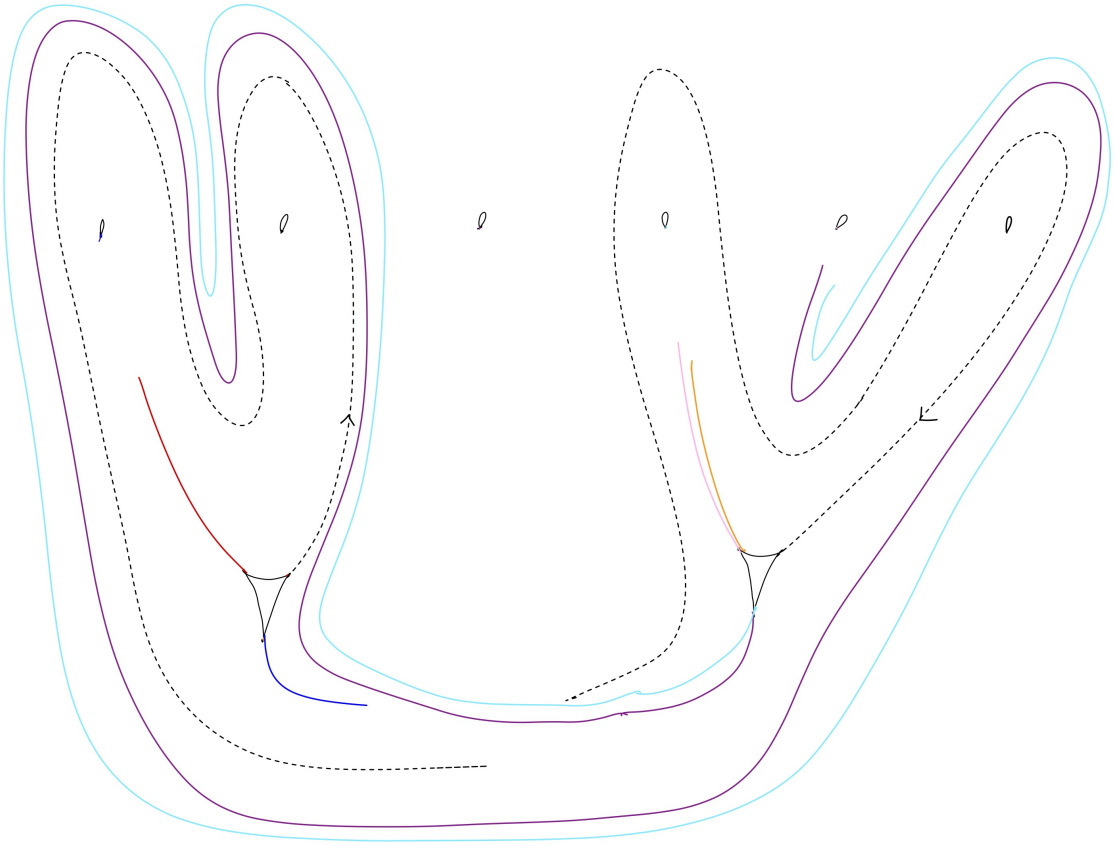


Figure H.9: RNT8

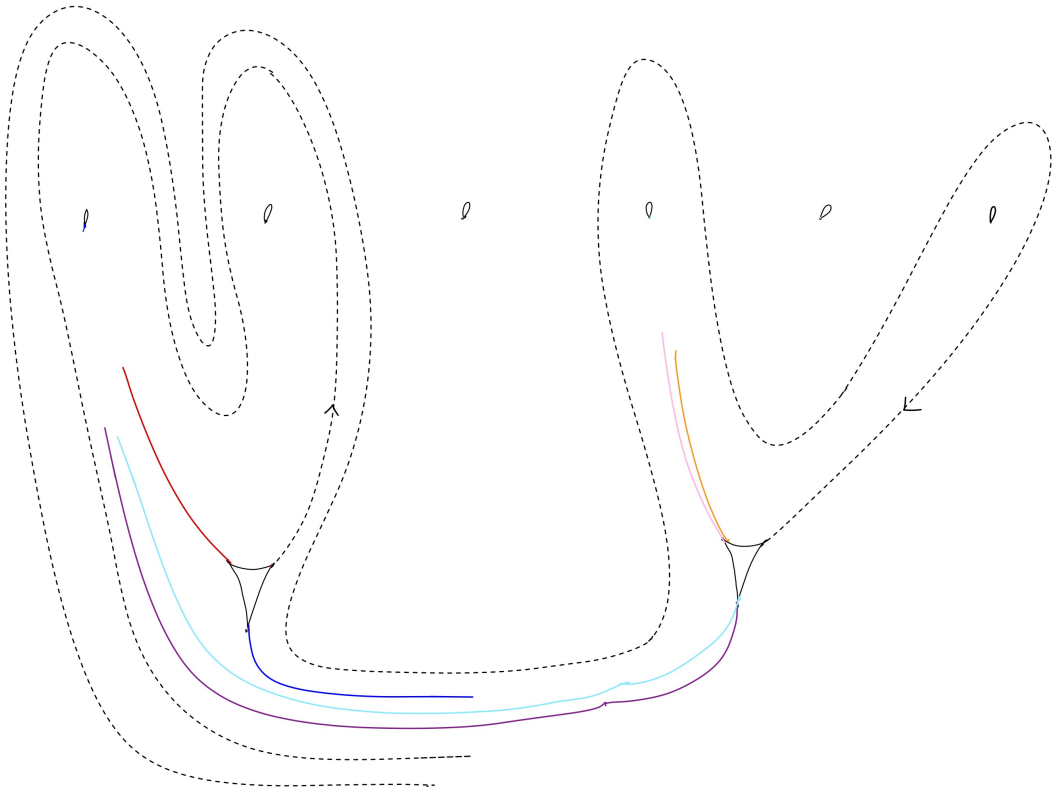


Figure H.10: RNT9

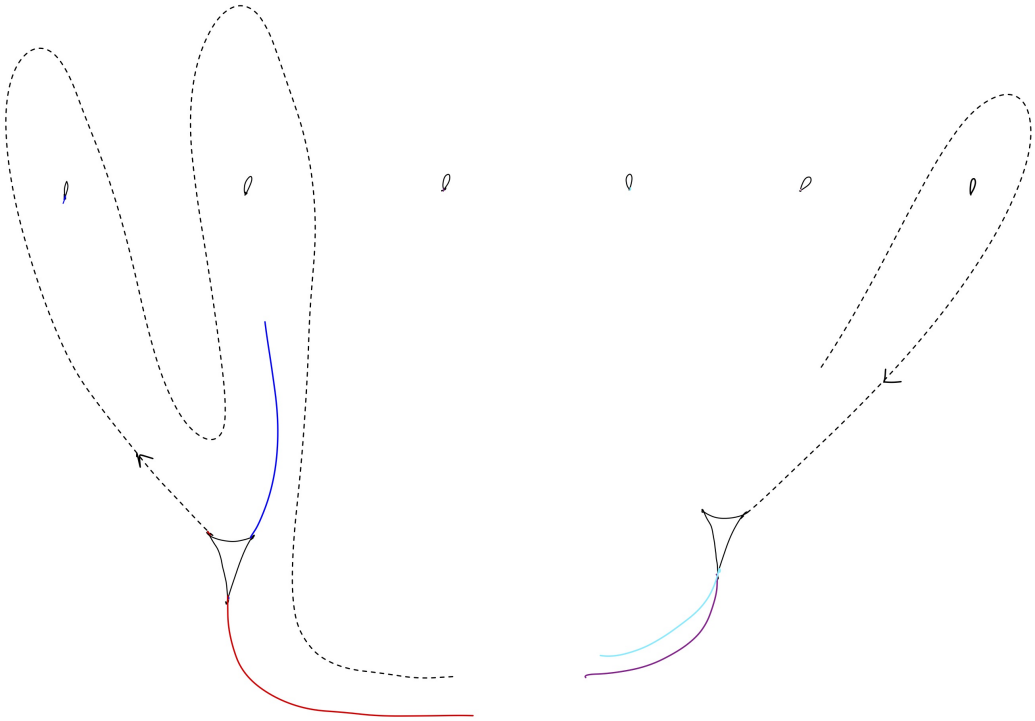


Figure H.11: RNT10



Figure H.12: Bort1

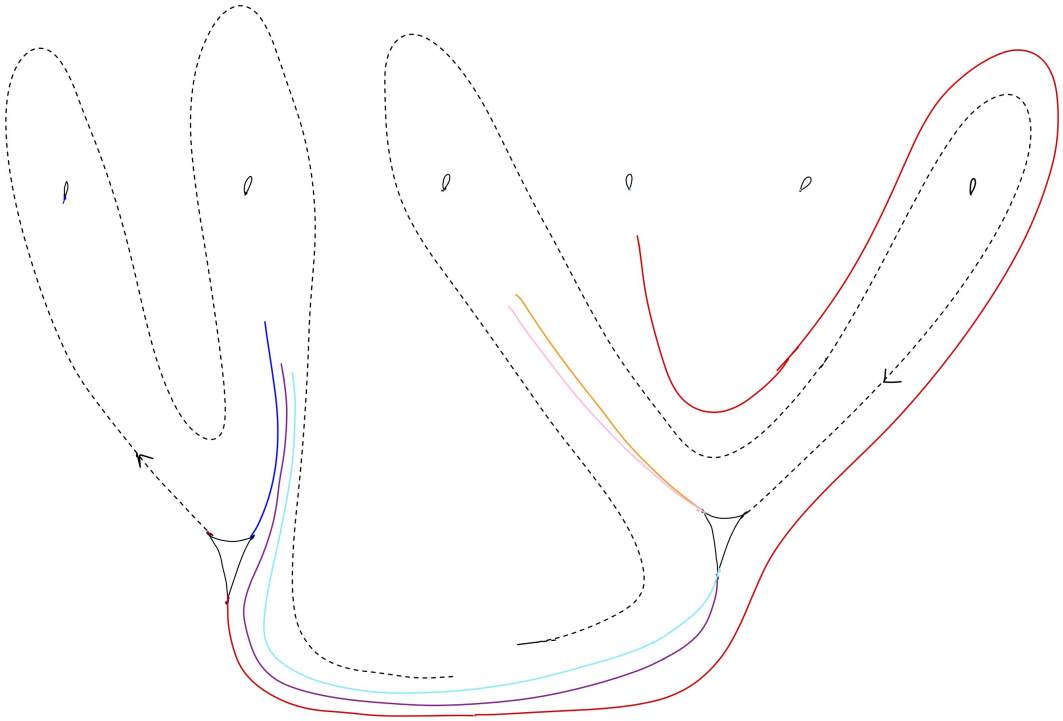


Figure H.13: Bort2

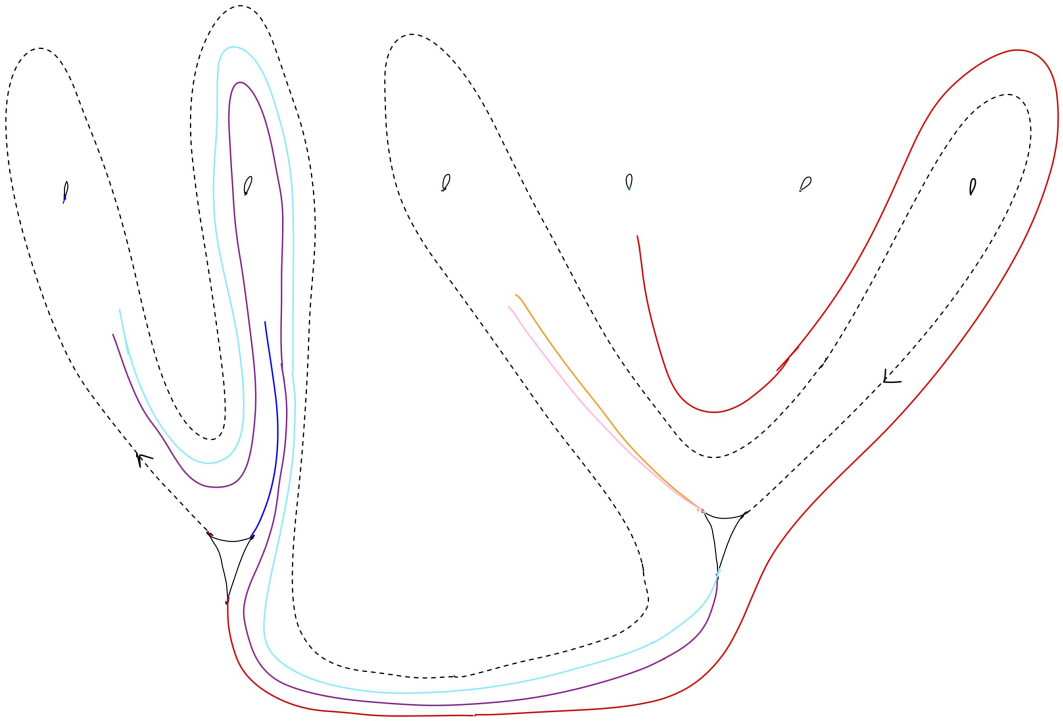


Figure H.14: Bort3

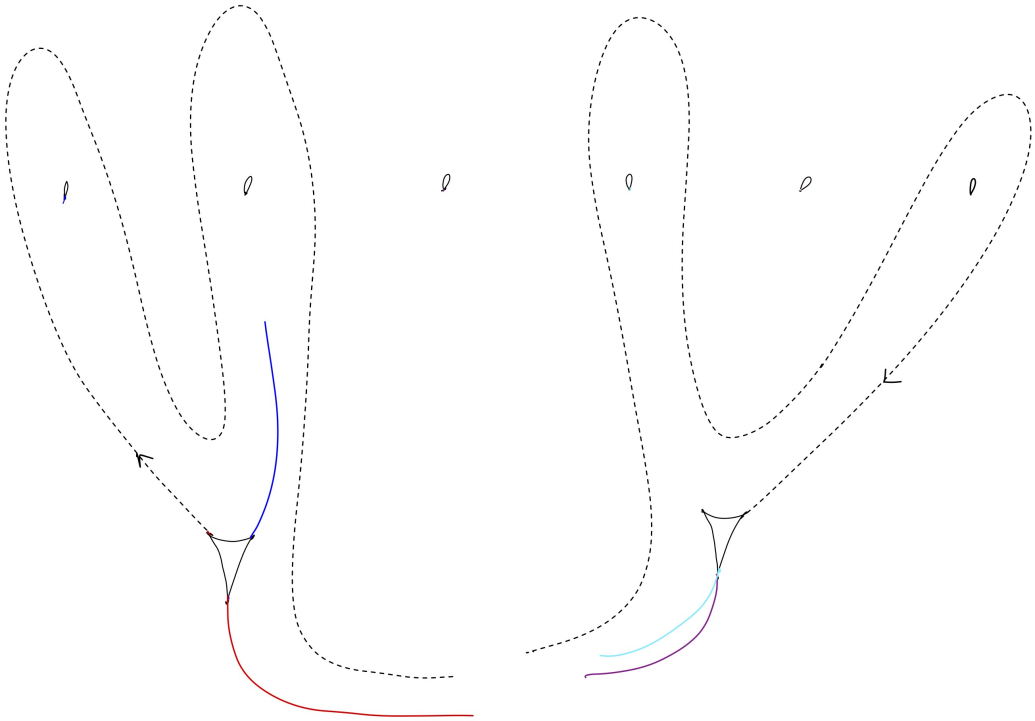


Figure H.15: Cess1

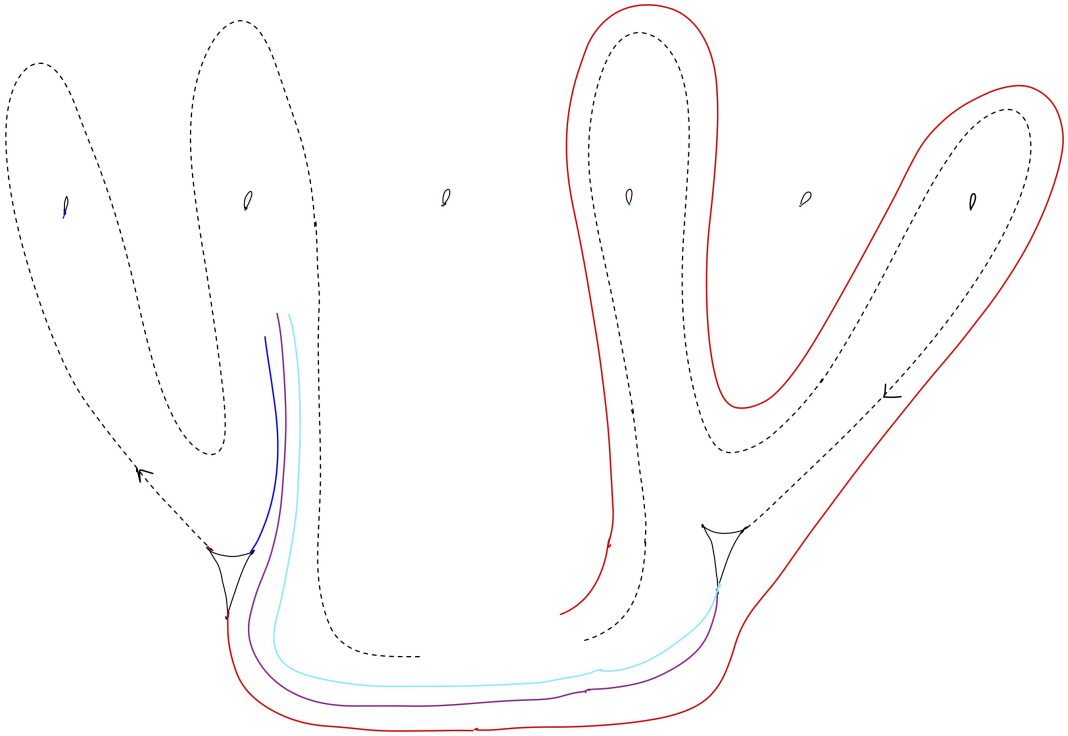


Figure H.16: Cess2

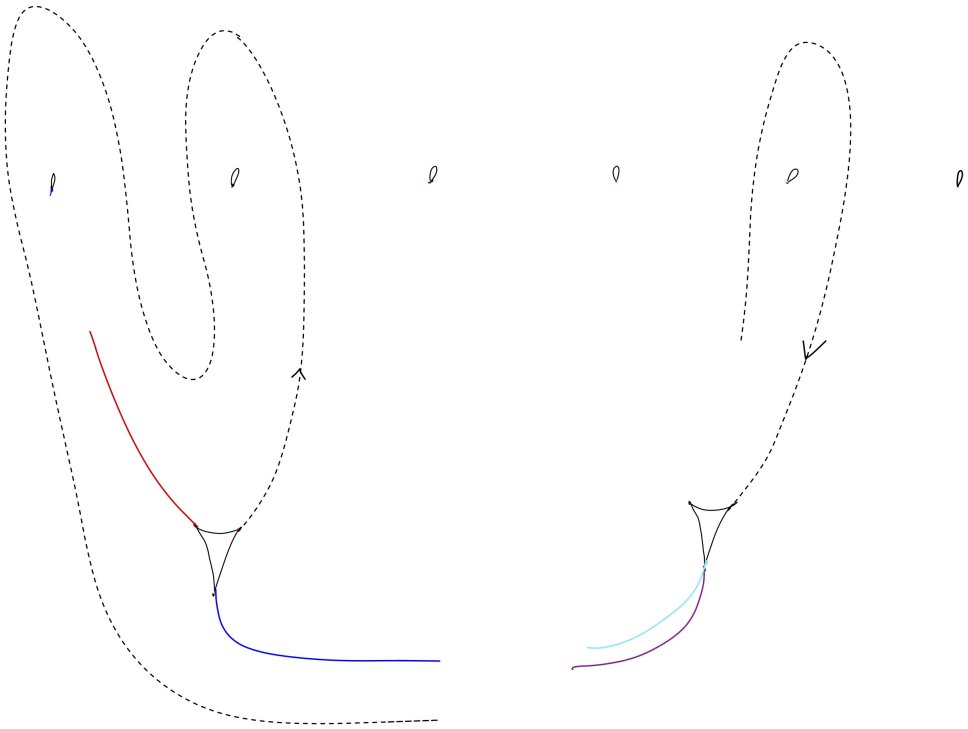


Figure H.17: PWK1

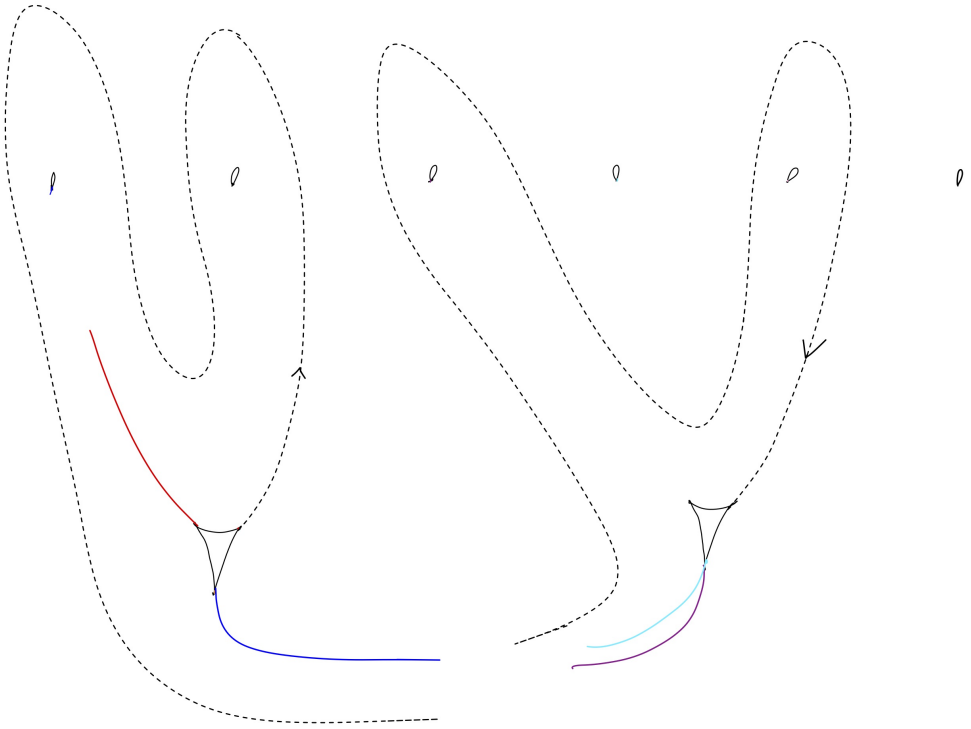


Figure H.18: Dowl1

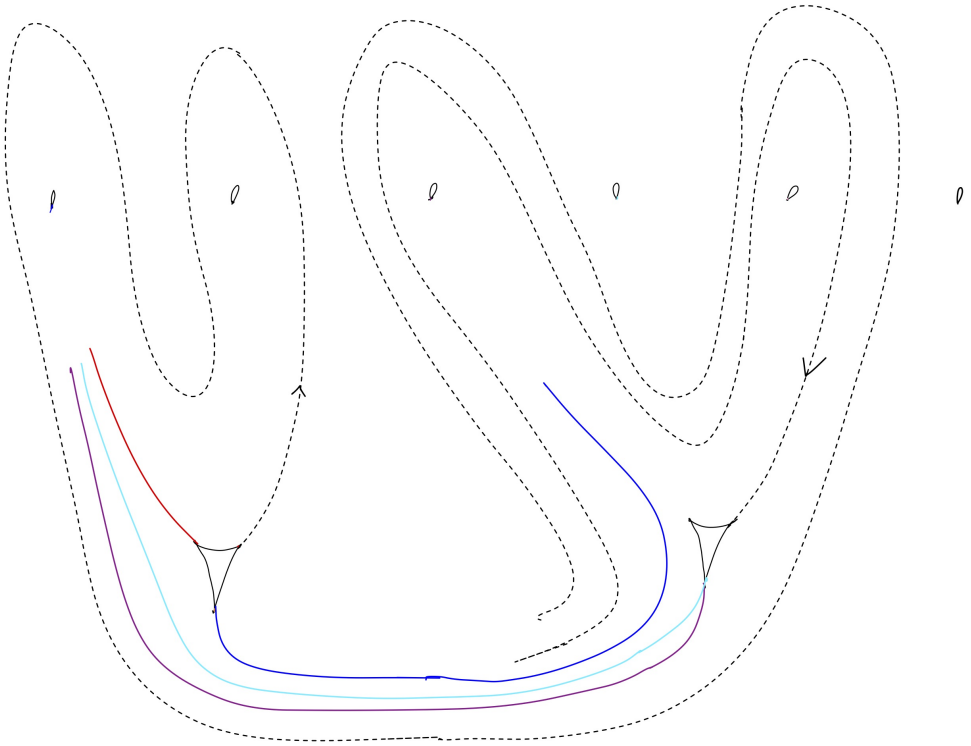


Figure H.19: Dowl2

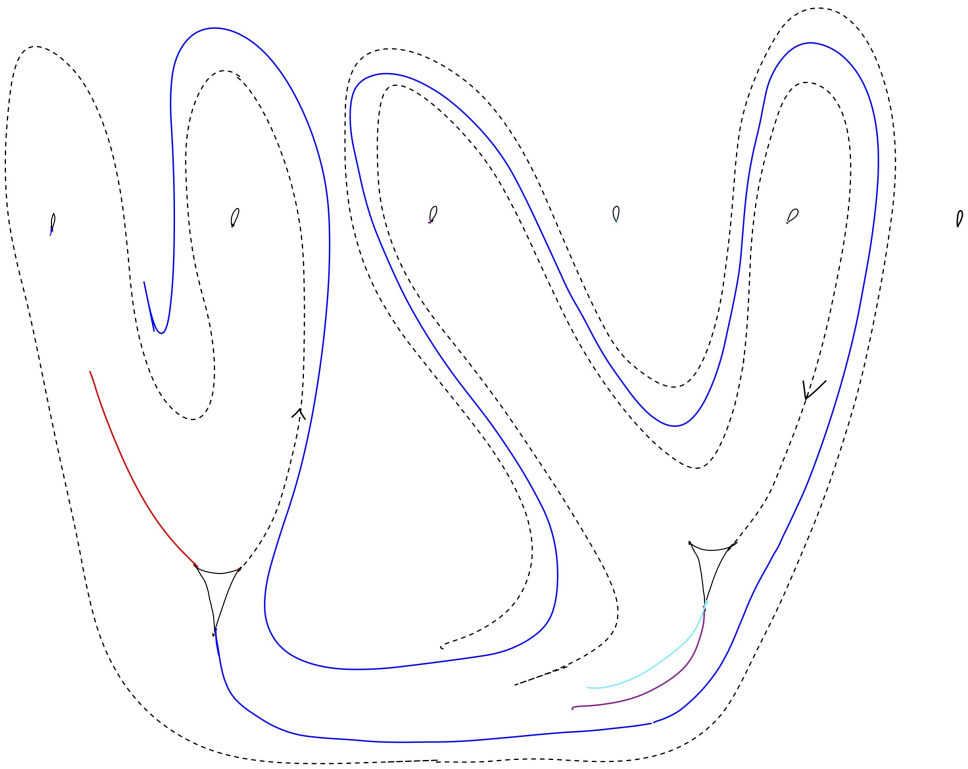


Figure H.20: Dowl3

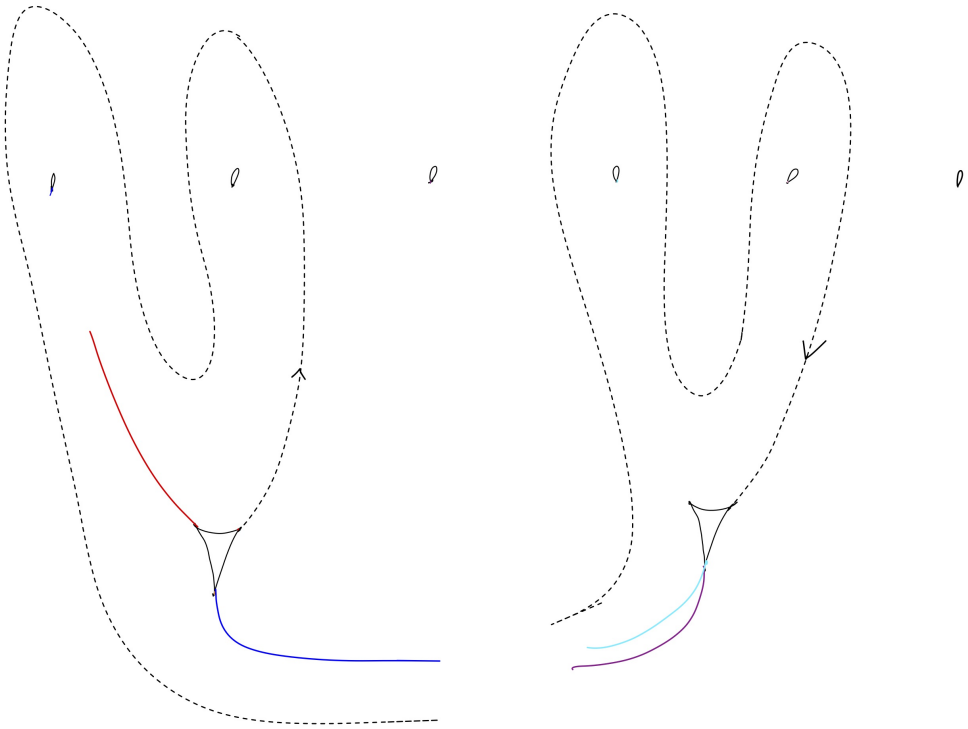


Figure H.21: Fubs1

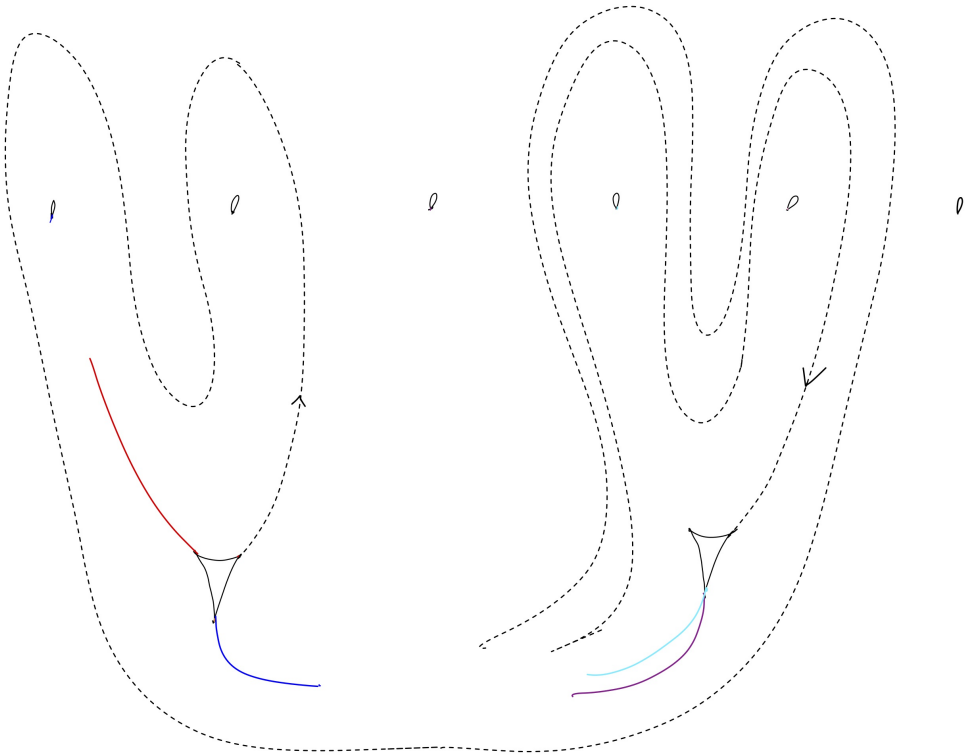


Figure H.22: Fubs2

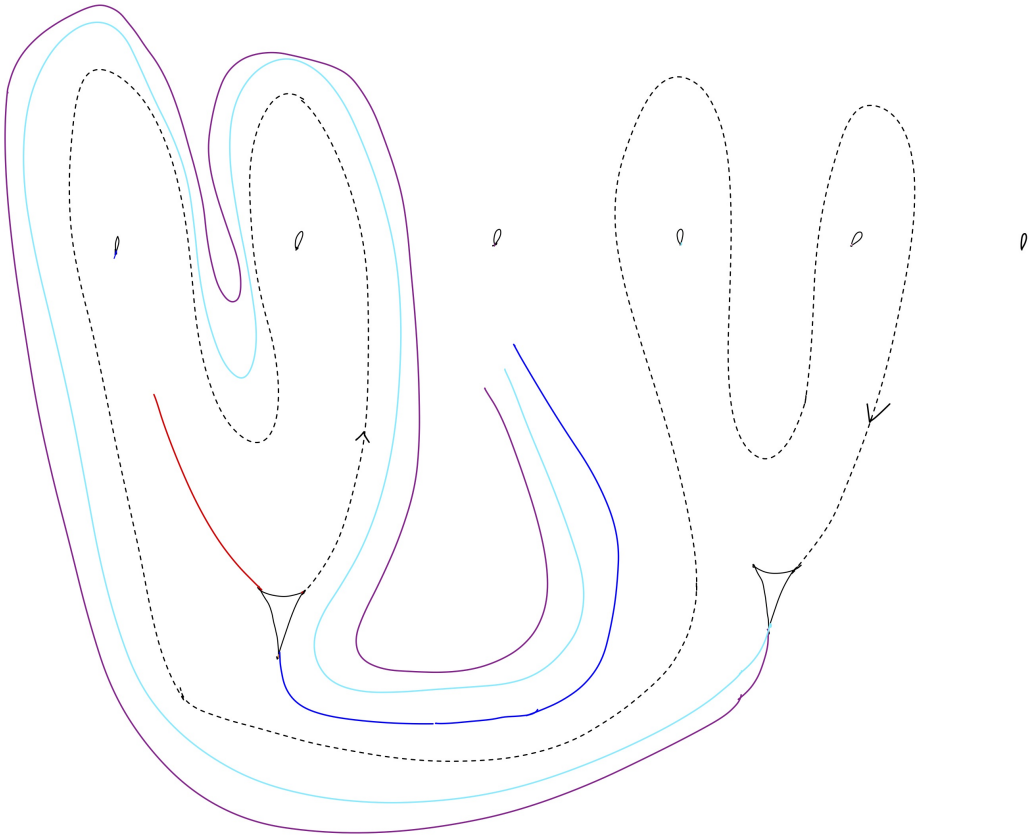


Figure H.23: Fubs3

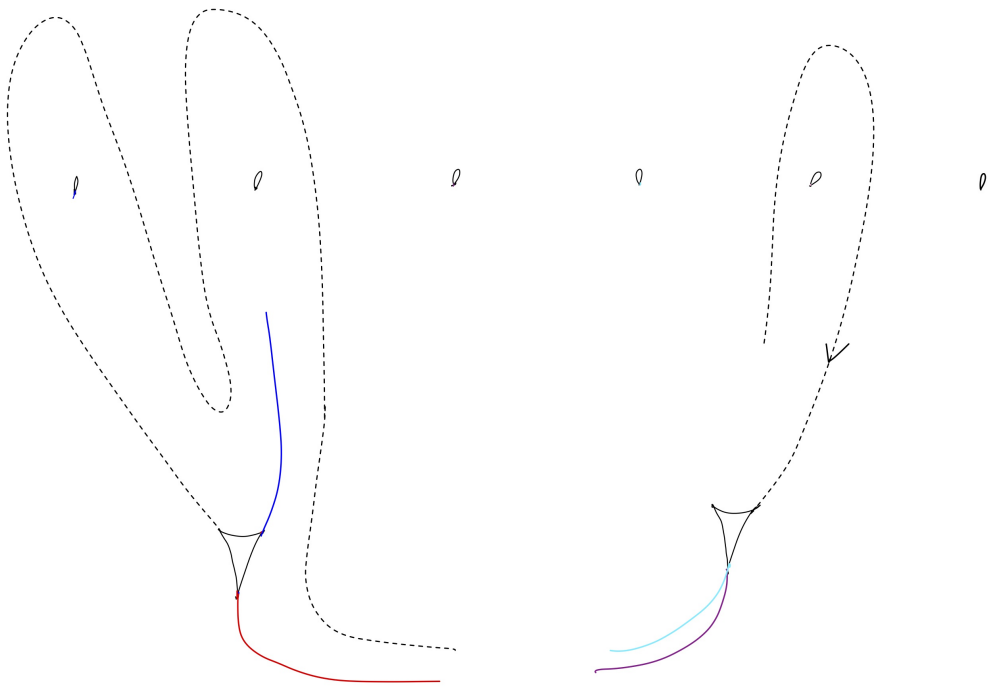


Figure H.24: BAF1

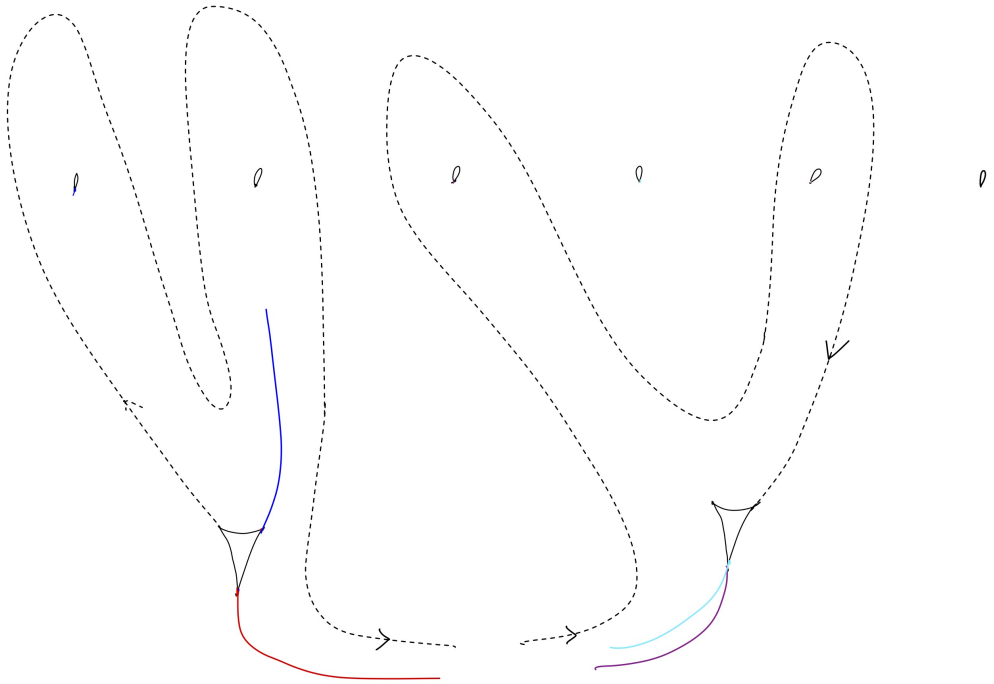


Figure H.25: Grig1

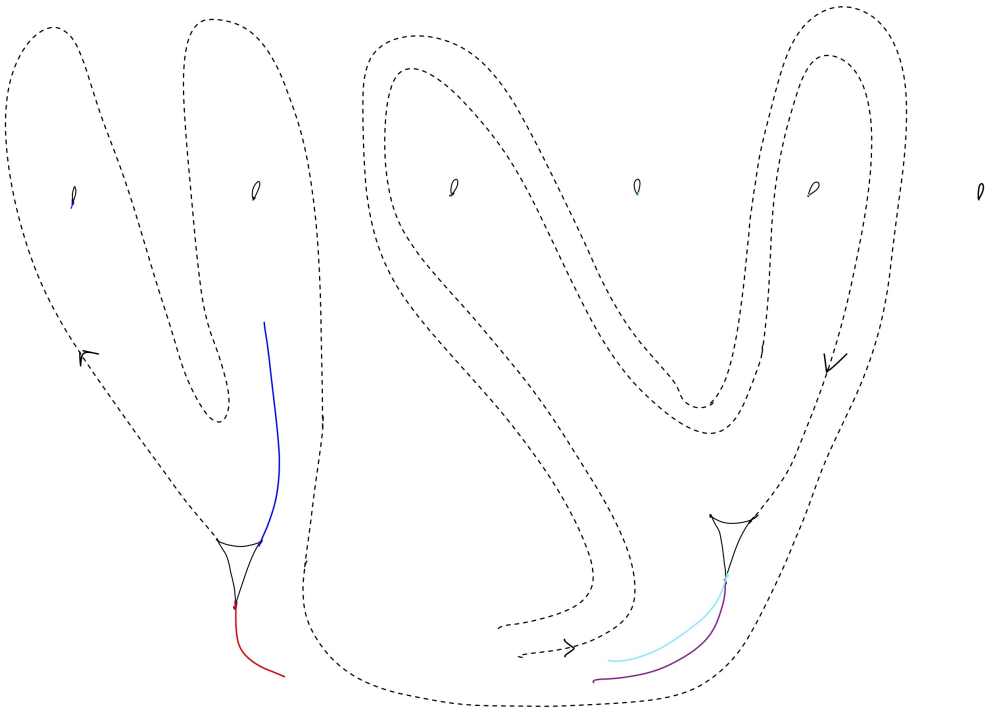


Figure H.26: Grig2

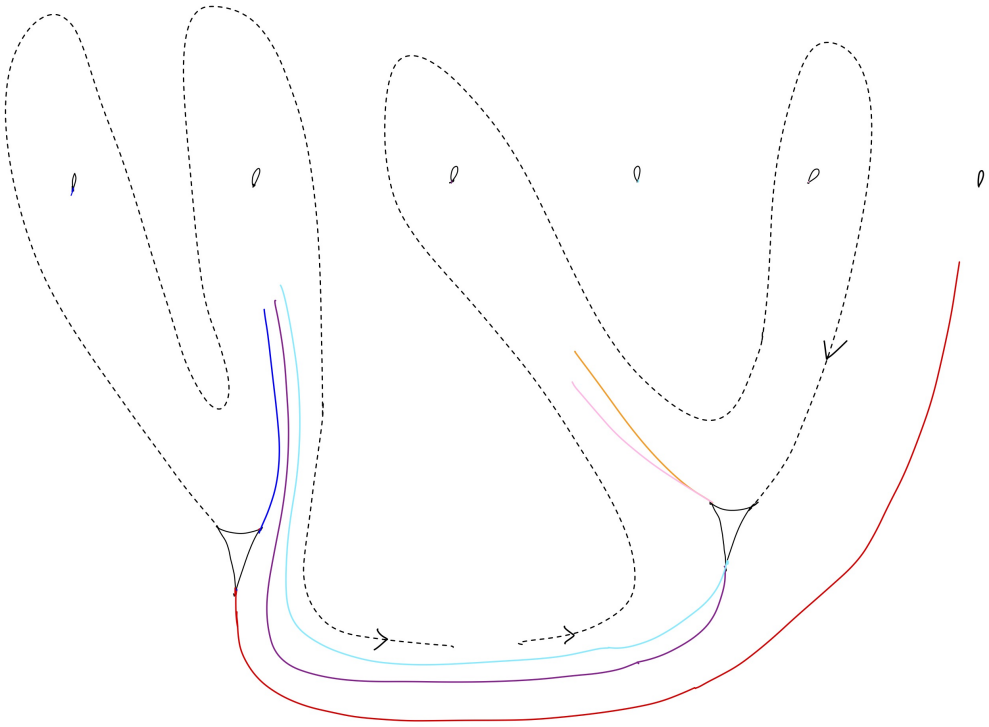


Figure H.27: Grig3

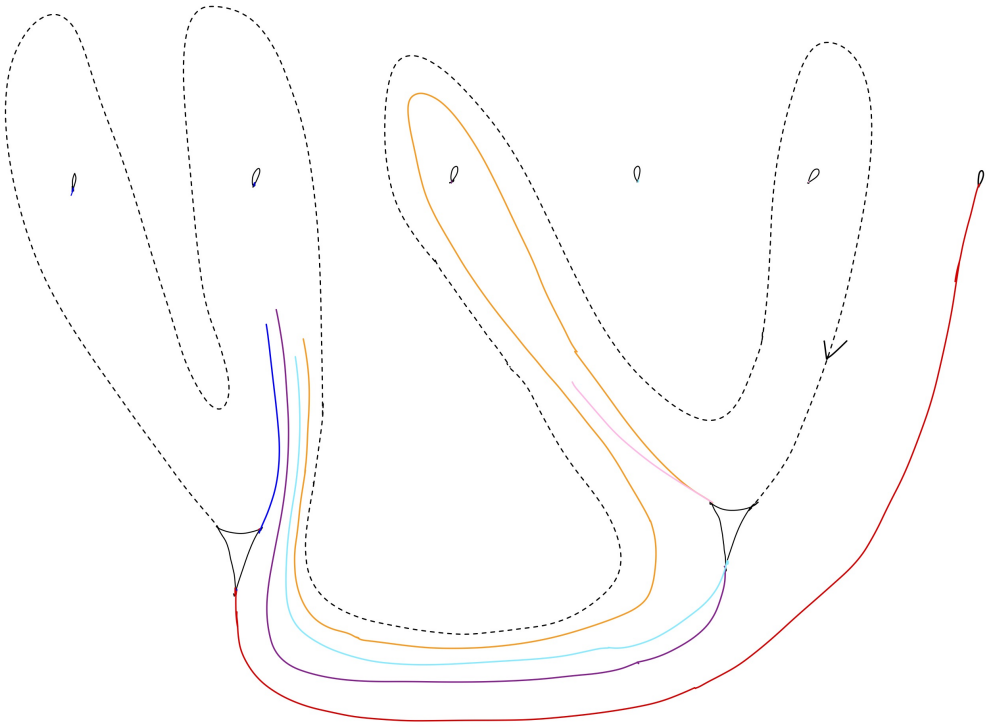


Figure H.28: Grig4

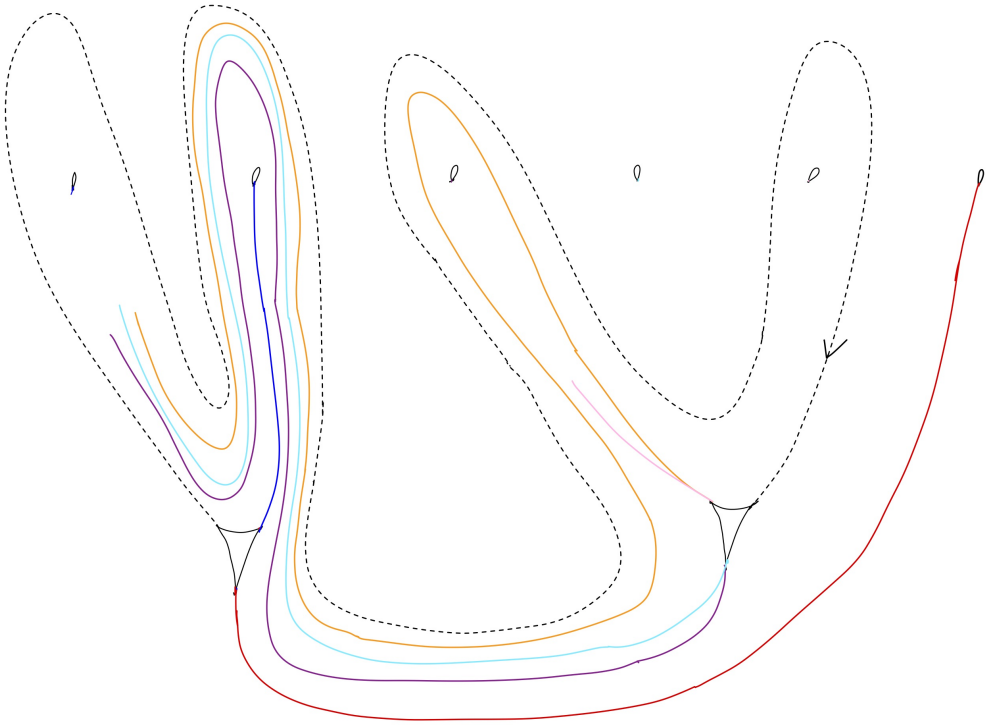


Figure H.29: Chirk1

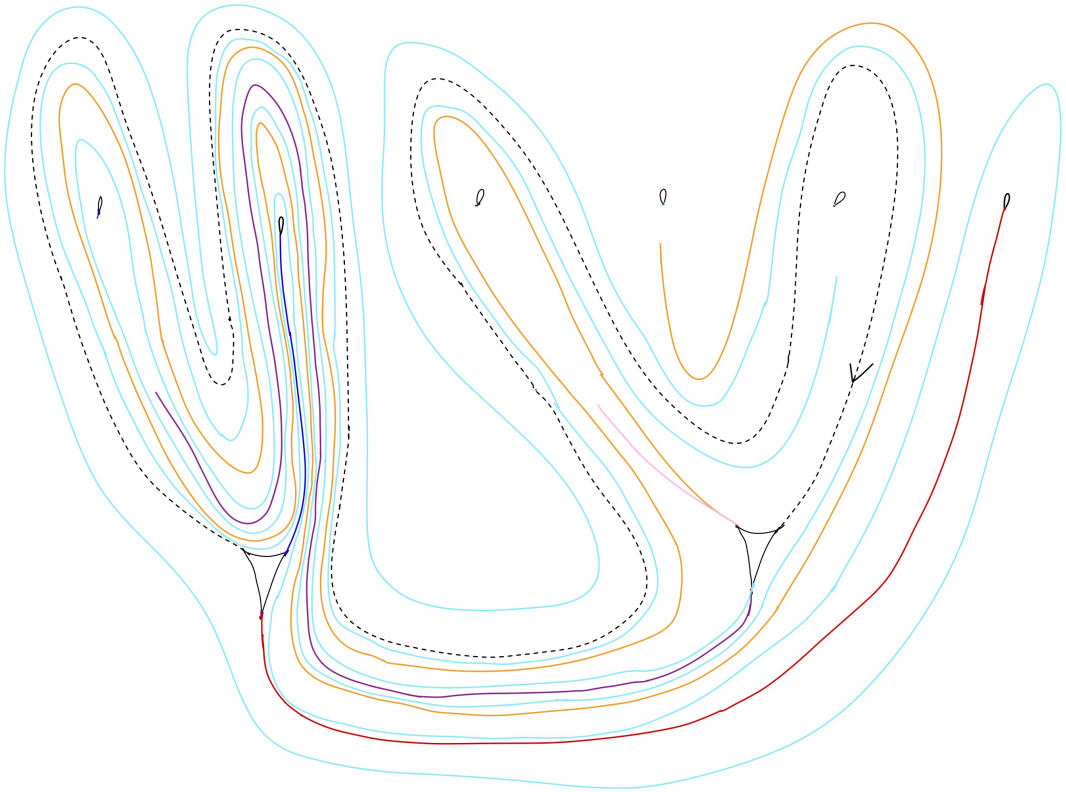


Figure H.30: Chirk2

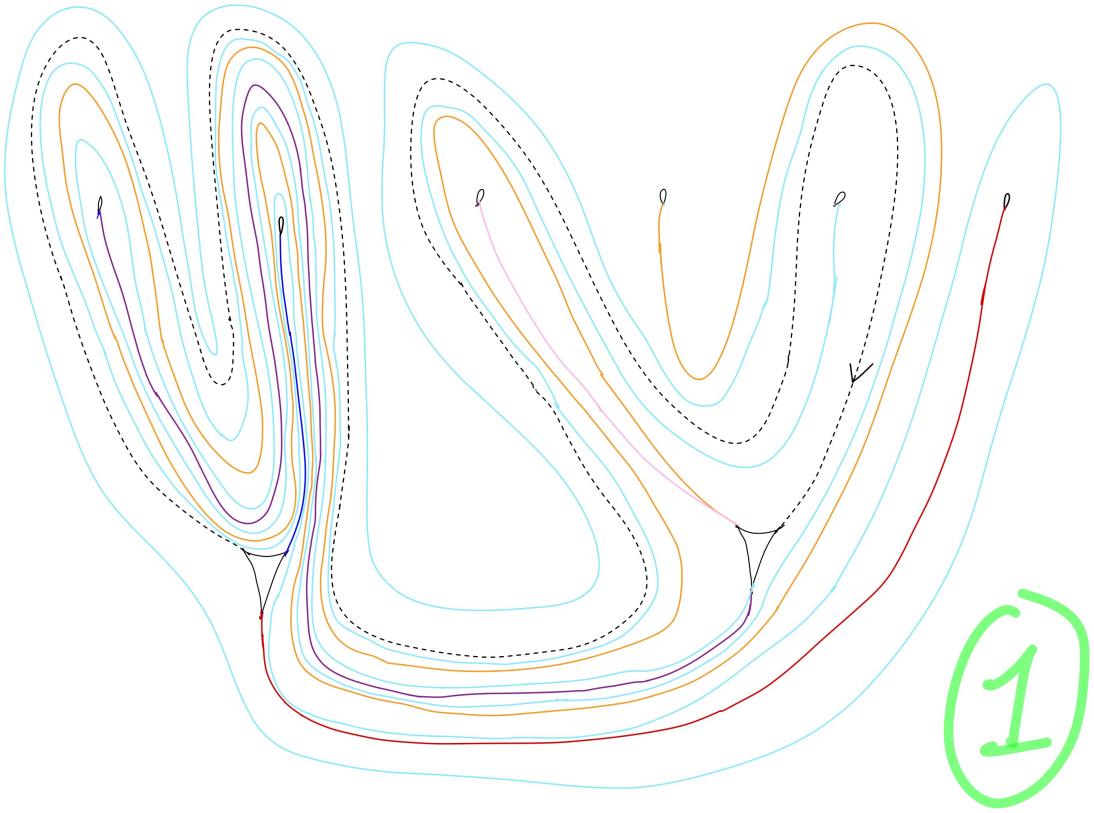


Figure H.31: Chirk3

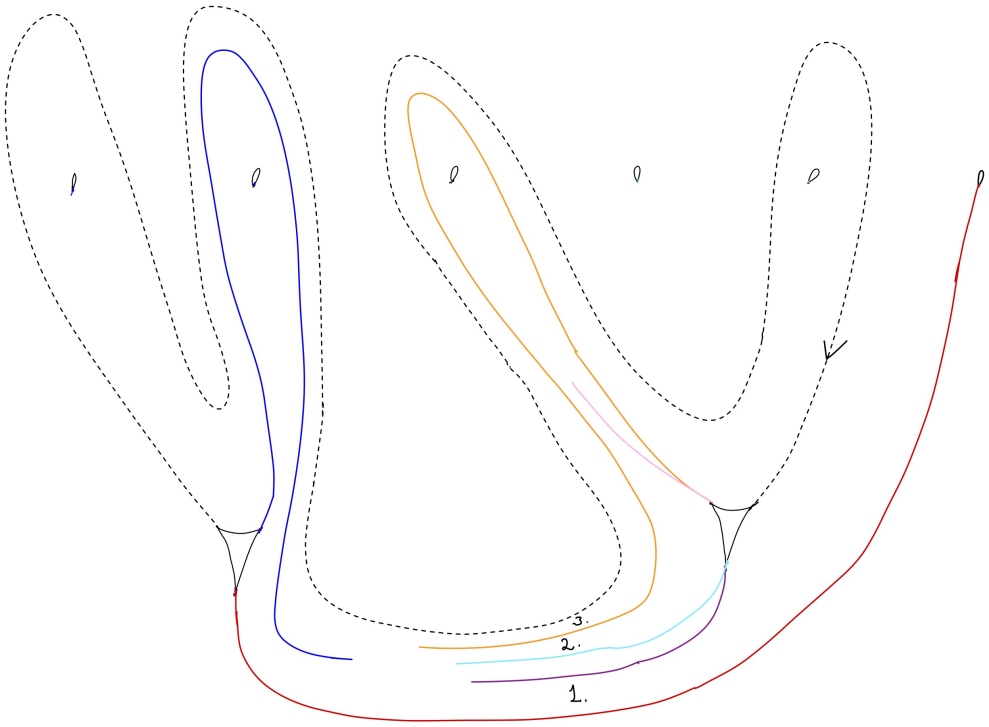


Figure H.32: Dwalm1

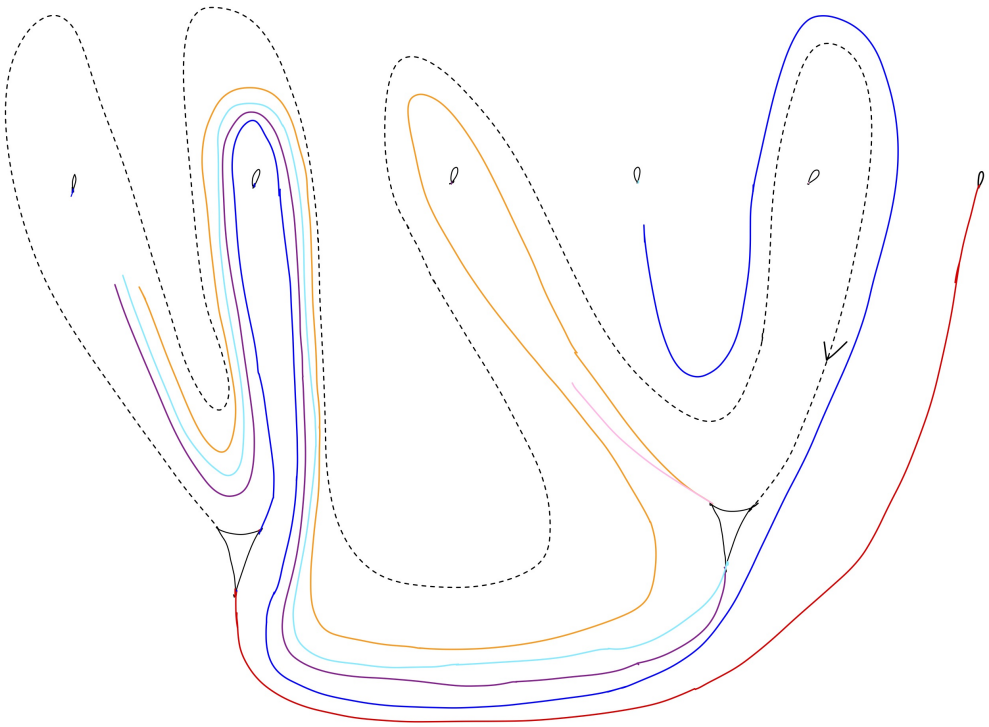


Figure H.33: Bocage1

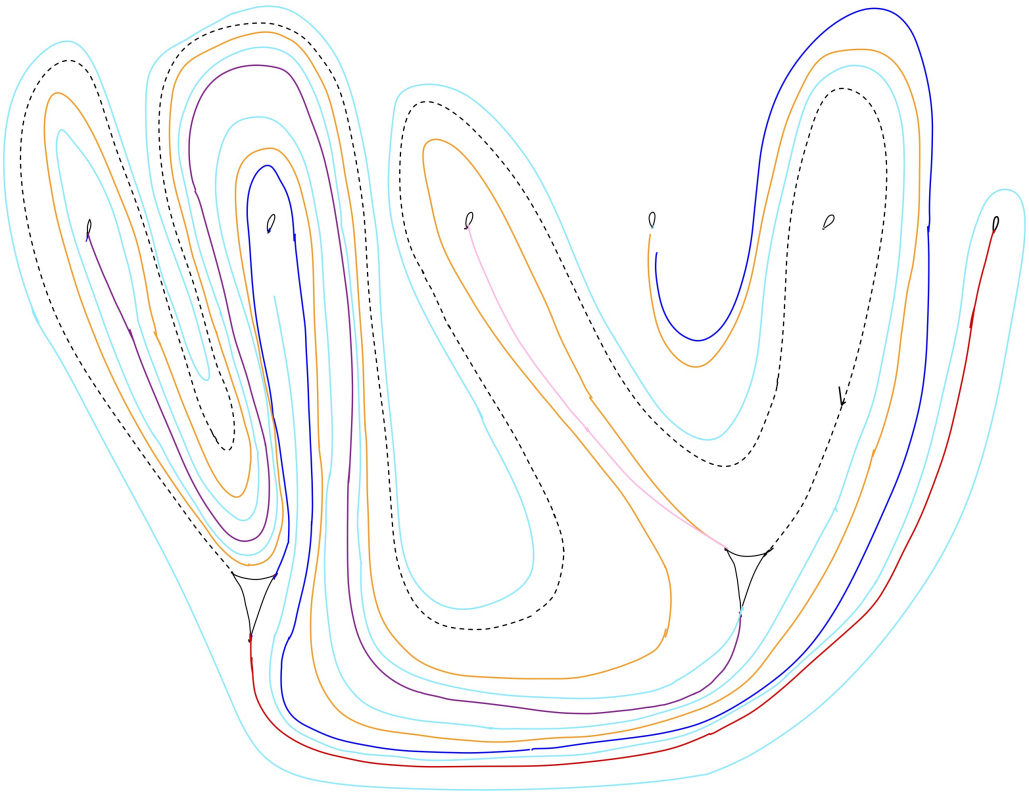


Figure H.34: Bocage2

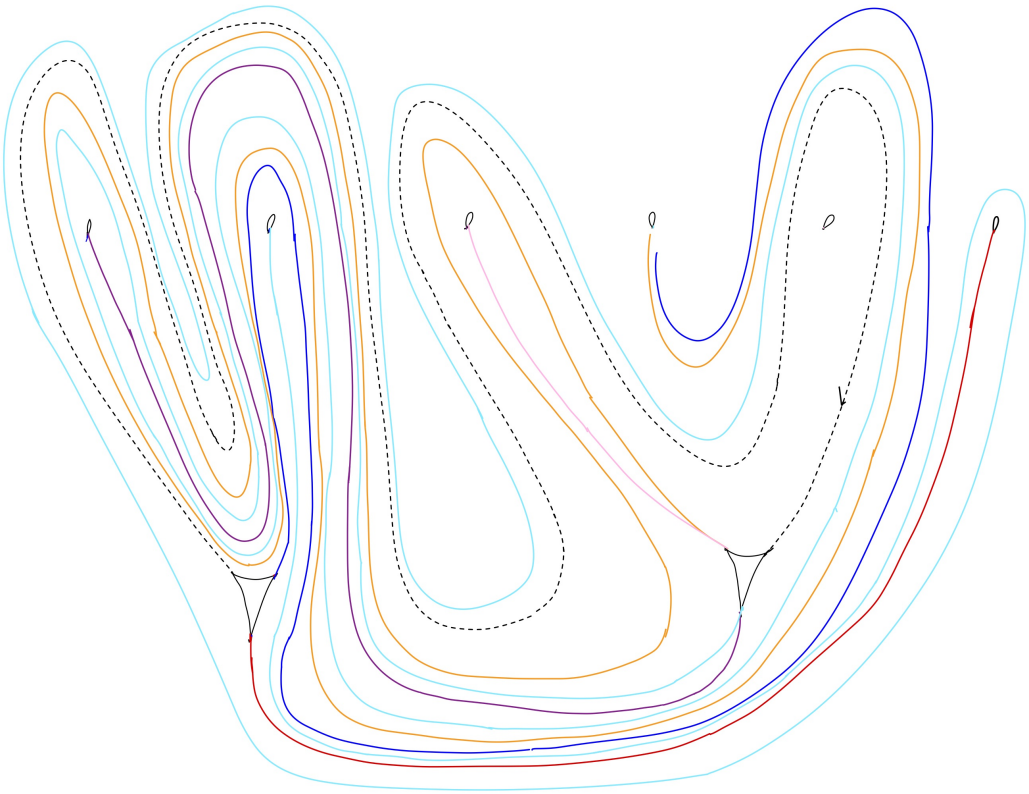


Figure H.35: Bocage3

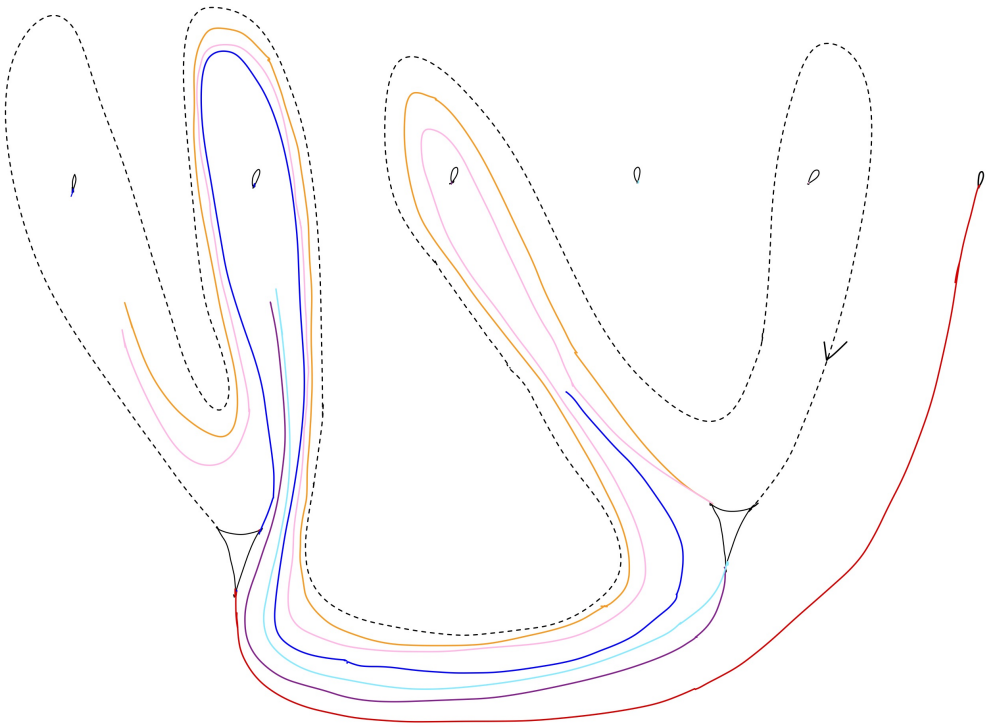


Figure H.36: Cagmag1

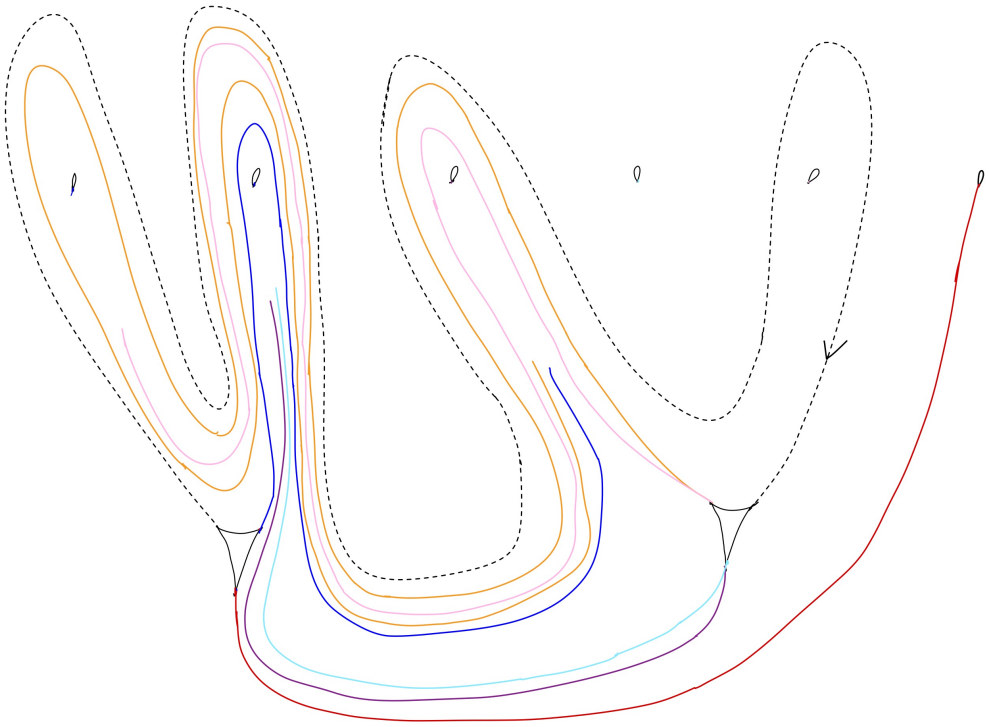


Figure H.37: Cagmag2

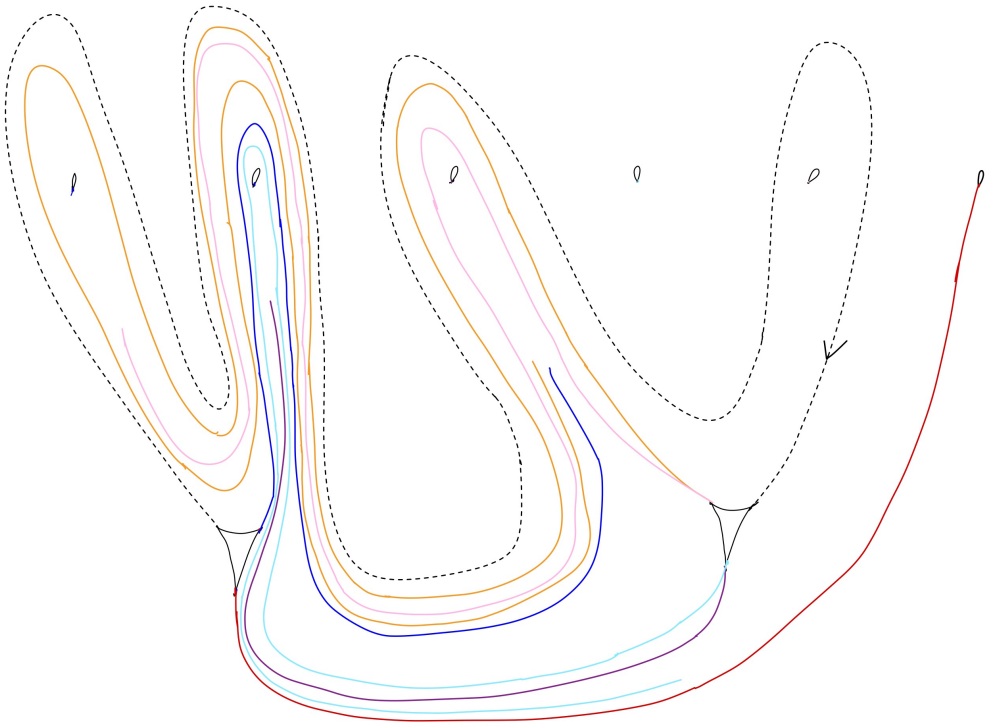


Figure H.38: Cagmag3

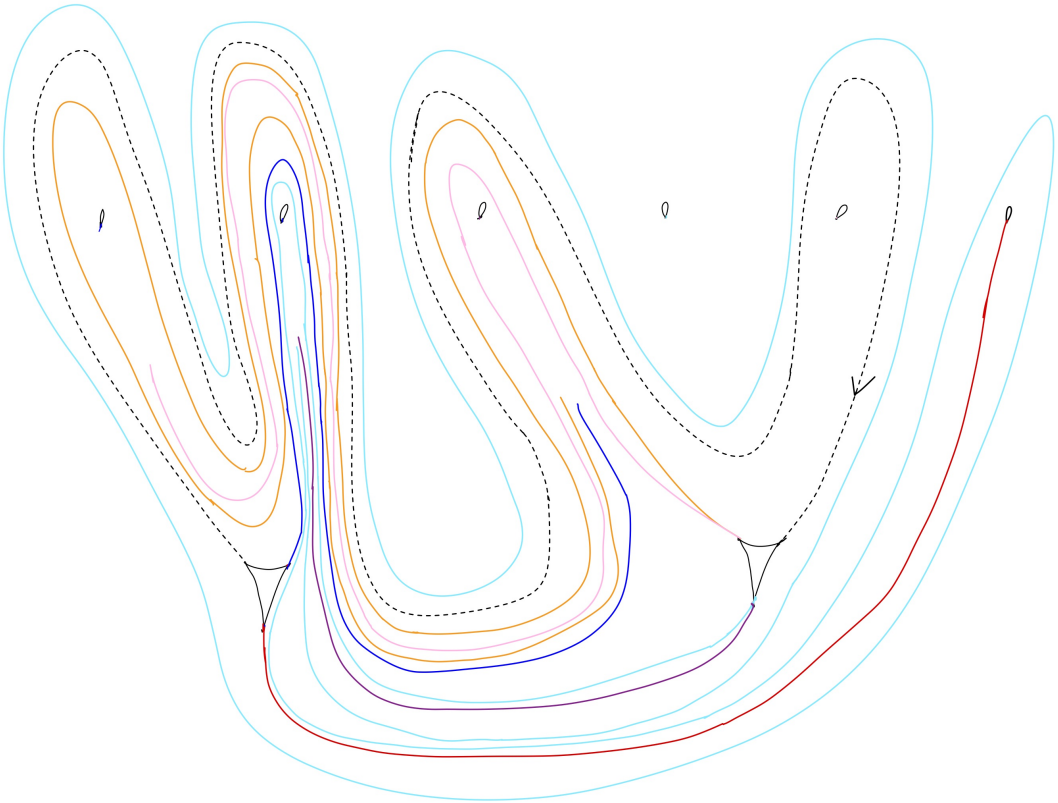


Figure H.39: Cagmag4

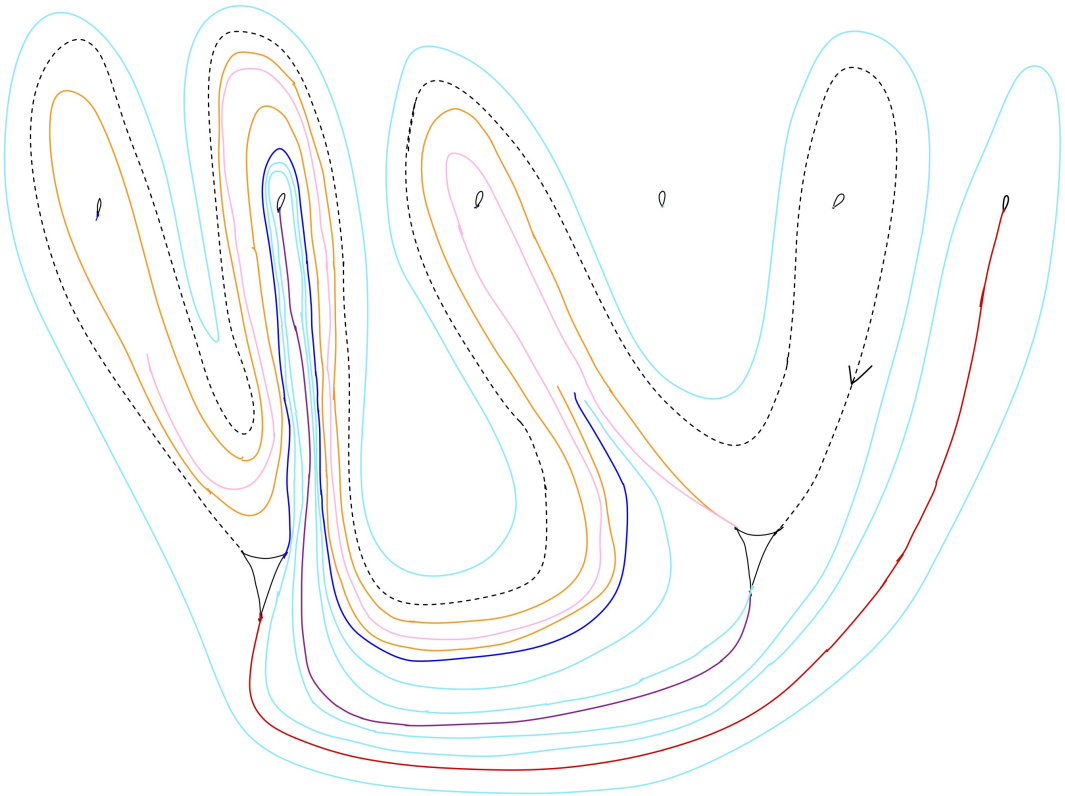


Figure H.40: Cagmag5

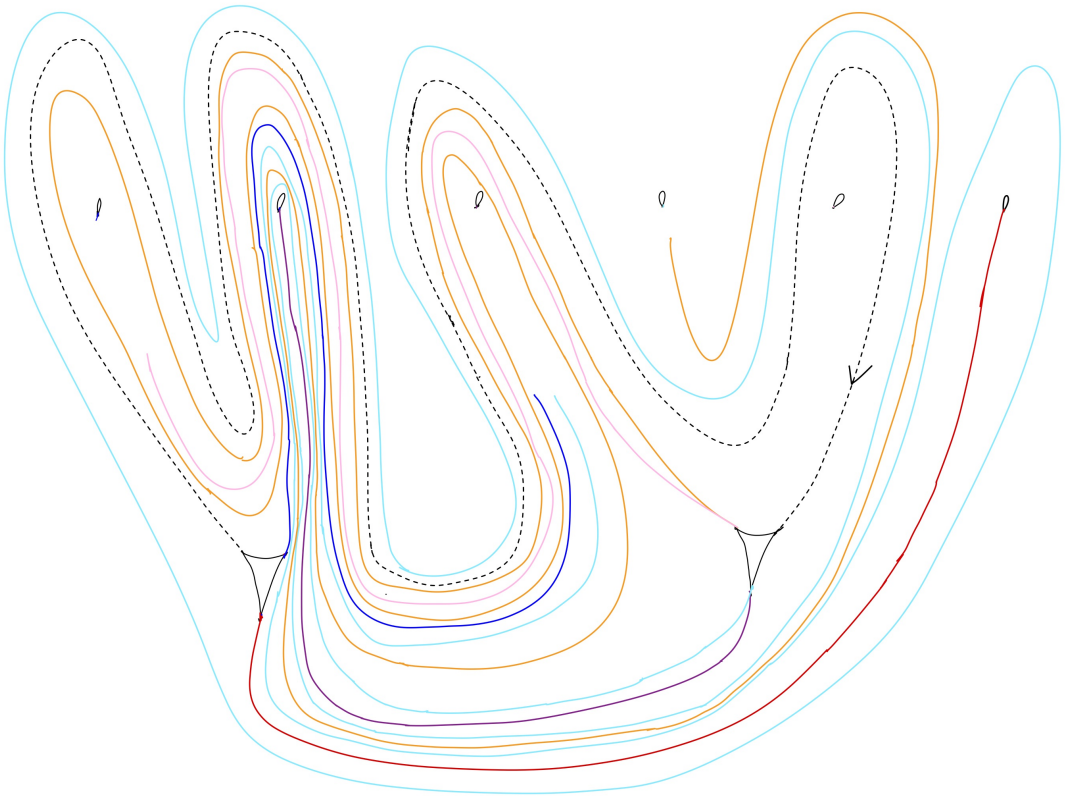


Figure H.41: Cagmag6

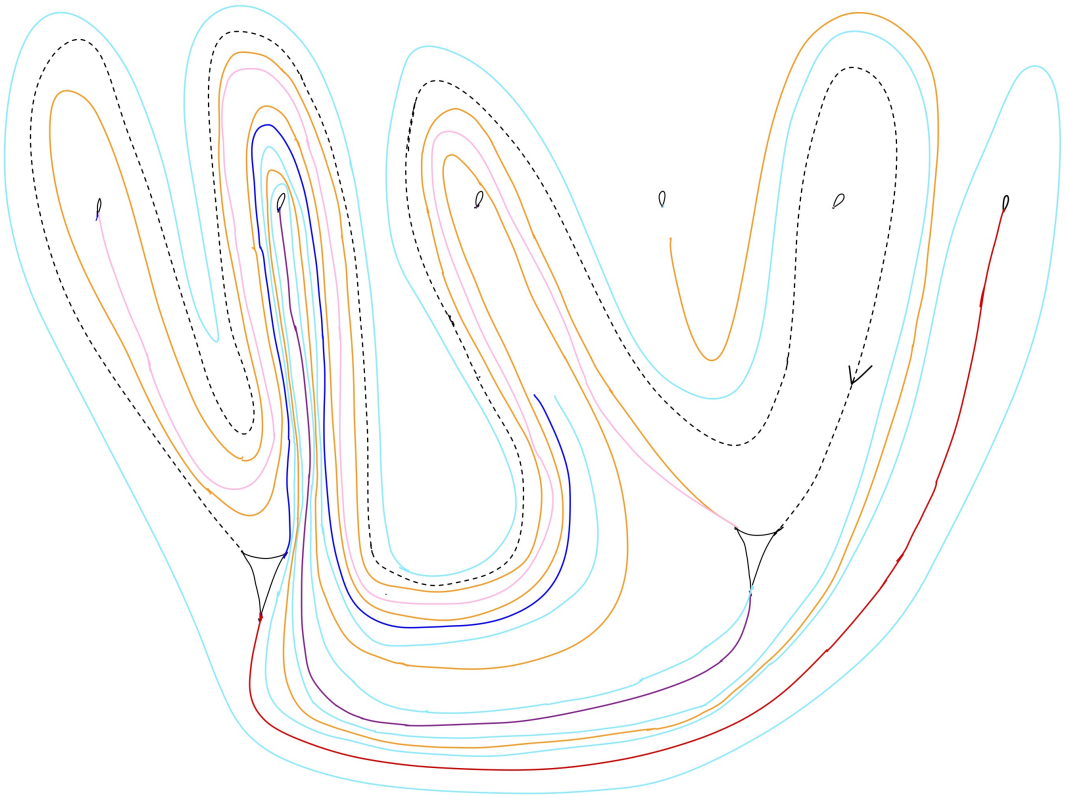


Figure H.42: Cagmag7

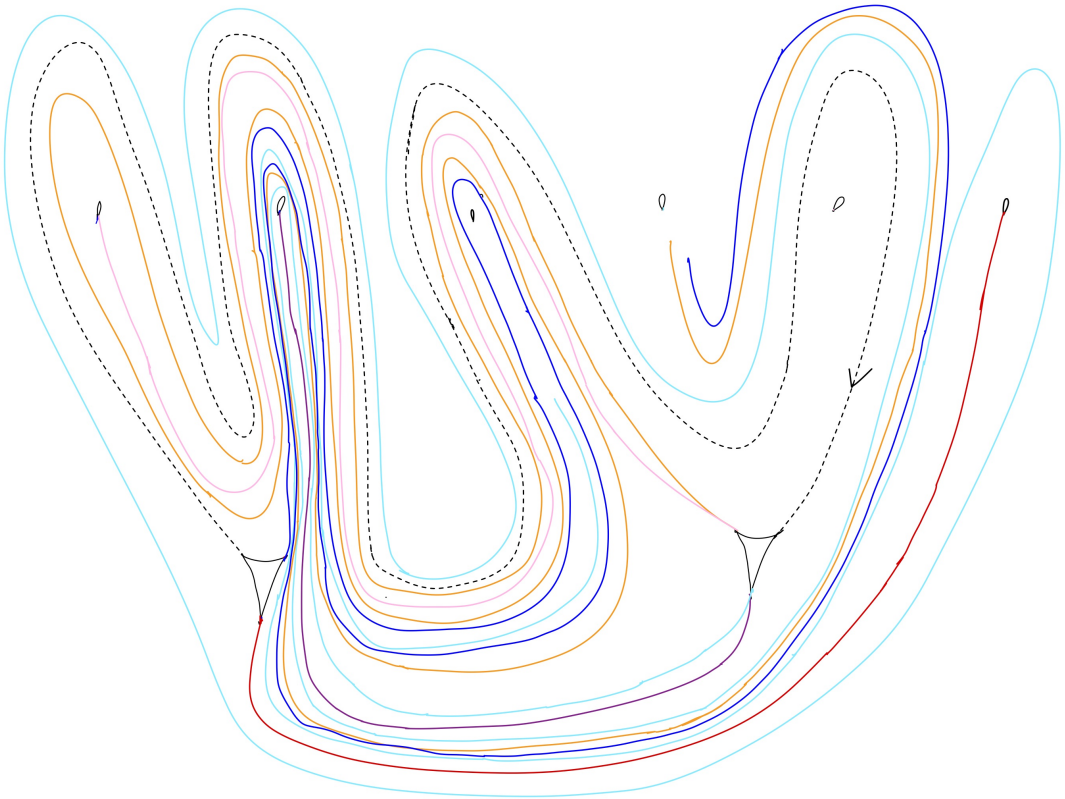


Figure H.43: Cagmag8

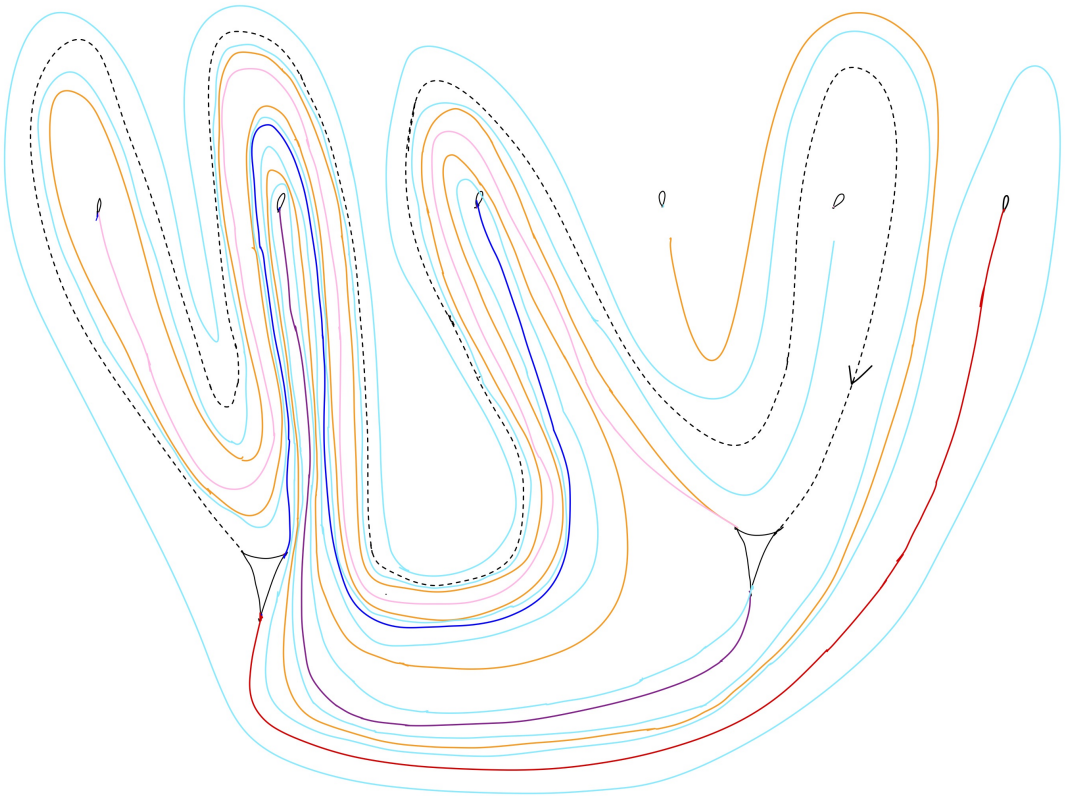


Figure H.44: Cagmag9

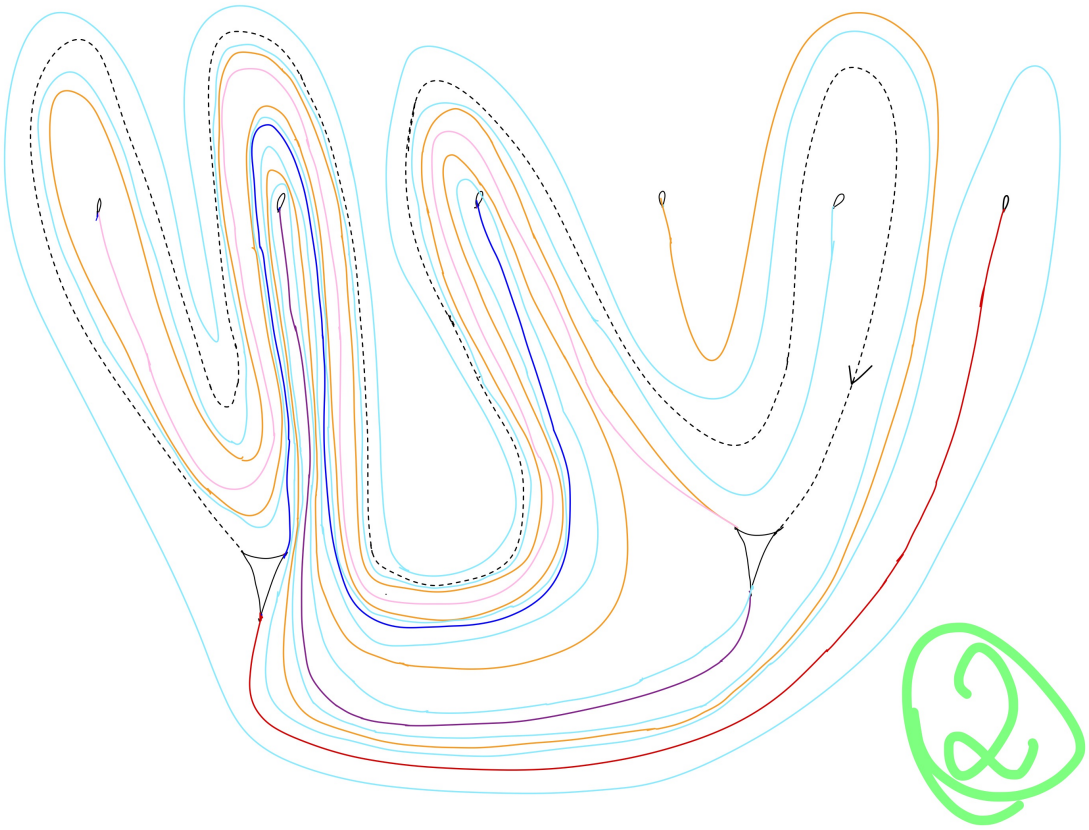


Figure H.45: Cagmag10

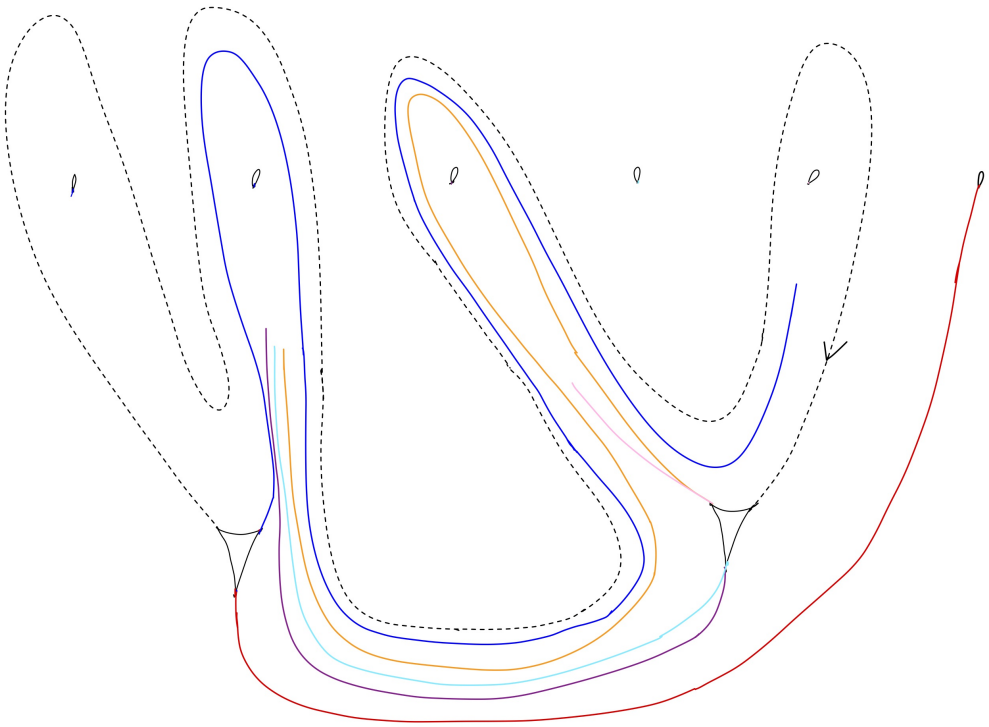


Figure H.46: Boofus1

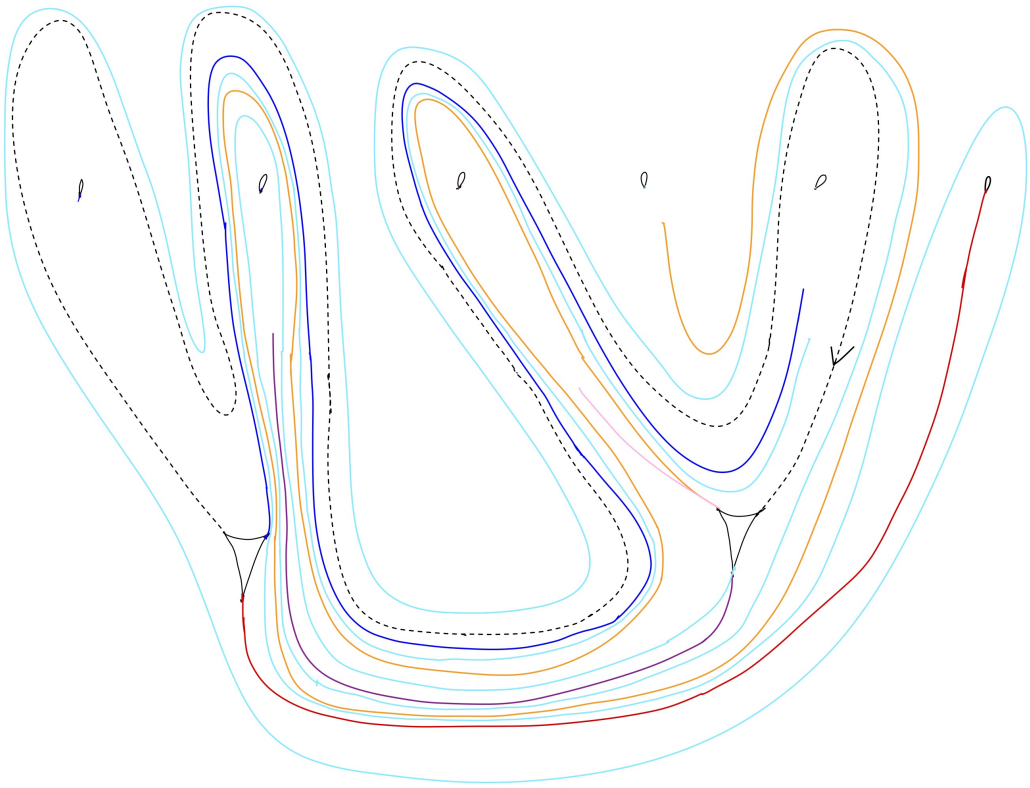


Figure H.47: Boofus2

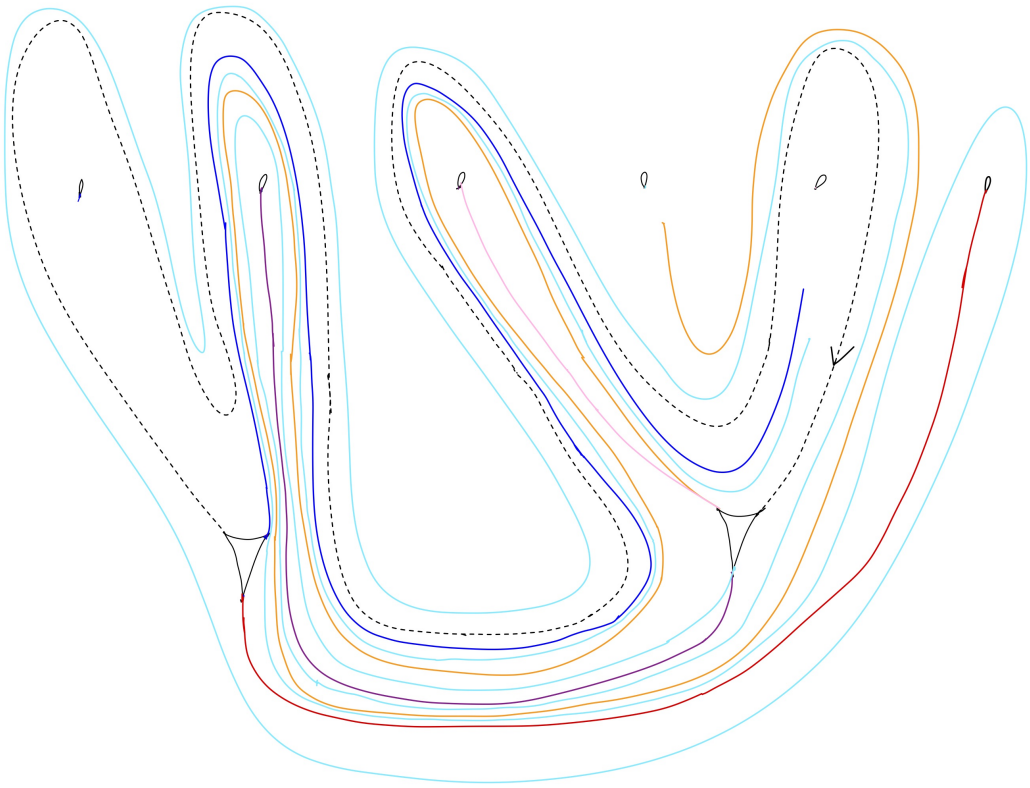


Figure H.48: Boofus3

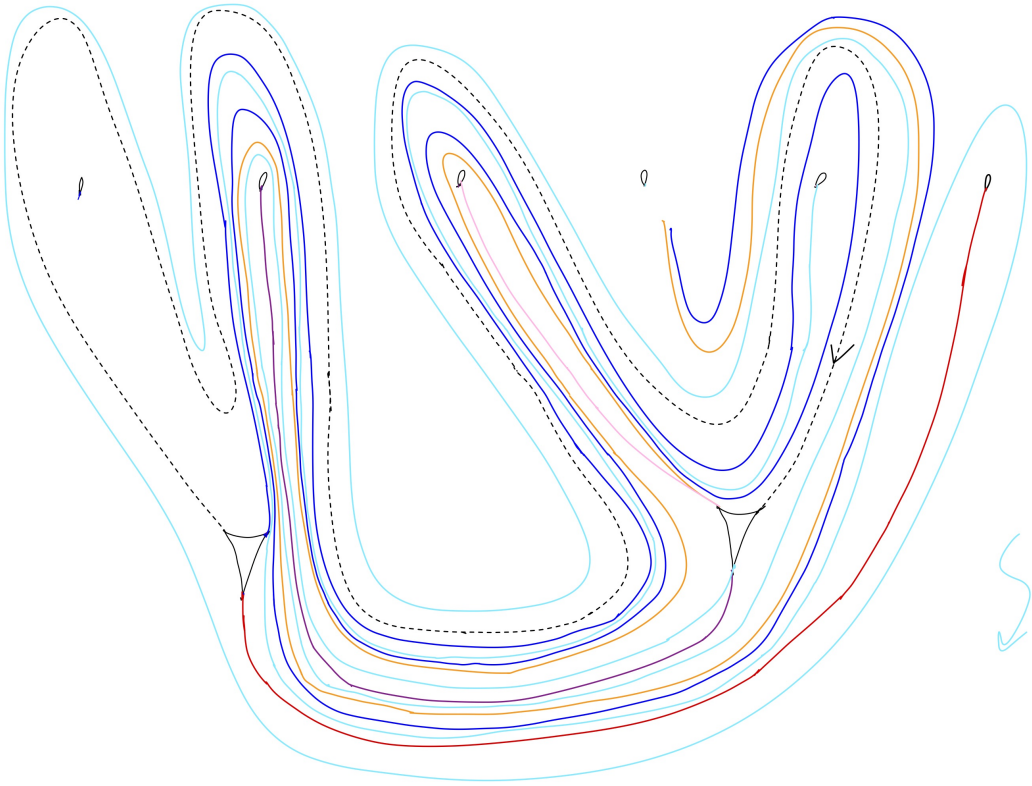


Figure H.49: Boofus4

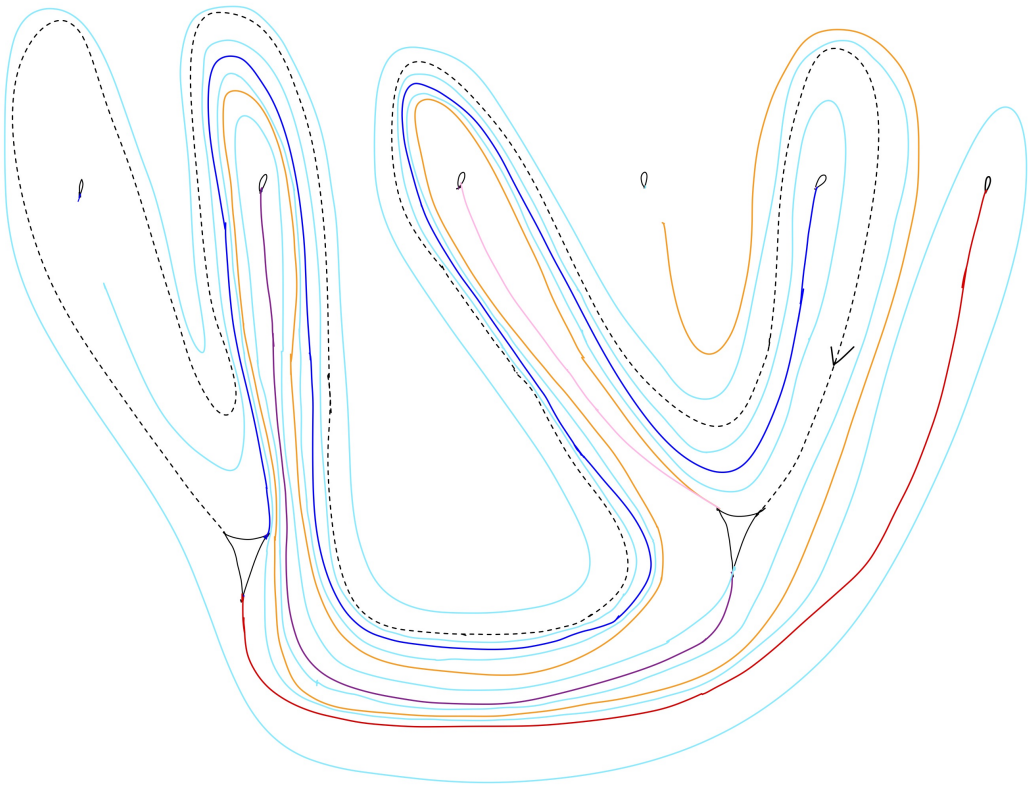


Figure H.50: Boofus5

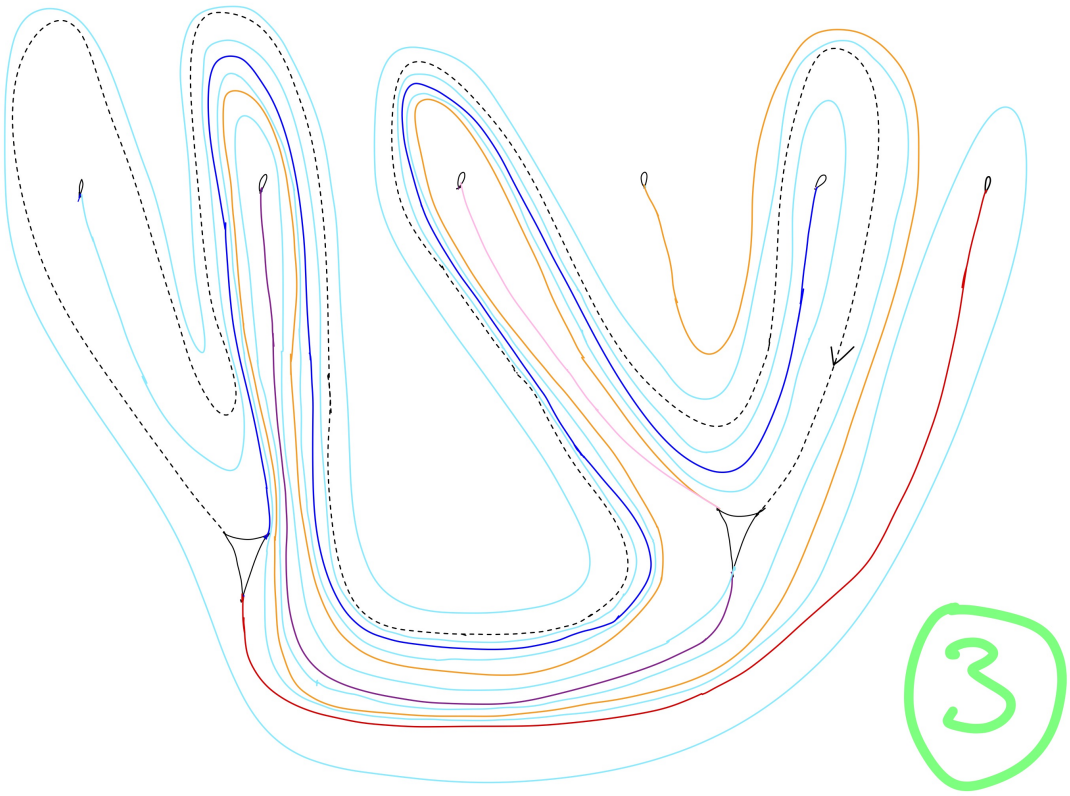


Figure H.51: Boofus6

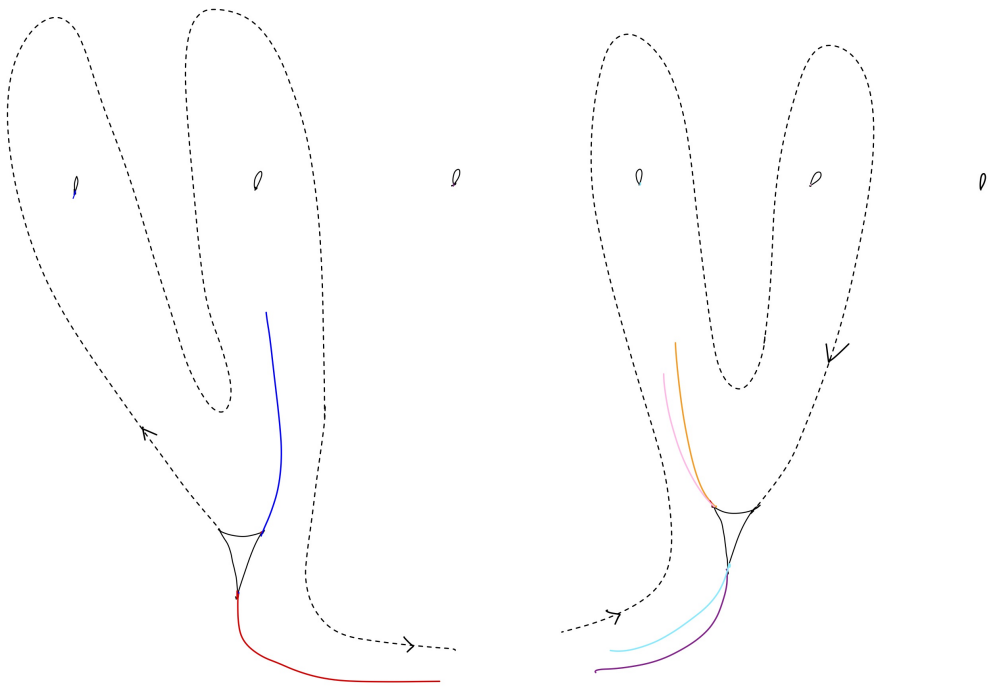


Figure H.52: Harl1

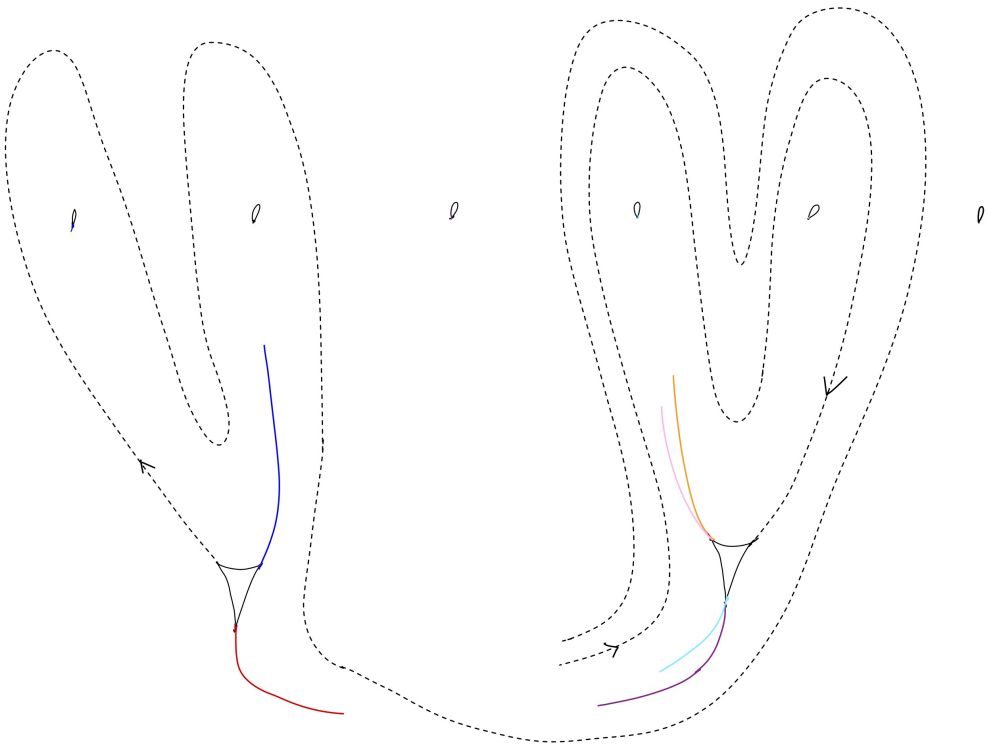


Figure H.53: Harl2

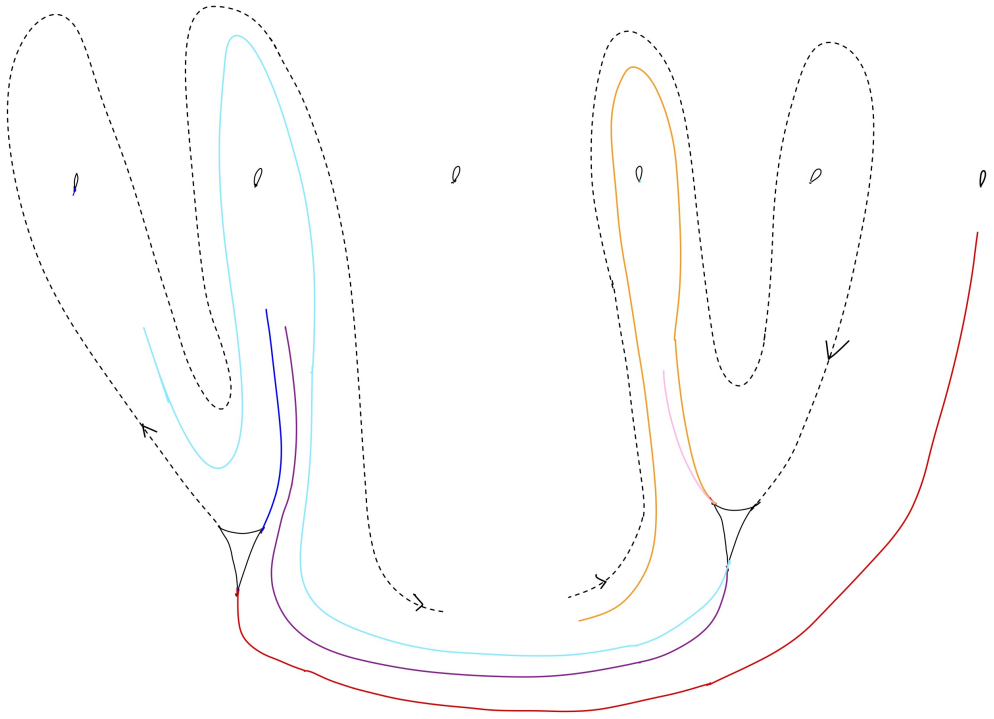


Figure H.54: Harl3

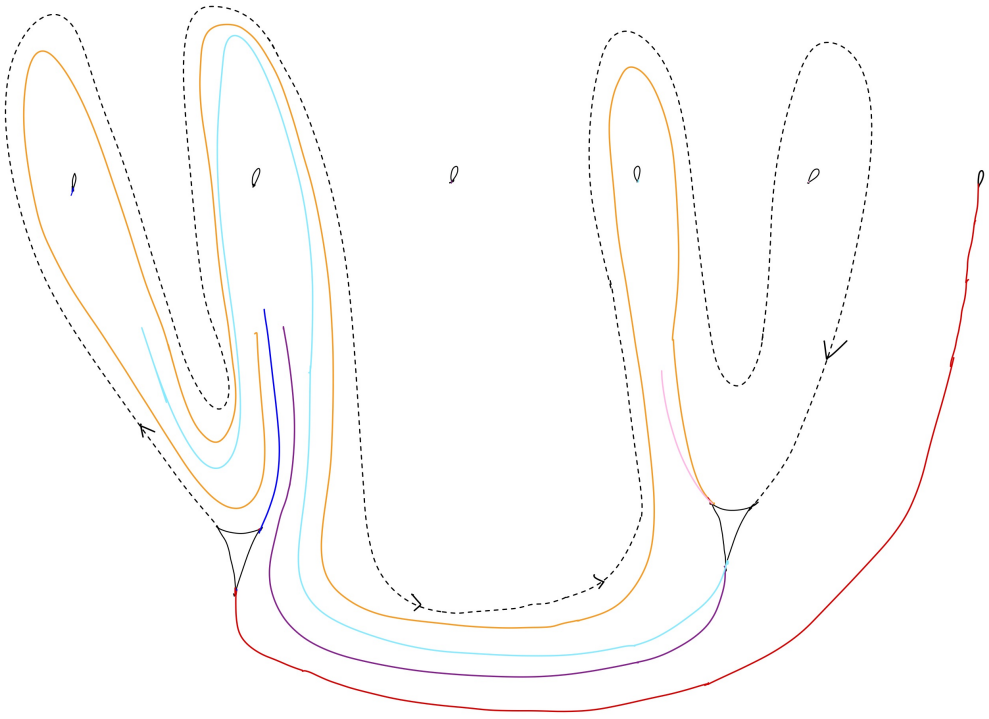


Figure H.55: Harl4

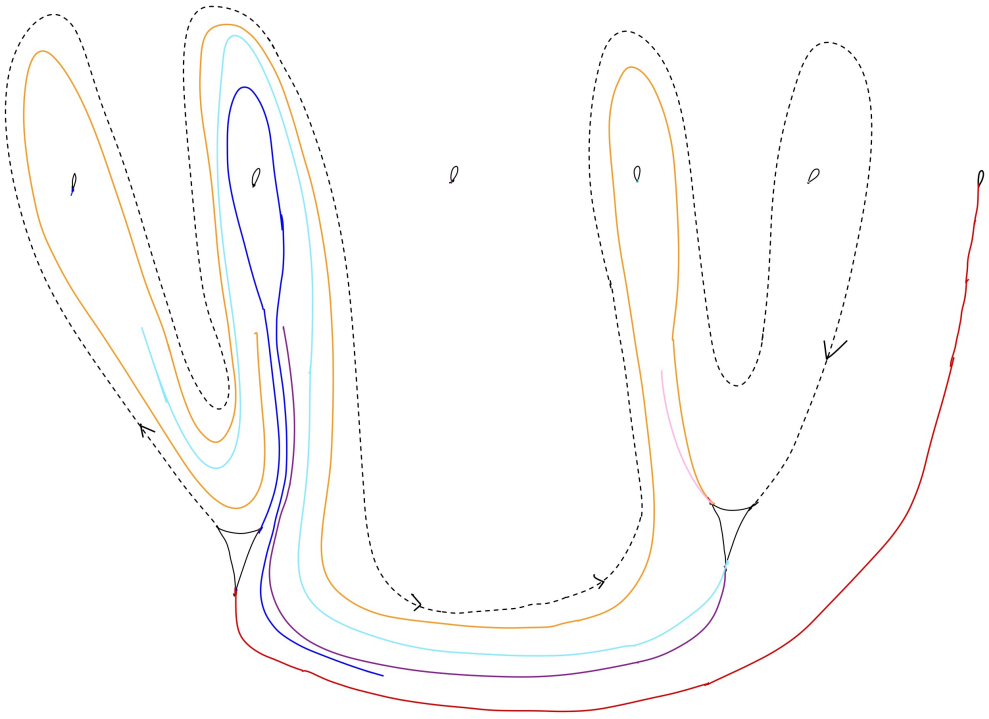


Figure H.56: Harl5

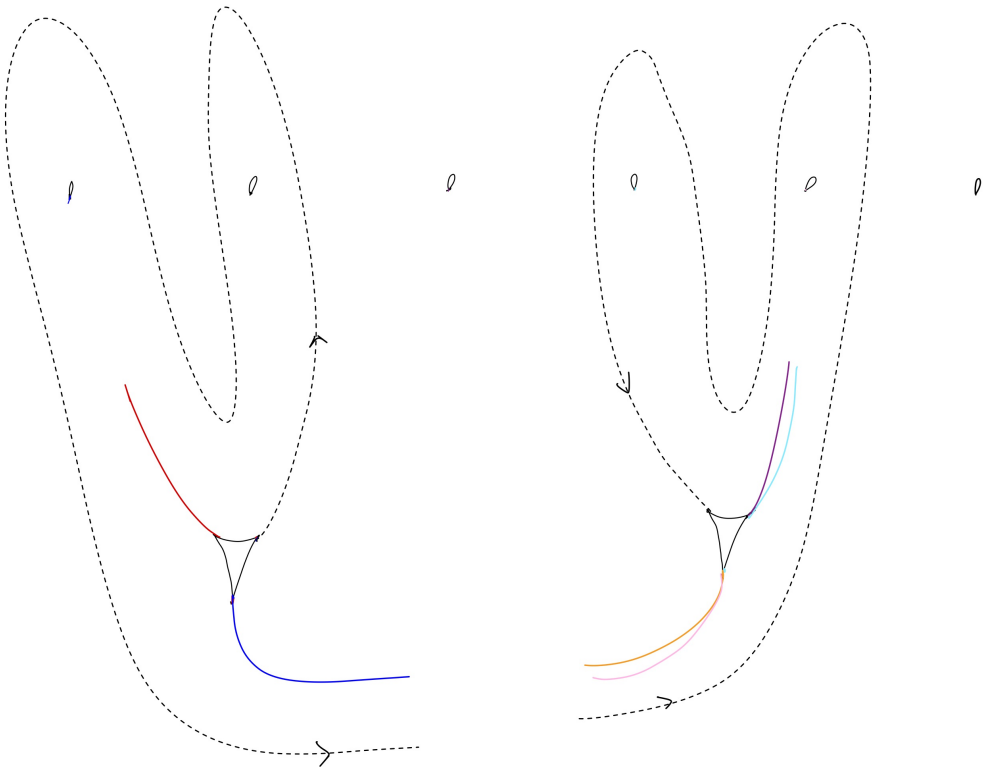


Figure H.57: SEN1

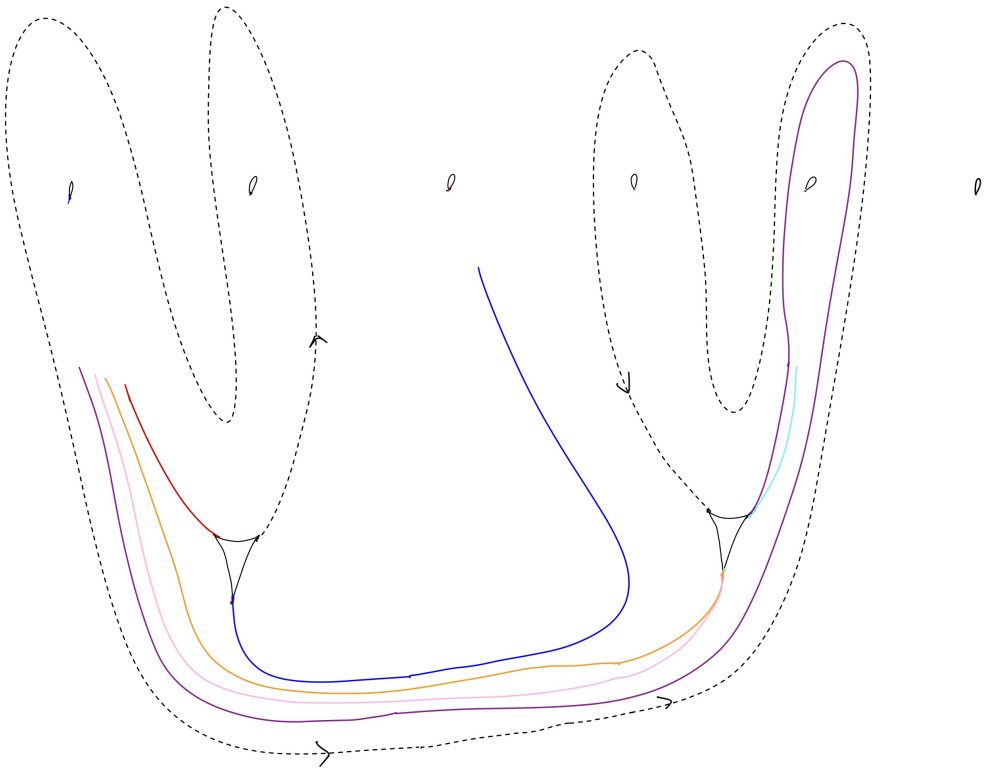


Figure H.58: SEN2

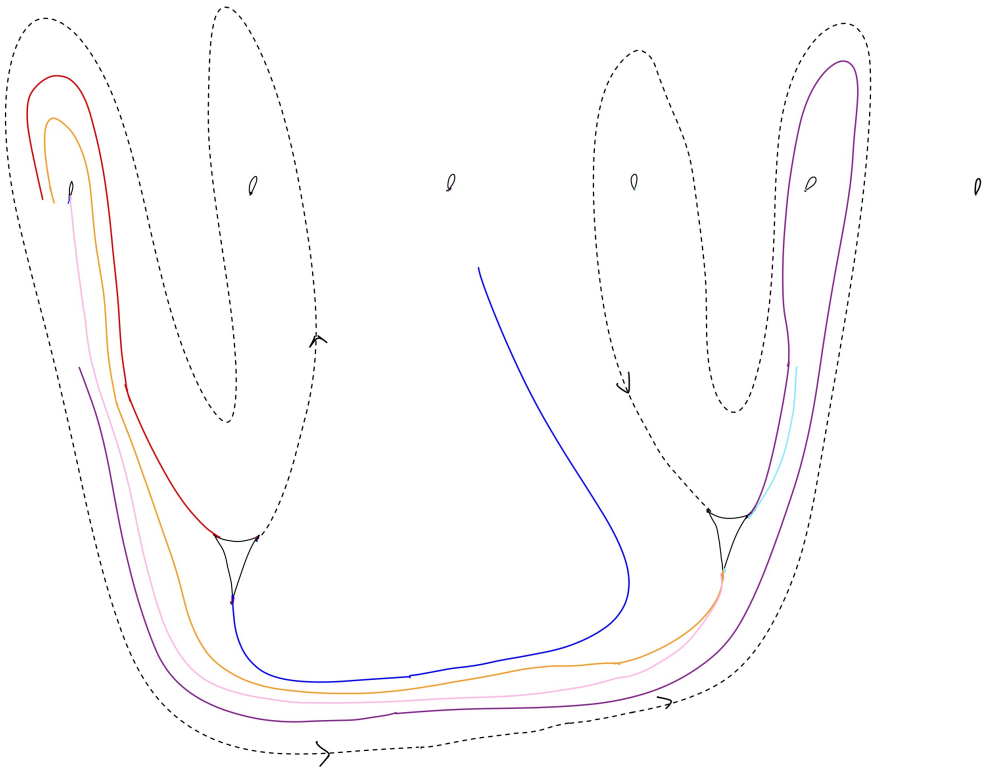


Figure H.59: Marl1

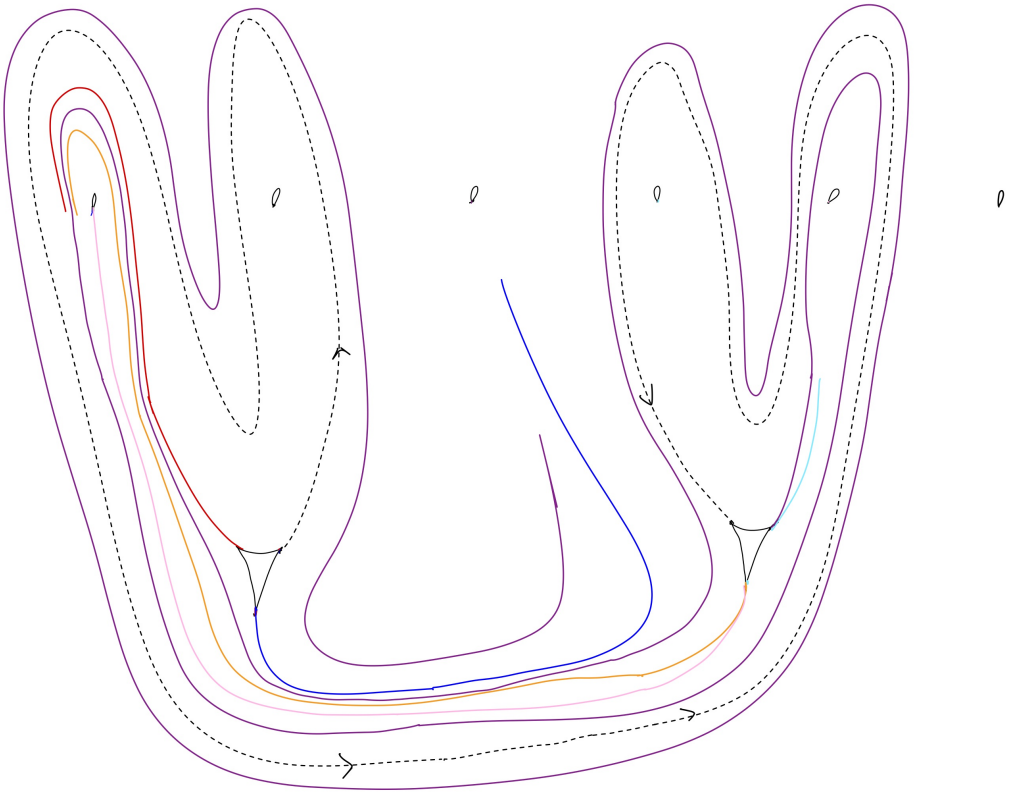


Figure H.60: Marl2

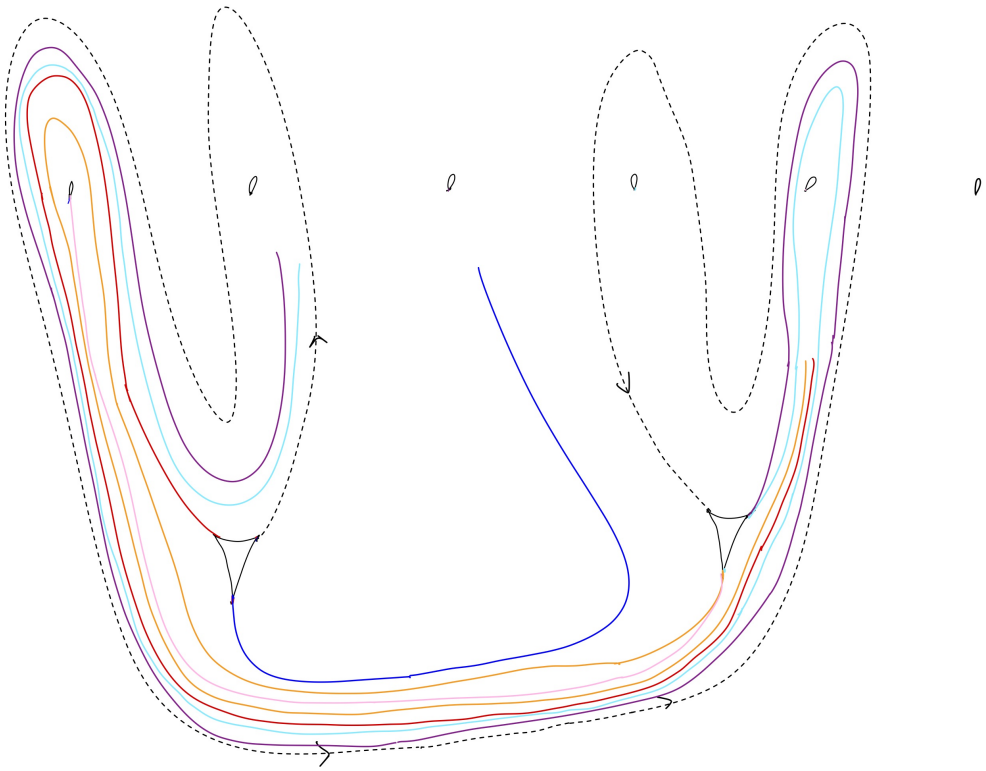


Figure H.61: Marl3

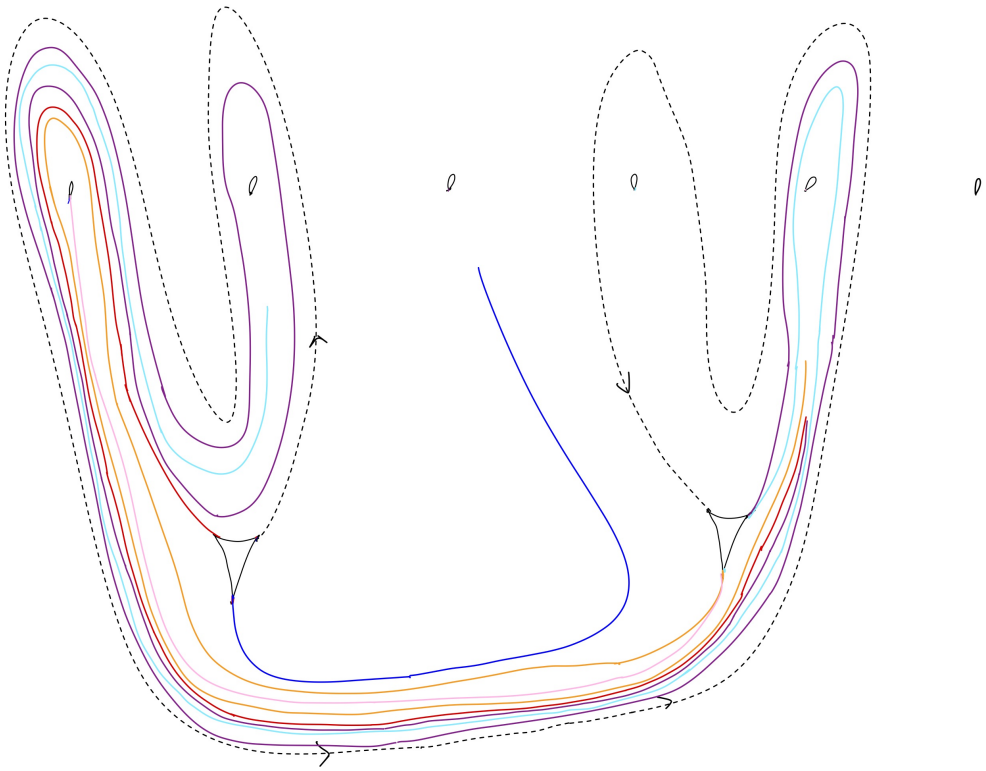


Figure H.62: Marl4

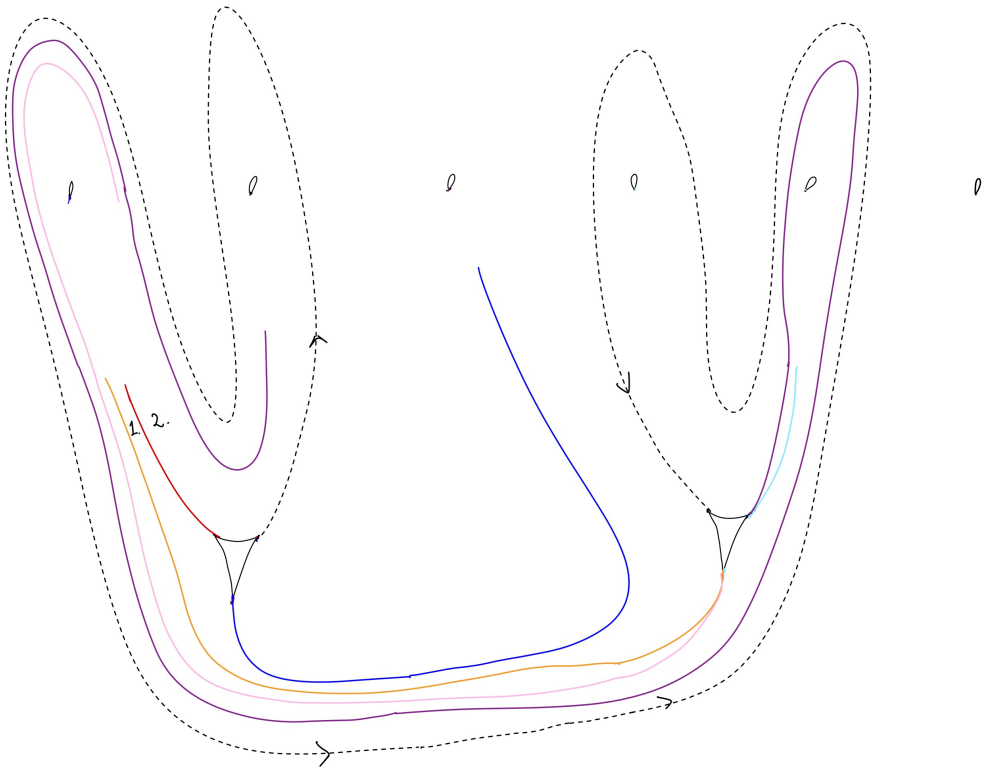


Figure H.63: Peen1

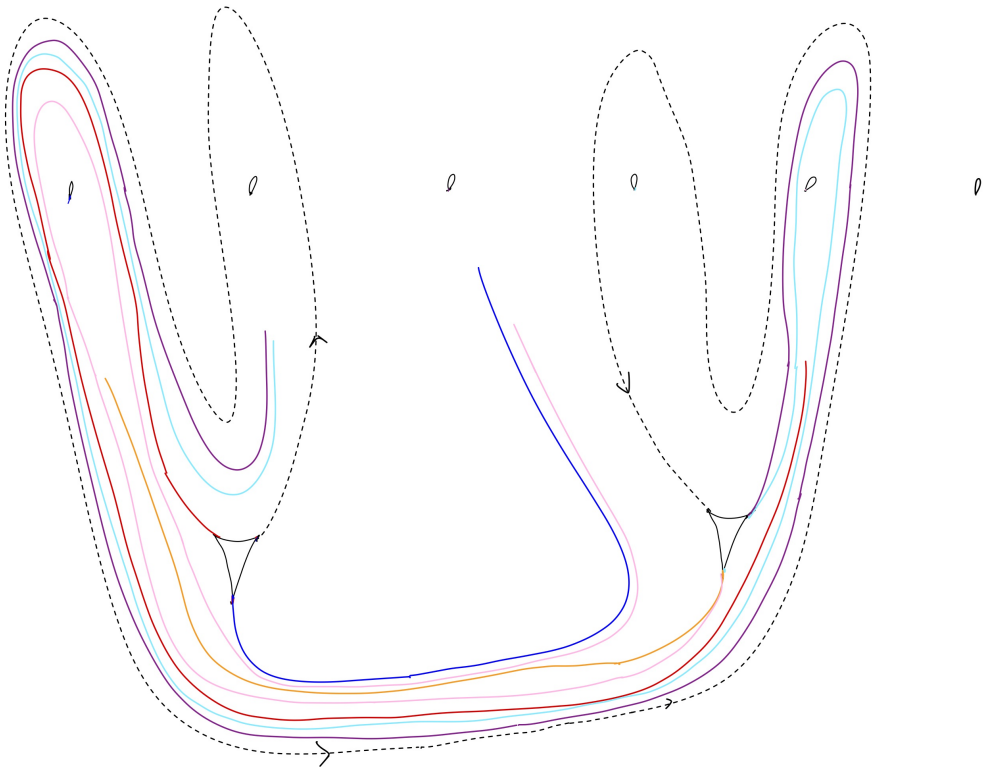


Figure H.64: Howff1

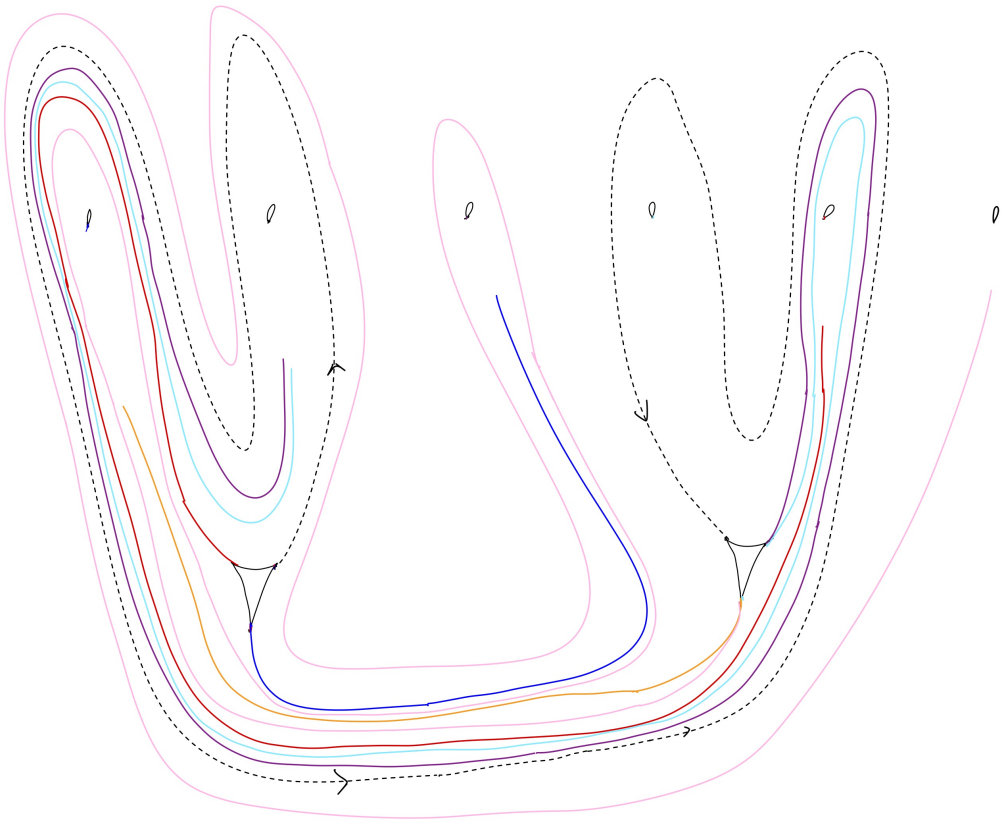


Figure H.65: Howff2

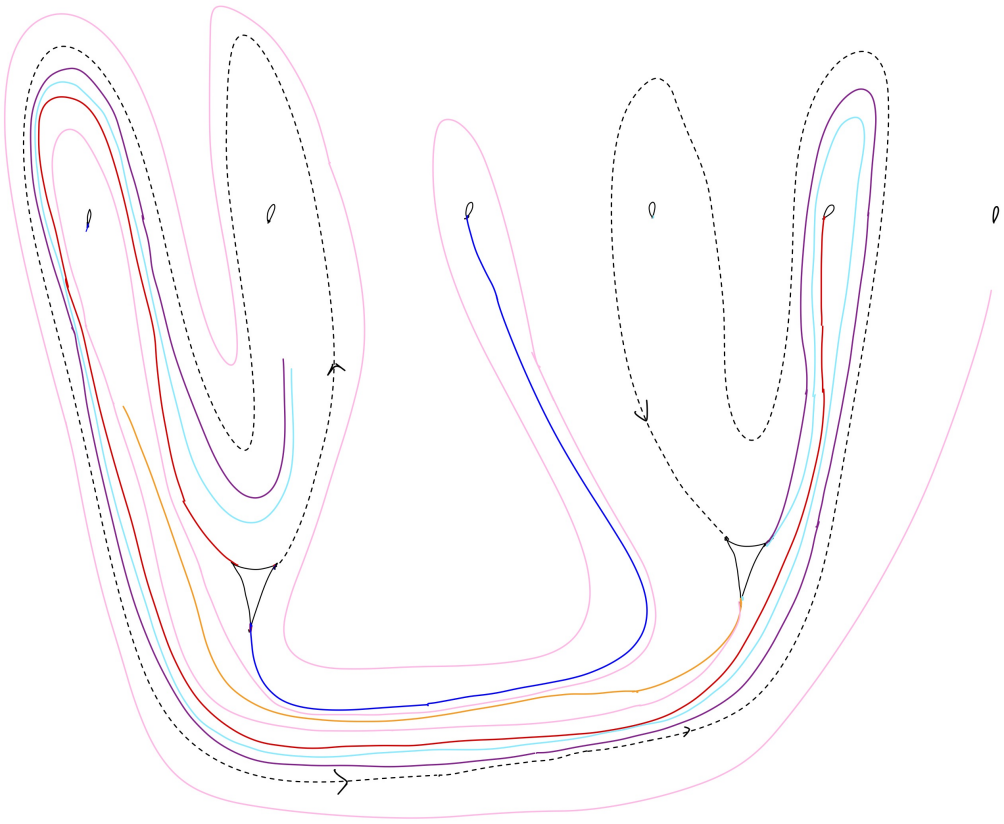


Figure H.66: Howff3

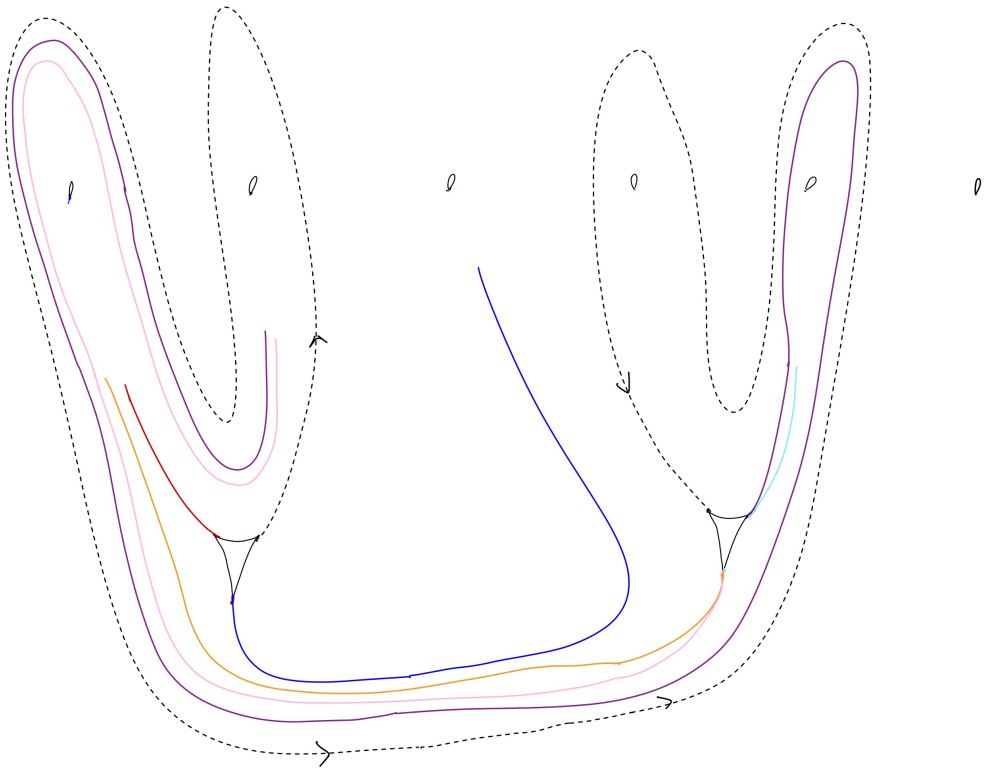


Figure H.67: Jasey1

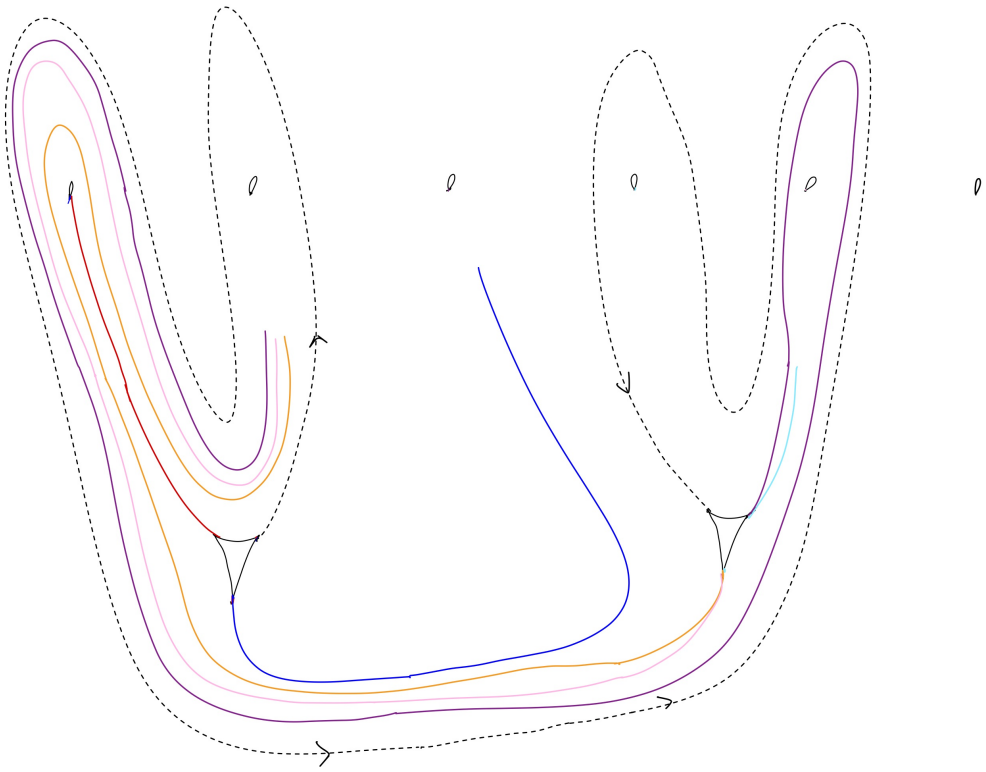


Figure H.68: Gimmer1

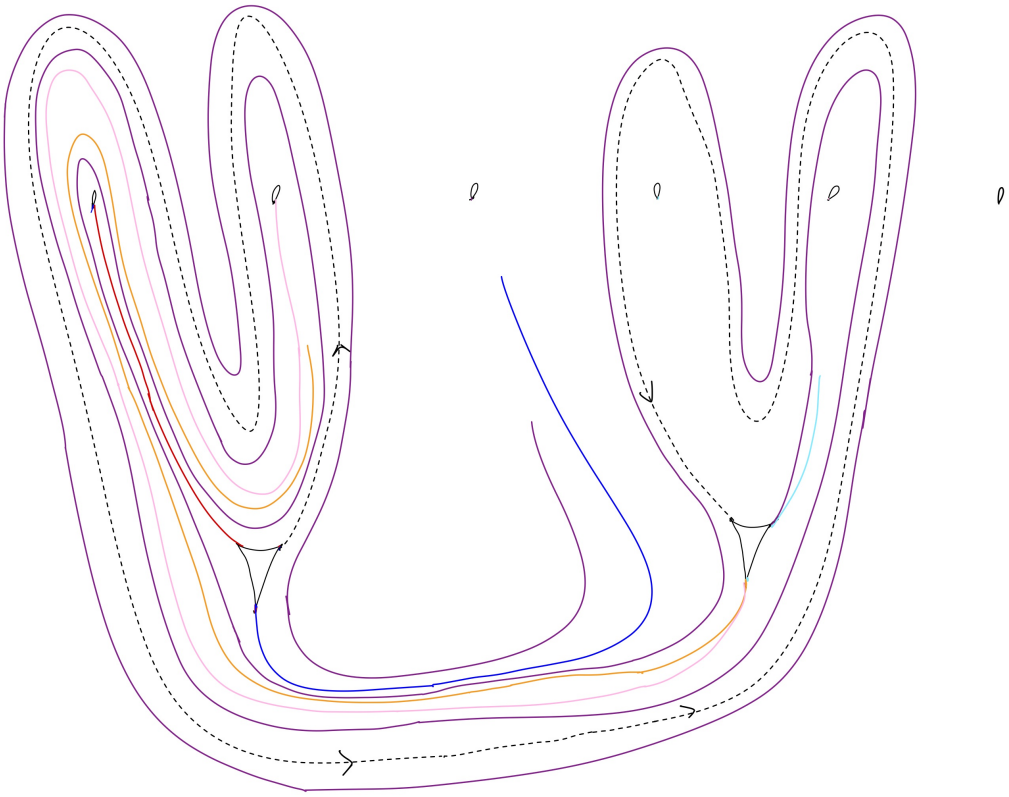


Figure H.69: Gimmer2

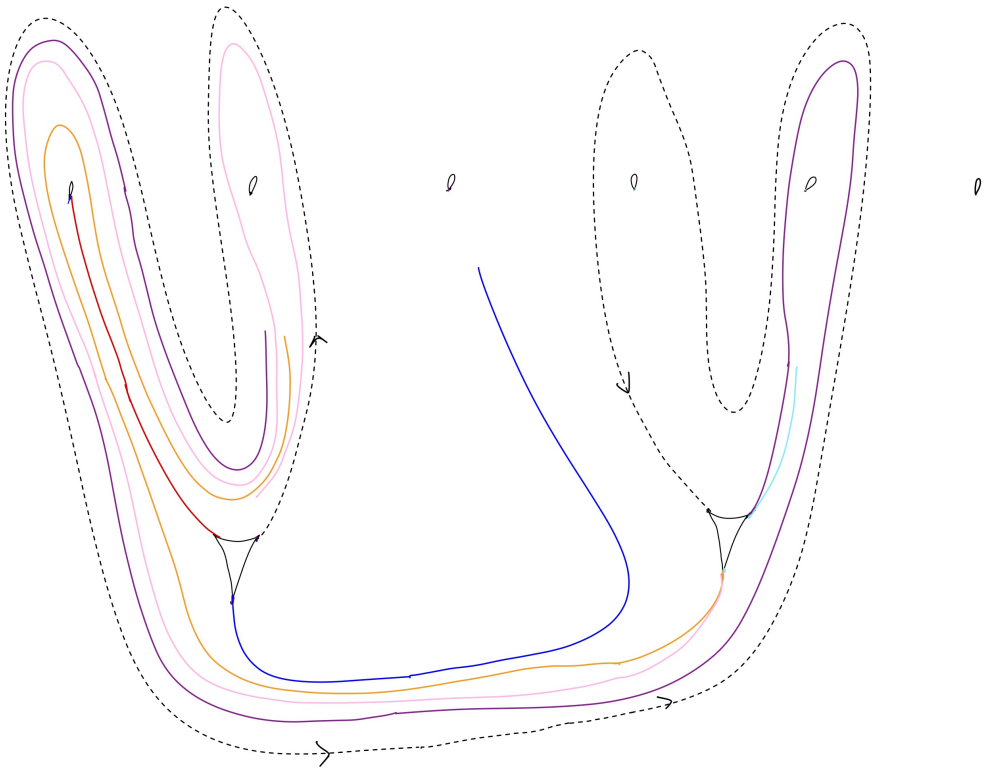


Figure H.70: Gimmer3

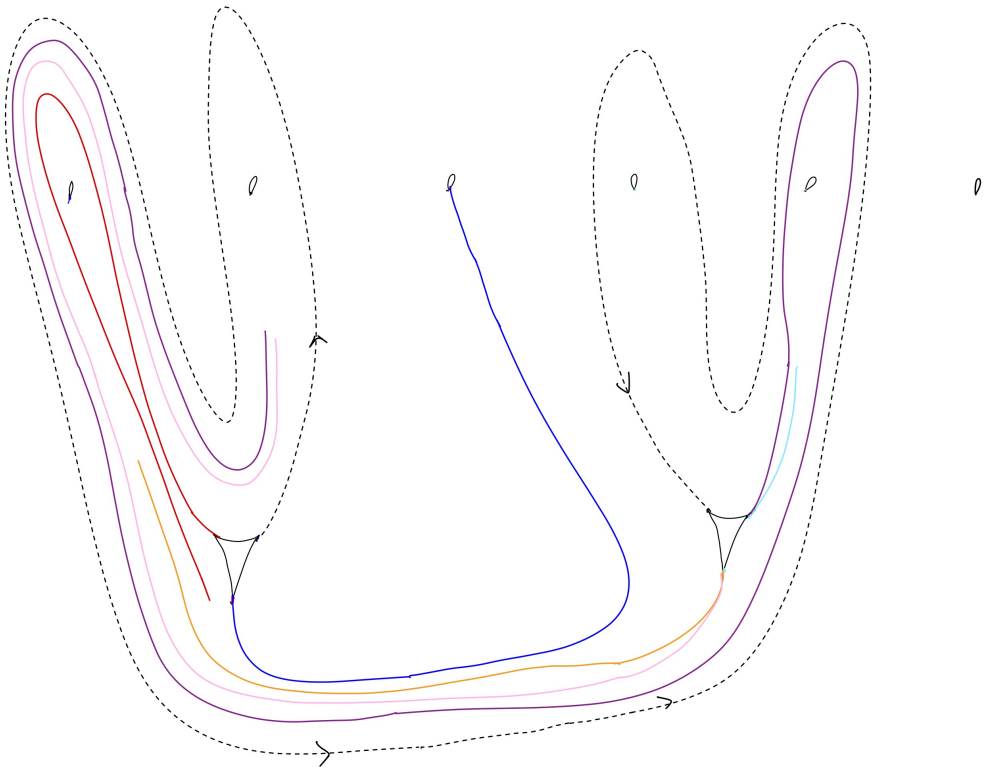


Figure H.71: Hantle1

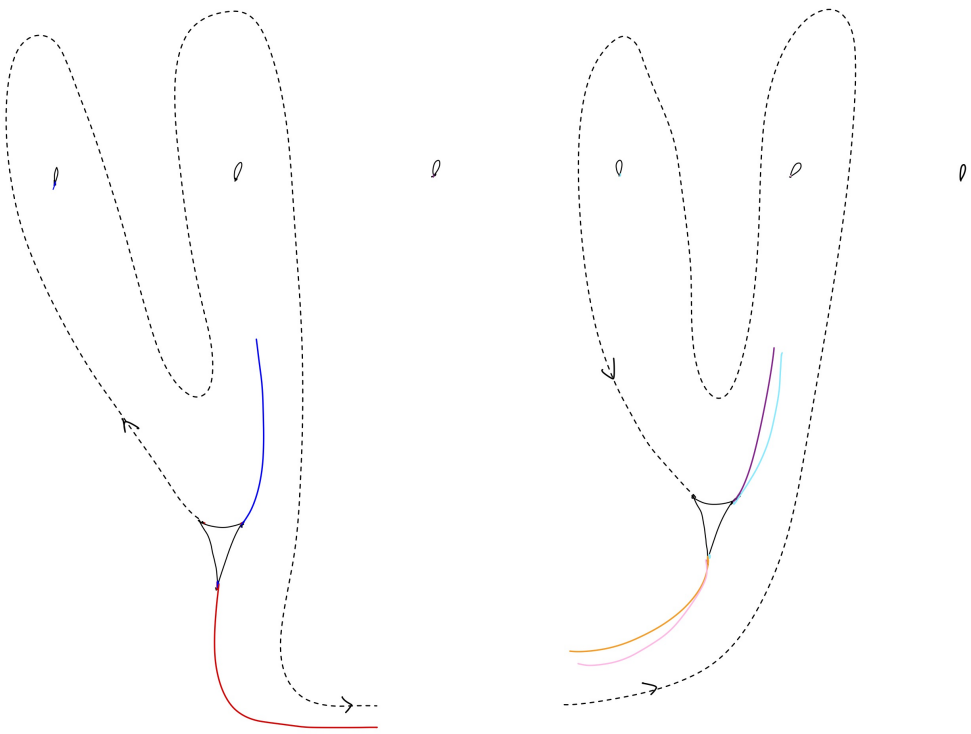


Figure H.72: HUN1

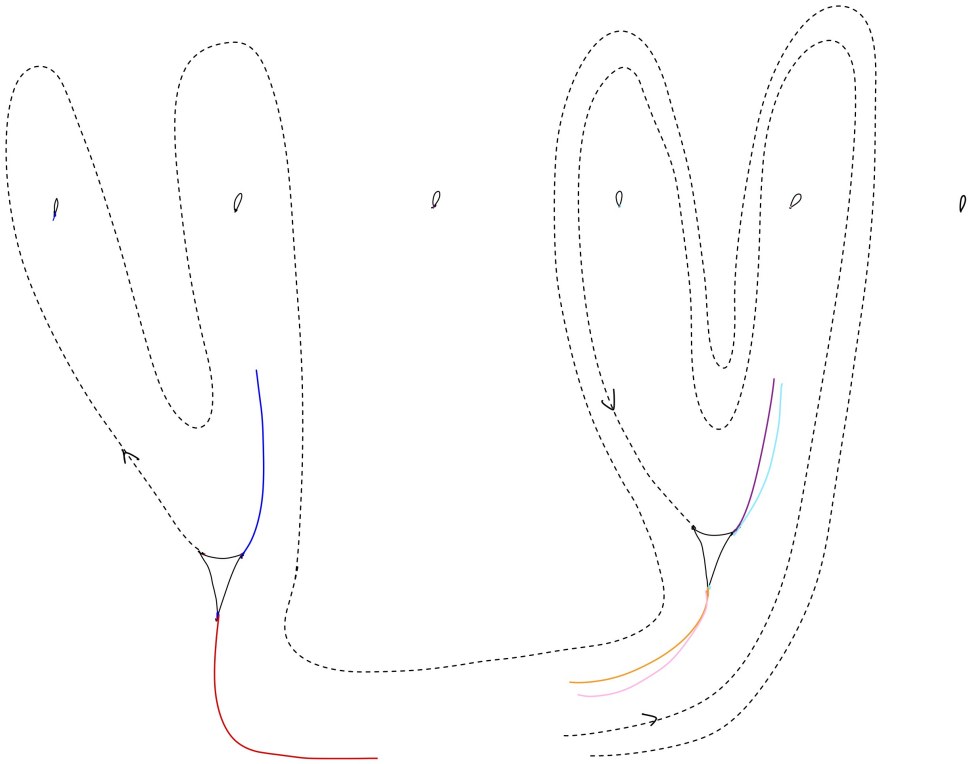


Figure H.73: HUN2

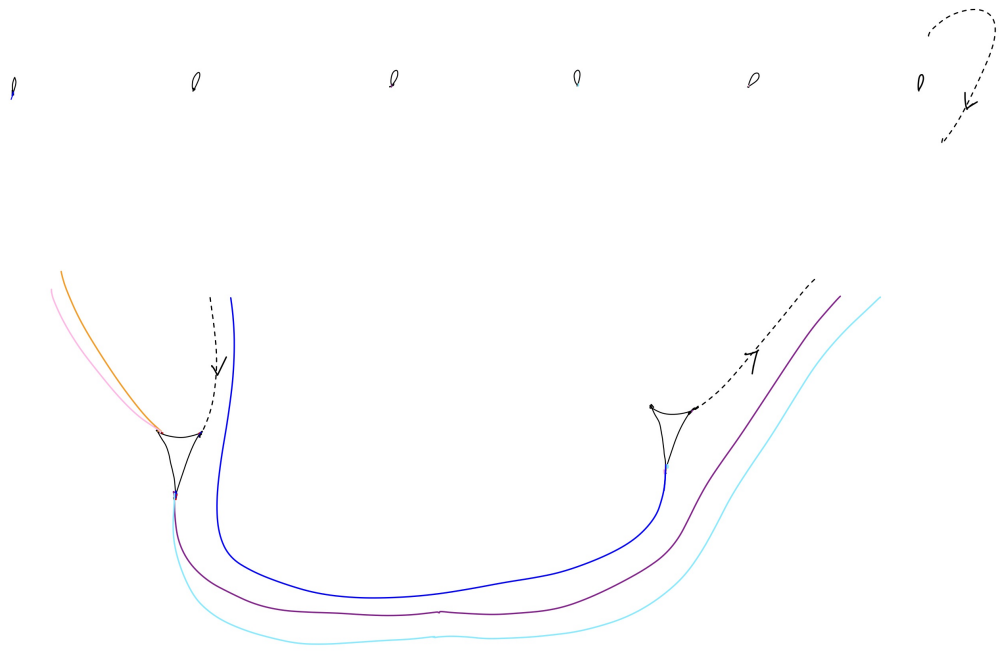


Figure H.74: GUW1

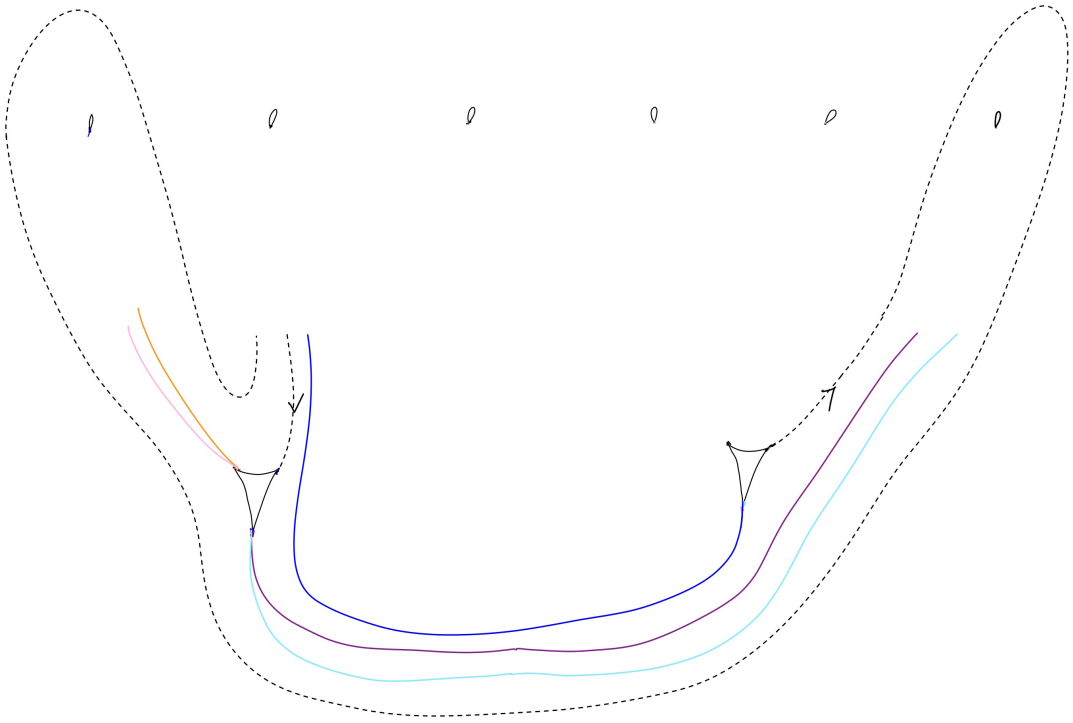


Figure H.75: GUW2

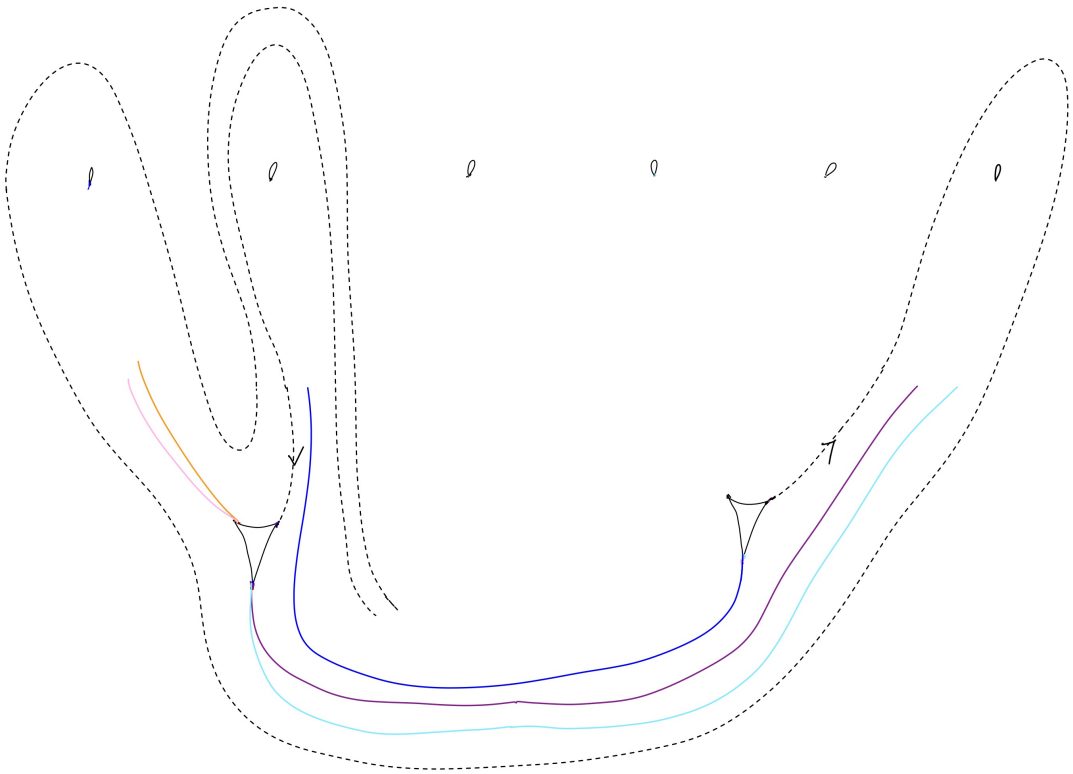


Figure H.76: GUW3

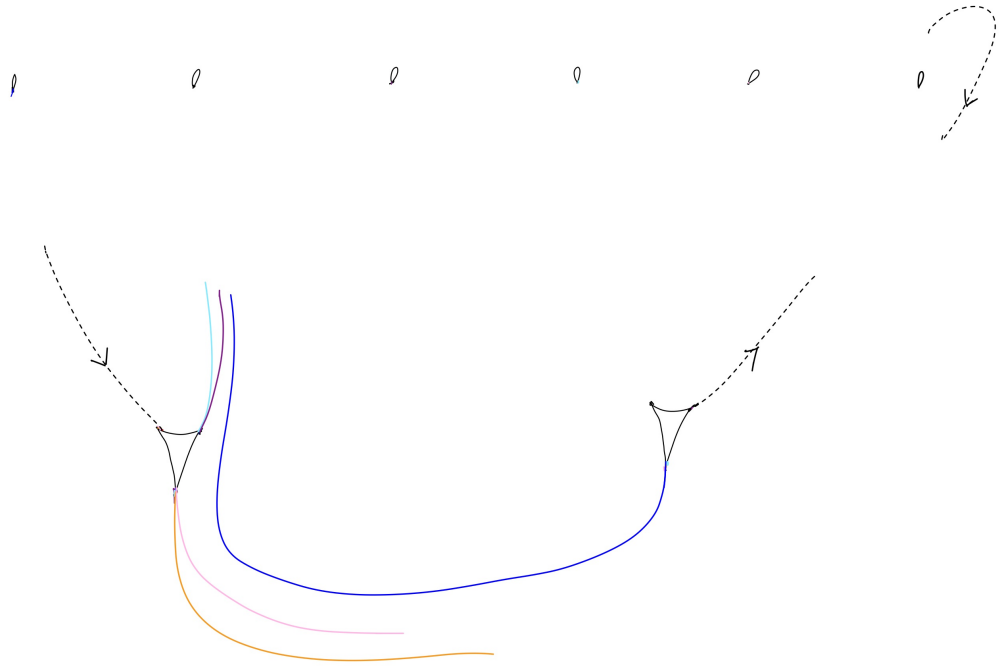


Figure H.77: CPX1

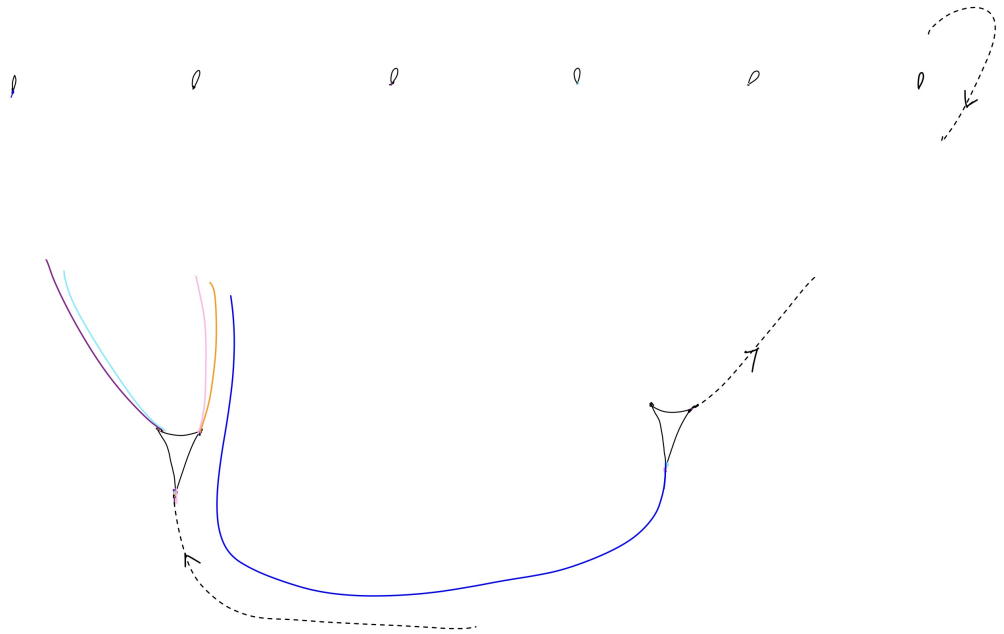


Figure H.78: SCC1

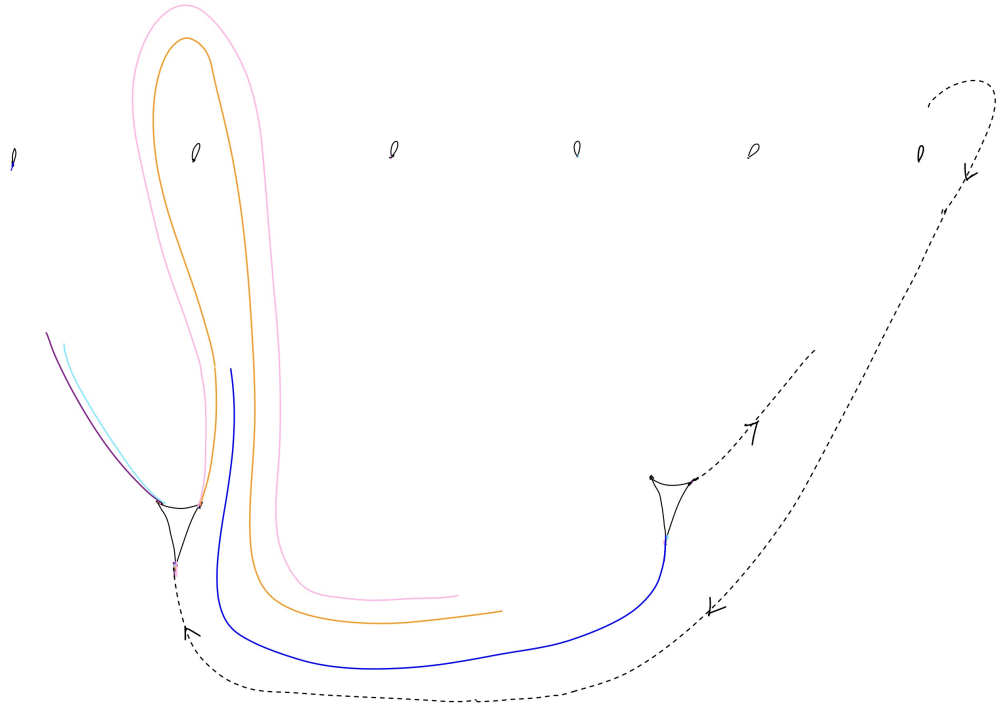


Figure H.79: SCC2

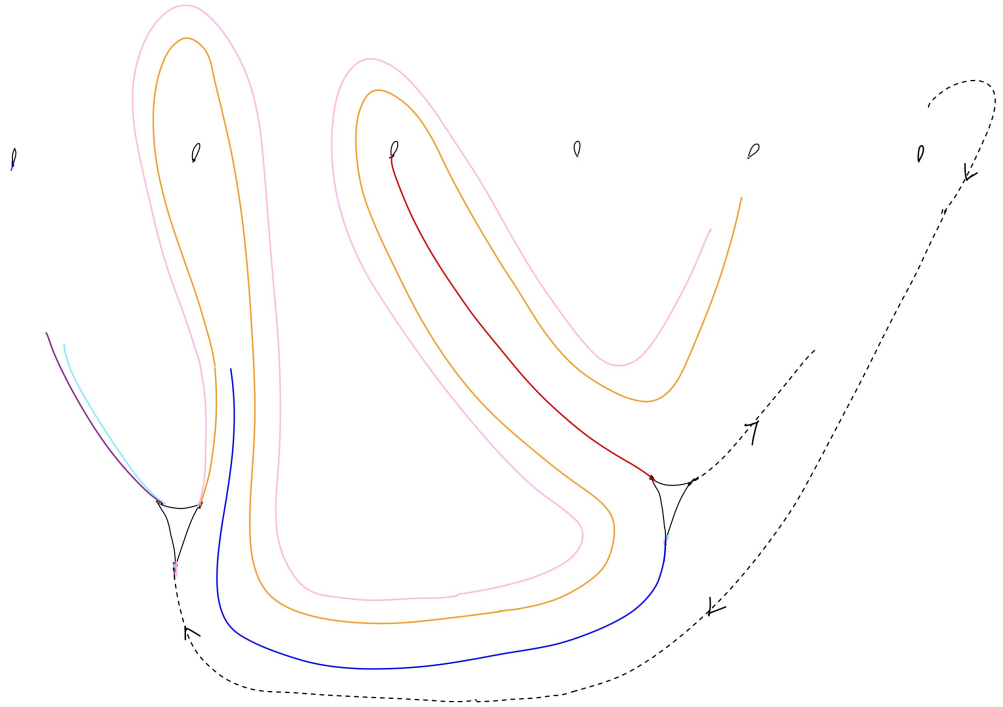


Figure H.80: SCC3

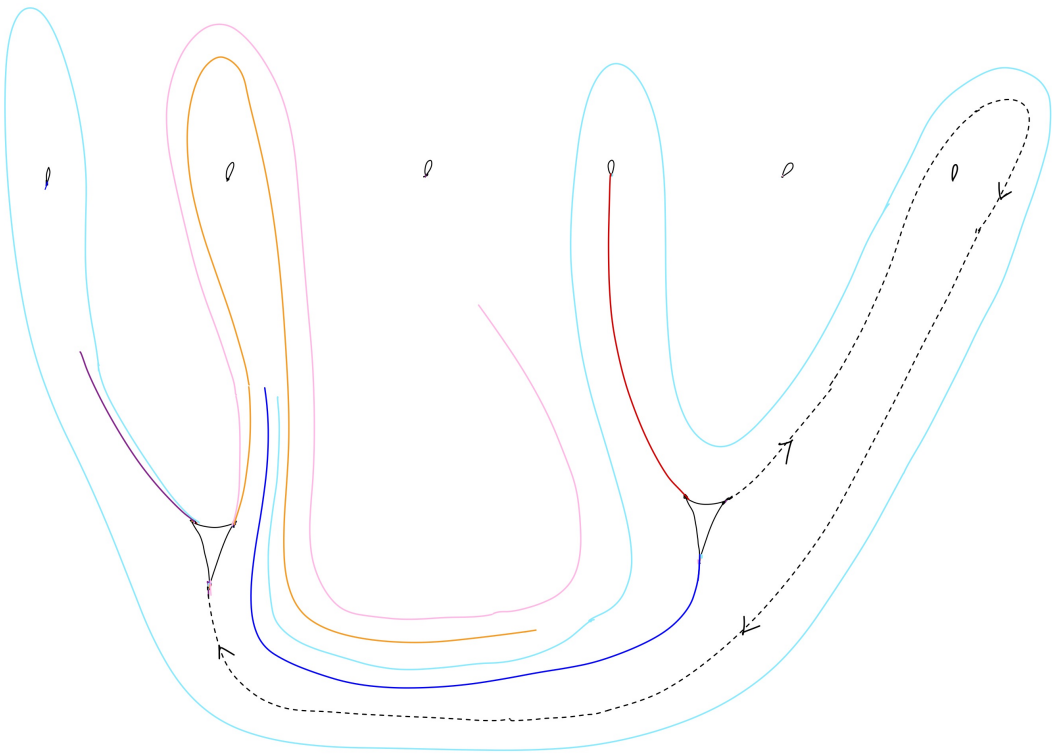


Figure H.81: SCC4

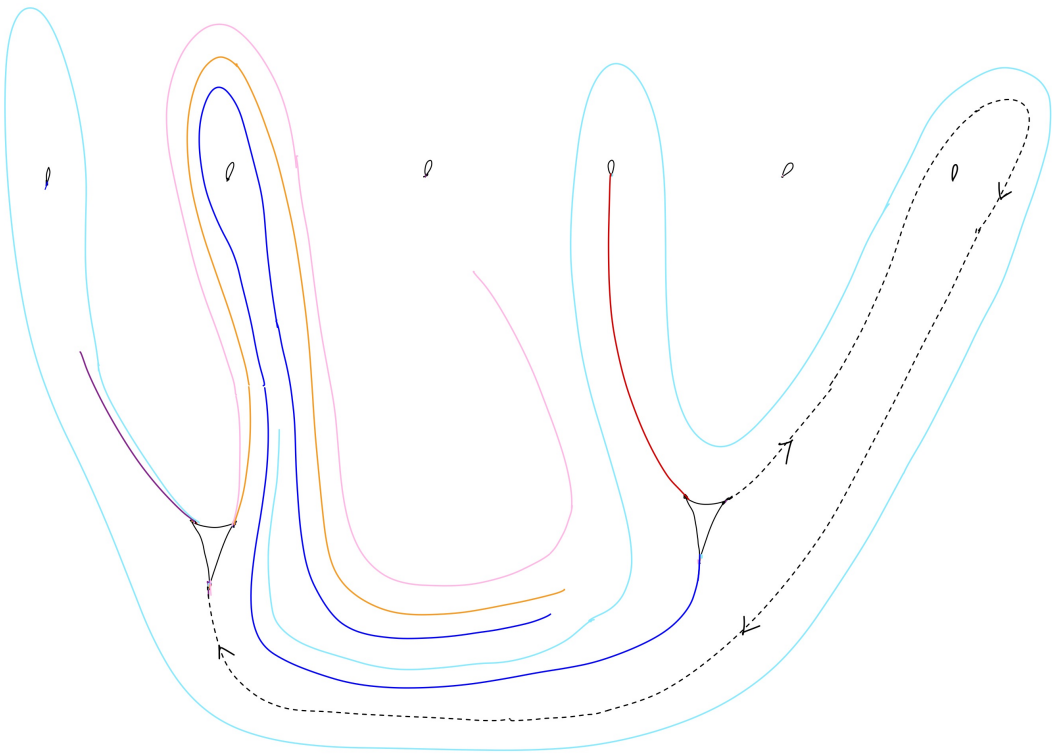


Figure H.82: SCC5

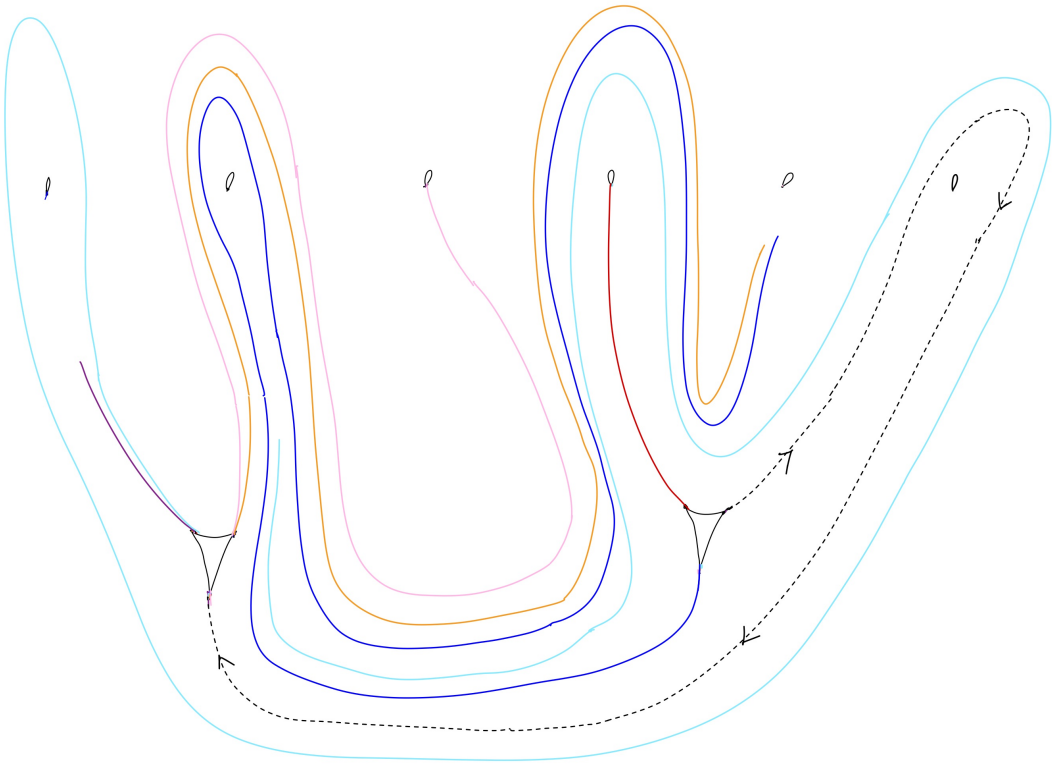


Figure H.83: SCC6

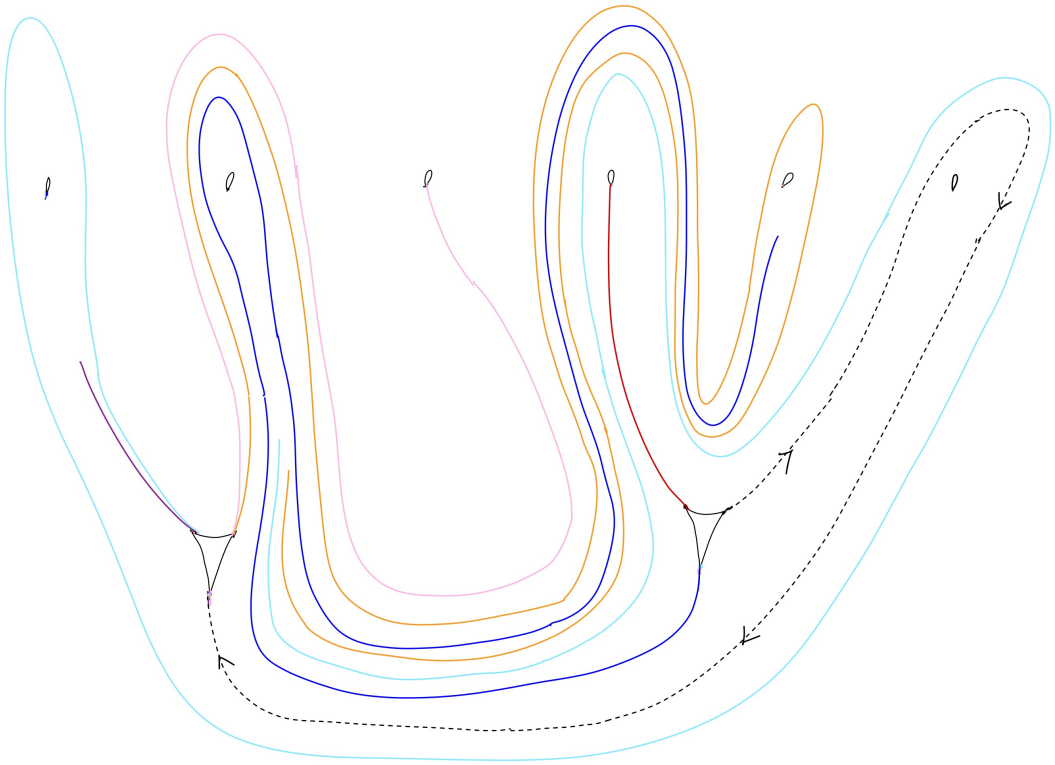


Figure H.84: SCC7

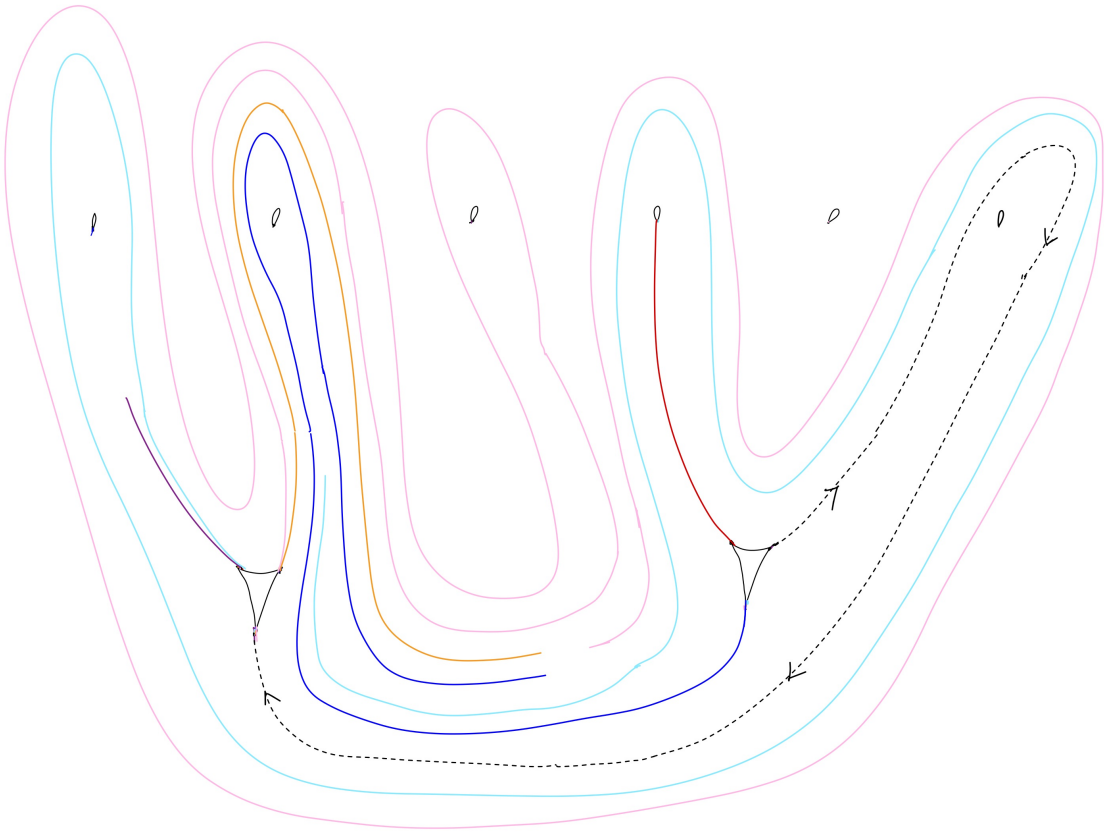


Figure H.85: SCC8

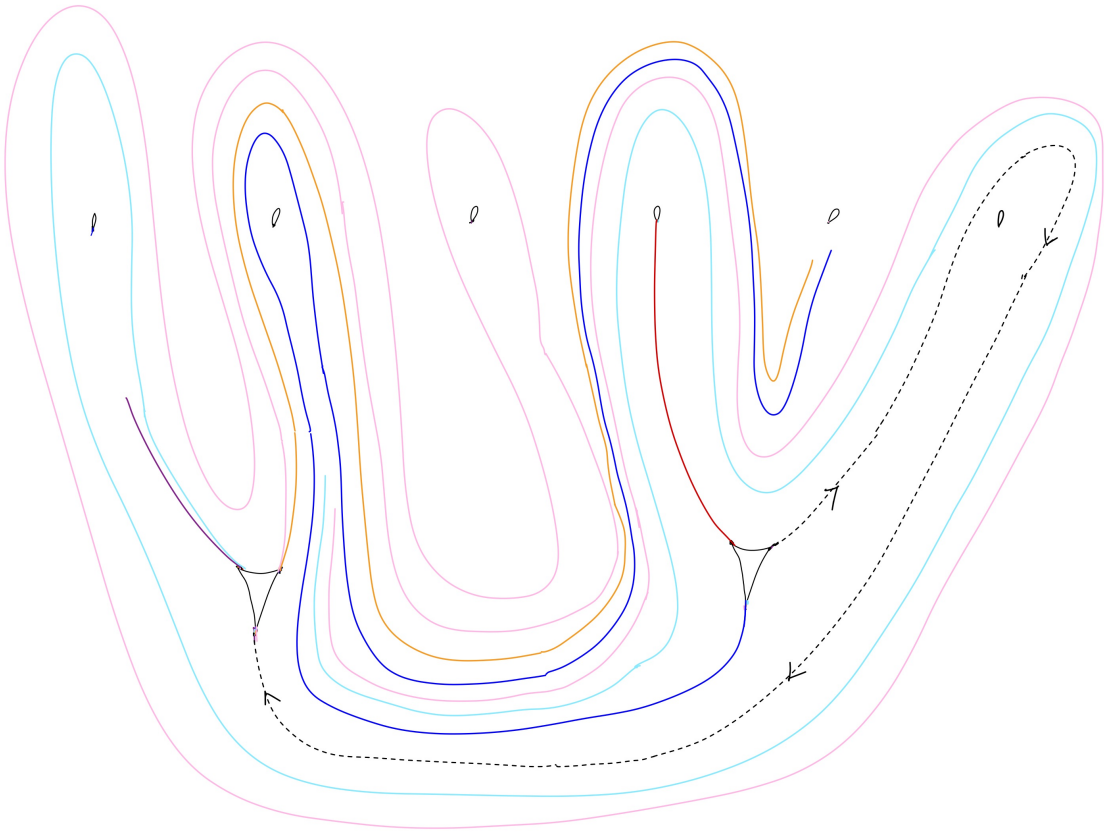


Figure H.86: SCC9

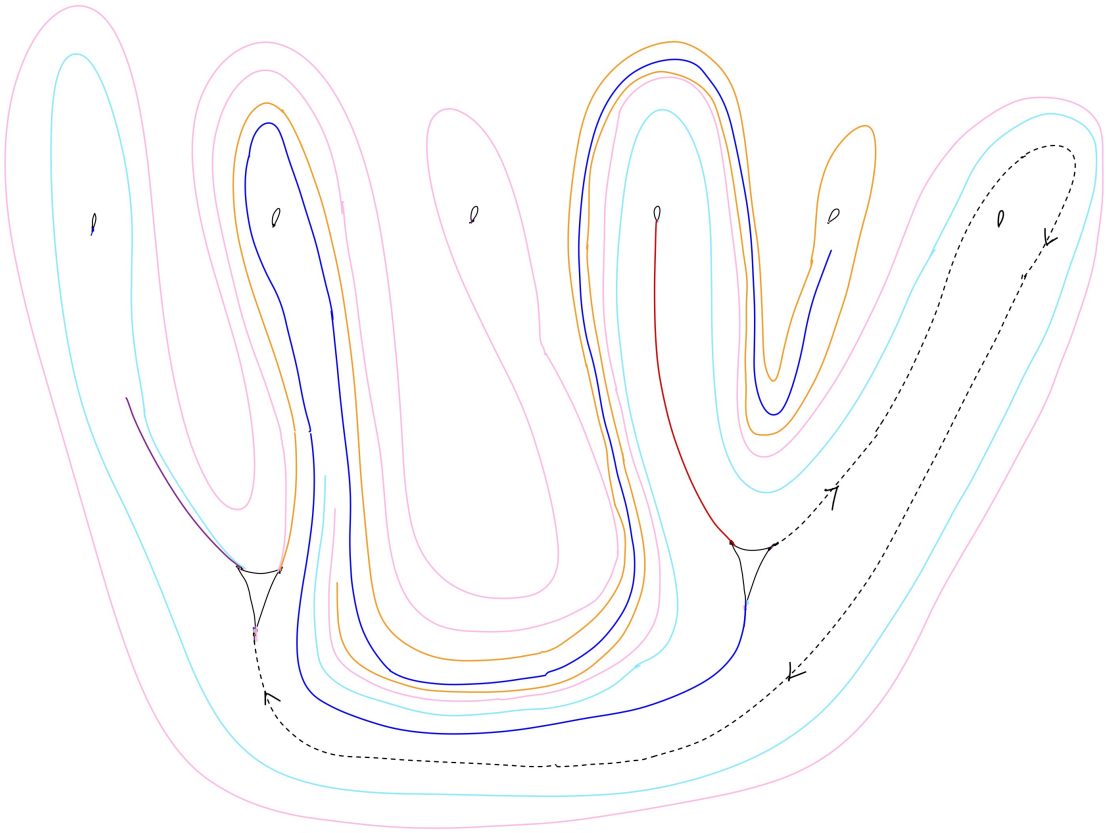


Figure H.87: SCC10

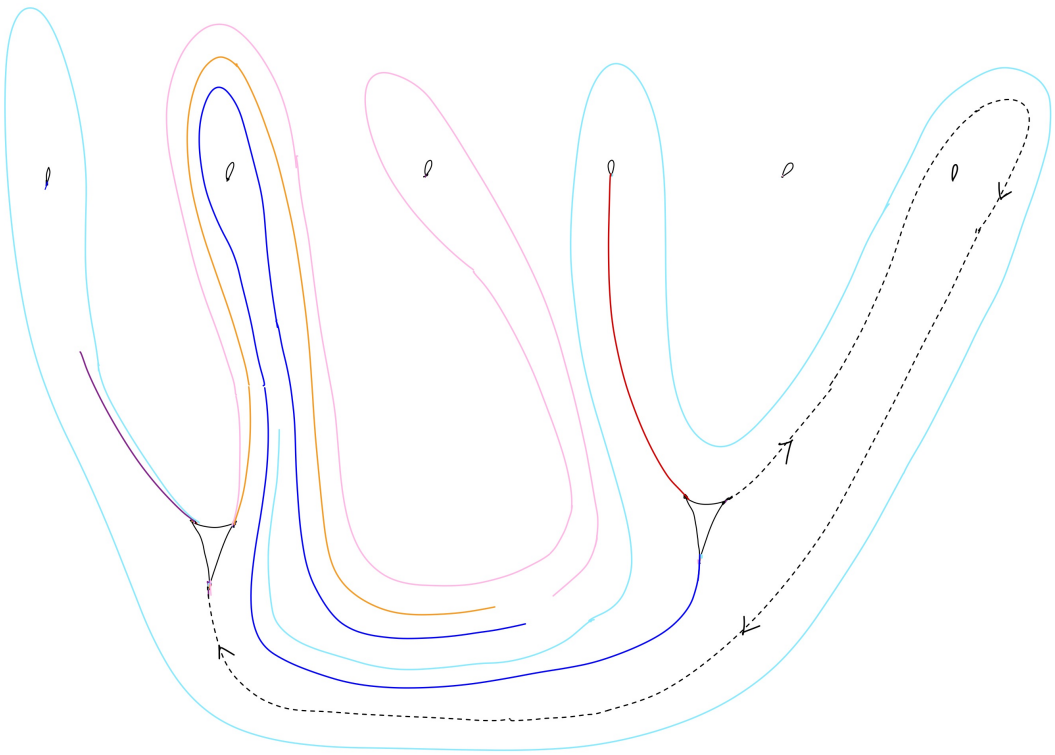


Figure H.88: SCC11

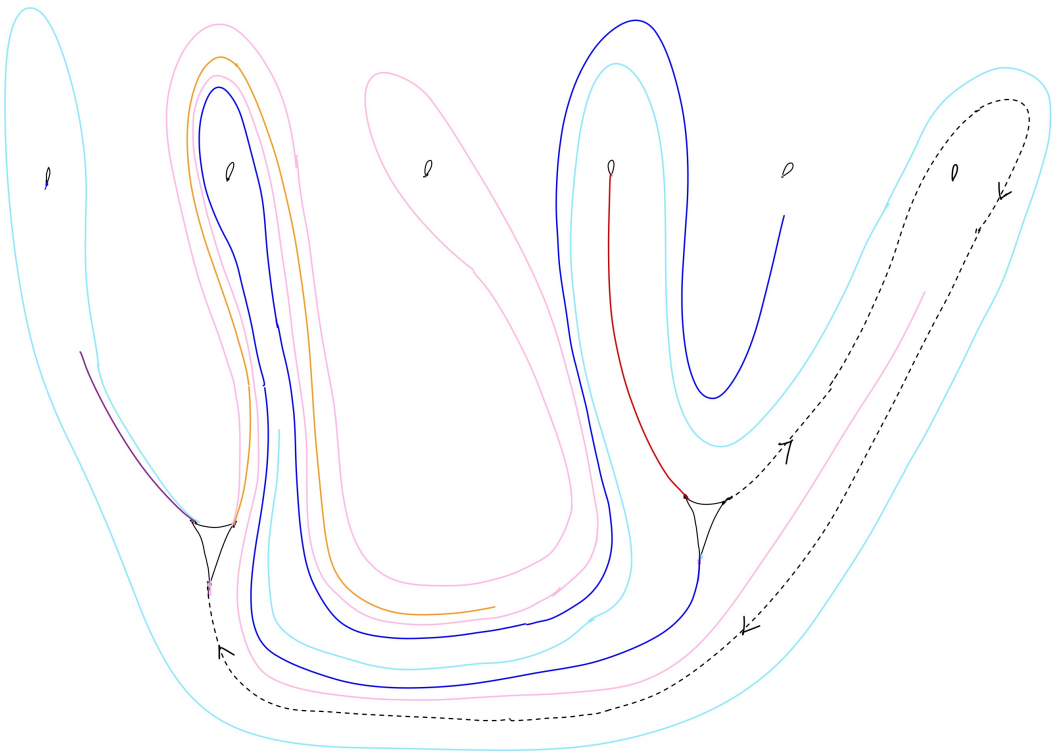


Figure H.89: SCC12

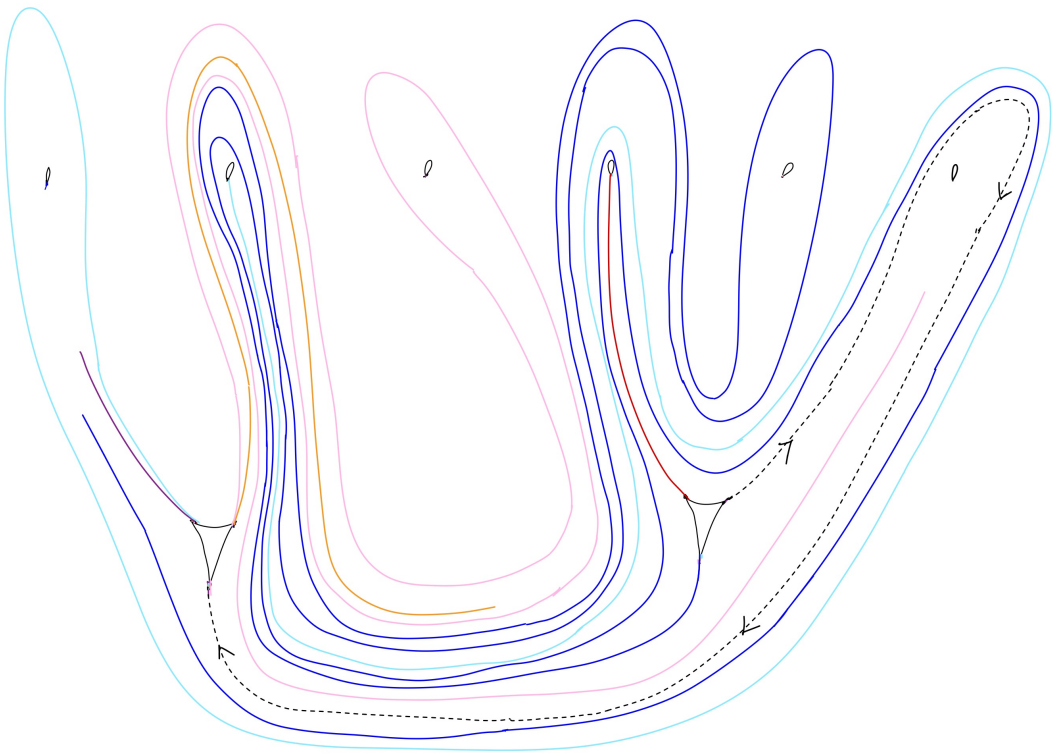


Figure H.90: SCC13

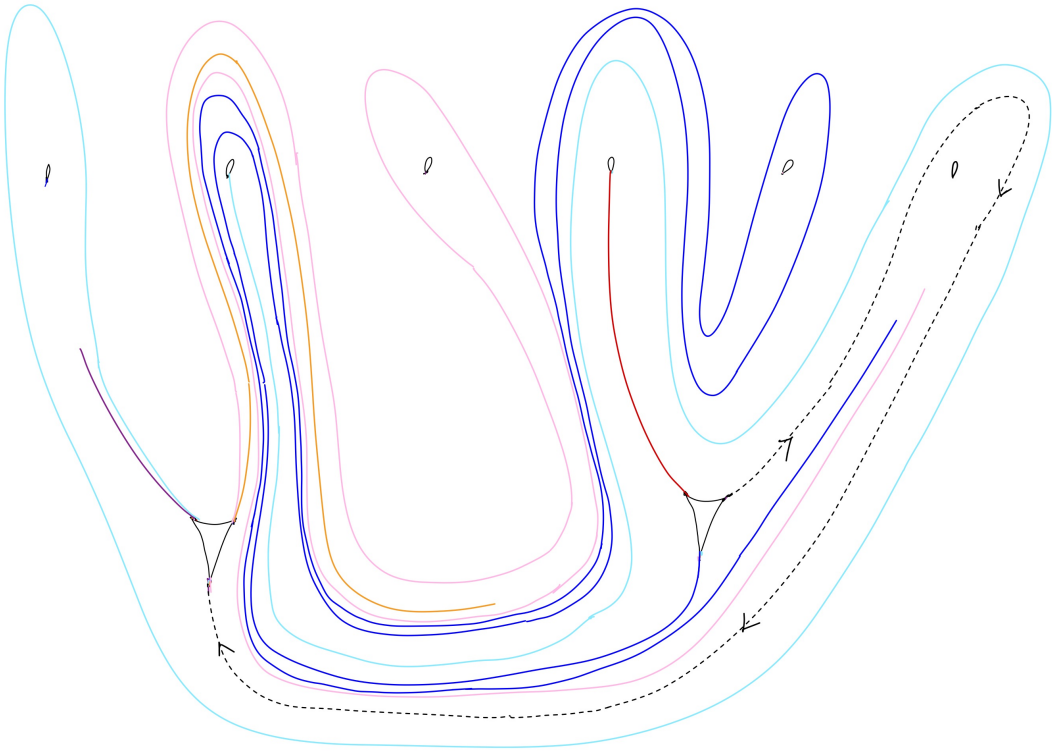


Figure H.91: SCC14

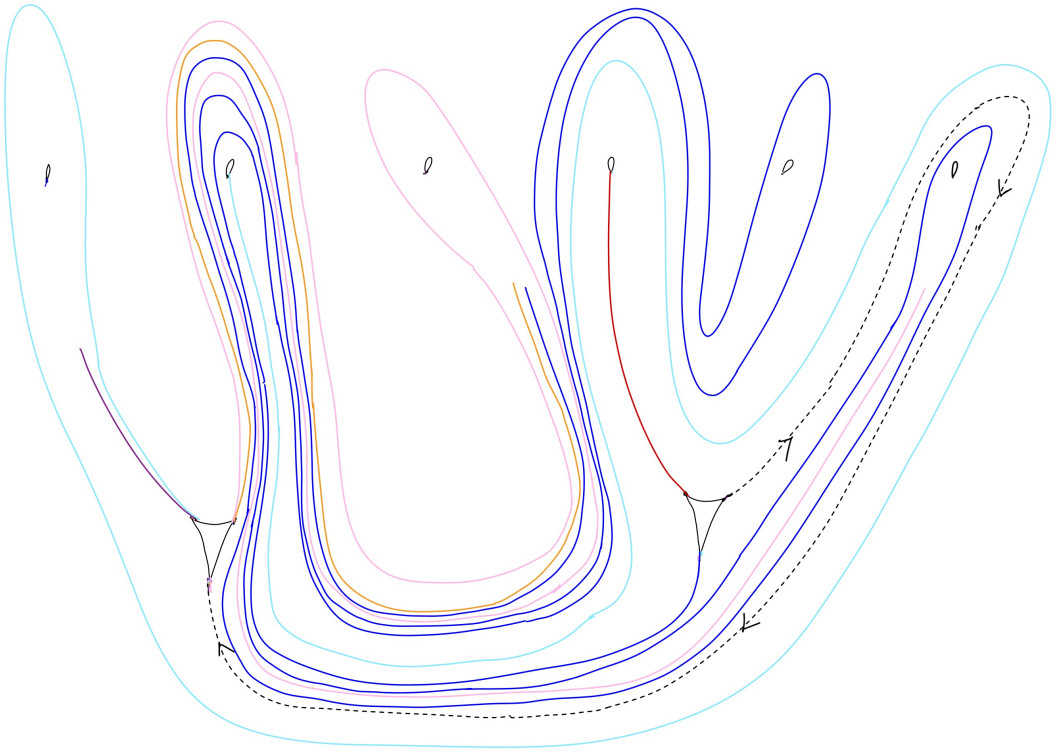


Figure H.92: SCC15

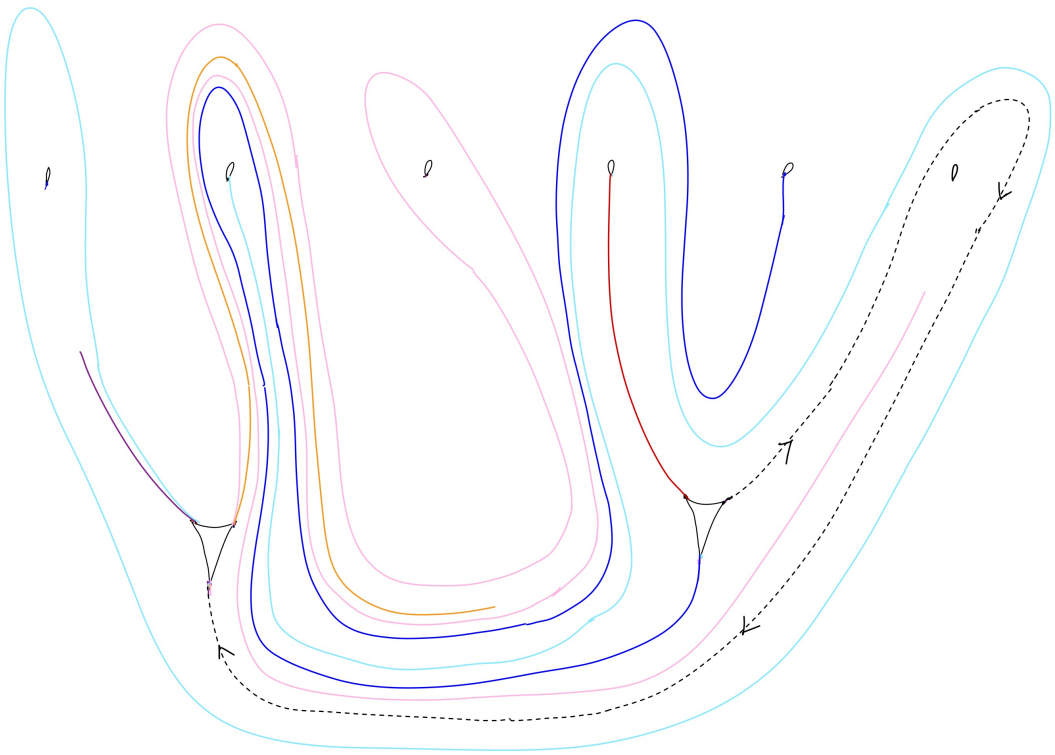


Figure H.93: SCC16

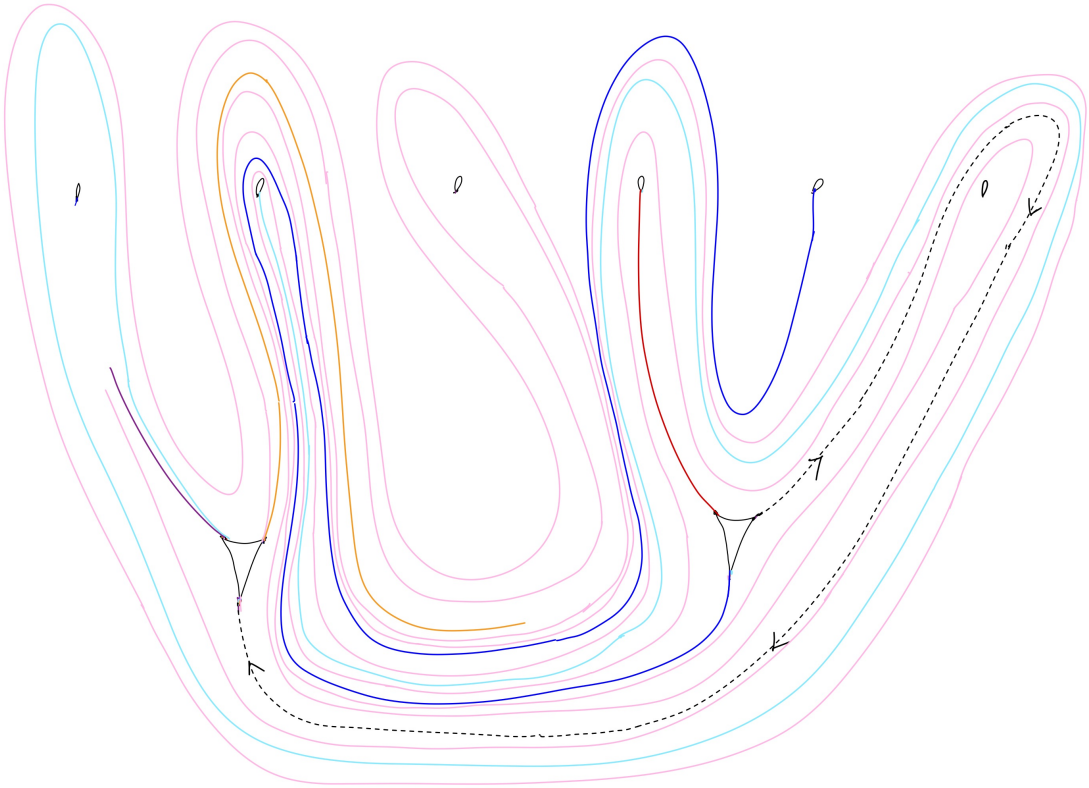


Figure H.94: SCC17

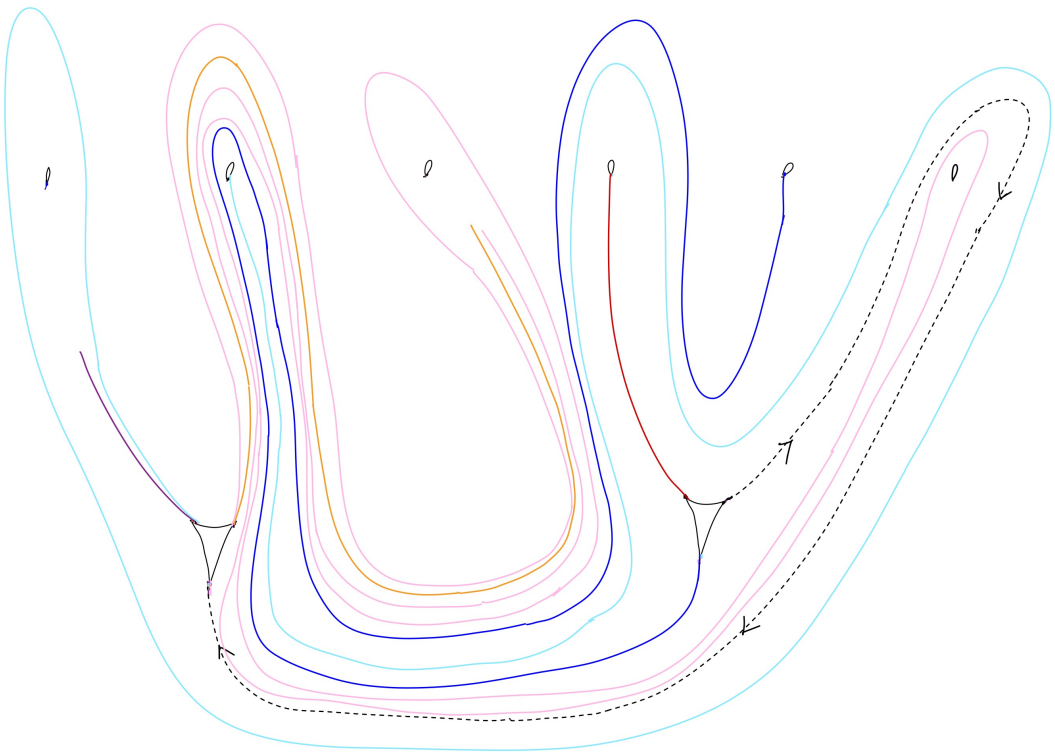


Figure H.95: SCC18

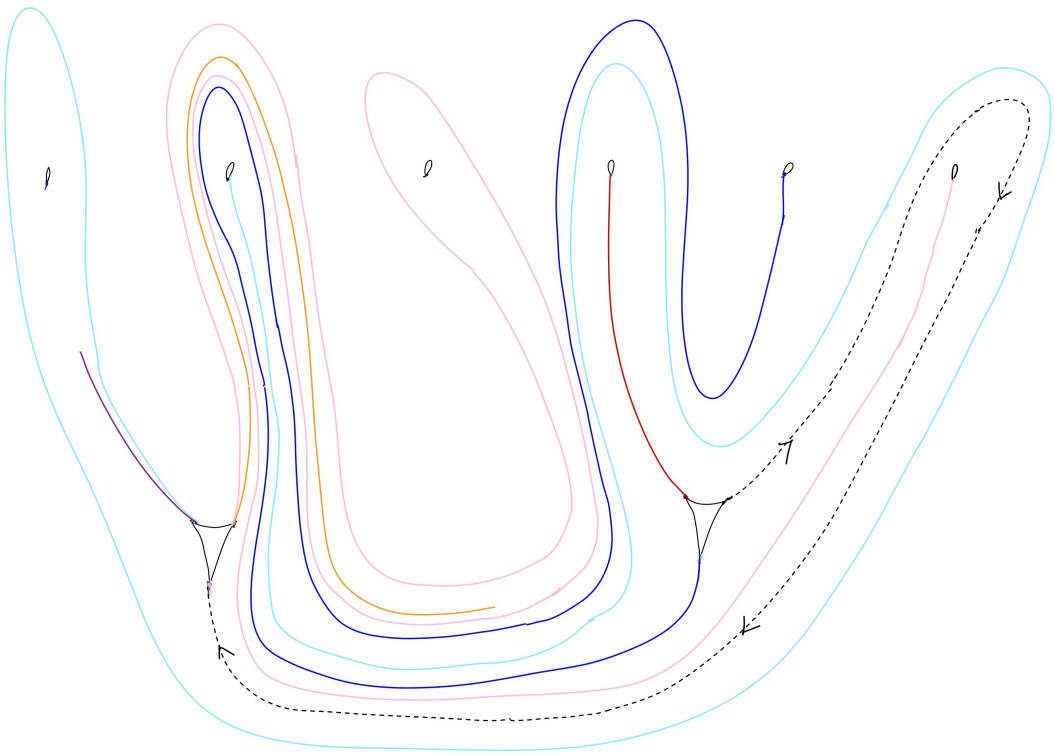


Figure H.96: SCC19

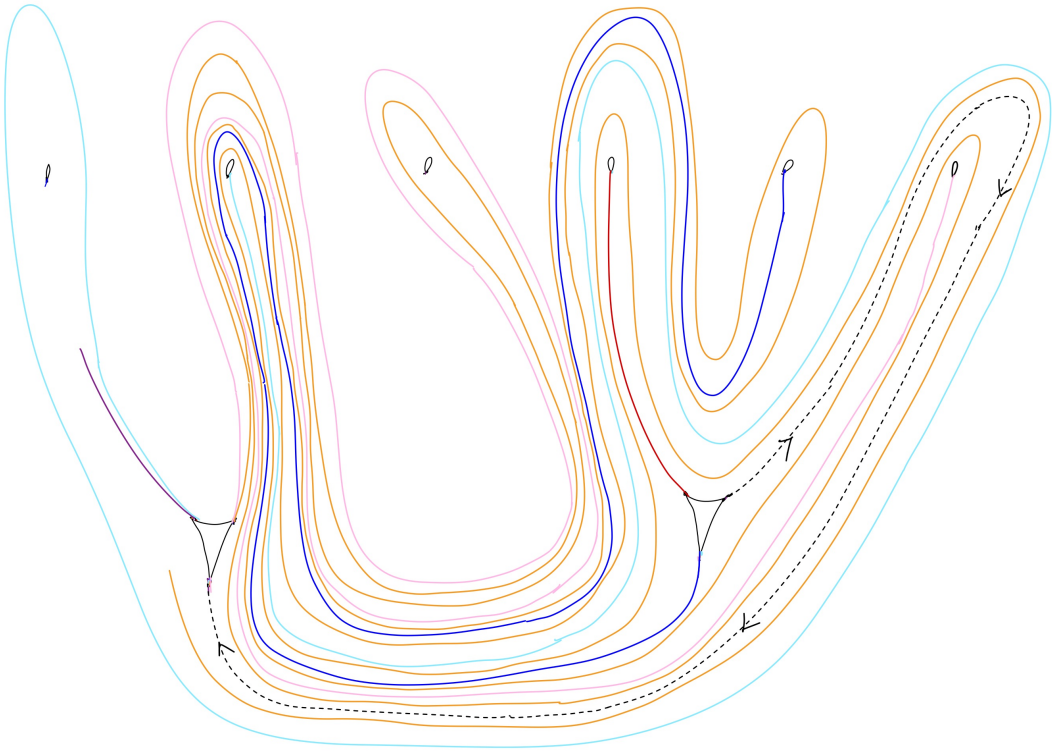


Figure H.97: SCC20

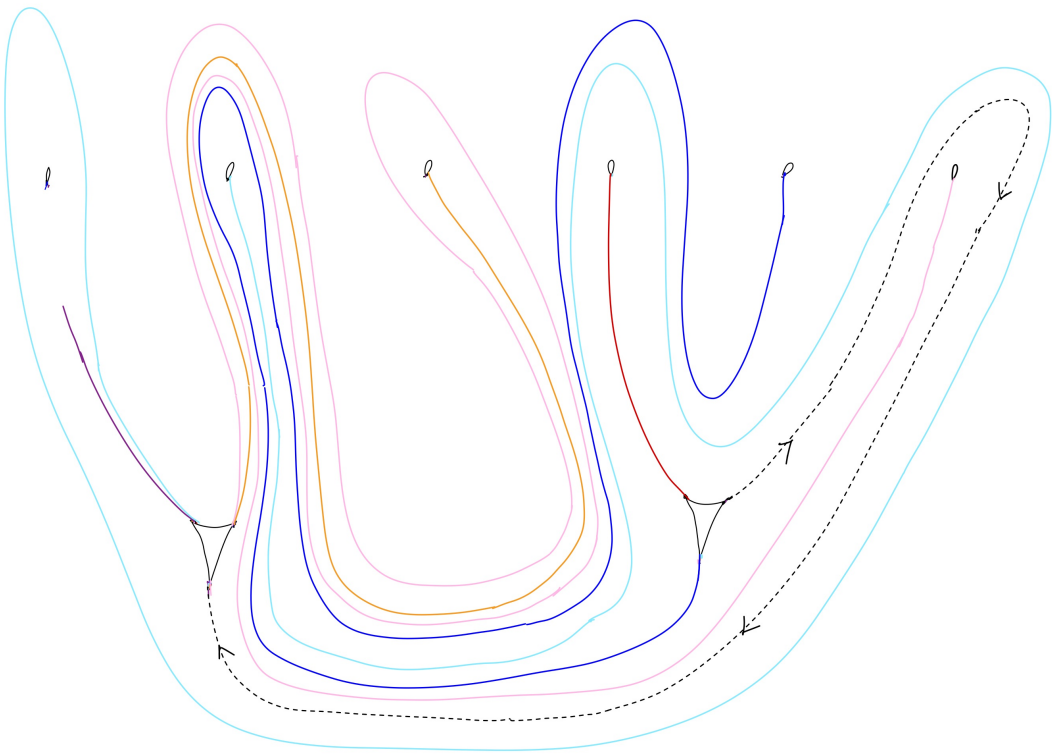


Figure H.98: SCC21

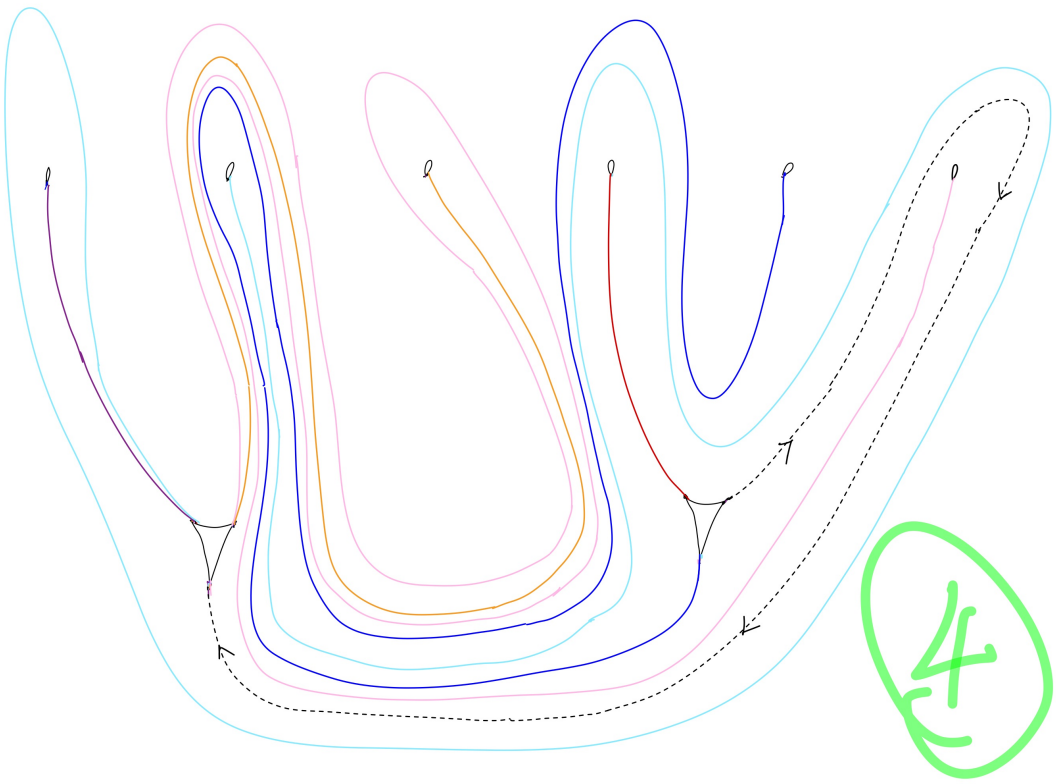


Figure H.99: SCC22

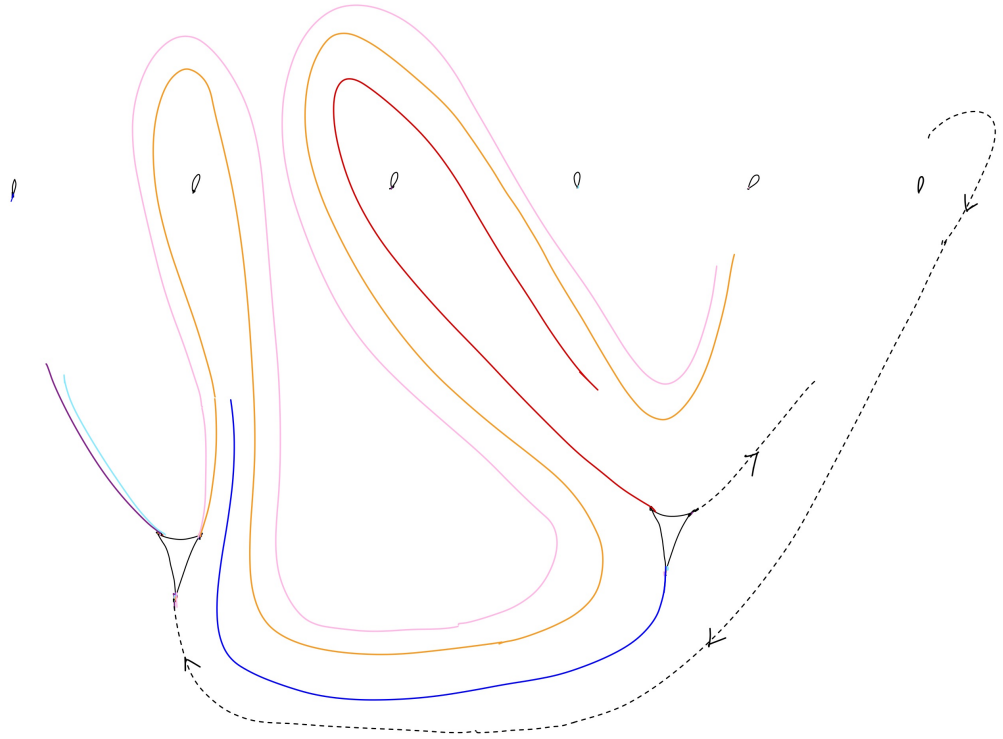


Figure H.100: SCC23

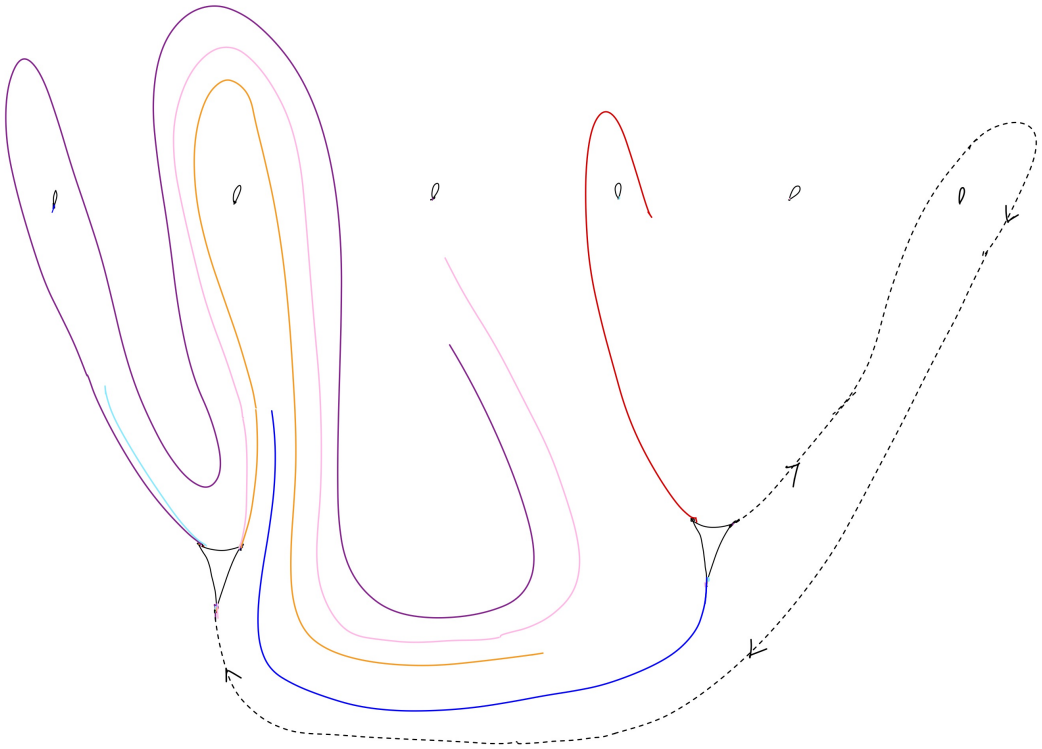


Figure H.101: SCC24

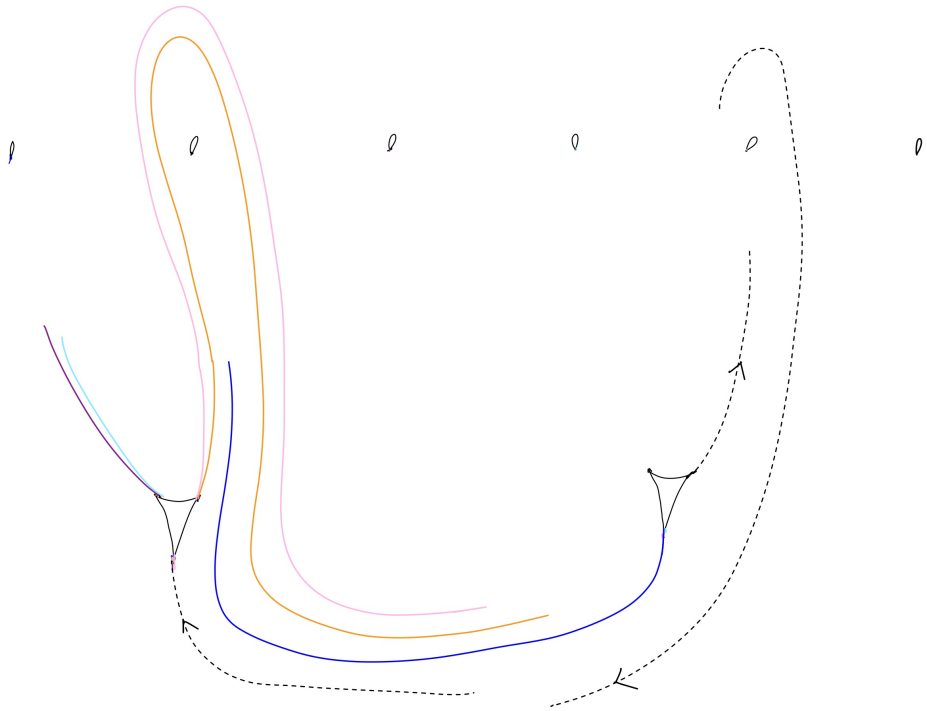


Figure H.102: LKE1

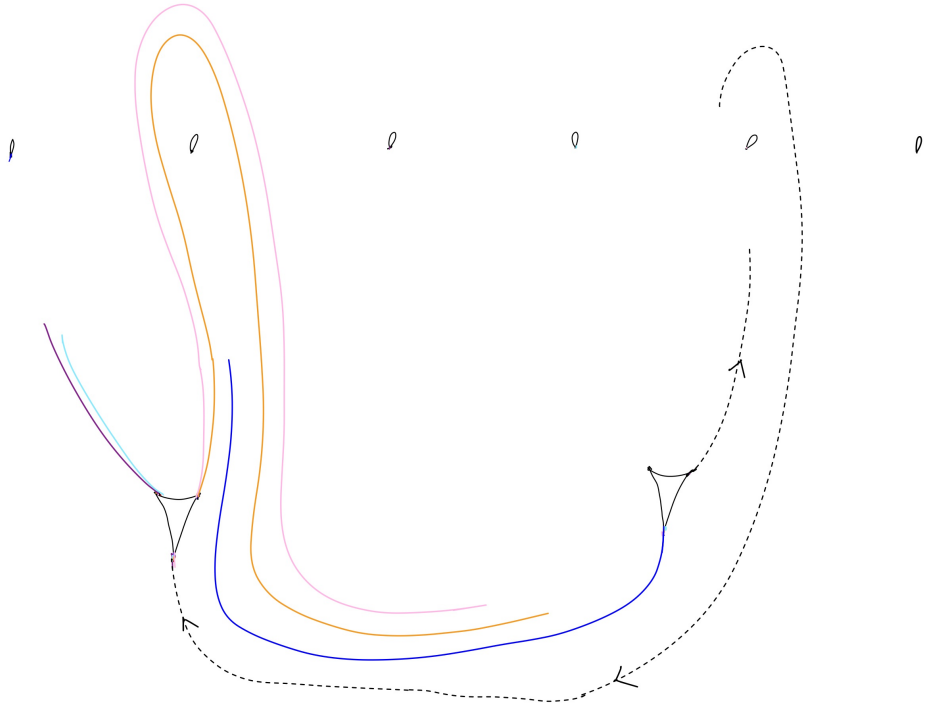


Figure H.103: LKE2

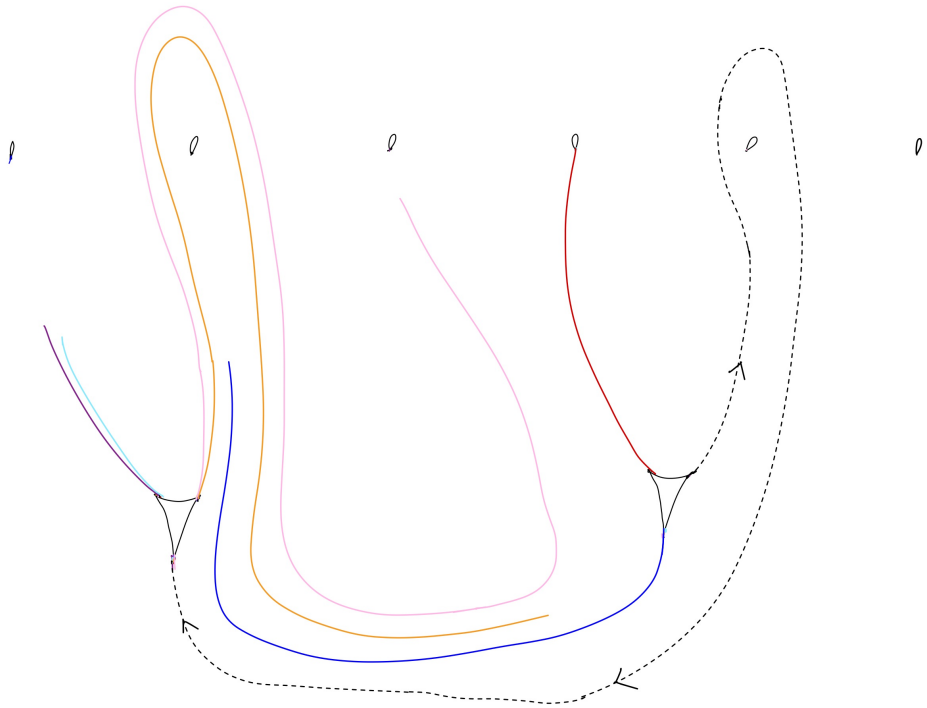


Figure H.104: LKE3

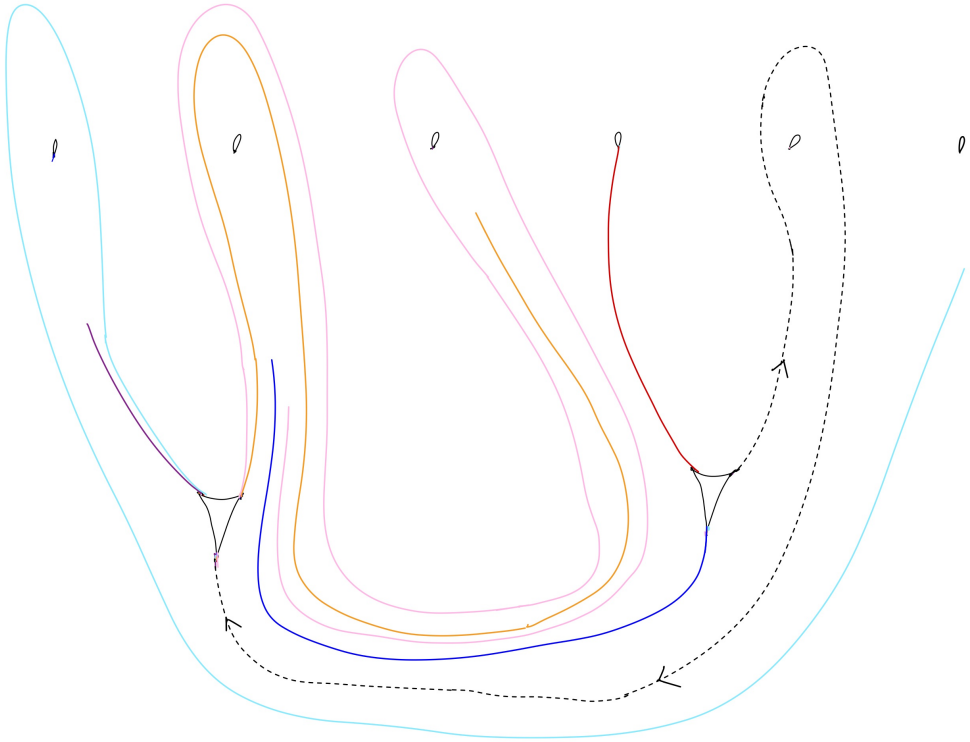


Figure H.105: LKE4

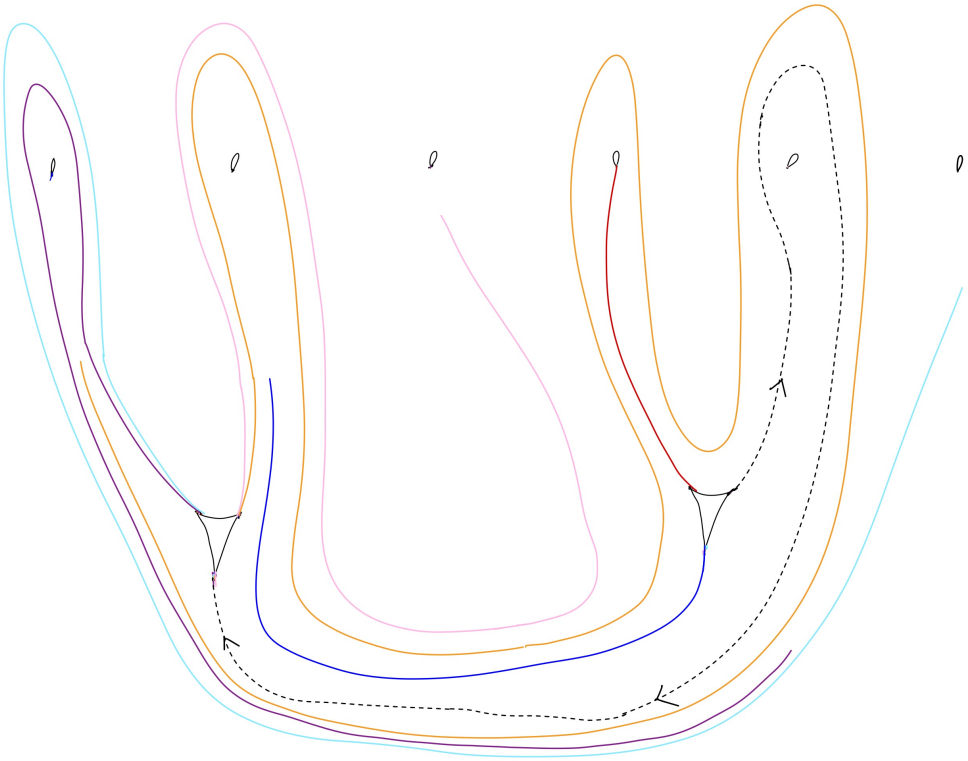


Figure H.106: LKE5

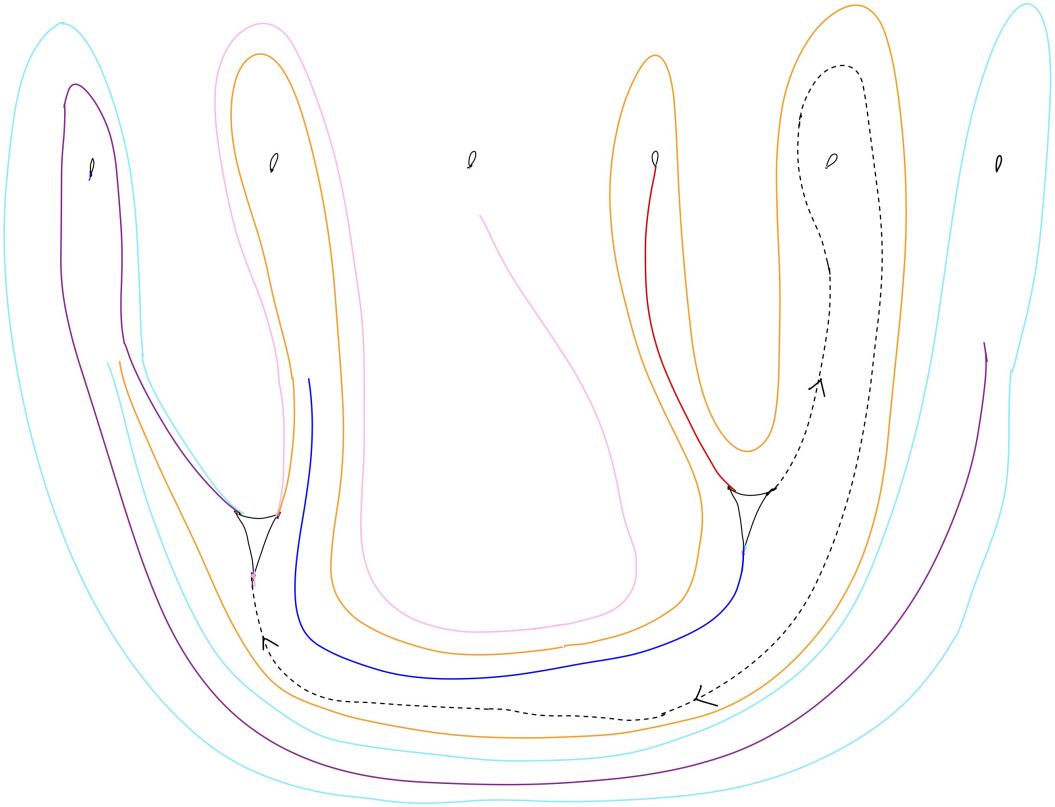


Figure H.107: LKE6

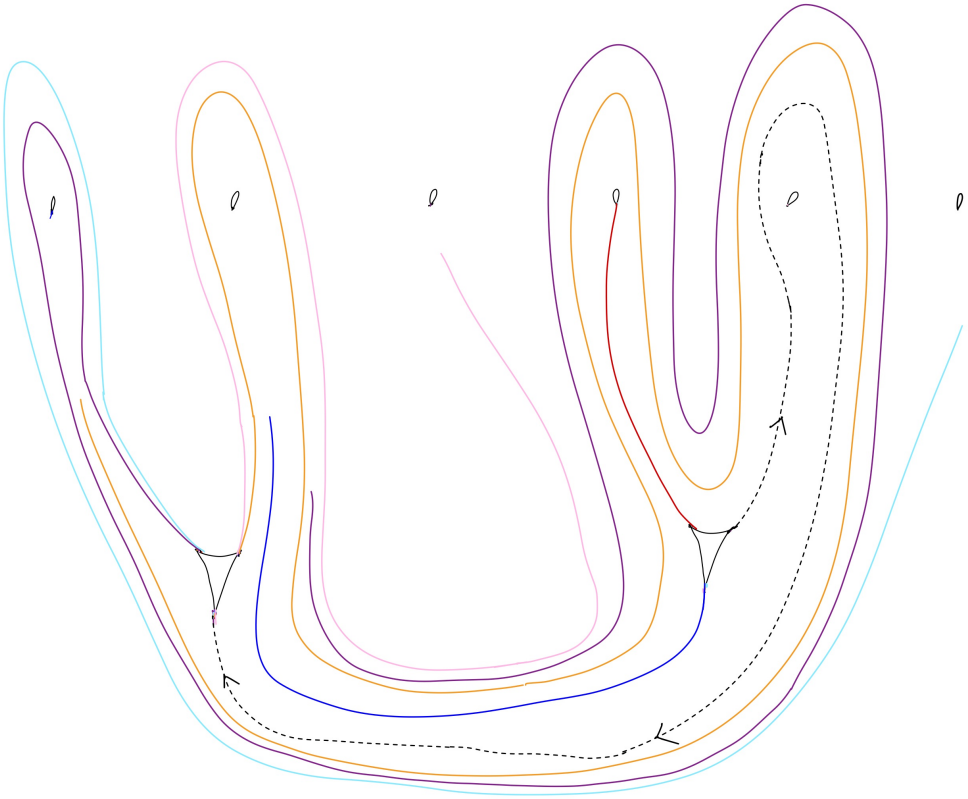


Figure H.108: LKE7

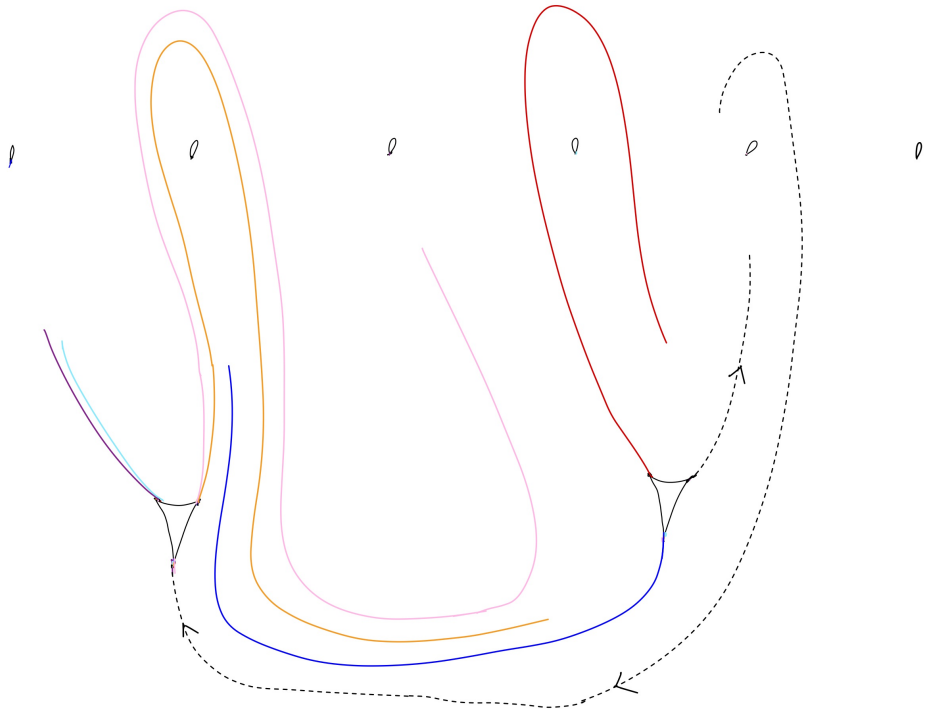


Figure H.109: LKE8

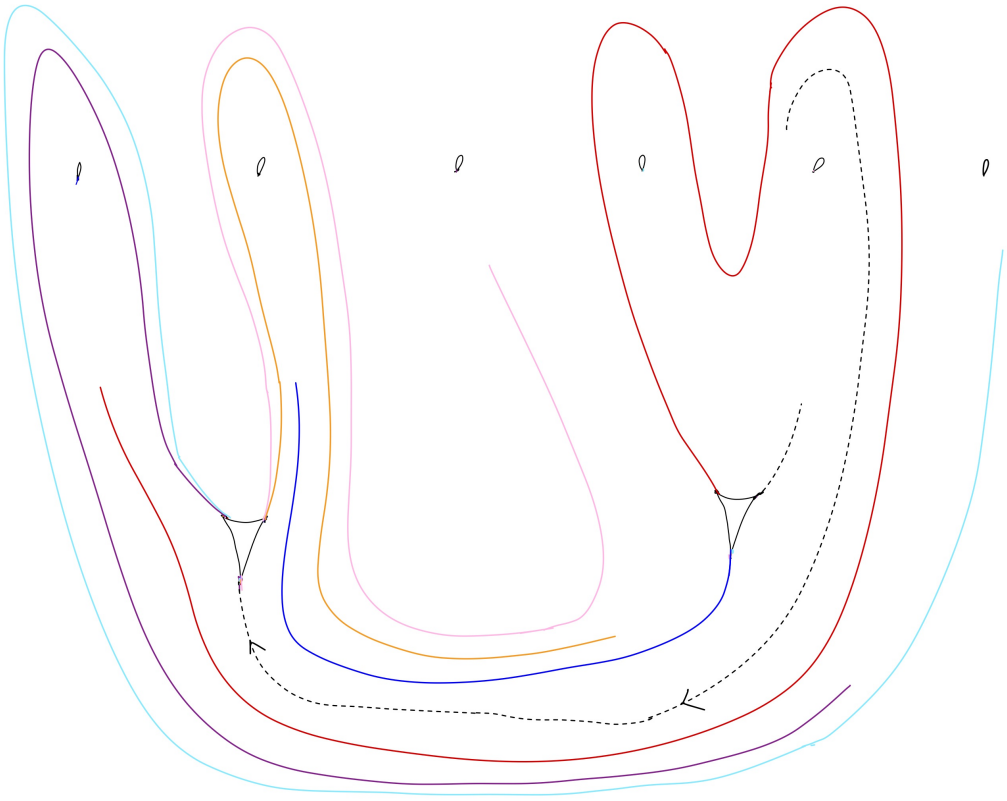


Figure H.110: LKE9

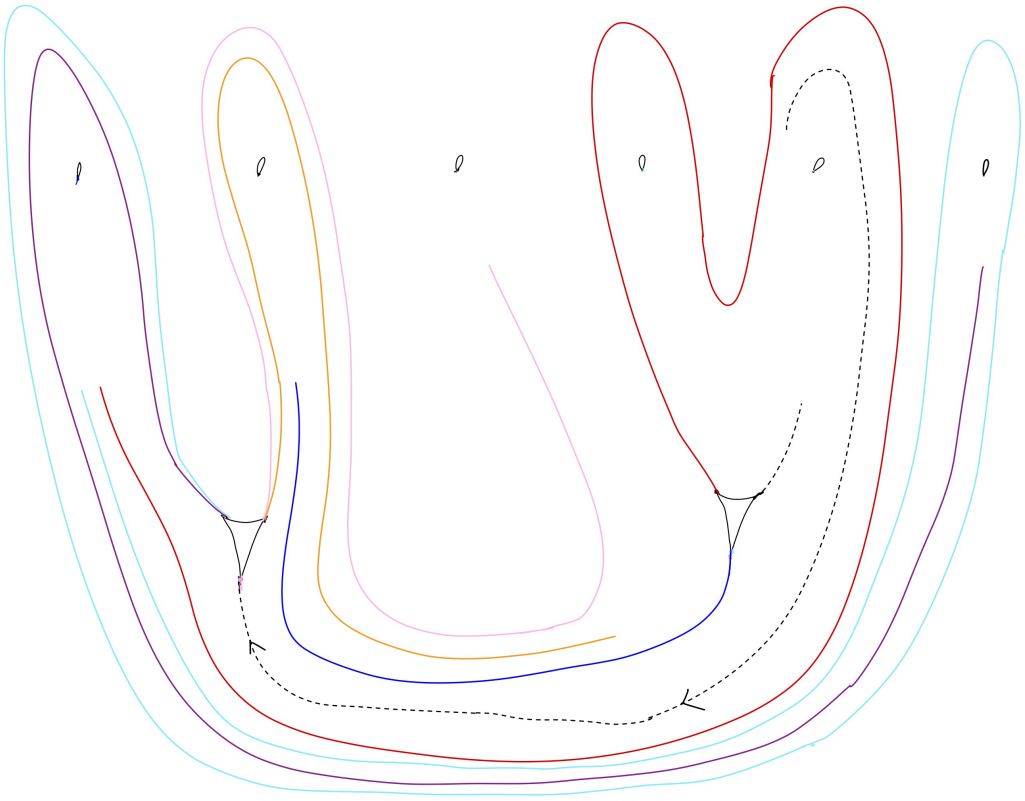


Figure H.111: LKE10

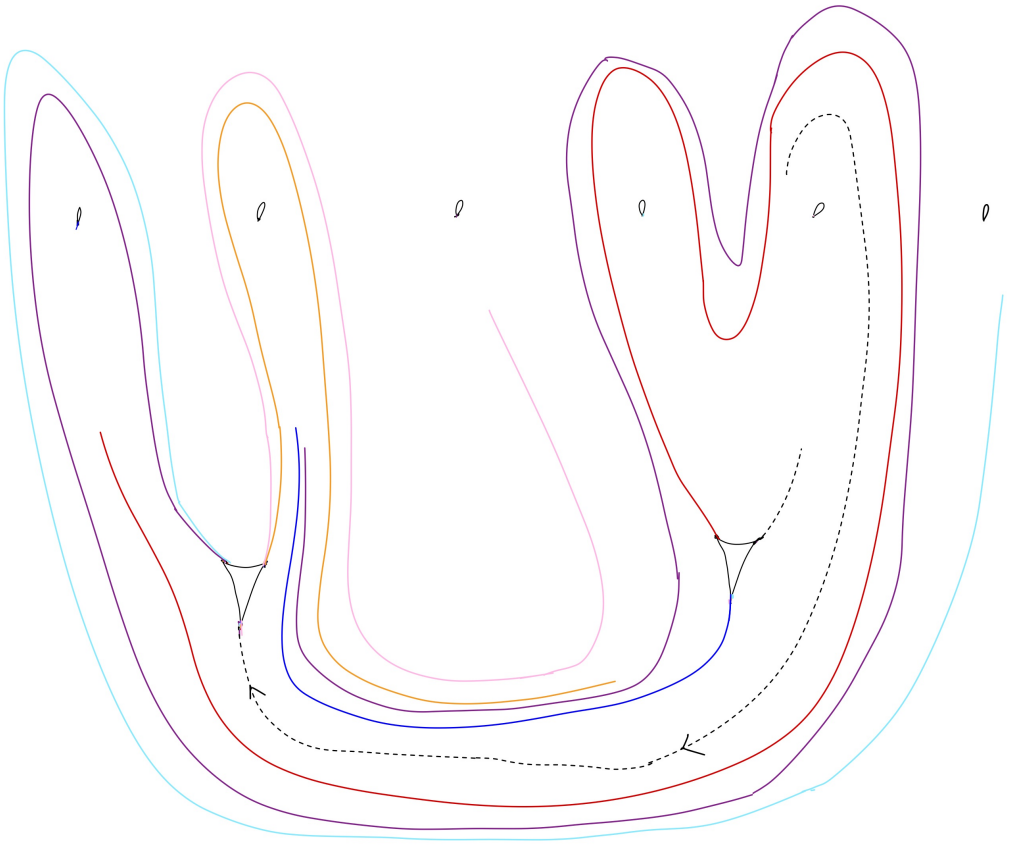


Figure H.112: LKE11

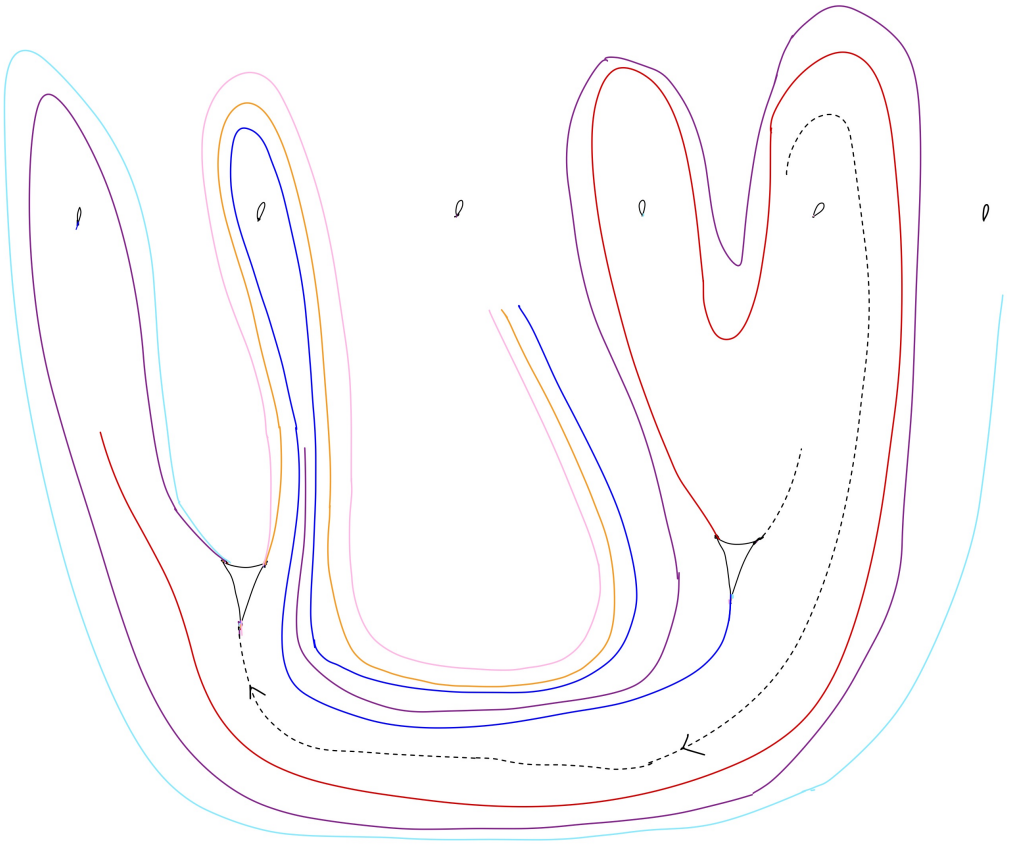


Figure H.113: LKE12

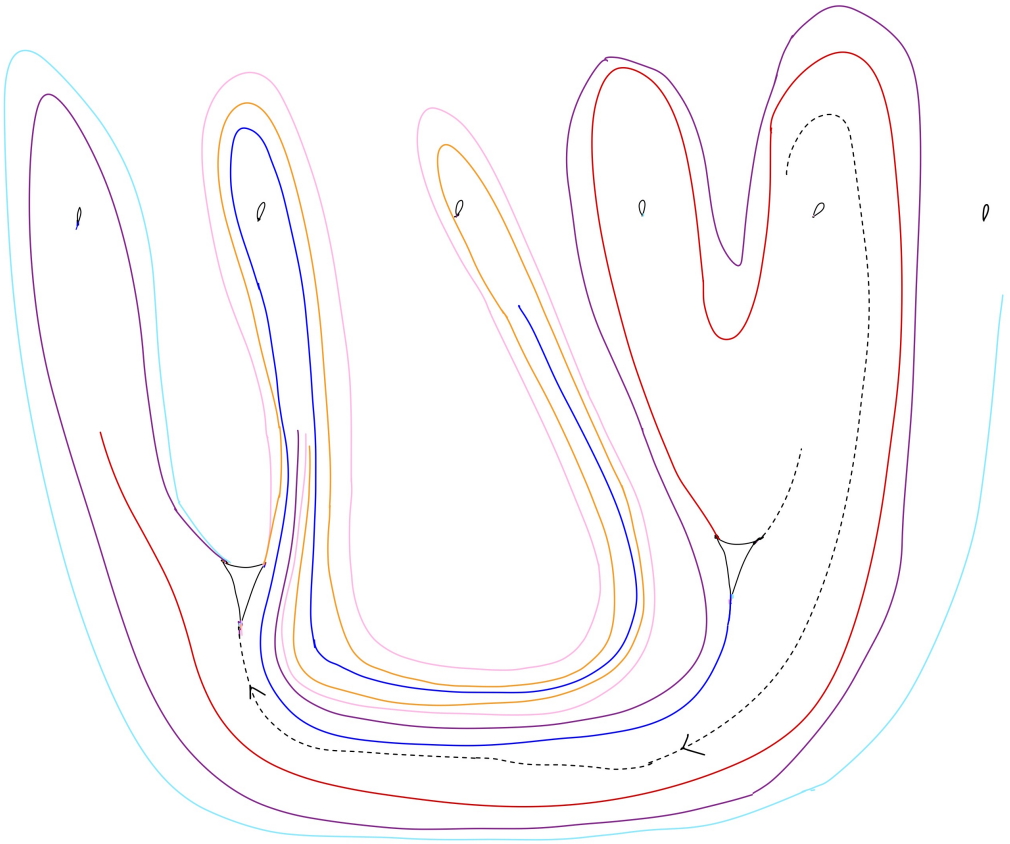


Figure H.114: LKE13

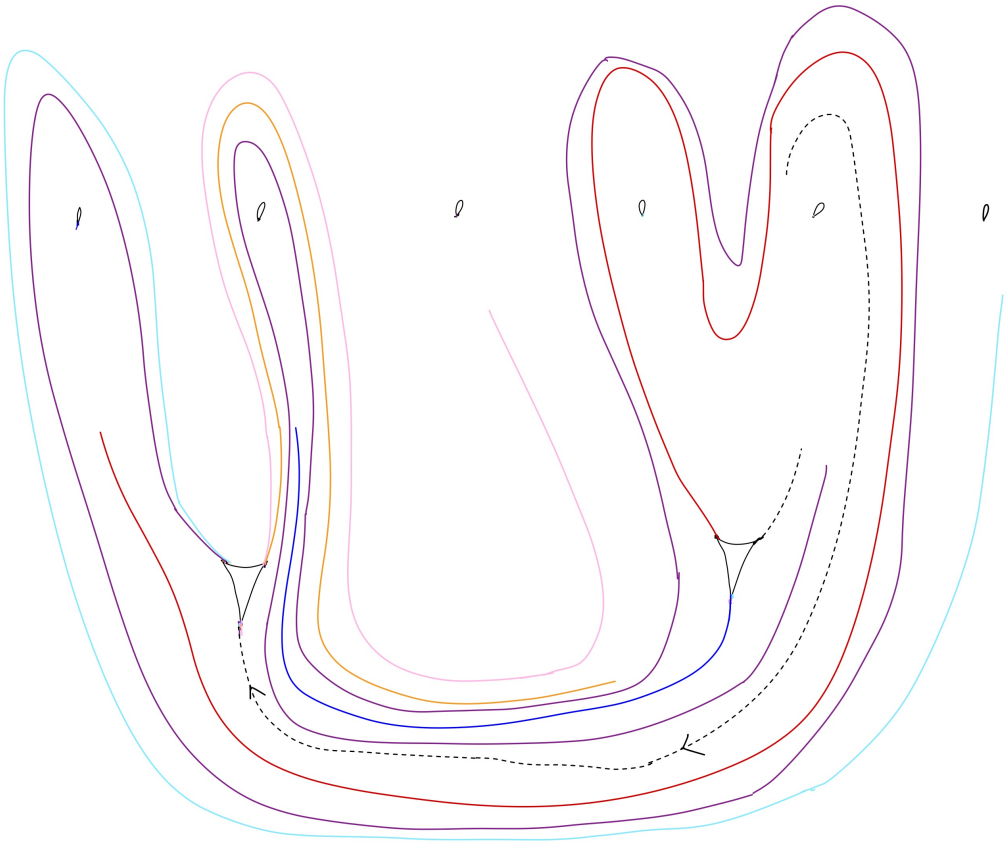


Figure H.115: LKE14

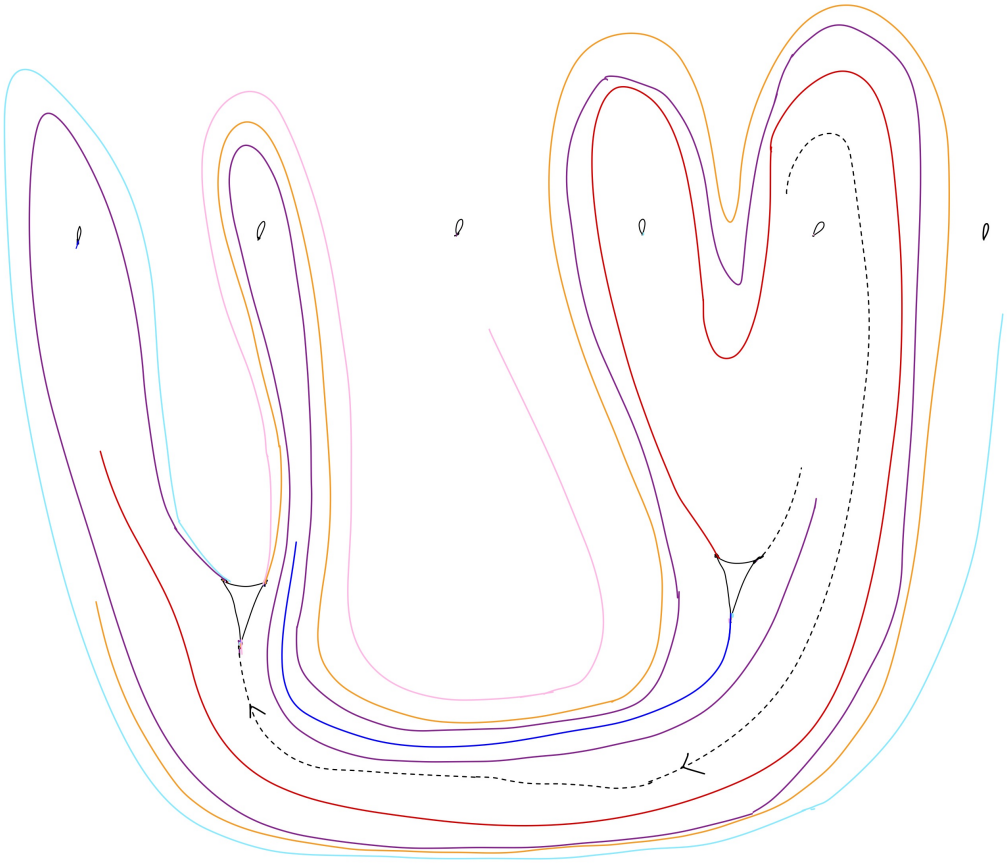


Figure H.116: LKE15

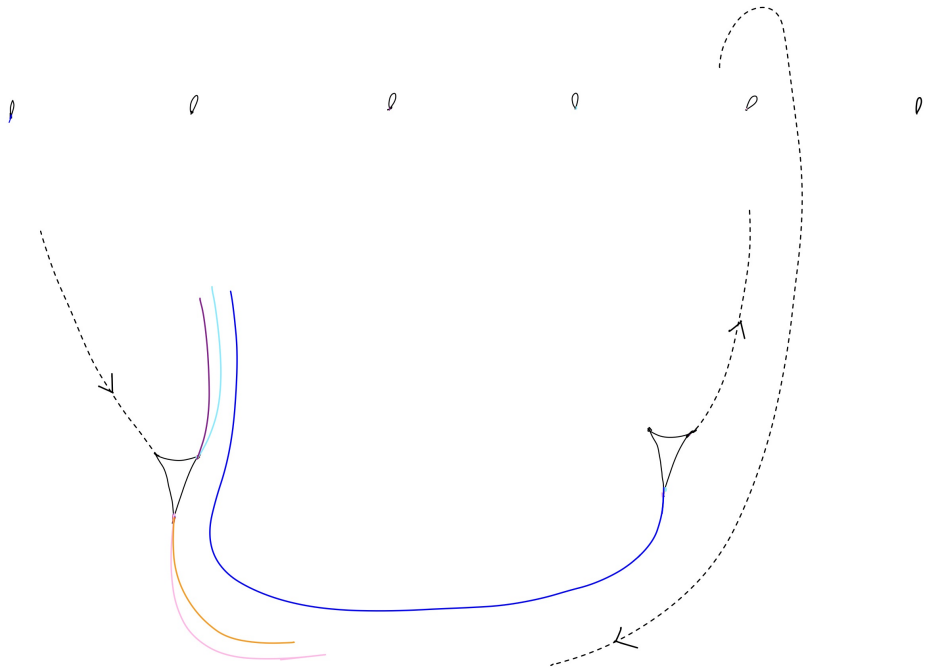


Figure H.117: YVQ1

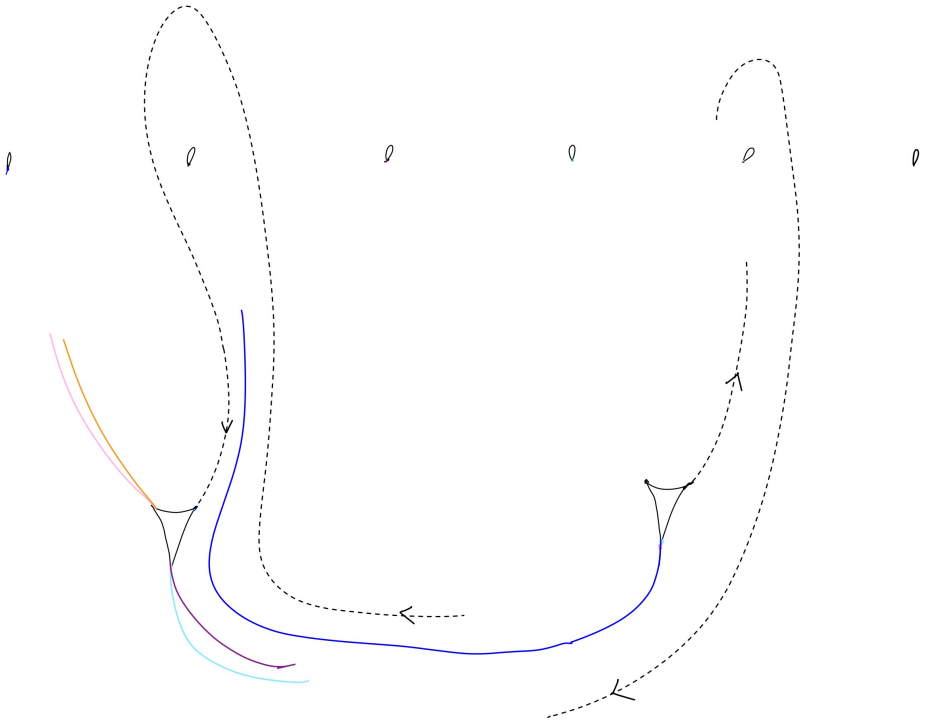


Figure H.118: SOB1

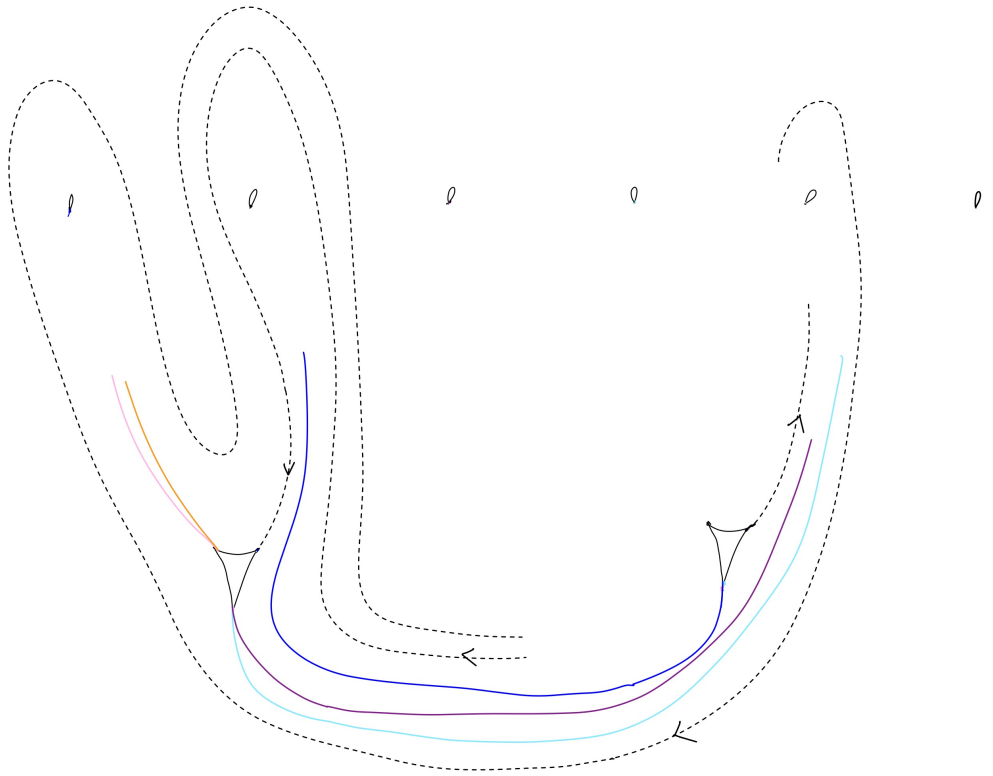


Figure H.119: SOB2

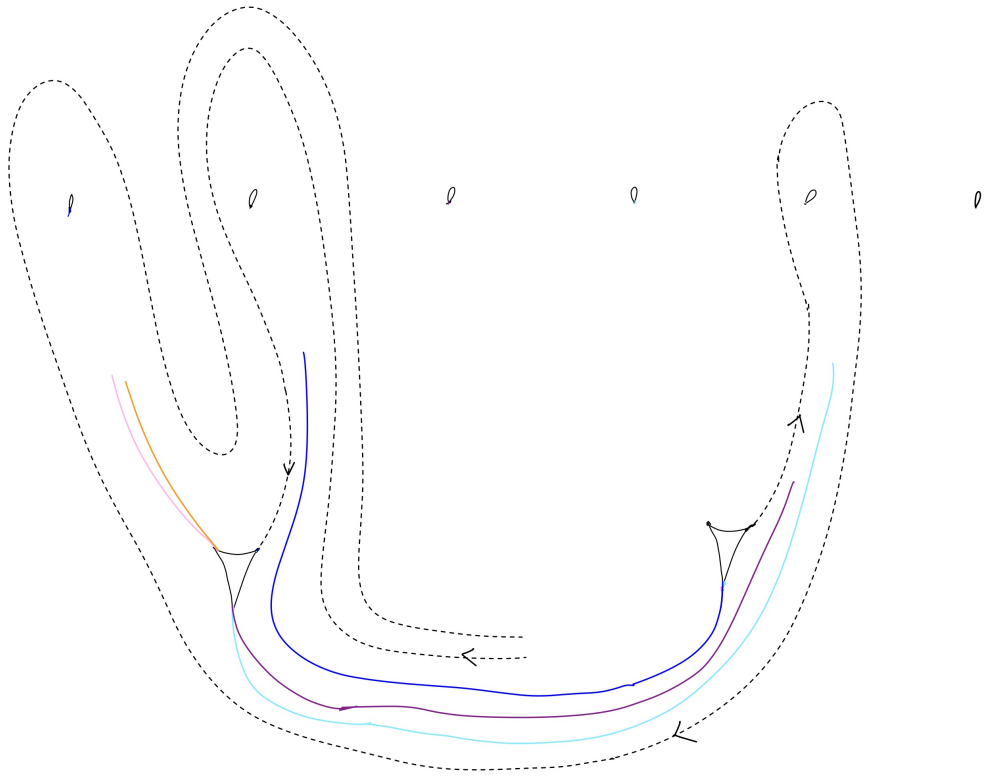


Figure H.120: SOB3

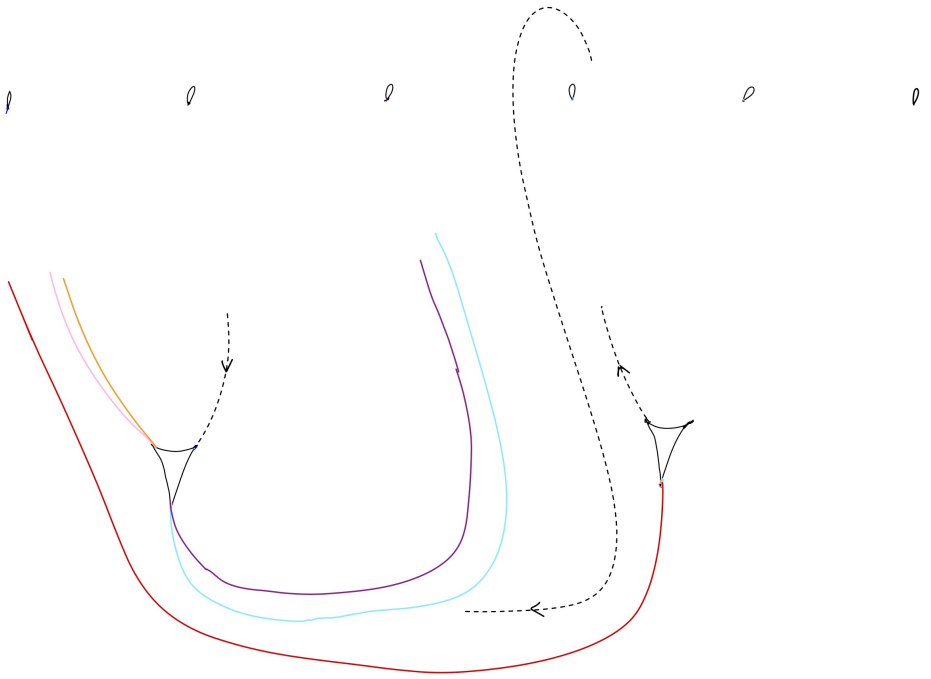


Figure H.121: BAM1

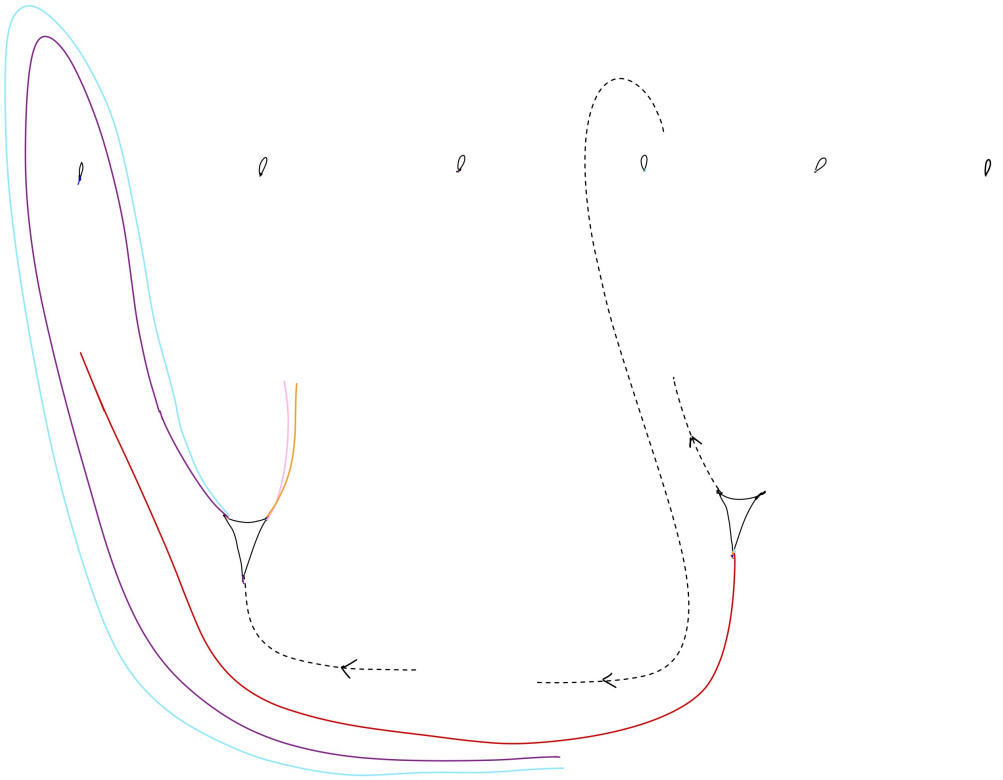


Figure H.122: PIZ1

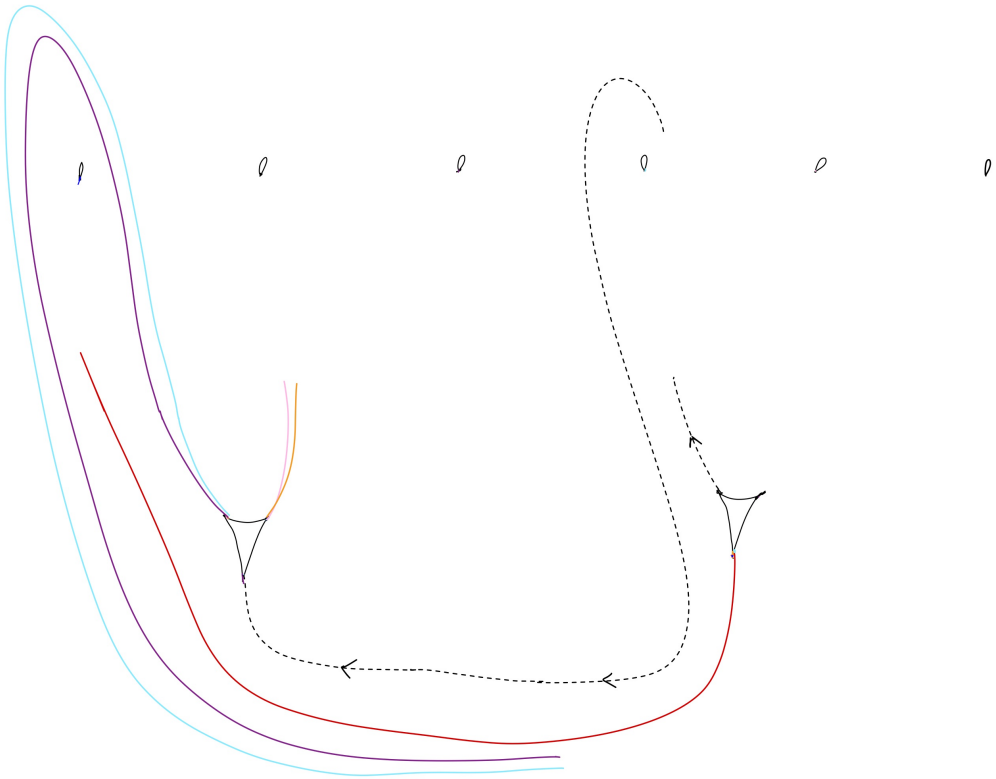


Figure H.123: PIZ2

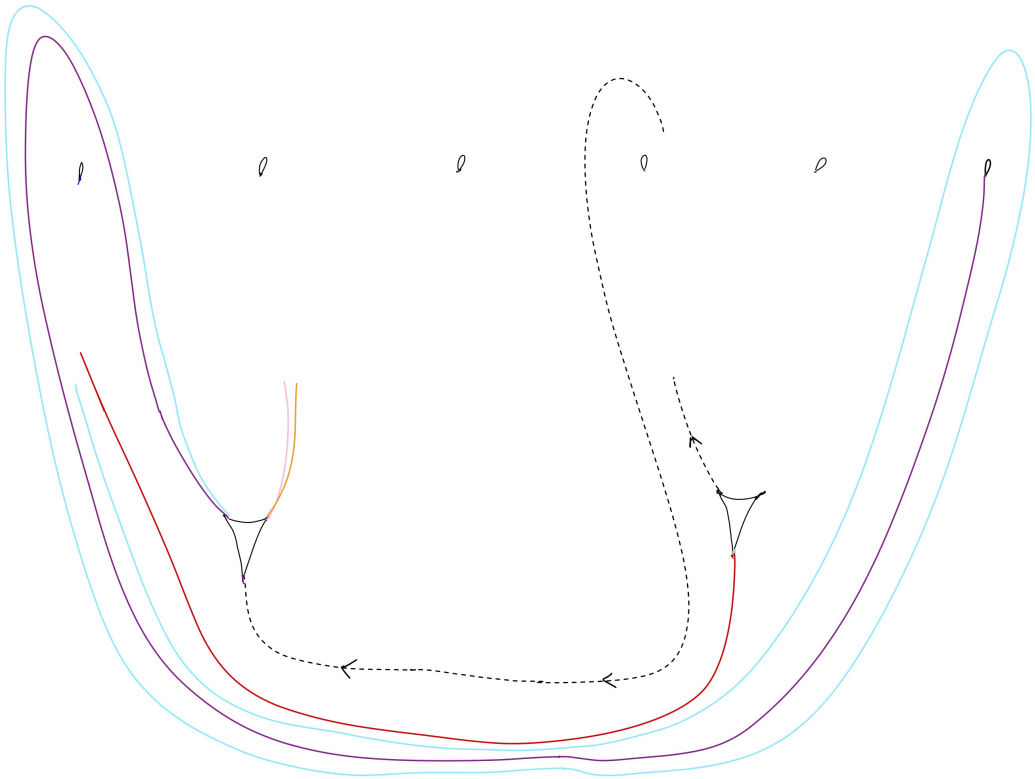


Figure H.124: Nurl1

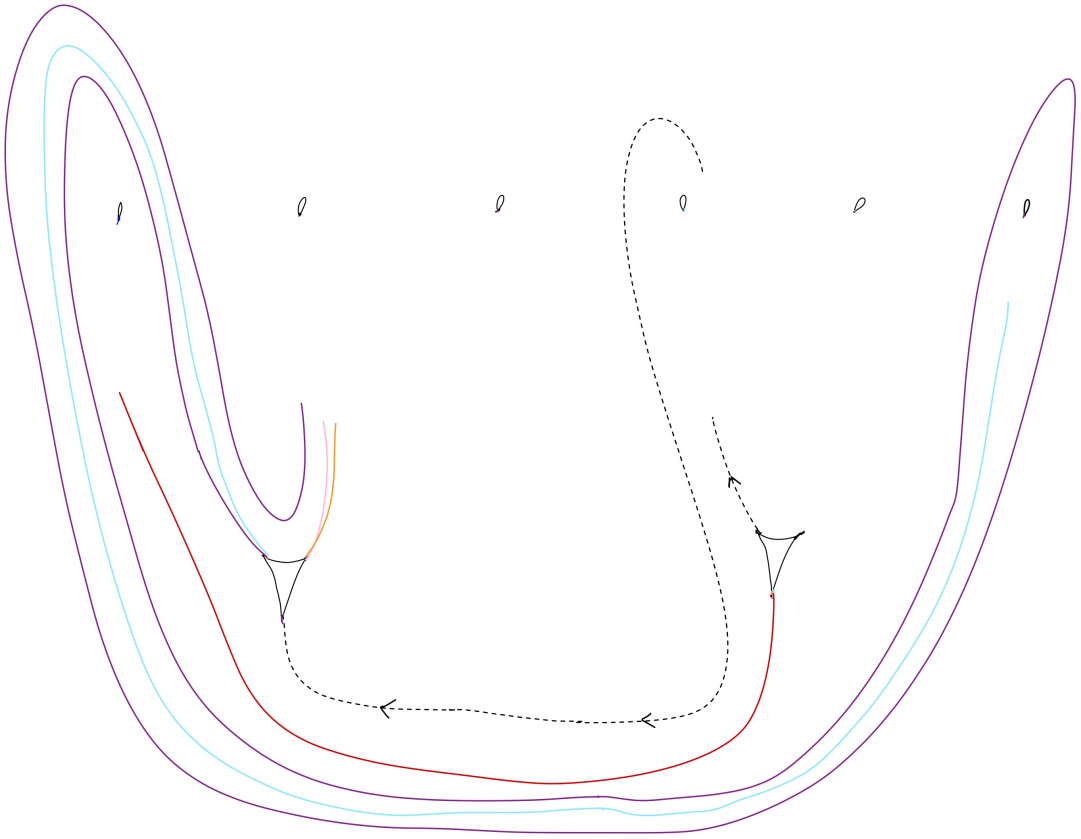


Figure H.125: Oast1

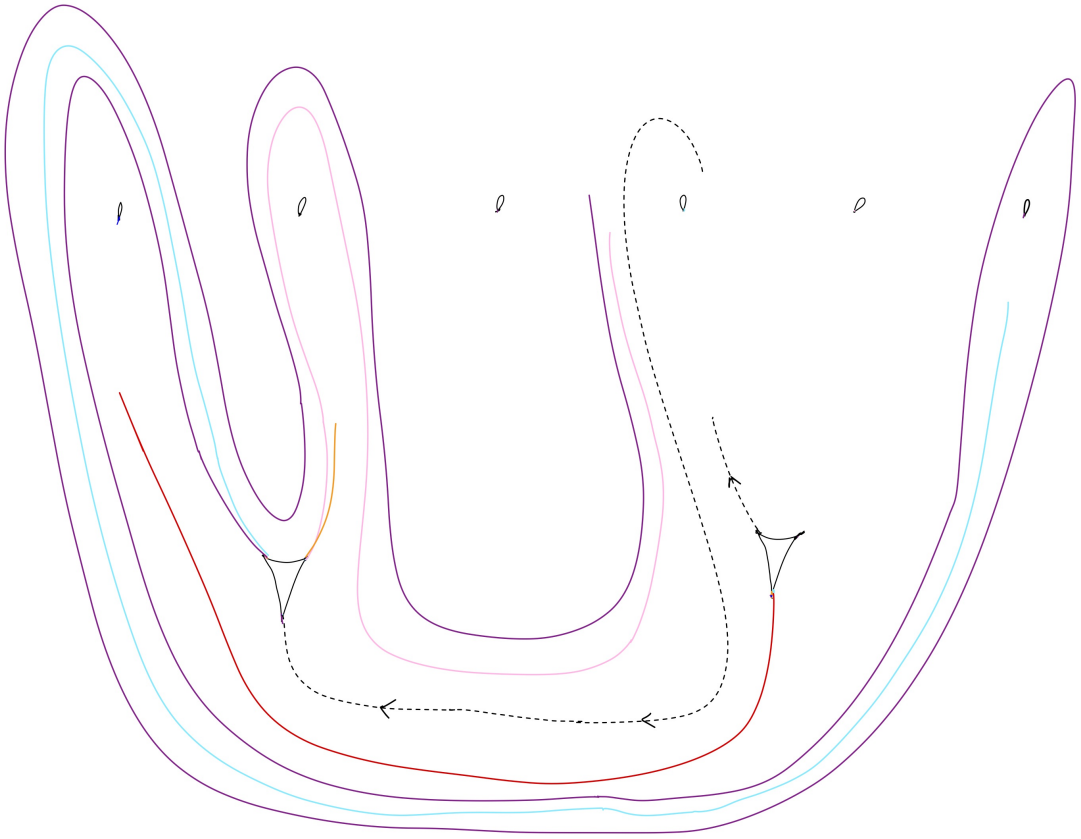


Figure H.126: Oast2

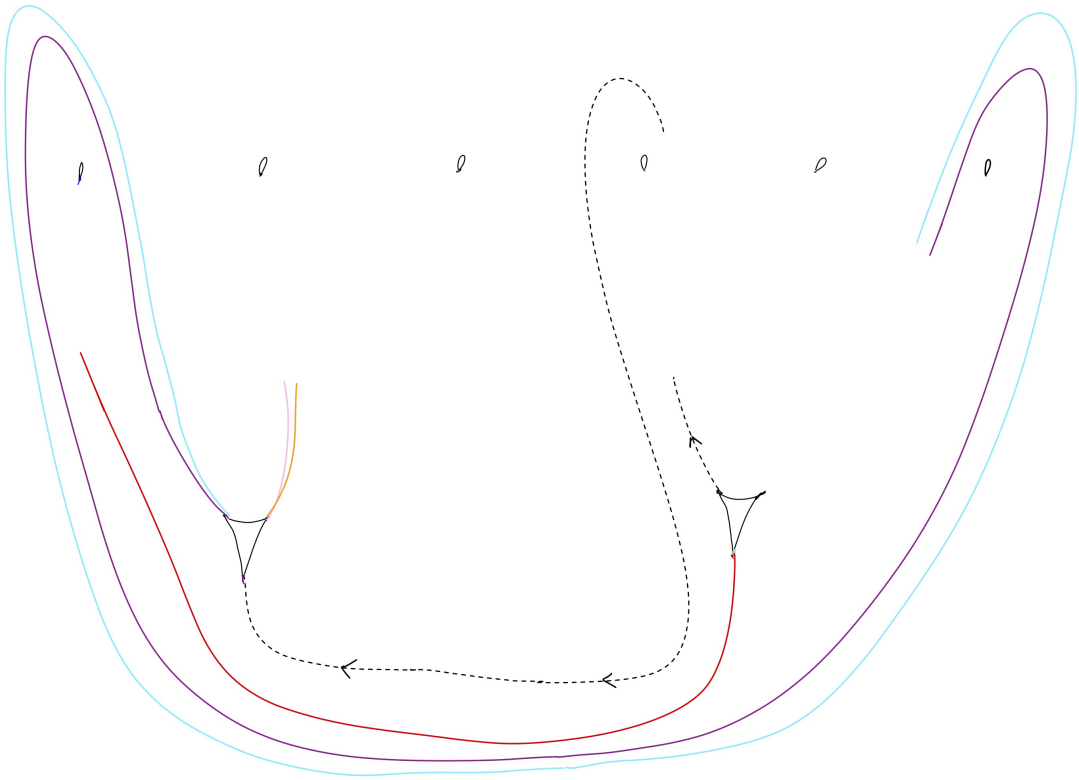


Figure H.127: Pilf1

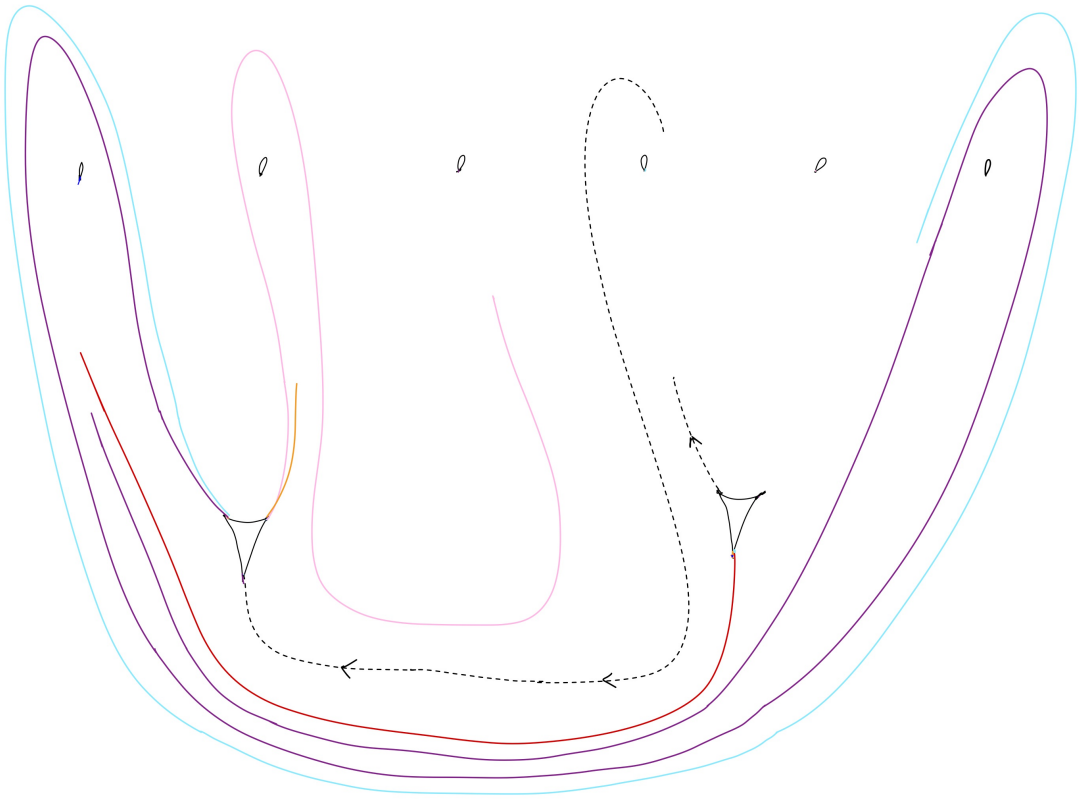


Figure H.128: Pilf2

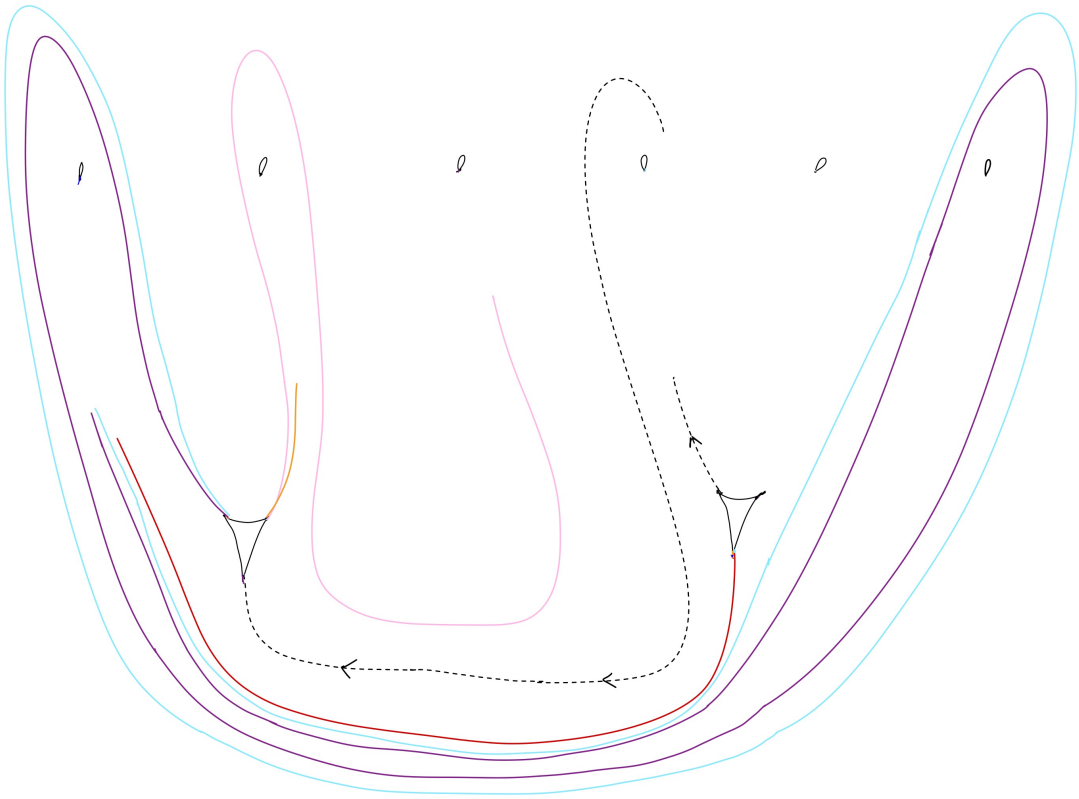


Figure H.129: Pilf3

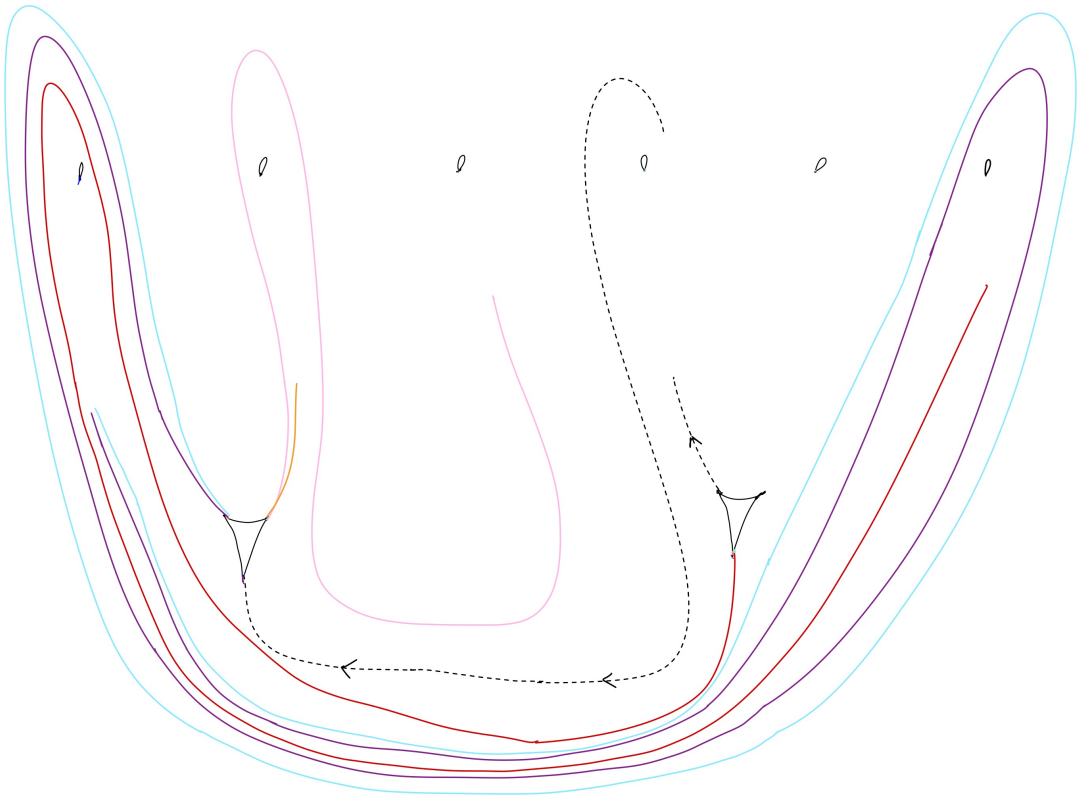


Figure H.130: Pilf4

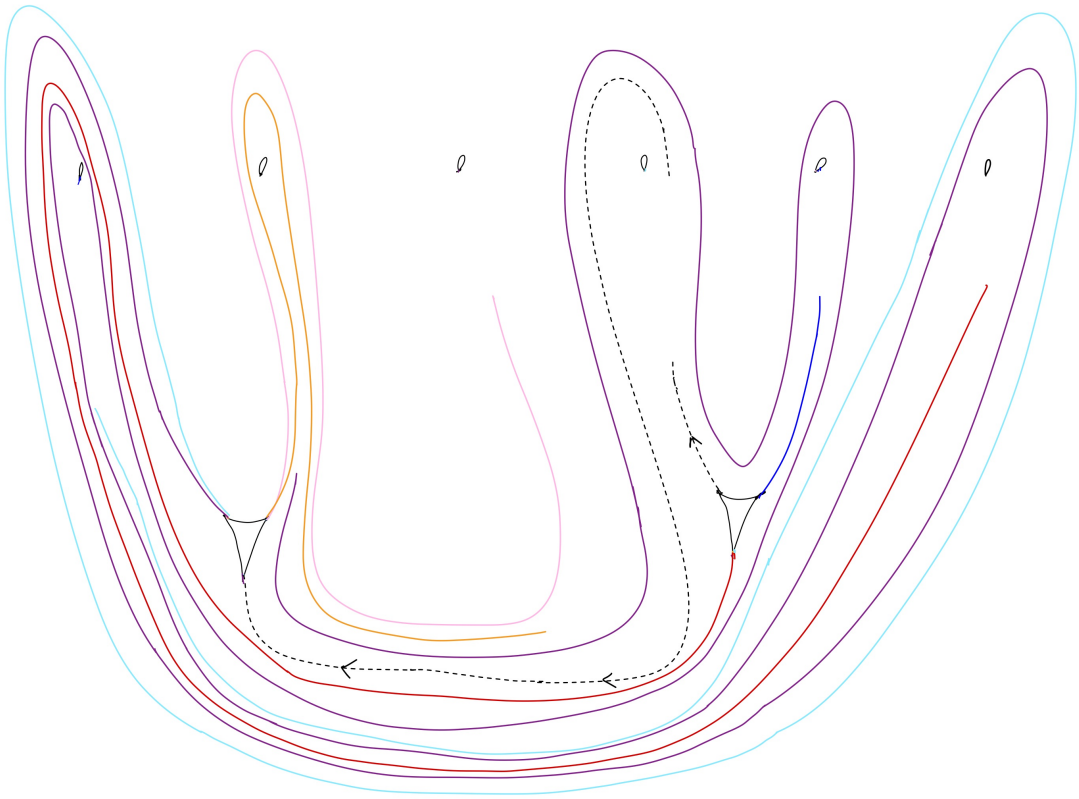


Figure H.131: Pilf5

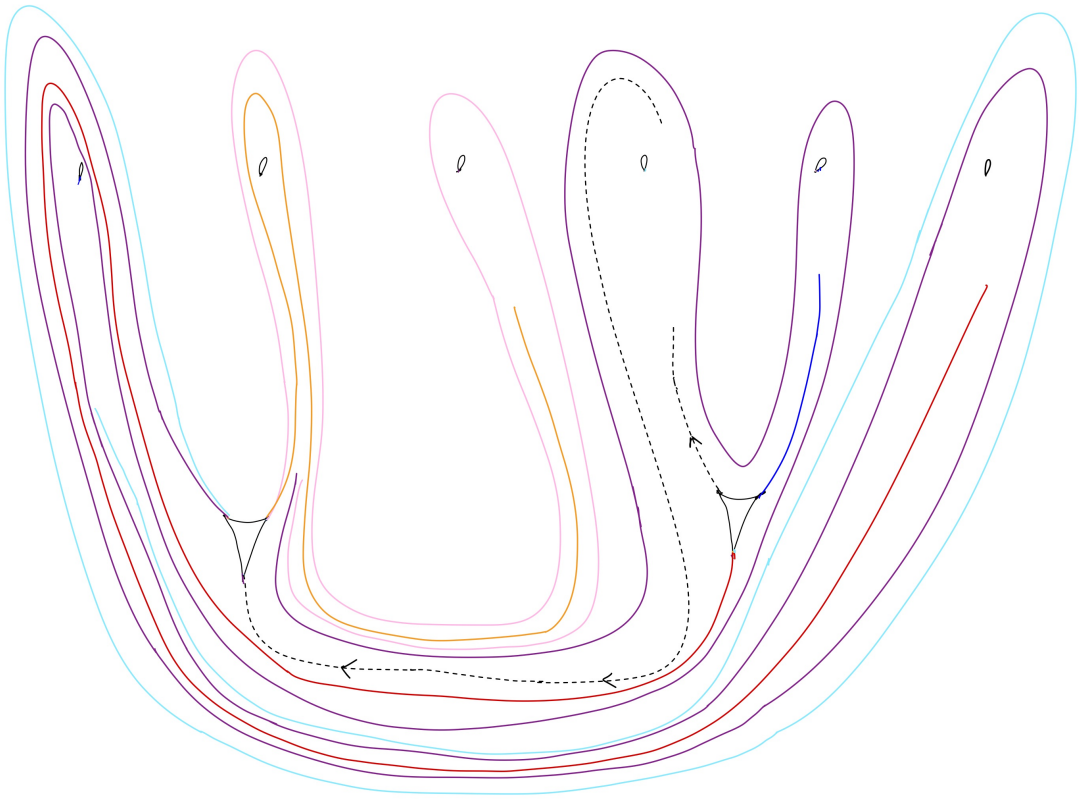


Figure H.132: Pilf6

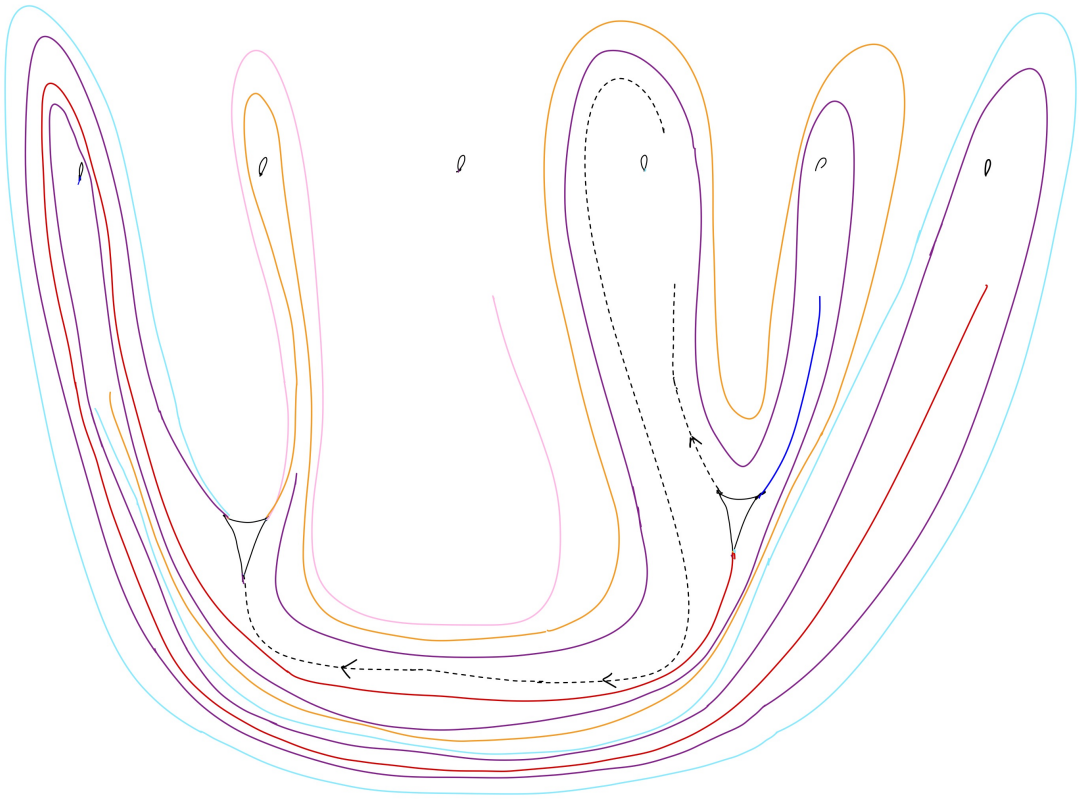


Figure H.133: Pilf7

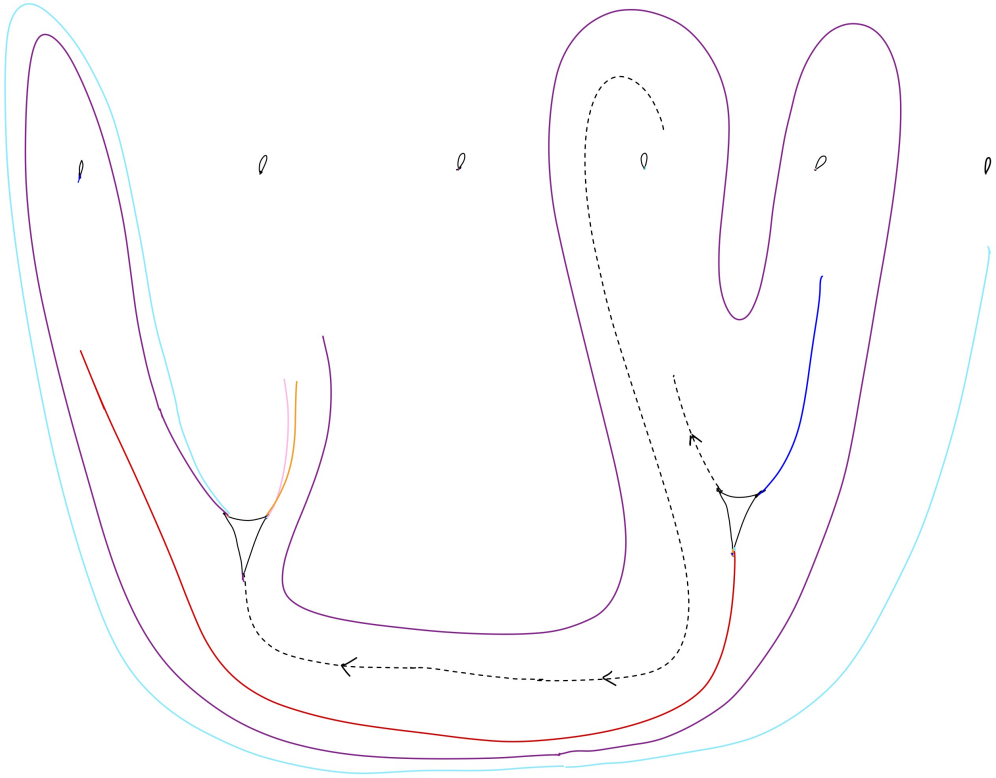


Figure H.134: Risp1

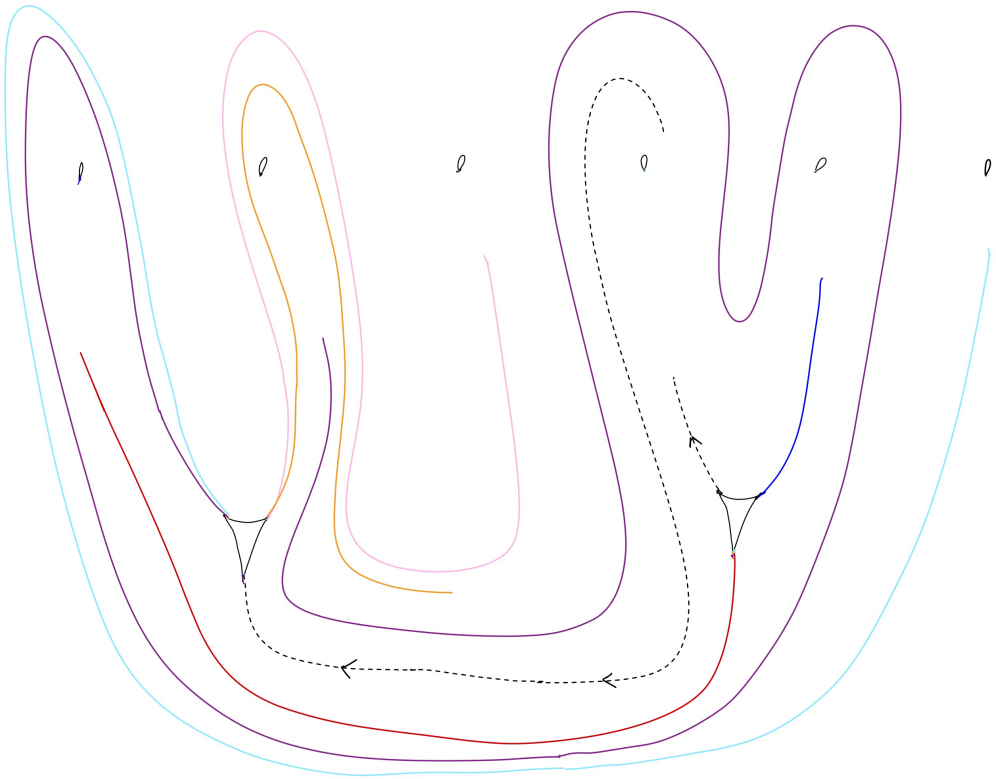


Figure H.135: Risp2

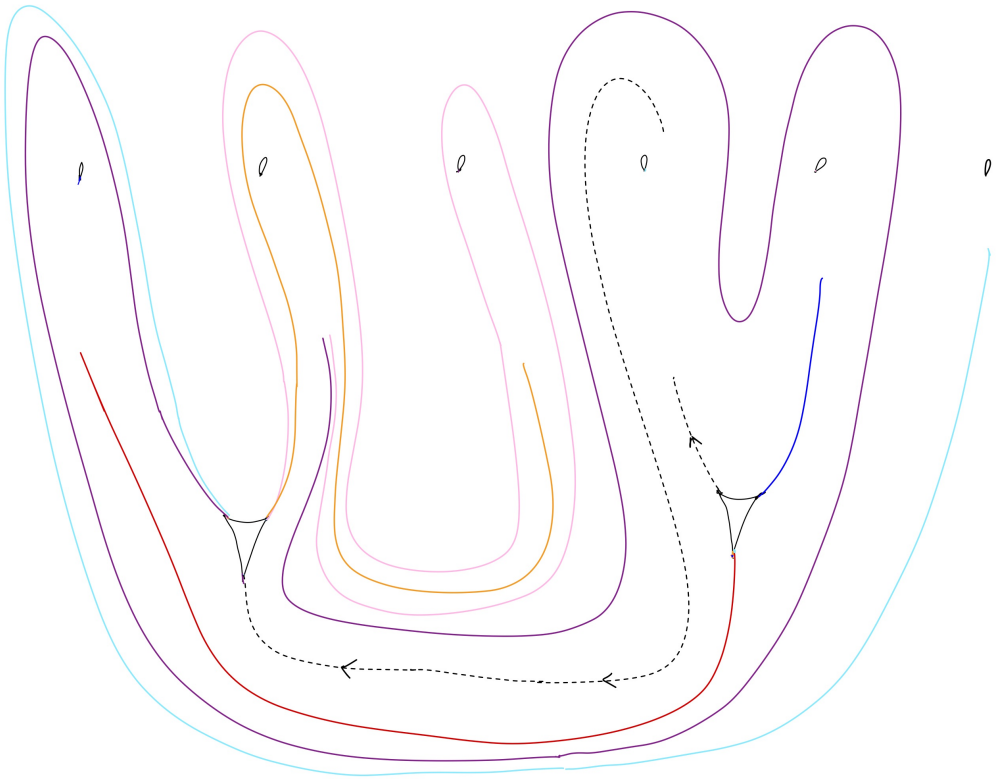


Figure H.136: Risp3

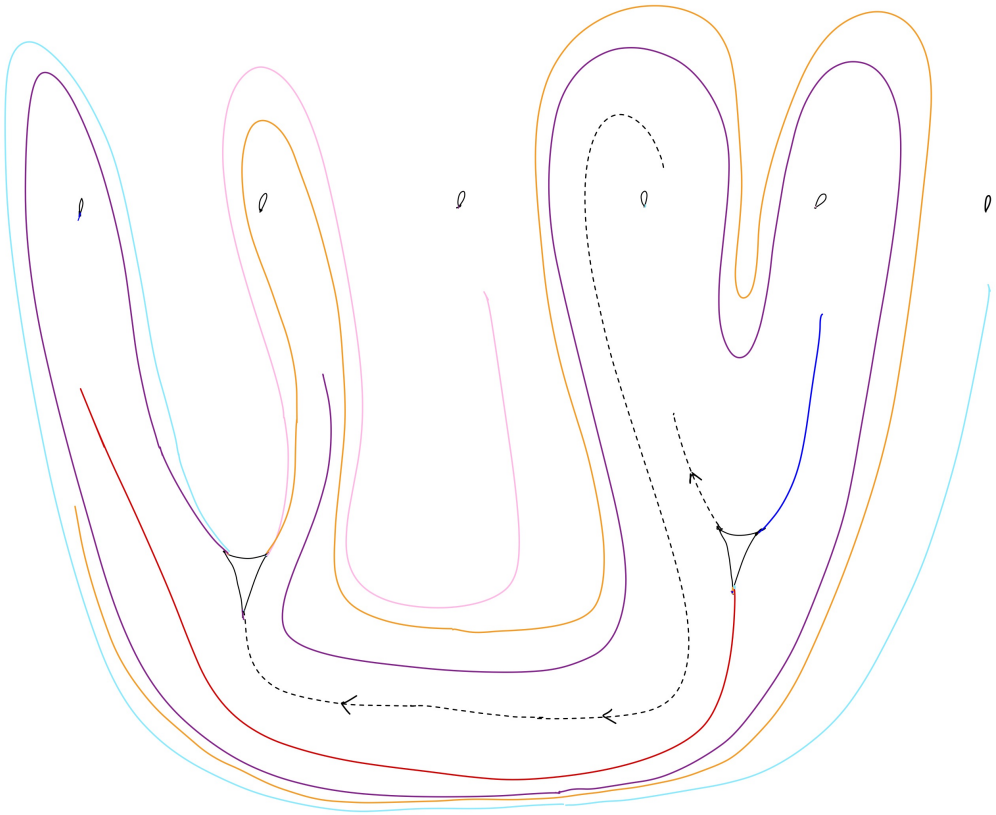


Figure H.137: Risp4

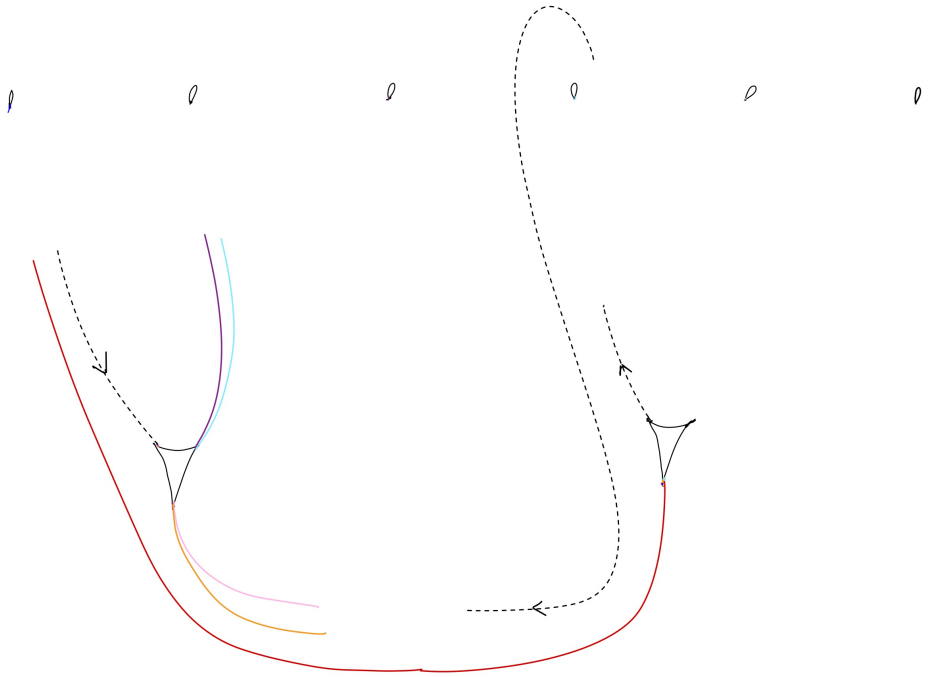


Figure H.138: RUT1

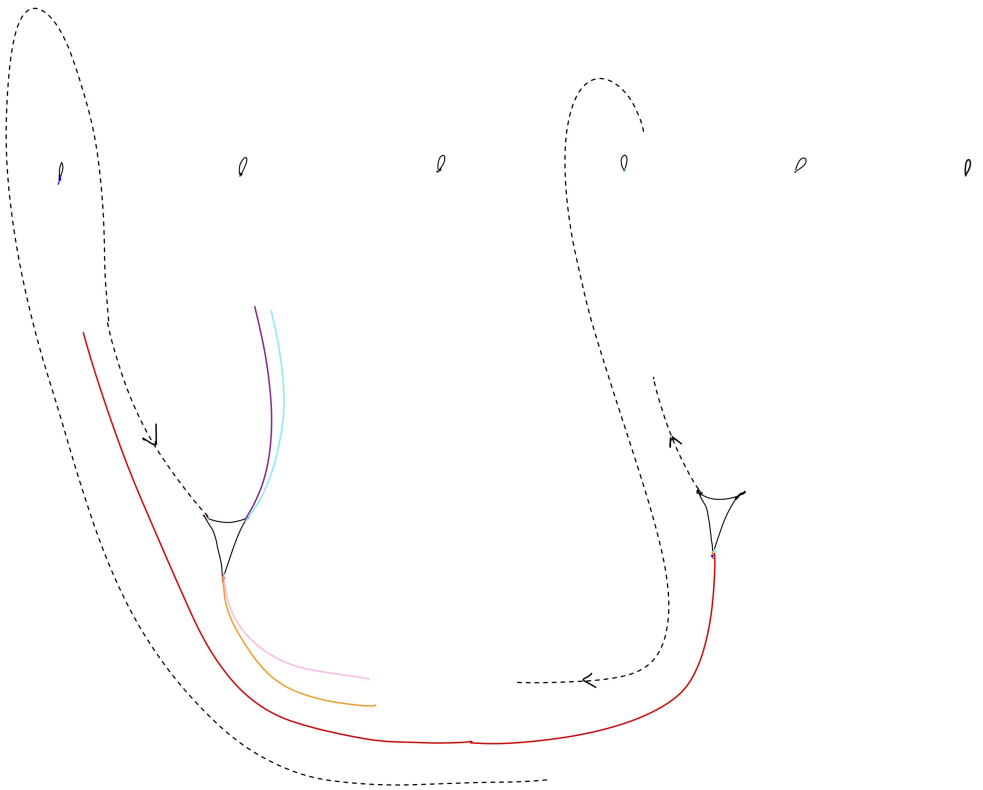


Figure H.139: RUT2

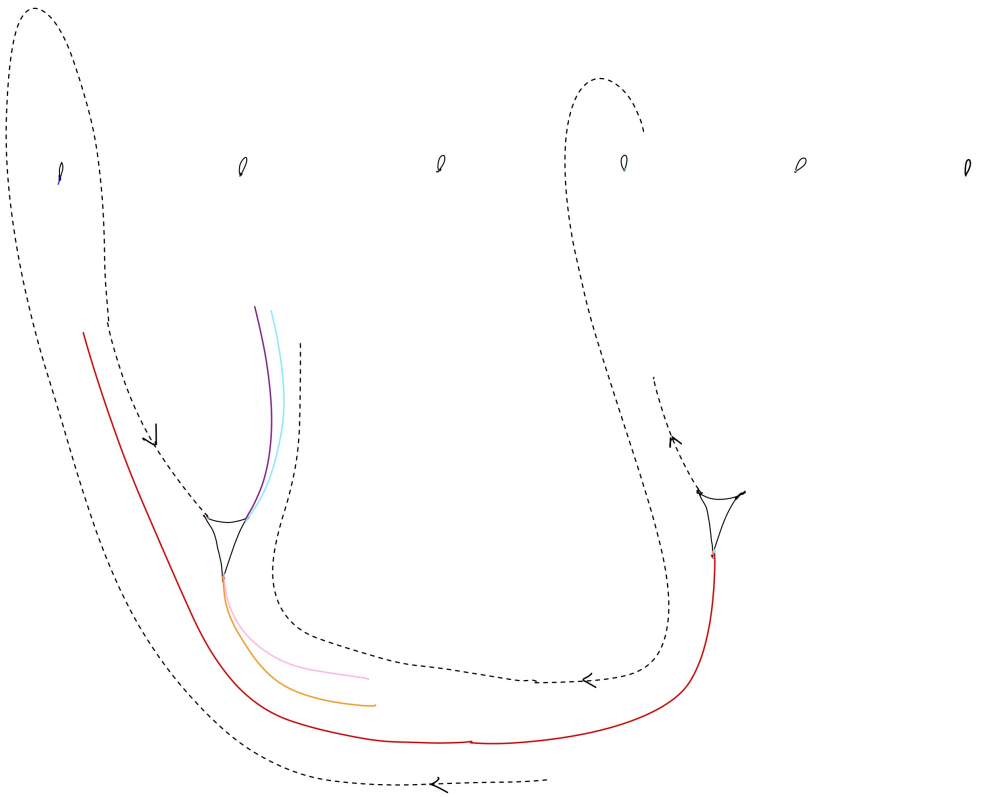


Figure H.140: RUT3

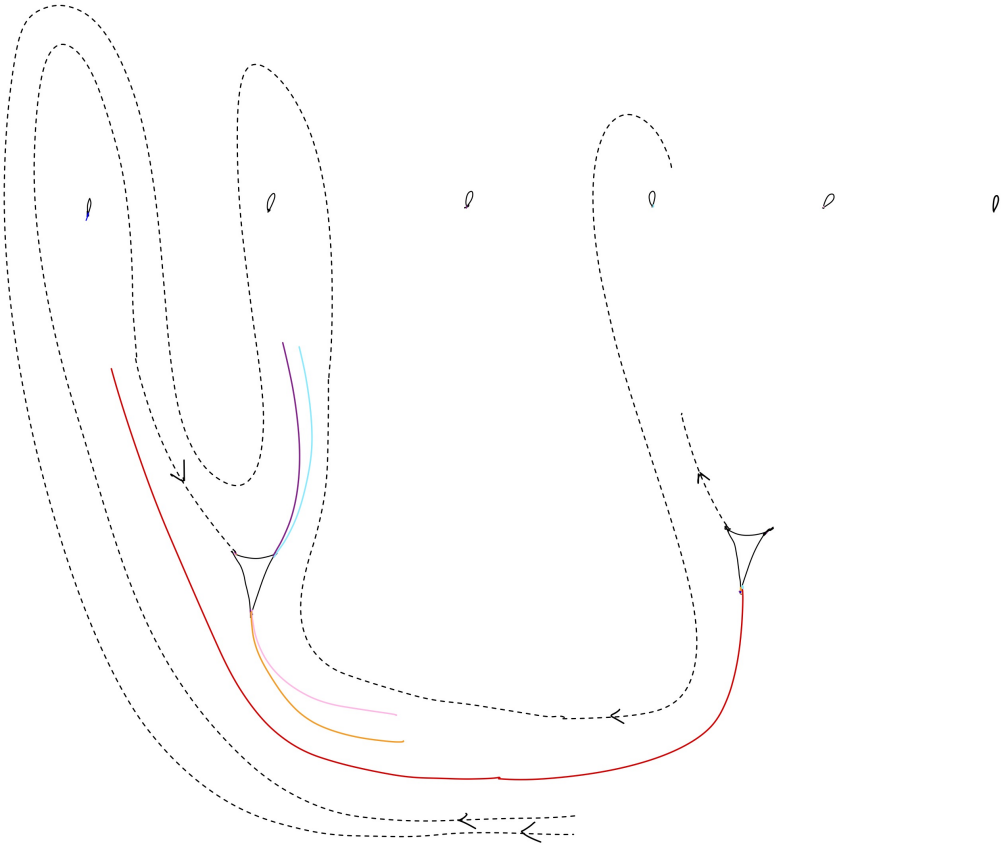


Figure H.141: RUT4

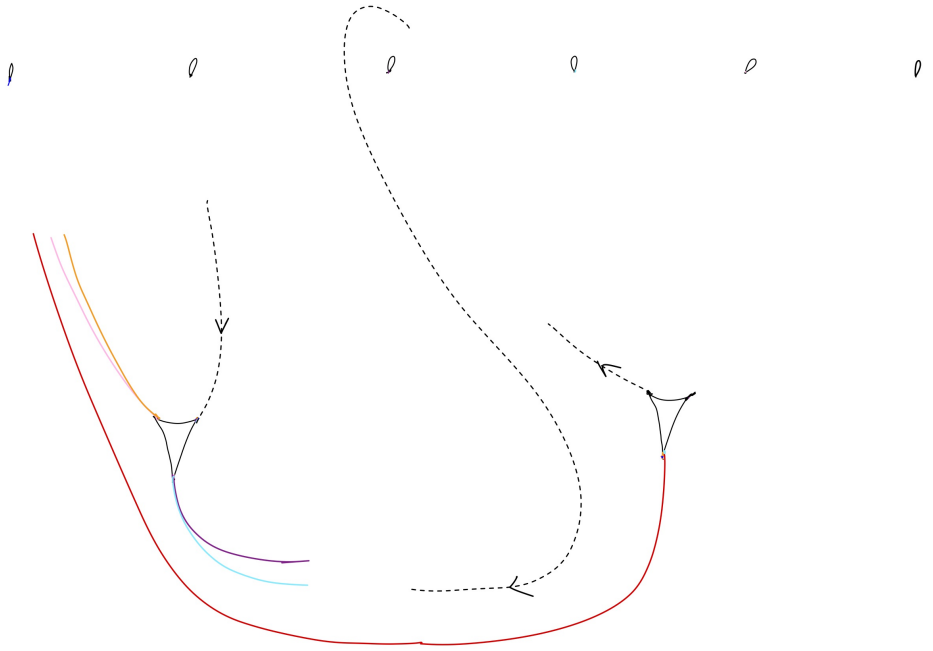


Figure H.142: ART1

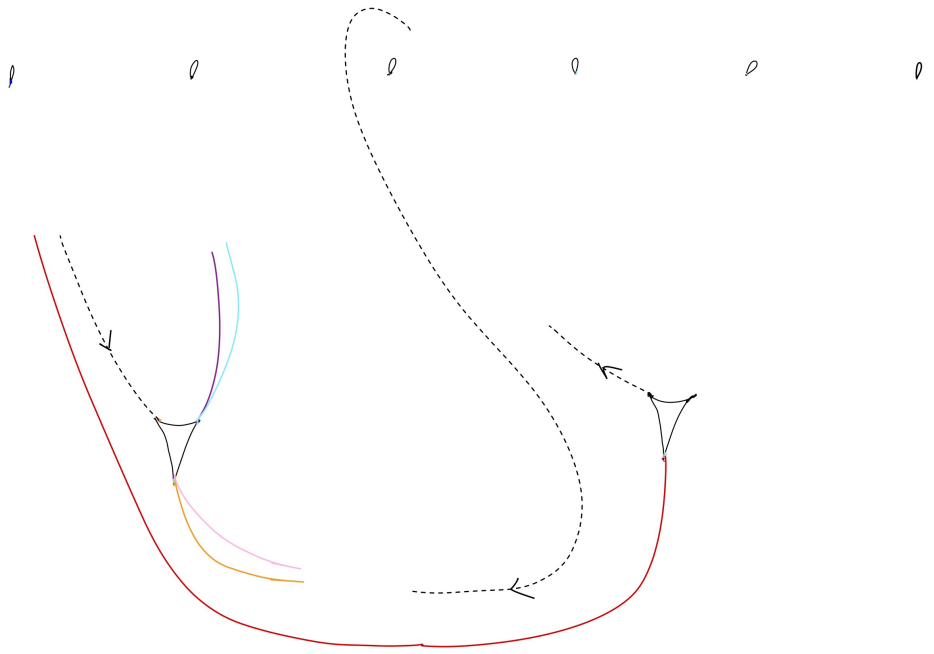


Figure H.143: WOT1

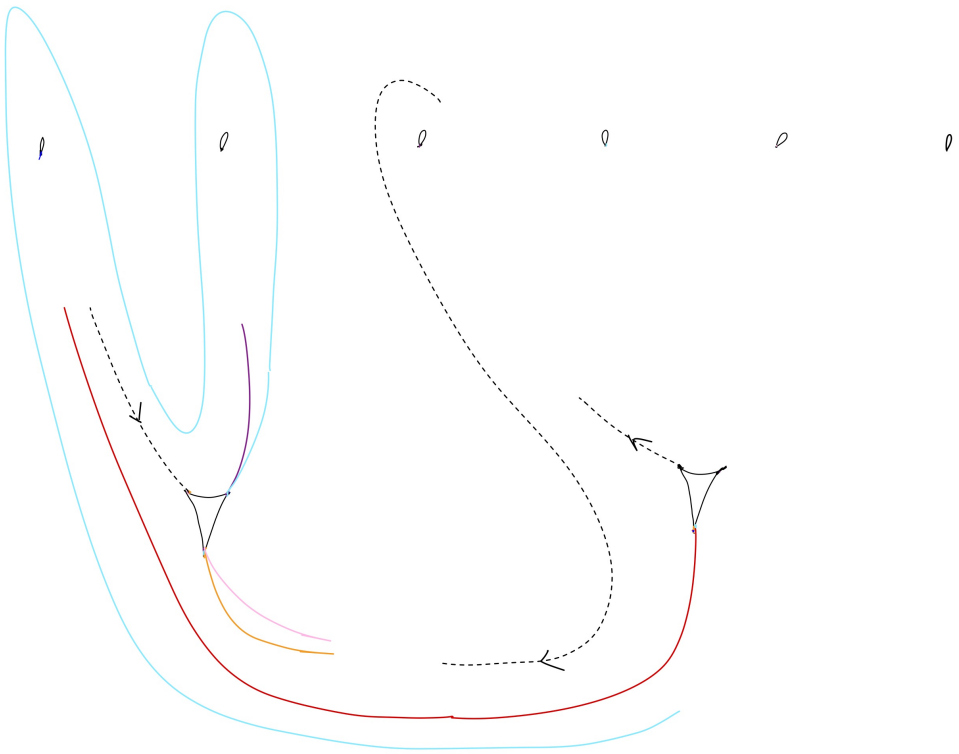


Figure H.144: WOT2

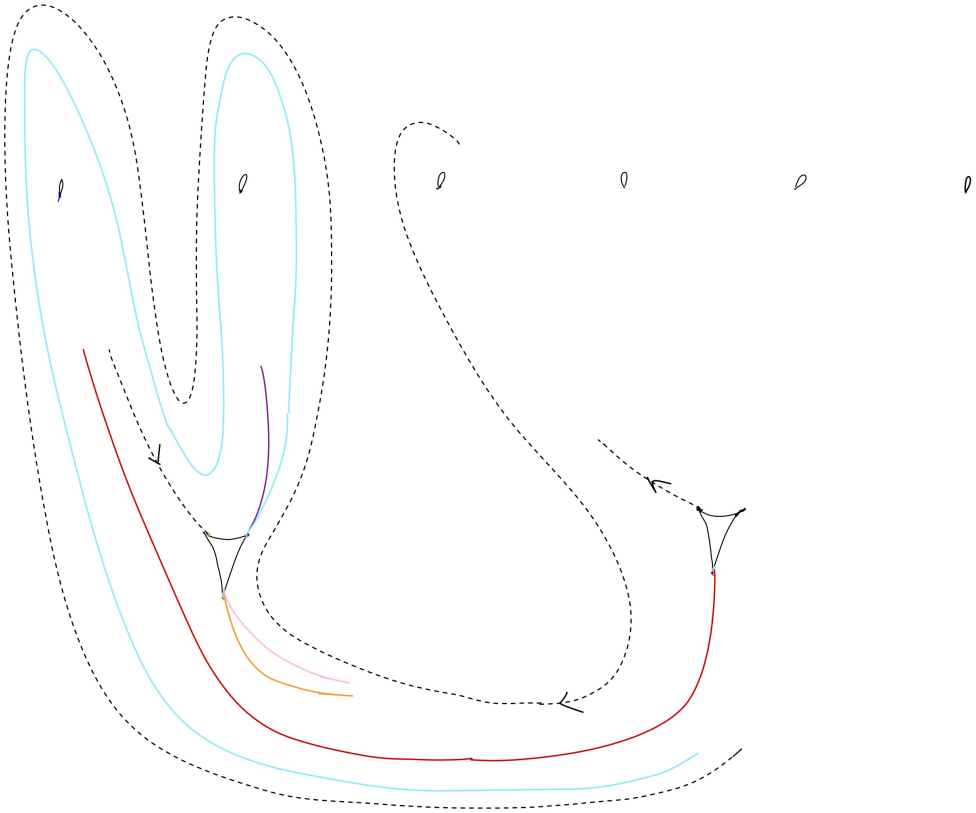


Figure H.145: WOT3

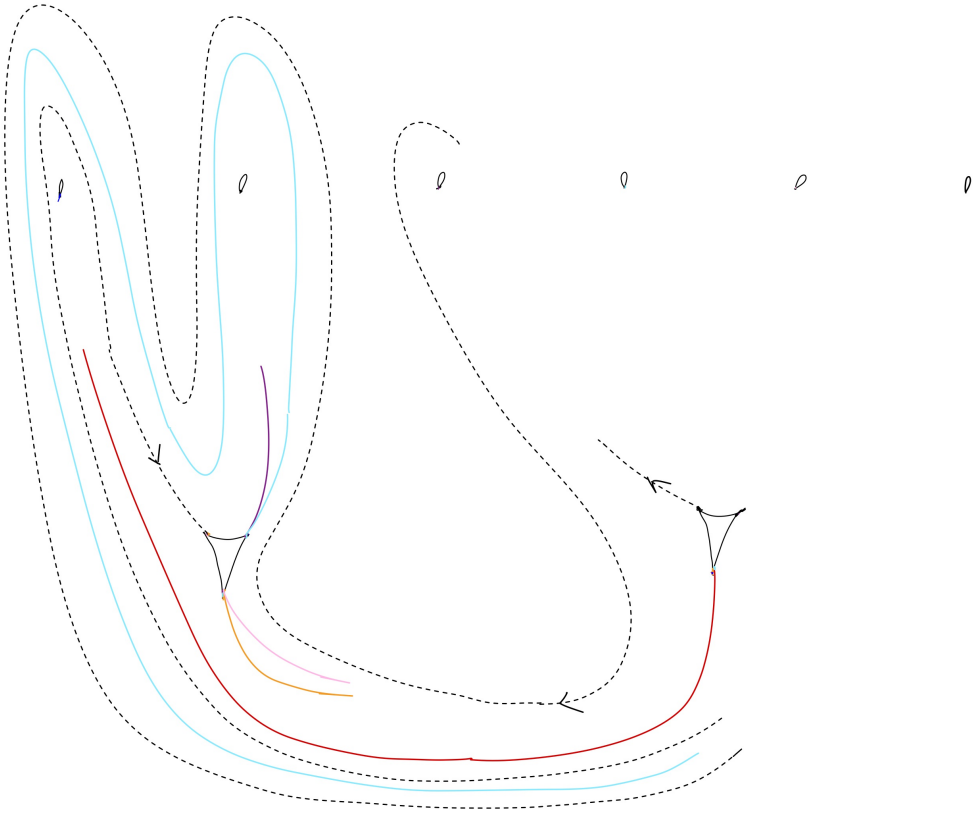


Figure H.146: WOT4

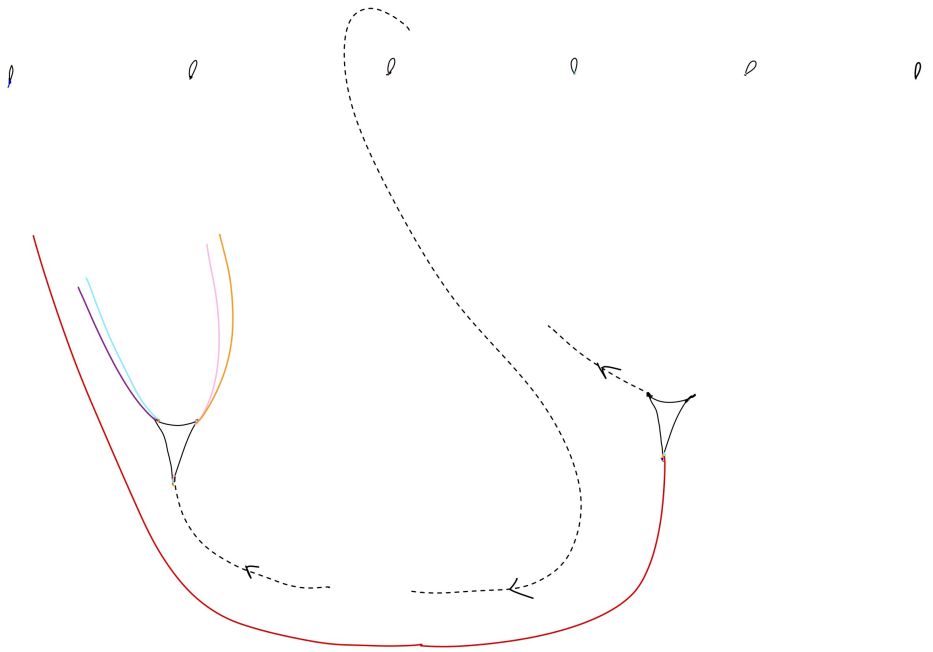


Figure H.147: ORE1

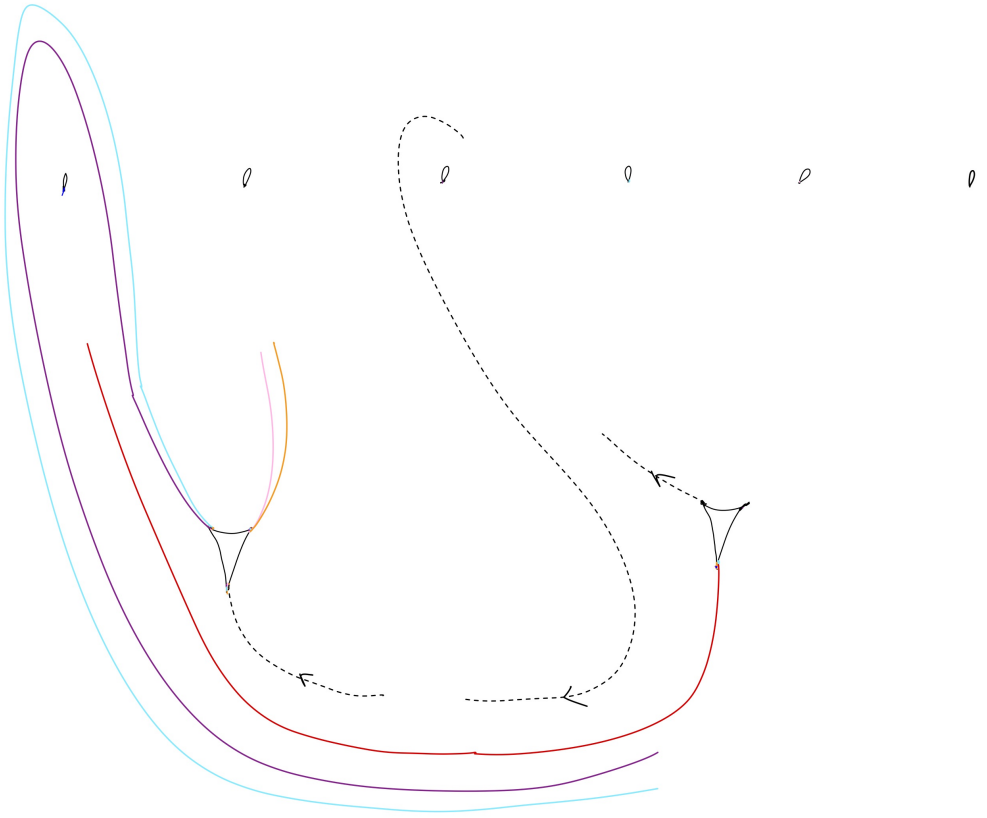


Figure H.148: ORE2

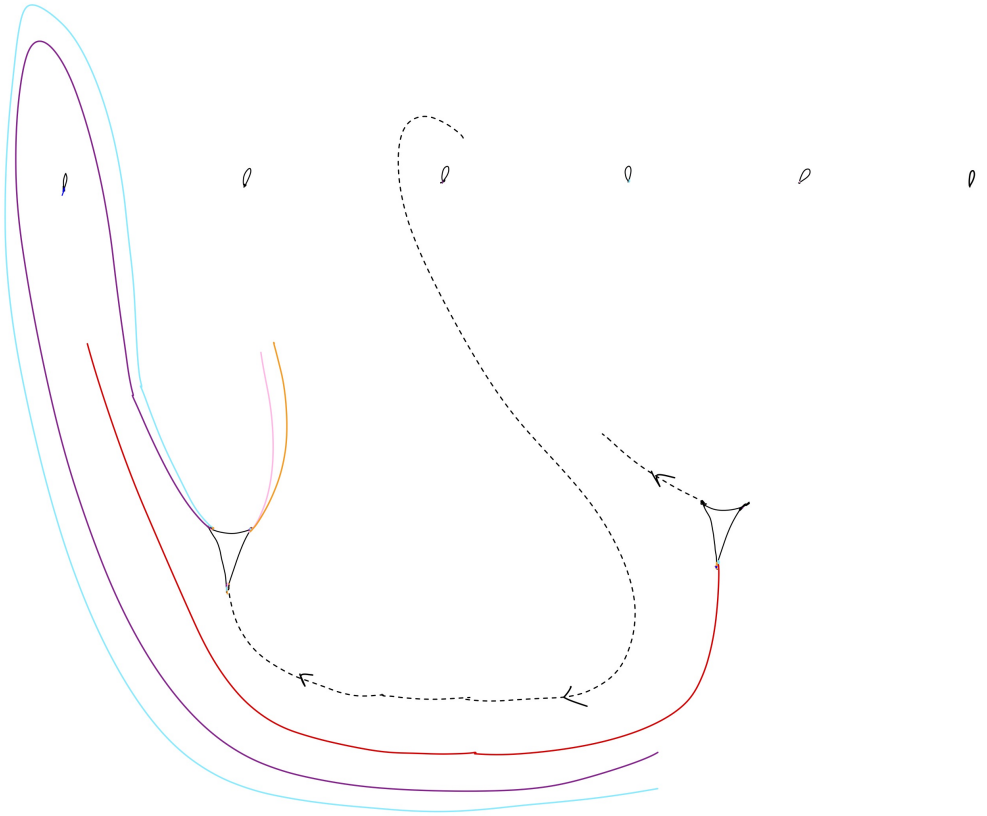


Figure H.149: ORE3

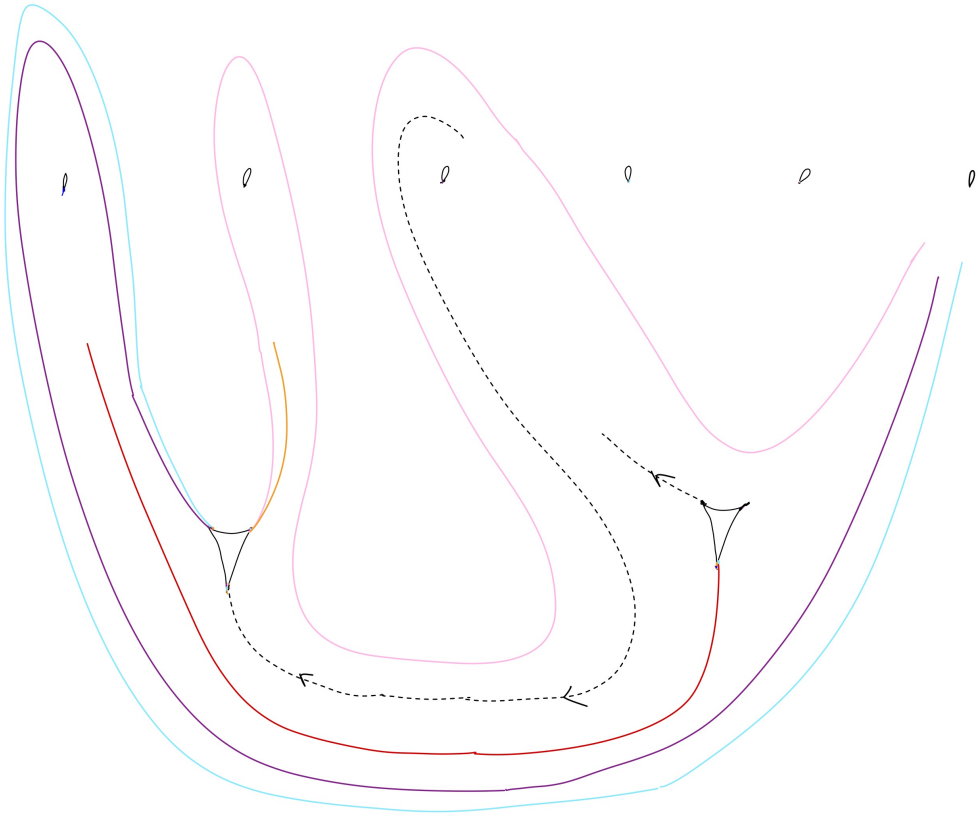


Figure H.150: ORE4

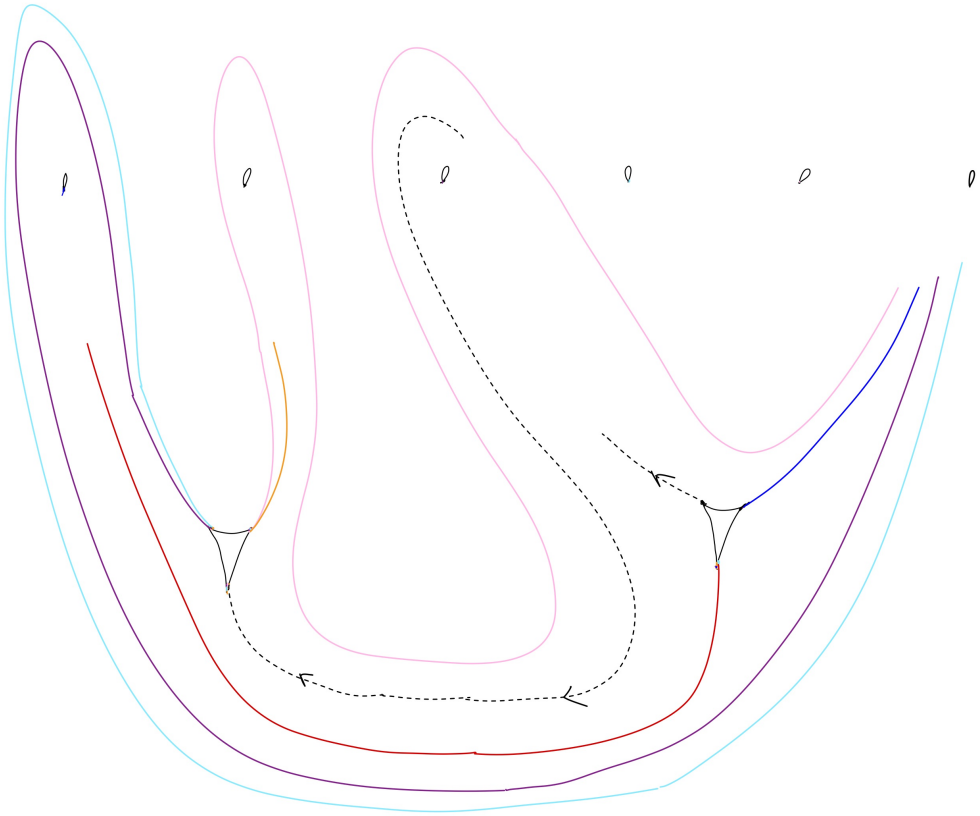


Figure H.151: ORE5

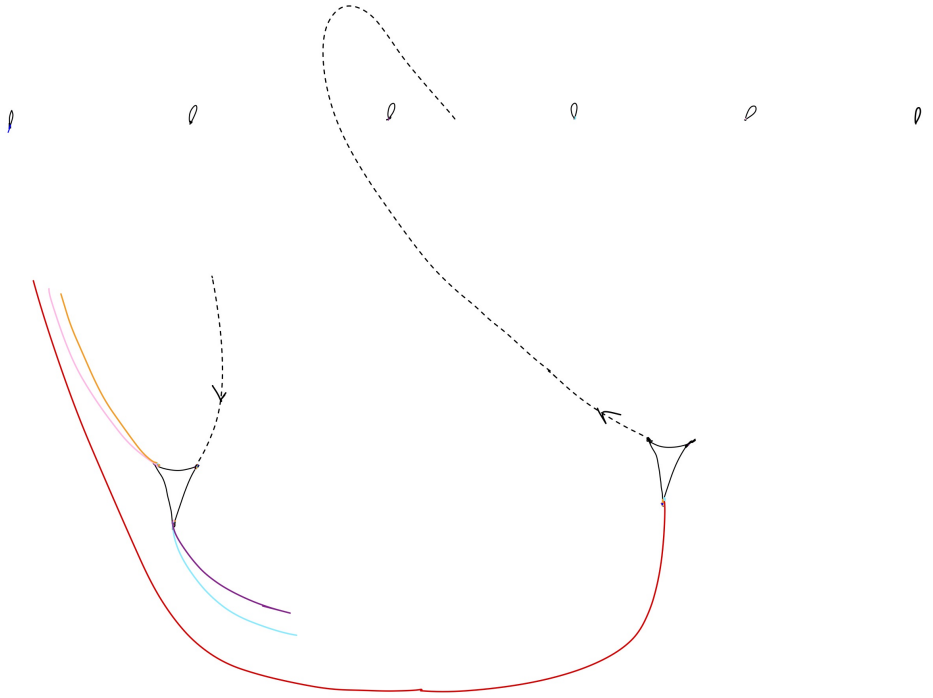


Figure H.152: BTV1

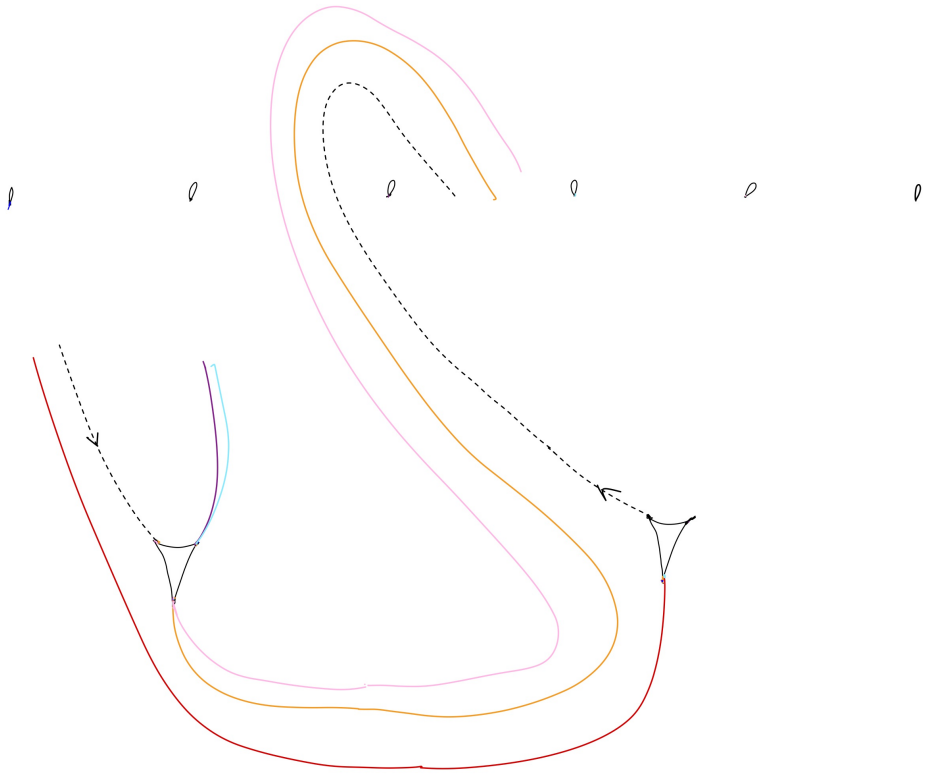


Figure H.153: AFN1

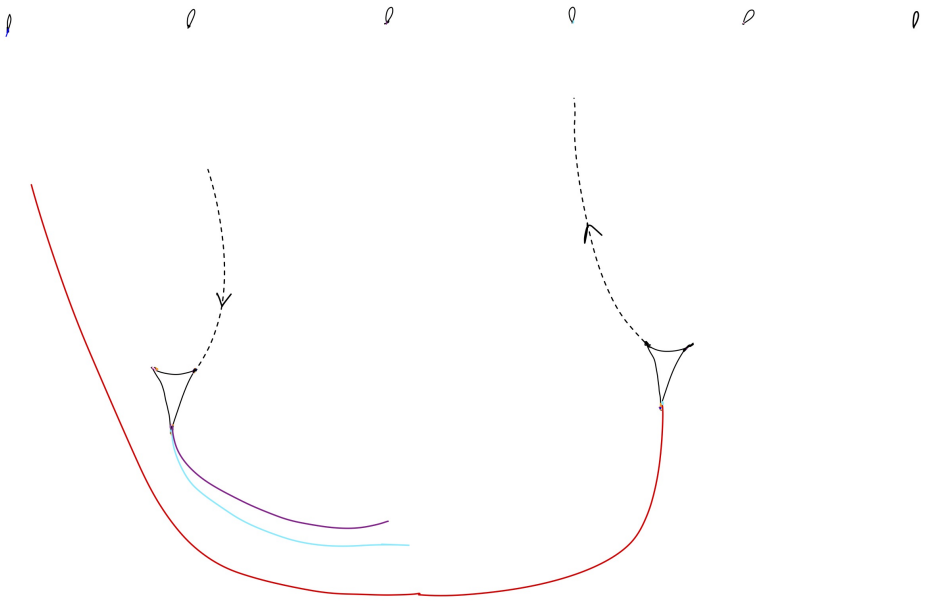


Figure H.154: CSS1

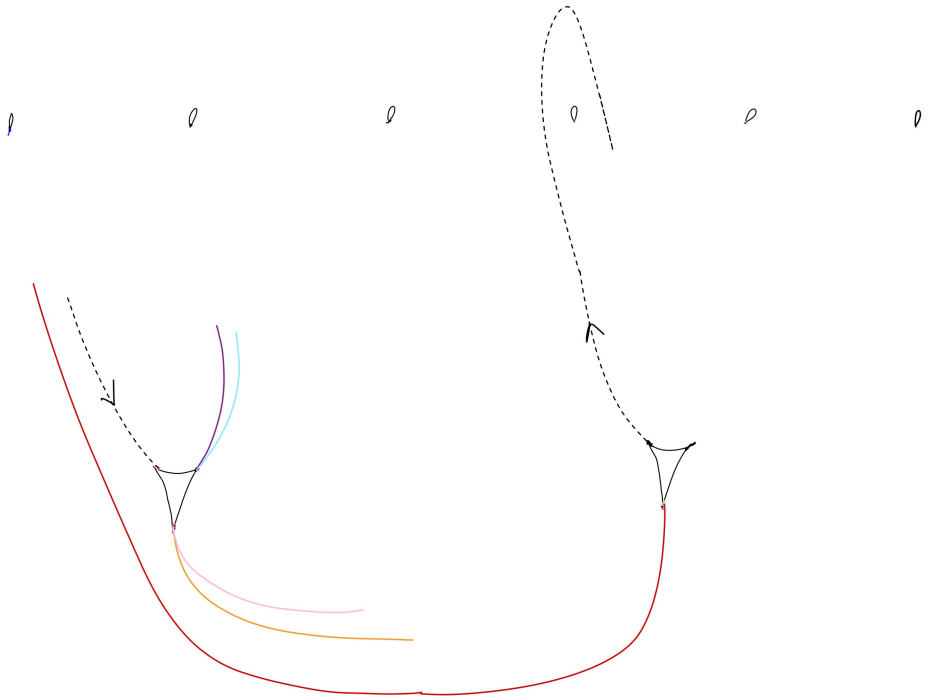


Figure H.155: UUU1

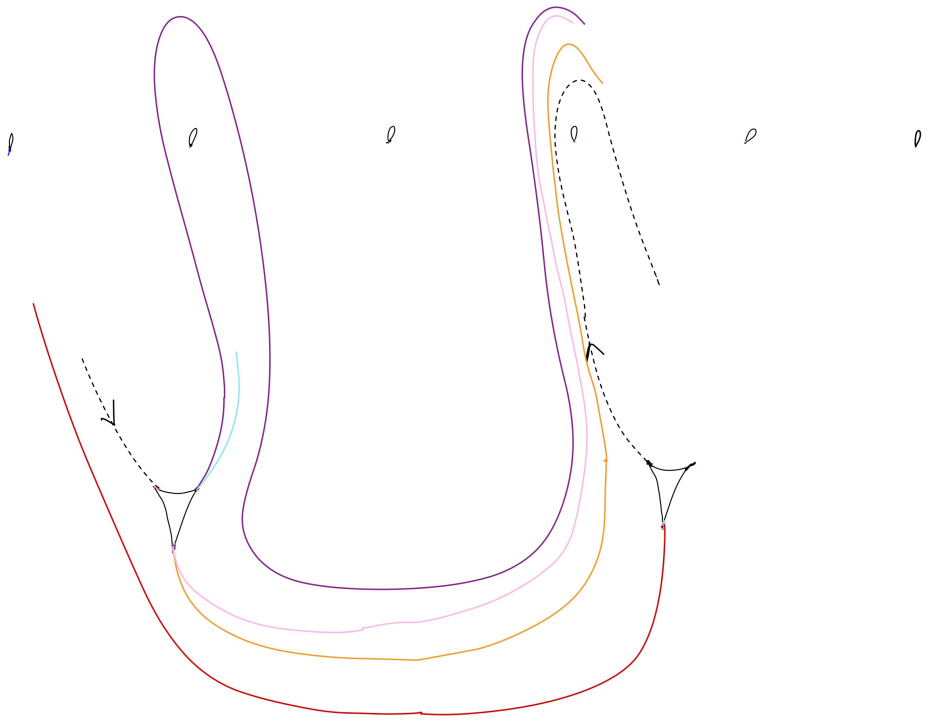


Figure H.156: UUU2

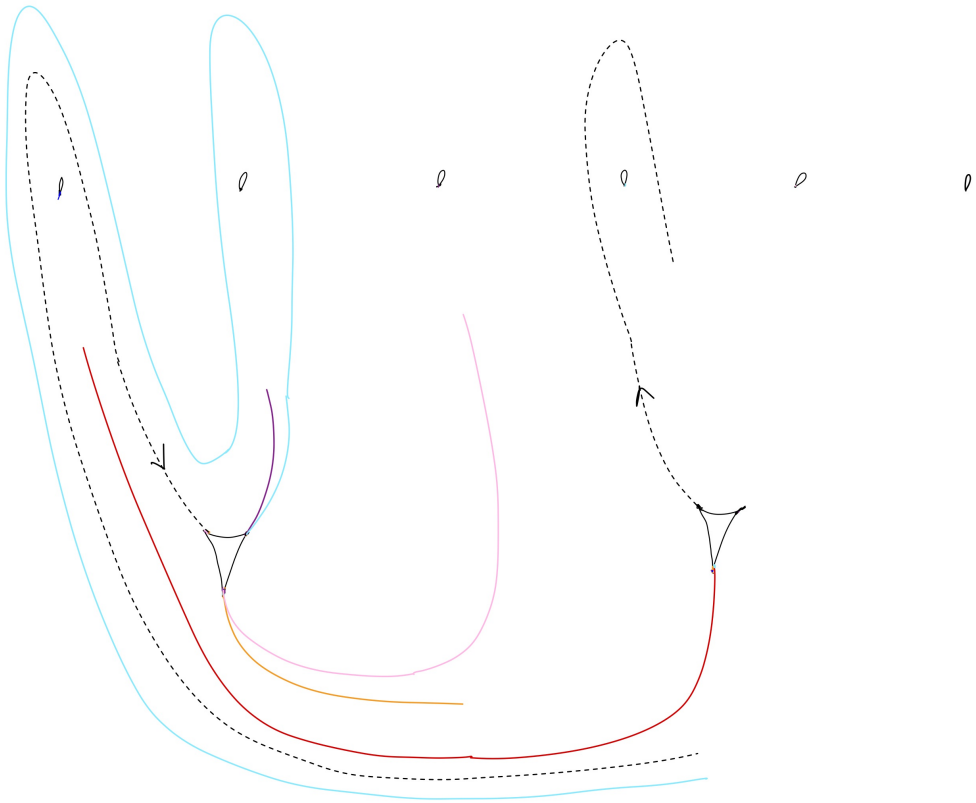


Figure H.157: UUU3

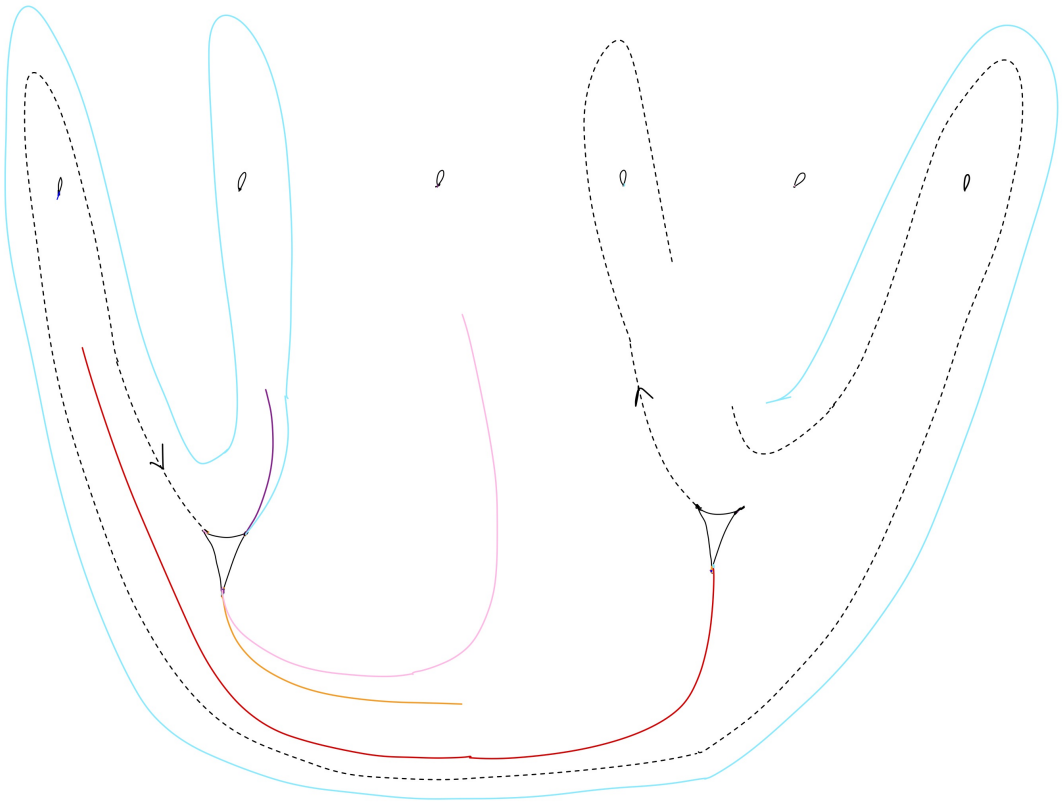


Figure H.158: UUU4

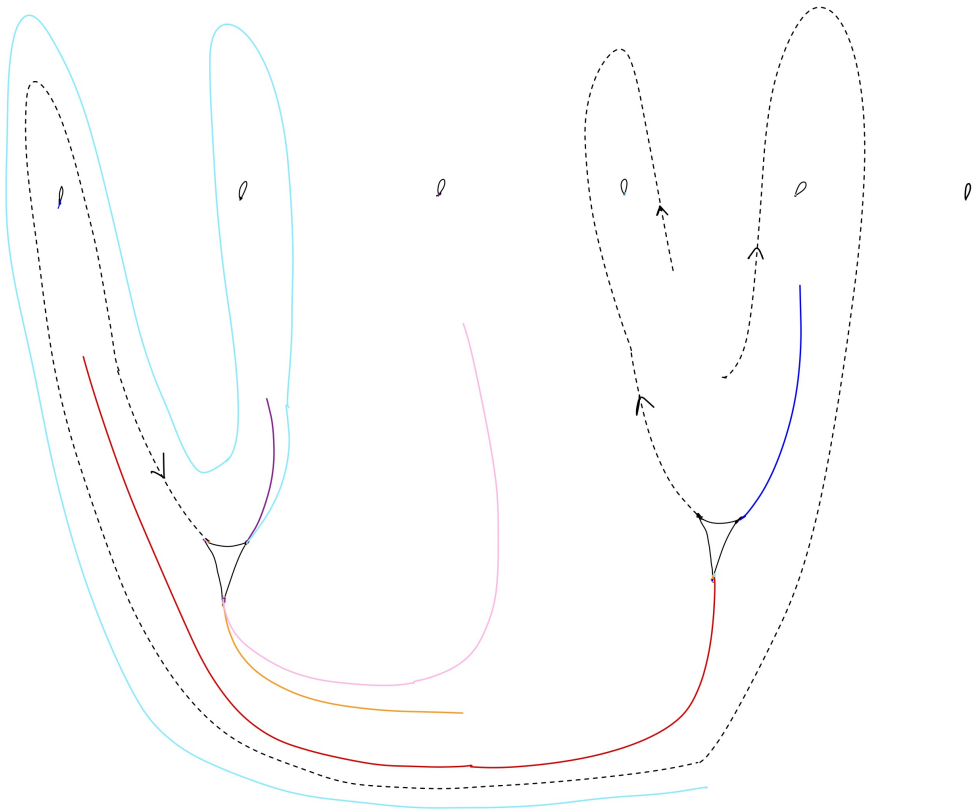


Figure H.159: UUU5

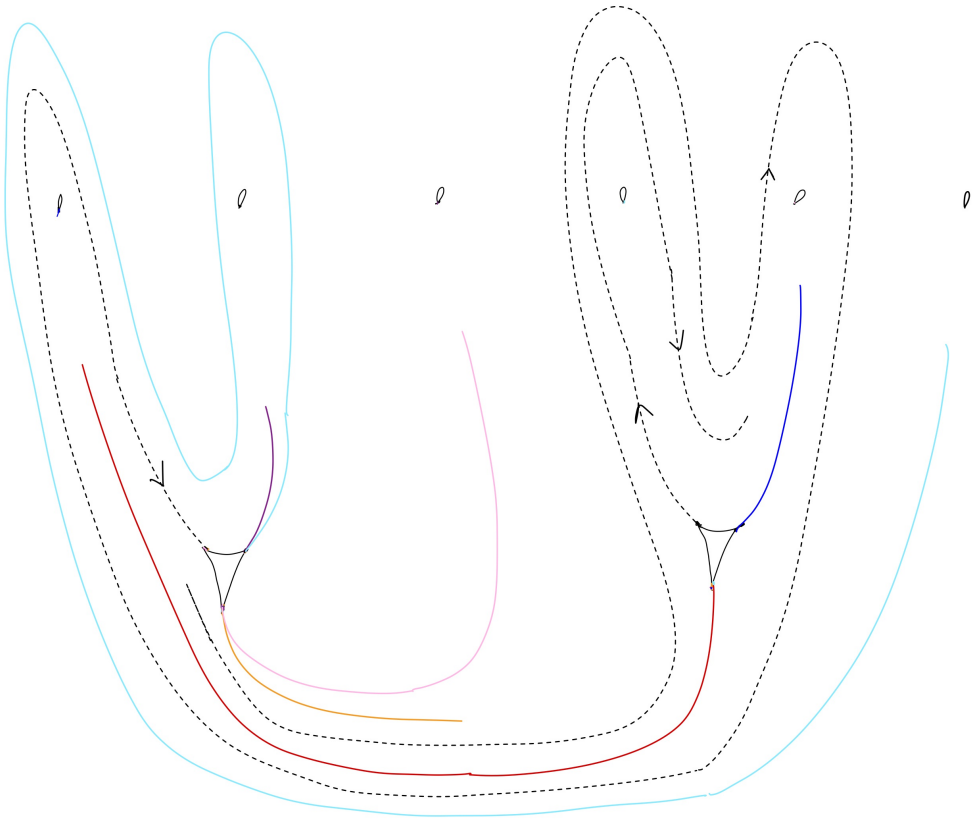


Figure H.160: UUU6

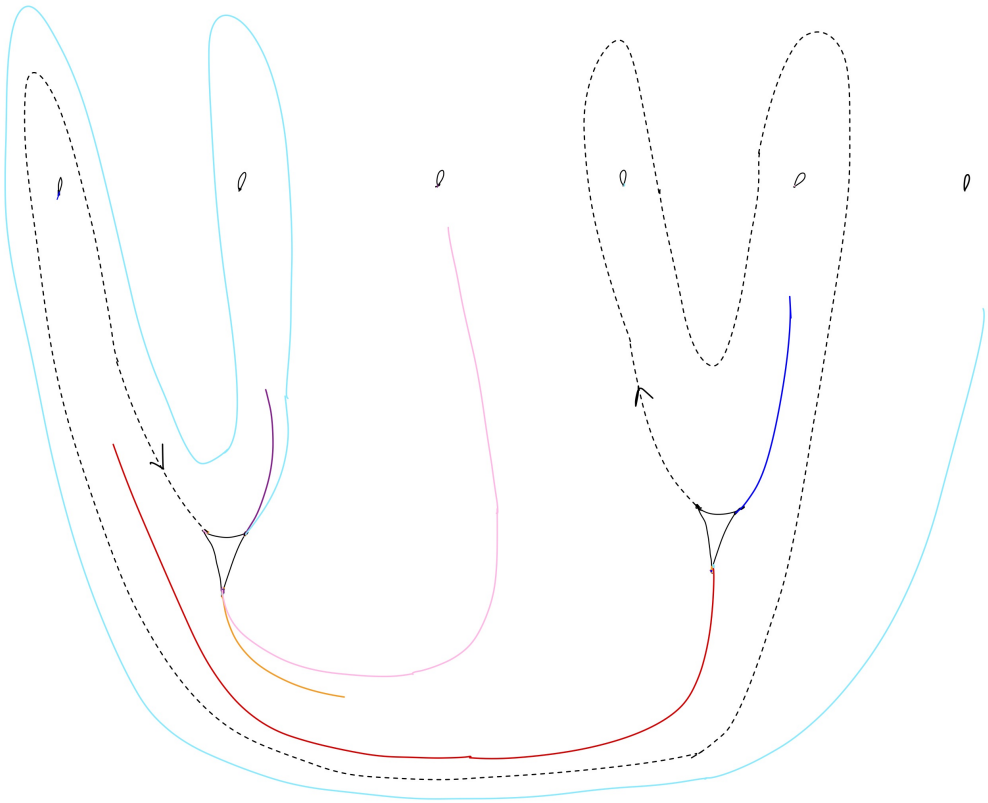


Figure H.161: UUU7

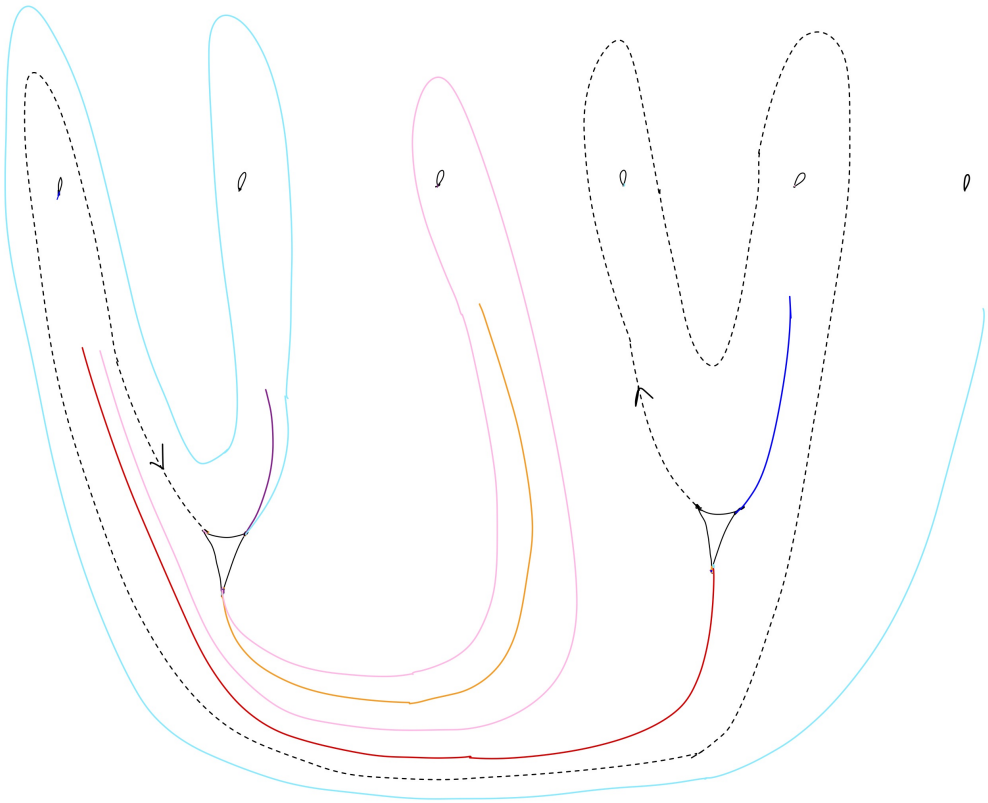


Figure H.162: UUU8

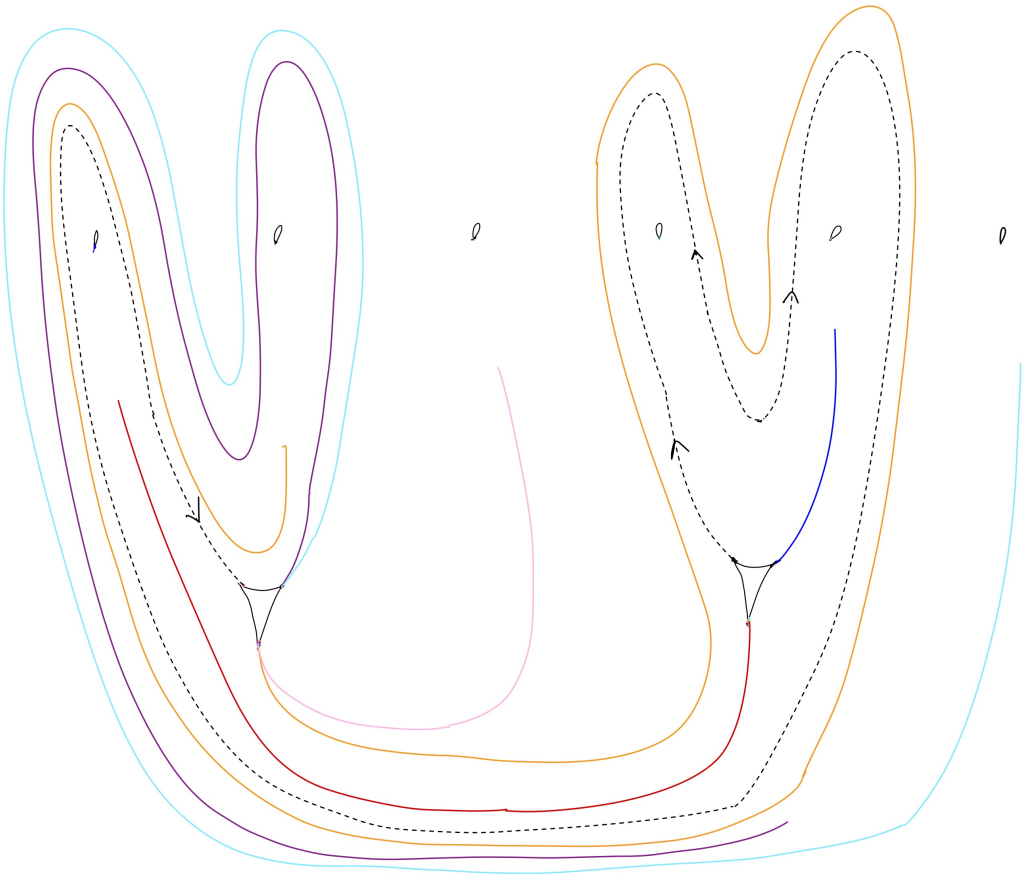


Figure H.163: UUU9

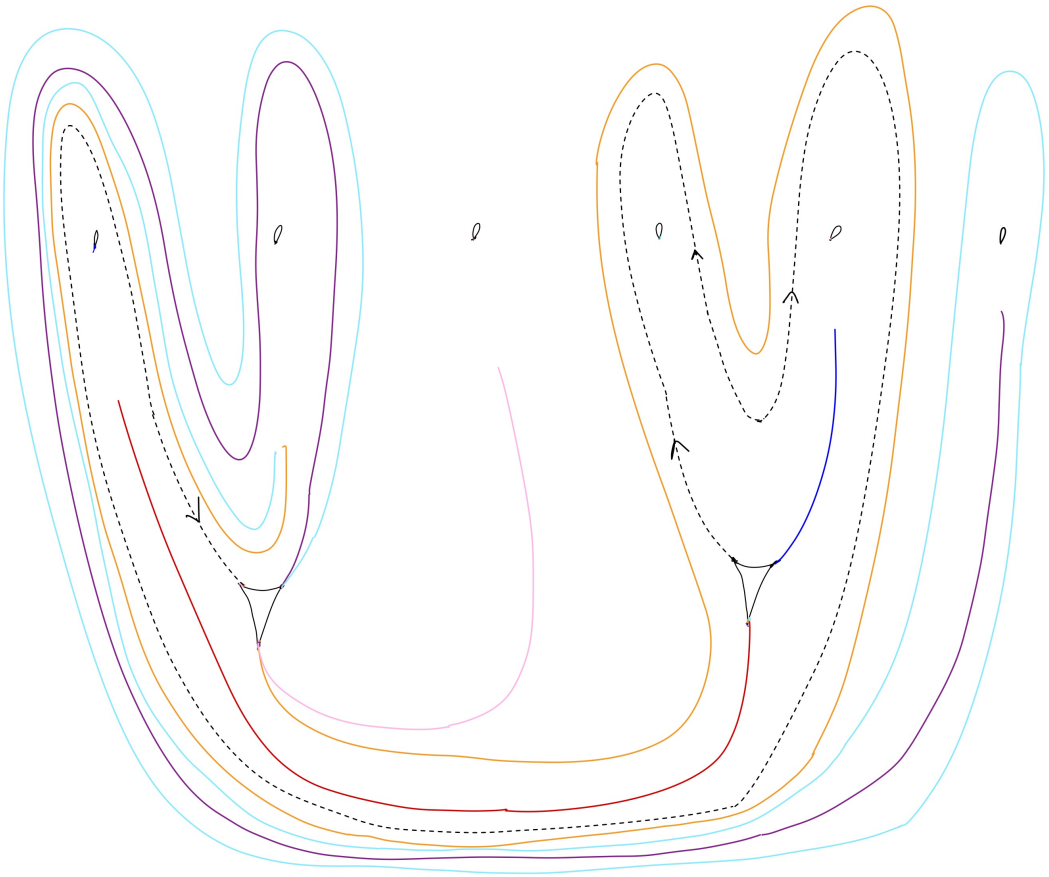


Figure H.164: UUU10

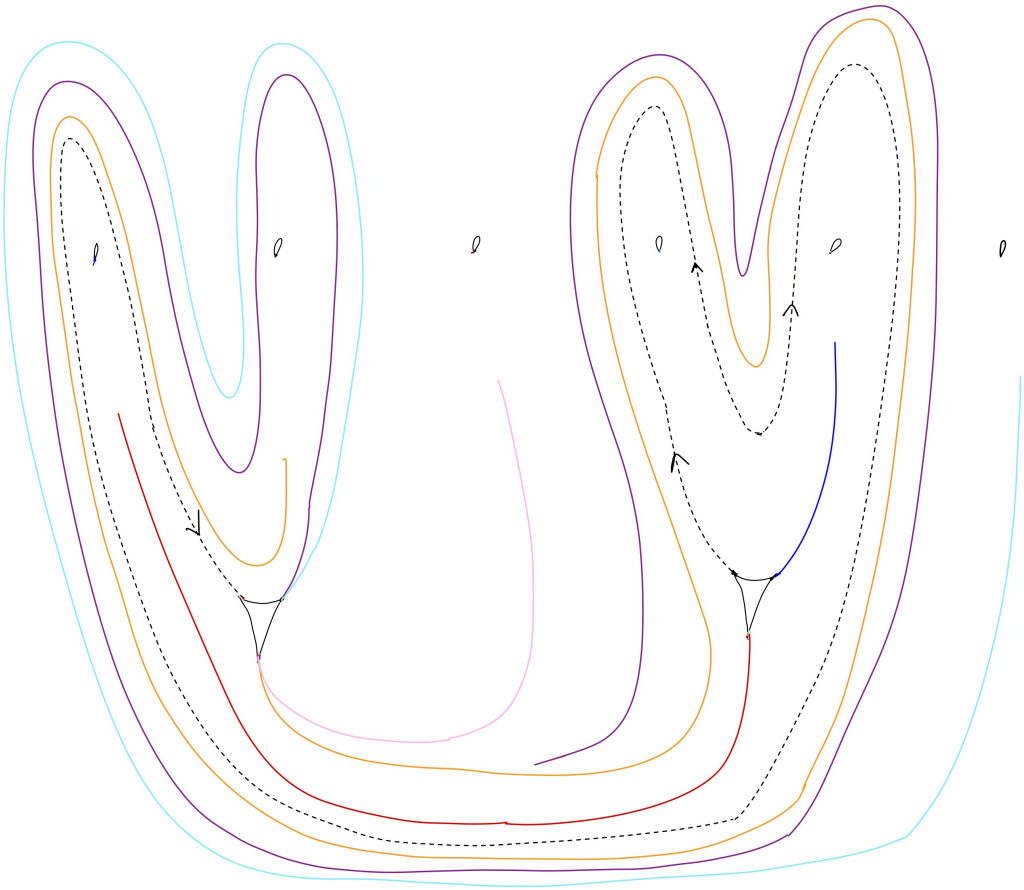


Figure H.165: UUU11

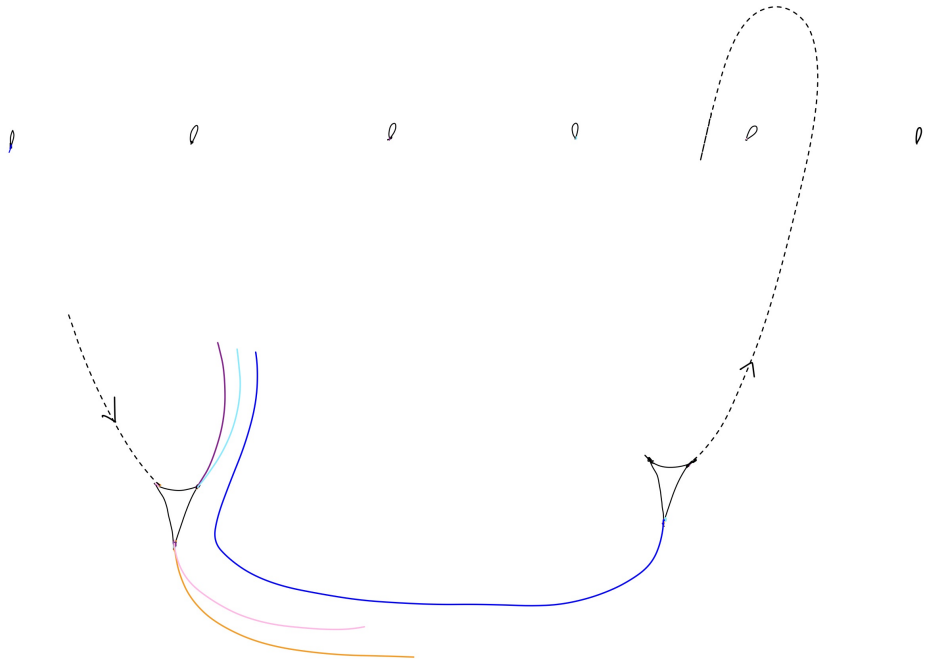


Figure H.166: GTK1

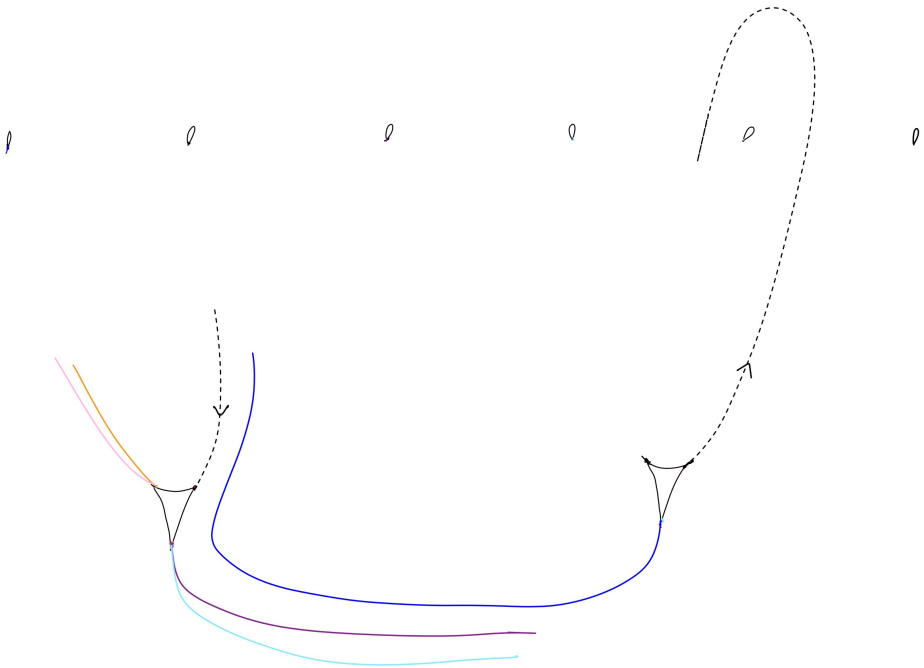


Figure H.167: CGI1

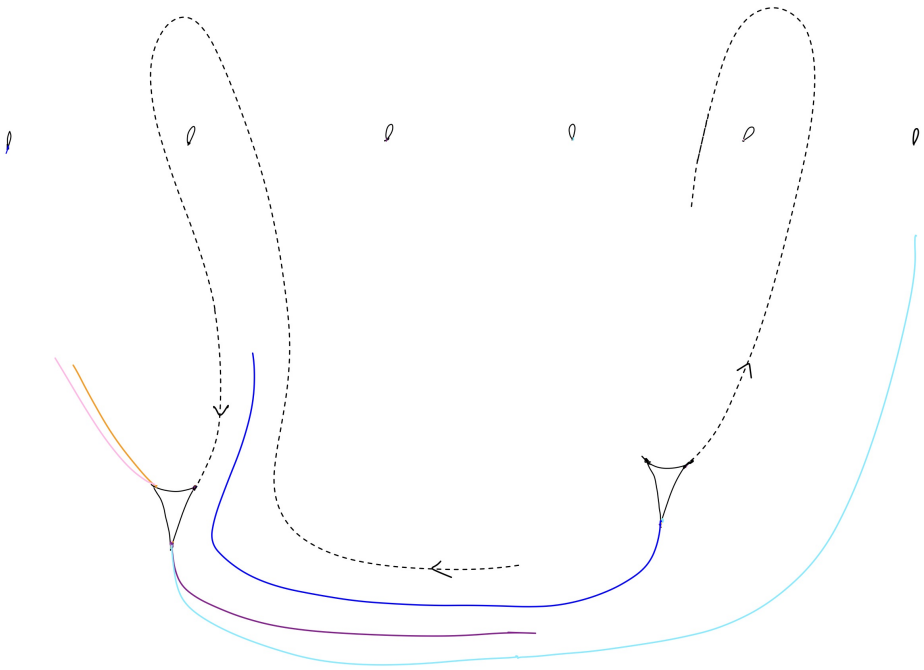


Figure H.168: CGI2

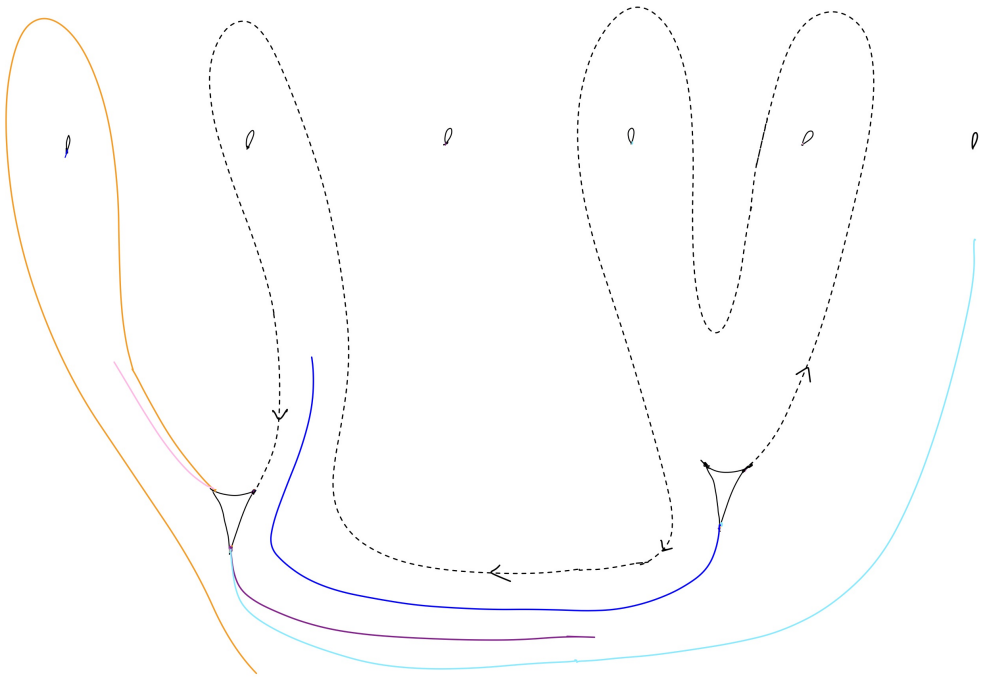


Figure H.169: CGI3

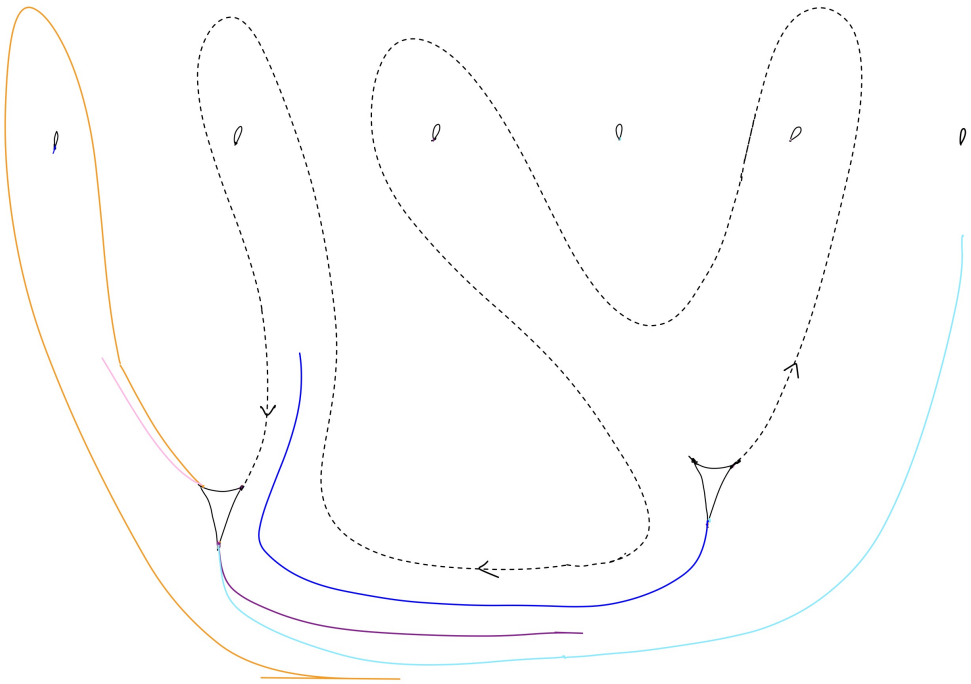


Figure H.170: CGI4

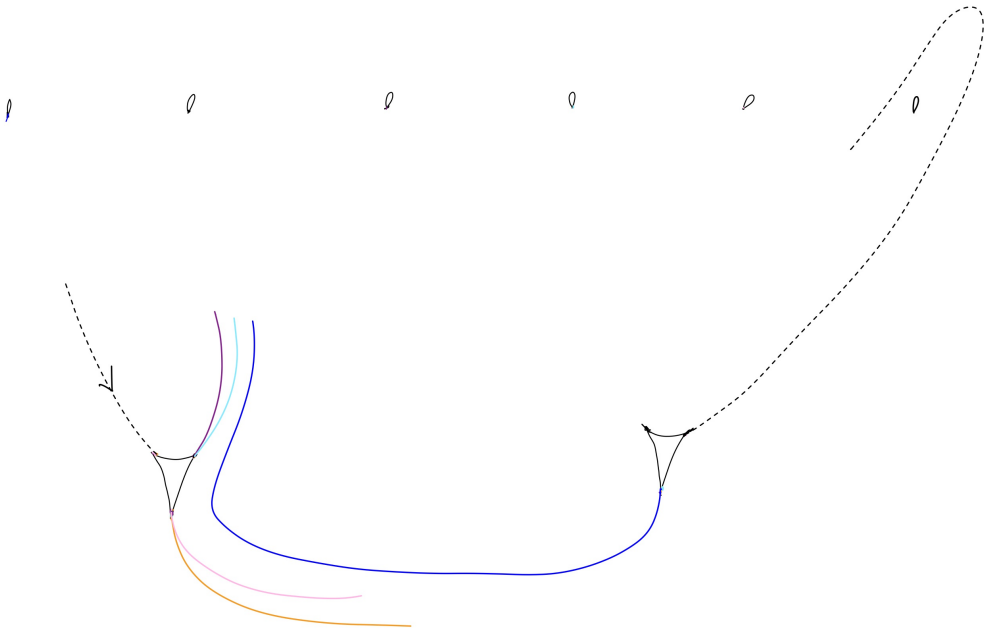


Figure H.171: GLD1

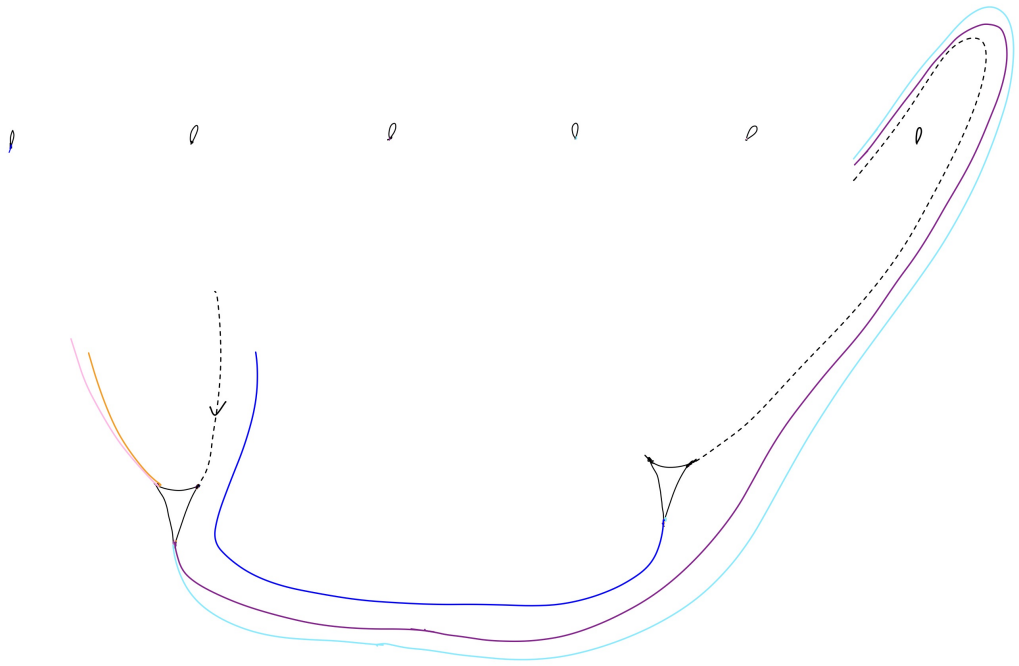


Figure H.172: UGN1

APPENDIX NINE

Train Track Case Analysis: Track 17

This is Track 17:

I.1 Case A: Triangles Fixed

Let us assume the triangles are fixed. Hence, both $f_\beta(d)$ and $f_\beta(\bar{d})$ both pass over $d/\bar{d}$ after an even number of letters. We shall call this *Assumption A*. Then $f_\beta(\bar{d})$ can begin with b, i, s, or o; and $f_\beta(d)$ can begin with r or p.

I.1.1 VSF

Suppose $f_\beta(\bar{d})$ began with b and $f_\beta(d)$ began with r.

This is Figure I.1.

Here there are two possibilities:

$$f_\beta(\bar{d}) = b^+ i^+ \bar{d}...$$

or

$$f_\beta(\bar{d}) = b^+ p^+ \bar{d}...$$

and any twists with o is not possible as that would cause $f_\beta(o)$ to trace.

I.1.1.1 Bawn

Suppose

$$f_\beta(\bar{d}) = b^+ i^+ \bar{d} ...$$

Then we have Figure I.2.

Here we claim that the dotted lines must join. Otherwise, either $f_\beta(\bar{d})$ has to go below $f_\beta(d)$ or $f_\beta(\bar{d})$ has to go above $f_\beta(p)$. It is not possible for $f_\beta(\bar{d})$ to go inbetween $f_\beta(p)$ and $f_\beta(d)$ as that would put it in Situation β.

Suppose it were the former case, then as Figure I.3 shows, the dotted lines are in Situation α.

Similarly, for the latter case, Figure I.4 shows the dotted lines also enter Situation α.

Thus the dotted lines must join, this is Figure I.5.

Here $f_\beta(p)$ can continue with i^- or s^*.

I.1.1.1.1 Blore

Suppose $f_\beta(p)$ continued with i^-:

$$f_\beta(p) = d i^- b^- o^* ...$$

This is Figure I.6.

Here in fact $f_\beta(p)$ must end at o°. Otherwise it will trace:

$$f_\beta(p) = d i^- b^- \hat{o}^+ b^+ i^+ \bar{d} r^+ p^\times$$

or

$$f_\beta(p) = di^- b^- \hat{o}^- b^+ i^+ \bar{d} p^\times$$

Thus we must have

$$f_\beta(p) = di^- b^- \hat{o}^\circ$$

Now consider $f_\beta(s)$. It cannot begin with $\bar{d}$, as that would also force $f_\beta(i)$ to begin with $\bar{d}$. In which case, one of them will trace after crossing d. So we must have $f_\beta(s)$ begin with o^+:

$$f_\beta(s) = o^+ b^+ i^+ \bar{d} r^+ p^+ di^* ...$$

On the other hand $f_\beta(i)$ must begin with $\bar{d}$ or it will trace:

$$f_\beta(i) = o^+ b^+ i^\times$$

So we have

$$f_\beta(i) = \bar{d} p^- r^- ds^\circ$$

This is Figure I.7.

And as shown $f_\beta(i)$ must end there at s° or it would either be abosrbed between itself and $f_\beta(s)$, or trace after crossing d.

Here $f_\beta(r)$ must end immediately at p°. Otherwise, if it began with p^- it immediately traces; while if it began with p^+, it would still trace:

$$f_\beta(r) = p^+ di^- b^- o^+ b^+ i^+ \bar{d} r^\times$$

Thus we must have

$$f_\beta(r) = p^\circ$$

This is Figure I.8.

Here we claim that $f_\beta(o)$ must end immediately at b°. Indeed, otherwise we have

$$f_\beta(o) = b^+ i^* ...$$

and here it must continue with i^+ and to the left of $f_\beta(s)$ and $f_\beta(b)$. Otherwise, either $f_\beta(b)$ would trace or $f_\beta(s)$ would immediately be absorbed between $f_\beta(o)$ and $f_\beta(\bar{d})$. Then $f_\beta(o)$ continues and traces:

$$f_\beta(o) = b^+ i^+ \bar{d} p^- r^- d i^- b^- o^\times$$

Thus we must have the situation depicted in Figure I.9. But here $f_\beta(b)$ must begin with i^+, otherwise $f_\beta(s)$ would be absorbed between $f_\beta(o)$ and $f_\beta(\bar{d})$. But now $f_\beta(b)$ will trace:

$$f_\beta(b) = i^+ \bar{d} p^- r^- d i^- b^\times$$

This is a contradiction.

I.1.1.1.2 Chark

Back to the end of Bawn I.1.1.1. Suppose $f_\beta(p)$ continued with s^*, then in fact it must be s°:

$$f_\beta(p) = d s^\circ$$

Otherwise it would trace:

$$f_\beta(p) = d s^+ r^+ p^\times$$

or

$$f_\beta(p) = ds^- \bar{d}p^\times$$

This is Figure I.10.

Now $f_\beta(i)$ can either begin with o^*, or $\bar{d}$. Suppose it were the former. Then it forces $f_\beta(s)$ to continue with o^- and to the right of the incoming $f_\beta(i)$. Otherwise, $f_\beta(i)$ would trace. So we have

$$f_\beta(s) = o^- i^* ...$$

This is Figure I.11.

Here $f_\beta(o)$ can either begin with b°, or with b^+.

I.1.1.1.2.1 Cudden

Suppose it were the former, that

$$f_\beta(o) = b^\circ$$

Then this forces $f_\beta(b)$ to begin with i^+ and to the left of the incoming $f_\beta(s)$. So we have

$$f_\beta(b) = i^+ \bar{d}p^- r^- ds^- \bar{d}p^- ...$$

This is Figure I.12.

Here $f_\beta(i)$ must end at o°. Otherwise it would immediately trace. This then forces $f_\beta(s)$ to also end, otherwise we would have

$$f_\beta(s) = o^- i^- o^- \operatorname{Abso}(f_\beta(i), f_\beta(s))^\times$$

or

$$f_\beta(s) = o^- i^+ o^+ b^+ i^+ \bar{d}$$

Now $f_\beta(s)$ can either end here at i° or continue with i^+. Suppose it were the former:

$$f_\beta(s) = o^- i^+ o^+ b^+ i^+ \bar{d} p^* ...$$

This is Figure I.13.

Here we claim that $f_\beta(r)$ must end immediately at p°. Indeed, if it began with p^- it immediately trace; while if it began with p^+, it either traces:

$$f_\beta(r) = p^+ ds^+ \bar{d} r^\times$$

or we would have the following:

$$f_\beta(r) = p^+ di^- b^- o^- i^* ...$$

as shown in Figure I.14.

Here if $f_\beta(s)$ were to continue with p° or p^+ then $f_\beta(b)$ would continue with p^+, and then trace:

$$f_\beta(b) = ...p^+ di^- b^\times$$

Whereas if instead $f_\beta(s)$ continued with p^- and to the right of $f_\beta(b)$, it would also trace:

$$f_\beta(s) = ...p^- ds^\times$$

Thus, we must have

$$f_\beta(r) = p^\circ$$

This gives Figure I.15.

Here $f_\beta(s)$ must continue with r^-, otherwise $f_\beta(s)$ would continue with r^+ and then eventually trace (and absorbed):

$$f_\beta(b) = ...r^+p^+di^-b^\times$$

But now $f_\beta(s)$ will trace:

$$f_\beta(s) = ...r^-p^+ds^\times$$

as shown in Figure I.16.

Thus going back to the situation depicted in Figure I.12, fbs must end here at i°, and also $f_\beta(i)$ ends at o° or it would immediately trace.

This is Figure I.17.

Here $f_\beta(b)$ must continue with p^-, otherwise $f_\beta(r)$ would continue with p^+ and then either trace:

$$f_\beta(r) = p^+ds^+\bar{d}r^\times$$

or absorbed:

$$f_\beta(r) = p^+di^-b^-o^-i^-o^+ \text{Abso}(f_\beta(i), f_\beta(s))^\times$$

This gives us Figure I.18.

Here it is clear that $f_\beta(r)$ must end, or it would trace, which then forces $f_\beta(b)$ to also end or it will trace, or escape to the outer perimeter and eventually be absorbed.

This is Figure **??**, which is Candidate 1.

I.1.1.1.3 Flisky

Back to the end of Chark I.1.1.1.2. Suppose $f_\beta(o)$ began with b^+. Then it continues:

$$f_\beta(o) = b^+ i^+ \bar{d} p^- r^- d s^- \bar{d} p * ...$$

This is Figure I.19.

Here $f_\beta(i)$ must end or it would immediately trace.

This is Figure I.20.

Here $f_\beta(b)$ can either continue with i^+ or end with i°. Suppose it were the former. Then it continues:

$$f_\beta(b) = i^+ \bar{d} p^- r^- d s^- \bar{d} p^* ...$$

This is Figure I.21.

Here $f_\beta(s)$ must end at i°, or it could continue with i^+. Suppose it were the latter case. This gives us the situation depicted in Figure I.22.

Here $f_\beta(r)$ cannot begin with p^- as it would trace; if it began with p^+, then it could only be done in between $f_\beta(d)$ and $f_\beta(s)$ as the other possibilities would cause it to eventually trace. This is Figure I.23. Here $f_\beta(o)$ must continue with p^+ and to the left of $f_\beta(s)$ otherwise $f_\beta(s)$ would immediately trace. But then $f_\beta(o)$ would trace:

$$f_\beta(o) = ...p6 + d i^- b^- o^\times$$

Thus we must have

$$f_\beta(r) = p^\circ$$

This is Figure I.24. But now again $f_\beta(o)$ must continue with r^+ and to the left of $f_\beta(s)$ otherwise $f_\beta(s)$ would trace. But then again $f_\beta(o)$ will eventually trace. This is a contradiction.

Thus $f_\beta(s)$ must in fact end at i° as shown in Figure I.25.

Now for the same reasoning as before, we can conclude that $f_\beta(r)$ must again end at p°, which then gives us the situation depicted in Figure I.26.

But now if $f_\beta(b)$ continued with r° or r^+, forcing $f_\beta(o)$ to continue with r^+, $f_\beta(o)$ would either trace:

$$f_\beta(o) = ...r^+p^+di^-b^-o^\times$$

or be absorbed:

$$f_\beta(o) = ...r^+p^+ds^+\bar{d}r^+p^+di^-o^\times$$

Thus going back to the situation depicted in Figure I.20, we must in fact have

$$f_\beta(b) = i^\circ$$

This gives us Figure I.27.

Here $f_\beta(s)$ can continue with b^+ or b°. Suppose it were the former. Then it continues:

$$f_\beta(s) = ...b^+i^+\bar{d}p^*...$$

as shown in Figure I.28.

Here if we claim that $f_\beta(r)$ must end at p°. Otherwise it would begin with p^+, and in between $f_\beta(d)$ and $f_\beta(s)$:

$$f_\beta(r) = p^+ di^- b^- o^- i^- b^* ...$$

as shown in Figure I.29.

Here if $f_\beta(s)$ were to continue with p° or p^+ then $f_\beta(o)$ would continue with p^+ and trace:

$$f_\beta(o) = ...p^+ di^- b^- o^\times$$

But then if $f_\beta(s)$ continues with p^- it would trace:

$$f_\beta(s) = ...p^- ds^\times$$

Thus we must in fact have

$$f_\beta(r) = p^\circ$$

This is Figure I.30.

But now again, if $f_\beta(s)$ continued with r° or r^+, forcing $f_\beta(o)$ to continue with r^+, then $f_\beta(o)$ would eventually trace; while if $f_\beta(s)$ continued with r^-, it would trace:

$$f_\beta(s) = ...r^- p^+ ds^\times$$

Thus in the situation depicted in Figure I.27, $f_\beta(s)$ must end:

$$f_\beta(s) = o^- i^- b^\circ$$

giving us Figure I.31.

Here $f_\beta(o)$ is forced to end as well, otherwise:

$$f_\beta(o) = ...r^+di^-b^-o^\times$$

or

$$f_\beta(o) = ...r^+dr^+p^+di^-b^-i^+o^\times$$

or

$$f_\beta(o) = ...r^-p^+ds^+r^+p^+di^-b^- \text{ Abso}(f_\beta(o), f_\beta(\bar{d}))^\times$$

Thus we must have the situation depicted in Figure I.32, which is Candidate 2.

I.1.1.1.3.1 Wanion

Back to the situation depicted in Figure I.33. Suppose instead that

$$f_\beta(i) = \bar{d}...$$

Then it continues:

$$f_\beta(i) = \bar{d}p^-r^-dp^*...$$

This is Figure I.33.

Here $f_\beta(r)$ must end at p°. Indeed, if in stead it began with p^- then it immediately traces. If instead it began with p^+, then either it traces:

$$f_\beta(r) = p^+dr^\times$$

or it is absorbed:

$$f_\beta(r) = p^+ di^- b^- o^- \operatorname{Abso}(f_\beta(i), f_\beta(s))^\times$$

Thus we must have

$$f_\beta(e) = p^\circ$$

This gives Figure I.34.

Here $f_\beta(i)$ must end at r°. Indeed, otherwise it either traces:

$$f_\beta(i) = ...r^+ p^+ di^\times$$

or

$$f_\beta(i) = ...r^- p^+ ds^+ r^+ p^+ di^\times$$

or is absorbed:

$$f_\beta(i) = ...r^+ p^+ dr^+ p^+ d \operatorname{Abso}(f_\beta(s), f_\beta(s))^\times$$

Thus we must have the situation depicted in Figure I.35.

Here $f_\beta(b)$ must end at i°. Indeed, if it began with i^- it would immediately trace. While if instead it began with i^+ it either traces:

$$f_\beta(b) = i^+ \bar{d} p^- r^- ds^- \bar{d} p^- r^+ p^+ di^- b^\times$$

or is absorbed:

$$f_\beta(b) = i^+ \bar{d} p^- r^- ds^- \bar{d} p^- r^+ p^+ ds^+ r^+ p^+ d \operatorname{Abso}(f_\beta(i), f_\beta(s))^\times$$

Thus we must have

$$f_\beta(b) = i^\circ$$

This is Figure I.36.

Here if $f_\beta(o)$ did not end, then we would have

$$f_\beta(o) = b^+ i^+ \bar{d} p^- r^- d s^- \bar{d} p^- r^+ p^+ d i^- b^- o^\times$$

or

$$f_\beta(o) = b^+ i^+ \bar{d} p^- r^- d s^- \bar{d} p^- r^+ p^+ d r^+ p^+ d \,\mathrm{Abso}(f_\beta(i), f_\beta(s))^\times$$

Thus we must have

$$f_\beta(o) = b^\circ$$

giving is Candidate 3, shown in Figure I.37.

I.1.1.2 Blet

Back to the end of VSF I.1.1. Suppose

$$f_\beta(\bar{d}) = b^+ p^+ \bar{d} ...$$

This is Figure I.38.

Here for the same reasoning as that of Bawn I.1.1.1, the dotted lines must join. But then $f_\beta(s)$ will trace, as shown in Figure I.39.

This is a contradiction.

I.1.2 HLE

Back to end of Case A I.1. Suppose that $f_\beta(\bar{d})$ began with b, and $f_\beta(d)$ began with p.

This is Figure I.40.

Here we either have

$$f_\beta(\bar{d}) = b^+ i^+ \bar{d} ...$$

or

$$f_\beta(\bar{d}) = b^+ s^+ \bar{d} ...$$

I.1.2.1 Dree

Suppose we have

$$f_\beta(\bar{d}) = b^+ i^+ \bar{d} ...$$

Then for a similar reasoning as that of Bawn I.1.1.1, the dotted lines must join. This is Figure I.41.

Here $f_\beta(s)$ and $f_\beta(i)$ must go above $f_\beta(r)$. Otherwise one of $f_\beta(s)$ or $f_\beta(i)$ would trace after crossing d again. Then $f_\beta(r)$ ends at o° as otherwise it would trace immediately after crossing $\bar{d}$. But now $f_\beta(r)$ would trace, as Figure I.42 shows.

I.1.2.2 Moke

Back to the end of HLE I.1.2. Suppose

$$f_\beta(\bar{d}) = b^+ s^+ \bar{d} ...$$

Then for the same reason as before, the dotted lines must join; and $f_\beta(i)$ and $f_\beta(s)$ must go

above $f_\beta(r)$ to give us

$$f_\beta(r) = db^+ i^* ...$$

This is Figure I.43.

Here $f_\beta(r)$ cannot continue with i^+:

$$f_\beta(r) = db^+ \hat{i}^+ b^- \bar{d} r^\times$$

so it either continues with i^- or i°. Suppose it were the former. Then it continues:

$$f_\beta(r) = db^+ \hat{i}^- b^- o^* ...$$

This is Figure I.44.

Here $f_\beta(i)$ must continue with r^+, otherwise $f_\beta(s)$ would trace immediately after crossing d. Also, $f_\beta(i)$ must go to the left of $f_\beta(p)$, otherwise if it went in between $f_\beta(p)$ and $f_\beta(s)$ then it would escape to the outer perimeter and eventually trace. This is Figure I.45.

Furthermore, $f_\beta(s)$ must also continue with r^+ and to the left of $f_\beta(p)$, as otherwise $f_\beta(p)$ would be absorbed between $f_\beta(s)$ and $f_\beta(i)$, shown in Figure I.46.

So we must have Figure I.47.

Here $f_\beta(i)$ must continue with p^+, otherwise $f_\beta(s)$ would trace immediately trace after d. This gives us Figure I.48.

Now $f_\beta(i)$ must continue with r^- and to the right of $f_\beta(p)$. Otherwise, $f_\beta(p)$ would trace

immediately. But now $f_\beta(i)$ will escape to the outer perimeter and eventually trace:

$$f_\beta(i) = ...r^- db^+ i^\times$$

or

$$f_\beta(i) = ...r^- db^+ s^+ \bar{d} r^+ p^+ db^+ i^\times$$

This is a contradiction. Thus $f_\beta(r)$ must end at b°. Now again for the same reasons as before, $f_\beta(i)$ and $f_\beta(s)$ must continue with r^+ and to the left of $f_\beta(p)$. This is Figure I.49.

Here $f_\beta(p)$ cannot begin with r^+ or it would immediately trace. However, if it began with r^- or r°, in both cases, $f_\beta(i)$ must continue with p^+ and would then escape to the outer perimeter and eventually trace.

This is shown in Figure I.50, Figure I.51, and Figure I.52.

This is a contradiction.

I.1.3 UAH

Back to end of Case A I.1. Suppose that $f_\beta(\bar{d})$ began with i, and $f_\beta(d)$ began with r.

This is Figure I.53.

Here we claim that the dotted lines must join. Indeed, otherwise suppose $f_\beta(\bar{d})$ went above $f_\beta(p)$. Then we would have the situation depicted in Figure I.54, where the dotted lines are in Situation β.

If instead $f_\beta(\bar{d})$ were to go in between $f_\beta(p)$ and $f_\beta(d)$ then it would be in Situation β.

If instead $f_\beta(\bar{d})$ were to go below $f_\beta(d)$, then again the dotted lines will be in Situation α, as shown in Figure I.55.

Thus we must have Figure I.56.

Here $f_\beta(b)$ must go below $f_\beta(p)$. Otherwise, it would trace immediately after crossing d. So we must have Figure I.57.

Here we must have

$$f_\beta(s) = b^- \bar{d} r^* ...$$

Otherwise $f_\beta(i)$ would immediately trace.

This gives us Figure I.58.

Here we claim that $f_\beta(o)$ must continue with s^*. Indeed, otherwise it must continue with

$$f_\beta(o) = ...di^- b^- \bar{d} p^- ...$$

which would force $f_\beta(p)$ to follow it and $f_\beta(p)$ will trace.

Thus we must have Figure I.59.

Here $f_\beta(p)$ can continue with $-$ or s^*.

I.1.3.1 Oche

Suppose $f_\beta(p)$ continued with d:

$$f_\beta(p) = d\hat{i}^- b^- o^* ...$$

This is Figure I.60.

Here $f_\beta(r)$ can begin and end with r°, or begin with r^+. Suppose it were the former case.

Then we have Figure I.61.

Here $f_\beta(b)$ must end. Otherwise,

$$f_\beta(b) = \bar{d}p^- \hat{r}^+ p^+ db^\times$$

or

$$f_\beta(b) = \bar{d}p^- \hat{r}^- p^+ di^- b^\times$$

Thus we must have

$$f_\beta(b) = \bar{d}p^- \hat{r}^\circ$$

which forces the situation depicted in Figure I.62. Here if $f_\beta(p)$ continued with o° or o^+, then $f_\beta(s)$ would continue with o^+:

$$f_\beta(s) = ...o^+ b^+ i^+ \bar{d}r^+ p^+ db^+ i^+ \text{ Abso}(f_\beta(o), f_\beta(\bar{d}))^\times$$

On the other hand, if $f_\beta(p)$ continued with o^- and to the right of $f_\beta(s)$ then:

$$f_\beta(p) = ...o^- b^+ i^+ \bar{d}p^\times$$

This is a contradiction.

Thus it must be the latter case, that $f_\beta(r)$ must begin with p^+.

This is Figure I.63. Here $f_\beta(r)$ cannot go into 1, as that would cause it to escape to the outer perimeter and trace (this is due to the fact that here $f_\beta(p)$ must end at o° or $f_\beta(p)$ would trace itself).

So it can go into 2, or 3.

I.1.3.1.1 Gurry

Suppose it were to go into 2. This is Figure I.64.

Here $f_\beta(b)$ must end. Otherwise, it would immediately trace after crossing d. Also, $f_\beta(i)$ is forced to begin with b^- due to the incoming $f_\beta(r)$:

$$f_\beta(i) = b^- \bar{d} p^- r^* ...$$

This is Figure I.65.

Here if $f_\beta(s)$ continued with r° or r^+, forcing $f_\beta(i)$ to continue with r^+, then:

$$f_\beta(i) = ...r^+ p^+ db^+ i^\times$$

So $f_\beta(s)$ must continue with r^-, but then

$$f_\beta(s) = ...r^- p^+ db^+ \bar{d} p^- di^- b^- o^+ b^+ i^+ \bar{d} r^+ p^+ db^+ i^+ \operatorname{Abso}(f_\beta(o), f_\beta(i))^\times$$

This is a contradiction.

I.1.3.1.2 Hanch

Back to the end of Oche I.1.3.1. Suppose $f_\beta(r)$ went into 3. This gives us Figure I.66.

Here iif $f_\beta(s)$ were to continue with p° or p^+, forcing $f_\beta(b)$ to continue with p^+, then:

$$f_\beta(b) = \bar{d} \hat{p}^+ db^\times$$

But if $f_\beta(s)$ continued with p^- and to the right of $f_\beta(b)$, then:

$$f_\beta(s) = ...p^- di^- b^- o^+ b^+ i^+ \bar{d} r^+ p^+ d b^+ i^+ \operatorname{Abso}(f_\beta(o), f_\beta(i))^\times$$

This is a contradiction.

I.1.3.2 Roop

Back to the end of UAH I.1.3. Suppose $f_\beta(p)$ continued with s^*. Then it forces $f_\beta(o)$ to continue with s^- otherwise $f_\beta(p)$ would escape to the outer perimeter and trace.

This is Figure I.67.

Here $f_\beta(s)$ must continue with p^-. Otherwise, $f_\beta(b)$ would trace after crossing d. Here $f_\beta(i)$ can either end at b° or begin with b^-. Suppose it were the former. Then this forces $f_\beta(b)$ and $f_\beta(o)$ to continue with p^- or they would be absorbed between $f_\beta(s)$ and $f_\beta(i)$.

This is Figure I.68.

Here $f_\beta(s)$ must continue with r^- otherwise $f_\beta(b)$ would trace. If it went in between $f_\beta(o)$ and $f_\beta(d)$ then we have Figure I.69, where $f_\beta(s)$ would trace. So instead it must go in between $f_\beta(b)$ and $f_\beta(o)$, and it continues:

$$f_\beta(s) = r^- p6 + di^- b^- o^* ...$$

This is Figure I.70.

Here $f_\beta(b)$ must end, or it would trace immediately after crossing d. Also, $f_\beta(r)$ must end as

well, or it would trace immediately if continuing with p^-, and trace if continuing with p^+:

$$f_\beta(r) = p^+ ds^+ r^\times$$

Thus we must have

$$f_\beta(r) = p^\circ$$

This is Figure I.71.

Here $f_\beta(o)$ both must end, otherwise it would eventually escape to the outer perimeter and trace; this in turn forces $f_\beta(s)$ to also end. This gives us Candidate 4, shown in Figure I.72.

Now suppose instead $f_\beta(i)$ were to begin with b^-:

$$f_\beta(i) = b^- \bar{d} p^* ...$$

Then here it must be p^- or $f_\beta(b)$ would trace.

This is Figure I.73.

Here $f_\beta(s)$ and $f_\beta(i)$, as a pair, must go into 1 or 2. No image path can go in between $f_\beta(s)$ and $f_\beta(i)$ because it would then be absorbed between the two. So suppose they go into 1.

This is Figure I.74.

Here $f_\beta(s)$ must continue with r^-, otherwise $f_\beta(i)$ would continue with r^+ and be absorbed between itself and $f_\beta(s)$.

This is Figure I.75.

Here $f_\beta(s)$ must continue with p^+ or $f_\beta(r)$ would immediately trace. As shown in Figure I.76, $f_\beta(s)$ can go into 1 or 2.

If it were 1, then we would be in the situation depicted in Figure I.77. Here if $f_\beta(b)$ were to continue with $r\circ$ or r^- then $f_\beta(i)$ would continue with r^- and then trace:

$$f_\beta(i) = r^- p^+ di^\times$$

But if $f_\beta(b)$ continued with r^+ and to the left of $f_\beta(i)$:

$$f_\beta(b) = r^+ p^+ db^\times$$

So instead suppose $f_\beta(s)$ went into 2. Then $f_\beta(r)$ must continue with p^+ as well to prevent $f_\beta(b)$ from eventually tracing. This is Figure I.78.

Here $f_\beta(s)$ must continue with b^+ and to the left of $f_\beta(r)$ otherwise $f_\beta(r)$ would trace after crossing $\bar{d}$.

This is Figure I.79.

Here $f_\beta(s)$, $f_\beta(b)$, $f_\beta(o)$, and $f_\beta(r)$ are in a four-way counterclockwise path mill between p and b.

Going back to the situation depicted in in Figure I.73. Suppose the pair go into 2.

This gives Figure I.80.

Here $f_\beta(s)$ and $f_\beta(i)$ escape to the outer perimeter, and $f_\beta(s)$ cannot continue here with s so it forces $f_\beta(i)$ to continue with i, thereby tracing.

This is a contradiction.

I.1.4 GKA

Back to end of Case A I.1. Suppose that $f_\beta(\bar{d})$ began with i, and $f_\beta(d)$ began with p.

This is Figure I.81.

Here for the same reasoning as before in the previous sections of this Appendix so far, the dotted lines must join (or else we would have Situation α). But now $f_\beta(b)$ will trace, as shown in Figure I.82.

This is a contradiction.

I.1.5 WGA

Back to end of Case A I.1. Suppose that $f_\beta(\bar{d})$ began with s, and $f_\beta(d)$ began with r.

This is Figure I.83.

Here again the dotted lines must join. Consider $f_\beta(o)$:

$$f_\beta(o) = s^- b^- \bar{d} p^- r^- ...$$

This is Figure I.84.

Here $f_\beta(b)$ must go below $f_\beta(p)$. Otherwise, it would trace:

$$f_\beta(b) = \bar{d} r^+ p6 + db^\times$$

This forces

$$f_\beta(p) = ds^- b^- o^* ...$$

where the fourth letter here must be o^* and not $\bar{d}$ or it would trace.

But now $f_\beta(o)$ will trace, as shown in Figure I.85.

I.1.6 LUA

Back to end of Case A I.1. Suppose that $f_\beta(\bar{d})$ began with s, and $f_\beta(d)$ began with p.

This is Figure **??**.

Here the same arguments of GKA I.1.4 will lead to a contradiction.

This concludes the cases analysis for the case where the triangles are swapped.

I.2 Case B,C,D: Triangles Swapped

Now suppose the triangles are swapped. Then at least one of $f_\beta(d)$ and $f_\beta(\bar{d})$ must go over an odd number of letters before crossing. We first assume this to be the case for $f_\beta(\bar{d})$, that is, $f_\beta(\bar{d})$ crosses an odd number of letters before crossing d.

Then $f_\beta(\bar{d})$ can begin with p or r; and $f_\beta(\bar{d})$ can begin with s, i, b, or o.

I.2.1 GBR

Suppose $f_\beta(\bar{d})$ began with p, and $f_\beta(d)$ began with s. We remind the reader that we are assuming $f_\beta(\bar{d})$ must go over an odd number of letters before crossing. This assumption necessitates that $f_\beta(\bar{d})$ must eventually travers p^+d...

Here $f_\beta(d)$ can begin with s, i, b, or o.

Suppose $f_\beta(d)$ began with s. This is Figure I.86. Here $f_\beta(d)$ must begin with s^+ or $f_\beta(b)$ would immediately trace.

This gives us Figure I.87.

Here the dotted lines are in Situation α.

So suppose $f_\beta(d)$ began with i. This is Figure I.88.

Here if $f_\beta(b)$ were to continue with i, then we would be in the situation depicted in Figure I.89, where the dotted lines are in Situation α.

So instead we must have

$$f_\beta(b) = s^*...$$

Here $f_\beta(i)$ must begin with r^+ otherwise $f_\beta(s)$ would begin with r^- and trace immediately after crossing. So we have

$$f_\beta(i) = r^+p^+db^*...$$

This is Figure I.90.

Here $f_\beta(p)$ msut begin with b^- and to the right of $f_\beta(i)$ or $f_\beta(i)$ would immediately trace. So we have

$$f_\beta(p) = b^-o^*...$$

This is Figure I.91.

Here consider $f_\beta(\bar{d})$. In order to not violate the Trace Lemma, it cannot continue with b^+, so we must have

$$f_\beta(\bar{d}) = p^+d\hat{b}^-o^+b^+i^*...$$

This is Figure I.92.

And in fact here the dotted lines must join, otherwise $f_\beta(\bar{d})$ will have no other option but to

violate the Trace Lemma.

So we have Figure I.93, where we have drawn

$$f_\beta(o) = p^+ db^* ...$$

which is forced.

Here $f_\beta(o)$ must continue with b^- and to the right of $f_\beta(i)$. Otherwise, $f_\beta(i)$ would continue with b^+ and be absorbed between $f_\beta(\bar{d})$ and $f_\beta(o)$. So we have

$$f_\beta(o) = p^+ d\hat{b}^- \bar{d} p^- r^- ds^* ...$$

as shown in Figure I.94.

Here $f_\beta(o)$ must continue with s^- or $f_\beta(b)$ would trace immediately after crossing $\bar{d}$. So we have:

$$f_\beta(o) = p^+ db^- \bar{d} p^- r^- d\hat{s}^- \bar{d} p^* ...$$

This is Figure I.95.

Here $f_\beta(o)$ must continue with p^+ or $f_\beta(r)$ would trace:

$$f_\beta(r) = \bar{d}\hat{p}^- ds^+ \bar{d} r^\times$$

But now $f_\beta(o)$ would trace:

$$f_\beta(o) = p^+ db^- \bar{d} p^- r^- ds^- \bar{d}\hat{p}^+ db^- o^\times$$

So now suppose $f_\beta(d)$ began with b^*.

This is Figure I.96.

Here $f_\beta(r)$ must go above $f_\beta(\bar{d})$. Otherwise, it would trace after crossing d, irregardless if $f_\beta(\bar{d})$ has any initial twists:

$$f_\beta(r) = \bar{d}p^*...$$

However, this position menas in fact $f_\beta(\bar{d})$ cannot have any initial twists or it would bring $f_\beta(r)$ along and make it trace. So we have

$$f_\beta(\bar{d}) = p^+db^*...$$

Trhis is Figure I.97.

Here Suppose $f_\beta(s)$ were to begin with r° or r^+, forcing

$$f_\beta(i) = r^+p^+db^*...$$

This is Figure I.98.

Here the dotted lines must both continue with b^- to prevent $f_\beta(i)$ from tracing, and then continue with o^* to not violate the Trace Lemma.

Now $f_\beta(o)$ will trace:

$$f_\beta(o) = p^+db^-o^\times$$

as shown in Figure I.99.

So suppose instead $f_\beta(s)$ began with r^- and to the right of $f_\beta(i)$:

$$f_\beta(s) = r^- d i^* ...$$

This is Figure I.100.

Here $f_\beta(p)$ cannot continue with i° or i^- or $f_\beta(b)$ will immediately trace. But if it began with i^+ it would trace immediately after crossing $\bar{d}$.

This is a contradiction.

So suppose now that $f_\beta(d)$ began with $\bar{d}$.

This is Figure I.101.

Here if the dotted lines did not join, then it must be done with $f_\beta(d)$ going below $f_\beta(\bar{d})$, otherwise $f_\beta(b)$ would be in Situation β. So we have

$$f_\beta(d) = \bar{d} p^- r^- d ...$$

as shown in Figure I.102.

But now it is clearthat the dotted lines are in Situation α.

So the dotted lines must join.

This is Figure I.103.

Here we claim that $f_\beta(s)$ must begin with r^- and to the right of $f_\beta(i)$. Otherwise, $f_\beta(i)$ would begin with r^+:

$$f_\beta(i) = r^+ p^+ d b^* ...$$

and here $f_\beta(s)$ can either begin with r° or r^+ forcing

$$f_\beta(i) = r^+p^+d...$$

or we could have $f_\beta(s)$ begin with r^-:

$$f_\beta(s) = r^-d...$$

I.2.1.1 Boke

Suppose

$$f_\beta(i) = r^+p^+d...$$

This is Figure I.104.

Here $f_\beta(b)$ must continue with s^*. Otherwise, if it continued with i° or i^+, $f_\beta(p)$ would trace immediately after crossing $\bar{d}$; while if $f_\beta(b)$ continued with i^- it would trace immediately.

Thus we must have Figure I.105.

Here $f_\beta(p)$ can begin with i^- or i°. Suppose it were the former:

$$f_\beta(p) = i^-b^-o^*...$$

as shown in Figure I.106. Here if $f_\beta(p)$ continued with o° or o^+, forcing $f_\beta(r)$ to continue with o^+, then we would have the situation depicted in Figure I.107, where it is clear that $f_\beta(o)$ would trace. So instead suppose $f_\beta(p)$ continued with o^-:

$$f_\beta(p) = i^-b^-o^-b^*...$$

This is Figure I.108.

Here $f_\beta(i)$, $f_\beta(p)$, and $f_\beta(r)$ are stuck in a three-way clockwise path mill between b and o. This is a contradiction. Hence, we must in fact have

$$f_\beta(p) = i^\circ$$

This is Figure I.109.

Here $f_\beta(r)$ can either continue with o^- or o°. Whereas if it continued with o^+:

$$f_\beta(r) = o^+ b^+ \bar{d} p^* ...$$

forcing

$$f_\beta(o) = p^+ d i^- b^- o^\times$$

So suppose $f_\beta(r)$ continued with o^-:

$$f_\beta(r) = b^- \hat{o}^- b^* ...$$

This is Figure I.110.

This forces $f_\beta(i)$ to continue with $b^- o^* ...$

This is Figure I.111.

Here $f_\beta(r)$ and $f_\beta(i)$ twist k times between b and o, and if any other image path were to enter into b or o, it would cause the three to either enter into a three-way path mill, or an image path might escape to the outer perimeter and trace. This observation immediately forces $f_\beta(o)$ to end, and subsequently $f_\beta(b)$ to end, and $f_\beta(s)$ to end immediately.

This is Candidate Family 5, shown in Figure I.112.

Now going back to the situation depicted in Figure I.109, we suppose now that

$$f_\beta(r) = b^- o^\circ$$

This is Figure I.113.

Consider $f_\beta(b)$. If it did not end here immediately at s°, then it could only continue with $s^- dp^*...$, thereby forcing

$$f_\beta(o) = p^+ ds^+ \bar{d}r^+ p^+ db^*...$$

shown in Figure I.114.

Here $f_\beta(s)$, $f_\beta(i)$, and $f_\beta(o)$ are stuck in a three-way counterclockwise path mill between p and b.

So we must have

$$f_\beta(b) = ds^\circ$$

This is Figure I.115.

Consider $f_\beta(o)$. Suppose it did not end immediately at p°, so similar to the previous case, we have

$$f_\beta(o) = p^+ ds^+ \bar{d}r^+ p^+ db^*...$$

again $f_\beta(s)$, $f_\beta(i)$, and $f_\beta(o)$ are stuck in a three-way counterclockwise path mill between p and b.

Hence, we must have

$$f_\beta(o) = p^\circ$$

This is Figure I.116. Here the remaining $f_\beta(s)$ and $f_\beta(i)$ twist between r and b (counter-clockwise) and eventually end there, giving us Candidate Family 6.

I.2.1.2 Clat

Back to the end of GBR I.2.1. Suppose

$$f_\beta(s) = r^- di^* ...$$

This forces

$$f_\beta(b) = di^* ...$$

which in turn forces

$$f_\beta(p) = i^+ d ...$$

or else $f_\beta(b)$ would trace. Moreover, $f_\beta(p)$ must go in between $f_\beta(s)$ and $f_\beta(b)$, otherwise it would trace.

this is Figure I.117.

Here $f_\beta(i)$ is forced to trace:

$$f_\beta(i) = r^- di^\times$$

This is a contradiction.

I.2.2 MMU

Suppose $f_\beta(\bar{d})$ began with r, and $f_\beta(d)$ began with s. We remind the reader that we are assuming $f_\beta(\bar{d})$ must go over an odd number of letters before crossing. This assumption necessitates that eventually $f_\beta(\bar{d})$ must eventually traverse r^- and then d, apriori with possible twists with p.

We must have $f_\beta(s)$ and $f_\beta(i)$ go below $f_\beta(r)$ otherwise $f_\beta(s)$ would immediately trace after crossing.

This is Figure I.118.

Here it is clear that $f_\beta(r)$ will trace after crossing.

The case when $f_\beta(d)$ began with i is identical. So suppose $f_\beta(d)$ began with b.

Here $f_\beta(p)$ must go below $f_\beta(\bar{d})$ or it would trace after crossing $\bar{d}$ regardless if $f_\beta(\bar{d})$ has any initial twists.

This is Figure I.119.

This means $f_\beta(\bar{d})$ cannot have any initial twists for $f_\beta(p)$ would trace. Consider $f_\beta(d)$. It must begin with b^- and to the right of the incoming $f_\beta(s)$ and $f_\beta(i)$ or one of them would immediately trace.

We have Figure I.120.

Here $f_\beta(r)$ can begin with s or i. If it were the former, then we would have the situation depicted in Figure I.121. Here if $f_\beta(r)$ began with s° or s^- then $f_\beta(o)$ and $f_\beta(\bar{d})$ would continue with s^- and then b^-, as shown in Figure I.122.

But here $f_\beta(o)$ cannot continue with o^* for obvious reasons, so it continues to cross $\bar{d}$ and

forces the dotted lines with it. But now the dotted lines will be in Situation α. On the other hand, $f_\beta(r)$ cannot begin with s^+ as it would trace immediately after crossing.

So $f_\beta(r)$ must begin with i^*, and for the same reasoning $f_\beta(o)$ cannot also continue with i so it must continue with s^*. On the other hand $f_\beta(\bar{d})$ cannot continue with s as that would cause it to violate the Trace Lemma. So we have

$$f_\beta(\bar{d}) = r^- d i^* ...$$

and here it must continue with i^- otherwise $f_\beta(r)$ would be forced to begin with i^+ and then trace immediately after crossing. So we have

$$f_\beta(\bar{d}) = r^- d i^* b^-$$

So we must have the situation depicted in Figure I.123.

Here consider $f_\beta(d)$. It can continue with $\bar{d}$ or o^*. Suppose it were the former, then we have Figure I.124, where $f_\beta(d)$ will violate the Trace Lemma at this position.

So it must be the latter, that $f_\beta(d)$ continues with o. So we have the situation depicted in Figure I.125.

Here we claim that the dotted lines must join. Indeed, if they did not, then the only possibility for $f_\beta(\bar{d})$ to not violate the Trace Lemma is to continue with:

$$f_\beta(\bar{d}) = o^- b^+ \bar{d} ...$$

But now it will be in Situation β, as shown in Figure I.126.

Thus the dotted lines must join to give us the situation depicted in Figure I.127.

Here $f_\beta(b)$ can either begin with p^- or p°. Suppose it were the former. Then we have

$$f_\beta(b) = p^- r^- ds^* ...$$

and here it forces $f_\beta(o)$ to continue with s^+ or $f_\beta(b)$ would be absorbed. So we have

$$f_\beta(o) = r^- d\hat{s}^+ \bar{d} r^+ p^+ db^* ...$$

as shown in Figure I.128.

Here $f_\beta(o)$ continues with b^+ and to the left of $f_\beta(s)$ and $f_\beta(i)$. Otherwise, $f_\beta(s)$ or $f_\beta(i)$ would eventually trace. So we have:

$$f_\beta(o) = r^- ds^+ \bar{d} r^+ p^+ d\hat{b}^+ \bar{d} r^* ...$$

as shown in Figure I.129.

Here $f_\beta(i)$ must continue with b^+ and to the left of $f_\beta(s)$. Otherwise, $f_\beta(s)$ would escape to the outer perimeter and eventually either trace or be absorbed between $f_\beta(o)$ and $f_\beta(\bar{d})$. So we have Figure I.130. Here $f_\beta(i)$, $f_\beta(o)$, $f_\beta(p)$, and $f_\beta(s)$ are stuck in a four-way counterclockwise path mill between r and b.

This is a contradiction. Thus in the situation depicted in Figure I.127, we must have

$$f_\beta(b) = p^\circ$$

In this situation, $f_\beta(i)$ still continues with b^+ otherwise $f_\beta(s)$ would again escape to the outer perimeter. This is Figure I.131.

Here if $f_\beta(o)$ were to end at s°, then $f_\beta(i)$, $f_\beta(p)$, and $f_\beta(s)$ are stuck in a three-way

counterclockwise path mill between r and b, as shown in Figure I.132. If instead $f_\beta(o)$ does not end, then it could only continue with s^+:

$$f_\beta(o) = r^- d\hat{s}^+ \bar{d}r^= b^+ db^+ \bar{d}r^* ...$$

as shown in Figure I.133.

Here $f_\beta(i)$, $f_\beta(o)$, $f_\beta(p)$, and $f_\beta(s)$ are stuck in a four-way counterclockwise path mill between r and b.

This is a contradiction.

So let us now assume that $f_\beta(d)$ began with o^*. In this case either $f_\beta(s)$ or $f_\beta(i)$ will immediately trace after crossing d.

So let us now assume that $f_\beta(d)$ began with $\bar{d}$.

This is Figure I.134.

Here if the dotted lines do not join, then $f_\beta(d)$ cannot go below $f_\beta(\bar{d})$ or $f_\beta(d)$ would be in Situation β. So if they did not join, then $f_\beta(d)$ must go above. Then we have

$$f_\beta(d) = \bar{d}r^+ p^+ db^* ...$$

as shown in Figure I.135.

But here the dotted lines are in Situation α.

Thus the dotted lines must join. This is Figure I.136, where we show that $f_\beta(r)$ must begin with b^- or either $f_\beta(s)$ or $f_\beta(i)$ will trace. It must then continue with o, as if it continued with $\bar{d}$ we would have Figure I.129, where if it continued with p° or p^+ then $f_\beta(b)$ would trace

immediately after crossing d, but if $f_\beta(r)$ continued instead with p^- it traces immediately. Thus we must instead have

$$f_\beta(r) = -b^- o^* ...$$

This is Figure I.138.

Here $f_\beta(b)$ can either begin with p^- or $p\circ$. Suppose it were the former. Then we have

$$f_\beta(b) = p^- r^- d ...$$

This is Figure I.139. Here regardless if $f_\beta(p)$ were to begin at s or i, it would lead to a contradiction: If $f_\beta(b)$ were to continue with s°/i° or s^+/i^+, then $f_\beta(p)$ must begin with counterclockwise traversal and thus cross $f_\beta(\bar{d})$ and then eventually trace. On the other hand, the alternative is for $f_\beta(b)$ to continue traversing clockwise, in which case it would immediately trace.

Thus we must have

$$f_\beta(b) = p^\circ$$

This is Figure I.141. This means $f_\beta(\bar{d})$ cannot have initial twists, forcing

$$f_\beta(o) = r^- d ...$$

as shown.

Here the same situation is repeated except between $f_\beta(o)$ and $f_\beta(p)$. This is a contradiction.

This concludes the case analysis for the situation where the triangles are swapped with the assumption that $f_\beta(\bar{d})$ goes over an odd number of letters before crossing. Now we assume that $f_\beta(\bar{d})$ goes over an even number of letters before crossing, which necessitates that $f_\beta(d)$

goes over an odd number of letters before crossing.

The possible places for $f_\beta(\bar{d})$ to begin are still r and p. While the possible places for $f_\beta(d)$ to begin are s, i, and b

I.2.3 TKE

Suppose $f_\beta(\bar{d})$ began with p, and $f_\beta(d)$ began with s. We remind the reader that we are assuming $f_\beta(\bar{d})$ must go over an even number of letters before crossing, and therefore $f_\beta(d)$ goes over an even number of letters before crossing. This assumption necessitates that $f_\beta(\bar{d})$ must traverse

$$f_\beta(\bar{d}) = p^- r^- d...$$

and we must have

$$f_\beta(b) = ds^*...$$

This forces $f_\beta(r)$ to trace:

$$f_\beta(r) = \bar{d}p^- r^\times$$

as shown in Figure I.142.

This is a contradiction.

Suppose now that $f_\beta(d)$ began with i^*. Then

$$f_\beta(b) = ds^*...$$

or

$$f_\beta(b) = di^*...$$

but irregardless the situation is identical to the previoous one, and $f_\beta(r)$ will trace, as shown in Figure I.143.

Suppose now that $f_\beta(d)$ began with b^*. Here $f_\beta(p)$ will trace, as shown in Figure I.144.

I.2.4 RKD

Suppose $f_\beta(\bar{d})$ began with r, and $f_\beta(d)$ began with s. We remind the reader that we are assuming $f_\beta(\bar{d})$ must go over an even number of letters before crossing, and therefore $f_\beta(d)$ goes over an even number of letters before crossing. This assumption necessitates that $f_\beta(\bar{d})$ must traverse

$$f_\beta(\bar{d}) = r^+p^+d...$$

Now $f_\beta(r)$ cannot go below $f_\beta(s)$ and $f_\beta(i)$ or it will immediately trace. But now $f_\beta(r)$ still traces, as shown in Figure I.145.

Now suppose $f_\beta(d)$ began with i. The situation is identical, as shown in Figure I.146.

Now suppose $f_\beta(d)$ began with b. This is Figure I.147. Here if $f_\beta(p)$ went below $f_\beta(i)$ and $f_\beta(s)$ then it immediately trace; but if it went above the pair, then one of the pair will immediately trace after crossing d.

Now suppose $f_\beta(s)$ began with o. This is Figure I.148. Here it is clear that either $f_\beta(s)$ or $f_\beta(i)$ will immediately trace after crossing d.

This concludes the case analysis for Track 17.

I.3 Figures

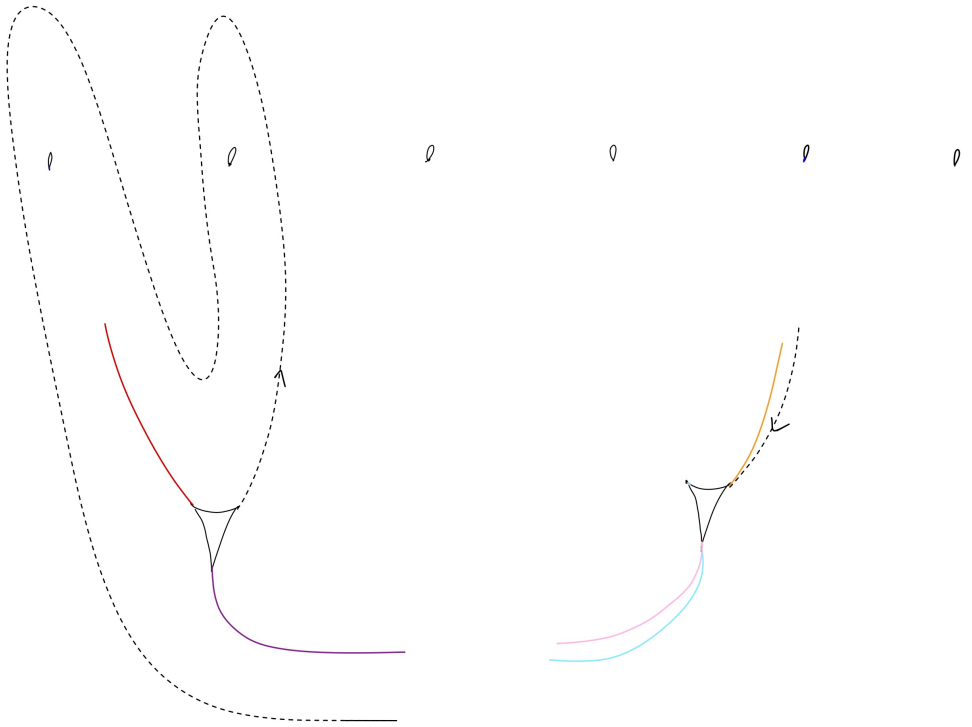


Figure I.1: VSF1

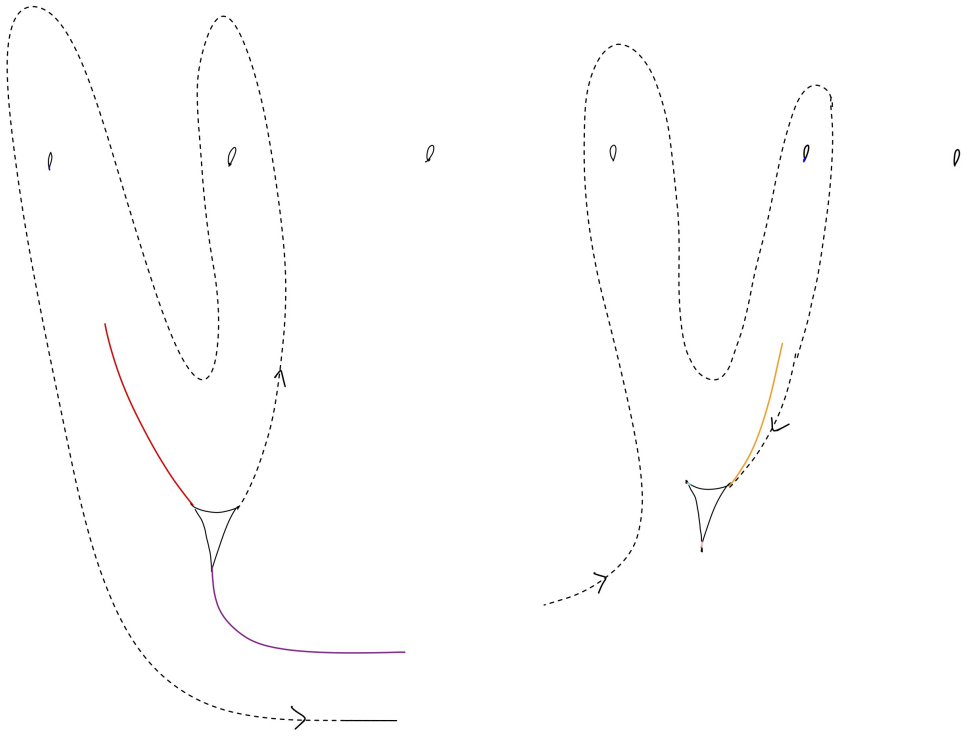


Figure I.2: Bawn1

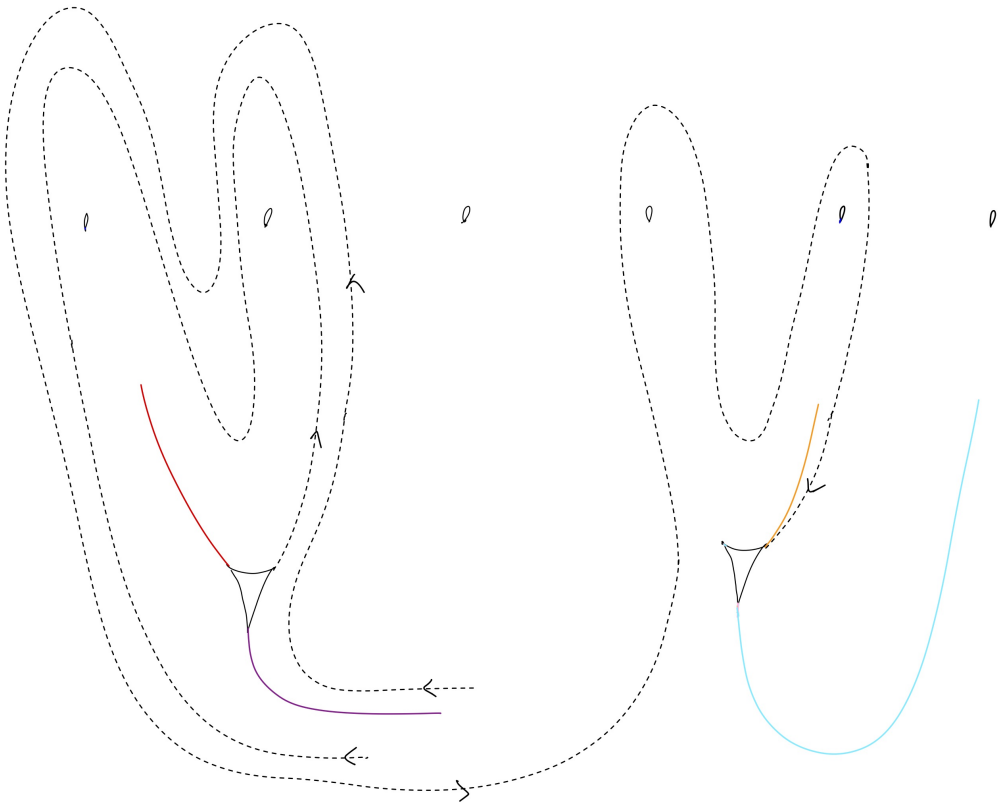


Figure I.3: Bawn2

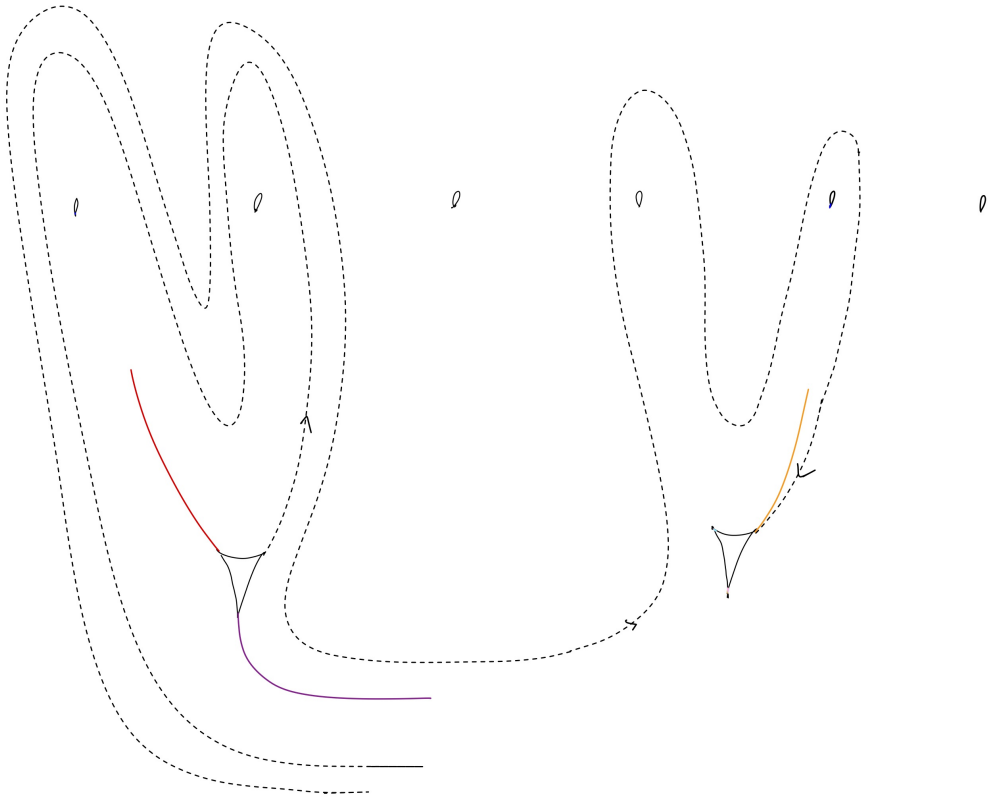


Figure I.4: Bawn3

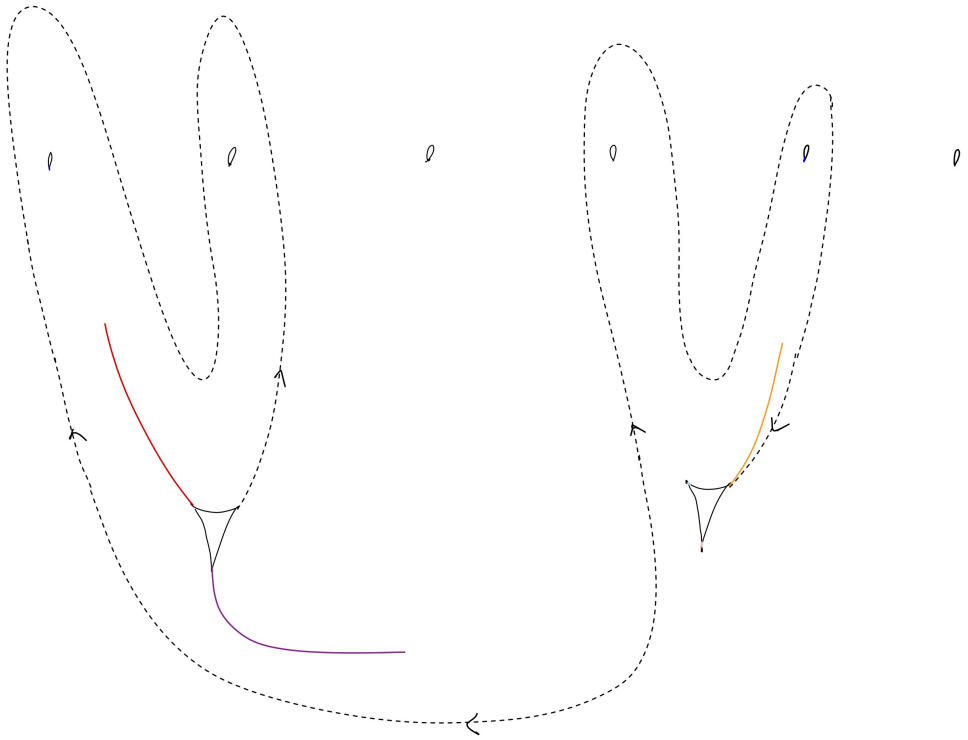


Figure I.5: Bawn4

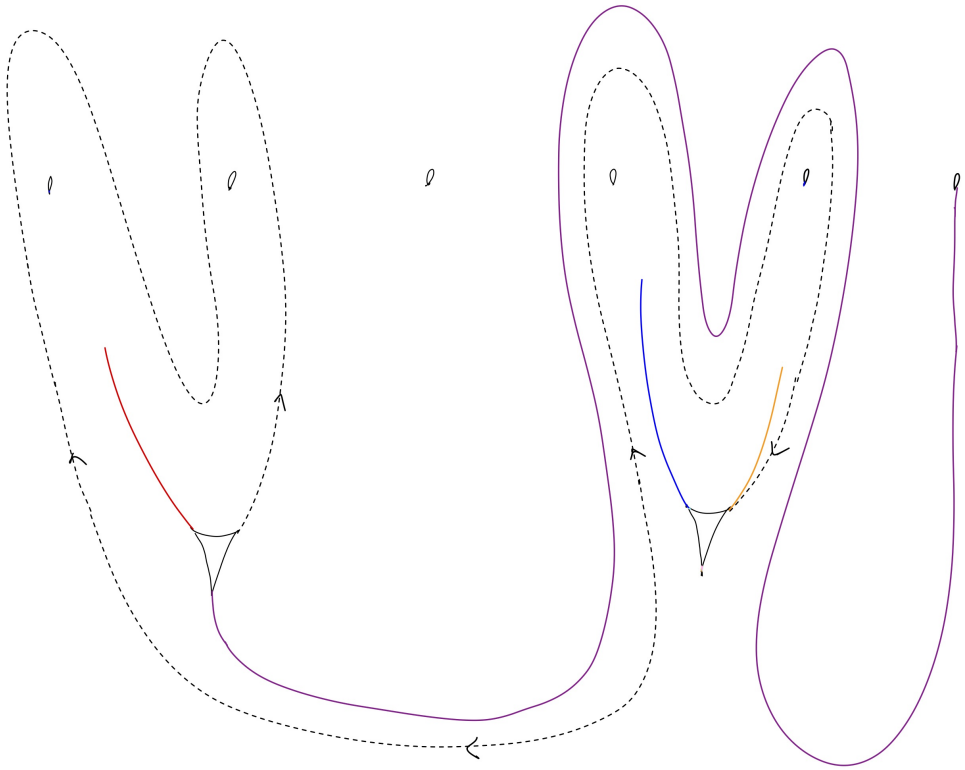


Figure I.6: Blore1

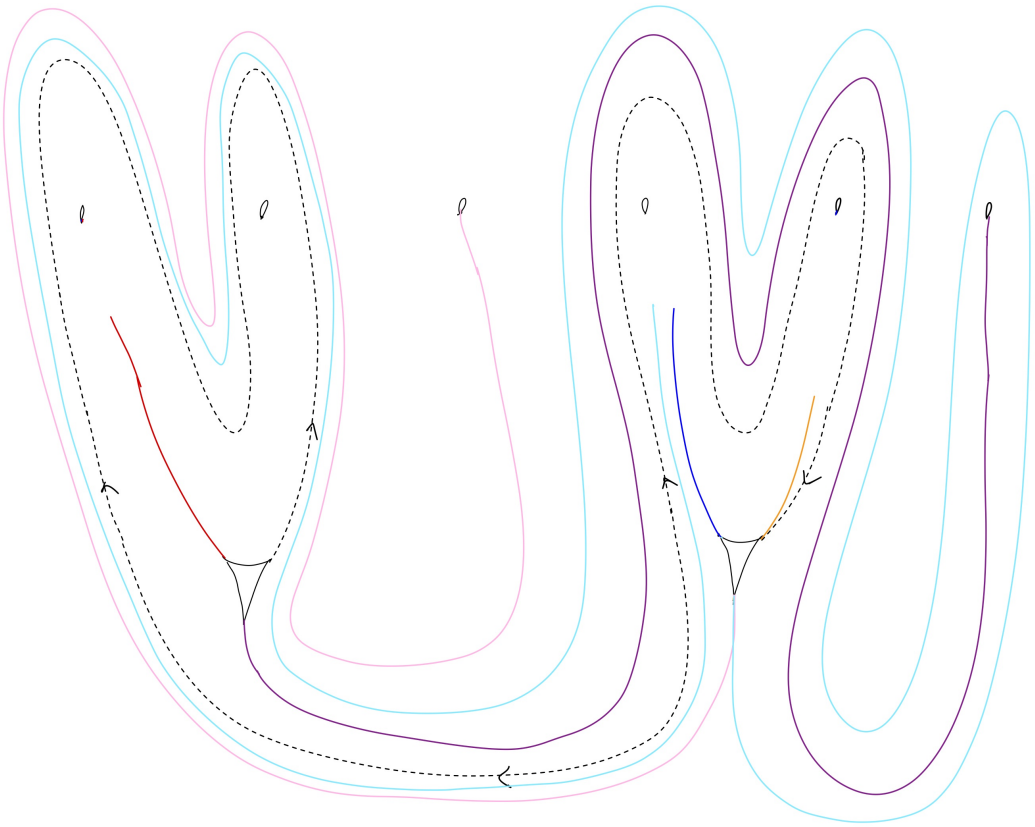


Figure I.7: Blore2

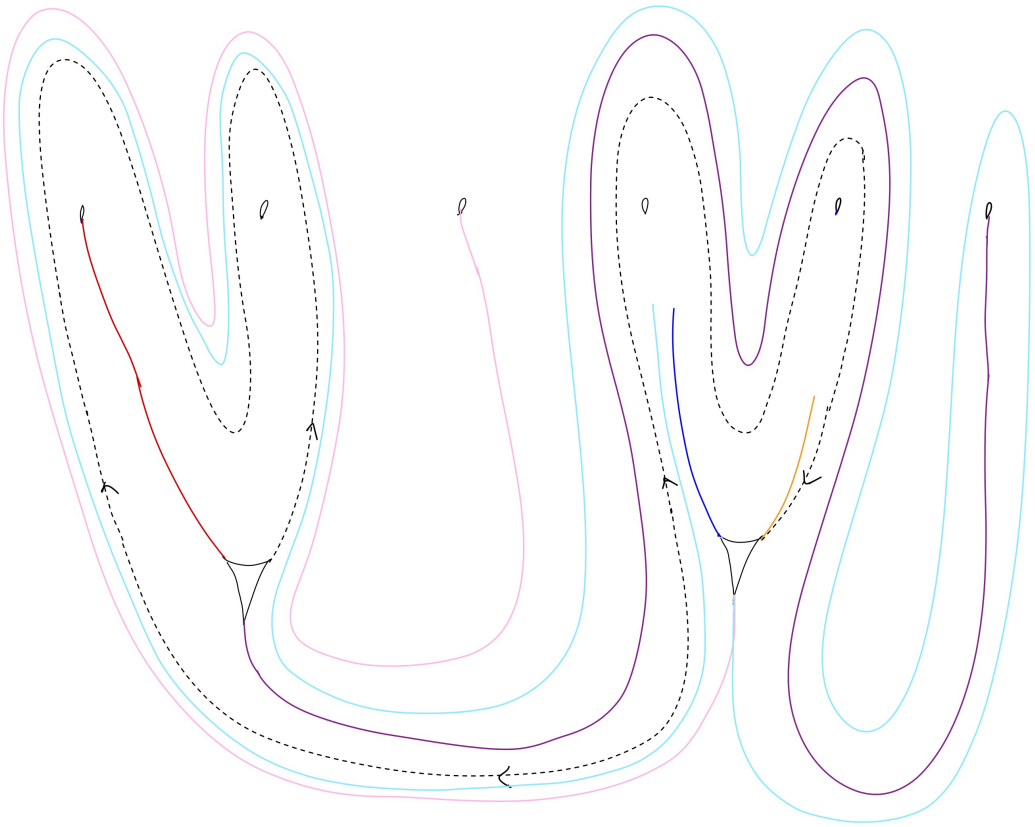


Figure I.8: Blore3

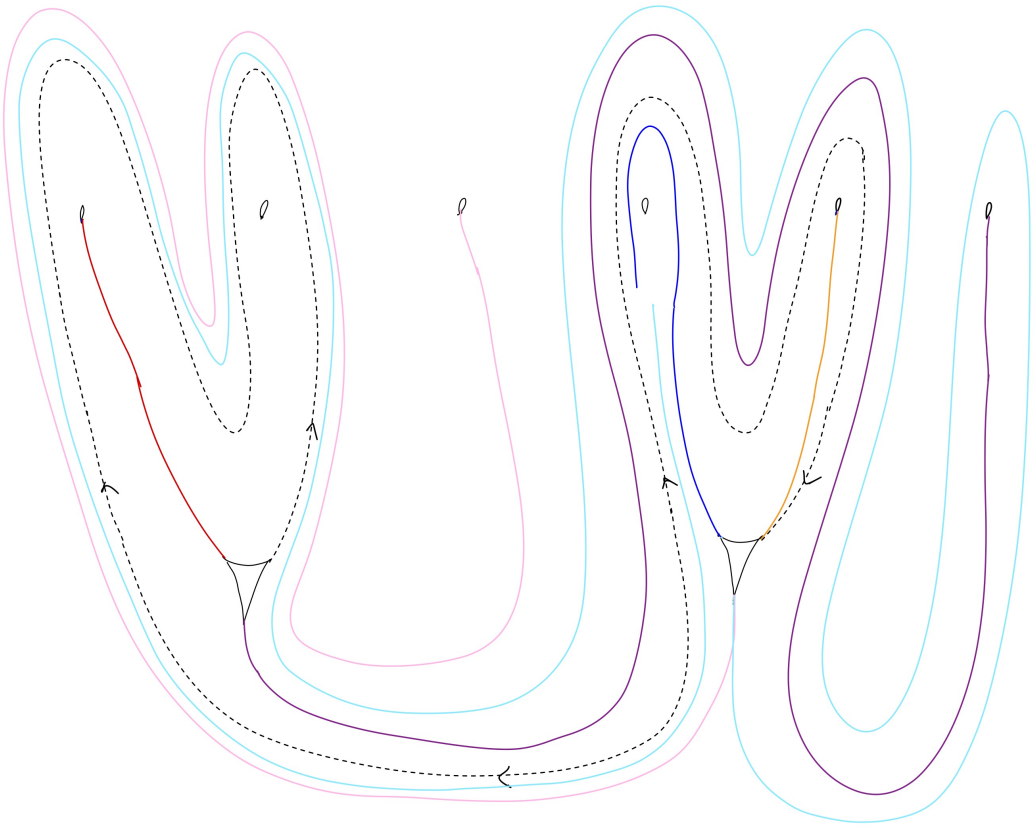


Figure I.9: Blore4

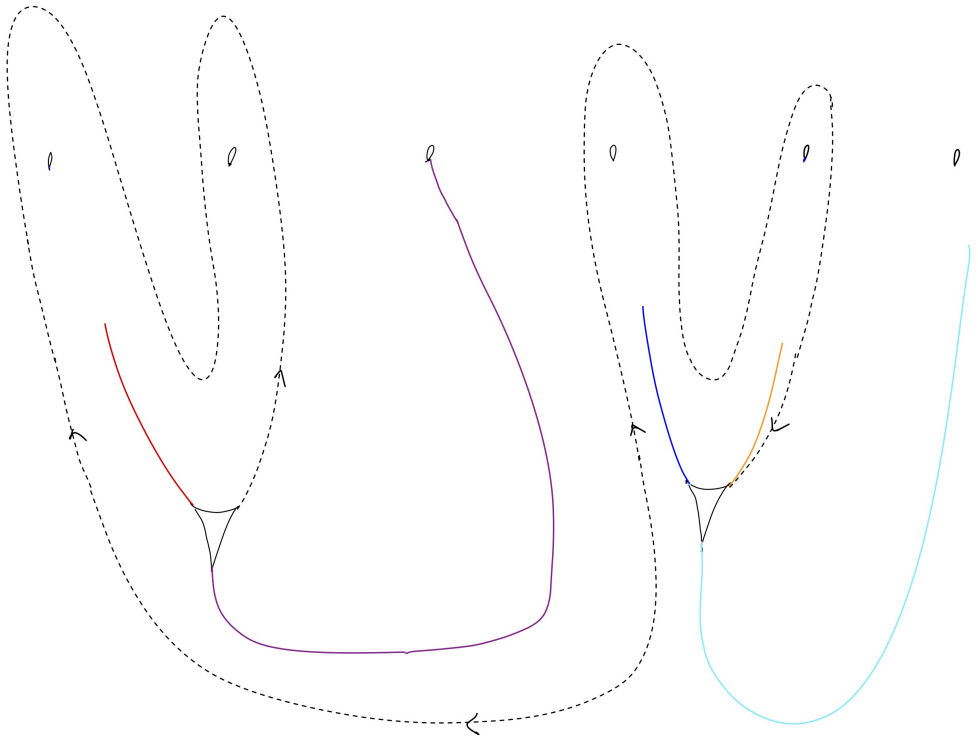


Figure I.10: Chark1

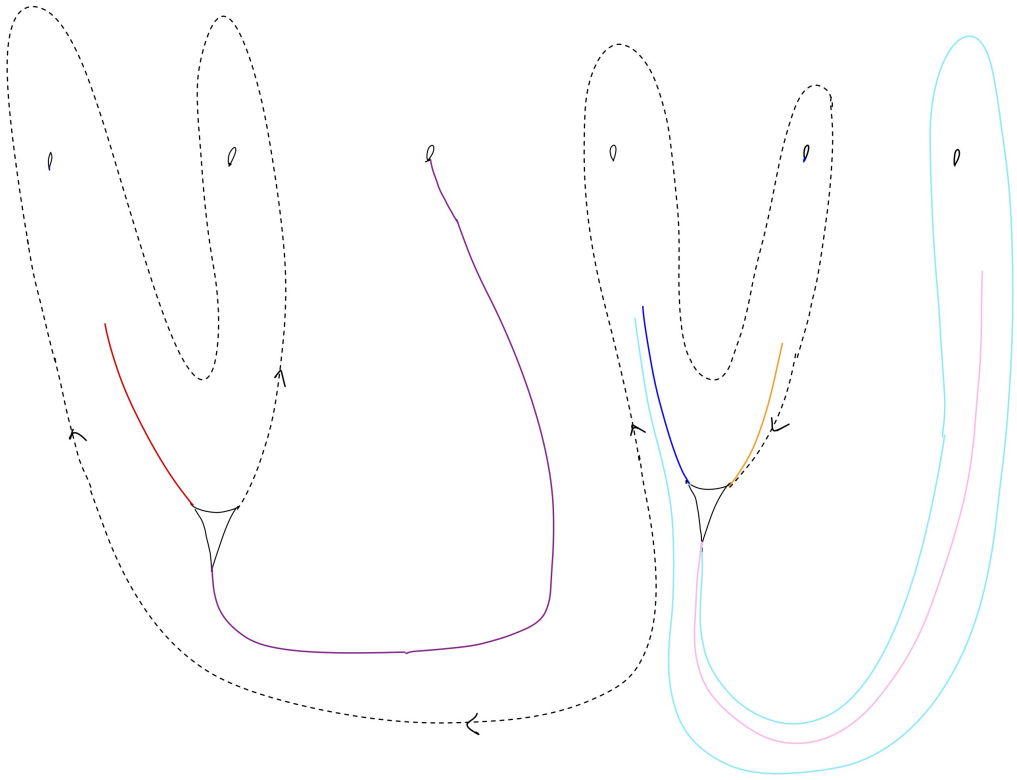


Figure I.11: Chark2

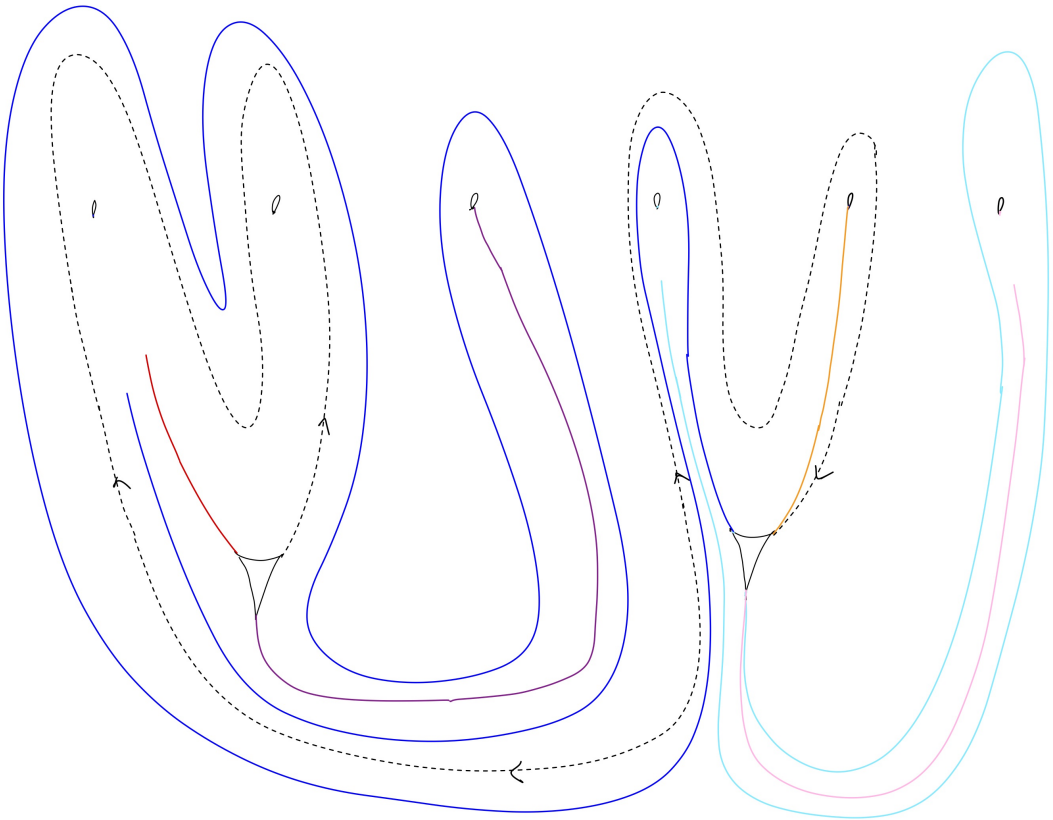


Figure I.12: Cudden1

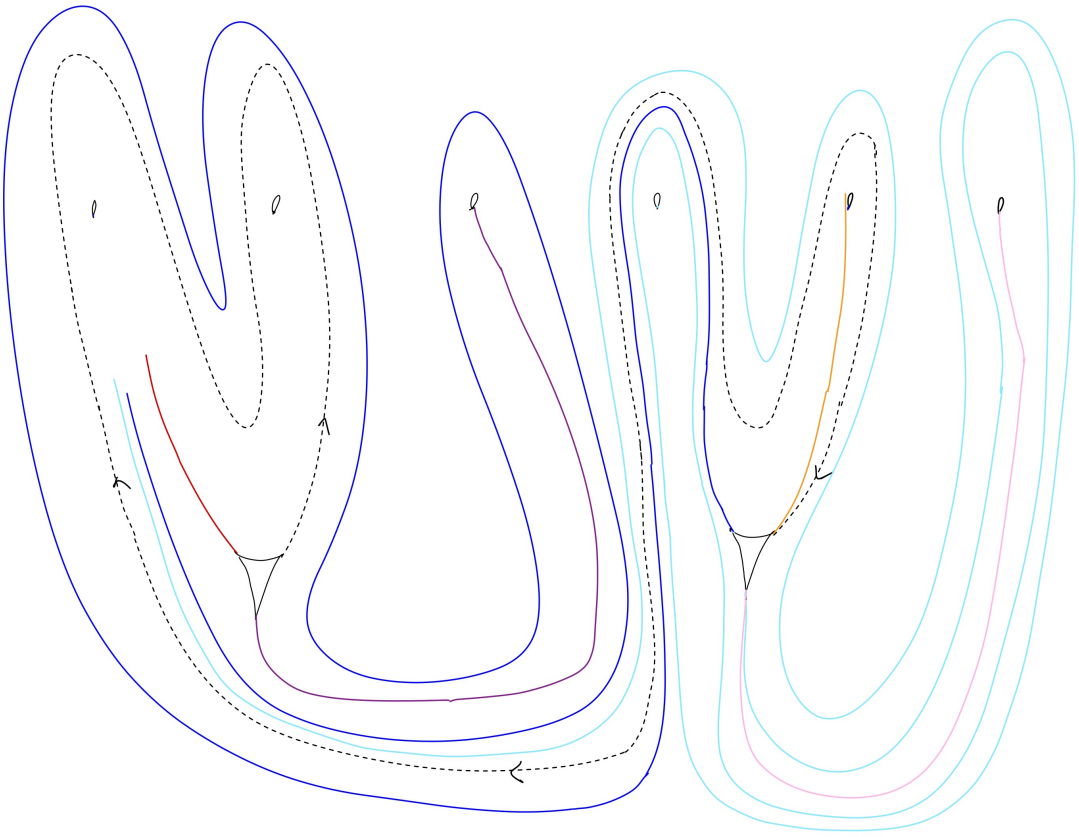


Figure I.13: Cudden2

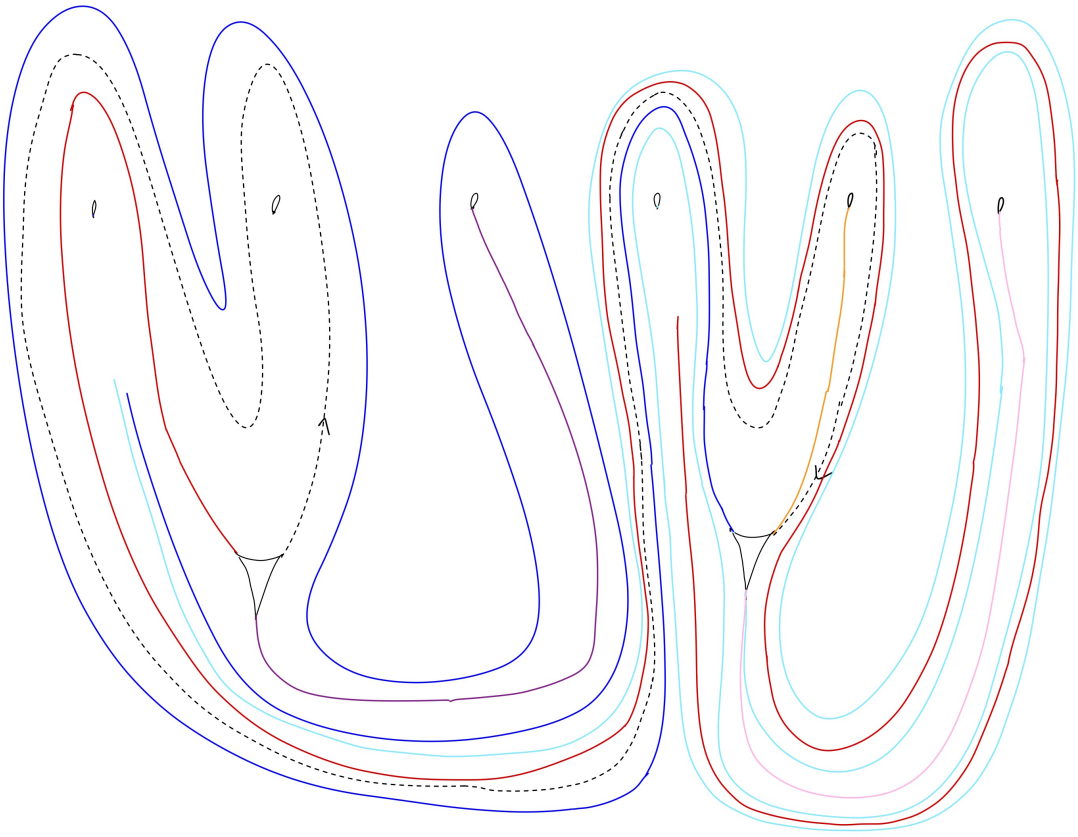


Figure I.14: Cudden3

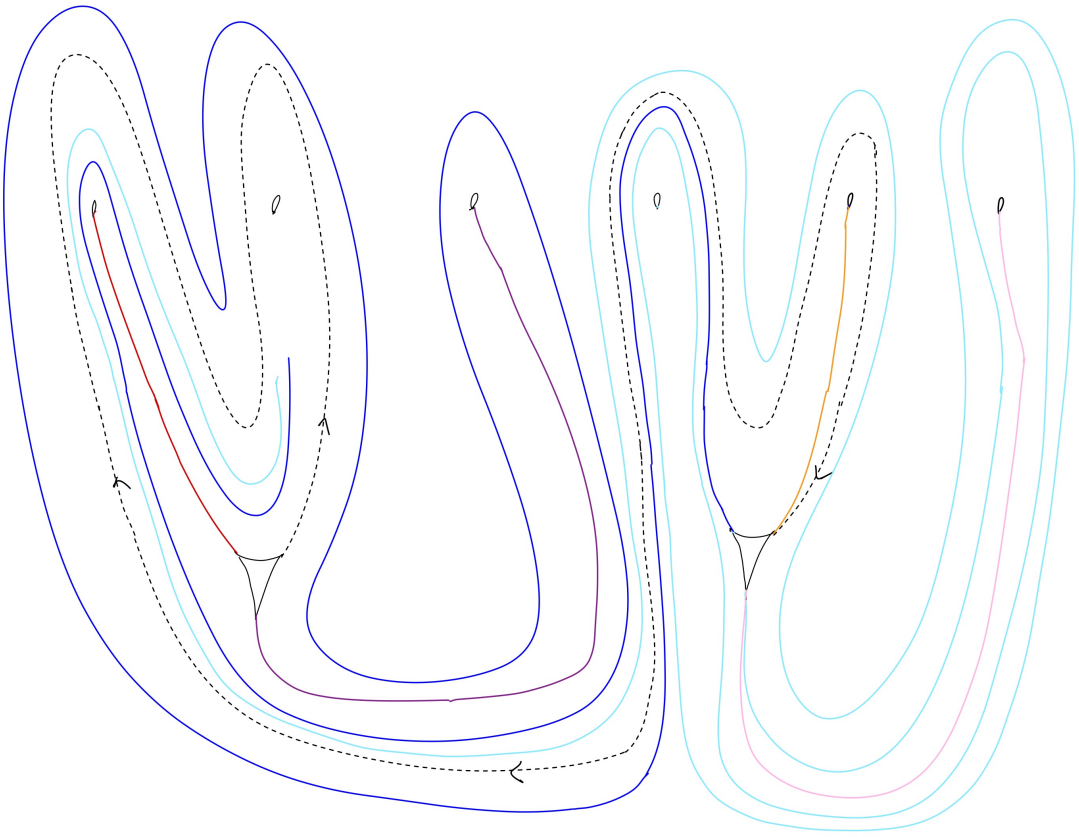


Figure I.15: Cudden4

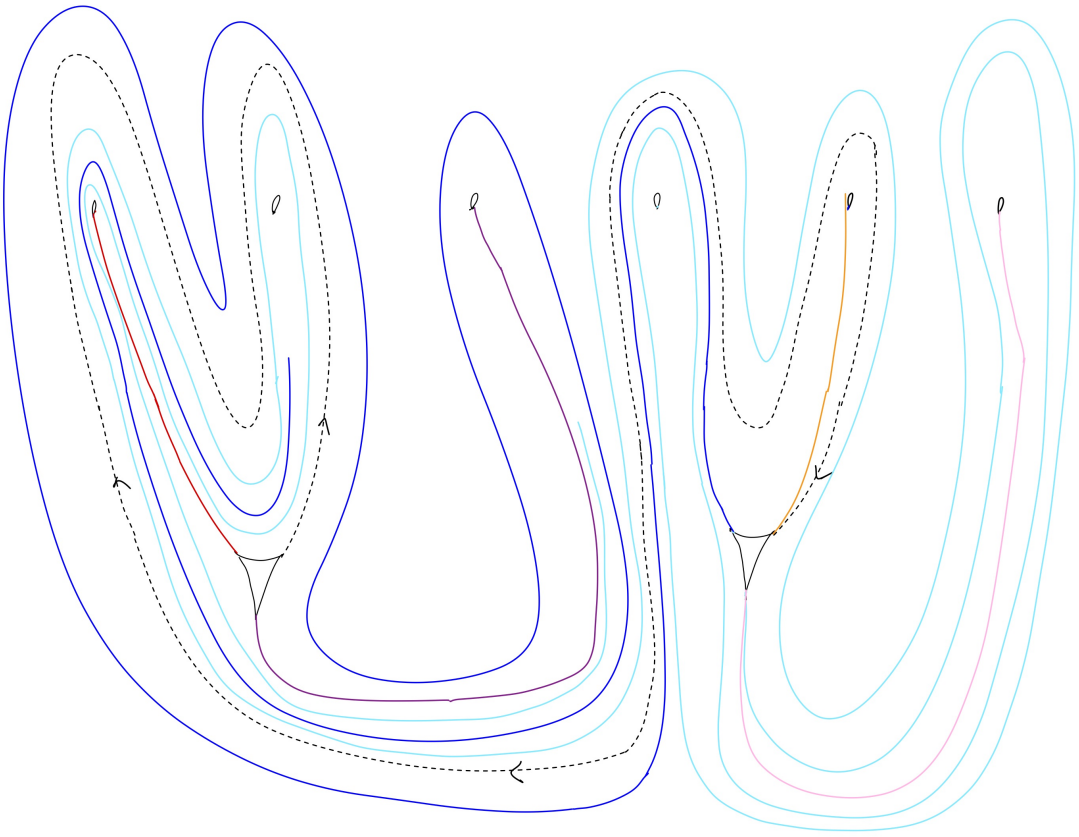


Figure I.16: Cudden5

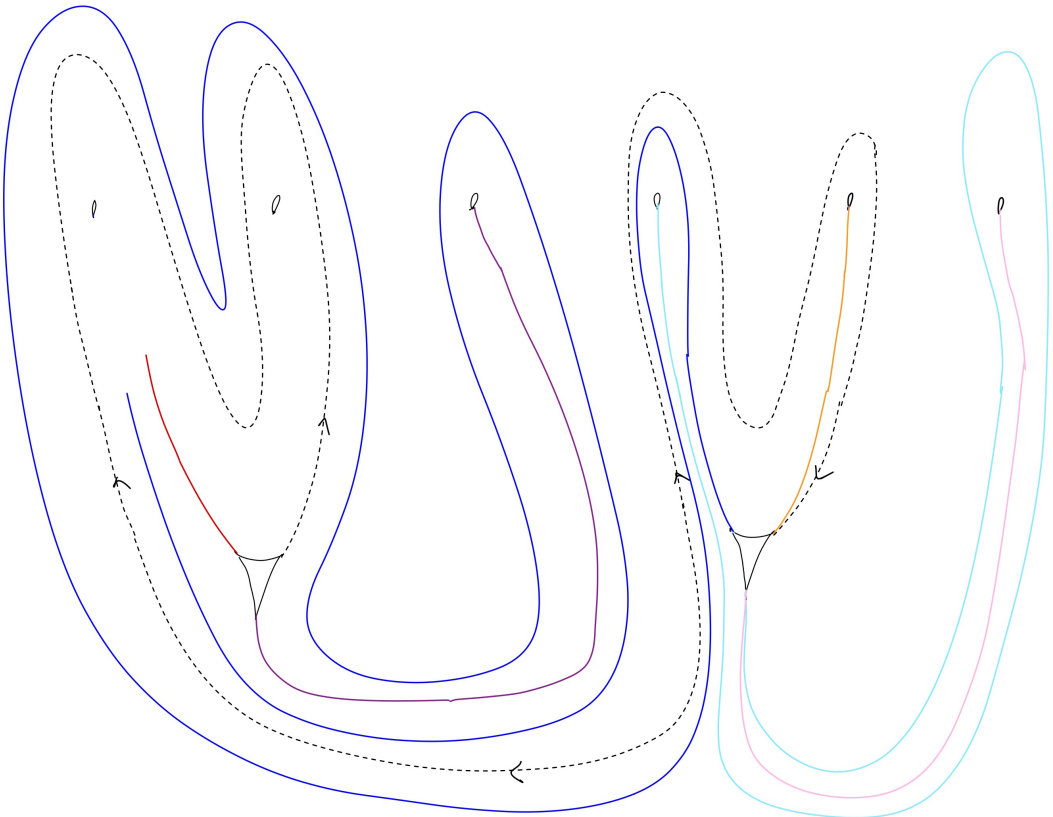


Figure I.17: Cudden6

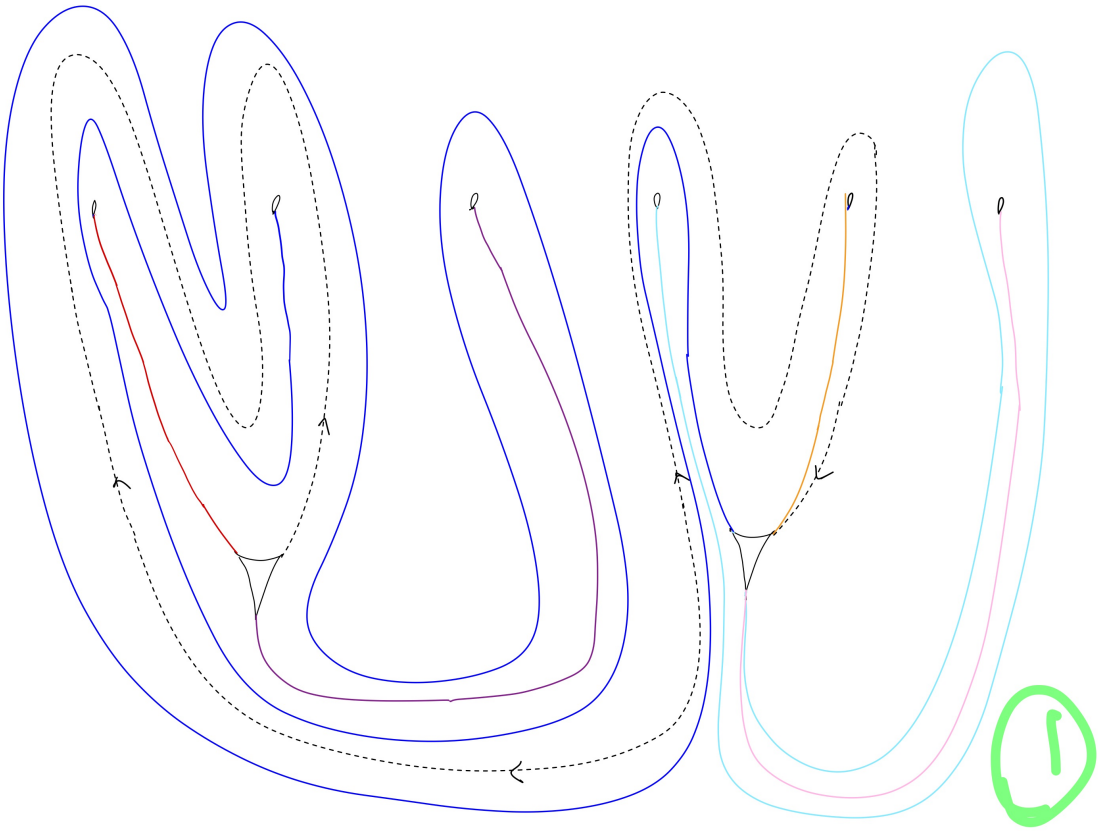


Figure I.18: Cudden7

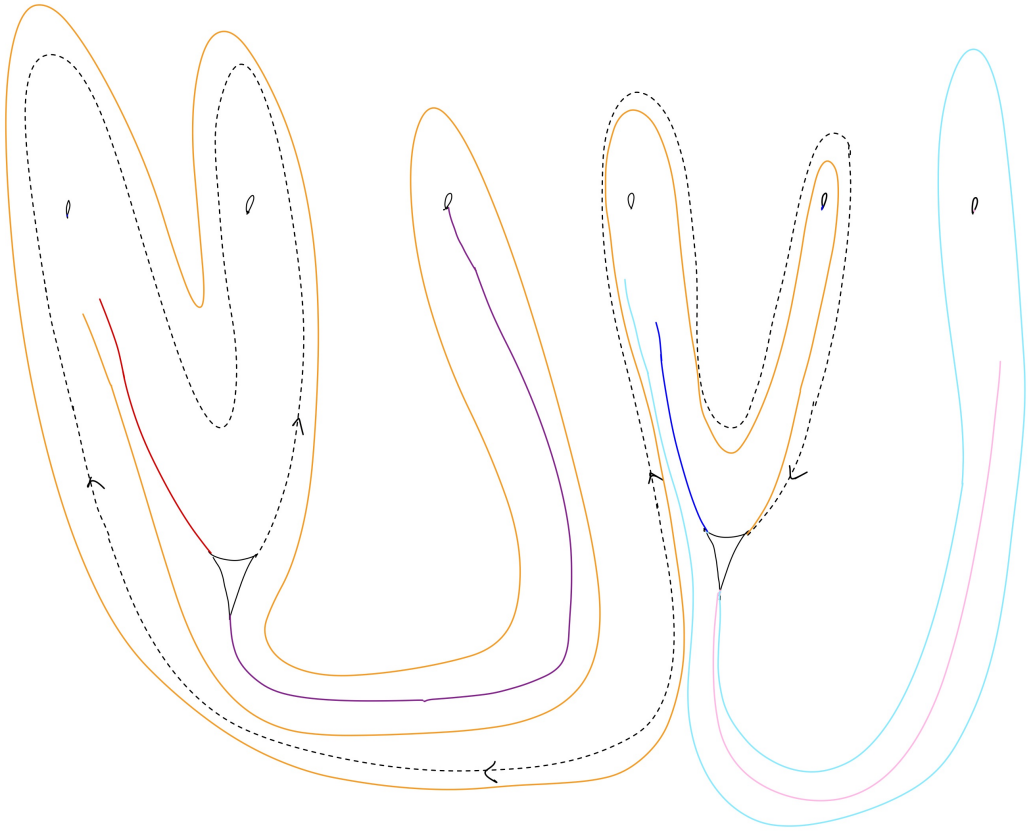


Figure I.19: Flisky1

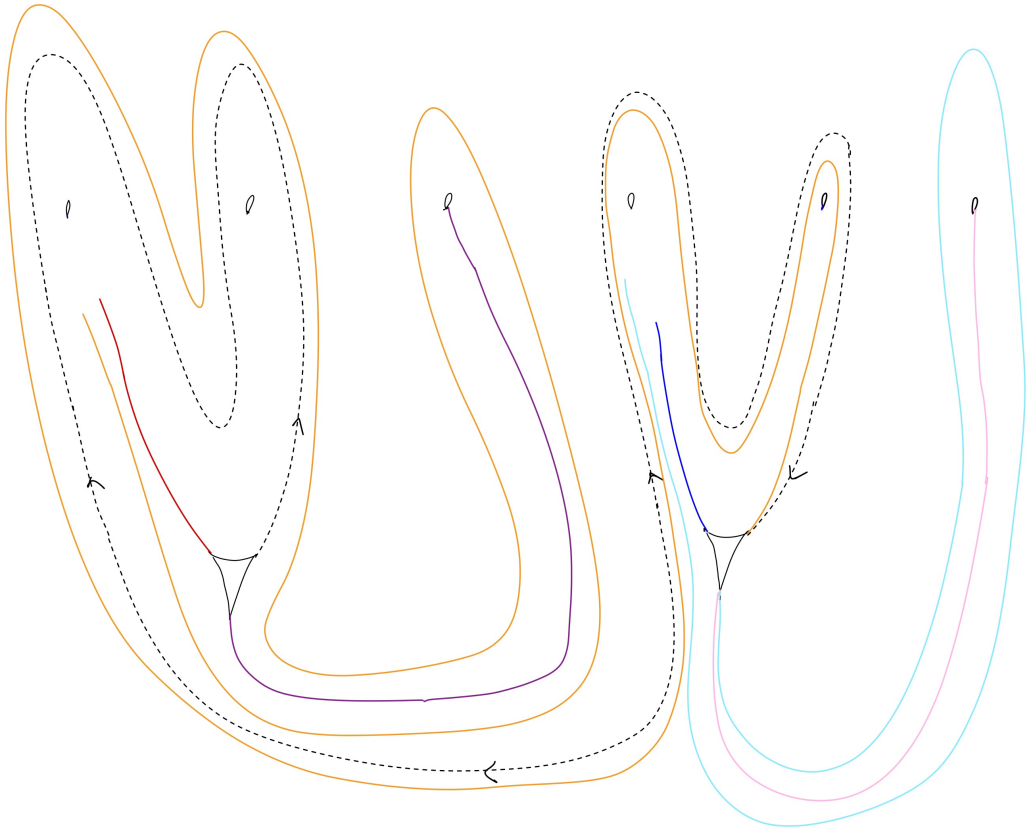


Figure I.20: Flisky2

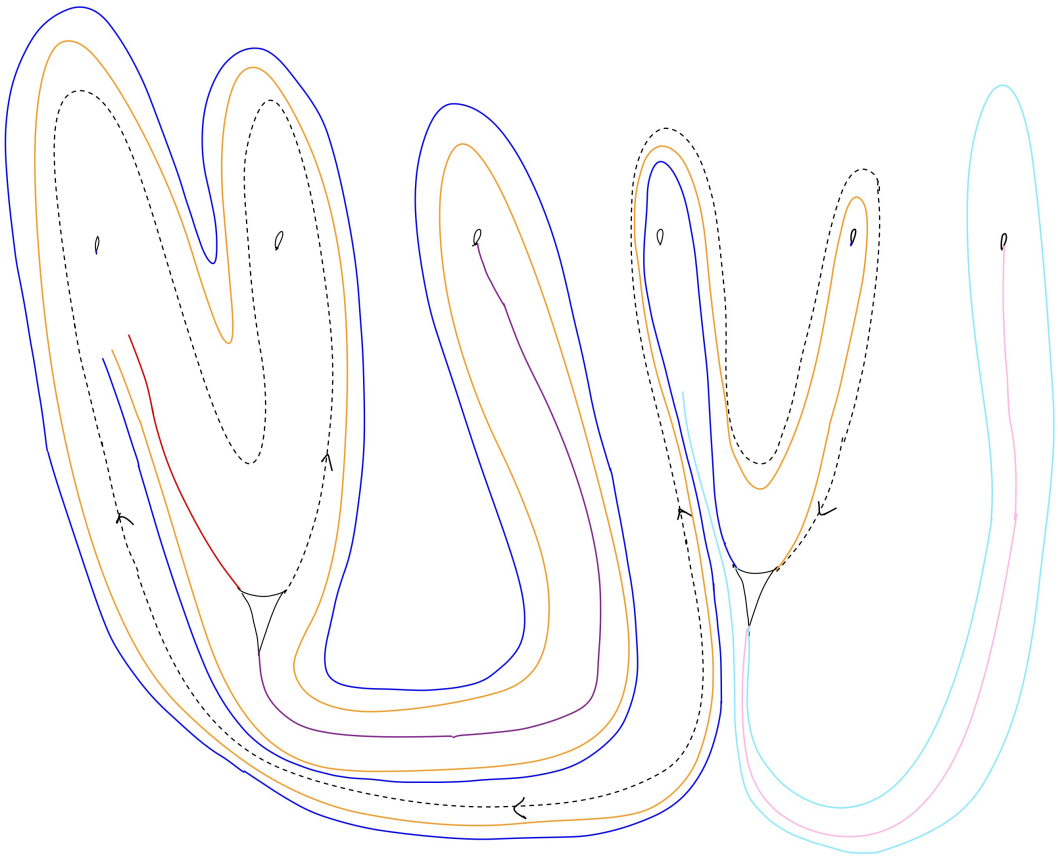


Figure I.21: Flisky3

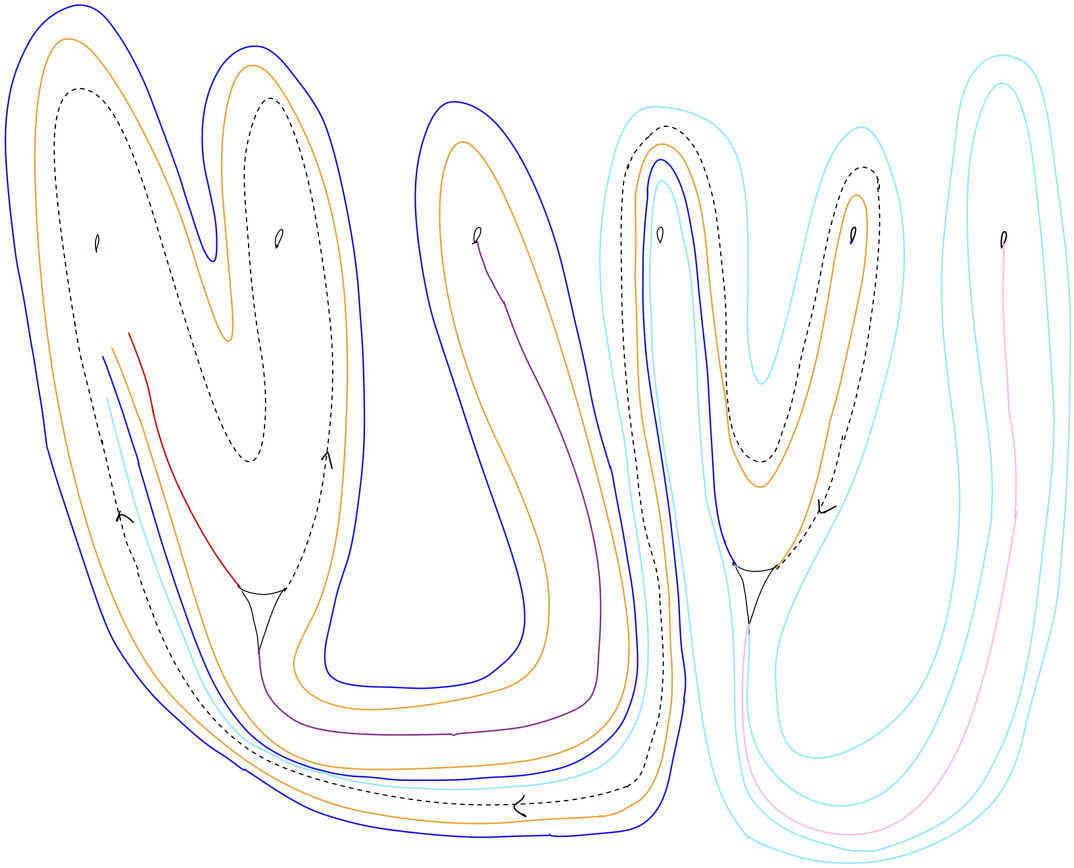


Figure I.22: Flisky4

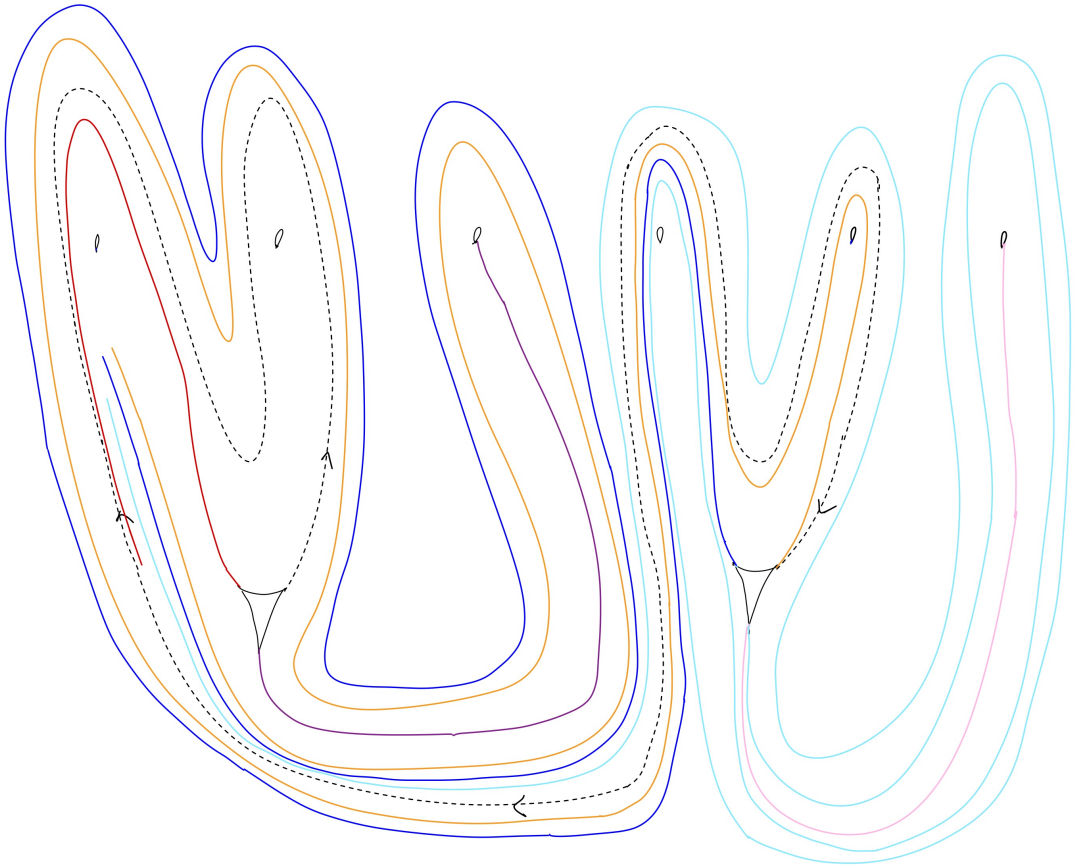


Figure I.23: Flisky5

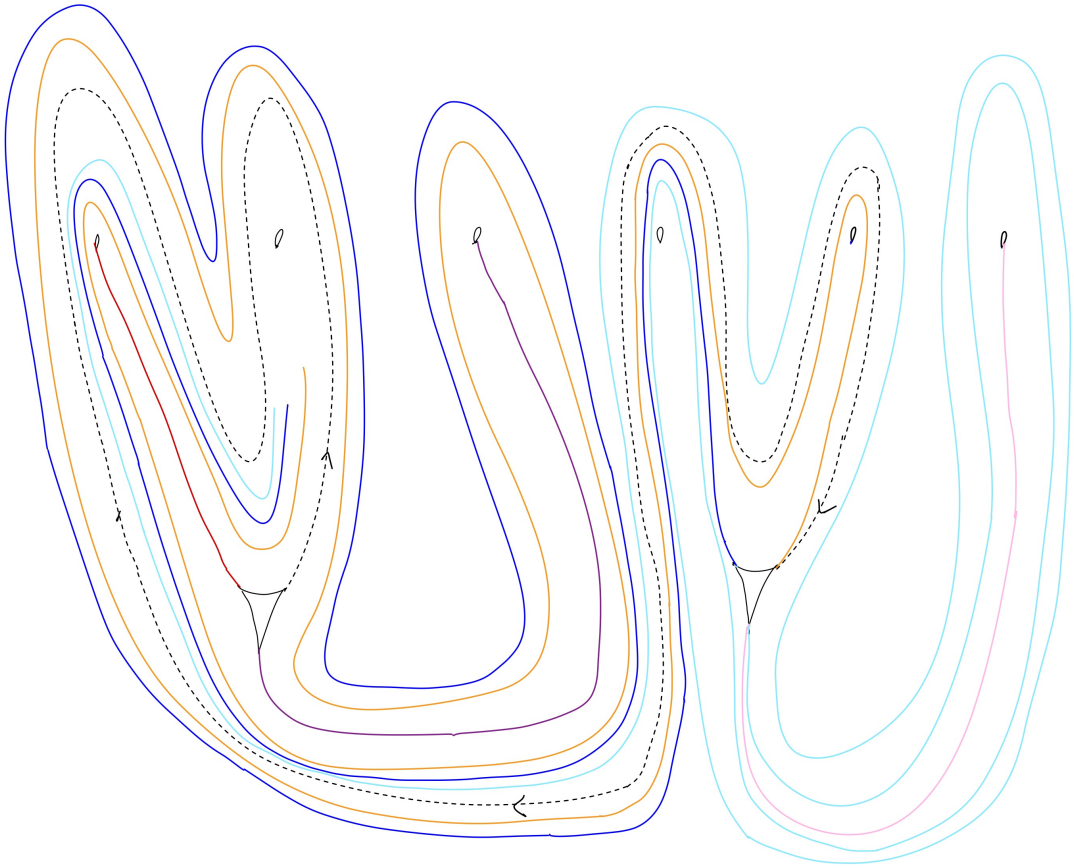


Figure I.24: Flisky6

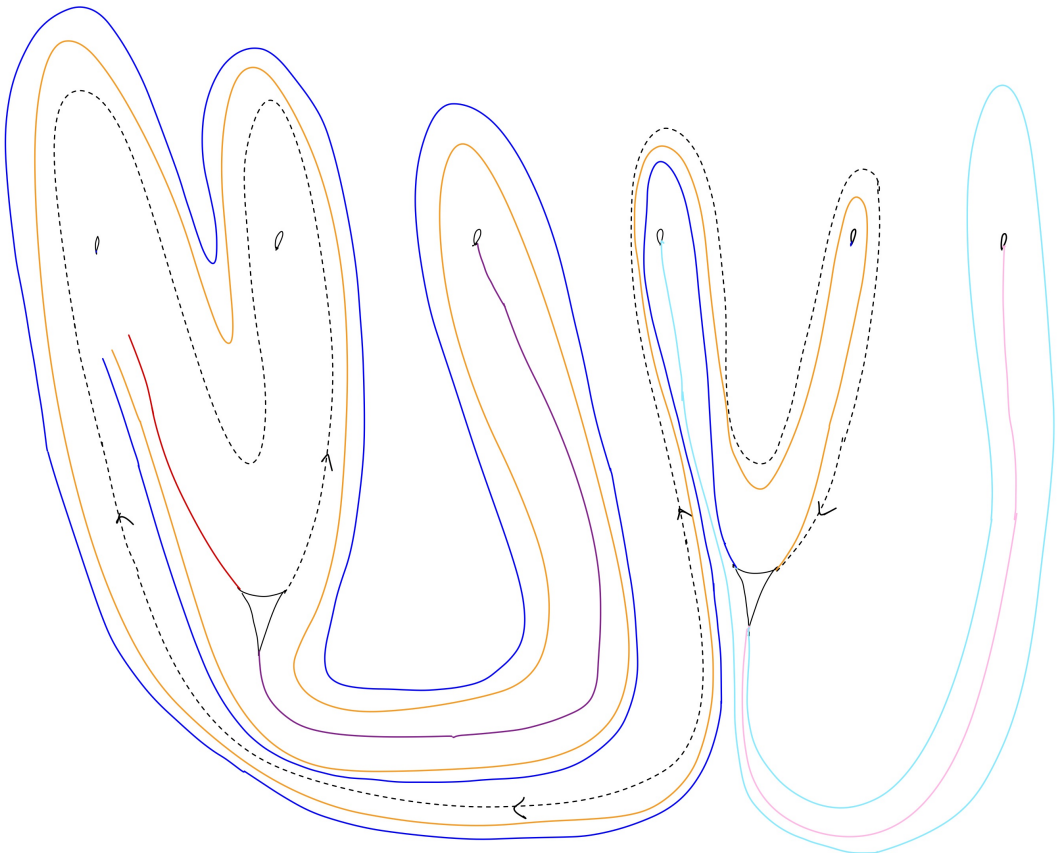


Figure I.25: Flisky7

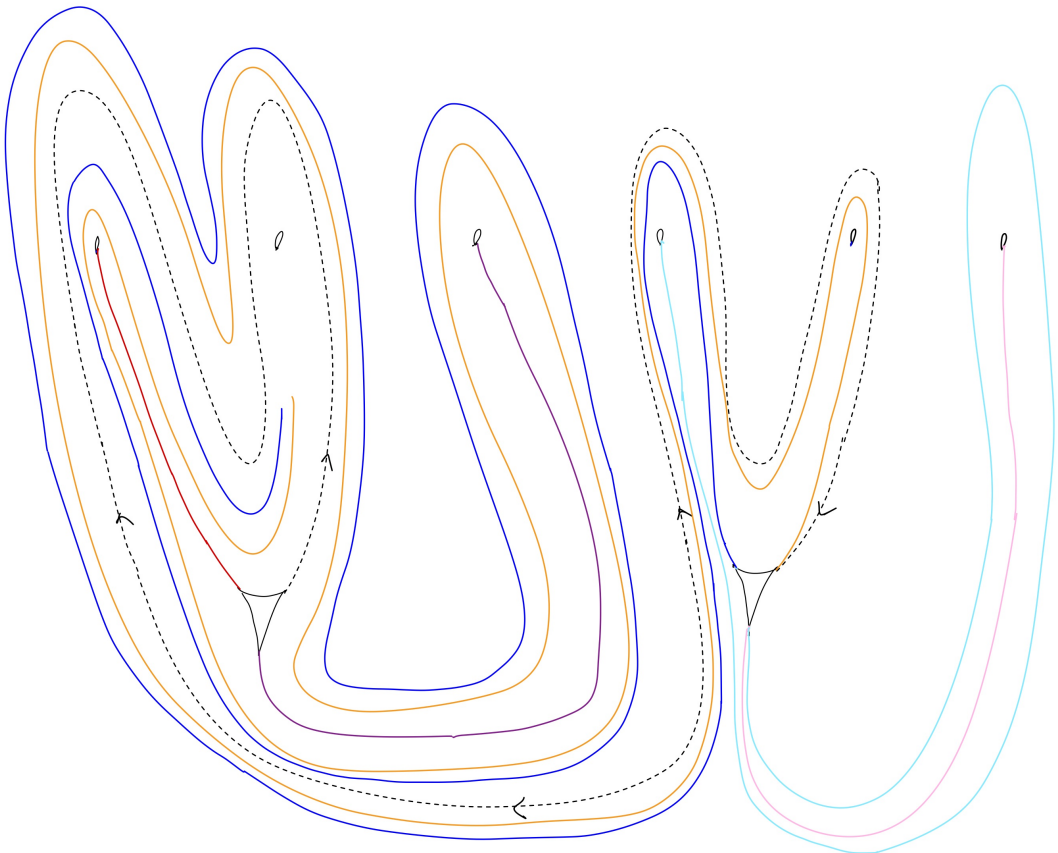


Figure I.26: Flisky8

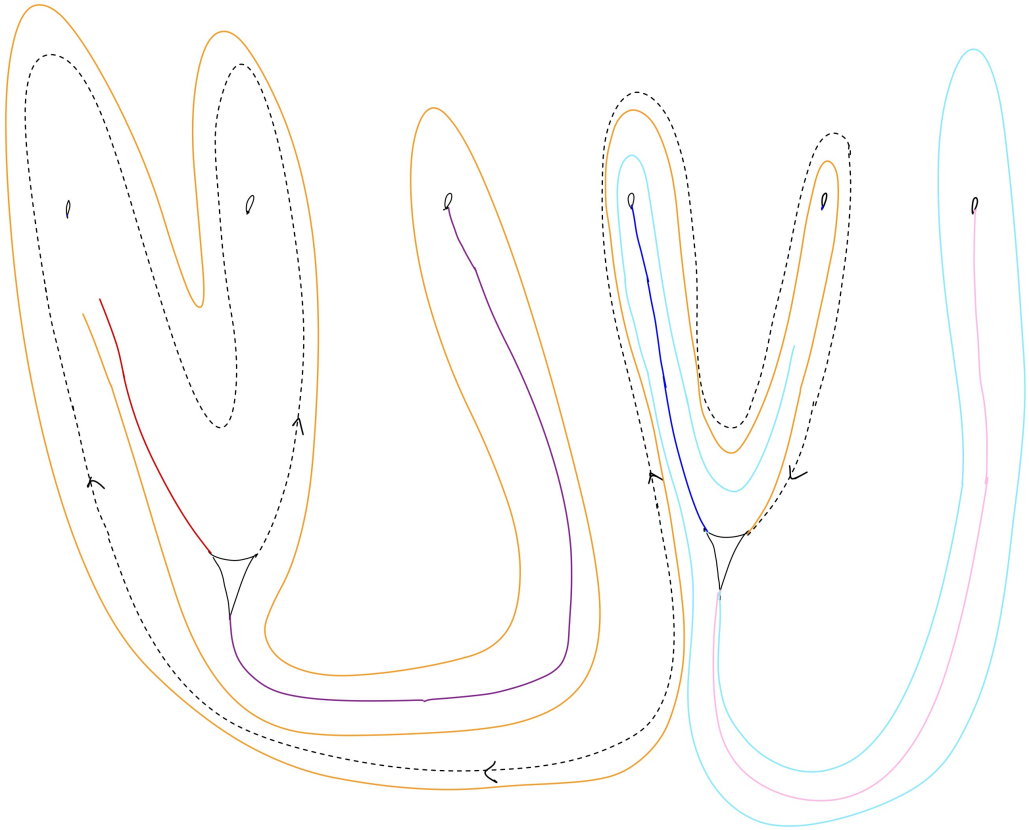


Figure I.27: Flisky9

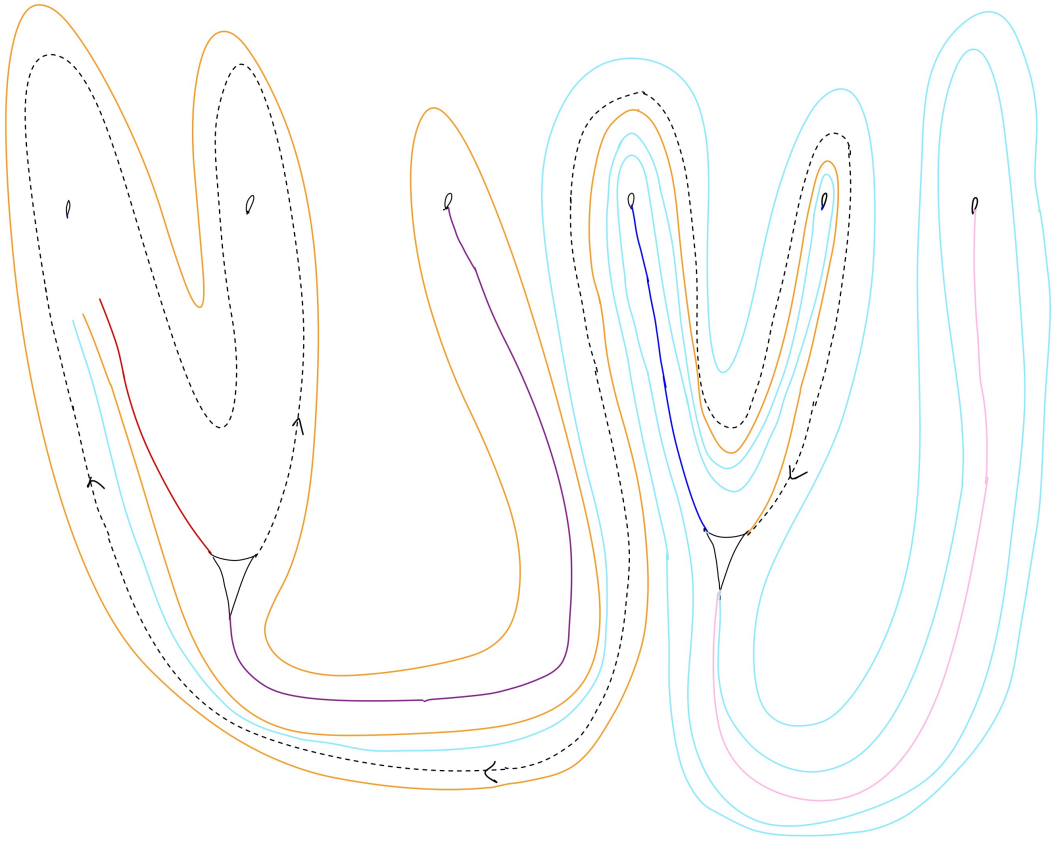


Figure I.28: Flisky10

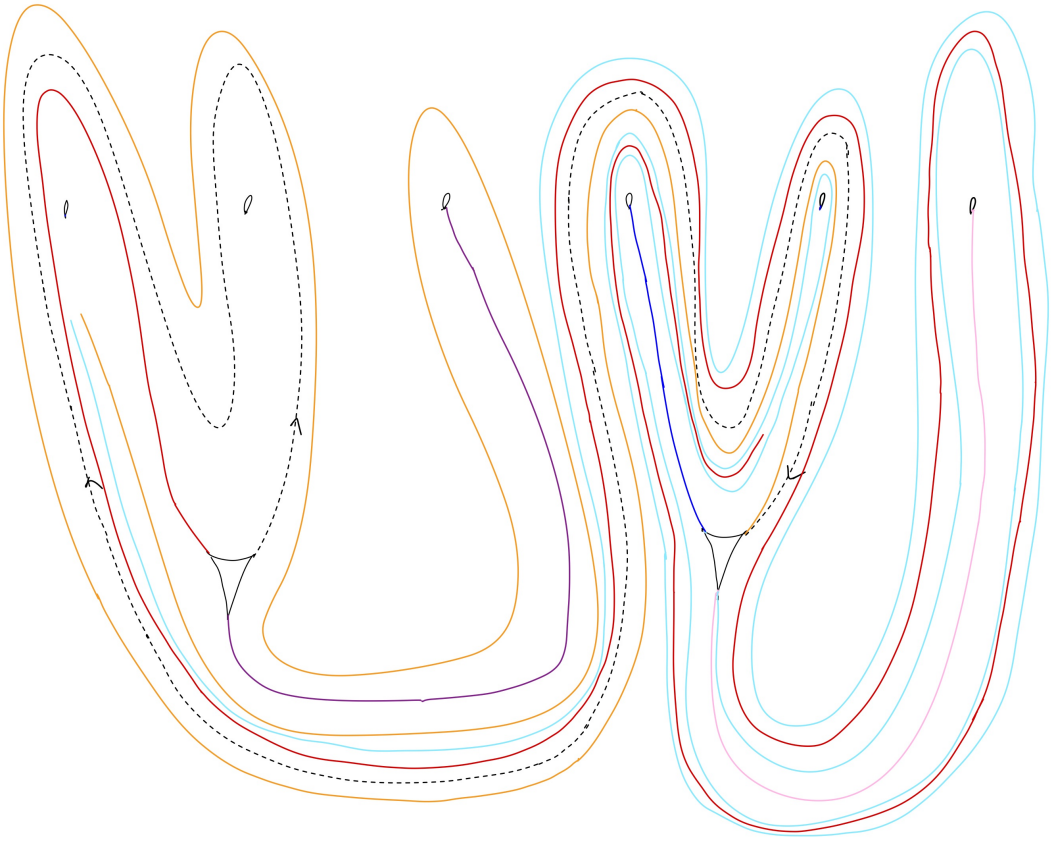


Figure I.29: Flisky11

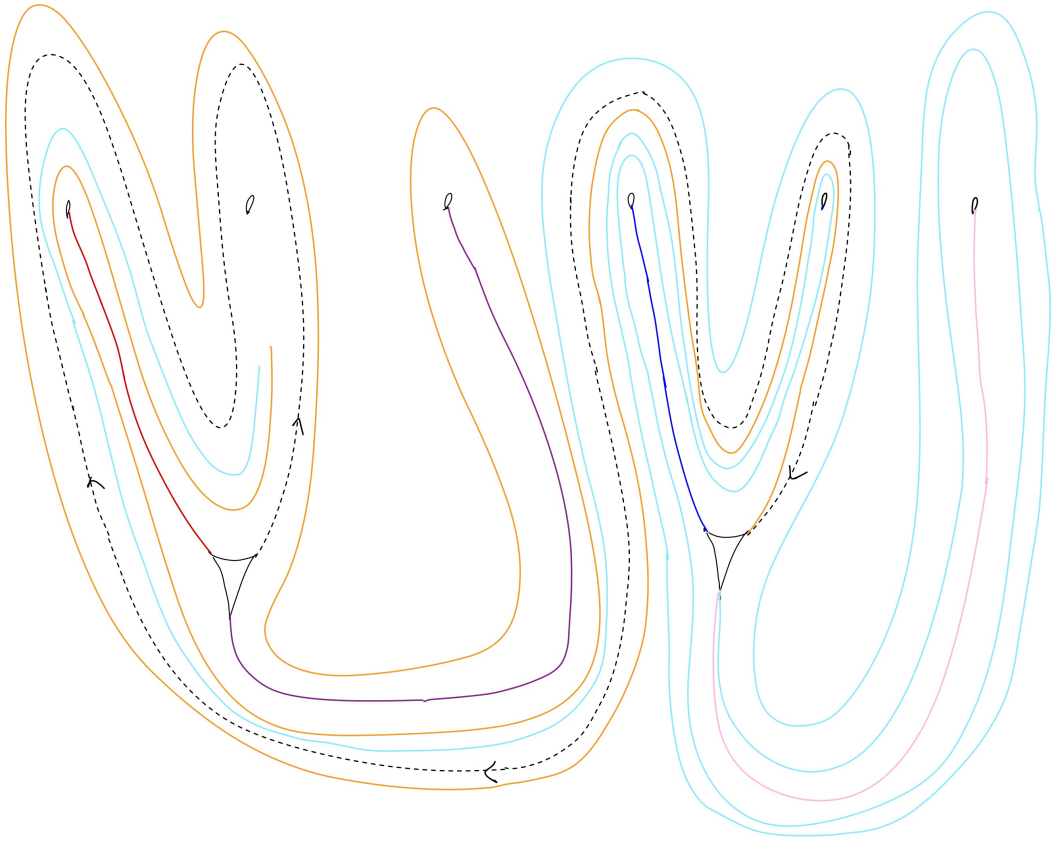


Figure I.30: Flisky12

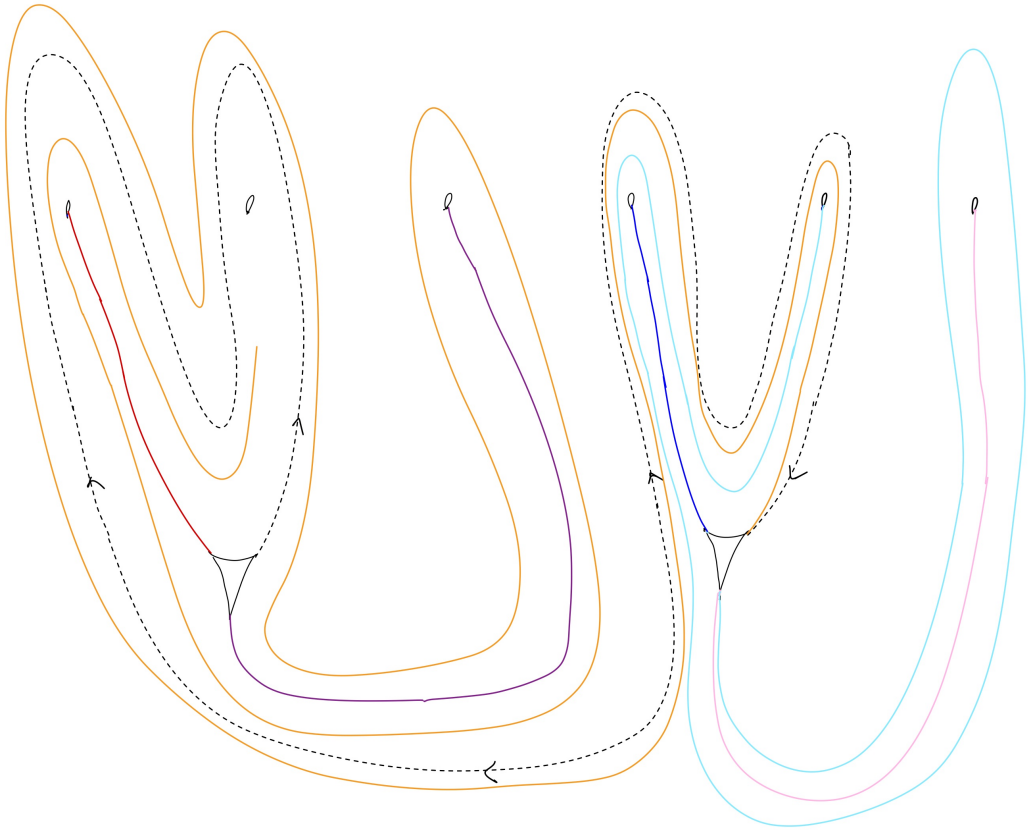


Figure I.31: Flisky13

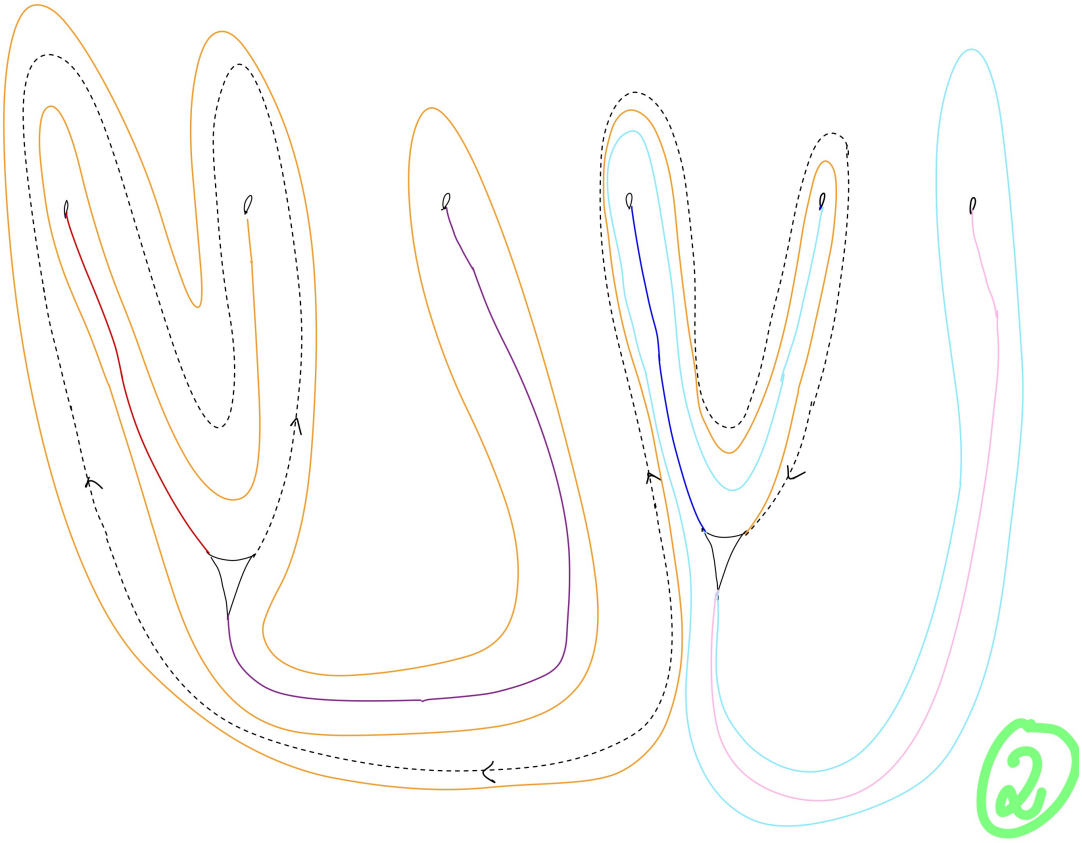


Figure I.32: Flisky14

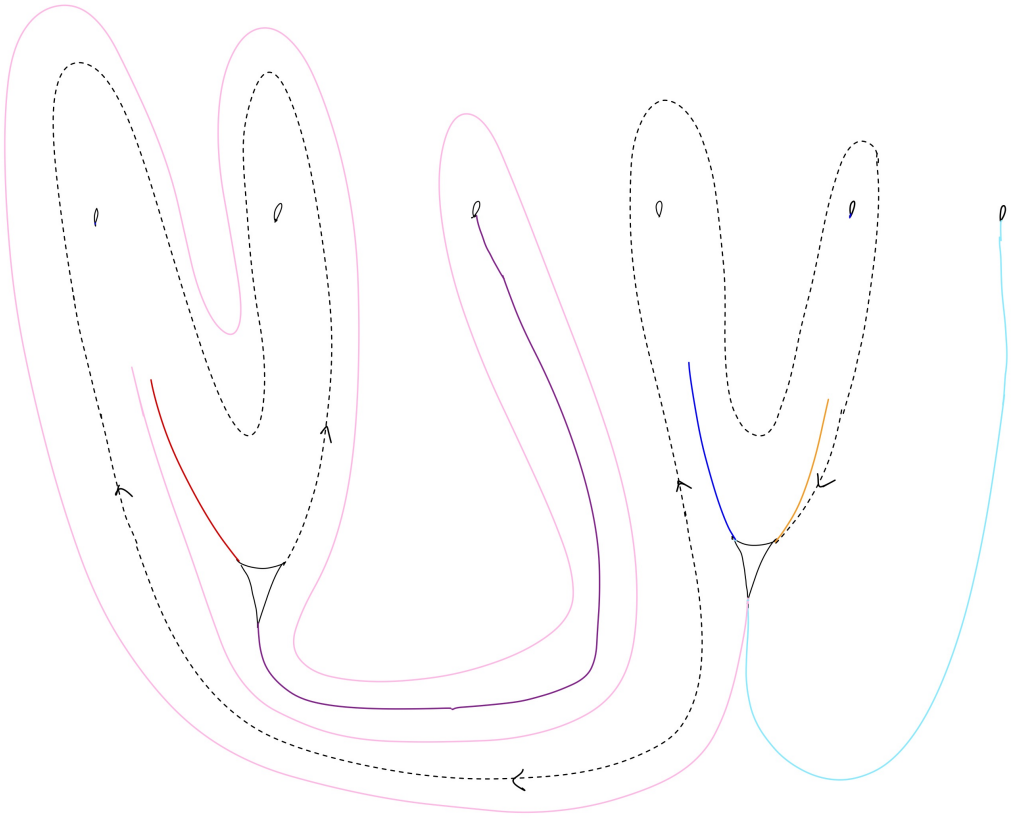


Figure I.33: Wanion1

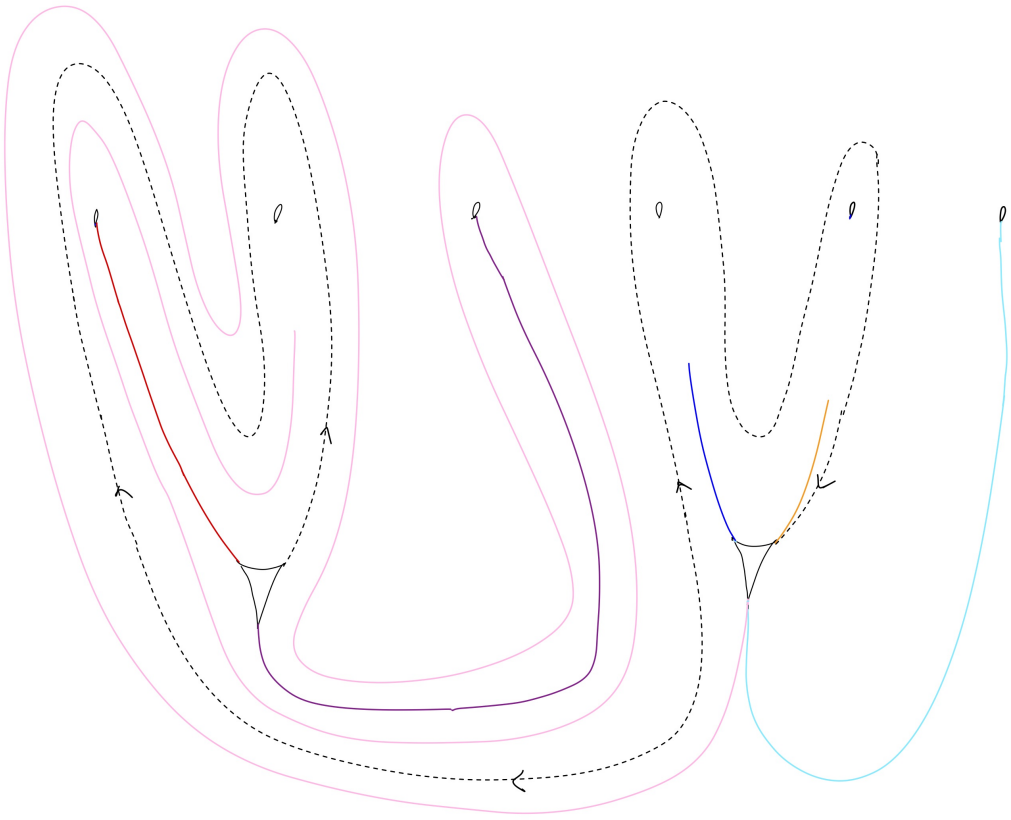


Figure I.34: Wanion2

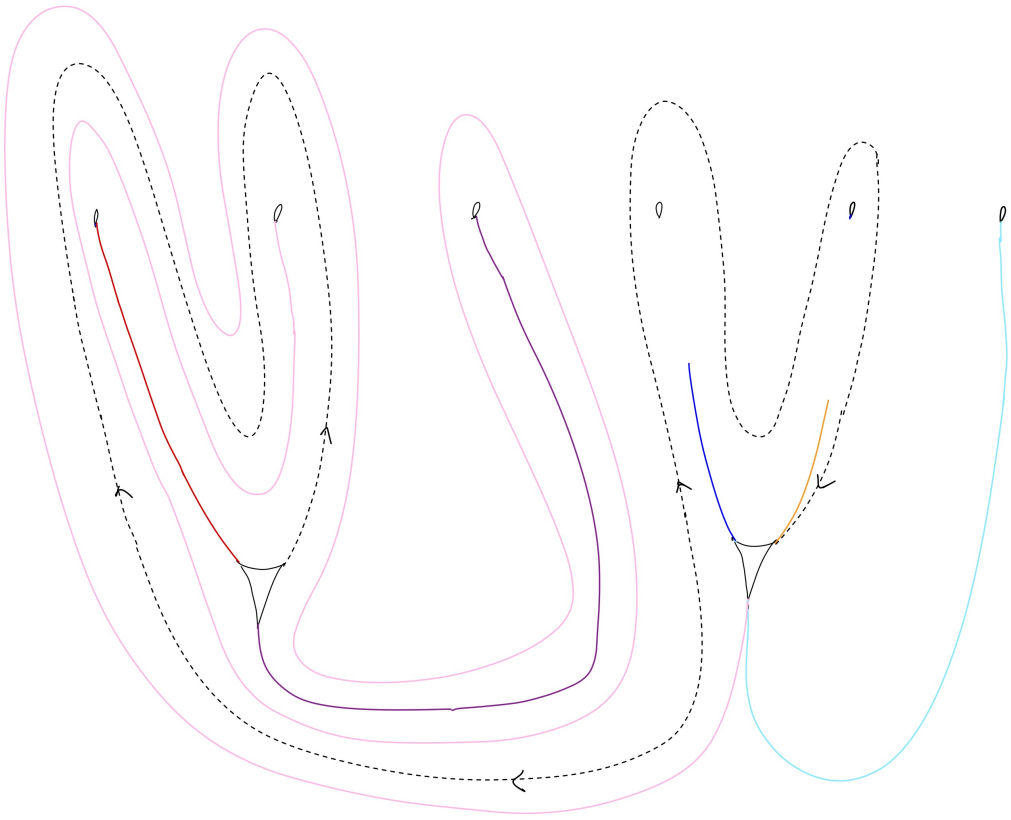


Figure I.35: Wanion3

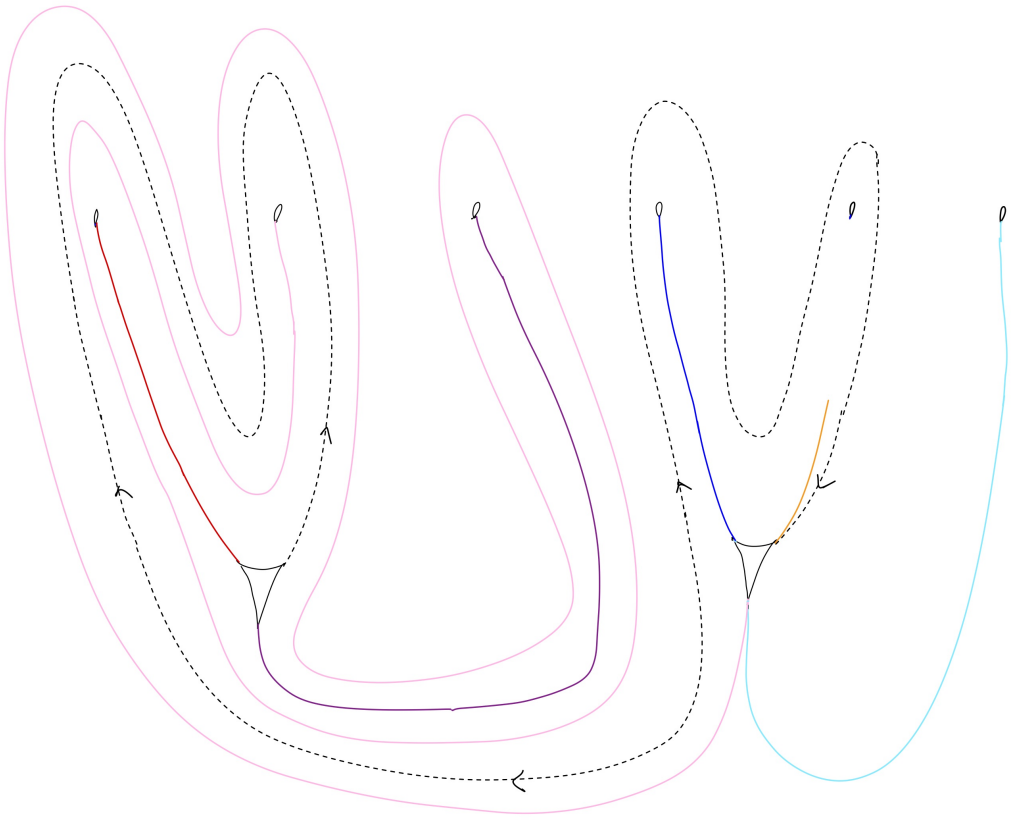


Figure I.36: Wanion4

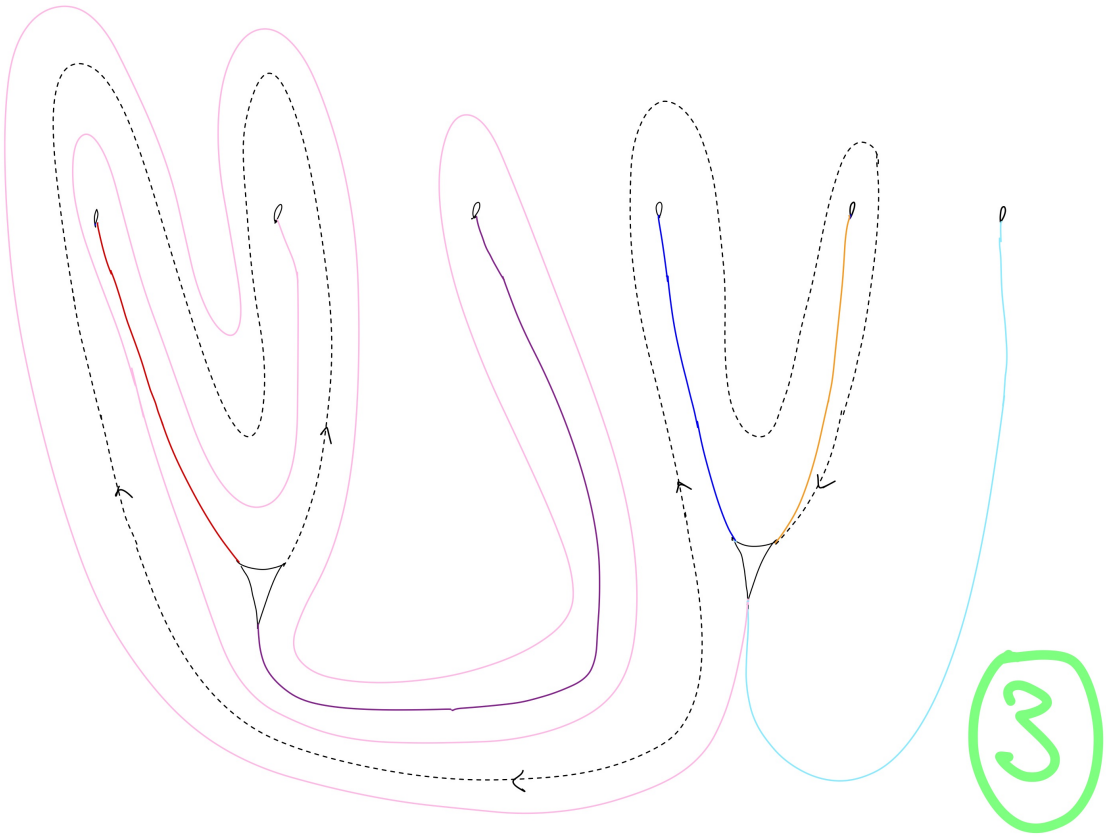


Figure I.37: Wanion5

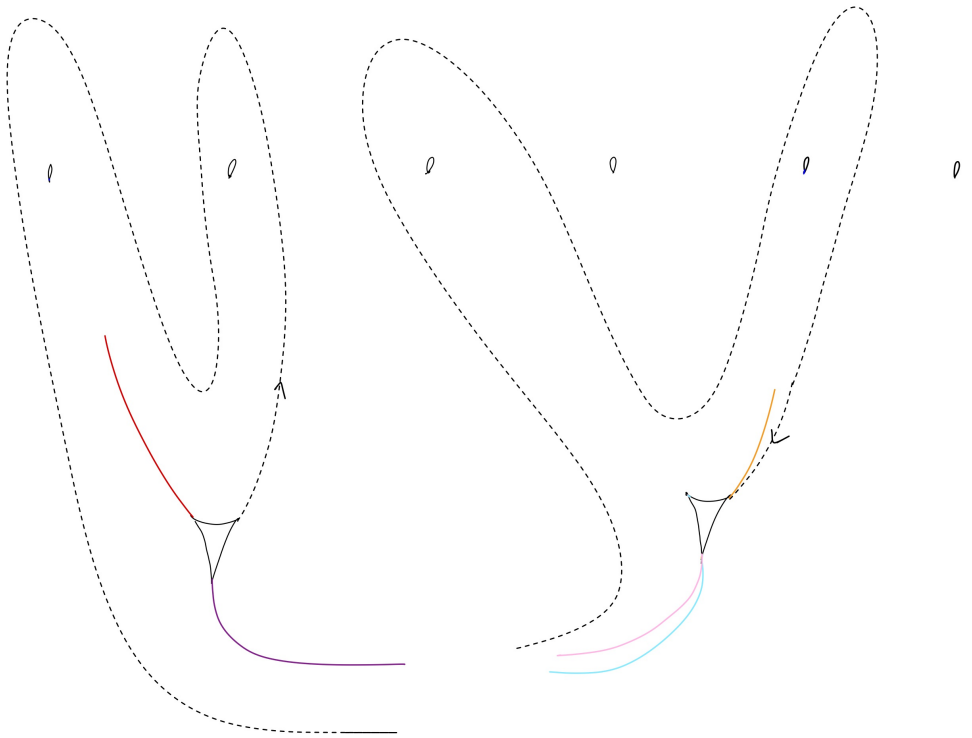


Figure I.38: Blet1

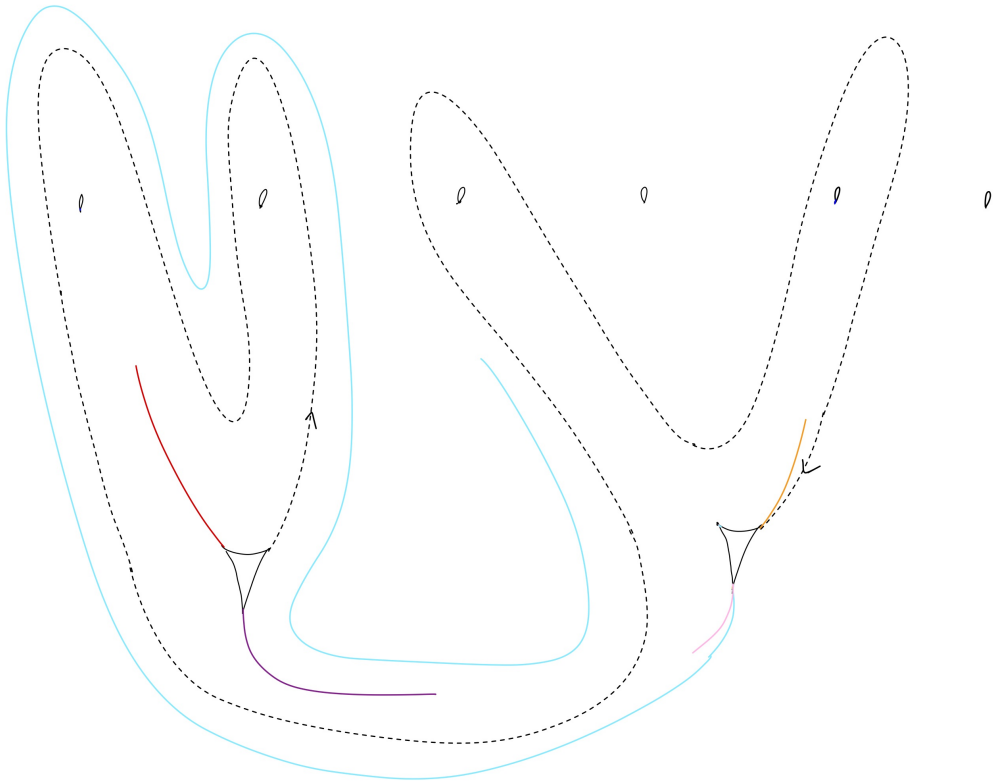


Figure I.39: Blet2

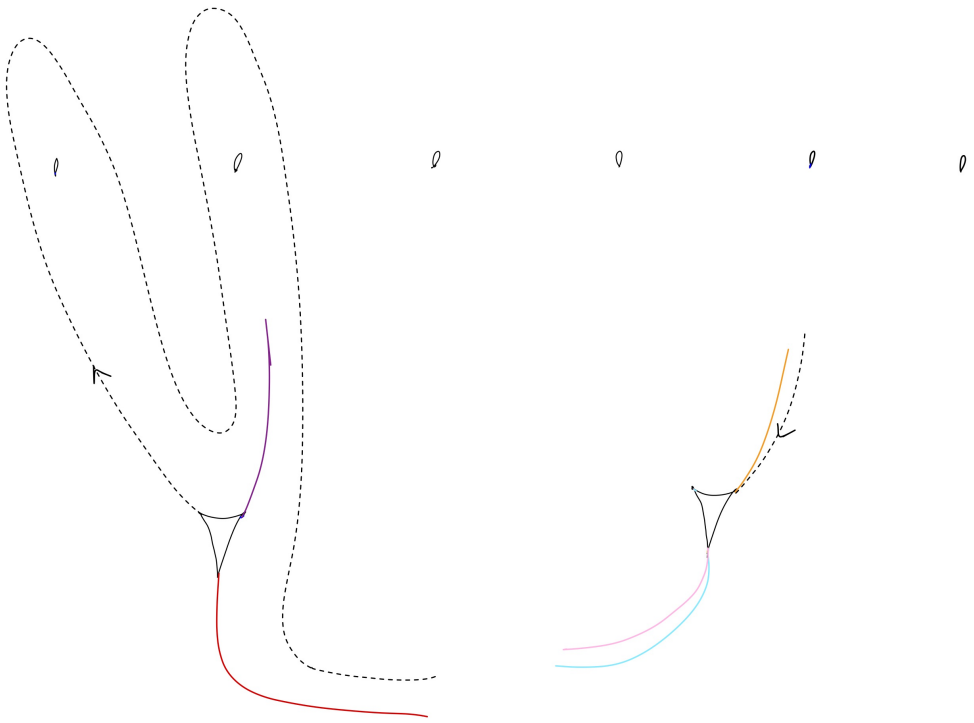


Figure I.40: HLE1

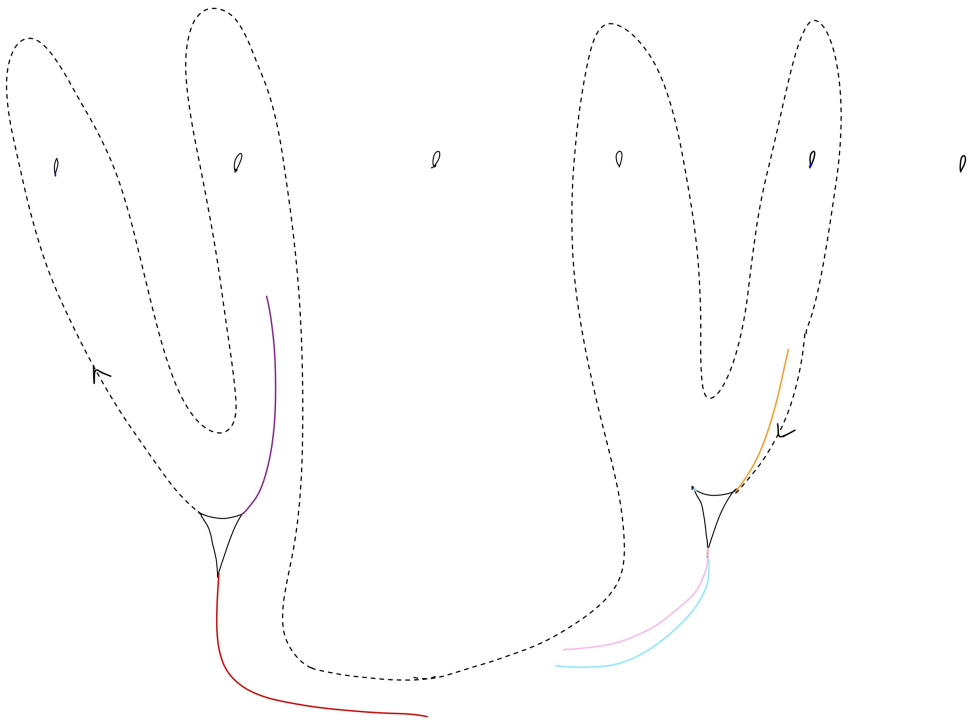


Figure I.41: Dree1

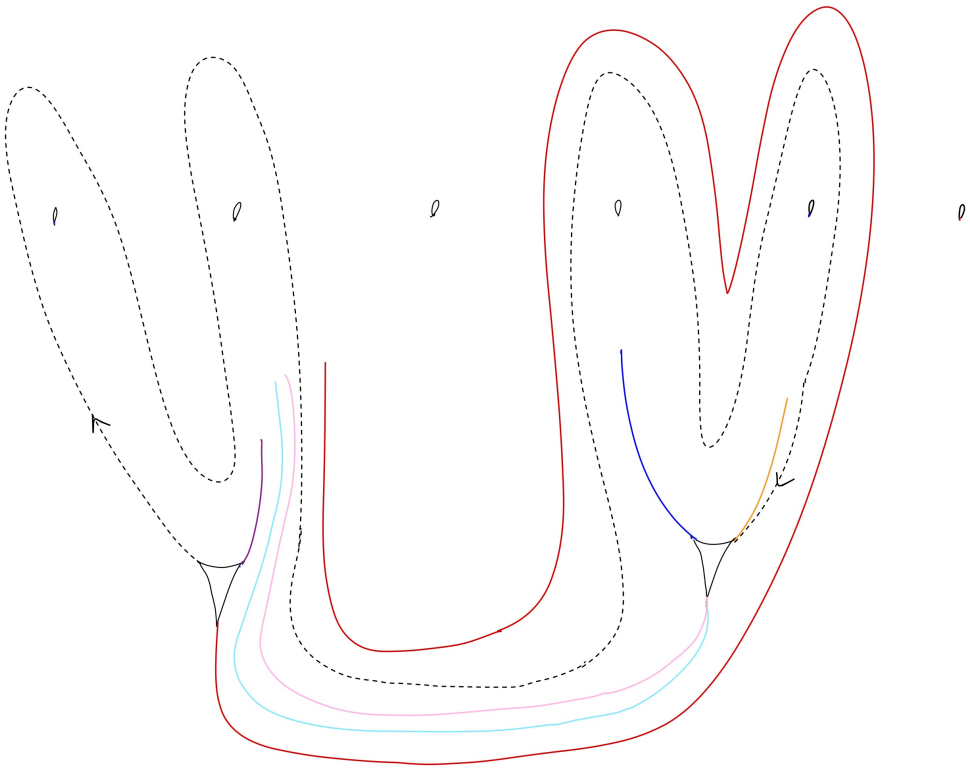


Figure I.42: Dree2

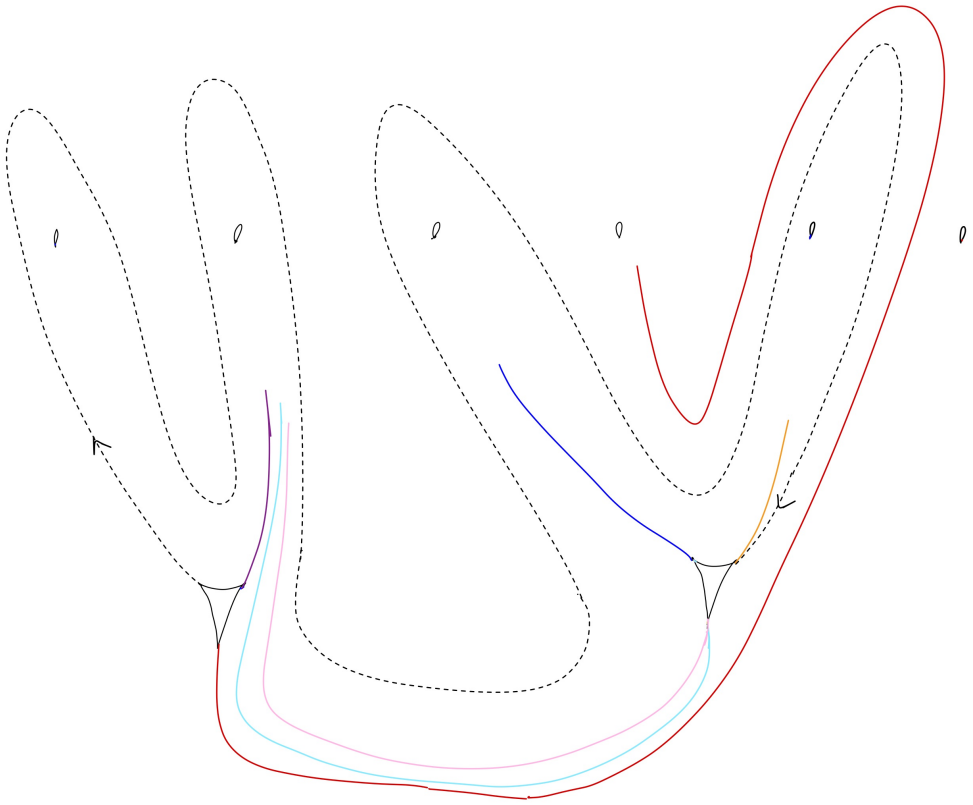


Figure I.43: Moke1

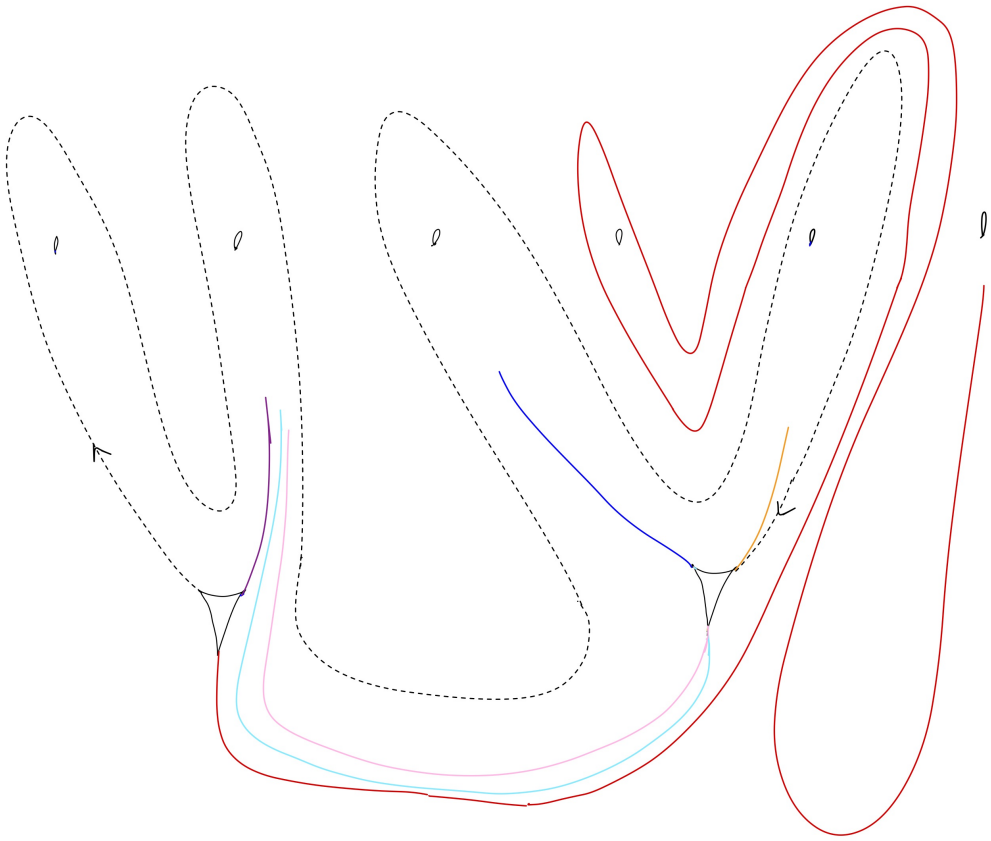


Figure I.44: Moke2

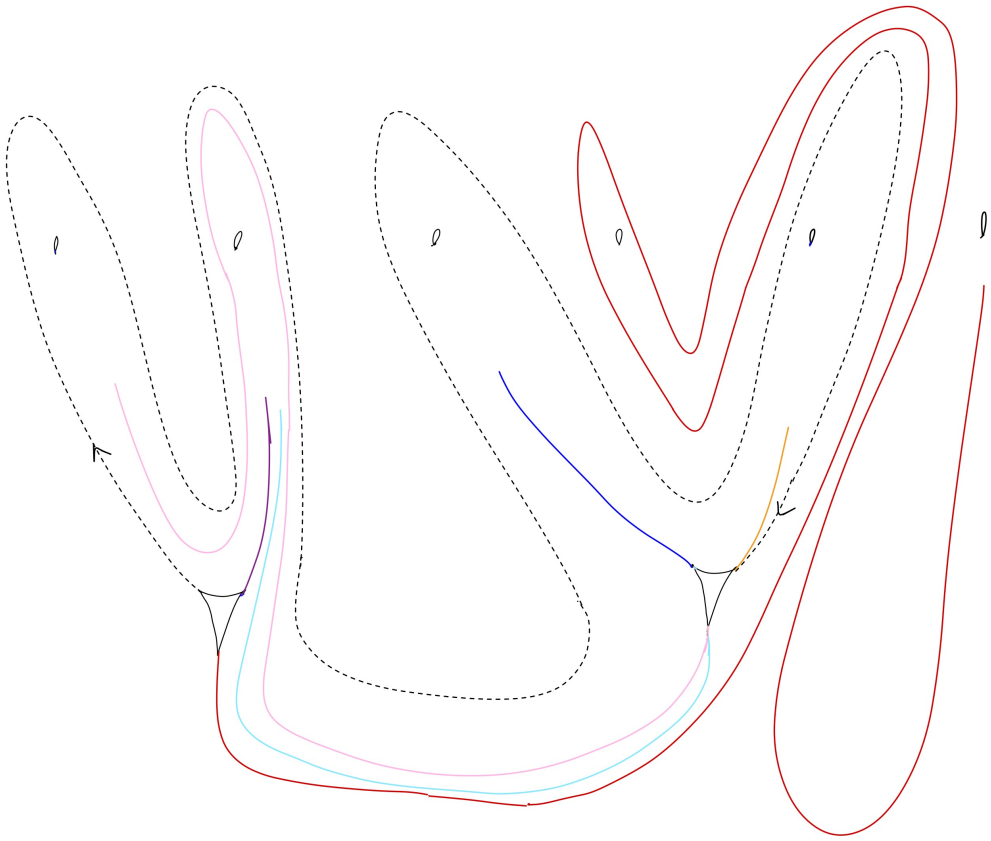


Figure I.45: Moke3

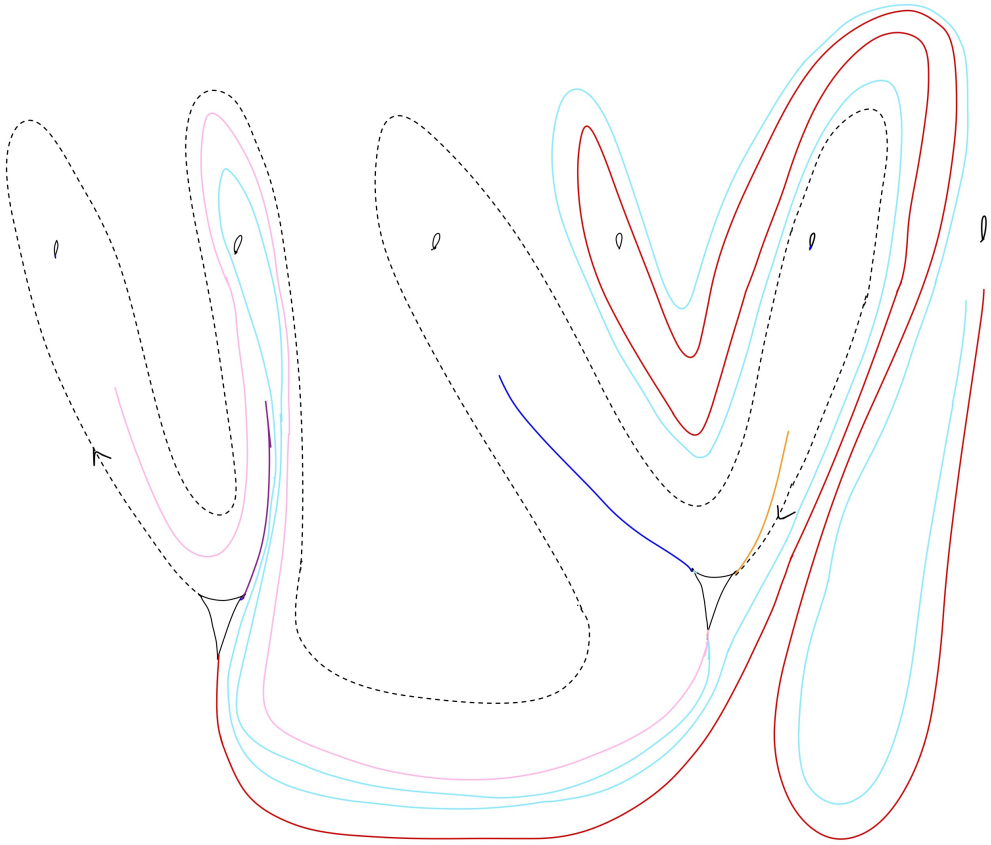


Figure I.46: Moke4

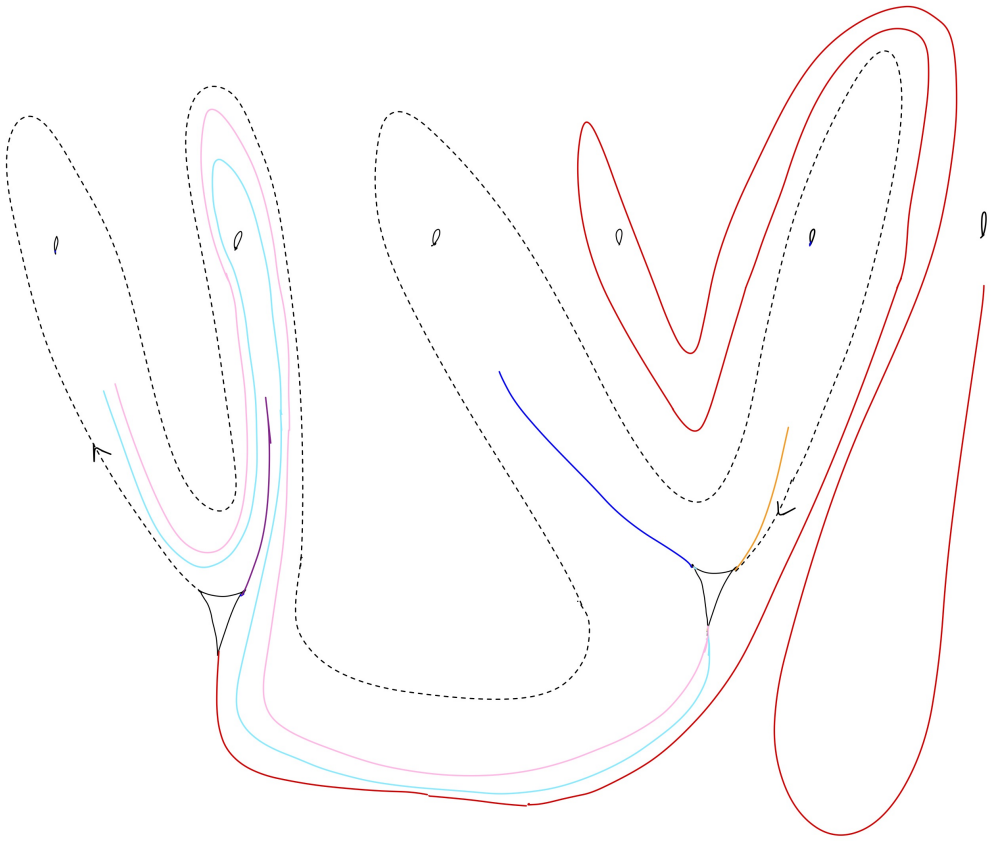


Figure I.47: Moke5

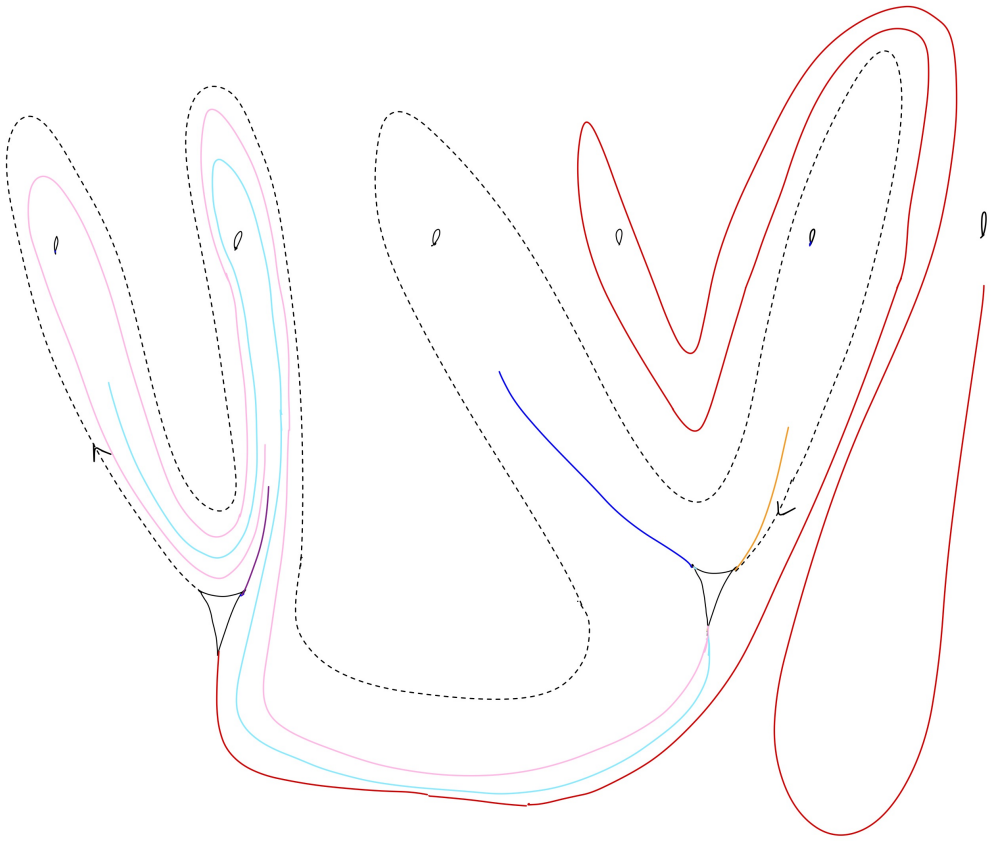


Figure I.48: Moke6

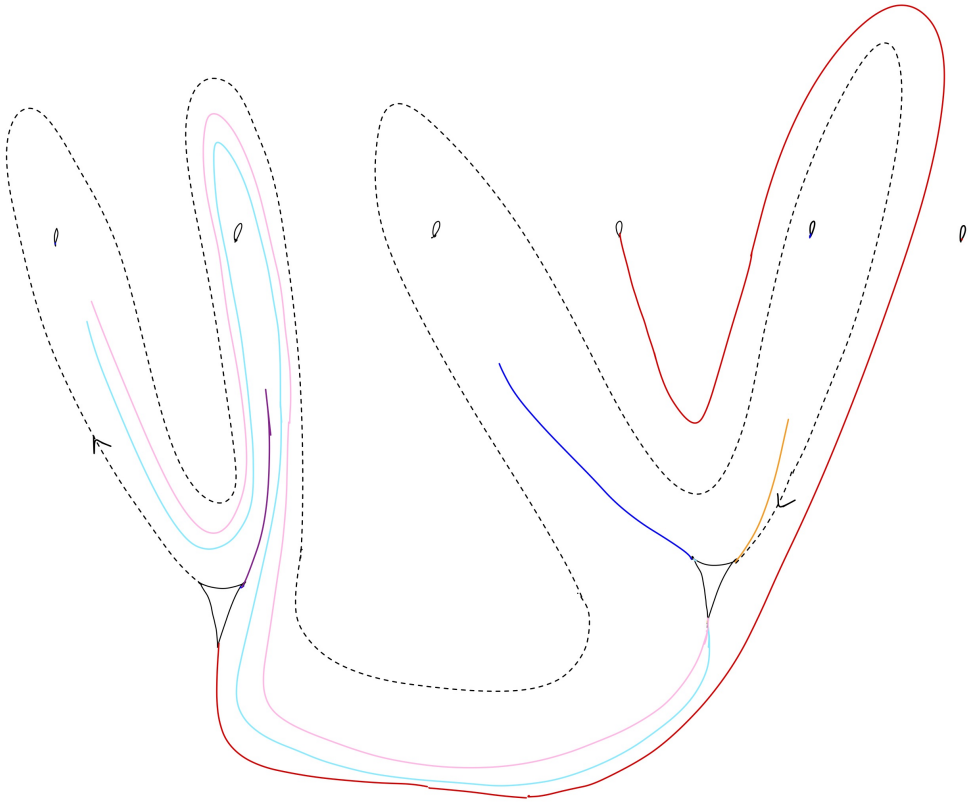


Figure I.49: Moke7

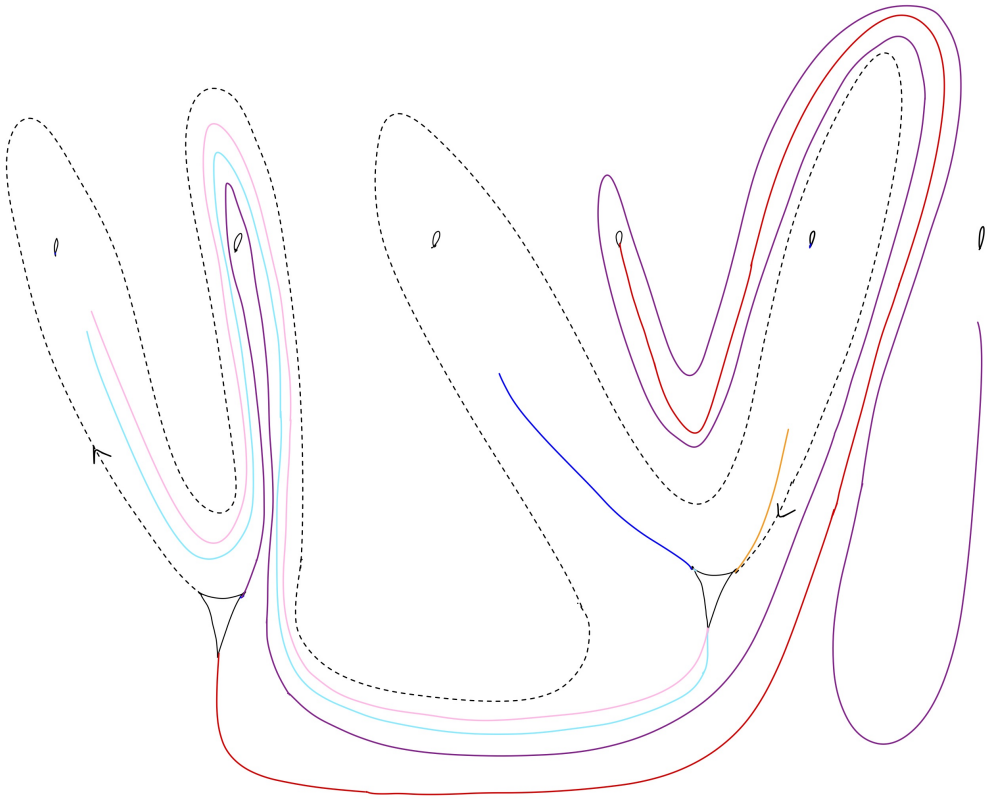


Figure I.50: Moke8

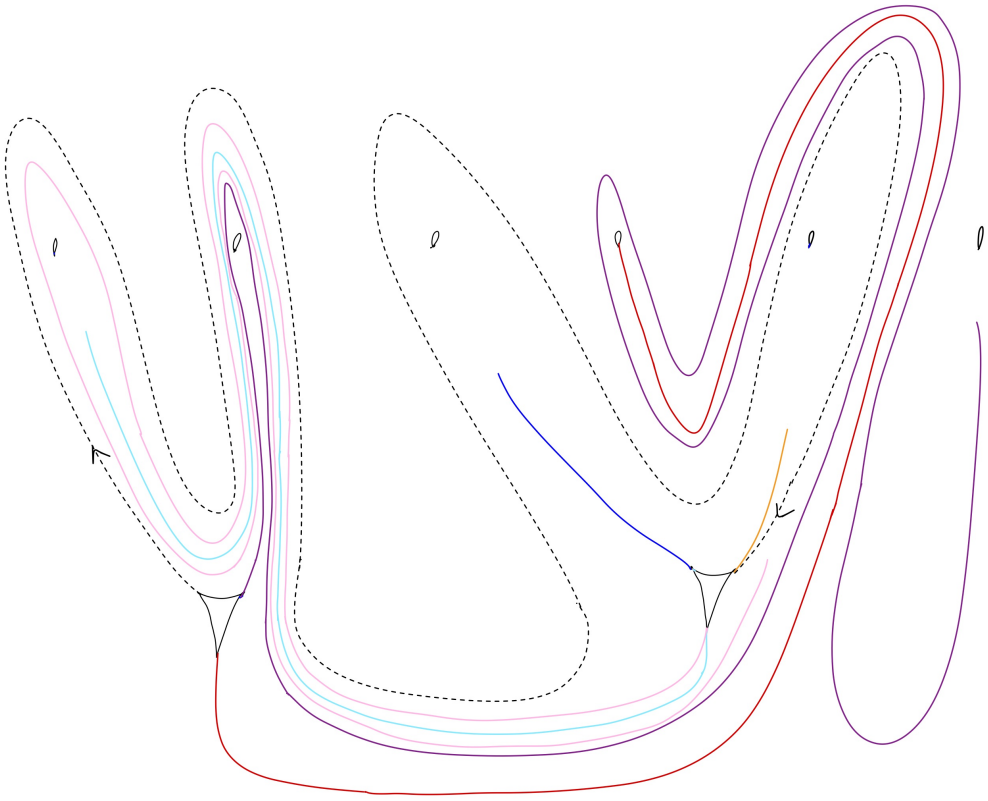


Figure I.51: Moke9

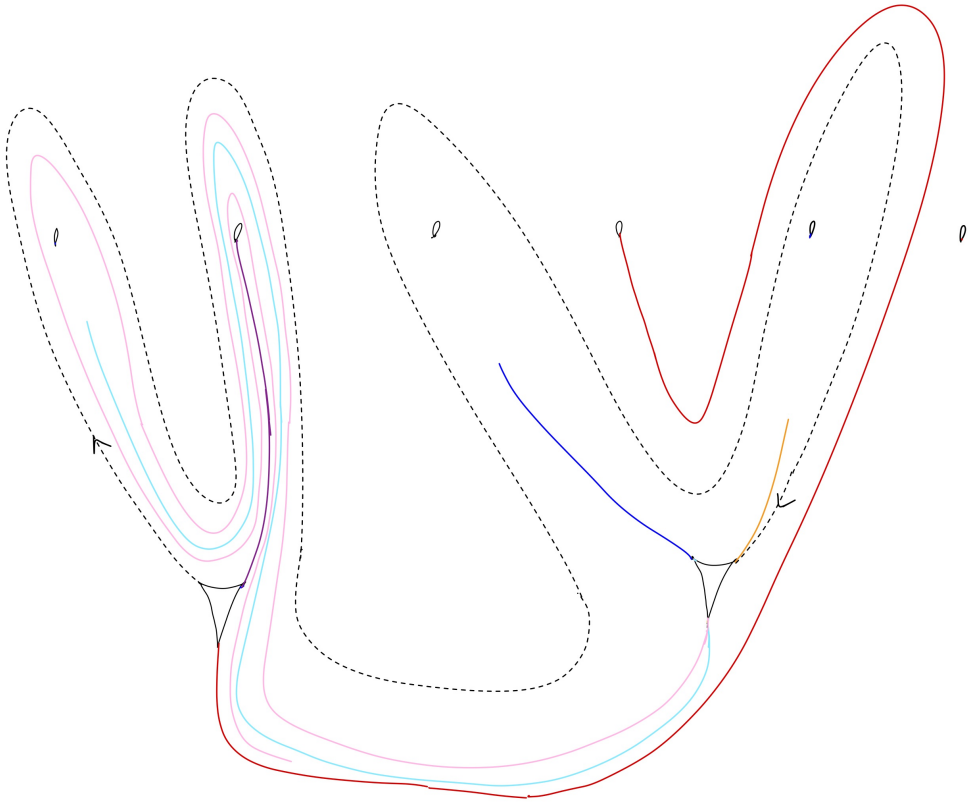


Figure I.52: Moke10

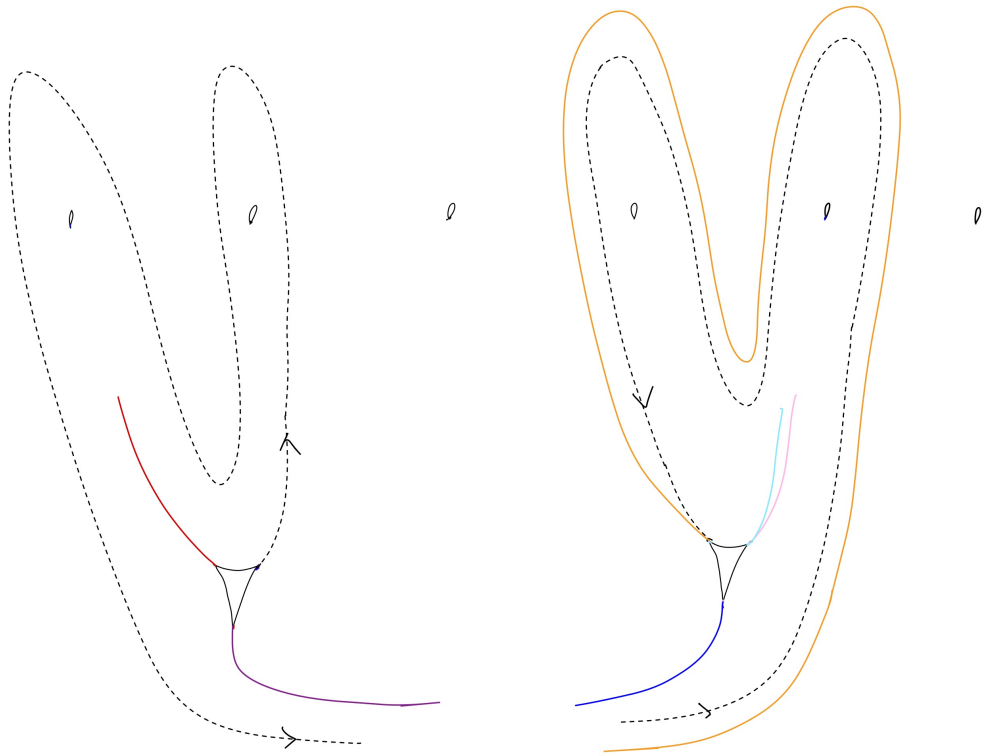


Figure I.53: UAH1

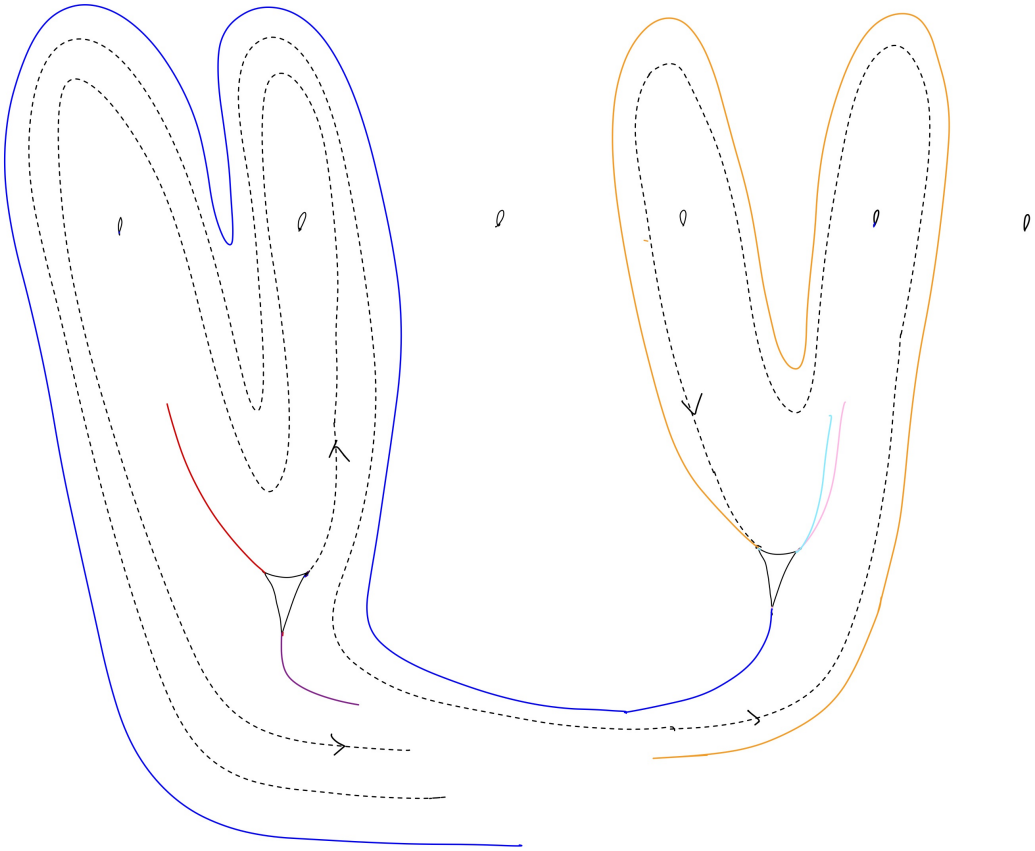


Figure I.54: UAH2

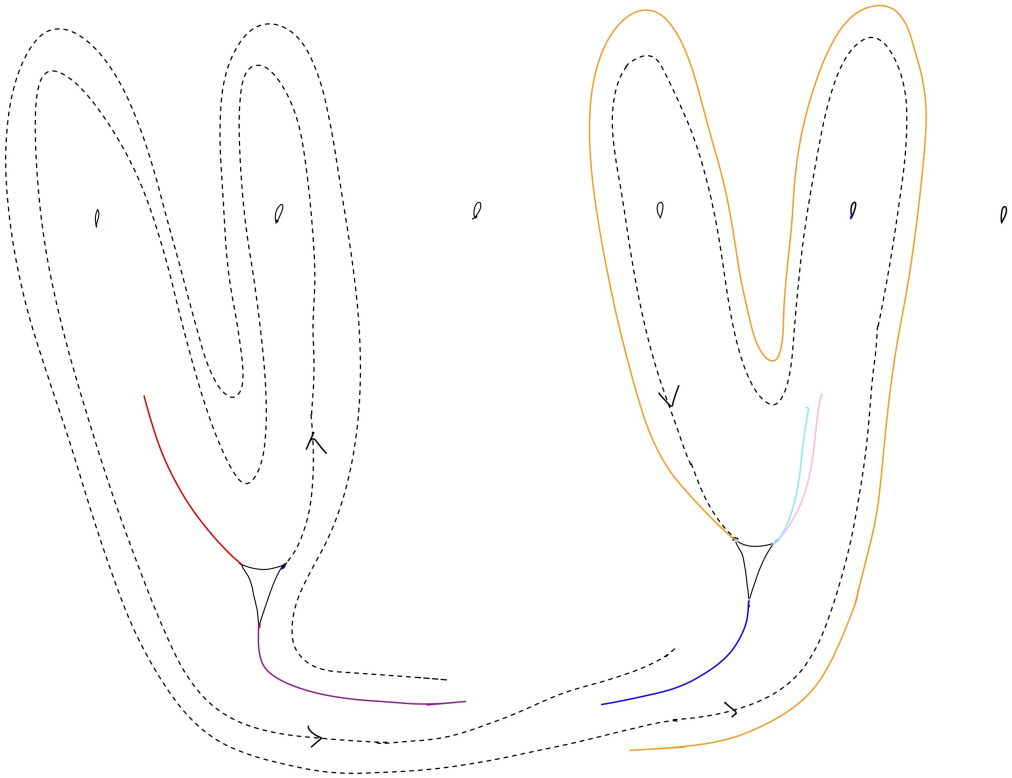


Figure I.55: UAH3

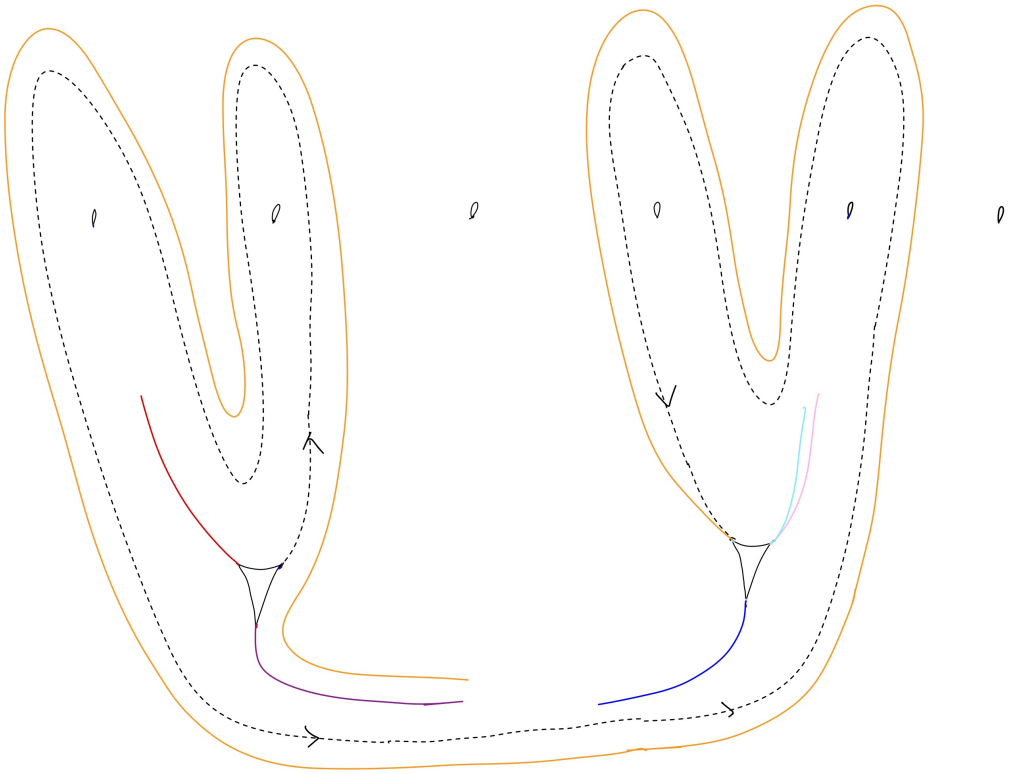


Figure I.56: UAH4

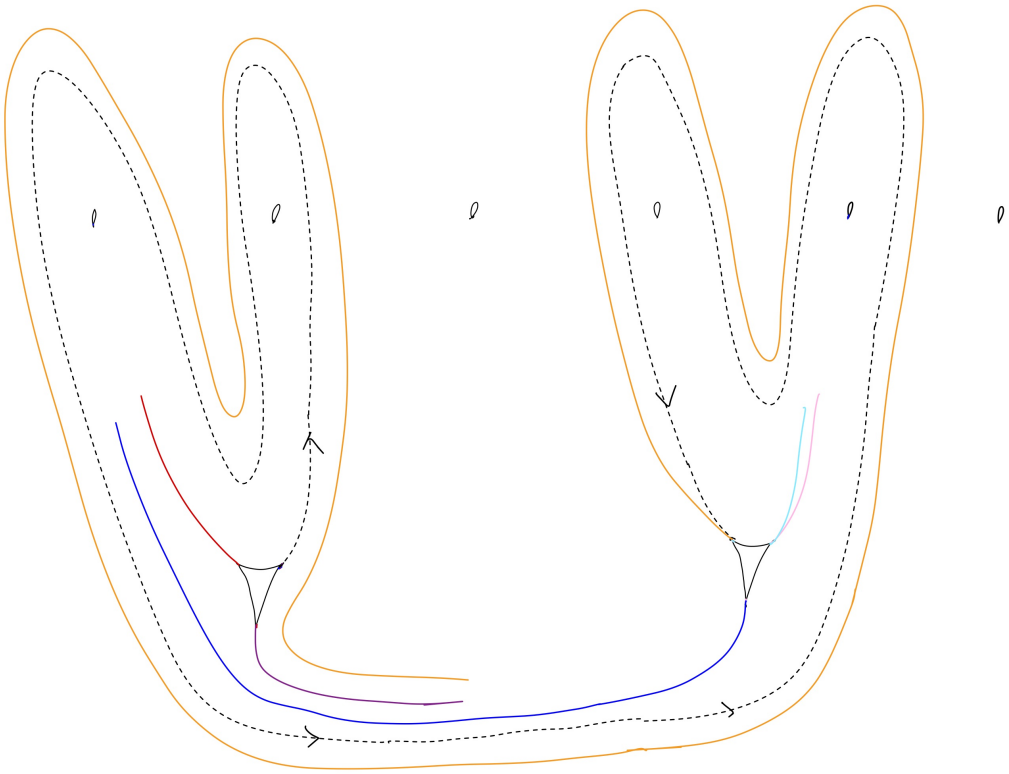


Figure I.57: UAH5

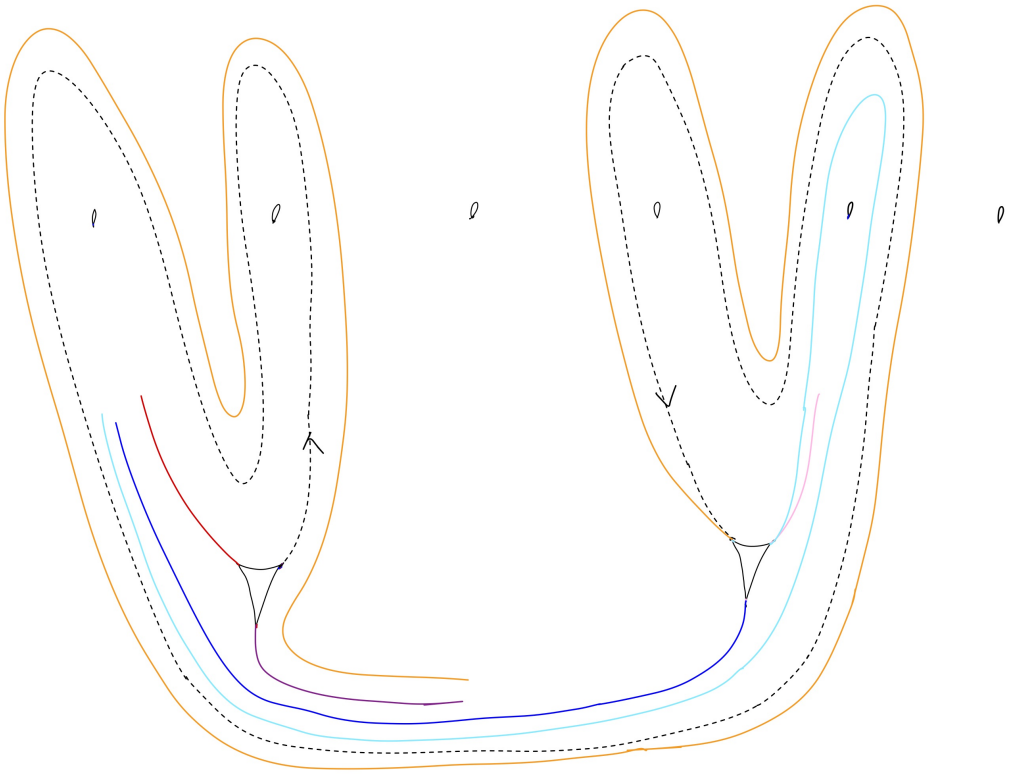


Figure I.58: UAH6

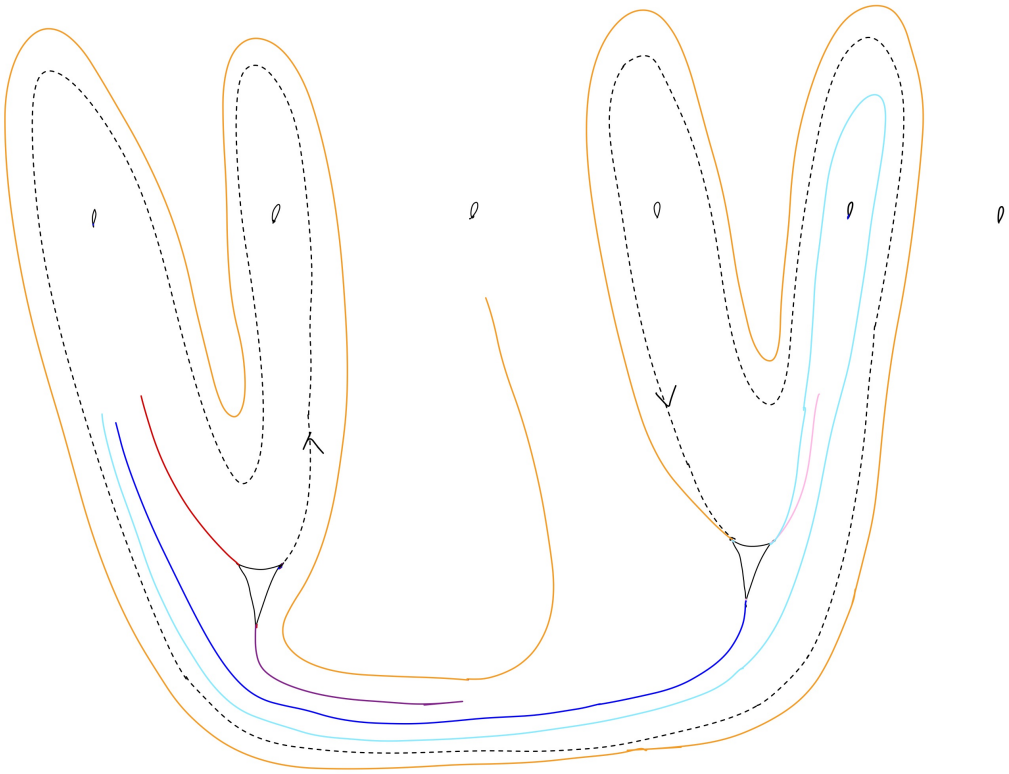


Figure I.59: UAH7

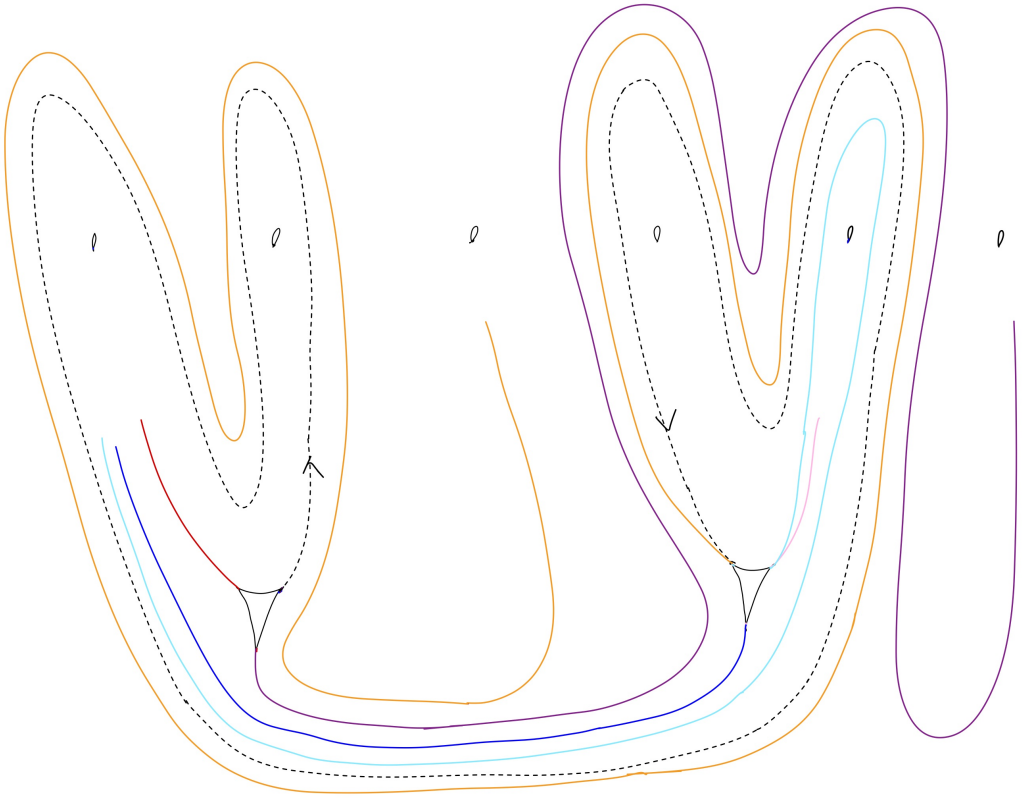


Figure I.60: Oche1

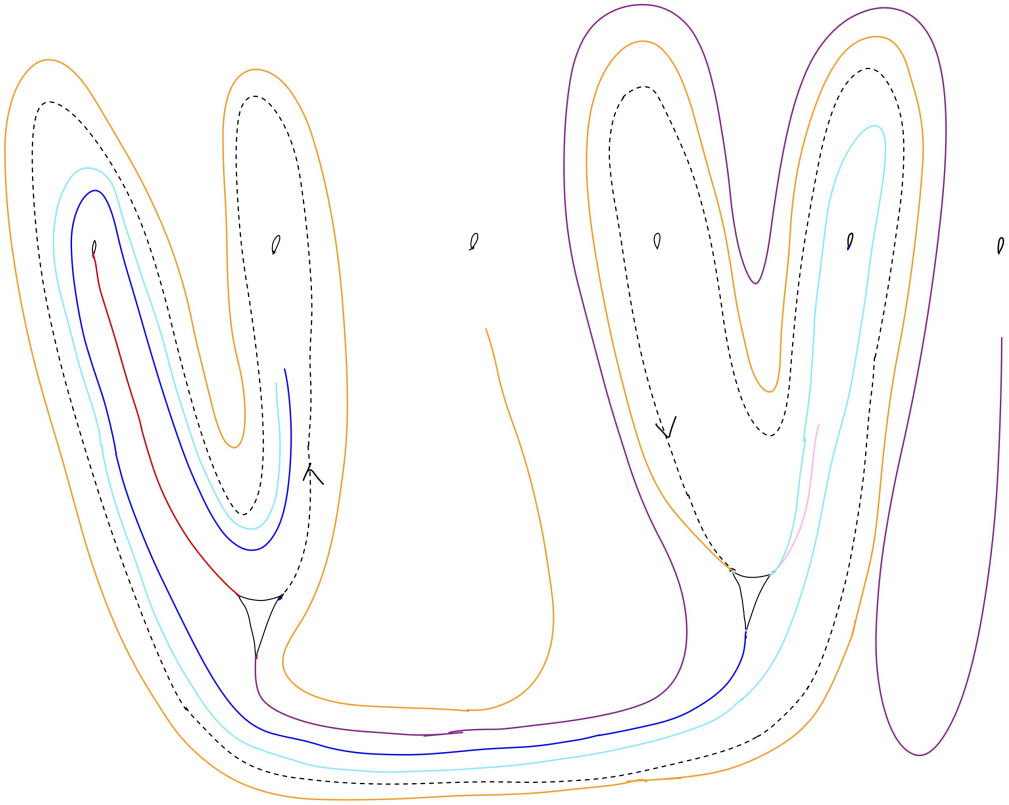


Figure I.61: Oche2

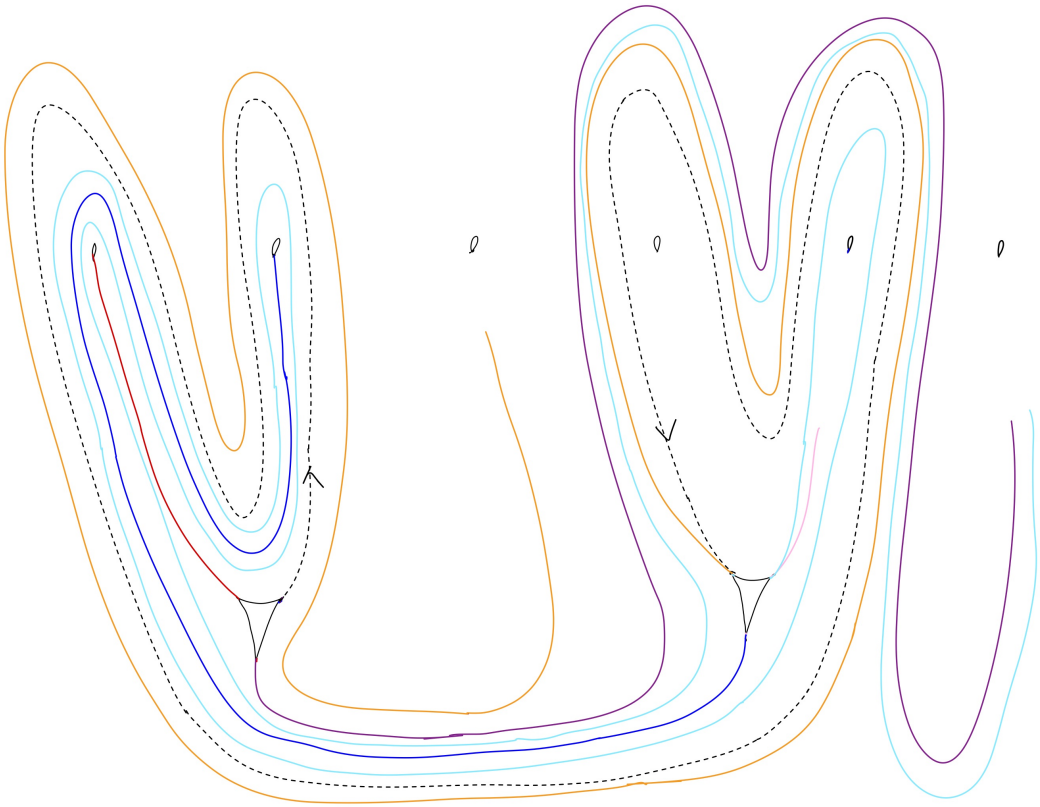


Figure I.62: Oche3

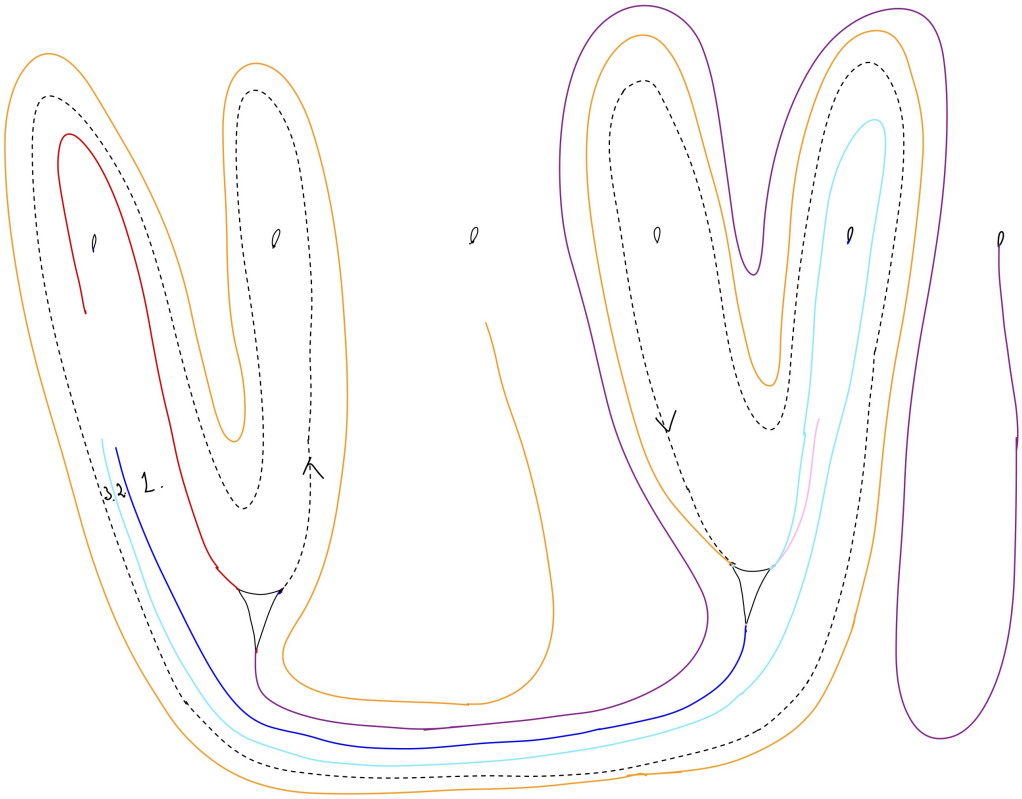


Figure I.63: Oche4

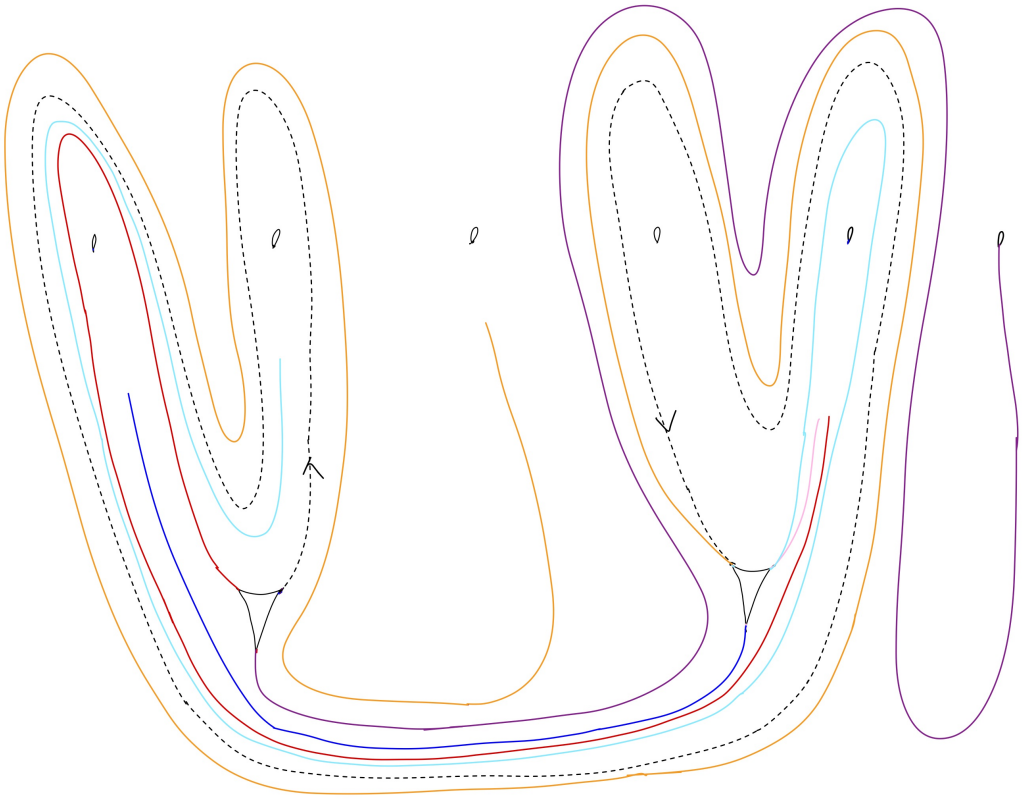


Figure I.64: Gurry1

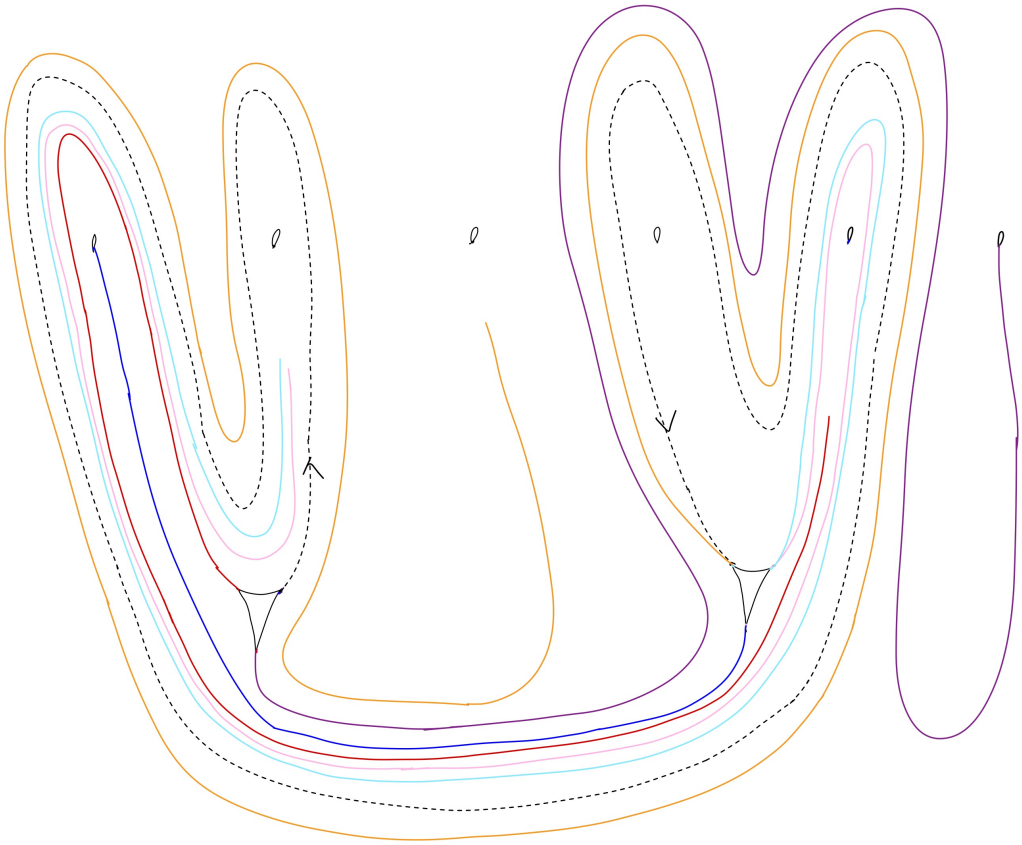


Figure I.65: Gurry2

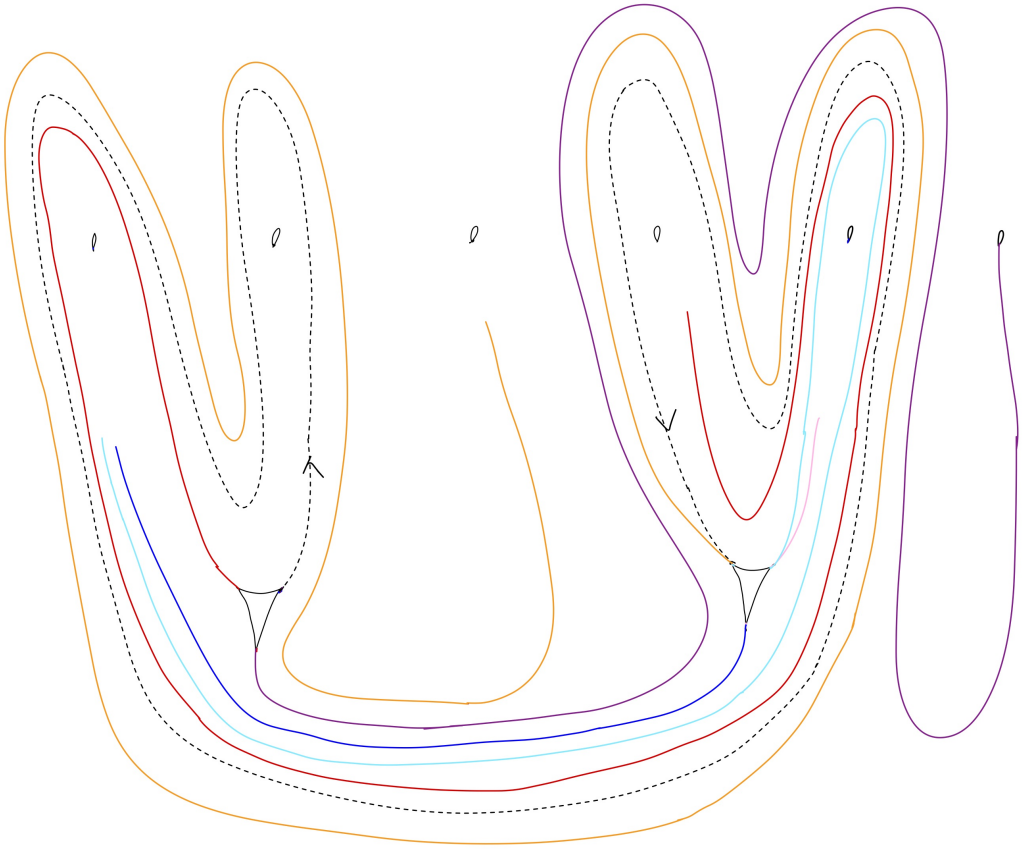


Figure I.66: Hanch1

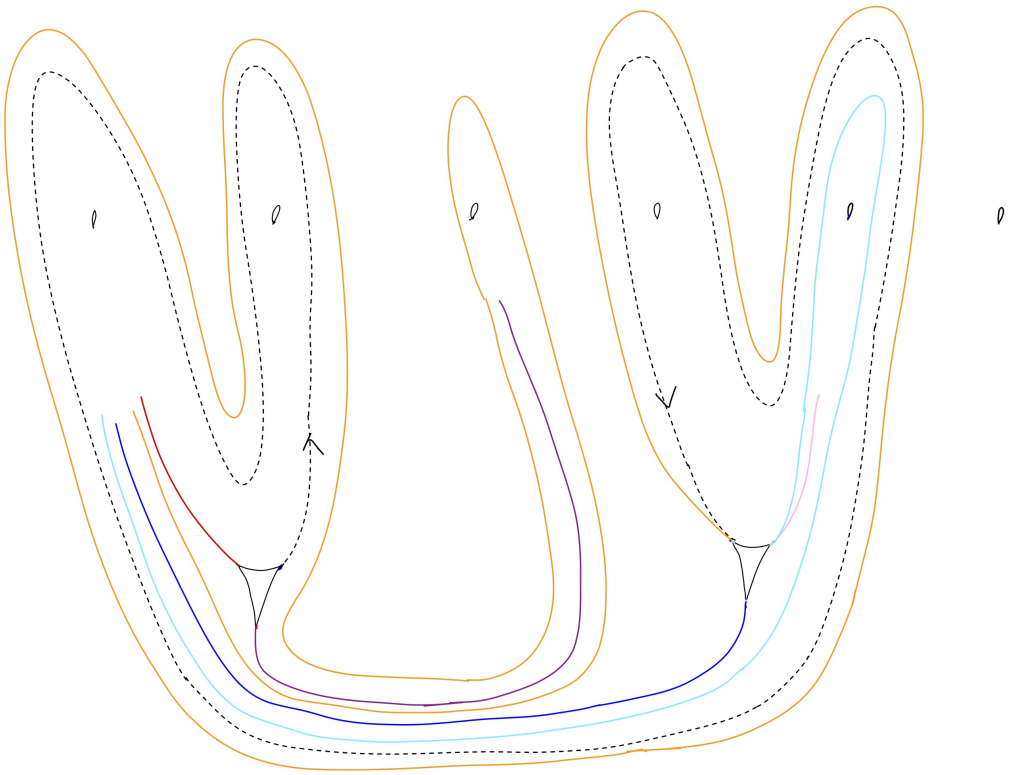


Figure I.67: Roop1

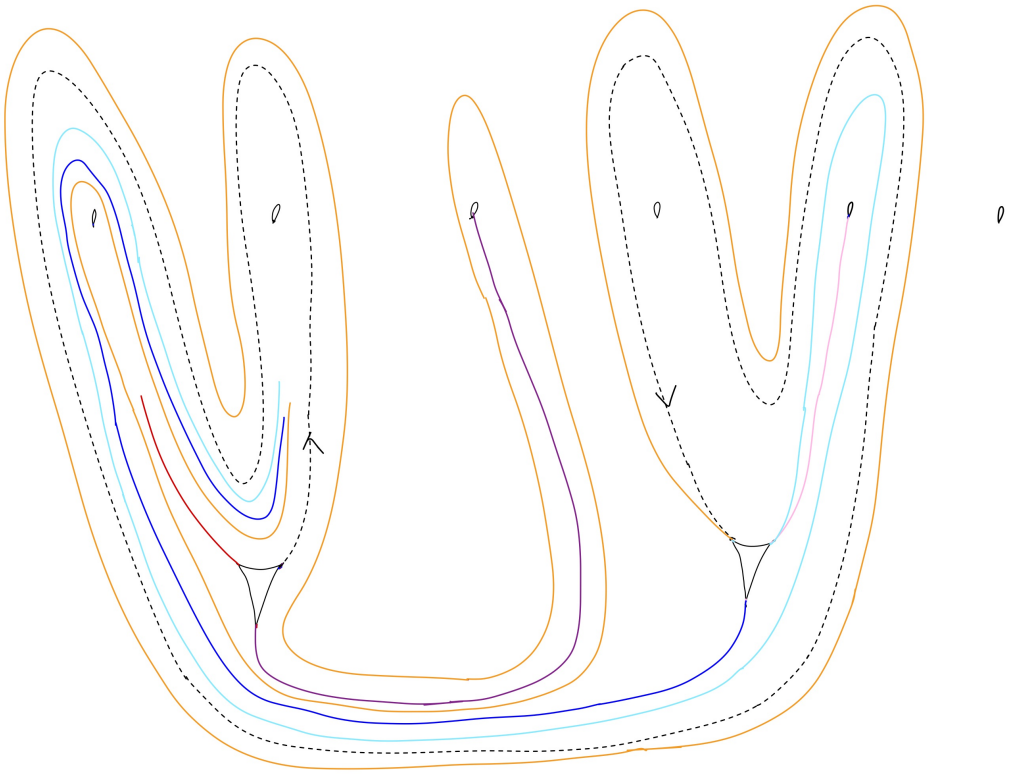


Figure I.68: Roop2

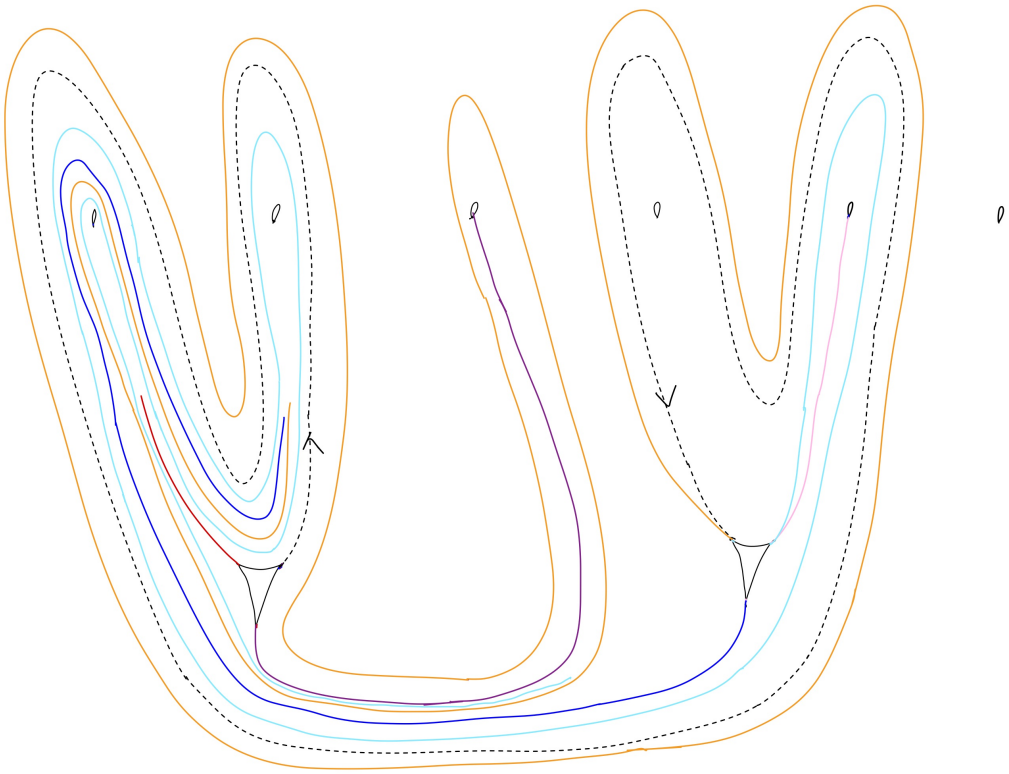


Figure I.69: Roop3

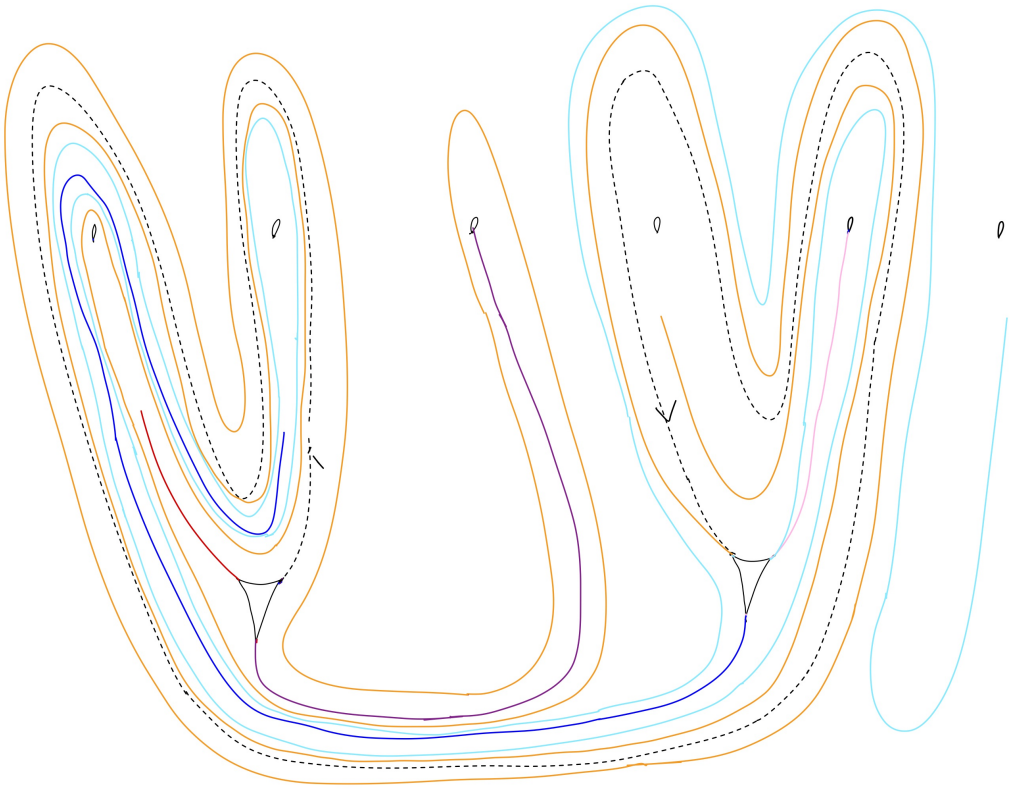


Figure I.70: Roop4

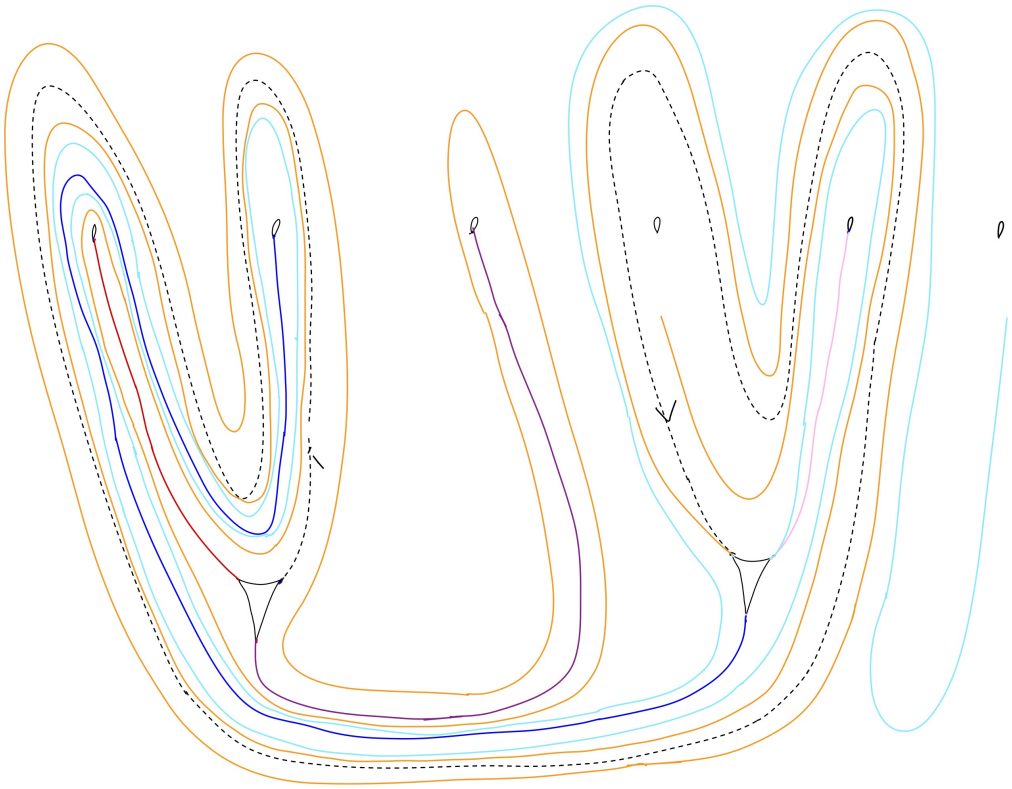


Figure I.71: Roop5

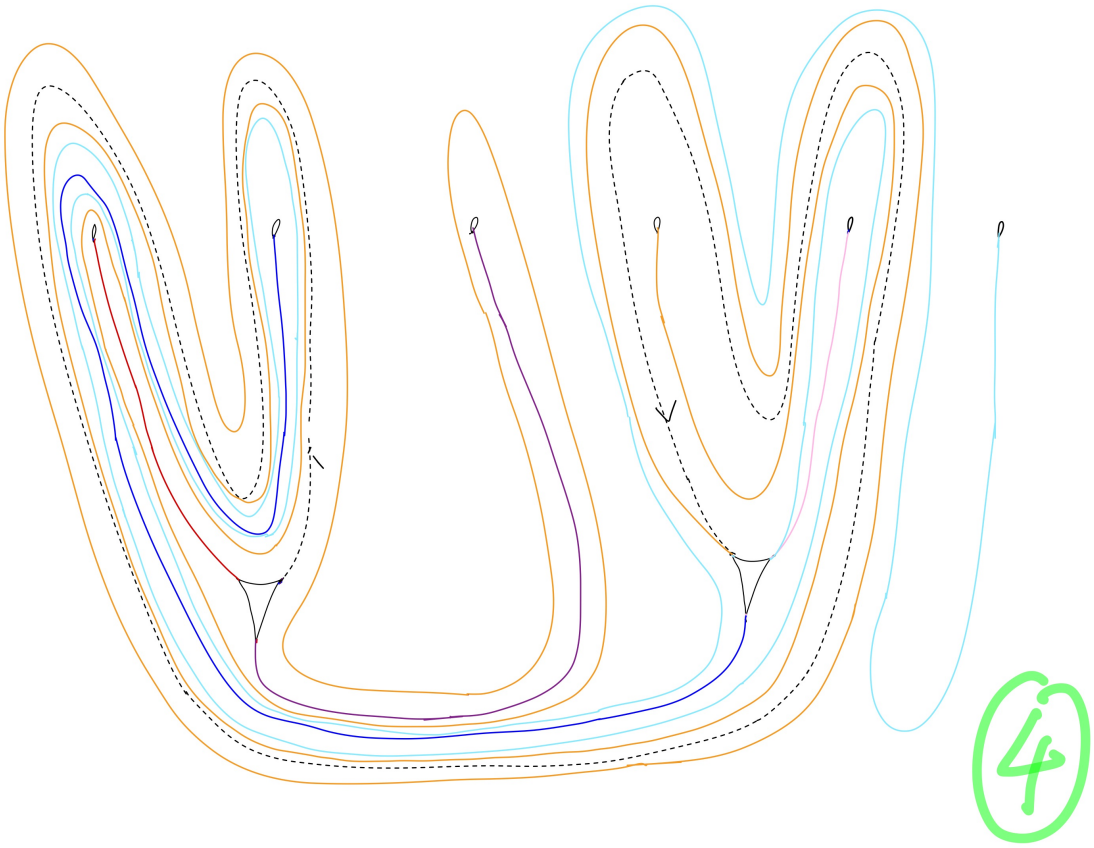


Figure I.72: Roop6

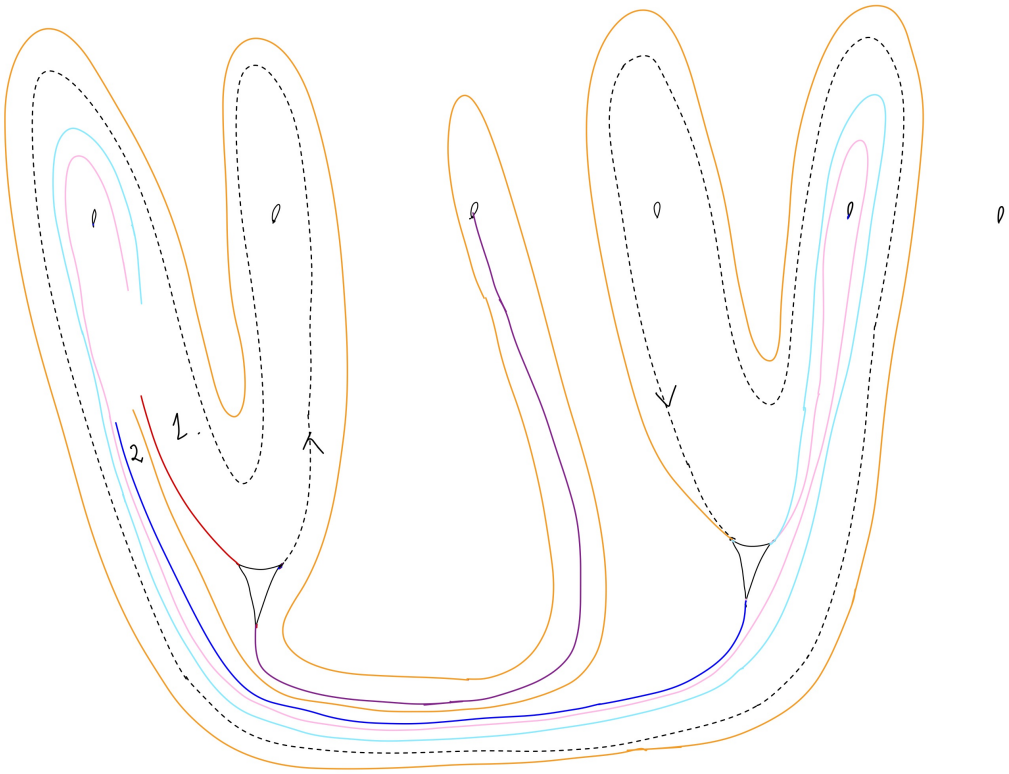


Figure I.73: Roop7

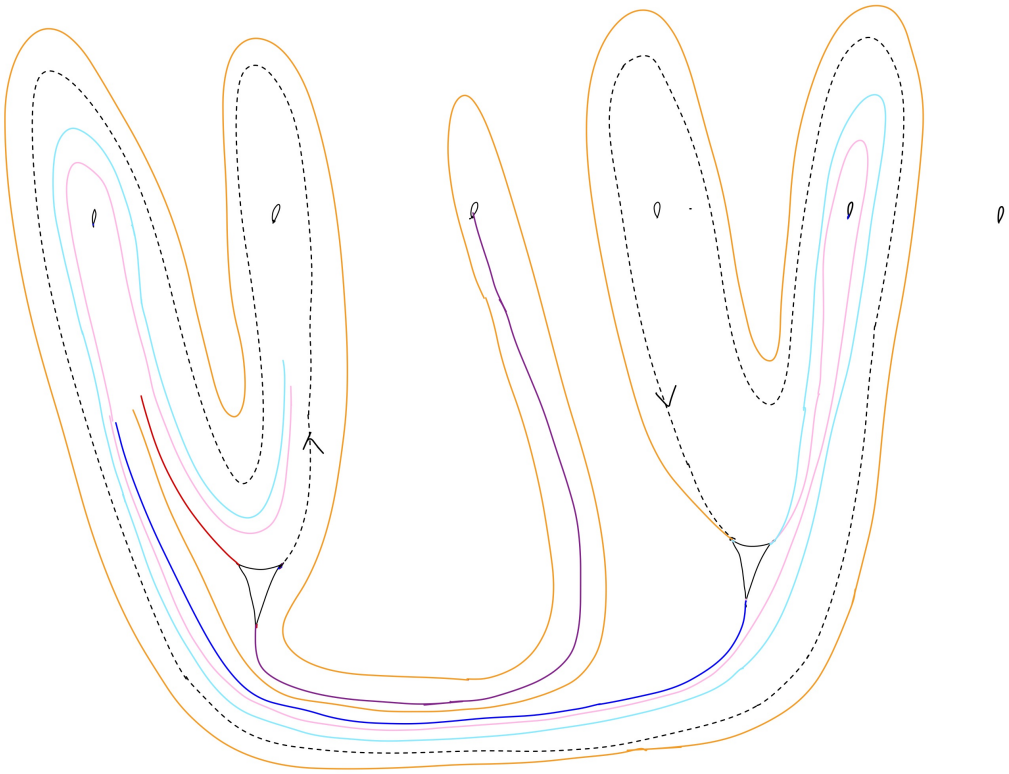


Figure I.74: Roop8

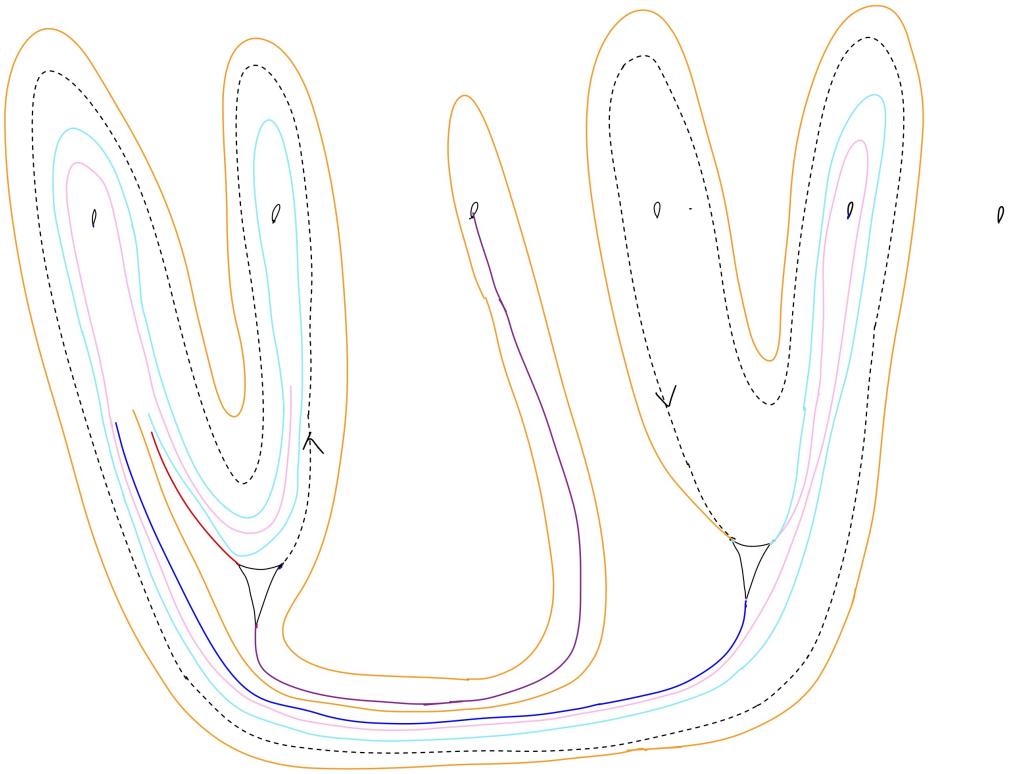


Figure I.75: Roop9

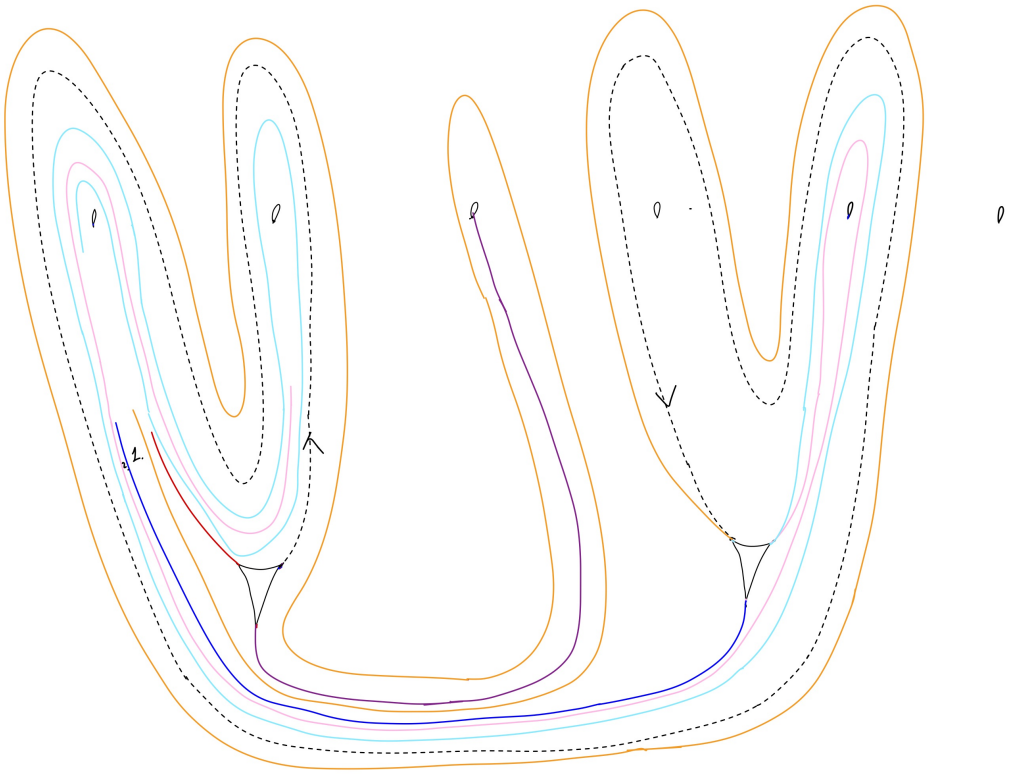


Figure I.76: Roop10

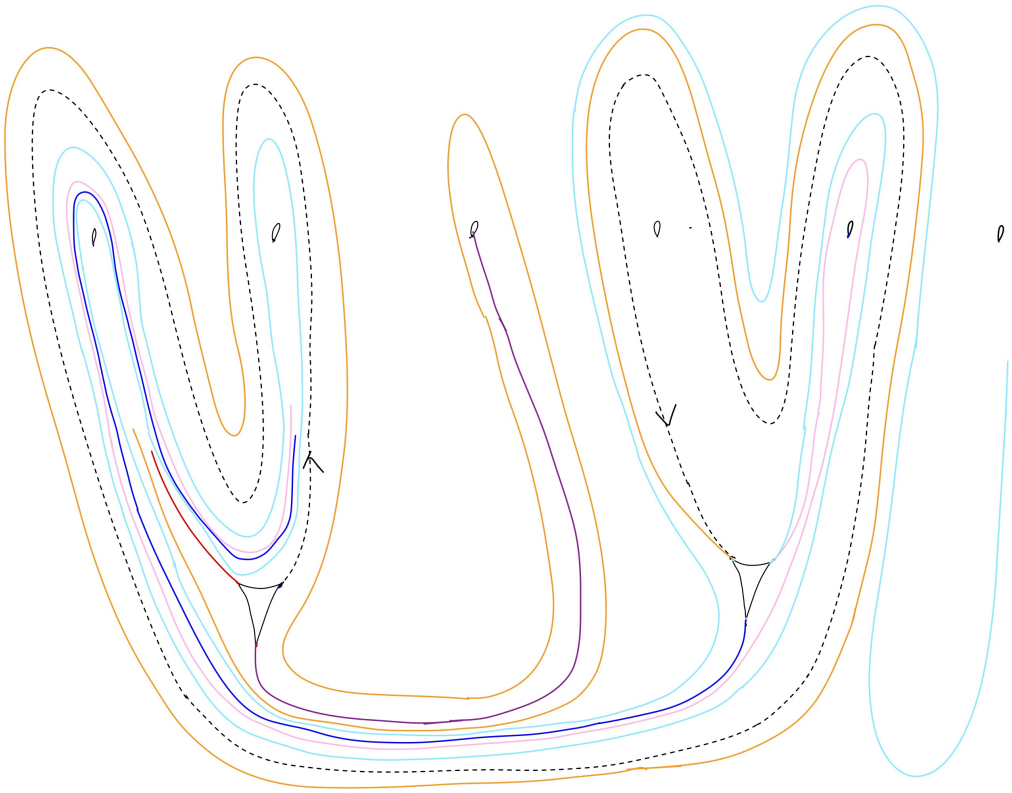


Figure I.77: Roop11

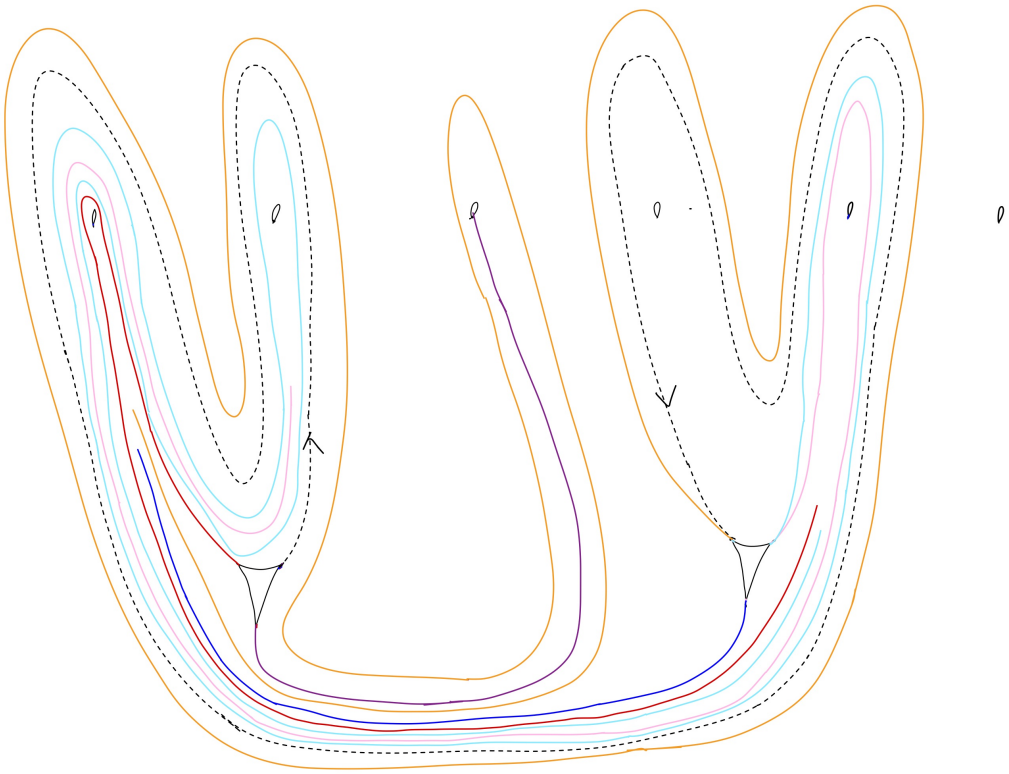


Figure I.78: Roop12

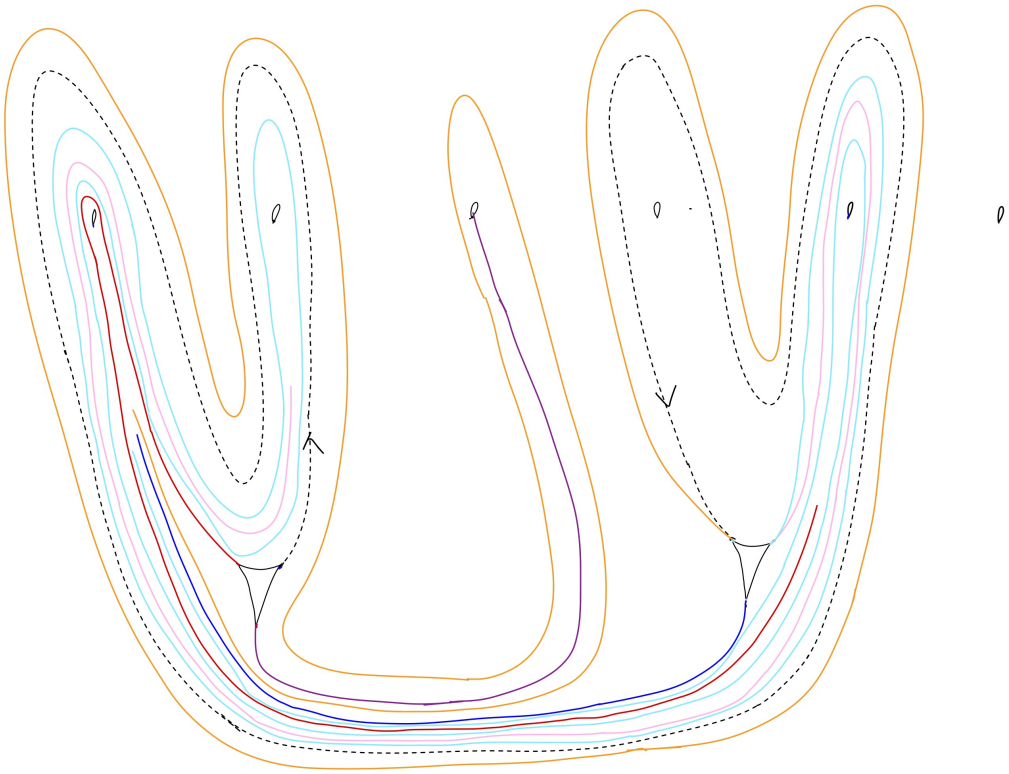


Figure I.79: Roop13

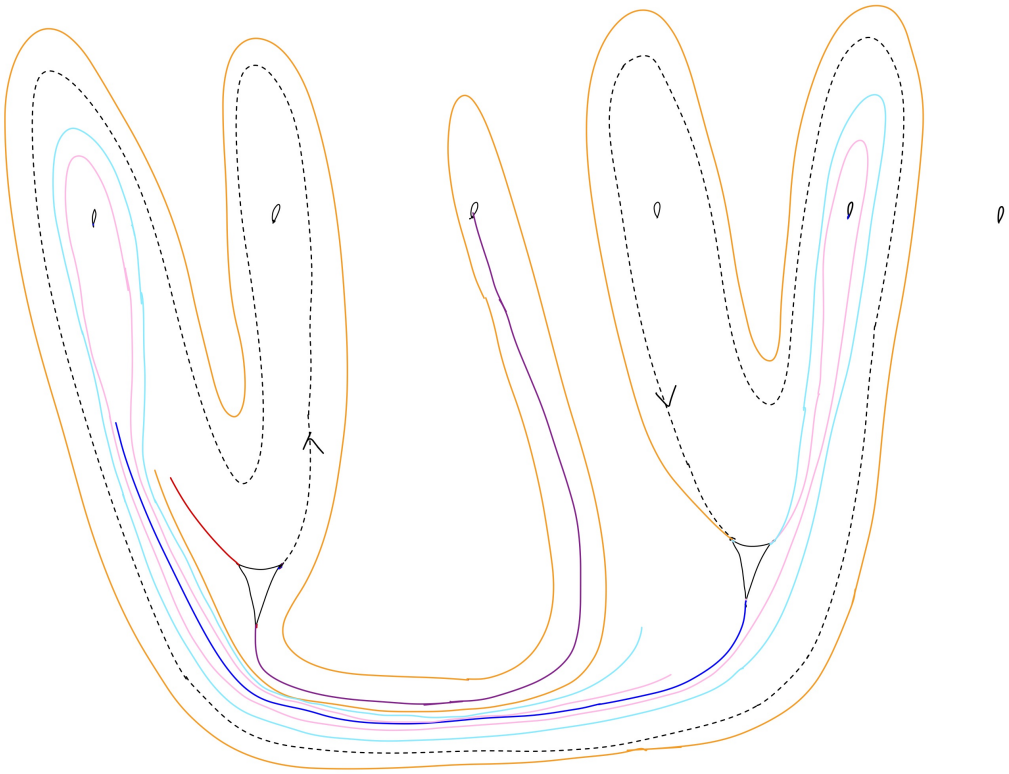


Figure I.80: Roop14

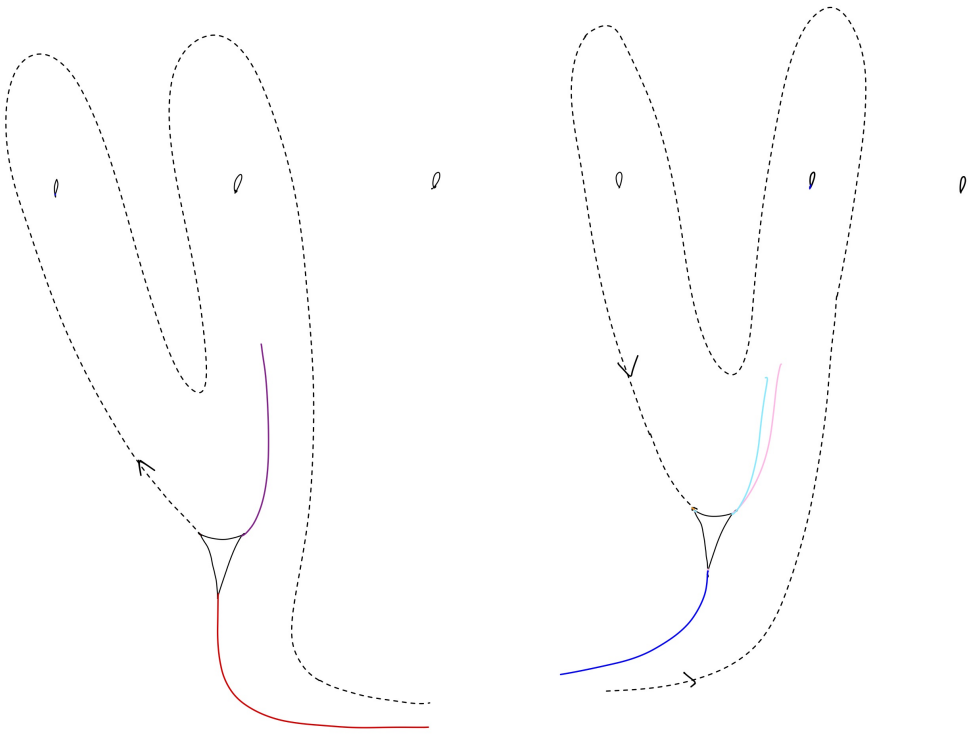


Figure I.81: GKA1

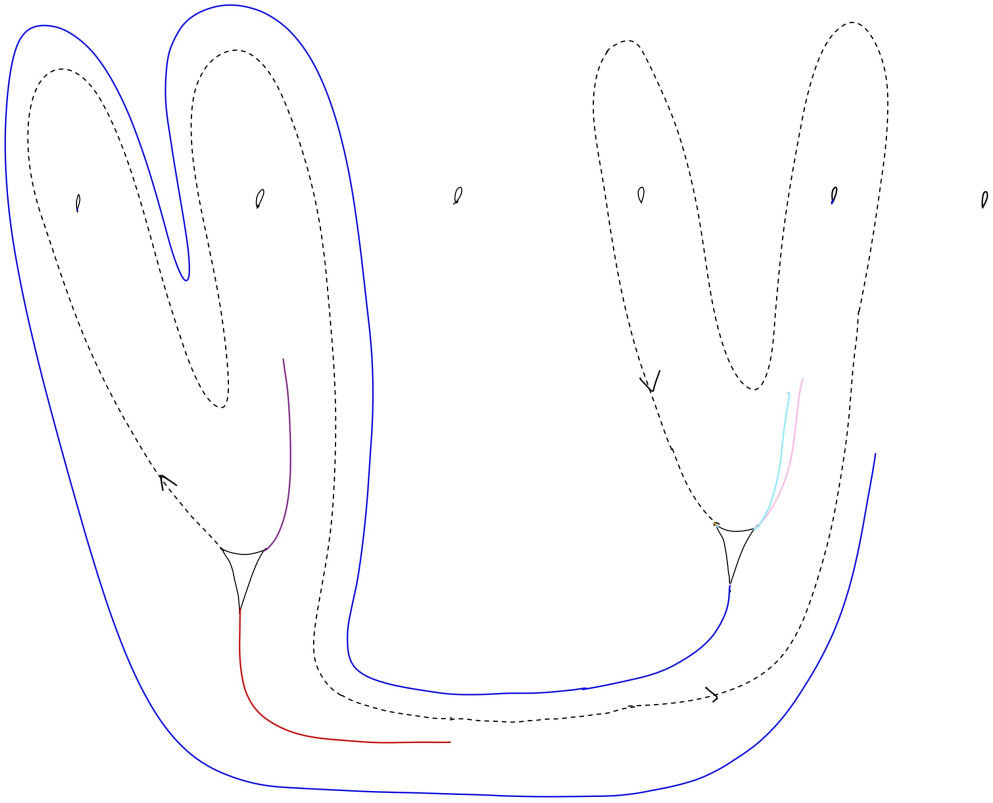


Figure I.82: GKA2

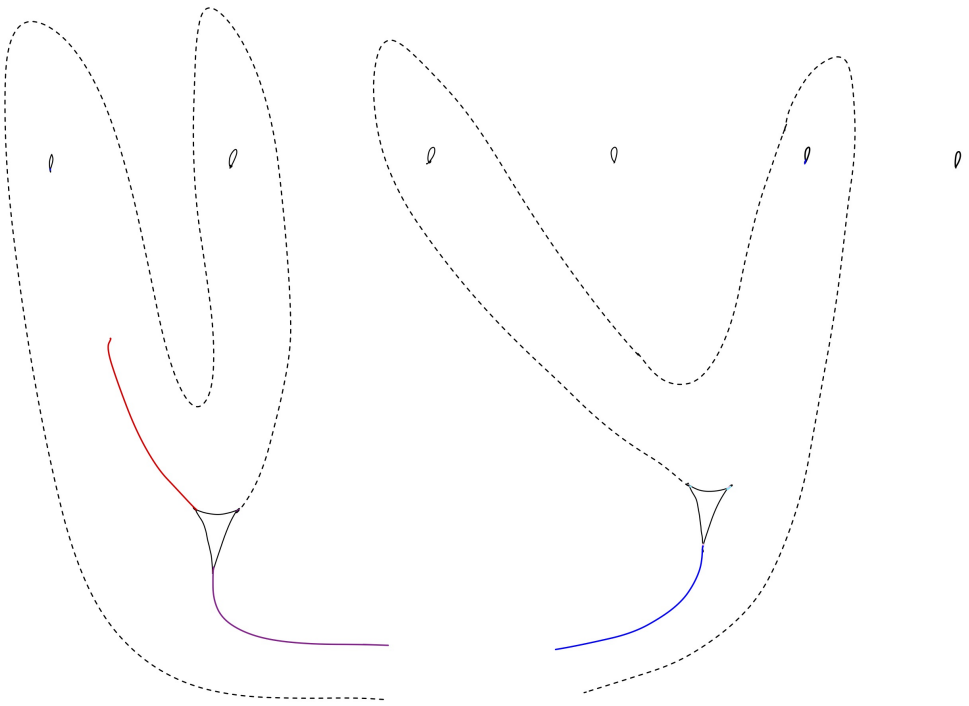


Figure I.83: WGA1

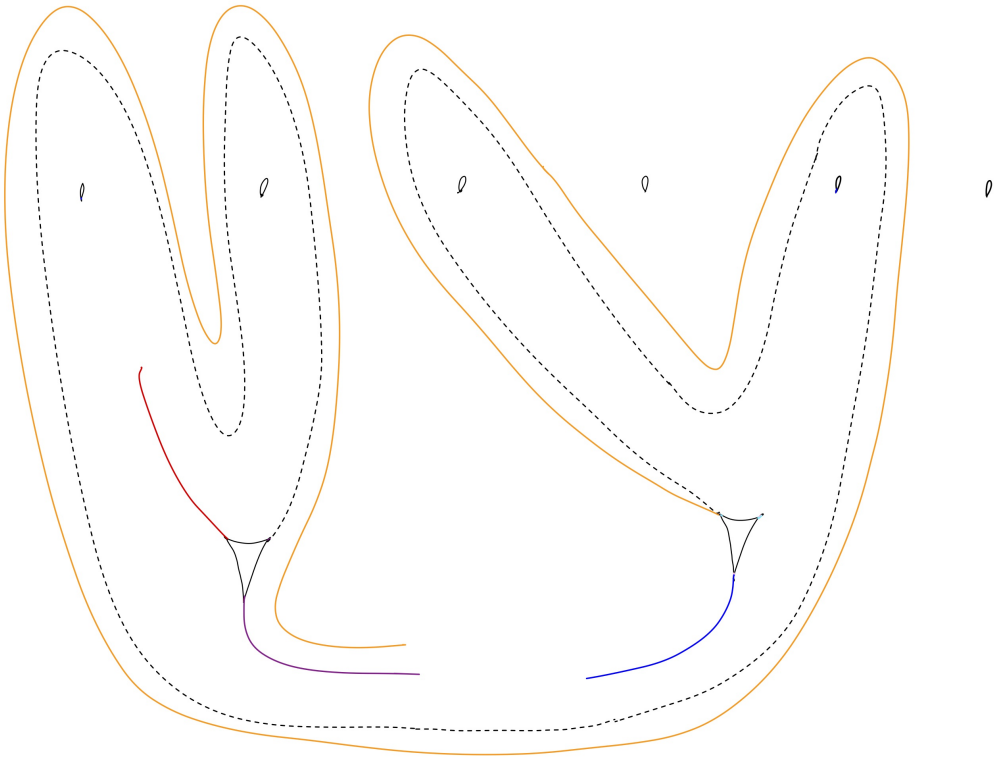


Figure I.84: WGA2

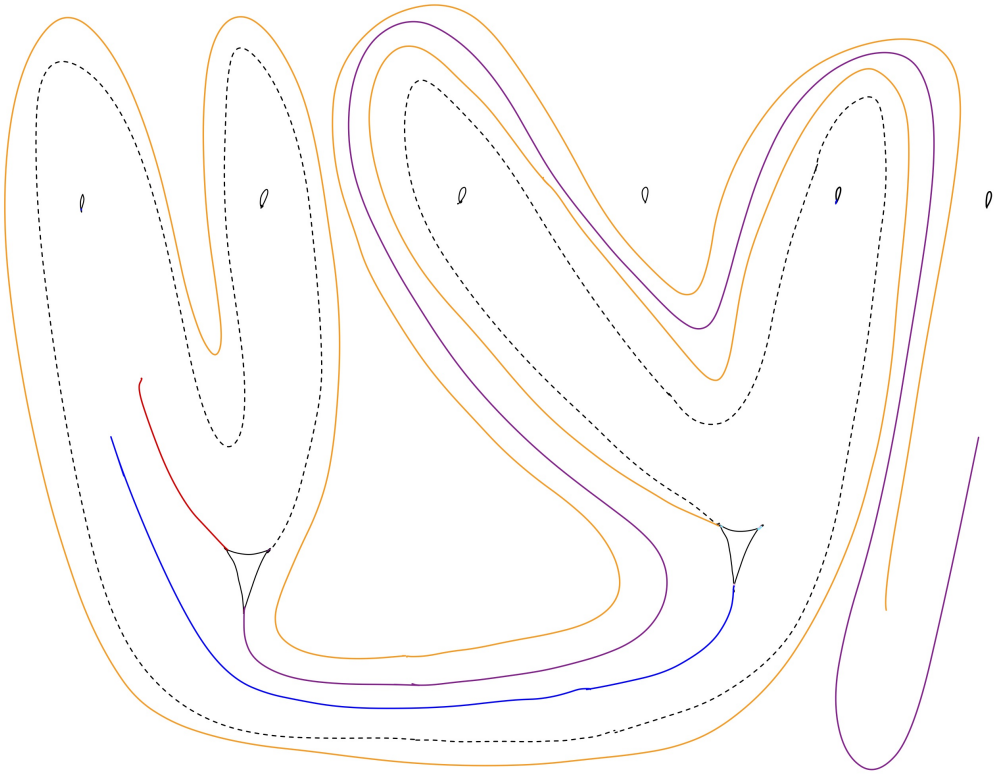


Figure I.85: WGA3

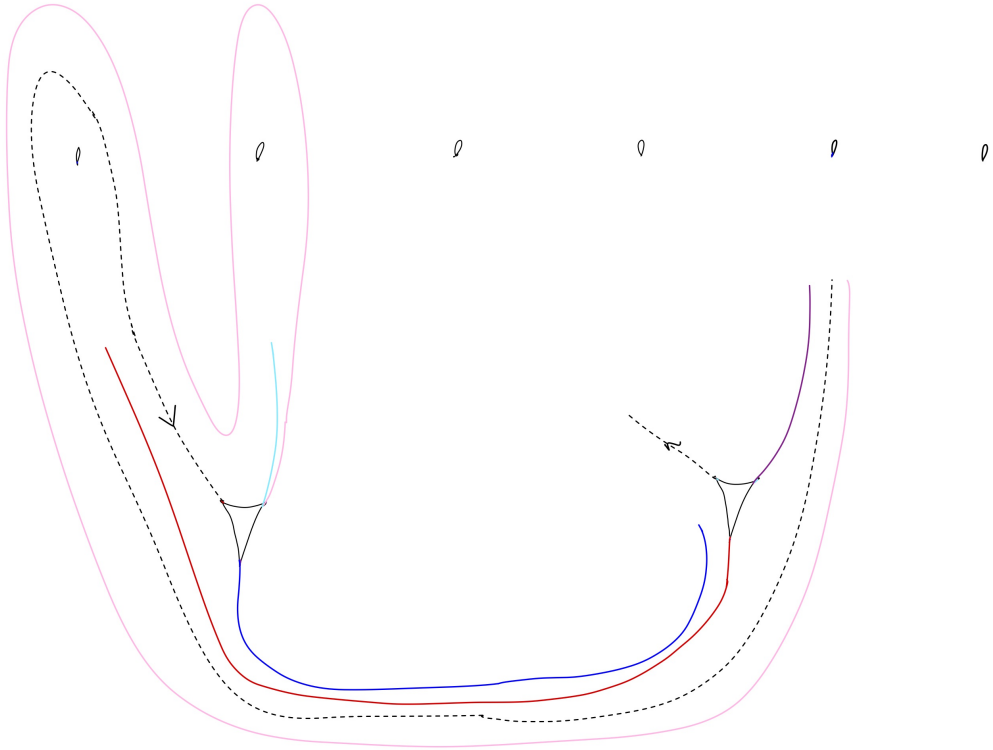


Figure I.86: GBR1

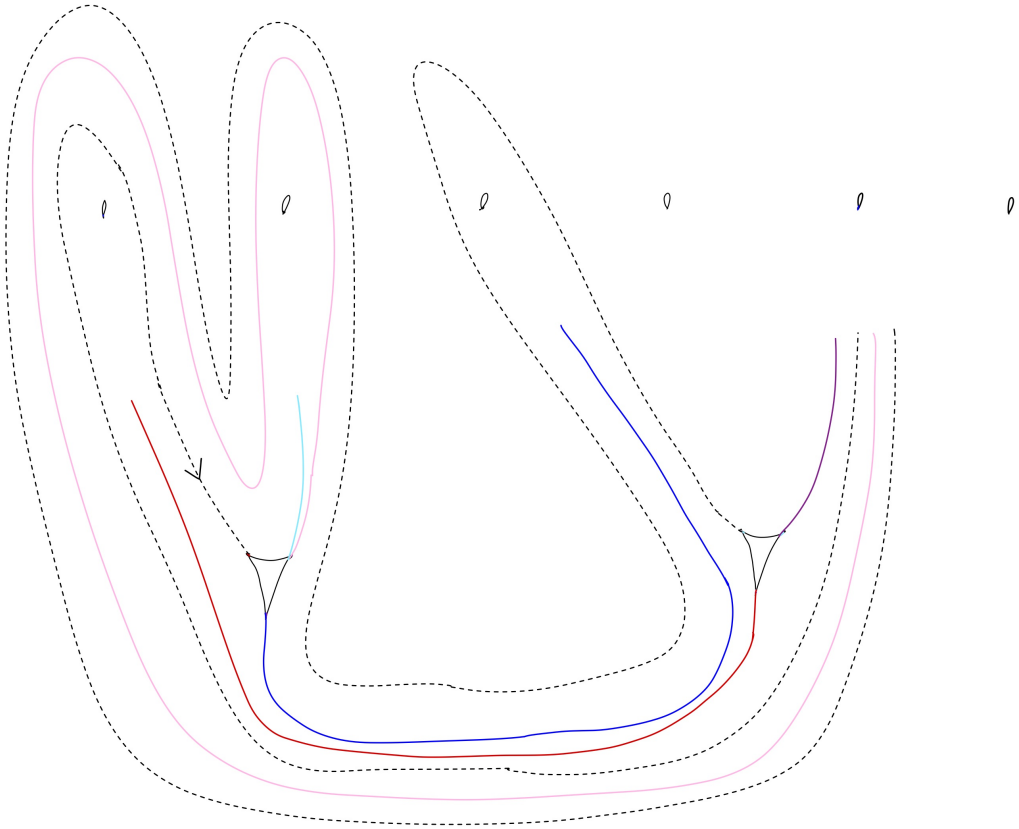


Figure I.87: GBR2

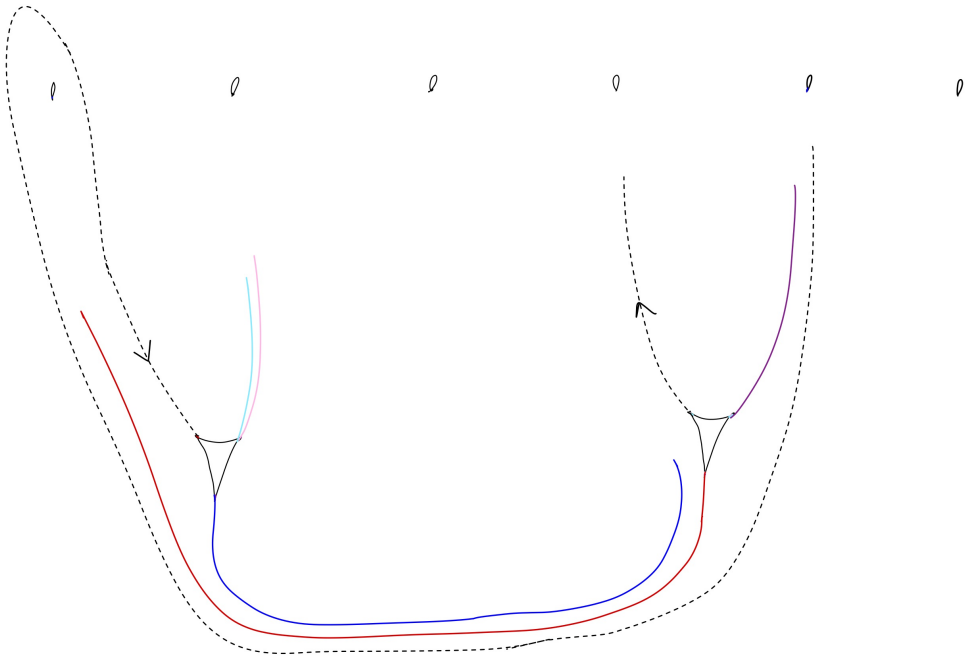


Figure I.88: GBR3

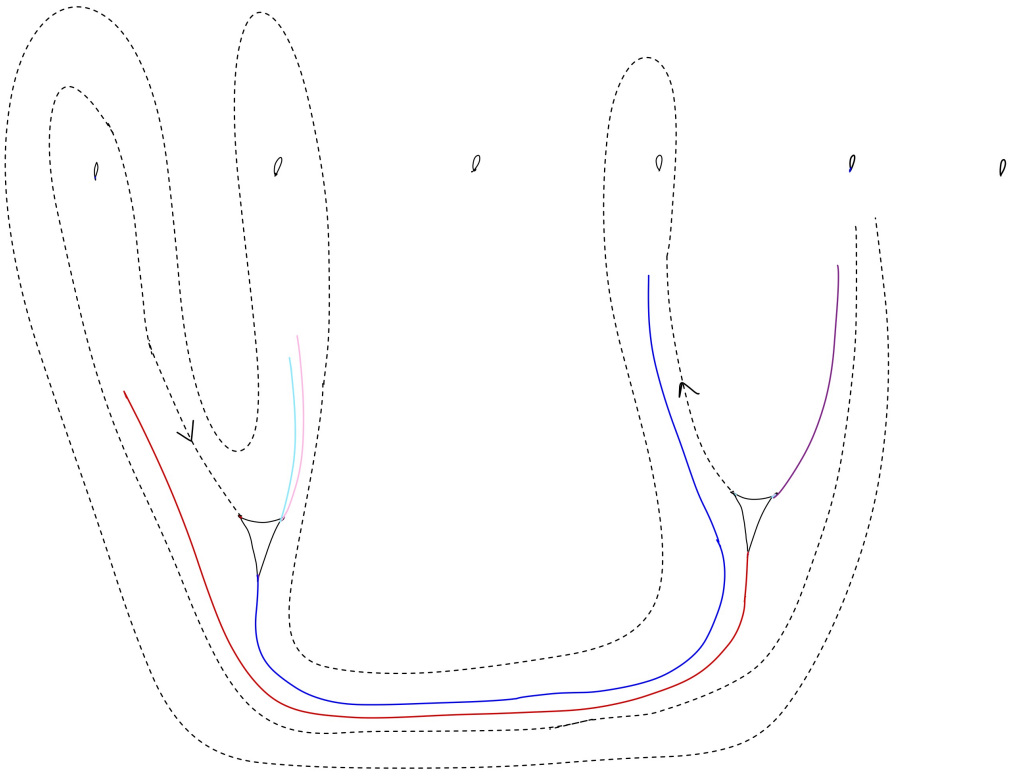


Figure I.89: GBR4

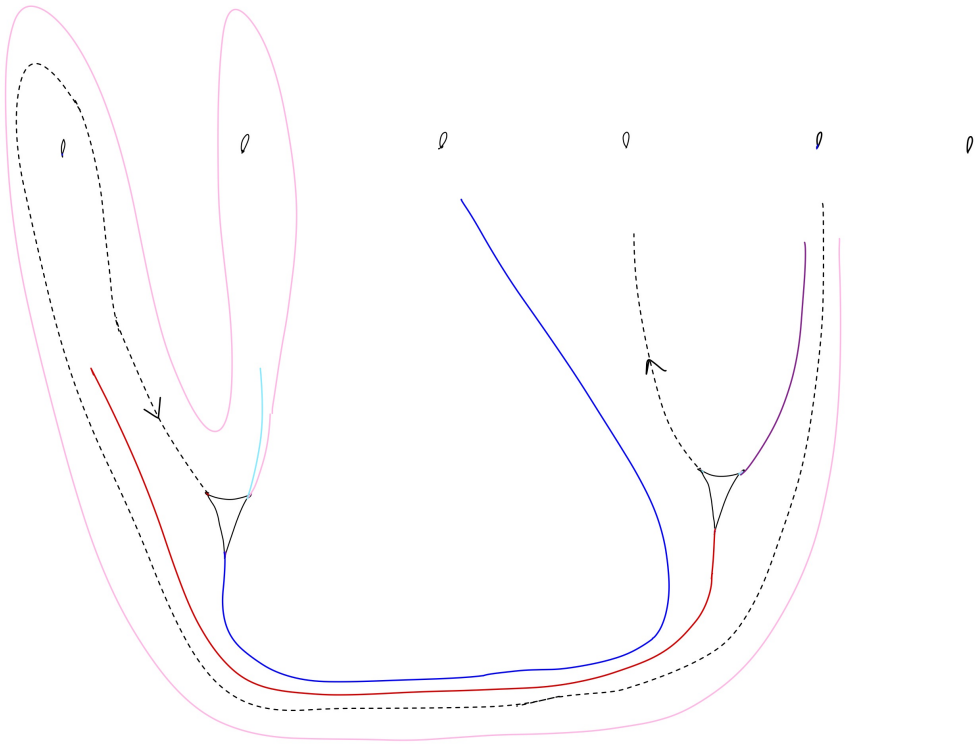


Figure I.90: GBR5

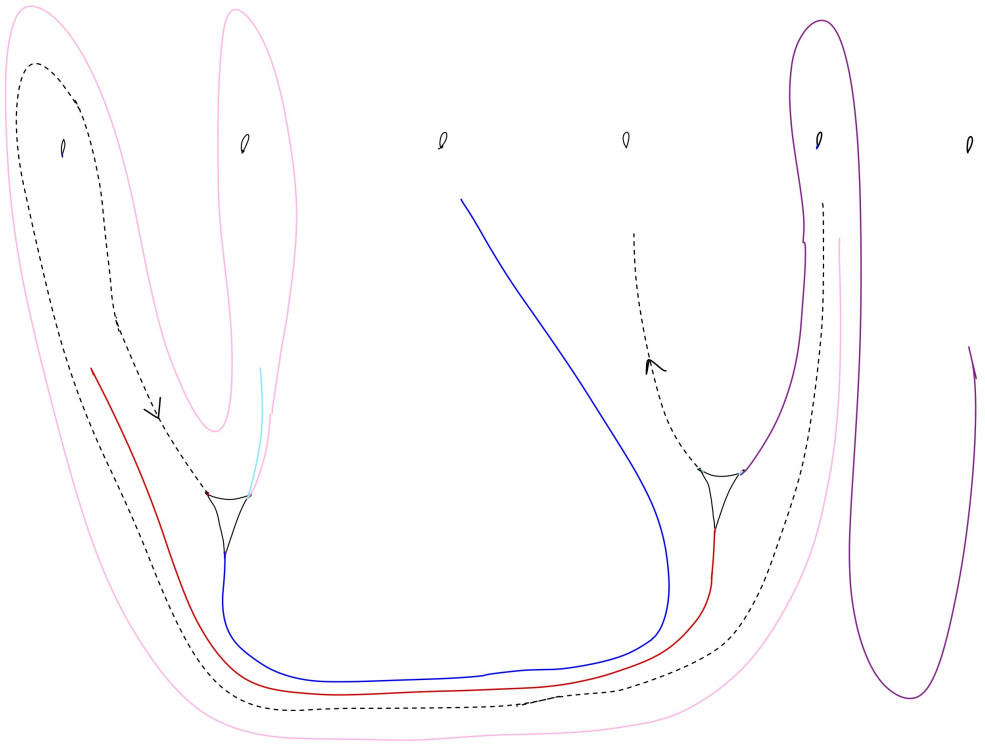


Figure I.91: GBR6

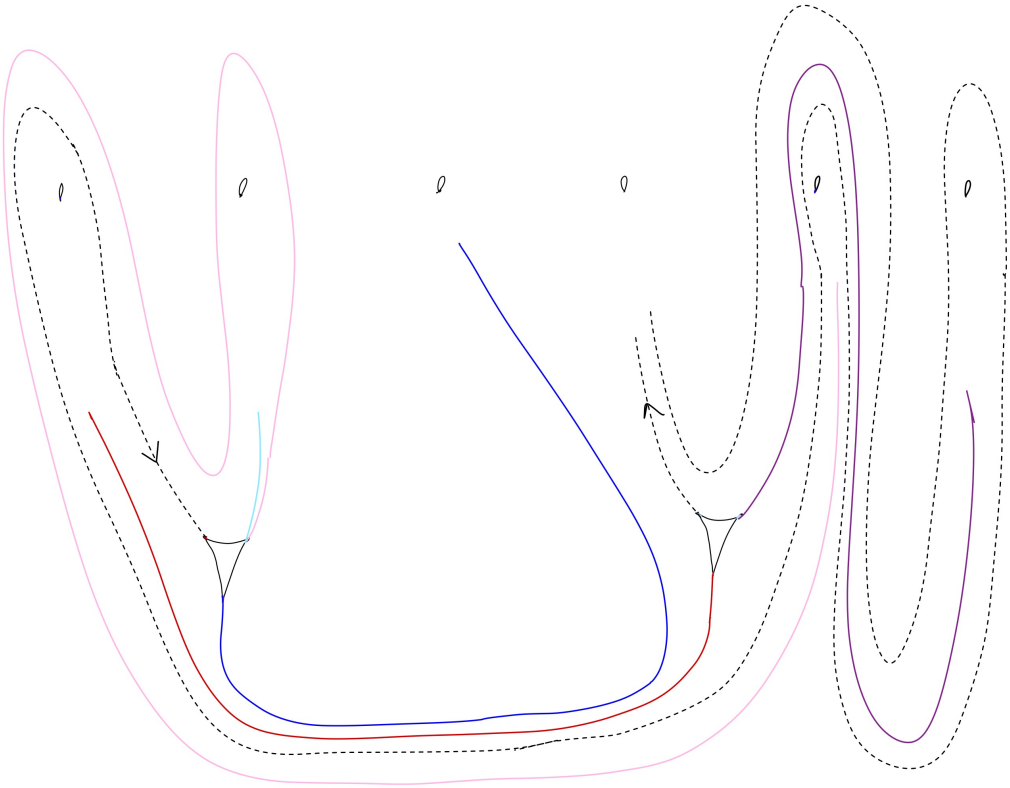


Figure I.92: GBR7

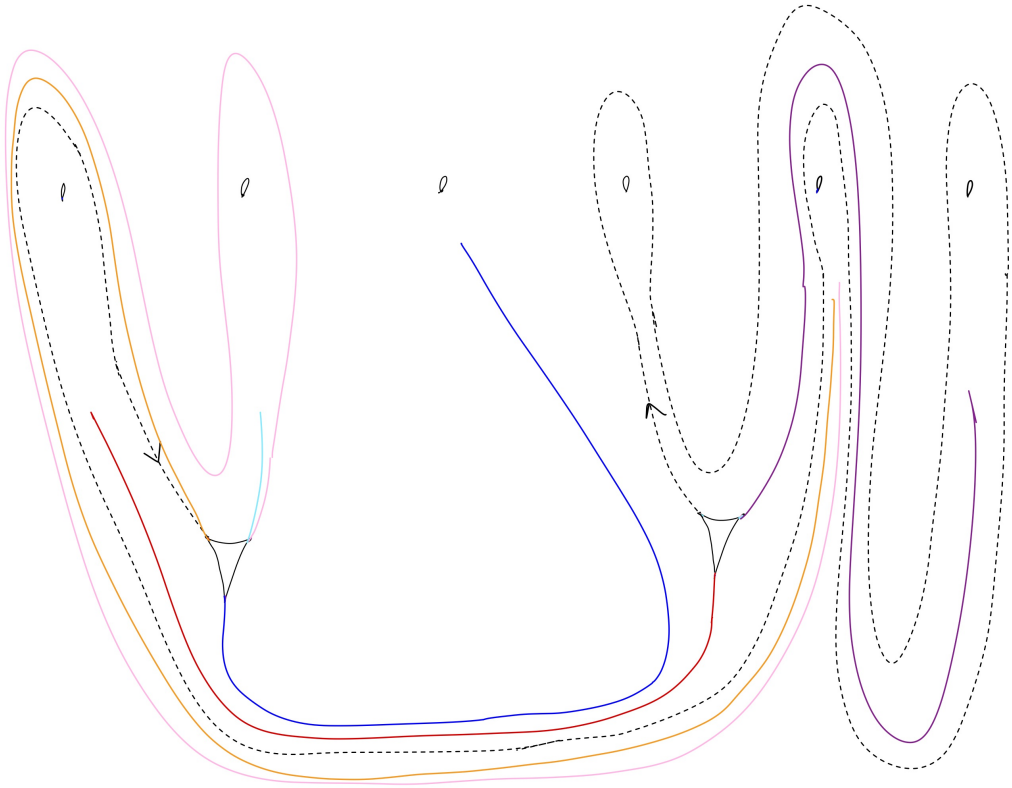


Figure I.93: GBR8

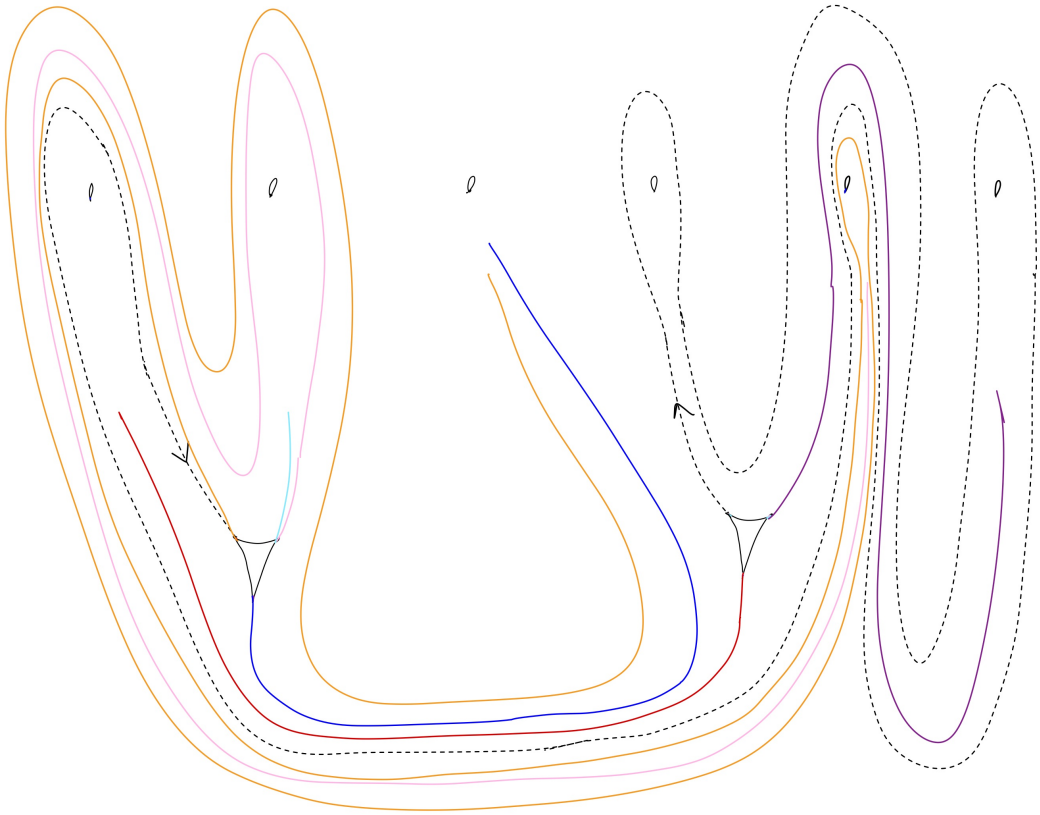


Figure I.94: GBR9

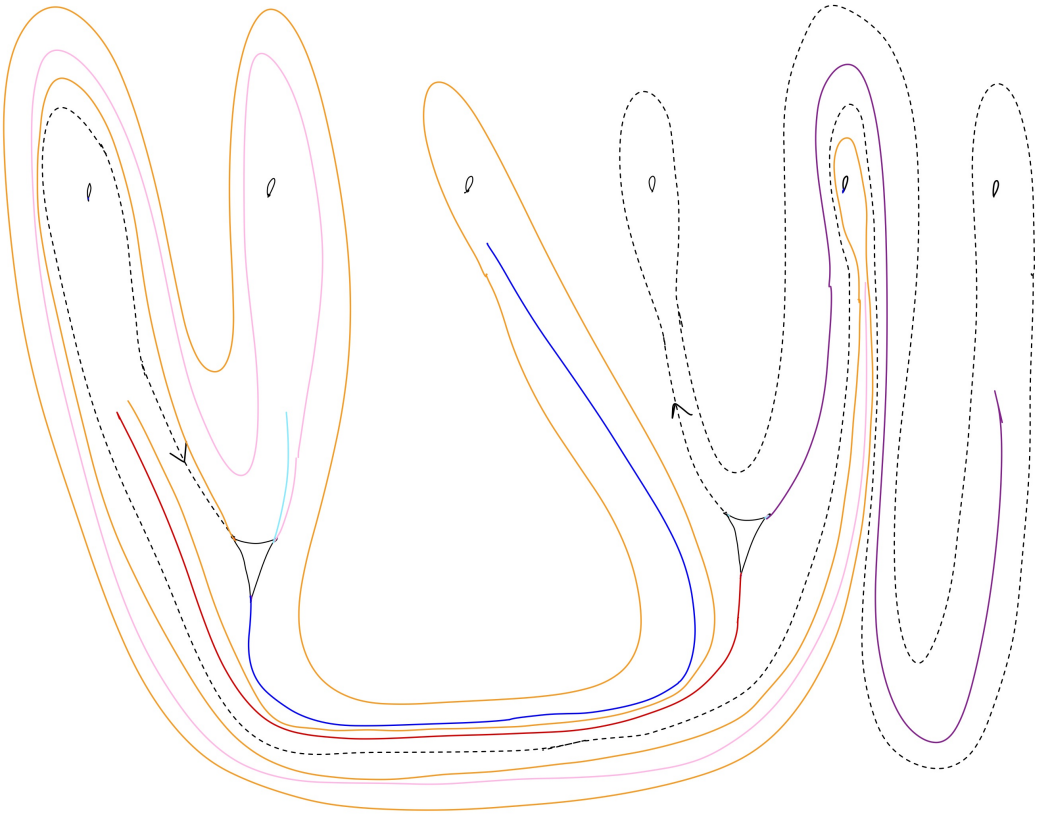


Figure I.95: GBR10

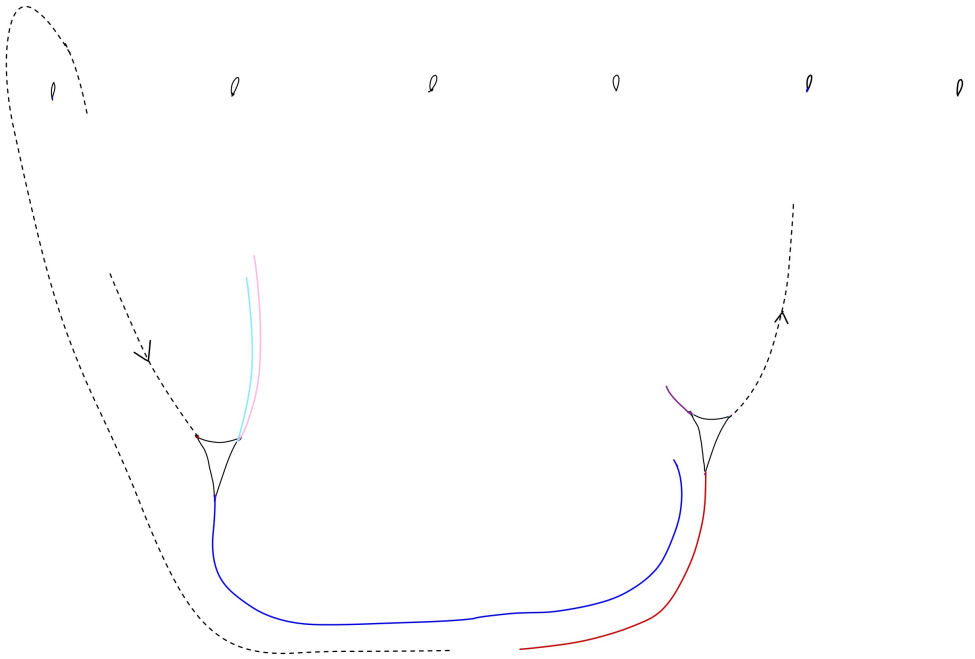


Figure I.96: GBR11

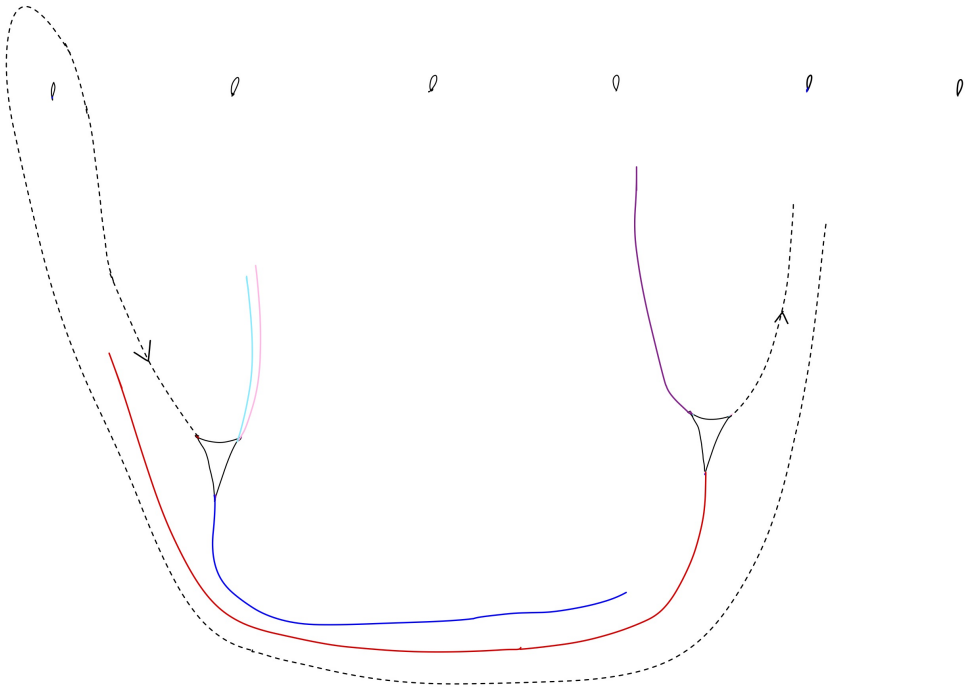


Figure I.97: GBR12

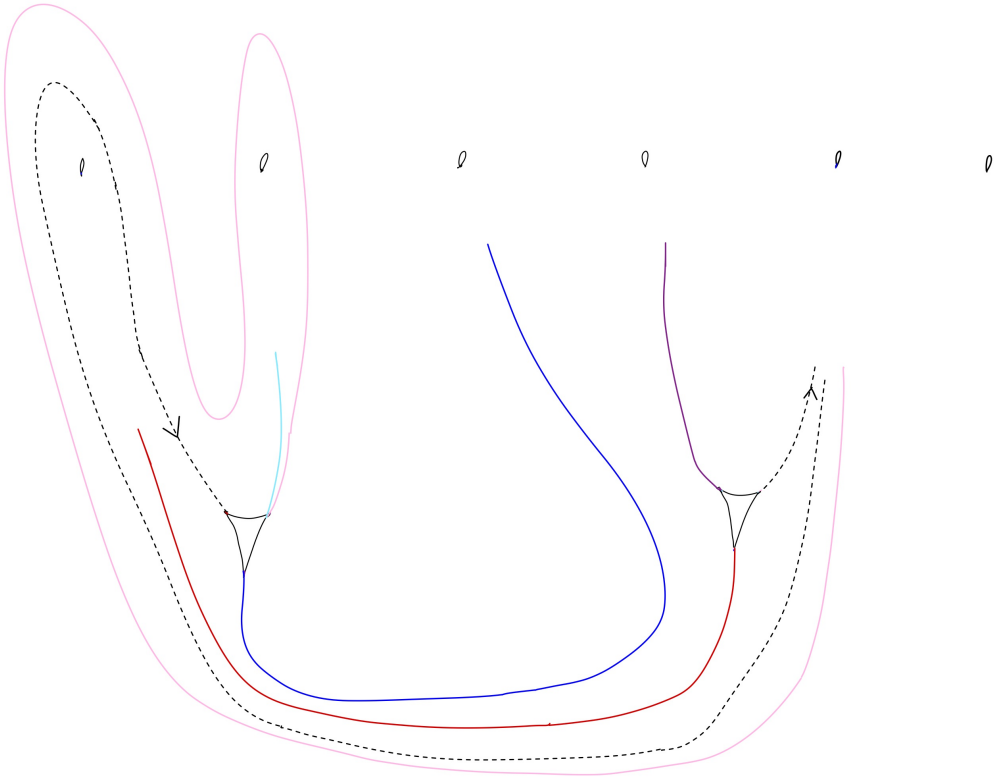


Figure I.98: GBR13

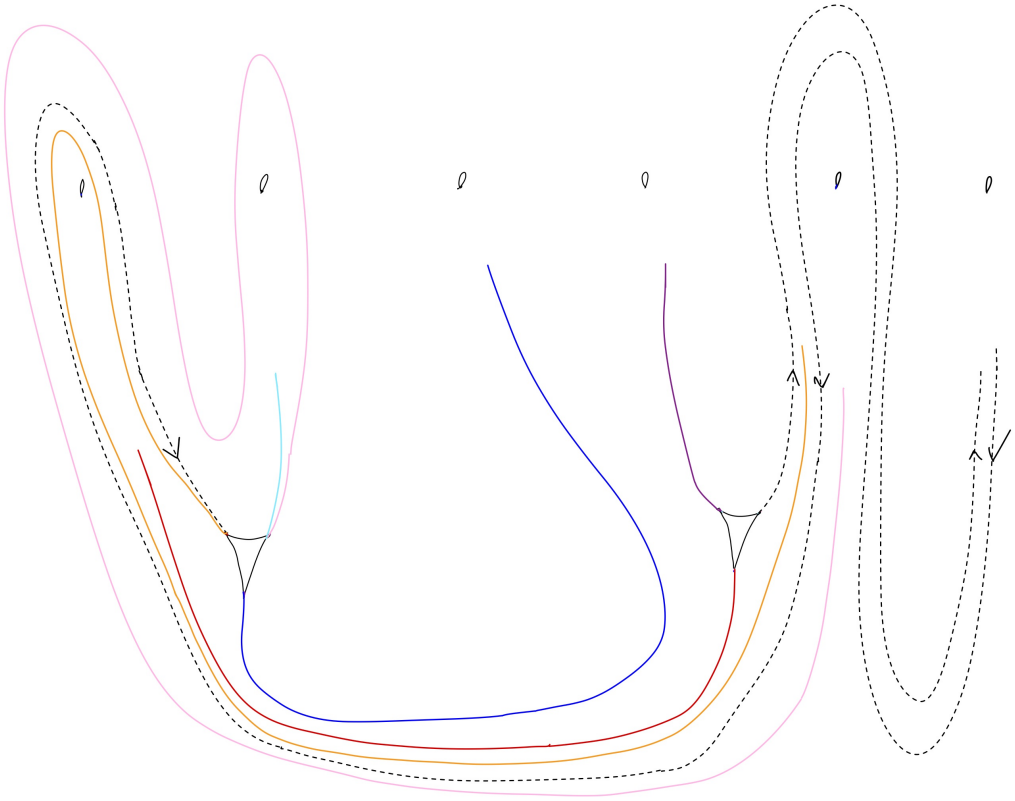


Figure I.99: GBR14

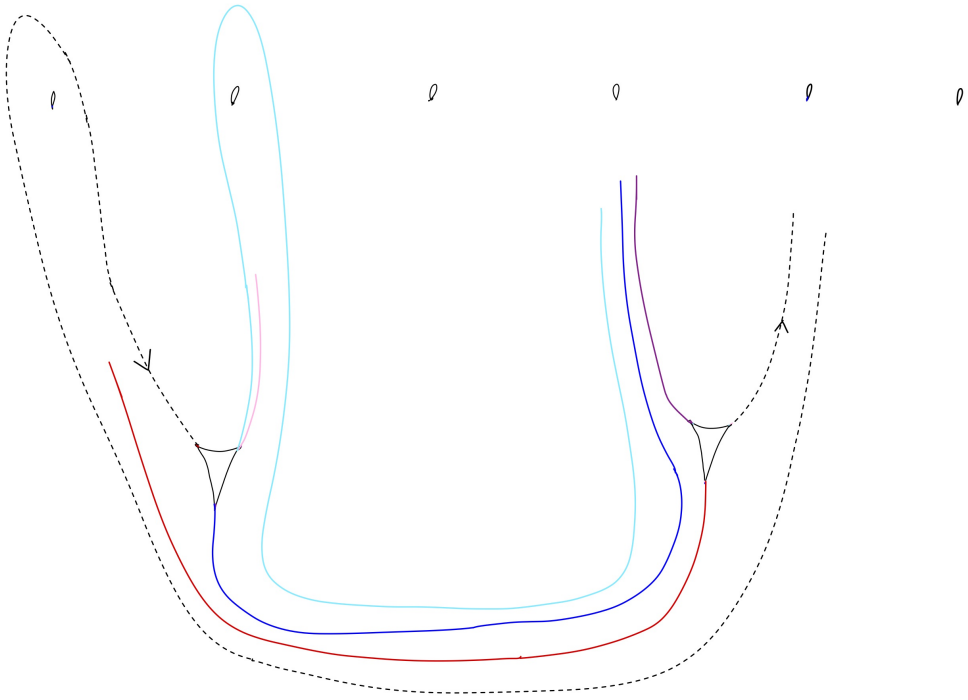


Figure I.100: GBR15

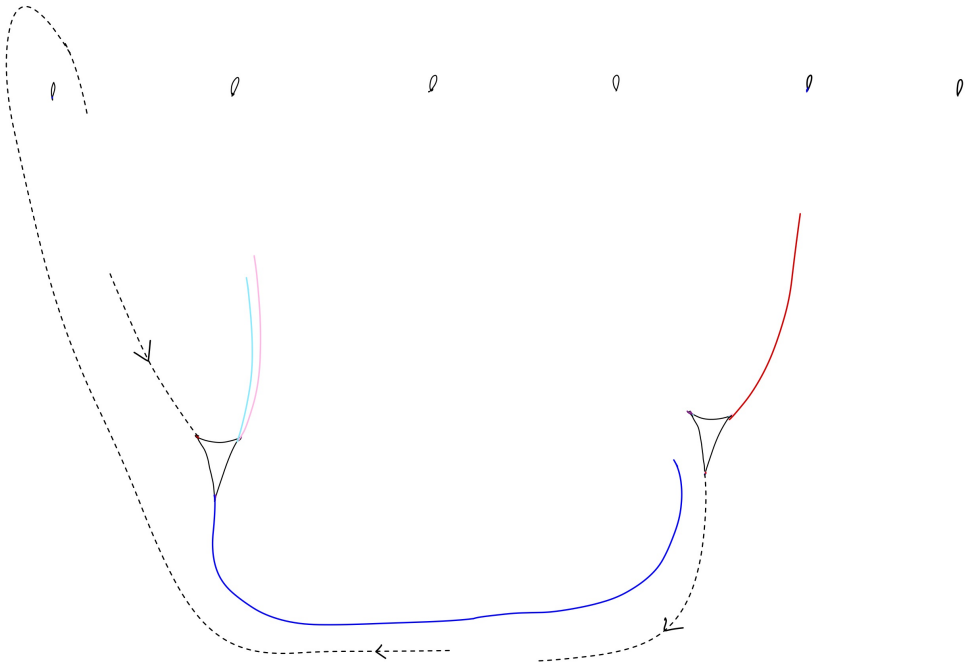


Figure I.101: GBR16

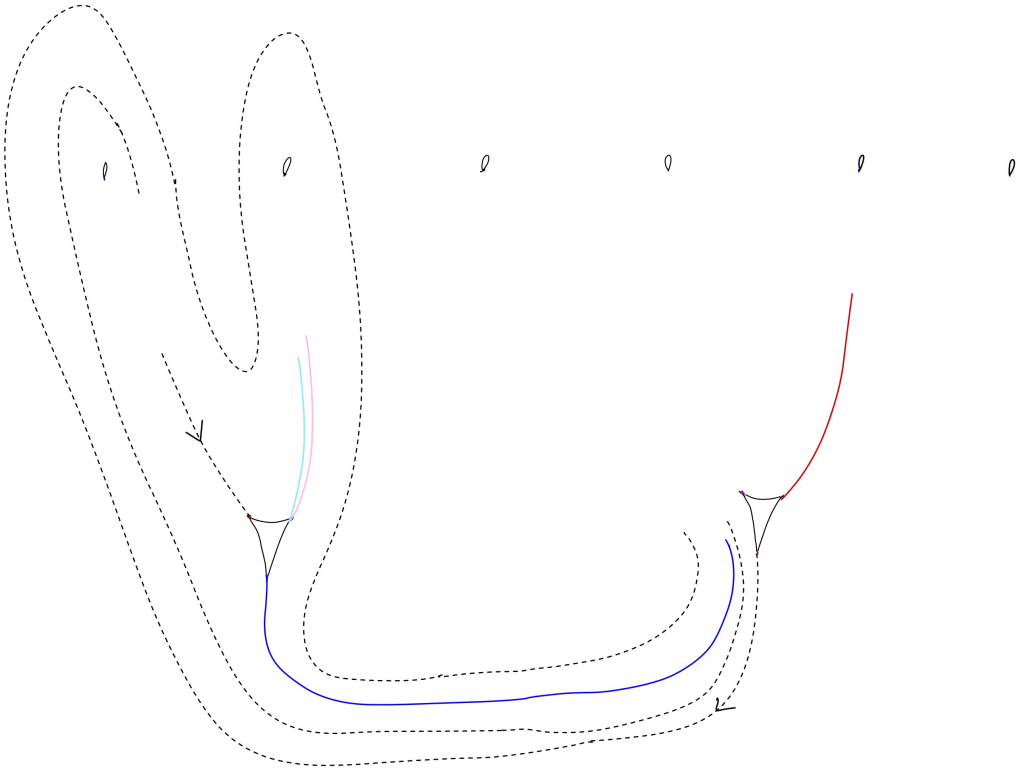


Figure I.102: GBR17

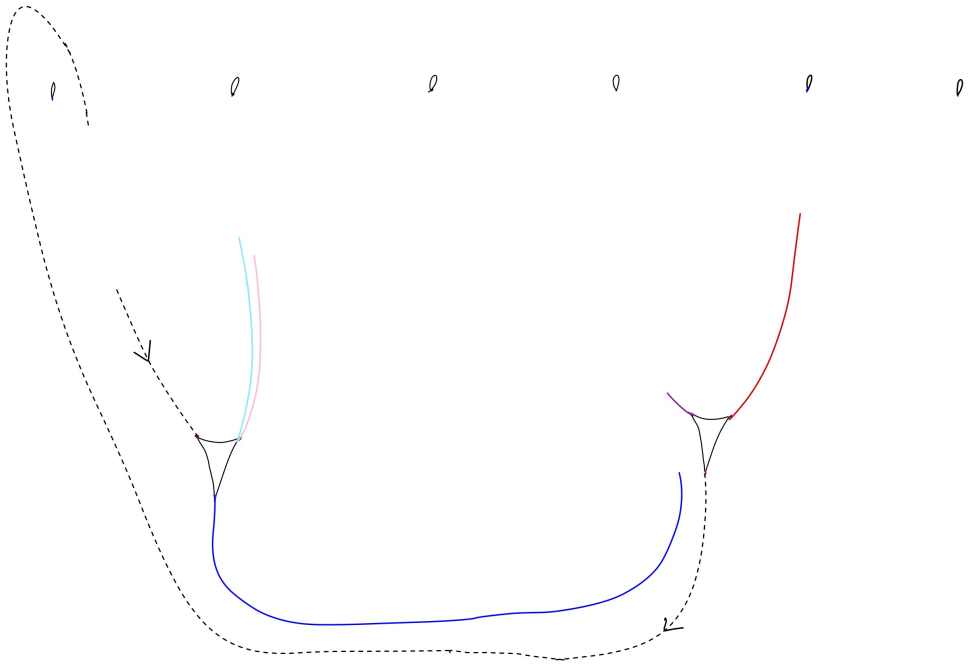


Figure I.103: GBR18

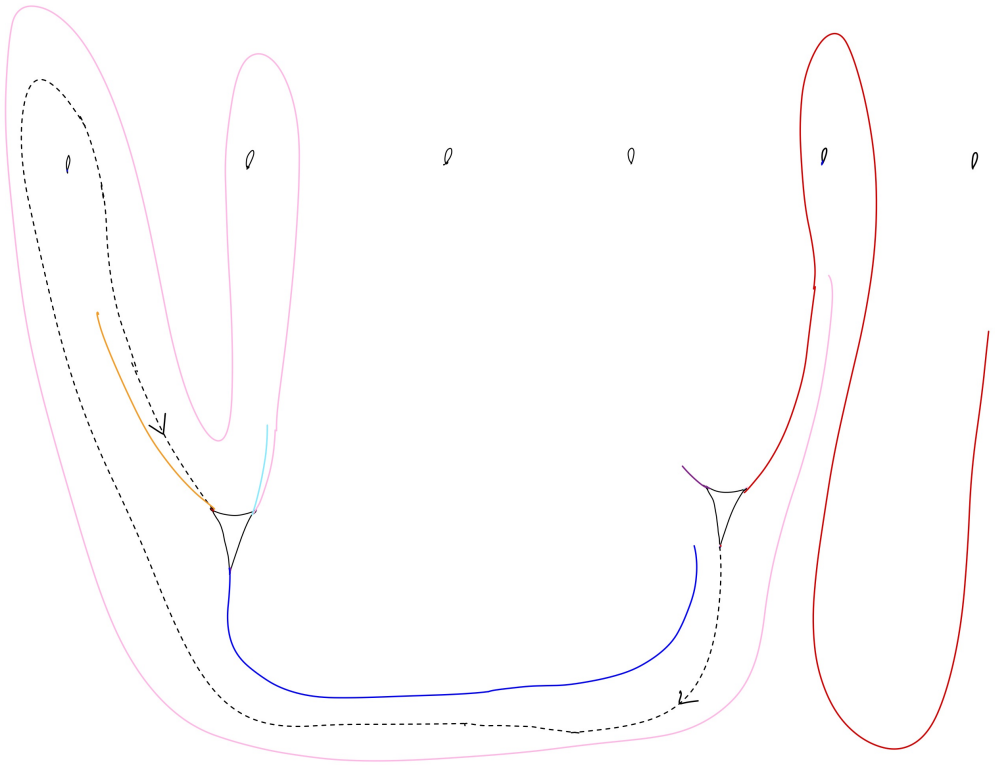


Figure I.104: Boke1

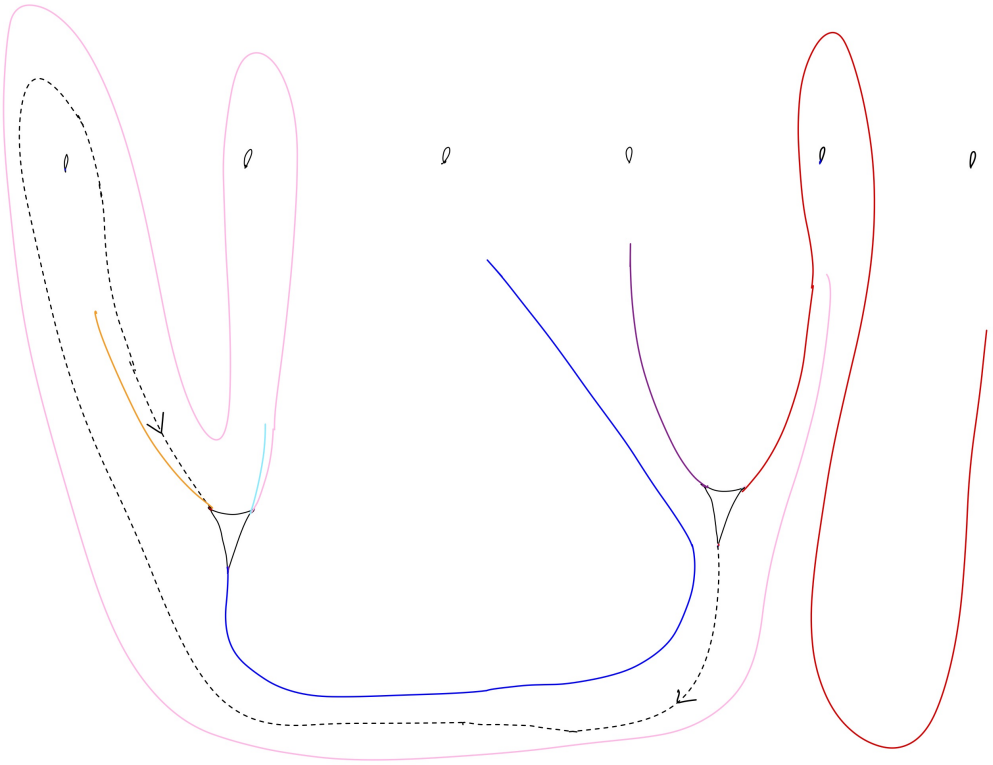


Figure I.105: Boke2

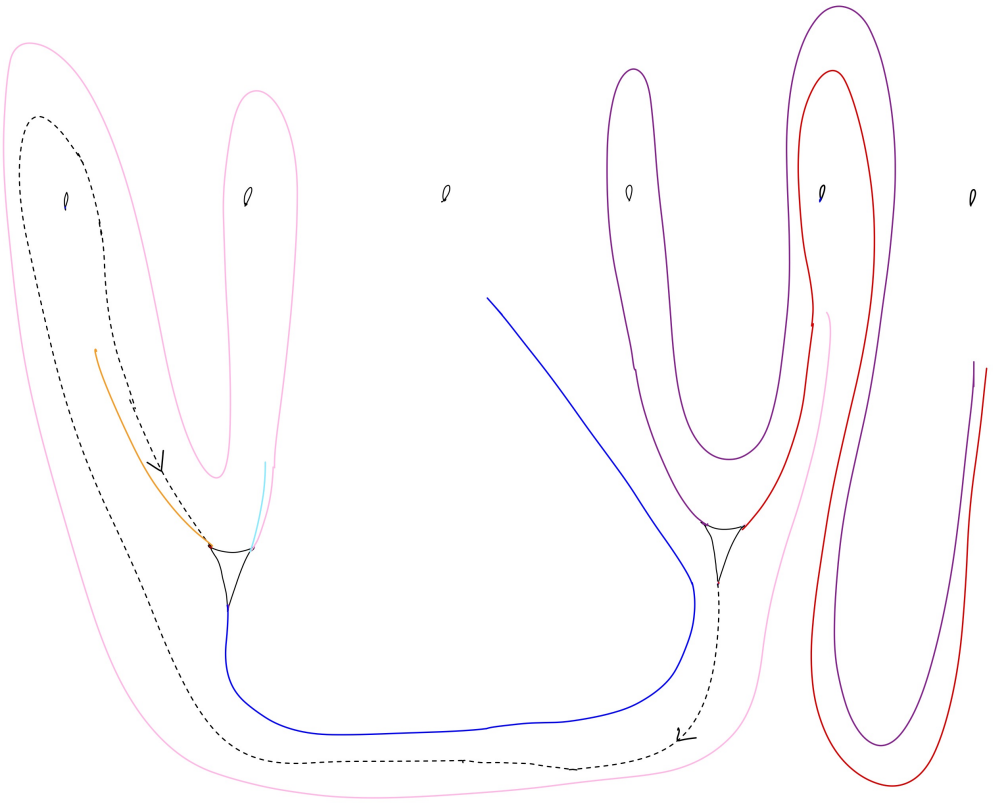


Figure I.106: Boke3

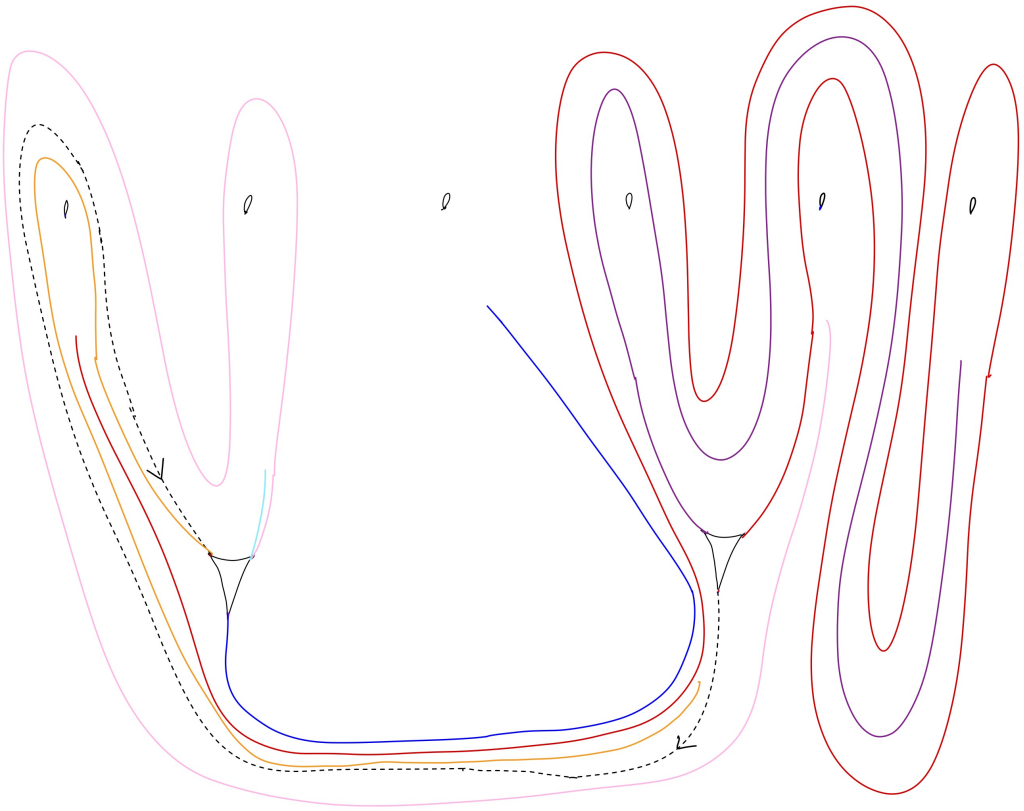


Figure I.107: Boke4

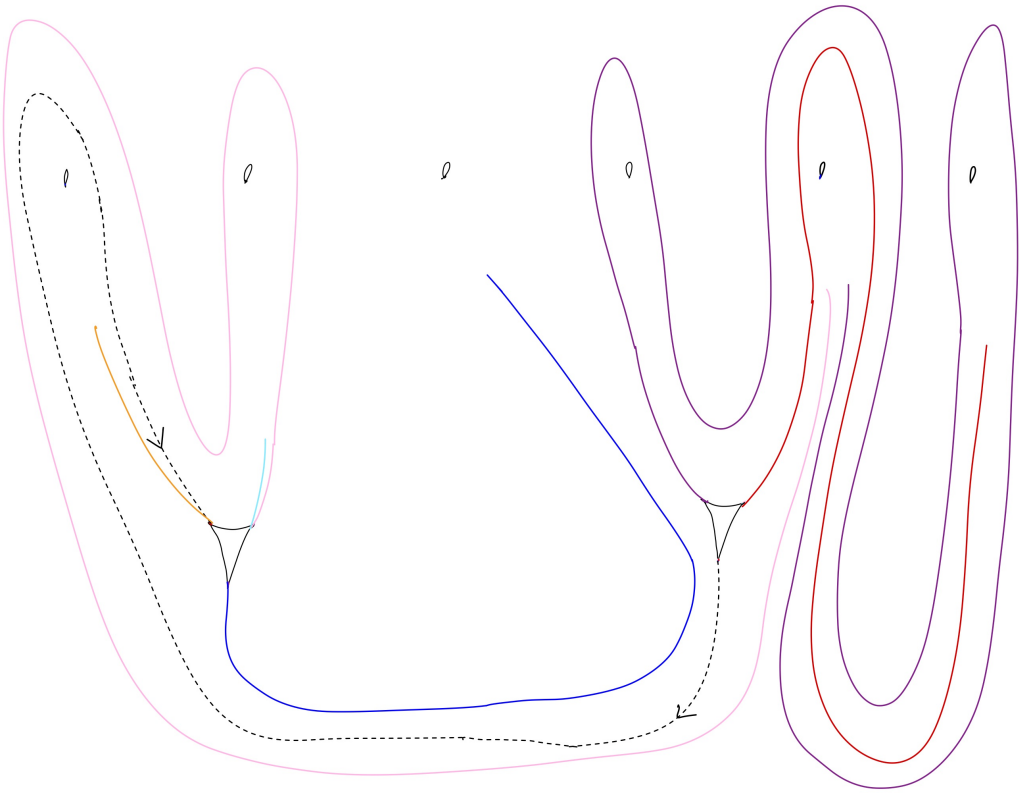


Figure I.108: Boke5

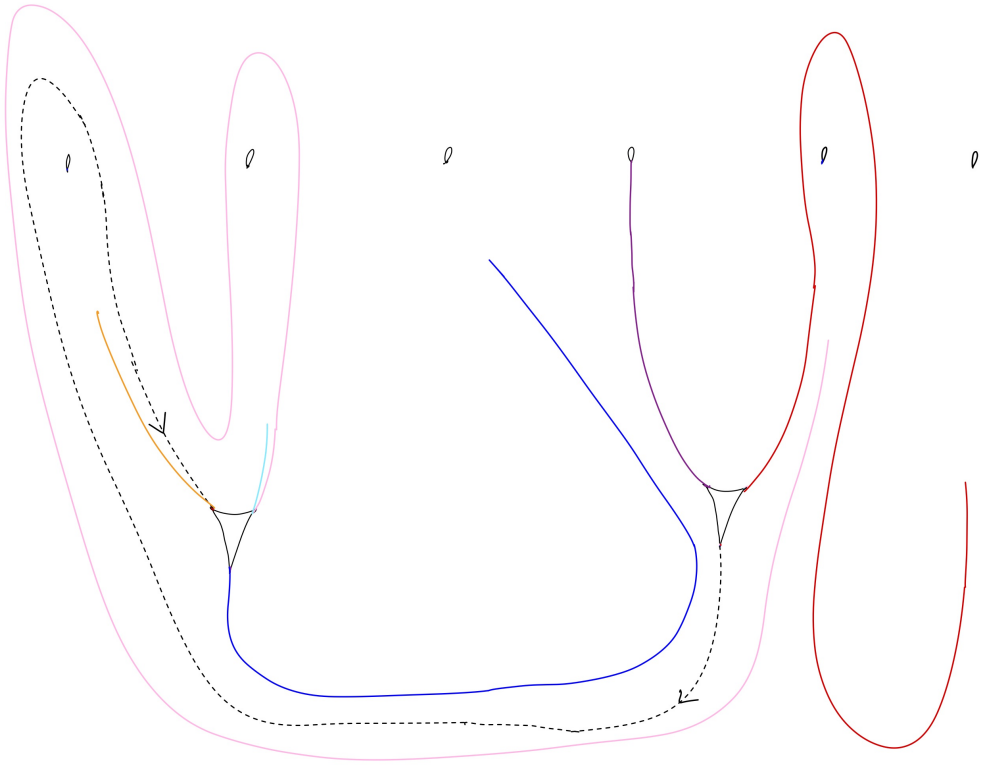


Figure I.109: Boke6

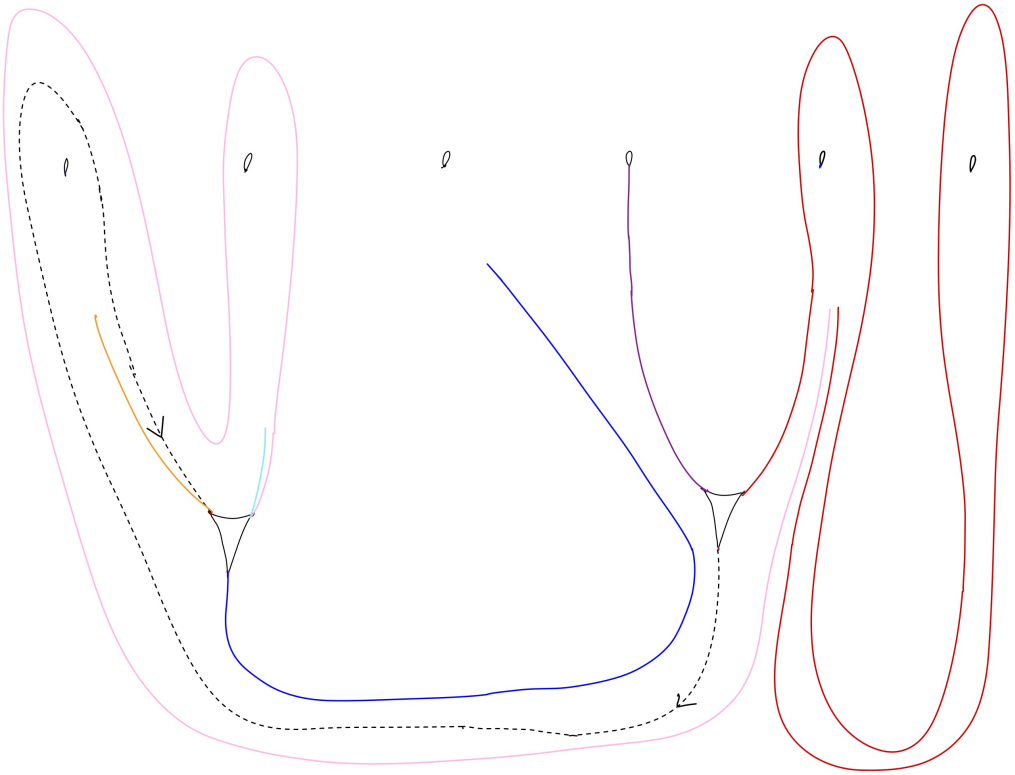


Figure I.110: Boke7

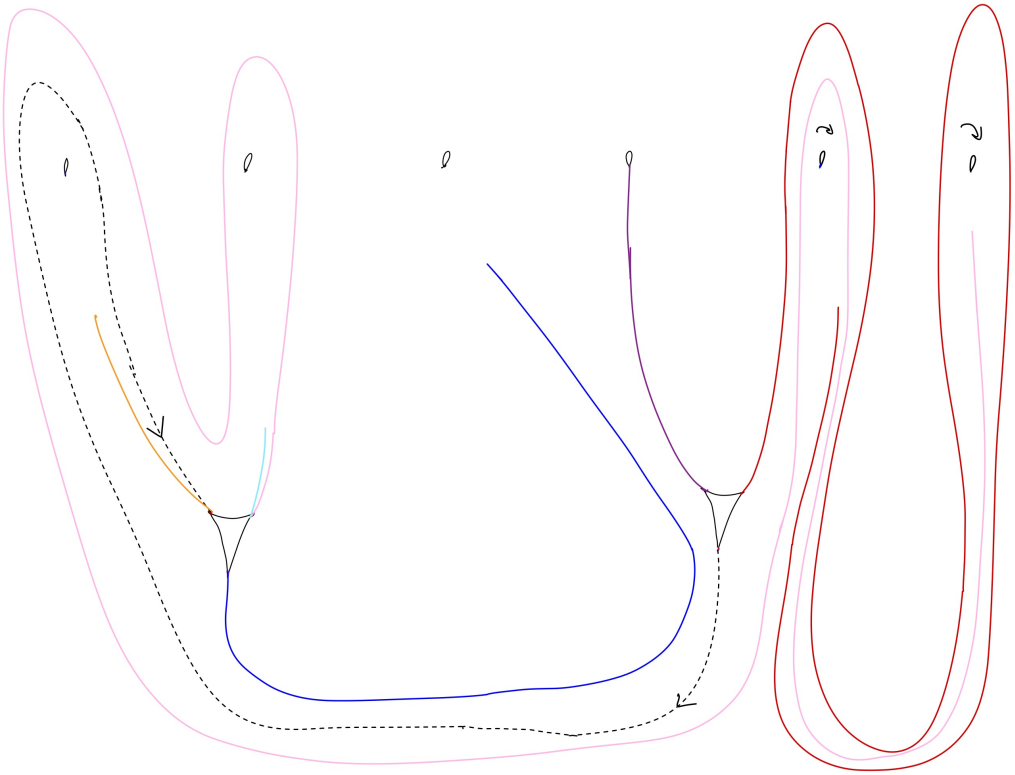


Figure I.111: Boke8

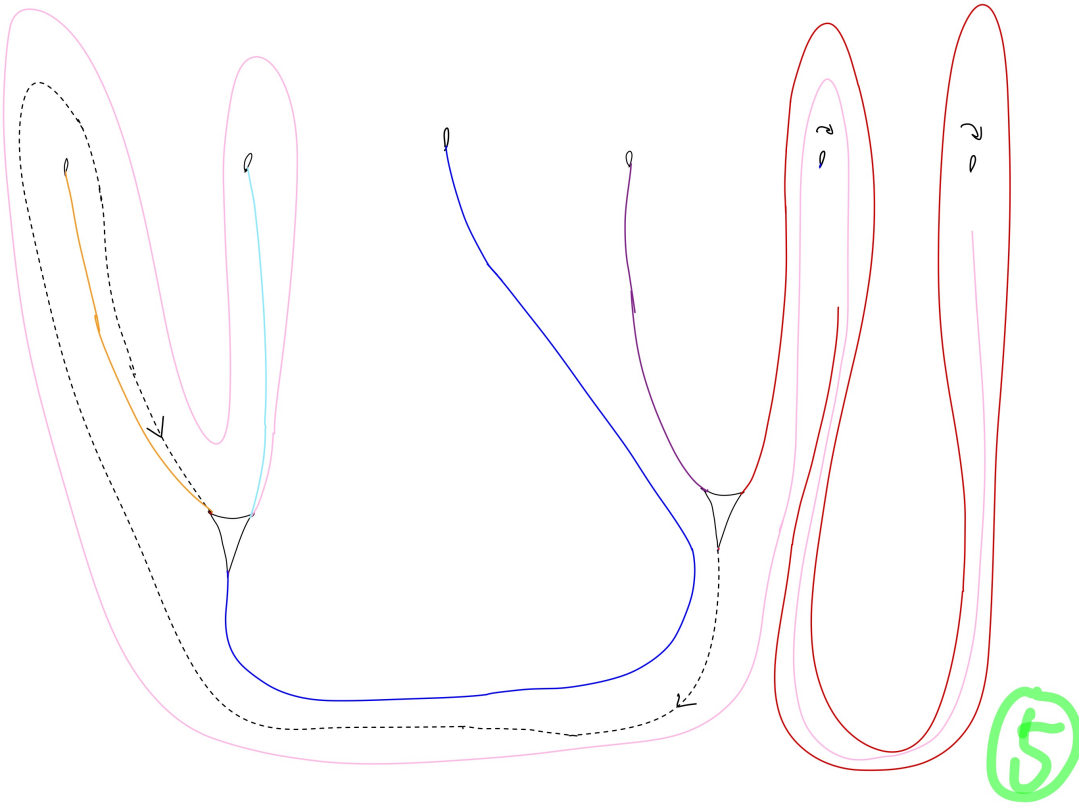


Figure I.112: Boke9

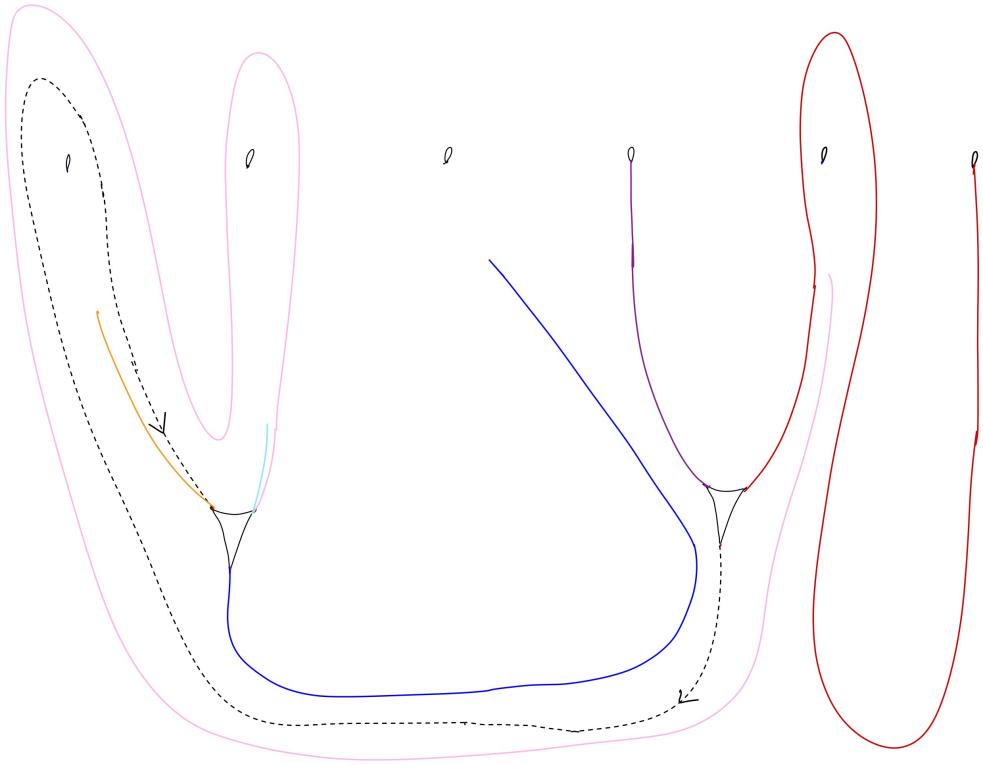


Figure I.113: Boke10

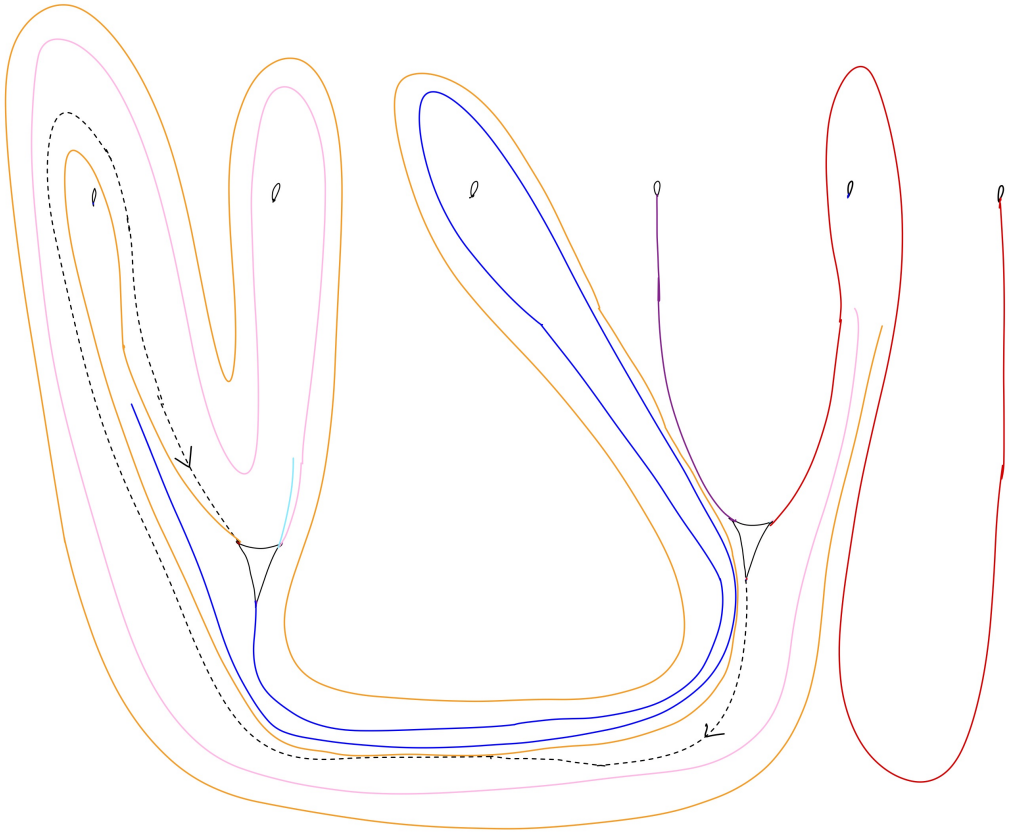


Figure I.114: Boke11

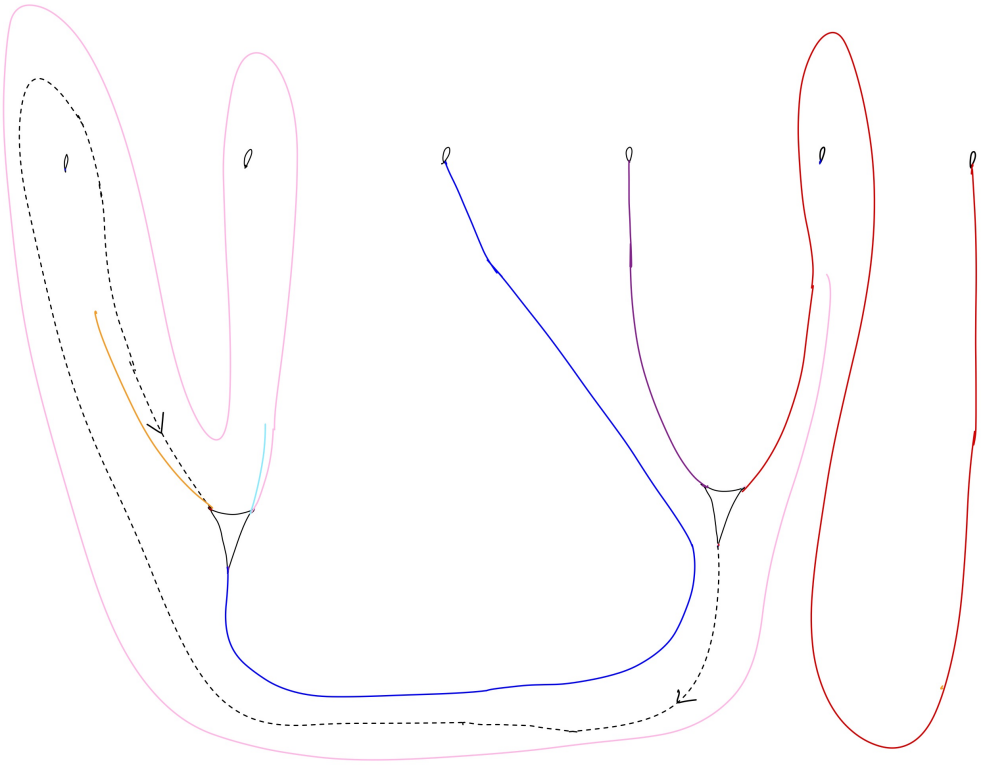


Figure I.115: Boke12

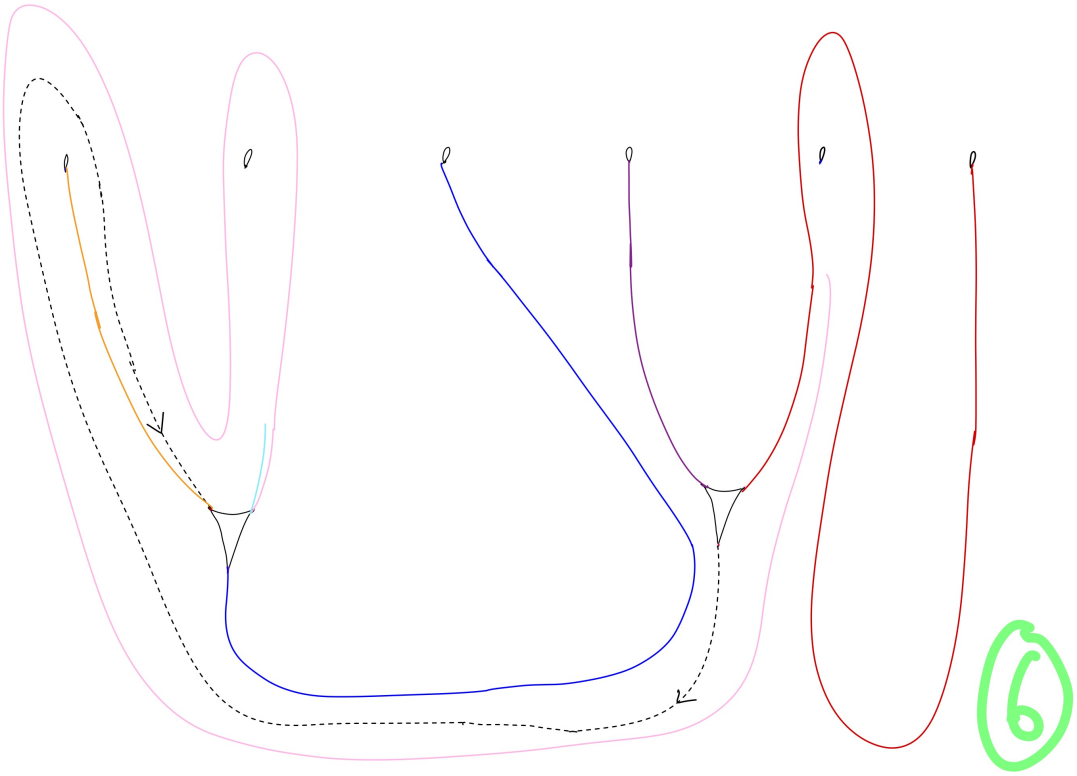


Figure I.116: Boke13

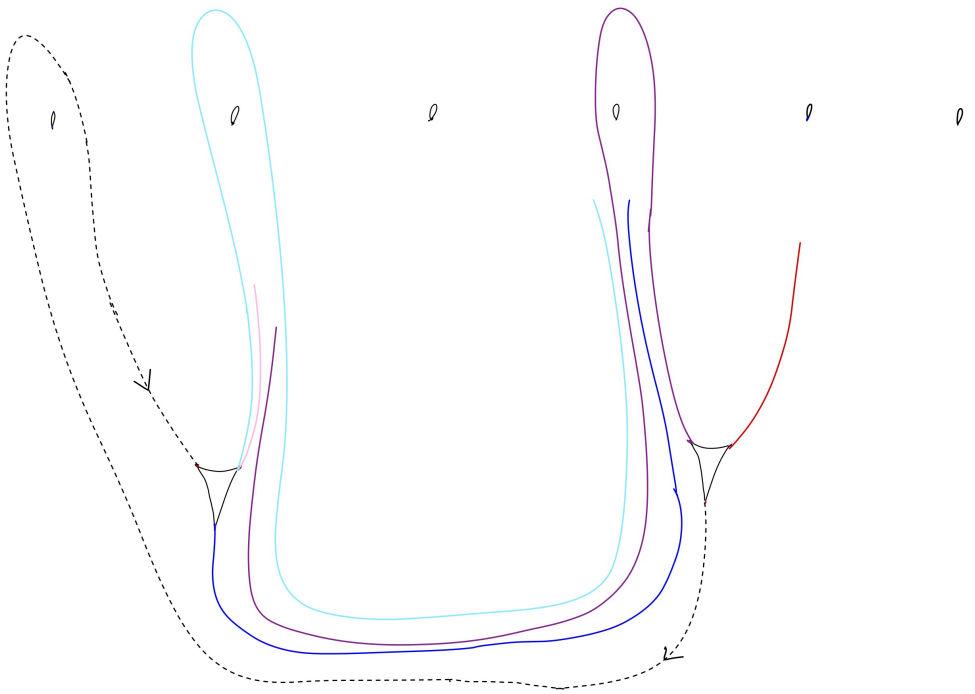


Figure I.117: Clat1

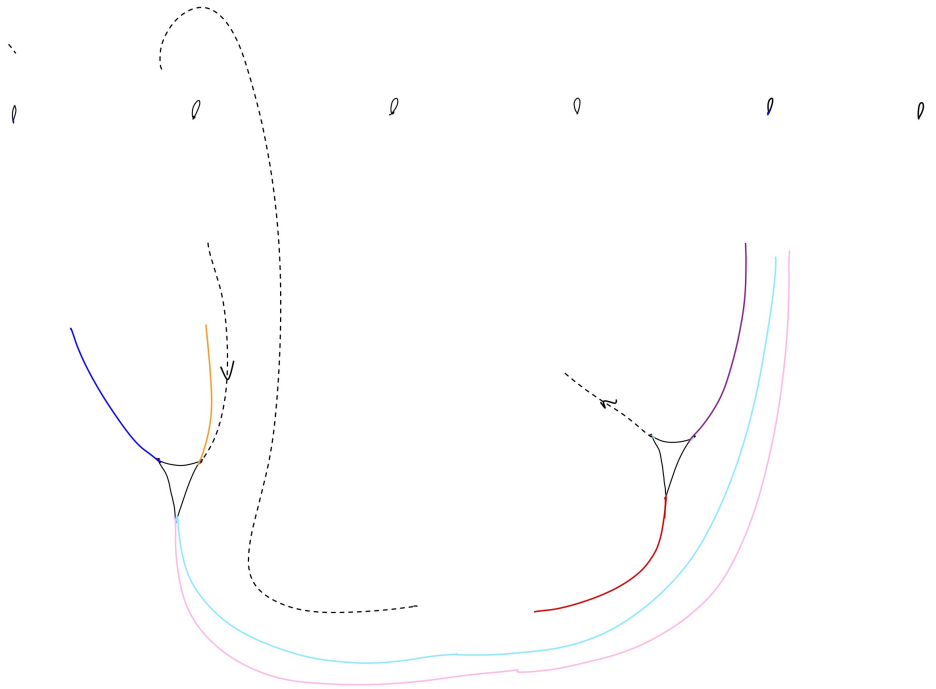


Figure I.118: MMU1

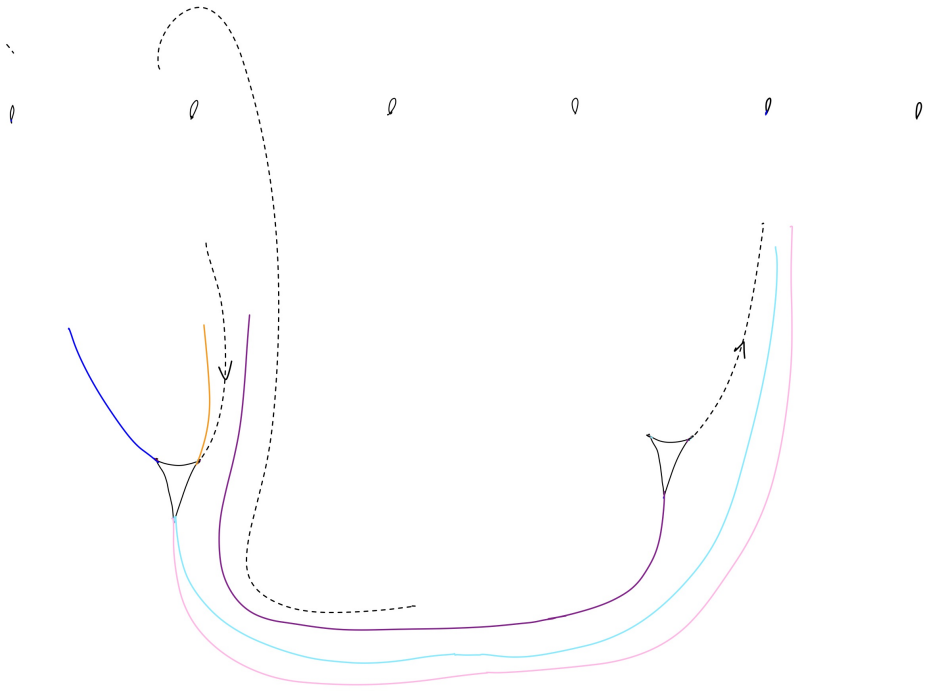


Figure I.119: MMU2

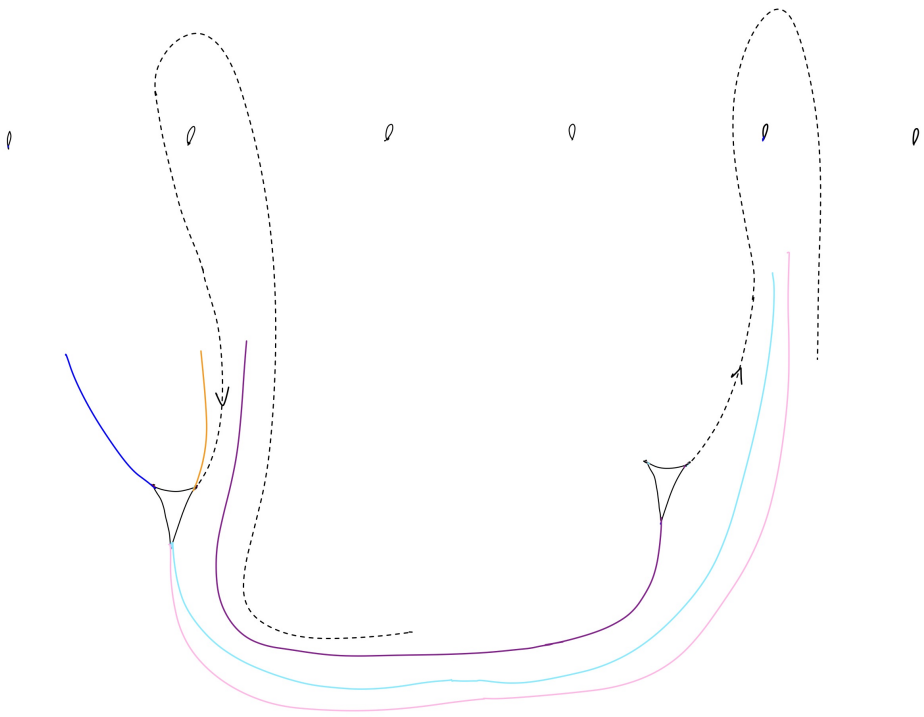


Figure I.120: MMU3

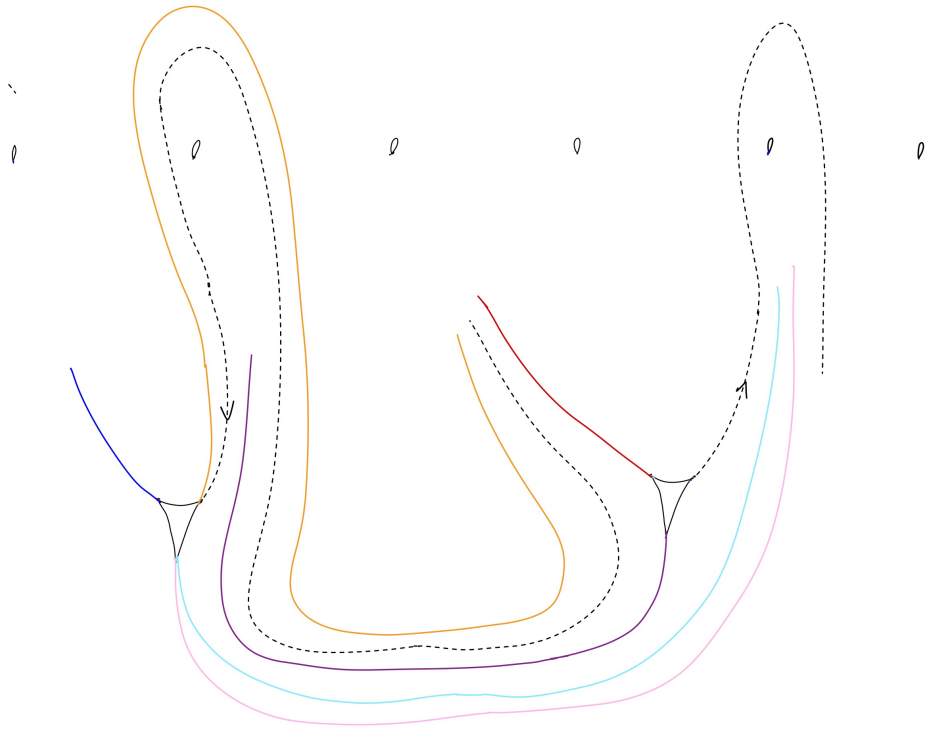


Figure I.121: MMU4

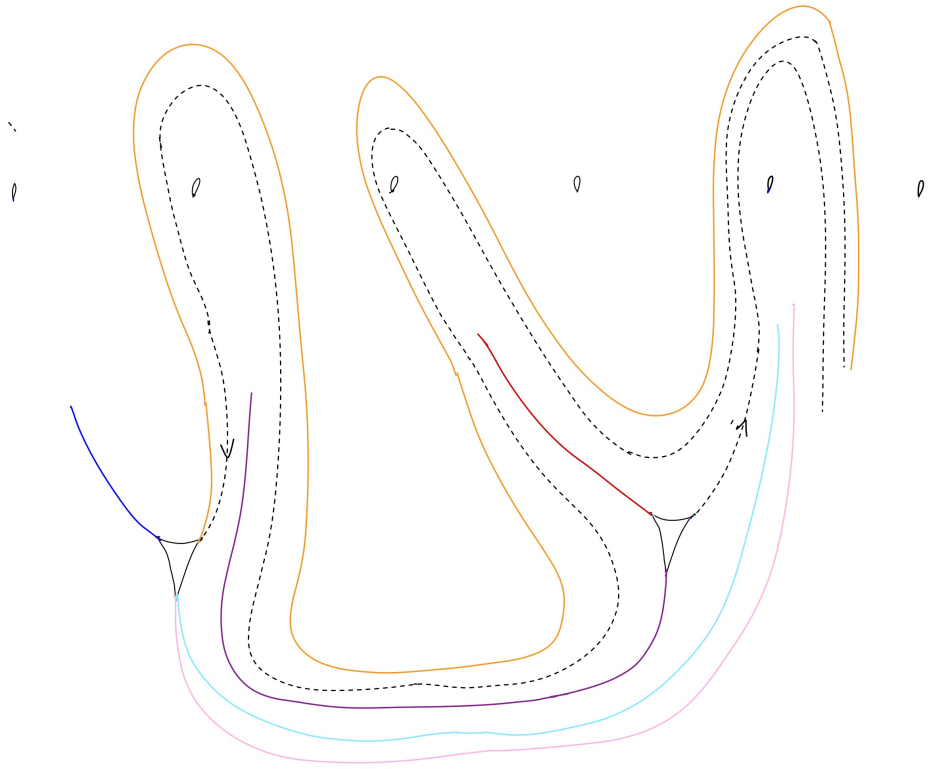


Figure I.122: MMU5

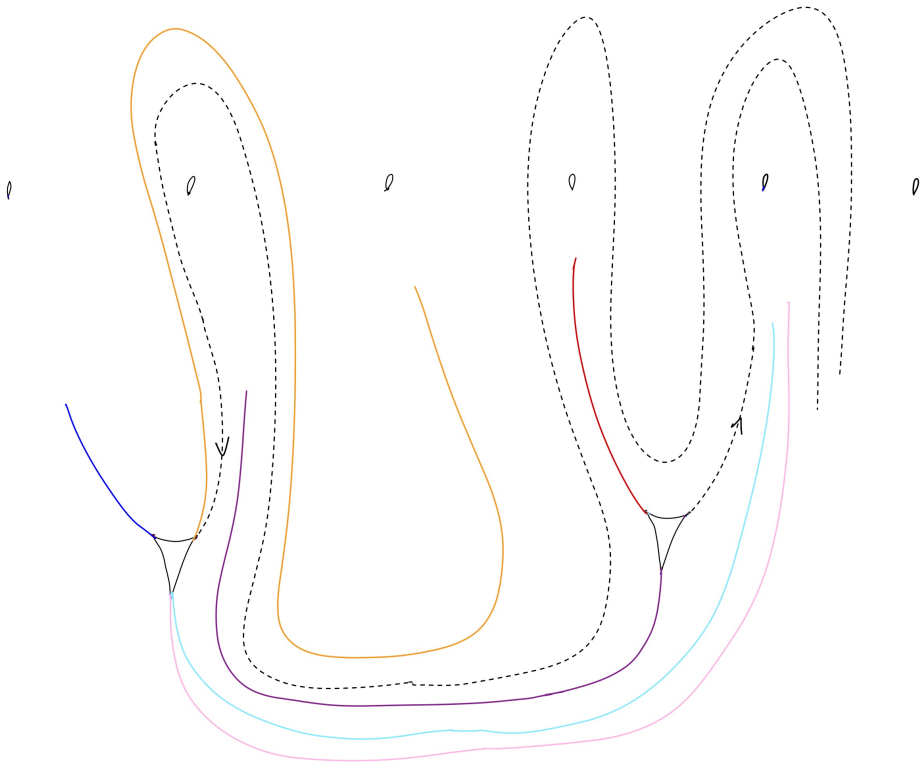


Figure I.123: MMU6

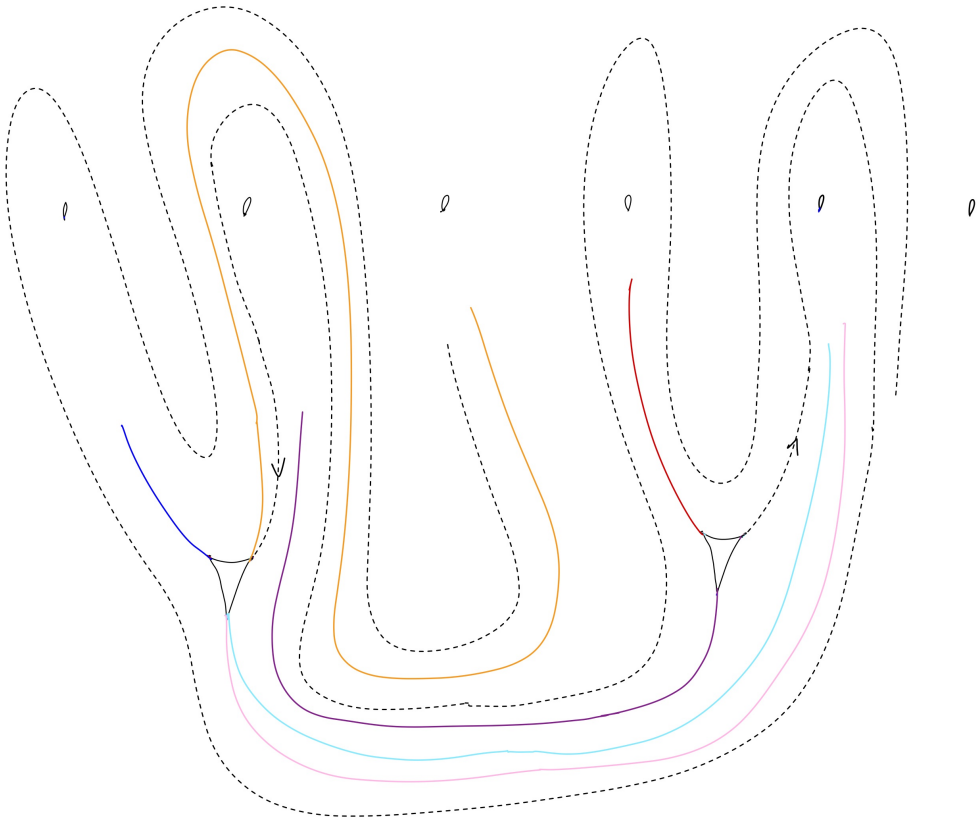


Figure I.124: MMU7

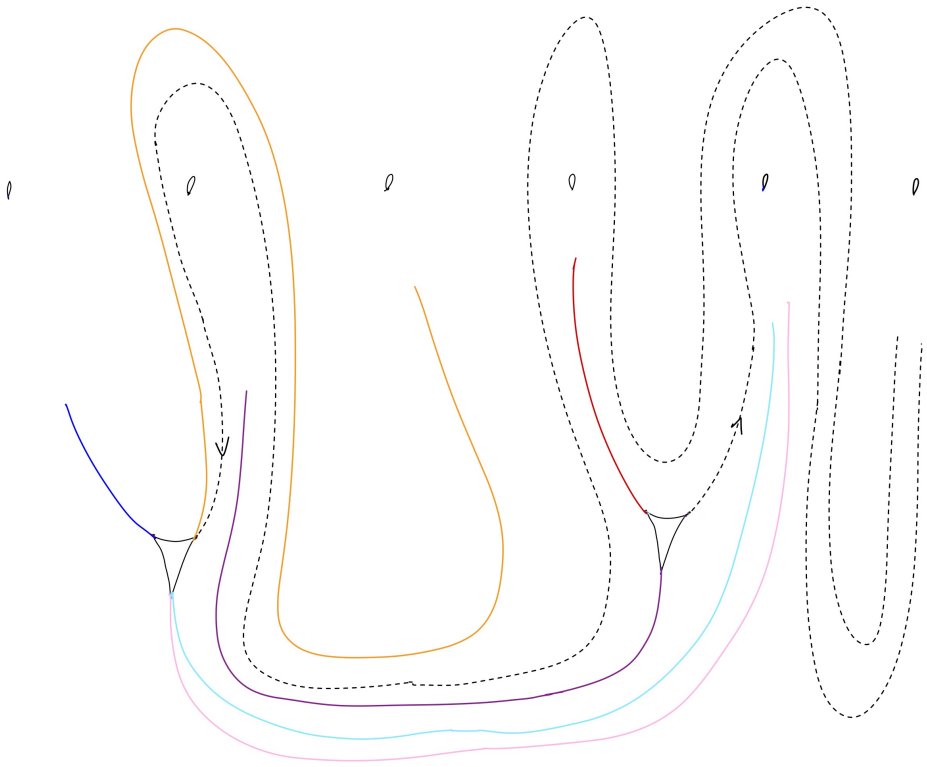


Figure I.125: MMU8

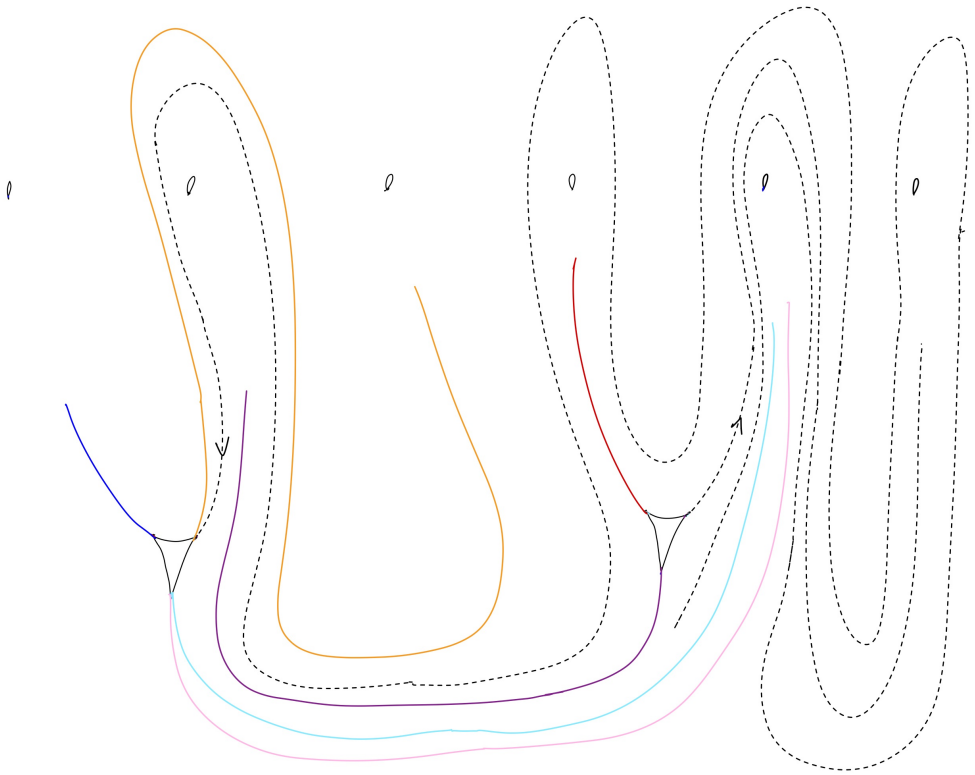


Figure I.126: MMU9

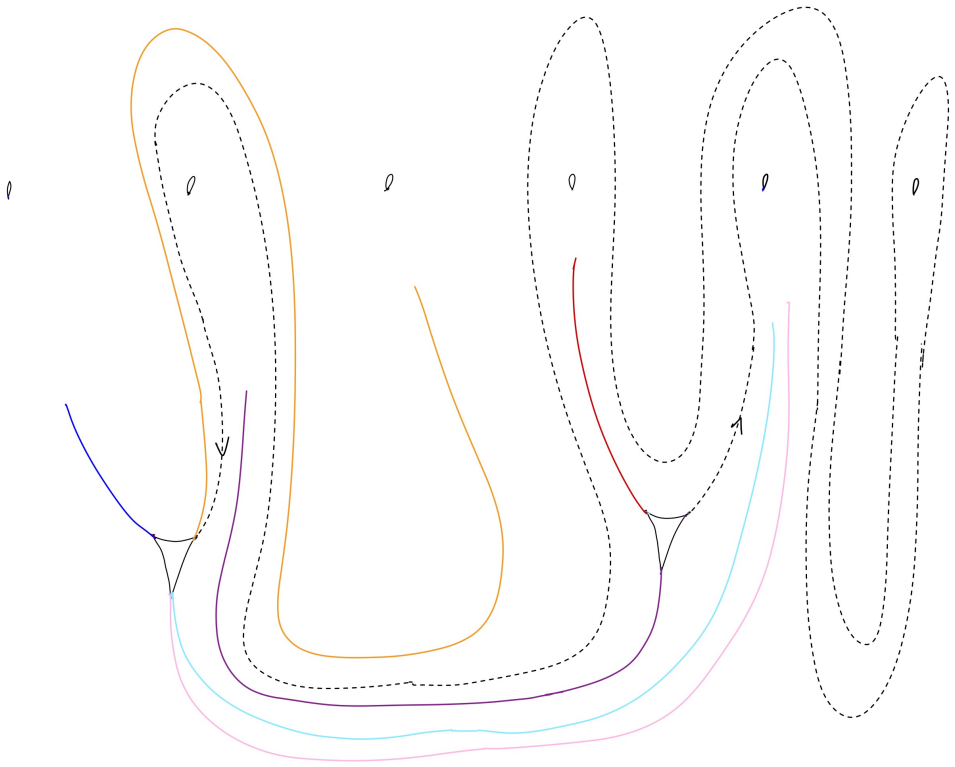


Figure I.127: MMU10

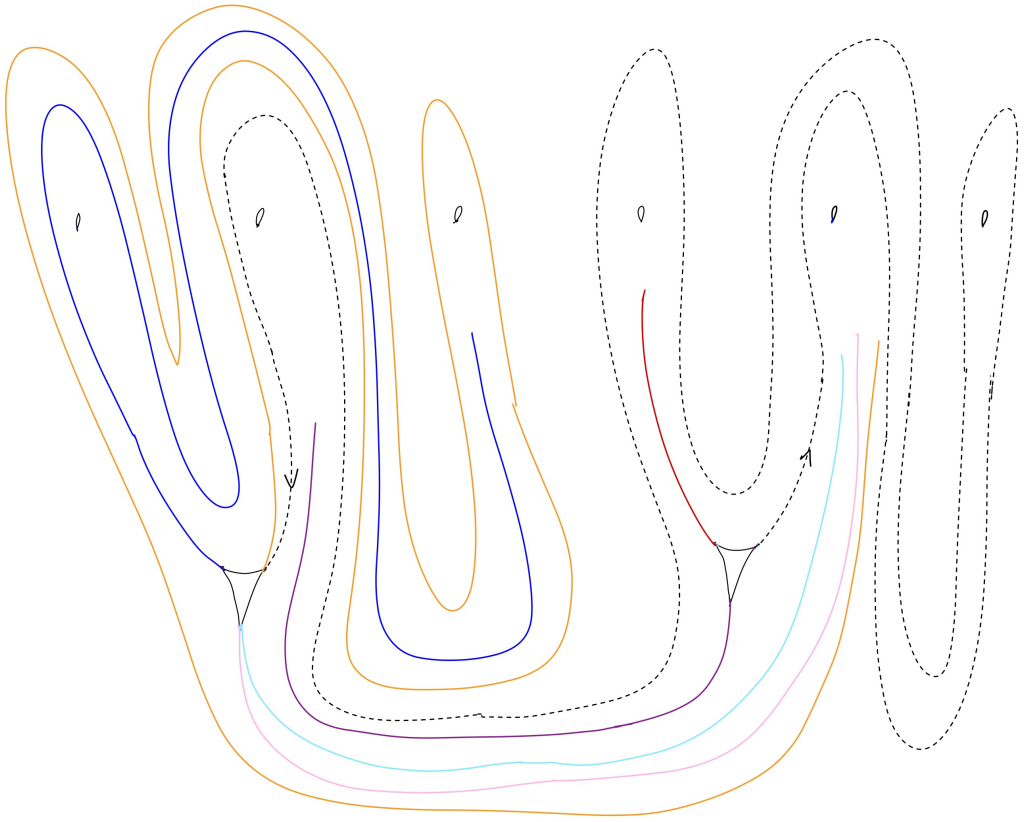


Figure I.128: MMU11

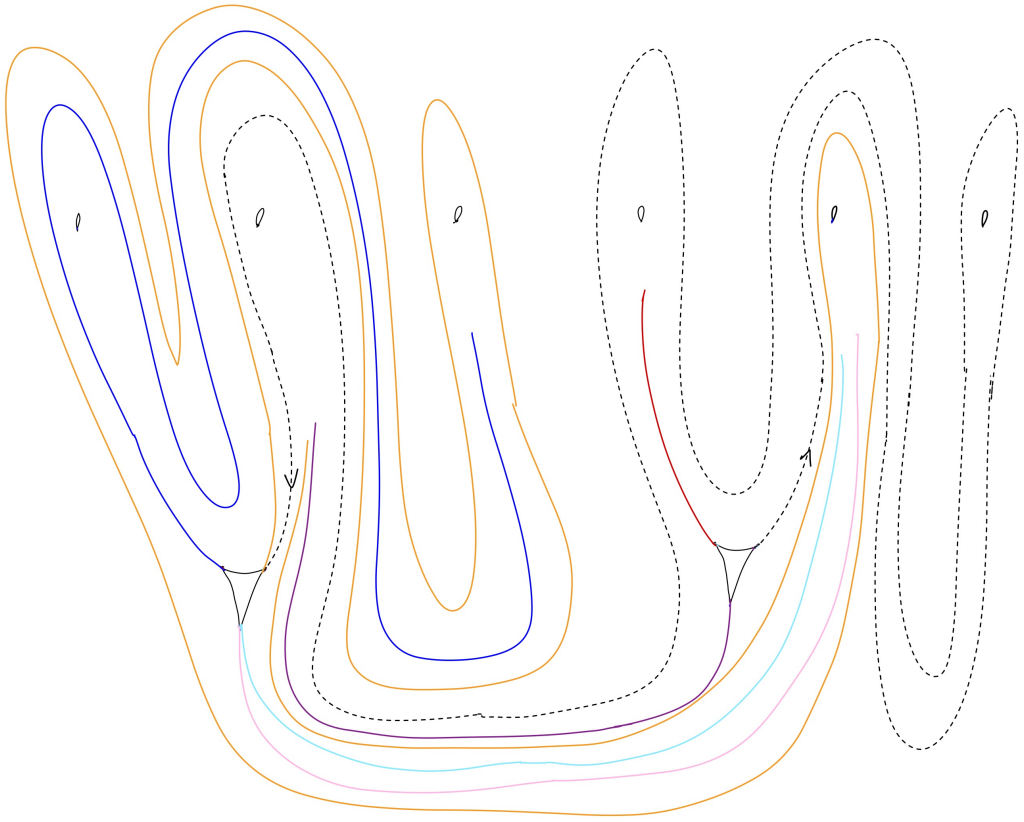


Figure I.129: MMU12

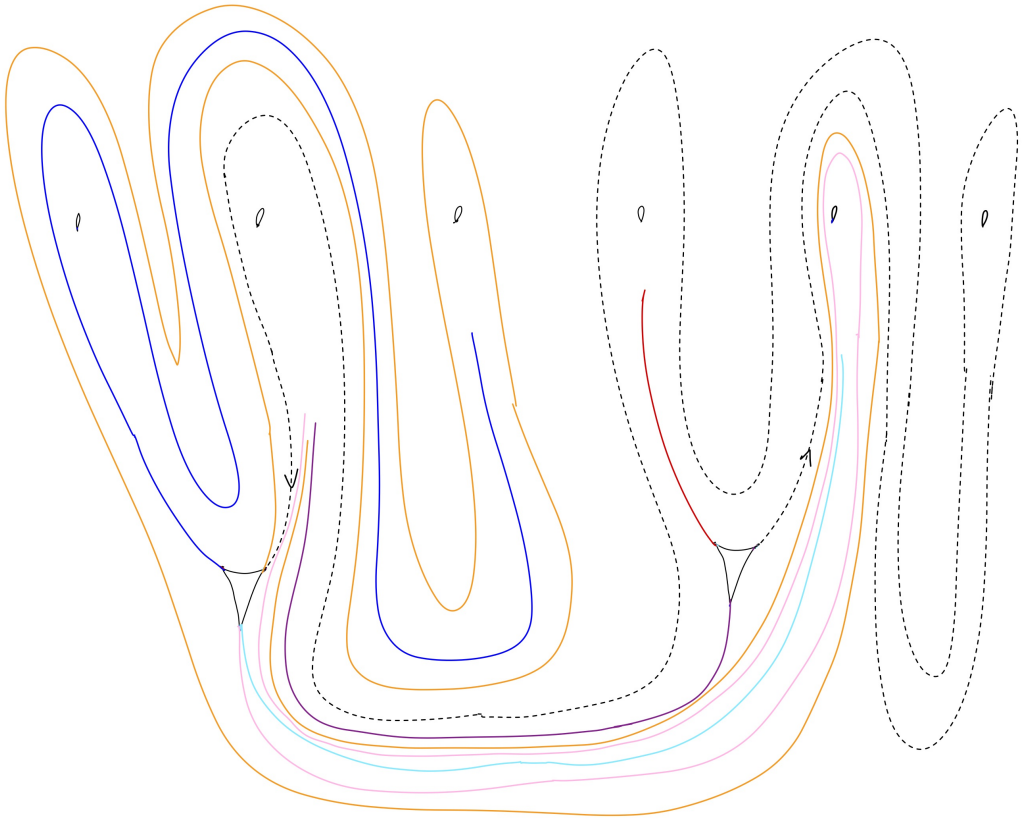


Figure I.130: MMU13

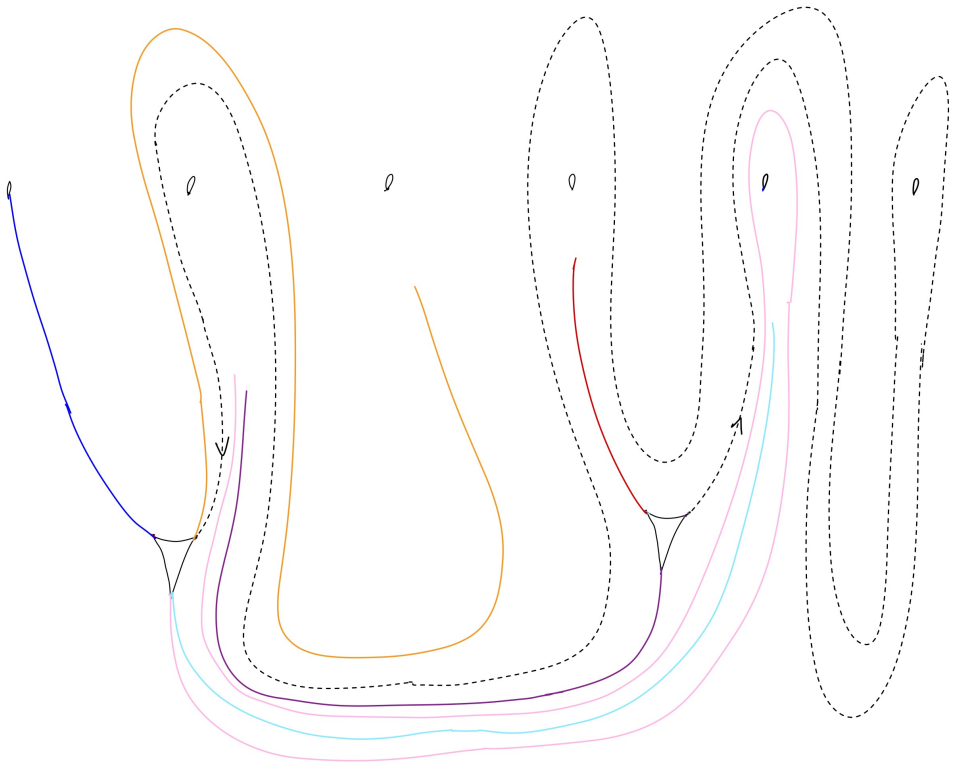


Figure I.131: MMU14

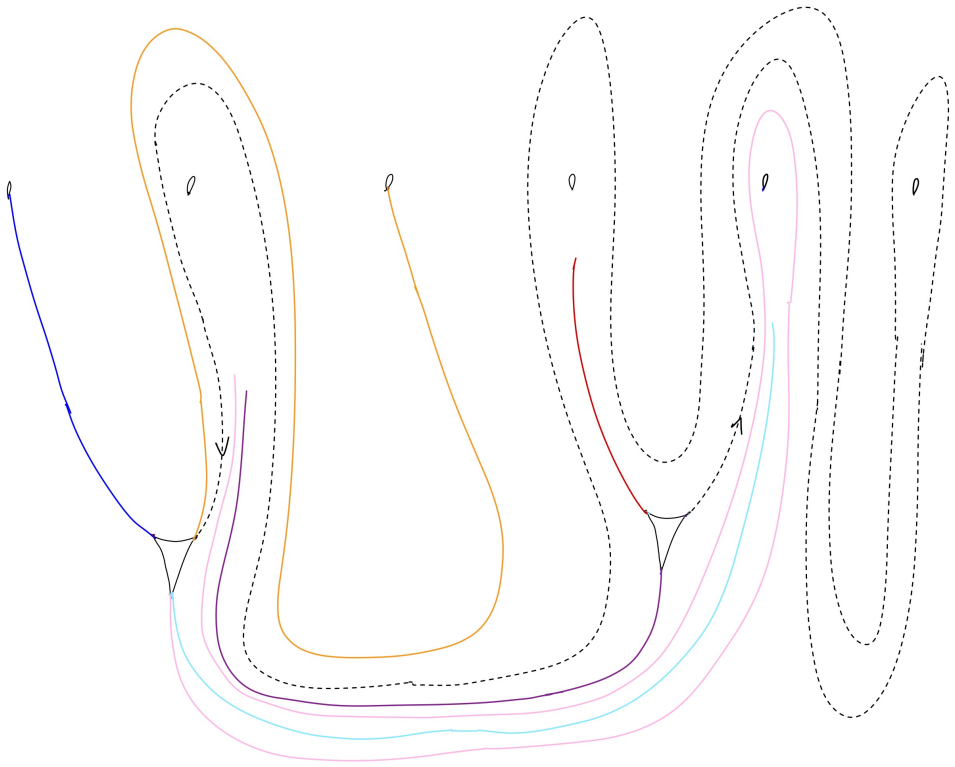


Figure I.132: MMU15

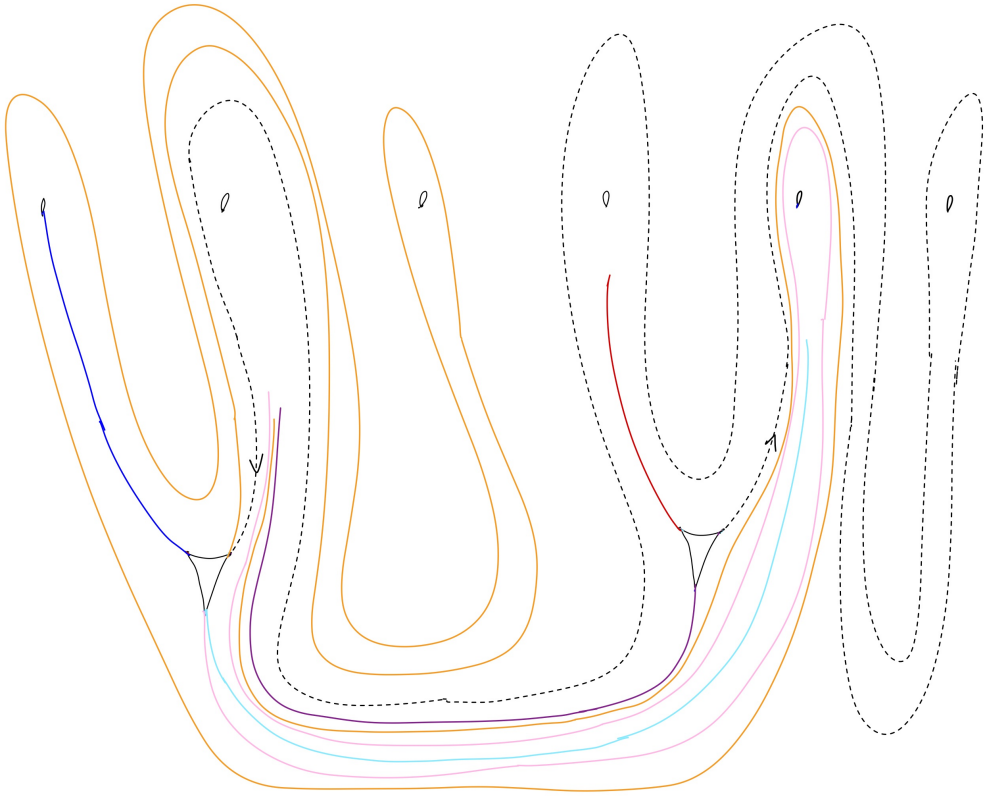


Figure I.133: MMU16

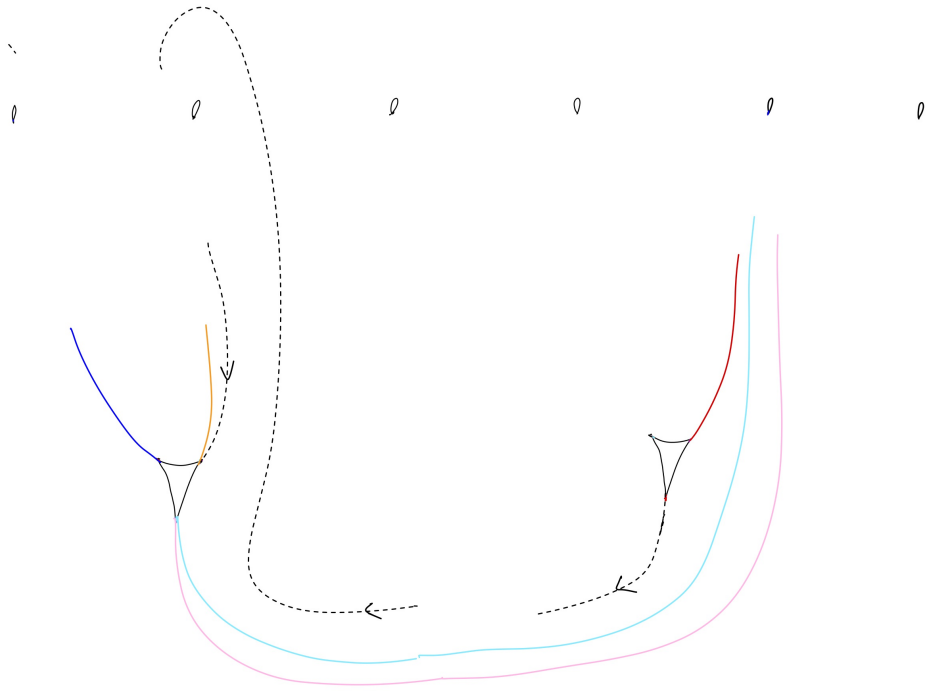


Figure I.134: MMU17

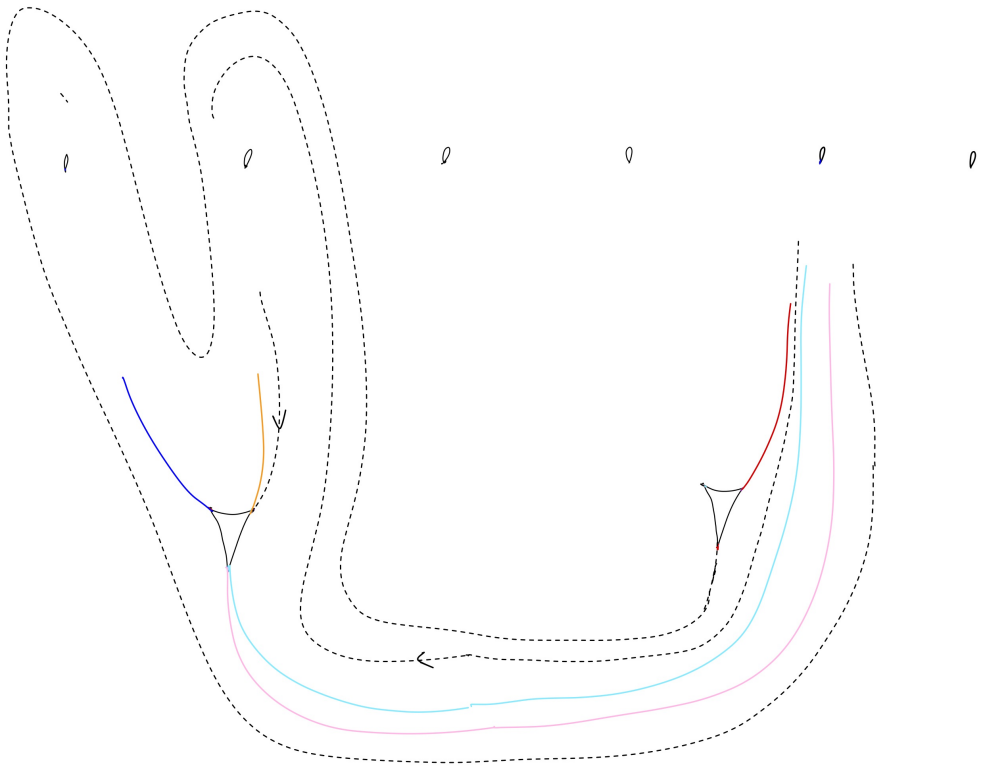


Figure I.135: MMU18

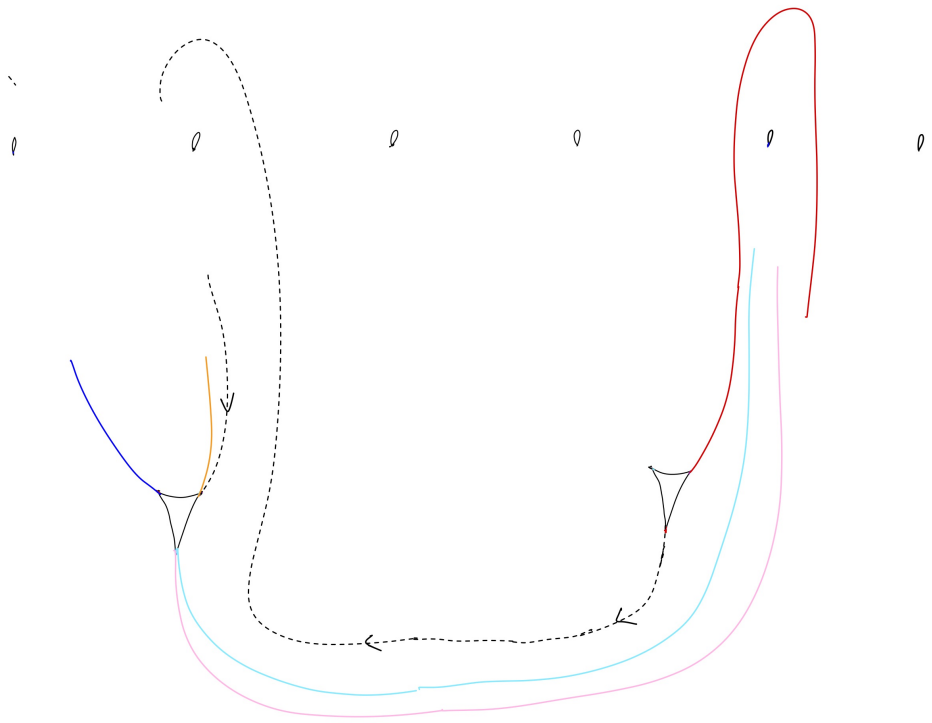


Figure I.136: MMU19

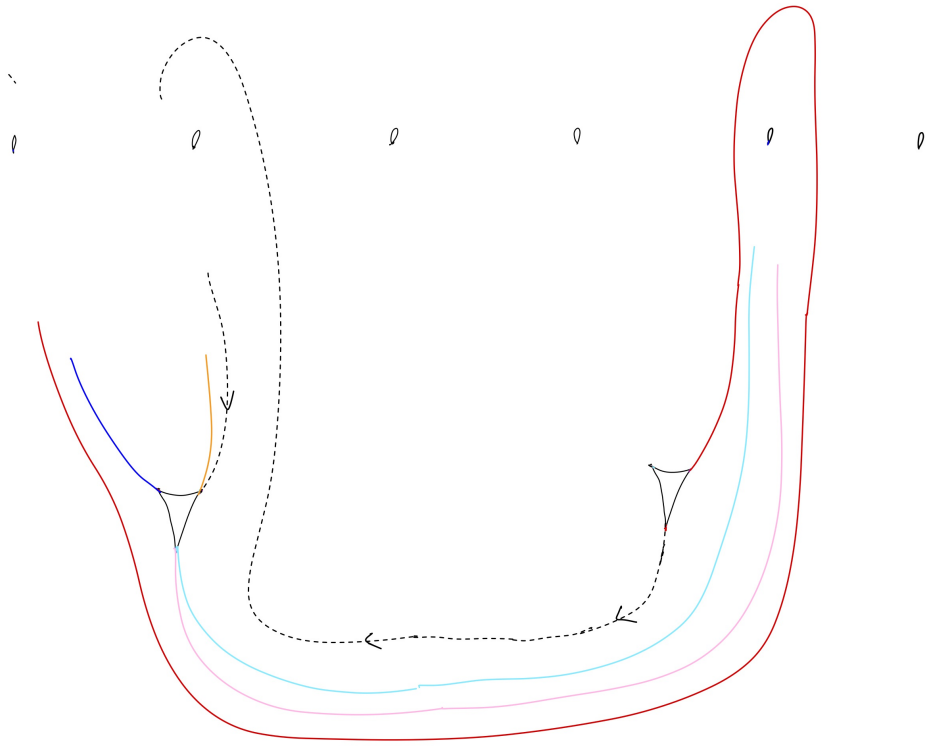


Figure I.137: MMU20

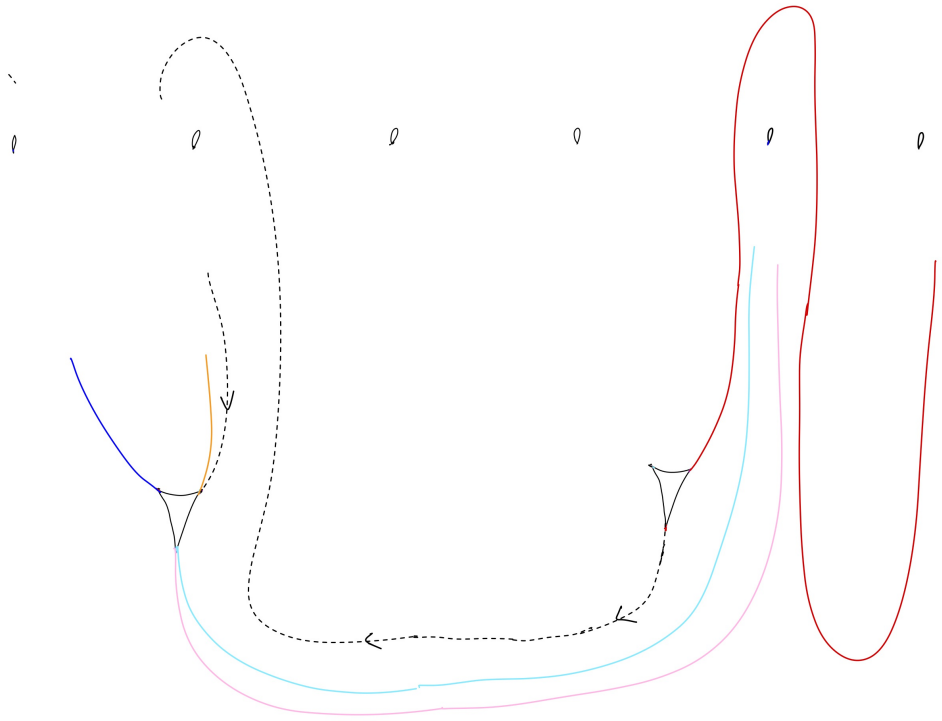


Figure I.138: MMU21

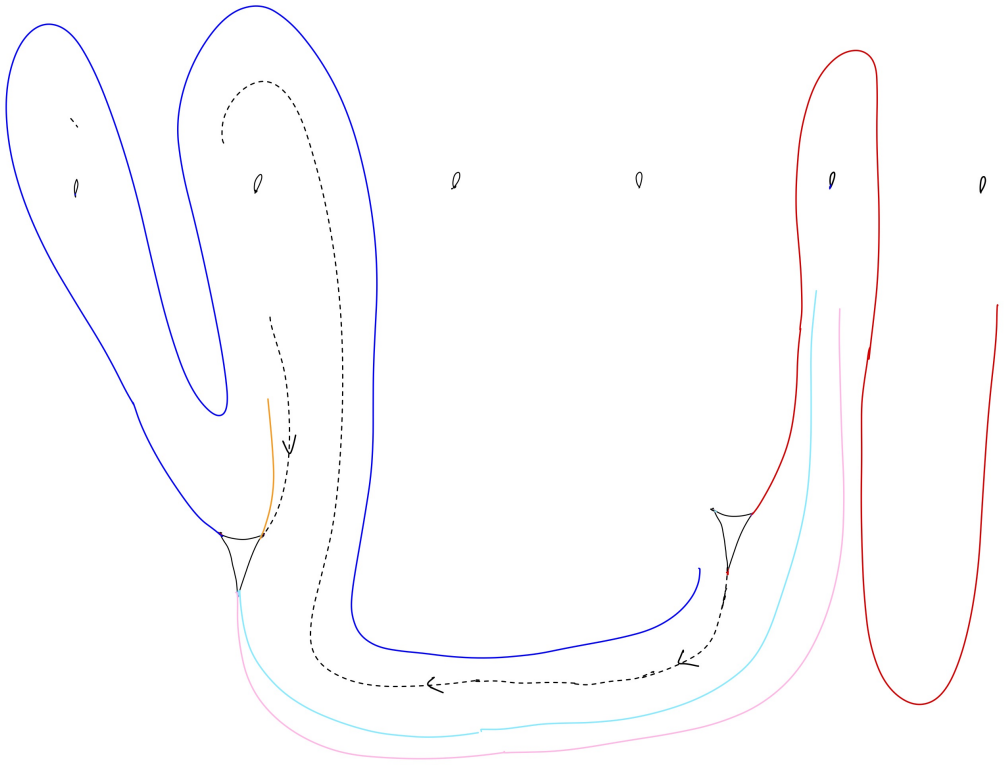


Figure I.139: MMU22

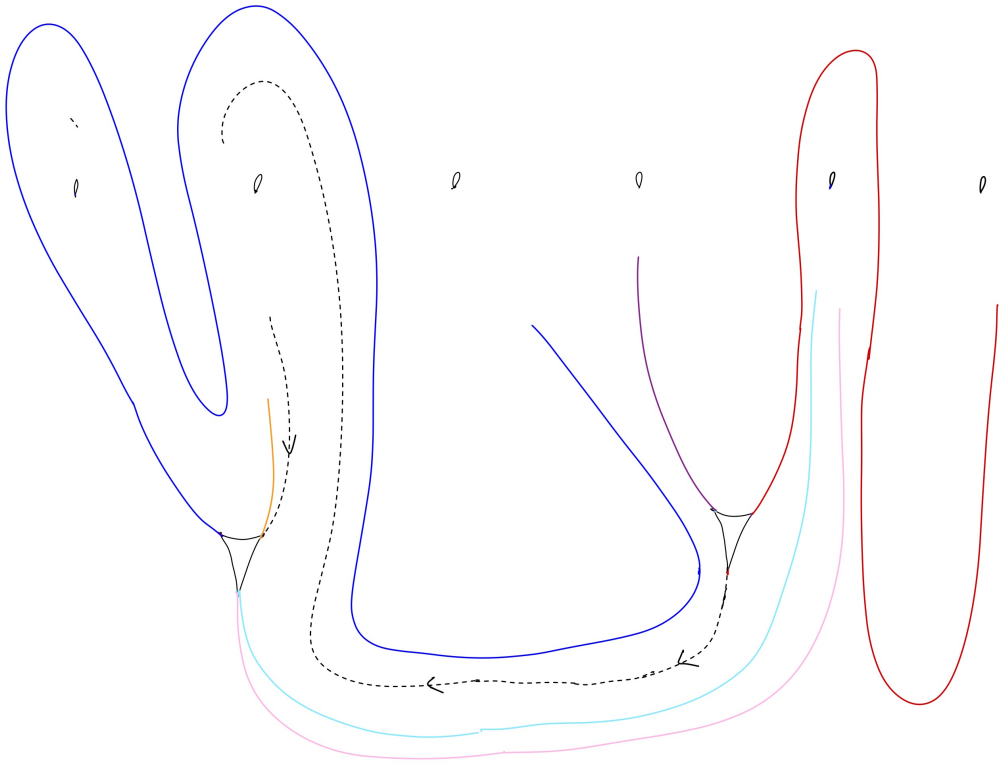


Figure I.140: MMU23

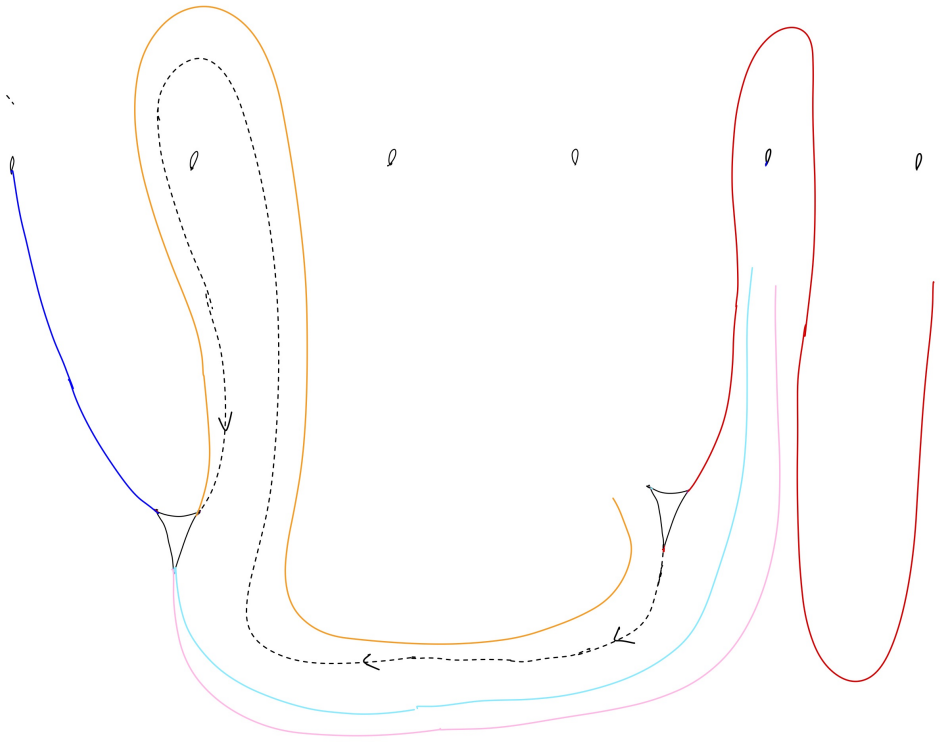


Figure I.141: MMU24

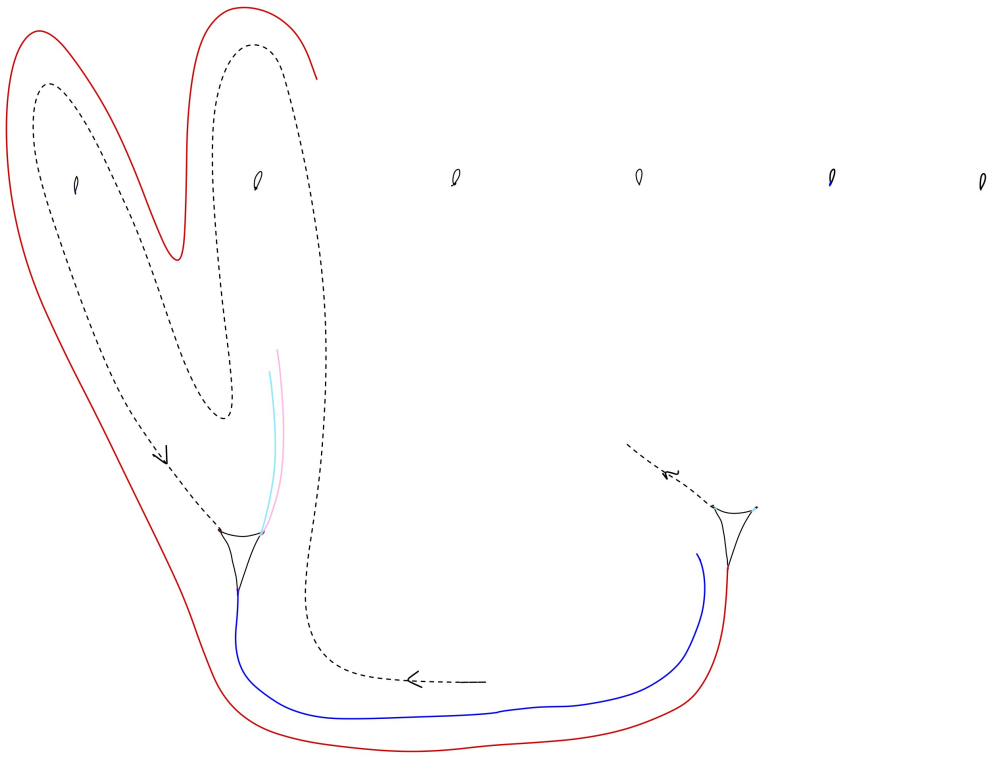


Figure I.142: TKE1

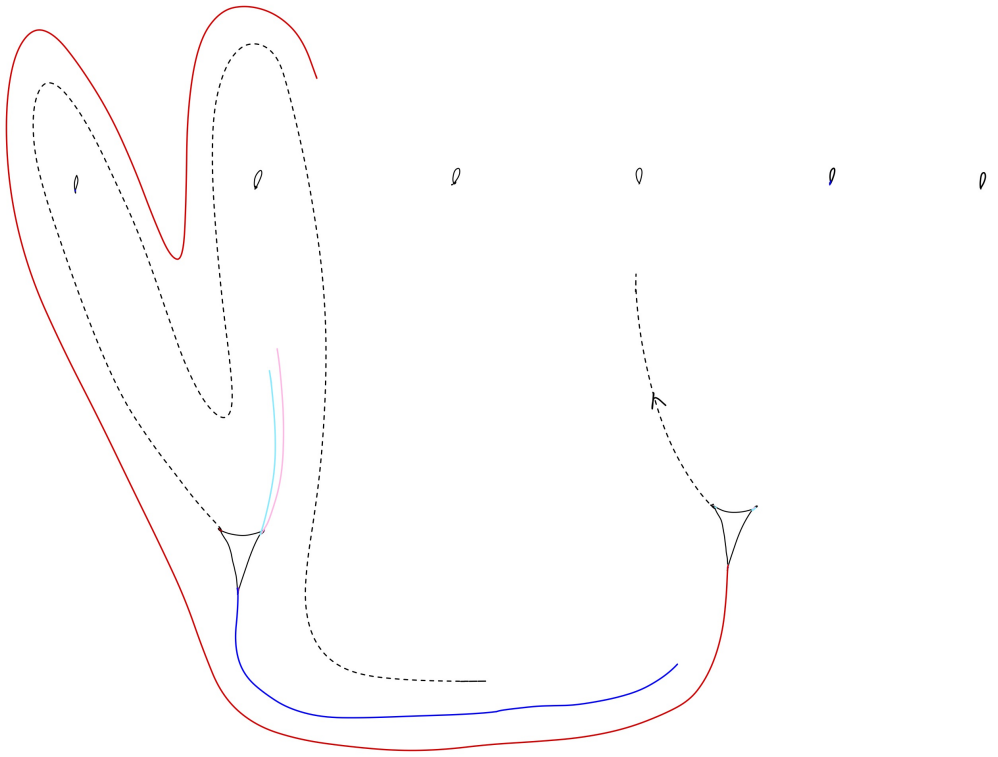


Figure I.143: TKE2

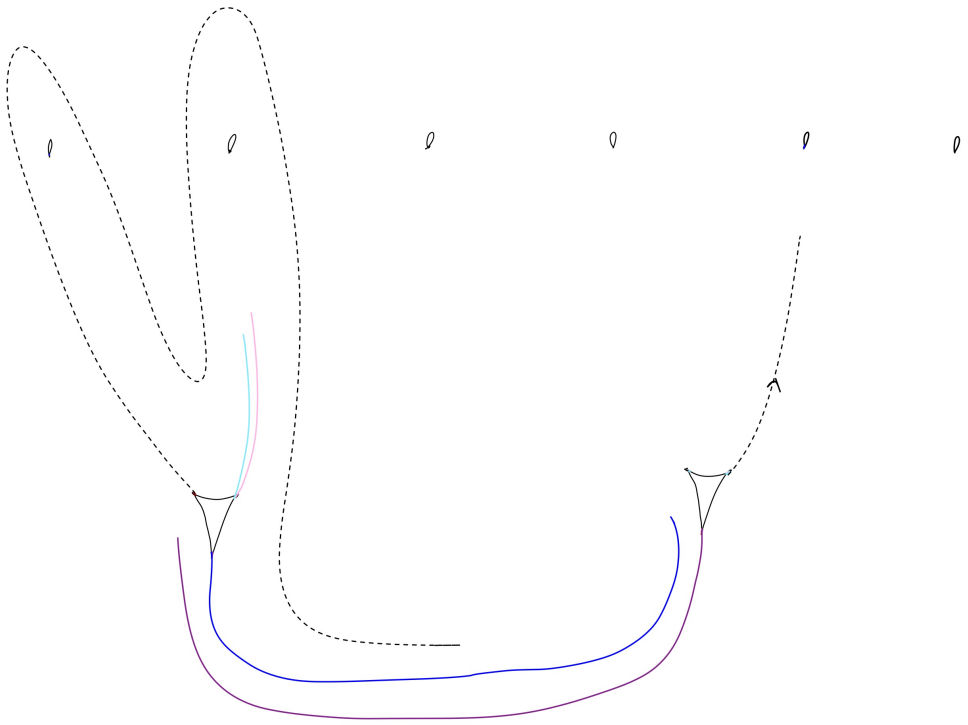


Figure I.144: TKE3

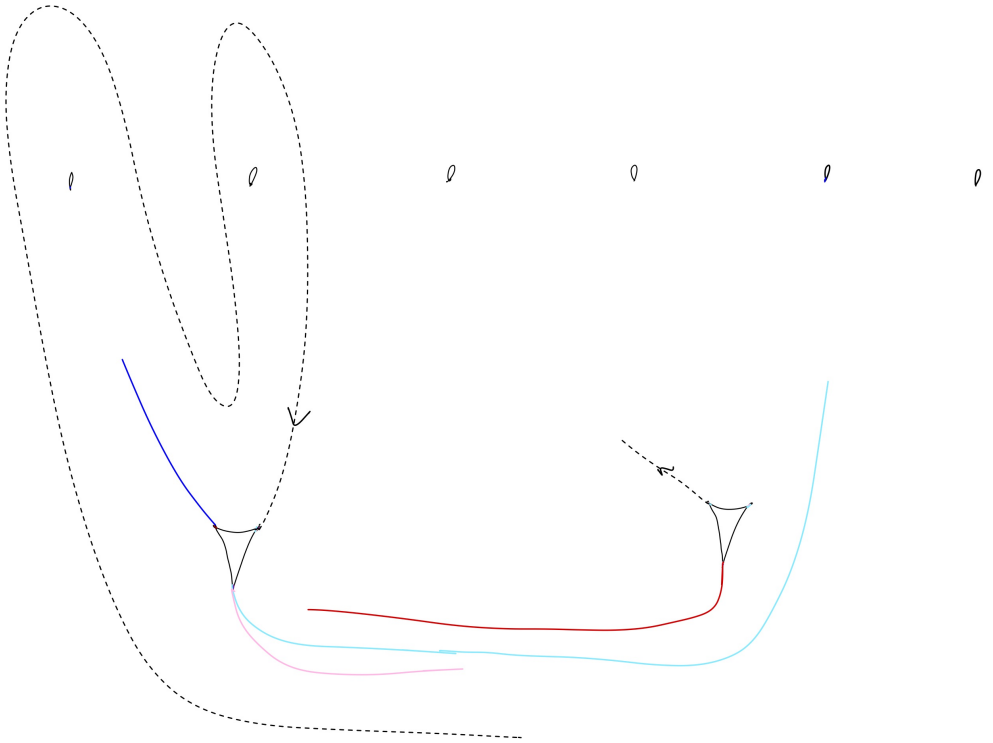


Figure I.145: RKD1

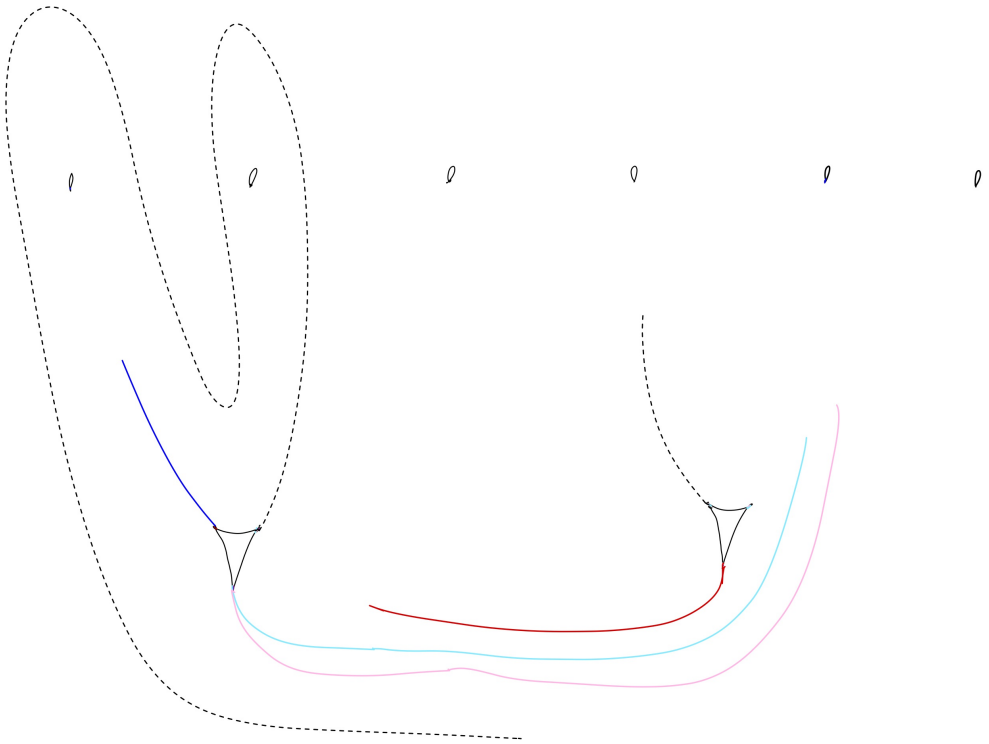


Figure I.146: RKD2

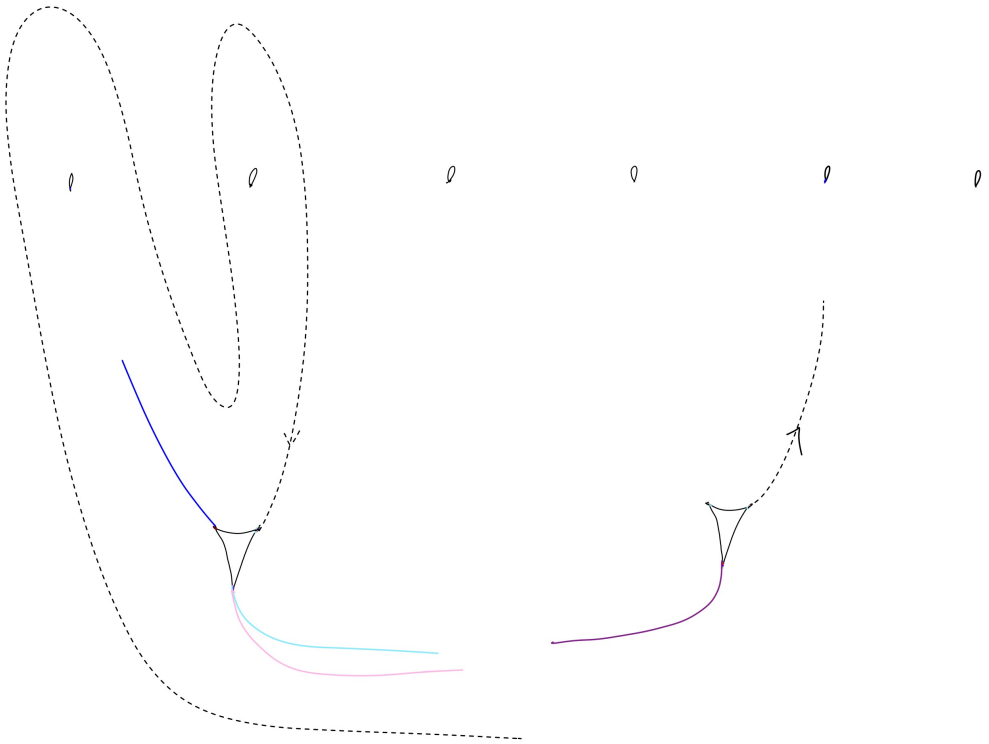


Figure I.147: RKD3

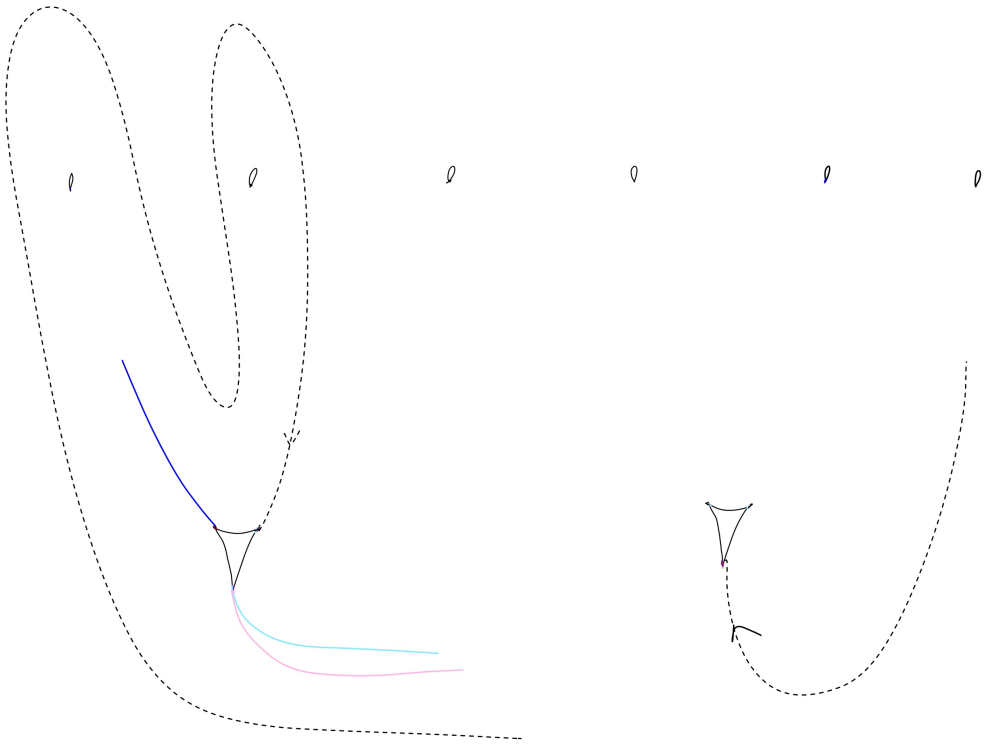


Figure I.148: RKD4

APPENDIX TEN

Appendix: Candidate Braids for the Candelabra

J.1 Summary of Candidate Braid Families

Through the train track case analysis of the Candelabra (stratum $(3; 1^6; 3)$), we isolate exactly 19 candidate families of train track maps for the one-click rotational state of the central triangle, listed as families $1, 1.1, 1.2, 2, 3, \ldots, 17$ below. The two-clicks rotational state is related to the one-click state by precomposition with the braid G realizing one rotational click, as discussed in Appendix C; the resulting parallel families $1', 1.1', 1.2', 2', 3', \ldots, 17'$ are listed thereafter. If the pseudo-Anosov representative ϕ_Φ has no interior fixed points, then its mapping class Φ must be conjugate to the lift of one of the following 38 braid families (enumerated below with their twist parameters).

1. $\Delta^{2i}(\sigma_3^{-1}\sigma_4^{-1}\sigma_2^{-1}\sigma_3^{-1}\sigma_1^{-1}\sigma_2^{-1}\sigma_3^{-1}\sigma_4^{-1}\sigma_3\sigma_4^{-1}\sigma_5^{-1}\sigma_4^{-1}\sigma_3^{-1}\sigma_4\sigma_5\sigma_2^{-1}\sigma_1^{-1}\sigma_1^{-1}\sigma_2^{-1}\sigma_1^{-1}\sigma_1^{-1} \cdot \sigma_5\sigma_4\sigma_3$
$\sigma_2\sigma_1\sigma_2\sigma_3\sigma_4\sigma_5\sigma_5\sigma_4\sigma_3\sigma_2\sigma_3\sigma_4\sigma_5\sigma_5\sigma_4\sigma_3\sigma_4\sigma_5\sigma_5\sigma_4\sigma_5\sigma_5)^{-1}$

(For the remainder of this list, we shall denote by G the braid word immediately following Δ^{2i} in item 1, inside the parenthesis and without the inversion).

1.1. $\Delta^{2i}(\sigma_3^{-1}\sigma_2 \cdot G)^{-1}$

1.2. $\Delta^{2i}(\sigma_3^{-k}\sigma_2^m \cdot G)^{-1}$

2. $\Delta^{2i}(\sigma_4^k\sigma_2^{-1}\sigma_3^{-1}\sigma_4 \cdot G)^{-1}$

3. $\Delta^{2i}(\sigma_5\sigma_4^{-k} \cdot G)^{-1}$

4. $\Delta^{2i}(\sigma_5^{-k}\sigma_4 \cdot G)^{-1}$

5. $\Delta^{2i}(\sigma_5^{-k}\sigma_4^m\sigma_4^{-1} \cdot G)^{-1}$

6. $\Delta^{2i}(\sigma_3^{-k}\sigma_2\sigma_3\sigma_4^{-1}\sigma_5^{-1}\sigma_4 \cdot G)^{-1}$

7. $\Delta^{2i}(\sigma_3^{-k}\sigma_2\sigma_3\sigma_4^{-1}\sigma_5^{-1}\sigma_4^m \cdot G)^{-1}$

8. $\Delta^{2i}(\sigma_5^k\sigma_3\sigma_4^{-1}\sigma_5^{-1} \cdot G)^{-1}$

9. $\Delta^{2i}(\sigma_5^m\sigma_3\sigma_4^{-k}\sigma_4^{-1}\sigma_5^{-1} \cdot G)^{-1}$

10. $\Delta^{2i}(\sigma_5^{-k}\sigma_4\sigma_5\sigma_1\sigma_2\sigma_3\sigma_4 \cdot F \cdot G)^{-1}$

11. $\Delta^{2i}(\sigma_4\sigma_5^m\sigma_4^k\sigma_1\sigma_2\sigma_3\sigma_4 \cdot F \cdot G)^{-1}$

12. $\Delta^{2i}(\sigma_5^{-k}\sigma_4\sigma_5\sigma_1\sigma_2\sigma_1\sigma_3\sigma_2\sigma_4\sigma_3\sigma_4\sigma_4)^{-1}$

13. $\Delta^{2i}(\sigma_5\sigma_1\sigma_2\sigma_1\sigma_3\sigma_2\sigma_4\sigma_3\sigma_4\sigma_4)^{-1}$

14. $\Delta^{2i}(\sigma_5^k\sigma_3^m\sigma_1\sigma_2\sigma_3\sigma_4 \cdot F \cdot G)^{-1}$

15. $\Delta^{2i}(\sigma_2\sigma_1\sigma_3\sigma_2\sigma_5\sigma_4\sigma_3\sigma_4\sigma_4\sigma_5^{-k}\sigma_4)^{-1}$

16. $\Delta^{2i}(\sigma_5^j\sigma_3^m\sigma_1^k \cdot H \cdot G)^{-1}$

17. $\Delta^{2i}(\sigma_1^k\sigma_2\sigma_1\sigma_5\sigma_4\sigma_3\sigma_2\sigma_4\sigma_3\sigma_4\sigma_5^{-m}\sigma_4)^{-1}$

$1'.\ \Delta^{2i}(\sigma_3^{-1}\sigma_4^{-1}\sigma_2^{-1}\sigma_3^{-1}\sigma_1^{-1}\sigma_2^{-1}\sigma_3^{-1}\sigma_4^{-1}\sigma_3\sigma_4^{-1}\sigma_5^{-1}\sigma_4^{-1}\sigma_3^{-1}\sigma_4\sigma_5\sigma_2^{-1}\sigma_1^{-1}\sigma_1^{-1}\sigma_2^{-1}\sigma_1^{-1}\sigma_1^{-1}\cdot\sigma_5\sigma_4\sigma_3$
$\sigma_2\sigma_1\sigma_2\sigma_3\sigma_4\sigma_5\sigma_5\sigma_4\sigma_3\sigma_2\sigma_3\sigma_4\sigma_5\sigma_5\sigma_4\sigma_3\sigma_4\sigma_5\sigma_5\sigma_4\sigma_5\sigma_5\cdot G)^{-1}$

$1.1'.\ \Delta^{2i}(\sigma_3^{-1}\sigma_2\cdot G\cdot G)^{-1}$

$1.2'.\ \Delta^{2i}(\sigma_3^{-k}\sigma_2^{m}\cdot G\cdot G)^{-1}$

$2'.\ \Delta^{2i}(\sigma_4^{k}\sigma_2^{-1}\sigma_3^{-1}\sigma_4\cdot G\cdot G)^{-1}$

$3'.\ \Delta^{2i}(\sigma_5\sigma_4^{-k}\cdot G\cdot G)^{-1}$

$4'.\ \Delta^{2i}(\sigma_5^{-k}\sigma_4\cdot G\cdot G)^{-1}$

$5'.\ \Delta^{2i}(\sigma_5^{-k}\sigma_4^{m}\sigma_4^{-1}\cdot G\cdot G)^{-1}$

$6'.\ \Delta^{2i}(\sigma_3^{-k}\sigma_2\sigma_3\sigma_4^{-1}\sigma_5^{-1}\sigma_4\cdot G\cdot G)^{-1}$

$7'.\ \Delta^{2i}(\sigma_3^{-k}\sigma_2\sigma_3\sigma_4^{-1}\sigma_5^{-1}\sigma_4^{m}\cdot G\cdot G)^{-1}$

$8'.\ \Delta^{2i}(\sigma_5^{k}\sigma_3\sigma_4^{-1}\sigma_5^{-1}\cdot G\cdot G)^{-1}$

$9'.\ \Delta^{2i}(\sigma_5^{m}\sigma_3\sigma_4^{-k}\sigma_4^{-1}\sigma_5^{-1}\cdot G\cdot G)^{-1}$

$10'.\ \Delta^{2i}(\sigma_5^{-k}\sigma_4\sigma_5\sigma_1\sigma_2\sigma_3\sigma_4\cdot F\cdot G\cdot G)^{-1}$

$11'.\ \Delta^{2i}(\sigma_4\sigma_5^{m}\sigma_4^{k}\sigma_1\sigma_2\sigma_3\sigma_4\cdot F\cdot G\cdot G)^{-1}$

$12'.\ \Delta^{2i}(\sigma_5^{-k}\sigma_4\sigma_5\sigma_1\sigma_2\sigma_1\sigma_3\sigma_2\sigma_4\sigma_3\sigma_4\sigma_4\cdot G)^{-1}$

$13'.\ \Delta^{2i}(\sigma_5\sigma_1\sigma_2\sigma_1\sigma_3\sigma_2\sigma_4\sigma_3\sigma_4\sigma_4\cdot G)^{-1}$

$14'.\ \Delta^{2i}(\sigma_5^{k}\sigma_3^{m}\sigma_1\sigma_2\sigma_3\sigma_4\cdot F\cdot G\cdot G)^{-1}$

$15'.\ \Delta^{2i}(\sigma_2\sigma_1\sigma_3\sigma_2\sigma_5\sigma_4\sigma_3\sigma_4\sigma_4\sigma_5^{-k}\sigma_4\cdot G)^{-1}$

16′. $\Delta^{2i}(\sigma_5^j\sigma_3^m\sigma_1^k \cdot H \cdot G \cdot G)^{-1}$

17′. $\Delta^{2i}(\sigma_1^k\sigma_2\sigma_1\sigma_5\sigma_4\sigma_3\sigma_2\sigma_4\sigma_3\sigma_4\sigma_5^{-m}\sigma_4 \cdot G)^{-1}$

J.2 The Auxiliary Braid H

Before we list the braids carrying candidate train track maps, we introduce the following braid, which we will call H:

$H = \sigma_1^{-1}\sigma_2^{-1}\sigma_3^{-1}\sigma_4^{-1}\sigma_5^{-1}\sigma_1^{-1}\sigma_2^{-1}\sigma_3^{-1}\sigma_4^{-1}\sigma_4^{-1}\sigma_3^{-1}\sigma_2^{-1}\sigma_1^{-1}\sigma_2^{-1}\sigma_3^{-1}\sigma_4^{-1}\sigma_2^{-1}\sigma_3^{-1}\sigma_2^{-1}\sigma_3^{-1}\sigma_4^{-1}\sigma_2^{-1}$
$\sigma_3^{-1}\sigma_4^{-1}$

As shown in Figure J.1, the inverse of the braid H can be thought of as "swinging" the right-most arm of the Candelabra all the way to the left. We shall make use of H occasionally in constructing candidate braids for the Candelabra.

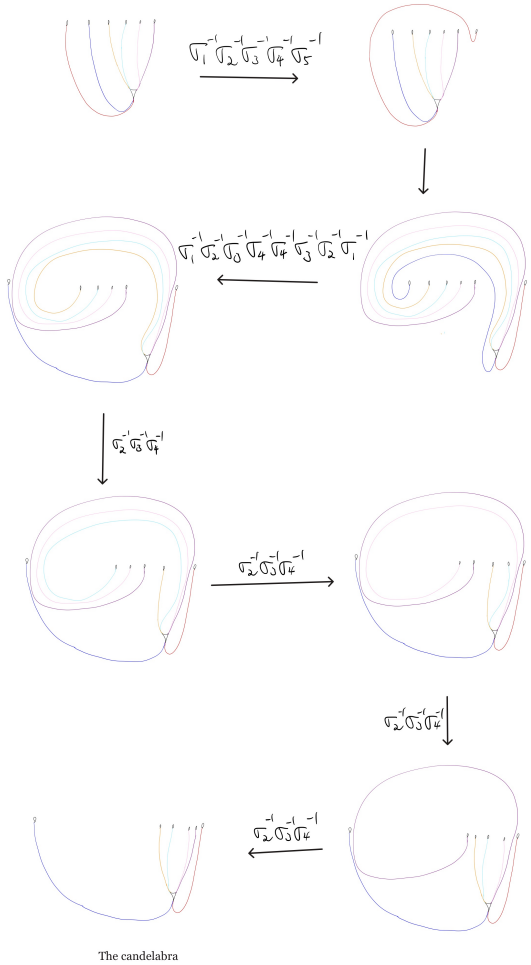


Figure J.1: This sequence shows the inverse of the braid H can be thought of as swinging the right-most arm of the Candelabra all the way to the left.

J.3 Candidate 1

The inverse of the following braid, which we call G, carries Candidate Train Track Map 1 of the Candelabra train track:

$$G = \sigma_3^{-1}\sigma_4^{-1}\sigma_2^{-1}\sigma_3^{-1}\sigma_1^{-1}\sigma_2^{-1}\sigma_3^{-1}\sigma_4^{-1}\sigma_3\sigma_4^{-1}\sigma_5^{-1}\sigma_4^{-1}\sigma_3^{-1}\sigma_4\sigma_5\sigma_2^{-1}\sigma_1^{-1}\sigma_1^{-1}\sigma_2^{-1}\sigma_1^{-1}\sigma_1^{-1} \cdot \sigma_5\sigma_4\sigma_3\sigma_2$$
$$\sigma_1\sigma_2\sigma_3\sigma_4\sigma_5\sigma_5\sigma_4\sigma_3\sigma_2\sigma_3\sigma_4\sigma_5\sigma_5\sigma_4\sigma_3\sigma_4\sigma_5\sigma_5\sigma_4\sigma_5\sigma_5$$

This is shown in Figure J.2.

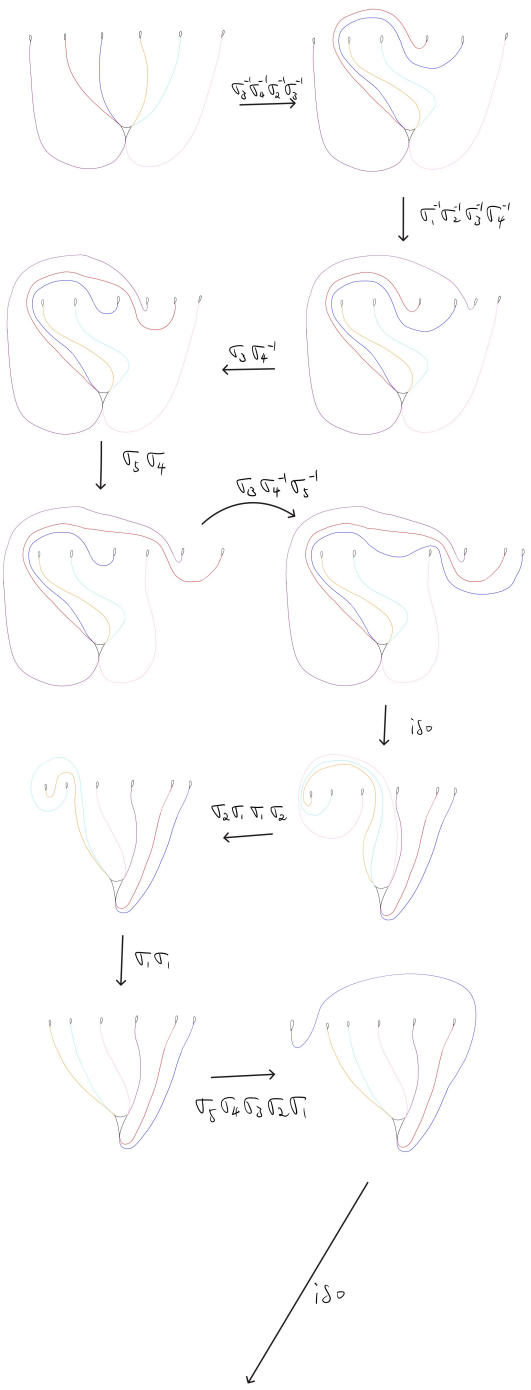


Figure J.2: This sequence shows the inverse of the braid G carries Train Track Candidate 1.

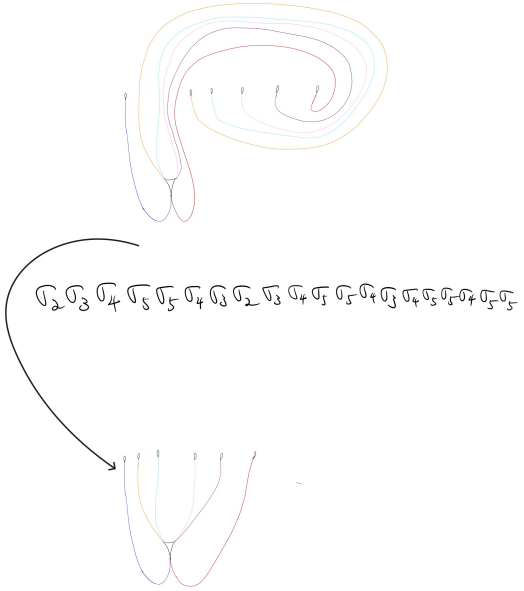


Figure J.2: This sequence shows the inverse of the braid G carries Train Track Candidate 1 (continued).

J.4 Candidate 1.1

Train Track Map Candidate 1.1 of the Candelabra train track is shown in Figure J.3. See Section C.0.1.1 of Appendix C for details.

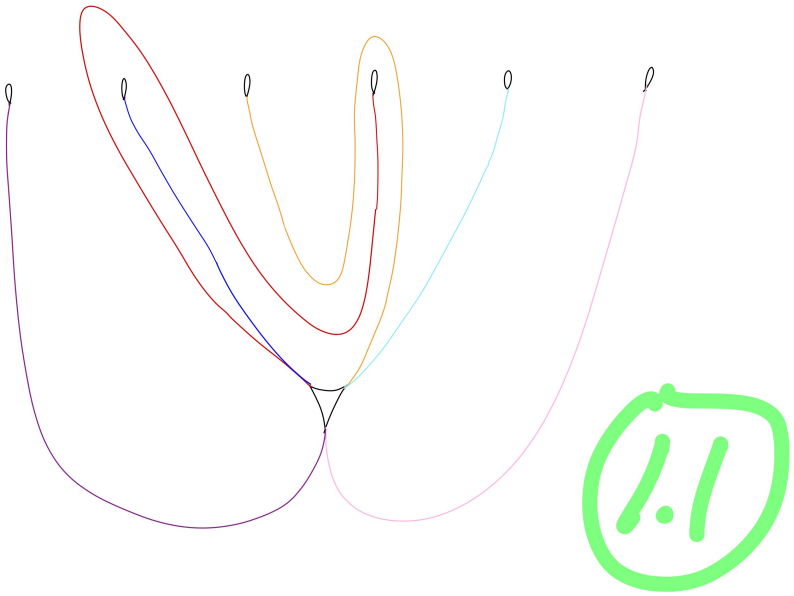


Figure J.3: Train Track Map Candidate 1.1 of the Candelabra.

The inverse of the following braid carries this train track map:

$$b^c_{1.1} = \sigma_3^{-1}\sigma_2 \circ G$$

where G is the braid of Section J.3. This is shown in Figure J.4.

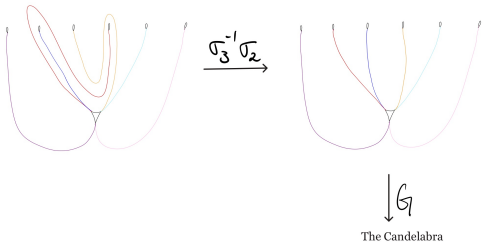


Figure J.4: This sequence shows the inverse of the braid $b^c_{1.1}$ carries Train Track Candidate 1.1.

J.5 Candidate Family 1.2

Train Track Map Candidate Family 1.2 of the Candelabra train track is shown in Figure J.5. Note there is twisting between $f_\beta(o)$ between i and s, and additional twisting between $f_\beta(r)$ and $f_\beta(b)$. See Section C.0.1.1 of Appendix C for details.

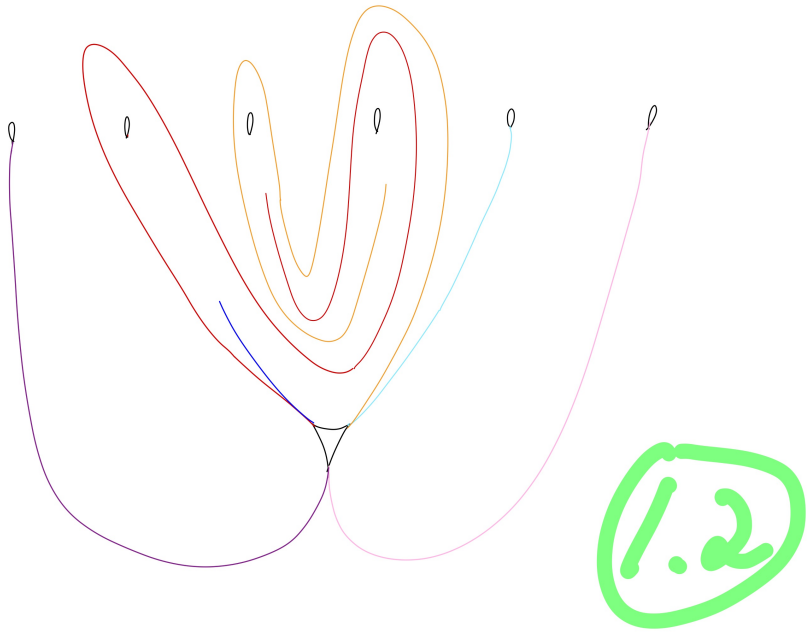


Figure J.5: Train Track Map Candidate Family 1.2 of the Candelabra.

The inverse of the following braid carries this family of train track maps:

$$b^c_{1.2} = \sigma_3^{-k}\sigma_2^m \circ G$$

where G is the braid of Section J.3, and $k, m \geq 1$ ($k, m \in \mathbb{Z}$) are the twisting parameters. This is shown in Figure J.6.

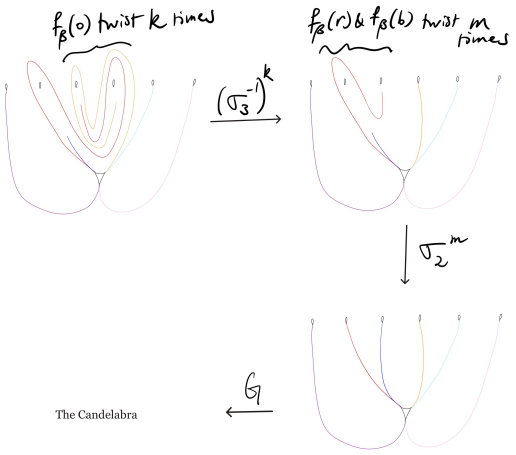


Figure J.6: This sequence shows the inverse of the braid $b^c_{1.2}$ carries Train Track Candidate Family 1.2.

J.6 Candidate 2

Train Track Map Candidate Family 2 of the Candelabra train track is shown in Figure J.7. Note there is twisting between $f_\beta(r)$ and $f_\beta(b)$. See C.0.1.1 for details.

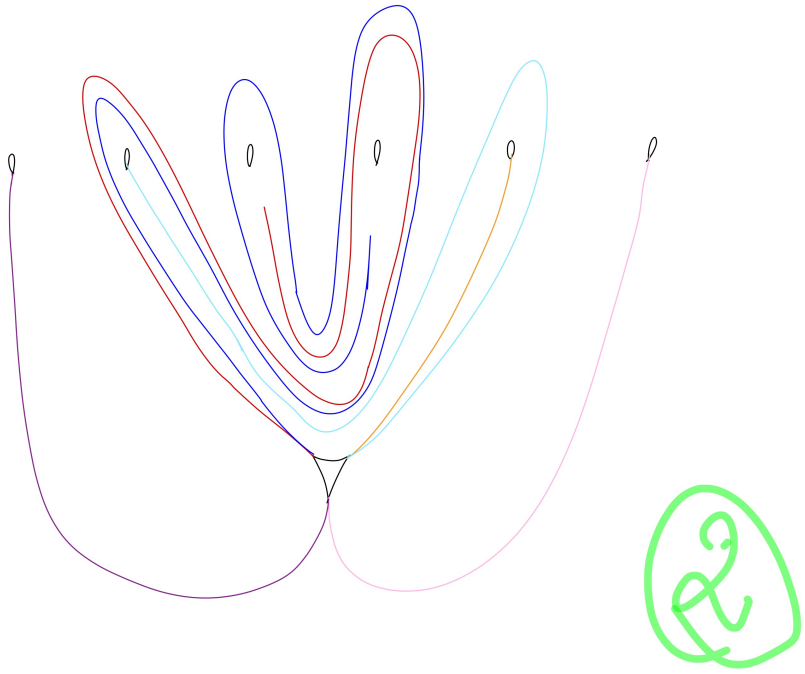


Figure J.7: Train Track Map Candidate Family 2 of the Candelabra.

The inverse of the following braid carries this family of train track maps:

$$b_2^c = \sigma_4^k \sigma_2^{-1} \sigma_3^{-1} \sigma_4 \circ G$$

where G is the braid of Section J.3, and $k \geq 1$ ($k \in \mathbb{Z}$) is the twisting parameter. This is shown in Figure J.8.

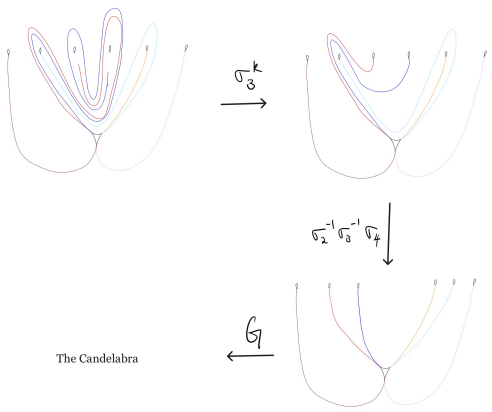


Figure J.8: This sequence shows the inverse of the braid b_2^c carries Train Track Candidate Family 2.

J.7 Candidate Family 3

Train Track Map Candidate Family 3 of the Candelabra train track is shown in Figure J.9. Note there is twisting between $f_\beta(s)$ and $f_\beta(o)$. See C.0.2.1.1.1 for details.

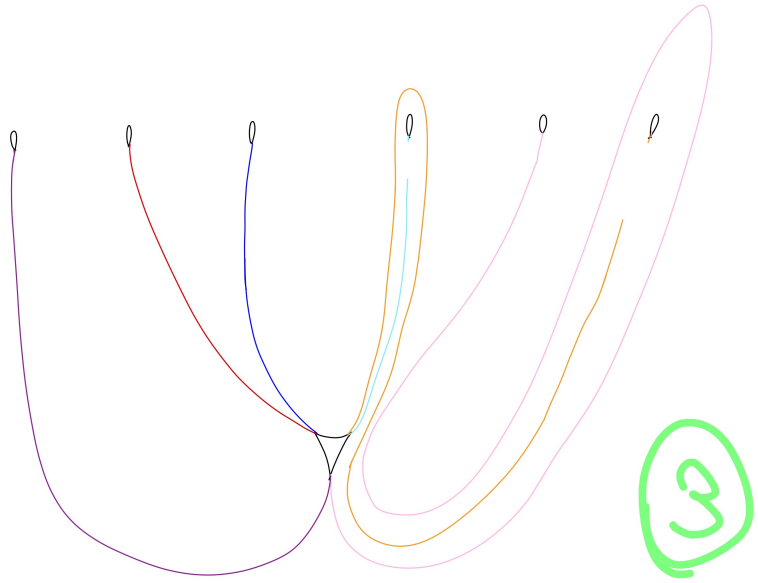


Figure J.9: Train Track Map Candidate Family 3 of the Candelabra.

The inverse of the following braid carries this family of train track maps:

$$b_3^c = \sigma_5(\sigma_4^{-1})^k \circ G$$

where G is the braid of Section J.3, and $k \geq 1$ ($k \in \mathbb{Z}$) is the twisting parameter. This is shown in Figure J.10

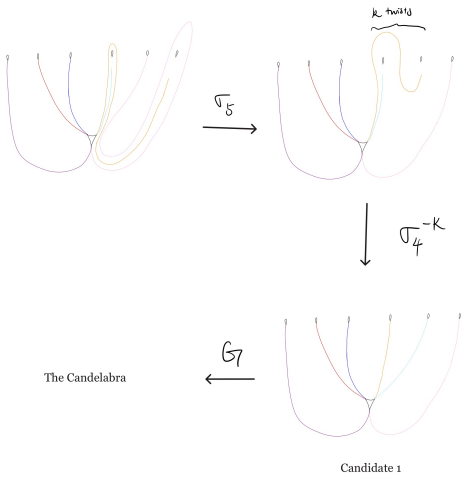


Figure J.10: This sequence shows the inverse of the braid b_3^c carries Train Track Candidate Family 3.

J.8 Candidate Family 4

Train Track Map Candidate Family 4 of the Candelabra train track is shown in Figure J.11. Note there is twisting between $f_\beta(o)$ and $f_\beta(i)$. See C.0.2.2.1.1 for details.

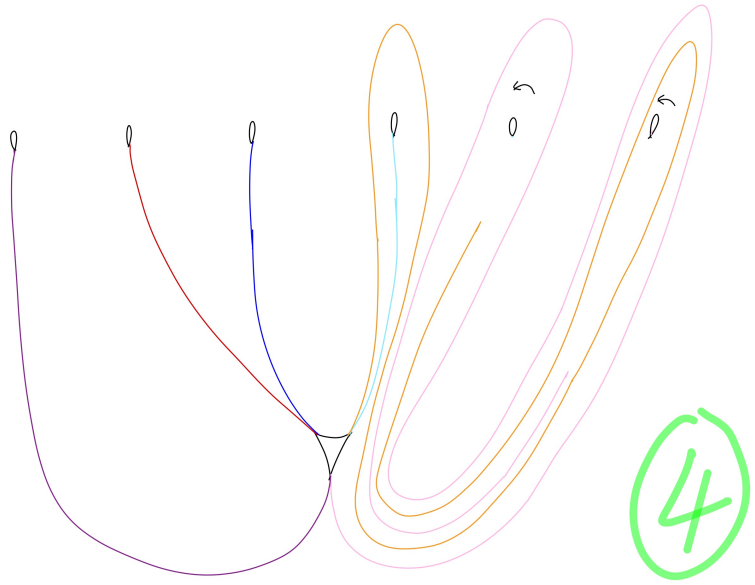


Figure J.11: Train Track Map Candidate Family 4 of the Candelabra.

The inverse of the following braid carries this family of train track maps:

$$b_4^c = (\sigma_5^{-1})^k \sigma_4 \circ G$$

where G is the braid of Section J.3, and $k \geq 1$ ($k \in \mathbb{Z}$) is the twisting parameter. This is shown in Figure J.12

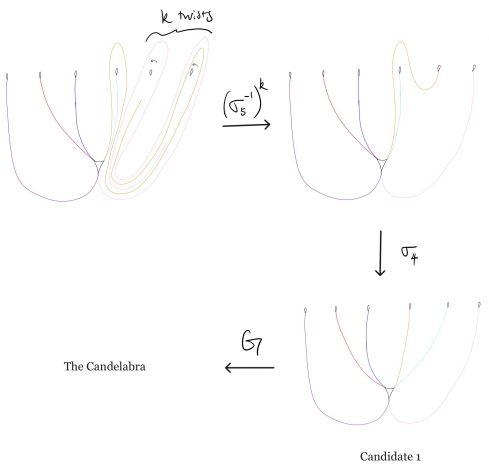


Figure J.12: This sequence shows the inverse of the braid b_4^c carries Train Track Candidate Family 4.

J.9 Candidate Family 5

Train Track Map Candidate Family 5 of the Candelabra train track is shown in Figure J.13. Note there is twisting among $f_\beta(s)$,$f_\beta(i)$, and $f_\beta(o)$. See C.0.2.2.1.1 for details.

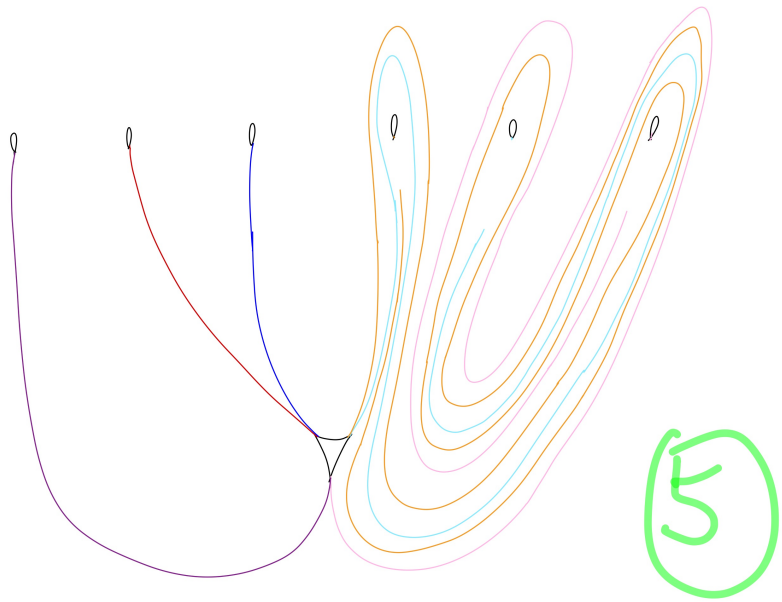


Figure J.13: Train Track Map Candidate Family 5 of the Candelabra.

The inverse of the following braid carries this family of train track maps:

$$b_5^c = (\sigma_5^{-1})^k \sigma_4^m \sigma_4^{-1} \circ G$$

where G is the braid of Section J.3, and $k, m \geq 1$ ($k, m \in \mathbb{Z}$) are the twisting parameters. This is shown in Figure J.14

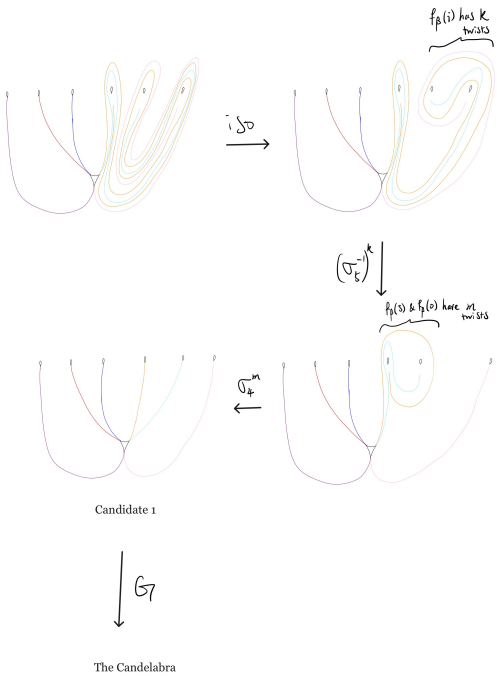


Figure J.14: This sequence shows the inverse of the braid b_5^c carries Train Track Candidate Family 5.

J.10 Candidate Family 6

Train Track Map Candidate Family 6 of the Candelabra train track is shown in Figure J.15. Note there is twisting between $f_\beta(b)$ and $f_\beta(r)$. See C.0.2.2.2.1.1 for details.

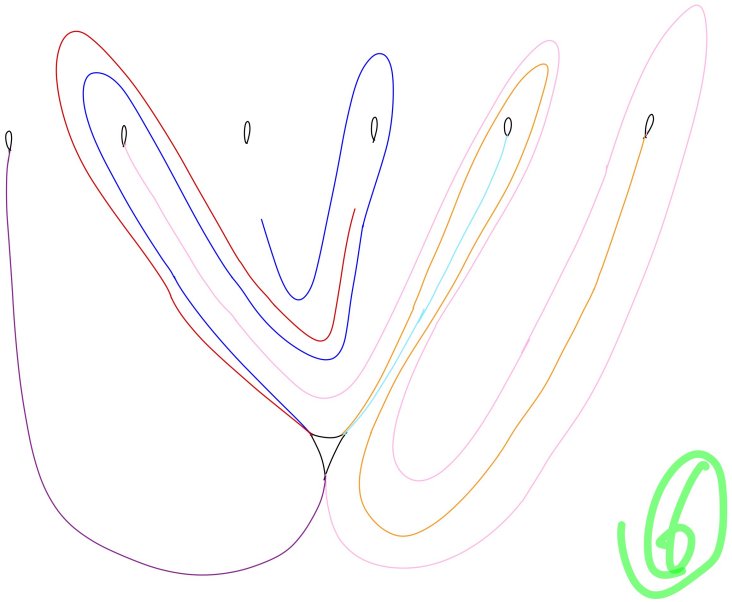


Figure J.15: Train Track Map Candidate Family 6 of the Candelabra.

The inverse of the following braid carries this family of train track maps:

$$b_6^c = (\sigma_3^{-1})^k \sigma_2 \sigma_3 \sigma_4^{-1} \sigma_5^{-1} \sigma_4 \circ G$$

where G is the braid of Section J.3, and $k \geq 1$ ($k \in \mathbb{Z}$) is the twisting parameter. This is shown in Figure J.16

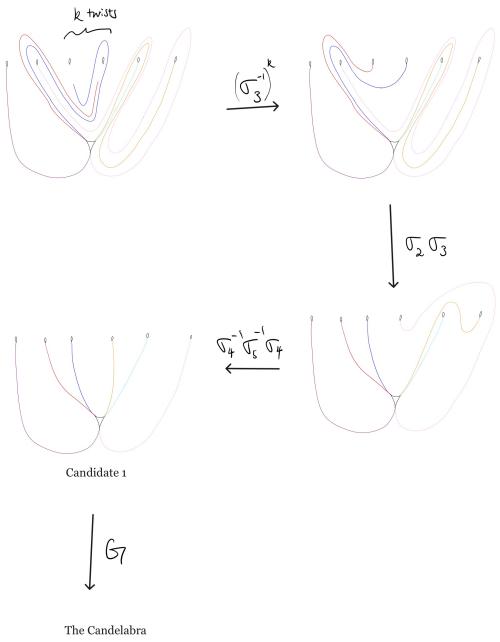


Figure J.16: This sequence shows the inverse of the braid b_6^c carries Train Track Candidate Family 6.

J.11 Candidate Family 7

Train Track Map Candidate Family 7 of the Candelabra train track is shown in Figure J.17. Note there is twisting between $f_\beta(b)$ and $f_\beta(r)$, and twisting between $f_\beta(o)$ and $f_\beta(s)$. See C.0.2.2.2.1.2 for details.

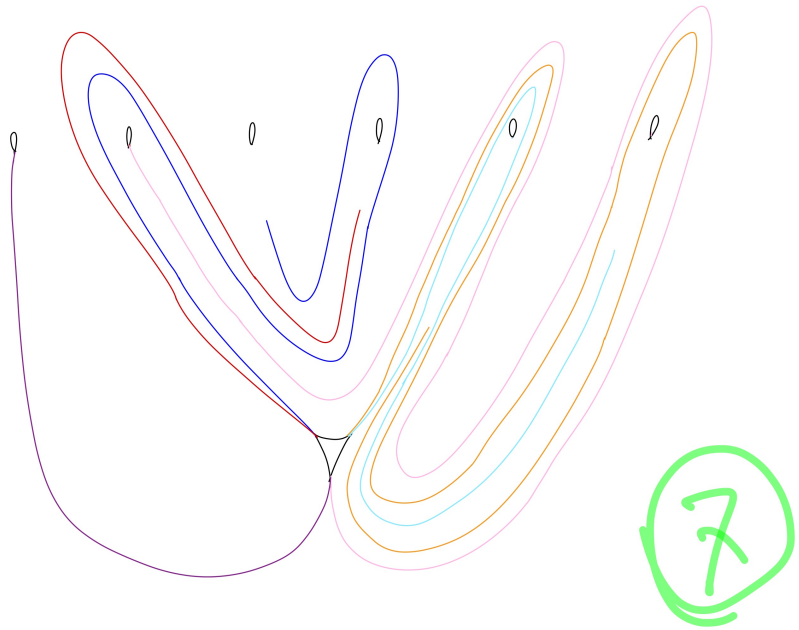


Figure J.17: Train Track Map Candidate Family 7 of the Candelabra.

The inverse of the following braid carries this family of train track maps:

$$b_7^c = (\sigma_3^{-1})^k \sigma_2 \sigma_3 \sigma_4^{-1} \sigma_5^{-1} \sigma_4^m \circ G$$

where G is the braid of Section J.3, and $k, m \geq 1$ ($k, m \in \mathbb{Z}$) are the twisting parameters. This is shown in Figure J.18

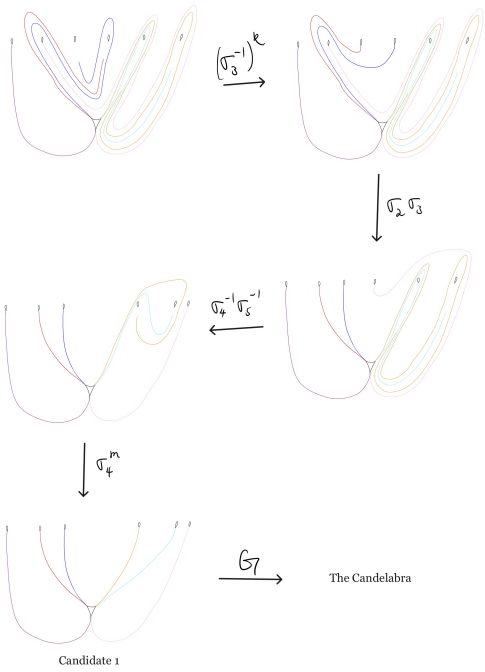


Figure J.18: This sequence shows the inverse of the braid b_7^c carries Train Track Candidate Family 7.

J.12 Candidate Family 8

Train Track Map Candidate Family 8 of the Candelabra train track is shown in Figure J.19. Note there is twisting between $f_\beta(o)$ and $f_\beta(s)$. See C.0.2.2.3.4.1 for details.

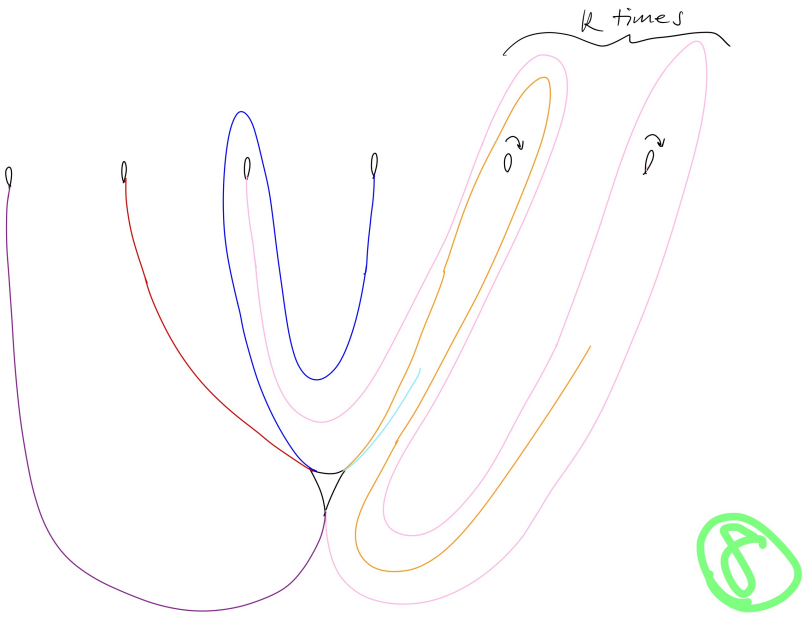


Figure J.19: Train Track Map Candidate Family 8 of the Candelabra.

The inverse of the following braid carries this family of train track maps:

$$b_8^c = \sigma_5^k \sigma_3 \sigma_4^{-1} \sigma_5^{-1} \circ G$$

where G is the braid of Section J.3, and $k \geq 1$ ($k \in \mathbb{Z}$) is the twisting parameter. This is shown in Figure J.20

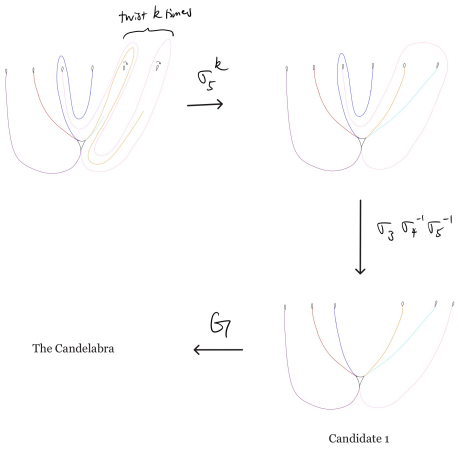


Figure J.20: This sequence shows the inverse of the braid b_8^c carries Train Track Candidate Family 8.

J.13 Candidate Family 9

Train Track Map Candidate Family 9 of the Candelabra train track is shown in Figure J.21. Note there is twisting among $f_\beta(i)$, $f_\beta(o)$ and $f_\beta(s)$. See C.0.2.2.3.4.2 for details.

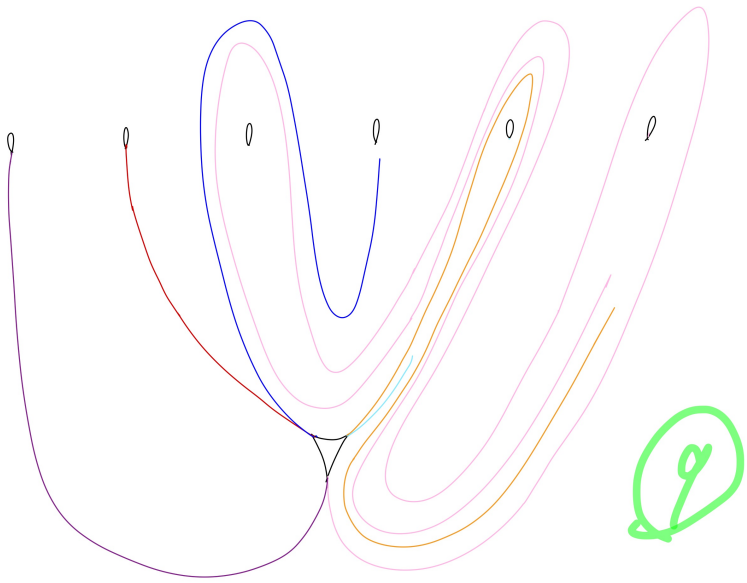


Figure J.21: Train Track Map Candidate Family 9 of the Candelabra.

The inverse of the following braid carries this family of train track maps:

$$b_9^c = \sigma_5^m \sigma_3 (\sigma_4^{-1})^k \sigma_4^{-1} \sigma_5^{-1} \circ G$$

where G is the braid of Section J.3, and $k, m \geq 1$ ($k, m \in \mathbb{Z}$) are the twisting parameters. This is shown in Figure J.22

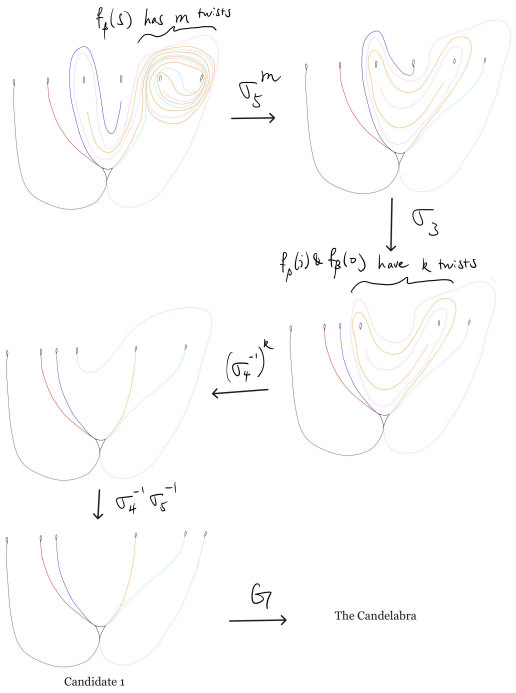


Figure J.22: This sequence shows the inverse of the braid b_9^c carries Train Track Candidate Family 9.

J.14 Candidate Family 10

Train Track Map Candidate Family 10 of the Candelabra train track is shown in Figure J.23. Note there is twisting between $f_\beta(o)$ and $f_\beta(s)$. See C.0.5.1.1.1 for details.

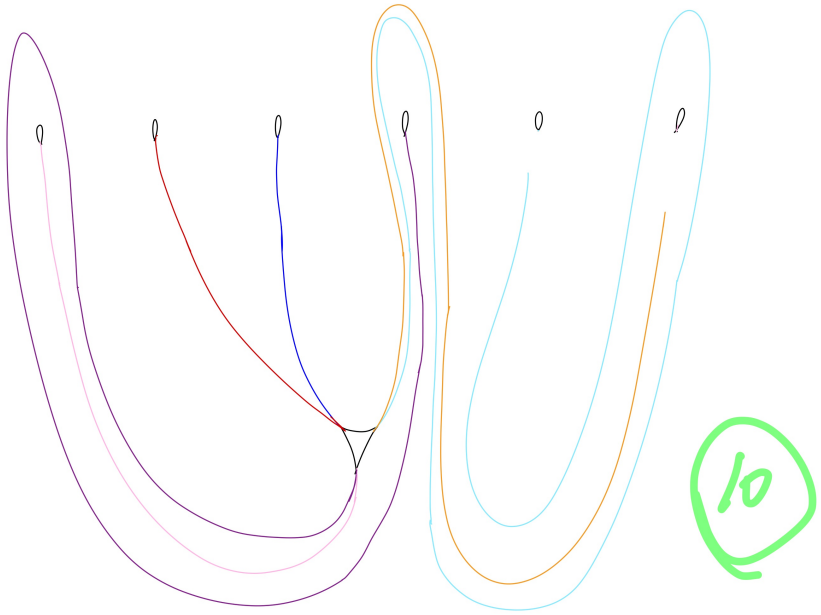


Figure J.23: Train Track Map Candidate Family 10 of the Candelabra.

For this and subsequent candidates, we define the auxiliary braid F:

$$F = \sigma_5\sigma_4\sigma_3\sigma_2\sigma_1\sigma_2\sigma_3\sigma_4\sigma_5\sigma_5\sigma_4\sigma_3\sigma_2\sigma_3\sigma_4\sigma_5\sigma_5\sigma_4\sigma_3\sigma_4\sigma_5\sigma_5\sigma_4\sigma_5\sigma_5$$

The inverse of the following braid carries this family of train track maps:

$$b_{10}^c = (\sigma_5^{-1})^k\sigma_4\sigma_5\sigma_1\sigma_2\sigma_3\sigma_4 \circ F \circ G$$

where G is the braid of Section J.3, and $k \geq 1$ ($k \in \mathbb{Z}$) is the twisting parameter. This is shown in Figure J.24.

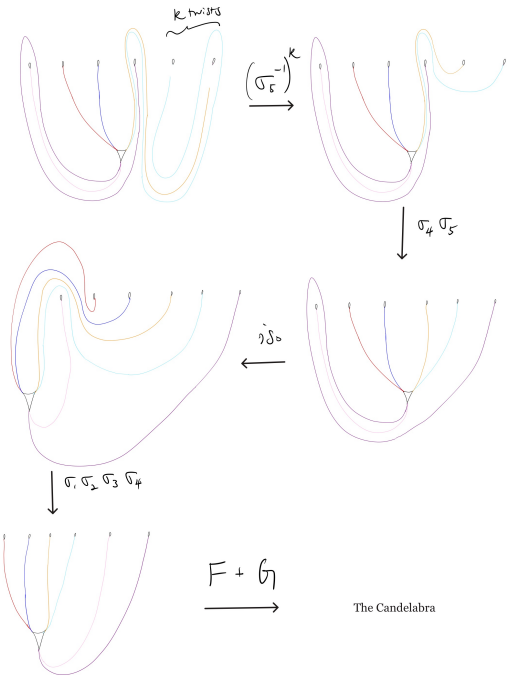


Figure J.24: This sequence shows the inverse of the braid b_{10}^c carries Train Track Candidate Family 10.

J.15 Candidate Family 11

Train Track Map Candidate Family 11 of the Candelabra train track is shown in Figure J.25. Note there is twisting among $f_\beta(p)$, $f_\beta(o)$ and $f_\beta(s)$. See C.0.5.1.1.2 for details.

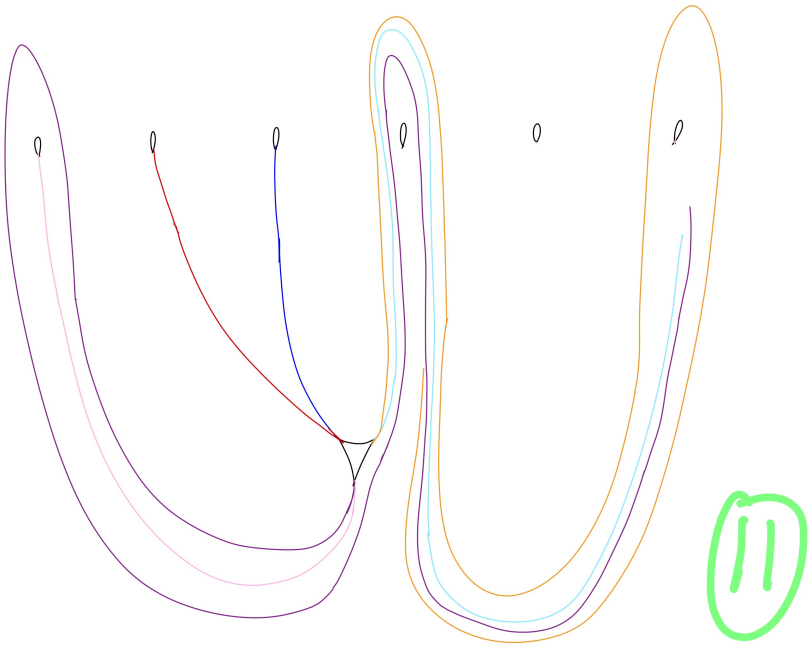


Figure J.25: Train Track Map Candidate Family 11 of the Candelabra.

The inverse of the following braid carries this family of train track maps:

$$b_{11}^c = \sigma_4\sigma_5^m\sigma_4^k\sigma_1\sigma_2\sigma_3\sigma_4 \circ F \circ G$$

where G is the braid of Section J.3, and $k, m \geq 1$ ($k, m \in \mathbb{Z}$) are the twisting parameters. This is shown in Figure J.26.

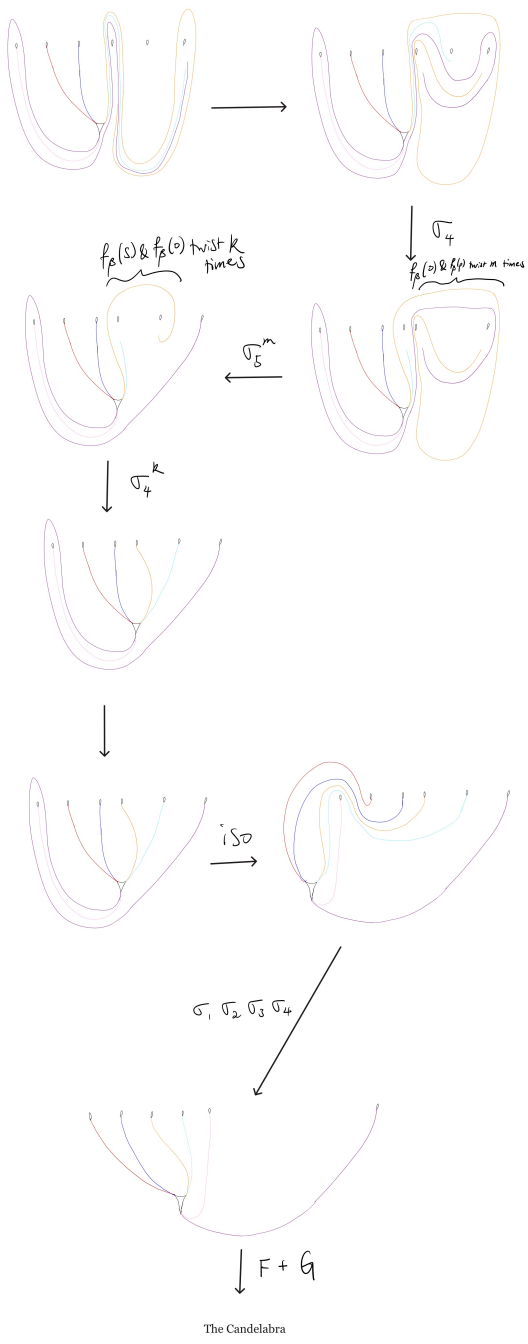


Figure J.26: This sequence shows the inverse of the braid b_{11}^c carries Train Track Candidate Family 11.

J.16 Candidate Family 12

Train Track Map Candidate Family 12 of the Candelabra train track is shown in Figure J.27. Note there is twisting between $f_\beta(o)$ and $f_\beta(s)$. See C.0.5.2.1.1.1 for details.

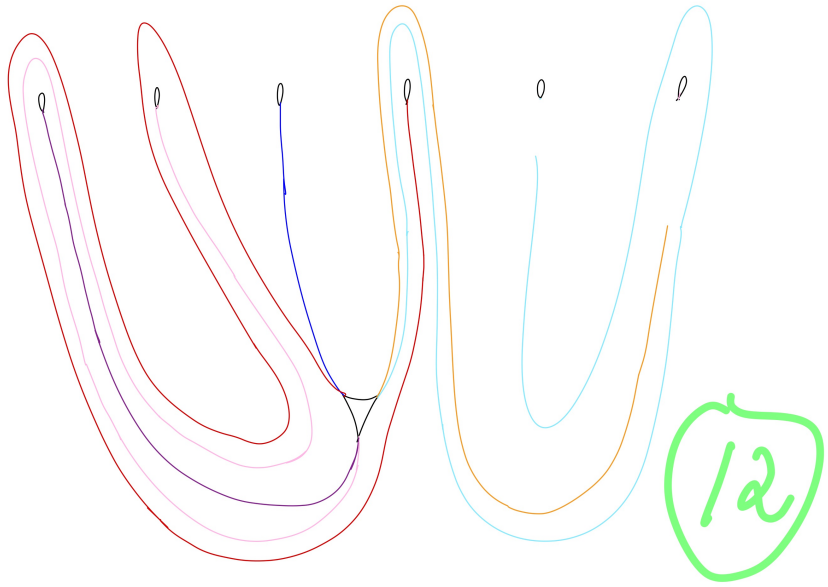


Figure J.27: Train Track Map Candidate Family 12 of the Candelabra.

The inverse of the following braid carries this family of train track maps:

$$b_{12}^c = (\sigma_5^{-1})^k \sigma_4\sigma_5\sigma_1\sigma_2\sigma_1\sigma_3\sigma_2\sigma_4\sigma_3\sigma_4\sigma_4$$

where $k \geq 1$ ($k \in \mathbb{Z}$) is the twisting parameter. This is shown in Figure J.28.

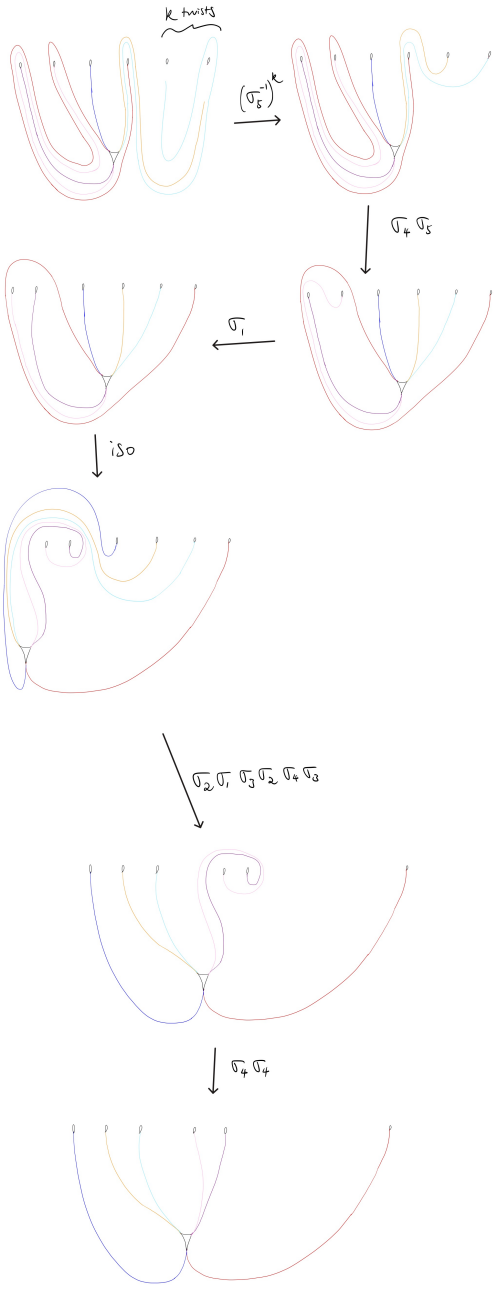


Figure J.28: This sequence shows the inverse of the braid b_{12}^c carries Train Track Candidate Family 12.

J.17 Candidate 13

Train Track Map Candidate 13 of the Candelabra train track is shown in Figure J.29.

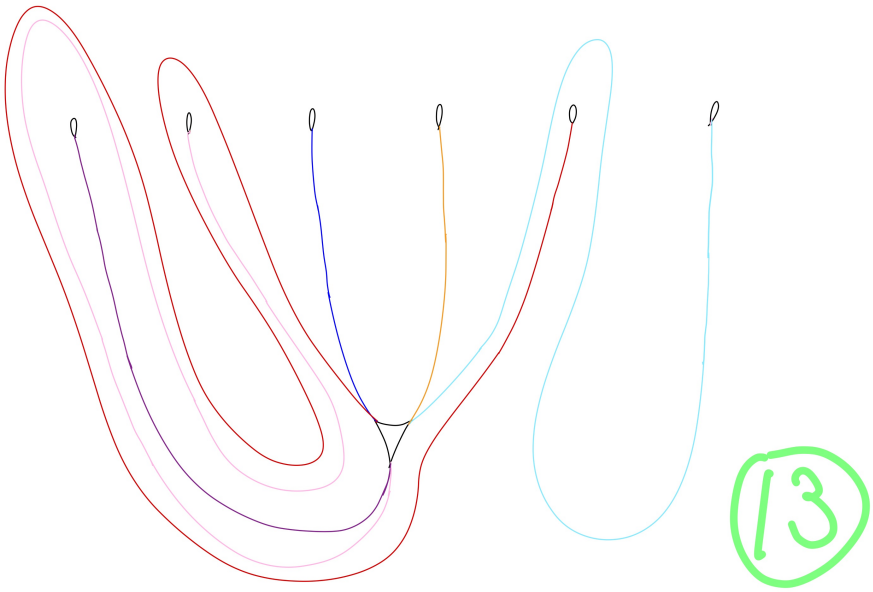


Figure J.29: Train Track Map Candidate 13 of the Candelabra.

The inverse of the following braid carries this train track map:

$$b_{13}^{c} = \sigma_5\sigma_1\sigma_2\sigma_1\sigma_3\sigma_2\sigma_4\sigma_3\sigma_4\sigma_4$$

This is shown in Figure J.30.

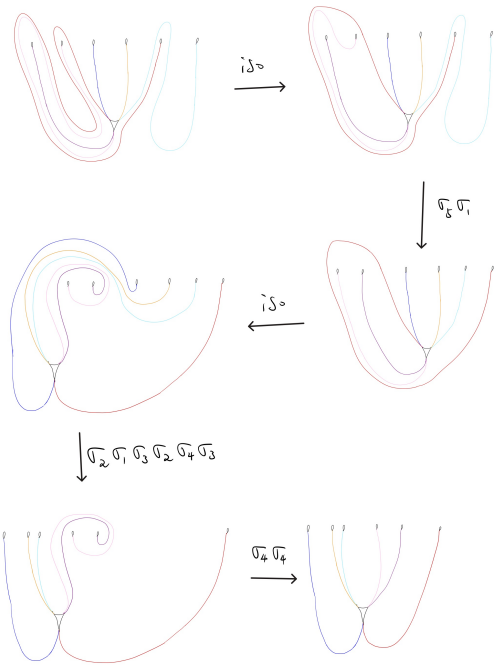


Figure J.30: This sequence shows the inverse of the braid b_{13}^{c} carries Train Track Map Candidate 13.

J.18 Candidate Family 14

Train Track Map Candidate Family 14 of the Candelabra train track is shown in Figure J.31. Note there is twisting between $f_\beta(o)$ and $f_\beta(s)$; and twisting between $f_\beta(r)$ and $f_\beta(b)$. See C.0.5.2.1.1.1 for details.

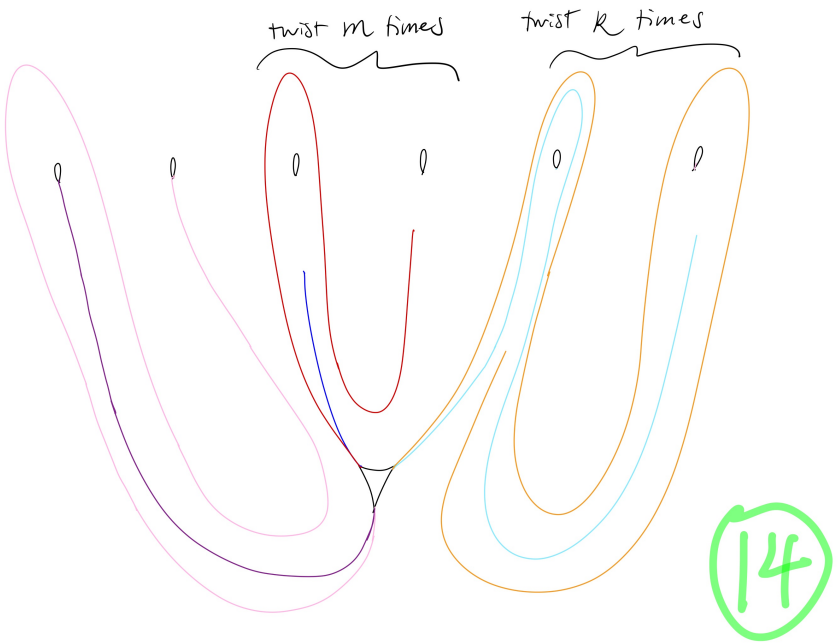


Figure J.31: Train Track Map Candidate Family 14 of the Candelabra.

The inverse of the following braid carries this family of train track maps:

$$b_{14}^c = \sigma_5^k \sigma_3^m \sigma_1 \sigma_2 \sigma_3 \sigma_4 \circ F \circ G$$

where $k, m \geq 1$ ($k, m \in \mathbb{Z}$) are the twisting parameters. This is shown in Figure J.32.

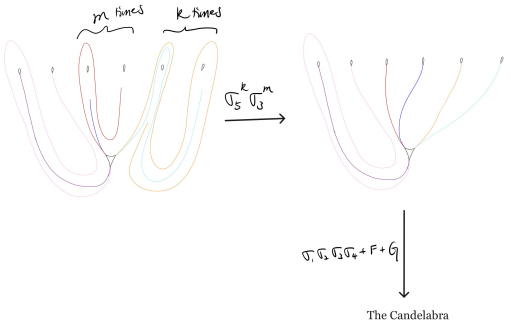


Figure J.32: This sequence shows the inverse of the braid b_{14}^c carries Train Track Candidate Family 14.

J.19 Candidate Family 15

Train Track Map Candidate Family 15 of the Candelabra train track is shown in Figure J.33. Note there is twisting between $f_\beta(i)$ and $f_\beta(r)$. See C.0.5.2.1.1.3 for details.

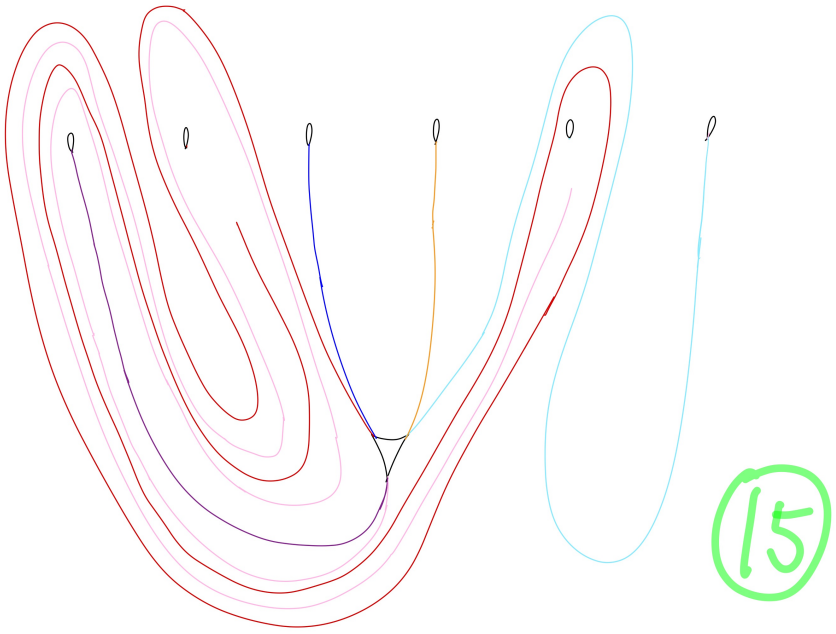


Figure J.33: Train Track Map Candidate Family 15 of the Candelabra.

The inverse of the following braid carries this family of train track maps:

$$b_{15}^c = \sigma_2\sigma_1\sigma_3\sigma_2\sigma_5\sigma_4\sigma_3\sigma_4\sigma_4(\sigma_5^{-1})^k\sigma_4$$

where $k \geq 1$ ($k \in \mathbb{Z}$) is the twisting parameter. This is shown in Figure J.34.

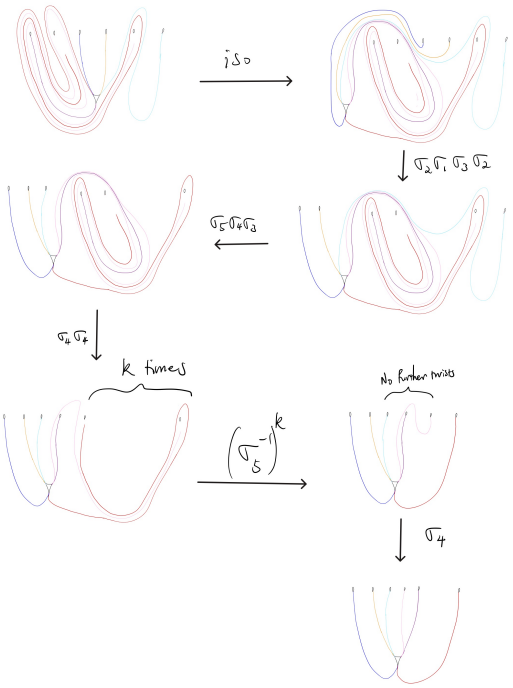


Figure J.34: This sequence shows the inverse of the braid b_{15}^c carries Train Track Candidate Family 15.

J.20 Candidate Family 16

Train Track Map Candidate Family 16 of the Candelabra train track is shown in Figure J.35. Note there is twisting between $f_\beta(p)$ and $f_\beta(i)$; between $f_\beta(r)$ and $f_\beta(b)$; and between $f_\beta(o)$ and $f_\beta(s)$. See C.0.5.3.1 for details.

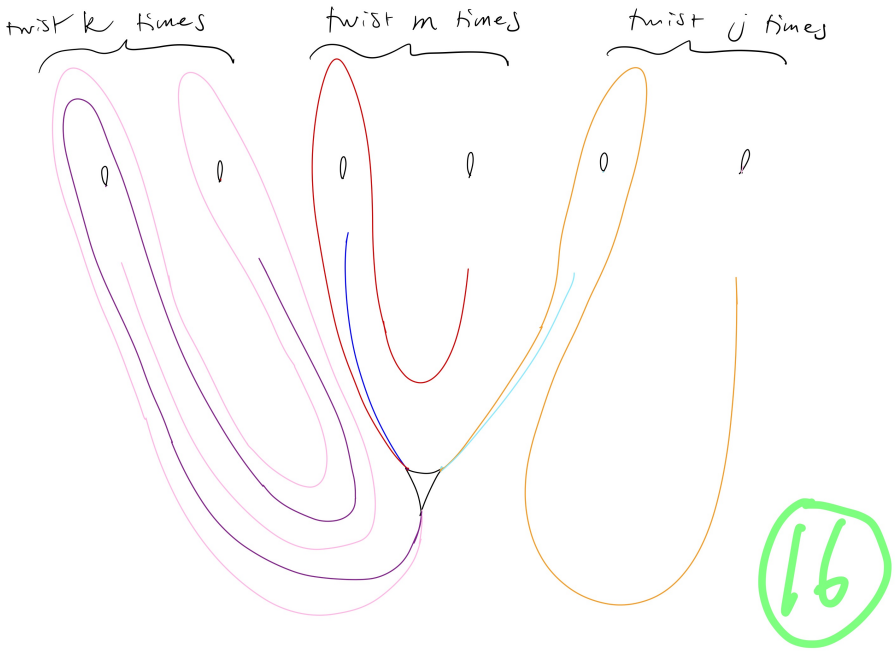


Figure J.35: Train Track Map Candidate Family 16 of the Candelabra.

The inverse of the following braid carries this family of train track maps:

$$b_{16}^c = \sigma_5^j \sigma_3^m \sigma_1^k \circ H \circ G$$

where $k, m, j \geq 1$ ($k, m, j \in \mathbb{Z}$) are the twisting parameters. This is shown in Figure J.36.

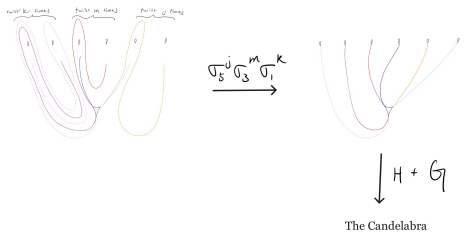


Figure J.36: This sequence shows the inverse of the braid b_{16}^c carries Train Track Candidate Family 16.

J.21 Candidate Family 17

Train Track Map Candidate Family 17 of the Candelabra train track is shown in Figure J.37. Note there is twisting among $f_\beta(i)$, $f_\beta(p)$, and $f_\beta(r)$. See C.0.5.3.2 for details.

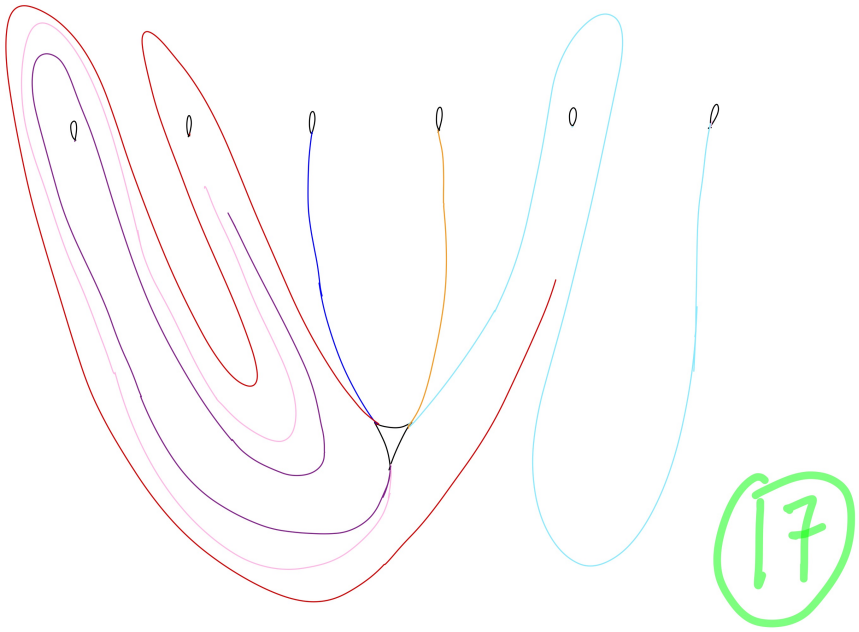


Figure J.37: Train Track Map Candidate Family 17 of the Candelabra.

The inverse of the following braid carries this family of train track maps:

$$b_{17}^c = \sigma_1^k \sigma_2 \sigma_1 \sigma_5 \sigma_4 \sigma_3 \sigma_2 \sigma_4 \sigma_3 \sigma_4 (\sigma_5^{-1})^m \sigma_4$$

where $k, m \geq 1$ ($k, m \in \mathbb{Z}$) are the twisting parameters. This is shown in Figure J.38.

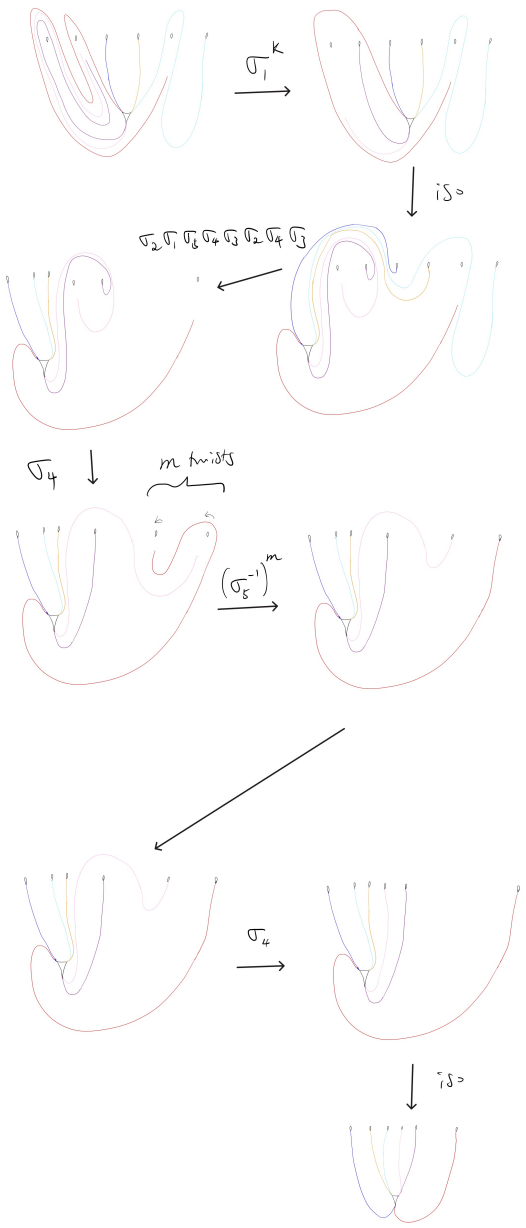


Figure J.38: This sequence shows the inverse of the braid b_{17}^c carries Train Track Candidate Family 17.

APPENDIX ELEVEN

Appendix: Candidate Braids for Track 0

K.1 Summary of Candidate Braid Families

Through the exhaustive train track case analysis of Track 0 in the stratum $(2; 1^6; 3^2)$ (the full details of which are presented in Appendix D), we isolate exactly 13 candidate families of train track maps. If the pseudo-Anosov representative ϕ_Φ has no interior fixed points, then its mapping class Φ must be conjugate to the lift of one of the following 13 braid families (enumerated below with their twist parameters).

1. $\Delta^{2i}(\sigma_2^{-1}\sigma_4^{-1}\sigma_1^{-1}\sigma_3\sigma_2\sigma_1\sigma_3\sigma_2\sigma_3\sigma_2\sigma_1\sigma_4\sigma_3\sigma_2\sigma_5\sigma_4\sigma_3)^{-1}$
2. $\Delta^{2i}(\sigma_2^{-1}\sigma_3^{-1}\sigma_4^{-1}\sigma_3\sigma_2\sigma_1^{-1}\sigma_4\sigma_3\sigma_2\sigma_1\sigma_2\sigma_1\sigma_3\sigma_2\sigma_1^{-1}\sigma_2^{-1}\sigma_3^{-1}\sigma_1\sigma_1 \cdot J \cdot \Lambda_6)^{-1}$
3. $\Delta^{2i}(\sigma_2^{-1}\sigma_3^{-1}\sigma_4^{-1}\sigma_2\sigma_1^{-1}\sigma_2^{-1}\sigma_3\sigma_2\sigma_4^{-1}\sigma_3^{-1}\sigma_2\sigma_1\sigma_4\sigma_3\sigma_2\sigma_1\sigma_4\sigma_3\sigma_2\sigma_1 \cdot J \cdot \Lambda_6)^{-1}$
4. $\Delta^{2i}(\sigma_2^{-1}\sigma_3^{-1}\sigma_4^{-1}\sigma_1^{-1}\sigma_3\sigma_2\sigma_4^{-1}\sigma_3^{-1}\sigma_2\sigma_1\sigma_4\sigma_4\sigma_3\sigma_2\sigma_1\sigma_4\sigma_3\sigma_2 \cdot J \cdot \Lambda_6)^{-1}$
5. $\Delta^{2i}(\sigma_4\sigma_2\sigma_5^{-1}\sigma_3\sigma_2\sigma_1\sigma_4^{-1}\sigma_5^{-1}\sigma_4^{-1}\sigma_3\sigma_2\sigma_3\sigma_2\sigma_1\sigma_4\sigma_5\sigma_5)^{-1}$
6. $\Delta^{2i}(\sigma_4\sigma_2\sigma_5^{-1}\sigma_5^{-1}\sigma_3\sigma_2\sigma_1\sigma_3\sigma_2\sigma_4^{-1}\sigma_5^{-1}\sigma_3\sigma_2\sigma_1\sigma_4\sigma_5\sigma_5)^{-1}$

7. $\Delta^{2i}(\sigma_4^m\sigma_3\sigma_4\sigma_5^{-k}\sigma_3\sigma_3\sigma_4^j\sigma_4\sigma_3\sigma_2\sigma_1\sigma_4\sigma_3\sigma_2\sigma_4\sigma_3\sigma_5\sigma_4\sigma_5\sigma_5)^{-1}$

8. $\Delta^{2i}(\sigma_4^k\sigma_3^m\sigma_3\sigma_4\sigma_4\sigma_3\sigma_4\sigma_4\sigma_2\sigma_1\sigma_3\sigma_2\sigma_4\sigma_3\sigma_5\sigma_4\sigma_5\sigma_5)^{-1}$

9. $\Delta^{2i}(\sigma_2^{-1}\sigma_1\sigma_3\sigma_4\sigma_5^{-k}\sigma_4\sigma_3\sigma_2\sigma_1\sigma_3\sigma_2\sigma_4\sigma_3\sigma_5\sigma_4\sigma_5\sigma_5)^{-1}$

10. $\Delta^{2i}(\sigma_2^{-j}\sigma_1^m\sigma_3\sigma_4\sigma_5^{-k}\sigma_4\sigma_3\sigma_2\sigma_1\sigma_3\sigma_2\sigma_4\sigma_3\sigma_5\sigma_4\sigma_5\sigma_5)^{-1}$

11. $\Delta^{2i}(\sigma_4\sigma_3\sigma_4^k\sigma_4\sigma_3\sigma_4\sigma_2\sigma_1\sigma_3\sigma_2\sigma_4\sigma_3\sigma_5\sigma_4\sigma_5\sigma_5)^{-1}$

12. $\Delta^{2i}(\sigma_4^{-k}\sigma_4^{-1}\sigma_3\sigma_4^m\sigma_4\sigma_3\sigma_4\sigma_1\sigma_3\sigma_2\sigma_4\sigma_3\sigma_5\sigma_4\sigma_5\sigma_5)^{-1}$

13. $\Delta^{2i}(\sigma_4^{-k}\sigma_4^{-1}\sigma_3\sigma_4\sigma_5^{-1}\sigma_4^m\sigma_3\sigma_4\sigma_2\sigma_1\sigma_3\sigma_2\sigma_4\sigma_3\sigma_5\sigma_4\sigma_5\sigma_5)^{-1}$

K.2 Base Braids Λ_6 and J

Before we detail the individual candidate families, we introduce the following auxiliary base braids, which we call Λ_6 and J:

$\Lambda_6 = \sigma_1\sigma_2\sigma_1\sigma_3\sigma_2\sigma_1\sigma_4\sigma_3\sigma_2\sigma_1\sigma_5\sigma_4\sigma_3\sigma_2\sigma_1$

$J = \sigma_1^{-1}\sigma_2^{-1}\sigma_1^{-1}\sigma_5\sigma_4\sigma_5$

We shall make use of Λ_6 and J occasionally in constructing candidate braids for Track 0.

K.3 Candidate Family 1 (Loblolly)

Train Track Map Candidate Family 1 of Track 0 is shown in Figure K.1. See D.1.1.2.1.1.2.2 for details.

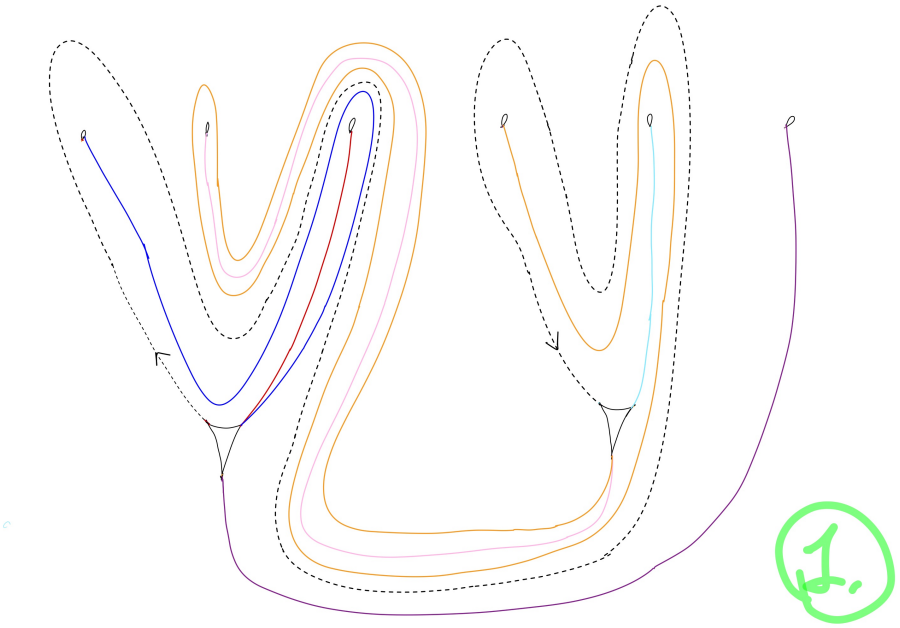


Figure K.1: Train Track Map Candidate Family 1 of Track 0.

The inverse of the following braid carries this family of train track maps:

$$b_1^0 = \sigma_2^{-1}\sigma_4^{-1}\sigma_1^{-1}\sigma_3\sigma_2\sigma_1\sigma_3\sigma_2\sigma_3\sigma_2\sigma_1\sigma_4\sigma_3\sigma_2\sigma_5\sigma_4\sigma_3$$

This is shown in Figure K.2.

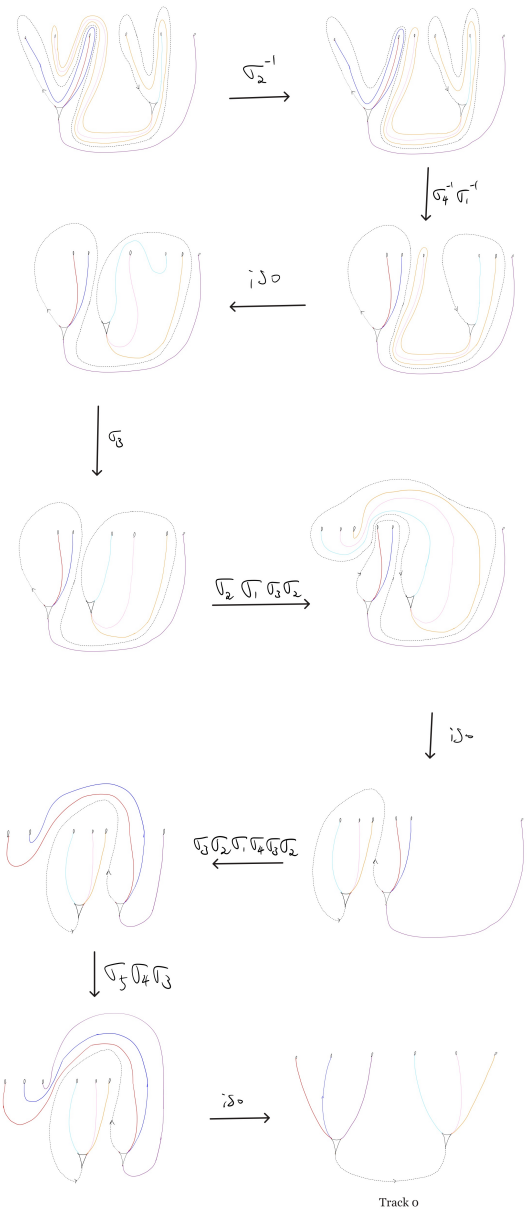


Figure K.2: This sequence shows the inverse of the braid b_1^0 carries Train Track Candidate Family 1.

K.4 Candidate Family 2 (Sloom)

Train Track Map Candidate Family 2 of Track 0 is shown in Figure K.3. See D.1.2.1.1 for details.

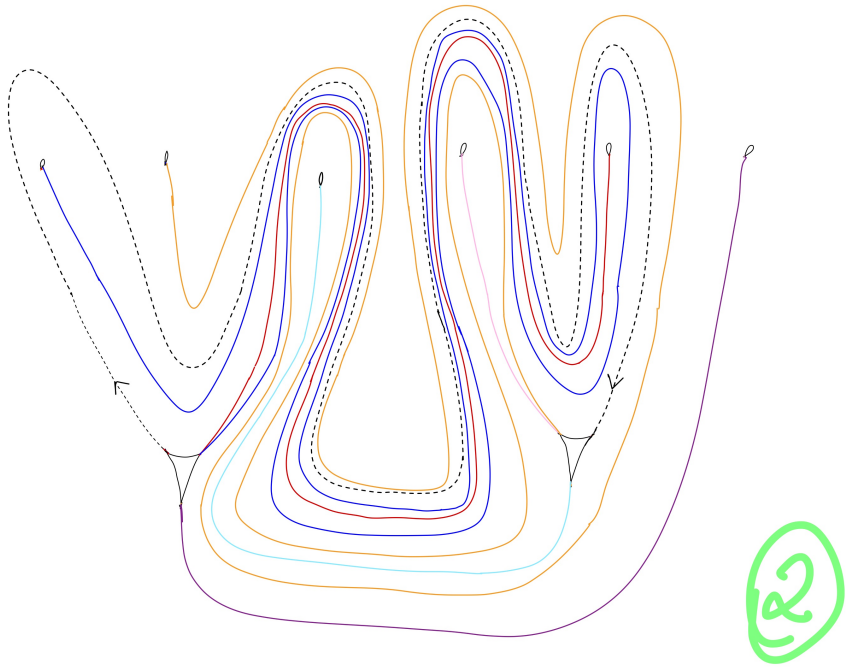


Figure K.3: Train Track Map Candidate Family 2 of Track 0.

The inverse of the following braid carries this family of train track maps:

$$b_2^0 = \sigma_2^{-1}\sigma_3^{-1}\sigma_4^{-1}\sigma_3\sigma_2\sigma_1^{-1}\sigma_4\sigma_3\sigma_2\sigma_1\sigma_2\sigma_1\sigma_3\sigma_2\sigma_1^{-1}\sigma_2^{-1}\sigma_3^{-1}\sigma_1\sigma_1 \cdot J \cdot \Lambda_6$$

This is shown in Figure K.4.

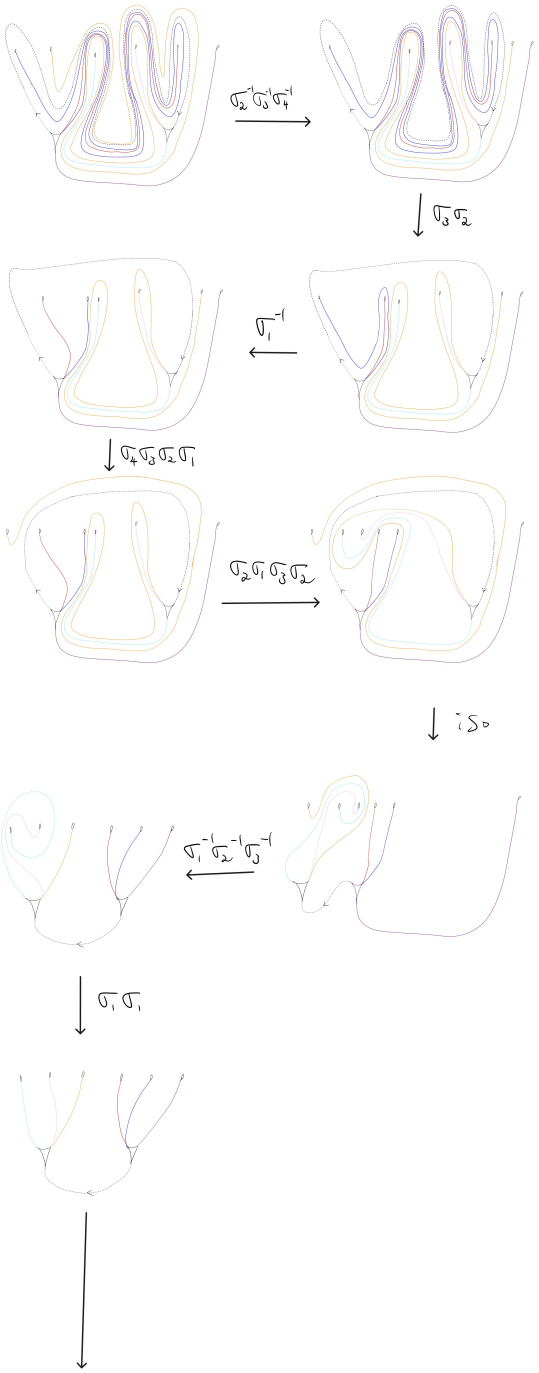


Figure K.4: This sequence shows the inverse of the braid b_2^0 carries Train Track Candidate Family 2.

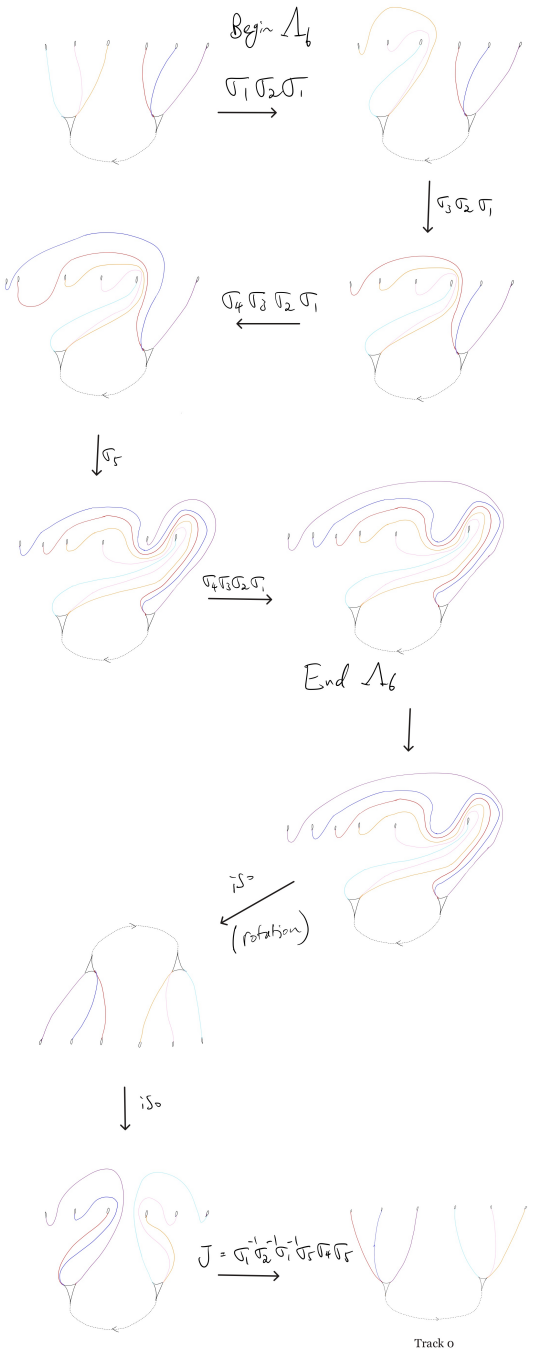


Figure K.4: This sequence shows the inverse of the braid b_2^0 carries Train Track Candidate Family 2 (continued).

K.5 Candidate Family 3 (Mooncalf)

Train Track Map Candidate Family 3 of Track 0 is shown in Figure K.5. See D.1.2.1.2.1.2 for details.

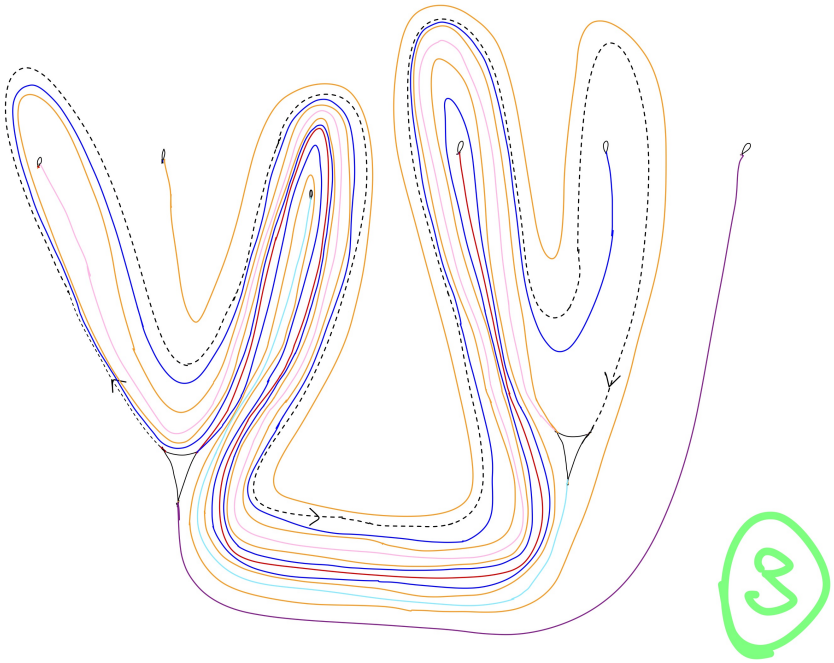


Figure K.5: Train Track Map Candidate Family 3 of Track 0.

The inverse of the following braid carries this family of train track maps:

$$b_3^0 = \sigma_2^{-1}\sigma_3^{-1}\sigma_4^{-1}\sigma_2\sigma_1^{-1}\sigma_2^{-1}\sigma_3\sigma_2\sigma_4^{-1}\sigma_3^{-1}\sigma_2\sigma_1\sigma_4\sigma_3\sigma_2\sigma_1\sigma_4\sigma_3\sigma_2\sigma_1 \cdot J \cdot \Lambda_6$$

This is shown in Figure K.6.

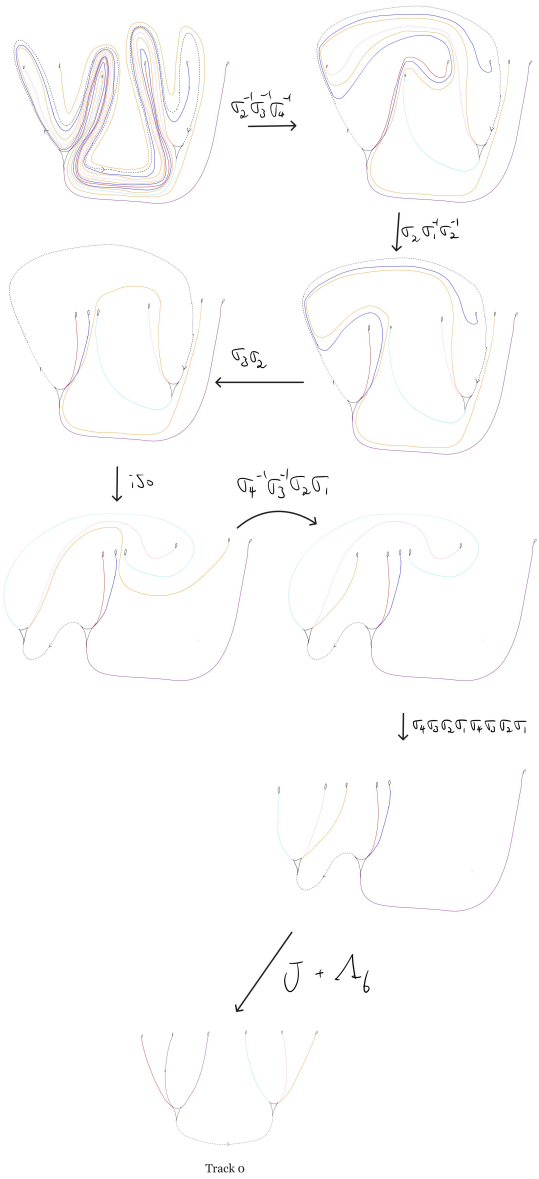


Figure K.6: This sequence shows the inverse of the braid b_3^0 carries Train Track Candidate Family 3.

K.6 Candidate Family 4 (Faffel)

Train Track Map Candidate Family 4 of Track 0 is shown in Figure K.7. See D.1.2.1.2.2 for details.

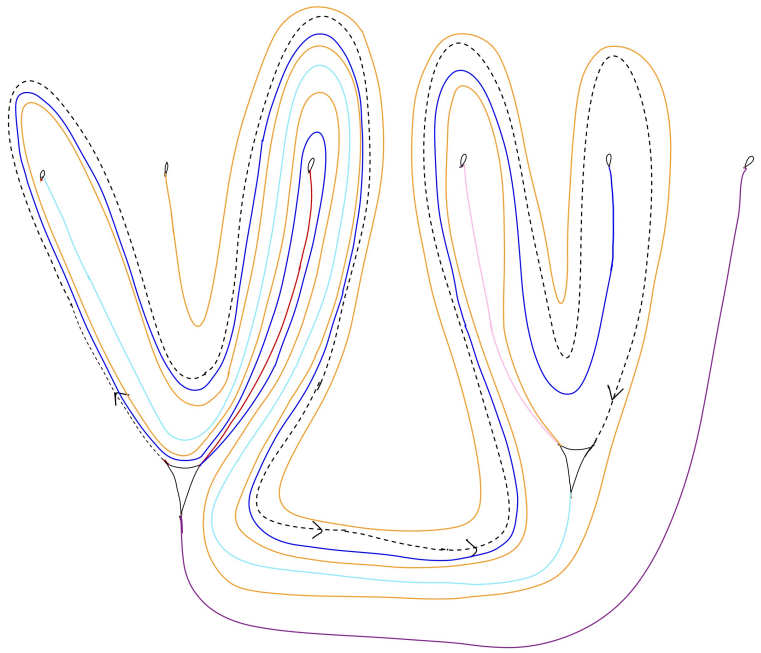


Figure K.7: Train Track Map Candidate Family 4 of Track 0.

The inverse of the following braid carries this family of train track maps:

$$b_4^0 = \sigma_2^{-1}\sigma_3^{-1}\sigma_4^{-1}\sigma_1^{-1}\sigma_3\sigma_2\sigma_4^{-1}\sigma_3^{-1}\sigma_2\sigma_1\sigma_4\sigma_4\sigma_3\sigma_2\sigma_1\sigma_4\sigma_3\sigma_2 \cdot J \cdot \Lambda_6$$

This is shown in Figure K.8.

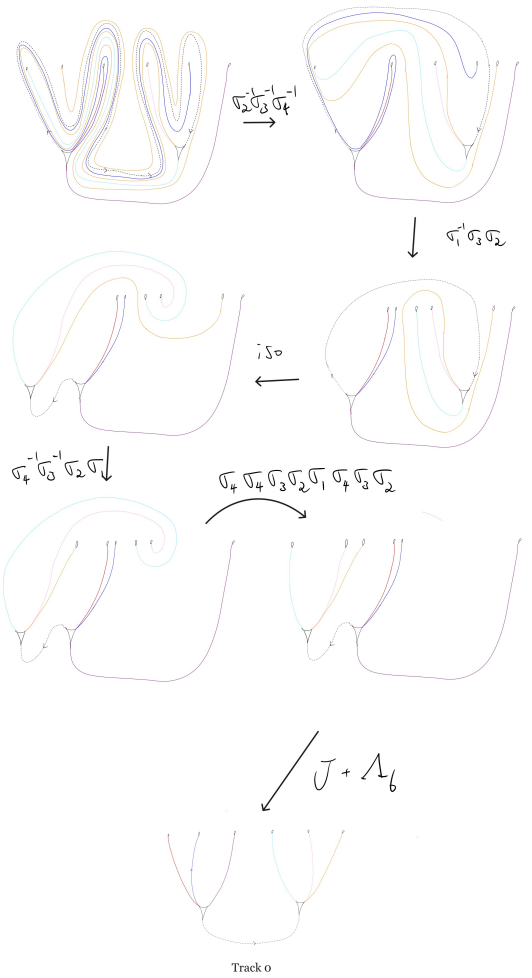


Figure K.8: This sequence shows the inverse of the braid b_4^0 carries Train Track Candidate Family 4.

K.7 Candidate Family 5 (Balance)

Train Track Map Candidate Family 5 of Track 0 is shown in Figure K.9. See D.1.6.1.2.1.1 for details.

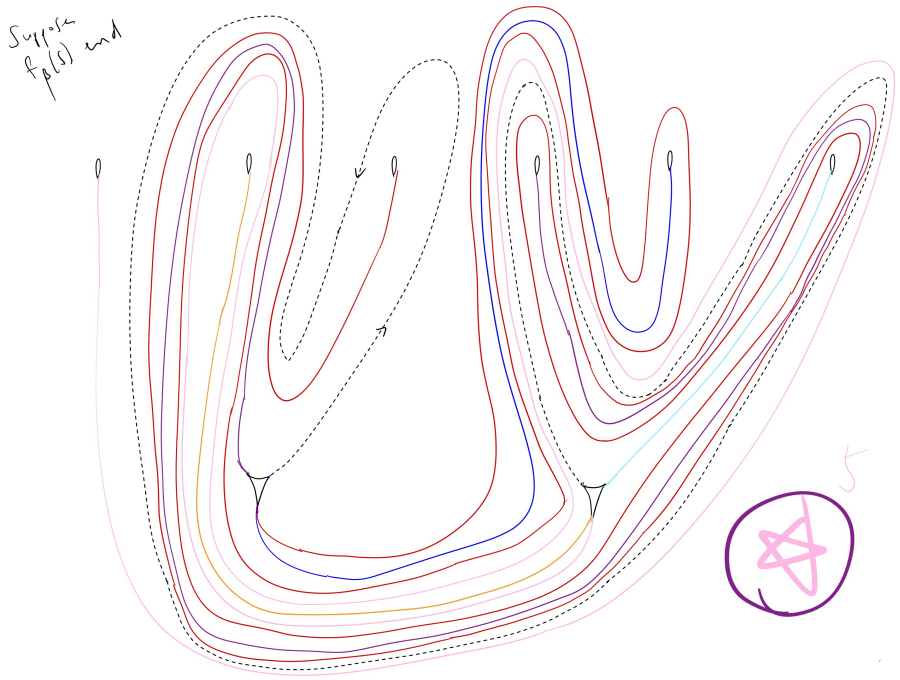


Figure K.9: Train Track Map Candidate Family 5 of Track 0.

The inverse of the following braid carries this family of train track maps:

$$b_5^0 = \sigma_4\sigma_2\sigma_5^{-1}\sigma_3\sigma_2\sigma_1\sigma_4^{-1}\sigma_5^{-1}\sigma_4^{-1}\sigma_3\sigma_2\sigma_3\sigma_2\sigma_1\sigma_4\sigma_5\sigma_5$$

This is shown in Figure K.10.

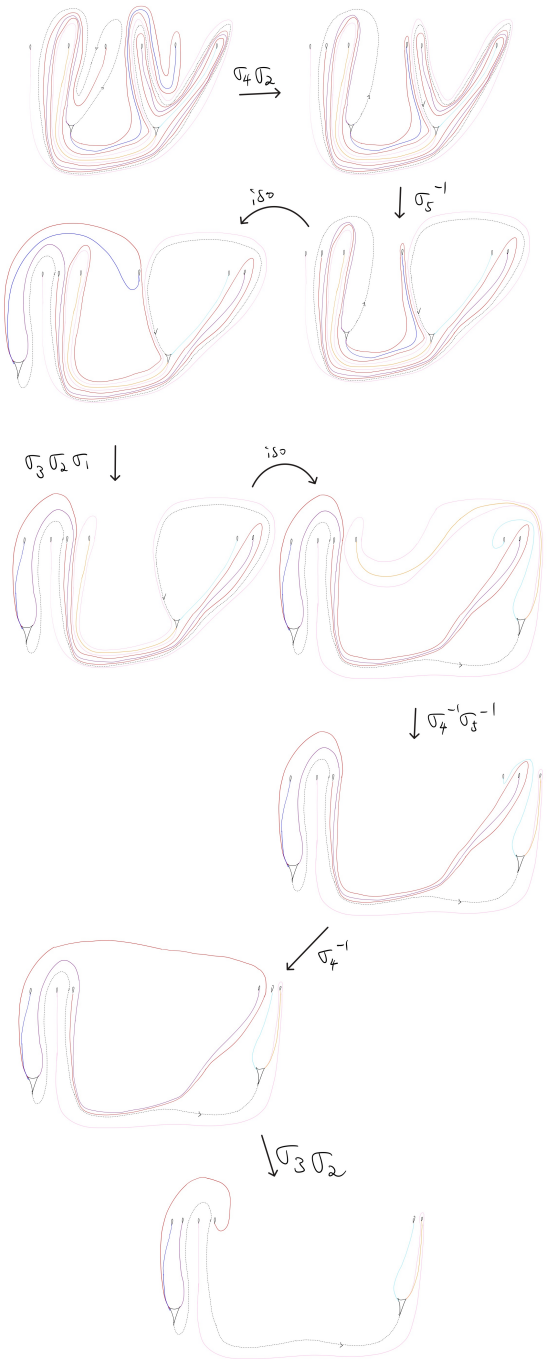


Figure K.10: This sequence shows the inverse of the braid b_5^0 carries Train Track Candidate 5.

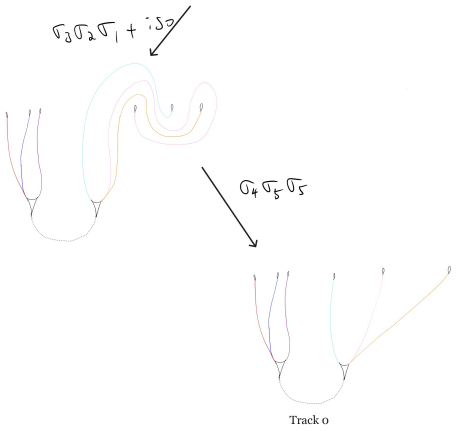


Figure K.10: This sequence shows the inverse of the braid b_5^0 carries Train Track Candidate 5 (continued).

K.8 Candidate Family 6 (Fiasco)

Train Track Map Candidate Family 6 of Track 0 is shown in Figure K.11. See D.1.6.1.2.3 for details.

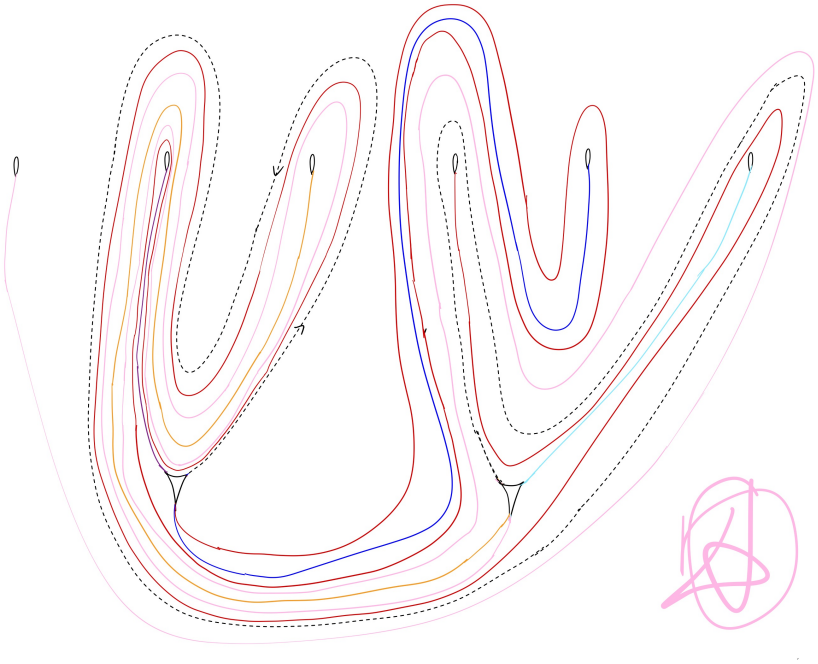


Figure K.11: Train Track Map Candidate Family 6 of Track 0.

The inverse of the following braid carries this family of train track maps:

$$b_6^0 = \sigma_4\sigma_2\sigma_5^{-1}\sigma_5^{-1}\sigma_3\sigma_2\sigma_1\sigma_3\sigma_2\sigma_4^{-1}\sigma_5^{-1}\sigma_3\sigma_2\sigma_1\sigma_4\sigma_5\sigma_5$$

This is shown in Figure K.12.

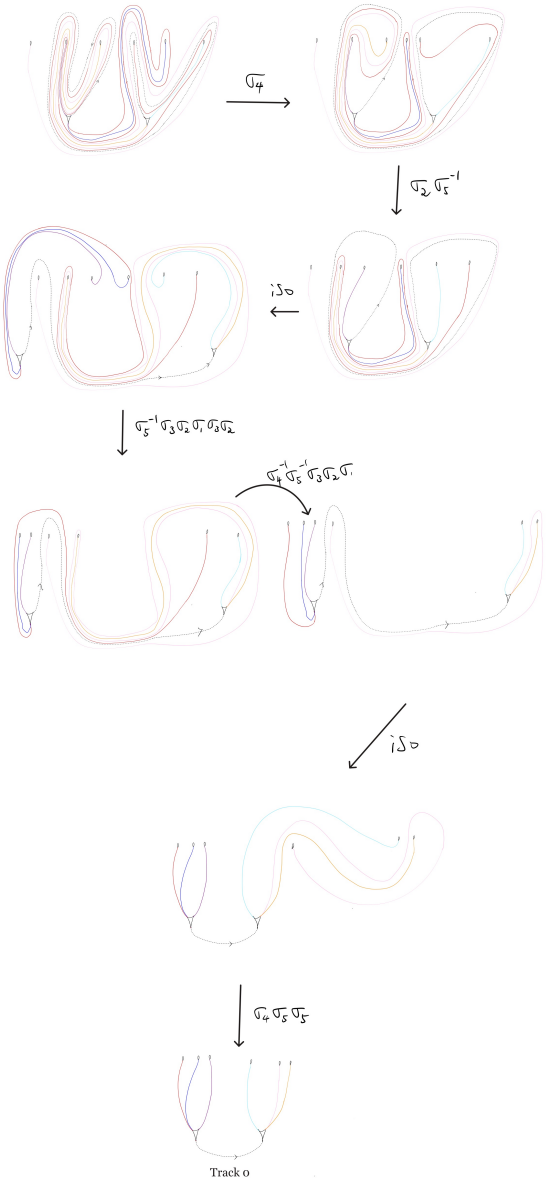


Figure K.12: This sequence shows the inverse of the braid b_6^0 carries Train Track Candidate Family 6.

K.9 Candidate Family 7 (Briefing)

Train Track Map Candidate Family 7 of Track 0 is shown in Figure K.13. See D.2.2.2.2.1.3 for details.

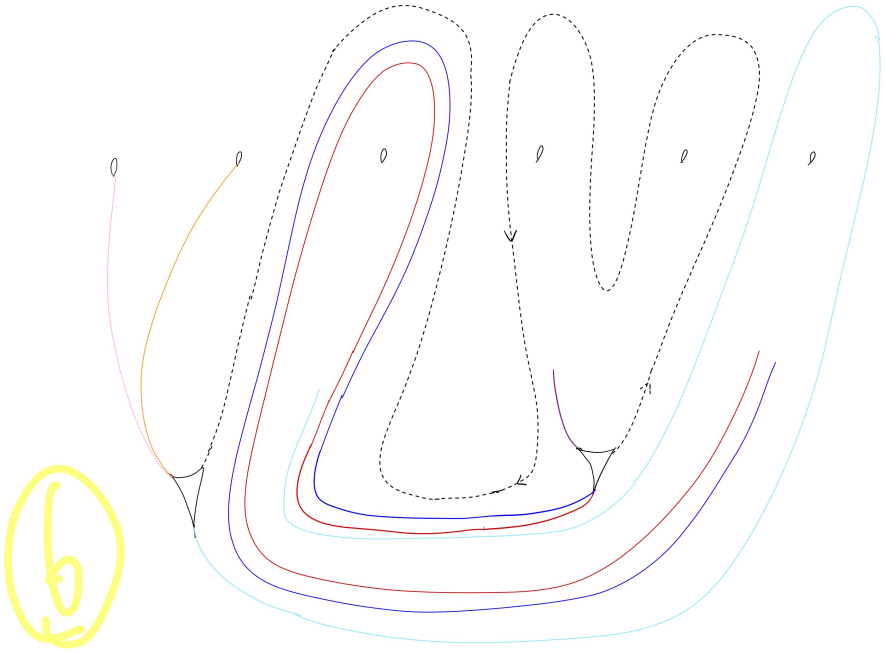


Figure K.13: Train Track Map Candidate Family 7 of Track 0.

The inverse of the following braid carries this family of train track maps:

$$b_7^0 = \sigma_4^m \sigma_3 \sigma_4 \sigma_5^{-k} \sigma_3 \sigma_3 \sigma_4^j \sigma_4 \sigma_3 \sigma_2 \sigma_1 \sigma_4 \sigma_3 \sigma_2 \sigma_4 \sigma_3 \sigma_5 \sigma_4 \sigma_5 \sigma_5$$

where $m, k, j \geq 1$ ($m, k, j \in \mathbb{Z}$) are the twisting parameters. This is shown in Figure K.14.

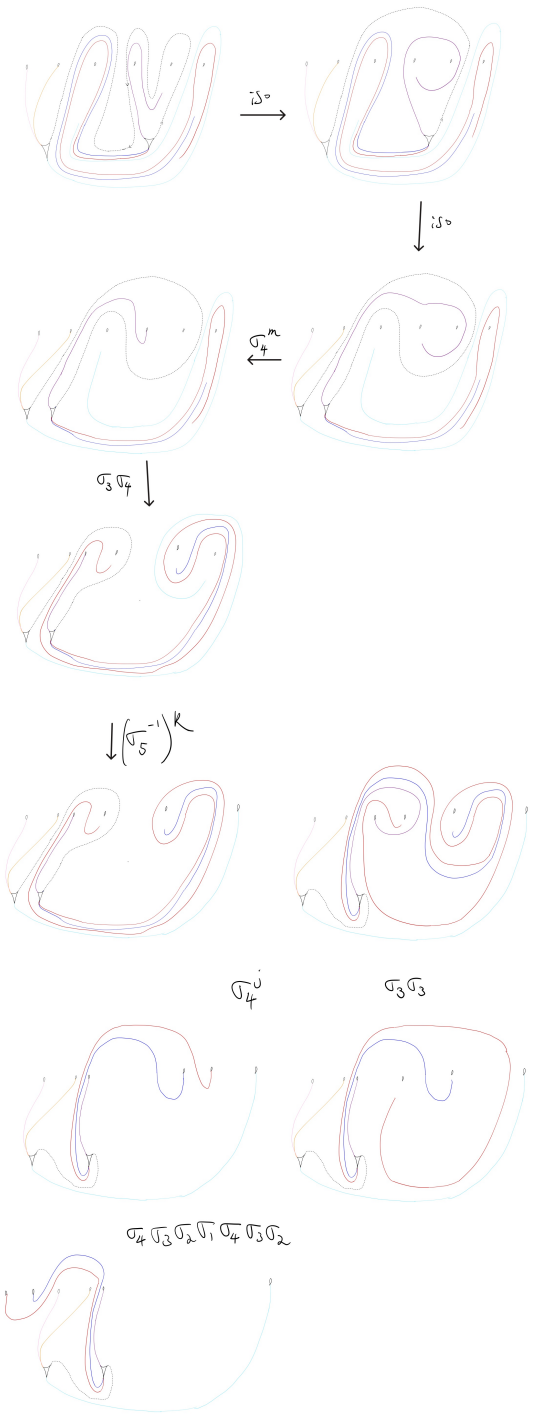


Figure K.14: This sequence shows the inverse of the braid b_7^0 carries Train Track Candidate Family 7.

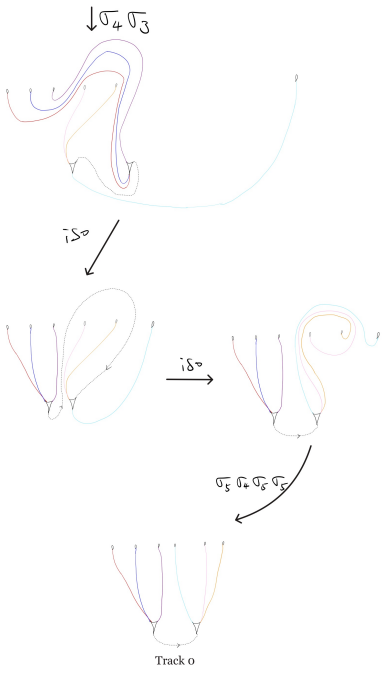


Figure K.14: This sequence shows the inverse of the braid b_7^0 carries Train Track Candidate Family 7 (continued).

K.10 Candidate Family 8 (Briefing)

Train Track Map Candidate Family 8 of Track 0 is shown in Figure K.15. See D.2.2.2.2.1.3 for details.

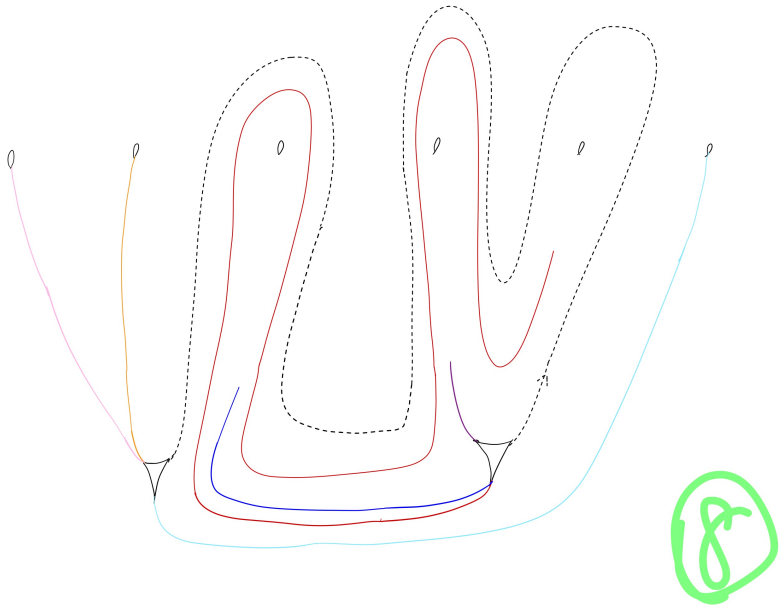


Figure K.15: Train Track Map Candidate Family 8 of Track 0.

The inverse of the following braid carries this family of train track maps:

$$b_8^0 = \sigma_4^k \sigma_3^m \sigma_3\sigma_4\sigma_4\sigma_3\sigma_4\sigma_4\sigma_2\sigma_1\sigma_3\sigma_2\sigma_4\sigma_3\sigma_5\sigma_4\sigma_5\sigma_5$$

where $k, m \geq 1$ ($k, m \in \mathbb{Z}$) are the twisting parameters. This is shown in Figure K.16.

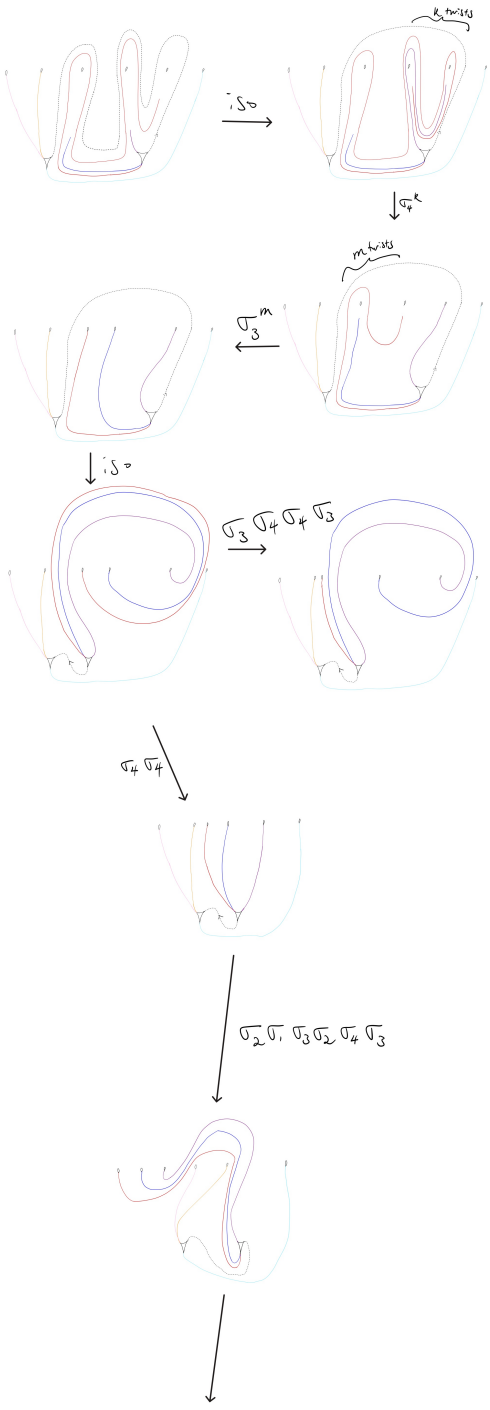


Figure K.16: This sequence shows the inverse of the braid b_8^0 carries Train Track Candidate Family 8.

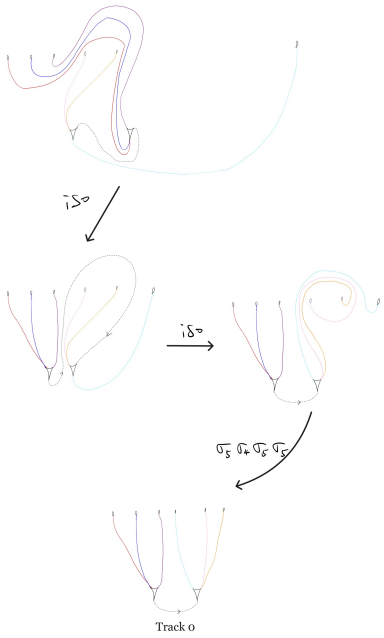


Figure K.16: This sequence shows the inverse of the braid b_8^0 carries Train Track Candidate Family 8 (continued).

K.11 Candidate Family 9 (Quail)

Train Track Map Candidate Family 9 of Track 0 is shown in Figure K.17. See D.2.4.2.1 for details.

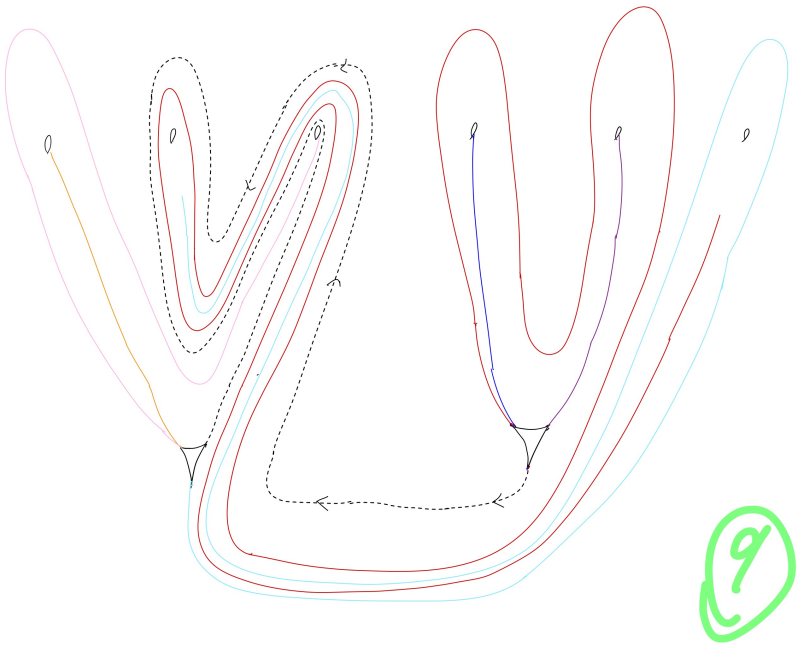


Figure K.17: Train Track Map Candidate Family 9 of Track 0.

The inverse of the following braid carries this family of train track maps:

$$b_9^0 = \sigma_2^{-1}\sigma_1\sigma_3\sigma_4\sigma_5^{-k}\sigma_4\sigma_3\sigma_2\sigma_1\sigma_3\sigma_2\sigma_4\sigma_3\sigma_5\sigma_4\sigma_5\sigma_5$$

where $k \geq 1$ ($k \in \mathbb{Z}$) is the twisting parameter. This is shown in Figure K.18.

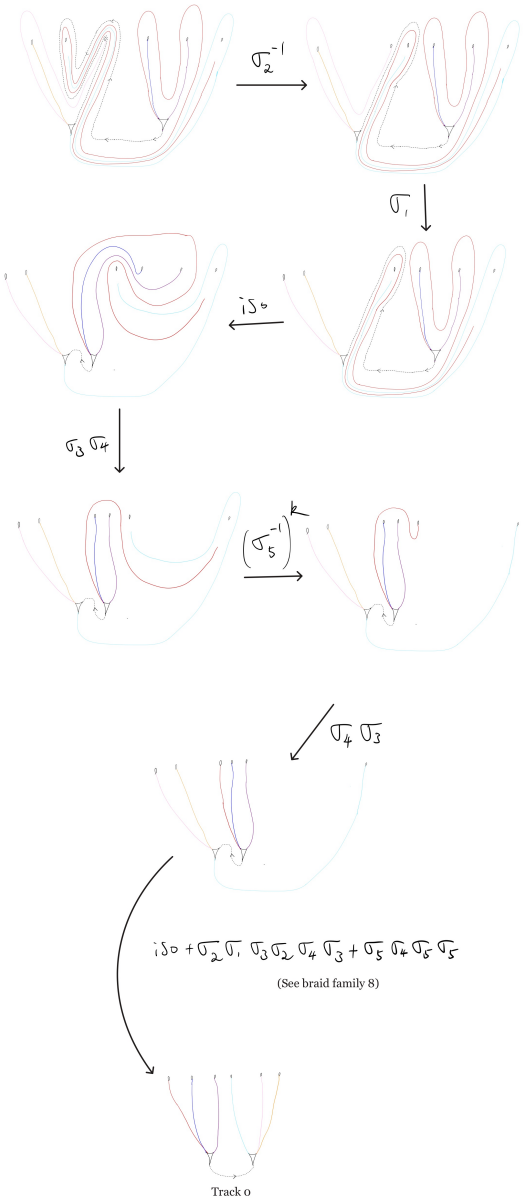


Figure K.18: This sequence shows the inverse of the braid b_9^0 carries Train Track Candidate Family 9.

K.12 Candidate Family 10 (Quail)

Train Track Map Candidate Family 10 of Track 0 is shown in Figure K.19. See D.2.4.2.1 for details.

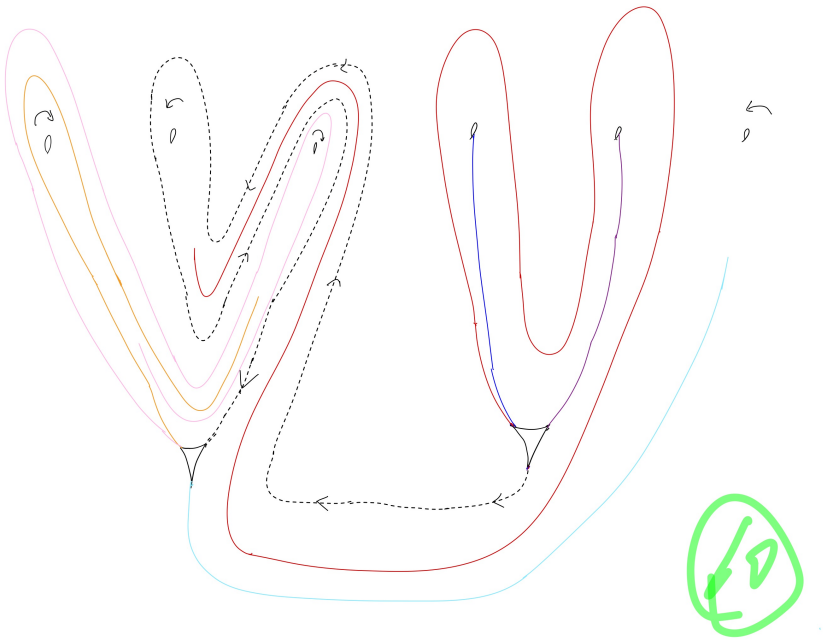


Figure K.19: Train Track Map Candidate Family 10 of Track 0.

The inverse of the following braid carries this family of train track maps:

$$b_{10}^{0} = \sigma_2^{-j}\sigma_1^{m}\sigma_3\sigma_4\sigma_5^{-k}\sigma_4\sigma_3\sigma_2\sigma_1\sigma_3\sigma_2\sigma_4\sigma_3\sigma_5\sigma_4\sigma_5\sigma_5$$

where $j, m, k \geq 1$ $(j, m, k \in \mathbb{Z})$ are the twisting parameters. This is shown in Figure K.20.

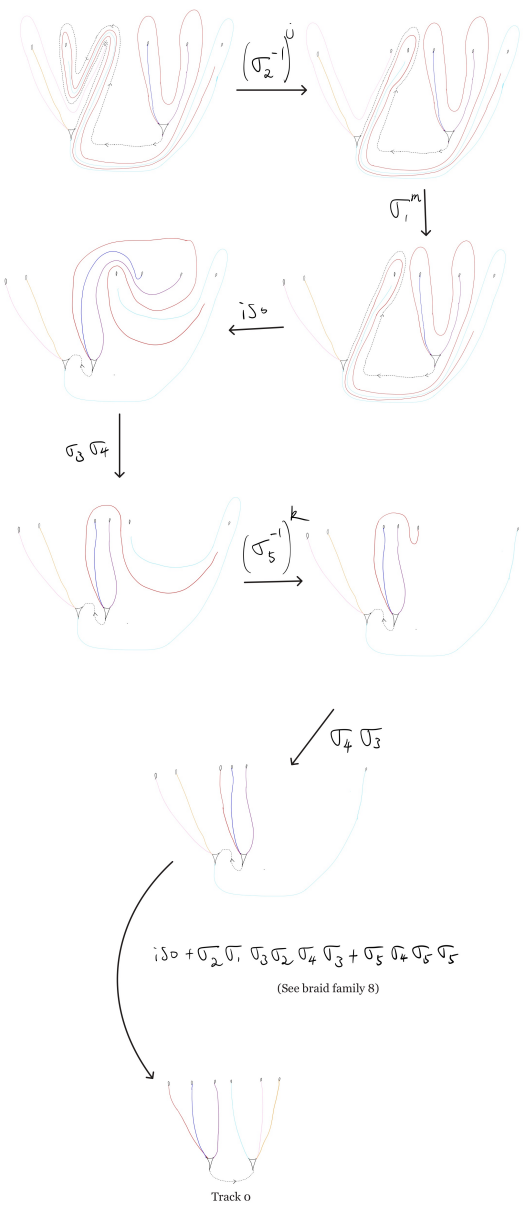


Figure K.20: This sequence shows the inverse of the braid b_{10}^0 carries Train Track Candidate Family 10.

K.13 Candidate Family 11 (Jubilant)

Train Track Map Candidate Family 11 of Track 0 is shown in Figure K.21. See D.2.4.2.2.1.1.1 for details.

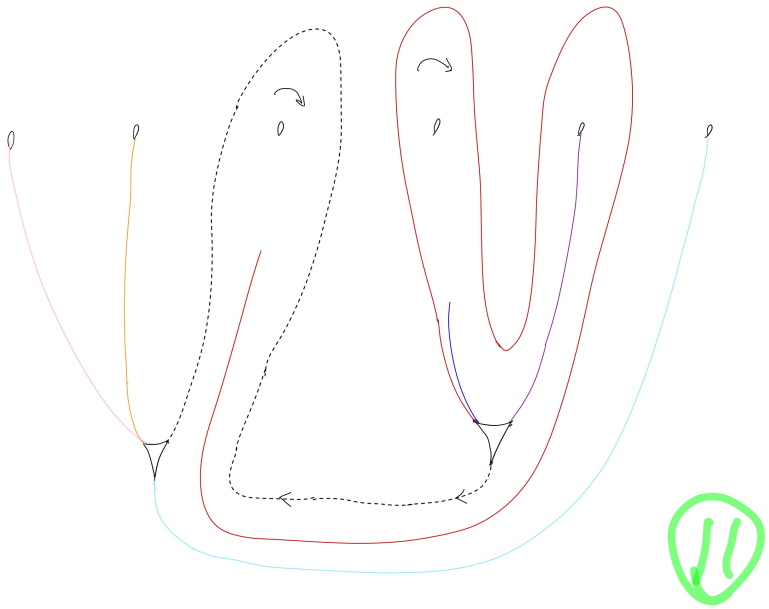


Figure K.21: Train Track Map Candidate Family 11 of Track 0.

The inverse of the following braid carries this family of train track maps:

$$b_{11}^{0} = \sigma_4\sigma_3\sigma_4^{k}\sigma_4\sigma_3\sigma_4\sigma_2\sigma_1\sigma_3\sigma_2\sigma_4\sigma_3\sigma_5\sigma_4\sigma_5\sigma_5$$

where $k \geq 1$ ($k \in \mathbb{Z}$) is the twisting parameter. This is shown in Figure K.22.

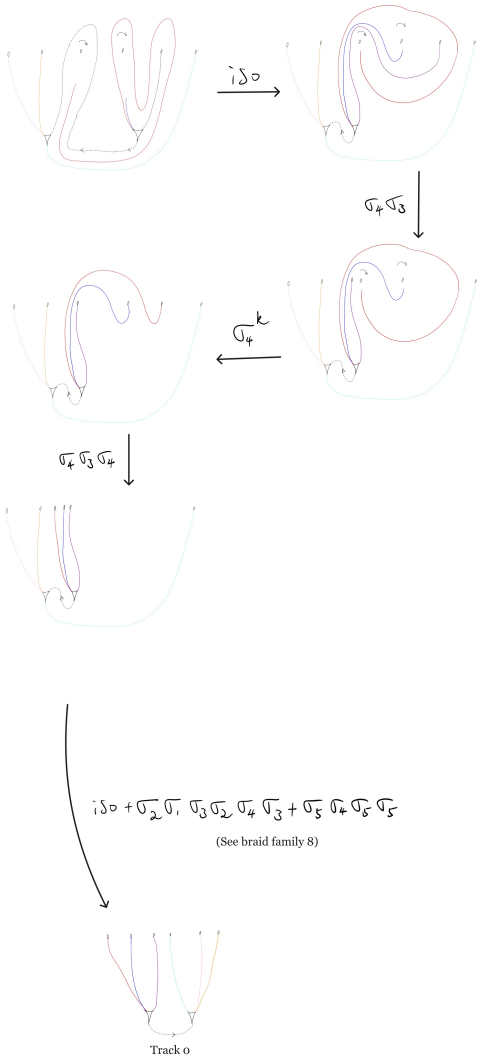


Figure K.22: This sequence shows the inverse of the braid b_{11}^0 carries Train Track Candidate Family 11.

K.14 Candidate Family 12 (Jubilant)

Train Track Map Candidate Family 12 of Track 0 is shown in Figure K.23. See D.2.4.2.2.1.1.1 for details.

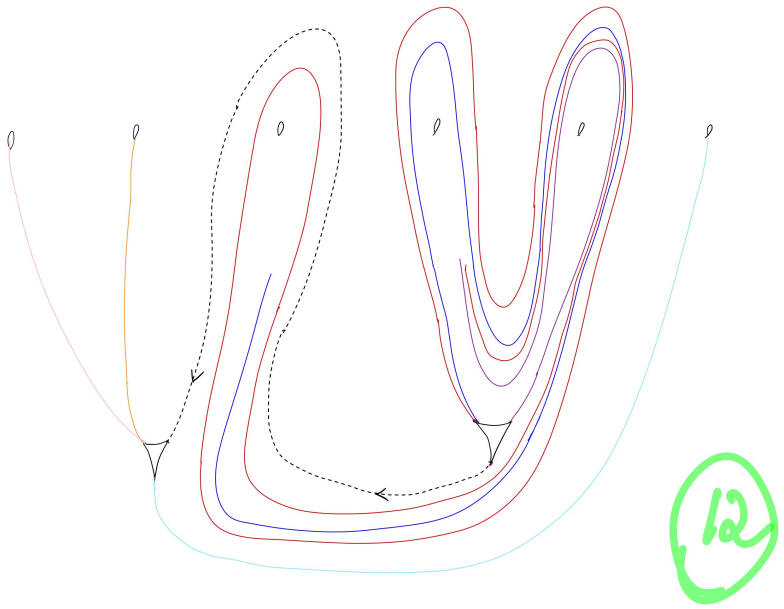


Figure K.23: Train Track Map Candidate Family 12 of Track 0.

The inverse of the following braid carries this family of train track maps:

$$b_{12}^{0} = \sigma_4^{-k}\sigma_4^{-1}\sigma_3\sigma_4^{m}\sigma_4\sigma_3\sigma_4\sigma_1\sigma_3\sigma_2\sigma_4\sigma_3\sigma_5\sigma_4\sigma_5\sigma_5$$

where $k, m \geq 1$ ($k, m \in \mathbb{Z}$) are the twisting parameters. This is shown in Figure K.24.

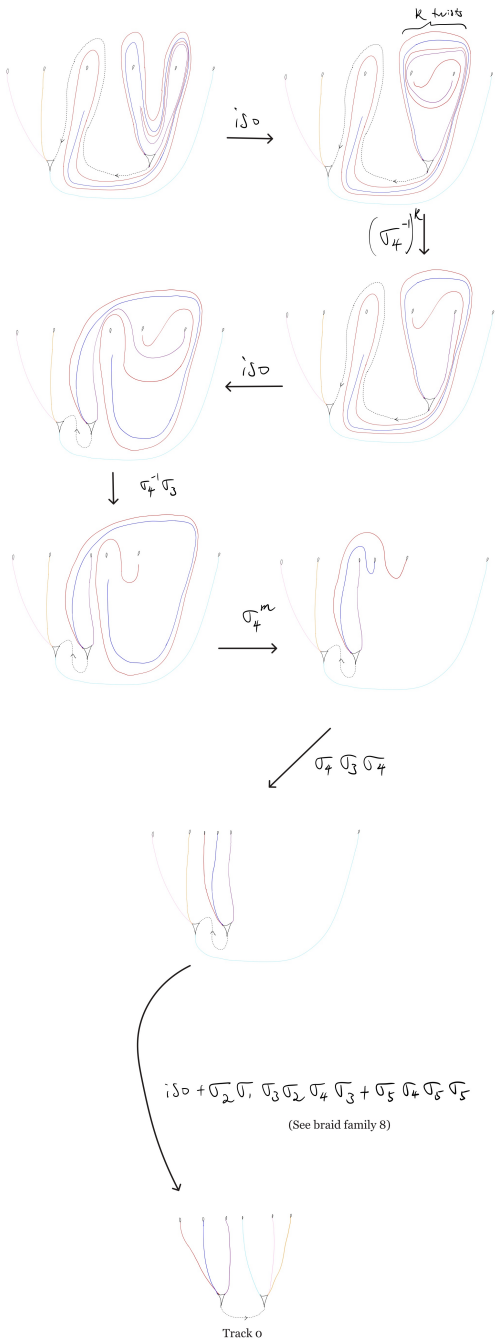


Figure K.24: This sequence shows the inverse of the braid b_{12}^0 carries Train Track Candidate Family 12.

K.15 Candidate Family 13 (Treasure)

Train Track Map Candidate Family 13 of Track 0 is shown in Figure K.25. See D.2.4.2.2.1.1.2.2 for details.

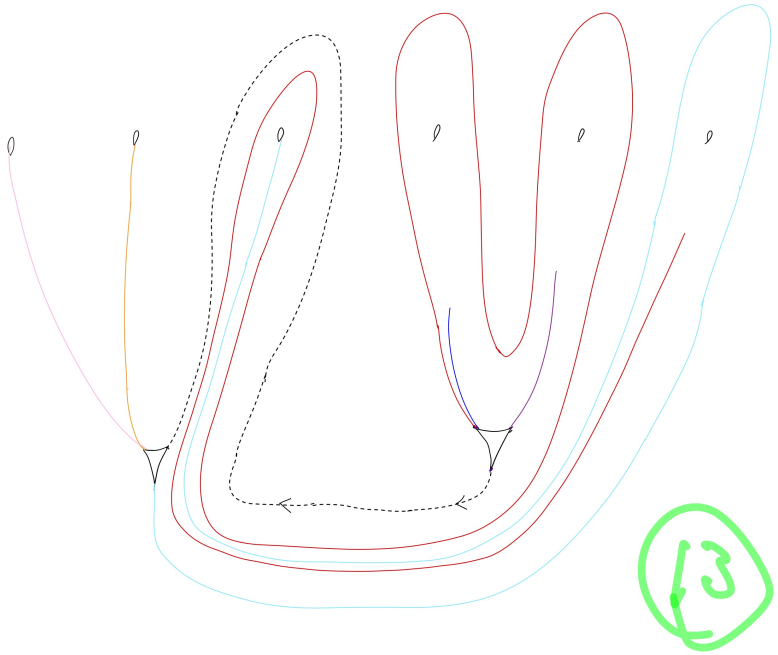


Figure K.25: Train Track Map Candidate Family 13 of Track 0.

The inverse of the following braid carries this family of train track maps:

$$b_{13}^{0} = \sigma_4^{-k}\sigma_4^{-1}\sigma_3\sigma_4\sigma_5^{-1}\sigma_4^{m}\sigma_3\sigma_4\sigma_2\sigma_1\sigma_3\sigma_2\sigma_4\sigma_3\sigma_5\sigma_4\sigma_5\sigma_5$$

where $k, m \geq 1$ ($k, m \in \mathbb{Z}$) are the twisting parameters. This is shown in Figure K.26.

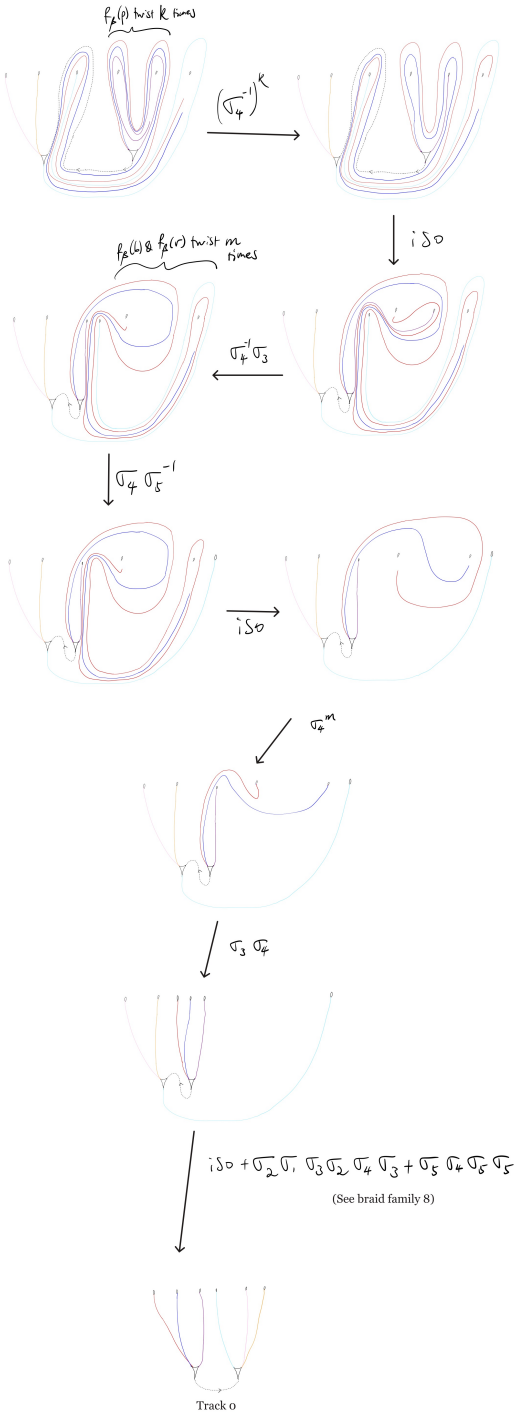


Figure K.26: This sequence shows the inverse of the braid b_{13}^0 carries Train Track Candidate Family 13.

APPENDIX TWELVE

Appendix: Candidate Braids for Track 1

L.1 Summary of Candidate Braid Families

Through the exhaustive train track case analysis of Track 1 in the stratum $(2; 1^6; 3^2)$ (the full details of which are presented in Appendix E), we isolate exactly 17 candidate families of train track maps. If the pseudo-Anosov representative ϕ_Φ has no interior fixed points, then its mapping class Φ must be conjugate to the lift of one of the following 17 braid families (enumerated below with their twist parameters).

1. $\Delta^{2i}(\sigma_2^{-1}\sigma_4\sigma_3\sigma_2\sigma_1\sigma_2^{-1}\sigma_3^{-1}\sigma_4^{-1}\sigma_5^{-1}\sigma_2^{-1}\sigma_3^{-1}\sigma_4^{-1}\sigma_1^{-1}\sigma_2^{-1} \cdot J \cdot \Lambda_6)^{-1}$
2. $\Delta^{2i}(\sigma_4\sigma_3\sigma_2\sigma_1\sigma_5\sigma_4\sigma_3\sigma_4^{-1}\sigma_5^{-1}\sigma_4\sigma_2^{-1}\sigma_3^{-1}\sigma_4^{-1}\sigma_5^{-1}\sigma_2^{-1}\sigma_2^{-1}\sigma_3^{-1}\sigma_4^{-1}\sigma_2^{-1}\sigma_3^{-1}\sigma_1^{-1}\sigma_2^{-1} \cdot J \cdot \Lambda_6)^{-1}$
3. $\Delta^{2i}(\sigma_4\sigma_3\sigma_2\sigma_1\sigma_5^k\sigma_5\sigma_4\sigma_2^{-1}\sigma_3^{-1}\sigma_4^{-1}\sigma_5^{-1}\sigma_2^{-1}\sigma_2^{-1}\sigma_3^{-1}\sigma_4^{-1}\sigma_2^{-1}\sigma_3^{-1}\sigma_1^{-1}\sigma_2^{-1} \cdot J \cdot \Lambda_6)^{-1}$
4. $\Delta^{2i}(\sigma_4\sigma_3\sigma_4\sigma_4\sigma_3\sigma_2\sigma_1\sigma_4\sigma_3\sigma_2\sigma_5\sigma_5\sigma_4\sigma_3\sigma_2^{-1}\sigma_1^{-1}\sigma_1^{-1}\sigma_2^{-1}\sigma_4\sigma_5 \cdot J \cdot \Lambda_6)^{-1}$
5. $\Delta^{2i}(\sigma_4\sigma_3\sigma_4\sigma_4\sigma_3\sigma_2\sigma_1\sigma_1\sigma_2\sigma_3\sigma_1^{-1}\sigma_2^{-1}\sigma_1^{-1}\sigma_1^{-1}\sigma_5\sigma_4\sigma_5)^{-1}$
6. $\Delta^{2i}(\sigma_4\sigma_3\sigma_4^k\sigma_4\sigma_4\sigma_3\sigma_2\sigma_1\sigma_4\sigma_3\sigma_2\sigma_5\sigma_4\sigma_3\sigma_1\sigma_2\sigma_1\sigma_3\sigma_4\sigma_5\sigma_5\sigma_4\sigma_3\sigma_1^{-1}\sigma_4\sigma_5 \cdot J \cdot \Lambda_6)^{-1}$

7. $\Delta^{2i}(\sigma_2^{-1}\sigma_3^{-1}\sigma_4^{-1}\sigma_3\sigma_2\sigma_4\sigma_3\sigma_4\sigma_4\sigma_3\sigma_2\sigma_1\sigma_4\sigma_3\sigma_2\sigma_4^{-1}\sigma_3^{-1}\sigma_2^{-1}\sigma_1^{-1}\sigma_1^{-1}\sigma_2^{-1}\sigma_5\sigma_4\sigma_5 \cdot J \cdot \Lambda_6)^{-1}$

8. $\Delta^{2i}(\sigma_4\sigma_3\sigma_2\sigma_4\sigma_3\sigma_4^{-1}\sigma_3^{-1}\sigma_4\sigma_4\sigma_3\sigma_2\sigma_1\sigma_4\sigma_3\sigma_2\sigma_5\sigma_4\sigma_3\sigma_3^{-1}\sigma_4^{-1}\sigma_5^{-1}\sigma_2^{-1}\sigma_3^{-1}\sigma_4^{-1}\sigma_2^{-1}\sigma_3^{-1}\sigma_2^{-1}\sigma_2^{-1}$
$\sigma_1\sigma_2\sigma_3\sigma_4\sigma_5)^{-1}$

9. $\Delta^{2i}(\sigma_4\sigma_3\sigma_2\sigma_3^{-1}\sigma_4\sigma_4\sigma_3\sigma_2\sigma_1\sigma_2^{-1}\sigma_3^{-1}\sigma_2^{-1}\sigma_2^{-1}\sigma_1\sigma_2\sigma_3\sigma_5\sigma_4\sigma_5)^{-1}$

10. $\Delta^{2i}(\sigma_4\sigma_3\sigma_2\sigma_3^{-1}\sigma_4\sigma_4\sigma_3\sigma_2\sigma_1\sigma_4\sigma_3\sigma_2\sigma_5\sigma_4\sigma_5^{-1}\sigma_5^{-1}\sigma_4^{-1}\sigma_3^{-1}\sigma_2^{-1}\sigma_1^{-1}\sigma_1^{-1}\sigma_2^{-1}\sigma_4\sigma_5 \cdot J \cdot \Lambda_6)^{-1}$

11. $\Delta^{2i}(\sigma_4\sigma_3\sigma_2\sigma_3^{-1}\sigma_4\sigma_4\sigma_3\sigma_2\sigma_1\sigma_4\sigma_3\sigma_2\sigma_4^{-1}\sigma_5^{-1}\sigma_3^{-1}\sigma_2^{-1}\sigma_1^{-1}\sigma_1^{-1}\sigma_2^{-1}\sigma_5\sigma_4\sigma_5 \cdot J \cdot \Lambda_6)^{-1}$

12. $\Delta^{2i}(\sigma_4\sigma_3\sigma_2\sigma_3^{-1}\sigma_4^{-1}\sigma_3\sigma_4\sigma_4\sigma_4\sigma_3\sigma_2\sigma_1\sigma_1\sigma_2\sigma_3\sigma_1^{-1}\sigma_2^{-1}\sigma_1^{-1}\sigma_1^{-1}\sigma_4\sigma_5)^{-1}$

13. $\Delta^{2i}(\sigma_4\sigma_3\sigma_2\sigma_3^{-1}\sigma_4^{-1}\sigma_3\sigma_2^{-1}\sigma_1^{-1}\sigma_1^{-1}\sigma_2^{-1}\sigma_3^{-1}\sigma_4^{-1}\sigma_3\sigma_4^{-1}\sigma_5^{-1}\sigma_3^{-1}\sigma_4^{-1}\sigma_3^{-1}\sigma_1^{-1}\sigma_2^{-1}\sigma_1^{-1}\sigma_1^{-1}\sigma_5\sigma_4\sigma_5)^{-1}$

14. $\Delta^{2i}(\sigma_4\sigma_3\sigma_2\sigma_3^{-1}\sigma_4^{-1}\sigma_2^{-1}\sigma_3^{-1}\sigma_2\sigma_3\sigma_2^{-1}\sigma_1^{-1}\sigma_1^{-1}\sigma_2^{-1}\sigma_3^{-1}\sigma_4^{-1}\sigma_5^{-1}\sigma_3\sigma_4^{-1}\sigma_5^{-1}\sigma_3^{-1}\sigma_4^{-1}\sigma_1^{-1}\sigma_2\sigma_1^{-1}\sigma_5$
$\sigma_4\sigma_5)^{-1}$

15. $\Delta^{2i}(\sigma_4\sigma_3\sigma_2\sigma_3^{-1}\sigma_4^{-1}\sigma_3\sigma_4\sigma_4\sigma_3\sigma_2\sigma_1\sigma_1\sigma_3^{-1}\sigma_2\sigma_3\sigma_1^{-1}\sigma_2^{-1}\sigma_1^{-1}\sigma_5\sigma_4\sigma_5)^{-1}$

16. $\Delta^{2i}(\sigma_4^{-1}\sigma_1^{-1}\sigma_2^{-1}\sigma_3^{-1}\sigma_4^{-1}\sigma_3^{-1}\sigma_3^{-1}\sigma_4^{-1}\sigma_1^{-1}\sigma_1^{-1}\sigma_5^{-1}\sigma_4^{-1}\sigma_3^{-1}\sigma_2^{-1}\sigma_1^{-1}\sigma_1^{-1}\sigma_2^{-1})^{-1}$

17. $\Delta^{2i}(\sigma_4^k\sigma_3^m\sigma_2^{-1}\sigma_1^{-1}\sigma_1^{-1}\sigma_2^{-1}\sigma_5\sigma_4\sigma_5 \cdot J \cdot \Lambda_6)^{-1}$

L.2 Base Braids Λ_6 and J

Before we detail the individual candidate families, we introduce the following auxiliary base braids, which we call Λ_6 and J:

$\Lambda_6 = \sigma_1\sigma_2\sigma_1\sigma_3\sigma_2\sigma_1\sigma_4\sigma_3\sigma_2\sigma_1\sigma_5\sigma_4\sigma_3\sigma_2\sigma_1$

$J = \sigma_1^{-1}\sigma_2^{-1}\sigma_1^{-1}\sigma_5\sigma_4\sigma_5$

We shall make use of Λ_6 and J occasionally in constructing candidate braids for Track 1.

L.3 Candidate Family 1 (Flute)

Train Track Map Candidate Family 1 of Track 1 is shown in Figure L.1. See E.1.1.1.1 for details.

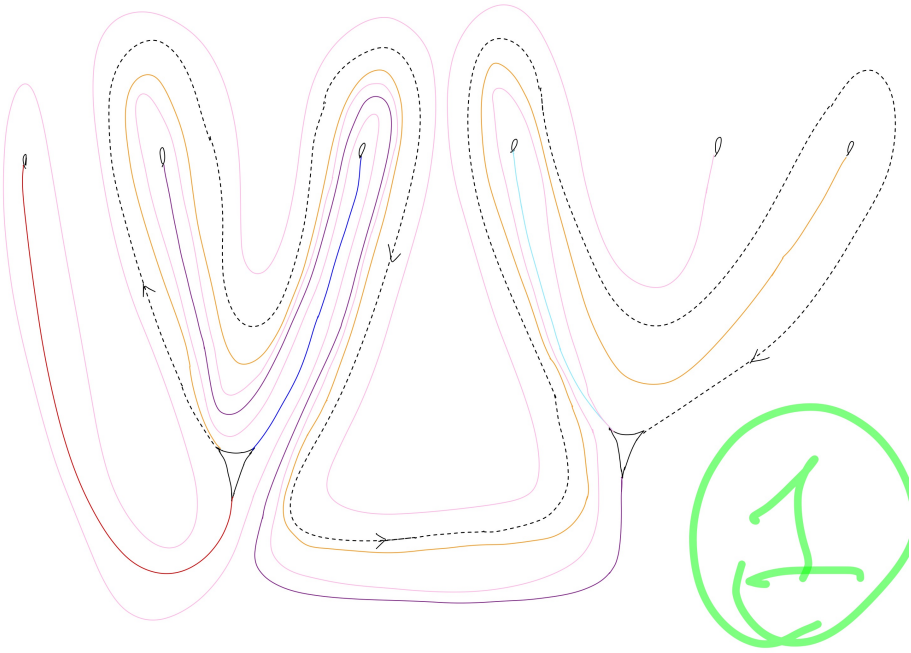


Figure L.1: Train Track Map Candidate Family 1 (Flute) of Track 1.

The inverse of the following braid carries this family of train track maps:

$$b_1^1 = \sigma_2^{-1}\sigma_4\sigma_3\sigma_2\sigma_1\sigma_2^{-1}\sigma_3^{-1}\sigma_4^{-1}\sigma_5^{-1}\sigma_2^{-1}\sigma_3^{-1}\sigma_4^{-1}\sigma_1^{-1}\sigma_2^{-1} \circ J \circ \Lambda_6$$

This is shown in Figure L.2.

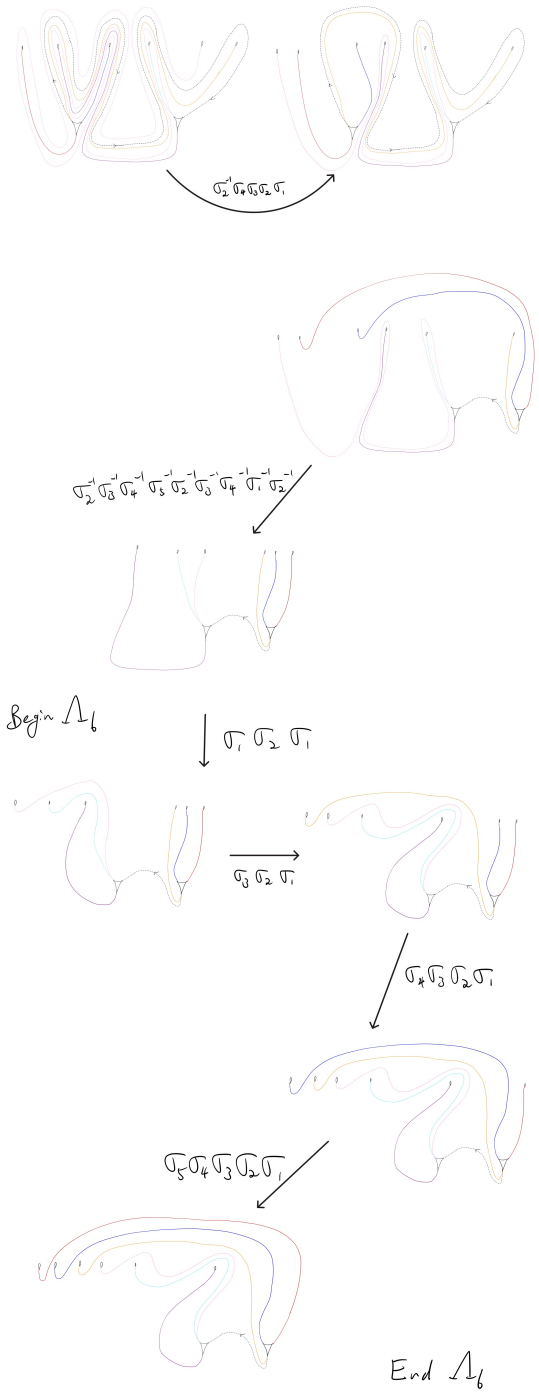


Figure L.2: This sequence shows the inverse of the braid b_1^1 carries Train Track Candidate Family 1.

L.4 Candidate Family 2 (Dolphin)

Train Track Map Candidate Family 2 of Track 1 is shown in Figure L.3. See E.1.1.1.2.1.1 for details.

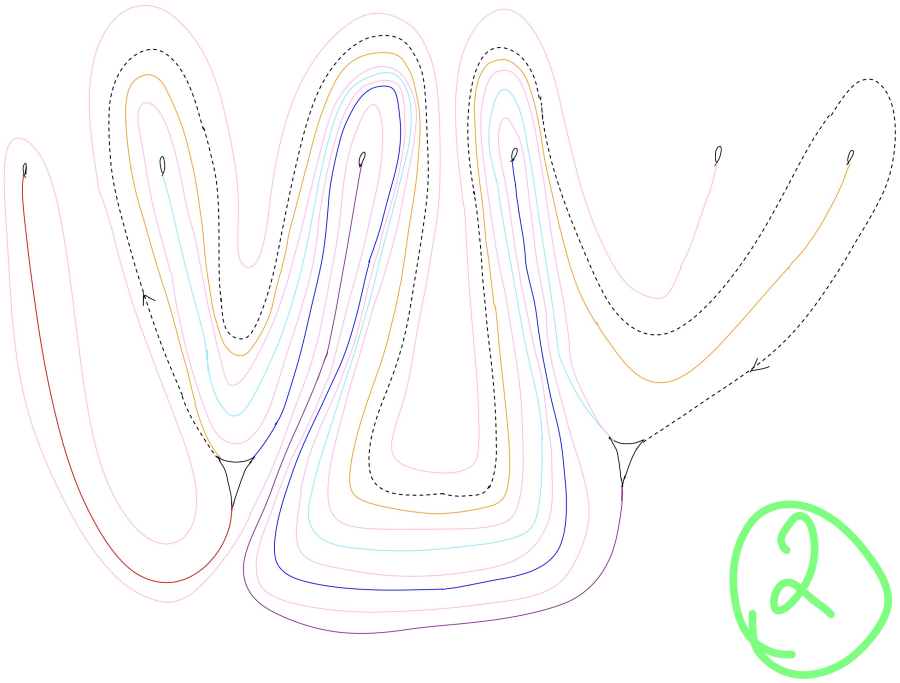


Figure L.3: Train Track Map Candidate Family 2 (Dolphin) of Track 1.

The inverse of the following braid carries this family of train track maps:

$$b_2^1 = \sigma_4\sigma_3\sigma_2\sigma_1\sigma_5\sigma_4\sigma_3\sigma_4^{-1}\sigma_5^{-1}\sigma_4\sigma_2^{-1}\sigma_3^{-1}\sigma_4^{-1}\sigma_5^{-1}\sigma_2^{-1}\sigma_2^{-1}\sigma_3^{-1}\sigma_4^{-1}\sigma_2^{-1}\sigma_3^{-1}\sigma_1^{-1}\sigma_2^{-1} \circ J \circ \Lambda_6$$

This is shown in Figure L.4.

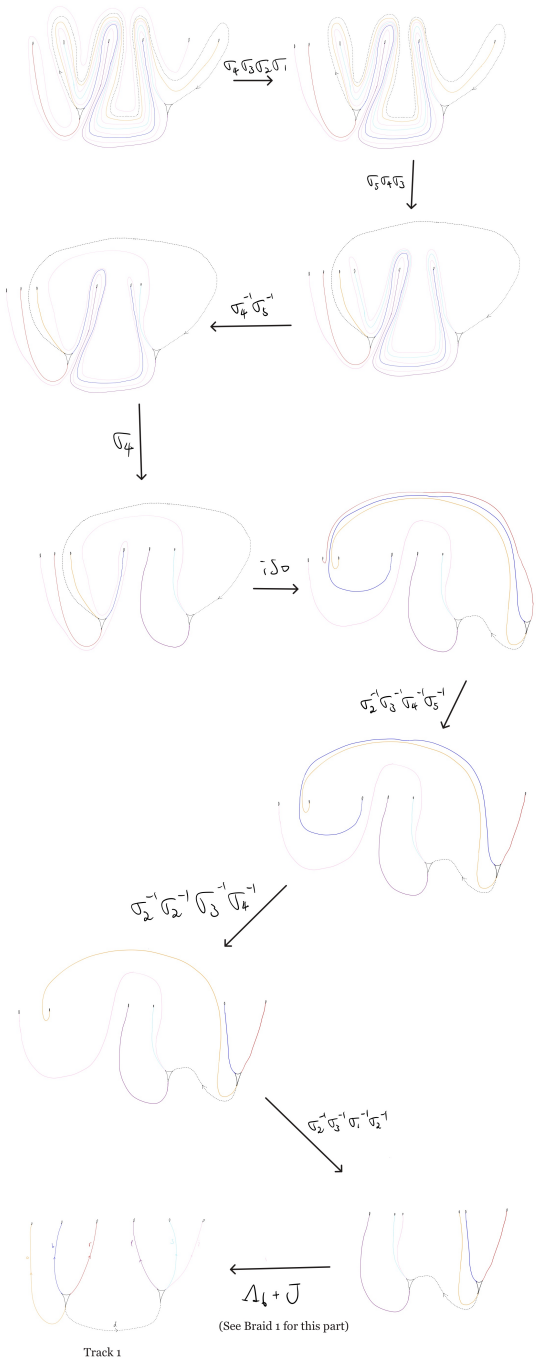


Figure L.4: This sequence shows the inverse of the braid b_2^1 carries Train Track Candidate Family 2.

L.5 Candidate Family 3 (Magpie)

Train Track Map Candidate Family 3 of Track 1 is shown in Figure L.5. See E.1.1.1.2.2 for details.

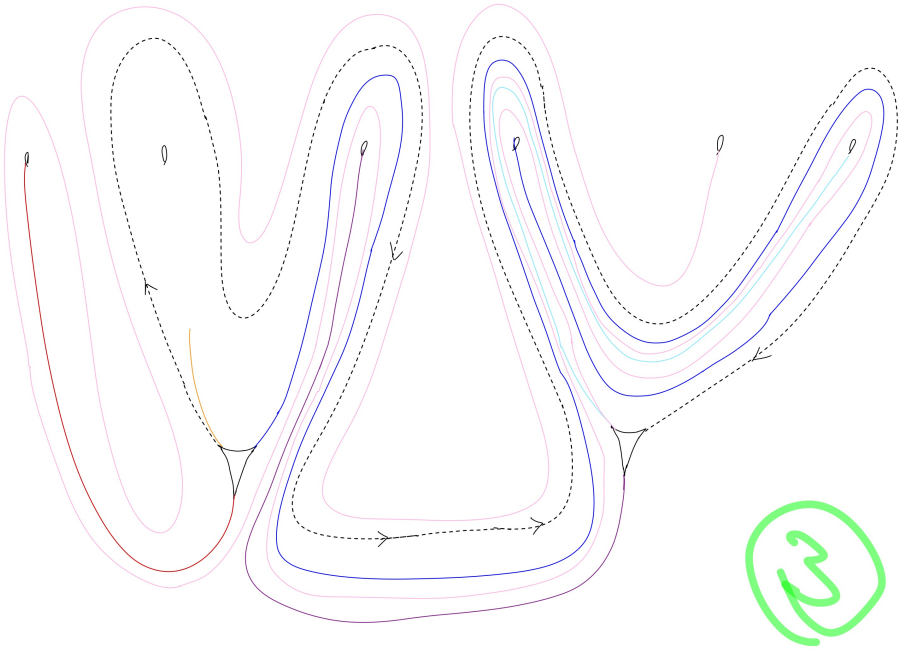


Figure L.5: Train Track Map Candidate Family 3 (Magpie) of Track 1.

The inverse of the following braid carries this family of train track maps:

$$b_3^1 = \sigma_4\sigma_3\sigma_2\sigma_1\sigma_5^k\sigma_5\sigma_4\sigma_2^{-1}\sigma_3^{-1}\sigma_4^{-1}\sigma_5^{-1}\sigma_2^{-1}\sigma_2^{-1}\sigma_3^{-1}\sigma_4^{-1}\sigma_2^{-1}\sigma_3^{-1}\sigma_1^{-1}\sigma_2^{-1} \circ J \circ \Lambda_6$$

where $k \geq 1$ ($k \in \mathbb{Z}$) is the twisting parameter. This is shown in Figure L.6.

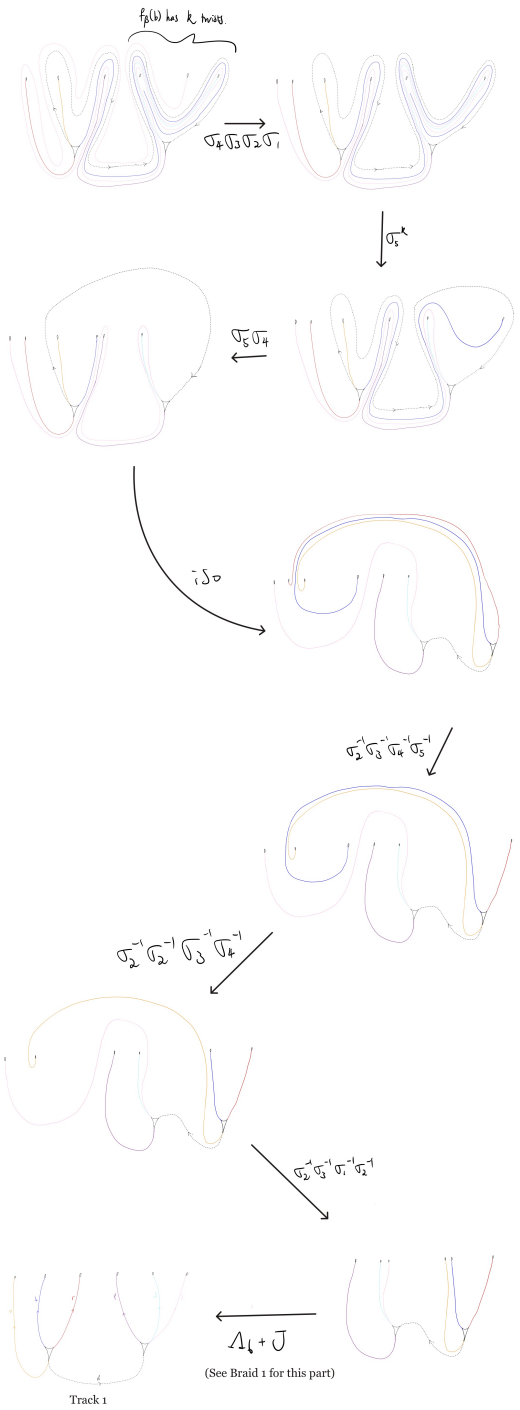


Figure L.6: This sequence shows the inverse of the braid b_3^1 carries Train Track Candidate Family 3.

L.6 Candidate Family 4 (Bezoar)

Train Track Map Candidate Family 4 of Track 1 is shown in Figure L.7. See E.1.2.2.1.1 for details.

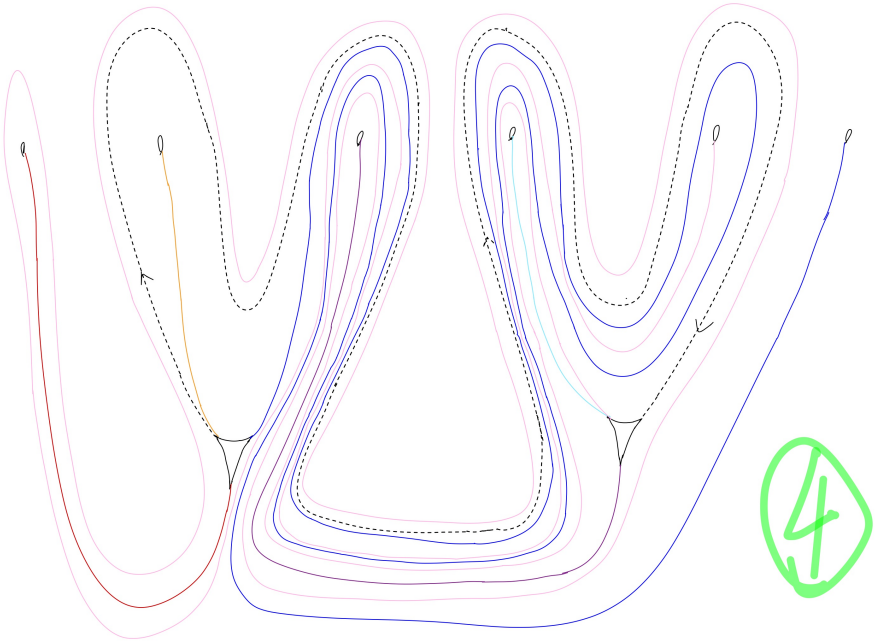


Figure L.7: Train Track Map Candidate Family 4 (Bezoar) of Track 1.

The inverse of the following braid carries this family of train track maps:

$$b_4^1 = \sigma_4\sigma_3\sigma_4\sigma_4\sigma_3\sigma_2\sigma_1\sigma_4\sigma_3\sigma_2\sigma_5\sigma_5\sigma_4\sigma_3\sigma_2^{-1}\sigma_1^{-1}\sigma_1^{-1}\sigma_2^{-1}\sigma_4\sigma_5 \circ J \circ \Lambda_6$$

This is shown in Figure L.8.

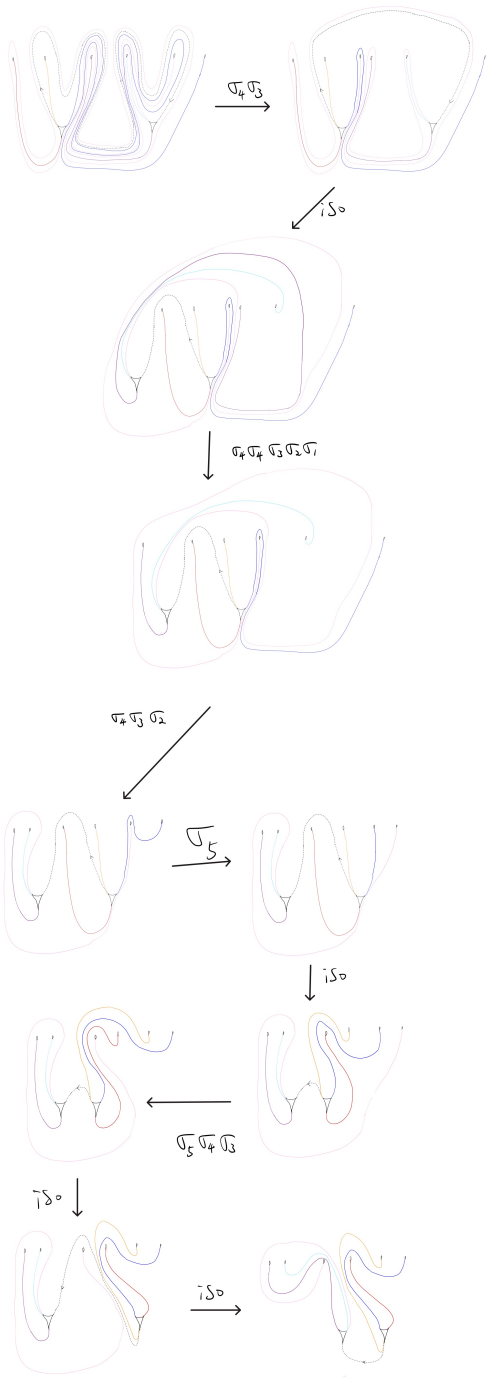


Figure L.8: This sequence shows the inverse of the braid b_4^1 carries Train Track Candidate Family 4.

L.7 Candidate Family 5 (Abscond)

Train Track Map Candidate Family 5 of Track 1 is shown in Figure L.9. See E.1.2.2.1.2.1 for details.

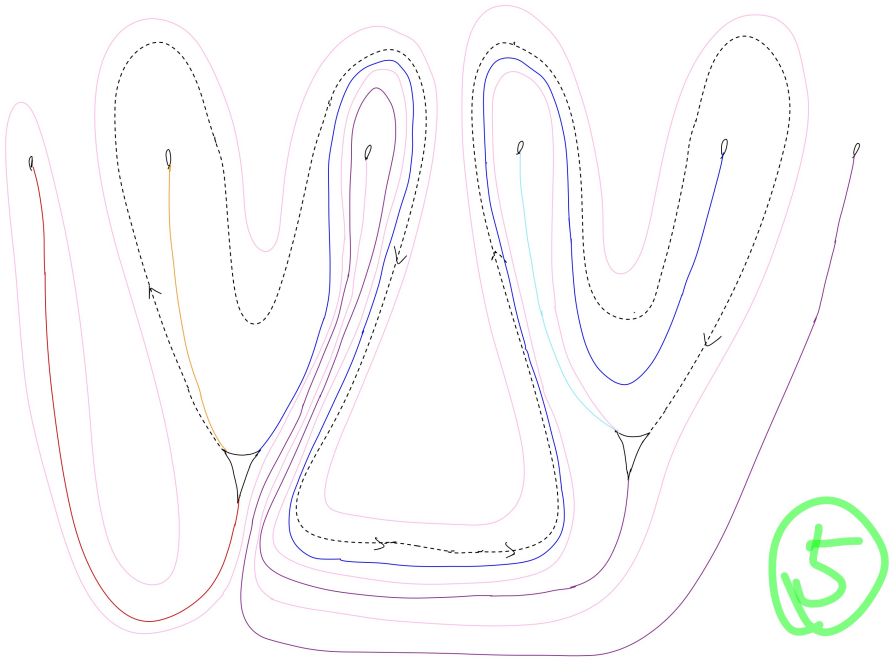


Figure L.9: Train Track Map Candidate Family 5 (Abscond) of Track 1.

The inverse of the following braid carries this family of train track maps:

$$b_5^1 = \sigma_4\sigma_3\sigma_4\sigma_4\sigma_3\sigma_2\sigma_1\sigma_1\sigma_2\sigma_3\sigma_1^{-1}\sigma_2^{-1}\sigma_1^{-1}\sigma_1^{-1}\sigma_5\sigma_4\sigma_5$$

This is shown in Figure L.10.

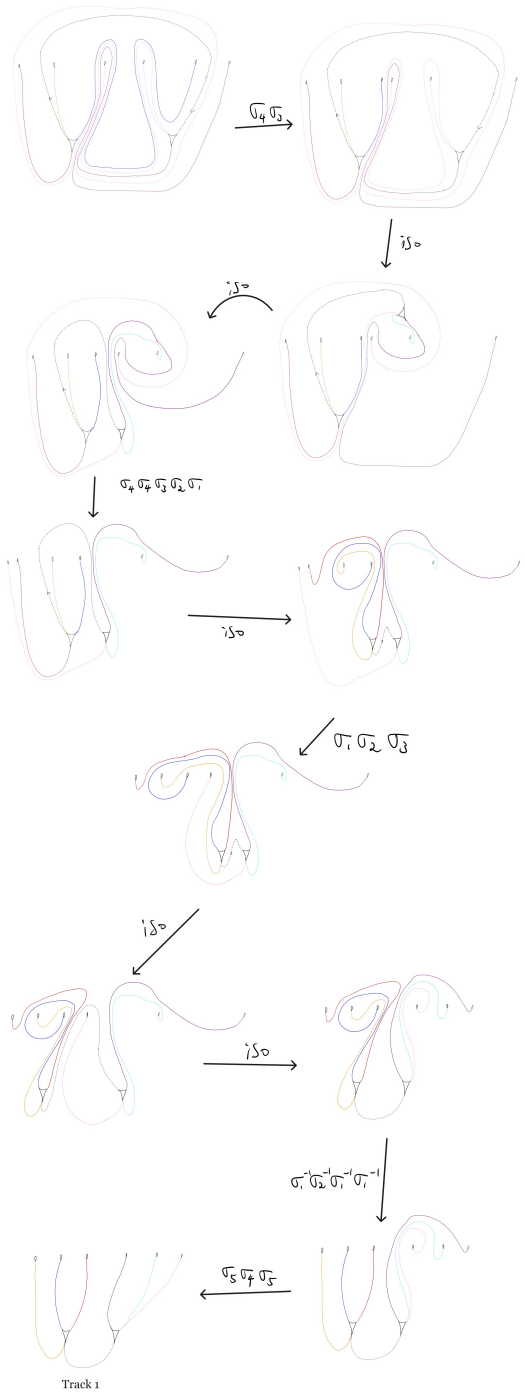


Figure L.10: This sequence shows the inverse of the braid b_5^1 carries Train Track Candidate Family 5.

L.8 Candidate Family 6 (Abscond)

Train Track Map Candidate Family 6 of Track 1 is shown in Figure L.11. See E.1.2.2.1.2.1 for details.

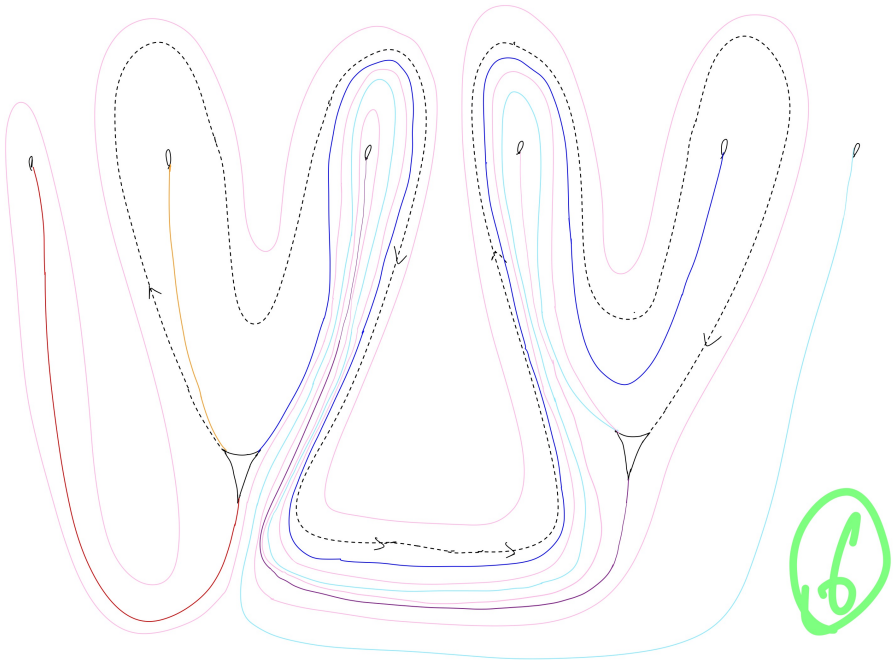


Figure L.11: Train Track Map Candidate Family 6 (Abscond) of Track 1.

The inverse of the following braid carries this family of train track maps:

$$b_6^1 = \sigma_4\sigma_3\sigma_4^k\sigma_4\sigma_4\sigma_3\sigma_2\sigma_1\sigma_4\sigma_3\sigma_2\sigma_5\sigma_4\sigma_3\sigma_1\sigma_2\sigma_1\sigma_3\sigma_4\sigma_5\sigma_5\sigma_4\sigma_3\sigma_1^{-1}\sigma_4\sigma_5 \circ J \circ \Lambda_6$$

where $k \geq 1$ ($k \in \mathbb{Z}$) is the twisting parameter. This is shown in Figure L.12.

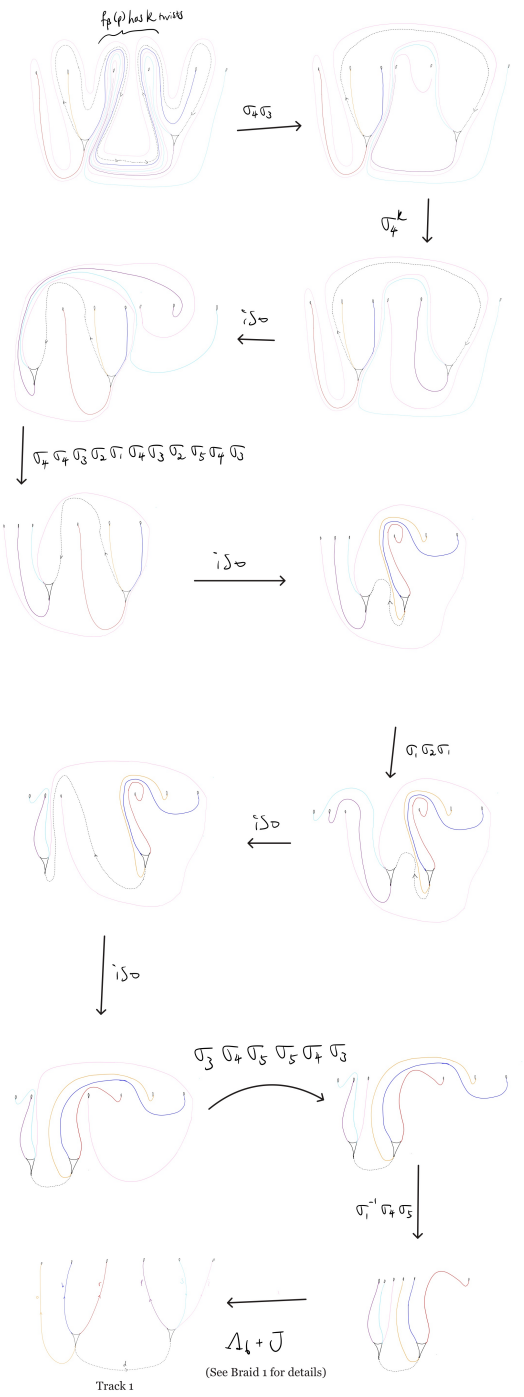


Figure L.12: This sequence shows the inverse of the braid b_6^1 carries Train Track Candidate Family 6.

L.9 Candidate Family 7 (Fervent)

Train Track Map Candidate Family 7 of Track 1 is shown in Figure L.13. See E.1.2.2.1.2.2 for details.

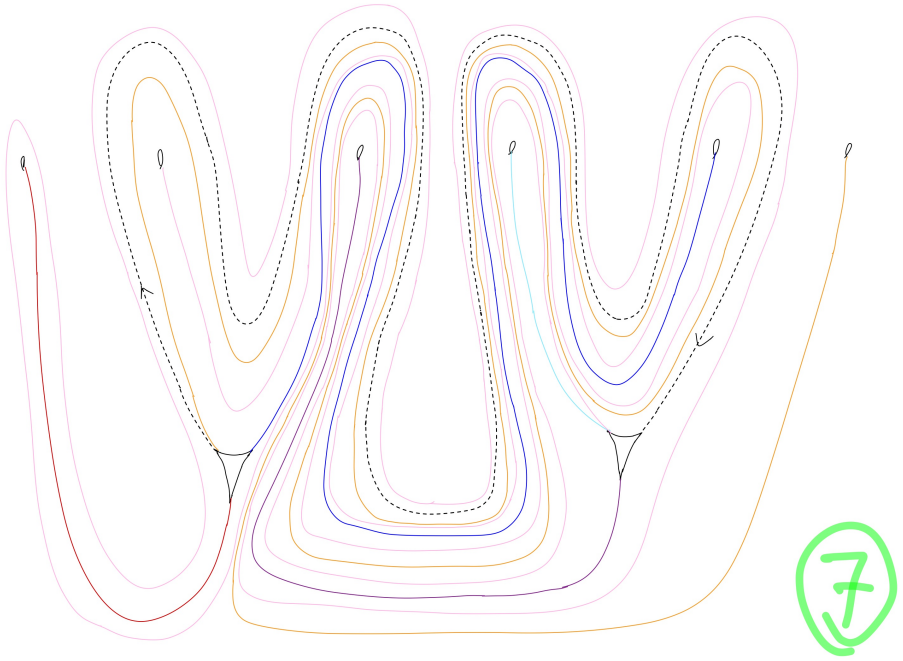


Figure L.13: Train Track Map Candidate Family 7 (Fervent) of Track 1.

The inverse of the following braid carries this family of train track maps:

$$b_7^1 = \sigma_2^{-1}\sigma_3^{-1}\sigma_4^{-1}\sigma_3\sigma_2\sigma_4\sigma_3\sigma_4\sigma_4\sigma_3\sigma_2\sigma_1\sigma_4\sigma_3\sigma_2\sigma_4^{-1}\sigma_3^{-1}\sigma_2^{-1}\sigma_1^{-1}\sigma_1^{-1}\sigma_2^{-1}\sigma_5\sigma_4\sigma_5 \circ J \circ \Lambda_6$$

This is shown in Figure L.14.

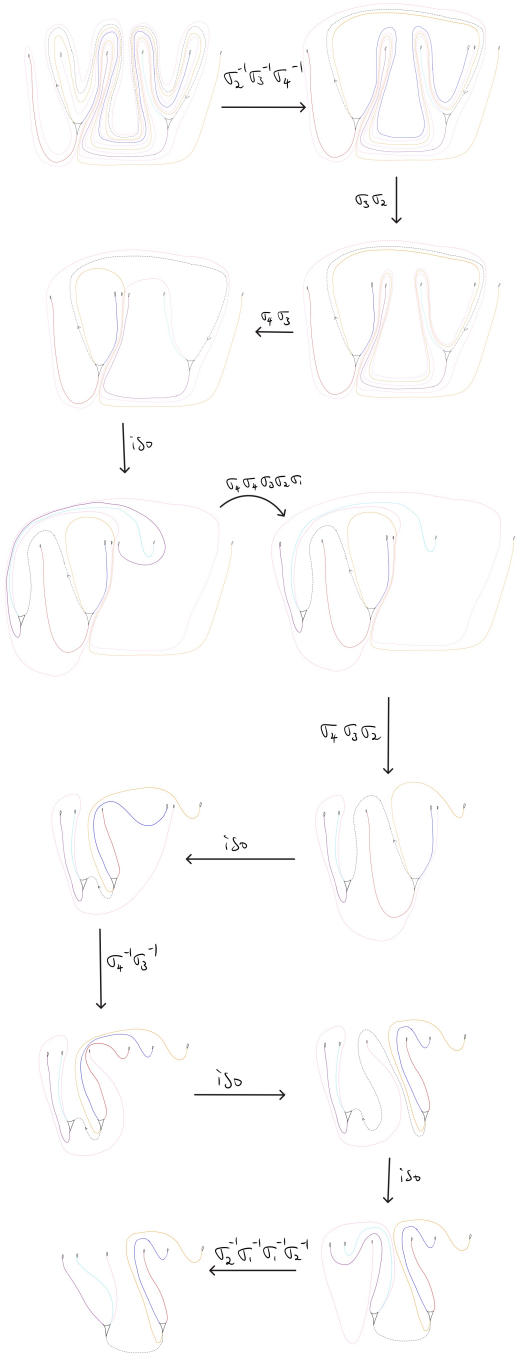


Figure L.14: This sequence shows the inverse of the braid b_7^1 carries Train Track Candidate Family 7.

L.10 Candidate Family 8 (Panorama)

Train Track Map Candidate Family 8 of Track 1 is shown in Figure L.15. See E.1.2.2.2.1.1.1 for details.

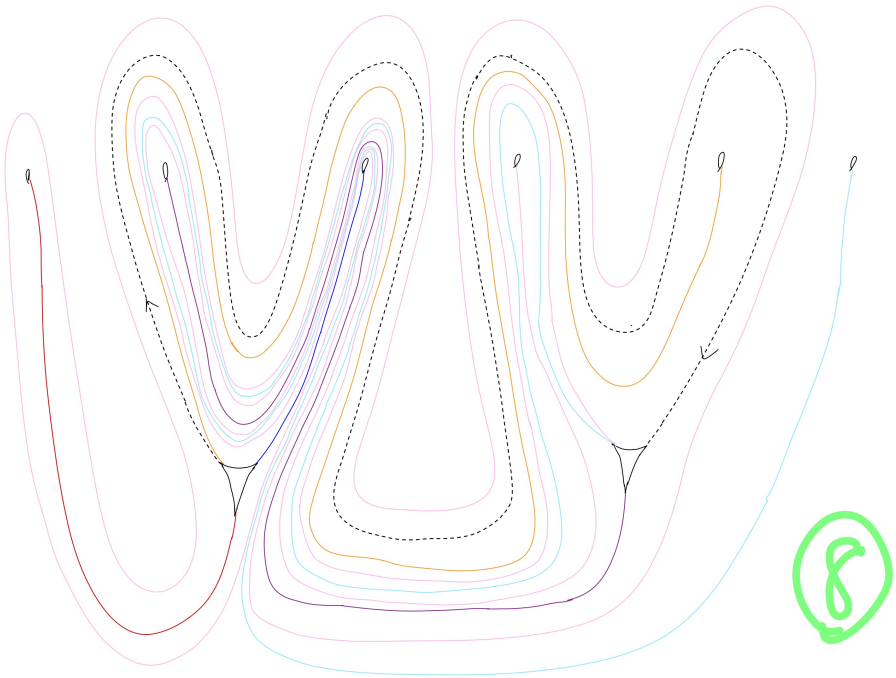


Figure L.15: Train Track Map Candidate Family 8 (Panorama) of Track 1.

The inverse of the following braid carries this family of train track maps:

$$b_8^1 = \sigma_4\sigma_3\sigma_2\sigma_4\sigma_3\sigma_4^{-1}\sigma_3^{-1}\sigma_4\sigma_4\sigma_3\sigma_2\sigma_1\sigma_4\sigma_3\sigma_2\sigma_5\sigma_4\sigma_3\sigma_3^{-1}\sigma_4^{-1}\sigma_5^{-1}\sigma_2^{-1}\sigma_3^{-1}\sigma_4^{-1}\sigma_2^{-1}\sigma_3^{-1}\sigma_2^{-1}\sigma_2^{-1}\sigma_1\sigma_2\sigma_3\sigma_4\sigma_5$$

This is shown in Figure L.16.

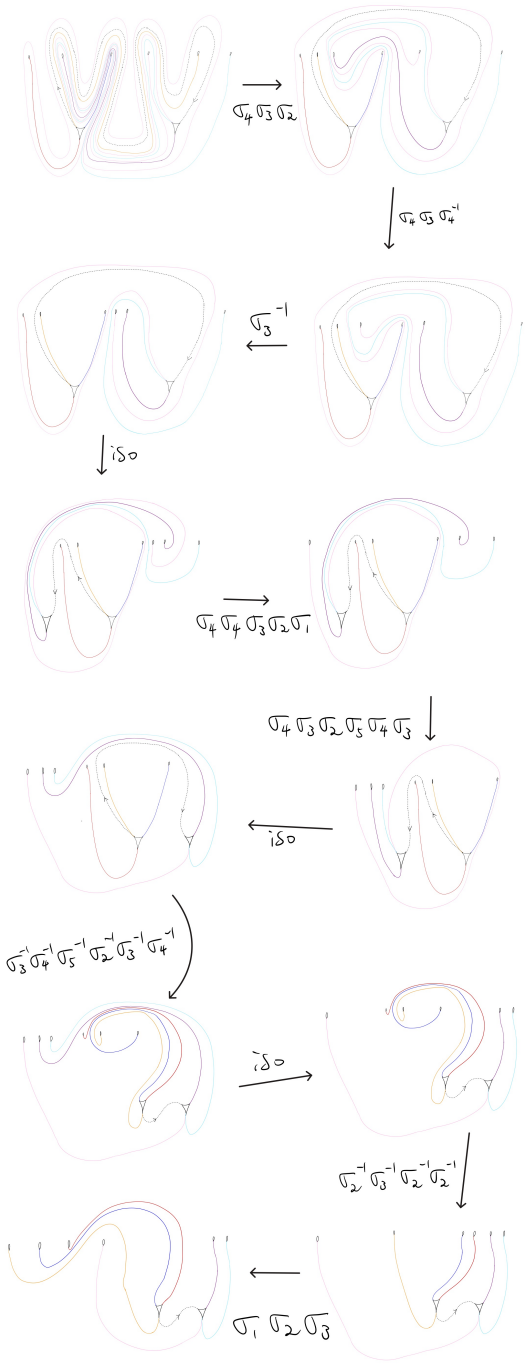


Figure L.16: This sequence shows the inverse of the braid b_8^1 carries Train Track Candidate Family 8.

L.11 Candidate Family 9 (Pristine)

Train Track Map Candidate Family 9 of Track 1 is shown in Figure L.17. See E.1.2.2.2.1.1.2 for details.

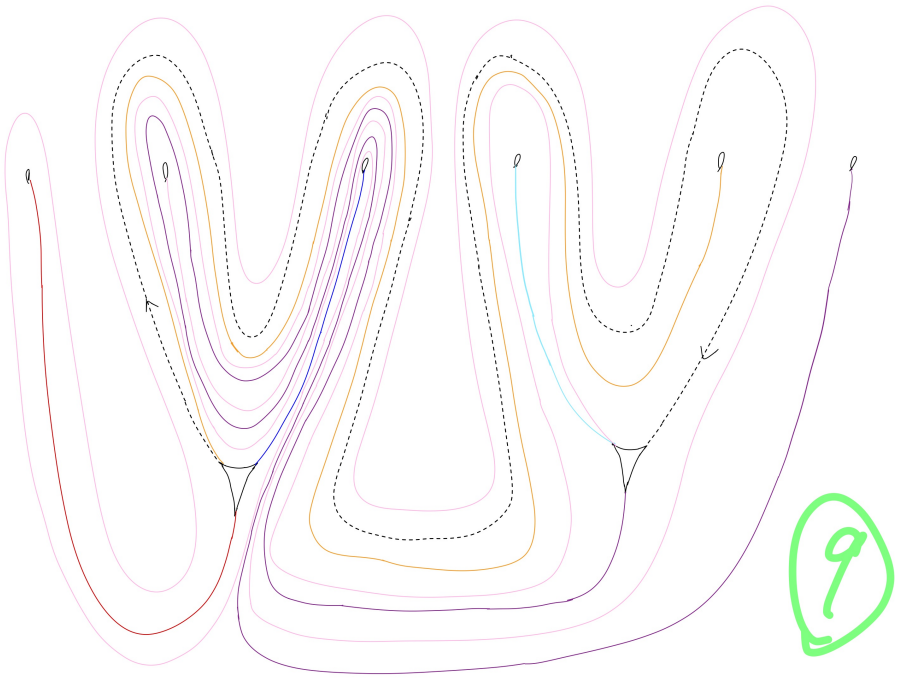


Figure L.17: Train Track Map Candidate Family 9 (Pristine) of Track 1.

The inverse of the following braid carries this family of train track maps:

$$b_9^1 = \sigma_4\sigma_3\sigma_2\sigma_3^{-1}\sigma_4\sigma_4\sigma_3\sigma_2\sigma_1\sigma_2^{-1}\sigma_3^{-1}\sigma_2^{-1}\sigma_2^{-1}\sigma_1\sigma_2\sigma_3\sigma_5\sigma_4\sigma_5$$

This is shown in Figure L.18.

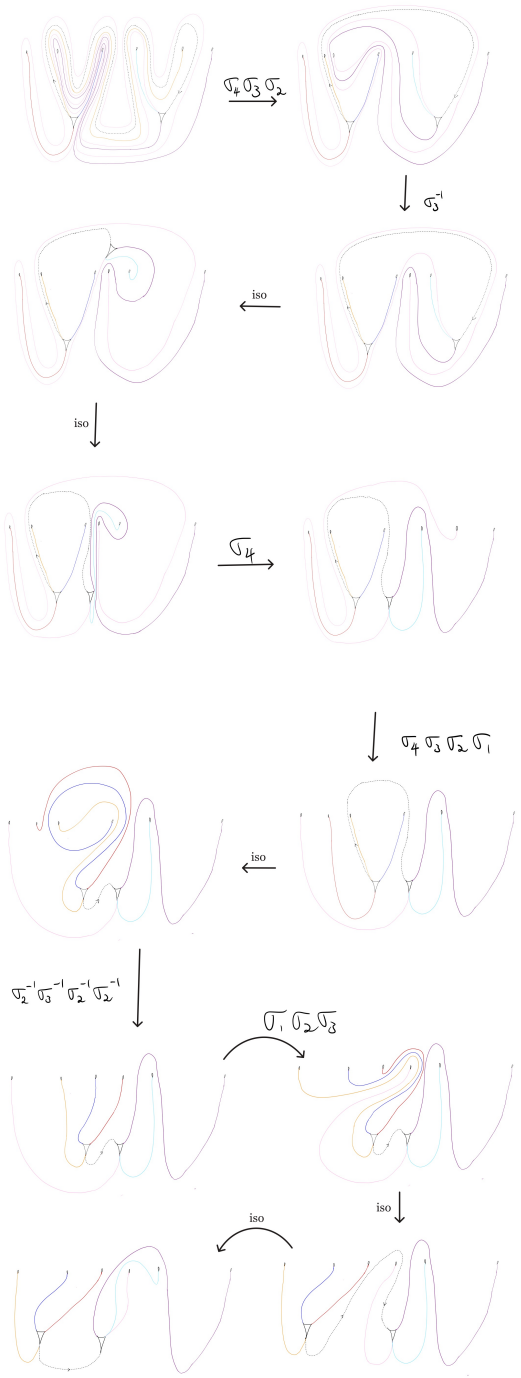


Figure L.18: This sequence shows the inverse of the braid b_9^1 carries Train Track Candidate Family 9.

L.12 Candidate Family 10 (Gingham)

Train Track Map Candidate Family 10 of Track 1 is shown in Figure L.19. See E.1.2.2.2.1.2 for details.

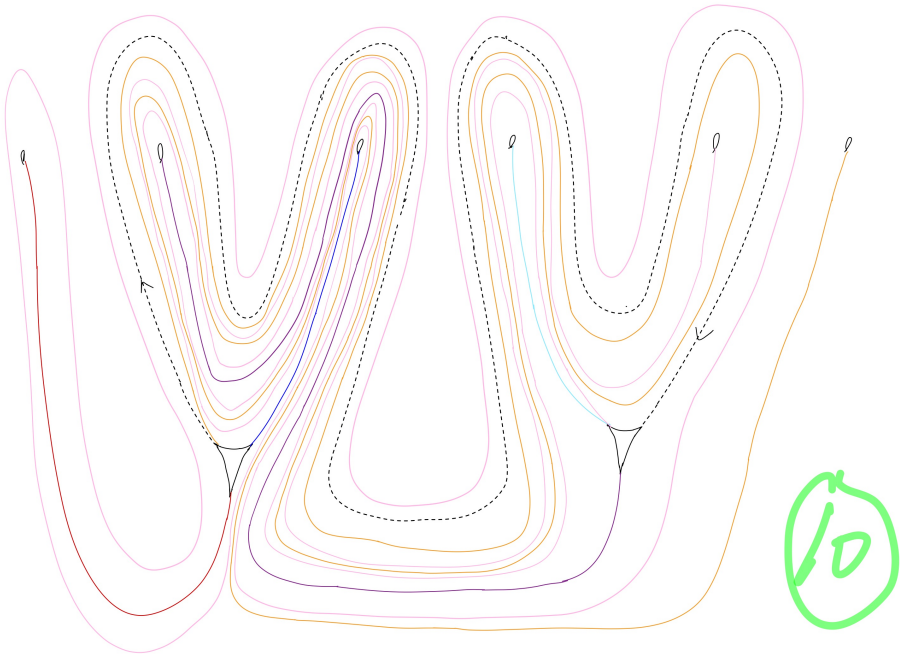


Figure L.19: Train Track Map Candidate Family 10 (Gingham) of Track 1.

The inverse of the following braid carries this family of train track maps:

$$b_{10}^{1} = \sigma_4\sigma_3\sigma_2\sigma_3^{-1}\sigma_4\sigma_4\sigma_3\sigma_2\sigma_1\sigma_4\sigma_3\sigma_2\sigma_5\sigma_4\sigma_5^{-1}\sigma_5^{-1}\sigma_4^{-1}\sigma_3^{-1}\sigma_2^{-1}\sigma_1^{-1}\sigma_1^{-1}\sigma_2^{-1}\sigma_4\sigma_5 \circ J \circ \Lambda_6$$

This is shown in Figure L.20.

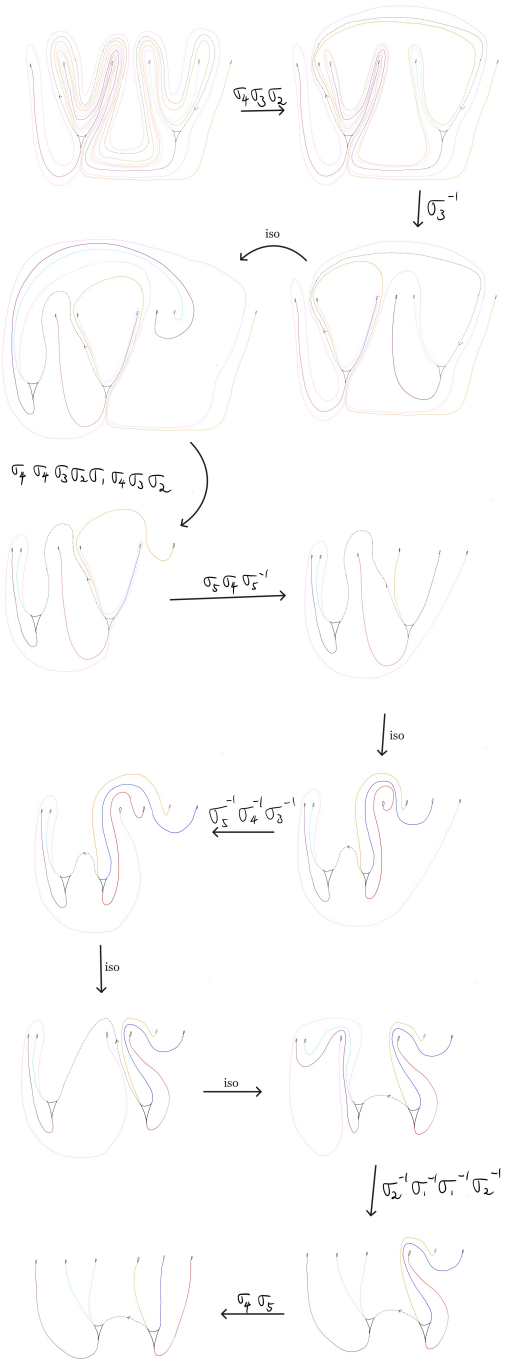


Figure L.20: This sequence shows the inverse of the braid b_{10}^1 carries Train Track Candidate Family 10.

L.13 Candidate Family 11 (Dossier)

Train Track Map Candidate Family 11 of Track 1 is shown in Figure L.21. See E.1.2.2.2.2.1 for details.

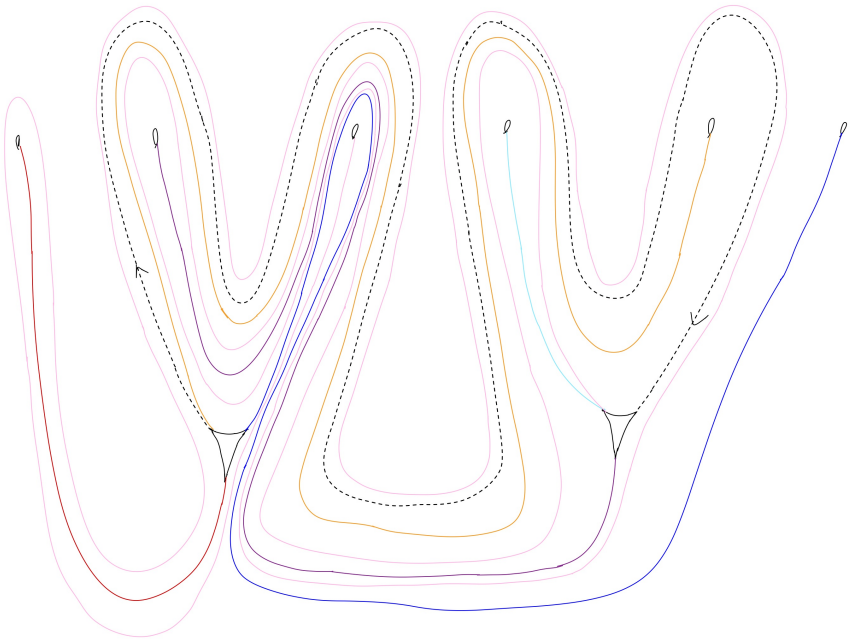


Figure L.21: Train Track Map Candidate Family 11 (Dossier) of Track 1.

The inverse of the following braid carries this family of train track maps:

$$b_{11}^{1} = \sigma_4\sigma_3\sigma_2\sigma_3^{-1}\sigma_4\sigma_4\sigma_3\sigma_2\sigma_1\sigma_4\sigma_3\sigma_2\sigma_4^{-1}\sigma_5^{-1}\sigma_3^{-1}\sigma_2^{-1}\sigma_1^{-1}\sigma_1^{-1}\sigma_2^{-1}\sigma_5\sigma_4\sigma_5 \circ J \circ \Lambda_6$$

This is shown in Figure L.22.

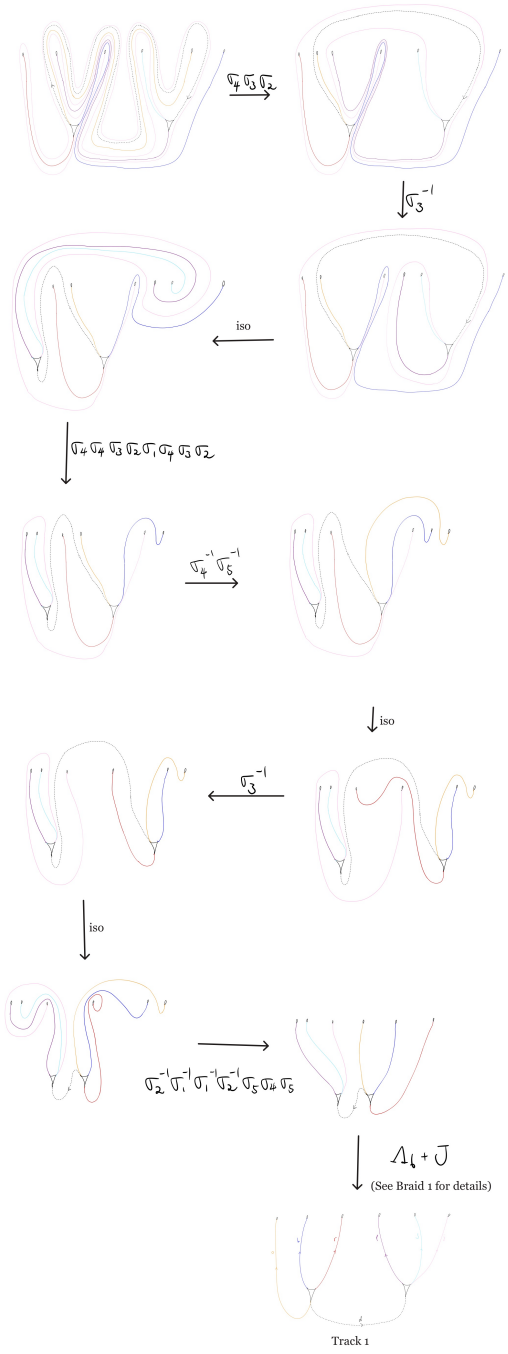


Figure L.22: This sequence shows the inverse of the braid b_{11}^1 carries Train Track Candidate Family 11.

L.14 Candidate Family 12 (Querulous)

Train Track Map Candidate Family 12 of Track 1 is shown in Figure L.23. See E.1.2.2.2.2.2.1.1 for details.

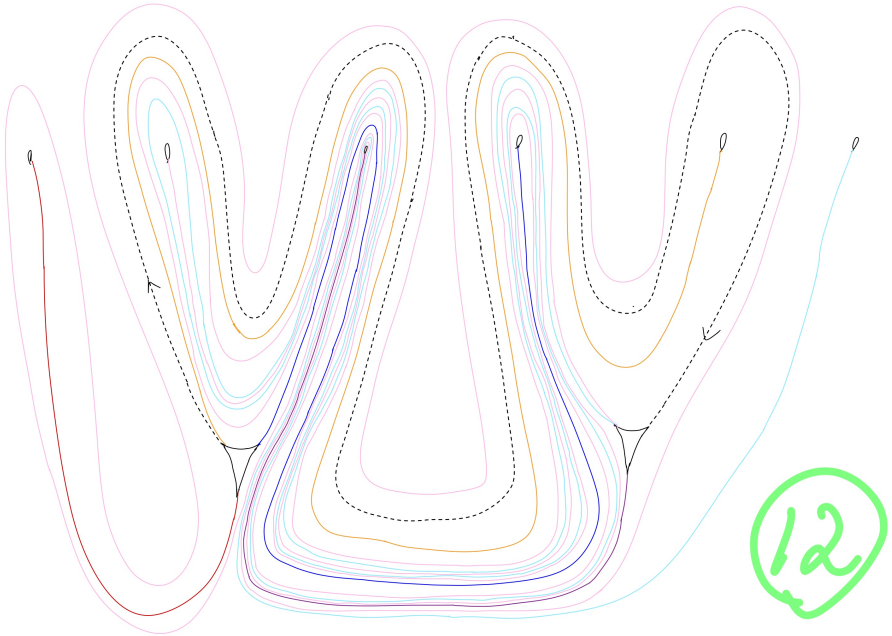


Figure L.23: Train Track Map Candidate Family 12 (Querulous) of Track 1.

The inverse of the following braid carries this family of train track maps:

$$b_{12}^{1} = \sigma_4\sigma_3\sigma_2\sigma_3^{-1}\sigma_4^{-1}\sigma_3\sigma_4\sigma_4\sigma_4\sigma_3\sigma_2\sigma_1\sigma_1\sigma_2\sigma_3\sigma_1^{-1}\sigma_2^{-1}\sigma_1^{-1}\sigma_1^{-1}\sigma_4\sigma_5$$

This is shown in Figure L.24.

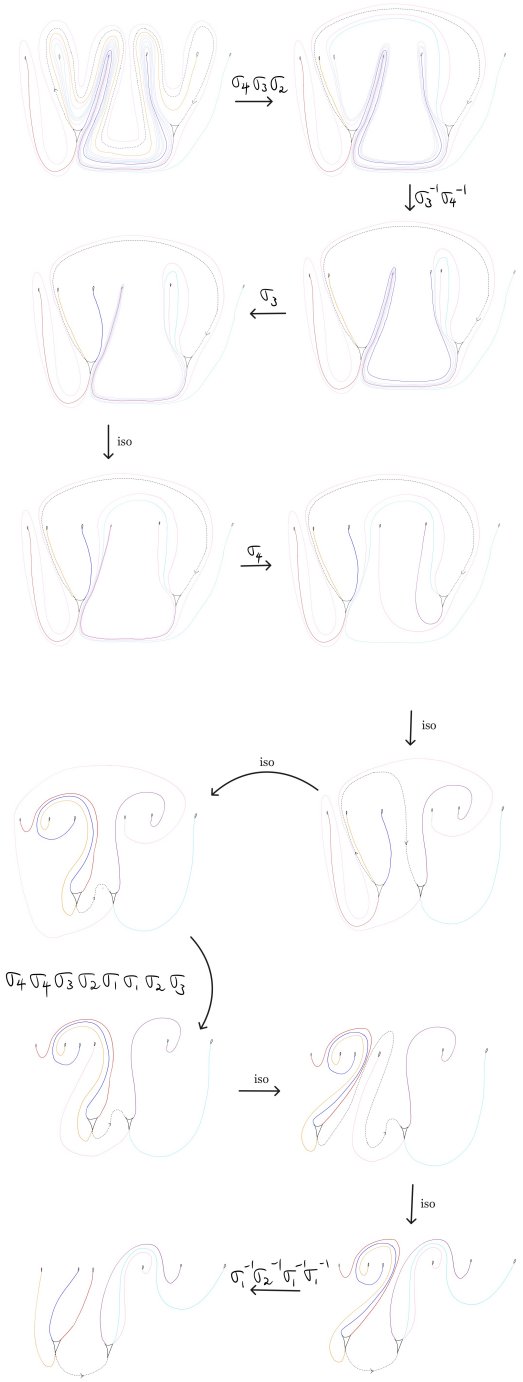


Figure L.24: This sequence shows the inverse of the braid b_{12}^1 carries Train Track Candidate Family 12.

L.15 Candidate Family 13 (Querulous)

Train Track Map Candidate Family 13 of Track 1 is shown in Figure L.25. See E.1.2.2.2.2.2.1.1 for details.

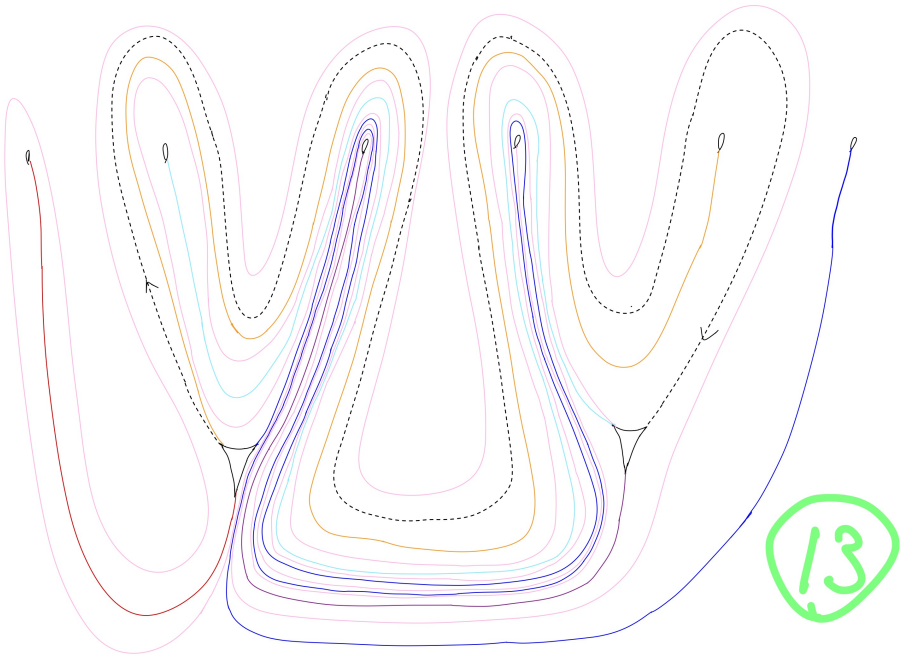


Figure L.25: Train Track Map Candidate Family 13 (Querulous) of Track 1.

The inverse of the following braid carries this family of train track maps:

$$b_{13}^{1} = \sigma_4\sigma_3\sigma_2\sigma_3^{-1}\sigma_4^{-1}\sigma_3\sigma_2^{-1}\sigma_1^{-1}\sigma_1^{-1}\sigma_2^{-1}\sigma_3^{-1}\sigma_4^{-1}\sigma_3\sigma_4^{-1}\sigma_5^{-1}\sigma_3^{-1}\sigma_4^{-1}\sigma_3^{-1}\sigma_1^{-1}\sigma_2^{-1}\sigma_1^{-1}\sigma_1^{-1}\sigma_5\sigma_4\sigma_5$$

This is shown in Figure L.26.

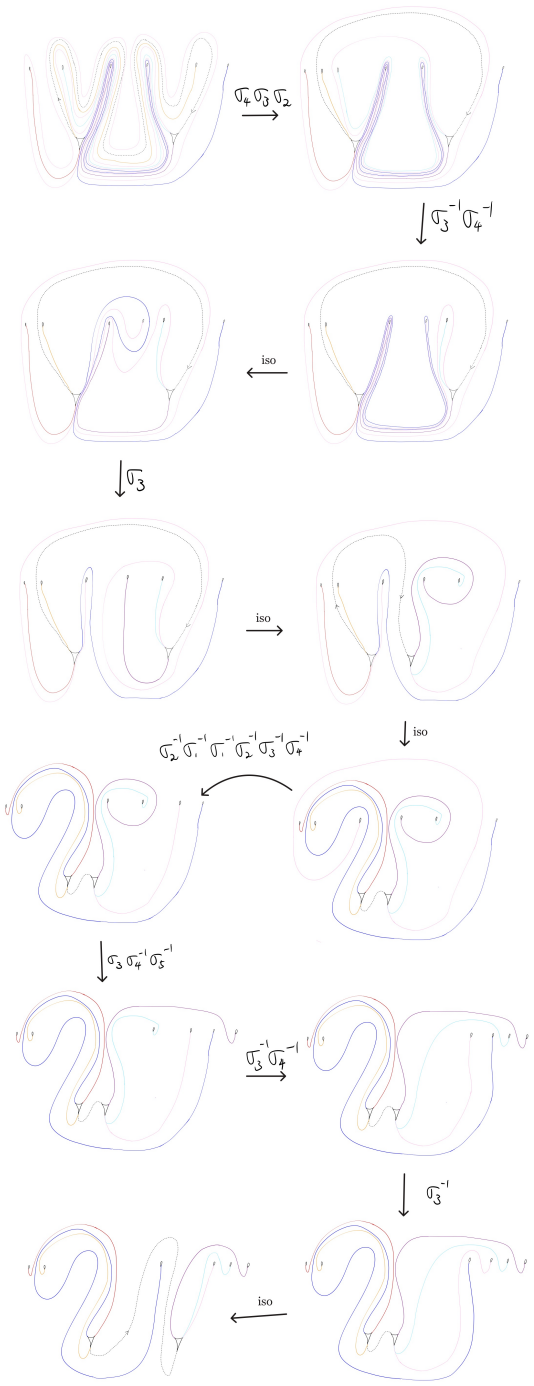


Figure L.26: This sequence shows the inverse of the braid b_{13}^1 carries Train Track Candidate Family 13.

L.16 Candidate Family 14 (Sybaritic)

Train Track Map Candidate Family 14 of Track 1 is shown in Figure L.27. See E.1.2.2.2.2.2.1.2 for details.

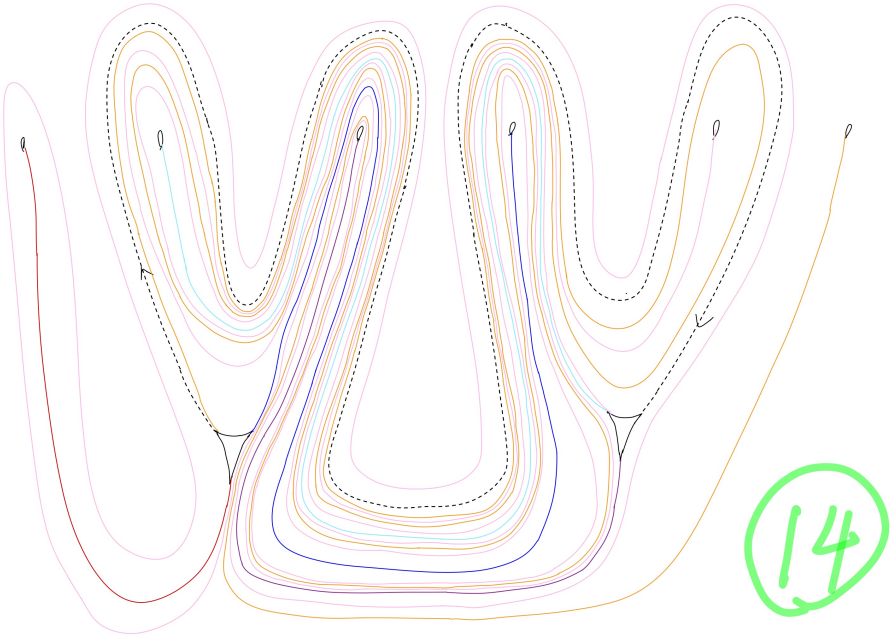


Figure L.27: Train Track Map Candidate Family 14 (Sybaritic) of Track 1.

The inverse of the following braid carries this family of train track maps:

$$b_{14}^{1} = \sigma_4\sigma_3\sigma_2\sigma_3^{-1}\sigma_4^{-1}\sigma_2^{-1}\sigma_3^{-1}\sigma_2\sigma_3\sigma_2^{-1}\sigma_1^{-1}\sigma_1^{-1}\sigma_2^{-1}\sigma_3^{-1}\sigma_4^{-1}\sigma_5^{-1}\sigma_3\sigma_4^{-1}\sigma_5^{-1}\sigma_3^{-1}\sigma_4^{-1}\sigma_1^{-1}\sigma_2\sigma_1^{-1}\sigma_5\sigma_4\sigma_5$$

This is shown in Figure L.28.

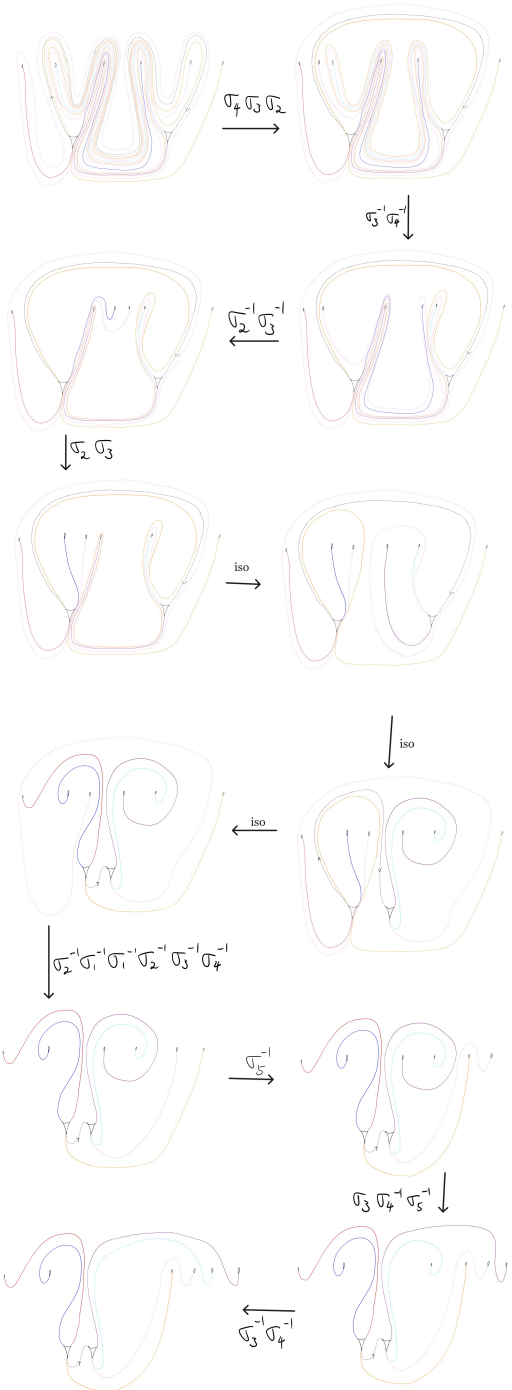


Figure L.28: This sequence shows the inverse of the braid b_{14}^1 carries Train Track Candidate Family 14.

L.17 Candidate Family 15 (Leverage)

Train Track Map Candidate Family 15 of Track 1 is shown in Figure L.29. See E.1.2.2.2.2.2.2 for details.

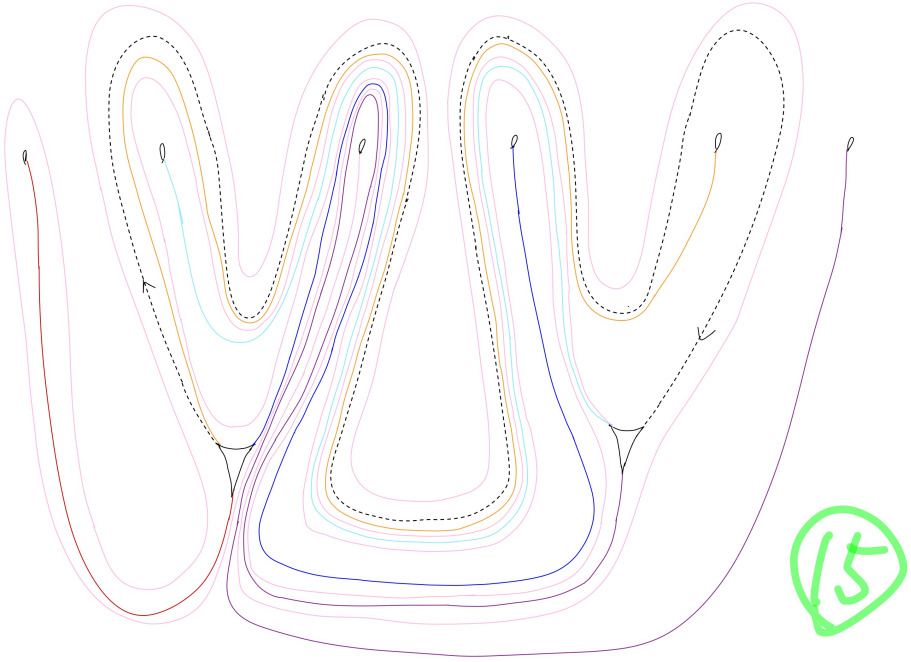


Figure L.29: Train Track Map Candidate Family 15 (Leverage) of Track 1.

The inverse of the following braid carries this family of train track maps:

$$b_{15}^{1} = \sigma_4\sigma_3\sigma_2\sigma_3^{-1}\sigma_4^{-1}\sigma_3\sigma_4\sigma_4\sigma_3\sigma_2\sigma_1\sigma_1\sigma_3^{-1}\sigma_2\sigma_3\sigma_1^{-1}\sigma_2^{-1}\sigma_1^{-1}\sigma_5\sigma_4\sigma_5$$

This is shown in Figure L.30.

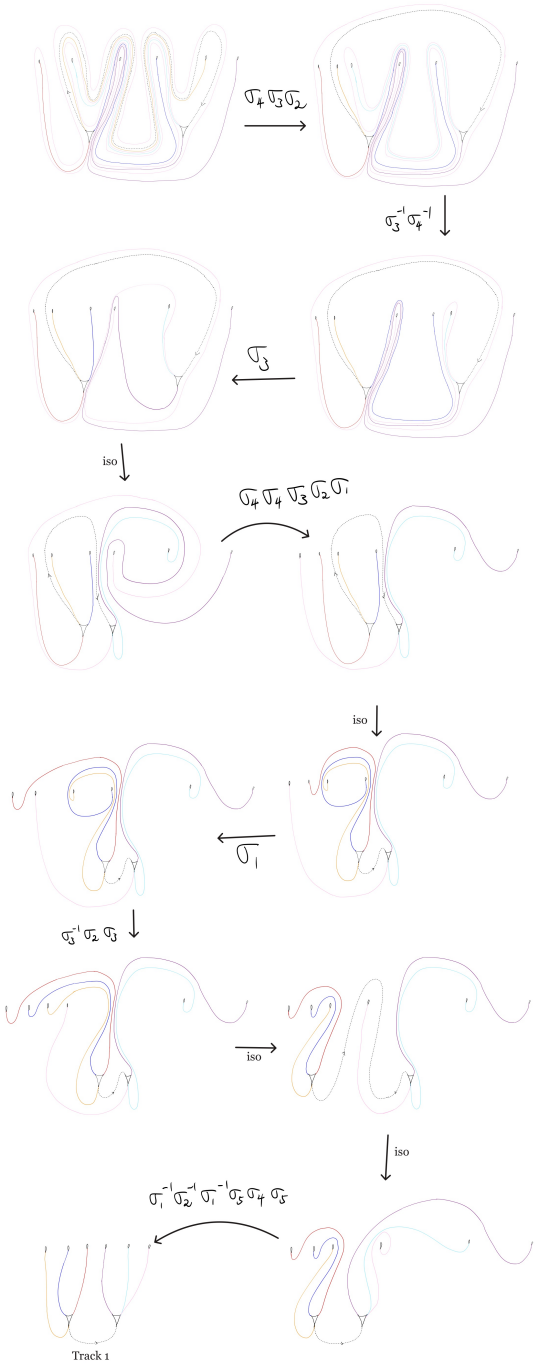


Figure L.30: This sequence shows the inverse of the braid b_{15}^1 carries Train Track Candidate Family 15.

L.18 Candidate Family 16 (Guddle)

Train Track Map Candidate Family 16 of Track 1 is shown in Figure L.31. See E.1.3.3.2.1 for details.

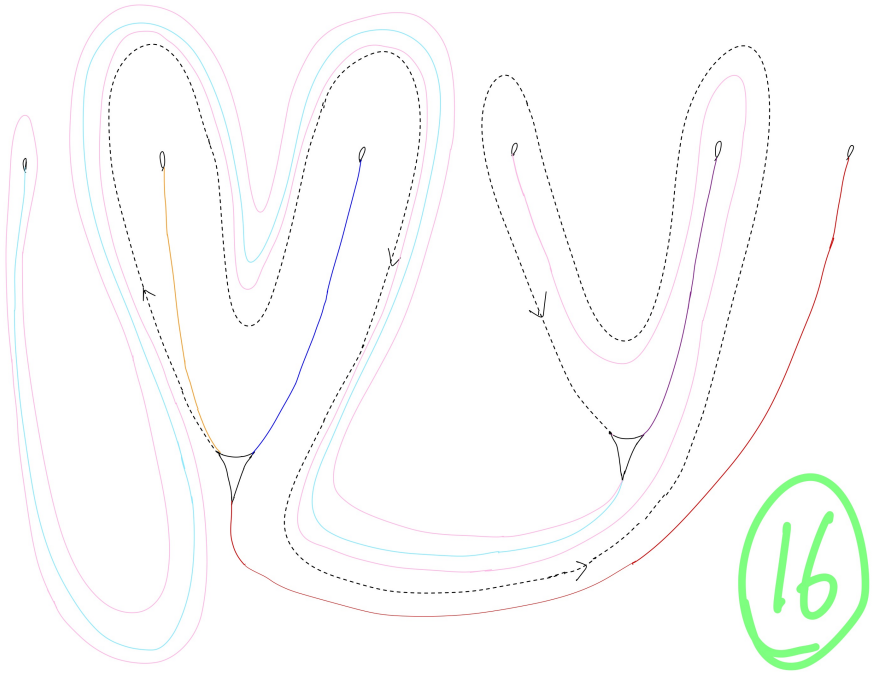


Figure L.31: Train Track Map Candidate Family 16 (Guddle) of Track 1.

The inverse of the following braid carries this family of train track maps:

$$b_{16}^{1} = \sigma_4^{-1}\sigma_1^{-1}\sigma_2^{-1}\sigma_3^{-1}\sigma_4^{-1}\sigma_3^{-1}\sigma_3^{-1}\sigma_4^{-1}\sigma_1^{-1}\sigma_1^{-1}\sigma_5^{-1}\sigma_4^{-1}\sigma_3^{-1}\sigma_2^{-1}\sigma_1^{-1}\sigma_1^{-1}\sigma_2^{-1}$$

This is shown in Figure L.32.

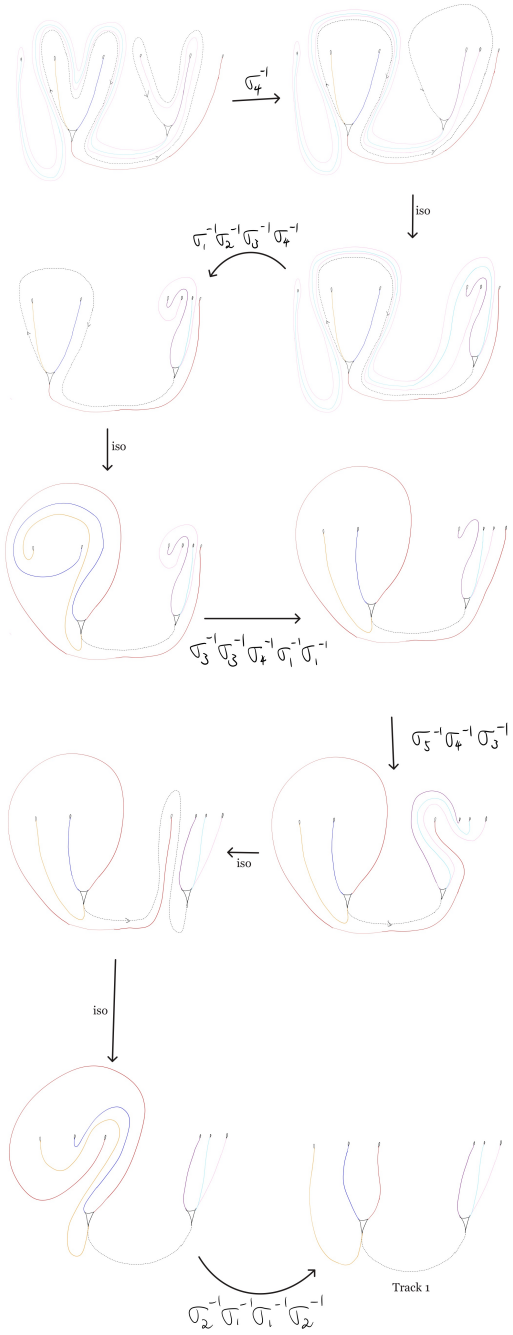


Figure L.32: This sequence shows the inverse of the braid b_{16}^1 carries Train Track Candidate Family 16.

L.19 Candidate Family 17 (Popjoy)

Train Track Map Candidate Family 17 of Track 1 is shown in Figure L.33. See E.2.10.1.2.1 for details.

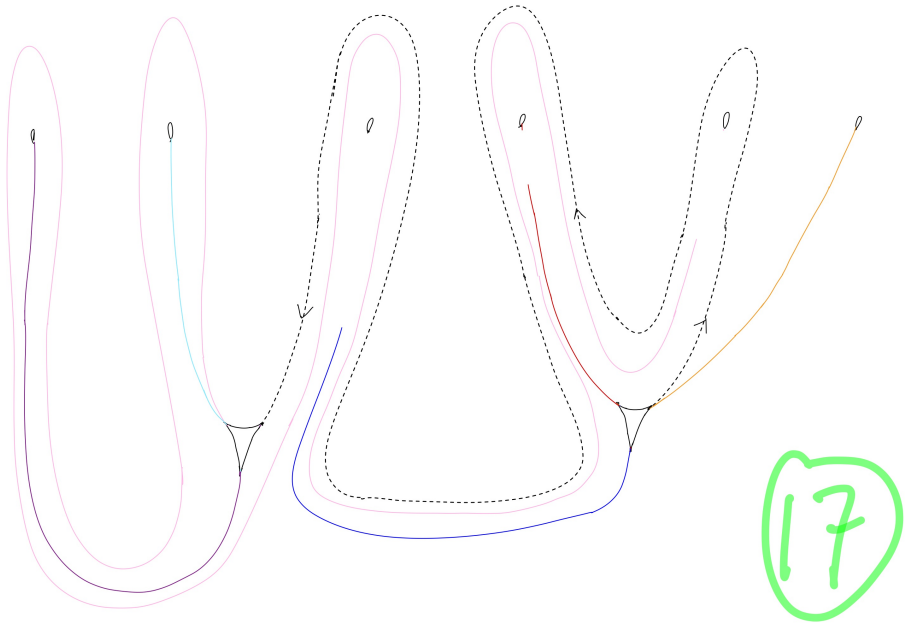


Figure L.33: Train Track Map Candidate Family 17 (Popjoy) of Track 1.

The inverse of the following braid carries this family of train track maps:

$$b^1_{17} = \sigma_4^k \sigma_3^m \sigma_2^{-1} \sigma_1^{-1} \sigma_1^{-1} \sigma_2^{-1} \sigma_5 \sigma_4 \sigma_5 \circ J \circ \Lambda_6$$

where $k, m \geq 1$ ($k, m \in \mathbb{Z}$) are the twisting parameters. This is shown in Figure L.34.

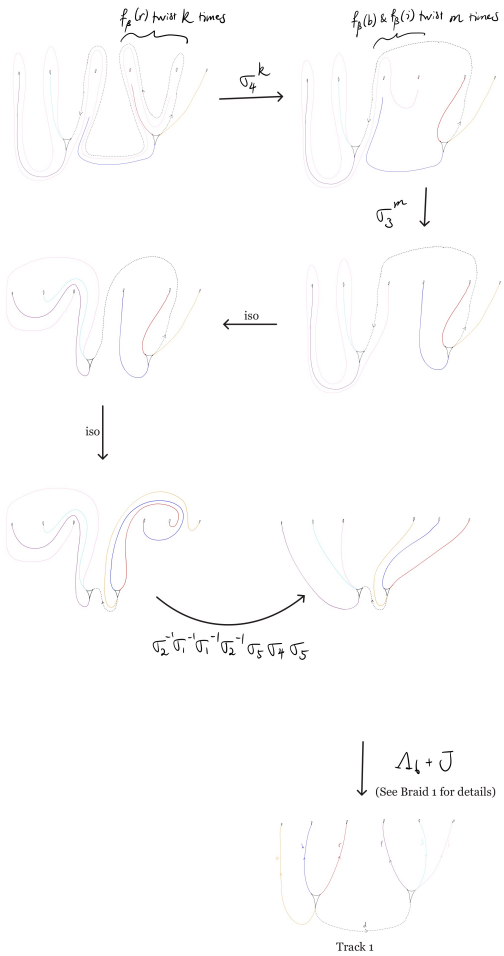


Figure L.34: This sequence shows the inverse of the braid b_{17}^1 carries Train Track Candidate Family 17.

APPENDIX THIRTEEN

Appendix: Candidate Braids for Track 8

M.1 Summary of Candidate Braid Families

Through the exhaustive train track case analysis of Track 8 in the stratum $(2; 1^6; 3^2)$ (the full details of which are presented in Appendix F), we isolate exactly 9 candidate families of train track maps. If the pseudo-Anosov representative ϕ_Φ has no interior fixed points, then its mapping class Φ must be conjugate to the lift of one of the following 9 braid families (enumerated below with their twist parameters).

1. $\Delta^{2i}(\sigma_5^{-1}\sigma_2\sigma_4^{-1}\sigma_1^{-1}\sigma_2^{-1}\sigma_3^{-1}\sigma_4^{-1}\sigma_5^{-1}\sigma_3^{-1}\sigma_4^{-1}\sigma_2\sigma_1\sigma_2\sigma_3^{-1}\sigma_4^{-1}\sigma_2^{-1}\sigma_1^{-1})^{-1}$
2. $\Delta^{2i}(\sigma_5^{-1}\sigma_2\sigma_4^{-1}\sigma_1^{-1}\sigma_2^{-1}\sigma_3^{-1}\sigma_4^{-1}\sigma_2\sigma_1\sigma_2\sigma_3^{-1}\sigma_5^{-1}\sigma_3^{-1}\sigma_4^{-1}\sigma_3^{-1}\sigma_2^{-1}\sigma_1^{-1})^{-1}$
3. $\Delta^{2i}(\sigma_5^{-1}\sigma_2\sigma_4^{-1}\sigma_1^{-1}\sigma_2^{-1}\sigma_3^{-1}\sigma_4^{-1}\sigma_5^{-1}\sigma_2\sigma_1\sigma_3^{-1}\sigma_4^{-1}\sigma_2\sigma_3^{-1}\sigma_4^{-1}\sigma_2^{-1}\sigma_1^{-1})^{-1}$
4. $\Delta^{2i}(\sigma_5^{-1}\sigma_2^{-1}\sigma_1^{-1}\sigma_1^{-1}\sigma_2^{-1}\sigma_3^{-1}\sigma_4^{-1}\sigma_3^{-1}\sigma_3^{-1}\sigma_3^{-1}\sigma_5^{-1}\sigma_4^{-1}\sigma_3^{-1}\sigma_1^{-1}\sigma_2^{-1}\sigma_1^{-1}\sigma_1^{-1})^{-1}$
5. $\Delta^{2i}(\sigma_5^{-1}\sigma_4^{-1}\sigma_1^{-1}\sigma_2^{-1}\sigma_1^{-1}\sigma_1^{-1}\sigma_1^{-1}\sigma_2^{-1}\sigma_3^{-1}\sigma_4^{-1}\sigma_3^{-1}\sigma_3^{-1}\sigma_5^{-1}\sigma_4^{-1}\sigma_3^{-1}\sigma_2^{-1}\sigma_1^{-1})^{-1}$
6. $\Delta^{2i}(\sigma_5^{-1}\sigma_1^{-1}\sigma_2^{-1}\sigma_4^{-1}\sigma_3^{-1}\sigma_4^{-1}\sigma_5^{-1}\sigma_3^{-1}\sigma_3^{-1}\sigma_4^{-1}\sigma_3^{-1}\sigma_2^{-1}\sigma_1^{-1}\sigma_1^{-1}\sigma_2^{-1}\sigma_1^{-1}\sigma_1^{-1})^{-1}$

7. $\Delta^{2i}(\sigma_5^{-1}\sigma_4^k\sigma_3\sigma_1^{-1}\sigma_2^{-1}\sigma_3^{-1}\sigma_4^{-1}\sigma_3\sigma_3\sigma_2\sigma_1\sigma_4\sigma_3\sigma_2\sigma_4\sigma_3 \cdot \Lambda_6 \cdot J)^{-1}$

8. $\Delta^{2i}(\sigma_5^{-1}\sigma_1^{-1}\sigma_2^{-1}\sigma_3^{-1}\sigma_4^{-1}\sigma_3\sigma_2\sigma_1\sigma_2^{-1}\sigma_3^{-1}\sigma_2\sigma_3\sigma_3\sigma_2\sigma_1\sigma_4\sigma_3\sigma_2\sigma_4\sigma_3 \cdot \Lambda_6 \cdot J)^{-1}$

9. $\Delta^{2i}(\sigma_1^{-1}\sigma_2^{-k}\sigma_3^{-1}\sigma_2^{-1}\sigma_2^{-1}\sigma_3^{-1}\sigma_2^{-1}\sigma_2^{-1}\sigma_1\sigma_2\sigma_3\sigma_4\sigma_5 \cdot \Lambda_6 \cdot J)^{-1}$

M.2 Base Braids Λ_6 and J

Before we list the braids carrying candidate train track maps for Track 8, we introduce the following base braids, which we will call Λ_6 and J:

$\Lambda_6 = \sigma_1\sigma_2\sigma_1\sigma_3\sigma_2\sigma_1\sigma_4\sigma_3\sigma_2\sigma_1\sigma_5\sigma_4\sigma_3\sigma_2\sigma_1$

$J = \sigma_1^{-1}\sigma_2^{-1}\sigma_1^{-1}\sigma_5\sigma_4\sigma_5$

We shall make use of Λ_6 and J occasionally in constructing candidate braids for Track 8.

M.3 Candidate Family 1 (Anomy)

Train Track Map Candidate Family 1 of Track 8 is shown in Figure M.1. See F.1.1.2.1 for details.

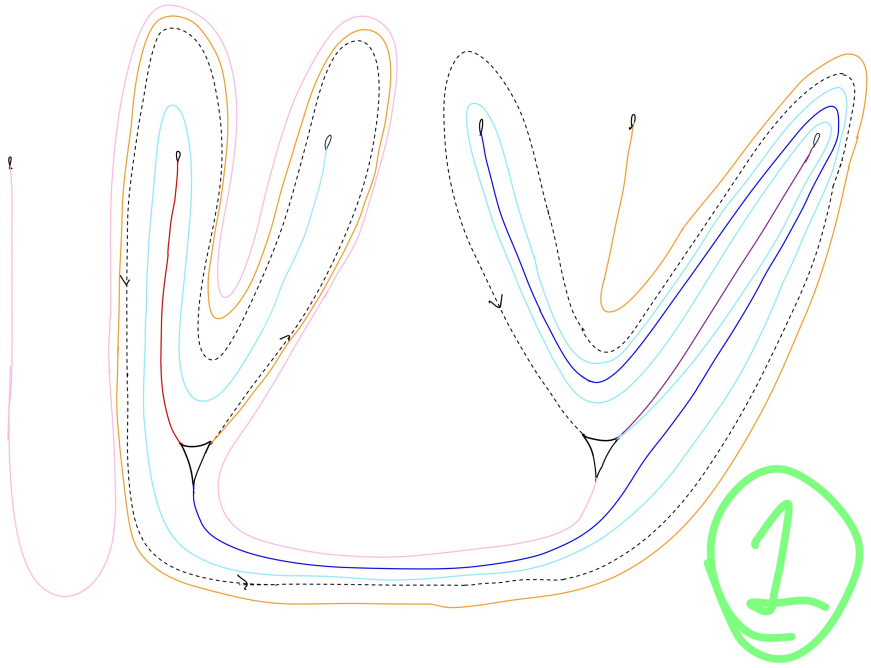


Figure M.1: Train Track Map Candidate Family 1 (Anomy) of Track 8.

The inverse of the following braid carries this family of train track maps:

$$b_1^8 = \sigma_5^{-1}\sigma_2\sigma_4^{-1}\sigma_1^{-1}\sigma_2^{-1}\sigma_3^{-1}\sigma_4^{-1}\sigma_5^{-1}\sigma_3^{-1}\sigma_4^{-1}\sigma_2\sigma_1\sigma_2\sigma_3^{-1}\sigma_4^{-1}\sigma_2^{-1}\sigma_1^{-1}$$

This is shown in Figure M.2.

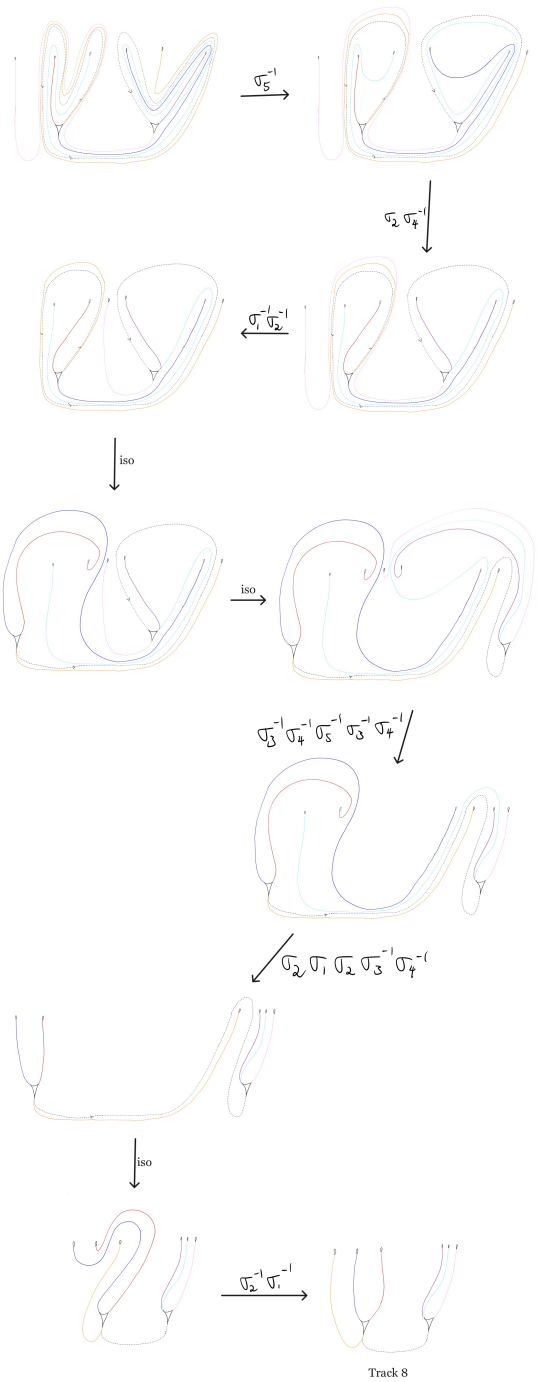


Figure M.2: This sequence shows the inverse of the braid b_1^8 carries Train Track Candidate Family 1.

M.4 Candidate Family 2 (Diatree)

Train Track Map Candidate Family 2 of Track 8 is shown in Figure M.3. See F.1.1.2.2.1 for details.

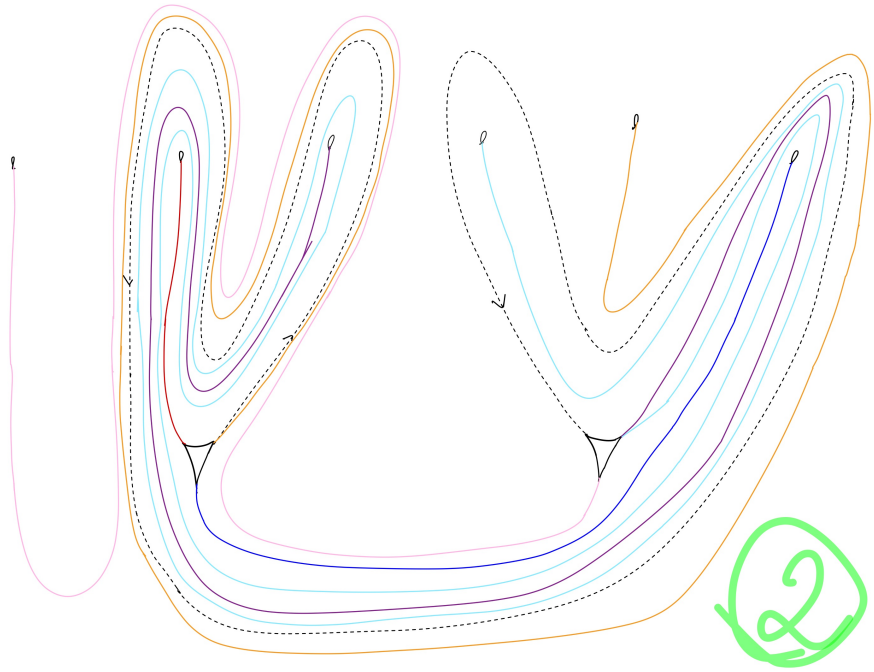


Figure M.3: Train Track Map Candidate Family 2 (Diatree) of Track 8.

The inverse of the following braid carries this family of train track maps:

$$b_2^8 = \sigma_5^{-1}\sigma_2\sigma_4^{-1}\sigma_1^{-1}\sigma_2^{-1}\sigma_3^{-1}\sigma_4^{-1}\sigma_2\sigma_1\sigma_2\sigma_3^{-1}\sigma_5^{-1}\sigma_3^{-1}\sigma_4^{-1}\sigma_3^{-1}\sigma_2^{-1}\sigma_1^{-1}$$

This is shown in Figure M.4.

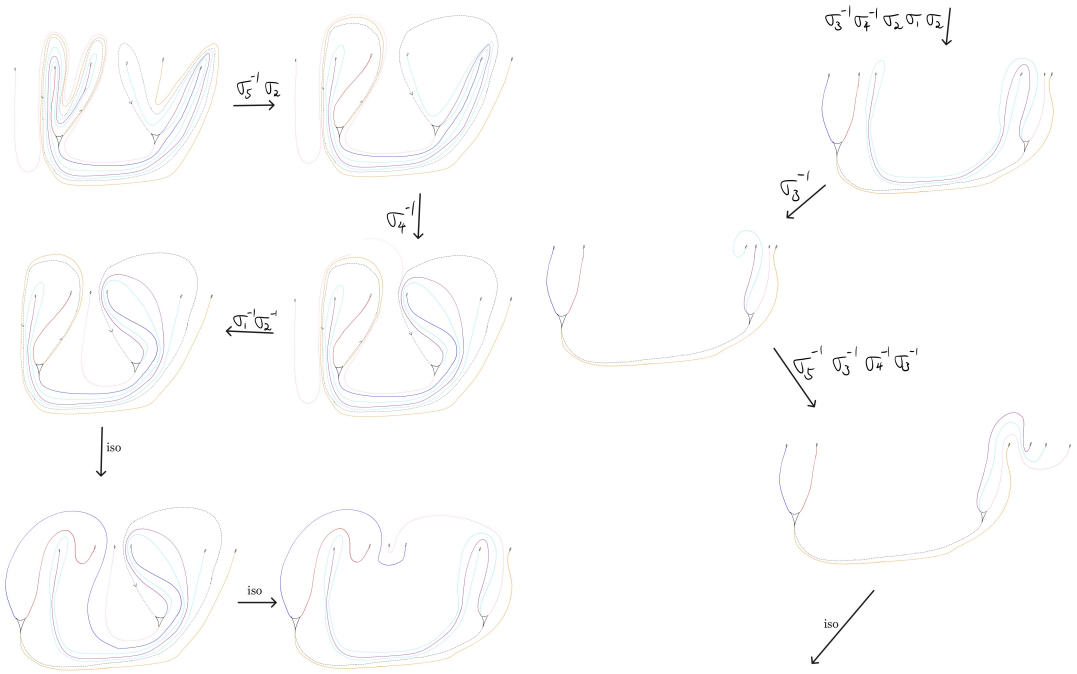


Figure M.4: This sequence shows the inverse of the braid b_2^8 carries Train Track Candidate Family 2.

M.5 Candidate Family 3 (Fulmine)

Train Track Map Candidate Family 3 of Track 8 is shown in Figure M.5. See F.1.1.2.2.2 for details.

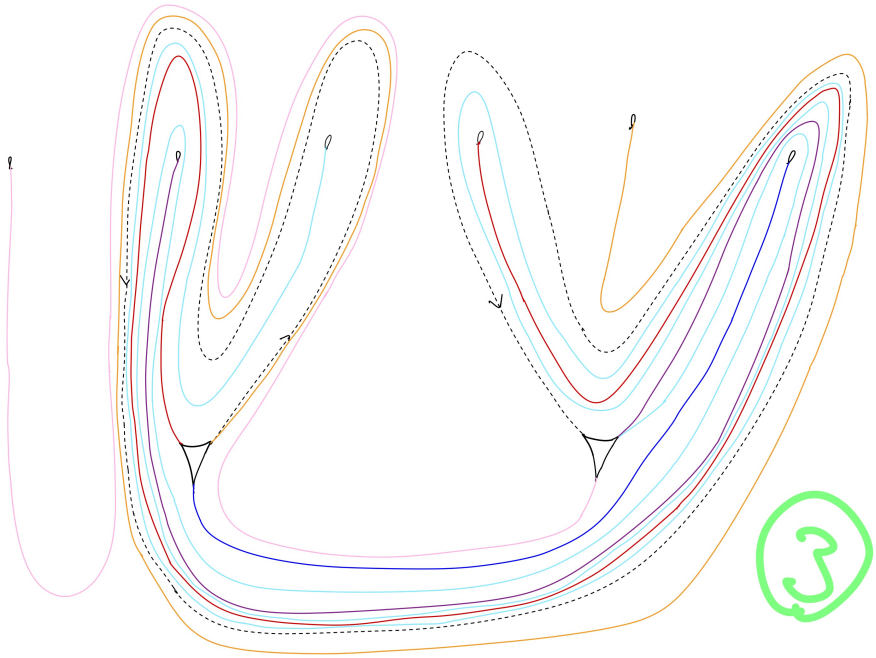


Figure M.5: Train Track Map Candidate Family 3 (Fulmine) of Track 8.

The inverse of the following braid carries this family of train track maps:

$$b_3^8 = \sigma_5^{-1}\sigma_2\sigma_4^{-1}\sigma_1^{-1}\sigma_2^{-1}\sigma_3^{-1}\sigma_4^{-1}\sigma_5^{-1}\sigma_2\sigma_1\sigma_3^{-1}\sigma_4^{-1}\sigma_2\sigma_3^{-1}\sigma_4^{-1}\sigma_2^{-1}\sigma_1^{-1}$$

This is shown in Figure M.6.

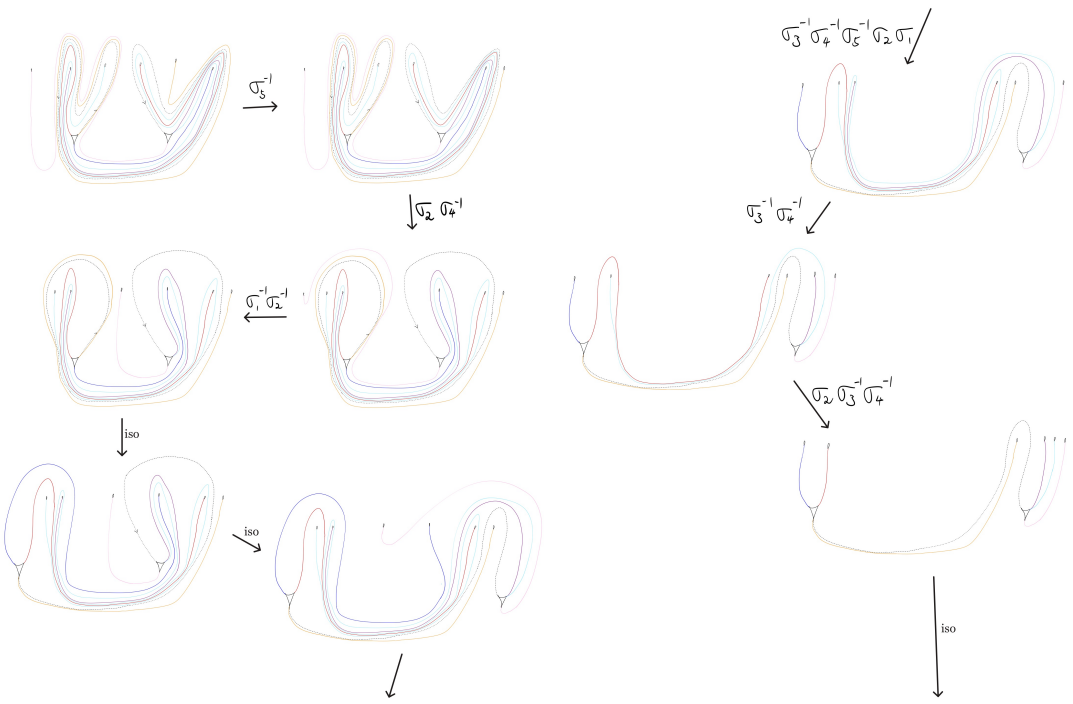


Figure M.6: This sequence shows the inverse of the braid b_3^8 carries Train Track Candidate Family 3.

M.6 Candidate Family 4 (Chine)

Train Track Map Candidate Family 4 of Track 8 is shown in Figure M.7. See F.1.5.1.1 for details.

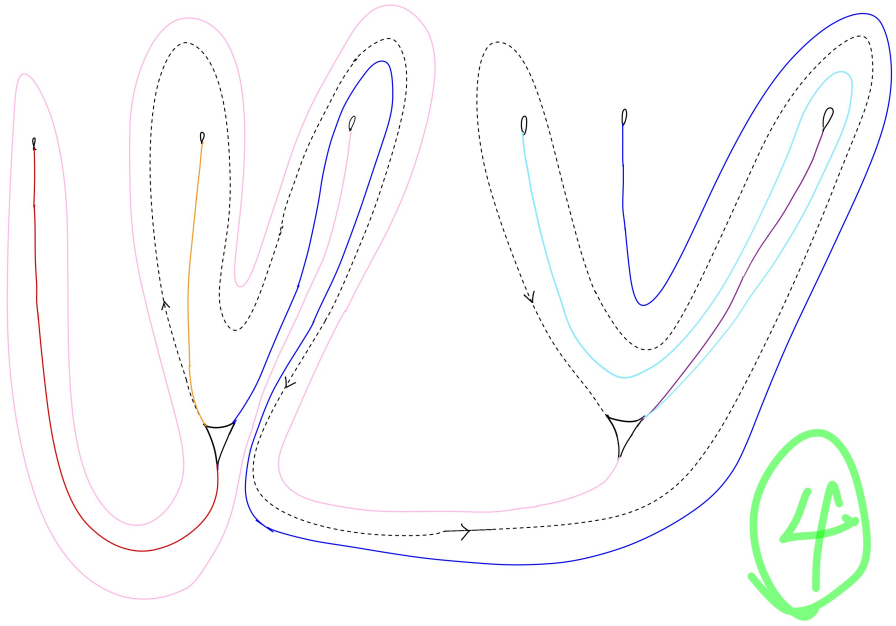


Figure M.7: Train Track Map Candidate Family 4 (Chine) of Track 8.

The inverse of the following braid carries this family of train track maps:

$$b_4^8 = \sigma_5^{-1}\sigma_2^{-1}\sigma_1^{-1}\sigma_1^{-1}\sigma_2^{-1}\sigma_3^{-1}\sigma_4^{-1}\sigma_3^{-1}\sigma_3^{-1}\sigma_3^{-1}\sigma_5^{-1}\sigma_4^{-1}\sigma_3^{-1}\sigma_1^{-1}\sigma_2^{-1}\sigma_1^{-1}\sigma_1^{-1}$$

This is shown in Figure M.8.

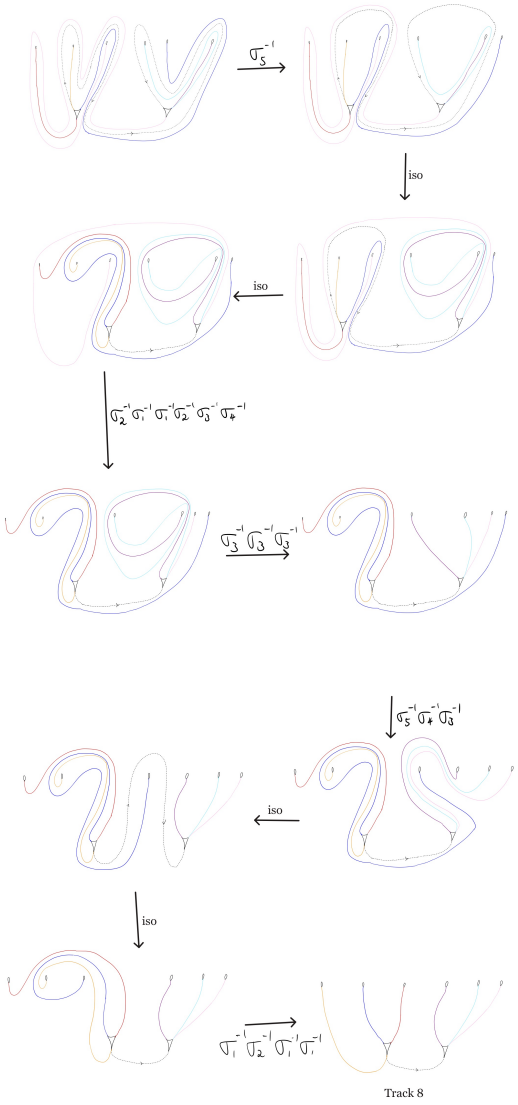


Figure M.8: This sequence shows the inverse of the braid b_4^8 carries Train Track Candidate Family 4.

M.7 Candidate Family 5 (Quaint)

Train Track Map Candidate Family 5 of Track 8 is shown in Figure M.9. See F.1.5.1.2.0.1 for details.

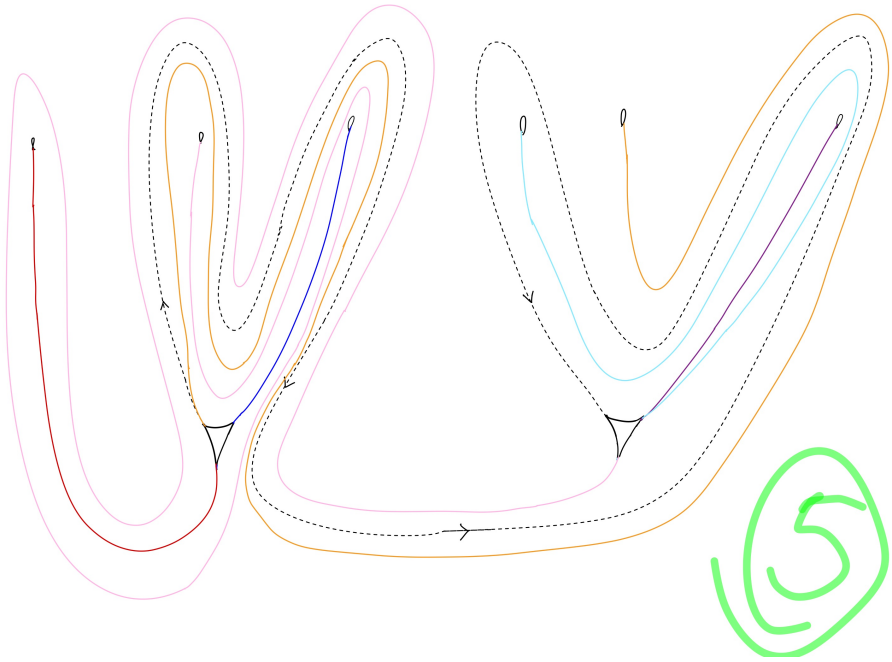


Figure M.9: Train Track Map Candidate Family 5 (Quaint) of Track 8.

The inverse of the following braid carries this family of train track maps:

$$b_5^8 = \sigma_5^{-1}\sigma_4^{-1}\sigma_1^{-1}\sigma_2^{-1}\sigma_1^{-1}\sigma_1^{-1}\sigma_1^{-1}\sigma_2^{-1}\sigma_3^{-1}\sigma_4^{-1}\sigma_3^{-1}\sigma_3^{-1}\sigma_5^{-1}\sigma_4^{-1}\sigma_3^{-1}\sigma_2^{-1}\sigma_1^{-1}$$

This is shown in Figure M.10.

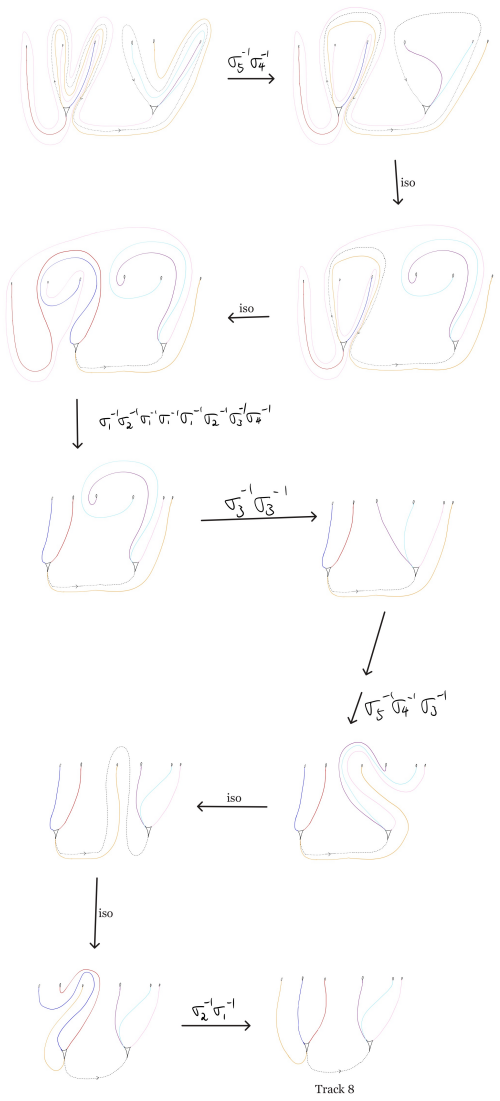


Figure M.10: This sequence shows the inverse of the braid b_5^8 carries Train Track Candidate Family 5.

M.8 Candidate Family 6 (Lacuna)

Train Track Map Candidate Family 6 of Track 8 is shown in Figure M.11. See F.1.5.2.1.1 for details.

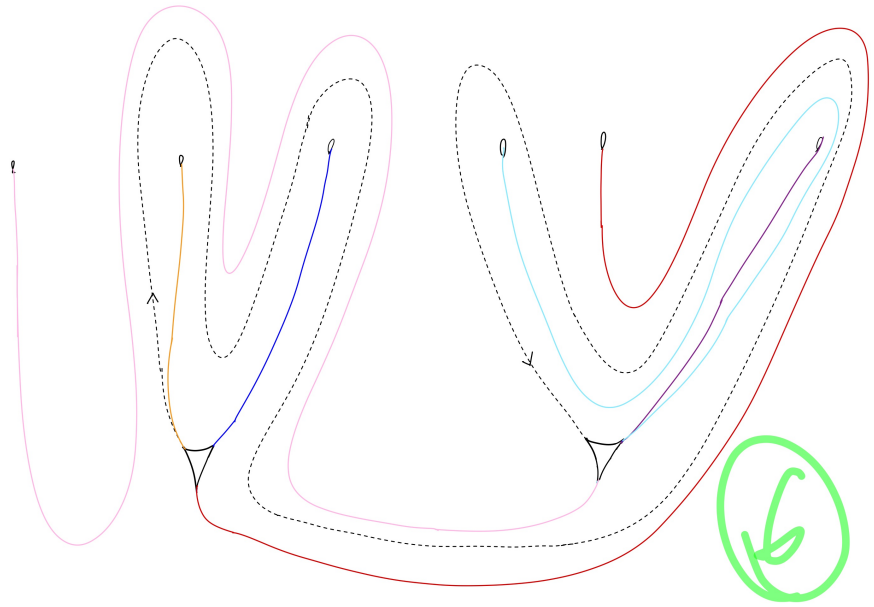


Figure M.11: Train Track Map Candidate Family 6 (Lacuna) of Track 8.

The inverse of the following braid carries this family of train track maps:

$$b_6^8 = \sigma_5^{-1}\sigma_1^{-1}\sigma_2^{-1}\sigma_4^{-1}\sigma_3^{-1}\sigma_4^{-1}\sigma_5^{-1}\sigma_3^{-1}\sigma_3^{-1}\sigma_4^{-1}\sigma_3^{-1}\sigma_2^{-1}\sigma_1^{-1}\sigma_1^{-1}\sigma_2^{-1}\sigma_1^{-1}\sigma_1^{-1}$$

This is shown in Figure M.12.

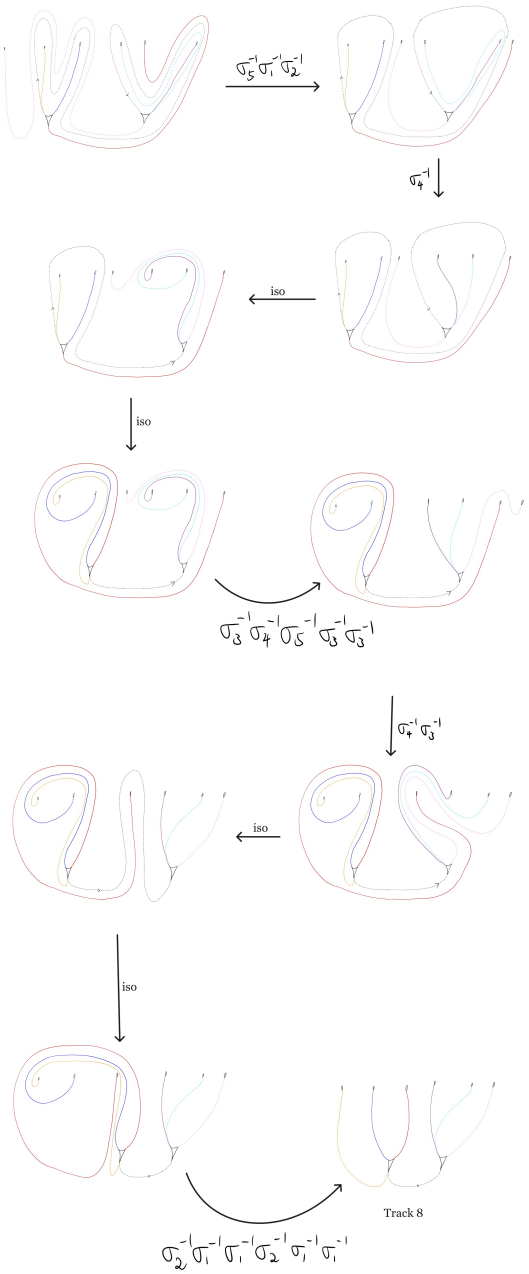


Figure M.12: This sequence shows the inverse of the braid b_6^8 carries Train Track Candidate Family 6.

M.9 Candidate Family 7 (Aulic)

Train Track Map Candidate Family 7 of Track 8 is shown in Figure M.13. See F.1.7.2.1 for details.

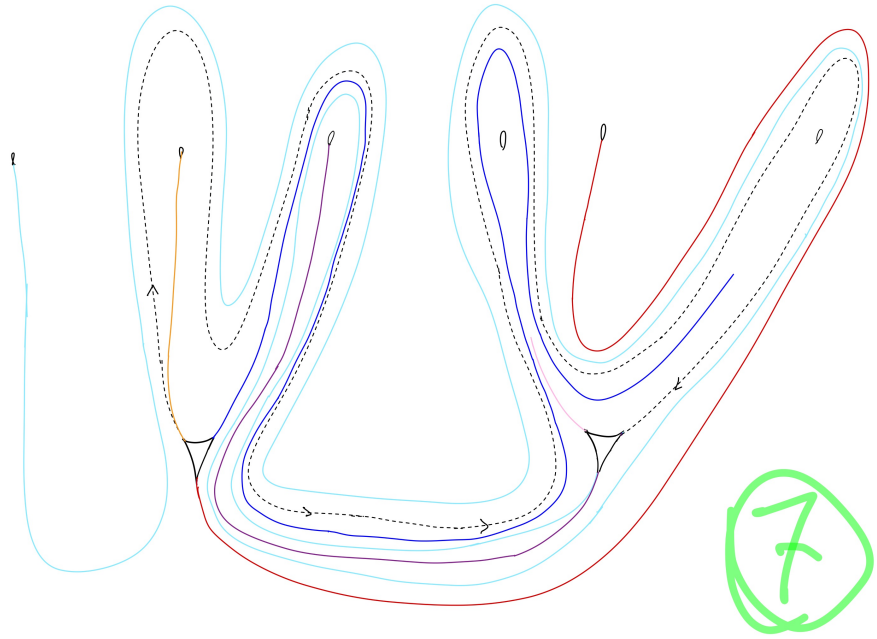


Figure M.13: Train Track Map Candidate Family 7 (Aulic) of Track 8.

The inverse of the following braid carries this family of train track maps:

$$b_7^8 = \sigma_5^{-1}\sigma_4^k\sigma_3\sigma_1^{-1}\sigma_2^{-1}\sigma_3^{-1}\sigma_4^{-1}\sigma_3\sigma_3\sigma_2\sigma_1\sigma_4\sigma_3\sigma_2\sigma_4\sigma_3 \circ \Lambda_6 \circ J$$

where $k \geq 1$ ($k \in \mathbb{Z}$) is the twisting parameter. This is shown in Figure M.14.

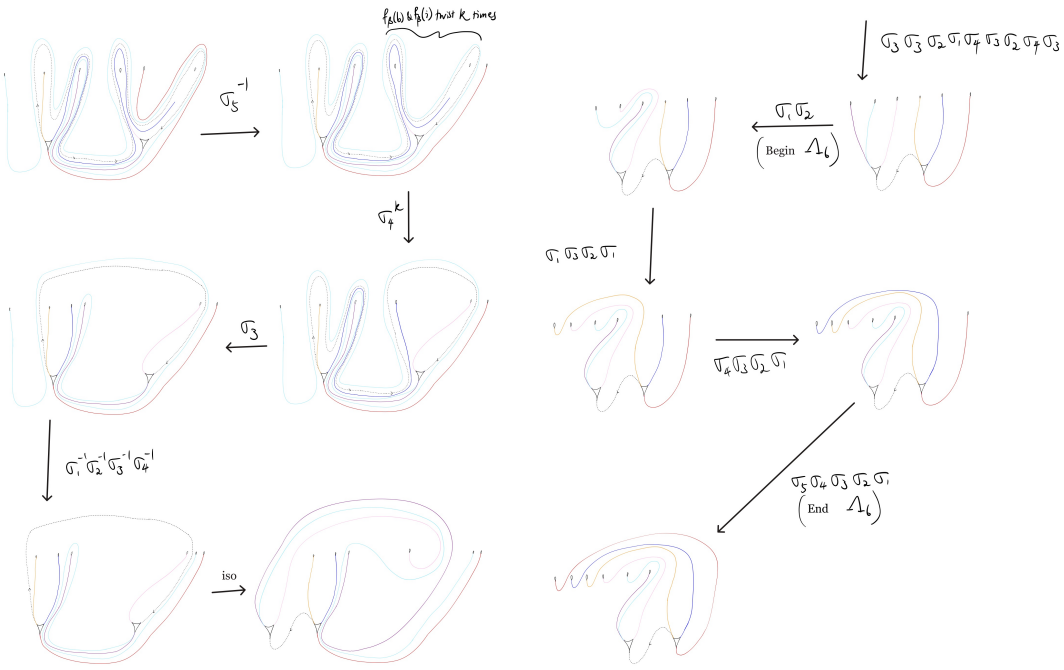


Figure M.14: This sequence shows the inverse of the braid b_7^8 carries Train Track Candidate Family 7.

M.10 Candidate Family 8 (Oread)

Train Track Map Candidate Family 8 of Track 8 is shown in Figure M.15. See F.1.7.2.2 for details.

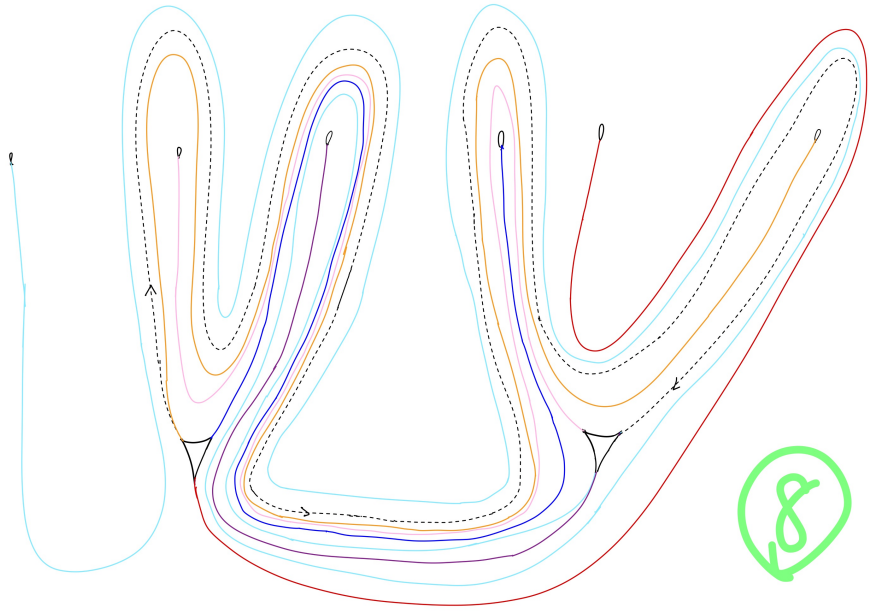


Figure M.15: Train Track Map Candidate Family 8 (Oread) of Track 8.

The inverse of the following braid carries this family of train track maps:

$$b_8^8 = \sigma_5^{-1}\sigma_1^{-1}\sigma_2^{-1}\sigma_3^{-1}\sigma_4^{-1}\sigma_3\sigma_2\sigma_1\sigma_2^{-1}\sigma_3^{-1}\sigma_2\sigma_3\sigma_3\sigma_2\sigma_1\sigma_4\sigma_3\sigma_2\sigma_4\sigma_3 \circ \Lambda_6 \circ J$$

This is shown in Figure M.16.

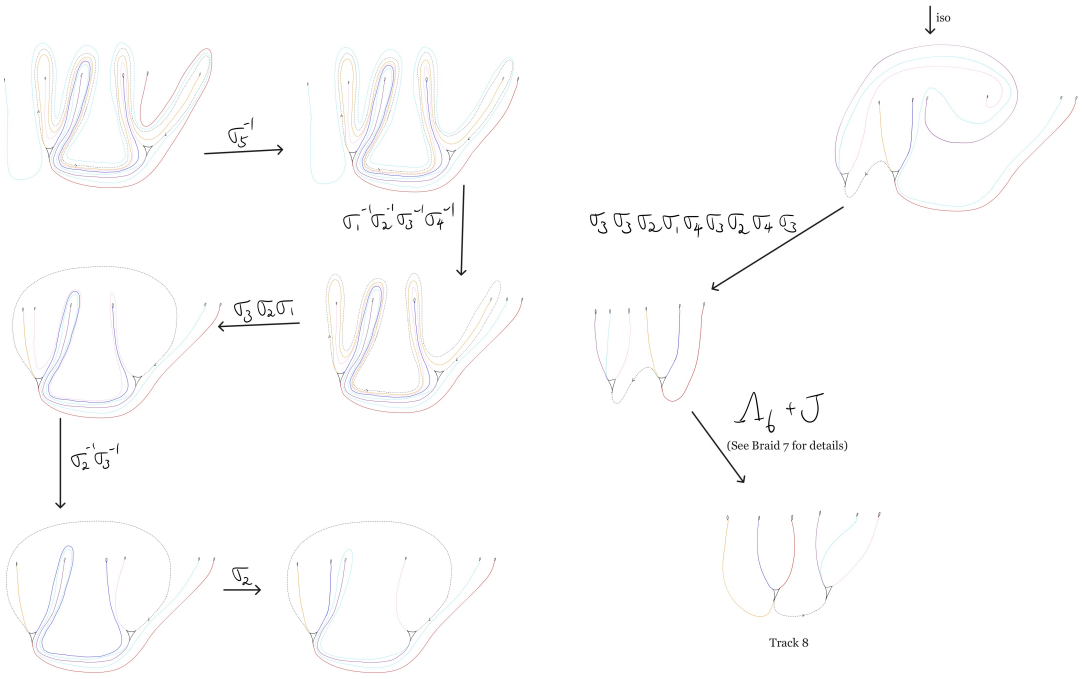


Figure M.16: This sequence shows the inverse of the braid b_8^8 carries Train Track Candidate Family 8.

M.11 Candidate Family 9 (FAT)

Train Track Map Candidate Family 9 of Track 8 is shown in Figure M.17. See F.2.3 for details.

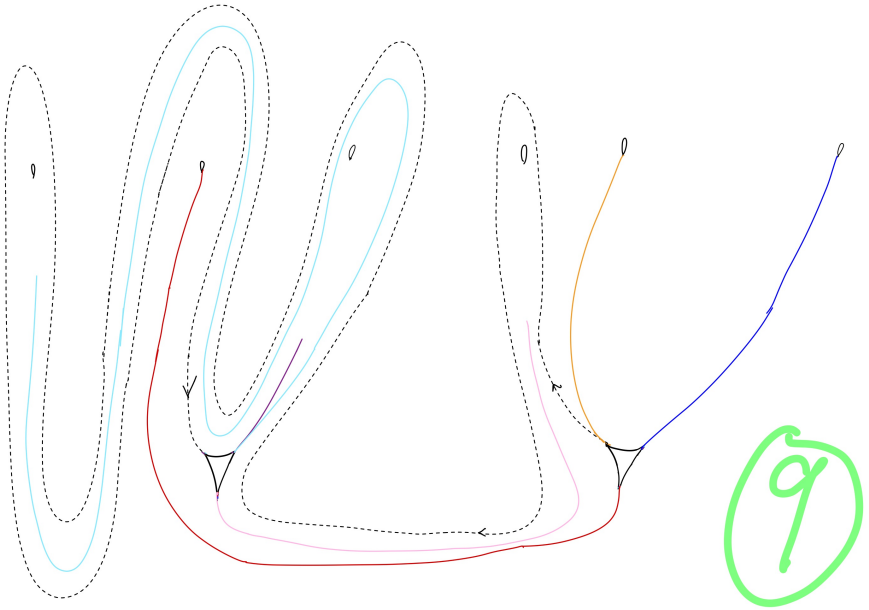


Figure M.17: Train Track Map Candidate Family 9 (FAT) of Track 8.

The inverse of the following braid carries this family of train track maps:

$$b_9^8 = \sigma_1^{-1}\sigma_2^{-k}\sigma_3^{-1}\sigma_2^{-1}\sigma_2^{-1}\sigma_3^{-1}\sigma_2^{-1}\sigma_2^{-1}\sigma_1\sigma_2\sigma_3\sigma_4\sigma_5 \circ \Lambda_6 \circ J$$

where $k \geq 1$ ($k \in \mathbb{Z}$) is the twisting parameter. This is shown in Figure M.18.

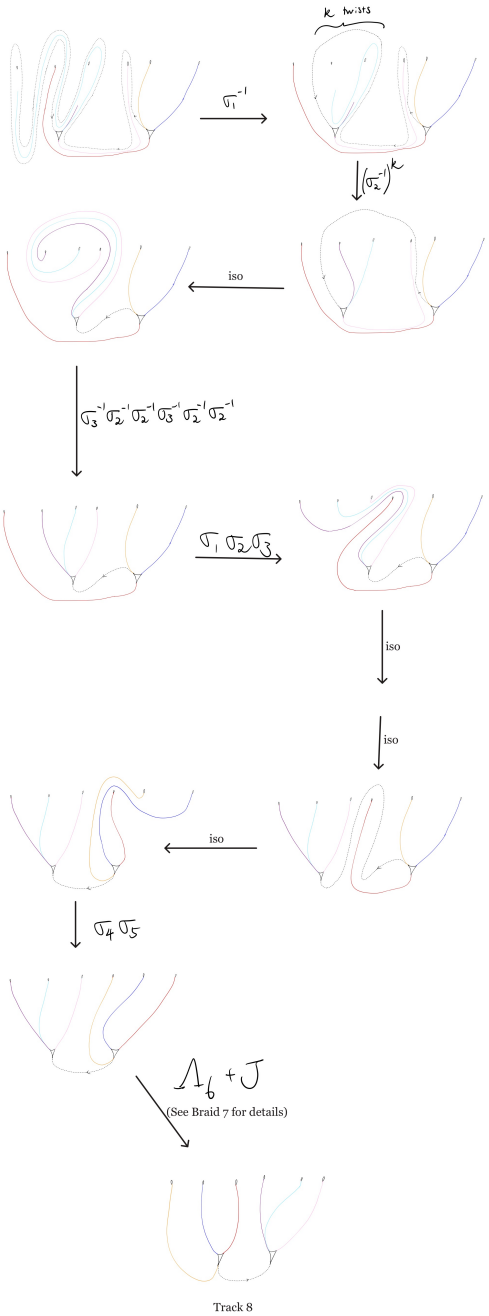


Figure M.18: This sequence shows the inverse of the braid b_9^8 carries Train Track Candidate Family 9.

APPENDIX FOURTEEN

Appendix: Candidate Braids for Track 13

N.1 Summary of Candidate Braid Families

Through the exhaustive train track case analysis of Track 13 in the stratum $(2; 1^6; 3^2)$ (the full details of which are presented in Appendix H), we isolate exactly 4 candidate families of train track maps. If the pseudo-Anosov representative ϕ_Φ has no interior fixed points, then its mapping class Φ must be conjugate to the lift of one of the following 4 braid families.

1. $\Delta^{2i}(\sigma_4^{-1}\sigma_3\sigma_2\sigma_1\sigma_2^{-1}\sigma_3\sigma_3\sigma_2\sigma_1\sigma_3\sigma_2\sigma_4\sigma_3\sigma_4^{-1}\sigma_5^{-1}\sigma_5^{-1}\sigma_4^{-1}\sigma_3^{-1}\sigma_2^{-1}\sigma_1^{-1}\sigma_1^{-1} \cdot L \cdot \Lambda_6)^{-1}$
2. $\Delta^{2i}(\sigma_4^{-1}\sigma_3\sigma_2\sigma_1\sigma_2^{-1}\sigma_3^{-1}\sigma_1^{-1}\sigma_2^{-1}\sigma_1\sigma_2\sigma_3\sigma_3\sigma_2\sigma_1\sigma_3\sigma_2\sigma_4\sigma_3\sigma_5^{-1}\sigma_5^{-1}\sigma_4^{-1}\sigma_3^{-1}\sigma_2^{-1}\sigma_1^{-1}\sigma_1^{-1}\cdot L\cdot\Lambda_6)^{-1}$
3. $\Delta^{2i}(\sigma_4^{-1}\sigma_3\sigma_2\sigma_1^{-1}\sigma_3\sigma_3\sigma_2\sigma_1\sigma_3\sigma_2\sigma_4\sigma_3\sigma_5^{-1}\sigma_1\sigma_2\sigma_3\sigma_2\sigma_1\sigma_4\sigma_3\sigma_2\sigma_4\sigma_3\sigma_5\sigma_4\sigma_5\sigma_5)^{-1}$
4. $\Delta^{2i}(\sigma_4\sigma_2\sigma_3\sigma_4^{-1}\sigma_5^{-1}\sigma_4^{-1}\sigma_5^{-1}\sigma_3^{-1}\sigma_4^{-1}\sigma_2\sigma_3^{-1}\sigma_2^{-1}\sigma_1^{-1}\sigma_1^{-1} \cdot L \cdot \Lambda_6)^{-1}$

N.2 Base Braids Λ_6 and L

Before we list the braids carrying candidate train track maps for Track 13, we introduce the following base braids, which we will call Λ_6 and L:

$\Lambda_6 = \sigma_1\sigma_2\sigma_1\sigma_3\sigma_2\sigma_1\sigma_4\sigma_3\sigma_2\sigma_1\sigma_5\sigma_4\sigma_3\sigma_2\sigma_1$

$L = \sigma_1^{-1}\sigma_5\sigma_4\sigma_3\sigma_5\sigma_4\sigma_5$

We shall make use of Λ_6 and L occasionally in constructing candidate braids for Track 13.

N.3 Candidate Family 1 (Chirk)

Train Track Map Candidate Family 1 of Track 13 is shown in Figure N.1. See H.1.3.1.1 for details.

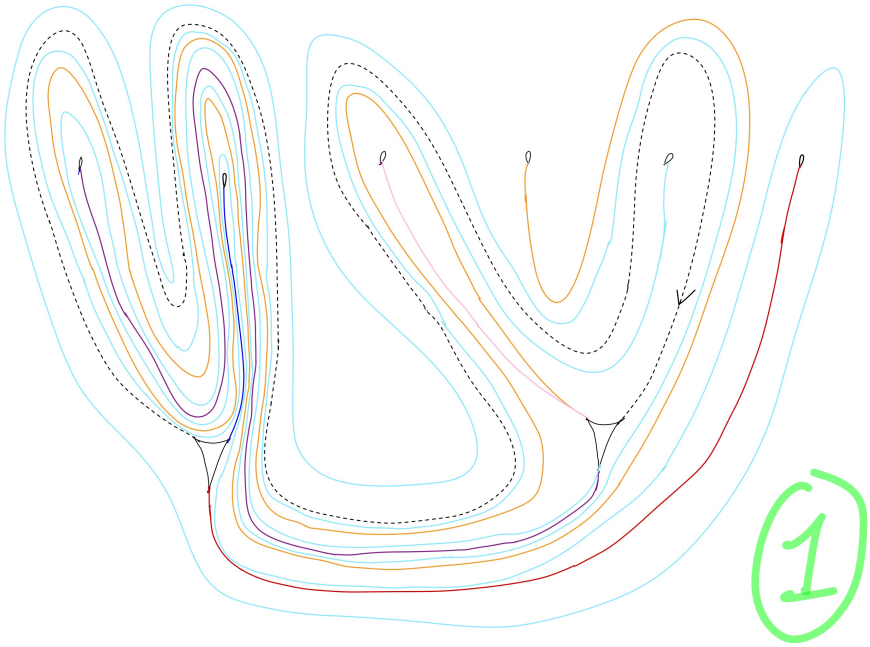


Figure N.1: Train Track Map Candidate Family 1 (Chirk) of Track 13.

The inverse of the following braid carries this family of train track maps:

$$b_1^{13} = \sigma_4^{-1}\sigma_3\sigma_2\sigma_1\sigma_2^{-1}\sigma_3\sigma_3\sigma_2\sigma_1\sigma_3\sigma_2\sigma_4\sigma_3\sigma_4^{-1}\sigma_5^{-1}\sigma_5^{-1}\sigma_4^{-1}\sigma_3^{-1}\sigma_2^{-1}\sigma_1^{-1}\sigma_1^{-1} \circ L \circ \Lambda_6$$

This is shown in Figure N.2.

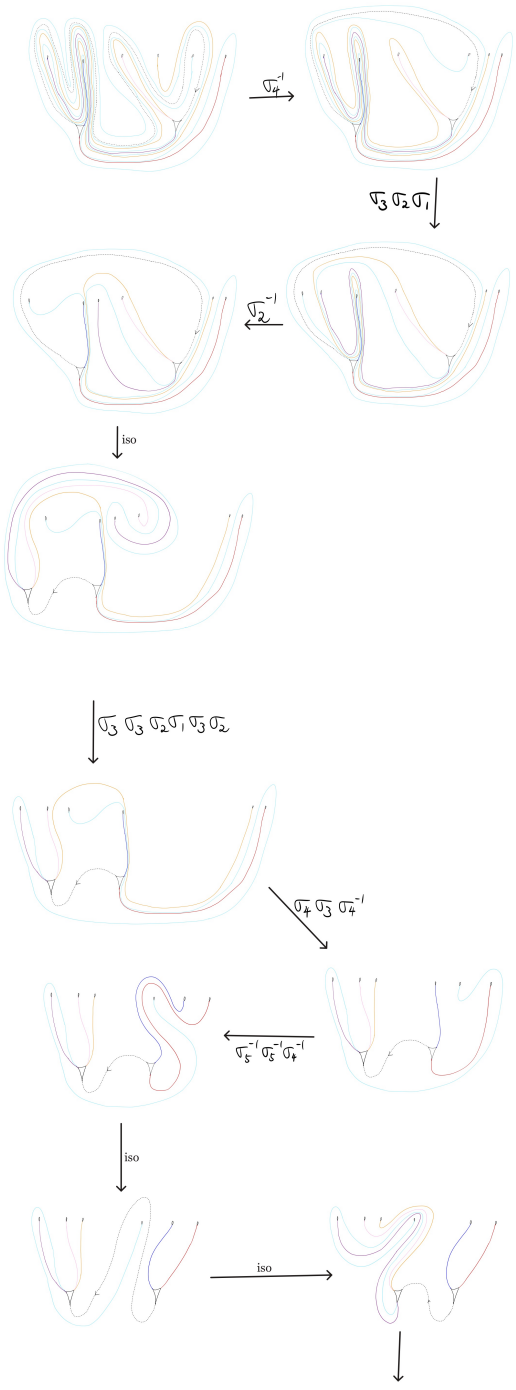


Figure N.2: This sequence shows the inverse of the braid b_1^{13} carries Train Track Candidate Family 1.

N.4 Candidate Family 2 (Cagmag)

Train Track Map Candidate Family 2 of Track 13 is shown in Figure N.3. See H.1.3.1.2.2 for details.

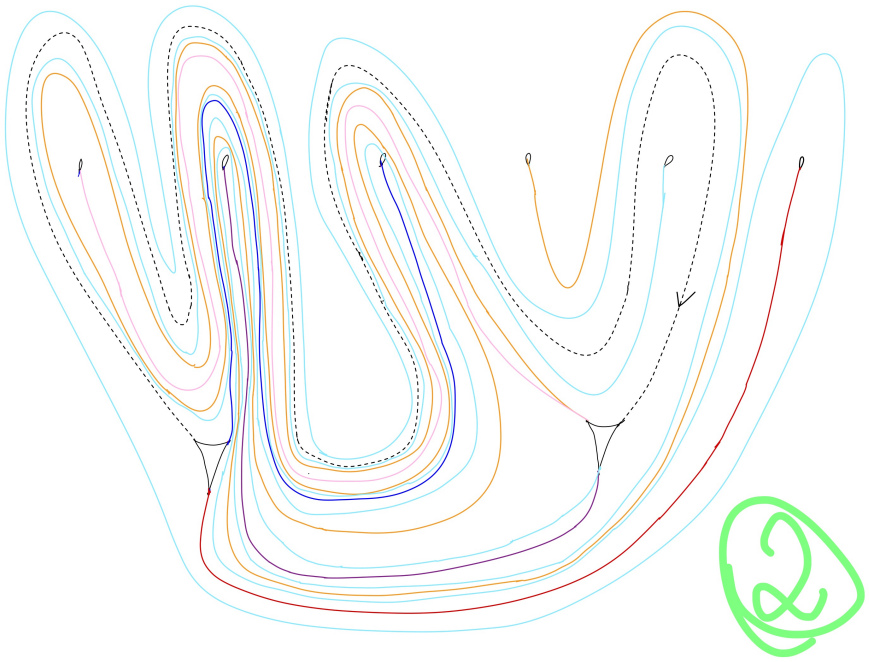


Figure N.3: Train Track Map Candidate Family 2 (Cagmag) of Track 13.

The inverse of the following braid carries this family of train track maps:

$$b_2^{13} = \sigma_4^{-1}\sigma_3\sigma_2\sigma_1\sigma_2^{-1}\sigma_3^{-1}\sigma_1^{-1}\sigma_2^{-1}\sigma_1\sigma_2\sigma_3\sigma_3\sigma_2\sigma_1\sigma_3\sigma_2\sigma_4\sigma_3\sigma_5^{-1}\sigma_5^{-1}\sigma_4^{-1}\sigma_3^{-1}\sigma_2^{-1}\sigma_1^{-1}\sigma_1^{-1} \circ L \circ \Lambda_6$$

This is shown in Figure N.4.

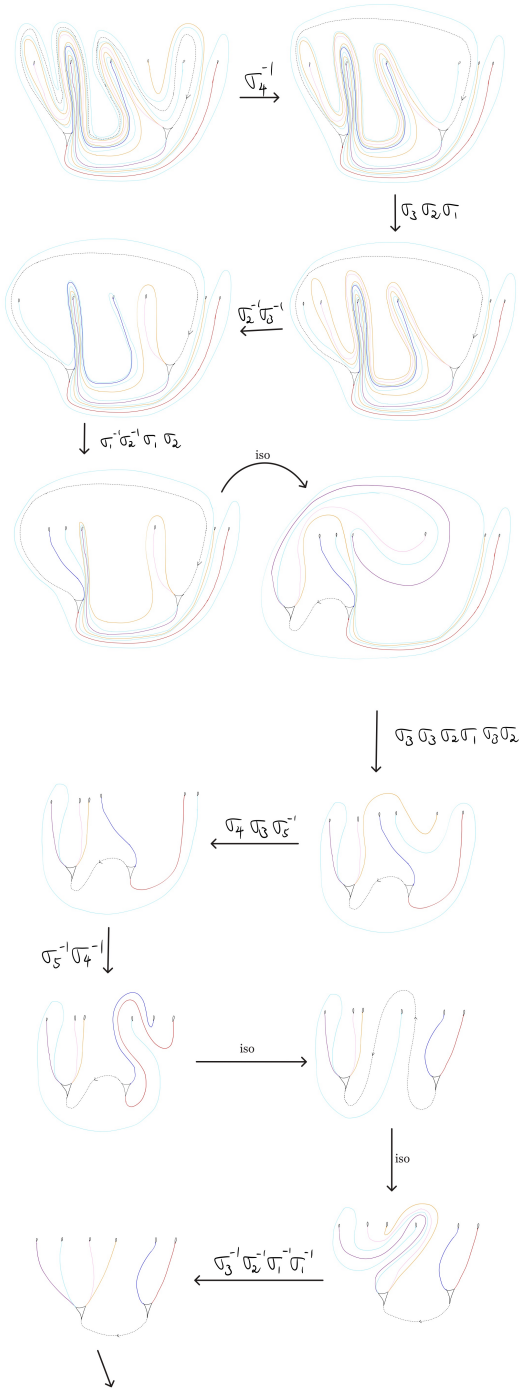


Figure N.4: This sequence shows the inverse of the braid b_2^{13} carries Train Track Candidate Family 2.

N.5 Candidate Family 3 (Boofus)

Train Track Map Candidate Family 3 of Track 13 is shown in Figure N.5. See H.1.3.1.2.3 for details.

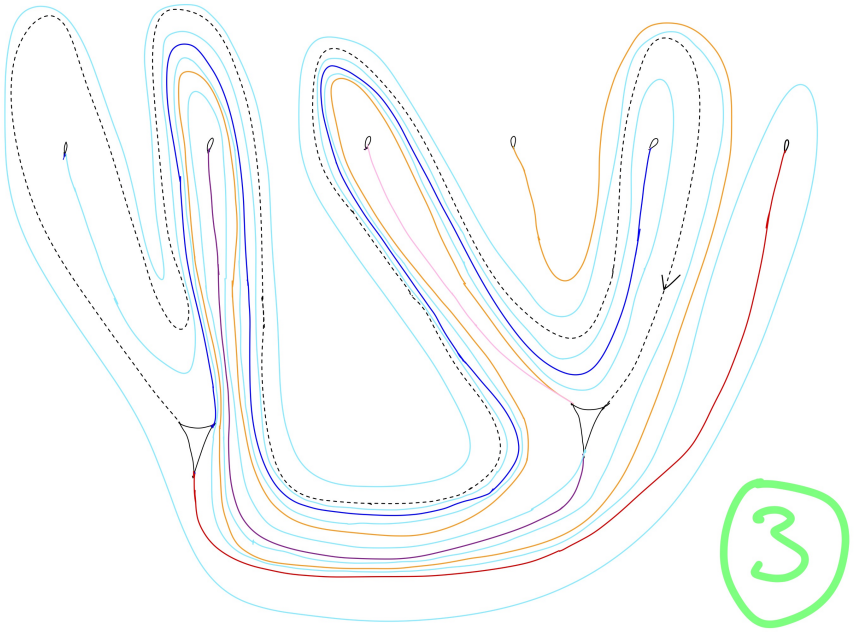


Figure N.5: Train Track Map Candidate Family 3 (Boofus) of Track 13.

The inverse of the following braid carries this family of train track maps:

$$b_3^{13} = \sigma_4^{-1}\sigma_3\sigma_2\sigma_1^{-1}\sigma_3\sigma_3\sigma_2\sigma_1\sigma_3\sigma_2\sigma_4\sigma_3\sigma_5^{-1}\sigma_1\sigma_2\sigma_3\sigma_2\sigma_1\sigma_4\sigma_3\sigma_2\sigma_4\sigma_3\sigma_5\sigma_4\sigma_5\sigma_5$$

This is shown in Figure N.6.

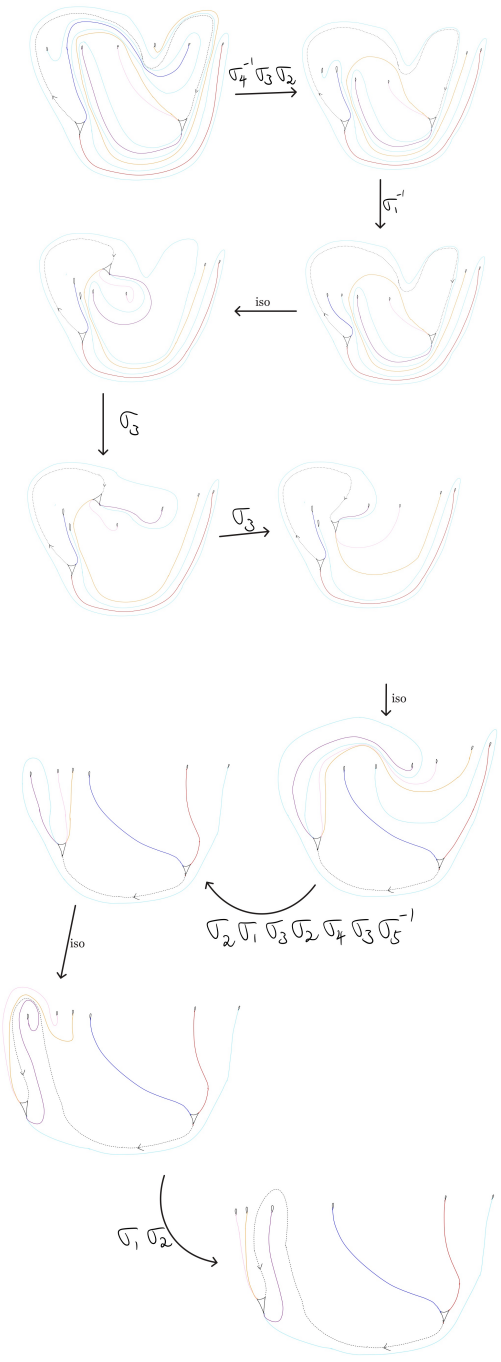


Figure N.6: This sequence shows the inverse of the braid b_3^{13} carries Train Track Candidate Family 3.

N.6 Candidate Family 4 (SCC)

Train Track Map Candidate Family 4 of Track 13 is shown in Figure N.7. See H.2.3 for details.

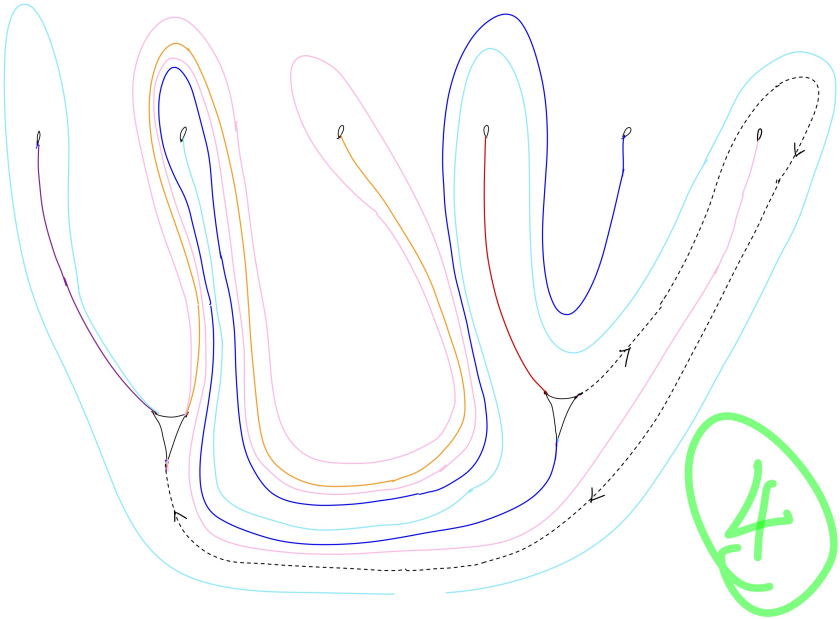


Figure N.7: Train Track Map Candidate Family 4 (SCC) of Track 13.

The inverse of the following braid carries this family of train track maps:

$$b_4^{13} = \sigma_4\sigma_2\sigma_3\sigma_4^{-1}\sigma_5^{-1}\sigma_4^{-1}\sigma_5^{-1}\sigma_3^{-1}\sigma_4^{-1}\sigma_2\sigma_3^{-1}\sigma_2^{-1}\sigma_1^{-1}\sigma_1^{-1} \circ L \circ \Lambda_6$$

This is shown in Figure N.8.

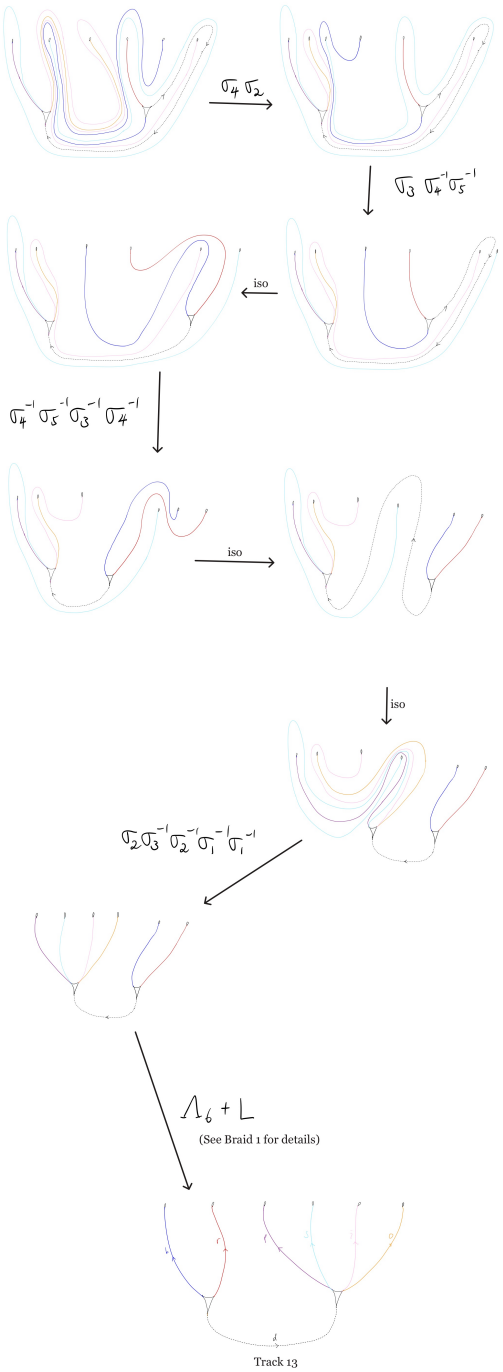


Figure N.8: This sequence shows the inverse of the braid b_4^{13} carries Train Track Candidate Family 4.

APPENDIX FIFTEEN

Appendix: Candidate Braids for Track 17

O.1 Summary of Candidate Braid Families

Through the exhaustive train track case analysis of Track 17 in the stratum $(2; 1^6; 3^2)$ (the full details of which are presented in Appendix I), we isolate exactly 6 candidate families of train track maps. If the pseudo-Anosov representative ϕ_Φ has no interior fixed points, then its mapping class Φ must be conjugate to the lift of one of the following 6 braid families (enumerated below with their twist parameters where applicable).

1. $\Delta^{2i}(\sigma_1\sigma_1\sigma_2\sigma_2\sigma_1\sigma_2\sigma_4\sigma_5\sigma_5\sigma_4\sigma_5\sigma_1\sigma_2\sigma_3\sigma_4\sigma_5\sigma_5)^{-1}$
2. $\Delta^{2i}(\sigma_1\sigma_4\sigma_1\sigma_2\sigma_2\sigma_1\sigma_2\sigma_4\sigma_5\sigma_5\sigma_4\sigma_5\sigma_1\sigma_2\sigma_3\sigma_4\sigma_5)^{-1}$
3. $\Delta^{2i}(\sigma_1\sigma_1\sigma_2\sigma_2\sigma_1\sigma_2\sigma_5\sigma_4\sigma_5\sigma_5\sigma_1\sigma_2\sigma_3\sigma_4\sigma_5\sigma_5\sigma_4)^{-1}$
4. $\Delta^{2i}(\sigma_1\sigma_5\sigma_4\sigma_2\sigma_1\sigma_2\sigma_3\sigma_5^{-1}\sigma_4^{-1}\sigma_5^{-1}\sigma_4^{-1}\sigma_3^{-1}\sigma_2\sigma_1\sigma_1\sigma_2\sigma_3\sigma_4\sigma_5)^{-1}$
5. $\Delta^{2i}(\sigma_5^k\sigma_1\sigma_2\sigma_5^{-1}\sigma_4^{-1}\sigma_3^{-1}\sigma_2^{-1}\sigma_1^{-1}\sigma_1^{-1}\cdot P\cdot\Lambda_6)^{-1}$
6. $\Delta^{2i}(\sigma_1\sigma_2\sigma_4^{-1}\sigma_1\sigma_2\sigma_3^{-k}\sigma_2\sigma_3\sigma_1\sigma_2\sigma_1\sigma_1\cdot P\cdot\Lambda_6)^{-1}$

O.2 Base Braids Λ_6 and P

Before we list the braids carrying candidate train track maps for Track 17, we introduce the following base braids, which we will call Λ_6 and P:

$\Lambda_6 = \sigma_1\sigma_2\sigma_1\sigma_3\sigma_2\sigma_1\sigma_4\sigma_3\sigma_2\sigma_1\sigma_5\sigma_4\sigma_3\sigma_2\sigma_1$

$P = \sigma_1^{-1}\sigma_5\sigma_4\sigma_3\sigma_5\sigma_4\sigma_5$

We shall make use of Λ_6 and P in constructing the parametric families of candidate braids for Track 17 (specifically families 5 and 6, both named Boke).

O.3 Candidate Family 1 (Cudden)

Train Track Map Candidate Family 1 of Track 17 is shown in Figure O.1. See I.1.1.1.2.1 for details.

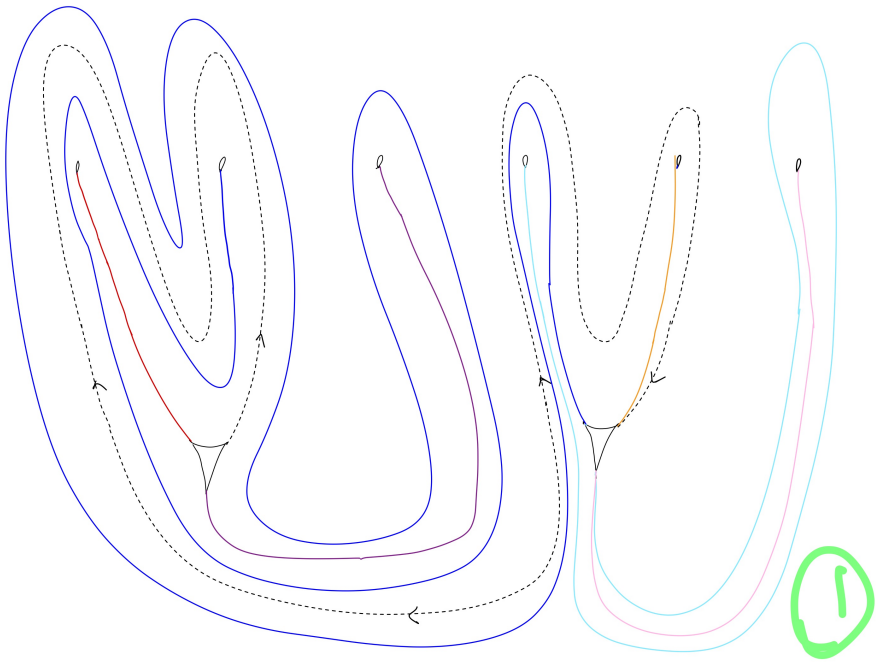


Figure O.1: Train Track Map Candidate Family 1 (Cudden) of Track 17.

The inverse of the following braid carries this family of train track maps:

$$b_1^{17} = \sigma_1\sigma_1\sigma_2\sigma_2\sigma_1\sigma_2\sigma_4\sigma_5\sigma_5\sigma_4\sigma_5\sigma_1\sigma_2\sigma_3\sigma_4\sigma_5\sigma_5$$

This is shown in Figure O.2.

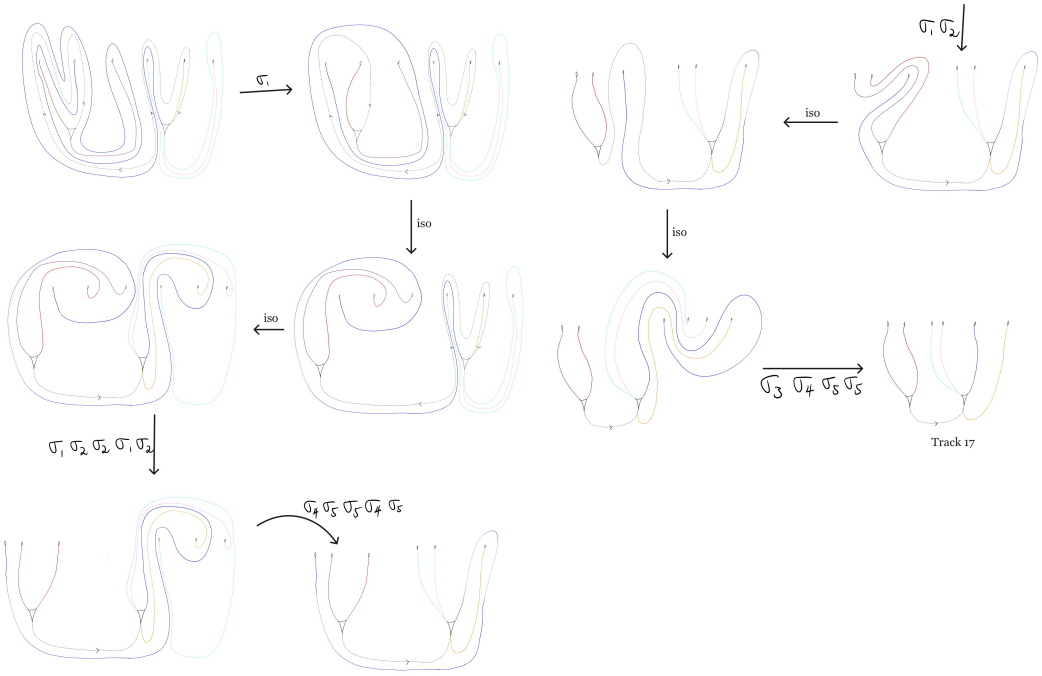


Figure O.2: This sequence shows the inverse of the braid b_1^{17} carries Train Track Candidate Family 1.

O.4 Candidate Family 2 (Flisky)

Train Track Map Candidate Family 2 of Track 17 is shown in Figure O.3. See I.1.1.1.3 for details.

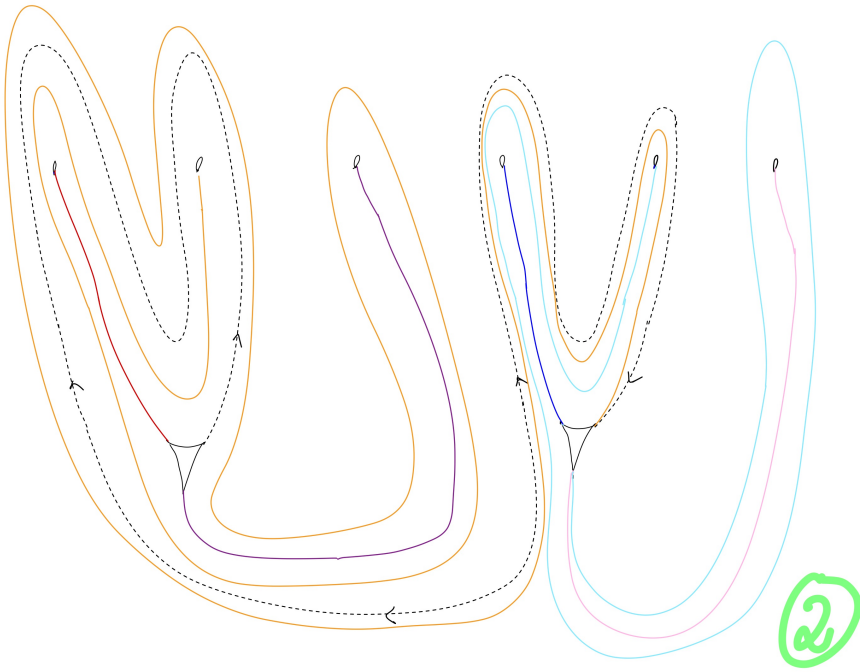


Figure O.3: Train Track Map Candidate Family 2 (Flisky) of Track 17.

The inverse of the following braid carries this family of train track maps:

$$b_2^{17} = \sigma_1\sigma_4\sigma_1\sigma_2\sigma_2\sigma_1\sigma_2\sigma_4\sigma_5\sigma_5\sigma_4\sigma_5\sigma_1\sigma_2\sigma_3\sigma_4\sigma_5$$

This is shown in Figure O.4.

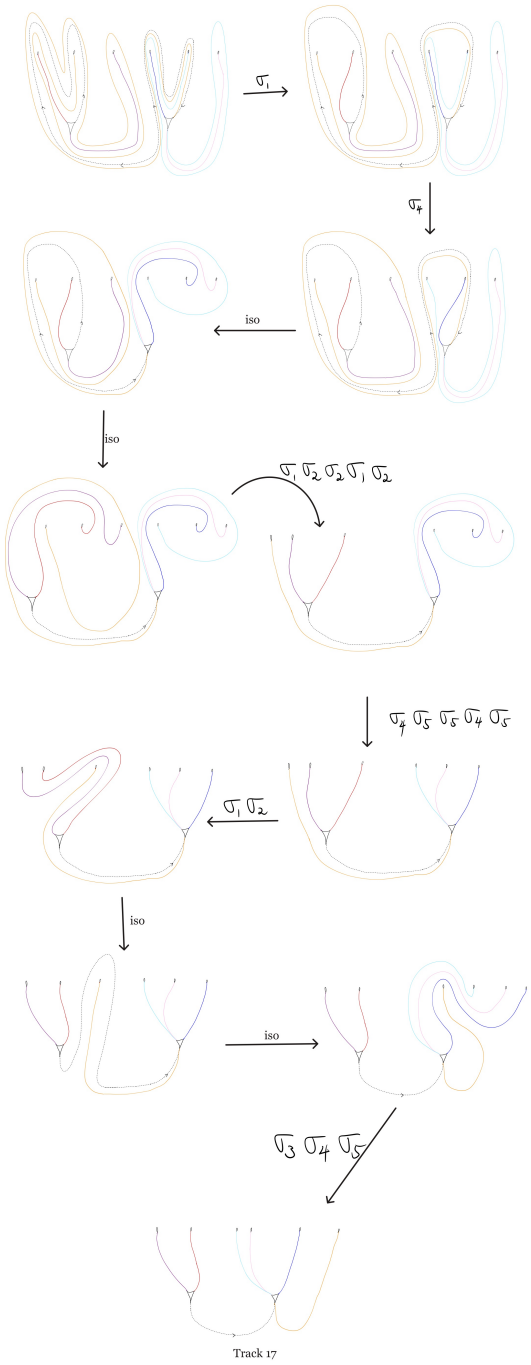


Figure O.4: This sequence shows the inverse of the braid b_2^{17} carries Train Track Candidate Family 2.

O.5 Candidate Family 3 (Wanion)

Train Track Map Candidate Family 3 of Track 17 is shown in Figure O.5. See I.1.1.1.3.1 for details.

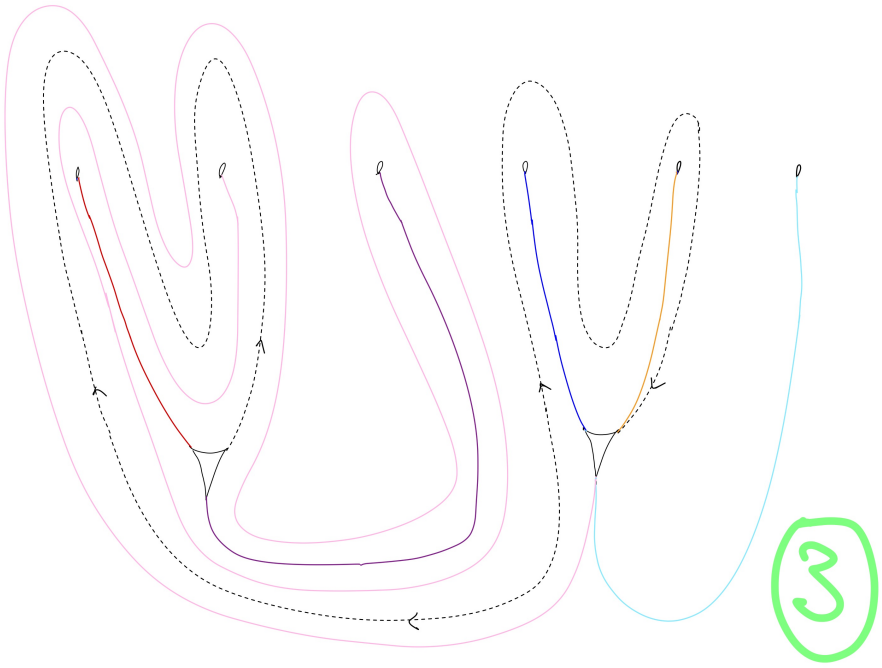


Figure O.5: Train Track Map Candidate Family 3 (Wanion) of Track 17.

The inverse of the following braid carries this family of train track maps:

$$b_3^{17} = \sigma_1\sigma_1\sigma_2\sigma_2\sigma_1\sigma_2\sigma_5\sigma_4\sigma_5\sigma_5\sigma_1\sigma_2\sigma_3\sigma_4\sigma_5\sigma_5\sigma_4$$

This is shown in Figure O.6.

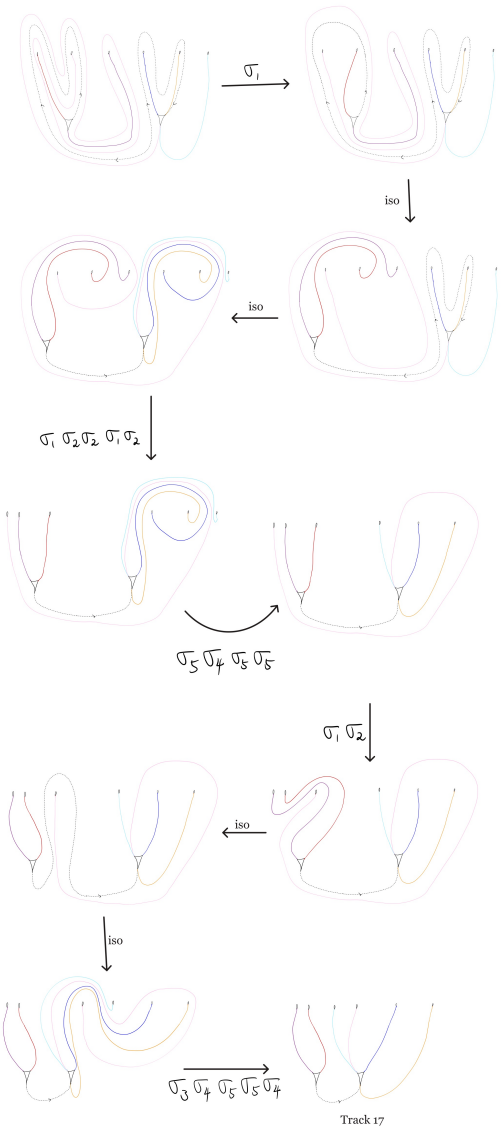


Figure O.6: This sequence shows the inverse of the braid b_3^{17} carries Train Track Candidate Family 3.

O.6 Candidate Family 4 (Roop)

Train Track Map Candidate Family 4 of Track 17 is shown in Figure O.7. See I.1.3.2 for details.

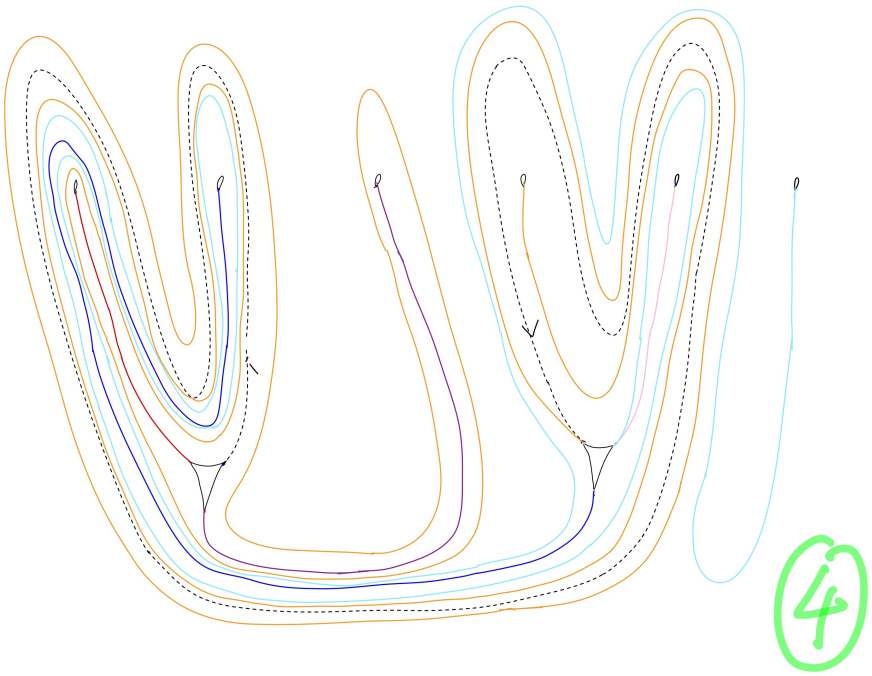


Figure O.7: Train Track Map Candidate Family 4 (Roop) of Track 17.

The inverse of the following braid carries this family of train track maps:

$$b_4^{17} = \sigma_1\sigma_5\sigma_4\sigma_2\sigma_1\sigma_2\sigma_3\sigma_5^{-1}\sigma_4^{-1}\sigma_5^{-1}\sigma_4^{-1}\sigma_3^{-1}\sigma_2\sigma_1\sigma_1\sigma_2\sigma_3\sigma_4\sigma_5$$

This is shown in Figure O.8.

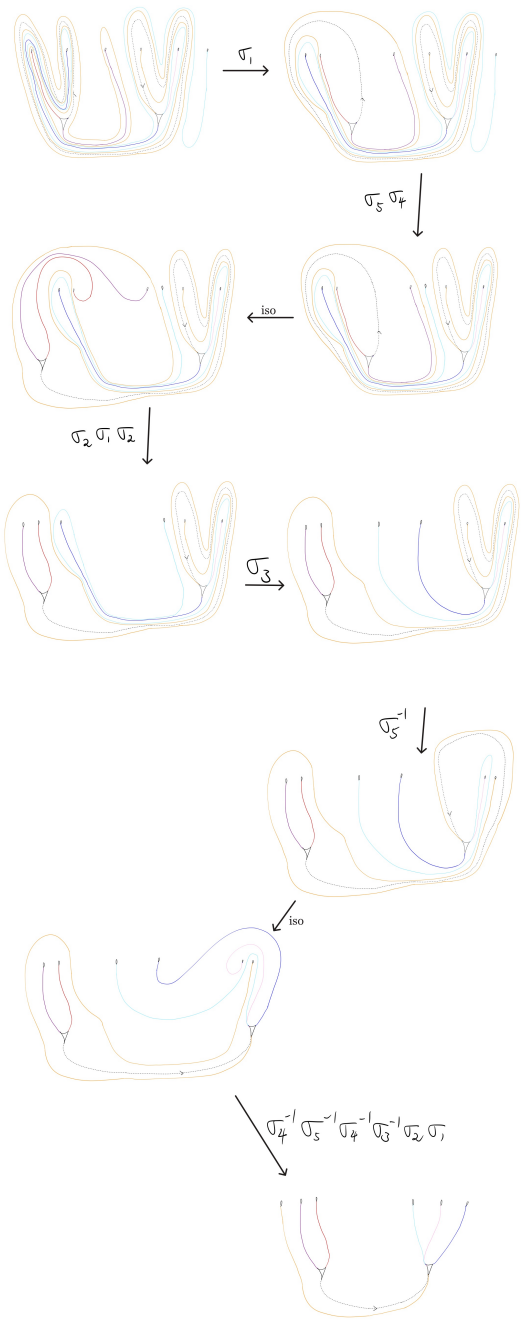


Figure O.8: This sequence shows the inverse of the braid b_4^{17} carries Train Track Candidate Family 4 (first half).

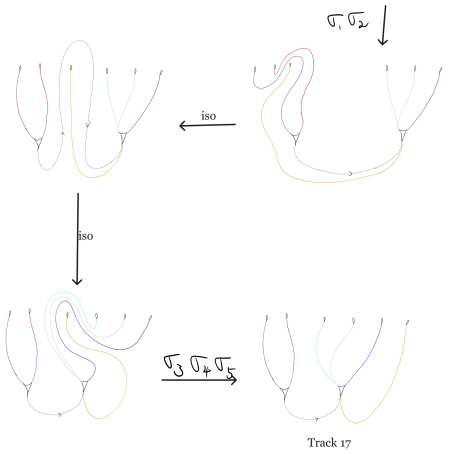


Figure O.9: Continuation of Figure O.8: the inverse of b_4^{17} carries Train Track Candidate Family 4 (second half).

O.7 Candidate Family 5 (Boke)

Train Track Map Candidate Family 5 of Track 17 is shown in Figure O.10. See Section I.2.1.1 for details. This is a parametric family indexed by an integer twist parameter $k \in \mathbb{Z}_{\geq 0}$.

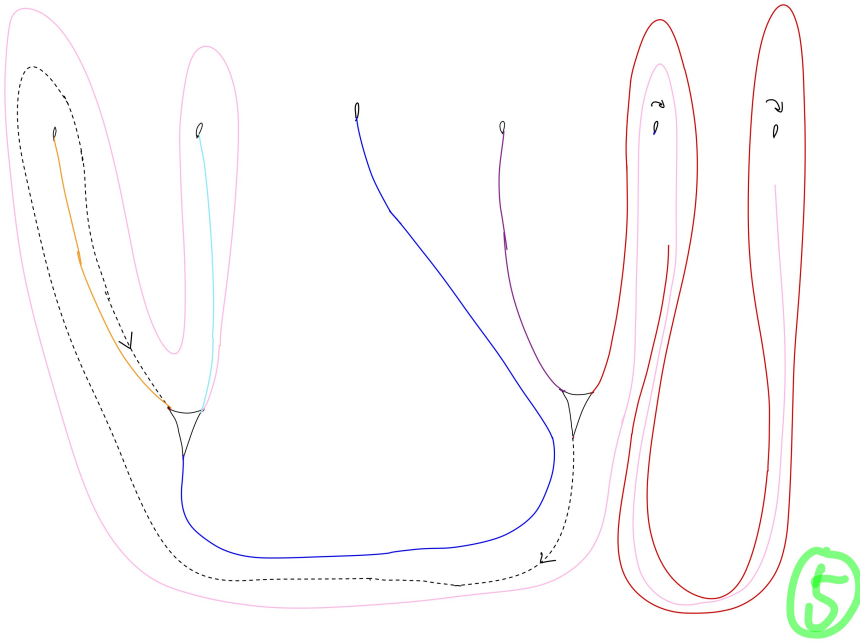


Figure O.10: Train Track Map Candidate Family 5 (Boke) of Track 17.

The inverse of the following braid carries this family of train track maps:

$$b_5^{17} = \sigma_5^k \sigma_1 \sigma_2 \sigma_5^{-1} \sigma_4^{-1} \sigma_3^{-1} \sigma_2^{-1} \sigma_1^{-1} \sigma_1^{-1} \circ P \circ \Lambda_6$$

This is shown in Figure O.11.

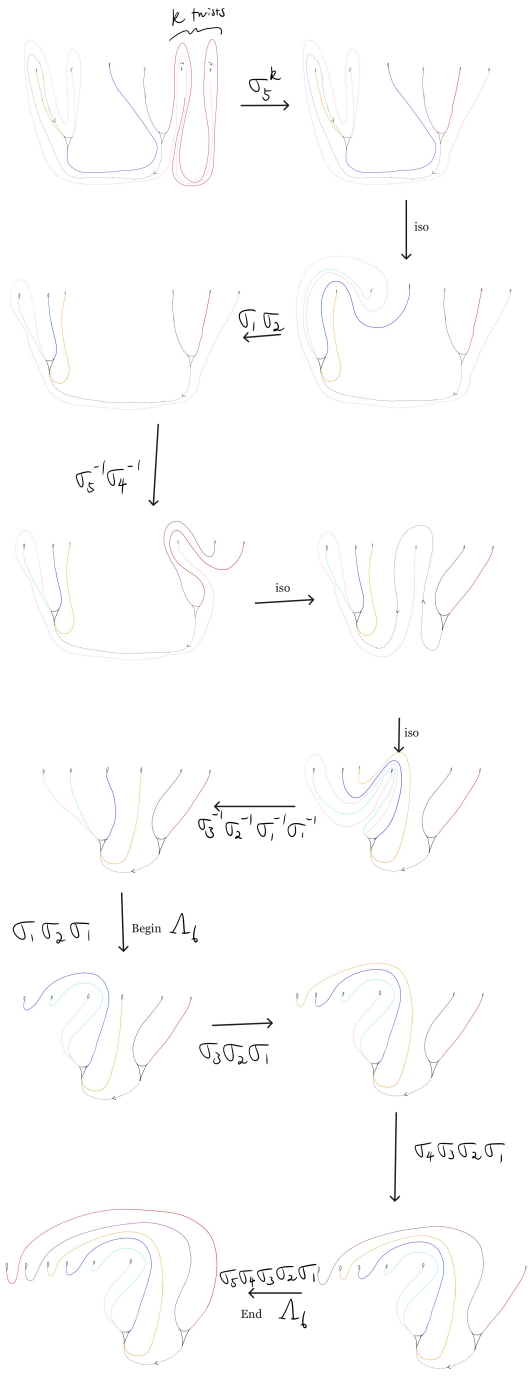


Figure O.11: This sequence shows the inverse of the braid b_5^{17} carries Train Track Candidate Family 5 (first half).

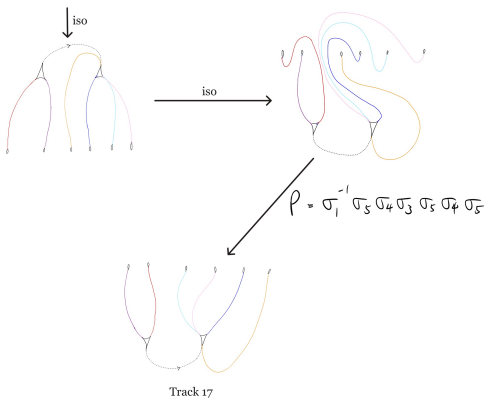


Figure O.12: Continuation of Figure O.11: the inverse of b_5^{17} carries Train Track Candidate Family 5 (second half).

O.8 Candidate Family 6 (Boke)

Train Track Map Candidate Family 6 of Track 17 is shown in Figure O.13. See Section I.2.1.1 for details. This is a parametric family indexed by an integer twist parameter $k \in \mathbb{Z}_{\geq 0}$.

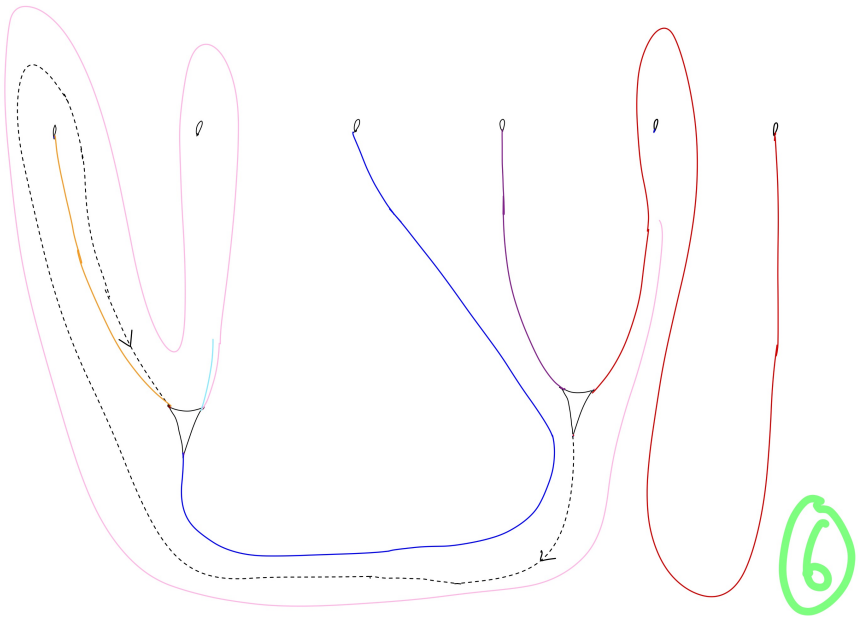


Figure O.13: Train Track Map Candidate Family 6 (Boke) of Track 17.

The inverse of the following braid carries this family of train track maps:

$$b_6^{17} = \sigma_1\sigma_2\sigma_4^{-1}\sigma_1\sigma_2\sigma_3^{-k}\sigma_2\sigma_3\sigma_1\sigma_2\sigma_1\sigma_1 \circ P \circ \Lambda_6$$

This is shown in Figure O.14.

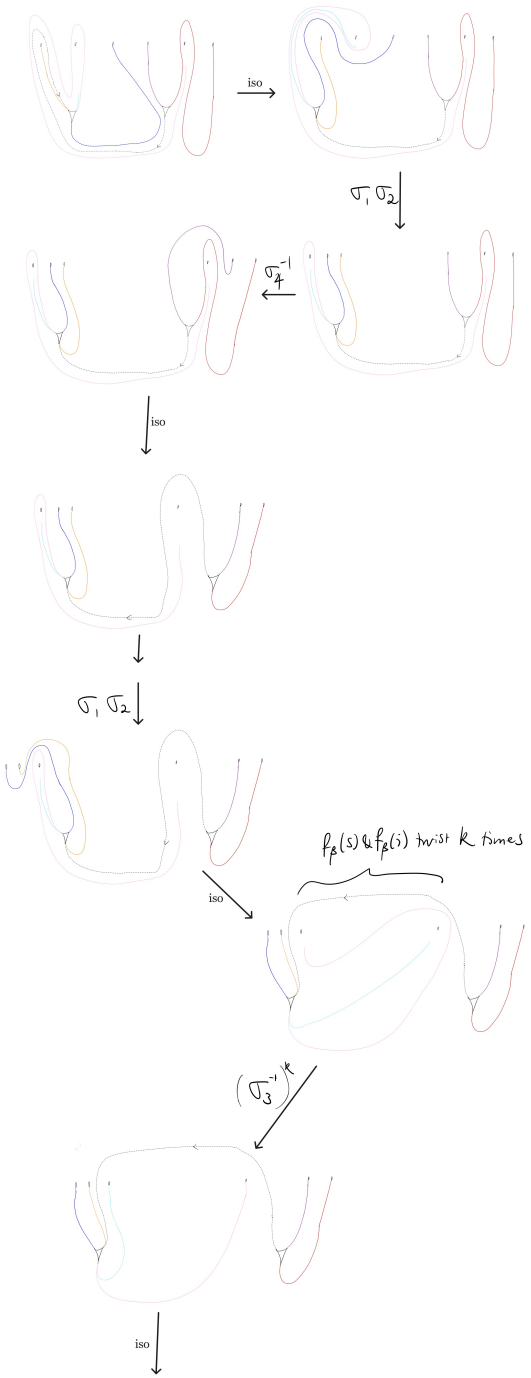


Figure O.14: This sequence shows the inverse of the braid b_6^{17} carries Train Track Candidate Family 6 (first half).

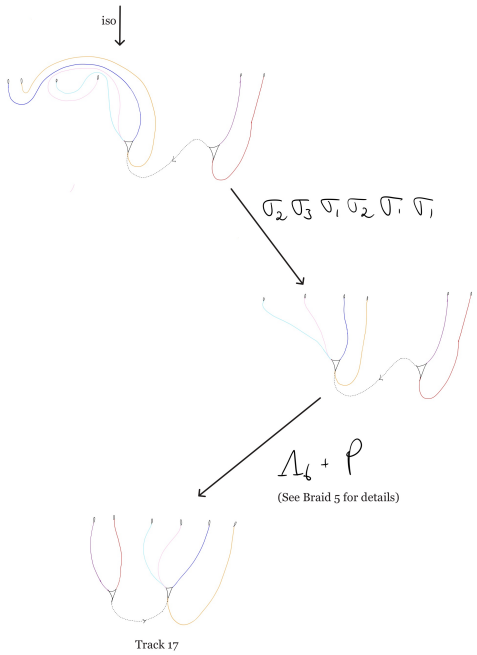


Figure O.15: Continuation of Figure O.14: the inverse of b_6^{17} carries Train Track Candidate Family 6 (second half).

APPENDIX SIXTEEN

Verdict Tables for the Granny Detection

This appendix tabulates the homological filtering verdicts for all 87 candidate braid families generated by the train-track analysis of Chapters 4 and 7, evaluated against the granny target Alexander polynomial $\Delta(t) = (t^2 - t + 1)^2$. The data here support the proof of Theorem 1.1, specifically the conclusions of Theorems 7.7 and 7.10.

For each family, we list:

- the family name (as recorded in Appendices J–O),
- the determinant $\det(I - A_{\mathrm{red}})$, expressed as a constant or a polynomial in the family's twist parameters k, m, j,
- the verdict, which records the means of elimination.

The verdicts are categorized as follows:

F1 Filter 1 fails outright: $\det(I - A_{\mathrm{red}})$ is a constant other than ± 1, so the open book does not bound an integer homology sphere.

F1* Filter 1 fails parametrically: $\det(I - A_{\mathrm{red}})$ is a non-constant polynomial in the family

parameters, and no assignment of non-negative integer values to those parameters yields $|\det| = 1$.

F2 Filter 1 admits at least one non-negative integer parameter value where $|\det(I - A_{\mathrm{red}})| = 1$, but at every such value the characteristic polynomial $\det(tI - A_{\mathrm{red}})$ fails to match the granny target $(t^2 - t + 1)^2$.

All verdicts were computed by direct evaluation of the matrices $M_1, \ldots, M_5$ from Section 7.3, using the parsing rules and execution pipeline described in the implementation of the homological filter. The reduced action is invariant under conjugation, full twists, and mirroring (Section 7.3), so testing a single representative braid word per family suffices. For parametric families that pass Filter 1 at some non-negative integer parameter value (verdict F2), the parameter search was conducted over the ranges $k, m \in [0, 14]$ (two parameters) or $k, m, j \in [0, 9]$ (three parameters), which exhaustively covers the small-twist solutions; the characteristic polynomial obstruction at those solutions then closes the case.

P.1 Stratum $(3; 1^6; 3)$: The Candelabra

We list the 38 candidate braid families on the Candelabra train track. The unprimed entries (1 through 17, including 1.1 and 1.2 in the Jehu subcase) correspond to the standard families derived from the train track maps in Appendix J; the primed entries ($1'$ through $17'$, including $1.1'$ and $1.2'$) are their counterparts under the rotational symmetry of the Candelabra (see Remark C.1 in Appendix C). Each primed family n' is obtained from its unprimed counterpart n by precomposition with the braid G (the rotation braid, which coincides with the braid of family 1).

Table P.1: Verdict table for the Candelabra (38 families).

Family	$\det(I - A_{\mathrm{red}})$	Verdict
1 (also called G)	13	F1 ($\lvert\det\rvert \neq 1$)
1.1 Jehu	18	F1 ($\lvert\det\rvert \neq 1$)
1.2 Jehu	$(k+2)m + 2k + 13$	F1* (no $(k,m) \in \mathbb{Z}_{\geq 0}$ gives $\lvert\det\rvert = 1$; minimum value 13 at $k = m = 0$)
2 Jehu	$3k + 15$	F1* (no $(k,m,j) \in \mathbb{Z}_{\geq 0}$ gives $\lvert\det\rvert = 1$)
3 Dindle	$-k + 11$	F2 (passes F1 at $k = 10$, etc.; $P(t)$ mismatches at all)
4 Keffel	$3k + 15$	F1* (no $(k,m,j) \in \mathbb{Z}_{\geq 0}$ gives $\lvert\det\rvert = 1$)
5 Keffel	$(k+2)m + k + 11$	F1* (no $(k,m,j) \in \mathbb{Z}_{\geq 0}$ gives $\lvert\det\rvert = 1$)
6 Epigone	9	F1 ($\lvert\det\rvert \neq 1$)
7 Farrago	$(k-1)m - k + 10$	F2 (passes F1 at $k = 0$, $m = 9$, etc.; $P(t)$ mismatches at all)
8 Jumbuck	$-k + 11$	F2 (passes F1 at $k = 10$, etc.; $P(t)$ mismatches at all)
9 Nithing	$(k-1)m - 2k + 11$	F2 (passes F1 at $k = 0$, $m = 10$, etc.; $P(t)$ mismatches at all)
10 Chouse	$k + 9$	F1* (no $(k,m,j) \in \mathbb{Z}_{\geq 0}$ gives $\lvert\det\rvert = 1$)
11 Fardel	$-(3k-2)m + 2k + 7$	F2 (passes F1 at $k = 1$, $m = 8$, etc.; $P(t)$ mismatches at all)
12 Tantivy	$2k + 11$	F1* (no $(k,m,j) \in \mathbb{Z}_{\geq 0}$ gives $\lvert\det\rvert = 1$)
13 Tantivy	10	F1 ($\lvert\det\rvert \neq 1$)
14 Tantivy	$-(2k-3)m + 2k + 5$	F2 (passes F1 at $k = 2$, $m = 8$, etc.; $P(t)$ mismatches at all)
15 Xiphias	$k + 10$	F1* (no $(k,m,j) \in \mathbb{Z}_{\geq 0}$ gives $\lvert\det\rvert = 1$)
16 Kieve	$(j+1)k + (j+k-2)m + 3j - 6$	F2 (passes F1 at $k = 1$, $m = 0$, $j = 1$, etc.; $P(t)$ mismatches at all)
17 Oorie	$km + 9$	F1* (no $(k,m,j) \in \mathbb{Z}_{\geq 0}$ gives $\lvert\det\rvert = 1$)
$1'$	65	F1 ($\lvert\det\rvert \neq 1$)
$1.1'$	109	F1 ($\lvert\det\rvert \neq 1$)
$1.2'$	$2(4k+9)m + 18k + 65$	F1* (no $(k,m) \in \mathbb{Z}_{\geq 0}$ gives $\lvert\det\rvert = 1$; minimum value 65 at $k = m = 0$)
$2'$	$82k + 27$	F1* (no $(k,m,j) \in \mathbb{Z}_{\geq 0}$ gives $\lvert\det\rvert = 1$)
$3'$	$-10k + 47$	F1* (no $(k,m,j) \in \mathbb{Z}_{\geq 0}$ gives $\lvert\det\rvert = 1$)
$4'$	$26k + 83$	F1* (no $(k,m,j) \in \mathbb{Z}_{\geq 0}$ gives $\lvert\det\rvert = 1$)
$5'$	$2(4k+9)m + 10k + 47$	F1* (no $(k,m,j) \in \mathbb{Z}_{\geq 0}$ gives $\lvert\det\rvert = 1$)
$6'$	$4k + 12$	F1* (no $(k,m,j) \in \mathbb{Z}_{\geq 0}$ gives $\lvert\det\rvert = 1$)
$7'$	$(k+3)m + 3k + 9$	F1* (no $(k,m,j) \in \mathbb{Z}_{\geq 0}$ gives $\lvert\det\rvert = 1$)
$8'$	$6k + 15$	F1* (no $(k,m,j) \in \mathbb{Z}_{\geq 0}$ gives $\lvert\det\rvert = 1$)
$9'$	$2(10k+3)m - 46k + 15$	F1* (no $(k,m,j) \in \mathbb{Z}_{\geq 0}$ gives $\lvert\det\rvert = 1$)
$10'$	$6k + 23$	F1* (no $(k,m,j) \in \mathbb{Z}_{\geq 0}$ gives $\lvert\det\rvert = 1$)

Family	$\det(I - A_{\mathrm{red}})$	Verdict
$11'$	$-4(5k+9)m + 14k + 59$	F2 (passes F1 at $k = 4$, $m = 1$, etc.; $P(t)$ mismatches at all)
$12'$	$4k + 12$	F1* (no $(k, m, j) \in \mathbb{Z}_{\geq 0}$ gives $\lvert\det\rvert = 1$)
$13'$	21	F1 ($\lvert\det\rvert \neq 1$)
$14'$	$-9k - 9m + 45$	F1* (no $(k, m, j) \in \mathbb{Z}_{\geq 0}$ gives $\lvert\det\rvert = 1$)
$15'$	$4k + 21$	F1* (no $(k, m, j) \in \mathbb{Z}_{\geq 0}$ gives $\lvert\det\rvert = 1$)
$16'$	$(j-1)k + (j+k-2)m - j + 1$	F2 (passes F1 at $k = 0$, $m = 0$, $j = 0$, etc.; $P(t)$ mismatches at all)
$17'$	$5(2k-1)m + 7k + 19$	F2 (passes F1 at $k = 0$, $m = 4$, etc.; $P(t)$ mismatches at all)

All 38 families are excluded.

P.2 Stratum $(2; 1^6; 3^2)$: The Two-Triangle Tracks

We list the candidate braid families for each of the five surviving two-triangle tracks (Tracks 0, 1, 8, 13, and 17). Track 12 contributes no families; see Appendix G for the case analysis showing this.

P.2.1 Track 0 (13 families)

Table P.2: Verdict table for Track 0.

Family	$\det(I - A_{\mathrm{red}})$	Verdict
1 Loblolly	-4	F1 ($\lvert\det\rvert \neq 1$)
2 Sloom	11	F1 ($\lvert\det\rvert \neq 1$)
3 Mooncalf	15	F1 ($\lvert\det\rvert \neq 1$)
4 Faffel	9	F1 ($\lvert\det\rvert \neq 1$)
5 Balance	9	F1 ($\lvert\det\rvert \neq 1$)
6 Fiasco	9	F1 ($\lvert\det\rvert \neq 1$)
7 Briefing	$-(j+3)k + (j-k)m + j - 1$	F2 (passes F1 at $k = 0$, $m = 0$, $j = 0$, etc.; $P(t)$ mismatches at all)
8 Briefing	$km - 1$	F2 (passes F1 at $k = 0$, $m = 0$, etc.; $P(t)$ mismatches at all)
9 Quail	-4	F1 ($\lvert\det\rvert \neq 1$)

Family	$\det(I - A_{\mathrm{red}})$	Verdict
10 Quail	$jk - (j + k + 2)m - 1$	F2 (passes F1 at $k = 0$, $m = 0$, $j = 0$, etc.; $P(t)$ mismatches at all)
11 Jubilant	-1	F2 ($\det = -1$; $P(t) \neq (t^2 - t + 1)^2$)
12 Jubilant	$-(k + 3)m + k + 2$	F2 (passes F1 at $k = 0$, $m = 1$, etc.; $P(t)$ mismatches at all)
13 Treasure	$-(k + 3)m + 2k + 2$	F2 (passes F1 at $k = 0$, $m = 1$, etc.; $P(t)$ mismatches at all)

P.2.2 Track 1 (17 families)

Table P.3: Verdict table for Track 1.

Family	$\det(I - A_{\mathrm{red}})$	Verdict
1 Flute	9	F1 ($\lvert\det\rvert \neq 1$)
2 Dolphin	15	F1 ($\lvert\det\rvert \neq 1$)
3 Magpie	$-k + 9$	F2 (passes F1 at $k = 8$, etc.; $P(t)$ mismatches at all)
4 Bezoar	-13	F1 ($\lvert\det\rvert \neq 1$)
5 Abscond	12	F1 ($\lvert\det\rvert \neq 1$)
6 Absocond	9	F1 ($\lvert\det\rvert \neq 1$)
7 Fervent	9	F1 ($\lvert\det\rvert \neq 1$)
8 Panorama	9	F1 ($\lvert\det\rvert \neq 1$)
9 Pristine	9	F1 ($\lvert\det\rvert \neq 1$)
10 Gingham	9	F1 ($\lvert\det\rvert \neq 1$)
11 Dossier	9	F1 ($\lvert\det\rvert \neq 1$)
12 Querulous	15	F1 ($\lvert\det\rvert \neq 1$)
13 Querulous	15	F1 ($\lvert\det\rvert \neq 1$)
14 Sybaritic	-13	F1 ($\lvert\det\rvert \neq 1$)
15 Leverage	15	F1 ($\lvert\det\rvert \neq 1$)
16 Guddle	3	F1 ($\lvert\det\rvert \neq 1$)
17 Popjoy	$-k - 4m$	F2 (passes F1 at $k = 1$, $m = 0$, etc.; $P(t)$ mismatches at all)

P.2.3 Track 8 (9 families)

Table P.4: Verdict table for Track 8.

Family	$\det(I - A_{\mathrm{red}})$	Verdict
1 Anomy	9	F1 ($\lvert\det\rvert \neq 1$)
2 Diatree	9	F1 ($\lvert\det\rvert \neq 1$)
3 Fulmine	15	F1 ($\lvert\det\rvert \neq 1$)
4 Chine	3	F1 ($\lvert\det\rvert \neq 1$)
5 Quaint	3	F1 ($\lvert\det\rvert \neq 1$)
6 Lacuna	3	F1 ($\lvert\det\rvert \neq 1$)
7 Aulic	$-2k + 11$	F2 (passes F1 at $k = 5$, etc.; $P(t)$ mismatches at all)
8 Oread	15	F1 ($\lvert\det\rvert \neq 1$)
9 FAT	$k - 1$	F2 (passes F1 at $k = 0$, etc.; $P(t)$ mismatches at all)

P.2.4 Track 13 (4 families)

Table P.5: Verdict table for Track 13.

Family	$\det(I - A_{\mathrm{red}})$	Verdict
1 Chirk	9	F1 ($\lvert\det\rvert \neq 1$)
2 Cagmag	15	F1 ($\lvert\det\rvert \neq 1$)
3 Boofus	9	F1 ($\lvert\det\rvert \neq 1$)
4 SCC	-2	F1 ($\lvert\det\rvert \neq 1$)

P.2.5 Track 17 (6 families)

Table P.6: Verdict table for Track 17.

Family	$\det(I - A_{\mathrm{red}})$	Verdict
1 Cudden	3	F1 ($\lvert\det\rvert \neq 1$)
2 Flisky	3	F1 ($\lvert\det\rvert \neq 1$)
3 Wanion	3	F1 ($\lvert\det\rvert \neq 1$)
4 Roop	4	F1 ($\lvert\det\rvert \neq 1$)
5 Boke	-1	F2 ($\det = -1$; $P(t) \neq (t^2 - t + 1)^2$)
6 Boke	$-3k + 3$	F1* (no $(k, m, j) \in \mathbb{Z}_{\geq 0}$ gives $\lvert\det\rvert = 1$)

P.3 Summary

Across all 87 candidate families:

- 44 families are eliminated by Filter 1 with $\det(I - A_{\text{red}})$ a constant other than ± 1 (verdict F1).
- 22 families are eliminated by Filter 1 parametrically: the determinant is a polynomial in the family parameters that admits no non-negative integer assignment giving $|\det| = 1$ (verdict F1*).
- 21 families admit non-negative integer parameter values at which $|\det(I - A_{\text{red}})| = 1$, but at every such value the characteristic polynomial $P(t)$ fails to match the granny target $(t^2 - t + 1)^2$ (verdict F2). Of these, 2 are constant cases ($\det = -1$ for the Jubilant family on Track 0 and the Boke family on Track 17, both yielding $P(t) = t^4 - 3t^2 + 1$), and 19 are parametric.

The new families 1.1 Jehu and 1.2 Jehu were identified as part of the Jehu subcase of the Candelabra case analysis (Appendix C), and their rotational counterparts 1.1$'$ and 1.2$'$ follow by Remark C.1. Of these, 1.1 and 1.1$'$ are excluded by Filter 1 (constant determinant), and 1.2 and 1.2$'$ are excluded by Filter 1* (parametric determinant with no integer solution).

In every case, the elimination is unconditional: at no non-negative integer parameter value does any of the 87 candidate braids satisfy both filters simultaneously. This completes the homological elimination of the hyperbolic case in the proof of Theorem 1.1.

APPENDIX SEVENTEEN

Residual Hyperbolic Candidates for the Cable Detection

This appendix records the homological filtering verdicts for all 87 candidate braid families against the cable target Alexander polynomial $\Phi_{12}(t) = t^4 - t^2 + 1$. The data here support Proposition 10.6 and clarify the residual gap in Theorem 10.2.

The structure of the analysis is identical to that of Appendix P: for each family we have a determinant $\det(I - A_{\mathrm{red}})$ and a characteristic polynomial $P(t) = \det(tI - A_{\mathrm{red}})$, both of which depend only on the family (not on the target polynomial). Only the comparison to the target changes: instead of $(t^2 - t + 1)^2$, we test against $t^4 - t^2 + 1$.

Q.1 Surviving Families

In contrast to the granny case (Appendix P), six families survive both filters at non-negative integer parameter values for the cable target; two of these six (Track 0 / 7 Briefing and Track 0 / 10 Quail) survive at infinitely many parameter values, while the remaining four survive only at finitely many. We list these explicitly.

Table Q.1: Candidate families surviving both homological filters at non-negative integer parameter values for the cable target $t^4 - t^2 + 1$.

Track	Family	$\det(I - A_{\mathrm{red}})$	Surviving non-negative parameters	$P(t)$ at those values
Candelabra	16 Kieve	$(j{+}1)k + (j{+}k{-}2)m + 3j - 6$	$(j,k,m) = (0,3,4)$ $(j,k,m) = (0,7,0)$ $(j,k,m) = (1,2,0)$	$t^4 - t^2 + 1$ $t^4 - t^2 + 1$ $t^4 - t^2 + 1$
Track 0	7 Briefing	$-(j{+}3)k + (j{-}k)m + j - 1$	infinitely many integer triples	$t^4 - t^2 + 1$
Track 0	8 Briefing	$km - 1$	$(k,m) = (1,2)$ $(k,m) = (2,1)$	$t^4 - t^2 + 1$ $t^4 - t^2 + 1$
Track 0	10 Quail	$jk - (j{+}k{+}2)m - 1$	infinitely many integer triples	$t^4 - t^2 + 1$
Track 0	13 Treasure	$-(k{+}3)m + 2k + 2$	$(k,m) = (2,1)$	$t^4 - t^2 + 1$
Track 8	9 FAT	$k - 1$	$k = 2$	$t^4 - t^2 + 1$

For family Track 0 / 7 Briefing, the equation

$$-(j+3)k + (j-k)m + j - 1 = 1$$

admits infinitely many non-negative integer solutions; representative values include $(j,k,m) = (1,0,1), (2,0,0), (2,1,5), (3,2,11), \ldots$ — at each, $P(t) = t^4 - t^2 + 1$.

For family Track 0 / 10 Quail, the equation

$$jk - (j+k+2)m - 1 = 1$$

likewise admits infinitely many non-negative integer solutions; representative values include $(j,k,m) = (1,2,0), (2,1,0), (2,6,1), (3,12,2), \ldots$ — at each, $P(t) = t^4 - t^2 + 1$.

Q.2 Excluded Families

The remaining 81 families (that is, $87 - 6$, the six residual families comprising four with finitely many surviving parameter values and two with infinitely many) are excluded by the same Filter 1 / Filter 1* / Filter 2 verdict as in the granny case. The detailed table is identical in structure to Appendix P, with the verdict re-evaluated against the cable target. The excluded families' polynomial mismatches with $t^4 - t^2 + 1$ may be verified directly from the characteristic polynomials recorded there. In particular, the new families 1.1 Jehu, 1.2 Jehu, 1.1′, and 1.2′ are excluded by Filter 1 against any target (the determinant is constant or admits no non-negative integer assignment giving $|\det| = 1$), so they do not contribute to the residual list.

Q.3 Discussion

The residual list above represents the precise gap in Theorem 10.2: any hypothetical hyperbolic knot K with $\widehat{HFK}(K) \cong \widehat{HFK}(C_{2,1}(T_{2,3}))$ must, by the analysis of Chapter 10, have its associated 6-braid lying in one of these six families at one of the surviving parameter values. For a complete cable detection theorem, each of these (family, parameter) pairs must be ruled out by an additional argument.

The candidate strategies for closing this gap are discussed in Section 10.4.

Bibliography

[AFT25] Tarik Aougab, David Futer, and Samuel J. Taylor. *On fixed points of pseudo-Anosov maps*. 2025. arXiv: 2509.07818 [math.GT].

[BHS25] John A. Baldwin, Ying Hu, and Steven Sivek. "Khovanov homology and the cinquefoil". In: *Journal of the European Mathematical Society* 27.6 (2025), pp. 2443–2465. DOI: 10.4171/JEMS/1415. arXiv: 2105.12102 [math.GT].

[BS24] John A. Baldwin and Steven Sivek. "Characterizing slopes for 5_2". In: *J. London Math. Soc.* 109.6 (2024), paper no. e12951, 64 pp. DOI: 10.1112/jlms.12951. arXiv: 2209.09805 [math.GT].

[BS25] John A. Baldwin and Steven Sivek. *L-spaces and knot traces*. 2025. arXiv: 2501.00914 [math.GT]. URL: https://arxiv.org/abs/2501.00914.

[BS26] John A. Baldwin and Steven Sivek. "[forthcoming title]". In preparation. 2026.

[Bal+21] John A. Baldwin et al. "Khovanov homology detects the figure-eight knot". In: *Bull. Lond. Math. Soc.* 53.3 (2021), pp. 871–876. DOI: 10.1112/blms.12467. arXiv: 2007.01269 [math.GT].

[BH95] Mladen Bestvina and Michael Handel. "Train tracks for surface homeomorphisms". In: *Topology* 34.1 (1995), pp. 109–140.

[Bin23] Fraser Binns. "The CFK^∞ type of almost L-space knots". In: (2023). arXiv preprint, v2 January 2025. arXiv: 2303.07249 [math.GT].

[BLM83] Joan S. Birman, Alex Lubotzky, and John McCarthy. "Abelian and solvable subgroups of the mapping class groups". In: *Duke Mathematical Journal* 50.4 (Dec. 1983), pp. 1107–1120. DOI: 10.1215/S0012-7094-83-05046-9.

[BZ03] Gerhard Burde and Heiner Zieschang. *Knots*. 2nd. Vol. 5. De Gruyter Studies in Mathematics. Walter de Gruyter & Co., Berlin, 2003, pp. xii+559. ISBN: 3-11-017005-1. DOI: 10.1515/9783110198034.

[Dow24] Nathan Dowlin. "A spectral sequence from Khovanov homology to knot Floer homology". In: *J. Amer. Math. Soc.* (2024). DOI: 10.1090/jams/1039. arXiv: 1811.07848 [math.GT].

[FM11] Benson Farb and Dan Margalit. *A primer on mapping class groups*. Princeton University Press, 2011.

[FM12] Benson Farb and Dan Margalit. *A Primer on Mapping Class Groups*. Vol. 49. Princeton Mathematical Series. Princeton, NJ: Princeton University Press, 2012, pp. xiv+472. ISBN: 978-0-691-14794-9.

[FRW24] M. Farber, Braeden Reinoso, and W. Wang. "Fixed-point-free pseudo-Anosovs and genus-two L-space knots". In: *arXiv preprint* (2024).

[Ghi08] Paolo Ghiggini. "Knot Floer homology detects genus-one fibred knots". In: *American Journal of Mathematics* 130.5 (2008), pp. 1151–1169.

[GS22] Paolo Ghiggini and M. Spano. "Heegaard Floer homology and fixed points of monodromy". In: *arXiv preprint* (2022).

[HS07] Ji-Young Ham and Won Taek Song. "The minimum dilatation of pseudo-Anosov 5-braids". In: *Experimental Mathematics* 16.2 (2007), pp. 167–179.

[Hed09] Matthew Hedden. "On knot Floer homology and cabling. II". In: *International Mathematics Research Notices* 2009.12 (2009), pp. 2248–2274. DOI: 10.1093/imrn/rnp015.

[Hed10] Matthew Hedden. "Notions of positivity and the Ozsváth–Szabó concordance invariant". In: *Journal of Knot Theory and Its Ramifications* 19.5 (2010), pp. 617–629. DOI: 10.1142/S0218216510008017.

[HM18] Matthew Hedden and Thomas Mark. "Floer homology and fractional Dehn twists". In: *Advances in Mathematics* 324 (2018), pp. 1–39.

[HW18] Matthew Hedden and Liam Watson. "On the geography and botany of knot Floer homology". In: *Selecta Math. (N.S.)* 24.2 (2018), pp. 997–1037. DOI: 10.1007/s00029-017-0351-5. arXiv: 1404.6913 [math.GT].

[HMS08] Mikami Hirasawa, Kunio Murasugi, and Daniel S. Silver. "When does a satellite knot fiber?" In: *Hiroshima Math. J.* 38.3 (2008), pp. 411–423.

[Hom14] Jennifer Hom. "Bordered Heegaard Floer homology and the tau-invariant of cable knots". In: *Journal of Topology* 7.2 (2014), pp. 287–326. DOI: 10.1112/jtopol/jtt030. arXiv: 1202.1463 [math.GT].

[HKM07] Ko Honda, William H. Kazez, and Gordana Matić. "Right-veering diffeomorphisms of compact surfaces with boundary". In: *Inventiones mathematicae* 169.2 (2007), pp. 427–449.

[Juh08] András Juhász. "Floer homology and surface decompositions". In: *Geometry & Topology* 12.1 (2008), pp. 299–350.

[LT11] Erwan Lanneau and Jean-Luc Thiffeault. "On the minimum dilatation of pseudo-Anosov homeomorphisms on surfaces of small genus". In: *Annales de l'Institut Fourier* 61.1 (2011), pp. 105–144.

[Los08] Jérôme Los. "Infinite sequence of fixed point free pseudo-Anosov homeomorphisms". In: *arXiv* (2008). DOI: 10.48550/arxiv.0806.4027.

[Los93] Jérôme E. Los. “Pseudo-Anosov maps and invariant train tracks in the disc: a finite algorithm”. In: *Proceedings of the London Mathematical Society* 3.2 (1993), pp. 400–430.

[Ni07] Yi Ni. “Knot Floer homology detects fibred knots”. In: *Inventiones mathematicae* 170.3 (2007), pp. 577–608.

[Ni22] Yi Ni. “A Note on Knot Floer Homology and Fixed Points of Monodromy”. In: *Peking Mathematical Journal* (2022). DOI: 10.1007/s42543-022-00051-3. URL: https://link.springer.com/article/10.1007/s42543-022-00051-3.

[OS03] Peter Ozsváth and Zoltán Szabó. “Heegaard Floer homology and alternating knots”. In: *Geometry & Topology* 7 (2003), pp. 225–254.

[OS04a] Peter Ozsváth and Zoltán Szabó. “Holomorphic disks and genus bounds”. In: *Geom. Topol.* 8 (2004), pp. 311–334. DOI: 10.2140/gt.2004.8.311. eprint: math/0306124.

[OS04b] Peter Ozsváth and Zoltán Szabó. “Holomorphic disks and knot invariants”. In: *Advances in Mathematics* 186.1 (2004), pp. 58–116.

[OS04c] Peter Ozsváth and Zoltán Szabó. “Holomorphic disks and topological invariants for closed three-manifolds”. In: *Annals of Mathematics* 159.3 (2004), pp. 1027–1158.

[PH92] Robert C. Penner and John L. Harer. *Combinatorics of train tracks*. Vol. 125. Princeton University Press, 1992.

[Ras03] Jacob Rasmussen. “Floer homology and knot complements”. PhD thesis. Harvard University, 2003.

[Rei23] Braeden Reinoso. “Fixed-point-free pseudo-Anosovs, and genus-two L-space knots in the Poincaré sphere”. In: *arXiv preprint arXiv:2304.13670* (2023).

[Rei24] Braeden Reinoso. “Pseudo-Anosov maps and genus-two L-space knots”. PhD thesis. Boston College, 2024.

[Sch53] Horst Schubert. “Knoten und Vollringe”. In: *Acta Mathematica* 90 (1953), pp. 131–286. DOI: 10.1007/BF02392437.

[SKL02] Won Taek Song, Ki Hyoung Ko, and Jérôme E. Los. “Entropies of braids”. In: *Journal of Knot Theory and Its Ramifications* 11.04 (2002), pp. 647–666.

[Thu82] William P. Thurston. “Three-dimensional manifolds, Kleinian groups and hyperbolic geometry”. In: *Bull. Amer. Math. Soc. (N.S.)* 6.3 (1982), pp. 357–381. DOI: 10.1090/S0273-0979-1982-15003-0.

[Thu88] William P. Thurston. “On the geometry and dynamics of diffeomorphisms of surfaces”. In: *Bulletin of the American Mathematical Society (New Series)* 19.2 (1988), pp. 417–431.

[Thu98] William P. Thurston. “Hyperbolic structures on 3-manifolds, II: Surface groups and 3-manifolds which fiber over the circle”. In: *arXiv preprint math/9801045* (1998).

[Wan22] Joshua Wang. “The cosmetic crossing conjecture for split links”. In: *Geom. Topol.* 26.7 (2022), pp. 2941–3053. DOI: 10.2140/gt.2022.26.2941. arXiv: 2006.01070 [math.GT].